MRI of Bone and Soft Tissue Tumors and Tumorlike Lesions

Differential Diagnosis and Atlas

Steven P. Meyers

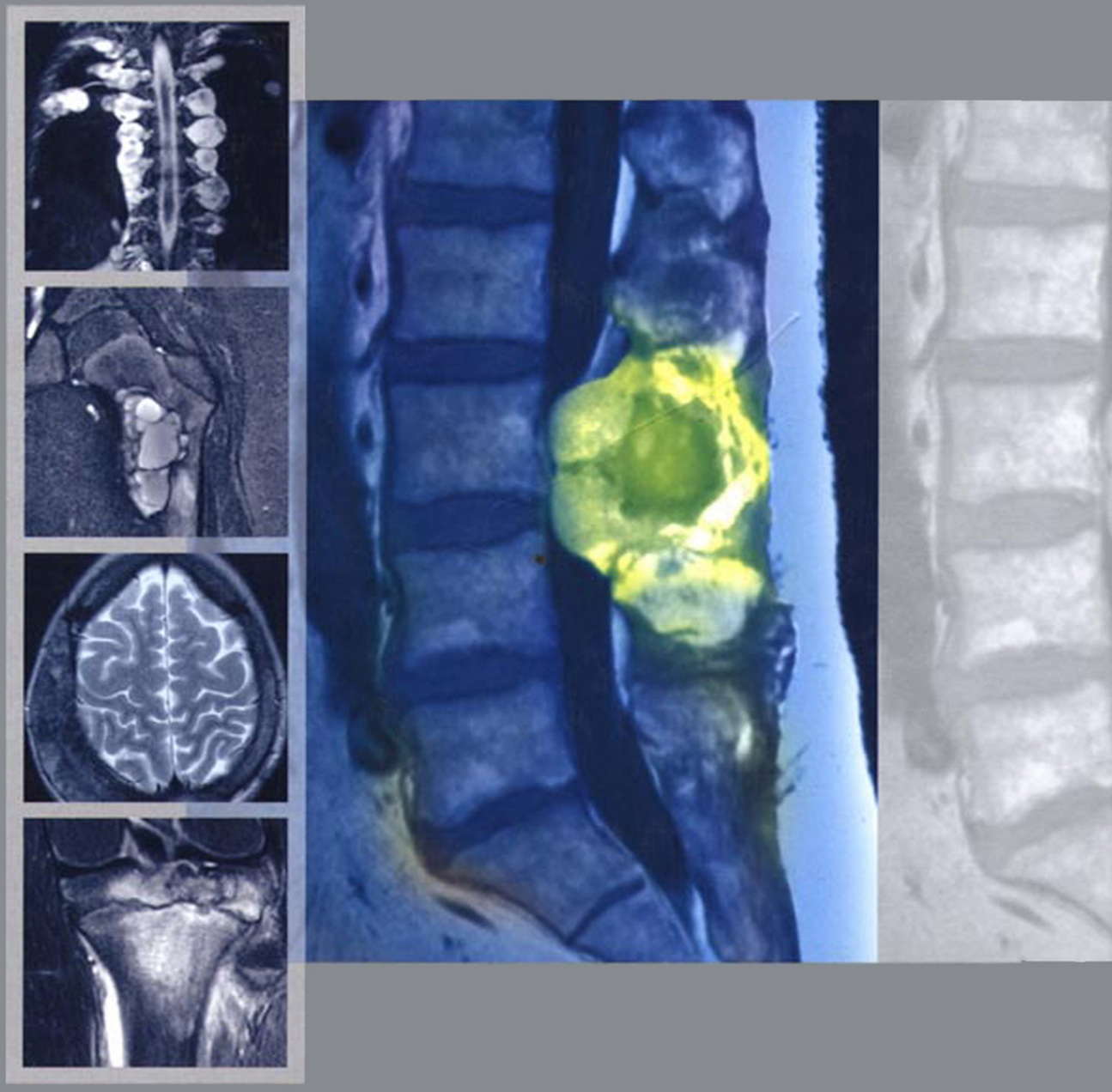

Thieme

Thieme

MRI of Bone and Soft Tissue Tumors and Tumorlike Lesions

Differential Diagnosis and Atlas

Steven P. Meyers, MD, PhD

Professor of Radiology,
Imaging Sciences, and Neurosurgery
University of Rochester
School of Medicine and Dentistry
Rochester, NY
USA

2976 illustrations

Thieme
Stuttgart • New York

Library of Congress Cataloging-in-Publication Data is available from the publisher.

Important note: Medicine is an ever-changing science undergoing continual development. Research and clinical experience are continually expanding our knowledge, in particular our knowledge of proper treatment and drug therapy. Insofar as this book mentions any dosage or application, readers may rest assured that the authors, editors, and publishers have made every effort to ensure that such references are in accordance with **the state of knowledge at the time of production of the book.**

Nevertheless, this does not involve, imply, or express any guarantee or responsibility on the part of the publishers in respect to any dosage instructions and forms of applications stated in the book. **Every user is requested to examine carefully** the manufacturers' leaflets accompanying each drug and to check, if necessary in consultation with a physician or specialist, whether the dosage schedules mentioned therein or the contraindications stated by the manufacturers differ from the statements made in the present book. Such examination is particularly important with drugs that are either rarely used or have been newly released on the market. Every dosage schedule or every form of application used is entirely at the user's own risk and responsibility. The authors and publishers request every user to report to the publishers any discrepancies or inaccuracies noticed. If errors in this work are found after publication, errata will be posted at www.thieme.com on the product description page.

© 2008 Georg Thieme Verlag,
Rüdigerstraße 14, 70469 Stuttgart, Germany
http://www.thieme.de
Thieme New York, 333 Seventh Avenue,
New York, NY 10001, USA
http://www.thieme.com

Typesetting by primustype Hurler GmbH, Notzingen
Printed in Germany by Grammlich, Pliezhausen

ISBN 978-3-13-135421-1 (TPS, Rest of World)
ISBN 978-1-58890-251-1 (TPN, The Americas)

1 2 3 4 5 6

Some of the product names, patents, and registered designs referred to in this book are in fact registered trademarks or proprietary names even though specific reference to this fact is not always made in the text. Therefore, the appearance of a name without designation as proprietary is not to be construed as a representation by the publisher that it is in the public domain.

This book, including all parts thereof, is legally protected by copyright. Any use, exploitation, or commercialization outside the narrow limits set by copyright legislation, without the publisher's consent, is illegal and liable to prosecution. This applies in particular to photostat reproduction, copying, mimeographing, preparation of microfilms, and electronic data processing and storage.

To my parents, Morton and Wilma Meyers,
and my uncle, Aaron Fox,
for their unwavering encouragement
along my long journey
through formal education.

And to my wife, Barbara, and son, Noah,
for their continuous love,
support, and patience during this project.

Foreword

MRI has become a widely accepted imaging modality in musculoskeletal radiology. Regarding bone tumors, MRI complements conventional radiography and CT in assessing tissue composition and is unsurpassed in the evaluation of the local tumor extension. For soft tissue lesions, MRI is the imaging modality of choice because of its high soft tissue contrast resolution.

Musculoskeletal tumor evaluation is dependent upon clinical and laboratory data and relevant imaging. Radiologists, clinicians, and pathologists with an interest in bone and soft tissue tumors must work in unison to achieve the best possible outcome for a patient affected with such a disease. This new text facilitates the understanding and interpretation of data provided by the various medical specialists.

I have known Dr. Meyers since he became a staff member of our department 15 years ago. Dr. Meyers is a radiologist with additional fellowship training in MRI and neuroradiology, and has always had a keen interest in musculoskeletal tumors with emphasis on MRI. Over the years he accumulated an outstanding collection of exquisite tumor cases ranging from a complete presentation spectrum of common lesions to the manifestation of the most unusual neoplasm. This collection forms the foundation of this new text.

A few years ago, when I was obliged to seek a new co-author for *Differential Diagnosis in MRI* at short notice, I was extremely fortunate that Dr. Meyers was kind enough to assume the task of writing the "Brain" and "Spine" sections of that text. Dr. Meyers performed this task admirably and at the same time developed a taste for further textbook writing that resulted in the conception and execution of *MRI of Bone and Soft Tissue Tumors and Tumorlike Lesions.*

The book is divided into three main sections. The first section includes an introductory chapter that presents a detailed overview of MRI of musculoskeletal tumors and tumorlike lesions. Multiple tables regarding the WHO classification of bone and soft tissue tumors, their relative frequencies and pertinent immunohistochemical and genetic data round up part one of the book.

The second section of the book contains 20 tables of differential diagnosis of lesions based on anatomic locations and/or specific MRI features. Pertinent radiographic and CT findings and key clinical data are summarized beside the MRI findings.

In the third section of the book, 77 bone and soft tissue lesions are listed in alphabetical order and analyzed in great detail with regard to clinical, pathologic, and imaging findings. A large number of superb state-of-the-art images complement the text throughout the entire book. The photographic quality of the illustrations in the book is outstanding.

Dr. Meyers is to be congratulated for his original approach to this text, the excellent and complete coverage of musculoskeletal tumors and tumorlike lesions, and his succinct presentation of the material. I believe the book will be an invaluable resource for residents, fellows, radiologists, pathologists, orthopedists, and clinicians with an interest in this topic. There is no doubt in my mind that this new text will receive extraordinary acceptance in the medical community.

Francis A. Burgener, MD
Professor of Radiology
University of Rochester Medical Center
Rochester, New York, NY, USA

Preface

Over many decades, conventional radiography has been an important and often critical imaging modality in the evaluation of bone tumors. The radiographic features of various osseous tumors and tumorlike lesions have been well described. Magnetic resonance imaging (MRI), being a relative newcomer to clinical radiology for slightly more than 20 years, has become a widely available imaging modality internationally. It is estimated that there are 20 000 MRI scanners worldwide performing approximately 60 million MRI examinations per year. With its high soft tissue contrast resolution, MRI has been shown to be a very powerful method in the detection of marrow pathology as well as in the evaluation of lesions within soft tissues.

In the daily routine of clinical practice and teaching of physicians-in-training in the medical disciplines of radiology, orthopedics, and neurosurgery, it has become apparent that a need exists for a modern reference book that covers both MRI and radiographic features of neoplasms and tumorlike lesions of bone and adjacent soft tissues as well as providing associated relevant clinical and pathologic data citing recent literature.

The goal of this book is to present the MRI features of bone and soft tissue tumors and tumor mimics in a single easy-to-use resource with extensive utilization of figures for illustration. For consistency purposes, the nomenclature and categorization of the various musculoskeletal tumors and tumorlike lesions in this book are based on the 2002 WHO classification. This book includes soft tissue tumors as well as osseous lesions involving both the appendicular and axial skeleton. For bone tumors and tumorlike lesions, efforts were also made to correlate the conventional radiographic features with the rapidly proliferating data from the published literature using MRI.

The book's unique organization helps the reader obtain desired information efficiently and quickly. It is divided into three main sections. The first portion includes a detailed introductory chapter which presents an overview of MRI in the evaluation of musculoskeletal tumors and tumor mimics. In addition, it contains multiple tables regarding the WHO classification of bone and soft tissue tumors, relative frequencies of malignant and non-malignant lesions, and pertinent immunohistochemical and genetic data.

The second portion of the book contains 20 lists of differential diagnosis of lesions based on anatomic locations and/or specific MRI features in a tabular format. Each of the lesions or musculoskeletal disorders listed in the tables has a column summarizing the MRI features and pertinent radiographic and/or CT findings with associated MR images for illustration, and a comments column summarizing key clinical data. The comments section contains references to the specific Atlas chapters in the subsequent third portion of the book for additional detailed information, or to the literature at the end of each table.

The third portion of the book contains 77 Atlas chapters organized into a routine format that enables the efficient acquisition of specific information regarding each lesion. For the majority of the Atlas chapters, multiple MR images, often with corresponding plain film and/or CT images, are provided to demonstrate the range of imaging findings and locations associated with the lesions. The arrangement of the Atlas chapters in alphabetical order also facilitates easy and quick reference. When using this book, familiarity of the MRI findings for various lesions will allow for a formulation of a reasonable differential diagnosis to guide the clinician.

Acknowledgements

I wish to acknowledge the Thieme staff, in particular Dr. Clifford Bergman, Ms. Rachel Swift, Ms. Stefanie Langner, and Ms. Elisabeth Kurz for their dedication, hard work, and attention to detail. I would also like to thank Ms. Colleen Cottrell for her outstanding secretarial work with this project.

In addition, I wish to acknowledge the following for their contribution of interesting cases: Arun Basu, MD, A. Oscar Beitia, MD, Allan Bernstein, MD, Timothy Bratz, MD, Francis A. Burgerner, MD, Christopher Cerniglia, DO, Gary M. Hollenberg, MD, James J. Lester, MD, Johnny U.V. Monu, MD, David Shrier, MD, Raymond K. Tan, MD, Eric P. Weinberg, MD, Vanessa Zayas, MD, and Andrea Zynda, MD.

I extend my special thanks and appreciation to all of my coworkers and physician colleagues (Drs. Bernstein, Hollenberg, Shrier, Weinberg, Zayas, and Zynda) at University Medical Imaging, the Outpatient Diagnostic Imaging Facility of the University of Rochester Medical Center. I could not ask for a greater group of dedicated people to work with in the clinical practice of Diagnostic Radiology.

Lastly, I would like to give thanks to my former teachers and mentors (Drs. Curtis J. Nelson, Larry E. Schrader, Stephen N. Wiener, and Emanuel Kanal) for their guidance and wisdom; and to the University of Vermont College of Medicine for the opportunity of entering into the great and noble field of Medicine.

Table of Contents

Introduction. 1

Differential Diagnosis Tables

1 Tumors and tumorlike lesions involving the skull and facial bones 18
2 Tumors and tumorlike lesions involving the spine 38
3 Paraspinal tumors and tumorlike lesions 64
4 Lesions involving the outer surface of bone 76
5 Lesions associated with thickening of bone cortex 104
6 Intramedullary lesions associated with expansion of intact cortical margins 117
7 Intramedullary lesions associated with cortical destruction and extraosseous extension 128
8 Solitary intramedullary lesions with well-circumscribed margins 140
9 Solitary intramedullary lesions with poorly defined margins of abnormal marrow signal 150
10 Solitary intramedullary lesions located near the ends of tubular bones 163
11 Solitary intramedullary metadiaphyseal lesions 176
12 Solitary intramedullary diaphyseal lesions 189
13 Osseous tumors and tumorlike lesions at the hands and feet 199
14 Diffuse, multiple, poorly defined and/or multifocal zones of abnormal marrow signal 211
15 Lesions that contain cartilage 236
16 Tumors and tumorlike lesions within joints 247
17 Solitary tumors and tumorlike lesions of the soft tissues located mostly deep to the subcutaneous fat 258
18 Tumors and tumorlike lesions of the superficial soft tissues including subcutaneous fat 280
19 Lesions involving peripheral nervous tissue 305
20 Lesions that contain fat 312

Atlas

A1 Adamantinoma (Also Referred to as Extragnathic Adamantinoma, Adamantinoma of Long Bones, Juvenile Intracortical Adamantinoma) 325
A2 Aneurysmal Bone Cyst 328
A3 Bone Cyst (Also Referred to as Simple Bone Cyst, Unicameral Bone Cyst, Solitary Bone Cyst) 334
A4 Angiofibroma (Also Referred to as Juvenile Nasopharyngeal Angiofibroma) 340
A5 Angiomatoid Fibrous Histiocytoma (Also Referred to as Angiomatoid Malignant Fibrous Histiocytoma) 342
A6 Angiosarcoma (Also Referred to as Malignant Hemangioendothelioma, High-Grade Hemangioendothelioma, Hemangiosarcoma, Angioendothelioma, Angiofibrosarcoma, and Hemangioendotheliosarcoma) 344
A7 Chondroblastoma 347
A8 Chondroma, Intramedullary Type: Enchondroma (Also Referred to as Intra-osseous Chondroma or Central Chondroma) 352
A9 Chondroma, Periosteal or Juxtacortical Type (Also Referred to as Periosteal or Juxtacortical Chondroma, Surface Chondroma, and Juxtacortical/Parosteal Chondroma) 359
A10 Chondromyxoid Fibroma 364
A11 Chondrosarcoma 368
A12 Chordoma 379
A13 Dermatofibrosarcoma and Dermatofibrosarcoma Protuberans 383
A14 Dermatomyositis 386
A15 Dermoid and Epidermoid 390
A16 Desmoid Tumor (Also Referred to as Fibromatosis, Superficial and Deep Types Involving Soft Tissues; Desmoplastic Fibroma; Desmoid Tumor within Bone). 396
A17 Elastofibroma 404
A18 Eosinophilic Granuloma (Also Referred to as Langerhans Cell Histiocytosis, Formerly Histiocytosis X) 406
A19 Erdheim-Chester Disease (Also Referred to as Chester-Erdheim Disease, Lipoid Granulomatosis, and Lipogranulomatosis) 413
A20 Ewing Sarcoma 416
A21 Nodular Fasciitis (Also Referred to as Pseudosarcomatous Fasciitis, Proliferative Fasciitis, Infiltrative Fasciitis, and Pseudosarcomatous Fibromatosis) 423
A22 Fibrolipomatous Hamartoma (Also Referred to as Nerve Lipoma, Neural Fibrolipoma, Lipofibromatous Hamartoma, Perineural Lipoma, Intraneural Lipoma, Lipofibroma, and Lipomatous Hamartoma) 426
A23 Fibroma of the Tendon Sheath 428
A24 Solitary Fibrous Tumor 430
A25 Fibrosarcoma 433
A26 Fibrous Cortical Defect and Nonossifying Fibroma (Also Referred to as Metaphyseal Fibrous Defect), Cortical Desmoid (Also Referred to as Periosteal Desmoid or Distal Femoral Cortical Irregularity), and Fibroxanthoma (Also Referred to as Benign Fibrous Histiocytoma) 438
A27 Fibrous Dysplasia (Also Referred to as Fibro-osseous Dysplasia, Fibrocartilaginous Dysplasia, and Lichtenstein-Jaffe Disease) 449
A28 Geode (Also Referred to as Subchondral Cyst and Osteoarthritic Cyst); Soft Tissue and Intra-osseous Ganglion (Also Referred to as Intra-osseous Ganglion, Juxta-articular Bone Cyst, and Periosteal Ganglion) 456
A29 Giant Cell Tumor of Bone 462
A30 Giant Cell Tumor of the Tendon Sheath and/or Soft Tissue (Also Referred to as Nodular Tenosynovitis, Fibrous Xanthoma, Tenosynovial Giant Cell Tumor, and Benign Synovioma) 469

A31 Glomus Tumor (Also Referred to as Glomangioma and Angioglomoid Tumor) 476
A32 Gout 479
A 33 Hemangioendothelioma (Also Referred to as Low-grade Hemangioendothelioma, Low-grade Hemangioendothelial Sarcoma, Low-grade Angiosarcoma, and Myxoid Angioblastoma) 484
A34 Hemangiomas (Also Referred to as Vascular Hamartomas) 491
A 35 Hemangiopericytoma 502
A 36 Hematoma, Morel-Lavallee Lesion, and Hemophilic Pseudotumor 507
A 37 Bone and Muscle Infarct (Also Referred to as Avascular Necrosis and Osteonecrosis) 512
A 38 Kaposi Sarcoma (Also Referred to as Angiosarcoma Multiplex, Kaposi Disease, Idiopathic Multiple Pigmented Sarcoma of the Skin, and Granuloma Multiplex Hemorrhagicum) 519
A39 Leiomyoma 521
A 40 Leiomyosarcoma 525
A41 Leukemia 531
A42 Lipoblastoma 540
A 43 Lipoma, Atypical Lipoma, and Hibernoma 543
A 44 Liposarcoma 554
A 45 Liposclerosing Myxofibrous Tumor (Also Referred to as Polymorphic Fibro-osseous Lesion of Bone and Polymorphic Fibrocystic Disease of Bone) 563
A 46 Lymphangioma (Also Referred to as Cystic Hygroma) 566
A47 Lymphoma 570
A48 Malignant Fibrous Histiocytoma (Also Referred to as Malignant Histiocytoma, Xanthosarcoma, Malignant Fibrous Xanthoma, and Fibroxanthosarcoma) 584
A49 Meningioma 594
A 50 Metastatic Lesions 601
A 51 Morton Neuroma 609
A 52 Multiple Myeloma (Also Referred to as Myeloma, Kahler Disease, and Plasma Cell Neoplasm; Plasmacytoma Represents a Solitary Neoplastic Variant) 611
A53 Myositis Ossifrcans (Also Referred to as Heterotopic Ossification, Reactive Mesenchymal Proliferation, Ossifying Hematoma, and Pseudomalignant Osseous Tumor of Soft Tissues) 618
A54 Myxoma 624
A 55 Neuroblastoma, Ganglioneuroblastoma, and Ganglioneuroma 627
A 56 Neurofibroma and Malignant Peripheral Nerve Sheath Tumor 633
A 57 Traumatic Neuroma 642
A 58 Osteochondroma (Also Referred to as Osteo-cartilaginous Exostosis) 645
A 59 Osteofibrous Dysplasia (Also Referred to as Ossifying Fibroma of the Tibia and/or Fibula, Cortical Fibrous Dysplasia) 654
A 60 Osteoid Osteoma 660
A61 Osteoblastoma (Also Referred to as Ossifying Giant Cell Tumor and Giant Osteoid Osteoma) 668
A 62 Osteoma, Enostosis, Osteopoikilosis, and Melorheostosis 674
A 63 Osteomyelitis 679
A 64 Osteosarcoma (Also Referred to as Osteogenic Sarcoma and Osteoblastic Sarcoma) 693
A 65 Paget Disease (Also Referred to as Osteitis Deformans) 713
A66 Paraganglioma (Also Referred to as Chemodectoma for Carotid Body Tumor and Glomus Jugulare Tumor for Jugulotympanic Paragangliomas) 721
A 67 Pigmented Villonodular Synovitis 726
A 68 Pleomorphic Hyalinizing Angiectatic Tumor 730
A 69 Rhabdomyosarcoma (Also Referred to as Myosarcoma, Malignant Rhabdomyoma, Rhabdosarcoma, and Embryonal Sarcoma) 732
A70 Rheumatoid Arthritis 738
A71 Sarcoid 744
A 72 Schwannoma (Also Referred to as Neurilemoma and Neurinoma) 747
A73 Synovial Chondromatosis (Also Referred to as Primary and Secondary Chondromatosis, and Synovial Chondrometaplasia), and Synovial Osteochondromatosis 753
A74 Synovial Cyst 758
A 75 Synovial Sarcoma (Also Referred to as Carcino-sarcoma and Spindle Cell Carcinoma of Soft Tissue) ... 762
A76 Teratoma 769
A 77 Xanthoma 773

Subject Index 775

Abbreviations

ABC	aneurysmal bone cyst
ABME	acute bone marrow edema
AIDS	acquired immune deficiency syndrome
ALL	acute lymphoblastic leukemia
AML	acute myelogenous leukemia
AP	anteroposterior
APUD	amine precursor uptake and decarboxylation
AVN	avascular necrosis
Ca	calcium
CLL	chronic lymphocytic leukemia
CML	chronic myelogenous leukemia
CMPD	chronic myeloproliferative disease
CNS	central nervous system
CPPD	calcium pyrophosphate dihydrate deposition
CSF	cerebrospinal fluid
CT	computed tomography
3DFT	three-dimensional Fourier transform
DFS	dermatofibrosarcoma
DFSP	dermatofibrosarcoma protuberans
DTPA	diethylene triamine pentacetic acid
DWI	diffusion-weighted imaging
EG	eosinophilic granuloma
EMA	epithelial membrane antigen
FCD	fibrous cortical defect
FISH	fluorescent in situ hybridization
FLAIR	fluid attenuated inversion recovery
FS	frequency selective
FS-DFSP	fibrosarcomatous variant of dermato-fibrosarcoma
FSE	fast spin echo
FSPDWI	fat-suppressed proton density-weighted imaging
FSPGR	fast spoiled gradient-recalled echo
FST1WI	fat-suppressed Tl-weighted imaging
GCSF	granulocyte colony-stimulating factor
Gd-contrast	gadolinium chelate contrast
GRE	gradient-refocused echo pulse sequence
HD	Hodgkin disease
HHV	human herpes virus
HPF	high power field
HU	Hounsfield unit
HVA	homovanillic acid
ICA	internal carotid artery
IL	interleukin
JRA	juvenile rheumatoid arthritis
LCH	Langerhans cell histiocytosis
MDP	methylene diphosphonate
MDS	myelodysplastic syndrome
MFH	malignant fibrous histiocytoma
MIBC	meta-iodobenzylguanidine
MIP	maximum intensity projection
MKI	mitosis karyorrhexis index
MPNST	malignant peripheral nerve sheath tumor
MR	magnetic resonance
MRA	magnetic resonance angiography
MRI	magnetic resonance imaging
NF1	neurofibromatosis type 1
NF2	neurofibromatosis type 2
NHL	non-Hodgkin lymphoma
NOF	nonossifying fibroma
PCV	polycythemia vera
PDWI	proton density weighted imaging
PET	positron emission tomography
PHAT	pleomorphic hyalinizing angiectatic tumor
PNET	primitive neuroectodermal tumor
PVNS	pigmented villonodular synovitis
RA	rheumatoid arthritis
RBC	red blood cell
RF	radio frequency
RSD	reflex sympathetic dystrophy
SE	spin echo
SFT	solitary fibrous tumor
SMA	smooth muscle actin
STIR	short tau (Tl) inversion recovery
Tl	spin-lattice or longitudinal relaxation time
T2	spin-spin or transverse relaxation time
T2*	effective spin-spin relaxation time using GRE
T1WI	Tl-weighted imaging
T2WI	T2-weighted imaging
TB	tuberculosis
TE	echo time
TI	inversion time
TOP	time-of-flight
TR	repetition time
UBC	unicameral bone cyst
VMA	vanillylmandelicacid
WHO	World Health Organization

Introduction

Overview of Magnetic Resonance Imaging and its Role in the Evaluation of Musculoskeletal Abnormalities

Magnetic resonance imaging (MRI) is a powerful medical imaging method that has been used extensively in the evaluation of musculoskeletal tumors and other lesions.[1-3,7-12,20,23-25,29,31,32,36,38-45,47,48] MRJ can provide "in vivo" anatomic images of the human body with high, soft tissue contrast resolution. The magnetic resonance (MR) images can be obtained in multiple planes, that is, sagittal, axial, coronal, or various oblique combinations. The "signal" used to generate an MR image comes from hydrogen nuclei (protons) within a human body. In essence, MRI is a hydrogen scan.

The hydrogen nucleus has a net charge of +1 and spins at a frequency that is dependent on the ambient magnetic field and its particular physical characteristic known as the gyromag¬netic ratio. The spinning charge of each hydrogen nucleus gives off a tiny magnetic field perpendicular to the axis of spin, thus acting like a tiny bar magnet. Outside the bore of a magnet, the net magnetic properties (magnetic moment) of a person will be zero because the spinning hydrogen nuclei will be oriented randomly, resulting in an overall cancellation of the sum total of tiny magnetic fields. Once placed into a high field-strength magnet, spinning hydrogen nuclei within the human body become aligned or magnetized along its magnetic field. This net magnetization of hydrogen nuclei is oriented in a low-energy alignment (ground state) that is parallel to the magnetic field of the magnet. The hydrogen nuclei spin (precess) at a frequency proportional to their specific gyromagnetic ratio and the magnetic field, in a relationship known as the Larmor equation. The precessional frequency of hydrogen nuclei at 1.5 tesla (T) is 64 megahertz (MHz).

To generate an MR signal, energy is transferred to the hydrogen nuclei within the magnet by using a radio frequency (RF) pulse at the Larmor frequency. The Larmor frequency is dependent on the field strength of the magnetic device and the gyromagnetic ratio, which is specific for the element or molecule of interest. For MRI, that element is the hydrogen nucleus. The hydrogen nuclei absorb this energy and move out of their ground-state alignment. When the RF pulse is turned off, the energy absorbed by the hydrogen nuclei is emitted at the same frequency. This emitted energy, or MR signal, can be detected by the receiver coils (which act like antennae) in the magnet, and used to produce an MR image. Soft tissue contrast results from: (1) the densities of protons (hydrogen nuclei) within different tissues, (2) the different rates which the protons in various tissues realign themselves with the magnetic field of the magnet (also referred to as Tl relaxation, longitudinal or spin lattice relaxation), and (3) rates of signal decay or dephas¬ing (also referred to as T2 relaxation, transverse or spin spin relaxation). Using these biophysical properties of different normal and abnormal tissues allows MRI to have greater soft tissue contrast than computed tomography (CT).

The main components of a typical MRI scanner include: (1) a large-bore magnet with high field strength (0.3-3.0T); (2) radio frequency (RF) coils within the magnet which can transmit and receive properly-tuned RF pulses, as well as set spatially-dependent magnetic fields (gradients) that allow localization of specific regions of anatomic interest; and (3) a computer which operates the device as well as processes the RF signal data received from the patient to form an anatomic image. To generate an MR image, a person is placed onto a table which can move into specific locations within the bore of the magnet. Once in the magnet, the operator selects programs which include the RF pulse sequences necessary to generate images with the desired contrast parameters based on the proton densities, Tl and T2 values of the various tissues. The data received from the subject or patient are processed by the computer using computer algorithms (2 D or 3 D Fourier transformation). The images are displayed on the monitor console and transferred to film or other computers. Many systems store the image data on digital tape or optical discs for easy retrieval.

Not all patients can have MRI examinations. Intracranial aneurysm clips, cardiac pacemakers, and metallic foreign bodies in the eyes are absolute contraindications for MRI. In addition, the presence of surgical clips, metallic rods, wires, and other orthopedic hardware can produce artifacts obscuring visualization of the anatomic structures in the region of interest.

Major advantages of MRI for musculoskeletal imaging include excellent soft-tissue contrast resolution, multiplanar imaging capabilities, dynamic rapid data acquisition, and various available contrast agents. MRI has proven to be a powerful imaging modality for abnormalities involving fat, muscles, nerves, bone and bone marrow, and has been used in the evaluation of:

- neoplasms of the muscles, fat, nerves, bone, and meninges
- response of neoplasms to neoadjuvant (preoperative chemotherapy) and postoperative chemotherapy and/or radiation treatment
- residual and/or recurrent tumor after surgery
- disorders of histogenesis
- congenital and developmental musculoskeletal anomalies
- traumatic lesions
- hemorrhage
- ischemia and infarction of muscles, fat and bone marrow
- infectious and noninfectious inflammatory diseases
- metabolic disorders.

MR data can also be used to generate images of arteries and veins (MR angiography) in displays similar to conventional angiography. The appearance of blood vessels on MR images depends on various factors such as the type of MRI pulse sequence, pulsatility and range of velocities in the vessels of interest, and size, shape, and orientation of the vessels relative to the image plane. Useful anatomic information of blood vessels can be gained by using spin echo pulse sequences which can display patent vessels as zones of signal void (black-blood images), or gradient recall echo (GRE) pulse sequences which display the moving hydrogen atomic-nuclei (protons) in blood as zones of high signal (bright-blood images). Other options with clinical MRI scanners include: magnetic resonance spectroscopy (acquisition of spectral data to characterize the biochemical properties of selected regions of interest in the soft tissues); diffusion-weighted imaging (evaluation of different rates of proton diffusion between normal and abnormal tissue); and perfusion imaging (evaluation of the differences in rates of contrast enhancement between normal and abnormal tissue).

The appearance of muscle, fascia, tendons, ligaments, and bone cortex and marrow depends on the MRI pulse sequence used as well as the age of the patient imaged. In addition to the

standard spin echo or fast spin echo sequences that are commonly used for evaluation of the musculoskeletal system, other MRI pulse sequences or imaging options are sometimes used such as: inversion recovery techniques (STIR-short Tan inversion recovery used for fat signal suppression, FLAIR-fluid attenuated inversion recovery used for fluid signal suppression); GRE imaging with or without MR angiography; magnetic transfer; diffusion/perfusion MR imaging; and frequency selective chemical saturation. Detailed discussions of these sequences and options can be found elsewhere in the literature.

Bone formation occurs by either enchondral or membranous ossification. Longitudinal growth occurs by enchondral bone formation in which a calcified cartilaginous matrix at the growth (physeal) plates is remodeled into bone.[41] The physeal plate contains four parallel zones oriented perpendicular to the long axis of bone. The four zones from peripheral (nearest the epiphysis) to proximal (nearest the metaphysis) are (1) resting zone, (2) proliferating zone, (3) hypertrophic zone, and (4) calcifying zone. Active cartilage cell division and maturation occurs in the proliferating and hypertrophic zones. Osteoid matrix formation and mineralization occurs in the calcifying zone, also referred to as the zone of provisional calcification. At the adjacent metaphyseal region (primary spongiosa), remodeling of bone occurs with osteoclastic activity.The resting, proliferating, and hypertrophic zones are radiolucent, and on MRI have high signal on T2-weighted imaging (WI) and frequency selective (FS) T2WI, whereas the zone of provisional calcification has attenuation similar to mature mineralized bone on radiographs and CT, and has low signal on T2WI and FST2WI.[41] With membranous bone formation, bone cells form directly from the periosteum (long bones, facial bones, clavicle) for axial growth, or dura (calvarium) without intervening growth plates. The periosteum has low signal on TlWI and T2WI and is attached to the outer surface of the bone cortex in the meta¬diaphyseal regions by collagen fibers (fibers of Sharpey), but is absent from the articular ends of the bones; it is composed of an outer fibrous layer and an inner cellular layer referred to as the cambrium.[48] Osteoblastic activity occurs in the cambrium, and is responsible for increasing the diameter of bone during growth in childhood. The periosteum is loosely attached to the cortex in children, whereas it is firmly attached in adults. Reactivation of the perisoteum in adults can occur as a result of trauma, infection, or neoplasms. Perisoteal membranous bone formation occurs with induction of fibroblasts (in the fibrous layer or adjacent soft tissues) into osteogenic precursor cells that eventually develop into acive osteogenic cells in the cambrium.[48] Hyperemia from fracture, infection or tumor can accelerate new periosteal bone formation which can be seen as a radiodense line superificial to the cortex on radiographs or CT.[48] Perisoteal reaction can have variable configurations related to the disease process.[48] MRI can demonstrate periosteal elevation from diseases as well as subperiosteal abnormalities such as hemorrhage, pus, or tumor.[48]

Within the medullary portion of bone, MRI signal is related to the the presence of hematopoeitic (red) marrow which contains 40 % fat, 40 % water, and 20 % protein, or hematopoeiti¬cally-inactive fatty (yellow) marrow containing 80% fat, 15% water, and 5 % protein. Fatty marrow usually has a similar signal to subcutaneous fat on T1WI and FST2WI. Red marrow typically has an intermediate signal on T1WI that is slightly lower than for fat, and an intermediate signal on FST2WI, which is often similar to muscle. In early childhood, bone marrow is predominantly composed of red (hematopoeitic) marrow.[41,49] Later in childhood, progressive conversion of red to yellow marrow occurs in the hands and feet followed by the distal long bones.[41] In long bones, progressive conversion from red to yellow marrow occurs in the diaphyseal regions during the first decade.[41] The marrow of ossified epiphyses and trochanters is typically fatty.[41] In adults, red marrow is typically found in the spine, flat bones, skull, and proximal portions of the femora and humeri. MRI can demonstrate the process of red to yellow marrow conversion because of the slightly differing signal characteristics on TlWI and FS T2WI.

Most pathologic processes increase the Tl and T2 relaxation coefficients of the involved tissues, resulting in decreased signal on T1WI and increased signal on T2WI relative to adjacent normal tissue. Such processes include ischemia, infarction, inflammation, infection, metabolic or toxic disorders, trauma, neoplasms, and radiation injury. Hemorrhage, however, can have variable appearances depending on the age of the hematoma, oxidation states of the iron in hemoglobin, hematocrit, protein concentration, clot formation and retraction, location, and size.[6] Oxyhemoglobin in a hyperacute blood clot has ferrous iron and is diamagnetic. Oxyhemoglobin does not significantly alter the Tl and T2 values of the tissue environment other than causing possible localized edema. After a few hours during the acute phase of the hematoma, the oxyhemoglobin loses its oxygen to form deoxyhemoglobin which also has ferrous iron, although it has unpaired electrons and becomes paramagnetic. As a result, deoxyhemoglobin shortens the T2 value of the acute clot but does not significantly change the Tl value. On MRI, deoxyhemoglobin in the clot will have intermediate Tl signal and low signal on T2-weighted spin echo or gradient echo images. Later in the early subacute phase of the hematoma, deoxyhemoglobin becomes oxidized to the ferric state in met¬hemoglobin, which is strongly paramagnetic. Methemoglobin shortens the Tl value of hydrogen nuclei resulting in high signal on TlWI. While the red blood cells in the clot are intact, the T2 values of the intracellular methemoglobin will also be decreased resulting in low signal on T2WI. In the late subacute phase, breakdown of the membranes of the red blood cells results in extracellular methemoglobin, which now results in high signal on both Tl - and T2WI. In the chronic phase, methemoglobin becomes further oxidized and broken down by macrophages into hemosiderin, which has prominent low signal on T2-weighted images and low-intermediate signal on Tl-weighted images.

Other processes which can result in zones of high signal on Tl-weighted images are fat, dermoids (intact or ruptured), teratomas, lipomas, cystic structures with high protein concentration or cholesterol, and pantopaque. Lesions or structures with low signal on Tl - and T2WI can result from calcifications, very high protein or gadolinium-chelate concentrations, magnetic susceptibility effect especially from metal fragments or surgical clips, and artifacts.

Classification of Bone Tumors and Tumors Involving Musculoskeletal Soft Tissues

The classification of the bone and soft tissue neoplasms has evolved with the combined and coordinated utilization of clinical, imaging, macroscopic, histologic, immunohistochemical cytogenetic, and molecular genetic information.[4,8,12,13,16,17,20,34,35] This book uses the World Health Organization (WHO) classification, which was derived from an Editorial and Consensus Conference of the International Academy of Pathology in Lyon, France, during April 2002. The WHO classification of bone tumors is listed in Table 1.**1** and that of soft tissue tumors is listed in Table 1**2** These classifications incorporate immunohistochemical reactivity profiles to distinguish between lesions that have overlapping morphologic features or have uncertain histogenesis.[14,16,20] Various enzyme-linked antibodies used to

Table 1.1 WHO classification of bone tumors

Tumor type	ICD-O Code*
Cartilage tumors	
Osteochondroma	9210/0
Chondroma	9220/0
Enchondroma	9220/0
Periosteal chondroma	9221/0
Multiple chondromatosis	9220/1
Chondroblastoma	9230/0
Chondromyxoid fibroma	9241/0
Chondrosarcoma	9220/3
Central, primary, and secondary	9220/3
Peripheral	9221/3
Dedifferentiated	9243/3
Mesenchymal	9240/3
Clear cell	9242/3
Osteogenic tumors	
Osteoid osteoma	9191/0
Osteoblastoma	9200/0
Osteosarcoma	9180/3
Conventional	9180/3
Chondroblastic	9181/3
Fibroblastic	9182/3
Osteoblastic	9180/3
Telangiectatic	9183/3
Small cell	9185/3
Low grade central	9187/3
Secondary	9180/3
Parosteal	9192/3
Periosteal	9193/3
High-grade surface	9194/3
Fibrogenic tumors	
Desmoplastic fibroma	8823/0
Fibrosarcoma	8810/3
Fibrohistiocytic tumors	
Benign fibrous histiocytoma	8830/0
Malignant fibrous histiocytoma	8830/3
Ewing sarcoma/primitive neuroectodermal tumor	
Ewing sarcoma	9260/3
Hematopoietic tumors	
Plasma cell myeloma	9732/3
Malignant lymphoma, NOS	9590/3
Giant cell tumor	
Giant cell tumor	9250/1
Malignancy in giant cell tumor	9250/3
Notochordal tumors	
Chordoma	9370/3
Vascular tumors	
Haemangioma	9120/0
Angiosarcoma	9120/3
Smooth muscle tumors	
Leiomyoma	8890/0
Leiomyosarcoma	8890/3
Lipogenic tumors	
Lipoma	8850/0
Liposarcoma	8850/3
Neural tumors	
Neurilemmoma	9560/0
Miscellaneous tumors	
Adamantinoma	9261/3
Miscellaneous lesions	
Aneurysmal bone cyst	
Simple cyst	
Fibrous dysplasia	
Osteofibrous dysplasia	
Langerhans cell histiocytosis	9751/1
Erdheim-Chester disease	
Joint lesions	
Synovial chondromatosis	9220/0

* Morphology codes of the International Classification of Diseases for Oncology (ICD-O) and the Systematized Nomenclature of Medicine (http://snomed.org). Behavior is coded /0 for benign tumors, /1 for unspecified, borderline or uncertain behavior, /2 for in-situ carcinomas and grade III intraepithelial neoplasia, and /3 for malignant tumors.
NOS: not otherwise specified.

Table 1.2 WHO classification of soft tissue tumors

Tumor type	ICD-O Code
Adipocytic tumors	
Benign	
Lipoma	8850/0
Lipomatosis	8850/0
Lipomatosis of nerve	8850/0
Lipoblastoma/lipoblastomatosis	8881/0
Angiolipoma	8861/0
Myolipoma	8890/0
Chondroid lipoma	8862/0
Extrarenal angiomyolipoma	8860/0
Extra-adrenal myelolipoma	8870/0
Spindle cell/	8857/0
Pleomorphic lipoma	8854/0
Hibernoma	8880/0
Intermediate (locally aggressive)	
Atypical lipomatous tumor/	
Well-differentiated liposarcoma	8851/3
Malignant	
Dedifferentiated liposarcoma	8858/3
Myxoid liposarcoma	8852/3
Round cell liposarcoma	8853/3
Pleomorphic liposarcoma	8854/3
Mixed-type liposarcoma	8855/3
Liposarcoma, not otherwise specified	8850/3

Table 1.2 (Continued) WHO classification of soft tissue tumors

Tumor type	ICD-O Code
Fibroblastic/myofibroblastic **tumors**	
Benign	
Nodular fasciitis	
Proliferative fasciitis	
Proliferative myositis	
Myositis ossificans	
Fibro-osseous pseudotumor of digits	
Ischemic fasciitis	
Elastofibroma	8820/0
Fibrous hamartoma of infancy	
Myofibroma/myofibromatosis	8824/0
Fibromatosis colli	
Juvenile hyaline fibromatosis	
Inclusion body fibromatosis	
Fibroma of tendon sheath	8810/0
Desmoplastic fibroblastoma	8810/0
Mammary-type myofibroblastoma	8825/0
Calcifying aponeurotic fibroma	8810/0
Angiomyofibroblastoma	8826/0
Cellular angiofibroma	9160/0
Nuchal-type fibroma	8810/0
Gardner fibroma	8810/0
Calcifying fibrous tumor	
Giant cell angiofibroma	9160/0
Intermediate (locally aggressive)	
Superficial fibromatoses (palmar/plantar)	
Desmoid-type fibromatoses	8821/1
Lipofibromatosis	
Intermediate (rarely metastasizing)	
Solitary fibrous tumor	8815/1
and hemangiopericytoma	9150/1
(incl. lipomatous hemangiopericytoma)	
Inflammatory myofibroblastic tumor	8825/1
Low-grade myofibroblastic sarcoma	8825/3
Myxoinflammatory	
fibroblastic sarcoma	8811/3
Infantile fibrosarcoma	8814/3
Malignant	
Adult fibrosarcoma	8810/3
Myxofibrosarcoma	8811/3
Low-grade fibromyxoid sarcoma	8811/3
Hyalinizing spindle cell tumor	
Sclerosing epithelioid fibrosarcoma	8810/3
So-called fibrohistiocytic tumors	
Benign	
Giant cell tumor of tendon sheath	9252/0
Diffuse-type giant cell tumor	9251/0
Deep benign fibrous histiocytoma	8830/0
Intermediate (rarely metastasizing)	
Plexiform fibrohistiocytic tumor	8835/1
Giant cell tumor of soft tissues	9251/1
Malignant	
Pleomorphic "MFH"/undifferentiated	
pleomorphic sarcoma	8830/3
Giant cell "MFH'/undifferentiated	
pleomorphic sarcoma with giant cells	8830/3
Inflammatory "MFH"/undifferentiated	
pleomorphic sarcoma with prominent inflammation	8830/3
Smooth muscle tumors	
Angioleiomyoma	8894/0
Deep leiomyoma	8890/0
Genital leiomyoma	8890/0
Leiomyosarcoma (excluding skin)	8890/3

Tumor type	ICD-O Code
Pericytic (perivascular) tumors	
Glomus tumor (and variants)	8711/0
malignant glomus tumor	8711/3
Myopericytoma	8713/1
Skeletal muscle tumors	
Benign	
Rhabdomyoma	8900/0
adult type	8904/0
fetal type	8903/0
genital type	8905/0
Malignant	
Embryonal rhabdomyosarcoma	8910/3
(incl. spindle cell,	8912/3
botryoid, anaplastic)	8910/3
Alveolar rhabdomyosarcoma	
(incl. solid, anaplastic)	8920/3
Pleomorphic rhabdomyosarcoma	8901/3
Vascular tumors	
Benign	
Hemangiomas of:	
subcut/deep soft tissue:	9120/0
capillary	9131/0
cavernous	9121/0
arteriovenous	9123/0
venous	9122/0
Intramuscular	9132/0
synovial	9120/0
Epithelioid hacmangioma	9125/0
Angiomatosis	
Lymphangioma	9170/0
Intermediate (locally aggressive)	
Kaposiform hemangioendothelioma	9130/1
Intermediate (rarely metastasizing)	
Retiform hemangioendothelioma	9135/1
Papillary intralymphatic angioendothelioma	9135/1
Composite hemangioendothelioma	9130/1
Kaposi sarcoma	9140/3
Malignant	
Epithelioid hemangioendothelioma	9133/3
Angiosarcoma of soft tissue	9120/3
Chondro-osseous tumors	
Soft tissue chondroma	9220/0
Mesenchymal chondrosarcoma	9240/3
Extraskeletal osteosarcoma	9180/3
Tumors of uncertain differentiation	
Benign	
Intramuscular myxoma	8840/0
(Incl. cellular variant)	
Juxta-articular myxoma	8840/0
Deep ("aggressive") angiomyxoma	8841/0
Pleomorphic hyalinizing	
angiectatic tumor	
Ectopic hamartomatous thymoma	8587/0
Intermediate (rarely metastasizing)	
Angiomatoid fibrous histiocytoma	8836/1
Ossifying fibromyxoid tumor	8842/0
(incl. atypical/malignant)	
Mixed tumor	8940/1
Myoepithelioma	8982/1
Parachordoma	9373/1

Table 1.2 (Continued) WHO classification of soft tissue tumors

Tumor type	ICD-O Code
Malignant	
Synovial sarcoma	9040/3
Epithelioid sarcoma	8804/3
Alveolar soft part sarcoma	9581/3
Clear cell sarcoma of soft tissue	9044/3
Extraskeletal myxoid chondrosarcoma	9231/3
("chordoid" type)	
PNET/extraskeletal Ewing tumor	
PNET	9364/3
extraskeletal Ewing tumor	9260/3
Desmoplastic small round cell tumor	8806/3
Extrarenal rhabdoid tumor	8963/3
Malignant mesenchymoma	8990/3
Neoplasms with perivascular epithelioid	
cell differentiation (PEComa)	
clear cell myomelanocytic tumor	
Intimai sarcoma	8800/3

PNET: primitive neuroectodermal tumor.

detect tissue antigens and their clinical applications for diagnosis are listed in Table 13 In addition, the new WHO classifications of bone and soft tissue tumors also utilize data from cytogenetic and molecular genetic analyses.[4,5,8,12,13,34,35,37] Cytogenetic and gene abnormalities of tumors of bone and soft tissues are listed in Table 1.4.

Table 1.3 Immunohistochemical markers used in the diagnosis of bone and soft tissue tumors

Marker		Positive immunoreactivity in:
Endothelial markers	**CD 31**-antigen gplla. PECAM-1: platelet endothelial cell adhesion	Angiosarcoma, hemangioendothelioma. Kaposi sarcoma. hemangioma
	CD 34; 110kDa transmembrane glycoprotein that occurs in skin and blood vessels on endothelium cells. stem cells and dendritic cells, marker for endothelial differentiation	Kaposi sarcoma, angiosarcoma, epithelioid hemangioendothelioma. dermatofibrosarcoma protuberans, solitary fibrous tumor, hemangiopericytoma, malignant peripheral nerve sheath tumor, other vascular and fibroblastic tumors
	CD 141	Variable in angiosarcoma, positive in mesothelioma, squamous carcinoma
	FLI-1; type of DNA-binding transcription factor	Angiosarcoma, Ewing sarcoma/PNET [translocation: t(11;22)(q24;q12)], lymphoblastic lymphoma
	Factor VIII antigen (von Willebrand factor); antigen expressed by endothelial cells within Weibel-Palade bodies and mekaryocytes	Endothelial neoplasms
Leukocyte differentiation antigens (CD; clusters of differentiation of monoclonal antibodies to human leukocyte and erythroid antigens)	**CD 1**	CD 1 a and S 100 in Langerhans cell histiocytosis
	CD 3	T-ALL/T-LBL (T *cell lymphoblastic lymphoma/leukemia),* NK *(natural killer)* cells
	CD 5	T-ALL/T-LBL. B-CLL *(chronic lymphoid leukemia).* mantle cell lymphoma
	CD 10	B-ALL *(acute lymphoid leukemia),* AML *(acute myeloid leukemia),* follicular lymphoma, Burkitt lymphoma
	CD 11	CD 11 c in hairy cell leukemia
	CD 15	Hodgkin disease, granulocytic sarcoma
	CD 20	B cell lymphomas
	CD 23	B cell lymphomas
	CD 25	Adult T-ALL. hairy cell leukemia
	CD 30	Hodgkin disease, anaplastic large cell lymphoma
	CD 38	Plasma cells are characteristically CD38+/CD45-
	CD 43	Neoplastic B cell positive, normal B cell negative
	CD 45	T and B lymphomas, plasma cells
	CD 79a	B lymphomas
	CD 99 (MIC-2 gene product): surface glycoprotein 30-32 kDa present in most tissues	Ewing sarcoma/PNET (90%), lymphoblastic lymphoma (90%), synovial sarcoma (75%), mesenchymal chondrosarcoma (50%), neuroepitheliomas, alveolar rhabdomyosarcoma, solitary fibrous tumor, hemangiopericytoma.
	CD 117	Mast cells, gastrointestinal stromal tumors

Table 1.3 (Continued) Immunohistochemical markers used in the diagnosis of bone and soft tissue tumors

Marker		Positive immunoreactivity to:
Leukocyte differentiation antigens	**CD 138**	Plasma cells
Muscle cell markers	**Actin,** consists of contractile filaments in smooth muscle	Smooth muscle and myofibroblastic tumors, primary or metastatic spndle cell and round cell tumors
	Actin, (sarcomeric) consists of contractile filaments in skeletal muscle	Skeletal muscle and rhabdomyosarcoma
	Desmin, intermediate filament protein present in smooth and striated muscle cells and myofibroblasts	Angiomatoid malignant fibrous histiocytoma, Smooth and skeletal muscle tumors, other tumors
	HCD	Smooth muscle and its tumors, myoepithelia. Gl stromal tumors
	Calponin: actin-binding protein in smooth muscle associated with regulation of smooth muscle contractility	Smooth muscle, myofibroblasts, myoepithelia, synovial sarcoma (often)
	MyoD 1, myogenin; represent intranuclear MyoD transcription factors that initiate differentiation of striated muscle	Rhabdomyosarcoma (reactive skeletal muscle)
	Myoglobin: an oxygen-binding heme protein in cardiac and skeletal muscle, but not in smooth muscle	Rhabdomyosarcoma (differentiated)
	Myosin	Isoforms for smooth and skeletal muscle tumors
Neural, nerve sheath, and neuroendocrine¬ specific markers	**Synaptophysin:** glycoprotein in synaptic vesicles. used for cells of neural or neuroendocrine origin	Neuroblastoma, ganglioneuroblastoma, paraganglioma, neuroendocrine carcinoma, rhabdomyosarcoma, peripheral neuroepithelioma
	Chromogranin: family of acidic glycoproteins located in neurosecretory granules	paraganglioma, neuroendocrine carcinoma (low grade)
	Neuron-specific enolase: enzyme of glycolytic pathway expressed in neural and non-neural tumors	General neuroendocrine marker (poor specificity), Ewing sarcoma
	Neurofilaments (NF proteins): useful in diagnosis of small round-cell tumors	Neuroblastoma, paraganglioma, malignant fibrous histiocytoma. rhabdomyosarcoma. Merkel cell carcinoma
	Glial fibrillary acidic protein (GFAP)	Glial tumors, schwannomas, myoepithelial tumors.
	CD 57 (Leu-7): 110 kDa antigen is present on the surface of natural killer cells and T-lymphocytes	Synovial sarcoma, leiomyosarcoma (relatively nonspecific), round and spindle cells with nerve sheath differentiation
S-100 Protein and other multispecific neural markers	**S-100 protein:** dimeric, acidic calcium-binding protein that is soluble in 100% ammonium sulfate, used for tumors of neural origin, melanoma, and cartilaginous differentiation	Melanoma, schwannoma, neurofibroma, chondroblastoma, chondromyxoid fibroma, ossifying fibromyxoid tumor, chordoma, chondrosarcoma, clear cell sarcomas, Langerhans cell histiocytosis
	Nerve growth factor receptor	Dermatofibrosarcoma protuberans and other nerve sheath tumors
	CD 56: 140 kDa membrane glycoprotein involved in neural cell adhesion molecule	Neuroendocrine carcinoma, rhabdomyosarcoma, synovial sarcoma, chondrosarcoma, osteosarcoma, neuroblastoma, malignant peripheral nerve sheath tumor, schwannoma. rhabdomyosarcoma, leiomyosarcoma, leiomyoma
Melanoma markers other than S-100 protein	**HMB45:** monoclonal antibody for Pmel gene product in immature melanosomes	Melanoma, clear cell sarcoma, angiomyolipoma. perivascular epithelioid cell tumors (PECOmas)
	Tyrosinase; enzyme involved in melanin synthesis	Nevi, melanoma
	Melan-A, marker for melanosomes	Nevi, melanoma, angiomyolipoma
	Microphthalmia-transcription factor; transcription factor involved in melanogenesis and expression of the tyrosinase gene	Melanoma, clear cell sarcoma, osteoclastic giant cells
	CD 63	Melanoma, some carcinomas, alveolar soft parts sarcoma
Histiocytic markers	**Lysozyme**	Histiocytes, myelomonocytic cells
	Factor Xiia	Histiocytes, especially dendritic ones
	CD68: 110 kDa glycoprotein found in tumors containing lysosomes or phagolysosomes	Histiocytes, melanoma, paraganglioma, schwannoma, granular cell tumor malignant fibrous histiocytoma (50%)
	CD 163	Histiocytes

Table 1.3 (Continued) Immunohistochemical markers used in the diagnosis of bone and soft tissue tumors

Marker		Positive immunoreactivity to:
Epithelial markers	**Cytokeratins:** acidic or basic proLeins of intermediate sized filaments ranging from 40 to 67 kDa, often allows distinction of epithelial from non-epithelial tu¬ mors	Carcinoma, metastatic epithelial carcinoma, synovial and epithelioid sarcoma, chordoma, Merkel cell tumor, adamantinoma
	Epithelial membrane antigen (EMA): transmembrane glycoprotein with high molecular weight that is expressed in epithelial cells and tumor derived from epithelial cells	Epithelial tumors, synovial sarcoma, epithelioid sarcoma, meningioma, perineural tumors, malignant peripheral nerve sheath tumors, leiomyosarcoma
	Carcinoembryonlc antigen (CEA)	Many adenocarcinomas, biphasic synovial sarcoma
	Desmoplakin	Epithelial tumors in general, meningioma, Ewing sarcoma
	HBME-1	Mesothelioma, some adenocarcinoma, synovial sarcoma, chondroma
	CD 117: proto-oncogene transmenbrane receptor for stem cell factor on mast cells, melanocytes, hemato¬ poeitic cells, and germ cells	GI stromal tumor, angiosarcoma, Ewing sarcoma, leiomyoma, leiomyosarcoma, nerve sheath tumors
Mesenchymal marker	**Vimentin:** widely distributed intermediate filament (57 kDa) expressed in mesenchymal cells	Sarcomas, melanoma,some carcinomas and lymphomas
Bone tissue markers	**Alkaline phosphatase:** enzyme associated with bone turnover	
	Osteonectin: secreted glycoprotein in the extracellular matrix by bone cells	Osteosarcoma. Malignant fibrous histiocytoma, meningioma. melanoma, breast carcinoma
	Osteocalcin: intraosseous protein associated with osteoblasts and osteoblastic differentiation	Osteosarcoma
	Collagen: many subtypes	Type X collagen is seen only in benign osteochondromas. Type IV seen with glomus tumor
Cell proliferation evaluation	**K_1-67:**395 kDa specific nuclear antigen only expressed in proliferating cells in late GI, S, G2 and M phases	For sarcomas; aggressive can be related to the K_1-67 index (number of positive cells per 10 high-power fields), > 50/ 10HPFs
	Mutated p53 protein: TP53 gene product consisting of a nuclear phosphorylation protein that suppresses transcription and proliferation of cells with damaged DNA; has **a** longer half life when mutated and more detectable than wild type	p53 overexpression has been associated with sarcomas with high tumor grade, prognostic utility not proven
	p16 and p27: cyclin-dependent kinase inhibitors	Loss of p16 expression from deletion of CDKN2A/p16 in malignant peripheral nerve sheath tumors but not in neurofibromas; loss of p27 seen with malignant transformation of neurofibromas

Source: Adapted from references 14, 16, and 20.

Table 1.4 Genetic abnormalities in bone and soft tissue tumors

Tumor/lesion	Cytogenetic (chromosomal) abnormality	Molecular abnormality	Frequency (%)	Diagnosticutility
Malignant bone tumors				
Osteosarcoma	Loss of heterozygosity (LOH) at 3 q, 13 q, 17 p. and 18 q and variable chromosomal changes			Unclear
Parosteal osteosarcoma	Supernumerary ring chromosomes, ring 12 q 13-15			Unclear
Chondrosarcoma	1, 5, 7, 8, 11, 12, 15, 18, 19, 20			Unclear
Ewing sarcoma and PNET	t(11;22)(q24;q12), t(21;22)(q22;q12). t(7;22)9p22;q22)			Yes
Chordoma	3, 4, 10, 13			No
Adamantinoma	Numerical changes in 2 cases			No

Table 1.4 (Continued) Genetic abnormalities in bone and soft tissue tumors

Tumor/lesion	Cytogenetic (chromosomal) abnormality	Molecular abnormality	Frequency (%)	Diagnosticutility
Benign **bone** lesions				
Chondroma	12q13-15			Unclear
Malignant soft tissue tumors				
Chondrosarcoma, extraskeletal myxoid	t(9;22)(q31;q12) t(9;17)(q22;q11) t(9;15)(q22:q21)	*EWS-CHN* fusion RBP56-CHN(TEC) TEC-TCF12	>75	Yes
Clear cell sarcoma	t(12;22)(q13:q12)	*EWS-ATF1* fusion	>75	Yes
Desmoplastic small round cell tumor	t(11;22)(p13;q12)	*EWS-WT1* fusion	>75	Yes
Dermatofibrosarcoma protuberans	Ring form of chromosomes 17 q and 22 q t(17;22)(q22;q13)	*COL1A1-PDGFD* fusion *COL 1A1-PDGFB* fusion	>75 10	Yes
Ewing sarcoma	t(11;22)(q21;q13) t(21;22)(p22;q12) t(2;22)(q33:q12) t(7;22)(p22;q12) t(17;22)(ql2;q12)	*EWS-FLI1* fusion *EWS-ERG* fusion *EWS-FEV* fusion *EWS-ETV1* fusion *EWS-E1AF* fusion	>80 5-10 <5 <5 <5	Yes Yes Yes Yes Yes
Fibrosarcoma, infantile	t(12;15)(p13;q25) Trisomies 8, 11, 17, and 20	*ETV6-NTRK3* fusion	>75 >75	Yes Yes
Gastrointestinal stromal tumor	Monosomies 14 and 22 Deletion of 1 p	*KIT* mutation	>75 >25 >90	Yes No Yes
Malignant Hemangiopericytoma	t(12;19)(q13;q13)			
Inflammatory myofibroblastic tumor	t(2;19)(p23;p13.1) t(1:2)(q22-23;p23)	ALK-TPM4 TPM3-ALK		
Leiomyosarcoma	Deletion of 1 p		>50	No
Liposarcoma				
Well differentiated	Ring form of chromosome 12q13-15. 12q21.3-22		>75	
Myxoid/round cell	t(12;16)(q13;p11) t(12;22)(q13;q12)	*US-CHOP* fusion *EWS-CHOP* fusion	>75 > 5	Yes Yes
Pleomorphic	Complex*		90	No
Malignant fibrous histiocytoma				
Myxoid	Ring form of chromosome 12		?	?
High-grade	Complex*		> 90	No
Myxofibrosarcoma	See malignant fibrous histiocytoma			
Malignant peripheral nerve sheath tumor				
Low-grade	None		> 90	No
High-grade	Complex*			
Mesothelioma	Deletion of 1 p Deletion of 9 p Deletion of 22 q Deletions of 3 p and 6 q	P15, p16, and p19 inactivation *NF2* inactivation	>50 >75 >50 >50	Yes Yes Yes Yes
Neuroblastoma				
Good prognosis	Hyperdiploid, no 1 p deletion		90	Yes
Poor prognosis	1 p deletion Double minute chromosomes	N-*myc* amplification	90 >25	Yes Yes
Primitive neuroectodermal tumor	(see Ewing sarcoma)			
Rhabdoid tumor	Deletion of 22 q	*INI1* inactivation	>90	Yes

Table 1.4 (Continued) Genetic abnormalities in bone and soft tissue tumors

Tumor/lesion	Cytogenetic (chromosomal) abnormality	Molecular abnormality	Frequency (%)	Diagnosticutility
Rhabdomyosarcoma				
Alveolar	T(2;13)(q35;q14) t(1;13)(p36;q14), double minutes	*PAX3-FKHR* fusion *PAX7-FKHR* fusion	>75 10-20	Yes Yes
Embryonal	Trisomies 21, 8, and 20	Loss of hetero-zygosity at 11 p15	>75 >75	Yes Yes
Synovial sarcoma				
Monophasic	T(X;18)(p11;q11)	*SYT-SSZ1* or SYT-*SSX2* fusion	>90	Yes
Biphasic	T(X;18)(p13;q11)	*SYT-SSX1* fusion	>90	Yes
Benign soft tissue tumors				
Desmoid tumor	Trisomies 8 and/or 20 Deletion of 5 q	*APC* deletion	25 10	No ?
Hibernoma	Translocation at 11 q13		>50	Yes
Leiomyoma, uterine	T(12;14)(q15;q24) Deletion of 7 q Trisomy 12	*HMGIC* and *RAD 51* translocation	20 20 10	Yes ? ?
Upoblastoma	Rearrangement of 8 q11-13	*PLAG1* fusions	>50	Yes
Lipoma				
Solitary	Rearrangement of 12 q13, t(13-15), t(3;12), 6p. 13 q	*HMGIC* fusions	75	Yes
Multiple	None			
Spindle cell lipoma	16 q, 10.13			
Atypical lipoma	Supernumerary ring chromo-somes			
Myxoma	Y, telomeric associations			
Neurofibroma	None			
Schwannoma, benign	Deletion of 22 q	*NF2* inactivation	>75	Yes

Source: Adapted from references 4, 5, 13, 20, 34, and 37.

Frequency of Occurrence of Bone Tumors

Bone neoplasms can be primary lesions arising from osseous structures or secondary to metastatic disease. Metastatic carcinoma is the most frequent malignant tumor involving bone.[33] In adults, metastatic lesions to bone occur most frequently from carcinomas of the lung, breast, prostate, kidney, thyroid, as well as from sarcomas.[30] The exact incidence of metastatic skeletal disease is unknown.[33] Up to 50% of patients who die from disseminated carcinoma have evidence of skeletal metastases at autopsy.[33] Almost 240 000 patients die in the United States each year from carcinoma of the lung, breast, prostate, kidney, and thyroid.[18] Using these data, up to 120 000 oncology patients who die each year may have metastatic skeletal disease. Metastatic skeletal disease has also been reported to occur in up to 30% of all cancer cases.[15] Thirty per cent of the 1 284 900 annual new cancer cases in the United States[17] is 385 470. In comparison, only 2400 primary malignant bone tumors occur in the United States per year.[19] Metastatic lesions may therefore occur from 50 to 161 times more frequently than primary malignant bone tumors.[15,18,26,31]

Primary bone sarcomas represent only 0.2% of all neoplasms.[8] The incidence of primary bone sarcomas has been reported to be 8 per million.[8] Primary bone sarcomas occur ten times less frequently than sarcomas in the soft tissues.[8] The most frequent type of primary bone sarcoma is osteosarcoma followed by chondrosarcoma and Ewing sarcoma.[8] Bone sarcomas have a bimodal incidence rate with one peak occurring in the second decade (osteosarcoma, chondrosarcoma) and the other in patients over 60 years (chordoma, chondrosarcoma, osteosarcoma).[8] The relative frequencies of primary malignant bone tumors and primary nonmalignant bone tumors are listed in Tables 1.5 and 1.6, respectively.[27,28,46] The relative frequencies of tumorlike bone lesions are listed in Table 1.7.[27,28] Other lesions or abnormalities involving bone are listed in Table 1.8. The imaging features of some of these abnormalities may overlap those of bone tumors.

Table 1.5 Primary malignant bone tumors

	Mayo Clinic		NCBT		Age range (years): median age
	% malignant (*N* = 8591)	% total (*N* =11 087)	% malignant (*N* = 3355)	% total (*N* = 5133)	
Myeloma	44%	34%	2%	1%	16-80:60
Osteosarcoma	19%	15%	34%	22%	2-92:16-39
Chondrosarcoma	12%	9%	21%	14%	7-91:26-59
Lymphoma	8%	6%	3%	2%	18-69
Ewing sarcoma	6%	5%	11%	7%	6-30:14
Chordoma	4%	3%	2%	1%	30-80:58
Fibrosarcoma	3%	2%	5%	4%	10-75:43
Malignant fibrous hist.	1%	<1%	5%	3%	11-80:48
Giant cell tumor	<1%	<1%	2%	1%	10-55:30
Angiosarcoma	<1%	<1%	1%	<1%	10-80:51
Hemangioendothelioma	<1%	<1%	<1%	<1%	15-60:34
Adamantinoma	<1%	<1%	<1%	<1%	10-60:25
Hemangiopericytoma	<1%	<1%	<1%	<1%	1-90:40
Liposarcoma	<1%	<1%	<1%	<1%	Not reported
Synovial sarcoma			2%	1%	5-60:25
Paget sarcoma			1%	<1%	50-80:66

Source: Data for the Mayo Clinic from reference 46. Data for the Netherlands Committee on Bone Tumors (NCBT) from references 27 and 28.

Table 1.6 Primary benign bone tumors

	Mayo Clinic		NCBT		Age range (years): median age
	% benign (*N* = 2496)	% total (*N*= 11087)	% benign (*N* = 1778)	% total (*N* = 5133)	
Osteochondroma	35%	8%	14%	5%	1-50:20
Giant cell tumor	23%	5%	22%	8%	10-55:30
Enchondroma	12%	3%	17%	6%	3-83:35
Osteoid osteoma	13%	3%	11%	4%	6-30:17
Chondroblastoma	5%	1%	9%	3%	10-30:17
Hemangioma	4%	1%	2%	<1%	1-84:33
Osteoblastoma	3%	<1%	6%	2%	1-30:15
Juxtacortical chondroma	2%	<1%	5%	2%	4-77:26
Chondromyxoid fibroma	2%	<1%	4%	1%	1-40:17
Neurilemoma	<1%	<1%	1%	<1%	2-65:30
Fibrous histiocytoma	<1%	<1%			
Lipoma	<1%	<1%	<1%	<1%	
Hamartoma	<1%	<1%			
Osteoma			<1%	<1%	
Lymphangioma			<1%	<1%	
Desmoplastic fibroma			<1%	<1%	1-71:21

Source: Data for the Mayo Clinic from reference 46. Data for the Netherlands Committee on Bone Tumors (NCBT) from references 27 and 28.

Frequency of Occurrence of Soft Tissue Tumors

Benign tumors of the soft tissues are 100 times more frequent than sarcomas.[13] The annual incidence of benign tumors has been estimated to be 3000 per million, and 30 per million for sarcomas.[12] Sarcomas of the musculoskeletal system account for less than one per cent of all malignant tumors.[12] The relative frequencies of primary malignant tumors and primary non-malignant tumors of the soft tissues are listed in Tables 19 and 1.10, respectively.[21-23]

Grading and Staging of Bone Tumors

Two systems that are currently used for staging of primary malignant bone tumors include the the American Joint Committee on Cancer (AJCC) system that was recently revised in 2002, and the Musculoskeletal Tumor Society (MSTS) system.[8,40]

For the revised AJCC system, four criteria are used for Stages 1A to IVB. Tl refers to tumors measuring less than 8 cm in greatest dimension and T2 for tumors greater than 8 cm. NO refers to no regional lymph node metastasis and Nl for the occurrence of regional lymph node metastasis. M0 refers to the

Table 1.7 Tumorlike bone lesions

	Relative frequency (%) (A/=2287)	Age range (years): median age
Fibrous dysplasia	18%	1-50:20
Osteomyelitis	14%	
Fibrous cortical defect / non-ossifying fibroma	13%	5-20:14
Aneurysmal bone cyst	11%	1-25:14
Traumatic injury (fracture/callus)	10%	
Solitary bone cyst	9%	1-62:11
Eosinophilic granuloma	8%	1-35:10
Heterotopic bone formation/reaction	5%	1-45:22
Pigmented villonodular synovitis	3%	15-60:32
Geode	1%	25-85:52
Brown tumor	1%	40-70:52
Ganglion	<1%	20-70:38
Epidermoid cyst	<1%	19-71:38
Neuropathic arthropathy	<!%	
Melorheostosis	<1%	

Source: Data for the Netherlands Committee on Bone Tumors (NCBT) from references 27 and 28.

Table 1.8 Other lesions involving bone

Malignant lesions
Metastatic disease
Leukemia
Desmoid tumors
Benign lesions
Aneurysmal bone cyst
Unicameral bone cyst
Fibrous cortical defect
Non-ossifying fibroma
Fibrous dysplasia
Eosinophilic granuloma
Osteofibrous dysplasia
Paget disease
Plexiform neurofibromas
Ganglion cysts
Geode
Bone island
Melorrheostosis
Metabolic disorders
Thalasemia
Sickle-cell disease
Hemophilia
Osteopetrosis
Gaucher disease
Hyperparathyroidism
Vitamin deficiencies
Radiation injury
Fat conversion
Bone Infarcts
Inflammatory diseases
Pyogenic osteomyelitis
TB osteomyelitis
Fungal osteomyelitis
Langerhans cell histiocytosis / Eosinophilic granuloma
Erdheim-Chester disease
Sarcoid
Traumatic lesions
Fractures
Hematomas
Pseudoarthrosis
Neuropathic joint
Bone infarct
Osteochondritis dissecans

Table 1.9 Malignant soft tissue tumors

	% malignant (*N* = 12370)	% total (*N* = 31 047)	Age range (years): median age
Malignant fibrous histiocytoma	24%	10%	32-80: 59
Liposarcoma	14%	6%	18-78; 47
Sarcoma (not further classified)	12%	5%	
Leiomyosarcoma	8%	3%	35-79: 58
Malignant schwannoma	6%	2%	17-70; 42
Dermatofibrosarcoma protuberans	6%	2%	19-60; 38
Synovial sarcoma	5%	2%	14-58: 32
Fibrosarcoma	4%	2%	14-72; 41
Extraskeletal chondrosarcoma	2%	<1 %	22-71; 49
Angiosarcoma	2%	<1 %	17-77; 49
Rhabdomyosarcoma	2%	<1 %	2-40; 18
Epitheloid sarcoma	1%	<1 %	15-54; 31
Kaposi sarcoma	1%	<1 %	34-84; 64
Malignant hemangiopericytoma	1%	<1%	22-73; 46
Extraskeletal Ewing	1%	<1 %	11-42; 25
Clear cell sarcoma	1%	<1 %	15-60; 37
Extraskeletal osteosarcoma	<1%	<1 %	33-77; 57
Neuroblastoma	<1%	<1 %	1-47; 19
Hemangioendothelioma	<1%	<1 %	17-60; 40
Malignant granular cell tumor	<1%	<1 %	14-70; 39

Source: Data from reference 22.

Table 1.10 Benign soft tissue tumors/lesions

	% benign (*N* = 18677)	% total (*N* = 31047)	Age range (years): median age
Lipoma	16%	10%	26-68: 48
Fibrous histiocytoma	13%	8%	13-57; 33
Nodular fasciitis	11%	7%	11-51: 31
Hemangioma	8%	7%	1-65; 32
Fibromatosis	7%	5%	13-65; 36
Neurofibroma	5%	4%	16-66; 37
Schwannoma	5%	3%	22-72; 46
Giant cell tumor of tendon sheath	4%	3%	18-64; 39
Myxoma	3%	2%	24-74; 52
Granuloma annulare	2%	2%	2-58; 23
Hemangiopericytoma	2%	1% 2%	23-70; 44
Granular cell tumor	2%	1%	15-56; 35
Leiomyoma	2%	1%	14-67; 40
Chondroma	1%	1%	16-70; 44
Fibroma of tendon sheath	1%	<1% <1%	15-75; 35
Fibroma	1%	<1%	11-67; 40
Myofibromatosis	1%	<1%	<1-52; 14
Glomus tumor	<1%	<1%	19-71; 47
PVNS	<1%	<1%	18-59; 38
Lymphangioma	<1%	<1%	1-50; 19
Ganglion	<1%	<1%	19-65; 40
Proliferative fasciitis	<1%	<1%	33-71; 54
Myositis ossificans	<1%	<1%	13-64; 35
Lipoblastoma	<1%	<1%	1-10; 4
Proliferative myositis	<1%	<1%	
Paraganglioma	<1%	<1%	24-70; 47
Synovial chondromatosis	<1%	<1%	
Ganglioneuroma	<1%	<1%	4-44; 22
Hibernoma	<1%	<1%	21-50; 32

Source: Data from reference 21.
PVNS: Pigmented villonodular synovitis.

absence of distant metastasis and Ml for the presence of distant metastasis. The last criterion is based on tumor grade: Gl assigned to low grade or well differentiated, G2 for moderately differentiated (also low grade), G3 for poorly differentiated (high grade), and G4 for undifferentiated (high grade) (Table I.11). The AJCC system is used for all primary malignant tumors of bone (osteosarcoma, Ewing sarcoma), except for primary malignant lymphoma or myeloma.[40]

For the MSTS system, three criteria are used for Stages 1A to III. T refers to whether the tumor is localized to a single compartment (Tl) or involves more than one compartment (T2); M0 designation for absence of metastases and Ml for the presence of metastases; and Gl for low-grade tumors and G2 for high-grade tumors.[40]

Table 1.11 American Joint Committee on Cancer Staging system for primary malignant tumors of bone for those tumors diagnosed on or after January 1, 2003[40]

Stage	Tumor	Lymph node	Metastases	Grade
IA	T1	NO	M0	G1 or G2
IB	T2	NO	M0	G1 or G2
IIA	T1	NO	M0	G3 or G4
IIB	T2	NO	M0	G3 or G4
III	T3	NO	M0	Any G
IVA	Any T	NO	M1 a	Any G
IVB	Any T	N1	Any M	Any G
IVB	Any T	Any N	Ml b	Any G

Classifications: Tx, primary tumor cannot be assessed; TO, no evidence of primary tumor; T1, tumor 8 cm or less in greatest dimension; T2, tumor more than 8 cm in greatest dimension; T3, discontinuous tumors in the primary bone; Nx, regional lymph nodes not assessed; NO, no regional lymph node metastases; N1, regional lymph node metastasis; Mx, distant metastasis cannot be assessed; M0, no distant metastasis; M1, distant metastasis; M1 a, lung; M1 b, other distant sites; and Gx, grade cannot be assessed; G1, well differentiated (low grade); G2, moderately differentiated (low grade); G3, poorly differentiated (high grade); G4, undifferentiated (high grade).

Grading and Staging of Soft Tissue Tumors

The WHO has developed a classification system for soft tissue tumors with lesions assigned to four groups; benign, intermediate (locally aggressive), intermediate (rarely metastasizing), and malignant.[12] Two systems currently used for grading of soft tissue sarcomas include the NCI (United States National Cancer Institute) system and the FNCLCC (French Federation Nationale des Centres de Lutte Contre le Cancer) system (Table I.12). The NCI grading system for tumors takes into account the histologic type, cellularity, pleomorphism, mitotic rate, and presence of necrosis.The FNCLCC system uses tumor differentiation, mitotic rate, and presence/extent of necrosis. Two important histologic features that have been associated with prognosis include high mitotic indices and presence of necrosis. The FNCLCC system has been reported to result in a better correlation with overall and metastasis-free survival than the NCI system.[12] Staging of malignant soft tissue tumors is based on the extent of tumor from imaging, histologic features of the tumors, and clinical data. The main system used for staging for soft tissue sarcomas is the TNM system developed by the American Joint Committee on Cancer (AJCC) and the International Union against Cancer (Table I.13). The TNM system has been shown to be clinically useful for prognostic purposes.[12] The TNM system utilizes data consisting of tumor size and depth, histologic tumor grade, regional lymph node involvement, and presence of distant metastases.

Table 1.12 FNCLCC grading system: definition of parameters[12]

Tumor differentiation	
Score 1:	
	Sarcomas closely resembling normal adult mesenchymal tissue (e.g., low-grade leiomyosarcoma).
Score 2:	
	Sarcomas for which histological typing is certain (e. g., myxoid liposarcoma).
Score 3:	
	embryonal and undifferentiated sarcomas, sarcomas of doubtful type, synovial sarcomas, osteosarcomas. PNET.
Mitotic count	
Score 1:	0-9 mitoses per 10 HPF"
Score 2:	10-19 mitoses per 10 HPF
Score 3:	> 20 mitoses per 10 HPF
Tumor necrosis	
Score 0:	no necrosis
Score 1:	< 50 % tumor necrosis
Score 2:	> 50 % tumor necrosis
Histological grade	
Grade 1:	total score 2, 3
Grade 2:	total score 4, 5
Grade 3:	total score 6. 7, 8

* A high power field (HPF) measures 0.1734 mm^2
PNET: primitive neuroectodermal tumor

Imaging Evaluation of Bone and Soft Tissue Tumors Tumorlike Lesions

The diagnosis of bone tumors is often made on conventional radiographs.[4] Osteolytic lesions from tumors, however, may not be visible on conventional radiographs until there is 30-50% loss of mineralization.[40] Because of superior soft tissue contrast, MRI can detect marrow based tumors before they are evident on radiographs. In addition, MRI can be used to further characterize lesions with regard to extent and extra-osseous extension. With progressive increased utilization of MRI for evaluation of musculoskeletal disorders, tumors and other bone lesions may also be found incidentally.

Features used to characterize bone tumors and other lesions on conventional radiographs include:

- o lesion location (metaphyseal/diaphyseal/epiphyseal, cortical, intramedullary, eccentric, central)
- o lesion size
- o lesion density (radiolucent, sclerotic, presence of matrix mineralization)
- o margins (well-defined geographic with or without sclerotic borders, poorly-defined geographic, "moth-eaten" and/or "permeative" radiolucent patterns)
- o presence of cortical destruction with or without extra-osseous tumor extension
- o presence of periosteal reaction (interrupted vs. noninterrupted pattern, lamellated/onion-skin pattern, perpendicular pattern, sunburst pattern, Codman triangles).[4,8,32,48]

Table 1.13 TNM classification of soft tissue sarcomas

Primary tumor (T)	TX	primary tumor cannot be assessed		
	TO:	no evidence of primary tumor		
	T1:	tumor <5 cm in greatest dimension		
		T1 a: superficial tumor*		
		T1 b: deep tumor		
	T2:	tumor > 5 cm in greatest dimension		
		T2 a: superficial tumor		
		T2 b: deep tumor		
Regional lymph nodes (N)	NX:	regional lymph nodes cannot be assessed		
	N0:	no regional lymph node metastasis		
	N1:	regional lymph node metastasis		
Distant metastasis (M)	M0:	no distant metastasis		
	M1:	distant metastasis		
G Hislopathological Grading				
Translation table for three- and four-grade to two-grade (low vs. high-grade) system				
TNM two-grade system	Three-grade systems		Four-grade systems	
Low-grade	Grade 1		Grade 1	
			Grade 2	
High-grade	Grade 2		Grade 3	
	Grade 3		Grade 4	
Stage IA	T1 a	NO. NX	M0	Low-grade
	T1 b	NO. NX	M0	Low-grade
Stage IB	T2 a	NO, NX	M0	Low-grade
	T2 b	NO, NX	M0	Low-grade
Stage IIA	T1 a	NO. NX	M0	High-grade
	T1 b	NO. NX	M0	High-grade
Stage IIB	T2 a	NO. NX	M0	High-grade
Stage III	T2 b	NO, NX	M0	High-grade
Stage IV	Any T	NI	M0	Any grade
	Any T	Any N	M1	Any grade

Source: Reference 12.
* Superficial tumor is located exclusively above the superficial fascia without invasion of the fascia: deep tumor is located either exclusively beneath the superficial fascia, or superficial to the fascia with invasion of or through the fascia. Retroperitoneal, mediastinal and pelvic sarcomas are classified as deep tumors.
Note: Regional node involvement is rare and cases in which nodal status is not assessed either clinically or pathologically could be considered NO instead of NX or pNX.

On conventional radiographs, most bone tumors are radiolucent.[8,32] The appearance of the tumor margins on conventional radiographs is often predictive of the aggressiveness of the neoplasms. Radiolucent lesions with margins that appear as abrupt zones of transition relative to normal-appearing bone are referred to as having a geographic destructive pattern (type 1), usually indicating a slow growing lesion.[8,32] A "moth-eaten" radiolucent pattern (type 2) consists of multiple radiolucent foci separated by normal-appearing bone. A "permeative" radiolucent pattern (type 3) consists of poorly defined radiolucent zones with indistinct margins. The "moth-eaten" and "permeative" radiolucent patterns are often associated with aggressive lesions, including malignant neoplasms.[8,32] There can be, however, occasional overlapping patterns of bone destruction with benign and malignant neoplasms.[8,32] The presence of matrix mineralization (calcification, ossification) in tumors may allow a narrowing of the differential diagnosis. The presence of arc or ring shaped calcifications is highly suggestive of a cartilaginous tumor, whereas amorphous, cloud-like, ill-defined densities can be seen with osteosarcomas.[8,32]

Patterns of periosteal reaction can also vary related to tumor growth as well as occur with other disorders.[8] Slow-growing tumors (osteoma, osteoid osteoma, etc.) and inflammatory lesions (osteomyelitis, Langerhans cell histiocytosis) that cross the cortex can elevate the periosteum, resulting in noninterrupted layers of periosteal formation and cortical thickening.[8,32,48] Single layered noninterrupted periosteal reaction can also occur with healing fractures, hypertrophic pulmonary osteoarthropathy, venous stasis, myositis ossificans, thyroid acropachy, and Gaucher disease. Zones of cortical destruction are commonly seen with malignant neoplasms as well as extra-osseous tumor extension.[8,32,48] Aggressive and/or malignant tumors (osteosarcoma, Ewing sarcoma, chondrosarcoma, lymphoma) can elevate the periosteum as well as eventually destroy and interrupt portions of the elevated periosteum.[8,32,48] Tumor-induced bone formation can occur within medullary bone as well as within extra-osseous portions of neoplasms. Tumor-induced bone formation within extra-osseous portions of the neoplasms, also referred to as periosteal reaction, can have various configurations. Tumor-induced bone formation from malignant neoplasms can be oriented perpendicular to the long axis of bone with "velvet," "hair on end," "sunburst," "cumulus cloud" or disorganized/complex configurations.[8,32,48] Multilayered zones of periosteal reaction with an "onion-peel" or lamellated appearance can also be seen with aggressive tumors and inflammatory lesions. Triangular zones of periosteal reaction may be seen at the borders of cortical destruction and extra-osseous tumor extension, and are referred to as Codman triangles.[8,32,48] Codman triangles can be seen with malignant primary bone neoplasms, osteomyelitis, or trauma.[48] Various types of interrupted periosteal may be coexistent in malignant bone tumors.

With MRI, features used to evaluate and characterize bone and soft tissue tumors include:

- lesion location
- lesion size
- margins (well-defined geographic with or without low signal margins versus poorly-defined margins)
- signal of the lesion on Tl-weighted images, proton-density weighted images with and/or without fat-suppression, T2-weighted images with and/or without fat-suppression, STIR images
- enhancement after intravenous administration of Gadolinium-based contrast material
- presence of cortical destruction.

For bone tumors, MRI can accurately demonstrate the size, configuration, and margins of extra-osseous neoplastic extension from the medullary canal through sites of cortical destruction.

MRI findings may be useful for diagnosis and narrowing the list of differential possibilities of bone and soft tissue tumors. For example, extra- and intra-osseous lipomas have signal similar to fat, and unicameral bone cysts usually have circumscribed margins and contain fluid signal. Nonossifying fibromas in bone often have circumscribed margins and have internal low signal on T2-weighted images, reflecting their histological features. The locations of lesions combined with MRI features may also be highly suggestive of specific lesions, such as with osteofibrous dysplasia, osteoid osteoma, juxtacortical chondroma, enchondroma, osteochondroma, chondroblastoma, fibrous dysplasia, chordoma, chondromyxoid fibroma, and Paget sarcoma. Features commonly associated with malignant bone tumors include: poorly-defined margins, extension of tumor from marrow through sites of cortical destruction, irregular contrast enhancement with zones of necrosis, and skip lesions. Overlapping MRI features of many malignant tumors require biopsies for diagnosis and treatment planning. MRI is, however, recommended and routinely used for staging of bone and soft tissue tumors because of its superior contrast resolution and multi-planar imaging capabilities in determining tumor size and extent.[8,32] MRI provides a more accurate assessment of tumor volume compared with radiographs and CT, and is also useful in detecting fluid-fluid levels in tumors as well as non-enhancing necrotic zones.[8] MRI also provides detailed information regarding tumor margins, presence of tumor invasion of neurovascular structures and bone;[12] MRI can also confirm the presence of hemorrhage, cystic, fibrotic and/or myxoid changes within tumors.[12]

Contrast-enhanced MRI often provides useful information in the evaluation of musculoskeletal lesions.[9-11,23,24,43-45] For evaluation of musculoskeletal neoplasms, dynamic MR imaging after bolus intravenous administration of gadolinium-chelate contrast can sometimes be useful in distinguishing between rapidly enhancing tumor and initially nonenhancing perineoplastic edema and/or necrosis.[9-11] Combining information from static and dynamic contrast-enhanced MRI with results from nonenhanced MRI may allow improved differentiation between benign and malignant soft tissue tumors.[44] The presence of liquefaction, large tumor size and early patterns of dynamic contrast enhancement were features that were commonly associated with malignant than benign soft tissue tumors.[44] Responses of malignant tumors such as osteosarcomas and Ewing sarcomas to chemotherapy can also be assessed by detecting nonenhancing zones of necrosis or sites of persistent early enhancement that are typically associated with remaining viable tumor. Newer MRI techniques, such as diffusion weighted imaging and MR spectroscopy, have been used in clinical research studies for the evaluation of musculoskeletal neoplasms, although their clinical relevance requires further study.[38,47]

The information provided by MRI is valuable for the planning of biopsies and surgical resection.[12] Knowledge of the MRI features and associated findings from conventional radiographs and/or CT scans can provide comprehensive and detailed evaluation of musculoskeletal tumors and tumorlike lesions.

This book is focussed on the description and categorization of the MRI features of both benign and malignant bone and soft tissue tumors of the musculoskeletal system. The actual definition of the English word "tumor" is derived from the Latin word "tumere," which is translated as "swelling." The lesions described in this book include both neoplasms and tumorlike

masses involving the appendicular skeleton/extremities as well as the axial skeleton (spine, paraspinal soft tissues, and skull).

The portion of this book immediately following this introductory chapter groups musculoskeletal lesions into 20 lists of differential diagnoses based on anatomic locations and/or MRI features illustrated with MR images. This approach is intended to provide the reader with an easy-to-use format to help guide the evaluation of lesions that can be encountered in clinical practice. It is similar to the author's prior collaboration for the book *Differential Diagnosis in Magnetic Resonance Imaging* by Frances Burgener, Steven P. Meyers, Raymond K. Tan, and Wolfgang Zaubauer (Thieme, 2002). One substantial change that has been made for the new book is that the references are supplied for each lesion listed in the Comments Section of the tables. References are either made to the last section of the book, wich includes 77 Atlas chapters with illustrations for various lesions, or to publications in the literature at the end of each table for uncommon lesions with no Atlas chapter dedicated to them. Efforts were made to provide the reader with the most current references in the literature at the time of publication. The last portion of this book is organized into an atlas format with chapters that include detailed demographic, pathologic, and clinical information for musculoskeletal lesions as well as multiple MRI examples, often with corresponding plain film and/or CT images, to demonstrate the range of imaging findings and locations associated with each of the lesions. Each Atlas chapter also has references to the literature for each lesion. Some tumors (lipoma, hemangioma, hemangioendothelioma, malignant fibrous histiocytoma, osteosarcoma, chondrosarcoma, leukemia, etc.) and tumorlike lesions (sarcoidosis, Erdheim-Chester, etc.) can occur as primary abnormalities in bone and/or soft tissue. When relevant, the Atlas chapters contain examples of lesions that are primarily located in bone as well as within soft tissue.

For this book, MRI signal of the various entities will be described as low, intermediate, high, or mixed on Tl-weighted imaging (TlWI), proton density weighted imaging (PDWI), and T2-weighted imaging (T2WI); and whether there is gadolinium-contrast (Gd-contrast) enhancement or not. When available, comments and examples will be given regarding MRI features with fat-suppression techniques such as frequency-selective (FS) fat-presaturation applied on T1WI, PDWI, T2WI, or utilization of the short T1 inversion recovery (STIR) sequence. Both techniques enable distinction of pathologic processes (neoplasm, infection, inflammation, edema, etc.) from normal anatomic structures with high signal from intrinsic fat, such as marrow and subcutaneous soft tissues.

References

1 Arndt CA, Crist WM. Common musculoskeletal tumors of childhood and adolescence. *N Engl J Med* 1999;341(5):342-352.

2 Berquist TH, Ehman RL, King BF, Hodgman CG, Ilstrup DM. Value of MR imaging in differentiating benign from malignant soft-tissue masses: study of 95 lesions. *AJR Am J Roentgenol* 1990; 155: 1251-1255.

3 Biondetti PR, Ehman RL Soft-tissue sarcomas: use of textural patterns in skeletal muscle as a diagnostic feature in postoperative MR imaging. *Radiology* 1992;183(3):845-848.

4 Bridge JA, Orndal C. Cytogenetic analysis of bone and joint neoplasms. In: Helliwell TR, ed. *Pathology of Bone and Joint Neoplasms* Philadelphia, Pa: W.B. Saunders; 1999:59-78.

5 Bridge JA, Sandberg AA. Cytogenetic and molecular genetic techniques as adjunctive approaches in thediagnosis of bone and soft tissue tumors. *Skeletal Radiol* 2000;29:249-258.

6 Bush CH. The MRI of hemorrhage. *Skeletal Radiol* 2000;29:1-9.

7 Choi H, Varma Datla GK, Fornage BD, Kim EE, Johnston DA. Soft-tissue sarcoma: MR imaging vs. sonography for detection of local recurrence after surgery. *AJR Am J Roentgenol* 1991;157:353-358.

8 Dorfman HD, Czerniak B, Kotz R, Vanel D, Park YK, Unni KK. WHO classification of tumours of bone: introduction. In: Fletcher CDM, Unni KK, Mertens F, eds. *World Health Organization Classification of Tumours. Pathology and Genetics of Tumours of Soft Tissue and Bone* Geneva: IARC Press; 2002:227-232.

9 Dyke JP, Panicek DM, Healy JH, et al. Osteogenic and ewing sarcomas: estimation of necrotic fraction during induction chemotherapy with dynamic contrast-enhanced MR imaging. *Radiology* 2003;228: 271-278.

10 Erlemann R, Reiser MF, Peters PE, et al. Musculoskeletal neoplasms: static and dynamic Gd-DTPA-enhanced MR imaging. *Radiology* 1989;171(3):767-773.

11 Erlemann R. Letters to the Editor - Dynamic, Gadolinium-enhanced MR imaging to monitor tumor response to chemotherapy. *Radiology* 1993;186(3):904-905.

12 Fletcher CDM, Ryholm A, Singer S, Sundaram M, Coindre IM. Soft tissue tumours: epidemiology, clinical features, histopathological typing and grading. In: Fletcher CDM, Unni KK, Mertens F, eds. *World Health Organization Classification of Tumours. Pathology and Genetics of Tumours of Soft Tissue and Bone*. Geneva: IARC Press; 2002:12-18.

13 Fletcher JA. Cytogenetic analysis of soft-tissue tumors. In: Weiss SW, Goldblum JR, eds. *Enzinger and Weiss's Soft Tissue Tumors* 4th ed. St. Louis, Mo: Mosby; 2001:125-146.

14 Folpe AL, Gown AM. Immunohistochemistry for analysis of soft tissue tumors. In Weiss SW, Goldblum JR, eds. *Enzinger and Weiss's Soft Tissue Tumors* 4th ed. St. Louis: Mosby 2001; 199-245.

15 Forest M. Bone metastases. In: Forest M, Tomeno B, Vanel D, eds. *Orthopedic Surgical Pathology: Diagnosis of Tumors and Pseudotumoral Lesions of Bone and Joints* Edinburgh: Churchill Living¬ stone;1998:501-516.

16 Gao Z, Kahn LB. The application of immunohistochemistry in the diagnosis of bone tumors and tumorlike lesions. *Skeletal Radiol* 2005;34:755-770.

17 Helliwell TR. Classification and diagnosis of bone neoplasms. In: Helliwell TR,ed. *Pathology of Bone and Joint Neoplasms*. Philadelphia, Pa: W.B. Saunders; 1999:1-14.

18 Jemal A, Thomas A, Murray T, Thun M. Cancer statistics 2002. *CA Cancer J Clin* 2002;52:23-47.

19 Kransdorf MJ, Meis JM. From the Archives of the AFIP - Extraskeletal osseous and cartilaginous tumors of the extremities. *Radiographics* 1993;13(4):853-884.

20 Kransdorf MJ, Murphey MD. Origin and classification of soft tissue tumors. In: *Imaging of Soft Tissue Tumors*. 2nd ed. Philadelphia, Pa: Lippincott, Williams & Wilkins; 2006:1-5.

21 Kransdorf MJ. Benign soft-tissue tumors in a large referral population: distribution of specific diagnoses by age, sex, and location. *AJR Am J Roentgenol* 1995;164:395-402.

22 Kransdorf MJ. Malignant soft-tissue tumors in a large referral population: distribution of diagnoses by age, sex, and location. *AJR Am J Roentgenol* 1995;164:129-134.

23 Kransdorf MJ. Questions and Answers - Is it necessary to routinely use gadolinium in the MR imaging evaluation of soft-tissue tumors of the extremities? *AJR Am J Roentgenol* 1995; 165(6): 1545.

24 Miller SL, Hoffer FA. Malignant and benign bone tumors. *Radiol Clin North Am* 2001;39(4):673-699.

25 Moore SG, Bisset GS III, Siegel MJ, Donaldson JS. Pediatric musculoskeletal MR imaging. *Radiology* 1991;179(2):345-360.

26 Moser RP, Madewell JE. Metastatic bone disease. In: Tavers JM, Ferrucci JT, eds. *Radiology Diagnosis-Imaging-Intervention* Vol 5. Philadelphia, PA: Lippincott Williams & Wilkins; 2002.

27 Mulder JD, Schutte HE, Kroon HM, Taconis WK. Introduction. In: *Radiologic Atlas of Bone Tumors*. Amsterdam: Elsevier; 1993:3-6.

28 Mulder JD, Schutte HE, Kroon HM, Taconis WK. The diagnosis of bone tumors. In: *Radiologic Atlas of Bone Tumors*. Amsterdam: Elsevier; 1993:9-46.

29 Murphey MD, Smith WS, Smith SE, Kransdorf MJ, Temple HT. From the Archives of the AFIP - Imaging of musculoskeletal neurogenic tumors: radiologic-pathologic correlation. *Radiographics* 1999; 19(5): 1253-1280.

30 Patel SR, Benjamin RS. Sarcomas of soft tissue and bone. In: Fauci AS, Braunwald E, Isselbacher KJ, et al. *Harrison's Principles of Internal Medicine.* 14th ed. New York: McGraw-Hill; 1998:611-615.

31 Pettersson H, Gillespy T III, Hamlin DJ, et al. Primary musculoskeletal tumors: examination with MR imaging compared with conventional modalities. *Radiology* 1987;164(1):237-241.

32 Ritchie DA, Davies AM. Imaging studies in bone neoplasia. In: Helli¬well TR, ed. *Pathology of Bone and Joint Neoplasms* Philadelphia, Pa: W.B. Saunders; 1999:106-27.

33 Salisbury JR. Bone neoplasms containing epithelial and epithelioid cells. In: Helliwell TR, ed. *Pathology of Bone and Joint Neoplasms.* Philadelphia, PA: WB Saunders; 1999:345-368.

34 Sandberg AA. Cytogenetic and molecular genetics of bone and soft-tissue tumors. *Am J Med Genet* 2002;115:189-193.

35 Scholz RB, Christiansen H, Kabisch H, Winkler K. Molecular markers in the evaluation of bone neoplasms. In: Helliwell TR, ed. *Pathology of Bone and Joint Neoplasms* Philadelphia, Pa: W.B. Saunders; 1999: 79-105.

36 Shuman WP, Patten RM, Baron RL, Liddell RM, Conrad EU, Richardson ML. Comparison of STIR and spin-echo MR imaging at 1.5 T in 45 suspected extremity tumors: lesion conspicuity and extent. *Radiology* 1991;179(1):247-252.

37 Slominski A, Wortsman J, Carlson A, Mihm M, Nickoloff B, McClatchey K. Molecular pathology of soft tissue and bone tumors, a review. *Arch Pathol Lab Med* 1999;123:1246-1259.

38 Sostman HD, Prescott DM, Dewhirst MW, et al. MR imaging and spectroscopy for prognostic evaluation in soft-tissue sarcomas. *Radiology* 1994;190(1):269-275.

39 Stacy GS, Heck RK, Peabody TD, Dixon LB. Pictorial Essay - Neoplastic and tumorlike lesions detected on MR imaging of the knee in patients with suspected internal derangement: Part 1, intraosseous entities. *AJR Am J Roentgenol* 2002;178:589-594.

40 Stacy GS, Mahal RS, Peabody TD. Staging of bone tumors: a review with illustrative examples. *AJR Am J Roentgenol* 2006;186:967-976.

41 States LJ. Imaging of metabolic bone disease and marrow disorders in children. *Radiol Clin North Am* 2001;39:749-772.

42 Vade A, Eissenstadt R, Schaff HB. MRI of aggressive bone lesions of childhood. *Magn Reson Imaging* 1992;10(1):89-96.

43 van der Woude HJ, Bloem JL, Pope TL. Magnetic resonance imaging of the musculoskeletal system: Part 9. Primary tumors. *Clin Orthop Relat Res* 1998;347:272-286.

44 Van Rijswijk CSP, Geirnaerdt MJA, Hogendoorn PCW, et al. Soft-tissue tumors: value of static and dynamic gadopentetate dimeglumine¬enhanced MR imaging in prediction of malignancy. *Radiology* 2004;233:493-502.

45 Vanel D, Shapeero LG, De Baere T, et al. MR imaging in the follow-up of malignant and aggressive soft-tissue tumors: results of 511 examinations. *Radiology* 1994;190(1):263-268.

46 Unni KK. Introduction and scope of study. In: *Dahlin's Bone Tumors. General Aspects and Data on 11087 Cases.* 5th ed. Philadelphia, PA: Lippincott, Williams & Wilkins; 1996:1-9.

47 Wang CK, Li CW, Hsieh SH, Liu GC, Tsai KB. Characterization of bone and soft-tissue tumors with in vivo 1 H MR spectroscopy: initial results. *Radiology* 2004;232:599-605.

48 Wenaden AET, Szyszko TA, Saifuddin. A Imaging of periosteal reactions associated with focal lesions of bone. *Clin Radiol* 2005;60: 439-456.

49 Zawin JK, Jaramillo D. Conversion of bone marrow in the humerus, sternum, and clavicle: changes with age on MR images. *Radiology* 1993;188(1):159-164.

Differential Diagnosis Tables

Table 1 Tumors and tumorlike lesions involving the skull and facial bones

Tumor/Tumorlike Lesion	MRI Findings	Comments
Malignant neoplasms		
Metastatic tumor (Figs. 1.1-1.3)	Single or multiple well-circumscribed or poorly defined lesions involving the skull, dura, leptomeninges, and/or choroid plexus; low-intermediate signal on T1WI, intermediate-high signal on T2WI, usually shows Gd-contrast enhancement, +/- bone destruction. +•/- compression of neural tissue or vessels. Leptomeningeal tumor often best seen on postcontrast images.	May have variable destructive or infiltrative changes involving single or multiple sites of involvement. Primary tumors are usually from outside of CNS. (See Atlas Chapter A 50)
Myeloma/plasmacytoma (Figs. 1.4,1.5)	Multiple (myeloma) or single (plasmacytoma) well-circumscribed or poorly defined lesions involving the skull, and dura; low-intermediate signal on T1WI, intermediate-high signal on T2WI. usually shows Gd-contrast enhancement + bone destruction.	May have variable destructive or infiltrative changes involving the axial and/or appendicular skeleton. (See Atlas Chapter A 52)
Lymphoma (Fig. 1.6)	Single or multiple well-circumscribed or poorly defined lesions involving the skull, dura, and/or leptomeninges; low-intermediate signal on T1WI, intermediate-high signal on T2WI, usually shows Gd-contrast enhancement, +/- bone destruction, leptomeningeal tumor often best seen on postcontrast images.	Extra-axial lymphoma may have variable destructive or infiltrative changes involving single or multiple sites of involvement. (See Atlas Chapter A 47)
Leukemia (Fig. 1.7)	Single or multiple well-circumscribed or poorly defined lesions involving the skull, dura, and/or leptomeninges: low-intermediate signal on T1 WI. intermediate-high signal on T2WI, may show Gd-contrast enhancement, +/- bone destruction. LeptomenIngeal tumor often best seen on postcontrast images.	Extra-axial leukemia may have variable destructive or infiltrative changes involving single or multiple sites of involvement (See Atlas Chapter A 41)

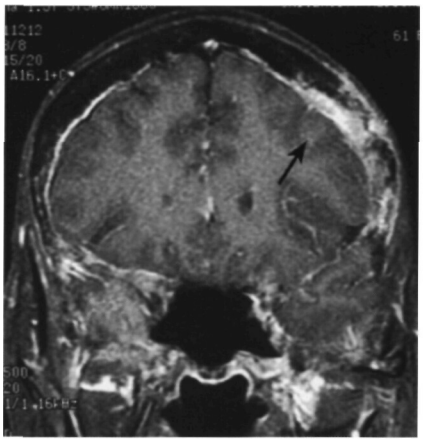

Figure 1.1 A 61-year-old woman with metastatic breast carcinoma involving the skull. The poorly defined metastatic disease shows Gd-contrast enhancement on coronal FST1WI and extends from the marrow through zones of bone destruction at the inner and outer tables of the skull to involve the intracranial dura and soft tissues of the scalp.

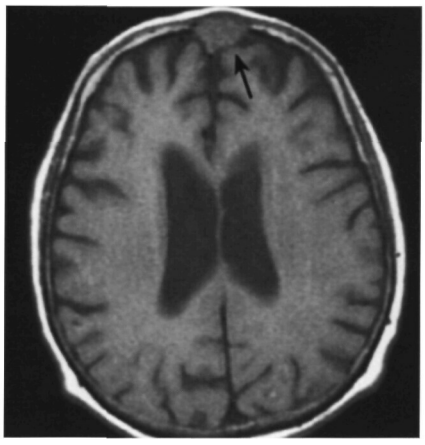

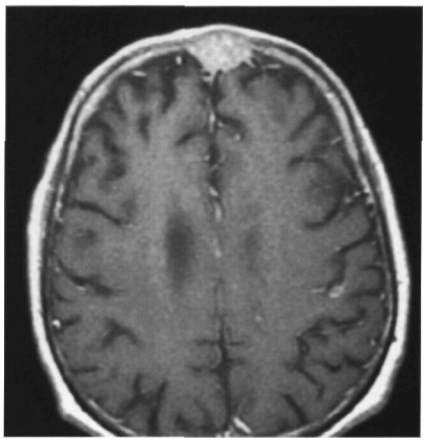

Figure 1.2 a. **b** Single metastatic lesion in the frontal bone from breast carcinoma has circumscribed margins and extends from the marrow through zones of bone destruction. The tumor has intermediate signal on axial T1WI (a) and shows prominent Gd-contrast administration on axial T1WI (b).

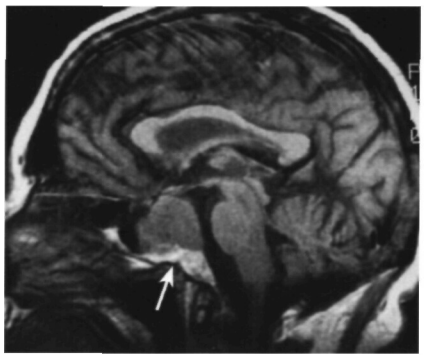

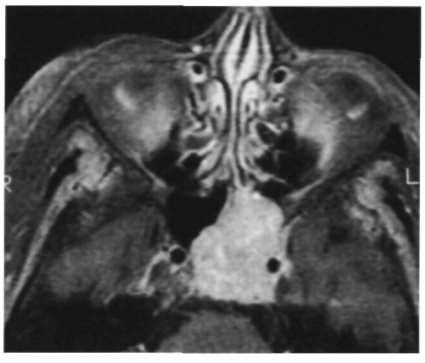

Figure 1.3 a, b Metastatic lesion in the clivus from breast carcinoma has circumscribed margins and extends from the marrow through zones of bone destruction. The tumor has intermediate signal on sagittal T1WI (a) and shows prominent Gd-contrast enhancement on axial FST1WI (b).

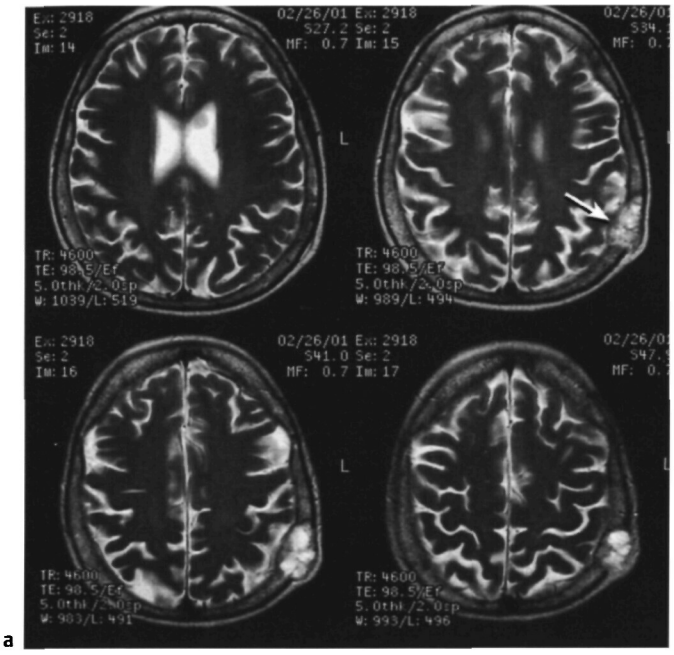

a

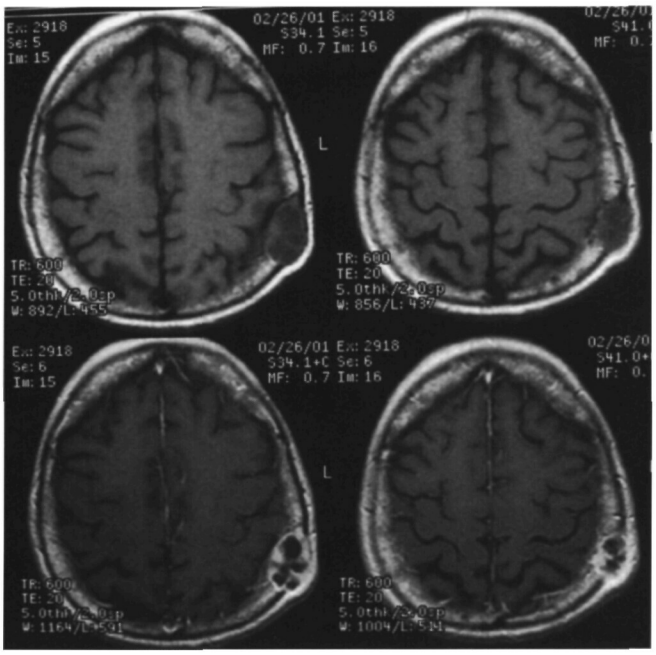

b

Figure 1.4a, b A 65-year-old woman with myeloma and a circumscribed lesion involving the skull that has heterogeneous high signal on axial T2WI (a). The tumor has low-intermediate signal on axial T1 WI (b, top *images)* and shows irregularGd-contrast enhancement on axial T1WI (b, bottom *images).*

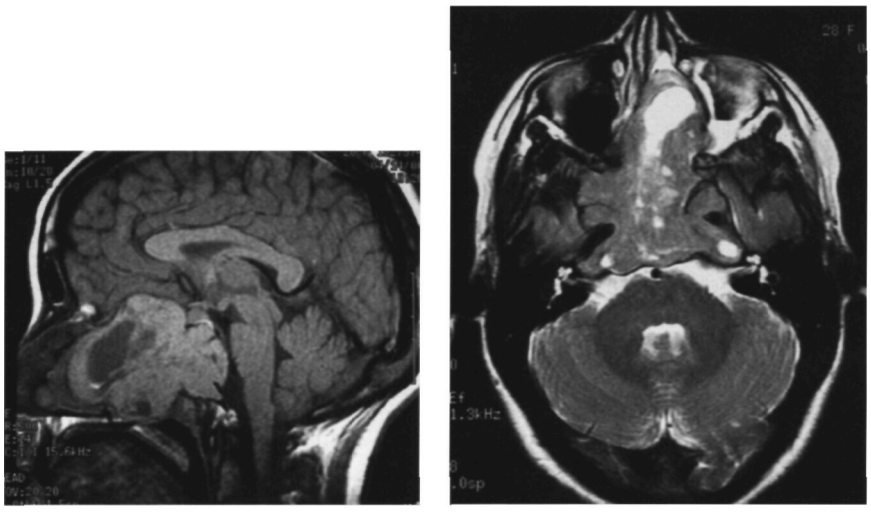

Figure 1.5 a, b Plasmacytoma involving the nasal cavity, ethmoid and sphenoid sinuses, and skull base in a 28-year-old woman. The tumor has mixed zones of low and intermediate signal on sagittal T1WI (a) and zones of intermediate to slightly high signal and high signal on axial T2WI (b).

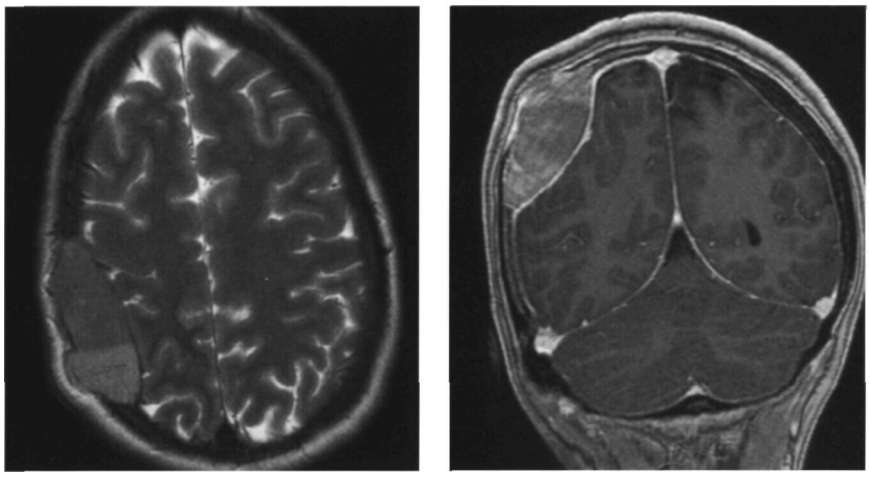

Figure 1.6a, b A 46-year-old woman with diffuse large B cell non-Hodgkin lymphoma involving the skull and dura. The lesion has low-intermediate signal on axial T2WI (a) and shows heterogeneous Gd-contrast enhancement on coronal T1WI (b).

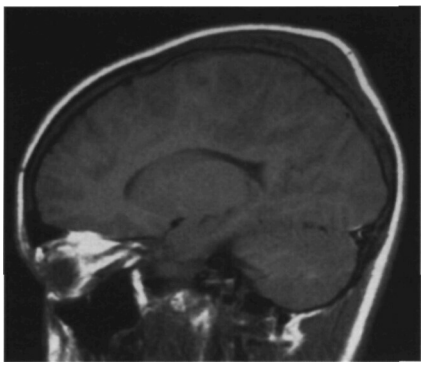

Figure 1.7 A 12-year-old female with leukemia (ALL) involving the skull, which is seen as zones of low-intermediate signal in the marrow as well as sites of destruction of the inner and outer tables on sagittal T1WI.

Table 1 (Continued) **Tumors and tumorlike lesions involving the skull and facial bones**

Tumor/Tumorlike Lesion	MRI Findings	Comments
Chordoma (Fig. 1.8)	Well-circumscribed tabulated lesions, low-intermediate signal on T1WI. high signal on T2WI, usually shows Gd-contrast enhancement (usually heterogeneous), locally invasive associated with bone erosion/destruction, encasement of vessels and nerves, skull base-clivus common location, usually in the midline.	Rare, slow-growing tumors at the skull base, detailed anatomic display of extension of chordomas by MRI is important for planning of surgical approaches. **(See Atlas Chapter A12)**
Chondrosarcoma (Fig. 1.9)	Lobulated lesions, low-intermediate signal on T1 WI, high signal on T2WI, +/- matrix mineralization-low signal on T2WI, usually shows Gd-contrast enhancement (often heterogeneous), locally invasive associated with bone erosion/destruction, encasement of vessels and nerves, skull base-petrous-occipital synchondrosis common location, usually off midline.	Rare, slow-growing tumors, detailed anatomic display of extension of chondrosarcomas by MRI is important for planning of surgical approaches. **(See Atlas Chapter A11)**
Osteogenic sarcoma (Fig. 1.10)	Destructive lesions involving the skull base, low-intermediate signal on T1WI, mixed low, intermediate, high signal on T2WI, usually + matrix mineralization/ossification-low signal on T2W images, typically shows Gd-contrast enhancement (usually heterogeneous).	Rare lesions involving the skull-base and calvaria, more common than chondrosarcomas and Ewing sarcoma, locally invasive, high metastalic potential. Occurs in children as primary tumors and adults (associated with Paget disease, irradiated bone, chronic osteomyelitis, osteoblastoma, giant cell tumor, fibrous dysplasia). **(See Atlas Chapter A 64)**
Ewing sarcoma (Fig. 1.11)	Destructive lesions involving the skull base, low-intermediate signal on T1WI, mixed low, intermediate, high signal on T2WI. typically shows Gd-contrast enhancement (usually heterogeneous).	Usually occurs between the ages of 5 and 30, males > females, rare lesions involving the skull-base, locally invasive, high metastatic potential. **(See Atlas Chapter A 20)**

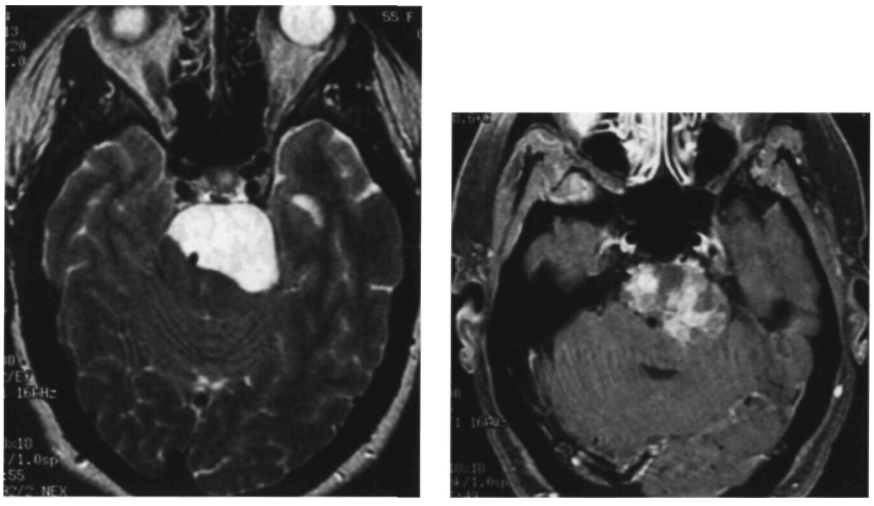

Figure 1.8 a, b A 55-year-old woman with a chordoma involving the endocranial surface of the clivus with intracranial extension causing compression of the brainstem. The tumor has high signal on axial T2WI (a) and shows heterogeneous Gd- contrast enhancement on axial FST1WI (b).

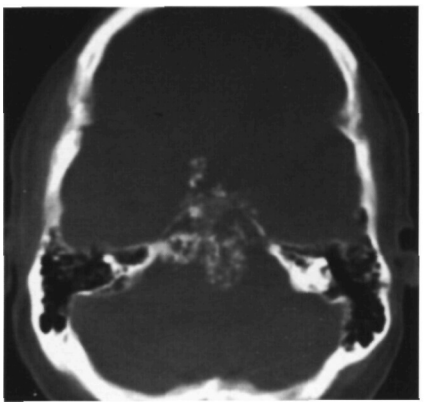

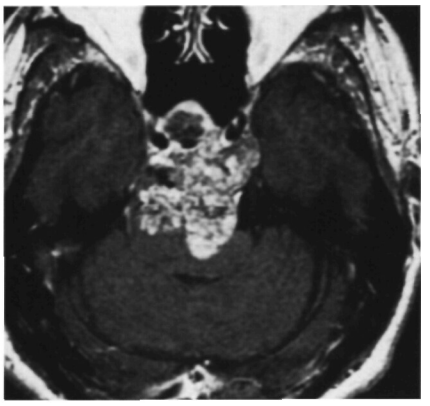

Figure 1.9a, b A 42-year-old woman with a chondrosarcoma involving the clivus. Axial CT image (a) shows the lesion to have prominent chondroid matrix mineralization. The tumor shows prominent heterogeneous Gd-contrast enhancement on axial T1WI (b).

Figure 1.10a, b A 16-year-old female with history of radiation and surgery for retinoblastoma and subsequent development of osteosarcoma involving the right sphenoid and frontal bones. The tumor has mixed intermediate, slightly high, and high signal on axial T2WI (a). The tumor is associated with bone destruction as well as intracranial extension resulting in compression and posterior displacement of the right temporal lobe, edema in the brain, and early uncal herniation. The tumor shows prominent heterogeneous Gd-contrast enhancement on axial T1WI(b).

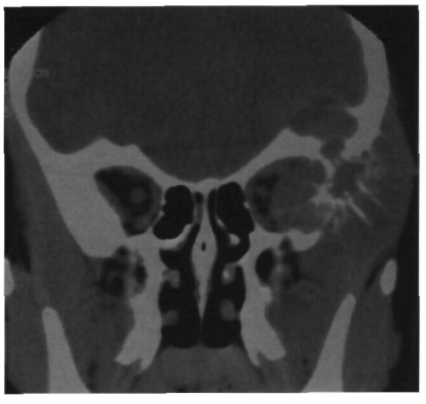

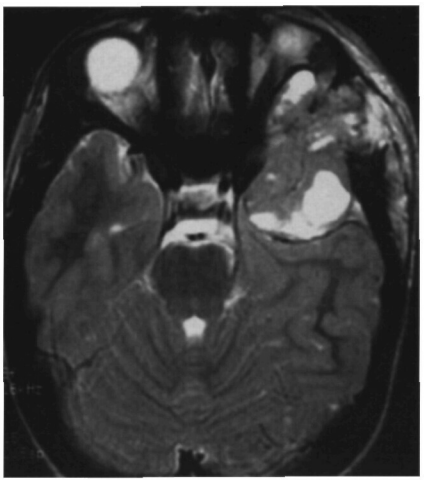

b, c

Figure 1.11a-c An 11-year-old girl with Ewing sarcoma involving the left frontal and zygomatic bones with tumor extension intracranially as well as into the left orbit. Coronal CT image (a) shows a soft tissue tumor containing perpendicular striated periosteal reaction associated with bone destruction. The tumor has heterogeneous intermediate and high signal on axial T2WI (b) with small foci of low signal. The tumor shows prominent irregular Gd-contrast enhancement on axial T1WI (c).

Table 1 (Continued) **Tumors and tumorlike lesions involving the skull and facial bones**

Tumor/Tumoriike Lesion	MRI *findings*	Comments
Sinonasal/nasopharyngeal carcinoma (Figs. 1.12,1.13)	Destructive lesions in the nasal cavity, paranasal sinuses, nasopharynx; +/- intracranial extension via bone destruction or perineural spread: intermediate signal on T1WI, intermediate-slightly high signal on T2WI; often shows Gd-contrast enhancement; large lesions (+/- necrosis and/or hemorrhage).	Occurs in adults usually > 55 years, males > females, associated with occupational or other exposure to: nickel, chromium, mustard gas, radium, manufacture of wood products.
Adenoid cystic carcinoma (Fig. 1.14)	Destructive lesions in the paranasal sinuses, nasal cavity, nasopharynx, +/- intracranial extension via bone destruction or perineural spread, intermediate signal on T1WI, intermediate-high signal on T2WI, variable mild, moderate, or prominent Gd-contrast enhancement.	Account for 10 % of sinonasal tumors, arise any location within sinonasal cavities, usually occurs in adults > 30 years.
Esthesioneuroblastoma (Figs. 1.15)	Locally destructive lesions with low-intermediate signal on T1WI, intermediate-high signal on T2WI, usually show prominent Gd-contrast enhancement, location: superior nasal cavity, ethmoid air cells with occasional extension into the other paranasal sinuses, orbits, anterior cranial fossa, cavernous sinuses.	Tumors also referred to as olfactory neuroblastoma, arise from olfactory epithelium in the superior nasal cavity. Occur in adolescents and adults, males > females.
Rhabdomyosarcoma (Atlas Fig. 459)	Lesions have low-intermediate signal on T1WI and FS-T1 WI with circumscribed and/or poorly defined margins. Signal changes from areas of hemorrhage may be present Lesions usually have heterogeneous signal (various combinations of intermediate, slightly high, and/or high signal) on T2WI and FS T2WI. Zones of edema may occur in the adjacent soft tissues. Tumors can be associated with destructive changes of adjacent bone. Tumors show variable degrees and patterns of contrast enhancement.	Malignant mesenchymal tumors with rhabdomyoblastic differentiation that occur primarily in soft tissue, and only very rarely in bone. Occurs most frequently in children. **(See Atlas Chapter A 69)**
Hemangiopericytoma (Fig. 1.16)	Extra-axial mass lesions, often well-circumscribed, intermediate signal on T1WI, intermediate-slightly high signal on T2WI, usually show prominent Gd-contrast enhancement (may resemble meningiomas), +/- associated erosive bone changes.	Rare neoplasms in young adults (males > females) sometimes referred to as angioblastic meningioma or meningeal hemangiopericytoma, arise from vascular cells-pericytes, frequency of metastases > meningiomas. **(See Atlas Chapter A 35)**

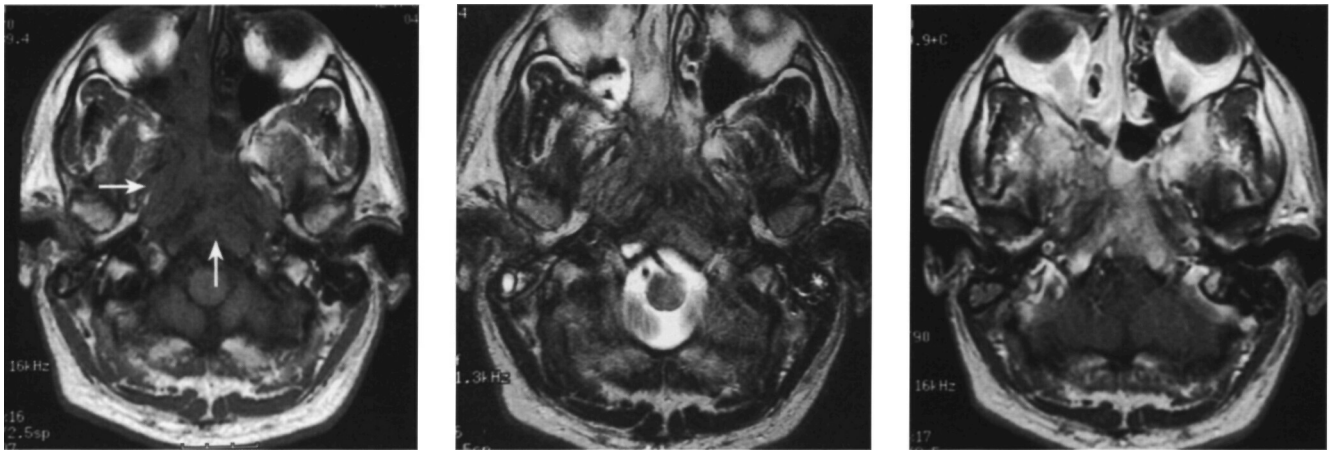

Figure 1.12 a-c Squamous cell carcinoma is seen as a poorly defined tumor in the posterior nasopharynx with invasion into the clival marrow. The tumor has intermediate signal on axial T1WI (a) and axial T2WI (b), and shows Gd-contrast enhancement on axial T1WI (c).

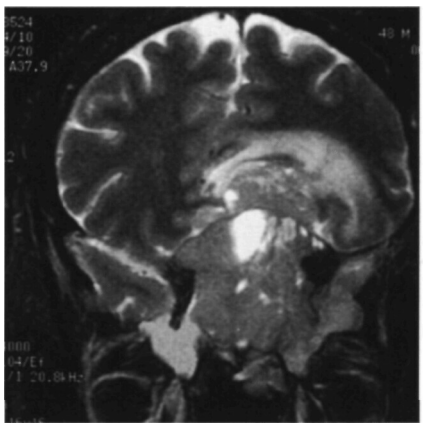

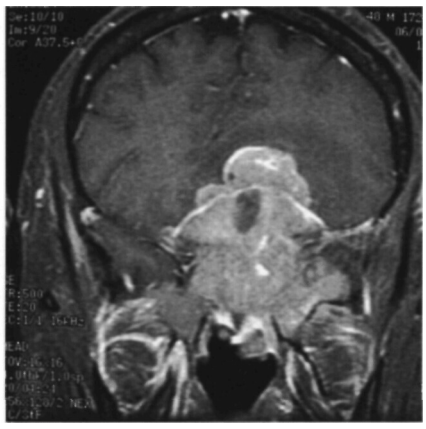

Figure 1.13a, b A 48-year-old man with a poorly differentiated nasopharyngeal carcinoma in the ethmoid sinus associated with bone destruction and intracranial and left infratemporal extension. The tumor has heterogeneous intermediate and high signal on coronal FS T2WI (a) and shows prominent irregular Gd-contrast enhancement on coronal FST1WI (b).

Figure 1.14 A 46-year-old woman with adenoid cystic carcinoma in the nasopharynx, which extends superiorly along the third division of the left fifth cranial nerve through a widened left foramen ovale into the left trigeminal cistern. The tumor shows prominent Gd-contrast enhancement on coronal FST1WI.

a

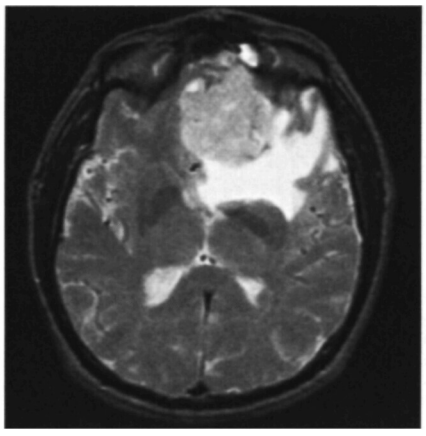

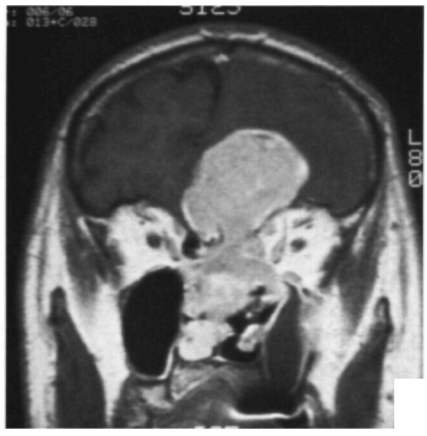

b

Figure 1.15 a, b Esthesioneuroblastoma in the anterior ethmoid air cells associated with bone destruction at the skull base and intracranial tumor extension. The tumor has heterogeneous slightly high to high signal on axial T2WI (a). The tumor shows prominent Gd-contrast enhancement on coronal T1 WI (b).

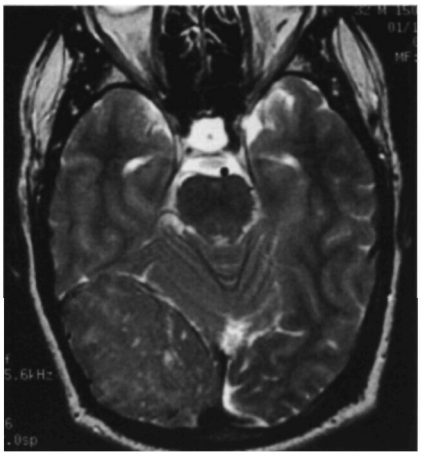

a

Figure 1.16a, b A 32-year-old man with a hemangiopericytoma involving the tentorium. The tumor has slightly lobulated margins and mostly intermediate signal on axial T2WI (a) as well as small zones with high signal. The tumor shows prominent Gd-contrast enhancement on coronal T1WI (b).

Table 1 (Continued) **Tumors and tumorlike lesions involving the skull and facial bones**

Tumor/Tumorlike Lesion	MR) Findings	Comments
Benign neoplasms		
Meningioma (Figs. 1.17-1.20)	Extra-axial dural-based lesions, well-circumscribed (supra- > infratentorial, parasagittal > convexity > sphenoid ridge > parasellar > posterior fossa > optic nerve sheath > intraventricular). intermediate signal on T1WI, intermediate-slightly high signal on T2WI, typically shows prominent Gd-contrast enhancement, +/- calcifications, +/- hyperostosis and/or invasion of adjacent skull.	Most common extra-axial tumor, usually benign neoplasms, typically occurs in adults (> 40 years), women > men, multiple meningiomas seen with NF2. can result in compression of adjacent brain parenchyma, encasement of arteries, and compression of dural venous sinuses, rarely invasive/malignant types. **(See Atlas Chapter A 49)**
Hemangioma (Fig. 1.21)	Circumscribed or poorly marginated structures (<4 cm in diameter) in marrow of skull (often frontal bone) with intermediate-high signal on T1WI (often isointense to marrow fat), high signal on T2WI and FST2WI, typically show Gd-contrast enhancement, +/- widening of diploic compartment.	Benign skull lesions, adults (> 30 years). **(See Atlas Chapter A 34)**
Ossifying hemangioma (Fig. 1.22)	Zone with low-intermediate signal on T1WI and slightly high to high signal on T2WI and FS T2WI. Lesions usually show prominent Gd-contrast enhancement on T1 WI and FST1WI.	Benign lesions within the temporal bone that involve the facial nerve, and on CT are usually radiolucent containing bone spicules. Lesions can be associated with slowly progressive or recurrent facial paralysis.

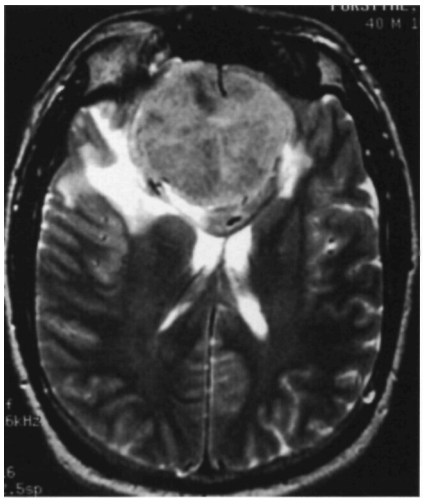

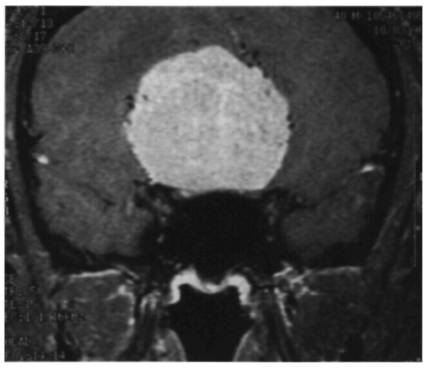

Figure 1.17 a, b A 40-year-old man with an olfactory groove meningioma that has heterogeneous slightly high signal on axial T2WI (a) as well as several small zones of low signal. Edematous high signal changes on T2WI are seen in the brain compressed by the meningioma. The tumor shows prominent Gd-contrast enhancement on coronal FS T1WI (b).

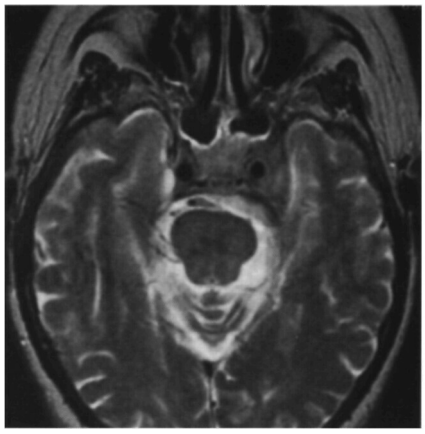

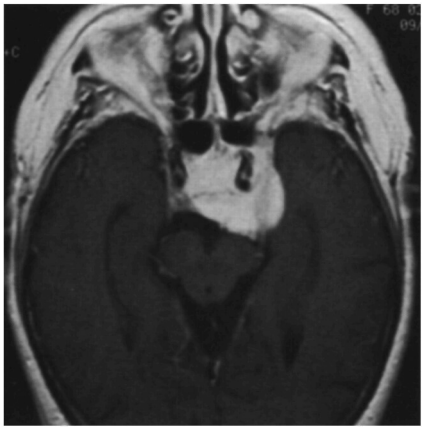

Figure 1.18a, b A 68-year-old woman with a meningioma involving the anteromedial left middle cranial fossa, clivus, left cavernous sinus with encasement of the left internal carotid artery, and left trigeminal cistern. The tumor has heterogeneous intermediate signal on axial T2WI (a). The tumor shows prominent Gd-contrast enhancement on axial T1WI(b).

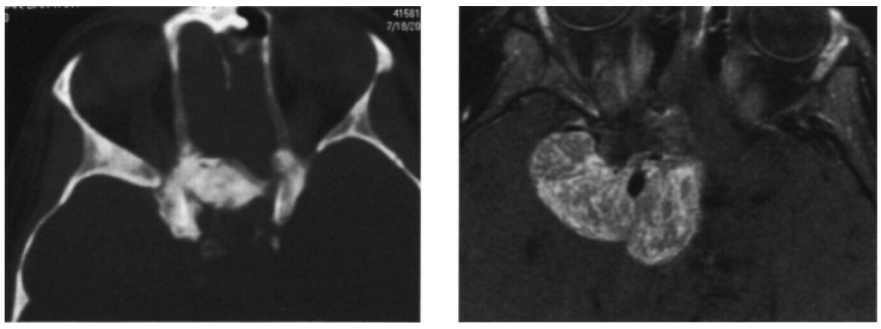

Figure 1.19a, b A 9-year-old girl with neurofibromatosis type II with a large meningioma involving the right sphenoid bone. Axial CT image (a) shows reactive hyperostosis at the greater wing and right anterior clinoid process of the sphenoid bone from osseous invasion of the meningioma. The meningioma shows prominent heterogeneous Gd-contrast enhancement on axial FS T1WI (b). Minimal irregular Gd-contrast enhancement is seen in the hyperostotic bone.

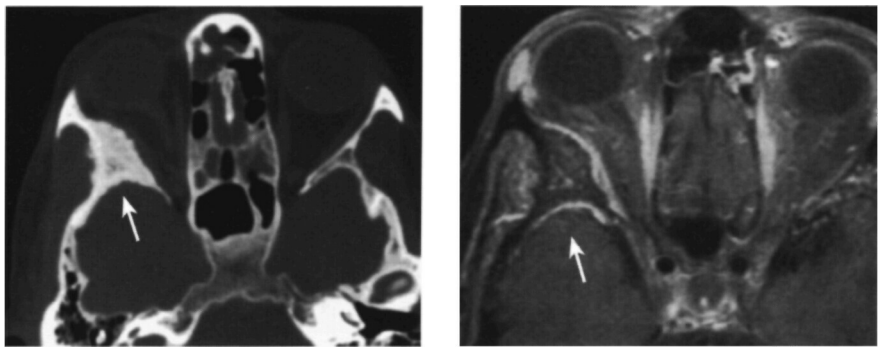

Figure 1.20a, b A 52-year-old woman with an intraosseous meningioma. Axial CT image (a) shows thickening and hyperostosis at the posterolateral wall of the right orbit. Small zones of extraosseous tumor at the lateral orbit and anterior middle cranial fossa show Cd-contrast enhancement on axial FST1WI (b).

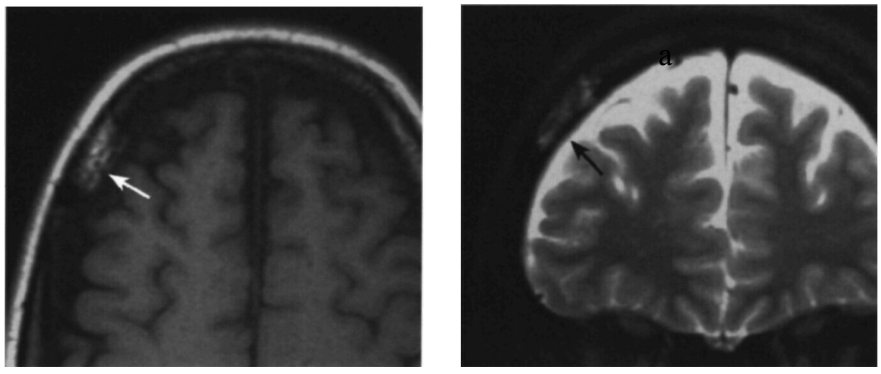

Figure 1.21 a, b A hemangioma in the marrow of the right frontal bone has high signal on axial T1WI (a) and coronal FST2WI (b).

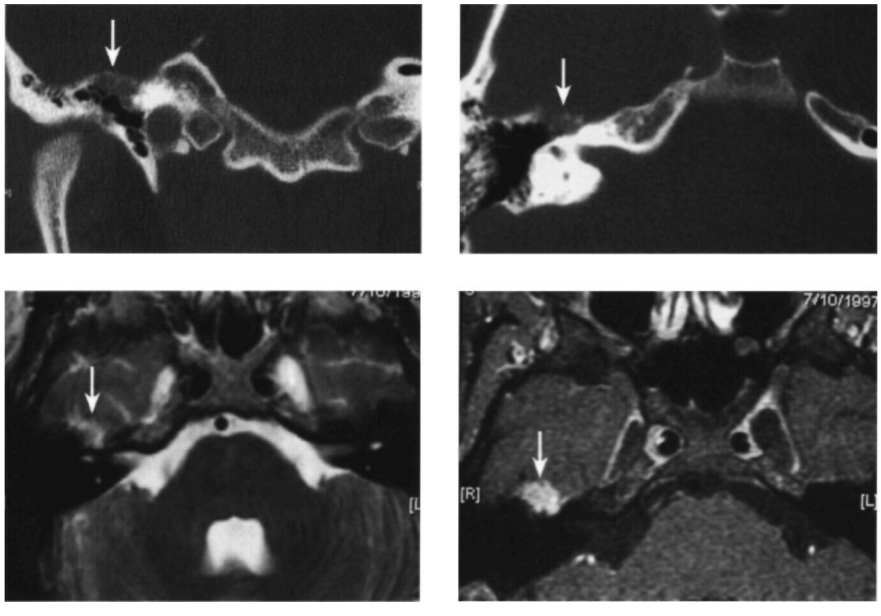

Figure **1.22a-d** An ossifying hemangioma in the right temporal bone is seen as a radiolucent lesion containing bone spicules on coronal (a) and axial (b) CT images. The lesion has slightly high to high signal on axial T2WI (c) and shows prominent Gd-contrast enhancement on axial FS T1WI (d).

Table 1 (Continued) **Tumors and tumorlike lesions involving the skull and facial bones**

Tumor/Tumorlike Lesion	MRI Findings	Comments
Osteold osteoma (Fig. 1.23)	Intraosseous circumscribed radiolucent lesion less than 1.5 cm in diameter surrounded by bone sclerosis. Lesions often have low-intermediate signal on T1WI and high signal on T2WI and FS T2WI with prominent Gd-contrast enhancement, surrounded by a peripheral rim of low signal on T1WI and T2WI (bone sclerosis).	Benign osseous lesion containing a nidus of vascularized osteoid trabeculae surrounded by osteoblastic sclerosis, rarely occurs in the skull. Usually occurs between ages of 5 and 25, males > females. Focal pain and tenderness, which is often worse at night, associated with lesion; relieved with aspirin. **(See Atlas Chapter A60)**
Osteoblastoma	Expansile radiolucent lesion often greater than 1.5cm surrounded by bone sclerosis. Lesions often have low-intermediate signal on T1WI and intermediate-high signal on T2WI and FST2WI. Usually show Gd-contrast enhancement, +/- high signal on T2WI and FST2WI in bone (edema) beyond zone of sclerosis or in adjacent softtissues.	Rare benign bone neoplasm (2% of bone tumors) usually occurs between ages of 6 and 30. Rarely involves the skull. **(See Atlas Chapter A 61)**
Enchondroma (Fig. 1.24)	Lobulated intramedullary that usually have low-intermediate signal on T1WI and intermediate signal on PDWI. On T2WI and fat-suppressed T2WI, lesions usually have predominantly high signal with foci and/or bands of low signal representing areas of matrix mineralization and fibrous strands. Lesions typically show Gd-contrast enhancement in various patterns (peripheral curvilinear lobular, central nodular/scptal, and peripheral lobular, or heterogeneous diffuse).	Benign intramedullary lesions composed of hyaline cartilage, represent -10% of benign bone tumors. Enchondromas can be solitary (88%) or multiple (12%).
Chondroblastoma	Tumors often have fine lobular margins, and typically have low-intermediate heterogeneous signal on T1WI, and mixed low, intermediate, and/or high signal on T2WI. Areas of low signal on T2WI are secondary to chondroid matrix mineralization, and/or hemosiderin. Lobular, marginal, or septal Gd-contrast enhancement patterns can be seen. Tumors may have thin margins of low signal on T2WI representing sclerotic borders. Cortical destruction is uncommon. Bone expansion can result in spinal cord compression.	Benign cartilaginous tumors with chondroblast-like cells and areas of chondroid matrix formation, rarely occur in the craniofacial bones. The squamous portion of the temporal bone is the most common location of these tumors involving the craniofacial bones. **(See Atlas Chapter A 7)**
Pituitary adenoma (Fig. 1.25)	Macroadenomas (> 10 mm): Commonly have intermediate signal on T1WI and T2WI and often similar to gray matter, +/- necrosis. +/- cyst. +/- hemorrhage, usually show prominent Gd-contrast enhancement, extension into suprasellar cistern with waist at diaphragma sella, +/- extension into cavernous sinus, occasionally invades skull base.	Common benign slow-growing tumors representing ~50% of sellar/parasellar neoplasms in adults. Can be associated with endocrine abnormalities related to oversecretion of hormones (prolactin > nonsecretory type > growth hormone > ACTH > others). Prolactinomas: females > males, growth hormone tumors: males > females.
Paraganglloma/glomus jugulare (Fig. 1.26)	Ovoid or fusiform lesions with low-intermediate signal on T1WI and PDWI, and intermediate to high signal on T2WI and FS T2WI. Punctate zones of signal void or low signal on PDWI, T2WI, and FST2WI can be seen within tumors as a "salt and pepper" pattern. Lesions typically show moderate to prominent Gd-contrast enhancement. Often erode adjacent bone.	Benign encapsulated neuroendocrine tumors that arise from neural crest cells associated with autonomic ganglia (paraganglia) throughout the body. Lesions are also referred to as chemodectomas, and are named according to location (glomus jugulare tympanicum, glomus vagale).
Endolymphatic sac cystadenoma (Fig. 1.27)	Extra-axial retrolabyrinthine lesions involving the posterior petrous bone extending into the cerebellopontine angle cistern. Lesions can have low, intermediate, and or high signal on T1WI and T2WI, and can show Cd-contrast enhancement. May contain blood products.	Rare solid and/or cystic benign or malignant papillary adenomatous tumors arising from the endolymphatic sac in children and adults. Tumors are slow growing and rarely metastasi/e. May be sporadic or associated with von Hippel-Lindau disease.

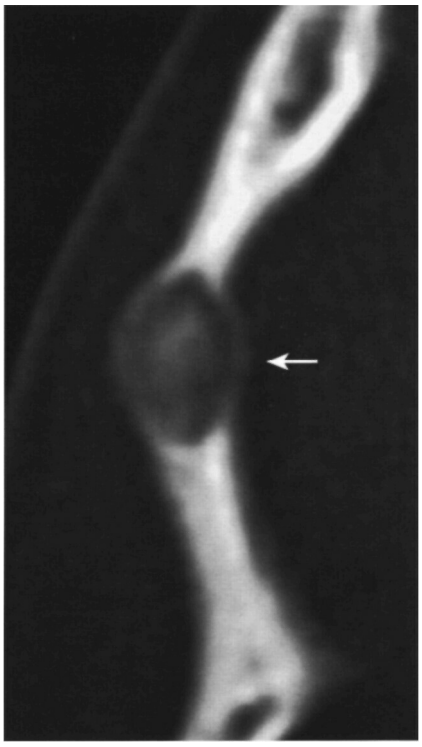

Figure 1.23 Osteoid osteoma in the right frontal bone in a 16-year-old male. Axial CTshows a small radiolucent lesion containing a central calcification associated with thinning and expansion of the inner and outer tables of the skull.

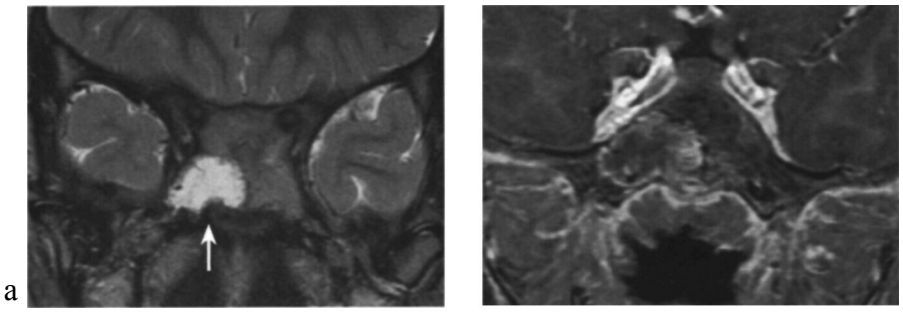

Figure 1.24a, b Enchondroma in the sphenoid bone has high signal on coronal T2WI (a) and shows mostly peripheral lobular Gd-contrast enhancement on coronal T1WI (b).

Figure 1.25 A pituitary macroadenoma is seen enlarging the sella with extension into the suprasellar cistern. The lesion shows prominent Gd-contrast enhancement on sagittal FST1WI.

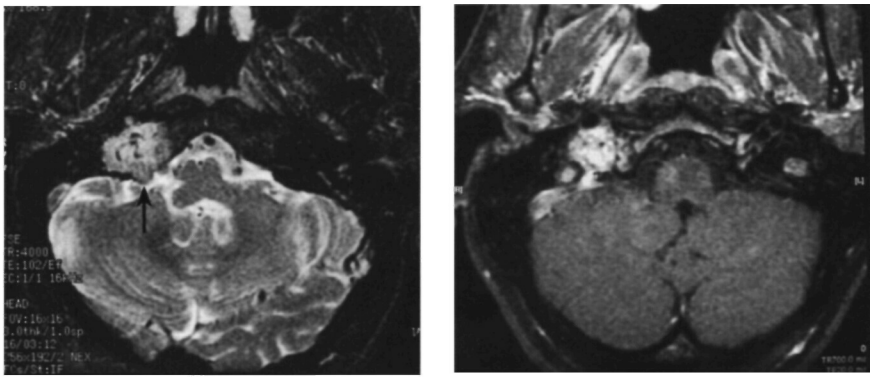

Figure 1.26 a, b A 55-year-old woman with a glomus jugulare at the right jugular foramen, which has heterogeneous slightly high signal on axial FST2WI (a). Multiple tortuous and punctate zones of signal void are seen representing intratumoral vessels. The tumor shows prominent Gd-contrast enhancement on axial (b) FST1WI.

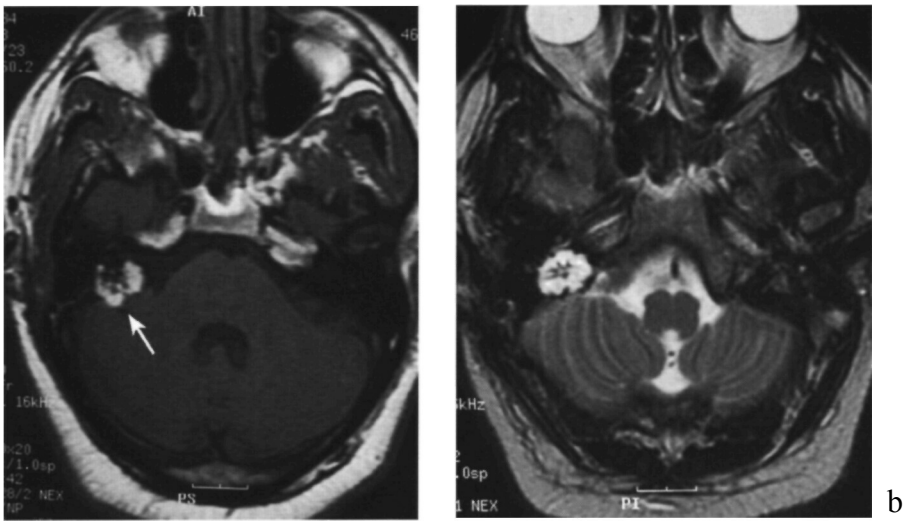

Figure 1.27 a, b Cystadenoma of the endolymphatic sac involving the right petrous bone has lobulated margins and contains mostly high signal on axial T1 WI (a) and T2WI (b).

Table 1 (Continued) **Tumors and tumorlike lesions involving the skull and facial bones**

Tumor/Tumorlike Lesion	MRI Findings	Comments
Ameloblastoma *(fig.* 1.28)	Lesions occur in the mandible and maxilla, are often radiolucent with associated bone expansion and cortical thinning on CT. Tumors often have circumscribed margins, and can show mixed low, intermediate, and/or high signal on T1WI, T2WI. and FST2WI. Lesions can show heterogeneous Gd-contrast enhancement.	Slow-growing solid and cystic tumors that contain epithelioid cells (basaloid and/or squamous types) associated with regions of spindle cells and fibrous stroma. These tumors typically lack metastatic potential.
Other lesions		
Osteoma (Fig. 1.29)	Well circumscribed lesions involving the skull with low-intermediate signal on T1 WI and T2WI, typically show no significant Gd-contrast enhancement.	Benign proliferation of bone located in the skull or paranasal sinuses (frontal > ethmoid > maxillary > sphenoid). **(See Atlas Chapter A 62)**
Epidermoid (Fig. 1.30)	Well-circumscribed spheroid ectodermal inclusion cystic lesions in the skull associated with chronic bone erosion, low-intermediate signal on T1WI, high signal on T2WI and diffusion weighted imaging, low signal on ADC maps, and no Gd-contrast enhancement.	Non-neoplastic lesions filled with desquamated cells and keratinaceous debris involving the skull. **(See Atlas Chapter A15)**
Dermoid (Fig. 1.31)	Well-circumscribed spheroid lesions in the skull associated with chronic bone erosion, usually with high signal on T1WI and variable low, intermediate, and/or high signal on T2WI, no Gd-contrast enhancement, +•/- fluid-fluid or fluid-debris levels.	Non-neoplastic ectodermal inclusion cystic lesions involving the skull filled with lipid material, cholesterol, desquamated cells, and keratinaceous debris. **(See Atlas Chapter A15)**

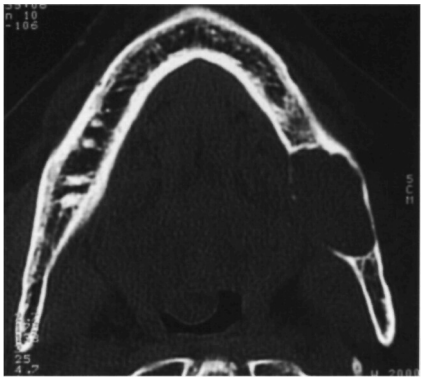

a

Figure 1.28a-c Ameloblastoma in the mandible is seen as a radiolucent lesion with associated bone expansion and cortical thinning on axial CT (a). The tumor has mixed high and intermediate signal on axial T2WI (b). A small fluid-fluid level is also seen. The tumor shows heterogeneous Gd-contrast enhancement on axial FST1WI (c)

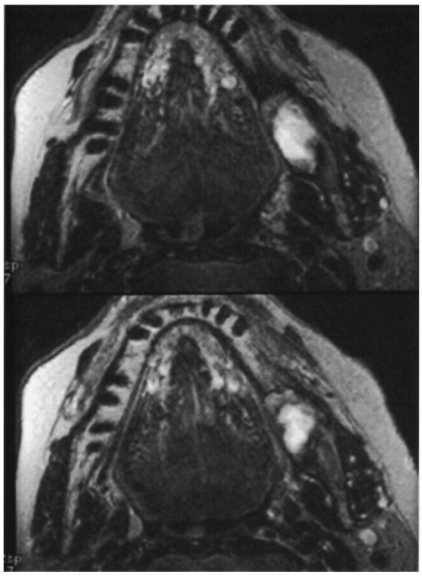

b

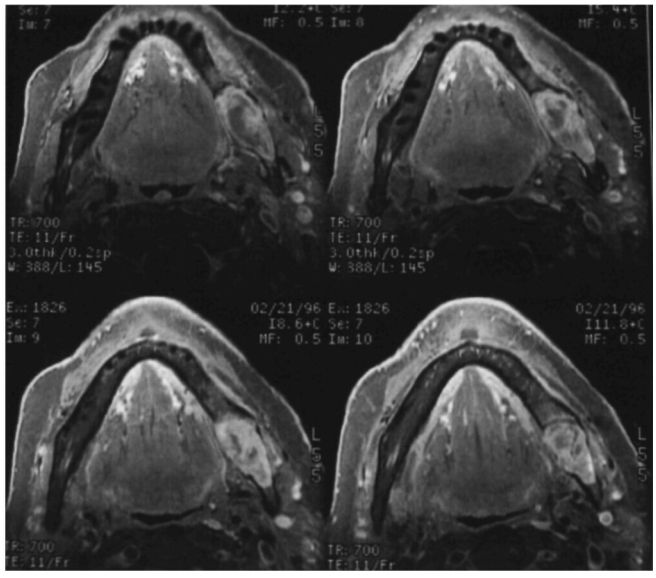

c

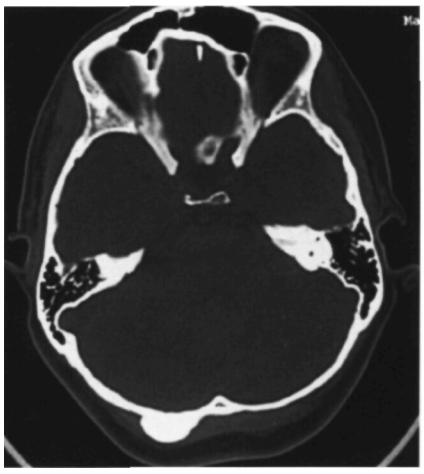

a

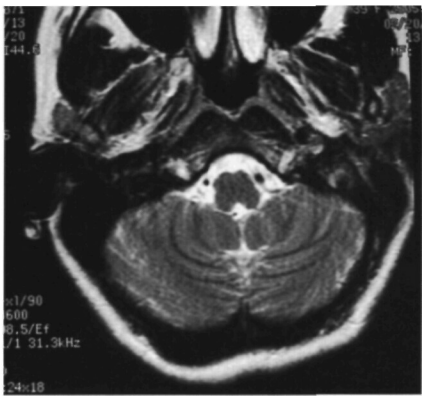

b

Figure 1.29a, b A 39-year-old woman with an osteoma involving the right occipital bone. Axial CT image (a) shows a well-circumscribed ovoid lesion with dense bone attenuation contiguous with the outer table of the right occipital bone via a broad base. The lesion has low signal on axial T2WI (b).

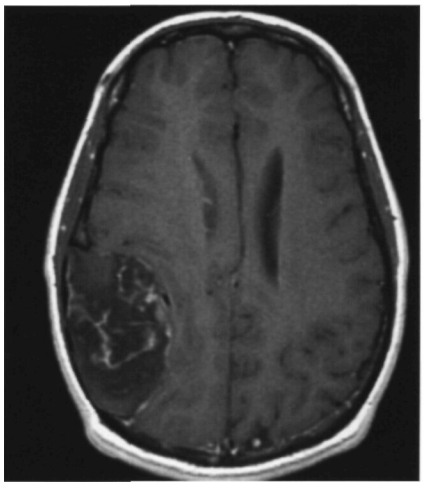

a

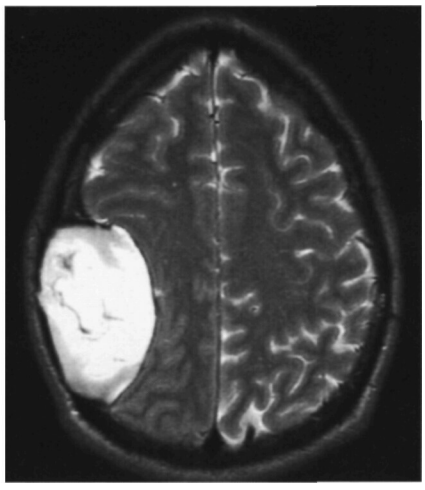

b

Figure 1.30a, b A 39-year-old man with an epidermoid involving the right parietal bone. The lesion has a mostly intermediate signal as well as zones of high signal on axial T1WI (a) associated with marked thinning of the inner and outer tables of the skull. The lesion has high signal centrally surrounded by a thin rim of low signal on axial T2WI (b).

a

b

Figure 1.31 a, b A 55-year-old man with a dermoid in the right middle cranial fossa. The extra-axial lesion has heterogeneous mostly high signal with a thin low signal septum on sagittal T1WI (a). The lesion has mixed low and high signal on axial T2WI (b).

Table 1 (Continued) **Tumors and tumorlike lesions involving the skull and facial bones**

Tumor/Tumorlike Lesion	MRI Findings	Comments
Aneurysmal bone cyst (Fig. 1.32)	Circumscribed lesion with variable low, intermediate, high, and/or mixed signal on T1WI and T2WI, +/- surrounding thin zone of low signal on T2WI, +/- lobulations, +/- one or multiple fluid-fluid levels.	Expansile blood/debris-filled lesions that may be primary lesions or occur secondary to other bone lesions such as giant cell tumor, fibrous dysplasia, chondroblastoma. Most occur in patients < 30 years. These lesions rarely involve the skull. **(See Atlas Chapter A 2)**
Giant cell reparative granuloma (Fig. 1.33)	Lesions are radiolucent, and can have heterogeneous low, intermediate, and/or high signal on T1WI, PDWI, and T2WI; as well as peripheral rim-like and central Gd-contrast enhancement on FST1WI.	Giant cell reparative granulomas are also referred to as solid ABCs. **(See Atlas Chapter A 2).** Histologic appearance resembles brown tumors.
Arachnoid cyst (Fig. 1.34)	Well-circumscribed extra-axial lesions with low signal on T1WI and FLAIR, and high signal on T2WI and FST2WI, similar to CSF, no Gd-contrast enhancement. Chronic erosive changes can be seen at the adjacent skull.	Non-neoplastic acquired, developmental, or congenital extra-axial cysts filled with CSF. Cysts can be small or large, asymptomatic or symptomatic.
Inflammatory lesions		
Pyogenic osteomyelitis (Figs. 1.35.1.36)	Abnormal low signal on T1WI and high signal on T2WI, FST2WI, diffusion-weighted imaging and low signal on ADC maps in marrow, focal sites of bone destruction, +/- complications including: subgaleal empyema. epidural empyema, subdural empyema, meningitis, cerebritis, intra-axial abscess, venous sinus thrombosis.	Osteomyelitis of the skull can result from surgery, trauma, hematogenous dissemination from another source of infection, or direct extension of infection from an adjacent site such as the paranasal sinuses. **(See Atlas Chapter A 63)**
Eosinophilic granuloma (Fig. 1.37)	Single or multiple circumscribed soft-tissue lesions in the marrow of the skull associated with focal bony destruction/erosion with extension extra-, intracranially or both. Lesions usually have low-intermediate signal on T1WI, mixed intermediate-slightly high signal on T2WI and FST2WI. usually show Gd-contrast enhancement +/- enhancement of the adjacent dura.	**Single lesion:** Commonly seen in males > females, <20years, proliferation of histiocytes in medullary cavity with localized destruction of bone with extension in adjacent soft tissues. **Multiple lesions:** Associated with syndromes such as: Letterer-Siwe disease (lymphadenopathy hepatosplenomegaly), children <2years; Hand-Schiiller-Christian disease (lymphadenopathy, exophthalmos, diabetes insipidus). children 5-10 years. **(See Atlas Chapter A18)**

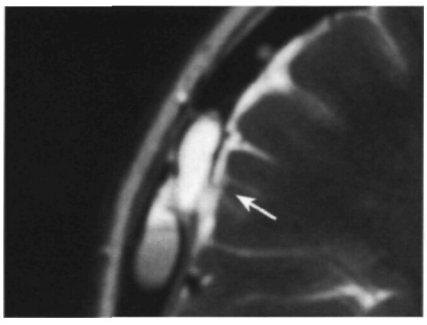

Figure 1.32 A 47-year-old woman with an aneurysmal bone cyst involving the right frontal bone. The lesion is associated with thinning and slight expansion of the inner and outer tables of the skull, and contains fluid-fluid levels on axial T2WI.

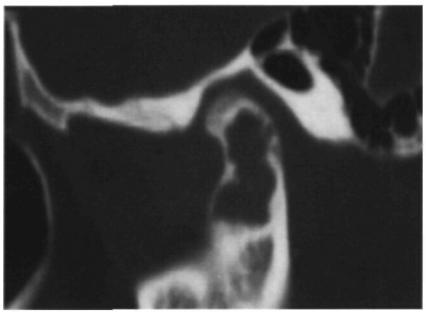

a

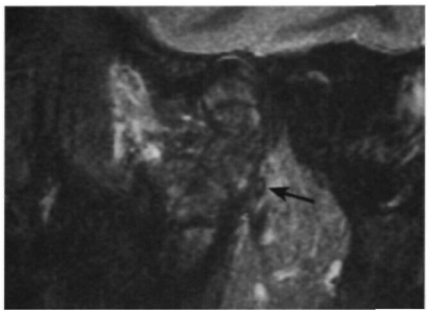

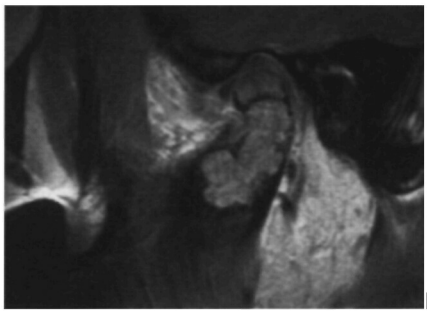

b, c

Figure 1.33a-c A 15-year-old female with a giant cell reparative granuloma involving the mandible. The radiolucent lesion has circumscribed margins on sagittal CT (a) and heterogeneous intermediate to slightly high signal on sagittal FST2WI (b). The lesion shows Gd-contrast enhancement on sagittal T1WI (c).

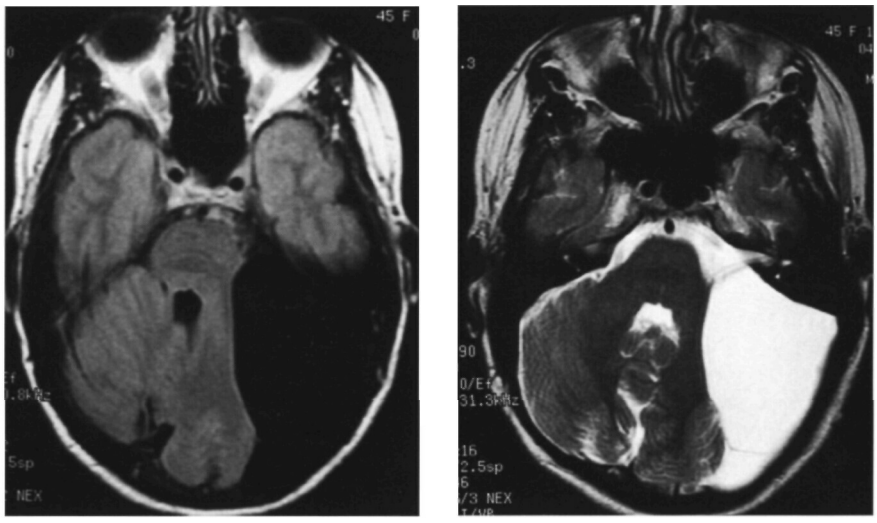

a, b

Figure 1.34a, b A large arachnoid cyst is seen in the left side of the posterior cranial fossa resulting in medial displacement and deformation of the left cerebellar hemisphere. The cyst contents have an MRI signal equal to CSF on axial FLAIR (a) and axial T2WI (b).

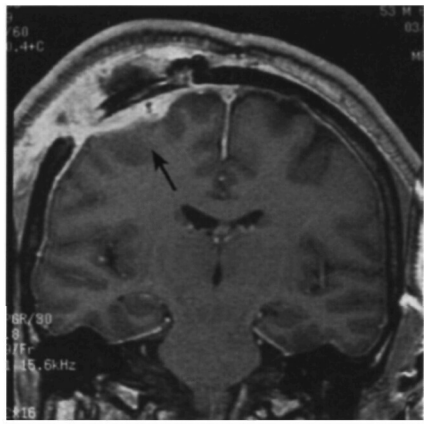

Figure 1.35 A 53-year-old man with pyogenic osteomyelitis involving a craniotomy flap associated with dural inflammation and scalp abscess. Prominent Gd-contrast enhancement is seen in the soft tissues superficial and deep to the infected bone, as well as at the margins and intramedullary portions of the craniotomy flap on coronal T1WI.

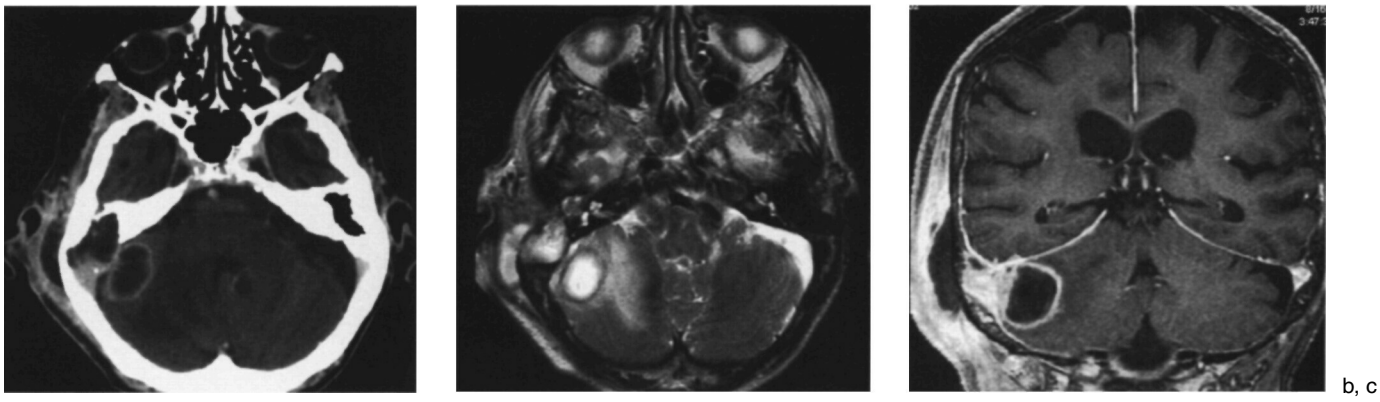

a

b, c

Figure 1.36a-c A 94-year-old woman with pyogenic osteomyelitis involving the mastoid portion of the right temporal bone associated with dural inflammation, and abscesses involving the right cerebellar hemisphere and scalp. Contrast-enhanced axial CT image (a) shows an irregular zone of bone destruction with associated dural enhancement, cerebellar and scalp abscesses. The region of osteomyelitis has heterogeneous mostly high signal on axial T2WI (b) and the cerebellar and scalp abscesses have high signal centrally surrounded by rims of low signal. The abscesses are surrounded by irregular zones of Gd-contrast enhancement on coronal T1WI (c).

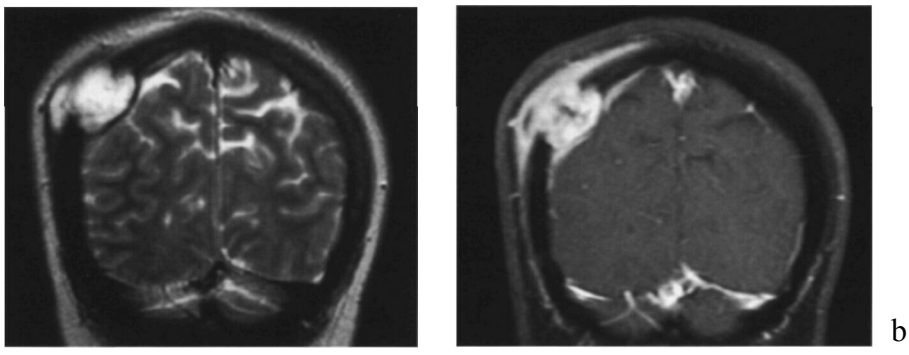

a

b

Figure 1.37 a, b A 20-year-old woman with an eosinophilic granuloma involving the right parietal bone. The lesion has high signal on coronal T2WI (a). Intra- and extracranial extension of the lesion is seen through areas of cortical disruption. The lesion shows prominent Gd-contrast enhancement in the marrow, intra- and extracranial portions of the lesion as well as the dura on coronal FST1 WI (b).

Table 1 (Continued) **Tumors and tumorlike lesions involving the skull and facial bones**

Tumor/Tumorlike Lesion	MRI Findings	Comments
Sarcoidosis (Fig. 1.38)	Sarcoid lesions within marrow may be multiple or solitary, with or without bone expansion and/or erosions or areas of destruction of the inner and/or outer tables with extension intracranially or into the extracranial soft tissues. Lesions can have circumscribed and/or indistinct margins, and usually have low to intermediate signal on T1WI, slightly high to high signal on T2WI and FST2WI, and show variable degrees of Gd-contrast enhancement.	Chronic systemic granulomalous disease of unknown etiology in which noncaseating granulomas occur in various tissues and organs including bone. **(See Atlas Chapter A71)**
Paranasal sinus mucocele (Fig. 1.39)	Circumscribed expansile lesion within a paranasal sinus that has variable low, intermediate, and/or high signal on T1WI. T2WI, and FST2WI depending on contents of mucous, inspissated mucous, and protein concentration.	Lesions occurring from chronic obstruction of a paranasal sinus ostium, results in outward expansion of the osseous margins from remodeling secondary to increased pressure from accumulated secretions from the sinus mucosa. Mucoceles occur most commonly in the frontal sinuses followed by the ethmoid, maxillary, and sphenoid sinuses.
Cholesterol granuloma (Fig. 1.40)	Circumscribed lesion measuring between 2 and 4cm in the marrow of the petrous bone often associated with mild bone expansion. Lesions usually have high signal on T1 WI and FST1 WI. Lesions may have high, intermediate, and/or low signal on T2WI and FST2WI. A peripheral rim of low signal on T2WI may also be seen from hemosiderin.	Lesions occur in young and middle-age adults and occur when there is obstruction of mucosal-lined air cells in the petrous bone. Multiple cycles of hemorrhage and granulomatous reaction result in accumulation of cyst contents with cholesterol granules, chronic inflammatory cells, red blood cells, hemosiderin. fibrous tissue, and debris.
Aneurysm (Fig. 1.41)	Focal circumscribed lesion with layers of low, intermediate, and/or high signal on T1WI and T2WI secondary to layers of thrombus, as well as a signal void representing a patent lumen if present.	Abnormal dilatation of artery secondary to acquired/degenerative cause, connective tissue disease, atherosclerosis, trauma, infection (mycotic), AVM, drugs, and vasculitis.
Acquired		
Postsurgical pseudomeningocele (Fig. 1.42)	CSF-filled collection contiguous with the subarachnoid space protruding through a surgical bony defect. Cliotic brain tissue may also accompany the dural protrusion.	Usually are not clinically significant unless they become large or infected.

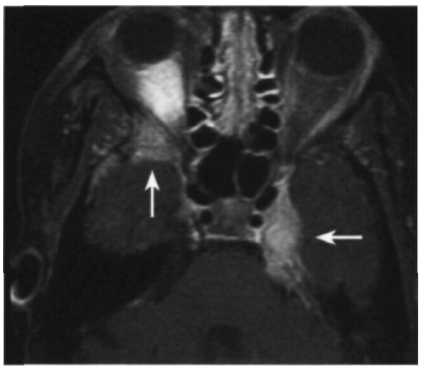

Figure 1.38 A 55-year-old woman with sarcoidosis and an intraosseous lesion involving the greater wing of the right sphenoid bone and in the subarachnoid space at the left cerebellopontine angle cistern and left trigeminal cistern. Both lesions show Gd-contrast enhancement on axial FST1WI.

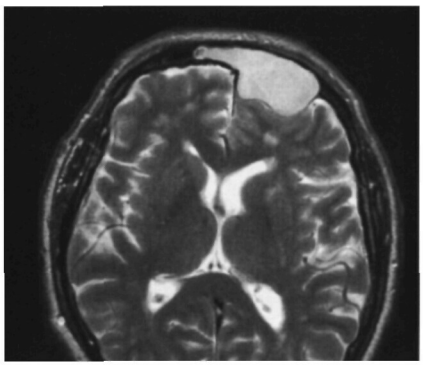

a

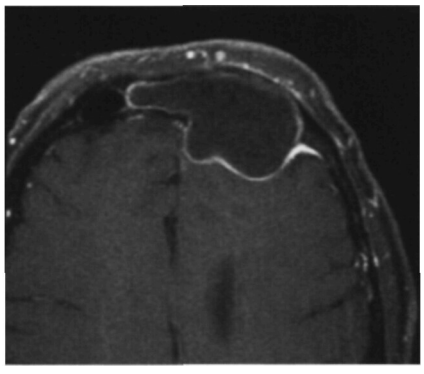

b

Figure 1.39a, b A mucocele is seen expanding the left frontal sinus associated with remodeling and thinning of the inner table and orbital roof. The mucocele contains high signal on axial T2WI (a). Thin peripheral Gd-contrast enhancement is seen surrounding low signal mucous on axial FS T1WI (b).

a b, c

Figure 1.40a-c A cholesterol granuloma is seen in the left petrous apex which has high signal on axial T1 WI (a) and axial FS T1 WI (b). The lesion has mixed high, intermediate, and low signal on axial T2WI (c). Mild bone expansion and a peripheral rim of low signal on T2WI are also seen.

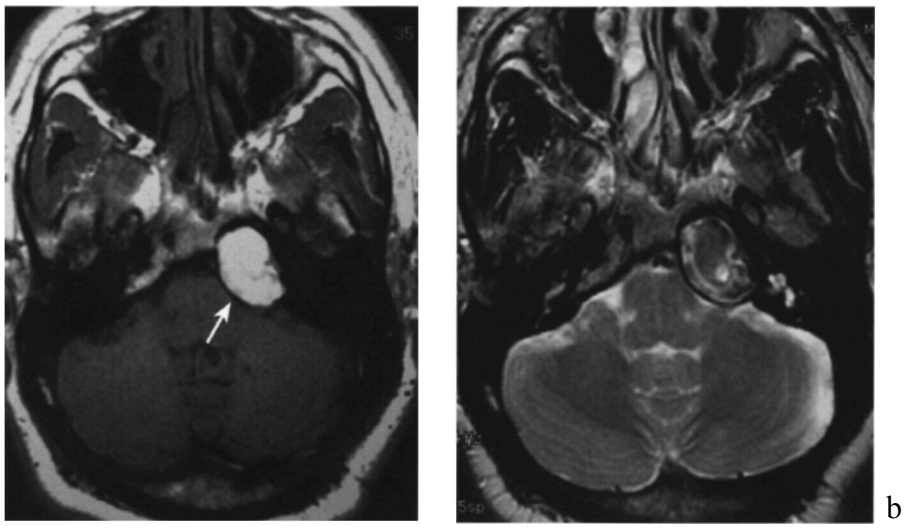

a b

Figure 1.41 a, b A 35-year-old man with an intraosseous aneurysm at the left petrous carotid canal, which erodes the petrous bone. The aneurysm has mostly high signal on axial T1WI (a) and mixed low, intermediate, and high signal on axial T2WI (b).

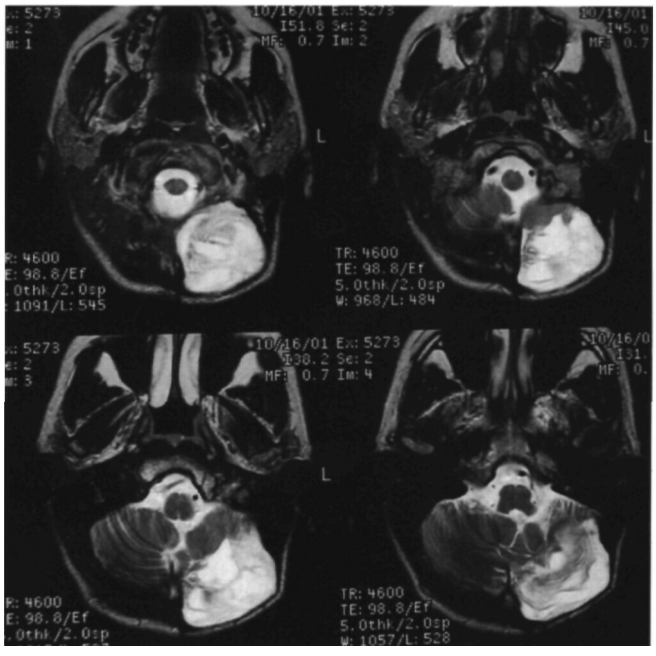

Figure 1.42 A pseudomeningocele is seen contiguous with the subarachnoid space protruding through a surgical bony defect from a left occipital craniectomy on axial T2WI. Damaged cerebellar tissue (gliosis and localized encephalomalacia) with high signal on T2WI is also seen.

Table 1 (Continued) **Tumors and tumorlike lesions involving the skull and facial bones**

Tumor/Tumorlike Lesion	MRI Findings	Comments
Paget disease (Fig. 1.43)	Expansile sclerotic/lytic process involving the skull with mixed low-intermediate signal on T1WI, variable mixed low, intermediate, high signal on T2WI, variable heterogeneous enhancement. Irregular/indistinct borders between marrow and inner margins of the outer and inner tables of the skull.	Usually seen in older adults, can result in narrowing of neuroforamina with cranial nerve compression, basilar impression +/- compression of brainstem. **(See Atlas Chapter A 65)**
Fibrous dysplasia (Fig. 1.44)	Expansile process involving the skull base with mixed low-intermediate signal on T1WI, variable mixed low, intermediate, high signal on T2WI, usually heterogeneous Gd-contrast enhancement.	Usually seen in adolescents and young adults, can result in narrowing of neuroforamina with cranial nerve compression, facial deformities, mono- and poly-ostotic forms (+/- endocrine abnormalities such as with McCune-Albright syndrome, precocious puberty). **(See Atlas Chapter A 27)**
Hematopoietic disorders (Fig. 1.45)	Enlargement of the diploic space with red marrow hyperplasia (low-intermediate signal on T1WI and intermediate to slightly high signal on T2WI and FST2WI) with thinning of the inner and outer tables.	Thickening of diploic space secondary to erythroid hyperplasia from anemia related to Sickle cell disease, thalassemia major, hereditary spherocytosis. Similar findings of red marrow expansion can be seen with polycythemia rubra.
Trauma		
Cephalohematoma	Hematoma located beneath periosteum of outer table, does not cross suture lines; +/- skull fracture; +/- subdural hematoma.	Results from birth trauma (complication of forceps delivery), associated with 1 % of births.
Fracture	**Nondisplaced/nondepressed skull fractures:** Abnormal low signal on T1WI and high signal on T2WI in marrow at the site of fracture, +/- subgaleal hematoma, +/- epidural hematoma, +/- subdural hematoma, +/- subarachnoid hemorrhage. **Depressed skull fracture:** Angulation and internal displacement of fractured skull, abnormal low signal on T1 WI and high signal on T2WI in marrow at the site of fracture, +/- subgaleal hematoma, +/- epidural hematoma, +/- subdural hematoma, +/- subarachnoid hemorrhage.	Traumatic fractures of the skull can involve the calvaria or skull base, significant complications that can result include: epidural hematoma, subdural hematoma. subarachnoid hemorrhage, CSF leakage/rhinorrhea, otorrhea.
Congenital abnormalities		
Cephaloceles (meningoceles or meningoencephaloceles) (Figs. 1.46.1.47)	Defect in skull through which there is either hemiation of meninges and CSF (meningocele); or meninges, CSF/ventricles, and brain tissue (meningoencephaloceles).	Congenital malformation involving lack of separation of neuroectoderm from surface ectoderm with resultant localized failure of bone formation. Occipital location most common in western hemisphere, frontoethmoidal location most common site in Southeast Asians. Other sites include parietal and sphenoid bones. Cephaloceles can also result from trauma or surgery.

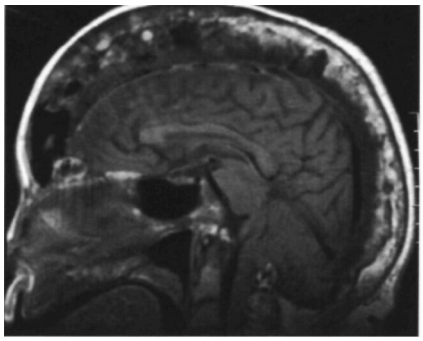

a

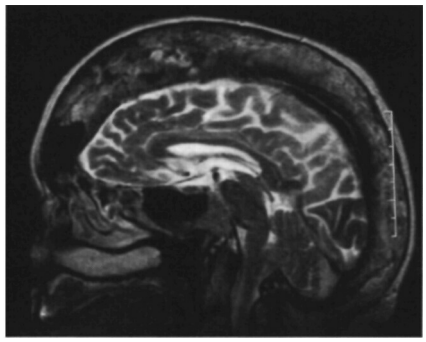

b

Figure 1.43a, b An 81-year-old woman with Paget disease involving the skull with associated basilar impression. The interface between the diploic space and the inner and outer tables is obscured, and there is marked osseous expansion. The marrow has mixed low, intermediate, and high signal on sagittal T1WI (a) and sagittal T2WI (b).

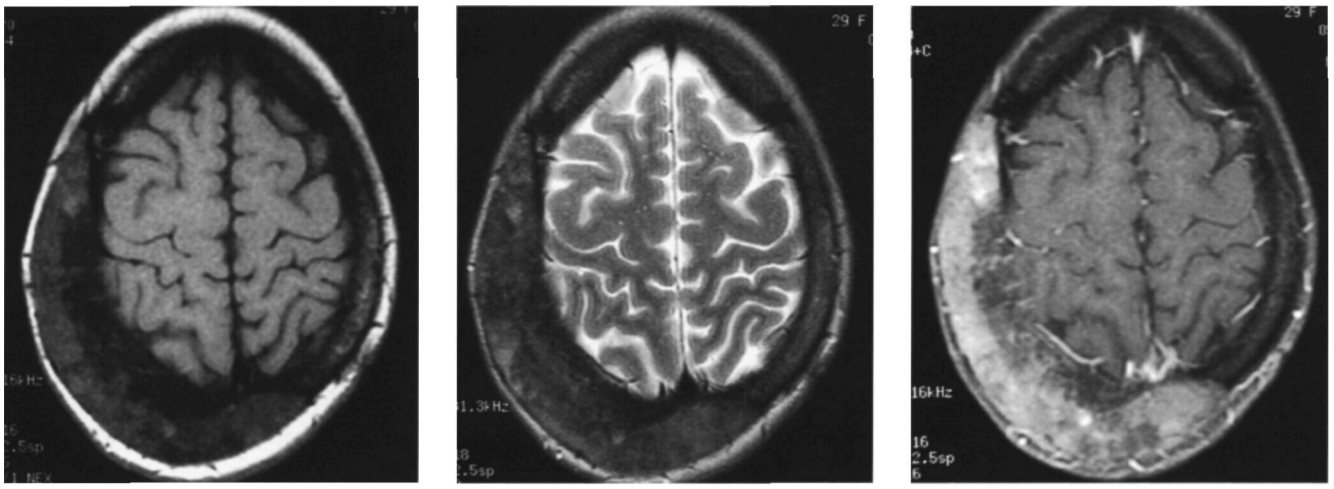

Figure 1.44a-c A 29-year-old woman with fibrous dysplasia expanding the right and posterior portions of the calvarium. The lesion has mixed low and intermediate signal on axial T1WI (a) and axial T2WI (b), and shows prominent Gd-contrast enhancement on axial FST1WI (c).

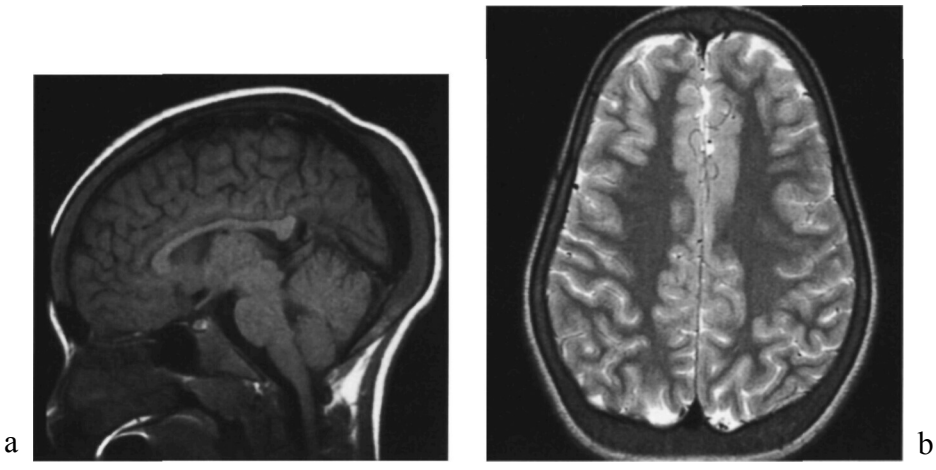

Figure 1.45 a, b Patient with sickle cell anemia who has enlargement of the diploic space with red marrow hyperplasia which has low-intermediate signal on sagittal T1WI (a) and intermediate signal on axial T2WI (b).

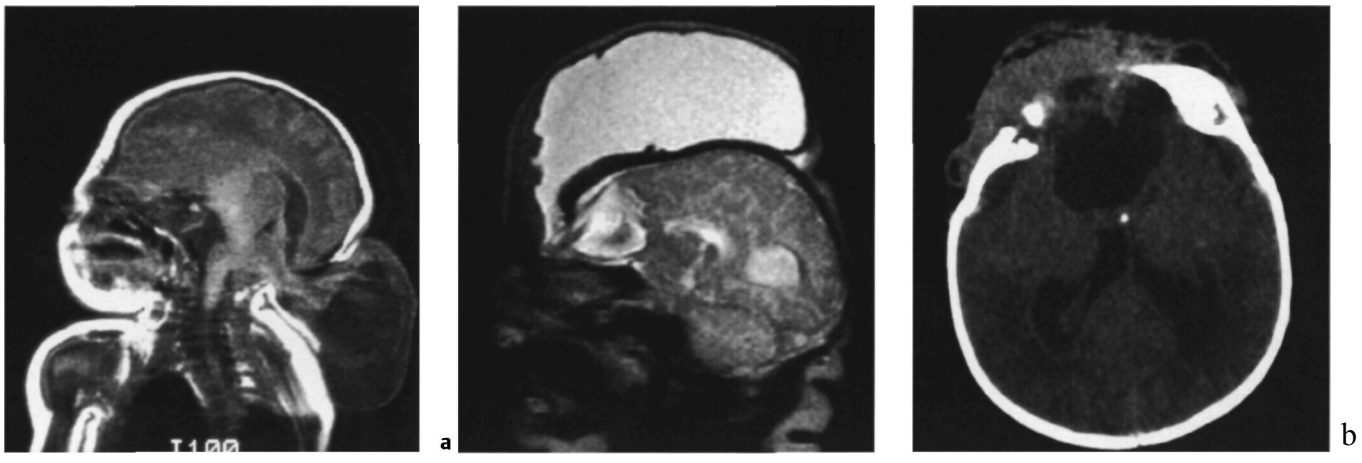

Figure 1.46 A 1-day-old neonate with an occipital meningoencephalocele containing meninges and damaged brain tissue as seen on sagittal T1WI.

Figure 1.47 a, b Neonate with a frontal meningoencephalocele containing meninges and damaged brain tissue as seen on sagittal (a) T2WI and axial CT image (b).

Table 1 (Continued) Tumors and tumorlike lesions Involving the skull and facial bones

Tumor/Tumorlike Lesion	MRI Findings	Comments
Neuroflbromatosis type 1 (Fig. 1.48)	NF1 associated with: focal ectasia of intracranial dura; widening of internal auditory canals from dural ectasia; dural and temporal lobe protrusion into orbit through bony defect, bony hypoplasia of greater sphenoid wing, bone malformation, or erosion from plexiform neurofibromas.	Autosomal dominant disorder (1/2500 births) representing the most common type of neurocutaneous syndromes, associated with neoplasms of central and peripheral nervous system and skin. Also associated with meningeal and skull dysplasias. (See Atlas Chapter A 56)

a

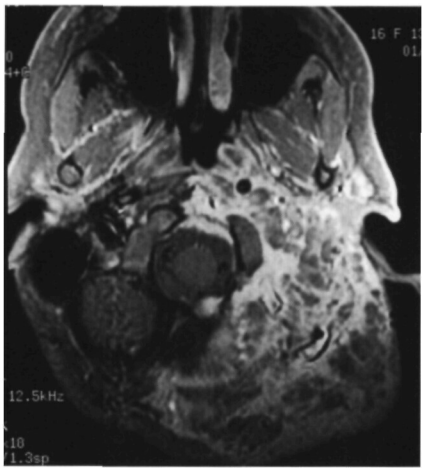

b

Figure 1.48a, b A 16-year-old female with a plexiform neurofibroma involving the posterior scalp and skull. The lesion appears as curvilinear and multinodular zones with intermediate, slightly high to high signal separated by curvilinear zones of low signal on axial T2WI (a). The plexiform neurofibroma shows heterogeneous Gd-contrast enhancement on axial FST1WI (b).

References

Nasopharyngeal Carcinoma

King AD, Vlantis AC, Tsang RKY, et al. Magnetic resonance imaging for the detection of nasopharyngeal carcinoma. *AJNR* Jun-Jul 2006; 27:1288-1291.

Loevner LA, Sonners Al. Imaging of neoplasms of the paranasal sinuses. *Magn Rcson Imaging Clin N Am* August 2002;10(3):467-493.

Adenoid Cystic Carcinoma

Sigal R, Monnet 0, de Baere T, et al. Adenoid cystic carcinoma of the head and neck: evaluation with MR imaging and clinical-pathologic correlation in 27 patients. Radiology 1992;184:95-101.

Triantafillidou K, DimitrapoulosJ, lordanidis F, Koufogiannis D. Management of adenoid cystic carcinoma of minor salivary glands. *J Oral Maxillofac Surg* 2006;64:1114-1120.

Esthesioneuroblastoma

Bradley PJ, Jones NS, Robertson I. Diagnosis and management of esthesioneuroblastoma. *Otolaryng Head Neck* 2003:11:112-118.

Chirico G, Pergolizzi S, Mazziotti S, Santacaterina A, Ascenti G. Primary sphenoid esthesioneuroblastoma studies with MR. *J Clin* /mag 2003:27:38-40.

Li C, Yousem DM. Hayden RE, Doty RL Olfactory ncuroblastoma: MR evaluation. *AJNR* Sep-Oct 1993;14(5):1167-1171.

Pickuth D, Heywang-Kobrunner SH, Spielmann RP. Computed tomography and magnetic resonance imaging features of olfactory neuroblastoma: an analysis of 22 cases. *Clin Otolaryngol* 1999;24:457-461.

Schuster JJ, Phillips CD, Levine PA. MR of esthesioneuroblastoma (olfactory neuroblastoma) and appearance after craniofacial resection. AJNR June 1994;15(6):1169-1177.

Ossifying Hemangioma

Brackman DE, Weisskopf PA, Lo WWM. Ossifying hemangioma of the internal auditory canal. *Otol Neurolol* 2005;26:1239-1240.

Curtin HD, Jensen JE, Barnes L, May M. Ossifying hemangiomas of the temporal bone: evaluation with CT. *Radiology* 1987:164:831-835.

Isaacson B, Telian SA, McKeever PE, Arts HA. Hemangiomas of the geniculate ganglion. *Otol Neurotol* 2005;26:796-802.

Pituitary Adenoma

Elster AD. Modern imaging of the pituitary. *Radiology* 1993:187:1-14.

FitzPatrick M, Tartaglino LM, Hollander MD, Zimmerman RA, Flanders AE. Imaging of sellar and parasellar pathology. Radio/ *Clin N Am* January 1999;37(1):101-121.

Pierallini A, Caramia F, Falcone C, et al. Pituitary macroadenomas: preoperative evaluation of consistency with diffusion-weighted MR imaging - initial experience. *Radiology* April 2006:239(1):223-231.

Pisaneschi M, Kapoor G. Imaging the sella and parasellar region. *NeuroimagClin N Am* February 2005;15(1):203-219.

Endolymphatic Sac Tumor

Baltacioglu F, Ekinci G, Ture U, Sav A, Pamyr N, Erzen C. MR imaging, CT, and angiography features of endolymphatic sac tumors: report of two cases. Neuroradio/ogy 2002;44:91-96.

Bonneville F, Sarrazin JL, Marsot-Dupuch K, et al. Unusual lesions of the cerebellopontine angle: a segmeiital approach. *RadioGraphics* 2002; 21:419-438.

Patel NP, Wiggins RH, Shelton C. The radiologic diagnosis of endolymphatic sac tumors. Laryngoscope 2006; 116:40-46.

Ameloblastoma

Asaumi J, Hisatomi M, Yanagi Y, et al. Assessment of ameloblastomas using MRI and dynamic contrast-enhanced MRI. *EurJ Radiol* 2005; 56:25-30.

Cihangiroglu M, Akfirat M, Yildirim H. CT and MRI findings of ameloblastoma in two cases. *Neuroradiology* 2002:44:434-437.

Arachnoid Cyst

Bonneville F, Sarrazin JL, Marsot-Dupuch K, et al. Unusual lesions of the cerebellopontine angle: a segmental approach. *RadioGraphics* 2002; 21:419-438.

Cakirer S. Arachnoid cyst of the craniospinal junction: a case report and review of the literature. *Acta Radial* 2004;45:460-463.

Mukherji SK, Chenevert TL, Castillo M. Diffusion-weighted magnetic resonance imaging. *J Neuro-Ophthalmol* 2002;22(2):118-122.

Rao G, Anderson RCE, Feldstein NA, Brockmeyer DL. Expansion of arachnoid cysts in children J *Neurosurg (Pediatrics 3)* 2005;102:314-317.

Tang L, Cianfoni A, Imbesi SG. Diffusion weighted imaging distinguishes recurrent epidermoid neoplasm from postoperative arachnoid cyst in the lumbosacral spine. J *Comput Assist Tomogr* 2006;30:507-509.

Paranasal Sinus Mucocele

Bonneville F, Cattin F, Marscot-Dupuch K, Dormont D, Bonneville JF, Chiras J. Tl hyperintensity in the sellar region: spectrum of findings. *RadioGraphics* 2006;26:93-113.

Cholesterol Cranuloma

Bonneville F, Sarrazin JL, Marsot-Dupuch K, et al. Unusual lesions of the cerebellopontine angle: a segmental approach. *RadioGraphics* 2002; 21:419-438.

Mosnier I, Cyna-Gorse F, Grayeli AB, et al. Management of cholesterol granulomas of the petrous apex based on clinical and radiologic evaluation. *Otol Neurotol* 2002;23(4):522-528.

Pisaneschi MJ, Langer B. Congenital cholesteatoma and cholesterol granuloma of the temporal bone: role of magnetic resonance imaging. *Top Magn Reson Imag* 2000;ll(2):87-97.

Hematologic Disorders

Lorand-Metze I, Santiago GF, Lima CSP, Zanardi VA, Torriani M. Magnetic resonance imaging of femoral marrow cellularity in hypocellular haemopoietic disorders. *Clin Radiol* 2001:56:107-110.

Loevner LA, Tobey JD, Yousem DM, Sonners Al, Hsu WC. MR imaging characteristics of cranial bone marrow in adult patients with underlying systemic disorders compared with healthy control subjects. *AJNR* February 2002; 23:248-254.

Tyler PA, Madani G, Chaudhuri R, Wilson LF, Dick EA. The radiological appearances of thalassaemia. *Clin Radial* 2006;61:40-52.

Table 2 Tumors and tumorlike lesions involving the spine

Tumor/tumorlil<e lesion	MRI Findings	Comments
Metastatic tumor (Figs. 2.1. 2.2)	Single or multiple well-circumscribed or poorly defined infiltrative lesions involving the vertebral marrow, dura, and/or leptomeninges; low-intermediate signal on T1 WI. low, intermediate, and/or high signal on T2WI and FST1WI. usually show Gd-contrast enhancement, +/-bone destruction. +/- pathologic vertebral fracture, +/- compression of neural tissue or vessels. Leptomeningeal tumor often best seen on postcontrast images.	May have variable destructive or infiltrative changes involving single or multiple sites of involvement. (See Atlas Chapter A 50)
Myeloma/plasmacytoma (Figs. 2.3. 2.4)	Multiple (myeloma) or single (plasmacytoma) well-circumscribed or poorly defined diffuse infiltrative lesions involving the vertebra(e), and dura; involvement of vertebral body typical, rarely involves posterior elements until late stages, low-intermediate signal on T1 WI, intermediate-high signal on T2WI. usually show Cd-contrast-enhancement + bone destruction.	May have variable destructive or infiltrative changes involving the axial and/or appendicular skeleton, **(see Atlas Chapter A 52)**

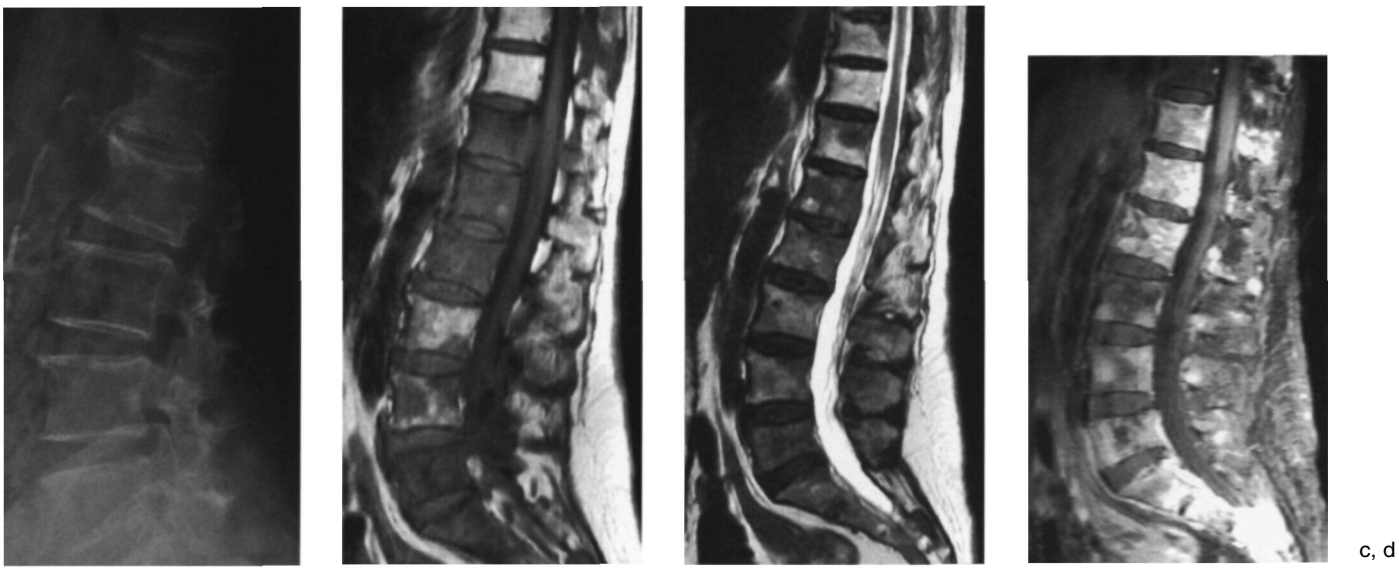

a, b c, d

Figure 2.1 a-d An 83-year-old woman with multiple metastases from breast carcinoma involving the lower spine. A lateral radiograph (a) shows multiple radiolucent lesions in the vertebrae. The metastatic lesions have low-intermediate signal on sagittal T1WI (b) and sagittal T2WI (c). and show Gd-contrast enhancement on sagittal FST1WI(d).

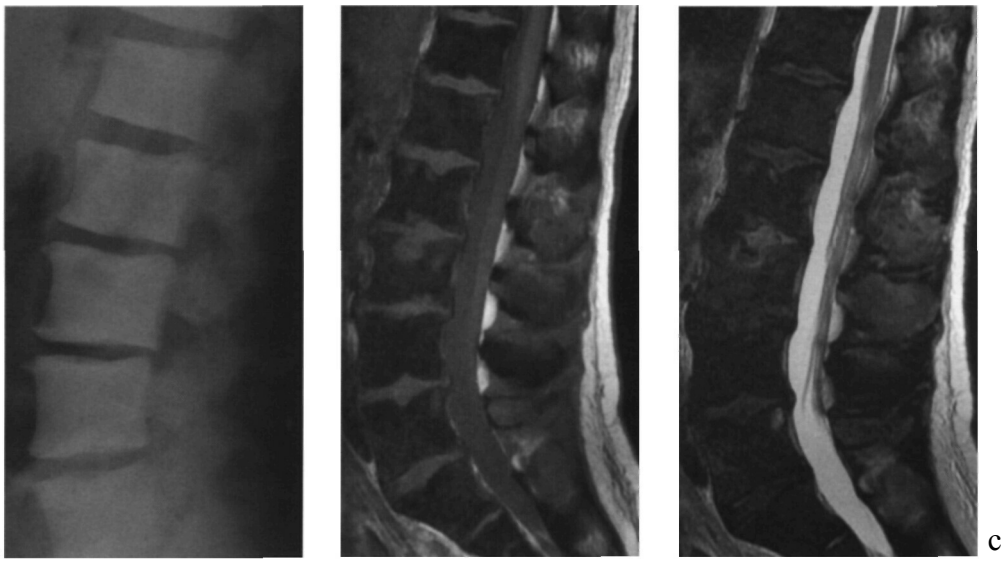

a, b c

Figure 2.2 a-c AST-year-old man with diffuse sclerotic metastases from prostate carcinoma involving the thoracic and lumbar spine seen as diffuse increased density on lateral radiograph (a). The neoplastic disease has mostly low signal on sagittal T1 WI (b) and sagittal T2WI (c).

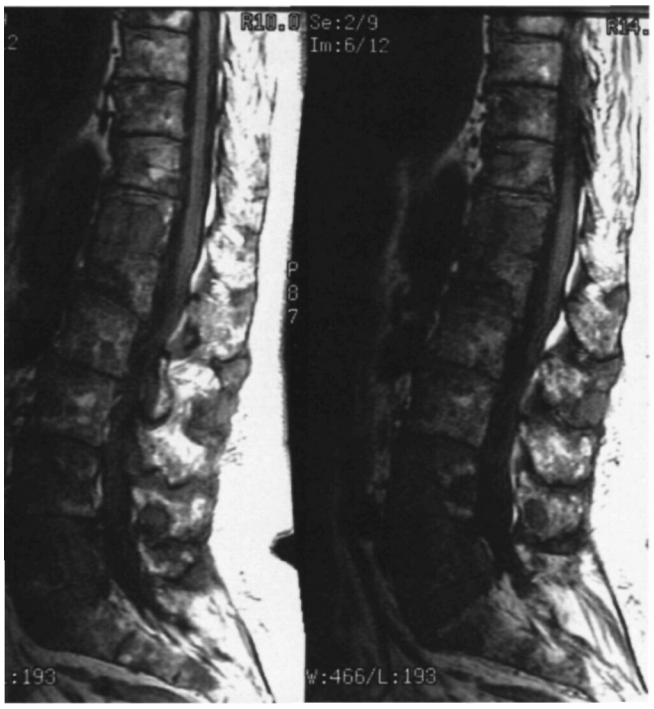

a

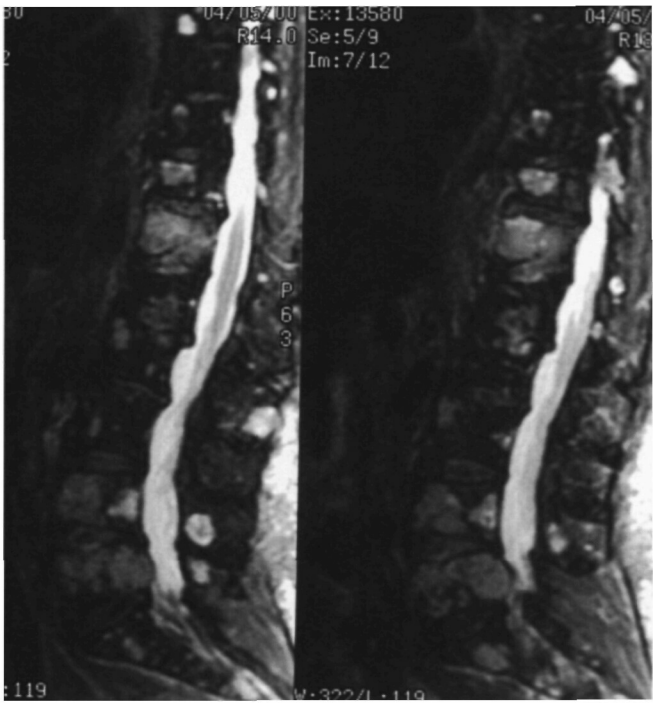

b

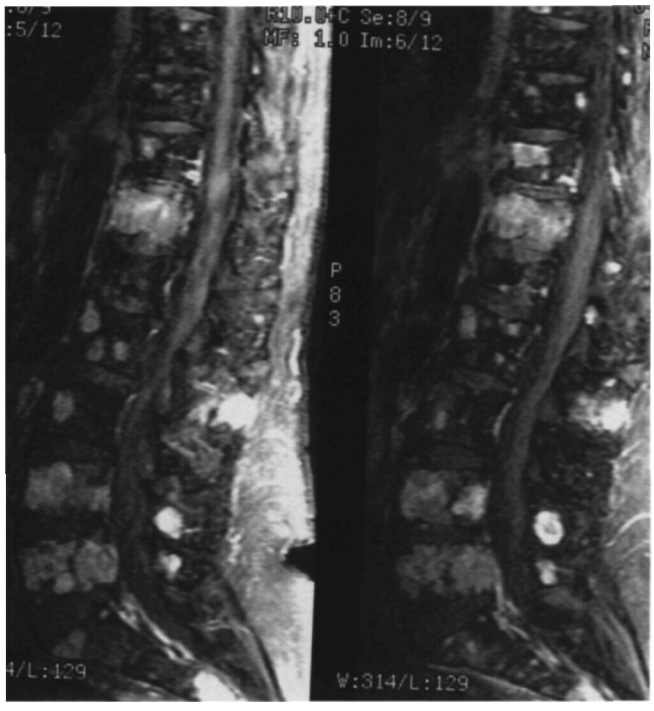

c

Figure **2.3a-c** Multiple myeloma involving multiple thoracic and lumbar vertebrae. The lesions have low-intermediate signal on sagittal T1WI (a) and high signal on sagittal FST2WI (b). The lesions show prominent Gd-contrast enhancement on sagittal FST1WI (c).

a

b, c

Figure **2.4a-c** Plasmacytoma involving a thoracic vertebral body with associated epidural extension and pathologic fracture. The tumor has diffuse low-intermediate signal on sagittal T1WI (a), and intermediate signal on sagittal (b) T2WI. The tumor shows prominent Gd-contrast enhancement on sagittal FST1WI(c).

Table 2 (Continued) Tumors and tumorlike lesions involving the spine

Tumor/Tumorlike Lesion	MRI Findings	Comments
Lymphoma and leukemia (Figs. 2.5-2.8)	Single or multiple well-circumscribed or poorly defined infiltrative lesions involving the vertebrae, dura, and/or leptomeninges; low-intermediate signal on T1WI, intermediate-high signal on T2WI and FST2WI. often shows Gd-contrast enhancement, +/- bone destruction. Diffuse involvement of vertebra with Hodgkin lymphoma can produce an "ivory vertebra" that has low signal on T1WI and T2WI. Leptomeningeal tumor often best seen on postcontrast images.	May have variable destructive or Infiltrative marrow/bony changes involving single or multiple sites of vertebral involvement. Lymphoma may extend from bone into adjacent soft tissues within or outside of the spinal canal; or initially involve only the epidural soft tissues or only the subarachnoid compartment. Can occur at any age (peak incidence 3rd to 5th decades). (See Atlas Chapters A 41 .A 47)

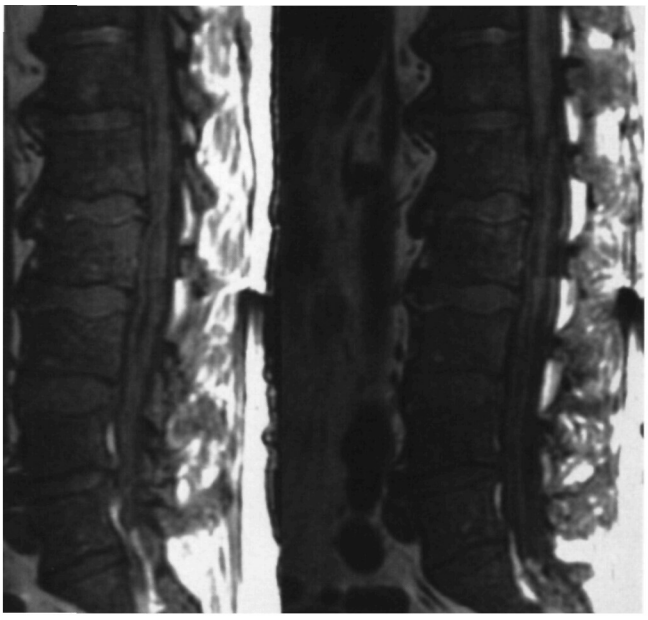

a

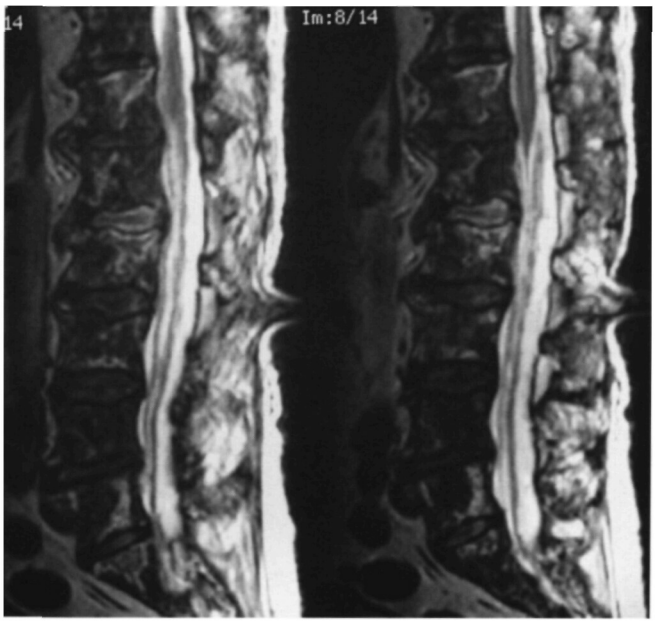

b

c

Figure 2.5 a-c Non-Hodgkin lymphoma involving vertebral marrow as well as within the lumbar subarachnoid space. Diffuse low-intermediate signal on sagittal T1WI (a) is seen throughout the marrow. Mostly low signal is seen in the marrow on sagittal T2WI (b). Heterogeneous Gd-contrast enhancement is seen throughout the marrow as well as within the thecal sac on sagittal (c) FST1WI.

Figure 2.6a, b A 41-year-old man with Hodgkin lymphoma involving multiple vertebrae. The lymphoma has intermediate signal on sagittal T1WI (a), and shows mild-moderate Gd-contrast enhancement on sagittal FST1WI (b).

Figure 2.7 Epidural non-Hodgkin lymphoma causing compression of the thoracic spinal cord. The epidural lesion has intermediate signal on sagittal T2WI.

Figure 2.8a, b A 28-year-old man with AML involving the marrow of the spine. The leukemic tissue has heterogeneous slightly high signal on sagittal FST2WI (a) and shows mild heterogeneous Gd-contrast enhancement on sagittal FS T1WI (b).

Table 2 (Continued) Tumors and tumorlike lesions involving the spine

Tumor/Tumorlike Lesion	MRI Findings	Comments
Chordoma (Fig. 2.9)	Well-circumscribed tabulated lesions, low-intermediate signal on T1WI, high signal on T2WI and FST2WI, usually show Gd-contrast enhancement (usually heterogeneous), locally invasive associated with bone erosion/destruction, usually involves the dorsal portion of the vertebral body with extension toward the spinal canal. Also occurs in sacrum.	Rare, slow-growing tumors (~3% of bone tumors); usually occur in adults 30 to 70 years; males > females (2/1); sacrum (50 %) > skull base (35 %) > vertebrae (15%). **(See Atlas Chapter A12)**
Enchondroma	Lobulated lesions, low-intermediate signal on T1WI, high signal on T2WI and FST2WI, +/- matrix mineralization, with low signal on T2WI, usually show Gd-contrast enhancement (usually heterogeneous), usually involve posterior elements.	Rare, slow-growing tumors (~12 % of bone tumors), usually occur in children and young adults (10-30 years), males = females. **(See Atlas Chapter AS)**
Chondrosarcoma (Fig.2.10)	Lobulated lesions, low-intermediate signal on T1 WI, high signal on T2WI, +/- matrix mineralization, with low signal on T2WI, usually show Gd-contrast enhancement (usually heterogeneous), locally invasive associated with bone erosion/destruction, encasement of vessels and nerves, can involve any portion of the vertebra.	Rare, slow-growing tumors (~16% of bone tumors), usually occur in adults (peak in 5th to 6th decades), males > females, sporadic (75%), malignant degeneration/ transformation of other cartilaginous lesion enchondroma. osteochondroma, etc *(25%).* **(See Atlas Chapter A11)**
Chondroblastoma	Tumors often have fine lobular margins and typically have low-intermediate heterogeneous signal on T1WI and mixed low, intermediate, and/or high signal on T2WI. Areas of low signal on T2WI are secondary to chondroid matrix mineralization, and/or hemosiderin. Lobular, marginal, or septal Gd-contrast enhancement patterns can be seen. Tumors may have thin margins of low signal on T2WI representing sclerotic borders. Cortical destruction is uncommon. Bone expansion can result in spinal cord compression.	Benign cartilaginous tumors with chondroblast-like cells and areas of chondroid matrix formation, rarely occur in the spine. Spinal tumors most often involve the thoracic vertebrae and usually involve both the body and pedicles. **(See Atlas Chapter A 7)**
Osteogenic sarcoma (Fig.2.11)	Destructive malignant lesions, low-intermediate signal on T1WI, mixed low. intermediate, high signal on T2WI, usually + matrix mineralization/ossification, with low signal on T2W images, usually show Gd-contrast enhancement (usually heterogeneous).	Malignant bone lesions rarely occur as primary tumor involving the vertebral column, locally invasive, high metastatic potential. Occur in children as primary tumors and adults (associated with Paget's Paget disease, irradiated bone, chronic osteomyelitis, osteoblastoma, giant cell tumor, and fibrous dysplasia). **(See Adas Chapter A 64)**

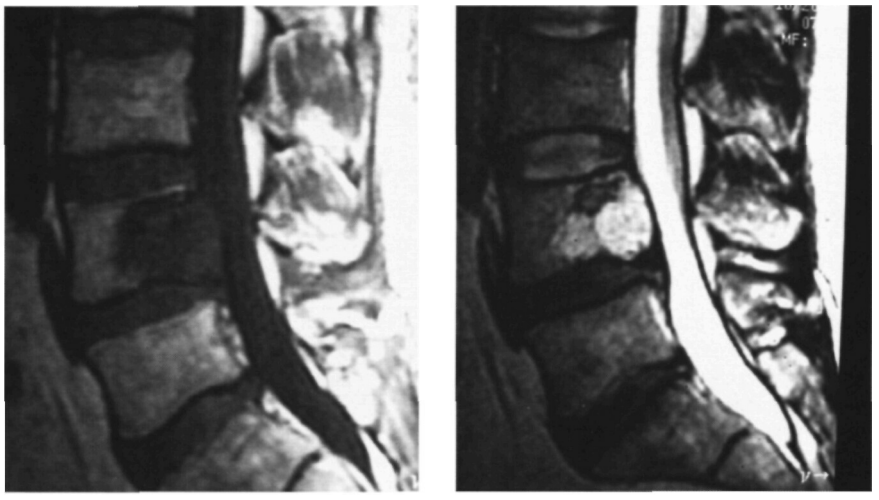

a, b

Figure 2.9a-c A 48-year-old man with a chordoma involving the dorsal portion of the L4 vertebral body. The tumor has low-intermediate signal on sagittal T1WI (a) and heterogeneous mostly high signal with small zones of low signal on sagittal T2WI (b). The tumor shows Gd-contrast enhancement on sagittal FST1WI (c).

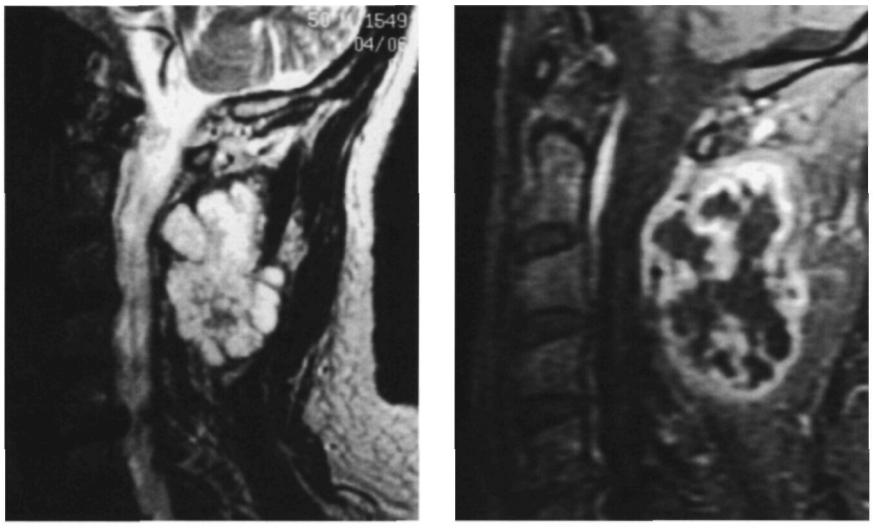

a b

Figure 2.10a, b A 50-year-old man with chondrosarcoma involving the posterior elements of C3. The tumor has high signal with thin bands of low signal on the sagittal view (a) and shows irregular nodular and curvilinear patterns of Gd-contrast enhancement on sagittal FST1WI (b).

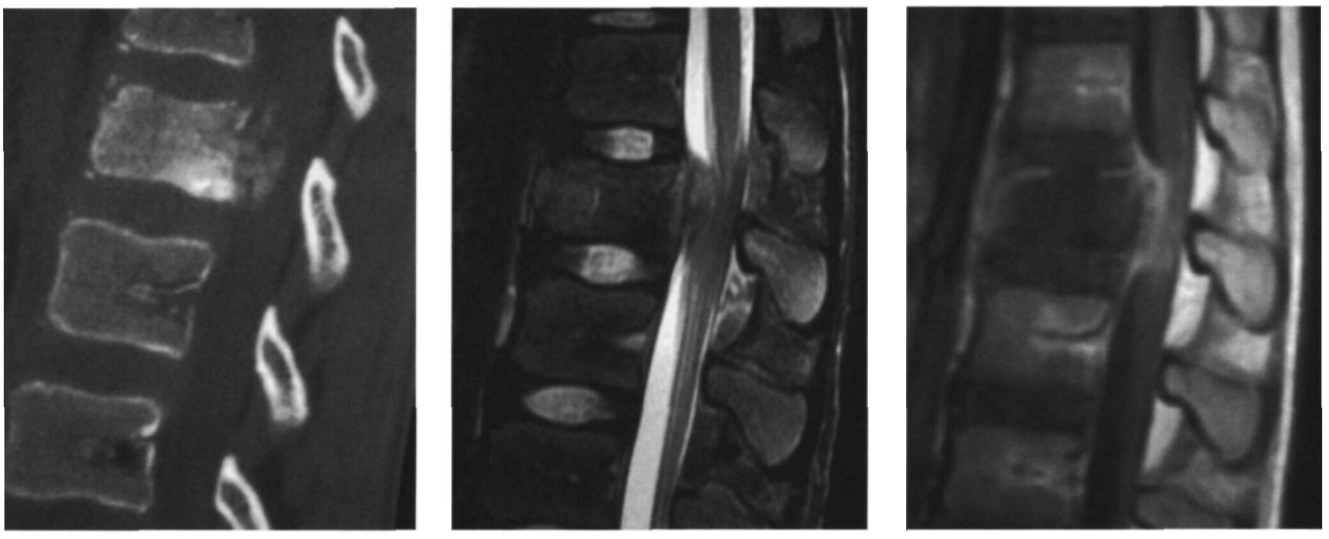

a, b c

Figure 2.11 a-c A 12-year-old boy with osteosarcoma involving the L1 vertebra. The tumor has heterogeneous mixed sclerotic and lucent zones within the vertebral body with cortical destruction and epidural tumor extension containing cumulus cloud-type matrix ossification on sagittal (a) CT. The tumor has mixed low and intermediate signal on sagittal FST2WI (b). The tumor shows heterogeneous Gd-contrast enhancement on sagittal T1WI (c). Enhancing tumor extending into the spinal canal compresses the spinal cord.

Table 2 (Continued) **Tumors and tumorlike lesions involving the spine**

Tumor/Tumorlike Lesion	MRI Findings	Comments
Ewing sarcoma (Fig. 2.12)	Destructive malignant lesions involving the vertebral column, low-intermediate signal on T1WI, mixed low, intermediate, and/or high signal on T2WI and FST2WI, usually show Gd-contrast enhancement (usually heterogeneous).	Usually occurs between the ages of 5 and 30, males > females, rarely occurs as primary tumor involving the spinal column, locally invasive, high metastatic potential. **(See Atlas Chapter A 20)**
Malignant fibrous histiocytoma(MFH)(Fig.2.13)	Tumors are often associated with zones of cortical destruction and extraosseous soft tissue masses. Tumors have low-intermediate signal on T1WI and heterogeneous intermediate-high signal on T2WI and FST2WI. Tumors show heterogeneous often prominent enhancement.	Malignant tumors involving soft tissue and rarely bone that are presumed to derive from undifferentiated mesenchymal cells. The World Health Organization (WHO) now uses the term undifferentiated pleomorphic sarcoma for pleomorphic MFH. **(See Atlas Chapter A 48)**
Osteoid osteoma (Fig. 2.14)	Intraosseous circumscribed vertebral lesion often less than 1.5cm in diameter located in posterior elements, central zone with low-intermediate signal on T1WI and high signal on T2WI and FST2WI with prominent Cd-contrast enhancement, surrounded by a peripheral rim of low signal on T1WI and T2WI (sclerosis); +/- high signal on T2WI and FST2WI in bone (edema) beyond zone of sclerosis or in adjacent soft tissues.	Benign osseous lesion containing a nidus of vascularized osteoid trabeculae surrounded by osteoblastic sclerosis, 14 % of osteoid osteomas are located in the spine, usually occurs between ages 5 and 25, males > females. Focal pain and tenderness associated with lesion that is often worse at night, relieved with aspirin. **(See Atlas Chapter A 60)**
Osteoblastoma (Fig. 2.15)	Expansile vertebral lesion often greater than 1.5cm in diameter located in posterior elements (90 %) +/- extension into vertebral body (30%), +/- epidural extension (40%), low-intermediate signal on T1WI and intermediate-high signal on T2WI and FST2WI, usually show Gd-contrast enhancement +/- spinal cord/spinal canal compression. +/- high signal on T2WI and FST2WI in bone (edema) beyond zone of sclerosis or in adjacent soft tissues.	Rare benign bone neoplasm (2 % of bone tumors) usually occurs from 6 to 30 years. One-third of osteoblastomas involve the spine. **(See Atlas Chapter A 61)**

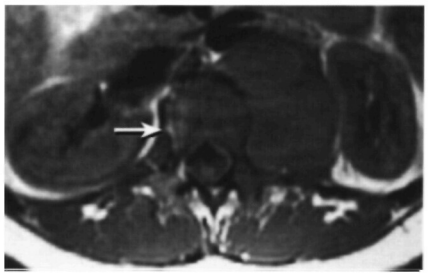

a

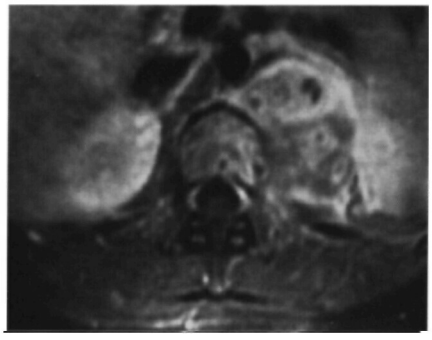

b

Figure 2.12 a, b A 16-year-old female with Ewing's sarcoma involving a vertebral body with extension laterally into the adjacent soft tissues on the left. Axial (a) T1WI shows the tumor to have low-intermediate signal. The tumor shows heterogeneous Gd-contrast enhancement on axial FST1WI (b).

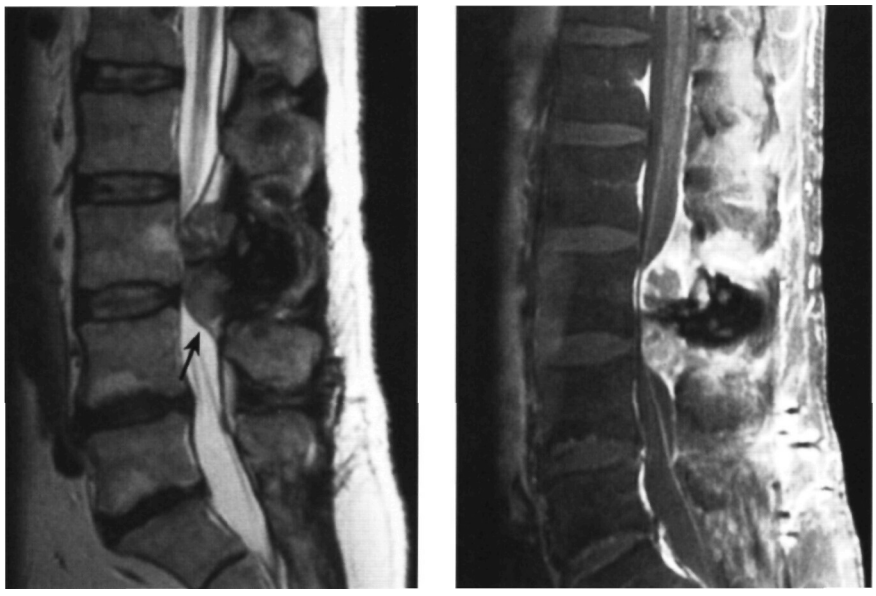

a b

Figure 2.13a, b A 56-year-old man with malignant fibrous histiocytoma involving the posterior elements at the L3 vertebra with extraosseous extension and spinal canal compression. The tumor has mixed low and intermediate signal on sagittal T2WI (a). The tumor shows heterogeneous Gd-contrast enhancement on sagittal FST1WI (b).

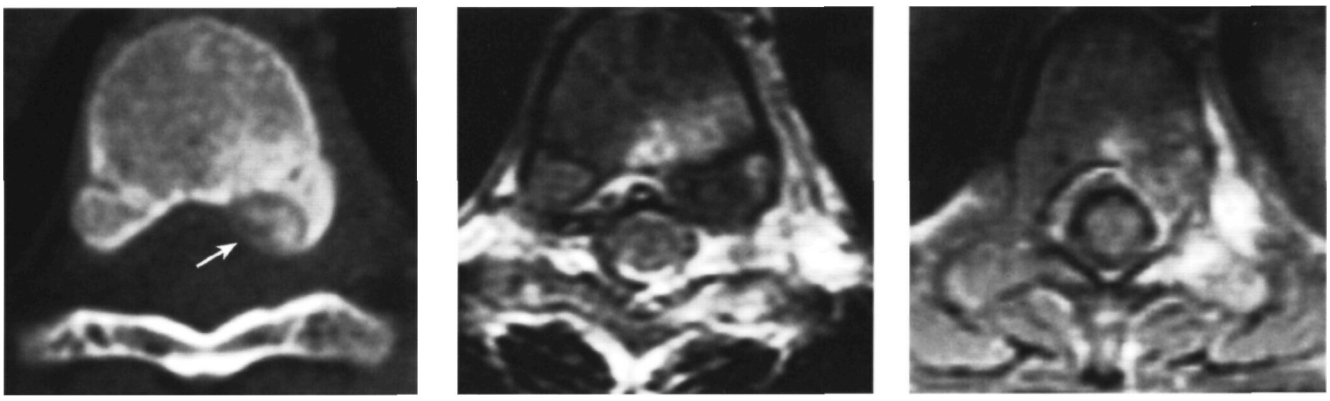

a, b c

Figure 2.14a-c A 5-year-old female with an osteoid osteoma involving the left pedicle of the T10 vertebra. Axial CT image (a) shows a circumscribed intramedullary lesion with low attenuation surrounding a zone of mineralization/calcification. Sclerotic increased attenuation is seen in the medullary bone adjacent to the lesion. The lesion has low and intermediate signal on axial T2WI (b) surrounded by high signal. The lesion shows prominent Gd-contrast enhancement on axial FST1WI (c). In addition, poorly defined zones of Gd-contrast enhancement are seen in the marrow adjacent to the lesion as well as in the extraosseous soft tissues.

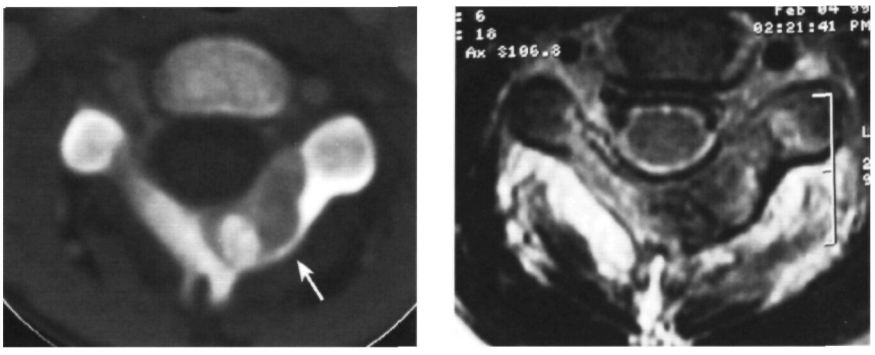

a, b

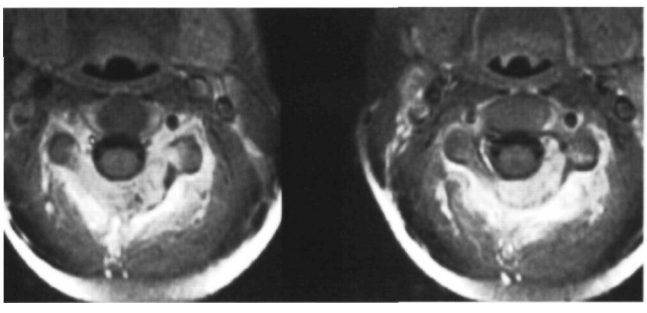

c

Figure 2.15 a-c A 4-year-old female with an Osteoblastoma involving the left lamina of the C3 vertebra. The axial CT image (a) shows a circumscribed radiolucent lesion with an internal calcification. Sclerotic reaction is seen in the adjacent bone. Bony expansion with thin peripheral sclerotic rims is seen. The lesion has heterogeneous low-intermediate signal on axial T2WI (b). The lesion shows prominent Gd-contrast enhancement on axial FST1WI (c). Poorly defined zones of high signal on T2WI and corresponding Gd-contrast enhancement are seen in the marrow and soft tissues adjacent to the Osteoblastoma.

Table 2 (Continued) **Tumors and tumorlike lesions involving the spine**

Tumor/Tumoriike Lesion	MRI Rndings	Comments
Giant cell tumor (Fig. 2.16)	Circumscribed extradural vertebral lesion with low-intermediate signal on T1WI, high signal on T2WI +/- surrounding thin zone of low signal on T2WI, usually show Gd-contrast enhancement; Location: vertebral body > vertebral body and vertebral arch > vertebral arch alone. +/- spinal cord / spinal canal compression.	Locally aggressive lesions that rarely metastasize. Account for 5% of primary bone tumors Usually involve lone bones, only 4 % involve vertebrae. Occur in adolescents and adults (20-40 years). **(See Atlas Chapter A 29)**
Aneurysmal bone cyst (Fig.2.17)	Circumscribed extradural vertebral lesion usually involving the posterior elements +/- involvement of the vertebral body; with variable low, intermediate, high, and/or mixed signal on T1WI and T2WI, +/- surrounding thin zone of low signal on T2WI, +/- lobulations, +/- one or multiple fluid-fluid levels.	Expansile blood/debris-filled lesions that may be primary lesions or occur secondary to other bone lesions such as giant cell tumor, fibrous dysplasia, chondroblastoma. Most occur in patients < 30 years. Locations: lumbar > cervical > thoracic. Clinical findings can include neurologic deficits and pain. **(See Atlas Chapter A 2)**
Osteochondroma (Fig. 2.18)	Circumscribed sessile lesion typically arising from posterior elements of vertebrae, central zone with intermediate signal on T1WI and T2WI similar to marrow surrounded by a peripheral zone of low signal on T1 WI and T2 WI, + cartilaginous cap. Increased malignant potential when cartilaginous cap is > 2 cm thick.	Benign cartilaginous tumors arising from defect at periphery of growth plate during bone formation with resultant bone outgrowth covered by a cartilaginous cap. Usually benign lesions unless associated with pain and increasing size of cartilaginous cap. **(See Atlas Chapter ASS)**
Hemangioma (Fig. 2.19)	Circumscribed or diffuse vertebral lesion usually located in the vertebral body +/- extension into pedicle or isolated within pedicle, typically have intermediate-high signal on T1WI, high signal on T2WI and FST2W, associated with thickened vertical trabeculae, usually show Gd-contrast enhancement, multiple in 30%, thoracic *(60%)* > lumbar (30%) > cervical (10%).	Most common benign lesions involving vertebral column, women > men, composed of endothelial-lined capillary and cavernous spaces within marrow associated with thickened vertical trabeculae and decreased secondary trabeculae, seen in 11 % of autopsies. Usually asymptomatic, rarely cause bone expansion and epidural extension resulting in neural compression (usually in thoracic region), increased potential for fracture with epidural hematoma. **(See Atlas Chapter A 34)**

a

b

Figure 2.16a, b Giant cell tumor involving a thoracic vertebra in a 15-year-old male. The lesion involves the vertebral body, left pedicle, left transverse process, and left lamina. Epidural tumor extension causes spinal cord compression. The tumor has well-defined margins, and has a central high signal on sagittal FST2WI (a) surrounded by a rim of low signal. The tumor shows prominent Gd-contrast enhancement on axial T1WI (b).

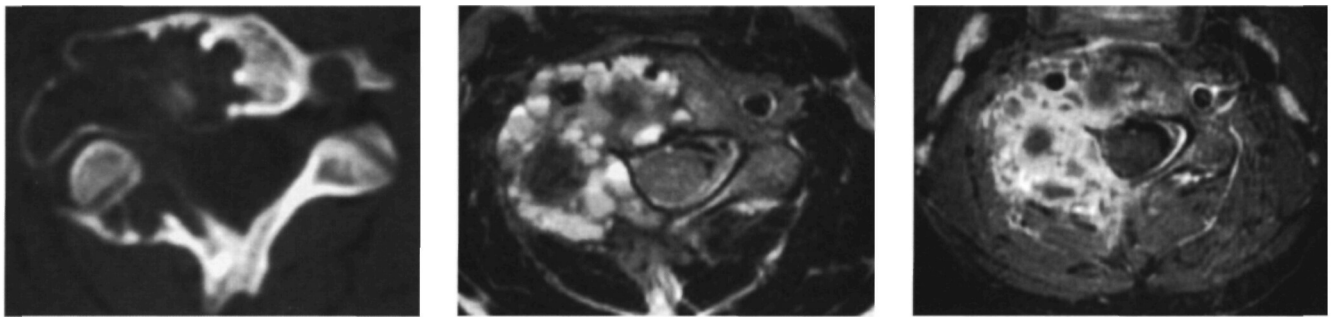

Figure 2.17a-c A 12-year-old girl with an aneurysmal bone cyst seen as a radiolucent expansile lesion involving the right side of the C 5 vertebral body, right transverse process, right pedicle, and lamina on axial CT (a). The MRI shows the lesion to have mixed low, intermediate, and high signal with multiple fluid-fluid levels on axial T2WI (b). The lesion shows multiple lobules with peripheral rim-like Gd-contrast enhancement on axial FST1WI (c).

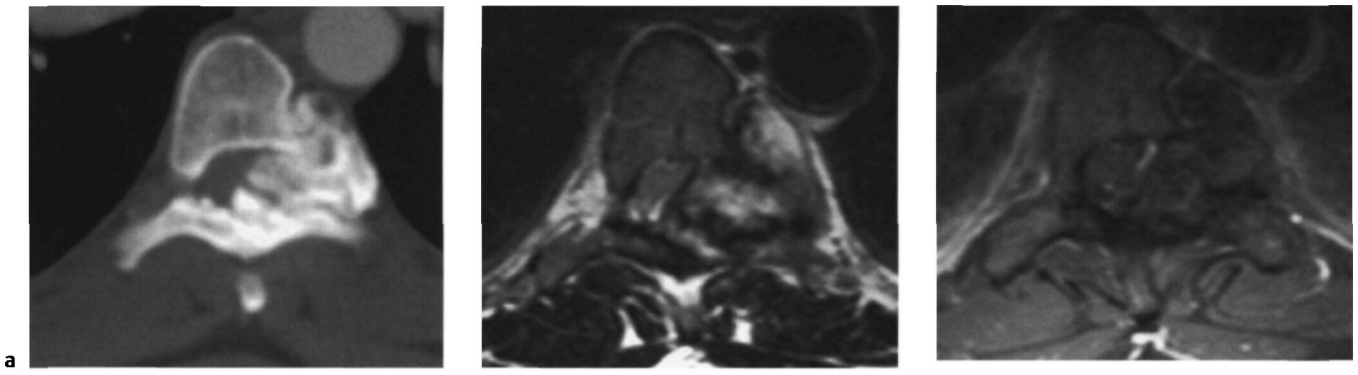

Figure 2.18a-c A 43-year-old woman with an osteochondroma involving the left pedicle of a thoracic vertebra with extension of the lesion into the spinal canal resulting in compression of the spinal cord as seen on axial CT image (a) and axial T2WI (b). The lesion has a central signal similar and slightly higher to marrow on T2WI surrounded by a thin rim of low signal from subchondral bone. The cartilaginous cap is very thin and shows minimal Gd-contrast enhancement on axial FST1WI (c).

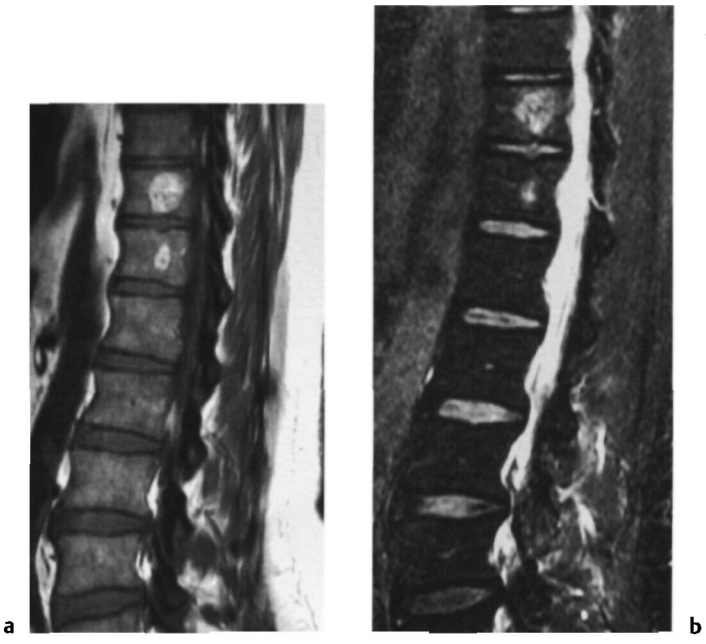

Figure 2.19a, b Hemangiomas in the T12 and L1 vertebral bodies. The hemangiomas have mostly high signal on sagittal (a) T1WI, and sagittal FST2WI (b).

Table 2 (Continued) **Tumors and tumorlike lesions involving the spine**

Tumor/Tumorlike Lesion	MRI Findings	Comments
Hemangioendothelioma (Fig. 2.20)	Lesions usually have sharp margins that may be slightly lobulated and often have low-intermediate signal on T1WI, and heterogeneous intermediate-high signal on T2WI and FS T2WI with zones of low signal. Lesions can be multifocal. Extraosseous extension of tumor through zones of cortical destruction can be seen. Lesions often show prominent heterogeneous Gd-contrast enhancement.	Vasoformative/endothelial low-grade malignant neoplasms thai are locally aggressive and rarely metastasize compared with high-grade angiosarcoma. **(See Atlas Chapter A 33)**
Hemangiopericytoma (Fig. 2.21)	Tumors usually have well-defined margins, with or without lobulations, low-intermediate signal on T1WI, intermediate or slightly high to high signal on T2WI, and heterogeneous high signal on FST2WI. On T2WI, lesions may contain tubular signal voids centrally or peripherally likely representing tumor vessels. Tumors can contain hemorrhagic zones with corresponding MR signal alteration. Tumors often show moderate to prominent Gd-contrast enhanrpmpnt.	Rare malignant tumors of pericytic origin that occur in soft tissues and less frequently in bone. **(See Atlas Chapter A 35)**
Other tumorlike lesions		
Arachnoid cyst (Fig. 2.22)	Well-circumscribed extra-axial lesions with low signal on T1WI and FLAIR, and high signal on T2WI and FST2WI, similar to CSF, no Gd-contrast enhancement. Usually cause mass effect on the adjacent spinal cord. Chronic erosive changes can be seen at the vertebrae adjacent to the cyst.	Non-neoplastic acquired, developmental, or congenital extra-axial cysts filled with CSF. Cysts can be small or large, asymptomatic or symptomatic.
Tarlov cyst (perineural cyst) (Fig. 2.23)	Well-circumscribed cysts with MRI signal comparable to CSF involving nerve root sleeves associated with chronic erosive changes involving adjacent bony structures. Sacral (+/- widening of sacral foramina) > lumbar nerve root sleeves. Usually range from 15 to 20 mm in diameter, but can be larger.	Typically represent incidental asymptomatic anatomic variants associated with prior dural injury.

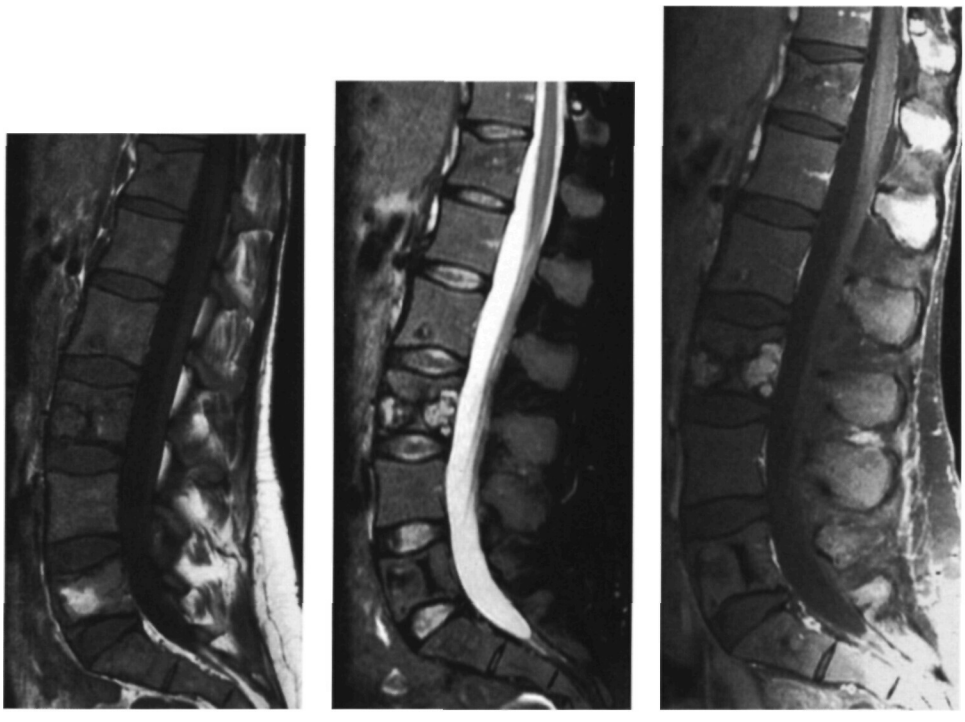

a b, c

Figure **2.20a-d** A 42-year-old woman with multifocal hemangioendotheliomas involving the *12, 13,* and L5 vertebral bodies. The lesions have mixed low-intermediate and high signal on sagittal T1WI (a), and sagittal FST2WI (b). Lesion in the L3 vertebral body shows Gd-contrast enhancement on sagittal FST1WI (c).

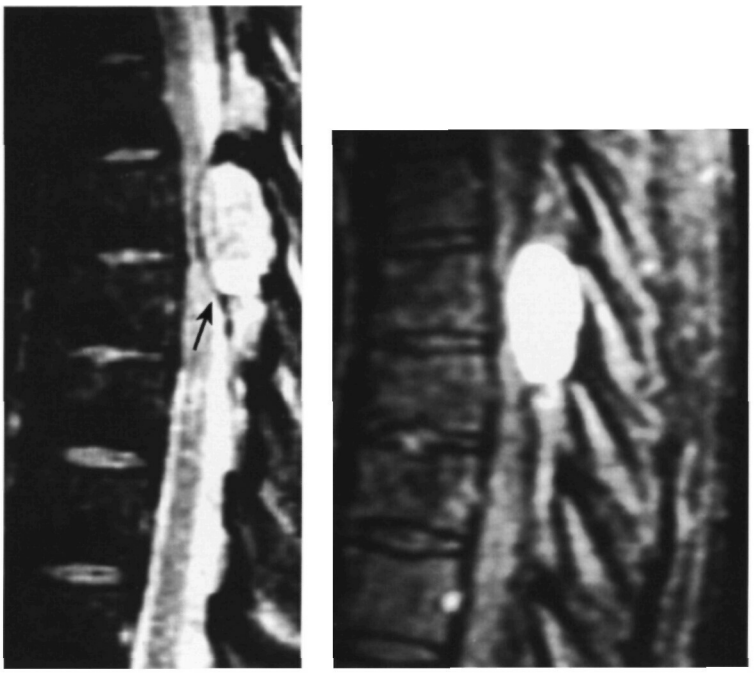

Figure 2.21 a, b Posterior epidural hemangiopericytoma involving the thoracic spine with spinal cord compression. The tumor has high signal on sagittal T2WI (a) and shows prominent Gd-contrast enhancement on sagittal FST1WI (b).

Figure 2.22a, b A 35-year-old woman with an arachnoid cyst at the dorsal portion of the spinal canal at the thoracolumbar junction. The cyst has circumscribed margins and contains fluid with low signal on sagittal T1 WI (a) and high signal on sagittal (b) T2WI.

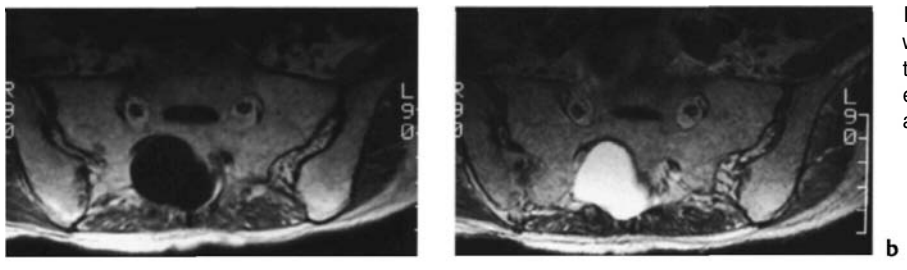

Figure 2.23 a, b A well-circumscribed cyst with MRI signal comparable to CSF is seen at the right S 3 nerve root sleeve with associated expansion of the adjacent sacral foramen on axial T1WI (a) and axial T2WI (b).

Table 2 (Continued) **Tumors and tumorlike lesions involving the spine**

Tumor/Tumorlike Lesion	MRI Findings	Comments
Dermoid (Fig. 2.24)	Well-circumscribed spheroid or multilobulated intradural extramedullary or intramedullary lesions, usually with intermediate-high signal on T1WI, and variable low, intermediate, and/or high signal on T2WI. Usually show no Gd-contrast enhancement, +/- fluid-fluid or fluid-debris levels. Lumbar region most common location in spine. Can cause chemical meningitis if dermoid cyst ruptures into the subarachnoid space. Commonly located: at or near midline.	Non-neoplastic congenital or acquired ectodermal inclusion cystic lesions filled with lipid material, cholesterol, desquamated cells, and keratinaceous debris, usually mild mass effect on adjacent spinal cord or nerve roots, adults: males slightly > females, +/- related clinical symptoms. **(See Atlas Chapter A15)**
Epidermoid	Well-circumscribed spheroid or multilobulated intradural extramedullary lesion with low-intermediate signal on T1WI, and high signal on T2WI and diffusion-weighted images, mixed low, intermediate, or high signal on FLAIR images, typically show no Gd-contrast enhancement.	Non-neoplastic extramedullary epithelial-inclusion lesions filled with desquamated cells and keratinaceous debris, usually mild mass effect on adjacent spinal cord and/or nerve roots. May be congenital (+/- associated with dorsal dermal sinus, spina bifida. hemivertebrae) or acquired (late complication of lumbar puncture). **(See Atlas Chapter A15)**
Neurenteric (endodermal) cyst (Fig. 2.25)	Well-circumscribed spheroid intradural extramedullary lesions, with low, intermediate, or high signal on T1WI and T2WI, and usually showing no Gd-contrast enhancement. Lesions may extend into the spinal cord in 10%.	A type of split cord malformation in which there is a persistent communication between ventrally located endoderm and dorsally located ectoderm secondary to developmental failure of separation of notochord and foregut, observed in patients <40 years. Obliteration of portions of a dorsal enteric sinus can result in cysts lined by endothelium, fibrous cords, or sinuses. Can occur within spinal canal (ventral > dorsal to the spinal cord), commonly in cervical and upper thoracic regions, and are often associated with vertebral anomalies such as hemivertebrae, butterfly vertebrae, clefts in vertebral bodies, and zones of incomplete segmentation. Patients can present with local and distal long tract symptoms and progressive spinal cord compression.

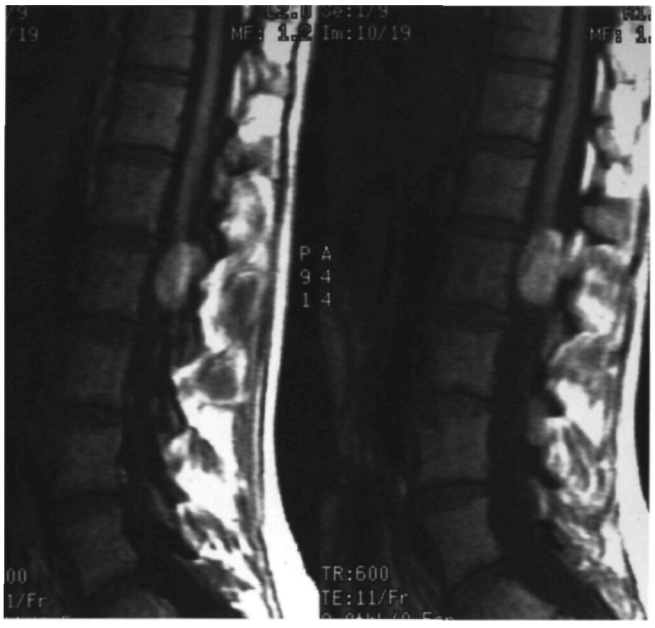

a

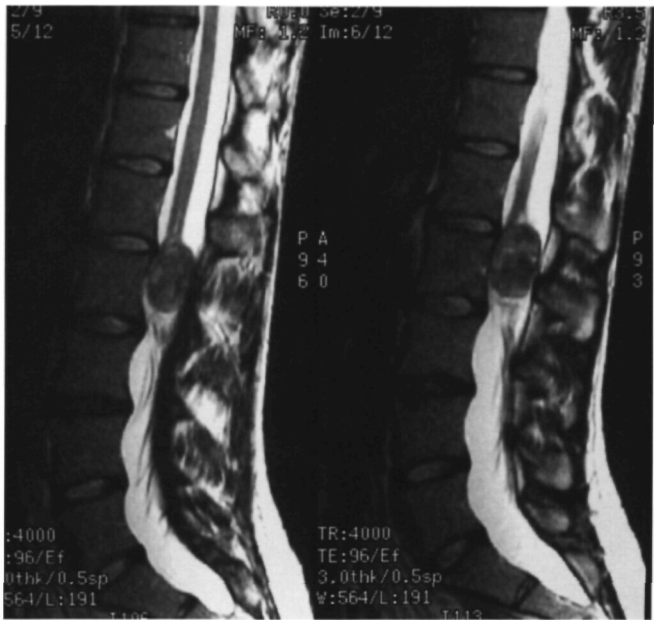

b

Figure 2.24a, b A 27-year-old woman with a dermoid in the posterior lumbar spinal canal. The lesion has high signal on sagittal T1WI (a), and low-intermediate signal on sagittal (b).

a

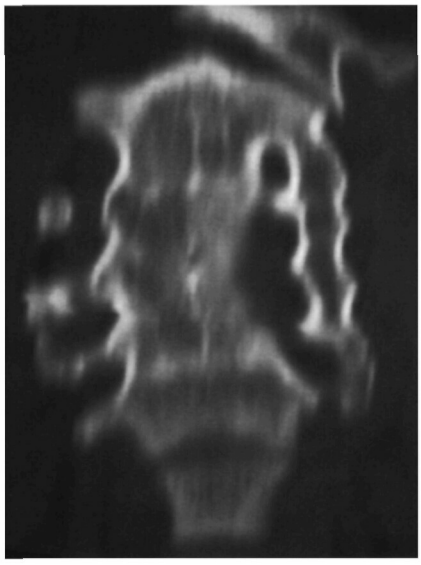

b

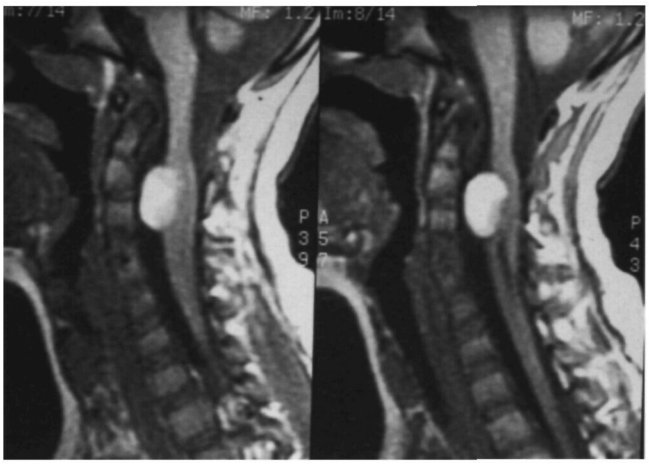

c

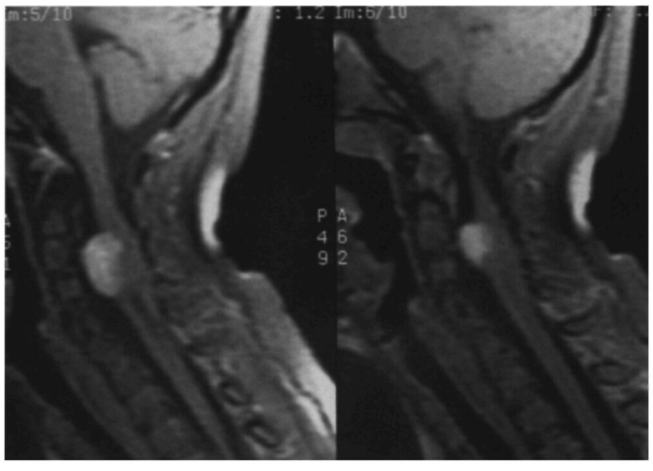

d

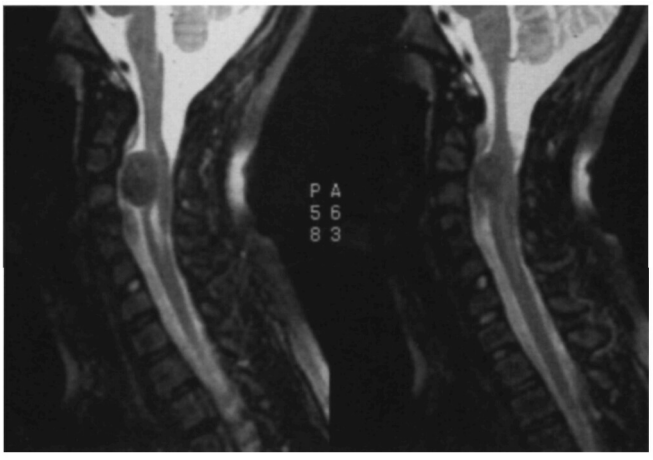

e

Figure 2.25 a-e A 7-year-old girl with a neurenteric cyst in the anterior portion of the cervical spinal canal which compresses the ventral margin of the spinal cord. The lateral radiograph (**a**) and coronal CT image (**b**) show segmentation anomalies and remnants of a midline cleft involving multiple vertebral bodies ventral to the neurenteric cyst. The cyst has high signal on sagittal T1WI (**c**) and FST1WI (**d**), and low-intermediate signal on FST2WI (**e**).

Table 2 (Continued) Tumors and tumorlike lesions involving the spine

Tumor/Tumorlike Lesion	MRI Findings	Comments
Synovial cyst (Fig. 2.26)	Circumscribed lesion located adjacent lo the facet joint. A thin rim of low signal on T2WI surrounds a central zone that may have low-intermediate signal on T1 WI, and low, intermediate, and or high signal on T2WI. No central Cd-contrast enhancement is usually seen, but a thin rim of peripheral enhancement may be observed.	Represents protrusion of synovium with fluid from degenerated facet joint into the spinal canal medially or dorsally into the posterior paraspinal soft tissues. Variable MRI signal is related to the contents that may include serous or mucinous fluid, blood, hemosiderin, and/or gas. **(See Atlas Chapter A 74)**
Bone island (Fig. 2.27)	Usually appear as a circumscribed radiodense ovoid or spheroid focus in medullary bone that may or may not contact the endosteal surface of cortical bone. Typically have low signal comparable to cortical bone on all pulse sequences.	Bone islands (enostoses) arc non-neoplastic intramedullary zones of mature compact bone composed of lamellar bone; considered lo be developmental anomalies resulting from localized failure of bone resorption during skeletal maturation. **(See Atlas Chapter A 62)**
Melorheostosis (Rg.2.28)	MRI signal varies based on the relative proportions of chondroicl, mineralized osteoid, and soft tissue components in these lesions. Mineralized zones typically have low signal on T1 WI and T2WI, no Cd-contrast enhancement. Nonmineralized portions can have low-intermediate signal on T1 WI, inlermediate to high signal on T2WI, and show Gd-contrast enhancement.	Rare bone dysplasia with cortical thickening that has a "flowing candle wax" configuration. Associated soft tissue masses occur in ~25 %. The soft tissue lesions often contain mixtures of chondroid material, mineralized osteoid, and fibrovascular tissue. Surgery is usually performed only for lesions causing symptoms. **(See Atlas Chapter A 62)**

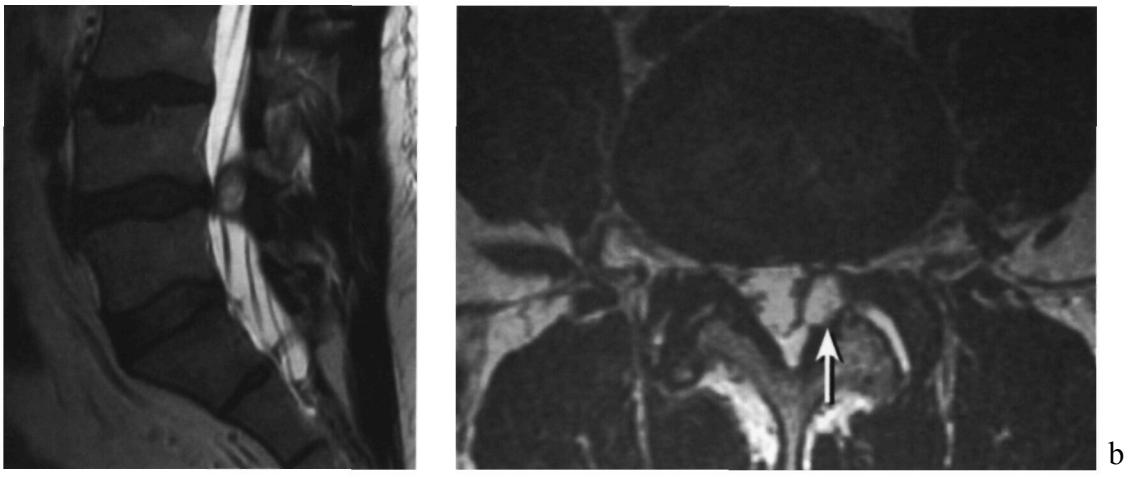

a b

Figure 2.26 a, b A 51-year-old man who has a synovial cyst extending from the medial aspect of the left L4-L5 facet joint, which mildly compresses the lateral margin of the thecal sac. The cyst lesion shows slightly high to high signal on sagittal (**a**) and axial (**b**)T2WI. A thin rim of low signal on T2WI is seen at the periphery of the lesion.

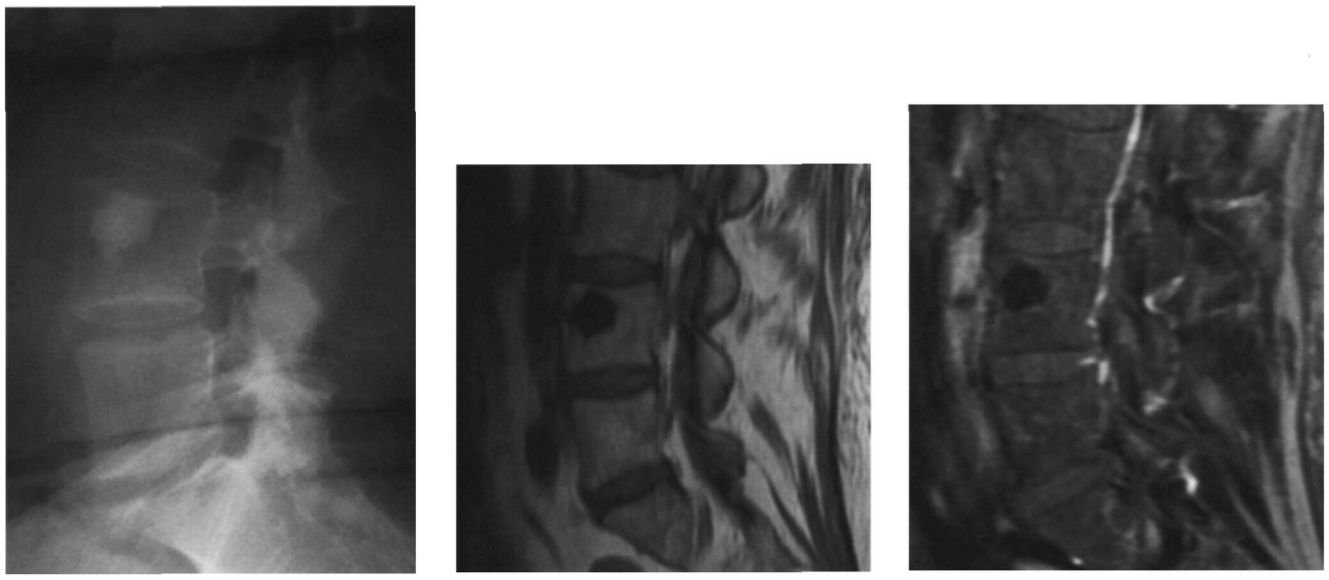

a b, c

Figure 2.27 a-c Bone island in a 70-year-old woman. A circumscribed dense lesion is seen in the L4 vertebral body on a lateral radiograph (**a**). The lesion has low signal on sagittal T1WI (**b**). The lesion shows no Gd-contrast enhancement on sagittal FST1WI (**c**).

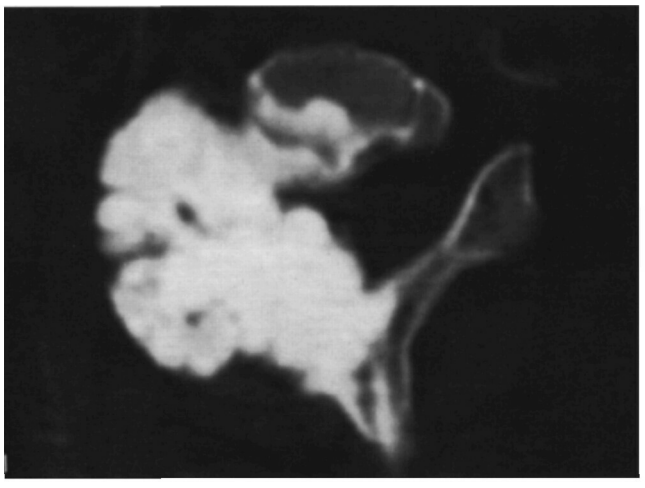

a

Figure 2.28 a-c A 53-year-old man with melorheostosis involving multiple vertebrae at the cervical and upper thoracic spine. The axial (**a**) CT image shows smooth zones of cortical hyperostosis with a "dripping candle wax" appearance at the right sides of the involved vertebrae. The zones of cortical hyperostosis show low signal on the axial (**b**) T2WI. No Gd-contrast enhancement is seen on the axial FSTIWI(**c**).

b

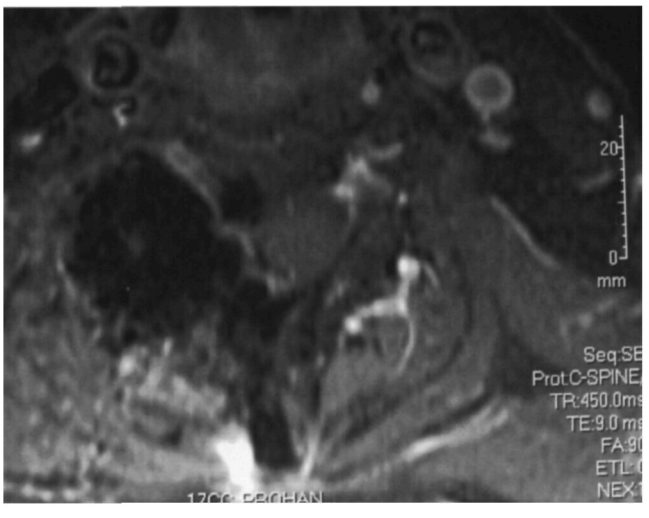

c

Table 2 (Continued) Tumors and tumorlike lesions involving the spine

Tumor/Tumorlike Lesion	MRI Findings	Comments
Trauma		
Fracture	**Traumatic and osteopenlc vertebral fracture (Fig. 2.29)** Acute/subacute fractures have sharply angulated cortical margins, near-complete or complete abnormal signal (usually low signal on T1 WI, high signal on T2WI, and FST2WI in marrow of affected vertebral body. Cd-contrast enhancement is seen in the early postfracture period, no destructive changes at cortical margins of fractured endplates. +/- convex outward angulated configuration of compressed vertebral bodies, +/- spinal cord and/or spinal canal compression related to fracture deformity, +/- retropulsed bone fragments into spinal canal. +/- subluxation, +/- kyphosis, +/-epidural hematoma, +/- high signal on T2WI and FST2WI involving marrow of posterior elements or between the inter-spinous ligaments. Chronic healed fractures usually have normal or near normal signal in compressed vertebral body. Occasionally persistence of signal abnormalities in vertebral marrow results from instability and abnormal axial loading. **Malignancy related vertebral fracture (Fig. 2.30)** Near-complete or complete abnormal marrow signal (usually low signal on T1WI, high signal on T2WI and FST2WI, occasionally low signal on T2WI for metastases with sclerotic reaction) in involved vertebra(**e**). Lesions usually show Gd-contrast enhancement, +/- destructive changes at cortical margins of vertebrae, +/-convex outward-bowed configuration of compressed vertebral bodies, +/- paravertebral mass lesions, +/- spheroid or diffuse signal abnormalities/lesions in other noncompressed vertebral bodies.	Vertebral fractures can result from trauma, primary bone tumors/lesions, metastatic disease, bone infarcts (steroids, chemotherapy, and radiation treatment), osteoporosis, osteomalacia, metabolic (calcium/phosphate) disorders, vitamin deficiencies, Paget disease, and genetic disorders (**e. g.**, osteogenesis imperfecta).
Degenerative changes		
Marrow changes related to degenerative disk disease	**Type 1:** Poorly defined zones with low-intermediate signal on T1WI (decreased relative to normal marrow), slightly high signal on T2WI (increased relative to normal marrow), and high signal on FST2WI in marrow next to intact endplates, often associated with Gd-contrast enhancement, intervening disk usually with degenerative changes. **(Fig. 2.31) Type 2:** Poorly defined zones with intermediate-slightly high signal on T1WI images (increased relative to normal marrow), intermediate-slightly high signal on T2WI (isointense or increased relative to normal marrow), and low or intermediate signal on FST2WI in marrow next to intact endplates, +/- Gd-contrast enhancement, intervening disk usually with degenerative changes. **(Fig. 2.32) Type 1 and 2 marrow changes** can also be focal in association with degenerative disk disease and SchmorPs nodes.	Reactive changes in marrow from degenerative disk disease can result from fissuring of endplates with edematous changes and/or replacement with fibrovascular tissue in the subjacent marrow. The endplate margins typically appear intact as thin linear zones of low signal on T1WI and T2WI adjacent to a degenerated disk with low signal on T2W images. These latter two findings differ from the MRI features of vertebral osteomyelitis where there is often destruction of the endplates and annulus, as well as high signal on T2WI within the disk.

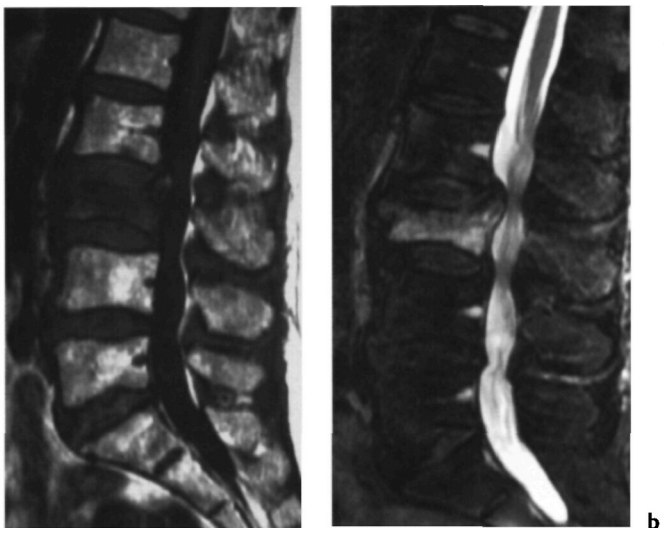

Figure 2.29 a, b An 82-year-old woman with a recent osteoporotic compression fracture involving the superior endplate of the L3 vertebral body. Sharply angulated cortical margins are seen at the fracture site, and the marrow has low signal on sagittal T1 WI (**a**) and high signal on sagittal FST2WI (**b**).

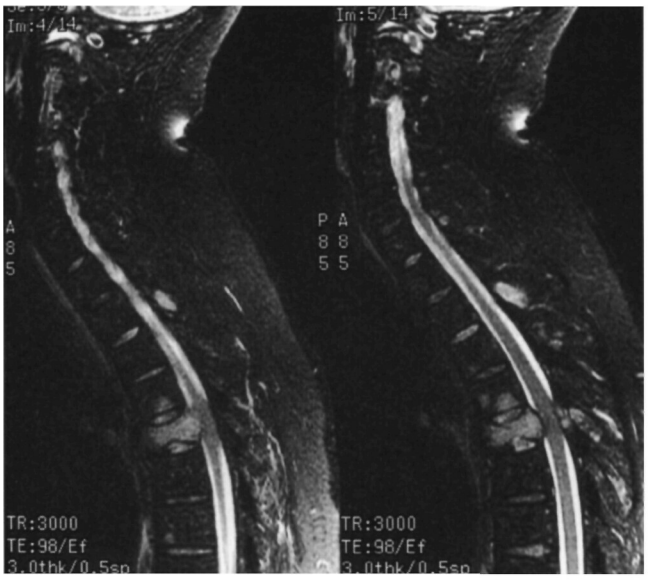

Figure 2.30 Multiple myeloma involving the spine including one lesion in a thoracic vertebral body that has a pathologic fracture causing spinal cord compression. The lesions including the fractured vertebral body have high signal on sagittal FST2WI.

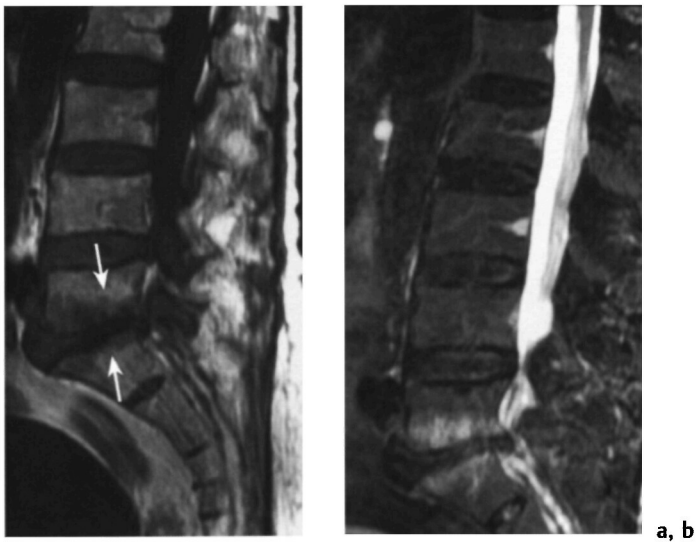

Figure 2.31 a, b Poorly defined zones of low- intermediate signal are seen in the marrow adjacent to the endplates at the L5-S 1 level on the sagittal T1WI (**a**), which have high signal on the sagittal FST2WI (**b**) representing reactive edematous changes secondary to the degenerative disk disease in this location.

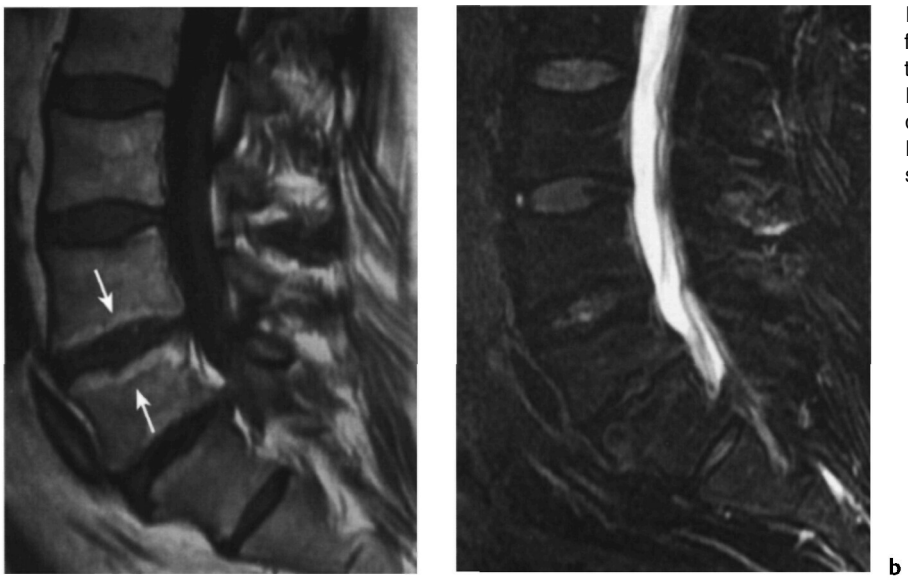

Figure 2.32 a, b Poorly defined zones of fatty signal are seen in the marrow adjacent to the endplates at the L4-L 5 and L 5-S1 levels secondary to chronic degenerative disk disease in these locations. The fatty marrow has high signal on sagittal T1WI (**a**), which is suppressed on sagittal T2WI (**b**).

Table 2 (Continued) Tumors and tumorlike lesions involving the spine

Tumor/Tumorlike Lesion	MRI Findings	Comments
Inflammation/Infection		
Pyogenic vertebral osteomyelitis/diskitis (Fig. 2.33)	Poorly defined /ones of low-intermediate signal on T1 WI and high signal on T2WI and FST2WI in marrow of two or more adjacent vertebral bodies and intervening disk(**s**), and +/- paravertebral soft tissues; +/- irregular deficiencies of endplates (loss of linear low signal on T1WI and T2WI); usually with prominent Gd-contrast enhancement in marrow and paravertebral soft tissues; variable enhancement of disk (patchy zones within disk, and/or thin or thick peripheral enhancement; +/- epidural abscess / paravertebral abscess (high signal collections on T2WI surrounded by a peripheral rim of gadolinium enhancement on T1WI. +/- vertebral compression deformity; +/- spinal cord or spinal canal compression.	Vertebral osteomyelitis represents 3% of osseous infections, results from hematogenous source (most common) from distant infection or intravenous drug abuse; complication of surgery, trauma, diabetes; spread from contiguous soft tissue infection. Initially involves end-arterioles in marrow adjacent to endplates with eventual destruction and spread to the adjacent vertebra through the disk. Children and adults > 50 years. Cram-positive organisms (Stoph. *aureus, S. epidermidis. Streptococcus,* etc) account for 70 % of pyogenic osteomyelitis and Gram-negative organisms *(Pseudomonas aeruginosa, Escherichia coli, Proteus,* etc) represent 30%. Fungal osteomyelitis can appear similar to pyogenic infection of spine. **(See Atlas Chapter A 63)**

a

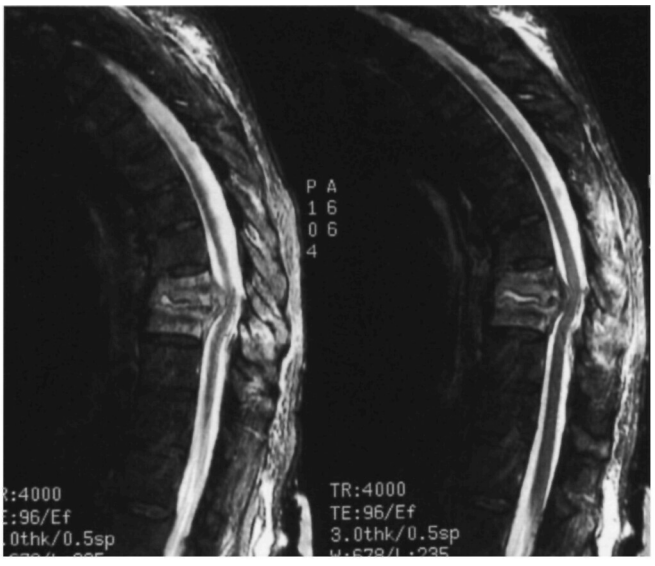

b

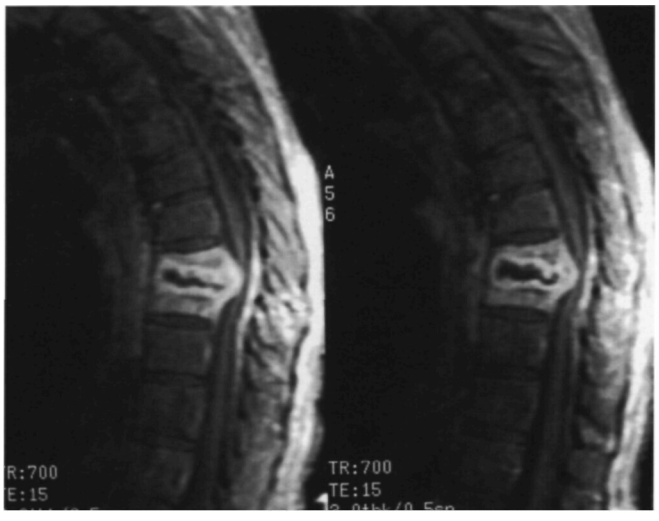

c

Figure 2.33 a-c A 77-year-old woman with pyogenic osteomyelitis involving two adjacent thoracic vertebral bodies and infection of the intervening disk. Poorly defined zones of low signal on sagittal T1WI (**a**) and high signal on sagittal FST2WI (**b**) are seen throughout the marrow of the vertebral bodies and intervening disk. Loss of definition of the low signal line of the end plates of the vertebral bodies is seen on T1WI and FST2WI. Prominent diffuse Gd-contrast enhancement is seen in the involved marrow on sagittal FST1WI (**c**).

Table 2 (Continued) Tumors and tumorlike lesions involving the spine

Tumor/Tumorlike Lesion	MRI Findings	Comments
Vertebral osteomyelitis-tuberculosis (Fig. 2.34)	Poorly defined zones of low-intermediate signal on T1WI and high signal on T2 Wand FST2W images in marrow of two or more adjacent vertebral bodies, Limited disk involvement early in the disease process tends to spare the disk until later in the disease process: +/- paravertebral soft tissues; +/- irregular deficiencies of endplates (loss of linear low signal on T1 W and T2W images); usually associated with Gd-contrast enhancement in marrow and paravertebral soft tissues; +/- epidural abscess, often paravertebral abscesses (high signal collections on T2WI surrounded by a peripheral rim(**s**) of Gd-contrast enhancement on T1WI. +/- vertebral compression deformity; +/- spinal cord or spinal canal compression.	Initially involves marrow in the anterior portion of the vertebral body with spread to the adjacent vertebrae along the anterior longitudinal ligament, often sparing the disk until later in the disease process; usually associated with paravertebral abscesses that may be more prominent than the vertebral abnormalities. **(See Atlas Chapter A 63)**

a

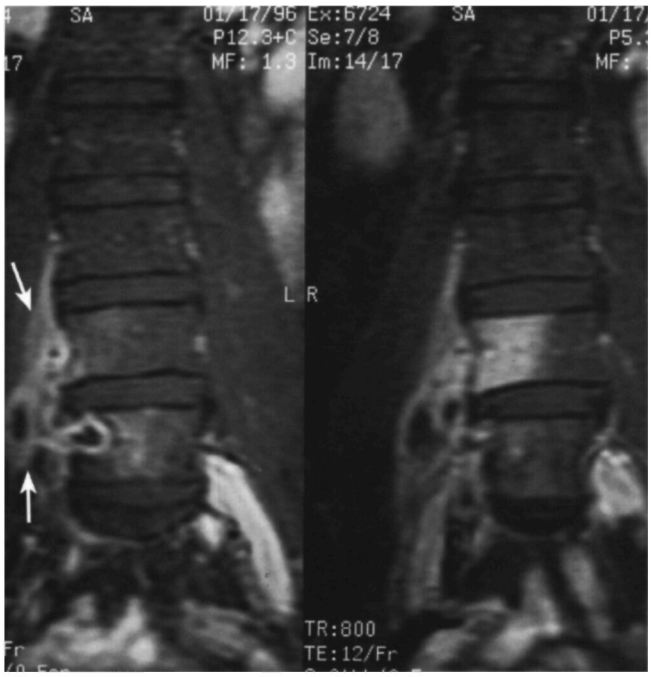

b

Figure 2.34a, b A 35-year-old man with tuberculous osteomyelitis involving the L4 and L5 vertebral bodies and paraspinal cold abscesses (arrows). Poorly defined zones of high signal on sagittal FST2WI (**a**) are seen in the marrow of adjacent vertebral bodies. No abnormal signal is seen at the intervening disk. The end plates appear intact. Irregular Gd-contrast enhancement is seen in the involved marrow and surrounding paraspinal "cold abscesses" on coronal (**b**) FST1WI.

Table 2 (Continued) Tumors and tumorlike lesions involving the spine

Tumor/Tumorlike Lesion	MRI Findings	Comments
Rheumatoid arthritis (Fig. 2.35)	Erosions of vertebral endplates, spinous processes, and uncovertebral and apophyseal joints. Irregular enlarged enhancing synovium (pannus low-intermediate signal on T1WI, intermediate-high signal on T2WI and FST2WI) at atlanto-dens articulation results in erosions of dens and transverse ligament, +/- destruction of transverse ligament with C1 on C2 subluxation and neural compromise. +/- basilar impression.	Most common type of inflammatory arthropathy that results in synovitis causing destructive/erosive changes of cartilage, ligaments, and bone. Cervical spine involvement in two-thirds of patients, juvenile and adult types. **(See Atlas Chapter A 70)**
Eosinophilic granuloma (Fig. 2.36)	Single or multiple circumscribed lesions in the vertebral marrow associated with focal bony destruction/erosion with extension into the adjacent soft tissues. Lesions usually involve the vertebral body and not the posterior elements, with low-intermediate signal on T1WI, mixed intermediate-slightly high signal on T2WI, usually with prominent Gd-contrast enhancement, +/- enhancement of the adjacent dura. Progression of lesion can lead to vertebra plana (collapsed flattened vertebral body) with minimal or no kyphosis and relatively normal-sized adjacent disks.	**Single lesion:** Commonly seen in males > females, < 20 years, proliferation of histiocytes in medullary cavity with localized destruction of bone with extension into adjacent soft tissues. **Multiple lesions:** Associated with syndromes such as: Letterer-Siwe disease (lymphadenopathy hepatosplenomegaly), children < 2 years; Hand-Schullcr-Christian disease (lymphadenopathy, exophthalmos, diabetes insipidus) children 5-10 years. **(See Atlas Chapter A18)**
Sarcoidosis (Fig. 2.37)	Sarcoid lesions can be multiple with variable sizes or solitary within marrow. Lesions can have circumscribed and/or indistinct margins within marrow and usually have low to intermediate signal on T1 WI, and intermediate or slightly high to high signal on T2WI and FST2WI. Lesions usually show variable degrees of Gd-contrast enhancement.	Chronic systemic granulomatous disease of unknown etiology in which noncaseating granulomas occur in various tissues and organs including bone. **(See Atlas Chapter A71)**
Hematopoietic		
Hematopoietic disorders (Fig. 2.38)	Red marrow hyperplasia can be seen as diffuse low-intermediate signal on T1WI; slightly high to high signal on FSET2WI; and low to intermediate signal on FST2WI with or without thinning of cortical bone.	Red marrow reconversion from erythroid hyperplasia can result from anemia secondary to sickle cell disease, thalassemia major, hereditary spherocytosis. Similar findings of red marrow expansion can be seen with polycythemia rubra. Medications (such as exogenous erythropoietin and granulocyle/macrophage colony-stimulating factor in patients with anemia and neutropenia, respectively) can also cause red marrow reconversion in adults and children.

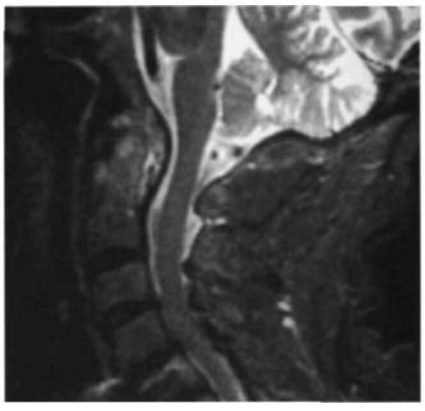

a

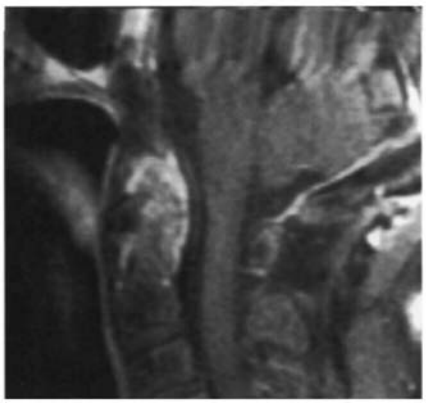

b

Figure 2.35a, b A 72-year-old woman with pannus from rheumatoid arthritis causing erosive changes at the upper dens and atlas as seen on sagittal FST2WI (**a**). The pannus and adjacent marrow have low-intermediate signal on T1WI and heterogeneous intermediate to slightly high signal on FST2WI. The pannus and adjacent marrow show Gd-contrast enhancement on sagittal FST1WI (**b**).

Figure 2.36a, b A 6-year-old boy with an eosinophilic granuloma involving the L3 vertebral body. The lesion has heterogeneous slightly high signal on sagittal FST2WI (**a**). The lesion shows Gd-contrast enhancement in the marrow as well as an extraosseous portion that extends into the anterior epidural soft tissues on sagittal FST1WI (**b**).

Figure 2.37a-c A 50-year-old man with sarcoidosis and multiple intraosseous spinal lesions. Multiple zones of low-intermediate signal on sagittal T1WI (**a**) and slightly high signal on sagittal FST2WI (**b**) are seen in multiple vertebrae. The lesions show Gd-contrast enhancement on sagittal FST1WI (**c**).

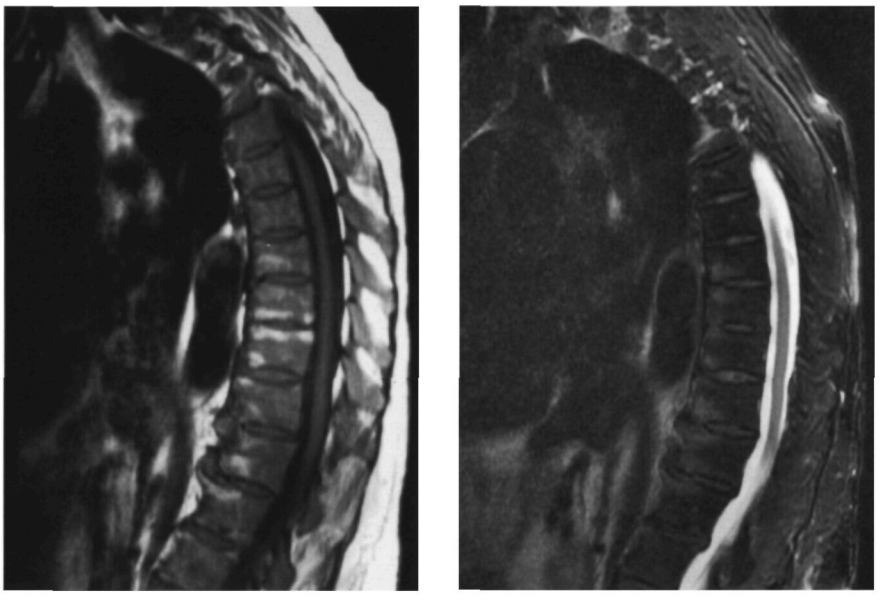

Figure 2.38 a, b A 60-year-old woman who has erythroid hyperplasia in the vertebral marrow from exogenous erythropoietin. Red marrow hyperplasia is seen as diffuse low-intermediate signal on sagittal T1WI (**a**) and FST2WI(**b**).

Table 2 (Continued) Tumors and tumorlike lesions involving the spine

Tumor/Tumorlike Lesion	MRI Findings	Comments
Extramedullary hematopoiesis (Fig. 2.39)	Lesions can have low, intermediate, and/or high signal on T1WI and T2WI depending on the proportions and distribution of fat and red marrow.	Represents proliferation of erythroid precursors outside of medullary bone secondary to physiologic compensation for abnormal medullary hematopoiesis from congenital disorders such as hemoglobinopathies (sickle cell, thalassemia, etc.) as well as acquired disorders such as myelofibrosis, leukemia, lymphoma, myeloma, or metastatic carcinoma.
Amyloidoma (Fig. 2.40)	Amyloid lesions in bone can occur as zones of osteopenia. permeative radiolucent destruction or uni- or multifocal radiolucency. Lesions can have low-intermediate signal on T1WI, and intermediate to slightly high signal on T2WI. Lesions can show Gd-contrast enhancement.	Uncommon disease in which various tissues (including bone, muscle, tendons, tendon sheaths, ligaments and synovium) are infiltrated with extracellular eosinophilic material composed of insoluble proteins with p-pleated sheet configurations (amyloid protein). Amyloidomas are single sites of involvement. Amyloidosis can be a primary disorder associated with an immunologic dyscrasia or secondary to a chronic inflammatory disease.
Bone infarcts (Atlas Figs. 209, 210)	Focal ring-like lesion or poorly defined zone with low-intermediate signal on T1WI, intermediate-high signal on T2WI centrally, variable or no Gd-contrast enhancement involving the marrow depending on age/stage of infarction/healing, +/- associated fracture.	Bone infarcts can occur after radiation treatment, surgery, chemotherapy, or trauma, **(see Atlas Chapter A 37)**
Congenital		
Myelomeningocele/myelocele (Figs. 2.41, 2.42)	MRI is usually performed after surgical repair of myeloceles or myelomeningoceles. Posterior protrusion of spinal contents and unfolded neural tube (neural placode) is seen through defects in the bony dorsal elements of the involved vertebrae or sacral elements. The neural placode is usually located at the lower lumbar-sacral region with resultant tethering of the spinal cord. If the neural placode is flush with the adjacent skin surface, the anomaly is labeled a **myelocele** If the neural placode extends above the adjacent skin surface, the anomaly is labeled a **myelomeningocele** +/- syringohydromyelia.	Failure of developmental closure of the caudal neural tube results in an unfolded neural tube (neural placode) exposed to the dorsal surface in the midline without overlying skin. Other features associated with myelomeningoceles and myeloceles include: dorsal bony dysraphism, deficient dura posteriorly at the site of the neural placode, and Chiari II malformations. By definition the spinal cords are tethered. Usually repaired surgically soon after birth.

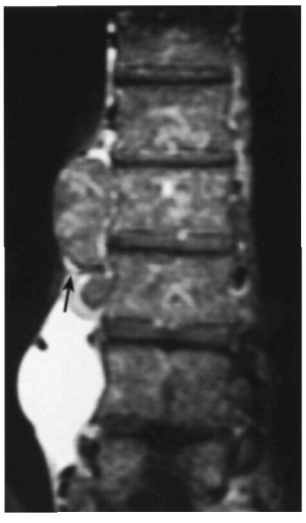

a

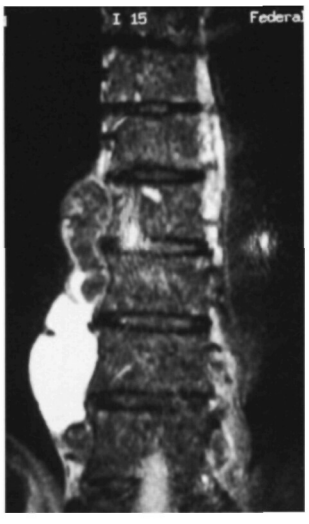

b

Figure 2.39 a, b A 56-year-old man with sickle cell disease and extramedullary hematopoiesis adjacent to a thoracic vertebra. A right paraspinal lesion is seen that has circumscribed margins and has intermediate signal on coronal T1 WI (**a**) and coronal T2WI (**b**) which is similar to the vertebral marrow.

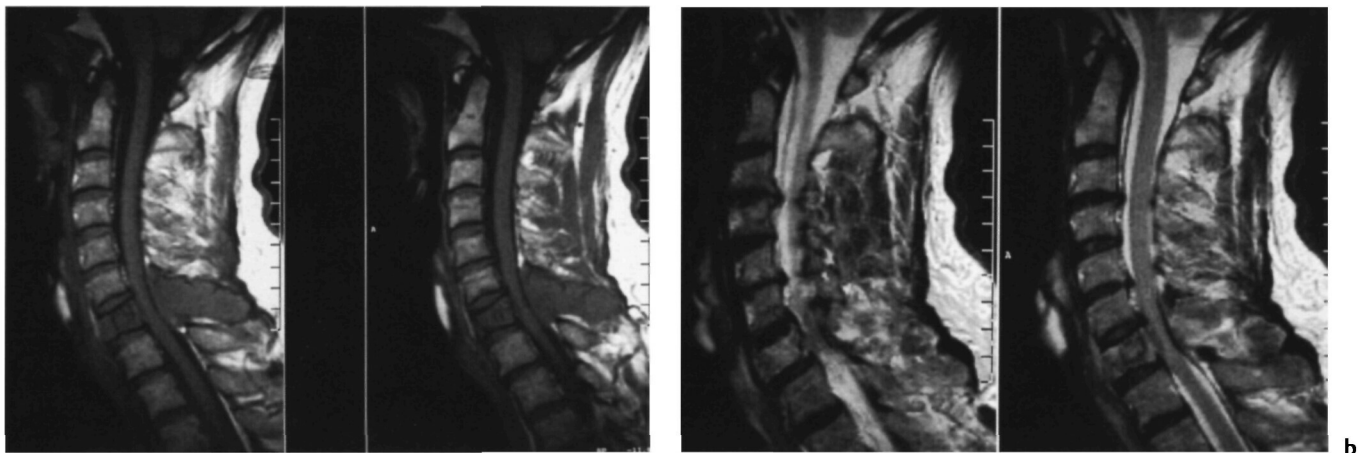

Figure 2.40a-c A 58-year-old man with an amyloidoma involving the C7 vertebra which has low-intermediate signal on sagittal T1WI (**a**), intermediate and slightly high signal on sagittal T2WI (**b**). Prominent Gd-contrast enhancement is seen in the involved vertebra as well as in epidural extension of the lesion on sagittal FST1 WI (**c**) which results in spinal cord compression.

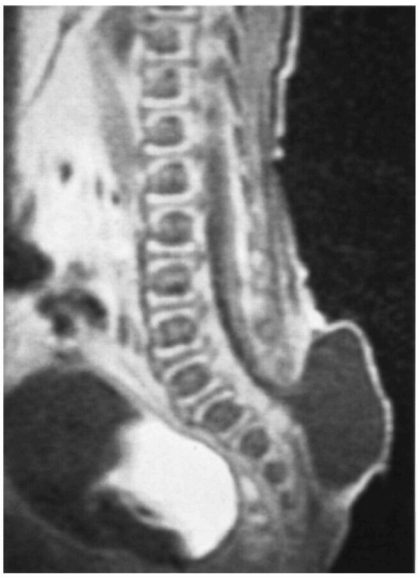

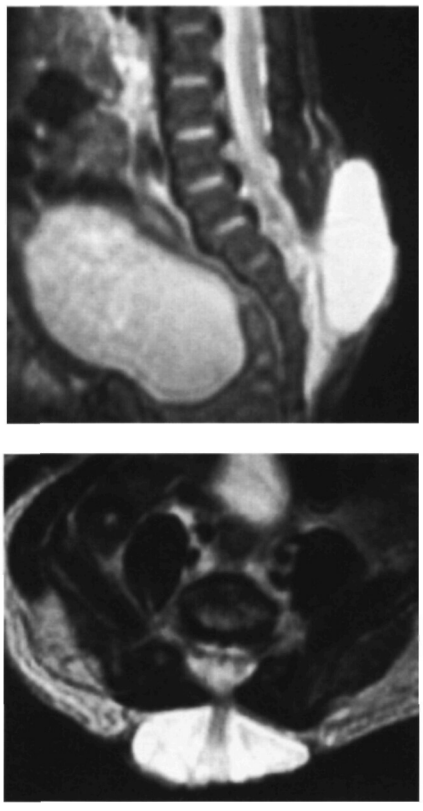

Figure 2.41 a-c Neonate with a sacral myelomeningocele that is seen as a posterior protrusion of spinal contents and unfolded neural tube (neural placode) through defects in the bony dorsal elements of the involved sacral elements on sagittal FST1WI (**a**) and sagittal FST2WI (**b**) and axial (**c**) T2WI.

Figure 2.42 Neonate with a thoracic myelomeningocele that is seen as a posterior protrusion of spinal contents and unfolded neural tube through defects in the bony dorsal elements of the involved thoracic vertebra on sagittal T1WI.

Table 2 (Continued) Tumors and tumorlike lesions involving the spine

Tumor/Tumorilke Lesion	MRI Findings	Comments
Meningoceles (Fig. 2.43)	Protrusion of CSF and meninges through a dorsal vertebral defect either from surgical laminectomies or congenital anomaly. Sacral meningoceles can alternatively extend anteriorly through a defect in the sacrum.	Acquired meningoceles are more common than meningoceles resulting from congenital dorsal bony dysraphism. Anterior sacral meningoceles can result from trauma or be associated with mesenchymal dysplasias (NF1. Marfan syndrome, syndrome of caudal regression).
Lipomyelomeningocele (Fig. 2.44)	Unfolded caudal neural tube (neural placode) covered by a lipoma, which is often contiguous with the dorsal subcutaneous fat through defects (spina bifida) involving the bony dorsal vertebral elements. The neural placode is usually located at the lower lumbar-sacral region with resultant tethering of the spinal cord, +/- syringohydromyelia.	Failure of developmental closure of the caudal neural tube results in an unfolded neural tube (neural placode) covered by a lipoma, which is continuous with the subcutaneous fat. The overlying skin is intact, although the lipoma usually protrudes dorsally. The nerve roots arise from the placode. Features associated with lipomyelomeningoceles and lipomyeloceles include: tethered spinal cords, dorsal bony dysraphism. and deficient dura posteriorly at the site of the neural placode. Not associated with Chiari II malformations. Diagnosis often in children, occasionally in adults.
Duralectasia (Fig. 2.43)	Scalloping of the dorsal aspects of vertebral bodies, dilatation of optic nerve sheaths, dilatation of intervertebral and sacral foraminal nerve sheaths, lateral meningoceles.	Dural dysplasia associated with NF1. Dural ectasia can also result from Marfan syndrome.

Figure 2.43 A 67-year-old woman with Marfan syndrome who has dural ectasia and an anterior sacral meningocele as seen on sagittal T2WI.

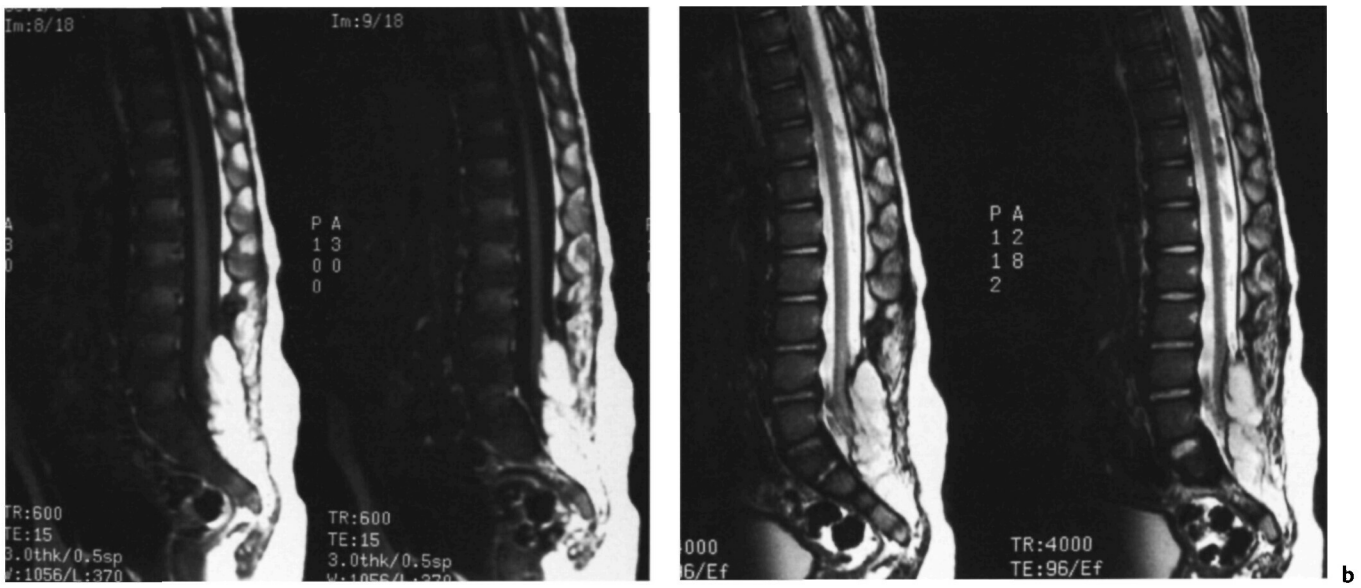

a b

Figure 2.44 a, b A lipomyelocele, representing an unfolded caudal neural tube covered by a lipoma, is seen located between congenital bony defects at the posterior elements (spina bifida) on sagittal T1 WI (**a**) and sagittal (**b**) T2WI. Also seen is tethering of the spinal cord.

References

Arachnoid Cyst

Mukherji SK, Chenevert TL, Castillo M. Diffusion-weighted magnetic resonance imagingJ *Neuro-Ophthalmol* 2002;22(2):118-122.

Tali ET, Ercan N, Kaymaz M, Pasaoglu A, Jinkins JR. Intrathecal gadolinium (gadopentetate dimeglumine)-enhanced MR cisternography used to determine potential communication between the cerebrospinal fluid pathways and intracranial arachnoid cysts. *Neuroradiology* 2004;46:744-754.

Tang L, Cianfoni A, Imbesi SG. Diffusion weighted imaging distinguishes recurrent epidermoid neoplasm from postoperative arachnoid cyst in the lumbosacral spine J *Comput Assist Tomogr* 2006:30:507-509.

Tarlov Cyst

Voyadzis JM, Bhargava P, Henderson FC. Tarlov cysts: a study of 10 cases with review of the literature. *J Neurosurg (Spinel)* 2001 ;95:25-32.

Neurenteric Cyst

Kumar R, Jain R, Rao KM, Hussain N. Intraspinal neurenteric cysts-report of three pediatric cases. *Child's Nerv Syst* 2001 ;17:585-588.

Menezes AH, Traynelis VC. Spinal neurenteric cysts in the magnetic resonance imaging era. *Neurosurgery* 2006:58:97-105.

Hematopoietic Disorders

Dibbern DA, Jr., Loevner LA, Lieberman AP, Salhany KE, Freese A, Marcotte PJ. MR of thoracic cord compression caused by epidural extramedullary hematopoiesis in myelodysplastic syndrome. *AJNR* February 1997:18:363-366.

Levin TL, Sheth SS, Hurlet A, et al. MR marrow signs of iron overload in transfusion-dependent patients with sickle cell disease. *Pediatr Radiol* 1995;25(8):614-619.

Niggemann P, Krings T, Hans F, Thron A. Fifteen-year follow-up of a patient with (S thalassaemia and extramedullary hematopoietic tissue compressing the spinal cord. *Neuroradiology* 2005:47:263-266.

Salehi SA, Koski T, Ondra SL. Spinal cord compression in |3-thalassemia: case report and review of the literature. *Spinal Cord* 2004;42: 117-123.

States LJ. Imaging of metabolic bone disease and marrow disorders in children. Radiof Clin Am July 2001;39(4):749-772.

Extramedullary Hematopoiesis

Capelastegui A, Astigarraga E, Garcia-Iturraspe C. MR findings in pulmonary hypertrophic osteoarthropathy. Cfin *Radiol* January 2000; 55(l):72-75.

Dibbern DA, Jr., Loevner LA, Lieberman AP, Salhany KE, Freese A, Marcotte PJ. MR of thoracic cord compression caused by epidural extramedullary hematopoiesis in myelodysplastic syndrome. *AJNR* February 1997;18:363-366.

Niggemann P, Krings T, Hans F, Thron A. Fifteen-year follow-up of a patient with (5 thalassaemia and extramedullary hematopoietic tissue compressing the spinal cord. *Neuroradiology* 2005:47:263-266.

Tan TC, Tsao J, Cheung FC. Extramedullary haemopoiesis in thalassemia intermedia presenting as paraplegia. *J Clin Neurosci* 2002;9(6): 721-725.

Amyloidoma

Haridas A, Basu S, King A, Pollock J. Primary isolated amyloidoma of the lumbar spine. *Neurosurgery* 2005;57(1):E196.

Meyers SP, Mullins J, Kazee AM. Unifocal primary amyloidoma of the spine causing compression of the cervical spinal cord: MR findings. *J ComputAsst Tomogr* 1996:20:592-593.

Unal A, Sutlap PN, Kyyk M. Primary solitary amyloidoma of the thoracic spine: a case report and review of the literature. *ClinNeurolNeurosur* 2003:105:167-169.

Table 3 Paraspinal tumors and tumorlike lesions

Tumors/tumorlike lesions	MRI Findings	Comments
Ependymoma (Fig. 3.1)	Intradural circumscribed tabulated lesions at conus medullaris and/or cauda equina / fllum terminale, rarely in sacrococcygeal region: lesions usually have low-intermediate signal on T1WI. intermediate-high signal on T2WI, +/- foci of high signal on T1WI from mucin or hemorrhage, +/- peripheral rim of low signal (hemosiderin) on T2WI, +/- lumoral cysts (high signal on T2WI). Lesions usually show Gd-contrast enhancement.	Ependymomas at conus medullaris or cauda equina / filum terminale usually are myxopapillary type, thought to arise from ependymal glia of filum terminale. Slight male predominance. Usually are slow-growing neoplasms associated with long duration of back pain, sensory deficits, motor weakness, bladder and bowel dysfunction. +/- chronic erosion of bone with scalloping of vertebral bodies and enlargement of intervertebral foramina.
Neurofibroma (Fig. 3.2)	tabulated extramedullary lesions +/- irregular margins, +/- cxtradural extension of lesion with dumbbell shape, low-intermediate signal on T1WI, slightly high to high signal on T2WI and FST2WI, usually show prominent Gd-contrast enhancement. High signal on T2WI and Gd-contrast enhancement can be heterogeneous in large lesions. +/- erosion of foramina, +/- scalloping of dorsal margin of vertebral body (chronic erosion or dural ectasia/NFI).	Unencapsulated neoplasms involving nerve and nerve sheath, common type of intradural extramedullary neoplasms often with extradural extension, usual presentation in adults with pain and radiculopathy, paresthesias and lower extremity weakness. Multiple neurofibromas seen with NF1. **(See Atlas Chapter A 56)**

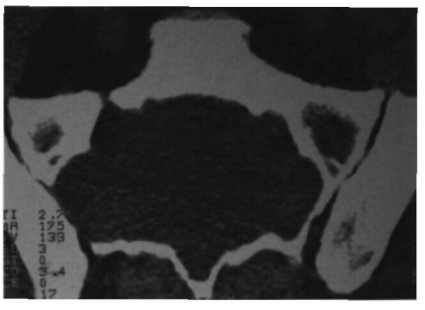

a

b

c, d

Figure 3.1 a-d A 41-year-old man with a myxopapillary ependymoma eroding the sacrum. The tumor has intermediate attenuation on axial CT (**a**) and intermediate signal on sagittal T1 WI (**b**). The tumor has mixed heterogeneous high, intermediate, and low signal on sagittal T2WI (**c**) and shows heterogeneous irregular Gd-contrast enhancement on sagittal FST1WI (**d**).

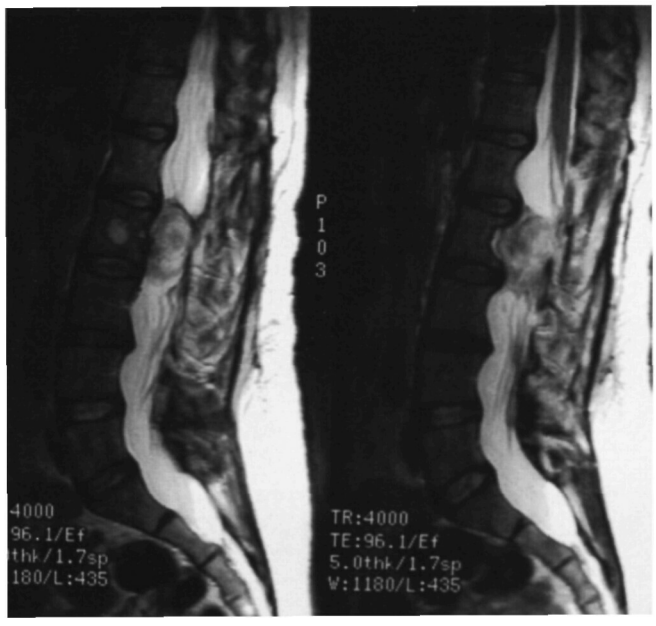

a

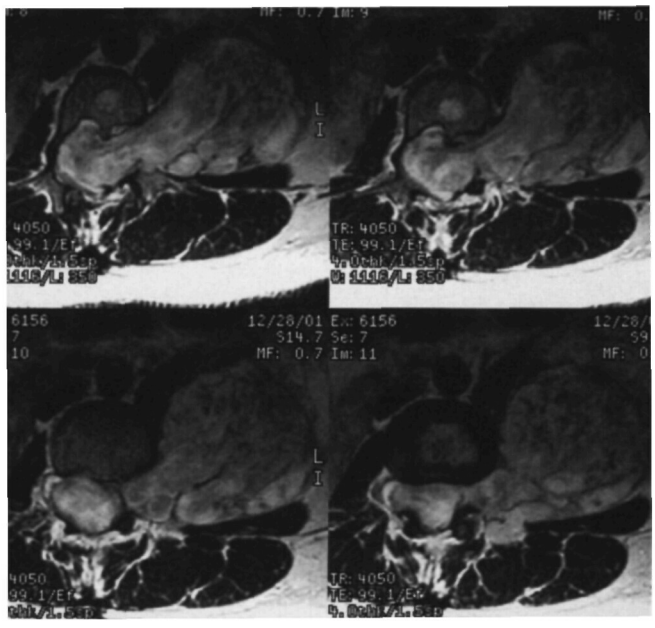

b

Figure 3.2 a-c A 45-year-old woman with a large left paraspinal neurofibroma extending through a widened intervertebral foramen and severely compressing the thecal sac. The lesion has intermediate, slightly high to high signal with foci of low signal on sagittal (**a**) and axial (**b**) T2WI. The lesion shows heterogeneous Gd-contrast enhancement on axial FST1WI (**c**). Note also the scalloping of the dorsal margins of the vertebral bodies from dural ectasia.

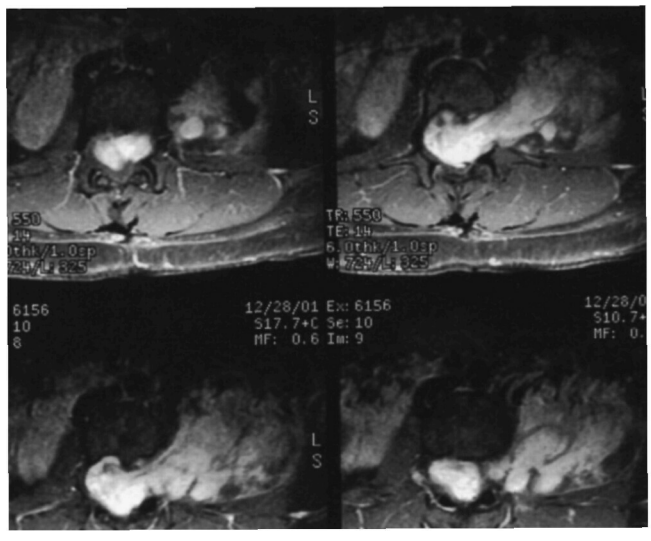

c

Table 3 (Continued) Paraspinal tumors and tumorlike lesions

Tumors/Tumorlike Lesion	MRI Findings	Comments
Schwannoma (neurinoma) (Rg.3.3)	Circumscribed or tabulated extramedullary lesions, low-intermediate signal on T1WI, high signal on T2WI and FST2WI, usually show prominent Gd-contrast-enhancement. High signal on T2WI and Gd-contrast enhancement can be heterogeneous in large lesions due to cystic degeneration and/or hemorrhage.	Encapsulated neoplasms arising asymmetrically from nerve sheath, most common type of intradural extramedullary neoplasms, usual presentation in adults with pain and radiculopathy, paresthesias and lower extremity weakness. Multiple schwannomas seen with NF2. **(See Atlas Chapter A 72)**

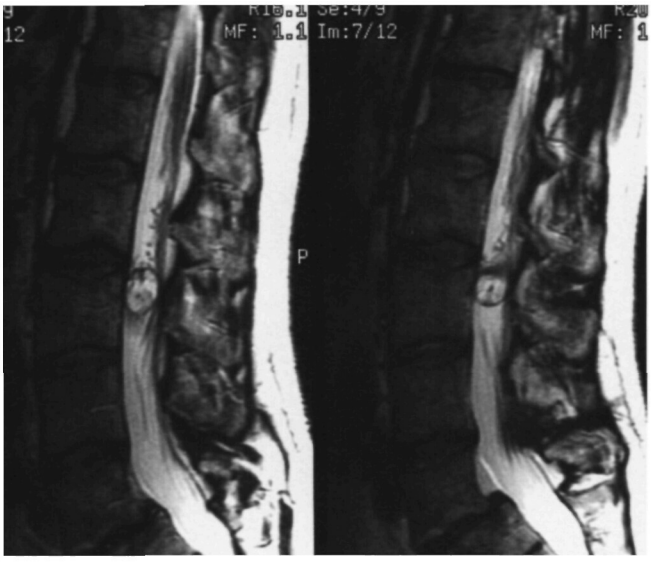

a

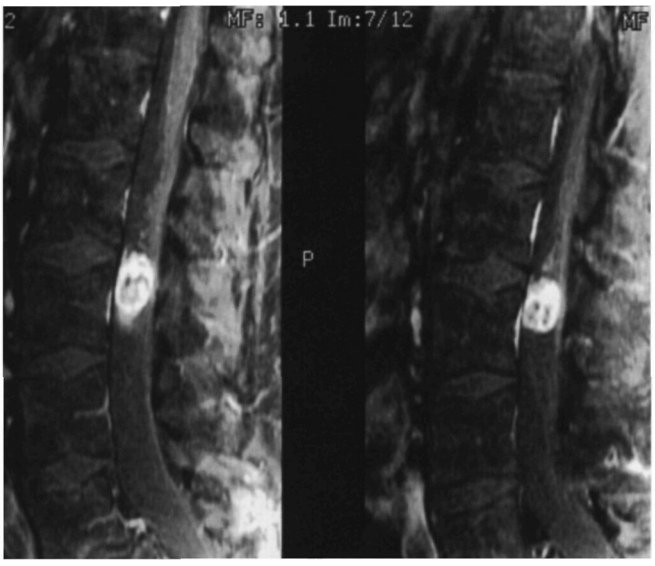

b

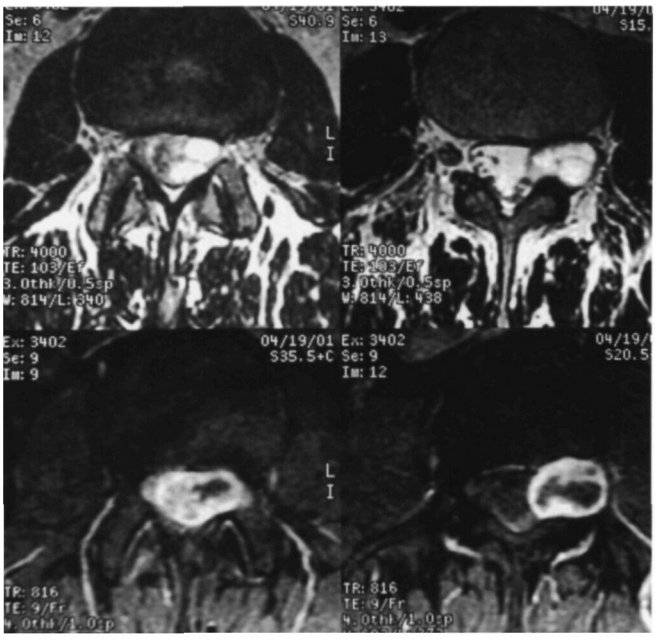

c

Figure 3.3 a-c Solitary schwannoma in the lumbar spine at the upper L3 level. The lesion has heterogeneous high signal on sagittal (**a**) and axial (c, *upper images)* T2WI, and shows heterogeneous Gd-contrast enhancement on sagittal (**b**) and axial (**c**), *lower images)* FST1WI.

Table 3 (Continued) **Paraspinal tumors and tumorlike lesions**

Tumors/Tumorlike Lesion	MRI Findings	Comments
Malignant peripheral nerve sheath tumor (Fig. 3.4)	These lesions usually have heterogeneous signal on T1 WI and T2WI; as well as heterogeneous Gd-contrast enhancement because of necrosis and hemorrhage. Some are similar in appearance to benign nerve sheath tumors.	Malignant tumors of the peripheral nerve sheath that contain mixtures of packed hyperchromatic spindle cells with elongated nuclei and slightly eosinophilic cytoplasm, mitotic figures, and zones of necrosis. Approximately 50% of malignant peripheral nerve sheath tumors occur in patients with NF1, followed by de novo evolution from peripheral nerves. Malignant peripheral nerve sheath tumors infrequently arise from schwannomas, ganglioneuroblastomas/ganglioneuromas, and pheochromocytomas. **(See Atlas Chapter A 56)**
Meningioma (Fig. 3.5)	Extradural or intradural extramedullary lesions, intermediate signal on T1WI, intermediate-slightly high signal on T2WI and FST2WI. usually show prominent Gd-contrast enhancement. +/- calcifications.	Usually benign neoplasms, typically occurs in adults (>40 years), women > men. multiple meningiomas seen with NF2, can result in compression of adjacent spinal cord and nerve roots, rarely invasive/malignant types. **(See Atlas Chapter A49)**

Figure 3.4 A 49-year-old man with a malignant peripheral nerve sheath tumor arising from a benign schwannoma. The large left paraspinal tumor shows irregular Gd-contrast enhancement on coronal FST1WI. Small zones of abnormal contrast enhancement are seen in two vertebral bodies secondary to tumor invasion.

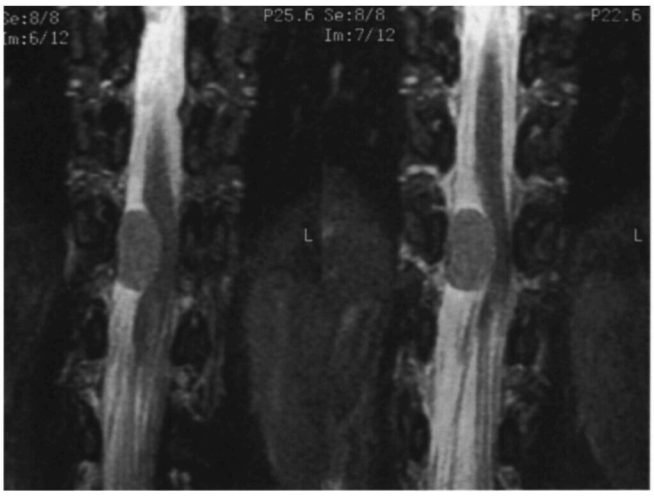

a

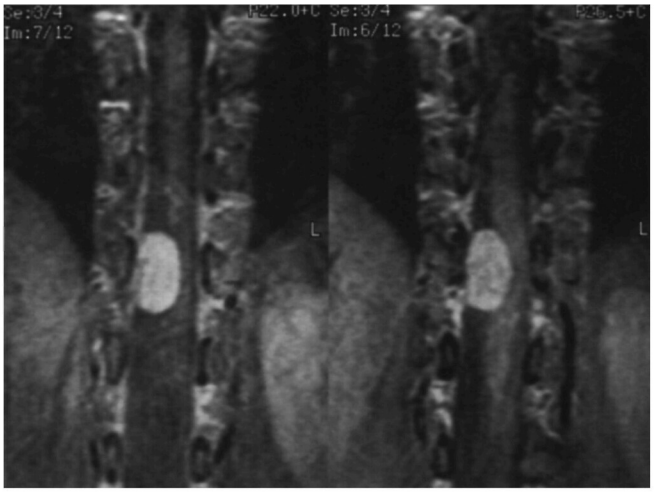

b

Figure 3.5 a, b A 43-year-old woman with a meningioma causing compression of the lower thoracic spinal cord. The tumor has intermediate signal on coronal FST2WI (**a**) and shows prominent Gd-contrast enhancement on coronal FST1WI (**b**).

Table 3 (Continued) **Paraspinal tumors and tumorlike lesions**

Tumors/Tumorlike Lesion	MRI Findings	Comments
Paraganglioma (Rg.3.6)	Spheroid or tabulated intradural-extramedullary lesion with intermediate signal on T1WI, intermediate-high signal on T2WI and FST2WI, +/- tubular zones of flow voids, usually show prominent Gd-contrast enhancement, +/- foci of high signal on T1WI from mucin or hemorrhage, +/- peripheral rim of low signal (hemosiderin) on T2WI, usually located in region of cauda equina and filum terminale.	Neoplasms that arise from paraganglion cells of neural crest origin usually occur at carotid body, jugular foramen, middle ear, and along vagus nerve. Rarely occur in spine. **(See Atlas Chapter A 66)**
Neuroblastoma/ganglioneuroblastoma (Fig. 3.7)	Tumors can have distinct or indistinct margins, and have low-intermediate signal on T1WI, homogeneous or heterogeneous intermediate, slightly high, and/or high signal on T2WI and FST2WI. Zones of high signal on T2WI may occur from sites of hemorrhage or necrosis. Foci of low signal on T2WI may be seen secondary to calcifications and blood products. Tumors can show mild to marked heterogeneous Gd-contrast enhancement. MRI can show extension of these tumors into the spinal canal as well as into bone marrow.	Neuroblastomas and ganglioneuroblastomas are malignant tumors of the sympathetic nervous system that consist of neuroectodermal cells derived from the neural crest. Neuroblastomas are highly malignant undifferentiated tumors whereas ganglioneuroblastomas are intermediate-grade malignant tumors. **(See Atlas Chapter A 55)**
Canglioneuroma (Fig. 3.8)	Tumors are well-circumscribed with low-intermediate signal on T1WI. and slightly high to high signal on T2WI and FST2WI. Small foci or strands of low signal on T2WI may be seen secondary to calcifications and fibrous tissue, respectively. Tumors show mild to marked heterogeneous Gd-contrast enhancement. MRI can show extension of these tumors into the spinal canal.	Rare benign lesions of the sympathetic nervous system composed of ganglion cells and Schwannian stroma and lacking neuroblasts and mitotic figures. **(See Atlas Chapter A 55)**
Lymphoma (Fig. 3.9)	Lymphadenopathy from lymphoma often has low-intermediate signal on T1 WI and intermediate to slightly high signal on T2WI. Variability in MRI signal characteristics may be related to differing histologic features (such as the degree of fibrosis). After Gd-contrast administration, extraosseous lymphoma can show Gd-contrast enhancement in varying degrees. Epidural lymphoma can show Gd-contrast enhancement and can cause spinal cord compression.	Lymphoma represents a group of lymphoid tumors whose neoplastic cells typically arise within lymphoid tissue (lymph nodes and reticuloendothelial organs). Unlike leukemia, lymphoma usually arises as discrete masses. **(See Atlas Chapter A 47)**

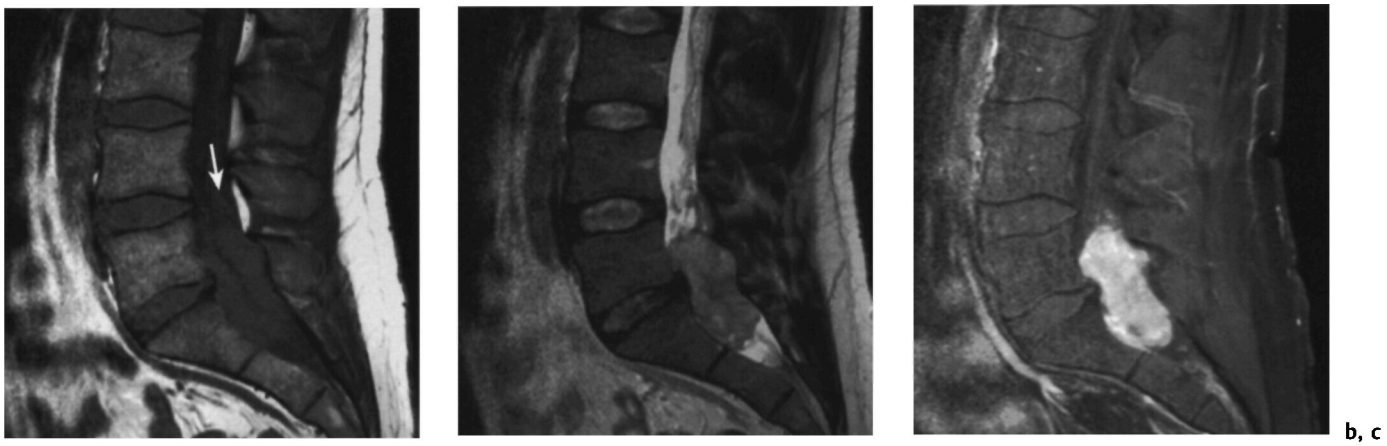

Figure 3.6 A 33-year-old man with an intradural paraganglioma in the distal lumbar thecal sac. The lesion has low-intermediate signal on sagittal T1WI (**a**), and heterogeneous intermediate to slightly high signal on sagittal T2WI (**b**). The tumor shows prominent Gd-contrast enhancement on sagittal FST1WI (**c**).

a

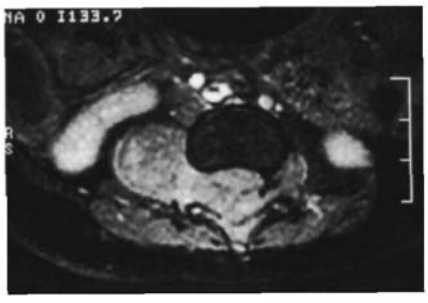

b

Figure 3.7 a, b A 9-month-old female infant with a right infra-renal paraspinal neuroblastoma with extension into the spinal canal resulting in spinal canal compression. The tumor has prominent slightly heterogeneous Gd-contrast enhancement on coronal (**a**) and axial (**b**)FSTIWI.

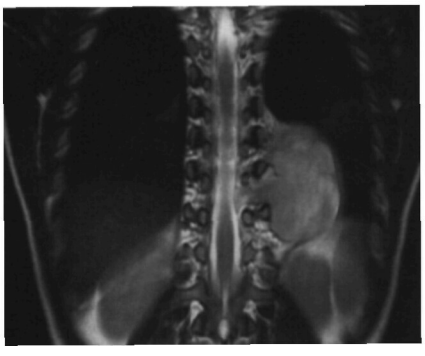

a

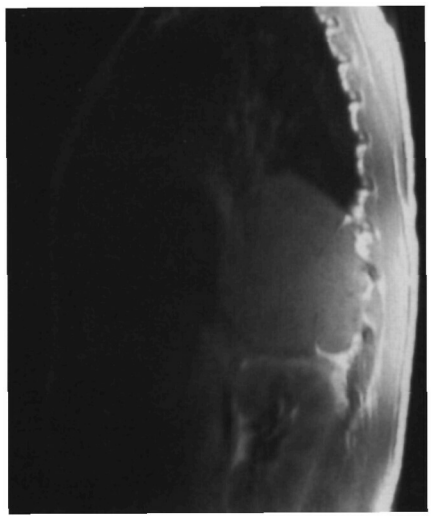

b, c

Figure 3.8a-c A 10-year-old boy with a left paraspinal ganglioneuroma. The tumor has heterogeneous intermediate, slightly high to high signal on coronal (**a**) and sagittal (**c**) T2WI and intermediate signal on sagittal T1WI (**b**).

a

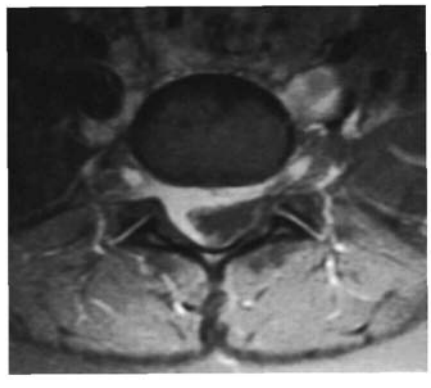

b

Figure 3.9a,b A 14-year-old female with epidural non-Hodgkin lymphoma that shows prominent Cd-contrast enhancement on sagittal (**a**) and axial (**b**) FST1WI.

Table 3 (Continued) Paraspinal tumors and tumorlike lesions

Tumors/Tumorlike Lesion	MRI Findings	Comments
Metastatic disease	Single or multiple well-circumscribed or poorly defined infiltrative lesions involving the paraspinal soft tissues with eventual involvement of vertebral marrow, dura, and leptomeninges. Lesions often have low-intermediate signal on T1WI, low. intermediate, and/or high signal on T2WI and FST1WI, and usually show Gd- contrast enhancement. +/- bone destruction, +/- pathologic vertebral fracture, +/- compression of neural tissue or vessels.	Metastatic tumor can involve the paraspinal tissues by direct extension from tumors such as retroperitoneal liposarcoma. lung and renal carcinomas; or from involved adjacent lymph nodes. Metastatic disease may also occur from hematogenous dissemination. **(See Atlas Chapter A 50)**
Hemangiopericytoma (Fig. 1.20)	Extradural or intradural extramedullary lesions, can involve vertebral marrow, often well circumscribed, intermediate signal on T1WI, intermediate-slightly high signal on T2WI and FST2WI, usually show prominent Gd-contrast enhancement (may resemble meningiomas), +/- associated erosive bone changes.	Rare neoplasms in young adults (males > females) sometimes referred to as angioblastic meningioma or meningeal hemangio-pericytoma. arise from vascular cell-pericytes **(See Atlas Chapter A 35)**
Desmoid tumor (Fig. 3.10)	Lesions can have distinct and/or poorly defined margins, homogeneous or heterogeneous low-intermediate signal on T1WI, and variable intermediate-high signal on T2WI, +/- zones of low signal. Myxoid zones in the lesions can have high signal on T1WI and T2WI. Tumors with high cellularity tend to show higher signal on T2WI than lesions with larger proportions of collagen. Lesions show variable degrees and patterns (heterogeneous versus homogenous) of Gd-contrast enhancement. Pattern or degree of Gd-contrast enhancement by desmoids does not enable prediction of rate of tumor recurrence.	Desmoid tumors or fibromatosis represent a group of soft tissue lesions comprised of benign fibrous tissue with elongated or spindle-shaped cells adjacent to collagen. **(See Atlas Chapter A16)**

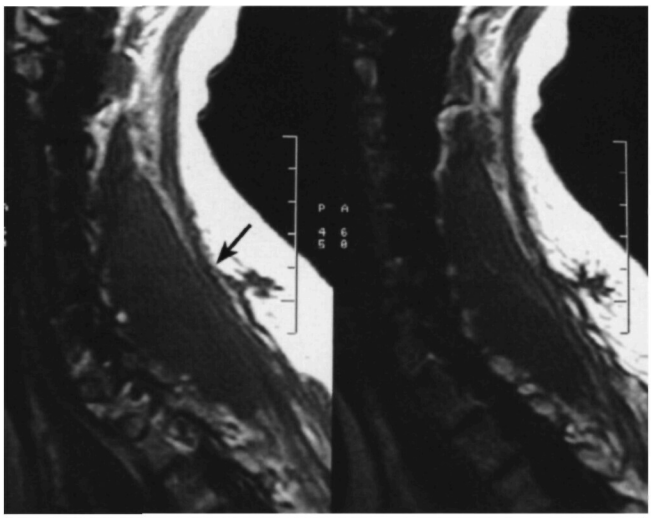

a

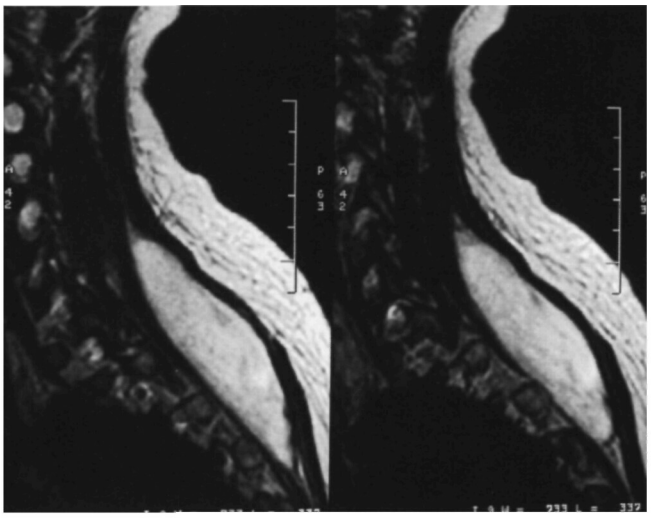

b

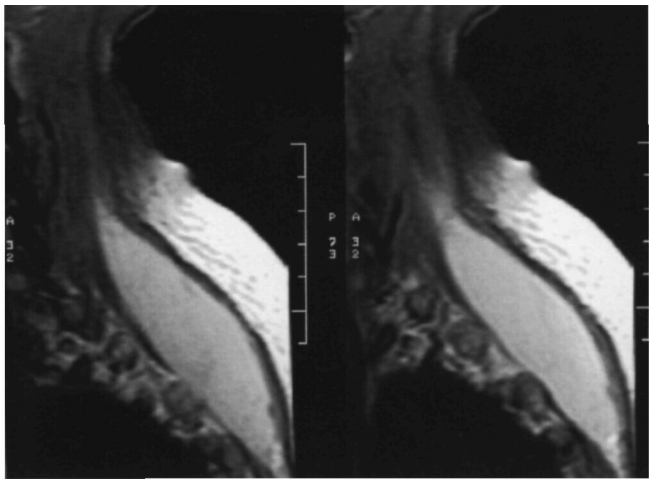

c

Figure 3.10a-c A 20-year-old woman with a desmoid tumor involving the posterior paraspinal muscles of the cervical and upper thoracic spine. The fusiform lesion has low-intermediate signal on sagittal T1WI (**a**) and high signal on sagittal T2WI (**b**). The lesion shows prominent Gd-contrast enhancement on sagittal FST1WI (**c**).

Table 3 (Continued) **Paraspinal tumors and tumorlike lesions**

Tumors/Tumorlike Lesion	MRI Findings	Comments
Primary sarcoma involving the paraspinal soft tissues (Fig. 3.11.3.12)	Tumors can have regular and/or irregular margins, and often have low-intermediate signal on T1WI, heterogeneous intermediate-high signal on T2WI, and show Cd-contrast enhancement. Signal heterogeneity on T1WI and T2WI is often related to the presence and extent of fibrous components (low signal on T1WI and T2WI), zones of hemorrhage (intermediate or high signal on T1WI; low. intermediate, and/or high signal on T2WI), zones of necrosis and/or myxoid material (low signal on T1WI and high signal on T2WI). Margins of lesions may be indistinct on T2WI for high-grade lesions. Tumors can be associated with erosion, destruction, and invasion of adjacent bone.	Various types of primary sarcomas can occur in the paraspinal soft tissues and subsequently invade the vertebrae, intervertebral foramina, and/or spinal canal.
Upoblastoma (Fig. 3.13)	Lesions often have mixed low, intermediate, and high signal on T1WI. T2WI, and FST2WI. Lesions often show heterogeneous Cd-contrast enhancement.	Rare benign mesenchymal tumors that contain embryonal fat. Typically occur in infancy and early childhood. (See Atlas Chapter A42)

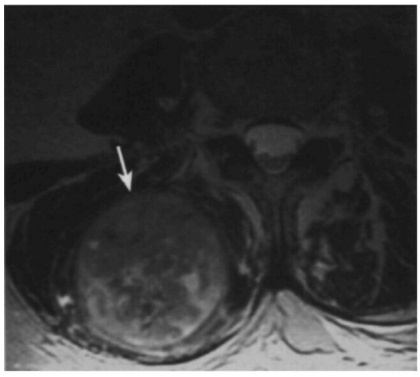

a

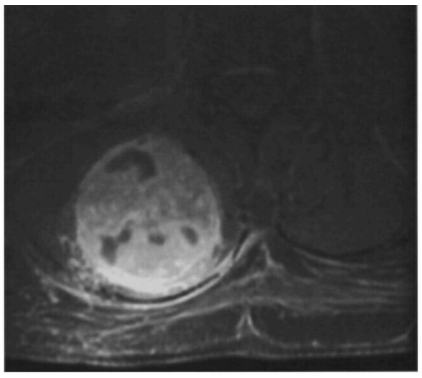

b

Figure 3.11 a, b A 56-year-old woman with a leiomyosarcoma involving the right paraspinal muscles in the lumbar region. The tumor has heterogeneous intermediate and slightly high signal on axial T2WI (**a**), and shows mostly prominent Gd-contrast enhancement on axial FST1WI (**b**).

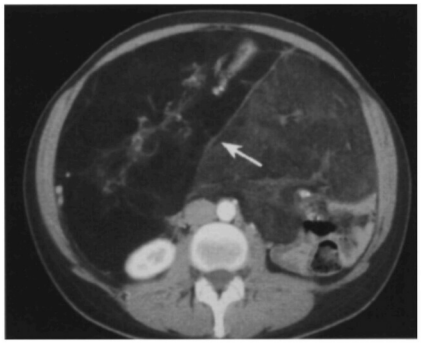

a

b

Figure 3.12a, b A 35-year-old woman with a liposarcoma in the right abdomen. The tumor has mostly low attenuation and contains thickened bands of enhancement on CT (**a**). The tumor has mostly a high fatty signal with irregular bands of low signal on axial T1WI(**b**)

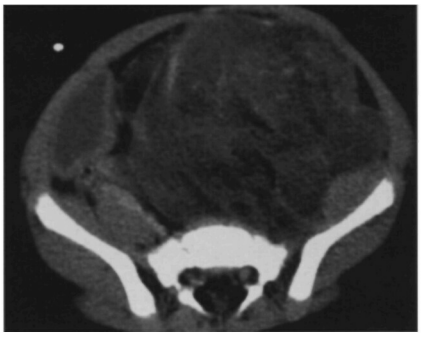

a

b

Figure 3.13 a, b A 1.5-year-old boy with a large intra-abdominal and pelvic lipoblastoma. The lesion has heterogeneous attenuation with zones of soft tissue, fluid and fat attenuation on axial CT (**a**). The lesion has mixed low-intermediate, intermediate, and high signal on axial T1WI (**b**).

Table 3 (Continued) Paraspinal tumors and tumorlike lesions

Tumors/Tumoriike Lesion	MRI Findings	Comments
Epidural abscess (Figs. 3.14,3.15)	Epidural collection with low signal on T1WI and high signal on T2WI and FST2WI surrounded by a peripheral rim (thin or thick) of Gd-contrast enhancement, +/- associated vertebral osteomyelitis/diskitis, +/- air collections (signal void on T1W and T2W images), often extend over two to four vertebral segments, can result in compression of spinal cord and spinal canal contents.	Epidural abscess can evolve from an inflammatory phlegmonous epidural mass, extension from paravertebral inflammatory process, or vertebral osteomyelitis/diskitis. May be associated with complications from surgery, epidural anesthesia, diabetes, distant source of infection, immuno-compromised status. Organisms commonly involved include *Staph. aureus,* Cram-negative bacteria, Mycobacteria, coccidiomycosis, candidiasis, aspergillosis, blastomycosis. Clinical findings include: back and radicular pain. +/- paresthesias and paralysis of lower extremities.
Epidural hematoma (Fig.3.16)	**Acute hematoma (< 48 hours):** Epidural collection with low-intermediate signal on T1WI and PDWI, heterogeneous high signal on T2WI. +/- spinal cord compression. +/- minimal central peripheral pattern of Cd-contrast enhancement at hematoma. **Subacute hematoma (>48 hours):** Epidural collection with intermediate-slightly high signal on T1WI, heterogeneous intermediate to high signal on T2WI. +/- spinal cord compression. +/- mixed central and/or peripheral patterns of Cd-contrast enhancement of hematoma as well as adjacent dura. **Older hematoma:** Epidural collection with variable/heterogeneous signal on T1WI and T2WI. +/- spinal cord compression.	The MR signal of acute epidural hematoma typically is secondary to deoxyhemoglobin. and with subacute hematoma secondary to methemoglobin. Older epidural hematomas have mixed MR signal related to the various states of hemoglobin and breakdown products. Can be spontaneous or result from trauma or complication from: coagulopathy, lumbar puncture, myelography, surgery. **(See Atlas Chapter A36)**
Teratoma(Fig.3.17)	Circumscribed lesions variable low, intermediate, and/or high signal on T1 WI and T2WI; +/- Cd-contrast enhancement. May contain calcifications, cysts, as well as fatty components that can cause chemical meningitis if ruptured.	Second most common type of germ cell tumors; occur in children, males > females; benign or malignant types, composed of derivatives of ectoderm, mesoderm, and/or endoderm. (See Atlas Chapter A 76)

Figure 3.14 A 34-year-old man with pyogenic osteomyelitis involving the L4 and L5 vertebral bodies and intervening disk associated with an epidural abscess. Irregular Gd-contrast enhancement is seen in the involved marrow on sagittal FST1WI as well as in the anterior epidural soft tissues causing spinal canal compression.

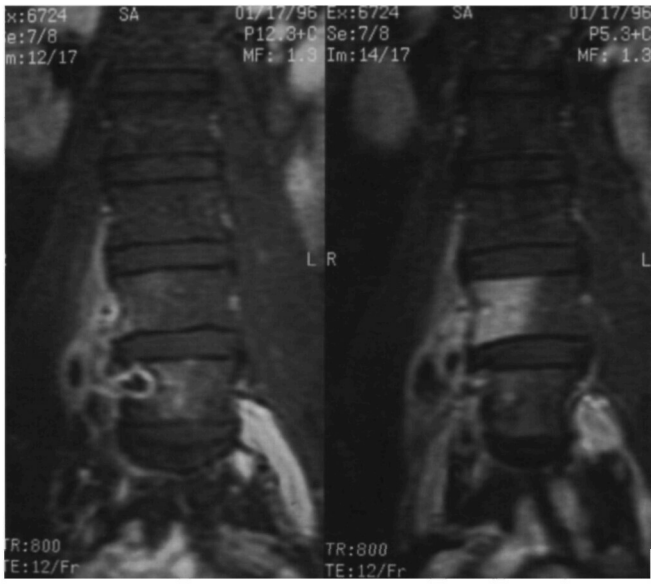

Figure 3.15 A 35-year-old man with tuberculous osteomyelitis involving the L4 and L5 vertebral bodies with right paraspinal cold abscesses. Irregular Gd-contrast enhancement is seen in the involved marrow on coronal FST1WI. Also seen is subligamentous spread of the paraspinal abscesses that show irregular peripheral zones of Gd-contrast enhancement.

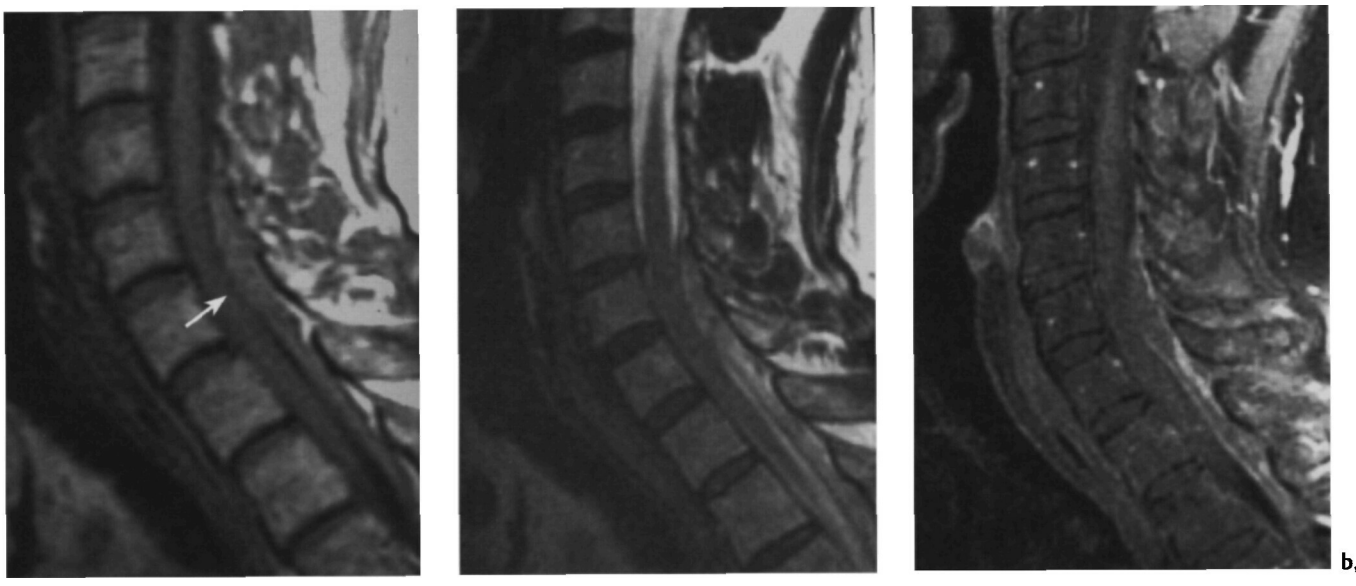

a b, c

Figure 3.16a-c A 60-year-old man with an epidural hematoma dorsally within the mid and lower cervical spinal canal as well as the upper thoracic spinal canal. The subdural hematoma has mostly intermediate signal and several small zones of slightly high signal on sagittal T1WI (**a**). The hematoma has intermediate, slightly high, and high signal on sagittal T2WI (**b**) and shows peripheral Gd-contrast enhancement on sagittal FST1WI (**c**).

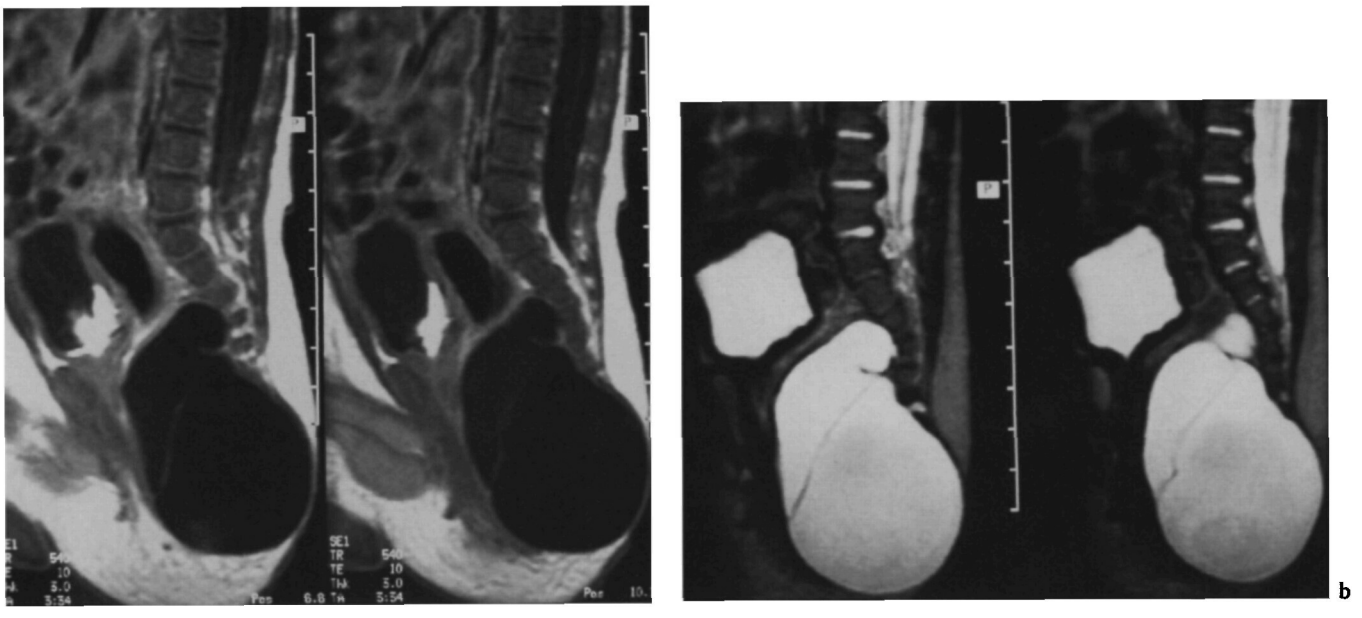

a b

Figure 3.17 a, b Sacrococcygeal teratoma in a 2-month-old male infant. The large lesion has low signal on sagittal T1 WI (**a**) and high signal on sagittal T2WI (**b**). Two thin septa are seen within the lesion.

Table 3 (Continued) Paraspinal tumors and tumorlike lesions

Tumon/Tumoriike Lesion	MRI Findings	Comments
Hiatal hernia (Fig. 3.18)	Circumscribed paraspinal structure contiguous with esophagus and gastric fundus and/or intra-abdominal fat. A low signal rim with rugae may be seen surrounding contents, which can have variable .low, intermediate, and/or high signal on T1WI and T2WI. Fluid-fluid or air-fluid levels may be present.	Represent trans-diaphragm communications through which abdominal contents extend into the thoracic cavity. Most occur posterolaterally through the foramen of Bochdalek (left greater than right sides). Anterior hernias occur less commonly through the foramen of Morgagni.
Retroperitoneal fibrosis	Bands or nodular lesions with low-intermediate signal on T1 WI, intermediate signal on T2WI. and intermediate to slightly high signal on FST2WI, can be seen adjacent to or surrounding the aorta, inferior vena cava, and/or ureters. Lesions usually show Gd-contrast enhancement.	Disorder in which there is proliferation of fibrous and inflammatory tissue in the retroperitoneum. Retroperitoneal fibrosis can be a primary disorder or occur secondary to malignancy, aortic aneurysm, or drugs such as methysergide and ergotamine.
Pneumonia (Fig. 3.19)	Infection of lung tissue adjacent to the spine can be seen as poorly defined zones of consolidation with low-intermediate signal on T1WI. intermediate to high signal on T2WI. Lesions can show Gd-contrast enhancement.	Infection of lung tissue adjacent to the spine is infrequently associated with direct extension to the spine.

a

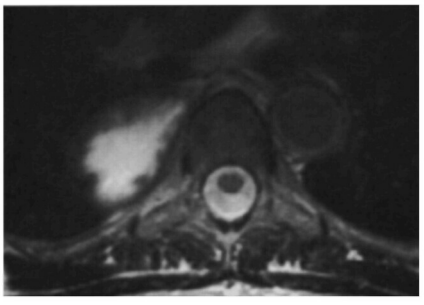

b

Figure 3.18a, b A hiatal hernia is seen on sagittal (**a**) and axial (**b**) T2WI as a right paraspinal structure that has a low signal wall with rugae, within which are high signal contents.

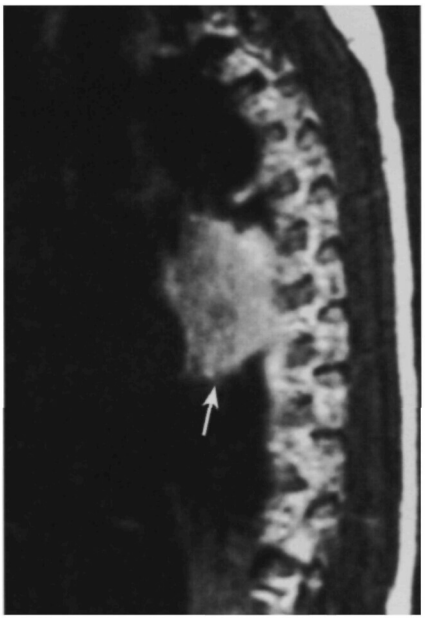

a

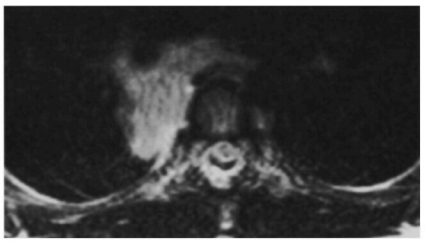

b

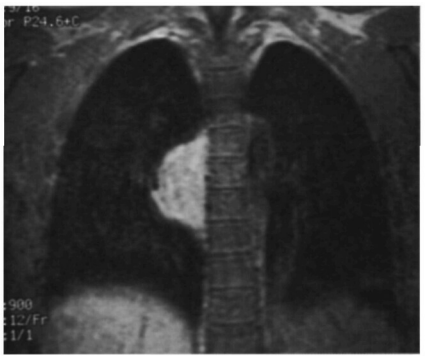

c

a A 9-year-old boy who is immunocompromised and has a right paravertebral cryptococcal pneumonia. The pulmonary consolidation has high signal on sagittal (**a**) and axial (**b**) T2WI, and shows Gd-contrast enhancement on coronal FST1WI (**c**).

References

Ependymoma

Biagini R, Demitri S, Orsini U, Bibiloni J, Briccoli A, Bertoni F. Osteolytic extra-axial sacral myxopapillary ependymoma. *Skeletal Radial* 1999; 28:585-589.

Ginsberg LE, Williams DW, Stanton C. Intrasacral myxopapillary ependymoma. *Neuroradiology* 1994;34:56-58.

Moelleken SM, Seeger LL, Eckardt JJ, Batzdorf U. Myxopapillary ependymoma with extensive sacral destruction: CT and MR findings. *J Comput Assist Tomogr* 1992;16:164-166.

Epidural Abscess

Baleriaux DL, Neugroschl C. Spinal and spinal cord infection. *Eur* Radio/ 2004;14:E72-E83.

Ledermann HP, Schweitzer ME, Morrison WB, Carrino JA. MR imaging findings in spinal infections: rules or myths? *Radiology* 2003;228: 506-514.

Soehle M, Wallenfang T. Spinal epidural abscesses: clinical manifestations, prognostic factors, and outcomes. *Neurosurgery* 2002:51: 79-87.

Table 4 Lesions involving the outer surface of bone

Lesion	MRI Findings	Comments
Benign		
Osteophyte(Fig.4.1)	Bone spurs (osteophytes) occur at the margins of synovial joints and have low peripheral signal on T1WI and T2WI overlying fatty marrow with or without edematous reaction. In the axial skeleton, smooth undulating zones of ossification involving the anterior longitudinal ligament can be seen along the anterior margins of the vertebral bodies and extending across the disks.	Bony outgrowths usually related to degenerative arthropathy at synovial joints, or degenerative disk disease adjacent to the anterior and posterior longitudinal ligaments. At synovial joints, these bony protrusions may be a response to increase the articular surface to reduce load. At the spine, osteophytes occur as a metaplastic bone response related to degenerative disk bulges displacing the longitudinal ligaments. Flowing or bridging osteophytes at four or more adjacent vertebral bodies have been referred to as diffuse idiopathic skeletal hyperostosis (DISH).
Synovia! cyst (Fig. 4.2)	Spinal lesions are spheroid or ovoid circumscribed collections that protrude beyond the margins of the facet joints. Spinal synovia! cysts typically show a site of communication with the adjacent degenerated facet joint. The contents of the spinal synovial cyst usually have low to intermediate signal on T1WI and PDWI. and high signal on T2WI and FST2WI. A thin or slightly thick rim of low signal on T2WI and FST2WI is typically seen at the periphery of the cysts. Some synovial cysts may have intermediate to high signal on T1WI. and/or intermediate or low signal on T2WI secondary to calcifications, cartilage formation, and/or hemorrhage. After Gd-contrast administration, thin marginal enhancement may be seen.	Synovium-lined fluid collections that frequently occur at or near joints of the extremities, occasionally occur at facet joints of the spine, as well as bursae and tendon sheaths. In adults, synovial cysts are often associated with osteoarthritis, rheumatoid arthritis, and trauma. **(See Atlas Chapter A74)**
Ganglion cyst (Fig. 4.3)	Sharply defined lesions with low signal on T1WI, low-intermediate signal on PDWI, and homogeneous high signal on T2WI. Peripheral rim-like Gd-contrast enhancement can be seen as well as complete lack of enhancement Lesions can erode and/or invade adjacent bone.	Ganglia are juxta-articular benign myxoid lesions that arise from degeneration of peri-articular connective tissue, prior trauma, or prior inflammation. Ganglia may be derived from tendons, tendon sheaths, joint capsules, bursae, or ligaments. **(See Atlas Chapter A 28)**

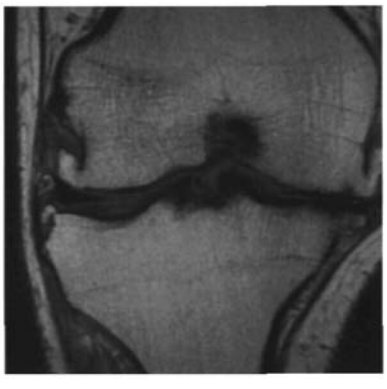

a

b

Figure 4.1 a, b A 54-year-old man with degenerative arthropathy at the knee with prominent osteophytes at the distal femur and proximal tibia on coronal PDWI (**a**). Sagittal T2WI showing bridging anterior osteophytes involving adjacent vertebral bodies (DISH) (**b**).

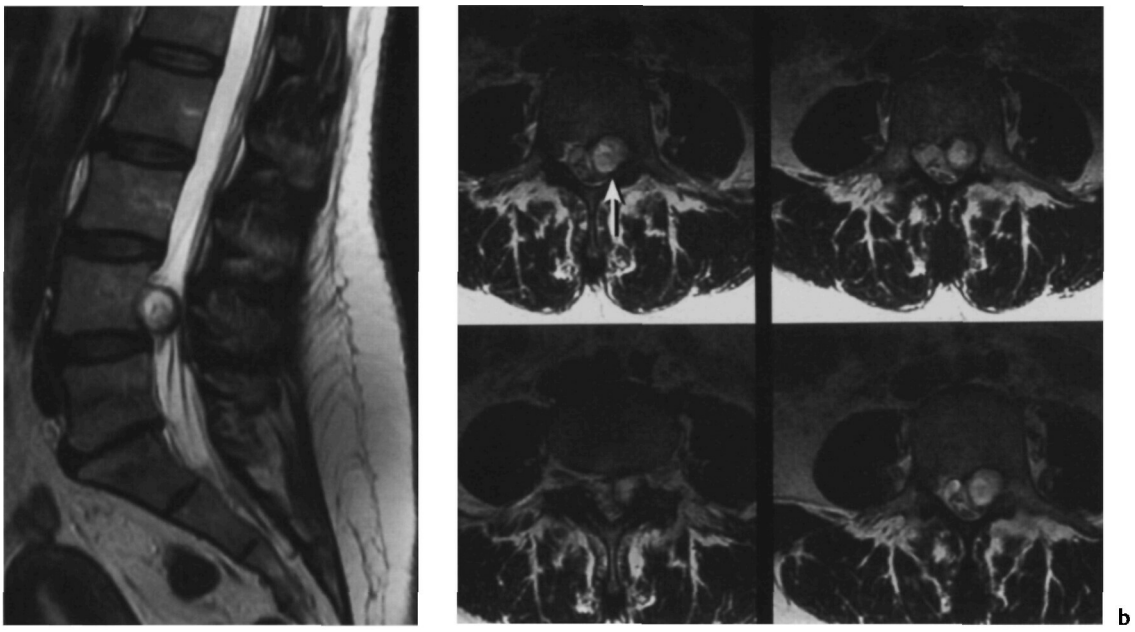

Figure 4.2 a, b Sagittal (**a**) and axial (**b**)T2WI shows a synovial cyst at the medial aspect of the left facet joint causing erosive changes at the vertebral body.

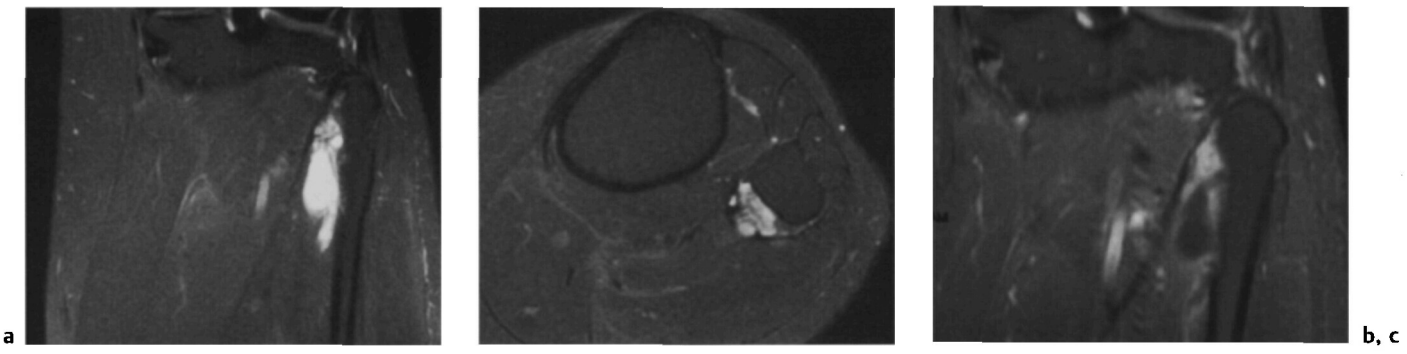

Figure 4.3 a, b Ganglion cyst along the outer surface of the fibula that has high signal on coronal (**a)** and axial (**b**) FST2WI. Thin peripheral Gd-contrast enhancement is seen at the margins on coronal FST1WI (**c)**.

Table 4 (Continued) Lesions involving the outer surface of bone

Lesion	MRI Hndings	Comments
Osteochondroma (Fig. 4.4)	Circumscribed protruding lesion arising from outer cortex with a central zone with intermediate signal on T1 WI and T2WI similar to marrow surrounded by a peripheral zone of low signal on T1 WI and T2WI, a cartilaginous cap is usually present in children and young adults. Increased malignant potential when cartilaginous cap is >2cm thick.	Benign cartilaginous tumors arising from defect at periphery of growth plate during bone formation with resultant bone outgrowth covered by a cartilaginous cap. Usually benign lesions unless associated with pain and increasing size of cartilaginous cap. Osteochondromas are common lesions, accounting for 14 to 35% of primary bone tumors. Occur with median age of 20 years, up to 75% of patients are less than 20years. **(See Atlas Chapter A58)**
Juxtacortical chondroma (Fig.4.5)	Lesions are located at the bone surface and are usually lobulated with low-intermediate signal on T1 WI, which is hypo- or isointense relative to muscle. Lesions usually have heterogeneous predominantly high signal on T2WI. Lesions are surrounded by low signal borders on T2WI representing thin sclerotic reaction. Areas of low signal on T2WI are secondary to matrix mineralization. Edema is not typically seen in nearby medullary bone. Lesions often show a peripheral patlern of Gd-contrast enhancement.	Benign protuberant hyaline cartilaginous tumors that arise from the periosteum and superficial to bone cortex. Juxtacortical chondromas account for < 1 % of bone lesions. Occur with median age of 26 years. **(See Atlas Chapter A 9)**
Chondromyxoid fibroma (Fig. 4.6)	Lesions are often slightly tabulated with low-intermediate signal on T1WI, intermediate signal on PDWI, and heterogeneous predominantly high signal on T2WI secondary to myxoid and hyaline chondroid components with high water content. MR signal heterogeneity on T2WI is related to the proportions of myxoid, chondroid. and fibrous components within the lesions. Thin low signal septa within lesions on T2WI are secondary to fibrous strands. Lesions are surrounded by low-signal borders representing thin sclerotic reaction. Edema is not typically seen in medullary bone. Lesions show prominent diffuse Gd-contrast enhancement.	Rare, benign, slow-growing bone lesions that contain chondroid, myxoid, and fibrous components. Chondromyxoid fibromas represent 2-4% of primary benign bone lesions, and < 1 % of primary bone lesions. Most chondromyxoid fibromas occur between the ages of 1 and 40 years, with a median of 17 years, and peak incidence in the 2nd to 3rd decades. **(See Atlas Chapter A10)**
Periostea! osteoid osteoma (Fig. 4.7)	Typically shows dense fusiform thickening of the cortex, which has low-intermediate signal on T1 W. PDWI, T2WI. and FST2WI. Within the thickened cortex, a spheroid or ovoid zone (nidus) measuring < 1.5 cm is seen in the region of the original external surface of bone cortex. The nidus can have irregular, distinct, or indistinct margins relative to the adjacent region of cortical thickening. The nidus can have low-intermediate signal on T1 WI and PDWI, and low-intermediate or high signal on T2WI and FST2WI. Calcifications in the nidus can be seen as low signal on T2WI. After Gd-contrast administration, variable degrees of enhancement are seen at the nidus and adjacent marrow and cortex.	Benign osteoblastic lesion comprised of a circumscribed nidus < 1.5 cm, and usually surrounded by reactive bone formation. These lesions are usually painful and have limited growth potential. Osteoid osteoma accounts for 11 to 13% of primary benign bone tumors. Occurs in patients 6 to 30 years, median=17years. Approximately 75 % occur in patients less than 25 years. **(See Atlas Chapter A 60)**

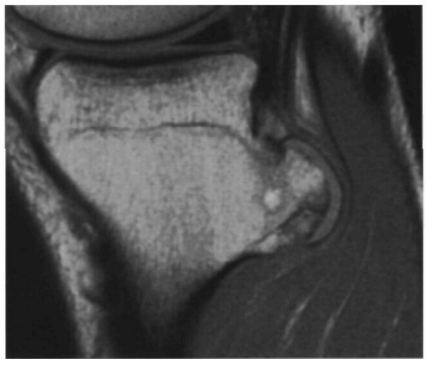

a

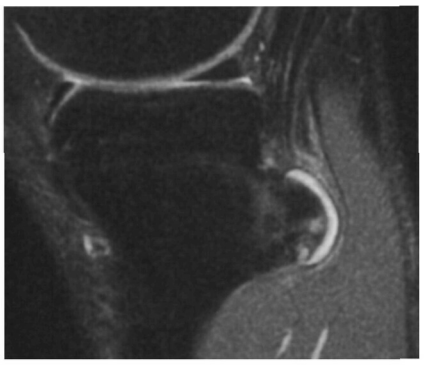

b

Figure 4.4a, b A 14-year-old male with an osteochondroma at the proximal dorsal surface of the tibia as seen on sagittal PDWI (**a**) and FST2WI (**b**).

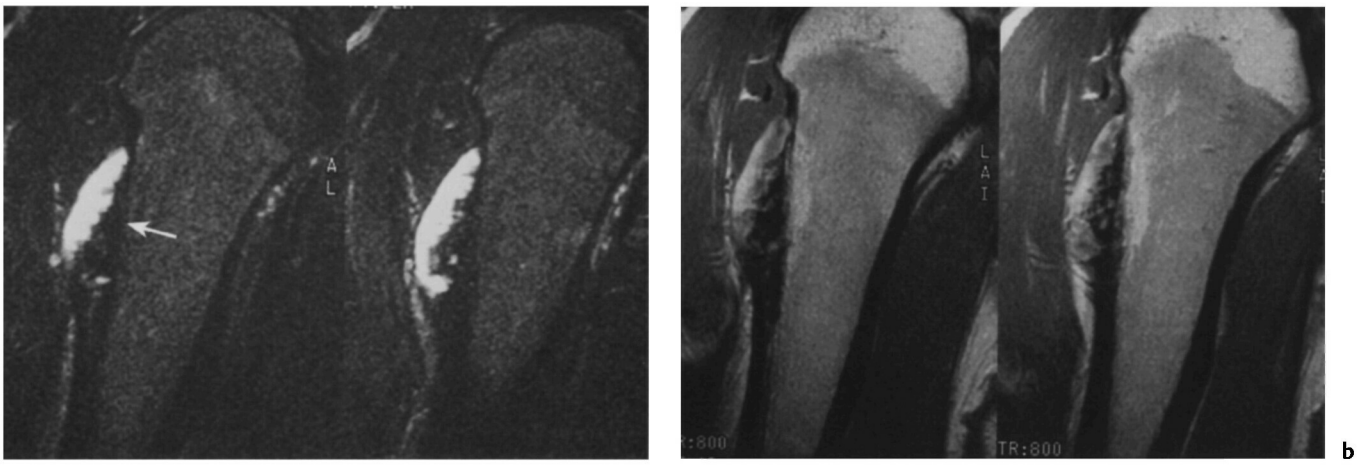

Figure 4.5 a, b Juxtacortical chondroma at the outer surface of the proximal humerus as seen on sagittal FST2WI **(a)**. The lesion shows Gd-contrast enhancement on sagittal T1WI (**b**).

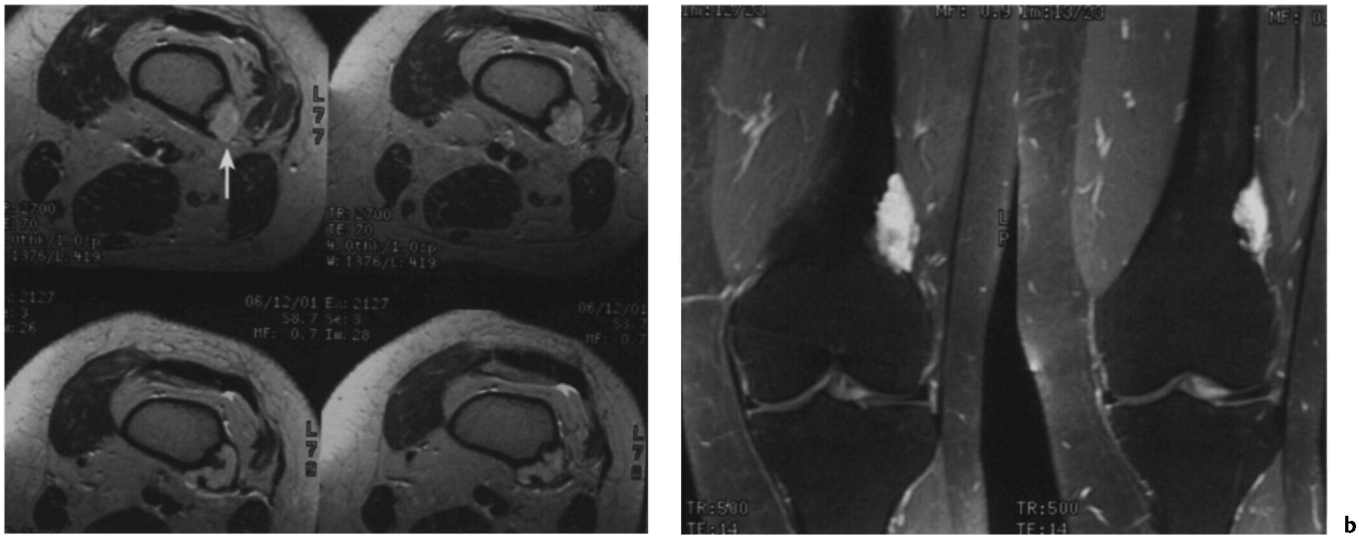

Figure 4.6 a, b Chondromyxoid fibroma involving the superficial portion of the distal femur. The expansile lesion has high signal on axial T2WI (**a**) and shows prominent Gd-contrast enhancement on coronal FST1WI (**b**).

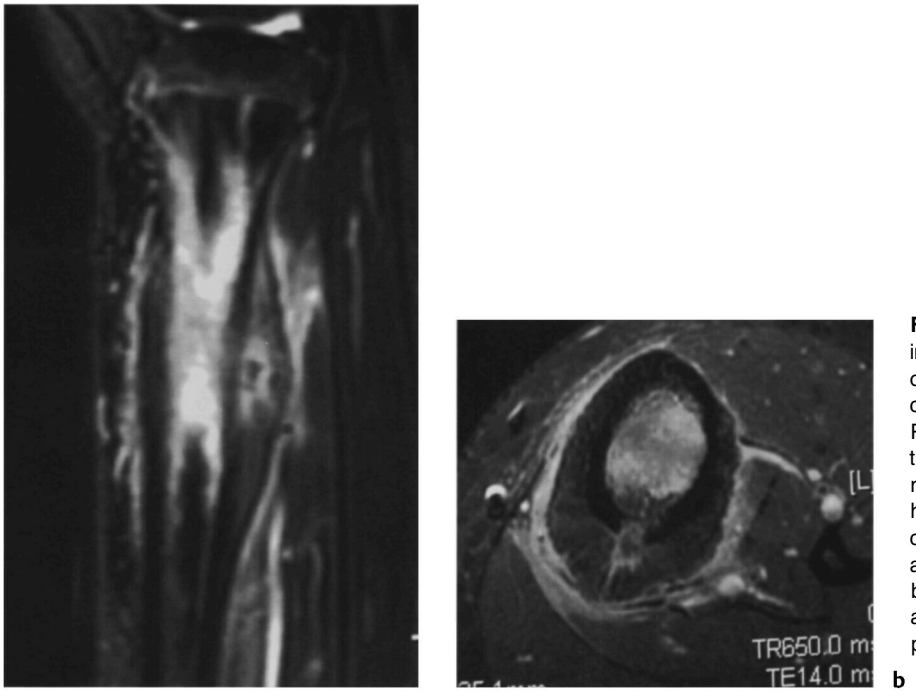

Figure 4.7 a, b Periosteal osteoid osteoma involving the tibia has a nidus with high signal on FST2WI (**a**) that shows prominent Gd-contrast enhancement on axial FST1WI (**b**). Prominent thickened periosteal bone formation is seen, which has heterogeneous intermediate and low signal on FS T2WI. Zones with high signal on FS T2WI with corresponding Gd-contrast enhancement are seen in the marrow and soft tissues superficial to the periosteal bone formation secondary to inflammatory and edematous changes from prostaglandin production by the lesion.

Table 4 (Continued) Lesions involving the outer surface of bone

Lesion	MRI Rndings	Comments
Fibrous cortical defect (FCD) and nonossifylng fibroma (NOF) (Figs. 4.8,4.9)	**FCDs:** Circumscribed oval lesions involving bone cortex of long bones, which have low to intermediate signal on T1WI and PDWI. and low. intermediate, and/or high signal on FST2WI surrounded by varying thickness of low signal from corresponding marginal sclerosis. FCDs with or without fracture can show variable degrees of Gd-contrast enhancement. **NOFs** have MRI features similar to FCDs, although they are larger and eccentrically involve the marrow in the metadiaphyseal regions of long bones. Cortical thinning or thickening, and bone expansion can be seen.	**FCDs** and **NOFs** are benign fibrohistiocytlc lesions in the metaphyseal portions of long bones, which are comprised of whorls of fibroblastic cells combined with smaller amounts of multinucleated giant cells and xanthomatous cells. Both lesions have similar pathologic findings although they differ in size. **FCDs** are small lesions in bone cortex, whereas the larger **NOFs** are located eccentrically in the medullary cavity. Both lesions are considered in the spectrum of the same disorder of fibrohistiocytic origins. **FCDs** and **NOFs** are common benign lesions that are usually asymptomatic, and are often detected as incidental findings. Incidence may be up to 30 to 40% of children. Both lesions occur in patients 1 to 45 years, median = 14 years, 95% occur between the ages of 5 and 20. **(See Atlas Chapter A26)**
Cortical desmoid (Fig. 4.10)	Cortical desmoids are located at the bone cortex at the distal posterior medial portions of the femur, and usually have low to intermediate signal on T1WI and PDWI, and intermediate to slightly high signal on T2WI. and slightly high to high signal on FST2WI. A thin border of low signal on T1WI and T2WI is often seen at the inner margin of the lesion, which corresponds to a thin zone of sclerosis seen on plain films and/or CT. Bone marrow deep and peripheral to the lesion may have slightly high signal on FST2WI. After Gd-contrast administration, enhancement can be seen at the lesion and occasionally in the adjacent marrow.	Cortical desmoids (also referred to as periosteal desmoid or distal femoral cortical irregularity) are fibrous defects at the distal posteromedial femur; may occur from an avulsive injury or stress reaction at the insertion site of the medial head of the gastrocnemius muscle or adductor magnus. Similar-appearing irregularities of bone cortex at sites where other tendons attach to bone are referred to as tug lesions. **(See Atlas Chapter A 26)**
Osteoma (Fig. 4.11)	Typically appear as well-circumscribed zones of dense bone with low signal on T1 WI. PDWI, T2WI. and FST2WI. No infiltration into the adjacent soft tissues is seen with osteomas. Zones of bone destruction or associated soft tissue mass-lesions are not associated with osteomas. Periostea! reaction is not associated with osteomas except in cases with coincidental antecedent trauma.	Benign primary bone tumors composed of dense lamellar, woven, and/or compact cortical bone usually located at the surface of bones. Multiple osteomas usually occur in Gardner syndrome, which is an autosomal dominant disorder associated with intestinal polyposis, fibromas, and desmoid tumors. Account for less than 1 % of primary benign bone tumors. Occurs in patients 16 to 74 years, most frequent in 6th decade. (See Atlas Chapter A62)

Figure 4.8 Fibrous cortical defect in the tibia on axial T1WI.

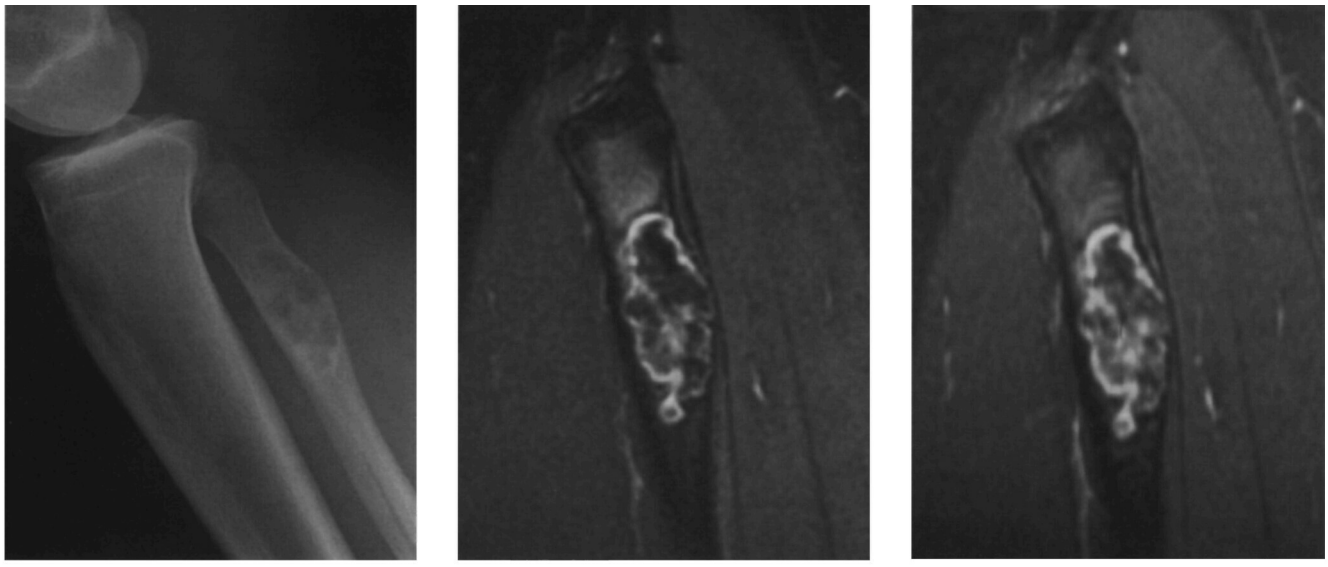

Figure **4.9a-c** Nonossifying fibroma in the marrow of the proximal fibula of a 15-year-old female. Oblique radiograph (**a**) shows a circumscribed radiolucent intramedullary lesion associated with thinning and expansion of the outer cortical margin. The lesion has mostly low signal centrally surrounded by thin zones with high signal on sagittal FST2WI (**b**) and Gd-contrast enhancement on sagittal FS T1 WI (**c**). The lesion expands and thins the outer cortical margin.

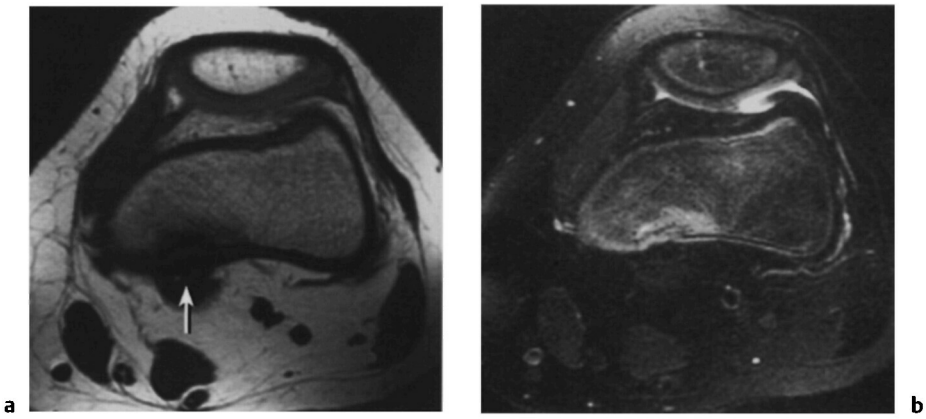

Figure 4.10 Cortical desmoid at the distal dorsal aspect of the femur medially adjacent to the insertion of the medial gastrocnemius muscle tendon as seen on axial T1WI (**a**) and axial FST2WI(**b**).

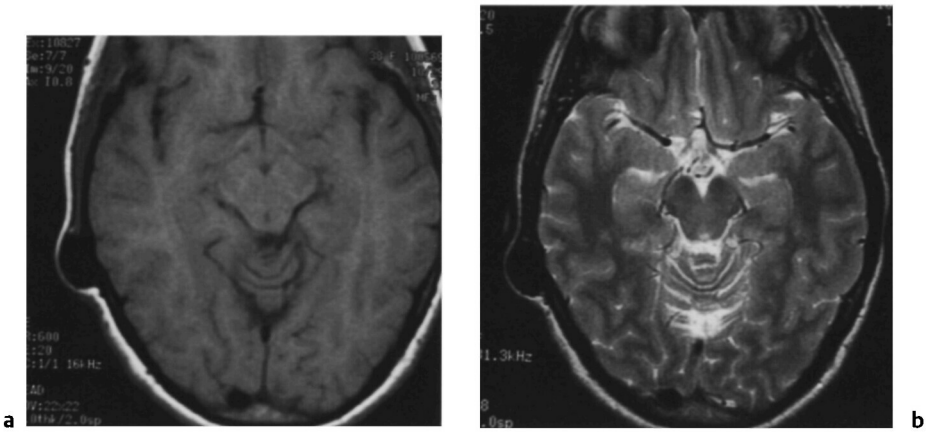

Figure 4.11 a, b Osteoma involving the outer table of the calvarium has low signal on axial T1WI (**a**) and T2WI (**b**).

Table 4 (Continued) Lesions involving the outer surface of bone

Lesion	MRI Findings	Comments
Parosteal lipoma	Lesions often have lobular margins and are immediately adjacent to the outer intact surface of adjacent bone. Lesions typically have fat signal on MRI, as well as zones of low signal on T1WI and T2WI from ossification changes that can occur within these lesions and at the junction with bone cortex. Zones with intermediate signal on T1WI and high signal on T2WI can occur in these lesions secondary to cartilaginous contents.	Rare, benign, slow-growing painless tumors with mature adipose tissue associated with the periosteum of bone. Account for 0.3 % of lipomas, typically occur in patients 40 to 60 years. Common sites include the femur, proximal radius, tibia, and humerus. Other sites have been reported. May be associated with compression of adjacent nerves causing sensory or motor deficits. **(See Atlas Chapter A 43)**
Melorheostosis (Fig. 4.12)	MRI signal varies based on the relative proportions of mineralized osteoid, chondroid, and soft tissue components in these lesions. Mineralized osteoid zones along bone cortex typically have low signal on T1 WI and T2WI, no Cd-contrast enhancement. Soft tissue lesions may also occur adjacent to the cortical lesions, which have a mixed signal on T1WI and T2WI.	Melorheostosis is a rare bone dysplasia with cortical thickening that has a "flowing candle wax" configuration. Associated soft tissue masses occur in -25 %. The soft tissue lesions often contain mixtures of chondroid material, mineralized osteoid, and fibrovascular tissue. **(See Atlas Chapter A 62)**
Heterotopic ossification (Fig.4.13)	Long-standing lesions can have variable low signal on T1WI, PDWI, and T2WI depending on the degree of mineralization/ossification, fibrosis, and hemosiderin deposition. Zones of high signal on T1WI and T2WI may occur from fatty marrow metaplasia. Gd-contrast enhancement in old mature lesions is often minimal or absent. Signal abnormalities within bone marrow are usually absent.	Represents localized non-neoplastic reparative lesions that are comprised of reactive hypercellular fibrous tissue, cartilage, and/or bone. Can arise secondary to trauma (myositis ossificans circumscripta, ossifying hematoma), although may also occur without a history of prior injury (pseudomalignant osseous tumor of the soft tissues). **(See Atlas Chapter A 53)**
Schwannoma (Fig. 4.14)	**Schwannomas** are circumscribed ovoid or fusiform lesions with low-intermediate signal on T1WI, intermediate signal on PDWI, and intermediate to high signal on T2WI and FST2WI. After Gd-contrast administration, lesions typically show moderate to prominent enhancement. Schwannomas involving spinal nerve roots may be associated with chronic erosive changes of adjacent vertebrae. Lesions may show signal heterogeneity on T2WI and heterogeneous Gd-contrast enhancement secondary to cyst formation, hemorrhage, fibrous/collagenous zones, and/or dense cellularity. Signal heterogeneity on T2WI tends to occur frequently in large Schwannomas. Malignant schwannomas (malignant peripheral nerve sheath tumors) can be large lesions that have heterogeneous signal on T1WI. T2WI, and FST2WI; as well as heterogeneous Gd-contrast enhancement because of necrosis and hemorrhage. These tumors can have irregular margins and associated invasion of adjacent structures.	Benign encapsulated tumors that contain differentiated neoplastic Schwann cells. Multiple schwannomas are often associated with NF2. Account for 5 % of benign primary soft tissue tumors and 3 % of all primary soft tissue tumors. Occur in patents 22 to 72 years, mean =46 years. Peak incidence is in the 4th to 6th decades. With NF2, many patients present in the 3rcl decade with bilateral vestibular schwannomas. **(See Atlas Chapter A 72)**

Figure 4.12 Melorheostosis involving multiple vertebrae as seen on sagittal T1WI (a) and T2WI (b).

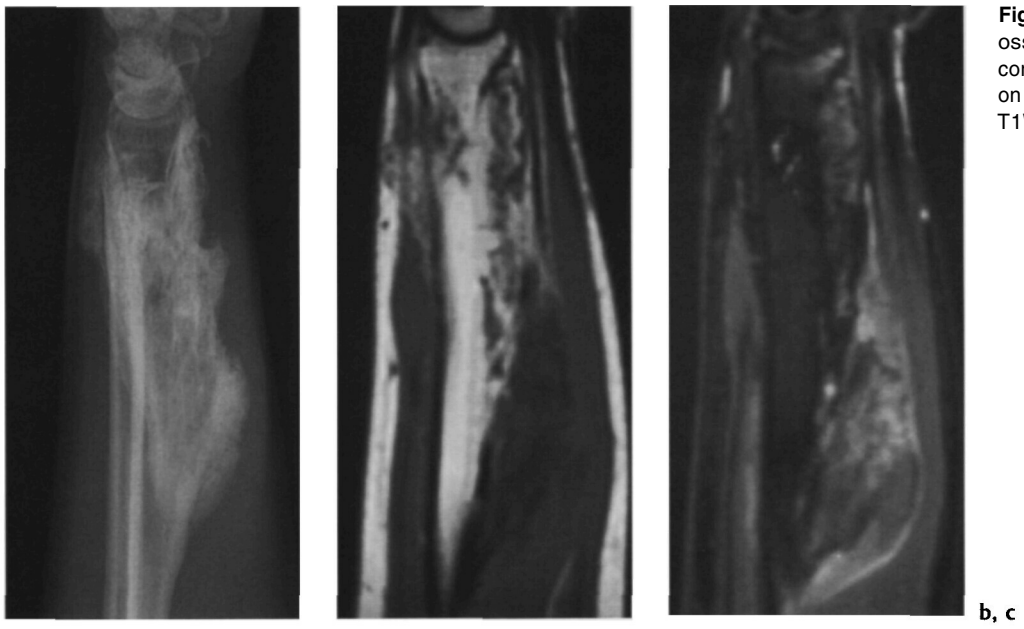

Figure 4.13 Extensive heterotopic ossification with involvement of the cortex of the distal radius as seen on lateral radiograph (**a**), sagittal T1WI(**b**), and FST2WI (**c**).

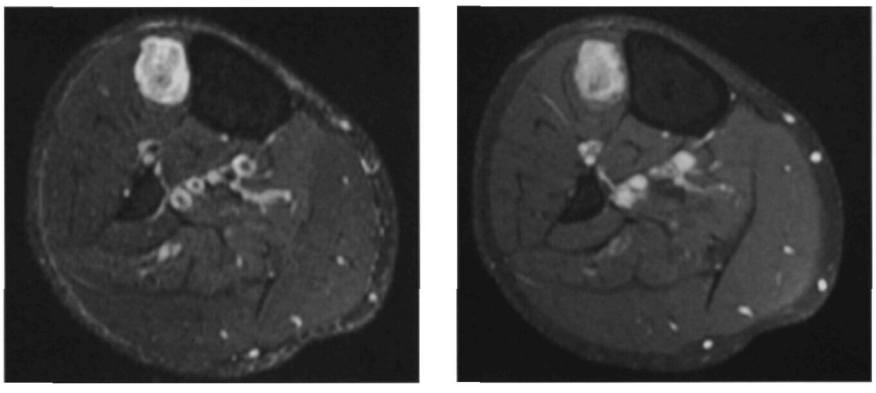

Figure 4.14 Schwannoma adjacent to the outer surface of the tibia as seen on axial FST2WI (**a**). The lesion shows prominent Gd-contrast enhancement on axial FST1WI (**b**).

Table 4 (Continued) **Lesions involving the outer surface of bone**

Lesion	MRI Findings	Comments
Neurofibroma (Fig. 4.15.4.16)	**Localized neurofibromas** are circumscribed ovoid or fusiform lesions with low-intermediate signal on T1WI and intermediate to high signal on T2WI and FST2WI. After Gd-contrast administration, lesions typically show moderate to prominent enhancement. Large lesions may show signal heterogeneity on T2WI and heterogeneous Gd-contrast enhancement. Neurofibromas involving spinal nerve roots may have a dumb-bell shape with or without associated chronic erosive changes of adjacent vertebrae. **(Fig. 4.15) Plexiform neurofibromas** appear as curvilinear and multinodular lesions involving multiple nerve branches. Lesions usually have low to intermediate signal on T1WI; and intermediate, slightly high to high signal on T2WI and FST2WI with or without bands or strands of low signal. On T2WI. lesions may show nodules with high signal surrounding a central region of low signal referred to as a "target sign." Lesions typically show Gd-contrast enhancement in a heterogenous pattern. Lesions can be associated with remodeling of adjacent bone **(Rg.4.16)**	Benign tumors of the peripheral nerve sheath that contain mixtures of Schwann cells, perineural-like cells, and interlacing fascicles of fibroblasts associated with abundant collagen. Unlike schwannomas, neurofibromas lack Antoni A and B regions and cannot be separated pathologically from the underlying nerve. Neurofibromas can be localized lesions (90%), or occur as diffuse or plexiform lesions. The presence of multiple neurofibromas is a typical feature of NF1, which is an autosomal dominant disorder resulting in mesodermal dysplasia affecting multiple organ systems. Plexiform neurofibromas are associated with an increased risk of malignant transformation into malignant peripheral nerve sheath tumors. Solitary neurofibromas account for 5% of primary benign soft tissue tumors and 3 % of all primary soft tissue tumors. Lesions occur in patients16 to 66years, mean = 37 years. Neurofibromas can also occur in younger children and older adults. NF1 often presents in childhood. **(See Atlas Chapter A 56)**
Meningioma (Fig.4.17)	Extra-axial dural-based lesions usually with intermediate signal on T1 WI. intermediate-slightly high signal on T2WI. typically show prominent Gd-contrast enhancement. +/- calcifications, +/- hyperostosis, and/or invasion of adjacent skull.	Most common extra-axial intracranial tumor, usually benign neoplasms, typically occurs in adults (> 40 years), women > men, multiple meningiomas seen with NF2. Can also occur in the spine with osseous erosion or invasion with or without associated hyperostosis. **(See Adas Chapter A 49)**
Arachnoid cyst (Fig. 4.18)	Well-circumscribed extra-axial lesions with low signal on T1WI and FLAIR, and high signal on T2WI and FST2WI. similar to CSF. no Gd-contrast enhancement. Chronic erosive changes can be seen at the adjacent skull.	Non-neoplastic acquired, developmental or congenital extra-axial cysts filled with CSF. Cysts can be small or large, asymptomatic or symptomatic.
Perineural, Tariov cysts (Fig.4.19)	Well-circumscribed cysts with MRI signal comparable to CSF involving nerve root sleeves associated with chronic erosive changes involving adjacent bony structures.	Typically represent incidental asymptomatic anatomic variants associated with prior dural injury.

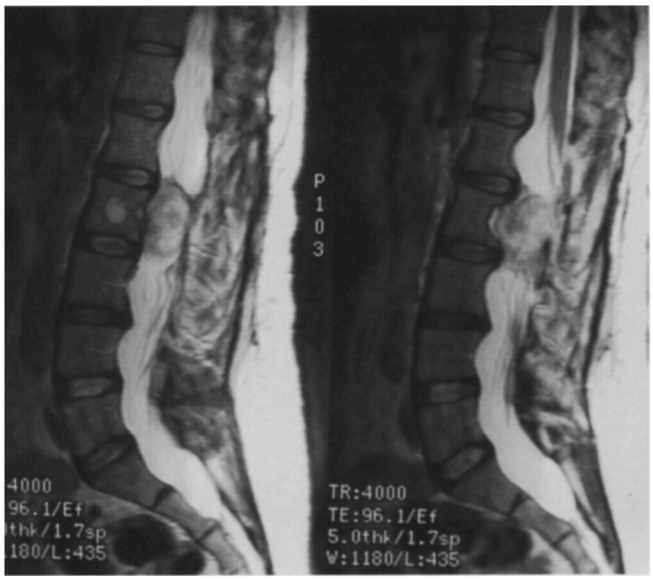

a

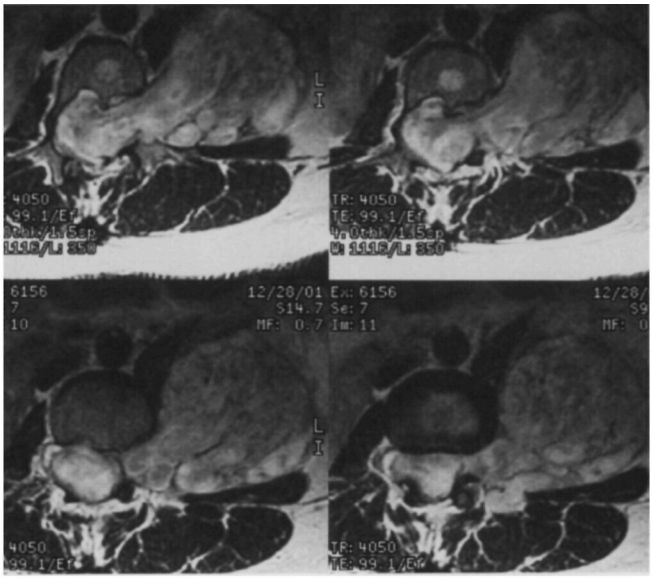

b

Figure 4.15 a, b Neurofibroma within the spinal canal at the L 2 level resulting in remodeling of the adjacent vertebra as seen on sagittal (**a**) and axial (**a**) T2WI.

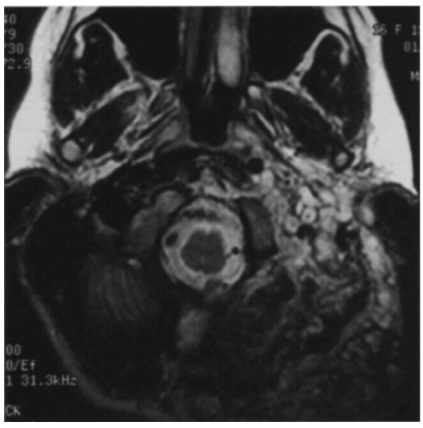

Figure 4.**16** Plexiform neurofibroma in the posterior left scalp and upper neck resulting in remodeling of the occipital bone as seen on axial T2WI.

a

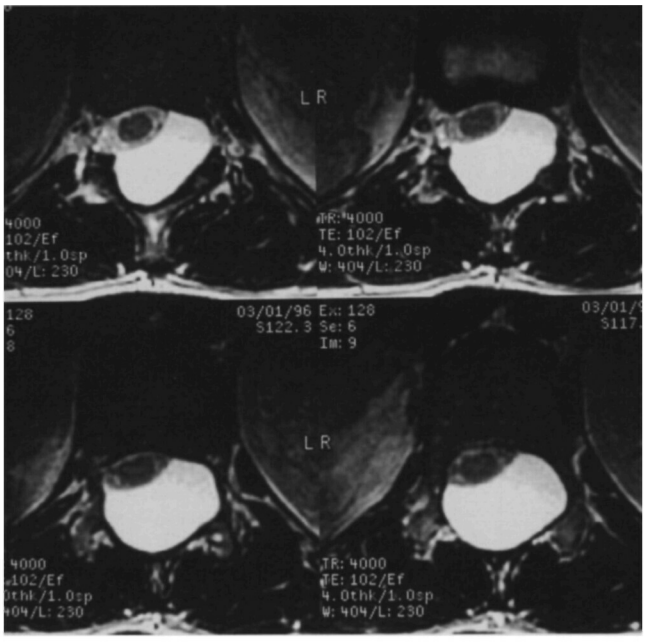

b

Figure 4.18a, b Arachnoid cyst in the dorsal portion of the spinal canal on sagittal (**a**) and axial (**b**) T2WI that displaces the thecal sac anteriorly and causes thinning and remodeling of the posterior elements.

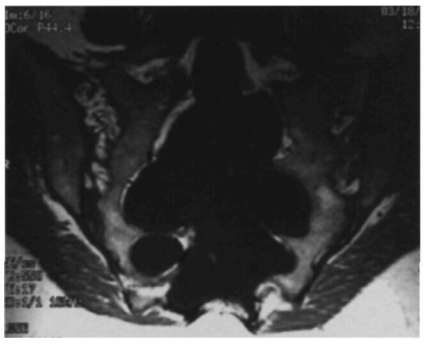

a

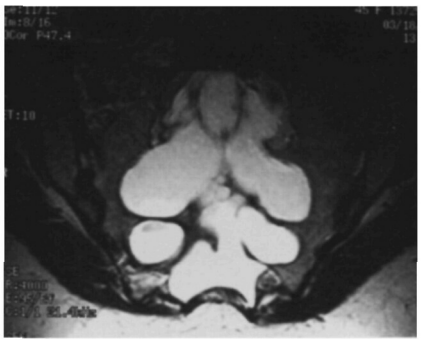

b

Figure 4.19 a, b Tarlov (perineural) cysts involving the sacral nerve root sleeves causing expansile remodeling of the sacral foramina as seen on coronal T1WI (**a**) and T2WI (**b**).

Table 4 (Continued) **Lesions involving the outer surface of bone**

Lesion	MRI Findings	Comments
Giant cell tumor of tendon sheath (Fig. 4.20)	Lesions usually have well-defined margins and are often adjacent to a tendon/tendon sheath. Lesions can be ovoid or multilobulated, and usually have low-intermediate or intermediate signal on T1WI and PDWI that is often similar to or less than muscle. On T2WI and FS T2WI, lesions can have mixed low, intermediate, and/or high signal. Zones of low signal on T2WI often correspond to sites of hemosiderin deposition. Lesions often show Gd-contrast enhancement in either homogeneous or heterogeneous pattern. Erosions of adjacent bone can be seen with some lesions.	Giant cell tumors of the tendon sheath and pigmented villonodular synovitis are benign proliferative lesions of synovium (tendon sheaths, joints, and bursae). Giant cell tumors of the tendon sheaths can occur as localized nodular lesions attached to tendon sheaths outside of joints (hands, feet) or within joints (infrapatellar portion of knee joint); or as a diffuse form near/outside of large joints such as the knee and ankle. Giant cell tumors of the tendon sheath represent 4 % of benign soft tissue tumors and 2 % of all soft tissue tumors. Occur in patients from 6 to 71 years, mean -39 to 46 years with peak ages in 3rd to 4th decades. **(See Adas Chapter A 30)**
Clomus tumor (Fig. 4.21)	Glomus tumors are well-circumscribed ovoid lesions measuring less than 1 cm and are often located under the nail beds at the distal phalanges of fingers and toes. Glomus tumors often have low-intermediate signal on nwi and PDWI, high signal on T2WI and FST2WI. A thin rim of low signal on T2WI may be seen secondary to a capsule from reactive tissue surrounding the glomus tumor. Lesions typically show Gd-contrast enhancement. MRI can show erosion of the underlying bone.	Benign mesenchymal hamartomas. composed of round cells derived from the neuromyoarterial apparatus (glomus bodies), that regulate arteriolar blood flow to the skin. **(See Atlas Chapter A 31)**
Nonmalignant giant cell tumor eroding through bone cortex (Fig. 4.22)	Usually well-defined lesions with thin low signal margins on T1WI, PDWI. and T2WI. Solid portions of giant cell tumors often have low to intermediate signal on T1WI and PDWI, intermediate to high signal on T2WI, and high signal on FSPDWI and FST2WI. Signal heterogeneity on T2WI is not uncommon. Zones of low signal on T2WI and T2* imaging may be seen secondary to hemosiderin. Aneurysmal bone cysts can be seen in 14% of giant cell tumors, resulting in cystic zones with variable signal and fluid-fluid levels. After Gd-contrast administration, mild to prominent enhancement of the solid intraosseous portions of the lesions is seen, as well as peripheral rim-like enhancement around cystic zones/aneurysmal bone cysts. Contrast enhancement is usually seen in the extraosseous portions of the tumors. Poorly defined zones of enhancement and high signal on FST2WI may also be seen in the marrow peripheral to the portions of the lesions associated with radiographic evidence of bone destruction, indicating reactive inflammatory and edematous changes associated with elevated tumor prostaglandin levels.	Aggressive tumors composed of neoplastic ovoid mononuclear cells and scattered multinucleated osteoclast-like giant cells (derived from fusion of marrow mononuclear cells). Up to 10% of all giant cell tumors are malignant. Benign giant cell tumors account for ~5 to 9.5% of all bone tumors and up to 23% of benign bone tumors. Occurs in patients 4 to 81 years (median =30 years), 75% occur in patients between 15 and 45 years. **(See Atlas Chapter A 29)**

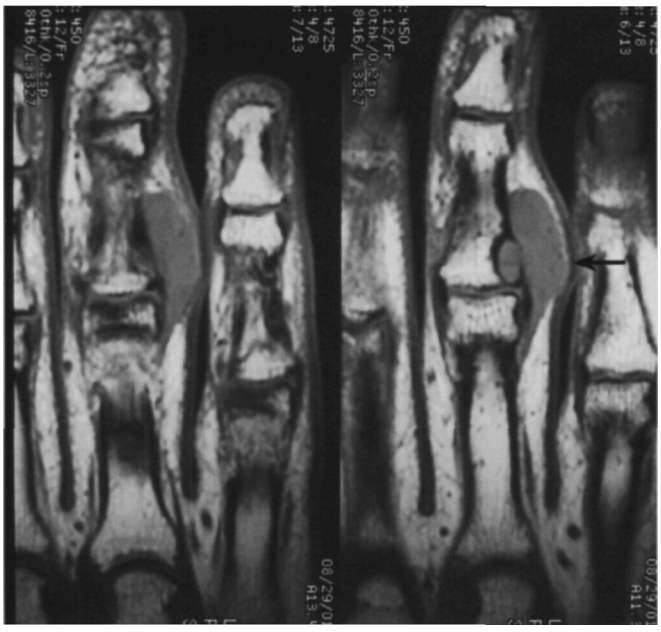

Figure 4.20 Giant cell tumor of the tendon sheath (nodular synovitis) causing focal erosion of the adjacent phalanx as seen on coronal T1WI.

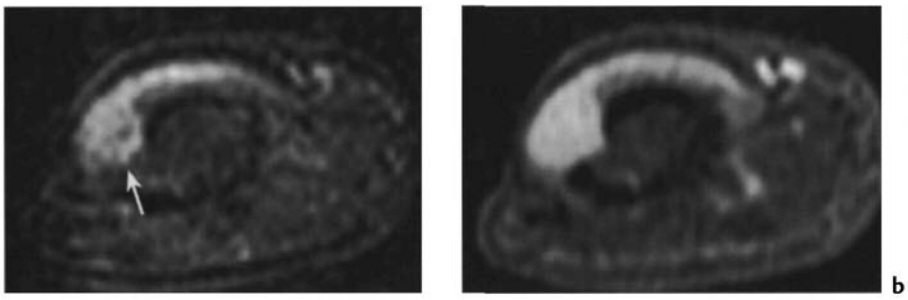

Figure 4.21 a, b Clomus tumor under the fingernail with slightly high signal on axial FST2WI (**a**) and Gd-contrast enhancement on axial FST1WI (**b**). The lesion erodes the cortical margin of the adjacent phalanx.

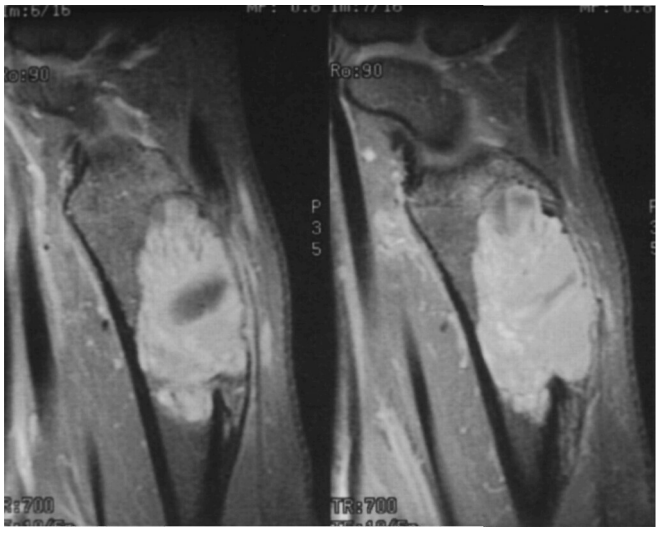

Figure 4.22 Giant cell tumor of bone involving the distal radius. The intramedullary lesion erodes cortical bone and extends into the extraosseous soft tissues. The lesion shows prominent Gd-contrast enhancement on sagittal FST1WI.

Table 4 (Continued) **Lesions involving the outer surface of bone**

Lesion	MRI Findings	Comments
Eosinophillc granuloma eroding through bone cortex (Fig. 4.23)	Focal intramedullary lesion(s) associated with trabecular and cortical bone destruction that typically have low-intermediate signal on T1WI and PDWI and heterogeneous slightly high to high signal on T2WI. Poorly defined zones of high signal on T2WI are usually seen in the marrow peripheral to the portions of the lesions associated with radiographic evidence of bone destruction, indicating reactive inflammatory and edematous changes. Extension of lesions from the marrow into adjacent soft tissues through areas of cortical disruption are commonly seen as well as linear periostea! zones of high signal on T2WI. Lesions typically show prominent Cd-contrast enhancement in marrow and in extraosseous soft tissue portions of the lesions.	Single or multiple eosinophilic granulomas are benign tumorlike lesions consisting of Langerhans' cells (histiocytes), and variable amounts of lymphocytes, polymorphonuclear cells, and eosinophils. Account for 1 % of primary bone lesions, and 8 % of tumorlike lesions. 5 to 20 per 1 000000 children per year in the USA. Occurs in patients 1 to60years, median =10years, average = 13.5 years, peak incidence is between 5 and 10 years, 80 to 85% occur in patients less than 30 years, and 60% occur in children less than 10 years. **(See Atlas Chapter A18)**
Osteomyelitis (Fig. 4.24)	Periostea! reaction associated with osteomyelitis is seen as a peripheral rim of high signal on T2WI and FST2WI and Gd-contrast enhancement on FST1WI adjacent to the low signal of cortical bone. A subperiosteal abscess with high signal on T2WI and FST2WI can be often seen elevating a single low signal thin band of periosteum. Within the underlying marrow, poorly defined zones with high signal on T2WI and FST2WI and Cd-contrast enhancement are seen with or without associated zones of cortical destruction.	Osteomyelitis refers to infection of bone and can result from hematogenous spread of microorganisms, trauma-direct inoculation, extension from adjacent tissues, and complications from surgery. *Staphylococcus ooreus* and *Streptococcus pyogenes* are the most common bacterial infections involving bone. Osteomyelitis can also result from other bacteria as well as from other organisms such as Mycobacteria tuberculosis, fungi, parasites, and viruses. (See Atlas Chapter A63)
Myositis/cellulitis associated with infection of bone (Fig.4.25)	Irregular poorly defined zones with slightly high to high signal on T2WI and FST2WI are typically seen with Cd-contrast enhancement. Circumscribed zones with high signal on T2WI and FST2WI may also be seen with abscess formation.	Infection of soft tissues can result in erosion, destruction, and invasion of adjacent bone.
Rheumatoid pannus adjacent to and eroding bone (Fig. 4.26)	Erosions of cortical bone in large and small joints, vertebral endplates, spinous processes, and uncovertebral and apophyseal joints. Irregular enlarged enhancing synovium (pannus low-intermediate signal on T1WI. intermediate-high signal on T2WI and FST2WI) in joints results in osseous erosions.	Most common type of inflammatory arthropathy that results in synovitis causing destructive/erosive changes of cartilage, ligaments, and bone. Cervical spine involvement two-thirds of patients, juvenile and adult types. **(See Atlas Chapter A 70)**
Pigmented villonodular synovitis (PVNS) (Fig.4.27)	Often appears as irregular, multinodular, and/or irregular thickening of synovium with low or low-intermediate signal on T1WI and T2WI. Solitary nodular lesions can also occur. Areas of low signal on T2WI and T2*WI in lesions are secondary to hemosiderin. Joint effusions are usually present, rarely with fluid-fluid levels. PVNS usually shows Gd-contrast enhancement in homogeneous, heterogeneous, and/or septal patterns.	Benign intra-articular lesions of proliferative synovium containing zones of recent or remote hemorrhage. Similar histopathologic features with giant cell tumors of the tendon sheath. Account for < 1 % of benign and all soft tissue tumors. Mean age - 38 years, median age - 32 years. **(See Atlas Chapter A67)**

a

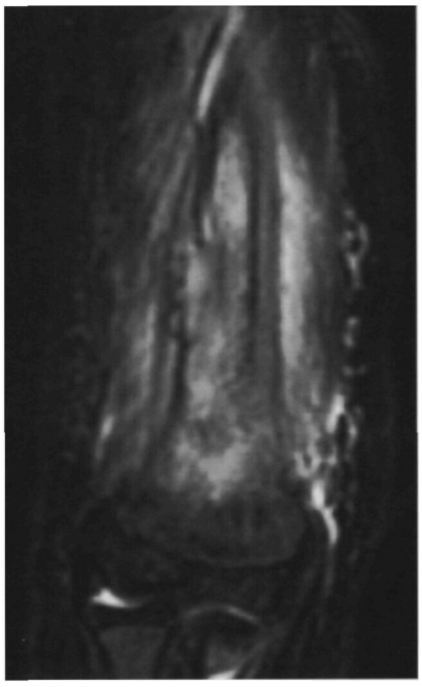

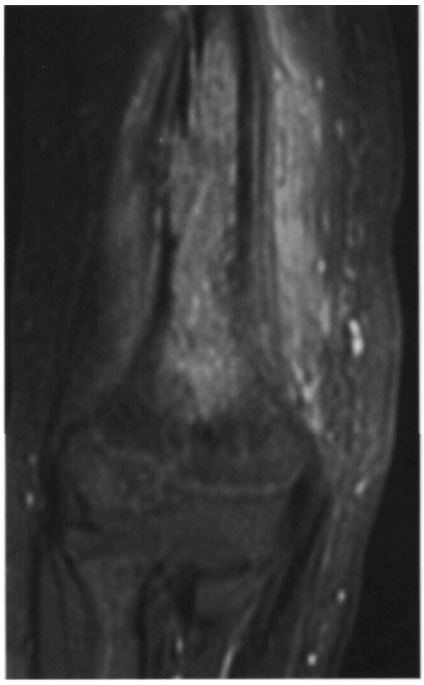

b, c

Figure 4.23 a-c Eosinophilic granuloma involving the distal humerus. AP radiograph (a) shows a radiolucent intramedullary lesion with irregular margins, cortical disruption medially, and a single layer of smooth periosteal reaction. A zone of disruption of the periosteum is seen medially. MRI shows an intramedullary poorly defined lesion with heterogeneous slightly high to high signal on coronal FST2WI (**b**) and corresponding Gd-contrast enhancement on coronal FST1WI (c). Extension of the lesion from the marrow into adjacent soft tissues is seen through areas of cortical disruption. Zones of high signal and Gd-contrast enhancement are seen superficial and deep to the elevated periosteum, which is seen as a linear zone of low signal.

Figure 4.24 Osteomyelitis involving the metaphysis and epiphysis of the distal tibia. The infection is seen as poorly defined zones of Gd-contrast enhancement in the marrow associated with periosteal elevation and poorly defined zones of Gd-contrast enhancement in the adjacent soft tissues on sagittal FST1WI.

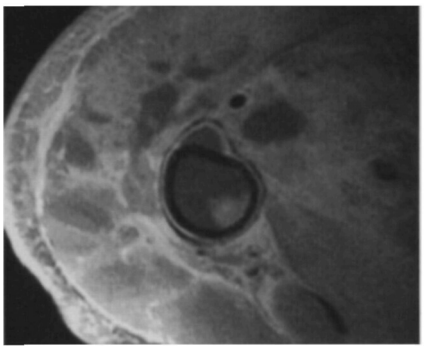

Figure 4.25 Myositis involving the muscles at the shoulder with erosion of cortical bone, intraosseous extension, periosteal reaction, and subperiosteal abscess as seen on post-contrast axial FST1WI.

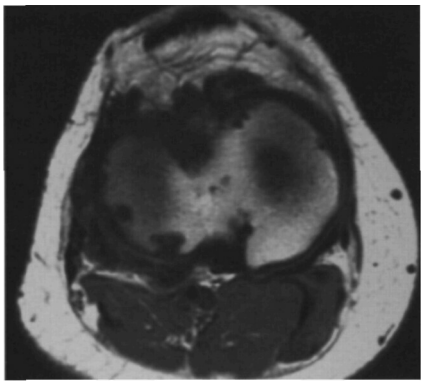

Figure 4.27 Pigmented villonodular synovitis in the knee associated with focal erosions of the adjacent tibia as seen on axial T1WI.

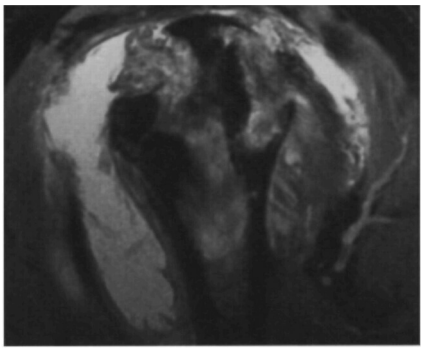

Figure **4.26** Rheumatoid arthritis at the shoulder with pannus eroding the humerus as seen on sagittal FST2WI. Pannus is seen as poorly defined synovium with mixed intermediate slightly high and low signal. A large joint fluid collection is also present.

Table 4 (Continued) Lesions involving the outer surface of bone

Lesion	MRI Findings	Comments
Calcific tendinitis eroding into bone (Fig. 4.28)	Zones with slightly high and low signal on T2WI and FST2WI are seen in tendons with or without erosion of bone cortex. Intramedullary zones with mixed low, intermediate, and/or high signal on T2WI and FST2WI may be seen in the adjacent marrow.	Degenerative disorder with amorphous calcifications in tendons or bursa associated with erosion of adjacent bone cortex, with or without marrow invasion. Most common in humerus and femur in patients 16 to 82 years, average - 50 years.
Nonintemipted periostea! reaction from fracture (Fig. 4.29)	Noninterrupted periosteal reaction from stress fractures and healing traumatic fractures typically appear as a linear thin single 1-2-mm band of low signal superficial to bone cortex, which is surrounded by poorly defined zones with high signal on FST2WI and Gd-contrast enhancement. Poorly defined intramedullary zones with high signal on FST2WI and Gd-contrast enhancement are usually seen in the underlying bone marrow. A thin linear radiodense line is seen at the elevated periosteum 7 to 10 days later.	48 hours after fracture, extravascular red blood cells lyse causing an intense inflammatory reaction followed by granulation tissue ingrowth. Periosteal reaction occurs when fibroblasts are induced to form osteoblasts in the outer periostea! layer secondary to trauma. Periosteal reaction occurs earlier in children compared with adults.
Subperiosteal hematoma (Fig.4.30)	Low signal thin bands of periosteum separated from underlying bone cortex can be seen surrounded by irregular zones with intermediate to high signal on T2WI and FST2WI, and irregular Gd-contrast enhancement.	Subperiosteal hematomas can result from bone fractures or avulsion of periosteum near sites of tendinous insertions.
Hemophilic pseudotumor	Subperiosteal pseudotumors elevate the periosteum from hemorrhage associated with cortical erosion and periostea! reaction. Lesions usually have mixed low. intermediate, and high signal on T1WI and T2WI. as well as fluid-fluid levels.	Lesions can occur within medullary bone or in a subperiosteal location, as well as within soft tissues in 1 -2 % of patients with severe factor VIII or IX deficiency. Enlarging lesions may require surgical resection.
Noninterrupted periostea! reaction from primary hypertrophic osteoarthropathy (pachydermoperiostosis)	Linear and/or irregular periosteal and cortical thickening seen in tubular bones of the extremities bilaterally (tibia, fibula, radius ulna are common sites, also seen in other bones and skull). Can involve epiphyseal, metaphyseal. and/or diaphyseal portions of long bones.	Rare clinical syndrome in adolescents or adults with swollen painful joints, enlargement of the extremities from osseous proliferation and periostitis, clubbing of digits, thickening of skin of the face and scalp with excessive sweating and sebaceous secretions. Can be hereditary (autosomal dominant with variable expression) or idiopathic.
Nonintemipted periostea! reaction from secondary hypertrophic osteoarthropathy	Smooth, wavy, and or irregular periostea! and cortical thickening seen in the diaphyseal and metaphyseal portions of long bones of the upper and lower extremities, as well as in other bones.	Clinical syndrome with clubbing of the digits, periostitis, hypertrophic osteoarthropathy, skin thickening, limb swelling, nail bed abnormalities (striations. increased curvature) related to extraskeletal lesions involving the lungs (bronchogenic carcinoma, metastasis, cystic fibrosis, bronchiectasis, infection, lymphoma). pleura (mesothelioma). abdomen (biliary atresia, cirrhosis, tumors, ulcerative colitis, Crohn disease), heart (cyanotic heart disease), or neoplasms at other sites. Regression of hypertrophic osteoarthropathy can occur after thoracotomy in patients with thoracic abnormalities, even in those without complete removal of the intrathoracic lesions.

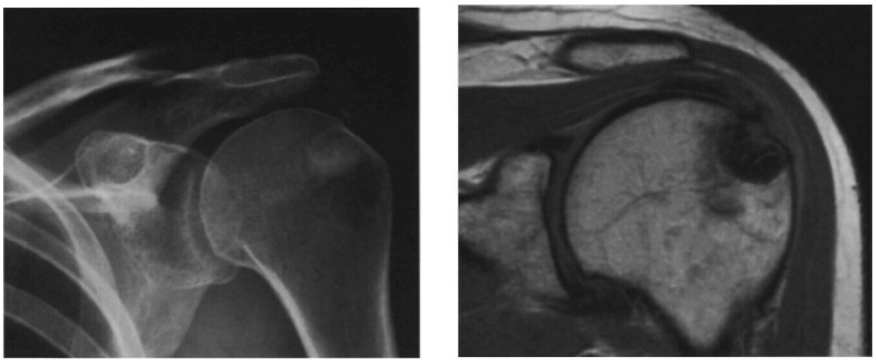

a, b

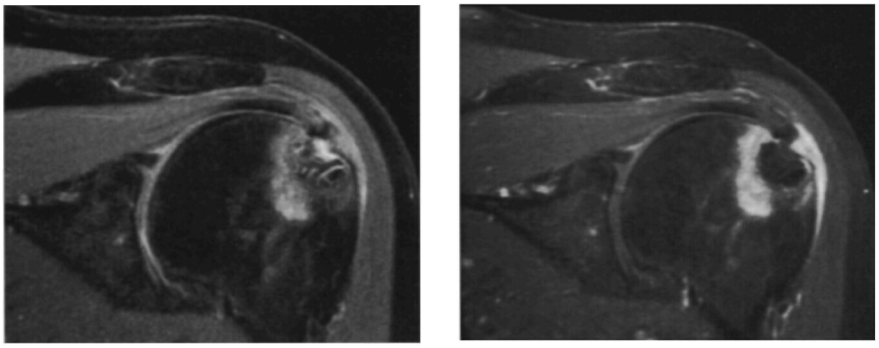

c d

Figure 4.28a-d Calcific tendonitis of the supraspinatus eroding into the humerus. The AP radiograph (**a**) shows calcifications in the supraspinatus tendon and within the humerus. Zones with low signal on coronal T1WI (**b**) and heterogeneous low, intermediate, and high signal on coronal FST2WI (**c**) are seen in the supraspinatus tendon associated with erosion of bone cortex and intramedullary extension. Intramedullary zones with mixed low, intermediate, and/or high signal on FST2WI are seen in the marrow. Poorly defined zones of Gd-contrast enhancement are seen in the marrow and tendon on coronal FST1WI (**d**).

a

b

c

Figure 4.29 a-c Noninterrupted single-layer periosteal reaction at the site of a healing stress fracture as seen on a lateral radiograph (**a**). A linear thin single 1-2-mm band of low signal superficial to bone cortex is seen surrounded by poorly defined zones of intermediate signal on sagittal T1WI (**b**) and high signal on sagittal FST2WI (**c**). Poorly defined intramedullary zones with high signal on FST2WI are seen, within which there is an irregular linear zone of low

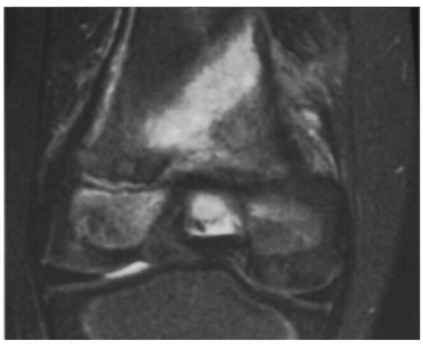

a

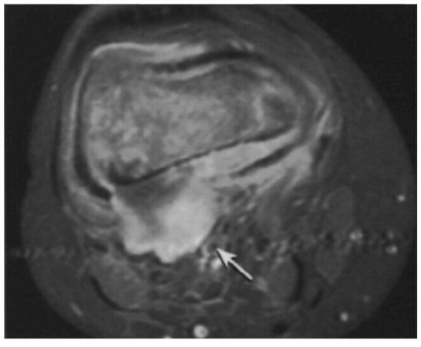

c

Figure 4.30a-c Traumatic fracture of the distal femur with periosteal elevation and subperiosteal hematoma as seen on coronal (**a**) and axial (**b**) FST2WI. Focal disruption of the periosteum is also seen dorsally on axial FST2WI and post-contrast axial FST1 WI (**c**).

Table 4 (Continued) Lesions involving the outer surface of bone

Lesion	MRI Findings	Comments
Noninterrupted periostea! reaction from venous stasis (Fig. 4.31)	Smooth and wavy periostea! and cortical thickening seen in the diaphyseal and metaphyseal portions of long bones of the lower extremities (tibia, fibula, metatarsal bones, phalanges).	Venous stasis is associated with edematous changes in the soft tissues as well as soft tissue ossification, periostitis, and cortical thickening.
Noninterrupted periostea! reaction from infantile cortical hyperostosis (Caffey disease)	Smooth, wavy, and/or irregular periosteal and cortical thickening seen in the diaphyseal and metaphyseal portions of one or multiple bones.	Clinical disorder that affects infants less than 5 months with findings of soft tissue swelling (commonly over the mandible), fever, hyperirritability, and cortical hyperostosis (ribs, ulna, tibia, fibula, humerus, femur, radius, metacarpal, and metatarsal bones). The clinical course is variable but regression of findings can occur over 3 to 4 years.
Noninterrupted periostea! reaction from thyroid acropachy	Asymmetric, irregular, spiculated periosteal thickening seen in the diaphyseal portions of one or multiple bones (metacarpal and metatarsal bones, phalanges, other bones).	This disorder represents an extreme form of autoimmune thyroid disease with clinical manifestations such as swelling of the digits and toes, digital clubbing, and periosteal reaction. Thyroid dermopathy (pretibial myxedema) occurs in 4 % of patients with Craves ophthalmopathy. Pronounced cases of thyroid dermopathy can be associated with thyroid acropachy in 1 % of patients with Craves ophthalmopathy.
Noninterrupted periostea! reaction from hypervitaminosis A	Smooth and wavy periosteal and cortical thickening seen in the diaphyseal portions of one or multiple bones (ulna, metatarsal bones, clavicle, tibia, fibula, other bones). Damage to the physeal plates can result in irregularities and premature fusion, as well as splaying and cupping deformities of the metaphyses.	Vitamin A intoxication in children can result in anorexia, dermatologic, and osseous disorders. In children, damage to the physeal plates may be irreversible despite cessation of vitamin A administration. In adults, anorexia, weight loss, and dermatologic disorders are frequently associated with hypervitaminosis A.

a

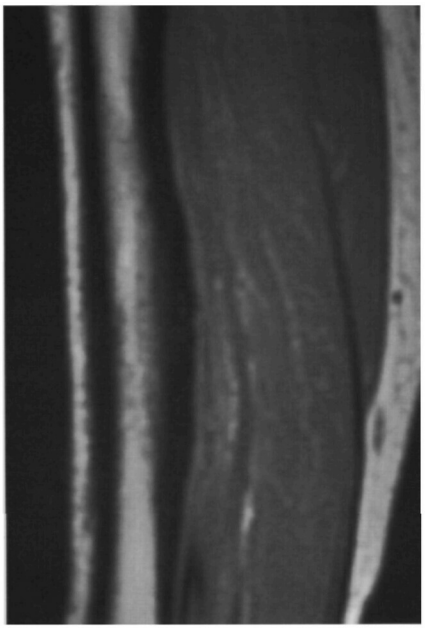

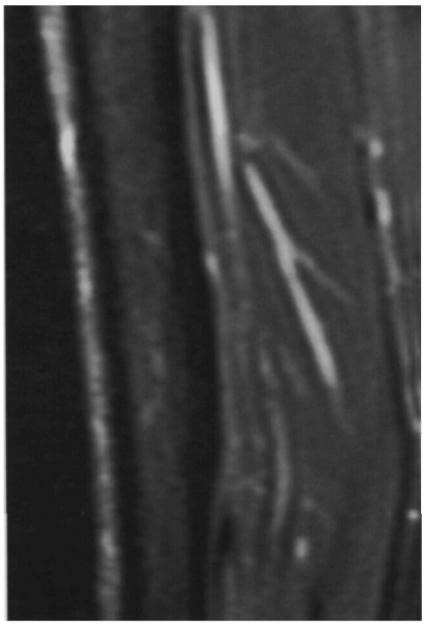

b, c

Figure 4.31 a-c Thickened noninterrupted periosteal reaction from venous stasis as seen on oblique radiograph (**a**). The periosteal bone formation has low signal on sagittal T1 WI (**b**) and post-contrast FST1WI (**c**).

Table 4 (Continued) **Lesions involving the outer surface of bone**

Lesion	MRI Findings	Comments
Noninterrupted periosteal reaction from hypovitaminosis A	Smooth and wavy periosteal and cortical thickening seen in the diaphyseal portions of one or multiple bones.	Vitamin A deficiency can result in anemia, dermatologic abnormalities (dry and scaly skin), growth retardation, osseous abnormalities, cranial nerve, and visual disorders.
Periosteal reaction from hypovitaminosis C (scurvy)	In children, periosleal elevation with new bone formation can be seen in the diaphyseal and metaphyseal portions of one or multiple bones from subperiosteal hemorrhage. Metaphyseal beak-like bone protrusions can occur from the abnormal zones of provisional calcification at the physeal plate, as well as subepiphyseal fractures. In adults, osteopenia with hemarthrosis can be associated with ischemic necrosis and fractures with mild periosteal reaction.	In young children, vitamin C deficiency after 4 to 10 months can result in infantile scurvy with clinical features including failure to thrive, petechial hemorrhages, ulcerated gingiva, hematemesis, melena. hematuria, and anemia. Clinical features associated with adult scurvy include anorexia, fatigue, weakness, petechial hemorrhages involving gingiva and skin, hemarthrosis, osteoporosis, ischemic necrosis, dermatologic disorders (dry and scaly skin), growth retardation, osseous and nerve disorders.
Syndromes of hyperostosis. osteitis, and skin lesions (SAPHO syndrome)	Periosteal elevation with cortical thickening can be seen as well as syndcsmophyte formation at one or multiple levels.	Syndrome that includes abnormalities such as synovitis, acne, pustulosis, hyperostosis with periosteal proliferation (sternum, clavicle, anterior ribs, symphysis pubis, femur, sacrum, iliac bones) and osteitis at the chest wall.
Neurofibromatosis type 1 (Fig. 4.32)	Undulating zones of periosteal bone formation can occur in the lower extremities in patients with NF1.	One of the most common genetic diseases with the involved locus on chromosome 17ql2 typically resulting in multiple neurofibromas. This is an autosomal dominant disorder resulting in mesodermal dysplasia affecting multiple organ systems. Can result in periosteal proliferation in the long bones of the lower extremities. **(See Atlas Chapter A 56)**

a

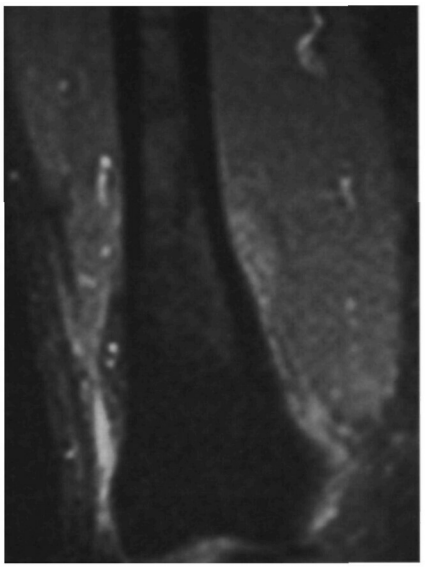

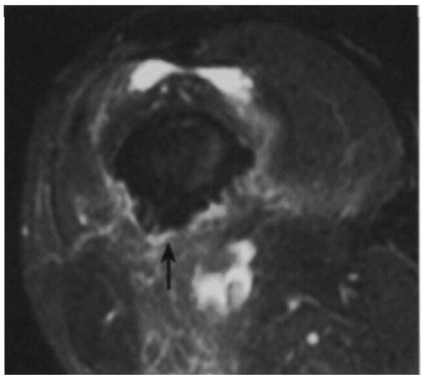

b, c

Figure 4.**32 a–c** Thickened irregular noninterrupted periosteal reaction in a patient with NF1 as seen on the AP radiograph (**a**). The periosteal bone formation has low signal on coronal (**b**) and axial (**c**) FS T2WI.

Table 4 (Continued) **Lesions involving the outer surface of bone**

Lesion	MRI Rndings	Comments
Periostitis associated with acute/subacute bone infarction (Fig. 4.33)	Acute and subacute bone infarcts typically show intramedullary zones with low-intermediate signal on T1WI and slightly high to high signal on FST2WI, often with heterogeneous Gd-contrast enhancement. Elevation of the periosteum surrounded by increased signal on FS T2WI and Gd-contrast enhancement on FS T1WI can also occur from associated periostitis.	Acute and subacute intramedullary bone infarcts can be associated with a periostitis that can be seen on MRI. **(See Atlas Chapter A 37)**

a, b

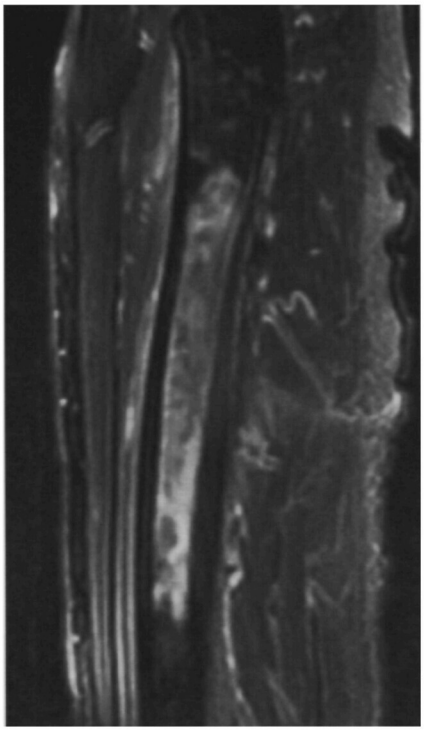

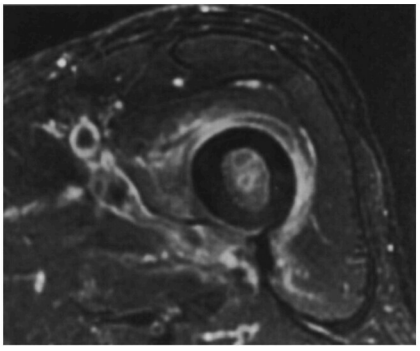

c

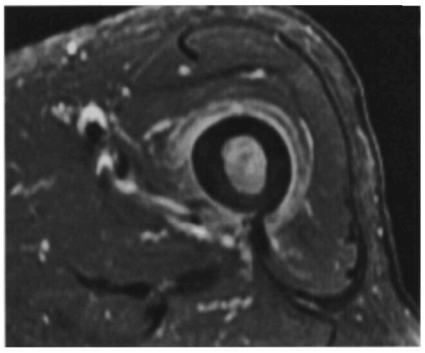

d

Figure 4.33 a-d Subacute bone infarct involving the diaphyseal marrow of the femur. The involved marrow has heterogeneous intermediate signal on sagittal T1WI (**a**), heterogeneous slightly high and high signal on sagittal (**b**) and axial (**c**) FST2WI, and shows Gd-contrast enhancement on axial FST1 WI (**d**). A thin linear zone with low signal is seen superficial to the cortex representing elevated periosteum, which is surrounded by zones of Gd-contrast enhancement and high signal on FST2WI.

Table 4 (Continued) Lesions involving the outer surface of bone

Lesion	MRI Findings	Comments
Malignant		
Parosteal osteosarcoma (Fig. 4.34)	Tumors occur at the surface of bone and extend outward with well-defined and/or indistinct margins. Tumors typically have mixed soft tissue and mineralized components. The mineralized portions of these tumors usually have low signal on T1WI, PDWI, T2WI, and FSPDWI and FST2WI. The soft tissue portions of these tumors often have low-intermediate signal on T1WI. intermediate to slightly high or high signal on T2WI, and high signal on FSPDWI and FST2WI. Areas of hemorrhage, cystic change, and/or necrosis with or without associated fluid-fluid levels may be present. Tumor extension into the medullary space can be seen in up to 50 % of cases. Nonnecrotic or nonmineralized soft tissue portions of these tumors usually show Gd- contrast enhancement as well as sites of invasion into the medullary space and adjacent soft tissues.	Malignant tumor, comprised of proliferating neoplastic spindle cells, that produce osteoid and/or immature tumoral bone. Parosteal osteosarcomas arise on the external surface of bone and account for 4 to 6 % of osteosa rcomas, occur in patients 6 to 80 years, median -27 years. **(See Atlas Chapter A 64)**

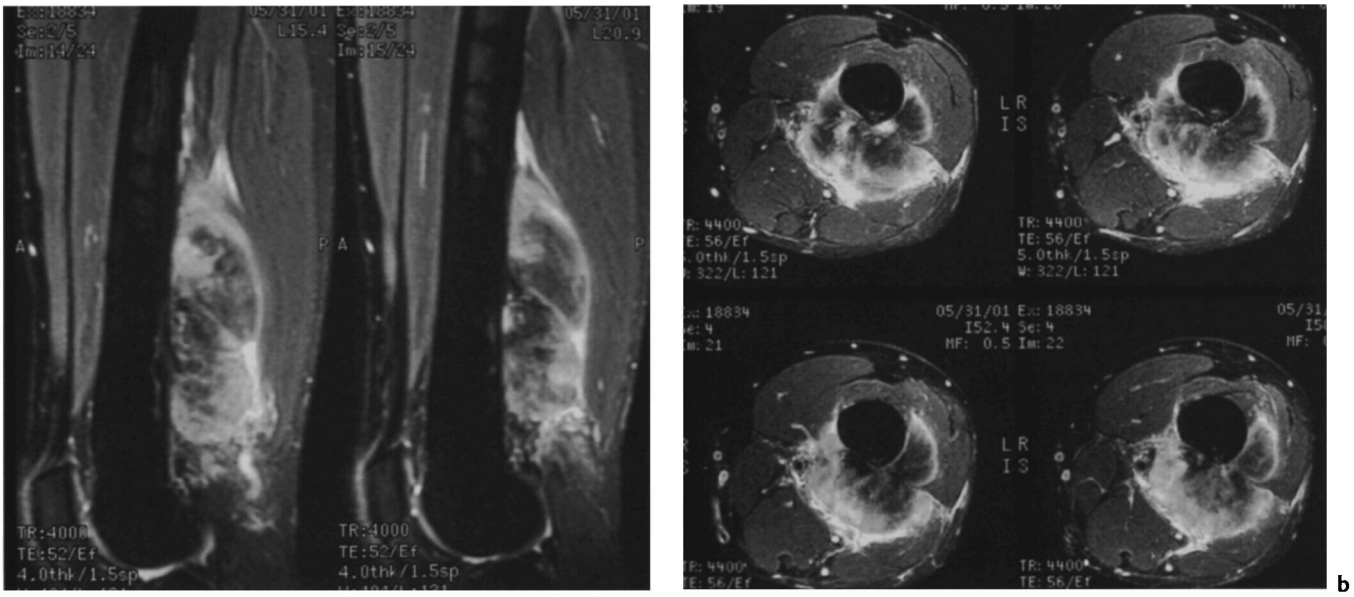

Figure 4.34 a, b Parosteal osteosarcoma along the outer dorsal surface of the distal femur that has heterogeneous low, slightly high, and high signal on sagittal (**a**) and axial (**b**) FST2WI.

Table 4 (Continued) Lesions involving the outer surface of bone

Lesion	MRI Findings	Comments
Periosteal osteosarcoma (Fig. 4.35)	Tumors usually involve the diaphyseal regions (femur > tibia > humerus > other bones) with associated cortical thickening and manifest as low signal on T1 WI and T2WI. Tumors often have a broad base along the outer cortex extending outward toward the adjacent soft tissues. Periosteal reaction, seen as linear zones of low signal on T1 WI and T2WI, can be associated with these tumors, as well as Codman's triangles. Tumors often have low-intermediate signal on T1WI and heterogenous slightly high to high signal on T2WI and FST2WI. Tumor extension into the marrow is uncommon, and when present is usually seen associated with a zone of cortical destruction.	Malignant tumor, comprised of proliferating neoplastic spindle cells, that produce osteoid and/or immature tumoral bone. Periostea! sarcoma has been proposed to represent a variant of parosteal osteogenic sarcoma that contains cartilaginous zones. Account for 1 to *2%* of osteosarcomas. occur in patients 11 to 57 years, median = 17 to 24 years. **(See Atlas Chapter A 64)**
Chondrosarcoma (Fig. 4.36)	MRI can easily demonstrate the thickness of cartilaginous caps of osteochondromas as well as erosive and/or destructive changes involving osteochondromas. Cartilage cap thickness exceeding 2cm is commonly associated with malignant degeneration or dedifferentiation of osteochondromas into secondary chondrosarcomas. Secondary chondrosarcomas from osteochondromas and periostea! chondrosarcomas have low-intermediate signal on T1WI, intermediate signal on PDWI, and heterogeneous intermediate-high signal on T2WI. Lesions show heterogeneous contrast enhancement, with or without Gd-contrast enhancement of adjacent soft tissues suggesting tumor invasion.	Malignant tumors containing cartilage formed within sarcomatous stroma. Primary chondrosarcomas represent neoplasms that occur without pre-existent lesions, whereas secondary chondrosarcomas arise from formerly benign cartilaginous lesions. Periosteal chondrosarcomas arc rare malignant cartilage tumors that occur on the surface of bone. Account for 12 to 21 % of malignant bone lesions, 21 to 26% of primary sarcomas of bone, 5 to 91 years, mean =40 years, median =26 to 59 years. **(See Atlas Chapter All)**
Chordoma (Fig. 4.37)	Chordomas are often midline in location, and usually have tabulated or slightly tabulated margins. Lesions can occur at the surface of bone, and often erode or destroy bone. Chondroid chordomas are either midline or off-midline in location. Chordomas typically have low-intermediate signal on T1WI and heterogeneous predominantly high signal on T2WI. Chordomas typically enhance with Gd-DTPA, often in a heterogeneous pattern.	Rare, locally aggressive, slow-growing low to intermediate malignant tumors derived from ectopic notochordal remnants along the axial skeleton. Account for 2-4% of primary malignant bone tumors, 1 -3 % of all primary bone tumors; and < 1 % of intracranial tumors. Patients range in age from 6 to 84 years, median = 58 years. **(See Atlas Chapter A12)**
Hemangioendothelloma (Fig. 4.38)	Intramedullary tumors usually have sharp margins that may be slightly tabulated. Lesions often have low-intermediate and/or high signal on T1WI and PDWI. and heterogeneous intermediate-high signal on T2WI and FST2WI with or without zones of low signal. Lesions can be multifocal. Extraosscous extension of tumor through zones of cortical destruction commonly occur. Lesions often show prominent heterogeneous Cd-contrast enhancement.	Low-grade malignant vasoformative/endothelial neoplasms that are locally aggressive and rarely metastasize compared with the high-grade endothelial tumors such as angiosarcoma. Account for < 1 % of primary malignant bone tumors. Patients range from 10 to 82 years, median = 36 to 47 years. Patients with multifocal lesions tend to be ~10 years younger on average than those with uni-focal tumors. **(See Atlas Chapter A 33)**

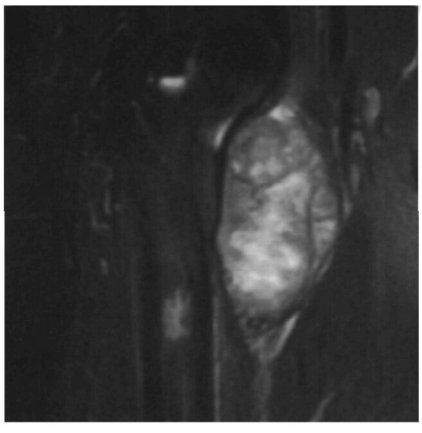

a

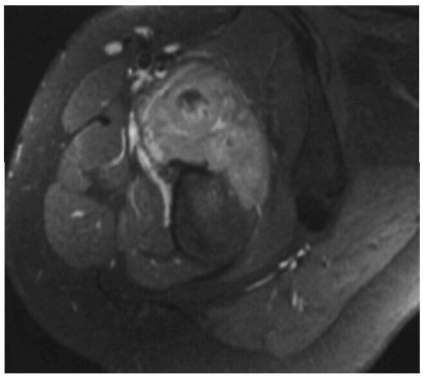

b

Figure 4.35 a, b Periosteal osteosarcoma along the outer anterior and medial margins of the proximal femur that has heterogeneous low, slightly high, and high signal on coronal FST2WI (**a**), and moderate Gd-contrast enhancement on axial FST1WI (**b**).

a

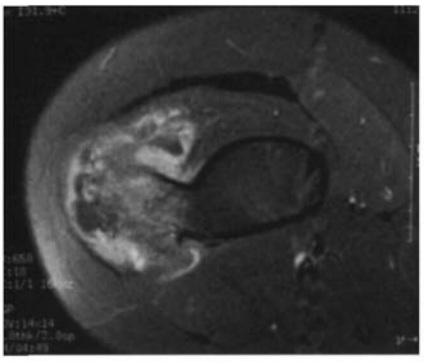

b

Figure 4.36 a, b Chondrosarcoma arising from an osteochondroma at the distal femur. The tumor has heterogeneous slightly high and high signal on coronal FST2WI (**a**) and shows heterogeneous Gd-contrast enhancement on axial FST1WI **(b**). Cortical destruction and intramedullary extension of tumor are also seen.

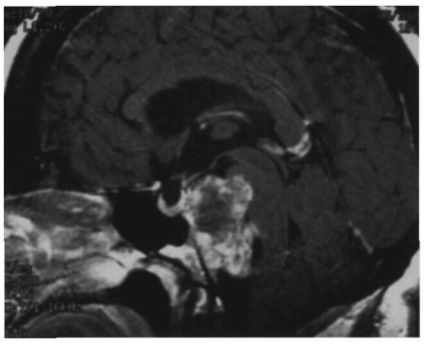

a

b

Figure *4.37 a, b* Chordoma along the endocranial surface of the clivus associated with bone erosion. The tumor shows heterogeneous Gd-contrast enhancement on sagittal T1WI (**a**), and has high signal on axial T2WI (**b**).

a

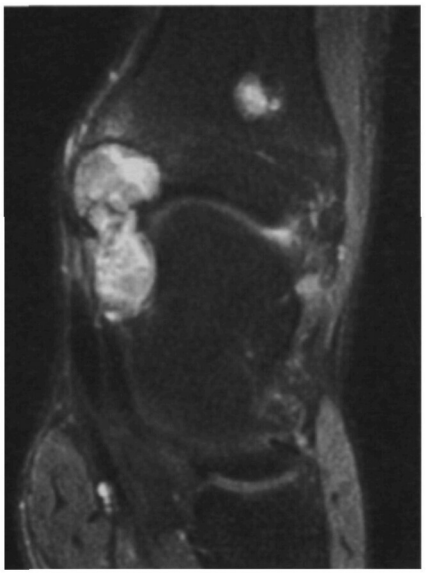

b

Figure 4.38 a, b Hemangioendothelioma involving the marrow of the distal tibia with cortical destruction, extension into the ankle joint and invasion of the talus as seen on sagittal PDWI (**a**) and coronal F5T2WI (**b**). Note that another focus of tumor is seen in the metaphyseal region.

Table 4 (Continued) Lesions involving the outer surface of bone

Lesion	MRI Findings	Comments
Sarcoma of soft tissue eroding into bone (Fig. 4.39)	Lesions with circumscribed or ill-defined margins may be associated with erosions and/or focal destruction of adjacent cortical bone with or without intraosseous extension of tumor.	Malignant tumors in extraosseous soft tissues can erode adjacent cortex and extend into the marrow.
Intramedullary primary sarcoma eroding through bone cortex (Fig. 4.40)	Poorly defined and/or circumscribed lesions in marrow with low-intermediate signal on T1WI; variable low, intermediate, and/or high signal on T2WI and FST2WI; and variable Gd-contrast enhancement associated with sites of cortical destruction and extraosseous tumor extension.	Malignant primary and metastatic tumors in marrow usually show trabecular bone destruction with frequent eventual cortical destruction and extraosseous tumor extension.
Metastatic lesions (Fig. 4.41)	Metastatic tumor within bone often appears as intramedullary zones with low-intermediate signal on T1 WI; low-intermediate to slightly high signal on PDWI; slightly high to high signal on T2WI and FST2WI. Sclerotic lesions often have low signal on T1WI; and mixed low, intermediate, and/or high signal on T2WI. Cortical destruction and tumor extension into the extraosseous soft tissues frequently occurs. Pathologic fractures can be associated with metastatic lesions involving tubular bones and vertebrae. Lesions show varying degrees of Gd-contrast enhancement. Periosteal reaction can occasionally be seen, but is uncommon.	Metastatic lesions typically occur in the marrow with or without cortical destruction and extraosseous tumor extension. Metastatic lesions occur rarely in the cortex alone. Metastatic lesions infrequently have associated single or multilayered periostea! reaction, (< 15 to 21 %). **(See Atlas Chapter A 50)**
Myeloma/plasmacytoma (Fig. 4.42)	Multiple (myeloma) or single (plasmacytoma) are well-circumscribed or poorly defined diffuse infiltrative lesions involving marrow, low-intermediate signal on T1WI. intermediate-high signal on T2WI, usually show Gd-contrast-enhancemenl, eventual cortical bone destruction and extraosseous extension.	Malignant tumors comprised of proliferating antibody-secreting plasma cells derived from single clones. Most common primary neoplasm of bone in adults. Most patients are older than 40 years, median =60 years. May have variable destructive or infiltrative changes involving the axial and/or appendicular skeleton. **(See Atlas Chapter A 52)**
Lymphoma (Fig. 4.43)	Single or multiple well-circumscribed or poorly defined infiltrative lesions involving marrow; low-intermediate signal on T1WI, intermediate-high signal on T2WI and FST2WI, often shows Gd-contrasl enhancement, +/- bone destruction and extraosseous extension. Diffuse involvement of vertebra with Hodgkin's lymphoma can produce an "ivory vertebra," which has low signal on T1WI and T2WI.	Lymphoid tumors with neoplastic cells typically within lymphoid tissue (lymph nodes and reticuloendolhelial organs). Unlike leukemia, lymphoma usually arises as discrete masses. Lymphomas are subdivided into Hodgkin disease (HD) and non-Hodgkin lymphoma (NHL). Almost all primary lymphomas of bone are B cell NHL. **(See Atlas Chapter A47)**

a

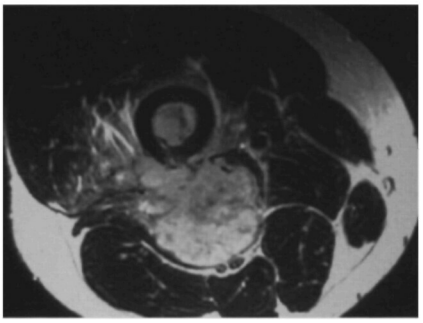

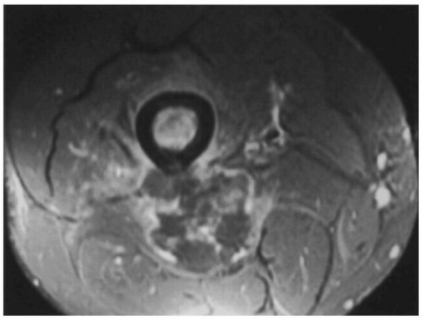

b, c

Figure 4.39a-c Clear cell sarcoma of soft tissue (formerly called malignant melanoma of soft parts) involving the deep soft tissue of the lower thigh. The tumor shows heterogeneous Gd-contrast enhancement on sagittal (**a**) and axial (**c**) FST1 WI, and has heterogeneous mostly high signal on axial T2WI (**b**). The tumor is associated with cortical destruction and intraosseous extension.

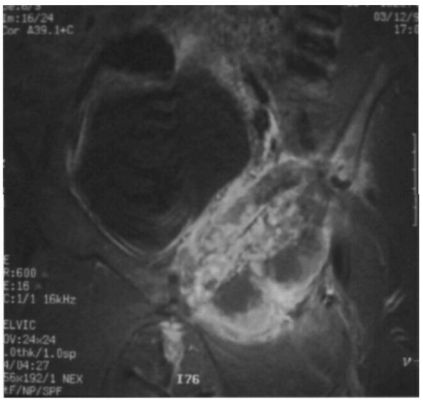

Figure 4.40 Ewing sarcoma involving the pubic bone, which extends from the marrow through destroyed cortical bone into the adjacent soft tissues. The tumor shows heterogeneous Gd-contrast enhancement on coronal FST1WI.

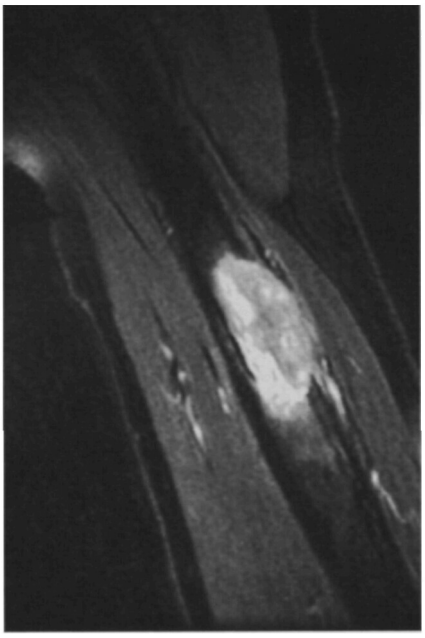

Figure 4.41 Metastatic lesion from lung carcinoma in the marrow of the humeral diaphysis associated with cortical destruction and extraosseous extension as seen on sagittal FST2WI.

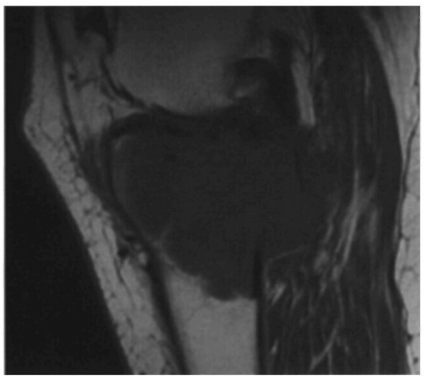

a

b

Figure 4.42 Myeloma involving the marrow of the proximal tibia with intermediate signal on sagittal T1WI (**a**) and heterogeneous high signal on FST2WI (**b**), associated with cortical destruction and extraosseous extension dorsally.

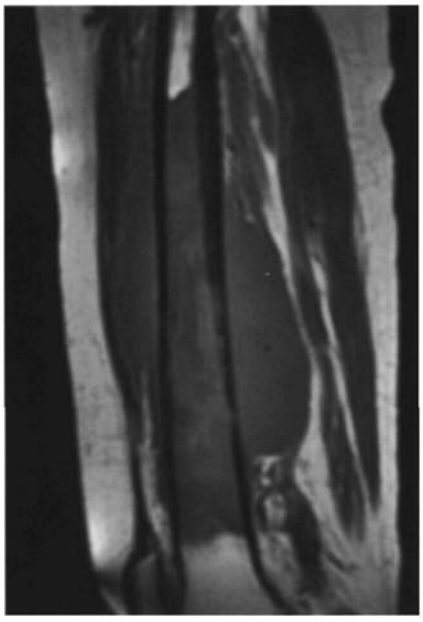

a

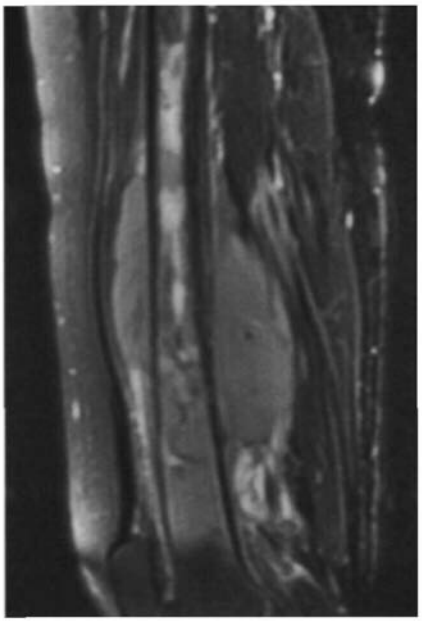

b

Figure 4.43 Large cell lymphoma involving the diaphyseal marrow of the femur, which has heterogeneous intermediate signal on sagittal T1WI (**a**) and heterogeneous slightly high and high signal on sagittal FST2WI (**b**). The tumor is associated with cortical destruction and extensive extraosseous extension.

Table 4 (Continued) **Lesions involving the outer surface of bone**

	MRI Rndings	Comments
Leukemia (Fig. 4.44)	Single or multiple well-circumscribed or poorly defined infiltrative lesions involving marrow; low-intermediate signal on T1WI, intermediate-high signal on T2WI and FST2WI, often shows Gd-contrast enhancement, +/- bone destruction and extraosseous extension.	Lymphoid neoplasms with involvement of bone marrow and with tumor cells in peripheral blood. In children and adolescents, acute lymphoblastic leukemia (ALL) is the most frequent type. In adults, chronic lymphocytic leukemia (small lymphocytic lymphoma) is the most common type of lymphocytic leukemia. Myelogenous leukemias are neoplasms derived from abnormal myeloid progenitor cells. Acute myelogenous leukemia (AML) occurs in adolescents and young adults, and represents ~20 % of childhood leukemia. Chronic myclogenous leukemia (CML) usually affects adults older than 25 years. **(See Atlas Chapter A 41)**
Malignant tumor with Interrupted periosteal reaction: sunburst or divergent pattern (Fig. 4.45)	Intramedullary neoplasm can be associated with zones of cortical destruction through which the lesion extends into the extraosseous soft tissues. Zones of reactive and/or tumoral bone formation under the elevated periosteum can have a divergent or "sunburst" appearance with low signal within the extraosseous tumor that often has slightly high to high signal on T2WI and FST2WI with corresponding Gd-contrast enhancement.	Periosteal elevation by tumor results in formation of a "sunburst or divergent pattern" of underlying bone spicules along vascular channels and fibrous bands (Sharpey's fibers) that are stretched out from the outer surface of bone cortex. Typically seen with osteosarcoma, rarely seen with osteoblastoma and osteoblastic metastasis (prostate carcinoma, lung carcinoma, carcinoid. breast carcinoma).
Malignant tumor with interrupted periosteal reaction: Codman's triangle (Fig. 4.46)	Intramedullary neoplasm or infection can be associated with zones of cortical destruction through which the lesions extend inlo the exlraosseous soft tissues. Lamellated and/or spiculated zones of periosteal reaction are often seen secondary to tumor invasion and perforation of bone cortex. Low signal from spicules of reactive and tumoral bone formation may have a "sunburst" appearance. Triangular zones of periosteal elevation (Codman's triangles) can be seen at the borders of zones of cortical destruction and tumor extension.	Codman's triangles are triangular zones of periosteal reaction or reactive bone at the borders of cortical destruction adjacent to extraosseous extension of neoplasms or infections from marrow. Can be seen with malignant primary bone neoplasms and lesions (osteosarcoma, Ewing sarcoma, chondrosarcoma, malignant fibrous histiocytoma, aneurysmal bone cyst, giant cell tumor), metastasis, osteomyelitis, or trauma.
Malignant tumor with interrupted periostea! reaction: disorganized pattern (Fig. 4.47)	Intramedullary neoplasm or infection seen with zones of cortical destruction through which the lesion extends into the extraosseous soft tissues. Irregular disorganized zones of periosteal reaction can be seen below the elevated periosteum.	Extraosseous extension of intramedullary tumor or infection results in disorganized lliin and/or thick irregular bone spicules under the elevated periosteum, Disorganized periosteal reaction is often seen with highly aggressive osteosarcomas, but can also be seen with other benign and malignant tumors that have associated complications of pathologic fracture or infection.

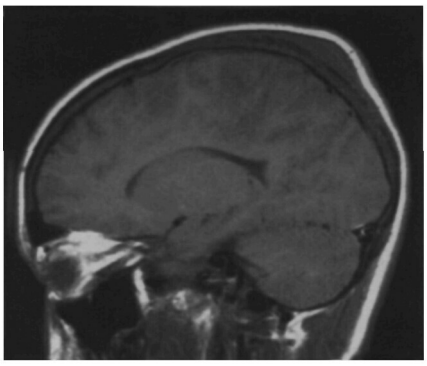

Figure 4.44 Acute lymphoblastic leukemia involving the marrow of the calvarium associated with cortical destruction and extraosseous extension on sagittal T1WI.

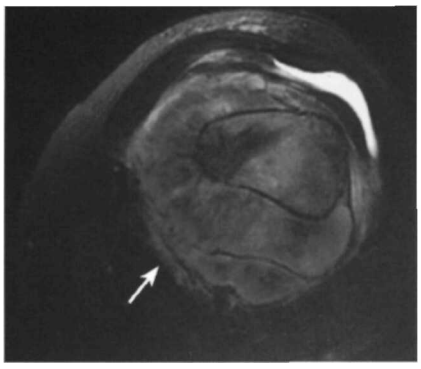

a

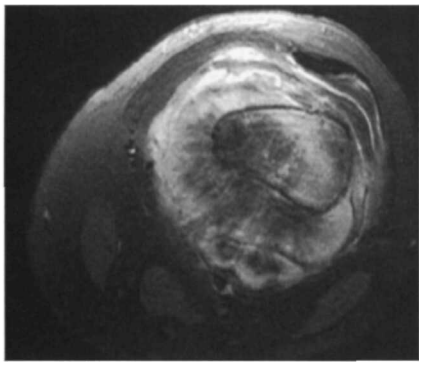

b

Figure 4.**45 a, b** Intramedullary osteogenic sarcoma with cortical destruction and extraosseous extension under an interrupted elevated periosteum. Beneath the elevated periosteum, divergent striated zones of low signal on FST2WI (**a**) and post-Gd-contrast FST1WI (**b**) are seen representing divergent or sunburst tumoral bone formation within the extraosseous neoplasm.

a

b, c

Figure 4.**46 a-c** Intramedullary osteogenic osteosarcoma with cortical destruction, extraosseous extension, and interrupted periosteal elevation. The AP radiograph (**a**) shows a destructive intraosseous lesion with mineralized ossified matrix, cortical destruction, extraosseous tumor extension with disorganized tumoral bone formation, and a Codman's triangle at the inferior borders. The tumor has mixed low, intermediate, and high signal on coronal T1WI (**b**), and shows prominent Gd-contrast enhancement on coronal FST1WI (**c**).

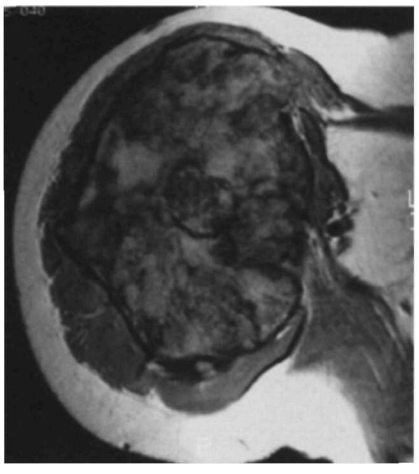

a

b

Figure 4.**47 a, b** Intramedullary osteogenic osteosarcoma with cortical destruction, extraosseous extension, and interrupted periosteal elevation. The destructive intraosseous tumor with extensive extraosseous extension contains irregular zones of low signal on axial PDWI (**a**) and axial T2WI (**b**) representing disorganized tumoral/ periosteal bone formation.

Table 4 (Continued) **Lesions involving the outer surface of bone**

Lesion	MRI Findings	Comments
Malignant tumor with interrupted periosteal reaction: "hair on end" or perpendicular-oriented spicules of periosteal reaction (Fig. 4.48)	Intramedullary neoplasm or infection seen with zones of cortical destruction through which the lesions extend into the extraosseous soft tissues. Parallel spiculated zones ("hair on end" pattern) of periosteal reaction oriented perpendicular to the long axis of bone can be seen within the extraosseous lesion often under an elevated periosteum.	Extraosseous extension of intramedullary tumor or infection results in a perpendicular ("hair on end," or "honeycomb") pattern of thin bone spicules radially oriented under the elevated periosteum. These bone spicules tend to be thin and oriented along radially oriented blood vessels extending from the cortical surface within the lesions. Most frequently seen with Ewing sarcoma, sometimes with osteosarcoma, and rarely with infection.
Malignant tumor with interrupted periosteal reaction: "onion skin" multilayered, or multilamellated periosteal reaction oriented parallel to the long axis of bone (Fig. 4.49)	Intramedullary neoplasm, inflammatory lesion, or infection seen with zones of cortical destruction through which the lesions extend into the extraosseous soft tissues. Multiple layers of periosteal reaction oriented parallel to cortical bone ("onion skin" pattern) can be seen within the extraosseous lesion often under an elevated periosteum.	Extraosseous extension of intramedullary tumor, noninfectious inflammatory lesions, or infection results in a multilayered periosteal reaction. Most frequently seen with Ewing sarcoma, sometimes with osteosarcoma, lymphoma, and rarely with infection.

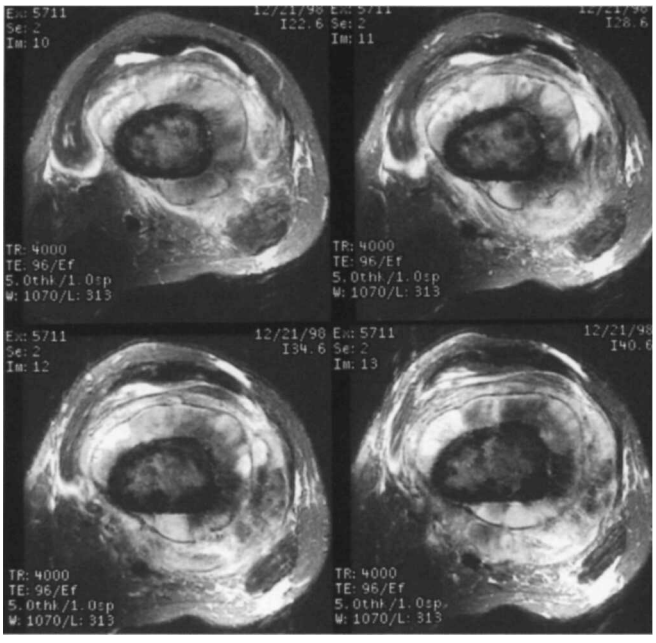

Figure **4.48** Intramedullary osteogenic sarcoma with cortical destruction and extraosseous extension under an interrupted elevated periosteum. Beneath the elevated periosteum, "hair on end" as well as divergent striated/ "sunburst-type" zones of low signal on FST2WI are seen representing tumoral bone formation within the extraosseous neoplasm.

a **b**

Figure 4.**49 a, b** Intramedullary telangiectatic osteosarcoma in the distal femur associated with cortical destruction with extraosseous tumor extension. Multiple layers of periosteal reaction oriented parallel to cortical bone *(onion skin* pattern) and a Codman's triangle inferiorly are seen on an AP radiograph (**a**). An intraosseous tumor is seen extending through destroyed cortical bone beneath an interrupted periosteum on coronal (**b**) FST2WI. Multiple thin layers or periosteal reaction are seen in the extraosseous tumor on axial FST2WI.

References

Calcific Tendinitis

Flemming DJ, Murphey MD, Shekitka KM, Temple HT, Jelinek JJ, Kransdorf MJ. Osseous involvement in calcific tendonitis: a retrospective review of 50 cases. *AJR* 2003; 181:965-972.

Periosteal Reaction

Resnick D. Enostosis, hyperostosis, and periostitis. In: Resnick D, ed. *Diagnosis of Bone and Joint Disorders,* 4th ed. Philadelphia, Pa: W.B. Saunders; 2002:5:4870-4919.

Wenaden AET, Szyszko TA, Saifuddin A. Imaging of periosteal reactions associated with focal lesions of bone. *Clin Radiol* 2005;60:439-456.

Hemophilic Pseudotumor

Geyskens W, Vanhoenacker FM, Van der Zijden T, Peerlinck K. MR imaging of intra-osseous hemophilic pseudotumor: case report and review of the literature *JBR-BTR* Nov-Dec 2004;87(6):289-293.

Jaovisidha S, Ryu KN, Hodler J, Schweitzer ME, Sartoris DJ, Resnick D. Hemophilic pseudotumor: spectrum of MR findings. *Skeletal Radiol* 1997;26:468-474.

Park JS, Ryu KN. Hemophilic pseudotumor involving the musculoskeletal system: spectrum of radiologic findings. *AJR* 2004;183:55-61.

Primary Hypertrophic Osteoarthropathy

Araki Y, Tsukaguchi I, Nakamura H. Pachydermoperiostosis involving the skull and spine: MR findings. *AJR* March 1993;160(3):664-665.

Capelastegui A, Astigarraga E, García-Iturraspe C. MR findings in pulmonary hypertrophic osteoarthropathy. *Clin Radiol* January 2000;55(1): 72-75.

Demirpolat G, Sener RN, Stun EE. MR imaging of pachydermoperiostosis. *J Neuroradiol* March 1999;26(l):61-63.

Loredo R, Pathria MN, Salonen D, Resnick D. Magnetic resonance imaging in pachydermoperiostosis. *Clin Imag* July-September 1996;20(3): 212-218.

Resnick D. Enostosis, hyperostosis, and periostitis. In: Resnick D, ed. *Diagnosis of Bone and Joint Disorders,* 4th ed. Philadelphia, Pa: W.B. Saunders; 2002:5:4870-4919.

Secondary Hypertrophic Osteoarthropathy

Capelastegui A, Astigarraga E, García-Iturraspe C. MR findings in pulmonary hypertrophic osteoarthropathy. *Clin Radiol* January 2000;55(1): 72-75.

Resnick D. Enostosis, hyperostosis, and periostitis. In: Resnick D, ed. Diagnosis *of Bone and Joint Disorders,* 4th ed. Philadelphia, Pa: W.B. Saunders; 2002:5:4870-4919.

Sainani Nl, Lawande MA, Parikh VP, Pungavkar SA, Patkar DP, Sase KS. MRI diagnosis of hypertrophic osteoarthropathy from a remote childhood malignancy. *Skeletal Radiol* 2007 Jun;36 Suppl 1:63-6. Epub Sep 5 2006.

Varan A, Kutluk T, Demirkazik FB, Akyüz C, Büyükpamukcu M. Hypertrophic osteoarthropathy in a child with nasopharyngeal carcinoma. *Pediatr Radiol* 2000:30:570-572.

Periosteal Reaction from Venous Stasis

Resnick D. Enostosis, hyperostosis, and periostitis. In: Resnick D, ed. *Diagnosis of Bone and Joint Disorders,* 4th ed. Philadelphia, Pa: W.B. Saunders; 2002:5:4870-4919.

Wenaden AET, Szyszko TA, Saifuddin A. Imaging of periosteal reactions associated with focal lesions of bone. *Clin Radiol* 2005;60:439-456.

Infantile Cortical Hyperostosis (Caffey Disease)

Katz DS, Eller DJ, Bergman G, Blankenberg FG. Caffey's disease of the scapula: CT and MR findings. *AJR* January 1997;168(l):286-287.

Resnick D. Enostosis, hyperostosis, and periostitis. In: Resnick D, ed. *Diagnosis of Bone and Joint Disorders,* 4th ed. Philadelphia, Pa: W.B. Saunders; 2002:5:4870-4919.

Saatci I, Brown JJ, McAlister WH. MR findings in a patient with Caffey's disease. *Pediatr Radiol* November 1996:26(1):68-70.

Thyroid Acropachy

Fatourechi V, Ahmed DDF, Schwartz KM. Thyroid acropachy: report of 40 patients treated at a single institution in a 26-year period. *J Clin Endocrin Metab* December 2002;87(12):5435-5441.

Vanhoenacker FM, Pelckmans MC, De Beuckeleer LH, Colpaert CG, De Schepper AM. Thyroid acropachy: correlation of imaging and pathology. *Eur Radiol* 2001 ;11(6):1058-1062.

Hypervitaminosis and Hypovitaminosis

Lips P. Hypervitaminosis A and fractures. *N Engl J Med* 2003;384: 347-349.

Romero JB, Schreiber A, Von Hochstetter AR, Wagenhauser FJ, Michel BA, Theiler R. Hyperostotic and destructive osteoarthritis in a patient with vitamin A intoxication syndrome: a case report. *Bull Hosp Jt Dis* 1996;54:169-174.

Jiang YB, Wang YZ, Zhao J, et al. Bone remodeling in hypervitaminosis D3. radiologic-microangiographic-pathologic correlations. *Invest Radiol* 1991;26:213-219.

Resnick D. Hypervitaminosis and hypovitaminosis. In: Resnick D, ed. *Diagnosis of Bone and Joint Disorders,* 4th ed. Philadelphia, Pa: W.B. Saunders; 2002:4:3456-3464.

Syndromes of Hyperostosis, Osteitis, and Skin Lesions (SAPHO Syndrome)

Boutin RD, Resnick D. The SAPHO syndrome: an evolving concept for unifying several idiopathic disorders of bone and skin. *AJR* 1998; 170:585-591.

Davies AM, Marino AJ, Evans N, Grimer RJ, Deshmukh N, Mangham DC. SAPHO syndrome: 20 year followup. *Skeletal Radiol* 1999;28: 159-162.

Kirchoff T, Merkesdal S, Rosenthal H, et al. Diagnostic management of patients with SAPHO syndrome: use of MR imaging to guide bone biopsy at CT for microbiological and histological work-up. *Eur Radiol* 2003:13:2304-2308.

Resnick D. Enostosis, hyperostosis, and periostitis. In: Resnick D, ed. *Diagnosis of Bone and Joint Disorders,* 4th ed. Philadelphia, Pa: W.B. Saunders; 2002:5:4870-4919.

Interrupted Periosteal Reaction

Resnick D. Enostosis, hyperostosis, and periostitis. In: Resnick D, ed. Diagnosis *of Bone and Joint Disorders,* 4th ed. Philadelphia, Pa: W.B. Saunders; 2002:5:4870-4919.

Wenaden AET, Szyszko TA, Saifuddin A. Imaging of periosteal reactions associated with focal lesions of bone. *Clin Radiol* 2005:60:439-456.

Table 5 Lesions associated with thickening of bone cortex

Lesion	MRI Findings	Comments
Benign		
Osteoid osteoma (Fig. 5.1)	Typically shows dense fusiform thickening of the cortex that has low to intermediate signal on T1 W, PDWI, T2WI, and FST2WI. Within the thickened cortex, a spheroid or ovoid zone (nidus) measuring < 1.5cm is typically seen. The nidus can have irregular, distinct or indistinct margins relative to the adjacent region of cortical thickening. The nidus can have low-intermediate signal on T1 WI and PDWI, and low-intermediate or high signal on T2WI and FST2WI. Calcifications in the nidus can be seen as low signal on T2WI. After Gd-contrast administration, variable degrees of enhancement are seen at the nidus.	Benign painful osteoblastic lesion comprised of a circumscribed nidus < 1.5 cm usually surrounded by reactive bone formation. Accounts for 11 to 13 % of primary benign bone tumors. Occurs in patients 6 to 30 years, median = 17 years. Approximately 75% occur in patients less than 25 years. **(See Atlas Chapter A60)**
Osteoblastoma (Fig. 5.2)	Lesions appear as spheroid or ovoid zone measuring >1.5 to 2cm located within medullary and/or cortical bone with low-intermediate signal on T1WI; low-intermediate to slightly high signal on PDWI; and low-intermediate and/or high signal on T2WI and FST2WI. Calcifications or areas of mineralization can be seen as zones of low signal on T2WI. After Gd-contrast administration, osteoblastomas show variable degrees of enhancement. Zones of thickened cortical bone and medullary sclerosis that are often seen adjacent to osteoblastomas typically show low signal on T1 W, T2WI, and FST2WI. Poorly defined zones of marrow signal alteration consisting of low-intermediate signal on T1WI, high signal on T2WI and FST2WI, and corresponding Gd-contrast enhancement can be seen in the marrow adjacent to osteoblastomas as well as within the extraosseous soft tissues.	Rare benign bone-forming tumors that are histologically related to osteoid osteomas. Osteoblastomas are larger than osteoid osteomas and show progressive enlargement. Account for 3 to 6% of primary benign bone tumors and < 1 to 2 % of all primary bone tumors. Occurs in patients 1 to 30years. median - 15 years, mean age -20 years. Approximately 90 % of lesions occur in patients less than 30 years. **(See Atlas Chapter A 61)**
Osteoma (Fig. 5.3)	Lesions typically appear as well-circumscribed zones of dense cortical bone with low signal on T1WI, PDWI, T2WI, and FST2WI. No infiltration into the adjacent soft tissues is seen by osteomas. Zones of bone destruction or associated soft tissue mass lesions are not associated with osteomas. Periosteal reaction is not associated with osteomas except in cases with coincidental antecedent trauma.	Benign primary bone lesions composed of dense lamellar, woven, and/or compact cortical bone usually located at the surface of bones. Account for less than 1 % of primary benign bone tumors. Occur in patients 16 to 74 years, most frequent in 6th decade. **(See Atlas Chapter A 62)**
Juxtacortical chondroma (Fig. 5.4)	Lesions are located at the bone surface and are usually tabulated with low-intermediate signal on T1 WI, which is hypo- or isointense relative to muscle. Lesions usually have heterogeneous predominantly high signal on T2WI. Lesions are surrounded by low signal borders on T2WI representing thin sclerotic reaction. Areas of low signal on T2WI are secondary to matrix mineralization. Edema is not typically seen in nearby medullary bone. Lesions often show a peripheral pattern of Gd-contrast enhancement that correlates to fibrovascular bundles surrounding the cartilage lobules.	Benign protuberant hyaline cartilaginous tumors that arise from the periosteum and superficial to bone cortex. Account for < 1 % of bone lesions. Juxtacortical chondromas represent ~5 to 12% of chondromas. Patients range from 4 to 77 years, median = 26 years. **(See Atlas Chapter A 9)**
Parosteal lipoma	Lesions often have lobular margins and are immediately adjacent to the outer intact surface of adjacent bone. Lesions typically have fat signal on MRI, as well as zones of low signal on T1WI and T2WI from ossification changes that can occur within these lesions and at the junction with bone cortex. Zones with intermediate signal on T1WI and high signal on T2WI can occur in these lesions secondary to cartilaginous contents.	Rare, benign, slow-growing painless tumors with mature adipose tissue associated with the periosteum of bone. Account for 0.3 % of lipomas; typically occur in patients 40 to 60 years. Common sites include the femur, proximal radius, tibia, and humerus. **(See Atlas Chapter A43)**

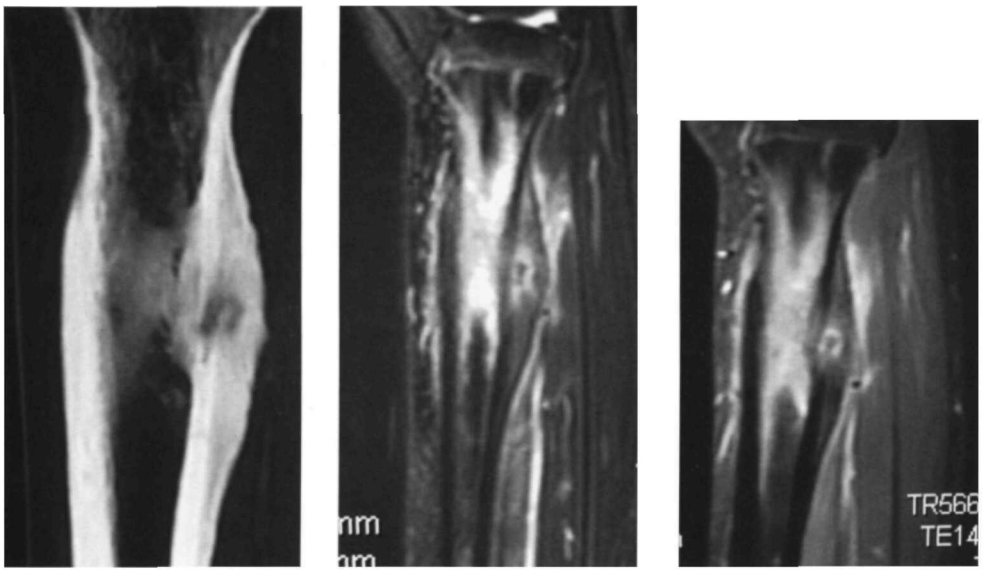

a b, c

Figure 5.**1 a-c** Osteoid osteoma involving the cortex of the proximal tibial shaft in a 15-year-old female. Sagittal CT image (**a**) shows dense fusiform osteosclerosis surrounding a small radiolucent zone (nidus) with a central calcification. The nidus has high signal on sagittal FST2WI (**b**) and the small central calcification has low signal. The thickened cortex has low-intermediate and slightly high signal on FST2WI, and is associated with periosteal reaction with high signal. The nidus shows Gd-contrast enhancement on sagittal FST1WI (**c**). Prominent Gd-contrast enhancement is seen at the periosteal reaction, and mild diffuse enhancement is seen in the cortical thickening adjacent to the nidus. Poorly defined zones of high signal on FST2WI and corresponding Gd-contrast enhancement on FST1WI are also seen in the marrow adjacent to the lesion.

a b, c

Figure 5.**2a-c** Osteoblastoma in the anterior left sacral alum in a 12-year-old boy. Prominent dense sclerotic reaction is seen in cortical and medullary bone adjacent to the mixed radiolucent and radiodense lesion on the axial CT image (**a**) and AP radiograph (**b**). The lesion has intermediate to slightly high signal peripherally surrounding a central zone with low and slightly high signal on coronal FST2WI (**c**). Poorly defined zones of high signal on FST2WI are seen in the marrow and soft tissues adjacent to the lesion.

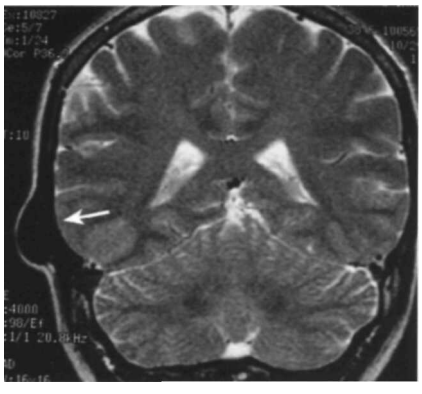

Figure 5.**3** Osteoma involving the outer table of the skull. A circumscribed lesion with low signal on coronal T2WI is seen protruding from the right side of the skull.

Figure 5.**4** Juxtacortical chondroma involving the outer surface of the proximal humerus of a 28-year-old man. Periosteal and cortical bone thickening is seen at the base of the lesion. The lesion shows irregular zones of Gd-contrast enhancement on sagittal FST1WI.

Table 5 (Continued) **Lesions associated with thickening of bone cortex**

Lesion	MRI Findings	Comments
Malignant		
Parosteal osteosarcoma (Fig. 5.5)	These tumors occur at the surface of bone and extend outward with well-defined and/or indistinct margins. Portions of these tumors that extend toward the juxtacortical soft tissues typically have mixed soft tissue and mineralized components. The mineralized portions of these tumors tend to be dense centrally and at the sites of contiguity (broad-based or stalk-like) with the outer cortical margins. The mineralized portions of these tumors usually have low signal on T1WI, PDWI, T2WI, FS PDWI and FST2WI. The soft tissue portions of these tumors often have low-intermediate signal on T1WI, intermediate to slightly high or high signal on T2WI, and high signal on FSPDWI and FST2WI. Tumor extension into the medullary space seen with MRI can occur in up to 50%. After Gd-contrast administration, non-necrotic or nonmineralized soft tissue portions of these tumors usually show enhancement as well as sites of invasion into the medullary space and adjacent soft tissues.	Malignant tumor comprising proliferating neoplastic spindle cells that produce osteoid and/or immature tumoral bone. Parosteal osteosarcomas arise on the external surface of bone and account for 4 to 6 % of osteosarcomas, occur in patients 6 to 80 years, median = 27 years. **(See Atlas Chapter A 64)**
Intraosseous osteosarcoma (Fig. 5.6)	Intramedullary osteosarcomas often have zones of cortical destruction through which tumors extend toward the extraosseous soft tissues under an elevated periosteum. Lamellated and/or spiculated zones of bone formation can occur under the periosteal elevation secondary to tumor invasion and perforation of bone cortex. Low signal from spicules of periosteal. reactive, and tumoral bone formation may have a divergent ("sunburst") pattern, perpendicular ("hair on end") pattern, or disorganized or complex appearance.	Malignant tumor comprised of proliferating neoplastic spindle cells which produce osteoid and/or immature tumoral bone. Intraosseous osteosarcoma accounts for 91 to 95% of osteosarcomas. Osteogenic sarcoma has two age peaks of incidence. The larger peak occurs between the ages of 10 and 20 and accounts for over half of the cases. The second smaller peak occurs in adults over 60 years and accounts for ~10 % of the cases. **(See Atlas Chapter A 64)**
Adamantinoma (Fig. 5.7)	Most frequently appear as a solitary labulated focus versus a multinodular pattern of signal alteration in thickened bone cortex. More than half involve bone cortex and marrow compared with only cortical involvement. Tumor foci in bone typically have low-intermediate signal on T1WI and PDWI, and slightly high to high signal on T2WI and FST2WI. Lesions usually show prominent Gd-contrasl enhancement. Adamantinomas with a multinodular pattern have enhancing nodules which have high signal on T2WI and FST2WI separated by zones of low signal from intervening cortical bone.	Rare low-grade malignant bone tumors consisting of epithelial cells surrounded by spindle cells and osteo-fibrous tissue that often involve the shaft of the tibia account for < 1 % of primary bone tumors. Patients range in age from 3 to 86 years, median = 19 to 25 years, average = 35 years, most common in 3rd and 4th decades. **(See Atlas Chapter A1)**

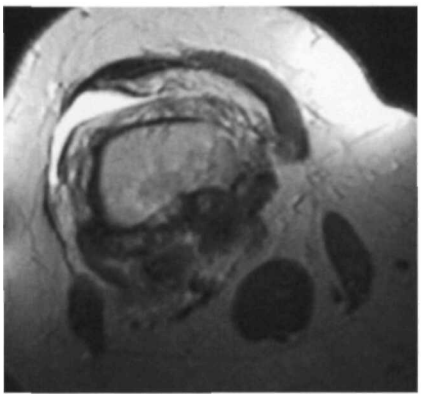

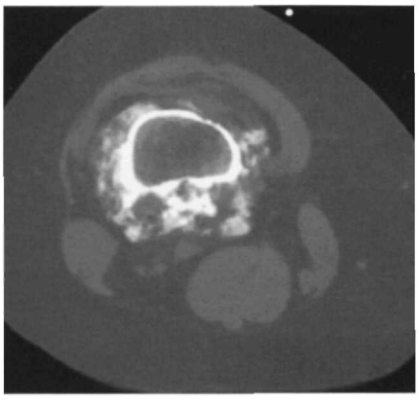

a **b, c**

Figure 5.**5 a-c** Parosteal osteosarcoma of the dorsal distal portion of the femur in a 45-year-old woman. The tumor has mixed low, intermediate, slightly high and high signal on sagittal (**a**) FST2WI and axial T2WI (**b**). The tumor extends into the marrow through a zone of cortical destruction. The mineralized portions of this tumor have low signal on T2WI and FST2WI. The axial CT image (**c**) shows a soft tissue tumor containing mineralized osteoid along the dorsal, medial, and lateral outer margins of the bone cortex. Small zones of cortical erosion are seen. Slight thickening of the bone cortex is also seen at several sites.

a **b**

Figure 5.**6 a, b** Conventional intramedullary osteosarcoma in the marrow of the distal metadiaphyseal portion of the femur in a 9-year-old boy. The tumor has heterogeneous intermediate signal on coronal T1WI (**a**) and heterogeneous high signal on coronal FST2WI (**b**). The intramedullary tumor is associated with zones of cortical destruction, periosteal elevation, and extraosseous extension.

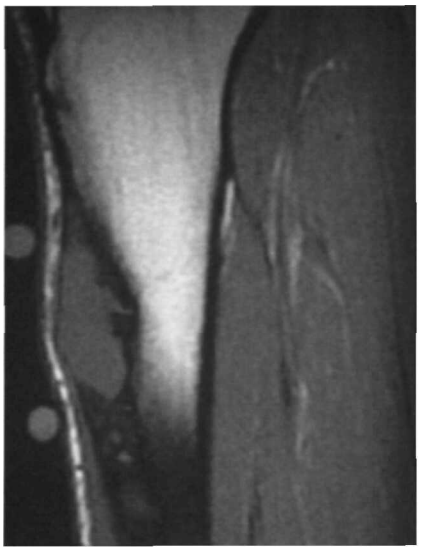

a **b**

Figure 5.**7 a, b** Adamantinoma involving the anterior cortex of the proximal shaft of the tibia. The lesion expands the cortex and has heterogeneous intermediate signal on sagittal T1WI (**a**) and high signal on sagittal FST2WI(**b**).

Table 5 (Continued) **Lesions associated with thickening of bone cortex**

Lesion	MRI Findings	Comments
Other lesions		
Heterotopic ossification (Fig. 5.8)	Long-standing lesions can have variable low signal on T1WI, PDWI, and T2WI depending on the degree of mineralization/ossification, fibrosis. and hemosiderin deposition. Zones of high signal on T1WI and T2WI may occur from fatty marrow metaplasia. Gd-contrast enhancement in old mature lesions is often minimal or absent. Signal abnormalities within bone marrow are usually absent.	Represents localized non-neoplastic reparative lesions that arc comprised of reactive hypercellular fibrous tissue, cartilage, and/or bone. Can arise secondary to trauma (myositis ossificans circumscripta, ossifying hematoma), although may also occur without a history of prior injury (pseudomalignant osseous tumor of the soft tissues). **(See Atlas Chapter A 53)**
Osteofibrous dysplasia (Fig. 5.9)	Osteofibrous dysplasia often shows multiple irregular inlracortical zones of low-intermediate signal on T1 W images, intermediate to slightly high signal on PDWI, and high signal on T2WI and FS T2WI separated by irregular zones of low signal on T1WI and T2WI, the latter representing thickened sclerotic cortical bone. The outer cortical margins can be expanded and thinned. Intracortical lesions usually show prominent Gd-contrast enhancement. Thin juxtacortical/periosteal enhancement may be seen in lesions with thinned and expanded cortical margins.	Rare self-limited benign fibro-osseous lesion primarily involving the anterior midshaft of the tibial cortex in children and adolescents. **(See Atlas Chapter A 59)**
Fibrous dysplasia (Figs. 5.10, 5.11)	MRI features depend on the proportions of bony spicules, collagen, fibroblastic spindle cells, hemorrhagic and/or cystic changes, and associated pathologic fracture if present. Lesions arc usually well-circumscribed, and have low or low-intermediate signal on T1WI and PDWI. On T2WI, lesions have variable mixtures of low, intermediate, and/or high signal often surrounded by a low signal rim of variable thickness. Internal septations and cystic changes are seen in a minority of lesions. Bone expansion and cortical thickening can be seen. Lesions show Gd-contrast enhancement that varies in degree and pattern. Periosteal and juxtacortical enhancement can be seen in lesions with associated pathologic fractures.	Benign medullary fibro-osseous lesion which can involve a single site (mono-ostotic) or multiple locations (poly-ostotic). Thought to occur from developmental failure in the normal process of remodeling primitive bone to mature lamellar bone with resultant zone or zones of immature trabeculae within dysplastic fibrous tissue. Lesions do not mineralize normally and result in loss of mechanical strength predisposing to deformity and pathologic fracture. Accounts for ~10% of benign bone lesions. Patients range in age from <1 to 76 years. 75% occur before the age of 30 years. **(See Atlas Chapter A 27)**

a

b

Figure 5.**8 a, b** Extensive pathologically proven heterotopic ossification that has blended into the outer cortical surface of the distal ulna as seen on the lateral radiograph (**a**) and sagittal T1WI (**b**).

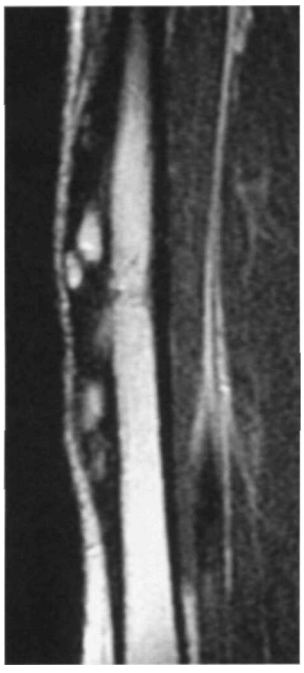

a

b

Figure 5.**9 a, b** Osteofibrous dysplasia involving the anterior cortex of the proximal shaft of the tibia. The lesion expands the cortex, within which are multiple zones of heterogeneous high signal on sagittal T2WI (**a**) that shows corresponding Gd-contrast enhancement on sagittal FST1WI (**b**).

a

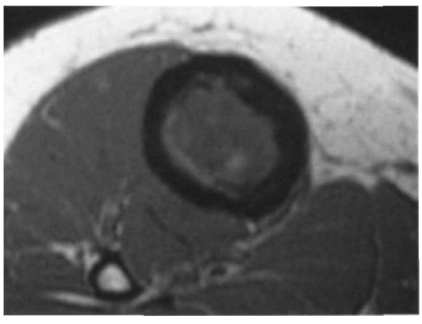

b

Figure 5.**10 a, b** Fibrous dysplasia involving the proximal shaft of the tibia with cortical thickening as seen on the AP radiograph (**a**) and axial T1WI (**b**). Also seen is the intermediate signal of the lesion within the marrow on axial T1WI.

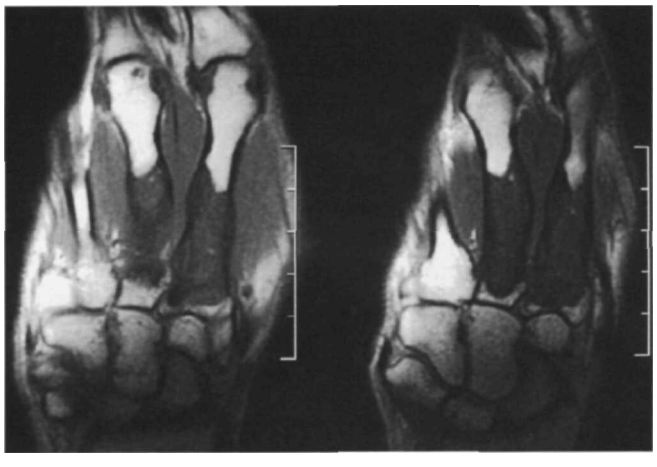

Figure 5.**11** Polyostotic fibrous dysplasia involving adjacent metacarpal bones with cortical thickening and intermediate marrow signal alteration on coronal T1WI.

Table 5 (Continued) **Lesions associated with thickening of bone cortex**

Lesion	MRI Findings	Comments
Focal fibrocartilaginous dysplasia (Fig. 5.12)	Cortical thickening seen along concave side of tibia vara, and asymmetric thickening of the epiphysis medially.	Uncommon benign condition causing deformities of long bones in children. Most frequent at proxial tibia in young children; typically unilateral; results in tibia vara. Also occurs less frequently in femur, humerus, and ulna. Lesions show dense collagenous tissue that may spontaneously regress. Corrective osteomy may be needed for severe and persistent lesions.
Melorheostosis (Fig. 5.13)	MRI signal varies based on the relative proportions of, mineralized osteoid, chondroid, and soft tissue components in these lesions. Mineralized osteoid zones involving bone cortex typically have low signal on T1WI and T2WI, no Gd-contrast enhancement. Soft tissue lesions may also occur adjacent to the cortical lesions, which have mixed signal on T1WI and T2WI.	Rare bone dysplasia with cortical thickening that has a "flowing candle wax" configuration. Associated soft tissue masses occur in ~25 %. The soft tissue lesions often contain mixtures of chondroid material, mineralized osteoid, and fibrovascular tissue. **(See Atlas Chapter A 62)**
Healing and healed fractures (Figs. 5.14, 5.15)	Healing stress or traumatic fractures can have periosteal elevation with associated adjacent high signal on T2WI and FST2WI, as well as poorly defined marrow zones with high signal on T2WI and FST2WI **(Fig. 5.14).** Poorly defined zones of Gd-contrast enhancement can be seen in the juxtacortical soft tissues and marrow. Maturation of the periosteal reaction can lead to cortical thickening **(Fig. 5.15).**	Fracture results in localized hemorrhage followed by an inflammatory response after 48 hours that leads to granulation tissue ingrowth, and activation of the osteoblasts in the periosteum. Periosteal bone formation results in cortical thickening. In addition endosteal sclerosis with stress fractures can be seen on radiographs, CT, and MRI.

a

b

Figure 5.12 **a, b** Focal fibrocartilaginous dysplasia with cortical thickening seen along the concave side of the tibia vara, and asymmetric thickening of the epiphysis medially on the AP radiograph (**a**) and coronal T1WI (**b**).

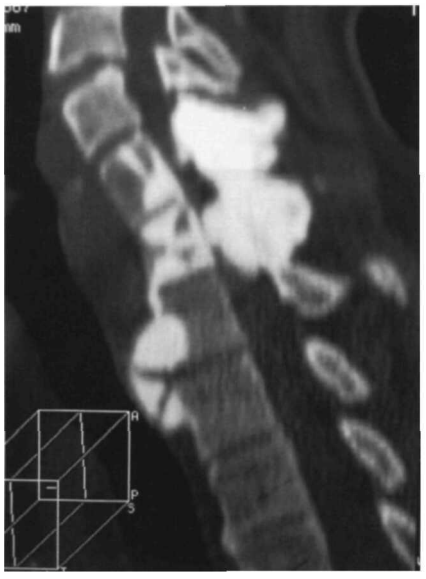

a

b

Figure 5**.13 a, b** Melorheostosis involving multiple vertebrae with extensive cortical thickening as seen on the sagittal CT image (**a**). Zones of cortical thickening have low signal on the sagittal T2WI (**b**).

a

b

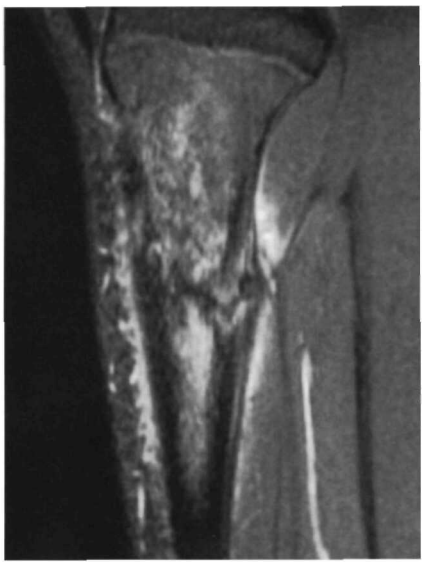

c

Figure 5**.14a-d** Healing stress fracture involving the proximal tibial diaphysis with cortical thickening and endosteal sclerosis as seen on an AP radiograph (**a**). The cortical thickening has mixed low and intermediate signal on sagittal T1WI (**b**) and mixed slightly high and low signal on sagittal (**c**) and axial (**d**) FST2WI. Zones with high signal are seen within the marrow and juxtacortical soft tissues on FST2WI. A thin zone of low signal is also seen within the marrow.

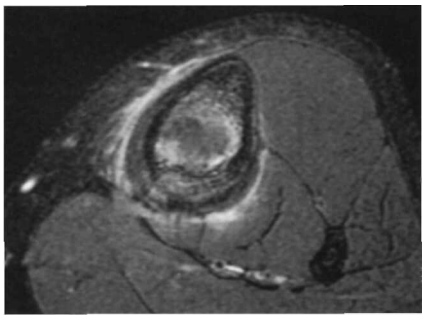

d

Figure 5**.15** Healed traumatic fracture deformity of the tibial shaft with thickened cortex as seen on sagittal T1WI.

Table 5 (Continued) **Lesions associated with thickening of bone cortex**

Lesion	MRI Findings	Comments
Subacute and chronic osteomyelitis (Fig. 5.16)	**A Brodle's abscess** represents a type of subacute osteomyelitis in long bones in which there is an intraosseous lesion (abscess) that can appear as a central zone with low to intermediate signal on T1WI and slightly high to high signal on T2WI surrounded by two rings, and an outer poorly defined zone or halo with low to intermediate signal on T1WI and high signal on T2WI, FST2WI. and STIR. The inner ring surrounding the abscess represents vascularized granulation tissue containing inflammatory cells connective tissues, and usually has low to intermediate signal on T1WI and high signal on T2WI. This inner ring usually shows Gd-contrast enhancement and has been referred to as the "penumbra sign." The outer ring often has low signal on T1WI and T2WI. Peripheral to these two rings, the poorly defined halo representing reactive edema often has low signal on T1WI, and low, intermediate, and/or high signal on T2WI and FST2WI. The peripheral halo typically shows contrast enhancement. A sinus tract may be seen extending through thickened cortex adjacent to the intraosseous abscess. **In chronic active osteomyelitis,** findings include: intraosseous abscess, sequestra, cloacae, subperiosteal fluid collections, cortical thickening. A narrow zone or rim of low signal on T1WI and T2WI is often seen separating the site of chronic osteomyelitis from normal adjacent bone marrow. Within this rim, a zone with low-intermediate signal on T1WI and heterogeneous intermediate, slightly high, to high signal is usually seen representing the intraosseous infection or abscess that may contain foci of low signal on T1WI and T2WI from sequestra. Irregular zones of Gd-contrast enhancement may be seen in active chronic osteomyelitis. Cloacae and sinus tracts can appear as linear or curvilinear zones with high signal on T2WI and Gd-contrast enhancement involving thickened cortex and extraosseous soft tissues.	Osteomyelitis refers to infection of bone and can result from hematogenous spread of microorganisms, trauma-direct inoculation, extension from adjacent tissues, and complications from surgery. A **Brodie's abscess** refers to a small abscess (subacule osteomyelitis) in long bones that are typically walled off by sclerotic bone and often involve the cortex. **Scierosing osteomyelitis of Carre** is a chronic bone infection, usually involving the mandible or shafts of long bones, that is associated with extensive new bone formation that often obscures the involved osseous structure. **(See Atlas Chapter A 63)**
Paget disease (Fig. 5.17)	In the late or inactive phases of Paget disease, findings include osseous expansion, cortical thickening, decreased diameter of the medullary canal, and coarsened trabeculae along stress lines The zones of cortical thickening usually have low signal on T1WI and T2WI. The inner margins of the thickened cortex can be irregular, indistinct, or slightly tabulated.	Chronic skeletal disease in which there is disordered bone resorption and woven bone formation resulting in osseous deformity. Typically occurs in adults, 90% of cases occurring in patients older than 40 years. **(See Atlas Chapter A 65)**
Neurofibromatosis type 1 (Fig. 5.18)	Irregular periosteal thickening of long bones of the lower extremities can be seen as zones of low signal.	Subperiosteal proliferation of bone can occasionally be seen involving long bones of the lower extremities in patients with NF1.
Noninterrupted periosteal reaction and bone formation from primary hypertrophic osteoarthropathy (pachydermoperiostosis)	Linear and /or irregular periosteal and cortical thickening seen in tubular bones of the extremities bilaterally (tibia, fibula, radius ulna are common sites, also seen in other bones and skull). Can involve epiphyseal, metaphyseal, and/or diaphyseal portions of long bones.	Rare clinical syndrome in adolescents or adults with swollen painful joints, enlargement of the extremities from osseous proliferation and periostitis, clubbing of digits, thickening of skin of the face and scalp with excessive sweating and sebaceous secretions. Can be hereditary (autosomal dominant with variable expression) or idiopathic.

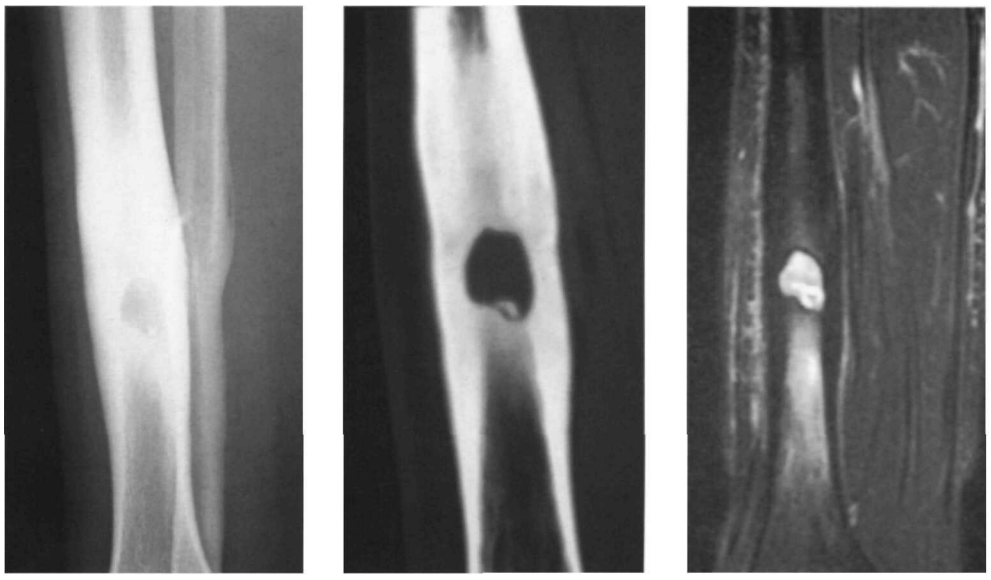

a b, c

Figure 5**.16a-c** Chronic osteomyelitis with abscess in the distal tibial shaft with dense sclerotic thickening of the cortex and medullary bone seen on a radiograph (**a**) and CT image (**b**). A radiolucent abscess is also seen in the medullary bone. The cortical thickening has mostly low signal on coronal FST2WI (**c**). Poorly defined zones with high signal on FST2WI are seen within the marrow surrounding a circumscribed high signal abscess.

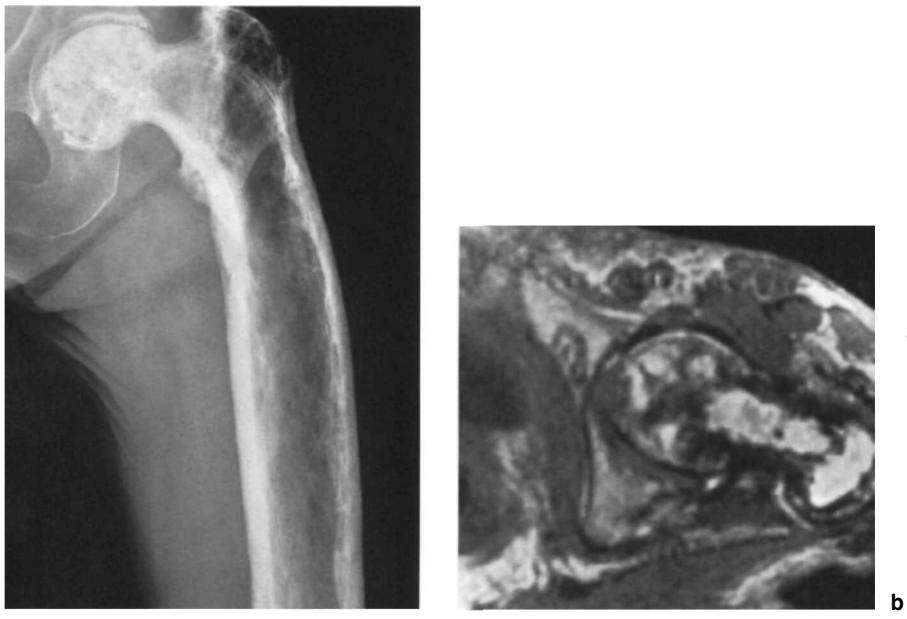

a b

Figure **5.17a, b** Paget disease involving the proximal femur in a 71-year-old woman with cortical thickening at the medial femoral shaft on an AP radiograph (**a**). Cortical thickening is seen as irregular zones with low signal on axial T1WI (**b**).

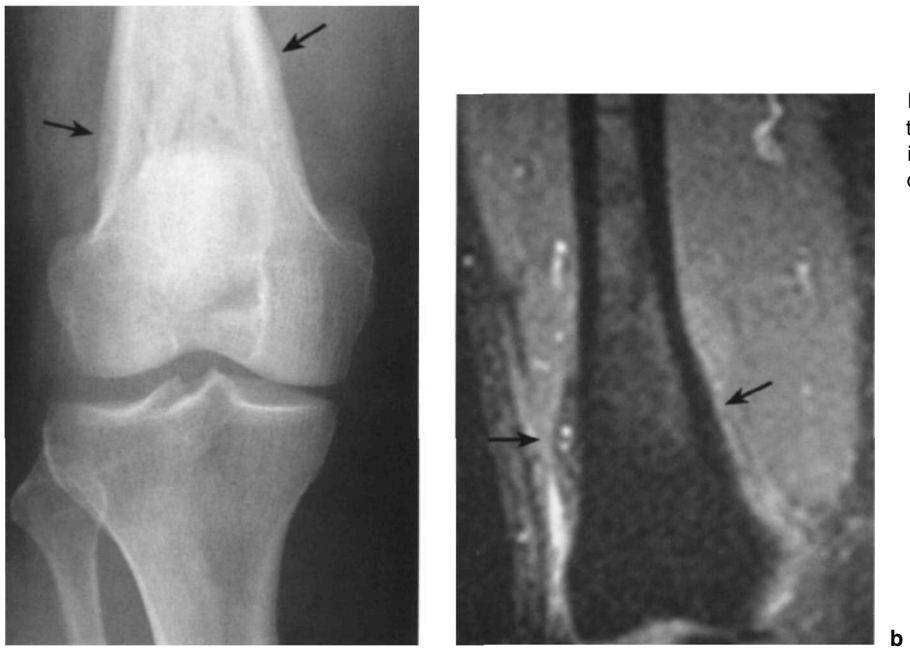

a b

Figure 5**.18** Periosteal bone formation at the distal femur in a patient with NF1 seen as intermediate and low signal on FST2WI at the outer cortical margin.

Table 5 (Continued) **Lesions associated with thickening of bone cortex**

Lesion	MRI Findings	Comments
Nonintemipted periosteal reaction and bone formation from secondary hypertrophic osteoarthropathy	Smooth, wavy, and/or irregular periosteal and cortical thickening seen in the diaphyseal and metaphyseal portions of long bones of the upper and lower extremities, as well as in other bones.	Clinical syndrome with clubbing of the digits, periostitis, hypertrophic osteoarthropathy. skin thickening, limb swelling, nail bed abnormalities (striations, increased curvature) related to extraskeletal lesions involving the lungs (bronchogenic carcinoma, metastasis, cystic fibrosis, bronchiectasis, infection, lymphoma), pleura (mesothelioma), abdomen (biliary atresia, cirrhosis, tumors, ulcerative colitis, Crohn disease), heart (cyanotic heart disease), or neoplasms at other sites. Regression of hypertrophic osteoarthropathy can occur after thoracotomy in patients with thoracic abnormalities, even in those without complete removal of the intrathoracic lesions.
Noninterrupted periosteal reaction and bone formation from venous stasis (Fig. 5.19)	Smooth and wavy periosteal and cortical thickening seen in the diaphyseal and metaphyseal portions of long bones of the lower extremities (tibia, fibula, metatarsal bones, phalanges).	Venous stasis is associated with edematous changes in the soft tissues as well as soft tissue ossification, periostitis, and cortical thickening.
Noninterrupted periosteal reaction and bone formation from infantile cortical hyperostosis (Caffey disease)	Smooth, wavy, and/or irregular periosteal and cortical thickening seen in the diaphyseal and metaphyseal portions of one or multiple bones.	Clinical disorder that affects infants less than 5 months with findings of soft tissue swelling (commonly over the mandible), fever, hyperirritability, and cortical hyperostosis (ribs, ulna, tibia, fibula, humerus, femur, radius, metacarpal, and metatarsal bones). The clinical course is variable but regression of findings can occur over 3-4 years.

a

b,c

Figure 5.**19a-c** Undulating solid periosteal bone formation along the tibial shaft as seen on a radiograph (**a**). The periosteal reaction and cortical thickening has low signal on sagittal T1WI (**b**) and post-contrast FST1WI (**c**).

Table 5 (Continued) **Lesions associated with thickening of bone cortex**

Lesion	MRI Findings	Comments
Nonintemipted periosteal reaction and bone formation from thyroid acropachy	Asymmetric, irregular, spiculated periosteal thickening seen in the diaphyseal portions of one or multiple bones (metacarpal and metatarsal bones, phalanges, other bones).	This disorder represents an extreme form of autoimmune thyroid disease with clinical manifestations such as swelling of the digits and toes, digital clubbing, and periosteal reaction. Thyroid dermopathy (pretibial myxedema) occurs in 4% of patients with Graves ophthalmopathy. Pronounced cases of thyroid dermopathy can be associated with thyroid acropachy in 1% of patients with Graves ophthalmopathy.
Nonintemipted periosteal reaction from hypervitaminosis A	Smooth and wavy periosteal and cortical thickening seen in the diaphyseal portions of one or multiple bones (ulna, metatarsal bones, clavicle, tibia, fibula, other bones). Damage to the physeal plates can result in irregularities and premature fusion, as well as splaying and cupping deformities of the metaphyses.	Vitamin A intoxication in children can result in anorexia, dermatologic and osseous disorders. In children, damage to the physeal plates may be irreversible despite cessation of vitamin A administration. In adults, anorexia, weight loss, and dermatologic disorders are frequently associated with hypervitaminosis A.
Noninterrupted periosteal reaction from hypovitaminosis A	Smooth and wavy periosteal and cortical thickening seen in the diaphyseal portions of one or multiple bones.	Vitamin A deficiency can result in anemia, dermatologic disorders (dry and scaly skin), growth retardation, osseous abnormalities, cranial nerve and visual disorders.
Noninterrupted periosteal reaction from hypovitaminosis C (scurvy)	In children, periosteal elevation with new bone formation can be seen in the diaphyseal and metaphyseal portions of one or multiple bones from subperiosteal hemorrhage. Metaphyseal beak-like bone protrusions can occur from the abnormal zones of provisional calcification at the physeal plate, as well as subepiphyseal fractures. In adults, osteopenia with hemarthrosis can be associated with ischemic necrosis and fractures with mild periosteal reaction.	In young children, vitamin C deficiency after 4 to 10 months can result in infantile scurvy with clinical features including failure to thrive, petechial hemorrhages, ulcerated gingiva, hematemesis, melena, hematuria. and anemia. Clinical features associated with adult scurvy include anorexia, fatigue, weakness, petechial hemorrhages involving gingiva and skin, hemarthrosis, osteoporosis, ischemic necrosis, dermatologic disorders (dry and scaly skin), growth retardation, osseous and nerve disorders.
Syndromes of hyperostosfs, osteitis, and skin lesions (SAPHO syndrome)	Periosteal elevation with cortical thickening can be seen as well as syndesmophyte formation at one or multiple levels.	Syndrome including abnormalities such as synovitis, acne, pustulosis, hyperostosis with periosteal proliferation (sternum, clavicle, anterior ribs, symphysis pubis, femur, sacrum, iliac bones) and osteitis at the chest wall.

References

Focal Fibrocartilaginous Dysplasia

Choi IH, Kim CJ, Cho TJ, et al. Focal fibrocartilaginous dysplasia of long bones: report of eight additional cases and literature review. *J Pediatr Orthoped* 2000:20:421-427.

Kim CJ, Choi IH, Chung CY, Chi JG. The histologic spectrum of subperiosteal fibrocartiiaginous pseudotumor of long bone (focal fibrocartilaginous dysplasia). *Pathol Int* 1999:49:1000-1006.

Neurofibromatosis

Resnick D. Enostosis, hyperostosis, and periostitis. In: Resnick D, ed. Diagnosis *of Bone and Joint Disorders,* 4th ed. Philadelphia, Pa: W.B. Saunders; 2002:5:4870-4919.

Primary Hypertrophic Osteoarthropathy

Araki Y, Tsukaguchi I, Nakamura H. Pachydermoperiostosis involving the skull and spine: MR findings. *AJR* March 1993;160(3):664-665.

Capelastegui A, Astigarraga E, García-Iturraspe C. MR findings in pulmonary hypertrophic Osteoarthropathy. *Clin Radiol* January 2000;55(1): 72-75.

Demirpolat G, Sener RN, Stun EE. MR imaging of pachydermoperiostosis. *J Neuroradiol* March 1999;26(l):61-63.

Loredo R, Pathria MN, Salonen D, Resnick D. Magnetic resonance imaging in pachydermoperiostosis. *Clin Imag* July-September 1996;20(3): 212-218.

Resnick D. Enostosis, hyperostosis, and periostitis. In: Resnick D, ed. *Diagnosis of Bone and Joint Disorders,* 4th ed. Philadelphia, Pa: W.B. Saunders; 2002:5:4870-4919.

Secondary Hypertrophic Osteoarthropathy

Capelastegui A, Astigarraga E, García-Iturraspe C. MR findings in pulmonary hypertrophic Osteoarthropathy. *Clin Radiol* January 2000:55(1): 72-75.

Resnick D. Enostosis, hyperostosis, and periostitis. In: Resnick D, ed. Diagnosis *of Bone and Joint Disorders,* 4th ed. Philadelphia, Pa: W.B. Saunders; 2002:5:4870-4919.

Sainani NI, Lawande MA, Parikh VP, Pungavkar SA, Patkar DP, Sase KS. MRI diagnosis of hypertrophic Osteoarthropathy from a remote childhood malignancy. *Skeletal Radiol* 2007 Jun;36 Suppl 1:63-6. Epub Sep 5 2006.

Varan A, Kutluk T, Demirkazik FB, Akyüz C, Büyükpamukcu M. Hypertrophic osteoarthropathy in a child with nasopharyngeal carcinoma. *Pediatr Radiol* 2000:30:570-572.

Periosteal Reaction from Venous Stasis

Resnick D. Enostosis, hyperostosis, and periostitis. In: Resnick D, ed. Diagnosis *of Bone and Joint Disorders,* 4th ed. Philadelphia, Pa: W.B. Saunders; 2002:5:4870-4919.

Wenaden AET, Szyszko TA, Saifuddin A. Imaging of periosteal reactions associated with focal lesions of bone. *Clin Radiol* 2005:60:439-456.

Infantile Cortical Hyperostosis (Caffey Disease)

Katz DS, Eller DJ, Bergman G, Blankenberg FG. Caffey's disease of the scapula: CT and MR findings. *AJR* January 1997;168(l):286-287.

Resnick D. Enostosis, hyperostosis, and periostitis. In: Resnick D, ed. Diagnosis *of Bone and Joint Disorders,* 4th ed. Philadelphia, Pa: W.B. Saunders; 2002:5:4870-4919.

Saatci I, Brown JJ, McAlister WH. MR findings in a patient with Caffey's disease. *Pediatr Radiol* November 1996;26(1):68-70.

Thyroid Acropachy

Fatourechi V, Ahmed DDF, Schwartz KM. Thyroid acropachy: report of 40 patients treated at a single institution in a 26-year period. *J Clin Endocrinol Metab* 2002:87:5435-5441.

Resnick D. Enostosis, hyperostosis, and periostitis. In: Resnick D, ed. Diagnosis *of Bone and Joint Disorders,* 4th ed. Philadelphia, Pa: W.B. Saunders; 2002:5:4870-4919.

Vanhoenacker FM, Pelckmans MC, De Beuckeleer LH, Colpaert CG, De Schepper AM. Thyroid acropachy: correlation of imaging and pathology. *EurRadiol* 2001;11(6):1058-1062.

Hypervitaminosis and Hypovitaminosis

Jiang YB, Wang YZ, Zhao J, Marchal G, Shen YL, Xing SZ, Li RG, Baert AL. Bone remodeling in hypervitaminosis D3. radiologic-microangiographic-pathologic correlations. *Invest Radiol* 1991:26:213-219.

Lips P. Hypervitaminosis A and fractures. *N Engl J Med* 2003;384: 347-349.

Resnick D. Hypervitaminosis and hypovitaminosis. In: Resnick D, ed. *Diagnosis of Bone and Joint Disorders,* 4th ed. Philadelphia, Pa: W.B. Saunders; 2002:4:3456-3464.

Romero JB, Schreiber A, Von Hochstetter AR, Wagenhauser FJ, Michel BA, Theiler R. Hyperostotic and destructive osteoarthritis in a patient with vitamin A intoxication syndrome: a case report. *Bull Hosp Jt Dis* 1996:54:169-174.

Syndromes of Hyperostosis, Osteitis, and Skin Lesions (SAPHO syndrome)

Boutin RD, Resnick D. The SAPHO syndrome: an evolving concept for unifying several idiopathic disorders of bone and skin. *AJR* 1998; 170:585-591.

Davies AM, Marino AJ, Evans N, Grimer RJ, Deshmukh N, Mangham DC. SAPHO syndrome: 20 year followup. *Skeletal Radiol* 1999;28: 159-162.

Kirchoff T, Merkesdal S, Rosenthal H, et al. Diagnostic management of patients with SAPHO syndrome: use of MR imaging to guide bone biopsy at CT for microbiological and histological work-up. *Eur Radiol* 2003:13:2304-2308.

Resnick D. Enostosis, hyperostosis, and periostitis. In: Resnick D, ed. *Diagnosis of Bone and Joint Disorders,* 4th ed. Philadelphia, Pa: W.B. Saunders; 2002:5:4870-4919.

Table 6 Intramedullary lesions associated with expansion of intact cortical margins

Lesion	MRI Findings	Comments
Benign		
Osteochondroma (Fig. 6.1)	Circumscribed protruding lesion arising from outer cortex with a central zone with intermediate signal on T1WI and T2WI similar to marrow surrounded by a peripheral zone of low signal on T1WI and T2WI, a cartilaginous cap is usually present in children and young adults. Increased malignant potential when cartilaginous cap is >2cm thick.	Benign cartilaginous tumors arising from defect at periphery of growth plate during bone formation with resultant bone outgrowth covered by a cartilaginous cap. Usually benign lesions unless associated with pain and increasing size of cartilaginous cap. Osteochondromas are common lesions, accounting for 14 to 35% of primary bone tumors. Occur with median age of 20 years, up to 75% of patients are less than 20 years old. **(See Atlas Chapter A 58)**
Fibrous dysplasia (Fig. 6.2)	MRI features depend on the proportions of bony spicules, collagen, fibroblastic spindle cells, hemorrhagic and/or cystic changes, and associated pathologic fracture if present. Lesions are usually well-circumscribed, and have low or low-intermediate signal on T1WI and PDWI. On T2WI, lesions have variable mixtures of low, intermediate, and/or high signal often surrounded by a low signal rim of variable thickness. Internal septations and cystic changes are seen in a minority of lesions. Bone expansion with thickened and/or thinned cortex can be seen. Lesions show Gd-contrast enhancement that varies in degree and pattern.	Benign medullary fibro-osseous lesion that can involve a single site **(mono-ostotic)** or multiple locations **(poly-ostotic).** Thought to occur from developmental failure in the normal process of remodeling primitive bone to mature lamellar bone with resultant zone or zones of immature trabeculae within dysplastic fibrous tissue. Account for ~10% of benign bone lesions. Patients range in age from <1 to 76 years. 75% occur before the age of 30 years. **(See Atlas Chapter A 27)**

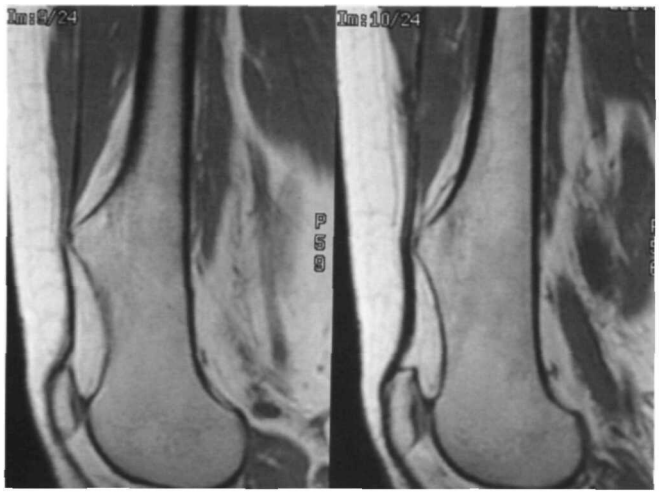

Figure 6.**1** A 20-year-old woman with an osteochondroma protruding from the anterior distal femur as seen on sagittal PDWI.

a

b

Figure 6.**2 a, b** A 39-year-old woman with fibrous dysplasia expanding the diaphyseal portion of the femur as seen on coronal T1WI (**a**), and showing Gd-contrast enhancement on sagittal FST1WI (**b**).

Table 6 (Continued) **Intramedullary lesions associated with expansion of intact cortical margins**

Leson	MRI Findings	Comments
Nonossifying fibroma (flbroxanthoma) (Fig. 6.3)	Well-circumscribed eccentric intramedullary lesions in the metadiaphyseal regions of long bones that have mixed low-intermediate signal on T1WI, and mixed low, intermediate, and/or high signal on T2WI, PDWI, and FST2WI. Zones of low signal on T1WI. PDWI. and T2WI can be seen in the central portions of the lesions. Zones with varying thickness of low signal on T1WI, PDWI, and T2WI are seen at the margins of the lesions representing bone sclerosis. Internal septations are commonly seen as zones of low signal on T2WI in these lesions. Cortical thinning or thickening and bone expansion can be seen. Lesions can show Gd-contrast enhancement (heterogeneous > homogeneous patterns). Linear periosteal Gd-contrast enhancement can be seen at lesions with associated fracture or marked cortical expansion/thinning.	**Fibrous cortical defects (FCDs)** and **nonossifying fibromas (NOFs)** are well-circumscribed common benign fibrohistiocytic lesions in the metadiaphyseal portions of long bones that are comprised of whorls of fibroblastic cells combined with smaller amounts of multinucleated giant cells and xanthomatous cells. Both **FCDs and NOFs** have similar pathologic findings although they differ in size and primary locations in long bones. **FCDs** are small lesions primarily located in bone cortex, whereas the larger **NOFs** are located eccentrically in the medullary cavity. **FCDs and NOFs** are usually asymptomatic and are often detected as incidental findings. The true incidence of these lesions is unknown, maybe up to 40% of children. 95% occur between the ages of 5 and 20, median = 14 years. **(See Atlas Chapter A 26)**
Unicameral bone cyst (Fig.6.4)	Unicameral bone cysts (UBCs) often have a peripheral rim of low signal on T1W, PDWI, and T2W images adjacent to normal medullary bone. UBCs usually contain fluid with low to low-intermediate signal on T1WI; low-intermediate, intermediate or slightly high signal on PDWI; and high signal on T2WI. Fluid-fluid levels may occur. In tubular bones, mild to moderate expansion of bone may occur with variable thinning of the overlying cortex. For UBCs without pathologic fracture, thin peripheral Gd-contrast enhancement can be seen at the margins of lesions. UBCs with pathologic fracture can have heterogeneous or homogeneous low-intermediate or slightly high signal on T1WI, and heterogeneous or homogeneous high signal on T2WI and FST2WI. UBCs complicated by fracture can have internal septations and fluid-fluid levels, as well as irregular peripheral Gd-contrast enhancement at internal septations.	Intramedullary non-neoplastic cavities filled with serous or serosanguineous fluid. Account for 9% of primary tumor-like lesions of bone. 85% occur in the first two decades, median = 11 years. **(See Atlas Chapter A 3)**
Aneurysmai bone cyst (Fig. 6.5)	Aneurysmai bone cysts (ABCs) often have a low signal rim on T1WI, PDWI, and T2WI adjacent to normal medullary bone, and between extraosseous soft tissues. Various combinations of low, intermediate, and/or high signal on T1WI, PDWI, and T2WI images are usually seen within aneurysmal bone cysts as well as fluid-fluid levels. Variable Gd-contrast enhancement is seen at the margins of lesions as well as involving the internal septae.	Tumor-like expansile bone lesions containing cavernous spaces filled with blood. ABCs can be primary bone lesions (two-thirds) or secondary to other bone lesions/tumors (such as giant cell tumors, chondroblastomas, osteoblastomas, osteosarcomas, chondromyxoid fibromas, nonossifying fibromas, fibrous dysplasia, fibrosarcomas, malignant fibrous histiocytomas, and metastatic disease). Account for ~11% of primary tumor-like lesions of bone. Patients usually range in age from 1 to 25 years, median = 14 years. **(See Atlas Chapter A 2)**

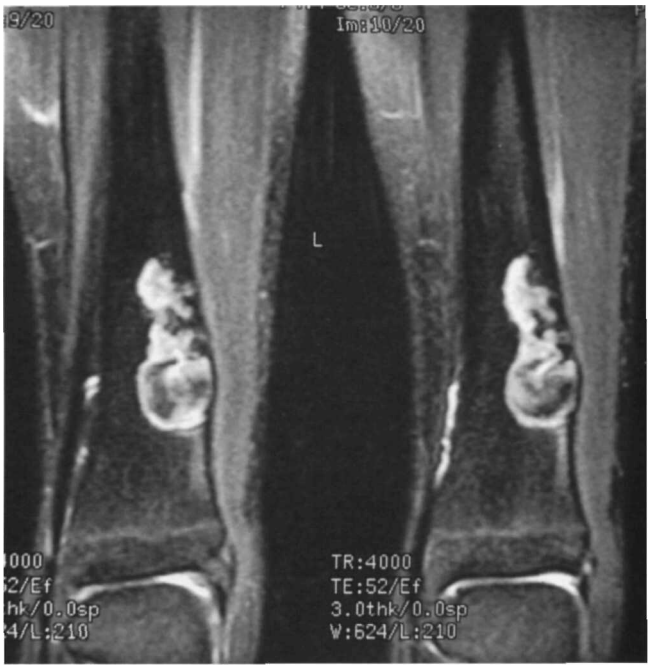

Figure 6.**3** A 16-year-old female with a nonossifying fibroma involving the posterior diaphyseal portion of the distal tibia. The lesion has circumscribed margins and has mixed low and high signal on coronal FST2WI. Cortical thinning and slight expansion are seen.

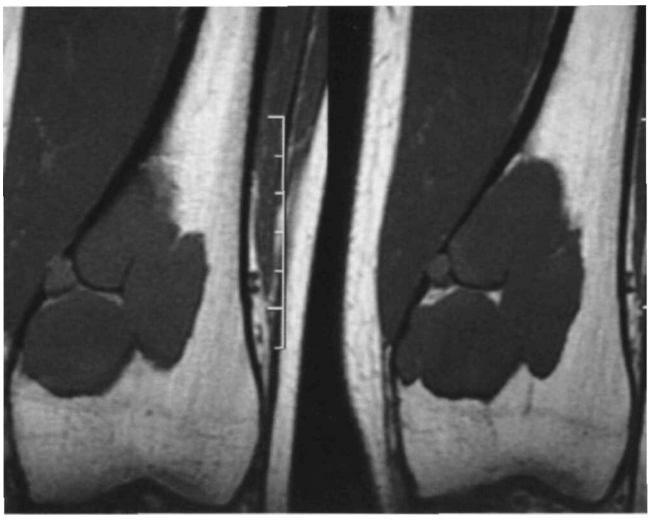

a

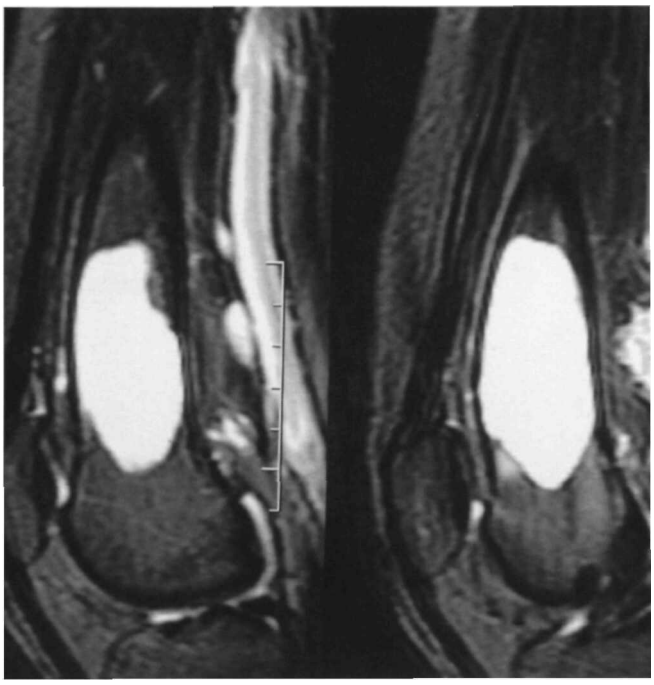

b

Figure 6.**4a, b** A 17-year-old female with a unicameral bone cyst within the distal metadiaphyseal portion of the femur as seen on coronal T1WI (**a**) and sagittal FST2WI (**b**). Cortical thinning and slight expansion are seen.

a

b

Figure 6.**5 a, b** An 11-year-old boy with an aneurysmal bone cyst involving the medial proximal shaft of the femur. Coronal T1WI (**a**) shows an expansile lesion with thinned cortex containing zones with intermediate and high signal. Coronal FST2WI (**b**) shows a multiseptated lesion with fluid-fluid levels containing high and low-intermediate signal.

Table 6 (Continued) **Intramedullary lesions associated with expansion of intact cortical margins**

Lesion	MRI Findings	Comments
Giant cell reparative granuloma (solid aneurysmal bone cyst) (Fig.6.6)	Radiolucent bone lesions on CT, typically occur in the metaphysis and/or diaphysis. Bone expansion may occur with or without intact thin cortical margins. Extraosseous extension of lesions may occur. Lesions can have heterogeneous low. intermediate, and/or high signal on T1WI, PDWI, and T2WI; as well as peripheral rim-like and central Gd-contrast enhancement on FST1WI.	Giant cell granulomas (also known as solid aneurysmal bone cysts) are reactive granulomatous lesions that have histologic features similar to Brown tumors. Lesions contain multinucleated giant cells adjacent to sites of hemorrhage, and fibroblasts. Osteoid formation adjacent to sites of hemorrhage can be seen. Lesions usually occur in patients less than 30 years, and are most frequently found in the mandible, maxilla, and small bones of the hands and feet. Lesions in long bones have also been referred to as solid variants of aneurysmal bone cysts. **(See Atlas Chapter A 2)**

a

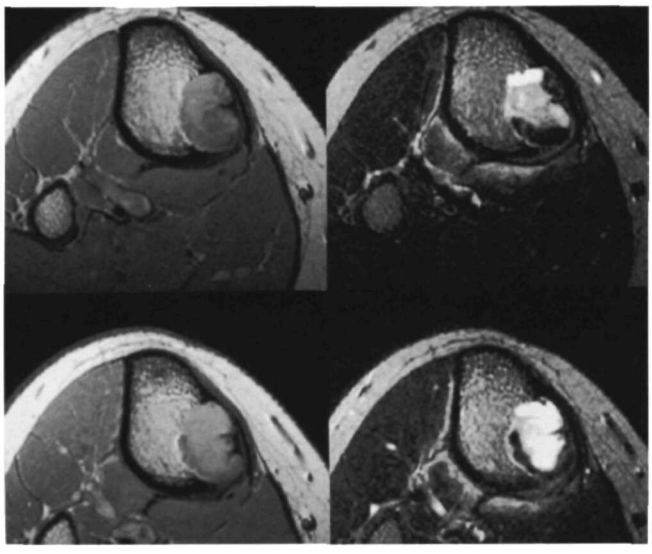
b

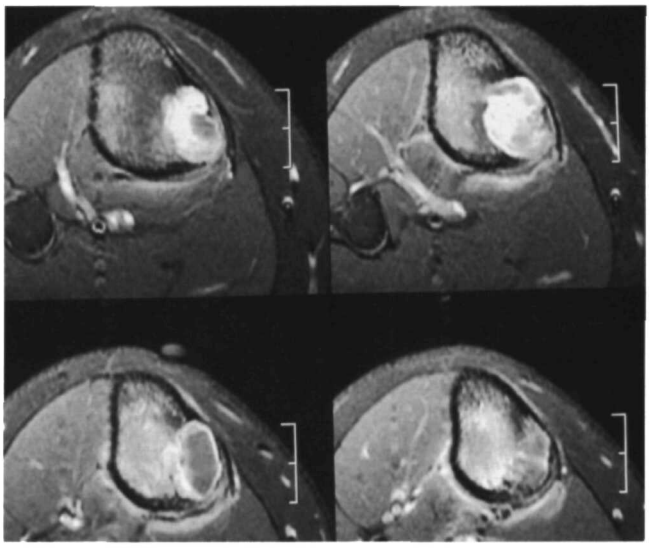
c

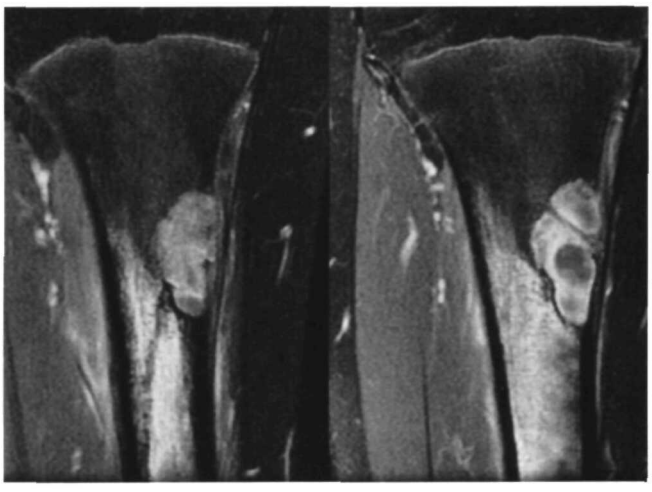
d

Figure 6.**6a-d** A 14-year-old girl with a giant cell reparative granuloma (solid aneurysmal bone cyst) involving the medial portion of the proximal tibial shaft. The AP radiograph (a) shows a well-circumscribed radiolucent lesion with thin sclerotic margins, thinning, and expansion of the bone cortex. The lesion has intermediate signal on axial PDWI (**b**, *images on left)* and mixed low, intermediate, and high signal on axial T2WI (**b**, *images on right).* The lesion shows prominent heterogeneous Gd-contrast enhancement on axial (**c**) and coronal (**d**) FST1WI. Poorly defined contrast enhancement is also seen in the marrow peripheral to the lesion.

Table 6 (Continued) **Intramedullary lesions associated with expansion of intact cortical margins**

Lesion	MRI Findings	Comments
Giant cell tumor of bone (Fig. 6.7)	Lesions may have expanded and thinned cortical margins on radiographs. Lesions may also show cortical disruption and extraosseous extension on MRI. Solid portions of giant cell tumors often have low to intermediate signal on T1WI and PDWI. intermediate to high signal on T2WI, and high signal on FSPDWI and FST2WI. Signal heterogeneity on T2WI is common. Aneurysmal bone cysts can be seen in 14% of giant cell tumors. Varying degrees of Gd-contrast enhancement can be seen. Peripheral rim-like Gd-contrast enhancement may be seen around cystic zones/aneurysmal bone cysts.	Aggressive tumors composed of neoplastic ovoid mononuclear cells and scattered multinucleated osteoclast-like giant cells (derived from fusion of marrow mononu clear cells). Up to 10% of all giant cell tumors are malignant. Benign giant cell tumors account for ~5 to 9.5% of all bone tumors and up to 23% of benign bone tumors. Occur in patients 4 to 81 years (median = 30 years), 75% occur in patients between the ages of 15 and 45 years. **(See Atlas Chapter A 29)**

a

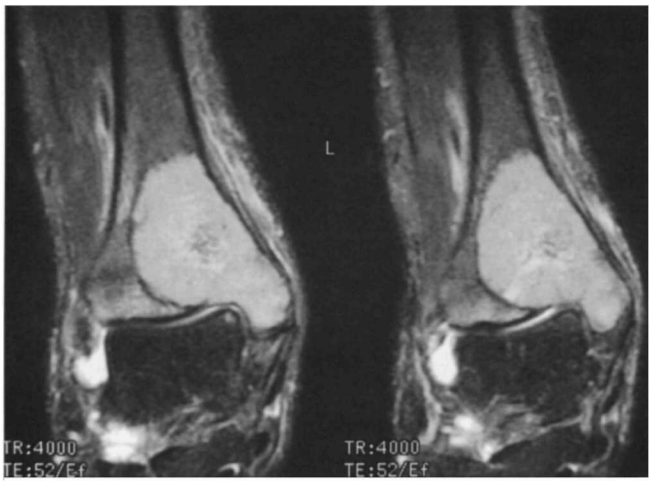

b

Figure 6.**7a-c** A 61-year-old man with a giant cell tumor involving the distal tibia with thinning and expansion of bone cortex as seen on coronal (**a**) and axial (**c**) T1WI and coronal FST2WI (**b**).

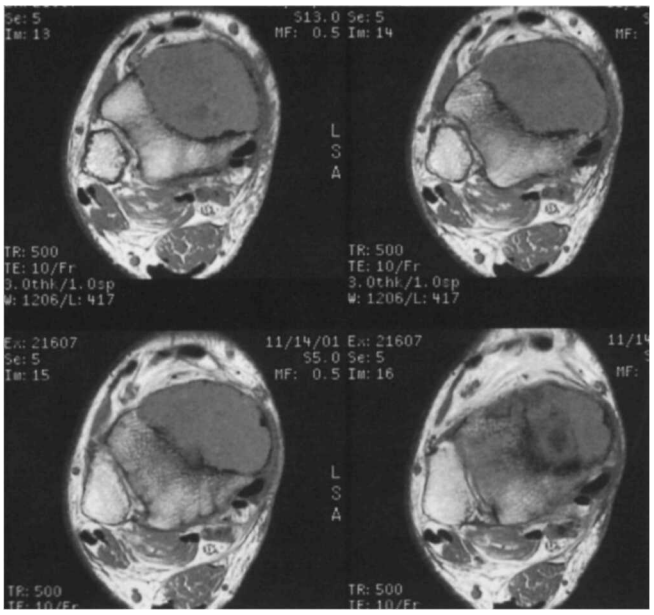

c

Table 6 (Continued) **Intramedullary lesions associated with expansion of intact cortical margins**

Lesion	MRI Findings	Comments
Brown tumor	Lesions are usually radiolucent on radiographs and CT. Lesions often have low-intermediate signal on T1WI, intermediate to slightly high signal on T2WI, and typically show Gd-contrast enhancement. Zones of low signal on T2WI may occur from hemosiderin. Expansion of cortical margins can occur with or without cortical disruption/destruction.	Lesions in bone contain multinucleated giant cells, fibrous tissue, blood vessels, and zones of hemorrhage/hemosiderin. Histologic and imaging features are similar to giant cell reparative granulomas. Most often involves ribs, mandible, clavicle, pelvis, craniofacial bones, and vertebrae. Can result from primary hypcrparathyroidism (3-7 %) (oversecretion of parathyroid hormone [PTH] from parathyroid adenoma associated with hypercalcemia). secondary type (vitamin D deficiency or chronic renal failure with hypocalcemia resulting in secretion of PTH and parathyroid gland hyperplasia) (1-2%), or tertiary type in which the secondary type leads to eventual autonomous elevated PTH secretion from parathyroid gland hyperplasia.
Enchondroma (Fig. 6.8)	Lobulated intrameclullary lesions with well-defined borders ranging in size from 3 to 16cm, mean = 5cm. Mild endosteal scalloping can be seen. Cortical bone expansion rarely occurs. Lesions usually have low-intermediate signal on T1WI and intermediate signal on PDWI. On T2WI and fat-suppressed T2WI, lesions usually have predominantly high signal with foci and/or bands of low signal representing areas of matrix mineralization and fibrous strands. No zones of abnormal high signal on T2WI are typically seen in the marrow outside the borders of the lesions. Lesions typically show Gd-contrast enhancement in various patterns (peripheral curvilinear lobular, central nodular/septal, and peripheral lobular, or heterogeneous diffuse).	Benign intramedullary lesions composed of hyaline cartilage, represent -10% of benign bone tumors. Enchondromas can be solitary (88%) or multiple (12%). Oilier disease is a dyschondroplasia involving endochondral-formed bone resulting in multiple enchondromas (enchondromatosis). Metachondromatosis is a combination of enchondromatosis and osleochondromatosis. and is rare. Maffucci disease refers to a syndrome with multiple enchondromas and soft tissue hemangiomas, and is very rare. Patients range in age from 3 to 83 years, median = 35 years, mean = 38 to 40 years, peak in 3rd and 4th decades. **(See Atlas Chapter A8)**
Chondromyxoid fibroma (Fig. 6.9)	Lesions are often slightly lobulated with low-intermediate signal on T1WI, intermediate signal on PDWI, and heterogeneous predominantly high signal on T2WI. Thin low signal septa within lesions on T2WI are secondary to fibrous strands. Lesions are surrounded by low signal borders representing thin sclerotic reaction. Edema is not typically seen in medullary bone. Lesions show prominent diffuse Gd-contrast enhancement.	Rare benign slow-growing bone lesions that contain chondroid, myxoid, and fibrous components. Chondromyxoid fibromas represent 2-4% of primary benign bone lesions, and < 1 % of primary bone lesions. Most Chondromyxoid fibromas occur between the ages of 1 to 40 years, with a median of 17 years, and peak incidence in the 2nd to 3rd decades. **(See Atlas Chapter A10)**
Osteoblastoma (Fig. 6.10)	Lesions appear as spheroid or ovoid zone measuring greater than 1.5 to 2cm located within medullary and/or cortical bone with low-intermediate signal on T1WI; low-intermediate to slightly high signal on PDWI; and low-intermediate and/or high signal on T2WI and FS T2WI. After Gd-contrast administration, osteoblastomas show variable degrees of enhancement. Expansion of thinned cortical margins can be seen as well as thickening of cortical bone and medullary sclerosis. Zones of sclerotic bone reaction adjacent to osteoblastomas typically show low signal on T1W, T2WI, and FST2WI. Poorly defined zones of marrow signal alteration consisting of low-intermediate signal on T1WI, high signal on T2WI and FST2WI, and corresponding Gd-contrast enhancement can be seen in the marrow adjacent to osteoblastomas as well as within the extraosseous soft tissues.	Rare benign bone-forming tumors that are histologically related to osteoid osteomas. Osteoblastomas are larger than osteoid osteomas and show progressive enlargement. Account for 3-6 % of primary benign bone tumors and <1-2% of all primary bone tumors. Occurs in patients from 1 to 30 years, median = 15 years, mean age = 20 years. Approximately 90% of lesions occur in patients less than 30 years. **(See Atlas Chapter A 61)**

a

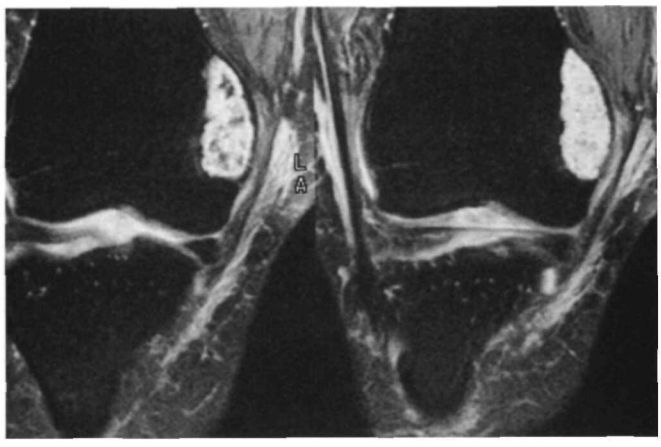

b

Figure 6.**8a, b** A 46-year-old woman with an enchondroma in the marrow of the distal medial femur. The circumscribed lesion has intermediate signal on coronal PDWI (**a**) and mostly high signal on coronal FST2WI (**b**). The lesion is associated with thinning and slight expansion of the adjacent bone cortex.

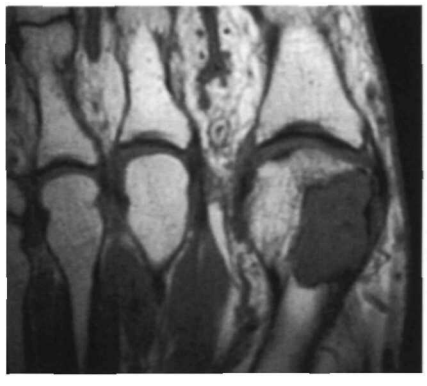

a

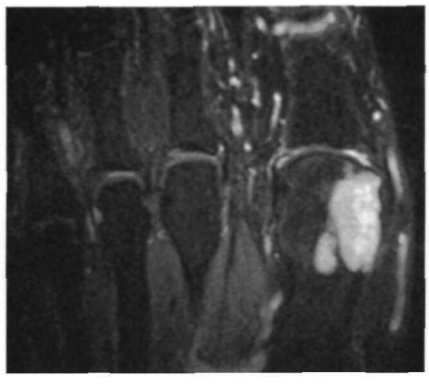

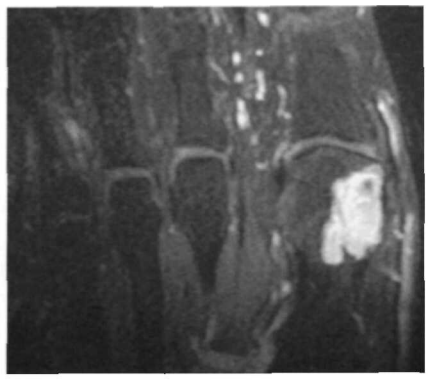

b, c

Figure 6.**9a-c** A 34-year-old man with a chondromyxoid fibroma involving the metatarsal head. The circumscribed lesion has intermediate signal on coronal PDWI (**a**), mostly high signal on coronal FST2WI (**b**), and shows prominent Gd-contrast enhancement on coronal FST1 WI (**c**). The lesion is associated with thinning and slight expansion of the adjacent bone cortex.

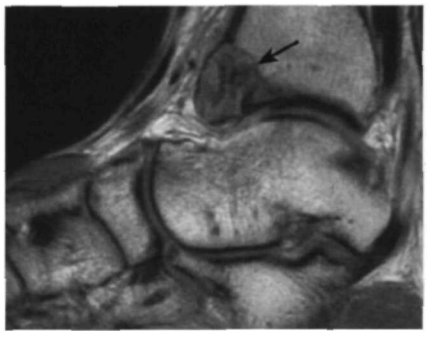

a

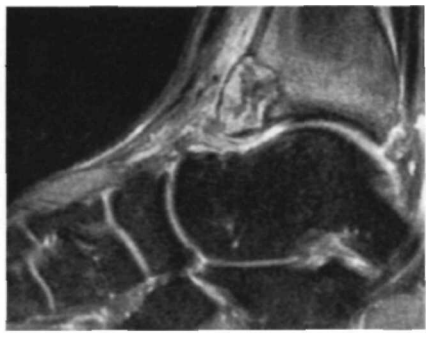

b

Figure 6.**10a, b** A 24-year-old man with an osteoblastoma involving the distal tibia. The lesion has heterogeneous low and intermediate signal on sagittal T1WI (**a**) and heterogeneous signal with zones of high and low signal on sagittal FST2WI (**b**). The tumor causes expansion and irregular thinning of the anterior margin of the distal tibia. Poorly defined zones of high signal on FST2WI are seen in the marrow and soft tissues adjacent to the lesion.

Table 6 (Continued) **Intramedullary lesions associated with expansion of intact cortical margins**

Lesion	MRI Findings	Comments
Hemangioma	Often well-circumscribed lesions that often have intermediate to high signal on T1WI, PDWI, T2WI, and FS T2WI. Hemangiomas usually show Gd-contrast enhancement (mild to prominent). Expansion of cortical margins can occasionally occur with intraosseous hemangiomas.	Benign lesions of bone and soft tissues comprised of capillary, cavernous, and/or malformed venous vessels. Considered to be a hamartomatous disorder, account for 2-4% of benign bone tumors and ~1 % of all bone tumors. **(See Atlas Chapter A 34)**
Chondroblastoma (Fig. 6.11)	Tumors often have fine lobular margins, and typically have low-intermediate heterogeneous signal on T1WI, and mixed low, intermediate, and/or high signal on T2WI. Areas of low signal on T2WI are secondary to chondroid matrix mineralization, and/or hemosiderin. Lobular, marginal, or septal Gd-contrast enhancement patterns can be seen. Tumors may have thin margins of low signal on T2WI representing sclerotic borders. Bone expansion can occasionally occur. Zones with high signal on FST2WI and Gd-contrast enhancement are seen in adjacent marrow.	Benign cartilaginous tumors with chondroblast-like cells and areas of chondroid matrix formation. Account for 5-9 % of benign bone lesions and 1 -3 % of all primary bone tumors, patients range from 10 to 30 years, median = 17 years. **(See Atlas Chapter A 7)**
Ameloblastoma (Fig. 6.12)	Lesions are often radiolucent with associated bone expansion and cortical thinning on CT. Tumors often have circumscribed margins, and can show mixed low, intermediate, and/or high signal on T1WI, T2WI, and FS T2WI. Lesions can show heterogeneous Gd-contrast enhancement.	Ameloblastomas are slow-growing solid and cystic tumors that contain epithelioid cells (basaloid and/or squamous types) associated with regions of spindle cells and fibrous stroma. These tumors occur in the mandible and maxilla and typically lack metastatic potential.
Desmoplastic fibroma (Fig. 6.13)	Lobulated lesions with abrupt zones of transition. Lesions usually have low-intermediate signal on T1WI, intermediate signal on PDWI, heterogeneous intermediate to high signal on T2WI. Lesions may have internal or peripheral zones of low signal on T1WI and T2WI secondary to dense collagenous parts of the lesions and/or foci with high signal onT2WI from cystic zones. Thin curvilinear zones of low signal on T2WI can be seen at the margins of the lesions. Lesions show variable degrees and patterns of Gd-contrast enhancement.	Represent rare intraosseous desmoid tumors that are comprised of benign fibrous tissue with elongated or spindle-shaped cells adjacent to collagen. Account for <1% of primary bone lesions. Occur in patients 1 to 71 years, mean = 20 years, median = 34 years, peak 2nd decade. **(See Atlas Chapter A16)**
Osteofibrous dysplasia (Fig. 6.14)	Multiple irregular intracortical zones of low-intermediate signal on T1WI, intermediate to slightly high signal on PDWI, and high signal on T2WI and FST2WI separated by irregular zones of low signal on T1WI and T2WI. the latter representing thickened sclerotic cortical bone. The outer cortical margins can be expanded and thinned. The intracortical lesions usually show prominent Gd-contrast enhancement. Thin juxtacortical/periosteal enhancement may be seen in lesions with thinned and expanded cortical margins. Prominent diffuse high signal on T2WI and marrow enhancement are seen for lesions with acute/subacute pathologic fractures.	Osteofibrous dysplasia represents rare benign fibro-osseous bone lesions that typically involve the cortex of the tibia and/or fibula in children and adolescents. **(See Atlas Chapter A 61)**

a

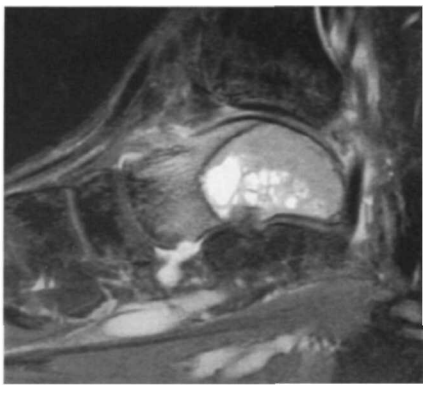

b

Figure 6.**11 a, b** A 20-year-old man with chondroblastoma in the talus. The lesion has a thin peripheral zone of low signal on sagittal PDWI (**a**) and sagittal FST2WI (**b**). The lesion has low-intermediate signal on PDWI, and both zones of intermediate and high signal on FST2WI, as well as in the adjacent marrow. Mild thinning and expansion of the cortex is seen.

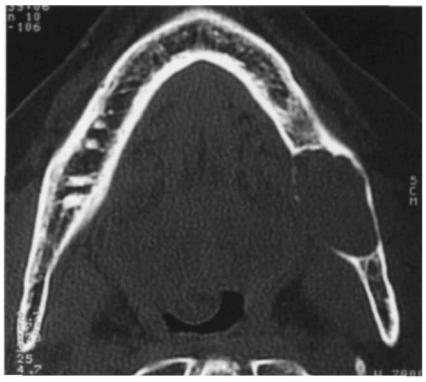

a

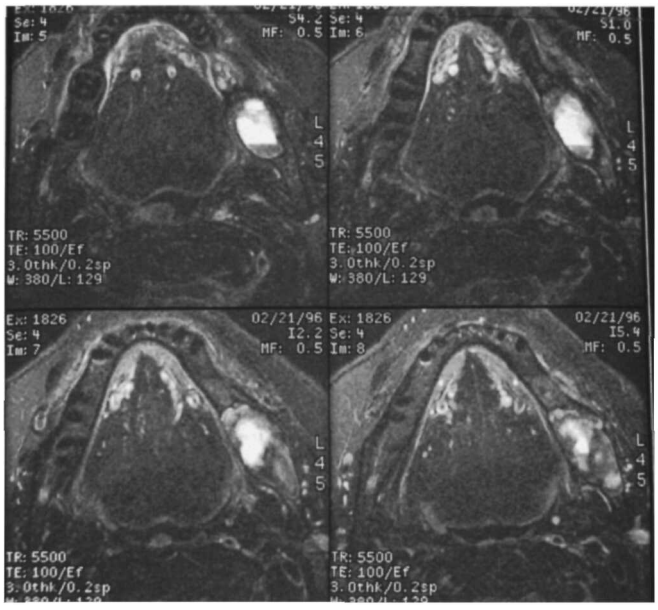

b

Figure 6.**12 a, b** A 70-year-old woman with ameloblastoma involving the mandible. The axial CT image (**a**) shows a radiolucent lesion with expansion and thinning of cortical bone. The lesion has mixed low, intermediate, and high signal on axial FST2WI (**b**).

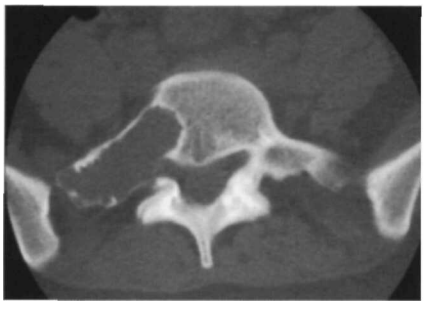

a

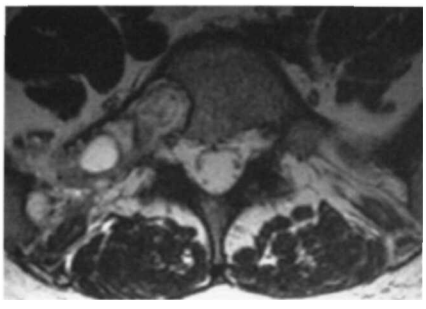

b

Figure 6.**13 a, b** Desmoplastic fibroma involving the L5 vertebral body, right pedicle, and transverse process. Axial CT image (**a**) shows an expansile radiolucent lesion with a thin peripheral shell of bone. The lesion has mixed signal with zones of intermediate, slightly high, high, and low signal on axial T2WI (**b**).

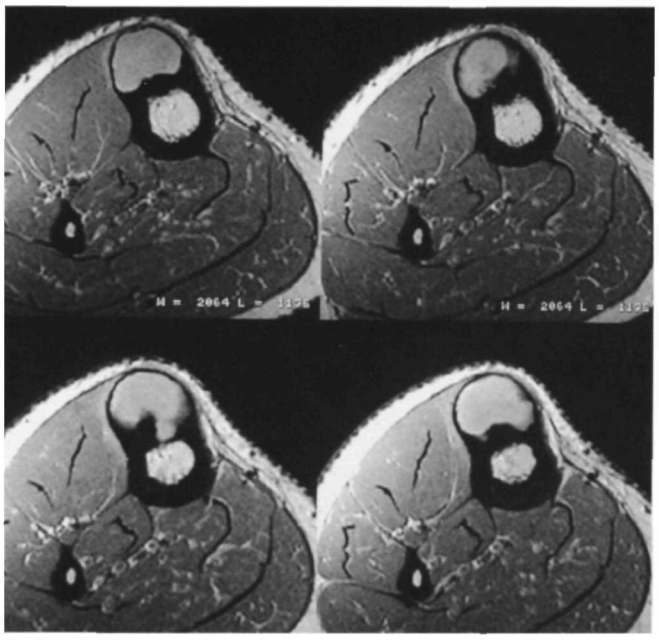

a

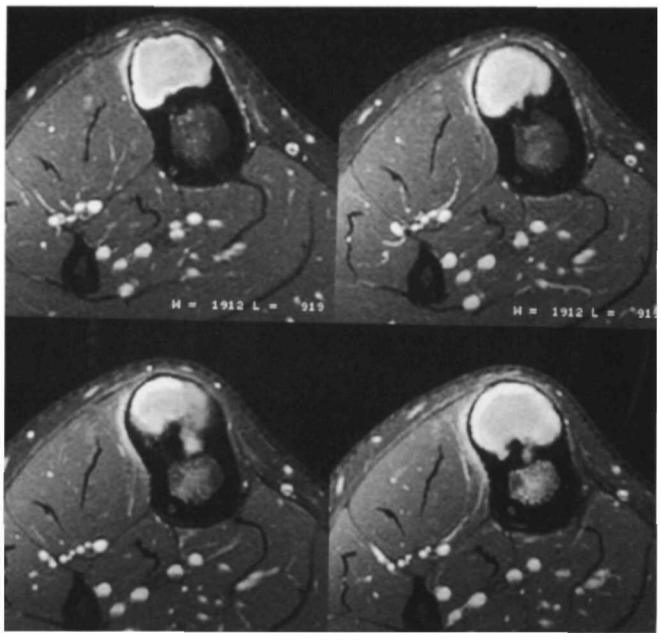

b

Figure 6.**14a, b** An 18-year-old female with osteofibrous dysplasia involving the anterior tibial cortex. Intracortical intermediate to slightly high signal is seen in the lesion on axial PDWI (**a**) with corresponding prominent Gd-contrast enhancement on axial FST1WI (**b**). The outer cortical margin is expanded and markedly thinned.

Table 6 (Continued) **Intramedullary lesions associated with expansion of intact cortical margins**

Lesion	MRI Findings	Comments
Gaudier disease (Fig. 6.15)	Diffuse and/or patchy heterogeneous zones with low-intermediate signal on T1WI, and intermecliale to slightly high heterogeneous signal on T2WI and FST2WI.	Rare, heritable metabolic disorder with deficient activity of the lysosomal enzyme-hydrolase β-glucosidase. Results in accumulation of the lipid-glucosylceramide within lysosomes of the monocyte-macrophage system (Gaucher cells) of the bone marrow, liver, and spleen. Marrow infiltration by Gaucher cells often results in zones of ischemia and bone infarction.
Hemophilic pseudotumor	Can appear as expansile radiolucent lesions on radiographs and CT. Lesions usually have mixed low, intermediate, and high signal on T1WI and T2WI, as well as fluid-fluid levels.	Lesions can occur within bone (femur, pelvis, tibia, hand) or soft tissue in 1-2% of patients with factor VIII or IX deficiency. Enlarging lesions may require surgical resection.
Malignant lesions		
Adamantinoma (Fig. 6.16)	Can appear as a solitary lobulated focus versus multinodular pattern of signal alteration in thickened bone cortex. More than half involve bone cortex and marrow compared with only cortical involvement. Bone cortex can be expanded and thinned. Tumor foci in bone typically have low-intermediate signal on T1WI and PDWI, and slightly high to high signal on T2WI and FST2WI. Lesions usually show prominent Gd-conlrasl enhancement. Adamanlinomas with a multinodular pattern have enhancing nodules which have high signal on T2WI and FST2WI separated by zones of low signal from intervening cortical bone.	Rare low-grade malignant bone tumors consisting of epithelial cells surrounded by spindle cells and osteo-fibrous tissue that often involve the shaft of the tibia. Account for < 1% of primary bone tumors. Patients range in age from 3 to 86 years, median = 19 to 25 years, average = 35 years, most common in 3rd and 4th decades. **(See Atlas Chapter A1)**
Other malignant lesions (Fig. 6.17)	Tumors may have poorly defined or sharp margins; and often have low-intermediate signal on T1WI with heterogeneous intermediate-high signal on T2WI and FS T2WI. Lesions often show prominent heterogeneous Gd-contrast enhancement.	Primary and melastatic tumors may initially show expansion of thinned intact cortical margins followed by eventual extraosseous extension of tumor through zones of cortical destruction. Hemangioendotheliomas and metastases from tumors such as renal cell carcinoma, breast, and lung carcinomas can show this pattern.

a

b

Figure 6.15 a, b A 34-year-old woman with Gaucher disease. Heterogeneous signal is seen in the marrow of the proximal femur on the coronal PDWI (**a**) and STIR (**b**), as well as trabecular disruption, and thinning and expansion of cortical bone laterally.

a

b

Figure 6.**16a, b** A 23-year-old woman with an adamantinoma of the tibial diaphysis. The lesion has intermediate signal on sagittal PDWI (**a**) and high signal on sagittal T2WI (**b**). There is thinning and expansion of cortical bone as well as tumor extension toward the

a

b

Figure 6.**17 a, b** Metastatic lesion in the proximal femur. The AP radiograph (**a**) shows a radiolucent lesion with partial sclerotic margins and cortical thinning. The coronal FST2WI (**b**) shows the lesion to have heterogeneous high signal that extends beyond the sclerotic margins and is associated with thinning and slight expansion of bone cortex medially.

References

Ameloblastoma

Asaumi J, Hisatomi M, Yanagi Y, et al. Assessment of ameloblastomas using MRI and dynamic contrast-enhanced MRI. *Eur J Radiol* 2005; 56:25-30.

Cihangiroglu M, Akfirat M, Yildirim H. CT and MRI findings of ameloblastoma in two cases. *Neuroradiology* 2002;44:434-437.

Caucher Disease

Maas M, Poll LW, Terk MR. Imaging and quantifying skeletal involvement in Gaucher disease. *Brit) Radiol* 2002;75 (Suppl. 1):A13-A24.

Poll LW, Koch JL, vom Dahl S, et al. Magnetic resonance imaging of bone marrow changes in Gaucher disease during enzyme replacement therapy: first German long-term results. *Skeletal Radiol* 2001 ;30: 496-503.

Roca M, Mota J, Alfonso P, Pocovi M, Giraldo P. S-MRI score: a simple method for assessing bone marrow in Gaucher disease. *Eur J Radiol* 2007;62:132-137.

Wenstrup RJ, Roca-Espiau M, Weinreb NJ, Bembi B. Skeletal aspects of Gaucher disease; a review. *Brit) Radiol* 2002;75(Suppl. 1):A2-A12.

Hemophilic Pseudotumor

Geyskens W, Vanhoenacker FM, Van der Zijden T, Peerlinck K. MR imaging of intra-osseous hemophilic pseudotumor: case report and review of the literature./BR-BTK Nov-Dec 2004;87(6):289-293.

Jaovisidha S, Ryu KN, Hodler J, Schweitzer ME, Sartoris DJ, Resnick D. Hemophilic pseudotumor: spectrum of MR findings. *Skeletal Radiol* 1997;26:468-474.

Park JS, Ryu KN. Hemophilic pseudotumor involving the musculoskeletal system: spectrum of radiologic findings. *AJR* 2004;183:55-61.

Table 7 Intramedullary lesions associated with cortical destruction and extraosseous extension

Lesion	MRI Findings	Comments
Nonmalignant		
Osteomyelitis (Fig. 7.1)	Poorly defined zones with high signal on T2WI and FST2WI and Gd-contrast enhancement are seen in marrow with associated zones of cortical destruction. Periosteal reaction can be seen as a peripheral rim of high signal on T2WI and FST2WI and Gd-contrast enhancement on FST1WI adjacent to the low signal of cortical bone. A subperiosteal abscess with high signal on T2WI and FS T2WI can often be seen elevating a single low signal thin band of periosteum.	Infection of bone which can result from hematogenous spread of microorganisms, trauma-direct inoculation, extension from adjacent tissues, and complications from surgery. *Staphyhcoccus aureus* and *Streptococcus pyogenes* are the most common bacterial infections involving bone. Osteomyelitis can also result from other bacteria as well as from other organisms such as tuberculosis, fungi, parasites, and viruses. **(See Atlas Chapter A 63)**
Eosinophilic granuloma (Fig. 7.2)	Focal intramedullary lesion(s) associated with trabecular and cortical bone destruction that typically have low-intermediate signal on T1WI and PDWI and heterogeneous slightly high to high signal on T2WI. Poorly defined zones of high signal on T2WI are usually seen in the marrow peripheral to the lesions secondary to inflammatory changes. Extension of lesions from the marrow into adjacent soft tissues through areas of cortical disruption are commonly seen as well as linear periosteal zones of high signal on T2WI. Lesions typically show prominent Gd-contrast enhancement in marrow and in extraosseous soft tissue portions of the lesions.	Benign tumor-like lesions consisting of Langerhans' cells (histiocytes) and variable amounts of lymphocytes, polymorphonuclear cells, and eosinophils. Account for 1 % of primary bone lesions, and 8 % of tumor-like lesions. Occur in patients with median age = 10 years, average = 13.5 years, peak incidence is between 5 and 10 years, 80-85 % occur in patients less than 30 years. **(See Atlas Chapter A18)**
Sarcoidosis (Fig. 7.3)	Lesions usually appear as intramedullary zones with low to intermediate signal on T1WI and slightly high to high signal on T2WI and FSPDWI and FST2WI. Erosions and zones of destruction involving adjacent bone cortex can occur with or without extraosseous extension of the granulomatous process. After Gd-contrast administration, lesions typically show moderate to prominent enhancement.	Chronic systemic granulomatous disease of unknown etiology in which noncaseating granulomas occur in various tissues and organs including bone. **(See Atlas Chapter A71)**

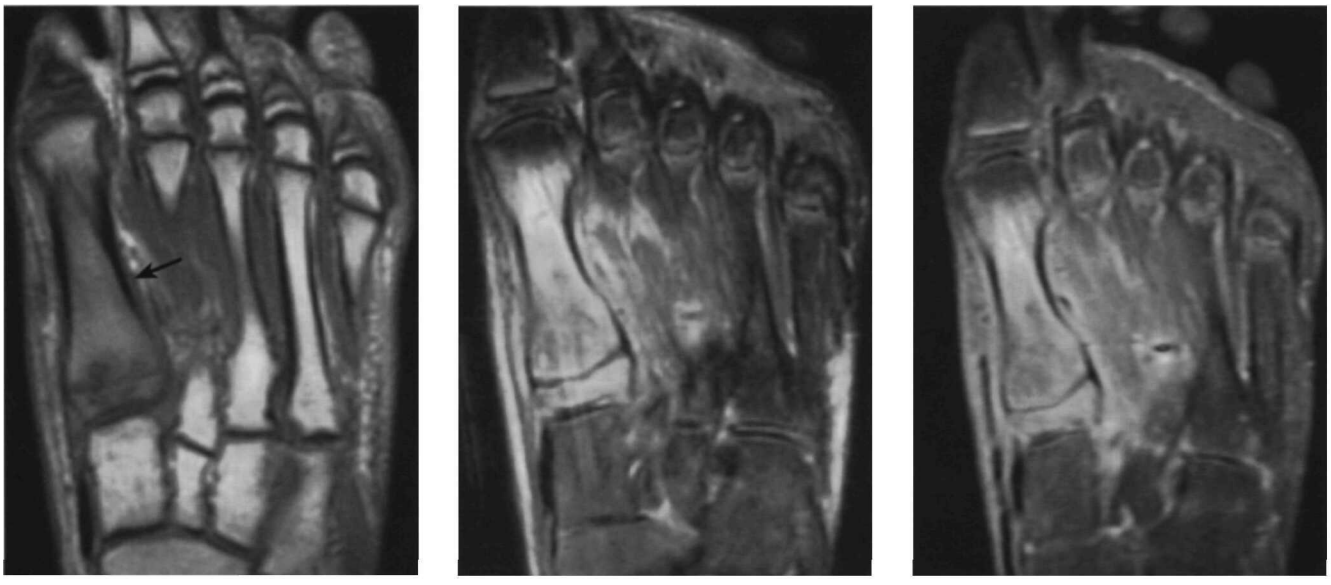

a b, c

Figure 7.**1a-c** A 14-year-old male with osteomyelitis involving the first metatarsal bone. Poorly defined zones of low-intermediate signal on coronal T1WI (**a**), high signal on coronal FST2WI (**b**) and Gd-contrast enhancement on FST1WI (**c**) are seen within the marrow as well as zones of cortical disruption and extraosseous extension.

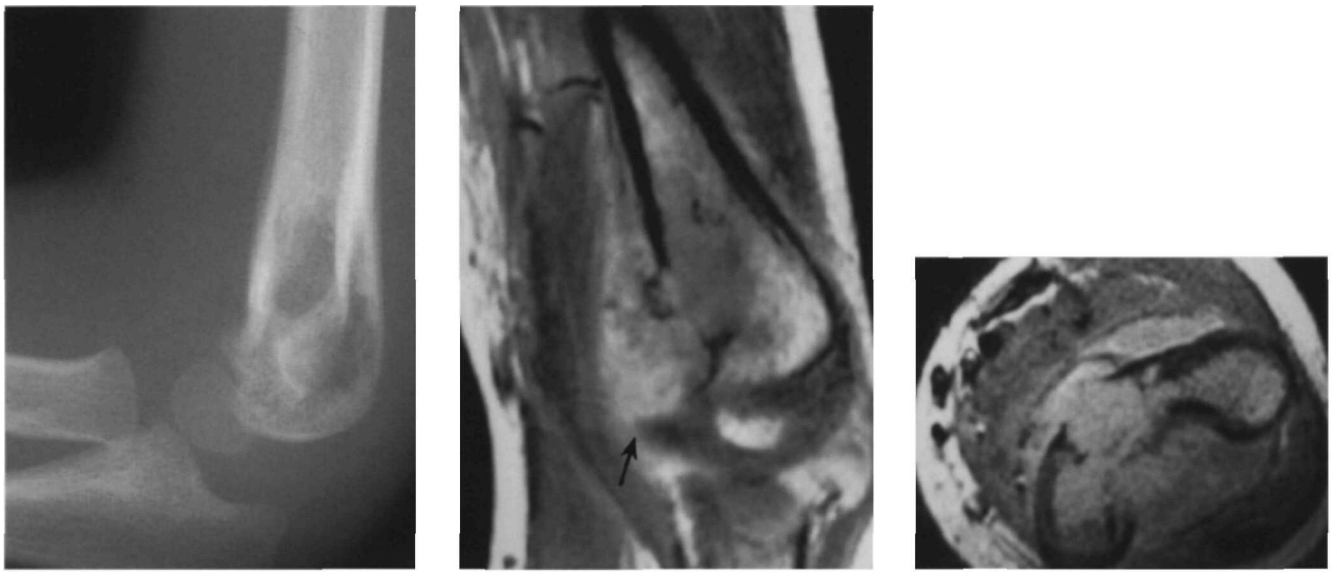

a **b, c**

Figure 7.**2a-c** A 5-year-old boy with an eosinophilic granuloma involving the distal humerus. Lateral radiograph (**a**) shows a radiolucent intramedullary lesion associated with a single layer of periosteal reaction. The lesion in the marrow is associated with cortical destruction and extraosseous extension into the adjacent soft tissues as seen on sagittal Gd-contrast enhanced T1WI (**b**) and axial (**c**) PDWI.

Figure 7.**3** A 55-year-old woman with sarcoidosis involving the right sphenoid bone. The lesion in the marrow shows Gd-contrast enhancement as well as erosion of cortical bone and extension into the anterior portion of the right middle cranial fossa on axial FST1WI. Also seen is abnormal subarachnoid contrast enhancement in the left trigeminal cistern surrounding the left fifth cranial nerve.

Table 7 (Continued) **Intramedullary lesions associated with cortical destruction and extraosseous extension**

Lesion	MRI Findings	Comments
Nonmalignant giant cell tumor (Fig. 7.4)	Usually well-defined lesions with thin low signal margins on T1WI, PDWI, and T2WI. Solid portions of giant cell tumors often have low to intermediate signal on T1WI and PDWI, intermediate to high signal on T2WI, and high signal on FSPDWI and FST2WI. Signal heterogeneity on T2WI is common. Aneurysmal bone cysts can be seen in 14% of giant cell tumors. Varying degrees of Gd-contrast enhancement can be seen in the lesions, as well as peripheral rim-like enhancement around cystic zones / aneurysmal bone cysts. Poorly defined zones of enhancement and high signal on FST2WI may also be seen in the marrow peripheral to the lesions secondary to reactive inflammatory changes from elevated tumor prostaglandin levels.	Aggressive tumors composed of neoplastic ovoid mononuclear cells and scattered multinucleated osteoclast-like giant cells (derived from fusion of marrow mononuclear cells). Up to 10% of all giant cell tumors are malignant. Benign giant cell tumors account for ~ 5 to 9.5% of all bone tumors and up to 23% of benign bone tumors. Occur in patients 4 to 81 years (median = 30 years), 75% occur in patients aged between 1 5 and 45 years. **(See Atlas Chapter A 29)**
Sickle cell disease with adjacent extramedullary hematopoiesis (Fig. 7.5)	Lesions can have low. intermediate, and/or high signal on T1WI and T2WI depending on the proportions and distribution of fat and red marrow. Lesions may be seen extending from marrow through zones of cortical disruption, or as isolated abnormalities.	Represents proliferation of erythroid precursors outside of medullary bone secondary to physiologic compensation for abnormal medullary hematopoiesis from congenital disorders such as hemoglobinopathies (Sickle cell, Thalassemia, etc.) as well as acquired disorders such as myelofibrosis, leukemia, lymphoma, myeloma, or metastatic carcinoma.
Brown tumor	Lesions are usually radiolucent on radiographs and CT. Lesions often have low-intermediate signal on T1WI, intermediate to slightly high signal on T2WI, and typically show Gd-contrast enhancement. Zones of low signal on T2WI may occur from hemosiderin. Expansion of cortical margins can occur with or without cortical disruption/destruction.	Lesions in bone containing multinucleated giant cells, fibrous tissue, blood vessels, and zones of hemorrhage/hemosiderin. Histologic and imaging features are similar to giant cell reparative granulomas.
Atypical hemangioma (Fig. 7.6)	Rare intraosseous hemangiomas may be associated with cortical disruption and extraosseous extension. Lesions can have low-intermediate signal on T1WI, and usually have high signal on T2WI and FST2WI. Lesions typically show prominent Gd-contrast enhancement.	Benign hamartomatous lesions of bone and soft tissues comprising capillary, cavernous, and/or malformed venous vessels. Account for 2-4% of benign bone tumors and - 1 % of all bone tumors. **(See Atlas Chapter A 34)**

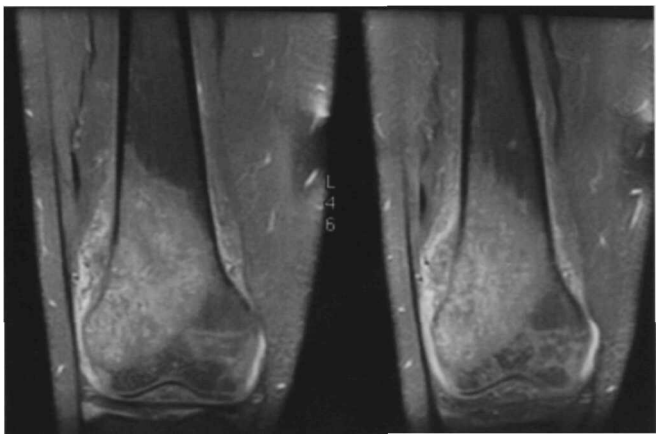

Figure 7.4 A 32-year-old woman with a giant cell tumor in the distal femur associated with cortical destruction and extraosseous extension. The tumor shows Gd-contrast enhancement on the coronal FST1WI.

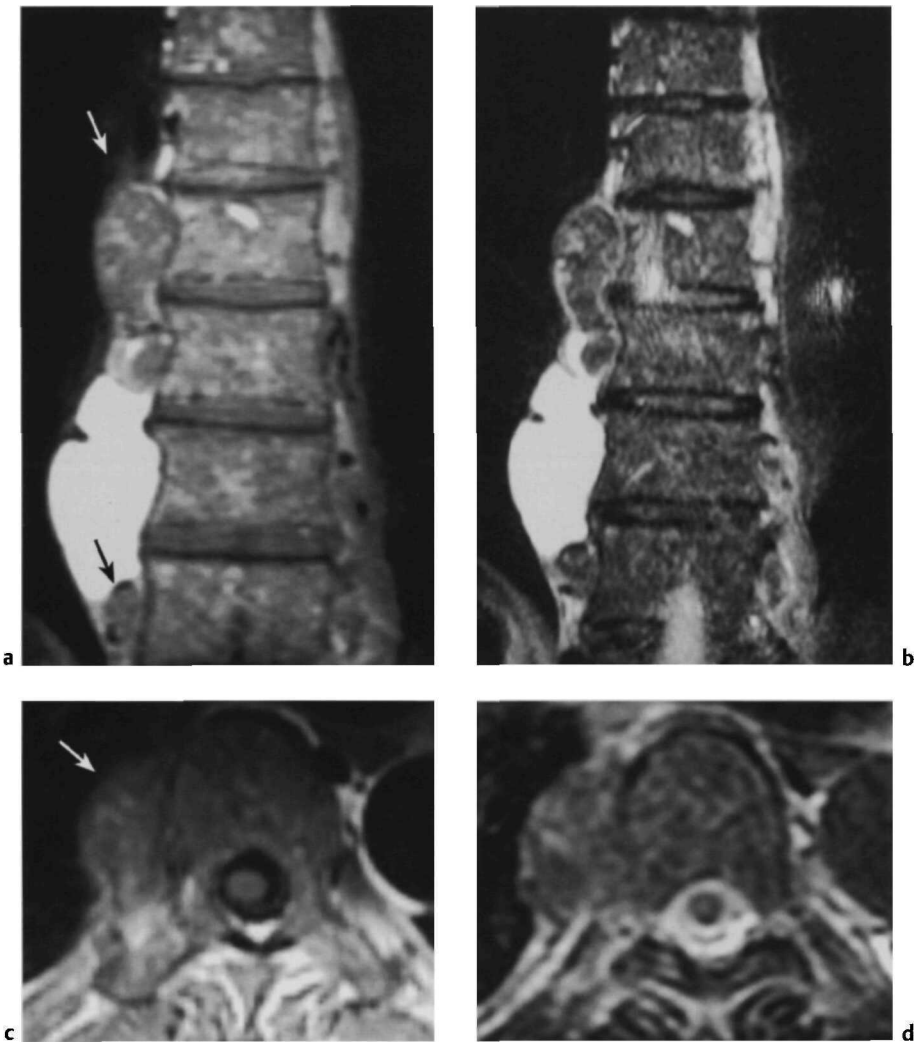

Figure 7.**5a-d** A 56-year-old man with sickle cell disease and extramedullary hematopoiesis. The lesions have a signal comparable to the intraosseous marrow on coronal (**a**) and axial (**c**) T1WI and coronal (**b**) and axial (**d**) T2WI. Small sites of cortical disruption are seen on the axial images.

Figure 7.**6a-c** A 43-year-old woman with an atypical hemangioma involving the posterior right marrow of the C6 vertebra associated with a zone of cortical disruption and extension into the right anterior epidural soft tissues. The lesion has high signal on the sagittal STIR image (**a**) and shows Gd-contrast enhancement on sagittal (**b**) and axial (**c**) FST1WI.

Table 7 (Continued) **Intramedullary lesions associated with cortical destruction and extraosseous extension**

Lesion	MRI Findings	Comments
Malignant		
Metastatic tumor (Fig. 7.7)	Single or multiple well-circumscribed or poorly defined infiltrative lesions involving marrow associated with cortical destruction and extraosseous extension. Lesions often have low-intermediate signal on T1WI, low, intermediate, and/or high signal on T2WI and FST2WI, usually show Gd-contrast enhancement. Cortical destruction and tumor extension into the extraosseous soft tissues frequently occurs. Pathologic fractures can be associated with metastatic lesions involving tubular bones and vertebrae. Periosteal reaction is uncommon.	Metastatic lesions typically occur in the marrow with or without cortical destruction and extraosseous tumor extension. **(See Atlas Chapter A 50)**
Myeloma/plasmacytoma (Fig. 7.8)	Multiple (myeloma) or single (plasmacytoma) are well-circumscribed or poorly defined diffuse infiltrative lesions involving marrow, low-intermediate signal on T1WI, intermediate-high signal on T2WI and FST2WI, usually show Gd-contrast-enhancement, eventual cortical bone destruction and extraosseous extension.	Malignant tumors comprised of proliferating antibody-secreting plasma cells derived from single clones. Most common primary neoplasm of bone in adults, median = 60 years. Most patients are older than 40 years. May have variable destructive or infiltrative changes involving the axial and/or appendicular skeleton. **(See Atlas Chapter A 52)**
Leukemia (Fig. 7.9)	Single or multiple well-circumscribed or poorly defined infiltrative lesions involving marrow; low-intermediate signal on T1WI, intermediate-high signal on T2WI and FST2WI, often shows Gd-contrast enhancement, +/- bone destruction and extraosseous extension.	Lymphoid neoplasms involving of bone marrow with tumor cells also in peripheral blood. In children and adolescents, acute lymphoblastic leukemia (ALL) is the most frequent type. In adults, chronic lymphocytic leukemia (small lymphocytic lymphoma) is the most common type of lymphocytic leukemia. Myelogenous leukemias are neoplasms derived from abnormal myeloid progenitor cells. Acute myelogenous leukemia (AML) occurs in adolescents and young adults, and represents ~20% of childhood leukemia. Chronic myelogenous leukemia (CML) usually affects adults older than 25 years. **(See Atlas Chapter A 41)**
Lymphoma (Fig. 7.10)	Non-Hodgkin lymphoma (NHL) and Hodgkin disease (HD) within bone typically appear as single or multifocal poorly defined or circumscribed intramedullary zones with low-intermediate signal on T1WI, and intermediate, slightly high, and/or high signal on T2WI and high signal on FST2WI; often show Gd-contrast enhancement. Zones of cortical destruction may occur associated with extraosseous soft tissue extension. HD involving bone with associated sclerosis seen on plain films or CT usually has low signal on T1WI and variable/mixed signal on T2WI. In some cases of NHL, intramedullary tumor may be associated with bulky extraosseous lesions without extensive cortical destruction. High resolution MRI in these cases shows thin penetrating channels of tumor extending through bone cortex into the extraosseous soft tissues.	Lymphoid tumors with neoplastic cells typically within lymphoid tissue (lymph nodes and reticuloendothelial organs). Unlike leukemia, lymphoma usually arises as discrete masses. Lymphomas are subdivided into HD and NHL. Almost all primary lymphomas of bone are B cell NHL. HD, mean age = 32 years. Osseous NHL, median = 35 years. **(See Atlas Chapter A 47)**

Figure 7.**7** A 50-year-old man with metastatic lung carcinoma to the iliac bone associated with cortical destruction and extraosseous extension as seen on axial FST2WI.

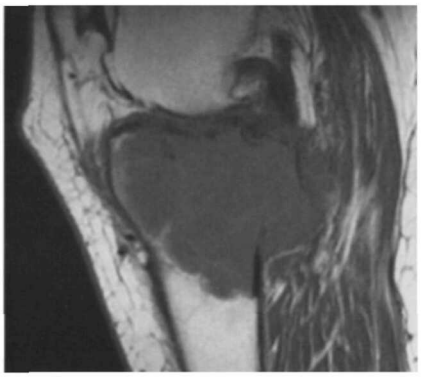

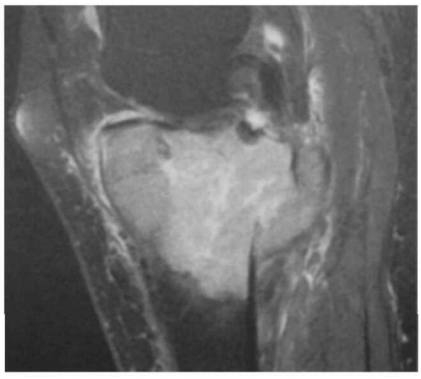

Figure 7.**8 a, b** A 77-year-old woman with myeloma in the proximal tibia. The intramedullary tumor has intermediate signal on sagittal T1WI (**a**) and high signal on FS T2WI (**b**). The tumor is seen extending through the destroyed bone cortex posteriorly.

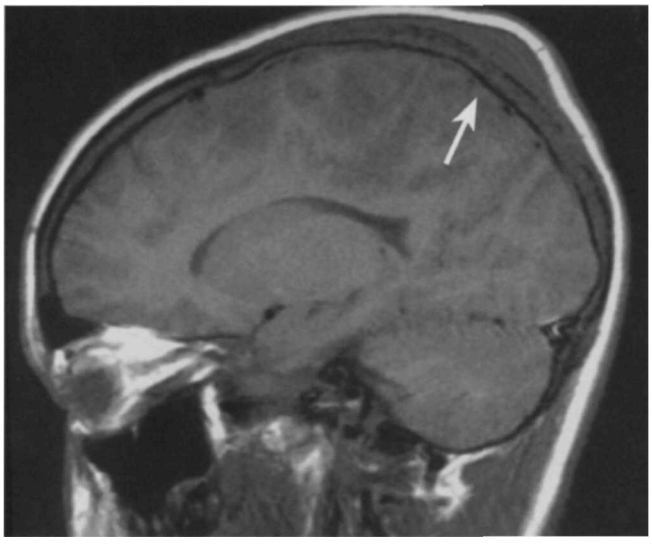

Figure 7.**9** A 12-year-old girl with leukemia (ALL) within the calvarial marrow associated with cortical destruction and extraosseous extension as seen on the sagittal T1WI.

Figure 7.**10** Large B cell NHL in the distal femoral marrow associated with cortical destruction and extraosseous extension as seen on the coronal FST2WI.

Table 7 (Continued) **Intramedullary lesions associated with cortical destruction and extraosseous extension**

Lesion	MRI Findings	Comments
Osteosarcoma (Fig. 7.11)	Destructive intramedullary malignant lesions, low-intermediate signal on T1WI, mixed low, intermediate, high signal on T2WI, usually with matrix mineralization/ossification, low signal on T2WI, typically show Gd-contrast enhancement (usually heterogeneous). Zones of cortical destruction are common, through which tumors extend into the extraosseous soft tissues under an elevated periosteum. Lamellated and/or spiculated zones of bone formation can occur under the periosteal elevation secondary to tumor invasion and perforation of bone cortex. Low signal from spicules of periosteal, reactive, and tumoral bone formation may have a divergent ("sunburst") pattern, perpendicular ("hair on end") pattern, or disorganized or complex appearance. Triangular zones of periosteal elevation (Codman's triangles) can be seen at the borders of zones of cortical destruction and tumor extension.	Malignant tumor comprising proliferating neoplastic spindle-cells that produce osteoid and/or immature tumoral bone, most frequently arising within medullary bone (meta-diaphyseal > metaphyseal > diaphyseal locations). Two age peaks of incidence. The larger peak occurs between the ages of 10 and 20 and accounts for over half of the cases. The second smaller peak occurs in adults over 60 years and accounts for ~10% of the cases. Occurs in children as primary tumors and adults (associated with Paget disease, irradiated bone, chronic osteomyelitis, ostcoblastoma, giant cell tumor, fibrous dysplasia). **(See Atlas Chapter A 64)**
Chondrosarcoma (Fig. 7.12)	Intramedullary tumors often have low-intermediate signal on T1WI, intermediate signal on PDWI, and heterogeneous intermediate-high signal on T2WI. Lesions usually show heterogeneous contrast enhancement. Zones of cortical destruction can be seen with extraosseous extension of tumor.	Chondrosarcomas are malignant tumors containing cartilage formed within sarcomatous stroma. Account for 12-21% of malignant bone lesions, 21-26% of primary sarcomas of bone, 5-91 years, mean = 40 years, median = 26-59 years. **(See Atlas Chapter A11)**
Ewing sarcoma (Fig. 7.13)	Destructive malignant lesions involving marrow, low-intermediale signal on T1WI, mixed low, intermediate, and/or high signal on T2WI and F5T2WI, typically show Gd-contrast enhancement (usually heterogeneous). Extraosseous tumor extension through sites of cortical destruction is commonly seen beneath an elevated periosteum. Thin striated zones of low signal on T2WI can be sometimes seen oriented perpendicular to the long axis of the involved bone under the elevated periosteum representing the "hair on end" appearance of reactive bone formation secondary to the tumor. In long bones, tumors are most often located in the diaphyseal region, followed by the meta-diaphyseal region.	Malignant primitive tumor of bone comprising of undifferentiated small cells with round nuclei. Account for 6-11% of primary malignant bone tumors, 5-7 % of primary bone tumors. Usually occur between the ages of 5 and 30, males > females, locally invasive, high metastatic potential. **(See Atlas Chapter A 20)**
Chordoma (Fig. 7.14)	Tumors are often midline in location, often have lobulated or slightly lobulated margins. Lesions can involve marrow with associated destruction of trabecular and cortical bone with extraosseous extension. Chondroid chordomas are either midline or off-midline in location. Chordomas typically have low-intermediate signal on T1WI and heterogeneous predominantly high signal on T2WI. Chordomas typically enhance with Gd-DTPA, often in a heterogeneous pattern.	Rare, locally aggressive, slow-growing low to intermediate malignant tumors derived from ectopic notochordal remnants along the axial skeleton. Chordomas account for 2-4% of primary malignant bone tumors, 1-3% of all primary bone tumors; and < 1 % of intracranial tumors. Patients range in age from 6 to 84 years, median = 58 years. **(See Atlas Chapter A12)**

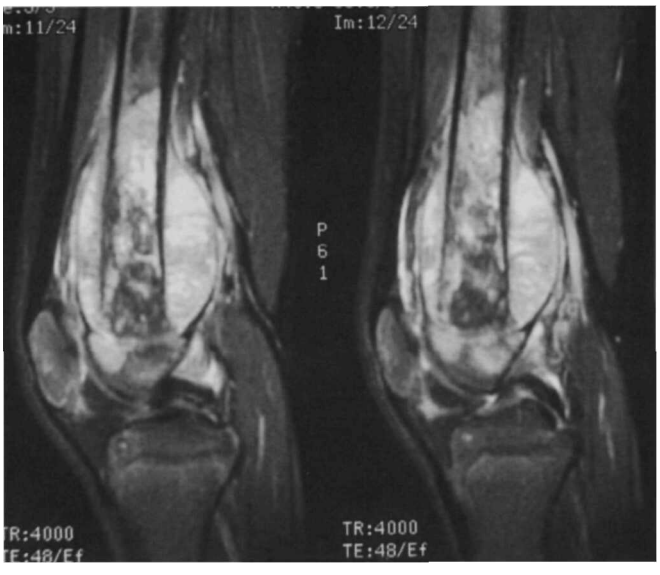

Figure 7.11 A 9-year-old girl with osteosarcoma in the distal femoral marrow associated with cortical destruction and extraosseous extension as seen on the sagittal FST2WI.

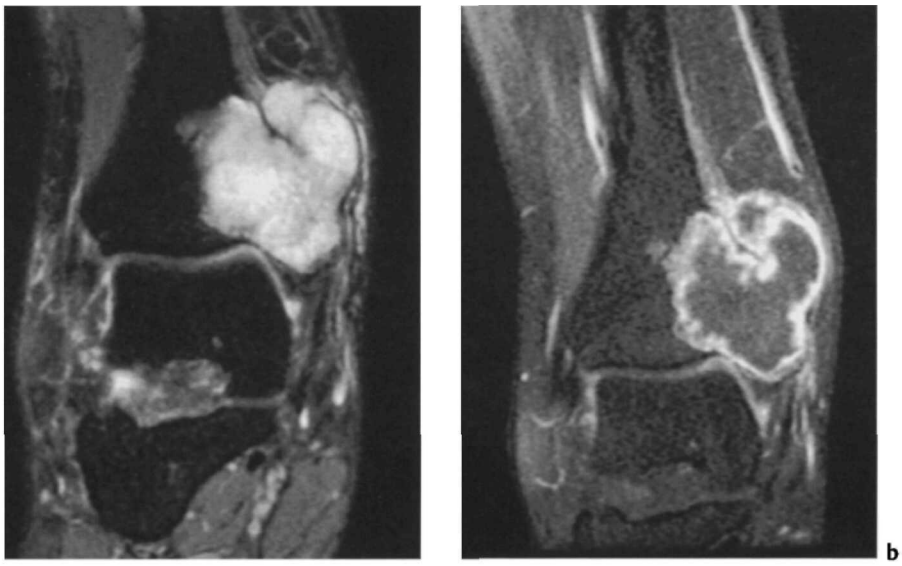

Figure 7**.12a, b** A 44-year-old woman with a chondrosarcoma in the marrow of the distal tibia associated with cortical destruction and extraosseous extension of tumor. The tumor has high signal on the coronal FST2WI (**a**) and shows peripheral lobular Gd-contrast enhancement on FST1WI (**b**).

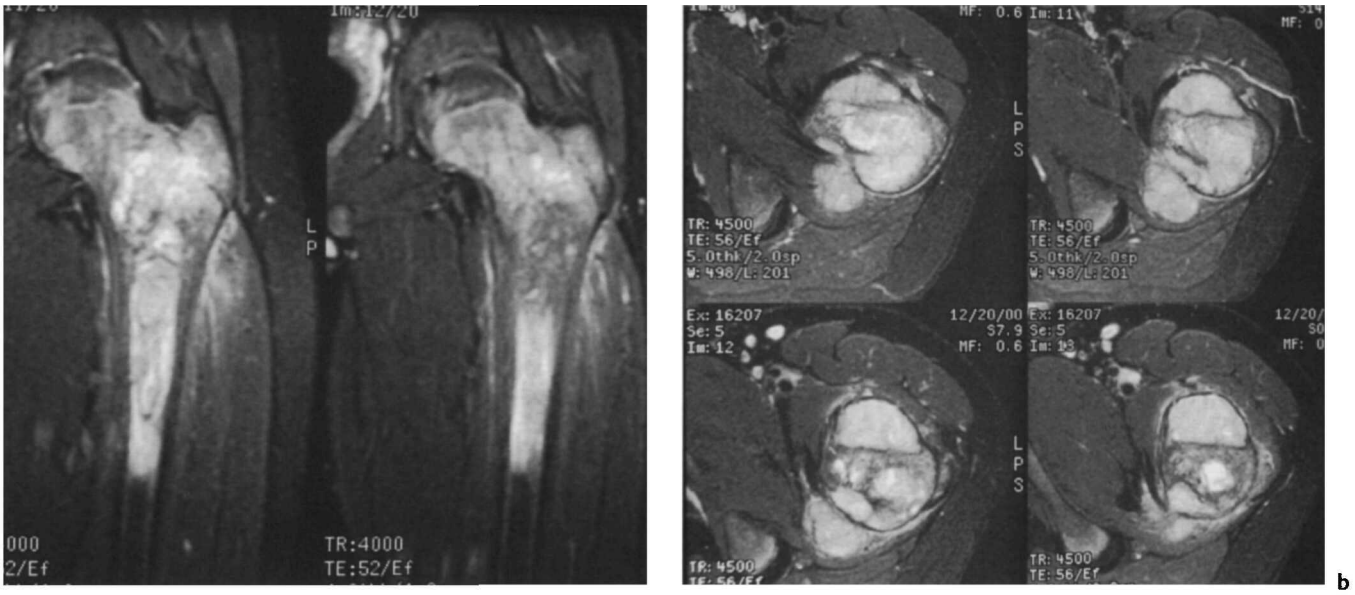

Figure **7.13a, b** A 15-year-old male with Ewing sarcoma in the marrow of the proximal femur associated with cortical destruction and extraosseous extension as seen on coronal (**a**) and axial (**b**) FST2WI.

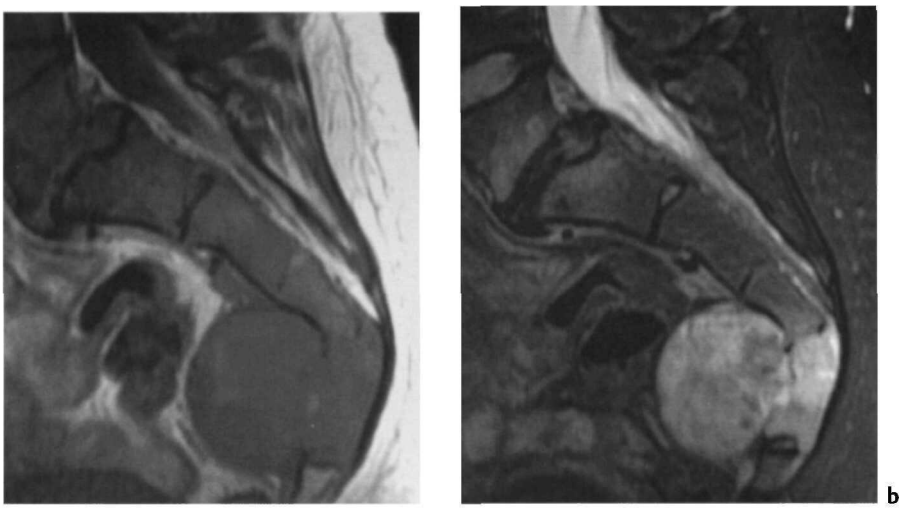

Figure **7.14a, b** A 30-year-old woman with a chordoma involving the lower sacrum associated with cortical bone destruction and tumor extension into the adjacent soft tissues. The tumor has mostly intermediate signal on sagittal T1WI (**a**) and heterogeneous mostly high signal on sagittal FST2WI (**b**).

Table 7 (Continued) **Intramedullary lesions associated with cortical destruction and extraosseous extension**

Lesion	MRI Findings	Comments
Fibrosarcoma (Fig. 7.15)	Intramedullary lesions with irregular margins, with or without associated cortical destruction and/or extraosseous soft tissue masses. Lesions usually have low-intermediate signal on T1WI and PDWI, and heterogeneous intermediate, slightly high, and/or high signal on T2WI. Lesions usually show heterogeneous Gd-contrast enhancement.	Fibrosarcomas are uncommon malignant tumors consisting of bundles of fibroblasts/spindle cells with varying proportions of collagen, lacking other tissue differentiating features such as tumor bone, osteoid, or cartilage. Can be primary lesions (75%) or arise as secondary tumors (25%) associated with prior irradiation, Paget disease, bone infarct, chronic osteomyelitis, fibrous dysplasia, giant cell tumor. Account for 3-5% of primary malignant bone tumors, and 2-4% of all bone tumors, median age = 43 years. **(See Atlas Chapter A 25)**
Malignant fibrous histiocytoma (Fig. 7.16)	Intramedullary lesions with irregular margins and zones of cortical destruction and extraosseous extension. Tumors often have low-intermediate signal on T1WI; low-intermediate signal on PDWI, and heterogeneous intermediate-high signal on T2WI and FST2WI. Invasion into joints occurs in 30%. May be associated with bone infarcts, bone cysts, chronic osteomyelitis, Paget disease, and other treated primary bone tumors. Lesions usually show heterogeneous Gd-contrast prominent enhancement.	Malignant tumor involving soft tissue and rarely bone derived from undifferentiated mesenchymal cells. Contains cells with limited cellular differentiation such as mixtures of fibroblasts, myofibroblasts, histiocyte-like cells, anaplastic giant cells, and inflammatory cells. Accounts for 1-5% of primary malignant bone tumors and < 1 -3 % of all primary bone tumors, patient ages range from 11 to 80 years, median = 48 years, mean = 55 years. **(See Atlas Chapter A 48)**
Malignant giant cell tumor (Fig. 7.17)	Well-defined lesions with or without thin low signal margins on T1WI and T2WI. Solid portions of giant cell tumors often have low to intermediate signal on T1WI and PDWI, intermediate to high signal on T2WI, and high signal on FSPDWI and FST2WI. Signal heterogeneity on T2WI is not uncommon. Aneurysmal bone cysts are seen with 14% of giant cell tumors. Lesions show mild to prominent variable and often heterogeneous Gel-contrast enhancement. Poorly defined zones of enhancement and high signal on FST2WI may occasionally be seen in the adjacent marrow secondary to inflammatory reaction from elevated tumor prostaglandin levels. Cortical destruction and extraosseous tumor extension are frequently seen.	Aggressive tumors composed of neoplastic ovoid mononuclear cells and scattered multinucleated osteoclast-like giant cells. Up to 10% of all giant cell tumors are malignant. Benign giant cell tumors account for ~ 5 to 9.5% of all bone tumors and up to 23% of benign bone tumors. Malignant giant cell tumors account for 5.8% of all giant cell tumors. 75% occur in patients between the ages of 15 and 45. **(See Atlas Chapter A 29)**
Hemangioendothelioma (Fig. 7.18)	Intramedullary tumors usually with sharp margins that may be slightly lobulated. Lesions often have low-intermediate and/or high signal on T1WI and PDWI, and heterogeneous intermediate-high signal on T2WI and FST2WI with or without zones of low signal. Lesions can be multifocal. Extraosseous extension of tumor through zones of cortical destruction commonly occur. Lesions often show prominent heterogeneous Gd-contrast enhancement.	Low-grade vasoformative/endothelial malignant neoplasms that are locally aggressive and rarely metastasize compared with the high-grade endothelial tumors such as angiosarcoma. Account for <1% of primary malignant bone tumors. Patients range from 10 to 82 years, median =36 to 47 years. Patients with multifocal lesions tend to be ~ 10 years younger on average than those with unifocal tumors. **(See Atlas Chapter A 33)**

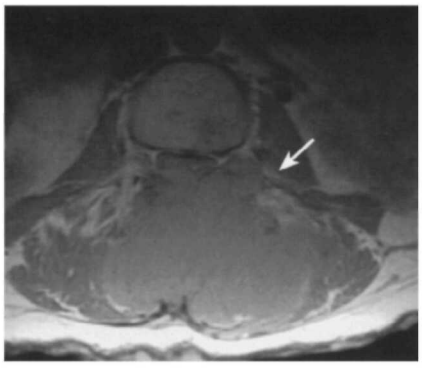

a

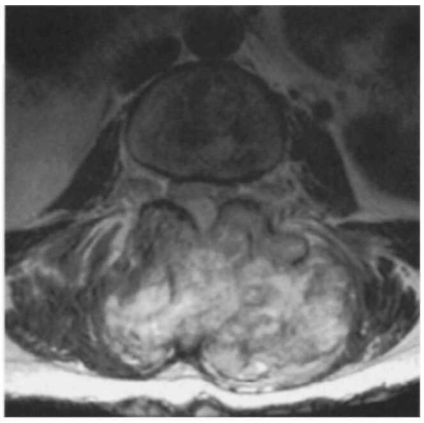

b

Figure **7.15a, b** A 25-year-old man with fibrosarcoma extending from the posterior elements of the L3 vertebra into the adjacent soft tissues through destroyed bone cortex. The tumor has intermediate signal on axial T1WI (**a**) and heterogeneous mostly high signal on axial T2WI (**b**).

a

Figure 7**.16** A 56-year-old man with a malignant fibrous histiocytoma extending from the posterior elements of the L3 vertebra into the adjacent soft tissues through destroyed bone cortex. The tumor involves the posterior elements of the L3 vertebra. The tumor shows heterogeneous Gd-contrast enhancement on sagittal FST1WI.

b

Figure 7**.17a, b** A 16-year-old male with a malignant giant cell tumor of the distal tibia associated with destruction of cortical bone with extraosseous extension as seen on coronal T1WI(**a**) and FST2WI (**b**).

a

Figure 7**.18a, b** A 19-year-old man with hemangioendothelioma involving the distal tibia with cortical disruption and tumor extension into the ankle joint, as seen on T2WI (**a**) and FST2WI (**b**). A second lesion with high signal is also seen in the metaphyseal marrow of the tibia (**b**).

b

Table 7 (Continued) **Intramedullary lesions associated with cortical destruction and extraosseous extension**

Lesion	MRI Findings	Comments
Liposarcoma (Fig. 7.19)	Tumors can have intermediate and/or slightly high to high signal on T1WI and T2WI, and show Gd-contrast enhancement.	Malignant mesenchymal tumors containing portions showing differentiation into adipose tissue. Primary liposarcoma in bone is very rare, median = 31 years. **(See Atlas Chapter A 44)**
Paget sarcoma (Fig. 7.20)	Irregular zones of medullary and cortical bone destruction associated with an extraosseous soft tissue mass lesion. The involved marrow typically has low to intermediate signal on T1WI and PDWI, and low to high signal on T2WI. Abnormal Gd-contrast enhancement is seen in the marrow as well as in the extraosseous tumor extension.	Paget disease is the most common bone disease in older adults after osteoporosis. Median age = 66 years. Disordered bone resorption and woven bone formation occurs, resulting in osseous deformity. Associated with <1% risk for developing secondary sarcomatous changes. **(See Atlas Chapter A 65)**

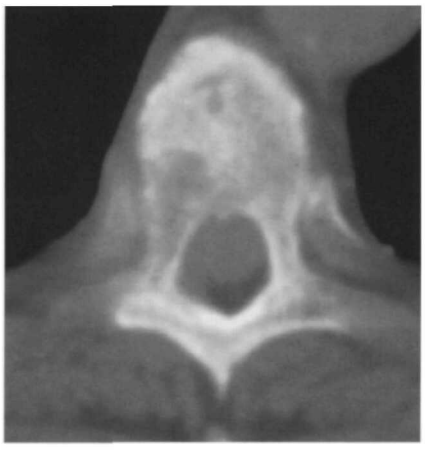

a

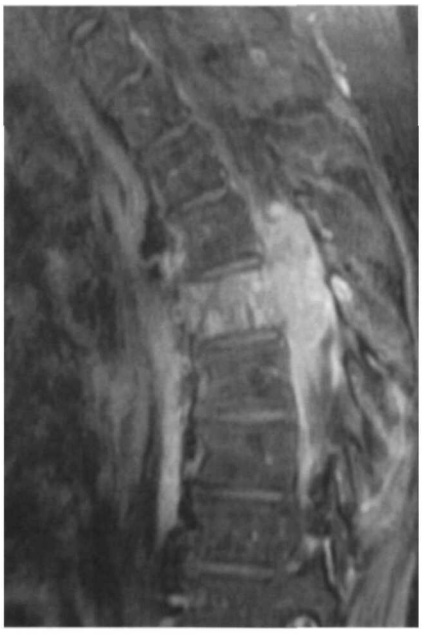

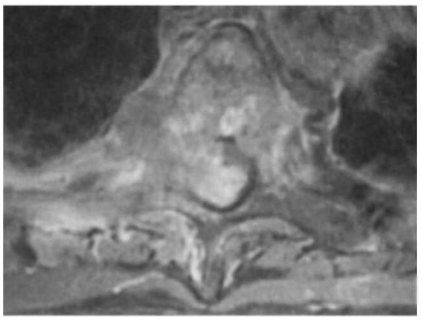

b, c

Figure 7.**19a-c** An 81-year-old man with an intraosseous liposarcoma involving a thoracic vertebra. Radiolucent and sclerotic changes are seen within the vertebra as well as cortical destruction on axial CT (**a**). The intraosseous tumor shows prominent Gd-contrast enhancement on sagittal (**b**) and axial (**c**) FST1WI. Also seen is cortical destruction with extraosseous tumor extension and spinal cord compression.

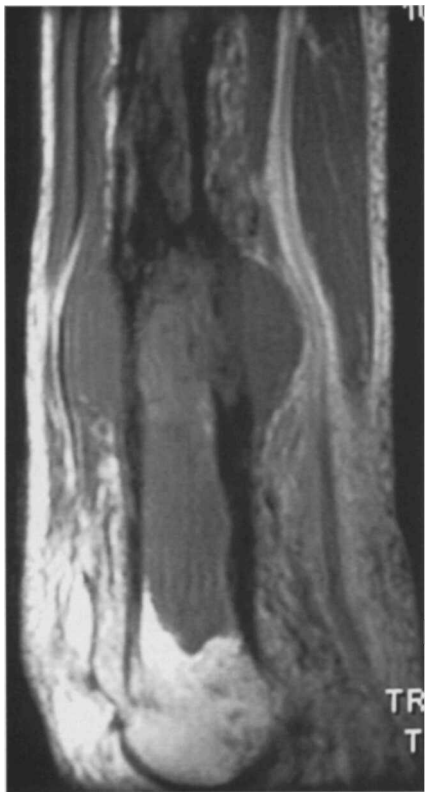

Figure 7.**20** A 71-year-old woman with Paget sarcoma extending from the marrow through destroyed bone cortex into the extraosseous soft tissues as seen on sagittal T1WI.

References

Sickle Cell Disease with Extramedullary Hematopoiesis

Castelli R, Graziadei G, Karimi M, Cappellini MD. Intrathoracic masses due to extramedullary hematopoiesis. *Am J Med Sci* 2004;328: 299-303.

Collins WO, Younis RT, Garcia MT. Extramedullary hematopoiesis of the paranasal sinuses in sickle cell disease. *Otolaryngol Head Neck Surg* 2005;132:954-956.

Table 8 Solitary intramedullary lesions with well-circumscribed margins

Lesion	MRI Findings	Comments
Benign		
Hemangioma (Fig. 8.1)	Often well-circumscribed lesions which typically have intermediate to high signal on T1WI, PDWI, T2WI, and FST2WI. On T1WI, hemangiomas usually have signal equal to or greater than adjacent normal marrow secondary to fatty components. Usually show Gd-contrast enhancement. Pathologic fractures associated with intraosseous hemangiomas usually result in low-intermediate marrow signal on T1WI.	Common benign lesions of bone comprised of capillary, cavernous, and/or malformed venous vessels. Hemangiomas have been considered to be a hamartomatous disorder. Account for 4 % of benign bone tumors and ~ 1 % of all bone tumors, likely underestimated. Occurs in all ages, median = 33 years. **(See Atlas Chapter A 34)**
Nonossifying fibroma (Fig. 8.2)	Well-circumscribed eccentric intramedullary lesions in the metadiaphyseal regions of long bones that have mixed low-intermediate signal on T1WI, and mixed low, intermediate, and/or high signal on T2WI, PDWI, and FST2WI. Zones of low signal on T1WI, PDWI, and T2WI can be seen in the central portions of the lesions. Zones with varying thickness of low signal on T1WI, PDWI, and T2WI are seen at the margins of the lesions representing bone sclerosis. Internal septations are commonly seen as zones of low signal on T2WI in these lesions. Lesions can show Gd-contrast enhancement (heterogeneous > homogeneous patterns).	Common benign fibrohistiocytic lesions in the metaphyseal portions of long bones that are comprised of whorls of fibroblastic cells combined with smaller amounts of multinucleated giant cells and xanthomatous cells. Usually asymptomatic, 95% occur between the ages of 5 and 20, median = 14 years. **(See Atlas Chapter A 26)**

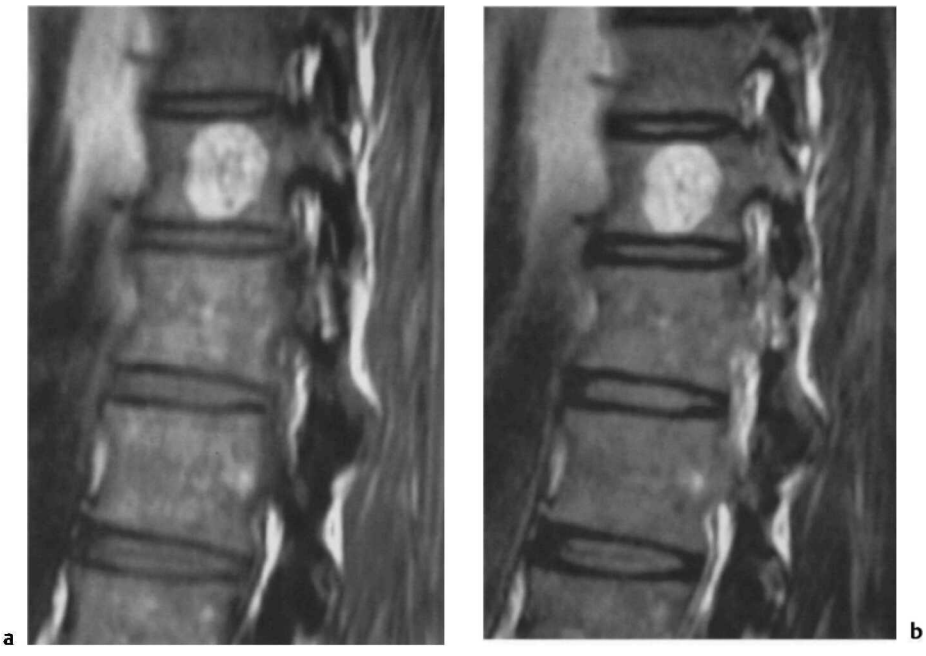

Figure 8.**1 a, b** Hemangioma within the T12 vertebral body has circumscribed margins and contains high signal on sagittal T1WI (**a**) and T2WI (**b**)

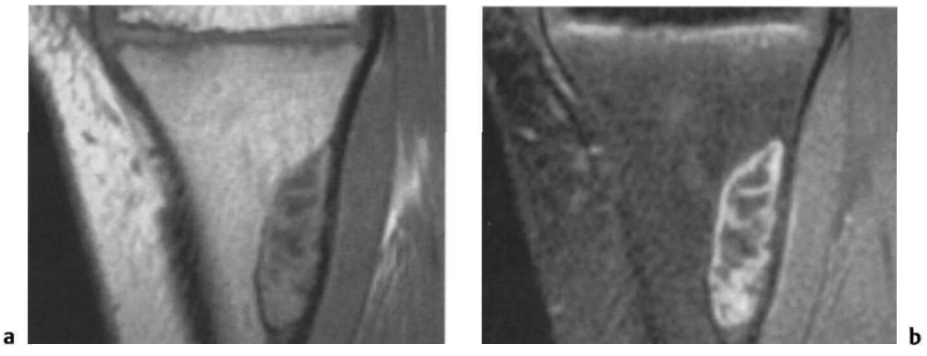

Figure 8.**2 a, b** Nonossifying fibroma in the dorsal proximal tibia of a 12-year-old girl has heterogeneous low and intermediate signal on sagittal T1WI (**a**) and mixed high and low signal on FST2WI (**b**)

Table 8 (Continued) **Solitary intramedullary lesions with well-circumscribed margins**

Lesion	MRI Findings	Comments
Enchondroma (Fig. 8.3)	Lobulated intramedullary lesions with well-defined borders, mean size = 5cm. Lesions usually have low-intermediate signal on T1WI and intermediate signal on PDWI. On T2WI and FST2WI, lesions usually have predominantly high signal with foci and/or bands of low signal representing areas of matrix mineralization and fibrous strands. Lesions typically show Gd-contrast enhancement in various patterns (peripheral curvilinear lobular, central nodular/septal and peripheral lobular, or heterogeneous diffuse).	Benign intramedullary lesions composed of hyaline cartilage, represent ~10% of benign bone tumors. Enchondromas can be solitary (88%) or multiple (12%). Median age = 35 years, peak in 3rd and 4th decades. **(See Atlas Chapter A5)**
Rbrous dysplasia (Fig. 8.4)	MRI features depend on the proportions of bony spicules, collagen, fibroblastic spindle cells, hemorrhagic and/or cystic changes, and associated pathologic fracture if present. Lesions are usually well-circumscribed and have low or low-intermediate signal on T1WI and PDWI. On T2WI, lesions have variable mixtures of low, intermediate, and/or high signal often surrounded by a low signal rim of variable thickness. Internal septations and cystic changes are seen in a minority of lesions. Bone expansion with thickened and/or thinned cortex can be seen. Lesions show Gd-contrast enhancement that varies in degree and pattern.	Benign medullary fibro-osseous lesion that can involve a single site **(mono-ostotic)** or multiple locations **(poly-ostotic).** Thought to occur from developmental failure in the normal process of remodeling primitive bone to mature lamellar bone with resultant zone or zones of immature trabeculae within dysplastic fibrous tissue. Accounts for ~10% of benign bone lesions. Patients range in age from < 1 to 76 years. 75% occur before age 30 years. **(See Atlas Chapter A 27)**

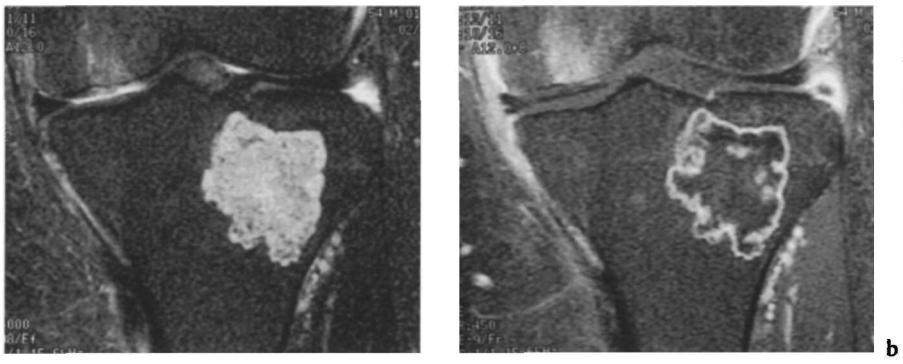

Figure 8.**3 a, b** Enchondroma in a 54-year-old man has slightly lobulated sharp margins. The lesion has high signal on coronal FST2WI (**a**) and shows thin peripheral Gd-contrast enhancement on FST1WI (**b**).

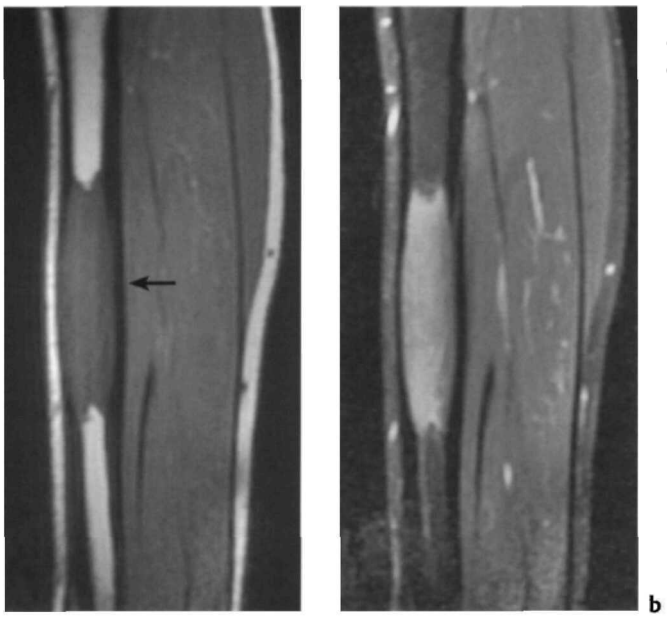

Figure 8.**4a, b** Fibrous dysplasia in the tibial diaphysis of a 19-year-old man has intermediate signal on sagittal T1WI (**a**) and shows Gd-contrast enhancement on FST1WI (**b**).

Table 8 (Continued) **Solitary intramedullary lesions with well-circumscribed margins**

Lesion	MRI Findings	Comments
Liposclerosing myxofibrous tumor (Fig. 8.5)	Lesions have well-defined margins with variable thickness of low signal borders on T1WI and T2WI. Lesions often have low to intermediate signal on T1WI, and intermediate to high signal on T2WI and FST2WI. Small zones with fat signal may be seen at the periphery of the lesions. Lesions usually lack Gd-contrast enhancement.	Uncommon benign fibro-osseous lesions with mixed histologic features of lipoma, fibroxanthoma, myxoma, fibrous dysplasia, bone cyst, myxofibroma, fat necrosis, and/or ischemic ossification. Most of these lesions occur in the intertrochanteric region of the femur. May represent a variant form of fibrous dysplasia. Patients range from 15 to 69 years, mean = 42 years. **(See Atlas Chapter A45)**
Unicameral bone cyst (Fig. 8.6)	Unicameral bone cysts (UBCs) often have a peripheral rim of low signal on T1WI and T2WI adjacent to normal medullary bone. UBCs usually contain fluid with low to low-intermediate signal on T1WI, low-intermediate and high signal on T2WI. Fluid-fluid levels may occur. For UBCs without pathologic fracture, thin peripheral Gd-contrast enhancement can be seen at the margins of lesions. UBCs with pathologic fracture can have heterogeneous or homogeneous low-intermediate or slightly high signal on T1WI, and heterogeneous or homogeneous high signal on T2WI and FST2WI. UBCs complicated by fracture can have internal septations and fluid-fluid levels, as well as irregular peripheral Gd-contrast enhancement at internal septations.	Intramedullary non-neoplastic cavities filled with serous or serosanguineous fluid. Account for *9%* of primary tumor-like lesions of bone. 85% occur in the first 2 decades, median = 11 years. **(See Atlas Chapter A 3)**
Aneurysmal bone cyst (Fig. 8.7)	ABCs often have a low signal rim on T1WI and T2WI adjacent to normal medullary bone and between extraosseous soft tissues. Various combinations of low, intermediate, and/or high signal on T1WI, PDWI, and T2WI are usually seen within aneurysmal bone cysts as well as fluid-fluid levels. Variable Gel-contrast enhancement is seen at the margins of lesions as well as involving the internal septae.	Tumor-like expansile bone lesions containing cavernous spaces filled with blood. ABCs can be primary bone lesions (two-thirds) or secondary to other bone lesions/tumors (such as giant cell tumors, chondroblastomas, osteoblastomas, osteosarcomas, chondromyxoid fibromas, nonossifying fibromas, fibrous dysplasia, fibrosarcomas, malignant fibrous histiocytomas, and metastatic disease). Account for ~11% of primary tumor-like lesions of bone. Patients usually range in age from 1 to 25 years, median = 14 years. **(See Atlas Chapter A 2)**
Giant cell reparative granuloma (Fig. 8.8)	Lesions can have heterogeneous low. intermediate, and/or high signal on T1WI, PDWI, and T2WI as well as peripheral rim-like and central Gd-contrast enhancement on FST1WI.	Giant cell reparative granulomas are also referred to as solid ABCs. **(See Atlas Chapter A 2).** Histologic appearance resembles brown tumors.

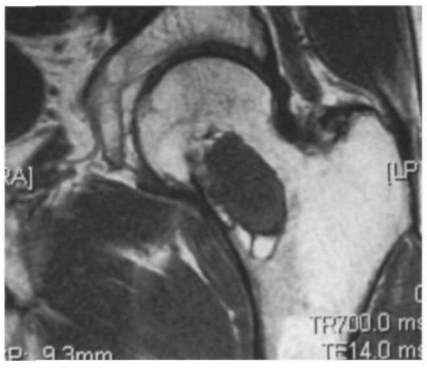

a

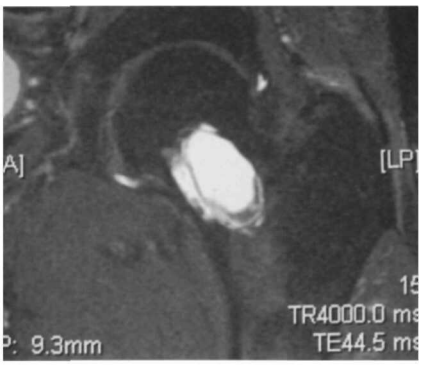

b

Figure 8.5 a, b Liposclerosing myxofibrous tumor in the femoral neck of a 61-year-old man. The circumscribed lesion has mostly low signal centrally as well as small peripheral zones with a high fat signal on coronal T1WI (**a**), and has mostly high signal on coronal FS T2WI (**b**).

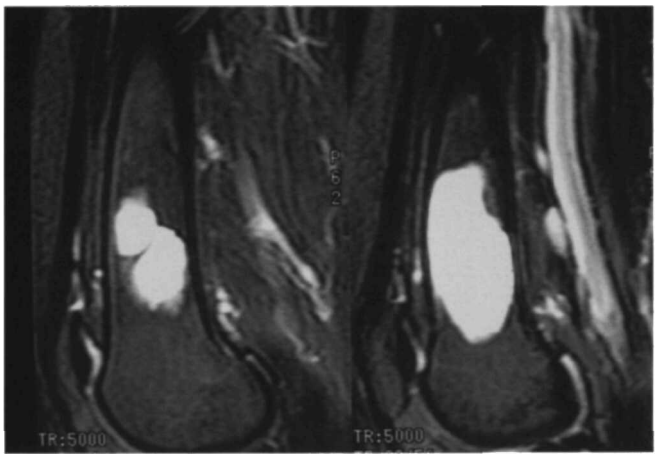

Figure 8.**6** Unicameral bone cyst in the distal femoral shaft of a 17-year-old female has high signal on sagittal FST2WI.

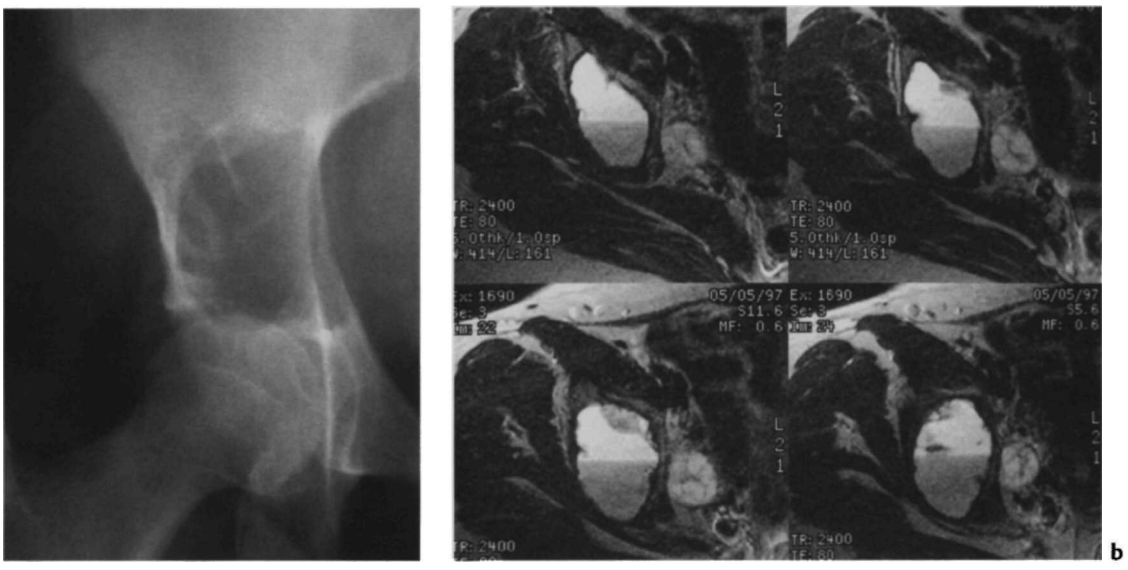

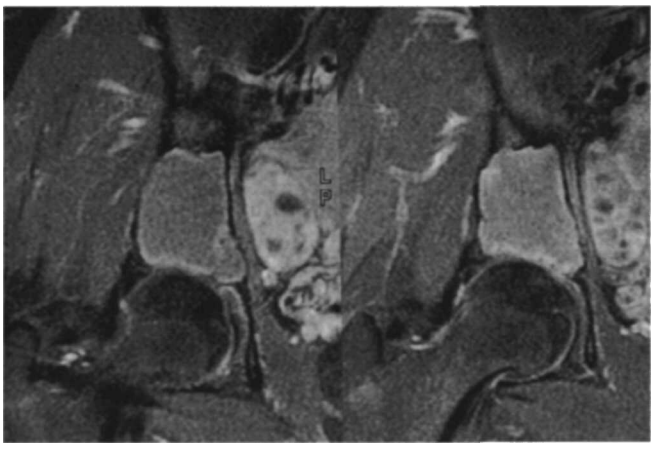

Figure 8.**7a-c** Aneurysmal bone cyst in a 10-year-old girl is seen as a radiolucent lesion in the right iliac bone on an AP radiograph (**a**). A fluid-fluid level is seen in the lesion on axial T2WI (**b**). A thin zone of peripheral Gd-contrast enhancement is seen on coronal FST1WI (**c**).

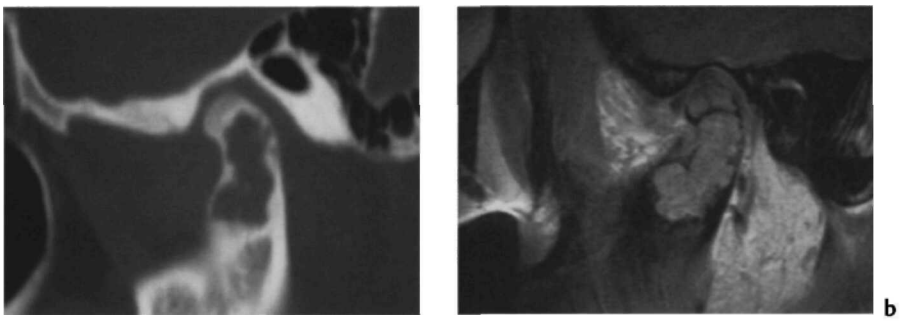

Figure 8.**8 a, b** Giant cell granuloma in a 15-year-old female is seen as a circumscribed radiolucent lesion in the mandible on the sagittal CT image (**a**) that shows Gd-contrast enhancement on sagittal T1WI (**b**).

Table 8 (Continued) **Solitary intramedullary lesions with well-circumscribed margins**

Lesion	MRI Findings	Comments
Intraosseous lipoma (Fig. 8.9)	Lesions can have heterogeneous high, intermediate, and/or low signal on T1WI, PDWI. and T2WI High signal from far is suppressed with FS T1WI, FST2WI, and STIR. Lesions may show no Gd-contrast enhancement. Peripheral rim-like and central Gd-contrast enhancement may occur occasionally on FST1WI. Calcifications, when present, usually appear as zones of low signal or signal void.	Uncommon benign hamartomas composed of mature white adipose tissue without cellular atypia. Osseous or chondroid metaplasia with myxoid changes can be associated with lipomas. Account for ~0.1% of bone tumors, likely underreported. **(See Atlas Chapter A 43)**
Brown tumor	Lesions are usually radiolucent on radiographs and CT. Lesions often have low-intermediate signal on T1WI, intermediate to slightly high signal on T2WI, and typically show Gd-contrast enhancement. Zones of low signal on T2WI may occur from hemosiderin. Expansion of cortical margins can occur with or without cortical disruption/destruction. Lesions may have circumscribed and/or poorly defined margins.	Lesions in bone contain multinucleated giant cells, fibrous tissue, blood vessels, and zones of hemorrhage/hemosiderin. Histologic and imaging features are similar to giant cell reparative granulomas. Most often involves ribs, mandible, clavicle, pelvis, craniofacial bones, and vertebrae. Can result from primary hyperparathyroidism (3-7%) (oversecretion of parathyroid hormone (PTH) from parathyroid adenoma associated with hypercalcemia), secondary type (vitamin D deficiency or chronic renal failure with hypocalcemia resulting in secretion of PTH and parathyroid gland hyperplasia) (1-2%), or tertiary type in which the secondary type leads to eventual autonomous elevated PTH secretion from parathyroid gland hyperplasia.
Geode (Fig. 8.10)	Typically have sharply defined margins and contains low signal on T1WI, low-intermediate signal on PDWI, and homogeneous high signal on T2WI. Poorly defined zones of Gd-contrast enhancement can be seen in the marrow adjacent to the subchondral cysts on FST1WI.	A geode or subchondral cyst is a cystic lesion located near the end of a long bone where there are changes of degenerative osteoarthropathy. Lesions can result from synovial fluid intrusion and/or bony contusion in the setting of degenerative joint disease. **(See Atlas Chapter A 28)**
Intraosseous ganglion (Fig. 8.11)	Can have round, oval, or serpiginous configurations with sharply defined margins. These lesions typically contain low signal on T1WI, low-intermediate signal on PDWI, and high signal on T2WI.	Benign cystic lesion usually located at or near the ends of long bones, and is not associated with degenerative osteoarthropathy. Lesions can result from intraosseous extension from a ganglion in the soft tissues or from intraosseous mucoid degeneration, synovial rests, or synovial intrusion. **(See Atlas Chapter A 28)**
Bone infarct (Fig. 8.12)	A double- line sign (curvilinear adjacent zones of low and high signal on T2WI) is commonly seen at the edges of the infarcts representing the borders of osseous resorption and healing. Irregular Gd-contrast enhancement can be seen from granulation tissue ingrowth.	Zones of ischemic death involving bone trabeculae and marrow which may be iciopathic or result from: trauma, corticosteroid treatment, chemotherapy, radiation treatment, occlusive vascular disease, collagen vascular and other autoimmune diseases, metabolic storage diseases (Gaucher etc.), sickle cell disease, thalassemia, hyperbaric events / Caisson disease, pregnancy, alcohol abuse, pancreatitis, infections, and lymphoproliferative diseases. **(See Atlas Chapter A 37)**

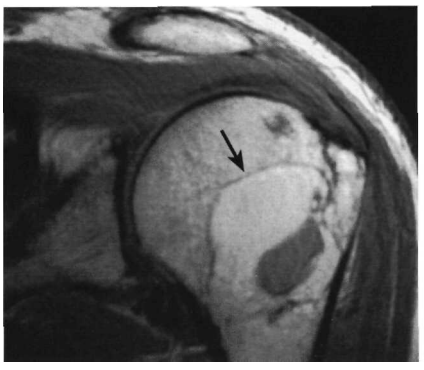

a

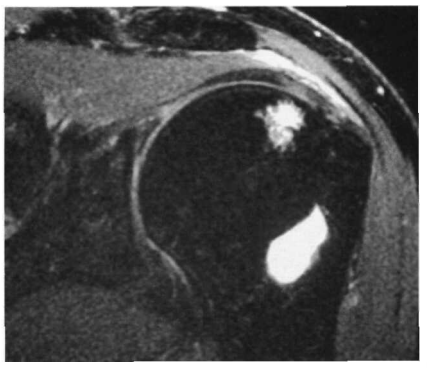

b

Figure 8.**9a, b** A 62-year-old man with a lipoma in the proximal humerus. The circumscribed lesion has a thin low signal margin and a signal similar to fat on coronal PDWI (**a**) and FST2WI (**b**). A small zone of cystic degeneration is also seen within the intraosseous lipoma.

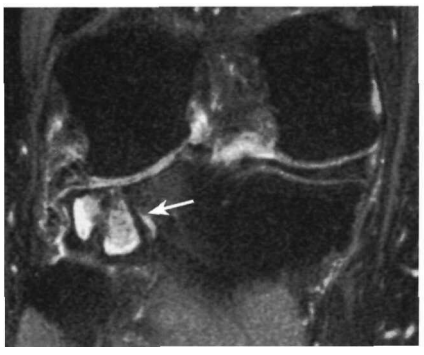

a

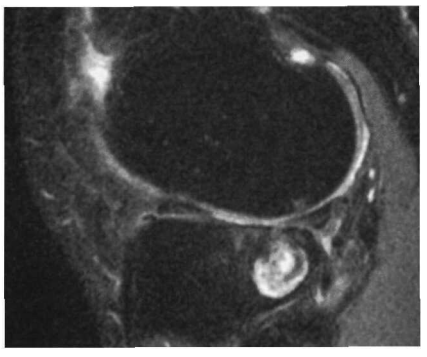

b

Figure 8.**10a, b** A 50-year-old man with a degenerative cystic lesion (geode) in the subchondral bone of the lateral proximal tibia related to articular damage. The circumscribed intraosseous lesion has mostly high signal on coronal (**a**) and sagittal (**b**) FST2WI.

a

b

Figure 8.**11 a, b** Intraosseous ganglion within the lateral metaphyseal region of the proximal tibia seen on coronal PDWI (**a**) and coronal FST2WI (**b**). The lesion has high signal on FST2WI and is contiguous with an extraosseous ganglion via a small defect in the cortex.

a

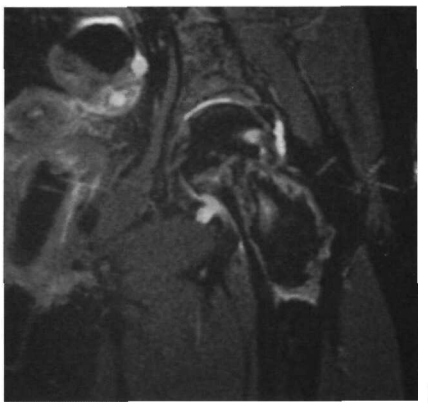

b

Figure 8.**12a, b** A 29-year-old woman with a nonacute bone infarct in the femoral neck after chemotherapy for leukemia. The circumscribed lesion has thin margins with intermediate signal on coronal T1WI (**a**) and high signal on coronal FST2WI (**b**).

Table 8 (Continued) **Solitary intramedullary lesions with well-circumscribed margins**

Lesion	MRI Findings	Comments
Enostosls/bone island (Fig. 8.13)	Typically appear as well-circumscribed zones of dense bone within marrow with low signal on T1WI, PDWI, T2WI, and FST2WI. Lesions typically show no Gd-contrast enhancement.	Non-neoplastic intramedullary zones of mature compact bone composed of lamellar bone, considered to be developmental anomalies resulting from localized failure of bone resorption during skeletal maturation. **(See Atlas Chapter A 62)**
Giant cell tumor (Fig. 8.14)	Often well-defined lesions with thin low signal margins on T1WI, PDWI, and T2WI. Solid portions of giant cell tumors often have low to intermediate signal on T1WI and PDWI, intermediate to high signal on T2WI, and high signal on FSPDWI and FST2WI. Zones of low signal on T2WI may be seen secondary to hemosiderin. Aneurysmal bone cysts can be seen in 14% of giant cell tumors. Areas of cortical thinning, expansion, and/or destruction can occur with extraosseous extension. Tumors show varying degrees of Gd-contrast enhancement.	Aggressive tumors composed of neoplastic mononuclear cells and scattered multinucleated osteoclast-like giant cells. Account for 23% of primary nonmalignant bone tumors, and 5-9% of all primary bone tumors, median age = 30 years. **(See Atlas Chapter A 29)**
Ameloblastoma (Fig. 8.15)	Lesions are often radiolucent with associated bone expansion and cortical thinning on CT. Tumors often have circumscribed margins, and can show mixed low, intermediate, and/or high signal on T1WI, T2WI, and FST2WI. Lesions can show heterogeneous Gd-contrast enhancement.	Ameloblastomas are slow-growing solid and cystic tumors that contain epithelioid cells (basaloid and/or squamous types) associated with regions of spindle cells and fibrous stroma. These tumors occur in the mandible and maxilla and typically lack metastatic potential.
Hemophillc pseudotumor	Can appear as expansile radiolucent lesions on radiographs and CT. Lesions usually have mixed low, intermediate, and high signal on T1WI and T2WI, as well as fluid-fluid levels.	Lesions can occur within bone (femur, pelvis, tibia, hand) or soft tissue in 1-2% of patients with factor VIII or IX deficiency. Enlarging lesions may require surgical resection.
Desmoplastic fibroma (Fig. 8.16)	Lobulated lesions with abrupt zones of transition. Lesions usually have low-intermediate signal on T1WI, intermediate signal on PDWI, heterogeneous intermediate to high signal on T2WI. Lesions may have internal or peripheral zones of low signal on T1WI and T2WI secondary to dense collagenous parts of the lesions and/or foci with high signal on T2WI from cystic zones. Thin curvilinear zones of low signal on T2WI can be seen at the margins of the lesions. Lesions show variable degrees and patterns of Gd-contrast enhancement.	Rare intraosseous desmoid tumors that comprise benign fibrous tissue with elongated or spindle-shaped cells adjacent to collagen. Account for < 1 % of primary bone lesions. Mean age = 20 years, median age = 34 years, peak 2nd decade. **(See Atlas Chapter A16)**
Malignant		
Metastatic tumor (Fig. 8.17)	Single or multiple well-circumscribed or poorly defined infiltrative lesions involving marrow associated with cortical destruction and extraosseous extension. Lesions often have low-intermediate signal on T1WI, low, intermediate, and/or high signal on T2WI and FST2WI, usually show Gd-contrast enhancement. Cortical destruction and tumor extension into the extraosseous soft tissues can occur. Pathologic fractures can be associated with metastatic lesions involving tubular bones and vertebrae. Periosteal reaction is uncommon.	Metastatic lesions typically occur in the marrow with or without cortical destruction and extraosseous tumor extension. **(See Atlas Chapter A 50)**

a

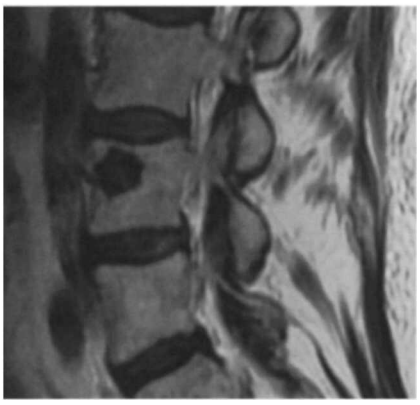

b

Figure 8.**13 a, b** A 70-year-old woman with a bone island in a lumbar vertebra that has high attenuation on a lateral radiograph (**a**). The circumscribed lesion has low signal on sagittal T2WI (**b**).

Figure 8.**14** A 22-year-old woman with a giant cell tumor in the proximal tibia that has circumscribed margins and shows Gd-contrast enhancement on coronal FST1WI.

a

Figure 8.**15 a, b** A 70-year-old woman with an ameloblastoma in the mandible, seen as a radiolucent expansile lesion on axial CT (**a**) that has mostly high signal on axial T2WI (**b**).

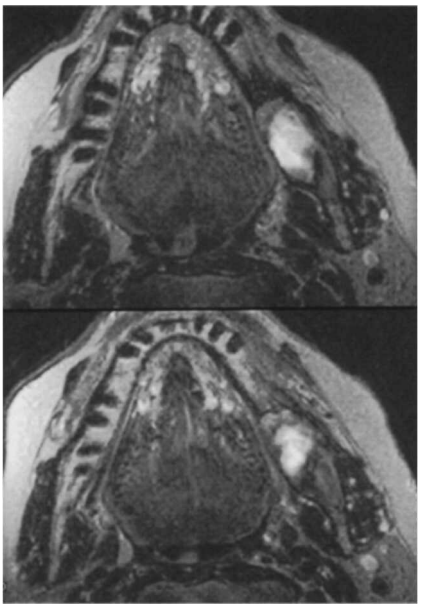

b

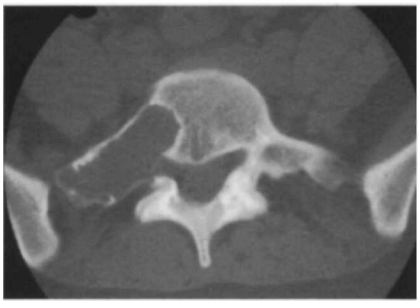

a, b

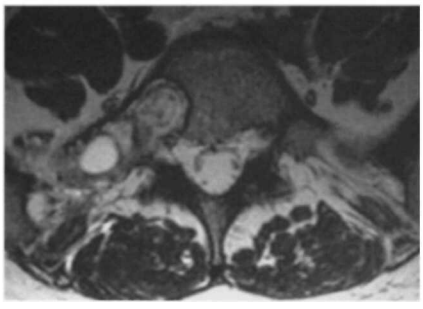

Figure 8.**16a, b** A 32-year-old woman with a desmoplastic fibroma involving the right lateral portion of the L5 vertebra. The radiolucent lesion has thinned, slightly expanded cortical margins on axial CT (**a**) and has mixed low, intermediate, slightly high, and high signal on axial T2WI (**b**).

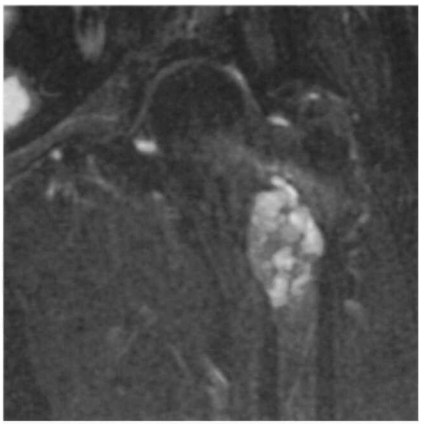

Figure 8.**17** A 56-year-old woman with a metastatic lesion from breast carcinoma involving the proximal shaft of the femur. The lesion has circumscribed margins and contains mixed intermediate and slightly high signal on coronal FST2WI.

Table 8 (Continued) **Solitary intramedullary lesions with well-circumscribed margins**

Lesion	MRI Findings	Comments
Plasmacytoma (Fig. 8.18)	Well-circumscribed or poorly defined infiltrative lesions involving marrow, low-intermediate signal on T1WI, intermediate-high signal on T2WI and FST2WI, usually show Gd-contrast enhancement, eventual cortical bone destruction and extraosseous extension.	Malignant tumors comprising proliferating antibody-secreting plasma cells derived from single clones. Most common primary neoplasm of bone in adults, median =60 years. Most patients are older than 40 years. May have variable destructive or infiltrative changes involving the axial and/or appendicular skeleton. **(See Atlas Chapter A 52)**
Lymphoma (Fig. 8.19)	Non-Hodgkin lymphoma (NHL) and Hodgkin Disease (HD) within bone typically appear as single or multifocal poorly defined or circumscribed intramedullary zones with low-intermediate signal on T1WI, and intermediate, slightly high, and/or high signal on T2WI and high signal on FST2WI; often show Gd-contrast enhancement. Zones of cortical destruction may occur, associated with extraosseous soft tissue extension.	Lymphoid tumors with neoplastic cells typically within lymphoid tissue (lymph nodes and reticuloendothelial organs). Unlike leukemia, lymphoma usually arises as discrete masses. Lymphomas are subdivided into HD and NHL. Almost all primary lymphomas of bone are B cell NHL. HD, mean age = 32 years. Osseous NHL. median = 35 years. **(See Atlas Chapter A 47)**
Low-grade chondrosarcoma (Fig. 8.20)	Intramedullary tumors often have low-intermediate signal on T1WI, intermediate signal on PDWI, and heterogeneous intermediate-high signal on T2WI. Lesions usually show heterogeneous contrast enhancement.	Malignant tumors containing cartilage formed within sarcomatous stroma. Account for 12-21% of malignant bone lesions, 21-26% of primary sarcomas of bone, mean age = 40 years, median = 26 to 59 years. **(See Atlas Chapter A11)**
Malignant giant cell tumor	Well-defined lesions with or without thin low signal margins on T1WI and T2WI. Solid portions of giant cell tumors often have low to intermediate signal on T1WI and PDWI, intermediate to high signal on T2WI, and high signal on FSPDWI and FST2WI. Signal heterogeneity on T2WI is not uncommon. Aneurysmal bone cysts are seen with 14% of giant cell tumors. Lesions show mild to prominent variable and often heterogeneous Gd-contrast enhancement. Cortical destruction and extraosseous tumor extension are frequently seen.	Aggressive tumors composed of neoplastic ovoid mononuclear cells and scattered multinucleated osteoclast-like giant cells. Up to 10% of all giant cell tumors are malignant. Benign giant cell tumors account for ~5 to 9.5% of all bone tumors and up to 23% of benign bone tumors. Malignant giant cell tumors account for 5.8% of all giant cell tumors. 75% occur in patients between the ages of 15 and 45. **(See Atlas Chapter A 29)**

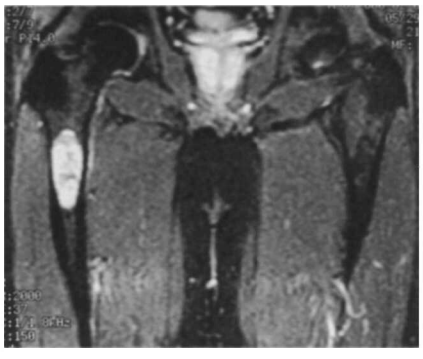

a

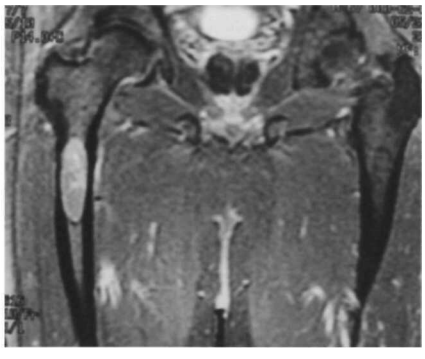

b

Figure 8.**18a, b** A 67-year-old man with a plasmacytoma involving the proximal shaft of the femur that has high signal on coronal STIR (**a**). The tumor shows moderate Gd-contrast enhancement on coronal FST1WI (**b**).

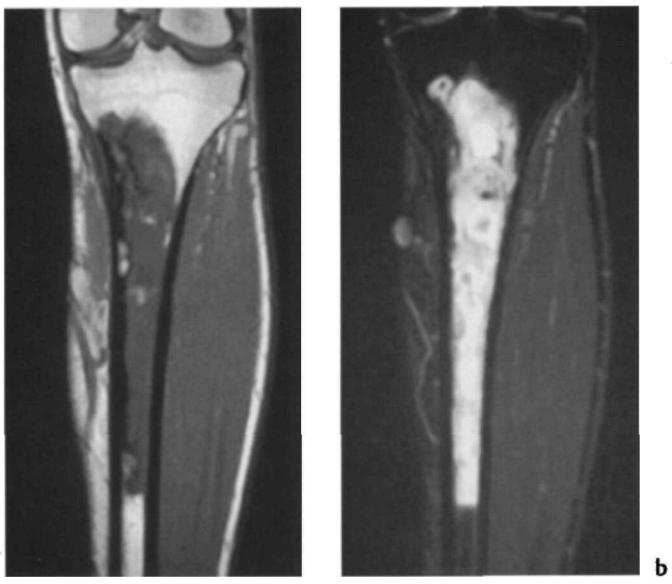

Figure 8.**19a, b** A 19-year-old man with large cell lymphoma in the marrow of the proximal tibia that has intermediate signal on coronal T1WI (**a**) and high signal on coronal FST2WI (**b**).

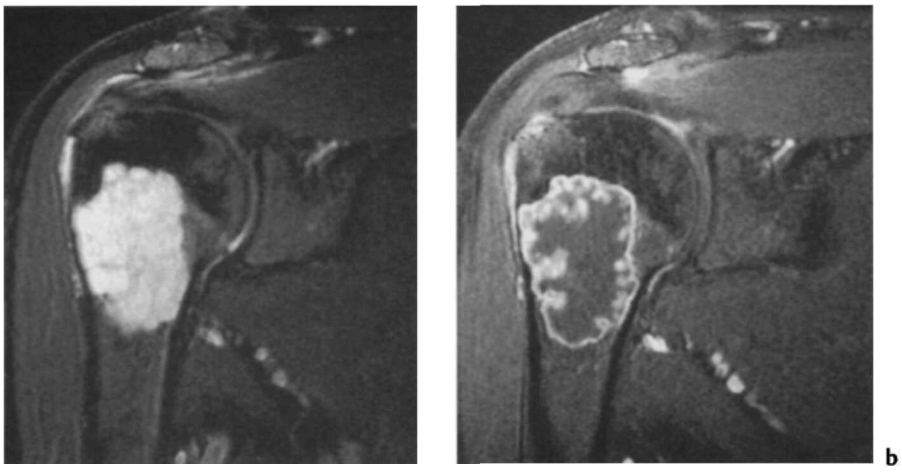

Figure 8.**20a, b** A 45-year-old woman with a low-grade chondrosarcoma involving the proximal humerus that has high signal on coronal FST2WI (**a**). The tumor shows peripheral lobular Gd-contrast enhancement on coronal FST1WI (**b**).

References

Ameloblastoma

Asaumi J, Hisatomi M, Yanagi Y, et al. Assessment of ameloblastomas using MRI and dynamic contrast-enhanced MRI. *Eur J Radiol* 2005;56:25-30.

Cihangiroglu M, Akfirat M, Yildirim H. CT and MRI findings of ameloblastoma in two cases. *Neuroradiology* 2002:44:434-437.

Hemophilic Pseudotumor

Geyskens W, Vanhoenacker FM, Van der Zijden T, Peerlinck K. MR imaging of intra-osseous hemophilic pseudotumor: case report and review of the literature. *JBR-BTR* Nov-Dec 2004;87(6):289-293.

Jaovisidha S, Ryu KN, Hodler J, Schweitzer ME, Sartoris DJ, Resnick D. Hemophilic pseudotumor: spectrum of MR findings. *Skeletal Radiol* 1997;26:468-474.

Park JS, Ryu KN. Hemophilic pseudotumor involving the musculoskeletal system: spectrum of radiologic findings. *AJR* 2004;183:55-61.

Table 9 Solitary intramedullary lesions with poorly defined margins of abnormal marrow signal

Lesion	MRI Findings	Comments
Benign		
Acute and subacute bone ischemia (Figs. 9.1,9.2)	In the early phases of ischemia, diffuse poorly defined zones of high signal may be seen on FST2WI, which can overlap the MRI features of transient bone marrow edema. In zones of bone infarction, curvilinear zones of low signal on T1WI and T2WI may occur in marrow from zones of fibrosis. Irregular zones of low signal on T1WI and high signal on T2WI may occur secondary to zones of fluid from edema, ischemia/infarction, or fracture. Zones with high signal on T1WI and T2WI may also occur from hemorrhage in combination with zones of fibrosis and fluid. A double-line sign (curvilinear adjacent zones of low and high signal on T2WI) is often seen at the edges of the infarcls representing the borders of osseous resorption and healing. Irregular Gd-contrast enhancement can be seen from granulation tissue ingrowth.	Bone infarcts are zones of ischemic death involving bone trabeculae and marrow which be idiopathic or result from: trauma, corticosteroid treatment, chemotherapy, radiation treatment, occlusive vascular disease, collagen vascular and other autoimmune diseases, metabolic storage diseases (Gaucher etc.), sickle cell disease, thalassemia, hyperbaric events / Caisson disease, pregnancy, alcohol abuse, pancreatitis, infections, and lymphoproliferative diseases. Osteonecrosis is more common in fatty compared with hematopoietic marrow. **(See Atlas Chapter A 37)**
Transient bone marrow edema; also referred to as: acute bone marrow edema syndromes, transient osteoporosis of the hip, regional migratory osteoporosis (Fig. 9.3)	Poorly defined zones with low-intermediate signal on T1WI and high signal on FST2WI and STIR are seen in the marrow of the proximal hip (femoral head and neck). The signal abnormalities may spare the subchondral marrow. MRI Findings can be seen within 48 hours from the onset of symptoms. Joint effusions may be present. With dynamic Gd-contrast administration, delayed peak enhancement can be seen with acute bone marrow edema (aBME). With osteonecrosis of the hip, crescentic zones of low signal on T1WI and FST2WI are seen in the marrow between the necrotic and normal areas. These crcscentic zones of low signal on T1WI and FST2WI are typically absent in aBME.	Acute bone marrow edema (aBME) is an idiopathic spontaneous process with transient edema in bone marrow that is not secondary to trauma, and may or may not be associated with osteoporosis. aBME frequently involves the proximal femur in men between 30 and 50 years, and women in the last trimester of pregnancy. aBME is typically associated with pain and limping disability. Biopsies show active osteoblasts and osteoid seams adjacent to thinned disconnected trabeculae, as well as mild fibrosis, edematous changes, vascular congestion with occasional hemorrhage in marrow without osteonecrosis. With conservative therapy such as analgesics, restricted weight-bearing and antiresortive agents such as bisphosphonates and calcitonin; symptoms resolve in 2 to 9 months. Similar clinical and imaging findings have been reported in other bones, often in juxta-articular locations in the lower extremities, and have been referred to as regional migratory osteoporosis.
Bone contusion (Fig. 9.4)	Contusions usually appear as poorly defined intramedullary zones with low-intermediate signal on T1WI and high signal on FST2WI, and corresponding Gd-contrast enhancement. Adjacent cortical margins are typically intact.	Also referred to as bone bruises, contusions represent trabecular microfractures without cortical fracture. In the knee, contusions at the lateral femoral condyle and posterolateral proximal tibia are commonly associated with injuries to the anterior cruciate ligament.

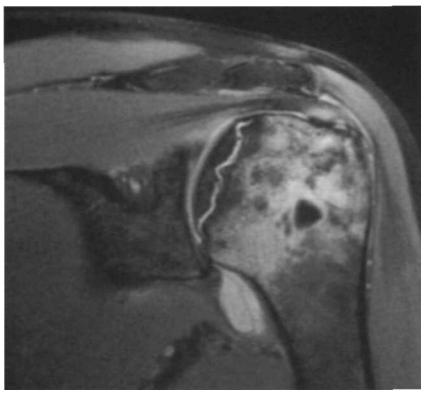

Figure 9.1 A 50-year-old woman with acute ischemia in the proximal humerus superimposed upon prior ischemia as seen on coronal FSPDWI. A poorly defined zone with increased signal is seen in the marrow adjacent to an old bone infarct at the medial aspect of the humeral head.

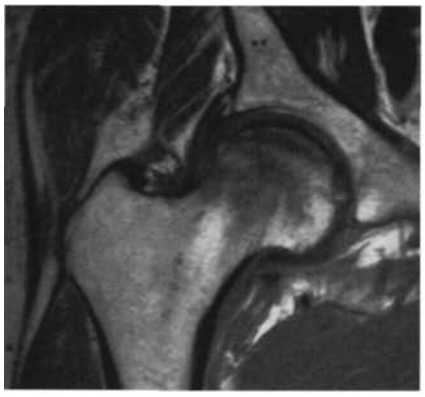

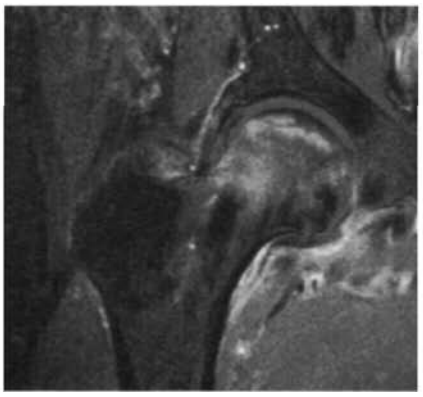

a **b, c**

Figure 9.**2a-c** A 50-year-old man with acute and subacute ischemia in the proximal femur. A poorly defined zone with low signal on coronal T1 WI (**a**), high signal on coronal FS T2WI (**b**), and corresponding abnormal Gd-contrast enhancement on FST1WI (**c**) is seen in the marrow. A thin linear zone of low signal is also seen in the subchondral marrow representing bone infarction.

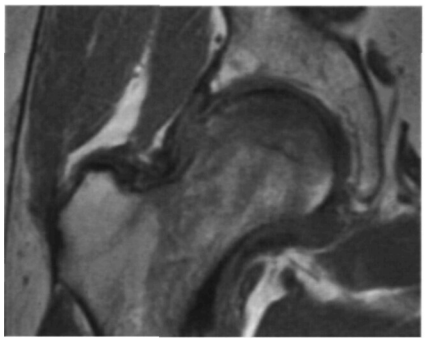

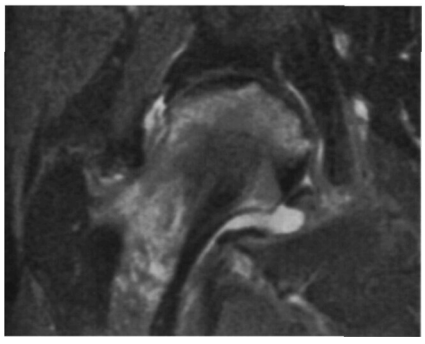

a **b**

Figure 9.**3a,b** A 53-year-old man with acute bone marrow edema in the proximal femur. A poorly defined zone with low-inter mediate signal on coronal T1WI (**a**) and high signal on coronal FST2WI (**b**) is seen in the marrow.

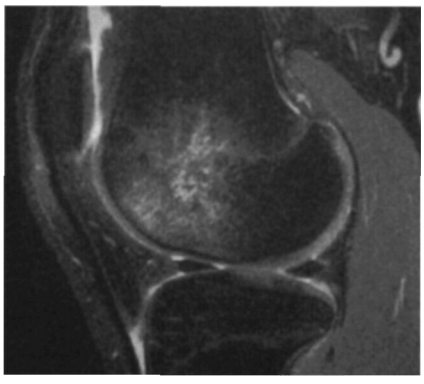

Figure 9.**4** Bone contusion in the distal femur is seen as a poorly defined zone with high signal on sagittal FST2WI.

Table 9 (Continued) **Solitary intramedullary lesions with poorly defined margins of abnormal marrow signal**

Lesion	MRI Findings	Comments
Fracture (Fig. 9.5)	Acute/subacute fractures typically have abnormal marrow signal (usually low signal on T1WI, high signal on T2WI and FST2WI). Gd-contrast enhancement is typically seen in the postfracture period. Angulated cortical margins and periosteal high signal on FST2WI can be seen with traumatic fractures. A curvilinear zone of low signal on T2WI and FST2WI may be seen within the marrow edema in stress fractures.	Fractures can result from trauma, primary bone tumors/lesions, metastatic disease, bone infarcts (steroids, chemotherapy, and radiation treatment), osteoporosis, osteomalacia, metabolic (calcium/phosphate) disorders, vitamin deficiencies, Paget disease, and genetic disorders (osteogenesis imperfecta, etc.)
Osteomyelitis (Fig. 9.6)	**In acute osteomyelitis,** poorly defined zones of low or low-intermediate signal on T1WI; and high signal on T2WI, STIR, and FST2WI are seen in the marrow. Loss of definition of the low signal line of the cortical margins is often observed on T1WI, T2WI, STIR, and FST2WI. After Gd-contrast administration, irregular zones of contrast enhancement are seen in the involved marrow on FST1WI. In the **subacute phase of osteomyelitis,** the pyogenic process becomes more localized. The zone of transition between normal and abnormal bone is sharper and more well-defined in subacute and chronic osteomyelitis than with acute osteomyelitis.	Osteomyelitis is a disorder in which there is infection of bone and commonly the adjacent soft tissues. Can result from hematogenous spread of microorganisms as well as from trauma-direct inoculation, extension from adjacent tissues, and complications from surgery. Bacteria such as *Staphy/ococcus aureus* and Streptococcus pyogenes are the most common infectious organisms. Can also result from other bacteria as well as /Wycobacter/um *tuberculosis,* fungi, parasites, and viruses. **(See Atlas Chapter A 63)**
Eosinophilic granuloma (Fig. 9.7)	Focal intramedullary lesion associated with trabecular and cortical bone destruction that typically has low-intermediate signal on T1WI and PDWI and heterogeneous slightly high to high signal on T2WI. Poorly defined zones of high signal on T2WI are usually seen in the marrow peripheral to the lesions secondary to inflammatory changes. Extension of lesions from the marrow into adjacent soft tissues through areas of cortical disruption are commonly seen as well as linear periosteal zones of high signal on T2WI. Lesions typically show prominent Gd-contrast enhancement in marrow and in extraosseous soft tissue portions of the lesions.	Benign tumor-like lesions consisting of Langerhans' cells (histiocytes), and variable amounts of lymphocytes, polymorphonuclear cells, and eosinophils. Account for 1 % of primary bone lesions, and 8% of tumor-like lesions. Occur in patients with median age =10 years, average =13.5 years, peak incidence is between 5 and 10 years, 80-85% occur in patients less **than 30 years. (See Atlas Chapter A18)**
Sarcoidosis	Lesions usually appear as intramedullary zones with low to intermediate signal on T1WI and slightly high to high signal on T2WI and FSPDWI and FST2WI. Erosions and zones of destruction of adjacent bone cortex as well as periosseous extension of the granulomatous process can occur. Fine perpendicular lines of low signal on T1 WI may be seen extending outward from the region of eroded or destroyed cortex. After Gd-contrast administration, lesions typically show moderate to prominent enhancement.	Chronic systemic granulomatous disease of unknown etiology in which noncaseating granulomas occur in various tissues and organs including bone. **(See Atlas Chapter** A 71)
Chondroblastoma (Fig. 9.8)	Tumors often have fine lobular margins, and typically have low-intermediate heterogeneous signal on T1WI, and mixed low, intermediate, and/or high signal on T2WI. Areas of low signal on T2WI are secondary to chondroid matrix mineralization, and/or hemosiderin. Lobular, marginal, or septal Gd-contrast enhancement patterns can be seen. Poorly defined zones with high signal on T2WI and FST2WI and corresponding Gd-contrast enhancement are typically seen in the marrow adjacent to the lesions representing inflammatory reaction from prostaglandin synthesis by these tumors.	Benign cartilaginous tumors with chondroblast-like cells and areas of chondroid matrix formation, usually occur in children and adolescents, median = 17years, mean = 16 years for lesions in long bones, mean = 28 years in other bones. Most cases are diagnosed between the ages of 5 and 25. **(See Atlas Chapter A7)**

a

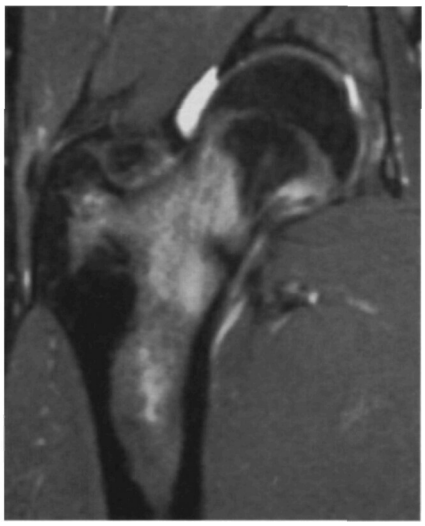

b

Figure **9.5a, b** A 17-year-old male with a fatigue-type stress fracture involving the femoral neck. The AP radiograph (**a**) shows a small linear zone of endosteal sclerosis. A poorly defined zone with high signal is seen in the marrow adjacent to a linear zone of low signal on FST2WI (**b**), as well as thin periosteal reaction with high signal medially.

a

b

Figure **9.6a, b** Pyogenic osteomyelitis seen as poorly defined zones of Gd-contrast enhancement in the marrow of the distal tibia of a 9-year-old girl on FS T1WI (a), and involving the first metatarsal marrow of a 14-year-old boy (**b**).

Figure 9.**7** An 18-year-old woman with an eosinophilic granuloma in the marrow of the femur seen as a poorly defined zone with high signal on coronal FS T2WI. Thin periosteal reaction with high signal is also seen.

Figure 9.**8** A 13-year-old girl with a chondroblastoma in the epiphysis of the proximal tibia seen as a lesion with thin low signal margins surrounding a central zone with a low, intermediate, slightly high, and high signal on coronal FST2WI. Poorly defined zones with high signal are seen in the epiphyseal and metaphyseal marrow peripheral to the lesion, as well as periosteal zones with high signal.

Table 9 (Continued) **Solitary intramedullary lesions with poorly defined margins of abnormal marrow signal**

Lesion	MRI Findings	Comments
Giant cell tumor (Fig. 9.9)	Lesions can have thin low signal margins on T1WI, PDWI, and T2WI. Solid portions of giant cell tumors often have low to intermediate signal on T1WI and PDWI, intermediate to high signal on T2WI, and high signal on FS PDWI and FST2WI. Zones of low signal on T2WI may be seen secondary to hemosiderin. Aneurysmal bone cysts can be seen in 14% of giant cell tumors. Areas of cortical thinning, expansion, and/or destruction can occur with extraosseous extension. Tumors show varying degrees of Cd-contrast enhancement. Poorly defined zones of Gd-contrast enhancement and high signal on FST2WI may also be seen in the marrow peripheral to the portions of the lesions associated with radiographic evidence of bone destruction, possibly indicating reactive inflammatory and edematous changes associated with elevated tumor prostaglandin levels.	Aggressive tumors composed of neoplastic mononuclear cells and scattered multinucleated osteoclast-like giant cells. Account for 23 % of primary nonmalignant bone tumors, and 5-9% of all primary bone tumors, median age = 30 years. **(See Atlas Chapter A 29)**
Giant cell reparative granuloma (Fig. 9.10)	Lesions can have heterogeneous low, intermediate, and/or high signal on T1WI, PDWI, and T2WI as well as peripheral rim-like and central Gd-contrast enhancement on FST1WI. May be surrounded by poorly defined zone of high signal on FST2WI and Gd-contrast enhancement in the adjacent marrow.	Giant cell reparative granulomas are also referred to as solid aneurysmal bone cysts (ABCs). **(See Atlas Chapter A 2).** Histologic appearance resembles brown tumors,
Aneurysmal bone cyst (Fig. 9.11)	ABCs often have a low signal rim on T1WI and T2WI adjacent to normal medullary bone, and between extraosseous soft tissues. Various combinations of low, intermediate, and/or high signal on T1WI, PDWI, and T2WI are usually seen within ABCs as well as fluid-fluid levels, Variable Gd-contrast enhancement is seen at the margins of lesions as well as involving the internal septae. Poorly defined zones with increased signal on FST2WI may be seen in marrow adjacent to these lesions.	Tumor-like expansile bone lesions containing cavernous spaces filled with blood, ABCs can be primary bone lesions (two-thirds) or secondary to other bone lesions/tumors. Account for ~ 11 % of primary tumor-like lesions of bone. Patients usually range in age from 1 to 25years, median = 14years. **(See Atlas Chapter A 2)**
Osteoid osteoma (Fig. 9.12)	Intraosseous circumscribed lesions often < 1.5 cm in diameter central zone with low-intermediate signal on T1WI and high signal on T2WI and FST2WI with prominent Gel-contrast enhancement, surrounded by a peripheral rim of low-intermediate signal on T1WI and T2WI (sclerosis). Lesions usually have poorly defined zones with high signal on T2WI and FST2WI and Gd-contrast enhancement in the marrow (edema, inflammation) beyond zone of sclerosis or in adjacent soft tissues from prostaglandin synthesis by these lesions.	Benign osseous lesion containing a nidus of vascularized osleoicl trabeculae surrounded by osteoblastic sclerosis, usually occurs between ages 5 and 25, males > females. Focal pain and tenderness associated with lesion, often worse at night, relieved with aspirin. **(See Atlas Chapter** A 60)

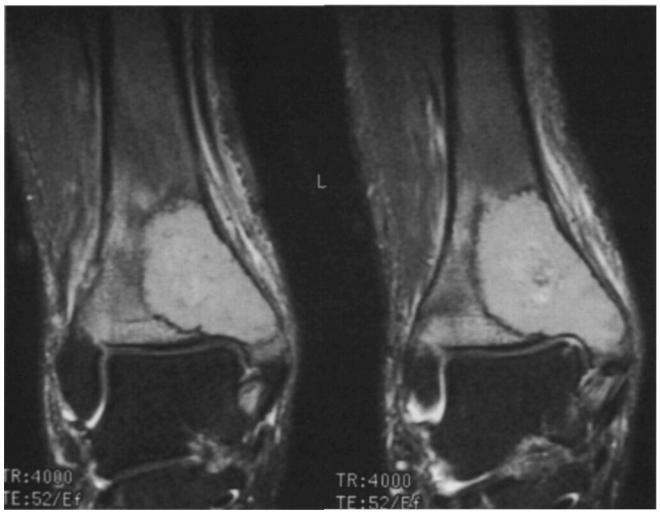

Figure 9.9 A 61-year-old man with a giant cell tumor in the distal medial tibia which has high signal centrally on coronal FST2WI surrounded by a thin rim of low signal, and a poorly defined peripheral zone of high signal in the marrow.

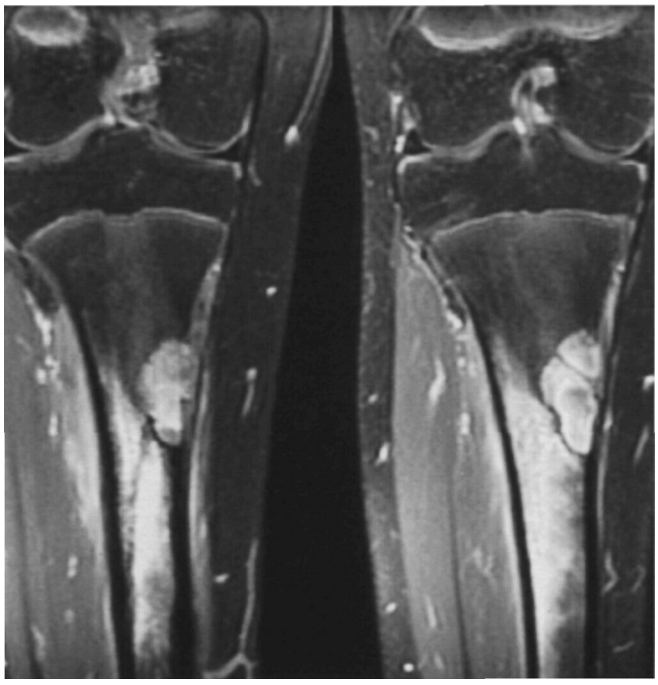

Figure 9.**10** **A** 14-year-old girl with a giant cell granuloma (solid aneurysmal bone cyst) involving the proximal metadiaphyseal region of the tibia. The lesion shows peripheral rim-like and central Gd-contrast enhancement as well as in the adjacent marrow on coronal FST1WI.

a

b

Figure 9.**11 a, b** A 14-year-old girl with an aneurysmal bone cyst in the proximal tibia that has low to intermediate signal as well as a small focus of high signal on coronal T1WI (**a**). The lesion contains multiple fluid-fluid levels on coronal FS T2WI (**b**). Poorly defined zones with increased signal on FST2WI are also seen in the adjacent marrow.

a

b

Figure 9.**12a, b** A 15-year-old female with a subperiosteal osteoid osteoma involving the proximal tibia. The nidus of the lesion has high signal on sagittal FST2WI (**a**). The small central calcification in the nidus has low signal on FST2WI. Thickened cortex adjacent to the nidus has low and intermediate-slightly high signal on FST2WI, and is associated with periosteal reaction with high signal. The nidus shows Gd-contrast enhancement on sagittal (**b**) FST1WI. Prominent Gd-contrast enhancement is seen at the periosteal reaction, and mild diffuse enhancement is seen in the cortical thickening adjacent to the nidus. Poorly defined zones of high signal on FST2WI and corresponding Gd-contrast enhancement on FST1WI are also seen in the marrow adjacent to the lesion.

Table 9 (Continued) **Solitary intramedullary lesions with poorly defined margins of abnormal marrow signal**

Lesion	MRI Findings	Comments
Osteoblastoma (Fig. 9.13)	Expansile lesion often > 1.5 cm in diameter with low-intermediate signal on T1WI and intermediate-high signal on T2WI and FST2WI, usually show Gd-contrast enhancement. Lesions usually have poorly defined zones with high signal on T2WI and FST2WI and Gd-contrast enhancement in the marrow (edema, inflammation) beyond zone of sclerosis or in adjacent soft tissues from prostaglandin synthesis by these lesions.	Rare benign bone neoplasm (2 % of bone tumors) usually occurs between 6 and 30 years. **(See Atlas Chapter A 61)**
Brown tumor	Lesions are usually radiolucent on radiographs and CT. Lesions often have low -intermediate signal on T1WI, intermediate to slightly high signal on T2WI, and typically show Gd-contrast enhancement. Zones of low signal on T2WI may occur from hemosiderin. Expansion of cortical margins can occur with or without cortical disruption/destruction. Lesions may have circumscribed and/or poorly defined margins.	Most often involves ribs, mandible, clavicle, pelvis, craniofacial bones, and vertebrae. Can result from primary hyperparathyroidism (3-7 %) (oversecretion of PTH from parathyroid adenoma associated with hypercalcemia), secondary type (vitamin D deficiency or chronic renal failure with hypocalcemia resulting in secretion of PTH and parathyroid gland hyperplasia) (1-2%), or tertiary type in which the secondary type leads to eventual autonomous elevated PTH secretion from parathyroid gland hyperplasia.
Malignant		
Metastatic tumor (Fig. 9.14)	Single or multiple well-circumscribed or poorly defined infiltrative lesions involving the marrow associated with cortical destruction and extraosseous extension. Lesions often have low-intermediate signal on T1WI, low, intermediate, and/or high signal on T2WI and FST2WI, usually show Gd-contrast enhancement. Cortical destruction and tumor extension into the extraosseous soft tissues can occur. Pathologic fractures can be associated with metastatic lesions involving tubular bones and vertebrae. Periosteal reaction is uncommon.	Metastatic lesions typically occur in the marrow with or without cortical destruction and extraosseous tumor extension. **(See Atlas Chapter A 50)**
Plasmacytoma (Fig. 9.15)	Multiple (myeloma) or single (plasmacytoma) are well-circumscribed or poorly defined infiltrative lesions involving marrow, low-intermediate signal on T1WI, intermediate-high signal on T2WI and FS T2WI, usually show Gd-conlrast-enhancement, eventual cortical bone destruction and extraosseous extension.	Malignant tumors comprising proliferating antibody-secreting plasma cells derived from single clones. Most common primary neoplasm of bone in adults, median -60 years. Most patients are older than 40 years. May have variable destructive or infiltrative changes involving the axial and/or appendicular skeleton. **(See Atlas Chapter A 52)**
Leukemia	Single or multiple well-circumscribed or poorly defined infiltrative lesions involving marrow; low-intermediate signal on T1WI, intermediate-high signal on T2WI and FST2WI, often show Gd-contrast enhancement, +/- cortical bone destruction and extraosseous extension.	Lymphoid neoplasms with involvement of bone marrow with tumor cells also in peripheral blood. In children and adolescents, acute lymphoblastic leukemia (ALL) is the most frequent type. In adults, chronic lymphocytic leukemia (CLL; small lymphocytic lymphoma) is the most common type of lymphocytic leukemia. Myelogenous leukemias are neoplasms derived from abnormal myeloid progenitor cells. Acute myelogenous leukemia (AML) occurs in adolescents and young adults, and represents -20% of childhood leukemia. Chronic myelogenous leukemia (CML) usually affects adults older than 25 years. **(See Atlas Chapter A 41)**

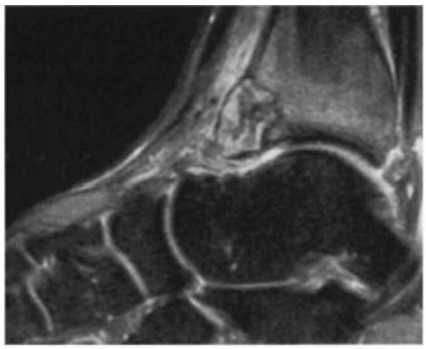

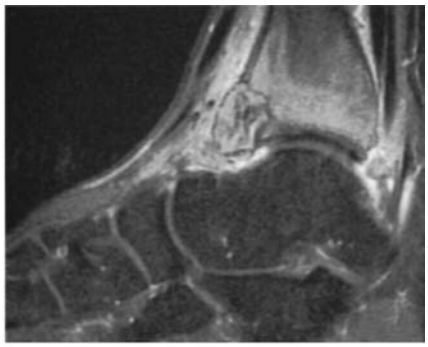

a, **b**

Figure 9.**13a, b** A 24-year-old man with an osteoblastoma involving the distal tibia that has heterogeneous high and low signal on sagittal FST2WI (**a**). A thin rim of low signal is seen at the periphery of the tumor and at the border with medullary bone. The tumor causes expansion and irregular thinning of the anterior margin of the distal tibia. The lesion shows prominent heterogeneous Gd-contrast enhancement on sagittal FST1WI (**b**). Poorly defined zones of high signal on T2WI and corresponding Gd-contrast enhancement are seen in the marrow and soft tissues adjacent to the osteoblastoma.

a

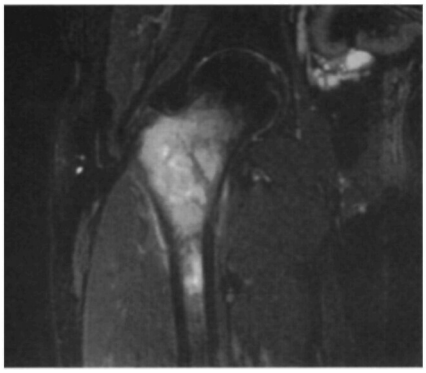

b

Figure 9.**14 a, b** Metastatic disease in the marrow of the femur seen as poorly defined zones with slightly high to high signal on coronal FS T2WI from breast carcinoma in a 57-year-old woman (**a**) and from seminoma in a 26-year-old man (**b**).

Figure 9.**15** Myeloma involving the humerus seen as a poorly defined zone of high signal in the marrow on sagittal FS T2WI.

Table 9 (Continued) **Solitary intramedullary lesions with poorly defined margins of abnormal marrow signal**

Lesion	MRI Findings	Comments
Lymphoma (Fig. 9.16)	Non-Hodgkin lymphoma (NHL) and Hodgkin disease (HD) within bone typically appear as single or multifocal poorly defined or circumscribed intramcdullary zones with low-intermediate signal on T1 WI, and intermediate, slightly high, and/or high signal on T2WI and high signal on FST2WI; often show Gd-contrast enhancement, Zones of cortical destruction may occur associated with extraosseous soft tissue extension.	Lymphoid tumors with neoplastic cells typically within lymphoid tissue (lymph nodes and reticuloendothelial organs). Unlike leukemia, lymphoma usually arises as discrete masses. Lymphomas are subdivided into HD and NHL. Almost all primary lymphomas of bone are B cell NHL. HD, mean age = 32 years. Osseous NHL, median = 35 years. **(See Atlas Chapter A 47)**
Chondrosarcoma (Fig. 9.17)	Inlramedullary tumors often have low-intermediate signal on T1WI, intermediate signal on PDWI, and heterogeneous intermediate-high signal on T2WI. Lesions usually show heterogeneous contrast enhancement.	Malignant tumors containing cartilage formed within sarcomatous stroma. Account for 12-21 % of malignant bone lesions, 21-26% of primary sarcomas of bone, mean age = 40 years, median = 26 to 59 years. **(See Atlas Chapter A 11)**
Osteosarcoma (Fig. 9.18)	Destructive intramedullary malignant lesions, low-intermediate signal on T1WI, mixed low, intermediate, high signal on T2WI, usually with matrix mineralization/ossification-low signal on T2WI, typically show Gd-contrast enhancement (usually heterogeneous). May have circumscribed and/or ill-defined margins. Zones of cortical destruction are typically seen, through which tumors extend into the extraosseous soft tissues under an elevated periosteum. Lamellated and/or spiculated zones of bone formation can occur under the periostea! elevation secondary to tumor invasion and perforation of bone cortex. Low signal from spicules of periosteal, reactive, and tumoral bone formation may have a divergent ("sunburst") pattern, perpendicular ("hair on end") pattern, or disorganized or complex appearance. Triangular zones of periosteal elevation (Codman's triangles) can be seen at the borders of zones of cortical destruction and tumor extension.	Malignant tumor comprising proliferating neoplastic spindle cells which produce osteoid and/or immature tumoral bone most frequently arising within medullary bone (metadiaphyseal > metaphyseal > diaphyseal locations). Two age peaks of incidence. The larger peak occurs between the ages of 10 and 20 and accounts for over half of the cases. The second smaller peak occurs in adults over 60years and accounts for ~ 10 %"of the cases. Occurs in children as primary tumors and adults (associated with Page! disease, irradiated bone, chronic osteomyelitis, osteoblastoma, giant cell tumor, fibrous dysplasia. **(See Atlas Chapter A 64)**

a b

Figure 9.**16a, b** A 13-year-old girl with Burkitt lymphoma involving the marrow of the proximal tibia seen as poorly defined zones with low-intermediate signal on sagittal T1WI (**a**) and high signal on FS T2WI (**b**).

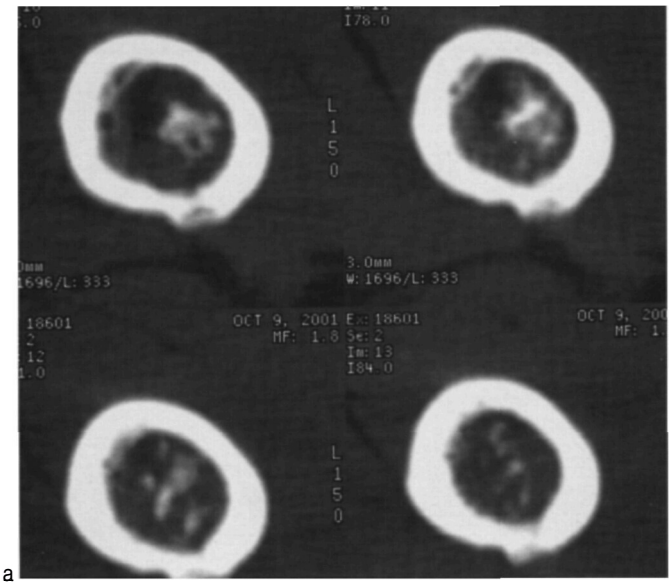

a

b

Figure **9.17a, b** A 44-year-old woman with a chondrosarcoma in the proximal shaft of the femur that has chondroid mineralization on the axial CT (**a**). The tumor has high signal with poorly defined margins on coronal FS T2WI (**b**).

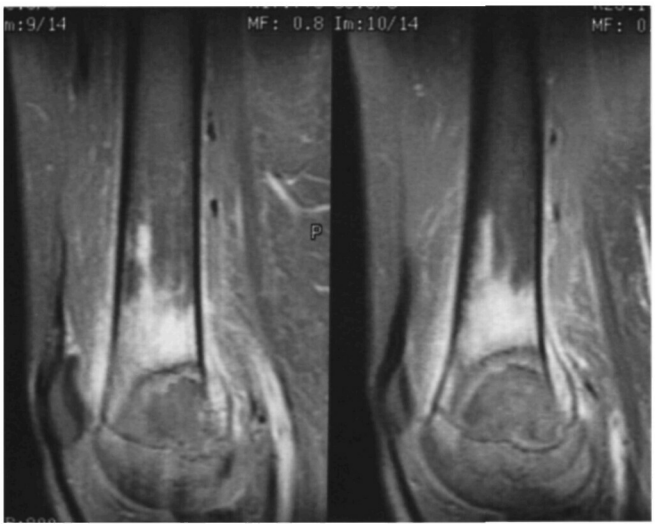

a

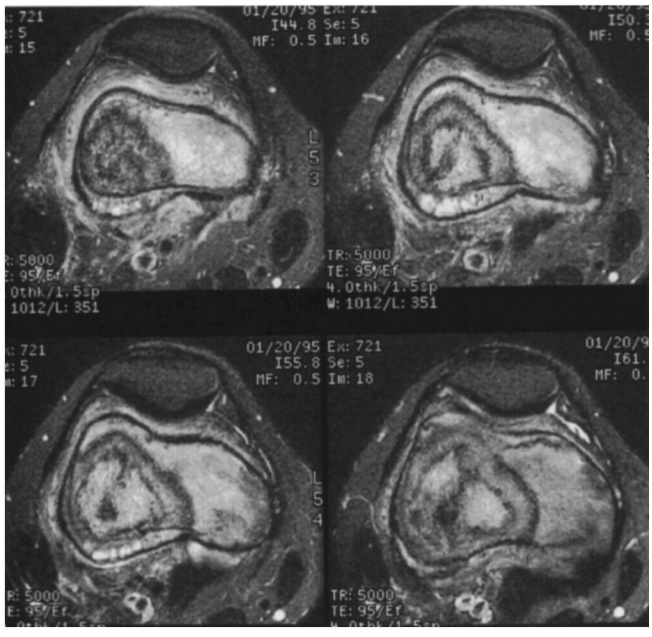

b

Figure 9.**18a, b** A 13-year-old girl with an osteosarcoma involving the marrow of the distal epi- and metaphyseal portions of the femur associated with disrupted periosteal elevation, cortical destruction, and extraosseous extension. The tumor has poorly defined margins and shows Gd-contrast enhancement on sagittal FST1WI (**a**) and has heterogeneous low and high signal on axial FS T2WI (**b**).

Table 9 (Continued) **Solitary intramedullary lesions with poorly defined margins of abnormal marrow signal**

Lesion	MRI Findings	Comments
Ewing sarcoma (Fig. 9.19)	Destructive malignant lesions involving marrow, low-intermediate signal on T1WI, mixed low, intermediate, and/or high signal on T2WI and FST2WI, typically shows Gd-contrast enhancement (usually heterogeneous). Extraosseous tumor extension through sites of cortical destruction is commonly seen beneath an elevated periosteum. Thin striated zones of low signal on T2WI can be somelimes seen oriented perpendicular to the long axis of the involved bone under the elevated periosteum representing the "hair on end" appearance of reactive bone formation secondary to the tumor. In long bones, tumors are most often located in the diaphyseal region, followed by the metadiaphyseal region.	Malignant primitive tumor of bone comprised of undifferentiated small cells with round nuclei. Accounts for 6-11 % of primary malignant bone tumors, 5-7% of primary bone tumors. Usually occurs between the ages of 5 and 30, males > females, locally invasive, high metastatic potential. **(See Atlas Chapter A 20)**
Malignant giant cell tumor (Fig. 9.20)	Well-defined or poorly-marginated lesions with or without thin low signal margins on T1WI and T2WI. Solid portions of giant cell tumors often have low to intermediate signal on T1WI and PDWI, intermediate to high signal on T2WI, and high signal on FS PDWI and FST2WI. Signal heterogeneity on T2WI is not uncommon. Aneurysmal bone cysts are seen with 14 % of giant cell tumors, Lesions show mild to prominent variable and often heterogeneous Gd-contrast enhancement. Cortical destruction and extraosseous tumor extension are frequently seen.	Aggressive tumors composed of neoplastic ovoid mononuclear cells and scattered multinucleated osteoclast-like giant cells, Up to 10 % of all giant cell tumors are malignant. Benign giant cell tumors account for ~5 to 9.5 % of all bone tumors and up to 23% of benign bone tumors. Malignant giant cell tumors account for 5.8 % of all giant cell tumors. 75 % occur in patients between the ages of 15 and 45 years. **(See Atlas Chapter A 29)**
Fibrosarcoma	Intramedullary lesions with irregular margins, with or without associated cortical destruction and/or extraosseous soft tissue masses. Lesions usually have low-intermediate signal on T1WI and PDWI. and heterogeneous intermediate, slightly high, and/or high signal on T2WI. Lesions usually show heterogeneous Gd-contrast enhancement.	Fibrosarcomas are uncommon malignant tumors consisting of bundles of fibroblasts/spindle cells with varying proportions of collagen, lacking other tissue differentiating features such as tumor bone, osteoid, or cartilage. Can be primary lesions (75%) or arise as secondary tumors (25 %) associated with prior irradiation, Paget disease, bone infarct, chronic osteomyelitis, fibrous dysplasia, giant cell tumor. Accounts for 3-5 % of primary malignant bone tumors, and 2-4% of all bone tumors, median age = 43 years. **(See Atlas Chapter A 25)**
Malignant fibrous histiocytoma (Fig. 9.21)	Intramedullary lesions with irregular margins and zones of cortical destruction and extraosseous extension. Tumors often have low-intermediate signal on T1WI; low-intermediate signal on PDWI and heterogeneous intermediate-high signal on T2WI and FST2WI. Invasion into joints occurs in 30 %. May be associated with bone infarcts, bone cysts, chronic osteomyelitis, Paget disease, and other treated primary bone tumors. Lesions usually show heterogeneous Gd-contrast prominent enhancement.	Malignant tumor involving soft tissue and rarely bone derived from undifferentiated mesenchymal cells. Contains cells with limited cellular differentiation such as mixtures of fibroblasts, myofibroblasts, histiocyte-like cells, anaplastic giant cells, and inflammatory cells. Accounts for 1-5 % of primary malignant bone tumors and < 1-3 % of all primary bone tumors, patient ages range from 11 to 80 years, median = 48 years, mean = 55 years. **(See Atlas Chapter A 48)**
Paget sarcoma (Fig. 9.22)	Irregular zones of medullary and cortical bone destruction associated with an extraosseous soft tissue mass lesion. The involved marrow typically has low to intermediate signal on T1WI and PDWI, and low to high signal on T2WI. Abnormal Gd-contrast enhancement is seen in the marrow as well as in the extraosseous tumor extension.	Paget disease is the second most common bone disease in older adults after osteoporosis. Median age = 66 years. Disordered bone resorption and woven bone formation occurs resulting in osseous deformity, Associated with less than 1 % risk for developing secondary sarcomatous changes. **(See Atlas Chapter A 65)**

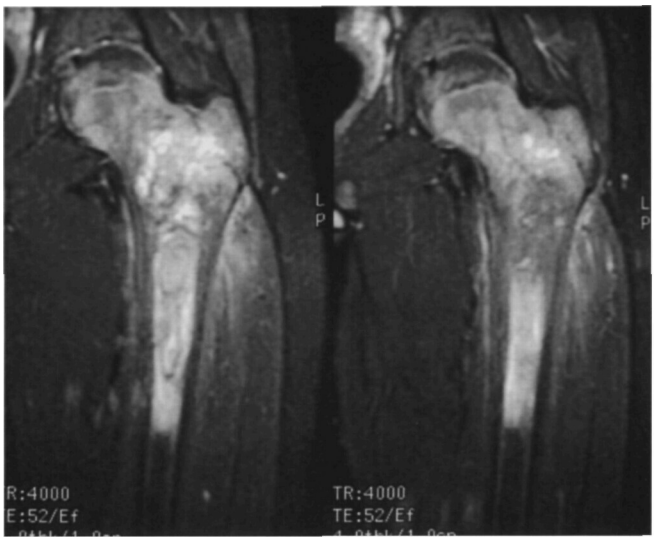

Figure 9.**19** **A** 15-year-old male with Ewing sarcoma in the proximal femur seen as a poorly defined zone with high signal in the marrow on coronal FS T2WI. Cortical disruption and extraosseous tumor extension are also present.

Figure 9.**20** A 16-year-old male with a malignant giant cell tumor in the marrow of the distal tibia associated with cortical destruction and extraosseous extension. The intramedullary portion of the tumor has high signal centrally on coronal FST2WI surrounded by a rim of low signal, and a poorly defined peripheral zone of high signal in the

a, b

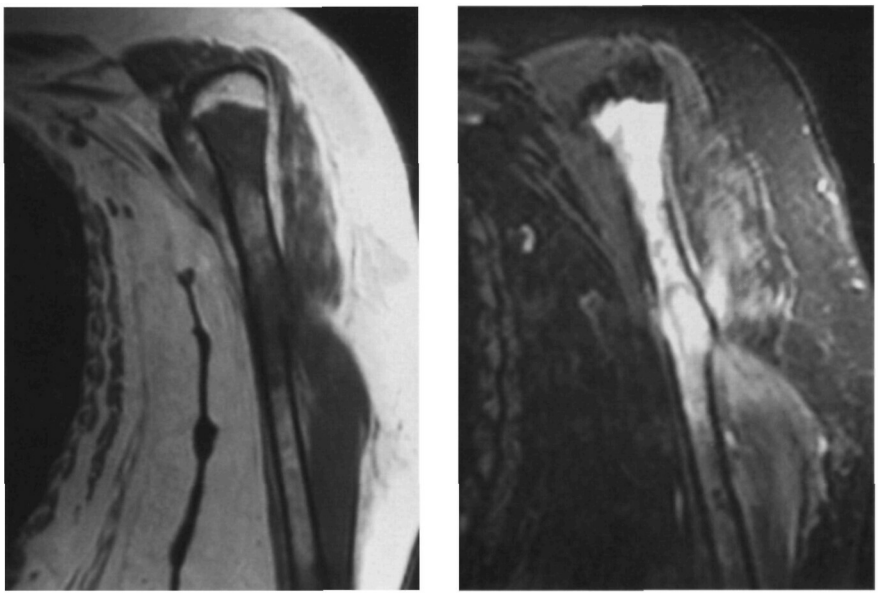

Figure 9.**21 a, b** A 55-year-old woman with a malignant fibrous histiocytoma involving the humerus seen as a poorly defined lesion in the marrow with low-intermediate signal on coronal T1WI (**a**) and high signal on coronal FS T2WI (**b**).

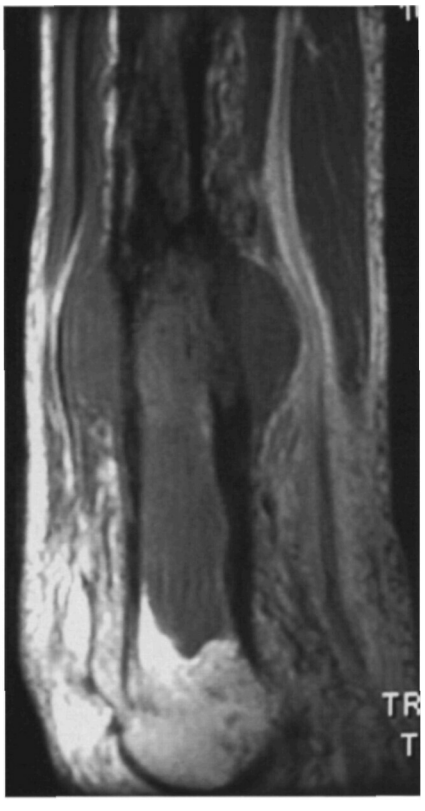

Figure 9.**22** A 71-year-old woman with Paget sarcoma involving the marrow of the distal femur associated with cortical destruction and extraosseous extension as seen on sagittal T1WI.

References

Transient Bone Marrow Edema

Balakrishnan A, Schemitsch EH, Pearce D, McKee MD. Distinguishing transient osteoporosis of the hip from avascular necrosis. *CanJSurg* June 2003;46(3):187-192.

zMalizosKN,ZibisAH,DailianaZ,HantesM,KarahaliosT,KarantanasAH. MR imaging findings in transient osteoporosis of the hip. *Eur] Radial* 2004;50:238-244.

Toms AP, Marshall TJ, Becker E, Donell ST, Lobo-Mueller EM, Barker T. Regional migratory osteoporosis: a review illustrated by five cases. Clin Radiof 2005:60:425-438.

Yamamoto T, Kubo T, Hirasawa Y, Noguchi Y, Iwamoto Y, Sueishi K. A clinicopathologic study of transient osteoporosis of the hip. *Skeletal* Radio/1999:28:621-627.

Intraosseous Cakific Tendinopathy

Hemming DJ, Murphey MD, Shekitka KM, Temple HT, Jelinek JJ, Kransdorf MJ. Osseous involvement in calcific tendonitis: a retrospective review of 50 cases. *AJR* 2003:181:965-972.

Table 10 Solitary intramedullary lesions located near the ends of tubular bones

Lesion	MRI Findings	Comments
Benign		
Enchondroma (Figs. 10.1,10.2)	Lobulated circumscribed intramedullary lesions that usually have low-intermediate signal on T1WI and intermediate signal on PDWI. On T2WI and FST2WI. lesions usually have predominantly high signal with foci and/or bands of low signal representing areas of matrix mineralization and fibrous strands. Lesions typically show Gd-contrast enhancement in various patterns (peripheral curvilinear lobular, central nodular/septal and peripheral lobular, or heterogeneous diffuse).	Benign intramedullary lesions comprising hyaline cartilage, represent ~-10 % of benign bone tumors. Enchondromas can be solitary *(88 %)* or multiple (12 %). Median age = 35 years, peak in 3rd and 4th decades. (See Atlas Chapter A 8).

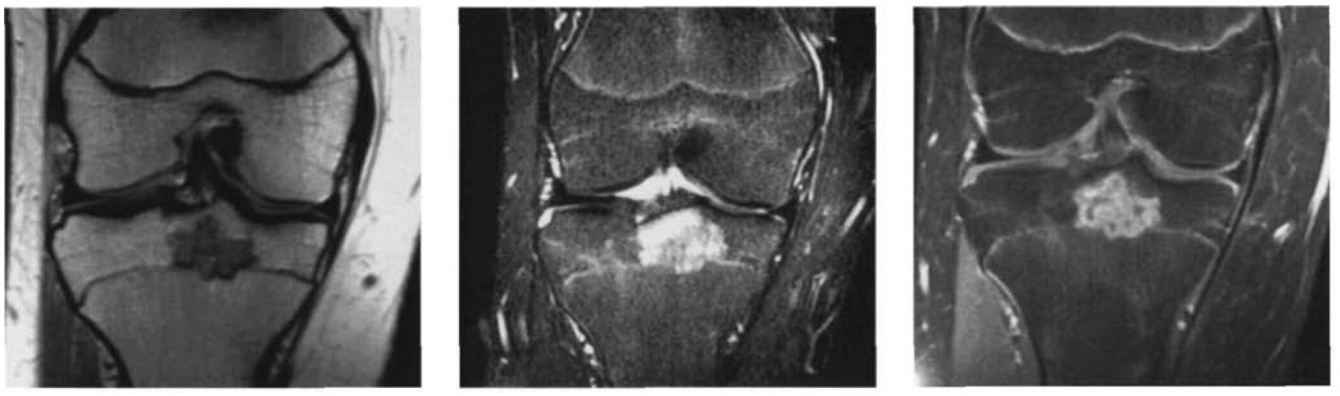

a b, c

Figure 10.**1 a-c** A 14 -year-old girl with an enchondroma in the epiphysis of the proximal tibia which has low -intermediate signal on coronal T1 WI (**a**), and high signal on FS T2WI (**b**). The lesion shows peripheral lobular Gd-contrast enhancement on FST1WI (**c**).

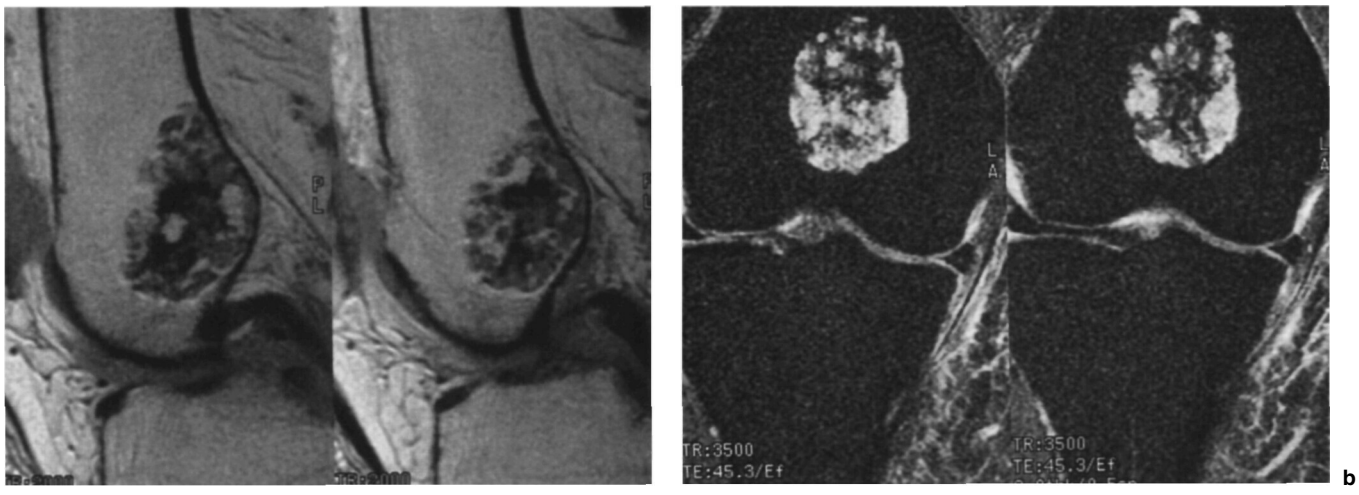

a b

Figure 10.**2 a, b** A 66-year-old woman with an enchondroma in the marrow of the distal femur that has mixed low, intermediate, and slightly high signal on sagittal PDWI (**a**), and mixed low and high signal on coronal FST2WI (**b**).

Table 10 (Continued) **Solitary intramedullary lesions located near the ends of tubular bones**

Lesion	MRI Findings	Comments
Giant cell tumor (Fig. 10.3)	Often well-defined lesions with thin low signal margins on T1WI, PDWI, and T2WI. Solid portions of giant cell tumors often have low to intermediate signal on T1WI and PDWI, intermediate to high signal on T2WI, and high signal on FS PDWI and FST2WI. Zones of low signal on T2WI may be seen secondary to hemosiderin. Aneurysmal bone cysts can be seen in 14% of giant cell tumors. Areas of cortical thinning, expansion, and/or destruction can occur with extraosseous extension. Tumors show varying degrees of Gd-contrast enhancement.	Aggressive tumors composed of ncoplastic mononuclear cells and scattered multinucleated osteoclast-like giant cells. Account for 23% of primary nonmalignant bone tumors and 5-9 % of all primary bone tumors, median age = 30 years. **(See Atlas Chapter A 29)**
Chondroblastoma (Fig. 10.4)	Tumors often have fine lobular margins, and typically have low-intermediate heterogeneous signal on T1WI, and mixed low, intermediate, and/or high signal on T2WI. Areas of low signal on T2WI are secondary to chondroid matrix mineralization, and/or hemosiderin. Lobular, marginal, or septal Gd-contrast enhancement patterns can be seen. Poorly defined /ones with high signal on T2WI and FST2WI and corresponding Gd-contrast enhancement are typically seen in the marrow adjacent to the lesions representing inflammatory reaction from prostaglandin synthesis by these tumors.	Benign cartilaginous tumors with chondroblast-like cells and areas of chondroid matrix formation, usually occur in children and adolescents, median = 17years, mean = 16 years for lesions in long bones, mean = 28 years in other bones. Most cases are diagnosed between the ages of 5 and 25. **(See Atlas Chapter A7)**
Chondromyxoid fibroma (Fig. 10.5)	Lesions are often slightly lobulated with low-intermediate signal on T1WI and heterogeneous predominantly high signal on T2WI. MR signal heterogeneity on T2WI is related to the proportions of myxoid, chondroid. and fibrous components within the lesions. Thin low signal septa on T2WI can be seen. Lesions are surrounded by low signal borders representing thin sclerotic reaction, Edema is not typically seen in adjacent medullary bone, Lesions show prominent diffuse Gd contrast enhancement.	Rare, benign, slow-growing bone lesions that contain chondroid, myxoicl, and fibrous components. Chondromyxoid fibromas represent 2-4% of primary benign bone lesions, and < 1 % of primary bone lesions. Most chondromyxoid fibromas occur between the ages of 1 to 40years, with a median of 17 years, and peak incidence in the 2nd to 3rd decades. **(See Atlas ChapterAIO)**
Osteoblastoma (Fig. 10.6)	Expansile lesion often > 1.5 cm in diameter with low-intermediate signal on T1WI and intermediate-high signal on T2WI and FST2WI, typically shows Gd-contrast enhancement. Lesions usually have poorly defined zones with high signal on T2WI and FST2WI and Gd-contrast enhancement in the marrow (edema, inflammation) beyond zone of sclerosis or in adjacent soft tissues from prostaglandin synthesis by these lesions.	Rare benign bone neoplasm (2% of bone tumors) usually occurs between the ages 6 and 3O years. **(See Atlas Chapter A61)**
Intraosseous lipoma (Fig. 10.7)	Lesions can have heterogeneous high, intermediate. and/or low signal on T1WI, PDWI, and T2WI. Fat signal in lesions is suppressed on FST1WI, FST2W and STIR. Lesions often show no Gd-contrast enhancement. Peripheral rim-like and central Gd-contrast enhancement may occasionally be seen on FST1WI.	Uncommon benign hamartomas composed of mature white adipose tissue without cellular atypia. Osseous or chondroid metaplasia with myxoicl changes can be associated with lipomas. Account for -0.1% of bone tumors, likely under-reported. **(See Atlas Chapter A 43)**

a, **b**

Figure 10.3a, **b** A 26-year-old woman with a giant cell tumor in the distal radius that has intermediate signal on coronal T1WI (a), and shows Gd-contrast enhancement on coronal FST1WI (**b**)

Figure 10.4 A 13-year-old girl with a chondroblastoma involving the epiphysis of the proximal tibia. A lesion with mixed low and high signal is seen with thin low signal margins on coronal FS T2WI. Poorly defined zones with high signal are seen in the adjacent marrow.

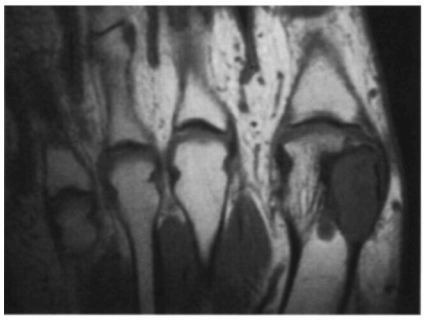

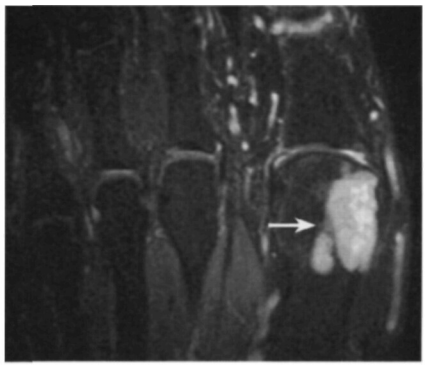

a **b**, c

Figure 10.5a-c A 34-year-old man with a chondromyxoid fibroma involving the first metatarsal head. The lesion has circumscribed low signal margins and contains intermediate signal on coronal T1WI (a) and high signal on coronal FST2WI (**b**). The lesion shows Gd-contrast enhancement on coronal FS T1WI (c).

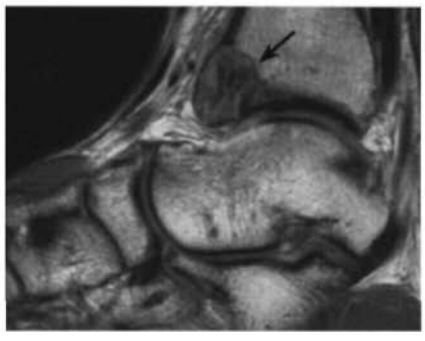

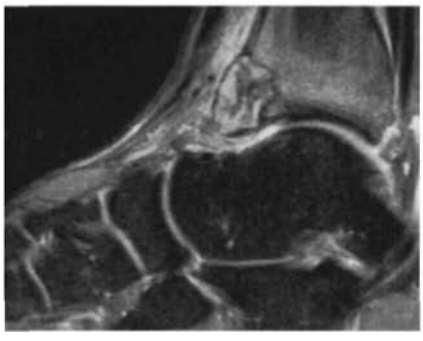

a, b

Figure 10.6a, **b** A 24-year-old man with an osteoblastoma in the distal tibia. The lesion is associated with cortical thinning and expansion, and has low-intermediate signal on sagittal PDWI (**a**), and heterogeneous high and low signal on sagittal FST2WI (**b**). Poorly defined high signal on FST2WI is also seen in the marrow adjacent to the lesion.

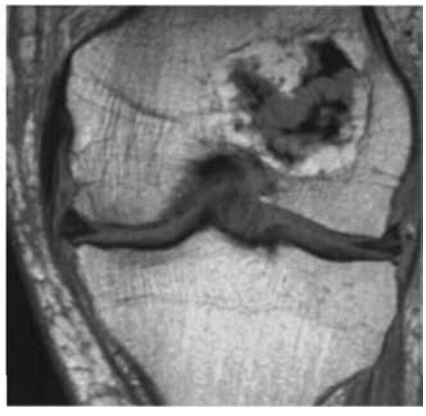

Figure 10.**7** A 74-year-old man with an intraosseous lipoma in the distal portion of the femur that has high signal peripherally surrounding a central zone with intermediate and low signal from cystic degeneration and dystrophic calcifications on PDWI.

Table 10 (Continued) **Solitary intramedullary lesions located near the ends of tubular bones**

Lesion	MRI Findings	Comments
Ceode/subchondral degenerative cyst (Fig. 10.8)	Typically have sharply defined margins and contains low signal on T1WI, low-intermediate signal on PDWI, and homogeneous high signal on T2WI. Poorly defined zones of Gd-contrast enhancement can be seen in the marrow adjacent to the subchondral cysts on FST1WI.	A geode or subchondral cyst is a cystic lesion located near the end of *a* long bone where there are changes of degenerative osteoarthropathy. Lesions can result from synovial fluid intrusion and/or bony contusion in the setting of degenerative joint disease. **(See Atlas Chapter A 28)**
Intraosseous ganglion (Fig. 10.9)	Can have round, oval, or serpiginous configurations with sharply defined margins. These lesions typically contain low signal on T1WI, low-intermediate signal on PDWI, and high signal on T2WI.	Benign cystic lesion usually located at or near the ends of long bones, and is not associated with degenerative osteoarthropathy. Lesions can result from intraosseous extension from a ganglion in the soft tissues; or from intraosseous mucoid degeneration, synovial rests, or synovial intrusion. **(See Atlas Chapter A 28)**
Intraosseous extension of inflammatory synovium/ pannus (Fig. 10.10)	Hypertrophied synovium can be diffuse, nodular and/or villous, and often has low to intermediate or intermediate signal on T1WI and PDWI, and low to intermediate, intermediate, and/or slightly high to high signal on T2WI. Erosive changes in subchondral bone appear as zones of low signal on T1 WI, and high signal on T2WI. Contrast enhancement is often seen within the erosions.	Inflammatory synovitis associated with rheumatoid arthritis can result in progressive destruction of cartilage and cortical bone leading with intraosseous extension and trabecular destruction. Prevalence ranges from 0.3 to 2.1 % of the world population. 80 % of adult patients present between the ages of 35 and 50. Incidence of juvenile rheumatoid arthritis (IRA) ranges from 6 to 19.6 cases per 100,000. Patients with JRA range from 5 to 16 years, mean = 10.2 years. **(See Atlas Chapter A 70)**
Intraosseous calcific tendinopathy (Fig. 10.11)	Zones with slightly high and low signal on T2WI and FS T2WI are seen in tendons with or without erosion of bone cortex. Intramedullary zones with mixed low, intermediate, and/or high signal on T2WI and FST2WI may be seen in the adjacent marrow.	Degenerative disorder with amorphous calcifications in tendons or bursa associated with erosion of adjacent bone cortex, with or without marrow invasion. Most common in humerus and femur in patients 16 to 82 years, average = 50 years.

a

b

Figure 10.**8 a, b** Geode or degenerative arthritic subchondral cyst in the proximal medial tibia beneath degenerated disrupted hyaline cartilage that has high signal centrally surrounded by a thin lobulated rim of low signal on axial T2WI (**a**). A poorly-defined zone of Gd-contrast enhancement is seen in the marrow medially on coronal FS T1WI (**b**); may be secondary to chronic pressure effects from the geode as well as reaction to overlying chondral damage.

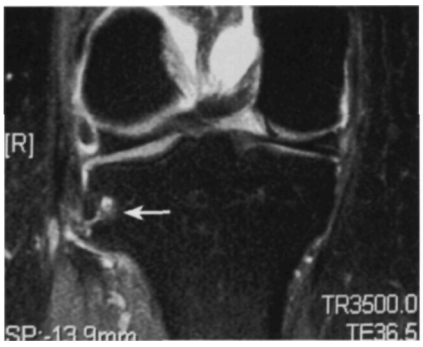

a

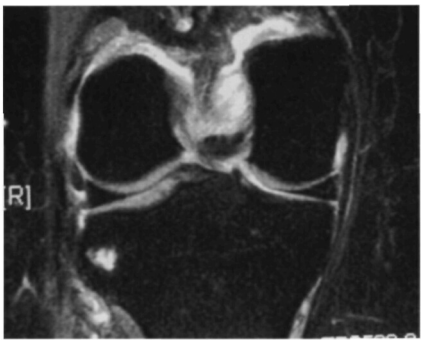

b

Figure 10.**9 a, b** Juxtacortical ganglion eroding bone cortex resulting in an intraosseous ganglion in the proximal lateral tibia that has high signal and circumscribed margins on coronal FS T2WI (**a**, **b**).

a

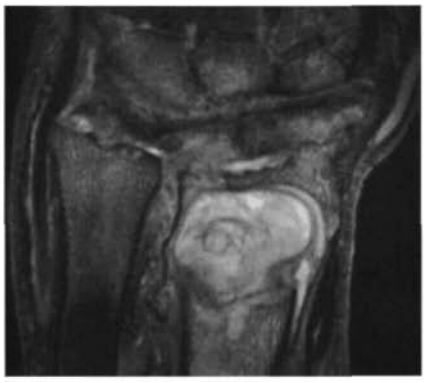

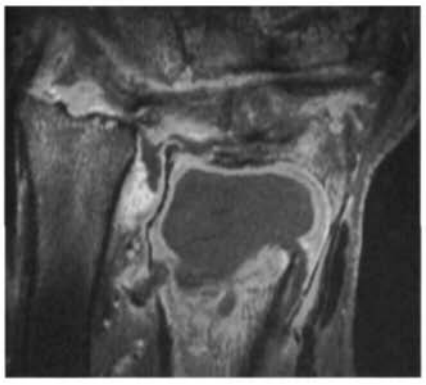

b, c

Figure 10.**10a-c** A 71-year-old man with pannus eroding into the distal radius resulting in destruction of trabecular bone and intraosseous cyst-like lesion. The intraosseous lesion has intermediate signal on coronal T1WI (**a**) and heterogeneous high signal on coronal T2WI (**b**). Cd-contrast enhancement is seen at the margins of the intraosseous lesion on coronal FS T1 WI (**c**) as well as in the hypertrophied synovium in the wrist. Also seen is destruction of hyaline cartilage at the carpal bones and distal ulna.

a, b

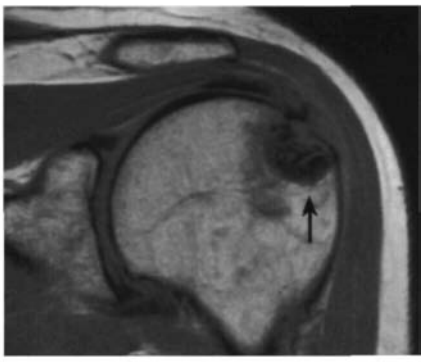

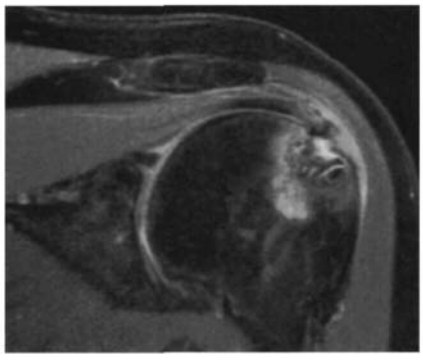

c

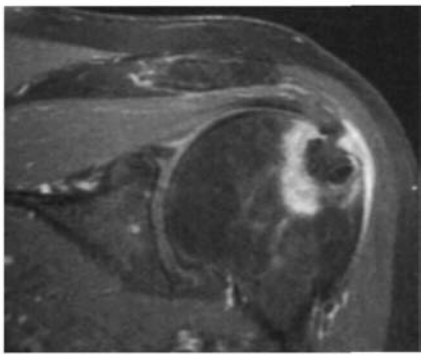

d

Figure 10.**11 a-d** A 57-year-old woman with intraosseous calcific tendinopathy in the humerus. Calcification is seen in the rotator cuff near the insertion site as well as an intraosseous zone of increased attenuation on the AP radiograph (**a**). Coronal PDWI (**b**) shows a circumscribed intraosseous zone with low and intermediate signal beneath a zone of cortical disruption. The intraosseous lesion has mixed high and low signal on Goronal FST2WI (**b**), as well as a poorly defined zone with high T2 signal in the adjacent marrow. The intraosseous lesion shows marginal Gd-contrast enhancement surrounding the circumscribed lesion, and a poorly defined zone of contrast enhancement is seen in the adjacent bone marrow on FST1WI (**d**).

Table 10 (Continued) **Solitary intramedullary lesions located near the ends of tubular bones**

Lesion	MRI Findings	Comments
Fracture (Fig. 10.12)	Acute/subacule fractures typically have abnormal marrow signal (usually low signal on T1WI, high signal on T2WI and FST2WI). Cd-contrast enhancement is typically seen in the postfracture period. Angulated cortical margins and periosteal high signal on FST2WI can be seen with traumatic fractures. A curvilinear zone of low signal on T2WI and FST2WI may be seen within the marrow edema in stress fractures.	Can result from trauma, primary bone tumors/lesions, metastatic disease, bone infarcts (steroids, chemotherapy, and radiation treatment), osteoporosis, osteomalacia, metabolic (calcium/ phosphate) disorders, vitamin deficiencies, Paget disease, and genetic disorders (osteogenesis imperfecta, etc.)
Bone contusion (Fig. 10.13)	Contusions usually appear as poorly defined intramedullary zones with low-intermediate signal on T1WI and high signal on FST2WI, and corresponding Cd-contrast enhancement. Adjacent cortical margins are typically intact.	Also referred to as bone bruises, contusions represent trabecular microfractures without cortical fracture. In the knee, contusions at the lateral femoral condyle and posterolateral proximal tibia are commonly associated with injuries to the anterior cruciate ligament.
Osteochondritis dissecans (Fig. 10.14)	Subchondral lesions in marrow ranging from 1 to 3 cm with low-intermediate signal on T1WI and T2WI. Small irregular zones with slightly high to high signal may be seen with FST2WI. A linear zone with high signal on T2WI along the margins can represent tracking of synovial fluid from a defect in the overlying hyaline cartilage, and is associated with an increased risk of fragmentation and separation.	Osteochondrosis in which there is localized necrosis followed by reossification and healing unless there is osteochondral fragmentation and separation. Lesions commonly occur at the lateral surface of the medial femoral condyle, aswellasthecapitellum, talardome, and femoral head,
Boneinfarct(Fig.IO.I5)	A double-line sign (curvilinear adjacent zones of low and high signal on T2WI) is commonly seen at the edges of the infarcts representing the borders of osseous resorption and healing. Irregular Gd-contrast enhancement can be seen from granulation tissue ingrowth.	Zones of ischemic death involving bone trabeculae and marrow which can be idiopathic or result from: trauma, corticosteroid treatment, chemotherapy, radiation treatment, occlusive vascular disease, collagen vascular and other autoimmune diseases, metabolic storage diseases (Caucher etc.), sickle cell disease, thalassemia, hyperbaric events / Caisson disease, pregnancy, alcohol abuse, pancreatitis, infections, and lymphoproliferative diseases. **(See Atlas Chapter A 37)**
Transient bone marrow edema (Fig. 10.16)	Poorly defined zones with low-intermediate signal on T1WI and high signal on FST2WI and STIR are seen in the marrow of the proximal hip (femoral head and neck). The signal abnormalities may spare the subchondral marrow. MRI Findings can be seen within 48 hours from the onset of symptoms. Joint effusions may be present. With dynamic Gd-contrast administration, delayed peak enhancement can be seen.	Idiopathic spontaneous process with transient edema in bone marrow that is not secondary to trauma, and may or may not be associated with osteoporosis. Transient bone marrow edema or acute bone marrow edema frequently involves the proximal femur in men between 30 and 50 years, and women in the last trimester of pregnancy.

a b, c

Figure 10.**12a-c** A traumatic fracture of the lateral tibial plateau is seen with subjacent poorly defined zones of low-intermediate signal in the marrow on coronal PDWI (**a**) and high signal on coronal (**b**) and sagittal (**c**) FST2WI. Also seen is a bone contusion in the marrow of the lateral femoral condyle.

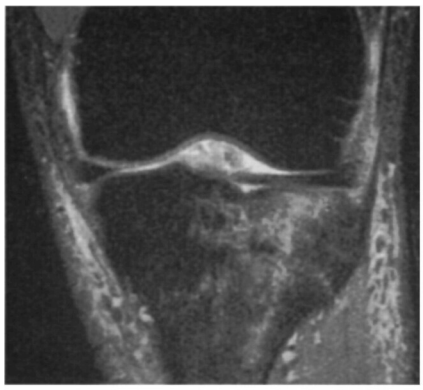

Figure 10.**13** A bone contusion is seen as a poorly defined zone with increased signal on coronal FS T2WI in the proximal tibia with intact overlying bone cortex.

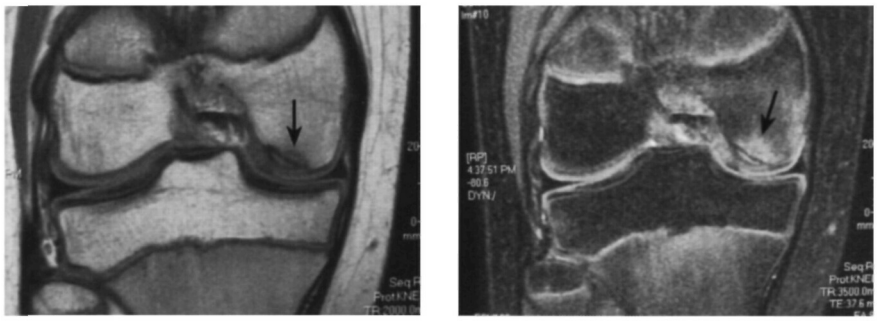

a, **b**

Figure 10.**14 a**, **b** Osteochondritis involving the lateral aspect of the medial femoral condyle in a 12-year-old boy that is seen as a poorly defined zone of low-intermediate signal in the subchondral marrow on coronal PDWI (**a**) and high signal on coronal FS T2WI (**b**).

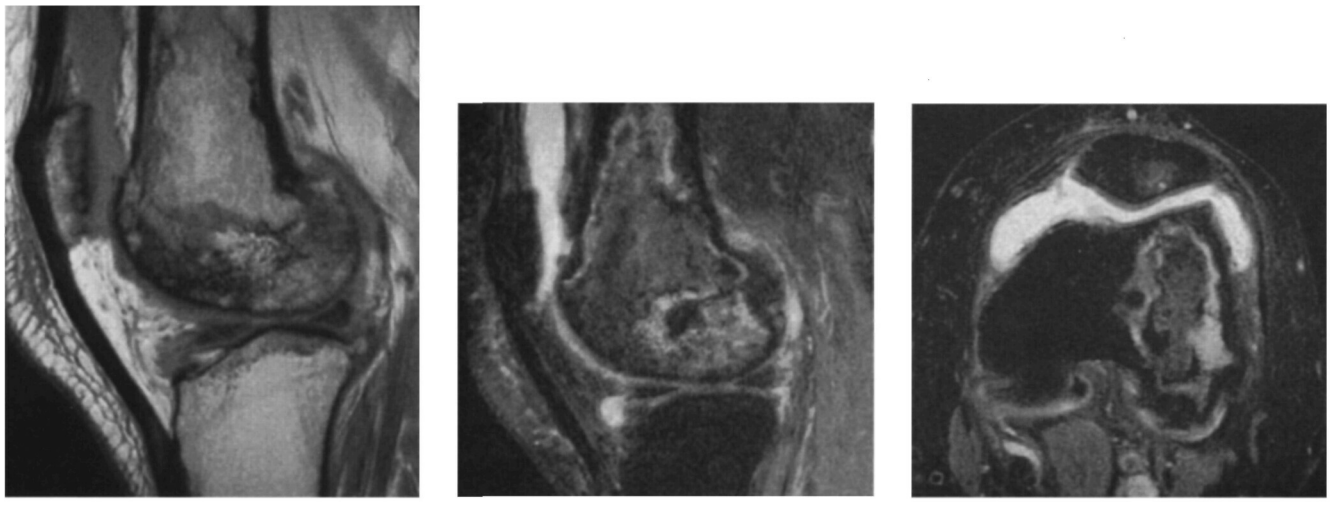

a **b**, c

Figure 10.**15a-c** A 49-year-old woman with a bone infarct in the distal femur as seen on sagittal PDWI (**a**), and sagittal (**b**) and axial (**c**) FST2WI.

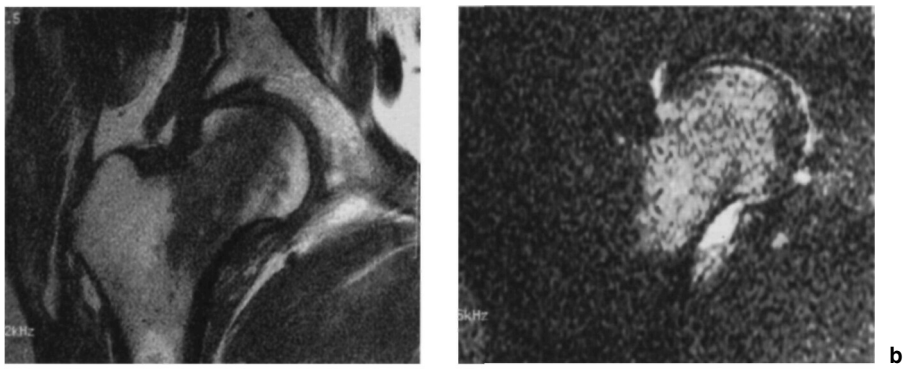

a **b**

Figure 10.**16a-d** A 51-year-old man with hip pain. MRI showing acute bone marrow edema with a poorly defined zone with low-intermediate signal in the marrow of the proximal femur on coronal T1WI (**a**) with corresponding high signal on coronal FS T2WI (**b**). The abnormal marrow signal resolved 2 months later, as seen on coronal T1 WI (**c**) and FST2WI (**d**).

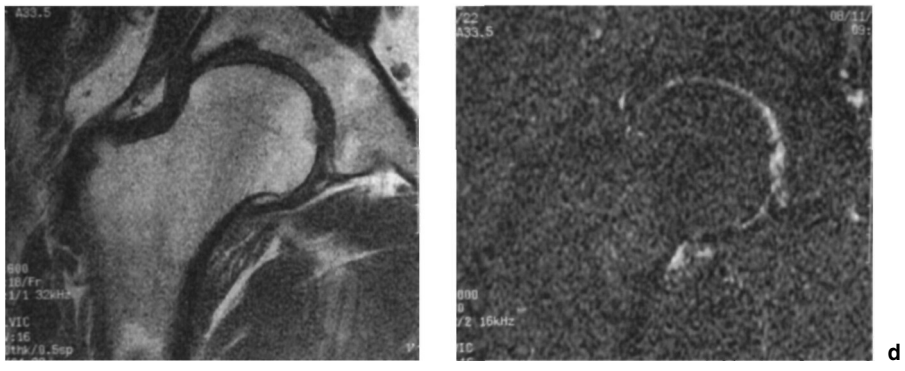

c **d**

Table 10 (Continued) **Solitary intrameduilary lesions located near the ends of tubular bones**

Lesion	MRI Findings	Comments
Osteomyelitis (Fig. 10.17)	In **acute osteomyelitis,** poorly defined zones of low or low-intermediate signal on T1WI; and high signal on T2WI, STIR, and FS T2WI are seen in the marrow. Loss of definition of the low signal line of the cortical margins is often observed on T1WI, T2WI, STIR, and FST2WI. After Gd-contrasl administration, irregular zones of contrast enhancement are seen in the involved marrow on FST1 WI. In the **subacute phase of osteomyelitis,** the pyogenic process becomes more localized. The zone of transition between normal and abnormal bone is sharper and more well-defined in subacute and chronic osteomyelitis than with acute osteomyelitis.	Infection of bone that can result from hematogenous spread of microorganisms as well as from trauma-direct inoculation, extension from adjacent tissues, and complications from surgery. Bacteria such as Stop/iy/ococcus *aureus* and *Streptococcus pyogenes* are the most common infectious organisms. Can also result from other bacteria as well as *Mycabacterium tuberculosis,* fungi, parasites, and viruses. **(See Atlas Chapter A 63)**
Eosinophilic granuloma (Fig. 10.18)	Intrameduilary lesion associated with trabecular and cortical bone destruction which typically has low-intermediate signal on T1WI and PDWI and heterogeneous slightly high to high signal on T2WI. Poorly defined zones of high signal on T2WI are usually seen in the marrow peripheral to the lesions secondary to inflammatory changes. F_xtension of lesions from the marrow into adjacent soft tissues through areas of cortical disruption are commonly seen as well as linear periosteal zones of high signal on T2WI. Lesions typically show prominent Cd-contrast enhancement in marrow and in extraosseous soft tissue portions of the lesions.	Benign tumor-like lesions consisting of Langerhans' cells (histiocytes) and variable amounts of lymphocytes, polymorphonuclear cells, and eosinophils. Account for 1 % of primary bone lesions and 8 % of tumor-like lesions. Occur in patients with median age = 10years, average = 13.5years, peak incidence is between 5 and 10 years, 80 to 85 % occur in patients less than 30 years. **(See Atlas Chapter A 18)**
Malignant		
Metastatic lesion	Single or multiple well-circumscribed or poorly defined infillralive lesions involving marrow associated with cortical destruction and extraosseous extension. Lesions often have low-intermediate signal on T1 WI, low, intermediate, and/or high signal on T2WI and FST2WI, usually showGd-contrast enhancement. Cortical destruction and tumor extension into the extraosseous soft tissues can occur. Pathologic fractures can be associated with metastatic lesions involving tubular bones and vertebrae. Periosteal reaction is uncommon.	Metastatic lesions typically occur in the marrow with or without cortical destruction and extraosseous tumor extension, **(See Atlas Chapter A50)**
Plasmacytoma (Fig. 10.19)	Well-circumscribed or poorly defined infiltrative lesions involving marrow, low-intermediate signal on T1WI, intermediate-high signal on T2WI and FST2WI, usually show Gd-contrast-enhancement, eventual cortical bone destruction and extraosseous extension.	Malignant tumors composed of proliferating antibody-secreting plasma cells derived from single clones. Most common primary neoplasm of bone in adults, median = 60 years. Most patients are older than 40 years. May have variable destructive or infiltrative changes involving the axial and/or appendicular skeleton. **(See Atlas Chapter A 52)**

a b, c

Figure 10.**17 a-c** An 11-year-old boy with septic arthritis and pyogenic osteomyelitis from *Staphylococcus aureus* involving the marrow of the femoral epiphysis. A poorly defined zone of low-intermediate signal is seen in the epiphyseal marrow on coronal T1WI (**a**) with corresponding high signal on coronal FST2WI (**b**). AbnormalGd-contrast enhancement is seen in the marrow on coronal FST1 WI (**c**) as well as within the septic joint collection.

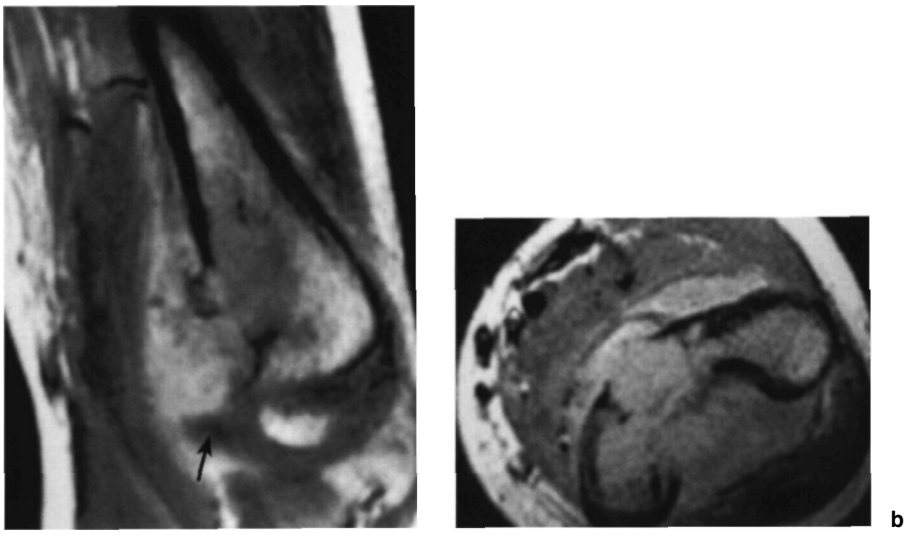

a b

Figure 10.**18a, b** A 5-year-old male with an eosinophilic granuloma involving the distal humerus. The lesion in the marrow is associated with cortical destruction and extraosseous extension into the adjacent soft tissues as seen on sagittal Gd-contrast-enhanced T1WI (**a**) and axial PDWI (**b**).

a b, c

Figure 10.**10a-c** a-c A 77-year-old woman with myeloma involving the marrow of the proximal tibia that has low-intermediate signal on coronal T1WI (**a**) and high signal on coronal FST2WI (**b**). The tumor showGd-contrast enhancement on FST1WI (**c**).

Table 10 (Continued) **Solitary intramedullary lesions located near the ends of tubular bones**

Lesion	MRI Rndings	Comments
Lymphoma (Fig. 10.20)	Non-Hodgkin lymphoma (NHL) and Hodgkin disease (HD) within bone typically appears as single or multifocal poorly defined or circumscribed intramedullary zones with low-intermediate signal on T1 WI. and intermediate, slightly high, and/or high signal on T2WI and high signal on FST2WI; often show Gd-contrast enhancement, Zones of cortical destruction may occur associated with extraosseous soft tissue extension.	Lymphoid tumors with neoplastic cells typically within lymphoid tissue (lymph nodes and reticuloendothelial organs). Unlike leukemia, lymphoma usually arises as discrete masses. Lymphomas are subdivided into HD and NHL. Almost all primary lymphomas of bone are B cell NHL. HD, mean age = 32 years. Osseous NHL, median = 35 years. **(See Atlas Chapter A 47)**
Leukemia	Single or multiple well-circumscribed or poorly defined infiltrative lesions involving marrow; low-intermediate signal on T1WI, intermediate-high signal on T2WI and FST2WI, often shows Gd-contrast enhancement, +/- cortical bone destruction and extraosseous extension.	Malignant lymphoid neoplasms with involvement of bone marrow and with tumor cells also in peripheral blood. **(See Atlas Chapter A41)**
Chondrosarcoma (Fig. 10.21)	Intramedullary tumors of ten have low-intermediate signal on T1WI, intermediate signal on PDWI, and heterogeneous intermediate-high signal on T2WI. Lesions usually show heterogeneous contrast enhancement.	Malignant tumors containing cartilage formed within sarcomatous stroma. Account for 12-21 % of malignant bone lesions, 21-26% of primary sarcomas of bone, mean age - 40 years, median = 26 to 59 years. Clear cell chondrosarcoma is commonly located near the ends of long bones. **(See Atlas Chapter A11)**
Osteosarcoma (Fig. 10.22)	Destructive intramedullary malignant lesions, low-intermediate signal on T1WI, mixed low, intermediate, high signal on T2WI, usually with matrix mineralization/ossification-low signal on T2 W images, typically show Gd-contrast enhancement (usually heterogeneous). Zones of cortical destruction are typically seen through which tumors extend into the extraosseous soft tissues under an elevated periosteum. Lamellated and/or spiculated zones of bone formation can occur under the periosteal elevation secondary to tumor invasion and perforation of bone cortex.	Malignant tumor comprising proliferating neoplastic spindle cells that produce osteoid and/or immature tumoral bone most frequently arising within medullary bone. Two age peaks of incidence. The larger peak occurs between the ages of 10 and 20 and accounts for over half of the cases. The second smaller peak occurs in adults over 60years and accounts for ~ 10 % of the cases. **(See Atlas Chapter** A 64)
Ewing sarcoma (Fig. 10.23)	Destructive malignant lesions involving marrow, low-intermediate signal on T1WI, mixed low, intermediate, and/or high signal on T2WI and FS T2WI, typically shows Gd-contrast enhancement (usually heterogeneous). Extraosseous tumor extension through sites of cortical destruction is commonly seen beneath an elevated periosteum. Thin striated zones of low signal on T2WI can be sometimes seen oriented perpendicular to the long axis of the involved bone under the elevated periosteum representing the "hair on end" appearance of reactive bone formation secondary to the tumor. In long bones, tumors are most often located in the diaphyseal region, followed by the metadiaphyseal region.	Malignant primitive tumor of bone comprising undifferentiated small cells with round nuclei. Accounts for 6-11 % of primary malignant bone tumors, 5-7% of primary bone tumors. Usually occurs between the ages of 5 and 30, males > females, locally invasive, high metastatic potential. **(See Atlas Chapter A 20)**

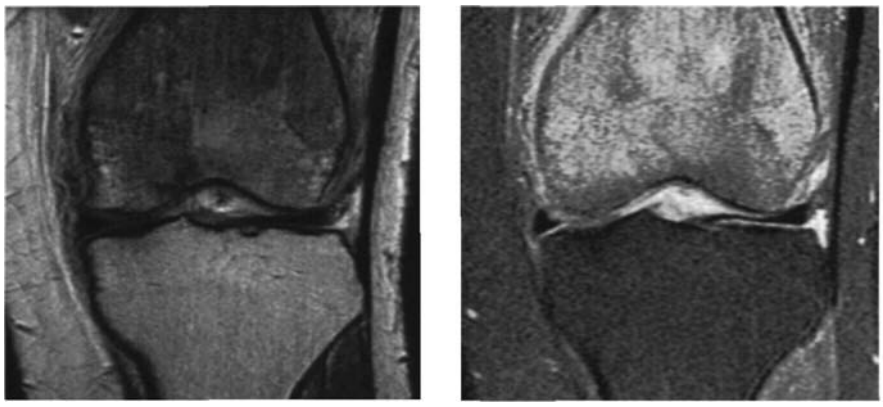

Figure 10.**20a**, **b** A 26-year-old man with large cell NHL involving the marrow of the distal femur as seen as diffuse low signal on coronal PDWI (**a**) and high signal on coronal FST2WI (**b**).

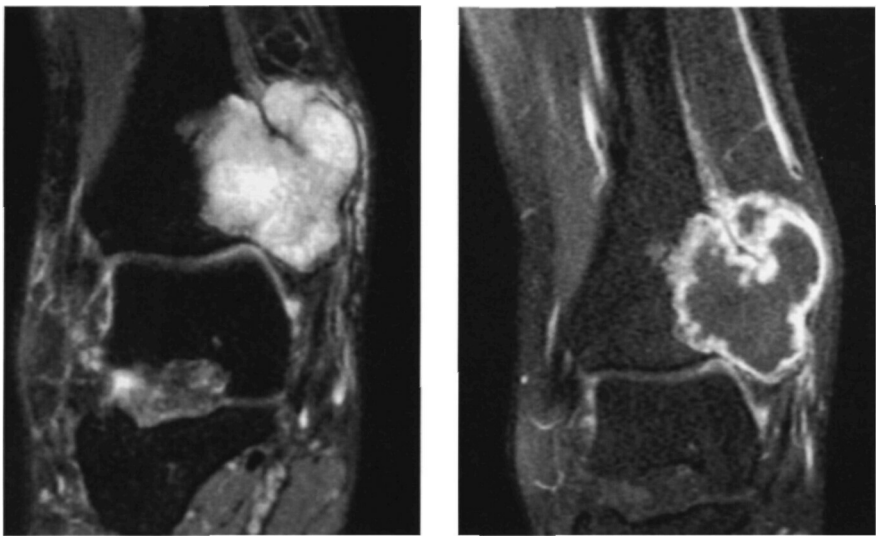

Figure 10.**21 a, b** A 44-year-old woman with a chondrosarcoma in the marrow of the distal tibia associated with cortical destruction and extraosseous extension of tumor. The tumor has high signal on coronal FST2WI (a) and shows peripheral lobular Gd-contrast enhancement on FS T1WI (**b**).

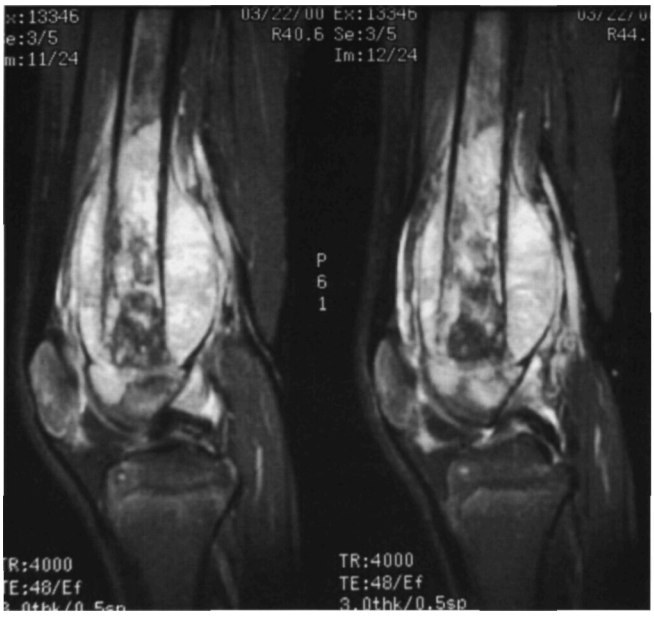

Figure 10.**22** A 9-year-old girl with osteosarcoma in the distal femoral marrow associated with cortical destruction and extraosseous extension as seen on sagittal FS T2WI.

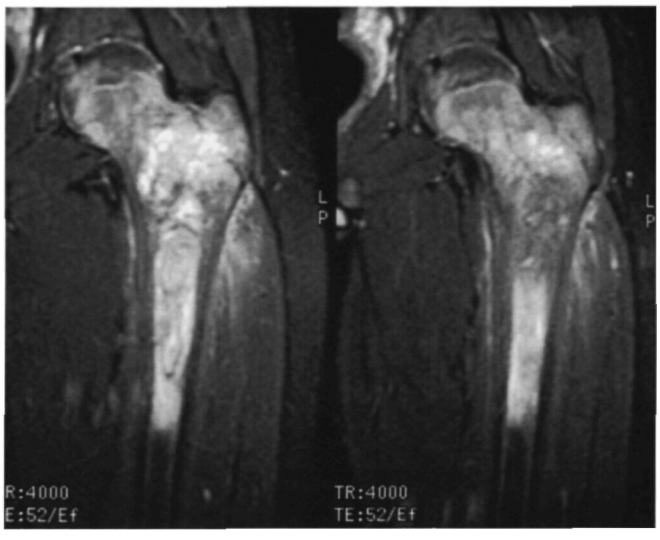

Figure 10.**23** A 15-year-old male with Ewing sarcoma in the marrow of the proximal femur that has high signal on coronal FS T2WI.

Table 10 (Continued) **Solitary intramedullary lesions located near the ends of tubular bones**

Lesion	MRI Findings	Comments
Malignant giant cell tumor (Fig. 10.24)	Well-defined lesions with or without thin low signal margins on T1WI and T2WI. Solid portions of giant cell tumors often have low to intermediate signal on T1WI and PDWI, intermediate to high signal on T2WI. and high signal on FS PDWI and FST2WI. Signal heterogeneity on T2WI is not uncommon. Aneurysmal bone cysts are seen with 14% of giant cell tumors. Lesions show mild to prominent variable and often heterogeneous Gd-contrast enhancement. Cortical destruction and extraosseous tumor extension are frequently seen.	Aggressive tumors composed of neoplastic ovoid mononuclear cells and scattered multinucleated osteoclast-like giant cells. Up to 10 % of all giant cell tumors are malignant. Benign giant cell tumors account for ~ 5 to 9.5 % of all bone tumors and up to 23 % of benign bone tumors, Malignant giant cell tumors account for 5.8% of all giant cell tumors. 75 % occur between the ages of 15 and 45. **(See Atlas Chapter A 29)**
Fibrosarcoma	Intramedullary lesions with irregular margins, with or without associated cortical destruction and/or extraosseous soft tissue masses. Lesions usually have low-intermediate signal on T1WI and PDWI, and heterogeneous intermediate, slightly high, and/or high signal on T2WI. Lesions usually show heterogeneous Gd-contrast enhancement.	Uncommon malignant tumors consisting of bundles of fibroblasts/spindle cells with varying proportions of collagen, lacking other tissue differentiating features such as tumor bone, osteoid, or cartilage. Can be primary lesions (75 %) or arise as secondary tumors (25%) associated with prior irradiation, Paget disease, bone infarct, chronic osteomyelitis, fibrous dysplasia, giant cell tumor. Account for 3-5 % of primary malignant bone tumors, and 2-4 % of all bone tumors, median age = 43 years. **(See Atlas Chapter A 25)**
Malignant fibrous histiocytoma	Intramedullary lesions with irregular margins and zones of cortical destruction and extraosseous extension. Tumors often have low-intermediate signal on T1 WI; low-intermediate signal on PDWI. and heterogeneous intermediate-high signal on T2WI and FS T2WI. Invasion into joints occurs in 30 %. May be associated with bone infarcts, bone cysts, chronic osteomyelitis, Paget disease, and other treated primary bone tumors. Lesions usually show heterogeneous Gd-contrast prominent enhancement.	Malignant tumor involving soft tissue and rarely bone derived from undifferentiated mesenchymal cells. Contains cells with limited cellular differentiation such as mixtures of fibroblasts, myofibroblasts, histiocyte-like cells, anaplastic giant cells, and inflammatory cells. Accounts for 1-5 % of primary malignant bone tumors and < 1-3 % of all primary bone tumors, patient ages range from 11 to 80 years, median = 48 years, mean = 55 years. **(See Atlas Chapter A 48)**
Hemangioendothelioma (Fig. 10.25)	Intramedullary tumors which often have low-intermediate and/or high signal on T1WI, and heterogeneous intermediate-high signal on T2WI and FST2WI with or without zones of low signal. Cortical expansion with or without extraosseous extension of tumor through zones of cortical destruction can occur. Lesions often show prominent heterogeneous Gd-contrast enhancement.	Low-grade vasoformative/endothelial malignant neoplasms that are locally aggressive and rarely metastasize compared with the high-grade endothelial tumors such as angiosarcoma. Account for less than 1 % of primary malignant bone tumors. Patients range from 10 to 82 years, median = 36 to 47 years. Patients with multifocal lesions tend to be ~ 10 years younger on average than those with unifocal tumors. **(See Atlas Chapter A 33)**

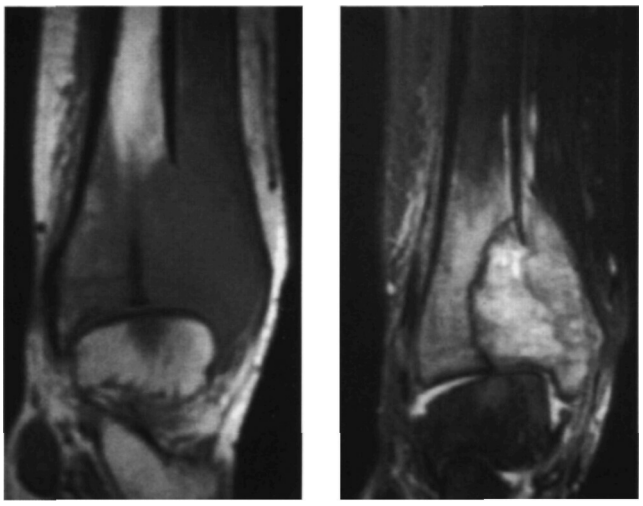

Figure 10.**24** **A** 16-year-old male with a malignant giant cell tumor of the distal tibia associated with destruction of cortical bone with extraosseous extension as seen on coronal T1 WI (a) and FS T2WI (**b**).

Figure 10.**25** A 19-year-old man with hemangioendothelioma involving the distal tibia with cortical disruption and tumor extension into the ankle joint as seen on coronal T2WI.

References

Fracture

Ahovuo JA, Kiuru MJ, Visuri T. Fatigue stress fractures of the sacrum: diagnosis with MR imaging. *Eur Radiol* March 2004;14(3):500-505. Epub October 24, 2003.

Berger FH, de Jonge MC, Maas M. Stress fractures in the lower extremity. The importance of increasing awareness amongst radiologists. *Eur J Radiol* 2007;62:16-26.

Grangier C, Garcia J, Howarth NR, May M, Rossier P. Role of MRI in the diagnosis of insufficiency fractures of the sacrum and acetabular roof. *Skeletal Radiol* !997;26:517-524.

Meyers SP, Wiener SN. Magnetic resonance imaging features of fractures using the short tau inversion recovery (STIR) sequence: correlation with radiographic findings. *Skeletal Radiol* 1991;20(7): 499-507.

Pham T, Azulay-Parrado J, Champsaur P, Chagnaud C, Legre V, Lafforgue P. Occult osteoporotic vertebral fractures. Vertebral body fractures without radiologic collapse. Spine 2005;30(21):2430-2435.

Takahara K, Kamimura M, Nakagawa H, Hashidate H, Uchiyama S. Radiographic evaluation of vertebral fractures in osteoporotic patients./ *Clin Neurosci* 2007:14:122-126.

Bone Contusion

Boks SS, Vroegindeweij D, Koes BW, Hunink MGM, Bierma-Zeinstra SMA. Follow-up of occult bone lesions detected at MR imaging: systematic review. *Radiology* March 2006;238(3):853-862.

Davies NH, Niall D, King LJ, Lavelle J, Healy JC. Magnetic resonance imaging of bone bruising in the acutely injured knee - short-term outcome. *Clin Radiol* 2004;59:439-445.

Osteochondritis Dissecans

Kijowski R, De Smet AA. MRI findings of Osteochondritis dissecans of the capitellum with surgical correlation. *AJR* December 2005;185: 1453-1459.

O'Connor MA, Palaniappan M, Khan N, Bruce CE. Osteochondritis dissecans of the knee in children. *J Bone Joint Surg* March 2002; 84-B(2):258-262.

Sanders TG, Paruchuri NB, Zlatkin MB. MRI of osteochondral defects of the lateral femoral condyle: incidence and pattern of injury after transient lateral dislocation of the patella. AJR November 2006; 187: 1332-1337.

Schmid MR, Hodler J, Vienne P, Binkert CA, Zanetti M. Bone marrow abnormalities of foot and ankle: STIR versus Tl-weighted contrast-enhanced fat-suppressed spin-echo MR imaging. *Radiology* August 2002;224(2):463-469.

Transient Bone Marrow Edema

Balakrishnan A, Schemitsch EH, Pearce D, McKee MD. Distinguishing transient osteoporosis of the hip from avascular necrosis. *Can] Surg* June 2003;46(3):187-192.

Malizos KN, Zibis AH, Dailiana Z, Hantes M, Karahalios T, Karantanas AH. MR imaging findings in transient osteoporosis of the hip. *Eur J Radiol* 2004;50:238-244.

Toms AP, Marshall TJ, Becker E, Donell ST, Lobo-Mueller EM, Barker T. Regional migratory osteoporosis: a review illustrated by five cases. *Clin Radiol* 2005;60:425-438.

Yamamoto T, Kubo T, Hirasawa Y, Noguchi Y, Iwamoto Y, Sueishi K. A clinicopathologic study of transient osteoporosis of the hip. *Skeletal Radiol* 1999;28:621-627.

Table 11 Solitary intramedullary metadiaphyseal lesions

Lesion	MRI Findings	Comments
Benign		
Nonossifying fibroma (Fig. 11.1)	Well-circumscribed eccentric intramedullary lesions in the metadiaphyseal regions of long bones that have mixed low-intermediate signal on T1WI, and mixed low, intermediale, and/or high signal on T2WI, PDWI, and FST2WI. Zones of low signal on T1WI, PDWI, and T2WI can be seen in the central portions of the lesions. Zones with varying thickness of low signal on T1WI, PDWI, and T2WI are seen at the margins of the lesions representing bone sclerosis. Internal septations are commonly seen as zones of low signal on T2WI in these lesions. Lesions can show Gd-contrast enhancement (heterogeneous > homogeneous patterns).	Common benign fibrohistiocytic lesions in the metaphyseal portions of long bones that are comprised of whorls of fibroblastic cells combined with smaller amounts of multinucleated giant cells and xanthomatous cells. Usually asymptomatic, 95 % occur between the ages of 5 and 20, median = 14 years. **(See Atlas Chapter A 26)**
Enchondroma (Fig. 11.2)	Lobulated intramedullary lesions with well-defined borders, mean size = 5 cm. Lesions usually have low-intermediate signal on T1WI and intermediate signal on PDWI. On T2WI and FST2WI, lesions usually have predominantly high signal with foci and/or bands of low signal representing areas of matrix mineralization and fibrous strands. Lesions typically show Gd-contrast enhancement in various patterns (peripheral curvilinear lobular, central nodular/septal and peripheral lobular, or heterogeneous diffuse).	Benign intramedullary lesions composed of hyaline cartilage, represent~10 % of benign bone lumors. Enchondromas can be solitary (88 %) or multiple (12 %). Median age = 35 years, peak in 3rd and 4th decades. **(See Atlas Chapter A 8)**
Unicameral bone cyst (Fig. 11.3)	Unicameral bone cysts (UBCs) often have a peripheral rim of low signal on T1 WI and T2WI adjacent to normal medullary bone. UBCs usually contain fluid with low to low-intermediate signal on T1WI; low-intermediate; and high signal on T2WI. Fluid-fluid levels may occur. For UBCs without pathologic fracture, Ihin peripheral Gd-contrast enhancement can be seen at the margins of lesions. UBCs with pathologic fracture can have heterogeneous or homogeneous low-intermediate or slightly high signal on T1WI, and heterogeneous or homogeneous high signal on T2WI and FS T2WI. UBCs complicated by fracture can have internal septations and fluid-fluid levels, as well as irregular peripheral Gd-contrast enhancement and at internal septations.	Inlramedullary non-neoplastic cavities filled with serous or serosanguineous fluid. Account for *9%* of primary tumor-like lesions of bone. 85 % occur in the first 2 decades, median = 11 years. **(See Atlas Chapter A 3)**

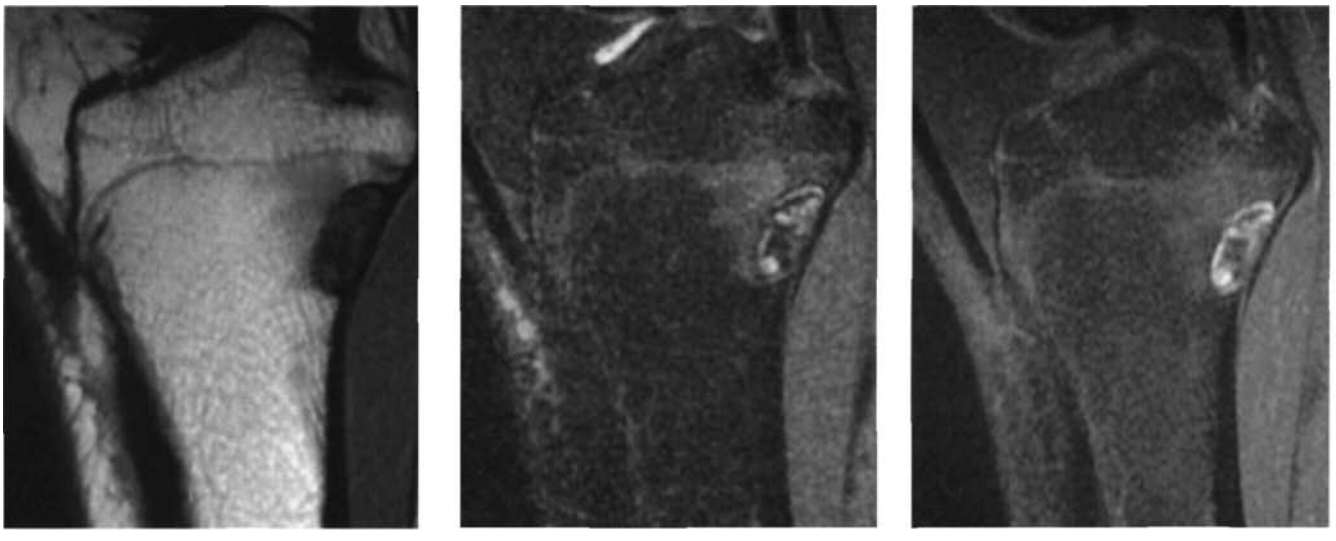

a b, c

Figure 11.1 **a-c** **A** 15-year-old female with a nonossifying fibroma in the dorsal proximal tibia that has a thin peripheral rim of low signal surrounding a central zone with low-intermediate signal on sagittal T1WI (**a**) and mixed low and high signal on FST2WI (**b**). The lesion shows thin marginal and central Gd-contrast enhancement on sagittal FST1WI (**c**).

a

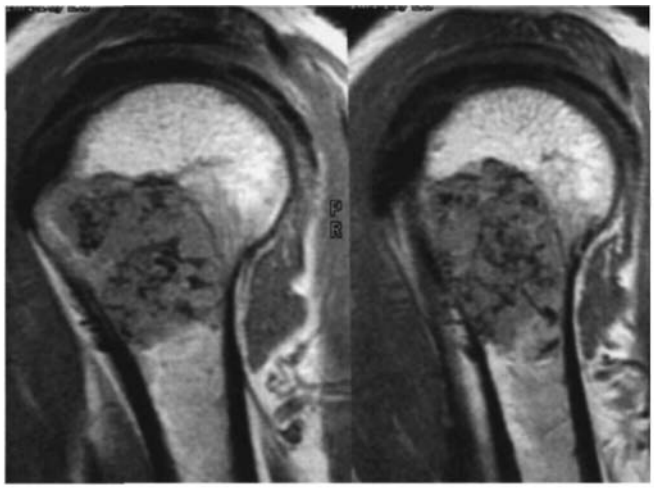

b

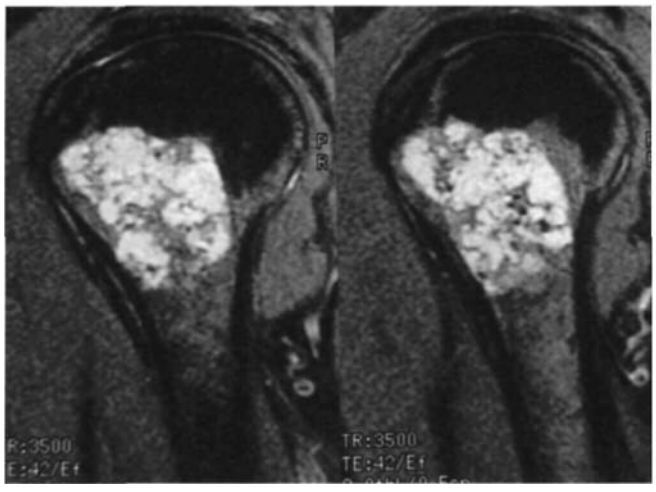

c

Figure 11.2a-c A 40-year-old woman with an enchondroma in the metadiaphyseal portion of the proximal humerus that has chondroid mineralization on the AP radiograph (a). The lesion has a predominantly intermediate signal on PDWI (**b**) and high signal on FST2WI (c) as well as zones of low signal corresponding to mineralized chondroid matrix.

a

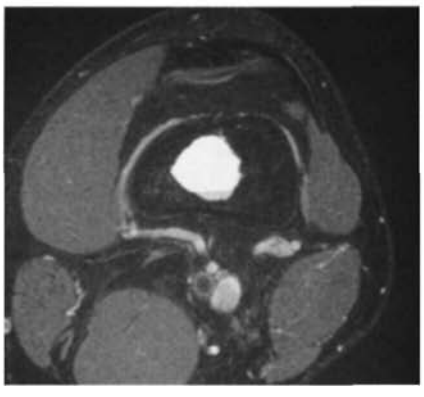

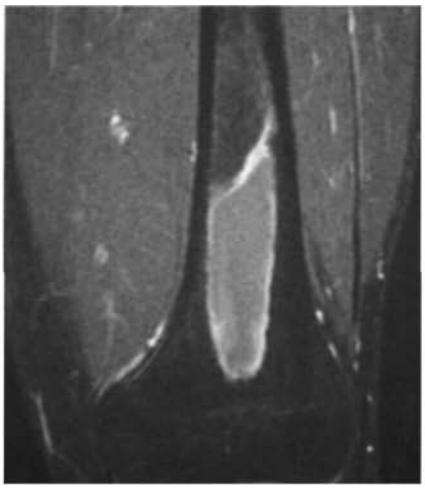

b, c

Figure 1**1.3a-c** A 16-year-old male with a unicameral bone cyst in the distal femur that has low-intermediate signal on coronal T1 WI (**a**) and high signal on axial FS T2WI (**b**). The lesion shows a thin peripheral rim of Gd-contrast enhancement on coronal FST1WI (**c**).

Table 11 (Continued) **Solitary intramedullary metadiaphyseal lesions**

Lesion	MRI Findings	Comments
Aneurysmal bone cyst (Fig. 11.4)	ABCs often have a low signal rim on T1WI and T2WI adjacent to normal medullary bone, and between extraosseous soft tissues. Various combinations of low, intermediate, and/or high signal on T1 WI, PDWI, and T2WI are usually seen within aneurysmal bone cysts as well as fluid-fluid levels. Variable Gd-contrast enhancement is seen at the margins of lesions as well as involving the internal septae.	Tumor-like expansile bone lesions containing cavernous spaces filled with blood, ABC s can be primary bone lesions (two-thirds) or secondary to other bone lesions/ tumors (such as giant cell tumors, chondroblastomas, osteoblastomas, osteosarcomas, chondromyxoid fibromas, nonossifying fibromas, fibrous dysplasia. fibrosarcomas, malignant fibrous histiocytomas, and metastatic disease). Account for ~11 % of primary tumor-like lesions of bone. Patients usually range in age from 1 to 25 years, median = 14years. **(See Atlas Chapter A 2)**
Giant cell tumor (prior to physeal plate closure) (Fig. 11.5)	Often well-defined lesions with thin low signal margins on T1WI, PDWI, and T2WI. Solid portions of giant cell tumors often have low to intermediate signal on T1WI and PDWI, intermediate to high signal on T2WI, and high signal on FS PDWI and FST2WI. Zones of low signal on T2WI may be seen secondary to hemosiderin. Aneurysmal bone cysts can be seen in 14 % of giant cell tumors. Areas of cortical thinning, expansion, and/or destruction can occur with extraosseous extension. Tumors show varying degrees of Gd-contrast enhancement.	Aggressive tumors composed of neoplastic mononuclear cells and scattered multinucleated osteoclast-like giant cells. Account for 23 % of primary nonmalignant bone tumors, and 5-9 % of all primary bone tumors, median age - 30 years. **(See Atlas Chapter A 29)**
Giant cell reparative granuloma (Fig. 11.6)	Lesions can have heterogeneous low, intermediate, and / or high signal on T1WI, PDWI. and T2WI; as well as peripheral rim-like and central Gd-contrast enhancement on FS T1 WI. May be surrounded by poorly defined zone of high signal on FS T2WI and Gd-contrast enhancement in the adjacent marrow.	**Giant cell reparative granulomas** are also referred to as solid ABC s. (See Atlas Chapter A 2). Histologic appearance resembles brown tumors.
Chondromyxoid fibroma (Fig. 11.7)	Lesions are often slightly lobulated with low-intermediate signal on T1WI, intermediate signal on PDWI, and heterogeneous predominantly high signal on T2WI. Thin low signal septa within lesions on T2WI are secondary to fibrous strands. Lesions are surrounded by low signal borders representing thin sclerotic reaction. Edema is not typically seen in adjacent medullary bone. Lesions show prominent diffuse Gd-contrast enhancement.	Rare, benign, slow-growing bone lesions that contain chondroid, myxoid, and fibrous components. Chondromyxoid fibromas represent 2-4% of primary benign bone lesions, and < 1 % of primary bone lesions. Most chondromyxoid fibromas occur between the ages of 1 and 40 years, with a median of 17 years, and peak incidence in the 2nd or 3rd decades. **(See Atlas Chapter A 10)**

a

b

Figure 11.**4 a, b** An 11 -year- old boy with an expansile aneurysmal bone cyst in the proximal femur that has multiple septations and compartments with high signal on coronal FST2WI (**a**). Gd-contrast enhancement is seen at the margins and between the fluid zones on coronal FST1WI (**b**).

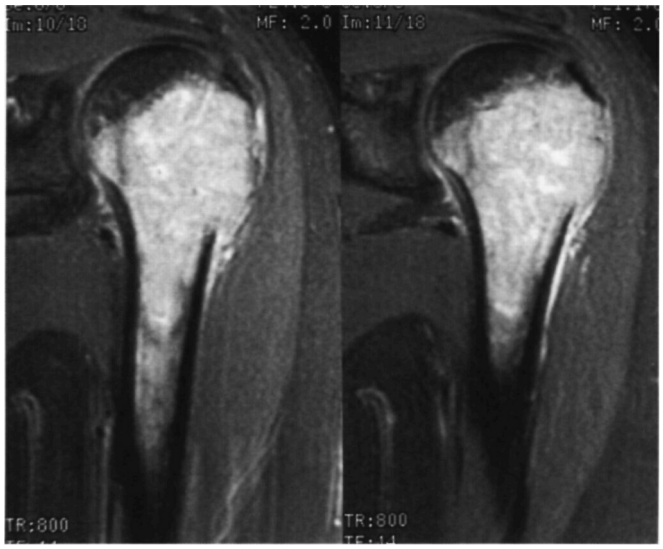

Figure 11.**5** A 14-year-old boy with a giant cell tumor within the metadiaphyseal portion of the proximal humerus that shows prominenGd-contrast enhancement on coronal FS T1WI, as well as cortical destruction and extraosseous extension.

a

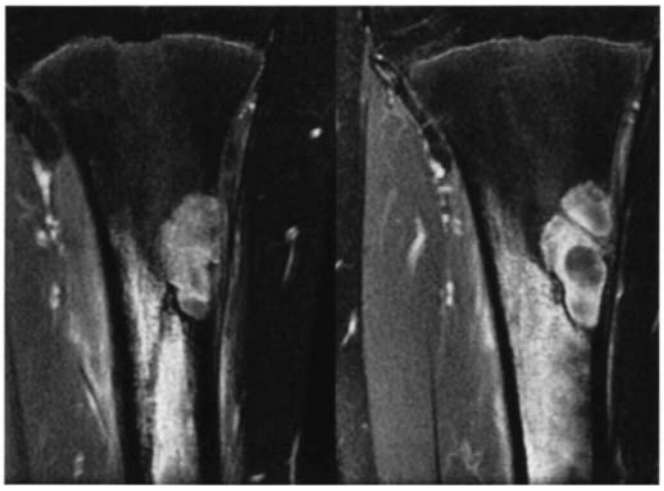

b

Figure 11.**6 a, b** A 14-year-old boy with a giant cell granuloma (also called solid aneurysmal bone cyst) in the metadiaphyseal portion of the proximal tibia that is seen as a radiolucent lesion with thin sclerotic margins on the AP radiograph (a). Gd-contrast enhancement is seen within the lesion as well as in the adjacent marrow on coronal FST1WI(**b**).

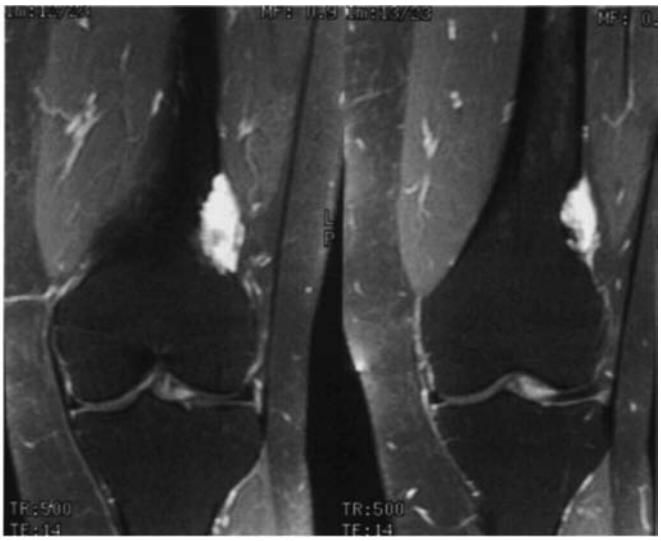

a

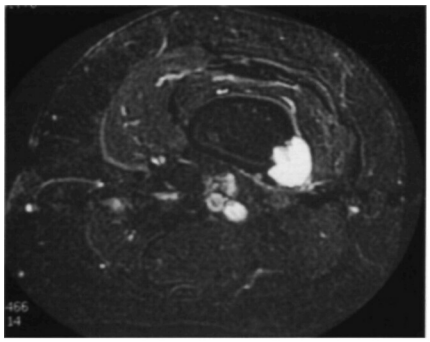

b

Figure 11.**7a**, **b** A 39-year-old woman with a chondromyxoid fibroma involving the metadiaphyseal portion of the distal femur laterally associated with cortical thinning and expansion. The lesion shows prominent Gd-contrast enhancement on coronal FST1WI (**a**) and has high signal on axial FST2WI (**b**).

Table 11 (Continued) **Solitary intramedullary metadiaphyseal lesions**

Lesion	MRI Findings	Comments
Hemangioma	Often well-circumscribed lesions thai typically have inlermecliate to high signal on T1WI, PDWI, T2WI, and FST2WI. On T1WI, hemangiomas usually have signal equal to or greater than adjacent normal marrow secondary to fatty components. Usually show Gel-contrast enhancement. Pathologic fractures associated with intraosseous hemangiomas usually result in low-intermediate marrow signal on T1WI.	Common benign lesions of bone compns-ing capillary, cavernous, and/or malformed venous vessels. Hemangiomas have been considered to be a hamartomatous disorder. Account for *4%* of benign bone tumors and~ 1 % of all bone tumors, likely underestimated. Occur in all ages, median =33 years. **(See Atlas Chapter A 34)**
Intraosseous lipoma (Fig. 11.8)	Lesions can have heterogeneous high, intermediate, and/or low signal on T1WI, PDWI, and T2WI. Fat signal in lesions is suppressed on FST1WI, FST2WI, andSTIR, Lesions usually show no Gd-contrast enhancement. Peripheral rim-like and central Gd-contrast enhancement may occasionally occur on FST1WI. ~0.1	Uncommon benign hamartomas composed of mature white adipose tissue without cellular atypia. Osseous or chondroid metaplasia with myxoid changes can be associated with lipomas. Account for % of bone tumors, likely under-reported. **(See Atlas Chapter A 43)**
Fibrous dysplasia (Fig. 11.9)	MRI features depend on the proportions of bony spicules, collagen, fibroblastic spindle cells, hemorrhagic and/or cystic changes, and associated pathologic fracture if present. Lesions are usually well-circumscribed, and have low or low-intermediate signal on T1WI and PDWI. On T2WI, lesions have variable mixtures of low, intermediate, and/or high signal often surrounded by a low signal rim of variable thickness. Internal septations and cystic changes are seen in a minority of lesions. Bone expansion with thickened and/or thinned cortex can be seen. Lesions show Gd-contrast enhancement that varies in degree and pattern.	Benign medullary fibro-osseous lesion that can involve a single site (**mono-ostotic**) or multiple locations **(poly-ostotic).** Thought to occur from developmental failure in the normal process of remodeling primitive bone to mature lamellar bone with resultant zone or zones of immature trabeculae within dysplastic fibrous tissue. Accounts for ~ 10 % of benign bone lesions. Patients range in age from <1 to 76 years. 75% occur before the age of 30 years. **(See Atlas Chapter A 27)**
Liposclerosing myxofibrous tumor (Fig. 11.10)	Lesions have well-defined margins with variable thickness of low signal borders on T1WI and T2WI. Lesions often have low to intermediate signal on T1WI, and intermediate to high signal on T2WI and FST2WI. Small zones with fat signal may be seen at the periphery of the lesions. Lesions usually lack Gd-contrast enhancement.	Uncommon benign fibro-osseous lesions with mixed histologic features of lipoma, fibroxanthoma, myxoma, fibrous dysplasia, bone cyst, myxofibroma, fat necrosis, and/or ischemic ossification. Most of these lesions occur in the intertrochanteric region of the femur. May represent a variant form of fibrous dysplasia. Patients range from 15 to 69 years, mean =42 years. **(See Atlas Chapter A 45)**
Stress fracture (Fig. 11.11)	Fractures typically have abnormal marrow signal (usually low signal on T1WI, high signal on T2WI and FST2WI). Gd-contrast enhancement is typically seen in the post-fracture period. Angulated cortical margins and periosteal high signal on FST2WI can be seen. A curvilinear zone of low signal on T2WI and FST2WI may be seen within the marrow edema, which is often perpendicular or oblique to the long axis of the involved bone.	Stress fractures can result from persistent chronic mechanical overload, as well as from osteoporosis or osteomalacia, primary bone tumors/lesions, metastatic disease, bone infarcts.

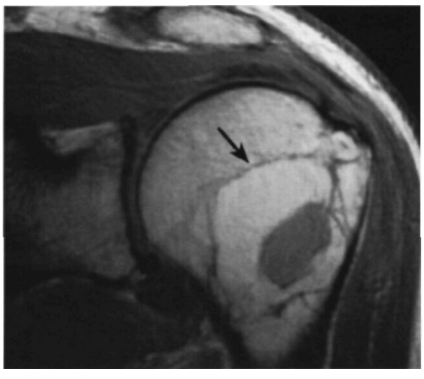

a

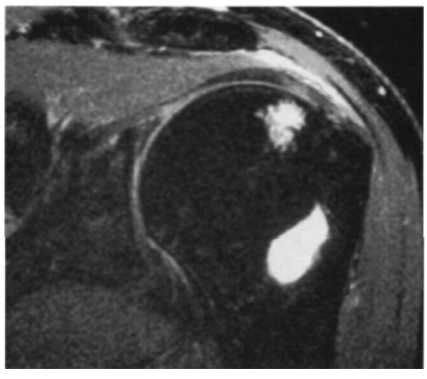

b

Figure 11.**8 a**, **b** Intraosseous lipoma in the metadiaphyseal portion of the proximal humerus that has high fat signal peripherally surrounding a central cyst-like zone with intermediate signal on coronal PDWI (**a**). The fat signal of the lesion is nulled on coronal FS T2WI (**b**) whereas the central cystic region has high signal.

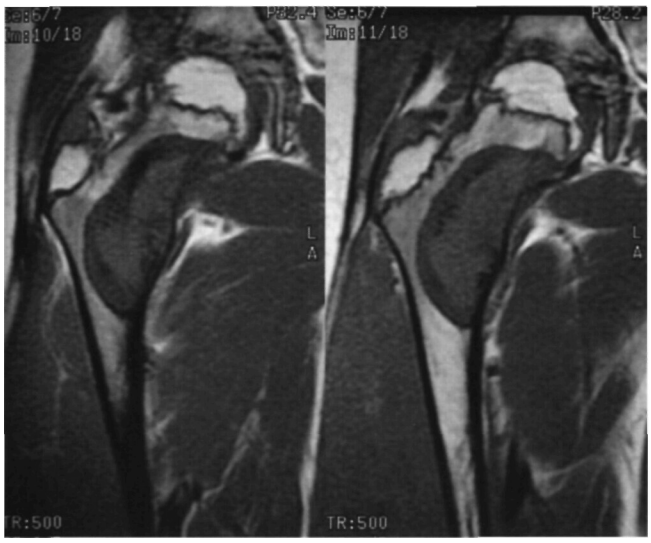

a

b

Figure 11.**9a, b** A 10-year-old boy with fibrous dysplasia involving the metadiaphyseal portion of the proximal femur. The circumscribed lesion has a margin of low signal surrounding a central zone with intermediate signal on coronal T1WI (**a**). The lesion has high signal on coronal FST2WI (**b**), and poorly defined high signal is also seen in the adjacent marrow.

Figure **11.10** A 61-year-old man with liposclerosing myxofibrous tumor in the metadiaphyseal portion of the proximal femur that has low- intermediate signal centrally surrounded by foci with fat signal on coronal T1WI.

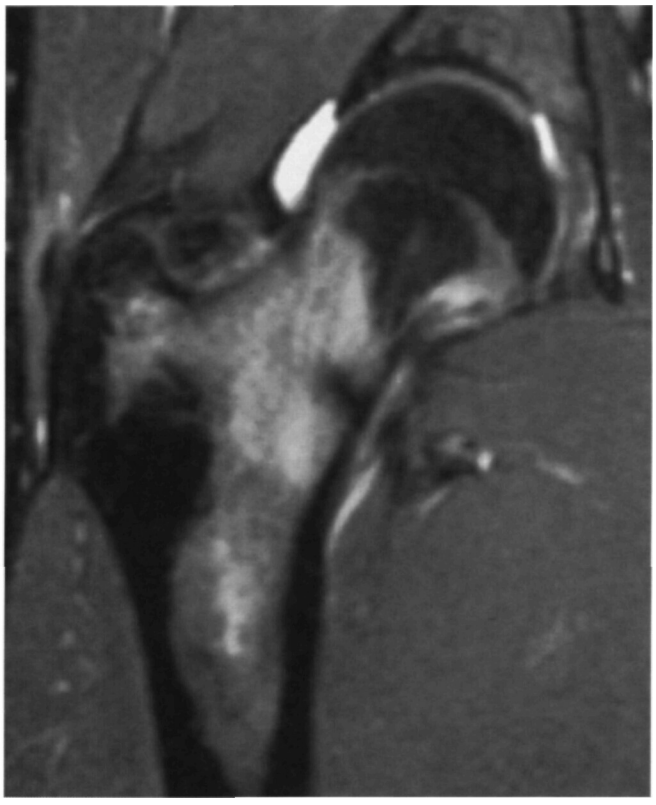

Figure **11.11** Stress fracture in the proximal femur seen as a poorly defined zone with high signal in the marrow surrounding a linear zone of low signal on coronal FS T2WI.

Table 11 (Continued) Solitary intramedullary metadiaphyseal lesions

Lesion	MRI Findings	Comments
Bone Infarct (Fig. 11.12)	A double-line sign (curvilinear adjacent zones of low and high signal on T2WI) is commonly seen at the edges of the infarcts representing the borders of osseous resorption and healing. Irregular Gd-contrast enhancement can be seen from granulation tissue in-growth.	Zones of ischemic death involving bone trabeculae and marrow that could be idiopathic or result from: trauma, corticosteroid treatment, chemotherapy, radiation treatment, occlusive vascular disease, collagen vascular and other autoimmune diseases, metabolic storage diseases (Gaucher etc.), sickle cell disease, thalassemia, hyperbaric events / Caisson disease, pregnancy, alcohol abuse, pancreatitis, infections, and lymphoproliferative diseases. **(See Atlas Chapter A 37)**
Eosinophilic granuloma (Fig. 11.13)	Focal intramedullary lesion(s) associated with trabecular and cortical bone destruction that typically have low-intermediate signal on T1WI and PDWI and heterogeneous slightly high to high signal on T2WI. Poorly defined zones of high signal on T2WI are usually seen in the marrow peripheral to the lesions secondary to inflammatory changes. Extension of lesions from the marrow into adjacent soft tissues through areas of cortical disruption are commonly seen as well as linear periosteal zones of high signal on T2WI. Lesions typically show prominent Gd-contrast enhancement in marrow and in extraosseous soft tissue portions	Benign tumor-like lesions consisting of Langerhans' cells (histiocytes), and variable amounts of lymphocytes, polymorphonuclear cells, and eosinophils. Account for 1 % of primary bone lesions and 8 % of tumor-like lesions. Occur in patients with median age =10years, average = 13.5 years, peak incidence is between 5 and 10 years, 80-85 % occur in patients less than 30 **years. (See Atlas Chapter A 18)**
Osteomyelitis (Fig. 11.14)	Poorly defined zones with high signal on T2WI and FS T2WI and Gd-contrast enhancement are seen in marrow with associated zones of cortical destruction. Periosteal reaction can be seen as a peripheral rim of high signal on T2WI and FST2WI and Gd-contrast enhancement on FST1WI adjacent to the low signal of cortical bone. A subperiosteal abscess with high signal on T2W1 and FS T2WI can be often seen elevating a single low signal thin band of periosteum.	Infection of bone that can result from hematogenous spread of microorganisms, trauma-direct inoculation, extension from adjacent tissues, and complications from surgery. *Staphylococcus aureus* and *Streptococcus pyogenes* are the most common bacterial infections involving bone. Osteomyelitis can also result from other bacteria as well as from other organisms such as tuberculosis, fungi, parasites, and viruses. **(See Atlas Chapter A 63)**

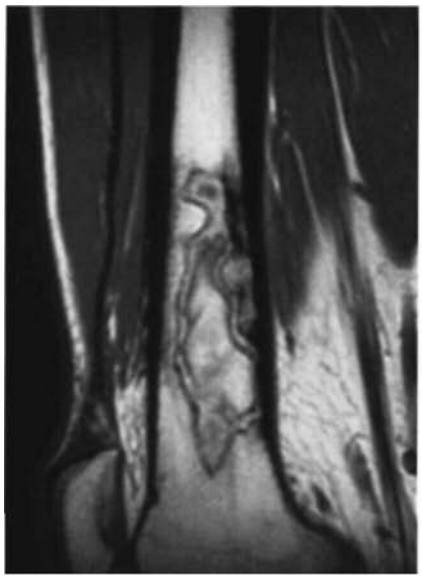

a

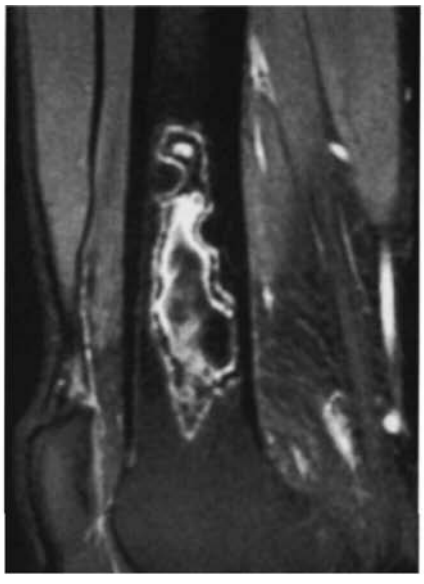

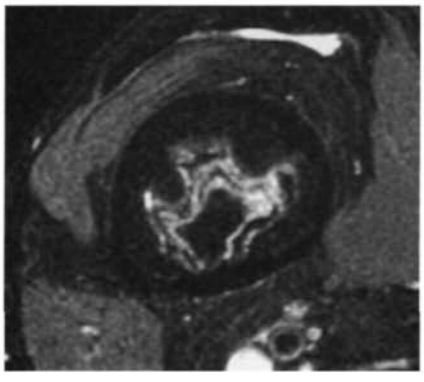

b, c

Figure 11.**12a-c** A 38-year-old man with sickle cell trait and a bone infarct in the distal metadiaphyseal portion of the distal femur as seen on sagittal T1WI (a) and sagittal (**b**) and axial (c) FST2WI. A double-line sign (curvilinear adjacent zones of low and high signal on T2WI) is seen at the edges of the infarct representing the borders of osseous resorption and healing.

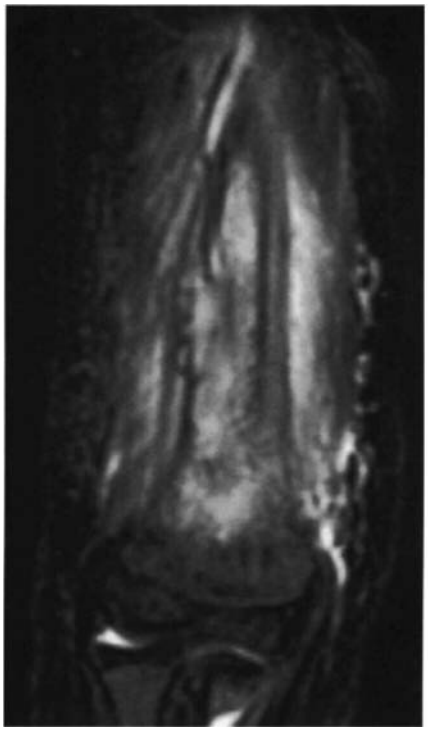

a

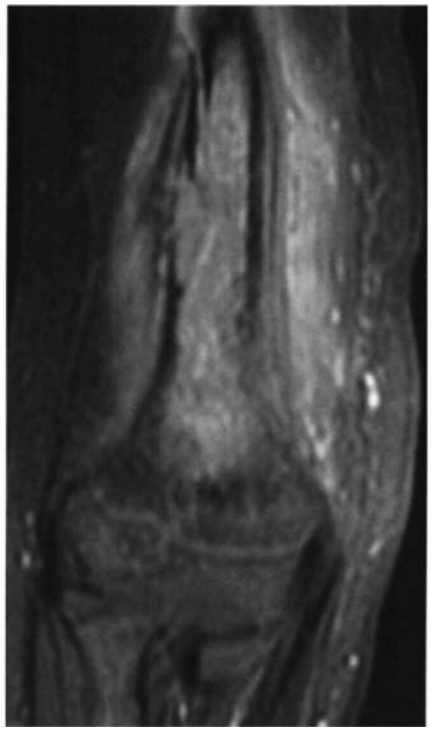

b

Figure 11.**13 a, b** A 5-year-old boy with an eosinophilic granuloma involving the metadiaphyseal portion of the distal humerus. The intramedullary lesion has high signal on coronal FS T2WI and is associated with cortical destruction, periosteal elevation, and extraosseous extension with abnormal high signal (**a**). The lesion shows prominent Gd-contrast enhancement on coronal FS T1WI (**b**).

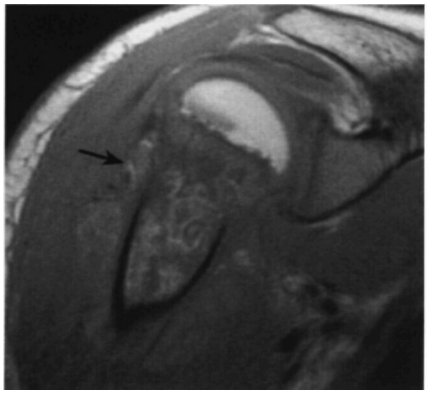

a

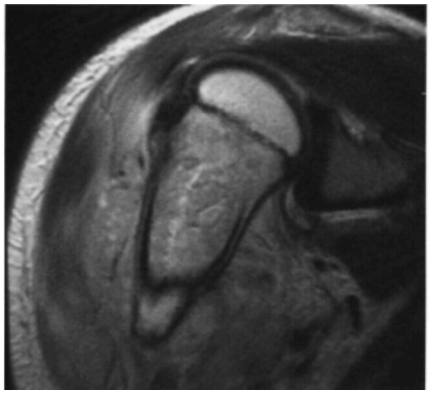

b

Figure 11.14a, **b** A 9-year-old boy with *Staphylococcus aureus* osteomyelitis, involving the metadiaphyseal portion of the humerus, that has heterogeneous mostly intermediate signal on coronal T1WI (a) and slightly high signal on T2WI (**b**). Poorly defined zones with high signal are seen in the extraosseous soft tissues secondary to the extension of the infection.

Table 11 (Continued) **Solitary intramedullary metadiaphyseal lesions**

Lesion	MRI Findings	Comments
Malignant		
Metastatic lesion (Fig. 11.15)	Single or multiple well-circumscribed or poorly defined infiltrative lesions involving marrow associated with cortical destruction and extraosseous extension. Lesions often have low-intermediate signal on T1 WI, low, intermediate, and/or high signal on T2WI and FS T2WI, usually show Gd-contrast enhancement. Cortical destruction and tumor extension into the extraosseous soft tissues frequently occurs. Pathologic fractures can be associated with metastatic lesions involving tubular bones and vertebrae. Periosteal reaction is uncommon.	Metastatic lesions typically occur in the marrow with or without cortical destruction and extraosseous tumor extension, **(See Atlas Chapter A50)**
Plasmacytoma/myeloma	Multiple (myeloma) or single (plasmacytoma) are well-circumscribed or poorly defined diffuse infiltrative lesions involving marrow, low-intermediate signal on T1WI, intermediate-high signal on T2WI and FST2WI, usually show Gd-contrast enhancement, eventual cortical bone destruction and extraosseous extension.	Malignant tumors comprised of proliferating antibody-secreting plasma cells derived from single clones. Most common primary neoplasm of bone in adults, median = 60 years. Most patients are older than 40 years. May have variable destructive or infiltrative changes involving the axial and/or appendicular skeleton. **(See Atlas Chapter A 52)**
Lymphoma (Fig. 11.16)	Non-Hodgkin lymphoma (NHL) and Hodgkin disease (HD) within bone typically appear as single or multifocal poorly defined or circumscribed intramedullary zones with low-intermediate signal on T1 WI, and intermediate, slightly high, and/or high signal on T2WI and high signal on FST2WI; often show Gd-contrast enhancement, Zones of cortical destruction may occur associated with extraosseous soft tissue extension. HD involving bone with associated sclerosis seen on plain films or CT usually have low signal on T1WI and variable/mixed signal on T2WI. In some cases of NHL, intramedullary tumor may be associated with bulky extraosseous lesions without extensive cortical destruction. High-resolution MRI in these cases shows thin penetrating channels of tumor extending through bone cortex into the extraosseous soft tissues.	Lymphoid tumors with neoplastic cells typically within lymphoid tissue (lymph nodes and reticuloendothelial organs). Unlike leukemia, lymphoma usually arises as discrete masses. Lymphomas are subdivided into HD and NHL. Almost all primary lymphomas of bone are B cell NHL. HD, mean age = 32 years. Osseous NHL, median = 35 years. **(See Atlas Chapter A 47)**
Osteosarcoma (Fig. 11.17)	Destructive intramedullary malignant lesions, low-intermediate signal on T1WI, mixed low, intermediate, high signal on T2WI, usually with matrix mineralization/ossification, low signal on T2WI, typically show Gd-contrast enhancement (usually heterogeneous). Zones of cortical destruction are common through which tumors extend into the extraosseous soft tissues under an elevated periosteum. Lamellatcd and/or spiculated zones of bone formation can occur under the periosteal elevation secondary to tumor invasion and perforation of bone cortex. Low signal from spicules of periosteal, reactive, and tumoral bone formation may have a divergent ("sunburst") pattern, perpendicular ("hair on end") pattern, or disorganized or complex appearance. Triangular zones of periosleal elevation (Codman's triangles) can be seen at the borders of zones of cortical destruction and tumor extension.	Malignant tumor comprising proliferating neoplastic spindle cells that produce osteoid and/or immature tumoral bone most frequently arising within medullary bone (metadiaphyseal > metaphyseal > diaphyseal locations). Two age peaks of incidence. The larger peak occurs between the ages of 10 and 20 and accounts for over half of the cases. The second smaller peak occurs in adults over 60 years and accounts for~ 10 % of the cases. Occurs in children as primary tumors and adults (associated with Paget disease, irradiated bone, chronic osteomyelitis, osteoblastoma, giant cell tumor, fibrous dysplasia). **(See Atlas Chapter A 64)**

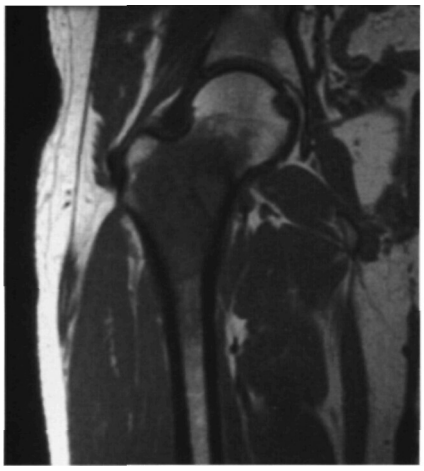

a

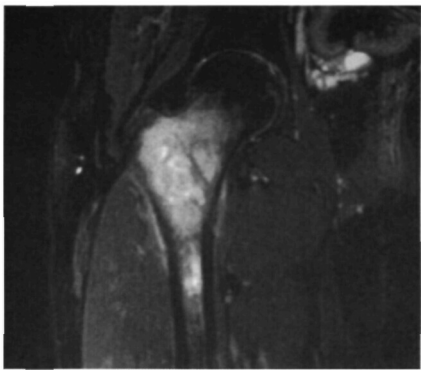

b

Figure 11.**15a**, **b** A 26-year-old man with a metastatic lesion in the metadiaphyseal portion of the proximal femur from seminoma that has low-intermediate signal on coronal T1WI (a) and high signal on coronal FST2WI (**b**). A thin zone of periosteal reaction with high signal on FST2WI is also seen laterally.

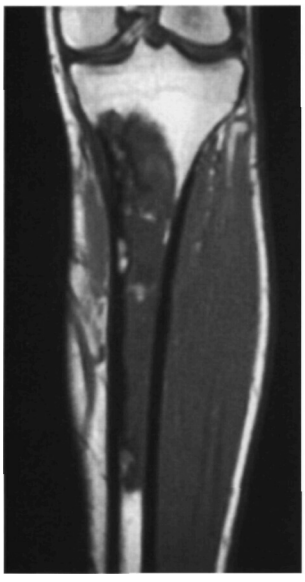

a

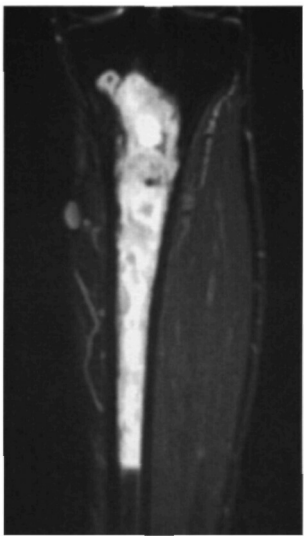

b

Figure 11.16a, **b** A 19-year-old man with a large B cell non-Hodgkin lymphoma in the metadiaphyseal marrow of the proximal tibia that has mostly intermediate signal on coronal T1WI (**a**) and high signal on coronal FST2WI (**b**).

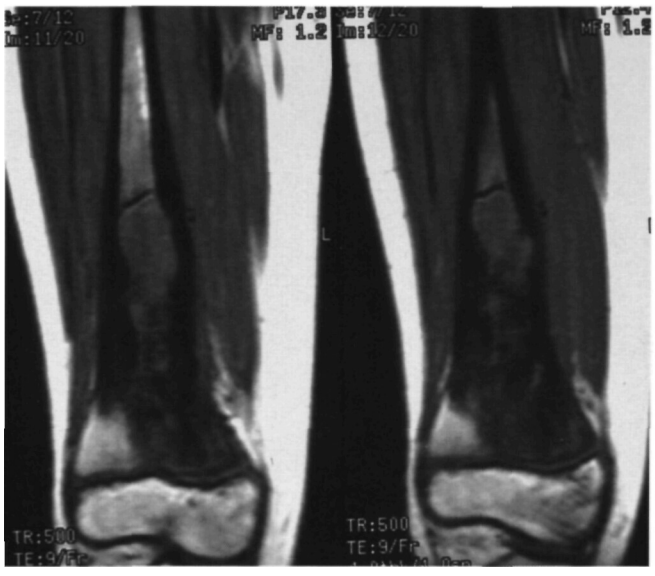

a

b

Figure 11.**17 a**, **b** A 9-year-old boy with a chondroblastic osteosarcoma in the metadiaphyseal marrow of the distal femur that has low and intermediate signal on coronal T1 WI (**a**) and heterogeneous high and low signal on coronal FST2WI (**b**).

Table 11 (Continued) **Solitary intramedullary metadiaphyseal lesions**

Lesion	MRI Findings	Comments
Ewing sarcoma (Fig. 11.18)	Destructive malignant lesions involving marrow, low-intermediate signal on T1WI, mixed low, intermediate, and/or high signal on T2WI and FS T2WI, typically shows Gd-contrast enhancement (usually heterogeneous). Extraosseous tumor extension through sites of cortical destruction is commonly seen beneath an elevated periosteum. Thin striated zones of low signal on T2WI can be sometimes seen oriented perpendicular to the long axis of the involved bone under the elevated periosteum representing the "hair on end" appearance of reactive bone formation secondary to the tumor. In long bones, tumors are most often located in the diaphyseal region, followed by the metadiaphyseal region.	Malignant primitive tumor of bone comprised of undifferentiated small cells with round nuclei. Accounts for 6-11 % of primary malignant bone tumors, 5-7% of primary bone tumors. Usually occurs between the ages of 5 and 30, males > females, locally invasive, high metastatic potential. **(See Atlas Chapter A 20)**
Chondrosarcoma (Fig. 11.19)	Intramedullary tumors often have low-intermediate signal on T1WI, intermediate signal on PDWI, and heterogeneous intermediate-high signal on T2WI. Lesions usually show heterogeneous contrast enhancement. Zones of cortical destruction can be seen with extraosseous extension of tumor.	Chondrosarcomas are malignant tumors containing cartilage formed within sarcomatous stroma. Account for 12-21 % of malignant bone lesions, 21-26% of primary sarcomas of bone, 5 to 91 years, mean = 40 years, median =26 to 59 years. **(See Atlas Chapter A 11)**
FIbrosarcoma	Intramedullary lesions with irregular margins, with or without associated cortical destruction and/or extraosseous soft tissue masses. Lesions usually have low-intermediate signal on T1WI and PDWI, and heterogeneous intermediate, slightly high, and/or high signal on T2WI. Lesions usually show heterogeneous Gd-contrast enhancement.	Fibrosarcomas are uncommon malignant tumors consisting of bundles of fibroblasts/spindle cells with varying proportions of collagen, lacking other tissue differentiating features such as tumor bone, osteoid, or cartilage. Can be primary lesions (75%) or arise as secondary tumors (25%) associated with prior irradiation. Pagel disease, bone infarct, chronic osteomyelitis, fibrous dysplasia, giant cell tumor. Account for 3-5% of primary malignant bone tumors, and 2-4% of all bone tumors, median age = 43 years. **(See Atlas Chapter A 25)**
Malignant fibrous hIstIocytoma(Fig.11.20)	Intramedullary lesions with irregular margins and zones of cortical destruction and extraosseous extension. Tumors often have low-intermediate signal on T1WI, low-intermediate signal on PDWI, and heterogeneous intermediate-high signal on T2WI and FST2WI. Invasion into joints occurs in 30%. May be associated with bone infarcts. bone cysts, chronic osteomyelitis, Paget disease, and other treated primary bone tumors. Lesions usually show heterogeneous Gd-contrast prominent enhancement.	Malignant tumor involving soft tissue and rarely bone derived from undifferentiated mesenchymal cells. Contains cells with limited cellular differentiation such as mixtures of fibroblasts, myofibroblasts, histiocyte-like cells, anaplastic giant cells, and inflammatory cells. Accounts for 1 -5 % of primary malignant bone tumors and < 1-3 % of all primary bone tumors, patient ages range from 11 to 80 years, median = 48 years, mean - 55 years. **(See Atlas Chap ter A 48)**

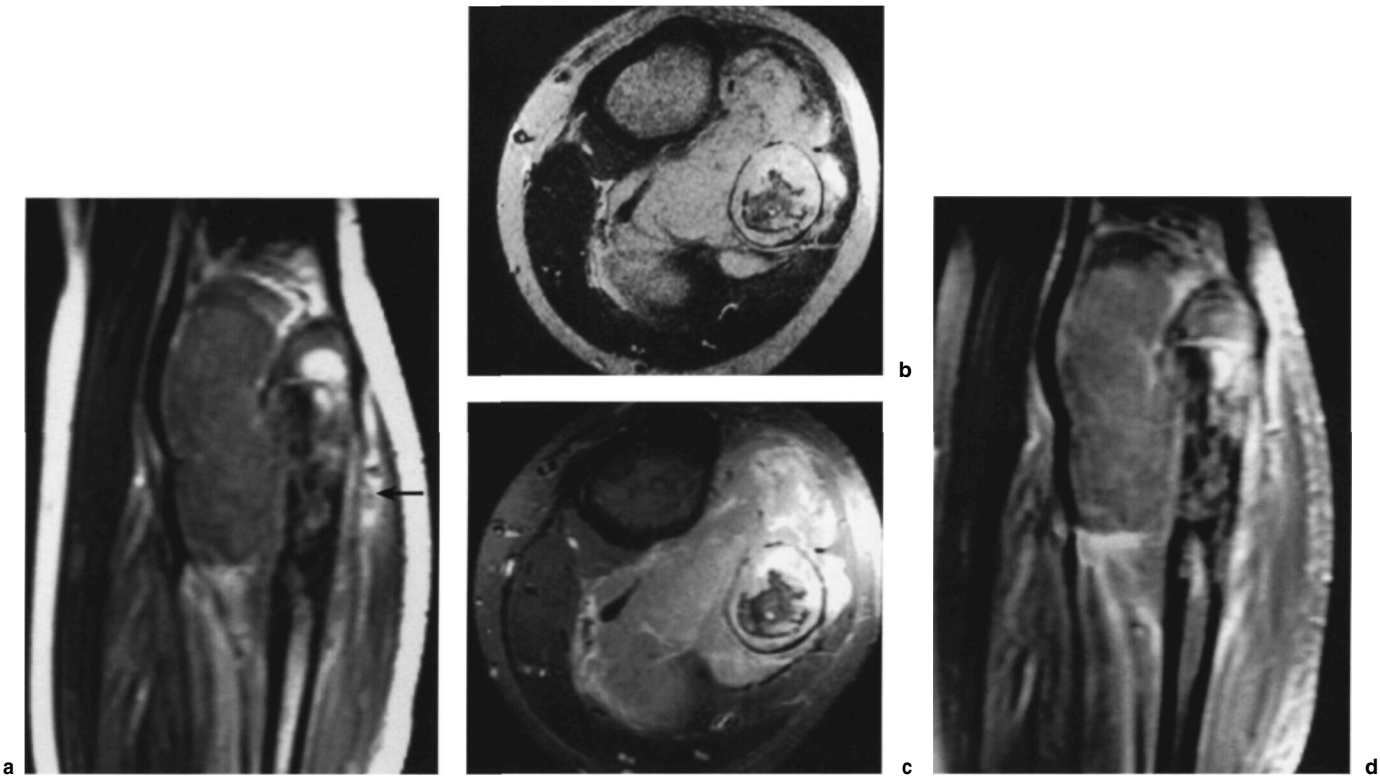

Figure 11.**18a-d** A 9-year-old boy with Ewing sarcoma in the metadiaphyseal portion of the proximal fibula that has intermediate signal on sagittal T1WI (**a**) and high signal in the marrow on axial T2WI (**b**), and has associated cortical destruction, periosteal elevation, and extraosseous tumor extension. The intra- and extraosseous tumor shows prominent Gd-contrast enhancement on axial (**c**) and sagittal (**d**) FS T1WI.

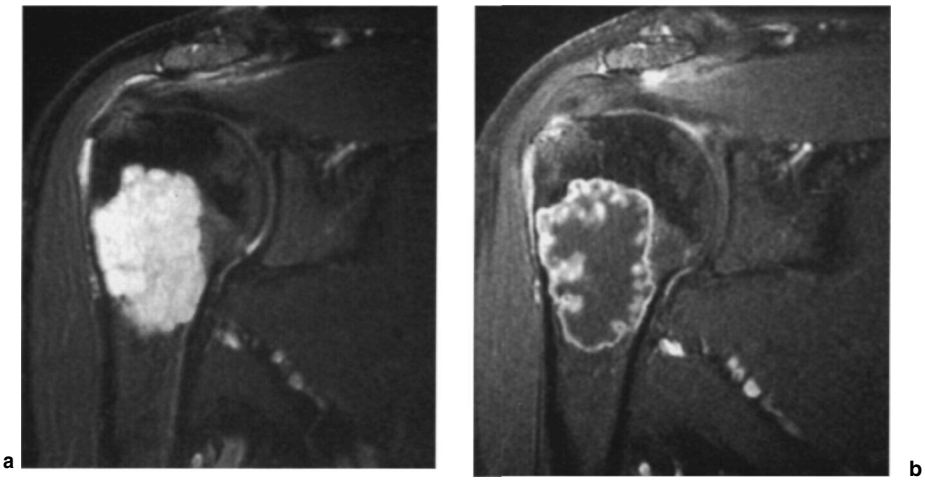

Figure 11.**19a, b** A 45-year-old woman with a low-grade chondrosarcoma in the metadiaphyseal portion of the proximal humerus that has high signal on coronal FS T2WI (a). The tumor shows thin peripheral lobular Gd-contrast enhancement on coronal FST1WI (**b**).

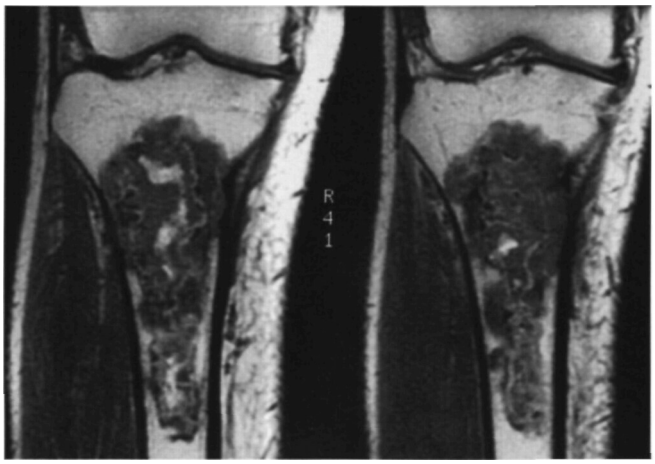

a

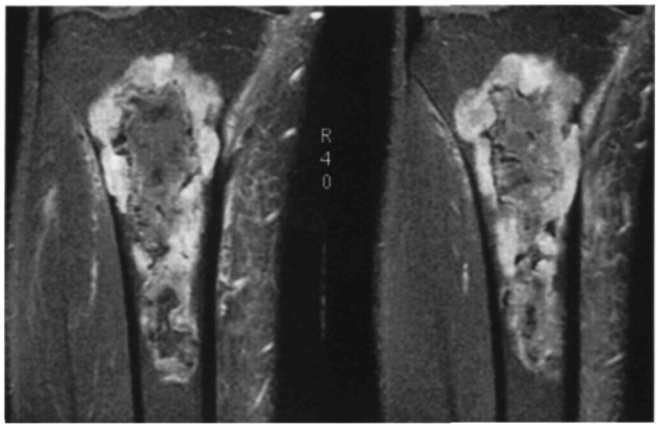

b

Figure 11.**20a**, **b** A 53-year-old man with a malignant fibrous histiocytoma in the metadiaphyseal region of the proximal tibia that arose from a bone infarct. The lesion has low, intermediate, and high signal on coronal T1WI (**a**), and shows heterogeneous Gd-contrast enhancement on coronal FS T1WI (**b**). The lesion is associated with cortical erosions.

References

Stress Fracture

Ahovuo JA, Kiuru MJ, Visuri T. Fatigue stress fractures of the sacrum: diagnosis with MR imaging. *Eur Radial* March 2004;14(3):500-505. Epub October 24, 2003.

Berger FH, de Jonge MC, Maas M. Stress fractures in the lower extremity. The importance of increasing awareness amongst radiologists. *EurJ* Radio/2007;62:16-26.

Grangier C, Garcia J, Howarth NR, May M, Rossier P. Role of MRI in the diagnosis of insufficiency fractures of the sacrum and acetabular roof. *Skeletal Radial* 1997;26:517-524.

Meyers SP, Wiener SN. Magnetic resonance imaging features of fractures using the short tau inversion recovery (STIR) sequence: correlation with radiographic findings. *Skeletal Radiol* 1991;20(7): 499-507.

Table 12 Solitary intramedullary diaphyseal lesions

Lesion	MRI Findings	Comments
Benign		
Stress fracture (Fig. 12.1)	Fractures often have associated poorly defined zones of abnormal marrow signal with low signal on T1WI, and high signal on T2WI and FST2WI. Gd-conlrasl enhancement is typically seen in the postfracture period. Angulated cortical margins and periosteal high signal on FS T2WI can be seen. A curvilinear zone of low signal on T2WI and FST2WI may be seen within the marrow edema, which is often perpendicular or oblique to the long axis of the involved bone.	Stress fractures can result from persistent chronic mechanical overload, as well as from osteoporosis or osteomalacia. Primary bone tumors/lesions, metastatic disease, bone infarcts.
Bone infarct (Fig. 12.2)	In the early phases of ischemia, poorly-defined zones with high signal on FST2WI or STIR are seen in the marrow. Later a double-line sign (curvilinear adjacent zones of low and high signal on T2WI) is commonly seen at the edges of the infarcts representing the borders of osseous resorption and healing. Irregular Gd-contrast enhancement can be seen from granulation tissue in-growth.	Zones of ischemic death involving bone trabeculae and marrow that may be idiopathic or result from: trauma, corticosteroid treatment, chemotherapy, radiation treatment, occlusive vascular disease, collagen vascular and other autoimmune diseases, metabolic storage diseases (Gaudier, etc.), sickle cell disease, thalassemia, hyperbaric events / Caisson disease, pregnancy, alcohol abuse, pancreatitis, infections, and lymphoproliferative diseases. **(See Atlas Chapter A 37)**

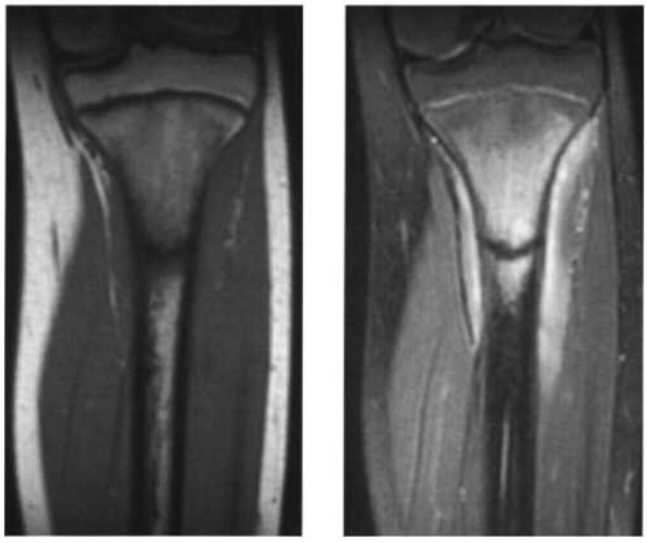

a, b

Figure 12.**1 a**, **b** A 12-year-old girl with a fatigue-type stress fracture in the proximal diaphysis of the tibia. A horizontal linear zone of low signal is seen within the marrow surrounded by a poorly defined zone of low-intermediate signal on coronal T1WI (**a**) and high signal on coronal FS T2WI (**b**). The high signal on ST **2FWI** from edema extends up into the metaphyseal marrow.

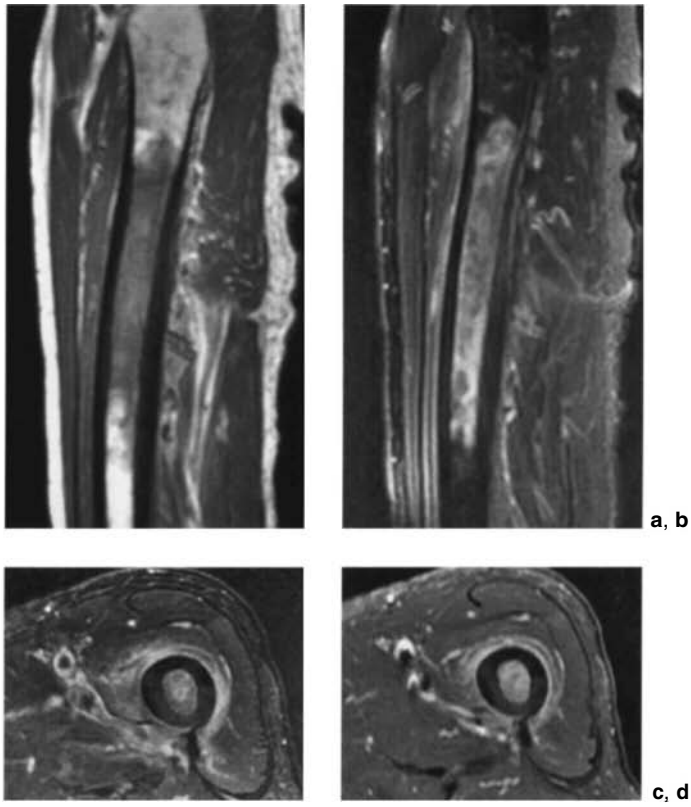

a, b

c, d

Figure 12.**2 a-d** A 76-year-old man with an acute bone infarct in the diaphysis of the femur that is seen as a poorly defined zone of low-intermediate signal in the marrow on sagittal T1 WI (a), heterogeneous high signal on sagittal (**b**) and axial (c) FST2WI with elevated thin periosteal reaction with adjacent high signal in the extraosseous soft tissues. The acute infarct shows Gd-contrast enhancement on axial FST1WI (**d**).

Table 12 (Continued) **Solitary intramedullary diaphyseal lesions**

Lesion	MRI Findings	Comments
Fibrous dysplasia (Fig. 12.3)	MRI features depend on the proportions of bony spicules, collagen, fibroblastic spindle cells, hemorrhagic and/or cystic changes, and associated pathologic fracture if present. Lesions are usually well-circumscribed, and have low or low-intermediate signal on T1WI and PDWI. On T2WI, lesions have variable mixtures of low, intermediate, and/or high signal often surrounded by a low signal rim of variable thickness. Internal septations and cystic changes are seen in a minority of lesions. Bone expansion with thickened and/or thinned cortex can be seen. Lesions show Gd-contrast enhancement that varies in degree and pattern.	Benign medullary fibro-osseous lesion that can involve a single site **(mono-ostotic)** or multiple locations **(poly-ostotic).** Thought to occur from developmental failure in the normal process of remodeling primitive bone to mature lamellar bone with resultant zone or zones of immature trabeculae within dysplastic fibrous tissue. Accounts for~ 10 % of benign bone lesions. Patients range in age from < 1 to 76 years. 75 % occur before the age of 30 years. **(See Atlas Chapter A 27)**
Fibroxanthoma	Well-circumscribed eccentric intramedullary lesions in the diaphyseal regions of long bones which have mixed low-intermediate signal on T1 WI, and mixed low, intermediate, and/or high signal on T2WI, PDWI, and FS T2WI. Zones of low signal on T1WI, PDWI, and T2WI can be seen in the central portions of the lesions. Zones with varying thickness of low signal on T1WI, PDWI, and T2WI are seen at the margins of the lesions representing bone sclerosis. Internal septations are commonly seen as zones of low signal on T2WI in these lesions. Lesions can show Gd-contrast enhancement (heterogeneous > homogeneous patterns).	Histologically identical to nonossifying fibromas but occur in diaphyseal portions of long bones. Lesions contain whorls of fibroblastic cells combined with smaller amounts of multinucleated giant cells and xanthomatous cells. Patients range in age from 6 to 74 years, 60 % of patients are older than 20 years at diagnosis. **(See Atlas Chapter A 26)**
Enchondroma (Fig. 12.4)	Lobulated intramedullary lesions with well-defined borders that usually have low-intermediate signal on T1WI and intermediate signal on PDWI. On T2WI and FS T2WI, lesions usually have predominantly high signal with foci and/or bands of low signal representing areas of matrix mineralization and fibrous strands. No zones of abnormal high signal on T2WI are typically seen in the marrow outside the borders of the lesions. Lesions typically show Gd-contrast enhancement in various patterns (peripheral curvilinear lobular, central nodular/septal and peripheral lobular, or heterogeneous diffuse).	Benign intramedullary lesions composed of hyaline cartilage, represent ~ 10 % of benign bone tumors. Enchondromas can be solitary (88 %) or multiple (12 %). Oilier disease is a dyschondroplasia involving endochondral-formed bone resulting in multiple enchondromas (enchondromatosis). Metachondromatosis is a combination of enchondromatosis and osteochondromatosis, and is rare. Maffucci disease refers to a syndrome with multiple enchondromas and soft tissue hemangiomas, and is very rare. Patients range in age from 3 to 83 years, median = 35 years, mean = 38 to 40 years, peak in 3rd and 4th decades. **(See Atlas Chapter A 8)**

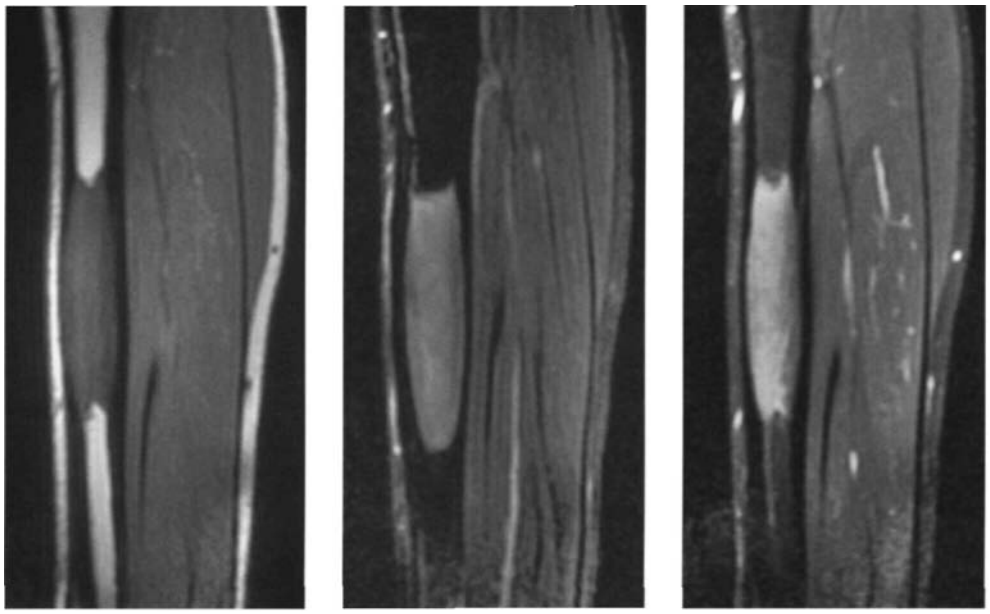

a b, c

Figure 12.**3a-c** A 19-year-old man with fibrous dysplasia involving the diaphysis of the tibia. The lesion is associated with slight expansion and thinning of adjacent cortical margins and has low-intermediate signal on sagittal T1WI (**a**), slightly high signal on sagittal FST2WI (**b**), and Cd-contrast enhancement on sagittal FS T1WI (**c**).

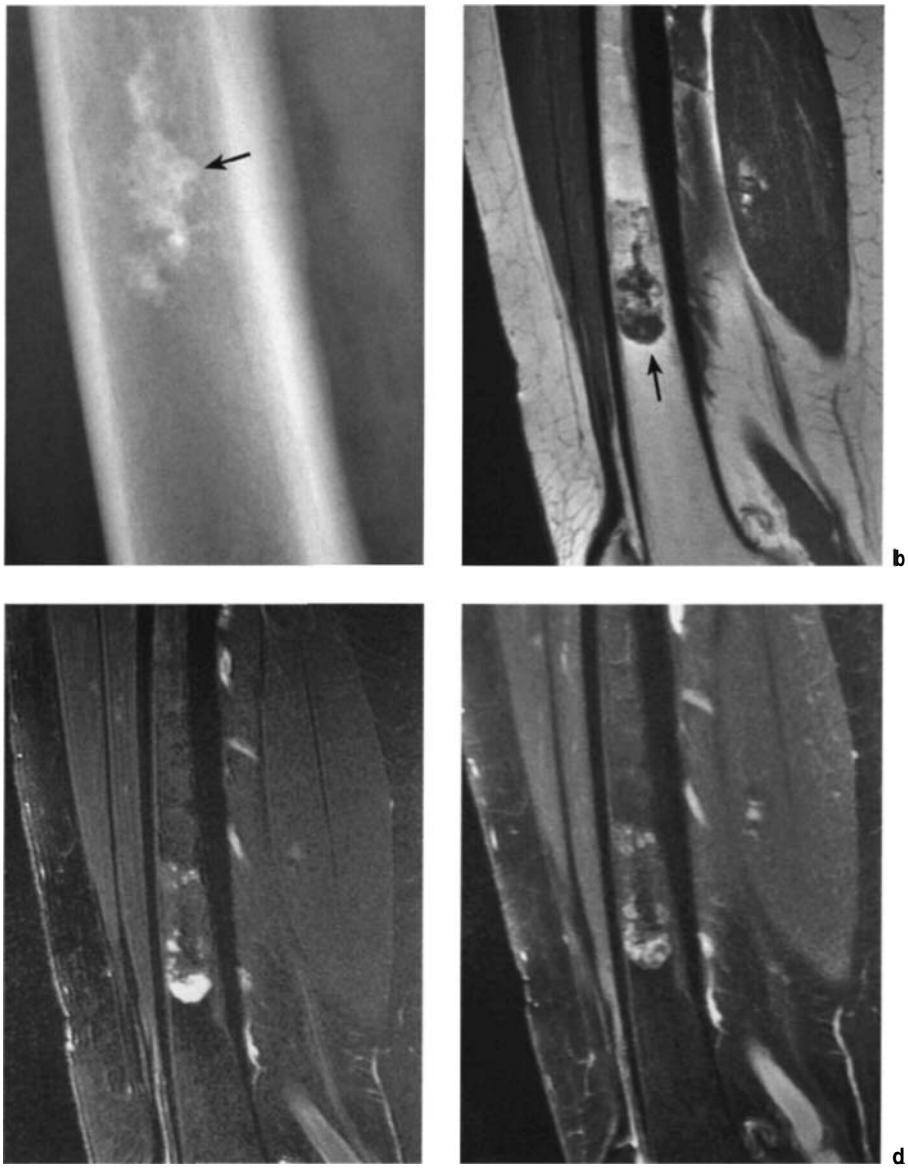

a b c d

Figure **12.4a-d** A 47-year-old woman with an enchondroma in the diaphyseal portion of the femur that contains chondroid matrix mineralization on the lateral radiograph (a). The lesion has mixed low-intermediate signal on sagittal T1WI (**b**) and mixed intermediate and high signal on sagittal FST2WI (c). The lesion shows heterogeneous Gd-contrast enhancement on sagittal FS T1WI (**d**).

Table 12 (Continued) **Solitary intramedullary diaphyseal lesions**

Lesion	MRI Findings	Comments
Eosinophilic granuloma (Fig. 12.5)	Focal intramedullary lesion(s) associated with trabecular and cortical bone destruction that typically have low-intermediate signal on T1WI and PDWI and heterogeneous slightly high to high signal on T2WI. Poorly defined zones of high signal on T2WI are usually seen in the marrow peripheral to the lesions secondary to inflammatory changes. Extension of lesions from the marrow into adjacent soft tissues through areas of cortical disruption are commonly seen as well as linear periosteal zones of high signal on T2WI. Lesions typically show prominent Gd-contrast enhancement in marrow and in extraosseous soft tissue portions.	Benign tumor-like lesions consisting of Langerhans' cells (histiocytes), and variable amounts of lymphocytes, polymorphonuclear cells, and eosinophils. Account for 1 % of primary bone lesions, and 8 % of tumor-like lesions. Occur in patients with median age = 10years, average = 13.5 years, peak incidence is between 5 and 10ycars, 80-85 % occur in patients less than 30 **years. (See Atlas Chapter A 18)**
Osteomyelitis (Fig. 12.6)	Poorly defined zones with high signal on I2WI and FS T2WI and Gd-contrast enhancement are seen in marrow with associated zones of cortical destruction. Periosteal reaction can be seen as a peripheral rim of high signal on T2WI and FST2WI and Gd-contrast enhancement on FS T1WI adjacent to the low signal of cortical bone. A subperiosteal abscess with high signal on T2WI and FS T2WI can be often seen elevating a single low signal thin band of periosteum.	Infection of bone that can result from hematogenous spread of microorganisms, trauma-direct inoculation, extension from adjacent tissues, and complications from surgery. Stop/iy/ococcus *aureus* and Sfrepto-coccus pyogenes are the most common bacterial infections involving bone. Osteomyelitis can also result from other bacteria as well as from other organisms such as *Mycobacterium tuberculosis,* fungi, parasites, and viruses. **(See Atlas Chapter A 63)**
Malignant		
Metastatic lesion (Fig. 12.7)	Single or multiple well-circumscribed or poorly defined intiltrative lesions involving marrow associated with cortical destruction and extraosseous extension. Lesions often have low-intermediate signal on T1 WI, low, intermediate, and/or high signal on T2WI and FST2WI. usually showGd-contrast enhancement. Cortical destruction and tumor extension into the extraosseous soft tissues frequently occurs. Pathologic fractures can be associated with metastatic lesions involving tubular bones and vertebrae. Periosteal reaction is uncommon.	Metastatic lesions typically occur in the marrow with or without cortical destruction and extraosseous tumor extension, **(See Atlas Chapter A 50)**

a b

Figure 12.5 a, **b** An 18-year-old woman with an eosinophilic granuloma involving the diaphyseal marrow of the femur, seen as a poorly defined zone of low-intermediate signal on coronal T1WI (a). A thin marginal rim of low signal is seen surrounding a central zone of high signal on coronal FST2WI (**b**), as well as a poorly defined zone of peripheral high signal in the adjacent marrow and thin periosteal reaction with high signal.

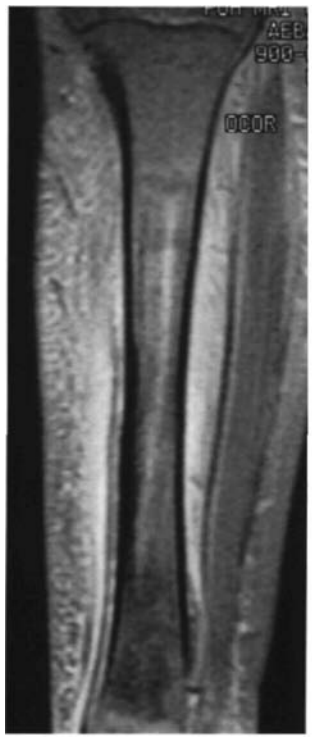

a

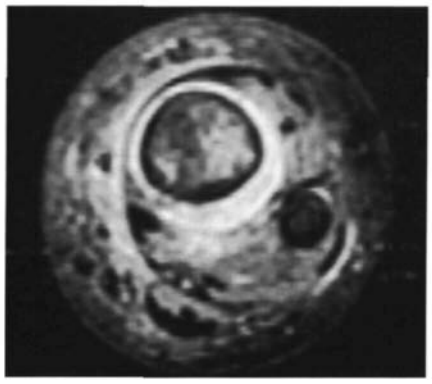

b

Figure 12.**6a, b** A 9-year-old girl with pyogenic osteomyelitis involving the diaphysis of the tibia, seen as a poorly defined zone of Gd-contrast enhancement in the marrow associated with periosteal elevation and juxtacortical enhancement on coronal FS T1WI (**a**). Abnormal increased signal is seen in the marrow on axial STIR (**b**) as well as unilayer periosteal elevation surrounded by high signal in the extraosseous soft tissues.

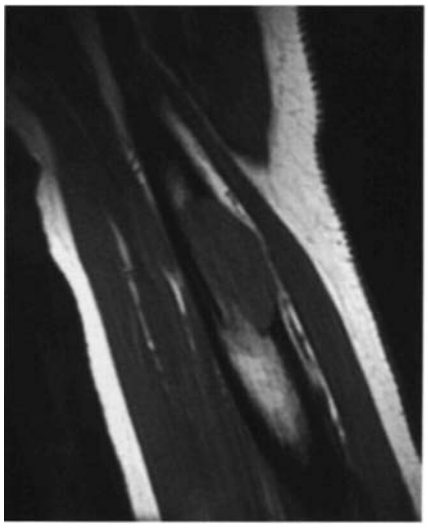

a

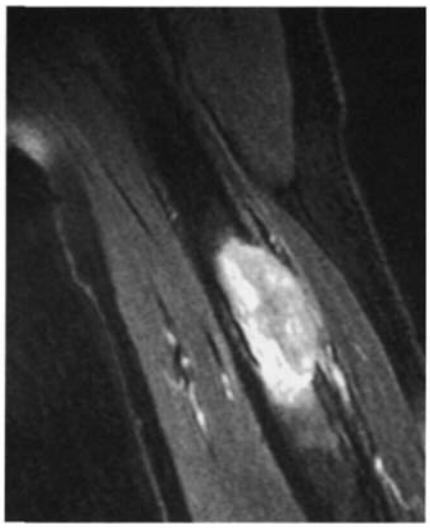

b

Figure 12.**7 a, b** A 63-year-old woman with metastatic lung carcinoma involving the diaphyseal portion of the humerus. The lesion has intermediate signal on sagittal T1WI (a) and high signal on sagittal FST2WI (**b**). The tumor is seen extending from the marrow into the extraosseous soft tissues through a zone of cortical destruction.

Table 12 (Continued) **Solitary intramedullary diaphyseal lesions**

Lesion	MRI Findings	Comments
Plasmacytoma/myeloma (Fig. 12.8)	Multiple (myeloma) or single (plasmacytoma) are well-circumscribed or poorly defined diffuse infiltrative lesions involving marrow, low-intermediate signal on T1 WI, intermediate-high signal on T2WI and FS T2WI, usually show Gd-contrast-enhancement, eventual cortical bone destruction and extraosseous extension.	Malignant tumors comprising proliferating antibody-secreting plasma cells derived from single clones. Most common primary neoplasm of bone in adults, median = 60 years. Most patients are older than 40 years. May have variable destructive or infiltrative changes involving the axial and/or appendicular skeleton. **(See Atlas Chapter A 52)**
Lymphoma (Fig. 12.9)	Non-Hodgkin lymphoma (NHL) and Hodgkin disease (HD) within bone typically appear as single or multifocal poorly defined or circumscribed inlramedullary zones with low-intermediate signal on T1 WI, and intermediate, slightly high, and/or high signal on T2WI and high signal on FST2WI; often show Gd-contrast enhancement, Zones of cortical destruction may occur associated with extraosseous soft tissue extension. HD involving bone with associated sclerosis seen on plain films or CT usually have low signal on T1WI and variable/mixed signal on T2WI. In some cases of NHL, intramedullary tumor may be associated with bulky extraosseous lesions without extensive cortical destruction. High-resolution MRI in these cases shows thin penetrating channels of tumor extending through bone cortex into the extraosseous soft tissues.	Lymphoid tumors with neoplastic cells typically within lymphoid tissue (lymph nodes and reticuloendothelial organs). Unlike leukemia, lymphoma usually arises as discrete masses. Lymphomas are subdivided into HD and non-Hodgkin lymphoma NHL. Almost all primary lymphomas of bone are B cell NHL. HD, mean age = 32 years. Osseous NHL, median = 35 years. **(See Atlas Chapter A 47)**

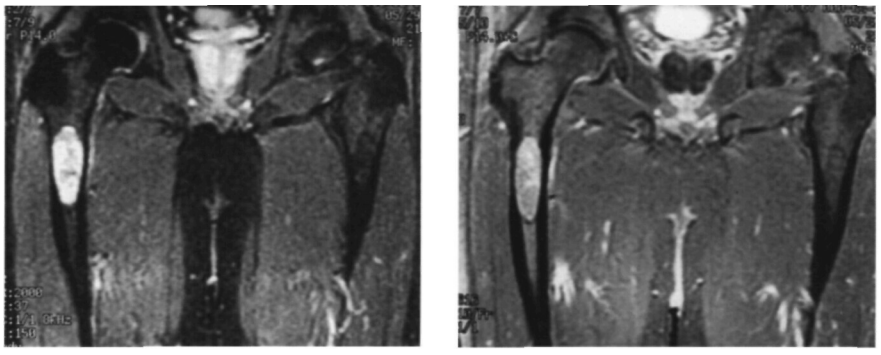

Figure 12.**8 a, b** Plasmacytoma in the proximal diaphysis of the femur that has high signal on coronal STIR (**a**) and shows Gd-contrast enhancement on coronal FST1WI (**b**).

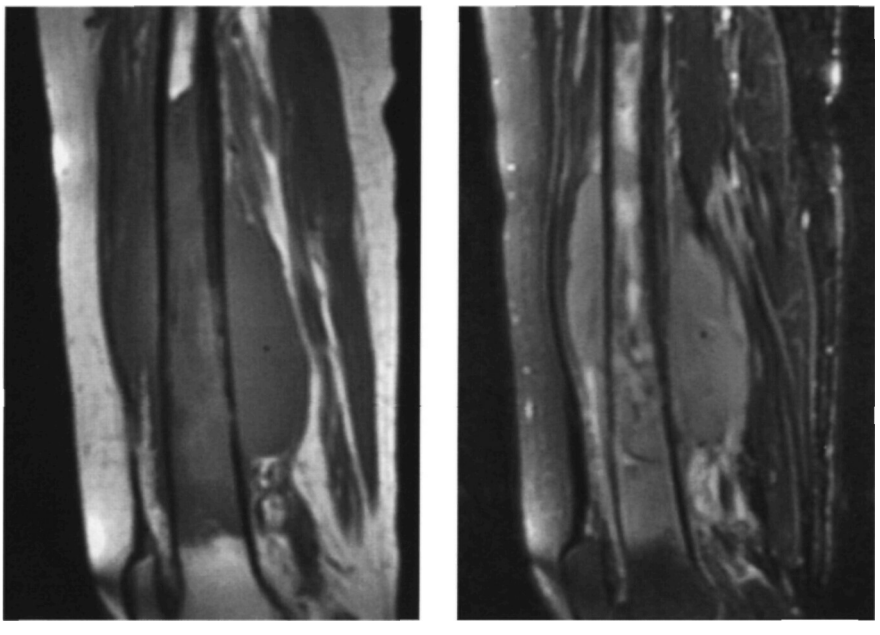

Figure 12.**9a, b** A 36-year-old woman with large cell non-Hodgkin lymphoma involving the marrow of the femur that has slightly indistinct margins and shows extensive extraosseous tumor extension relative to the degree of cortical disruption. The tumor has heterogeneous intermediate signal on sagittal T1WI (**a**) and heterogeneous slightly high and high signal on sagittal FST2WI (**b**).

Table 12 (Continued) **Solitary intramedullary diaphyseal lesions**

Lesion	MRI Findings	Comments
Osteosarcoma (Fig. 12.10)	Destructive intramedullary malignant lesions, low-intermediate signal on T1WI, mixed low, intermediate, high signal on T2WI, usually with matrix mineralization/ossification, low signal on T2WI, typically show Gd-contrast enhancement (usually heterogeneous). Zones of cortical destruction are common through which tumors extend into the extraosseous soft tissues under an elevated periosteum. Lamellated and/or spiculated zones of bone formation can occur under the periosteal elevation secondary to tumor invasion and perforation of bone cortex. Low signal from spicules of periosteal, reactive and tumoral bone formation may have a divergent ("sunburst") pattern, perpendicular ("hair on end") pattern, or disorganized or complex appearance. Triangular zones of periosteal elevation (Codman's triangles) can be seen at the borders of zones of cortical destruction and tumor extension.	Malignant tumor comprising proliferating neoplastic spindle cells that produce osteoid and/or immature tumoral bone most frequently arising within medullary bone (metadiaphyseal > metaphyseal > diaphyseal locations). Two age peaks of incidence. The larger peak occurs between the ages of 10 and 20 and accounts for over half of the cases. The second smaller peak occurs in adults over 60 years and accounts for ~ 10 % of the cases. Occurs in children as primary tumors and adults (associated with Paget disease, irradiated bone, chronic osteomyelitis, osteoblastoma, giant cell tumor, fibrous dysplasia). **(See Atlas Chapter A 64)**

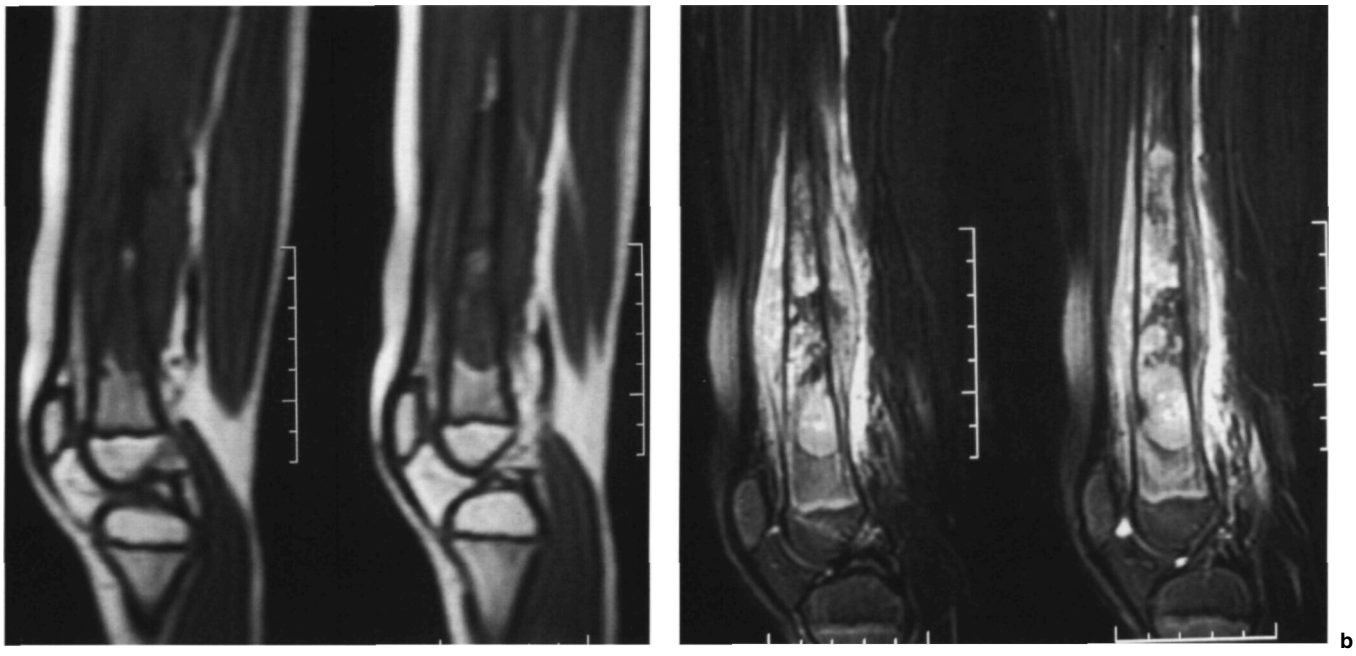

a b

Figure 12.**10 a, b** A 6-year-old girl with an osteosarcoma in the marrow of the distal femur that has low-intermediate signal on sagittal T1WI (**a**) and high signal on sagittal FS T2WI (**b**). The tumor is associated with cortical destruction, periosteal elevation, and extraosseous extension.

Table 12 (Continued) **Solitary intramedullary diaphyseal lesions**

Lesion	MRI Findings	Comments
Ewing sarcoma (Fig. 12.11)	Destructive malignant lesions involving marrow, low-intermediate signal on T1WI, mixed low, intermediate, and/or high signal on T2WI and FS T2WI, typically shows Gd-contrast enhancement (usually heterogeneous). Extraosseous tumor extension through sites of cortical destruction is commonly seen beneath an elevated periosteum. Thin striated zones of low signal on T2WI can be sometimes seen oriented perpendicular to the long axis of the involved bone under the elevated periosteum representing the "hair on end" appearance of reactive bone formation secondary to the tumor. In long bones, tumors are most often located in the diaphyseal region, followed by the metadiaphyseal region.	Malignant primitive tumor of bone comprising undifferentiated small cells with round nuclei. Accounts for 6-11 % of primany malignant bone tumors, 5-7% of primary bone tumors. Usually occurs between the ages of 5 and 30, males > females, locally invasive, high metastatic potential. **(See Atlas Chapter A 20)**
Chondrosarcoma (Fig. 12.12)	Intramedullary tumors often have low-intermediate signal on T1WI, intermediate signal on PDWI, and heterogeneous intermediate-high signal on T2WI. Lesions usually show heterogeneous contrast enhancement. Zones of cortical destruction can be seen with extraosseous extension of tumor.	Chondrosarcomas are malignant tumors containing cartilage formed within sarcomatous stroma. Account for 12-21 % of malignant bone lesions, 21-26% of primary sarcomas of bone, 5 to 91 years, mean = 40 years, median = 26 to 59 years. **(See Atlas Chapter A 11**
Fibrosarcoma	Intramedullary lesions with irregular margins, with or without associated cortical destruction and/or extraosseous soft tissue masses. Lesions usually have low-intermediate signal on T1WI and PDWI, and heterogeneous intermediate, slightly high, and/or high signal on T2WI. Lesions usually show heterogeneous Gd-contrast enhancement.	Fibrosarcomas are uncommon malignant tumors consisting of bundles of fibroblasts/spindle cells with varying proportions of collagen, lacking other tissue differentiating features such as tumor bone, osteoid, or cartilage. Can be primary lesions (75 %) or arise as secondary tumors (25 %) associated with prior irradiation, Paget disease, bone infarct, chronic osteomyelitis, fibrous dysplasia, giant cell tumor. Account for 3-5 % of primary malignant bone tumors, and 2-4 % of all bone tumors, median age = 43 years. **(See Atlas Chapter A 25)**
Malignant fibrous histiocytoma	Intramedullary lesions with irregular margins with zones of cortical destruction and extraosseous extension. Tumors often have low-intermediate signal on T1WI; low-intermediate signal on PDWI, and heterogeneous intermediate-high signal on T2WI and FS T2WI. Invasion into joints occurs in 30%. May be associated with bone infarcts, bone cysts, chronic osteomyelitis, Paget disease, and other treated primary bone tumors. Lesions usually show heterogeneous Gd-contrast prominent enhancement.	Malignant tumor involving soft tissue and rarely bone derived from undifferentiated mesencliymal cells. Contains cells with limited cellular differentiation such as mixtures of fibroblasts, myofibroblasts, histiocyte-like cells, anaplastic giant cells, and inflammatory cells. Accounts for 1 -5 % of primary malignant bone tumors and < 1-3 % of all primary bone tumors, patient ages range from 11 to 80 years, median =48 years, mean =55 years. **(See Atlas Chapter A 48)**
Paget sarcoma (Fig. 12.13)	Irregular zones of medullary and cortical bone destruction associated with an extraosseous soft tissue mass lesion. The involved marrow typically has low to intermediate signal on T1 WI and PDWI, and low to high signal on T2WI. Abnormal Gd-contrast enhancement is seen in the marrow as well as in the extraosseous tumor extension.	Paget disease is most common bone disease in older adults after osteoporosis. Median age = 66 years. Disordered bone resorption and woven bone formation occurs resulting in osseous deformity. Associated with less than 1 % risk for developing secondary sarcomatous changes. **(See Atlas Chapter A 65)**

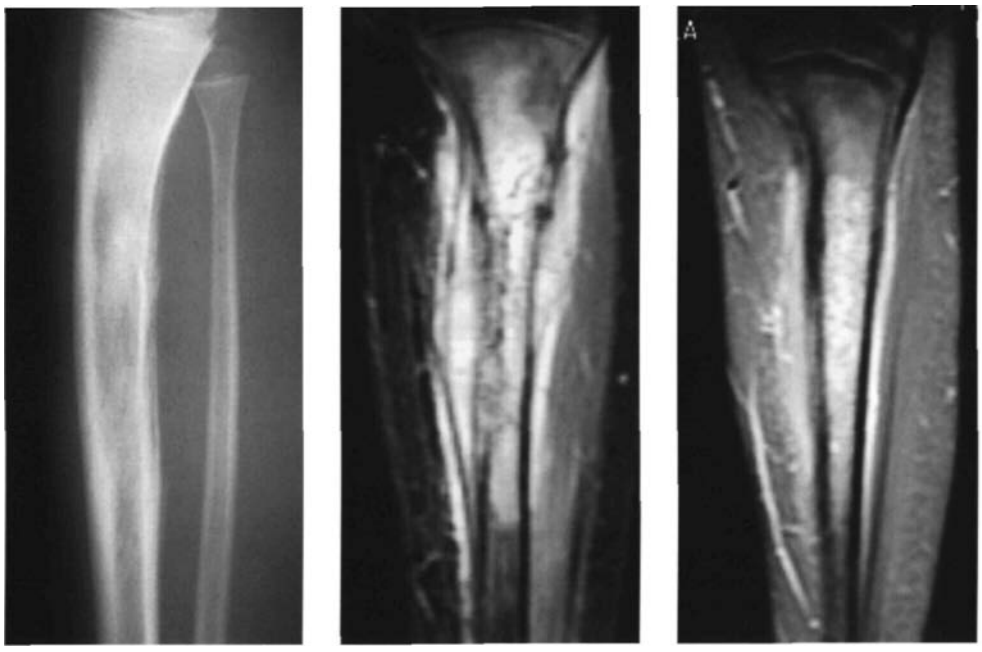

a b, c

Figure 12.**11 a-c** An 11-year-old boy with Ewing sarcoma involving the shaft of the proximal tibia. The tumor has permeative radiolucent intrameduliary changes, zones of cortical destruction, periosteal elevation, and a Codman's triangle inferiorly on the oblique radiograph (**a**). The intrameduliary tumor has high signal on coronal FST2WI (**b**) and shows Gd-contrast enhancement on coronal FST1WI (**c**). The tumor is associated with cortical destruction, periosteal elevation, and extraosseous extension.

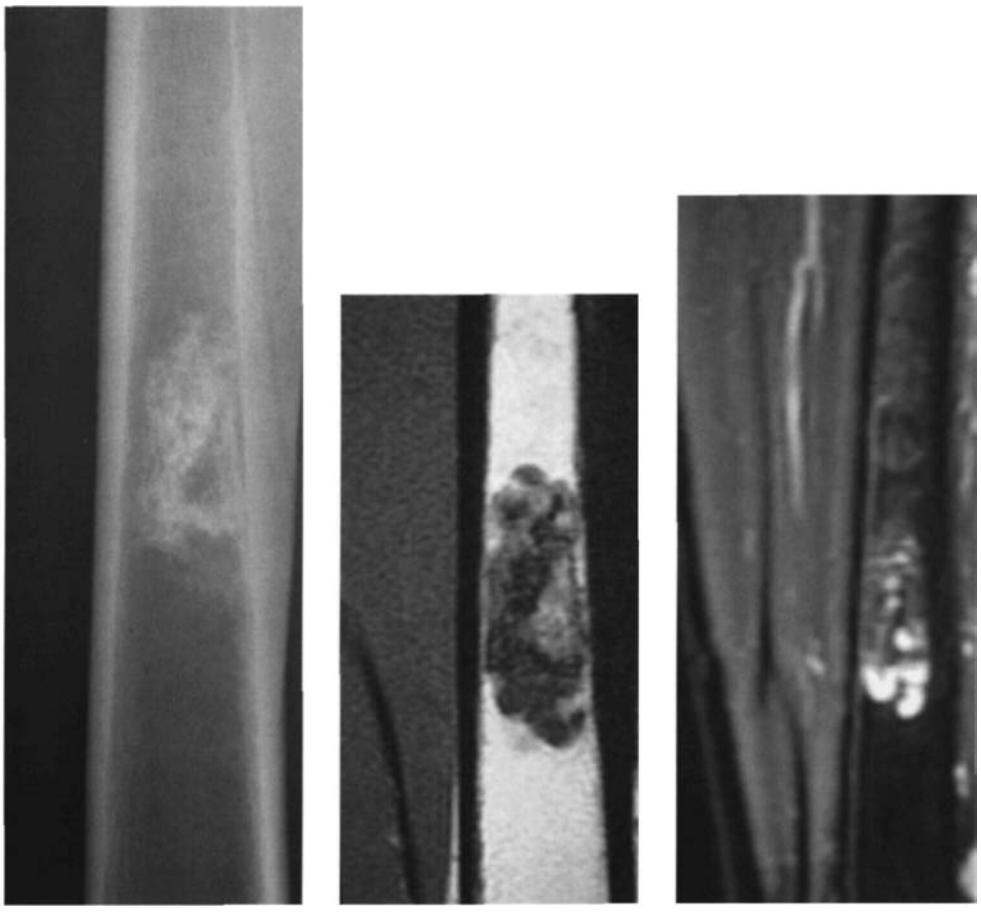

a, b c

Figure 12.**12 a-c** A 39-year-old man with a chondrosarcoma in the marrow of the distal tibial shaft that has chondroid matrix mineralization on a lateral radiograph (**a**). The tumor has mixed low and intermediate signal on sagittal T1WI (**b**) and heterogeneous slightly high and high signal on FS T2WI (**c**).

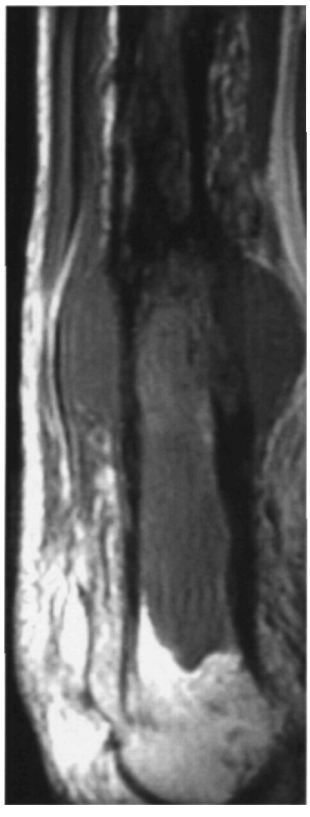

Figure 12.**13** A 71-year-old woman with Paget sarcoma involving the marrow of the distal femur associated with cortical destruction and extraosseous extension as seen on sagittal T1WI.

References

Stress Fracture

Ahovuo JA, Kiuru MJ, Visuri T. Fatigue stress fractures of the sacrum: diagnosis with MR imaging. *Eur* Radio/ March 2004;14(3):500-505. Epub October 24, 2003.

Berger FH, de Jonge MC, Maas M. Stress fractures in the lower extremity. The importance of increasing awareness amongst radiologists. *Eur] Radiol* 2007;62:16-26.

Grangier C, Garcia J, Howarth NR, May M, Rossier P. Role of MRI in the diagnosis of insufficiency fractures of the sacrum and acetabular roof. *Skeletal Radiol* 1997;26:517-524.

Meyers SP, Wiener SN. Magnetic resonance imaging features of fractures using the short tau inversion recovery (STIR) sequence: correlation with radiographic findings. Skeletal Radiol 1991;20(7): 499-507.

Table 13 Osseous tumors and tumorlike lesions at the hands and feet

Tumor/tumorlike Lesion	MRI Findings	Comments
Benign		
Enchondroma (Figs. 13.1,13.2)	tabulated intramedullary lesions with well-defined borders that usually have low-intermediate signal on T1WI and intermediate signal on PDWI. On T2WI and FS T2WI, lesions usually have predominantly high signal. Lesions typically show Gd-contrast enhancement in various patterns (peripheral curvilinear lobular, central nodular/septal and peripheral lobular, or heterogeneous diffuse).	Benign intramedullary lesions composed of hyaline cartilage, represent ~10 % of benign bone tumors. Enchondromas can be solitary (88 %) or multiple (12 %). Oilier disease is a dyschondroplasia involving endochondral-formed bone resulting in multipie enchondromas (enchondromatosis). Maffucci disease refers to a syndrome with multiple enchondromas and soft tis sue hemangiomas, and is very rare. Median age = 35 years, peak in 3rd and 4th decades. **(See Atlas Chapter A 8)**

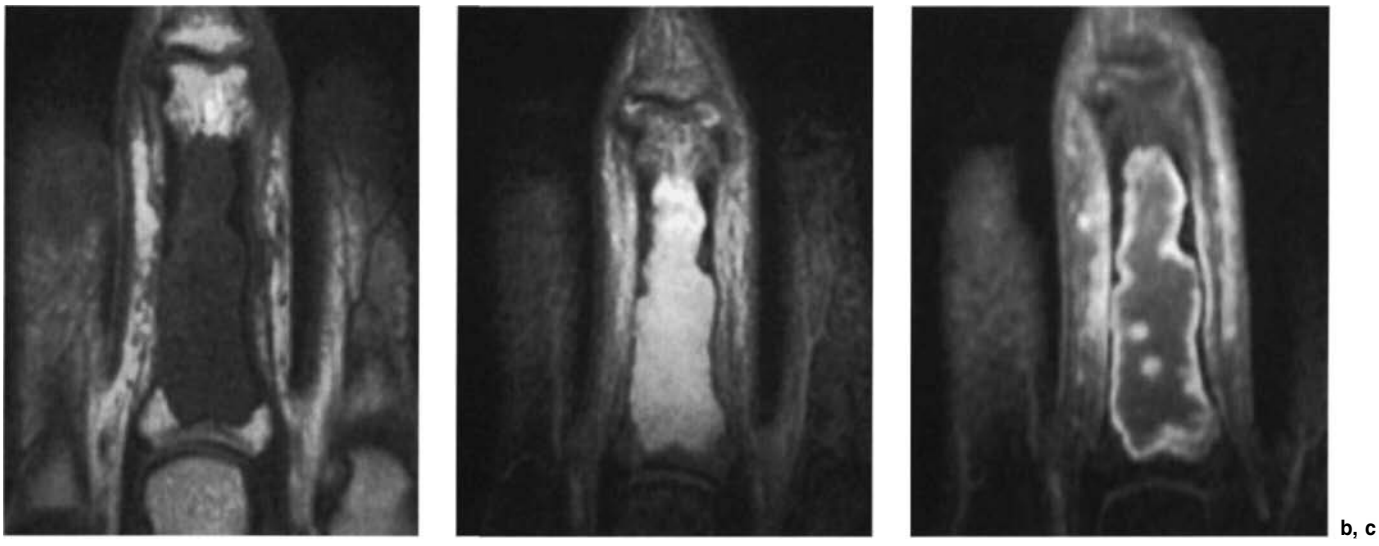

b, c

Figure 13.**1 a-c** A 39-year-old woman with an enchondroma in a proximal phalanx that has intermediate signal on coronal T1WI (**a**) and high signal on coronal FS T2WI (**b**). The lesion shows thin peripheral and central nodular Gd-contrast enhancement on coronal FST1WI (**c**). The lesion is associated with thinning and slight expansion of adjacent cortical bone.

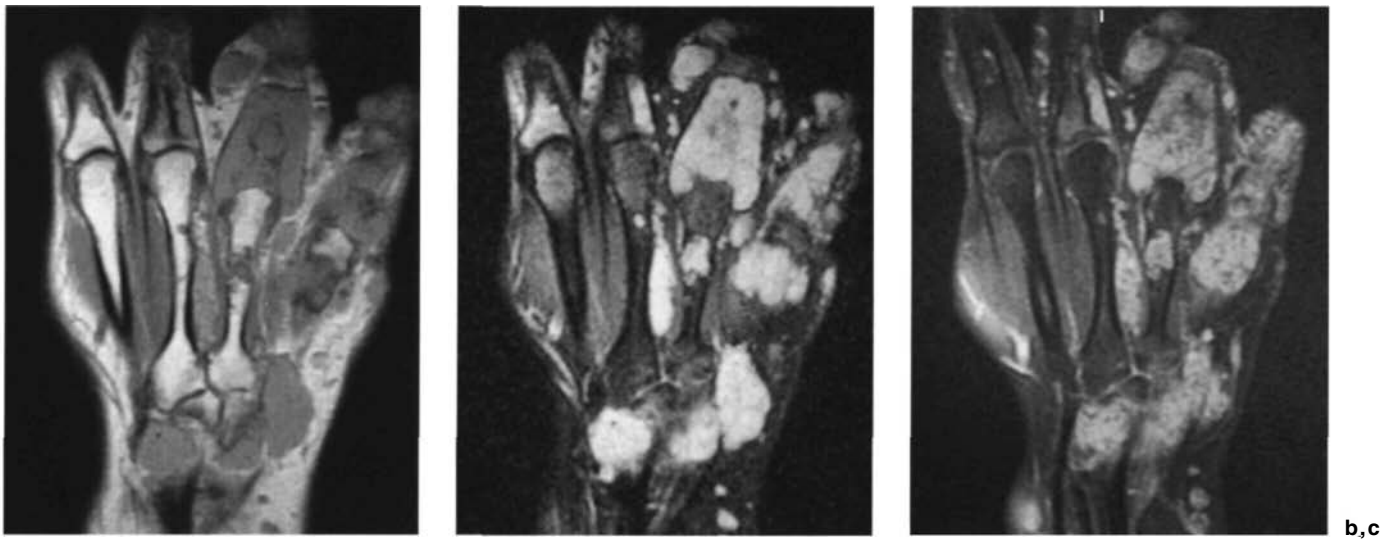

a b, c

Figure 13.**2a-c** A 20-year-old woman with Maffucci disease with multiple enchondromas within bones of the hand that have intermediate signal on coronal T1WI (**a**) and high signal on coronal FST2WI (**b**). The enchondromas and soft tissue hemangiomas show Gd-contrast enhancement on coronal FS T1 WI (**c**).

Table 13 (Continued) **Osseous tumors and tumorlike lesions at the hands and feet**

Tumor/tumorlike Lesion	MRI Findings	Comments
Osteochondroma (Fig. 13.3)	Circumscribed protruding lesion arising from outer cortex with a central zone with intermediate signal on T1 WI and T2WI similar to marrow surrounded by a peripheral outer zone of low signal on T1WI and T2WI, over which a cartilaginous cap is usually present in children and young adults. Increased malignant potential when cartilaginous cap is > 2 cm thick.	Benign cartilaginous tumors arising from defect at periphery of growth plate during bone formation with resultant bone outgrowth covered by a cartilaginous cap. Usually benign lesions unless associated with pain and increasing size of cartilaginous cap. Osteochondromas are common lesions, accounting for 14-35 % of primary bone tumors. Occur with median age of 20years, up to 75 % of patients are less than 20 years. **(See Atlas Chapter A 58)**
Bizarre parosteal osteochondromatous proliferation (Fig. 13.4)	Smooth and/or lobulated calcified and/or ossified lesions often with a broad base or stalk of attachment to an intact outer cortical surface of bone. Remodeling of adjacent bone cortex can occur. Typically does not invade adjacent extraosseous soft tissues.	Lesions adjacent to or attached to the outer periosteal surface of bone consisting of disorganized conglomerations of bone with short trabeculae, cartilage containing enlarged dysmorphic binucleate chondrocytes, spindle cells, fibrous tissue, and/or myxoid regions. Commonly occurs in the hands and feet (70%). less commonly in long bones. Peak age = 4th decade. May represent a type of heterotopic ossification vs. benign tumor. Can be cured by surgical excision although local recurrence is common.
Juxtacortical chondroma	Lesions are located at the bone surface and are usually lobulated with low-intermediate signal on T1WI which is hypo- or isointense relative to muscle. Lesions usually have heterogeneous predominantly high signal on T2WI. Lesions are surrounded by low signal borders on T2WI representing thin sclerotic reaction. Areas of low signal on T2WI are secondary to matrix mineralization. Edema is not typically seen in nearby medullary bone. Lesions often show a peripheral pattern of Gd-contrast enhancement.	Benign protuberant hyaline cartilaginous tumors that arise from the periosteum and superficial to bone cortex. Juxtacortical chondromas account for < 1 % of bone lesions. Occur with median age of 26 years, **(See Atlas Chapter A 9)**
Osteoblastoma (Fig. 13.5)	Expansile radiolucent lesions often greater than 1.5 cm in diameter with or without matrix mineralization and peripheral bone sclerosis seen on radiographs and CT. Lesions often have low-intermediate signal on T1WI and intermediate-high signal on T2WI and FST2WI, usually show Gd-contrast enhancement. Lesions usually have poorly defined zones with high signal on T2WI and FS T2WI and Gd-contrast enhancement in the marrow (edema, inflammation) beyond zone of sclerosis or in adjacent soft tissues from prostaglandin synthesis by these lesions.	Rare benign bone neoplasm (2 % of bone tumors) usually occurs between the ages 6 and 30years. **(See Atlas Chapter A61)**
Osteoid osteoma (Fig. 13.6)	Typically shows dense fusiform thickening of the cortex that has low to intermediate signal on T1WI. PDWI, T2WI, and FST2WI. Within the thickened cortex, a spheraid or ovoid zone (nidus) measuring < 1.5 cm is seen, The nidus can have irregular, distinct, or indistinct margins relative to the adjacent region of cortical thickening, The nidus can have low-intermediate signal on T1WI, and low-intermediate or high signal on T2WI and FST2WI. Calcifications in the nidus can be seen as low signal on T2WI. After Gd-contrast administration, variable degrees of enhancement are seen at the nidus.	Benign osteoblastic lesion with a circumscribed nidus < 1.5 cm and usually surrounded by reactive bone formation. These lesions are usually painful and have limited growth potential. Osteoid osteoma accounts for 11-13 % of primary benign bone tumors. Occurs in patients 6 to 30 years, median =17years. Approximately 75 % occur in patients less than 25 years, **(See Atlas Chapter A60)**

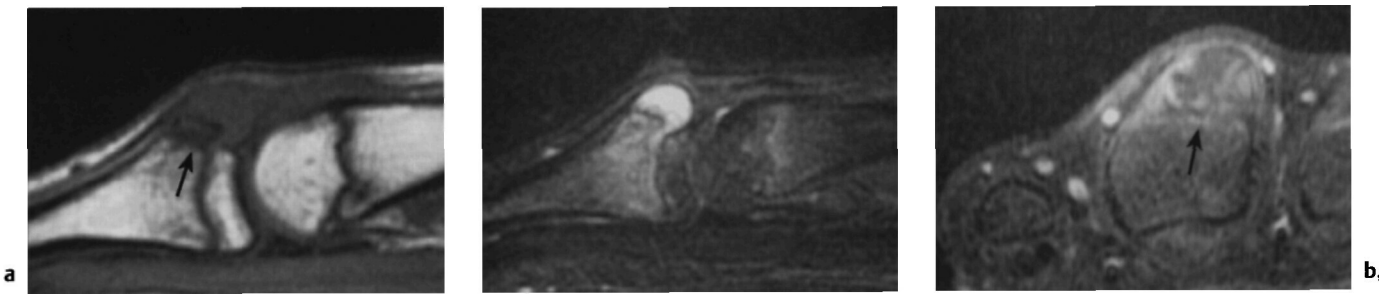

Figure 13.**3a-c** A 14-year-old boy with an osteochondroma involving the proximal metaphyseal surface of a phalanx that has intermediate signal on sagittal T1WI (**a**) and high signal on sagittal FS T2WI (**b**). The lesion shows thin peripheral Gd-contrast enhancement on axial FST1WI (**c**).

Figure 13.4 A 10-year-old boy with a bizarre parosteal osteochondromatous proliferation involving a proximal phalanx as seen on a radiograph. The ossified lesion has smooth margins and a broad base along the phalanx, and is associated with erosive remodeling of the adjacent cortical bone.

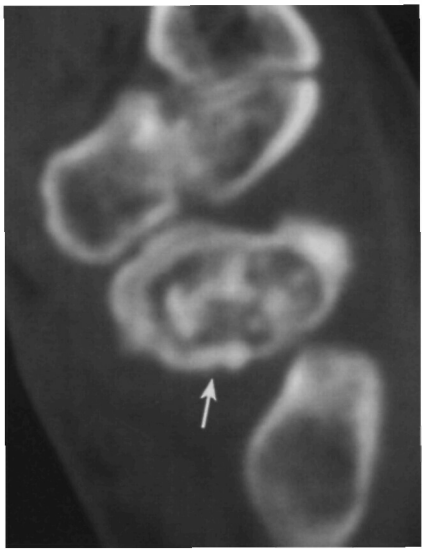

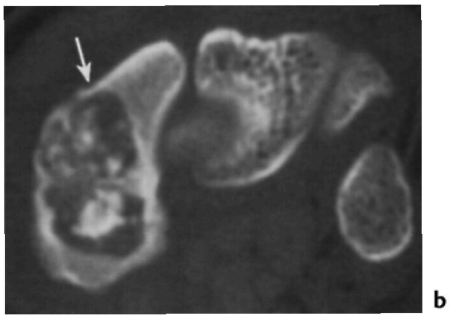

Figure **13.5 a, b** A 16-year-old male with an osteoblastoma within the scaphoid bone in the wrist, seen as a radiolucent lesion containing mineralized matrix on sagittal (**a**) and axial (**b**) CT.

Figure **13.6a, b** An 18-year-old woman with an osteoid osteoma in the calcaneus. The lesion has low signal on sagittal PDWI (**a**) and low signal peripheral to a central area of intermediate signal on axial T2WI (**b**).

Table 13 (Continued) **Osseous tumors and tumorlike lesions at the hands and feet**

Tumor/tumoriike Lesion	MRI Findings	Comments
Chondromyxoid fibroma (Fig. 13.7)	Lesions are often slightly lobulated with low-intermediate signal on T1WI, and heterogeneous predominantly high signal on T2WI secondary to myxoid and hyaline chondroid components with high water content. MR signal heterogeneity on T2WI Is related to the proportions of myxoid. chondroid. and fibrous components within the lesions. Thin low signal septa within lesions on T2WI are secondary to fibrous strands. Lesions are surrounded by low signal borders representing thin sclerotic reaction. Lesions show prominent diffuse Gd-contrast enhancement.	Rare, benign, slow-growing bone lesions that contain chondroid, myxoid, and fibrous components. Chondromyxoid fibromas represent 2-4% of primary benign bone lesions, and < 1 % of primary bone lesions. Most chondromyxoid fibromas occur between the ages of 1 and 40 years, with a median of 17 years, and peak incidence in the 2nd to 3rd decades. **(See Atlas Chapter A10)**
Lipoma (Fig. 13.8)	Lesions can have heterogeneous high. Intermediate, and/or low signal on T1WI, PDWI, and T2WI. Fat signal of lesions is suppressed on FST1WI. FST2WI. and STIR. Lesions usually show no Gd-contrast enhancement. Peripheral rim-like and central Gd-contrast enhancement on FST1WI may occassionally occur.	Uncommon benign hamartomas composed of mature white adipose tissue without cellular atypia. Osseous or chondroid metaplasia with myxoid changes can be associated with lipomas. Account for -0.1% of bone tumors, likely under-reported. **(See Atlas Chapter A 43)**
Enostosis/bone island	Typically appear as well-circumscribed zones of dense bone with low signal on T1 WI. PDWI. T2WI, and FS T2WI. No infiltration into the adjacent soft tissues is seen by osteomas. Zones of bone destruction or associated soft tissue mass lesions are not associated with osteomas. Periosteal reaction is not associated with osteomas except in cases with coincidental antecedent trauma.	Benign primary bone lesion composed of dense lamellar, woven and/or compact cortical bone usually located at the surface of bone. Multiple osteomas usually occur in Gardner syndrome, which is an autosomal dominant disorder that is associated with intestinal polyposis. fibromas. and desmoid tumors. Accounts for < 1 % of primary benign bone tumors. Occurs in patients 16 to 74 years, most frequent in 6th decade. **(See Atlas Chapter A 62)**
Aneurysmal bone cyst (Fig. 13.9)	Aneurysmal bone cysts (ABCs) often have a low signal rim on T1WI and T2WI adjacent to normal medullary bone, and between extraosseous soft tissues. Various combinations of low, intermediate, and/or high signal on T1WI, PDWI, and T2WI are usually seen within aneurysmal bone cysts as well as fluid-fluid levels. Variable Gd-contrast enhancement is seen at the margins of lesions as well as involving the internal septae.	Tumor-like expansile bone lesions containing cavernous spaces filled with blood. ABCs can be primary bone lesions (two-thirds) or secondary to other bone lesions/tumors (such as giant cell tumors, chondroblastomas. osteoblastomas. osteosarcomas. chondromyxoid fibromas. nonossifying fibromas. fibrous dysplasia, fibrosarcomas, malignant fibrous histiocytomas, and metastatic disease). Account for -11% of primary tumor-like lesions of bone. Patients usually range in age from 1 to 25 years, median -14 years. **(See Atlas Chapter A 2)**
Giant cell reparative granuloma (Fig. 13.10)	Lesions can have heterogeneous low, intermediate, and/or high signal on T1WI, PDWI. and T2WI; as well as peripheral rim-like and central Gd-contrast enhancement on FS T1WI.	Giant cell reparative granulomas are also referred to as solid ABCs. **(See Atlas Chapter A 2).** Histologic appearance resembles brown tumors.

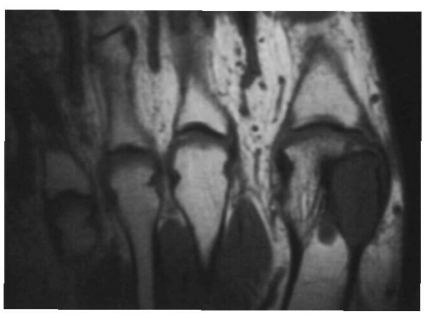

a

b

Figure 13.7a, b A 34-year-old man with chondromyxoid fibroma in the distal first metatarsal bone. The lesion has low-intermediate signal on coronal T1WI (a) and heterogeneous high signal on FST2WI (b).

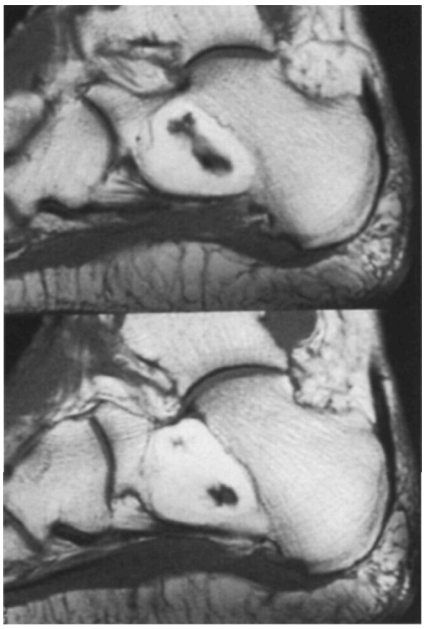

Figure 13.8 A 47-year-old woman with an intraosseous lipoma in the calcaneus that has thin low signal margins and mostly high signal on sagittal T1 WI as well as several small zones of intermediate signal from cystic degeneration.

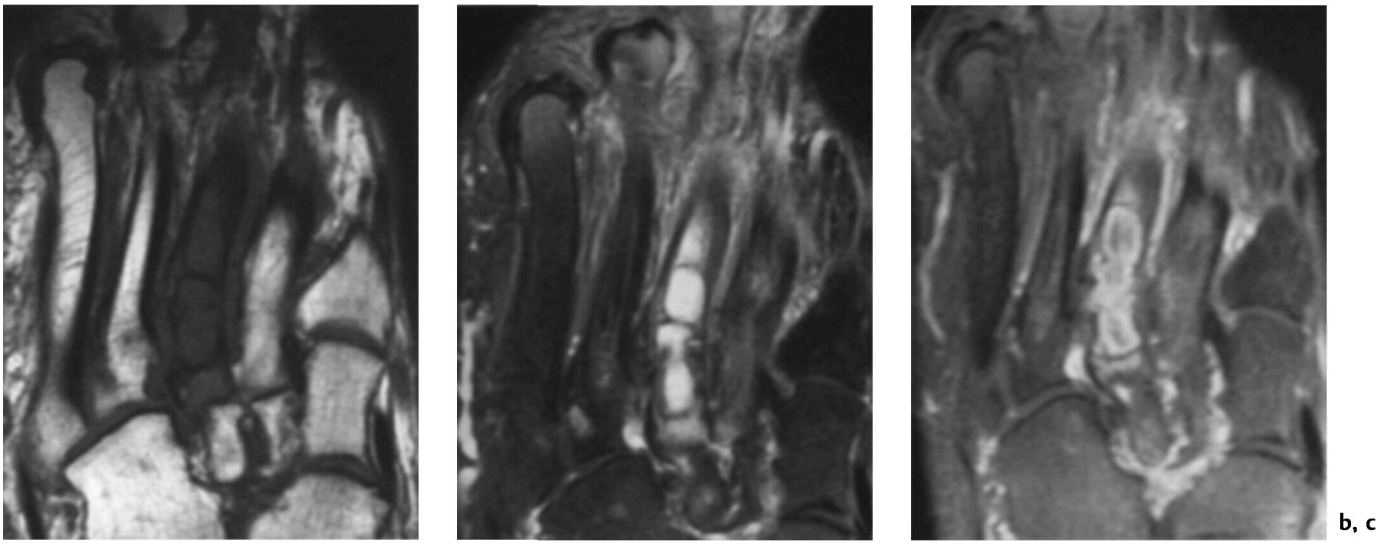

Figure 13.**9a-c** A 48-year-old man with an aneurysmal bone cyst in the proximal portion of the third metatarsal bone that has low-intermediate signal on coronal T1WI (**a**) and mostly high signal on coronal FST2WI (**b**). The lesion shows thin, mostly peripheral Gd-contrast enhancement on coronal FST1WI (**c**). Also seen are slight expansion and thinning of the adjacent cortical margins, and poorly defined zones of increased signal on FST2WI and Gd-contrast enhancement in the adjacent bone marrow.

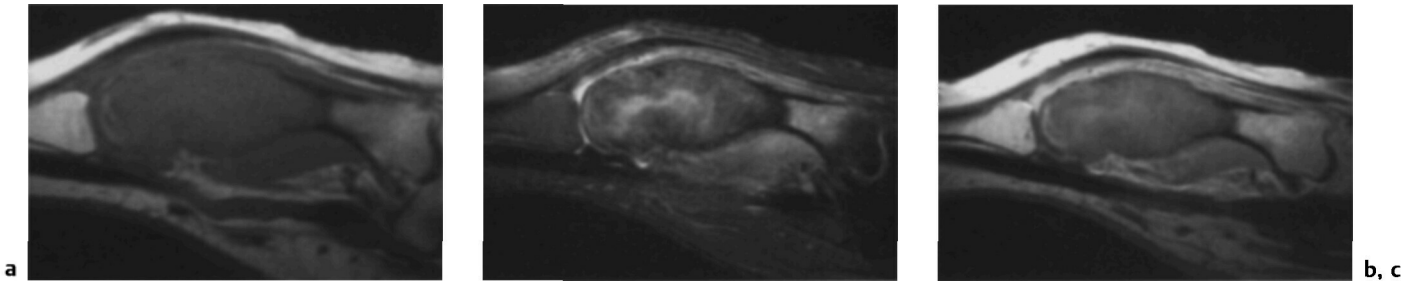

Figure 13.**10a-c** A 39-year-old woman with a giant cell granuloma involving a metacarpal bone. The intramedullary lesion expands and thins bone cortex, and has intermediate signal on sagittal T1WI (**a**), heterogeneous low, intermediate, slightly high, and high signal on sagittal FST2WI (**b**). The lesion shows Gd-contrast enhancement on sagittal T1WI (**c**).

Table 13 (Continued) Osseous tumors and tumorlike lesions at the hands and feet

Tumor/tumoriike Lesion	MRI Findings	Comments
Unicameral bone cyst (Fig. 13.11)	Unicameral bone cysts (UBCs) often have a peripheral rim of low signal on T1WI and T2WI adjacent to normal medullary bone. Usually contain fluid with low to low-intermediate signal on T1 WI. low-intermediate and high signal on T2WI. Fluid-fluid levels may occur. For UBCs without pathologic fracture, thin peripheral Gd-contrast enhancement can be seen at the margins of lesions. UBCs with pathologic fracture can have heterogeneous or homogeneous low-intermediate or slightly high signal on T1WI, and heterogeneous or homogeneous high signal on T2WI and FS T2WI. UBCs complicated by fracture can have internal septations and fluid-fluid levels, as well as irregular peripheral Gd-contrast enhancement at internal septations.	Intramedullary non-neoplastic cavities filled with serous or serosanguineous fluid. Account for 9% of primary tumor-like lesions of bone. 85% occur in the first 2 decades, median -11 years. **(See Atlas Chapter A 3)**
Chondroblastoma (Fig. 13.12)	Tumors often have fine lobular margins, and typically have low-intermediate heterogeneous signal on T1WI, and mixed low, intermediate, and/or high signal on T2WI. Lobular, marginal septal or diffuse Gd-contrast enhancement patterns can be seen. Poorly defined zones with high signal on T2WI and FS T2WI and corresponding Gd-contrast enhancement are typically seen in the marrow adjacent to the lesions representing inflammatory reaction from prostaglandin synthesis by these tumors.	Benign cartilaginous tumors with chondroblast-like cells and areas of chondroid matrix formation, usually occur in children and adolescents, median -17 years, mean - 16 years for lesions in long bones, mean - 28 years in other bones. Most cases are diagnosed between the ages of 5 and 25. **(See Atlas Chapter A 7)**
Hemangioma	Often well-circumscribed lesions that typically have intermediate to high signal on T1WI, PDWI. T2WI, and FST2WI. On T1WI, hemangiomas usually have signal equal to or greater than adjacent normal marrow secondary to fatty components. Usually show Gd-contrast enhancement. Pathologic fractures associated with intraosseous hemangiomas usually result in low-intermediate marrow signal on T1WI.	Benign lesions of bone comprising capillary, cavernous, and/or malformed venous vessels. Considered to be a hamartomatous disorder. Account for 4% of benign bone tumors and -1 % of all bone tumors, likely underestimated. Occur in all ages, median - 33 years. **(See Adas Chapter A 34)**
Clomus body tumor (Fig**. 13.13)**	Glomus body tumors are well-circumscribed ovoid lesions measuring < 1 cm and are often located under the nail beds at the distal phalanges of fingers and toes. Glomus body tumors often have low- intermediate signal on T1WI and PDWI, although may be hypointense or hyperintense on T1WI relative to the adjacent dermis layers. Glomus tumors usually have high signal T2WI and FST2WI. and typically show Gd-contrast enhancement.	Benign mesenchymal hamartomas derived from the neuromyoarterial apparatus (glomus bodies) that regulate arteriolar blood flow to the skin, and are normally present throughout the reticular dermis throughout the body. Glomus bodies occur in large numbers under the nail beds of the fingers and toes. **(See Adas Chapter A 31)**
Giant cell tumor (Fig. 13.14)	Often well-defined lesions with thin low signal margins on T1WI. PDWI. and T2WI. Solid portions of giant cell tumors often have low to intermediate signal on T1WI and PDWI, intermediate to high signal on T2WI, and high signal on FS PDWI and FST2WI. Zones of low signal on T2WI may be seen secondary to hemosiderin. Aneurysmal bone cysts can be seen in **14**% of giant cell tumors. Areas of cortical thinning, expansion, and/or destruction can occur with extraosseous extension. Tumors show varying degrees of Gd-contrast enhancement.	Aggressive tumors composed of neoplastic mononuclear cells and scattered multinucleated osteoclast-like giant cells. Account for 23% of primary nonmalignant bone tumors, and 5-9% of all primary bone tumors, median age -30 years. **(See Adas Chapter A 29)**

a

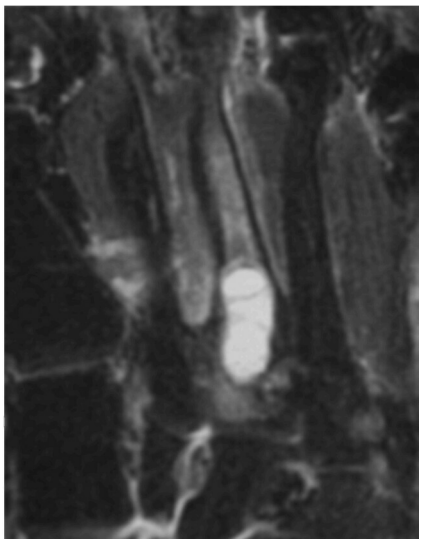

b

Figure 13.**11 a, b** A 60-year-old woman with a unicameral bone cyst in the proximal portion of a metatarsal bone. The lesion has low-intermediate signal on coronal T1WI (**a**) and mostly high signal on coronal FST2WI (**b**). Also seen are poorly defined zones of slightly increased signal on FST2 W in the adjacent bone marrow.

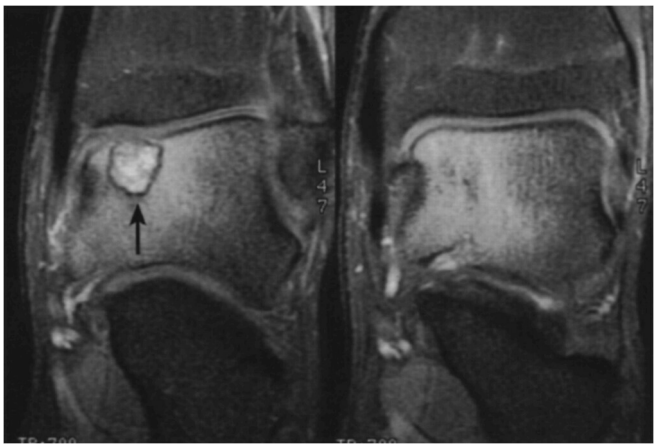

c

Figure **13.12** A 15-year-old female with a chondroblastoma involving the talus. The lesion shows prominent Gd-contrast centrally surrounded by a thin rim of low signal on coronal FST1WI. Poorly defined zones of contrast enhancement are also seen in the marrow adjacent to the lesion.

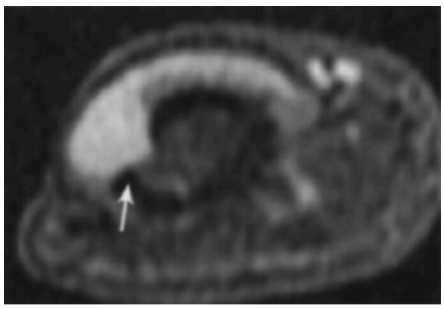

d

Figure **13.13** A 24-year-old woman with a glomus tumor under the nail bed laterally associated with erosion of the adjacent cortex of the distal phalanx. The lesion shows prominent Gd-contrast enhancement on coronalFST1WI.

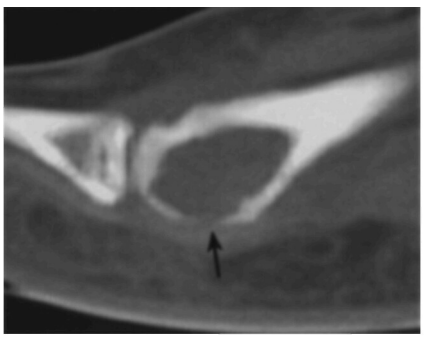

a

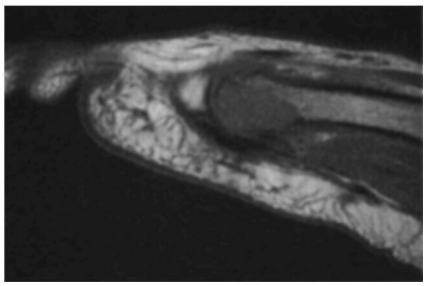

b

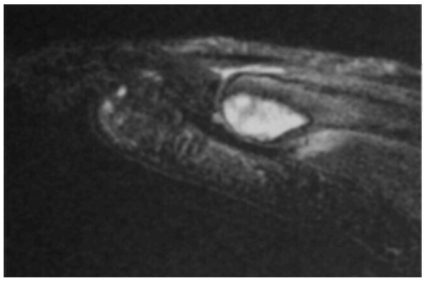

c

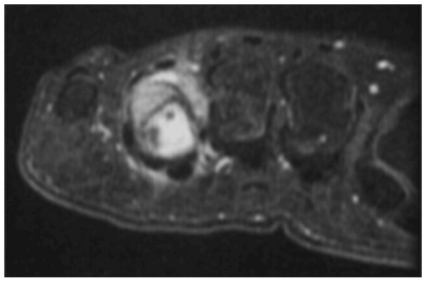

d

Figure **13.14a-d** A 29-year-old man with a giant cell tumor involving the distal end of the fourth metatarsal bone. The radiolucent lesion is associated with cortical thinning and disruption on sagittal CT (**a**). The lesion has intermediate signal on sagittal T1WI (**b**) and high signal on sagittal FST2WI (**c**). The lesion shows Gd-contrast enhancement on axial FS TIWI(**d**).

Table 13 (Continued) Osseous tumors and tumorlike lesions at the hands and feet

Tumor/tumoriike Lesion	MRI Findings	Comments
Fibrous dysplasia (Fig. 13.15)	MRI features depend on the proportions of bony spicules, collagen, fibroblastic spindle cells, hemorrhagic and/or cystic changes, and associated pathologic fracture if present. Lesions are usually well-circumscribed, and have low or low-intermediate signal on T1WI and PDWI. On T2WI, lesions have variable mixtures of low, intermediate, and/or high signal often surrounded by a low signal rim of variable thickness. Internal septations and cystic changes are seen in a minority of lesions. Bone expansion wilh thickened and/or thinned cortex can be seen. Lesions show Cd-contrast enhancement that varies in degree and pattern.	Benign medullary fibro-osseous lesion that can involve a single site **(mono-ostotic)** or multiple locations **(poly-ostotic).** Thought to occur from developmental failure in the normal process of remodeling primitive bone to mature lamellar bone with resultant zone or zones of immature trabeculae within dysplastic fibrous tissue. Accounts for - 10% of benign bone lesions. Patients range in age from <1 to 76 years. 75% occur before the age of 30 years. **(See Atlas Chapter A 27)**
Osteomyelitis (Fig. 13.16)	In **acute osteomyelitis,** poorly defined /ones of low or low-intermediate signal on T1WI and high signal on T2WI, STIR, and FST2WI are seen in the marrow. Loss of definition of the low signal line of the cortical margins is often observed on T1WI, T2WI, STIR, and FST2WI. After Gd-contrast administration, irregular zones of contrast enhancement are seen in the involved marrow on FST1WI. In the **subacute phase of osteomyelitis,** the pyogenic process becomes more localized. The zone of transition between normal and abnormal bone is sharper and more well-defined in subacute and chronic osteomyelitis than with acute osteomyelitis.	Osteomyelitis is a disorder in which there is infection of bone and commonly the adjacent soft tissues. Can result from hematogenous spread of microorganisms as well as from trauma-direct inoculation, extension from adjacent tissues, and complications from surgery. Bacteria such as *Staphylococcus aureus* and Streptococcus pyo*genes are* the most common infectious organisms. Can also result from other bacteria as well as *Mycobactcrium tuberculosis,* fungi, parasites, and viruses. **(See Atlas Chapter A 63)**
Eosinophilic granuloma	Focal intramedullary lesion associated with trabecular and cortical bone destruction that typically has low-intermediate signal on T1WI and PDWI and heterogeneous slightly high to high signal on T2WI. Poorly defined zones of high signal on T2WI are usually seen in the marrow peripheral to the lesions secondary to inflammatory changes. Extension of lesions from the marrow into adjacent soft tissues through areas of cortical disruption are commonly seen as well as linear periosteal zones of high signal on T2WI. Lesions typically show prominent Gd-contrast enhancement in marrow and in extraosseous soft tissue portions of the lesions.	Benign tumor-like lesions consisting of Langerhans' cells (histiocytes), and variable amounts of lymphocytes, polymorphonuclear cells, and eosinophils. Account for 1 % of primary bone lesions and 8 % of tumor-like lesions. Occur in patients with median age =10years, average =13.5years, peak incidence is between 5 and 10years, 80 to 85% occur in patients less than 30 years. **(See Atlas Chapter A 18)**
Sarcoidosis	Lesions usually appear as intramedullary zones with low to intermediate signal on T1WI and slightly high to high signal on T2WI and FS PDWI and FST2WI. Erosions and zones of destruction of adjacent bone cortex as well as periosseous extension of the granulomatous process can occur. Fine perpendicular lines of low signal on T1 WI may be seen extending outward from the region of eroded or destroyed cortex representing collagen separating periosseous extension of granulomas. After Gd-contrast administration, lesions typically show moderate to prominent enhancement.	Chronic systemic granulomatous disease of unknown etiology in which noncaseating granulomas occur in various tissues and organs including bone. **(See Atlas Chapter A71)**
Gout (Fig. 13.17)	Tophi have variable sizes and shapes, and have low-intermediate signal on T1WI, FST2WI, and T2WI. Zones of high signal on T2WI can also be seen in tophi. Erosions of bone, synovial pannus, joint effusion, bone marrow, and soft tissue edema can be seen with MRI. Tophi may show heterogeneous, diffuse, or peripheral/marginal Gd-contrast enhancement patterns.	Gout is an inflammatory disease involving synovium resulting from deposition of monosodium urate crystals and occurs when the serum urate level exceeds its solubility in various tissues and body fluid. **(See Atlas Chapter A 32)**

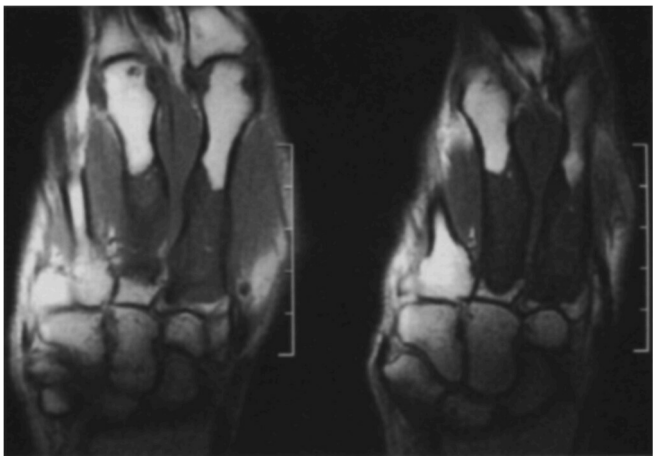

a

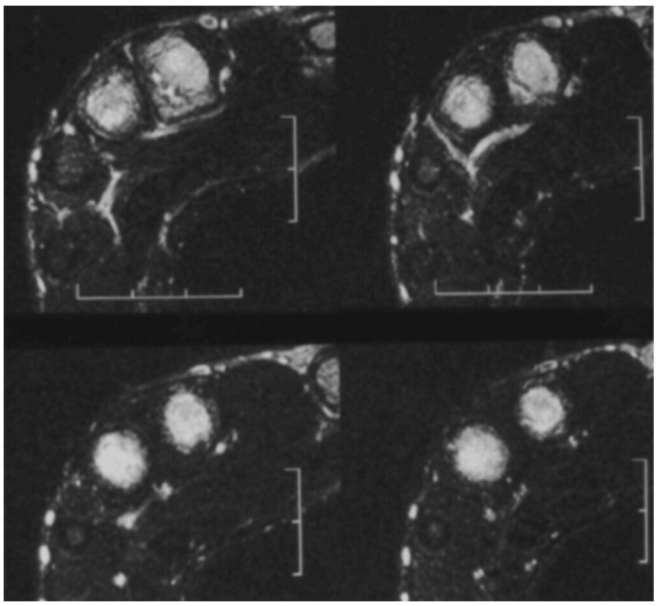

b

Figure 13.15 a, b Polyostotic fibrous dysplasia involving two adjacent metacarpal bones. The intramedullary lesions have low-intermediate signal on coronal T1WI (a), and mostly high signal on axial T2WI (b). Slight cortical thickening and expansion are also seen.

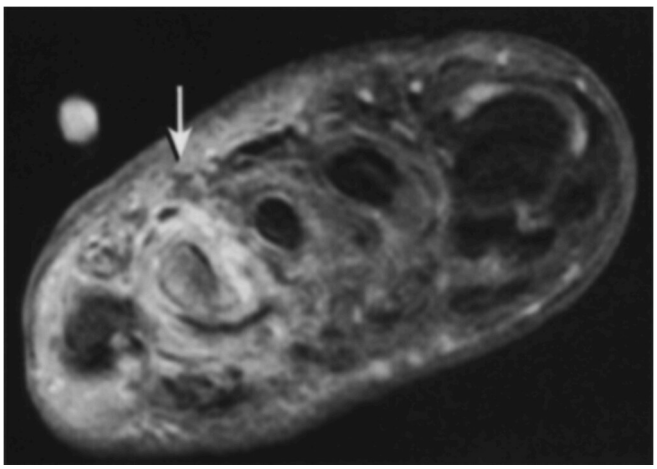

Figure 13.16 A 54-year-old woman with pyogenic osteomyelitis involving the fourth metatarsal bone with abnormal high signal in the marrow and adjacent soft tissues on coronal FS T2WI.

a

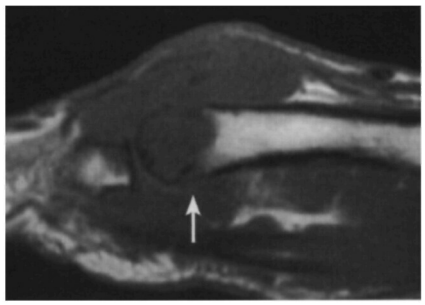

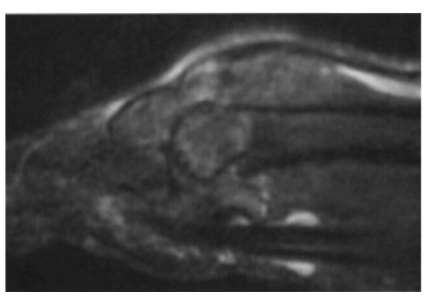

c

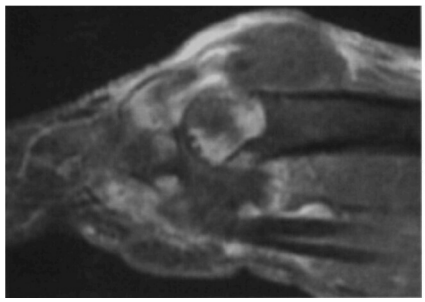

b, d

Figure 13.**17a-d** A 53-year-old man with gout involving the metatarsal-phalangeal joint with bone erosions seen on a radiograph (**a**). MRI shows a soft tissue lesion (tophus) with intermediate signal on sagittal T1WI (**b**), and heterogeneous intermediate, slightly high, and high signal on FS T2WI (**c**). The lesion erodes cortical bone and extends into the marrow of the metatarsal head. Only peripheral irregular Gd-contrast enhancement is seen with the intraosseous and extraosseous lesions on sagittal FST1WI (**d**).

Table 13 (Continued) Osseous tumors and tumorlike lesions at the hands and feet

Tumor/tumorlike Lesion	MRI Findings	Comments
Bone infarct (Fig. 13.18)	A double-line sign (curvilinear adjacent zones of low and high signal on T2WI) is commonly seen at the edges of the infarcts representing the borders of osseous resorption and healing. Irregular Gd-contrast enhancement can be seen from granulation tissue ingrowth.	Zones of ischemic death involving bone trabeculae and marrow that may be idiopathic or result from: trauma, corticosteroid treatment, chemotherapy, radiation treatment, occlusive vascular disease, collagen vascular and other autoimmune diseases, metabolic storage diseases (Gaucher, etc.), sickle cell disease, thalassemia. hyperbaric events / Caisson disease, pregnancy, alcohol abuse, pancreatitis, infections, and lymphoproliferative diseases. **(See Atlas Chapter A 37)**
Malignant		
Metastatic lesion	Single or multiple well-circumscribed or poorly defined infiltrative lesions involving marrow associated with cortical destruction and extraosseous extension. Lesions often have low-intermediate signal on T1WI, low, intermediate, and/or high signal on T2WI and FST2WI. and usually show Gd- contrast enhancement. Cortical destruction and tumor extension into the extraosseous soft tissues can occur. Pathologic fractures can be associated with metastatic lesions involving tubular bones and vertebrae. Periostea! reaction is uncommon.	Metastatic lesions typically occur in the marrow with or without cortical destruction and extraosseous tumor extension. **(See Adas Chapter A 50)**
Ptasmacytoma/myeloma	Well-circumscribed or poorly defined infiltrative lesions involving marrow, low-intermediate signal on T1WI. intermediate-high signal on T2WI and FST2WI. usually show Cd-contrast enhancement, eventual cortical bone destruction and extraosseous extension.	Malignant tumors comprised of proliferating antibody-secreting plasma cells derived from single clones. Most common primary neoplasm of bone in adults, median -60 years. Most patients are older than 40 years. May have variable destructive or infiltrative changes involving the axial and/or appendicular skeleton. **(See Adas Chapter A 52)**

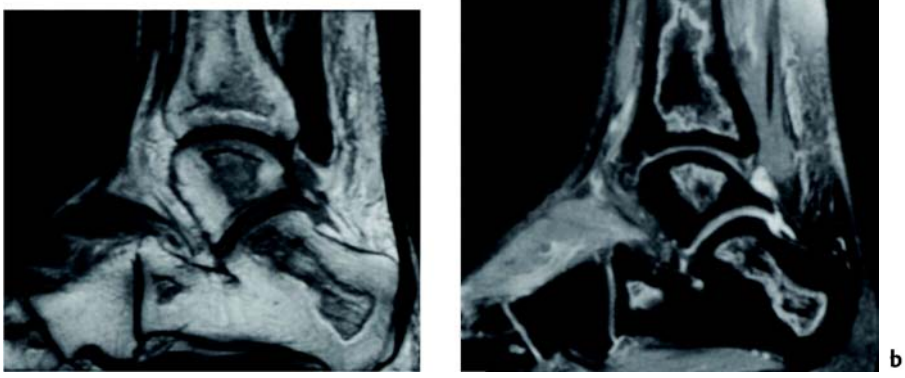

Figure 13.18 a, b A 36-year-old man with sickle cell trait and bone infarcts in the distal tibia, talus, and calcaneus as seen on sagittal T1WI (a) and sagittal FS T2WI (b).

Table 13 (Continued) Osseous tumors and tumorlike lesions at the hands and feet

Tumor/tumoriike Lesion	MRI Hndings	Comments
Chondrosarcoma (Fig. 13.19)	Intramedullary tumors often have low-intermediate signal on T1WI. intermediate signal on PDWI, and heterogeneous intermediate-high signal on T2WI. Lesions usually show heterogeneous contrast enhancement.	Malignant tumors containing cartilage formed within sarcomatous stroma. Account for 12-21 % of malignant bone lesions, 21-26% of primary sarcomas of bone, mean age -40 years, median -26 to 59 years. **(See Atlas Chapter A 11)**
Osteosarcoma	Destructive intramedullary malignant lesions, low-intermediate signal on T1WI, mixed low, intermediate, high signal on T2WI, usually with matrix mineralization/ossification-low signal on T2WI, usually show Gd-contrast enhancement. Zones of cortical destruction are typically seen through which tumors extend into the extraosseous soft tissues. Low signal from spicules of periosteal, reactive, and tumoral bone formation may be seen.	Malignant tumor comprising proliferating neoplastic spindle cells that produce osteoid and/or immature tumoral bone, most frequently arising within medullary bone. Two age peaks of incidence. The larger peak occurs between the ages of 10 and 20 and accounts for over half of the cases. The second smaller peak occurs in adults over 60 years and accounts for -10% of the cases. Occurs in children as primary tumors and adults (associated with Paget disease, irradiated bone, chronic osteomyelitis, osteoblastoma, giant cell tumor, fibrous dysplasia. **(See Atlas Chapter A 64)**
Ewing sarcoma	Destructive malignant lesions involving marrow, low-intermediate signal on T1WI, mixed low, intermediate, and/or high signal on T2WI and FST2WI. usually shows Gd-contrast enhancement (usually heterogeneous). Extraosseous tumor extension through sites of cortical destruction is commonly seen. Thin striated zones of low signal on T2WI can be sometimes seen oriented perpendicular to the long axis of the involved bone under the elevated periosteum representing the "hair on end" appearance of reactive bone formation secondary to the tumor.	Malignant primitive tumor of bone comprised of undifferentiated small cells with round nuclei. Accounts for 6-11 % of primary malignant bone tumors, 5-7% of primary bone tumors. Usually occurs between the ages of 5 and 30, males > females, locally invasive, high metastatic potential. **(See Atlas Chapter A 20)**

a

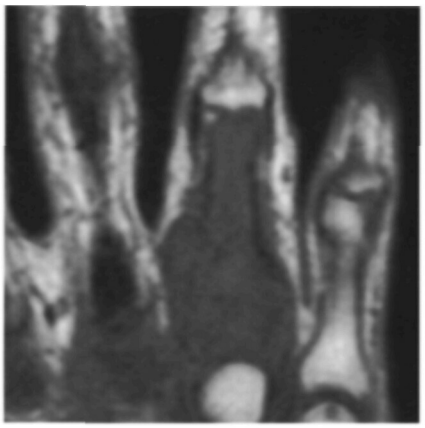

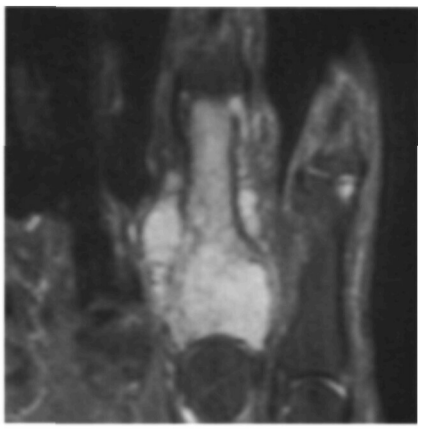

b, c

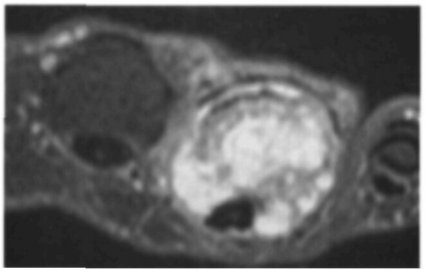

d

Figure **13.19a-d** A 56-year-old man with a chondrosarcoma involving a metacarpal bone. The radiograph (**a**) shows an intramedullary lesion with chondroid matrix and cortical destruction. The lesion has intermediate signal on coronal T1WI (**b**) and high signal on coronal FST2WI (**c**). The tumor shows Gd-contrast enhancement on axial FST1WI (**d**). Cortical destruction and extraosseous tumor extension is seen with MRI.

References

Bizarre Parosteal Osteochondromatous Proliferation

Ambramovid L, Steiner GC. Bizarre parosteal Osteochondromatous proliferation (Nora's Lesion): a retrospective study of 12 cases, 2 arising in long bones. Hum *Pathol* 2002;33:1205-1210.

Michelsen H, Abramovici L, Steiner G, Posner MA. Bizarre parosteal Osteochondromatous proliferation (Nora's Lesion) in the hand. J *Hand Surg* May 2004;29A(3):520-525.

Orui H, Ishikawa A, Tsuchiya T, Ogino T. Magnetic resonance imaging characteristics of bizarre parosteal Osteochondromatous proliferation of the hand: a case report. *] Hand Surg* November 2002; **27**A(6):1104-1108.

Torreggiani WC, Munk PL, Al-Ismail K, et al. MR imaging features of bizarre parosteal Osteochondromatous proliferation of bone (Nora's Lesion). *Eur] Radiol* 2001 ;40:224-231.

Table 14 Diffuse, multiple, poorly defined and/or multifocal zones of abnormal marrow signal

Disorder	MRI Findings	Comments
Nonmalignant		
Red marrow reconversion (Fig. 14.1,14.2.14.3)	Involved marrow has slightly to moderately decreased signal relative to fat on T1WI and PDWI. isointense signal relative to muscle and slightly increased signal relative to fat on FS T2WI.	Hyperplasia of normal marrow elements at sites that were previously composed mostly of yellow marrow. May be seen in obese middle-aged patients, tobacco smokers, marathon runners, and those living in high altitudes.

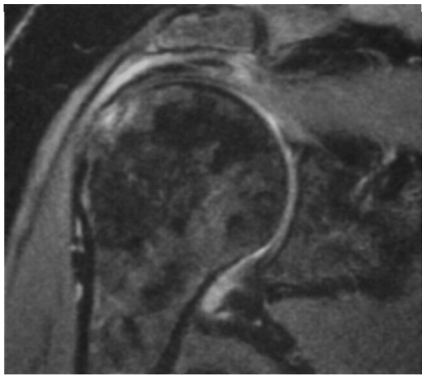

Figure 14.1 A 48-year-old woman with red marrow reconversion in the proximal humerus seen as irregular zones with isointense signal relative to muscle and slightly increased signal relative to fat on coronal FST2WI.

Figure 14.2 A 40-year-old woman with red marrow reconversion in the metadiaphyseal marrow of the femur as seen on coronal FST2WI.

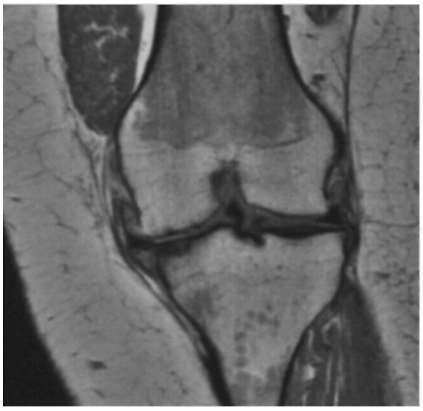

a

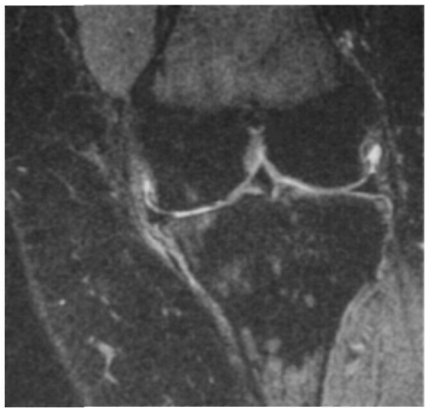

b

Figure 14.**3 a, b** A 36-year-old woman with red marrow reconversion in the metadiaphyseal marrow of the distal femur and proximal tibia as seen on coronal PDWI (**a**) and coronal FST2WI (**b**).

Table 14 (Continued) Diffuse, multiple, poorly defined and/or multifocal zones of abnormal marrow signal

Disorder	MRI Findings	Comments
Inherited anemias (sickle cell anemia, thalassemia, sideroblastic anemia) ***(Figs.*** **14.4-14.7)**	Involved marrow has slightly to moderately decreased signal relative to fat on T1WI and T2WI, isointense to slightly hyperintense signal relative to muscle and increased signal relative to fat on FST2WI.	Inherited anemias result in hyperplasia of normal marrow elements. Sickle cell disease is the most common hemoglobinopathy in which abnormal hemoglobin S is combined with itself, or other hemoglobin types such as C, D, E, or thalassemia. Hemoglobin SS, SC, and S-thalassemia have the most sickling of erythrocytes. In addition to marrow hyperplasia seen in sickle cell disease, bone infarcts and extramedullary hematopoiesis can also occur. (5-thalassemia is a disorder in which there is deficient synthesis of p chains of hemoglobin resulting in excess a chains in erythrocytes and erythrocytes causing dysfunctional hematopoiesis and hemolysis. The decrease in p chains can be severe as in the major type homozygous), moderate in the intermediate type (heterozygous), or mild in the minor type (heterozygous).

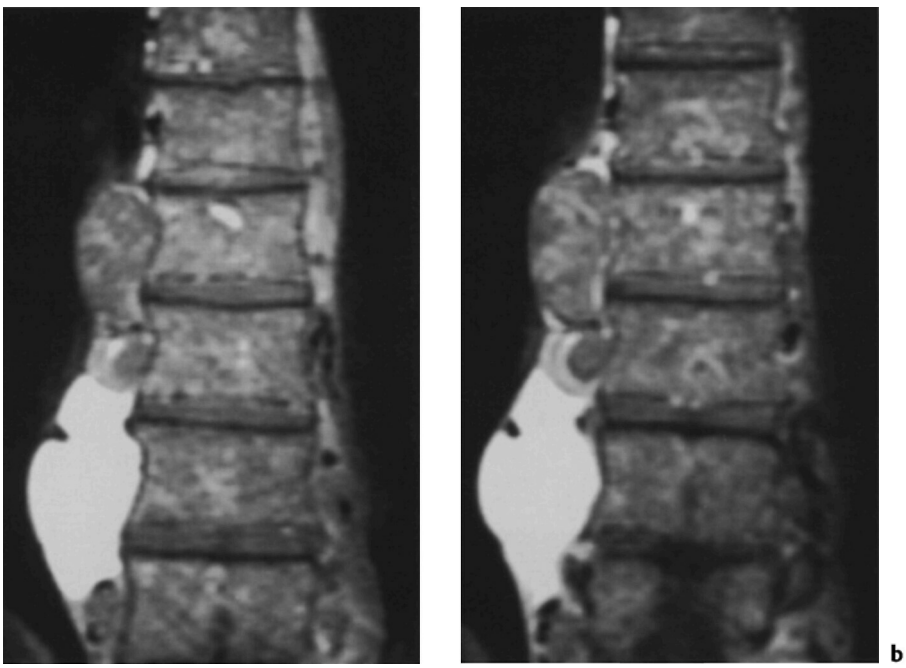

Figure 14.**4a**, **b** A 54-year-old man with sickle cell disease and extramedullary hematopoiesis. The marrow has heterogeneous mixed low-intermediate signal and slightly high signal on coronal T1WI (a) and coronal T2WI (b) that is hypointense to fat.

Figure 14.**5a, b** A 14-year-old girl with sickle cell disease with marrow signal alteration in the metaphyseal regions of the knee, and to a lesser extent within epiphyseal marrow. Marrow signal is low-intermediate on coronal T1WI (**a**) and hypointense relative to fat. The marrow signal is slightly high on coronal FS T2WI (**b**), which is hyperintense relative to fat and muscle.

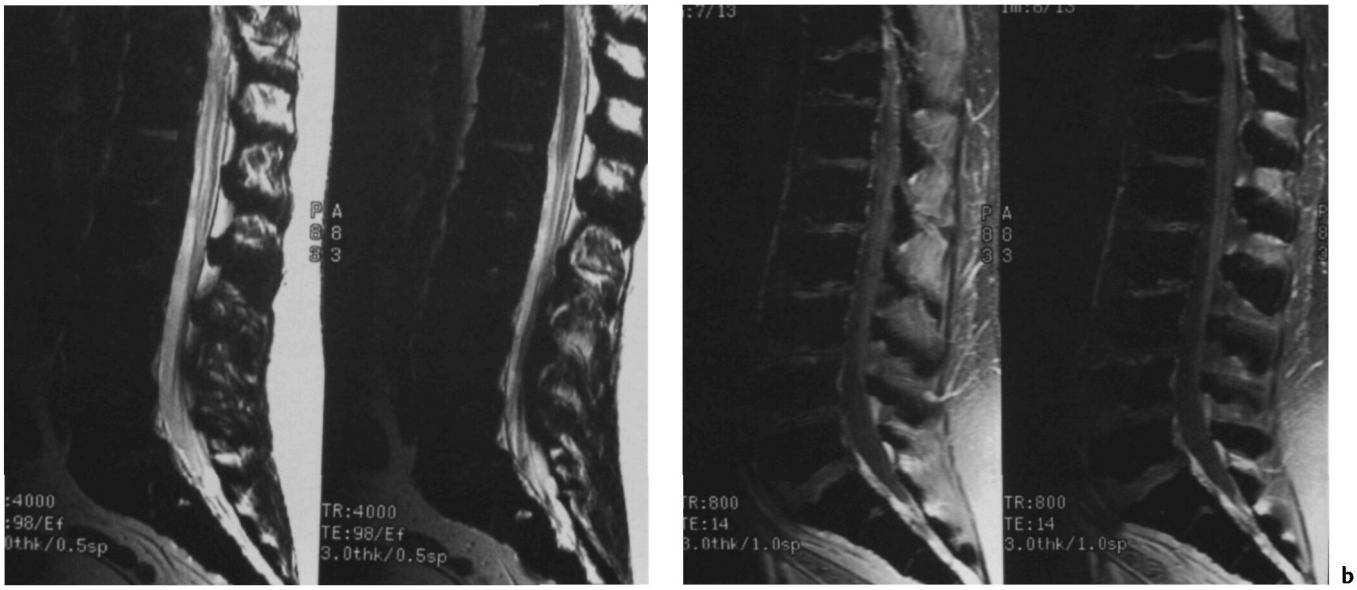

a b

Figure 14.**6a, b** A 22-year-old man with β thalassemia major. Marrow signal is low on sagittal T2WI (**a**) and post-Gd-contrast FS T1WI (**b**) secondary to iron overload.

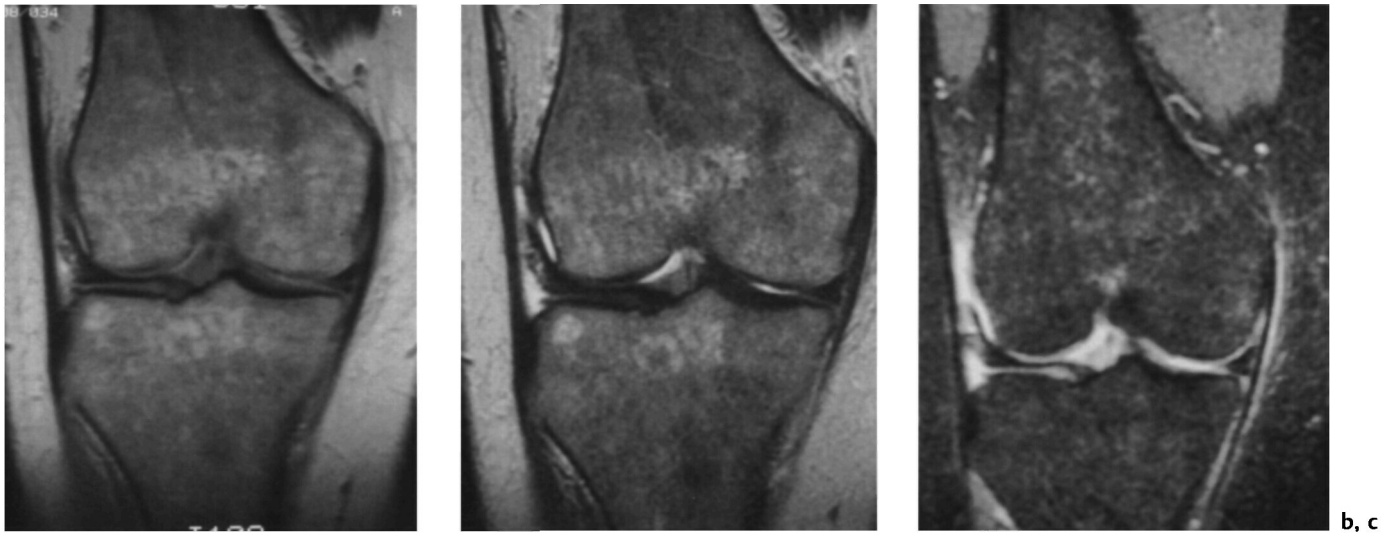

a b, c

Figure 14.**7a-c** A 49-year-old woman with β thalassemia minor. The marrow has heterogeneous mixed low-intermediate signal on coronal PDWI (**a**) and coronal T2WI (**b**), which is hypointense relative to fat, and slightly high signal on coronal FST2WI (**c**), which is hyperintense relative to fat.

Table 14 (Continued) Diffuse, multiple, poorly defined and/or multifocal zones of abnormal marrow signal

Disorder	MRI Findings	Comments
Marrow hyperplasia from exogenous erythropoietin (Fig. 14.8)	Involved marrow has slightly to moderately decreased signal relative to fat on T1 WI and T2WI; isointense signal relative to muscle and slightly increased signal relative to fat on FS T2WI.	Exogenous source (medication) of erythropoietin used for treatment of anemia.
Granulocyte/macrophage colony stimulating factor (G/M-CSF) (Fig. 14.9)	Use of these medications induces red marrow reconversion, which occurs more commonly in a diffuse pattern compared with focal sites. Involved marrow has slightly decreased signal relative to fat on T1WI and T2WI; isointense signal relative to muscle and slightly increased signal relative to fat on FS T2WI.	G-CSF is used as an adjunct for chemotherapy to minimize or correct treatment-related neutropenia by regulating the proliferation and differentiation of hematopoietic progenitor cells.
Hemochromatosis and iron deposition from multiple transfusions (Fig. 14.10)	Involved marrow has low signal on T1WI. PDWI, and T2WI.	Hemochromatosis is an iron storage disorder with abnormal increased deposition of iron in various tissues. Hemochromatosis can be a primary autosomal recessive disorder in which there is increased intestinal absorption of iron resulting in a 10 to 50-fold increase in total body iron. The primary disorder is associated with a gene on chromosome 6. and occurs with an incidence of 3-5 per 1000. Usually presents in adults, and occasionally in children. Secondary hemochromatosis occurs from iron overload from transfusions for sickle cell disease and thalassemia, alcoholic liver disease, and excessive dietary iron.

a

b

Figure 14.**8a, b** A 60-year-old woman treated with exogenous erythropoietin for anemia. Marrow has slightly to moderately decreased signal relative to fat on sagittal T1 WI (**a**) and sagittal (**b**) T2WI.

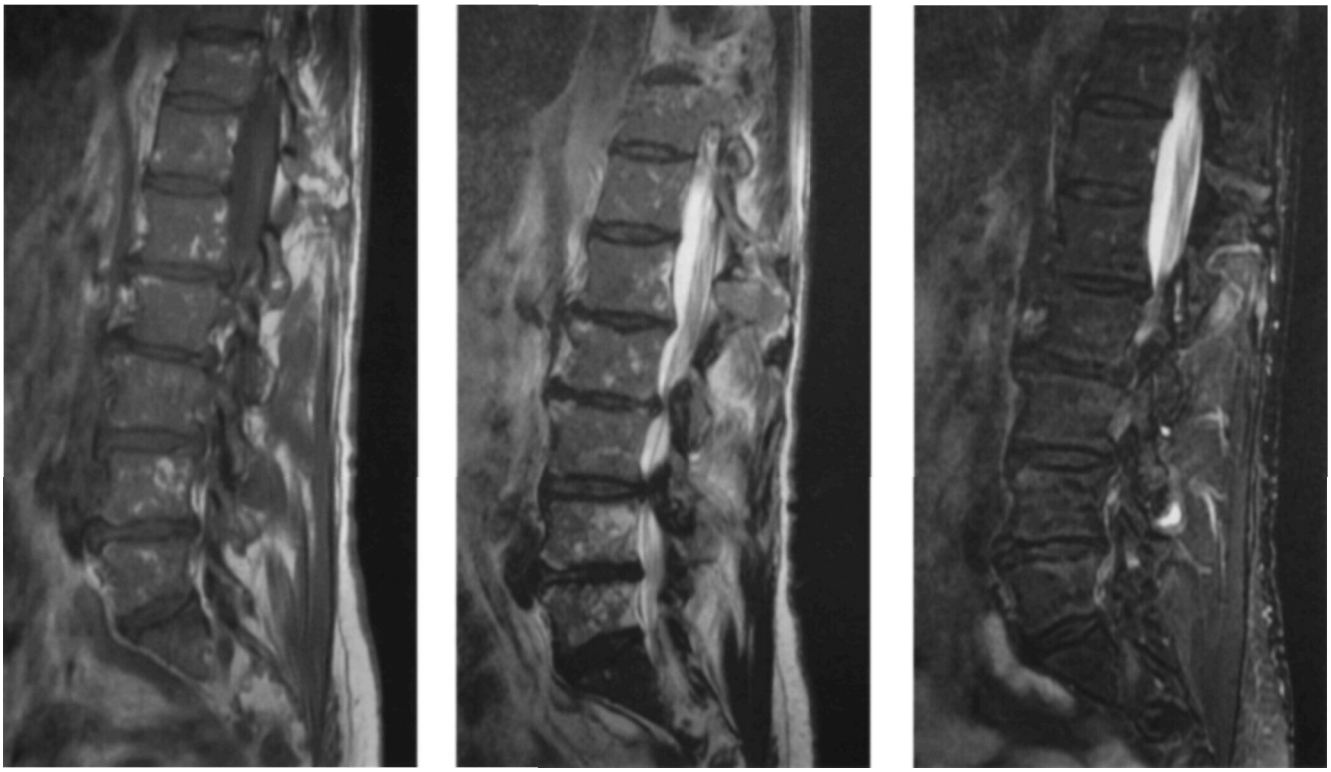

a b, c

Figure 14.**9a-c** A 79-year-old woman with neutropenia treated with granulocyte colony stimulating factor. Marrow has heterogeneous slightly to moderately decreased signal relative to fat on sagittal T1 WI (**a**) and sagittal T2WI (**b**). Marrow signal is minimally increased relative tofatonFST2WI(**c**).

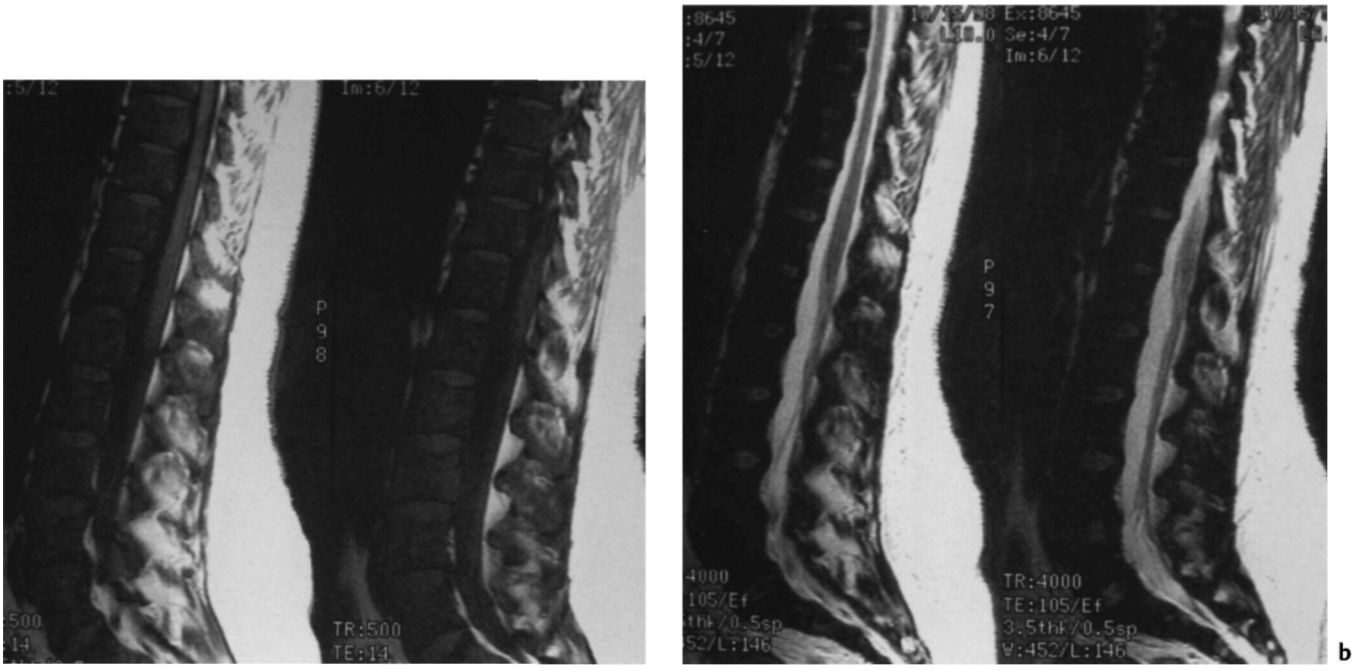

a b

Figure 14.**10 a, b** Iron overload in a patient with sickle cell disease from multiple transfusions. Marrow signal is low on sagittal T1WI (**a**) and T2WI (**b**).

Table 14 (Continued) Diffuse, multiple, poorly defined and/or multifocal zones of abnormal marrow signal

Disorder	MRI Findings	Comments
Paget disease	In the initial phases, thickening of the involved cortex is seen, which has low to intermediate signal on T1 WI and PDWI and often has various combinations of low, intermediate, slightly high, and/or high signal on T2WI and FST2WI. Irregular Gd-contrast enhancement can be seen in the thickened cortex. Marrow signal during the initial phases of Paget disease can be within normal limits, or slightly increased in a V-shape on FST2WI secondary to fibrovascular tissue replacement of normal marrow, and/or dilated blood vessels with slow flow. In the late or inactive phases of the disease, findings include osseous expansion, cortical thickening, decreased diameter of the medullary canal, and coarsened trabeculae along stress lines. Zones of cortical thickening usually have low signal on T1WI and T2WI. Thick linear intramedullary zones of low signal on T1WI and T2WI can be seen secondary to thickened bone trabeculae. Marrow in late or inactive phases of Paget disease can: 1) have signal similar to normal marrow. 2) contain focal areas of fat signal. 3) have low signal on T1WI and T2WI secondary to regions of sclerosis, 4) have areas of high signal on FS T2WI from edema or persistent fibrovascular tissue, or 5) have various combinations of the aforementioned.	Paget disease is a chronic skeletal disease in which there is disordered bone resorption and woven bone formation resulting in osseous deformity. A paramyxovirus may be an etiologic agent for Paget disease. Can be poly-ostotic in up to 66% of patients. Paget disease is associated with a risk of less than 1 % for developing secondary sarcomatous changes. **(See Atlas Chapter A 65)**
Renal osteodystrophy (Fig. 14.11)	Zones of low signal on T1WI and T2WI corresponding to regions of bone sclerosis are seen. In the spine, bands of low signal on T1WI and T2WI can be seen at bands of sclerosis that occur parallel to endplates *(rugger jersey vertebrae).*	Osteoblastic and osteoclastic changes can occur in bone as a result of chronic end-stage renal disease, secondary hyperparathyroidism (hyperplasia of parathyroid glands), and osteomalacia (abnormal vitamin D metabolism). Can result in pathologic fracture. Unlike secondary hyperparathyroidism, diffuse or patchy bone sclerosis infrequently occurs.

a

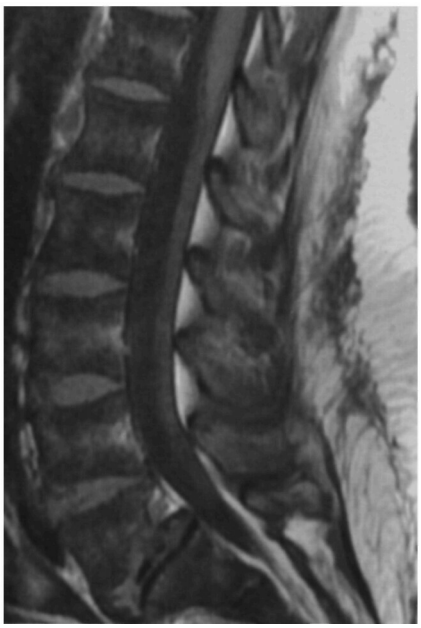

b, c

Figure 14.**11 a-c** A 34-year-old woman with renal osteodystrophy. Lateral radiograph (**a**) shows bands of sclerosis parallel to end plates *(ruggerjersey vertebrae).* Zones of low signal on sagittal T1 WI (**b**) and T2WI (**c**) correspond to regions of bone sclerosis.

Table 14 (Continued) Diffuse, multiple, poorly defined and/or multifocal zones of abnormal marrow signal

Disorder	MRI Findings	Comments
Hypoparathyroidism	Localized or generalized osteosclerosis can be seen in bone on radiographs and CT, with corresponding low signal on T1WI and T2WI.	Deficiency in functional parathyroid hormone formation (surgical excision, radiation, trauma, autoimmune disease) results in hypocalcemia and generalized or localized osteosclerosis.
Pseudohypoparathyroidism	Bone density can be normal or diffusely increased or decreased as seen on radiographs. Other features include premature physeal plate closure resulting in short stature, calvarial thickening, shortening of the 1 st, 4th, and 5th metacarpal bones, soft tissue calcifications, and ossification of the posterior longitudinal ligament.	Heritable disorder with end-organ resistance to parathyroid hormone resulting in hypocalcemia, hyperphosphatemia with deposition of calcium in soft tissues and basal ganglia in the brain. More common in females, X - linked dominant trait.
Pseudo- pseudohypoparathyroidism	Imaging findings similar to pseudohypoparathyroidism.	Similar clinical and imaging features to pseudohypoparathyroidism except patients are normocalcemic.
Osteitis condensans (Fig.14.12)	Zones of subchondral osteosclerosis usually have corresponding zones of low signal on T1WI and T2WI. In addition, small irregular zones of slightly high signal may be seen in the marrow on FST2WI, as well as mild irregular Gd-contrast enhancement.	Unilateral or asymmetric or symmetric bilateral osteosclerotic process in the subchondral marrow adjacent to the sacroiliac joints (iliac bone more pronounced than the sacral marrow) and/or pubic symphysis. usually occurs in women and is often associated with pregnancy. The subchondral bone is usually well defined, and the sacroiliac joint is typically intact. Findings may persist or regress.

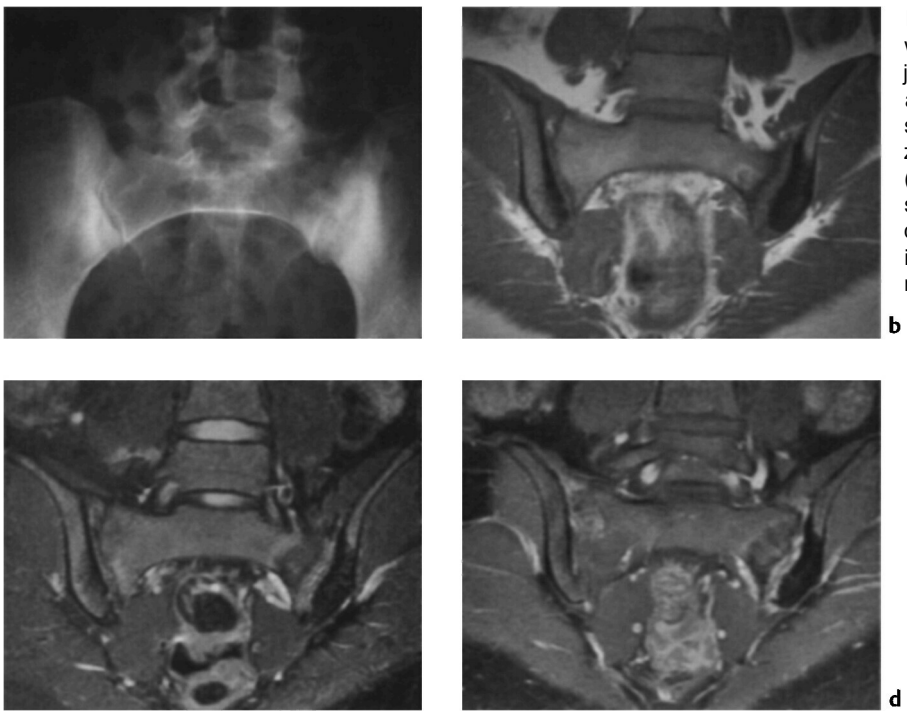

Figure 14.**12a-d** A 35-year-old woman with osteitis condensans ilii at both sacroiliac joints. Zones of subchondral osteosclerosis are seen on the AP radiograph (**a**) at both sacroiliac joints. They have corresponding zones of mostly low signal on coronal T1 WI (**b**) and FS T2WI (**c**). Small irregular zones of slightly high signal are seen in the subchondral marrow on FST2WI (**c**) and show mild irregular Cd-contrast enhancement on coronal FST1WI (**d**).

Table 14 (Continued) Diffuse, multiple, poorly defined and/or multifocal zones of abnormal marrow signal

Disorder	MRI Findings	Comments
Bilateral sacroiliitis (Fig. 14.13)	Asymmetric or symmetric poorly defined zones with high signal on T2WI and FS T2 WI and corresponding Gd-contrast enhancement in the subchondral marrow of the iliac and sacral bones adjacent to the sacroiliac joints.	Commonly occurs in ankylosing spondylitis, which is an autoimmune inflammatory disorder associated with HLA-B27 that frequently involves both sacroiliac joints in most patients, as well as the hips in 35% of patients.
Bilateral sacral insufficiency fractures (Fig. 14.14)	Asymmetric or symmetric poorly defined zones with low signal on T1WI. high signal on T2WI and FST2WI. and corresponding Gd-contrast enhancement are seen in the marrow of both sacral ala within which may be serpiginous curvilinear zones of low signal. No zones with abnormal signal are typically seen in the iliac bones or sacroiliac joints.	Axial forces to sacral bone can result in insufficiency-type stress fractures in osteopenic bone in older patients or from osteomalacia, or fatigue-type stress fractures in athletes (runners, gymnasts, etc.). May be associated with pubic bone fractures. Patients can have point tenderness, pain with weight bearing and movement.
Bone infarction (Fig. 14.15)	In the early phases of ischemia, diffuse poorly defined zones of high signal may be seen on FST2WI that can overlap the MRI features of transient painful bone marrow edema. In zones of bone infarction, curvilinear zones of low signal on T1WI and T2WI representing zones of fibrosis are usually seen in the marrow. In addition to the above findings, irregular zones of low signal on T1 WI and high signal on T2 WI and FS T2WI may be seen in the marrow representing zones of fluid from edema, ischemia/infarction, or fracture if present. Irregular zones with high signal on T1WI and T2WI can occasionally be seen resulting from hemorrhage in combination with zones of fibrosis and fluid. A double-line sign (curvilinear adjacent zones of low and high signal on T2WI) is often seen at the edges of the infarcts representing the borders of osseous resorption and healing. After Gd-contrast administration, irregular enhancement can be seen from granulation tissue ingrowth.	Bone infarcts are zones of ischemic death involving bone trabeculae and marrow, which may be idiopathic or result from: trauma, corticosteroid treatment, chemotherapy, radiation treatment, occlusive vascular disease, collagen vascular and other autoimmune diseases, metabolic storage diseases (Gaucher etc.), sickle cell disease, thalassemia, hyperbaric events / Caisson disease, pregnancy, alcohol abuse, pancreatitis, infections, and lymphoproliferative diseases. Osteonecrosis is more common in fatty compared with hematopoietic marrow. Avascular necrosis involving specific bones may have names such as: Legg-Calve-Perthes disease (femoral head), Kienbock disease (lunate), Preiser disease (scaphoid). Kohler disease (tarsal navicular), Freiberg infarction (metatarsal head), Panner disease (capitulum of humerus), and Thiemann disease (phalanges of hand). **(See Atlas Chapter A 37)**
Reflex sympathetic dystrophy (also referred to as Sudek atrophy. algodystrophy. complex regional pain syndromes type I)	Poorly defined zones with increased signal on FST2WI may be seen in the bone marrow of one or more bones in some cases during the warm phase of RSD, but signal abnormalities are typically absent in the dystrophic cold phases of this disorder. Findings of increased signal on FST2WI may also occur in the adjacent soft tissues in some cases.	Syndromes in which there are clinical findings such as abnormal sensation (continuing pain in the absence of external stimuli, hyperesthesia), and altered vasomotor (skin temperature asymmetry, skin color asymmetry) and autonomic function (edema, sweating changes or sweating asymmetry). In Chronic regional pain syndrome type 1 (RSD), no nerve damage can be detected. RSD can occur in a limb after fracture or other injury, or in immobilized limbs of patients who have had cerebral infarcts. Chronic regional pain syndrome type 2 (causalgia) differs from type 1 (RSD) in that the former is associated with nerve damage detectable with electromyography.

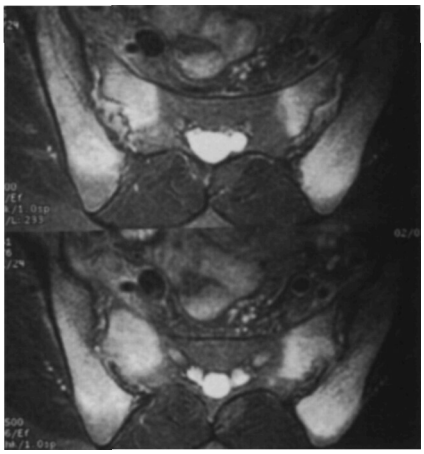

Figure 14.13 A 35-year-old woman with bilateral sacroiliitis seen as symmetric poorly defined zones with high signal on axial FST2WI. Zones with high signal are also seen in the sacroiliac joints.

a

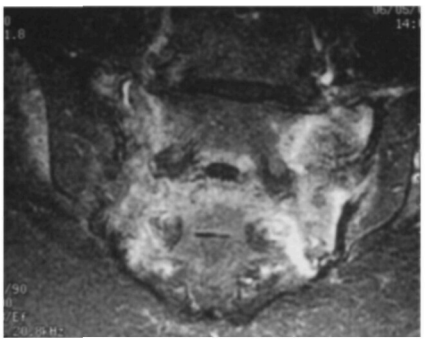

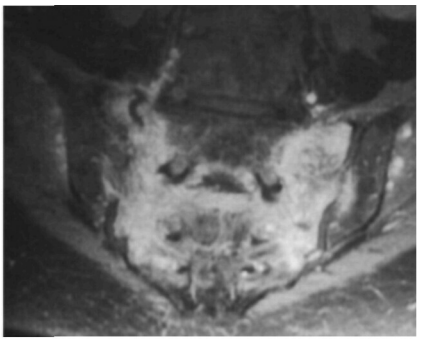

b, c

Figure 14.**14a-c** An 85-year-old woman with bilateral sacral insufficiency fractures that have poorly defined zones of abnormal marrow signal consisting of low signal on coronal T1WI (**a**) and high signal on FST2WI (**b**), with corresponding Gd-contrast enhancement on coronal FST1WI (**c**). Serpiginous thin curvilinear zones of low signal are also seen at the fracture sites on FST2WI.

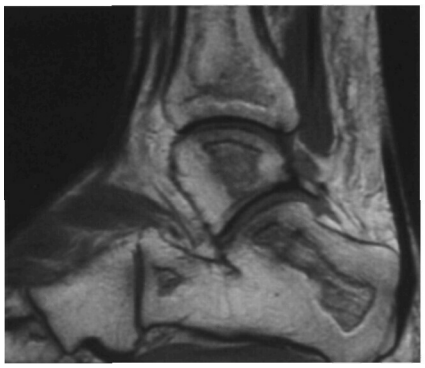

a

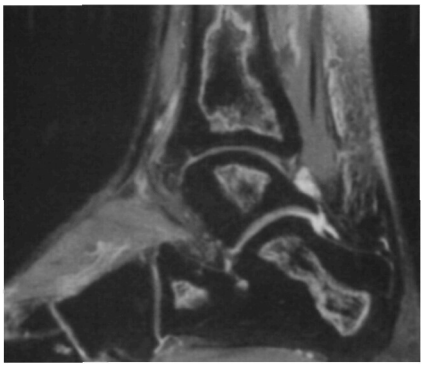

b

Figure 14.**15a, b** A 36-year-old man with bone infarcts in the distal tibia, talus, and calcaneus bones seen as serpiginous zones of low signal on sagittal PDWI (**a**) and high signal on FST2WI (**b**).

Table 14 (Continued) Diffuse, multiple, poorly defined and/or multifocal zones of abnormal marrow signal

Disorder	MRI Findings	Comments
Serous atrophy of marrow from malnutrition (Figs. 14.16.14.17)	Depending on the severity of the malnutrition, involved marrow can have low-intermediate signal on T1WI and high signal on T2WI and FST2WI. No Gd-contrast enhancement is usually seen. The marrow signal abnormalities may be localized or diffuse.	In emaciated patients from various causes (malnutrition, malabsorption, anorexia nervosa/bulimia. chronic renal insufficiency, HIV infection, and cancer), decreases in adipose tissue progressively occurs in bone marrow and subcutaneous tissue followed by orbital fat. With progression of malnutrition, serous atrophy occurs in marrow in which there is accumulation of extracellular matrix containing hyaluronic acid associated with adipose and hematopoietic cell atrophy. The degree and extent of serous atrophy in marrow are related to body mass index and hemoglobin concentration. The lower limbs are frequent sites of serous atrophy, often being more prominent distally than proximally.
Gaudier disease (Fig. 14.18)	Diffuse and/or patchy heterogeneous zones with low-intermediate signal on T1WI and heterogeneous intermediate to high signal on T2WI and FST2WI.	Rare, heritable metabolic disorder with deficient activity of the lysosomal enzyme-hydrolase β-glucosidase. Results in accumulation of the lipid-glucosylceramide within lysosomes of the monocyte-macrophage system (Gaucher cells) of the bone marrow, liver, and spleen. Marrow infiltration by Caucher cells often results in zones of ischemia and bone infarction.
Glycogen storage disease type 1B	Myeloid hyperplasia present in this disorder results in inhomogeneous decreased signal of marrow on T1WI compared with fat, and inho mogeneous hyperintense signal on FST2WI or STIR.	Disorder affecting children and young adults in which there is deficiency of functional microsomal glucose-6-phosphatase activity causing impairment of glycogenolysis and gluconeogenesis. As a result. Patients suffer from postprandial and fasting hypoglycemia, increased production of lactic acid, uric acid, and triglycerides. Patients have increased susceptibility to bacterial infections secondary to chronic neutropenia, abnormal myeloid maturation, and dysfunction of circulating neutrophils and monocytes. Patients are often treated with G-CSF for neutropenia.
Glycogen storage disease type 1A	Marrow in this disorder is typically fatty.	Disorder affecting children and young adults in which there is deficiency of functional microsomal glucose-6-phosphatase activity causing impairment of glycogenolysis and gluconeogenesis. As a result, patients suffer from postprandial and fasting hypoglycemia, increased production of lactic acid, uric acid, and triglycerides. Unlike Glycogen storage disease type 1B, patients do not have increased susceptibility to bacterial infections.
Osteopetrosis (Fig. 14.19)	Radiographs show diffuse and/or band-like zones of osteosclerosis that appear as zones of low signal on T1WI and T2WI.	Osteopetrosis consists of four types (precocious type: autosomal recessive form that is usually lethal: delayed type: autosomal dominant form described by Albers-Schonberg that can be asymptomatic until there is a pathologic fracture or anemia; intermediate recessive type in which patients have short stature, hepatomegaly, and anemia; and tubular acidosis autosomal recessive form in which cerebral calcifications occur as well as renal tubular acidosis, mental retardation, muscle weakness, and hypotonia.

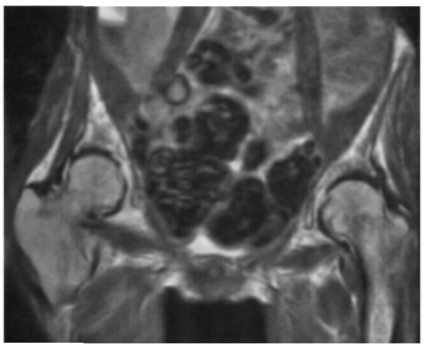

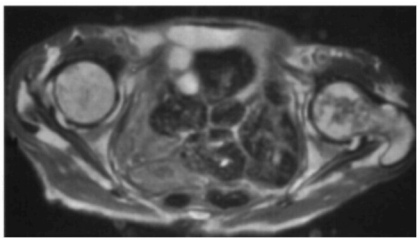

a b, c

Figure 14.**16a-c** A 66-year-old woman with malabsorption syndrome and cachexia with extensive diffuse serous atrophy of marrow seen as loss of normal fat signal in the soft tissues and marrow on coronal (**a**) T1WI. Diffuse abnormal high signal is seen in the marrow on coronal (**b**) and axial (**c**) T2WI.

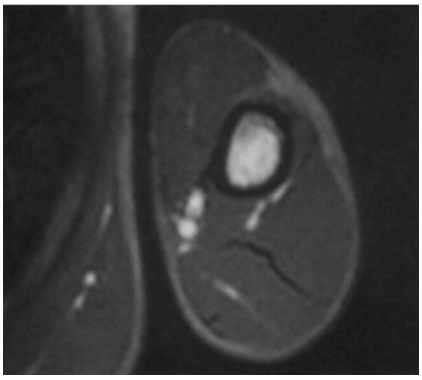

Figure 14.**17** A 16-year-old male with anorexia and serous atrophy involving the marrow of the humerus seen as high signal on axial FS T2WI. Note diminished subcutaneous fat.

Figure 14.**18** A 34-year-old woman with Gaucher disease with diffuse and patchy heterogeneous zones with intermediate to high signal in the marrow on coronal STIR.

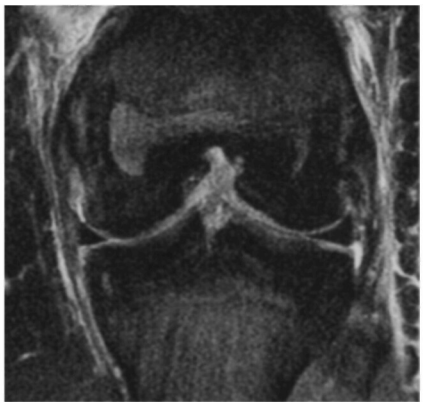

a b, c

Figure 14.**19a-c** A 28-year-old woman with osteopetrosis. The AP (**a**) radiograph shows diffuse osteosclerosis that appears as zones with low signal on coronal (**b**) T1 WI and FS T2WI (**c**).

Table 14 (Continued) Diffuse, multiple, poorly defined and/or multifocal zones of abnormal marrow signal

Disorder	MRI Findings	Comments
Hypervitamosis A and D	Hyperostosis and cortical thickening may be seen involving tubular bones of children on plain films and CT.	Intoxication of vitamins A and D can lead to hyperostosis in children from cortical thickening from increased periosteal bone formation.
Fluorosis	Often seen as dense diffuse osteosclerosis associated with osteophytes involving the spine, thorax, and pelvis. Limited osseous changes are seen in tubular bones of the extremities and the skull. MRI can show corresponding low signal in the spine on T1WI and T2WI.	Disease caused by excessive intake of fluoride via water containing more than 4 ppm. Fluorosis is associated with increased ossification and sclerosis of bone, as well as the posterior longitudinal ligament with resultant myelopathy. Hypertrophy of joints and bones can occur with osteoarthropathy.
Osteomyelitis (Fig. 14.20)	In **acute osteomyelitis,** poorly defined zones of low or low-intermediate signal on T1WI; and high signal on T2WI. STIR, and FS T2WI are seen in the marrow. A wide zone of transition between normal bone and edematous and infected bone is typically seen in acute osteomyelitis. Loss of definition of the low signal line of the cortical margins is often observed on T1WI, T2WI, STIR, and FST2WI. After Gd-contrast administration, irregular zones of contrast enhancement are seen in the involved marrow on FST1WI.	Osteomyelitis is a disorder in which there is infection of bone and commonly the adjacent soft tissues. Can result from hematogenous spread of microorganisms as well as from trauma-direct inoculation, extension from adjacent tissues, and complications from surgery. Bacteria such *as Stophy-*/ococcus o*ureus* and Streptococcus pyogenes are the most common infectious organisms. Can also result from other bacteria as well as *Mycobacterium tuberculosis,* fungi, parasites, and viruses. **(See Atlas Chapter A 63)**
Eosinophilic granuloma (Langerhans cell histiocytosis)	Focal intramedullary lesion(s) associated with trabecular and cortical bone destruction that typically have low-intermediate signal on T1WI and PDWI and heterogeneous slightly high to high signal on T2WI. Poorly defined zones of high signal on T2WI are usually seen in the marrow peripheral to the lesions secondary to inflammatory changes, txtension of lesions from the marrow into adjacent soft tissues through areas of cortical disruption are commonly seen as well as linear periosteal zones of high signal on T2WI. Lesions typically show prominent Gd-contrast enhancement in marrow and in extraosseous soft tissue portions of the lesions.	Benign tumor-like lesions consisting of Langerhans cells (histiocytes), and variable amounts of lymphocytes, polymorphonuclear cells, and eosinophils. Account for 1 % of primary bone lesions, and 8 % of tumor-like lesions. Occur in patients with median age =10years, average =13.5 years, peak incidence is between 5 and 10 years, 80-85% occur in patients less than 30 years. Multifocal subtypes (Letterer-Siwe disease and Hand-Schiiller-Christian disease) account for 30% of cases. **(See Atlas Chapter A 18)**
Sarcoidosis (Fig. 14.21)	In **small bones,** lesions usually appear as intramedullary zones with low to intermediate signal on T1WI and slightly high to high signal on T2WI, FS PDWI, and FS T2WI. After Gd-contrast administration, lesions typically show moderate to prominent enhancement. In **long bones and axial skeleton,** sarcoid lesions are often multiple with variable sizes or solitary within marrow. Zones of cortical destruction associated with intramedullary lesions are uncommon, unlike with sarcoid involving small bones. Lesions can have circumscribed and/or indistinct margins within marrow. Irregular confluent or patchy zones as well as a diffuse stippled pattern of signal alteration in marrow have also been described for skeletal sarcoid lesions. Lesions usually have low to intermediate signal on T1WI and PDWI, and often have slightly high to high signal on T2WI and FST2WI. Occasional lesions *may* also have low or intermediate signal on T2WI. Focal areas with MRI signal similar to fat are seen in some lesions in long bones. Lesions with low signal on T2WI correspond to plain film and CT findings of osteosclerosis. After Gd-contrast administration, variable enhancement can be seen.	Sarcoidosis is a chronic systemic granulomatous disease of unknown etiology in which noncaseating granulomas occur in various tissues and organs. Sarcoidosis appears to be related to an abnormal or exaggerated T helper-induced cellular immune response to antigens or self-antigens resulting in the collection of large numbers of activated T cells in the affected tissue. Bones of the hands and feet are common sites of involvement, but any bone can be affected. **(See Atlas Chapter A71)**

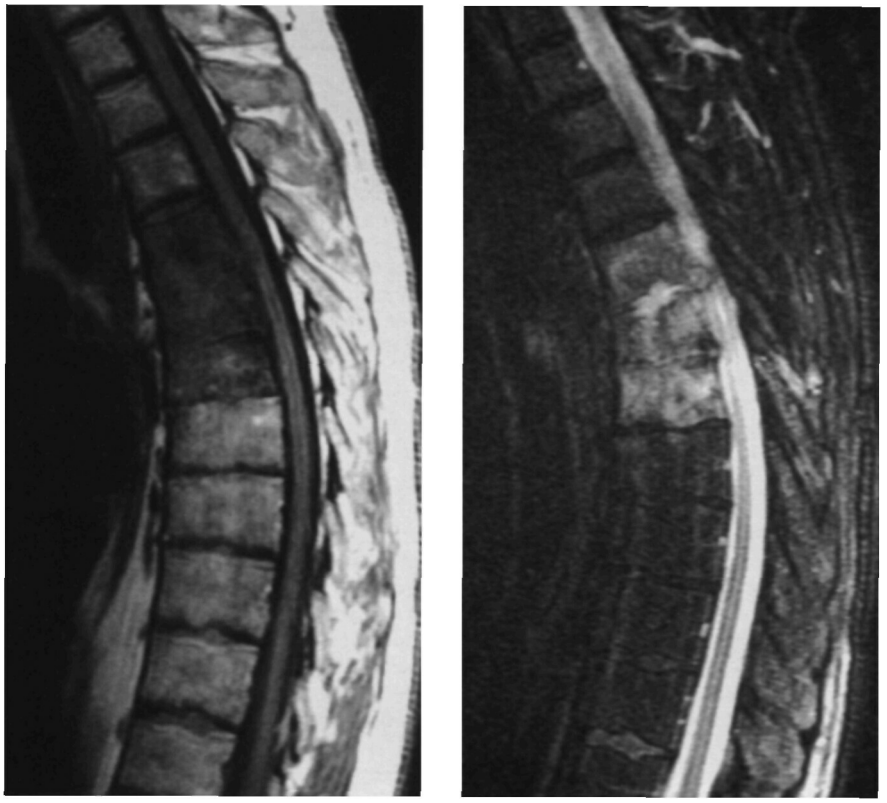

Figure 14.**20 a, b** Coccidioidal osteomyelitis involving three adjacent thoracic vertebrae and intervening disks seen as poorly defined zones of low-intermediate signal on sagittal T1 WI (**a**) and high signal on FS T2WI (**b**) in the marrow and disks. Loss of definition of the low signal line of the vertebral end plates is seen on T1WI and FS T2WI.

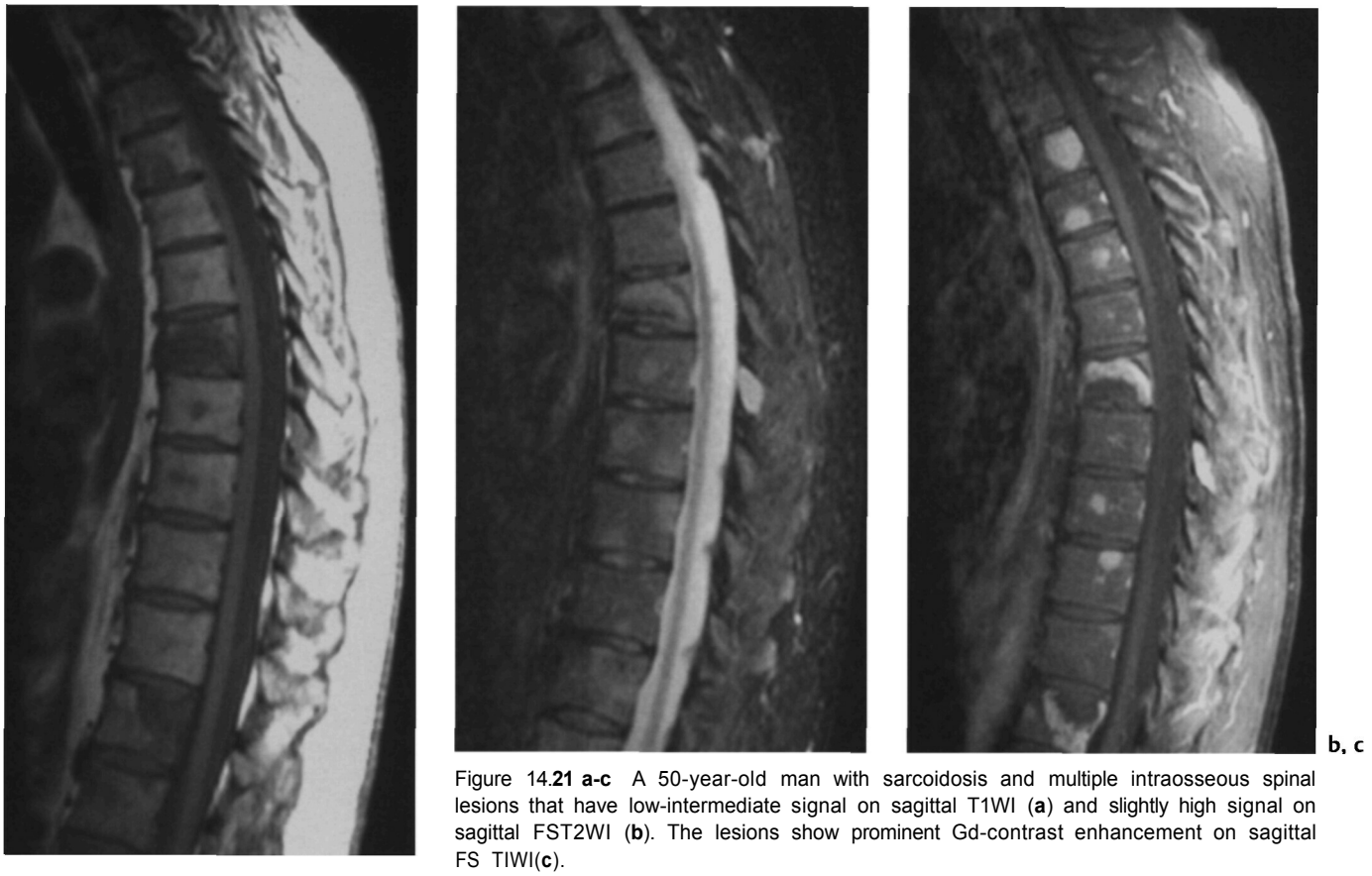

Figure 14.**21 a-c** A 50-year-old man with sarcoidosis and multiple intraosseous spinal lesions that have low-intermediate signal on sagittal T1WI (**a**) and slightly high signal on sagittal FST2WI (**b**). The lesions show prominent Gd-contrast enhancement on sagittal FS TIWI(**c**).

Table 14 (Continued) Diffuse, multiple, poorly defined and/or multifocal zones of abnormal marrow signal

Disorder	MRI Findings	Comments
Erdheim-Chester disease (fig. 14.22)	Lesions can appear as Irregular zones with low and/or intermediate signal on T1WI and PDWI, and mixed low. intermediate, and/or high signal on T2WI and FST2WI within marrow. Zones of cortical destruction with or without extraosseous lesion extension may be seen occasionally with lesions in long bones. After Gd-contrast administration, heterogeneous enhancement may be seen in the involved marrow and zones of extraosseous extension if present.	Erdheim-Chester disease is a rare multisystem non-Langerhans cell histiocytic disorder of unknown etiology that usually affects adults. Collections of foamy macrophages can be seen within various tissues and organs of the musculoskeletal, pulmonary, cardiac, gastrointestinal, and central nervous systems. **(See Atlas Chapter A19)**
Radiation Injury (Fig. 14.23)	Involved marrow has a signal similar to fat. Bone infarcts may be present.	Radiation treatment or exposure typically converts red marrow to yellow due to damage to myeloid and erythroid producing cells.
Multiple enchondromatosis (Oilier disease, metadiondromatosis, and Maffucci syndrome (Figs. 14.24, 14.25)	Lobulated intramedullary lesions with well-defined borders with mean size = 5 cm. Mild endosteal scalloping can be seen. Lesions usually have low-intermediate signal on T1WI and intermediate signal on PDWI. On T2WI and FST2WI, lesions usually have predominantly high signal with foci and/or bands of low signal representing areas of matrix mineralization and fibrous strands. No zones of abnormal high signal on T2WI are typically seen in the marrow outside the borders of the lesions. Lesions typically show Gd-contrast enhancement in various patterns.	**Oilier disease** results from anomalies of endochondral bone formation with multiple enchondromas located predominantly or only in limbs on one side. Short and long tubular bones of the limbs are primarily affected. Median age =12 years. **Metachondromatosis** is a rare disorder that includes the combination of enchondromatosis and osteochondromatosis. **Maffucci syndrome** is a very rare disease that occurs in children and adults with simultaneous occurrence of multiple enchondromas and soft tissue cutaneous or visceral hemangiomas. **(See Atlas Chapter A 8)**

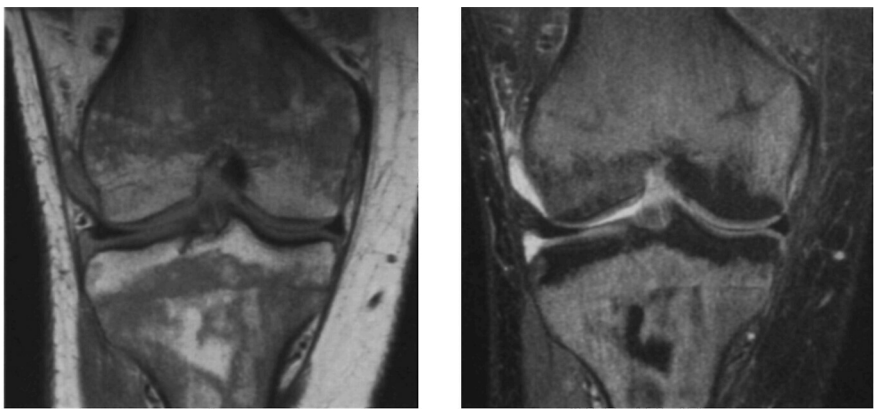

a, b

Figure 14.**22 a, b** A 39-year-old man with Erdheim-Chester disease with bone marrow involvement. Irregular zones with intermediate signal on coronal PDWI (**a**) and slightly high signal on coronal FS T2WI (**b**) are seen within the marrow in the epiphyseal, metaphyseal, and metadiaphyseal regions.

Figure 14.**23** A 21-year-old woman who has been treated with craniospinal radiation for medulloblastoma shows fatty marrow as well as multiple bone infarcts on sagittal T1WI.

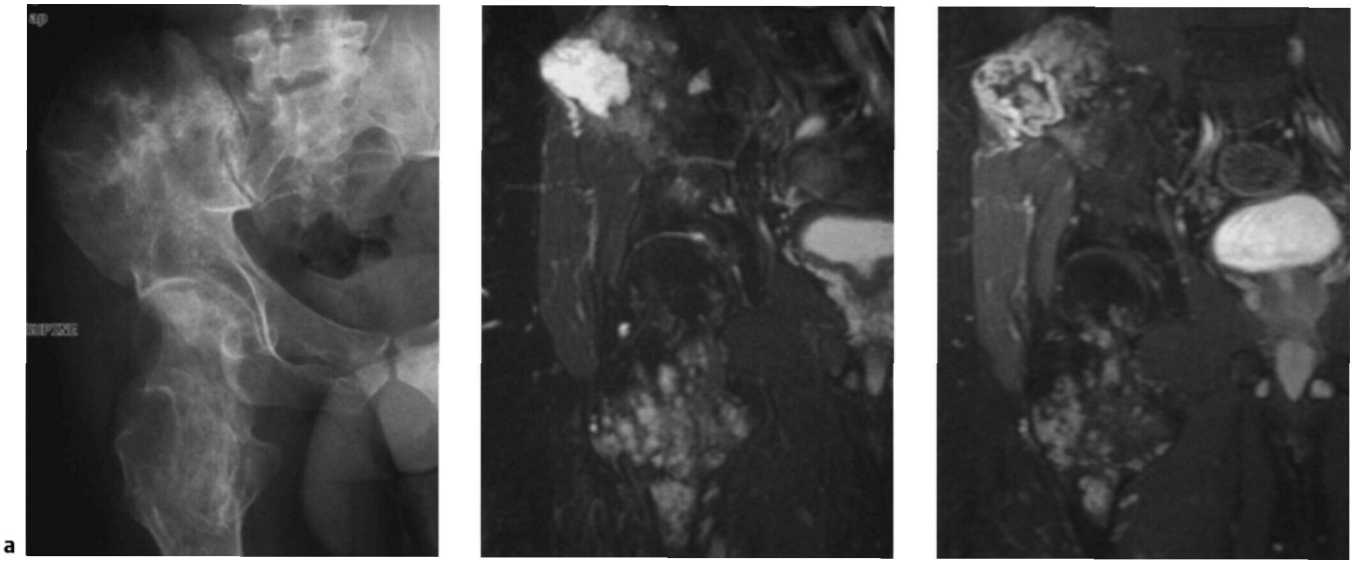

Figure **14.24a-c** A 29-year-old man with Oilier disease. The AP radiograph (**a**) shows multiple enchondromas involving the iliac bone, ischium, pubic bone, and femur. The lesions show high signal on coronal FS T2WI (**b**). The lesions show nodular and lobulated peripheral Gd-contrast enhancement on coronal FS T1 WI (**c**).

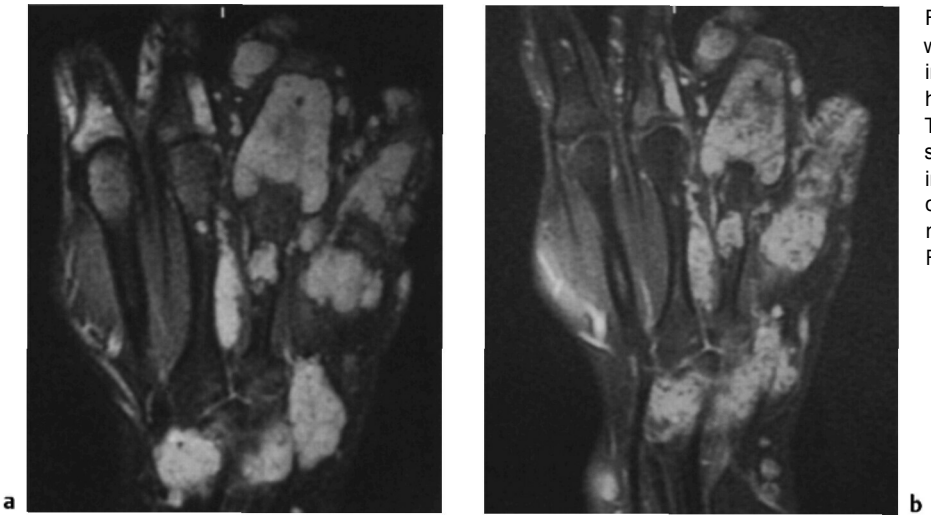

Figure 14.**25 a, b** A 20-year-old woman with Maffucci syndrome who has multiple intraosseous enchondromas and soft tissue hemangiomas involving the wrist and hand. The intra- and extraosseous lesions have high signal on coronal FST2WI (**a**). Some of the intraosseous lesions are associated with cortical expansion. The lesions show prominent Gd-contrast enhancement on coronal FS TIWI(**b**).

Table 14 (Continued) Diffuse, multiple, poorly defined and/or multifocal zones of abnormal marrow signal

Disorder	MRI Findings	Comments
Poly-ostotic fibrous dysplasia (Fig. 14.26)	MRI features depend on the proportions of bony spicules, collagen, fibroblastic spindle cells, hemorrhagic and/or cystic changes, and pathologic fracture if present. Lesions are usually well-circumscribed and have low or low-intermediate signal on T1 WI and PDWI. On T2WI, lesions have variable mixtures of low, intermediate, and/or high signal often surrounded by a low signal rim of variable thickness. Internal septations and cystic changes arc seen in a minority of lesions. Bone expansion is commonly seen. All or portions of the lesions can show Gd-contrast enhancement that varies from mild to marked in degree.	Benign medullary fibro-osseous lesion of bone that can occur as a solitary lesion **(mono-ostotic type)** (80-85%); or as multiple lesions **(poly-ostotic fibrous dysplasia** type). Results from developmental failure in the normal process of remodeling primitive bone to mature lamellar bone with resultant zone or zones of immature trabeculae within dysplastic fibrous tissue. Lesions do not mineralize normally with predisposition to pathologic fracture. **(See Atlas Chapter A 27)**
Osteopoikilosis (Fig. 14.27)	Multiple foci with low signal comparable to cortical bone are seen on all pulse sequences within marrow	**Osteopoikilosis (osteopathia condensans disseminate or spotted bone disease)** is a sclerosing bone dysplasia in which numerous small round or oval radiodense foci are seen in medullary bone giving the appearance of multiple bone islands. **(See Atlas Chapter A 62)**

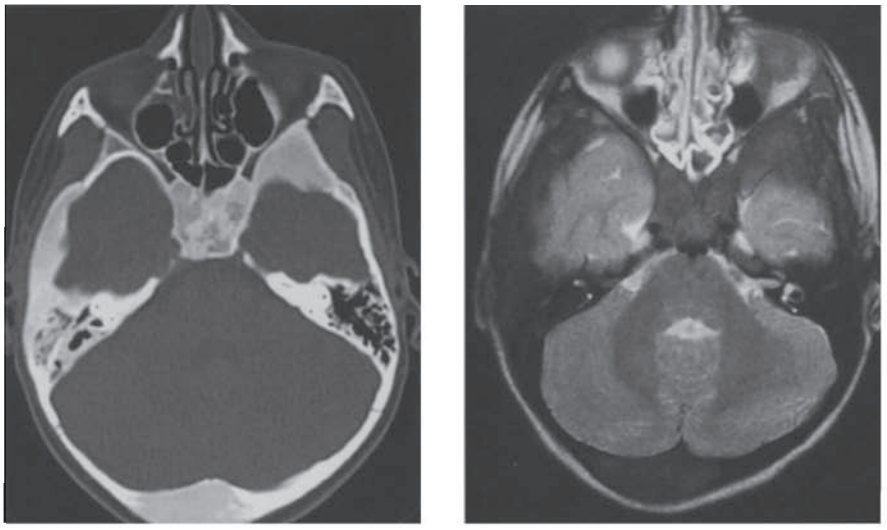

a, b

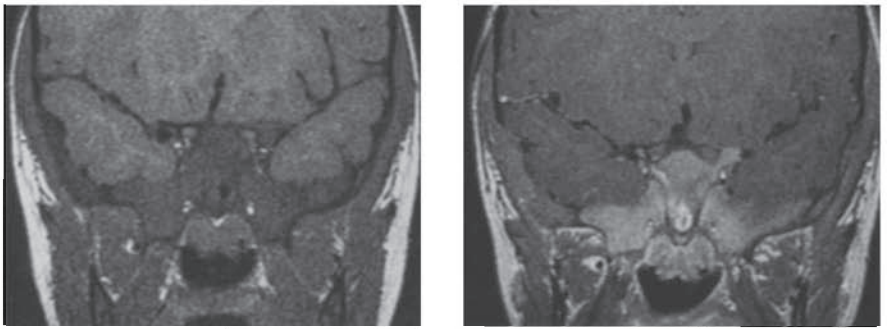

c, d

Figure 14.**26a-d** An 8-year-old girl with McCune-Albright syndrome of polyostotic fibrous dysplasia. Axial CT image (**a**) shows multiple lesions involving the calvaria and sphenoid bone that have an expansile "ground glass" appearance. The lesions have low signal on axial T2WI (**b**) and coronal T1WI (**c**). The lesions shows Gd-contrast enhancement on coronal T1WI (**d**).

Figure 14.**27** A 41-year-old woman with osteopoikilosis seen as multiple foci with low signal in the marrow of the distal femur and proximal tibia, on coronal T1WI.

Table 14 (Continued) Diffuse, multiple, poorly defined and/or multifocal zones of abnormal marrow signal

Disorder	MRI Findings	Comments
Malignant		
Metastatic disease (Figs. 14.28. 14.29)	Metastatic tumor within bone often appears as intramedullary zones with low-intermediate signal on T1WI, low-intermediate to slightly high signal on PDWI, and slightly high to high signal on T2WI and FST2WI. Sclerotic lesions often have low signal on T1WI and mixed low. intermediate, and/or high signal on T2WI. Metastatic spinal lesions may be focal or involve most of a vertebra. In tubular bones, metastatic lesions are usually intramedullary with frequent cortical destruction and tumor extension into the extraosseous soft tissues. Metastatic skeletal lesions usually show varying degrees of Gd-contrast enhancement.	Metastatic lesions represent proliferating neoplastic cells that are located in sites or organs separated or distant from their origins. Metastatic lesions can disseminate hematogenously via arteries or veins, along CSF pathways, along surgical tracts, and along lymphatic structures. Metastatic carcinoma is the most frequent malignant tumor involving bone. In adults, metastatic lesions to bone occur most frequently from carcinomas of the lung, breast, prostate, kidney, thyroid, as well as from sarcomas. Primary malignancies of the lung, breast, and prostate account for 80% of bone mctastascs. **(See Atlas Chapter A 50)**

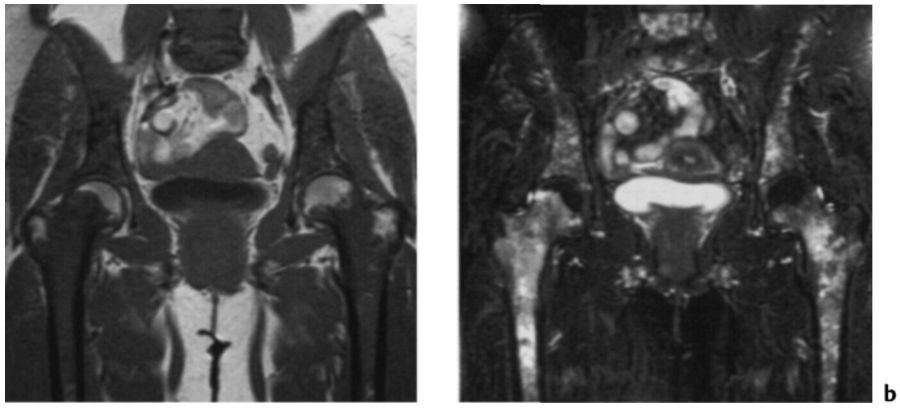

Figure 14.**29** A 63-year-old woman with extensive diffuse metastatic breast carcinoma involving the marrow of the spine seen as poorly defined zones with high signal on sagittal FST2WI (**a**) and Gd-contrast enhancement on FS T1WI (**b**).

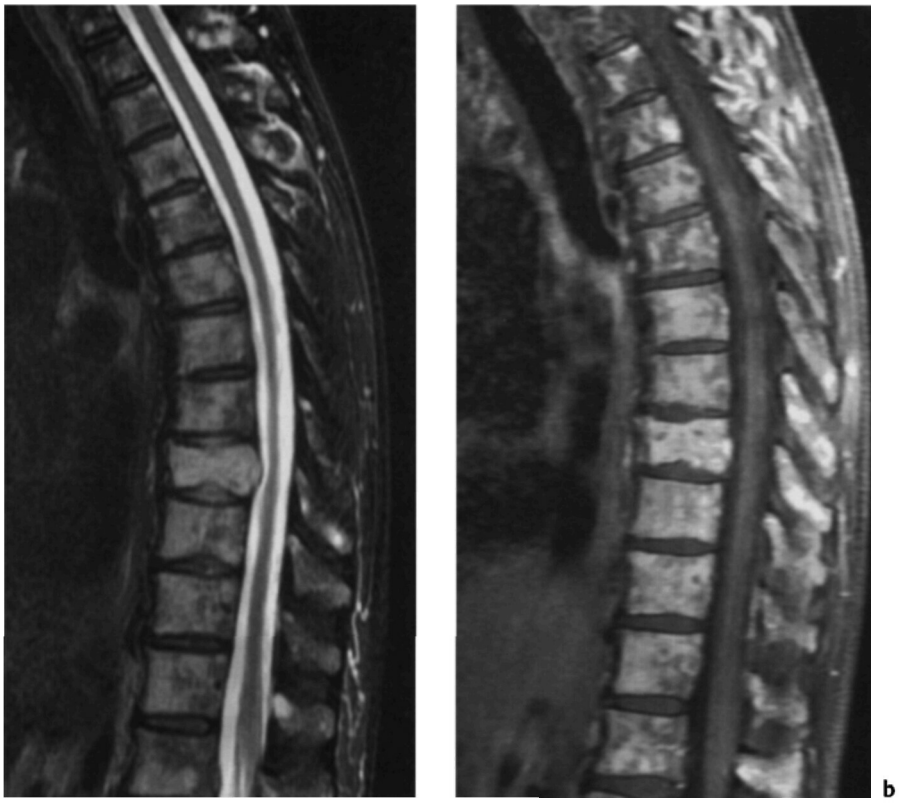

Figure 14.**28a, b** A 53-year-old woman with metastatic breast carcinoma involving the marrow of spine, pelvis, and femur seen as poorly defined zones with low-intermediate signal on coronal T1 WI (**a**) and high signal on coronal STIR (**b**).

Table 14 (Continued) Diffuse, multiple, poorly defined and/or multifocal zones of abnormal marrow signal

Disorder	MRI Findings	Comments
Multiple myeloma (Fig. 14.30)	Multiple myeloma typically appears as multiple intiamedullary zones with low-intermediate signal on T1WI and PDWI. intermediate, slightly high to high signal on T2WI, and slightly high to high signal on FST2WI. FST2WI is important for detecting myeloma because intermediate and high signal heterogeneity on T1WI from red and yellow marrow, respectively, can be seen in normal vertebral marrow in elderly patients. Intramcdullary lesions and corresponding signal abnormalities may be diffuse, focal with poorly defined or distinct margins, and/or in an extensive variegated pattern. Multifocal lesions can be seen in long bones. Zones of cortical destruction may occur associated with extraosseous soft tissue lesions. Lesions usually show Gd-contrast enhancement.	Multiple myelomas are malignant tumors comprising proliferating antibody-secreting plasma cells derived from single clones. Multiple myeloma is primarily located in bone mairow. A solitary myeloma or plasmacytoma is an infrequent variant in which a neoplastic mass of plasma cells occurs at a single site of bone or soft tissues. **(See Atlas Chapter A 52)**
Non-Hodgkin lymphoma (Fig. 14.31)	Non-Hodgkin lymphoma (NHL) within bone typically appears as intramedullary zones with low-intermediate signal on T1 WI and PDWI, slightly high to high signal on T2WI, and high signal on FST2WI. Zones of low signal on T1 WI and T2WI may he secondary to fibrosis. Zones of cortical destruction may occur associated with extraosseous soft tissue lesions. NHL typically shows Gd-contrast enhancement. Destruction of cortical and medullary bone may also occur from invasion from adjacent extraosseous NHI.	Lymphoma represents a group of lymphoid tumors whose neoplastic cells typically arise within lymphoid tissue (lymph nodes and reticuloendothelial organs). Unlike leukemia, lymphoma usually arises as discrete masses. Almost all primary lymphomas of bone are B cell NHL. NHL frequently originates at extranodal sites and spreads in an unpiedictable pattern. **(See Atlas Chapter A 47)**
Hodgkin lymphoma (Fig. 14.32)	Hodgkin disease (HD) within bone typically appears as intramedullary zones with low-intermediate signal on T1WI, and intermediate, slightly high, and/or high signal on T2WI and high signal on FST2WI. Intramedullary lesions may have poorly defined or distinct margins. Multifocal lesions can be seen in long bones and vertebrae. Zones of cortical destruction may occur associated with extraosseous soft tissue lesions. Most lesions show Gd-contrast enhancement. HD involving bone with associated sclerosis seen on plain films or CI usually has low signal on TIWI and variable/mixed signal on T2WI. Destruction of cortical and medullary bone may also occur from invasion from adjacent extraosseous lymphadenopathy from HD.	Lymphoma represents a group of lymphoid tumors whose neoplastic cells typically arise within lymphoid tissue (lymph nodes and reticuloendothelial organs). Unlike leukemia, lymphoma usually arises as discrete masses. HD typically arises in lymph nodes and often spreads along nodal chains. **(See Atlas Chapter A 47)**

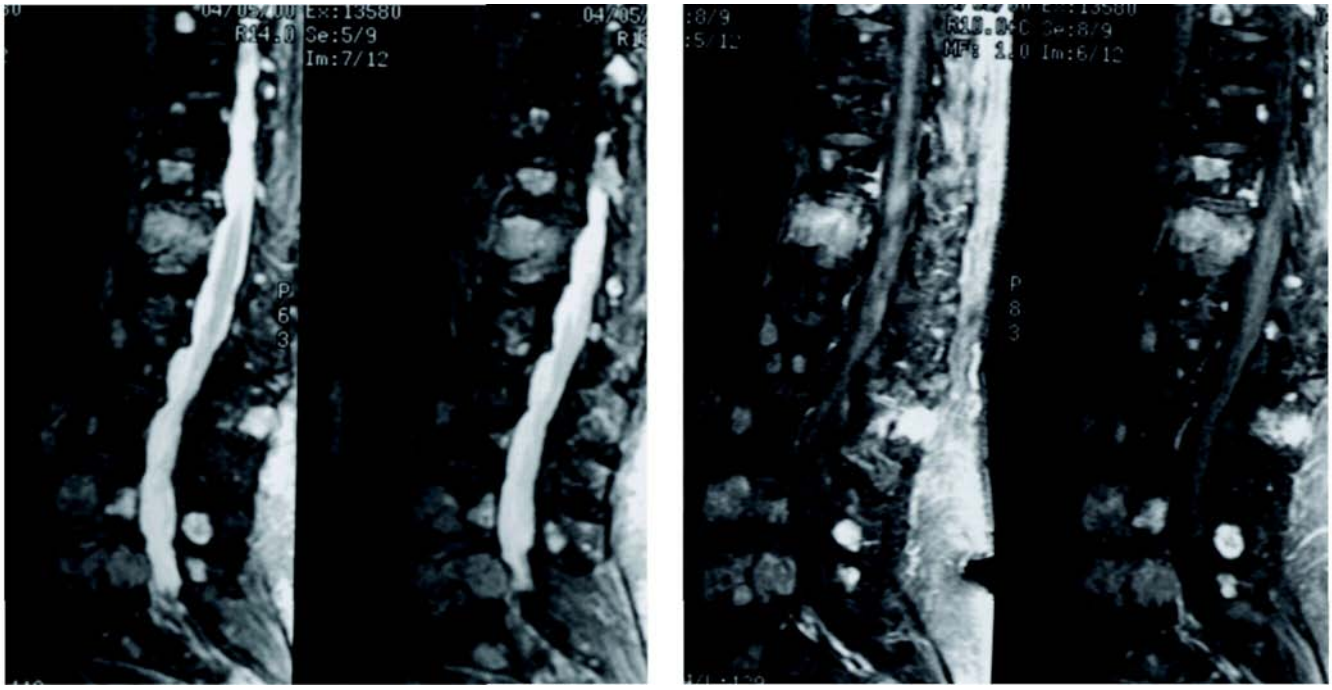

a b

Figure 14.**30 a, b** Multiple myeloma seen as numerous lesions in the vertebral marrow with high signal on sagittal FS T2WI (a) and Gd-contrast enhancement on FST1WI (**b**).

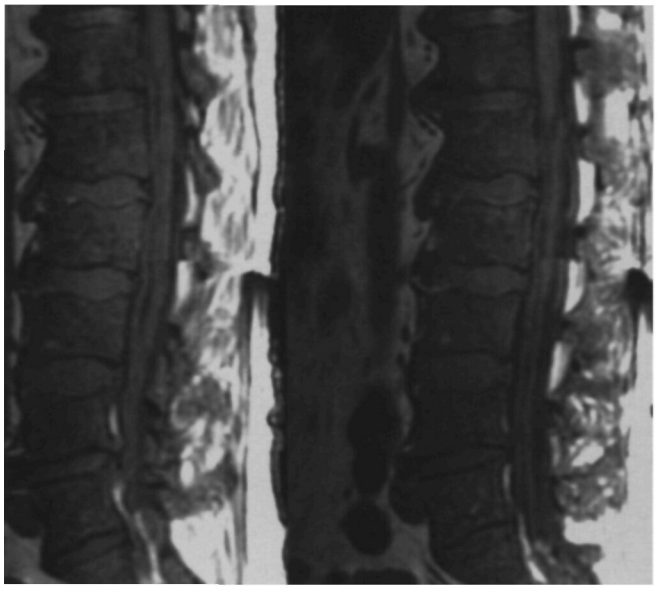

a

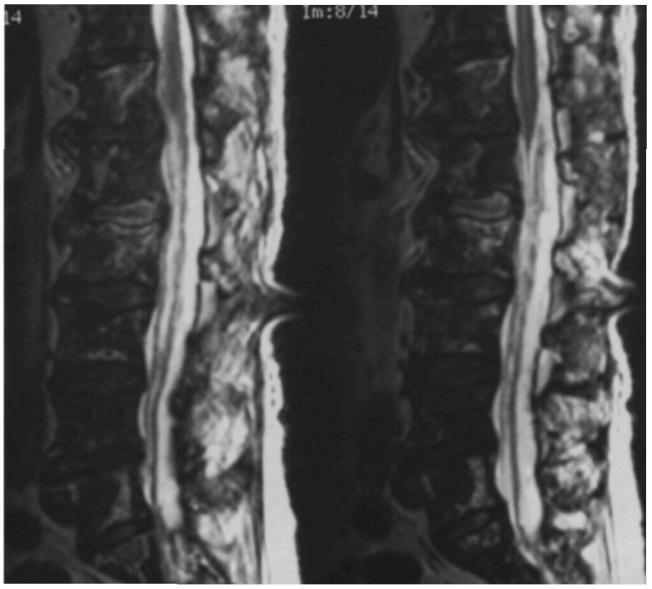

b

Figure 14.**31 a-c** NHL involving vertebral marrow as well as within the lumbar subarachnoid space. Diffuse low-intermediate signal on sagittal T1WI (**a**) is seen throughout the marrow. Heterogeneous mostly low signal is seen in the marrow on sagittal T2WI (**b**). Heterogeneous Gd-contrast enhancement is seen throughout the marrow as well as within the thecal sac on sagittal FS T1WI **(c)**.

c

a, b

c, d

Figure **14.32a-d** A 46-year-old man with Hodgkin lymphoma with osteosclerotic lesions involving many thoracic and lumbar vertebrae on sagittal reconstructed CT (**a**). Multiple poorly defined lesions in the marrow have low-intermediate signal on sagittal T1WI (**b**), slightly high signal on sagittal FST2WI (**c**), and mild-moderate Gd-contrast enhancement on sagittal FS T1WI (**d**).

Table 14 (Continued) Diffuse, multiple, poorly defined and/or multifocal zones of abnormal marrow signal

Disorder	MRI Findings	Comments
Leukemia (Figs. 14.33-14.36)	Acute lymphoblastic leukemia (ALL), chronic lymphocytic leukemia (CLL), acute myelogenous leukemia (AML), and chronic myelogenous leukemia (CML) infiltration in marrow can appear as diffuse or poorly defined zones of low-intermediate signal on I1WI and PDWI, intermediate-slightly high to high signal on FST2WI. Focal or geographic regions with similar signal alteration can also be seen. After Gd-contrast administration, ALL, CLL, AML, and CML may show Gd-contrast enhancement on T1WI and FST1WI. Note should be made that Gd-contrast enhancement may be seen in normal vertebral marrow in children less than 7 years.	Lymphoid neoplasms that have widespread involvement of the bone marrow as well as tumor cells in peripheral blood. ALL is the most frequent type in children and adolescents. In adults, CLL is the most common type. Myelogenous leukemias represent neoplasms derived from abnormal myeloid progenitor cells that, if normal, would form erythrocytes, monocytes, granulocytes, and platelets. AML usually occurs in adolescents and young adults, and accounts for - 20 % of childhood leukemia. CML occurs in adults older than 25 years. **(See Atlas Chapter A 41)**
Myelodysplastic syndromes (Fig. 14.37)	Marrow signal on FS T2WI and STIR can be isointense or hyperintense to muscle depending on the degree of cellular hyperplasia in the marrow and stage of the disease. Can progress to myelofibrosis and myelosclerosis.	Myelodysplastic syndromes (MDS) are clonal hematopoietic stem cell diseases associated with dysplasias of myeloid cell lines resulting in decreased functional hematopoicsis. Myeloblasts can occur up to 20% in MDS. Progressive marrow failure occurs in MDS as well as eventual progression to acute myeloid leukemia. Usually occurs in older adults over the age of 60 years, incidence up to 30 per million. MDS includes chronic myelomonocytic leukemia, atypical chronic myeloid leukemia, juvenile myelomonocytic leukemia, and myelodysplastic/myeloproliferative disease.

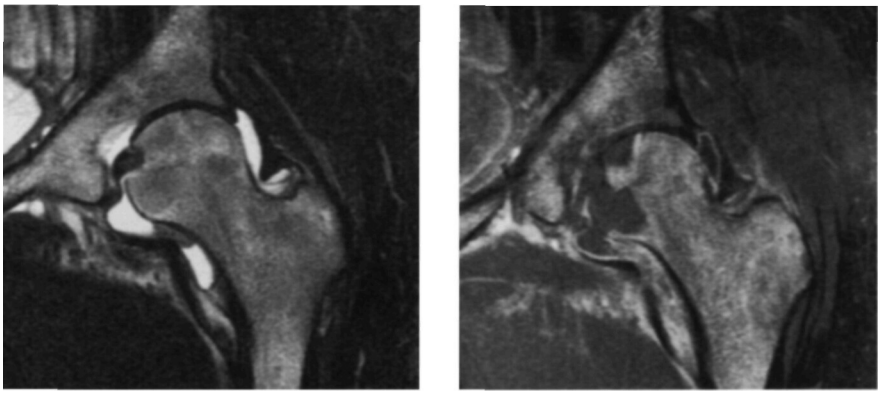

Figure **14.33 a, b** A 16-year-old male with ALL involving the femur and bony pelvis. Leukemic infiltration in the marrow of the pelvis and femur has heterogeneous slightly high signal on coronal FST2WI (**a**) and Gd-contrast enhancement on coronal FST1WI (**b**). Zones with no Gd-contrast enhancement in the femoral head represent sites of bone marrow ischemia/infarction.

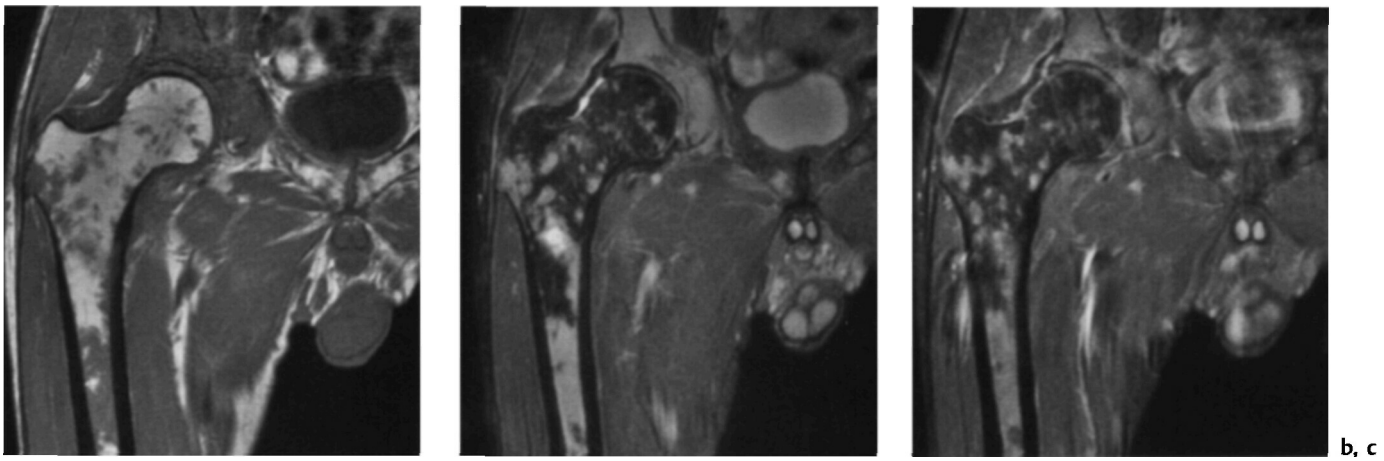

Figure **14.34a-c** CLL involving the marrow of a 61-year-old man. Leukemic deposits are seen as irregular zones with low-intermediate signal on coronal T1 WI (**a**) and slightly high or high signal on coronal FST2WI (**b**). Lesions show Gd-contrast enhancement on coronal FST1WI (**c**).

Figure **14.35a, b** A 28-year-old man with AMI involving the marrow of the spine. The leukemic deposits have heterogeneous intermediate and slightly high signal on sagittal FST2WI (**a**), and mild heterogeneous Gd-contrast enhancement on sagittal FST1WI (**b**).

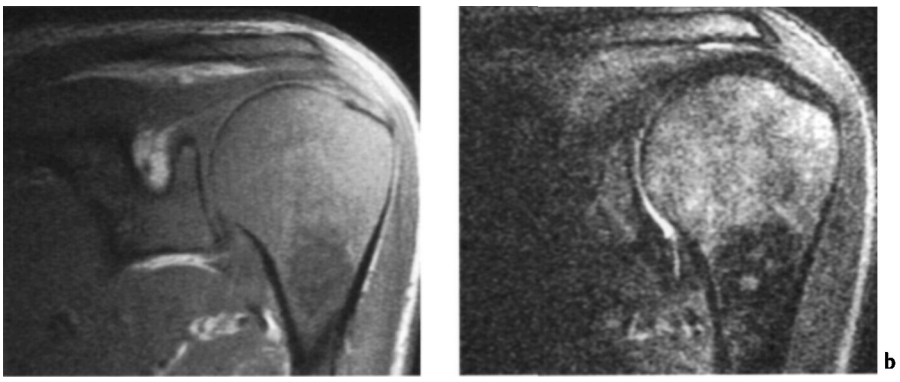

Figure **14.36a, b** A 39-year-old man with CML involving the marrow of the humerus and scapula. The leukemic deposits have heterogeneous low-intermediate signal on coronal PDWI (**a**) and heterogeneous high signal on coronal FST2WI (**b**).

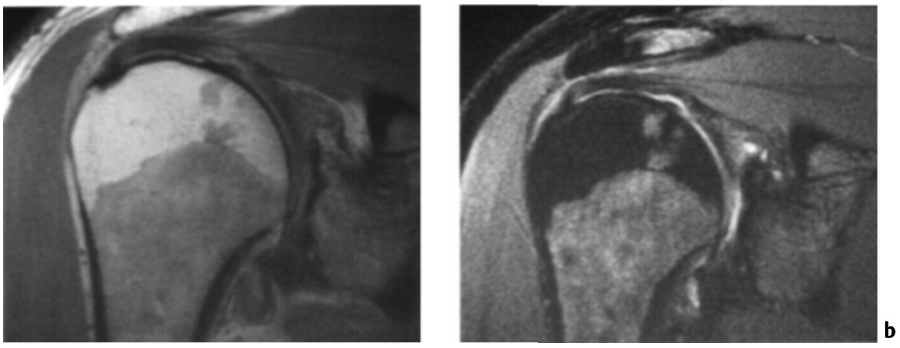

Figure **14.37 a, b** A 45-year-old man with chronic myelodysplastic syndrome with metaphyseal marrow signal that is hypointense to fat on coronal PDWI (**a**) and hyperintense relative to fat on coronal FS T2WI (**b**).

Table 14 (Continued) Diffuse, multiple, poorly defined and/or multifocal zones of abnormal marrow signal

Disorder	MRI Findings	Comments
Chronic myeloproliferative disease (Fig. 14.38)	Involved bone marrow often has low or low- intermediate signal on T1WI and slightly high signal on T2WI and FST2WI. CPMDs typically have an insidious onset, but can progress to myelofibrosis, myelosclerosis, and acute leukemia.	Chronic myeloproliferative diseases (CMPDs) represent bone marrow disorders in which there is proliferation of one or more hematopoietic stem cells (granulocytic, erythrocytic. and/or megakaryocytic). Unlike myelodysplastic syndromes, there is relatively normal maturation of the blood cells and platelets along with increased numbers of the cells from the derivatives of the abnormal clonal proliferations in CMPD. Incidence of CMPD is 90 per million, usually involves adults older than 40 years. Percent of marrow blasts is less than 10%. CPMD includes polycythemia vera (PCV), chronic idiopathic myelofibrosis. essential thrombocytopenia, chronic eosinophilic leukemia, chronic neutrophilic leukemia, and chronic early phases of myelogenous leukemia (Philadelphia chromosome t(9;22) (q34;q11). BCR/ABL positive). PCV occurs in up to 13 per million per year, and results from proliferation of a clonal hematopoietic stem cell lacking the normal regulatory mechanism for erythropoiesis. Other myeloid clonal proliferations can occur concurrently. PCV occurs in two phases. The initial phase is followed by a postpolycythemic phase that is associated with anemia and cytopenia, myelofibrosis, and potential development of acute leukemia.
Waldenstrom macroglobulinemia (lymphoplasmacytic lymphoma) (Fig. 14.39)	Marrow may have no associated abnormal signal or have irregular and/or diffuse findings similar to red marrow reconversion. Signal changes in the marrow may become more prominent as well as Gd-contrast enhancement with increasing lymphoplasmacytoid infiltration of bone marrow.	Waldenstrom macroglobulinemia, also referred to as Lymphoplasmacytic lymphoma, is a rare neoplasm of plasmacytoid lymphocytes, plasma cells and small B lymphocytes that usually involves bone marrow, spleen, and lymph nodes. Typically associated with a serum monoclonal IgM protein in concentrations >3g/dl, often with hyperviscosity and cryoglobulinemia. Occurs in older adults, mean age = 63 years. Median survival is - 5 years.
Mastocytosis	Radiographs and CT can show indistinctly marginated sclerotic lesions, radiolucent zones, or mixed sclerotic and radiolucent lesions in medullary bone. Sclerotic lesions usually have low signal on T1 WI and T2WI, whereas radiolucent lesions may have intermediate, slightly high to high signal on T2WI and FST2WI. Marrow signal abnormalities also include varying degrees of nonfatty homogeneous or heterogeneous zones of low signal on T1WI and intermediate, slightly high, and/or high signal on FS T2WI or STIR. In some cases, marrow signal may be normal or have intermediate signal on T1 WI and FS T2WI or STIR.	Heterogeneous uncommon disorders with pathologic accumulation of mast cells in various tissues (age ranges from 1 st to 7th decades, mean in 4th decade) and can be classified into four clinical categories. Category 1 is the most common and includes 1A which involves the skin (cutaneous mastocytosis or urticaria pigmentosa), and 1B or systemic mastocytosis with mast cells occurring in various tissues (bone marrow, spleen, gastrointestinal tract, and lymph nodes). Category 1 usually has a favorable prognosis. Category II includes mastocytosis associated with a myeloproliferative or myelodysplastic disorder. Prognosis depends on the associated degree of myelodysplasia. Category III (lymphadenopathic mastocytosis with eosinophilia or aggressive mastocytosis) is associated with a poor prognosis related to large mast cell burdens. Category IV results from mast cell leukemia and has a very poor prognosis.

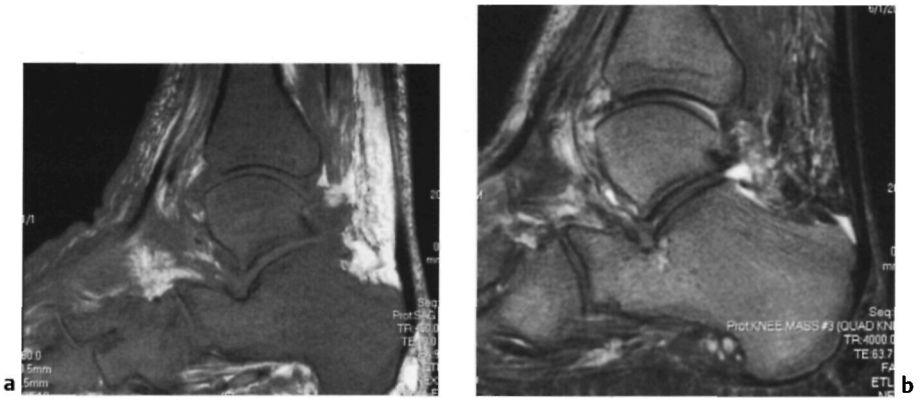

Figure **14.38 a, b** A 49-year-old man with polycythemia rubra with diffuse low-intermediate signal in the marrow on sagittal T1WI (**a**) and slightly high signal on sagittal T2WI (**b**) that is slightly hyperintense relative to muscle.

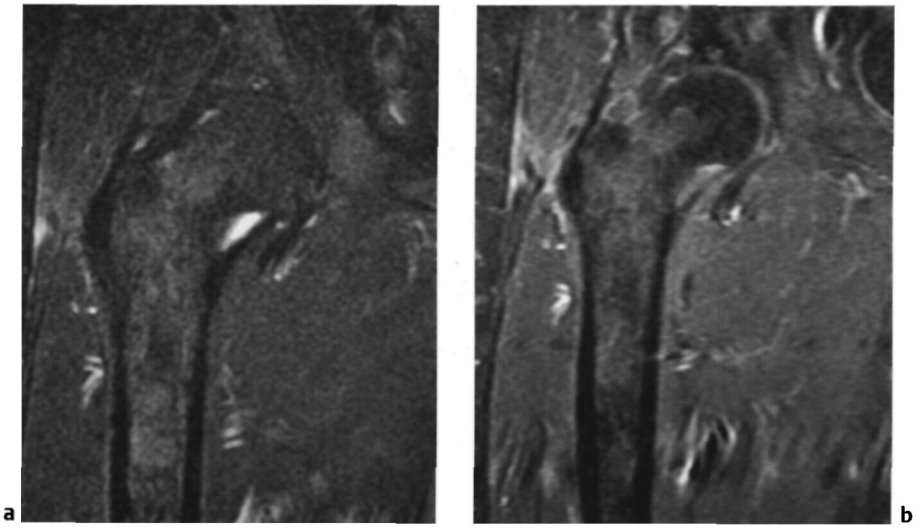

Figure **14.39** A 61-year-old man with Waldenstrom macroglobulinemia with irregular zones of intermediate signal in the metadiaphyseal marrow on coronal FST2WI (**a**) and post-Cd-contrast FST1WI (**b**).

References

Red Marrow Reconversion

Barnewolt CE, Shapiro F, Jaramillo D. Normal gadolinium-enhanced MR images of the developing appendicular skeleton: Part 1. Cartilaginous epiphysis and physis. *AJR* July 1997;169:183-189.

Dwek JR, Shapiro F, Laor T, Barnewolt CE, Jaramillo D. Normal gadolinium-enhanced MR images of the developing appendicular skeleton: Part 2. Epiphyseal and metaphyseal marrow. *AJR* July 1997; 169:191-196.

Moore SG, Dawson KL. Red and yellow marrow in the femur: age-related changes in appearance at MR imaging. *Radiology* 1990;175: 219-223.

Waitches G, Zawin JK, Poznanski AK. Sequence and rate of bone marrow conversion in the femora of children as seen on MR imaging: are accepted standards accurate? *AJR* June 1994;162(6):1399-1406.

Inherited Anemias

Aydmgoz 0, Oto A, Cila A. Spinal cord compression due to epidural extramedullary hematopoiesis in thalassaemia: MRI. *Neuroradiology* 1997;39:870-872.

Lorand-Metze I, Santiago GF, Lima CSP, Zanardi VA, Torriani M. Magnetic resonance imaging of femoral marrow cellularity in hypocellular haemopoietic disorders. Clin Radiol 2001:56:107-110.

Niggemann P, Krings T, Hans F, Thron A. Fifteen-year follow-up of a patient with |3 thalassaemia and extramedullary hematopoietic tissue compressing the spinal cord. *Neuroradiology* 2005;47:263-266.

Salehi SA, Koski T, Ondra SL Spinal cord compression in β-thalassemia: case report and review of the literature. *Spinal Cord* 2004;42: 117-123.

States LJ. Imaging of metabolic bone disease and marrow disorders in children. Radio/ *Clin N Am* July 2001;39(4):749-772.

Tan TC, Tsao J, Cheung FC. Extramedullary haemopoiesis in thalassemia intermedia presenting as paraplegia. *J Clin Neurosci* 2002:9(6): 721-725.

Tyler PA, Madani G, Chaudhuri R, Wilson LF, Dick EA. The radiological appearances of thalassaemia. *Clin Radiol* 2006;61:40-52.

Marrow Hyperplasia from Exogenous Erythropoietin

Biljanovic-Paunovic L, Djukanovic, Lezaic V, Stojanovic N, Marisavljevic D, Pavlovic-Kentera V. In vivo effects of recombinant human erythropoietin on bone marrow hematopoiesis in patients with chronic renal failure. *EurJ Med Res* 1998:16:564-570.

Horina JH, Schmid CR, Roob , et al. Bone marrow changes following treatment of renal anemia with erythropoietin. *Kidney Int* 1991; 40:917-922.

Jensen KE, Stenver D, Jensen M, et al. Magnetic resonance imaging of bone marrow following treatment with recombinant human erythropoietin in patients with end-stage renal disease. *Int j Artif Organs* 1990:13:477-481.

Cranulocyte/Macrophage Colony Stimulating Factor

Altehoefer C, Bertz H, Ghanem NA, Langer M. Extent and time course of morphologic changes of bone marrow induced by granulocyte-colony stimulating factor as assessed by magnetic resonance imaging of healthy blood cell donors. J Mag *Reson Imaging* 2001; 14:141 -146.

Chabanova E, Johnsen HE, Knudsen LM, et al. Magnetic resonance investigation of bone marrow following priming and stem cell mo bilization. *J Magn Reson Imaging* 2006;24:1364-1370.

Ciray I, Lindman H, Astrom GKO, Wanders A, Bergh J, Ahlstrom HK. Effect of granulocyte colony-stimulating factor (G-CSF)-supported

chemotherapy on MR imaging of normal red bone marrow in breast cancer patients with focal bone metastases. *Acta Radiologica* 2003:44:472-484.

Hartman RP, Sundaram M, Okuno SH, Sim FH. Effect of granulocyte-stimulating factors on marrow of adult patients with musculoskeletal malignancies: incidence and MRI findings. *AJR* 2004:183: 645-653.

Hemochromatosis/Iron Overload

Emy PY, Levin TL, Sheth SS, Ruzal-Shapiro C, Garvin J, Berdon WE. Iron overload in reticuloendothelial systems of pediatric oncology patients who have undergone transfusions: MR observations. *AJR* April 1997;168(4):1011-1015.

Kornreich L, Horev G, Yaniv I, Stein J, Grunebaum M, Zaizov R. Iron overload following bone marrow transplantation in children: MR findings. *Pediatr Radiol* 1997;27:869-872.

Levin TL, Sheth SS, Hurlet A, et al. MR marrow signs of iron overload in transfusion-dependent patients with sickle cell disease. *Pediatr Radiol* 1995;25(8):614-619.

Renal Osteodystrophy

Al-Gahtany M, Cusimano M, Singer W, Bilbao J, Kovacs K, Marotta T. Brown tumors of the skull base. Case report and review of the literature.J *Neurosurg* February 2003:98:417-420.

Davies AM, Evans N, Mangham DC, Grimer RJ. MR imaging of brown tumor with fluid-fluid levels: a report of three cases. *Eur Radiol* 2001;11(8):1445-1449.

Mustonen AOT, Kiuru MJ, Stahls A, Bohling T, Kivioja A, Koskinen SK. Radicular lower extremity pain as the first symptom of primary hyperparathyroidism. *Skeletal Radiol* 2004:33:467-472.

Hypoparathyroidism, Pseudo-, Pseudo- Pseudo-Hypo parathyroidism

Koch CA. Rapid increase in bone mineral density in a child with osteoporosis and autoimmune hypoparathyroidism treated with PTH 1-34. *Exp din* Endocrino/ *Diabetes* 2001;109(6):350-354.

Rastogi R, Beauchamp NJ, Ladenson PW. Calcification of the basal ganglia in chronic hypoparathyroidism. *J Clin Endrocrin Metab* April 2003:88(4): 1476-1477.

Resnick D. Parathyroid disorders and renal Osteodystrophy. In: Resnick D, ed. *Diagnosis of Bone and Joint Disorders,* 4th ed. Philadelphia, Pa: W.B. Saunders; 2002:3:2043-2111.

van Oostenbrugge RJ, Herpers MJ, de Kruijk JR. Spinal cord compression caused by unusual location and extension of ossified ligamenta flava in a Caucasian male: a case report and literature review. Spine March 1,1999;24(5):486-488.

Xiong L, Zeng QY, Jinkins JR. CT and MRI characteristics of ossification of the ligamenta flava in the thoracic spine. *Eur Radiol* 2001:11(9): 1798-1802.

Yamamoto Y, Noto Y, Saito M, Ichizen H, Kida H. Spinal cord compression by heterotopic ossification associated with pseudohypoparathyroidism. J *Int Med Res* Nov-Dec 1997;25(6):364-368.

Osteitis Condensans

Clarke DP, Higgins JN, Valentine AR, Black C. Magnetic resonance imaging of osteitis condensans ilii. Brit *J Rheumatol* June 1994; 33(6): 599-600.

Major NM, Helms CA. Pelvic stress injuries: the relationship between osteitis pubis (symphysis pubis stress injury) and sacroiliac abnormalities in athletes. *Skeletal Radiol* 1997:26:711-717.

Olivieri I, Ferri S, Barozzi L. Osteitis condensans ilii. *Brit J Rheumatol* March 1996;35(3):295-297.

Bilateral Sacroiliitis

Bredella MA, Steinbach LS, Morgan S, Ward M, Davis JC. MRI of the sacroiliac joints in patients with moderate to severe ankylosing spondylitis. *AJR* December 2006:187:1420-1426.

Bennett DL, Ohashi K, El-Khoury GY. Spondyloarthropathies: ankylosing spondylitis and psoriatic arthritis. *Radiol Clin North Am* January 2004;42(1):121-134.

Heuft-Dorenbosch L, Landewe R, Weijers R, et al. Combining information obtained from magnetic resonance imaging and conventional radiographs to detect sacroiliitis in patients with recent onset inflammatory back pain. *Ann Rheum Dis* 2006:65:804-808.

Levine DS, Forbat SM, Saifuddin A. MRI of the axial skeletal manifestations of ankylosing spondylitis. *Clin Radiol* 2004:59:400-413.

Oostveen J, Prevo R, den Boer J, van de Laar M. Early detection of sacroiliitis on magnetic resonance imaging and subsequent development of sacroiliitis on plain radiography. A prospective, longitudinal study. *J Rheumatol* September 1999;26(9):1953-1958.

Puhakka KB, Jurik AG, Egund N, et al. Imaging of sacroiliitis in early seronegative spondylarthropathy. Assessment of abnormalities by MR in comparison with radiography and CT. *Acta Radiologica* 2003; 44:218-229.

Sacral Insufficiency Fractures

Ahovuo JA, Kiuru MJ, Visuri T. Fatigue stress fractures of the sacrum: diagnosis with MR imaging. *Eur Radiol* March 2004;14(3):500-505. Epub October 24, 2003.

Grangier C, Garcia J, Howarth NR, May M, Rossier P. Role of MRI in the diagnosis of insufficiency fractures of the sacrum and acetabular roof. Skeletal Radiol 1997;26:517-524.

Reflex Sympathetic Dystrophy

Bennett DS, Brookoff D. Complex regional pain syndromes (reflex sympathetic dystrophy and causalgia) and spinal cord stimulation. Pain *Med* May-Jun 2006;7(Suppl 1):64-96.

Crozier F, Champsaur P, Pham T, et al. Magnetic resonance imaging in reflex sympathetic dystrophy syndrome of the foot. Joint *Bone Spine* 2003;70:503-508.

Lechevalier D, Banal F, Damiano J, Imbert I, Magnin J. Correspondence. Reflex sympathetic dystrophy of the foot: MRI with fat suppression is essential (letter with the drafting). Joint Bone Spine 2004;71: 446-447.

Quisel A, Gill JM, Witherell P. Complex regional pain syndrome: which treatments show promise? *J Fam* Practjuly 2005;54(7):599-603.

Quisel A, Gill JM, Witherell P. Complex regional pain syndrome underdiagnosed. J Fam Pracr June 2005:54(6):524-532.

Sintzoff S, Sintzoff S Jr, Stallenberg B, Matos C. Imaging in reflex sympathetic dystrophy. *Hand Clin* August 1997;13(3):431-442.

Serous Atrophy of Marrow

Kuwashima S, Nishimura G, Yamato M, Fujioka M. Magnetic resonance imaging of clival marrow in patients with anorexia nervosa. *Acta Paediatrjpn* 1996;38(2):114-117.

Okamoto K, Ito J, Ishikawa K, Sakai K, Tokiguchi S. Change in signal intensity on MRI of fat in the head of markedly emaciated patients. Neuroradiology 2001:43:134-138.

Vande Berg BC, Malghem J, Devuyst, 0, Malgague BE, Lambert MJ. Anorexia nervosa: correlation between MR appearance of bone marrow and severity of disease. *Radiology* 1994;193:859-864.

Vande Berg BC, Malghem J, Lecouvet FE, Lambert M, Malgague BE. Distribution of serouslike bone marrow changes in the lower limbs of patients with anorexia nervosa: predominant involvement of the distal lower extremities. *AJR* 1996 :166:621-625.

Gaucher Disease

Hermann G, Pastores GM, Abdelwahab IF, Lorberboym AM. Gaucher disease: assessment of skeletal involvement and therapeutic responses to enzyme replacement. *Skeletal Radiol* 1997:26:687-696.

Maas M, Poll LW, Terk MR. Imaging and quantifying skeletal involvement in Gaucher disease. Brit J Radiol 2002;75 (Suppl. 1):A13-A24.

Poll LW, Koch JL, vom Dahl S, et al. Magnetic resonance imaging of bone marrow changes in Gaucher disease during enzyme replacement therapy: first German long-term results. *Skeletal Radiol* 2001 ;30: 496-503.

Roca M, Mota J, Alfonso P, Pocovi M, Giraldo P. S-MRI score: a simple method for assessing bone marrow in Gaucher disease. *Eur J Radiol* 2007:62:132-137.

Wenstrup RJ, Roca-Espiau M, Weinreb NJ, Bembi B. Skeletal aspects of Gaucher disease; a review. *Brit J Radiol* 2002;75(Suppl. 1):A2-A12.

Clycogen Storage Disease

Scherer A, Engelbrecht V, Neises G, et al. MR imaging of bone marrow in glycogen storage disease type IB in children and young adults. *AJR* 2001:177:421-425.

Osteopetrosis

Cure JK, Key LL, Goultra DP, VanTassel P. Cranial MR imaging of osteopetrosis. *AJNR* 2000:21:1110-1115.

Elster AD, Theros EG, Key LL, Chen MYM. Cranial imaging in autosomal recessive osteopetrosis. Part I. Facial bones and calvarium. *Radiology* 1992:183:129-135.

Tolar J, Teitelbaum SL, Orchard PJ. Osteopetrosis. *N Engl J Med* 2004: 351:2839-2849.

Hypervitaminosis A and D

Lips P. Hypervitaminosis A and fractures. N *Engl J Med* 2003;384: 347-349.

Jiang YB, Wang YZ, Zhao J, et al. Bone remodeling in hypervitaminosis D3. Radiologic-microangiographic-pathologic correlations. Invest Radio/1991:26:213-219.

Resnick D. Hypervitaminosis and hypovitaminosis. In: Resnick D, ed. *Diagnosis of Bone and Joint Disorders,* 4th ed. Philadelphia, Pa: W.B. Saunders; 2002:4:3456-3464.

Romero JB, Schreiber A, Von Hochstetter AR, Wagenhauser FJ, Michel BA, Theiler R. Hyperostotic and destructive osteoarthritis in a patient with vitamin A intoxication syndrome: a case report. *Butt Hasp JtDis* 1996:54:169-174.

Fluorosis

Haettich B, Lebreton C, Prier A, Kaplan G. Magnetic resonance imaging of fluorosis and stress fractures due to fluoride. *Rev Rhum Mai Osteoartic* November 1991;58(11):803-808.

Muthukumar N. Ossification of the ligamentum flavum as a result of fluorosis causing myelopathy: report of two cases. *Neurosurgery* March 2005:56(3):622.

Reddy DR, Srikanth RD, Misra M. Fluorosis. *Surg Neural* 1998;49: 635-636.

Myelodysplastic Syndromes

Kusumoto S, Jinnai I, Matsuda A, et al. Bone marrow patterns in patients with aplastic anemia and myelodysplastic syndrome: observations with magnetic resonance imaging. *Eur J Haematol* September 1997;59(3):155-161.

Moulopoulos LA, Dimopoulos MA. Magnetic resonance imaging of the bone marrow in hematologic malignancies. *Blood* 1997;90(6): 2127-2147.

Olipitz W, Beham-Schmid C, Aigner R, et al. Acute myelofibrosis: multifocal bone marrow infiltration detected by scintigraphy and magnetic resonance imaging. *Ann Hematol* 2000:79:275-278.

Takagi S, Tanaka 0, Origasa H, Miura Y. Prognostic significance of magnetic resonance imaging of femoral marrow in patients with myelodysplastic syndromes. *J Clin Oncol* January 1999;17(1): 277-283.

Vardiman JW. Myelodysplastic/myeloproliferative diseases: introduction. In: Jaffe ES, Harris NL, Sein H, Vardiman JW, eds. *World Health Organization Classification of Tumors. Pathology and Genetics of Tumors of Hematopoietic and Lymphoid Tissues.* Lyon, France: IARC Press; 2001:47-48.

Chronic Myeloproliferative Disease

Amano Y, Onda M, Amano M, Kumazaki T. Magnetic resonance imaging of myelofibrosis stir and gadolinium-enhanced MR images. *Clin Imag* July/August 1997;21(4):264-268.

Bock 0, Loch G, Schade U, et al. Osteosclerosis in advanced chronic idiopathic myelofibrosis is associated with endothelial overexpression of osteoprotegerin. Brit *J Haematol* 2005:130:76-82.

Diamond T, Smith A, Schnier R, Manoharan A. Syndrome of myelofibrosis and osteosclerosis: a series of case reports and review of the literature. *Bone* March 2002;30(3):498-501.

Moulopoulos LA, Dimopoulos MA. Magnetic resonance imaging of the bone marrow in hematologic malignancies. *Blood* 1997:90(6): 2127-2147.

Sale GE, Deeg HJ, Porter BA. Regression of myelofibrosis and osteoscle rosis following hematopoietic cell transplantation assessed by magnetic resonance imaging and histologic grading. *Biol Blood Marrow Transplant* 2006:12:1285-1294.

Sideris P, Tassiopoulos S, Sakellaropoulos N, et al. Unusual radiological findings in a case of myelofibrosis secondary to polycythemia vera. *Ann Hematol* 2006:85:555-556.

Thiele J, Pierre R, Imbert M, Vardiman JW, Brunning RD, Flandrin G. Chronic idiopathic myelofibrosis. In: Jaffe ES, Harris NL, Sein H, Vardiman JW, eds. *World Health Organization Classification of Tumors. Pathology and Genetics of Tumors of Hematopoietic and Lymphoid Tissues.* Lyon, France: IARC Press; 2001:35-38.

Waldenstrom Macroglobulinemia

Berger F, Isaacson PG, Piris MA, Harris NL. Lymphoplasmacytic lymphoma/Waldenstrom macroglobulinemia. In: Jaffe ES, Harris NL, Sein H, Vardiman JW, eds. *World Health Organization Classification of Tumors. Pathology and Genetics of Tumors of Hematopoietic and Lymphoid Tissues.* Lyon, France: IARC Press; 2001:132-34.

Moulopoulos LA, Dimopoulos MA. Magnetic resonance imaging of the bone marrow in hematologic malignancies. Blood 1997;90(6): 2127-2147.

Mastocytosis

Arias M, Villalba C, Requena I, Vazquez-Veiga H, Sesar A, Pereiro I. Acute spinal epidural hematoma and systemic mastocytosis. *Spine* April 15, 2004;29(8):E161-3.

Avila NA, Ling A, Metcalfe DD, Worobec AS. Mastocytosis: magnetic resonance imaging patterns of marrow disease. *Skeletal Radiol* 1998:27:119-126.

Boncoraglio GB, Brucato A, Carriero MR, et al. Systemic mastocytosis: a potential neurologic emergency. *Neurology* July 2005:65:332-333.

Myers B, Grimley C, Jones SG, Clark D, Kerslake R. Skin, bone marrow and magnetic resonance imaging appearances in systemic mastocytosis. Brit J *Haematol* 2003:122:876.

Roca M, Mota J, Giraldo P, Garcia Erce JA. Systemic mastocytosis: MRI of bone marrow involvement. *Eur Radiol* 1999;9(6):1094-1097.

Siegel S, Sadler MA, Yook C, Chang V, Miller J. Systemic mastocytosis with involvement of the pelvis: a radiographic and clinicopathologic study - a case study. *Clin Imag* 1999:23:245-248.

Valent P., Horny HP, Li CY, et al. Mastocytosis. In: Jaffe ES, Harris NL, Sein H, Vardiman JW, eds. *World Health Organization Classification of Tumors. Pathology and Genetics of Tumors of Hematopoietic and Lymphoid Tissues.* Lyon, France: IARC Press; 2001:293-302.

Table 15 Lesions that contain cartilage

Lesion	MRI Findings	Comments
Benign		
Osteochondroma (Fig. 15.1)	Circumscribed protruding lesion arising from outer cortex with a central zone with intermediate signal on T1 WI and T2WI similar to marrow surrounded by a peripheral outer zone of low signal on T1 WI and T2WI images over which, a cartilaginous cap is usually present in children and young adults. Increased malignant potential when cartilaginous cap is > 2 cm thick.	Benign cartilaginous tumors arising from defect at periphery of growth plate during bone formation with resultant bone outgrowth covered by a cartilaginous cap. Usually benign lesions unless associated with pain and increasing size of cartilaginous cap. Osteochondromas are common lesions, accounting for 14-35% of primary bone tumors. Occur with median age of 20years, up to 75% of patients are less than 20years. **(See Atlas Chapter A 58)**
Enchondroma *(Fig.* 15.2)	Lobulated intramedullary lesions with well-defined borders ranging in size from 3 cm to 16 cm. mean -5cm. Mild endosteal scalloping can be seen. Cortical bone expansion rarely occurs. Lesions usually have low-intermediate signal on T1WI and intermediate signal on PDWI. On T2WI and FST2WI, lesions usually have predominantly high signal with foci and/or bands of low signal representing areas of matrix mineralization and fibrous strands. No zones of abnormal high signal on T2WI are typically seen in the marrow outside the borders of the lesions. Lesions typically show Gd-contrast enhancement in various patterns (peripheral curvilinear lobular, central nodular/septal and peripheral lobular, or heterogeneous diffuse).	Benign intramedullary lesions composed of hyaline cartilage, represent -10% of benign bone tumors. Enchondromas can be solitary (88 %) or multiple (12 %). Oilier disease is a dyschondroplasia involving endochondral-formed bone resulting in multiple enchondromas (enchondromatosis). Metachondromatosis is a combination of enchondromatosis and osteochondromatosis, and is rare. Maffucci disease refers to a syndrome with multiple enchondromas and soft tissue hemangiomas and is very rare. Patients range in age from 3 to 83 years, median -35 years, mean =38 to 40 years, peak in 3rd and 4th decades. **(See Atlas Chapter A 8)**
Juxtacortical chondroma (Fig. 15.3)	Lesions are located at the bone surface and are usually lobulated with low-intermediate signal on T1 WI, which is hypo- or isointense relative to muscle. Lesions usually have heterogeneous predominantly high signal on T2WI. Lesions are surrounded by low-signal borders on T2WI representing thin sclerotic reaction. Areas of low signal on T2WI are secondary to matrix mineralization. Edema is not typically seen in nearby medullary bone. Lesions often show a peripheral pattern of Gd-contrast enhancement.	Benign protuberant hyaline cartilaginous tumors that arise from the periosteum and superficial to bone cortex. Juxtacortical chondromas account for < 1 % of bone lesions. Occur with median age of 26 years. **(See Atlas Chapter A 9)**
Chondroblastoma (Fig. 15.4)	Tumors often have fine lobular margins and typically have low-intermediate heterogeneous signal on T1WI, and mixed low, intermediate, and/or high signal on T2WI. Areas of low signal on T2WI are secondary to chondroid matrix mineralization and/or hemosiderin. Lobular, marginal or septal Gd-contrast enhancement patterns can be seen. Poorly defined zones with high signal on T2WI and FS T2WI and corresponding Gd-contrast enhancement are typically seen in the marrow adjacent to the lesions representing inflammatory reaction from prostaglandin synthesis by these tumors.	Benign cartilaginous tumors with chondroblast-like cells and areas of chondroid matrix formation, usually occur in children and adolescents, median =17 years, mean - 16 years for lesions in long bones, mean • 28 years in other bones. Most cases are diagnosed between the ages of 5 and 25. **(See Atlas Chapter A 7)**

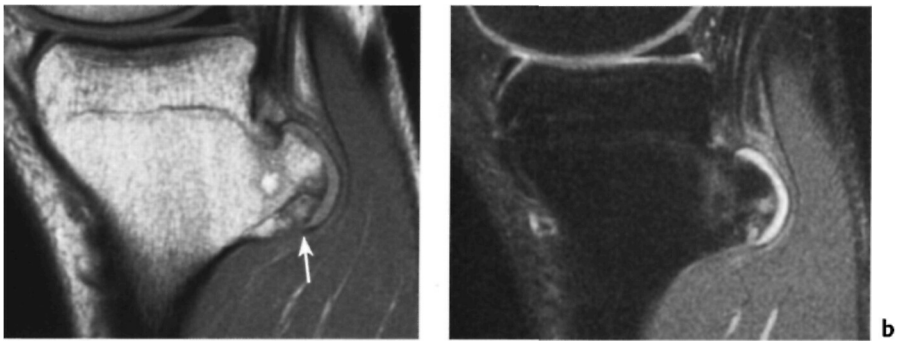

Figure **15.1 a, b** A 14-year-old boy with an osteochondroma at the proximal dorsal surface of the tibia as seen on sagittal PDWI (**a**) and FST2WI (**b**).

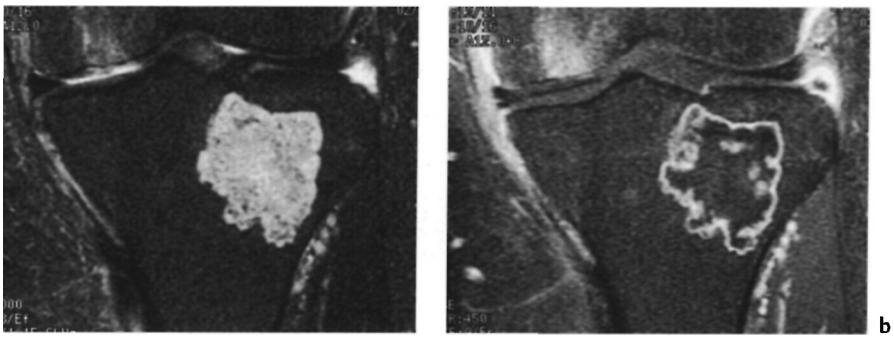

Figure **15.2 a, b** A 54-year-old man with an enchondroma in the marrow of the proximal tibia that has mostly high signal on coronal FST2WI (**a**) and thin peripheral lobulated Gd-contrast enhancement on FS T1WI (**b**).

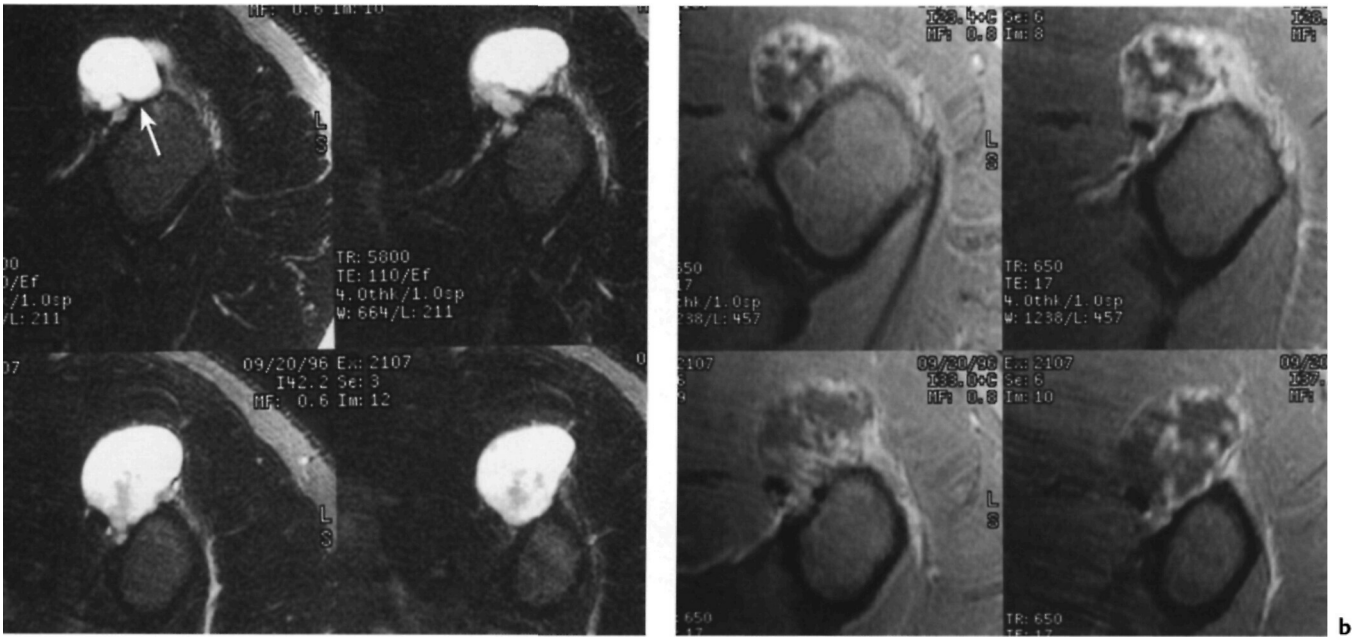

Figure **15.3 a, b** A 28-year-old man with a juxtacortical/periosteal chondroma involving the proximal humerus. The lesion has high signal on axial FST2WI (**a**) and shows nodular and lobulated peripheral Gd-contrast enhancement on axial FST1WI (**b**).

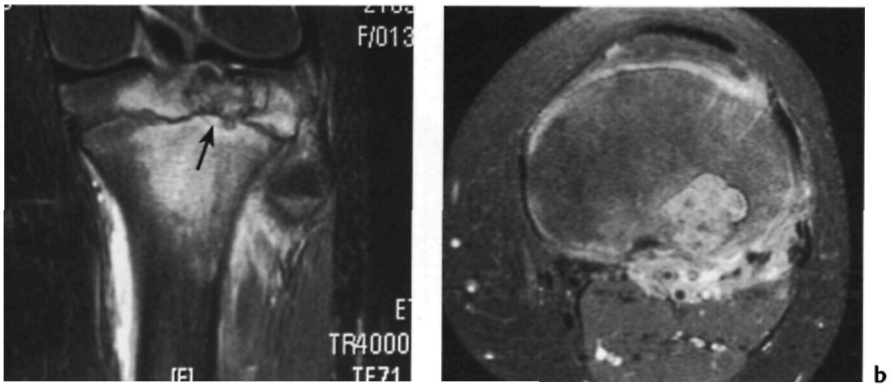

Figure **15.4a, b** A 13-year-old girl with a chondroblastoma in the epiphysis of the proximal tibia that has slightly lobulated margins. The lesion has high signal on coronal FS T2WI (**a**) as well as in the adjacent marrow. The lesion shows Gd-contrast enhancement on axial FST1WI **(b**) as well as poorly defined enhancement in the adjacent marrow.

Table 15 (Continued) Lesions that contain cartilage

Lesion	MRI Findings	Comments
Chondromyxoid fibroma (Fig.15.5)	Lesions are often slightly lobulated with low-intermediate signal on T1WI, intermediate signal on PDWI, and heterogeneous predominantly high signal on T2WI secondary to myxoid and hyaline chondroid components with high water content. MR signal heterogeneity on T2WI is related to the proportions of myxoid. chondroid, and fibrous components within the lesions. Thin low signal septa within lesions on T2WI are secondary to fibrous strands. Lesions are surrounded by low-signal borders representing thin sclerotic reaction. Edema is not typically seen in medullary bone. Lesions show prominent diffuse Gd-contrast enhancement.	Rare, benign, slow-growing bone lesions that contain chondroid, myxoid, and fibrous components. Chondromyxoid fibromas represent 2-4 % of primary benign bone lesions, and < 1 % of primary bone lesions. Most Chondromyxoid fibromas occur between the ages of 1 and 40 years, with a median of 17 years, and peak incidence in the 2nd to 3rd decades. **(See Atlas Chapter A 10)**
Synovial chondroma, chondromatosis/osteochondroma, osteochondromatosis (Figs. 15.6, 15.7)	MRI features depend on the relative proportions of cartilage, calcified cartilage, and mineralized osseous tissue within the lesions. Calcifications result in low signal on T1WI. PDWI. T2WI. and FST2WI. Synovial osteochondromas with ossification can have peripheral low signal on T1WI and T2WI surrounding a central region with fat/marrow signal. Noncalcified portions of the lesions typically have low to intermediate signal on T1 WI, intermediate signal on PDWI, and slightly high to high signal on T2WI and FS T2WI. Low signal septae on T2WI can be seen within the lesions. Synovial chondromas/osteochondromas can show irregular, thin-peripheral and/or septal Gd-contrast enhancement.	**Primary synovial chondromatosis** is a benign disorder resulting from nodular metaplastic cartilaginous proliferation in synovium of joints. The cartilaginous nodules can become detached forming intra-articular loose bodies. Metaplasia of connective tissue into cartilage can also occur in bursae and in tendon sheaths. **Secondary synovia! chondromatosis** is associated with joint disorders (degenerative osteoarthrosis, avascular necrosis, osteonecrosis, osteochondritis dissecans, trauma/osteochondral fractures). In the secondary type, osteocartilaginous loose bodies arise from avulsion of hyaline cartilage into the joint, which can enlarge via nutrients supplied from synovial fluid. Soli tary lesions can occur in both primary and secondary disorders and are referred to as synovial chondromas. Synovial chondromas with osseous metaplasia are referred to as **primary or secondary synovial osteochondromas** Account for < 1 % of benign soft tissue tumors. Occur most frequently between the ages of 25 to 65 years, mean - 44 years. **(See Atlas Chapter A 73)**

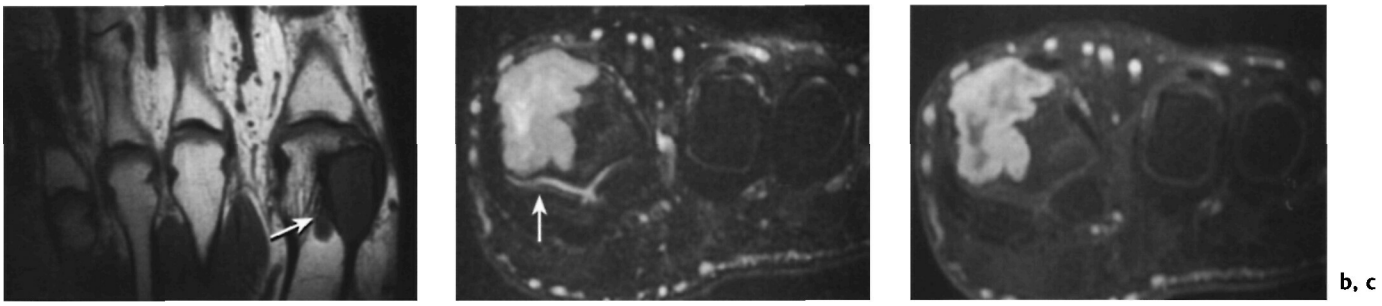

Figure **15.5a-c** A 34-year-old man with chondromyxoid fibroma in the distal first metatarsal bone that has low-intermediate signal on coronal T1WI (**a**) and heterogeneous high signal on axial FST2WI (**b**). The lesion shows Gd-contrast enhancement on axial FST1 WI (**c**).

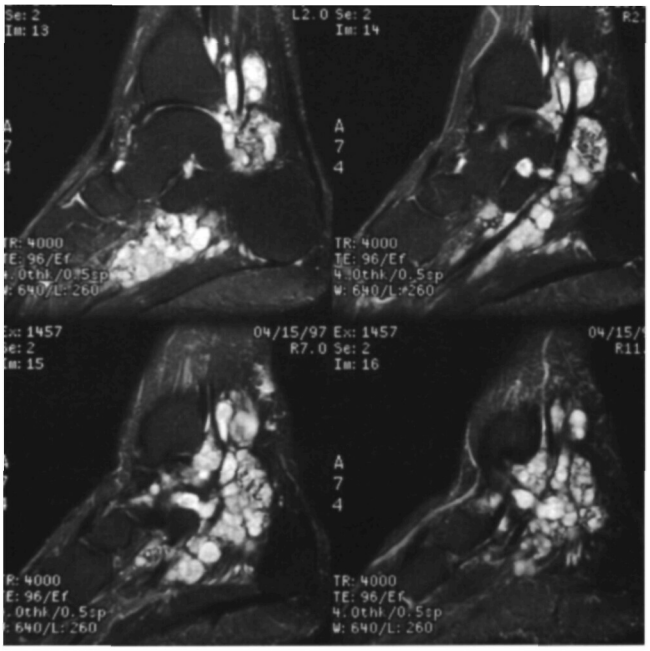

a

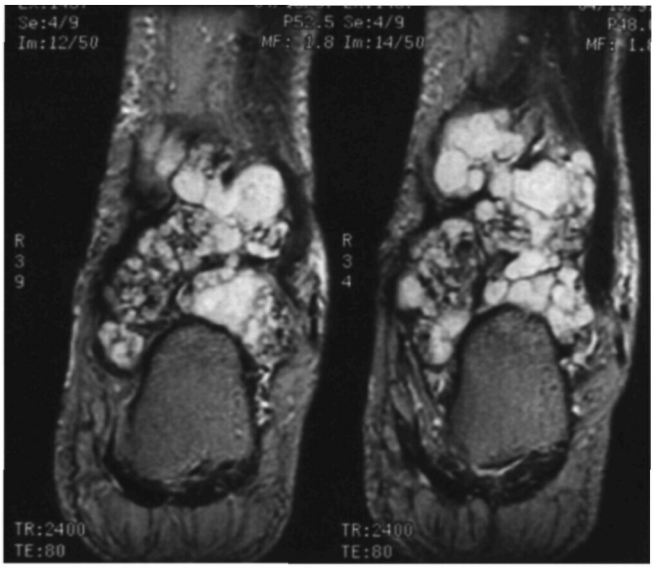

b

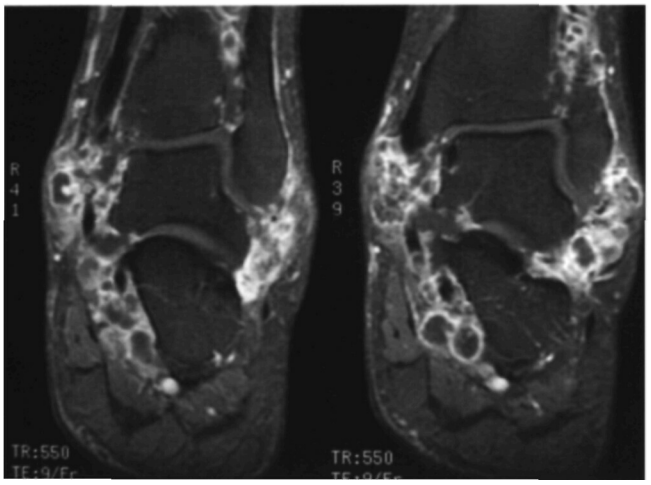

c

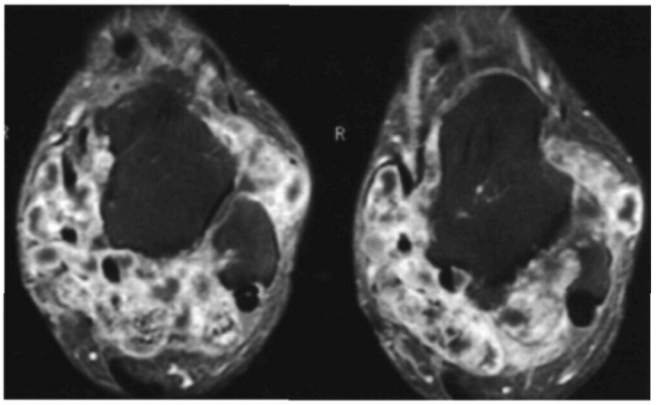

d

Figure **15.6a-d** Primary synovial chondromatosis at the ankle. Multiple lobulated zones are seen at the ankle joint and tendon sheaths that have high signal on sagittal FST2WI (**a**) and coronal T2WI (**b**). Lesions show irregular peripheral-lobular and septal patterns of Gd-contrast enhancement on coronal (**c**) and axial (**d**) FS T1WI.

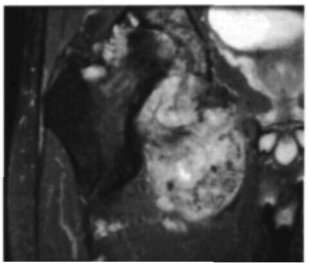

a

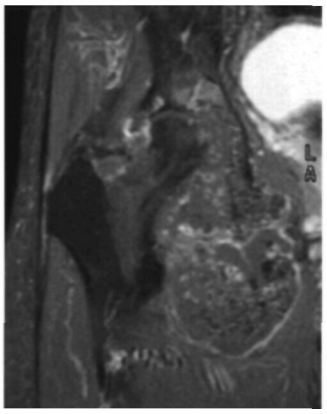

b, c, d

Figure **15.7 a-c** A 51 -year-old man with extensive primary synovial osteochondromatosis at the right hip. The AP radiograph (**a**) shows multiple nodules with chondroid-type calcifications within the hip joint with secondary osteoarthritic changes. Noncalcified portions of the lesion have high signal on coronal FS T2WI (**b**). Low signal septa on T2WI and multiple foci with low signal correspond to calcified cartilage nodules. The lesion shows irregular peripheral-lobular and septal patterns of Gd-contrast enhancement on coronal FST1WI (**c, d**).

Table 15 (Continued) Lesions that contain cartilage

Lesion	MRI Findings	Comments
Chondroid lipoma (Fig. 15.8)	Chondroid lipomas are much less common than the classic benign lipomas. Lesions can show irregular zones of nonfatty signal on T1WI and T2WI resulting from chondroid zones, calcifications, and thick septa which may or may not show Gd-contrast enhancement. Most atypical lipomas contain more than 75% fat, whereas liposarcomas often have less than 75% fat. Distinguishing between atypical lipomas and low grade liposarcomas with MRI, however, can be difficult and challenging.	Osseous or chondroid metaplasia with myxoid changes can be associated with lipomas. These **atypical lipomas** have been labeled as **chondroid lipomas, osteolipomas, or benign mesenchymomas** Chondroid lipomas are benign adipose tumors that contain mature fat, lipoblasts, and chondroid matrix. **(See Atlas Chapter A 43)**
Malignant		
Conventional chondrosarcoma (Figs. 15.9, 15.10)	Lesions usually have low-intermediate signal on T1WI, intermediate signal on PDWI, and heterogeneous predominantly high signal on T2WI. Zones of low signal on T2WI can occur from matrix mineralization and/or fibrous tissue. Lesions often have lobulated margins, with or without internal septations. Peritumoral high signal on T2WI in marrow and periosteal soft tissues may be seen associated with chondrosarcomas, and typically not with enchondromas. Chondrosarcomas usually show Gd-contrast enhancement in patterns ranging from lobulated peripheral and/or septal, or homogeneous versus heterogeneous depending on the degree of matrix mineralization and/or necrosis. MRI can readily show sites of cortical destruction and extension of tumor into the adjacent soft tissues.	Malignant tumors containing cartilage formed within sarcomatous stroma. Can contain areas of calcification/mineralization, myxoid material, and/or ossification. Primary chondrosarcomas (62-86%) represent lesions occurring without pre-existent lesions, whereas secondary chondrosarcomas arise from formerly benign cartilaginous lesions (enchondroma, osteochondroma, etc.) or other lesions (Paget disease, fibrous dysplasia, prior irradiation, repetitive trauma). Account for 12-21 % of malignant bone lesions, 21-26% of primary sarcomas of bone, 9-14% of all bone tumors. Mean age = 40 years, median age= 26 to 59 years. **(See Atlas Chapter A11)**

a

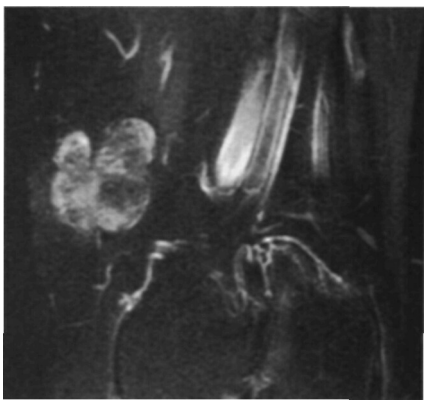

b

Figure **15.8a, b** A 57-year-old woman with a chondroid/myxoid lipoma in the soft tissues of the distal lateral thigh. The lesion has lobulated well-defined margins, and has heterogeneous low, intermediate, and high signal on coronal T1WI (**a**) and coronal FST2WI (**b**).

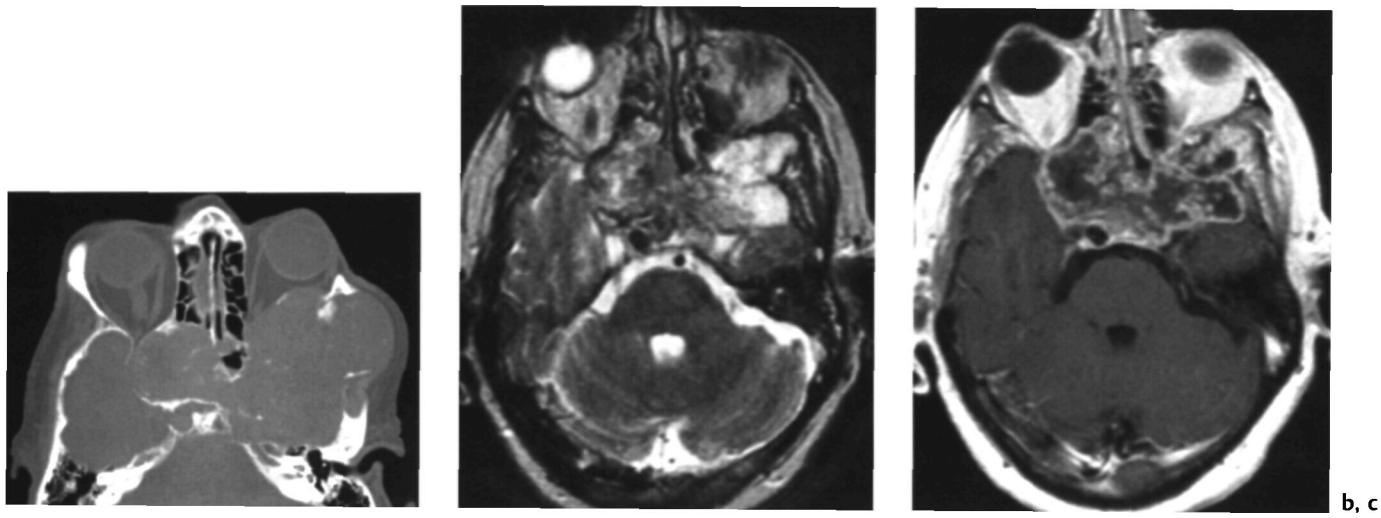

Figure 15.**9a-c** An 81-year-old woman with a large low-grade conventional chondrosarcoma involving the sphenoid bone with extension into both middle cranial fossae. The tumor contains chondroid mineralization and is associated with extensive destruction and remodeling of bone as seen on axial CT (**a**). The tumor has heterogeneous intermediate high and low signal on axial T2WI (**b**) and shows peripheral lobular and central nodular Gd-contrast enhancement on axial T1WI (**c**).

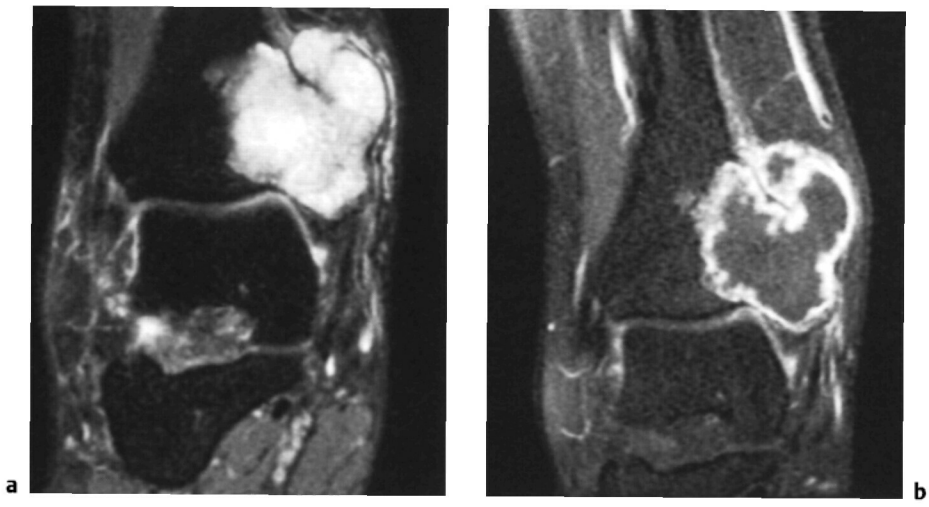

Figure **15.10a, b** A 44-year-old woman with a grade 2 conventional chondrosarcoma involving the distal tibia. The tumor has mostly high signal on coronal FS T2WI (**a**) and extends into the adjacent soft tissues through a zone of cortical destruction. The tumor shows irregular peripheral lobular Gd-contrast enhancement on coronal FS T1WI (**b**).

Table 15 (Continued) Lesions that contain cartilage

Lesion	MRI Findings	Comments
Myxoid chondrosarcoma (Figs. 15.11.15.12)	These tumors can arise in bone or soft tissues. In soft tissues, tumors often have tabulated margins and range in size from 4 to 7cm. Lesions usually have low-intermediate signal on T1WI and PDWI, and predominantly high signal on T2WI. Hemorrhagic foci in myxoid chondrosarcomas can show intermediate to high signal on T1 WI and T2WI. Myxoid chondrosarcomas show heterogeneous Gd-contrast enhancement.	Patients range in age from 6 to 89 years, median -52 years, mean -49 years. Considered low-grade tumors, and are also known as chordoid sarcoma. Tumors can contain abundant myxoid/mucoid stroma with strands and/or foci of cells with small hyperchromatic nuclei and moderate cytoplasm containing glycogen granules. Well-differentiated cartilage cells are also seen. Areas of hemorrhage and cysts often seen in extraosseous tumors. Matrix mineralization/calcification is rarely seen. Typically, minimal or no mitotic activity is seen in tissue samples. These tumors often arise in soft tissues of the extremities (thigh most common), and rarely in bone.
Dedifferentiated chondrosarcoma (Fig. 15.13)	Tumors usually have low-intermediate signal on T1WI and PDWI, heterogeneous predominantly high signal on T2WI. Zones of low signal on T2WI are related to the presence and degree of matrix mineralization and/or fibrous tissue. Lesions often have irregular poorly defined margins and associated cortical destruction. Lesions usually show heterogeneous contrast- enhancement. MRI can readily show sites of extension of the lesion into the adjacent soft tissues.	Occurs as both primary and secondary chondrosarcomas in patients ranging in age from 29 to 85 years, with the average between 50 and 60 years. Tumors have mixtures of high-grade spindle cells and low-grade or high-grade malignant cartilage cells. **(See Atlas Chapter A11)**
Clear cell chondrosarcoma	Lesions usually are seen near the ends of long bones +/- extension into metaphyseal and diaphyseal regions. Smaller lesions may be well circumscribed, larger lesions may have associated cortical disruption and extension into adjacent soft tissues. Lesions typically have low-intermediate signal on T1WI and heterogeneous intermediate-high signal on T2WI. Lesions usually show prominent Gd-contrast enhancement.	These slow-growing tumors have been referred to as "malignant chondroblastoma." Patients range in age from14 to 84 years, mean =37 years, peak in 4th and 5th decades. Occur two to three times more frequently in males compared with females. Tumor cells have clear cytoplasm with centrally positioned nuclei with few mitotic figures. Multinucleated osteoclast-like giant cells may also be seen. Tumor matrix and/or zones with histology similar to conventional chondrosarcoma are often present. Tumor cartilage may be calcified/ ossified. **(See Adas Chapter A11)**
Periostea! chondrosarcoma (also referred to as juxtacortical chondrosarcoma) (Fig. 15.14)	Tumors vary in size from 4 to 11 cm. Bone cortex is either thinned or thickened but not destroyed. Lesions occasionally involve medullary bone. Tumors have low-intermediate signal on T1WI, intermediate signal on PDWI, and heterogeneous intermediate-high signal on T2WI. Tumors show heterogeneous Gd-contrast enhancement.	Low-grade tumors that account for 1-2% of chondrosarcomas. Tumors occur on the surface of bones and are often large (> 5 cm). Typically have histologic features similar to conventional chondrosarcomas.

a

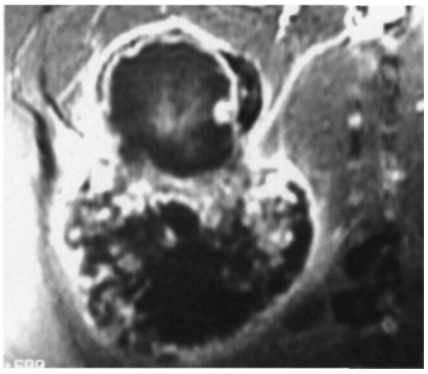

b

Figure 15.**11 a, b** A 34-year-old man with a high-grade myxoid chondrosarcoma involving the proximal femur with cortical destruction and extraosseous extension of tumor dorsally. The lesion has irregular circumscribed margins and contains high signal on axial T2WI (**a**). The tumor shows lobulated irregular peripheral Gd-contrast enhancement on axial FST1WI (**b**).

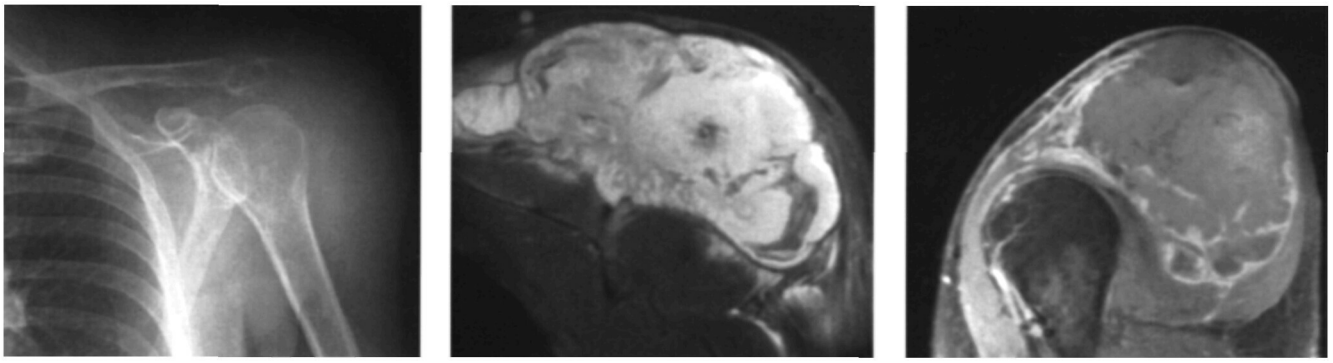

a b, c

Figure **15.12a-c** A 63-year-old man with an extraosseous myxoid chondrosarcoma involving the soft tissues at the left shoulder. The radiograph (a) shows chondroid mineralization associated with the tumor. The large tumor has mostly high signal on coronal FST2WI (**b**) as well as irregular zones of low signal. The tumor shows lobulated irregular peripheral Gd-contrast enhancement on sagittal FST1WI (c).

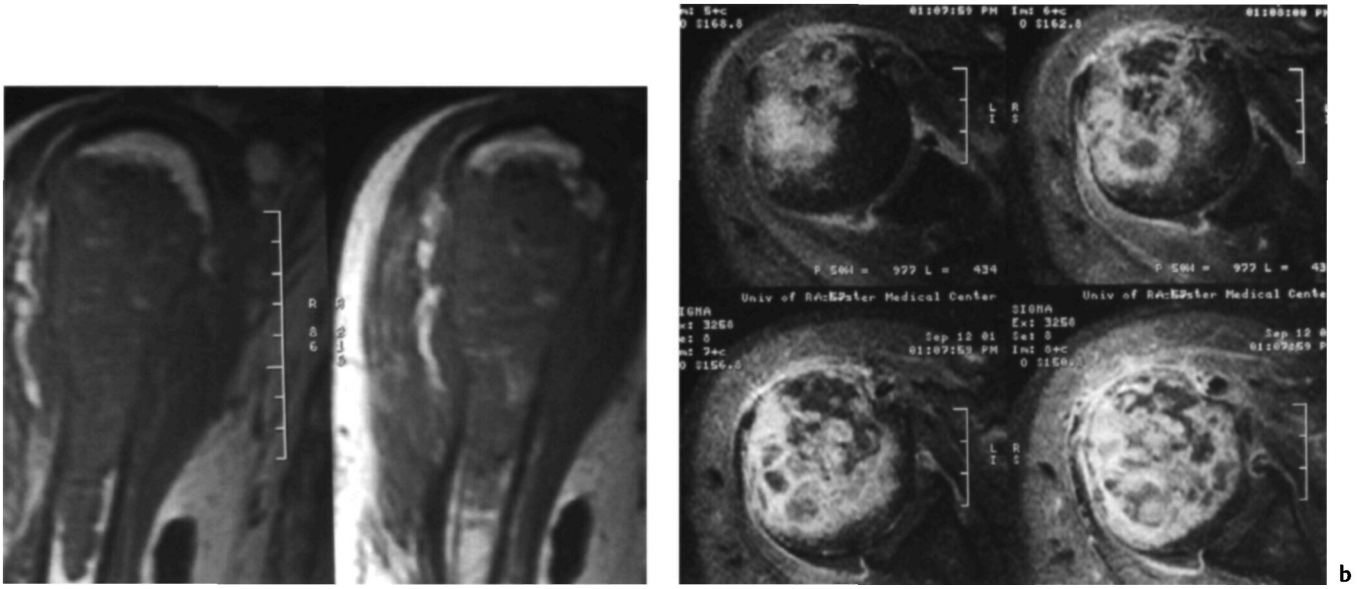

a b

Figure 15.**13 a, b** An 88-year-old man with a dedifferentiated chondrosarcoma involving the proximal humerus that has low-intermediate signal on sagittal T1WI (a). The lesion shows prominent heterogeneous Gd-contrast enhancement on axial FST1WI (**b**) that extends through disrupted cortex,

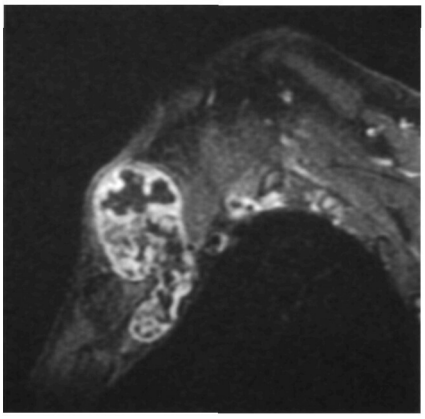

Figure **15.14** A 40-year-old man with a low-grade periosteal chondrosarcoma along the cortical surface of the clavicle. The lesion has circumscribed margins and shows irregular peripheral and central lobular Gd-contrast enhancement on sagittal FST1WI.

Table 15 (Continued) **Lesions that contain cartilage**

	MRI Findings	Comments
Mesenchymal diondrosarcoma (Fig. 15.15)	These tumors can arise in bone or soft tissue. Tumors in bone are usually destructive lesions commonly associated with extraosseous soft tissue masses. Lesions have low-intermediate signal on T1WI, intermediate signal on PDWI, and heterogeneous intermediate-high or slightly high signal on T2WI. Foci of low signal on T1WI and T2WI can be seen secondary to chondroid matrix mineralization. Lesions typically show heterogeneous Gd-contrast enhancement.	Patients range in age from 5 to 74 years, with peak occurrences in the 2nd and 3rd decades. Tumors contain undifferentiated small cells with oval nuclei associated with an extracellular reticulin network. Small to large foci of cartilage are seen in the in sions, with or without reactive osteoid and bone formation. This type can also arise in soft tissues. **(See Atlas Chapter A11)**
Secondary chondrosarcoma from osteochondroma (Fig. 15.16)	MRI can demonstrate the thickness of cartilaginous caps of osteochondromas as well as erosive and/or destructive bone changes involving osteochondromas. Cartilage cap thickness exceeding 2 cm is associated with malignant degeneration of osteochondromas into secondary chondrosarcomas. Lesions have low-intermediate signal on T1WI, intermediate signal on PDWI, and heterogeneous intermediate-high signal on T2WI. Lesions show heterogeneous contrast enhancement, with or without Gd-contrast enhancement in adjacent soft tissues.	Peripheral chondrosarcomas refer to secondary chondrosarcomas that arise from osteochondromas, and usually have histologic features similar to a conventional intraosseous chondrosarcomas. **(See Atlas Chapter A11)**
Chondroblastic osteosarcoma (Fig. 15.17)	Tumors usually have low-intermediate signal on T1WI. Tumors can have variable MRI signal on T2WI, and FS T2WI depending upon the relative proportions of calcified/mineralized osteoid, chondroid, fibroid, hemorrhagic, and necrotic components. Zones of necrosis typically have high signal on T2WI, whereas mineralized zones usually have low signal on T2WI. Zones of cortical destruction are often seen through which tumors extend into the extraosseous soft tissues. Zones of low signal from spicules of periosteal, reactive, and tumoral bone formation may be seen under an elevated periosteum. Tumors typically show prominent Gd-contrast enhancement in nonmineralized/calcified portions of the tumors.	Chondroblastic osteosarcomas account for 25 % of osteosarcomas. These tumors contain chondroid zones with malignant spindle-shaped cells. Endochondral ossification and metaplastic bone formation are commonly seen.
Periosteal osteosarcoma (Fig.15.18)	Often involves the diaphyseal regions with associated cortical thickening seen as low signal on T1WI and T2WI. Tumors can have a broad base along the outer cortex with tumor seen extending outward toward the adjacent soft tissues. Cortical thickening associated with these tumors is often thinner or eroded at the center or base of the protruding mass. Periosteal reaction, seen as linear zones of low signal on T1WI and T2WI, can be associated with these tumors, as well as Codman's triangles. Can involve 50 % *or* more of the bone circumference. Tumors often have low-intermediate signal on T1WI, heterogeneous slightly high to high signal on T2WI and FST2WI, and show Gd-contrast enhancement. Tumor extension into the marrow is uncommon, and when present is usually seen associated with a zone of cortical destruction.	Histologic features are often similar to moderately differentiated chondroblastic osteosarcoma. Tumors are often covered by periosteum associated with immature cells. Tumors consist of lobules of malignant-appearing cartilage separated and surrounded by malignant spindle-shaped cells within an osteoid matrix. Endochondral ossification can be seen in the central portions of the chondroid lobules. Tumor may extend into Haversian canals and bone marrow. Occurs in patients aged from 11 to 57years, median = 17 to 24years.

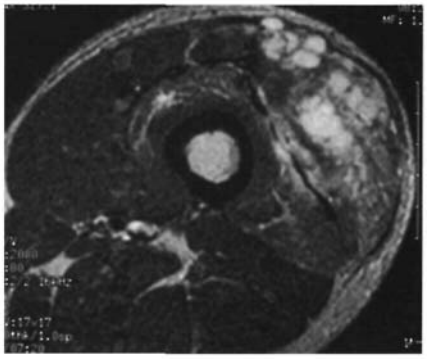

a

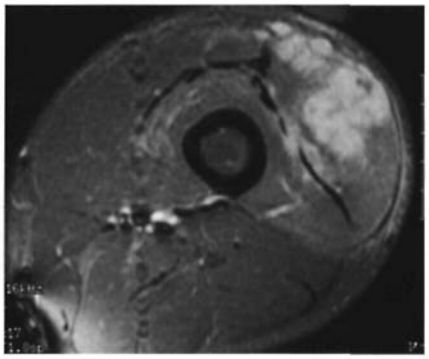

b

Figure 15.**15 a. b** An 18-year-old man with an extraosseous mesenchymal chondrosarcoma involving the vastus lateralis and adjacent soft tissues in the distal thigh. The tumor has poorly defined margins and has heterogeneous mostly high signal on axial T2WI (a). The tumor shows irregular Gd-contrast enhancement on axial FST1WI (**b**).

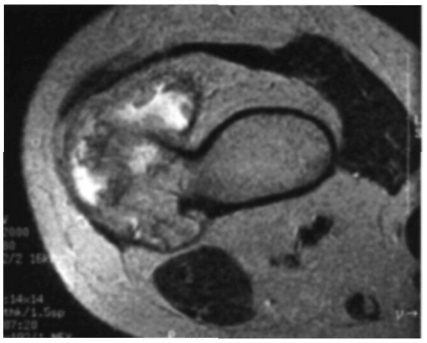

a

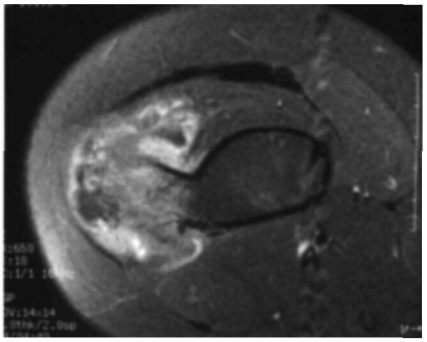

b

Figure 15.16a, b An 18-year-old woman with a secondary low-grade chondrosarcoma arising from an osteochondroma at the distal femur. The thickened cartilaginous cap of the tumor has irregular margins and contains heterogeneous slightly high and high signal with small foci of low signal on axial T2WI (a). Zones of cortical destruction are seen at the osteochondroma adjacent to the malignant cartilaginous cap. The lesion shows irregular heterogeneous Gd-contrast enhancement on axial FSTIWI(b).

a

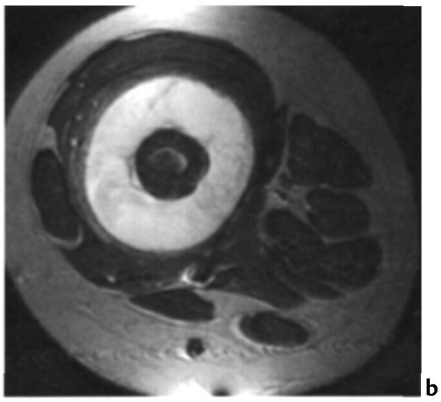

b

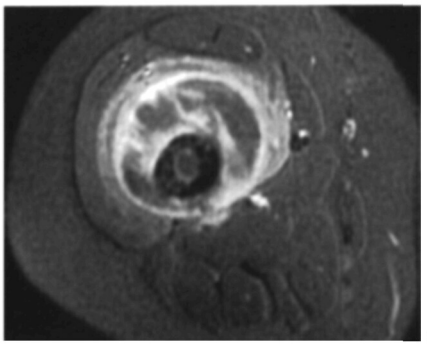

c

Figure 15.17a-c A 10-year-old female with a chondroblastic osteosarcoma involving the proximal diaphysis of the femur. The AP radiograph (a) shows osteoid matrix mineralization from intramedullary tumor associated with interrupted perpendicular, lamellated periosteal reaction, and a Codman's triangle at the upper border of tumor extension. The intramedullary tumor has mostly low signal on axial T2WI (b), whereas the circumferential extraosseous tumor has mostly high signal. Irregular thin strands of low signal are seen in the extraosseous tumor representing perpendicular periosteal reaction. Irregular Gd-contrast enhancement is seen mostly in the extraosseous tumor on axial FST1 WI (c).

a

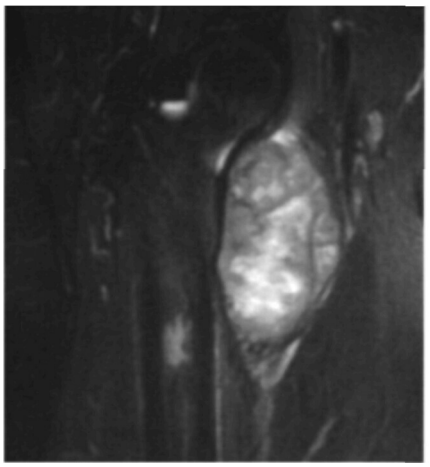

b, c

Figure 15.18a-c A 26-year-old man with a periosteal osteosarcoma involving the anteromedial surface of the proximal femur. The AP radiograph (a) shows an extraosseous tumor containing mineralized matrix as well as interrupted lamellated periosteal reaction adjacent to the femur. The tumor has mixed intermediate, slightly high, and high signal on coronal FST2WI (b) and shows heterogeneous Gd-contrast enhancement on coronal FST1WI (c).

Table 15 (Continued) Lesions that contain cartilage

Lesion	MRI Findings	Comments
Chondroid chordoma	Chondroid chordomas are either midline or off-midline in location, and typically have low-intermediate signal on T1WI and heterogeneous predominantly high signal on T2WI. Typically show Gd-contrast enhancement. Lesions can displace and encase blood vessels, and extend into adjacent structures such as the cavernous sinus, sella, nasopharynx, and hypoglossal canal.	Rare, locally aggressive, slow-growing malignant tumors derived from ectopic notochordal remnants along the axial skeleton. Chondroid chordomas (5-15% of chordomas) show both chordomatous and chondromatous differentiation. Average survival for chondroid chordomas (16years) is greater than conventional chordomas (4 years). Morbidity and mortality are usually secondary to local recurrence and extension. Distant metastasis is uncommon. **(See Atlas Chapter A12)**

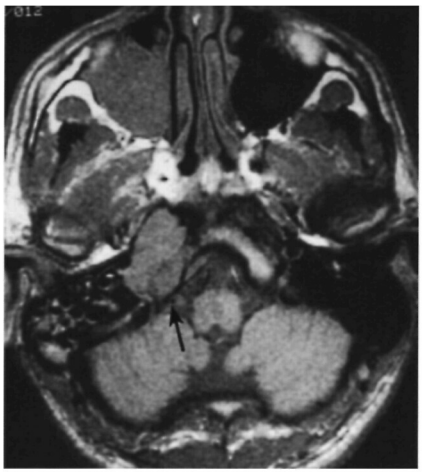
a

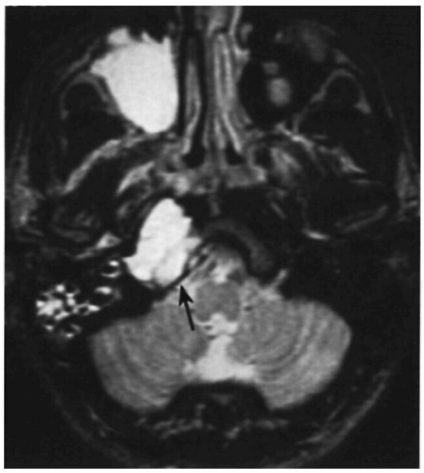
b

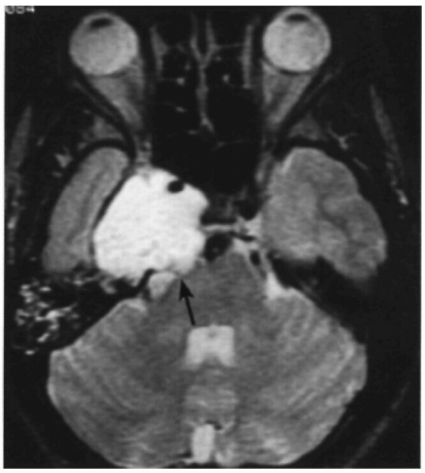
c

Figure 15.19a-c A 21-year-old man with chondroid chordoma at the right petro-occipital synchondrosis. The lesion is associated with bone destruction and extraosseous extension, and has intermediate signal on axial T1WI (a) and high signal on axial T2WI (b, c).

Table 16 Tumors and tumorlike lesions within joints

Lesion	MRI Findings	Comments
Benign		
Synovial osteochondroma/ osteochondromatosis (Figs. 16.1,16.2)	MRI features of osteochondromatosis are dependent on the relative proportions of cartilage, calcified cartilage, and mineralized osseous tissue within the lesions. Calcifications result in low signal on T1WI. PDWI, T2WI, and FST2WI. Lesions with extensive calcification can have signal voids. Mature ossifications can have peripheral low signal on T1WI and T2WI surrounding a central region with fat signal. Noncalcified portions of the lesions can have low to intermediate signal on T1WI, intermediate signal on PDWI, and slightly high to high signal on T2WI and FST2WI. Lesions can show irregular, thin-peripheral and/or scptal enhancement.	**Primary synovial osteochondromatosis** is a benign disorder that results from cartilaginous and osseous metaplastic proliferation in synovium of joints. The osteocartilaginous nodules can become detached forming intra-articular loose bodies. **Secondary synovial osteochondromatosis** occurs from avulsion of osteochondral fragments into the joint, forming loose bodies that can enlarge via nutrient supply from synovial fluid. **(See Atlas Chapter A 73)**

a

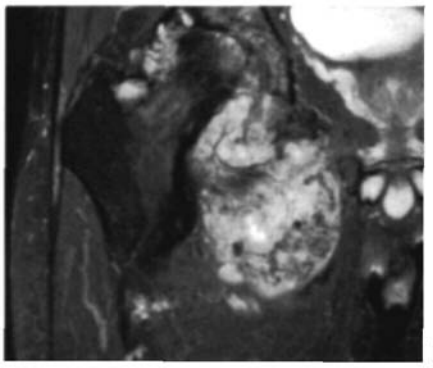

b

Figure 16.1 a, b A 51-year-old man with extensive primary synovial osteochondromatosis at the right hip. The AP radiograph (a) shows multiple nodules with chondroid-type calcifications within the hip joint with associated osteoarthritic changes. Noncalcified portions of the lesion have high signal on coronal FST2WI (b). Low signal septa on T2WI are seen within the lesion. Multiple foci of low signal and signal void on FST2WI correspond to calcified cartilage nodules seen on the radiograph.

a

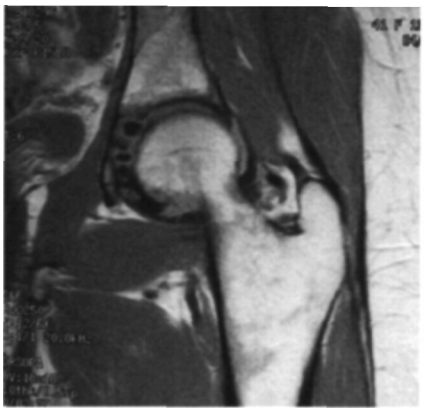

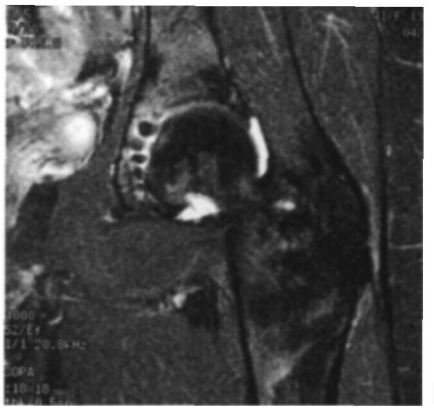

b, c

Figure 16.2 a-c A 41 -year-old woman with secondary synovial osteochondromatosis at the left hip. The AP radiograph (a) shows multiple calcified nodules within the medial portion of the left hip joint. Foci of low signal on coronal T1 WI (b) and coronal FS T2WI (c) are seen within the medial portion of the hip joint, which correspond to calcified cartilage nodules.

Table 16 (Continued) **Tumors and tumorlike lesions within joints**

Lesion	MRI Findings	Comments
Synovial chondroma/ chondromatosis *(figs.* 16.3.16.4)	Synovial chondromas are typically radiolucent and have low to intermediate signal on T1 WI (that is iso- or hyperintense relative to muscle), intermediate signal on PDWI, and slightly high to high signal on T2WI and FST2WI. Low signal septae on T2WI can be seen within the lesions. Synovial chondromas can show irregular, thin-peripheral and/or septal Gd-contrast enhancement.	**Primary synovial chondromatosis** accounts for < 1 % of benign soft tissue tumors and is a disorder that results from cartilaginous metaplastic proliferation in synovium of joints. Usually occurs in patients from 25 to 65years, mean -44years. The cartilaginous nodules can become detached forming intra-articular loose bodies. Metaplasia of connective tissue into cartilage can also occur in bursae and in tendon sheaths. **Secondary synovial chondromatosis** occurs from avulsion of hyaline cartilage into the joint, forming loose bodies that can enlarge via nutrient supply from synovial fluid. **(See Atlas Chapter A 73)**
Pigmented villonodular synovKis (Fig. 16.5)	Often appears as irregular, multinodular, and/or diffuse thickening of synovium. Occasionally occurs as single nodular intra-articular lesions. Lesions often have low or low-intermediate signal on T1WI, PDWI, and T2WI. Areas of low signal on T2WI and T2*WI are secondary to hemosiderin in Pigmented villonodular synovitis (PVNS). Areas of slightly high to high signal on T2WI and FS T2WI can also occur from edema and/or inflammatory reaction. joint effusions are usually present, rarely with fluid-fluid levels. PVNS can show Gd-contrast enhancement in irregular heterogeneous and/or homogeneous patterns.	Benign intra-articular lesions of proliferative synovium (tendon sheaths, joints. and bursae) containing zones of recent or remote hemorrhage. PVNS has similar histopathologic features with giant cell tumors of the tendon sheath/nodular synovitis; although PVNS lesions have frond- like or villous growth patterns and contain large amounts of hemosiderin. Accounts for < 1 % of benign and all soft tissue tumors. Patients range in age from 9 to 74 years, mean -38 years, median age - 32 years. **(See Atlas Chapter A 67)**
Nodular synovKis (also referred to as giant cell tumors of the tendon sheath and soft tissue) (Fig. 16.6)	Lesions can be ovoid or multilobulated and usually have low-intermediate or intermediate signal on T1WI and PDWI that is often similar to or less than muscle. On T2WI and FST2WI, lesions can have mixed intermediate and/or high signal. Small zones of low signal on T2WI can represent small sites of hemosiderin deposition. Lesions often show Gd-contrast enhancement in either homogeneous or heterogeneous pattern. Erosions of adjacent bone can be seen with some lesions.	Benign proliferative lesions of synovium (tendon sheaths, joints, and bursae). Can occur as localized nodular lesions attached to tendon sheaths outside of joints (hands, feet) or within joints (infrapatellar portion of knee joint); or as a diffuse form near/outside of large joints such as the knees, ankles, etc. Nodular synovitis accounts for 4 % of benign soft tissue tumors and 2 % of all soft tissue tumors. Occurs in patients aged from 6 to 71 years, mean -39 to 46 years, peak ages in 3rd to 4th decades. **(See Atlas Chapter A 30)**

a

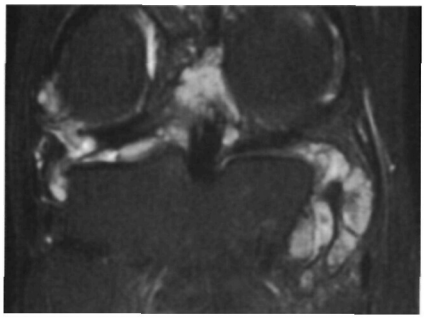

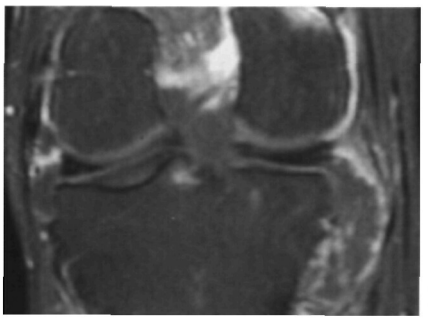

b, c

Figure 16.3a-c A 37-year-old woman with primary synovial chondromatosis at the knee. Multiple lobulated zones are seen that have intermediate signal on coronal PDWI (a) and high signal on coronal FST2WI (b). The lobules have thin margins of low signal. The lesions show irregular peripheral-lobular and septal patterns of Gd-contrast enhancement on coronal FST1WI (c). No mineralized zones were seen on the radiographs (not shown).

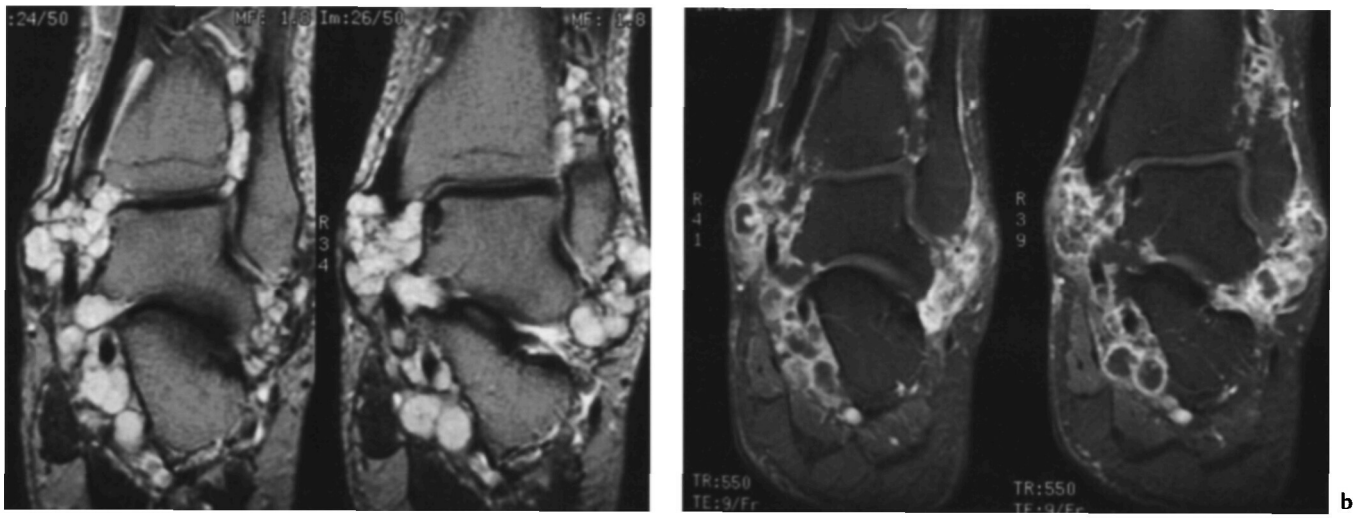

a b

Figure 16.4a, b A 57-year-old man with primary synovial chondromatosis at the ankle. Multiple lobulated zones are seen at the ankle joint and tendon sheaths that have high signal on coronal T2WI (a). The lobules have thin margins of low signal on T2WI. The lesion shows irregular peripheral-lobular and septal patterns of Gd-contrast enhancement on coronal FST1WI (b). No mineralized zones were seen on the radiographs (not shown).

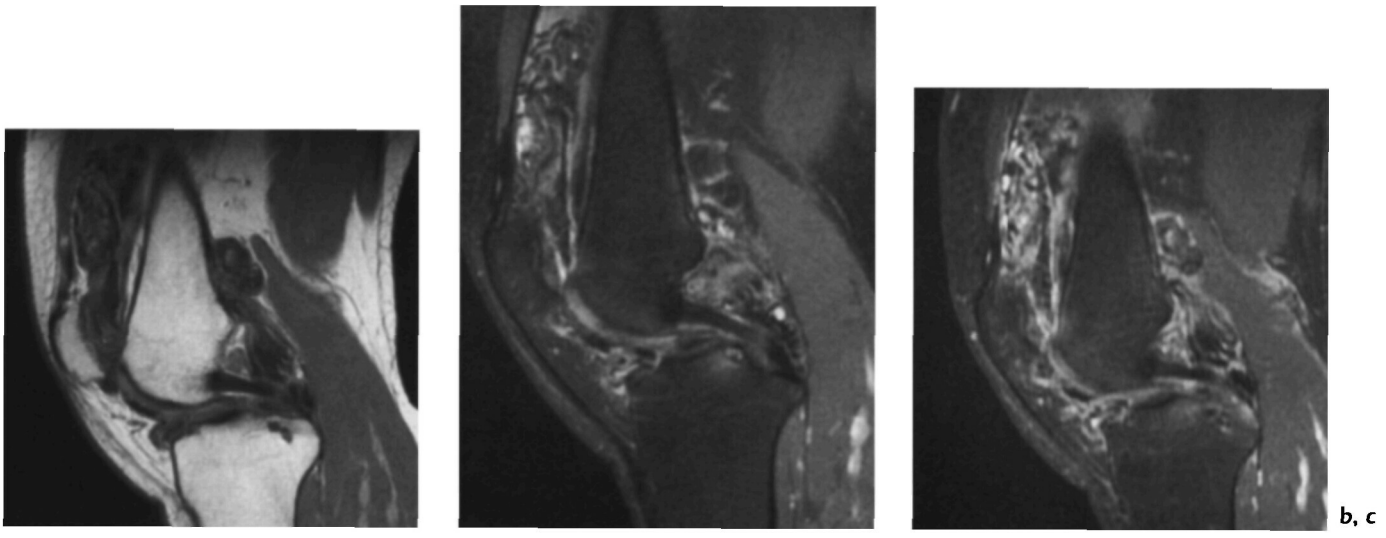

a b, c

Figure 16.5a-c A 36-year-old woman with PVNS involving the knee. Poorly defined and ovoid zones with heterogeneous intermediate and low signal on sagittal T1WI (a), and heterogeneous intermediate, slightly high, and low signal on sagittal FST2WI (b) are seen in the anterior and posterior portions of the knee joint. Heterogeneous Gd-contrast enhancement of the lesions is seen on sagittal FST1WI (c).

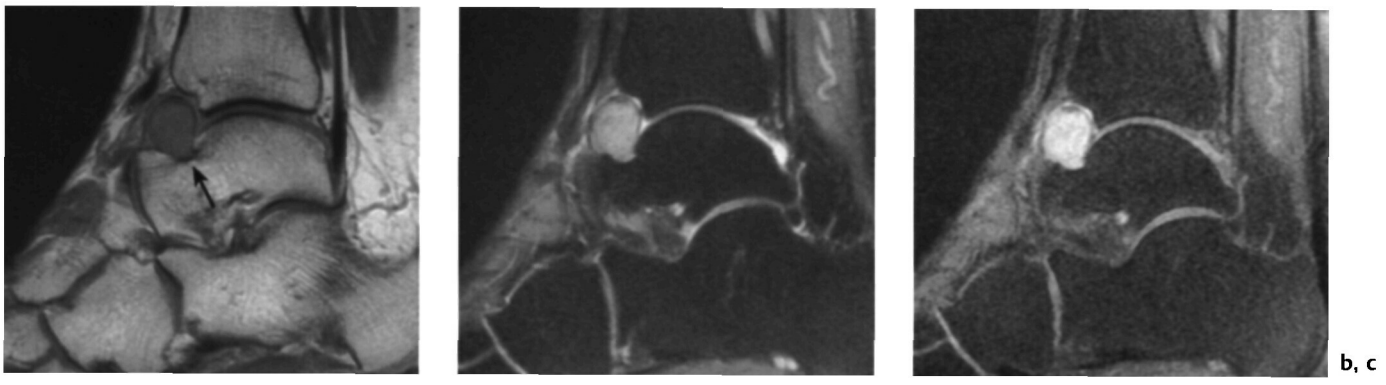

a b, c

Figure 16.6a-c A 68-year-old woman with a giant cell tumor of the tendon sheath/nodular synovitis at the ankle. An ovoid lesion with well-defined margins is seen that has mostly intermediate signal on sagittal T1WI (a) and high signal on sagittal FST2WI (b). The lesion shows prominent Gd-contrast enhancement on sagittal FST1WI (c).

Table 16 (Continued) **Tumors and tumorlike lesions within joints**

Lesion	MRI Findings	Comments
Rheumatoid arthritis (Figs. 16.7, 16.8.16.9)	Hypertrophied synovium seen with rheumatoid arthritis can be diffuse, nodular, and/or villous, and usually has low to intermediate or intermediate signal on T1 WI and PDWI. On T2WI, hypertrophied synovium can have low to intermediate, intermediate, and/or slightly high to high signal that is typically lower than joint fluid. Signal heterogeneity of hypertrophied synovium on T2WI can result from variable amounts of fibrin, hemosiderin, and fibrosis. Chronic fibrotic nonvascular synovium usually has low signal on T1WI and T2WI. Hypertrophied synovium can show prominent homogeneous or variable heterogeneous Gd-contrast enhancement. Joint effusions can be seen. Zones of erosion and/or destruction of hyaline cartilage and subchondral bone, meniscal damage; bursal and joint fluid collections containing "rice bodies," other extra-articular cysts; intraosseous cystic-like areas, joint effusion, and rheumatoid nodules can eventually occur.	Chronic multisystem disease of unknown etiology with persistent inflammatory synovitis involving peripheral joints in a symmetric distribution. Can result in progressive destruction of cartilage and bone leading to joint dysfunction. Affects ~1 % of the world population. Eighty percent of adult patients present between the ages of 35 and 50 years. In patients with juvenile rheumatoid arthritis, patients range from 5 to 16 years, mean = 10.2 years. **(See Atlas Chapter A 70)**
Gout/tophi (Fig. 16.10)	Tophi have variable sizes and shapes, and often have low-intermediate signal on T1WI, FST2WI, and T2WI. Zones of high signal on T2WI can be seen secondary to regions with increased hydration and proteinaceous zones associated with the deposits of urate crystals. Erosions of bone, synovial pannus, joint effusion, bone marrow and soft tissue edema can be seen with MRI. Tophi may be associated with heterogeneous, diffuse, or peripheral/marginal Gd-contrast enhancement patterns. Contrast enhancement seen with tophi is likely secondary to the hypervascular granulation tissue and reactive inflammatory cells in the synovium and/or adjacent soft tissues.	Inflammatory disease involving synovium resulting from deposition of monosodium urate crystals when serum urate levels exceed its solubility (7mg/dL in men and 6mg/dL in women) in various tissues and body fluids. Can be a primary disorder (inherited metabolic defects in purine metabolism or abnormal renal tubular secretion of urate) or secondary disorder (alcohol and medications; thiazide diuretics, salicylates, cyclosporin) that results from diminished renal excretion of uric acid salts, or from increased metabolic turnover of nucleic acids associated with malignancy, chemotherapy, endocrine, vascular, and/or myeloproliferative diseases. Prevalence of gout ranges from 0.5 to 2.8% of men and 0.1 to 0.6% of women in the United States. Accounts for 5% of arthritis cases. Usually occurs in middle-aged and elderly patients. **(See Atlas Chapter A 32)**

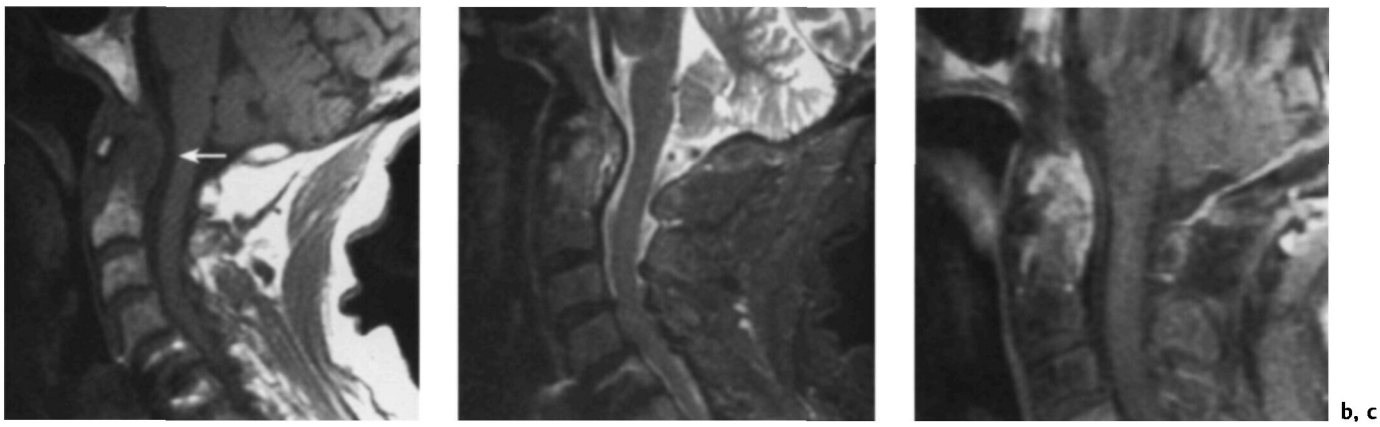

Figure 16.7a-c A 72-year-old woman with pannus from rheumatoid arthritis at the upper dens and atlas. The low signal line of bone cortex at the upper dens is markedly thinned and eroded on sagittal T1WI (a) and sagittal FST2WI (b). The pannus and adjacent marrow have low-intermediate signal on T1WI and heterogeneous intermediate to slightly high signal on FST2WI. The pannus and adjacent marrow show Gd-contrast enhancement on sagittal FS T1WI (c).

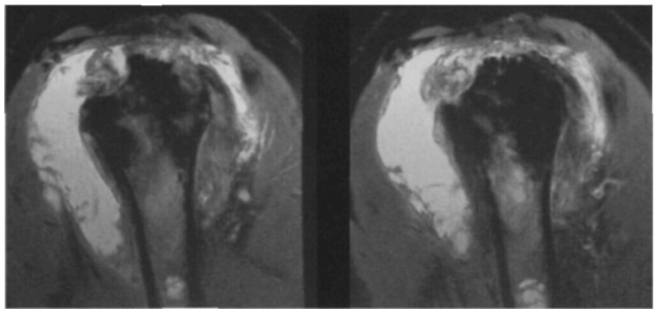

Figure 16.**8** Rheumatoid arthritis involving the shoulder with pannus formation associated with erosions into the humeral head. Pannus has mixed intermediate, slightly high, high, and low signal on sagittal FST2WI. A large effusion with high signal is also seen.

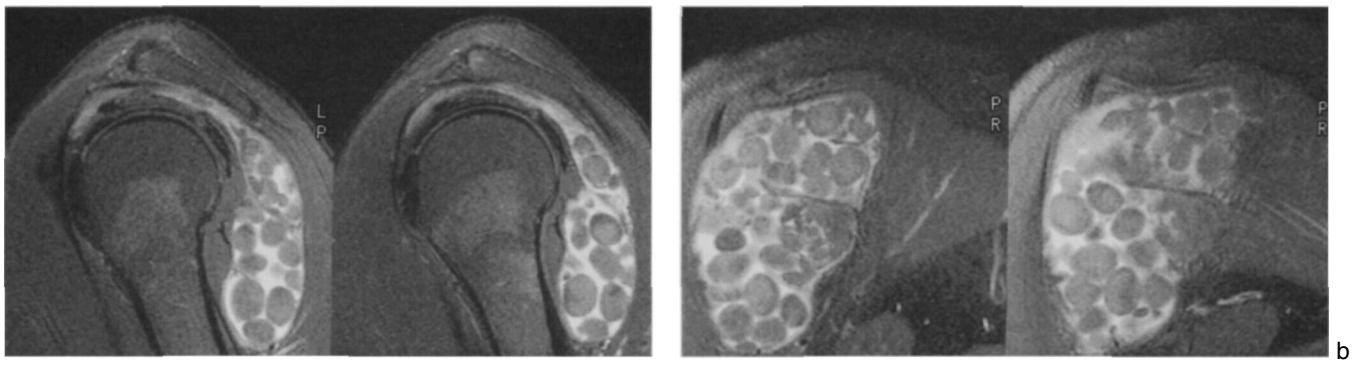

a b

Figure 16.9**a, b** A 56-year-old woman with rheumatoid arthritis involving the bursa of the shoulder with hypertrophied synovium appearing as "rice bodies." The ovoid and spheroid zones of synovial proliferation have intermediate signal on sagittal (**a**) and coronal (**b**) FST2WI and are located within a large effusion in the subdeltoid bursa.

a b

Figure 16.**10a, b** A 53-year-old man with gout involving a metatarsal-phalangeal joint. Bone erosions are seen associated with soft tissue lesions (tophus) with heterogeneous intermediate, slightly high, and high signal on FST2WI (**a**). Only peripheral irregular Gd-contrast enhancement is seen with the intraosseous and extraosseous gout lesions on sagittal FST1WI (**b**).

Table 16 (Continued) Tumors and tumorlike lesions within joints

Lesion	MRI Findings	Comments
Calcium pyrophosphate dlhydrate deposition disease (Fig. 16.11)	Radiographs and CT show chondrocalcinosis, which is typically difficult to visualize with MRI except at the C1-odontoid articulation. At C1-C2, hypertrophy of synovium may occur that can have low-intermediate signal on T1WI and T2WI. Small zones of low signal may correspond to calcifications seen with CT.	Calcium pyrophosphate dihydrate deposition (CPPD) disease is a common disorder in older adults in which there is deposition of CPPD crystals resulting in calcifications of hyaline and fibrocartilage, and is associated with cartilage degeneration, subchondral cysts, and osteophyte formation. Symptomatic CPPD is referred to as pseudogout because of overlapping clinical features with gout. Usually occurs in the knee, hip, shoulder, elbow, and wrist, and rarely at the odontoid-C1 articulation.
Eosinophilic granuloma (Fig. 16.12)	Intramedullary lesions associated with trabecular and cortical bone destruction that typically have low-intermediate signal on T1WI and PDWI and heterogeneous slightly high to high signal on T2WI. Poorly defined zones of high signal on T2WI are usually seen in the marrow peripheral to the lesions secondary to inflammatory changes. Extension of lesions from the marrow into adjacent soft tissues through areas of cortical disruption are commonly seen as well as linear periosteal zones of high signal on T2WI. Lesions typically show prominent Gd-contrast enhancement in marrow and in extraosseous soft tissue portions of the lesions.	Benign tumorlike lesions consisting of Langerhans cells (histiocytes), and variable amounts of lymphocytes, polymorphonuclear cells, and eosinophils. Account for 1 % of primary bone lesions, and 8% of tumorlike lesions. Occur in patients with median age =10years, average =13.5years, peak incidence is between 5 and 10 years, 80-85% occur in patients less than 30 years. **(See Atlas Chapter A 18)**
Fracture and hemarthrosis (Fig. 16.13)	Fluid-fluid levels and debris can be seen with zones of mixed low, intermediate, and/or high signal on T1WI and T2WI within joints.	Fractures involving articular surfaces of bone can result in loose osteochondral fragments, marrow fat, hemorrhage, and inflammatory reaction within joints.
Synovial hemangioma (Fig. 16.14)	Lesions can have well-circumscribed margins with or without tobulation. Usually have low-intermediate signal or heterogeneous low-intermediate and high signal on T1WI and PDWI. The high-signal regions on T1WI and PDWI can range from thin linear zones to thick irregular zones, and are most often secondary to fat and occasionally from slow-flowing blood within these lesions. On T2WI. hemangiomas usually have distinct margins with or without tobulation, and slightly high to high signal. On FST2WI, hemangiomas typically have high signal except for zones of fat within the lesions. Lesions usually show prominent Gd-contrast enhancement. Prominent adjacent veins may be seen.	Benign hamartomatous lesions comprised of capillary, cavernous, and/or malformed venous vessels with varying amounts of mature adipose tissue. **(See Atlas Chapter A 34)**

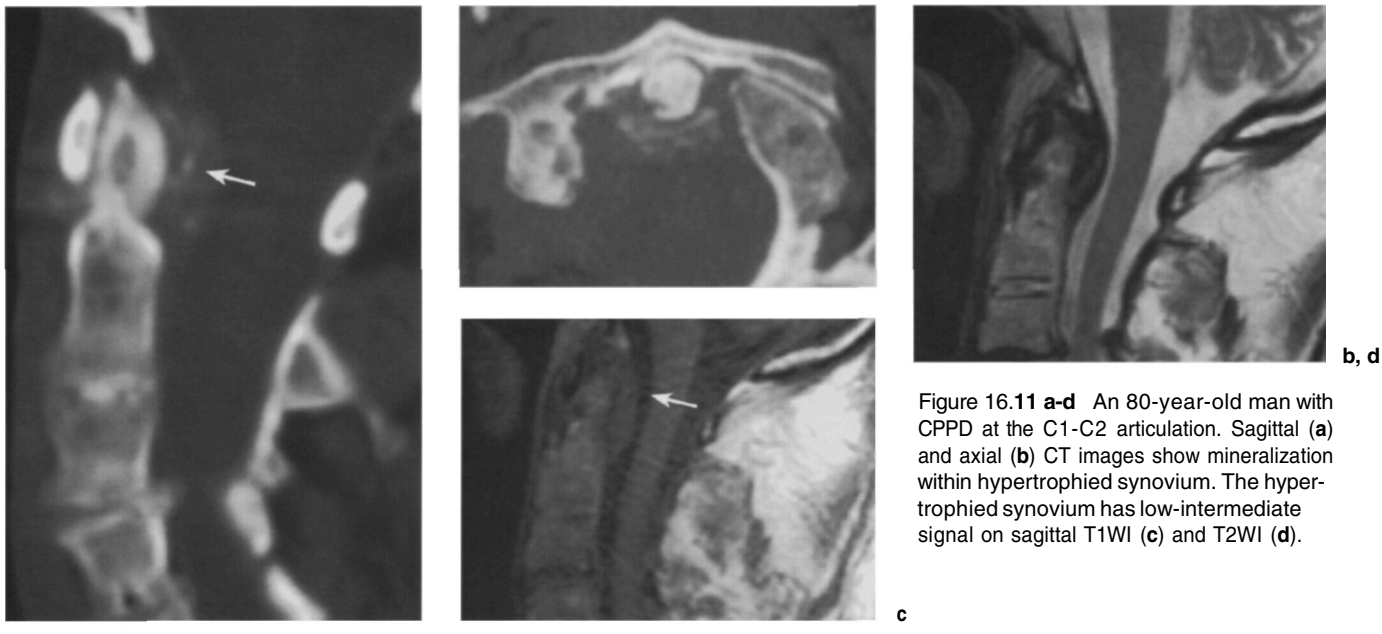

a c b, d

Figure 16.**11 a-d** An 80-year-old man with CPPD at the C1-C2 articulation. Sagittal (**a**) and axial (**b**) CT images show mineralization within hypertrophied synovium. The hypertrophied synovium has low-intermediate signal on sagittal T1WI (**c**) and T2WI (**d**).

a

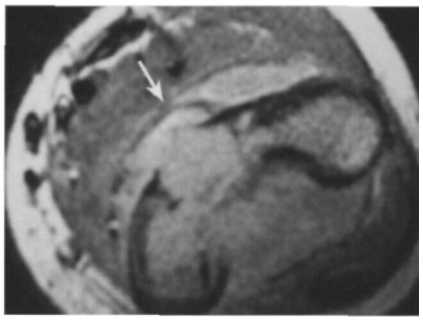

b

Figure 16.**12a, b** A 5-year-old boy with an eosinophilic granuloma involving the distal humerus. The lesion in the marrow is associated with cortical destruction and extraosseous extension into the adjacent soft tissues and elbow joint as seen on sagittal Gd-contrast enhanced T1WI (**a**) and axial PDWI (**b**).

a

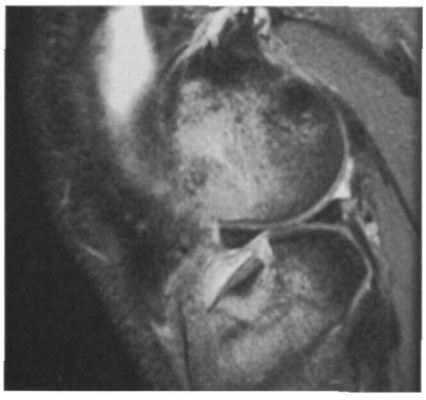

b

Figure 16.**13 a, b** A traumatic fracture of the lateral tibial plateau is seen with subjacent poorly defined zones of low-intermediate signal in the marrow on coronal PDWI (**a**) and high signal on sagittal FST2WI (**b**). Also seen is a bone contusion in the marrow of the lateral femoral condyle.

a

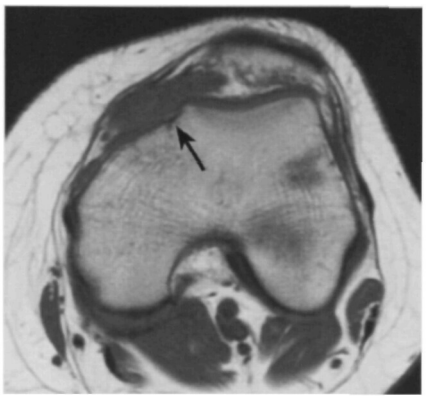

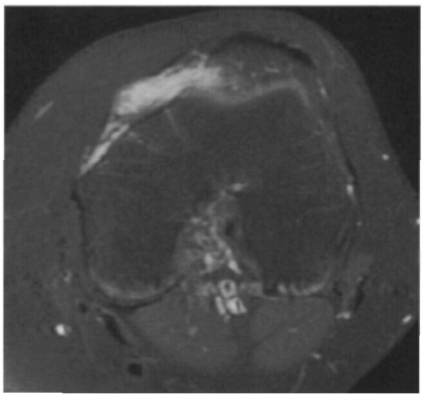

b. c

Figure 16.**14a-c** A 13-year-old girl with a synovial hemangioma in the knee. The lesion has high signal on sagittal FST2WI (**a**). Multiple enlarged veins are seen adjacent to the hemangioma. The hemangioma has intermediate signal on axial T1 WI (**b**) and shows prominent Gd-contrast enhancement on axial FST1WI (**c**).

Table 16 (Continued) Tumors and tumorlike lesions within joints

Lesion	MRI Findings	Comments
Lipoma arborescens (Fig. 16.15)	Appears as multiple nodular or frond-like deposits with fat signal within hypertrophied synovium, often associated with a joint effusion.	Disorder with multiple villous or frond-like zones of fatty deposition in synovium within a joint, tendon sheath, and/or bursa. Most frequently involves the knee. May be idiopathic, or occur in the setting of degenerative arthritis, collagen vascular disorders, or trauma. Occurs in patients aged from 9 to 66 years. **(See Atlas Chapter A43)**
Intra-articular lipoma (Fig.16.16)	Lesions usually have circumscribed margins and have MRI signal comparable to subcutaneous fat on T1WI, PDWI, T2WI, and FST2WI. Often do not show Gd-contrast enhancement except for minimal to mild enhancement along the thin nonfatty septa.	Common benign hamartomas composed of mature white adipose tissue without cellular atypia. Most common soft tissue tumor, representing 10% of all soft tissue tumors and 16% of benign soft tissue tumors. **(See Atlas Chapter A43)**
Giant cell tumor of bone with joint extension (Fig. 16.17)	Intraosseous lesions near the ends of long bones that often have low to intermediate signal on T1WI and PDWI. intermediate to high signal on T2WI. and high signal on FSPDWI and FST2WI. Aneurysmal bone cysts can be seen in 14% of giant cell tumors, resulting in cystic zones with variable signal and fluid-fluid levels. Lesions frequently have areas of cortical destruction with extraosseous extension, including into joints. Tumors show mild to prominent Gd-contrast enhancement.	Aggressive tumors composed of neoplastic ovoid mononuclear cells and scattered multinucleated osteoclast-like giant cells. Account for - 5 to 9.5 % of all bone tumors and up to 23% of benign bone tumors. Malignant giant cell tumors account for 5.8% of all giant cell tumors. Occur in patients aged from 4 to 81 years, median = 30 years, mean =33 years. **(See Atlas Chapter A29)**
Chondroblastoma (Fig. 16.18)	Lesions typically involve the physeal plate, adjacent epiphysis, and metaphysis. Lesions often have fine lobular margins, and typically have low-intermediate heterogeneous signal on T1WI and mixed low, intermediate, and/or high signal on T2WI. Areas of low signal on T2WI are secondary to chondroid matrix mineralization, and/or hemosiderin. Lesions can show marginal or septal Gd-contrast enhancement patterns. Cortical disruption and extraosseous extension into joints is uncommon. Perilesional zones with high signal on T2WI and Gd-contrast enhancement are commonly seen in bone marrow as well as periosteal location indicating reactive hyperemia and/or edema.	Benign cartilaginous tumors with chondroblast-like cells and areas of chondroid matrix formation usually involving the epiphysis. Usually present before cessation of endochondral bone growth. Account for 5-9% of benign bone lesions, 1-3% of all bone lesions. Occur in patients with median age =17years, mean age =16years for lesions in long bones, mean age -28 years in other bones. **(See Atlas Chapter A7)**
Malignant		
Intra-articular extension from metastatic tumor Involving bone	Intramedullary lesions with low-intermediate signal on T1WI; low-intermediate to slightly high signal on PDWI; slightly high to high signal on T2WI and FST2WI. Sclerotic lesions often have low signal on T1WI; and mixed low. intermediate, and/or high signal on T2WI. Tumors frequently cause cortical destruction with extension into the extraosseous soft tissues, including joints. Most lesions show Gd-contrast enhancement.	Proliferating neoplastic cells that are located in sites or organs separated or distant from their origins. Intraosseous metastatic lesions can have associated bone destruction and extraosseous extension, including into joints. **(See Atlas Chapter A50)**
Intra-articular extension from myeloma (Fig. 16.19)	Appear as multiple or single intramedullary zones with low-intermediate signal on T1WI and PDWI; and intermediate, slightly high to high signal on T2WI and slightly high to high signal on FST2WI. Intramedullary lesions and corresponding signal abnormalities may be diffuse, focal with poorly defined or distinct margins, and/or in an extensive variegated pattern. Lesions usually show Gd-contrast enhancement. Tumors frequently cause cortical destruction with extension into the extraosseous soft tissues, including joints.	Malignant tumors comprised of proliferating antibody-secreting plasma cells derived from single clones within bone marrow. Plasma cells normally account for <5% of the cells in bone marrow. Most common primary neoplasm of bone in adults, accounts for 44 % of primary malignant bone tumors and 34% of all primary bone tumors. Occurs in patients aged from 16 to 80 years, median =60 years. Most patients are older than 40 years. **(See Atlas Chapter A52)**

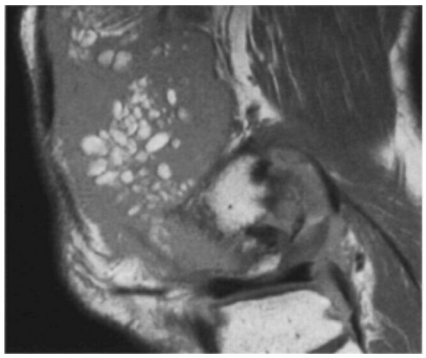

a

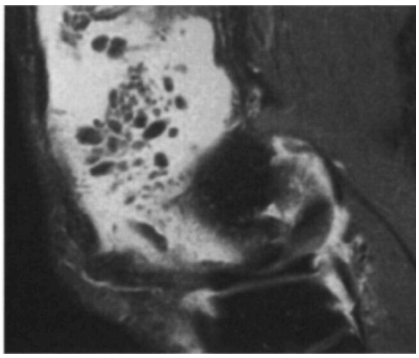

b

Figure 16.**15a, b** A 37-year-old man with lipoma arborescens at the knee. Multiple nodular and frond-like/villous deposits with fat signal are seen within hypertrophied synovium on sagittal PDWI **(a)**. The fat signal is suppressed on sagittal FST2WI **(b)**. The hypertrophied fatty synovium is seen within a large joint effusion.

Figure 16.**16** A 56-year-old man with a lipoma in Hoffa's fat pad that has high signal on sagittal T1WI.

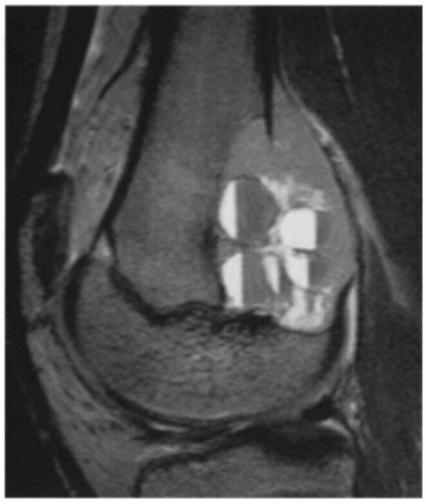

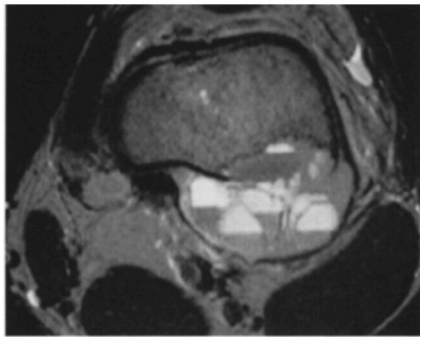

a, b

Figure 16.**17 a, b** A 17-year-old male with a giant cell tumor involving the distal metaphyseal portion of the femur associated with a secondary aneurysmal bone cyst. The tumor has mixed intermediate and high signal on sagittal (**a**) and axial (**b**) T2WI. Multiple fluid-fluid levels are seen at the aneurysmal cyst associated with the tumor within bone and at the extraosseous portion which extends through disrupted cortex dorsally into the knee joint.

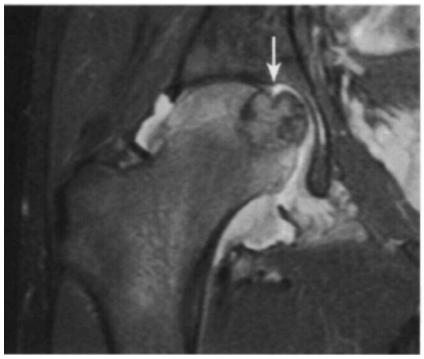

Figure 16.**18** A 17-year-old male with chondroblastoma in the proximal femur. The lesion is located mostly in the epiphysis, but also involves the physeal plate and a small portion of the metaphysis. The lesion has expanded and thinned the medial margin of the femoral head with resultant extension into the hip joint. The lesion has slightly lobulated margins, and has slightly high signal on coronal FST2WI as well as in the adjacent marrow. A joint effusion is also present.

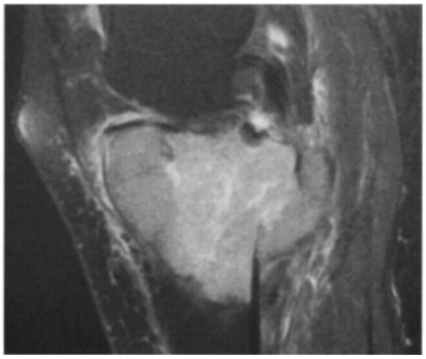

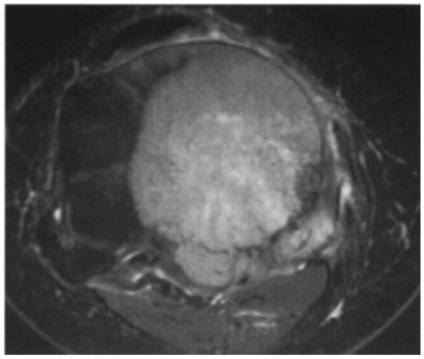

a, b

Figure 16.**19a, b** A 77-year-old woman with myeloma involving the marrow of the proximal tibia associated with cortical destruction and extraosseous extension, including the knee joint. The tumor has high signal on sagittal (**a**) and axial **(b)** FST2WI.

Table 16 (Continued) Tumors and tumorlike lesions within joints

Lesion	MRI Findings	Comments
Intra-articular extension from lymphoma involving bone (Fig. 16.20)	Appear as multiple or single intramedullary zones with low-intermediate signal on T1WI and PDWI; and intermediate, slightly high to high signal on T2WI and slightly high to high signal on FST2WI. Intramedullary lesions and corresponding signal abnormalities may be diffuse, focal with poorly defined or distinct margins, and/or in an extensive variegated pattern. Lesions usually show Gd-contrast enhancement. Tumors frequently cause cortical destruction with extension into the extraosseous soft tissues, including joints.	Lymphoma represents a group of lymphoid tumors whose neoplastic cells typically arise within lymphoid tissue (lymph nodes and reticuloendothelial organs). Unlike leukemia, lymphoma usually arises as discrete masses. Almost all primary lymphomas of bone are B cell non-Hodgkin lymphomas (NHL). NHL frequently originates at extranodal sites and spreads in an unpredictable pattern. **(See Atlas Chapter A47)**
Intra-articular extension from leukemia	Leukemic infiltration in marrow can appear as diffuse or poorly defined zones of low-intermediate signal on T1 WI and PDWI, intermediate-slightly high to high signal on FST2WI. Focal or geographic regions with similar signal alteration can also be seen. After Gd-contrast administration, leukemia can show Gd-contrast enhancement on T1 WI and FST1WI. It should be noted that Gd-contrast enhancement may be seen in normal vertebral marrow in children less than 7 years. Tumors can cause cortical destruction with extension into the extraosseous soft tissues, including joints.	Lymphoid neoplasms that have widespread involvement of the bone marrow as well as tumor cells in peripheral blood. Acute lymphoblastic leukemia (ALL) is the most frequent type in children and adolescents. In adults, chronic lymphocytic leukemia (CLL) is the most common type. Myelogenous leukemias represent neoplasms derived from abnormal myeloid progenitor cells that, if normal, would form erythrocytes, monocytes, granulocytes, and platelets. Acute myelogenous leukemia (AML) usually occurs in adolescents and young adults and accounts for ~20% of childhood leukemia. Chronic myelogenous leukemia (CML) occurs in adults older than 25 years. **(See Atlas Chapter A 41)**
Intra-articular extension from primary malignant bone tumors (Figs. 16.21, 16.22)	Appear as intramedullary zones with low-intermediate signal on T1WI; and intermediate, slightly high to high signal on T2WI and slightly high to high signal on FST2WI. Lesions usually show Gd-contrast enhancement. Tumors frequently cause cortical destruction with extension into the extraosseous soft tissues, including joints.	Primary sarcomas involving bone (osteosarcoma, chondrosarcoma, fibrosarcoma, etc.) can cause cortical destruction with extraosseous extension of tumor, including into joints.
Synovial chondrosarcoma	Lesions usually have low-intermediate signal on T1WI and heterogeneous predominantly high signal on T2WI. Zones of low signal on T2WI are related to the presence and degree of matrix mineralization and/or fibrous tissue. Lesions often have lobulated margins, with or without internal septations. Tumors usually show contrast enhancement in patterns ranging from lobulated peripheral and/or septal. or homogeneous versus heterogeneous depending on the degree of matrix mineralization and/or necrosis.	Chondrosarcomas rarely arise within synovium. **(See Atlas Chapter A11).**

a

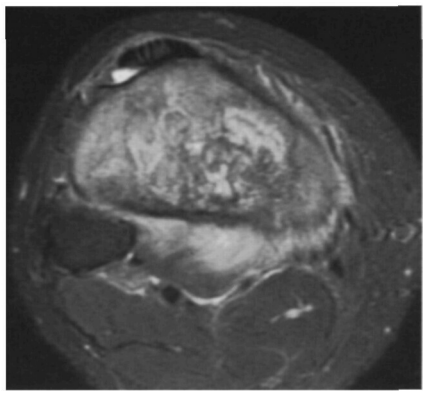

b

Figure 16.**20a, b** A 32-year-old woman with large B cell NHL involving the marrow of the proximal tibia associated with cortical destruction and extraosseous extension into the knee joint. The lymphoma has heterogeneous high signal on sagittal (**a**) and axial (**b**) FST2WI. A nodular lymphoma lesion is also seen dorsal and superior to the posterior cruciate ligament.

a, b

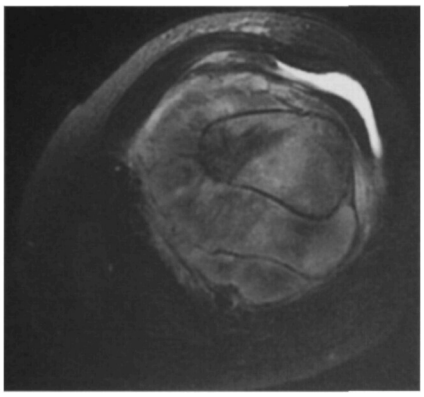

Figure 16.**21 a, b** Primary osteosarcoma in the distal metaphysis and epiphysis of the femur that extends from the marrow into adjacent extraosseous tissues and knee joint via multiple zones of cortical disruption. The intramedullary and extraosseous tumor has heterogeneous slightly high, intermediate, and low signal on sagittal (**a**) and axial (**b**) FST2WI. Irregular amorphous, divergent, and perpendicular bands and strands of low signal are seen in the extraosseous tumor representing tumor-induced bone formation/ periosteal reaction. A thin slightly irregular zone of low signal on T1WI is seen at portions of the peripheral border of the extraosseous tumor representing a partially intact elevated periosteum.

a, b

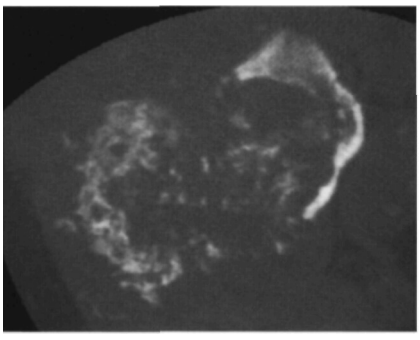

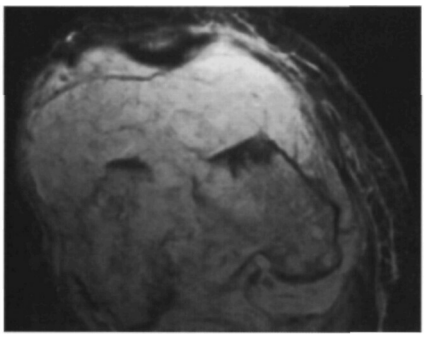

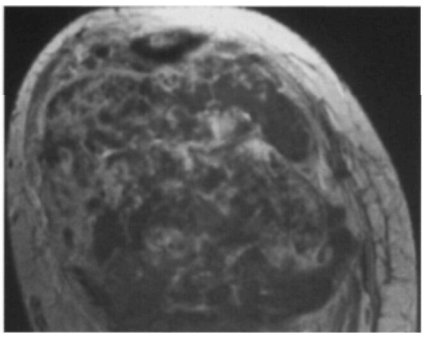

c

Figure 16.**22a-c** A 60-year-old woman with a dedifferentiated chondrosarcoma involving the distal femur. Axial CT image (**a**) shows a radiolucent lesion with chondroid matrix mineralization and associated zones of cortical destruction. The tumor has heterogeneous high signal on axial (**b**) FST2WI. Extensive cortical destruction is seen with tumor extension from the marrow into the knee joint and adjacent soft tissues. The lesion shows irregular heterogeneous Gd-contrast enhancement on axial T1WI (**c**).

References

Calcium Pyrophosphate Deposition Disease

Abreu M, Johnson K, Chung CB, et al. Calcification in calcium pyrophosphate dehydrate (CPPD) crystalline deposits in the knee: anatomic, radiographic, MR imaging, and histologic study in cadavers. *Skeletal Radiol* 2004;33:392-398.

Lin SH, Hsieh ET, Wu TY, Chang CW. Cervical myelopathy induced by pseudogout in ligamentum flavum and retro-odontoid mass: a case report. *Spinal Cord* 2006:44:692-694.

Mahmud T, Basu D, Dyson PHP. Crystal arthropathy of the lumbar spine - a series of six cases and a review of the literature.*J Bone Joint Surg* April 2005;87-B(4):513-517.

Table 17 Solitary tumors and tumorlike lesions of the soft tissues located mostly deep to the subcutaneous fat

Lesion	MRI Findings	Comments
Neoplastic-malignant		
Malignant fibrous histiocytoma (Fig. 17.1)	Tumors have poorly defined and or circumscribed margins, and often have low-intermediate signal on T1WI and heterogeneous intermediate-high signal on T2WI and FST2WI. Tumors show heterogeneous, often prominent Gd-contrast, enhancement.	Malignant tumors involving soft tissue and rarely bone that are presumed to derive from undifferentiated mesenchymal cells. The World Health Organization (WHO) now uses the term undifferentiated pleomorphic sarcoma for malignant fibrous histiocytoma (MFH). **(See Atlas Chapter A48)**
Fibrosarcoma/myxofibrosarcoma (Fig. 17.2)	Tumors can have slightly irregular margins, with or without associated destruction and invasion of adjacent bone. High-grade fibrosarcomas may have an infiltrative pattern with respect to adjacent soft tissues. Lesions usually have low-intermediate signal on T1WI, intermediate to slightly high signal on PDWI, and heterogeneous intermediate-high signal on T2WI. Margins of lesions may be indistinct on T2WI for high-grade lesions. Zones with high signal on T2WI can be seen in myxoid regions of myxofibrosarcoma. For sclerosing epithelioid fibrosarcoma, zones of low signal on T1WI and T2WI can be seen from regions of decreased cellularity and dense collagen deposition in these neoplasms. Tumors usually show heterogeneous Gd-contrast enhancement. Enhancing margins may be indistinct for high-grade lesions.	Uncommon malignant tumors consisting of bundles of fibroblasts/spindle cells with varying proportions of collagen, lacking other tissue differentiating features such as tumor bone, osteoid, or cartilage. Infantile fibrosarcoma accounts for < 1 % of all malignant soft tissue tumors and 12% of soft tissue tumors in infants, and occurs in young patients with mean age =2 years. Adult fibrosarcomas account for 4 % of malignant soft tissue tumors, mean age of patients -41 years. Variants of fibrosarcoma include: myxofibrosarcoma, low-grade fibromyxoid sarcoma, and sclerosing epithelioid fibrosarcoma. **(See Chapters A25 and A48)**

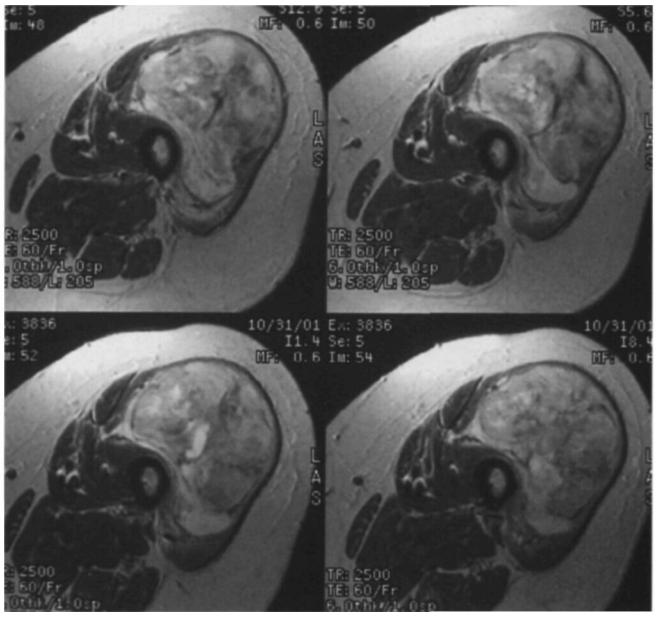

a

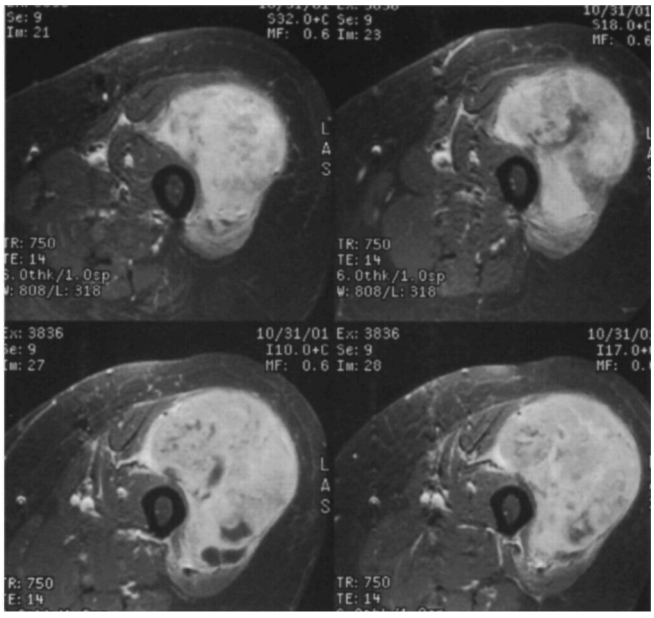

b

Figure 17.**1a, b** A 66-year-old woman a malignant fibrous histiocytoma involving the vastus lateralis muscle of the proximal thigh. The tumor has heterogeneous slightly high and high signal on axial T2WI (**a**) and shows irregular prominent Gd-contrast enhancement as well as several nonenhancing zones of necrosis on axial FST1WI (**b**).

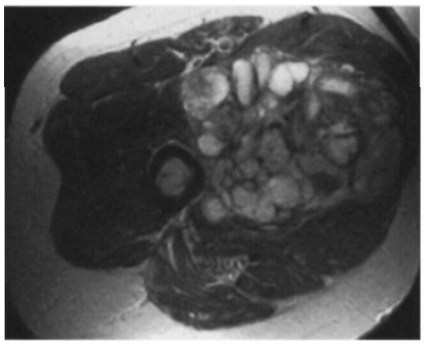

a

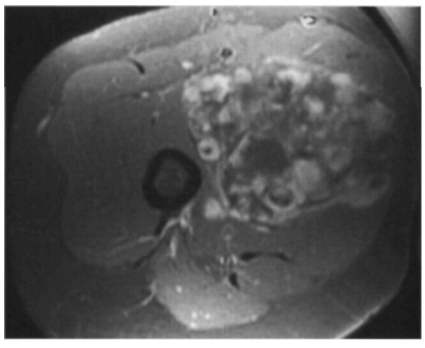

b

Figure 17.**2a, b** A 37-year-old man with a myxofibrosarcoma involving the adductor muscles in the proximal thigh, showing mixed zones of low, intermediate, and high signal on axial T2WI (**a**). The tumor shows prominent heterogeneous Gd-contrast enhancement on axial FST1WI(**b**).

Table 17 (Continued) Solitary tumors and tumorlike lesions of the soft tissues located mostly deep to the subcutaneous fat

Lesion	MRI Findings	Comments
Liposarcoma, well differentiated (Fig. 17.3)	Tumors contain up to 75 % overall fat signal, and contain thick nonadipose septae, and/or nodular nonadipose zones. The nonadipose zones can have low-intermediate signal on T1WI and PDWI; and low, intermediate, and/or high signal on T2WI. Nonadipose tumor portions show variable degrees of Gd-contrast enhancement.	Malignant mesenchymal tumors containing portions showing differentiation into adipose tissue. Compared with benign lipomas, these tumors have thicker and more numerous fibrous septae containing fibroblastic spindle cells, atypical cells and vacuolated lipoblasts surrounding various-sized lobules of fat. Fat cells have nuclear atypia, and hyperchromatic stromal cells are seen in fibrous septa. Account for 40-54 % of liposarcomas. Occur in patients 39 to 77 years, mean - 50 years **(See Atlas Chapter A44)**
Myxoid liposarcoma (Fig. 17.4)	Tumors usually have mostly low signal on T1WI, and may contain small zones of high fat signal in lacy, amorphous, and/or linear configurations. Most myxoid liposarcomas contain less than 25 % fat. Some myxoid liposarcomas do not contain fatty zones. Tumors can have heterogeneous or homogeneous high signal on PDWI, T2WI, and some have a multi-loculated pattern. Low signal septa may be present on T2WI. Tumors usually show Gd-contrast enhancement in varying degrees and patterns, or rarely none at all.	Composed of proliferating stellate and/or fusiform lipoblasts in varying stages of differentiation, signet cells containing lipids, variable myxoid matrix, and plexiform capillary network. Mitotic activity is usually low. Osseous, cartilaginous, and/or leiomyomatous metaplasia may occur in these tumors. Fat content in these myxoid liposarcomas is usually < 10 -25% of tumor volume. Account for 23 % of liposarcomas. Occur in patients 18 to 67 years, mean = 42 years. **(See Atlas Chapter A44)**

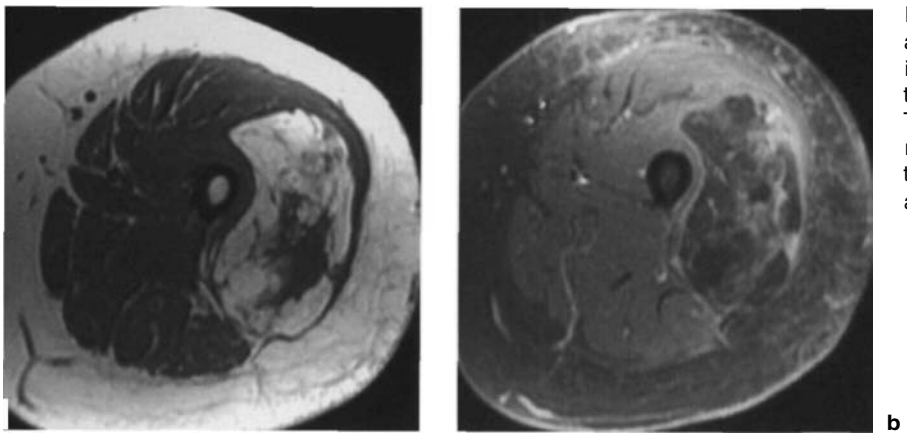

a b

Figure 17.**3 a, b** A 57-year-old woman with a well-differentiated low-grade liposarcoma involving the vastus lateralis muscle of the thigh. The tumor has high fat signal on axial T1WI (**a**) as well as zones with low-intermediate signal. The nonfatty portions of the tumor show Gd-contrast enhancement on axial FST1WI(**b**).

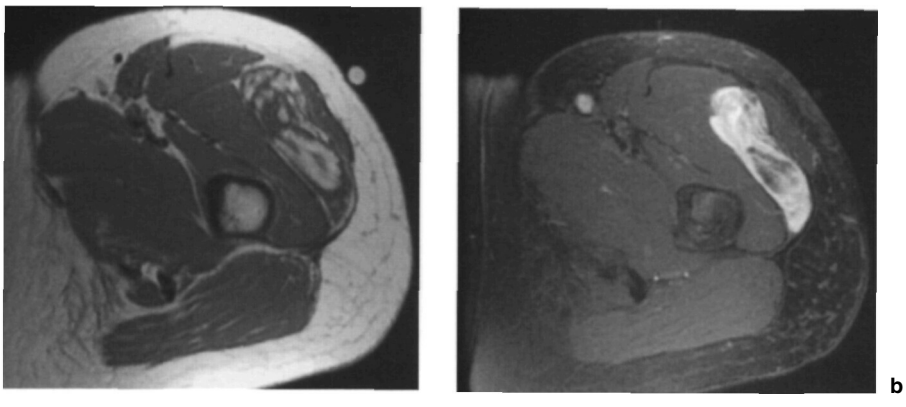

a b

Figure 17.**4a, b** A 13-year-old female with a myxoid liposarcoma involving the vastus lateralis muscle in the upper thigh. This tumor has circumscribed margins and contains both low-intermediate signal and high signal on axial T1WI (**a**). Some of the zones with high signal on T1WI secondary to fat are suppressed on axial FST2WI (**b**) whereas most of the tumor has high signal from the myxoid components.

Table 17 (Continued) Solitary tumors and tumorlike lesions of the soft tissues located mostly deep to the subcutaneous fat

Lesion	MRI Findings	Comments
Pleomorphic liposarcoma (Fig. 17.5)	Tumors often have relatively well-defined margins, and have heterogeneous/mixed low, intermediate, and/or high signal on T1WI, PDWI, and T2WI. Less than 26% of the tumor volumes have fat signal. Tumors usually show prominent Gd-contrast enhancement in a heterogeneous pattern.	Tumors contain lipogenic and nonlipogenic zones that have features similar to malignant fibrous histiocytoma, round cell liposarcoma, and/or epithelioid carcinoma. Tumors have prominent cellular pleomorphism with malignant pleomorphic lipoblasts, pleomorphic spindle cells, and occasional giant cells. Mitoses are common. Variable degrees of necrosis are seen. Most tumors have infiltrative borders microscopically. Account for 5-7 % of liposarcomas. Occur in patients 41 to 78 years, mean =60 years **(See Atlas Chapter A44)**
Round cell liposarcoma	Tumors can have relatively well-defined margins *(72%)* or poorly defined margins (28%), and have heterogeneous/mixed low, intermediate, and/or high signal on T1WI, PDWI, and T2WI. Most round cell liposarcomas contain <26% fat. Tumors usually show prominent Gd-contrast enhancement (61 %) in a heterogeneous pattern that may be globular or nodular.	Contain round small cells with single naked round or slightly oval nuclei, scarce cytoplasm containing vacuoles with minimal intracellular lipid. Tumor cells have low mitotic activity and occur within a myxoid matrix. Have been considered to represent poorly differentiated myxoid liposarcomas. Account for 6 % of liposarcomas. Occur in patients 30 to 64 years, mean =43 years. **(See Atlas Chapter A44)**
Dedifferentiated liposarcoma (Fig. 17.6)	Tumors can contain portions with features of a well-differentiated liposarcoma as well as a focal nonlipomatous mass. Frequently occur in the retroperitoneum and can be large (mean = 19.3 cm). Tumors can have circumscribed, and/or irregular/poorly defined margins. Tumors often have heterogeneous/mixed low, intermediate, and/or high signal on T1WI, PDWI, and T2WI. Hemorrhage and necrosis can be seen in the nonlipomatous portions. Tumors often show prominent Gd-contrast enhancement in nonlipomatous portions in a heterogeneous or homogeneous pattern.	Occur most frequently in the retroperitoneum and often contain both well-differentiated and poorly differentiated zones. The poorly differentiated component is usually a high-grade sarcoma. Account for 10% of liposarcomas. Occur in patients 42 to 78 years, mean =63 years **(See Atlas Chapter A44)**
Metastatic disease (Fig. 17.7)	Tumors can occur as lymphadenopathy or as focal lesions. Lesions have low-intermediate signal on T1 WI; and intermediate to slightly high signal or high signal on T2WI and FST2WI. Variability in MRI signal characteristics may be related to differing histologic features of the metastatic lesions. Tumors can show variable degrees of Gd-contrast enhancement.	Metastatic lesions are proliferating neoplastic cells that are located in sites or organs separated or distant from their origins. **(See Atlas Chapter A50)**
Myeloma	Lesions usually have low-intermediate signal on T1WI and slightly high to high signal on T2WI and high signal on FST2WI. Extraosseous tumors can occur from extension from intraosseous lesions, or from within the soft tissues. Lesions may have poorly defined or distinct margins. Most lesions show Gd-contrast enhancement. Zones of high signal on T2WI peripheral to the Gd-contrast enhancing portion of the lesion may represent zones of tumor invasion or perilesional edema.	Malignant tumors comprising proliferating antibody-secreting plasma cells derived from single clones. Usually occur in bone and occasionally in soft tissue. **(See Atlas Chapter A52)**
Lymphoma (Fig. 17.8)	Lymphadenopathy from Hodgkin lymphoma (HL) and lesions of non-Hodgkin lymphoma (NHL) have low-intermediate signal on T1WI and intermediate to slightly high signal on T2WI. Variability in MRI signal may be related to differing histologic features (such as the degree of fibrosis) for the subtypes of HL. After Gd-contrast administration, HL and NHL can show variable Gd-contrast enhancement.	Lymphomas are tumors in which neoplastic cells arise within lymphoid tissue. HL usually occurs in lymph nodes and spreads along nodal chains, whereas NHL frequently originates at extranodal sites and spreads in an unpredictable pattern. Mycosis fungoides is a T-cell lymphoma that involves the skin. **(See Atlas Chapter A47)**

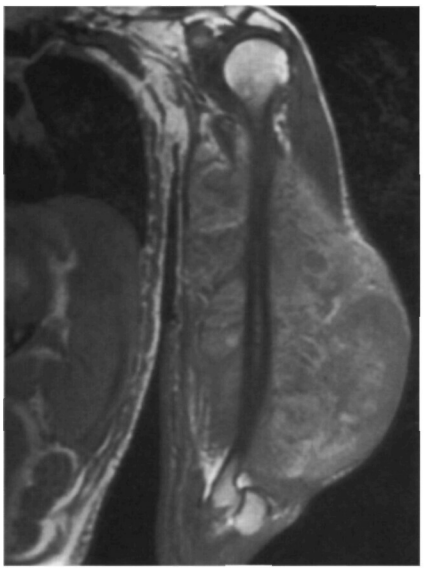

Figure 17.**5** A 43-year-old man with a large high-grade pleomorphic liposarcoma involving the left arm that has heterogeneous intermediate and slightly high signal on coronal T1WI.

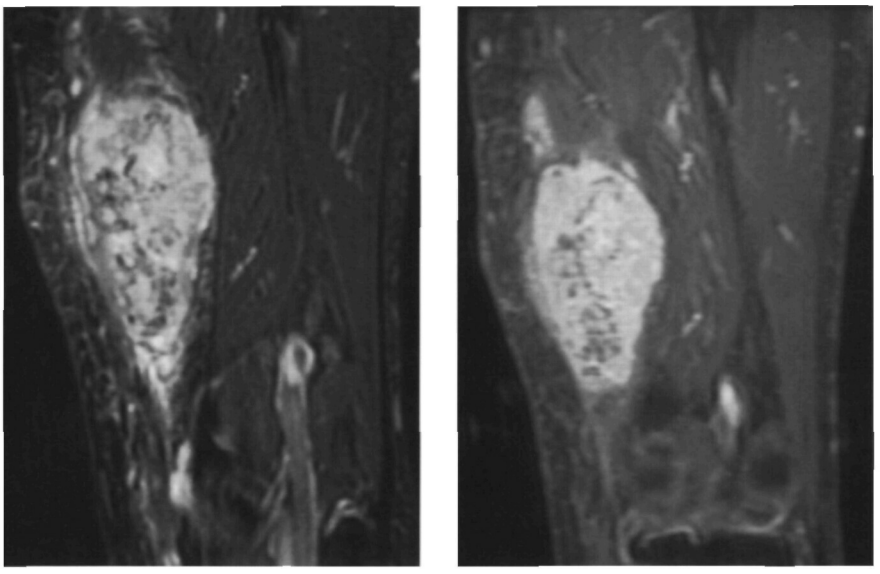

a, b

Figure 17.**6a, b** A 71-year-old woman with a dedifferentiated liposarcoma in the distal thigh. A large mass lesion involving the soft tissues of the medial thigh that has circumscribed margins and contains mostly high signal on coronal (**a**) FS T2WI as well as small zones with low signal. The tumor shows prominent slightly heterogeneous Gd-contrast enhancement on coronal FST1WI (**b**).

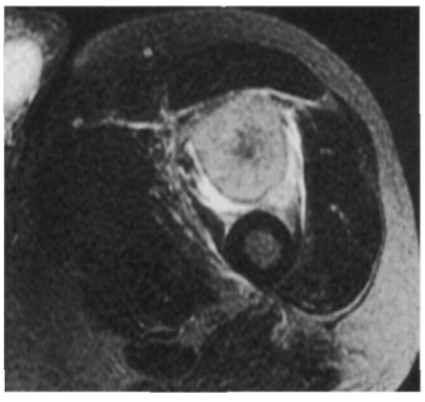

a

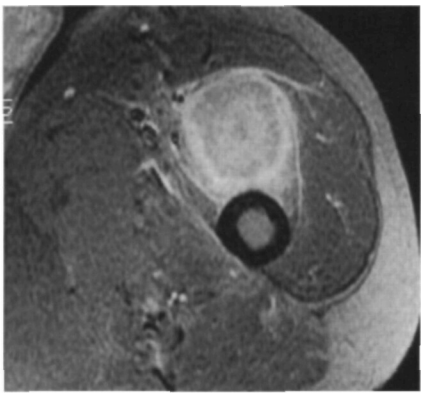

b

Figure 17.**7 a, b** A 51-year-old man with a metastatic lesion from lung carcinoma involving the vastus intermedius muscle of the upper thigh, showing high signal on axial T2WI (**a**). The tumor shows prominent Gd-contrast enhancement on axial FST1WI (**b**).

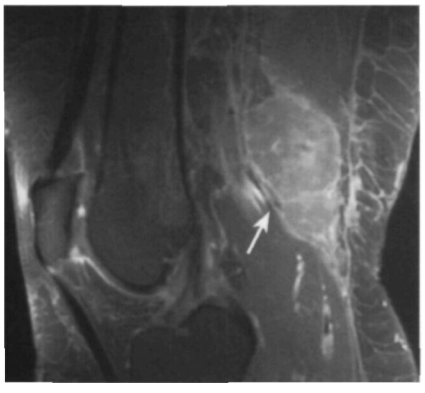

a

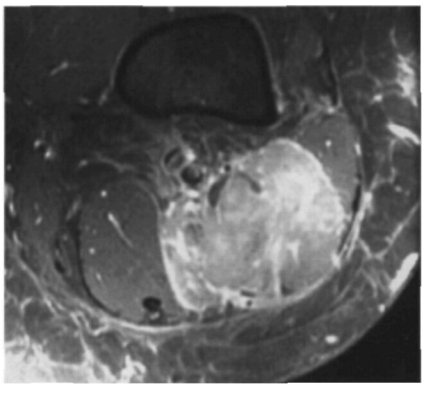

b

Figure 17.**8a, b** A 51-year-old woman with diffuse large B cell NHL involving the posterior soft tissues at the distal thigh, showing slightly heterogeneous Gd-contrast enhancement on sagittal (**a**) and axial (**b**) FST1WI.

Table 17 (Continued) Solitary tumors and tumorlike lesions of the soft tissues located mostly deep to the subcutaneous fat

Lesion	MRI Findings	Comments
Leukemia (Fig. 17.9)	Appear as single or multiple well-circumscribed or poorly defined infiltrative lesions; low-intermediate signal on T1WI, intermediate-high signal on T2WI and FST2WI, often shows Gd-contrast enhancement, +/- cortical bone destruction and extraosseous extension from lesions in marrow.	Malignant lymphoid neoplasms with involvement of bone marrow with tumor cells also in peripheral blood and in soft tissues. **(See Atlas Chapter A41)**
Synovial cell sarcoma (Fig. 17.10)	Tumors are often ovoid and/or lobulated lesions that often have low-intermediate signal on T1WI and heterogeneous signal (various combinations of intermediate, slightly high, high, and/or low signal) on T2WI. Multiloculated cystic zones are present in 77 %. Calcifications may occur in up to 30 %. Tumors show various patterns of Gd-contrast enhancement.	Mesenchymal tumors comprised of spindle cells and cells with varying degrees of epithelial differentiation. Account for 5% of primary malignant soft tissue tumors. Occur in patients 14 to 58 years, mean -32 years. **(See Atlas Chapter A75)**
Malignant peripheral nerve sheath tumor (Fig. 17.11)	These lesions usually have heterogeneous signal on T1 WI and T2WI; as well as heterogeneous Gd-contrast enhancement because of necrosis and hemorrhage. Some malignant peripheral nerve sheath tumors (MPNSTs) are similar in appearance to benign nerve sheath tumors.	MPNSTs are malignant tumors of the peripheral nerve sheath that contain mixtures of packed hyperchromatic spindle cells with elongated nuclei and slightly eosinophilic cytoplasm, mitotic figures and zones of necrosis. Approximately 50 % of MPNSTs occur in patients with neurofibromatosis type 1 (NF1), followed by de novo evolution from peripheral nerves. Malignant peripheral nerve sheath tumors infrequently arise from schwannomas, ganglioneuroblastomas/ganglioneuromas, and pheochromocytomas. **(See Atlas Chapter A 56)**
Clear cell sarcoma (also referred to as melanoma of soft parts) (Fig. 17.12)	Tumors can have well defined or irregular margins, and usually have low-intermediate signal on T1WI; and intermediate to slightly high or high signal on T2WI and FST2WI. Tumors usually show Gd-contrast enhancement. Erosion into bone can occur.	Rare malignant tumors with melanocytic differentiation (immunoreactive to SI00 protein, HMB45) that occur in patients between 10 and 50 years. Usually occur in the deep soft tissues involving aponeuroses and tendons.
Leiomyosarcoma (Fig. 17.13)	Lesions may have well-defined or irregular margins, and often have intermediate signal on T1 WI and PDWI. which can be hyperintense relative to muscle, and intermediate to slightly high or high signal on T2WI and FST2WI. Large lesions often have zones of necrosis or cystic change that have low signal on T1WI and high signal on T2WI. Solid portions of the lesions usually show Gd-contrast enhancement.	Malignant mesodermal tumors associated with smooth muscle differentiation that can arise de novo or occur after radiation treatment. Account for 8 % of primary malignant soft tissue tumors and 3% of all primary soft tissue tumors. Patients range in age from 35 to 79 years, mean =58 years. **(See Atlas Chapter A 40)**

a

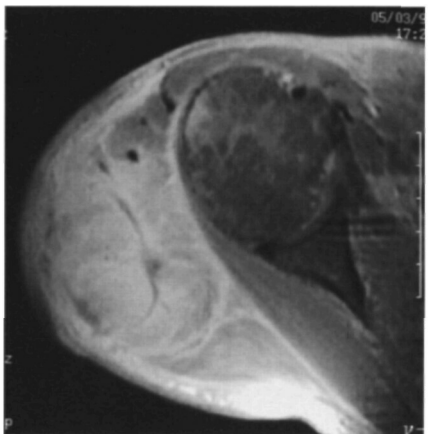

b

Figure 17.**9a, b** A 69-year-old man with acute myelogenous leukemia involving the soft tissues at the right shoulder and right humerus. Leukemic involvement in the soft tissues has slightly high signal on axial FST2WI (**a**) and irregular indistinct margins. Leukemic tissue in the marrow of the humerus has heterogeneous slightly high signal on axial FST2WI. The leukemic tissue in marrow shows minimal Gd-contrast enhancement, whereas the leukemic involvement in the extraosseous soft tissues shows prominent Gd-contrast enhancement on axial FST1WI (**b**).

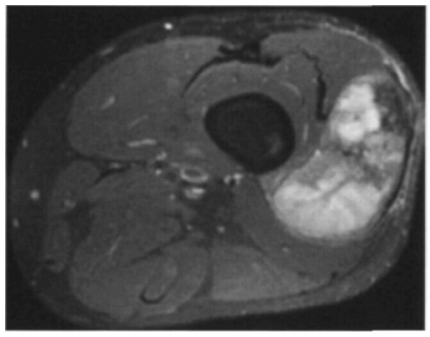

a

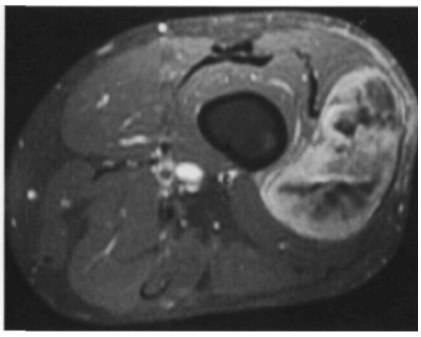

b

Figure 17.**10a, b** A 59-year-old man with a synovial sarcoma in the lateral lower thigh involving the vastus lateralis muscle, showing heterogeneous mostly high signal with zones of low and intermediate signal on axial FST2WI (**a**). The tumor shows prominent heterogeneous Gd-contrast enhancement on axial FST1WI(**b**).

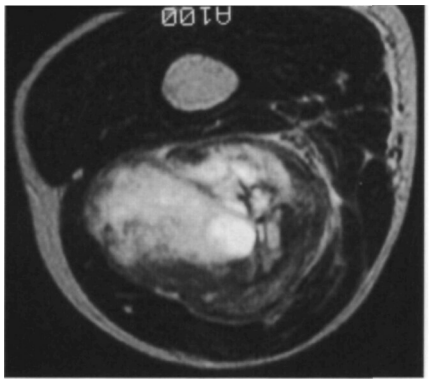

a

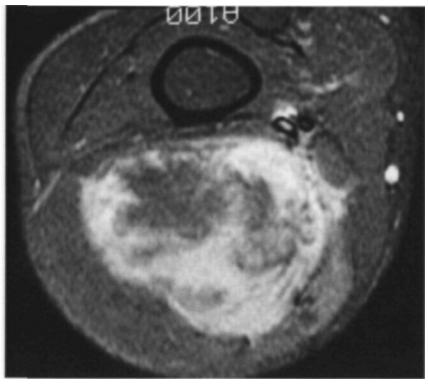

b

Figure 17.**11 a, b** Malignant peripheral nerve sheath tumor in the posterior soft tissues of the thigh in a 19-year-old man with NF1 and multiple neurofibromas in both thighs. A large lesion is seen in the right thigh that has mixed high, low, and intermediate signal on axial T2WI (**a**). The tumor shows heterogeneous irregular Gd-contrast enhancement on axial FST1WI (**b**).

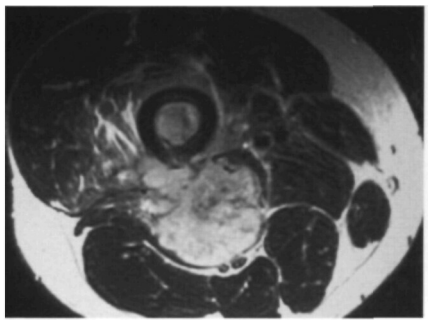

a

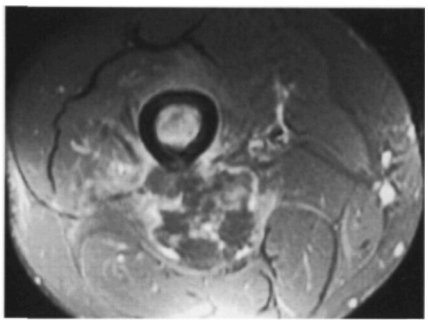

b

Figure 17.**12 a, b** A 52-year-old man with clear cell sarcoma involving the muscles of the thigh that has mostly high signal on axial T2WI (**a**). The tumor shows heterogeneous Gd-contrast enhancement on axial FST1WI (**b**). The tumor erodes adjacent cortical bone and extends into the marrow.

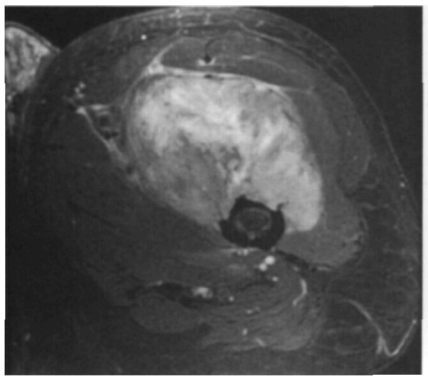

a

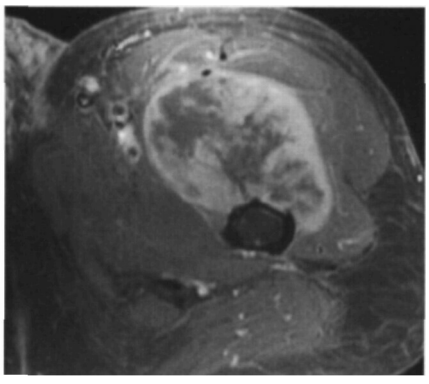

b

Figure 17.**13a, b** A 55-year-old man with a leiomyosarcoma involving the muscles of the thigh that has heterogeneous mostly high signal on axial FST2WI (**a**) as well as small zones of low signal. The tumor shows mostly prominent Gd-contrast enhancement except at several sites of necrosis on axial FST1WI (**b**). Erosion of the outer cortical margin of the femur by the tumor is present.

Table 17 (Continued) Solitary tumors and tumorlike lesions of the soft tissues located mostly deep to the subcutaneous fat

Lesion	MRI Findings	Comments
Rhabdomyosarcoma (Fig. 17.14)	Tumors can have circumscribed and/or poorly defined margins, and typically have low-intermediate signal on T1WI and heterogeneous signal (various combinations of intermediate, slightly high, and/or high signal) on T2WI and FST2WI. Tumors show variable degrees of Gd-contrast enhancement.	Malignant mesenchymal tumors with rhabdomyoblastic differentiation that occur primarily in soft tissue. Account for *2%* of primary malignant soft tissue tumors and < 1 % of all primary soft tissue tumors. Account for 19% of soft tissue sarcomas in children. **(See Atlas Chapter A69)**
Hemangioendothelioma	Tumors have lobulated well-defined or irregular margins, and have intermediate signal on T1WI, and heterogeneous predominantly high signal on T2WI with or without internal low signal septations. Flow voids may be seen with the lesions. Tumors show heterogeneous Gd-contrast enhancement.	Low-grade malignant neoplasms composed of vasoformative/endothelial elements that occur in soft tissues and bone. These tumors are locally aggressive and rarely metastasize, compared with the high-grade endothelial tumors such as angiosarcoma. Account for < 1 % of malignant and all soft tissue tumors. Patients range in age from 17 to 60 years, mean =40 years. **(See Atlas Chapter A33)**
Hemangiopericytoma (Fig. 17.15)	Usually have well-defined margins, often have low-intermediate signal on T1WI, intermediate or slightly high-high signal on T2WI, and heterogeneous high signal on FST2WI. On T2WI, lesions may contain tubular signal voids centrally or peripherally likely representing tumor vessels. Can contain hemorrhagic zones with corresponding MR signal alteration. Typically show Gd-contrast enhancement.	Rare malignant tumors of presumed pericytic origin that contain various shaped pericytic cells (oval, round, spindle-like) and adjacent irregular branching vascular spaces lined by endothelial cells. Usually occur in soft tissues and less frequently in bone. Account for < 1 % of primary tumors in the soft tissues. Most tumors, 90-95 %, occur in adults, and 5-10% occur in children. **(See Atlas Chapter A35).**
Angiosarcoma (Fig. 17.16)	Tumors have low-intermediate signal on T1WI, mixed low, intermediate, and/or high signal on T2WI, and show prominent Gd-conlrast enhancement in a homogeneous or heterogeneous pattern.	Malignant tumors composed of neoplastic blood vessels in bone and/or soft tissues. These tumors can be associated with Paget disease, radiation treatment, bone infarcts, knee and hip prostheses, synthetic vessel grafts, prior trauma or surgery, osteomyelitis, and hereditary disorders (NF1, Maffucci disease, achondroplasia). Represent < 1 % of malignant bone tumors. Account for 2% of malignant soft tissue tumors. Patients range in age from 5 to 97 years, mean =49 years (8. 9, 11). **(See Atlas Chapter A6)**
Extraosseous osteosarcoma (Fig. 17.17)	Tumors have irregular poorly defined or slightly well-circumscribed margins and heterogeneous signal on most MRI pulse sequences. Various combinations of low, intermediate, and/or high signal on T1WI, T2WI, and FST2WI can be seen depending on the presence and extent of hemorrhage and/or necrosis within the lesions. On T2WI and FST2WI, tumors often have heterogeneous predominantly high signal. Fluid-fluid levels may be present at sites of hemorrhage or necrosis. Peripheral nonenhancing high signal on T2WI may be present and represent zones of edema and/or tumor invasion within adjacent tissues. Tumors often show heterogeneous patterns of Gd-contrast enhancement.	Malignant tumor comprised of proliferating neoplastic spindle cells that produce osteoid and/or immature tumoral bone. Osteosarcoma most commonly occurs within bone and less frequently on the external surface of bone. Rarely, osteogenic sarcomas can also occur as extraskeletal primary lesions in the soft tissues. **(See Atlas Chapter A64)**

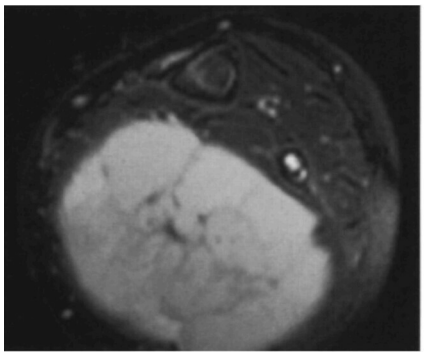

a

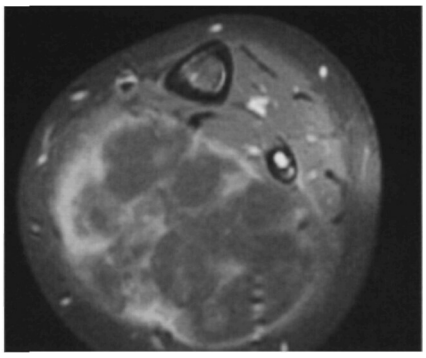

b

Figure 17.**14a, b** A 2.5-year-old girl with an embryonal rhabdomyosarcoma involving the posterior calf. The tumor has mostly high signal with strands of low signal on axial FS T2WI (**a**). The tumor shows heterogeneous irregular peripheral and central Gd-contrast enhancement on axial FS T1 WI (**b**). The tumor is associated with signal alteration of the adjacent fibula.

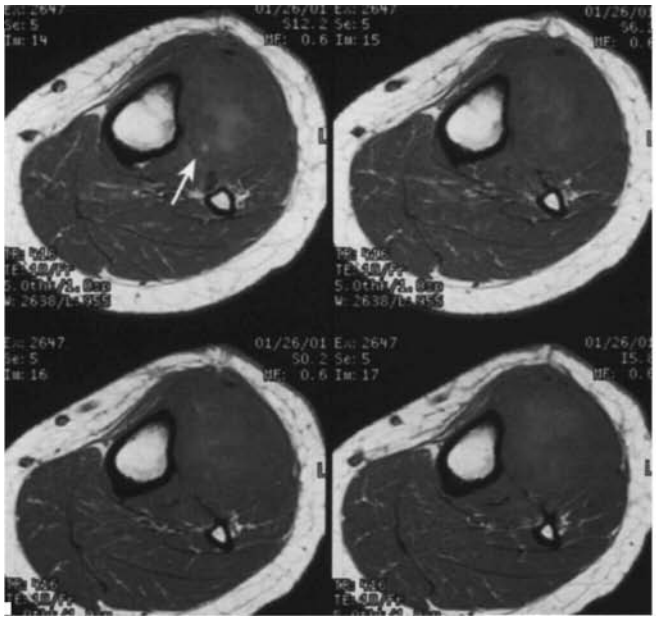

a

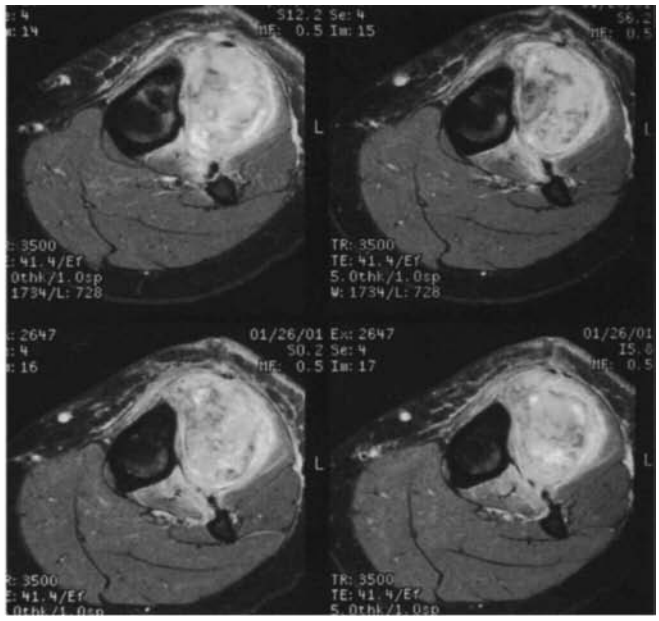

b

Figure 17.**15a, b** A 29-year-old woman with a hemangiopericytoma involving the tibialis anterior, tibialis posterior, extensor digitorum longus, and popliteus muscles. The tumor has mostly intermediate signal on axial (**a**) T1 WI as well as several zones of high signal at sites of hemorrhage. The tumor has mixed intermediate and mostly high signal on axial FST2WI (**b**) as well as foci and curvilinear zones of low signal.

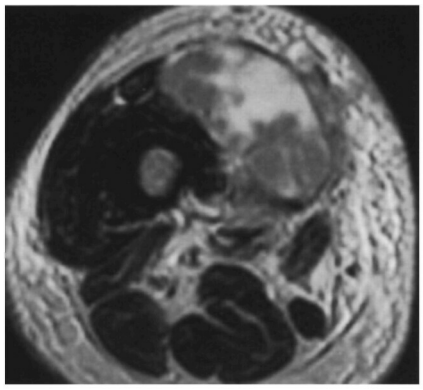

a

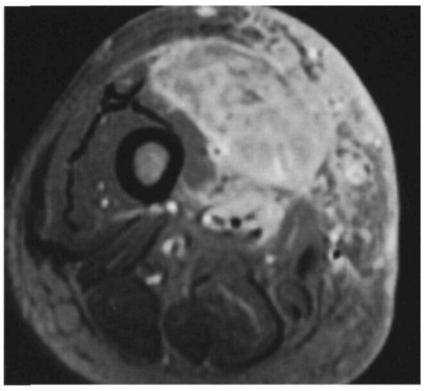

b

Figure 17.**16a, b** A 74-year-old man with an angiosarcoma in the medial anterior thigh involving the vastus medialis muscle. The tumor has mixed low, intermediate, and/or high signal on axial T2WI (**a**) and shows prominent Gd-contrast enhancement on FST1WI (**b**).

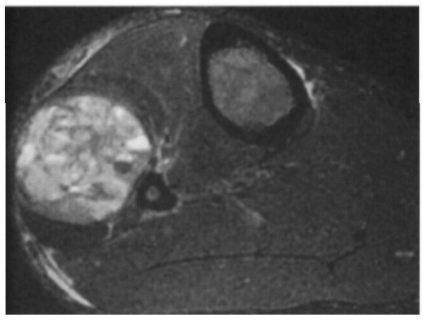

a, b

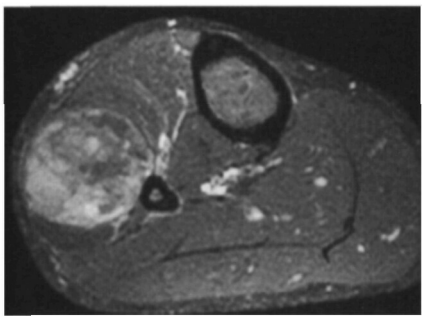

Figure 17.**17a, b** A 32-year-old man with an extraosseous osteosarcoma involving the extensor digitorum longus muscle and peroneus longus and brevis muscles of the proximal lateral leg. The tumor has heterogeneous mostly high signal on axial FST2WI (**a**) as well as septa with low signal and fluid-fluid levels with high and low signal. Fluid-fluid levels represent sites of hemorrhage within the tumor. The tumor shows heterogeneous Gd-contrast enhancement on axial FST1WI (**b**).

Table 17 (Continued) Solitary tumors and tumorlike lesions of the soft tissues located mostly deep to the subcutaneous fat

Lesion	MRI Findings	Comments
Extraosseous Ewing sarcoma (Fig. 17.18)	Tumors usually have low-intermediate signal on T1WI, and heterogeneous slightly high to high signal on T2WI and FST2WI. Tumors often show prominent irregular Gd-contrast enhancement.	Malignant primitive tumors of bone and occasionally soft tissue that are comprised of undifferentiated small cells with round nuclei. **(See Atlas Chapter A20)**
Extraosseous chondrosarcoma (Fig. 17.19)	Tumors have low-intermediate signal on T1WI, intermediate signal on PDWI, and heterogeneous intermediate, slightly high and/or high signal on T2WI. Foci of low signal on T1WI and T2WI can be seen secondary to chondroid matrix mineralization. Lesions typically show heterogeneous Gd-contrast enhancement.	Malignant tumors containing cartilage formed within sarcomatous stroma, with or without areas of calcification/mineralization, myxoicl material, and/or ossification. **(See Atlas Chapter A11)**
Neoplastic-benign		
Lipoma (Fig. 17.20)	Often have circumscribed margins and have MRI signal comparable to subcutaneous fat on T1WI, PDWI, T2WI, and FST2WI. Often do not show Gd-contrast enhancement except for minimal to mild enhancement along the thin nonfatty septa.	Common benign hamartomas composed of mature white adipose tissue without cellular atypia. Most common soft tissue tumor, representing 10% of all soft tissue tumors and 16% of benign soft tissue tumors. **(See Atlas Chapter A43)**
Lipomatosis (Fig. 17.21)	Infiltrating adipose tissue or multiple lobules of fat can be seen in muscles, fascial planes, and/or subcutaneous fat.	Diffuse proliferation of mature adipose tissue. Can occur as several types. The diffuse type typically occurs in the soft tissues of an extremity or trunk in children with or without associated osseous hypertrophy. Multiple symmetric lipomatosis (Madelung disease) usually occurs in the neck, trunk, and pelvis of adult men (peak incidence in the 5th decade). Shoulder girdle lipomatosis usually occurs in women and involves the muscles at one shoulder and adjacent chest wall. Adiposis dolorosa (Dercum syndrome) usually occurs in obese postmcnopausal women who have multiple painful fatty lesions in the extremities or trunk.
Atypical lipoma (Fig. 17.22)	Atypical lipomas may contain cystic/necrotic zones, calcifications, thick septa, and/or nodular zones that may or may not show Gd-contrast enhancement. Most atypical lipomas contain >75% fat, whereas liposarcomas often have <75% fat. Distinguishing between atypical lipomas and low-grade liposarcomas with MRI can be difficult and challenging.	Atypical lipomas account for up to 31 % of lipomas. Lesions contain zones with osseous, chondroid, or fibrous metaplasia with myxoid changes. Atypical lipomas have been labeled as chondroid lipomas, osteolipomas, or benign mescnchymomas. Chondroid lipomas contain mature fat, lipoblasts, and chondroid matrix. Spindle cell and pleomorphic lipomas are variants that have varying proportions of mature fat cells, spindle cells, collagen, and multinucleated giant cells. Lipomas with high content of fibrous tissue have been labeled as fibrolipomas. **(See Atlas Chapter A43)**

a

b

Figure 17.**18 a, b** An 11-year-old girl with an extraosseous Ewing sarcoma in the soft tissues adjacent to the right clavicle. The tumor has intermediate signal on coronal PDWI (**a**) and high signal on axial FST2WI (**b**).

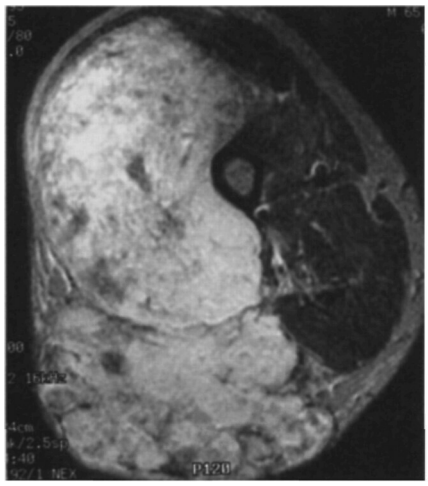

a

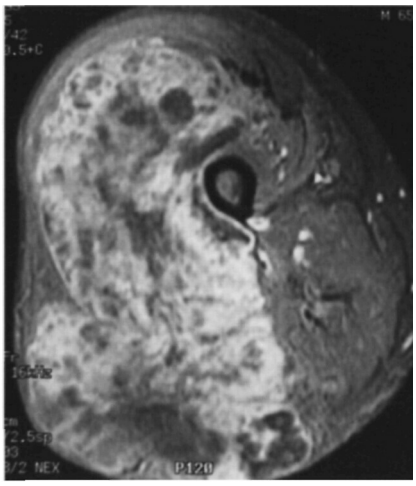

b

Figure 17.**19a, b** A 65-year-old man with an extraosseous myxoid chondrosarcoma in the distal thigh that has circumscribed margins and contains heterogeneous mostly high signal with small foci of low signal on axial T2WI (**a**). The lesion shows prominent irregular heterogeneous Gd-contrast enhancement on axial FST1WI (**b**).

a

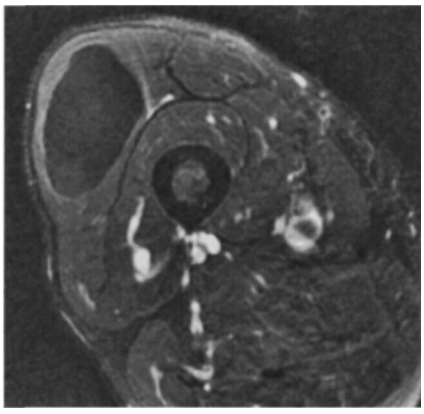

b

Figure 17.**20a, b** A 71-year-old woman with an intramuscular lipoma in the thigh. The lipoma has high signal on axial T1WI (**a**). The fat signal of the lipoma is suppressed on axial FST2WI (**b**).

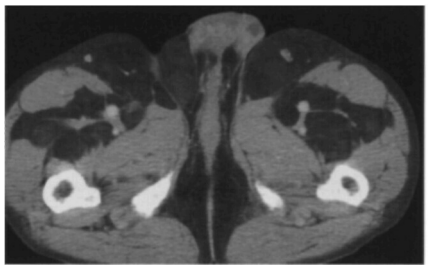

a

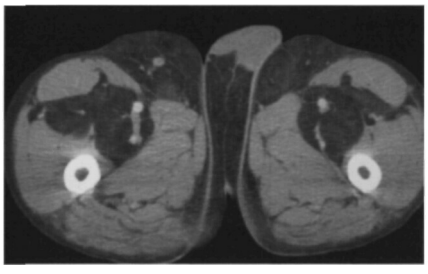

b

Figure 17.**21 a, b** A 42-year-old man with bilateral symmetric lipomatosis involving the inguinal regions, subcutaneous and intermuscular soft tissues of both proximal thighs. Multiple fatty lobules are seen with thin peripheral nonfatty septa on axial CT images (**a**, **b).** Poorly defined zones with attenuation slightly higher than fat are also seen in the fatty lobules.

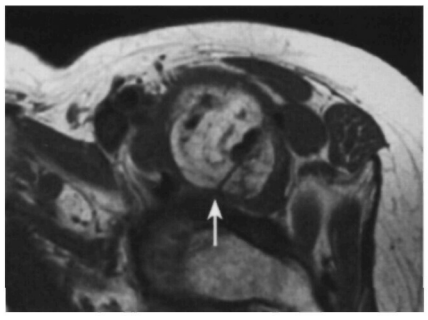

a

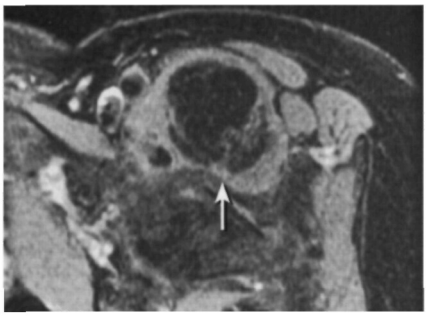

b

Figure 17.**22 a, b** A 55-year-old woman with an atypical lipoma/osteolipoma involving the iliopsoas muscle ventral to the proximal femur The lesion contains mostly fat signal on axial T1WI (**a**) as well as curvilinear and small nodular zones of low signal. The signal of the fatty portions of the lesion is suppressed on axial FST2WI (**b**), whereas several of the small nonfatty portions show intermediate to high signal.

Table 17 (Continued) Solitary tumors and tumorlike lesions of the soft tissues located mostly deep to the subcutaneous fat

Lesion	MRI Findings	Comments
Hibernoma (Fig. 17.23)	Well-defined lesions that often have intermediate to high signal on T1WI (hypo- or isointense relative to fat), and slightly high signal on T2WI. Lesions can have slightly hyperintense signal relative to fat on FST2WI and STIR. Internal septations, and/or branching-serpentine slow-flow vascular channels may be seen on T1WI and T2WI. Lesions can show Gd-contrast enhancement within branching vascular channels.	Rare benign lesions derived from brown adipose tissue intermixed with white adipose tissue. Account for <2% of fatty tumors. Occur in patients aged from 2 to over 75 years, mean =32 to 38 years. **(See Atlas Chapter A43)**
Lipoblastoma (Fig. 17.24)	Lesions often have mixed low, intermediate, and high signal on T1WI, T2WI, and FST2WI. Lesions often show heterogeneous Gd-contrast enhancement.	Rare benign mesenchymal tumors that contain embryonal fat. Account for <1 % of benign soft tissue tumors. Occur in patients from less than 1 to 10 years, mean = 4 years. **(See Atlas Chapter A42)**
Hemangioma (Fig. 17.25)	Hemangiomas have circumscribed margins with or without lobulations, and have low-intermediate signal or heterogeneous low-intermediate and high signal on T1WI and PDWI; and high signal on T2WI. On FST2WI, hemangiomas typically have high signal except for zones of fat within the lesions. Zones of hemorrhage can sometimes be present in hemangiomas as well as phleboliths. Hemangiomas usually show prominent Gd-contrast enhancement.	Benign hamartomatous lesions of bone and soft tissues comprised of capillary, cavernous, and/or malformed venous vessels. **(See Atlas Chapter A34)**
Lymphangioma (Figs. 273-275 In Atlas section)	Can be circumscribed lesions or occur in infiltrative pattern with extension within and between muscles. Often contain single or multiple cystic zones that have predominantly low signal on T1WI and high signal on T2WI and FS T2WI. Fluid-fluid levels and zones with high signal on T1WI and variable signal on T2WI may result from cysts containing hemorrhage, high protein concentration, and/or necrotic debris. Septa between the cystic zones can vary in thickness and Gd-contrast enhancement, and usually have low signal on T1WI and low to intermediate signal on T2WI and FST2WI. Nodular zones within the lesions can have variable degrees of Gd-contrast enhancement.	Benign vascular tumors that typically occur in soft tissue and only rarely in bone that result from abnormal proliferation of lymphatic vessels. Lesions are composed of endothelium-lined lymphatic channels interspersed within connective tissue stroma. Account for < 1 % of benign soft tissue tumors, 5.6% of all benign lesions of infancy and childhood. Can occur in association with Turner syndrome and Proteus syndrome. Patients usually range in age from 1 to 50 years, mean =19years. Can be congenital, with ~50% present at birth. Approximately 85 % are detected by age 2. **(See Atlas Chapter A46)**
Nodular fasciitis (Fig. 17.26)	Lesions can have mildly irregular or stellate borders. Lesions usually have intermediate signal on T1WI and PDWI; and homogeneous or mildly heterogeneous high signal on T2WI and FS T2WI. Surrounding edema is occasionally seen. Older lesions with high fibrous content may have intermediate signal on T2WI. Lesions can show homogeneous or peripheral rim- like patterns of Gd- contrast enhancement.	Benign reactive lesion comprised of proliferating fibroblasts, usually occur in the subcutaneous tissue or muscle. Account for 11 % of benign soft tissue tumors and 7 % of all soft tissue tumors. Patients range from 11 to 51 years, mean =31 years. **(See Atlas Chapter A21)**

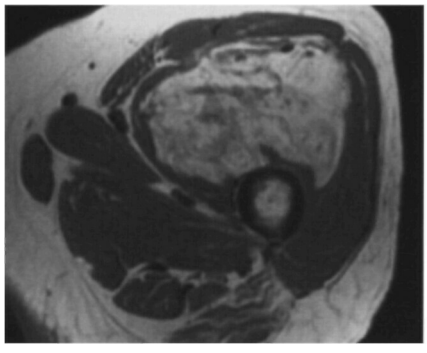

a

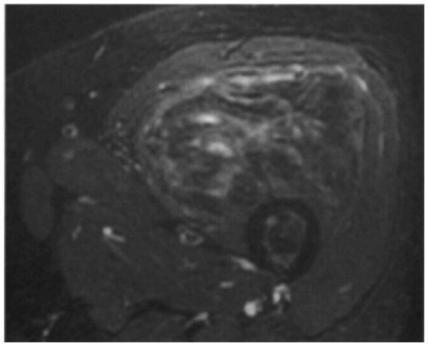

b

Figure **17.23a, b** A 71-year-old woman with a hibernoma involving the vastus muscles of the proximal thigh. The lesion has well-defined margins and contains mostly fat signal on axial T1WI (**a**) as well as curvilinear and small nodular zones of low signal. The signal of the fatty portions of the lesion is suppressed on axial FST2WI (**b**), whereas nonfatty portions show intermediate to high signal on FST2WI.

a b, c

Figure 17.**24a-c** A 1.5-year-old boy with a large intra-abdominal and pelvic lipoblastoma that has heterogeneous attenuation with zones of soft tissue, fluid, and fat attenuation on axial CT **(a**). The lesion has mixed low-intermediate, intermediate, and high signal on axial T1WI (**b**) and heterogeneous mostly high signal with thin strands of low signal on axial FST2WI (**c**).

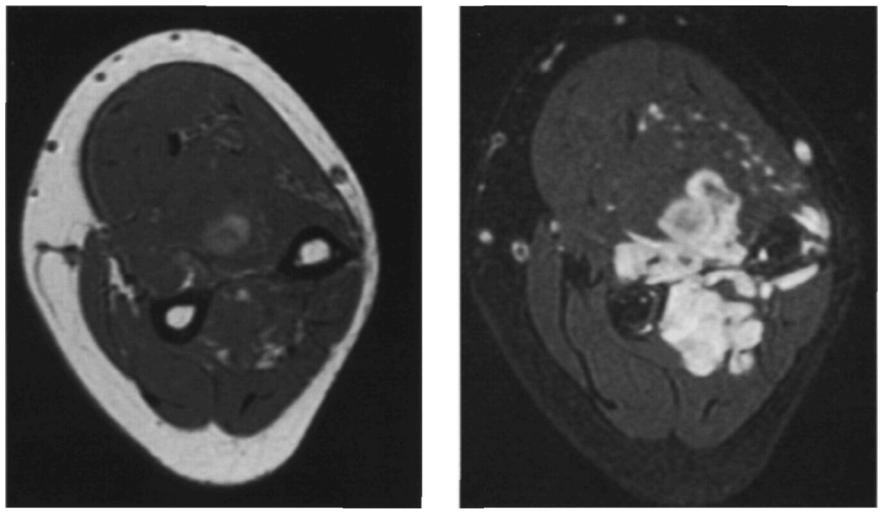

a b

Figure 17.**25a, b** A 14-year-old female with a hemangioma in the soft tissues of the forearm that has mostly intermediate signal on axial T1 WI (**a**) and contains a zone of high signal from an area of hemorrhage. The lesion has mostly high signal on axial FST2WI (**b**). Several prominent veins are also seen.

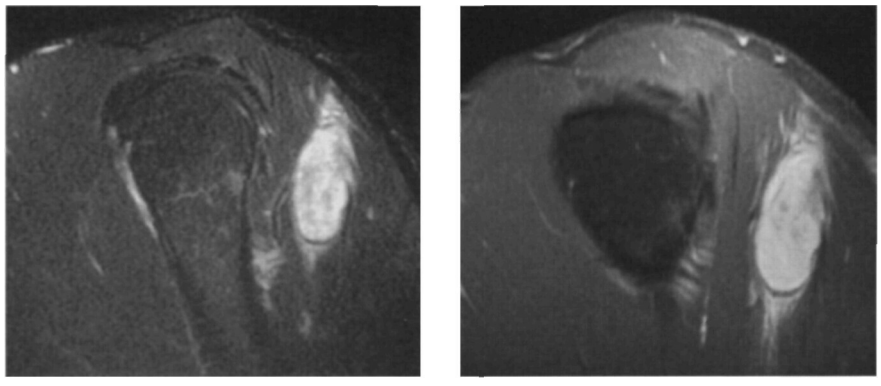

a b

Figure 17.**26 a, b** A 43-year-old man with intramuscular nodular fasciitis involving the deltoid muscle at the left shoulder. The lesion has high signal on sagittal FST2WI (**a**) that is surrounded by a thin rim of low signal and poorly defined zones of high signal in the adjacent soft tissues. The lesion shows prominent Gd-contrast enhancement on sagittal FST1WI (**b**).

Table 17 (Continued) Solitary tumors and tumorlike lesions of the soft tissues located mostly deep to the subcutaneous fat

Lesion	MRI Findings	Comments
Nerve sheath tumor (schwannoma, neurofibroma) (Figs. 17.27-17.29)	**Localized neurofibromas and Schwannomas** are circumscribed ovoid or fusiform lesions with low-intermediate signal on T1WI, intermediate signal on PDWI, and intermediate to high signal on T2WI and FST2WI. Lesions typically show moderate to prominent Gd-contrast enhancement. Multiple neurofibromas and schwannomas are frequently seen with NF1 and NF2, respectively. Neurofibromas can occur in various soft tissues. **Plexiform neurofibromas** appear as curvilinear and multinodular lesions involving multiple nerve branches. They have low to intermediate signal on T1 WI and intermediate, slightly high to high signal on T2WI and FS T2WI with or without bands or strands of low signal. Lesions usually show Gd-contrast enhancement.	Benign nerve sheath tumors include schwannomas and neurofibromas. Schwannomas are benign encapsulated tumors that contain differentiated neoplastic Schwann cells. Neurofibromas contain mixtures of Schwann cells, perineural-like cells, and interlacing fascicles of fibroblasts associated with abundant collagen. Unlike schwannomas, neurofibromas lack Antoni A and B regions and cannot be separated pathologically from the underlying nerve. Neurofibromas can be localized lesions, or occur as diffuse or plexiform lesions. Multiple neurofibromas are typically seen with NF1. Multiple schwannomas are typically seen with NF2. **(See Atlas Chapters A56, A72)**
Neurothekeoma (Fig. 17.30)	Occurs as circumscribed lesions with low-intermediate signal on T1 WI, high signal on T2WI, and heterogeneous Gd-contrast enhancement.	Neurothekeoma, also referred to as nerve sheath myxoma, is considered to be a neurofibroma with prominent myxoid matrix separated into lobules by fibrous connective tissue. **(See Atlas Chapter A 56)**
Paraganglioma (Fig. 17.31)	Paragangliomas are circumscribed ovoid or fusiform lesions with low-intermediate signal on T1WI and PDWI, and intermediate to high signal on T2WI and FST2WI. Multiple tortuous and/or punctate zones of signal void or low signal on PDWI, T2WI, and FST2WI can be seen within tumors as a "salt and pepper" pattern. Lesions typically show moderate to prominent Cd-contrast enhancement.	Extra-adrenal paragangliomas are benign encapsulated neuroendocrine tumors that arise from neural crest cells associated with autonomic ganglia (paraganglia) throughout the body. In the superficial soft tissues, paragangliomas can occur at the carotid body in the neck or near the vagus nerve. Patients range from 24 to 70 years, mean = 47 years. **(See Atlas Chapter A 66)**
Solitary fibrous tumor (Fig. 17.32)	SFTs often have circumscribed margins. Often have low to intermediate signal on T1WI and PDWI, low, intermediate, and/or slightly high signal on T2WI, and heterogeneous slightly high to high signal on FST2WI. Usually show Gd-contrast enhancement.	Rare benign spindle-cell mesenchymal neoplasms that occur in a wide range of anatomic sites including the extremities. Tumors typically show a hemangiopericytoma-like branching vascular pattern and resemble pleural SFTs. Account for < 2 % of soft tissue tumors. Median patient age from 50 to 60 years. **(See Atlas Chapter A24)**

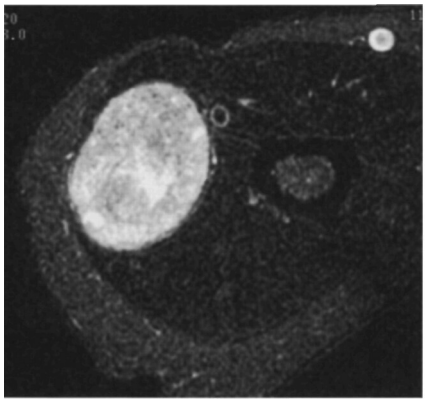

a

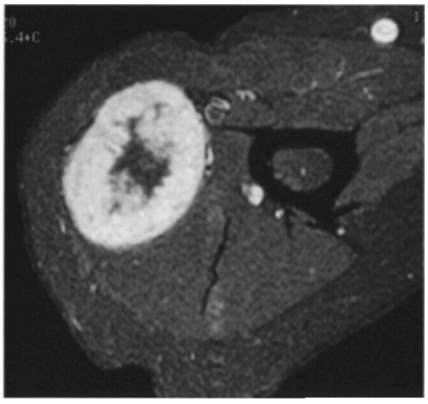

b

Figure 17.**27 a. b** A 61-year-old woman with an intramuscular schwannoma in the arm that has high signal on axial T2WI (a) and shows heterogeneous Gd-contrast enhancement on axial FST1WI (**b**).

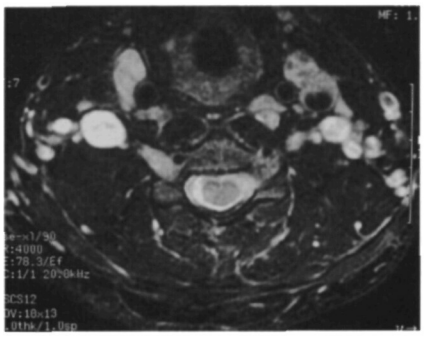

Figure 17.**28** A 22-year-old man with NF1 with multiple neurofibromas in the soft tissues in the neck, showing high signal on axial FST2WI.

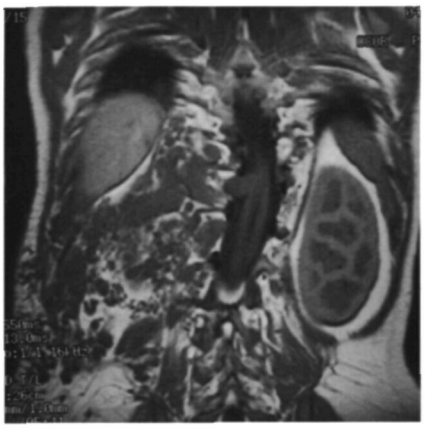

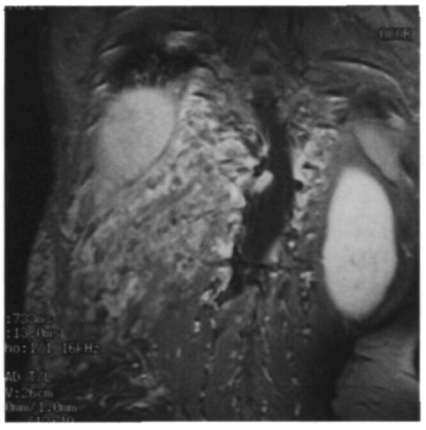

a, b

Figure 17.**29a, b** A 2-year-old girl with NF1 and a plexiform neurofibroma posterior and medial to the right kidney with extension into the spinal canal. The tumor appears as curvilinear and multinodular zones with intermediate signal on coronal T1 WI (**a**) and heterogeneous Gd-contrast enhancement on coronal FST1WI (**b**).

a

b

Figure 17.**30a, b** A 38-year-old man with a neurothekeoma involving the flexor digitorum superficialis muscle of the proximal forearm. The lesion has high signal on axial T2WI (**a**) and shows moderate heterogeneous Gd-contrast enhancement on sagittal FST1WI(**b**).

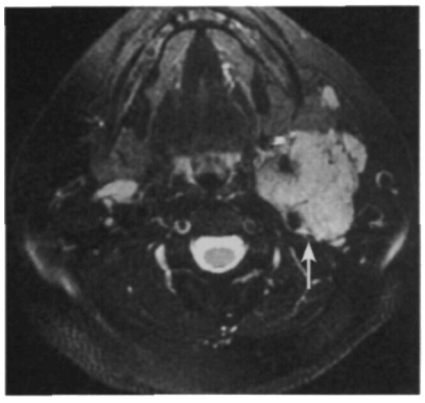

a

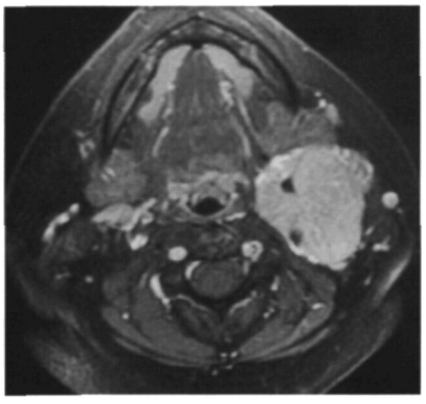

b

Figure 17.**31 a, b** A 27-year-old woman with a paraganglioma (carotid body tumor) at the left common carotid artery bifurcation. The lesion has heterogenous mostly high signal on axial FST2WI (**a**) and shows prominent Gd-contrast enhancement on axial FST1WI (**b**). The tumor splays the proximal external carotid artery from the internal carotid artery.

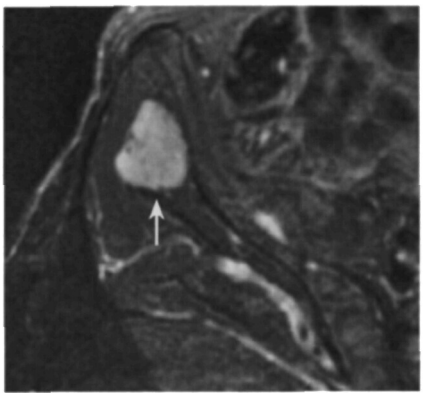

a

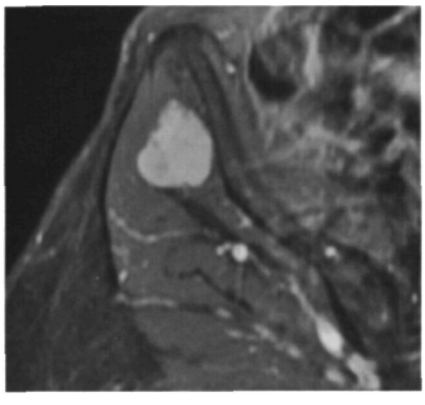

b

Figure 17.**32a, b** An 81-year-old man with a solitary fibrous tumor involving the gluteus minimus muscle. The lesion has circumscribed margins, high signal on axial FST2WI (**a**), and shows Gd-contrast enhancement on axial FST1WI (**b**).

Table 17 (Continued) Solitary tumors and tumorlike lesions of the soft tissues located mostly deep to the subcutaneous fat

Lesion	MRI Findings	Comments
Desmold tumor (Fig. 17.33)	Lesions can have distinct and/or poorly defined margins, homogeneous or heterogeneous low-intermediate signal on T1WI, and variable intermediate-high signal on T2WI, +/- zones of low signal. Myxoid zones in the lesions can have high signal on T1 WI and T2WI. Tumors with high cellularity tend to show higher signal on T2WI than lesions with larger proportions of collagen. Lesions show variable degrees and patterns (heterogeneous versus homogenous) of Gd-contrast enhancement. Pattern or degree of Gd-contrast enhancement by desmoids does not enable prediction of rate of tumor recurrence.	Desmoid tumors or fibromatosis represent a group of soft tissue lesions comprised of benign fibrous tissue with elongated or spindle-shaped cells adjacent to collagen. **(See Atlas Chapter A16)**
Myxoma (Fig. 17.34)	Lesions usually have low or low-intermediate signal on T1WI and PDWI, and high signal on T2WI and FST2WI. Myxomas can have heterogeneous mild or moderate degrees of enhancement in noncystic portions.	Benign lesions that contain fibroblasts (spindle cells) and abundant mucoid material (glycosaminoglycans, other mucopolysaccharides). Account for 3 % of benign soft tissue tumors/lesions and 2 % of all soft tissue tumors/lesions. Occur in adults aged from 24 to 74 years, mean = 52 years. **(See Atlas Chapter A54)**
Tumorlike lesions		
Ganglion cyst (Fig. 17.35)	Ganglia are sharply defined lesions with low signal on T1WI, low-intermediate signal on PDWI. and homogeneous high signal on T2WI. Some ganglia may have intermediate signal on T1WI secondary to elevated proteinaceous or fibrous content. Low signal septa on T2WI can be seen. Peripheral rim-like Gd-contrast enhancement can be seen as well as complete lack of enhancement.	Ganglia are juxta-articular benign myxoid lesions that arise from degeneration of peri-articular connective tissue, prior trauma, or prior inflammation. Ganglia may be derived from tendons, tendon sheaths, joint capsules, bursae, or ligaments. **(See Atlas Chapter A28)**
Hematoma/seroma (Fig. 17.36)	Acute hematomas (< 3-7 days) have mostly intermediate signal similar to muscle on T1WI and mixed low-intermediate and/or high signal relative to muscle on PDWI, T2WI, and FST2WI. Poorly defined zones of high signal on PDWI, T2WI, and FST2WI may also be seen peripheral to the hematoma representing adjacent edema. Subacute hematomas (1 week to 3 months) have high and/or intermediate signal on T1WI, and high signal on FST1WI, PDWI, T2WI, and FST2WI. Peripheral and central zones of low signal on PDWI, T2WI, and FS T2WI can be seen in mid to late subacute hematomas secondary to the presence of hemosiderin from breakdown of blood cells and oxidation/metabolism of hemoglobin. Mild peripheral Gd-contrast may be seen Chronic hematomas (>3 months) usually have high signal on T1WI, PDWI, T2WI, and FST2WI. A thick peripheral rim of low signal on T2WI from hemosiderin is often seen with chronic hematomas. Chronic hematomas often evolve eventually into zones with low-intermediate signal on T1 WI and T2WI secondary to fibrosis and residual hemosiderin.	Hematomas are extravascular collections of red and white blood cells that can result from trauma, surgery, coagulopathy (hemophilia, thrombocytopenia, medications/coumadin/heparin, and sepsis). **(See Atlas Chapter A36)**

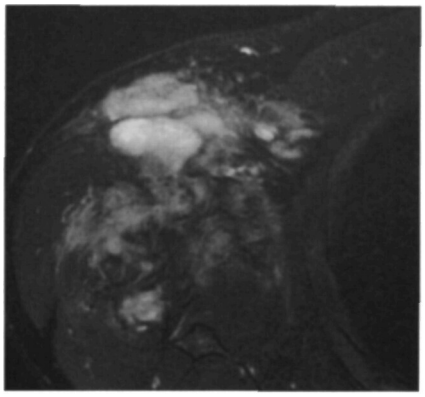

a

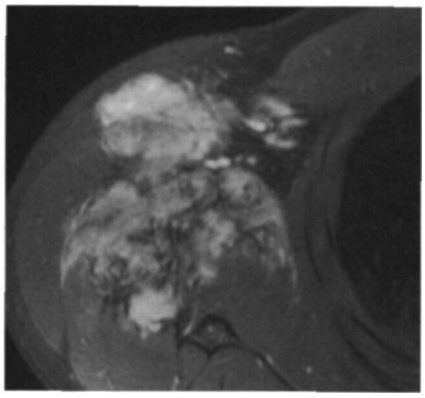

b

Figure 17.**33a, b** A 32-year-old man with aggressive fibromatosis involving the soft tissues in the right axilla. MRI shows a lobulated lesion with indistinct margins that has slightly high and high signal on axial FST2WI (**a**). Foci and thin curvilinear zones of low signal are also seen. The lesion shows prominent heterogeneous Gd-contrast enhancement on axial FST1WI (**b**).

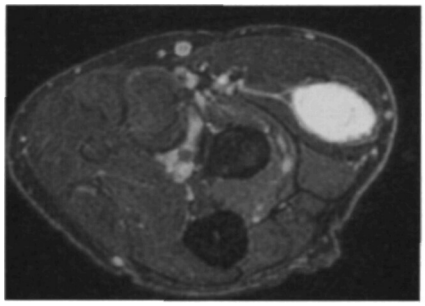

a

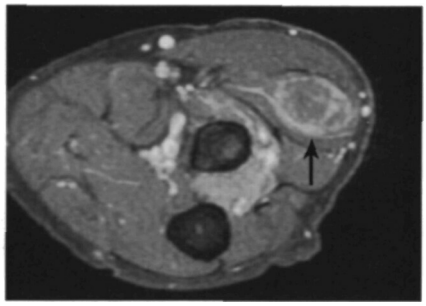

b

Figure 17.**34a, b** A 77-year-old man with an intramuscular myxoma involving the extensor carpi radialis longus and brevis muscles of the proximal forearm. The lesion has high signal on axial FS T2WI (**a**) and shows mild irregular Gd-contrast enhancement on axial FST1WI (**b**).

Figure 17.**35** Periosteal ganglion along the posterolateral proximal tibia of a 30-year-old man. The lesion has sharply defined margins, and has high signal on sagittal FST2WI. The lesion causes erosion and concave deformity of the tibial cortex.

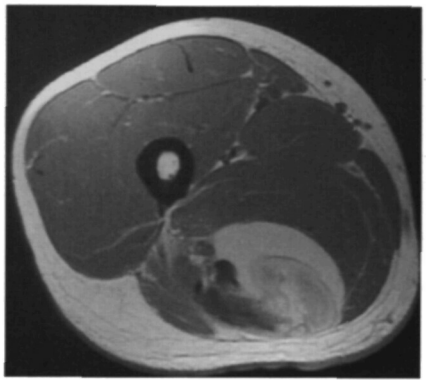

a

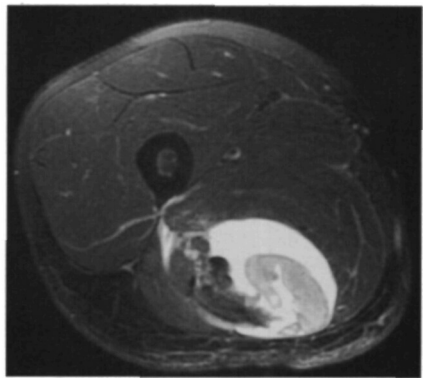

b

Figure 17.**36a, b** Subacute intramuscular hematoma involving the semitendinosus muscle in the upper thigh. The hematoma has heterogeneous slightly high, intermediate, and low signal on axial PDWI (**a**), and heterogeneous high, slightly high, and low signal on axial FST2WI (**b**).

Table 17 (Continued) Solitary tumors and tumorlike lesions of the soft tissues located mostly deep to the subcutaneous fat

Lesion	MRI Findings	Comments
Heterotopic ossification (Fig. 17.37)	MRI features vary depending on the age, location, and degree of mineralization/ossification. Lesions < 2 weeks have localized mass effect with poorly defined margins, heterogeneous low-intermediate or slightly high signal on T1 WI, and heterogeneous slightly high to high signal on T2WI and FST2WI. Poorly defined zones of high signal on T2WI may be seen in the adjacent soft tissues. After 2 weeks, curvilinear and/or amorphous zones of low signal on T2WI and FST2WI can be seen at the peripheral portions of the subacute lesions resulting from mineralization/ossification. Subsequent progressive centripetal mineralization/ossification appears as irregular zones of low signal on T2WI with heterogeneous Gd-contrast enhancement. Old lesions have well-defined margins, and variable low signal on T1WI, PDWI, and T2WI depending on the degree of mineralization/ossification, fibrosis, and hemosiderin deposition. Zones of high signal on T1WI and T2WI may occur from fatty marrow metaplasia. Gd-contrast enhancement in old mature lesions is often minimal or absent.	Heterotopic ossification or myositis ossificans are non-neoplastic reparative extraosseous lesions that are comprised of reactive hypercellular fibrous tissue, cartilage, and/or bone. These lesions can arise secondary to trauma (myositis ossificans circumscripta, ossifying hematoma), although may also occur without a history of prior injury (pseudomalignant osseous tumor of the soft tissues). **(See Atlas Chapter A53)**

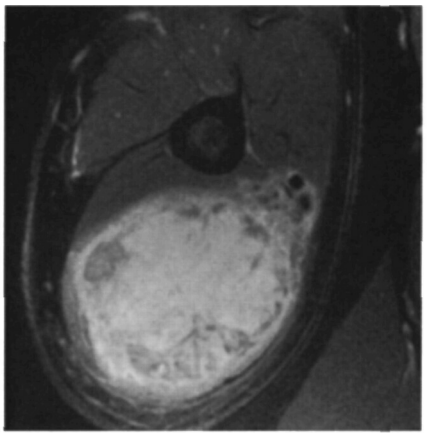

a, b

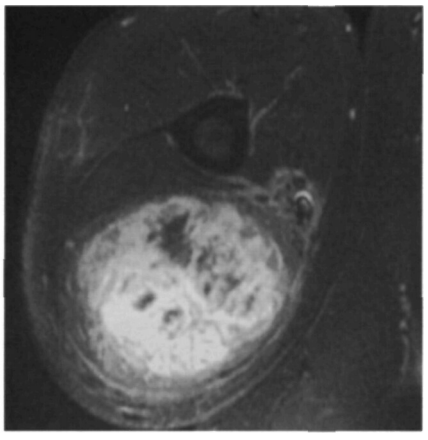

c

Figure 17.**37a-c** A 19-year-old man with myositis ossificans involving the triceps brachii muscle of the upper arm that has heterogeneous high signal on axial FS T2WI (**a**). The lesion shows prominent slightly heterogeneous Gd-contrast enhancement on axial FST1WI (**b**). Poorly defined zones of Gd-contrast enhancement are also seen in the soft tissues adjacent to the nodular mass-like portion of the lesion. The radiograph (c) obtained 10 days after the MRI examination shows predominantly peripheral mineralization of a localized soft tissue swelling.

Table 17 (Continued) Solitary tumors and tumorlike lesions of the soft tissues located mostly deep to the subcutaneous fat

Lesion	MRI Findings	Comments
Tumoral calcinosis (Fig. 17.38)	Radiographs and CT show lobular and/or multiloculated opacities that may contain radiolucent strands secondary to fibrous septate and calcium fluid levels. Erosion of bone adjacent to the tumoral calcinosis can occur. Lesions have variable signal on MRI with mixed low and intermediate signal on T1WI, and mixed low, intermediate, and/or high signal on T2WI. Gd-contrast may occur in septae or surrounding the lesions secondary to inflammatory reaction.	Rare metabolic disorder related to abnormal phosphate metabolism with elevated levels of 1,25-dihydroxyvitamin D resulting in hyperphosphatemia with precipitation of calcium salts in juxta-articular soft tissues. Common locations include the soft tissues near bursae at the hips, shoulders, elbows, buttocks, and scapula. Can be hereditary in up to 33 % as autosomal dominant with variable penetrance. Lesions consist of deposits of hydroxyapatite with or without fibrous septae, macrophages and chronic inflammatory cells, and multinucleated giant cells.
Amyloidoma	Lesions in soft tissue can have low-intermediate signal on T1WI, and intermediate to slightly high signal on T2WI. Lesions can show Gd-contrast enhancement.	Uncommon disease in which various tissues (including bone, muscle, tendons, tendon sheaths, ligaments, and synovium) are infiltrated with extracellular eosinophilic material composed of insoluble proteins with β-pleated sheet configurations (amyloid protein). Amyloidomas are single sites of involvement. Amyloidosis can be a primary disorder associated with an immunologic dyscrasia or secondary to a chronic inflammatory disease.
Aneurysm	Saccular aneurysms are focal well-circumscribed structures contiguous with arteries. Signal voids are usually seen where there is fast blood flow in nonthrombosed portions of the aneurysms. Variable mixed signal on T1WI and T2WI can be seen in thrombosed portions of the aneurysms.	Focal or diffuse zones of arterial dilatation that are associated with wall abnormalities and increased risk of rupture. Focal aneurysms are also referred to as saccular aneurysms that typically occur at arterial branch points. Giant aneurysms are saccular aneurysms that measure > 2.5 cm in diameter.

a

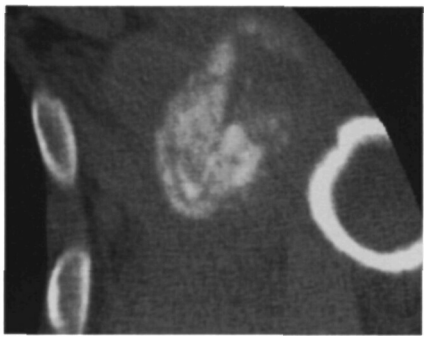

b

Figure 17.**38 a, b** Oblique sagittal (**a**) and axial (**b**) CT images show amorphous opacities in the soft tissues at the shoulder and axillary region in a 76-year-old man.

Table 17 (Continued) Solitary tumors and tumorlike lesions of the soft tissues located mostly deep to the subcutaneous fat

Lesion	MRI Findings	Comments
Inflammatory		
Abscess/myositis (Fig. 17.39)	Deep infections and myositis typically show poorly defined zones of decreased signal on T1WI, and slightly high to high signal on T2WI and FST2WI with corresponding Gd-contrast enhancement. Progression to abscess formation occurs with circumscribed zones that have low signal on T1WI and high signal on T2WI (with or without an air-fluid level) that are surrounded by a rim of low signal on T2WI. Rim-like Gd-contrast enhancement is usually seen. Peripherally, a poorly defined zone of high signal may be seen secondary to edema and/or inflammation.	Infection of muscles (myositis) and deep soft tissues from bacteria, fungi, and mycobacteria can eventually progress to liquefaction with necrosis (abscess formation) enclosed by a pseudocapsule surrounded by zones of edema and inflammatory reaction.
Parasitic infection (Fig. 17.40)	Parasitic infections can vary from cystic-appearing lesions to poorly marginated or circumscribed solid lesions depending on the infectious organism and stage of its life cycle.	Parasitic infections can occur in soft tissues in endemic regions or in immunocompromised patients.
Sarcoid (Fig. 17.41)	Sarcoid granulomas can occur in subcutaneous fat and may be associated with superficial adenopathy. Lesions are often nodular with low to intermediate signal on T1WI. and intermediate to high signal on T2WI. Lesions usually show Gd-contrast enhancement. Sarcoid can also involve muscles as discrete or poorly-defined lesions.	Chronic systemic granulomatous disease of unknown etiology in which noncaseating granulomas occur in various tissues and organs. Common sites of involvement include the lungs, lymph nodes, liver, spleen, skin, and eyes. **(See Atlas Chapter A71)**
Giant cell reaction to foreign body	Lesions usually occur in soft tissue and often have low-intermediate signal on T1 WI, and low, intermediate, and/or high signal on T2WI. Lesions can show Gd-contrast enhancement. Sites of bone erosion and/or destruction may be seen particularly with penetrating trauma. The MRI signal of the foreign body varies based on its composition.	Reactive granulomatous lesions can form adjacent to foreign bodies, and may simulate neoplasm.
Gout	Tophi have variable sizes and shapes, and have low-intermediate signal on T1WI, FST2WI, and T2WI. Zones of high signal on T2WI can also be seen in tophi. Erosions of bone, synovial pannus, joint effusion, bone marrow, and soft tissue edema can be seen with MRI. Tophi may show heterogeneous, diffuse, or peripheral/marginal Gd-contrast enhancement patterns.	Gout is an inflammatory disease involving synovium resulting from deposition of monosodium urate crystals and occurs when the serum urate level exceeds its solubility in various tissues and body fluid. **(See Atlas Chapter A32)**
Rheumatoid arthritis (Fig. 17.42)	MRI can show diffuse and/or localized zones of synovial hypertrophy; soft tissue swelling; zones of erosion and/or destruction of hyaline cartilage, menisci/fibrocartilage, subchondral bone, tendons, ligaments; bursal fluid collections containing "rice bodies", other extra-articular cysts; intraosseous cystic-like areas, joint effusion, and rheumatoid nodules. With tendon and ligament involvement, abnormal increased signal is seen on PDWI and T2WI. Tendons and ligaments may be thickened from partial tearing or thinned. Tenosynovitis is usually seen with fluid and hypertrophied synovium within tendon sheaths.	Chronic multi-system disease of unknown etiology in which there is a persistent inflammatory synovitis that typically involves peripheral joints in a symmetric distribution. The inflammatory synovitis can result in progressive destruction of cartilage and bone leading to joint dysfunction. **(See Atlas Chapter A70)**

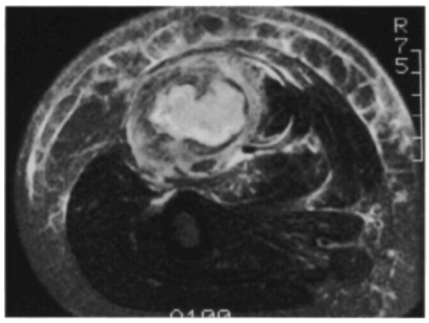

a

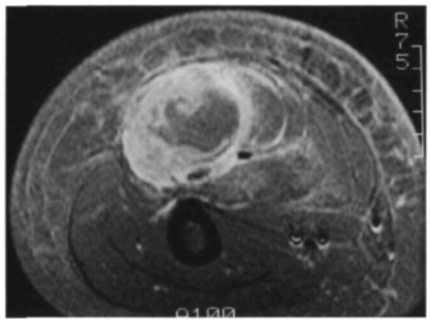

b

Figure 17.**39a, b** A 15-year-old male with myositis and abscess involving the anterior thigh muscles seen as a poorly defined zone with slightly high to high signal surrounding a circumscribed central zone (abscess) with high signal on axial T2WI (**a**). Irregular peripheral Gd-contrast enhancement is seen in the soft tissues surrounding the abscess on axial FSTIWI(**b**).

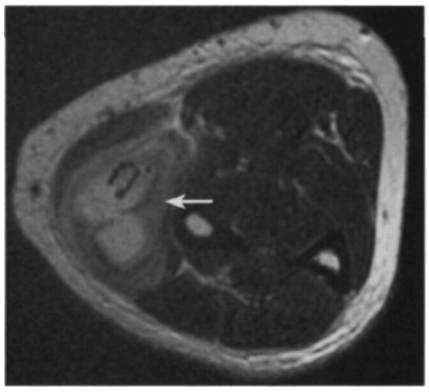

a

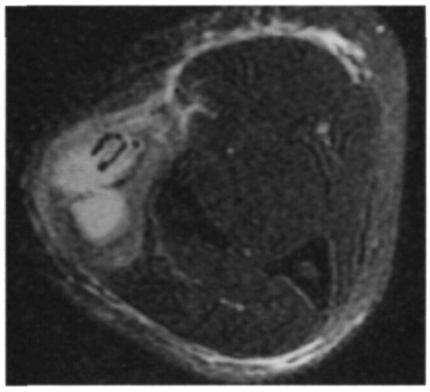

b

Figure 17.**40 a, b** A 34-year-old woman with intramuscular infection from cysticercosis in the forearm. A curvilinear zone with low signal representing the senescent parasite is surrounded by an abscess and solid inflammatory reaction with slightly high signal and high signal on axial T2WI (**a**) and high signal on axial FST2WI (**b**).

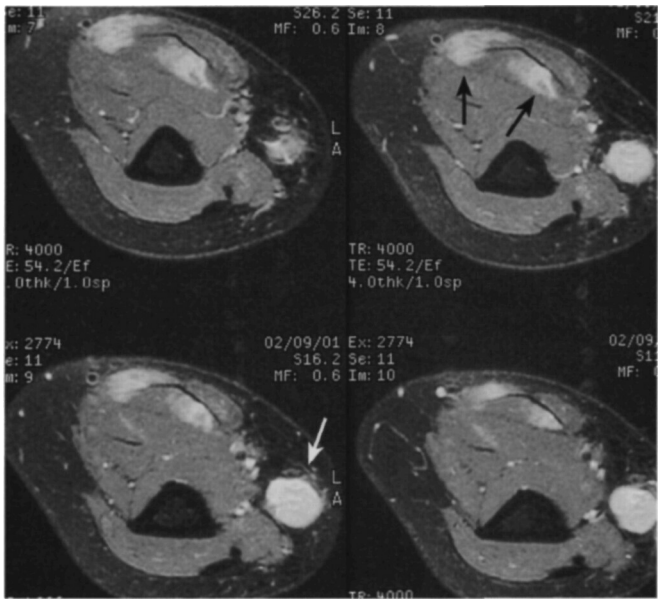

Figure 17.**41** A 49-year-old woman with sarcoid granulomas in the subcutaneous fat and within the biceps brachii muscle at the distal arm. The intramuscular lesions have slightly irregular margins and have high signal on axial FST2WI.

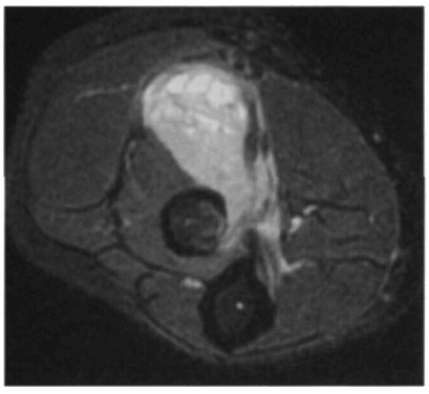

a

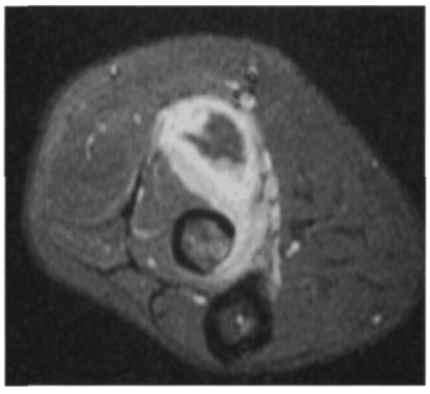

b

Figure 17.**42a, b** A 37-year-old woman with an inflammatory lesion from rheumatoid arthritis involving the antecubital bursa and biceps brachii muscle and tendon. The lesion has heterogeneous high signal on axial FS T2WI (**a**) and shows heterogeneous Gd-contrast enhancement on axial FST1WI (**b**). The lesion causes erosion of the cortex of the adjacent radius.

Table 17 (Continued) Solitary tumors and tumorlike lesions of the soft tissues located mostly deep to the subcutaneous fat

Lesion	MRI Findings	Comments
Dermatomyositis (Fig. 17.43)	In acute and subacute phases, poorly defined zones of high signal on T2WI are seen in muscles, subcutaneous fat, and fascia secondary to ischemic or infarcted muscle resulting from vasculitis. Zones of low signal on T2WI can result from calcifications seen on radiographs and CT scans. "Milk of calcium" collections may occur which have variable signal on T1WI and T2WI depending on the relative proportions of fluid and fluid-calcium levels. Poorly defined zones of Gd-contrast enhancement can be seen in muscles, fascia, and/or subcutaneous fat if there is active inflammation and/or ischemia infarction. Muscle atrophy with fatty infiltration can be seen in the chronic phases	Nonsupperative autoimmune systemic vasculopathy involving muscle fibers, skin, and blood vessels. Can be associated with other connective tissue diseases such as scleroderma, and mixed connective tissue disease. Incidence: 2-8 per million, prevalence: 4-60 per million. Juvenile dermatomyositis occurs in children between 2 and 15 years. Adult dermatomyositis occurs with peak incidence in 5th decade. **(See Atlas Chapter A14).**
Other		
Giant cell tumor of the tendon sheath (Fig. 17.44)	Lesions usually have well-defined margins and are often adjacent to a tendon/tendon sheath. Lesions have low-intermediate or intermediate signal on T1WI and PDWI, and mixed low. intermediate and/or high signal on T2WI and FST2WI. Zones of low signal on T2WI often correspond to sites of hemosiderin deposition. Lesions often show Gd-contrast enhancement in either a homogeneous or heterogeneous pattern.	Giant cell tumors of the tendon sheath and pigmented villonodular synovitis represent benign proliferative lesions of synovium (tendon sheaths, joints, and bursae). Giant cell tumors of the tendon sheaths can occur as localized nodular lesions attached to tendon sheaths outside of joints (hands, feet) or within joints (infrapatellar portion of knee joint), or as a nodular or diffuse form near/outside of large joints such as the knee, ankles, etc. **(See Atlas Chapter A 30)**
Fibroma of the tendon sheath	Lesions are ovoid or fusiform and well-circumscribed, and are located adjacent to tendons of the fingers, hands, wrists, feet, and other locations. Lesions usually have low-intermediate signal on T1WI. On T2WI, lesions can have a slightly heterogeneous low-intermediate signal in half, intermediate signal in a third, or mixed low and intermediate signal and/or high signal in the remainder. Lesions can show diffuse or peripheral Gd-contrastG enhancement.	Fibromas of the tendon sheath are benign, small fibrous nodules involving tendons and tendon sheaths of the fingers, hands, wrists, or feet. **(See Atlas Chapter A 23)**
Xanthoma	Xanthomas in tendons often appear as zones of fusiform enlargement with diffuse heterogeneous signal. Xanthomas usually contain multiple longitudinally oriented linear zones or striations with intermediate signal on T1WI and PDWI, and intermediate to slightly high signal on T2WI and FST2WI interspersed among bands of low signal within the enlarged tendons. On axial images, xanthomas often have a stippled or reticulated pattern on T1WI and T2WI resulting from collagen bundles with low signal surrounded by higher signal from lipid deposits, foamy histiocytes. and inflammatory reaction.	Xanthomas are localized accumulations of lipids within normal structures such as tendons, skin, and bone. Considered reactive lesions and are not true neoplasms. Often occur in the setting of types I, II. and III hyperlipoproteinemia. **(See Atlas Chapter A 77)**

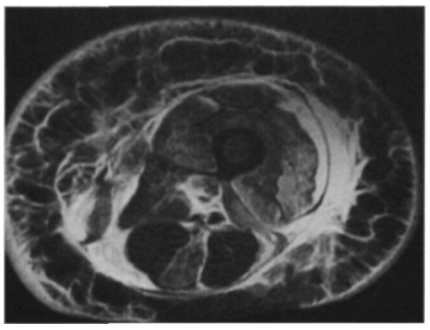

a

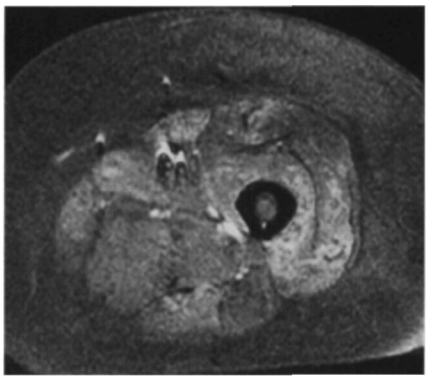

b

Figure 17.**43a, b** A 78-year-old woman with dermatomyositis involving the thigh. Poorly defined zones of abnormal high signal on FST2WI (**a**) and abnormal Gd-contrast enhancement on FST1WI (**b**) are seen in the thigh muscles secondary to active inflammation. Zones of abnormal high signal on axial FST2WI are also seen in the subcutaneous fat.

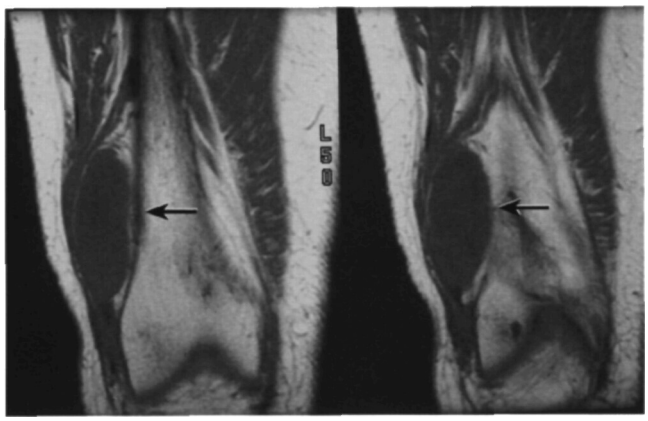

a

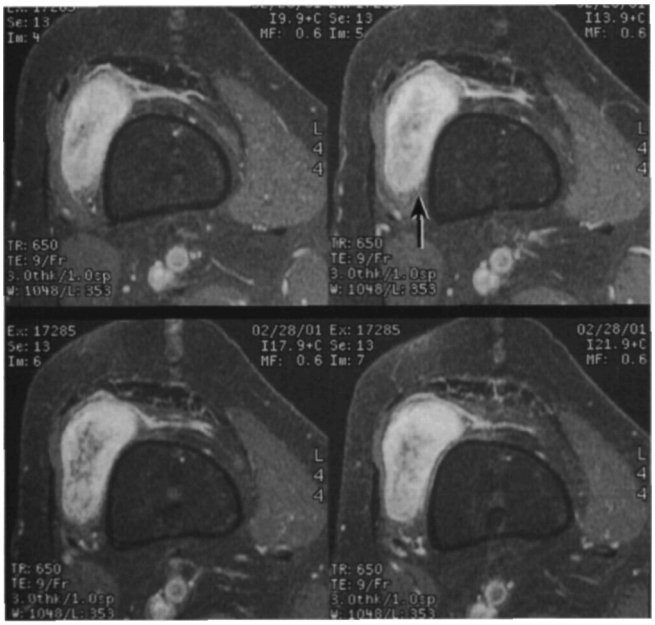

b

Figure 17.**44a, b** A 60-year-old woman with a giant cell tumor of the tendon sheath/nodular synovitis at the knee. An ovoid lesion with well-defined margins is seen adjacent to the iliotibial band. The lesion has low-intermediate signal on coronal T1WI (**a**) and shows prominent Gd-contrast enhancement on axial FST1WI (**b**).

References

Clear Cell Sarcoma

De Beuckeleer LH, De Schepper AM, Vandevenne JE, et al. MR imaging of clear cell sarcoma (malignant melanoma of the soft parts): a multicenter correlative MRI-pathology study of 21 cases and literature review. *Skeletal Radial* 2000;29:187-195.

Lipomatosis

Amine B, Leguilchard F, Benhamou CL. Dercum's disease (adiposis dolorosa): a new case *report. Joint Bone Spine* 2004;71:147-149.

Drevelegas A, Pilavald M, Chourmouzi D. Lipomatous tumors of soft tissue: MR appearance with histological correlation. Eur *J Radial* 2004;50:257-267.

Haloi AK, Ditchfield M, Penington A, Phillips R. Facial infiltrative lipomatosis. *Pediatr Radial* 2006;36:1159-1162.

Klein FA, Smith MJ, Kasenetz I. Pelvic lipomatosis: 35-year experience. *J Urol* May 1988;139(5):998-1001.

Murphy MD, Carroll JF, Flemming DJ, Pope TL, Gannon FH, Kransdorf MJ. Benign musculoskeletal lipomatous lesions. *RadioGraphics* September-October 2004;24(5): 1433-1466.

Sener RN. Epidural, paraspinal, and subcutaneous lipomatosis. *Pediatr Radial* 2003;33:655-657.

Torigian DA, Siegelman ES. CT findings of pelvic lipomatosis of nerve. *AJR* March 2005:184:94-96.

Tumoral Calcinosis

Durant DM, Riley LH, III, Burger PC, McCarthy EF. Tumoral calcinosis of the spine. A study of 21 cases. *Spine* 2001;26(15):1673-1679.

Martinez S, Vogler JB, III, Harrelson JM, Lyles KW. Imaging of tumoral calcinosis: new observations. Radiology January 1990;174(1): 215-222.

Olsen KM, Chew FS. Tumoral calcinosis: pearls, polemics, and alternative possibilities. *RadioGraphics* May-June 2006;26(3):871-885.

Şenol U, Karaali K, Çevikol C, Dinçer A. MR imaging findings of recurrent tumoral calcinosis. *J Clin Imag* 2000:24:154-156.

Table 18 Tumors and tumorlike lesions of the superficial soft tissues including subcutaneous fat

Lesion	MRI Findings	Comments
Neoplastic- malignant		
Dermatofibrosarcoma and dermatofibrosarcoma protuberans (Fig. 18.1)	Dermatofibrosarcoma (DFS) are small lesions with circumscribed and/or poorly defined margins involving the skin and/or subcutaneous adipose tissue. Tumors can have low-intermediate signal on T1WI, and intermediate to high signal on T2WI and FST2WI. DFS show variable degrees of Gd-contrast enhancement, dermatofibrosarcoma protuberans (DFSP) are usually circumscribed lesions in the skin and subcutaneous adipose tissues that can measure up to 25cm. Ten percent of DFSP have poorly defined margins. DFSP tumors have low-intermediate signal on T1WI, intermediate, slightly high, and/or high signal on T2WI. DFSP show heterogeneous or homogeneous Gd-contrast enhancement.	DFS and DFSP are dermal tumors containing malignant fibroblastic cells with spindle-shaped nuclei. **(See Atlas Chapter A13)**
Malignant fibrous histiocytoma (Fig. 18.2)	Tumors have poorly defined and or circumscribed margins, and often have low-intermediate signal on T1WI and heterogeneous intermediate-high signal on T2WI and FST2WI. Tumors show heterogeneous often prominent enhancement.	Malignant tumors involving soft tissue and rarely bone that are presumed to derive from undifferentiated mesenchymal cells. The World Health Organization (WHO) now uses the term undifferentiated pleomorphic sarcoma. **(See Atlas Chapter A48)**
Liposarcoma (Fig. 18.3)	**Well-differentiated liposarcomas** contain up to 75% overall fat signal, and contain thick nonadipose septae and/or nodular nonadipose zones. The nonadipose zones can have low-intermediate signal on T1WI and PDWI; and low, intermediate, and/or high signal on T2WI. Nonadipose tumor portions show variable degrees of Gd-contrast enhancement. **Myxoid liposarcomas:** These tumors usually contain myxoid material with low signal on T1WI, heterogeneous or homogeneous high signal on T2WI. Tumors may or may not contain fat seen with MRI. Tumors show variable degrees of Gd-contrast enhancement. **Pleomorphic, round cell and dedifferentiated liposarcomas** often have heterogeneous/mixed low, intermediate, and/or high signal on T1 WI and T2WI. Less than 26% of pleomorphic liposarcomas have fat signal. Tumors show variable degrees of Gd-contrast enhancement.	Malignant mesenchymal tumors containing portions showing differentiation into adipose tissue. Liposarcomas represent ~ 14% of malignant soft tissue tumors and 6 % of all soft tissue tumors. **(See Atlas Chapter A44)**
Metastatic disease (Fig. 18.4)	Tumors can occur as lymphadenopathy or as focal lesions. Lesions have low-intermediate signal on T1WI and intermediate to slightly high signal or high signal on T2WI and FST2WI. Variability in MRI signal characteristics may be related to differing histologic features of the metastatic lesions. Tumors can show variable degrees of Gd-contrast enhancement.	Metastatic lesions are proliferating neoplastic cells that are located in sites or organs separated or distant from their origins. **(See Atlas Chapter A50)**

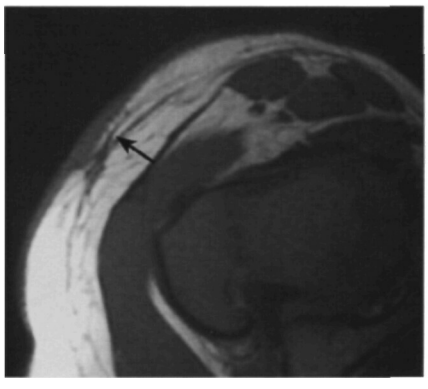

a

b

Figure 18.**1 a, b** A 2-year-old boy with a dermatofibrosarcoma in the upper thigh. The lesion is associated with skin thickening, as well as a poorly defined zone of intermediate signal on axial T1WI (**a**) in the subcutaneous fat that shows Gd-contrast enhancement on FST1WI(**b**).

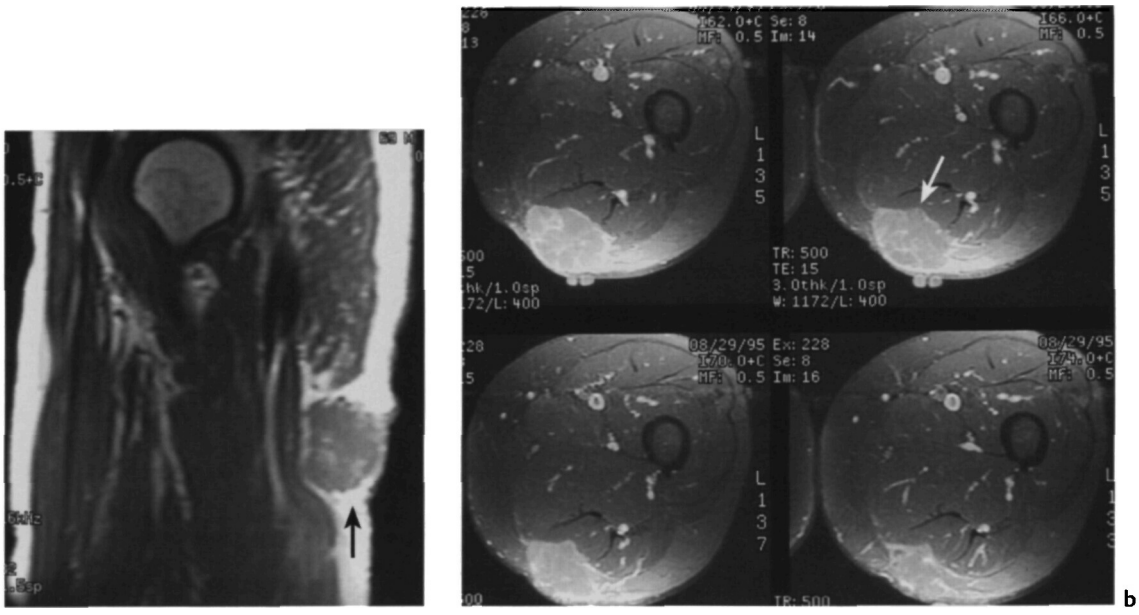

Figure 18.**2a, b** A 69-year-old man with a malignant fibrous histiocytoma involving the subcutaneous fat of the posterior thigh. The tumor has intermediate signal on sagittal (**a**) T1 WI and shows slightly heterogeneous Gd-contrast enhancement on axial FST1WI (**b**).

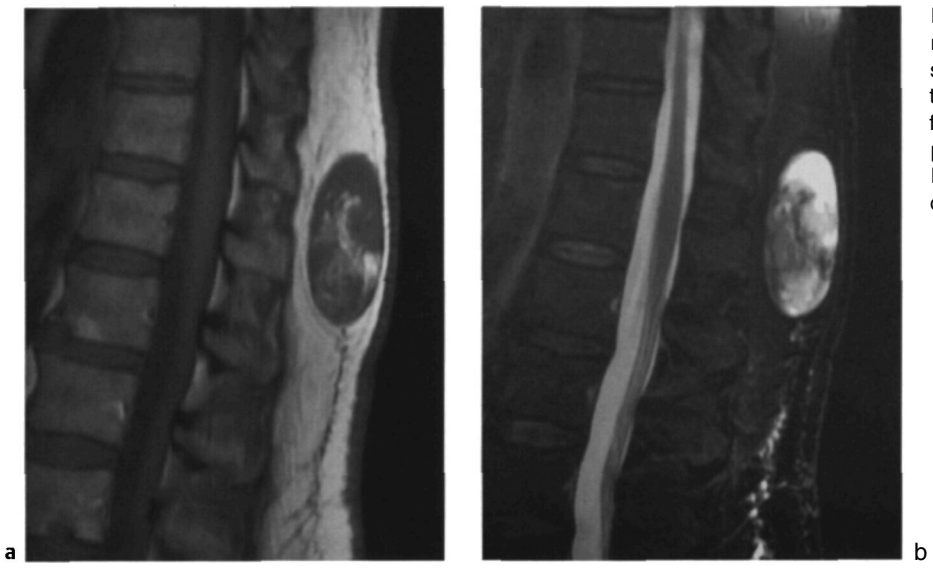

Figure 18.**3a, b** A 65-year-old man with a myxoid liposarcoma involving the dorsal subcutaneous fat in the lumbar region. The tumor contains mixed intermediate and high fat signal on sagittal T1WI (**a**). Myxoid portions of the tumor have high signal on FST2WI (**b**). The signal from the small zones of fat is suppressed on sagittal FST2WI.

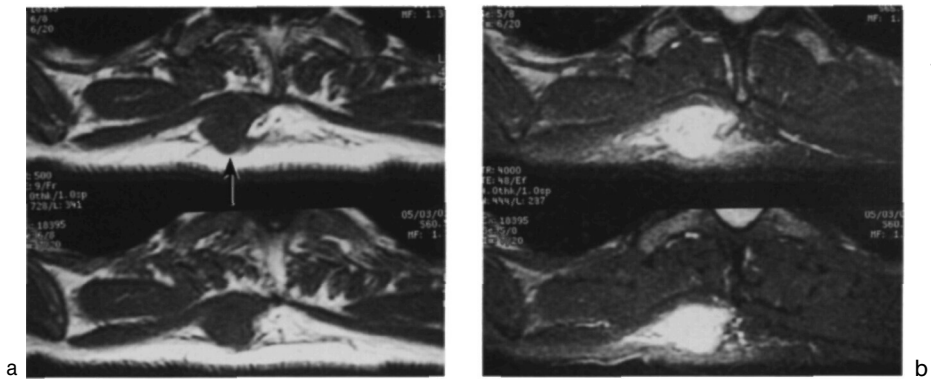

Figure 18.**4a, b** Metastatic lesion from lung carcinoma involving the deep subcutaneous fat of the upper dorsal back. The tumor has low-intermediate signal on axial (**a**) T1WI, and high signal on axial (**b**) FST2WI.

Table 18 (Continued) Tumors and tumorlike lesions of the superficial soft tissues including subcutaneous fat

Lesion	MRI Findings	Comments
Lymphoma (Figs. 18.5, 18.6)	Lymphadenopathy from Hodgkin lymphoma (HL) and lesions of non-Hodgkin lymphoma (NHL) have low-intermediate signal on T1WI and intermediate to slightly high or high signal on T2WI. Variability in MRI signal may be related to differing histologic features (such as the degree of fibrosis) for the subtypes of HL. After Gd-contrast administration, HL and NHL can show variable Gd-contrast enhancement.	Lymphomas are tumors in which neoplastic cells arise within lymphoid tissue. HL usually occurs in lymph nodes and spreads along nodal chains, whereas NHL frequently originates at extranodal sites and spreads in an unpredictable pattern. Mycosis fungoides is a T cell lymphoma that involves the skin. **(See Atlas Chapter A47)**
Leukemia cutis	Lesions with circumscribed or poorly defined margins with low-intermediate signal on T1WI, intermediate to high signal on T2WI, variable degrees of Gd-contrast enhancement.	Collections of leukemic cells in the epidermis, dermis, and/or subcutaneous fat, associated with poor prognosis. **(See Atlas Chapter A41)**
Melanoma	Tumors can have low-intermediate signal on T1WI, or slightly high signal on T1WI. Tumors can have low, intermediate, or high signal on T2WI and FST2WI. Slightly high signal on T1WI and low-intermediate signal on T2WI in melanoma can occur secondary to the presence of melanin (which has T1 and T2 shortening effects). Tumors usually show Gd-contrast enhancement.	Malignant tumors of melanocytes that frequently occur in the skin, and less frequently in the eye and mucosal surfaces. Melanomas can metastasize to brain, bone, cutaneous and subcutaneous tissues.
Squamous cell sarcoma (Fig. 18.7)	Tumors can have irregular margins, and often have low-intermediate signal on T1 WI and PDWI, and intermediate to slightly high signal on T2WI and FST2WI. Tumors can show Gd-contrast enhancement.	Common tumors occurring on sun-exposed sites in older adults. Tumor cells have hyperchromatic and large nuclei, and can break through the basement membrane invading adjacent tissue.
Synovial cell sarcoma (Fig. 18.8)	Tumors are often ovoid and/or lobulated lesions that often have low-intermediate signal on T1WI, and heterogeneous signal (various combinations of intermediate, slightly high, high, and/or low signal) on T2WI. Multiloculated cystic zones are present in 77 %. Calcifications may occur in up to 30 %. Tumors show various patterns of Gd-contrast enhancement.	Mesenchymal tumors comprised of spindle cells and cells with varying degrees of epithelial differentiation. Account for 5% of primary malignant soft tissue tumors. **(See Atlas Chapter A75)**

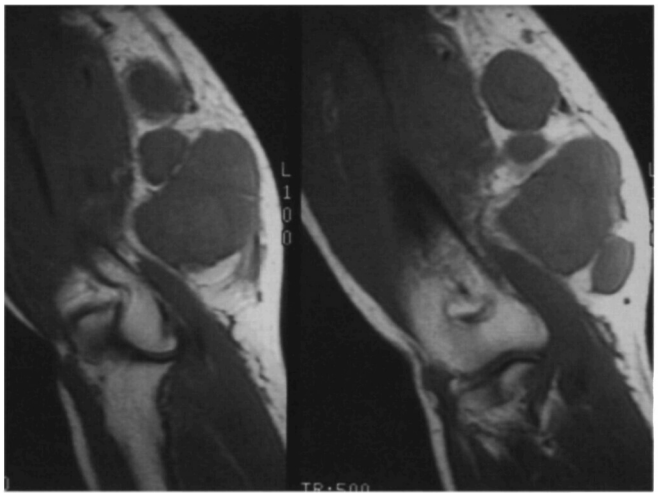

a

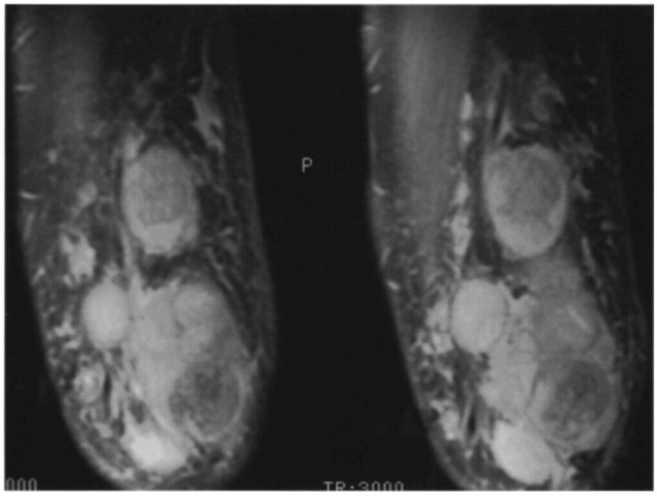

b

Figure 18.**5a, b** A 66-year-old man with diffuse large cell NHL involving the subcutaneous fat, biceps brachii muscle, medial head of the triceps muscle, and neurovascular bundle in the elbow region. Multiple nodular lesions with intermediate signal on coronal T1 WI (**a**) are seen which have heterogeneous high signal on coronal FST2WI (**b**).

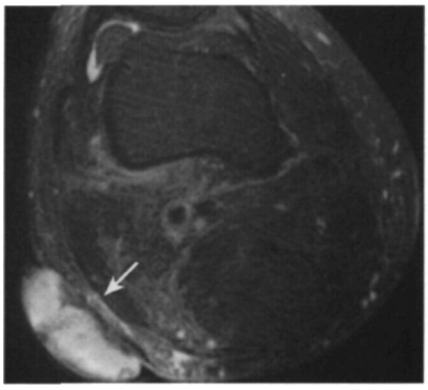

a

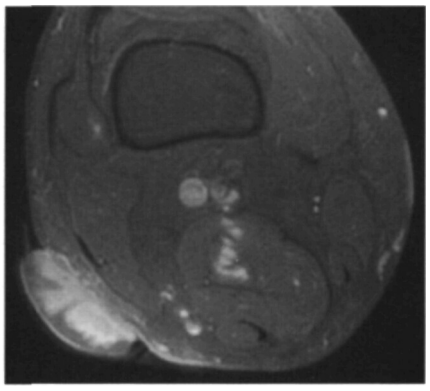

b

Figure 18.**6a, b** A 62-year-old man with Tcell lymphoma (mycosis fungoides) involving the skin. The nodular lesion involves the epidermis and has heterogeneous high signal on axial (**a**) FST2WI and shows heterogeneous Gd-contrast enhancement on axial (**b**) FS T1WI.

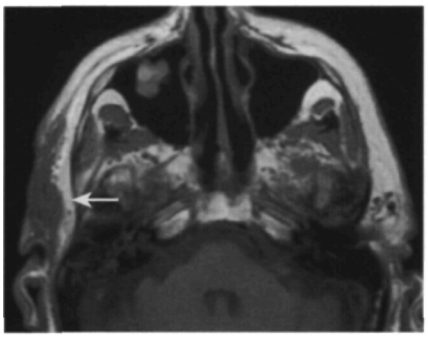

a

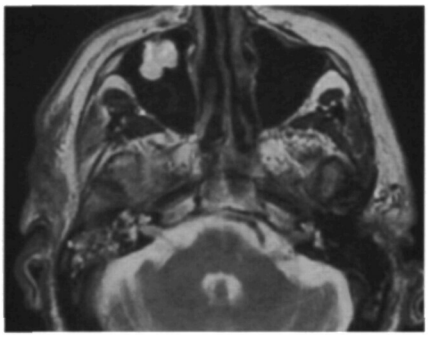

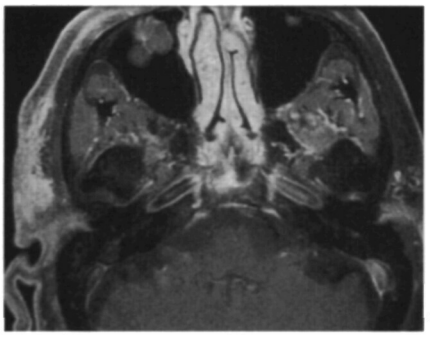

b, c

Figure 18.**7a-c** An 80-year-old man with squamous cell carcinoma involving the right side of the face. The tumor has irregular margins, and has intermediate signal on axial T1WI (**a**) and axial T2WI (**b**). The tumor shows Gd-contrast enhancement on axial FST1WI (**c**).

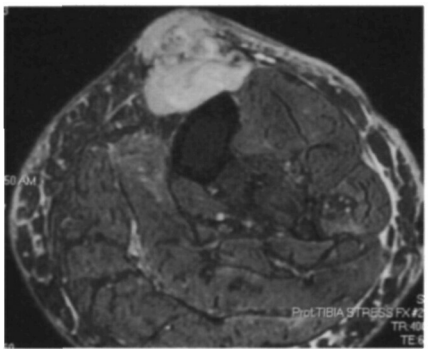

a

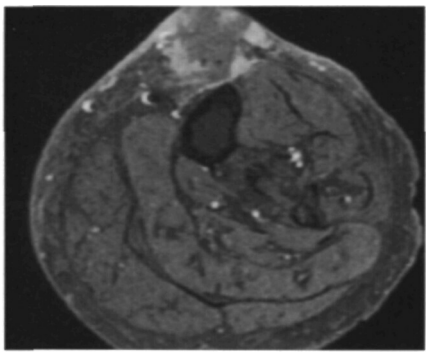

b

Figure 18.**8a, b** An 82-year-old woman with a synovial sarcoma involving the subcutaneous fat of the anterior leg. The tumor has high signal on axial (**a**) FST2WI and shows heterogeneous Gd-contrast enhancement on axial FST1WI(**b**).

Table 18 (Continued) Tumors and tumorlike lesions of the superficial soft tissues including subcutaneous fat

Lesion	MRI Findings	Comments
Malignant peripheral nerve sheath tumor (Fig. 18.9)	These lesions usually have heterogeneous signal on T1 WI and T2WI; as well as heterogeneous Gd-contrast enhancement because of necrosis and hemorrhage. Some malignant peripheral nerve sheath tumors (MPNSTs) are similar in appearance to benign nerve sheath tumors.	MPNSTs are malignant tumors of the peripheral nerve sheath containing mixtures of packed hyperchromatic spindle cells with elongated nuclei and slightly eosinophilic cytoplasm, mitotic figures and zones of necrosis. Approximately 50 % of MPNSTs occur in patients with neurofibromatosis type 1 (NF1), followed by de novo evolution from peripheral nerves. MPNSTs infrequently arise from schwannomas, ganglioneuroblastomas/ganglioneuromas, and pheochromocytomas. **(See Atlas Chapter A56)**
Leiomyosarcoma (Fig. 18.10)	Lesions may have well-defined or irregular margins and usually have low-intermediate signal on T1 WI and PDWI; and intermediate to slightly high or high signal on T2WI and FST2WI. Large lesions often have zones of necrosis or cystic change that have low signal on T1WI and high signal on T2WI. Solid portions of the lesions usually show Gd-contrast enhancement.	Malignant mesodermal tumors associated with smooth muscle differentiation. Can arise de novo or occur after radiation treatment. **(See Atlas Chapter A40)**
Rhabdomyosarcoma (Fig. 18.11)	Tumors can have circumscribed and/or poorly defined margins, and typically have low-intermediate signal on T1 WI and heterogeneous signal (various combinations of intermediate, slightly high, and/or high signal) on T2WI and FST2WI. Tumors show variable degrees of Gd-contrast enhancement.	Malignant mesenchymal tumors with rhabdomyoblastic differentiation; occur primarily in soft tissue. **(See Atlas Chapter A69)**
Hemangioendothelioma (Fig. 18.12)	Tumors have lobulated well-defined or irregular margins, and have intermediate signal on T1WI and heterogeneous predominantly high signal on T2WI with or without internal low signal septations. Flow voids may be seen with the lesions. Tumors show heterogeneous Gd-contrast enhancement.	Low-grade malignant neoplasms composed of vasoformative/endothelial elements that occur in soft tissues and bone. These tumors are locally aggressive and rarely melastasize, compared with high-grade endothelial tumors such as angiosarcoma. **(See Atlas Chapter A33)**
Angiosarcoma	Tumors have low-intermediate signal on T1WI, mixed low, intermediate, and/or high signal on T2WI, and show prominent Gd-contrast enhancement in a homogeneous or heterogeneous pattern.	Malignant tumors composed of neoplastic blood vessels in bone and/or soft tissues. These tumors can be associated with Paget disease, radiation treatment, bone infarcts, knee and hip prostheses, synthetic vessel grafts, prior trauma or surgery, osteomyelitis, and hereditary disorders (NF1, Maffucci disease, achondroplasia). **(See Atlas Chapter A6)**

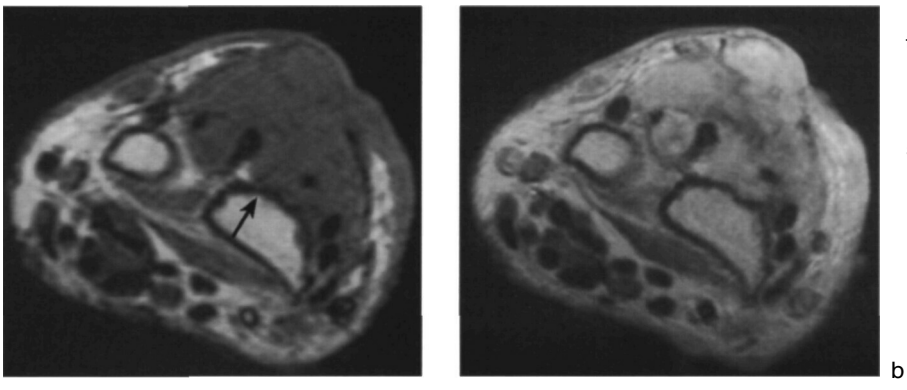

a b

Figure 18.**9 a, b** MPNST in the soft tissues of the wrist in a patient with NF1. The tumor has poorly defined margins and envelops multiple extensor tendons. The tumor has low-intermediate signal on coronal T1WI (**a**) and shows heterogeneous Gd-contrast enhancement on axial T1WI (b).

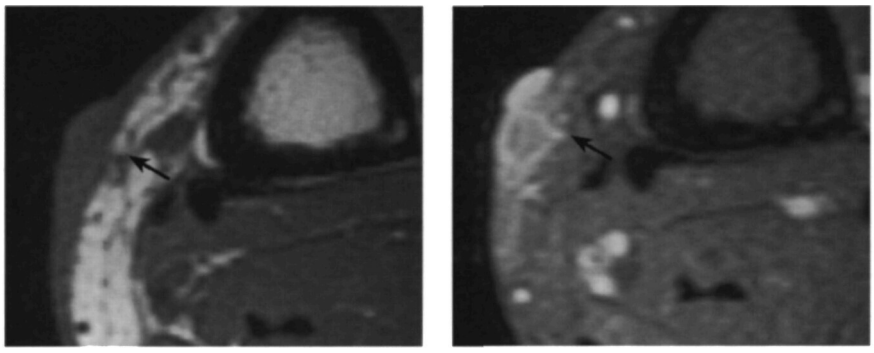

Figure 18.**10 a, b** A 72-year-old man with a leiomyosarcoma involving the dermis with extension into subcutaneous fat. The tumor has intermediate signal on axial T1WI (**a**) and shows heterogeneous Gd-contrast enhancement on axial FST1WI (**b**).

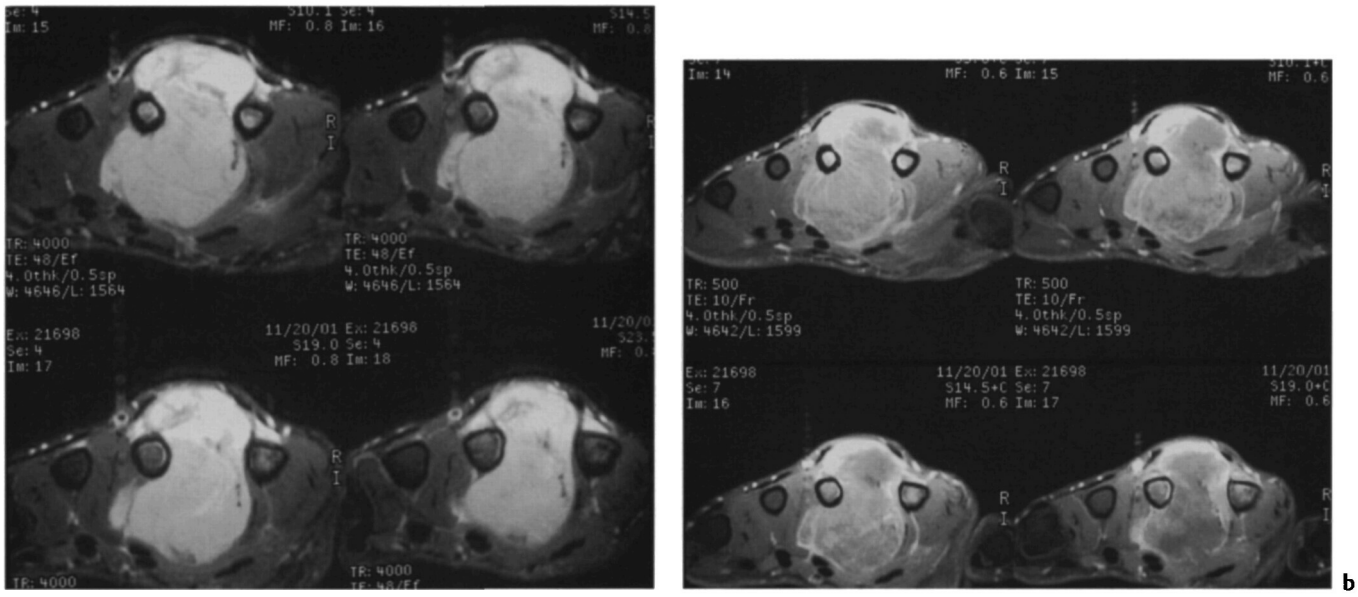

Figure 18.**11 a, b** A 23-year-old man with an alveolar rhabdomyosarcoma involving the soft tissues between the second and third metacarpal bones. The tumor has high signal on coronal FST2WI (**a**) and shows heterogeneous Gd-contrast enhancement on coronal FST1WI (**b**).

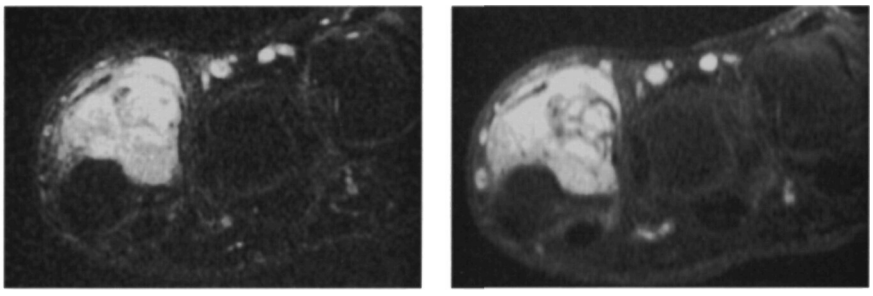

Figure 18.**12a, b** A 36-year-old man with a hemangioendothelioma involving the dorsal soft tissues of the foot. The tumor has high signal on coronal FST2WI (**a**) and shows prominent Gd-contrast enhancement on coronal FST1WI (**b**).

Table 18 (Continued) Tumors and tumorlike lesions of the superficial soft tissues including subcutaneous fat

Lesion	MRI Findings	Comments
Extraosseous osteosarcoma (Fig. 18.13)	Tumors have irregular poorly defined or slightly well-circumscribed margins and heterogeneous signal on most MRI pulse sequences. Various combinations of low, intermediate, and/or high signal on T1WI, T2WI, and FST2WI can be seen depending on the presence and extent of hemorrhage and/or necrosis within the lesions. On T2WI and FST2WI, tumors often have heterogeneous predominantly high signal. Fluid-fluid levels may be present at sites of hemorrhage or necrosis. Peripheral nonenhancing high signal on T2WI may be present and represent zones of edema and/or tumor invasion within adjacent tissues. Tumors often show heterogeneous patterns of Gd-contrast enhancement.	Malignant tumor comprised of proliferating neoplastic spindle cells that produce osteoid and/or immature tumoral bone. Osteosarcoma most commonly occurs within bone and less frequently on the external surface of bone. Rarely, osteogenic sarcomas can also occur as extraskeletal primary lesions in the soft tissues. **(See Atlas Chapter A64)**
Extraosseous Ewing Sarcoma	Tumors usually have low-intermediate signal on T1WI and heterogeneous slightly high to high signal on T2WI and FST2WI. Tumors often show prominent irregular Gd-contrast enhancement.	Malignant primitive tumors of bone and occasionally soft tissue that contain undifferentiated small cells with round nuclei. **(See Atlas Chapter A20)**
Extraosseous chondrosarcoma (Fig. 18.14)	Tumors have low-intermediate signal on T1WI, intermediate signal on PDWI, and heterogeneous intermediate-high or slightly high signal on T2WI. Foci of low signal on T1WI and T2WI can be seen secondary to chondroid matrix mineralization. Lesions typically show heterogeneous Gd-contrast enhancement.	Malignant tumors containing cartilage formed within sarcomatous stroma, with or without areas of calcification/mineralization, myxoid material and/or ossification. **(See Atlas Chapter A11)**
Merkel cell tumor (Fig. 18.15)	Tumors can have circumscribed margins, and have low-intermediate signal on T1WI and PDWI, and slightly high to high signal on T2WI. Zones of necrosis with high signal on T2WI may occur within the tumors. Tumors can show Gd-contrast enhancement.	Tumors are rare primary malignant neuroendocrine neoplasms involving the skin and dermis, typically occurring in adults over 60 years. Small round tumor cells contain neurosecretory cytoplasmic granules and are thought to have neural crest origins.
Kaposi Sarcoma (Fig. 18.16)	Tumors can appear as lesions with circumscribed or irregular margins that commonly involve the skin and superficial soft tissues. Tumors often have low to intermediate signal on T1WI and slightly high to high signal on T2WI and FST2WI. Tumors usually show moderate to marked Gd-contrast enhancement.	Endothelial tumor that is associated with human herpes virus 8 (HHV-8) infections. These tumors are locally invasive and often are located in the cutaneous tissues, mucosa, lymph nodes, and/or visceral organs. **(See Atlas Chapter A 38)**

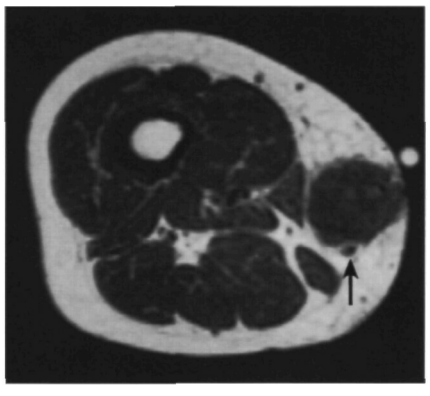

a

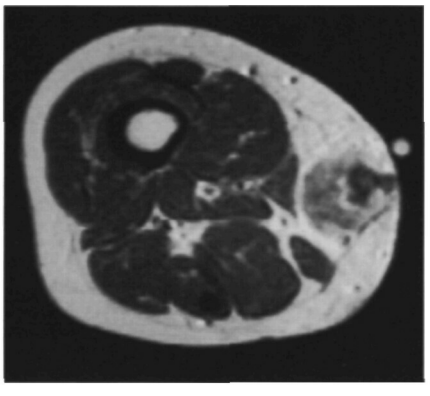

b

Figure 18.**13 a, b** A 47-year-old woman with an extraosseous osteosarcoma in the subcutaneous fat of the medial thigh. The tumor has low signal on axial T1WI (**a**) and shows heterogeneous Gd-contrast enhancement on axial T1WI (**b**).

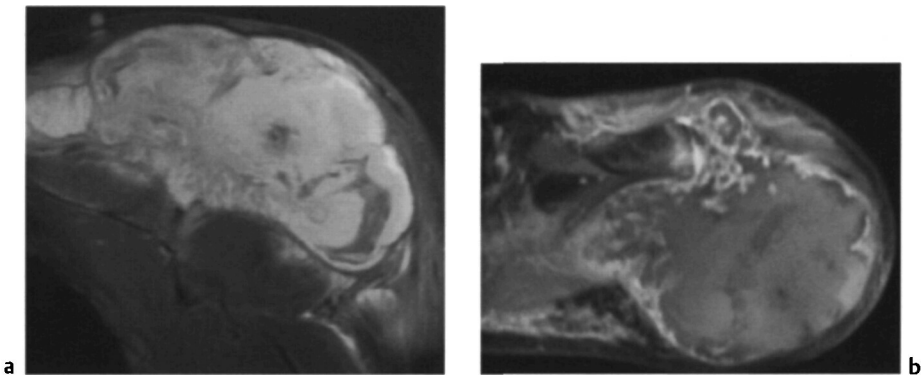

Figure **18.14a, b** A 63-year-old man with an extraosseous myxoid chondrosarcoma involving the soft tissues at the left shoulder. The tumor has mostly high signal on coronal FST2WI (a) as well as irregular zones of low signal. The tumor shows lobulated irregular peripheral Gd-contrast enhancement on axial FST1WI (b).

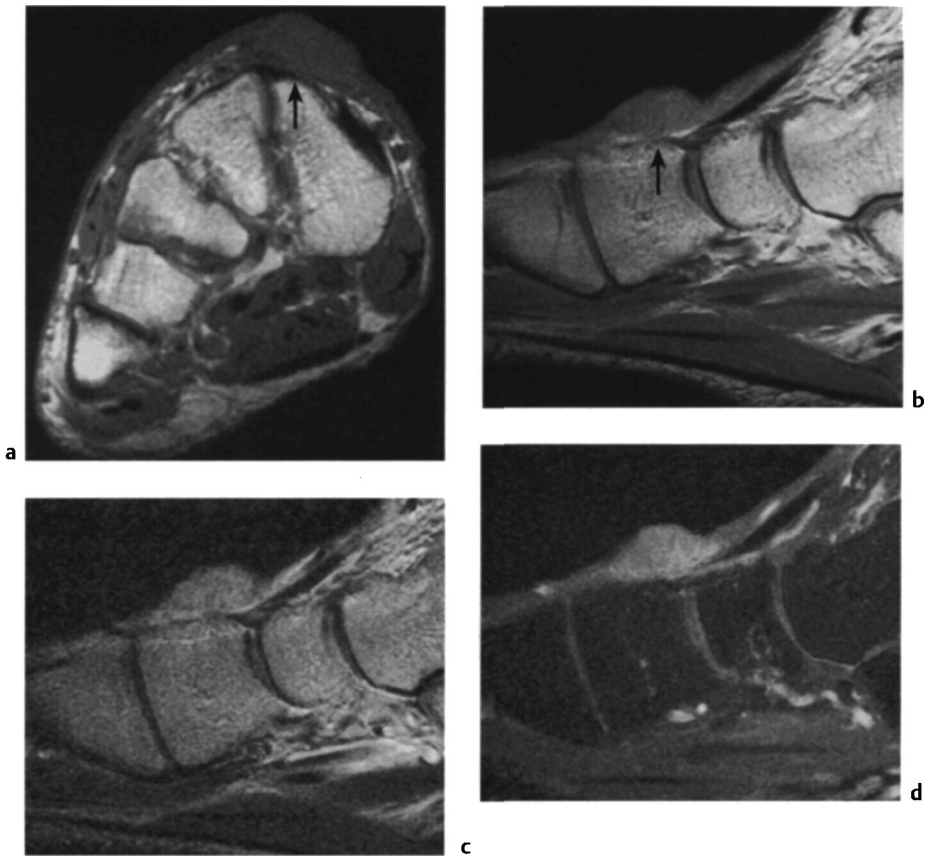

Figure **18.15a-d** A 72-year-old man with a Merkel cell tumor involving the dorsal superficial soft tissues of the foot. The tumor has low-intermediate signal on coronal T1WI (a) and intermediate signal on sagittal PDWI (b) and sagittal T2WI (c). The tumor shows moderate Gd-contrast enhancement on sagittal FST1WI (d).

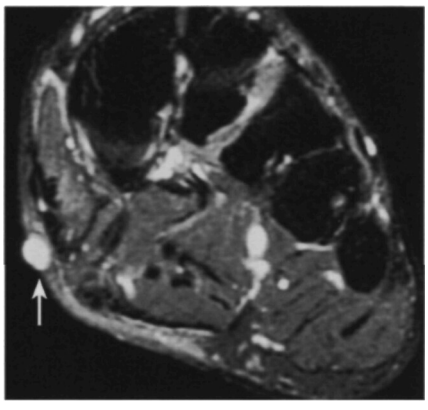

Figure 18.**16** A 70-year-old man with Kaposi sarcoma involving the superficial soft tissues of the foot. The small tumor has high signal on coronal FST2WI.

Table 18 (Continued) Tumors and tumorlike lesions of the superficial soft tissues including subcutaneous fat

Lesion	MRI Findings	Comments
Epithelioid sarcoma (Fig. 18.17)	Tumors can appear as lesions with circumscribed or irregular margins that commonly involve the skin and superficial soft tissues. Tumors often have low to intermediate signal on T1WI; and mixed low intermediate and/or high signal on T2WI and FST2WI. Tumors can be solid or can have single or multiple fluid-filled portions with or without hemorrhage or associated inflammatory reaction. Solid portions of tumors can show Gd-contrast enhancement. Marginal Gd-contrast enhancement can be seen at cystic zones.	These sarcomas are firm, slow-growing, aggressive tumors that involve the superficial soft tissues as well as tendons and tendon sheaths. Tumors contain mixtures of eosinophilic epithelioid and spindle cells with nuclear atypia, and occur in young adults (median age =29 years, female/male ratio 2:1). Recurrence rate of 80 % at 10 years, and 5 and 10 year survival rates ranging from 50 to 80 %.
Myoepithelial carcinoma (Fig. 18.18)	Tumors can appear as lesions with circumscribed or irregular margins that commonly involve the subcutis and adjacent superficial soft tissues. Tumors often have low to intermediate signal on T1 WI; and slightly high to high signal on T2WI and FST2WI. Tumors usually show Gd-contrast enhancement.	Myoepitheliomas and mixed tumors *(pleomorphic adenomas and carcinomas)* are tumors that usually occur in salivary glands, but can rarely occur in other soft tissues such as the subcutis or deeper soft tissues. Extrasalivary tumors occur in patients with a mean age of 38 years, with near equal gender frequency. Tumors contain epithelioid, ovoid, and/or spindle cells. Unlike benign myoepithelial tumors, malignant tumors have cellular atypia, nuclear pleomorphism, increased mitotic activity, coarse chromatin, and prominent nucleoli.Tumors are typically immunoreactive to keratins (AE1/AE3. PAN-K). and S-100 protein.
Neoplastic- benign		
Lipoblastoma (Fig. 18.19)	Lesions often have mixed low, intermediate, and high signal on T1WI, T2WI, and FST2WI. Lesions often show heterogeneous Gd-contrast enhancement.	Rare benign mesenchymal tumors that contain embryonal fat. Typically occur in infancy and early childhood. **(See Atlas Chapter A42)**
Lipoma (Fig. 18.20)	Lipomas in subcutaneous fat often have circumscribed margins and have MRI signal comparable to subcutaneous fat on T1WI, PDWI. T2WI, and FST2WI. Nonencapsulated superficial lipomas have also been described. Lipomas often show mostly no Gd-contrast enhancement except for minimal to mild enhancement along thin nonfatty septa.	Common benign hamartomas composed of mature white adipose tissue without cellular atypia. Lipomas are the most common soft tissue tumor, representing 10% of all soft tissue tumors and 16 % of benign soft tissue tumors. **(See Atlas Chapter A 43)**

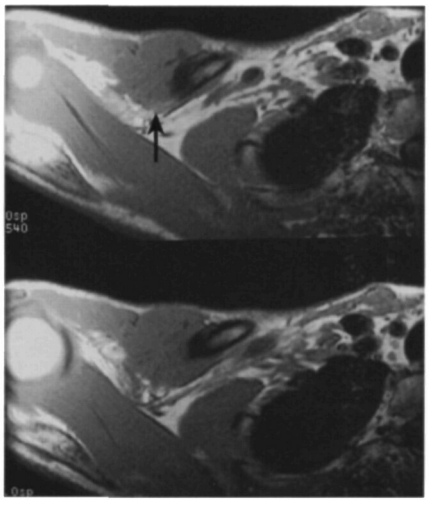

a

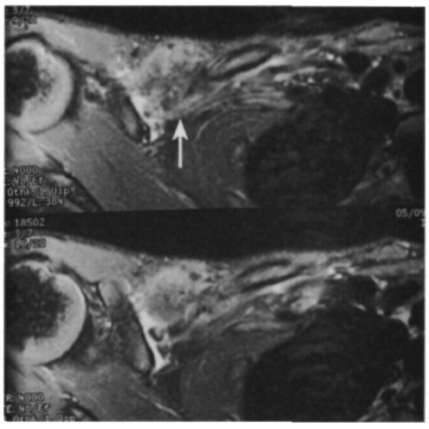

b

Figure **18.**17a, b A 14-year-old boy with an epithelioid sarcoma in the superficial soft tissues adjacent to the right clavicle. The tumor has intermediate signal on axial T1WI (**a**) and mixed intermediate and slightly high signal on axial FST2WI (**b**).

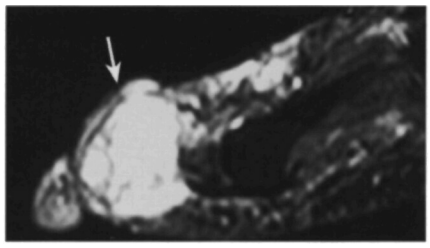

a

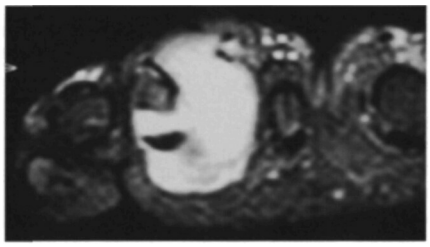

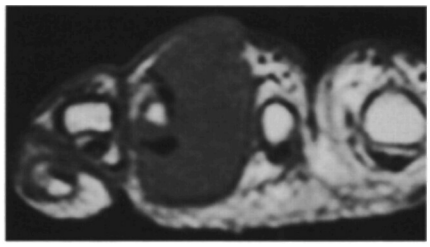

b, c

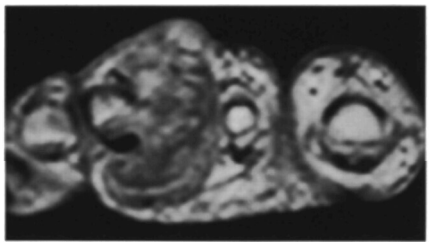

d

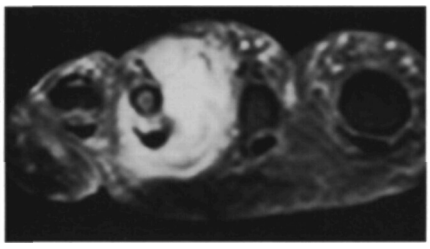

e

Figure 18.**18a-e** A 63-year-old man with a myoepithelial carcinoma involving the superficial and subcutaneous tissue between the toes. The tumor has high signal on sagittal (**a**) and axial (**b**) FST2WI, and intermediate signal on axial T1WI (**c**). The tumor shows Gd-contrast enhancement on axial T1WI (**d**) and axial FST1WI (**e**).

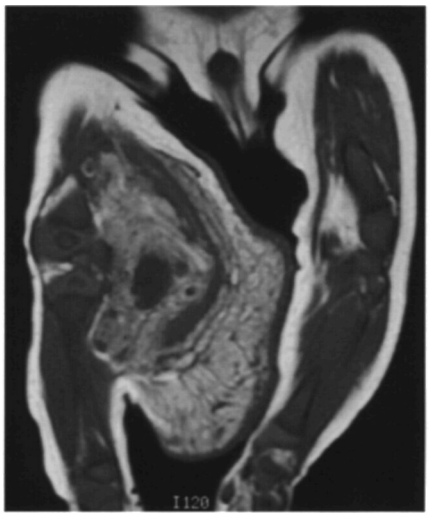

a

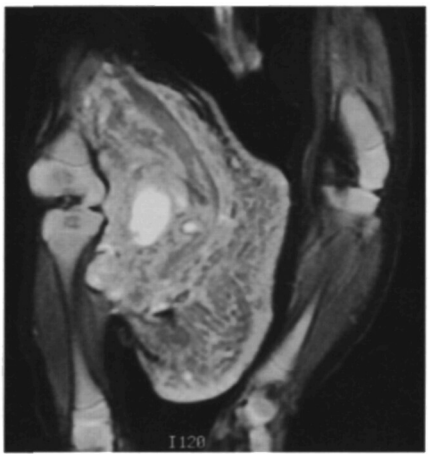

b

Figure 18.**19a, b** A 3-month-old boy with a large lipoblastoma that infiltrates the subcutaneous soft tissues and muscles of the thigh. The lesion contains signal approximating that of fat on coronal T1 WI (**a**). Many of the fatty zones have signal slightly lower than subcutaneous fat on T1WI as well as higher signal on coronal STIR (**b**). Intralesional bands, septa, and/or nodular zones are seen with low-intermediate signal on T1WI and intermediate-slightly high and high signal on STIR.

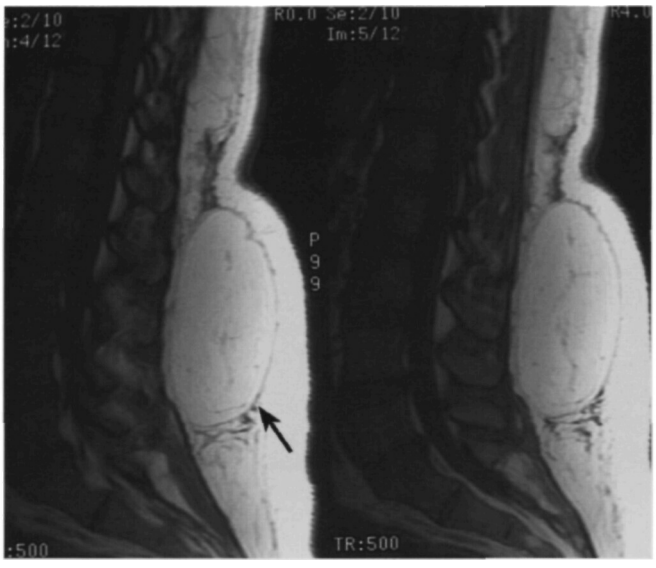

a

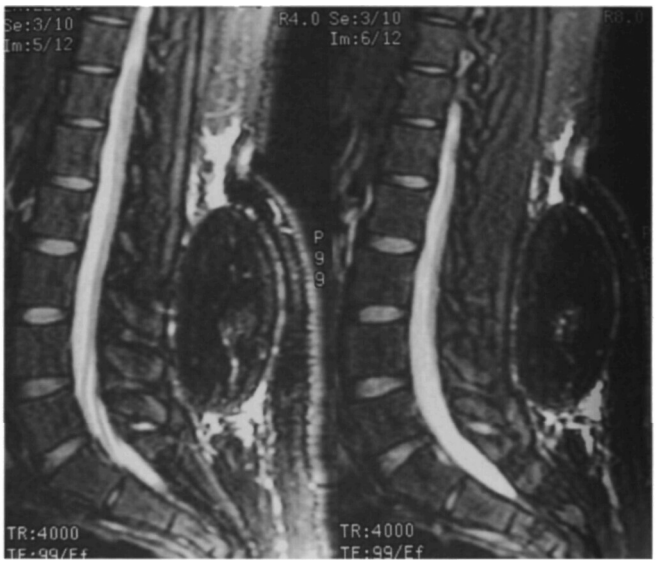

b

Figure 18.**20a, b** A 28-year-old woman with a lipoma in the dorsal subcutaneous fat superficial to the lumbar spine. The lipoma has high signal on sagittal T1WI (**a**). The lipoma has a thin capsule of low signal. The signal of the lipoma is suppressed on sagittal FST2WI (**b**).

Table 18 (Continued) Tumors and tumorlike lesions of the superficial soft tissues including subcutaneous fat

Lesion	MRI Findings	Comments
Hemangioma (Fig. 18.21)	Hemangiomas have circumscribed margins with or without lobulations, and have low-intermediate signal or heterogeneous low-intermediate and high signal on T1WI and PDWI; and high signal on T2WI. On FST2WI, hemangiomas typically have high signal except for zones of fat within the lesions. Zones of hemorrhage can sometimes be present in hemangiomas as well as phleboliths. Hemangiomas usually show prominent Gd-contrast enhancement.	Benign hamartomatous lesions of bone and soft tissues composed of capillary, cavernous, and/or malformed venous vessels. **(See Atlas Chapter A34)**
Lymphangioma (Fig. 272 in Atlas section)	Can be circumscribed lesions or occur in infiltrative pattern with extension within and between muscles. Often contain single or multiple cystic zones that have predominantly low signal on T1WI and high signal on T2WI and FST2WI. Fluid-fluid levels and zones with high signal on T1WI and variable signal on T2WI may result from cysts containing hemorrhage, high protein concentration, and/or necrotic debris. Septa between the cystic zones can vary in thickness and Gd-contrast enhancement, and usually have low signal on T1WI and low to intermediate signal on T2WI and FS T2WI. Nodular zones within the lesions can have variable degrees of Gd-contrast enhancement.	Benign vascular tumors that typically occur in soft tissue and only rarely in bone. They result from abnormal proliferation of lymphatic vessels. Lesions are composed of endothelium-lined lymphatic channels interspersed within connective tissue stroma. Account for less than 1 % of benign soft tissue tumors, 5.6% of all benign lesions of infancy and childhood. Can occur in association with Turner syndrome and Proteus syndrome. Patients usually range in age from 1 to 50 years, mean = 19 years. Can be congenital, with ~ 50 % present at birth. Approximately 85 % are detected by age 2 **(See Atlas Chapter A46).**
Nodular fasciitis (Atlas Figs. 109,110)	Lesions can have mildly irregular or stellate borders. They usually have intermediate signal on T1WI and PDWI and homogeneous or mildly heterogeneous high signal on T2WI and FST2WI. Surrounding edema is occasionally seen. Older lesions with high fibrous content may have intermediate signal on T2WI. Lesions can show homogeneous or peripheral rim-like patterns of Gd-contrast enhancement.	Benign reactive lesion comprised of proliferating fibroblasts, usually occurring in the subcutaneous tissue or muscle in young adults. **(See Atlas Chapter A21)**

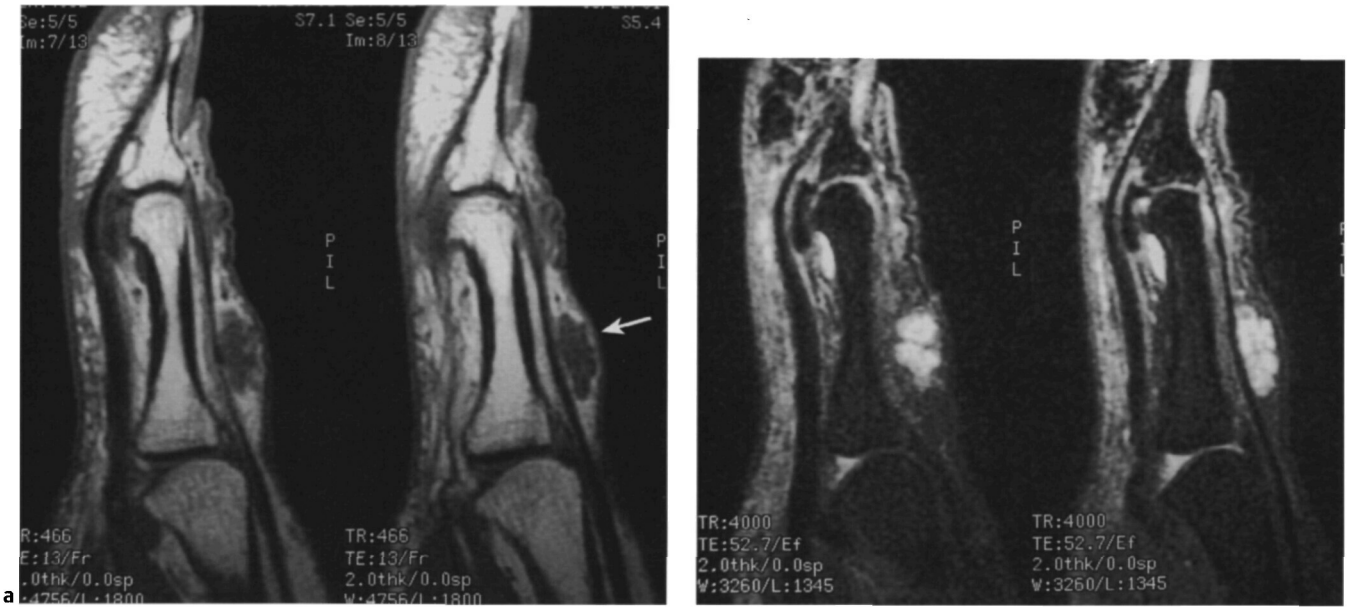

a b

Figure 18.**21 a, b** A 44-year-old woman with a hemangioma in the dorsal soft tissues of a finger. The hemangioma has circumscribed slightly lobulated margins, and has intermediate signal on sagittal T1WI (**a**) and high signal on sagittal FST2WI (**b**).

Table 18 (Continued) Tumors and tumorlike lesions of the superficial soft tissues including subcutaneous fat

Lesion	MRI Findings	Comments
Nerve sheath tumor (schwannoma, neurofibroma)	**Localized neurofibromas (Figs. 18.22, 18.23) and schwannomas (Fig. 18.24)** are circumscribed ovoid or fusiform lesions with low-intermediate signal on T1WI, intermediate signal on PDWI. and intermediate to high signal on T2WI and FST2WI. Lesions typically show moderate to prominent Gd-contrast enhancement. Multiple neurofibromas and schwannomas are frequently seen with neurofibromatosis type 1 and 2 (NF1 and NF2), respectively. Neurofibromas can occur in various soft tissues including the skin. **Plexiform neurofibromas (Fig. 18.25)** usually appear as curvilinear and multinodular lesions involving multiple nerve branches. They have low to intermediate signal on T1WI and intermediate, slightly high to high signal on T2WI and FST2WI with or without bands or strands of low signal. Lesions usually show Gd-contrast enhancement.	Benign nerve sheath tumors include schwannomas and neurofibromas. Schwannomas are benign encapsulated tumors that contain differentiated neoplastic Schwann cells. Neurofibromas are benign tumors of the peripheral nerve sheath that contain mixtures of Schwann cells, perineural-like cells, and interlacing fascicles of fibroblasts associated with abundant collagen. Unlike schwannomas, neurofibromas lack Antoni A and B regions and cannot be separated pathologically from the underlying nerve. Neurofibromas can be localized lesions, or occur as diffuse or plexiform lesions. The presence of multiple neurofibromas is a typical feature of NF1. Multiple schwannomas typically occur in patients with NF2. **(See Atlas Chapters A56, A72)**
Paraganglioma	Paragangliomas are circumscribed ovoid or fusiform lesions with low-intermediate signal on T1WI and PDWI, and intermediate to high signal on T2WI and F5T2WI. Multiple tortuous and/or punctate zones of signal void or low signal on PDWI, T2WI, and FS T2WI can be seen within tumors as a "salt and pepper" pattern. Lesions typically show moderate to prominent Gd-contrast enhancement.	Extra-adrenal paragangliomas are benign encapsulated neuroendocrine tumors that arise from neural crest cells associated with autonomic ganglia (paraganglia) throughout the body. In the superficial softtissues, paragangliomas can occur at the carotid body in the neck or near the vagus nerve. **(See Atlas Chapter A66)**
Granular cell tumor (Fig. 18.26)	Tumors can have circumscribed and/or irregular margins, and contain low-intermediate signal on T1WI and PDWI, and intemediate, slightly high to high signal on T2WI and FS T2WI. Tumors can also have low-intermediate signal on T2WI. Tumors can show prominent Gd-contrast enhancement.	Rare benign schwannian neoplasms that conlain cells with diffuse granular cytoplasm and are immunoreactive to S-100, but not to HMB-45. Tumors are often located in the dermis/subcutis, and occasionally within muscle. Occur more commonly in females compared with males, adults over 30 years old.
Clomus body tumor (Fig. 18.27)	Glomus body tumors are well-circumscribed ovoid lesions measuring less than 1 cm and are often located under the nail beds at the distal phalanges of fingers and toes. Glomus body tumors often have low-intermediate signal on T1WI and PDWI, although may be hypointense or hyperintense on T1WI relative to the adjacent dermis layers. Glomus tumors usually have high signal T2WI and FST2WI, and typically show Gd-contrast enhancement.	Benign mesenchymal hamartomas derived from the neuromyoarlerial apparatus (glomus bodies) that regulate arteriolar blood flow to the skin and are normally present in the reticular dermis throughout the body. Glomus bodies occur in large numbers under the nail beds of the fingers and toes. **(See Atlas Chapter A31)**
Leiomyoma (Fig. 18.28)	Lesions may have well-defined or irregular margins, and have low-intermediate signal on T1WI and intermediate to slightly high or high signal on T2WI and FST2WI. Lesions usually show moderate to marked Gd-contrast enhancement.	Benign spindle cell tumors composed of mature smooth muscle bundles. Ninety-five percent of leiomyomas involve the female genitourinary tract, and 3 % occur in the skin with the remainder in the gastrointestinal tract, bladder, and other sites. Cutaneous leiomyomas (leiomyoma cutis) arise from the pilar arrector muscles of the skin, or from the network of muscle fibers in the deep dermis. Angioleiomyomas are tumors that contain mixtures of vascular channels and smooth muscle cells. **(See Atlas Chapter A39)**
Desmoid tumor (Fig. 18.29)	Lesions can have distinct and/or poorly defined margins, homogeneous or heterogeneous low-intermediate signal on T1WI, and variable intermediate-high signal on T2WI, +/- zones of low signal. Myxoid zones in the lesions can have high signal on T1WI and T2WI. Tumors with high cellularity tend to show higher signal on T2WI than lesions with larger proportions of collagen. Lesions show variable degrees and patterns (heterogeneous versus homogenous) of Gd-contrast enhancement. Pattern or degree of Gd-contrast enhancement by desmoids does not enable prediction of rate of tumor recurrence.	Desmoid tumors or fibromatosis represent a group of soft tissue lesions composed of benign fibrous tissue with elongated or spindle-shaped cells adjacent to collagen. **(See Atlas Chapter A16)**

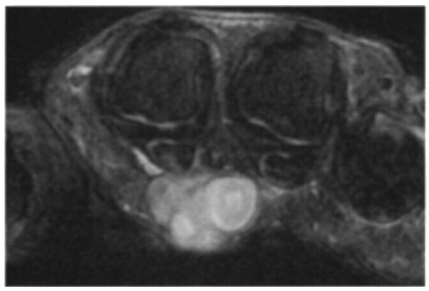

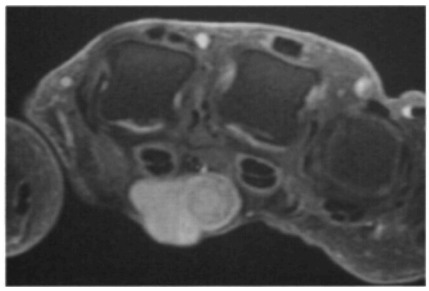

Figure 18.**22a, b** An 81-year-old woman with a neurofibroma involving the soft tissues ventral to the metacarpophalangeal joint in the hand. The lesion has high signal on axial FST2WI (**a**) and shows slightly heterogeneous Gd-contrast enhancement on axial FST1WI (**b**).

Figure 18.**23 a, b** A 68-year-old woman with NF1 and multiple cutaneous neurofibromas that have intermediate signal on sagittal T1WI (**a**) and mixed intermediate to high signal on sagittal T2WI (**b**).

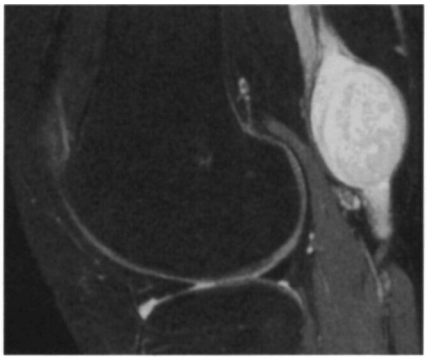

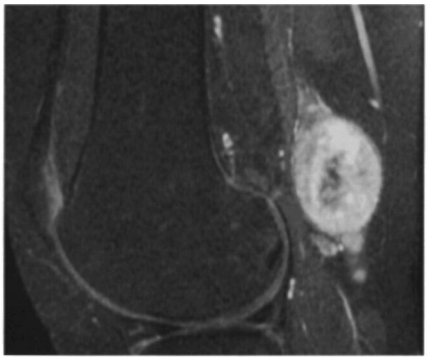

Figure 18.**24a, b** A 17-year-old woman with a schwannoma involving the tibial nerve at the dorsal knee. The lesion has high signal on sagittal FST2WI (**a**) and shows prominent Gd-contrast enhancement on sagittal FST1WI (**b**).

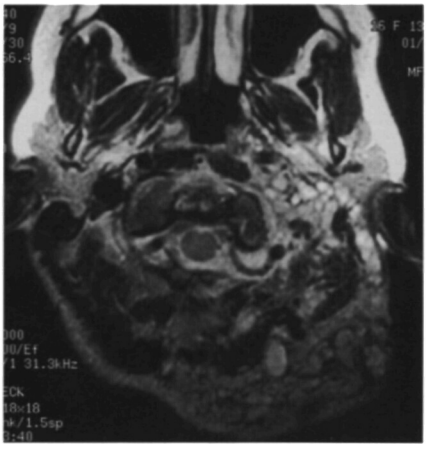

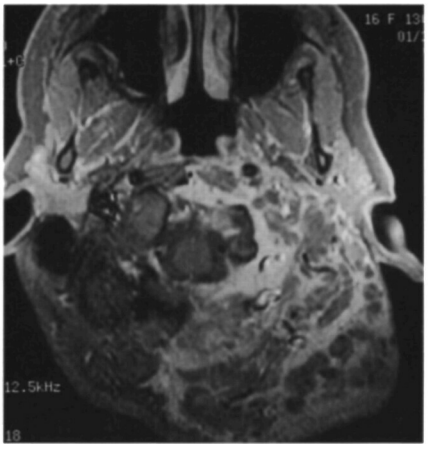

Figure 18.**25 a, b** A 16-year-old female with a plexiform neurofibroma involving the posterior scalp and skull. The lesion appears as curvilinear and multinodular zones with intermediate, slightly high to high signal separated by curvilinear zones of low signal on axial T2WI (**a**). The plexiform neurofibroma shows heterogeneous Gd-contrast enhancement on axial FST1WI (**b**).

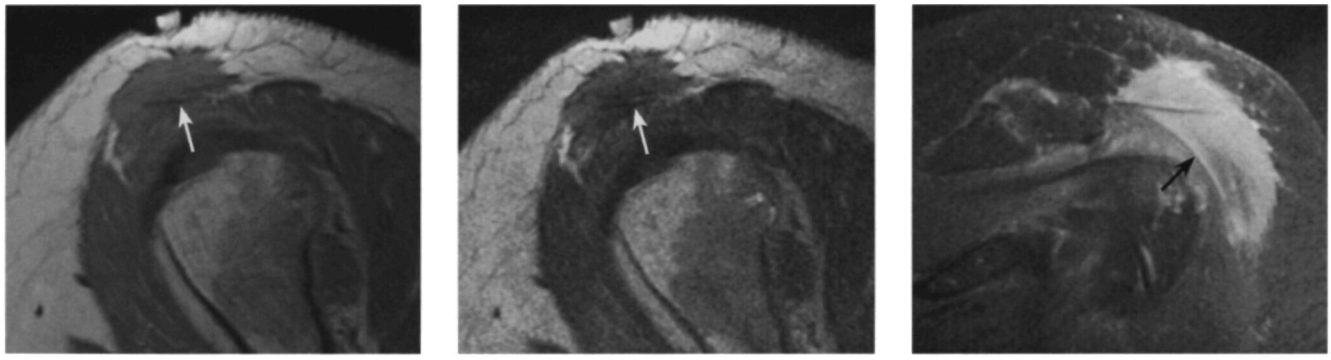

Figure 18.**26a-c** A 56-year-old woman with a granular cell tumor involving the subcutaneous fat and superficial portion of the deltoid muscle. The tumor has irregular margins and contains low-intermediate signal on sagittal PDWI (**a**) and T2WI (**b**). The tumor shows prominent Gd-contrast enhancement on coronal FST1WI (**c**).

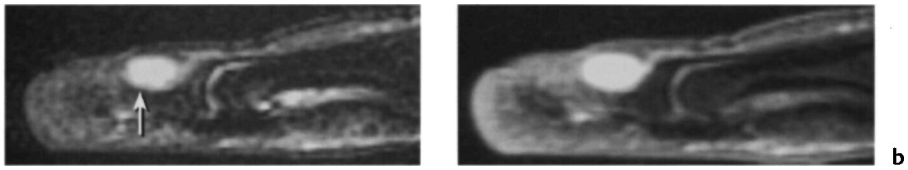

Figure 18.**27 a, b** Clomus tumor in a subungual location of a finger in a 43-year-old woman. The lesion has high signal on sagittal FST2WI (**a**) and shows prominent Gd-contrast enhancement on sagittal FST1WI (**b**).

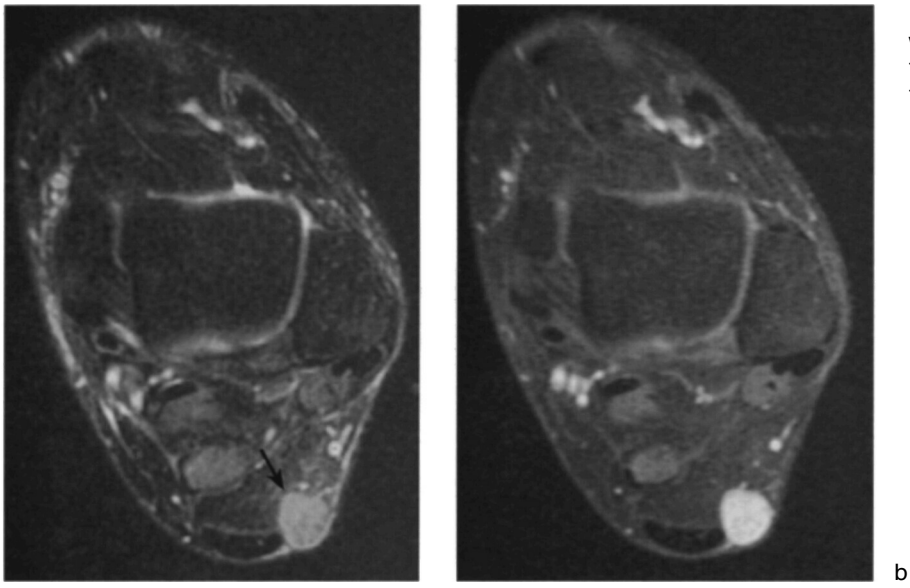

Figure 18.**28a, b** A 60-year-old woman with a leiomyoma in the subcutaneous fat in the ankle region. The lesion has slightly high to high signal on axial FST2WI (**a**) and shows prominent Gd-contrast enhancement on axial FST1WI (**b**).

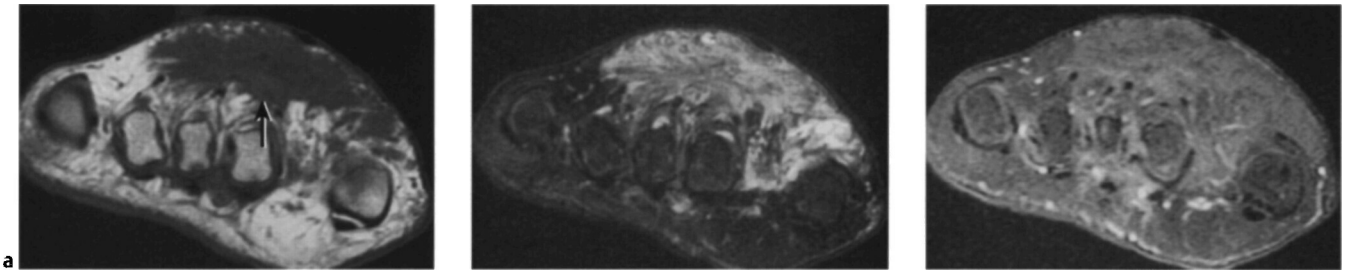

Figure 18.**29a-c** A 16-year-old male with aggressive fibromatosis (desmoid tumor) involving the dorsal subcutaneous soft tissues of the foot. The lesion has irregular margins and infiltrates adjacent tissue. The lesion has intermediate signal on coronal T1WI (**a**) and heterogeneous high signal on coronal FST2WI (**b**), and shows only minimal Gd-contrast enhancement on coronal FST1WI (**c**).

Table 18 (Continued) Tumors and tumorlike lesions of the superficial soft tissues including subcutaneous fat

Lesion	MRI Findings	Comments
Myxoma (Atlas Figs. 349-351)	Lesions usually have low or low-intermediate signal on T1WI and PDWI and high signal on T2WI and FST2WI. Myxomas can have heterogeneous mild or moderate degrees of enhancement in noncystic portions.	Benign lesions containing fibroblasts (spindle cells) and abundant mucoid material (glycosaminoglycans. other mucopolysaccharides). **(See Atlas Chapter A 54)**
Angiomatoid fibrous histiocytoma (Fig. 18.30)	Tumors can appear as multinodular lesions in the superficial soft tissues wilh heterogeneous low-intermediate signal on T1 WI and PDWI, and heterogeneous high signal on T2WI. Fluid-fluid levels may be seen secondary to hemorrhage. Thin septa with low signal on T2WI may be seen between the multiple nodular zones with high signal. Tumors can show prominent heterogeneous Gd-contrast enhancement.	Low-grade fibrohistiocytic neoplasms that are often located in the deep dermis and subcutis. **(See Atlas Chapter A 5)**
Pleomorphic hyalinizing angiectatlc tumor (Fig. 18.31)	Tumors in the superficial soft tissues can have lobulated and/or irregular/indistinct margins, and have low to intermediate signal on T1 WI and PDWI, and slightly high to high signal on T2WI and FST2WI. Linear or curvilinear zones of low signal on T2WI and FST2WI can be seen within these tumors. Tumors can show prominent Gd-contrast enhancement.	Pleomorphic hyalinizing angiectatic tumors (PHATs) are rare nonmetastasizing tumors. They contain a spindle cell neoplastic stroma lacking mitotic activity that surrounds aggregates of thin-walled ectatic vessels lined with fibrin. More than 50% involve the subcutaneous tissues of the lower extremity. **(See Atlas Chapter A68)**
Tumorlike lesions		
Ganglion cyst (Fig. 18.32)	Ganglia are sharply defined lesions with low signal on T1WI, low-intermediate signal on PDWI, and homogeneous high signal on T2WI. Some ganglia may have intermediate signal on T1WI secondary to elevated proteinaceous or fibrous content. Low signal septa on T2WI can be seen. Peripheral rim-like Gd-contrast enhancement can be seen as well as complete lack of enhancement.	Ganglia are juxta-articular benign myxoid lesions that arise from degeneration of peri-articular connective tissue, prior trauma, or prior inflammation. Ganglia may be derived from tendons, tendon sheaths, joint capsules, bursae, or ligaments. **(See Atlas Chapter A28)**
Sebaceous cyst (Figs. 18.33.18.34)	Lesions usually occur in the subcutaneous fat and have circumscribed margins. Cyst contents often have low-intermediate signal on T1WI, and variable low, intermediate, and/or high signal on T2WI and FST2WI. Lesions typically do not show Gd-contrast enhancement.	Sebaceous glands are holocrine glands that occur mostly on the face and scalp. These glands shed cells into the excretory stream whose sebum contents include squalene, triglycerides, and wax esters.

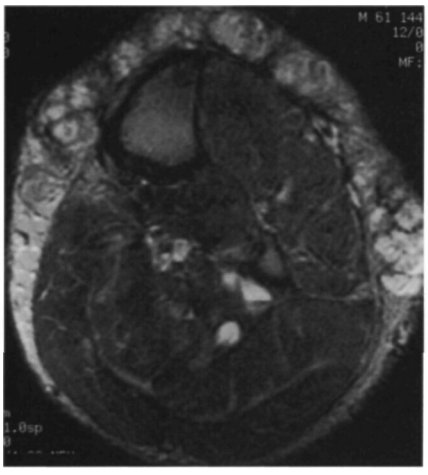

a

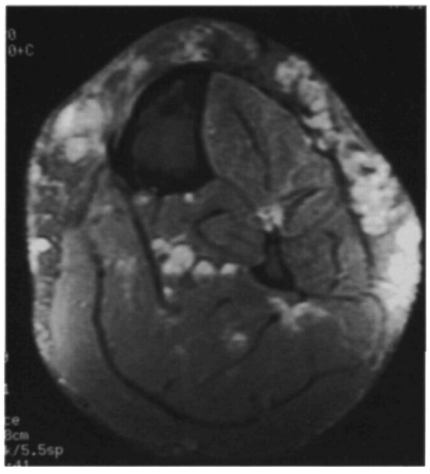

b

Figure 18.**30a, b** A 61-year-old man with an angiomatoid fibrous histiocytoma in the subcutaneous fat of the leg. The multinodular lesions in the subcutaneous fat have heterogeneous high signal on axial T2WI (**a**) and show Gd-contrast enhancement on axial FST1WI(**b**).

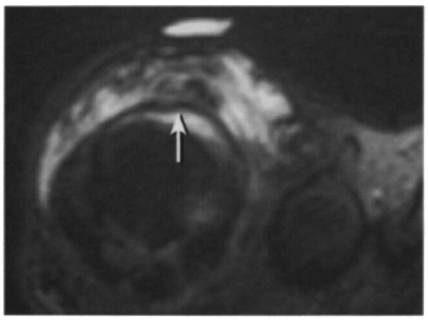

a

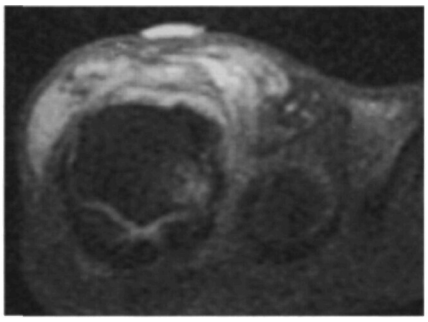

b

Figure 18.**31 a, b** A 42-year-old woman with a pleomorphic hyalinizing angiectatic tumor involving the dorsal superficial soft tissues of the foot. The tumor has heterogeneous slightly high and high signal on coronal FST2WI (**a**). Linear and curvilinear zones of low signal on FST2WI are seen in the lesion. The tumor shows prominent Gd-contrast enhancement on coronal FST1WI (**b**).

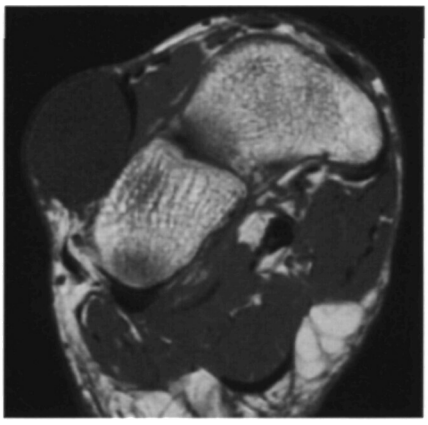

a

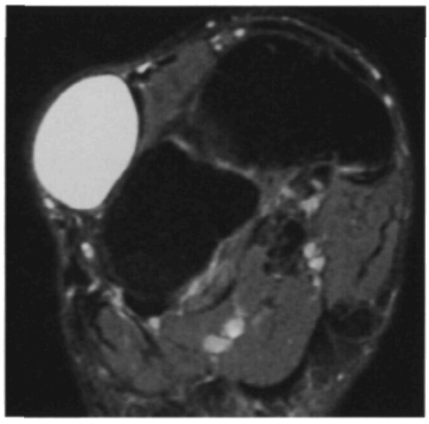

b

Figure 18.**32 a, b** Ganglion in the dorsal soft tissues of the foot. The lesion has sharply defined margins and has low signal on coronal T1WI (**a**) and high signal on coronal FST2WI(**b**).

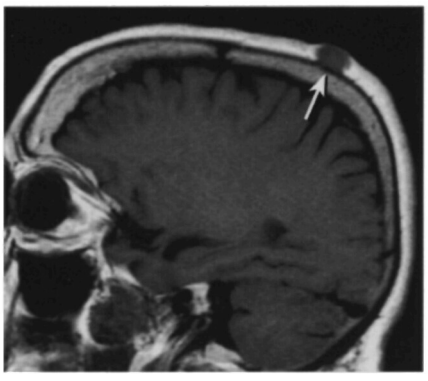

a

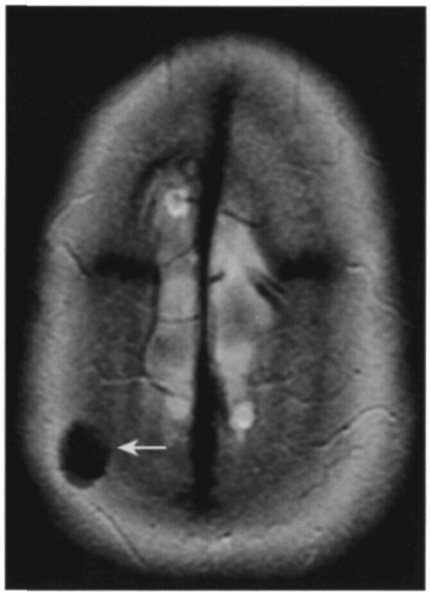

b

Figure 18.**33 a, b** Sebaceous cyst in the subcutaneous fat of the scalp that has intermediate signal on sagittal T1WI (**a**) and low signal on axial T2WI (**b**).

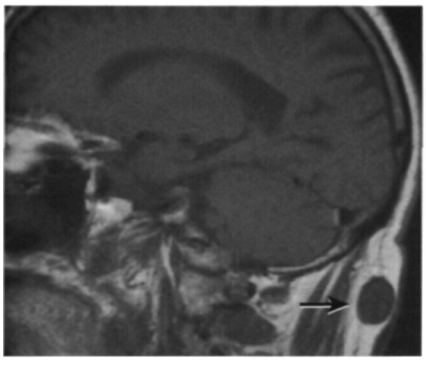

a

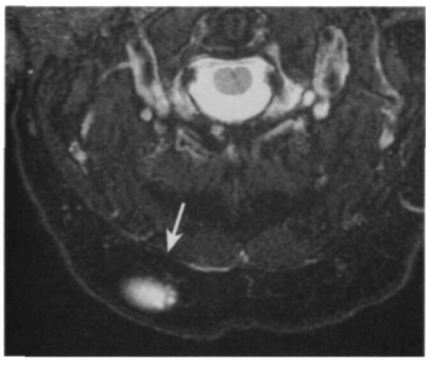

b

Figure 18.**34 a, b** Sebaceous cyst in the subcutaneous fat of the scalp that has intermediate signal on sagittal T1WI (**a**) and high signal on axial FST2WI (**b**).

Table 18 (Continued) Tumors and tumorlike lesions of the superficial soft tissues including subcutaneous fat

Lesion	MRI Findings	Comments
Epidermoid (Fig. 18.35)	Epidermoids are circumscribed lesions with or without lobulated margins, and usually have low signal or low-intermediate signal on T1WI and high signal on T2WI and FS T2WI that may approximate CSF. Lesions occasionally contain foci of high signal on T1WI Epidermoids may show minimal peripheral Gd-contrast enhancement, but no enhancement is typically seen centrally.	Epidermoids are ectoderm-lined inclusion cysts that contain only squamous epithelium. Epidermoids often slowly enlarge, but are not considered to be neoplasms. **(See Atlas Chapter A15)**
Dermoid	Dermoid cysts are circumscribed lesions with walls with low signal on T1WI and T2WI. The contents of dermoid cysts can have low, intermediate, and/or high signal on T1 WI and T2WI **(Atlas Figs. 73-76)** Dermoids may show Gd-contrasl enhancement at the wall margins, but not centrally.	Dermoids are ectoderm-lined inclusion cysts that contain hair, sebaceous and sweat glands, and squamous epithelium. Dermoids slowly enlarge, although are not considered to be neoplasms. **(See Atlas Chapter A15)**
Hematoma/seroma	Acute hematomas (< 3-7 days) have mostly intermediate signal similar to muscle on T1 WI and mixed low-intermediate and/or high signal relative to muscle on PDWI, T2WI, and FST2WI. Poorly defined zones of high signal on PDWI, T2WI, and FST2WI may also be seen peripheral to the hematoma representing adjacent edema. Subacute hematomas (1 week to 3 months) have high and/or intermediate signal on T1WI. and high signal on FST1WI. PDWI, T2WI, and FST2WI **(Fig. 18.36)** Peripheral and central zones of low signal on PDWI, T2WI, and FST2WI can be seen in mid to late subacute hemalomas secondary to the presence of hemosiderin from breakdown of blood cells and oxidation/metabolism of hemoglobin. Mild peripheral Gd-contrast may be seen **(Fig. 18.37)** Chronic hematomas (> 3 months) usually have high signal on T1 WI, PDWI, T2WI, and FS T2WI. A thick peripheral rim of low signal on T2WI from hemosiderin is often seen with chronic hematomas. Chronic hematomas often evolve eventually into zones with low-intermediate signal on T1 WI and T2WI secondary to fibrosis and residual hemosiderin.	Hematomas are extravascular collections of red and white blood cells. They can result from trauma, surgery or coagulopathy (hemophilia, thrombocytopenia, medications/coumadin/heparin, and sepsis). **(See Atlas Chapter A36)**
Morel-Lavallee lesion (Atlas Fig. 202)	Circumscribed collection in the subcutaneous fat often with low to intermediate signal on T1WI, and high signal on T2WI. A thin or slightly thick rim of low signal on T2WI is often present.	High-velocity injury to the superficial soft tissues in which there is internal degloving or separation of the skin and subcutis from the fascia resulting in a collection filled with fluid and debris. Most often occurs in the pelvic subcutaneous fat. **(See Atlas Chapter A36)**
Heterotopic ossification (Fig. 18.38)	The MRI features vary depending on the age, location, and degree of mineralization/ossification. Lesions < 2 weeks have localized mass effect with poorly defined margins, heterogeneous low-intermediate or slightly high signal on T1WI, and heterogeneous slightly high to high signal on T2WI and FST2WI. Poorly defined zones of high signal on T2WI may be seen in the adjacent soft tissues. After 2 weeks, curvilinear and/or amorphous zones of low signal on T2WI and FST2WI can be seen at the peripheral portions of the subacute lesions resulting from mineralization/ossification. Subsequent progressive centripetal mineralization/ossification appears as irregular zones of low signal on T2WI. During this process, heterogeneous Gd-contrast enhancement is typically seen. Old lesions usually have well-defined margins, and have variable low signal on T1WI, PDWI, and T2WI depending on the degree of mineralization/ossification, fibrosis, and hemosiderin deposition. Zones of high signal on T1WI and T2WI may occur from fatty marrow metaplasia. Gd-contrast enhancement in old mature lesions is often minimal or absent.	Heterotopic ossification or myositis ossificans are non-neoplastic reparative extraosseous lesions that are composed of reactive hypercellular fibrous tissue, cartilage, and/or bone. These lesions can arise secondary to trauma (myositis ossificans circumscripta, ossifying hematoma), though may also occur without a history of prior injury (pseudomalignant osseous tumor of the soft tissues). **(See Atlas Chapter A53)**

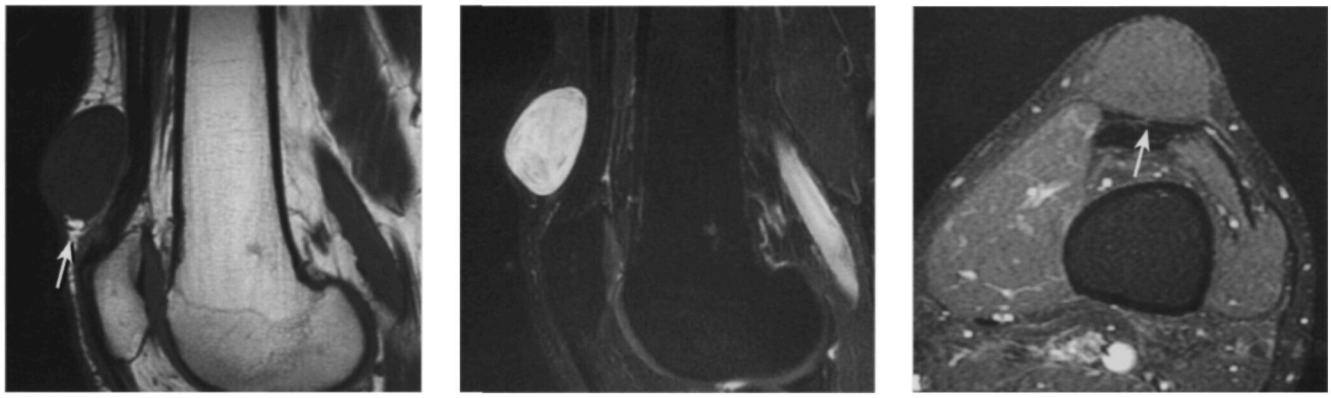

Figure 18.**35a-c** A 25-year-old man with an epidermoid involving the anterior soft tissues at the knee. The lesion has low-intermediate signal on sagittal PDWI (**a**) and high signal on sagittal FST2WI (**b**). The lesion shows no Gd-contrast enhancement on axial FST1WI (**c**).

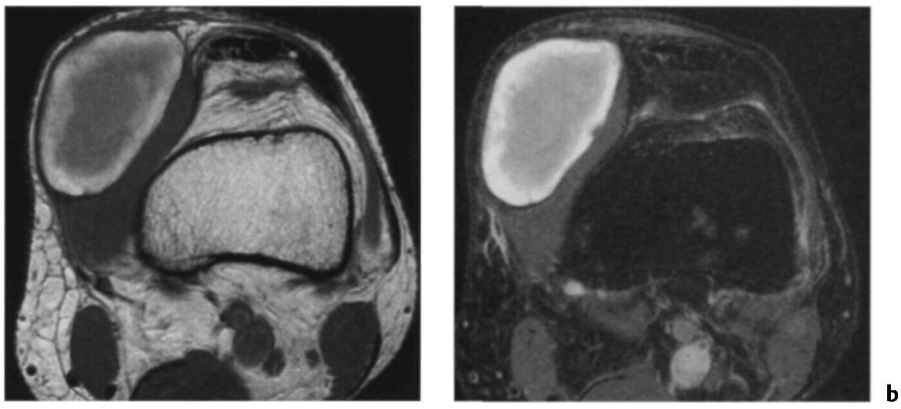

Figure 18.**36a, b** A 40-year-old woman with a hematoma in the soft tissues at the medial knee. The tumor has mixed high and intermediate signal on axial PDWI (**a**) and high and slightly high signal on axial FST2WI (**b**). The hematoma is surrounded by a rim of low signal on PDWI and FST2WI.

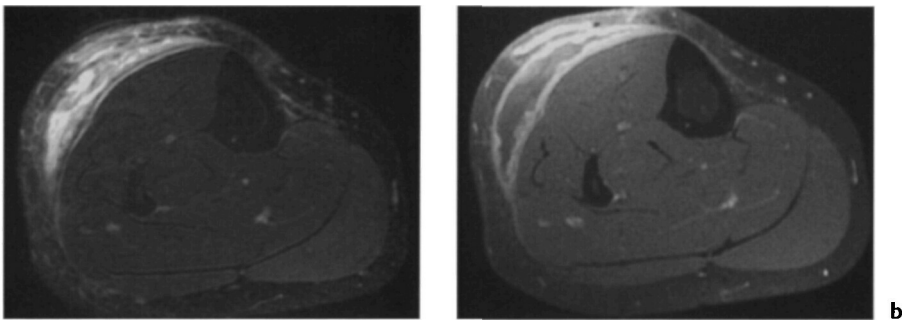

Figure 18.**37 a, b** A 14-year-old girl with a subacute hematoma in the subcutaneous fat of the medial leg. The tumor has heterogeneous high and slightly high signal on axial FST2WI (**a**). The hematoma has intermediate signal centrally and shows irregular peripheral zones of Gd-contrast enhancement on axial FST1WI (**b**).

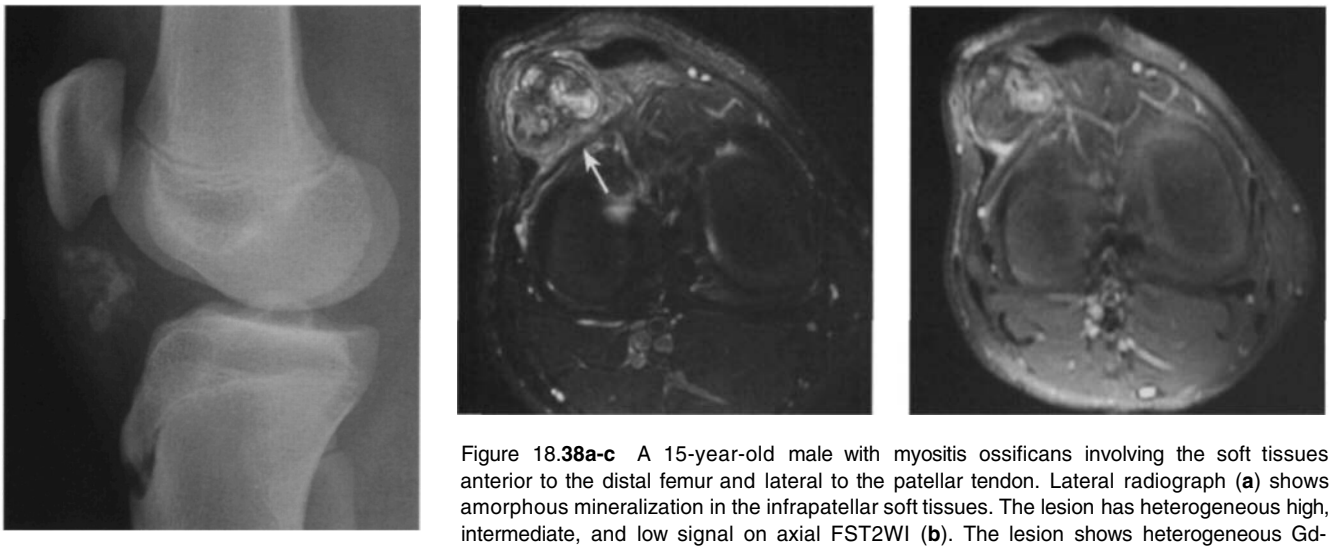

Figure 18.**38a-c** A 15-year-old male with myositis ossificans involving the soft tissues anterior to the distal femur and lateral to the patellar tendon. Lateral radiograph (**a**) shows amorphous mineralization in the infrapatellar soft tissues. The lesion has heterogeneous high, intermediate, and low signal on axial FST2WI (**b**). The lesion shows heterogeneous Gd-contrast enhancement on axial FST1WI (**c**).

Table 18 (Continued) Tumors and tumorlike lesions of the superficial soft tissues including subcutaneous fat

Lesion	MR Findings	Comments
Amyloidoma	Lesions in soft tissue can have low-intermediate signal on T1WI, and intermediate to slightly high signal on T2WI. Lesions can show Gd-contrast enhancement.	Uncommon disease in which various tissues (including bone, muscle, tendons, tendon sheaths, ligaments, and synovium) are infiltrated with extracellular eosinophilic material composed of insoluble proteins with β-pleated sheet configurations (amyloid protein). Amyloidomas are single sites of involvement. Amyloidosis can be a primary disorder associated with an immunologic dyscrasia or secondary to a chronic inflammatory disease.
Aneurysm (Figs. 18.39,18.40)	Saccular aneurysms are focal well-circumscribed structures contiguous with arteries. Signal voids are usually seen where there is fast blood flow in nonthrombosed portions of the aneurysms. Variable mixed signal on T1WI and T2WI can be seen in thrombosed portions of the aneurysms.	Aneurysms are focal or diffuse zones of arterial dilatation that are associated with wall abnormalities and increased risk of rupture. Focal aneurysms are also referred to as saccular aneurysms; they typically occur at arterial branch points. Giant aneurysms are saccular aneurysms that measure > 2.5 cm in diameter.
Hypothenar hammer injury (Fig. 18.41)	Thrombosis of the distal ulnar artery can be seen as lack of intraluminal signal void. The thrombosed vessel can have intermediate to high signal on T1WI, and heterogeneous high signal on FST2WI.	Thrombosis of the superficial branch of the distal ulnar artery can occur from trauma as it travels along the hypothenar muscles after exiting from Guyon canal. Emboli into the superficial palmar arch can result in symptoms.
Inflammatory		
Abscess (Fig. 18.42)	Lesions usually contain a circumscribed portion that has low signal on T1WI and high signal on T2WI (with or without an air-fluid level) that is surrounded by a rim of low signal on T2WI. Rim-like Gd-contrast enhancement is usually seen. Peripherally, a poorly defined zone of high signal may be seen secondary to edema and/or inflammation.	Abscesses are inflammatory lesions that are formed when liquefaction and necrosis occurs at sites of infection, are often enclosed by a pseudocapsule and surrounded by zones of edema and inflammatory reaction. Infectious organisms commonly include bacteria and fungi.

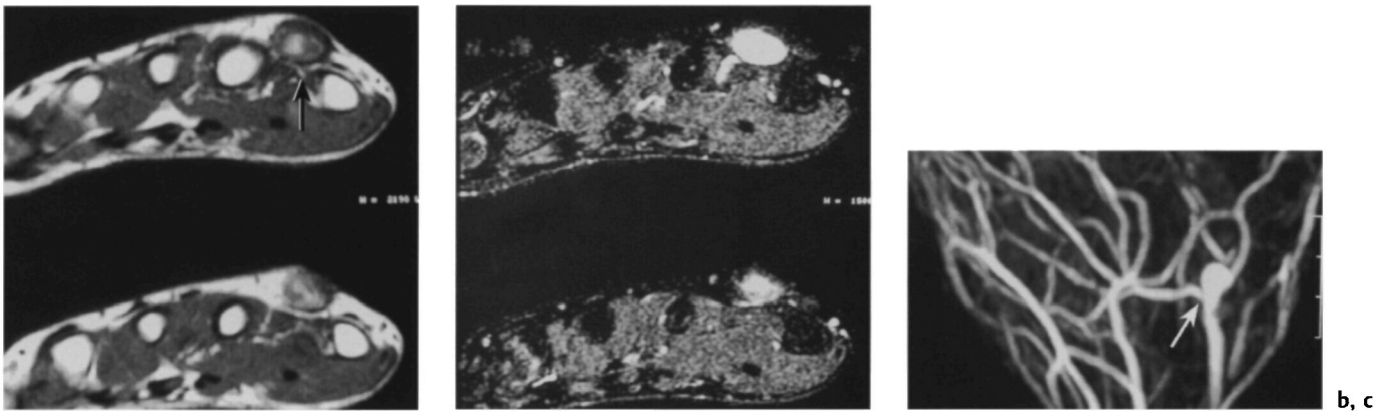

Figure 18.**39a-c** Aneurysm of the radial artery has mixed intermediate and high signal on axial PDWI (**a**) and high signal on axial FST2WI (**b**). The aneurysm is seen on the 3 D time-of-flight MRA (**c**).

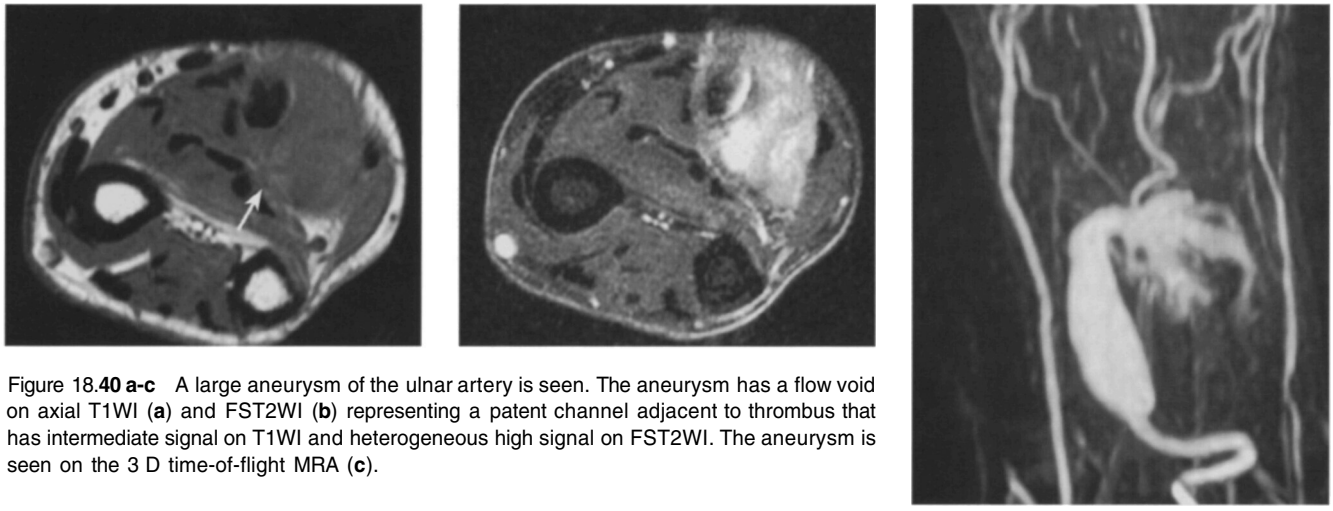

a, b

Figure 18.**40 a-c** A large aneurysm of the ulnar artery is seen. The aneurysm has a flow void on axial T1WI (**a**) and FST2WI (**b**) representing a patent channel adjacent to thrombus that has intermediate signal on T1WI and heterogeneous high signal on FST2WI. The aneurysm is seen on the 3 D time-of-flight MRA (**c**).

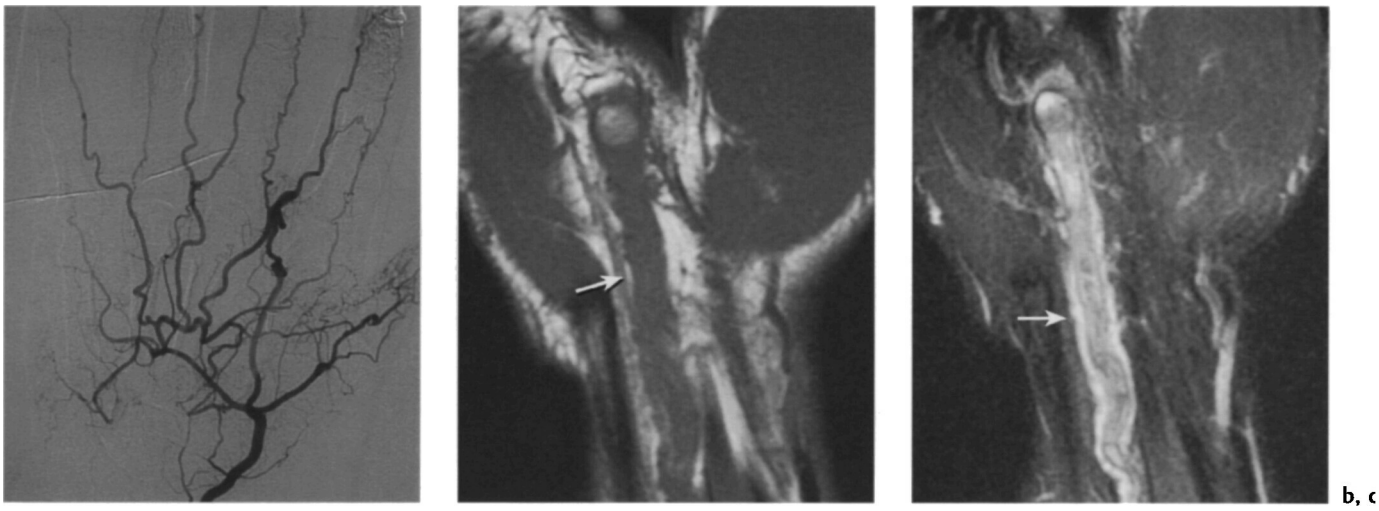

a

b, c

Figure 18.**41 a-d** Hypothenar hammer injury in a 46-year-old man resulting in thrombosis of the ulnar artery. The arteriogram (**a**) shows occlusion of the ulnar artery and patency of the radial artery. The occluded ulnar artery contains intermediate and high signal on coronal T1 WI (**b**) and heterogeneous mostly high signal on coronal (**c**) and axial (**d**) FST2WI.

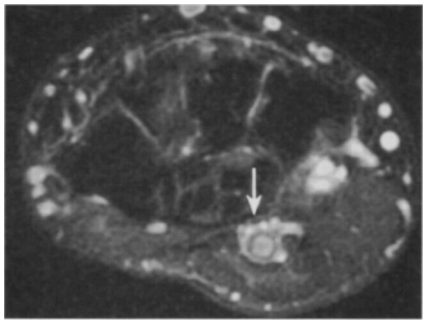

d

Figure 18.**42** A 75-year-old man with an abscess in the superficial soft tissues at the elbow. The abscess has irregular peripheral margins of Gd-contrast enhancement surrounding nonenhancing fluid/pus on sagittal FST1WI.

Table 18 (Continued) Tumors and tumorlike lesions of the superficial soft tissues including subcutaneous fat

Lesion	MRI Findings	Comments
Cat-scratch disease (Fig. 18.43)	Single or multiple enlarged lymph nodes are often seen, as well as localized granulomatous lesions. Lesions often occur in the epitrochlear and axillary regions, have low-intermediate signal on T1WI and intermediate to high signal on T2WI. Lesions can have irregular margins with peripheral edematous changes. Lesions can show Gd-contrast enhancement.	Infection by the Cram-negative bacillus *Bartonella henselae* can result in self-limited regional adenitis. This infection usually occurs in patients < 30 years and is often related to contact with cats.
Parasitic infection	Parasitic infections can vary from cystic-appearing lesions to poorly marginated or circumscribed solid lesions depending on the infectious organism and stage of its life cycle.	Parasitic infections can occur in soft tissues in endemic regions or in immunocompromised patients.
Cranuloma annulare	Poorly defined subcutaneous lesion with intermediate signal on T1WI, and heterogeneous low to slightly high signal on T2WI.	Benign inflammatory disorder that can involve the epidermis, dermis, and subcutaneous fat. Often occurs in children and young adults. Lesions can occur as localized, generalized, or subcutaneous forms. The localized type can appear as one or more lesions. The generalized type has a slightly wider distribution than the localized type. The subcutaneous type often affects children between 2 and 5 years.
Sarcoid (Fig. 18.44)	Sarcoid granulomas can also occur in subcutaneous fat and may be associated with superficial adenopathy. Lesions are often nodular with low to intermediate signal on T1WI, and intermediate to high signal on T2WI. Lesions usually show Gd-contrast enhancement. Sarcoid can also involve muscles as discrete lesions.	Chronic systemic granulomatous disease of unknown etiology in which noncaseating granulomas occur in various tissues and organs. Common sites of involvement include the lungs, lymph nodes, liver, spleen, skin, and eyes. **(See Atlas Chapter A71)**
Giant cell reaction to foreign body	Lesions usually occur in soft tissue and often have low-intermediate signal on T1WI and low, intermediate, and/or high signal on T2WI. Lesions can show Gd-contrast enhancement. Sites of bone erosion and/or destruction may be seen, particularly with penetrating trauma. The MRI signal of the foreign body varies based on its composition.	Reactive granulomatous lesions can form adjacent to foreign bodies, and may simulate neoplasm.
Gout (Fig. 18.45)	Tophi have variable sizes and shapes, and have low-intermediate signal on T1WI. FST2WI, and T2WI. Zones of high signal on T2WI can also be seen in tophi. Erosions of bone, synovial pannus, joint effusion, bone marrow, and soft tissue edema can be seen with MRI. Tophi may show heterogeneous, diffuse, or peripheral/marginal Gd-contrast enhancement patterns.	Gout is an inflammatory disease involving synovium resulting from deposition of monosodium urate crystals and occurs when the serum urate level exceeds its solubility in various tissues and body fluid. **(See Atlas Chapter A32)**

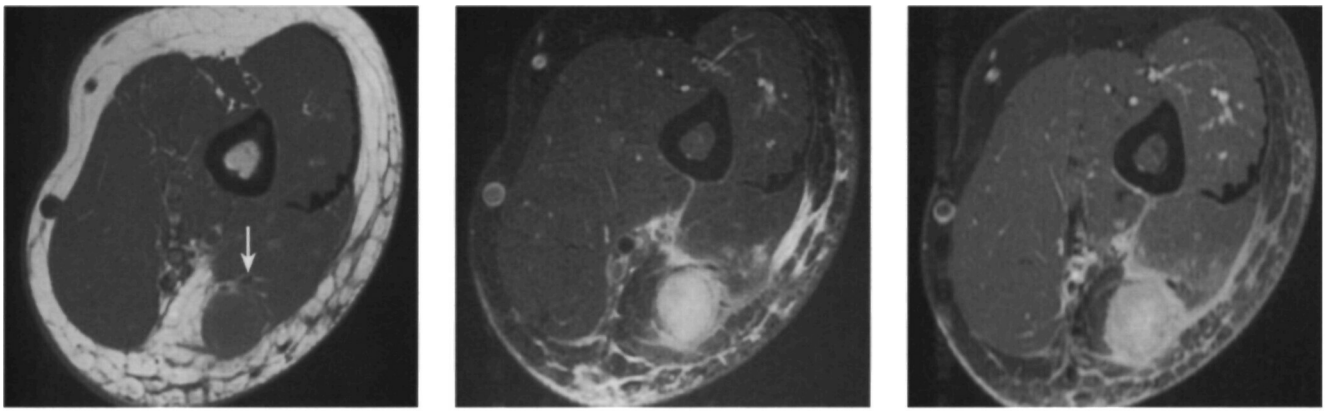

Figure **18.43a-c** A 45-year-old man with cat scratch disease with a granuloma involving a lymph node in the distal arm. The nodular lesion has intermediate signal on axial T1 WI (**a**) and slightly high to high signal on axial FST2WI (**b**). The lesion shows Cd-contrast enhancement on axial FST1WI (**c**). Irregular zones of inflammatory reaction are seen in the soft tissues peripheral to the nodular lesion.

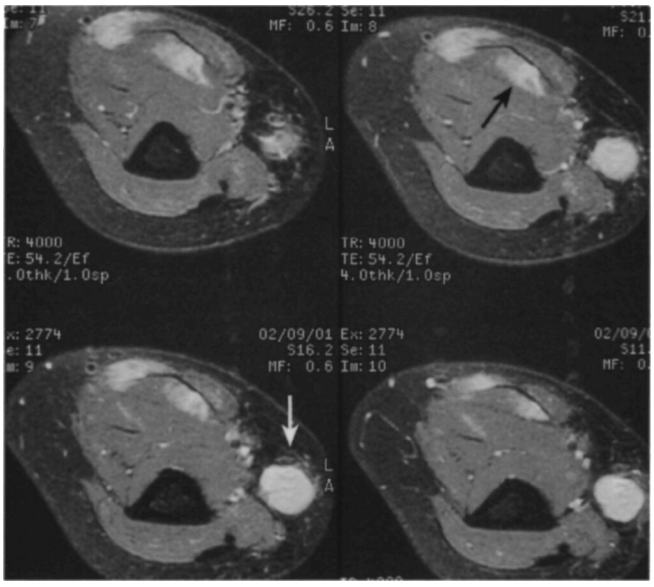

Figure **18.44** A 49-year-old woman with sarcoid granulomas in the subcutaneous fat and within the biceps brachii muscle at the distal arm. The lesions have slightly irregular margins, and have high signal on axial FST2WI.

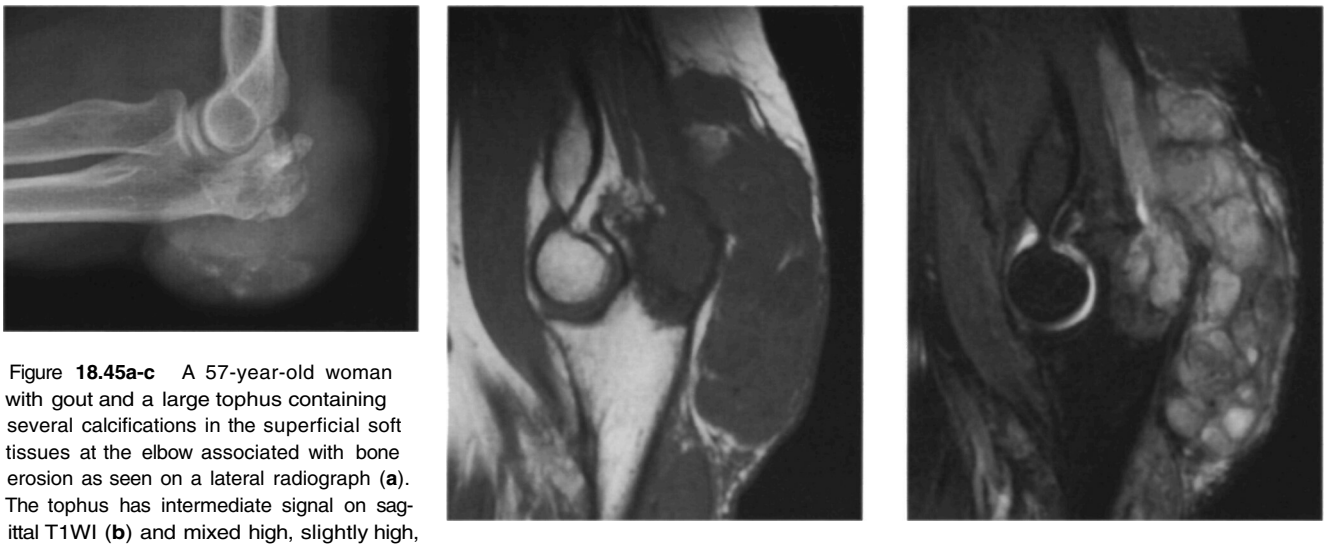

Figure **18.45a-c** A 57-year-old woman with gout and a large tophus containing several calcifications in the superficial soft tissues at the elbow associated with bone erosion as seen on a lateral radiograph (**a**). The tophus has intermediate signal on sagittal T1WI (**b**) and mixed high, slightly high, intermediate, and low signal on sagittal FST2WI(**c**).

Table 18 (Continued) **Tumors and tumorlike lesions of the superficial soft tissues including subcutaneous fat**

Lesion	MRI Findings	Comments
Rheumatoid arthritis (Fig. 18.46)	MRI can show diffuse and/or localized zones of synovial hypertrophy; soft tissue swelling; zones of erosion and/or destruction of hyaline cartilage, menisci, subchondral bone, tendons and/or ligaments; bursal fluid collections containing "rice bodies," other extra-articular cysts; intraosseous cystic-like areas, joint effusion, and rheumatoid nodules. With tendon and ligament involvement, abnormal increased signal is seen on PDWI and T2WI. Tendons and ligaments may be thickened from partial tearing or thinned. Tenosynovitis is usually seen with fluid and hypertrophied synovium within tendon sheaths.	Rheumatoid arthritis is a chronic multisystem disease of unknown etiology in which there is a persistent inflammatory synovitis that typically involves peripheral joints in a symmetric distribution. The inflammatory synovitis associated with rheumatoid arthritis typically results in progressive destruction of cartilage and bone, leading to joint dysfunction. **(See Atlas Chapter** A 70)
Kimura disease	Poorly marginated subcutaneous lesions with intermediate signal on T1WI and slightly high to high signal on T2WI. Lesions often show prominent Cd-contrast enhancement.	Inflammatory autoimmune disorder involving the superficial soft tissues composed of enlarged lymph nodes with eosinophilic infiltration, often occurs in Asian males between 10 and 30 years.
Other		
Giant cell tumor of the tendon sheath (Fig. 18.47)	Lsions usually have well-defined margins and are often adjacent to a tendon/tendon sheath. Lesions have low-i n t e r a t e signal on T1WI and PDWI and mixed low, intermediate and/or high signal on T2WI and FST2WI. Zones of low signal on T2WI often correspond to sites of hemosiderin deposition. Lesions often show Gd-contrast enhancement in either homogeneous or heterogeneous pattern.	Giant cell tumors of the tendon sheath and pigmented villonodular synovitis (PVNS) represent benign proliferative lesions of synovium (tendon sheaths, joints, and bursae). Giant cell tumors of the tendon sheaths can occur as localized nodular lesions attached to tendon sheaths outside of joints (hands, feet) or within joints (infrapatellar portion of knee joint); or as a diffuse form near/outside of large joints such as the knee, ankles, etc. **(See Atlas Chapter A 30)**
Fibroma of the tendon sheath (Fig. 18.48)	Lesions are ovoid or fusiform and well-circumscribed, and are often located adjacent to tendons of the fingers, hands, wrists, and feet. Lesions usually have low-intermediate signal on T1WI. On T2WI, lesions can have a slightly heterogeneous low-intermediate signal in half, intermediate signal in a third, or mixed low and intermediate signal and/or high signal in the remainder. Lesions can show diffuse or peripheral Gd-contrast enhancement.	Fibromas of the tendon sheath are benign, small fibrous nodules involving tendons and tendon sheaths of the fingers, hands, wrists, or feet. **(See Atlas Chapter A 23)**
Xanthoma	Xanthomas in tendons often appear as zones of fusiform enlargement with diffuse heterogeneous signal **(Atlas Figs. 505, 506)** Xanthomas usually contain multiple longitudinally oriented linear zones or striations with intermediate signal on T1WI and PDWI, and intermediate to slightly high signal on T2WI and FST2WI interspersed among bands of low signal within the enlarged tendons **(Atlas Fig. 506)** On axial images, xanthomas often have a stippled or reticulated pattern on T1WI and T2WI resulting from collagen bundles with low signal surrounded by higher signal from lipid deposits, foamy histiocytes, and inflammatory reaction. **(Atlas Fig. 506)**	Xanthomas represent localized accumulations of lipids within normal structures such as tendons, skin, and bone. Xanthomas are considered reactive lesions and are not true neoplasms. They often occur in the setting of types I, II, and III hyperlipoproteinemia. **(See Atlas Chapter A 77)**

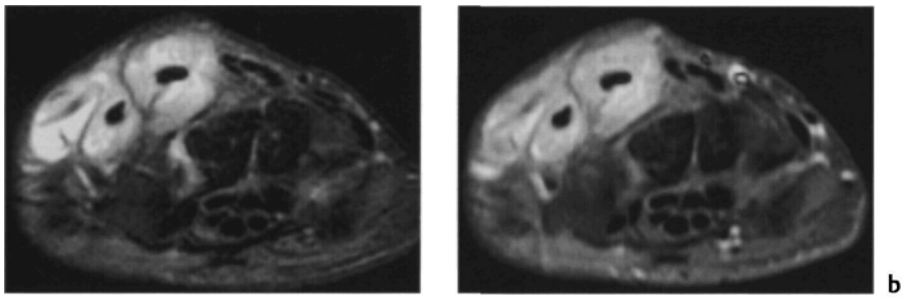

Figure **18.46a, b** A 48-year-old woman with rheumatoid arthritis. Pannus is seen in the tendon sheaths of 3 extensor tendons which has high signal on axial FST2WI (**a**), and shows prominent Gd-contrast enhancement on axial FST1WI(**b**).

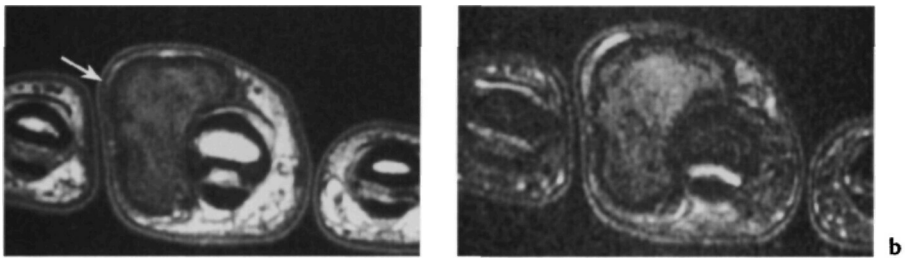

Figure **18.47 a, b** A 28-year-old man with a giant cell tumor of the tendon sheath involving a finger. An ovoid lesion with well-defined margins is seen adjacent to a flexor tendon sheath and middle phalanx. The lesion has low-intermediate signal on axial (**a**) T1WI, and mixed high, intermediate, and low signal on axial FST2WI (**b**).

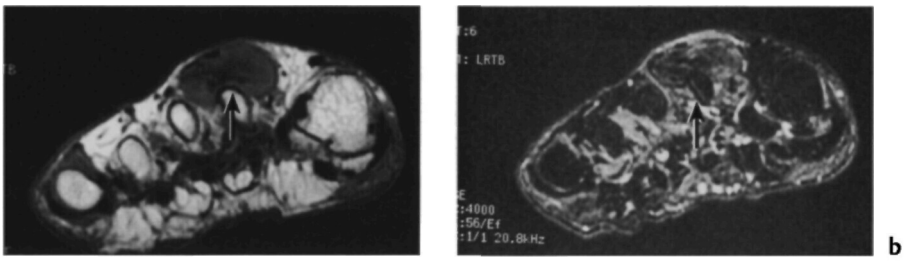

Figure **18.48a, b** A 63-year-old woman with a fibroma involving an extensor tendon sheath in the foot. The lesion has zones of low and intermediate signal on coronal (**a**) T1WI as well as on coronal FST2WI (**b**).

References

Melanoma

Kalkman E, Baxter G. Melanoma. *Clin Radiol* 2004;59:313-326.

Squamous Cell Carcinoma

Bolzoni A, Cappiello J, Piazza C, et al. Diagnostic accuracy of magnetic resonance imaging in the assessment of mandibular involvement in oral-oropharyngeal squamous cell carcinoma. *Arch Otolaryngol Head Neck* Surg July 2004;130:837-843.

Goo HW, Kim EAR, Pi SY, Yoon CH. MR imaging of squamous cell carcinoma complicating chronic osteomyelitis of the femur. *AJR* February 2002:178:512-516.

Merkel Cell Carcinoma

Anderson SE, Beer KT, Banic A, et al. MRI of Merkel cell carcinoma: histologic correlation and review of the literature. *AJR* 2005;185: 1441-1448.

O'Rourke H, Meyers SP, Katzman PJ. Merkel cell carcinoma of the foot: case report and review of the literature. *J Foot Ankle Surg* May-June 2007;46(3): 196-200.

Epithelioid Sarcoma

Dion E, Forest M, Brasseur JL, Amoura Z, Grenier P. Epithelioid sarcoma mimicking abscess: review of the MRI appearances. *Skeletal Radiol* 2001:30:173-177.

Herr MJ, Hamsen WS, Amadio PC, Scully SP. Epithelioid sarcoma of the hand. *Clin Orthop Relat R* 2005;431:193-200.

Kato H, Hatori M, Watanabe M, Kokubun S. Epithelioid sarcomas with elevated serum CA125: report of two cases. *Jpn J Clin Oncol* 2003;33: 141-144.

Myoepithelial Carcinoma

Darvishian F, Lin 0. Myoepithelial cell-rich neoplasms. Cytologic features of benign and malignant lesions. *Cancer (Cancer Cytopathology)* December 25, 2004;102(6):355-361.

Hornick JL, Fletcher CDM. Myoepithelial tumors of soft tissue. A clinicopathologic and immunohistochemical study of 101 cases with evaluation of prognostic parameters. *Am J Surg Pathol* September 2003;27(9):1183-1196.

Hornick JL, Fletcher CDM. Cutaneous myoepithelioma: a clinicopathologic and immunohistochemical study of 14 cases. *Human Pathol* January 2004;35(1): 14-24.

Venkatraman L, Sinnathuray AR, Raut V, Brooker DS, McCluggage WG. Soft tissue myoepithelioma: a case report. *Pathology* 2002;34: 451-454.

Granular Cell Tumor

Blacksin MF, White LM, Hameed M, Kandel R, Patterson FR, Benevenia J. Granular cell tumor of the extremity: magnetic resonance imaging characteristics with pathologic correlation. *Skeletal Radiol* 2005; 34:625-631.

Elkousy H, Harrelson J, Dodd L, Martinez S, Scully S. Granular cell tumors of the extremities. *Clin Orthop Relat R* 2000:380:191-198.

Pleomorphic Hyalinizing Angiectatic Tumor

Folpe AL, Weiss SW. Pleomorphic hyalinizing angiectatic tumor. Analysis of 41 cases supporting evolution from a distinctive precursor lesion. *Am J Surg Pathol* 2004;28:1417-1425.

Lee JC, Jiang WY, Karpinski RHS, Moore ED. Pleomorphic hyalinizing angiectatic tumor of soft parts. *Surgery* 2005:137:119-121.

Weiss SW. Pleomorphic hyalinizing angiectatic tumor of soft parts. In: Fletcher CDM, Unni KK, eds. *World Health Organization Classification of tumors. Pathology and Genetics of Tumors of Soft Tissue and Bone.* Lyon, France: IARC Press; 2002:191.

Hypothenar Hammer Injury of the Dinar Artery

Blum AG, Zabel JP, Kohlmann R, et al. Pathologic conditions of the hypothenar eminence: evaluation with multidetector CT and MR imaging. *RadioGraphics* 2006:26:1021-1044.

Drape JL, Feydy A, Guerini H, et al. Vascular lesions of the hand. *Eur]* Radio/2005:56:331-343.

Cat Scratch Disease

Dong PR, Seeger LL, Yao L, Panosian CB, Johnson BL, EckhardtJJ. Uncomplicated cat-scratch disease: findings at CT, MR imaging and radiography. *Radiology* 1995;195:837-839.

Gielen J, Wang XL, Vanhoenacker F, et al. Lymphadenopathy at the medial epitrochlear region in cat-scratch disease. *Eur Radial* 2003;13: 1363-1369.

Mele FM, Friedman M, Reznik AM. MR imaging of the knee: findings in cat scratch disease. ***AJR*** 1996;166:1232-1233.

Cranuloma Annulare

Bancroft LW, Perniciaro C, Berquist TH. Granuloma annulare: radiographic demonstration of progressive mutilating arthropathy with vanishing bones. *Skeletal Radial* 1998;27:211-214.

Chung S, Frush DP, Prose NS, Shea CR, LaorT, Bisset GS. Subcutaneous granuloma annulare: MR imaging features in six children and literature review. *Radiology* 1999:210:845-849.

KransdorfMJ, Murphey MD, Temple HT. Subcutaneous granuloma annulare: radiologic appearance. *Skeletal* Radio/1998:27:266-270.

Kimura Disease

Choi AH, Lee GK, Kong KY, et al. Imaging findings of Kimura's disease in the soft tissue of the upper extremity. *AJR* 2005:184:193-199.

Huang GS, Lee HS, Chiu YC, Yu CC, Chen CY. Kimura's disease of the elbows. *Skeletal* Radio/ 2005:34:555-558.

Table 19 Lesions involving peripheral nervous tissue

Lesion	MRI Findings	Comments
Benign lesions		
Schwannoma (Fig. 19.1)	Circumscribed or tabulated lesions, low-intermediate signal on T1 WI. high signal on T2WI and FST2WI, usually show prominent Gd-contrast enhancement. High signal on T2WI and Gd-contrast enhancement can be heterogeneous in large lesions due to cystic degeneration and/or hemorrhage.	Encapsulated neoplasms arising asymmetrically from nerve sheath, most common type of intradural extramedullary neoplasms involving the spine, usual presentation in adults with pain and radiculopathy. paresthesias, and lower extremity weakness. Multiple schwannomas seen with neurofibromatosis type 2 (NF2). **(See Atlas Chapter A72)**
Neurofibroma (Figs. 19.2,19.3)	Solitary neurofibromas are spheroid or tabulated lesions +/~ irregular margins, low-intermediate signal on T1WI, high signal on T2WI and FST2WI, usually show prominent Gd-contrast enhancement. High signal on T2WI and Gd-contrast enhancement can be heterogeneous in large lesions +/- erosion of adjacent bone. **Plexiform neurofibromas** usually appear as curvilinear and multinodular lesions involving multiple nerve branches, and have low to intermediate signal on T1 WI and intermediate, slightly high to high signal on T2WI and FST2WI +/- bands or strands of low signal. Lesions usually show Gd-contrast enhancement.	Unencapsulated neoplasms involving nerve and nerve sheath, usual presentation in adults with pain and radiculopathy, paresthesias, and lower extremity weakness. Multiple neurofibromas seen with neurofibromatosis type 1 (NF1). **(See Atlas Chapter A56)**
Neurothekeoma ***(fig.*** **19.4)**	Neurothekeomascan occur as circumscribed lesions with low-intermediate signal on T1WI. high signal on T2WI, and heterogeneous Gd-contrast enhancement.	Neurothekeoma, also referred to as nerve sheath myxoma, is considered to be a neurofibroma with prominent myxoid matrix separated into lobules by fibrous connective tissue. **(See Atlas Chapter A 56)**
Granular cell tumor (Fig. 19.5)	Tumors can have circumscribed and/or irregular margins, and contain low-intermediate signal on T1WI and PDWI, and slightly high to high signal on T2WI and FS T2WI. Tumors can also have low-intermediate signal on T2WI. Tumors can show prominent Gd-contrast enhancement.	Rare benign schwannian neoplasms that contain cells with diffuse granular cytoplasm, and are immunoreactive to S-100, but not to HMB-45. Tumors are often located in the dermis/subcutis, and occasionally within muscle. Occur more commonly in females compared with males, adults over 30 years old.
Traumatic neuroma (Fig. 19.6)	Traumatic neuromas can appear as bulbous lesions at the end of a transected nerve (terminal neuroma) or as fusiform swelling of an intact nerve (spindle neuroma). Lesions often have low-intermediate signal on T1WI, intermediate signal on PDWI, and mildly heterogeneous intermediate to high signal on T2WI and FST2WI	Non-neoplastic lesions that result from complete or partial transection of nerves. The proximal end of the damaged or transected nerve undergoes a benign proliferative process that can be painful. Terminal neuromas refer to traumatic neuromas that result from transection or avulsion of nerves and occur 1 -12 months after injury. Spindle neuromas refer to focal swelling of intact nerves damaged by chronic friction or irritation. **(See Atlas Chapter A 57)**
Avulsed nerve root (Fig. 19.7)	Nerve root avulsions may be seen as discontinuous nerves with bulbous ends within dura or extradural fluid collections. Post-traumatic nerve root pouch cysts may also be seen.	Spinal injury can affect the integrity of bone, ligaments, disks, spinal cord, as well as the connection of the nerve roots to the spinal cord.
Morton neuroma (Fig. 19.8)	Lesions located in neurovascular bundle within the intermetatarsal space on the plantar side of the transverse metatarsal ligament. Lesions appear as nodular zones with low-intermediate signal on T1WI and PDWI that is isointense or slightly hyperintense relative to muscle. Lesions often have low to intermediate signal on T2WI that is hypointense or isointense relative to fat. Lesions can have intermediate, slightly high, or high signal on FST2WI. Lesions can show Gd-contrast enhancement that is often more conspicuous with fat-suppression.	Non-neoplastic lesions that result from perineural fibrosis of a plantar digital nerve near the metatarsal head. **(See Atlas Chapter A51)**

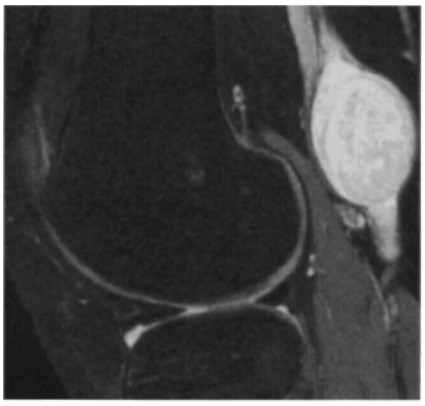

a

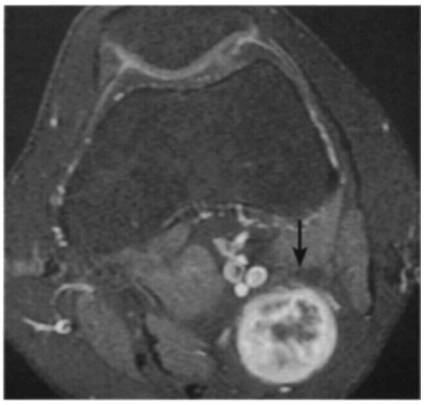

b

Figure **19.1 a, b** A 17-year-old female with a schwannoma involving the tibial nerve at the dorsal knee. A well-circumscribed ovoid lesion is seen along the nerve that has high signal on sagittal FST2WI (**a**) and shows prominent Cd-contrast enhancement on axial FST1WI(**b**).

a

b

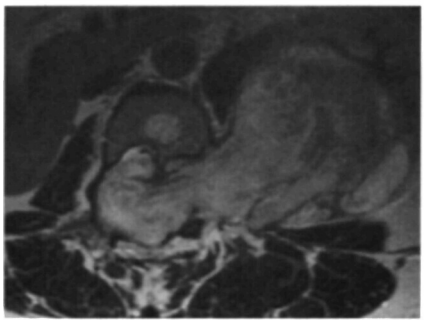

c

d

Figure **19.2a-d** A 52-year-old woman with NF1 and a large left paraspinal neurofibroma extending through a widened intervertebral foramen resulting in compression of the thecal sac. Note also the scalloping of the dorsal margins of the vertebral bodies from dural ectasia. The lesion has heterogeneous intermediate and slightly high signal on sagittal (**a**) and axial (**c**) T2WI, and shows heterogeneous Cd-contrast enhancement on sagittal (**b**) and axial (**d**) FST1WI.

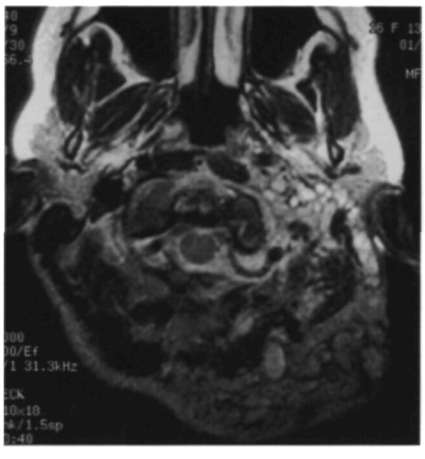

a

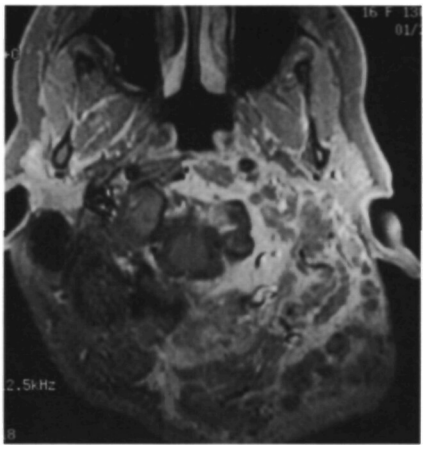

b

Figure **19.3 a, b** A 16-year-old female with a plexiform neurofibroma involving the posterior scalp and skull. The tumor appears as curvilinear and multinodular zones with intermediate, slightly high to high signal separated by curvilinear zones of low signal on axial T2WI (**a**) and shows heterogeneous Gd-contrast enhancement on axial FST1 WI

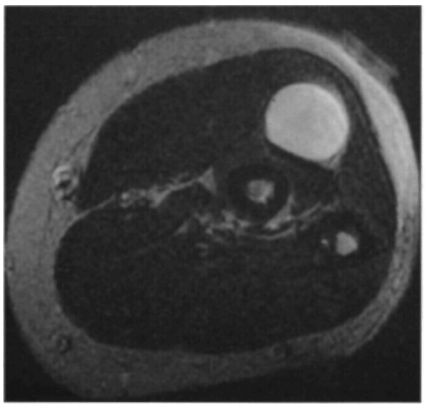

a

b

Figure **19.4a, b** A 38-year-old man with a neurothekeoma involving the flexor digitorum superficial muscle of the proximal forearm. The lesion has high signal on axial T2WI (**a**) and shows moderate heterogeneous Gd-contrast enhancement on sagittal FS T1WI (**b**).

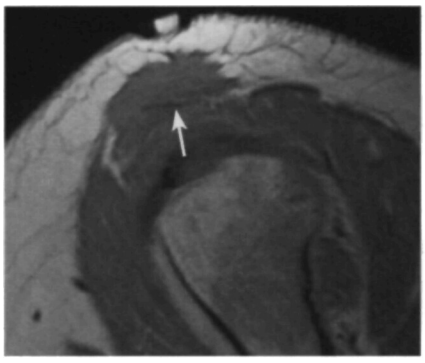

a

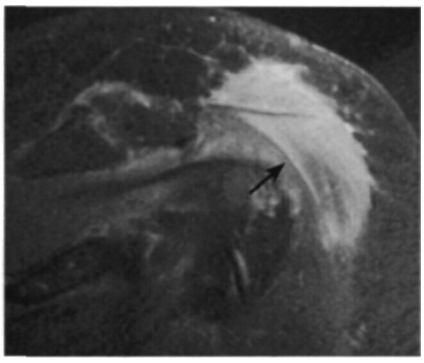

b

Figure **19.5 a, b** A 56-year-old woman with a granular cell tumor involving the subcutaneous fat and superficial portion of the deltoid muscle. The tumor has irregular margins and contains low-intermediate signal on sagittal PDWI (**a**) and shows prominent Gd-contrast enhancement on coronal FST1WI (**b**).

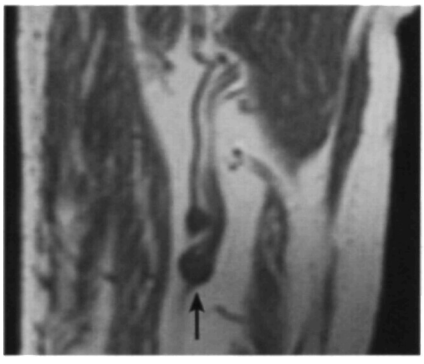

a

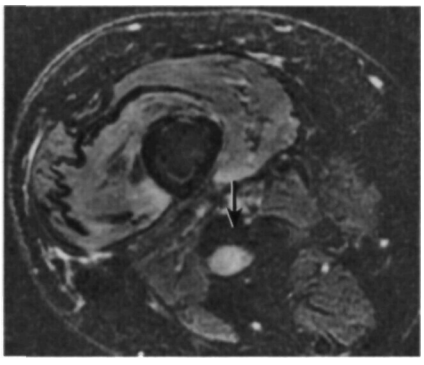

b

Figure **19.6a, b** A 60-year-old man with a traumatic neuroma involving the sciatic nerve in the thigh after an amputation of the leg. Bulbous dilatation of the distal transected sciatic nerve is seen that has low-intermediate signal on sagittal T1WI (**a**) and high signal on axial FST2WI (**b**).

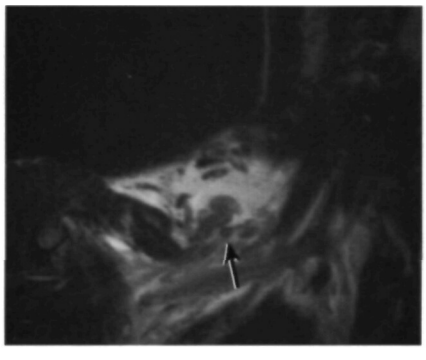

a, b

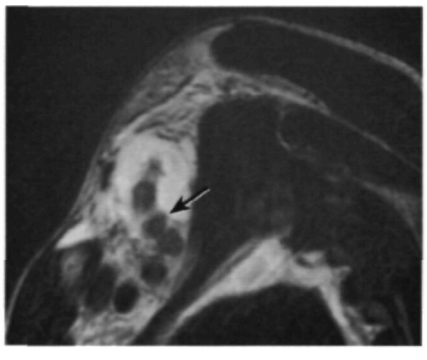

Figure **19.7 a, b** A 15-year-old male with traumatic avulsion of multiple nerves of the right brachial plexus. Multiple nodular low signal structures representing retracted torn nerve endings are seen within high signal fluid on coronal (**a**) and sagittal (**b**) FST2WI.

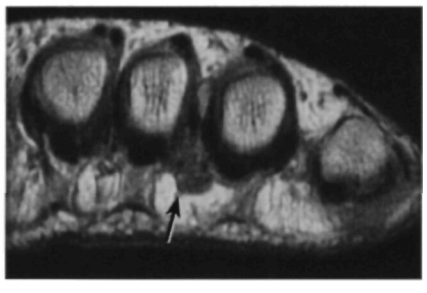

Figure **19.8** Morton neuroma between the third and fourth digits. The nodular lesion has low-intermediate signal on coronal T1WI.

Table 19 (Continued) **Lesions involving peripheral nervous tissue**

Lesion	MRI Findings	Comments
Lipoma of nerve (fibrolipomatous hamartoma) (Fig. 19.9)	Well-circumscribed fusiform-shaped lesions involving nerves. On T1WI. PDWI, and T2WI a network of cylindrical longitudinally oriented thin curvilinear signal voids with 1 -3 mm diameters is seen within a background of intermediate to high signal. This "coaxial cable-like" appearance is secondary to the combination of nerve fascicles with varying degrees of fatty infiltration, and epineural and perineural fibrosis. The degree of fatty proliferation varies among patients. Lesions may follow the branching patterns of nerves.	Rare benign lesions with varying degrees of fibrous and fatty (mature adipocytes) infiltration of the epineurium (nerve sheath) of peripheral nerves as well as within the interfascicular connective tissue (perineurium) of nerves. **(See Atlas Chapter A 22)**
Paraganglioma (Fig. 19.10)	Spheroid or lobulated lesion with intermediate signal on T1WI, intermediate-high signal on T2WI and FST2WI. +/- tubular zones of flow voids, usually show prominent Gd-contrast enhancement, +/- foci of high signal on T1WI from mucin or hemorrhage, +/- peripheral rim of low signal (hemosiderin) on T2WI.	Neoplasms that arise from paraganglion cells of neural crest origin. Usually occur at carotid body, jugular foramen, middle ear, and along vagus nerve. Rarely occur in spine. **(See Atlas Chapter A 66)**
Ganglioneuroma (Fig. 19.11)	Tumors are well-circumscribed with low-intermediate signal on T1WI and slightly high to high signal on T2WI and FST2WI. Small foci or strands of low signal on T2WI may be seen secondary to calcifications and fibrous tissue, respectively. Tumors show mild to marked heterogeneous Gd-contrast enhancement. MRI can show extension of these tumors into the spinal canal.	Rare benign lesions of the sympathetic nervous system composed of ganglion cells and schwannian stroma, and typically lack neuroblasts and mitotic figures. **(See Atlas Chapter A 55)**
Malignant lesions		
Malignant peripheral nerve sheath tumor (MPNST) (Fig. 19.12)	These lesions usually have heterogeneous signal on T1WI and T2WI; as well as heterogeneous Gd-contrast enhancement because of necrosis and hemorrhage. Some malignant peripheral nerve sheath tumors (MPNSTs) are similar in appearance to benign nerve sheath tumors.	Malignant tumors of the peripheral nerve sheath that contain mixtures of packed hyperchromatic spindle cells with elongated nuclei and slightly eosinophilic cytoplasm, mitotic figures, and zones of necrosis. Approximately 50% of MPNSTs occur in patients with NF1, followed by de novo evolution from peripheral nerves. Malignant peripheral nerve sheath tumors infrequently arise from schwannomas, ganglioneuroblastomas/ganglioneuromas, and pheochromocytomas. **(See Atlas Chapter A 56)**
Primitive neuroectodermal tumor/extraskeletal Ewing sarcoma (Fig. 19.13)	Tumors usually have low-intermediate signal on T1WI and PDWI, heterogeneous slightly high to high signal on T2WI and FST2WI. Margins of the lesions are often ill-defined. Lesions typically show prominent irregular Gd-contrast enhancement.	Extracranial primitive neuroectodermal tumors (extracranial PNETs) are malignant tumors of bone and soft tissue composed of undifferentiated small cells with round nuclei. These tumors are similar to Ewing sarcoma, except that extracranial PNETs usually show varying degrees of neural differentiation. **(See Atlas Chapter A 20)**

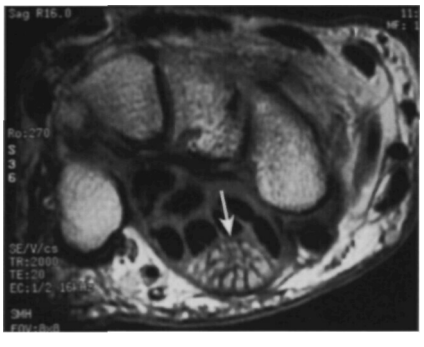

Figure 19.9 A 9-year-old boy with a fibrolipomatous hamartoma (lipomatosis of the nerve) involving the median nerve at the wrist. Cylindrical, longitudinally oriented, thin, curvilinear zones of low signal are seen against a background of intermediate to high signal on axial PDWI.

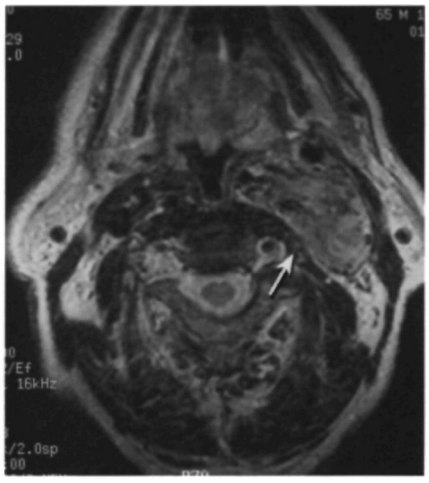

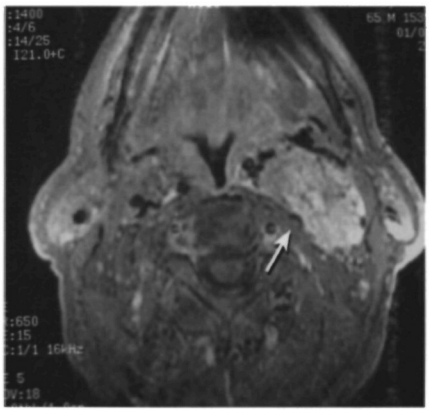

a, b

Figure **19.10a, b** A 65-year-old man with a paraganglioma at the left common carotid artery bifurcation in the neck, also referred to as a carotid body tumor. The ovoid tumor splays the proximal external carotid artery from the internal carotid artery, and has heterogenous slightly high and intermediate signal on axial T2WI (**a**). The tumor shows prominent Gd-contrast enhancement on axial FST1WI (**b**). Multiple tortuous and punctate zones of signal void are seen within the peripheral and central portions of the tumor.

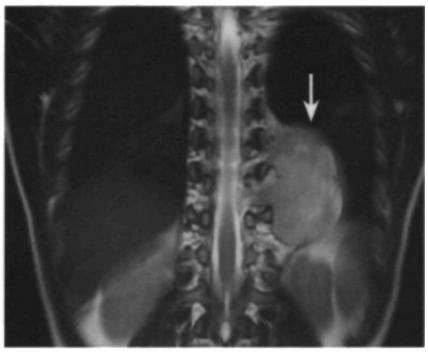

Figure **19.11** A 10-year-old boy with a left paraspinal ganglioneuroma. The tumor has well-circumscribed margins and has heterogeneous intermediate, slightly high to high signal on coronal T2WI.

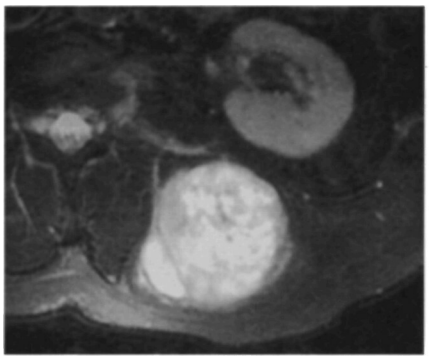

a

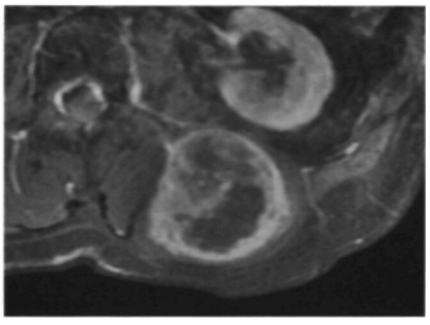

b

Figure **19.12 a, b** Malignant peripheral nerve sheath tumor in the left posterior paraspinal muscles of a 51-year-old man. The tumor has high signal on axial FST2WI (**a**) and shows heterogeneous Cd-contrast enhancement on axial FST1WI (**b**) as well as zones of central necrosis.

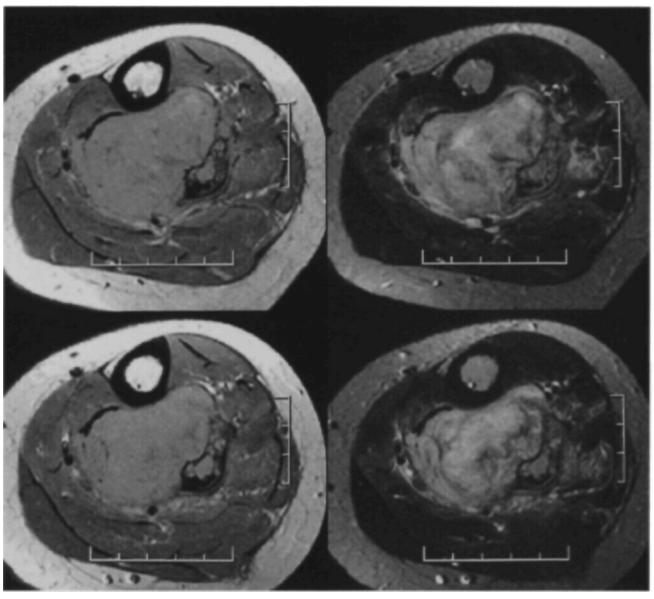

a

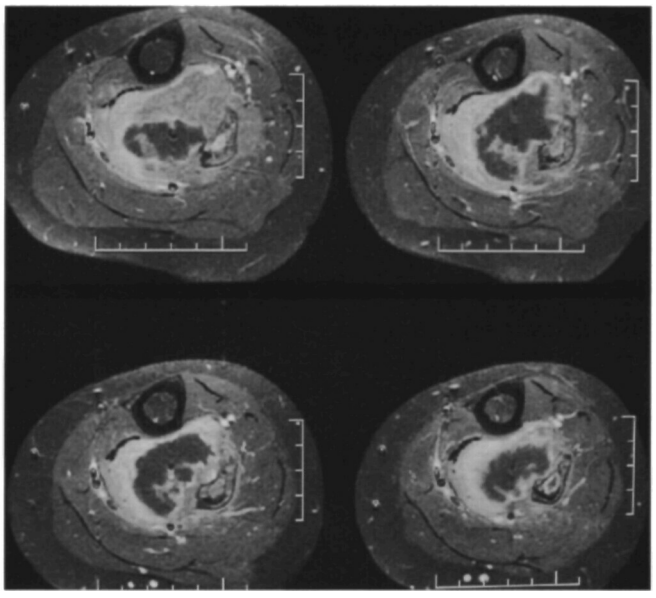

b

Figure **19.13a, b** An 11-year-old boy with Ewing sarcoma/PNET involving the proximal fibula. The tumor has poorly defined margins and is associated with cortical destruction and prominent extraosseous tumor extension. The tumor contains zones with intermediate and slightly high signal on axial PDWI (**a**, *images on left)* and slightly high to high signal on axial T2WI (**a**, *images on right).* The tumor shows prominent irregular Gd-contrast enhancement on axial FS T1WI (**b**) as well as zones of central necrosis.

Table 19 (Continued) **Lesions involving peripheral nervous tissue**

Lesion	MRI Findings	Comments
Neuroblastoma/ganglio-neuroblastoma (Fig. 19.14)	Tumors can have distinct or indistinct margins, and have low-intermediate signal on T1WI, homogeneous or heterogeneous intermediate, slightly high, and/or high signal on T2WI and FST2WI. Zones of high signal on T2WI may occur from sites of hemorrhage or necrosis. Foci of low signal on T2WI may be seen secondary to calcifications and blood products. Tumors can show mild to marked heterogeneous Cd-contrast enhancement. MRI can show extension of these tumors into the spinal canal as well as into bone marrow.	Neuroblastomas and ganglioneuroblastomas are malignant tumors of the sympathetic nervous system that consist of neoplastic neuroectodermal cells derived from the neural crest. Neuroblastomas are highly malignant undifferentiated tumors whereas ganglioneuroblastomas are intermediate-grade malignant tumors. **(See Atlas Chapter A 55)**
Lymphoma of nerve (Fig. 19.15)	Lymphoma involving nerves can have intermediate signal on T1WI, high signal on FST2WI, and show Cd-contrast enhancement.	Non-Hodgkin lymphoma (NHL) represents a group of lymphoid tumors whose neoplastic cells frequently originate at extranodal sites and spread in an unpredictable pattern. NHL can infiltrate soft tissues such as muscle, nerves, dermis, and epidermis. **(See Atlas Chapter A 47)**
Merkel cell tumor (Fig. 19.16)	Tumors can have circumscribed margins, and have low-intermediate signal on T1WI and PDWI and slightly high to high signal on T2WI. Zones of necrosis with high signal on T2WI may occur within the tumors. Tumors can show Cd-contrast enhancement.	Rare primary malignant neuroendocrine neoplasms that involve the skin and dermis usually in adults over 60 years. Tumor cells are small and contain neurosecretory cytoplasmic granules secondary to neural crest origin.

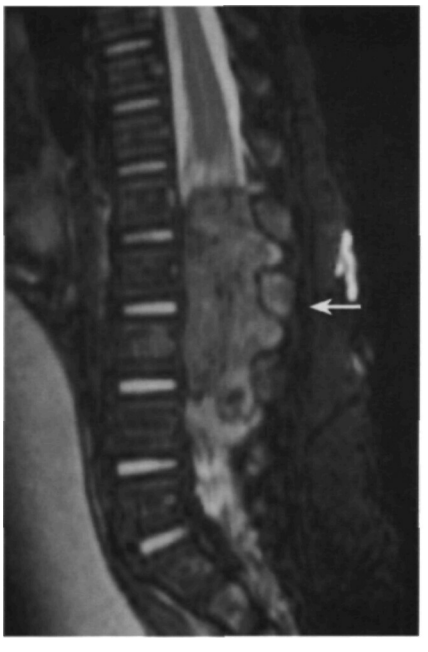

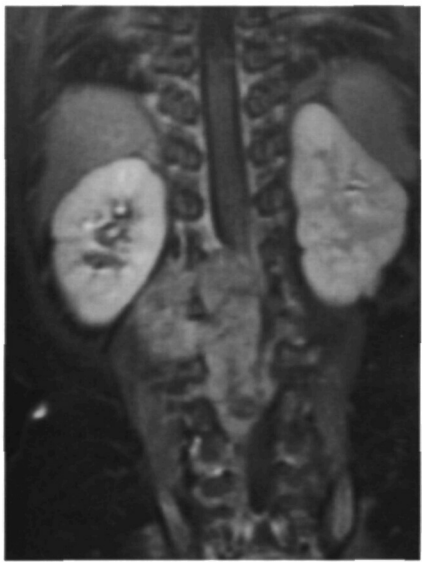

b

Figure **19.14a, b** A 10-month-old boy with a right paraspinal neuroblastoma that extends into the spinal canal resulting in spinal cord compression. The tumor has heterogeneous intermediate and slightly high signal on sagittal FST2WI (**a**) and shows heterogeneous Cd-contrast enhancement on coronal FST1WI (**b**).

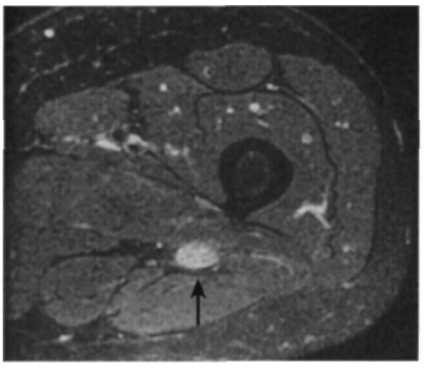

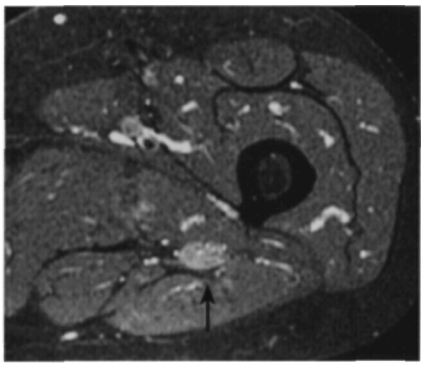

b

Figure **19.15a, b** A 70-year-old woman with B cell NHL involving the sciatic nerve. The lymphoma has high signal on axial FST2WI (**a**) and shows Cd-contrast enhancement on axial FST1WI (**b**).

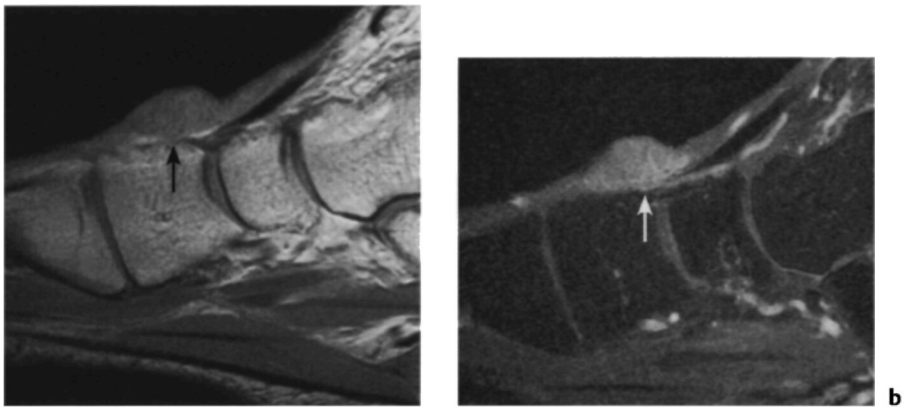

Figure **19.16a, b** A 72-year-old man with a Merkel cell tumor involving the dorsal superficial soft tissues of the foot. The tumor has low-intermediate signal on sagittal PDWI (**a**) and shows moderate Gd-contrast enhancement on sagittal FST1WI (**b**).

References

Granular Cell Tumor

Blacksin MF, White LM, Hameed M, Kandel R, Patterson FR, Beneveni a J. Granular cell tumor of the extremity: magnetic resonance imaging characteristics with pathologic correlation. *Skeletal* Radio/ 2005;34: 625-631.

Elkousy H, Harrelson J, Dodd L, Martinez S, Scully S. Granular cell tumors of the extremities. *Clin Orthop RelatR* 2000:380:191-198.

Merkel Cell Carcinoma

Anderson SE, Beer KT, Banic A, et al. MRI of Merkel cell carcinoma: histologic correlation and review of the literature. *AJR* 2005; 185: 1441-1448.

O'Rourke H, Meyers SP, Katzman PJ. Merkel cell carcinoma of the foot: case report and review of the literature. *J Foot Ankle Surg* May-June 2007;46(3): 196-200.

Table 20 Lesions that contain fat

Lesion	MRI Findings	Comments
Congenital		
Upomyelocele/lipomyelo-meningocele (Fig. 20.1)	Unfolded caudal neural tube (neural placode) covered by a lipoma. Usually contiguous with the dorsal subcutaneous fat through congenital defects (spina bifida) in the posterior elements of the involved vertebrae and/or sacrum. With lipomyelomeningocele. the dorsal lipoma that extends into the spinal canal is asymmetric resulting in rotation of the placode and meningocele.	Failure of closure of the caudal neural tube results in an unfolded neural tube covered by a lipoma which is typically contiguous with the dorsal subcutaneous fat. The subcutaneous fat is intact, although the lipoma often protrudes dorsally. Features associated with lipomyeloceles and lipomyelomeningoceles include: tethered spinal cord, dorsal bony dysraphism, and deficient dura posteriorly at the site of the neural placode. Not associated with Chiari II malformations. Diagnosis usually in childhood, occasionally as adults.
Intradural lipoma/spinal lipoma (Fig. 20.2)	Focal dorsal dysraphic spinal cord attached to a lipoma; has high signal on T1WI. Lipoma often extends from the central canal of the spinal cord to the pial surface, intact dorsal dural margins and posterior vertebral elements.	Intradural lipomas often occur in the cervical or thoracic regions. **(See Atlas Chapter A43)**
Benign lesions		
Lipoma—intraosseous (Fig. 20.3)	Lesions are typically well-circumscribed intramedullary lesions that often have a peripheral thin border of low signal on T1WI. PDWI, and T2WI. Lesions often have high signal on T1WI and PDWI and intermediate-high signal on T2WI, which is isointense to subcutaneous fat. Suppression of fat signal typically occurs with short Tan inversion recovery (STIR) and frequency selective FS T1WI or FST2WI. Cystic zones are seen in approximately two-thirds of intraosseous lipomas and range from 2 to 35 mm. Calcifications, when present, usually appear as zones of low signal or signal void.	Lipomas in bone are uncommon benign hamartomas composed of mature white adipose tissue without cellular atypia. **(See Atlas Chapter A 43)**
Lipoma—soft tissue (Fig. 20.4)	Superficial lipomas in subcutaneous fat often have circumscribed margins and have MRI signal comparable to subcutaneous fat on T1WI, PDWI, T2WI, and FST2WI. Lipomas may also be localized within and/or between muscles. Nonfatty thin septa may be present within superficial or deep-seated lipomas. These thin septa may show slightly high to high signal on FST2WI. Lipomas often show no Cd-contrast enhancement. Minimal to mild Gd-contrast enhancement may, however, be seen along the thin nonfatty septae.	Lipomas are common benign hamartomas in soft tissue that are composed of mature white adipose tissue without cellular atypia. **(See Atlas Chapter A43)**
Upomatosls (Fig. **17.21)**	Infiltrating adipose tissue or multiple lobules of fat can be seen in muscles, fascial planes, and/orsubcutaneousfat.	Diffuse proliferation of mature adipose tissue. Can occur as several types. The diffuse type typically affects the soft tissues of an extremity or trunk in children with or without associated osseous hypertrophy. Multiple symmetric lipomatosis (Madelung disease) usually occurs in the neck, trunk, and pelvis of adult men (peak incidence in the 5th decade. Shoulder girdle lipomatosis usually occurs in women and involves the muscles at one shoulder and adjacent chest wall. Adiposis dolorosa (Dercum syndrome) usually occurs in obese postmenopausal women who have multiple painful fatty lesions in the extremities or trunk.

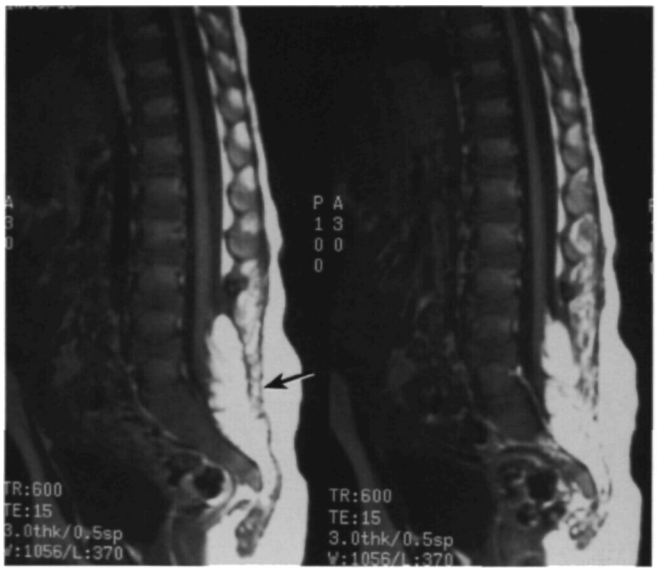

a

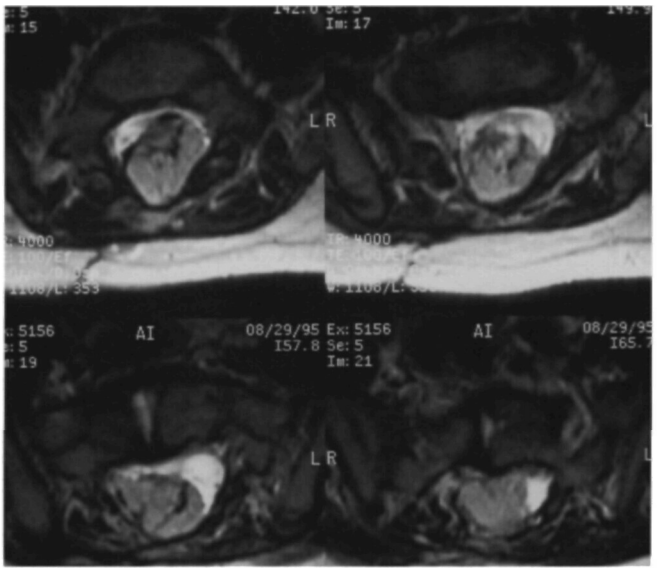

b

Figure **20.1 a, b** A lipomyelocele, which represents an unfolded neural tube covered by a lipoma, is seen between congenital bony defects at the posterior elements on sagittal T1WI (**a**) and axial T2WI (**b**).

Figure **20.2** Intradural lipoma involving the dorsal portion of the cervical and upper thoracic spinal cord. The lipoma has high signal on sagittal T1WI.

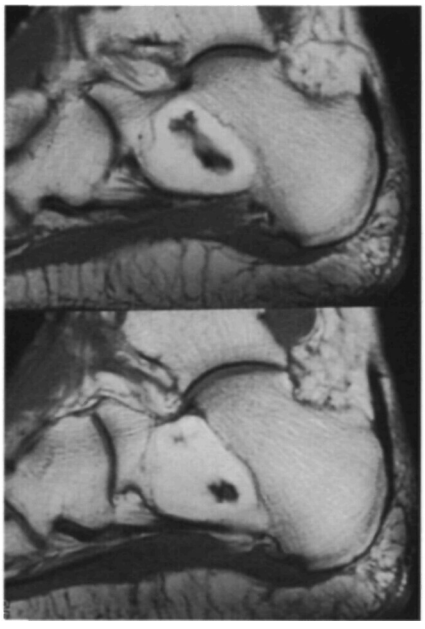

Figure **20.3** **A** 47-year-old woman with an intraosseous lipoma of the calcaneus that has thin margins of low signal surrounding a central zone of mostly high fat signal as well as several zones of low signal on sagittal T1WI.

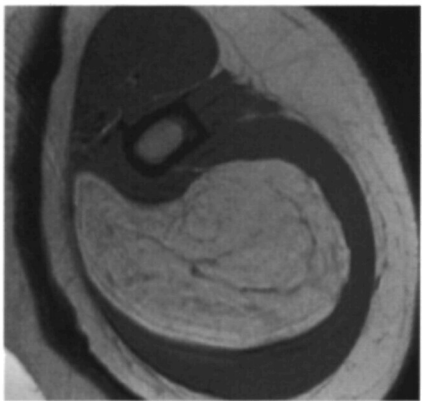

Figure **20.4** **A** 43-year-old woman with an intramuscular lipoma in the triceps brachii muscle of the arm that has high signal on axial T1WI.

Table 20 (Continued) **Lesions that contain fat**

Lesion	MRI Findings	Comments
Lapoma—atypical lipoma (Fig. 20.5)	Atypical lipomas are less common than the classic benign lipoma. They often contain cystic/necrotic zones, calcifications, thick septa, and/or nodular zones that may or may not show Cd-contrast enhancement. Most atypical lipomas contain >75% fat, whereas liposarcomas often have <75% fat. Distinguishing between atypical lipomas and low-grade liposarcomas with MRI, however, can he difficult *and* challenging.	Osseous or chondroid metaplasia with myxoid changes can be associated with lipomas. These **atypical lipomas** have been labeled as **chondroid lipomas. osteolipomas. or benign mesenchymomas. Chondroid lipomas** nign adipose tumors that contain mature fat, lipoblasts, and chondroid matrix. **Spindle cell and pleomorphic lipomas** are lipoma variants that have overlapping histologic features of varying proportions of mature fat cells, spindle cells, hyperchromatic spheroid cells, collagen and multinucleated giant cells. Lipomas with high fibrous tissue content have been labeled as fibrolipomas. **(See Atlas Chapter A 43)**
Hibernoma (Fig. 20.6)	Well-defined soft tissue lesions that often have intermediate to high signal on T1WI (hypo- or isointense relative to fat), slightly high signal on T2WI, slightly hyperintense signal relative to fat on FST2WI and STIR. Mild signal heterogeneity, internal septations, and/or branching-serpentine, slow-flow vascular channels may be seen on T1WI and T2WI. Lesions can show Gd-contrast enhancement within branching-serpentine vascular channels.	Rare benign lesions derived from brown adipose tissue intermixed with white adipose tissue. **(See Atlas Chapter A 43)**
Flbrolipomatous hamartoma of nerve (Fig. 20.7)	Fusiform-shaped lesions involving nerves containing a network of cylindrical, longitudinally oriented, thin, curvilinear signal voids with 1-3 mm diameters are seen against a background of intermediate to high signal on T1WI, PDWI, and T2WI. This "coaxial cable-like" lesion may follow the branching patterns of nerves.	Fibrolipomatous hamartomas are rare benign lesions with varying degrees of fibrous and fatty infiltration of the epineurium of peripheral nerves as well as within the interfascicular connective tissue of nerves. Frequently involve the median nerve followed by the ulnarnerve, radial nerve, brachialplexus, sciatic nerve, nerves of the lower extremity. **(See Atlas Chapter A 22)**
Upoblastoma (Fig. 20.8)	Lesions are often circumscribed, although some have margins that infiltrate adjacent muscle or subcutaneous tissues. Lesions typically contain zones with MRI signal approximating that of fat on 11 WI and T2WI. Fatty zones within the lesions may have signal slightly lower than normal fat on T1WI as well as higher signal on FST2WI and STIR resulting from the differing fat contents and shapes of immature lipoblasts compared with mature adipocytes. Intralesional bands and/or nodular zones with low-intermediate to slightly high signal on T1WI and T2WI may he seen in large lesions. Variable degrees of Cd-contrast enhancement can be seen, particularly in the nonlipomatosis portions.	Rare benign mesenchymal tumors that contain embryonal white fat. and typically occur during infancy and early childhood. **(See Atlas Chapter A 42)**

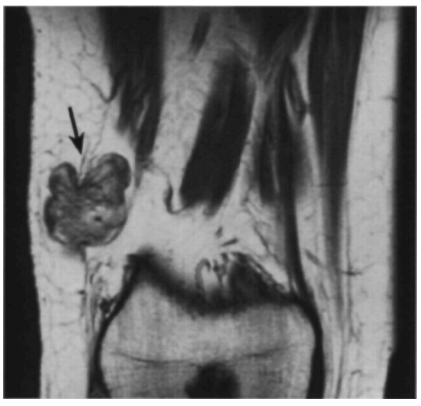

Figure 20.5 A 57-year-old woman with a chondroid/myxoid lipoma in the soft tissues of the distal lateral thigh. The lesion has lobulated well-defined margins and has heterogeneous low, intermediate, and high signal on coronal T1WI.

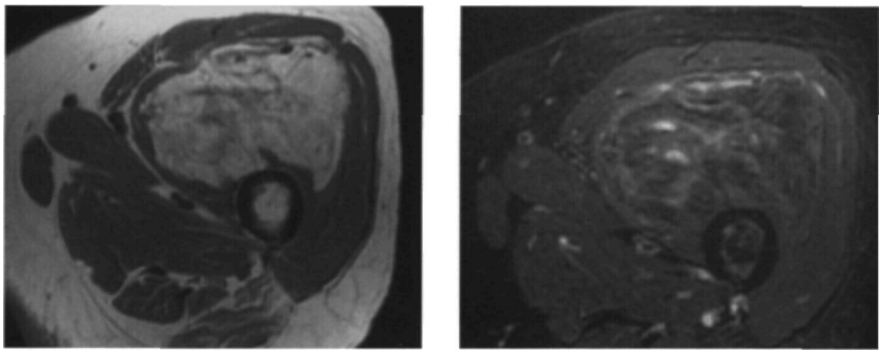

Figure **20.6a, b** A 71-year-old woman with a hibernoma involving the vastus muscles of the proximal thigh. The lesion has well-defined margins and contains mostly fat signal on axial T1WI (**a**) as well as curvilinear and small nodular zones of low signal. The signal of the fatty portions of the lesion is suppressed on axial FST2WI (**b**).

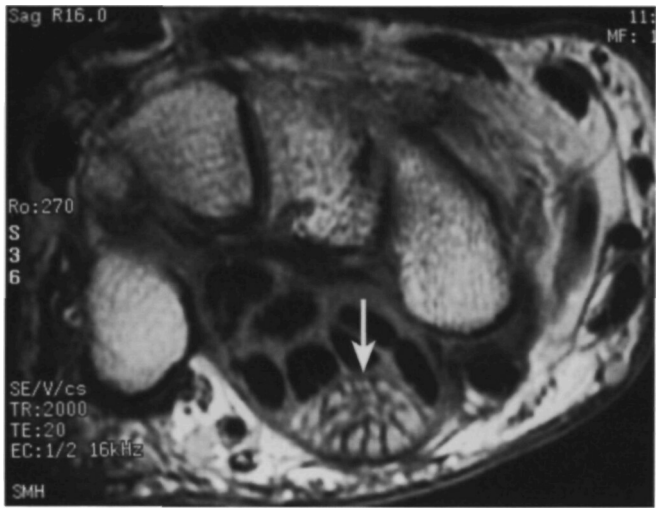

Figure **20.7** A 59-year-old man with a fibrolipomatous hamartoma involving the median nerve at the wrist. Cylindrical, longitudinally oriented, thin, curvilinear zones of low signal are seen against a background of intermediate to high signal on axial PDWI.

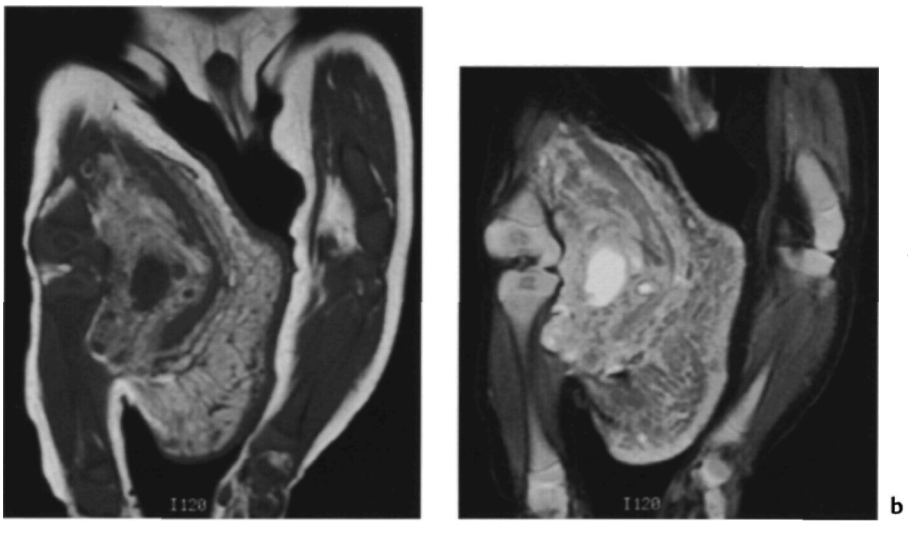

Figure **20.8 a, b** A 3-month-old boy with a large lipoblastoma involving the thigh. The lesion infiltrates adjacent muscles and subcutaneous tissues, and contains zones with MRI signal approximating that of fat on coronal T1WI (**a**). Many of the fatty zones have signal slightly lower than subcutaneous fat on T1WI as well as higher signal on coronal STIR (**b**).

Table 20 (Continued) **Lesions that contain fat**

Lesion	MRI Findings	Comments
Epidural lipomatosis (Fig. 20.9)	Increased extradural fat is seen within the spinal canal with resultant narrowing of the thecal sac.	Epidural lipomatosis is a condition in which there is prominent deposition of unencapsulated mature adipose tissue in the epidural space. May be related to obesity, chronic use of steroid medication, or endogenous hypercortisolemia. Thoracic 60%, lumbar 40%. (**See Atlas Chapter A 43**)
Spinal angiolipoma	Lesions are typically epidural, and often have intermediate to high signal on T1WI and high signal on T2WI. Usually show prominent Gd-contrast enhancement.	Very rare benign lesions composed of mature adipocytes and various-sized blood vessels ranging from capillaries, small to large veins, and arteries.
Hemangioma (Figs. 20.10, 20.11)	**Hemangiomas in bone:** Lesions are often well-circumscribed and often have intermediate to high signal on T1WI, PDWI.T2WI, and FST2WI. On T1WI, hemangiomas usually have signal equal to or greater than adjacent normal marrow secondary to fatty components. Hemangiomas usually show Gd-contrast enhancement (mild to prominent). Extraosseous extension of hemangiomas may lack adipose tissue, with resulting intermediate signal on T1WI. Pathologic fractures associated with intraosseous hemangiomas usually result in low-intermediate marrow signal on T1WI. **Hemangiomas in soft tissue:** Lesions can have either well-circumscribed margins or irregular margins. They usually have low-intermediate signal or heterogeneous low-intermediate and high signal on T1WI and PDWI. Hemangiomas often have defined margins with high signal on T2WI, and high signal on FST2WI except for zones offat within the lesions. Lesions usually show prominent Gd-contrast enhancement.	Benign hamartomatous lesions of bone and soft tissues composed of capillary, cavernous, and/or malformed venous vessels, with or without varying amounts of mature adipose tissue. (**See Atlas Chapter A 34**)
Dermoid(Fig.20.12)	Circumscribed lesions that may have identifiable walls with low signal on T1WI and T2WI. The contents of dermoid cysts can have low, intermediate, and/or high signal on T1WI and T2WI. Fluid-fluid and fat-fluid levels may be seen within dermoids. Lesions may show enhancement at the wall margins, but not centrally. Dermoids may be associated with anomalies such as skeletal dysraphism and dorsal dermal sinus.	Ectoderm-lined inclusion cysts that contain hair, sebaceous and sweat glands, and squamous epithelium. These lesions slowly enlarge, but are not considered to be neoplasms. (**See Atlas Chapter A15**)

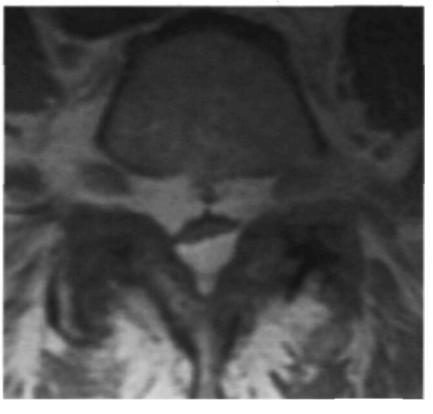

Figure **20.9 a, b** Epidural lipomatosis in a 52-year-old man. Prominent epidural fat is seen in the lumbar spinal canal causing narrowing of the thecal sac on sagittal T1WI (**a**) and axial PDWI (**b**).

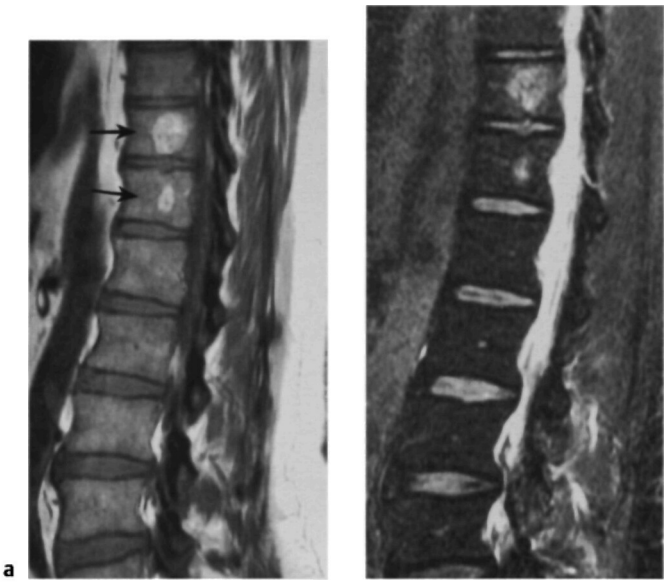

Figure **20.10 a, b** Hemangiomas in theT12 and L1 vertebral bodies. The hemangiomas have spheroid configurations and have mostly high signal on sagittal (**a**) and sagittal FST2WI (**b**).

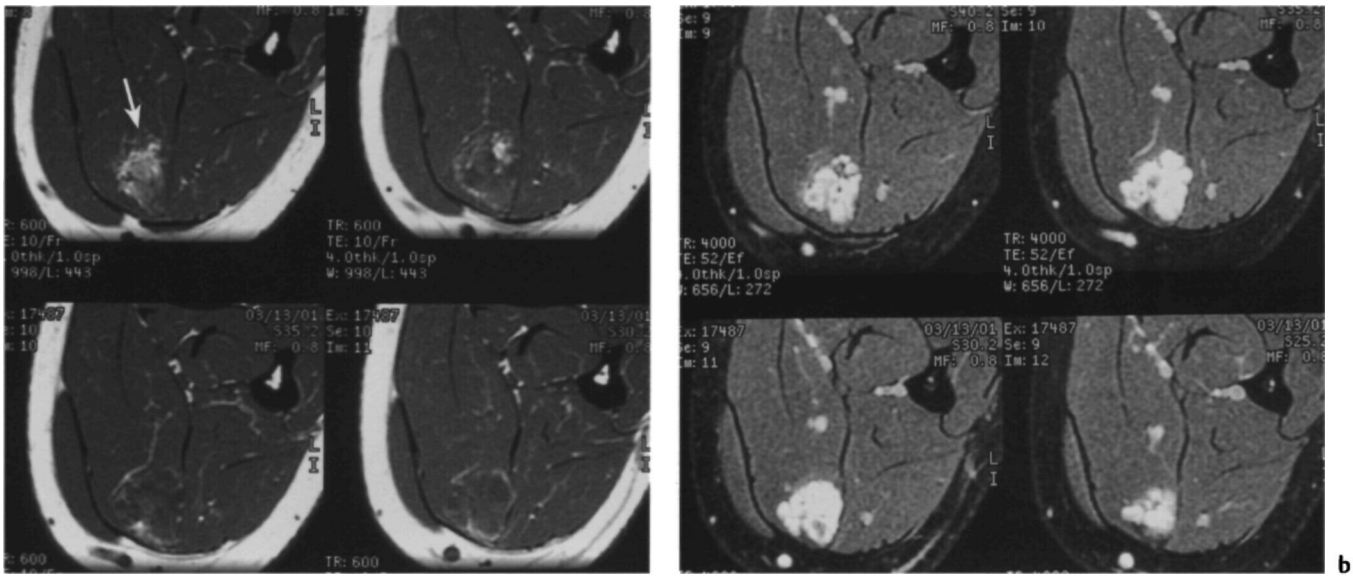

Figure **20.11 a, b** Intramuscular hemangioma in the soleus muscle of the leg. The lesion has slightly lobulated margins and contains zones of intermediate and high signal on axial T1WI (**a**) and high signal on axial FST2WI (**b**).

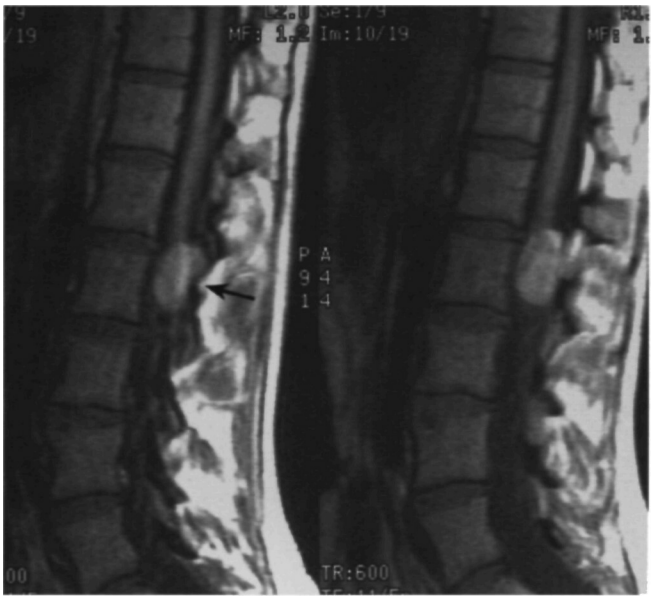

Figure **20.12** A 27-year-old woman with a dermoid in the posterior lumbar spinal canal. The lesion has high signal on sagittal T1WI.

Table 20 (Continued) **Lesions that contain fat**

Lesion	MRI Findings	Comments
Teratoma (Fig. 20.13)	Lesions usually have circumscribed margins and can contain various combinations and proportions of zones with low. intermediate, and/or high signal on T1WI, **PDWI,** T2WI, and **FST2WI.** Lesions can contain teeth and zones of bone formation, as well as amorphous, **clump-like,** and/or curvilinear calcifications with low signal on T1 **WI,** PDWI, T2WI, and **FST2WI.** Fluid-fluid and fat-fluid levels may be seen within teratomas. Gd-contrast enhancement is usually seen in solid portions and septa. Invasion of adjacent tissue and bone destruction, as well as **metastases** are findings associated with malignant teratomas.	Teratomas are neoplasms that arise from displaced embryonic germ cells (multipotential germinal **cells),** and contain various combinations of cells and tissues derived from more than one germ layer (endo**derm,** mesoderm, ectoderm). **(See Atlas Chapter A 76)**
Muscle infarct(Fig. 20.14)	In the early phases of ischemia and **infarction,** poorly defined zones of increased signal on T2WI and **FST2WI** can be seen in the involved muscles. Remote **infarcts are** seen as fatty replacement of muscle tissue.	Zones of ischemic injury and death involving muscle can result from trauma, **corti**costeroid treatment, chemotherapy, radiation treatment, diabetes, occlusive vascular disease, collagen vascular and other autoimmune **diseases. (See Atlas Chapter A 37)**
Denervatlon of muscle (Fig. 20.15)	In the early phases of **denervation** within **15 days,** involved muscles can have low signal on **T1WI,** and slightly high to high signal on T2WI and **FST2WI** without involvement of the adjacent fascia and subcutaneous fat. After one year, fatty replacement of the involved muscles with atrophy can be seen.	Early phases of denervation results in neurogenic edema. In chronic and complete muscle denervation after 1 year, atrophy and fatty replacement of muscle typically occurs. Parsonage-Turner syndrome is one type of denervation that results in an acute painful shoulder from injury of the brachial plexus and damage to the suprascapular nerve **(C5, C6)** with involvement of the supraspinatus and/or infraspinatus muscles. Quadrilateral space syndrome results from damage or injury to the axillary nerve **(C5. C6)** that can affect the teres minor and deltoid muscles.
Lipoma arborescens (Fig. 20.16)	Usually appears as multiple nodular or **frond-like** deposits with fat signal within **hypertrophied** synovium, often associated with a joint effusion.	Lipoma arborescens, also referred to as diffuse synovia! lipoma, represents a disorder in which there are multiple villous or **frond-like** zones of fatty deposition in synovium within a joint, tendon sheath, and/or bursa. **(See Atlas Chapter A43)**
Liposclerosing myxofibrous tumor (Fig. 20.17)	Lesions have well-defined margins with variable thickness of low signal on T1WI and T2WI. Lesions often have low to intermediate signal on T1WI and intermediate to high signal on T2WI and FST2WI. Small zones with signal equal to fat can be seen at the periphery of these lesions.	Uncommon benign fibro-osseous lesions that contain varying proportions with histologic features of lipoma, fibroxanthoma. **myxoma,** fibrous **dysplasia,** bone **cyst, myxofibroma,** fat necrosis, and/or ischemic ossification. Most of the lesions occur in the **intertrochanteric** region of the femur. **(See Atlas Chapter A 45)**
Xanthoma (Fig.20.18)	Often appear as zones of fusiform enlargement of tendons with diffuse heterogeneous signal **(Atlas Figs. 505, 506).** Usually contain multiple longitudinally oriented linear zones or striations with intermediate signal on T1WI and PDWI, and intermediate to slightly high signal on T2WI and **FST2WI** interspersed among bands of low signal within the enlarged tendons **(Atlas Fig. 506)** On axial images, xanthomas often have a stippled or reticulated pattern on T1WI and T2WI resulting from collagen bundles with low signal surrounded by higher signal from lipid deposits, foamy histiocytes, and inflammatory reaction. **(Atlas Fig. 506)**	Xanthomas represent localized accumulations of lipids within normal structures such as tendons, skin, and bone. Xanthomas are considered reactive lesions and are not true neoplasms, and often occur in the setting of types I, II, and III hyperlipoproteinemia. **(See Atlas Chapter A 77).**

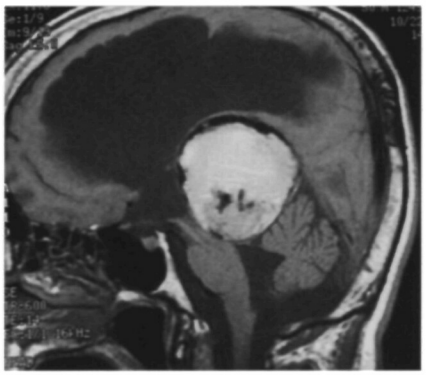

Figure **20.13** A 50-year-old man with an intracranial teratoma in the pineal recess. The lesion has a peripheral rim of low signal surrounding internal contents with mostly high signal as well as small zones of low signal on T1WI.

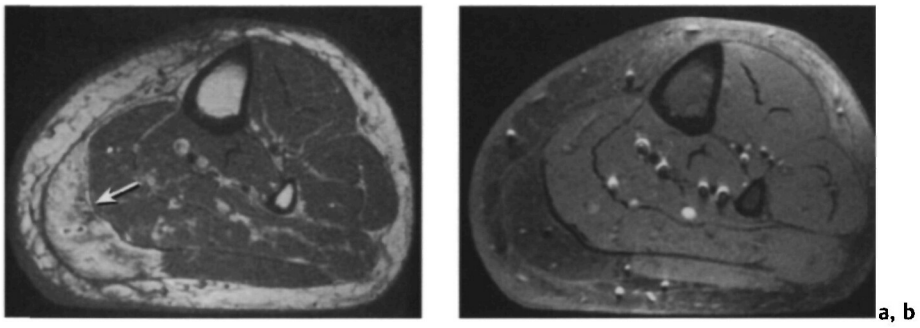

a, b

Figure **20.14a, b** A 60-year-old man with a remote infarct involving the medial gastrocnemius muscle. There is diffuse high signal on axial T1WI (**a**) in the muscle secondary to fatty atrophy resulting from the infarct which has corresponding low signal on axial FST1WI (**b**).

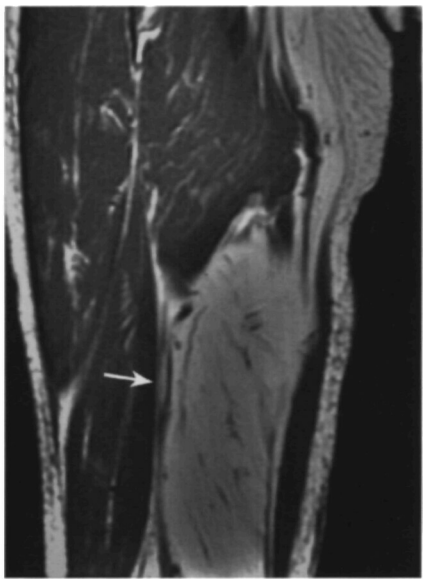

a, b

Figure **20.15 a, b** Denervation in an 82-year-old man with a history of polio. Extensive fatty replacement is seen involving the semimembranosus muscle on coronal (**a**) and axial (**b**)T1WI.

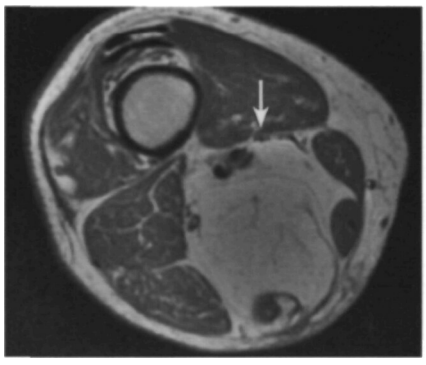

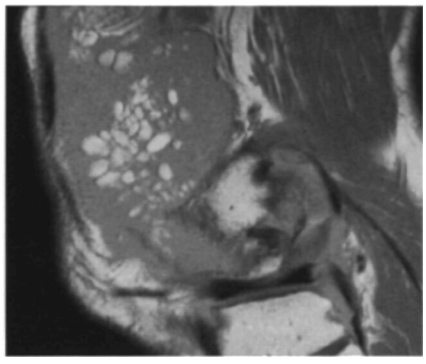

Figure **20.16** A 37-year-old man with lipoma arborescens at the knee. Multiple nodular and frond like/villous deposits with fat signal are seen within hypertrophied synovium on sagittal PDWI.

Figure **20.17** A 61-year-old man with a liposclerosing myxofibrous tumor in the intertrochanteric portion of the femur. The lesion has well-defined margins with thin low signal margins on coronal T1WI. The internal portion of the lesion has mostly low-intermediate signal as well as small peripheral zones with high fat signal.

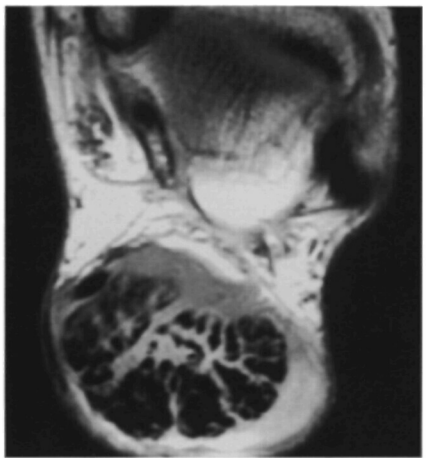

a, b

Figure **20.18a, b** Xanthoma involving the Achilles' tendon. Sagittal (**a**) and axial (**b**) T1WI shows striated zones with increased signal within an enlarged tendon.

Table 20 (Continued) **Lesions that contain fat**

Lesion	MRI Findings	Comments
Malignant		
Liposarcoma (Figs. 20.19-20.21)	**Well-differentiated type:** tumors contain up to 75% overall fat signal, as well as thick nonadipose septae and/or nodular nonadipose zones. Nonadipose zones can have low-intermediate signal on T1WI and PDWI and low, intermediate, and/or high signal on T2WI. Tumor margins are usually smooth, well-defined, and/or lobulated. Nonadipose portions of these tumors can show varying degrees of Gd-contrast enhancement. MRI features that are more commonly associated with well-differentiated liposarcomas compared with lipomas include large tumor size and presence of Gd-contrast enhancing nonadipose thick septa or nodular/patchy zones. **Myxoid type:** These tumors usually have predominantly low signal on T1WI, and may contain smaller proportions of high fat signal in lacy, amorphous, and/or linear configurations. Most myxoid liposarcomas contain <26% fat. Some myxoid liposarcomas do not contain fatty zones. Tumors can have heterogeneous or homogeneous high signal on PDWI, T2WI, and some have a multiloculated pattern. Low signal septa may be present on T2WI. Tumors usually show Gd-contrast enhancement in varying degrees and patterns, or rarely none at all. **Pleomorphic type:** Tumors often have relatively well-defined margins, and have heterogeneous/mixed low, intermediate, and/or high signal on T1WI, PDWI, and T2WI. Less than 26% of the tumor volumes have fat signal. Tumors usually show prominent Gd-contrast enhancement in a heterogeneous pattern. **Round cell liposarcomas:** Tumors can have relatively well-defined margins (72 %) or poorly defined margins (28%), and have heterogeneous/mixed low, intermediate, and/or high signal on T1WI, PDWI, and T2WI. Most round cell liposarcomas contain <26%fat. Tumors usually show prominent Gd-contrast enhancement (61 %) in a heterogeneous pattern that may be globular or nodular. **De-differentiated liposarcomas:** Tumors have a component with features of a well-differentiated liposarcoma as well as a focal nonlipomatous mass. These tumors frequently occur in the retroperitoneum and are large (mean = 19.3cm). Tumors can have well-defined, relatively well-defined, and/or irregular/poorly defined margins. Tumors often have heterogeneous/mixed low, intermediate, and/or high signal on T1WI, PDWI, and T2WI. Hemorrhage and necrosis can be seen in the nonlipomatous portions. Tumors often show prominent Gd-contrast enhancement in nonlipomatous portions in a heterogeneous or homogeneous pattern.	Malignant mesenchymal tumors containing portions showing differentiation into adipose tissue. Liposarcomas are classified into five sub-types (well-differentiated [40-54%], myxoid [23%], pleomorphic [5-7%], dedifferentiated [10%], and round cell [6%]). **(See Atlas Chapter A 44)**

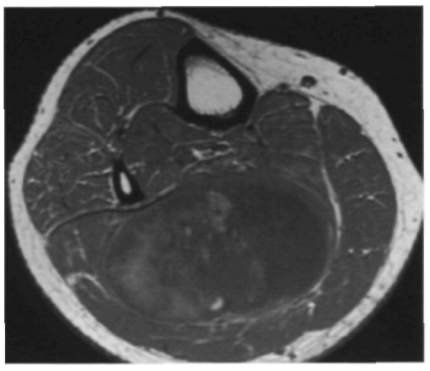

a

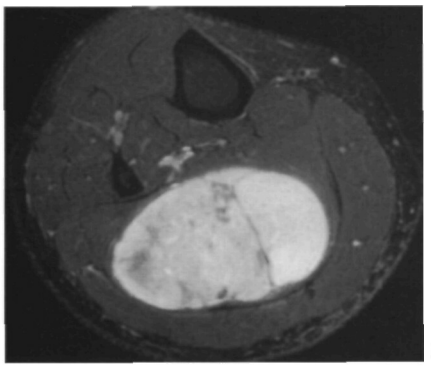

b

Figure **20.20a, b** A 34-year-old woman with a myxoid liposarcoma in the posterior calf. The tumor has circumscribed margins and contains mostly low-intermediate signal on axial T1WI (**a**) as well as small irregular zones of high fat signal. Most of the tumor has high signal on axial (**b**) FST2WI secondary to the myxoid components. The signal from the zones of fat is suppressed on FST2WI.

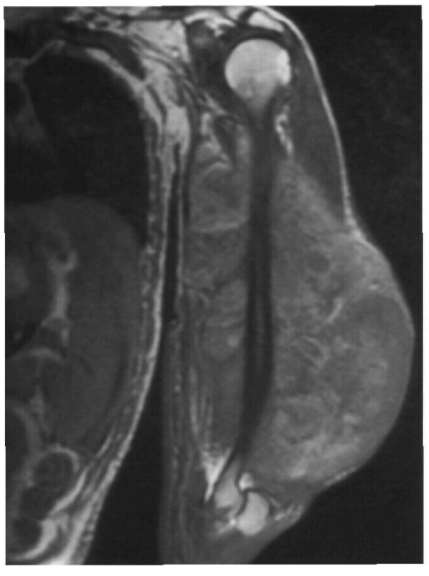

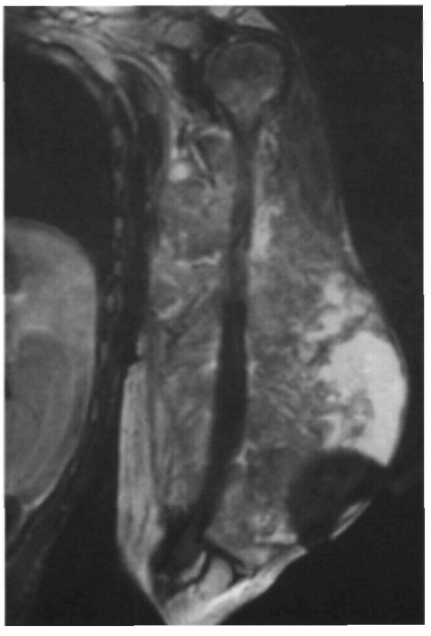

b

Figure **20.21 a, b** A 43-year-old man with a high-grade pleomorphic liposarcoma involving the left arm. The tumor has heterogeneous intermediate and slightly high signal on coronal T1 WI (**a**) and mixed low-intermediate, slightly high, and high signal on coronal FST2WI (**b**).

References

Lipomatosis

Amine B, Leguilchard F, Benhamou CL. Dercum's disease (adiposis dolorosa): a new case - *report. Joint Bone Spine* 2004;71:147-149.

Drevelegas A, Pilavaki M, Chourmouzi D. Lipomatous tumors of soft tissue: MR appearance with histological correlation. *Eur J Radial* 2004;50:257-267.

Haloi AK, Ditchfield M, Penington A, Phillips R. Facial infiltrative lipomatosis. *Pediatr Radio!* 2006:36:1159-1162.

Klein FA, Smith MJ, Kasenetz I. Pelvic lipomatosis: 35-year experience. *J Urol* May 1988;139(5):998-1001.

Murphy MD, Carroll JF, Flemming DJ, Pope TL, Gannon FH, Kransdorf MJ. Benign musculoskeletal lipomatous lesions. *RadioGraphics* September-October 2004;24(5): 1433-1466.

Sener RN. Epidural, paraspinal, and subcutaneous lipomatosis. *Pediatr Radial* 2003:33:655-657.

Torigian DA, Siegelman ES. CT findings of pelvic lipomatosis of nerve. *AJR* March 2005:184:94-96.

Spinal Angiolipoma

Leu NH, Chen CY, Shy CG, et al. MR imaging of an infiltrating spinal epidural angiolipoma. *AJNR* May 2003:24:1008-1011.

Gelabert-Gonzalez M, Agulleiro-DiazJ, Reyes-Santias RM. Spinal extradural angiolipoma, with a literature review. *Childs Nerv Syst* 2002: 18:725-728.

Klisch J, Spreer J, Bloss HG, Baborie A, Hubbe U. Radiological and histological findings in spinal intramedullary angiolipoma. *Neuroradiology* 1999:41:584-587.

Denervation of Muscle

Bredella MA, Tirman PFJ, Fritz RC, Wischer TK, Stork A, Genant HK. Denervation syndromes of the shoulder girdle: MR imaging with electrophysiologic correlation. *Skeletal Radial* 1999:28:567-572.

Cothan RL, Helms C. Quadrilateral space syndrome: incidence of imaging findings in a population referred for MRI of the shoulder. *AJR* 2005:184:989-992.

Atlas

A1 Adamantinoma (Also Referred to as Extragnathic Adamantinoma, Adamantinoma of Long Bones, Juvenile Intracortical Adamantinoma)[3]

ICD-O Code

9261/3

Definition

Adamantinomas are rare, low-grade malignant bone tumors consisting of epithelial cells surrounded by spindle cells and osteofibrous tissue that often involve the shaft of the tibia[2-4,9,10,12,13]

Frequency of Occurrence

Adamantinomas of long bones account for < 1 % of primary bone tumors.[3,4,7,8,12,13]

Age at Presentation

From 3 to 86 years, median = 19-25 years, average = 35 years, most common in 3rd and 4th decades.[3,4,7,8,12,13]

Gender Ratio (M / F)

1/1 to 2/1 [3,4,3,9,12]

Location

Lesions usually occur in the tibia (mid-diaphysis > distal metaphysis), but much more rarely in the fibula, ulna, femur, radius, humerus, metatarsals, capitate, ischium, andribs.[2-4,9,12,13] Tumors in the tibia involve the anterior cortex in 86 % of cases.[13] Tumors occasionally involve only the posterior or posteromedial tibial cortex.[13]

Signs and Symptoms[2-4]

Tumors can present as localized swelling with or without pain. Pathologic fractures occur in up to 10 % of cases.[13] The duration of symptoms ranges from months to years.

Cross Pathologic Findings

These tumors are considered as low-grade, malignant neoplasms of epithelial origin. Tumors are well-circumscribed, fleshy, fibrous lesions, which are often more than 5 cm in length and may contain cystic zones with or without hemorrhage.[2-6,10,12,13] Tumors can involve bone cortex, with or without marrowinvolvement.[2-6,10,12,13]

Histopathologic Findings[2-6,10,12,13]

Tumors often have variable proportions of epithelial-like and mesenchymal-like components. Tumor cells can appear as large polygonal cells with euchromatin, fusiform cells, and/or small cells with poorly defined cytoplasm. Mitotic figures are usually uncommon. Collagenized zones may be present, and regions of giant cell reaction can be seen in hemorrhagic portions.[2,3] Two major histologic patterns have also been described which are at the opposite ends of a spectrum: the classic adamantinoma type and the osteofibrous dysplasia-like type.[13] The classic type contains aggregates of epithelial cells which proportionally dominate the osteofibrous background.[13] There are four differentiation patterns of the classic form:basiloid, squamoid, tubular, and spindle cell.[2,3] More than one of these patterns often occurs in a single lesion.[2,3] The basiloid pattern is made up of lobules of cuboid or columnar cells.[2,3] The squamoid type contains zones of squamous differentiation with keratinization.[23] The tubular pattern consists of loose fascicles of elongated cells adjacent to bone trabeculae lined by osteoblasts.[2,3] The spindle cell pattern includes cells in storiform, herringbone, or cartwheel arrangements, often with abundant collagen.[2,3] The osteofibrous dysplasia-type adamantinoma contains proportionally dominant osteofibrous tissue relative to minimal scattered keratin-positive epithelial tumor cells.[2,3,13] Lesions can be associated with fibrous dysplasia-like regions.[2,3,13] Tumors have been reported to show immunoreactivity to basal epithelial keratins 1, 5,13,14, and 19, vimentin in spindle cells, and carcinoembryonic antigen.[2,3]

Tumor Genetics

Tumors may show two balanced translocations, t(l;13;22)(q22:p!3) and t(15;17)(ql2;pl3),[2,10] and another translocation has been reported, t(7;13)(q32q!4).[2] Gains of chromosomes 7, 8, 12, and 19 have also been reported.[3] Aneuploid zones and TP53 gene abnormalities have been observed in the epithelial portions of the tumors.[2,3]

Findings on Plain Films (Roentgenograms)[1-3,5,6,13,14]

Lesions appear as eccentric circumscribed zones of radiolucency involving the cortex, which occur as either a solitary focus or in a "saw-tooth" and/or multinodular pattern (Fig. 1). The involved cortex is often thickened.[13] Tumors can extend into the marrow resulting in a honeycomb radiolucent appearance. Extra-osseous soft tissue lesions and periosteal bone formation may occasionally be seen with adamantinomas.

MRI Findings[1,5,13]

Adamantinomas can appear either as a solitary tabulated focus (73 %) or in a multinodular pattern of signal alteration in bone cortex (27%), with or without marrow involvement (Fig. 1). Tumors can extend longitudinally within bone from 2 to 21 cm, mean = 9 cm.[13] With MRI, 60 % of adamantinomas have been shown to involve bone cortex and marrow compared with 40% that showed only cortical involvement.[13] Tumor foci in bone typically have low-intermediate signal on T1WI and PDWI, and slightly high to high signal on T2WI and FST2WI. Tumor signal on T2WI and FS T2WI can be homogeneous (62 %) or heterogeneous (38 %).[13] After Gd-contrast administration, lesions usually show prominent enhancement.[13] Adamantinomas with a multinodular pattern have enhancing nodules which have high signal on T2WI and FST2WI separated by zones of low signal from intervening cortical bone.[13] Tumor destruction of the outer cortical margins was observed in 32 % of cases.[13] Only 9 % of adamantinomas showed tumor extension into the adjacent soft tissues.[13]

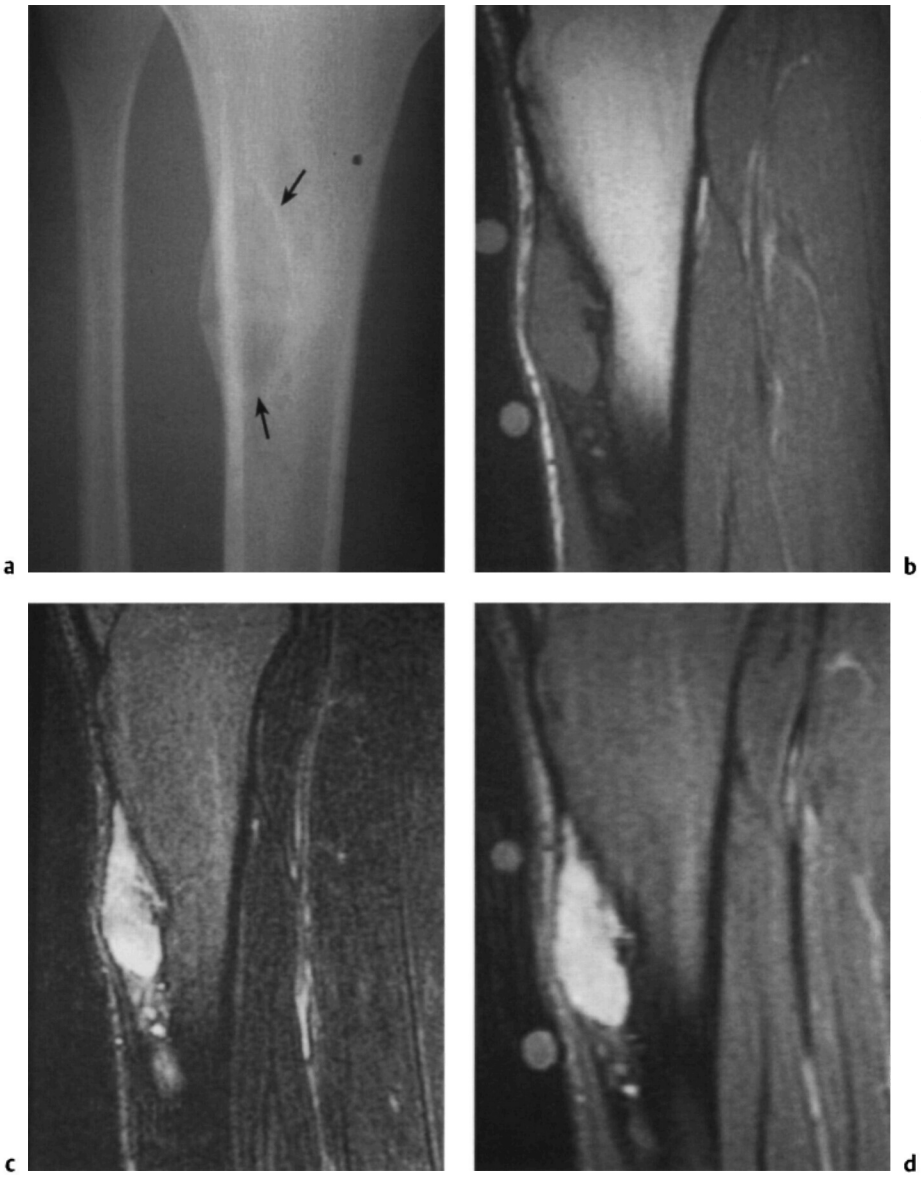

Figure **1 a-d** A 23-year-old woman with an adamantinoma of the tibial diaphysis. AP radiograph (**a**) shows a radiolucent lesion in the tibia. MRI shows the tumor to have low-intermediate signal on T1WI (**b**), high signal on T2WI (**c**), and Gd-contrast enhancement on FST1WI (**d**). There is expansion of the cortical bone at the site of the tumor, as well as tumor extension toward the marrow.

Differential Diagnosis

Osteofibrous dysplasia, fibrous dysplasia, metastatic disease, eosinophilic granuloma, aneurysmal bone cyst, chondromyxoid fibroma, non-ossifying fibroma, osteomyelitis.

Treatment and Prognosis[2-4,12,13]

Wide excision with bone grafting is the optimal treatment. Where resection is incomplete, local recurrence has been reported to occur in 32 % of cases and lung metastases in 25 %.[13] Metastatic disease and paraneoplastic syndromes have also been reported. Lesions are considered to be resistant to radiation treatment. The mortality rate is ~ 15 % of patients suffering from adamantinomas.

References

1 Conway WF, Hayes CW. Miscellaneous lesion of bone. *Radiol Clin North Am* 1993;31(2):339-358.

2 Forest M. Adamantinoma. In: Forest M, Tomeno B, Vanel D, eds. Orthopedic *Surgical Pathology: Diagnosis of Tumors and Pseudotumoral Lesions of Bone and Joints* Edinburgh: Churchill Livingstone; 1998:385-393.

3 Hogendoorn PCW, Hashimoto H. Adamantinoma. In: Fletcher CDM, Unni KK, Mertens F, eds. *World Health Organization Classification of Tumours. Pathology and Genetics of Tumours of Soft Tissue and Bone* Geneva: lARC Press; 2002:333-334.

4 Huvos AG. Adamantinoma of extragnathic bones. In: Huvos, AG, ed. *Bone Tumors: Diagnosis, Treatment, and Prognosis* 2nd ed. Philadelphia, Pa: W.B. Saunders; 1991:677-693.

5 Judmaier W, Peer S, Krejzi T, Dessl A, Kuhberger R. MR findings in tibial adamantinoma—a case report. *Acta Radiol* 1998;39:276-278

6 Kumar D, Mulligan ME, Levine AM, Dorfman HD. Classic adamantinoma in a 3-year-old. *Skeletal Radial* 1998;27:406-409.

7 Mulder JD, Schutte HE, Kroon HM, Taconis WK. Introduction. In: *Radiologic Atlas of Bone Tumors* Amsterdam: Elsevier; 1993:3-6.

8 Mulder JD, Schutte HE, Kroon HM, Taconis WK. The Diagnosis of Bone Tumors. In: *Radiologic Atlas of Bone Tumors* Amsterdam: Elsevier; 1993:9-46.

9 Mulder JD, Schutte HE, Kroon HM, Taconis WK. Adamantinoma. In: *Radiologic Atlas of Bone Tumors* Amsterdam: Elsevier; 1993: 255-262.

10 Salisbury JR. Bone neoplasms containing epithelial and epitheloid cells. In: Helliwell TR, ed. *Pathology of Bone and Joint Neoplasms* Philadelphia, Pa: W.B. Saunders; 1999:345-368.

11 Unni KK. Introduction and scope of study. In: *Dahlin's Bone Tumors: General Aspects and Data on 11087 Cases* 5th ed. Philadelphia, Pa: Lippincott, Williams & Wilkins; 1996:1-9.

12 Unni KK. Adamantinoma of long bones. In: *Dahlin's Bone Tumors: General Aspects and Data on 11087 Cases* 5th ed. Philadelphia, Pa: Lippincott, Williams & Wilkins; 1996:333-342.

13 Van der Woude HJ, Hazelbag HM, Bloem JL, Taminiau AHM, Hogendoorn PCW. MRI of adamantinoma of long bones in correlation with histopathology. *AJR Am J Roentgenol* 2004;183:1737-1744.

14 Young JWR, Aisner SC, Resnik CS, Levine AM, Dorfman HD, Whitley NO. Case Report 660. *Skeletal Radial* 1991:20:152-156.

A 2 Aneurysmal Bone Cyst

Definition

Aneurysmal bone cysts (ABCs) are tumor-like expansile bone lesions containing cavernous spaces filled with blood.[1,10,13,21,27,30,32,40] Two-thirds of ABCs are primary bone lesions but may otherwise be secondary to other bone lesions/tumors such as giant cell tumors, chondroblastomas, osteoblastomas, osteosarcomas. chondromyxoid fibromas, nonossifying fibromas, fibrous dysplasia, fibrosarcomas, malignant fibrous histiocytomas, and metastatic disease.[10,13,32,40] Solid ABCs are also referred to as **giant cell reparative granulomas**[14,32]

Frequency of Occurrence

ABCs account for ~11 % of primary tumor-like lesions of bone.[25-27,40]

Age at Presentation

From 1 to 25 years, median = 14 years.[13,25-27,32] As many as 75-85 % occur in patients below 25 years.[13,25,26] Patients with aneurysmal bone cysts tend to be younger than patients with giant cell tumors.[40] ABCs occasionally occur in older adults up to 67 years of age.[25,26]

Gender Ratio (M IF)

1/1 to l/1.3 [13,16,32]

Location[8,10,13,16,19,21,22,29,32,-40]

ABCs occur in many different bones, often involving the metaphyseal regions of long bones, and posterior elements of vertebrae. Long bones represent ~50-60% of cases, vertebrae ~20-30%, and short tubular and flat bones ~20%. Distal femur or proximal tibia > cervical vertebrae > thoracic vertebrae > proximal femur > sacrum, proximal fibula, carpal bones > proximal humerus, distal tibia, distal fibula > scapula, iliac bones > craniofacial bones. Most lesions are eccentric within medullary bone, although cortically centered lesions occur in up to 18 % of cases.[16,33] In the spine, the posterior elements are usually involved in nearly all cases (lamina in 80 %, pedicles in 59 %), and the vertebral bodies in 71 %.[29] Lesions in the sacrum usually involve more than one segment.[29] Multiple sites of involvement occur in 8 % of cases.[16] Solid ABCs (giant cell reparative granulomas) occur in the femur > ulna > tibia > humerus, radius, fibula > other bones; metaphyseal > diaphyseal > juxtaarticular > metadiaphyseal locations; most often they are eccentric within medullary bone.[14] Aneurysmal cysts rarely occur in soft tissues[19,34]

Signs and Symptoms[10,13,16,27,32,40]

Patients can present with local pain and swelling (weeks to months), or with pathologic fractures in up to 25% of cases. Spinal lesions can be associated with spinal cord compression[13,32]

Cross Pathologic Findings[6,8,10,13,14,21,27,30,32,40]

Lesions often appear as sponge-like tissue in bone with cavities ranging in size from millimeters to 2 cm, filled with unclotted blood. A thin layer of periosteal bone covers the lesion. Solid components of aneurysmal bone cysts have friable and/or fibrous tissue with zones of hemorrhage.

Histopathologic Findings[6,8,10,13,14,21,27,30,32,40]

Primary ABCs typically have cavernous spaces filled with blood. Fibrous septae lined by fibroblastic cells as well as strands of woven bone are present between dilated capillaries or sinusoids. Osteoclastic giant cells and hemosiderin-laden macrophages are also often present in the septae lining the blood channels. The outer expansile margins of the lesion are limited by periosteal connective tissue and/or periosteal bone. A solid variant of ABC (or giant cell reparative granuloma) contains spindle-cells and osteoclasts surrounding zones of hemorrhage and necrosis.[14,32] Zones of woven bone are also present.[14,32] Careful evaluation of all ABCs should be made for the presence of coexistent bone tumors to enable appropriate treatment planning.

Lesion Genetics

Chromosomal rearrangements involving the short arm of chromosome 17 with five different chromosomes have been reported.[32] Many ABCs probably result from acquired chromosomal rearrangements with clonal proliferations from activation of a 17 p oncogene.[32]

Findings on Plain Films (Roentgenograms) and Computed Tomography[1-5,7-13,15-18,21,22,27,28,31-33,35,36,40]

Lesions often appear as solitary, expansile radiolucent lesions that are often eccentric within medullary bone with narrow zones of transition, with or without sclerotic borders adjacent to normal bone (Figs. 2-7). Outer expanded margins of lesions often have a thin shell of bone which may partially demineralize. Lesions may have associated extra-osseous soft tissue components. Invasion of the growth plate can occur in children. CT can show subtle subperiosteal calcification and internal features such as small trabeculae and fluid-fluid levels.

Findings on Radionuclide Bone Scans

ABCs are usually associated with increased radiopharmaceutical accumulation, often with a rim-like pattern.

MRI Findings[2-5,7-9,11,12,15,16,18,22,23,27,28,31-33,35-38,40]

ABCs often have a low signal rim on Tl-, PD-, and T2-weighted images adjacent to normal medullary bone, and between extraosseous soft tissues (Figs. 2-6). Various combinations of low, intermediate, and/or high signal on these images are usually seen within ABCs as well as fluid-fluid levels. Variable Gd-contrast enhancement is seen at the margins of lesions as well as involving the internal septae. The solid types of ABCs (or giant cell reparative granuloma) can also have heterogene-

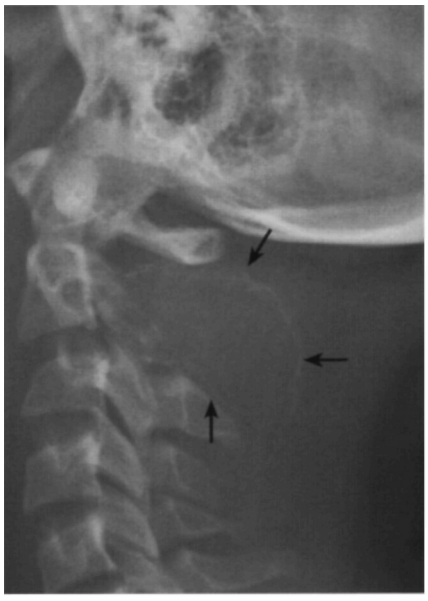

a

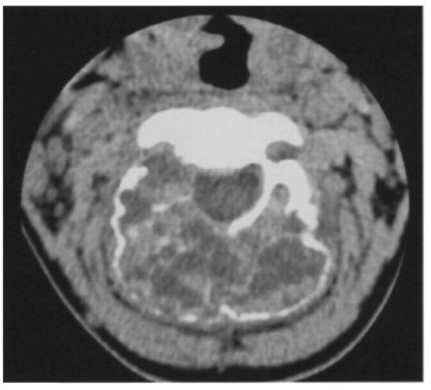

b, c

d

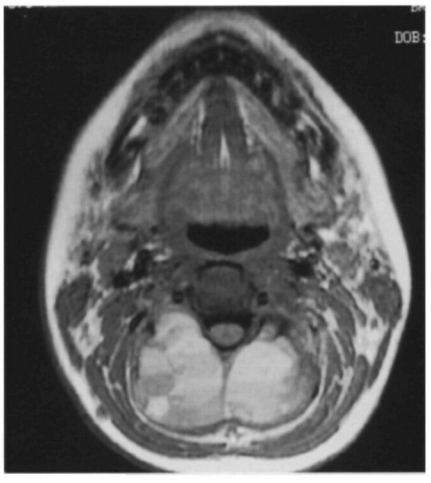

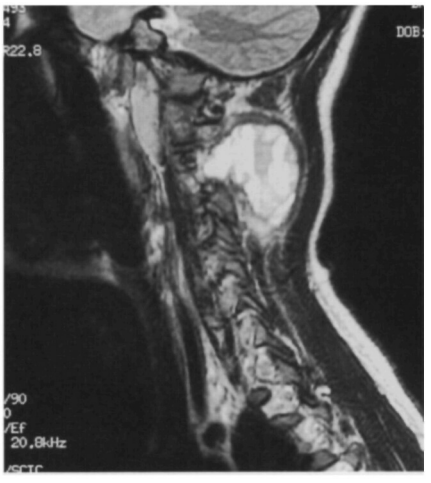

e, f

g

Figure **2a-g** A 13-year-old female with an aneurysmal bone cyst involving the posterior elements of C2. Lateral radiograph (**a**), and sagittal (**b**) and axial (**c**) CT scans show an expansile radiolucent lesion involving the posterior elements of C2. Fluid-fluid levels in the lesion are seen on the CT images. MRI shows the expansile lesion to contain multiple fluid-fluid levels on sagittal (**d**) and axial (**e**) T1WI, and sagittal (**f**) T2WI. The lesion shows multiple lobules with peripheral rimlike Gd-contrast enhancement on sagittal (**g**) T1WI.

a

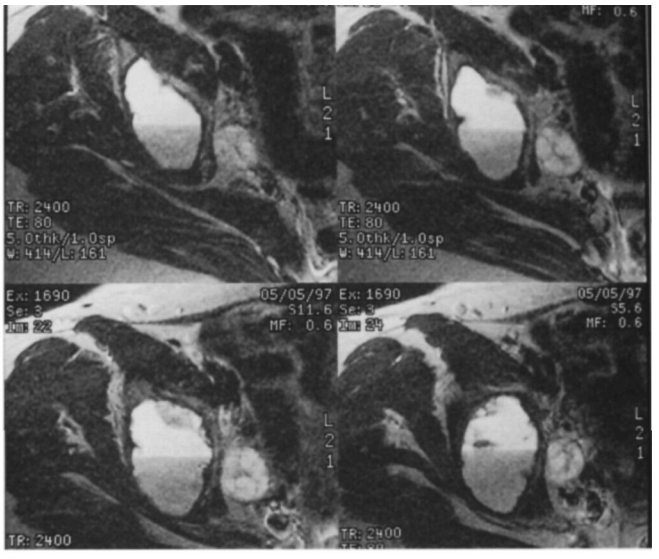

b

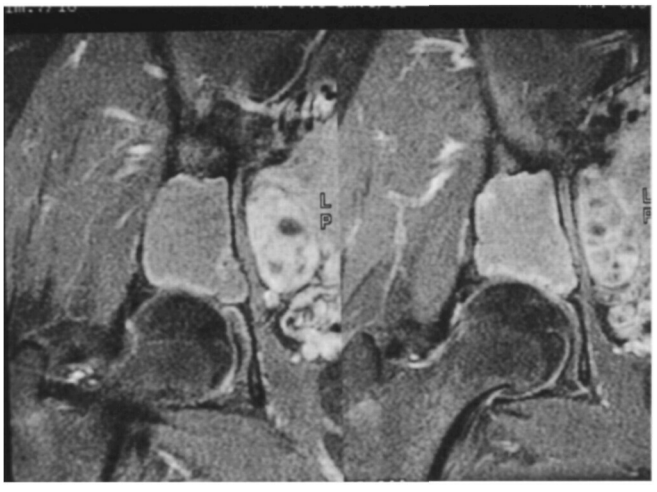

c

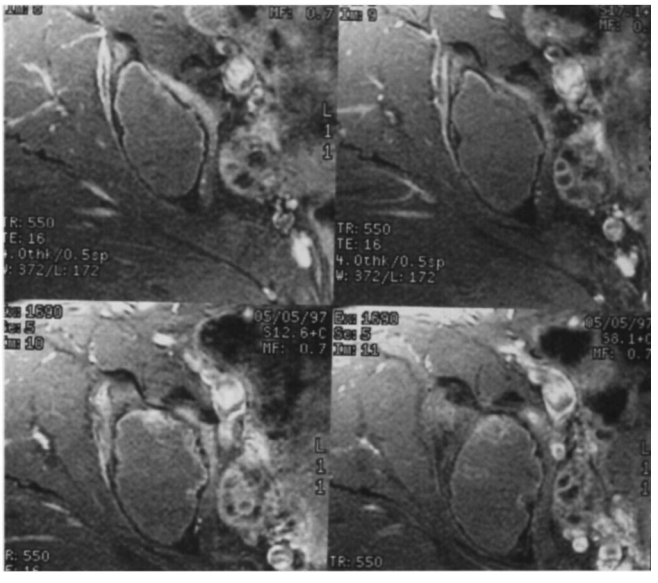

d

Figure **3 a-d** **A** 10-year-old female with an aneurysmal bone cyst in the right acetabulum. AP radiograph (**a**) shows a geographic radiolucent lesion. MRI shows the lesion to contain a fluid-fluid level on axial (**b**) T2WI. The lesion shows thin, peripheral rimlike Gd-contrast enhancement on coronal (**c**) and axial (**d**) FST1WI.

ous low, intermediate, and/or high signal on T1WI, PDW1, and T2WI, as well as peripheral rim-like and central Gd-contrast enhancement on FST1WI (Fig. 7).

Differential Diagnosis[9,10,16,20,21,24,37,38]

Giant cell tumor, unicameral bone cyst with hemorrhage, osteoblastoma, brown tumor-hyperparathyroidism, fibrous dysplasia, eosinophilic granuloma, enchondroma, chondroblastoma, metastasis, plasmacytoma, chondromyxoid fibroma, telangiectatic osteosarcoma, osteomyelitis, hemophilia pseudotumor, juxta-articular cysts in rheumatoid arthritis.

Treatment and Prognosis[5,7,8,10,13,16,28,29,40]

Resection or curettage are the most common methods of treatment. Local recurrence can occur in 10-44 % of patients.[16] Up to 90 % of recurrences occur in the first 2 years.[16] Embolization of ABCs has also been performed as a primary treatment or in preparation for surgical excision.

a

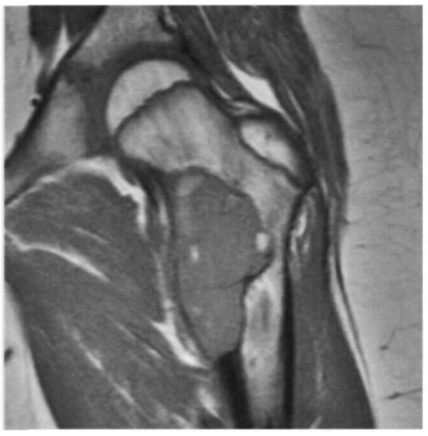

b, c

d, e

Figure 4a-e An 11-year-old male with an aneurysmal bone cyst involving the medial proximal shaft of the femur. AP radiograph (**a**) shows a geographic radiolucent expansile lesion. Coronal (**b**) T1WI shows the lesion to have circumscribed margins, and contains mostly intermediate signal with several foci of high signal. Coronal (**c**) and sagittal (**d**) FS T2WI shows the lesion to be multiseptated with fluid-fluid levels containing high and low-intermediate signal. The lesion has expanded and thinned cortical margins as well as high signal in the adjacent soft tissues. The lesion shows peripheral rimlike and septal Cd-contrast enhancement on coronal (**e**) FST1WI.

a

b, c

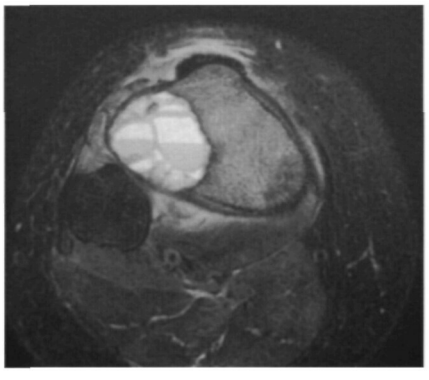

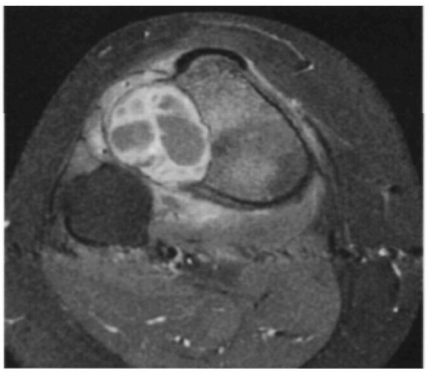

d, e

Figure **5a-e** A 14-year-old female with an aneurysmal bone cyst in the proximal lateral right tibia. AP radiograph (**a**) shows a geographic radiolucent lesion. MRI shows the lesion to have low to intermediate signal as well as a small focus of high signal on coronal (**b**) T1WI. The lesion contains multiple fluid-fluid levels on coronal (**c**) and axial (**d**) FST2WI. The lesion shows multiple lobules with peripheral rimlike Gd-contrast enhancement on axial (**e**) FST1WI.

a

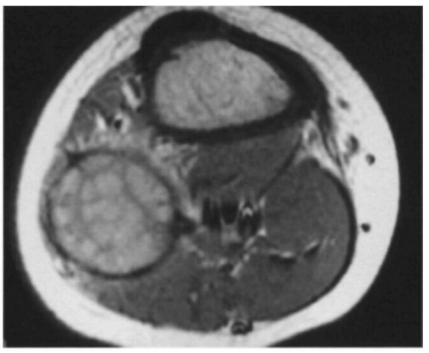

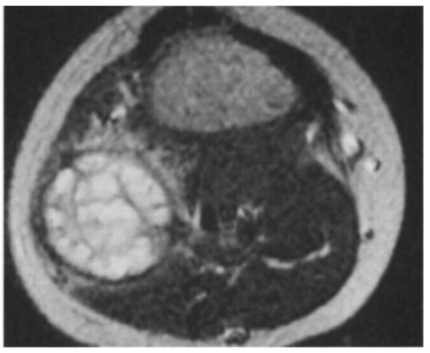

b, c

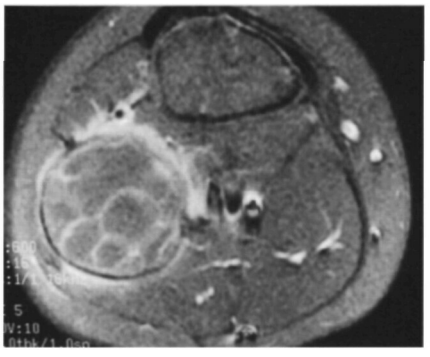

d

Figure **6a-d** A 5-year-old male with an aneurysmal bone cyst involving the proximal fibula. AP radiograph (**a**) shows a geographic radiolucent expansile lesion in the proximal fibula. MRI shows the lesion to contain multiple fluid-fluid levels on axial (**b**) PDWI and axial (**c**) T2WI. The lesion shows multiple lobules with peripheral rimlike Cd-contrast enhancement on axial (**d**) FST1WI.

a

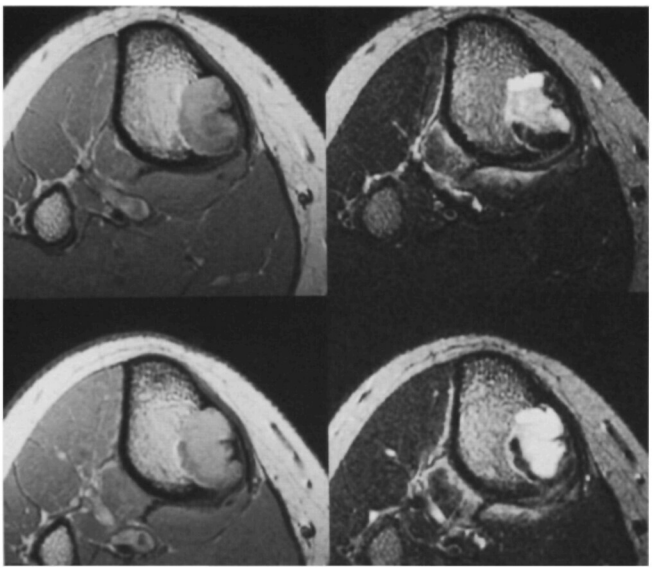

b

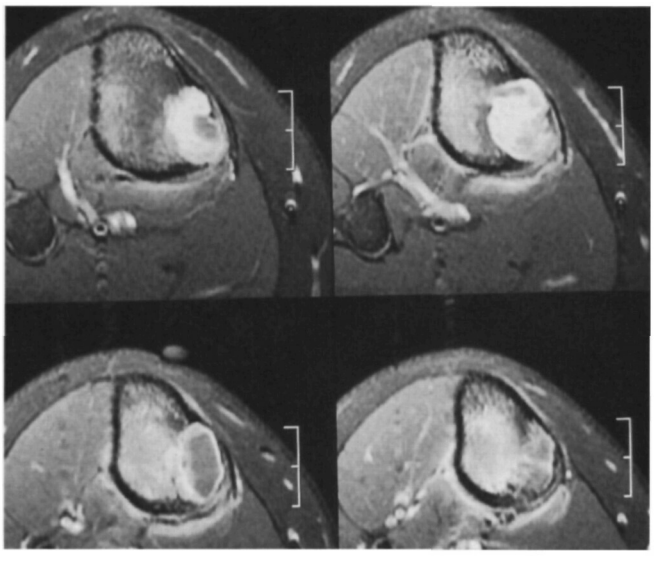

c

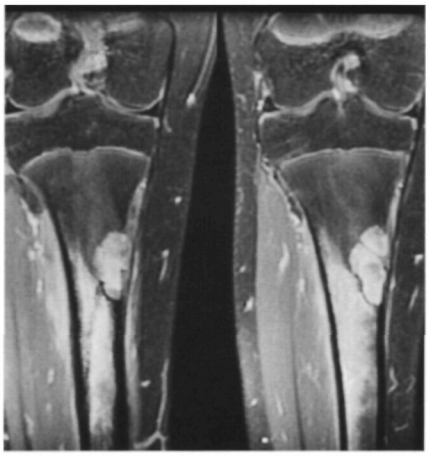

d

References

1 Bollini G, Jouve JL, Cottalorda J, Petit P, Panuel M, Jacquemier M. Aneurysmal bone cyst in children: analysis of twenty-seven patients. *J Pediatr Orthop B* 1998;7(4):274-285.

2 Capanna R, Van Horn JR, Biagini R, Ruggieri P. Aneurysmal bone cyst of the sacrum. *Skeletal Radiol* 1989;18:109-113.

3 Caro PA, Mandell GA, Stanton RP. Aneurysmal bone cyst of the spine in children. MRI imaging at 0.5 Tesla. Pediatr *Radiol* 1991;21(2): 114-116.

4 Conway WF, Hayes CW. Miscellaneous lesion of bone. *Radiol Clin North Am* 1993;31(2):339-358.

5 Cybulski GR, Anson J, Gleason T, Homsi MF, Reyes MG. Aneurysmal bone cyst of the thoracic spine: treatment by excision and segmental stabilization with luque rods. *Neurosurgery* 1989;24(2):273-276.

6 Darby AJ. Vascular neoplasms of bone. In: Helliwell TR, ed. *Major Problems in Pathology: Pathology of Bone and Joint Neoplasms* 1st ed. Philadelphia, Pa: W.B. Saunders; 1999:37:339-342.

7 de Kleuver M, van der Heul RO, Veraart Ben EEMJ. Aneurysmal bone cyst of the spine: 31 cases and the importance of the surgical approach J Pediatr *Orthop B* 1998;7(4):286-292.

8 Dicaprio MR, Murphy MJ, Camp RL Aneurysmal bone cyst of the spine with familial incidence. *Spine* 2000;25(12):1589-1592.

9 Fletcher BD, Hanna SL. Pediatric musculoskeletal lesions simulating neoplasms. *Magn Reson Imaging Clin N Am* 1996;4(4):724-727.

10 Forest M. Aneurysmal bone cyst. In: Forest M, Tomeno B, Vanel D, eds. Orthopedic Surgical *Pathology: Diagnosis of Tumors and Pseudotumoral Lesions of Bone and Joints* Edinburgh: Churchill Livingstone; 1998:531-544.

11 Guida F, Rapana A, Conti C, Cagliari E, Civelli F, Trincia G. Cranial aneurysmal bone cyst: a diagnostic problem. With a review of the literature. *Childs Nerv Syst* 2001; 17:297-301.

12 Hudson TM, Hamlin DJ, Fitzsimmons JR. Magnetic resonance imaging of fluid levels in an aneurysmal bone cyst and in anticoagulated human blood. *Skeletal Radial* 1985:13:267-270.

13 Huvos AG. Simple bone cyst and aneurysmal bone cyst. In: Huvos AG, ed. *Bone Tumors: Diagnosis, Treatment, and Prognosis* 2nd ed. Philadelphia, Pa: W.B. Saunders; 1991:727-738.

14 Ilaslan H, Sundaram M, Unni KK. Solid variant of aneurysmal bone cysts in long tubular bones: giant cell reparative granuloma..*AJR Am] Roentgenol* 2003;180:1681-1687.

15 JansenJ, Terwey B, Rama B, Markakis E. MRI diagnosis of aneurysmal bone cyst. *NeurosurgRev* 1990;13(2):161-166.

16 Kransdorf MJ, Sweet DE. Review Article-Aneurysmal bone cyst: concept, controversy, clinical presentation, and imaging. *AJR Am J Roentgenol* 1995;164:573-580.

17 Lee JH Edmund, Reinus WR, Wilson AJ. Quantitative analysis of the plain radiographic appearance of unicameral bone cysts. *Invest Radio*/1999;34(l):28-37.

18 Lippman CR, Jallo GI, Feghali JG, Jimenez E, Epstein F. Aneurysmal bone cyst of the temporal bone. Pediatr *Neurosurg* 1999;31:219-223. Lopez-Barea F, Rodriguez-Peralto JL, Alvarez-Linera J. Primary aneurysmal cyst of soft tissue: serial magnetic resonance imaging study. *Hum* Patho/1998;29(6):656-657.

20 Margau R, Babyn P, Cole W, Smith C, Lee F. MR imaging of simple bone cysts in children: not so simple. *Pediatr Radial* 2000; 30:551-557.

21 Martinez V, Sissons HA. Aneurysmal bone cyst: a review of 123 cases including primary lesions and those secondary to other bone pathology. *Cancer* 1988:61:2291-2304.

22 Menon J, Brosnahan DM, Jellinek DA. Aneurysmal bone cyst of the orbit: a case report and review of literature. *Eye* 1999:13:764-768.

23 Meyer JS, Dormans JP. Differential diagnosis of pediatric musculoskeletal masses. *Magn Reson Imaging Clin N Am* 1998;6(3):561-577.

24 Miller SL, Hoffer FA. Malignant and benign bone tumors. *Radiol Clin North Am* 2001;39(4):688-690, 692.

25 Mulder JD, Schutte HE, Kroon HM, Taconis WK. Introduction. In: *Radiologic Atlas of Bone Tumors* Amsterdam: Elsevier; 1993:3-6.

26 Mulder JD, Schutte HE, Kroon HM, Taconis WK. The Diagnosis of Bone Tumors. In: *Radiologic Atlas of Bone Tumors* Amsterdam: Elsevier; 1993:9-46.

27 Mulder JD, Schutte HE, Kroon HM, Taconis WK. Aneurysmal bone cyst. In: *Radiologic Atlas of Bone Tumors* Amsterdam: Elsevier; 1993: 557-577.

28 Munk PL, Helms CA, Holt RG, Johnston J, Steinbach L, Neumann C. Pictorial Essay—MR imaging of aneurysmal bone cysts. *AJR Am] Roentgenol* 1989:153:99-101.

29 Papagelopoulos PJ, Currier BL, Shaughnessy WJ, et al. Aneurysmal bone cyst of the spine management and outcome. Spine 1998:23(5): 621-628.

30 Reid RP. Bone neoplasms and tumor-like lesions on the bone surface. In: Helliwell TR, ed. Major *Problems in Pathology: Pathology of Bone and Joint Neoplasms* 1st ed. Philadelphia, Pa: W.B. Saunders; 1999: 37:220-235.

31 Revel MP, Vanel D, Sigal R, et al. Aneurysmal bone cysts of the jaws: CT and MR findings. *J Comput Assist Tomogr* 1992;16(1):84-86.

32 Rosenberg AE, Nielsen GP, Fletcher JA. Aneurysmal bone cyst. In: Fletcher COM, Unni KK, Mertens F, eds. *World Health Organization Classification of Tumours. Pathology and Genetics of Tumours of Soft Tissue and Bone* Geneva: IARC Press; 2002:338-339.

33 Schoedel K, Shankman S, Desai P. Intracortical and subperiosteal aneurysmal bone cysts: a report of three cases. *Skeletal Radiol* 1996:25:455-459.

34 Shannon P, Bedard Y, Bell R, Kandel R. Aneurysmal cyst of soft tissue: report of a case with serial magnetic resonance imaging and biopsy. *Hum* Patho/1997;28(2):255-257.

35 Shimizu T, Ukai K, Hayashi T, Imanishi Y, Sakakura Y. Aneurysmal bone cyst of the temporal bone: magnetic resonance imaging as a valuable tool for preoperative diagnosis. *Am J Otolaryngol* 1998; 19(6):379-382.

36 Som PM, Schatz CJ, Flaum EG, Lanman TH. Case Report—Aneurysmal bone cyst of the paranasal sinuses associated with fibrous dysplasia: CT and MR findings.; *Comput Assist Tomogr* 1991;15(3):513-515.

37 Sullivan RJ, Meyer JS, Dormans JP, Davidson RS. Diagnosing aneurysmal and unicameral bone cysts with magnetic resonance imaging. *Clin Orthop Relat Res* 1999:366:186-190.

38 Tsai JC, Dalinka MK, Fallen MD, Zlatkin MB, Kressel HY. Fluid-fluid level: a nonspecific finding in tumors of bone and soft tissue. Radi*ology* 1990;175:779-782.

39 Unni KK. Introduction and scope of study. In: *Dahlin's Bone Tumors: General Aspects and Data on 11087 Cases* 5th ed. Philadelphia, Pa: Lippincott, Williams & Wilkins;1996:l-9.

40 Unni KK. Osteosarcoma. In: *Dahlin's Bone Tumors: General Aspects and Data in 11087 Cases* 5th ed. Philadelphia, Pa: Lippincott, Williams & Wilkins;1996:143-183.

41 Unni KK. Conditions that commonly simulate primary neoplasms of bone. In: *Dahlin's Bone Tumors: General Aspects and Data on 11087 Cases* 5th ed. Philadelphia, Pa: Lippincott, Williams & Wilkins; 1996: 355-432.

Figure **7a-d** A 14-year-old female with an aneurysmal bone cyst involving the proximal di-metaphyseal region of the tibia. The lesion had predominant histologic findings of a solid type of aneurysmal bone cyst as well as smaller portion, which resembled a unicameral bone cyst. AP radiograph (**a**) shows a geographic radiolucent slightly expansile lesion. Axial (**b**) PDWI and T2WI show the lesion to have intermediate signal and heterogeneous low, intermediate, and high signal, respectively. The lesion shows peripheral rimlike and central Gd-contrast enhancement as well as in the adjacent marrow on axial (**c**) and coronal (**d**) FST1WI.

A3 Bone Cyst (Also Referred to as Simple Bone Cyst, Unicameral Bone Cyst, Solitary Bone Cyst)

Definition

Bone cysts are intramedullary cavities filled with serous or serosanguinous fluid.[1,3,4]

Frequency of Occurrence

Simple or unicameral bone cysts (UBCs) represent 9% of primary tumor-like lesions of bone.[7]

Age at Presentation

From 1 to 30 years, median = 11 years.[8] Approximately 85% of cases occur in the first two decades.[4] Lesions can also occur in older adults up to 62 years of age.[8,9]

Gender Ratio (M / F)

2/1 to 3/1.[3,4,9]

Location

Lesions are located in the proximal humerus > distal femur > proximal femur > iliac bone > tibia > fibula, calcaneus > radius, ulna > other sites.[3,9]

Signs and Symptoms

UBCs may be initially seen as incidental findings on radiographs or present from pathologic fractures in up to 70% of cases.[3,9] Locations within bone: metadiaphyseal > diaphyseal > metaphyseal.[9] Only 3 % of UBCs involve the epiphysis.[9]

Gross Pathologic Findings

UBCs often show a slight bulge in the overlying thinned bone cortex with intact periosteum.[1,3,9] The underlying cyst may have a bluish appearance under the thinned cortex.[9] UBC content is usually clear, yellow-green, and serous, and when associated with pathologic fracture is sero-sanguineous.[1,3,9,11] The inner walls of the UBCs often have a thin glistening, whitish or reddish-brown appearance.[3,9] The inner surface frequently has ridges.[11] Partial or complete septa may be occasionally seen.[11] Usually, one cystic compartment is seen, except for lesions associated with prior fracture or recurrent lesions which may have several compartments.[1,3,9] When complete septa are present, these bone cysts have been referred to as multicameral.[11]

Histopathologic Findings

The cyst walls are composed of a thin continuous or wavy layer of fibrous tissue with fibroblasts, collagen fibers, multinucleated giant cells, with or without zones of hemorrhage or hemosiderin.[1,3,9,11] Immature bone or osteoid trabeculae surrounded by osteoblasts may be seen at the cyst walls.[1] Focal deposits of eosinophilic material in the inner cyst walls derived from fibrin may be seen with calcifications and occasional ossification resembling cementum.[1,9,11] Cyst fluid often contains prostaglandins, interleukin-1, proteolytic enzymes, and alkaline and acid phosphatases.[1] UBCs with pathologic fractures usually show callus and granulation tissue, as well as giant cells, cholesterol crystals, and hemosiderin.[1,9,11]

Lesion Genetics

Cells in these lesions are typically diploid.[1] A complex chromosomal rearrangement involving chromosomes 4, 6, 8, 12, 16, and 21 has been reported in a single case[14]

Findings on Plain Films (Roentgenograms) and Computed Tomography

UBCs are geographic, medullary, radiolucent lesions with well-defined margins that are typically located in the metaphysis and/or diaphysis[1-4,6,9-11] (Figs. **8,11-13).** UBCs rarely involve the epiphysis.[1,2,9] The margins may be smooth or slightly lobulated.[1,9] Lobulated or trabeculaed margins of UBCs result from ridges on the inner surface of the cortex.[1] In tubular bones, mild to moderate expansion of bone may occur with thinning of the overlying cortex.[1-4,6,9-11] The thinned cortex results in increased susceptibility to pathologic fracture[1-4,6,9-11] (Figs. **12-14).** Periosteal reaction and a "fallen-leaf fracture fragment are often seen with UBCs complicated by pathologic fracture[1,2,6] (Figs. **12-14).** No matrix mineralization is present in UBCs. No extra-osseous soft tissue mass is associated with UBCs.[1-4,6,9-11]

CT scans may show fluid-fluid levels and fibrous septa.[1]

MRI Findings

UBCs often have a peripheral rims of low signal on Tl-, PD-, and T2-weighted images adjacent to normal medullary bone, and between extra-osseous soft tissues[1,2,6,9,10] (Figs. **8-14).** UBCs usually contain fluid with low to low-intermediate signal on T1WI; low-intermediate, intermediate, or slightly high signal on PDW1, and high signal on T2WI.[1,2,6,9,10] Fluid-fluid levels may occur.[1] In tubular bones, mild to moderate expansion of bone may occur with variable thinning of the overlying cortex.[2] For UBCs without pathologic fracture, thin, peripheral Gd-contrast enhancement can be seen at the margins of lesions.[6]

UBCs with pathologic fracture can have heterogeneous or homogeneous low-intermediate to high signal on T1WI, and heterogeneous or homogeneous high signal on T2WI and FS T2WI[6] (Figs. **12-14).** MRI features associated with UBCs complicated by fracture include internal septations in 100%, and fluid-fluid levels or hemorrhage in 61 %.[6] After Gd-contrast administration, UBCs with fracture can show irregular peripheral enhancement up to 1-cm thick, nodular enhancing zones, and enhancement at internal septations.[6] Juxtacortical soft tissue and periostea! enhancement also commonly occur with recent pathologic fractures of UBCs.[6]

Differential Diagnosis

Enchondroma, aneurysmal bone cyst, fibrous dysplasia, non-ossifying fibroma, Brodie abscess, chondromyxoid fibroma, giant cell tumor, chondrosarcoma.

a

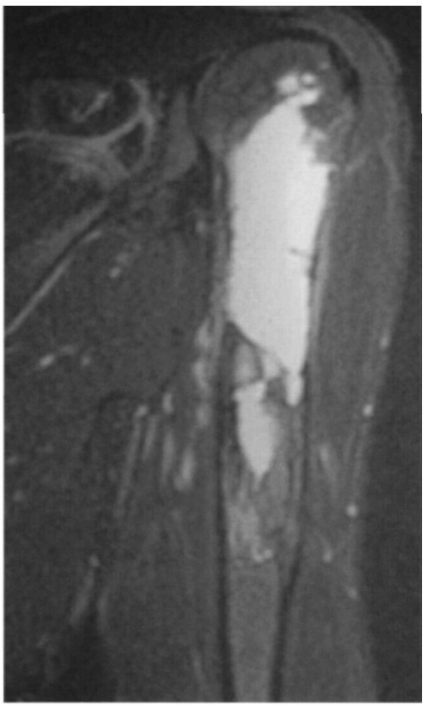

b, c

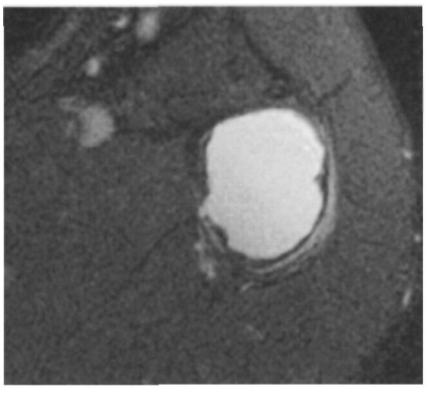

d

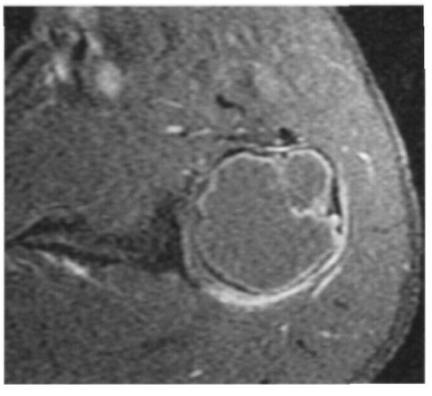

e

Figure **8a-e** A 17-year-old male with a unicameral bone cyst involving the proximal di-metaphyseal portion of the humerus. AP radiograph (**a**) shows a geographic radiolucent slightly expansile lesion. Coronal (**b**) T1WI shows the lesion to have intermediate signal, and coronal (**c**) and axial (**d**) FST2WI shows the lesion to have high signal with expanded and thinned cortical margins as well as thin, high periosteal signal. The intramedullary lesion shows peripheral rimlike Cd-contrast enhancement, as well as at the periosteum on axial (**b**) FST1WI.

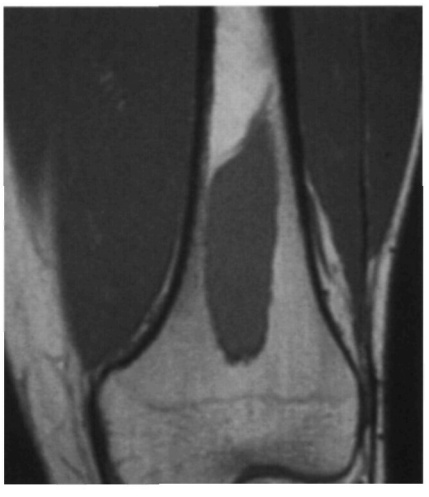

a

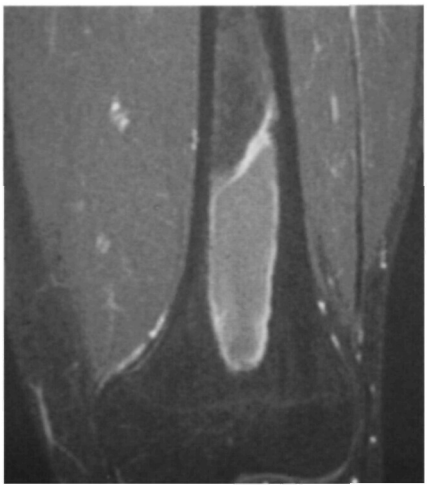

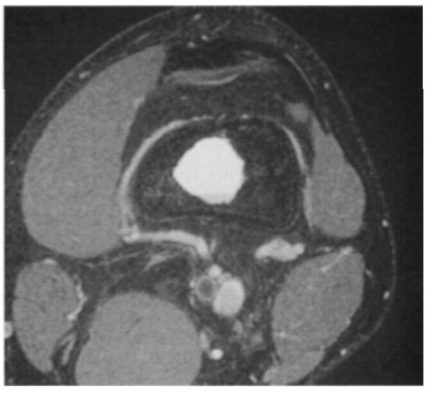

b, c

Figure **9a-c** A 16-year-old male with a unicameral bone cyst in the distal di-metaphyseal portion of the femur. Coronal PDWI (**a**) shows a well-circumscribed lesion with intermediate signal. The lesion shows peripheral rimlike Cd-contrast enhancement on coronal FST1WI (**b**). The lesion has high signal on FST2WI (**c**) and contains a fluid-fluid level.

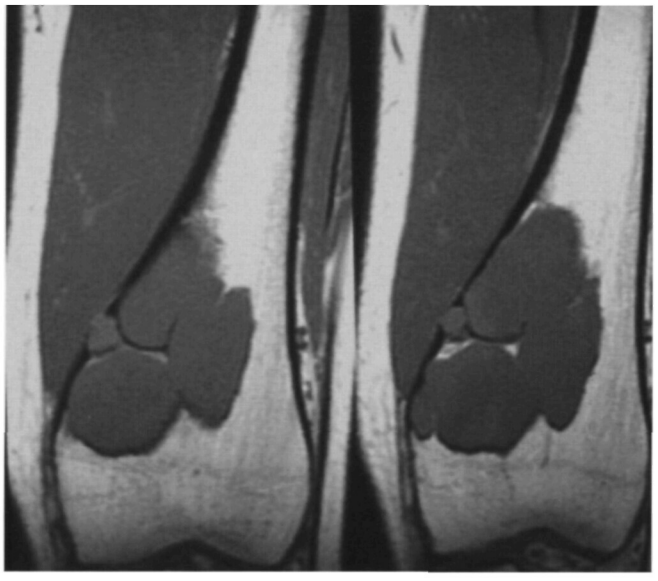

a

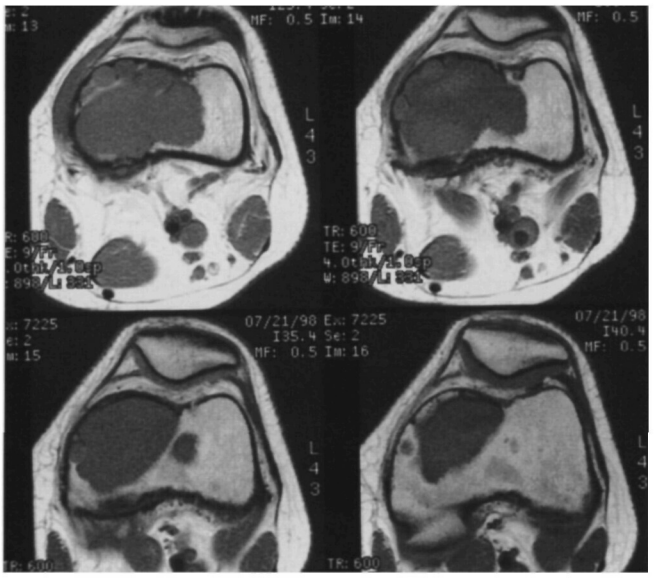

b

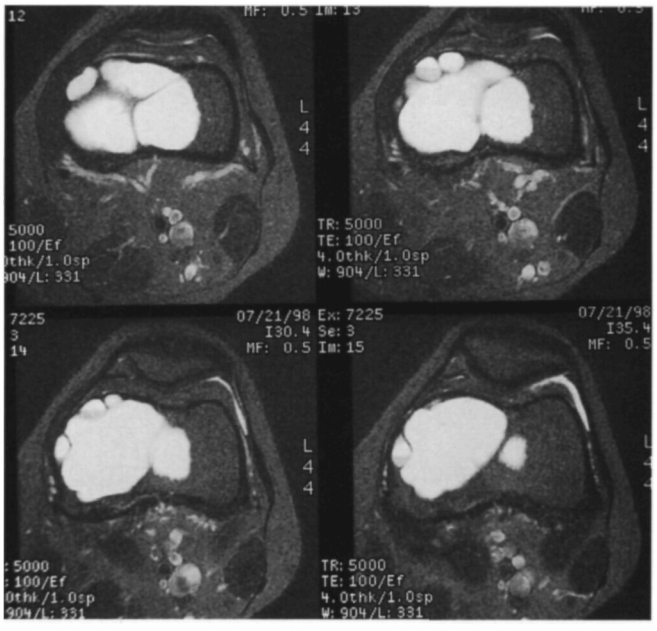

c

Figure **IOa-c** A 17-year-old female with a unicameral bone cyst in the distal di-metaphyseal portion of the femur. Coronal (**a**) and axial (**b**) T1WI shows a well-circumscribed lesion with low-intermediate signal, and high signal on axial (**c**) FST2WI. Several thin septa are seen as well as several small fluid-fluid levels. Thinning of the cortex with slight expansion is also noted.

a

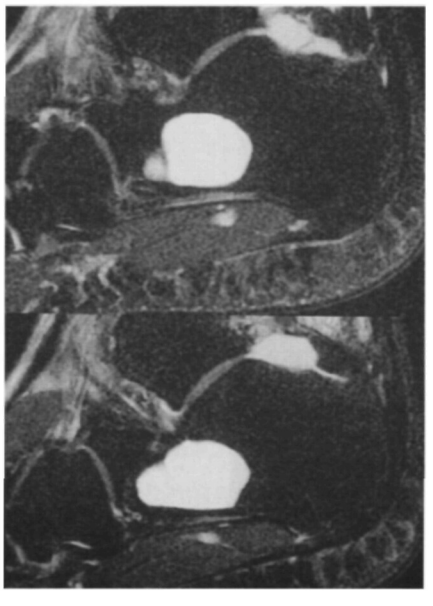

b, c

Figure **11 a, b** A 17-year-old male with a unicameral bone cyst in the calcaneus bone. Lateral radiograph shows a geographic radiolucent lesion. The lesion has intermediate signal on sagittal PDWI (**a**), and high signal on sagittal FST2WI (**b**), as well as a small fluid-fluid level.

a

b

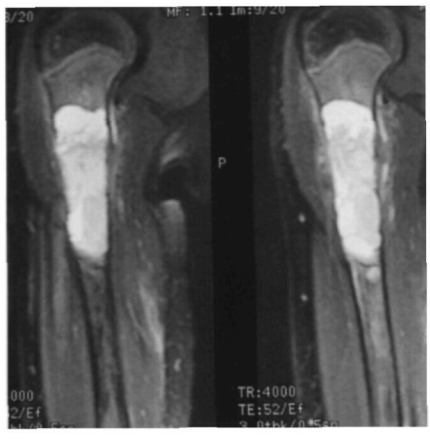

c

Figure **12a-e** A 9-year-old male with a pathologic fracture at a unicameral bone cyst involving the proximal di-metaphyseal portion of the humerus. AP radiograph (**a**) shows a radiolucent geographic lesion with a "fallen fragment." The lesion has heterogeneous intermediate and high signal on coronal (**b**) and axial (**d**) T1WI, and coronal (**c**) and axial (**e**) FST2WI. The "fallen fragments" are also seen (**d, e**).

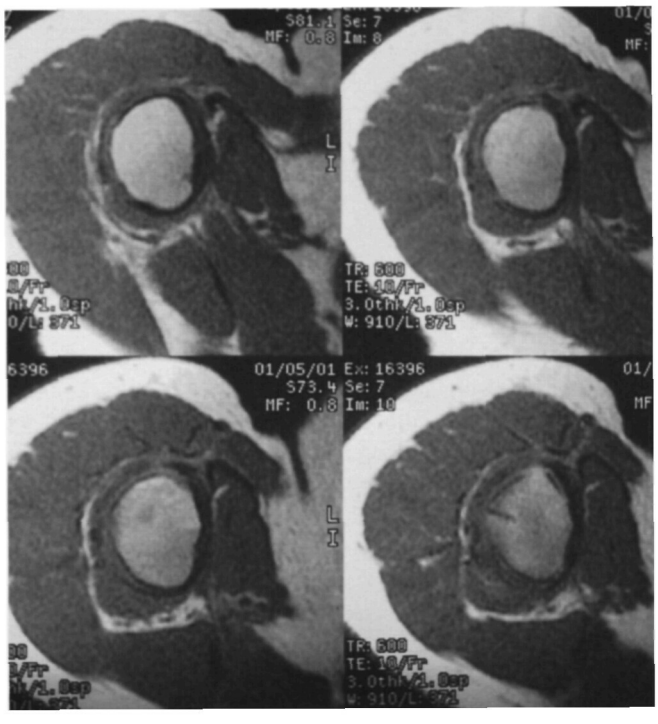

d

e

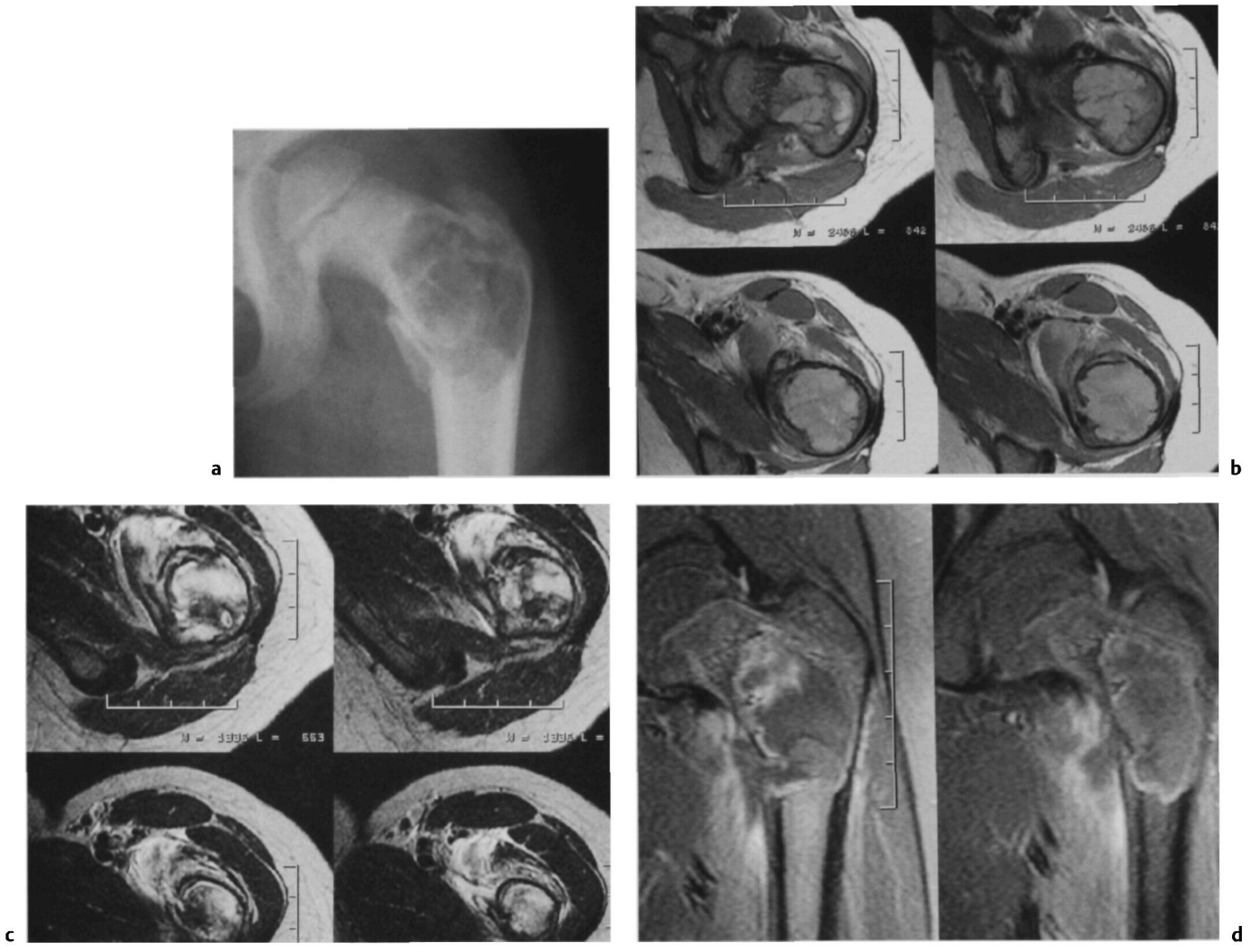

Figure **13a-d** A 4-year-old female with a pathologic fracture at a unicameral bone cyst involving the intertrochanteric region of the femur. AP radiograph (**a**) shows a radiolucent geographic lesion with cortical fracture. The lesion has heterogeneous intermediate and slightly high signal on axial PDWI (**b**) mixed low, intermediate, and high signal on axial T2WI (**c**). The lesion shows irregular peripheral Gd-contrast enhancement on coronal FST1WI (**d**), as well as in the adjacent soft tissues.

Prognosis and Treatment

Up to 70% of UBCs are associated with pathologic fracture.[3,9] Surgical treatment consists of curettage and placement of bone graft material.[9,12] In patients with pathologic fractures secondary to UBCs, surgery is usually performed after ample callus has formed.[9] Local recurrence after surgery may occur in 15-40% of cases.[1] Injection of steroids, such as methylprednisolone into the lesion after drainage of cyst contents has given similar results.[1,9,11,12] Percutaneous grafting with allograft and/or bone substitutes has also been recently utilized in the treatment of bone cysts.[12]

a, b

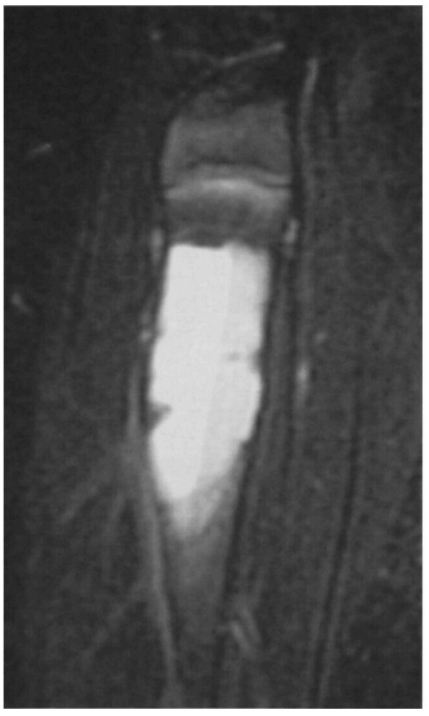

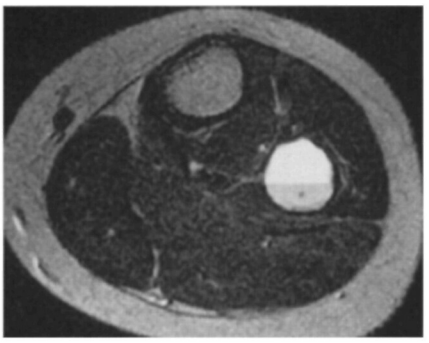

c

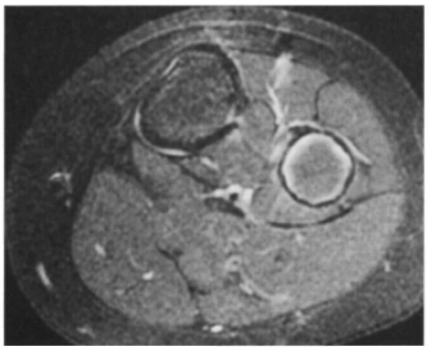

d

Figure **14a-d** A 1-year-old female with a pathologic fracture at a unicameral bone cyst involving the proximal di-metaphyseal portion of the fibula. AP radiograph (**a**) shows a fracture at a geographic radiolucent slightly expansile lesion. The lesion has high signal on sagittal FST2WI (**b**) and axial T2WI (**c**) with a fluid-fluid level. The lesion shows peripheral rimlike Gd-contrast enhancement on axial FST1WI (**d**), as well as thin periosteal enhancement.

References

1 Forest M Simple bone cyst. In: Forest M, Tomeno B, Vanel D, eds. *Orthopedic Surgical Pathology: Diagnosis of Tumors and Pseudotumoral Lesions of Bone and Joints* Edinburgh: Churchill Livingstone; 1998:519-529.

2 Haims AH, Desai P, Present D, Beltran J. Epiphyseal extension of a unicameral bone cyst. *Skeletal Radial* 1997;26:51-54.

3 Huvos AC. Simple bone cyst and aneurysmal bone cyst. In: Huvos AG, ed. *Bone Tumors: Diagnosis, Treatment, and Prognosis* 2nd ed. Philadelphia, Pa: W.B. Saunders; 1991:727-738.

4 Kalil RK, Araujo ES. Simple bone cyst. In: Fletcher COM, Unni KK, Mertens F, eds. *World Health Organization Classification of Tumours. Pathology and Genetics of Tumours of Soft Tissue and Bone* Geneva: 1ARCPress;2002:340.

5 Lee JH, Reinus WR, Wilson AJ. Quantitative analysis of the plain radiographic appearance of unicameral bone cysts. *Invest* Radio/ 1999;34:28-37.

6 Margau R, Babyn P, Cole W, Smith C, Lee F. MR imaging of simple bone cysts in children: not so simple. *Pediatr Radial* 2000; 30: 551-557.

7 Mulder JD, Schutte HE, Kroon HM, Taconis WK. Introduction. In: *Radiologic Atlas of Bone Tumors* Amsterdam: Elsevier; 1993:3-6.

8 MulderJD, Schutte HE, Kroon HM, Taconis WK. The diagnosis of bone tumors. In: *Radiologic Atlas of Bone Tumors* Amsterdam: Elsevier; 1993:9-46.

9 MulderJD, Schutte HE, Kroon HM, Taconis WK. Solitary bone cyst. In: *Radiologic Atlas of Bone Tumors* Amsterdam: Elsevier; 1993:579-590.

10 Sullivan RJ, Meyer JS, Dormans JP, Davidson RS. Diagnosing aneurysmal and unicameral bone cysts with magnetic resonance imaging. *Clin Orthop RelatRes* 1999:366:186-190.

11 Unni KK. Conditions that commonly simulate primary neoplasms of bone. In: *Dahlin's Bone Tumors: General Aspects and Data on 11087 Cases* 5th ed. Philadelphia, Pa: Lippincott, Williams & Wilkins; 1996: 355-432.

12 Wilkins RM. Unicameral bone cysts. J Am *Acad Orthop Surg* 2000;8: 217-224.

A 4 Angiofibroma (Also Referred to as Juvenile Nasopharyngeal Angiofibroma)

Definition

Angiofibromas are benign fibrovascular tumors that are locally destructive and typically occur in male adolescents[3,4]

Frequency of Occurrence

Occurrence is 1 in 5000, and accounts for 0.05 % of neoplasms of the head and neck.[4,6] Angiofibromas are the most common benign tumor of the nasopharynx.[6]

Age at Presentation

From 8 to 25 years, mean = 15.3-15.5 years.[4,11]

Gender Ratio (M / F)

Angiofibromas almost exclusively involve male adolescents.[3,4] Rare cases have been reported in females.[5]

Location

These lesions typically occur in the nasopharynx near and/or within the pterygopalatine fossa and pterygomaxillary fissure.[3] Lesions may show locally aggressive growth patterns with bone remodeling and extension into adjacent paranasal sinuses, infratemporal fossa, orbit via the inferior orbital fissure, and intracranially via the foramen rotundum, pterygoid canal, or superior orbital fissure.[3] Tumor extension into the pterygoid canal with invasion of the pterygoid process and greater wing of the sphenoid has been reported to occur in up to 60% of cases.[8] Sphenoid sinus invasion has been reported to occur in up to two-thirds of cases.[6] Intracranial extension occurs in up to 36 % of cases and is typically extradural.[4] Extracranial extension usually occurs toward the nasal cavity and infratemporal fossa, and occasionally toward the nasopharyngeal mucosa, base of the pterygoids, and/or vascular spaces of the clivus.[4]

Signs and Symptoms

These lesions are frequently associated with epistaxis and/or nasal obstruction.[3]

Cross Pathologic Findings

Lesions are firm, pink-white lesions.[14] The cut surface is yellow-white with white trabeculations.[14]

Histopathologic Findings

Angiofibromas contain cells with round, ovoid, and/or short spindle-shaped nuclei[14] as well as stromal cells with stellate nuclei.[14] Lesions typically also contain fibrous tissue and prominent vascular channels.[14]

Findings on Plain Films (Roentgenograms) and Computed Tomography

Angiofibromas often have circumscribed margins, and usually have soft tissue attenuation.[3,6-8,10,13,14] These lesions usually show contrast enhancement.[1,3,4,6,7,13,14] Lesions are commonly associated with erosion and/or remodeling of adjacent bone, particularly the pterygopalatine fossa.[3,4,6-8,13,14]

MRI Findings

Angiofibromas are usually circumscribed lesions with sharp margins which may be tabulated.[1,4,5,7,8,10,13,14] Lesions typically have low-intermediate signal on T1WI, and heterogeneous slightly high to high signal on T2WI[1,4,5,7,8,10,13,14] (Figs. **15, 16).** Flow voids on T2W1 may be seen in the lesions representing blood vessels.[1,4,5,7,8,10,13,14] After Gd-contrast administration, lesions show prominent enhancement.[1,4,5,7,8,10,13,14]

Differential Diagnosis

Hypervascular nasal polyps, lymphoma, nasopharyngeal carcinoma, rhabdomyosarcoma, parotid neoplasm, hemangioma, metastatic disease.[14]

Prognosis and Treatment

Conventional arteriography is often used for diagnosis as well as for embolization with or without subsequent surgery.[3,5,11-13,15] Endoscopically assisted surgical techniques have been used.[4,9,10] Large, late-stage angiofibromas have been treated with preoperative embolization, surgical excision, and radiosurgery.[2] New craniofacial or subcranial techniques and infratemporal fossa approaches with osteotomies can allow greater surgical access to large angiofibromas, including those which involve the skull base and intracranial compartment.[15] Findings associated with recurrence of angiofibromas include high tumor growth rate at the time of surgery and incomplete surgical resection because of sphenoid invasion.[8] Residual lesions seen with MRI after treatment can undergo spontaneous resolution.[1,10] Advanced angiofibromas can be treated with radiotherapy, after which they tend to regress slowly over several months.[12] Angiofibromas that regress slowly have an increased recurrence risk.[12]

References

1 Chagnaud C, Petit P, Bartoli J, et al. Postoperative follow-up of juvenile nasopharyngeal angiofibromas: assessment by CT scan and MR imaging. *Eur Radial* 1998;8(5):756-764.

2 Dare AO, Gibbons KJ, Proulx GM, Fenstermaker RA. Resection followed by radiosurgery for advanced juvenile nasopharyngeal angiofibroma: report of two cases. *Neurosurgery* 2003;52(5):1207-1211.

3 Eich GF, Hoeffel JC, Tschappeler H, Gassner I, Willi UV. Fibrous tumours in children: imaging features of a heterogeneous group of disorders. *Pediatr Radial* 1998;28:500-509.

4 El-Banhawy OA, El-Dien A, El-Hafiz S, Am T. Endoscopic-assisted midfacial degloving approach for type III juvenile angiofibroma. *Int J Pediatr Otorhinolaryngol* 2004:68:21-28.

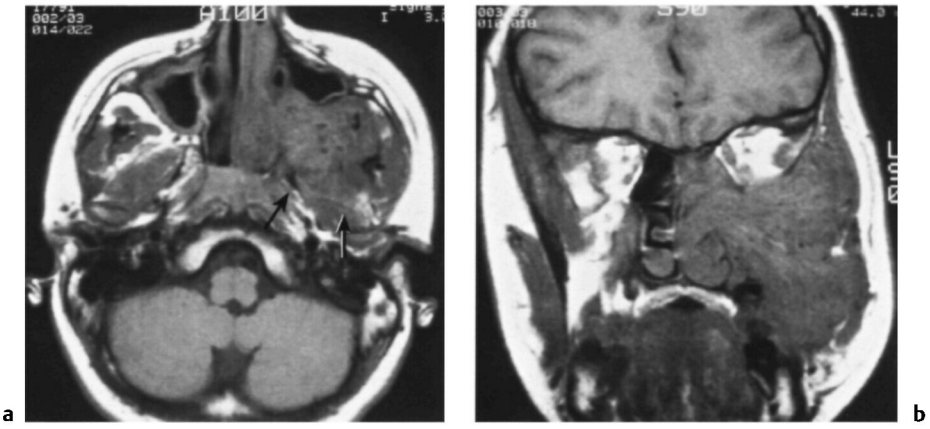

a b

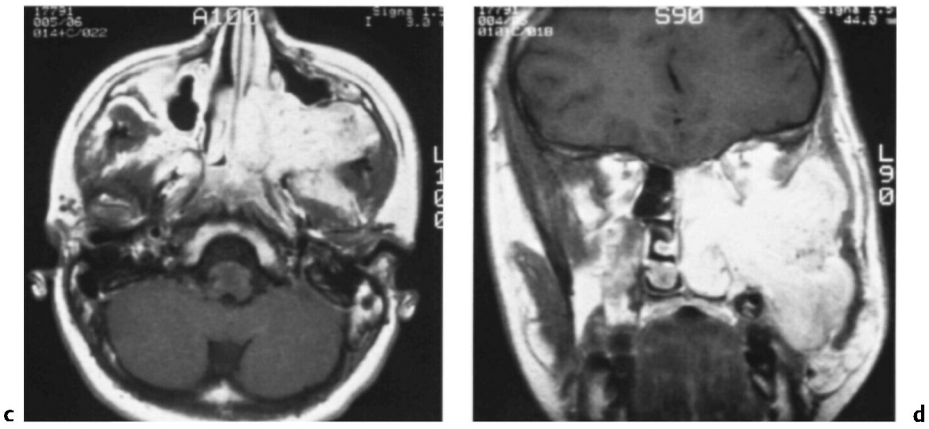

c d

Figure **15a-d** A 15-year-old male with an angiofibroma involving the left nasal cavity, left sphenopalatine foramen, and left pterygomaxillary fissure associated with bone remodeling and erosion at the orbit and maxillary sinus. The lesion has intermediate signal on axial (**a**) and coronal (**b**) T1WI, and contains several flow voids. The lesion shows prominent Gd-contrast enhancement on axial (**c**) and coronal (**d**) T1WI.

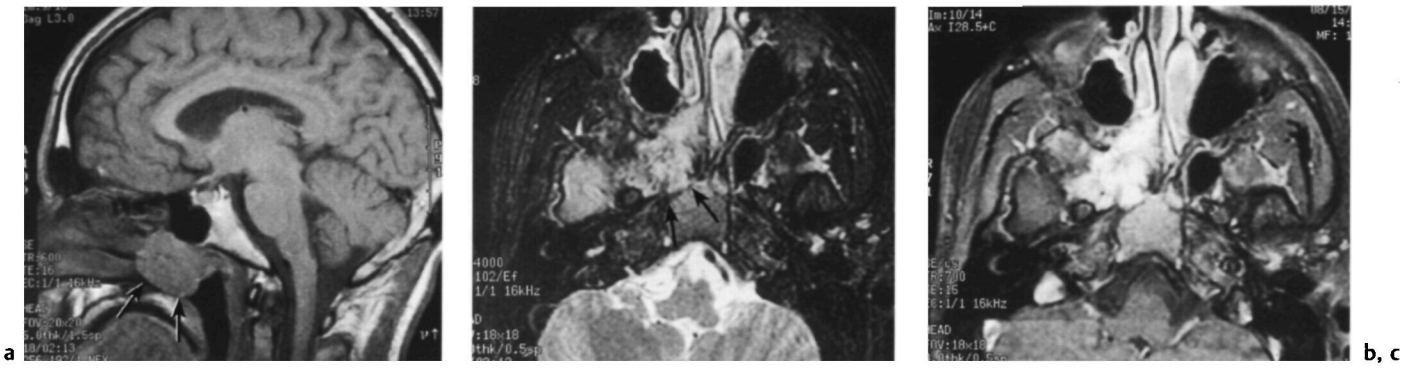

a b, c

Figure **16a-c** An 18-year-old man with angiofibroma involving the right nasal cavity, right sphenopalatine foramen, and right pterygomaxillary fissure with bone erosion and remodeling of the dorsal portion of the right maxillary sinus. The lesion has intermediate signal on sagittal FST2WI (**a**), check edited text.and predominantly high signal with small foci of low signal on axial FST2WI (**b**). The lesion shows prominent Gd-contrast enhancement on axial FST1WI (**c**).

5 Jones BV, Koch BL. Magnetic resonance imaging of the pediatric head and neck. *Top Magn Reson Imaging* 1999;10(6):348-361.

6 Laine FJ, Nadel L, Braun IF. CT and MR imaging of the central skull base. Part 2. Pathologic spectrum. *Radiographics* 1990;10(5): 797-821.

7 Lloyd G, Howard D, Lund VJ, Savy L Imaging for juvenile angiofibroma. *J Laryngol Otol* 2000;114(9):727-730.

8 Lloyd G, Howard D, Phelps P, Cheesman A. Juvenile angiofibroma: the lessons of 20 years of modern imaging. *J Laryngol Otol* 1999; 113(2): 127-134.

9 Nicolai P, Berlucchi M, Tomenzoli D, et al. Endoscopic surgery for juvenile angiofibroma: when and how. *Laryngoscope* 2003;113(5): 775-782.

10 Onerci TM, Yucel OT, 09retmenofllu 0. Endoscopic surgery in treatment of juvenile nasopharyngeal angiofibroma. *IntJ Pediatr Otorhinolaryngol* 2003;67:1219-1225.

11 Paris J, Guelfucci B, Moulin G, Zanaret M, Triglia JM. Diagnosis and treatment of juvenile nasopharyngeal angiofibroma. *Eur Arch Oto*-r/imofaryngo(2001;258(3):l20-l24.

12 Reddy KA, Mendenhall WM, Amdur RJ, Stringer SP, Cassisi NJ. Long-term results of radiation therapy for juvenile nasopharyngeal angiofibroma. *AmJOtolaryngol* 2001 ;22(3):172-175.

13 Schick B, Kahle G. Radiological findings in angiofibroma. *Acta Radial* 2000;41(6):585-593.

14 Seo CS, Han MH, Chang KH, Yeon KM. Angiofibroma confined to the pterygoid muscle region: CT and MR demonstration. *AJNR Am J Neuroradiol* 1996;17:374-376.

15 Tewflk TL, Tan AK, al Noury K, et al. Juvenile nasopharyngeal angiofibroma. J Otolaryngol 1999;28(3):145-151.

A 5 Angiomatoid Fibrous Histiocytoma (Also Referred to as Angiomatoid Malignant Fibrous Histiocytoma)

ICD-O Code

8836/1

Definition

Angiomatoid fibrous histiocytoma (AFH) is considered to be a low-grade fibrohistiocytic neoplasm.[1-3,5]

Frequency of Occurrence

AFH accounts for 1.6% of primary, malignant soft tissue tumors.[7]

Age at Presentation

From 2 to 71 years, mean = 20 years.[2,3]

Gender Ratio (M / F)

1/1.3[3]

Location

Lesions occur in the upper extremity > lower extremity > trunk > hand and wrist > proximal limb girdle > hip and buttocks > head and neck.[3,6,7] Lesions are often located in the deep dermis and subcutis.[2,4,6]

Signs and Symptoms

AFH often presents as painless slow-growing masses in the superficial soft tissues.[2,6] Rarely, systemic signs of anemia, weight loss, and fever may occur from tumor production of cytokines.[2]

Cross Pathologic Findings

AFH ranges from less than 1cm to 12cm, median = 2 cm.[2,3] Lesions can be firm, tan-gray, and multinodular with circumscribed margins.[2] Blood-filled cystic spaces are often present within these neoplasms.[2]

Histopathologic Findings

AFH typically contains nodules of spindle-shaped or epithelioid cells with ovoid vesicular nuclei associated with increased mitotic activity, as well as blood-filled cystic spaces that are not lined by endothelial cells (pseudoangiomatoid spaces). Lesions may have a thick, fibrous pseudocapsule and a pericapsular lymphoplasmacytic response.[2,3]

Tumor Genetics

A deletion involving chromosome 11 (q24) and rearrangements involving chromosomes 2,12,16, and 17 have been reported in a single case.[2] A gene fusion product (FUS/ATF1 protein) has

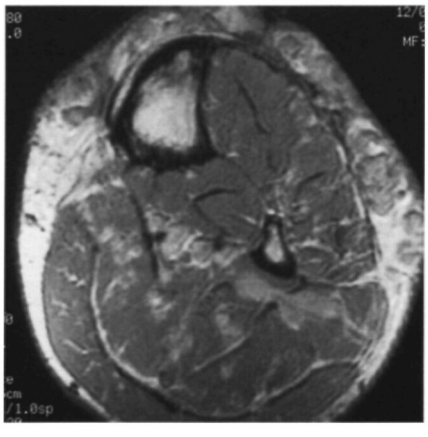

a

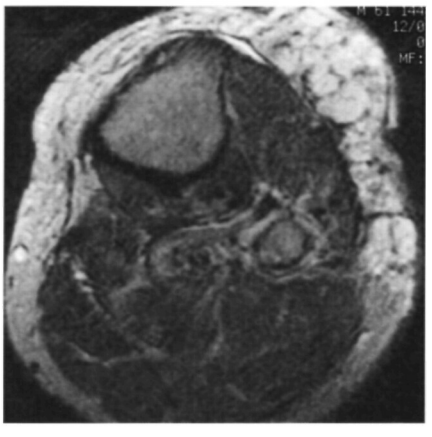

b, c

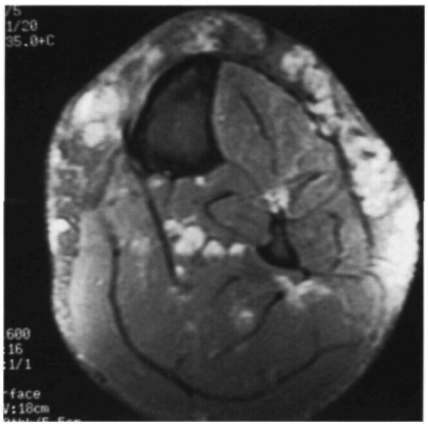

d

e

Figure **17a-e** A 61-year-old man with an angiomatoid fibrous histiocytoma in the subcutaneous fat of the leg. Axial PDWI (**a**) and T2WI (**b, c**) show multinodular lesions in the subcutaneous fat which have intermediate signal on PDWI, and heterogeneous high signal on T2WI. The multinodular lesions show prominent Cd-contrast enhancement on FST1WI (**d, e**).

been found resulting from translocation of the chromosome band 16pll (FUS gene) to chromosome band 12ql3 (ATF1 gene).[2]

MRI Findings

AFH can appear as multinodular lesions in the dermis or superficial soft tissues (Fig. 17). Lesions can have heterogeneous low-intermediate signal on T1WI and PDWI, and heterogeneous high signal on T2WI. Fluid-fluid levels may be seen secondary to hemorrhage. Thin septa with low signal on T2WI may be seen between the multiple nodular zones with high signal. After Gd-contrast administration, AFH can show prominent heterogeneous enhancement.

Differential Diagnosis

Malignant fibrous histiocytoma, myxoid liposarcoma, lymphangioma, hemangioma, hemangioendothelioma, angiosarcoma.

Prognosis and Treatment

Cases of AFH typically have a non-aggressive clinical course, unlike malignant fibrous histiocytomas.[2,3] AFH is treated by surgical excision with wide margins.[2] Local recurrence ranges from 2 to 11 % of cases.[2] Metastatic disease is uncommon, occurring in less than 1 %.[2]

References

1 Daw NC, Billups CA, Pappo AS, et al. Malignant fibrous histiocytoma and other fibrohistiocytic tumors in pediatric patients: the St Jude Children's research hospital experience. *Cancer* 2003;97:2839-2847

2 Fanburg-Smith JC, Cin PD. Angiomatoid fibrous histiocytoma. In: Fletcher COM, Unni KK, Mertens F, eds. *World Health Organization Classification of Tumours. Pathology and Genetics of Tumours of Soft Tissue and Bone* Geneva: IARC Press; 2002:194-195.

3 Fanburg-Smith JC, Miettinen M. Angiomatoid "malignant" fibrous histiocytoma: a clinicopathologic study of 158 cases and further exploration of the myoid type. *Hum Pathol* 1999;30:1336-1343.

4 Hasegawa T, Seki K, Ono K, Hirohashi S. Angiomatoid (malignant) fibrous histiocytoma: a peculiar low-grade tumor showing immunophenotypic heterogeneity and uitrastructural variations. *Pathol Int* 2000:50:731-738.

5 Lagace R, Aurias A. Does malignant fibrous histiocytoma exist? *Ann Pathol* 2002:22:29-34.

6 Kransdorf MJ, Murphey MD. Malignant fibrous and fibrohistiocytic tumors. In: *Imaging of Soft Tissue Tumors* 2nd ed. Philadelphia, Pa: Lippincott, Williams & Wilkins; 2006:257-297.

7 Kransdorf MJ. Malignant soft-tissue tumors in a large referral population: distribution of diagnoses by age, sex, and location. *AJR Am J Roentgenol* 1995:164:129-134.

A6 Angiosarcoma (Also Referred to as Malignant Hemangioendothelioma, High-Grade Hemangioendothelioma, Hemangiosarcoma, Angioendothelioma, Angiofibrosarcoma, and Hemangioendotheliosarcoma)

ICD-OCode

9120/3

Definition

Angiosarcomas are primary malignant tumors composed of neoplastic blood vessels in bone and/or soft tissues.[1,4-7,10,11,14,15,17,18] These tumors can be associated with Paget disease, radiation treatment, bone infarcts, knee and hip prostheses, synthetic vessel grafts, prior trauma or surgery, osteomyelitis, and hereditary disorders (neurofibromatosis type 1, Maffucci disease, achondroplasia).

Frequency of Occurrence

Angiosarcomas represent less than 1 % of malignant bone tumors,[7,12,13,16,17] and account for 2 % of malignant soft tissue tumors.[8,9]

Age at Presentation

Bone: from 10 to 82 years, median = 47 years.[12-14,16]

Soft tissue lesions: from 5 to 97years, mean = 49 years.[8,9,11]

Gender Ratio (M / F)

Bone: 1.4/1 to 2 /1.[3,7,14,17]

Soft tissue lesions: 1.1 /1 to 1.7 /1.[9,11]

Location

Bone. Common locations include: vertebrae, pelvic bones, tibia, humerus, femur, skull, and others.[14-16] Tumors are multifocal in 20-30 % of cases.[15,16] In tubular bones, tumors are often diaphyseal or metadiaphyseal, and rarely are epiphyseal alone.[14]

Soft tissue. Angiosarcomas of soft tissue occur most commonly in the skin, subcutaneous tissues, breast, liver spleen, and bone.[10,11] Such angiosarcomas occur less frequently in skeletal muscle, retroperitoneum, mesentery, and mediastinum.[10,11] Locations of these angiosarcomas have been reported in order of decreasing frequency as follows: head and neck, trunk, lower extremity, hip and buttocks, upper extremity, hand and wrist, foot and ankle, retroperitoneum.[8,9]

Signs and Symptoms

Bone lesions. Tumors can be associated with localized tenderness and dull pain, from several weeks' to several years' duration.

Soft tissue lesions. Tumors often present as enlarging painful mass-lesions of several weeks' duration, which may contain zones of hemorrhage, and may be associated with anemia or coagulopathy.[10,11,18]

Cross Pathologic Findings

Angiosarcomas are soft, bloody, fleshy and spongy tumors in bone cortex, medulla, and/or soft tissues.[6,7,11]

Histopathologic Findings[1-7,11,15,17,18]

Tumors contain neoplastic cells with varying atypia lining vascular spaces and channels. Endothelial cells are often pleomorphic with hyperchromatic nuclei and prominent nucleoli. Undifferentiated zones containing spindle and/or epithelioid cells may be present. Angiosarcomas are often immunoreactive to von Willebrand factor, CD 31, CD 34, vimentin, and Ulex Europaeus.[11,15,18]

Tumor Genetics

Angiosarcomas in soft tissues typically show various complex cytogenetic aberrations.[18] Of the various chromosomal rearrangements that have been reported, the most frequent involve gains of 5 pter-pll, 8 p!2-qter, and 20 pter-q!2; losses involving 4 p, 7 pl5-pter, and Y, as well as 22 q abnormalities.[18] KRAS 2 and TP53 mutation have been reported for angiosarcomas that result from exposure to vinyl chloride and thorium dioxide.[18] Translocations involving chromosomes 1 and 3 have been reported for epithelioid hemangioendotheliomas of bone.[15]

Findings on Plain Films (Roentgenograms) and Computed Tomography

Bone.[1-3,6,14,15] Tumors are typically osteolytic lesions. Zones of sclerosis and reactive bone formation occur in 10 %.[14] Broad, poorly-defined zones of transition and presence of an extraosseous soft tissue tumor are features commonly seen with higher grades of malignancy. Multifocal lesions in adjacent bones may occur. Angiosarcomas may be associated with bone infarcts.[1]

Soft tissue. Tumors can have low-intermediate attenuation on CD

MRI Findings

Bone. Tumors have low-intermediate signal on T1WI, and mixed low, intermediate, and/or high signal on T2W1.[2,15] Tumors can show prominent Gd-contrast enhancement.[2]

Soft tissue. Tumors have low-intermediate signal on TlWl, and mixed low, intermediate, and/or high signal on T2WI[10] (Fig. **18).** Tumors can show prominent Gd-contrast enhancement in a homogeneous or heterogeneous pattern.[10]

Differential Diagnosis

Bone. Metastases, myeloma/plasmacytoma, lymphoma, eosinophilic granuloma, osteomyelitis, Kaposi sarcoma, cystic angiomatosis, fibrosarcoma, aneurysmal bone cyst.

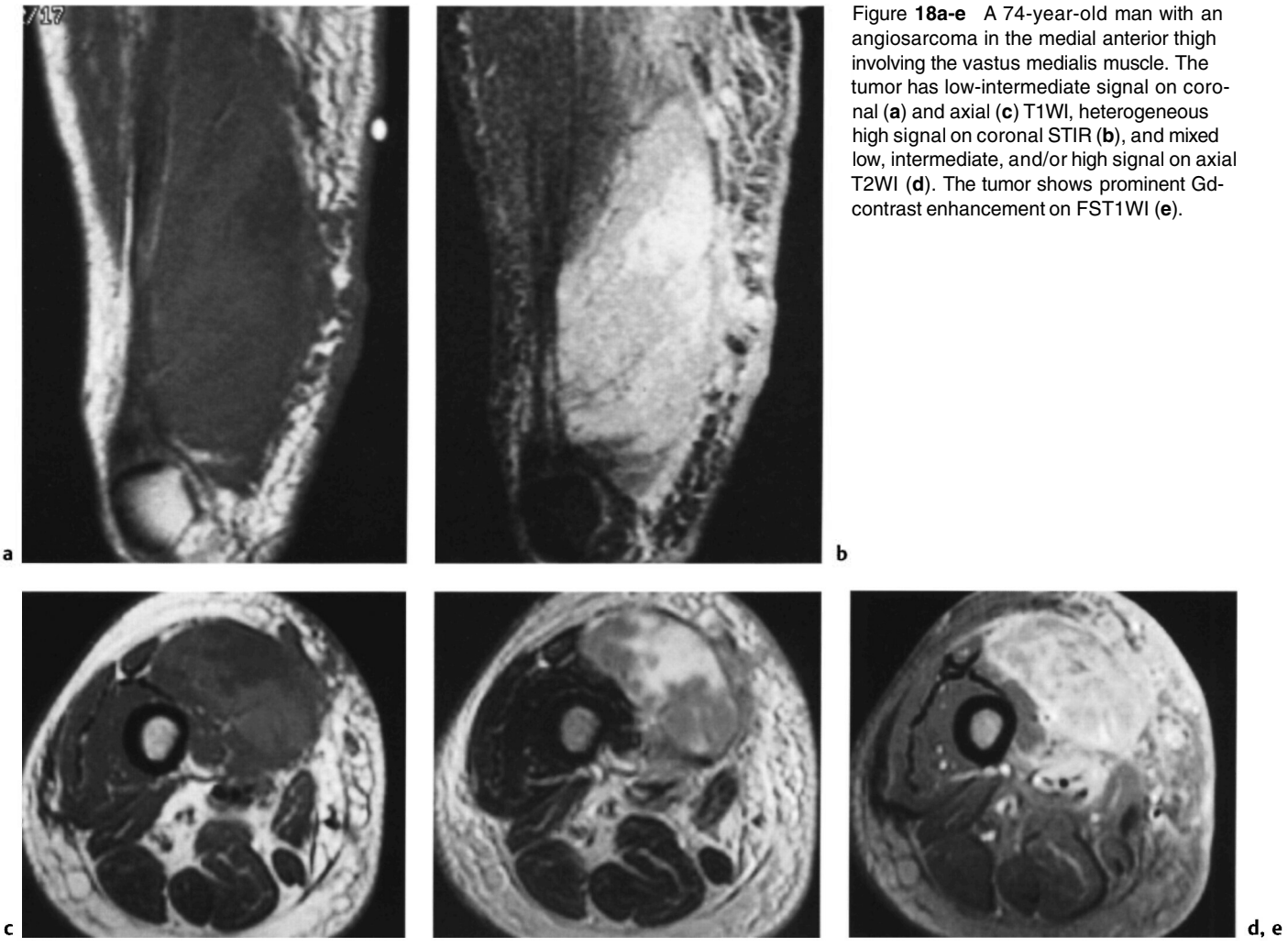

Figure **18a-e** A 74-year-old man with an angiosarcoma in the medial anterior thigh involving the vastus medialis muscle. The tumor has low-intermediate signal on coronal (**a**) and axial (**c**) T1WI, heterogeneous high signal on coronal STIR (**b**), and mixed low, intermediate, and/or high signal on axial T2WI (**d**). The tumor shows prominent Gd-contrast enhancement on FST1WI (**e**).

Soft tissue. Liposarcoma, dermatofibrosarcoma, malignant peripheral nerve sheath tumor, malignant fibrous histiocytoma, synovial sarcoma, melanoma, leiomyosarcoma, lymphoma, metastatic disease, sarcoid, granular cell tumor.

Prognosis and Treatment

Angiosarcomas in bone. Prognosis depends on histologic grade of angiosarcomas.[7,15] High-grade lesions typically have a poor prognosis.[7] Metastases occur in the skeleton, pleura, lung, and lymphatics.[6,7] Treatment is typically surgery with adjuvant chemotherapy.[6,7] Angiosarcomas are moderately responsive to radiation treatment.[6,7] The overall survival rate has been reported to be ~ 20 % for high-grade lesions.[6] Multifocal tumors can have a higher survival rate.[15]

Angiosarcomas in soft tissue. Angiosarcomas in soft tissue are very aggressive tumors that are locally invasive and can result in metastatic disease to the lungs, lymph nodes, bone, and soft tissues.[10,11,18] Poor prognosis is associated with older patient ages, larger tumor size, retroperitoneal tumor location, and/or high Ki67 values.[11,18] Tumors are treated with surgery, and up to 20 % have local recurrence.[10,18]

References

1 Abdelwahab IF, Klein MJ, Hermann G, Springfield D. Angiosarcomas associated with bone infarcts. *Skeletal Radiol* 1998;27:546-551.

2 Bourekas EC, Cohen ML, Kamen CS, Tarr RW, Lanzieri CF, Lewin JS. Malignant hemangioendothelioma (angiosarcoma) of the skull: plain film, CT, and MR appearance. *AJNR Am J Neuroradiol* 1996; 17: 1946-1948.

3 Conway WF, Hayes CW. Miscellaneous lesion of bone. *Radial Clin North Am* 1993;31(2):339-358.

4 Darby AJ. Vascular neoplasms of bone. In: Helliwell TR, ed. *Major Problems in Pathology: Pathology of Bone and Joint Neoplasms* 1st ed. Philadelphia, Pa: W.B. Saunders; 1999:37:337.

5 Das Gupta TK, Chaudhuri PK. Tumors of vascular and perivascular tissue. In: Das Gupta TK, Chaudhuri PK, eds. *Tumors of the Soft Tissues.* 2nd ed. Stamford, Conn.: Appleton & Lange; 1998:420-425.

6 Forest M. Vascular tumors. In: Forest M, Tomeno B, Vanel D, eds. *Orthopedic Surgical Pathology: Diagnosis of Tumors and Pseudotumoral Lesions of Bone and Joints.* Edinburgh: Churchill Livingstone; 1998:345-362.

7 Huvos AG. Angiosarcoma of Bone (Epithelioid Hemangioendothelioma; Malignant Hemangioendothelioma). In: Huvos AG, ed. *Bone Tumors: Diagnosis, Treatment, and Prognosis* 2nd ed. Philadelphia, Pa: WB Saunders; 1991:579-594.

8 Kransdorf MJ, Murphey MD. Soft tissue tumors in a large referral population: prevalence and distribution of diagnoses by age, sex, and location. In: *Imaging of Soft Tissue Tumors* 2nd ed. Philadelphia, Pa: WB Saunders; 2006:6-37.

9 Kransdorf MJ. Malignant soft-tissue tumors in a large referral population: distribution of diagnoses by age, sex, and location. *AJR Am] Roentgenol* 1995:164:129-134.

10 Kransdorf MJ, Murphey MD. Vascular and Lymphatic Tumors. In: *Imaging of Soft Tissue Tumors* 2nd ed. Philadelphia, Pa: Lippincott, Williams & Wilkins; 2006:150-188.
11 Meis-Kindblom JM, Kindblom LG. Angiosarcoma of soft tissue: a study of 80 cases. *Am J Surg Pathol* 1998;22(6):683-697.
12 Mulder JD, Schutte HE, Kroon HM, Taconis WK. Introduction. In: *Radiologic Atlas of Bone Tumors* Amsterdam: Elsevier; 1993:3-6.
13 Mulder JD, Schutte HE, Kroon HM, Taconis WK. The diagnosis of bone tumors. In: *Radiologic Atlas of Bone Tumors* Amsterdam: Elsevier; 1993:9-46.
14 Mulder JD, Schutte HE, Kroon HM, Taconis WK. Hemangio-endothelioma and Hemangio-endotheliosarcoma. In: *Radiologic Atlas of Bone* Tumors Amsterdam: Elsevier; 1993:241-248.
15 Roessner A, Boehling T. Angiosarcoma. In: Fletcher COM, Unni KK, Mertens F, eds. *World Health Organization Classification of Tumours. Pathology and Genetics of Tumours of Soft Tissue and Bone* Geneva: IARC Press; 2002:322-323.
16 Unni KK. Introduction and scope of study. In: *Dahlin's Bone Tumors: General Aspects and Data on 11087 Cases* 5th ed. Philadelphia, Pa: Lippincott, Williams & Wilkins; 1996:1-9.
17 Unni KK. Hemangioendothelioma (Hemangiosarcoma) and Hemangiopericytoma. In: *Dahlin's Bone Tumors: General Aspects and Data on 11087 Cases* 5th ed. Philadelphia, Pa: Lippincott, Wiliams & Wilkins; 1996:317-331.
18 Weiss SW, Lasota J, Miettinen MM. Angiosarcoma of soft tissue. In: Fletcher CDM, Unni KK, Mertens F, eds. *World Health Organization Classification of Tumours. Pathology and genetics of tumours of soft tissue and bone* Geneva: IARC Press; 2002:175-177.

A 7 Chondroblastoma

ICD-O Code

9230/0

Definition

Chondroblastomas are benign cartilaginous tumors with chondroblast-like cells and areas of chondroid matrix formation usually involving the epiphysis.[2,4,5,9,12,16,19] Chondroblastomas usually present before cessation of endochondral bone growth.[2,4,5,9,12,16,19]

Frequency of Occurrence

From 5 to 9 % of benign bone lesions, 1 -3 % of all bone lesions.[5,9,14-16,18,19]

Age at Presentation[4,5,9,14-16,18,19]

From 3 to 73 years, median = 17 years; mean = 16 years for lesions in long bones; mean = 28 years in other bones. Most cases are diagnosed between the ages of 5 and 25 years.[8,9] Chondroblastomas are rare in children below 10 years old and adults older than 60 years.[4]

Gender Ratio (M IF)

1.5 to2/l.[5,14-16,19,21]

Location[5,6,16,19]

Lesions are located in the epiphyseal regions of long bones (40%), or involve both the epiphyseal and adjacent metaphyseal regions (60%). More than 70% occur in long bones but may also occur in apophyses (such as greater trochanter, etc.) Most lesions are mono-ostotic. Proximal humerus > proximal and distal femur > proximal tibia > talus >calcaneus > bony pelvis > ribs > vertebrae > skull. Chondroblastomas rarely occur in the spine and craniofacial bones.[1,6] Spinal tumors most often involve the thoracic vertebrae and usually involve both the body and pedicles.[6]

Signs and Symptoms[1,2,4-6,9-11,16,19,21]

Tumors can be associated with swelling and pain in the region of the lesion for several months to years in duration. Pathologic fractures are uncommon. Spinal tumors can be associated with spinal cord compression.[6]

Cross Pathologic Findings[2,4,5,9,11,16,19,21]

Chondroblastomas are relatively small, well-demarcated neoplasms ranging in size from 1 to 7 cm. Chondroblastomas are mottled gritty and/or soft lesions that range from gray-yellow to gray-brown. Lesion can contain calcifications, areas of hemorrhage and/or cystic changes. Chondroblastomas can be associated with aneurysmal bone cysts in 10-40% of cases.

Histopathologic Findings[2,4,5,7-11,16,19,21]

Chondroblastomas are composed of nearly uniform oval or polyhedral cells with oval grooved nuclei and small volumes of pink cytoplasm separated by scant interstitial matrix. Pericellular fine calcifications are often seen in a "chicken wire" or "lattice-like" pattern. In most cases, normal mitotic activity is observed. Most chondroblastomas show chondroid differentiation ranging from multiple small foci to extensively distributed. Areas of necrosis and hemorrhage may be present surrounded by multinucleated giant cells. Vascular invasion is rare. Cystic regions and secondary aneurysmal bone cysts may represent small or large proportions of the entire lesions. Lesions are often immunoreactively positive for S-100 protein (expressed by chondrocytes and chondroblasts), vimentin, and fibronectin; and occasionally positive for cytokeratin, actin, and epithelial membrane protein.

Tumor Genetics

Most chondroblastomas are diploid tumors with low proliferative fractions.[9] Structural anomalies involving chromosomes 5 and 8 have been reported.[2,9] Structural abnormalities involving 11 p!5, similar to giant cell tumors, have also been reported.[2] Aggressive chondroblastomas are associated with unbalanced translocations involving chromosomes 2, 5, 8, and 21; and rearrangements involving chromosome band 8 q21.[2,9]

Findings on Plain Films (Roentgenograms) and Computed Tomography[1-11,13,16,17,19]

Chondroblastomas are geographic lytic lesions that often involve the epiphysis with or without metaphyseal involvement (Figs. **19-22,24**). Tumors are often eccentric, ranging from 1 to 7cm in diameter. Lesions may have thin sclerotic margins, cortical bone expansion, endosteal expansion, and/or periosteal reaction. Matrix mineralization (punctate, ring-like, or arc-like) may be seen in 25 to 33 % of cases on plain films.[2,21] A higher percentage of mineralization can be seen with CT.[2] Chondroblastomas can also occur in apophyses.

Findings on Radionuclide Bone Scans[3]

Lesions usually are associated with increased radiopharmaceutical accumulation.

MRI Findings[1,6-8,10,13,16,17,20]

Chondroblastomas often have fine lobular margins, and typically have low-intermediate heterogeneous signal on T1WI, and mixed low, intermediate, and/or high signal on T2WI (Figs. 19-25). Areas of low signal on T2WI are secondary to chondroid matrix mineralization, and/or hemosiderin (Figs. **22, 23, 25**). Lobular, marginal or septal Gd-contrast enhancement patterns can be seen. Tumors may have thin margins of low signal on T2WI representing sclerotic borders. Cortical destruction is uncommon. Perilesional zones with high signal on T2WI and Gd-contrast enhancement are commonly seen in bone marrow as well as periosteal locations, indicating reactive hyperemia and/or edema[21] (Figs. **20-25**). These perilesional MRI

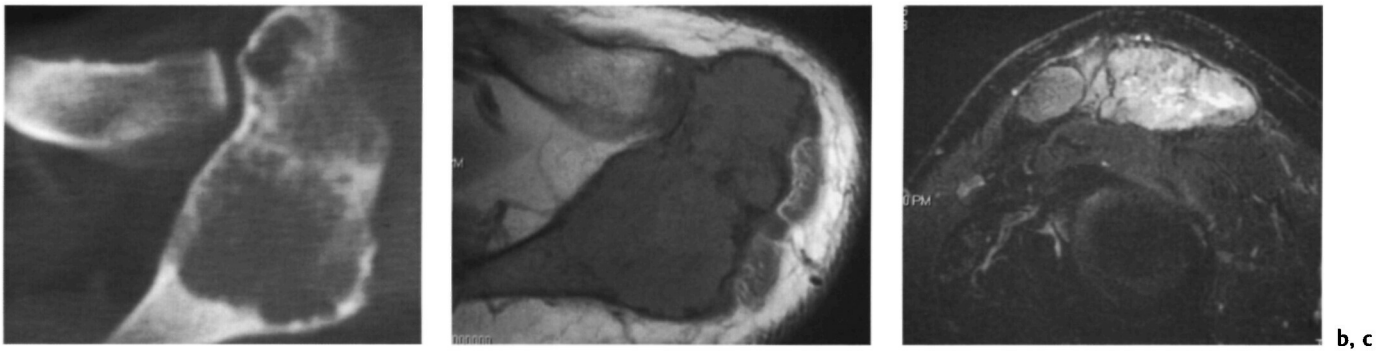

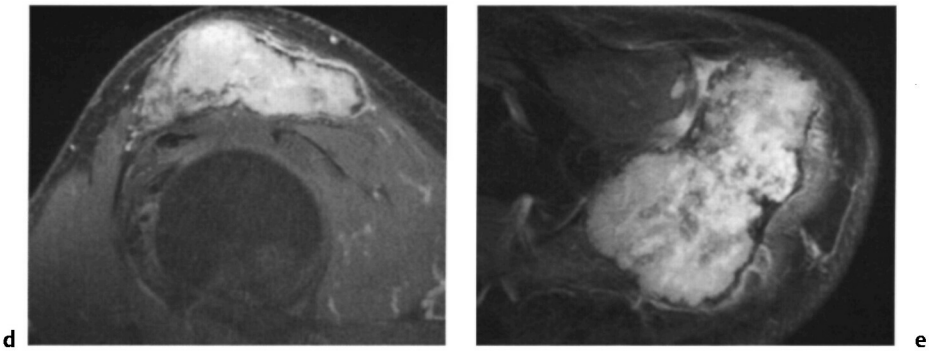

Figure **19a-e** A 50-year-old man with chondroblastoma in the acromion. Axial CT shows a radiolucent expansile lesion in the acromion (**a**). The lesion has fine lobular margins, and low-intermediate heterogeneous signal on axial T1WI (**b**), and mixed low, intermediate, and high signal on sagittal FST2WI (**c**). The lesion shows prominent Gd-contrast enhancement on sagittal (**d**) and axial (**e**) FST1WI.

Figure **20a-d** A 15-year-old male with chondroblastoma involving the physeal plate, epiphysis, and metaphysis of the proximal humerus. Axial CT shows a radiolucent lesion in the humerus (**a**). The lesion has low-intermediate signal on coronal T1WI (**b**), and mixed intermediate and high signal on coronal T2WI (**c**), and is surrounded by high signal on T2WI in the adjacent marrow. The lesion shows moderate Gd-contrast enhancement on coronal FST1WI (**d**), as well as prominent enhancement in the adjacent marrow.

findings have been shown to be correlated with inflammatory reaction associated with elevated tumor prostaglandin levels.[22] Aneurysmal bone cysts can be seen associated with chondroblastomas (Figs. **23, 24**). In spinal tumors, bone expansion can result in spinal cord compression.[6]

Differential Diagnosis

Giant cell tumor, clear cell chondrosarcoma, enchondroma, aneurysmal bone cyst, chondromyxoid fibroma, enchondroma, eosinophilic granuloma, degenerative or post-traumatic cyst/intra-osseous ganglion, ischemic necrosis.

Treatment and Prognosis[2,4,5,9,11,16,19,21]

Standard treatment is curettage with or without bone grafts, which produces successful results in 80-90% of patients.[9,21] Local recurrence typically ranges from 5 to 38 % of cases, and usually occurs within 2 years. Because of difficulty in complete surgical resection, chondroblastomas may recur in up to 50 % of patients.[9] Recurrences can be treated with repeat curettage or resection. Although chondroblastomas are sensitive to radiation, this type of treatment is not used because of the risk of malignant transformation into sarcoma. Rare metastases have been reported to the lungs.[9]

a

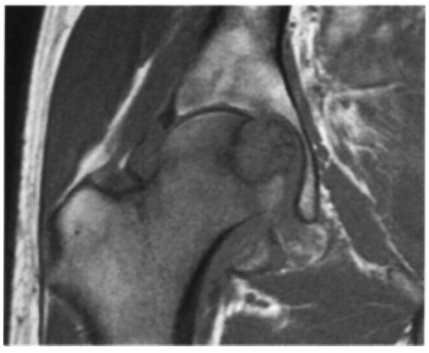

b

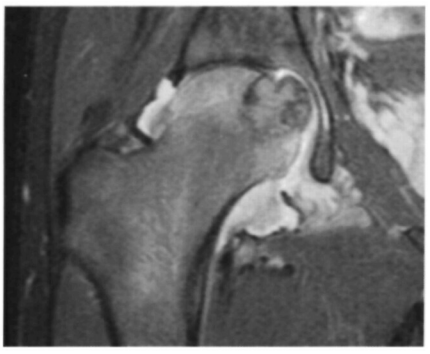

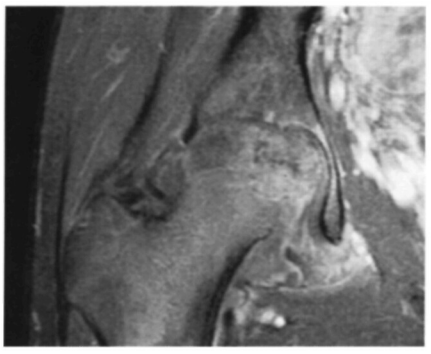

c, d

Figure **21 a-d** A 17-year-old male with chondroblastoma in the proximal femur. AP radiograph (**a**) shows a geographic radiolucent lesion in the epiphysis medially. With MRI, the lesion is located mostly in the epiphysis, but also involves the physeal plate and a small portion of the metaphysis. The lesion has expanded and thinned the medial margin of the femoral head. The lesion has slightly lobulated margins, and has low-intermediate signal on coronal T1WI (**b**), and slightly high signal on coronal FST2WI (**c**), as well as in the adjacent marrow. The lesion shows moderate heterogeneous Cd-contrast enhancement on coronal FST1WI (**d**), as well as prominent enhancement in the adjacent marrow.

a

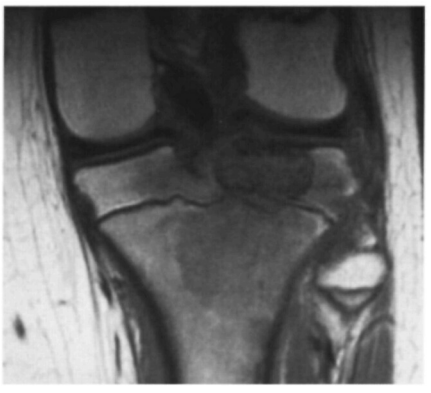

b, c

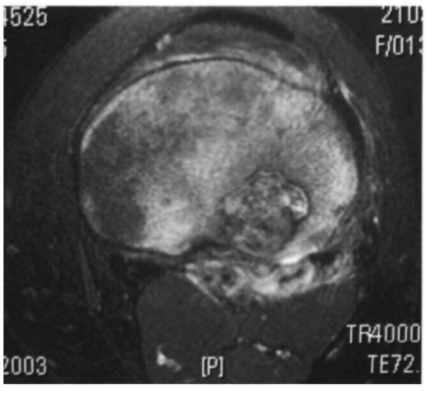

d

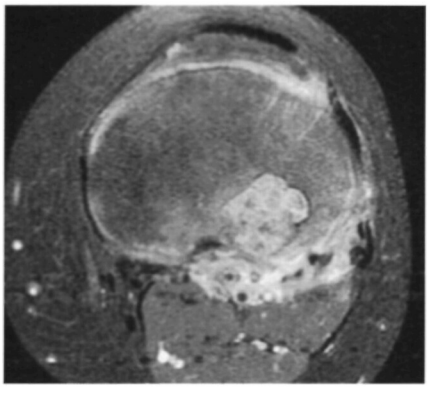

e

Figure **22a-e** A 13-year-old female with chondroblastoma in the tibia. The lesion has slightly lobulated margins and is located at the physeal plate with extension into both the epiphysis and metaphysis. AP radiograph (**a**) shows a slightly radiolucent zone in the epiphysis with thin sclerotic margins. The lesion has low-intermediate signal on coronal (**b**) T1 WI, and high and low signal on coronal (**c**) and axial (**d**) FST2WI, as well as in the adjacent marrow. The lesion shows zones of prominent Gd-contrast enhancement on axial (**e**) FST1WI, as well as mild enhancement in the adjacent marrow.

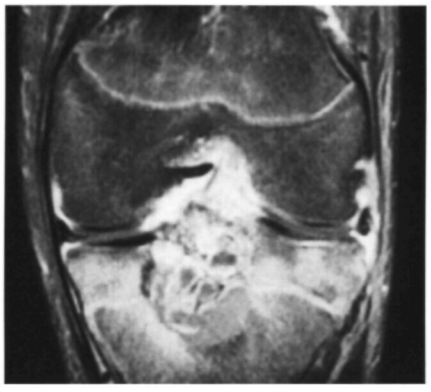

a b

Figure **23a, b** A 17-year-old male with chondroblastoma in the tibia with a secondary aneurysmal bone cyst. The lesion has slightly lobulated margins and is located at the physeal plate with extension into both the epiphysis and metaphysis. The lesion has mixed low, intermediate, and high signal on sagittal T2WI (**a**). Multiple lobules with high signal on T2WI are seen in both the metaphyseal and epiphyseal regions of the lesion, representing a secondary aneurysmal bone cyst. The lesion shows lobular and septal zones of prominent Cd-contrast enhancement on coronal FST1 WI (**b**), as well as in the adjacent marrow.

a

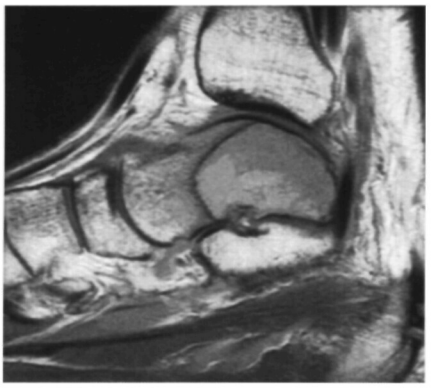

b, c

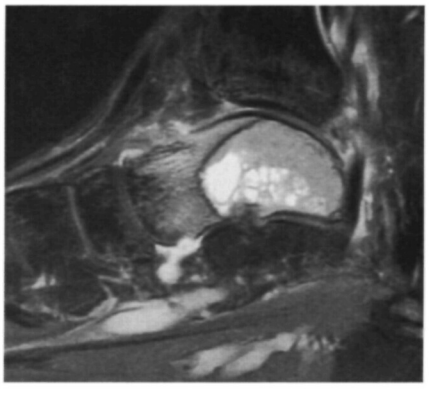

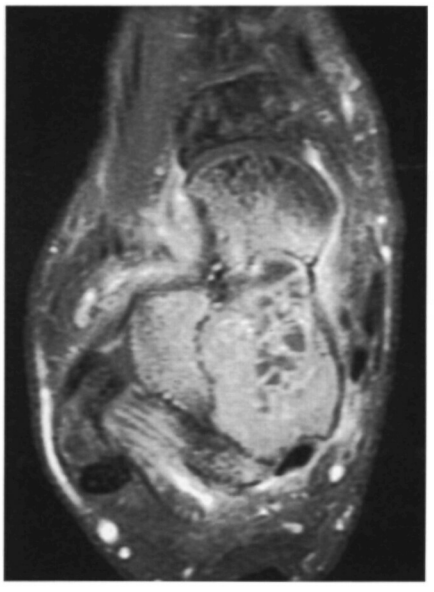

d e,f

Figure **24a-f** A 20-year-old man with chondroblastoma in the talus with a secondary aneurysmal bone cyst. Lateral (**a**) and AP (**b**) radiographs shows a radiolucent zone in the thin sclerotic margins in the talus. The lesion has a thin peripheral zone of low signal on sagittal (**c**) PDWI, and sagittal (**d**) and axial (**e**) FST2WI. The lesion has low-intermediate signal on PDWI (**c**), and zones of both intermediate and high signal on FST2WI (**d, e**), as well as high signal in the adjacent marrow. Multiple locules of high signal on FS T2WI represent secondary aneurysmal bone cyst. The lesion shows zones of prominent Gd-contrast enhancement on axial FST1 WI (**f**), as well as in the adjacent marrow.

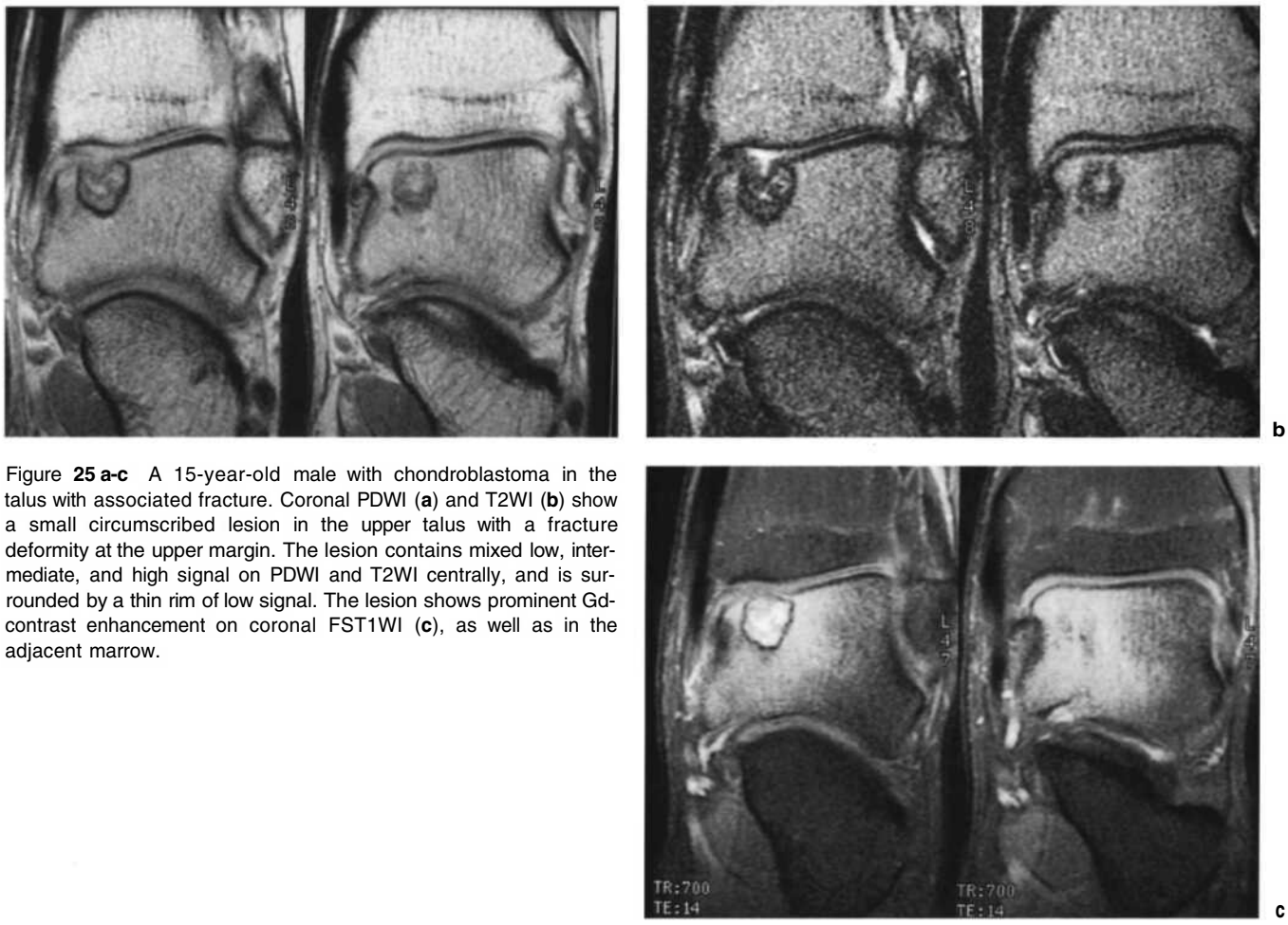

Figure **25 a-c** A 15-year-old male with chondroblastoma in the talus with associated fracture. Coronal PDWI (**a**) and T2WI (**b**) show a small circumscribed lesion in the upper talus with a fracture deformity at the upper margin. The lesion contains mixed low, intermediate, and high signal on PDWI and T2WI centrally, and is surrounded by a thin rim of low signal. The lesion shows prominent Gd-contrast enhancement on coronal FST1WI (**c**), as well as in the adjacent marrow.

References

1 Flowers CH, Rodriguez J, Naseem M, Reyes MM, Verano AS. MR of benign chondroblastoma of the temporal bone. *AJNR Am] Neuroradiol* 1995;16:414-416.

2 Forest M. Chondroblastoma. In: Forest M, Tomeno B, Vanel D, eds. *Orthopedic Surgical Pathology: Diagnosis of Tumors and Pseudotumoral Lesions of Bone and Joints* Edinburgh: Churchill Livingstone; 1998:207-218.

3 Giudici MA, Moser RP, Kransdorf MJ. Cartilaginous bone tumors. *Radiol Clin North Am* 1993;31(2):237-259.

4 Helliwell TR. Central cartilaginous neoplasms of bone. In: Helliwell TR, ed. *Major Problems in Pathology: Pathology of Bone and Joint Neoplasms.* Vol 37. 1st ed. Philadelphia, Pa: W.B. Saunders; 1999: 209-210.

5 Huvos AG. Chondroblastoma and clear-cell chondrosarcoma. In: Huvos AG, ed. Bone *Tumors: Diagnosis, Treatment, and Prognosis* 2nd ed. Philadelphia, Pa. W.B. Saunders; 1991:295-315.

6 Ilaslan H, Sundaram M, Unni KK. Vertebral chondroblastoma. *Skeletal Radiol* 2003;32:66-71.

7 Jee WH, Park YK, McCauley TR, et al. Chondroblastoma: MR characteristics with pathologic correlation. *J Comput Assist Tomogr* 1999; 23(5):721-726.

8 Kaim AH, Hügli R, Bonél HM, Jundt G. Chondroblastoma and clear-cell chondrosarcoma: radiological and MRI characteristics with histopathological correlation. *Skeletal Radiol* 2002;31:88-95.

9 Kilpatrick SE, Parisien M, Bridge JA. Chondroblastoma. In: Fletcher CDM, Unni KK, Mertens F, eds. *World Health Organization Classification of Tumours. Pathology and Genetics of Tumours of Soft Tissue and Bone* Geneva: IARC Press; 2002:241-242.

10 Ly JQ, LaGatta LM, Beall DP. Calcaneal chondroblastoma with secondary aneurysmal bone cyst. *A]R Am] Roentgenol* 2004;182:130.

11 Mangham DC. Giant cell tumor of bone and giant cell-containing lesions of bone. In: Helliwell TR, ed. *Major Problems in Pathology: Pathology of Bone and Joint Neoplasms.* Vol 37. 1st ed. Philadelphia, Pa: W.B. Saunders; 1999:37:315-319.

12 Meyer JS, Dormans JP. Differential diagnosis of pediatric musculoskeletal masses. *Magn Reson Imaging Clin N Am* 1998;6(3):561-577

13 Miller SL, Hoffer FA. Malignant and benign bone tumors. *Radiol Clin North Am* 2001;39(4):673-699.

14 Mulder JD, Schutte HE, Kroon HM, Taconis WK. Introduction. In: *Radiologic Atlas of Bone Tumors* Amsterdam: Elsevier; 1993:3-6.

15 Mulder JD, Schutte HE, Kroon HM, Taconis WK. The diagnosis of bone tumors. In: *Radiologic Atlas of Bone Tumors* Amsterdam: Elsevier; 1993:9-46.

16 Mulder JD, Schutte HE, Kroon HM, Taconis WK. Chondroblastoma. In: *Radiologic Atlas of Bone Tumors* Amsterdam: Elsevier; 1993: 461-473.

17 Muntané A, Vails C, de Miquel MA, Pons LC. Chondroblastoma of the temporal bone: CT and MR appearance. *AJNR Am J Neuroradiol* 1993;14:70-71.

18 Unni KK. Introduction and scope of study. In: *Dahlin's Bone Tumors: General Aspects and Data on 11 087 Cases* 5th ed. Philadelphia, Pa: Lippincott, Williams & Wilkins; 1996:1-9.

19 Unni KK. Benign chondroblastoma. In: *Dahlin's Bone Tumors: General Aspects and Data in 11 087 Cases* 5th ed. Lippincott, Williams & Wilkins;1996:47-57.

20 Weatherall PT, Maale GE, Mendelsohn DB, Sherry CS, Erdman WE, Pascoe HR. Chondroblastoma: classic and confusing appearance at MR imaging. *Radiology* 1994;190(2):467-474.

21 Wold LE, Adler CP, Sim FH, Unni KK. Chondroblastoma. In: *Atlas of Orthopedic Pathology.* 2nd ed. Philadelphia, Pa: W.B. Saunders; 2003: 232-237.

22 Yamamura S, Sato K, Sugiura H, et al. Prostaglandin levels of primary bone tumor tissues correlate with peritumoral edema demonstrated by magnetic resonance imaging. *Cancer* 1997;79:255-261.

A 8 Chondroma, Intramedullary Type: Enchondroma (Also Referred to as Intra-osseous Chondroma or Central Chondroma)

ICD-O code

9220/0

Definitions

Solitary enchondromas are benign lesions composed of hyaline cartilage located in the medullary portion of bones.[2,5,6,8,12,13,15]

Multiple enchondromatosis / Oilier disease.[2,5,6,8,9,12,13,15] Multiple enchondromatosis is a genetic cartilage dysplasia involving endochondral formed bone resulting in multiple enchondromas. Oilier disease results from anomalies of endochondral bone formation with enchondromas located predominantly, or only, in limbs on one side. Short and long tubular bones of the limbs are primarily affected.

Metachondromatosis is a rare disorder that includes the combination of enchondromatosis and osteochondromatosis.[2,5,6,8,12,13,15]

Maffucci syndrome refers to a very rare disease with simultaneous occurrence of multiple enchondromas and cutaneous or visceral hemangiomas of soft tissue.[2,5-9, 12,13,15]

Frequency of Occurrence

Chondromas represent 10-25 % of benign bone tumors.[5,6,8,10-12,14,15] Enchondromas are intramedullary chondromas, and represent ~24 to 40% of all chondromas; they can be solitary (88%) or multiple (12%). Oilier disease is a dyschondroplasia involving endochondrally formed bone resulting in multiple enchondromas (enchondromatosis). Metachondromatosis is a combination of enchondromatosis and osteochondromatosis, and is rare. Maffucci disease refers to a syndrome with multiple enchondromas and soft tissue hemangiomas, and is very rare.

Age at Presentation

Enchondroma: from 3 to 83 years, median = 35 years, mean = 38 40 years, peaks in 3rd and 4th decades[8,10-12,14,15]

Oilier disease: from 1 to 63 years, median = 12 years.[2,9,12]

Maffucci syndrome: occurs in children and adults.[7,8]

Gender Ratio (M / F)

Enchondroma: 0.8 / 1 to 1.1 / 1.[5,6,8,10-12,14,15]

Oilier disease: 1 / 1.[2,9]

Maffucci syndrome: 1 / 1.[2,7,9]

Location

Solitary enchondroma.[6,10-12] Locations include: phalanx (hands) (~30%)> femur > metacarpals > humerus > tibia > ribs > metatarsals > phalanx (feet) > fibula > ulna > other sites. Intra-osseous locations: diaphyseal (58%) > meta-diaphyseal (39%) > epiphyseal-equivalent zones (3%). Central (80%) > eccentric location within bone.

Multiple enchondromatosis / Oilier disease, Maffucci syndrome. Lesions are most frequently located in the small bones of the hands and feet.[7,9,12] In Oilier disease, lesions are usually located predominantly or only in limbs on one side.[9,12] In Maffucci syndrome, hemangiomas in the soft tissues may be near or distant from the enchondromas.[7,12]

Signs and Symptoms[2,5,6,12,13,15]

Solitary enchondromas are usually asymptomatic unless bone cortex is fractured or eroded causing focal pain (40%). Lesions in hands or feet are often associated with deformities and/or pathologic fractures.

Cross Pathologic Findings[2,5-8,12,15]

Enchondromas are typically lobulated or nodular, bluish-white, firm lesions with varying degrees of matrix mineralization causing gritty texture.

Histopathologic Findings[2,5-8,12,15]

Lesions contain varying-sized lobules of hyaline cartilage separated by normal marrow (fat and trabeculae) and fibrous strands. Cartilage cells are relatively few among the abundant intercellular matrix, which is comprised of varying proportions of hyaline chondroid and mucinous/myxoid components. Chondrocytes are relatively uniform in size with small, rounded nuclei in vacuolated cytoplasm. Mitotic figures are rare or absent. Varying degrees of matrix mineralization are usually seen. Lesions are immunoreactive to S-100 protein, and types I, II, and VI collagen.[2]

Lesion Genetics

These lesions have been reported to have diploid or near-diploid cells with structural abnormalities involving chromosomes 6 and 12.[8] Patients with Oilier disease have been reported to have mutations involving the PTHR1 gene which encodes a receptor for parathyroid hormone.[9] Maffucci syndrome is a nonhereditary mesodermal dysplasia.[7]

Findings on Plain Films (Roentgenograms) and Computed Tomography[2,4,5,9,12,13,15]

Enchondromas are usually well-circumscribed radiolucent lesions, often containing chondroid matrix mineralization (Figs. **26, 27, 30, 31, 33-35).** In small bones, cortex can be eroded and thinned on the endosteal side, with or without associated bone expansion. In large bones, expansion is minimal or not seen. CT is more sensitive than plain films in detecting subtle matrix mineralization and erosion of cortex (Fig. **33**). In patients with Maffucci syndrome, hemangiomas in the soft tissues may contain phleboliths.[7,12]

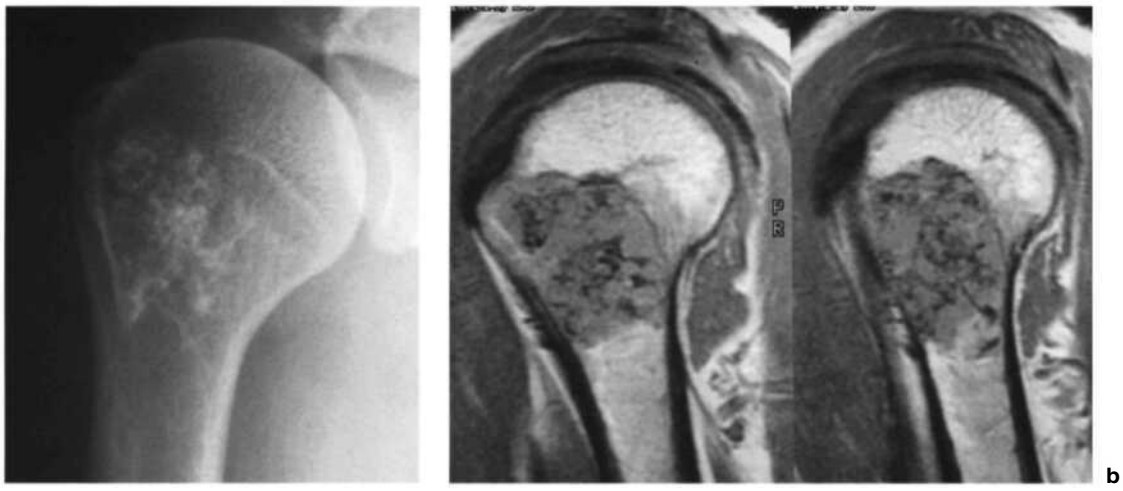

Figure **26 a-c** A 40-year-old woman with an enchondroma in the proximal humerus. AP radiograph (**a**) shows chondroid matrix mineralization in the lesion. The lesion has lobulated circumscribed margins and contains nodular zones with intermediate signal separated by thin curvilinear zones of low signal on sagittal PDWI (**b**). On sagittal FS T2WI (**c**), the lesion has predominantly high signal with foci and bands of low signal.

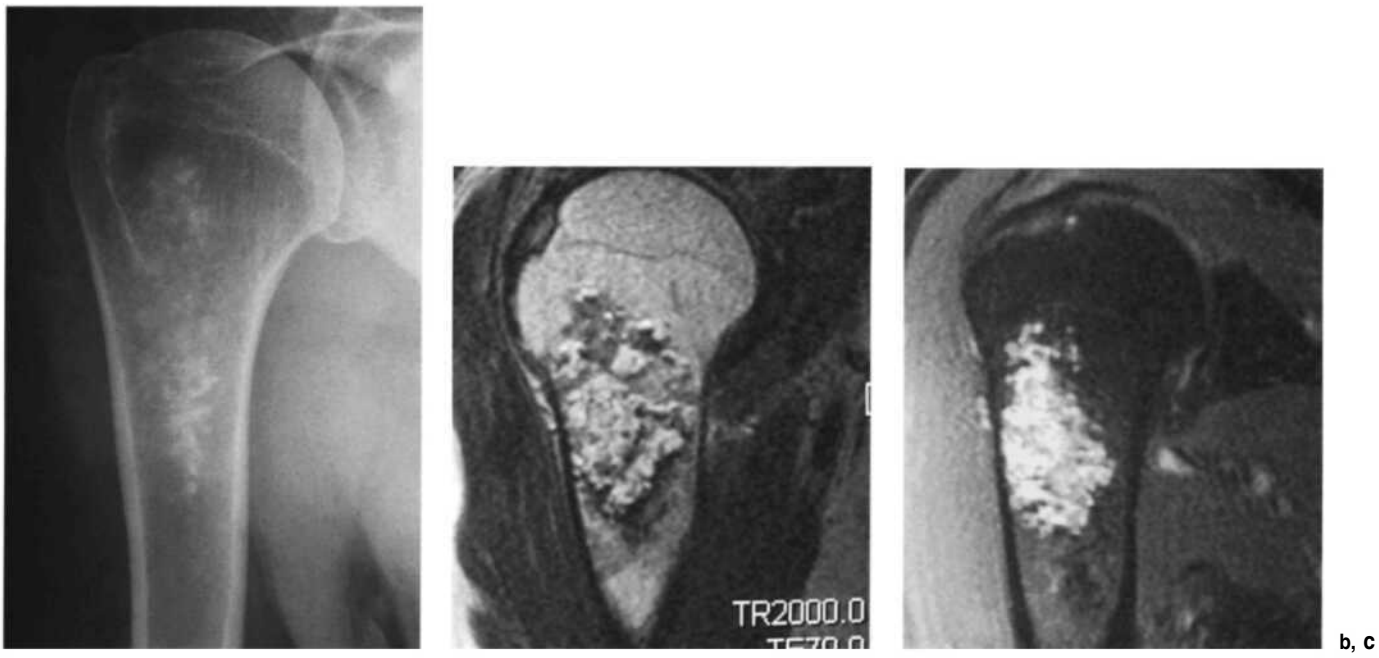

Figure **27 a-c** A 50-year-old man with an enchondroma in the proximal humerus. AP radiograph (**a**) shows chondroid matrix mineralization in the lesion. On coronal T2WI (**b**), the lesion has predominantly high signal with foci and bands of low signal. The lesion shows prominent Gd-contrast enhancement on FS T1WI (**c**).

a b

Figure **28 a, b** A 44-year-old woman with an enchondroma in the proximal humerus. The lesion has lobulated circumscribed margins and has high signal on coronal T2WI (**a**) surrounded by a thin rim of low signal. The lesion shows thin lobulated peripheral Gd-contrast enhancement on coronal FS T1WI (**b**).

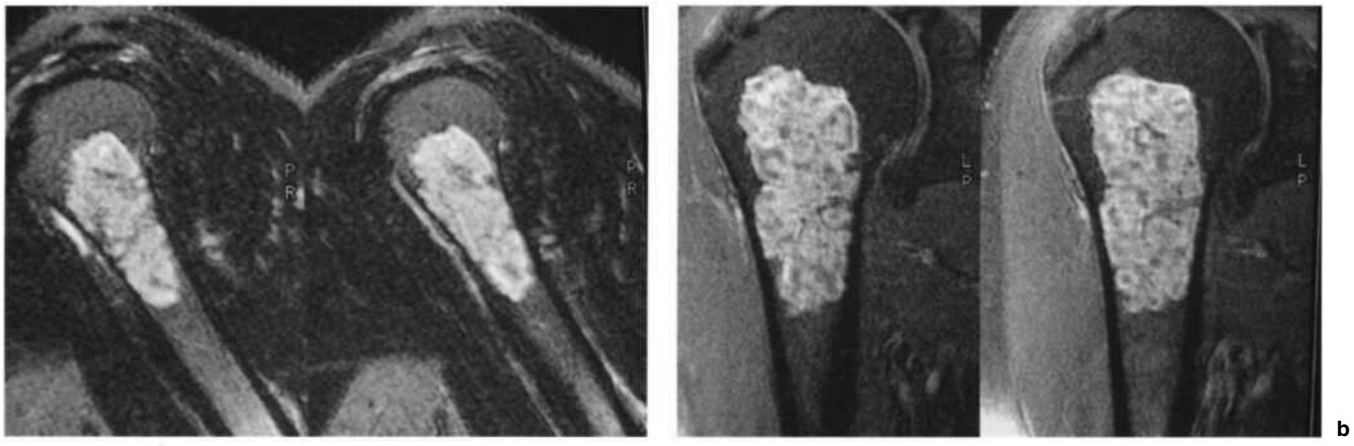

a b

Figure **29 a, b** A 48-year-old man with an enchondroma in the proximal humerus. The lesion has lobulated circumscribed margins and contains predominantly high signal with curvilinear zones of low signal on sagittal T2WI (**a**). The lesion shows both heterogeneous central and peripheral curvilinear patterns of Gd-contrast enhancement on coronal FS T1WI (**b**).

a

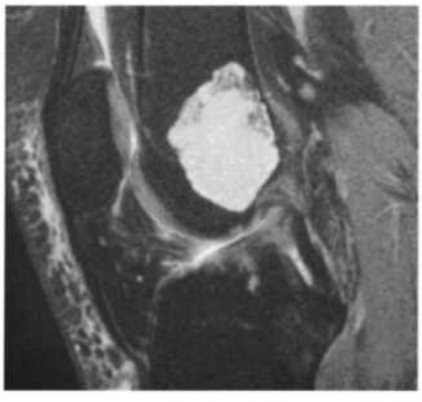

b

Figure **30 a, b** A 39-year-old woman with an enchondroma in the distal femur. Lateral radiograph (**a**) shows faint chondroid matrix mineralization in the lesion. The lesion has lobulated circumscribed margins and contains high signal on sagittal FS T2WI (**b**).

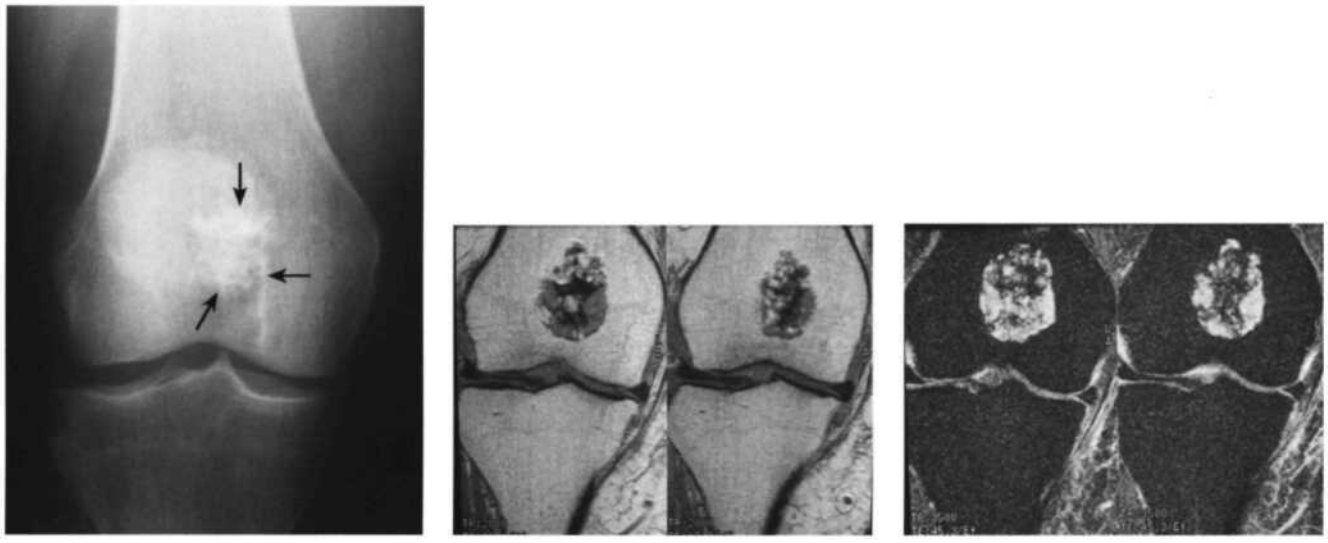

a b, c

Figure **31 a, b** A 66-year-old woman with an enchondroma in the distal femur. AP radiograph (**a**) shows chondroid matrix mineralization in the lesion. The lesion has lobulated circumscribed margins and contains zones of low, intermediate, and slightly high signal on coronal (**b**) PDWI, and zones of high and low signal on coronal (**c**) FS T2WI.

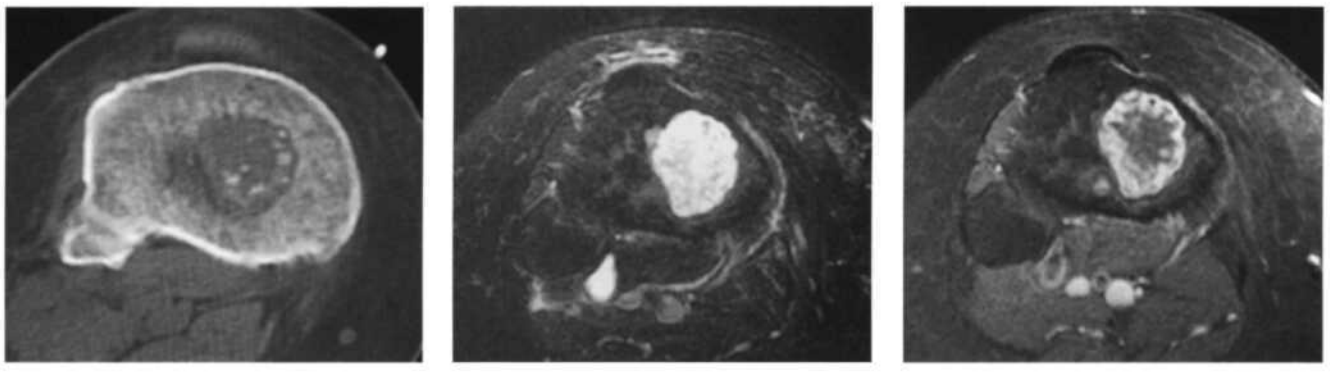

a b, c

Figure **32 a-c** A 45-year-old woman with an enchondroma in the proximal tibia. Axial CT image (**a**) shows a circumscribed radiolucent lesion containing chondroid matrix. The lesion has lobulated circumscribed margins and contains high signal on axial (**b**) FS T2WI. The lesion shows lobulated peripheral Gd-contrast enhancement on axial (**c**) FS T1WI.

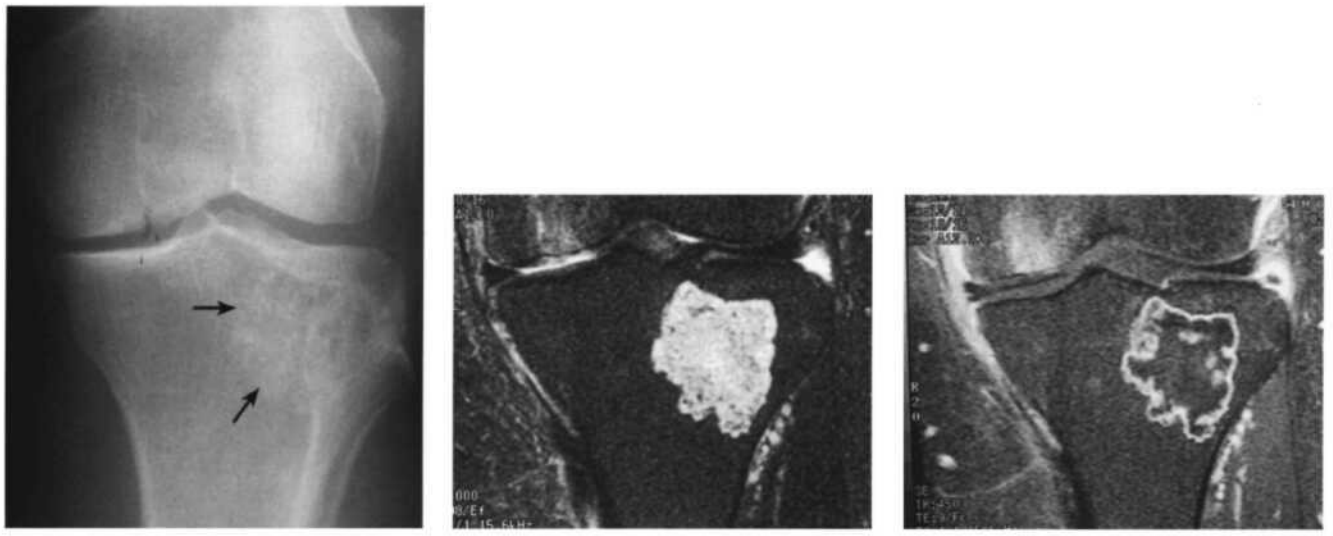

a b, c

Figure **33 a-c** A 54-year-old man with an enchondroma in the proximal tibia. AP radiograph (**a**) shows a lesion containing chondroid matrix. The lesion has lobulated circumscribed margins and contains high signal on coronal (**b**) FS T2WI. The lesion shows lobulated peripheral Gd-contrast enhancement on coronal (**c**) FS T1WI.

a

b

Figure **34 a, b** An 11-year-old female with an Oilier disease. Sagittal (**a**) T1WI shows single enchondromas in the metacarpal bone, proximal and middle phalanges, which have low-intermediate signal. The lesions show nodular and lobulated peripheral Gd-contrast enhancement on sagittal (**b**) FS T1WI.

a

b

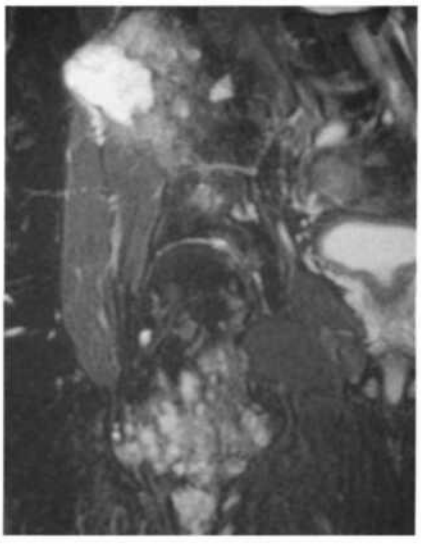

c

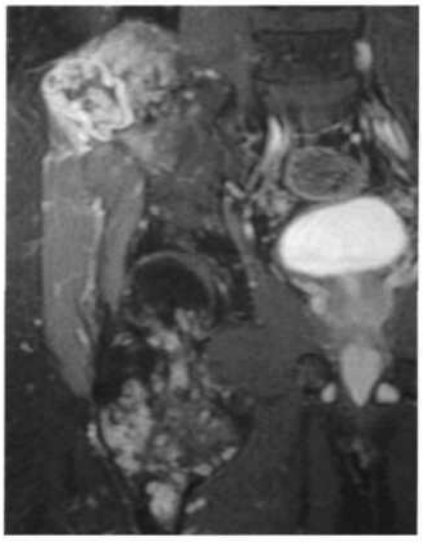

d

Figure **35 a-c** A 29-year-old man with Oilier disease. AP radiograph (**a**) shows multiple enchondromas involving the iliac bone, ischium, pubic bone, and femur. The lesions have low-intermediate signal on coronal (**b**) T1WI, and high signal on coronal (**c**) FS T2WI. The lesions show nodular and lobulated peripheral Gd-contrast enhancement on coronal (35 d) FS T1WI

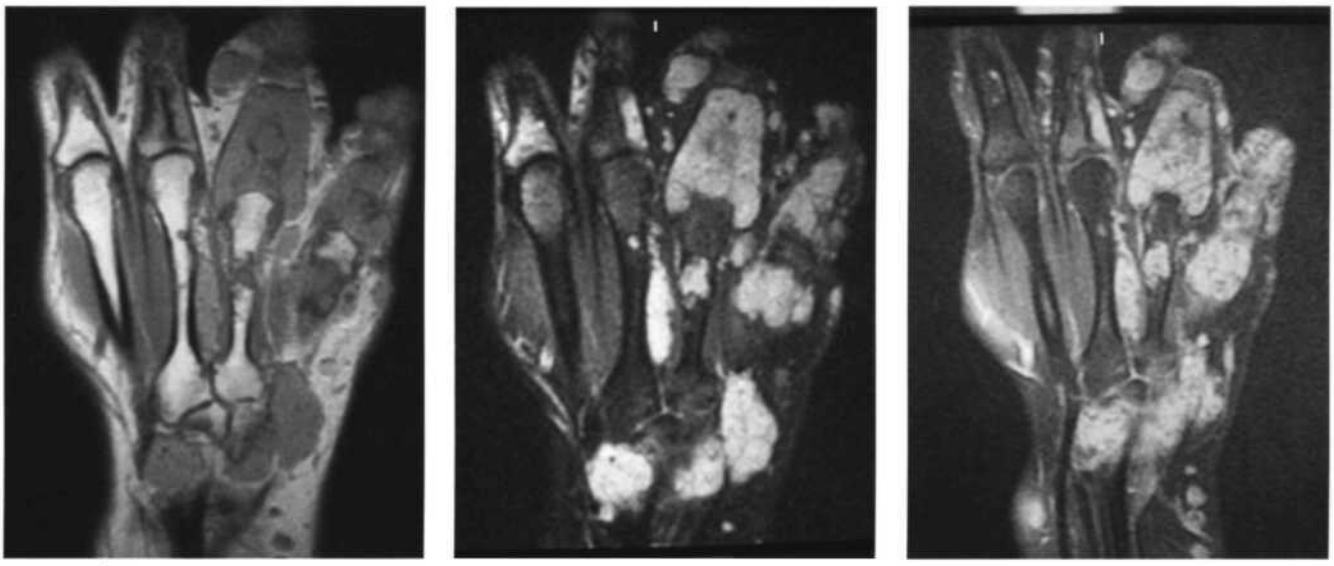

a b, c

Figure **36 a-c** A 20-year-old woman with Maffucci syndrome who has multiple intra-osseous enchondromas and soft tissue hemangiomas involving the wrist and hand. Multiple intra-osseous lesions and circumscribed extra-osseous soft tissue lesions are seen, which have mostly intermediate signal on coronal PDWI (**a**) and high signal on coronal FS T2 W (**b**). Some of the intra-osseous lesions are associated with cortical expansion. The lesions show prominent Gd-contrast enhancement on coronal FS T1WI (**c**).

MRI Findings[1,3,4,13]

Enchondromas often appear as lobulated, intramedullary lesions with well-defined borders ranging in size from 3 to 16 cm, mean = 5 cm (Figs. **26-36).** Mild endosteal scalloping can be seen. Lesions usually have low-intermediate signal on T1W1 and intermediate signal on PDWI. On T2WI and fat-suppressed T2WI, lesions usually have predominantly high signal with foci and/or bands of low signal representing areas of matrix mineralization and fibrous strands. No zones of abnormal high signal on T2WI are typically seen in the marrow outside the borders of the lesions. Lesions typically show Gd-contrast enhancement in various patterns (peripheral curvilinear lobular, central nodular/septal and peripheral lobular, or heterogeneous diffuse). Patients with Maffucci syndrome usually have multiple enchondromas as well as multiple hemangiomas in the soft tissues, which typically have high signal on FST2W1 and prominent Gd-contrast enhancement (Fig. **36**).

Deep endosteal scalloping (greater than two-thirds cortical thickness), cortical destruction, extrao-sseous soft tissue mass, and periosteal reaction are features commonly associated with chondrosarcoma and not with enchondroma. Pathologic fractures are less common with enchondromas compared with chondrosarcomas. Using fast, contrast-enhanced MRI, enchondromas reportedly have delayed enhancement (after 10s to 2 min from the start of arterial enhancement) compared with chondrosarcomas, which show enhancement in the first 10 seconds. Using early and exponential features of dynamic contrast enhancement may enable confirmation of the diagnosis of chondrosarcoma and exclusion of enchondroma.

Differential Diagnosis

Chondrosarcoma, bone infarct, unicameral bone cyst, aneurysmal bone cyst, fibrous dysplasia, giant cell tumor, chondroblastoma, chondromyxoid fibroma.

Treatment and Prognosis[2,5,6,8,9,12,15]

Solitary enchondromas are benign lesions that can increase in size during childhood and adolescence. After completion of endochondral bone growth, enchondromas typically do not enlarge. If growth of enhcondromas occurs in adults, low-grade chondrosarcoma should be excluded. Degeneration of enchondromas to chondrosarcoma may occur in 1% of solitary enchondromas and up to 56 % in patients with multiple enchondromas (multiple enchondromatosis, Oilier disease, and Maffucci syndrome).[2.5-9,12,15] The risk of developing chondrosarcoma is greater for patients with Maffucci syndrome than for patients with Oilier disease.[8] Chondrosarcomas have been reported in15-56% of patients with Maffucci syndrome.[7] The hemangiomas in Maffuci syndrome can also degenerate into sarcomas in 3-5% of cases.[7] Removal can be accomplished by en-bloc resection or curettage with or without bone grafts.

References

1 Aoki J, Sone S, Fujioka F, et al. MR of enchondroma and chondrosarcoma: rings and arcs of Gd-DTPA enhancement. *J Comput Assist Tomogr* 1991;15:1011-1016.

2 Forest M. Chondroma. In: Forest M, Tomeno B, Vanel D, eds. *Orthopedic Surgical Pathology: Diagnosis of Tumors and Pseudotumoral Lesions of Bone and Joints* Edinburgh: Churchill Livingstone; 1998: 191-205.

3 Geirnaerdt MJ, Hogendoorn Pancras CW, Bloem JL, Taminiau Antonie HM, van der Woude HJ. Cartilaginous tumors: fast contrast-enhanced MR imaging. *Radiology* 2000;214(2):539-546.

4 Giudici MA, Moser RP, Kransdorf MJ. Cartilaginous bone tumors. *Radiol Clin North Am* 1993;31(2):237-259.

5 Helliwell TE. Central cartilaginous neoplasms of bone. In: Helliwell TR, ed. *Major Problems in Pathology: Pathology of Bone and Joint Neoplasms* 1st ed. Philadelphia, Pa: W.B. Saunders; 1999;37: 193-214.

6 Huvos AG. Solitary and multiple osteochondromas and enchondromas; juxtacortical chondroma; Maffucci's disease. In: Huvos AG, ed. *Bone Tumors: Diagnosis, Treatment, and Prognosis* 2nd ed. Philadelphia, Pa: W.B. Saunders Co.; 1991:276-279.

7 Kransdorf MJ, Murphey MD. Vascular and lymphatic tumors. In: Kransdorf MJ, Murphey MD. *Imaging of Soft Tissue Tumors* 2nd ed. Philadelphia, Pa: W.B. Saunders 2006:150-188.

8 Lucas DR, Bridge JA. Chondromas, enchondroma, periosteal chondroma, and enchondromatosis. In: Fletcher CDM, Unni KK, Mertens F, eds. *World Health Organization Classification of Tumours. Pathology and Genetics of Tumours of Soft Tissue and Bone* Geneva: IARC Press; 2002:237-240.

9 Mertens F, Unni KK. Enchondromatosis: Ollier's disease and Maffucci syndrome. In: Fletcher CDM, Unni KK, Mertens F, eds. *World Health Organization Classification of Tumours. Pathology and Genetics of Tumours of Soft Tissue and Bone* Geneva: IARC Press: 2002:356-357.

10 Mulder JD, Schutte HE, Kroon HM, Taconis WK. Introduction. In: *Radiologic Atlas of Bone Tumors* Amsterdam: Elsevier; 1993:3-6.

11 Mulder JD, Schutte HE, Kroon HM, Taconis WK. The diagnosis of bone tumors. In: *Radiologic Atlas of Bone Tumors.* Amsterdam: Elsevier; 1993:9-46.

12 Mulder JD, Schutte HE, Kroon HM, Taconis WK. Intraosseous chondroma. In: *Radiologic Atlas of Bone Tumors* Amsterdam: Elsevier; 1993:421-434.

13 Murphey MD, Flemming DJ, Boyea SR, Bojescul JA, Sweet DE, Temple HT. From the archives of the AFIP. Enchondroma versus chondrosarcoma of the appendicular skeleton: differentiating features. *Radiographics* 1998;18:1213-1237.

14 Unni KK. Introduction and scope of study. In: *Dahlin's Bone Tumors: General Aspects and Data on 11 087* Cases 5th ed. Philadelphia, Pa: Lippincott, Williams & Wilkins; 1996:1-9.

15 Unni KK. Chondroma. In: *Dahlin's Bone Tumors: General Aspects and Data on 11 087 Cases* 5th ed. Philadelphia, Pa: Lippincott, Williams & Wilkins;1996:25-45.

A 9 Chondroma, Periosteal or Juxtacortical Type (Also Referred to as Periosteal or Juxtacortical Chondroma, Surface Chondroma, and Juxtacortical/Parosteal Chondroma)

ICD-O Code

9221/0

Definition

Juxtacortical chondromas are benign protuberant hyaline cartilaginous tumors that arise from the periosteum and are superficial to bone cortex.[1-4,7-9,12]

Frequency of Occurrence[5-7,11,12]

Juxtacortical chondromas account for <1 % of bone lesions. Juxtacortical chondromas represent ~5-12% of chondromas, which also include enchondroma, osteochondroma (exostosis), and capsular, synovial, and tendon-sheath types.

Age at Presentation

From 4 to 77 years, median = 26 years.[7]

Gender Ratio (M / F)

1.3 / 1 to 2 / 1[2,7]

Location

Lesions occur in the hand and foot bones > femur > tibia > humerus > others.[1,3,4,7] Juxtacortical chondromas occur most frequently at the surface of the diaphyseal portions of bone, followed by the metadiaphyseal and metaphyseal regions.[7] Lesions rarely occur in the epiphyseal region alone.[7]

Signs and Symptoms

Juxtacortical chondromas can be present as slow-growing, painless or dull-aching, bony protrusions.[2-4,7-10,12,13]

Gross Pathologic Findings[1-4,7,8,12,13]

Juxtacortical chondromas contain lobules of bluish-white hyaline cartilage adjacent to the cortex with variable calcification. Lesions range in size from 1 to 14 cm, although most are less than 5cm. The mean size of Juxtacortical chondromas is 2.6-4 cm, median size = 2.5 cm.

Histopathologic Findings[1-4,7,8,12,13]

Juxtacortical chondromas contain lobulated hyaline cartilage that lacks nuclear atypia. Lesions often contain foci of calcification (50%), ossification, and myxoid material. Peripheral areas of cellular pleomorphism may be seen occasionally.[3]

Tumor Genetics

Lesions typically show a diploid pattern with low proliferative activity.[4] Structural alterations involving chromosomes 6 and 12 have been reported.[4]

Findings on Plain Films (Roentgenograms) and Computed Tomography[1-3,7-10,12,13]

Juxtacortical chondromas often appear as soft tissue lesions with or without calcifications (Figs. **37, 39**). Lesions are associated with erosion and radiolucent scalloping of the underlying cortex. Periosteal thickening is seen at the base and at the periphery of the lesion adjacent to normal cortex and trabeculae (saucer-configuration). Rarely, a thin shell of periosteal bone can be seen along the outer margin of the lesion. Lesions typically do not prominently extend into the medullary space.

MRI Findings[1,9,10,13]

Lesions are located at the bone surface and are usually lobulated with low-intermediate signal on TlWI, which is hypo- or isointense relative to muscle (Figs. **37-41**). Lesions usually have heterogeneous predominantly high signal on T2WI. Lesions are surrounded by low signal borders on T2WI representing thin sclerotic reaction. Areas of low signal on T2WI are secondary to matrix mineralization. Edema is not typically seen in nearby medullary bone.[13] Lesions often show a peripheral pattern of Gd-contrast enhancement which correlates to fibrovascular bundles surrounding the cartilage lobules.[13] Chondromas can also occur in a subperiosteal location (Fig. **41**).

Differential Diagnosis

Fibrous cortical defect, periosteal chondrosarcoma, periosteal osteosarcoma, parosteal osteosarcoma, periosteal/cortical desmoid, synovial chondroma, aneurysmal bone cyst.

Treatment and Prognosis

Standard treatment is en-bloc resection or local excision that includes the periosteum, lesion, and fibrous capsule.[1,2,8] Recurrence is treated by en-bloc excision with bone grafting if necessary.

a

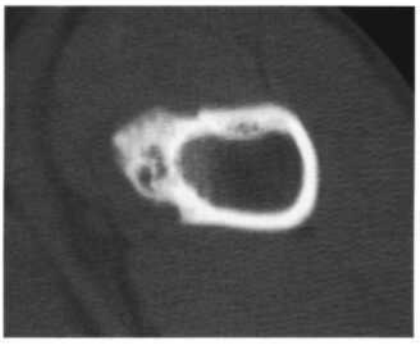
b

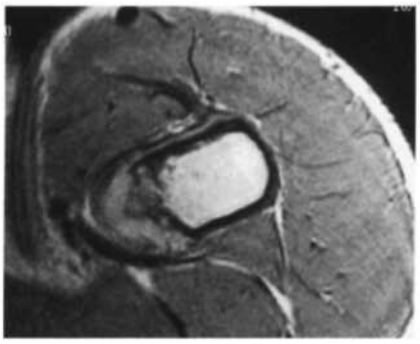
c

d

e

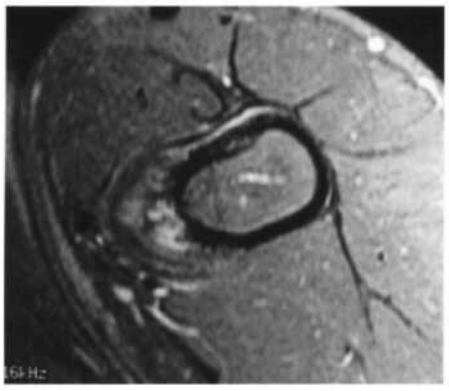
f

Figure **37 a-f** A 14-year-old male with a sessile type of juxtacortical/periosteal chondroma involving the humerus. AP radiograph (**a**) and axial CT image (**b**) show a lesion with chondroid matrix at the medial outer cortical surface of the proximal humeral diaphysis. Irregular cortical thickening is seen at the base of the lesion. The lesion has intermediate signal on axial (**c**) PDWI, and heterogeneous predominantly high signal as well zones of intermediate and low signal on axial (**d**) T2WI, and sagittal (**e**) FS T2WI. Periosteal thickening at the base of the lesion is seen as irregular zones of low signal at the outer cortical margin. The lesion shows irregular zones of Gd-contrast enhancement on axial (**f**) FS T1WI.

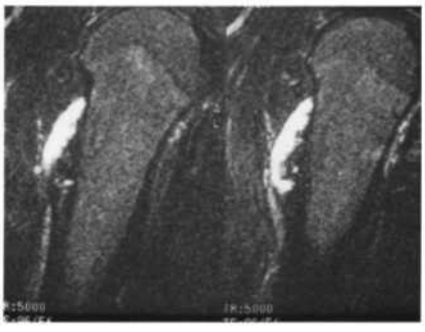
a

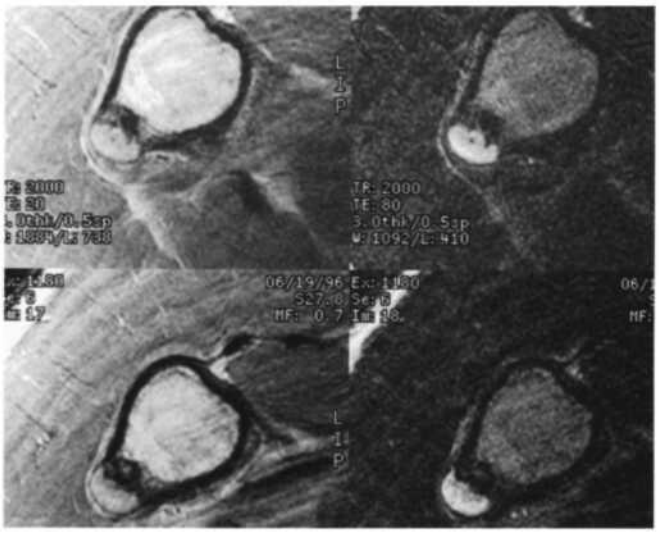
b

Figure **38 a-e** A 28-year-old man with a sessile-type Juxtacortical/periosteal chondroma involving the metadiaphyseal region of the humerus. The lesion has heterogeneous predominantly high signal as well zones of intermediate and low signal on sagittal (**a, c**) FS T2WI and axial (**b**) T2WI. The lesion has intermediate signal on axial (**b**) PDWI. Periosteal thickening at the base of the lesion is seen as irregular zones of low signal at the outer cortical margin. The lesion shows irregular zones of Gd-contrast enhancement on sagittal (**d**) T1WI and sagittal (**e**) FS T1WI.

Figure **38 c–e** ▷

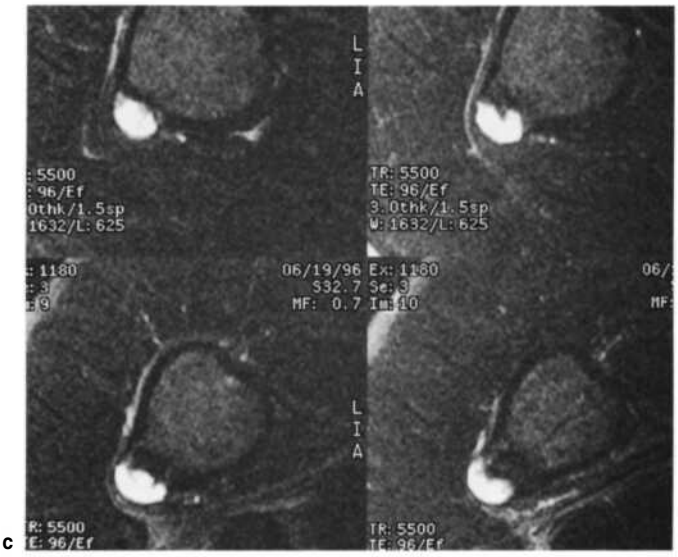

c

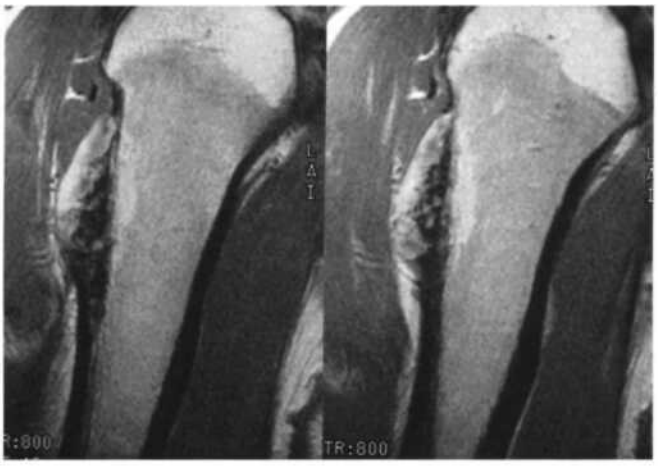

d

e

Figure **38 c-e**

a

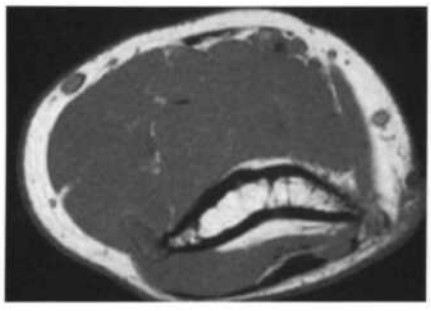

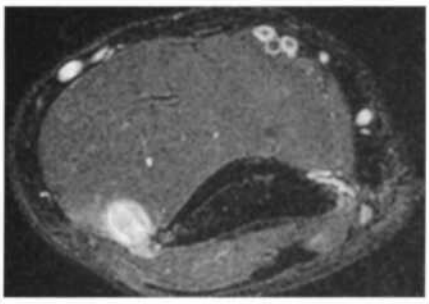

c

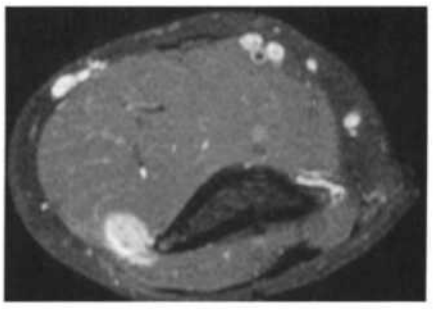

b, d

Figure **39 a-d** A 40-year-old man with a juxtacortical/periosteal chondroma involving the distal humerus. AP radiograph (**a**) shows a pedunculated mineralized lesion arising from an intact outer cortical surface. The lesion has low-intermediate signal on axial (**b**) T1WI, and high signal on axial (**c**) FS T2WI. Slight periosteal thickening is seen at the base of the lesion. The lesion shows prominent Gd-contrast enhancement on axial (**d**) FS T1WI.

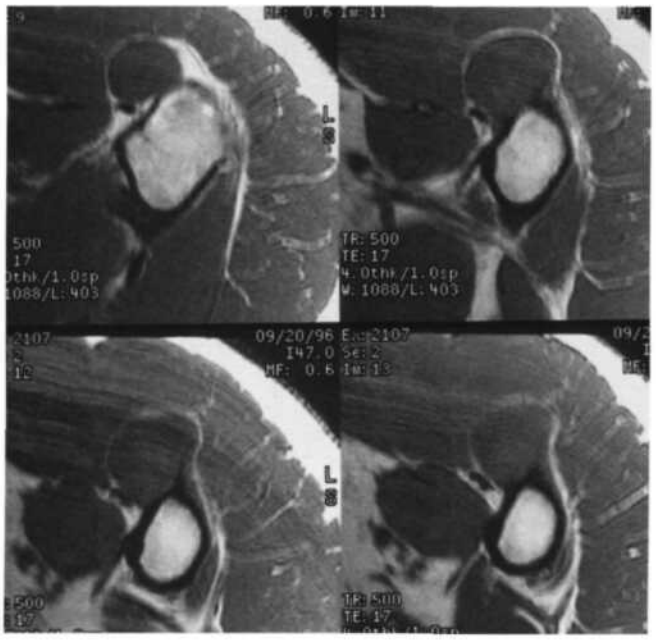

a

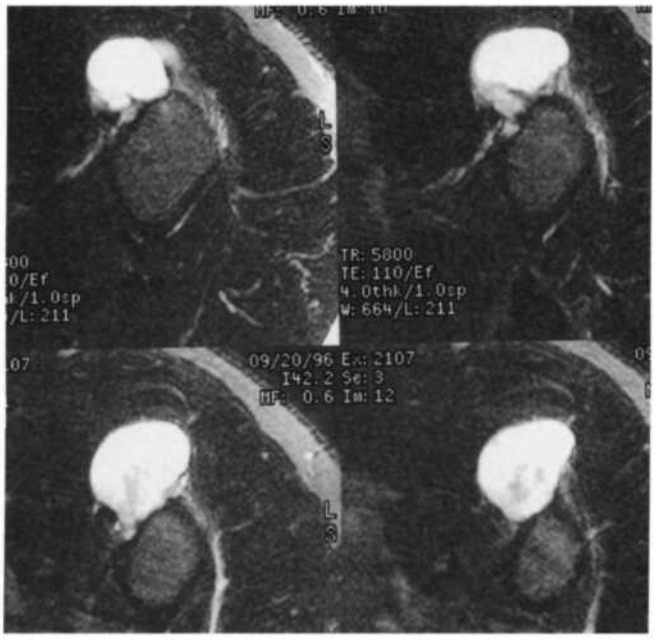

b

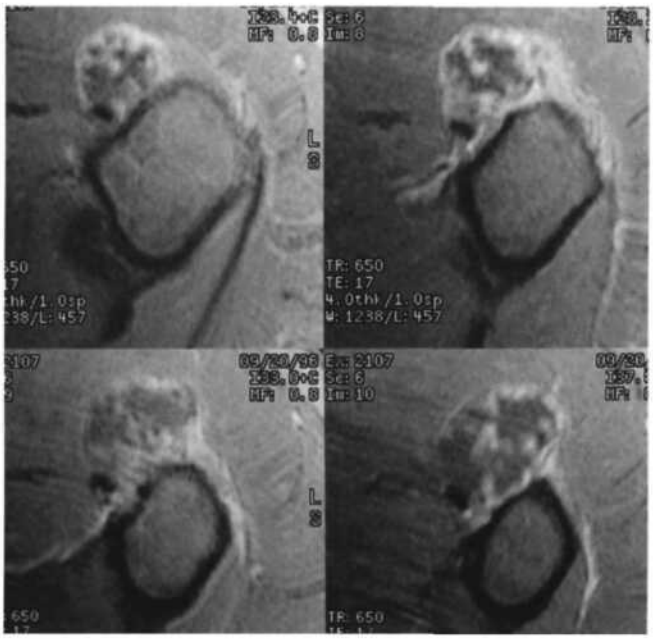

c

Figure **40 a-c** A 28-year-old man with a juxtacortical/periosteal chondroma involving the proximal humerus. The lesion has low-intermediate signal on axial (**a**) T1WI, and high signal on axial (**b**) FS T2WI. The lesion shows nodular and lobulated peripheral Gd-contrast enhancement on axial (**c**) FS T1WI.

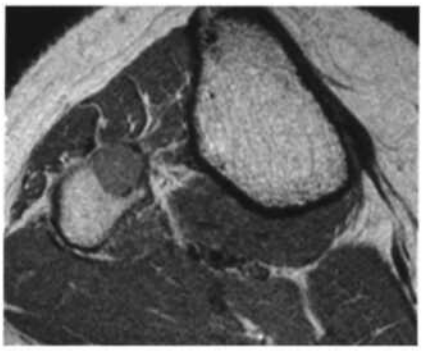

a

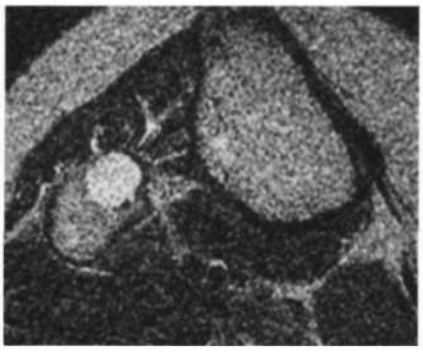

b

Figure **41 a-e** A 29-year-old woman with a subperiosteal chondroma involving the proximal fibula. The lesion has intermediate signal on axial (**a**) PDWI, and high signal on axial (**b**) T2WI and axial (**c**) FST2WI. The lesion shows lobulated peripheral Gd-contrast enhancement on axial (**d**) and sagittal (**e**) FS T1WI.

Figure **38c-e** ▷

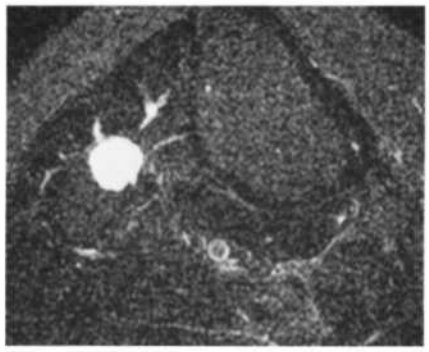

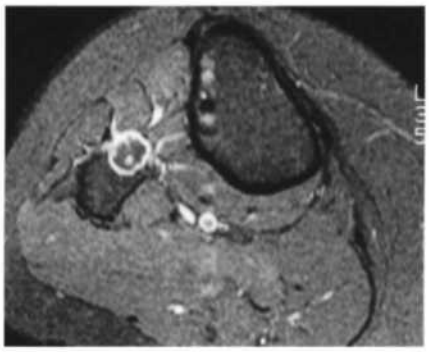

c, d

e

Figure **41 c-e**

References

1 Brien EW, Mirra JM, Luck JV Jr. Benign and malignant cartilage tumors of bone and joint: their anatomic and theoretical basis with an emphasis on radiology, pathology and clinical biology. II. Juxtacortical cartilage tumors. *Skeletal Radiol* 1999;28:1-20.

2 Forest M. Chondroma. In: Forest M, Tomeno B, Vanel D, eds. *Orthopedic Surgical Pathology: Diagnosis of Tumors and Pseudotumoral Lesions of Bone and Joints.* Edinburgh: Churchill Livingstone; 1998: 200-201.

3 Huvos AG. Solitary and multiple osteochondromas and enchondromas; Juxtacortical chondroma; Maffucci's disease. In: Huvos AG, ed. *Bone Tumors: Diagnosis, Treatment, and Prognosis* 2nd ed. Philadelphia, Pa: W.B. Saunders; 1991:276-279.

4 Lucas DR, Bridge JA. Chondromas: enchondroma, periosteal chondroma, and enchondromatosis. In: Fletcher CDM, Unni KK, Mertens F, eds. *World Health Organization Classification of Tumours. Pathology and Genetics of Tumours of Soft Tissue and Bone* Geneva: IARC Press; 2002:237-240.

5 Mulder JD, Schutte HE, Kroon HM, Taconis WK. Introduction. In: *Radiologic Atlas of Bone Tumors* Amsterdam: Elsevier; 1993:3-6.

6 Mulder JD, Schutte HE, Kroon HM, Taconis WK. The diagnosis of bone tumors. In: *Radiologic Atlas of Bone Tumors* Amsterdam: Elsevier; 1993:9-46.

7 Mulder JD, Schutte HE, Kroon HM, Taconis WK. Surface chondroma. In: *Radiologic Atlas of Bone Tumors* Amsterdam: Elsevier; 1993: 435-437.

8 Reid RP. Bone neoplasms and tumor-like lesions on the bone surface. In: Helliwell TR, ed. *Major Problems in Pathology: Pathology of Bone and Joint Neoplasms* Vol 37. 1st ed. Philadelphia, Pa: W.B. Saunders; 1999:230-231.

9 Robinson P, White LM, Sundaram M, et al. Periosteal chondroid tumors: radioiogic evaluation with pathologic correlation. *AJR Am J Roentgenol* 2001;177:1183-1188.

10 Tillich M, Lindbichler F, Reittner P, Weybora W, Linhart W, Fotter R. Childhood periosteal chondroma: femoral neck thickening and remote hyperostosis as clues to plain film diagnosis. *Pediatr Radiol* 1998;28:899.

11 Unni KK. Introduction and scope of study. In: *Dahlin's Bone Tumors: General Aspects and Data in 11087 Cases* 5th ed. Philadelphia, Pa: Lippincott, Williams & Wilkins; 1996:1-9.

12 Unni KK. Chondroma. In: *Dahlin's Bone Tumors: General Aspects and Data on 11 087 Cases* 5th ed. Philadelphia, Pa: Lippincott, Williams & Wilkins; 1996:25-45.

13 Woertler K, Blasius S, Brinkschmidt C, Hillmann A, Link TM, Heindel W. Periosteal chondroma: MR characteristics. *J Comput Assist Tomogr* 2001;25(3):425-430.

A 10 Chondromyxoid Fibroma

ICD-O Code

9241/0

Definition

Chondromyxoid fibromas are rare, benign, slow-growing bone lesions that contain chondroid, myxoid, and fibrous components.[4-6,11,18,20,26,27]

Frequency of Occurrence

Chondromyxoid fibromas represent 2 to 4 % of primary benign bone lesions, and < 1 % of primary bone lesions[1-18,25,26,27]

Age at Presentation

Most Chondromyxoid fibromas occur between the ages of 1 and 40 years, median = 17 years, and peak incidence in the 2nd to 3rd decades.[16-18,25-27] Eighty percent of these tumors occur in patients less than 30 years old.[18] Tumors occasionally occur in older patients up to 79 years.[18]

Gender Ratio (M / F)

1/1 to 1.6/1[16,17,25-27]

Location[4-6,11,17,18,20,26,27]

Chondromyxoid fibromas occur in the tibia> femur > pelvic bones > ankle and foot > fibula > ulna > ribs > humerus > skull > other bones, including vertebrae. In tubular bones, tumors occur most frequently in the metadiaphyseal and metaphyseal regions.[18]

Signs and Symptoms

Gradual onset of localized swelling and pain with or without restriction of movement; duration can be from 2 weeks to 10 years.[4-6,11,18,20,26,27]

Cross Pathologic Findings[4,6,11,18,20,26,27]

Lesions range in size from 1 to 13 cm, with an average of 3 cm. Chondromyxoid fibromas appear as lobulated, white to gray-white, firm and semitranslucent lesions with smooth surfaces and circumscribed borders. Erosion of the overlying bone is commonly seen.

Histopathologic Findings[4,6-8,10-15,18-22,26,27]

Chondromyxoid fibromas appear as a mixture of various proportions of myxoid, chondroid, and fibrous components with lobular patterns of growth. Scattered giant cells can be seen at the periphery of the lobules. Mitotic figures are uncommon. Small foci of calcification can be seen in a minority of lesions. Abrupt demarcation of the lesion with adjacent noninvolved bone is commonly seen.

Lesion Genetics

Abnormalities involving bands q13 and q25 of chromosome 6 have been reported.[20] Rearrangements involving chromosomes 2 and 5 have also been reported.[4] Chondromyxoid fibromas are associated with a unique genetic expression pattern composed of extensive diffuse hydrated proteoglycans, and focal regions of collagen types II, I, III, and VI.[20]

Findings on Plain Films (Roentgenograms) and Computed Tomography[1-4,6,9,11-15,18,19,21,22,24,26,27]

Chondromyoid fibromas are radiolucent, well-circumscribed lesions containing apparent "ridges" and "septa" with abrupt zones of transition (Figs. **42, 43**). The apparent ridges and septa represent erosions and indentations on normal bone from the adjacent lesions. Tumors may have thin sclerotic margins, with or without peripheral thick reactive sclerotic margins. Expansion and thinning of overlying cortex is commonly seen, with or without periosteal reaction. Lesions are usually eccentric in long bones. In small bones, lesions often involve the full bone diameter. Matrix mineralization is uncommon (seen in 13 % of lesions, best seen with CT).

Findings on Radionuclide Bone Scans

Lesions usually are associated with increased radiopharmaceutical accumulation.

MRI Findings[1-3,8-10,12-15,18,19,21-24,27]

Lesions are often slightly tabulated with low-intermediate signal on T1WI, intermediate signal on PDWI, and heterogeneous predominantly high signal on T2WI secondary to myxoid and hyaline chondroid components with high water content (Figs. **42, 43**). MR signal heterogeneity on T2WI is related to the proportions of myxoid, chondroid, and fibrous components within the lesions. Thin, low signal septa within lesions on T2W1 are secondary to fibrous strands. Lesions are surrounded by low signal borders representing thin sclerotic reaction. Edema is not typically seen in adjacent medullary bone. Lesions show prominent diffuse Gd-contrast enhancement.

Differential Diagnosis

Giant cell tumor, aneurysmal bone cyst, unicameral bone cyst, nonossifying fibroma / fibrous cortical defect, fibrous dysplasia, enchondroma, eosinophilic granuloma, chondroblastoma, desmoplastic fibroma.

Treatment and Prognosis

Standard treatment is block resection or curettage and bone grafting.[4,5,9,11,18,20,26] Recurrence is seen in 10-25% of cases.[6,20,26]

a b

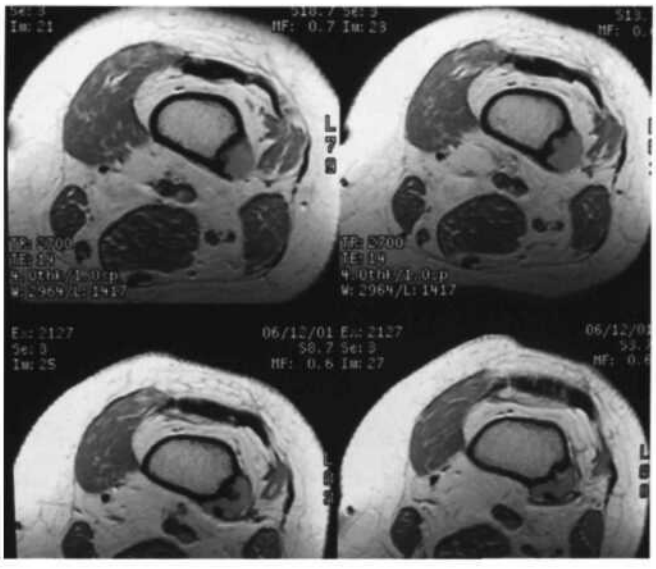

c

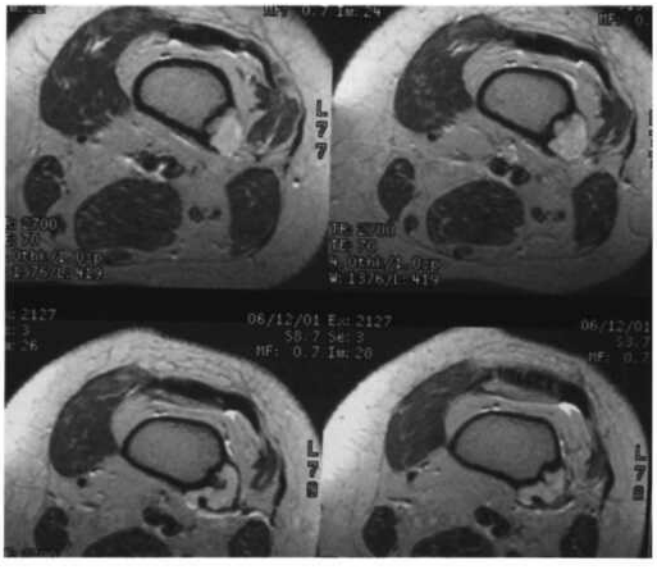

d

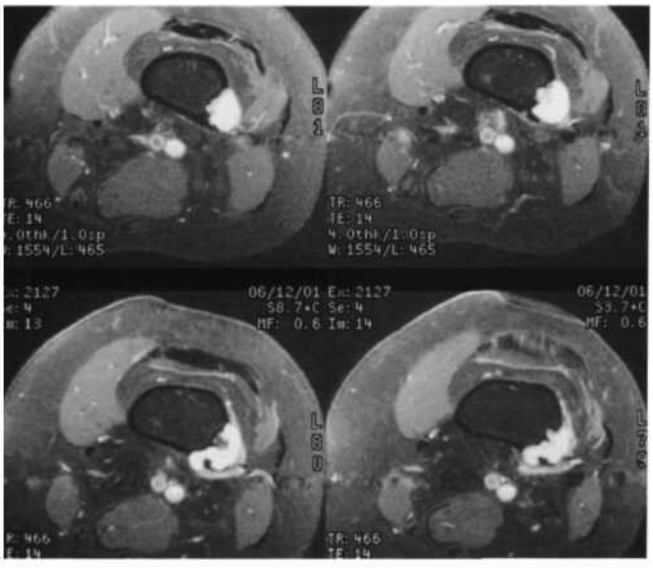

f

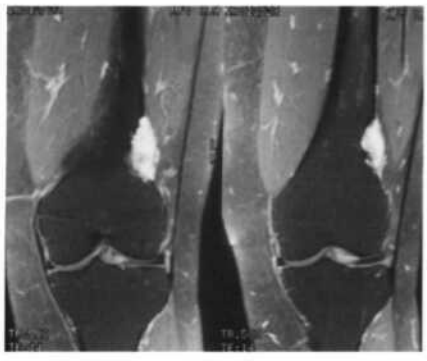

e

Figure **42 a-f** A 39-year-old woman with chondromyxoid fibroma in the distal femur. AP (**a**) and lateral (**b**) radiographs show a radiolucent, well-circumscribed, eccentric lesion in the femur with ridges associated with slight expansion and thinning of the overlying cortex. The lesion has intermediate signal on axial (**c**) PDWI, and high signal on axial (**d**) I2WI. The lesion shows prominent diffuse Gd-contrast enhancement on coronal (**e**) and axial (**f**) FS T1WI.

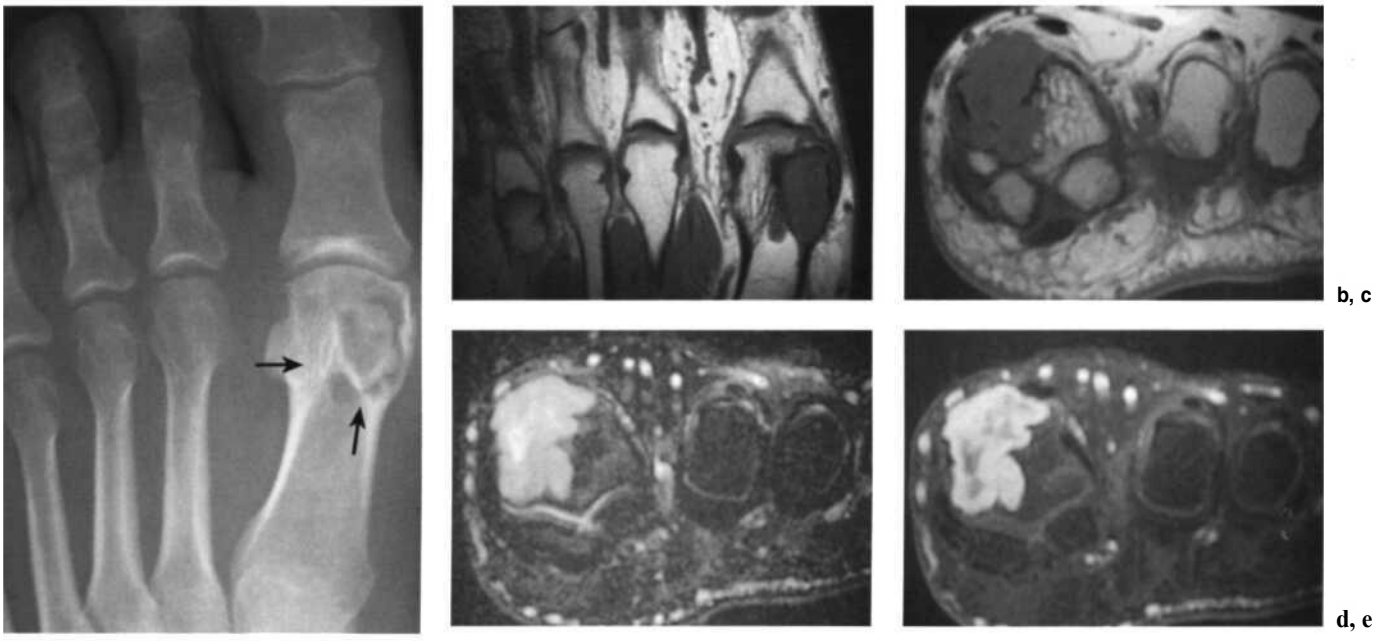

Figure **43 a-f** A 34-year-old man with chondromyxoid fibroma in the distal 1st metatarsal bone. AP radiograph (**a**) shows a radiolucent, well-circumscribed lesion in the metatarsal head with thin sclerotic margins associated with slight expansion and thinning of the overlying cortex. The lesion has low-intermediate signal on coronal (**b**) and axial (**c**) T1WI, and heterogeneous high signal on axial (**d**) FS T2WI. The lesion shows prominent diffuse Gd-contrast enhancement on axial (**e**) and coronal (**f**) FS T1WI.

References

1 Adams MJ, Spencer GM, Totterman S, Hicks DG. Quiz: Case Report 776. *Skeletal Radiol* 1993;22:358-361.

2 Brat HG, Renton P, Sandison A, Cannon S. Chondromyxoid fibroma of the sacrum. *Eur Radiol* 1999;9:1800-1803.

3 Bruder E, Zanetti M, Boos N, von Hochstetter AR. Chondromyxoid fibroma of two thoracic vertebrae. *Skeletal Radiol* 1999:28:286-289.

4 Forest M. Chondromyxoid fibroma. In: Forest M, Tomeno B, Vanel D, eds. *Orthopedic Surgical Pathology: Diagnosis of Tumors and Pseudotumoral Lesions of Bone* and Joints. Edinburgh: Churchill Livingstone; 1998:223-231.

5 Helliwell TR. Central cartilaginous neoplasms of bone. In: Helliwell TR, ed. *Major Problems in Pathology: Pathology of Bone and Joint Neoplasms* Vol 37. 1 st ed. Philadelphia, Pa: W.B. Saunders; 1999:193-214.

6 Huvos AG. Chondromyxoid fibroma; myxoma of the facial skeleton; myxoma and fibromyxoma of extragnathic bones. In: Huvos AG, ed. *Bone Tumors Diagnosis, Treatment, and Prognosis* 2nd ed. 1991: 319-330.

7 Keel SB, Bhan AK, Liebsch NJ, Rosenberg AE. Chondromyxoid fibroma of the skull base: a tumor which may be confused with chordoma and chondrosarcoma: a report of three cases and review of the literature. *Am J SurgPathol*(1997;21(5):577-582.

8 LeMay DR, Sun JK, Mendel E, Hinton DR, Giannotta SL. Chondromyxoid fibroma of the temporal bone. *Surg Neurol* 1997;48:148-152.

9 Lopez-Ben R, Siegal GP, Hadley MN. Chondromyxoid fibroma of the cervical spine: case report. *Neurosurgery* 2002;50(2):409-411.

10 Macdonald D, Fornasier V, Holtby R. Chondromyxoid fibroma of the acromium with soft tissue extension. *Skeletal Radiol* 2000;29: 168-170.

11 Mangham DC. Giant cell tumor of bone and giant cell-containing lesions of bone. In: Helliwell TR, ed. *Major Problems in Pathology: Pathology of Bone and Joint Neoplasms* Vol 37. 1st ed. Philadelphia, Pa: W.B. Saunders; 1999:304-329.

12 Marin C, Gallego C, Manjón P, Martinez-Tello FJ. Juxtacortical chondromyxoid fibroma: imaging findings in three cases and a review of the literature. *Skeletal Radiol* 1997;26:642-649.

13 Mehta S, Szklaruk J, Faria SC, Raymond AK, Whitman GJ. Chondromyxoid fibroma of the sacrum and iliac bone. *AJR Am J Roentgenol* 2006;186:467-469.

14 Mitchell M, Sartoris DJ, Resnick D. Case report 713. *Skeletal Radiol* 1992:21:252-255.

15 Mizuno K, Sasaki T, Prado G, et al. Chondromyxoid fibroma of the scapula associated with aneurysmal bone cyst. *Radiat Med* 1999; 17(5):383-387.

16 Mulder JD, Schutte HE, Kroon HM, Taconis WK. Introduction. In: *Radiologic Atlas of Bone Tumors* Amsterdam: Elsevier; 1993:3-6.

17 Mulder JD, Schutte HE, Kroon HM, Taconis WK. The diagnosis of bone tumors. In: *Radiologic Atlas of Bone Tumors.* Amsterdam: Elsevier; 1993:9-46.

18 Mulder JD, Schutte HE, Kroon HM, Taconis WK. Chondromyxoid fibroma. In: *Radiologic Atlas of Bone Tumors* Amsterdam: Elsevier; 1993:475-482.

19 O'Connor PJ, Gibbon WW, Hardy G, Butt WP. Chondromyxoid fibroma of the foot. *Skeletal Radiol* 1996:25:143-148.

20 Ostrowski ML, Spjut HJ, Bridge JA. Chondromyxoid fibroma. In: Fletcher CDM, Unni KK, Mertens F, eds. *World Health Organization Classification of Tumours. Pathology and Genetics of Tumours of Soft Ttissue and Bone* Geneva: IARC Press; 2002:243-245.

21 Park SH, Kong KY, Chung HW, Kim CJ, Lee SH, Kang HS. Juxtacortical chondromyxoid fibroma arising in an apophysis. *Skeletal Radiol* 2000;29:466-469.

22 Patino-Cordoba JI, Turner J, McCarthy SW, Pagan P. Chondromyxoid fibroma of the skull base. *Otolaryngol Head Neck Surg* 1998:118(3): 415-418.

23 Soler R, Rodríguez E, Suárez I, Gayol A. Magnetic resonance imaging of chondromyxoid fibroma of the fibula. *Eur J Radiol* 1994;18: 210-211.

24 Tarhan NC, Yologlu Z, Tutar NU, Coskun M, Agildere AM, Arikan U. Chondromyxoid fibroma of the temporal bone: CT and MRI findings. *Eur Radiol* 2000;10:1678-1680.

25 Unni KK. Introduction and scope of study. In: *Dahlin's Bone Tumor: General Aspects and Data on 11 087 Cases* 5th ed. Philadelphia, Pa: Lippincott, Williams & Wilkins; 1996:1-9.

26 Unni KK. Chondromyxoid Fibroma. In: *Dahlin's Bone Tumors: General Aspects and Data on 11 087 Cases* 5th ed. Philadelphia, Pa: Lippincott, Williams & Wilkins; 1996:59-69.

27 Wu CT, Inwards CY, O'Laughlin S, Rock MG, Beabout JW, Unni KK. Chondromyxoid fibroma of bone: a clinicopathologic review of 278 cases. *Hum Pathol* 1998;29(5):438-446.

A 11 Chondrosarcoma

ICD-O Codes

Central, primary, and secondary: 9220/3

Peripheral: 9221/3

Dedifferentiated: 9243/3

Mesenchymal: 9240/3

Clear cell: 9242/3

Definition

Chondrosarcomas are malignant tumors containing cartilage formed within sarcomatous stroma. Chondrosarcomas can contain areas of calcification/mineralization, myxoid material, and/or ossification. Primary Chondrosarcomas (62-86 %) represent lesions occurring without pre-existent lesions, whereas secondary Chondrosarcomas arise from formerly benign cartilaginous lesions (enchondroma, enchondromatosis / Oilier disease, Maffucci syndrome / multiple enchondromas [soft tissue hemangiomas], osteochondroma, multiple osteochondromas / exostoses, synovial chondromatosis), or other lesions (Paget disease, fibrous dysplasia, prior irradiation, repetitive trauma).[15,39] Periosteal Chondrosarcomas are rare malignant cartilage tumors that occur on the surface of bone.[2,9,15] Chondrosarcomas rarely arise within synovium.[37]

Chondrosarcomas are also classified according to their (1) site of origin (osseous vs. extra-osseous); (2) locations in bone (central or intramedullary [75%] or peripheral or surface/cortical based [25%]); and (3) histology. There are five major histologic variants of Chondrosarcomas: conventional, clear cell, dedifferentiated, mesenchymal, and myxoid.[1,2,8,9,15,23,25,27,29-31,33-35,39]

Frequency of Occurrence

Bone: Chondrosarcomas represent from 12 to 21 % of malignant bone lesions, 21-26% of primary sarcomas of bone, 9-14% of all bone tumors, 6% of skull base tumors, and 0.15% of all intracranial tumors.[1,8,29,30,33,39] Chondrosarcomas are predominantly osseous lesions (96%), and rarely occur as primary extra-osseous tumors (4%)[15] or arise within synovium.[37]

Soft tissue: Chondrosarcomas represent 2.1 % of malignant soft tissues, and < 1% of all soft tissue tumors.[19,20]

Age at Presentation

Bone: from 5 to 91 years, mean = 40 years, median = 26-59 years.[1,15,28-30,33,38]

Soft tissue: from 22 to 71 years, mean = 49 years.[20]

Gender Ratio (M / F)

Bone: 1.3 / 1 to 2 / 1.[8,15,29,30,33,38,39]

Soft tissue: 1.4 / 1.[20]

Location

Bone:

- For **conventional intra-osseous Chondrosarcomas,** tumors occur in the femur > pelvic bones > humerus > ribs > tibia > craniofacial bones > sternum > scapula > vertebrae > feet > hands.[8,15,29,30,33,39] In long bones, Chondrosarcomas involve the metaphysis (49%), diaphysis (36%), or epiphysis (15%).[31]
- **Peripheral Chondrosarcoma** refers to a chondrosarcoma that arises from a cartilaginous exostosis or osteochondroma.[31] Common locations include the scapula, iliac bone, tibia, femur, pubic bone, and rib.[31]
- **Periosteal Chondrosarcomas (juxtacortical Chondrosarcomas)** have histologic features of a low-grade conventional chondrosarcoma, and occur on the surface of bones (distal femoral metadiaphysis > proximal humeral metadiaphysis > proximal femoral meta-diaphysis > iliac wing).[31,33,39,40]
- For **dedifferentiated Chondrosarcomas,** common sites include pelvic bones, femur, and humerus.[28,39]
- The rare, **clear cell chondrosarcoma** usually involves the epiphyseal region of long bones, (proximal femur > proximal humerus > distal femur > proximal tibia > other sites.[4,9,33,39]
- For **mesenchymal Chondrosarcomas,** common sites of involvement include: craniofacial bones, iliac bone, ribs, and vertebrae.[9,33,34]

Soft tissue: Tumors occur in the lower extremity > trunk > hip and buttocks > foot and ankle > upper extremity > proximal limb girdle > head and neck > hand and wrist > retroperitoneum.[20,23,26] Myxoid Chondrosarcomas often occur in the deep subcutis or deeper soft tissues (80% are located in proximal extremities or limb girdles, and 20 % involve the trunk).[26] Up to one-third of mesenchymal Chondrosarcomas occur as primary tumors in the soft tissues.[9,33,34] Chondrosarcomas rarely arise within synovium.[37]

Signs and Symptoms

Bone: Chondrosarcomas can be painless or result in local pain, swelling, and tenderness; with or without pathologic fracture.[2,8,13,15,25,28,31,33,34,39]

Soft tissue: Extraskeletal Chondrosarcomas often present as enlarging soft tissue masses which may be associated with pain and tenderness, as well as restricted range of motion for tumors near joints.[19,23]

Cross Pathologic Findings[2,3,5,6,8,9,13,15,19,21,25,26,28,31,33-35,39]

Chondrosarcomas often appear as lobulated, pearly, bluish-white, translucent tumors, associated with areas of calcification/ossification and slimy mucoid material. Destructive changes are often seen in the involved bone. Clear cell Chondrosarcomas are usually gray-red and soft, with or without cystic spaces, and can involve the epiphysis. Periosteal Chondrosarcomas are typically large (>5cm) tumors covered by a fibrous layer, which is located on the surfaces of bones and usually appears as lobulated gray-white tissue with or without yellowish calcifications or ossifications.[2,9,15] For extraskeletal

myxoid chondrosarcomas, tumors range in size from 1 to 25 cm, with a median size of 7 cm[26]

Histopathologic Findings[3,5-9,13-15,19,25,26,28,31,33-35]

Histologic findings of chondrosarcoma need to be correlated with radiographic findings for appropriate diagnosis and treatment because of the discordance between biologic behavior and histologic features.

Conventional chondrosarcoma (70-75%).[1-3] Tumors contain multiple atypical chondrocytes which vary in size and often contain large hyperchromatic nuclei, as well as large cartilage cells with large single nuclei or multiple nuclei. Nuclear atypia is often mild to moderate. Tumor cells permeate and surround bony trabeculae in the marrow compartment. Hyaline cartilage is present in lesions as well as extracellular matrix, usually containing mucinous material and/or myxoid changes. Necrosis may be present in high-grade tumors. Mitotic figures are uncommon. Grade 1 lesions (27-61%) have moderate cytologic atypia and are hypercellular compared with enchondromas. Grade 2 chondrosarcomas (33-60%) are hypercellular relative to grade 1 lesions. Nuclei in grade 2 lesions are hyperchromatic and enlarged. Grade 3 (3-31%) chondrosarcomas are less common and have marked hypercellularity with bizarrely shaped nuclei. Conventional chondrosarcomas are typically intra-osseous tumors. Peripheral chondrosarcomas refer to chondrosarcomas that arise from osteochondromas, and usually have histologic features similar to a conventional intra-osseous chondrosarcoma.[31]

Clear cell chondrosarcoma (1-2%).[3,4,9,15,18,25,33,39] These tumors typically occur in patients older than 18 years after cessation of endochondral bone growth, age range 14-84 years, mean = 37 years, peaking in the 4th and 5th decades.[3,9,15,18,25,33,39] These tumors occur two to three times more frequently in males than females.[9,25] Tumor cells vary in appearance from immature chondroblasts to mature chondrocytes. Neoplastic cells have clear cytoplasm and centrally positioned nuclei with few mitotic figures. Multinucleated osteoclast-like giant cells may also be seen. Tumor matrix and/or zones having histology similar to conventional chondrosarcoma are often present. The cartilage may be calcified or ossified. Woven bone may form in the stroma. Clear cell chondrosarcomas are sometimes referred to as "malignant chondroblastoma." Clear cell chondrosarcomas are slow-growing neoplasms.

Dedifferentiated chondrosarcoma (6-11%).[1,3,9,28,33] This tumor type occurs as either primary and secondary chondrosarcomas, usually in patients ranging in age from 29 to 85 years, with the average between 50 and 60 years.[1,9,15,28] Male to female ratios of 1.5 / 1 to 2 / 1 have been reported.[9] Lesions have mixtures of high-grade spindle cells and low-grade or high-grade malignant cartilage cells.

Mesenchymal chondrosarcoma (2-10%).[1,3,5,6,33,34] Patients with these tumors range in age from 5 to 74 years, with peak occurrences in the 2nd and 3rd decades. Both genders are equally affected.[33,34] Tumors contain sheets of undifferentiated small cells with oval nuclei associated with an extracellular reticulin network. Small to large foci of cartilage are seen in the lesions, with or without reactive osteoid and bone formation. This type can also occur as extra-osseous tumors in soft tissues.

Myxoid chondrosarcoma (12%).[5-7,26,33] Patients with these tumors range in age from 6 to 89 years, median = 52 years, and mean = 49 years.[7,26,33] A male to female ratio of 2 / 1 has been reported[26,33] Lesions are considered low-grade tumors, and are also known as chordoid sarcoma. Tumors can contain abundant myxoid/mucoid stroma with strands and/or foci of cells with small hyperchromatic nuclei and moderate cytoplasm containing glycogen granules. In addition, relatively well-differentiated cartilage cells are usually seen. Areas of hemorrhage and cysts are often seen in extra-osseous tumors. Matrix mineralization/calcification is rarely seen. Typically, minimal or no mitotic activity is seen in tissue samples. These tumors often occur as extra-osseous tumors in the soft tissues of the extremities (thigh most common), and rarely in bone.[26] Extraskeletal myxoid chondrosarcomas are associated with a chromosomal translocation: t(9;22) (q22-31;q11-12).[14,33]

Periosteal chondrosarcoma (1-2%). These tumors are also referred to as juxtacortical chondrosarcomas. They are located on the surfaces of bones, are typically large (>5cm), and have histologic features similar to conventional chondrosarcomas[2,9,15,21,33,40]

Tumor Genetics

Chondrosarcomas have been reported to be associated with loss of chromosomes or chromosome segments including: 1 p36, 1p13-22, 4, 5q13-31, 6q22-qter, 9p22-pter, 10p, 10q24-qter, 11 p13-pter, 18 p, 18q22-qter, and 22q13.[2] Chromosomal gains have also been reported at 7p13-pter, 12q15-qter, 19, 20pter-q11, and 21 q.[2] Deletions from chromosome 13 q have been shown to be associated with increased risk of metastatic disease.[2] Trisomy 22 has been detected in primary conventional chondrosarcomas.[2]

Findings on Plain Films (Roentgenograms) and Computed Tomography[2-4,8-13,15,17,18,25,28,31-34,36,39,40]

Central conventional chondrosarcoma. Tumors usually appear as areas of radioluceny involving medullary bone secondary to destruction, and endosteal scalloping. Areas of cortical bone destruction occur late and periosteal reaction is usually minimal. Cartilaginous matrix mineralization, variously described as "arcs," "rings," "punctate," "popcorn," "flocculent," "fluffy," and/or "cotton wool" configurations, is common. Margins of the tumor tend to become less well-defined with increasing grade of tumor. Tumors may be associated with expansion of bone (Figs. **44, 46, 47, 49, 52-54).**

Peripheral chondrosarcoma. These tumors are associated cartilaginous cap thicknesses of osteochondromas exceeding 2 cm, as well as erosive and/or destructive bony changes, soft tissue mass, chondroid mineralization, and/or thickening of cortex at sites of attachment to bone (Fig. **57**).

Periosteal chondrosarcoma.[21,33,40] These tumors vary in size from 5 to 11 cm. The bone cortex is either thinned or thickened but not destroyed. Lesions occasionally involve medullary bone. Juxtacortical soft tissue components of the lesion can have chondroid calcifications, with or without radial periosteal bone formation, and/or a thin peripheral rim of periosteal bone.

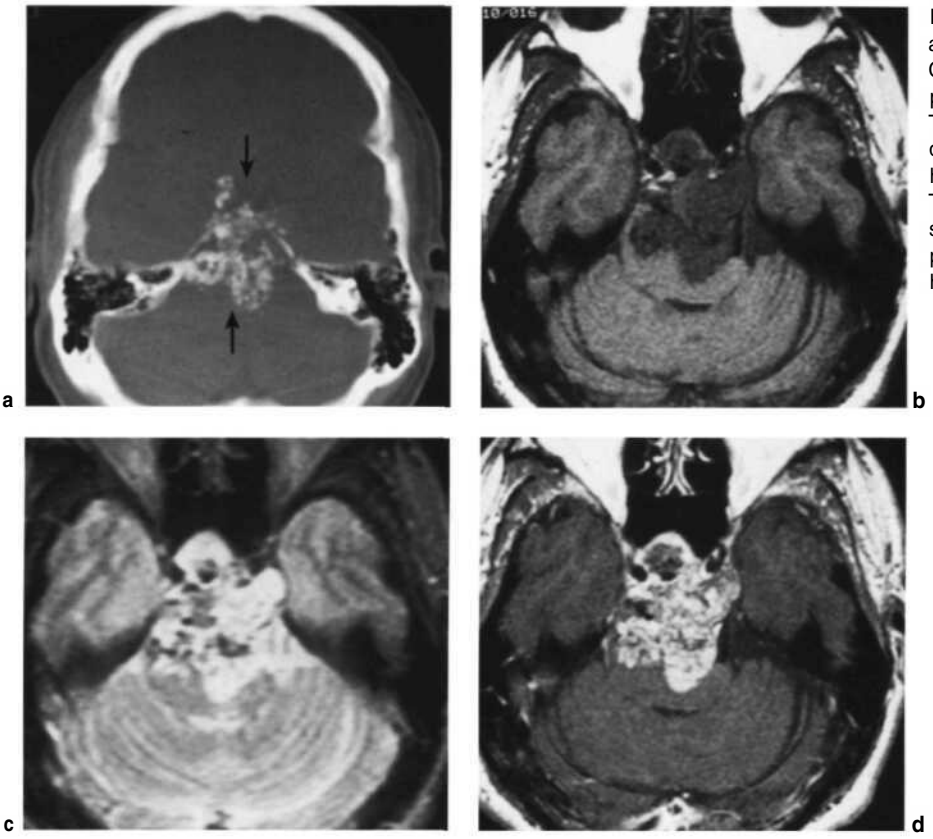

Figure **44 a-d** A 42-year-old woman with a chondrosarcoma involving the clivus. Axial CT image (**a**) shows the lesion to have prominent chondroid matrix mineralization. The lesion erodes the clivus and extends dorsally compressing the pons. The tumor has low-intermediate signal on axial (**b**) T1WI, and mostly high signal with foci of low signal on axial (**c**) T2WI. The tumor shows prominent heterogeneous Gd-contrast enhancement on axial (**c**) T1WI.

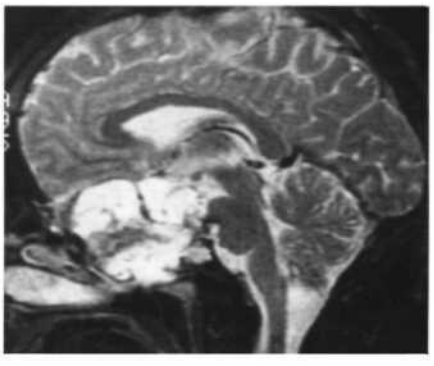

Figure **45** Chondrosarcoma involving the ethmoid and sphenoid paranasal sinuses with extension into the nasal cavity. The lesion has mostly high signal with bands of low signal on sagittal FS T2WI.

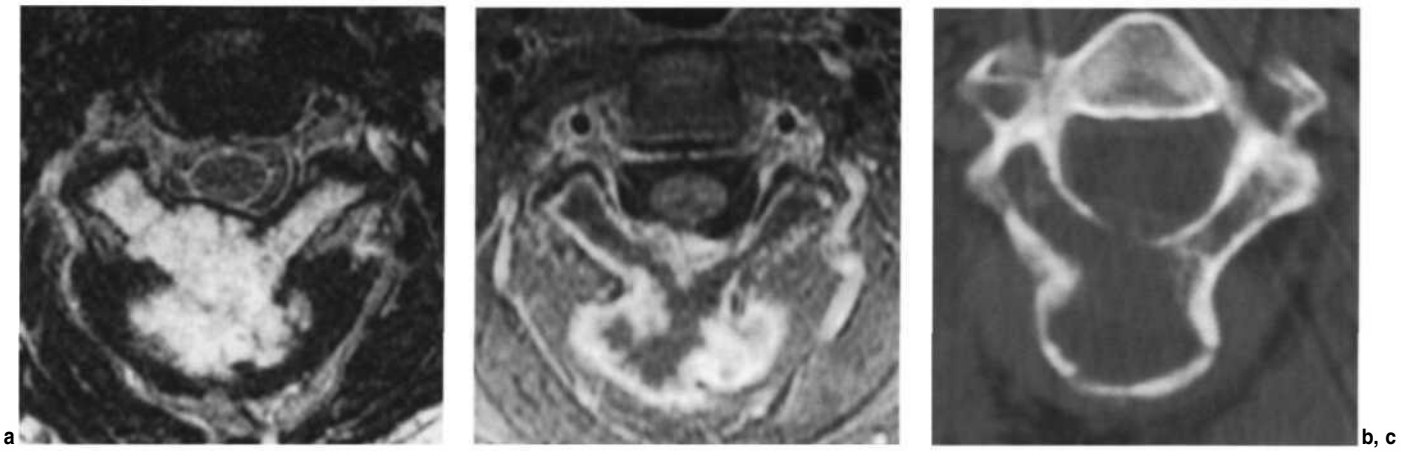

Figure **46 a-c** A 50-year-old man with chondrosarcoma involving the posterior elements of C3. The tumor has high signal with thin bands of low signal on axial T2WI (**a**). The lesion shows irregular nodular and curvilinear patterns of Gd-contrast enhancement on axial FS T1WI (**b**). Axial CT image (**c**) shows a radiolucent expansile lesion involving the posterior elements.

a

b, c

Figure **47 a-c** A 45-year-old woman with a low-grade chondrosarcoma involving the proximal humerus. AP radiograph (**a**) shows a radiolucent lesion with chondroid matrix mineralization. The lesion has lobulated, circumscribed margins and contains high signal on coronal (**b**) FS T2WI. The lesion shows lobulated peripheral Gd-contrast enhancement on coronal (**c**) FS T1WI.

a

b

Figure **48 a, b** A 55-year-old woman with a low-grade chondrosarcoma involving the proximal humerus. The lesion has lobulated, circumscribed and irregular margins, and contains low, intermediate, and high signal on coronal T2WI (**a**). The lesion shows heterogeneous diffuse Gd-contrast enhancement on coronal (**b**) FS T1WI.

Clear cell chondrosarcoma. Tumors appear as lytic lesions involving the epiphyseal regions/ends of long bone, and usually range from 3 to 7.5 cm, mean 5 cm. Lesions can also occur in or extend into metaphyseal or diaphyseal regions. Matrix mineralization is seen in 30% of cases. Lesions may have a sclerotic rim. Large lesions (>3 cm) often are associated with cortical destruction. Lesions are most commonly located in the proximal humerus or proximal femur. Lesions occur in patients who are typically older than those with chondroblastoma.

Dedifferentiated chondrosarcoma. These tumors usually appear as multifocal radiolucent zones in medullary bone with endosteal scalloping. Cartilaginous matrix mineralization is common. Areas of cortical bone destruction are commonly seen with extension into adjacent soft tissues (Fig. **54**).

Mesenchymal chondrosarcoma. These tumors are often large, predominantly lytic lesions with irregular borders. Minimal matrix mineralization is seen in 75%. These neoplasms can also occur as extra-osseous tumors.

Extra-osseous myxoid chondrosarcoma. These tumors appear as soft tissue masses, usually without matrix mineralization (Fig. **59**).

Findings on Radionuclide Bone Scans

Lesions are typically associated with increased radiopharmaceutical accumulation.

MRI Findings[2-4,10,11,13,16-19,21,26-28,31-34,36-40]

Conventional chondrosarcomas. Lesions range from 3 to 28 cm in size, mean = 8 cm. Lesions usually have low-intermediate signal on T1WI, intermediate signal on PDWI, and heterogeneous predominantly high signal on T2WI (Figs. **44-53, 58**). Zones of low signal on T2W1 are related to the presence and degree of matrix mineralization and/or fibrous tissue. Lesions often have lobulated margins, with or without internal septations. Peritumoral high signal on T2WI in marrow and periosteal soft tissues may be seen associated with chondrosarcomas, and typically not with enchondromas.[16] Chondrosarcomas usually show contrast-enhancement in patterns ranging from lobulated peripheral and/or septal, or homogeneous versus het-

a

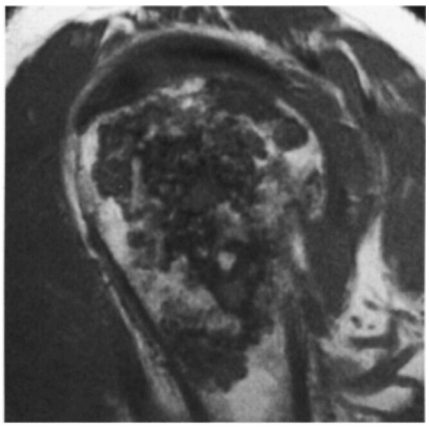

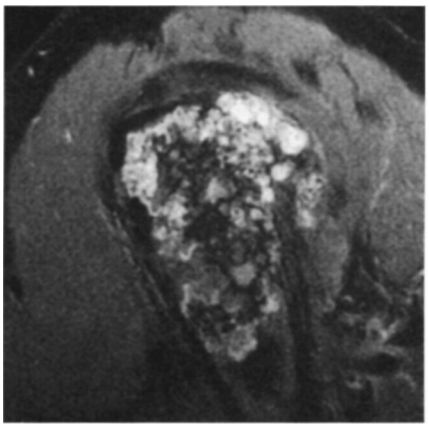

b, c

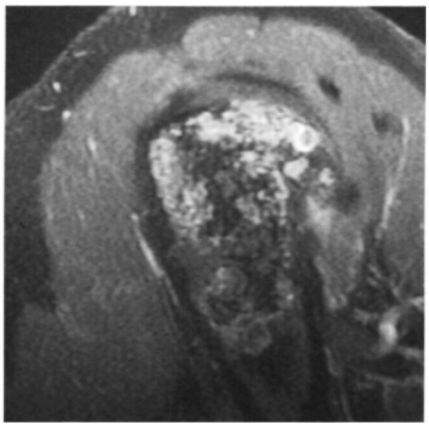

d

Figure **49 a-d** A 70-year-old man with a chondrosarcoma involving the proximal humerus. Oblique lateral radiograph (**a**) shows a lesion containing prominent chondroid matrix mineralization. The lesion has lobulated, circumscribed and irregular margins, and contains low-intermediate signal on sagittal (**b**) T1WI, and heterogeneous low, intermediate, and high signal on sagittal (**c**) FS - T2WI. The lesion shows heterogeneous diffuse Gd-contrast enhancement on sagittal (**d**) FS T1WI.

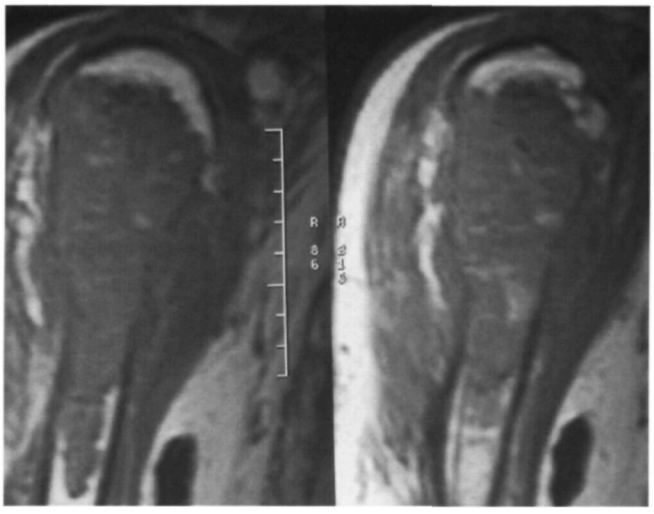

a

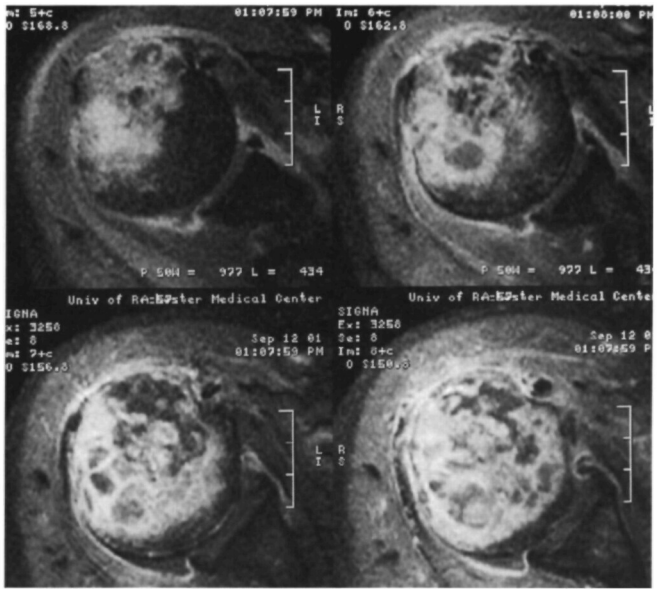

b

Figure **50 a, b** An 88-year-old man with a dedifferentiated chondrosarcoma involving the proximal humerus. The lesion has both lobulated circumscribed and irregular margins, and contains low-intermediate signal on sagittal (**a**) T1WI. The lesion shows prominent heterogeneous Gd-contrast enhancement on axial (**b**) FST1WI which through the cortex. Sense unclear, something missing?

a

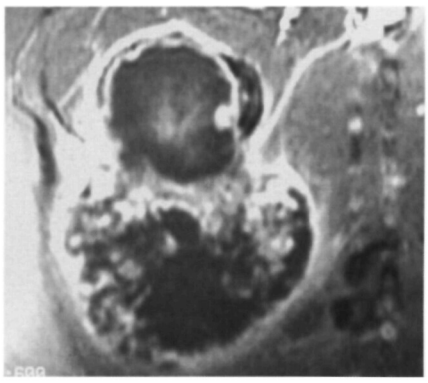

b, c

Figure **51 a-c** A 34-year-old man with a high-grade, myxoid chondrosarcoma involving the proximal femur, with cortical destruction and extra-osseous extension of tumor dorsally. AP radiograph (a) shows a radiolucent lesion containing mineralized chondroid matrix. The lesion has irregular circumscribed margins and contains high signal on axial (**b**) FS T2WI. The lesion shows lobulated irregular peripheral Gd-contrast enhancement on axial (**c**) FS T1WI.

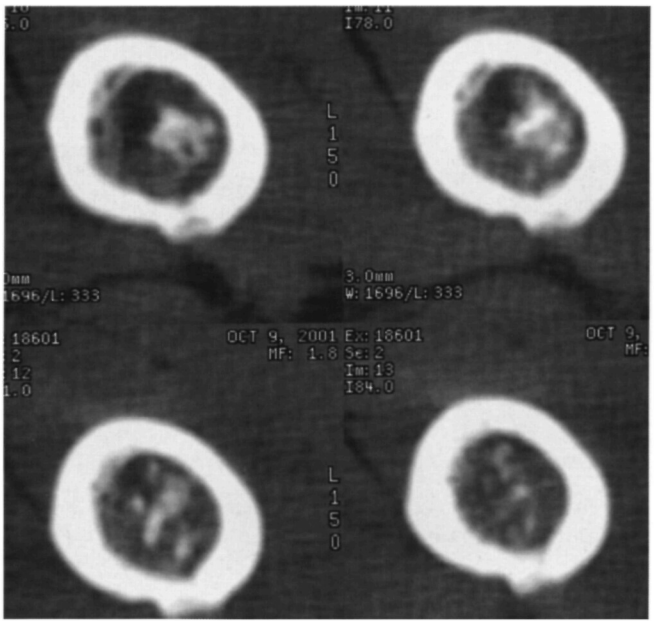

a

b

Figure **52 a, b** A 41-year-old man with a low-grade chondrosarcoma involving the proximal diaphysis of the femur. Axial CT images (**a**) show intramedullary chondroid matrix mineralization. The lesion has lobulated circumscribed margins and contains high signal on coronal (**b**) FS T2WI.

erogeneous depending on the degree of matrix mineralization and/or necrosis.[10,11,27] MRI can readily show sites of cortical destruction and extension of tumor into the adjacent soft tissues.

Peripheral chondrosarcomas. MRI can easily demonstrate the thickness of cartilaginous caps of osteochondromas, as well as erosive and/or destructive changes involving osteochondromas. Cartilage cap thickness exceeding 2 cm is commonly associated with malignant degeneration or dedifferentiation of osteochondromas into secondary chondrosarcomas. Lesions have low-intermediate signal on T1WI, intermediate signal on PDWI, and heterogeneous intermediate-high signal on T2WI (Figs. **56, 57**). Lesions show heterogeneous contrast enhancement, with or without Gd-contrast enhancement of adjacent soft tissues, suggesting tumor invasion.

Periosteal chondrosarcomas.[21,33,40] These tumors vary in size from 4 to 11 cm. The bone cortex is either thinned or thickened but not destroyed. Lesions occasionally involve medullary bone. Juxtacortical soft tissue components of the lesion can have chondroid calcifications, with or without radial periosteal bone formation, and/or a thin peripheral rim of periosteal bone. Lesions have low-intermediate signal on T1W1, intermediate signal on PDWI, and heterogeneous intermediate-high signal on T2WI (Fig. **55**). Lesions show heterogeneous contrast enhancement. Gd-contrast enhancement of adjacent soft tissues may be seen from tumor invasion.

Clear cell chondrosarcomas.[4,18,33] Lesions usually are seen near the ends of long bones, with or without extension into metaphyseal and diaphyseal regions. Smaller lesions may be well circumscribed; larger lesions may have associated cortical disruption and extension into adjacent soft tissues. Lesions typically have low-intermediate signal on T1WI and heterogeneous intermediate-high signal on T2WI. Lesions usually show prominent Gd-contrast enhancement.

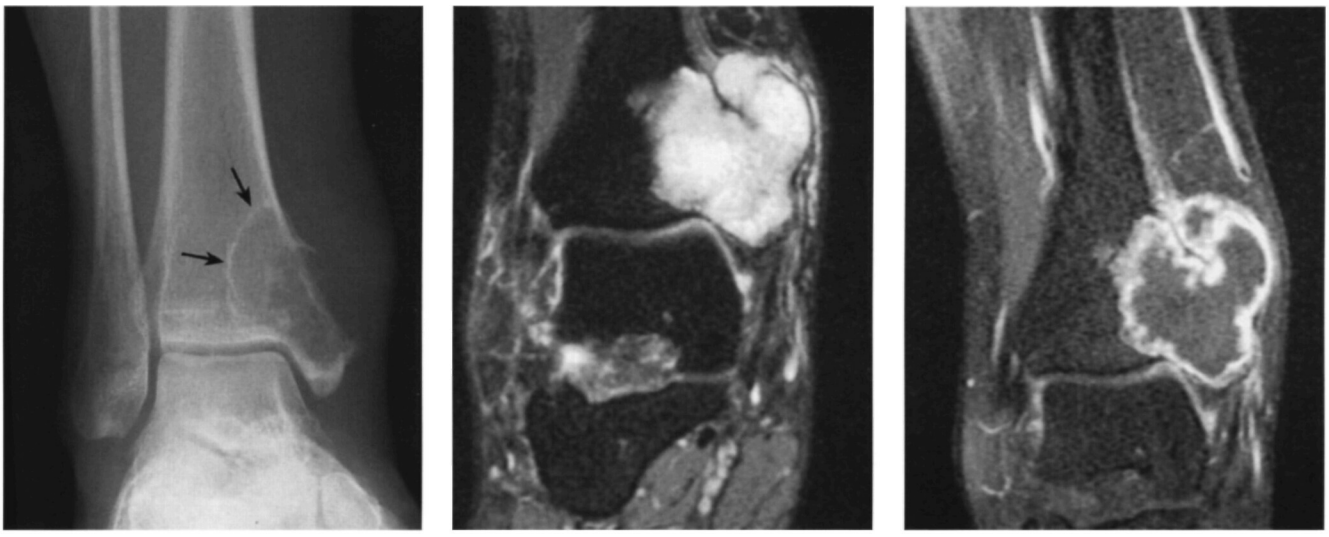

Figure **53 a-c** A 44-year-old woman with a grade 2 chondrosarcoma involving the distal tibia. AP radiograph (**a**) shows a radiolucent intramedullary lesion with erosion and destruction of cortical bone. The tumor has lobulated, circumscribed margins and contains mostly high signal on coronal (**b**) FS T2WI. The tumor extends into the adjacent soft tissues through a zone of cortical destruction. The tumor shows irregular peripheral lobular Gd-contrast enhancement on coronal (**c**) FS T1WI.

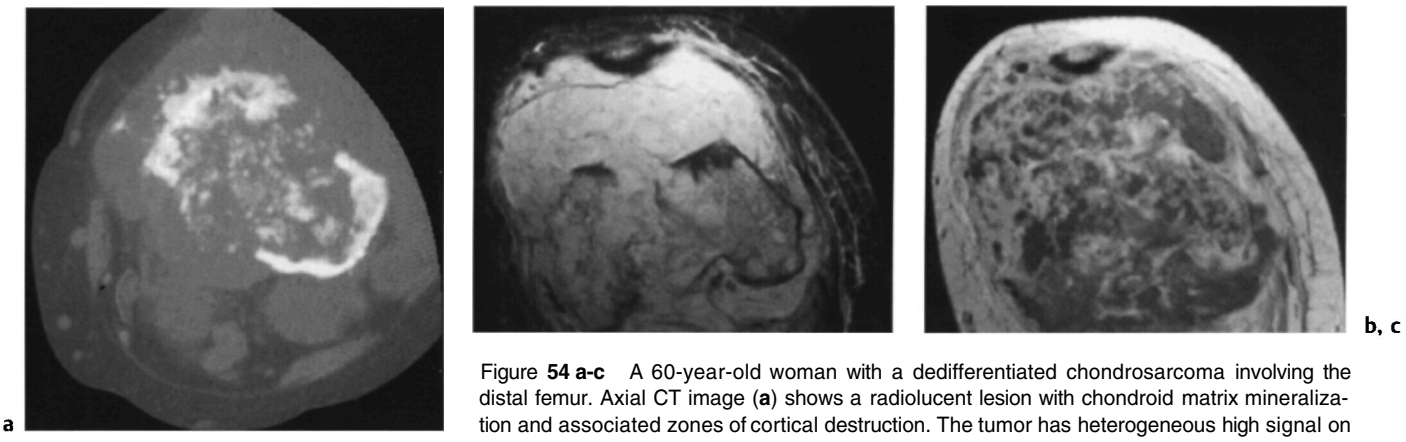

Figure **54 a-c** A 60-year-old woman with a dedifferentiated chondrosarcoma involving the distal femur. Axial CT image (**a**) shows a radiolucent lesion with chondroid matrix mineralization and associated zones of cortical destruction. The tumor has heterogeneous high signal on axial (**b**) FS T2WI. Extensive cortical destruction is seen with tumor extension from the marrow into the knee joint and adjacent soft tissues. The lesion shows irregular heterogeneous Gd-contrast enhancement on axial (**c**) T1WI.

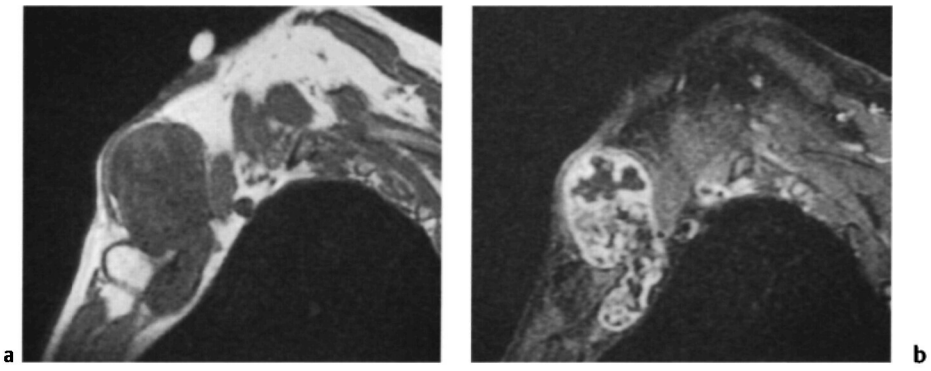

Figure **55** A 40-year-old man with a low-grade, perisoteal chondrosarcoma along the cortical surface of the clavicle. The lesion has circumscribed margins and contains intermediate signal on sagittal (**a**) T1WI, and shows irregular peripheral and central lobular Gd-contrast enhancement on axial sagittal (**b**) FS T1WI.

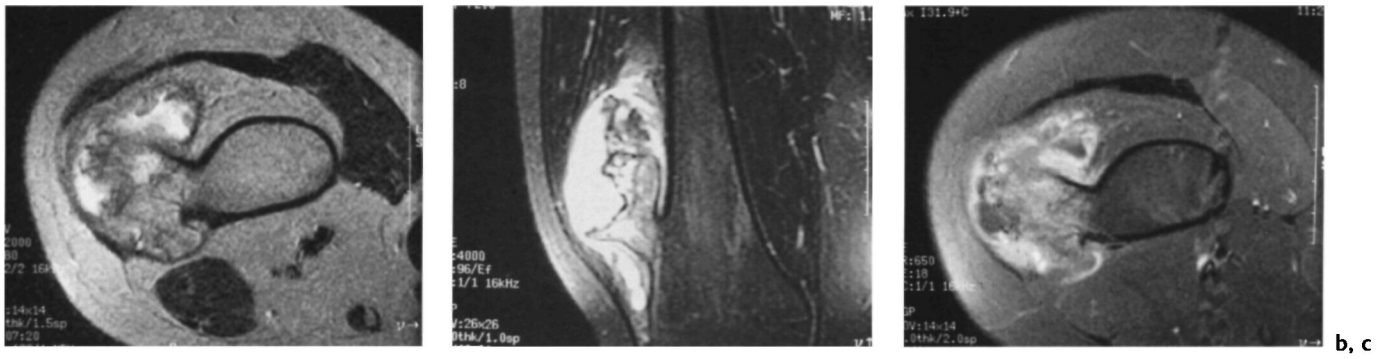

Figure **56 a-c** An 18-year-old woman with a secondary low-grade chondrosarcoma arising from an osteochondroma at the distal femur. The thickened cartilaginous cap of the tumor has irregular circumscribed margins and contains heterogeneous slightly high and high signal with small foci of low signal on axial (**a**) T2WI, and high signal on coronal (**b**) FS T2W1. Zones of cortical destruction are seen at the osteochondroma adjacent to the malignant cartilaginous cap. The lesion shows irregular heterogeneous Gd-contrast enhancement on axial (**c**) FS T1WI.

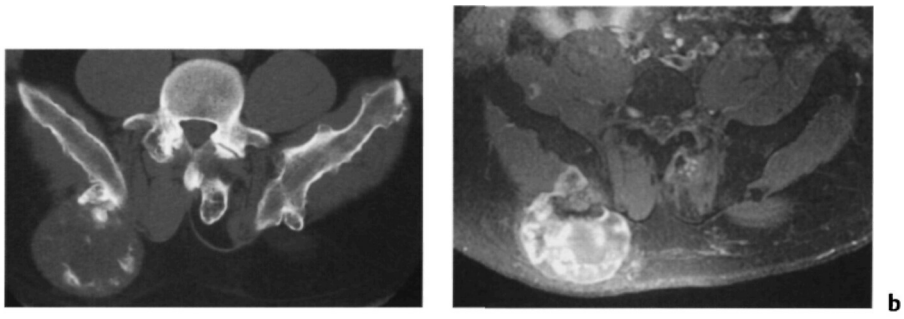

Figure **57 a, b** A 30-year-old man who has multiple hereditary exostoses (osteochondromas) and a secondary low-grade chondrosarcoma arising from an osteochondroma at the posterior right iliac bone. Axial CT image (**a**) shows the tumor to have soft tissue attenuation as well as foci of chondroid mineralization. The thickened cartilaginous cap of the tumor has circumscribed margins and shows irregular heterogeneous Gd-contrast enhancement on axial (**b**) FS T1WI.

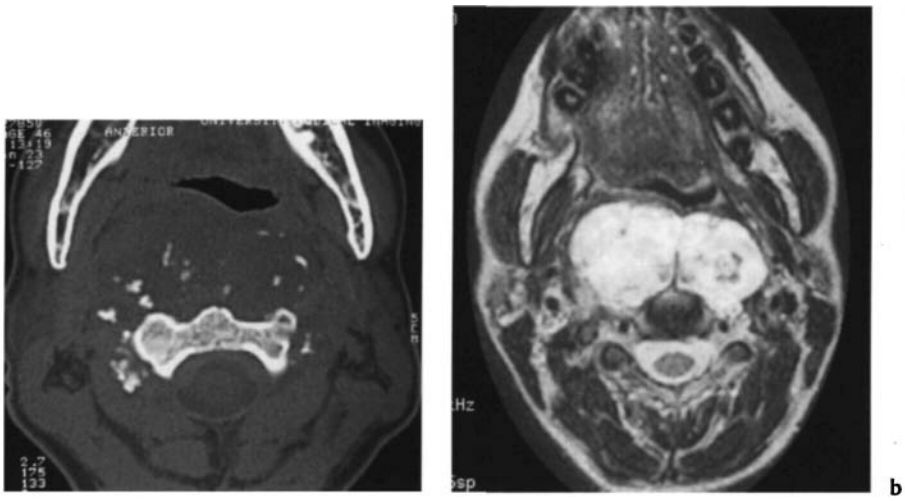

Figure **58** A 44-year-old woman with a well-differentiated extra-osseous chondrosarcoma located ventral to the cervical spine. Axial CT image (**a**) shows the tumor to have soft tissue attenuation as well as foci of chondroid mineralization. The tumor has circumscribed margins and contains mostly high signal on axial T2WI (**b**) as well as small zones of low signal.

Dedifferentiated chondrosarcomas.[28,33] Lesions usually have low-intermediate signal on T1WI and PDWI, and heterogeneous predominantly high signal on T2W1 (Figs. **50, 54**). Zones of low signal on T2WI are related to the presence and degree of matrix mineralization and/or fibrous tissue. Lesions often have irregular poorly-defined margins and associated cortical destruction. Lesions usually show heterogeneous contrast enhancement. MRI can readily show sites of extension of the lesion into the adjacent soft tissues.

Mesenchymal chondrosarcomas.[17,28,33,36] Tumors are usually destructive lesions commonly associated with extra-osseous soft tissue masses. Lesions have low-intermediate signal on T1WI, intermediate signal on PDWI, and heterogeneous intermediate-high or slightly high signal on T2WI. Foci of low signal on T1WI and T2WI can be seen secondary to chondroid matrix mineralization. Lesions typically show heterogeneous Gd-contrast enhancement.[36] Mesenchymal chondrosarcomas can arise in soft tissues (Fig. **60)** or bone.[36]

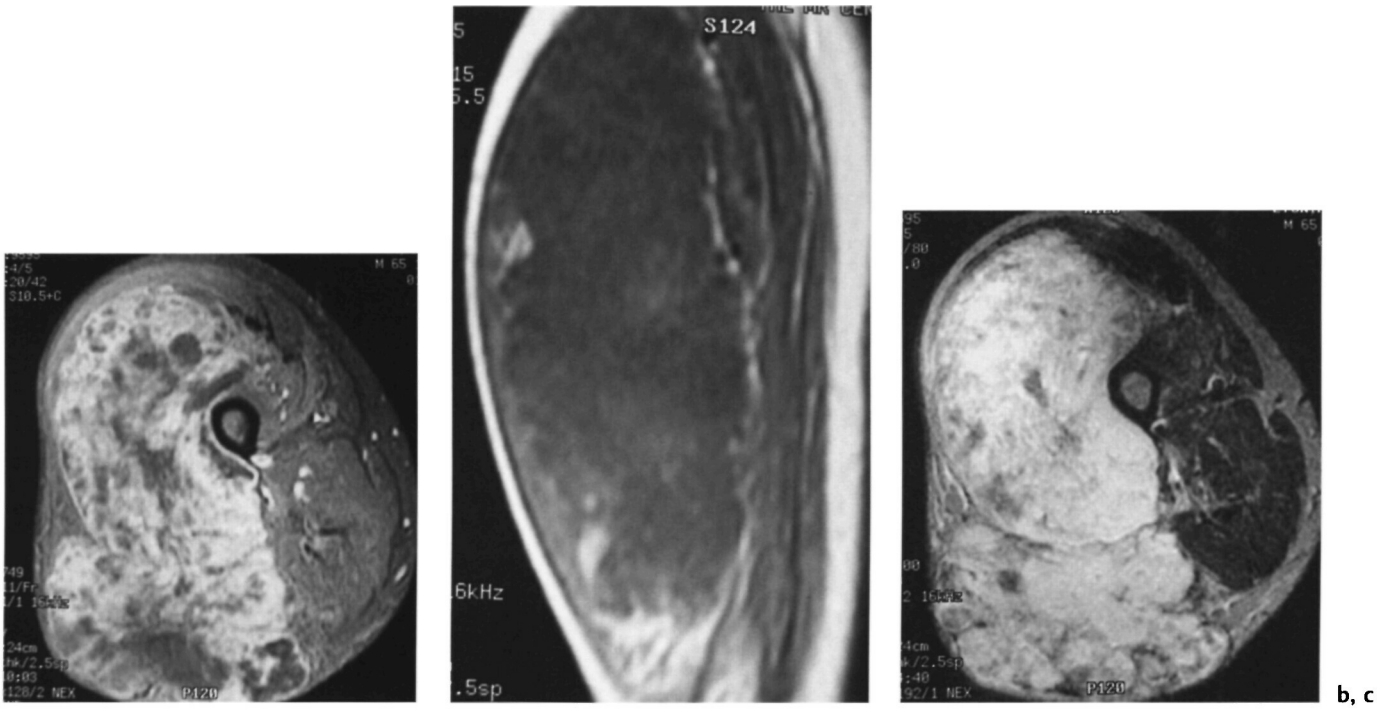

a b, c

Figure **59 a, b** A 65-year-old man with an extra-osseous myxoid chondrosarcoma in the distal thigh. The lesion has circumscribed margins and contains heterogeneous mostly high signal with small foci of low signal on axial (**a**) T2WI. The lesion shows prominent irregular heterogeneous Gd-contrast enhancement on axial (**b**) FS T1WI.

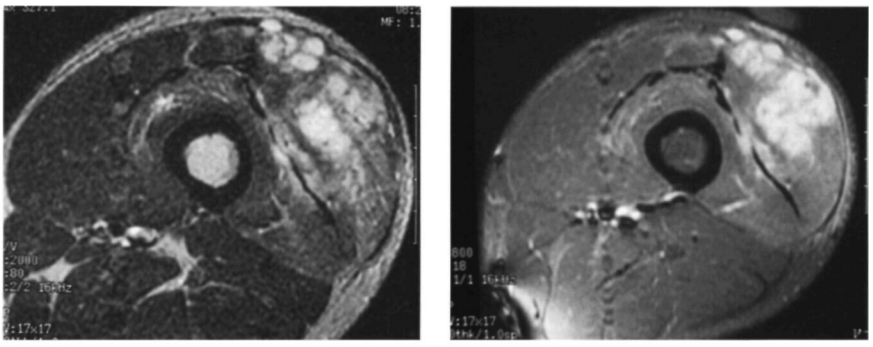

a b

Figure **60 a, b** An 18-year-old man with an extra-osseous mesenchymal chondrosarcoma involving the vastus lateralis and adjacent soft tissues in the distal thigh. The tumor has poorly defined margins and has heterogeneous mostly high signal on axial T2WI (**a**). The lesion shows prominent irregular Gd-contrast enhancement on axial FS TIWI(**b**).

Myxoid chondrosarcomas.[19,33] These tumors can occur in bone (Fig. **51**) or arise in soft tissues (Fig. **59**). In soft tissues, tumors often have lobulated margins and range in size from 4 to 7 cm. Lesions usually have low-intermediate signal on T1WI and PDWI, and predominantly high signal on T2WI. Hemorrhagic foci in myxoid chondrosarcomas can show intermediate to high signal on T1WI and T2WI. Myxoid chondrosarcomas show heterogeneous contrast enhancement.

Differential Diagnosis

Enchondroma, fracture callus, fibrous dysplasia, chondroblastoma, chondromyxoid fibroma, chondroblastic osteosarcoma, osteoblastoma, bone infarct, chordoma. The distinction between an enlarging symptomatic enchondroma and a low-grade chondrosarcoma can be difficult based on imaging features.

Treatment and Prognosis

Conventional chondrosarcomas.[1,3,8,13,33] Treatment often consists of en-bloc surgical resection, with or without limb salvage procedures in long bones.[1,3,8,38] These tumors are usually resistant to radiation.[8] Fractionated proton beam radiation has also been used.[1] The prognosis for grade 1 and 2 lesions is related to the extent of resection. The 5-year survival rates for grade 1 tumors range from 71 to 94%, 40 to 75% for grade 2 tumors, and 15 to 44% for grade 3 tumors.[1,2,8,33] Local recurrence usually occurs within 3 years after surgery.[1] Metastatic risk is high for grade 3 lesions with rates of 75-85% at 5 years.[8]

Peripheral chondrosarcomas. These tumors are treated with en bloc resection.[31] The 5-year survival rate ranges from 80 to 90%.[31]

Periosteal chondrosarcomas. Treatment typically consists of wide resection.[9,31,33] These tumors are usually well-differentiated chondrosarcomas and often have a favorable prognosis.[9,31]

Clear cell chondrosarcomas. These tumors are considered a low-grade malignancy.[4,9,13,31,33] Treatment is en bloc or wide resection, which is associated with a 16% recurrence rate and 8% mortality.[4,9,31,33] A 5-year survival rate of 92% has been reported.[9] Local recurrence may occur up to 15 years after initial surgery.[38] Metastases occur in 15-25% of patients and are commonly located in the lungs, brain, and bone.[9,13,33]

Dedifferentiated chondrosarcomas. These are aggressive malignant neoplasms with 5-year survival of 8 to 13%, median survival of 6 months.[1,2,9,13,38] Metastases are common and are often located in the lungs, bones, and visceral organs.[9,13] Standard treatment is radical resection, followed by radiation and chemotherapy.[9,13]

Mesenchymal chondrosarcomas. These tumors are aggressive sarcomas with 5-year survival rates between 40 and 60% and 10-year survival rates of 25-30%.[1,9,16,33] A mean survival rate of 38 months has been reported.[15,17] Metastases occur in 60% of cases, and occur most frequently in lung, lymph nodes, and bone.[1] Treatment usually consists of wide surgical excision.[6,9,17,33]

Myxoid chondrosarcomas. The 5-year survival rate is 90%, and the 10-year survival rate ranges from 45 to 78%.[19,26,33] Metastases occur in 46% of patients.[26] Histologic grading is not reliable for prognosis.[26] Treatment usually consists of wide surgical excision.[6,33] Radiation and chemotherapy have not been effective to date.[6]

References

1 Barnes L. Pathobiology of selected tumors of the base of the skull. *Skull Base Surg* 1991;1:207-216.

2 Bertoni F, Bacchini P, Hogendoorn PCW. Chondrosarcoma. In: Fletcher CDM, Unni KK, Mertens F, eds. *World Health Organization Classification of Tumours. Pathology and Genetics of Tumours of Soft Tissue and Bone* Geneva: IARC Press; 2002:247-251.

3 Brien EW, Mirra JM, Kerr R. Benign and malignant cartilage tumors of bone and joint: their anatomic and theoretical basis with an emphasis on radiology, pathology and clinical biology. *Skeletal Radiol* 1997;26:325-353.

4 Cannon CP, Nelson SD, Seeger SD, Eckardt JJ. Clear cell chondrosarcoma mimicking chondroblastoma in a skeletally immature patient. *Skeletal Radiol* 2002;31:369-372.

5 Das Gupta TK, Chaudhuri PK. Pathology of soft tissue sarcoma. In: Das Gupta TK, Chaudhuri PK, eds. Tumors *of the Soft Tissues* 2nd ed. New York, NY: Appleton and Lange; 1998:63-200.

6 Das Gupta TK, Chaudhuri PK. Heterotopic bone and cartilage. In: Das Gupta TK, Chaudhuri PK, eds. Tumors *of the Soft Tissues* 2nd ed. New York, NY: Appleton and Lange; 1998:465-469.

7 Dei Tos AP, Wadden C, Fletcher Christopher DM. Extraskeletal myxoid chondrosarcoma: an immunohistochemical reappraisal of 39 cases. *Appl Immunohistochem Mol Morphol* 1997;5(2):73-77.

8 Forest M. Chondrosarcoma. In: Forest M, Tomeno B, Vanel D, eds. *Orthopedic Surgical Pathology: Diagnosis of Tumors and Pseudotumoral Lesions of Bone and Joints* Edinburgh: Churchill Livingstone; 1998:233-256.

9 Forest M. Chondrosarcoma: variants. In: Forest M, Tomeno B, Vanel D, eds. *Orthopedic Surgical Pathology: Diagnosis of Tumors and Pseudotumoral Lesions of Bone and Joints.* Edinburgh: Churchill Livingstone; 1998:261-288.

10 Geirnaerdt MJ, Hogendoorn PC, Bloem JL, Taminiau AH, van der Woude HJ. Cartilaginous tumors: fast contrast-enhanced MR imaging. *Radiology* 2000;214(2):539-546.

11 Hanna SL, Magill HL, Parham DM, Bowman LC, Fletcher BD. Childhood chondrosarcoma: MR imaging with gadolinium-DTPA. *Magn Reson Imaging* 1990;8(5):669-672.

12 Hassounah M, Al-Mefty 0, Akhtar M, Jinkins JR, Fox JL. Primary cranial and intracranial chondrosarcoma-a survey. *Acta Neurochir (Wien)* 1985;78:123-132

13 Helliwell TR. Central cartilaginous neoplasms of bone. In: Helliwell TR, ed. *Major Problems in Pathology: Pathology of Bone and Joint Neoplasms.* Vol 37. 1st ed. Philadelphia, Pa: W.B. Saunders 1999: 193-214.

14 Hieken TJ, Levine EA. Molecular biology of soft tissue tumors. In: Das Gupta TK, Chaudhuri PK, eds. Tumors *of the Soft Tissues.* 2nd ed. New York, NY: Appleton and Lange; 1998:201-225.

15 Huvos AG. Chondrosarcoma including spindle-cell (dedifferentiated) and myxoid chondrosarcoma; mesenchymal chondrosarcoma. In: Huvos AG, ed. *Bone Tumors: Diagnosis, Treatment, and Prognosis* 2nd ed. Philadelphia, Pa: W.B. Saunders; 1991:343-362.

16 Janzen L, Logan PM, O'Connell JX, Connell DG, Munk PL. Intramedullary chondroid tumors of bone: correlation of abnormal peritumoral marrow and soft-tissue MRI signal with tumor type. *Skeletal Radiol* 1997;26:100-106.

17 Johnson DBS, Breidahl W, Newman JS, Devaney K, Yahanda A. Extraskeletal mesenchymal chondrosarcoma of the rectus sheath. *Skeletal Radiol* 1997;26:501-504.

18 Kaim AH, Hugli R, Borel HM, Jundt G. Chondroblastoma and clear cell chondrosarcoma: radiological and MRI characteristics with histopathologic correlation. *Skeletal Radiol* 2002;31:88-95.

19 Kransdorf MJ, Murphey MD. Extraskeletal osseous and cartilaginous tumors. In: *Imaging of Soft Tissue Tumors* 2nd ed. Philadelphia, Pa: W. B. Saunders; 2006:437-480.

20 Kransdorf MJ. Malignant soft-tissue tumors in a large referral population: distribution of diagnoses by age, sex, and location. *AJR Am J Roentgenol* 1995;164:129-134.

21 Kumta SM, Griffith JF, Chow Louis TC, Leung PC. Primary juxtacortical chondrosarcoma dedifferentiating after 20 years. *Skeletal Radiol* 1998;27:569-573.

22 Lee YY, Van Tassel P. Craniofacial chondrosarcomas: imaging findings in 15 untreated cases. *AJNR Am J Neuroradiol* 1989;10:165-170.

23 Lucas DR, Heim S. Extraskeletal myxoid chondrosarcoma. In: Fletcher CDM, Unni KK, Mertens F, eds. *World Health Organization Classification of Tumours. Pathology and Genetics of Tumours of Soft Tissue and Bone* Geneva: IARC Press; 2002:213-215.

24 Mack MG, Vogl TJ. MR-guided ablation of head and neck tumors. *Magn Reson Imaging Clin N Am* 2002;10(4):707-713.

25 McCarthy EF, Freemont A, Hogendoorn PCW. Clear cell chondrosarcoma. In: Fletcher CDM, Unni KK, Mertens F, eds. *World Health Organization Classification of Ttumours. Pathology and Genetics of Tumours of Soft Tissue and Bone* Geneva: IARC Press; 2002:257-258.

26 Meis-Kindblom JM, Bergh P, Gunterberg B, Kindblom LG. Extraskeletal myxoid chondrosarcoma: a reappraisal of its morphologic spectrum and prognostic factors based on 117 cases. *Am J Surg Pathol* 1999;23(6):636-650.

27 Meyers SP, Hirsch WL Jr, Curtin HD, Barnes L, Sekhar LN, Sen C. Chondrosarcomas of the skull base: MR imaging features. *Radiology* 1992;184(l):103-108.

28 Milchgrub S, Hogendoorn PCW. Dedifferentiated chondrosarcoma. In: Fletcher CDM, Unni KK, Mertens F, eds. *World Health Organization Classification of Tumours. Pathology and Genetics of Tumours of Soft Tissue and Bone* Geneva: IARC Press; 2002:252-254.

29 Mulder JD, Schutte HE, Kroon HM, Taconis WK. Introduction. In: *Radiologic Atlas of Bone* Tumors Amsterdam: Elsevier; 1993:3-6.

30 Mulder JD, Schutte HE, Kroon HM, Taconis WK. The diagnosis of bone tumors. In: *Radiologic Atlas of Bone Tumors* Amsterdam: Elsevier; 1993:9-46.

31 Mulder JD, Schutte HE, Kroon HM, Taconis WK. Chondrosarcoma. In: *Radiologic Artaso/Bone Tumors* Amsterdam: Elsevier; 1993:139-191.

32 Murphey MD, Flemming DJ, Boyea SR, Bojescul JA, Sweet DE, Temple HT. From the archives of the AFIP. Enchondroma versus chondrosarcoma of the appendicular skeleton: differentiating features. *Radiographics* 1998;18:1213-1237.

33 Murphey MD, Walker EA, Wilson AJ, Kransdorf MJ, Temple HT, Gannon FH. From the archives of the AFIP. Imaging of primary chondrosarcoma: radiologic-pathologic correlation. *Radiographics* 2003;23:1245-1278.

34 Nakashima Y, Park YK, Sugano O. Mesenchymal Chondrosarcoma. In: Fletcher CDM, Unni KK, Mertens F, eds. *World Health Organization Classification of Tumours. Pathology and Genetics of Tumours of Soft Tissue and Bone* Geneva: IARC Press; 2002:255-256.

35 Salisbury JR. Bone neoplasms containing epithelial and epithelioid cells. In: Helliwell TR, ed. *Major Problems in Pathology: Pathology of Bone andJoint Neoplasms* Vol 37. 1st ed. Philadelphia, Pa: W.B. Saunders; 1999:359-360.

36 Shinaver CN, Mafee MF, Choi KH. MRI of mesenchymal Chondrosarcoma of the orbit: case report and review of the literature. *Neuroradiology* 1997;39:296-301.

37 Taconis WK, van der Heul RO, Taminiau AMM. Synovial Chondrosarcoma: report of a case and review of the literature. *Skeletal Radiol* 1997;26:682-685.

38 Unni KK. Introduction and scope of study. In: *Dahlin's Bone Tumors: General Aspects and Data in 11087 Cases* 5th ed. Philadelphia, Pa: Lippincott, Williams & Wilkins; 1996:1-9.

39 Unni KK. Chondrosarcoma (primary, secondary, dedifferentiated, and clear cell). In: *Dahlin's Bone Tumors: General Aspects and Data in 11087 Cases* 5th ed. Philadelphia, Pa: Lippincott, Williams & Wilkins; 1996:71-106.

40 Vanel D, De Paolis M, Monti C, Mercuri M, Picci P. Radiological features of 24 periosteal chondrosarcomas. *Skeletal Radiol* 2001; 30:208-212.

A 12 Chordoma

ICD-O Code

Chordoma: 9370/3
Chondroid chordoma: 9371/3
Dedifferentiated chordoma: 9372/3

Definition

Chordomas are rare, locally aggressive, slow-growing, low to intermediate malignant tumors derived from ectopic notochordal remnants along the axial skeleton.[2,6-9,14,15,17,9,20,28] Chordomas that contain high sarcomatous components are referred to as dedifferentiated chordomas or sarcomatoid chordomas.[14]

Frequency of Occurrence

Chordomas account for 2-4% of primary malignant bone tumors, 1-3% of all primary bone tumors; and less than 1% of intracranial tumors.[2,5,6,14-17,27,28] The annual incidence has been reported to be 0.18-0.3 per million.[20] Dedifferentiated chordomas or sarcomatoid chordomas account for less than 5% of all chordomas.[14]

Age at Presentation

From 6 to 84 years, median = 58 years[16,17;] mean = 48-55 years for sacrococcygeal chordomas; mean = 37-40 years for cranial chordomas.[16,17,27,28] Less than 5% of chordomas occur in patients below 20 years of age.[2]

Gender Ratio (M / F)

1.5 / 1 to 2 / 1 [2,8,14,17,28]

Location

Tumors occur in the sacrococcygeal region (29-47%), spheno-occipital region (basisphenoid > basiocciput > petrous apex) (32-38%), vertebrae (15-33%).[2,5,6,8,14] Locations for vertebral chordomas: cervical > lumbar > thoracic.[25] The vertebral body is the most common tumor site.[25] Eighty percent of the vertebral tumors extend into the epidural space.[25]

Signs and Symptoms

Sacrococcygeal. Patients can have pain and constipation.[14]

Spheno-occipital. Patients may have headaches, cranial neuropathies (diplopia from involvement of the VIth cranial nerve is the most common symptom, followed by neuropathies related to involvement of cranial nerves V, VII to XII), pituitary dysfunction[2,6,8,13,14] The duration of symptoms can range from weeks to 14 years.[8] Vertebral. Signs and symptoms may be related to spinal canal or nerve root compression.[14]

Cross Pathologic Findings

Chordomas are usually soft, lobulated encapsulated tumors, often gray and translucent.[2,6-9,14,17,19,20,25,28] Hemorrhagic zones may be present.[25] Cranial chordomas usually range in size from 1 to 8 cm with mean tumor size of 3.8 x 3.9 x 4.1 cm.[13]

Histopathologic Findings[2,6-9,14,17,19,20,28]

Chordomas can be divided into three types: conventional chordomas, chondroid chordomas, and dedifferentiated chordomas.

Conventional chordomas (80 to 85%) are observed as a lobular cellular pattern composed of epithelioid cells with vacuolated cytoplasm (physaliferous cells) containing glycogen within a mucoid matrix. Tumor cells are positive to immunohistochemical determinations for keratin and epithelial membrane antigen, allowing distinction from chondrosarcomas.

Chondroid chordomas (5-15%) show both chordomatous and chondromatous differentiation.

Dedifferentiated chordomas (5%) show zones of both conventional chordoma and malignant mesenchymal cells (malignant fibrous histiocytoma, fibrosarcoma, osteosarcoma). Dedifferentiated chordomas can occur de novo, in chordoma after radiation treatment, or within a long-extant chordoma.

Tumor Genetics

Tumors often contain hypodipolid cells with chromosome numbers ranging from 33 to 44.[14] Losses of chromosomes 3, 4, 10, and 13 are often seen.[14] Commonly deleted segments include: 1 p31-pter, 3p21-pter, 3q21-qter, 9p24-pter, and 17q11-qter.[14]

Findings on Plain Films (Roentgenograms) and Computed Tomography[4-6,9,12,13,17,18,24,28]

Chordomas are typically destructive, radiolucent lesions involving the skull-base and sacrum/coccyx, usually associated with a soft tissue mass (Fig. **63, 65**). Vertebral lesions are usually located at the dorsal portions of the vertebral bodies.

Findings on Radionuclide Bone Scans

Soft tissue components of chordomas usually show minimal or no radiopharmaceutical accumulation. Areas of bone erosion or destruction resulting from chordoma typically have increased radiopharmaceutical accumulation.

MRI Findings[3-7,11-14,17,18,25,26,28]

Sacrococcygeal chordomas.[4,7,14,17] These tumors are often large, destructive lesions involving the sacrum with presacral and/or postsacral soft tissue masses. Lesions often have low-intermediate signal on T1WI, with or without foci of high signal (Fig. **65**). On T2WI, lesions often have heterogeneous predominantly high signal, with or without septa or bands of low signal. Chordomas typically enhance with Gd-contrast in a heterogeneous pattern.

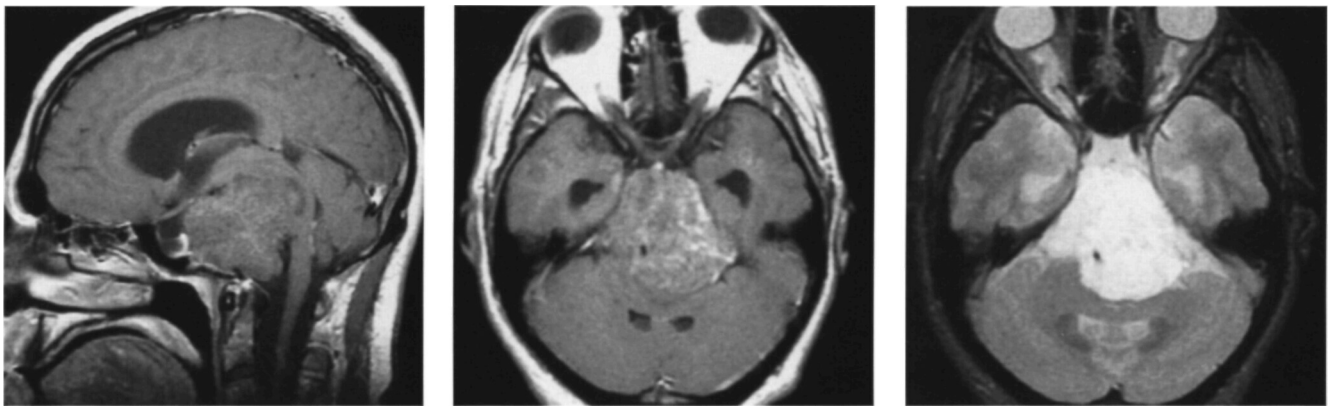

Figure **61 a-c** A 33-year-old man with a chordoma involving the clivus with intracranial extension causing compression of the brainstem. Irregular Gd-contrast enhancement is seen in only portions of the tumor on sagittal (**a**) and axial (**b**) T1WI. The tumor has high signal on axial T2WI (**c**)

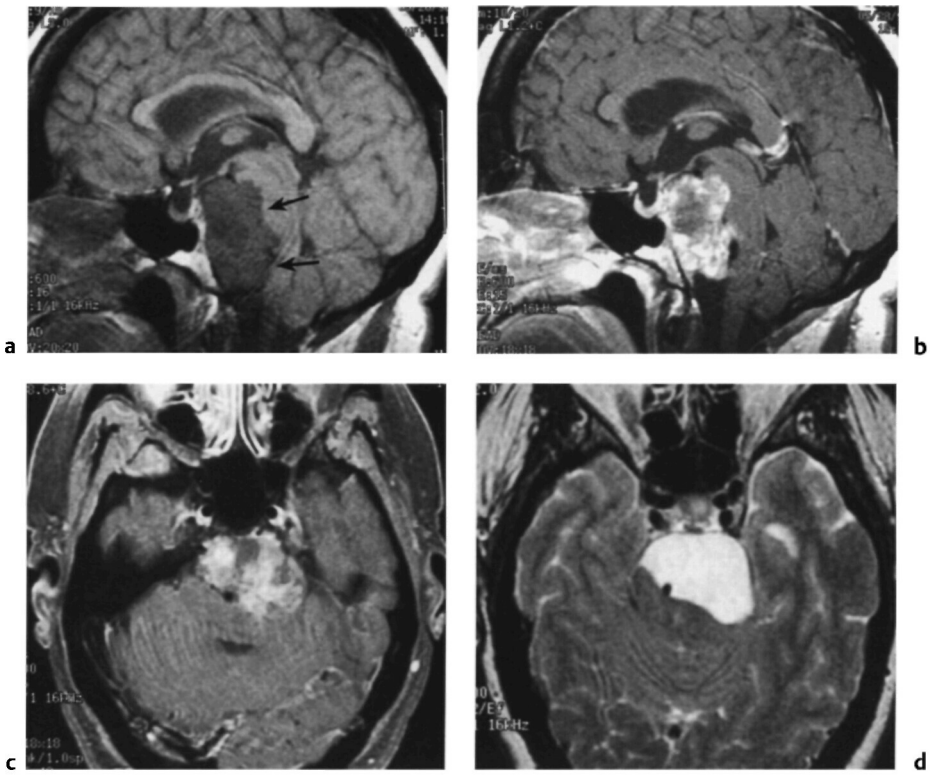

Figure **62 a-d** A 55-year-old woman with a chordoma involving the endocranial surface of the clivus with intracranial extension causing compression of the brainstem. The tumor has low-intermediate signal on sagittal (**a**) T1WI, and shows heterogeneous Gd-contrast enhancement on sagittal (**b**) and axial (**c**) T1WI. The tumor has high signal on axial (**d**) T2WI.

Spheno-occipital chordomas.[5,6,11-13,18] Lesions range from 1 to 8cm in size, mean 4cm. Conventional chordomas are often midline in location, and usually have lobulated or slightly lobulated margins (Figs. **61-63**). Lesions usually erode or destroy bone with an associated soft tissue mass. Chondroid chordomas are either midline or off-midline in location. Chordomas typically have low-intermediate signal on TlWI and heterogeneous predominantly high signal on T2WI with or without sepate with low signal. Chordomas typically enhance with Gd-contrast, often in a heterogeneous pattern. Lesions can displace and encase blood vessels, and extend into adjacent structures such as the cavernous sinus, sella, nasopharynx, and hypoglossal canal.

Vertebral chordomas.[3,7,25] Lesions often involve the posterior portion of the vertebral body and are usually associated with destructive bony changes and soft tissue mass, with or without spinal canal compression. Lesions may rarely involve the epidural soft tissues with chronic bony erosion without internal bony involvement. Lesions often have low-intermediate signal on TlWl, and heterogeneous high signal on T2WI with or without septa of low signal (Fig. **64**). Lesions usually show moderate Gd-contrast enhancement. Chordomas in the spine typically do not involve the disks, despite the fact that the nucleus pulposis portions of the intervertebral disks are the last parts of the fetal notochord to involute.

Differential Diagnosis

Chondrosarcoma, metastases, plasmacytoma/myeloma, chordoid meningioma, osteomyelitis, eosinophilic granuloma, lymphoma. Additional considerations for skull base lesions include: pituitary adenoma, epidermoid, squamous cell carcinoma, adenoid cystic carcinoma, trigeminal neuroma, meningioma.

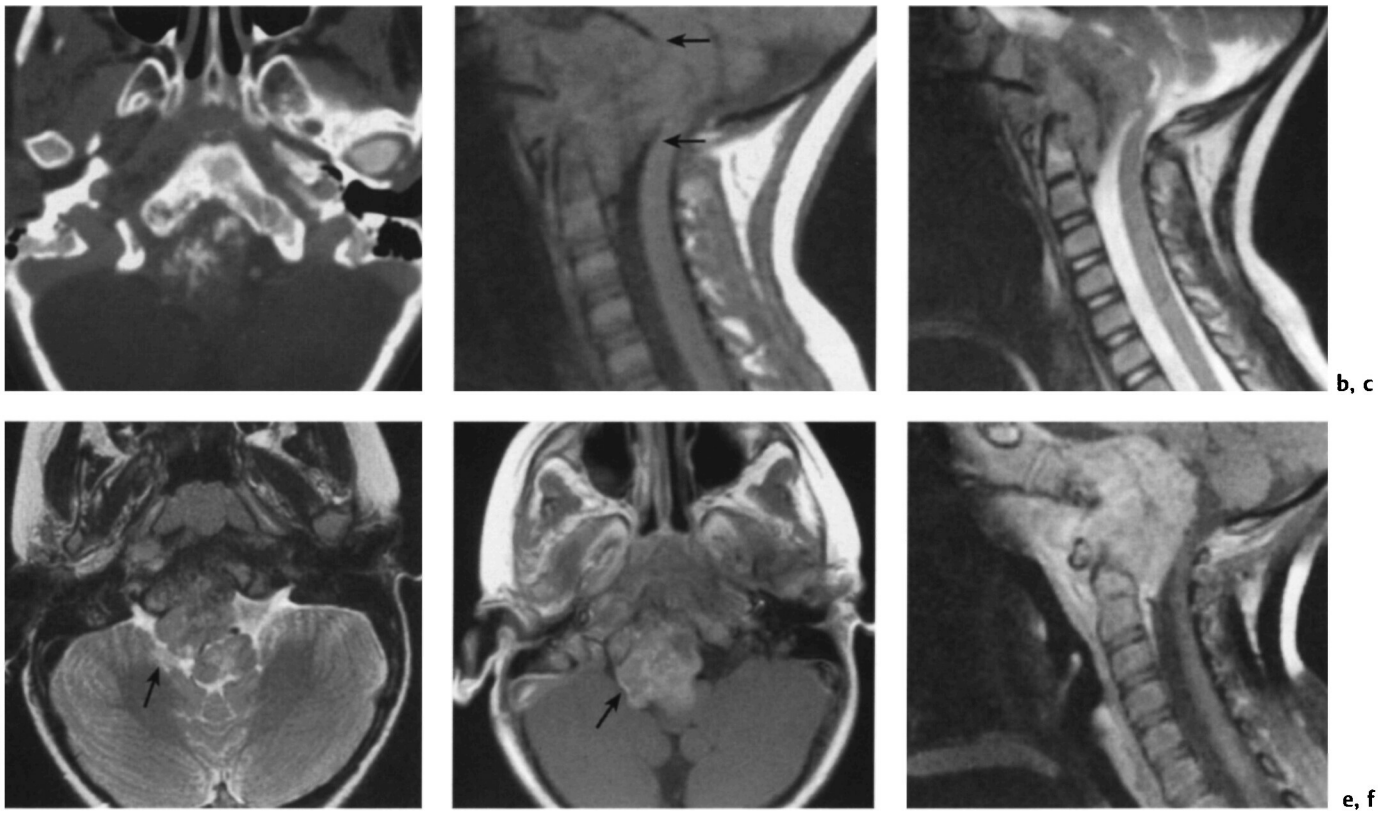

Figure **63 a-f** A 4-year-old female with a sarcomatoid chordoma involving the lower clivus and upper dens as well as the adjacent soft tissues at the craniovertebral junction, with extension dorsally causing compression of the medulla and upper spinal cord. Axial CT image (**a**) shows mineralization within the tumor and erosive changes at the dorsal margin of the clivus. The tumor has intermediate and low signal on sagittal (**b**) T1WI and sagittal (**c**) and axial (**d**) T2WI. The tumor shows heterogeneous moderate Gd-contrast enhancement on axial (**e**) T1WI and sagittal (**f**) FS T1WI.

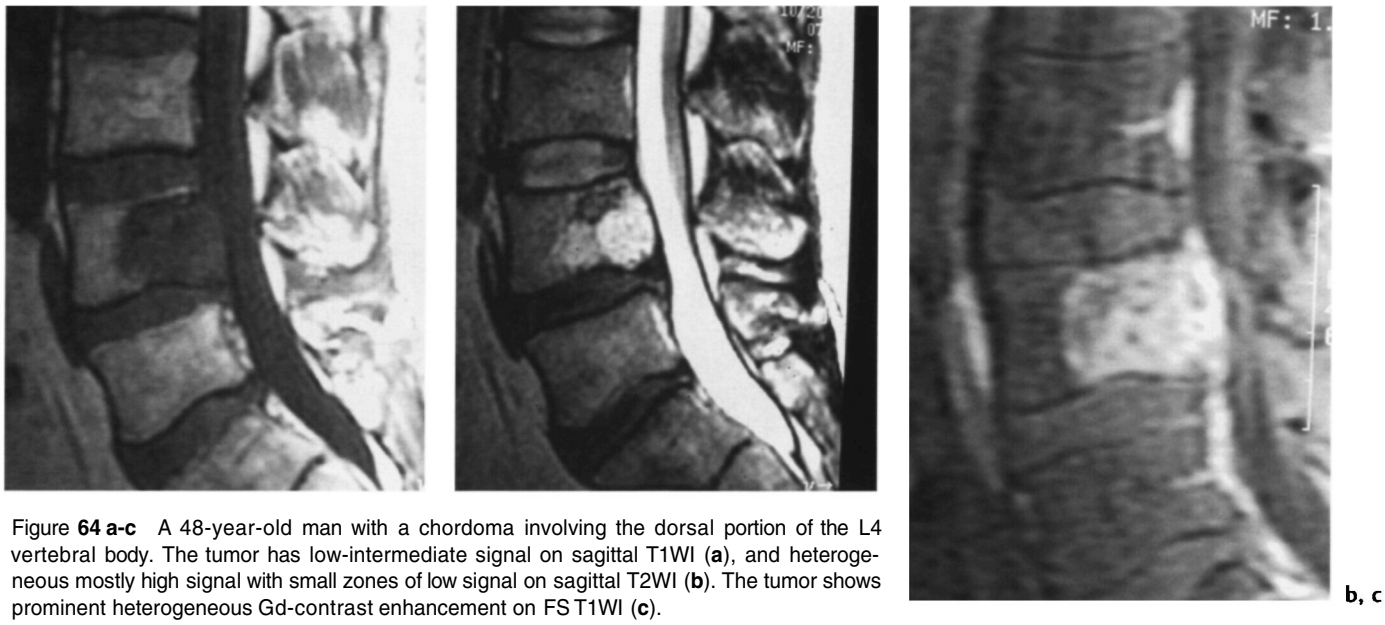

Figure **64 a-c** A 48-year-old man with a chordoma involving the dorsal portion of the L4 vertebral body. The tumor has low-intermediate signal on sagittal T1WI (**a**), and heterogeneous mostly high signal with small zones of low signal on sagittal T2WI (**b**). The tumor shows prominent heterogeneous Gd-contrast enhancement on FS T1WI (**c**).

Treatment and Prognosis[1,10,13,14,17,21-23,25,27,28]

Average survival for chondroid chordomas (16 years) is greater than for conventional chordomas (4 years). Morbidity and mortality are usually secondary to local recurrence and extension. Distant metastasis is uncommon. Systemic metastases occur in 7-14% of cases and are frequently located in lung, bone, lymph nodes, liver, and skin.[2,6] New aggressive surgical approaches have shown improved outcome.[6,13,21-23] Combined treatment of surgery and radiation is routinely used.[2,6] Proton beam radiation and stereotactic radiosurgery have also been used to treat chordomas of the skull base.[1,10]

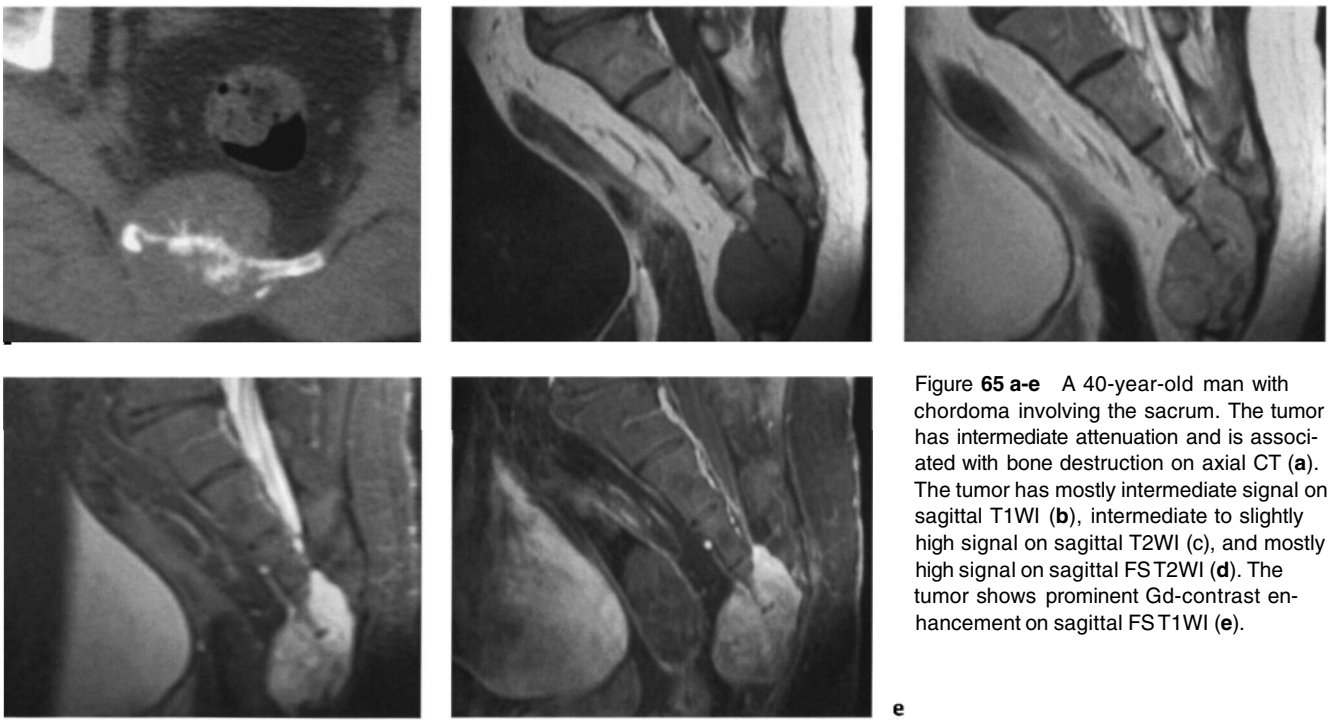

Figure **65 a-e** A 40-year-old man with chordoma involving the sacrum. The tumor has intermediate attenuation and is associated with bone destruction on axial CT (**a**). The tumor has mostly intermediate signal on sagittal T1WI (**b**), intermediate to slightly high signal on sagittal T2WI (c), and mostly high signal on sagittal FS T2WI (**d**). The tumor shows prominent Gd-contrast enhancement on sagittal FS T1WI (**e**).

References

1 Austin-Seymour M, Munzenrider J, Goitein M, et al. Fractionated proton radiation therapy of chordoma and low-grade chondrosarcoma of the base of the skull. *J Neurosurg* 1989;70:13-17.

2 Barnes L Pathobiology of selected tumors of the base of the skull. *Skull Base Surg* 1991;1(4):207-216.

3 Delank KS, Kriegsmann J, Drees P, Eckardt A, Eysel P. Metastasizing chordoma of the lumbar spine. *Eur Spine J* 2002;11:167-171.

4 Diel J, Ortiz 0, Losada RA, Price DB, Hayt MW, Katz DS. The sacrum: pathologic spectrum, multi-modality imaging, and subspecialty approach. *Radiographics* 2001;21:83-104.

5 Doucet V, Peretti-Viton P, Figarella-Branger D, Manera L, Salamon G. MRI of intracranial chordomas. Extent of tumour and contrast enhancement: criteria for differential diagnosis. *Neuroradiology* 1997; 39:571-576.

6 Erdem E, Angtuaco EC, Van Hemert R, Park JS, Al-Mefty 0. Comprehensive review of intra-cranial chordoma. *Radiographics* 2003;23: 995-1009.

7 Forest M. Chordoma. In: Forest M, Tomeno B, Vanel D, eds. *Orthopedic Surgical Pathology: Diagnosis of Tumors and Pseudotumoral Lesions of Bone and Joints* Edinburgh: Livingstone Churchill; 1998:397-410.

8 Heffelfinger MJ, Dahlin DC, MacCarty CS, Beabout JW. Chordomas and cartilaginous tumors at the skull base. *Cancer* 1973;32:410-420.

9 Huvos AG Chordoma. In: Huvos AG, ed. *Bone Tumors: Diagnosis, Treatment, and Prognosis* 2nd ed. Philadelphia, Pa: W.B. Saunders; 1991:599-617.

10 Kondziolka D, Lunsford LD, Flickinger JC. The role of radiosurgery in the management of chordoma and chondrosarcoma of the cranial base. *Neurosurgery* 1991;29(l):38-46.

11 Laine FJ, Nadel L, Braun IF. CT and MR imaging of the central skull base. Part 2. Pathologic spectrum. *Radiographics* 1990;10(5): 797-821.

12 Larson TC III, Houser OW, Laws ER Jr. Imaging of Cranial Chordomas. *Mayo Clin Proc* 1987:62:886-893.

13 Meyers SP, Hirsch WL Jr, Curtin HD, Barnes L, Sekhar LN, Sen C. Chordomas of the skull base: MR features. *AJNR Am J Neuroradiol* 1992;13:1627-1636.

14 Mirra JM, Nelson SD, Rocca CD, Mertens F. Chordoma. In: Fletcher CDM, Unni KK, Mertens F, eds. *World Health Organization Classification of Tumours. Pathology and Genetics of Tumours of Soft Tissue and Bone* Geneva: IARC Press; 2002:316-317.

15 Mulder JD, Schutte HE, Kroon HM, Taconis WK. Introduction. In: *Radiologic Atlas of Bone Tumors* Amsterdam: Elsevier; 1993:3-6.

16 Mulder JD, Schutte HE, Kroon HM, Taconis WK. The diagnosis of bone tumors. In: *Radiologic Atlas of Bone Tumors* Amsterdam: Elsevier; 1993:9-46.

17 Mulder JD, Schutte HE, Kroon HM, Taconis WK. Chordoma. In: *Radiologic Atlas of Bone Tumors* Amsterdam: Elsevier; 1993: 267-274.

18 Oot RF, Melville GE, New Paul FJ, et al. The role of MR and CT in evaluating clival chordomas and chondrosarcomas. *AJR Am J Roentgenol* 1988;l51:567-575.

19 Rich TA, Schiller A, Suit HD, Mankin HJ. Clinical and pathologic review of 48 cases of chordoma. *Cancer* 1985;56:182-187.

20 Salisbury JR. Bone neoplasms containing epithelial and epithelioid cells. In: Helliwell TR, ed. *Major Problems in Pathology: Pathology of Bone and Joint Neoplasms* Vol 37. 1st ed. Philadelphia, Pa: W.B. Saunders 1999:352-360.

21 Sekhar LN, Schramm VL, Jones NF. Subtemporal-preauricular infratemporal fossa approach to large lateral and posterior cranial base neoplasms. *J Neurosurg* 1987;67:488-499.

22 Sekhar LN, Janecka IP, Jones NF. Subtemporal—infratemporal and basal subfrontal approach to extensive cranial base tumours. *Acta Neurochir (Wien)* 1988;92:83-92.

23 Sen CN, Sekhar LN, Schramm VL, Janecka IP. Chordoma and Chondrosarcoma of the cranial base: an 8-year experience. *Neurosurgery* 1989;25(6):931-941.

24 Smith J, Ludwig RL, Marcove RC. Sacrococcygeal chordoma: a clinicoradiological study of 60 patients. *Skeletal Radial* 1987; 16:37-44.

25 Smolders D, Wang X, Drevelengas A, Vanhoenacker F, DeSchepper AM. Value of MRI in the diagnosis of non-clival, non-sacral chordoma. *Skeletal Radiol* 2003;32:343-350.

26 Sze G, Uichanco LS III, Brant-Zawadzki MN, et al. Chordomas: MR imaging. *Radiology* 1988;166(1):187-191.

27 Unni KK. Introduction and scope of study. In: *Dahlin's Bone Tumors: General Aspects and Data on 11087 Cases* 5th ed. Philadelphia, Pa: Lippincott, Williams & Wilkins; 1996:1-9.

28 Unni KK. Chordoma. In: *Dahlin's Bone Tumors: General Aspects and Data on 11 087 Cases* 5th ed. Philadelphia, Pa: Lippincott, Williams & Wilkins; 1996:291-303.

A 13 Dermatofibrosarcoma and Dermatofibrosarcoma Protuberans

Definition

Dermatofibrosarcoma (DFS) and dermatofibrosarcoma protuberans (DFSP) are dermal tumors containing fibroblastic cells with spindle-shaped nuclei arranged into interwoven fascicles forming storiform patterns.[1,4,5] DFSP is associated with the chromosomal translocation t(17:22) which involves fusion of the COL1A1 and PDGF-β genes.[6] The COL1A1 is a collagen type I, alpha 1 gene and PDGF-β is a platelet-derived growth factor beta gene.[6]

Frequency of Occurrence

These tumors account for ~ 6% of primary malignant soft tissue tumors, and 2% of all primary soft tissue tumors.[3]

Age at Presentation

From 19 to 60 years, mean = 38 years.[3]

Gender Ratio(M / F)

1.1 / 1[1,3] to 4 / 1.[8,9]

Location

These tumors involve the dermis.[1,2,4,5,7-9] Most tumors are located above the investing fascia.[19] DFSP extends from 8 to 60mm, mean = 17 mm, deep to the skin margin.[9] Approximately 30 % of these tumors may extend into or involve soft tissue deep to the superficial fascia.[9] Trunk > head and neck > proximal limb girdle > lower extremity > hip and buttocks > foot and ankle > upper extremity > hand and wrist.[3]

Signs and Symptoms

Patients often present with solitary, slow-growing, painless nodules in the superficial soft tissues / dermis.[1,4,5,8]

Gross Pathologic Findings

Lesions are often firm, reddish-brown, bluish, or gray-white; single or multiple nodules and/or plaques within the dermis.[4,5] Tumors can range from 1 to 25 cm in size.[4,8,9] Eighty-four percent, however, are less than 5 cm.[1,10]

Histopathologic Findings

These tumors are fibroblastic cells with spindle-shaped nuclei arranged into interwoven fascicles forming storiform patterns.[1,4,5,10] Tumor cells often show little nuclear pleomorphism, and low to moderate mitotic activity.[10] DFSP can contain areas of fibrosarcoma in up to 27% of cases, and are referred to as the fibrosarcomatous variant of DFSP, abbreviated as FS-DFSP.[1,4,5] The fibrosarcomatous zones of FS-DFSP contain zones with increased cellularity and mitotic activity arranged in fascicular herringbone patterns.[1] The FS-DFSP often shows tentacle-like projections of tumor cells invading adjacent tissue.[1] Tumors usually are immunoreactive to CD 34.[10]

Tumor Genetics

DFS is commonly associated with supernumerary ring chromosome 11, often with amplified sequences from chromosomes 17 and 22.[10] The resulting gene products involve the fusion of the platelet-derived growth factor beta-chain (PDGF-β) with collagen type 1 alpha 1 gene (COL1A1), placing the PDGF-β under the COL1A1 promotor.[10] Overproduction of PDGF-β has been reported to play a role in the development of dermatofibrosarcoma.[10]

Findings on Plain Films (Roentgenograms) and Computed Tomography[4,5,7]

DFS can have well-defined or poorly defined margins and are located in the skin and adjacent adipose tissue. DFSPs are typically nodular or lobular lesions located in the skin and subcutaneous adipose tissue, usually with well-defined margins.[4,5] These tumors typically have soft tissue CT attenuation similar to muscle.[4,5] On plain films, DFSP can be seen as a soft tissue mass or swelling without bone erosion.[4] DFSPs usually show moderate contrast enhancement with CT, and typically lack calcifications.[4,5]

MRI Findings[4,5,7,9]

DPS usually appears as small lesions with circumscribed and/or poorly defined margins involving the skin and/or subcutaneous adipose tissue. Tumors can have low-intermediate signal on T1WI, intermediate signal on PDWI, and intermediate to high signal on T2W1 and FS T2W1 (Figs. **66, 67**). DFS usually shows variable degrees of Gd-contrast enhancement.

DFSPs are usually circumscribed lesions in the skin and subcutaneous adipose tissue, which can measure up to 25cm.[4,8,9] A small percentage (10%) of DFSPs have poorly defined margins.[9] DFSP tumors often have low-intermediate signal on T1WI (iso- or hypointense relative to muscle in 80%, and hypointense to fat in 100%)[4,9] (Fig. **68**). Zones of high signal on T1WI in DFSP occasionally occur from hemorrhage or necrosis.[4,9] DFSP tumors can have intermediate, slightly high, and/or high signal on T2WI; and slightly high and/or high signal on FS T2WI.[4,9] DFSPs usually show Gd-contrast enhancement in either a heterogeneous or homogeneous manner.[9]

Differential Diagnosis

Melanoma, lymphoma, metastatic disease, sarcoid, liposarcoma, malignant fibrous histiocytoma, granular cell tumor, mycosis fungoides.[7]

Prognosis and Treatment

DFSPs are slow-growing lesions that may be ignored by patients for several years.[9] The vast majority of DFSPs involve the superficial soft tissues, although up to 30 % may extend into or involve soft tissue deep to the superficial fascia.[9] These tumors are treated with wide resection.[1,2,4,6,8,9] Inadequate primary resection often results in larger deeper recurrent tumors.[2,4]

Patients with DFS who had wide resection with negative microscopic margins have a 7% recurrence rate at 5 years,

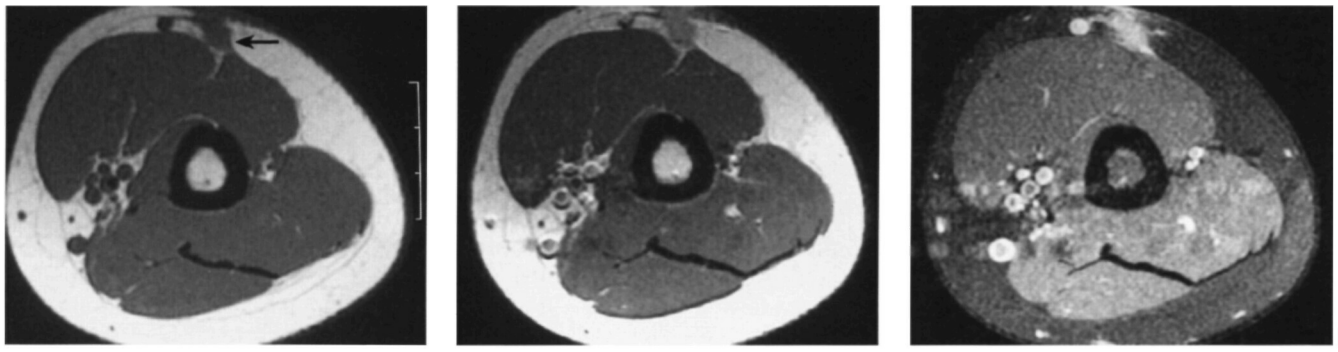

Figure **66 a-c** A 27-year-old woman with dermatofibrosarcoma in the thigh. The tumor has irregular margins and has low-intermediate signal on axial T1WI (**a**), and intermediate signal on axial PDWI (**b**). The tumor shows moderate Gd-contrast enhancement on axial FS T1WI (**c**).

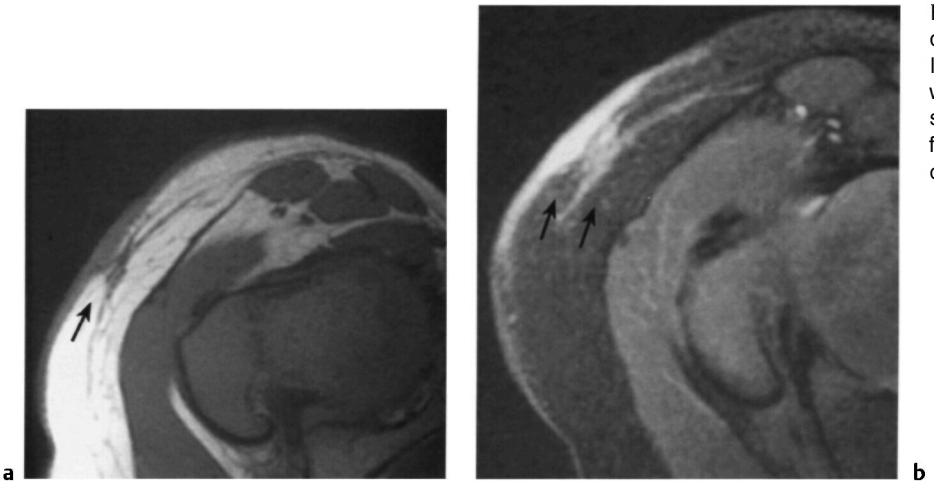

Figure **67 a, b** A 2-year-old male with a dermatofibrosarcoma in the upper thigh. The lesion is associated with skin thickening, as well as a poorly defined zone of intermediate signal on axial T1WI (**a**) in the subcutaneous fat which shows Gd-contrast enhancement on FS T1WI (**b**).

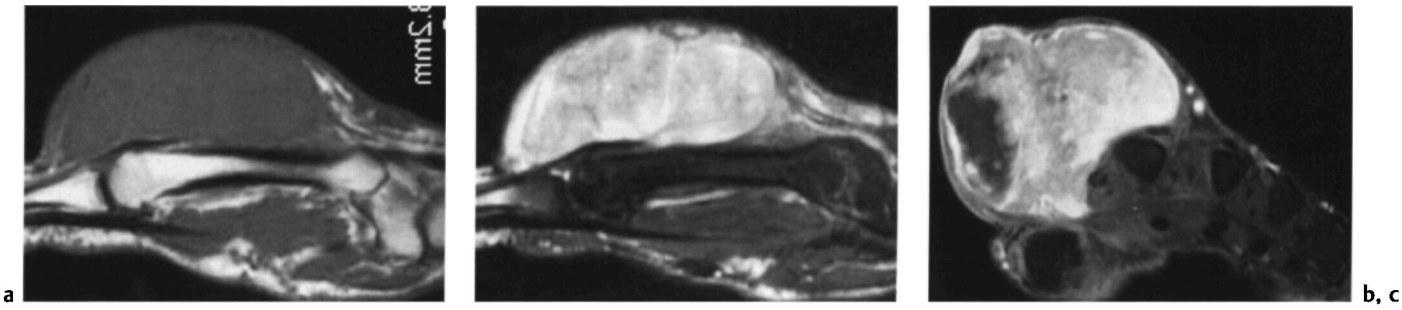

Figure **68 a, b** A 52-year-old man with a dermatofibrosarcoma protuberans at the dorsal aspect of the hand involving the skin and subcutaneous fat. The tumor has intermediate signal on sagittal (**a**) T1WI, and heterogeneous mostly high signal on sagittal (**b**) FS T2WI. The tumor shows prominent heterogeneous Gd-contrast enhancement and a nonenhancing necrotic zone on axial (**c**) FS T1WI.

whereas those with DFS who had wide resection and near-positive microscopic margins have a 27% recurrence rate at 5 years.[1]

Patients with FS-DFSP who had wide resection with negative microscopic margins have a 28% recurrence rate at 5 years, whereas those with FS-DFSP who had wide resection and near-positive microscopic margins have a 100% recurrence rate at 5 years.[1]

To minimize recurrence, Mohs' microscopic surgery has been recommended for DFS, DFSP, and FS-DFSP.[1] Radiation may be beneficial for patients with residual microscopic disease.[1,6,8] FS-DFSP may rarely be associated with metastatic pulmonary disease.[1,6]

References

1 Bowne WB, Antonescu CR, Leung Denis HY, et al. Dermatofibrosarcoma protuberans. A clinicopathologic analysis of patients treated and followed at a single institution. *Cancer* 2000;88(12):2711-2720.

2 Khatri VP, Galante JM, Bold RJ, Schneider PD, Ramsamooj R, Goodnight JE Jr. Dermatofibrosarcoma protuberans: reappraisal of wide local excision and impact of inadequate initial treatment. *Ann Surg Oncol* 2003;10(9):1118-1122.

3 Kransdorf MJ. Malignant soft-tissue tumors in a large referral population: distribution of diagnoses by age, sex, and location. *AJR Am J Roentgenol* 1995;164:129-134.

4 Kransdorf MJ, Meis-Kindblom JM. Dermatofibrosarcoma protuberans: radiologic appearance. *AJR Am J Roentgenol* 1994;163:39l-394.

5 Kransdorf MJ, Murphey MD. Malignant fibrous and fibrohistiocytic tumors. In: *Imaging ofSoft Tissue Tumors* 2nd ed. Philadelphia, Pa: W. B. Saunders; 2006:257-297.

6 Linn SC, West RB, Pollack JR, et al. Gene expression patterns and gene copy number changes in dermatofibrosarcoma protuberans. *Am] Pathol* 2003;163(6):2383-2395.

7 Ono I, Kaneko F. Magnetic resonance imaging for diagnosing skin tumors, *Clin Dermatol* 1995:13:393-399.

8 Sun LM, Wang CJ, Huang CC, et al. Dermatofibrosarcoma protuberans: treatment results of 35 cases. *Radiother Oncol* 2000:57:175-181.

9 Torreggiani WC, Al-Ismail K, Munk PL, Nicolaou S, O'Connell JX, Knowling MA. Dermatofibrosarcoma protuberans: MR imaging features. *AJR Am J Roentgenol* 2002;178:989-993.

10 Weiss SW, Goldblum JR. Fibrohistiocytic Tumors of Intermediate Malignancy. In: Weiss SW, Goldblum JR, eds. *Enzinger and Weiss' Soft Tissue Tumors* 4th ed. St. Louis, Mo: Mosby; 2001:491-534.

A 14 Dermatomyositis

Definition

Dermatomyositis is a nonsupperative, autoimmune inflammatory disease of unknown etiology, involving muscle fibers, skin, and blood vessels. This disorder is considered a systemic vasculopathy. Dermatomyositis can be associated with other connective tissue diseases such as scleroderma and mixed connective tissue disease.

Frequency of Occurrence

Incidence 2-8 per million, prevalence 4-60 per million.[9]

Age at Presentation

Juvenile dermatomyositis: children between 2 and 15 years.[5,13]

Adult dermatomyositis: peak incidence in 5th decade.[10]

Gender Ratio

Dermatomyositis occurs more often in females than males.

Location

Muscles of shoulder and pelvis are the most common locations, often symmetric.[5]

Signs and Symptoms

Patients may have these signs and symptoms: proximal lower extremity muscle weakness followed by proximal upper extremity weakness; myalgia and muscle tenderness; heliotropic rash (upper eyelids) with periorbital edema; scaling erythematous eruptions or red patches (Gottron papules on knuckles, elbows, and knees); and elevated levels of serum creatine phospholdnase.[2,4,9,13] Skin rashes can also be observed on the elbows, neck, upper chest, and shoulders.[9]

Cross Pathologic Findings

Swelling, edema, and/or ischemia are seen in affected muscles in the early stages of the disease.[4] Muscle atrophy and fatty infiltration are seen in the late or chronic phases.

Histopathologic Findings

In the active phase of this disease, a humoral immune response occurs against vascular endothelium with deposition of the C5b-9 membrane component of complement. Associated with these Findings are resultant abnormalities of the endomysial capillary bed and ischemic muscle injury.[1,4,9] Inflammatory infiltrates with collections of B cells can be observed at vessels in skeletal muscle.[4,8] Positive reactions with antibodies to the Mi-2 antigen are relatively specific for dermatomyositis.[9] In later phases of the disease, fatty infiltration occurs in the ischemic muscles as well as muscle atrophy.[2,6,9,10]

Findings on Plain Films (Roentgenograms) and Computed Tomography

In the acute stages, soft tissue swelling and subcutaneous edema may be observed as indistinctness of fat and soft tissue planes (Fig. **71**). In the chronic phases, irregular or amorphous deposits of calcium/minerals are seen in the subcutaneous soft tissues in up to 50% of cases, which is associated with muscle atrophy(Figs. **69, 70, 72**).[5] The subcutaneous calcifications are sometimes referred to as milk of calcium (Fig. **72**).[13] Radiographic findings of arthritis are usually absent.

MRI Findings

In the acute and subacute phases of the disease, poorly defined zones of high signal on T2WI and FS T2WI are seen in muscles, subcutaneous fat, and fascia resulting from ischemic or infarcted muscle secondary to vasculitis (Figs. **70,71**).[2,5,7] Enlargement of the involved muscles often occurs. Zones of low signal on T2WI in subcutaneous fat can be seen corresponding to areas of calcifications seen on radiographs and CT scans (Figs. **69, 70, 72**). Milk of calcium collections have variable signal on T1WI and T2WI, depending on the relative proportions of fluid and fluid-calcium levels (Fig. **72**).[13]

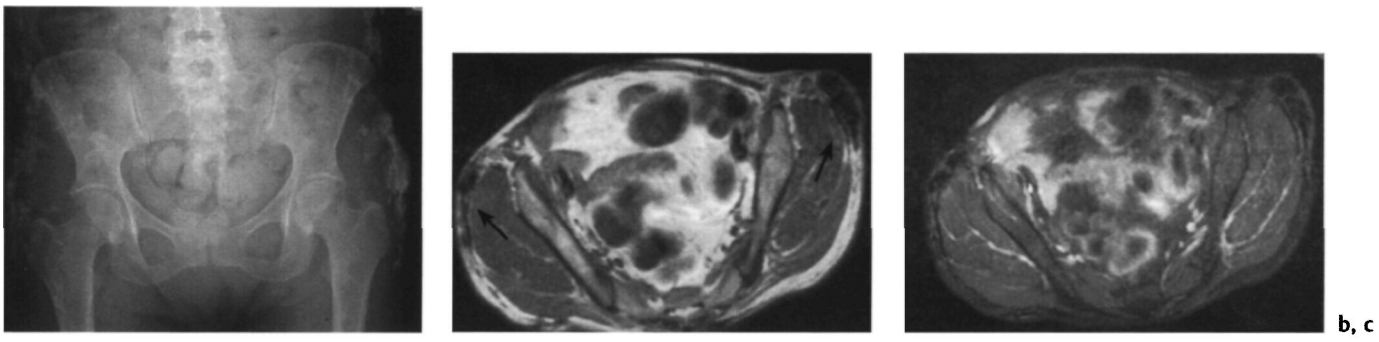

Figure **69 a-c** A 42-year-old man with dermatomyositis involving the pelvic and thigh regions. AP radiograph (**a**) shows irregular amorphous deposits of calcium/minerals in the subcutaneous soft tissues. Zones of low signal on axial T1WI (**b**) and axial FS T2WI (**c**) are seen in the subcutaneous fat corresponding to areas of calcification seen on the radiograph.

a

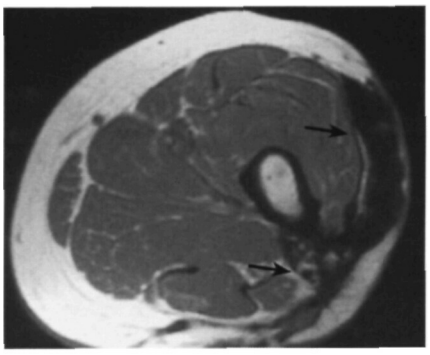

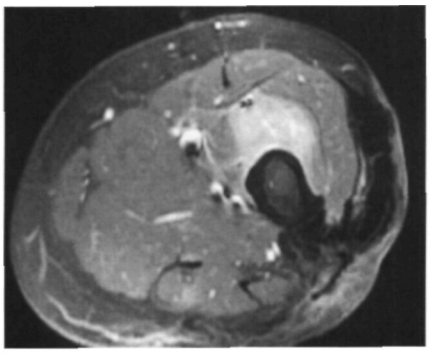

b, c

Figure **70 a-c** A 60-year-old man with dermatomyositis involving the thigh. AP radiograph (**a**) shows irregular amorphous deposits of calcium/minerals in the subcutaneous soft tissues. Zones of low signal on axial T1WI (**b**) are seen in the subcutaneous fat corresponding to areas of calcification seen on the radiograph. After Gd-contrast administration, a poorly defined zone of enhancement is also seen in the vastus intermedius muscle on axial FS T1WI (**c**) secondary to active inflammation.

a

b

Figure **71 a-e** A 78-year-old woman with dermatomyositis involving the thigh. AP radiographs (**a, b**) show edematous changes in the soft tissues without calcification. Zones of abnormal low signal on axial T1WI (**c**) are seen in the subcutaneous fat, which have corresponding high signal on axial FS T2WI (**d**). Poorly defined zones of abnormal high signal on FS T2WI (d) and abnormal Gd-contrast enhancement on FS T1WI (**e**) are seen in the thigh muscles secondary to active inflammation.

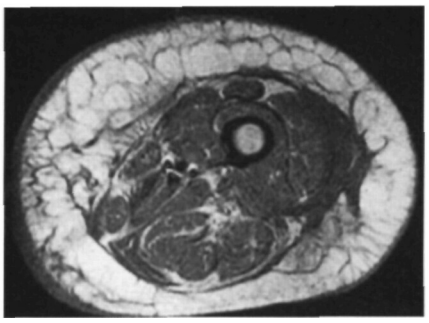

c

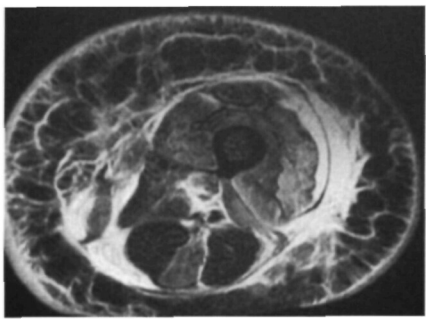

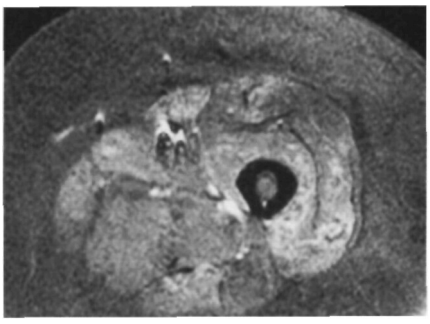

d, e

Poorly defined zones of low signal can occur in the subcutaneous fat on Tl WI (Figs. **69-72**). After Gd-contrast administration, poorly defined zones of enhancement can be seen in muscles, fascia, and/or subcutaneous fat if there is active inflammation and/or ischemia-infarction (Figs. **70, 71**). Subcutaneous and intermuscular calcium-containing collections often have mild peripheral enhancement.[2,13] Muscle atrophy with fatty infiltration can be seen in the chronic phases. Patients with inactive disease may have no signal abnormalities evident with MRI.[6]

Hydrogen MR spectroscopy can show decreased choline-to-lipid and creatine-to-lipid ratios in chronic phases.[3] P-31 MR spectroscopy shows inefficient energy metabolism or impaired oxidative metabolism indices in muscles of patients with myopathic dermatomyositis, and during exercise in muscles of patients with amyopathic variant of dermatomyositis.[1,11]

Differential Diagnosis

Healed necrotizing fasciitis, radiation injury, post-traumatic injury, cellulitis, pyomyositis, polymyositis, graft versus host disease, deep venous thrombosis, rhabdomyolysis, acute denervation, sickle cell crisis, Duchenne muscular dystrophy (chronic dermatomyositis), Becker muscular dystrophy (chronic dermatomyositis), congenital muscular dystrophy (chronic dermatomyositis), spinal muscular atrophy (chronic dermatomyositis).

a

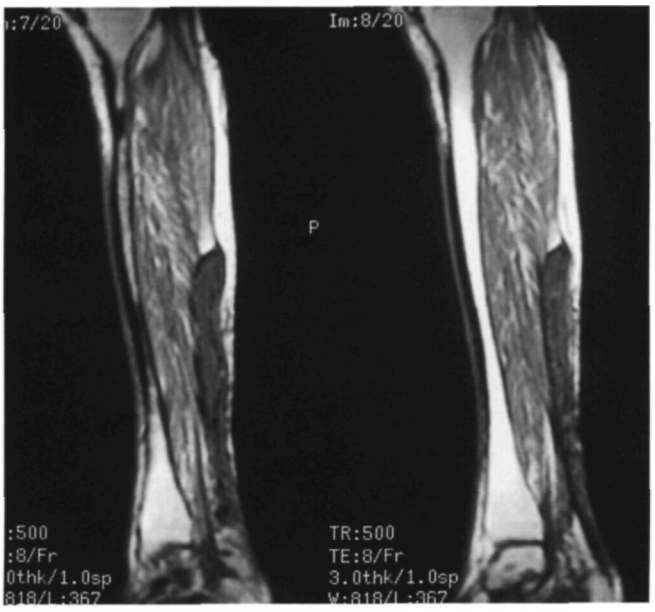

b

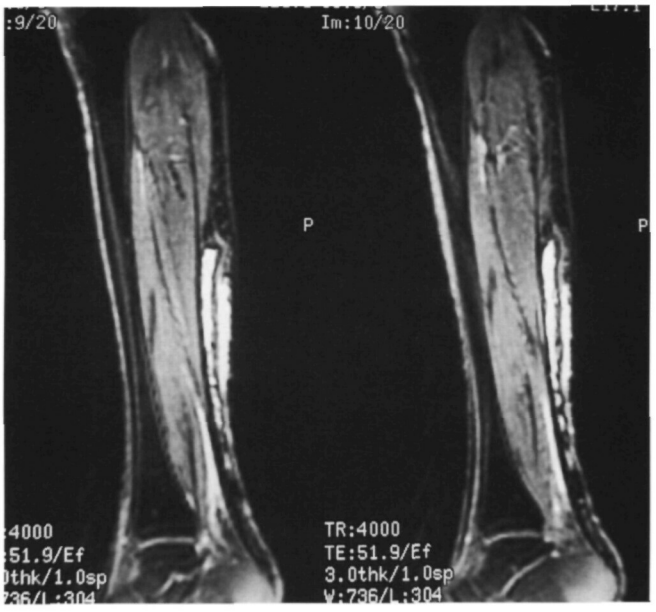

c

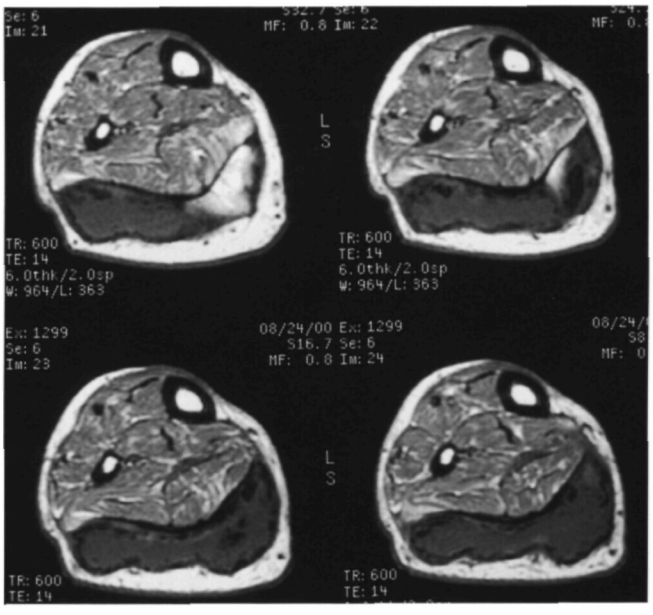

d

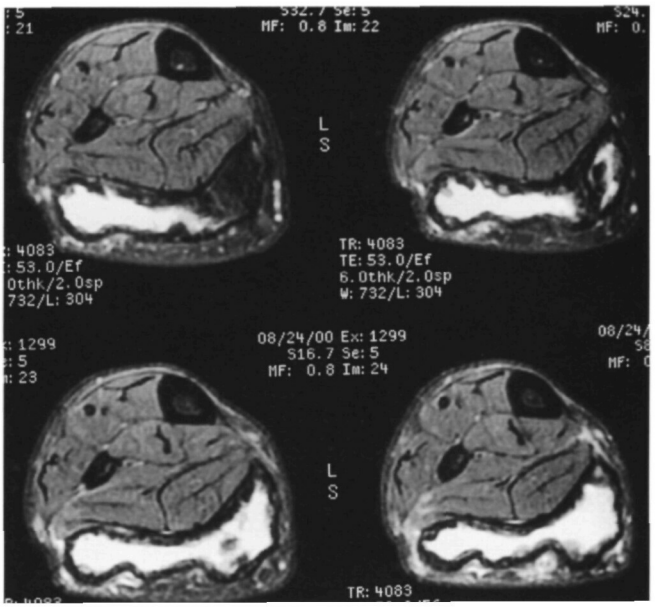

e

Figure **72 a-e** A 49-year-old woman with dermatomyositis involving the leg. Lateral radiograph (**a**) shows irregular amorphous deposits of calcium/minerals in the dorsal subcutaneous soft tissues. A zone of abnormal intermediate and low signal surrounded by a shaggy rim of low signal is seen on sagittal (**b**) and axial (**d**) T1WI. This zone has mostly high signal with irregular zones of low signal centrally surrounded by a thick irregular rim of low signal on sagittal (**c**) and axial (**e**) FS T2WI.

Prognosis and Treatment

MRI is useful in determining the extent and degree of active and chronic disease, as well as response to therapy.[5,6,12] Treatment often consists of corticosteroids and other immunosuppressive drugs.[9] Monoclonal antibodies directed toward the B-cells involved in the aberrant immune response are under investigation.[9] Patients with dermatomyositis have an increased risk of developing cancer relative to the general population.[4,14]

References

1 Cea G, Bendahan D, Manners D, et al. Reduced oxidative phosphorylation and proton efflux suggest reduced capillary blood supply in skeletal muscle of patients with dermatomyositis and polymyositis: a quantitative SIP-magnetic resonance spectroscopy and MRI study. *Brain* 2002;125(7):1635-1645.

2 Chan WP, Liu GC. Pictorial Essay: MR imaging of primary skeletal muscle diseases in children. *AJR Am J Roentgenol* 2002;179(4): 989-997.

3 Chung YL, Smith EC, Williams SC, et al. In vivo proton magnetic resonance spectroscopy in polymyositis and dermatomyositis: a preliminary study. *Eur J Med Res* 1997;2(11):483-487.

4 Cotran RS, Kumar V, Collins T, Aster J, Kumar V. Diseases of immunity. In: Cotran RS, Kumar V, Collins T, eds. *Pathologic Basis of Disease* 6th ed. Philadelphia, Pa: W.B. Saunders; 1999:188-259.

5 Hanlon R, King S. Overview of the radiology of connective tissue disorders in children. *Eur J Radiol* 2000;33(2):74-84.

6 Hernandez RJ, Sullivan DB, Chenevert TL, Keim DR. MR imaging in children with dermatomyositis: musculoskeletal findings and correlation with clinical and laboratory findings. *AJR Am J Roentgenol* 1993;161(2):359-366.

7 Kimball AB, Summers RM, Turner M, et al. Magnetic resonance imaging detection of occult skin and subcutaneous abnormalities in juvenile dermatomyositis. Implications for diagnosis and therapy. *Arthritis Rheum* 2000;43(8):1866-1873.

8 Lofberg M, Liewendahl K, Lamminen A, Korhola O, Somer H. Antimyosin scintigraphy compared with magnetic resonance imaging in inflammatory myopathies. *Arch Neurol* 1998;55(7):987-993.

9 Mastaglia FL, Garlepp MJ, Phillips BA, Zilko PJ. Inflammatory myopathies: clinical, diagnostic and therapeutic aspects. Muscle *Nerve* 2003;27(4):407-425.

10 May DA, Disler DG, Jones EA, Balkissoon AA, Manaster BJ. Abnormal signal intensity in skeletal muscle at MR imaging: patterns, pearls, and pitfalls. *Radiographics* 2000;20:S295-S315.

11 Park JH, Vital TL, Ryder NM, et al. Magnetic resonance imaging and P-31 magnetic resonance spectroscopy provide unique quantitative data useful in the longitudinal management of patients with dermatomyositis. *Arthritis Rheum* 1994;37(5):736-746.

12 Revelon G, Rahmouni A, Jazaerli N, et al. Acute swelling of the limbs: magnetic resonance pictorial review of fascial and muscle signal changes. *Eur J Radiol* 1999;30:11-21.

13 Samson C, Soulen RL, Gursel E. Milk of calcium fluid collections in juvenile dermatomyositis: MR characterisitics. *Pediatr Radiol* 2000; 30:28-29.

14 Weiss SW, Goldblum JR. Osseous soft tissue tumors. In: Weiss SW, Goldblum JR, eds. *Enzinger and Weiss Soft Tissue Tumors* 4th ed. St. Louis, Mo: Mosby; 2001:1389-1417.

A 15 Dermoid and Epidermoid

Definition

Dermoids are ectoderm-lined inclusion cysts that contain hair, sebaceous and sweat glands, and squamous epithelium.[9] Dermoids slowly enlarge, although are not considered to be neoplasms.[9] Dermoids can be congenital lesions that arise between 3 and 5 weeks of gestation when surface ectoderm fails to separate completely from the adjacent neural tube.[3,9] Dermoids can also form as a result of invagination or sequestration of surface ectoderm at sites of dermal fusion (face, eyes, ears) during gestation.[3,9] In older patients, dermoids may occur from displacement of skin into deeper structures from trauma, surgery, or lumbar puncture.[3,9]

Epidermoids are ectoderm-lined inclusion cysts that contain only squamous epithelium.[9] Epidermoids slowly enlarge, although are not considered to be neoplasms.[9] Congenital epidermoid cysts arise later in gestation than dermoids, and tend to be more superficial and lateral relative to dermoids.[9] In older patients, epidermoids may occur from displacement of skin into deeper structures from trauma, surgery, or lumbar puncture.[9]

Frequency of Occurrence

Dermoids and epidermoids account for up to 5% of intracranial masses and up to 2% of intraspinal tumors.[3,9] Dermoid cysts are the most common orbital lesions in children.[9] Dermoids also commonly occur as ovarian lesions.

Age at Presentation

Dermoids and epidermoids can be congenital lesions, or can occur in children or adults as acquired lesions resulting from displacement of skin elements into deeper tissues from trauma, surgery, or other medical procedures such as lumbar puncture.[9] Dermoid cysts are often diagnosed in the 2nd to 3rd decades, whereas epidermoids often present in the 3rd to 4th decades.[3,9]

Gender Ratio

Males are slightly more affected than females.[9]

Location

Dermoids: orbits (zygomaticofrontal and frontoethmoidal sutures, supraorbital ridge, lateral eyebrow), posterior cranial fossa (cisterna magna, 4th ventricle, prepontine cistern), suprasellar cistern, spine, ovary, and other soft tissues.[3,9] Spinal dermoids can be extradural, intradural-extramedullary, or intramedullary.[3] Spinal dermoids are located in the lumbosacral region (60%), followed by the thoracic and cervical regions.[3] Some spinal dermoids are associated with a dorsal dermal sinus.[9] Dermoid cysts rarely occur within the cerebral ventricles, brain parenchyma, and brainstem.[4]

Epidermoids: intradiploic space (often involving the temporal or parietal bones), intradural extra-axial intracranial lesions (cerebellopontine angle cistern / congenital cholesteatoma, middle cranial fossa), extramedullary spinal lesions, soft tissues of the extremities.[9] Acquired cholesteatomas are secondary epidermoids that occur in the middle ear from retraction pockets or displaced epithelium from outside to inside the pars flaccida of the tympanic membrane.[9] Epidermoid cysts rarely occur within the cerebral ventricles, brain parenchyma, and brainstem.[4]

Signs and Symptoms

Dermoids are slow-growing lesions that are often asymptomatic.[3,9] Dermoids may be associated with chronic erosive changes involving adjacent bones. Rupture of dermoids within the central nervous system can result in seizures and other significant neurologic events because of severe chemical meningitis.[9] Large dermoids in the posterior cranial fossa may cause hydrocephalus.[9] Dermoids in the spinal canal can be associated with progressive lower extremity neurologic deficits and bladder sphincter dysfunction.[7] Approximately 20% of dermoids involving the spine are associated with a dorsal dermal sinus.[7] Other clinical features associated with spinal dermoids include sacral dimple, tufts of hair, and spina bifida.[7]

Epidermoids are slow-growing lesions that are often asymptomatic.[9] Epidermoids may be associated with chronic erosive changes involving adjacent bones. Rupture of epidermoids within the central nervous system can result in seizures and other significant neurologic events because of severe chemical meningitis.[9] Epidermoids typically do not cause hydrocephalus. Acquired cholesteatomas in the middle ear are often associated with conductive hearing loss that results from erosions of the ossicular chain.

Gross Pathologic Findings

Dermoids. Lesions typically appear as unilocular cysts containing viscous yellow, green, and/or brown fluid containing keratin, hair, and various fat metabolites and cholesterol crystals.[3]

Epidermoids. Lesions are nodular or multilobulated, with a capsule containing a thin lining of stratified squamous epithelium.[4,9] The cyst's contents often appear waxy, shiny, and smooth due to keratin.[9]

Histopathologic Findings

Dermoids. Lesions usually have a capsule containing connective tissue lined by stratified squamous epithelium with dermal appendages such as hair follicles, hair, sebaceous glands, and sweat glands.[3] Calcifications may occur in the cyst walls.[3] Cyst contents often include keratin, hair, and various fat metabolites and cholesterol crystals.[3] Occasionally bone and/or cartilage may be present inside these lesions.[3]

Epidermoids. Lesions have thin walls with flat squamous cells.[9] The contents of an epidermoid arise from debris from the desquamated squamous epithelial cells and include keratin, cholesterol, and other lipids.[9]

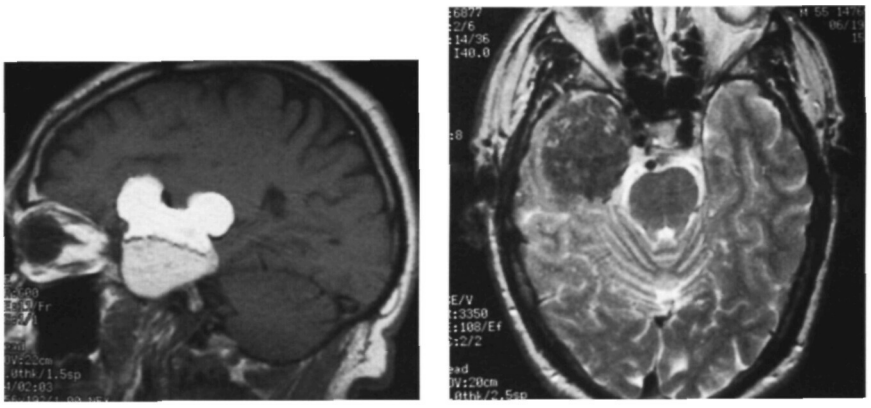

Figure **73 a, b** A 55-year-old man with a dermoid in the right middle cranial fossa. Sagittal (**a**) T1WI show a circumscribed extra-axial lesion, which has heterogeneous mostly high signal with a thin low signal septum. The lesion has mixed low and high signal on axial (**b**) T2WI.

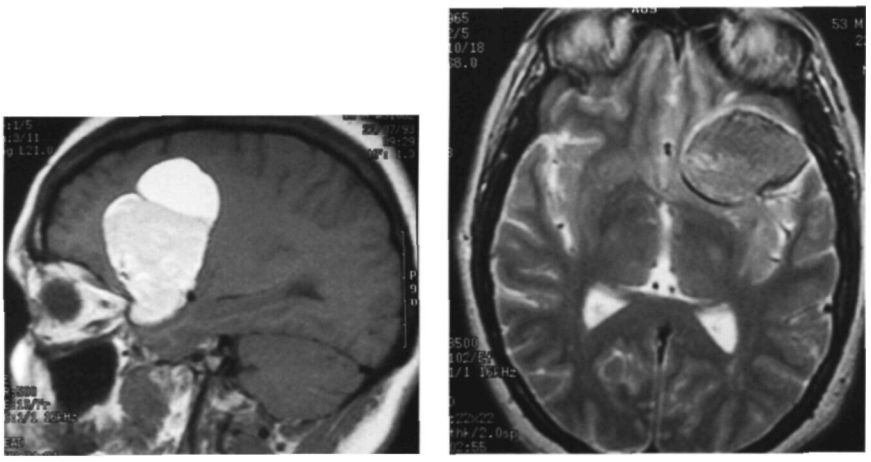

Figure **74 a, b** A 53-year-old man with a dermoid in the left middle and anterior cranial fossae, as well as the suprasellar cistern. Sagittal (**a**) T1WI shows a circumscribed, lobulated, extra-axial lesion which has heterogeneous high, intermediate, and low signal surrounded by a thin rim of low signal. The lesion has mixed low and high signal on axial T2WI and is surrounded by a thin rim of low signal (**b**).

Findings on Plain Films (Roentgenograms) and Computed Tomography

Dermoids.[2-4,9,11] Dermoid cysts can produce erosions of adjacent bone.[9] Dermoids within bone can cause erosion and/or expansion of the involved bone, with or without sclerotic margins.[9] On CT, dermoids are often circumscribed unilocular lesions which usually have thick walls that may or may not contain calcifications[9] (Fig. **76**). The contents of dermoids can have low attenuation (-60 HU to -90 HU) similar to fat, resulting from sebaceous and other lipid material.[2,9] Fat-fluid levels can occur within dermoids.[9] Dermoids may rupture, and zones of low attenuation similar to fat can be seen near or distant to the primary lesion.[3] Less frequently, some dermoids may have low attenuation similar to water, or high attenuation similar to hemorrhage.[4,9,11]

Epidermoids.[9,13] Epidermoid cysts can produce erosions of adjacent bone.[9] Epidermoids within bone can cause erosion and/or expansion of the involved bone, with or without sclerotic margins[9] (Fig. **78**). On CT, epidermoids are circumscribed and/or lobulated lesions that have thin imperceptible walls.[9] Epidermoids typically have low attenuation similar to water.[9] Infrequently, some epidermoids have high attenuation similar to hemorrhage from high protein content and high viscosity.[13]

MRI Findings

Dermoids.[3,4,7,9,11] Dermoid cysts are circumscribed lesions which may have identifiable walls with low signal on T1WI and T2WI.[9] The contents of dermoid cysts can have low, intermediate and/or high signal on T1WI and T2WI[3,4,7,9,11] (Figs. **73-76).** After Gd-contrast administration, dermoids may show enhancement at the wall margins, but not centrally.[9] Dermoids may be associated with anomalies such as skeletal dysraphism and dorsal dermal sinus.[9] Dermoids may rupture into the subarachnoid space, and zones of high signal on T1W1 similar to fat can be seen near or distant to the primary lesion[3] (Fig. **75**). Ruptured dermoids may incite an inflammatory meningitis and may be associated with adhesive arachnoiditis involving the cauda equina.[3,9]

Epidermoids.[1,2,4-6,8,12-14] Epidermoid cysts are circumscribed lesions which may have slightly lobulated margins. Epidermoids usually have low signal or low-intermediate signal on T1WI, and high signal on T2WI and FST2W1 that may approximate cerebrospinal fluid (CSF)[1,2,4-6,8,12,14] (Figs. **77-81).** Lesions occasionally contain foci of high signal on T1WI (Fig. **81**). With FLAIR, epidermoids typically show higher signal than CSF.[5] Epidermoids typically show very high signal on diffusion-weighted images,[1,5,12] which may result from T2 shine-through effect or diffusion restriction.[5] Apparent diffusion coefficient mapping can allow distinction between these possibilities (Fig. **77**). Infrequently, epidermoids have been shown to have high signal on T1WI, and/or low signal on T2WI secondary to cyst contents with high protein content and high viscosity.[13] Epidermoids may show minimal peripheral Gd-contrast enhancement, but no enhancement is typically seen centrally.[6,9] Intracranial epidermoids are soft lesions which may be associated with displacement of adjacent brain tissue and other neurologic structures, but hydrocephalus does not typically occur.[6] Ruptured epidermoids may incite an inflammatory meningitis and may be associated with adhesive arachnoiditis involving the cauda equina.[9]

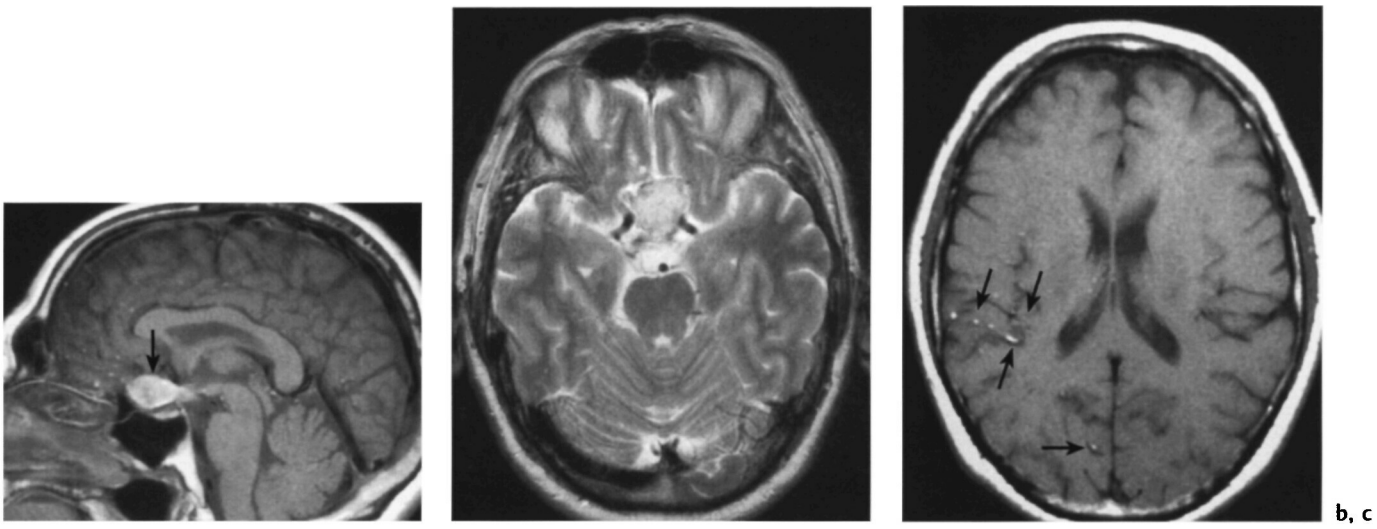

a b, c

Figure **75 a-c** A 53-year-old man with a leaking dermoid in the suprasellar cistern. Sagittal (**a**) and axial (**c**) T1WI show an extra-axial lesion, which has heterogeneous slightly high signal. Check as edited. The lesion has heterogeneous slightly high signal on axial T2WI (**b**). Multiple small foci with high signal on T1WI are seen in the subarachnoid space representing droplets from the leaking dermoid.

a b

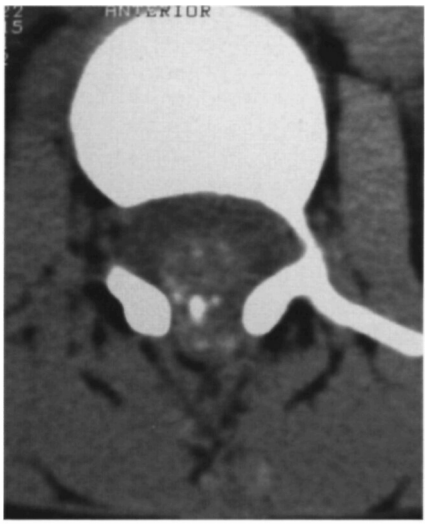

c

Figure **76 a-c** A 27-year-old woman with a dermoid in the posterior lumbar spinal canal. The lesion has high signal on sagittal T1WI (**a**), and low-intermediate signal on sagittal (**b**) T2WI. Axial CT image (**c**) shows the lesion to contain multiple calcifications.

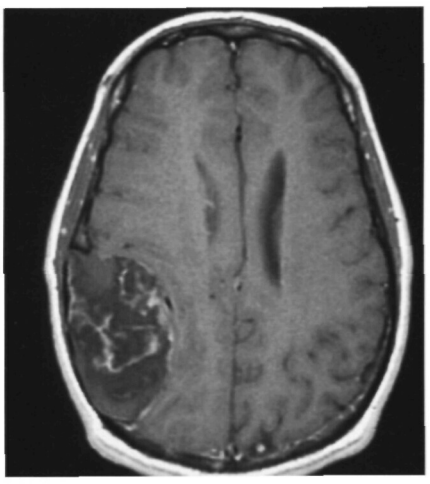

a

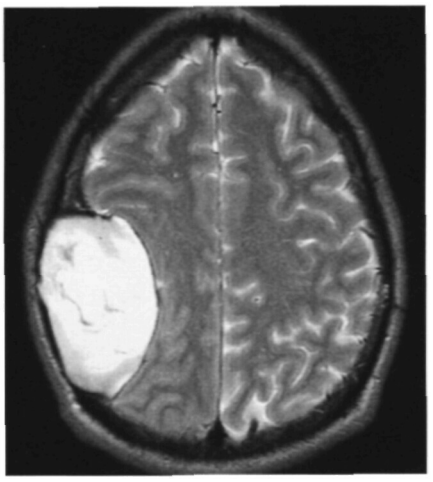

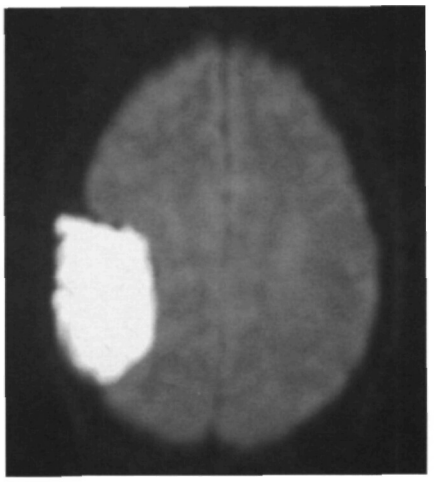

b, c

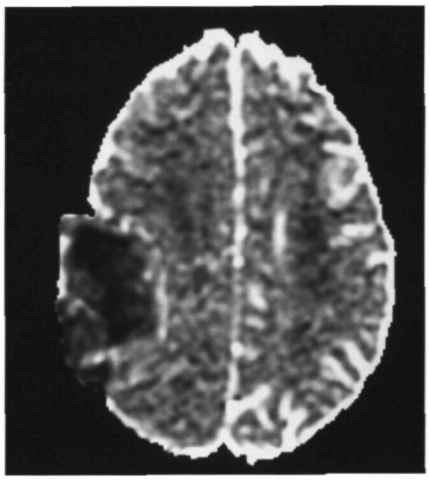

d

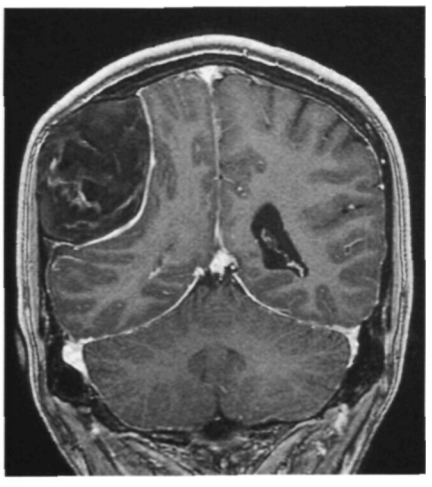

e

Figure **77 a-e** A 39-year-old man with an epidermoid involving the right parietal bone. Axial (**a**) T1WI shows a large extra-axial lesion with mostly intermediate signal as well as zones of high signal associated with marked expansion and thinning of the inner and outer tables of the skull. The lesion has high signal centrally surrounded by a thin rim of low signal on axial (**b**) T2WI. The lesion has high signal on diffusion-weighted imaging (**c**) and low signal on apparent diffusion coefficient mapping (**d**), indicating restricted diffusion within the lesion. No definite Gd-contrast enhancement is seen in the lesion on coronal (**e**) T1WI. Mild dural thickening is seen at the dura displaced medially by the epidermoid.

a

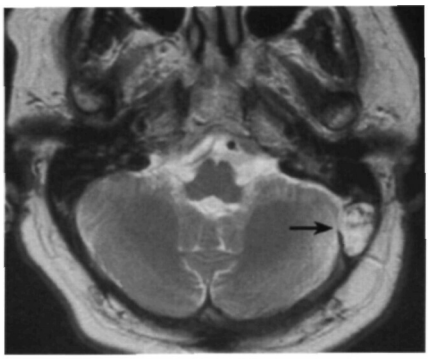

b

c

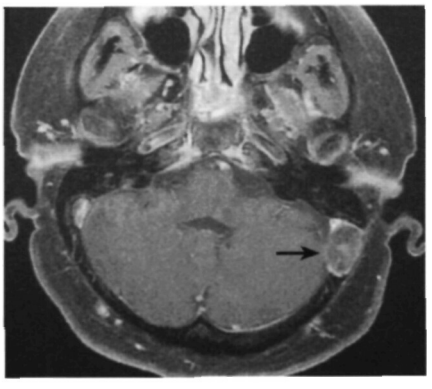

d

Figure **78 a-d** A 68-year-old woman with an intra-osseous epidermoid in the left temporal-occipital region. Axial CT image (**a**) shows an expansile lesion with low-intermediate attenuation associated with thinning and erosion of the inner and outer tables. The lesion has heterogeneous mostly high signal on axial T2WI (**b**) and axial diffusion weighted imaging (c). A thin rim of Gd-contrast enhancement is seen surrounding the lesion on axial FS T1WI (**d**).

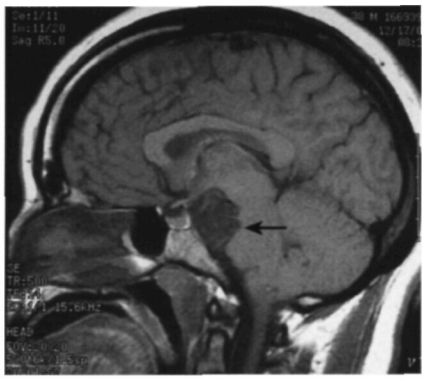

a

Figure **79 a-c** A 38-year-old man with an epidermoid along the endocranial surface of the clivus. The lesion has slightly lobulated margins and has low-intermediate signal on sagittal T1WI (**a**) and high signal on axial T2WI (**b**). The lesion has mixed, mostly intermediate signal on axial FLAIR images (**c**).

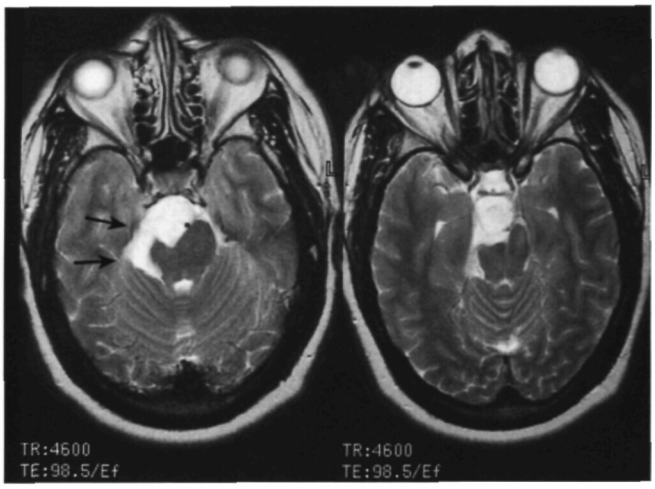

b

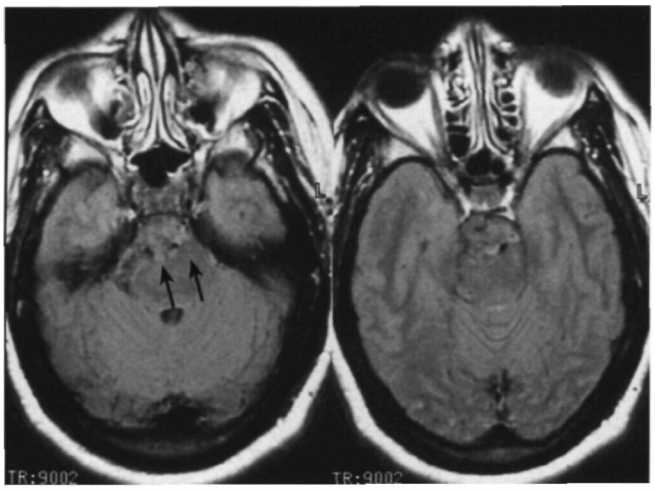

c

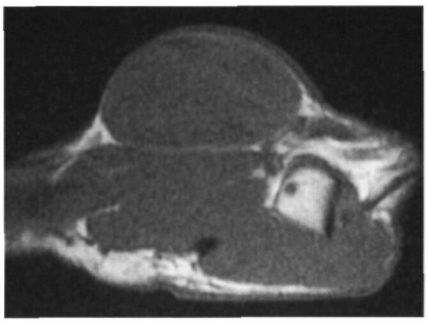

a

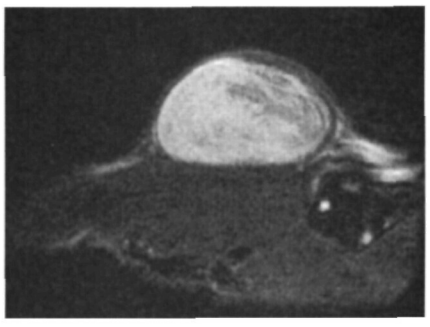

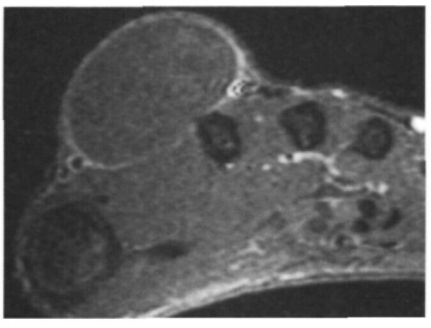

b, c

Figure **80 a-c** A 35-year-old man with an epidermoid involving the dorsal soft tissues of the hand. The lesion has intermediate signal on sagittal (**a**) T1WI, and heterogeneous mostly high signal on sagittal (**b**) FST2WI. The lesion shows no Gd-contrast enhancement on axial (**c**) T1WI.

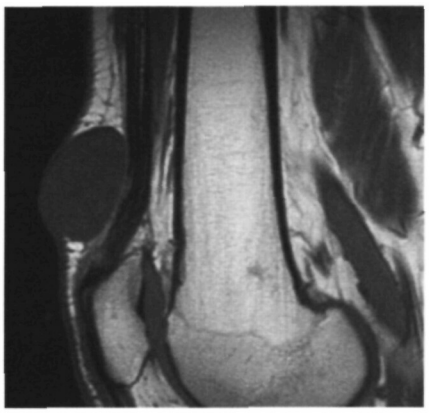

a

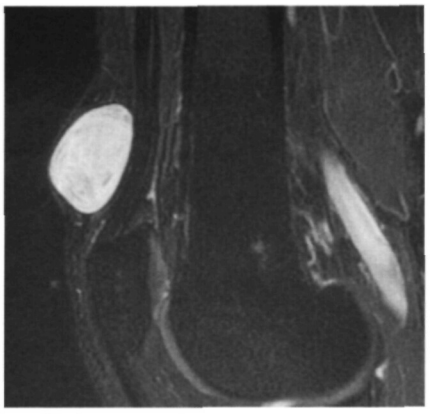

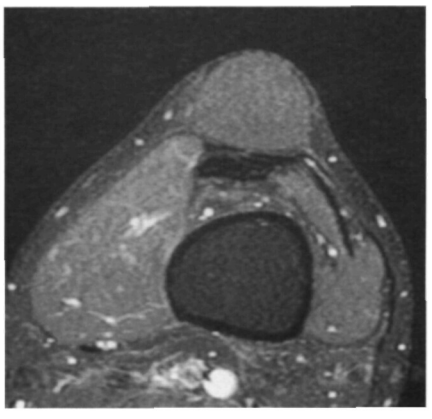

b, c

Figure **81 a-c** A 25-year-old man with an epidermoid involving the anterior soft tissues at the knee. The lesion has low-intermediate signal on sagittal (**a**) Saggital what?and high signal on sagittal (**b**) FST2WI. The lesion shows no Gd-contrast enhancement on axial (**c**) T1WI.

Differential Diagnosis

Teratomas, lipomas, liposarcomas, granulomas, fat necrosis, sebaceous cyst.[3]

Prognosis and Treatment

Both dermoids and epidermoids are usually treated with gross total resection.[4,7,8,12,13] Postoperative steroids may be beneficial to minimize the potential of meningitis when these lesions involve the central nervous system.[8]

References

1 Bergui M, Zhong J, Bradac GB, Sales S. Diffusion-weighted images of intracranial cyst-like lesions. *Neuroradiology* 2001;43:824-829.

2 Bonneville F, Sarrazin JL, Marsot-Dupuch K, et al. Unusual lesions of the cerebellopontine angle: a segmental approach. *Radiographics* 2001;21(2):419-438.

3 Calabro F, Capellini C, Jinkins JR. Rupture of spinal dermoid tumors with spread of fatty droplets in the cerebrospinal fluid pathways. *Neuroradiology* 2000;42:572-579.

4 Caldarelli M, Colosimo C, Di Rocco C. Intra-axial dermoid/epidermoid tumors of the brainstem in children. *Surg Neurol* 2001;56(2):97-105.

5 Chen S, Ikawa F, Kurisu K, Arita K, Takaba J, Kanou Y. Quantitative MR evaluation of intracranial epidermoid tumors by fast fluid-attenuated inversion recovery imaging and echo-planar diffusion-weighted imaging. *AJNR Am J Neuroradiol* 2001 ;22(6): 1089-1096.

6 Kallmes DF, Provenzale JM, Cloft HJ, McClendon RE. Typical and atypical MR imaging features of intracranial epidermoid tumors. *AJR Am J Roenrgenol* 1997;169(3):883-887.

7 Mhatre P, Hudgins PA, Hunter S. Dermoid cyst in the lumbosacral region. Radiographic findings. *AJR Am J Roentgenol* 2000; 174(3): 874-875.

8 Scarrow AM, Levy El, Gerszten PC, Kulich SM, Chu CT, Welch WC. Epidermoid cyst of the thoracic spine: case history. *Clin Neurol Neurosurg* 2001;103(4):220-222.

9 Smirniotopoulos JG, Chiechi MV. Teratomas, dermoids, and epidermoids of the head and neck. *Radiographics* 1995;15:1437-1455.

10 Szklaruk J, Tamm EP, Choi H, Varavithya V. MR imaging of common and uncommon large pelvic masses. *Radiographics* 2003;23(2): 403-424.

11 Tateshima S, Numoto RT, Abe S, Yasue M, Abe T. Rapidly enlarging dermoid cyst over the anterior fontanel: a case report and review of the literature. *Childs Nerv Syst* 2000;16:875-878.

12 Teksam M, Casey SO, Michel E, Benson M, Truwit CL Intraspinal epidermoid cyst: diffusion-weighted MRI. *Neuroradiology* 2001; 43:572-574.

13 Timmer FA, Sluzewski M, Treskes M, van Rooij WJJ, Teepen JLJM, Wijnalda D. Chemical analysis of an epidermoid cyst with unusual CT and MR characteristics. *AJNR Am J Neuroradiol* 1998;19:1111-1112.

14 Zamani AA. Cerebellopontine angle tumors: role of magnetic resonance imaging. *Top Magn Reson Imaging* 2000;11(2):98-107.

A 16 Desmoid Tumor (Also Referred to as Fibromatosis, Superficial and Deep Types Involving Soft Tissues; Desmoplastic Fibroma; Desmoid Tumor within Bone)

Desmoid is derived from the Greek word "desmos" meaning band or tendon.[3]

ICD-O Code

Palmar/plantar fibromatosis: 8821/1

Aggressive fibromatosis: 8821/1

Abdominal (mesenteric) fibromatosis: 8822/1

Desmoplastic fibroma of bone: 8823/0

Definition

Desmoid tumors or fibromatoses represent a group of soft tissue lesions comprised of benign fibrous tissue with elongated or spindle-shaped cells adjacent to collagen.[2,3,5,7,8,10-14,17,27,31,32,39,41] Lesions are categorized by location as superficial (palmar—Dupuytren contracture, plantar—Ledderhose disease, penile-Peyronie disease) or deep (extra-abdominal, abdominal, or intra-abdominal).[1,3,5,10,11,14,15,17,20,22,31-33,35,37,39,43,44] Aggressive fibromatosis is a type that usually occurs in the deep soft tissues and consists of proliferation of fibrous tissue that infiltrates adjacent tissues.[11,20,31] Aggressive fibromatosis has a greater tendency to recur locally after surgery compared with circumscribed desmoid tumors.[11,20,31] Desmoids rarely occur in bone and are referred to as desmoplastic fibroma.[2,4,6-9,12,13,16,26,28,30,36,41,42] Desmoid tumors can occur in association with Gardner syndrome and Turcot syndrome.[3,17,28,30,34] Fibromatosis coli is a benign form of infantile fibromatosis involving the distal sternocleidomastoid muscle, which can occur after abnormal intrauterine positioning or difficult deliveries.[17,29]

Frequency of Occurrence

Bone: Desmoplastic fibromas account for < 1% of bone lesions[9,23,24,40,41]

Soft tissue:

- **Superficial fibromatosis.** These lesions account for 1.5% of benign soft tissue tumors.[19]
- **Dupuyten contracture (palmar fibromatosis).** These lesions affect 1-2% of the population, up to 20% of patients older than 60 years of age.[17]
- **Plantar fibromatosis.** These lesions account for ~1 % of benign soft tissue tumors.[18,19]
- **Deep fibromatosis (adults).** These lesions account for 5 % of benign soft tissue tumors.[18,19] The incidence is 2-4 per million per year[11,20]
- **Deep fibromatosis (children).** These lesions are rare.[39]
- **Fibromatosis coli.** These lesions are rare and occur in 0.4 % of live births.[17,29]

Age at Presentation

Superficial fibromatosis: from 17 to 65 years, mean = 41 years.[18,19]

Dupuyten contracture (palmar fibromatosis): usually affects adults > 60 years.[10,17]

Plantar fibromatosis: from 20 to 60 years.[10,17]

Deep fibromatosis (adults): from 13 to 60 years, mean = 34 years, peak age between 25 and 35 years.[20]

Deep fibromatosis (children): from 6 months to 8 years, mostly in first 2 years.[14,39]

Fibromatosis coli: most cases are diagnosed in infants below 6 months.[29]

Desmoplastic fibroma: from 1 to 71 years, mean = 20 years, median = 34 years, peaks in 2nd decade.[9,12,13,25,26,41]

Gender Ratio (M / F)

Superficial fibromatosis: 2 / 1.[19]

Dupuytren contracture: 3-4 / 1.[10,17]

Plantar fibromatosis: 1 / 1.[10,17]

Deep fibromatosis (adults): 1 / 1.4 to 1 / 2.[19,31]

Deep fibromatosis (children): predominantly occurs in males.[14]

Fibromatosis coli: 1 / 1.[29]

Desmoplastic fibroma: 1 / 1 to 2 / 1.[9,13,41]

Location

Bone:

- **Desmoplastic fibroma** is a rare bone tumor that represents the intra-osseous version of desmoid tumor (fibromatosis). These lesions are usually present in the dimetaphyseal region, although can be seen in the diaphyseal or epiphyseal regions.[9,13] Mandible > iliac bone > humerus > tibia > vertebrae > ulna > scapula > femur.[13,16] Lesions in the skull have also been reported.[4,30]

Soft tissue:

- **Superficial fibromatosis.** Lesions occur in the foot and ankle > hand and wrist > trunk.[19] Duputyren contracture involves the palmar aponeurosis, often at the distal palmar crease (fourth > fifth > third > second rays, bilateral in 50%); plantar fibromatosis involves the plantar aponeurosis (usually medial, bilateral in 35%), and Peyronie / fibromatosis involves the penis.[10,17]
- **Deep fibromatosis (adults) / abdominal desmoids.** These lesions occur in the mesentery, retroperitoneum.[3,20] Desmoid tumors also occur in the abdominal wall at musculoaponeurotic structures.[3,20] Common sites include the rectus, oblique, and tranversalis muscles, and/or fascia.[3]
- **Deep fibromatosis / extra-abdominal desmoids (adults).** These lesions occur in the chest wall, paraspinal tissues, pelvic wall, mediastinum, extremities (lower extremity > foot and ankle > hand and wrist > upper extremity), head and neck, and mediastinum.[3,11] Locations for deep fibromatosis have been reported in order of decreasing frequency as:

trunk > lower extremity > foot and ankle > retroperitoneum > head and neck, hip and buttocks, hand and wrist, upper extremity.[19] For aggressive fibromatosis, involvement occurs in the upper extremity in 25 to 40% of cases, lower extremity in 20-30%, head and neck in 20-30%, and trunk in 10-15%.[27]

- **Deep fibromatosis (children).** Common sites include: head and neck (tongue, mandible, maxilla, mastoid), trunk, and proximal extremities.[14] Intra-abdominal desmoids in children are uncommon.[14]
- **Fibromatosis coli.** Lesions are characteristically located at the distal lower portion of the sternocleidomastoid muscle.[17,29]

Signs and Symptoms

Dupuytren contracture. These lesions occur as subcutaneous soft tissue nodules in the palmar aspect of hand, usually at the distal skin crease.[17] These lesions can restrict movement.[17]

Plantar Fibromatosis. These lesions occur as subcutaneous firm soft-tissue nodule or nodules (~33%) in the plantar aspect of the foot.[17]

Deep fibromatosis (adults and children). Patients can have solitary firm lesions noticed in skeletal muscle and/or adjacent fascia or aponeurosis.[3,11,17] Lesions are usually not painful.[3,11,17,31,32] Lesions can also be seen in the trunk, tongue, head, and neck.[3,17,31]

Fibromatosis coli. Infants often present with a firm mass in the lower third of the sternocleidomatoid muscle 2-4 weeks after birth.[17,29] The affected muscle is thickened and shortened in length, resulting in cervicofacial asymmetry.[29] Torticollis is seen in up to 20% of infants with fibromatosis coli.[17] Fibromatosis coli can be seen in association with other developmental abnormalities such as forefoot anomalies (metatarsus adductus, talipes equinovarus) and hip dysplasia with congenital hip dislocation.[17,29]

Desmoplastic fibromas. These lesions are usually asymptomatic until they become large, or because of pathologic fracture.[12,41] Pathologic fractures occur in 12% of desmoplastic fibromas.[2]

Gross Pathologic Findings

Dupuytren contracture. Lesions can appear as nodules or poorly defined nodular aggregates of gray-white or yellow firm tissue.[10,17]

Plantar fibromatosis. Lesions can appear as nodules or poorly defined nodular aggregates of gray-white or yellow firm tissue.[10,17]

Deep fibromatosis. These lesions are usually firm and gritty, and on cut surface are glistening white to light gray.[11,17] Lesions lack a true capsule. Lesions range from 2 to 20 cm in size.[11]

Fibromatosis coli. Lesions typically appear as fusiform, tan gritty masses involving the lower sternocleidomastoid muscle, and usually measure < 5 cm in length and < 2 cm in width.[29]

Desmoplastic fibroma. Lesions are usually firm, rubbery, and gray-white with a variegated whorled pattern.[8,13]

Histopathologic Findings

Dupuytren contracture. Lesions typically consist of benign fibrous tissue with elongated or plump spindle-shaped cells with little variability in appearance containing normochromatic nuclei with small nucleoli.[10] Mitotic figures are infrequent.[10] The spindle-shaped cells are usually associated with moderate or large amounts of collagen.[10,17]

Plantar fibromatosis. Lesions typically consist of benign fibrous tissue with elongated or plump spindle-shaped cells of little variability in appearance, which contain normochromatic nuclei with small nucleoli.[10] Mitotic figures are infrequent.[10] The spindle-shaped cells are often associated with moderate to large amounts of collagen.[10,17] Occasional multinucelated giant cells may be seen.[10]

Deep fibromatosis (adults and children). These lesions are often poorly marginated with infiltrative margins, and contain varying proportions of elongated spindle-shaped or fibroblast-like cells surrounded by dense bands of collagen.[3,11,14,31] Nuclei are usually small and pale, and contain between one and three nucleoli.[11,31] Mitoses are infrequent[3,11,14] Lesions can infiltrate adjacent tissue including muscle, which may result in reactive multinucleated giant cells.[11,31] Lesions tend to be more invasive/aggressive in children than in adults.[17] These lesions may be associated with Gardner syndrome and Turcot syndrome.[3,17,28,31] These tumors are immunoreactive to vimentin, muscle specific and smooth muscle actin as well as beta-catenin.[11]

Fibromatosis coli. Lesions contain groups of plump, spindle-shaped cells within myxoid and/or collagenous ground substance.[29] The relative proportions of spindle cells, myxoid material, and collagen can vary depending on the time of evaluation.[29] Long standing lesions often have less spindle cells and relatively larger amounts of collagen compared with earlier stage lesions.[29] Multinucleated skeletal myocytes, plump fibroblastic and myofibroblastic cells may also be seen in fine needle aspirates or surgical specimens.[29]

Desmoplastic fibroma. These lesions contain varying proportions of wavy bands of collagen and elongated spindle-shaped cells containing spindly-appearing nuclei. Mitotic figures are typically absent or rare.[8,13]

Lesion Genetics

Superficial fibromatoses often have near-diploid kartyotypes, as well as gains of chromosomes 7 or 8.[10] Desmoid-type fibromatoses and desmoplastic fibromas of bone can have cells with trisomies for chromosomes 8 and/or 20 in ~30% of lesions.[8,11] Inactivation of the APC tumor suppressor gene on chromosome 5 q has been reported in patients with familial polyposis, and occasionally in patients with sporadic desmoid tumors.[11] Patients with sporadic desmoid tumors have been reported to have mutations affecting beta-catenin, altering the normal inhibiting influence of the APC gene product effect.[11]

Findings on Plain Films (Roentgenograms) and Computed Tomography

Superficial fibromatosis. On plain films a small soft tissue lesion may be seen, whereas on CT a focal lesion with soft tissue attenuation may be observed.

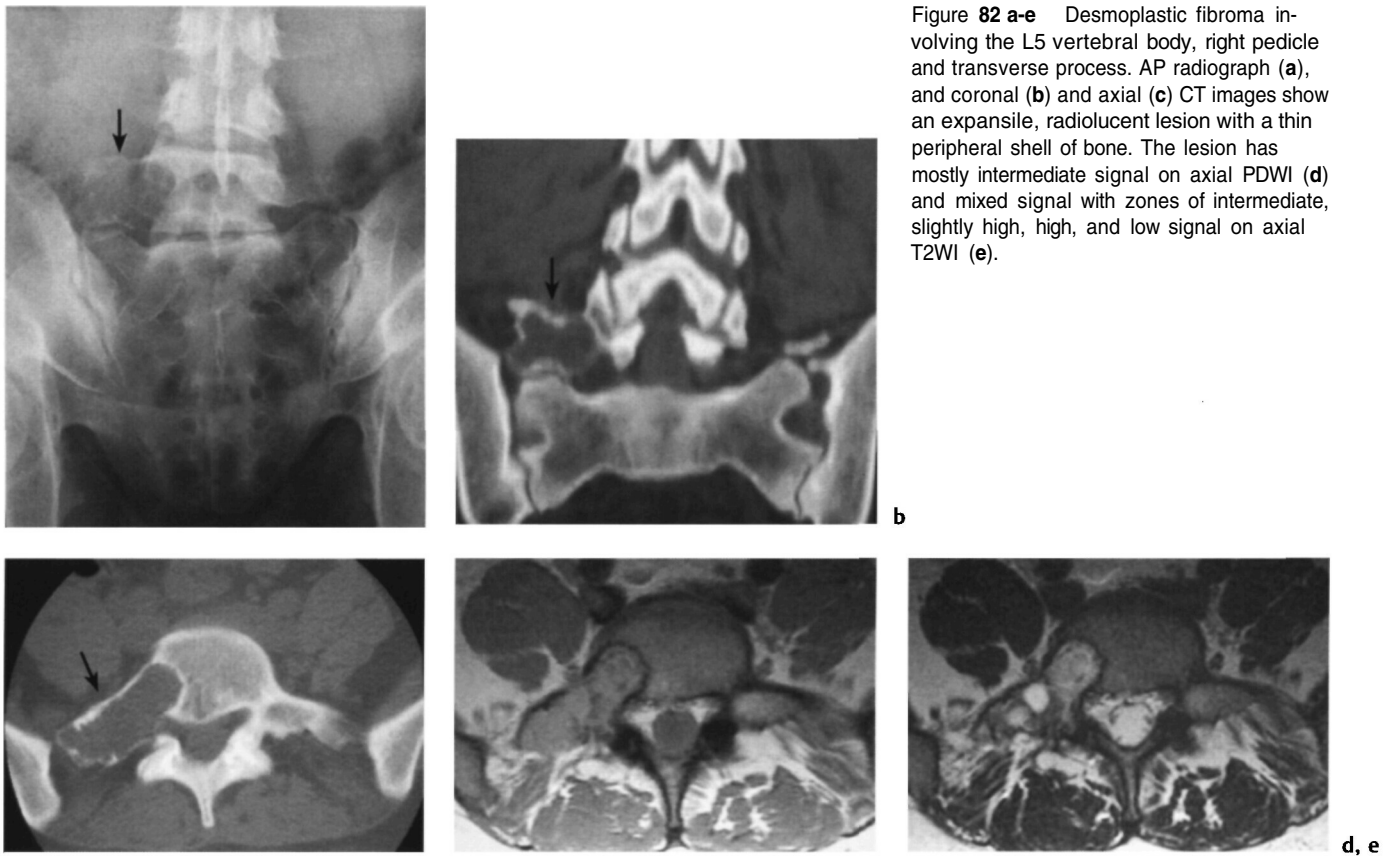

Figure **82 a-e** Desmoplastic fibroma involving the L5 vertebral body, right pedicle and transverse process. AP radiograph (**a**), and coronal (**b**) and axial (**c**) CT images show an expansile, radiolucent lesion with a thin peripheral shell of bone. The lesion has mostly intermediate signal on axial PDWI (**d**) and mixed signal with zones of intermediate, slightly high, high, and low signal on axial T2WI (**e**).

Deep fibromatosis (adults and children). Desmoids may appear on plain films as poorly-defined soft tissue lesions, which may cause bone erosion, periosteal reaction, and/or bone deformation.[17,27] In children, bowing of bone can occur.[17,27] Calcifications are uncommon.[20] On CT, desmoids can appear as soft tissue lesions with attenuation usually similar to or slightly increased relative to muscle.[3,5,14,27] Occasionally, attenuation of the lesions may be lower than muscle. Margins of lesions can be distinct and/or poorly defined.[3,5,14,27] Lesions show variable enhancement.[27] CT readily shows sites of bone erosion.[2,7,31]

Fibromatosis coli. On CT, fusiform swelling of the lower sternocleidomastoid muscle is usually seen.[17]

Desmoplastic fibroma.[6-9,12,13,23,41] Desmoplastic fibromas are typically radiolucent, lobulated, centrally located lesions with abrupt zones of transition, with or without: trabeculated appearance at borders, bone expansion with thinning of cortex, reactive sclerosis, and/or periosteal reaction (Fig. **82**). The lesions typically do not have matrix mineralization. CT is more accurate than plain films in defining the extent of bone destruction.[23]

MRI Findings

Dupuytren contracture. Lesions (10-55 mm) are seen along the flexor tendons. Lesions have low-intermediate signal on T1WI and T2W1.

Plantar fibromatosis. Lesions are usually present along the medial portion of the plantar aponeurosis. Lesions often have well-defined borders to superficial fat and somewhat ill-defined margins with adjacent deep muscles. Invasion of muscles is seen in 15% of cases. Lesions have heterogeneous low-intermediate signal on T1WI, PDWI, and T2WI, slightly high to high signal on fat suppressed T2WI or STIR (Fig. **83**). Lesions show various degrees of heterogeneous Gd-contrast enhancement.

Deep fibromatosis (adults and children).[1,3,14,15,17,20,21,27,31,33,34,39,43,44] Lesions can have distinct and/or poorly defined margins and can cross fascial compartments.[20] Lesions usually have homogeneous or heterogeneous low-intermediate signal on T1WI, intermediate signal on PDWI, and variable intermediate-high signal on T2WI (with or without zones of low signal) and slightly high to high signal on FST2WI (Figs. **84-86).** Myxoid zones in the lesions can have high signal on T1WI and T2WI. Tumors with high cellularity tend to show higher signal on T2WI than lesions with larger proportions of collagen. Lesions show variable degrees and patterns (heterogeneous vs. homogenous) of Gd-contrast enhancement. Pattern or degree of Gd-contrast enhancement by desmoids does not enable prediction of rate of tumor recurrence.

Fibromatosis coli.[17] Lesions usually appear as fusiform enlargement of the lower sternocleidomastoid muscle.[17] No discrete focal lesions are usually seen in the enlarged lower sternocleidomastoid muscle.[17] The involved muscle can have low-intermediate signal on T1WI, PDWI, and T2WI; and low, intermediate and/or slightly high signal on FS T2WI[17] (Fig. **87**).

Desmoplastic fibroma.[2,4,9,16,23,41,42] Desmoplastic fibromas are lobulated lesions with abrupt zones of transition. Lesions usually have low-intermediate signal on T1WI, intermediate signal on PDWI, and heterogeneous intermediate to high signal on T2W1 (Fig. **82**). Lesions may have internal or peripheral zones of low signal on T1WI and T2WI secondary to dense collagenous parts of the lesions and/or foci with high signal on T2WI from cystic zones. Thin curvilinear zones of low signal on T2WI can be seen

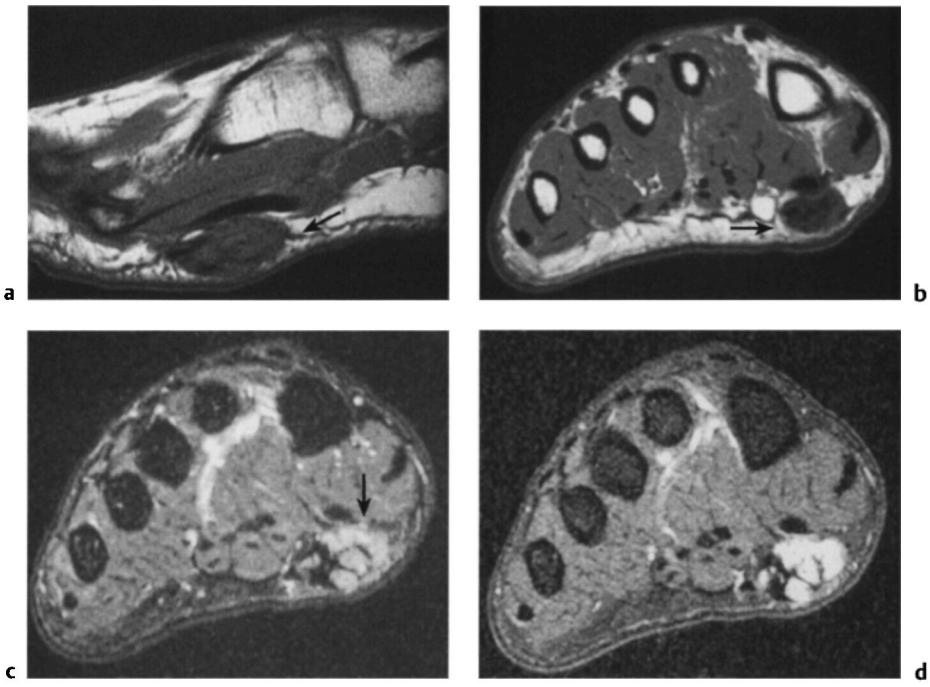

Figure **83 a-d** Desmoid tumor (plantar fibromatosis) involving the superficial soft tissues at the plantar aspect of the foot. The lesion has intermediate and low signal on sagittal (**a**) and axial (**b**) T1WI, and heterogeneous mostly high signal on axial FS T2WI (**c**). The lesion shows prominent Gd-contrast enhancement on axial FS T1WI (**d**).

at the margins of the lesions. Lesions show variable degrees and patterns of Gd-contrast enhancement.[9,23] Gd-contrast enhancement typically occurs in the more cellular portions of the lesions compared with the hypocellular and collagenous parts. Cortical disruption and soft tissue extension are commonly seen.

Differential Diagnosis

Superficial fibromatosis. Post-traumatic scar involving tendon or aponeurosis, giant cell tumor of tendon sheath, fibroma of tendon sheath, granuloma, gout.

Deep fibromatosis. Malignant fibrous histiocytoma, liposarcoma, leiomyosarcoma, malignant Schwannoma, synovial sarcoma, fibrosarcoma, rhabdomyosarcoma, epitheloid sarcoma, Kaposi sarcoma, clear cell sarcoma, malignant granular cell tumor, nodular fasciitis, neurofibroma, Schwannoma, giant cell tumor of tendon sheath, granular cell tumor, leiomyoma, fibroma of tendon sheath, proliferative fasciitis, dermatomyositis, hematoma, proliferative myositis, heterotopic bone formation.

Desmoplastic fibroma. Nonossifying fibroma, fibrous dysplasia, low-grade fibrosarcoma, unicameral or aneurysmal bone cyst, chondromyxoid fibroma, giant cell tumor, lymphoma, myeloma, metastatic lesion.

Treatment and Prognosis

Dupuytren contracture. These lesions are slow-growing.[10] Surgical excision is the standard treatment.[10] The risk of local recurrence is related to the extent of surgical resection.[10] Dermatofasciectomy with subsequent skin grafting usually produces the lowest recurrence rate.[10]

Plantar fibromatosis. These lesions are slow-growing.[10] Surgical excision is the standard treatment.[10] The risk of local recurrence is related to the extent of surgical resection, presence of multiple nodules, and presence of bilateral lesions.[10] Dermatofasciectomy with subsequent skin grafting usually produces the lowest recurrence rate.[10]

Deep fibromatosis. These lesions are more aggressive and infiltrative than superficial fibromatosis with regard to growth rate, size, and invasion of adjacent tissues.[13,14,27,31] Deep fibromatosis in children tends to be more aggressive and invasive than in adults.[14,17] Surgical excision with wide margins of normal-appearing tissue is the optimal treatment to include areas of tumor invasion not palpable at surgery or defined with imaging.[11,14,17] Local recurrence ranges from 25 to 77% of patients.[17,32] Radiation has been used as adjuvant therapy.[14,31,32] Chemotherapy has also been used as adjuvant treatment in children.[14,31,38,39] Lesions typically do not metastasize.[11,17,20,32,39] Lesions can invade neurovascular bundles and joints causing contractures. Severe morbidity from prolonged recurrences may require limb amputation.[32,39]

Fibromatosis coli. Lesions can initially grow rapidly, followed by progressively slower growth rates.[17] Lesions can then regress from 5 months to 2 years after diagnosis.[17] Most lesions are successfully treated with passive stretching and physiotherapy.[29] However, persistent masses are found in 10-15% of patients with associated abnormal cervicocranial posture despite passive stretching; and surgical tenotomy may be needed.[29] Up to 90% of patients have normal function after treatment with either passive stretching, physiotherapy, and/or tenotomy.[29] Patients older than 1 year with fibromatosis coli are typically less responsive to treatment than younger infants.[29]

Desmoplastic fibroma. These tumors are slowly progressive and locally aggressive.[2,7,8,26,30] The lesions can be treated with en bloc resection and/or definitive curettage with or without bone grafts.[7,8,26,30] Local recurrence has been reported to be 17% for en bloc resection,[2] and up to 47-72% for curettage.[2,7,8] Local recurrence can occur up to 8 years after treatment.[8] Radiation is not recommended because of the potential for dedifferentiation and/or malignant degeneration.[13]

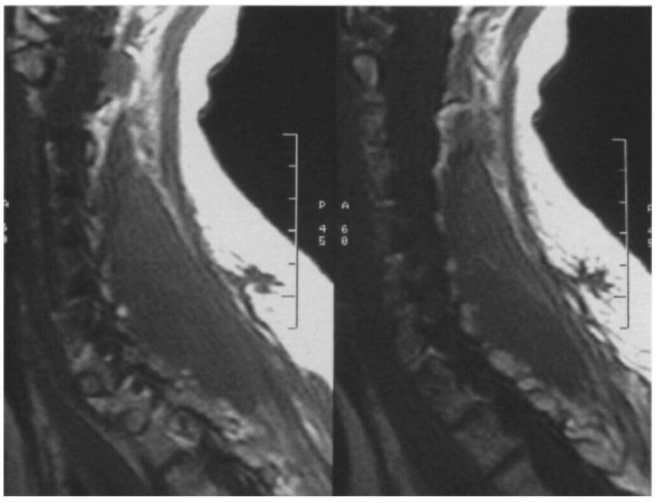

a

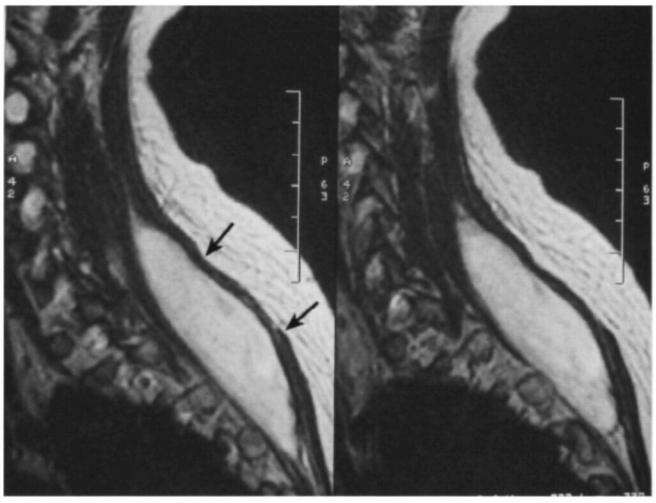

b

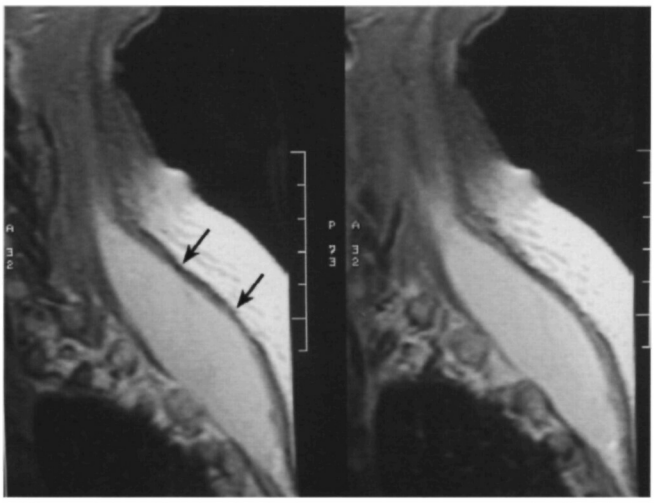

c

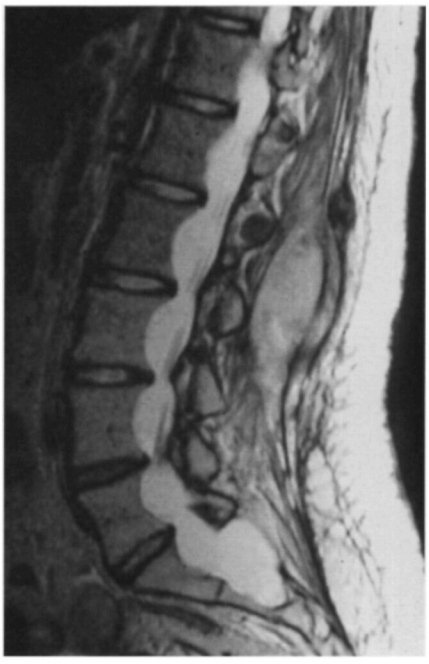

d

e, f

Figure **84 a-f** A 20-year-old woman with Turcot syndrome and multiple desmoid tumors involving the posterior paraspinal muscles of the cervical and upper thoracic spine (**a, b, c**) and lumbar spine (**d, e, f**). Sagittal (**a, d**) T1WI shows fusiform lesions with low-intermediate signal which have high signal on sagittal (**b, e**) T2WI. The lesions show prominent Gd-contrast enhancement on sagittal (**c, f**) FS T1WI.

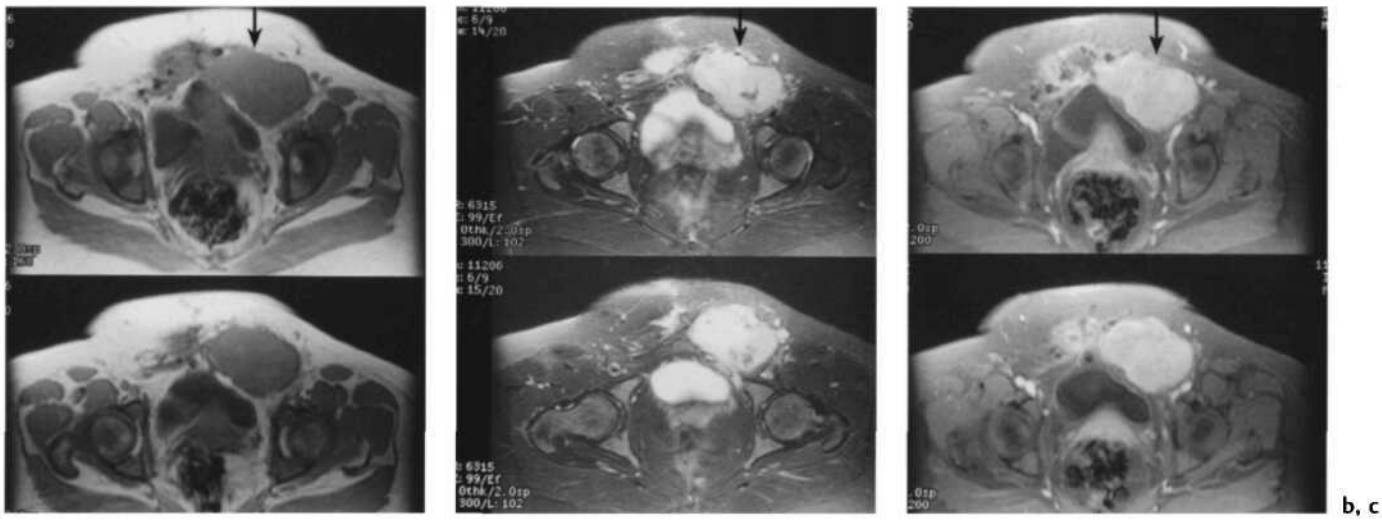

Figure **85 a-c** A 31 -year-old woman with a desmoid tumor involving the anterior soft tissues at the pelvis. The lesion has intermediate signal on axial PDWI **(a)**, and high signal on axial FST2WI **(b).** The lesion shows prominent Gd-contrast enhancement on axial FST1WI **(c)**.

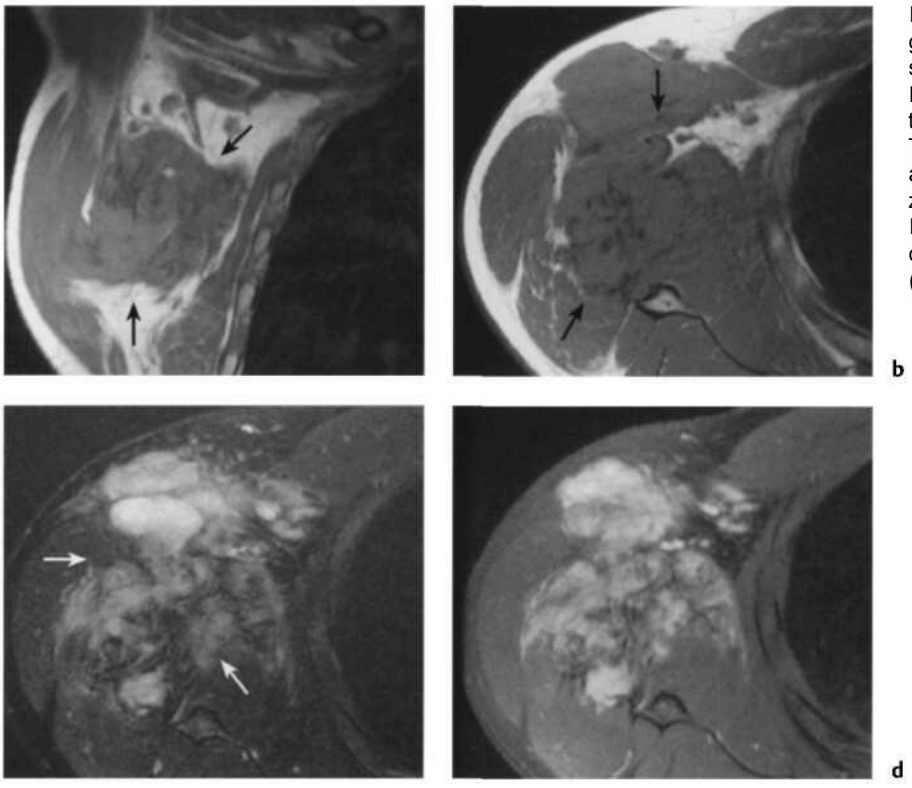

Figure **86a-d** A 32-year-old man with aggressive fibromatosis involving the soft tissues in the right axilla. MRI shows a lobulated lesion with indistinct margins which has intermediate signal on coronal **(a)** and axial **(b)** T1WI, and slightly high and high signal on axial **(c)** FST2WI. Foci and thin curvilinear zones of low signal are also seen on T1 WI and FS T2WI. The lesion shows prominent heterogeneous Gd-contrast enhancement on axial **(d)** FST1WI.

References

1 Bissett GS III. MR imaging of soft-tissue masses in children. Magn *Reson Imaging Clin N Am* 1996;4(4):697-719.

2 Bohm P, Krober S, Greschniok A, Laniado M, Kaiserling E. Desmoplastic fibroma of the bone. A report of two patients, review of the literature, and therapeutic implications. *Cancer* 1996;78:1011-1023.

3 Casillas J, Sais GJ, Greve JL, Iparraguirre MC, Morillo G. Imaging of intra- and extraabdominal desmoid tumors. *Radiographics* 1991; ll(6):959-968.

4 Celli P, Cervoni L, Trillo G. Desmoplastic fibroma of the skull. Case report and review of the literature. *Neurochimrgie* 1997;43: 260-264.

5 Chaudhuri B, Das Gupta TK. Pathology of soft tissue sarcoma. In: Das Gupta TK, Chaudhuri PK, eds. *Tumors of the Soft Tissues* 2nd ed. New York, NY: Appleton and Lange; 1998:88-95.

6 Crim JR, Gold RH, Mirra JM, Eckardt JJ, Bassett LW. Desmoplastic fibroma of bone: radiographic analysis. *Radiology* 1989;172: 827-832.

7 Forest M. Desmoplastic fibroma of bone. In: Forest M, Tomeno B, Vanel D, eds. *Orthopedic Surgical Pathology: Diagnosis of Tumors and Pseudotumoral Lesions of Bone and Joints* Edinburgh: Churchill Livingstone; 1998:303-316.

8 Fornasier V, Pritzker KPH, Bridge JA. Desmoplastic fibroma of bone. In: Fletcher CDM, Unni KK, Mertens F, eds. *World Health Organization Classification of Tumours. Pathology and Genetics of Tumours of Soft Tissue and Bone* Geneva: IARC Press; 2002:288.

9 Frick MA, Sundaram M, Unni KK, et al. Imaging findings in desmoplastic fibroma of bone: distinctive T2 characteristics. *AJR Am J Roentgenol* 2005;184:1762-1767.

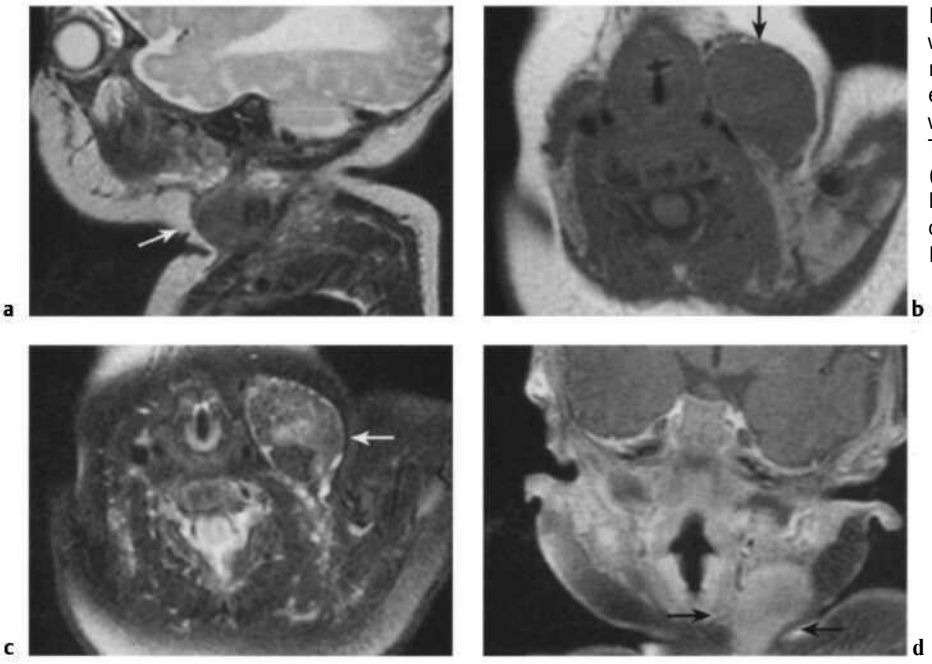

Figure **87a-d** A 5-week-old male infant with fibromatosis coli involving the left sternoclavicular muscle. There is fusiform thickening of the left sternoclavicular muscle which has low-intermediate signal on sagittal T2WI (**a**), intermediate signal on axial T1WI (**b**), and mixed low, intermediate, and slightly high signal on axial FST2WI (**c**). Minimal Gd-contrast enhancement is seen on coronal FST1WI (**d**).

10 Goldblum J, Fletcher JA. Superficial fibromatoses. In: Fletcher CDM, Unni KK, Mertens F, eds. *World Health Organization Classification of Tumours. Pathology and Genetics of Tumours of Soft Tissue and Bone* Geneva: 1ARC Press; 2002:81-82.

11 Goldblum J, Fletcher JA. Desmoid-type fibromatoses. In: Fletcher CDM, Unni KK, Mertens F, eds. *World Health Organization Classification of Tumours. Pathology and Genetics of Tumours of Soft Tissue and Bone* Geneva: IARC Press; 2002:83-84.

12 Huvos AG. Desmoplastic fibroma and periosteal "desmoid". In: Huvos AG, ed. *Bone Tumors: Diagnosis, Treatment, and Prognosis,* 2nd ed. Philadelphia, Pa: W.B. Saunders; 1991:404-405.

13 Kilpatrick SE, Unni KK. Spindle cell lesions of bone. In: Helliwell TR, ed. *Major Problems in Pathology: Pathology of Bone and Joint Neoplasms.* Vol 37. 1st ed. Philadelphia, Pa: W.B. Saunders, 1999: 239-240.

14 Kingston CA, Owens CM, Jeanes A, Malone M. Pictorial essay—Imaging of desmoid fibromatosis in pediatric patients. *AJR Am J Roentgenol* 2002;178:191-199.

15 Kobayashi H, Kotoura Y, Hosono M, et al. MRI and scintigraphic features of extraabdominal desmoid tumors. *Clin Imaging* 1997; 21(l):35-39.

16 Kong KY, Kang HS, Jung HW, Kim JJ, Lee CK. MR findings of desmoplastic fibroma of the spine. A case report. *Acta Radial* 2000;41: 89-91.

17 Kransdorf MJ, Murphey MD. Benign fibrous and fibrohisiocytic tumors. In: *Imaging of Soft Tissue Tumors* 2nd ed. Philadelphia, Pa: W.B. Saunders; 2006:189-256.

18 Kransdorf MJ, Murphy MD. Soft tissue tumors in a large referral population: prevalence and distribution of diagnoses by age, sex, and location. In: *Imaging of Soft Tissue Tumors* 2nd ed. Philadelphia, Pa: W.B. Saunders; 2006:6-37.

19 Kransdorf MJ. Benign soft-tissue tumors in a large referral population: distribution of specific diagnoses by age, sex, and location. *AJR AmJRoentgenol* 1995;164:395-402.

20 Lee JC, Thomas JM, Phillips S, Fisher C, Moskovic E. Aggressive fibromatosis: MRI features with pathologic correlation. *AJR Am J Roentgenol* 2006;186:247-254.

21 Lee JK, Glazer HS. Controversy in the MR imaging appearance of fibrosis. *Radiology* 1990;177:21-22.

22 Lewis JJ, Boland PJ, Leung DH, Woodruff JM, Brennan MF. The enigma of desmoid tumors. Ann *Surg* 1999;229:866-873.

23 Mahnken AH, Nolte-Ernsting CC, Wildberger JE, Wirtz DC, Gunther RW. Cross-sectional imaging patterns of desmoplastic fibroma. *Eur Radiol* 2001; 11:1105-1110.

24 Mulder JD, Schutte HE, Kroon HM, Taconis WK. Introduction. In: *Radiologic Atlas of Bone Tumors* Amsterdam: Elsevier; 1993:3-6.

25 Mulder JD, Schutte HE, Kroon HM, Taconis WK. The diagnosis of bone tumors. In: *Radiologic Atlas of Bone Tumors* Amsterdam: Elsevier ; 1993:9-46.

26 Mulder JD, Schutte HE, Kroon HM, Taconis WK. Desmoplastic fibroma. In: *Radiologic Atlas of Bone Tumors* Amsterdam: Elsevier; 1993:541-547.

27 Mulder JD, Schutte HE, Kroon HM, Taconis WK. Fibromatosis. In: *Radiologic Atlas of Bone Tumors* Amsterdam: Elsevier; 1993:639-646.

28 Mullins KJ, Rubio A, Meyers SP, Korones DN, Pilcher WH. Malignant ependymomas in a patient with Turcot's syndrome: case report and management guidelines. *Surg Neurol* 1998;49:290-294.

29 O'Connell. Fibromatosis coli. In: Fletcher CDM, Unni KK, Mertens F, eds. *World Health Organization Classification of Tumours. Pathology and Genetics of Tumours of Soft Tissue and Bone* Geneva: IARC Press; 2002:61-62.

30 Pensak ML, Nestok BR, VanLoveren H, Shumrick KA. Desmoplastic fibroma of the temporal bone. *AmJOtol* 1997;18:627-631.

31 Perez-Cruet MJ, Burke JM, Weber R, DeMonte F. Aggressive fibromatosis involving the cranial base in children. *Neurosurgery* 1998; 43(5):1096-1102.

32 Pignatti G, Barbanti-Brodano G, Ferrari D, et al. Extraabdominal desmoid tumor: a study of 83 cases. *Clin Orthop Relat Res* 2000; 375:207-213.

33 Quinn SF, Erickson SJ, Dee PM, et al. Walling MR imaging in fibromatosis: results in 26 patients with pathologic correlation. *AJR Am J Roentgenol* 1991;156:539-542.

34 Rai AT, Nguyen TP, Hogg JP, Gabriele FJ. Aggressive fibromatosis of the neck in a patient with Gardner's syndrome. Neuroradiology 2001;43:650-652.

35 Romero JA, Kim EE, Kim CG, Chung WK, Isiklar I. Different biologic features of desmoid tumors in adults and juvenile patients: MR demonstration. *JComput Assist Tomogr* 1995;19:782-787.

36 Shuto R, Kiyosue H, Hori Y, Miyake H, Kawano K, Mori H. CT and MR imaging of desmoplastic fibroma *Eur Radiol* 2002;12:2474-2476.

37 Siegel MJ. Magnetic resonance imaging of musculoskeletal soft tissue masses. *Radiol Clin North Am* 2001 ;39(4):714-715.

38 Skapek SX, Hawk BJ, Hoffer F, et al. Combination chemotherapy using vinblastine and methotrexate for the treatment of progressive desmoid tumor in children. *Clin Oncol* 1998;16:3021-3027.

39 Spiegel DA, Dormans JP, Meyer JS, et al. Aggressive fibromatosis from infancy to adolescence. *J Pediatr Orthop* 1999;19(6):776-784.

40 Unni KK. Introduction and scope of study. In: *Dahlin's Bone Tumors: General Aspects and Data on 1J087 Cases* 5th ed. Philadelphia, Pa: Lippincott, Williams & Wilkins; 1996:1-9.

41 Unni KK. Fibrosacroma and desmoplastic fibroma. In: *Dahlin's Bone Tumors: General Aspects and Data on 11087 Cases* 5th ed. Philadelphia, Pa: Lippincott, Williams & Wilkins; 1996:197-210.

42 Vanhoenacker FM, Hauben E, De Beuckeleer LH, Willemen D, Van Marck E, De Schepper AM. Desmoplastic fibroma of bone: MRI features. *Skeletal Radiol* 2000;29:171-175.

43 Van Slyke MA, Moser RPJr, Madewell JE. MR imaging of periarticular soft-tissue lesions. *Magn Reson Imaging Clin N Am* 1995;3(4): 662-664.

44 Weatherall FT. Benign and malignant masses. *Magn Reson Imaging Clin NAm* 1995;3(4):669-694.

A17 Elastofibroma

ICD-O Code

8820/0

Definition

Elastofibromas are benign, slow-growing fibroblastic tumorlike lesions that contain large amounts of enlarged coarse elastic fibers.[3-6,9-13] These lesions typically occur in patients over 50 years old, and most are located between the lower scapula and chest wall.[1-6,9-13] The etiology of these lesions is uncertain.[2] It has been suggested that these lesions are not true neoplasms but are fibroblastic pseudotumors that result from repetitive trauma or friction between the lower scapula and adjacent chest wall, or result from focal abnormal elastogenesis.[2,6] A genetic predisposition to these lesions has been shown in some cases.[2,6,9]

Frequency of Occurrence

Elastofibromas are rare and account for 0.3 % of benign soft tissue tumors.[5-8] These lesions are typically asymptomatic and have been suggested to be more common than previously reported." Lesions smaller than 3cm have been found at autopsy in 24 % of women and 11 % of men older than 55 years."

Age at Presentation

From 48 to 74 years, mean = 61 years,[8] median = 70 years.[3] Peak occurrence is in the 7th and 8th decades.[2]

Gender Ratio (M/F)

1/1 to 1/2[6,8]

Location

The most common sites are the trunk between lower scapula and chest wall (96%) > lower extremity (2%), hip and buttock (2%).[8] Bilateral parascapular lesions are not uncommon.[4,6,9] Other reported sites include the deltoid muscle, thoracic wall, axilla, infra-olecranon fossa, thigh, hand, foot, spinal canal, joints, greater trochanter region, viscera, gastrointestinal tract, and sclera.[1,2,9,10]

Signs and Symptoms

Elastofibromas are slow-growing lesions that rarely cause pain and tenderness.[2,6] Parascapular lesions may be associated with limitation in range of motion of the shoulder.[1]

Cross Pathologic Findings[1,2,4-6]

Elastofibromas are usually gray-white or gray-tan rubbery lesions with internal zones of yellow fat, and often range from 2 to 15cm in size.[1,2,4-6] Lesions typically have ill-defined margins.[1,2,4,5]

Histopathologic Findings[1,2,4-6,9-11]

Elastofibromas contain mixtures of hyalinized collagenous tissue with scattered fibroblasts, large numbers of elastic fibers, entrapped mature fat cells, and small amounts of mucoid stroma.[1,2,4,5,9-11] The elastic fibers are typically hypereosinophilic.[2,6] Elastic fibers can be branched or unbranched, large and coarse, and/or organized into linear arrangements of small globules or serrated disks which may have a "pipe-cleaner" or "beads on a string" appearance.[2,6]

Lesion Genetics

These lesions have been found to commonly have abnormalities involving the short arm of chromosome I.[2]

Findings on Plain Films (Roentgenograms) and Computed Tomography[1,4,5,9,10]

These lesions frequently have a lenticular shape with or without well-defined margins. They often have mostly soft tissue attenuation similar to skeletal muscle, as well as variable amounts of low attenuation from intralesional fatty deposits. Chronic erosions may be seen in adjacent bones.[1]

MRI Findings[1, 3-5, 9-13]

Lesions often range from 5 to 10cm, and frequently have a lenticular shape with or without well-defined margins. On T1WI and T2WI, lesions often have mostly intermediate signal that is isointense to muscle, as well as variable amounts of high signal from intralesional fatty deposits (Fig. 88). After Gd-contrast administration, lesions usually show variable degrees of enhancement, often in a heterogeneous pattern.

Differential Diagnosis

Atypical lipoma, liposarcoma, hemangioma, hematoma, desmoid, neurofibroma, lymphangioma, hamartoma, cicatricial fibroma, malignant fibrous histiocytoma.[9,11]

Treatment and Prognosis

Elastofibromas are slow-growing benign lesions that are cured by complete excision.[2] Local recurrence is rare.[2,9] These lesions have been reported to have no malignant potential[9] Core or fine-needle biopsies can be useful in excluding the diagnosis of sarcoma and avoiding surgery.[3,4,13]

References

1 Bae SJ, Shin MJ, Kim SM, Cho KJ. Intra-articular elastofibroma of the shoulder joint. *Skeletal Radiol* 2002;31:171-174.

2 Hashimoto H, Bridge JA. Elastofibroma. In: Fletcher COM, Unni KK, Mertens F, eds. *World Health Organization Classification of Tumours. Pathology and Genetics of Tumours of Soft Tissue and Bone* Geneva: IARC Press; 2002:56-57.

3 Hayes AJ, Alexander N, Clark MA, Thomas JM. Elastofibroma: a rare soft tissue tumour with a pathognomonic anatomical location and clinical symptom. *Eur J Surg Oncol* 2004:30:450-453.

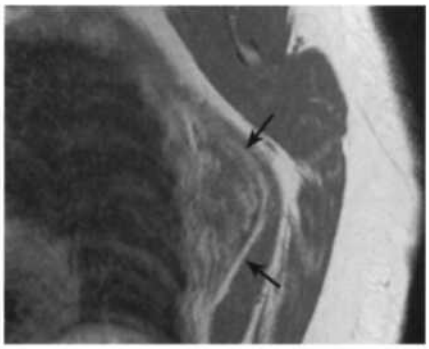

a

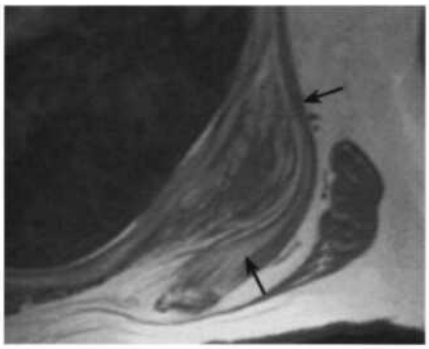

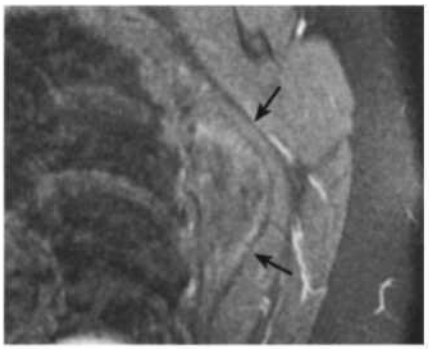

b, c

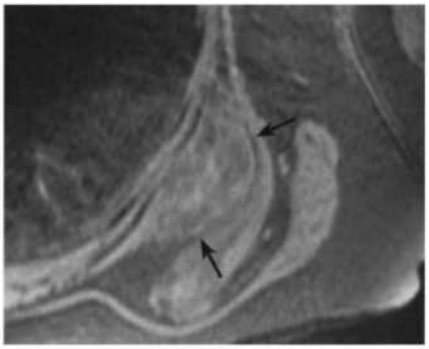

d

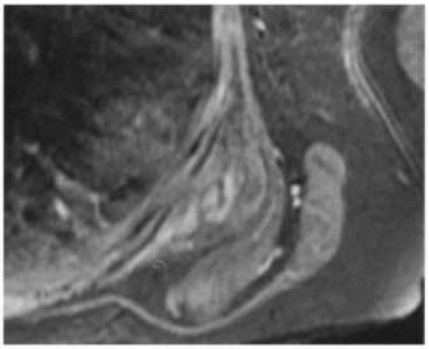

e

Figure **88a-d** Elastofibroma located between the lower scapula and chest wall in a 68-year-old woman. Coronal (**a**) and axial (**b**) T1WI show a lens-shaped lesion, which has mixed intermediate and high signal. The high signal zones represent intralesional fat as seen on coronal (**c**) FST1WI and axial (**d**) FST1WI. The lesion shows a heterogeneous pattern of Gd-contrast enhancement on FST1WI (**e**).

4 Hsieh SC, Shih Tiffany TF, Li YW. Bilateral elastofibroma dorsi two case reports. Clin *Imaging* **1999;23(1):47-50.**

5 Kransdorf MJ, Meis JM, Montgomery E. Elastofibroma: MR and CT appearance with radiologic-pathologic correlation. *AJR AmJ Roentgenol* 1992:159:575-579.

6 Kransdorf MJ, Murphey MD. Benign fibrous and fibrohistiocytic tumors. In: Kransdorf MJ, Murphey MD, eds. *Imaging of Soft Tissue Tumors* 2nd ed. Philadelphia, Pa: W.B. Saunders; 2006:189-256.

7 Kransdorf MJ, Murphy MD. Soft tissue tumors in a large referral population: prevalence and distribution of diagnoses by age, sex, and location. In: Kransdorf MJ, Murphey MD, eds. *Imaging of Soft Tissue Tumors* 2nd ed. Philadelphia, Pa: W.B. Saunders; 2006:6-37.

8 Kransdorf MJ. Benign soft-tissue tumors in a large referral population: distribution of specific diagnoses by age, sex, and location. *AJR Am J Roentgenol* 1995;164:395-402.

9 Naylor MF, Nascimento AC, Sherrick AD, McLeod RA. Elastofibroma dorsi: radiologic findings in 12 patients. *AJR Am] Roentgenol* 1996:167:683-687.

10 Nishida A, Uetani M, Oldmoto T, Hayashi K, Hirano T. Bilateral elastofibroma of the thighs with concomitant subscapular lesions. *Skeletal Radial* 2003:32:116-118.

11 Schick S, Zembsch A, Gahleitner A, et al. Atypical appearance of elastofibroma dorsi on MRI: case report and review of the literature. *Comput Assist Tomogr* 2000;24(2):288-292.

12 Yu JS, Weis LD, Vaughan LM, Resnick D. MRI of elastofibroma dorsi. *J Comput Assist Tomogr* 1995:19(4):601-603.

13 Zembsch A, Schick S, Trattnig S, Walter J, Amann G, Ritschl P. Elastofibroma dorsi. Study of two cases and magnetic resonance imaging findings. *Clin Orthop Relat Res* 1999; (364):213-219.

A18 Eosinophilic Granuloma (Also Referred to as Langerhans Cell Histiocytosis, Formerly Histiocytosis X)

ICD-OCode

Langerhans cell histiocytosis: 9751/1

Langerhans cell histiocytosis (unifocal): 9752/1

Langerhans cell histiocytosis (multifocal): 9753/1

Langerhans cell histiocytosis (disseminated): 9754/3

Definition[8,9,13,21,23,25]

Single or multiple eosinophilic granulomas are benign, tumor-like lesions consisting of Langerhans cells (histiocytes) and variable amounts of lymphocytes, polymorphonuclear cells, and eosinophils. Langerhans cells are mononuclear cells involved in both immune and nonimmune inflammatory responses. Langerhans cells are derived from bone marrow stem cells (CD 34+) and perform important roles in immune regulation. There are three types of Langerhans cell histiocytosis: a localized type involving bone or lung, **eosinophilic granuloma;** and two systemic types, the acute-subacute fulminant **Letterer-Siwe disease,** and a chronic disseminated form, **Hand-Schiiller-Christian disease**

Frequency of Occurrence

Eosinophilic granulomas[8,9,13,19,23-25] account for 70 % of Langerhans cell histiocytosis, 1 % of primary bone lesions, and 8% of tumor-like lesions; 5-20 per million children per year in the United States, 1-2 per million in the Netherlands, 1 per 200000 children per year younger than 15 years.

Letterer-Siwe disease accounts for 10% of Langerhans cell histiocytosis.[23]

Hand-Schiiller-Christian disease accounts for 20 % of Langerhans cell histiocytosis.[23]

Age at Presentation

Eosinophilic granuloma. From 1 to 60 years, median = 10 years, average = 13.5 years, peak incidence is between 5 and 10 years; 80-85 % occur in patients less than 30 years, and 60% occur in children less than 10 years.[8,9,13,17-19,23-25] Lesions involving the mandible tend to occur in older patients, average age = 26 years.[13]

Letterer-Siwe disease. This usually occurs in children younger than 3 years.[1923]

Hand-Schuller-Christian disease. This occurs in children from 1 to 5 years.[23]

Gender Ratio (M / F)

Eosinophilic granuloma: 1.1/1 to 2/1.[13,19,23]

Letterer-Siwe disease: 1 /1.[23]

Hand-Schuller-Christian disease: 1.3 /1.[23]

Location

Eosinophilic granuloma.[1,3,8,9,12,13,19,23] Lesions occur in the skull / craniofacial bones > femur > iliac bone > rib > vertebrae > humerus > tibia > other bones. Intra-osseous locations are diaphyseal (two-thirds) > metadiaphyseal > metaphyseal > epi-metaphyseal.[19] In vertebrae, the vertebral body is the most common location for eosinophilic granulomas.[1,3,19,20,22] Involvement of the posterior elements is rare.[1,3,19,20,22]

Letterer-Siwe disease. This disease often involves multiple organs such as the liver, spleen, lymph nodes, lungs, and bone.[23]

Hand-Schuller-Christian disease. Lesions are located in the liver, spleen, lymph nodes, skin, and bones.[23]

Signs and Symptoms

Eosinophilic granuloma.[1-4,8-13,15,19-23,25] The clinical manifestations depend on the sites of bony involvement. Signs and symptoms include localized pain and swelling, exophthalmos (orbital lesion), otitis media (temporal bone), diabetes insipidus (sella turcica), and spinal or neural compression (vertebral lesions). Pathologic fractures of long bones are uncommon.

Letterer-Siwe disease. This disease is associated with hepatosplenomegaly, lymphadenopathy, anemia, petechiae, osseous lesions, and/or skin rashes.[23]

Hand-Schuller-Christian disease. This disease is associated with otitis media, exophthalmos (25%), polyuria / diabetes insipidus (<50%) from lesions at the skull base or direct involvement of the pituitary gland or stalk, palpable skull lesions, bleeding and loosening of teeth from mandibular or maxillary lesions, hepatosplenomegaly, lymphadenopathy, eczema, xanthomatosis, anemia, low-grade fevers, and elevated erythrocyte sedimentation rates.[23,25] The clinical triad of this disease includes exophthalmos, diabetes insipidus, and radiolucent bone lesions.[25]

Cross Pathologic Findings

Eosinophilic granulomas are often soft yellow-brown lesions, with or without areas of hemorrhage or cysts associated with zones of bone destruction.[8,9,13,19,21,23,25]

Letterer-Siwe disease occurs as osseous / soft tissue lesions plus hepatosplenomegaly and lymphadenopathy.[23,25]

Hand-Schuller-Christian disease occurs as osseous / soft tissue lesions plus hepatosplenomegaly and lymphadenopathy.[23,25]

Histopathologic Findings

Lesions of Langerhans cell histiocytosis have variable cellular compositions of Langerhans cells, macrophages, osteoclast-like giant cells, polymorphonuclear cells, and eosinophilic leukocytes.[8,9,13,14,16,19,21,23,25] Langerhans cells have folded or indented nuclei with homogeneous pink granular cytoplasm. Eosinophilic leukocytes have irregular bilobed or indented nuclei and are a prominent feature of the lesions. Langerhans cell histiocytes are typically immunoreactive to S-100, CD 1 a, and CD 68.[8,13,14] CD 1 a is a membrane glycoprotein that is a marker for Langerhans cells.[8,14] CD 68 is a glycoprotein in lysosomes of histiocytes and monocytes/macrophages, and positive immunoreactivity can be seen with Langerhans cell histiocytosis as well as non-Langerhans histiocyte subpopulations, such as with Erdheim-Chester disease.[8,14] With electron microscopy, 20 % of Langerhans cell histiocytes have cytoplasm that contains X bodies, also referred to as Birbeck granules.[8,13,14,25]

Findings on Plain Films (Roentgenograms) and Computed Tomography

Langerhans cell histiocytosis involving bone.[4,6,8,9,12,13,20,22,23,25]**:** Lesions are typically radiolucent with either well-circumscribed or poorly-defined margins, with or without sclerotic margins, and with or without associated soft tissue mass (Figs. **89, 92,** 94-97). In the healing phases, lesions may have sclerotic margins.

- **Long Bones.** Lesions usually are radiolucent zones in diaphyseal or metadiaphyseal regions, endosteal scalloping and cortical lucent are common. Periosteal reaction is common, with or without extension into adjacent soft tissues. Lesions may be associated with pathologic fractures.[4,6,8,9,12,13,15,19,21-23,25]
- **Flat bones.** Eosinophilic granulomas in flat bones often appear as poorly-defined radiolucent lesions.[23]
- **Skull.** Lesions can have unequal erosion of the inner and outer tables giving a "beveled edge" appearance, with or without a central small sclerotic zone referred to as a "button sequestrum."[12,20,22,23]
- **Mandible.** Zones of lucency with "floating teeth" may be seen.[6,23]
- **Spine.** Lesions are typically located in the vertebral bodies and occasionally in the posterior elements.[3,12,22,23] Occasional collapse of the vertebral body may result.[22,23] Lesions rarely cause significant spinal canal compression. Disk spaces are usually preserved.

Findings on Radionuclide Bone Scans

Lesions show variable radiopharmaceutical accumulation (55 % show increased uptake, 35% show normal uptake, and 10% show decreased uptake).

MRI Findings[1-3,5-7,11,12,16,19,20,22,23,26]

Langerhans cell histiocytosis usually appears as focal intramedullary lesion(s) associated with trabecular and cortical bone destruction. Lesions typically have low-intermediate signal on T1W1 and PDWI; and heterogeneous slightly-high to high signal on T2WI[1-3,5-7,11,12,16,19,20,22,23,26] (Figs. **89-97).** Poorly defined zones of high signal on T2WI are usually seen in the marrow peripheral to the portions of the lesions associated with radiographic evidence of bone destruction, indicating reactive inflammatory and edematous changes.[2,5,26]

Extension of lesions from the marrow into adjacent soft tissues through areas of cortical disruption are commonly seen as well as linear periosteal zones of high signal on T2WI[1-3,5,7,11,12,16,19,20,22,23]

Lesions typically show prominent Gd-contrast enhancement in marrow and in extra-osseous soft tissue portions of the lesions.[6,11,12,20,23] Poorly defined zones of Gd-contrast enhancement are also seen in the marrow peripheral to the portions of the lesions associated with radiographic evidence of bone destruction, indicating reactive inflammatory and edematous changes.[2,5,11,12,16,22,23] These perilesional MRI findings have been shown to be correlated with inflammatory reaction associated with elevated tumor prostaglandin levels.[26]

Lesions involving the skull often are associated with scalp and dural enhancement representing reactive inflammation[12,20] (Figs. **89, 90).**

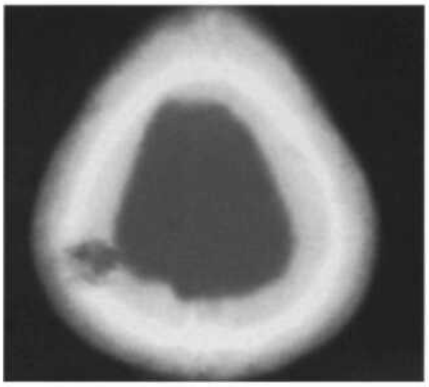

a

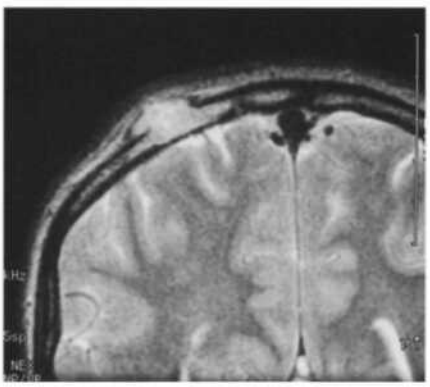

b, c

Figure **89a-c** A 14-year-old female with an eosinohilic granuloma involving the skull. Axial CT image (**a**) shows a radiolucent lesion with slightly irregular margins. The lesion has high signal on coronal T2WI **(b**), and extends from the marrow into the scalp through a zone of cortical destruction. Poorly defined zones of high signal on T2WI are seen in the marrow peripheral to the portions of the lesions associated with radiographic evidence of bone destruction. The lesion shows prominent Cd-contrast enhancement in marrow and in the extra-osseous soft tissue portion of the lesion on coronal T1WI (**c**). Poorly defined zones of Gd-contrast enhancement are also seen in the marrow peripheral to the portions of the lesion that are associated with radiographic evidence of bone destruction.

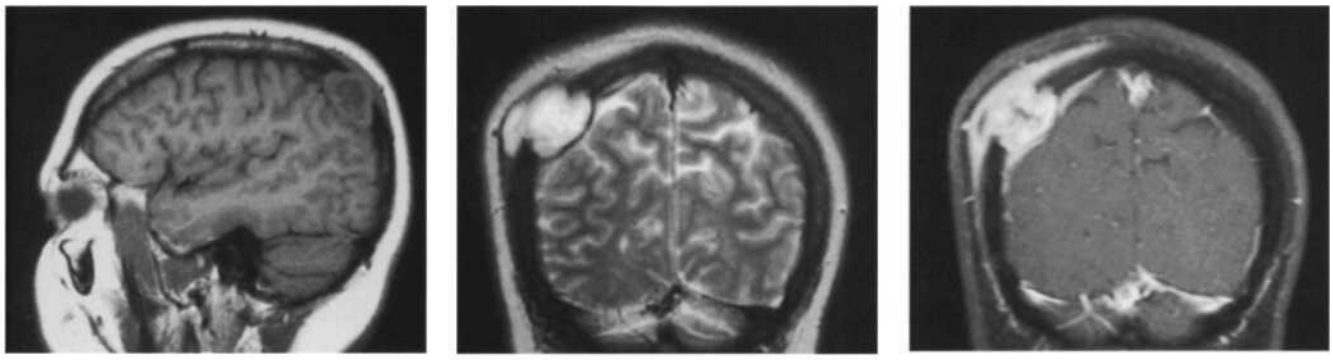

a b, c

Figure **90 a–c** 20-year-old woman with an eosinophilic granuloma involving the right parietal bone. The lesion has low-intermediate signal on sagittal (**a**) T1WI, and high signal on coronal (b) T2WI. Intracranial and extracranial extension of the lesion is seen through areas of cortical disruption. The lesion shows prominent Gd-contrast enhancement in the marrow, intracranial and extracranial portions of the lesion as well as the dura on coronal (c) FST1WI.

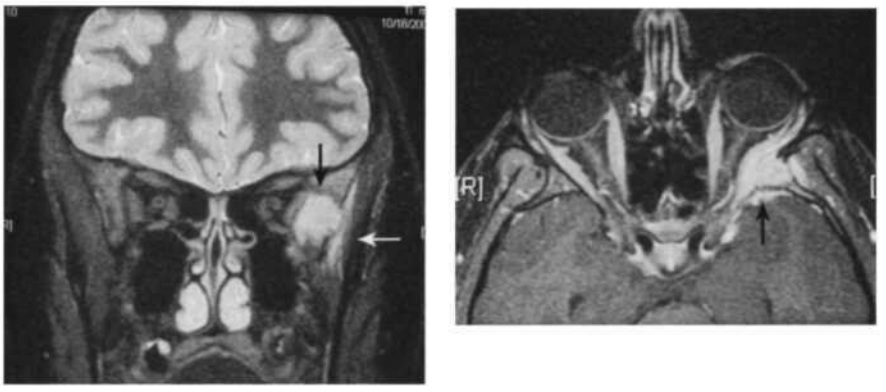

a b

Figure **91 a, b** A 13-year-old female with an eosinophilic granuloma involving the left zygoma, with associated bone destruction and extra-osseous extension into the orbit and lateral soft tissues. The lesion has high signal on coronal STIR (a), and shows prominent Gd-contrast enhancement on axial FST1WI (**b**).

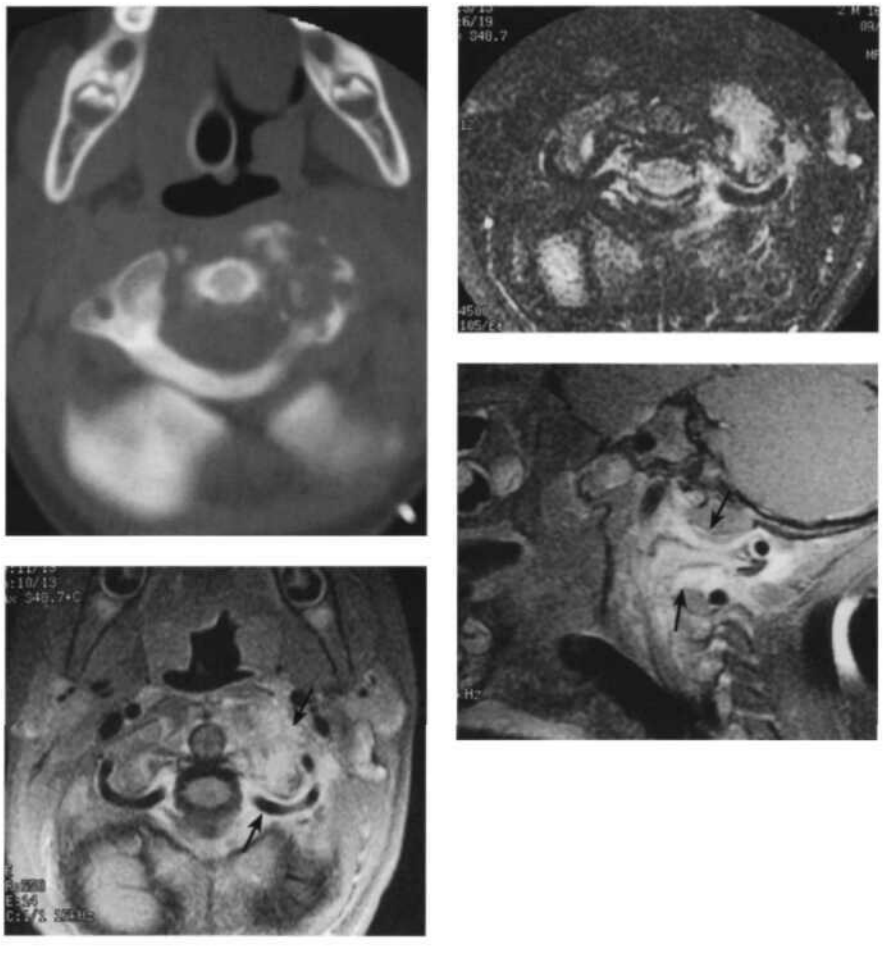

a b d c

Figure **92 a–d** A 2-year-old male with an eosinophilic granuloma involving the articular mass and pedicle of C 1. The lesion is radiolucent with poorly defined margins on axial CT (a). The lesion has high signal on axial FS T2WI (b). The lesion shows prominent Gd-contrast enhancement in marrow and in the extra-osseous soft tissue portions on axial (c) and sagittal (d) FST1WI.

a

b

Figure **93** a, b An 11-year-old female with an eosinophilic granuloma involving the T9 vertebral body with collapse. The lesion has low-intermediate signal on sagittal T1WI (**a**), and heterogeneous slightly high to high signal on sagittal T2WI (**b**).

a

b

c

Figure **94a-d** A 6-year-old male with an eosinophilic granuloma involving the L3 vertebral body. Sagittal CT image (**a**) shows a radiolucent lesion with poorly defined margins and cortical destruction. The lesion has low-intermediate signal on sagittal T1WI (**b**), and heterogeneous slightly high to high signal on sagittal FST2WI (**c**).

Figure **94 d** ▷

d

Figure **94 d** The lesion shows prominent Gd-contrast enhancement in the marrow as well as an extra-osseous portion, which extends into the anterior epidural soft tissues on sagittal FST1WI (**d**).

a

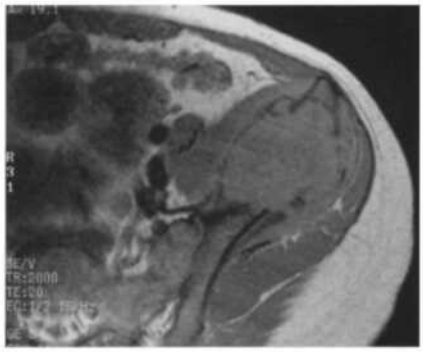

b

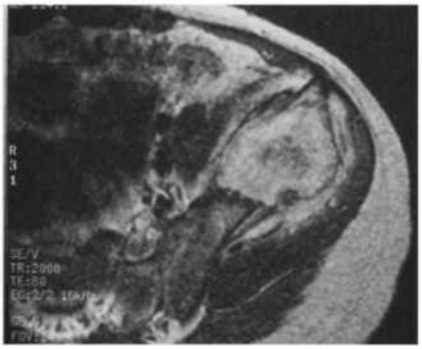

c

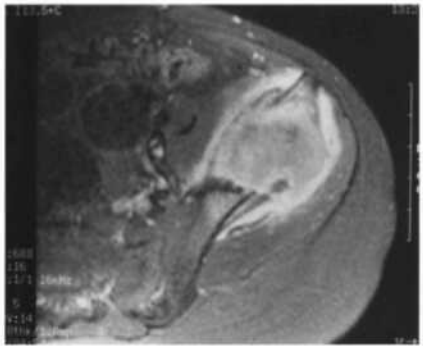

d

Figure **95a-d** A 4-year-old male with an eosinophilic granuloma involving the left iliac bone. AP radiograph (a) shows a radiolucent lesion with thin sclerotic margins. The lesion has intermediate signal on axial PDWI (**b**), and heterogeneous slightly high to high signal on axial T2WI (**c**). The lesion expands the bone and is associated with cortical disruption and extra-osseous extension. The lesion shows prominent Gd-contrast enhancement in marrow and in extra-osseous soft tissue portions on axial FST1WI (**d**).

Differential Diagnosis

For Langerhans cell histiocytosis: osteomyelitis, Ewing sarcoma, lymphoma, telangiectatic osteosarcoma, giant cell tumor, desmoplastic fibroma, chondromyxoid fibroma, plasmacytoma/myeloma, metastatic lesion. In healing phases: fibrous cortical defect, nonossifying fibroma.

Treatment and Prognosis

Eosinophilic granuloma.[1,3,8-10,13,19,21,23,25] Lesions with low morbidity can be followed conservatively by observation. Spontaneous regression and reactivation can occur.[13] Prognosis for lesions involving the skull base is worse than for other craniofacial locations.[13] Treatment of more clinically symptomatic lesions may include excision, curettage, steroid injection, and radiation.[1,3,8,10-13,19,21,23,25] For cervical lesions, immobilization can often result in successful outcomes.[3,22] Progression of eosinophilic granuloma involving the spine may require radiation.[3] In the spinal cases with instability or neurologic deficits, surgery is often required.[3,22] Chemotherapy has also been used.[22]

Letterer-Siwe disease. This disease can have a rapidly progressive clinical course with high morbidity and mortality from involvement of multiple organ systems.[23] Patients usually receive chemotherapy.[23] Death is often secondary to sepsis within **1** to **2** years.[23]

Hand-Schiiller-Christian disease. Prognosis depends on extent and distribution of organ systems involved.[23] In severe cases, mortality can be 15 %, often resulting from anemia, thrombocytopenia/hemorrhage, pneumonia, and pulmonary fibrosis.[24] Disease may be chronic and may extend over 25 years.[23]

a

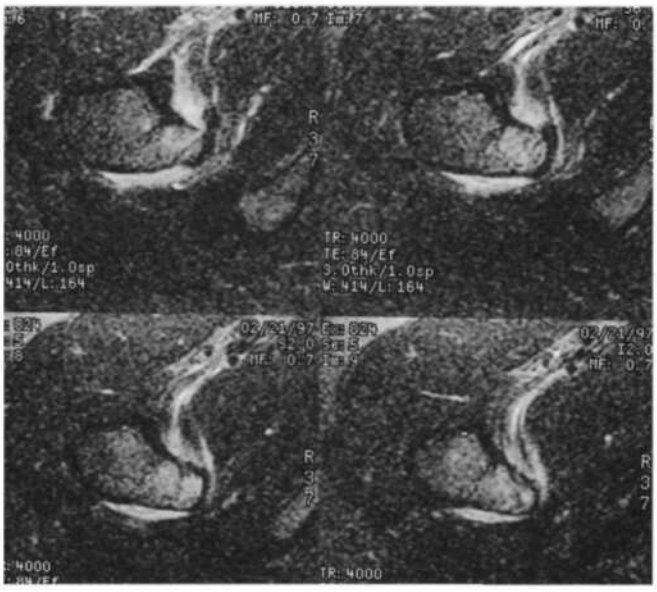

b

c

Figure **96a-c** A 13-year-old female with an eosinophilic granuloma involving the lesser trochanter. A radiolucent focus is seen at the lesser trochanter on an AP radiograph (**a**). A poorly defined zone of signal alteration is seen in the marrow associated with cortical disruption and extra-osseous extension. The lesion has heterogeneous slightly high to high signal on axial FST2WI (**b**). The lesion shows prominent Cd-contrast enhancement on coronal FST1WI (**c**).

References

1 Acciarri N, Paganini M, Fonda C, Gaist G, Padovani R. Langerhans' cell histiocytosis of the spine causing cord compression: case report. *Neurosurgery* 1992;31:965-968.

2 Beltran J, Aparisi F, Bonmati LM, Rosenberg ZS, Present D, Steiner GC. Eosinophilic granuloma: MRI manifestations. *Skeletal Radial* 1993; 22:157-161.

3 Bertram C, MadertJ, Eggers C. Eosinophilic granuloma of the cervical spine. *Spine* 2002;27:1408-1413.

4 Conway WF, Hayes CW. Miscellaneous lesions of bone. *Radial Clin North Am* 1993;31:339-358.

5 Davies AM, Pikoulas C, Griffith]. MRI of eosinophilic granuloma. *EurJ Radio/* 1994;18:205-209.

6 David R, Oria RA, Kumar R, et al. Radiologic features of eosinophilic granuloma of bone. *AJR Am] Roentgenol* 1989; 153:1021-1026.

7 De Schepper AM, Ramon F, Van Marck E. MR imaging of eosinophilic granuloma: report of 11 cases. *Skeletal* Radio/1993;22:163-166.

8 DeYoung BR, Unni KK. Langerhans' cell histiocytosis. In: Fletcher COM, Unni KK, Mertens F, eds. *World Health Organization Classification of Tumours. Pathology and Genetics of Tumours of Soft Tissue and Bone* Geneva: IARC Press; 2002:345-346.

9 Forest M. Eosinophilic granuloma. In: Forest M, Tomeno B, Vanel D. eds. *Orthopedic Surgical Pathology: Diagnosis of Tumors and Pseudotumoral Lesions of Bone and Joints* Edinburgh: Churchill Livingstone; 1998:555-566.

10 Ghanem I, Tolo VT, D'Ambra P, Malogalowkin MH. Langerhans' cell histiocytosis of bone in children and adolescents. *] Pediatr Orthop* 2003;23:124-130.

11 Hayes CW, Conway WF, Sundaram M. Misleading aggressive MR imaging appearance of some benign musculoskeletal lesions. *Radiographics* 1992;12:1119-1134.

12 Hindman BW, Thomas RD, Yound LW, Yu L. Langerhans' cell histiocytosis: unusual skeletal manifestations observed in thirty-four cases. *Skeletal* Radiol 1998:27:177-181.

13 Huvos AG. Langerhans' cell granulomatosis; Langerhans' cell histiocytosis; solitary and multifocal eosinophilic granuloma of bone. In: Huvos AG, ed. *Bone Tumors: Diagnosis, Treatment, and Prognosis* 2nd ed. Philadelphia, Pa: W.B. Saunders; 1991:695-706.

14 Kenn W, Eck M, Allolio B, et al. Erdheim-Chester disease: evidence for a disease entity different from Langerhans' cell histiocytosis? Three cases with detailed radiological and immunohistochemical analysis. *Hum Pathol* 2000;31(6):734-739.

15 Miller SL, Hoffer FA. Malignant and benign bone tumors. Radio*l Clin North Am* 2001;39(4):693-694.

16 Monroe M Ducou le Pointe H, Haddad S, Josset P, Montagne JP. Soft tissue signal abnormality associated associated with eosinophilic granuloma. Correlation of MR imaging with pathologic findings. Pediatr Radio*l* 1994;24:328-332.

17 Mulder JD, Schutte HE, Kroon HM, Taconis WK. Introduction. In: *Radiologic Atlas of Bone Tumors* Amsterdam: Elsevier; 1993:3-6.

18 Mulder JD, Schutte HE, Kroon HM, Taconis WK. The diagnosis of bone tumors. In: *Radiologic Atlas of Bone Tumors* Amsterdam: Elsevier; 1993:9-46.

19 Mulder JD, Schutte HE, Kroon HM, Taconis WK. Langerhans' histiocytosis (histiocytosis X). In: *Radiologic Atlas of Bone Tumors* Amsterdam: Elsevier; 1993:653-670.

Figure **97a-d** A 5-year-old male with an eosinophilic granuloma involving the distal humeral diaphysis. AP radiograph (a) shows a radiolucent, intramedullary lesion with irregular margins and prominent periosteal reaction. The periosteal reaction medially contains several zones of lucency. The lesion has low-intermediate signal on coronal T1WI (**b**) and heterogeneous high signal on coronal FST2WI (**c**). A zone of cortical destruction is seen, as well as poorly defined extra-osseous zones with high signal on FST2WI. Prominent abnormal Cd-contrast enhancement is seen in the marrow, periosteal reaction, and extra-osseous soft tissues on coronal FST1WI (**d**).

20 Okamoto K, Ito J, Furusawa T, Sakai K, Tokiguchi S. Imaging of calvarial eosinophilic granuloma. *Neuroradiology* 1999;41:723-728.

21 Perlman EJ. Ewing's sarcoma, lymphoma, and Langerhans' cell proliferations. In: Helliwell TR, ed. *Major Problems in Pathology: Pathology of Bone and Joint Neoplasms.* Vol 37.1st ed. Philadelphia, Pa: W.B. Saunders; 1999:279-303.

22 Scarpinati M, Artico M, Artizzu S. Spinal cord compression by eosinophilic granuloma of the cervical spine. Case report and review of the literature. *NeurosurgRev* 1995;18:209-212.

23 Stull MA, Kransdorf MJ, Devaney KO. From the archives of the AFIP - Langerhans' cell histiocytosis of bone. *Radiographics* 1992:12(4): 801-823.

24 Unni KK. Introduction and scope of study. In: Unni KK, ed. *Dahlin's Bone Tumors: General Aspects and Data on 11087 Cases* 5th ed. Philadelphia, Pa: Lippincott, Williams & Wilkins; 1996:1-9.

25 Unni KK. Conditions that commonly simulate primary neoplasms of bone. In: Unni KK, ed. *Dahlin's Bone Tumors: General Aspects and Data on 11087 Cases* 5th ed. Philadelphia, Pa: Lippincott, Williams & Wilkins; 1996:355-432.

26 Yamamura S, Sato K, Sugiura H, et al. Prostaglandin levels of primary bone tumor tissues correlate with peritumoral edema demonstrated by magnetic resonance imaging. *Cancer* 1997;79:255-261.

A 19 Erdheim-Chester Disease (Also Referred to as Chester-Erdheim Disease, Lipoid Granulomatosis, and Lipogranulomatosis)

Definition

Erdheim-Chester disease is a rare, multisystem, non-Langerhans cell histiocytic disorder of unknown etiology that usually affects adults.[1-13] In this disease, collections of foamy macrophages can be seen within various tissues and organs of the musculoskeletal, pulmonary, cardiac, gastrointestinal, and central nervous systems.[1-13] Lesions have also been reported in lymph nodes, retroperitoneum, kidneys, breast, aorta, and orbits.[2,3,5]

Frequency of Occurrence

Erdheim-Chester disease is rare.[1,2,13]

Age at Presentation

From 7 to 84 years,[1,7,13] average = 53 years.[4,7,13] Most common in 4th to 7th decades.[3,6]

Gender Ratio (M/F)

1/1 to 1.3/l.[2,13]

Location

Common sites in bone include the femur, tibia, radius, humerus, elbow, ulna, carpus.[1,2,4,13] Lesions infrequently involve flat bones and the axial skeleton." Skeletal abnormalities are often bilateral, and usually involve the diaphyseal and metaphyseal regions.[2] Epiphyseal abnomalities are uncommon.[3] Lesions are less frequently seen in the axial skeleton.[7] Lesions in the central nervous system can occur in the cerebrum, hypothalamus, cerebellum, and choroid plexus; they rarely involve the spinal or cranial dura.[1,2,4,5,13] Orbital lesions can be intraconal or extraconal, or involve eyelids the periorbital soft tissues.[3,6,13]

Signs and Symptoms

Lesions can present as a localized asymptomatic mass.[1] Intraosseous lesions can be associated with bone pain, which occurs in up to 50 % of patients and usually in the lower extremities.[2,13] Patients may also have joint pain and keloid formation.[3,4] Extensive infiltration of tissues or organs with foamy macrophages can result in organ failure or multisystem dysfunction.[1-4] Patients may have fever, weight loss, and/or malaise.[7,13] Lesions in the brain can produce symptoms (limb weakness, paraplegia, ataxia, numbness, nystagmus, etc.) mimicking multiple sclerosis.[4,5] Involvement of the hypothalamus and pituitary stalk can result in diabetes insipidus.[2,4,5,7] Involvement of the heart and/or pericardium can produce cardiac failure.[2] Lesions in the orbit can cause exophthalmos.[2,7,13] Orbital involvement is often bilateral and painless.[13] Xanthoma-like lesions involving the eyelids can occur and are referred to as xanthelasmas.[13] Shortness of breath secondary to pulmonary fibrosis from lung involvement can progress to cardiorespiratory failure.[2,7]

Cross Pathologic Findings

In bone, there is usually replacement of fatty marrow with varying degrees of fibrous tissue and collections of lipid-laden macrophages.[2,6] Infiltration of bone with foamy lipid-laden histiocytes of Erdheim-Chester disease often results in intramedullary zones of osteosclerosis.[2]

Histopathologic Findings

Specimens show xanthomatous or xanthogranulomatous lesions containing foamy lipid-laden histiocytes with small bland nuclei; also Touton-like giant cells, multinucleated giant cells, fibrosis/dense collagen, chronic inflammatory cells lymphocytes and histiocytes), and occasional scattered eosinophils.[1,4-6,13] Zones of osteonecrosis may be present.[9] Foamy histiocytes are usually immunoreactive to the histiocytic antigen CD 68, and show variable or no reactivity to S100.[2,5,7-9,12,13] Unlike Langerhans cell histiocytosis, Erdheim-Chester lesions lack immunoreactivity to CD 1 a and OKT6, and also lack intracytoplasmic Birbeck bodies on electron microscopy.[1,2]

Findings on Plain Films (Roentgenograms) and Computed Tomography

Bone. Abnormalities often consist of diffuse and/or poorly-defined zones of coarsened trabecular thickening, increased medullary density, and cortical thickening, primarily involving the diaphyses and metaphyses[2-5710-13] (Fig. 98). The epiphyseal regions are less commonly affected.[3,5,13] Up to one-third of patients have a mixed osteosclerotic and osteolytic pattern.[3,10,13] Zones of cortical destruction may be seen occasionally with lesions in long bones.[10] Lesions are often osteolytic in flat bones such as the skull, ribs, and mandible.[7]

Orbits. On CT, intraobital lesions may be intraconal or extraconal and usually have low and/or intermediate attenuation.[3,5] Lesions may have circumscribed margins or occur as diffuse infiltrative abnormalities within orbital fat.[3] Lesions may also cause eyelid xanthelasmas.[3]

MRI Findings

Bone. Lesions can appear as irregular zones with low and/or intermediate signal on T1WI and PDWI, and mixed low, intermediate and/or high signal on T2WI and FST2WI within marrow[3,6,7] (Fig. **98).** Zones of cortical destruction with or without extra-osseous lesion extension may be seen occasionally with lesions in long bones.[10] After Gd-contrast administration, heterogeneous enhancement may be seen in the involved marrow and zones of extra-osseous extension if present.[10]

Orbits. Abnormalities can appear as intraconal or extraconal lesions with low to intermediate signal on TlWI and PDWI, and variable low, intermediate and/or high signal on T2WI and FST2WT[6,7] (Fig. **99).** After Gd-contrast administration, enhancement is often seen in the involved marrow or soft tissue lesion zones.

a

b, c

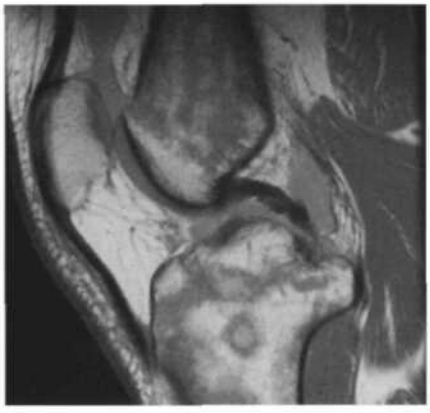

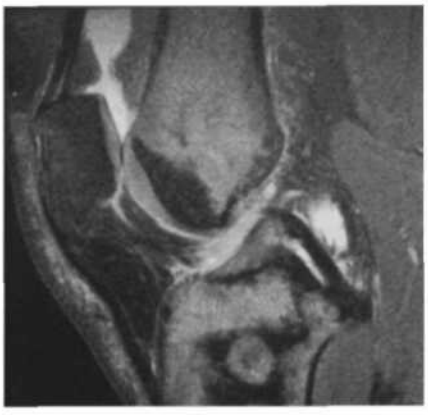

d

e, f

Figure **98a-f** A 39-year-old man with Erdheim-Chester disease with bone marrow involvement. AP (**a**) and lateral (**b**) radiographs show increased medullary density, coarsened trabecular thickening, and cortical thickening. Irregular zones with intermediate signal on coronal (**c**) and sagittal (e) PDWI, and slightly high signal on coronal (**d**) and sagittal (**f**) FST2WI are seen within the marrow in the epiphyseal, metaphyseal, and metadiaphyseal regions.

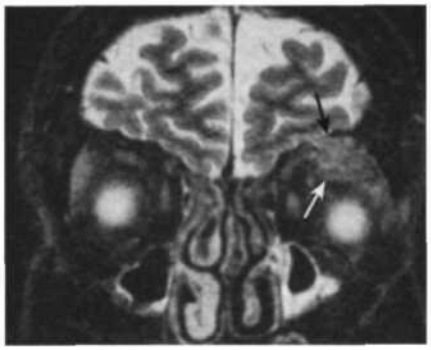

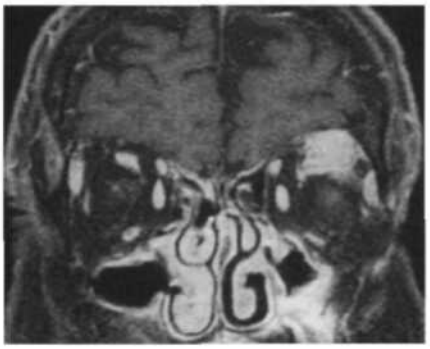

a

b

Figure **99 a, b** Erdheim-Chester disease in the upper left orbit involving the superior rectus muscle and intraconal fat. The lesion has slightly high signal on coronal STIR (**a**), and shows prominent Gd-contrast enhancement on coronal FST1WI (**b**).

Dura. Abnormalities can appear as circumscribed epidural, intradural, and/or subdural lesions with low to intermediate signal on T1WI, and variable low, intermediate and/or high signal on T2WI and FS T2WI.[1] After Gd-contrast administration, cranial and spinal dural lesions may or may not show contrast enhancement.[15]

Differential Diagnosis

Langerhans cell histiocytosis, Hand-Schuller-Christian disease, lymphoma, Castelman disease, sarcoidosis, Wegener granulomatosis, tuberculosis, chronic osteomyelitis, fibrous dysplasia, bone infarct, Gaudier disease, mucopolysaccharidoses, Paget disease.[1,3,10,12]

Prognosis and Treatment

The prognosis of Erdheim-Chester disease depends on the extent and location of disease.[2] Erdheim-Chester disease has been treated with surgical debulking, prednisone, cyclosporine, vincristine, vinblastine, cyclophosphamide, and/or doxorubicin.[2,6,7,12,13] Radiator, treatment may be useful for lesions in the brain parenchyma and other locations.[4,6,12,13] Immunotherapy with agents such as interferon-[alpha]2 a has also been used.[6,7,12,13] Multisystem disease can progress to result in death from respiratory distress, pulmonary fibrosis, renal and/or heart failure.[3,4,6,7,12] Thirty-seven percent of patients died after a mean follow-up interval of 32 months.[13]

References

1 Albayram S, Kizilkilic 0, Zulfikar Z, Islak C, Kocer N. Spinal dural involvement in Erdheim-Chester disease: MR1 findings. *Neuroradiology* 2002;44:1004-1007.

2 Al-Quran S, Reith J, Bradley J, Rimsza L Erdheim-Chester disease: case report, PCR-based analysis of clonality, and review of literature. *Mod Pathol* 2002;15(6):666-672.

3 Bancroft LW, Berquist TH. Erdheim-Chester disease: radiographic findings in five patients. *Skeletal Radio!* 1998;27:127-132.

4 Bohlega S, Alwatban J, Tulbah A, Bakheet SM, Powe J. Cerebral manifestation of Erdheim-Chester disease: clinical and radiologic findings. *Neurology* 1997;49(6):1702-1705.

5 Caparros-Lefebvre D, Pruvo JP, Remy M, Wallaert B, Petit H. Neuroradiologic asoects of Erdheim-Chester disease. *AJNR Am J Neuroradiol* 1995:16:735-740.

6 De Abreu MR, Chung CB, Biswal S, Haghighi P, Hesselink J, Resnick D. Erdheim-Chester disease: MR imaging, anatomic, and histopathologic correlation of orbital involvement. *AJNR Am J Neuroradiol* 2004;25:627-630.

7 Gottlieb R, Chen A. MR findings of Erdheim Chester diseasej *Comput Assist Tomogr* 2002;26(2):257-261.

8 Kenn W, Eck M, Allolio B, et al. Erdheim-Chester disease: evidence for a disease entity different from Langerhans' cell histiocytosis? Three cases with detailed radiological and immunohistochemical analysis. *Hum Pathol* 2000;31 (6):734-739.

9 Kim NR, Ko YH, Choe YH, Lee HG, Huh B, Ahn GH. Erdheim-Chester disease with extensive marrow necrosis: a case report and literature review. *IntJSurg Pathol* 2001;9(l):73-79.

10 Kushihashi T, Munechika H, Sekimizu M, Fujimaki E. Erdheim-Chester disease involving bilateral lower extremities. MR features. *AJR Am J Roentgenol* 2000;174(3):875-876.

11 Murray D, Marshall M, England E, Mander J, Chakera TMH. Erdheim-Chester disease. *Clin Radial* 2001 ;56:481-484.

12 Shamburek RD, Brewer HB, Gochuico BR. Erdheim-Chester disease: a rare multisystem histiocytic disorder associated with interstitial lung disease. *AmJMed Sci* 2001 ;321(1):66-75.

13 Veyssier-Belot C, Cacoub P, Caparros-Lefebvre D, et al. Erdheim-Chester disease: clinical and radiology characteristics of 59 cases. *Medicine* 1996:75(3): 157-169.

A 20 Ewing Sarcoma

ICD-O Code

9260/3

Definition

Ewing sarcoma is a malignant primitive tumor of bone comprised of undifferentiated small cells with round nuclei.[3,7,8,20,21,25,26] **Extracranial primitive neuroectodermal tumors (extracranial PNETs)** of bone and soft tissue are mostly similar to Ewing sarcoma, except that extracranial PNETs usually show varying degrees of neural differentiation.[3,7,8,20,21,25,26]

Frequency of Occurrence

Ewing sarcoma accounts for 6-11 % of primary malignant bone tumors, and 5-7% of primary bone tumors.[18-20,24-26] Ewing sarcoma usually occurs in Caucasians and Hispanics, and rarely occurs in Blacks and Asians.[7,8,26] The annual incidence in the United States is 2.1 per million.[7] Ewing sarcoma rarely occurs in the soft tissues, representing 1 % of malignant soft tissues and < 1 % of all soft tissue tumors.[7,11]

Age at Presentation

Ewing sarcoma in bone: usually occurs in patients ranging from 1 to 30 years, median = 14 years; 75 % in first 2 decades, > 90 % in patients <25 years; peaks in 2nd decade.[7,8,18 20,24-26]

Extraskeletal Ewing sarcoma: from 11 to 42 years, mean = 25 years."

Gender Ratio (M/F)

3 / 2 [8,11,25,26]

Location

Bone. Tumors are located in the femur > iliac bone > rib > tibia > humerus > fibula > vertebra, sacrum > scapula > radius, ulna > craniofacial bones.[4,7,8,18-20-24-26] Ewing sarcoma rarely involves the phalanges, bones of the feet, or calcaneous.[8] Ewing sarcoma occurs most frequently within the central medullary portions of bone (84%), versus eccentric locations within bone (11 %), intracortical locations (5%) or subperiosteal locations (<1 %).[20] In long bones, tumors are located in the diaphyseal region (57%), metadiaphyseal region (33%), metaphyseal region (6%), epi-metadiaphyseal zone (3 %), or epi-metaphyseal region (1 %).[20] In vertebrae, tumors involve the body (54%), arch (23 %), body and arch (23 %).[20]

Soft tissues. Tumors occur in the trunk > lower extremity > retroperitoneum > hip, buttocks > proximal limb girdle > upper extremity, head and neck."

Signs and Symptoms

Pain and swelling for several months are common clinical symptoms[7,8,21,25,26] Fever may result from tumor necrosis.[7,21-25] Patients may also have anemia, leukocytosis, and elevated erythrocyte sedimentation rates.[7,21,25,26] Pathologic fracture is uncommon.[25,26] Up to 35 % of patients have metastases at presentation.[7]

Cross Pathologic Findings

Ewing sarcoma occurs typically as soft gray-white moist tumors, often with areas of hemorrhage and/or necrosis associated with bone destruction and extra-osseous soft tissue mass.[2,3,7,8,26] Periosteal reactive ossification, "Codman Triangles," are commonly seen in Ewing tumors in long bones.[3,7,8,25,26]

Histopathologic Findings[2,3,7-9,20,21,25,26]

Ewing sarcoma consists of sheets of at least two cell populations. Cells can have spherical to ellipsoid shapes with round to oval nuclei and finely granular, ill-defined or well-defined cytoplasm. In addition, smaller cells with hyperchromatic nuclei and eosinophilic cytoplasm are also commonly seen. The mitotic rate tends to be low. Little intercellular stroma is common, except for widely separated strands of fibrous tissue. Lesions show little to no reticulin fibers within the cellular portions of the lesions. Zones of acute and/or chronic inflammation, necrosis, reactive fibrous and osseous tissue in Ewing tumors may complicate histopathologic interpretation.

Extracranial PNET shows histology similar to Ewing sarcoma except for evidence of neural differentiation (Homer Wright pseudorosettes), as well as by immunohistochemistry (higher rate of reactivity to neuron-specific enolase, synaptophysin, chromogranin, and S-100 compared with undifferentiated Ewing sarcoma) and electron microscopy (occasional cytoplasmic processes containing neurosecretory granules.)[3,7,8,21,26]

Other Ewing tumors have histopathologic and immunohistochemical features that are intermediate between the most undifferentiated forms of Ewing sarcoma and extracranial PNET.[3,7,8,21,26]

Ewing tumors / extracranial PNET show positive immunohistochemical reaction to the MIC 2 (CD 99) gene product in up to 95 % of cases.[17,21,26] The MIC 2 gene product is a membrane-bound glycoprotein that is probably involved in cell adhesion processes.[21] The MIC 2 gene is located on the sex chromosomes and is not related to the t(11;22) translocation.[3,21]

Tumor Genetics

Ewing tumors and extracranial PNET commonly show translocations involving chromosomes 11 and 22 at. t(11;22) (q24:ql2).[3,7,21,26] Using reverse transcriptase with the polymerase chain reaction, the genes and gene products at the translocation break points on chromosomes 11 and 22 have been identified.[3,21] The t(11;22) translocation results in the fusion of the FLI-1 gene at 11 q24 to the EWS gene at 22ql2.[3,21,26] The hybrid protein that results from translation of the gene fusion has been detected in almost all Ewing sarcomas and extracranial PNETs.[3,21,26] This translocation is also seen in peripheral neuroepithelioma, Askin tumor (extracranial PNET involving the thoracic wall) and extra-osseous Ewing sarcoma.

Findings on Plain Films (Roentgenograms) and Computed Tomography[1,3,5,6,8,16,20-22,25,26-29]

Ewing sarcoma often appears as a central radiolucent lesion with poorly defined margins (permeative > "moth-eaten" appearance), irregular zones of cortical destruction, and interrupted lamellated ("onion skin") or perpendicular ("hair on end") periosteal reaction (Figs. **100,102-106).** Codman triangles can be seen at the borders of tumor periosteal reaction with zones of cortical destruction and extra-osseous tumor extension (Figs. **105,106).** Lesions occur in diaphysis > metadiaphysis. Sclerosis can be seen in combination with lytic regions in a minority of cases. CT can show a thin striated periosteal reaction perpendicular to the long axis of bones, also referred to as the "hair on end" appearance (Figs. 100,104).

Extra-osseous soft tissue masses and extent of lesions are better seen with CT than with plain films. Extra-osseous soft tissue masses typically do not show ossification or calcification (Figs. **107,108).**

Findings on Radionuclide Bone Scans

Ewing sarcoma typically shows increased radiopharmaceutical accumulation of both technetium-99 m methylene diphosphonate and gallium-67-citrate. Soft tissue components of the lesions may show mild uptake.

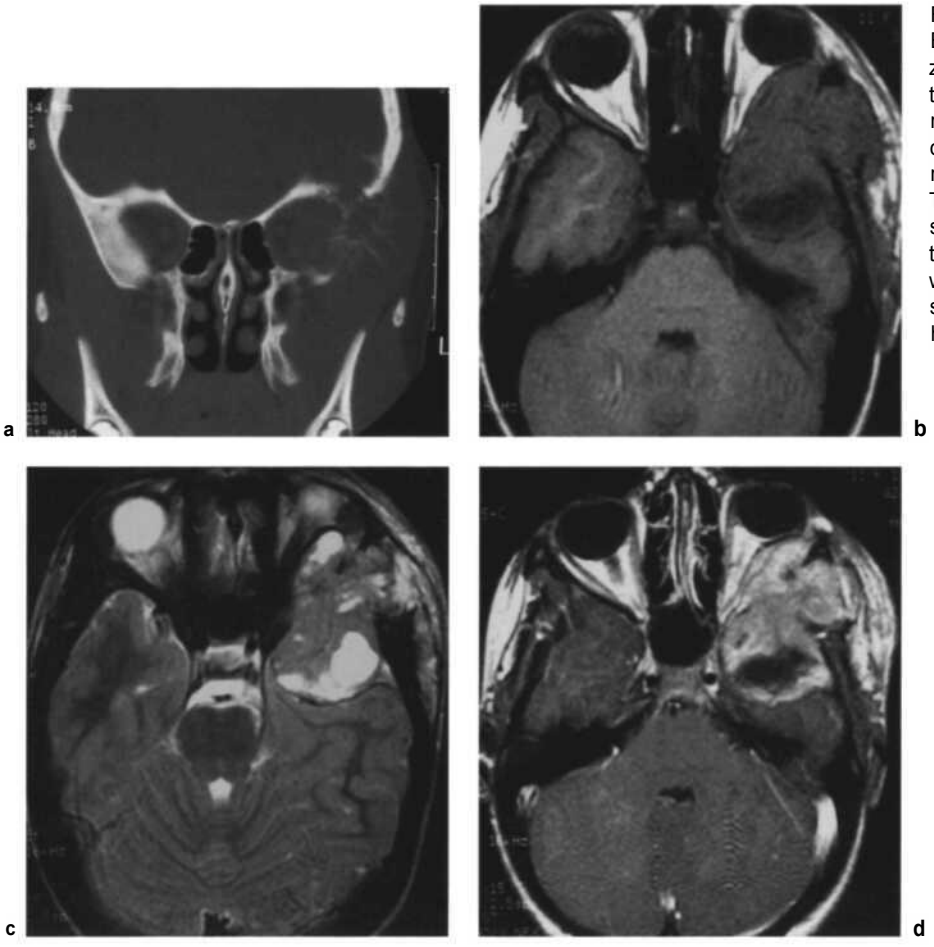

Figure **100a-d** An 11-year-old female with Ewing sarcoma involving the left frontal and zygomatic bones with tumor extension intracranially as well as into the left orbit. Coronal (**a**) CT image shows a soft tissue tumor, containing perpendicular striated periosteal reaction associated with bone destruction. The tumor has zones of low and intermediate signal on axial (**b**) T1WI, heterogeneous intermediate and high signal on axial (**c**) T2WI with small foci of low signal. The tumor shows prominent irregular Gd-contrast enhancement on axial T1WI (**d**).

Figure **101 a-c** A 16-year-old female with Ewing sarcoma involving a vertebral body with extension laterally into the adjacent soft tissues on the left. Axial (**a**) T1 WI shows the tumor to have low-intermediate signal. The tumor has heterogeneous mostly slightly high and high signal on axial (**b**) FST2WI, and shows heterogeneous Gd-contrast enhancement on axial (**c**) FST1WI.

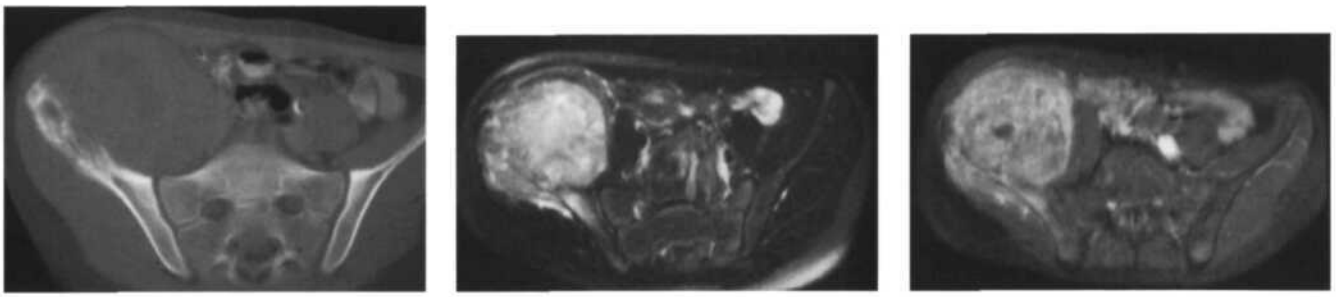

a **b, c**

Figure **102a-c** A 10-year-old male with Ewing sarcoma involving the right iliac bone associated with bone destruction and extra-osseous tumor extension. Axial CT image (**a**) shows a permeative, radiolucent lesion involving the iliac bone associated with a large extra-osseous mass. The tumor has heterogeneous mostly slightly high and high signal on axial FST2WI (**b**). The tumor shows heterogeneous Gd-contrast enhancement on axial FST1WI (**c**).

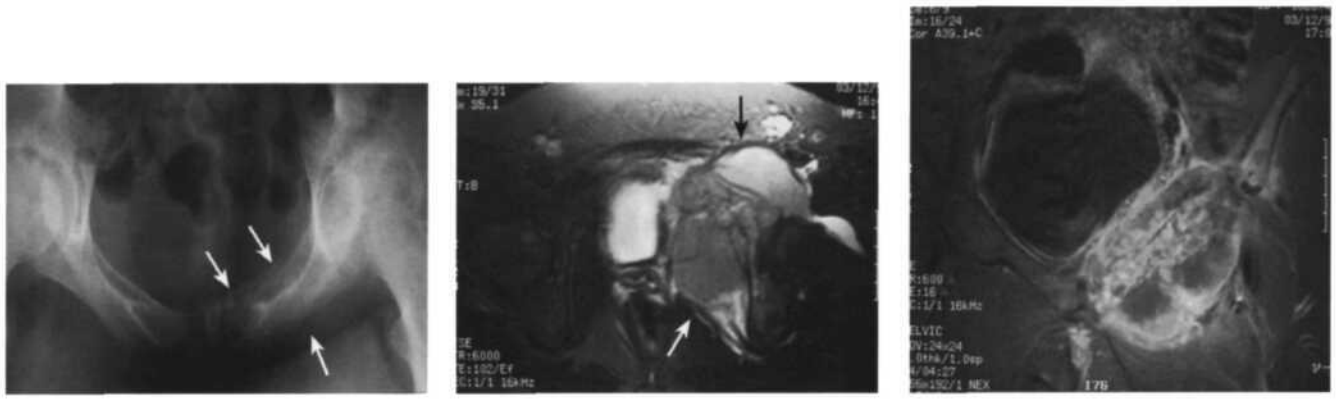

a **b, c**

Figure **103a-c** A 13-year-old female with Ewing sarcoma involving the left pubic bone. AP radiograph (**a**) shows a permeative, radiolucent lesion with periosteal reaction. The tumor is associated with cortical destruction and extra-osseous tumor extension (**b, c**). The tumor has heterogeneous slightly high to high signal on axial FS T2WI (**b**). The tumor shows prominent irregular Gd-contrast enhancement on coronal FST1WI (**c**).

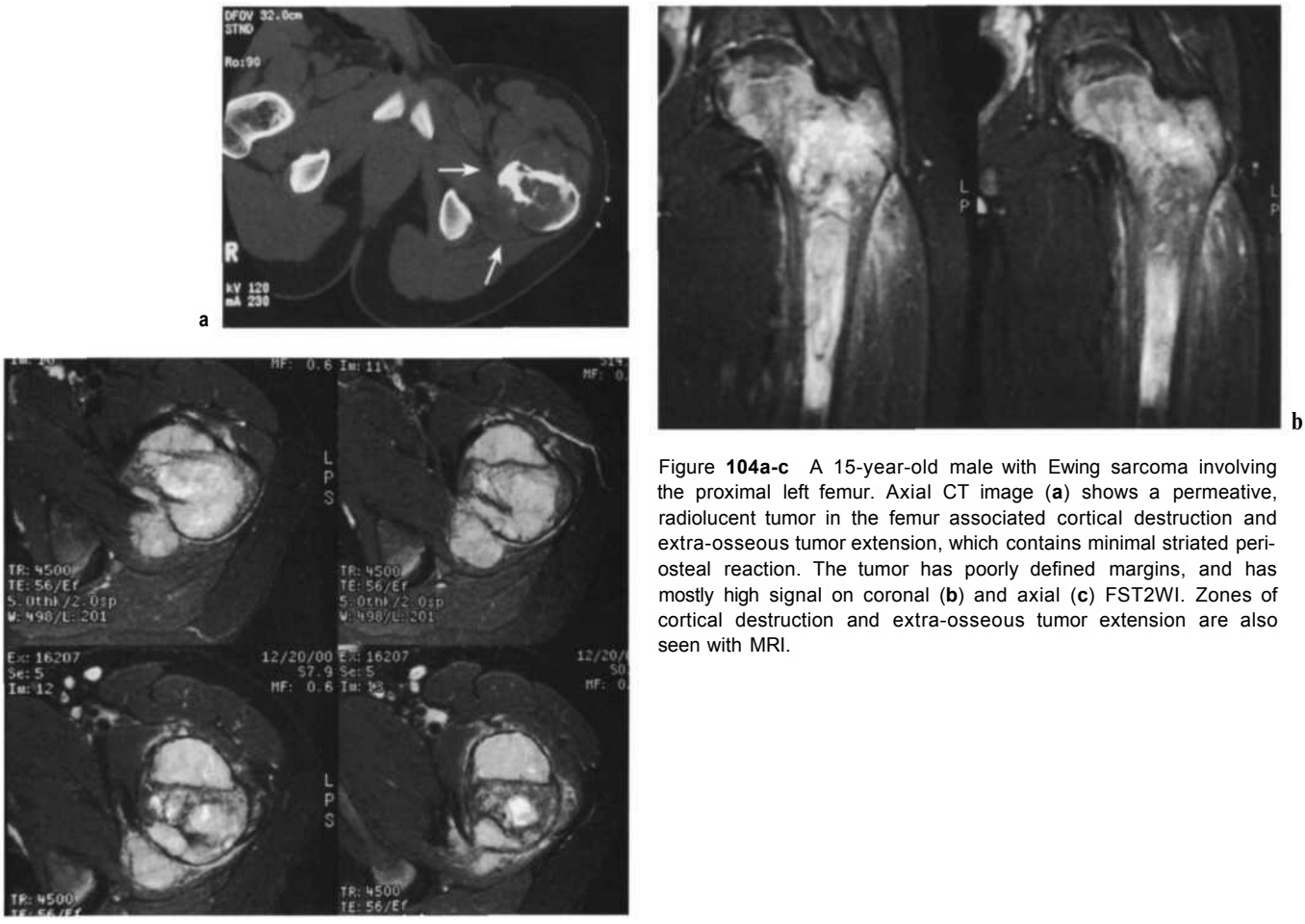

a **b** **c**

Figure **104a-c** A 15-year-old male with Ewing sarcoma involving the proximal left femur. Axial CT image (**a**) shows a permeative, radiolucent tumor in the femur associated cortical destruction and extra-osseous tumor extension, which contains minimal striated periosteal reaction. The tumor has poorly defined margins, and has mostly high signal on coronal (**b**) and axial (**c**) FST2WI. Zones of cortical destruction and extra-osseous tumor extension are also seen with MRI.

a

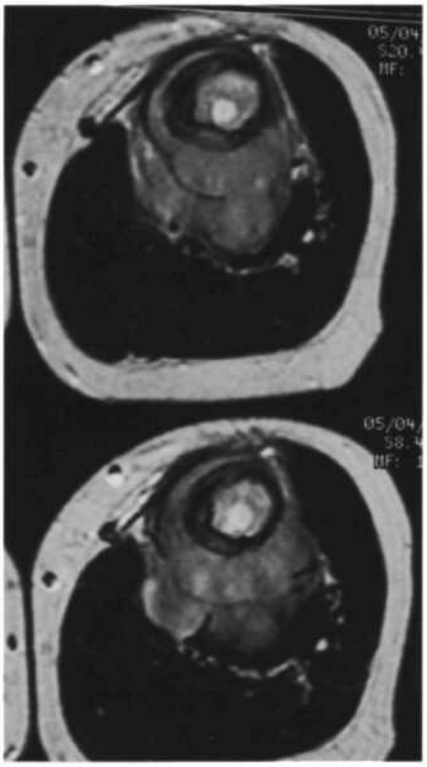

b, c

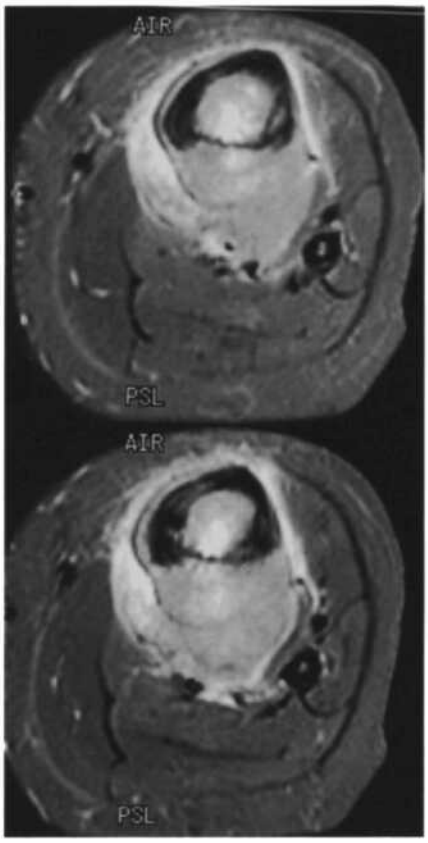

d

e

Figure **105a-e** A 9-year-old male with Ewing sarcoma involving the proximal tibia. AP (**a**) and lateral (**b**) radiographs show a permeative, radiolucent lesion in the proximal diaphyseal and metadiaphyseal portions of the tibia associated with irregular zones of cortical destruction and lamellated "onion skin" periosteal reaction. Codman triangles are seen at the proximal and distal borders of tumor periosteal reaction (**a, b**). The tumor has poorly defined margins and has heterogeneous slightly high to high signal on axial T2WI (**c**). Curvilinear thin zones of low signal on axial T2WI (**c**) represent elevated periosteum. The tumor shows prominent irregular Cd-contrast enhancement on axial (**d**) and coronal (**e**) FST1 WI. Zones of cortical destruction and extra-osseous tumor extension are also seen with MRI.

MRIFindings[1,3,4,6,10,12-17,20,22,23-25,29]

Lesions usually have low-intermediate signal on T1WI and PDWI, heterogeneous slightly high to high signal on T2W1 and FST2WI (Figs. **100-108).** Margins of the lesions are often ill defined. Lesions typically show prominent irregular Gd-contrast enhancement. MRI shows areas of cortical destruction; as well as the size, extent, and configuration of extra-osseous soft tissue masses (Figs. **100-103,105-107).** Dynamic Gd-contrast enhancement can allow differentiation between rapidly-enhancing tumors with higher mean initial slope values compared with reactive intramedullary and non-neoplastic soft tissue edema. On T2WI, thin striated zones of low signal can be sometimes be seen oriented perpendicular to the long axis of the involved bone, representing the "hair on end" appearance of periosteal or reactive bone formation within extra-

a

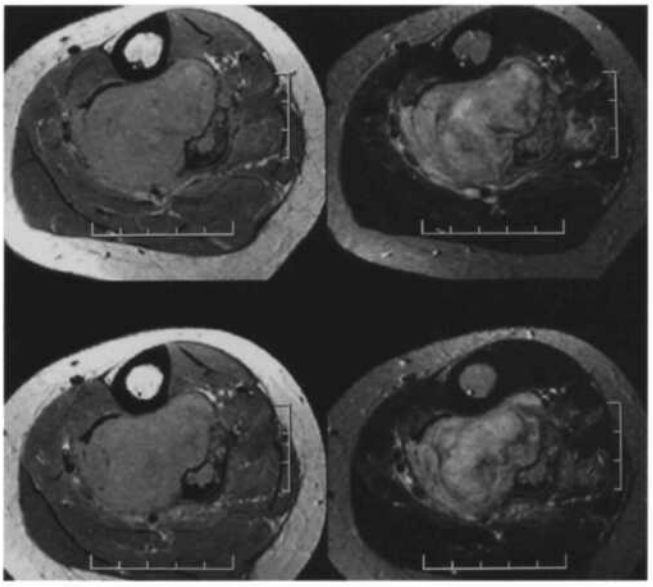

b

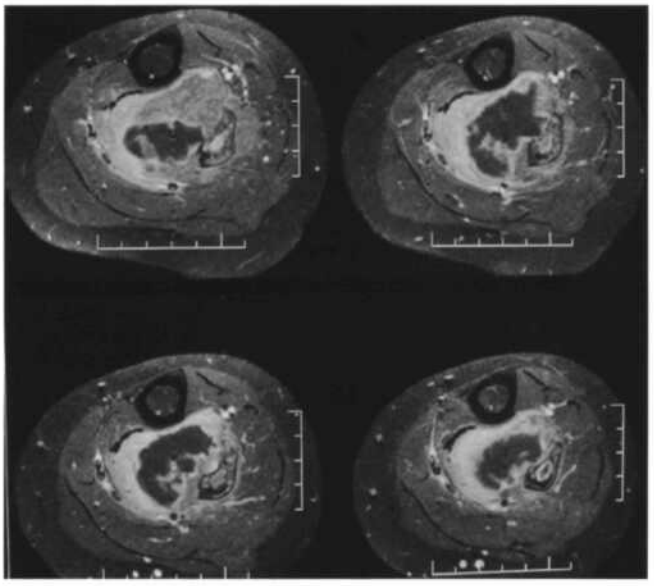

c

Figure **106a-c** An 11-year-old male with Ewing sarcoma/PNET involving the proximal fibula. AP radiograph (**a**) shows a permeative, radiolucent lesion in the proximal diaphyseal and metadiaphyseal portions of the fibula associated with irregular zones cortical destruction and lamellated "onion skin" periosteal reaction. Codman triangles are seen at the proximal and distal borders of tumor periosteal reaction (**a**). The tumor has poorly defined margins and is associated with cortical destruction and prominent extra-osseous tumor extension. The tumor contains zones with intermediate and slightly high signal on axial PDWI (**b**, images on left), and slightly high to high signal on axial T2WI (**b**, images on right). Curvilinear thin zones of low signal represent elevated periosteum and tumor periosteal reaction (**b**). The tumor shows prominent irregular Gd-contrast enhancement on axial FST1WI (**c**), as well as zones of central necrosis.

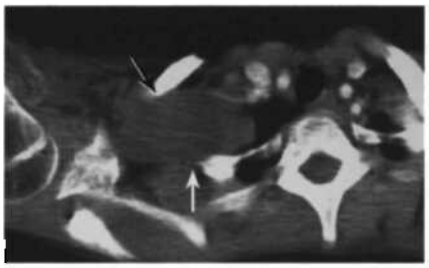

a

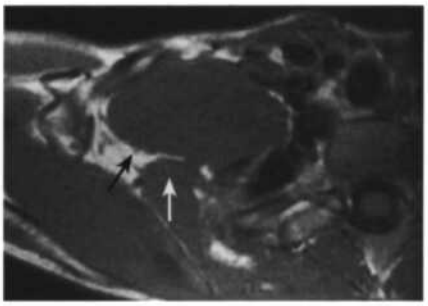

b

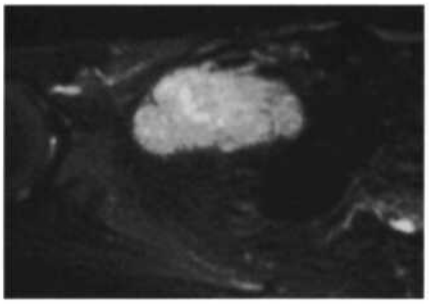

c

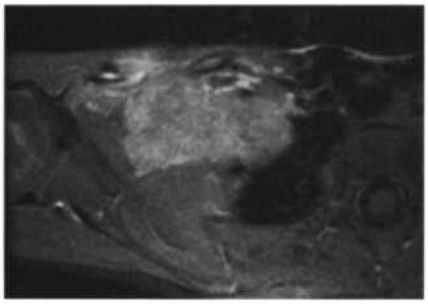

d

Figure **107a-d** An 11-year-old female with an extra-osseous Ewing sarcoma in the soft tissues adjacent to the right clavicle. Axial CT image (**a**) shows a circumscribed lesion with intermediate attenuation. The tumor has intermediate signal on axial T1WI (**b**), and high signal on axial FST2WI (**c**). The tumor shows moderate Gd-contrast enhancement on axial FST1WI (**d**).

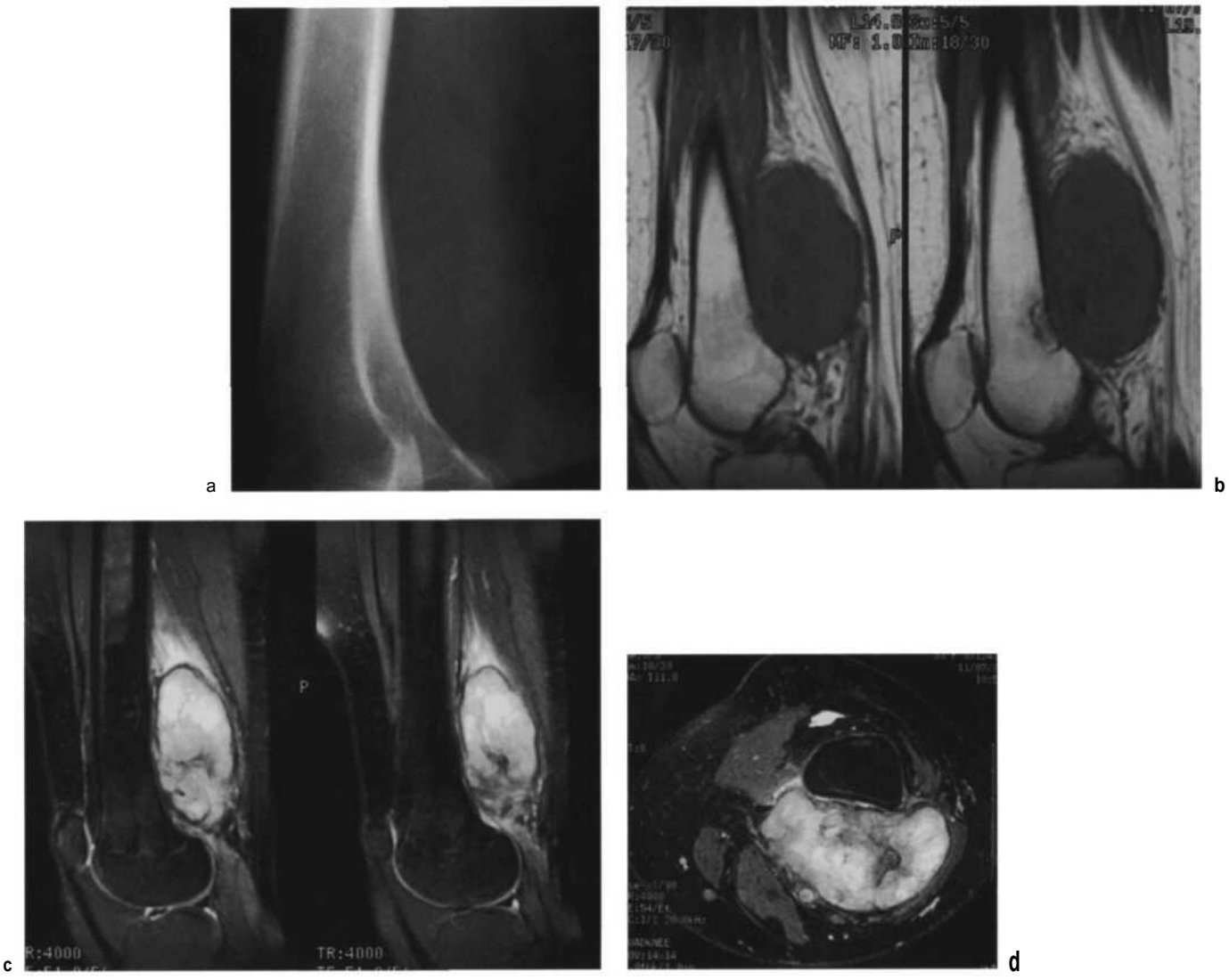

Figure **108a-d** 54-year-old woman with an extra-osseous Ewing sarcoma in the distal posterior thigh, tateral radiograph (**a**) shows a mass with soft tissue opacity dorsal to the distal femur. The tumor has mostly intermediate signal with several small foci of low signal on sagittal (**b**) T1WI. The tumor has mostly high signal on sagittal (**c**) and axial (**d**) FST2WI, and also contains curvilinear zones of low signal. Poorly defined zones of high signal on FS T2WI are seen in the soft tissues peripheral to the tumor. The tumor extends up to the femoral cortex and is associated with minimal periosteal reaction but no cortical destruction or intramedullary invasion.

osseous tumor extension, which may or may not be under an elevated layer of periosteum[29] These findings correspond to those seen with CT.[29] The soft tissue components of Ewing sarcoma in flat bones tend to be larger than in long bones.

After chemotherapy and/or radiation treatment, dynamic Gd-contrast enhanced MRI can be used to evaluate treatment response by defining remaining viable tumor from zones of necrosis by initial enhancement slope analysis and/or shapes of the time-intensity enhancement curves in regions of interest.[4,15,27,28] Viable tumor typically has rapid, early Gd-DTPA enhancement compared with areas of necrosis.

Differential Diagnosis

Osteomyelitis, myeloma, metastatic disease, osteosarcoma, non-Hodgkin lymphoma, giant cell tumor, eosinophilic granuloma, giant cell tumor, chondrosarcoma, fibrosarcoma, malignant fibrous histiocytoma.[20]

Treatment and Prognosis

Ewing sarcoma is a highly malignant tumor.[3,7,8,20,21,26] Important prognostic features include the tumor size, stage, and anatomic location.[26] Up to 35 % of patients have metastases at presentation.[37] Metastatic disease is common to the lungs, bone, and lymph nodes.[3,7,8,26] The presence of metastases at diagnosis is associated with poor survival (5-year survival of ~25% compared with 65 % for localized disease at diagnosis).[3] Large tumors and those that arise in the pelvis also have poor outcomes.[26] Treatment is based on primary (neoadjuvant) chemotherapy, radiation, resection of the primary tumor, as well as postsurgical adjuvant chemotherapy and/or radiation.[3,7,8,20,21,26] Histologic response to neoadjuvant chemotherapy has been shown to be useful for estimating prognosis[3,21] After neoadjuvant chemotherapy, tumors that show 100% necrosis show 3-year survival rates up to 100%.[21] Tumors that show more than 70% necrosis after chemotherapy have 87% survival with median follow-up of 3.5 years.[21] Tumors that show less than 70% necrosis after chemotherapy have 35% survival.[21] Patients with Ewing sarcoma have an 8.5-fold increased risk

for developing other types of cancer, and a 100-fold increase for developing a bone or soft tissue sarcoma within the radiated field.[3]

References

1 Carlotti CG Jr, Drake J, Hladky JP, Teshima I, Becker LE, Rutka JT. Primary Ewing's sarcoma of the skull in children. *Pediatr Neurosurg* J999;31:307-315.

2 Chaudhuri B, Das Gupta TIC Pathology of soft tissue sarcoma. In: Das Gupta TK, Chaudhuri PK, eds. Tumors *of the Soft Tissues* 2nd ed. New York, NY: Appleton and Lange 1998:155.

3 Coindre JM. Ewing sarcoma. In: Forest M, Tomeno B, Vanel D, eds. *Orthopedic Surgical Pathology: Diagnosis of Tumors and Pseudotumoral Lesions of Bone and Joints* Edinburgh: Churchill Livingstone: 1998:441-457.

4 DykeJP, Panicek DM, HealeyJH, et al. Osteogenic and Ewing's sarcomas: estimation of necrotic fraction during induction chemotherapy with dynamic contrast-enhanced MR imaging. *Radiology* 2003;228: 271-278.

5 Eggli KD, Quiogue T, Moser RP. Ewing's sarcoma. *Radio! Clin North Am* 1993;31:325-337.

6 Fletcher BD. Imaging pediatric bone sarcomas: diagnosis and treatment-related issues. Radio/ *Clin North Am* 1997:35(6):1477-1486.

7 Grier HE. The Ewing family of tumors-Ewing's sarcoma and primitive neuroectodermal tumors. *Pediatr Clin North Am* 1997:44(4): 991-1004.

8 Huvos AC. Ewing's Sarcoma. In: Huvos AG, ed. *Bone Tumors: Diagnosis, Treatment, and Prognosis* 2nd ed. Philadelphia, Pa: W.B. Saunders; 1991:523-542.

9 Jaffe N. Soft tissue sarcomas in children. In: Das Gupta TK, Chaudhuri PK, eds. *Tumors of the Soft Tissues* 2nd ed. New York, NY: Appleton and Lange: 1998:589-591.

10 Kransdorf MJ, Murphey MD. Neurogenic tumors. In: *Imaging of Soft Tissue Tumors* 2nd ed. Philadelphia, Pa: W.B. Saunders; 2006: 328-380.

11 Kransdorf MJ. Malignant soft-tissue tumors in a large referral population: distribution of specific diagnoses by age, sex, and location. *AJR Am J Roentgenol* 1995:164:129-134.

12 Lang P, Honda G, Roberts T, et al. Musculoskeletal neoplasm: perineoplastic edema versus tumor on dynamic postcontrast MR images with spatial mapping of instantaneous enhancement rates. *Radiology* 1995:197:831-839.

13 MacVicar AD, Olliff JF, Pringle J, Pinkerton CR, Husband Janet ES. Ewing's sarcoma: MR imaging of chemotherapy-induced changes with histologic correlation. *Radiology* 1992;184(3):859-864.

14 Meyer JS, Dormans JP. Differential diagnosis of pediatric musculoskeletal masses. *Magn Reson Imaging Clin N Am* 1998;6(3):570-571.

15 Miller SL, Hoffer FA, Reddick WE, et al. Tumor volume or dynamic contrast-enhanced MRI for prediction of clinical outcome of Ewing's sarcoma family of tumors. *Pediatr Radial* 2001:31:518-523.

16 Miller SL, Hoffer FA. Malignant and benign bone tumors. *Radial Clin North Am* 2001 ;39(4):682-684.

17 Mukhopadhyay P, Gairola M, Sharma MC, Thulkar S, Julka PK, Rath GK. Primary spinal epidural extraosseous Ewing's sarcoma: report of five cases and literature review. *Australas* Radio/ 2001;45:372-379.

18 Mulder JD, Schutte HE, Kroon HM, Taconis WK. Introduction. In: *Radiologic Atlas of Bone Tumors.* Amsterdam: Elsevier; 1993:3-6.

19 MulderJD, Schutte HE, Kroon HM, Taconis WK. The diagnosis of bone tumors. In: *Radiologic Atlas of Bone Tumors* Amsterdam: Elsevier; 1993:9-46.

20 MulderJD, Schutte HE, Kroon HM, Taconis WK. Ewing's Sarcoma. In: *Radiologic Atlas of Bone Tumors* Amsterdam: Elsevier; 1993:193-214.

21 Perlman EJ. Ewing's sarcoma, lymphoma, and Langerhans' cell proliferations. In: Helliwell TR, ed. *Major Problems in Pathology: Pathology of Bone and Joint Neoplasms* Vol 37.1 st ed. Philadelphia, Pa: W.B. Saunders; 1999:279-299.

22 Saifuddin A, Whelan J, Pringle Jean AS, Cannon SR. Malignant round cell tumours of bone: atypical clinical and imaging features. *Skeletal Radial* 2000:29:646-651.

23 Shin JH, Lee HK, Rhim SC, Cho KJ, Choi CG, Sun DC. Spinal epidural extraskeletal Ewing sarcoma: MR findings in two cases. *AJNR Am J Neuroradiol* 2001;22:795-798.

24 Unni KK. Introduction and scope of study. In:Dah/in's *Bone Tumors: General Aspects and Data on U087 Cases* 5th ed. Philadelphia, Pa: Lippincott, Williams & Wilkins; 1996:1-9.

25 Unni KK. Ewing's Tumor. In: *Dahlin's Bone Tumors: General Aspects and Data on 11087 Cases* 5th ed. Philadelphia, Pa: Lippincott, Williams & Wilkins; 1996:249-260.

26 Ushigome S, Machinami R, Sorensen PH. Ewing's sarcoma/primitive neuroectodermal tumour (PNET). In: Fletcher COM, Unni KK, Mertens F, eds. *World Health Organization Classification of Tumours. Pathology and Genetics of Tumours of Soft Tissue and Bone* IARC Press; 2002:298-300.

27 Van der Woude HJ, Bloem JL, Verstraete KL, Taminiau AH, Nooy MA, Hogendoorn PC. Osteosarcoma and Ewing's sarcoma after neoadjuvant chemotherapy: value of dynamic MR imaging in detecting viable tumor before surgery. *AJR Am J Roentgenol* 1995;165: 593-598.

28 Van der Woude HJ, Bloem JL, Hogendoorn PC, Pancras CW. Preoperative evaluation and monitoring chemotherapy in patients with high-grade osteogenic and Ewing's sarcoma: review of current imaging modalities. *Skeletal* Radio/1998;27:57-71.

29 Wenaden AET, Szyszko TA, Saifuddin A. Imaging of periosteal reactions associated with focal lesions of bone. *Clin Radial* 2005;60: 439-456.

A 21 Nodular Fasciitis (Also Referred to as Pseudosarcomatous Fasciitis, Proliferative Fasciitis, Infiltrative Fasciitis, and Pseudosarcomatous Fibromatosis)

Definition

Nodular fasciitis is a benign, reactive soft tissue lesion comprised of proliferating fibroblasts.[2-4,6] These lesions usually occur in the subcutaneous tissue or muscle.[4,6] Less common forms of nodular fasciitis are lesions that extend into vessel lumens (intravascular fasciitis) or skull and adjacent soft tissues (cranial fasciitis).[4,6]

Frequency of Occurrence

Nodular fasciitis is a common lesion that accounts for 11 % of benign soft tissue tumors and 7 % of all soft tissue tumors.[6-8]

Age at Presentation

From 11 to 51 years, mean = 31 years.[6-8] Nodular fasciitis typically occurs in young adults aged less than 30 years, but can occur in children and older adults.[458] Cranial fasciitis often occurs in infants less than *1* years old.[4]

Gender Ratio (M / F)

1/1[1,4] to 1.2/1[8]

Location

Subcutaneous (80-90%) location predominates over intramuscular or fascial subtypes.[5-9] Nodular fasciitis occurs most frequently in the upper extremity, followed by the head and neck, trunk, lower extremity, hand and wrist, proximal limb, and hip/buttock.[8] Lesions that involve adjacent periosteum have been referred to as parosteal fasciitis. Nodular fasciitis that contains metaplastic bone has been referred to as ossifying fasciitis[6] Cranial fasciitis is a version of nodular fasciitis that involves the scalp and usually presents in infancy.[469] Intravascular fasciitis is a rare form that involves medium-sized to small-sized arteries or veins.[46]

Signs and Symptoms

Nodular fasciitis often occurs as an enlarging palpable soft tissue lesion.[46] Lesions may show rapid growth over several weeks followed by slower rates of enlargement.[46] Lesions may or may not be associated with pain (50%).

Cross Pathologic Findings

Lesions usually range from 2 to 5cm and often contain firm fibrous regions, myxoid zones, and occasional cystic zones.[2-4,6,11] Intravascular fasciitis may be nodular or plexiform.[4] Cranial fasciitis lesions can be circumscribed and firm, with or without myxoid of cystic zones.[4]

Histopathologic Findings

Lesions contain bland, plump, spindle-like cells (fibroblastic and myofibroblastic), often in a myxoid matrix. The spindle-like cells usually lack pleomorphism and nuclear hyperchromasia. [2-4.6,9] -phe mitotic rate can be moderate to high, simulating a sarcoma, although atypical mitoses are not usually seen.[2-4,6,3] Portions of the lesion may be highly cellular or less cellular in loose organization with myxoid material[4,6] Multiple capillaries and inflammatory cells can be seen at the periphery of the lesions.[4,6] The histologic features of nodular fasciitis can mimic sarcoma.[2-4,6,9]

Nodular fasciitis can have positive immunohistochemical reactions to smooth muscle actin, muscle-specific actin, actin, and vimentin.[2,4] Nodular fasciitis rarely shows immunoreactivity to desmin, and typically does not show positive immunohistochemical reactions to S-100 or keratin.[2,4]

Lesion Genetics

Cells are typically diploid.[4] Rearrangements of 3 q21, losses of chromosomes 2 and 13, and a 2; 15 translocation have been reported for these lesions.[4]

Findings on Plain Films (Roentgenograms) and Computed Tomography[1,4,6]

Nodular fasciitis can be seen as soft tissue lesions. Intramuscular lesions can have attenuation slightly less than muscle, as well as areas of low attenuation on CT secondary to myxoid zones when present (Fig. **109).** Cranial fasciitis may be associated with erosions of the outer and inner tables of the skull, with or without thin sclerotic margins.[46]

MRI Findings[1,5,6,10]

Nodular fasciitis often appears as well-circumscribed lesions in subcutaneous fat, muscles, or fascia (Figs. **109,110).** Lesions are often 4 cm or less in size. Lesions in subcutaneous fat or fascia may have mildly irregular or even stellate borders.

Lesions usually have intermediate signal on T1WI (slightly hyperintense relative to muscle) and PDWI; and homogeneous or mildly heterogeneous high signal on T2WI and FST2W1 (Figs. **109, 110).** Surrounding edema is occasionally seen. Older lesions with high fibrous content may have intermediate signal on T2WI.

After Gd-contrast, lesions can show homogeneous or peripheral rim-like patterns of enhancement.

Differential Diagnosis

Sarcoma, hematoma, benign or malignant fibrous histiocytoma, Schwannoma, dermatofibroma (skin lesions).

Treatment and Prognosis

Nodular fasciitis lesions are usually self-limited.[4,6] Intravascular fasciitis and cranial fasciitis have similar indolent courses as nodular fasciitis.[4] Surgical excision is often utilized.[4,6] Recurrence after excision is rare (<2%).[4]

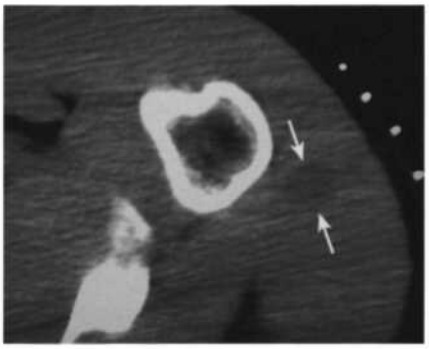

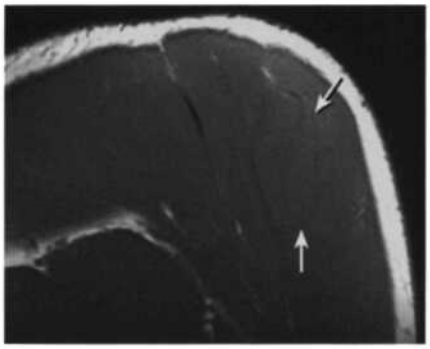

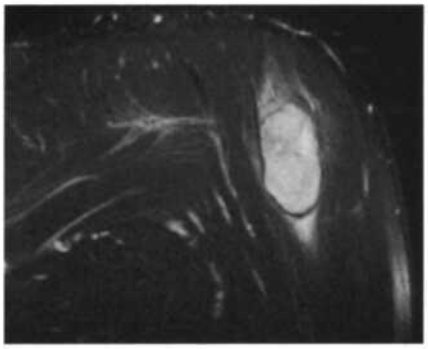

a

b, c

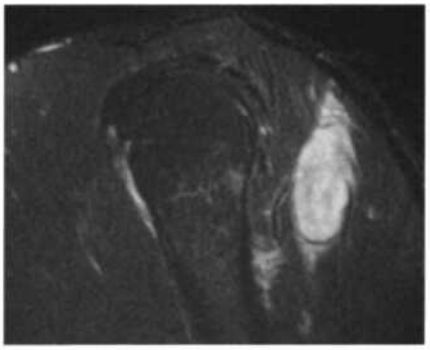

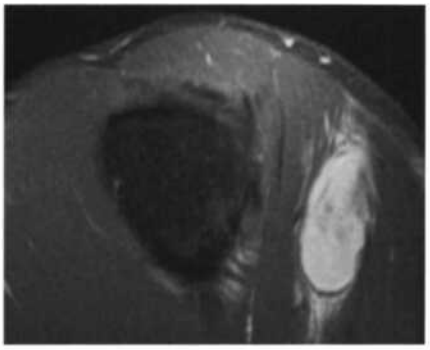

d

e

Figure **109 a–e** A 43-year-old man with intramuscular nodular fasciitis involving the deltoid muscle at the left shoulder. Axial CT image (**a**) shows the lesion to have attenuation that is slightly less than muscle, as well as areas of low attenuation. The lesion has intermediate signal on coronal (**b**) PDWI. The lesion has high signal on coronal (**c**) and sagittal (**d**) FS T2WI, which is surrounded by a thin rim of low signal and poorly defined zones of high signal in the adjacent soft tissues. The lesion shows prominent Cd-contrast enhancement on sagittal (**e**) FS T1WI.

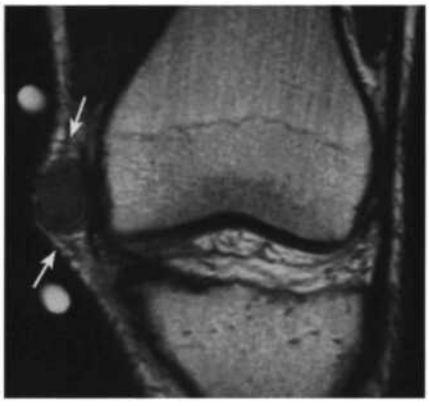

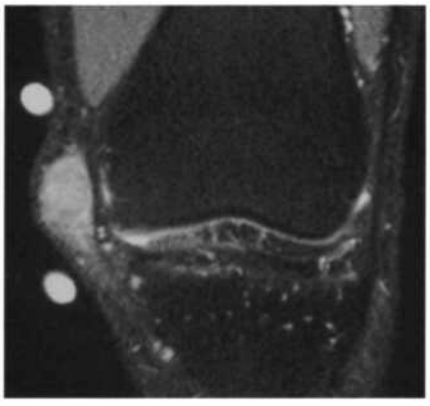

a

b

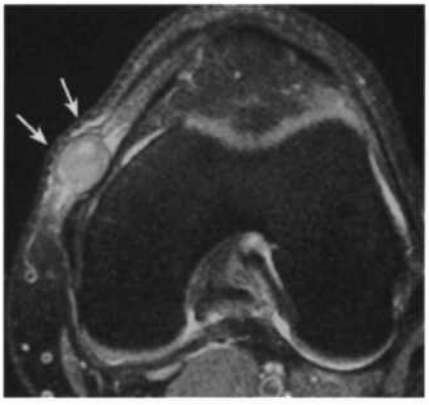

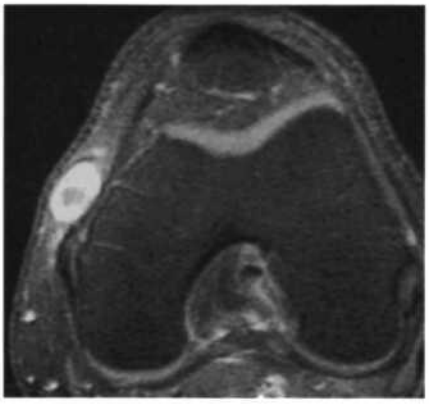

c

d

Figure **110 a–d** A 39-year-old man with nodular fasciitis involving the superficial soft tissues of the distal medial thigh. The lesion has circumscribed margins, and has intermediate signal on coronal **(a)** T1WI, and mildly heterogeneous high signal on coronal (**b**) and axial (**c**) FST2WI. The lesion shows prominent Gd-contrast enhancement on axial (**d**) FST1WI.

References

1 Bancroft LW, Peterson JJ, Kransdorf MJ, Nomikos GC, Murphey MD. Soft tissue tumors of the lower extremities. Radio/ *Clin North Am* 2002;40:991-1011.

2 Das Gupta TK, Chaudhuri PK. Nodular fasciitis (pseudosarcomatous fasciitis). In: Das Gupta TK, Chaudhuri PK, eds. Tumors *of the Soft Tissues.* 2nd ed. New York, NY: Appleton and Lange; 1998:87-88.

3 Das Gupta TK, Chaudhuri PK. Tumors of the fibrous tissue. In: Das Gupta TK, Chaudhuri PK, eds. *Tumors of the Soft Tissues* 2nd ed. Appleton and Lange Pubs.: 1998:265-308.

4 Evans H, Bridge JA. Nodular fasciitis. In: Fletcher COM, Unni KK, Mertens F, eds. *World Health Organization Classification of Tumours. Pathology and Genetics of Tumours of Soft Tissue and Bone* Geneva: IARC Press; 2002:48-49.

5 JelinekJ, Kransdorf MJ. MR imaging of soft-tissue masses: mass-like lesions that simulate neoplasms. *Magn Reson Imaging Clin N Am* 1995;3(4):727-741.

6 Kransdorf MJ, Murphey MD. Benign fibrous and fibrohistiocytic tumors. In: *Imaging of Soft Tissue Tumors* 2nd ed. Philadelphia, Pa: W.B. Saunders: 2006:189-256.

7 Kransdorf MJ, Murphey MD. Soft tissue tumors in a large referral population: prevalence and distribution of diagnoses by age, sex, and location. In: *Imaging of Soft Tissue Tumors* 2nd ed. Philadelphia Pa: W.B. Saunders; 2006:6-37.

8 Kransdorf MJ. Benign soft-tissue tumors in a large referral population: distribution of specific diagnoses by age, sex, and location. *AJR AmJRoentgenol* 1995;164:395-402.

9 Reid RP. Bone neoplasms and tumor-like lesions on the bone surface. In: Helliwell TR, ed. *Major Problems in Pathology: Pathology of Bone and Joint Neoplasms.* Vol 37.1st ed. Philadelphia, Pa: W.B. Saunders; 1999:215-235.

10 Sundaram M, Sharafuddin Melhem JA. MR imaging of benign soft-tissue masses. *Magn Reson Imaging Clin N Am* 1995;3(4):609-627.

A 22 Fibrolipomatous Hamartoma (Also Referred to as Nerve Lipoma, Neural Fibrolipoma, Lipofibromatous Hamartoma, Perineural Lipoma, Intraneural Lipoma, Lipofibroma, and Lipomatous Hamartoma)

ICD-OCode

8850/0

Definition

Fibrolipomatous hamartomas are rare, benign lesions with varying degrees of fibrous and fatty (mature adipocytes) infiltration of the epineurium (nerve sheath) of peripheral nerves as well as within the interfascicular connective tissue (perineurium] of nerves.[1-3,5-10]

Frequency of Occurrence

These lesions are rare and account for less than 1 % of benign soft tissue tumors, and less than 1 % of lipomas and lipoma variants.[3,4,9]

Age at Presentation

From 4 to 75 years,[5] mean = 24 to 40 years.[2,4,5] These lesions can also be congenital or occur in early childhood.[1,6]

Gender Ratio (M / F)

1.3/1[4] to 1/1.1[9]

Location

Lesions most frequently involve the median nerve and its digital branches (80%) followed by the ulnar nerve, radial nerve, brachial plexus, sciatic nerve, nerves of the lower extremity, ankle (superficial peroneal nerve), and feet (medial plantar nerve).[13-111] Lesions involving the median and ulnar nerves are usually solitary in 80% of cases.[9] Lesions involving the brachial plexus may be multifocal.[9]

Signs and Symptoms

Fibrolipomatosis hamartomas are soft, slowly enlarging lesions that often occur along the volar aspects of the wrist, hand, distal forearm, and foot.[1-35-10] Associated ipsilateral macrodactyly (macrodystrophia lipomatosa) may occur in up to two-thirds of patients (females > males) near the sites of fibrolipomatosis hamartomas.[1,2,6,10] The macrodactyly often involves the second or third digits of the hands or feet which are inervated by the involved nerves.[3,6,10] Initially, these lesions are usually painless without neurologic signs.[1,3,6,10] Eventually, these lesions can be associated with nerve compression resulting in pain, paresthesia, and motor deficit.[1,3,6,10] Lesions in the wrist can cause carpal tunnel syndrome[1,3,6,9]

Cross Pathologic Findings

Lesions are often yellow-tan, rubbery fusiform masses within the involved nerve sheaths.[1-3-6,7,9,10] Lesions may range from 5 to 30cm in length, and up to 2.5cm in diameter.[2,,9]

Histopathologic Findings[6,7,10]

Infiltration of fat cells within the interfascicular connective tissue (perineurium) of enlarged nerves is typically seen, often in association with perineural and epineural fibrosis.[6,7,10] The perineural fibrous tissue is usually concentric around the nerve bundles.[6] Atrophy of nerve fibers can occur after many years. Fibrolipomatous hamartoma differs from neural sheath lipoma in that the latter does not have fatty cells intervening between the nerve fascicles. Rarely, metaplastic bone formation may occur in these lesions.[56]

Findings on Plain Films (Roentgenograms) and Computed Tomography

Lesions can appear as a subcutaneous fusiform mass with fatty tissue attenuation containing serpentine structures with soft tissue attenuation representing thickened nerve bundles.[2,10] Bone hypertrophy (macrodactyly) may be seen adjacent to the lesion.[10] Rarely, metaplastic bone formation may occur in these lesions and appear as calcifications on radiographs or CT examinations.[5]

MRI Findings

Lesions are well-circumscribed and fusiform-shaped, involving nerves.[1-3,5,7,10] On Tl WI, PDW1, and T2WI a network of cylindrical, longitudinally-oriented, thin curvilinear zones of low signal of 1 to 3 mm in diameter is seen within a background of intermediate to high signal[1-3,5,7,10] (Figs. Ill, 112). This typical appearance, likened to a coaxial cable, is secondary to the combination of nerve fascicles with varying degrees of fatty infiltration, and epineural and perineural fibrosis.[1-3,5,7,10] The enlarged median nerves often contain 15 to 16 of these "coaxial cables," representing bundles of axons encased in epineural fibrous tissue.[9] Fibrolipomatous hamartomas of the ulnar nerve are usually smaller and contain fewer neural bundles (usually three or four) than lesions involving median nerves.[9] The degree of fatty proliferation varies among patients.[2,10] Lesions may follow the branching patterns of nerves.[2]

Lesions can show moderate to prominent Gd-contrast enhancement in fibrous tissue components of the lesions adjacent to spiculated low signal foci representing nerve fibers.[10]

Differential Diagnosis

Neural sheath lipoma, traumatic neuroma, plexiform neurofibroma, ganglion cyst, vascular malformation, atypical Schwannoma, hereditary hypertrophic interstitial neuritis of Dejerine-Sottas disease.[1,2,5,10]

Treatment and Prognosis

Surgical exploration with diagnostic biopsy is frequently performed for symptomatic lesions.[1-3,5,6,10] For patients with carpal tunnel syndrome, carpal release is commonly performed.[1,3,5,6,10] Complete resection can result in significant motor and sensory deficits.[1,3,6,7,10] Using MRI, preoperative diagnosis can usually be made, obviating the need for biopsy.[57]

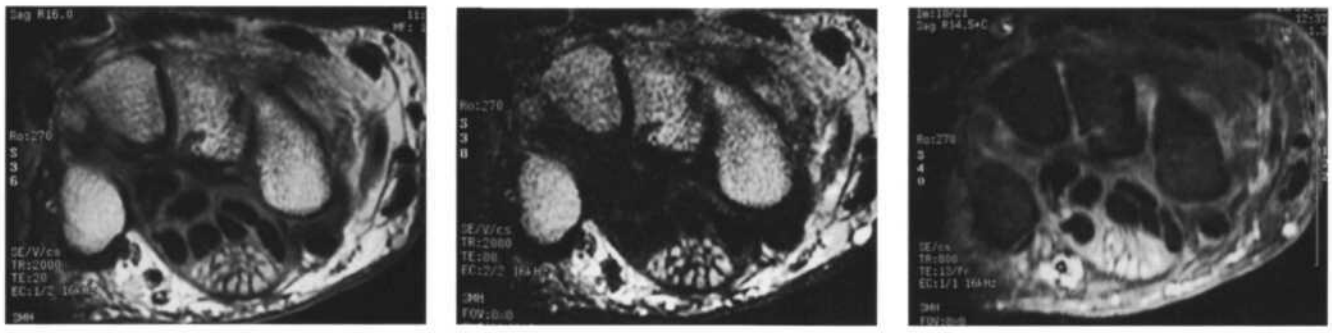

a **b, c**

Figure **111 a-c** A 59-year-old man with a fibrolipomatous hamartoma involving the median nerve at the wrist. Cylindrical, longitudinally oriented, thin curvilinear zones of low signal are seen within a background of intermediate to high signal on axial PDWI (**a**), and slightly high signal on axial T2WI (**b**). The lesion shows Gd-contrast enhancement on axial FST1WI (**c**).

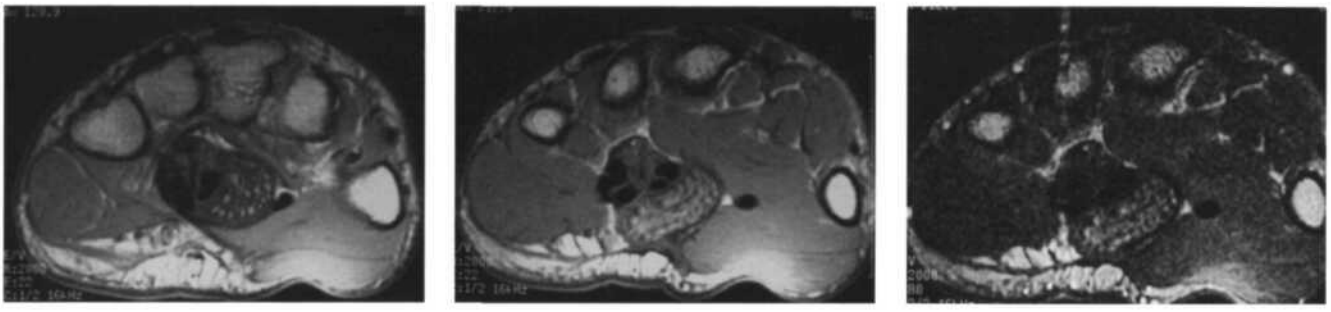

a **b, c**

Figure **112a-c** A 16-year-old male with a fibrolipomatous hamartoma involving the median nerve at the wrist. Cylindrical, longitudinally oriented, thin curvilinear zones of low signal are seen within a background of intermediate to high signal on axial PDWI (**a, b**), and slightly high signal on axial T2WI (**c**).

References

1 Cavallaro MC, Taylor JA, Gorman JD, Haghighi P, Resnick D. Imaging findings in a patient with fibrolipomatous hamartoma of the median nerve. *AJR Am J Roentgenol* 1993;161:837-838.

2 De Maeseneer M, Jaovisidha S, Lenchik L, et al. Fibrolipomatous hamartoma: MR imaging findings. *Skeletal Radial* 1997:26:155-160.

3 Kransdorf MJ, Murphey MD. Lipomatous tumors. In: *Imaging of Soft Tissue Tumors.* 2nd ed. Philadelphia, Pa: W.B. Saunders; 2006: 80-149.

4 Kransdorf MJ. Benign soft-tissue tumors in a large referral population: distribution of specific diagnoses by age, sex, and location. *AJR Am J Roentgenol* 1995:164:395-402.

5 Marom EM, Helms CA. Fibrolipomatous hamartoma: pathognomonic on MR imaging. *Skeletal Radiol* 1999:28:260-264.

6 Nielsen GP. Lipomatosis of nerve. In: Fletcher COM, Unni KK, Mertens F, eds. *World Health Organization Classification of Tumours. Pathology and Genetics of Tumours of Soft Tissue and Bone* Geneva: IARC Press; 2002:24-25.

7 Ogose A, Hotta T, Higuchi T, Katsumi N, Koda H, Umezu H. Fibrolipomatous hamartoma in the foot: magnetic resonance imaging and surgical treatment. A report of two cases./ *Bone Joint SurgAm* 2002; 84-A(3):432-436.

8 Silverman TA, Enzinger FM. Fibrolipomatous hamartoma of nerve. A clinicopathologic analysis of 26 cases. *Am J SurgPathol* 1985;9:7-14.

9 Toms AP, Anastakis D, Bleakney RR, Marshall TJ. Lipofibromatous hamartoma of the upper extremity: a review of the radiologic findings for 15 patients. *AJR Am J Roentgenol* 2006:186:805-811.

10 Van Breuseghem I, Scviot R, Pans S, Geusens E, Brys P, De Wever I. Fibrolipomatous hamartoma in the foot: atypical MR imaging findings. *Skeletal Radiol* 2003;32:651-655.

A 23 Fibroma of the Tendon Sheath

ICD-O Code

8810/0

Definition

Fibromas of the tendon sheath are benign, small, fibrous nodules involving tendons and tendon sheaths of the fingers, hands, wrists, or feet.[3,4]

Frequency of Occurrence

Fibromas of the tendon sheath represent ~ 1 % of benign soft tissue tumors.[5,6]

Age at Presentation

From 15 to 81 years, mean = 35 years.[5,6]

Gender Ratio (M / F)

1.5/1 to 3 /I.[3,5-7]

Location

As much as 98% of these lesions occur in the extremities, and 82 % occur in the upper extremities.[2,3] Lesions are usually found along tendons of fingers (thumb, index, middle finger (49%), hands (21 %), or wrist (12%).[3-6]Many of the remaining lesions involve the tendons at the plantar aspects of the feet, and anterior knee.[3-6] Rare sites of involvement include the arms, elbows, toes, temporomandibular joint, neck, and trunk[3-9]

Signs and Symptoms[1-4,7-10]

Fibromas of the tendon sheath are typically slow-growing, with durations of months to years.[1-4,7-10] The lesions are often painless, although are occasionally associated with mild tenderness or pain.[3,7] Lesions are sometimes associated with trauma or limitation of tendon motion;[7] those involving the wrist may cause carpal tunnel syndrome.[3]

Cross Pathologic Findings

Lesions often range in size from 1 to 5 cm, mean = 2 cm.[7] Most lesions are less than 3 cm in diameter[3] and may have a multilobulated configuration.[3] Lesions are firm, circumscribed, gray-white nodular masses adjacent to tendon sheaths.[3,4,7] Erosion of adjacent bone may rarely occur[3,7,10]

Histopathologic Findings

Lesions are composed of dense nodules of hypocellular fibrous connective tissue containing spindle-shaped fibroblasts in collagenous stroma separated by clefts.[3,4,7] Slitlike vascular channels may also be seen in these lesions.[3,4,7] Hypercellular regions may be seen in addition to the typical hypocellular areas, but these hypercellular zones lack nuclear hyperchromasia or coagulative necrosis.[3] Less frequently, other features such as myxoid change, cyst formation, stellate cells, dense hyalinization, chondroid and/or osseous metaplasia may be observed.[3]

Lesion Genetics

One of these lesions has been reported to have a translocation: t(2;ll)(q31-32;q!2).[3]

Findings on Plain Films (Roentgenograms) and Computed Tomography

Lesions may appear as ovoid or fusiform, superficial soft tissue masses which are infrequently associated with mild scalloping or remodeling of adjacent bone.[1,4,7,10] Lesions are usually seen at flexor tendons.[3,4]

MRI Findings[1,4,7,S]

Lesions are typically ovoid or fusiform, well circumscribed and located adjacent to tendons of the fingers, hands, wrists, feet, and other locations (Figs. **113,114).** Lesions are more common at the flexor tendons than at the extensor tendons.[3,4]

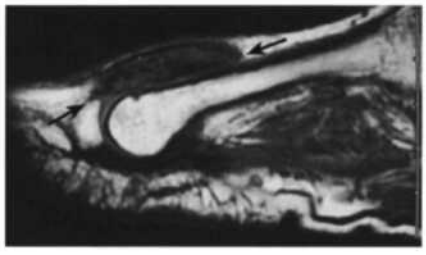

a

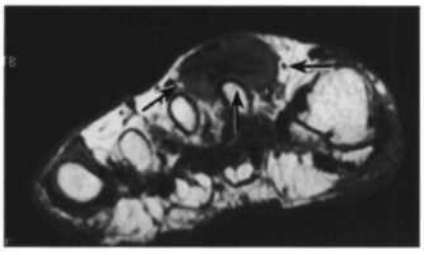

b

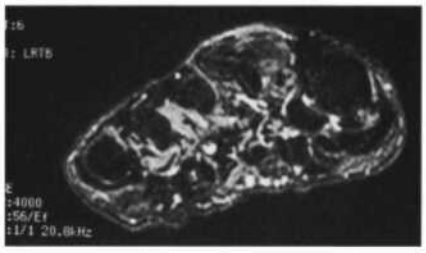

c

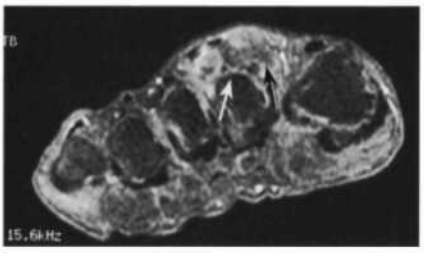

d

Figure **113a-d** A 63-year-old woman with a fibroma involving an extensor tendon sheath in the foot. The lesion has a fusiform shape with well-circumscribed margins, and has zones of low and intermediate signal on sagittal (a) and axial (b) T1WI, as well as on axial FST2WI (c). The lesion shows heterogeneous Gd-contrast enhancement on axial FST1WI (d).

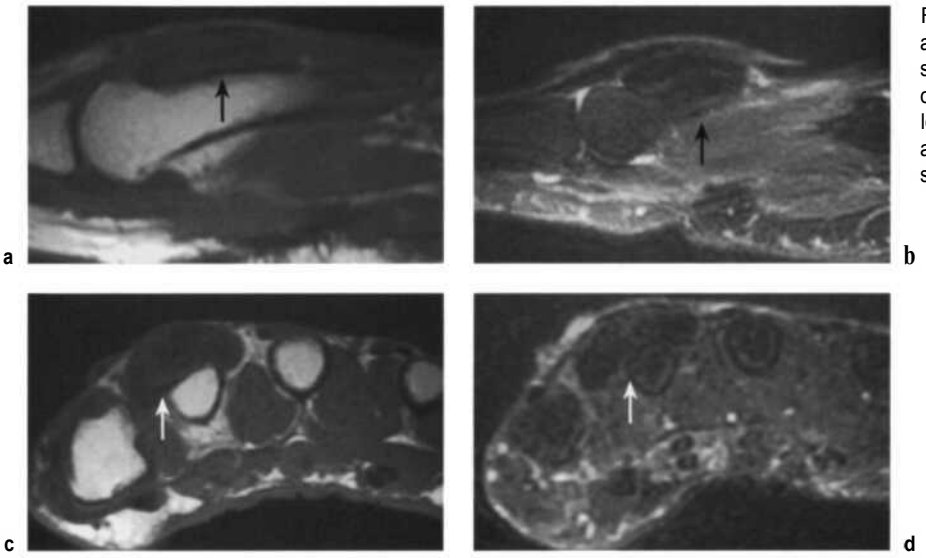

Figure **114a-d** An 89-year-old woman with a fibroma involving an extensor tendon sheath in the hand. The lesion has well-circumscribed margins; and contains zones of low and intermediate signal on sagittal (**a**) and axial (**c**) T1WI, and mostly low signal on sagittal (**b**) and axial (**d**) FST2WI.

Lesions usually have low-intermediate signal on T1WI (equal to or less than skeletal muscle, 83 %).[4] On T2WI, lesions have slightly heterogeneous low-intermediate signal in 50% of cases (equal to or less than skeletal muscle), intermediate signal that is hyperintense relative to muscle (33 %), or mixed low and intermediate (17%).[4] Lesions can also have areas of high signal on FST2WI. Lesions may be associated with remodeling or erosions of adjacent bone cortex (Fig. **114).** After Gd-contrast administration, lesions can show diffuse or peripheral enhancement patterns, or no discernable enhancement[4] (Fig. **113, 114).**

Differential Diagnosis

Giant cell tumor of the tendon sheath (which is 2.7 times more common than fibroma of the tendon sheath),[4] hematoma, xanthoma, gout.

Treatment and Prognosis

Surgical resection is a common treatment for flbromas of the tendon sheath, usually for cosmetic reasons, pain, and/or limitation of motion.[3] Local recurrence can occur in up to 24% of patients from months to years after surgery.[57]

References

1 Bertolotto M, Rosenberg I, Parodi RC, et al. Case report: fibroma of the tendon sheath in the distal forearm with associated median nerve neuropathy—US, CT, and MR appearances. *Clin Radial* 1996:51:370-372.

2 Chung EB, Enzinger FM. Fibroma of the tendon sheath. *Cancer* 1979:44:1945-1954.

3 Farshid G, Bridge JA. Fibroma of the tendon sheath. In: Fletcher COM, Unni KK, Mertens F, eds. *World Health Organization Classification of Tumours. Pathology and Genetics of Tumours of Soft Tissue and Bone* Geneva: IARC Press: 2002:66.

4 Fox MG, Kransdorf MJ, Bancroft LW, Peterson JJ, Flemming DJ. MR imaging of fibroma of the tendon sheath. *AJR Am J Roentgenol* 2003; 180:1449-1453.

5 Kransdorf MJ. Benign soft-tissue tumors in a large referral population: distribution of specific diagnoses by age, sex, and location. *AJR Am J Roentgenol* 1995;164:395-402.

6 Kransdorf MJ, Murphey MD. Soft tissue tumors in a large referral population: prevalence and distribution of diagnoses by age, sex, and location. In: *Imaging of Soft Tissue Tumors* 2nd ed. Philadelphia, Pa: W.B. Saunders; 2006:6-37.

7 Kransdorf MJ, Murphy MD. Benign fibrous and fibrohistiocytic tumors. In: *Imaging of Soft Tissue Tumors* 2nd ed. Philadelphia: Pa: W.B. Saunders; 2006:189-256.

8 McGrory JE, Rock MG. Fibroma of the tendon sheath involving the patellar tendon. *AmJ Orthop* 2000:29:465-467.

9 Misawa A, Okada K, Hirano Y, et al. Fibroma of the tendon sheath arising from the radio-ulnar joint. *Pathol Int* 1999;49:1089-1092.

10 Southwick GJ, Karamoskos P. Fibroma of the tendon sheath with bone involvement.*J Hand Surg* 1990;15(3):373-375.

A 24 Solitary Fibrous Tumor

ICD-O Code

8815/1

Definition

Solitary fibrous tumors (SFTs) are rare benign spindle-cell mesenchymal neoplasms that occur in a wide range of anatomic sites.[1-3] These fibroblastic tumors typically show a hemangiopericytoma-like branching vascular pattern.[13] Extrapleural SFTs morphologically resemble pleural SFTs, and have been termed hemangiopericytomas in the past.[13]

Frequency of Occurrence

These tumors are rare and have been reported to account for less than 2 % of soft tissue tumors.[2,3]

Age at Presentation

From 20 to 77 years, median = 50 to 60 years.[2,3]

Gender Ratio (M / F)

1/1.[2,3]

Location

These lesions occur in the thoracic cavity (pleura > lung > mediastinum > diaphragm) > peritoneal/visceral/retroperitoneal > pelvis > head and neck > extremity > trunk.[2] Extrapleural SFTs occur in the subcutaneous tissue > deep soft tissues.[3]

Signs and Symptoms

Most SFTs are slow-growing, painless lesions.[3] Large SFTs may cause compression of adjacent anatomic structures, producing signs and symptoms based on location.[3,4] Extrathoracic SFTs are more likely to be symptomatic than thoracic lesions.[2] Osteoarthropathy (clubbing of fingers and arthritis) occurs in 10%, and symptomatic hypoglycemia occurs in 5% from tumoral secretion of insulin-like growth factors.[5]

Cross Pathologic Findings

SFTs are usually well-circumscribed, partially encapsulated lesions, which frequently have a whitish, firm, multinodular appearance.[1,3] Zones of hemorrhage and myxoid changes may be present.[2] Indistinct tumor margins and areas of tumor necrosis are associated with the infrequent, locally aggressive or malignant SFTs.[3]

Histopathologic Findings

SFTs contain short, round to spindle-shaped cells containing single vesicular nuclei with dispersed chromatin within scant cytoplasm.[1-3] Mitotic activity is typically low and rarely exceeds 3 per 10 high-power fields.[3,5] The spindle cells are separated by bands of hyalinized dense collagen intermixed with branching small- and medium- sized hemangiopericytoma-like vessels.[1-3,5] SFTs typically have a patternless architecture with various combinations of hypercellular (tumor-cell rich) areas and hypocellular (collagen rich) zones.[1-3,5]

Malignant SFTs are hypercellular lesions with moderate or marked cellular atypia, increased mitotic activity (>4 mitoses per 10 high-power fields), necrosis, and/or infiltrative tumor margins.[1,3,5]

Tumor cells are often immunoreactive to CD 34 (up to 95%) and CD99 (70 %).[3] Tumor cells can be immunoreactive to epithelial membrane antigen (35%), occasionally to Bcl-2 and smooth muscle actin, and rarely to desmin.[3,5] Lesions are usually negative for S100 and cytokeratins.[1,5]

Lesion Genetics

These lesions are cytogenetically heterogeneous.[3] SFT has been associated with trisomy 21 and gains and losses in chromosomes[5]

Findings on Plain Films (Roentgenograms) and Computed Tomography

SFTs often have circumscribed margins on CT.[3] When present in the chest, SFTs can appear as a localized opacity on roentgenograms.[3] SFTs can have soft tissue attenuation that is slightly heterogeneous on CT.[3] SFTs can show contrast enhancement (Fig. **115).**

MRI Findings

SFTs usually have circumscribed margins. SFTs can have low to intermediate signal on T1WI and PDWI; low, intermediate, and/or slightly high signal on T2WI;[3] and heterogeneous slightly high to high signal on FS T2WI (Figs. **115,116).** After Gd-contrast administration, SFTs can show prominent, slightly heterogeneous enhancement.

Differential Diagnosis

Hemangiopericytoma, synovia! cell sarcoma, neurofibroma, Schwannoma, malignant or benign fibrous histiocytoma, fibrosarcoma, leiomyoma, angiosarcoma, rhabdomyosarcoma, epitheloid sarcoma, Kaposi sarcoma, hemangioendothelioma, clear cell sarcoma, nodular fasciitis.

Prognosis and Treatment

Thoracic and extrathoracic SFTs have similar clinical and pathologic features.[1] Treatment usually consists of surgical excision.[1,2] Most SFTs are benign, although up to 15% have aggressive behavior, [125] and typically have low rates of recurrence and metastasis after surgery.' SFTs in the extremities tend to have less aggressive behavior than SFTs elsewhere.[2] Surveillance is typically more intense for SFTs that are larger than 10cm and those which contain histologically malignant portions (increased cellularity and mitotic activity).[1] Metastatic disease most frequently occurs in the lungs, bone, and liver.[2]

a

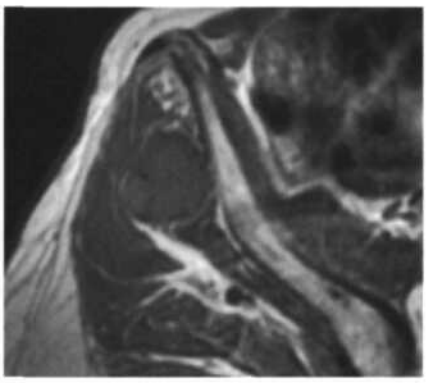

b

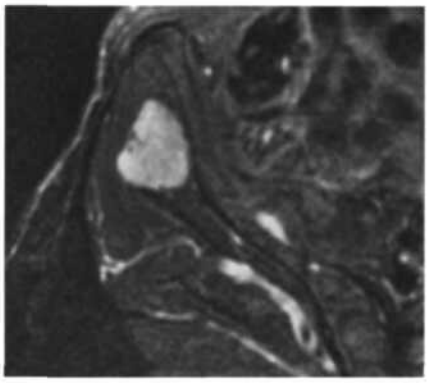

c

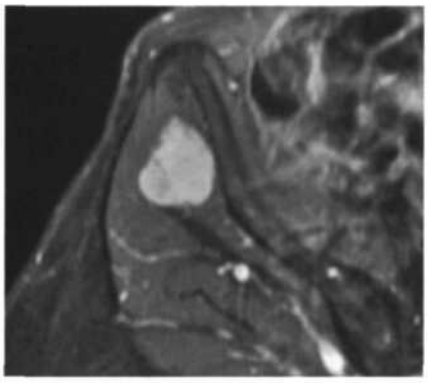

d

Figure **115 a–d** An 81-year-old man with a solitary fibrous tumor involving the gluteus mnimus muscle. The lesion has circumscribed margins, and shows contrast enhancement on axial CT (**a**). The lesion has intermediate signal on axial T1WI (**b**), high signal on axial FST2WI (c), and shows prominent Cd-contrast enhancement on axial FST1WI (**d**).

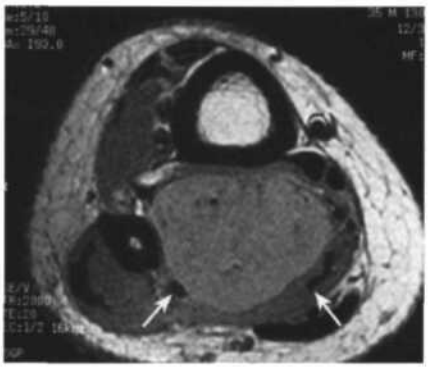

a

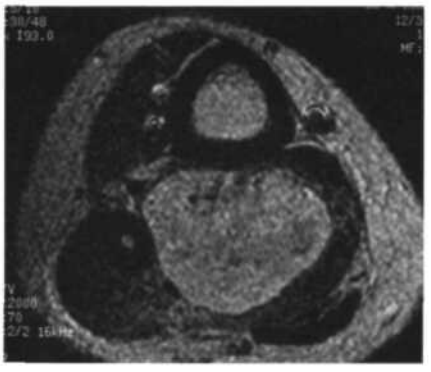

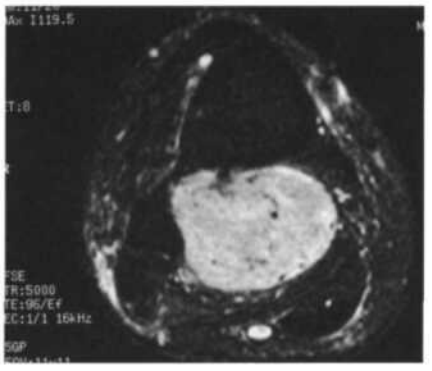

b, c

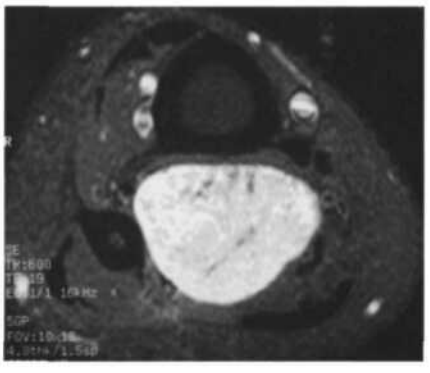

d

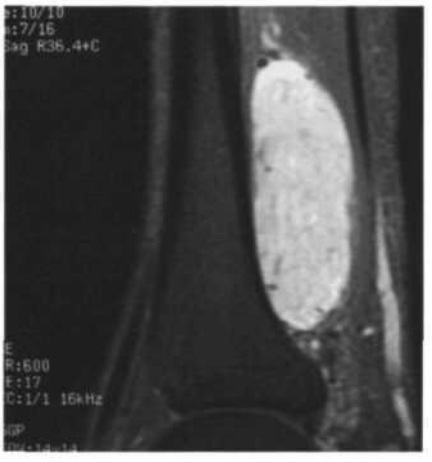

e

Figure **116a-e** A 35-year-old man with a solitary fibrous tumor involving the soft tissues dorsal to the distal tibia. The lesion has circumscribed margins, and has intermediate signal on axial PDWI (**a**), slightly high signal on axial T2WI (**b**), and heterogeneous high signal on axial FST2WI (**c**). The lesion shows prominent Gd-contrast enhancement on axial (**d**) and sagittal (**e**) FST1WI.

References

1 Gengler C, Guillou L. Solitary fibrous tumor and haemangiopericytoma: evolution of a concept. *Histopathology* 2006;48:63-74.

2 Gold JS, Antonescu CR, Hajdu C, et al. Clinicopathologic correlates of solitary fibrous tumors. *Cancer* 2002;94:1057-1068. Mo:

3 Guillou L, Fletcher JA, Fletcher CDM, Mandahl N. Extrapleural solitary fibrous tumour and hemangiopericytoma. In: Fletcher CDM, Unni KK, Mertens F, eds. *World Health Organization Classification of Tumours. Pathology and Genetics of Tumours of Soft Tissue and Bone* Geneva: IARC Press: 2002:86-90.

4 Lim SW, Chiang C. Radiological case of the month. *Appl Radiol* 2004;33:29-32.

5 Weiss SW, Goldblum JR. Perivascular tumors. In: Weiss SW, Goldblum JR, eds. *Enziger and Weiss Soft Tissue Tumors,* 4th ed. St. Louis, Mosby; 2001:985-1035.

A 25 Fibrosarcoma

ICD-OCode

Adult fibrosarcoma: 8810/3

Infantile fibrosarcoma: 8814/3

Myxofibrosarcoma: 8811/3

Low-grade fibromyxoid sarcoma: 8811/3

Sclerosing epithelioid fibrosarcoma: 8810/3

Definition

Fibrosarcomas are uncommon malignant tumors consisting of bundles of fibroblasts / spindle cells with varying proportions of collagen, lacking other tissue differentiating features such as tumor bone, osteoid, or cartilage.[2-7,9-11,13,15,16-19-21] Fibrosarcomas occur in soft tissues as well as in bone.[1-20] Infantile fibrosarcoma of soft tissue is often associated with a chromosomal translocation, t(12;15)(pl3;q26), which results in oncogenic activation of the NTRK3 gene.[2] Adult fibrosarcomas often have various different types of chromosomal rearrangements.[5]

Variants of fibrosarcoma include myxofibrosarcoma, low-grade fibromyxoid sarcoma, and sclerosing epithelioid fibrosarcoma.[1,6,15,16] Myxofibrosarcoma, also referred to as myxoid malignant fibrous histiocytoma (see Chapter A48), is a common sarcoma in elderly patients and is composed of malignant spindle cells, myxoid stroma, and curvilinear, thin-walled blood vessels.[16] Low-grade fibromyxoid sarcomas are rare sarcomas which contain whorled patterns of bland spindle cells, dense collagen, myxoid zones, and curvilinear blood vessels[6] Sclerosing epithelioid fibrosarcomas are rare sarcomas which contain epithelioid tumor cells arranged in nests and cords within sclerotic collagenous matrix.[115]

Fibrosarcomas can be primary lesions (75%) or arise as secondary tumors (25 %) associated with prior irradiation, Paget disease, bone infarct, chronic osteomyelitis, fibrous dysplasia, giant cell tumor, neurofibroma, or Schwannoma.[7,10,11]

Frequency of Occurrence

Fibrosarcomas of bone account for 3-5 % of primary malignant bone tumors, and 2-4% of all bone tumors.[10,17-21]

Fibrosarcomas of soft tissues (adult type) account for 4 % of malignant soft tissue tumors, and 2 % of all soft tissue tumors.[12-14]

Fibrosarcomas of soft tissues (infantile type) account for less than 1 % of malignant soft tissue tumors,[12] and for 12 % of soft tissue malignancies in infants.[2] Up to 80% are congenital, and mostly occur in the first year.[2]

Age at Presentation

Fibrosarcomas of bone: from 1 to 85 years, median = 43 years, average = 38 years.[9,19-21]

Fibrosarcomas of soft tissues (adult type): from 14 to 72 years, mean = 41 years.[12]

Fibrosarcomas of soft tissues (infantile type): from less than 1 year to 4 years, mean = 2 years[12];36-80% are congenital.[2,13] These tumors usually occur in neonates and infants[2,12,13] and are rarely present after the age of 2 years.[2]

Gender Ratio (M / F)

Fibrosarcomas of bone: 1 / 1 to 1.3 / 1.[9-11,19,21]

Fibrosarcomas of soft tissues (adult type): 1 / 1.[12]

Fibrosarcomas of soft tissues (infantile type): 1 / 1.[12]

Location

Fibrosarcomas of bone. Tumors are located in the distal femur > proximal tibia > iliac bone > mandible > sacrum > proximal humerus > otherbones.[7,9-11,19,21] In long bones, tumors are typically intramedullary; and occur most frequently in the metadiaphyseal region (38%), followed by diaphyseal (29%), epimetadiaphyseal (14%), epi-metaphyseal (11%), and metaphyseal sites (8 %).[19] In long bones, tumors are most often centrally located (89%) versus eccentric (11 %).[19] Tumors have also been reported to occur in a periosteal location.[9] Fibrosarcomas involving the spine are rare.[7]

Fibrosarcomas of soft tissues (adults). These tumors occur in the lower extremity > trunk > upper extremity > head and neck > foot and ankle > hand and wrist > other locations.[12]

Fibrosarcomas of soft tissues (infants, young children). These tumors occur in the lower extremity > head and neck > trunk > upper extremity > other locations.[12]

Signs and Symptoms

Fibrosarcomas of bone. Patients often have pain and swelling at the affected site.[7,10] Pathologic fractures can occur in up to 33 % of cases.[7,10]

Fibrosarcomas of soft tissues (adult type). Tumors can occur as localized soft tissue masses, with or without pain that is usually of short duration.[5]

Fibrosarcomas of soft tissues (infantile type). Fibrosarcomas in infancy can be painless, rapidly enlarging soft tissue lesions which measure up to and exceed 30cm^2 The overlying skin may be tense, ulcerated, and/or erythematous, with or without purplish skin discoloration[2]

Cross Pathologic Findings

Fibrosarcomas of bone. Lesions often are gray-white or tan-mixed tumors associated with bone destruction.[7,9-11,19,21] Low-grade tumors are often firm and fibrous, whereas high-grade fibrosarcomas are often soft and fleshy.[7,9-11,21] Zones of hemorrhage, myxoid changes, necrosis and/or cystic degeneration can

also be associated with these tumors.[7,9-11,19,21] Low-grade lesions tend to be more circumscribed than higher-grade lesions.[7,9-11,19,21]

Fibrosarcomas of soft tissues. In adults, fibrosarcomas are firm masses, often gray-white and/or tan with relatively defined margins.[2,5,6,13,15,16] Zones of necrosis and/or hemorrhage can be seen in high-grade fibrosarcomas in adults.[5,6,13,15,16] Fibrosarcomas in young children are usually lobulated, firm and rubbery tumors, often with poorly defined margins, with or without areas of necrosis, hemorrhage, cystic degeneration, mucinous and/or myxoid changes.[2]

Histopathologic Findings

Fibrosarcomas of bone. Lesions are composed of intertwined bundles of fibroblast-like spindle cells often arranged in a "herringbone pattern."[7,9-11,19,21] The intercellular substance contains varying amounts of collagen fibers. Lesions are graded on the basis of the cytologic features of the tumor cells and cellularity of the tumors.[7,9-11,19,21]

- **Grade 1 tumors** (5%) are well-differentiated neoplasms composed of elongated fibroblastic spindle cells with ovoid or elongated nuclei with only very few mitoses. Abundant collagen fibers are present in the intercellular substance.
- **Grade 2 tumors** (65%) are moderately differentiated neoplasms with greater cellularity than grade 1 lesions. The nuclei of the spindle cells are more atypical in appearance with more mitoses than grade 1 lesions. Less collagen is seen than in grade 1 tumors.
- **Grade 3 and 4 tumors** (30%) have greater cellularity than the lower-grade fibrosarcomas. The spindle cells are greater in number with higher mitotic activity compared with lower-grade fibrosarcomas. Small tumor cells may also be seen in some of the high-grade lesions. Tumor cells have pleomorphic and hyperchromatic nuclei. Areas of necrosis are often seen in the lesions. Intercellular collagen is usually minimal for grade 3 lesions or not visualized in grade 4 lesions.

Fibrosarcomas of soft tissues.[2,4,6,13,15,16] Lesions have anaplastic fibroblastic spindle cells with varying degrees of nuclear pleomorphism, and mitotic activity. Amounts of intercellular collagen and reticulin are also variable. Congenital and infantile fibrosarcomas have similar histologic features compared with the adult types, except that the lesions tend to have a more fasciculated pattern. Immunohistochemical reactivity to vimentin is usually observed for both infantile and adult types, whereas immunoreactivity to smooth muscle actin is less frequent.[2,5]

- **Differentiated soft tissue fibrosarcomas (grades 1 and** 2). The spindle-shaped tumor cells are present in an interwoven intercellular substance of abundant collagen. Mitotic figures are rare.
- **Undifferentiated soft tissue fibrosarcomas (grades 3 and** 4). The tumor cells have atypical features/anaplasia and multiple mitotic figures. The amounts of intercellular collagen and reticulin are markedly diminished compared with the more well-differentiated fibrosarcomas. Giant cells with single or multiple nuclei are also seen in grade 3 and 4 tumors. Unlike malignant fibrous histiocytomas, the giant cells in fibrosarcomas do not have growth patterns such as matted, storiform, or pinwheel configurations.
- **Myxofibrosarcoma.** These tumors have a myxoid component containing hyaluronic acid, which occupies more than 50% of the lesion volume; as well as spindle cells, bizarre giant cells, and spheroid histiocytic cells with foamy cytoplasm.[16] Low-grade tumors have infrequent mitotic figures.[16] These tumors often have curvilinear, thin-walled blood vessels with adjacent aggregates of tumor cells, lymphocytes, and plasma cells.[16] High-grade tumors contain fascicles and/or sheets of malignant pleomorphic and spindle cells with frequent atypical mitoses, zones of necrosis, and hemorrhage.[16]
- **Low-grade fibromyxoid sarcoma.**[6] These tumors contain whorled patterns of bland spindle cells, dense collagenous zones, and myxoid nodules.[6] Mitoses are uncommon.[6] Arcades of small blood vessels are often observed as well as small arteriole-sized vessels with adjacent sclerosis.[6] In ~40% of cases, dense zones of hyaline collagen are surrounded by cuffs of spindle cells, referred to as giant collagen rosettes.[6]
- **Sclerosing epithelioid fibrosarcoma.**[115] These tumors contain small epithelioid cells with spheroid, ovoid, or angulated nuclei within clear to eosinophilic cytoplasm.[15] Few mitoses are typically observed.[15] The tumor cells are often arranged in nests, cords, strands, or acini within abundant acidophilic collagen matrix.[15] The collagen matrix can occur as thick bands, in lace-like configurations, and/or hyalinized fibrous zones.[15]
- **Postradiation fibrosarcomas.** Lesions are often seen 4-15 years after radiation treatment of greater than 4000 cGy.[3] Histologic features are similar to other fibrosarcomas of soft tissue and bone.[3] Additional postradiation findings are often seen in the adjacent tissue, such as bone infarcts, fat and muscle necrosis/atrophy, and intimal vascular proliferation.

Tumor Genetics

Infantile fibrosarcoma of soft tissue is often associated with a chromosomal translocation, t(12;15) (p!3;q26), which results in oncogenic activation of the NTRK3 gene.[2] Adult fibrosarcomas often have various different types of chromosomal rearrangements.[5] Myxofibrosarcomas and low-grade fibromyxoid sarcomas often have supernumerary ring chromosomes.[616]

Findings on Plain Films (Roentgenograms) and Computed Tomography

Fibrosarcomas of bone.[7-11,19,21] Tumors are usually radiolucent with permeative or "moth-eaten" appearance, sometimes in combination with a more geographic pattern. Tumor margins are usually irregular and indistinct, although some of the borders may be more sharply defined. Typically no sclerotic margins are seen. Areas of cortical destruction are usually present, with or without associated extra-osseous soft tissue masses.

Fibrosarcomas of soft tissues (adults). Tumors appear as soft tissue lesions without matrix mineralization; with or without associated bone erosion, destruction or deformity[13]

Fibrosarcomas of soft tissues (infants and young children). Tumors appear as soft tissue lesions without matrix mineralization, rarely associated bone destruction.[4,13]

MRI Findings

Fibrosarcomas of bone.[21] Fibrosarcomas are often intramedullary lesions with irregular margins, with or without associated cortical destruction and/or extra-osseous soft tissue masses. Lesions usually have low-intermediate signal on T1WI and PDWI, and heterogeneous intermediate, slightly high, and/or high signal on T2WI (Fig. **117**). After Gd-contrast administration, lesions usually show heterogeneous prominent enhancement.

a

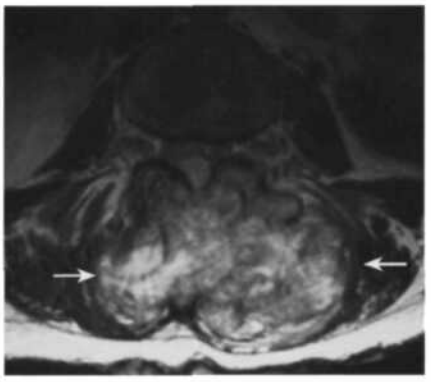

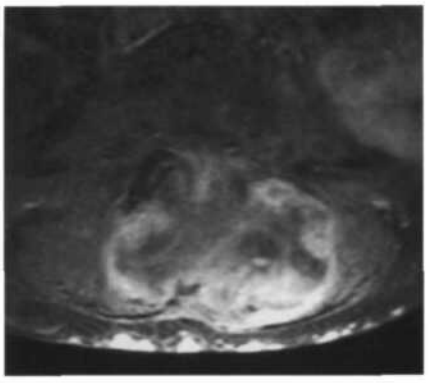

b, c

Figure 117a-c 25-year-old man with neurofibromatosis type I and fibrosarcoma involving the L3 and L 4 vertebrae. Sagittal (**a**) T1WI shows a tumor with intermediate signal, destroying bone and has extension into the adjacent soft tissues, including the dorsal epidural portion of the spinal canal resulting in spinal canal compression. The neoplasm has heterogeneous high and slightly high signal on axial (**b**) T2WI. The tumor shows heterogeneous Gd-contrast enhancement on axial (**c**) FS T1WI.

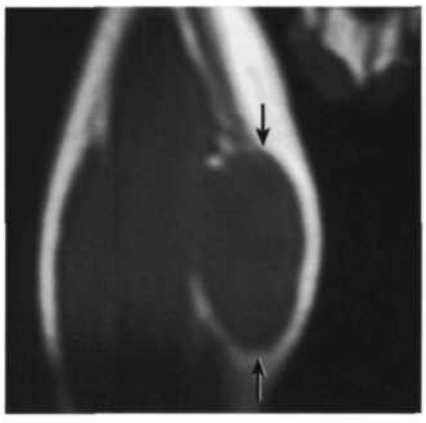

a

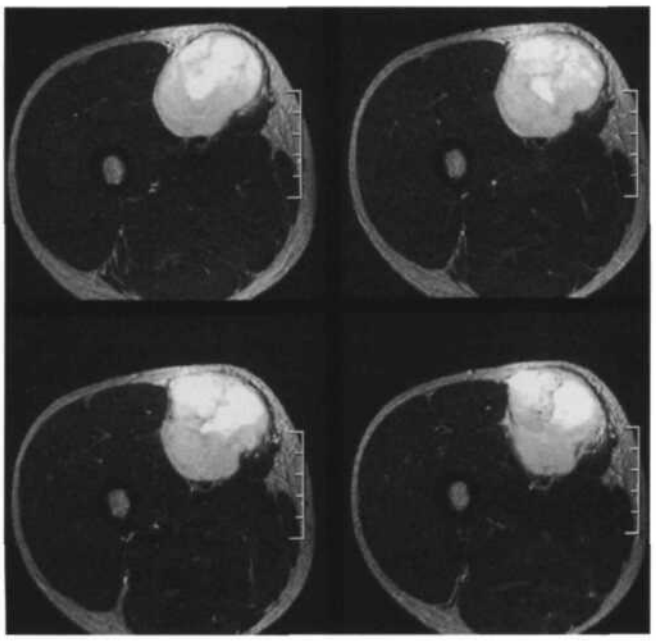

b

Figure **118a-c** A 13-year-old male with a fibrosarcoma in the vastus medialis muscle. Coronal T1 WI (**a**) shows a circumscribed tumor with low-intermediate signal. The tumor has high signal on axial T2WI (**b**), and shows prominent heterogeneous Gd-contrast enhancement on axial (**c**) FST1WI. An irregular, central, nonenhancing zone of necrosis is present.

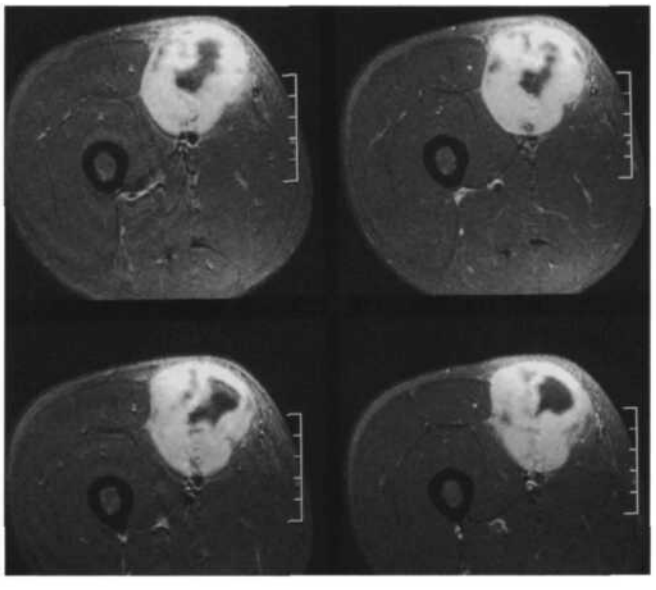

c

Fibrosarcomas of soft tissues.[4,13] Fibrosarcomas are often ovoid lesions with slightly irregular margins, with or without associated destruction and invasion of adjacent bone (Figs. **118, 119).** High-grade fibrosarcomas may have an infiltrative pattern with respect to adjacent soft tissues. Lesions usually have low-intermediate signal onT1WI, intermediate to slightly high signal on PDWI, and heterogeneous intermediate-high signal on T2WI. Margins of lesions may be indistinct on T2WI for high-grade lesions. Zones with high signal on T2W1 can be seen in myxoid regions of myxofibrosarcoma (Fig. **119).** For the tumor subtype of sclerosing epithelioid fibrosarcoma, zones of low signal on T1WI and T2WI can be seen from regions of decreased cellularity and dense collagen deposition in these neoplasms.' After Gd-contrast administration, lesions usually show heterogeneous enhancement. Enhancing margins of lesions may be indistinct for high-grade lesions. MRI shows the relationship of tumor enhancement to nearby neurovascular bundles and adjacent bone.

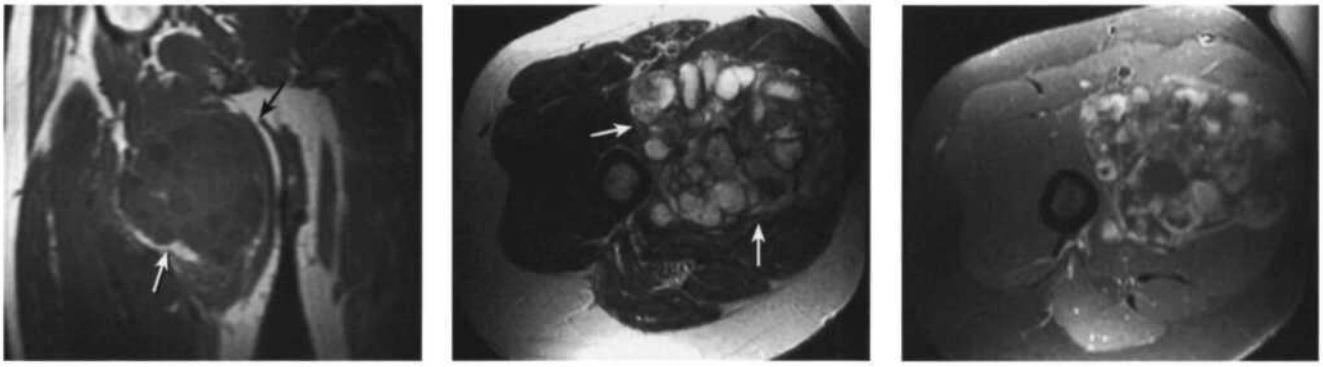

a b, c

Figure **119a-c** A 37-year-old man with a myxofibrosarcoma involving the adductor muscles in the proximal thigh. Coronal T1WI (**a**) shows a circumscribed tumor with zones of low and intermediate signal. The tumor has mixed zones of low, intermediate, and high signal on axial T2WI (**b**). The tumor shows prominent heterogeneous Cd-contrast enhancement on axial FST1WI (**c**).

Differential Diagnosis for Fibrosarcoma

Bone lesions:

- **Children.** Ewing sarcoma, osteosarcoma, lymphoma, chondrosarcoma, malignant fibrous histiocytoma, eosinophilic granuloma, osteomyelitis.
- **Adults.** Myeloma/plasmacytoma, metastatic disease, giant cell tumor, osteosarcoma, lymphoma, chondrosarcoma, malignant fibrous histiocytoma, desmoplastic fibroma, eosinophilic granuloma, osteomyelitis.

Soft tissue lesions: Malignant fibrous histiocytoma, liposarcoma, leiomyosarcoma, malignant peripheral nerve sheath tumor, synovial sarcoma, angiosarcoma, rhabdomyosarcoma, epitheloid sarcoma, hemangiopericytoma, clear cell sarcoma, malignant granular cell tumor, nodular fasciitis, hemangioma, hemangiopericytoma, granular cell tumor, proliferative fasciitis, dermatomyositis, hematoma, proliferative myositis.

Treatment and Prognosis

Fibrosarcoma of bone. Surgical resection with wide margins is the usual treatment. Prognosis is often dependent on tumor grade and staging.[7,9-1119,21] Favorable imaging findings related to prognosis include a geographic pattern of bone destruction, and involvement of less than two quadrants of the bone circumference.[7] For low-grade tumors, surgery is usually adequate, although local recurrence occurs in 11 % of patients. High-grade lesions often require preoperative or adjuvant chemotherapy after surgery to enhance survival. Amputation may be necessary in some cases. Local recurrences after amputation are associated with poor prognosis.[7,21] Metastatic disease is not infrequent (lungs > other bones > lymph nodes) and has been reported to occur in up to 45 % of patients.[7,10] Lesions are usually resistant to radiation treatment. Five-year and 10-year survival rates of 34% and 21-34%, respectively, have been reported.[7,10,11,19,21] In patients with grade 1 tumors, 10-year survival rates can be greater ranging from 64 to 83 %.[7,10,21] In children, periosteal fibrosarcomas have a better prognosis than medullary lesions.

Fibrosarcoma of soft tissue (adult type). Prognosis depends on tumor grade and staging.[5] Features associated with poor prognosis include high tumor grade, high cellularity with minimal collagen, necrosis, and mitotic rates greater than 20 per high power field.[5] Metastases occur in up to 63 %.[513] Surgical resection with wide margins for nondisseminated primary tumors is usually performed, with recurrence rates of ~ 18 %.[13] Five-year survival rates range from 39 to 54 %.[5] Adjuvant chemotherapy may be beneficial.

Fibrosarcoma of soft tissue (infantile type). Congenital fibrosarcomas can be cured with resection.[2,13] Infantile fibrosarcomas have rapid growth rates, although rarely metastasize.[2,4,13] Local recurrence after resection has been reported to range from 5 to 50 %.[2,13] Amputations may be necessary for recurrent lesions that are difficult to control.[13] Tumors in the head, neck, and trunk have a worse prognosis than lesions in the extremities.[13] Mortality rates of 4-25 % have been reported.[2] Chemotherapy has been reported to be beneficial.[2]

References

1 Christensen DR, Ramsamooj R, Gilbert TJ. Sclerosing epithelioid fibrosarcoma: short T2 on MR imaging. *Skeletal Radio!* 1997;26: 619-621.

2 Coffin CM, Fletcher JA. Infantile fibrosarcoma. In: Fletcher COM, Unni KK, Mertens F, eds. *World Health Organization Classification of Tumours. Pathology and Genetics of Tumours of Soft Tissue and Bone* Geneva: 1ARC Press: 2002:98-100.

3 Das Gupta TK, Chaudhuri PK. Pathology of soft tissue sarcoma. In: Das Gupta TK, Chaudhuri PK, eds. *Tumors of the Soft Tissues* 2nd ed. New York, NY: Appleton and Lange; 1998:63-200.

4 Eich GF, Hoeffel JC, Tschappeler H, Ggassner I, Willi UV. Fibrous tumours in children: imaging features of a heterogeneous group of disorders. *Pediatr Radiol* 1998:28:500-509.

5 Fisher C, van den Berg E, Molenaar WM. Adult fibrosarcoma. In: Fletcher COM, Unni KK, Mertens F, eds. *World Health Organization Classification of Tumours. Pathology and Genetics of Tumours of Soft Tissue and Bone* Geneva: IARC Press; 2002:100-101.

6 Folpe A, van den Berg E, Molenaar WM. Low grade fibromyxoid sarcoma. In: Fletcher COM, Unni KK, Mertens F, eds. *World Health Organization Classification of Tumours. Pathology and Genetics of Tumours of Soft Tissue and Bone* Geneva: IARC Press; 2002:104-105.

7 Forest M. Fibrosarcoma. In: Forest M, Tomeno B, Vanel D, eds. Orthopedic *Surgical Pathology: Diagnosis of Tumors and Pseudotumoral Lesions of Bone and Joints* Edinburgh: Churchill Livingstone; 1998: 311-316.

8 Hudson TM, Stiles RG, Monson DK. Fibrous lesions of bone. *Radiol Clin North Am* 1993 ;31:279-297.

9 Huvos AC. Fibrosarcoma of bone. In: Huvos AG, ed. *Bone Tumors: Diagnosis, Treatment, and Prognosis* 2nd ed. Philadelphia, Pa: W.B. Saunders; 1991:413-427.

10 Kahn LB, Vigorita V. Fibrosarcoma of bone. In: Fletcher CDM, Unni KK, Mertens F, eds. *World Health Organization Classification of Tumours. Pathology and Genetics of Tumours of Soft Tissue and Bone* Geneva: IARC Press; 2002:289-290.

11 Kilpatrick SE, Unni KK. Spindle cell lesions of bone. In: Helliwell TR, ed. *Major Problems in Pathology: Pathology of Bone and Joint Neoplasms* Vol 12. 1st ed. Philadelphia, Pa: W.B. Saunders; 1999: 237-255.

12 Kransdorf MJ. Malignant soft-tissue tumors in a large referral population: distribution of diagnoses by age, sex, and location. *AJR Am] Roentgenol* 1995;164:129-134.

13 Kransdorf MJ, Murphey MD. Malignant fibrous and fibrohistiocytic tumors. In: *Imaging of Soft Tissue Tumors* 2nd ed. Philadelphia: Pa: W. B. Saunders; 2006:257-297.

14 Kransdorf MJ, Murphy MD. Soft tissue tumors in a large referral population: prevalence and distribution of diagnoses by age, sex, and location. In: *Imaging of Soft Tissue Tumors* 2nd ed. Philadelphia, Pa: W.B. Saunders; 2006:3-37.

15 Meis-Kindblom JM, Kindblom LG, van den Berg E, Molenaar WM. Sclerosing epithelioid fibrosarcoma. In: Fletcher COM, Unni KK, Mertens F, eds. *World health organization classification of tumours. Pathology and genetics of tumours of soft tissue and bone* IARG Press; 2002:106-107.

16 Mentzel T, van den Berg E, Molenaar WM. Myxofibrosarcoma. In: Fletcher COM, Unni KK, Mertens F, eds. *World Health Organization Classification of Tumours. Pathology and Genetics of Tumours of Soft Tissue and Bone* Geneva: IARC Press; 2002:102-103.

17 Mulder JD, Schutte HE, Kroon HM, Taconis WK. Introduction. In: *Radiologic Atlas of Bone Tumors* Amsterdam: Elsevier; 1993:3-6.

18 Mulder JD, Schutte HE, Kroon HM, Taconis WK. The diagnosis of bone tumors. In: *Radiologic Atlas of Bone Tumors* Amsterdam: Elsevier; 1993:9-46.

19 Mulder JD, Schutte HE, Kroon HM, Taconis WK. Fibrosarcoma. In: *Radiologic Atlas of Bone Tumors* Amsterdam: Elsevier; 1993: 215-226.

20 Unni KK. Introduction and scope of study. In: *Dahlin's Bone Tumors: General Aspects and Data on 11 087 Cases* 5th ed. Philadelphia, Pa: Lippincott, Williams & Wilkins; 1996:1-9.

21 Unni KK. Fibrosarcoma and desmoplastic fibroma. In: *Dahlin's Bone Tumors: General Aspects and Data on 11 087 Cases* 5th ed. Philadelphia, Pa: Lippincott, Williams & Wilkins; 1996:197-210.

A 26 Fibrous Cortical Defect and Nonossifying Fibroma (Also Referred to as Metaphyseal Fibrous Defect), Cortical Desmoid (Also Referred to as Periostea! Desmoid or Distal Femoral Cortical Irregularity), and Fibroxanthoma (Also Referred to as Benign Fibrous Histiocytoma)

ICD-O Code

8830/0

Definition

Fibrous cortical defects and **nonossifying fibromas** are benign, well-circumscribed radiolucent lesions in the metaphyseal portions of long bones.[1-7,11,14] These lesions are comprised of whorls of fibroblastic cells combined with smaller amounts of multinucleated giant cells and xanthomatous cells.[3,5,7,11,14] Both **fibrous cortical defects** and **nonossifying fibromas** have similar pathologic findings, although they differ in size and primary locations in long bones. **Fibrous cortical defects** are small lesions primarily located in bone cortex, whereas the larger **nonossifying fibromas** are located eccentrically in the medullary cavity. Both lesions are considered to be in the spectrum of the same disorder of fibrohistiocytic origin. Less than 5 % of nonossifying fibromas are multiple. Multifocal nonossifying fibromas can be familial, or related to the clinicopathologic syndrome referred to as the Jaffe-Campanacci syndrome, which also includes some or all of the following: cafe-au-lait spots (without neurofibromatosis), mental retardation, congenital blindness, kyphoscoliosis, and/or precocious puberty.[3,7,14]

Cortical desmoid, also referred to as periosteal desmoid or distal femoral cortical irregularity, refers to a fibrous defect at the distal posteromedial femur, which may occur from an avulsive injury or stress reaction at the insertion site of the medial head of the gastrocnemius muscle or adductor magnus.[5,7,12,14] **Benign fibrous histiocytoma of bone** and **fibroxanthoma of bone** are lesions that are histologically identical to nonossifying fibromas but occur in nonmetaphyseal portions of long bones or in other bones.[8]

Frequency of Occurrence

Fibrous cortical defects and nonossifying fibromas are common benign lesions that are usually asymptomatic and are often detected as incidental findings[5,9,13]. The true incidence of these lesions is unknown, but may be up to 30-40% of children.[5,11]

Cortical desmoids can occur in up to 50% of knees evaluated by MRI.[12]

Benign fibrous histiocytomas of bone are rare.[8]

Age at Presentation

Fibrous cortical defects and nonossifying fibromas: from 1 to 45 years,[11,14] mean = 16-19 years, median = 14 years[11:] 95% occur between the ages of 5 and 20 years, 70-75 % occur in the second decade.[8,10,11]

Cortical desmoid: from 4 to 64 years, average = 34 years.[12]

Fibroxanthoma (benign fibrous histiocytoma): from 6 to 74 years; 60% of patients are older than 20 years at diagnosis.[8]

Gender Ratio (M / F)

Fibrous cortical defect and nonossifying fibroma: 1.1 /1 to 3/1.[5,11,14]

Cortical desmoid: 1.4/I.[12]

Benign fibrous histiocytoma: slight female predominance.[8]

Location

Fibrous cortical defects and nonossifying fibromas. These lesions occur in the distal femur > distal tibia > proximal tibia > proximal fibula > distal fibula > humerus > other bones.[11,14] Fibrous cortical defects are typically located in metaphyses of long bones.[5,11,14] Nonossifying fibromas are usually located in the metadiaphyseal regions of long bones.[5,11,14]

Cortical desmoids. These lesions are located at the posterior cortex of the distal medial femur at the attachment site of the medial gastocnemius muscle.[12]

Benign fibrous histiocytomas. Long bones (femur and tibia are common sites) account for 40 % of the locations of these lesions, followed by pelvic bones (iliac bone is the most common site) which account for 25 %.[8] These lesions can occur in almost any bone.[8] In long bones, these lesions occur in the epiphyseal or diaphyseal locations.[8]

Signs and Symptoms

Fibrous cortical defects are typically asymptomatic.[2,3,5,7,14] **Nonossifying fibromas** are often asymptomatic, except for larger lesions which can have associated pain, focal bony enlargement, and pathologic fracture.[2,3,5,7,11,14] Pathologic fractures have been reported to occur in up to 20 % of nonossifying fibromas.[11]

Cortical desmoids are typically asymptomatic.[12]

Benign fibrous histiocytomas are associated with pain in 65 %, and occasionally are associated with pathologic fracture.[8]

Cross Pathologic Findings

Fibrous cortical defects, nonossifying fibromas, and benign fibrous histiocytomas.[3,5,7,8,11,14] Specimens are usually obtained from curettage and consist of firm tissue with varying combinations of gray, yellow, brown, or red coloration. The outer margins of the lesion may be covered by a fibrous periosteum or thin shell of expanded cortex.

Cortical desmoids (distal femoral cortical irregularities). Cortical desmoids appear as irregular excavations or erosions involving the cortex at the distal posterior medial portions of the femur.[1214]

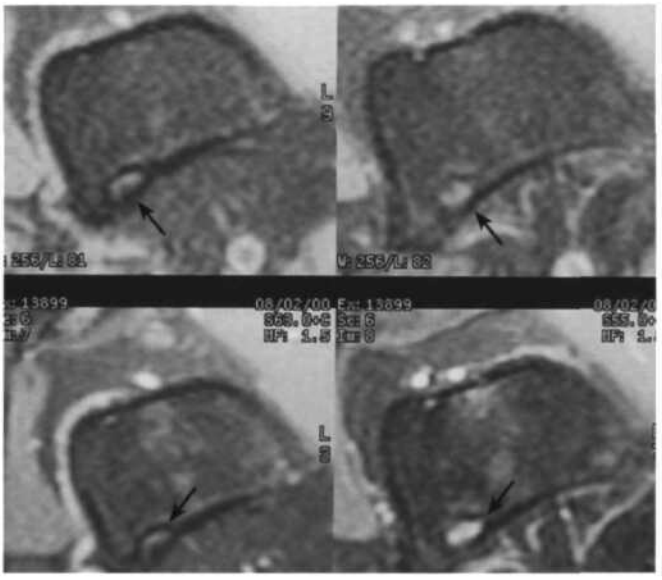

Figure **120a-c** An 18-year-old man with a fibrous cortical defect involving the distal posterior lateral femur. Lateral radiograph (**a**) shows an oval, sharply marginated, radiolucent zone in the metaphyseal cortex surrounded by a thin rim of sclerotic bone. Centrally, the lesion has intermediate signal on axial (**b**) T1WI, and intermediate to high signal on axial (c) FS T2W1. A thin zone of low signal is seen at the medullary border of the lesion (**b, c**).

Histopathologic Findings

Fibrous cortical defects, nonossifying fibromas, and benign fibrous histiocytomas.[3,5-8,11,14] Lesions are hypercellular consisting of fibroblastic spindle cells without nuclear pleomorphism arranged in a whorled or loose storiform pattern. Variable amounts of interlacing bundles of thin collagen fibers can be present. Mild mitotic activity lacking atypical mitoses is often seen in the fibroblastic spindle cells. Osteoclast-type giant cells, foamy and hemosiderin-laden macrophages, and lymphocytes are often scattered throughout the lesions. The foamy macrophages (xanthoma cells) contain lipid and small dark nuclei. Small zones of hemorrhage may be present surrounded by giant cells. Reactive new bone formation with associated osteoblasts can occur. Mature trabecular bone can be seen in the lesions over time. Areas of ischemic necrosis can be seen in areas of fracture.

Cortical desmoids (distal femoral cortical irregularities). Cortical desmoids appear as areas of osteoclastic resorption and remodeling of bone cortex with dense fibrous replacement at the distal posterior medial portions of the femur.[3,12,14] Scattered fragments of bone may be present within the dense fibrous tissue.[3] Sclerotic reaction can be seen at the inner margins of eroded cortex.

Findings on Plain Films (Roentgenograms) and Computed Tomography

Fibrous cortical defects are oval or rounded, sharply marginated, radiolucent zones in metaphyseal cortex of long bones, usually ranging in size from 1 to4cm[1,3,11] (Figs. **120-122).** A thin rim of sclerotic bone can be seen convex toward the adjacent medullary cavity as well as at the outer cortical margin.[1,3,11]

Nonossifying fibromas are well-circumscribed intramedullary radiolucent lesions ranging from 1 to 7 cm in diameter.[2-7,11,14] Lesions have lobulated borders with thin sclerotic margins against cancellous bone[11] (Figs. **123, 124).** Varying degrees of endosteal scalloping and cortical thinning are often seen.[2-7,11,14] Expansion of bone with a thinned cortex can be seen with nonossifying fibromas.[2-7,11,14] **Benign fibrous histiocytomas of bone** have findings similar to those of nonossifying fibromas, and differ only in location[8] (Fig. **130).**

a

b, c

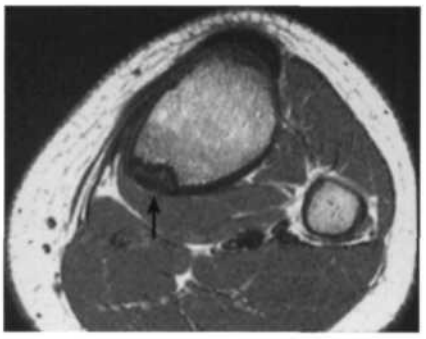

d

Figure **121 a-d** A 13-year-old male with a fibrous cortical defect involving the posterior medial tibia in the di-metaphyseal region. AP radiograph (**a**) shows an oval, sharply marginated, radiolucent zone in the cortex surrounded by a thin rim of sclerotic bone. Centrally, the lesion has low-intermediate signal on coronal (**b**) and axial (**d**) T1WI similar to muscle, and intermediate to slightly high signal on coronal (c) FST2WI. A thin zone of low signal is seen at the medullary border of the lesion (**b, c, d**).

a

b, c

Figure **122 a-c** A 17-year-old female with a fibrous cortical defect involving the posteromedial cortex of the distal femur associated with a stress fracture. AP radiograph (**a**) shows an oval, sharply marginated, radiolucent zone in the cortex surrounded by a rim of sclerotic bone, as well as a curvilinear sclerotic zone in adjacent medullary bone representing the fracture. Centrally, the fibrous cortical defect has intermediate signal on coronal (**b**) PDWI, and low-intermediate signal on coronal (**c**) FST2WI. An irregular zone of low signal is seen at the medullary border of the lesion as well as a linear zone of low signal in the adjacent marrow surrounded by high signal on FS T2WI representing a fracture.

a

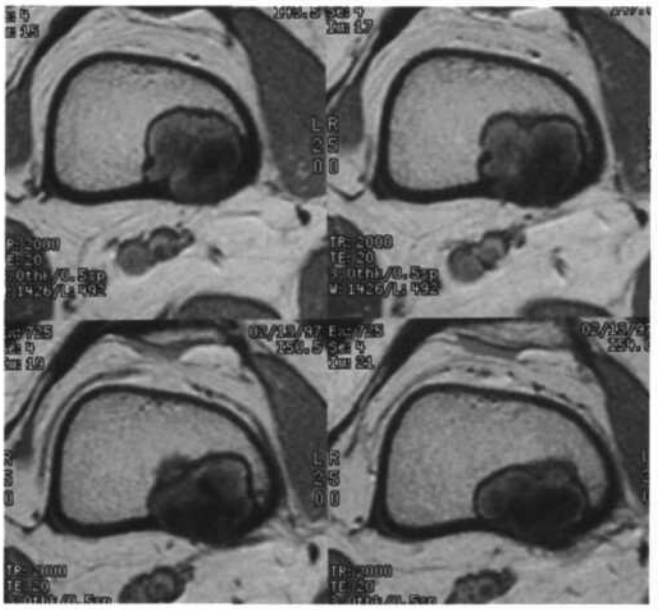

b

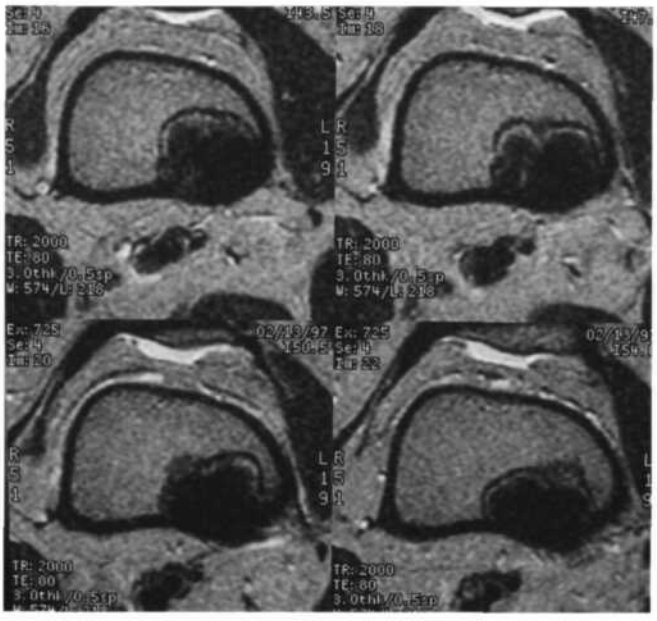

c

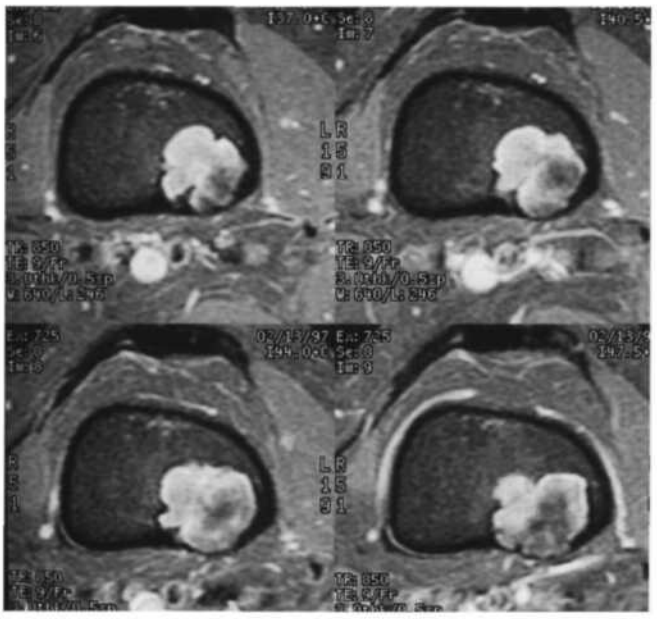

d

e

Figure **123**a-e A 16-year-old female with a nonossifying fibroma involving the distal posteromedial di-metaphyseal portion of the femur. AP radiograph (**a**) shows a well-circumscribed radiolucent lesion involving cortex and medullary bone with lobulated thin sclerotic margins. Centrally, the lesion has mixed low-intermediate signal on axial PDWI (**b**), and mostly low and intermediate signal on axial T2WI (**c**). A thin zone of low signal on T1WI and T2WI is seen at the margin of the lesion. The lesion shows heterogeneous Gd-contrast enhancement on axial (**d**) and coronal (**e**) FST1WI.

a

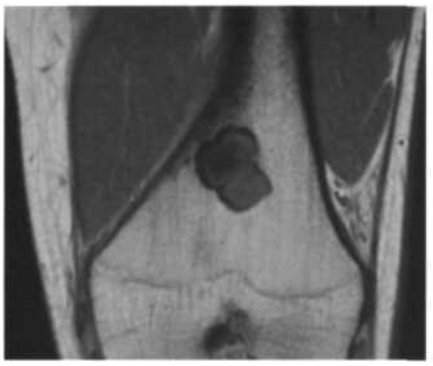

b

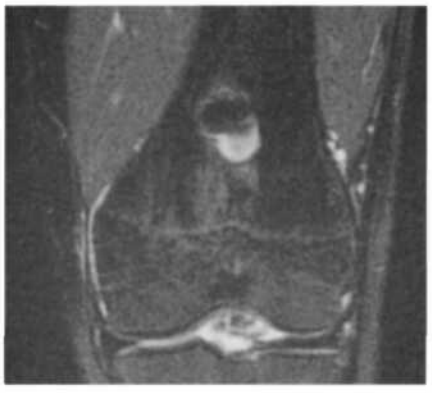

c

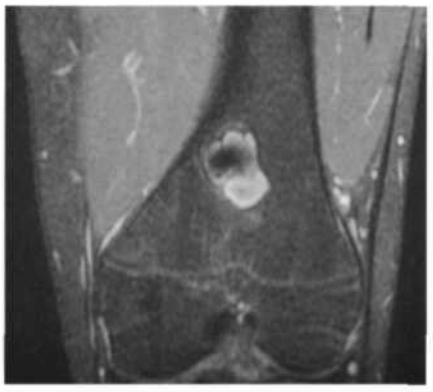

d

Figure **124a-d** A 16-year-old male with a nonossifying fibroma involving the distal metaphyseal portion of the femur. AP radiograph (**a**) shows a well-circumscribed radiolucent lesion involving medullary bone with lobulated thin sclerotic margins. Centrally, the lesion has mixed low-intermediate signal on coronal (**b**) PDWI, and low and high signal on coronal (**c**) FST2WI. A thin zone of low signal on T1 WI and T2WI is seen at the medullary margin of the lesion. The lesion shows heterogeneous Gd-contrast enhancement on coronal (**d**) FST1WI.

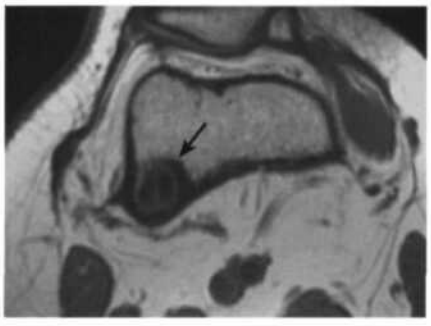

a

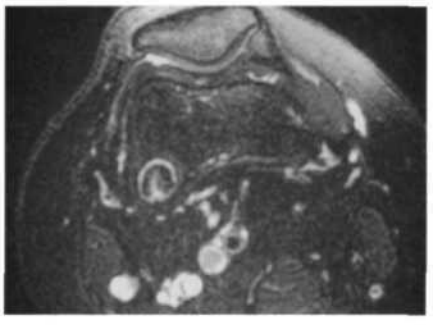

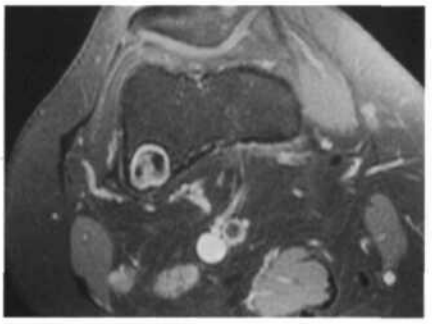

b, c

Figure **125a-c** A 19-year-old woman with a nonossifying fibroma involving the di-metaphyseal region of the femur posteriorly. The lesion has circumscribed margins with low signal on axial T1W1 (**a**). Centrally, the lesion has mostly low signal as well as a small zone of high signal on axial FS T2WI (**b**). A thin peripheral rim of high signal on axial FST2WI (**b**) is also seen which shows corresponding Gd-contrast enhancement on axial FST1WI (**c**).

Cortical desmoids (distal femoral cortical irregularities) appear most frequently as areas of radiolucency at the distal posterior medial portions of the femur[12,14] (Figs. **131-133),** of which 82 % have convex shapes, 9 % have concave shapes and 9 % have divergent shapes.[12] An inner zone of thin sclerosis is often seen deep to the zone of cortical erosion.[12,14] A compact periosteal reaction may be associated with these lesions.[3]

MRI Findings

Fibrous cortical defects are well-circumscribed, oval lesions involving bone cortex of long bones ranging in size from 8x6mm to 15x29mm, with average dimensions of 14mm.[1] Lesions usually have low to intermediate signal on T1WI and PDWI similar to muscle, and low, intermediate, and/or high signal on FST2W1 surrounded by varying thickness of low signal from corresponding marginal sclerosis[1] (Figs. **120-122).** Adjacent bone has normal signal except in rare cases of fibrous cortical defects associated with fractures[1] (Fig. **122).** After Gd-contrast administration, fibrous cortical defects with or without fracture can show variable degrees of enhancement.[1]

Nonossifying fibromas are well-circumscribed, intramedullary lesions in the dimetaphyseal regions of long bones.[2,6] Nonossifying fibromas have mixed low-intermediate signal on T1WI, and mixed low, intermediate, and/or high signal on T2WI, PDWI, and FS T2WI[2,6] (Figs. 123-129). Zones of low signal

a

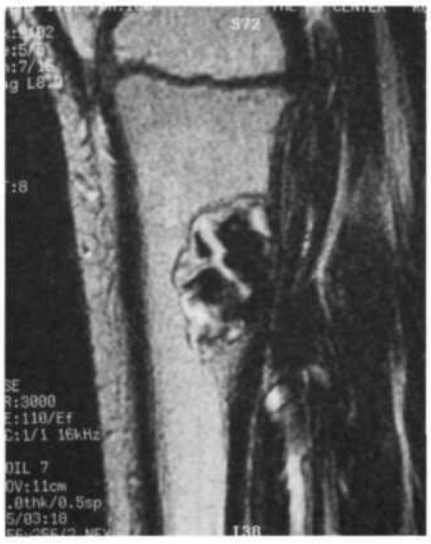

b

Figure **126a, b** A 9-year-old male with a nonossifying fibroma involving the di-metaphyseal region of the tibia posteriorly. The lesion has circumscribed margins with low signal on MRI. Centrally the lesion has mixed low and intermediate to slightly high signal on axial PDWI (**a**), and mixed low and high signal on sagittal T2WI (**b**). Cortical thickening and slight dorsal expansion are seen.

a

b

Figure ***127 a, b*** A 9-year-old male with a nonossifying fibroma involving the posterior metadiaphyseal portion of the proximal tibia. The lesion has circumscribed margins with low signal. Centrally, the lesion has mixed low and intermediate signal on sagittal (a) PDWI, and mixed low and high signal on sagittal (**b**) T2WI.

on T1WI, PDWI, and T2WI can be seen in the central portions of the lesions.[2,6] Zones with varying thickness of low signal on T1WI, PDWI, and T2WI are seen at the margins of the lesions representing bone sclerosis.[2,6] Internal septations are commonly seen as zones of low signal on T2WI in these lesions.[6] Zones of low signal on T2WI corresponded to sites of hypercellular fibrous tissue and/or hemosiderin.[6] Cortical thinning or thickening, and bone expansion can be seen.[2,6] **Benign fibrous histiocytomas of bone** have findings similar to those of nonossifying fibromas, and differ only in location[8] (Fig. **130).** After Gd-contrast administration, enhancement is usually seen (heterogeneous > homogeneous patterns)[6] (Figs. **123-125, 128,129).** Bone marrow peripheral to the lesions usually has normal MRI signal and lacks abnormal Gd-contrast enhancement unless lesions are associated with trauma or fracture[6] (Fig. **130).** Linear periosteal Gd-contrast enhancement can be seen at lesions with associated fracture or marked cortical expansion/thinning (Fig. **130).**

Cortical desmoids (distal femoral cortical irregularities) are located at the bone cortex at the distal posterior medial portions of the femur,[12,14] of which 82 % have convex shapes, 9 % have concave shapes, and 9 % have divergent shapes.[12] These lesions usually have low to intermediate signal on T1WI and PDWI, and intermediate to slightly high signal on T2WI, and slightly high to high signal on FS T2WI[12] (Figs. **131-134).** A thin border of low signal on T1WI and T2WI is often seen at the inner margin of the lesion, which corresponds to a thin zone of sclerosis seen on plain films and/or CT.[12] Bone marrow deep and peripheral to the lesion may have slightly high signal on FST2WI. After Gd-contrast administration, enhancement can be seen at the lesion and occasionally in the adjacent marrow.[12]

Differential Diagnosis

For fibrous cortical defects and nonossifying fibromas: distal medial femoral cortical irregularity (cortical desmoid—which occurs at the sites of attachment of the medial gastrocnemius muscle), fibrous dysplasia, desmoplastic fibroma, chondromyxoid fibroma, aneurysmal bone cyst, giant cell tumor, stress reaction/injury.

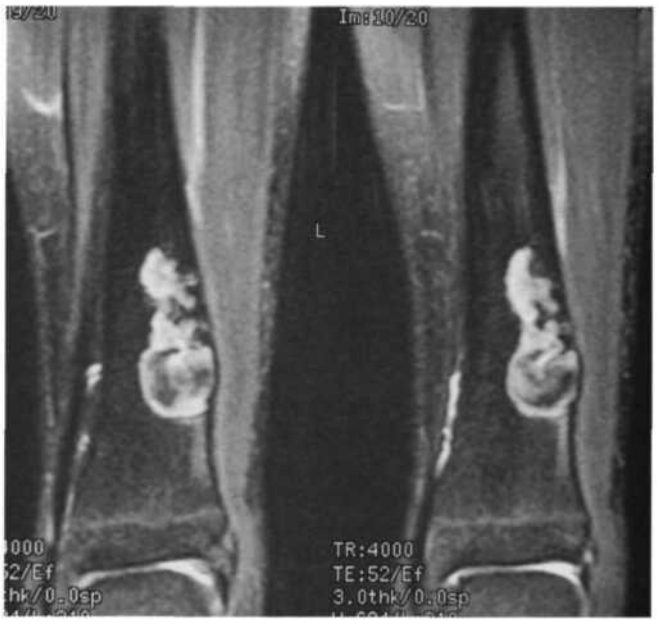

a

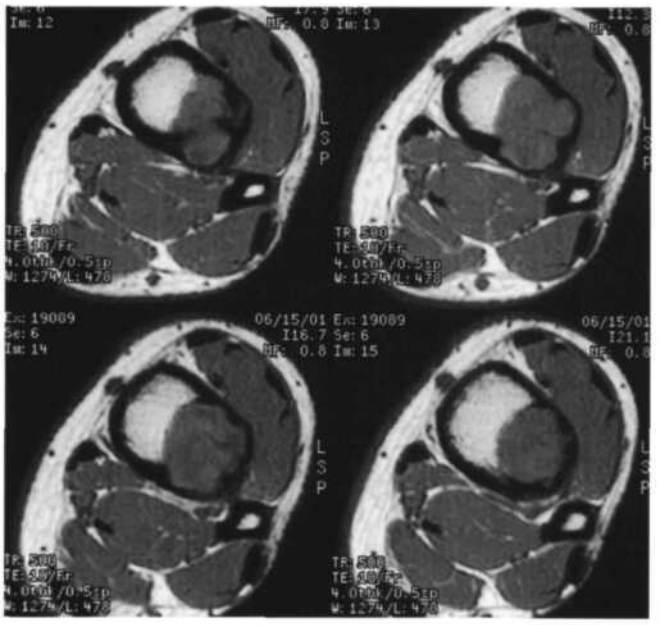

b

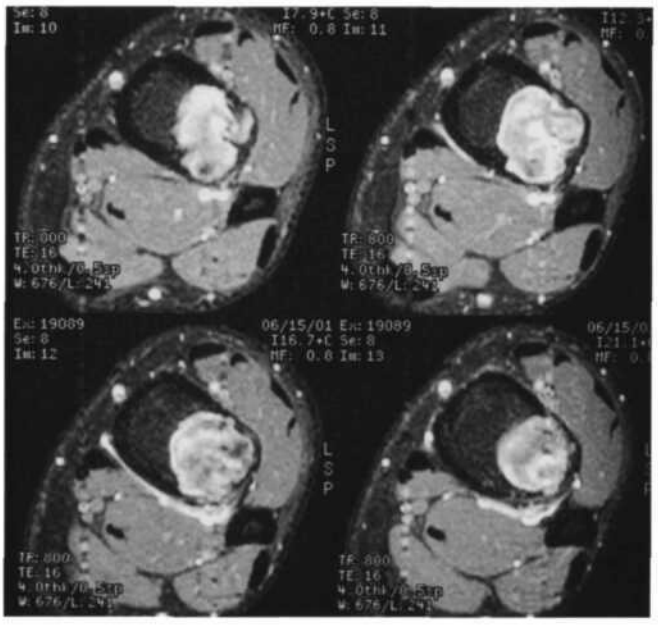

c

Figure 128 A 16-year-old female with a nonossifying fibroma involving the posterior portion of the distal tibia. The lesion has circumscribed margins with low signal. Centrally, the lesion has mixed low and high signal on coronal FST2WI (**a**), and intermediate signal with small zones of low signal on axial T1WI (**b**). The lesion shows prominent heterogeneous Cd-contrast enhancement on axial FST1 WI (**c**). Cortical thinning and slight dorsal expansion are seen.

Treatment and Prognosis

Nearly all **fibrous cortical defects** regress spontaneously from peripheral ossification.[3,11,14] **Nonossifying fibromas** also tend to regress, although pathologic fractures occur in up to 20 % of the largest lesions.[2,3,6,7,11,14] Lesions that involve more than 50 % of the bone width have the greatest risk for fracture.[2] Curettage and bone grafting are done for lesions that have associated fracture or for lesions that exceed more than half of the width of the involved bone.[2,3,6,7,11,14]

Cortical desmoids (distal femoral cortical irregularities) are typically asymptomatic and are incidentally detected on imaging examinations obtained for other reasons.[3,12,14]

For **benign fibrous histiocytomas of bone,** curettage and bone grafting of these lesions usually results in cure.[8]

a

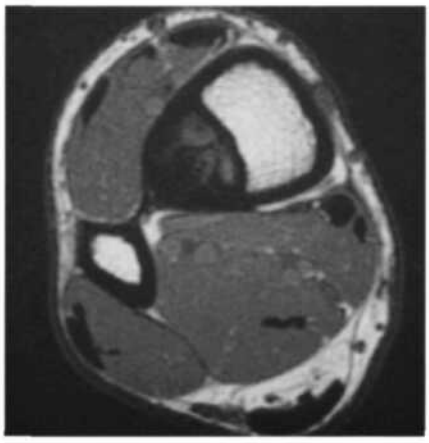

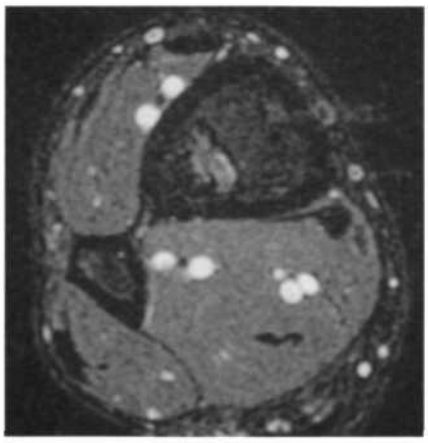

b, c

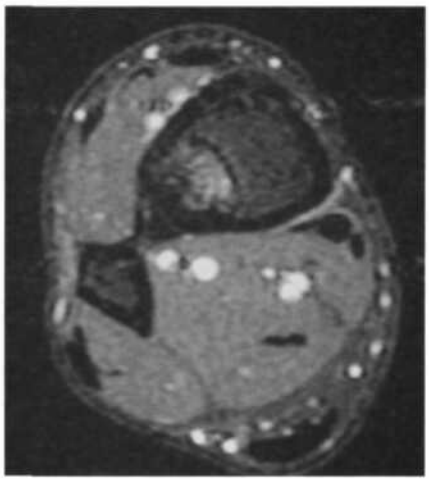

d

Figure **129a-d** A 17-year-old male with a nonossifying fibroma involving the di-metaphyseal portion of the distal tibia posterolaterally. AP radiograph (**a**) shows a slightly expansile, well-circumscribed sclerotic lesion. The lesion has circumscribed margins with low signal on MRI. Centrally the lesion has mixed low and intermediate signal on axial (**b**) T1WI, and mixed low, intermediate, and high signal on axial (**c**) FST2WI. The lesion shows heterogeneous Gd-contrast enhancement on axial (d) FS T1WI.

a, b

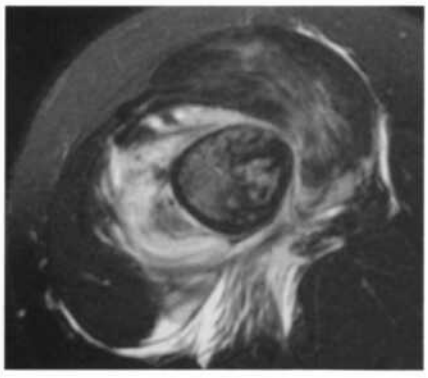

c

d

Figure 130a-d A 4-year-old male with a pathologic fracture associated with a fibroxanthoma / nonossifying fibroma involving the posterior di-metaphyseal portion of the distal femur. AP radiograph (**a**) shows a pathologic fracture involving a well-circumscribed, radiolucent, expansile lesion involving medullary bone with lobulated thin sclerotic margins. Centrally, the lesion has low, intermediate, and high signal on sagittal (**b**) and axial (**c**) FS T2WI. The lesion shows heterogeneous Gd-contrast enhancement on sagittal (**d**) FST1WI. Zones of high signal on FST2WI and Gd-contrast enhancement on FST1WI are seen in the adjacent soft tissues secondary to the fracture.

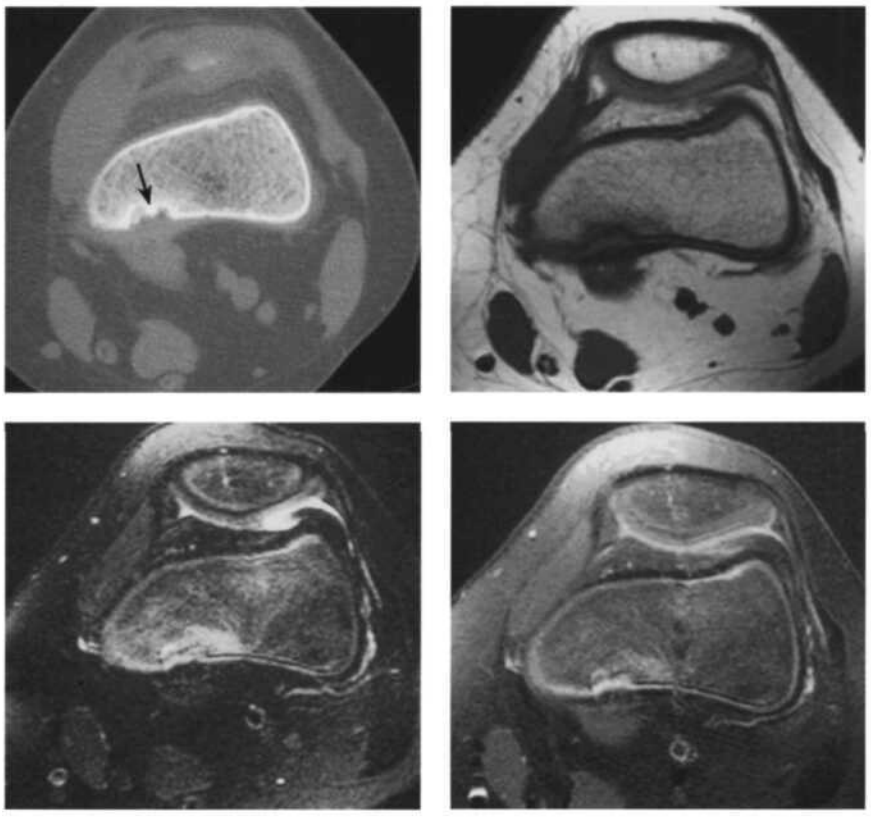

Figure **131 a-d** Cortical desmoid at the posterior distal medial femur. Axial CT (**a**) shows an erosion of bone cortex with a base of sclerotic bone oriented convex toward the medullary cavity. Soft tissue attenuation is seen superficial to the zone of remodeled cortex. The lesion has low to intermediate signal on axial T1WI (**b**) and heterogeneous high signal on FST2WI (**c**). A thin border of low signal on T1WI and T2WI is seen at the inner margin of the lesion, which corresponds to a thin zone of sclerosis seen on CT. Bone marrow deep and peripheral to the lesion has slightly high signal on FST2WI. **b** After Gd-contrast administration, enhancement is seen at the lesion on axial FS T1WI (**d**).

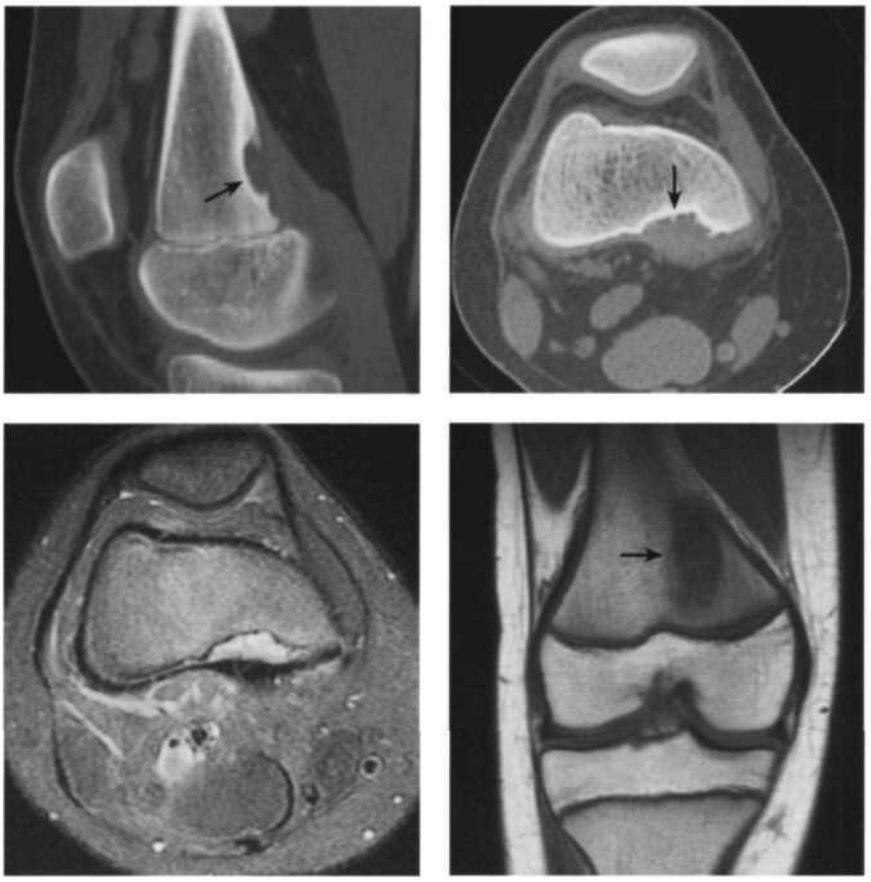

Figure **132 a-d** Cortical desmoid at the posterior distal medial femur in a 10-year-old female. Sagittal (**a**) and axial (**b**) CT images show an erosion of bone cortex with a base of sclerotic bone oriented convex toward the medullary cavity. Soft tissue attenuation is seen superficial to the zone of remodeled cortex. The lesion has high signal on axial (**c**) FS PDWI; and low to intermediate signal on coronal (**d**) T1WI. A thin border of low signal on T1 WI and T2WI is seen at the inner margin of the lesion, which corresponds to a thin zone of sclerosis seen on CT.

Figure 133 A 13-year-old female with a cortical desmoid at the posterior distal medial femur. Lateral radiograph (**a**) shows a small zone of periosteal reaction. The lesion has low to intermediate signal on sagittal T1WI (**b**), and heterogeneous high signal on sagittal (**c**) and axial (**d**) FS T2WI. A small zone of high signal on FST2WI is also seen at the site of periosteal reaction.

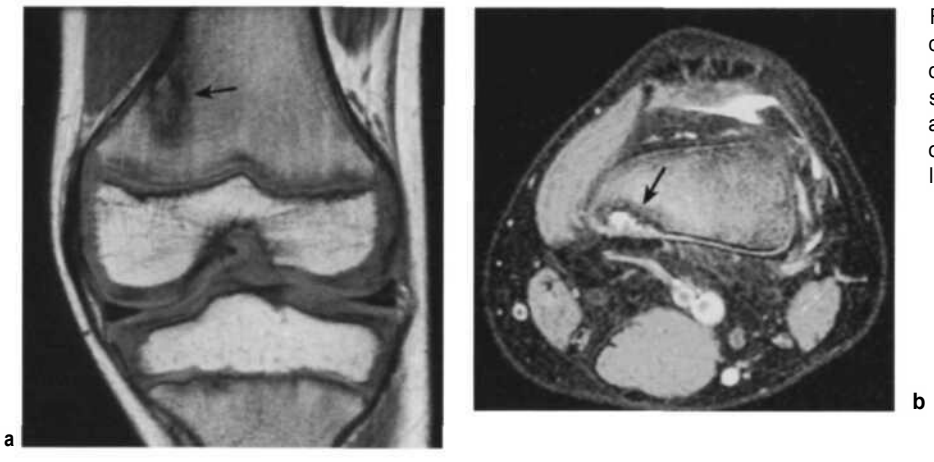

Figure **134a, b** An 8-year-old male with a cortical desmoid at the posterior distal medial femur. The lesion has low to intermediate signal on coronal (**a**) PDWI; and high signal on axial (**b**) FST2WI. A thin border of low signal on FS T2WI is seen at the inner margin of the lesion (**b**).

References

1 Araki Y, Tanaka H, Yamamoto H, et al. MRI of fibrous cortical defect of the femur. *Radiat Med* 1994;12(3):93-98.

2 Biermann JS. Common benign lesions of bone in children and adolescents.; *Pediatr Orthop* 2002;22:268-273.

3 Forest M. Fibrous cortical defect and non-ossifying fibroma. In: Forest M, Tomeno B, Vanel D, eds. *Orthopedic Surgical Pathology: Diagnosis of Tumors and Pseudotumoral Lesions of Bone and Joints* Edinburgh: Churchill Livingstone: 1998:293-301.

4 Hudson TM, Stiles RG, Monson DK. Fibrous lesions of bone. Radio/ *Clin North Am* 1993;31:279-297.

5 Huvos AG. Nonossifying fibroma, benign fibrous histiocytoma, and xanthoma of bone. In: Huvos AG, ed. *Bone Tumors: Diagnosis, Treatment, and Prognosis* 2nd ed. Philadelphia, Pa: W.B. Saunders: 1991: 481-495.

6 Jee WH, Choe BY, Kang HS, et al. Nonossifying fibroma: characteristics at MR imaging with pathologic correlation. *Radiology* 1998; 209:197-202.

7 Kilpatrick SE, Unni KK. Spindle cell lesions of bone. In: Helliwell TR, ed. *Major Problems in Pathology: Pathology of Bone and Joint Neoplasms* 1st ed. Philadelphia, Pa: W.B. Saunders; 1999:237-255.

8 Kyriakos M. Benign fibrous histicytoma of bone. In: Fletcher COM, Unni KK, Mertens F, eds. *World Health Organization Classification of Tumours. Pathology and Genetics of Tumours of Soft Tissue and Bone* Geneva: IARC Press; 2002:292-293.

9 Mulder JD, Schutte HE, Kroon HM, Taconis WK. Introduction. In: *Radiologic Atlas of Bone Tumors* Amsterdam: Elsevier; 1993:3-6.

10 Mulder JD, Schutte HE, Kroon HM, Taconis WK. The diagnosis of bone tumors. In: *Radiologic Atlas of Bone Tumors* Amsterdam: Elsevier; 1993:9-46.

11 Mulder JD, Schutte HE, Kroon HM, Taconis WK. Fibrous cortical defect and non-ossifying fibroma. In: *Radiologic Atlas of Bone Tumors* Amsterdam: Elsevier; 1993:627-638.

12 Suh JS, Cho JH, Shin KH, et al. MR appearance of distal femoral cortical irregularity (cortical desmoid). *J Comput Assist Tomogr* 1996; 20(2): 328-332.

13 Unni KK. Introduction and scope of study. In: *Dahlin's Bone Tumors-General Aspects and Data on 11087 Cases* 5th ed. Philadelphia, Pa: Lippincott, Williams & Wilkins; 1996:1-9.

14 Unni KK. Conditions that commonly simulate primary neoplasms of bone. In: *Dahlin's Bone Tumors—General Aspects and Data in 11087 Cases* 5th ed. Philadelphia, Pa: Lippincott, Williams & Wilkins; 1996: 355-432.

A 27 Fibrous Dysplasia (Also Referred to as Fibro- osseous Dysplasia, Fibrocartilaginous Dysplasia, and Lichtenstein-Jaffe Disease)

Definition

Fibrous dysplasia is a benign, medullary fibro-osseous lesion of bone.[1,3-9,11,20,22-24] Fibrous dysplasia is most often sporadic, involving a single site and referred to as **mono-ostotic** (80-85%), or in multiple locations as **polyostotic fibrous** dysplasia[3-5,7,9,15,20] Fibrous dysplasia is thought to occur from developmental failure in the normal process of remodeling primitive bone to mature lamellar bone, with resultant zone or zones of immature trabeculae within dysplastic fibrous tissue.[4] These lesions do not mineralize normally which results in loss of mechanical strength, predisposing to deformity and pathologic fracture[4]

McCune-Albright syndrome accounts for 3 % of polyostotic fibrous dysplasia and may include the presence of pigmented cutaneous macules (sometimes referred to as café-au-lait spots) with irregular indented borders which are ipsilateral to bone lesions, precocious puberty, and/or other endocrine disorders such as acromegaly, hyperthyroidism, hyperparathyroidism, and Gushing syndrome.[2,4,5,7,9,13,22]

Leontiasis ossea is a rare form of polyostotic fibrous dyplasia that involves the craniofacial bones, resulting in facial enlargement and deformity.[5]

Cherubism is an autosomal dominant disorder in which there is benign fibro-osseous enlargement of gnathic bony structures, primarily the mandible and maxilla.[5,9,13] Cherubism has been reported to represent a variant of fibrous dysplasia or occur as a variant of giant cell granuloma.[5] Fibrous dysplasia may also be associated with basal cell nevus syndrome, intramuscular myxoma, and sickle cell disease.[9]

Mazabraud syndrome is a rare disorder in which polyostotic fibrous dysplasia is associated with intramuscular myxomas. [3,4,9,10,14,22]

Frequency of Occurrence

Fibrous dysplasia is one of the most common nontumor and nontraumatic primary lesions involving bone. Fibrous dysplasia represents ~10% of benign bone lesions.[18-20] Mono-ostotic fibrous dysplasia is six times more common than the polyostotic type.[13,22] McCune-Albright syndrome occurs in ~3 % of polyostotic fibrous dysplasias.[2] Mazabraud syndrome is rare.[10,14]

Age at Presentation

Fibrous dysplasia has been reported in patients ranging in age from less than 1 year to 76 years,[18-20] and 75 % of cases occur before the age of 30 years.[7,13] Median age for mono-ostotic fibrous dysplasia has been reported to be 21 years[20]; mean and median ages for polyostotic fibrous dysplasia have been reported to be 8 years and 17 years, respectively.[9,13,20] Most cases are diagnosed in patients between the ages of 3 and 20 years.[3] Lesions involving the ribs can occur in older adults.[24]

Gender Ratio (M / F)

Mono-ostotic fibrous dysplasia: 1/1.[3,9,13,20,22]

Polyostotic fibrous dysplasia: 1/1.[3,9,13,20,22]

McCune-Albright syndrome: < 1 / 1.[3]

Location

Mono-ostotic fibrous dysplasia. The three most common locations are the craniofacial bones, proximal femur, and ribs; these are followed by the tibia > pelvis > humerus > radius, ulna, vertebrae > other bones.[3,7,9,13,20] In long bones, lesions are typically intramedullary.[3,7,9,11,13,20] Up to 86% of lesions from fibrous dysplasia occur in diaphyseal and metadiaphyseal locations of long bones.[20] After growth plate closure, fibrous dysplasia can extend from the diaphysis to the end of long bones.[8,13] Prior to growth plate closure, fibrous dysplasia rarely occurs in the epiphyseal region.[8,13] Lesions in the skull are often unilateral, and are often located in the frontal, sphenoid, maxillary, ethmoid, and temporal bones.[5,8,13]

Polyostotic fibrous dysplasia. The number of sites of involvement ranges from two bones to more than 75 % of the skeleton.[5,13] Lesions tend to be larger than mono-ostotic lesions and have higher rates of fractures and deformities.[5] Approximately 50 % of patients with polyostotic fibrous dysplasia have lesions involving the skull and facial bones.[1] Up to 63 % of patients with polyostotic fibrous dysplasia have lesions in the spine,[15] where the lesions occur most frequently in the lumbar and thoracic vertebrae, and infrequently in cervical vertebrae and sacrum.[15] Lesions in the spine can involve the vertebral bodies and posterior elements.[12]

Mazabraud syndrome. Intramuscular myxomas are often located in muscles near sites of fibrous dysplasia.[5] Myxomas in Mazabraud syndrome are often located in the thigh, and can be multiple.[10]

Signs and Symptoms

Fibrous dysplasia is often asymptomatic, although may be associated with bone deformities (varus or "shepherd's crook" deformity involving the proximal femur), discrepant leg lengths, tibial bowing, craniofacial deformities, and scoliosis.[3,4,7,9,13,15,20] When present, symptoms associated with fibrous dysplasia include pain, swelling, and tenderness.[3-5,7,9,13,20] In female patients, pain may increase during pregnancy or different phases of the menstrual cycle, secondary to the presence of estrogen receptors in fibrous dysplasia.[4] Fibrous dysplasia in the spine can result in scoliosis.[4] Fibrous dysplasia often results in expansion and weakening of bone.[15] Pathologic fractures occur in 17% of patients with mono-ostotic fibrous dysplasia.[20] Pathologic fractures are more frequent in the polyostotic type relative to the mono-ostotic type of fibrous dysplasia.[4,13] Cafe-au-lait spots (brown or yellow nonelevated zones of cutaneous pigmentation) can be seen in up to 50% of patients with polyostotic fibrous dysplasia.[3,7,9,13] Mono-ostotic lesions typically mature after cessation of skeletal growth.[4]

McCune-Albright syndrome refers to an uncommon disorder in which polyostotic fibrous dysplasia is associated with pigmented cutaneous macules (sometimes referred to as café-au-lait spots) with irregular indented borders, precocious puberty, and/or other endocrine disorders such as acromegaly, hyperthyroidism, hyperparathyroidism, and/or Cushing syndrome.[2-4,7,9,13,15,22] The complete clinical triad of polyostotic fibrous dysplasia, café-au-lait spots, and precocious puberty associated with McCune-Albright syndrome is uncommon and occurs in 3% of patients with polyostotic fibrous dysplasia.[7,13] Lesions involving the craniofacial bones may be associated with cranial neuropathies from neuroforaminal narrowing, facial deformities, sinonasal drainage disorders, and sinusitis.[1,12] Lesions in the spine are often associated with scoliosis.[14] Malignant degeneration of fibrous dysplasia is usually associated with pain and swelling.[5,7,9,13,20,24]

Cross Pathologic Findings

Lesions replace and expand normal bone and are usually well-defined, firm with gritty texture, yellowish, and/or gray-white.[3,4,7,9,13,20,22,24] Cystic and/or hemorrhagic zones may be present.[3,7,9,20,22,24] Lesions may contain blue-tinged, translucent zones of cartilage.[22]

Histopathologic Findings[4-8,11-13,15,20,22,24]

Multiple fibroblastic spindle cells are seen in a dense collagenous matrix-stroma. The spindle cells have no cytologic atypia and mitotic figures are very uncommon. Thin wavy spicules or trabeculae of woven nonlamellar bone are usually seen without osteoblastic rimming. The bony spicules have irregular sizes and shapes, as well as varying density and degrees of mineralization. Mineralization of the bony trabeculae results in "ground glass" appearance on radiographs. Clusters of giant cells are often seen in the lesions. Myxoid changes may also be seen in fibrous dysplasia.

Lesion Genetics

Somatic mutations involving the GNAS1 gene located on chromosome band 20ql3.2-13.3 have been associated with mono-ostotic and polyostotic fibrous dysplasia, including the McCune-Albright syndrome.[2,4,20] The GNAS1 gene (guanine nucleotide binding protein, alpha-stimulating activity polypeptide 1) encodes a stimulating protein component of the heterotrimeric G-protein complexes.[2] These G-proteins interact with adenylyl cyclase to result in formation of cyclic AMP from ATP.[2] The abnormal G-proteins associated with GNAS 1 mutations result in abnormal increased binding to adenylyl cyclase causing abnormal elevated cyclic AMP activity.[2] Abnormally elevated cyclic AMP activity has been proposed to cause the pathologic changes associated with mono-ostotic and polyostotic fibrous dysplasia, including the McCune-Albright syndrome.[2]

Findings on Plain Films (Roentgenograms) and Computed Tomography[1-13,15-17,20-24]

Lesions are well circumscribed and are usually eccentric in the medullary space of long bones[13] (Figs. **137, 138, 139).** Those lesions involving the skull are often associated with bone expansion[1] (Figs. **135,136,140).** Lesions have variable density and

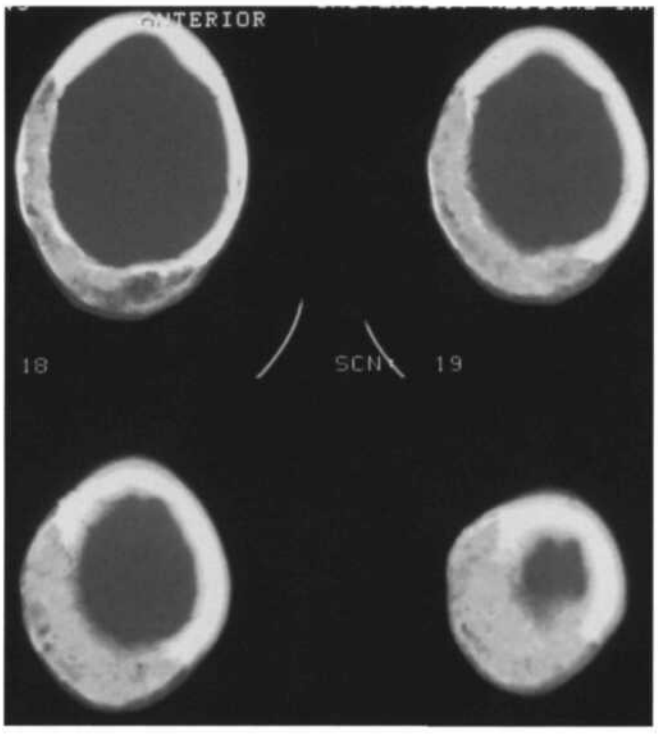

a

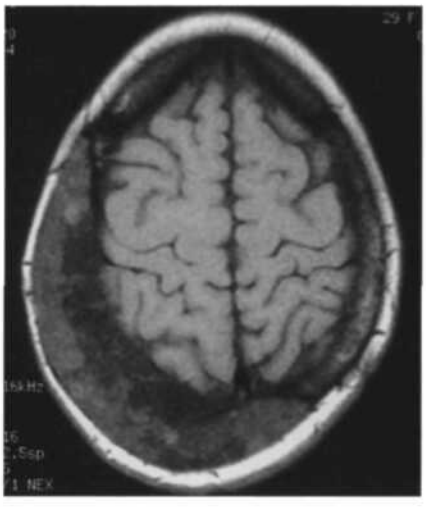

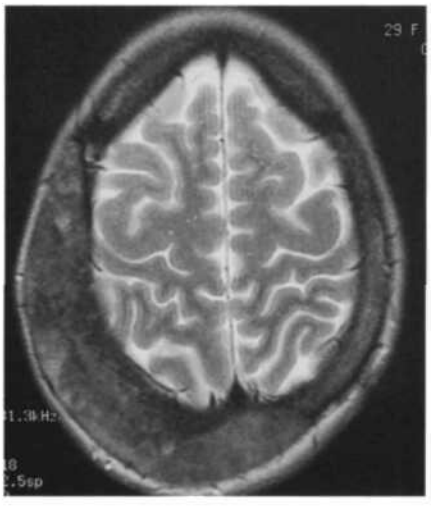

b, c

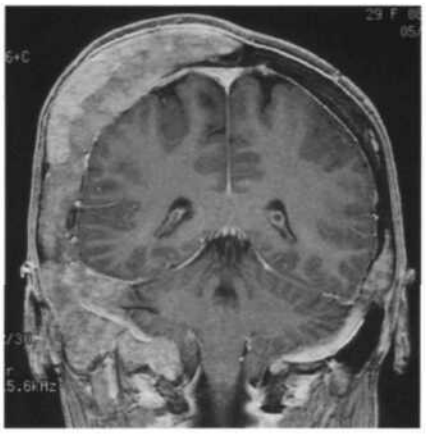

d

Figure **135a-d** A 29-year-old woman with fibrous dysplasia expanding the right and posterior portions of the calvarium. The lesion has mixed high and intermediate attenuation on axial CT (**a**), as well as zones with a "ground glass" appearance. The lesion has mixed low and intermediate signal on axial T1WI (**b**) and axial T2WI (**c**). The lesion shows prominent heterogeneous Gd-contrast enhancement on coronal T1WI (**d**).

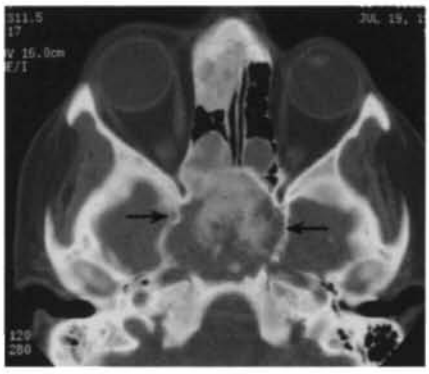

a, b

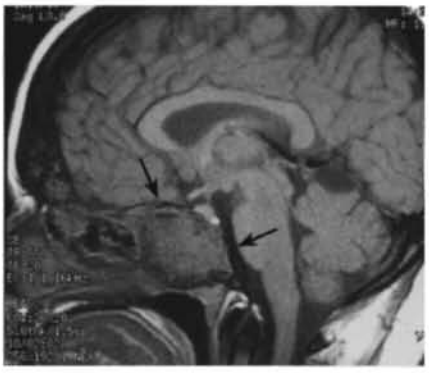

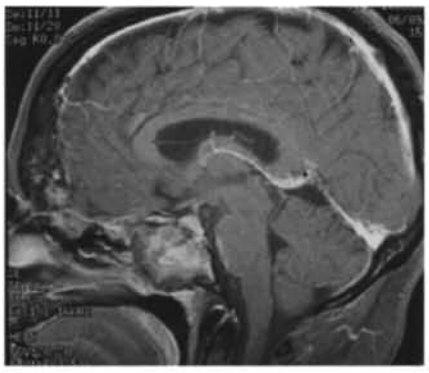

c

Figure **136a-d** A 31-year-old woman with fibrous dysplasia involving the sphenoid bone. Axial CT image (**a**) shows bone expansion which has a "ground glass" appearance. The lesion has mixed low and intermediate signal on sagittal T1WI (**b**), and mixed low, intermediate, and high signal on axial T2WI (**d**). The lesion shows prominent heterogeneous Gd-contrast enhancement on sagittal FS T1WI (**c**).

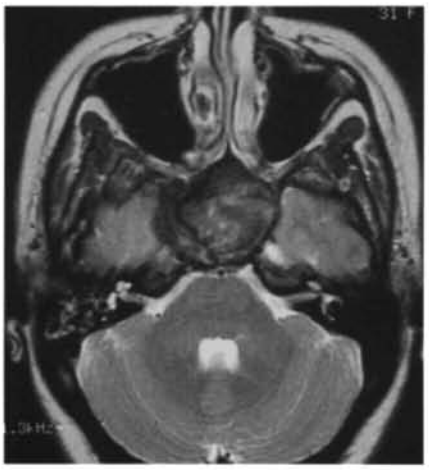

d

a

b

Figure **137a-c** A 10-year-old male with fibrous dysplasia involving the proximal right femur. AP radiograph (**a**) shows a well-defined zone of increased density with a "ground glass" appearance in medullary bone. The lesion has mixed low and intermediate signal on coronal (**b**) T1WI. The lesion has heterogeneous mostly high signal on coronal *(c)* FS T2WI. A zone of low signal is seen at the medullary borders of the lesion.

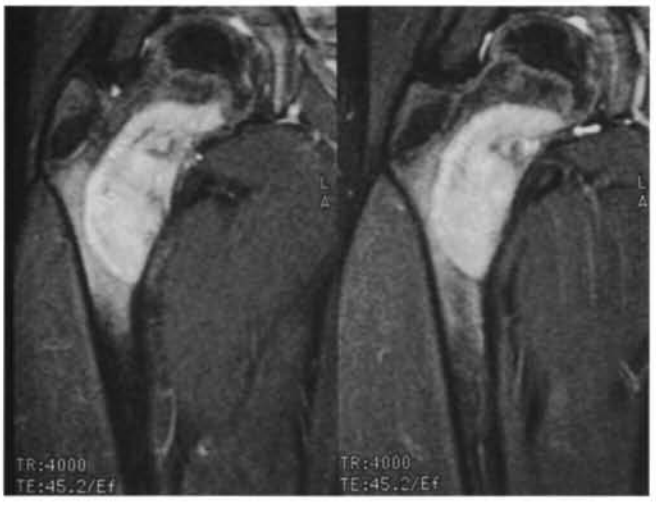

c

attenuation on radiographs and CT, respectively, depending on the degree of mineralization and number of the bony spicules in the lesions. Attenuation coefficients can range from 70 to 400 Hounsfield units.[8] Lesions can have a "ground glass" radiographic appearance secondary to the mineralized spicules of immature woven bone in fibrous dysplasia. Sclerotic borders of varying thickness can be seen surrounding parts or all of the lesions. Endosteal scalloping is commonly seen, with or without bone expansion and thinning of the cortex.

Fibrous dysplasia involving the proximal femur can be associated with a prominent varus deformity, referred to as a "shepherd's crook deformity," which results from altered biophysical loading on the involved bone.[13] Lesions involving the skull are usually expansile with a "ground glass" appearance (56%), although can have homogeneously dense (23%) or cystic-like patterns (21 %).' Lesions may narrow the paranasal sinuses and neuroforamina, and deform the orbits.[1,12] Findings associated with malignant degeneration of fibrous dysplasia include the presence of a soft tissue mass associated with bone destruction.[12]

Findings on Radionuclide Bone Scans

Fibrous dysplasia is typically associated with mild to prominent radiopharmaceutical uptake.[4,5,7,8,13,15,23]

MRI Findings[1,4-6,8,10-13,15-17,20,21,23]

The MRI features of fibrous dysplasia depend on the proportions of bony spicules, collagen, fibroblastic spindle cells, hemorrhagic and/or cystic changes, and associated pathologic fracture if present. Lesions are usually well circumscribed, and have low or low-intermediate signal on T1WI and PDWI (Figs. **135-141).** On T2WI, lesions have variable mixtures of low, intermediate, and/or high signal, often surrounded by a low signal rim of variable thickness. Internal septations and cystic changes are seen in a minority of lesions. Bone expansion is commonly seen.

After Gd-contrast administration, all or portions of the lesions can show contrast enhancement that varies from mild to marked in degree.[1,5,11,21,23] Lesions can show enhancement in a

Figure **138a-d** A 27-year-old woman with fibrous dysplasia involving the proximal femur. AP radiograph (**a**) shows a well-defined expansile lesion with zones of radiolucency and "ground glass" density. The lesion has mixed low, intermediate, and high signal on coronal T1WI (**b**) and coronal FST2WI (**c**). The lesion shows prominent heterogeneous Gd-contrast enhancement on coronal FST1WI (**d**).

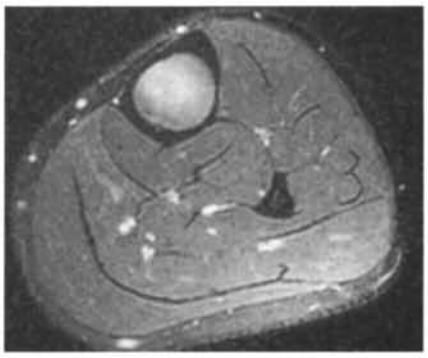

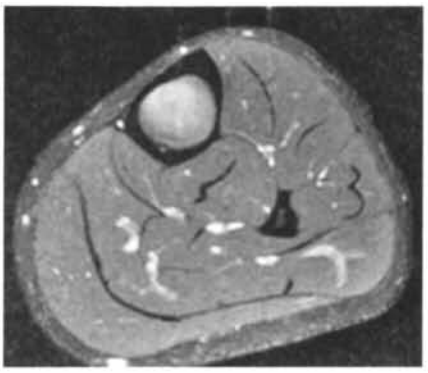

a, b

c

d

Figure **139a-d** A 19-year-old man with fibrous dysplasia involving the diaphysis of the tibia. AP radiograph (**a**) shows an expansile, well-defined lesion with a "ground glass" appearance in medullary bone. The lesion has mixed low and intermediate signal on sagittal (**b**) T1WI, and has heterogeneous slightly high signal on axial (**c**) FST2WI. The lesion shows Gd-contrast enhancement on axial (**d**) FST1WI.

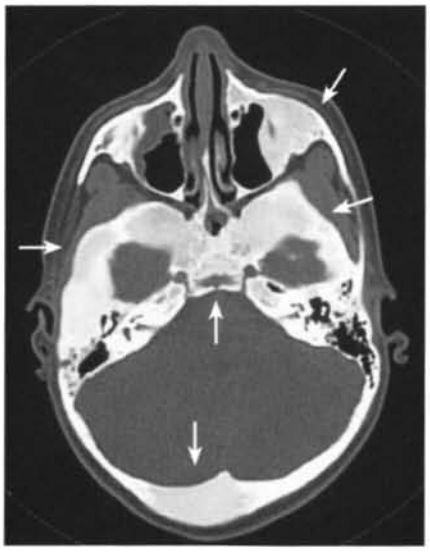

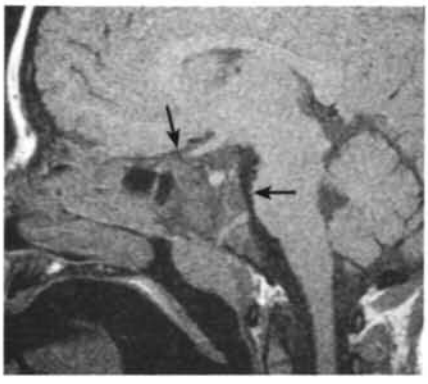

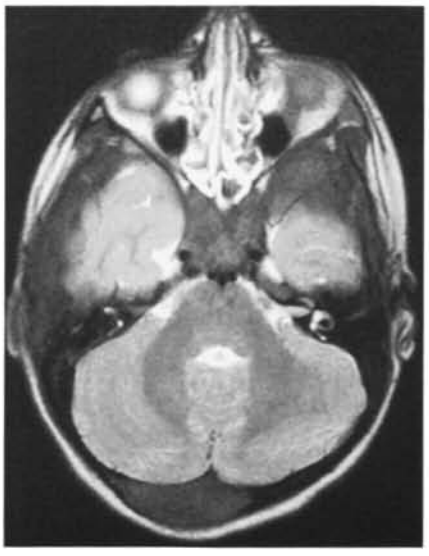

a, b

c

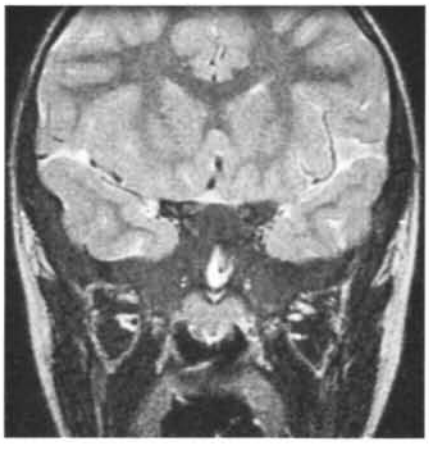

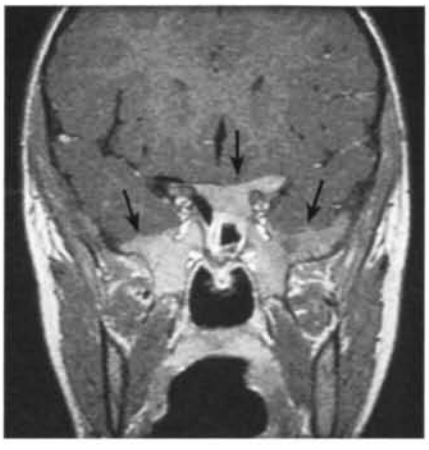

d

e

Figure **140a-e** A 5-year-old female with McCune Albright syndrome and polyostotic fibrous dysplasia involving the calvarium and skull base. Axial (**a**) CT image shows lesions with bone expansion and "ground glass" attenuation in the left maxilla, sphenoid, temporal, and occipital bones. The lesions have mixed low and intermediate signal on sagittal (**b**)T1WI, and on axial (**c**)and coronal (**d**) T2WI. The lesions show heterogeneous Gd-contrast enhancement on coronal (**e**) FST1WI.

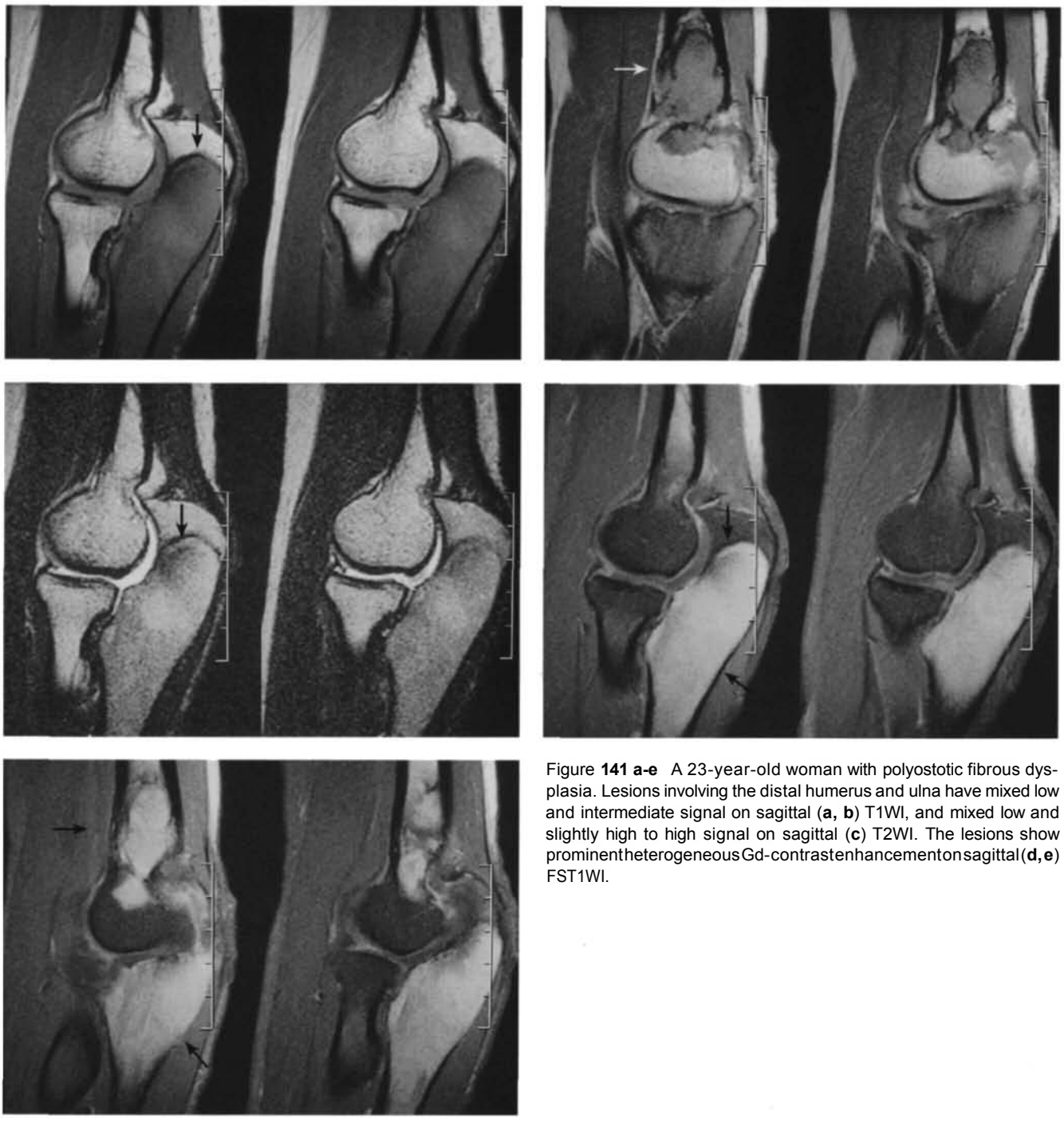

Figure **141 a-e** A 23-year-old woman with polyostotic fibrous dysplasia. Lesions involving the distal humerus and ulna have mixed low and intermediate signal on sagittal (**a, b**) T1WI, and mixed low and slightly high to high signal on sagittal (**c**) T2WI. The lesions show prominent heterogeneous Gd-contrast enhancement on sagittal (**d, e**) FST1WI.

heterogeneous, diffuse, or peripheral pattern.[1,5,11,21,23] A central enhancement pattern has been reported in 73 % of cases, and a peripheral rim pattern of enhancement in 27 %.[11] Periosteal and juxtacortical enhancement can be seen in lesions with associated pathologic fractures.

Differential Diagnosis

Bone cyst, metastatic lesion, eosinophilic granuloma, enchondroma, nonossifying fibroma, giant cell tumor, aneurysmal bone cyst, fibroxanthoma, Paget disease, chronic osteomyelitis, low-grade osteosarcoma, hyperostosis associated with meningioma.[4,13]

Treatment and Prognosis

Lesions are usually treated conservatively.[3,4,7,9,20,24] Most lesions cease or diminish growth at puberty.[5] Fibrous dysplasia often results in expansion and weakening of bone.[15] Fractures and deformities of long bones may need corrective surgery for alignment issues.[3,5,7,9,20] Lesions involving the craniofacial bones may need surgery for problems associated with mastication and compression of nerves, as well as for cosmetic reasons.[5] Radiation is not recommended, because of the potential of initiating sarcomatous changes.[20] Malignant changes have been reported to occur from 0.4 to 4 % of both solitary and polyostotic fibrous dysplasias.[4,5,9,13,20] Malignant lesions occurring with fibrous dysplasia include: osteosarcoma (38%), fibrosarcoma (38%), chondrosarcoma (9%), malignant fibrous his-

tiocytoma, and other high-grade sarcomas.[3-5,9,13] Malignant lesions often occur in patients over 30 years old, and most frequently arise in the craniofacial region followed by the femur, tibia, and pelvis.[4] Mazabraud syndrome is associated with an increased risk (up to 8.3 %) for malignant degeneration of fibrous dysplasia to osteosarcoma.[4,5,10] Sarcomas arising within fibrous dysplasia tend have worse prognoses than the corresponding primary sarcomas.[4]

References

1 Chong VF, Khoo JB, Fan YF. Pictorial Essay—Fibrous dysplasia involving the base of the skull. *AJR AmJ Roentgenol* 2002;178:717-720.

2 Cohen MM, Siegal GP. McCune Albright syndrome. In: Fletcher CDM, Unni KK, Mertens F, eds. *World Health Organization Classification of Tumours. Pathology and Genetics of Tumours of Soft Tissue and Bone* Geneva: IARC Press; 2002:357-359.

3 Devaney K. Benign fibro-osseous lesions of bone. In: Helliwell TR, ed. *Major Problems in Pathology: Pathology of Bone and Joint Neoplasms* 1st ed. Vol.37. Philadelphia, Pa: W.B. Saunders; 1999:256-264.

4 DiCaprio MR, Enneking WF. Fibrous dysplasia: pathophysiology, evaluation and treatment. J*Bone Joint Surg Am* 2005;87:1848-1864.

5 Fitzpatrick KA, Taljanovic MS, Speer DP, et al. Imaging findings of fibrous dysplasia with histopathologic and intraoperative correlation. *AJR Am J Roentgenol* 2004;182:1389-1398.

6 Fletcher BD, Hanna SL. Pediatric musculoskeletal lesions simulating neoplasms. *Magn Reson Imaging Clin N Am* 1996;4(4):721-747.

7 Forest M. Fibrous dysplasia. In: Forest M, Tomeno B, Vanel D, eds. *Orthopedic Surgical Pathology: Diagnosis of Tumors and Pseudotumoral Lesions of Bone and Joints* Edinburgh: Churchill Livingstone; 1998:595-610.

8 Hudson TM, Stiles RG, Monson DK. Fibrous lesions of bone. *Radiol Clin North Am* 1993;31:279-297.

9 Huvos AG. Ossifying fibroma and fibrous dysplasia. In: Huvos AG, ed. *Bone Tumors: Diagnosis, Treatment, and Prognosis* 2nd ed. Philadelphia, Pa: W.B. Saunders; 1991:30-43.

10 Iwasko N, Steinbach LS, Disler D, et al. Imaging findings in Mazabraud's syndrome: seven new cases. *Skeletal Radiol* 2002;31:81-87.

11 Jee WH, Choi KH, Choe BY, ParkJM, Shinn KS. Fibrous dysplasia: MR imaging characteristics with radiopathologic correlation. *AJR Am J Roentgenol* 1996;167:1523-1527.

12 Kaushik S, Smoker WRK, Frable WJ. Malignant transformation of fibrous dysplasia into chondroblastic osteosarcoma. *Skeletal Radiol* 2002;31:103-106.

13 Kransdorf MJ, Moser RP Jr, Gilkey FW. From the Archives of the AFIP-Fibrous dysplasia. *Radiographics* 1990;10(3):519-537.

14 Kransdorf MJ, Murphey MD. Tumors of uncertain histogenesis. In: *Imaging of Soft Tissue Tumors* 2nd ed. Philadelphia, Pa: W.B. Saunders; 2006:481-510.

15 Leet Al, Magur E, Lee JS, Weintroub S, Robey PG, Collins MT. Fibrous dysplasia in the spine: prevalence of lesions and association with scoliosis.J *Bone Joint Surg Am* 2004;86(3):531-537.

16 Meyer JS, Dormans JP. Differential diagnosis of pediatric musculoskeletal masses. *Magn Reson Imaging Clin N Am* 1998;6(3):561-577.

17 Miller SL, Hoffer FA. Malignant and benign bone tumors. *Radiol Clin North Am* 2001;39(4):673-699.

18 Mulder JD, Schutte HE, Kroon HM, Taconis WK. Introduction. In: *Radiologic Atlas of Bone Tumors* Amsterdam: Elsevier; 1993:3-6.

19 MulderJD, Schutte HE, Kroon HM, Taconis WK. The diagnosis of bone tumors. In: *Radiologic Atlas of Bone Tumors* Amsterdam: Elsevier; 1993:9-46.

20 MulderJD, Schutte HE, Kroon HM, Taconis WK. Fibrous dysplasia. In: *Radiologic Atlas ofBone Tumors* Amsterdam: Elsevier; 1993:607-625.

21 Shah ZK, Peh WCG, Koh WL, Shek TWH. Magnetic resonance imaging appearances of fibrous dysplasia. *Br J Radiol* 2005;78:1104-1115.

22 Siegal G, Dal Cin P, Araujo ES. Fibrous dysplasia. In: Fletcher CDM, Unni KK, Mertens F, eds. *World Health Organization Classification of Tumours. Pathology and Genetics of Tumours of Soft Tissue and Bone* Geneva: IARC Press; 2002:341-342.

23 Sirvanci M, Karaman K, Onat L, Duran C, Ulusoy OL Monostotic fibrous dysplasia of the clivus: MR and CT findings. *Neuroradiology* 2002;44:847-850.

24 Unni KK. Conditions that commonly simulate primary neoplasms of bone. In: *Dahlin's Bone Tumors—General Aspects and Data on 11087 Cases* 5th ed. Philadelphia, Pa: Lippincott, Williams & Wilkins; 1996: 367-376.

A 28 Geode (Also Referred to as Subchondral Cyst and Osteoarthritic Cyst); Soft Tissue and Intra-osseous Ganglion (Also Referred to as Intra-osseous Ganglion, Juxta-articular Bone Cyst, and Periosteal Ganglion)

Definition

Geode. A geode or subchondral cyst is a cystic lesion located near the end of a long bone, where there are changes of degenerative osteoarthropathy.[10,14,17] These lesions can result from synovial fluid intrusion and/or bony contusion in the setting of degenerative joint disease.[10,14,17]

Intra-osseous ganglion. An intra-osseous ganglion is a cystic lesion usually located at or near the ends of long bones, and is not associated with degenerative osteoarthropathy.[1,4,11,13,14,17] These lesions can result from intra-osseous extension from a ganglion in the soft tissues; or from intra-osseous mucoid degeneration, synovial rests, or synovial intrusion.[11,14]

Periosteal ganglion. Periosteal ganglia are small cystic lesions located at the surface of long bones associated with cortical erosion.[1,2,4,11,15]

Soft tissue ganglion. Nonosseous ganglia are benign, juxta-articular, myxoid lesions that arise from degeneration of peri-articular connective tissue, prior trauma, or prior inflammation.[2,5,12,15,16] Ganglia may be derived from tendons, tendon sheaths, joint capsules, bursae, or ligaments.[5,15]

Frequency of Occurrence

Geodes are common lesions at sites of degenerative arthritis or inflammatory arthritis.

Intra-osseous ganglia are rare lesions.[11,17]

Periosteal ganglia are rare lesions.[1,3]

Soft tissue ganglia account for less than 1 % of nonmalignant soft tissue lesions.[6,7]

Age at Presentation

Geode: usually occurs in adults.

Intra-osseous ganglion: from 19 to 77 years, mean = 44 years, median = 38 years.[8,9,11]

Periosteal ganglion: mean = 47 years.[3]

Soft tissue ganglion: from 19 to 65 years, mean = 40 years.[7]

Gender Ratio (M / F)

Intra-osseous ganglion: M > F.[11]

Periosteal ganglion: 1 /1 to 10 /1.[1,3]

Soft tissue ganglion: 1.3 /1.[7]

Location

Geodes. These lesions commonly occur in weight-bearing bones at the hip, knee, and ankle.[10]

Intra-osseous ganglia. Lesions are located in the proximal or distal tibia > proximal femur > proximal fibula > talus > acetabulum > distal femur > humerus > ulna > carpal bones > phalanx > other bones,[8,9,11,17] Lesions in long bones occur in epiphyseal-metaphyseal > metaphyseal > epiphyseal locations.[8,9,11]

Periosteal ganglia. Lesions are located at the outer cortical surface:[1,3] proximal shaft of tibia > distal shaft of tibia > distal shaft of ulna > other bones.[1,3]

Soft tissue ganglia. Lesions occur in the hand and wrist > lower extremity > foot and ankle > other sites.[7]

Signs and Symptoms

Geodes. These lesions are often seen at sites of symptomatic degenerative arthropathy.

Intra-osseous ganglia. Lesions can be asymptomatic or associated with mild, localized, intermittent pain of long duration near a joint.[4,11,14]

Periosteal ganglia. Lesions can be asymptomatic or associated with localized swelling and mild tenderness.[1,3]

Soft tissue ganglia. Palpable, soft tissue lesions are often observed which are asymptomatic.[2,5,12,16] Ganglia can occasionally be associated with neural compression.

Cross Pathologic Findings

Geodes. These lesions can have central cavitation with contents of proteinaceous material surrounded by fibrous margins, or can be noncavitary, with various combinations of myxoid, fibrous, and adipose contents.[10,14,17] Geodes can occur as single or multiple lesions often ranging from 2 to 20 mm in size.[10,14]

Intra-osseous ganglia.[4,11,13,14,17] Intraosseous ganglia appear as unilocular or multilocular cystic lesions in the medullary space, ranging from < 1 cm to 7 cm in size, with most being between 1 and 2 cm. A white fibrous outer capsule is often seen with contents ranging from a yellow, thin or viscous fluid, to gelatinous material.

Periosteal ganglia.[1,3] These appear as cystic lesions along the outer cortical surface of long bones, ranging from < 1 cm to 4 cm in size. A white fibrous outer capsule is often seen with contents ranging from a yellow, thin or viscous fluid, to gelatinous material.

Soft tissue ganglia.[5,16] These are unilocular or multilocular cystic lesions, often seen near joint capsules or tendon sheaths. Ganglia range from < 1 cm to 5 cm in size, with most being between 1.5 and 2.5 cm. Lesions occasionally extend into muscle.

Histopathologic Findings

Geodes. These lesions usually appear as spheric zones of bone rarefaction, which are filled with degenerative fibromyxoid

material.[14,17] No epithelial lining is seen along the margins of these lesions.[14]

Intra-osseous ganglia.[4,11,13,17] Ganglia are surrounded by a layer of connective tissue. Unlike synovial cysts, ganglia are not lined with synovium. The inner margins of the connective tissue have fibroblast-like cells associated with abundant mucoid ground substance. Thick-walled cystic and myxoid zones are seen filled with gelatinous material containing mucopolysaccharides.

Periosteal ganglia.[1,3] Ganglia are surrounded by a layer of connective tissue. The inner margins of the connective tissue have fibroblast-like cells associated with abundant mucoid ground substance. Periosteal ganglia are associated with cortical bone erosion, with or without periosteal reaction.

Soft tissue ganglia.[5,16] Ganglia have an outer layer comprised of dense connective tissue. The inner margins of the connective tissue have fibroblast-like cells associated with abundant mucoid ground substance. Thick-walled cystic and myxoid zones are seen filled with gelatinous material containing mucopolysaccharides.

Findings on Plain Films (Roentgenograms) and Computed Tomography

Geodes. Lesions typically appear as round or oval zones of radiolucency with sharp, thin, sclerotic margins, and measure up to 2 cm[10,14] (Figs. **142,143).** Concomitant findings of degenerative arthropathy such as decreased joint space and bony eburnation are typically seen.[10,14]

Intra-osseous ganglia.[4,11,13,14] Lesions typically appear as round, oval, or serpiginous zones of radiolucency with sharp, thin, sclerotic margins, usually from 1 to 2 cm in size. Thinning of the endosteal cortex can be seen. Periosteal reaction may be associated with these lesions.

Periosteal ganglia.[1,3] Sharply defined, soft tissue lesions with CT attenuation similar to fluid are located adjacent to the periosteum. Variable degrees of erosion and remodeling of the outer cortex are seen associated with the soft tissue periosteal lesion (Fig. **148).** Periosteal reaction may be seen with plain films or CT.

Soft tissue ganglia.[2,5,12,16] Ganglia are often not seen with plain films, although they can sometimes be detected as small, soft tissue lesions without matrix mineralization.

Findings with Ultrasonography

Ganglion cysts often appear as homogeneous, well-defined anechoic cystic structures. Complex ganglia may have internal echoes.[12]

MRI Findings

Geodes. A geode typically has sharply defined margins and contains low signal on T1WI, low-intermediate signal on PDWI, and homogeneous high signal on T2WI (Figs. **142,143).** Poorly defined zones of Gd-contrast enhancement can be seen in the marrow adjacent to the subchondral cysts on FST1WI (Fig. **143).**

Intra-osseous ganglia.[4,11,13] An intra-osseous ganglion can have round, oval, or serpiginous configurations with sharply defined margins. These lesions typically contain low signal on T1WI, low-intermediate signal on PDWI, and high signal on T2WI (Figs. **144,145,146).** Endosteal thinning may be seen with MRI.

Periosteal ganglia.[1,3] A periosteal ganglion has sharply defined margins and contains low signal on T1WI, low-intermediate signal on PDWI, and high signal on T2WI (Fig. **148).** Outer cortical thinning and erosion with remodeling may be seen with MRI.

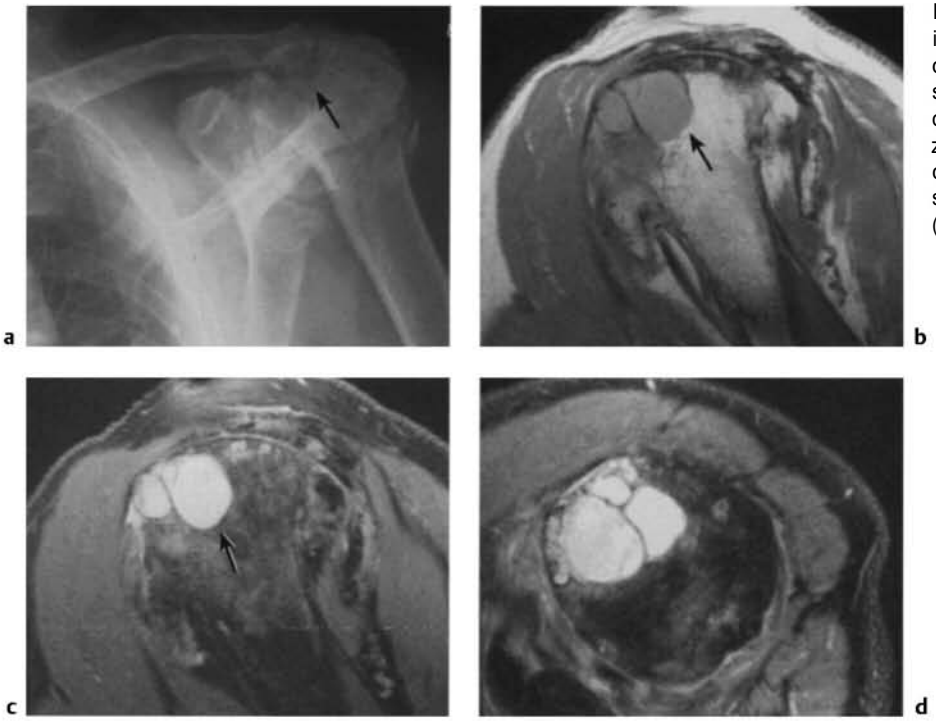

Figure **142a-d** Geode (subchondral cyst) in the proximal humerus related to severe degenerative arthropathy. AP radiograph (**a**) shows severe osteoarthritis with prominent osteophytes and subchondral radiolucent zones. MRI shows circumscribed subchondral cystic lesions with intermediate signal on sagittal PDWI (**b**) and high signal on sagittal (**c**) and axial (**d**) FST2WI.

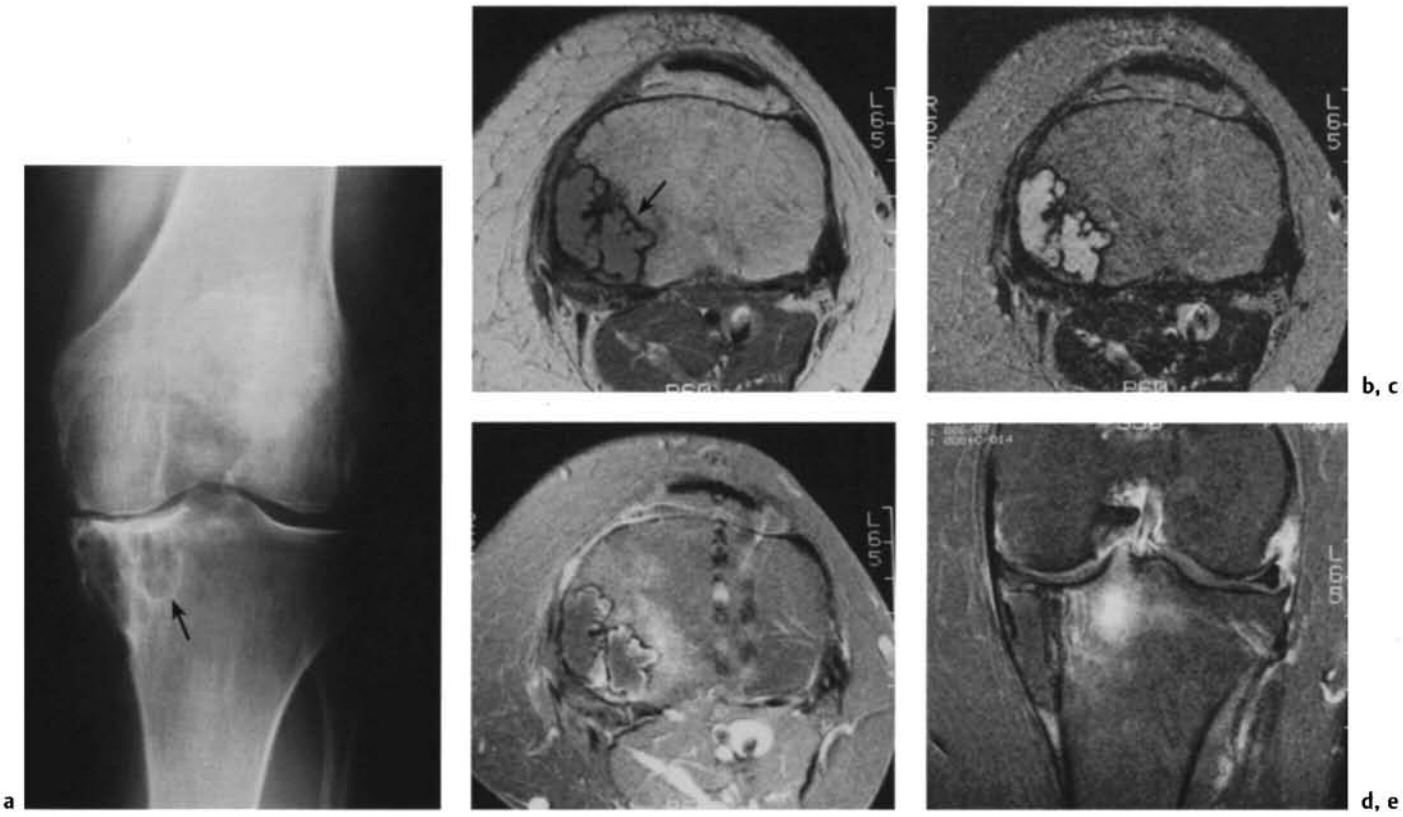

Figure **143 a-e** **G**eode in the proximal tibia of a 77-year-old woman. AP radiograph (**a**) shows prominent degenerative arthropathy at the medial knee compartment with circumscribed subchondral radiolucent zones with thin sclerotic margins. MRI shows circumscribed subchondral cystic lesions with intermediate signal on axial PDWI (**b**) and high signal on axial T2WI (**c**) with thin margins of low signal. Small, poorly defined zones of Gd-contrast enhancement are seen in the marrow adjacent to the subchondral cysts on axial (**d**) and coronal (**e**) FST1WI.

Figure **144a-c** Intra-osseous ganglion in the proximal lateral tibia of a 40-year-old woman. A circumscribed, small zone with intermediate signal on coronal PDWI (**a**) and high signal on coronal FST2WI (**b**, **c**) is seen extending from the outer cortical margin into the marrow. A small extra-osseous ganglion with high signal on FST2WI is also seen in the soft tissue adjacent to the small zone of cortical disruption.

Soft tissue ganglia.[2,5,12,16] Ganglia are sharply defined lesions, usually with low signal on T1WI, low-intermediate signal on PDWI, and homogeneous high signal on T2W1 (Figs. **147,149, 150).** Some ganglia may have intermediate signal on T1WI secondary to elevated proteinaceous or fibrous content. Low signal septa on T2WI can be seen. After Gd-contrast administration, peripheral rimlike or irregular enhancement can be seen as well as lack of enhancement.

Differential Diagnosis

Geode. Bone cyst, intra-osseous ganglion, aneurysmal bone cyst, chondroblastoma, fibrous dysplasia, nonossifying fibroma, chondromyxoid fibroma.

Intra-osseous ganglion. Bone cyst, osteoarthritic cyst (geode), aneurysmal bone cyst, chondroblastoma, fibrous dysplasia, nonossifying fibroma, chondromyxoid fibroma.

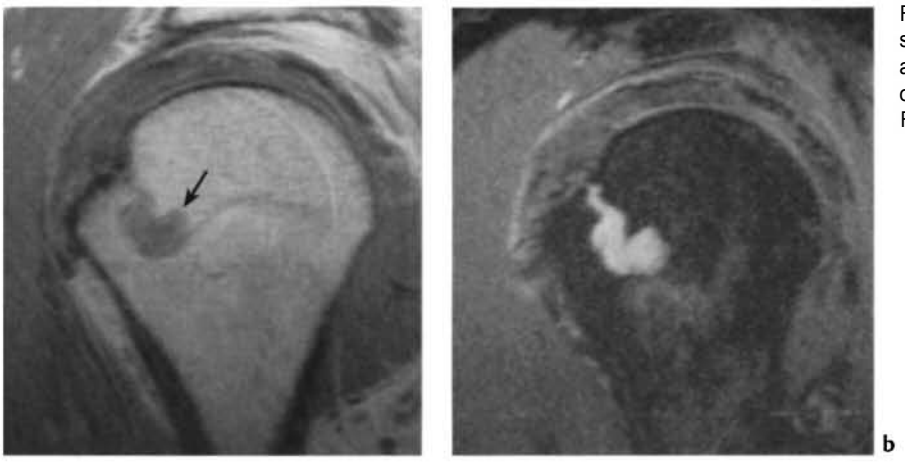

Figure **145a, b** An intra-osseous ganglion is seen in the proximal humerus which appears as a serpiginous zone with intermediate signal on sagittal PDWI (**a**) and high signal on sagittal FST2WI(**b**).

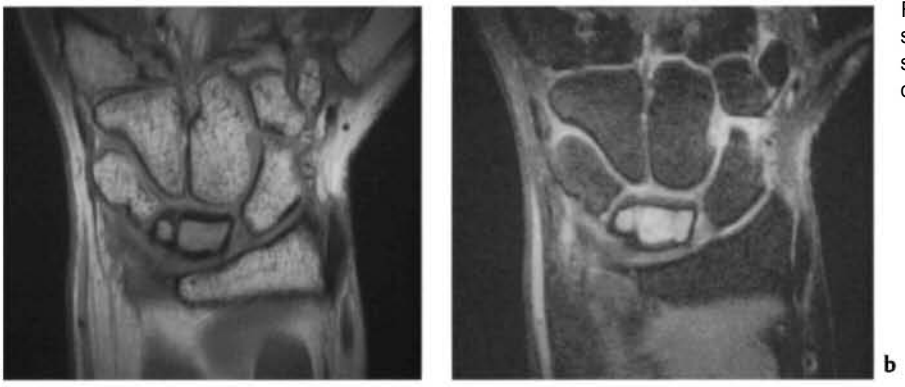

Figure **146a, b** An intra-osseous ganglion is seen in the lunate which has intermediate signal on coronal PDWI (**a**) and high signal on coronal FST2WI (**b**).

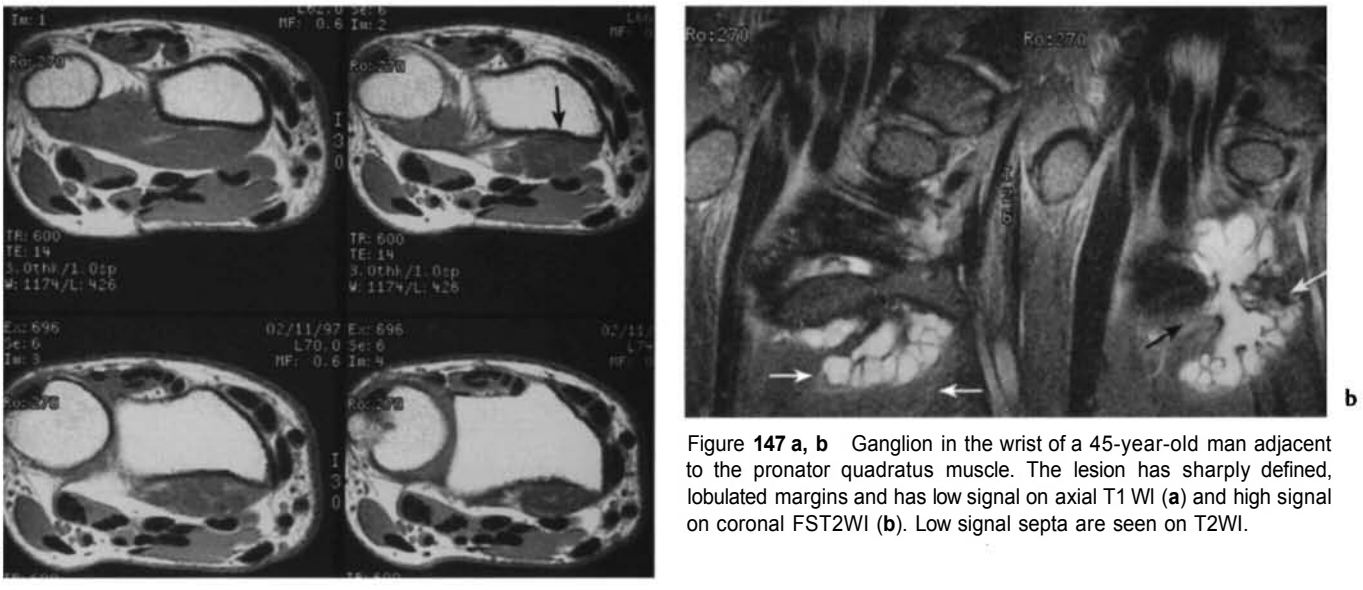

Figure **147 a, b** Ganglion in the wrist of a 45-year-old man adjacent to the pronator quadratus muscle. The lesion has sharply defined, lobulated margins and has low signal on axial T1 WI (**a**) and high signal on coronal FST2WI (**b**). Low signal septa are seen on T2WI.

Periostea! ganglion. Juxtacortical chondroma, hematoma/seroma.

Soft tissue ganglion. Myxoma, seroma, hematoma, synovial cyst, synovial sarcoma.

Treatment and Prognosis

Intra-osseous and periosteal ganglia are benign, nontumor lesions that are often asymptomatic and detected as incidental findings with medical imaging. Symptomatic lesions can be treated by surgical excision with or without bone grafting.[1,4,11]

Soft tissue ganglia are benign lesions that can be treated with surgical exploration and excision.

Figure **148 a-d** Periosteal ganglion along the posterolateral proximal tibia of a 30-year-old man. AP radiograph (**a**) shows a radiolucent lesion with thin sclerotic margins. The lesion has sharply defined margins, and has intermediate signal on coronal (**b**) and sagittal (**c**) PDWI and high signal on sagittal (**d**) FST2WI. The lesion causes erosion and concave deformity of the tibial cortex.

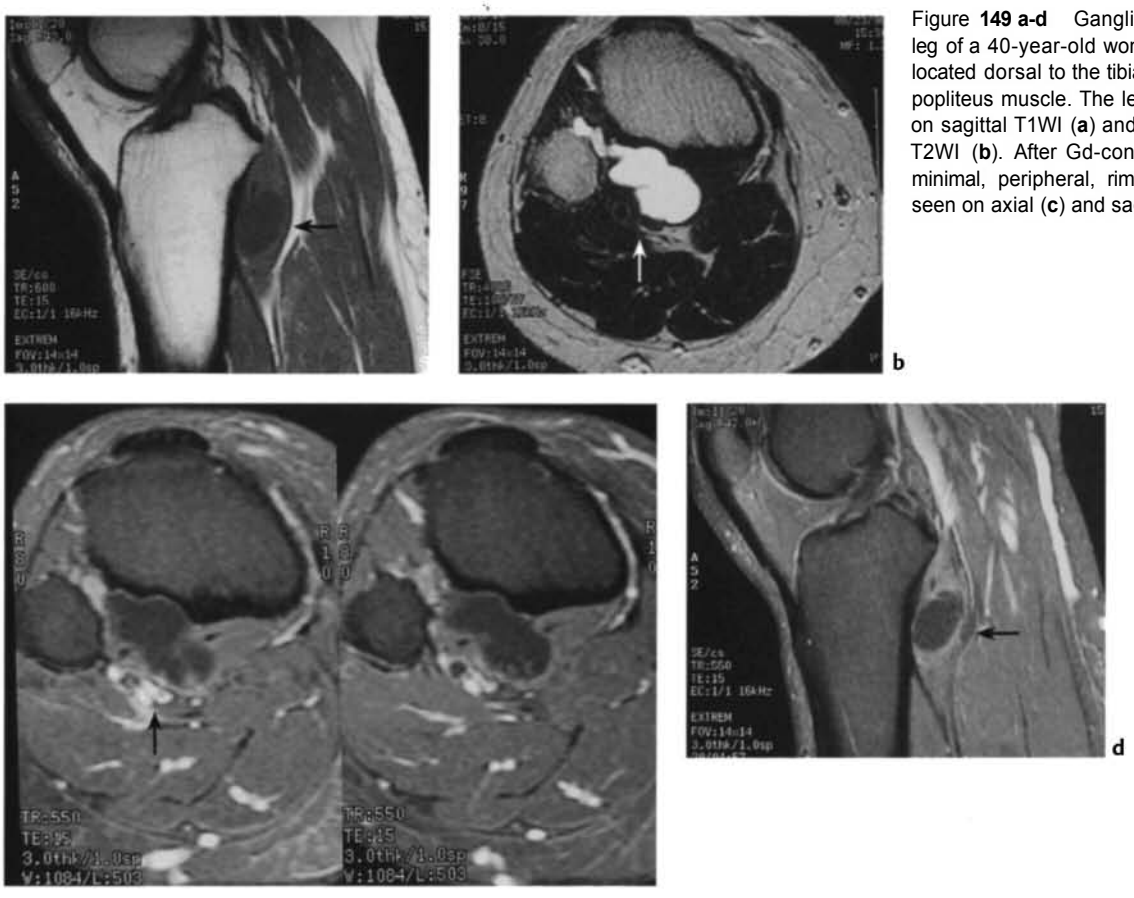

Figure **149 a-d** Ganglion in the proximal leg of a 40-year-old woman. The lesion is located dorsal to the tibia and adjacent to the popliteus muscle. The lesion has low signal on sagittal T1WI (**a**) and high signal on axial T2WI (**b**). After Gd-contrast administration, minimal, peripheral, rimlike enhancement is seen on axial (**c**) and sagittal (**d**) FST1WI.

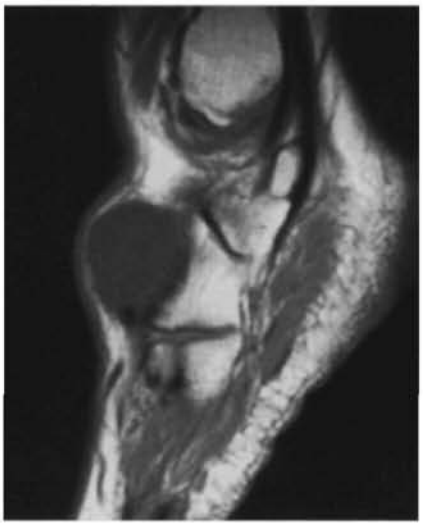

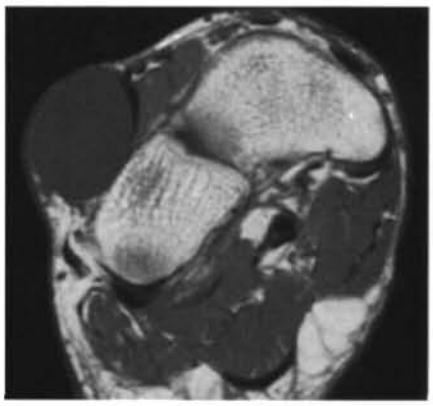

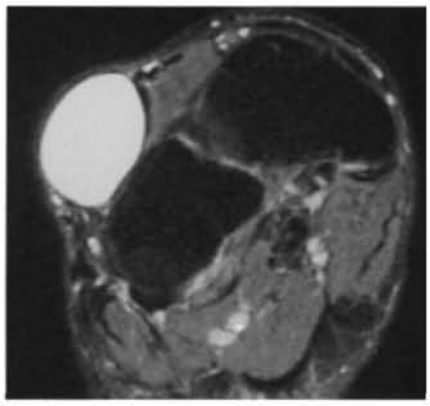

a

b, c

Figure **150a-c** Ganglion in the dorsal soft tissues of the foot. The lesion has sharply defined margins, and has low signal on sagittal (**a**) and coronal (**b**) T1 WI, and high signal on coronal (**c**) FST2WI.

References

1 Abdelwahab IF, Kenan S, Hermann G, Klein MJ, Lewis MM. Periosteal ganglia: CT and MR imaging features. *Radiology* 1993;188(1): 245-248.

2 Bisset GS. MR imaging of soft-tissue masses in children. *MRl Clin North Am* 1996:4:697-719.

3 Blanco JF, DePedro JA, Paniagua JC. Periosteal ganglion in a child. *Arch Orthop Trauma Surg* 2003:123:115-117.

4 Forest M. Ganglion and epidermoid cyst. In: Forest M, Tomeno B, Vanel D, eds. *Orthopedic Surgical Pathology: Diagnosis of Tumors and Pseudotumoral Lesions of Bone and Joints* Edinburgh: Churchill Livingstone; 1998:547-553.

5 Kransdorf MJ, Murphey MD. Synovial tumors. In: *Imaging of Soft Tissue Tumors* 2nd ed. Philadelphia, Pa: W.B. Saunders; 2006: 381-436.

6 Kransdorf MJ, Murphey MD. Soft tissue tumors in a large referral population: prevalence and distribution of diagnoses by age, sex, and location. In: *Imaging of Soft Tissue Tumors* 2nd ed. Philadelphia, Pa: W.B. Saunders; 2006:6-37.

7 Kransdorf MJ. Benign soft-tissue tumors in a large referral population: distribution of specific diagnoses by age, sex, and location. *AJR Am J Roentgenol* 1995;164:395-402.

8 Mulder JD, Schutte HE, Kroon HM, Taconis WK. Introduction. In: *Radiologic Atlas of Bone Tumors* Amsterdam: Elsevier; 1993:3-6.

9 Mulder JD, Schutte HE, Kroon HM, Taconis WK. The diagnosis of bone tumors. In Radiologic *Atlas of Bone Tumors* Amsterdam: Elsevier; 1993:9-46.

10 Mulder JD, Schutte HE, Kroon HM, Taconis WK. Osteo-arthritic cyst. In: *Radiologic Atlas of Bone Tumors* Amsterdam: Elsevier; 1993: 591-594.

11 Mulder JD, Schutte HE, Kroon HM, Taconis WK. Ganglion. In: Radio-*logic Atlas of Bone Tumors* Amsterdam: Elsevier; 1993:595-606.

12 Pham H, Fessell DP, Femino JE, Sharp S, Jacobson JA, Hayes CW. Sonography and MR imaging of selected benign masses in the ankle and foot. *AJR Am] Roentgenol* 2003;180:99-107.

13 Reid RP. Bone neoplasms and tumor-like lesions on the bone surface. In: Helliwell TR, ed. *Major Problems in Pathology: Pathology of Bone and Joint Neoplasms* 1st ed. Vol.37. Philadelphia, Pa: W.B. Saunders; 1999:215-235.

14 Resnick D. Degenerative disease of extraspinal locations. In: Resnick D, ed. *Diagnosis of Bone and Joint Disorders* 4th ed. Philadelphia, Pa: W.B. Saunders; 2002:1271-1381.

15 Resnick D. Tumors and tumor-like lesions of soft tissues. In: Resnick D, ed. Diagnosis *of Bone and Joint Disorders* 4th ed. Philadelphia, Pa: W.B. Saunders; 2002:4129-4273.

16 Sundaram M, Sharafuddin MJ. MR imaging of benign soft-tissues masses. *Magn Reson Imaging Clin N Am* 1995;3:609-627.

17 Unni KK. Conditions that commonly simulate primary neoplasms of bone. In; *Dahlin's Bone Tumors—General Aspects and Data on 11 087 Cases* 5th ed. Philadelphia, Pa: Lippincott, Williams & Wilkins; 1996:367-376.

A 29 Giant Cell Tumor of Bone

ICD-O Code

Giant cell tumor: 9250/1

Malignant giant cell tumor: 9250/3

Definition

Giant cell tumors are aggressive tumors composed of neoplastic, ovoid, mononuclear cells and scattered multinucleated osteoclastlike giant cells (derived from fusion of marrow mononuclearcells).[3,4,7,9,13,17,20,21,23,27] Giantcelltumorscanoccasionallybe seen associated with Paget disease in older patients.[5,22] Up to 10 % of all giant cell tumors are malignant.[21,28]

Frequency of Occurrence

Benign giant cell tumors account for ~ 5 to 9.5 % of all bone tumors and up to 23 % of benign bone tumors.[17-21,26,27] Malignant giant cell tumors account for 5.8 % of all giant cell tumors.[28]

Age at Presentation

From 4 to 81 years,[9,18-20,26,27] median = 30 years,[9,18-20] mean = 33 years[9]; 80% occur in patients older than 20 years[9] and 75% occur in patients between the ages of 15 and 45 years.[21] Giant cell tumors are rare in children less than 15 years old and adults older than 50 years.[9,23] Approximately 6 % of giant cell tumors occur in skeletally immature patients.[10]

Gender Ratio (M / F)

1 /1.1 to 1 /1.5 for all giant cell tumors,[9,21,23,26,27] although malignant giant cell tumors have a 3 /1 male predominance.[9,21]

Location

Tumors are located in the distal femur > proximal tibia > distal radius > sacrum > distal tibia > proximal humerus > vertebrae > iliac bone > proximal fibula > other bones.[9,20,21,2S] Up to 75 % occur at the knee involving the distal femur, proximal tibia, or proximal fibula.[9,17,20,21,28] More than 75 % of these tumors occur at the ends of long bones.[9] Giant cell tumors arise in the metaphyseal region, and grow toward the ends of long bones / epiphyseal equivalent regions.[10,21] Approximately 90 % of giant cell tumors are located withinl cm ofthe subarticular cortex.[20,21] In children, prior to closure of the physeal plate, giant cell tumors are located in the metaphyseal region.[10] In long bones, 62% are eccentric within the bone and 38 % are centrally located.[20] In vertebrae, giant cell tumors involve the vertebral body and arch in 52%, vertebral body alone in 44%, and arch in 4% of cases.[20]

Signs and Symptoms[4-7,9,13,17,20,21,23,28]

Giant cell tumors can be associated with localized pain, tenderness, and swelling. The duration of pain often ranges from weeks to months.[20] Tumors may be associated with pathologic fractures in ~ 10 % of patients.[21] A painful mass may be palpated. Joint effusion and muscle atrophy from disuse may be associated with giant cell tumors.[28]

Cross Pathologic Findings[3- 7,9,17,20,21,23,28]

Specimens of lesions can be soft/elastic and/or friable. Lesions are brown, gray-brown, or gray-red in color. Cyst-like zones and hemorrhage may be present in the lesions.

HistopathologicFindings[3-7,9,10,13,17,20,21,23,28,29]

Tumors are composed of neoplastic, ovoid, and/or spindle-shaped mononuclear stromal cells, CD 68-positive monocytes, and multinucleated osteoclastlike giant cells. The multinucleated giant cells scattered within the lesions usually have from 30 to a 100 or more nuclei. The ovoid and spindle-shaped mononuclear stromal cells contain single, round or oval nuclei and poorly defined cytoplasmic margins, and are the neoplastic component of giant cell tumors.[23,29] These neoplastic stromal cells secrete cytokines which cause migration and fusion of monocytes to form the multinucleated giant cells.[29] The stroma of giant cell tumors usually contains many thin-walled capillaries. Areas of hemorrhage are commonly seen in giant cell tumors, often surrounded by clusters of foamy histiocytes. Secondary aneurysmal bone cysts are present in 10-14% of giant cell tumors.

In conventional giant cell tumors, stromal cells have varying degrees of mitotic activity indicating active tumor growth. The mitotic activity of stromal cells does not often correlate with the frequency of metastases in giant cell tumors. Histologic features may not always predict rate of recurrence or metastases in giant cell tumors.

Giant cell tumors have been categorized into three or four grades.[7,9,20,28] **Grade I tumors** (23 %), also referred to as conventional giant cell tumors, have a large ratio of giant cells to spindle-shaped stromal cells. **Grade II tumors** (62%) have a higher ratio of stromal to giant cells, as well as moderate mitotic activity and cellular atypia. **Grades HI** (12%) and **IV** (3%) **tumors** have a high ratio of sarcomatous spindle-cell stroma to giant cells. Multiple samples of giant cell tumors should be evaluated because of the possibility of multiple tumor grades in different locations. The prognostic significance of the grading system for giant cell tumors is questionable and often unreliable.[23]

Metastatic lesions from benign giant cell tumors have also been reported.[7,9,14,28] Metastases to lung occur in ~2 to 10% of "benign" giant cell tumors.[23,27] Giant cell tumors have been reported to be occasionally co-existent in patients with Paget disease, often in atypical locations for giant cell tumors.[22]

Malignant transformation of benign giant cell tumors has been reported, with or without prior radiation treatment.[7,9,14,23,28] The three most common tumors that result from malignant transformation of giant cell tumors are fibrosarcoma, osteosarcoma, and malignant fibrous histiocytoma.[2728]

Tumor Genetics

The distal ends of chromosomes are referred to as telomeres. Giant cell tumors have been reported to have end-to-end fusion of chromosomes, which has been given the term telomeric association (tas).[2, 23] Reductions in telomere length of -500 base pairs have been reported in giant cell tumors with and without telomeric association.[2,7,23] Telomeres that have been

reported to be affected include: 11 p, 13 p, 14 p, 15 p, 19 p, 20 q, and 21 p.[7,23] Chromosomal rearrangements involving 16 q22 and 17pl3 have also been reported.[23] Two oncogenes, JUN and NME2, have been found in the neoplastic stromal cells of giant cell tumors.[29] These oncogenes may play a role in tumor formation.[29]

Findings on Plain Films (Roentgenograms) and Computed Tomography[4-14,16.17.20-23.25.27.28.30]

Giant cell tumors are radiolucent and predominantly geographic lesions with relatively narrow zones of transition (Figs. **154, 157, 159).** Wide zones of transition occur in less than 20% of giant cell tumors. Lesions are often eccentric. Margins of lesions usually lack a sclerotic margin on radiographs. Peripheral sclerosis can be occasionally seen with CT in ~20 % of cases. No matrix mineralization is seen. Trabeculated features on plain films result from uneven growth patterns of giant cell tumors and not from internal, bony septa.

Lesions are located near the ends of long bones, most often after cessation of endochondral bone growth. Zones of cortical thinning are typical. Expansion and zones of cortical destruction are seen in up to 50 % of cases. Periosteal reaction is uncommon. Pathologic fractures may be observed in ~25% of patients.

CTcan define areas of cortical destruction and extra-osseous soft tissue extension, as well as confirming the absence of subtle matrix mineralization.

Findings on Radionuclide Bone Scans[4,11,21]

Giant cell tumors usually have moderate to marked radiopharmaceutical uptake at the peripheral portions of the lesions in bone, with lesser uptake centrally.

MRI Findings[1,4,7,8,12,14–16,20–23,25,27,28,30,31]

Giant cell tumors are often well-defined lesions with thin, low-signal margins on T1WI, PDWI, and T2WI. Solid portions of giant cell tumors often have low intermediate signal on T1W1 and PDWI, intermediate to high signal on T2WI, and high signal on FSPDWI and FST2WI (Figs. **151-159).** Signal heterogeneity on T2W1 is not uncommon.

Zones of low signal on T2WI and T2* imaging may be seen secondary to hemosiderin.[1] Aneurysmal bone cysts can be seen in 14% of giant cell tumors, resulting in cystic zones with variable signal and fluid-fluid levels[21] (Fig. **156).** MRI clearly defines areas of cortical destruction and extension of extra-osseous portions of giant cell tumors.

After Gd-contrast administration, giant cell tumors show mild to prominent enhancement of the solid intra-osseous portions of the lesions, and peripheral rimlike enhancement around cystic zones / aneurysmal bone cysts.[1,14,15,21,31] Contrast enhancement is usually seen in the extra-osseous portions of the tumors.[21]

Poorly defined zones of enhancement and high signal on FST2WI may also be seen in the marrow that is peripheral to the portions of the lesions associated with radiographic evidence of bone destruction, possibly indicating reactive inflammatory and edematous changes[30] (Figs. **158,159).** These perilesional MRI findings have been shown to be correlated with an inflammatory reaction associated with elevated prostaglandin levels in tumors.[30]

Differential Diagnosis[24]

Aneurysmal bone cyst, lymphoma, nonossifying fibroma, chondrosarcoma, chondroblastoma, osteoblastoma, chondromyxoid fibroma, Ewing sarcoma, eosinophilic granuloma, osteosarcoma, fibrosarcoma, fibrous dysplasia, metastatic disease, mye-

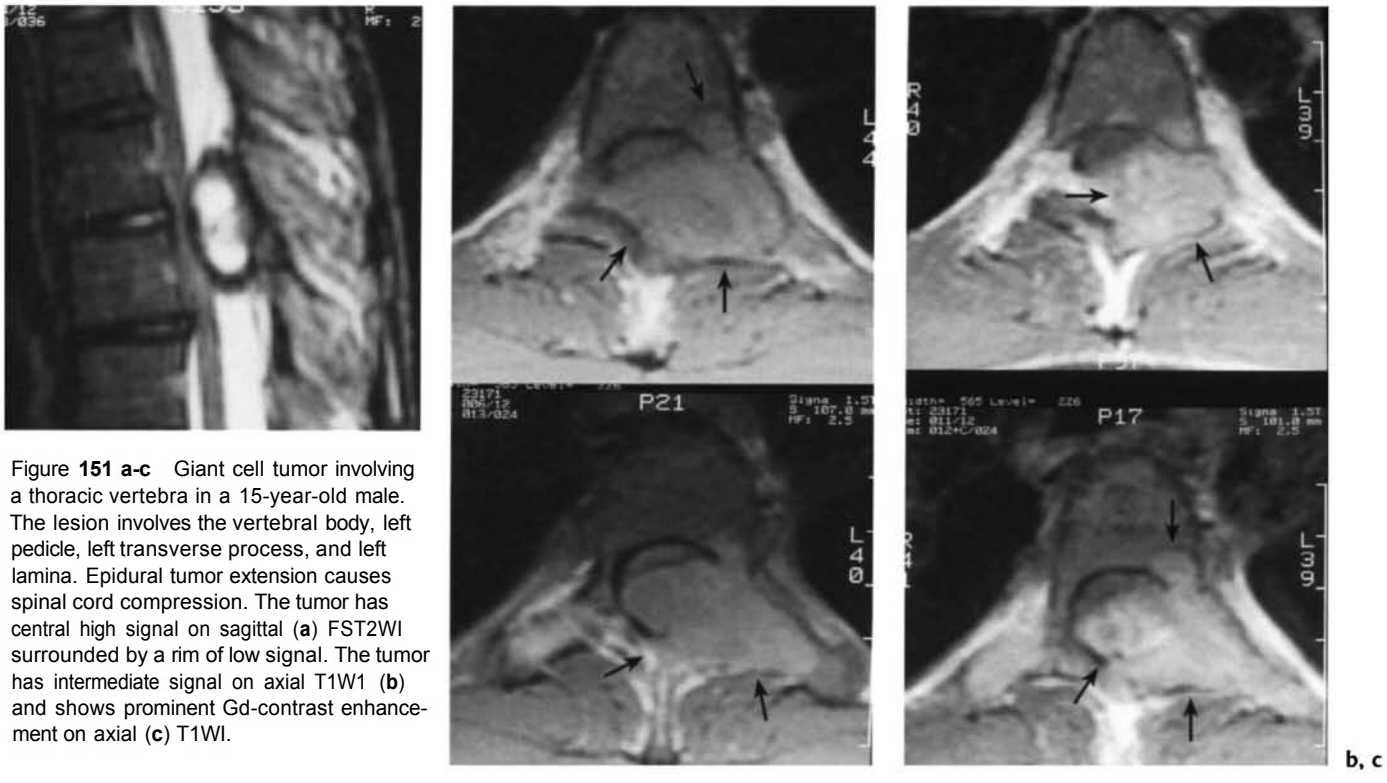

Figure **151 a-c** Giant cell tumor involving a thoracic vertebra in a 15-year-old male. The lesion involves the vertebral body, left pedicle, left transverse process, and left lamina. Epidural tumor extension causes spinal cord compression. The tumor has central high signal on sagittal (**a**) FST2WI surrounded by a rim of low signal. The tumor has intermediate signal on axial T1W1 (**b**) and shows prominent Gd-contrast enhancement on axial (**c**) T1WI.

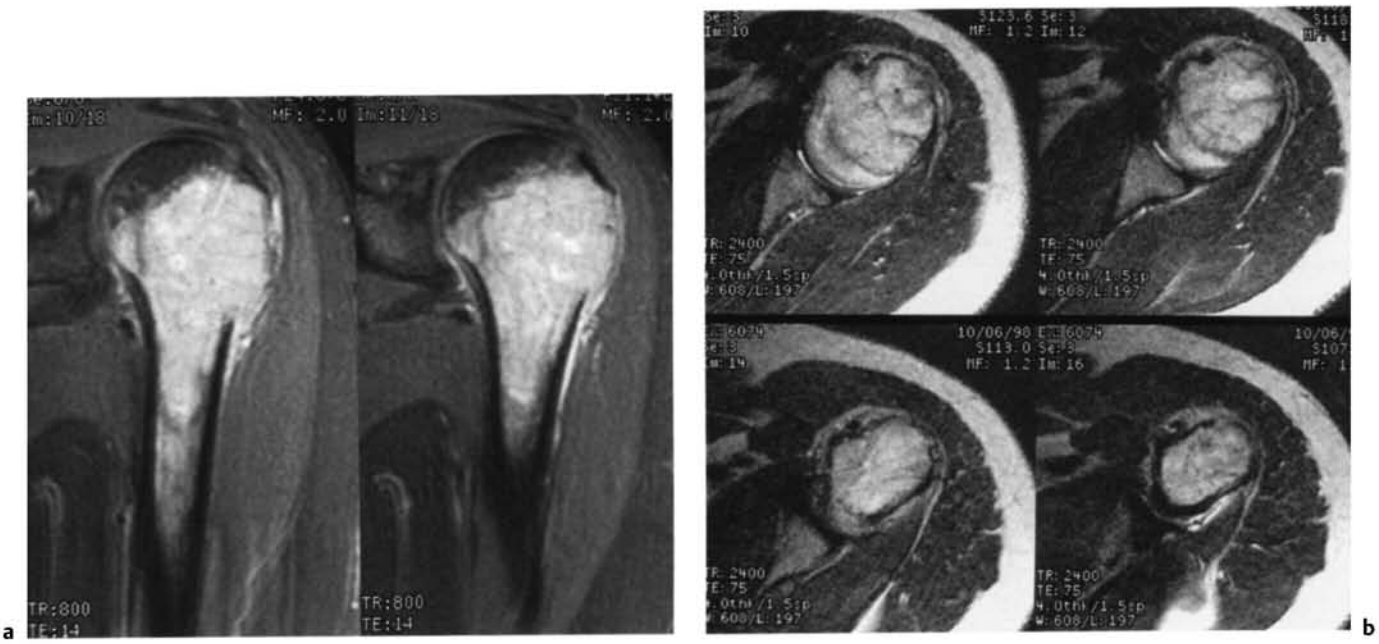

Figure **152a, b** Giant cell tumor involving the meta-diaphyseal portion of the proximal humerus in a 14-year-old female. The tumor shows prominent Gd-contrast enhancement on coronal (**a**) FST1WI; and has heterogeneous high signal on axial (**b**) T2WI. The margins of the lesion are irregular, and there is evidence of cortical disruption and extra-osseous tumor extension.

Figure **153a-d** Giant cell tumor involving the distal radius in a 26-year-old woman. The tumor has circumscribed margins, and has intermediate signal on coronal T1WI (**a**) and axial PDWI (**b**). The tumor has heterogeneous slightly high to high signal on axial T2WI (**c**). The tumor shows prominent Gd-contrast enhancement on coronal FST1WI (**d**). There is evidence of bone expansion, cortical thinning, small zones of cortical disruption, and extra-osseous tumor extension.

loma/plasmacytoma, brown tumor of hyperparathyroidism, pseudotumor of hemophilia.

Treatment and Prognosis[4,5,7,9,11,20,23,27,28,32]

Histologic grading has been shown to be unreliable in predicting which nonsarcomatous giant cell tumors will metastasize.[9,23] Giant cell tumors can be treated by extensive curettage, cryotherapy with liquid nitrogen, instillation of phenol and packing with bone graft and/or methyl methacrylate.[4,7,9,11,20,23,27] Bone curettage with instillation of 50 % aqueous zinc chloride solution followed by bone grafting has also been effective.[32] En-bloc resection with allograft or endoprosthetic replacement is often necessary for larger giant cell tumors which have prominent cortical destruction and soft tissue extension.[4,5,7,9,20,27] Local recurrence ranges from 10 to 40%, and is often associated with radiologic features of large-sized lesions, cortical destruction, and soft tissue extension.[4,7,20,23,27]

Radiation treatment is not commonly used for giant cell tumors of long bones because of the risk of malignant degeneration into sarcoma.[4,5,7,20,23,27] Radiation treatment and embolization may be necessary for local control of partially resected

a

b, c

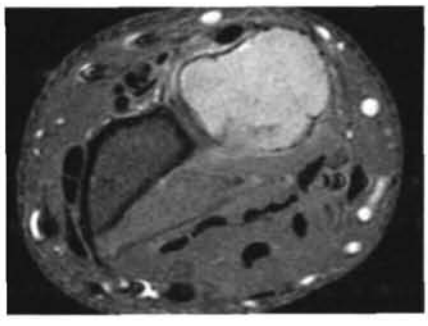

d

Figure **154a-d** Giant cell tumor involving the distal ulna in a 52-year-old man. AP radiograph (**a**) shows an expansile, radiolucent lesion with a narrow zone of transition. The tumor has circumscribed margins, and has high signal on coronal FST2WI (**b**). The tumor shows prominent Gd-contrast enhancement on coronal (**c**) and axial (**d**) FS T1 WI. There is evidence of bone expansion, cortical thinning, small zones of cortical disruption and extra-osseous tumor extension.

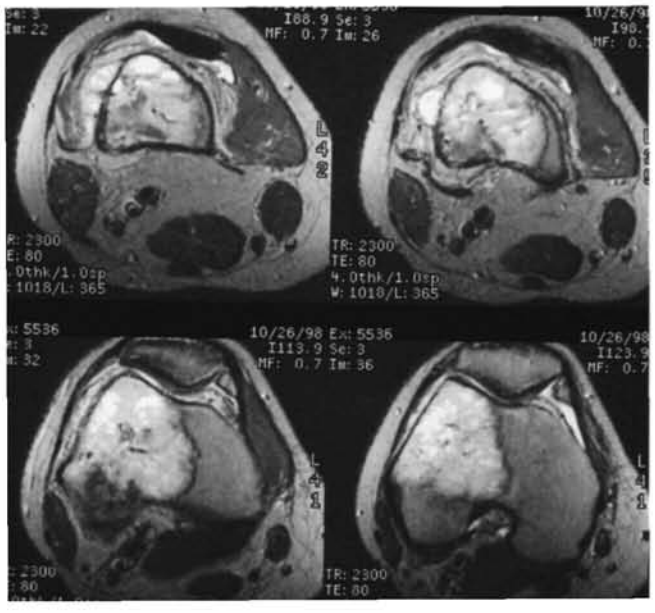

a

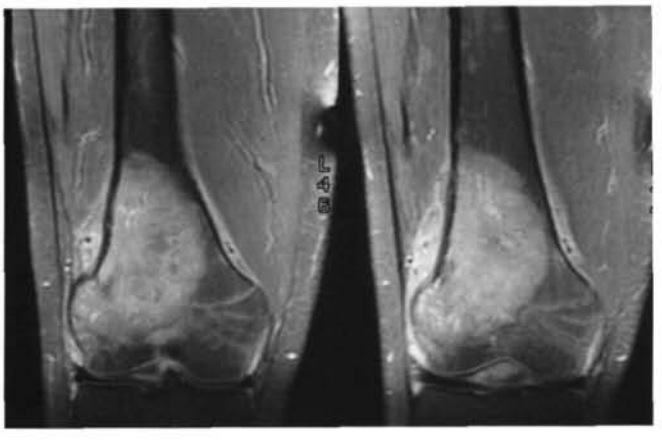

b

Figure **155 a, b** Giant cell tumor involving the distal femur in a 32-year-old woman. The tumor has circumscribed margins, and has heterogeneous mostly high signal on axial T2WI (**a**), with multiple circumscribed high-signal cystic zones. The tumor shows prominent Gd-contrast enhancement on coronal FST1WI (**b**). The peripheral margins of Gd-contrast enhancement are poorly defined. There is evidence of cortical thinning and zones of cortical disruption with extra-osseous tumor extension.

giant cell tumors from surgically challenging locations such as vertebrae and sacrum.[4,7,9,27]

Metastases to lung have been reported to occur in up to 3.5 % of benign giant cell tumors.[7,23] Patients with pulmonary metastases may have improved survival with resection, owing to the usually slow growth rates of the metastatic lesions. Mortality rates have been reported to range from 4 % for grade I lesions to 29% for grade II lesions.[20]

The prognosis for patients with primary malignant giant cell tumors is better than for patients with secondary malignant giant cell tumors.[3,28] The prognosis for patients with secondary malignant giant cell tumors is similar to high-grade, spindle cell sarcomas, and a survival rate of 32 % has been reported.[3,28]

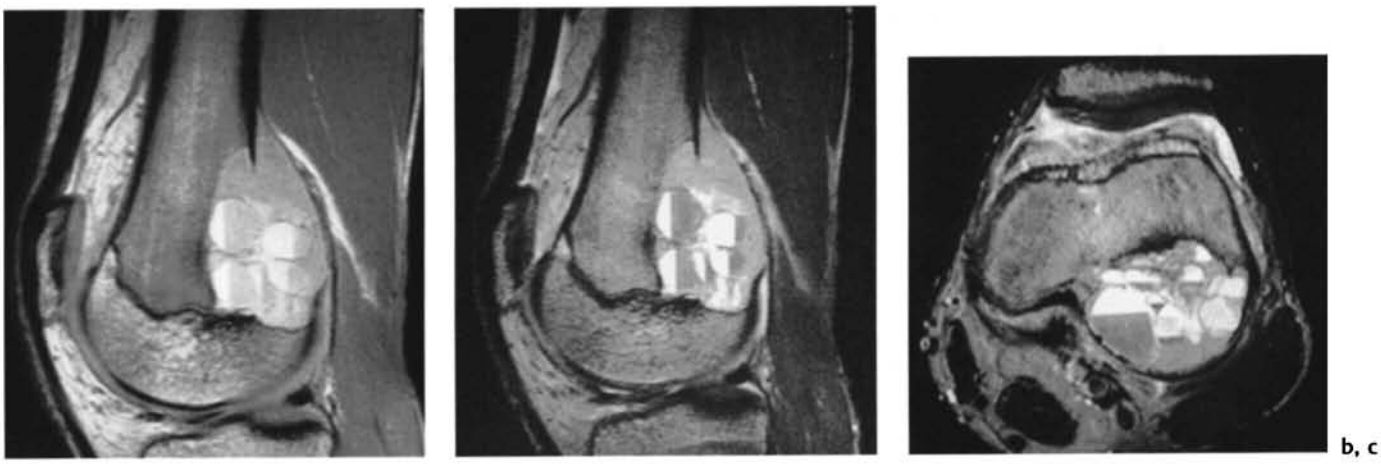

Figure **156a-c** 17-year-old male with a giant cell tumor involving the distal metaphyseal portion of the femur associated with a secondary aneurysmal bone cyst. The tumor has circumscribed and ill-defined margins, and has mixed intermediate and high signal on sagittal PDWI (**a**), and sagittal (**b**) and axial (**c**) T2WI. Multiple fluid-fluid levels are seen at the aneurysmal cyst associated with the tumor within bone and at the extra-osseous portion, which extends through disrupted cortex dorsally.

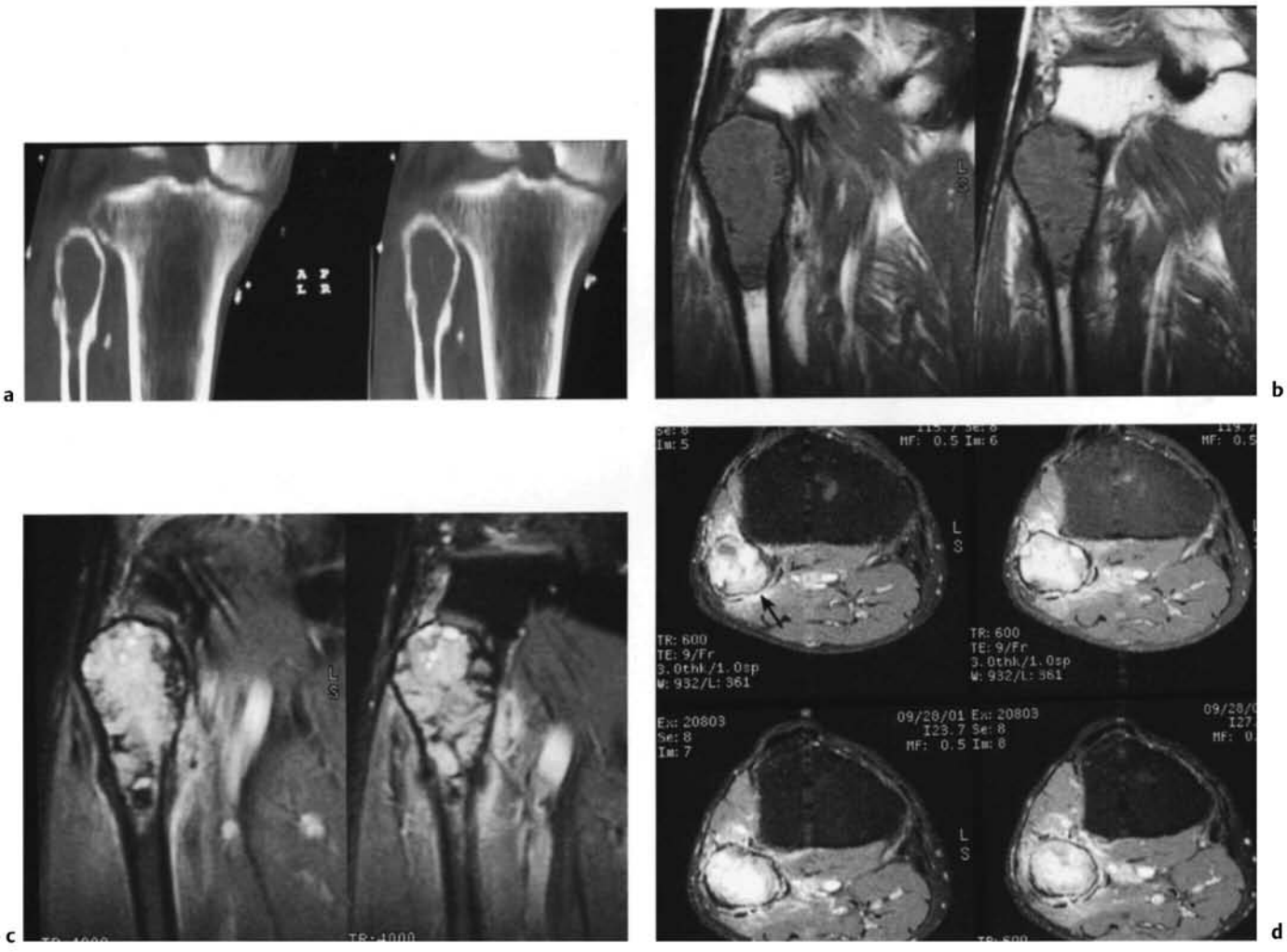

Figure **157a-d** Giant cell tumor involving the proximal fibula in a 58-year-old man. Coronal CT image (**a**) shows an expansile, radiolucent lesion. The tumor has low-intermediate signal on coronal PDWI (**b**), and heterogeneous high and low signal on coronal FST2WI (**c**). The tumor shows prominent Gd-contrast enhancement on axial FST1WI (**d**). There is evidence of cortical thinning and zones of cortical disruption with extra-osseous tumor extension and contrast enhancement in the adjacent soft tissues.

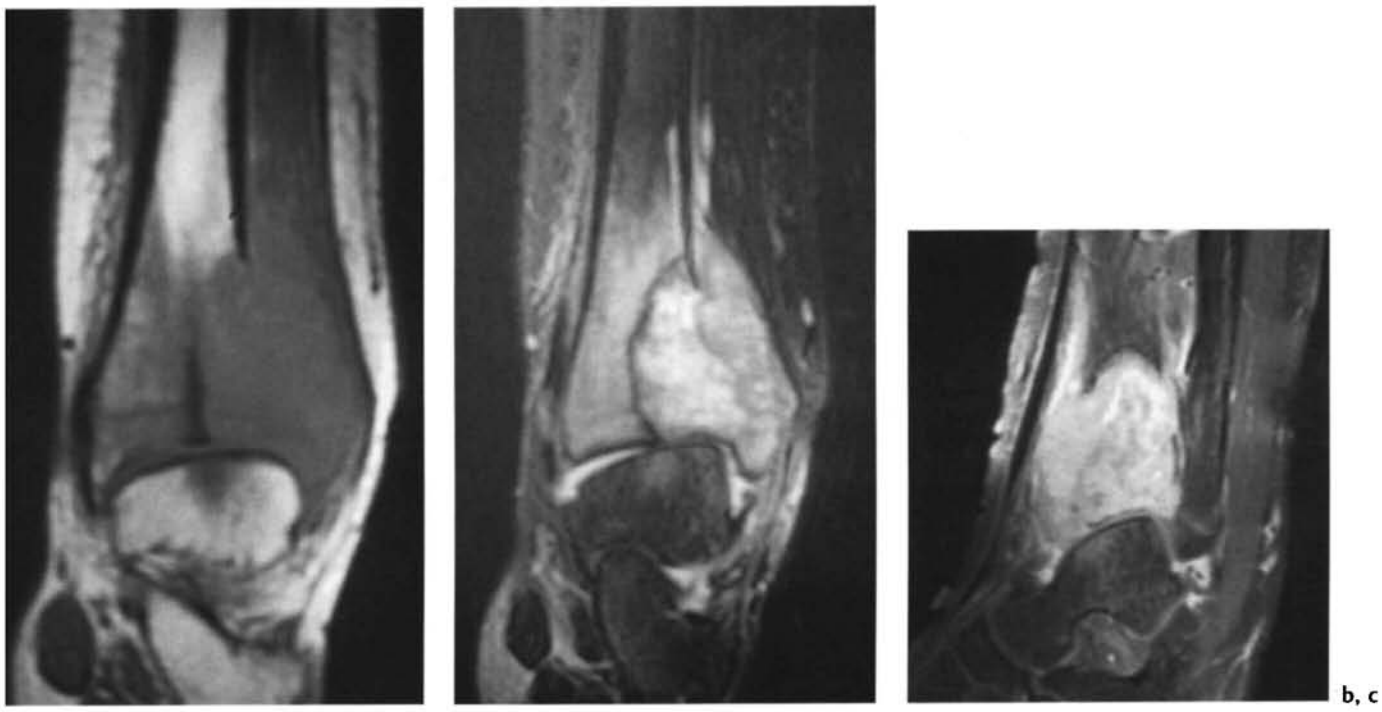

Figure **158a-c** Malignant giant cell tumor involving the distal tibia in a 16-year-old male. The patient subsequently had metastatic lesions in the lungs. The tumor has low-intermediate signal on coronal (**a**) T1 WI, and slightly heterogeneous high signal on coronal (**b**) FST2WI. The tumor shows prominent Gd-contrast enhancement on sagittal (**c**) FST1WI. There is evidence of cortical thinning and zones of cortical disruption with extra-osseous tumor extension and contrast enhancement in the adjacent soft tissues. A thin rim of low signal is seen at the medullary border of the lesion. Poorly defined zones of high signal on FST2WI and Gd-contrast enhancement are seen in the marrow adjacent to the lesion,

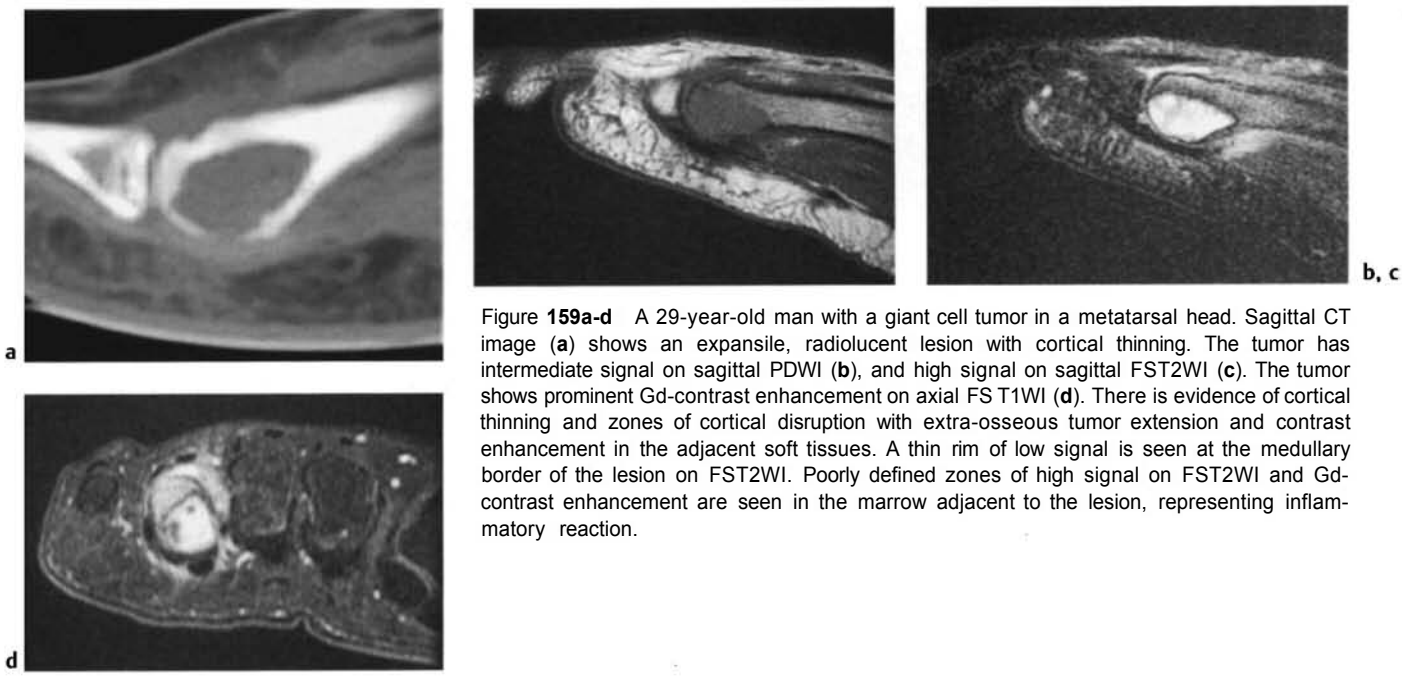

Figure **159a-d** A 29-year-old man with a giant cell tumor in a metatarsal head. Sagittal CT image (**a**) shows an expansile, radiolucent lesion with cortical thinning. The tumor has intermediate signal on sagittal PDWI (**b**), and high signal on sagittal FST2WI (**c**). The tumor shows prominent Gd-contrast enhancement on axial FS T1WI (**d**). There is evidence of cortical thinning and zones of cortical disruption with extra-osseous tumor extension and contrast enhancement in the adjacent soft tissues. A thin rim of low signal is seen at the medullary border of the lesion on FST2WI. Poorly defined zones of high signal on FST2WI and Gd-contrast enhancement are seen in the marrow adjacent to the lesion, representing inflammatory reaction.

References

1 Aoki J, Tanikawa H, Ishii K, et al. MR findings indicative of hemosiderin in giant-cell tumor of bone: frequency, cause, and diagnostic significance. *AJR AmJ Roentgenol* 1996;166:145-148.

2 Bridge JA, Ordnal C. Cytogenetic analysis of bone and joint neoplasms. In: Helliwell TR, ed. *Major Problems in Pathology: Pathology of Bone and Joint Neoplasms* 1st ed. Vol 4. Philadelphia, Pa: W.B. Saunders; 1999:59-78.

3 Bullough PG, Bansal M. Malignancy in giant cell tumour. In: Fletcher CDM, Unni KK, Mertens F, eds. *World Health Organization Classification of Tumours. Pathology and Genetics of Tumours of Soft Tissue and Bone* Geneva: IARC Press; 2002:313.

4 Carrasco CH, Murray JA. Giant cell tumors. *Orthop Clin North Am* 1989;20(3):395-405.

5 Dahlin DC, Cupps RE, Johnson EW Jr. Giant-cell tumor: a study of 195 cases. *Cancer* 1970;25:1061-1070.

6 Dahlin DC. Giant-cell tumor of vertebrae above the sacrum—A review of 31 cases. *Cancer* 1977;39(3):1350-1356.

7 Forest M. Giant cell tumor. In: Forest M, Tomeno B, Vanel D, eds. *Orthopedic Surgical Pathology: Diagnosis of Tumors and Pseudotumoral Lesions of Bone and Joints* Edinburgh: Churchill Livingstone; 1998:415-436.

8 Herman SD, Mesgarzadeh M, Bonakdarpour A, Dalinka MK. The role of magnetic resonance imaging in giant cell tumor of bone. *Skeletal* Radiol1987:16:635-643.

9 Huvos AG. Giant-cell tumor of bone. In Huvos AG, ed. Bone *Tumors Diagnosis, Treatment, and Prognosis* 2nd ed. Philadelphia, Pa: W.B. Saunders; 1991:429-456.

10 Kransdorf MJ, Sweet DE, Buetow PC, Giudici Michaela AI, Moser RP Jr. Giant cell tumor in skeletally immature patients. *Radiology* 1992; 184(1):233-237.

11 Levine E, De Smet AA, Neff JR. Role of radiologic imaging in management planning of giant cell tumor of bone. *Skeletal Radiol* 1984; 12: 79-89.

12 Manaster BJ, Doyle AJ. Giant cell tumors of bone. Radio/ *Clin North Am* 1993;31(2):299-323.

13 Mangham DC. Giant cell tumor of bone and giant cell-containing lesions of bone. In: Helliwell TR, ed. Major *Problems in Pathology: Pathology of Bone and Joint Neoplasms* 1st ed. Vol.37. Philadelphia, Pa: W.B. Saunders; 1999:304-329.

14 McEnery KW, Raymond AK. Radiologic-Pathologic Conferences of the University of Texas M.D. Anderson Cancer Center-Giant cell tumor of the fourth metacarpal.AJR AmJRoentgeno/1999;172:1092.

15 Meyers SP, Yaw K, Devaney K. Giant cell tumor of the thoracic spine: MR appearance. *AJNR Am J Neuroradiol* 1994:15:962-964.

16 Miller SL, Hoffer FA. Malignant and benign bone tumors. Radiol *Clin North Am* 2001;39(4):673-699.

17 Moser RP Jr, Kransdorf MJ, Gilkey FW, Manaster BJ. From the archives of the AFIP-Giant cell tumor of the upper extremity. *Radiographics* 1990;10(1):83-102.

18 Mulder JD, Schutte HE, Kroon HM, Taconis WK. Introduction. In: *Radiologic Atlas of Bone Tumors* Amsterdam: Elsevier; 1993:3-6.

19 Mulder JD, Schutte HE, Kroon HM, Taconis WK. The diagnosis of bone tumors. In: *Radiologic Atlas of Bone Tumors* Amsterdam: Elsevier; 1993:9-46.

20 Mulder JD, Schutte HE, Kroon HM, Taconis WK. Giant cell tumor. In: *Radiologic Atlas of Bone Tumors* Amsterdam: Elsevier; 1993:483-506.

21 Murphey MD, Nomikos GC, Flemming DJ, Gannon FH, Temple HT, Kransdorf MJ. From the archives of the AFIP—Imaging of giant cell tumor and giant cell reparative granuloma of bone: radiologic-pathologic correlation. *Radiographics* 2001;21(5):1283-1302.

22 Potter HG, Schneider R, Ghelman B, Healey JH, Lane JM. Multiple giant cell tumors and Paget's disease of bone: radiographic and clinical correlations. *Radiology* 1991 ;180(1):261-264.

23 Reid R, Banerjee SS. Sciot R. Giant cell tumour. In: Fletcher CDM, Unni KK, Mertens F, eds. *World Health Organization Classification of Tumours. Pathology and Genetics of Tumours of Soft Tissue and Bone* Geneva: IARC Press; 2002:310-312.

24 Stacy GS, Peabody TD, Dixon LB. Mimics on radiography of giant cell tumor of bone. *AJR AmJ Roentgenol* 2003:181:1583-1589.

25 Tehranzadeh J, Murphy BJ, Mnaymneh W. Giant cell tumor of the proximal tibia: MR and CT appearance. J Comput Assist *Tomogr* 1989; 13(2):282-286.

26 Unni KK. Introduction and scope of study. In: *Dahlin's Bone Tumors-General Aspects and Data on 11087 Cases* 5th ed. Philadelphia, Pa: Lippincott, Williams & Wilkins; 1996:1-9.

27 Unni KK. Giant cell tumor (osteoclastoma). In: *Dahlin's Bone Tumors— General Aspects and Data on 11087 Cases* 5th ed. Philadelphia, Pa: Lippincott, Williams & Wilkins. 1996:263-282.

28 Unni KK. Malignancy in giant cell tumor of bone. *Dahlin's Bone Tumors—General Aspects and Data on 11087 Cases* 5th ed. Philadelphia, Pa: Lippincott, Williams & Wilkins; 1996:285-289.

29 Wuelling M, Delling G, Kaiser E. Differential gene expression in stromal cells of human giant cell tumor of bone. *Virchow's Archiv* 2004:445:621-630.

30 Yamamura S, Sato K, Sugiura H, et al. Prostaglandin levels of primary bone tumor tissues correlate with peritumoral edema demonstrated by magnetic resonance imaging. *Cancer* 1997;79:255-261.

31 Yao L, Mirra JM, Seeger LL, Eckardt JJ. Case report 715. *Skeletal* Radiol 1992;21:124-127.

32 Zhen W, Yaotian H, Songjian L, Ge L, Qingliang W. Giant-cell tumour of bone. The long-term results of treatment bone curettage and bone graft.J *Bone Joint SurgBr* 2004;86:212-216.

A 30 Giant Cell Tumor of the Tendon Sheath and/or Soft Tissue (Also Referred to as Nodular Tenosynovitis, Fibrous Xanthoma, Tenosynovial Giant Cell Tumor, and Benign Synovioma)

ICD-OCode

Localized giant cell tumor of the tendon sheath: 9252/0

Diffuse-type giant cell tumor of the tendon sheath: 9251/0

Definition

Giant cell tumors of the tendon sheath and soft tissue, and pigmented villonodular synovitis, represent benign, proliferative lesions of synovium (tendon sheaths, joints, and bursae).[1,3-11.14-16.18-20] Giant cell tumors of the tendon sheath can occur as localized nodular lesions attached to tendon sheaths outside of joints (hands, feet) or within joints (infrapatellar portion of the knee joint); or can occur as a diffuse type near/outside of large joints such a the knee, ankle, etc.[1,3-11,14-16,1S-20] The diffuse type of giant cell tumor of the tendon sheath is also referred to as florid or proliferative synovitis.[1,3-11,14-16,18-20] The diffuse-type giant cell tumors are typically larger and more irregular than the nodular giant cell tumors involving the fingers.[20]

Pigmented villonodular synovitis (PVNS) has histopathologic features that are similar to giant cell tumors of the tendon sheath, although PVNS only occurs in joints and differs in that these lesions have frondlike or villous growth patterns and contain large amounts of hemosiderin.[7,9, 14]

Frequency of Occurrence

Giant cell tumors of the tendon sheath and soft tissue represent 4% of benign, soft tissue tumors and 2% of all soft tissue tumors.[11-13]

Age at Presentation

From 6 to 71 years,[11-13,16] mean = 39 years,"-[13] 46 years;[16] peak ages in 3rd to 4th decades.[16]

Gender Ratio (M / F)

1/1.5 to 1/2[1,11-13.16.18,20]

Location

Nodular (localized) type of giant cell tumor of soft tissue Lesions can be extra- or intra-articular. Extra-articular lesions are attached to tendon sheaths of hands and wrists > feet and ankles > lower extremity > upper extremity > other sites.[11-13,16,19,20] The tendons at the volar aspects of the first three fingers are the most common locations (up to 85% of cases).[11-13,16,19,20] Intra-articular lesions are most often present in the knee (infrapatellar fat pad in 67 %, suprapatellar pouch in 24 %, and posterior intercondylar notch region in 6%).[7,14]

Diffuse type of giant cell tumor of the tendon sheath. Lesions are located mostly outside of large joints." Extra-articular lesions occur in periarticular soft tissues, as well as in muscles or subcutaneous tissue.[20] The knee is a common periarticular site.[20] Other common extra-articular locations include the thigh and foot.[20] Uncommon extra-articular sites include the finger, wrist, groin, elbow, and toe.[20] Intra-articular sites include the knee (75%) and hip (15%), followed by the ankle, elbow, and shoulder.[20]

Signs and Symptoms

Localized lesions are often slowly enlarging, firm, nodular soft tissue masses attached to tendon sheaths.[11,19] Lesions can occur as painless swelling (80-90%) or are occasionally associated with mild pain, often worsened by activity.[11,16,19] Lesions in the knee often have pain, joint swelling, and a palpable mass.[7] Duration of symptoms ranges from 2 to 60 months, mean = 6 months to 1 year.[1,7,16,18] Lesions may be associated with a prior history of trauma.[16,19]

Patients with **diffuse-type giant cell tumors** are commonly associated with swelling, pain, tenderness, and limitation of range of motion.[20] Duration of symptoms ranges from months to years.[20]

Gross Pathologic Findings

Nodular giant cell tumors are polypoid or well-defined rubbery, white, tan-yellow and/or brown nodules attached to tendon sheaths.[1,7,11,18,19] Lesions appear encapsulated and have smooth and/or lobulated contours.[18] These lesions usually range in size from < 1 cm to 4.5 cm, mean = 1.5 cm.[11,16,18,19] Lesions located in the fingers can extend from 63 to 360 around a phalanx, mean = 169°.[10]

Diffuse-type giant cell tumors have irregular infiltrative features and can measure up to 9 cm.[11,20] Lesions can have various combinations of white, yellow, or brown coloration, and can be firm and/or sponge-like.[20]

Histopathologic Findings

Lesions consist of synovial proliferation with fibrous collagenous tissue and varying amounts of scattered multinucleated giant cells, foamy macrophages, xanthoma cells, round-polygonal and/or spindle-shaped mononuclear cells.[1,3,5,8,11,14-16,18,19] Multinucleated giant cells are often immunohistochemically reactive to CD 68 and CD45.[19] The round to spindle-shaped mononuclear cells have round or reniform, grooved nuclei within pale cytoplasm, and often are immunohistochemically reactive to CD68.[16,19] Mitotic activity can range from 2 to 21 mitoses per 10 HPF (high power field).[1,16,19] Mitotic activity has also been reported to absent in up to 40 % of cases.[1] Lesions typically show no cellular atypia.[1] Osteoclastlike cells with 3 to 50 nuclei are often present.[16,19] Siderophages and variable amounts of hemosiderin are usually present in these lesions.[1,7,11,16,18,19] Xanthoma cells frequently occur at the periphery of the lesions and may be associated with cholesterol clefts.[19] Varying degrees of collagenized stroma (fibrosis, hyalinization) are seen within these lesions.[1,19] Zones of necrosis are usually absent.[19] These lesions can been classified as type I when the tumor is surrounded by one pseudocapsule, and as type II when the tumor is not surrounded by one pseudocapsule.[1]

Intra-articular nodular synovitis can be differentiated from pigmented villonodular synovitis because the former lacks the frondlike projections of synovium and abundant hemosiderin seen with the latter.[7,11]

The diffuse form of giant cell tumors has similar histologic features to the nodular type, but may also have several peripheral layers of synovial cells as well as pseudoglandular spaces.[20] These lesions are usually located outside of joints and do not share the villous or frondlike growth patterns commonly associated with pigmented villonodular synovitis.[20] Blood-filled spaces are seen in 10% of these lesions.[20]

Rarely, giant cell tumors may contain malignant sarcomatous zones.[11,19,20,22] In one reported case, giant cells with bizarre nuclei, pleomorphic spindle cells with nuclear atypia, and tumor osteoid were seen at a site of recurrent giant cell tumor.[22]

Lesion Genetics

Nodular lesions commonly have a pseudodiploid karyotype.[19] Structural changes with breakpoints in the pll-p13 regions of the short arm of chromosome 1 have been reported.[17,19] The t(1;2)(p11;q35-36) change has also been reported with several additional variations involving 3q21, 5q22-31, llqll-12, 8 q21-22, and 16q24.[17,19] Using the fluorescent in situ hybridization (FISH) technique, abnormalities involving the RDC1 gene may play a role in the development of these lesions."

Diffuse-type lesions often have a pseudodiploid karyotype.[20] Trisomies for chromosomes 5 and 7 have also been reported in these lesions, as well as rearrangement of the 1 pll-13 region, and t(l;2)(p22;q35-37).[20]

Findings on Plain Films (Roentgenograms) and Computed Tomography

A soft tissue mass may be seen, without or with erosions of adjacent bone cortex (15-20 %)[11,14,15] (Fig. **167).** Cystic bone change, periosteal reaction, and calcifications occur in less than 10% of lesions.[13,14,15]

MRI Findings

Nodular or localized type of giant cell tumor of the tendon sheath. Lesions usually have well-defined margins and are often adjacent to a tendon or tendon sheath.[2,7,9-11,14,15,21] Lesions can be ovoid or multilobulated[7,9-11] (Figs. **160-166).** Lesions in the knee range in size from 2 to 9 cm[7] (Fig. **164).** Lesions elsewhere usually range in size from 2 to 4cm.[9] Lesions usually have low-intermediate or intermediate signal on T1WI and PDWI, which is often similar to or less than muscle.[2,7,9-11,14,15,21] On T2WI and FST2WI, lesions can have mixed intermediate and/or high signal.[2,7,9-11,14,15,21] Small zones of low signal on T2WI often correspond to small sites of hemosiderin deposition.[7,9,10,14] Lesions often show Gd-contrast enhancement in either or homogeneous or heterogeneous pattern.[2,7,10,11,14] Erosions of adjacent bone can be seen with some lesions (Figs. **162, 163, 166).**

Diffuse type of giant cell tumor of the tendon sheath. Lesions are larger and have more irregular or lobular margins than the nodular type.[9,14] The MR signal characteristics of the diffuse type are similar to the nodular type.[9,14] Malignant giant cell tumors of the tendon sheath have MRI features similar to the diffuse type (Fig. **167).**

Differential Diagnosis

Fibroma of the tendon sheath, pigmented villonodular synovitis, desmoid tumors/fibromatosis, neurofibroma, Schwannoma, hematoma, ganglion, synovial cyst, chondroma, granuloma, malignant fibrous histiocytoma, synovial cell sarcoma, tophaceous gout.[10,14-16]

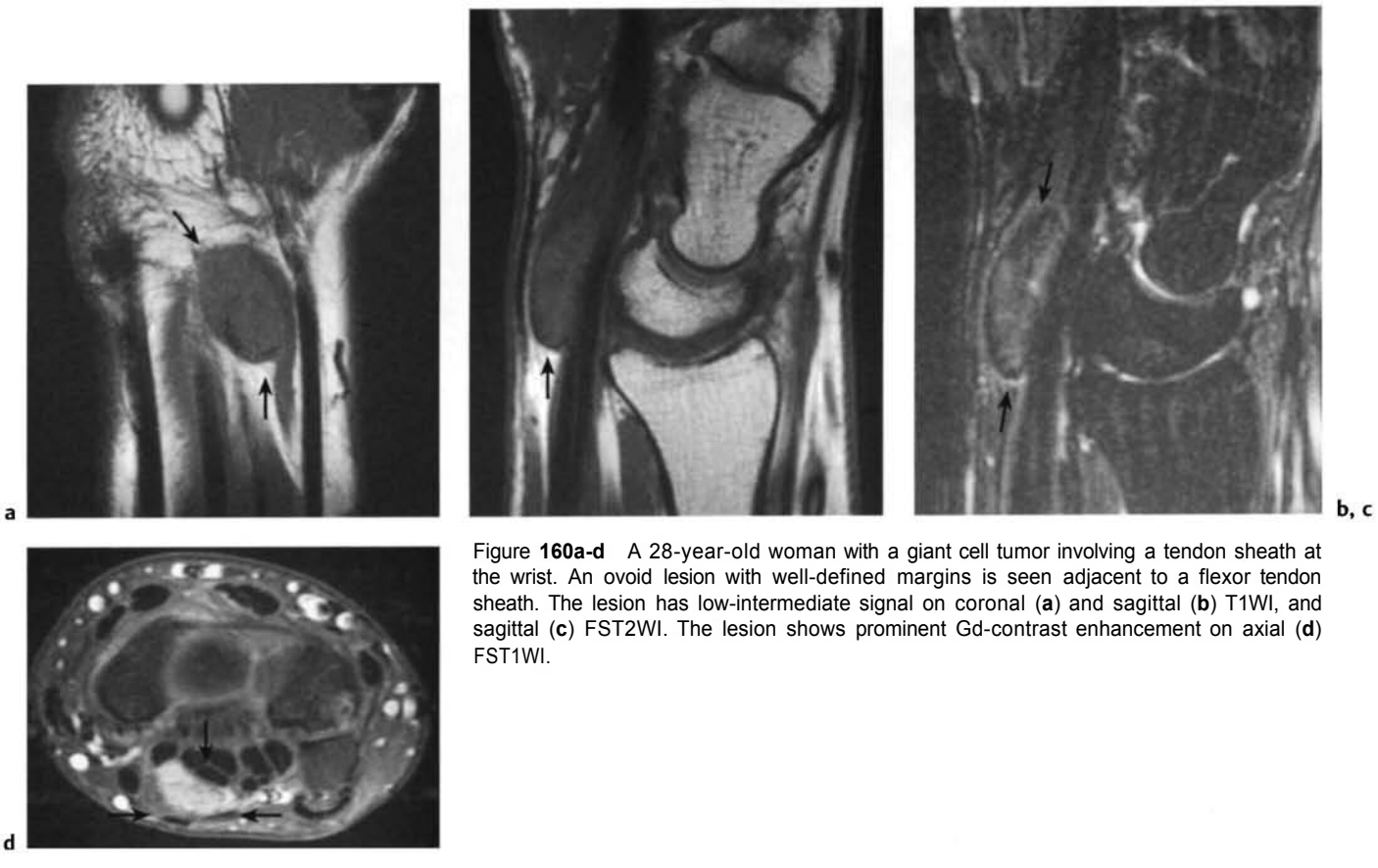

Figure **160a-d** A 28-year-old woman with a giant cell tumor involving a tendon sheath at the wrist. An ovoid lesion with well-defined margins is seen adjacent to a flexor tendon sheath. The lesion has low-intermediate signal on coronal (**a**) and sagittal (**b**) T1WI, and sagittal (**c**) FST2WI. The lesion shows prominent Gd-contrast enhancement on axial (**d**) FST1WI.

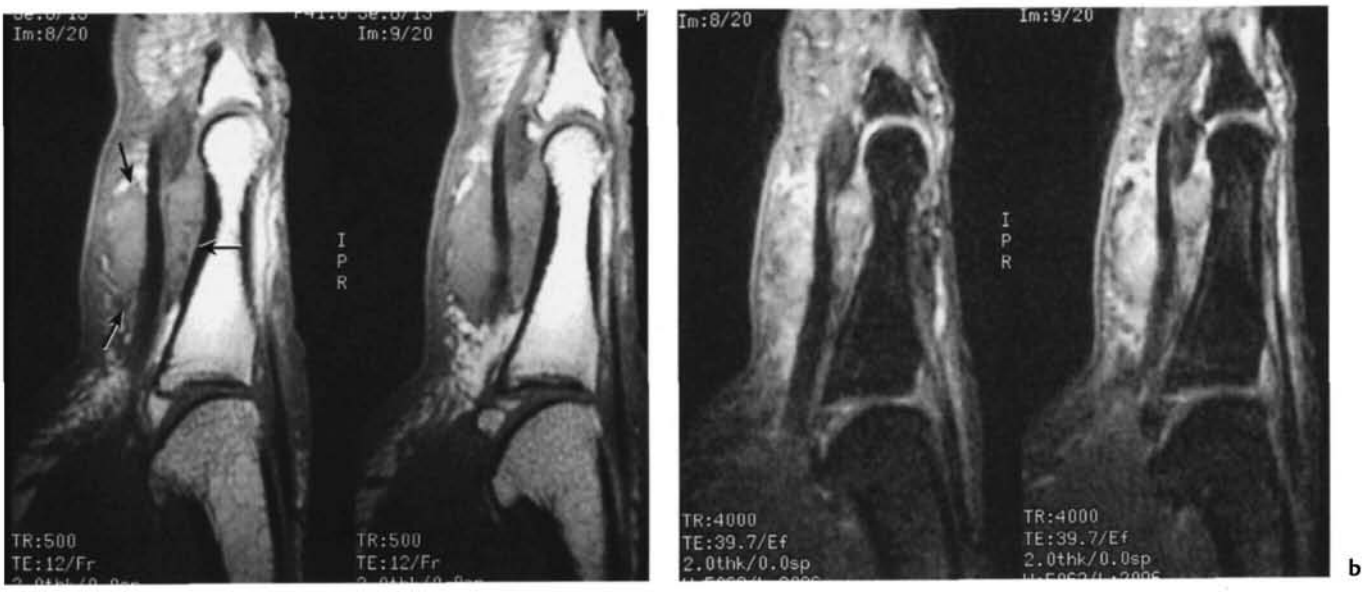

a **b**

Figure **161 a, b** A 39-year-old man with a giant cell tumor of the tendon sheath involving a finger. An ovoid lesion with well-defined margins is seen adjacent to a flexor tendon sheath. The lesion has intermediate signal on sagittal T1WI (**a**), and high signal on sagittal FST2WI (**b**).

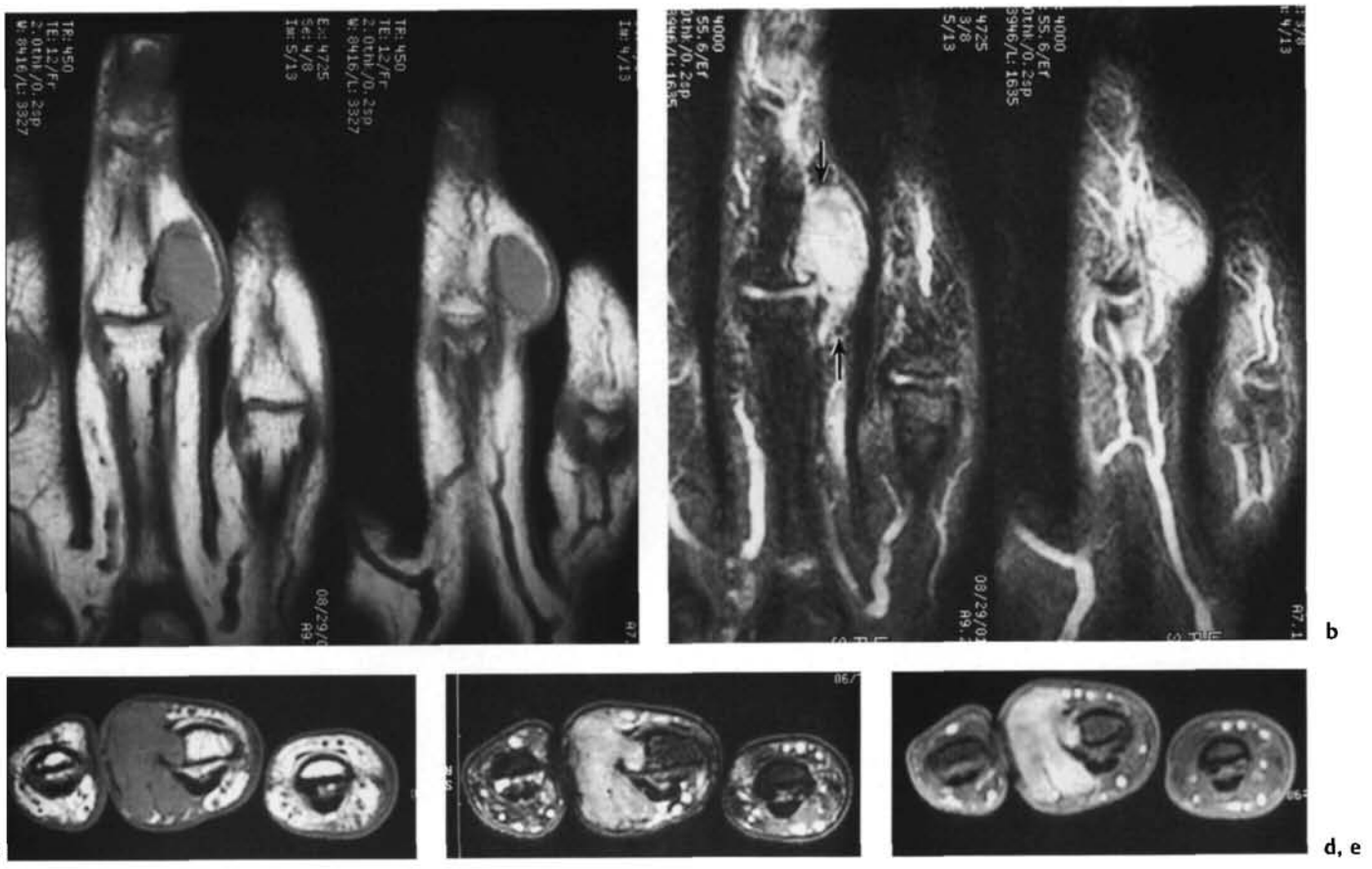

a **b** **c** **d, e**

Figure **162 a-e** A 46-year-old woman with a giant cell tumor of the tendon sheath involving a finger. An ovoid lesion with well-defined margins is seen adjacent to a flexor tendon sheath and middle phalanx. The lesion has low-intermediate signal on coronal (**a**) and axial (**c**) T1WI, and high signal on coronal (**b**) and axial (**d**) FST2WI. The lesion shows prominent Gd-contrast enhancement on axial (**e**) FST1WI. The lesion is associated with focal erosion of the adjacent bone.

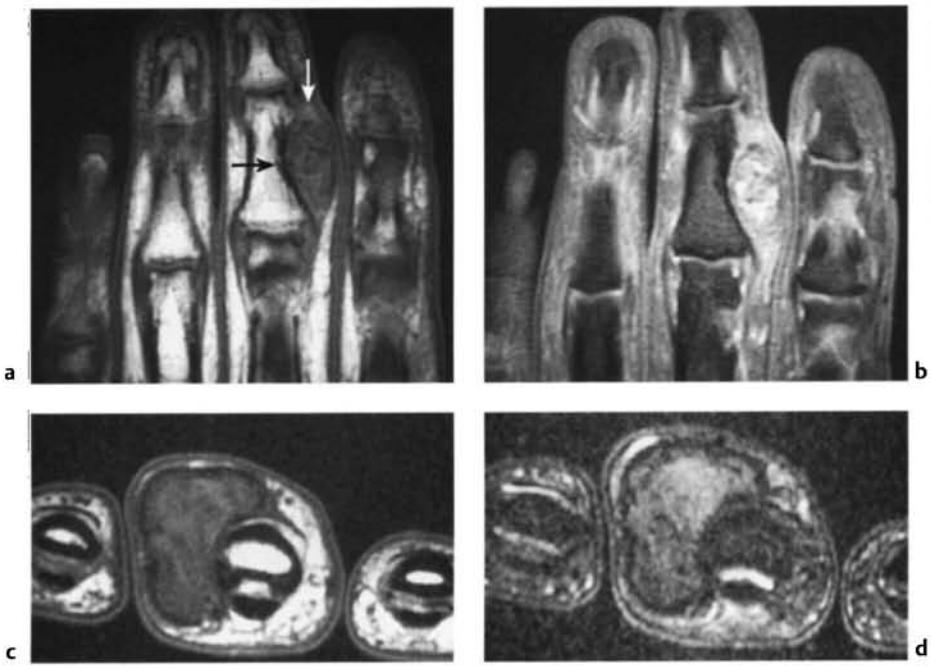

Figure **163 a-d** A 28-year-old man with a giant cell tumor of the tendon sheath involving a finger. An ovoid lesion with well-defined margins is seen adjacent to a flexor tendon sheath and middle phalanx. The lesion has low-intermediate signal on coronal (**a**) and axial (**c**) T1WI, and mixed high, intermediate, and low signal on coronal (**b**) and axial (**d**) FST2WI.

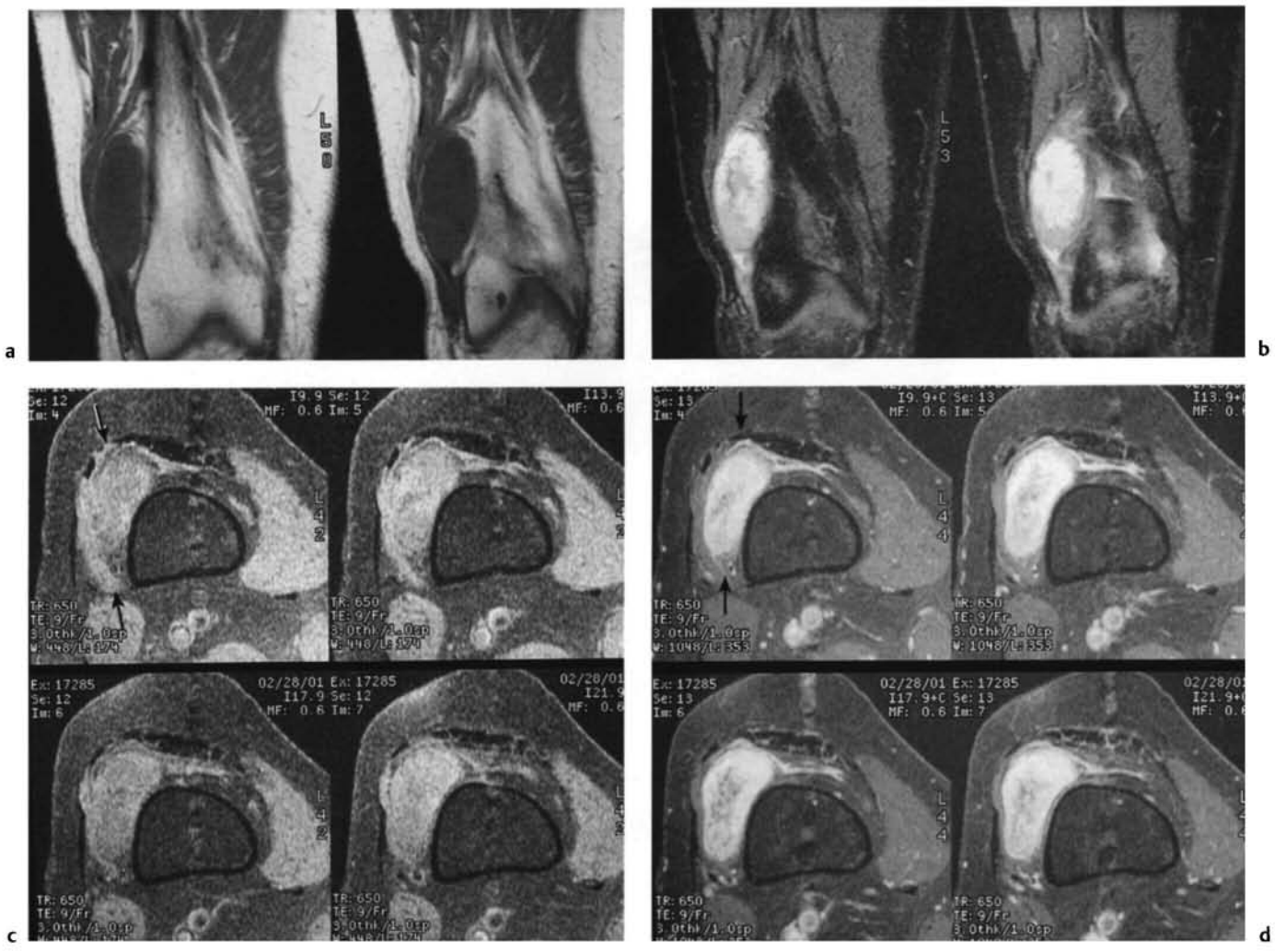

Figure **164a-d** A 60-year-old woman with a giant cell tumor/nodular synovitis at the knee. An ovoid lesion with well-defined margins is seen adjacent to the iliotibial band. The lesion has low-intermediate signal on coronal T1WI (**a**), and high signal on coronal FST2WI (**b**). The lesion has intermediate signal on axial FST1WI (**c**), and shows prominent Gd-contrast enhancement on axial FST1WI (**d**).

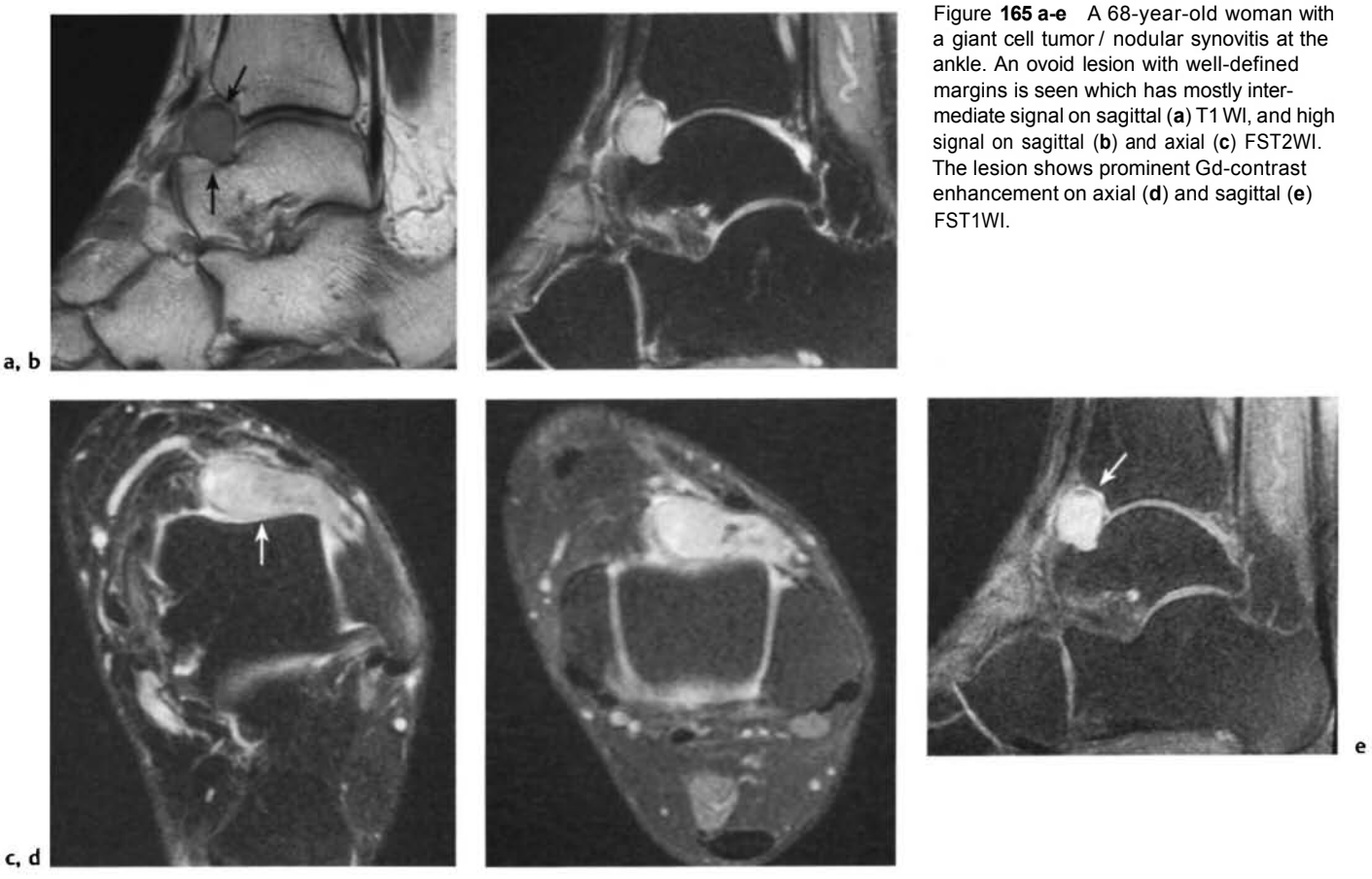

Figure **165 a-e** A 68-year-old woman with a giant cell tumor / nodular synovitis at the ankle. An ovoid lesion with well-defined margins is seen which has mostly intermediate signal on sagittal (**a**) T1 WI, and high signal on sagittal (**b**) and axial (**c**) FST2WI. The lesion shows prominent Gd-contrast enhancement on axial (**d**) and sagittal (**e**) FST1WI.

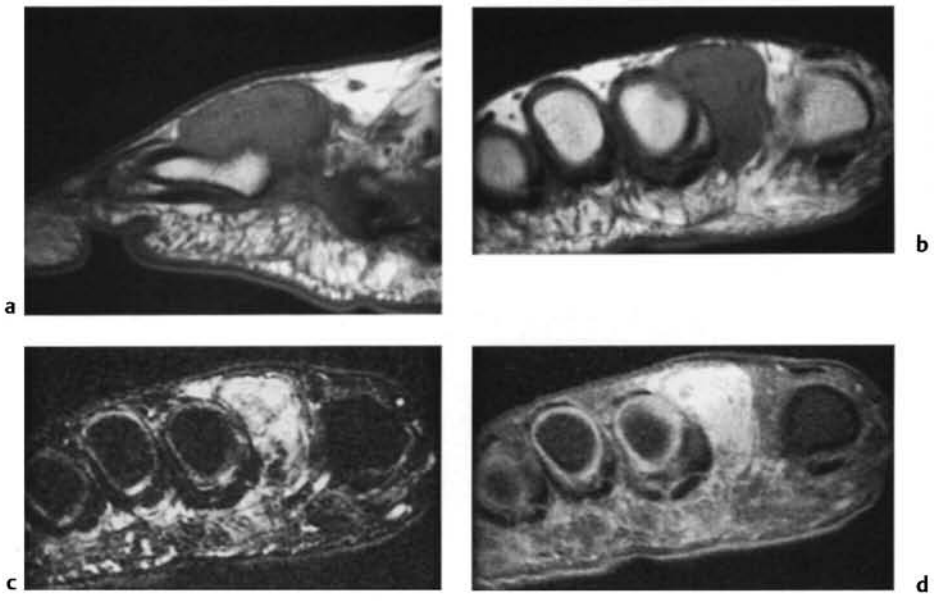

Figure **166a-d** A 39-year-old man with a giant cell tumor of the tendon sheath / nodular synovitis at the foot dorsally. An ovoid lesion with well-defined margins is seen which has mostly intermediate signal on sagittal (**a**) and axial (**b**) T1WI, and heterogeneous high signal on axial (**c**) FS T2WI. The lesion shows prominent Gd-contrast enhancement on axial (**d**) FST1WI.

Treatment and Prognosis

Nodular lesions are benign and can often be surgically resected.[1,2,11,14,16,18,19] Recurrence rates range from 7 to 30 %.[1,14,19] Incomplete surgical removal is the most important factor associated with recurrence.[1] Intra-osseous invasion is associated with a higher rate of recurrence, whereas mild bone erosion or remodeling of the outer cortical surface of bone is not.[1] Lesions with high cellularity and increased mitotic activity also have been reported to be associated with recurrences[1,19] Type II lesions have higher recurrence rate than type I lesions.[1] Diffuse lesions are more aggressive than the localized type and are more difficult to completely resect.[20] Recurrence for the diffuse form can be up to 50 %.[9-11,14,20] Recurrent lesions are usually seen within 2 years of surgery and are typically treated with repeat excision.[1] Malignant giant cell tumors of the tendon sheath are very rare and have aggressive behavior with high potential for pulmonary metastasis.[19,20]

Figure **167 a-f** A 60-year-old man with a malignant giant cell tumor of the tendon sheath at the wrist. AP radiograph (**a**) shows a soft tissue mass at the distal forearm and wrist. MRI shows a large multilobulated tumor with both well-defined and indistinct margins in the soft tissues of the distal forearm and wrist. The tumor has low-intermediate signal on sagittal (**b**) and axial (**c**) T1WI, and has heterogeneous intermediate, low, and slightly high signal on axial FS T2WI (**d**). The lesion shows prominent heterogeneous Gd-contrast enhancement on axial (**e**) and sagittal (**f**) FST1WI.

References

1 Al-Qattan MM. Giant cell tumours of tendon sheath: Classification and recurrence rate. *J Hand Surg* 2001 ;26(1):72-75.

2 Bancroft LW, Peterson JJ, Kransdorf MJ, Nomikos GC, Murphey MD. Soft tissue tumors of the lower extremities. Radiol *Clin North Am* 2002;40:991-1011.

3 Dingle SR, Flynn JC, Flynn JC Jr, Stewart G. Giant-cell tumor of the cervical spine. *J Bone Joint Surg Am* 2002;84-A(9):1664-1667.

4 Gibbons CL, Khwaja HA, Cole AS, Cooke PH, Athanasou NA. Giant-cell tumour of the tendon sheath in the foot and *ankle. J Bone Joint Surg Br* 2002;84:1000-1003.

5 Gupta K, Dey P, Goldsmith R, Vasishta RK. Comparison of cytologic features of giant-cell tumor and giant cell tumor of tendon sheath. *Diagn Cytopathol* 2004;30:14-18.

6 Helliwell TR, Ritchie DA. Tumors and tumor-like lesions ofjoints and juxta-articular bone. In: Helliwell TR, ed. *Major Problems in Pathology: Pathology of Bone and Joint Neoplasms* 1st ed. Vol.37. Philadelphia, Pa: W.B. Saunders: 1999:369-393.

7 Huang GS, Lee CH, Chan CY, Yu JS, Resnick D. Localized nodular synovitis of the knee: MR imaging appearance and clincial correlates in 21 patients. *AJR Am J Roentgenol* 2003;181:539-543.

8 Iyer VK, Kapila K, Verma K. Fine-needle aspiration cytology of giant cell tumor of tendon sheath. *Diagn Cytopathol* 2003;29:105-110.

9 JelinekJS, Kransdorf MJ, Shmookler BM, Aboulafia AA, Malawer MM. Giant cell tumor of the tendon sheath: MR findings in nine cases. *AJR Am J Roentgenol* 1994;162:919-922.

10 Kitagawa Y, Ito H, Amano Y, Sawaizumi T, Takeuchi T. MR imaging for preoperative diagnosis and assessment of local tumor extent on localized giant cell tumor of tendon sheath. *Skeletal Radiol* 2003; 32:633-638.

11 Kransdorf MJ, Murphey MD. Synovial tumors. In: *Imaging of Soft Tissue Tumors* 2nd ed. Philadelphia, Pa: W.B. Saunders; 2006: 381-436.

12 Kransdorf MJ, Murphey MD. Soft tissue tumors in a large referral population: prevalence and distribution of diagnoses by age, sex, and location. In: *Imaging of Soft Tissue Tumors* 2nd ed. Philadelphia, Pa: W.B. Saunders; 2006:6-37.

13 Kransdorf MJ. Benign soft-tissue tumors in a large referral population: distribution of specific diagnoses by age, sex, and location. *AJR Am J Roentgenol* 1995;164:395-402.

14 Llauger J, Palmer J, Roson N, Cremades R, Hague S. Pictorial Essay - Pigmented villonodular synovitis and giant cell tumors of the tendon sheath: radiologic and pathologic features. *AJR Am J Roentgenol* 1999; 172:1087-1091.

15 Ly JQ, Carlson CL, LaGatta LM, Beall DP. Giant cell tumor of the peroneus tendon sheath. *AJR Am J Roentgenol* 2003:180:1442.

16 Monaghan H, Salter DM, Al-Nafussi A. Giant cell tumor of tendon sheath (localized nodular synovitis): clinicopathologic features of 71 cases. J *Clin Pathol* 2001;54:404-407.

17 Nilsson M, Hoglund M, Panagopoulos I, et al. Molecular cytogenetic mapping of recurrent chromosomal breakpoints in tenosynovial giant cell tumors. *Virchows Arch* 2002;441:475-480.

18 Rodrigues C, Desai S, Chinoy R. Giant cell tumor of the tendon sheath: a retrospective study of 28 cases. *J Surg Oncol* 1998;68: 100-103.

19 Somerhausen N, Cin PD. Giant cell tumor of the tendon sheath. In: Fletcher CDM, Unni KK, Mertens F, eds. *World Health Organization Classification of Tumours. Pathology and Genetics of Tumours of Soft Tissue and Bone* Geneva: IARC Press: 2002:110-111.

20 Somerhausen N, Cin PD. Diffuse-type giant cell tumor of the tendon sheath. In: Fletcher CDM, Unni KK, Mertens F, eds. *World Health Organization Classification of Tumours. Pathology and Genetics of Tumours of Soft Tissue and Bone* Geneva: IARC Press; 2002:112-114.

21 Weatherall PT. Benign and malignant masses. *Magn Reson Imaging Clin N Am* 1995;3:669-694.

22 Wu NL, Hsiao PF, Chen BF, Chen HC, Su HY. Malignant giant cell tumor of the tendon sheath. *Int J Dermatol* 2004;43:54-55.

A 31 Glomus Tumor (Also Referred to as Glomangioma and Angioglomoid Tumor)

ICD-OCode

Glomus tumor: 8711/0

Glomus tumor of uncertain malignant potential: 8711/1

Malignant glomus tumor: 8711/3

Definition

Glomus tumors are benign, mesenchymal hamartomas that are composed of round cells derived from the neuromyoarterial apparatus (glomus bodies), which regulates arteriolar blood flow to the skin for temperature homeostasis.[2-4,7-13,15,18-20] Glomus bodies consist of: an afferent arteriole, a tortuous arteriovenous anastomotic vessel (Sucquet-Hoyer canal) without an intervening capillary bed; collecting veins; and a neurovascular reticulum that regulates the blood flow through the anastomosis.[2-4,7-13,15,18-20] Glomus bodies are usually 300pm long, and are normally present throughout the reticular dermis (deepest dermal layer) throughout the body, but are mostly concentrated under the nail beds of the fingers and toes.[2-4,7-13,15,18-20] Up to 500 glomus bodies occur per square centimeter in the nail beds of the fingers and toes.[9] Glomus tumors have been subcategorized into solid glomus tumor, glomangioma, or glomangiomyoma, based on the relative proportions of small round glomus cells, smooth muscle, and vascular structures.[10] Multiple glomus tumors occur in 2.3 % of cases and have been reported to be associated with an autosomal dominant inheritance pattern.[6,10] Malignant glomus tumors are rare and account for 1 % of all glomus body tumors.[10]

Frequency of Occurrence

Glomus tumors account for < 1 % of primary benign soft tissue tumors.[10,16,17,20] Glomus tumors account for 1-4.5% of tumors in the hands.[12,20]

Age at Presentation

From 19 to 71 years, mean = 47 years, peak ages in the 3rd to 5th decades.[12,16-18,20]

Gender Ratio (M / F)

1/1 to 1.9/1.[6,10,16,17] Subungual lesions are more common in women.[10]

Location

Glomus bodies are normally present throughout the reticular dermis (deepest dermal layer) of the body, and are most concentrated under nail beds of the fingers and toes.[2-4,7-13,15,18-20] Tumors of glomus bodies typically occur in the soft tissues.[2-4,7-13,15,18-20] Glomus tumors are most commonly seen in the hand and wrist followed by the upper and lower extremities > foot and ankle > hip, buttock, trunk > other sites.[10,16,17] Approximately 66 % of glomus tumors involve the upper extremities.[12] Lesions frequently occur in a subungual location of fingers (thumb, second and fourth fingers > fourth finger > fifth finger) > subungual region of toes.[10] Lesions also occur in the lateral folds of the nails. Multiple glomus tumors occur in 2.3 % of cases.[20] Up to 35 % of glomus tumors are extradigital and have been reported at the juxtacortical region of the femoral metaphysis, suprapatellar subcutaneous tissue within the joint capsule, Hoffa fat pad, and coccyx.[12,19] Erosions at the surface of bone adjacent to glomus tumors have been reported to occur in up to 82 % of cases evaluated with MRI.[9] Primary intra-osseous glomus tumors are very rare and have been reported in the medulla of a terminal phalanx, middle phalanx, ulna, femur, fibula, mandible, pubis, sacrum, and coccyx.[7,12,13]

Signs and Symptoms

Lesions can be associated with tenderness and pain, exacerbated by changes in temperature, often with cold sensitivity.[2,9,10] The duration of symptoms can be up to several years, with an average of 1.9 years.[2] Most lesions are deep within the dermis and are not evident on visual inspection. Superficial lesions may present as a blue or purple-reddish nodule.[1,9] Lesions in the nail bed are usually not palpable and may occasionally be seen as tiny blue spots.[9] Gentle pressure on the lesions using the blunt end of a pin typically elicits severe pain, known as Love's test.[2] Application of a tourniquet on the arm proximal to the lesion will often alleviate the pain associated with a glomus tumor: the Hildreth sign.[2] Placing the affected hand into cold water also causes pain at the lesion: the cold-sensitivity test.[2]

Cross Pathologic Findings

Lesions are typically small nodules, ranging in size from 1.4 to 8mm, mean = 3.5 mm.[9] Lesions appear as red or blue, nodular vascular tissue.[1,6,18]

Histopathologic Findings[1,3-5, 7-14,19,22]

Glomus tumors are comprised of oval, polygonal or spindle-shaped cells that are relatively uniform and distributed in sheets among reticulin fibers adjacent to numerous capillaries and sometimes larger vessels. Glomus cells typically contain a centrally located spheroid nucleus within amphophilic to slightly eosinophilic cytoplasm. Glomus cells are surrounded by a basal lamina that is visualized with toludine blue or periodic acid-Schiff stains.[10]

Glomus tumors have been subcategorized into solid glomus tumor, glomangioma, or glomangiomyoma, based on the relative proportions of small round glomus cells, vascular structures, and smooth muscle. Solid glomus tumors account for 75 % of these lesions and are comprised of nests of glomus cells adjacent to capillary-sized blood vessels, and stroma which can contain zones of myoid changes or hyalinization.[10] Glomangiomas account for 20 % of these lesions and contain aggregates of glomus cells surrounding dilated veins.[10] Glomangiomas are the most common lesion-type seen in patients with multiple lesions. Glomangiomyomas are the least common type, and have histologic features that overlap those of solid glomus tumors and glomangiomas, except that they also contain elongated cells resembling mature smooth muscle. Solitary glomus tumors are encapsulated, whereas multiple glomus tumors (autosomal dominant inheritance) are usually unencapsulated.[9]

These lesions can show immunoreactivity to smooth muscle actin, type IV collagen, and H-caldesmon.[10]

Malignant glomus tumors (glomangiosarcomas) are very rare and are often larger than 2 cm in size.[10] These tumors often contain glomus cells as well as neoplastic cells with nuclear atypia and atypical mitoses.

Lesion Genetics

An autosomal dominant inheritance pattern has been reported for patients with multiple familial glomus tumors.[10] The gene associated with multiple glomus tumors is linked to chromosome 1 p21-22.[10]

Findings on Plain Films (Roentgenograms) and Computed Tomography

Glomus tumors can be associated with focal erosion of bone cortex with abrupt zones of transition (14-80% reported), although plain radiographs may show no abnormalities.[3,6,15,18,22]

MRI Findings[3, 6,9,12,15,18-20]

Glomus tumors are well-circumscribed, ovoid lesions measuring less than 1 cm and often located under the nail beds at the distal phalanges of fingers and toes (Fig. **168).** Glomus tumors often have low-intermediate signal on T1WI and PDWI, although may be hypointense or hyperintense on Tl WI relative to the adjacent dermis layers (Figs. **168, 169).** Glomus tumors usually have high signal on T2WI and FS T2WI. A thin rim of low signal on T2WI may be seen secondary to a capsule from reactive tissue surrounding the glomus tumor.

Lesions typically show Gd-contrast enhancement[9,12,19,20] (Figs. **168,169).** MRI can show erosion of the underlying bone when similar findings are not evident on plain films.[9] Contrast-enhanced time-of-flight MR angiography can show enhancing glomus tumors during the arterial phase.[3]

Glomus tumors are usually well-circumscribed when solitary. Multiple glomus tumors often have ill-defined margins on T1WI, T2WI, and Gd-contrast enhanced T1WI.

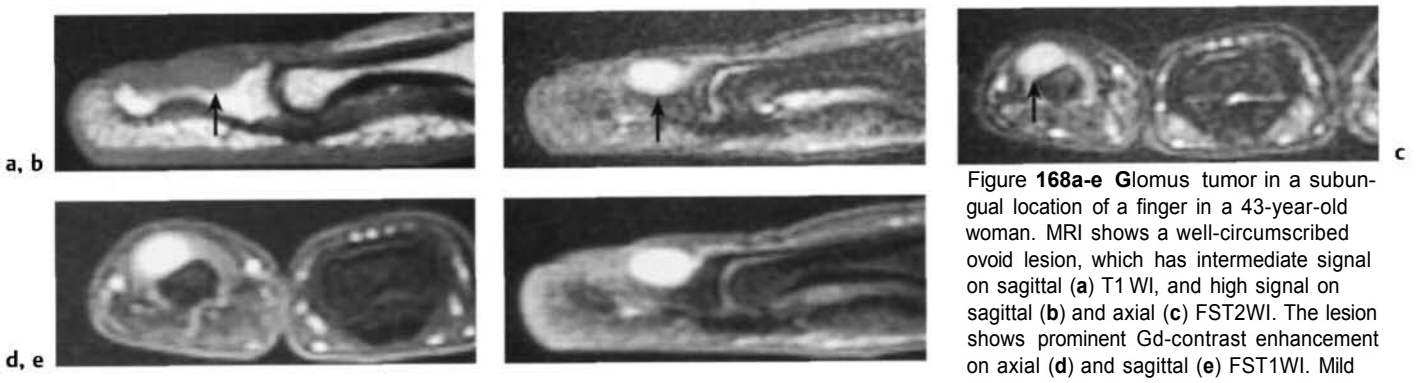

Figure **168a-e** Glomus tumor in a subungual location of a finger in a 43-year-old woman. MRI shows a well-circumscribed ovoid lesion, which has intermediate signal on sagittal (**a**) T1 WI, and high signal on sagittal (**b**) and axial (**c**) FST2WI. The lesion shows prominent Gd-contrast enhancement on axial (**d**) and sagittal (**e**) FST1WI. Mild erosion of the underlying bone is seen.

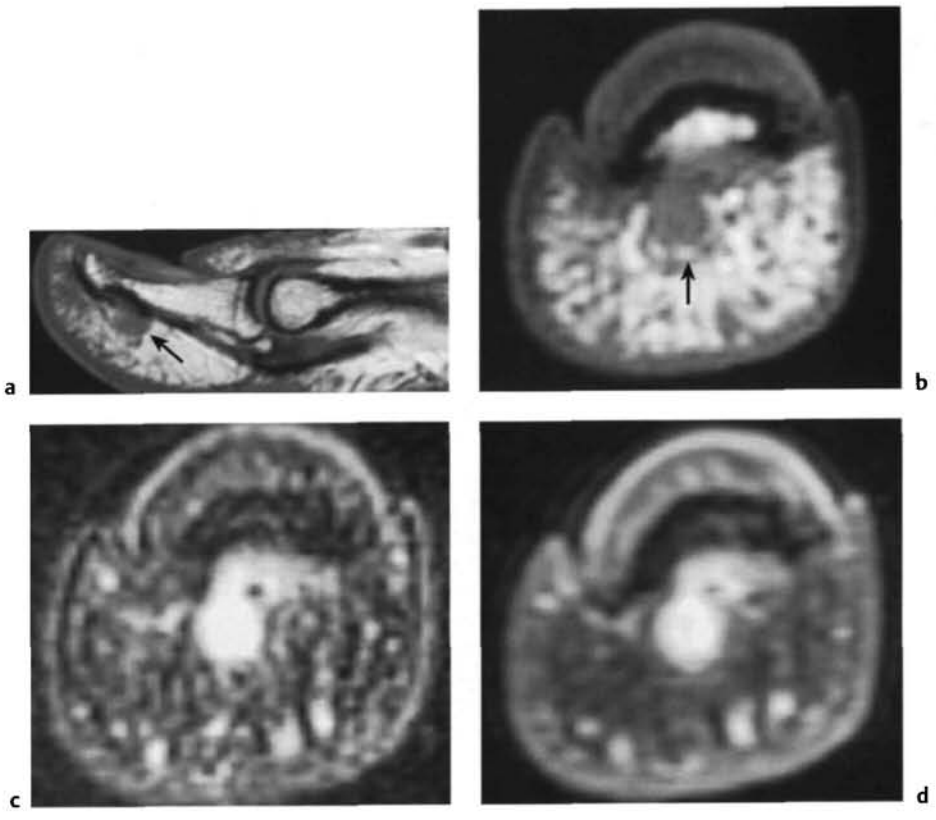

Figure **169a-d** Glomus tumor adjacent to the ventral surface of a distal phalanx. MRI shows a well-circumscribed ovoid lesion, which has intermediate signal on sagittal (**a**) and axial (**b**) T1WI, and high signal on axial (**c**) FST2WI. The lesion shows prominent Gd-contrast enhancement on axial (**d**) FS T1WI. Mild erosion of adjacent bone is seen.

Differential Diagnosis

Benign hemangiopericytoma, angioma, epithelial inclusion cyst/mucoid cyst, metastasis, xanthoma, juxtacortical chondroma, sarcoidosis, tuberous sclerosis.

Treatment and Prognosis

Complete surgical excision is usually curative for glomus tumors.[1,2,9,12,18-21] Accurate location of the lesion prior to surgery is important to avoid nail dystrophy. Pulsed dye laser treatment has also been shown to be effective for hereditary multiple glomus tumors.[1] Recurrence of symptoms and lesions occurs in 5-50 % of patients, who require additional surgery.[9,20] Recurrent lesions result from inadequate initial excision.[9,21]

Patients with the rare form of malignant glomus tumor have a 40 % rate of metastasis, which is associated with high mortality.[10,14]

References

1 Antony FC, Cliff S, Cowley N. Complete pain relief following treatment of a glomangiomyoma with the pulsed dye laser. *Clin Exp Dermatol* 2003;28:617-619.

2 Bhaskaranand K, Navadgi BC. Glomus tumour of the hand. *J Hand Surg* 2002;27(3):229-231.

3 Boudghene FP, Gouny P, Tassart M, Callard P, Le Breton C, Vayssairat M. Subungual glomus tumor: combined use of MRI and three-dimensional contrast MR angiography. *J Magn Reson Imaging* 1998; 8(6):1326-1328.

4 Chaudhuri B, Das Gupta TK. Pathology of soft tissue sarcoma. In: Das Gupta TK, Chaudhuri PK, eds. Tumors *of the Soft Tissues* 2nd ed. Stamford, Conn: Appleton & Lange; 1998:172-173.

5 Conway WF, Hayes CW. Miscellaneous lesions of bone. *Radiol Clin North Am* 1993:31:339-358.

6 Dalrymple NC, Hayes J, Bessinger VJ, Wolfe SW, Katz LD. MRI of multiple glomus tumors of the finger. *Skeletal Radiol* 1997;26: 664-666.

7 Darby AJ. Vascular neoplasms of bone. In: Helliwell TR, ed. *Major Problems in Pathology: Pathology of Bone and Joint Neoplasms* 1st ed. Vol.37. Philadelphia, Pa: W.B. Saunders; 1999:330-343.

8 Das Gupta TK, Chaudhuri PK. Tumors of vascular and perivascular tissue. In: Das Gupta TK, Chaudhuri PK, eds. Tumors *of the Soft Tissues* 2nd ed. Appleton and Lange Pubs.: 1998:407-448.

9 Drape JL, Idy-Peretti I, Goettmann S, et al. Subungual glomus tumors: evaluation with MR imaging. *Radiology* 1995;195(2):507-515.

10 Folpe AL. Glomus tumours. In: Fletcher CDM, Unni KK, Mertens F, eds. *World Health Organization Classification of Tumours. Pathology and Genetics of Tumours of Soft Tissue and Bone* Geneva: IARC Press; 2002:136-137.

11 Forest M. Vascular tumors. In: Forest M, Tomeno B, Vanel D, eds. *Orthopedic Surgical Pathology: Diagnosis of Tumors and Pseudotumoral Lesions of Bone and Joints* Edinburgh: Churchill Livingstone; 1998:345-362.

12 Hermann G, Klein MJ, Springfield D, Abdelwahab IF, Hoch BL Glomus tumor of the thigh: confluent with the periosteum of the femur. *Skeletal Radiol* 2005:34:116-120.

13 Huvos AC. Hemangioma of bone; lymphangioma of bone; diffuse skeletal angiomatosis and lymphangiomatosis; glomus tumor; "disappearing bone disease." In Huvos AG, ed. *Bone Tumors: Diagnosis, Treatment, and Prognosis* 2nd ed. Philadelphia, Pa: W.B. Saunders; 1991:566-567.

14 Kayal JD, Hampton RW, Sheehan DJ, Washington CV. Malignant glomus tumor: a case report and review of the literature. *Dermatol Surg* 2001;27:837-840.

15 Kransdorf MJ, Murphey MD. Vascular and lymphatic tumors. In: *Imaging of Soft Tissue Tumors* 2nd ed. Philadelphia, Pa: W.B. Saunders; 2006:150-188.

16 Kransdorf MJ, Murphey MD. Soft tissue tumors in a large referral population: prevalence and distribution of diagnoses by age, sex, and location. In: *Imaging of Soft Tissue Tumors* 2nd ed. Philadelphia, Pa: W.B. Saunders; 2006;6-37.

17 Kransdorf MJ. Benign soft-tissue tumors in a large referral population: distribution of specific diagnoses by age, sex, and location. *AJR Am J Roentgenol* 1995;164:395-402.

18 Opdenakker G, Gelin G, Palmers Y. MR imaging of a subungual glomus tumor. *AJR Am J Roentgenol* 1999;172:250-251.

19 Perks FJ, Beggs I, Lawson GM, Davie R. Juxtacortical glomus tumor of the distal femur adjacent to the popliteal fossa. *AJR Am J Roentgenol* 2003;181:1590-1592.

20 Theumann NH, Goettmann S, LeViet D, et al. Recurrent glomus tumors of the fingertips: MR imaging evaluation. *Radiology* 2002; 223:143-151.

21 Tomak Y, Akcay I, Dabak N, Eroglu L. Subungual glomus tumours of the hand: diagnosis and treatment in 14 cases. *ScandJPlastReconstr Surg Hand Surg* 2003:37:121-124.

22 Unni KK. Benign vascular tumors. In: *Dahlin's Bone Tumors—General Aspects and Data on 11* 087 Cases 5th ed. Philadelphia, Pa: Lippincott, Williams & Wilkins; 1996:307-316.

A 32 Gout

Definition

Gout is an inflammatory disease involving synovium resulting from deposition of monosodium urate crystals.[1,4,6-9,11,12] Gout occurs when the serum urate level exceeds its solubility in various tissues and body fluid. Patients with gout often have a serum urate level of 7 mg/dL in men and 6 mg/dL in women.[8] Gout can be a primary disorder of hyperuricemia resulting from inherited metabolic defects in purine metabolism or inherited abnormalities involving renal tubular secretion of urate.[8] Primary gout accounts for up to 90 % of cases in men.[8] Secondary gout results from acquired metabolic alterations caused by medications (thiazide diuretics, alcohol, salicylates, cyclosporin) that diminish renal excretion of uric acid salts.[8] Secondary gout can also occur from increased urate production that results from increased metabolic turnover of nucleic acids associated with malignancy, chemotherapy, endocrine, vascular, and/or myeloproliferative diseases such as polycythemia vera, leukemia, myeloid metaplasia, and multiple myeloma.[8] Four clinical phases of gout include: (1) asymptomatic hyperuricemia, (2) acute gouty arthritis, (3) intercritical gout, and (4) chronic tophaceous gout.[4,8,12]

Frequency of Occurrence

The prevalence of gout in the United States ranges from 0.5 to 2.8 % of men and between 0.1 to 0.6 % of women in the United States.[8] Gout accounts for 5 % of arthritis cases.[12]

Age at Presentation

Gout usually occurs in middle-aged and elderly patients.[8] The peak ages of initial occurrence of gout have been reported to lie between the ages of 30 and 50 years.[8] Patients with gout involving the spine range from 33 to 76 years.[1]

Gender Ratio (M / F)

5/1.[8]

Locations

Early stages of gouty arthritis are often are monoarticular.[8] The most common location is the first metatarsophalangeal joint followed by the ankle joint, tarsal joints, and knee joint.[8,11]

Chronic tophaceous gout is usually polyarticular and asymmetric.[8] Common locations include the feet > hands > wrists > elbows > knees > ankles > shoulders > hips > sacro-iliac joints > spine (disks: facets and uncovertebral joints).[18] Tophaceous deposits can also occur in periarticular ligaments and tendons, bursa, bone, nasal cartilage, ear-lobes, skin, and kidneys.[18] Lesions involving the spine can involve disks, vertebral bodies, facet and uncovertebral joints, posterior elements, and paravertebral soft tissues.[1,2] Spinal gout has been reported to involve any vertebral segment or location.[1,6]

Signs and Symptoms

Patients with hyperuricemia may be asymptomatic[8] Patients with acute gouty arthritis often have intermittent episodes of joint pain and swelling for hours to 10 days that results from acute inflammation.[8] Systemic features such as fever, elevated erythrocyte sedimentation rate, and leukocytosis can occur with acute gouty arthritis.[8] In the early phases of this disease, patients often have one to three exacerbations per year.[8] The symptom-free periods between attacks is referred to as intercritical gout.[8]

Long-standing or chronic arthritis from gout is often associated with continuous chronic pain with intermittent exacerbations.[8] Chronic gout is often associated with deposition of monosodium urate into nodules/tophi associated with protein matrix, inflammatory cells, and giant cells.[8] Tophi may be associated with weakening and rupture of tendons, restriction of movement, and carpal tunnel syndrome.[8] Spinal involvement by gout can result in back pain, fever, spinal canal or foraminal compression.[1,2,5,6,8]

Cross Pathologic Findings

Lesions can appear as irregularly shaped masses associated with hypertrophied synovium.

Histopathologic Findings[2,5,7,12]

Tophi are masses of monosodium urate crystals surrounded by inflammatory reaction consisting of macrophages, lymphocytes, fibroblasts, and foreign body giant cells. Synovial granulomas with epithelioid and giant cells are seen among granular debris. Polarizing microscopy of synovial fluid and synovial granulomas show negative birefringence from urate crystals.

Findings on Plain Films (Roentgenograms) and Computed Tomography

Early phase. Plain films often show asymmetric swelling at joints without mineralization[8] (Fig. **173)** Subsequent episodes may occasionally result in fine calcium deposits producing a poorly defined, hazy increase in density. Articular cartilage damage does not occur until later stages of the disease. Bone mineral density in the early phase is usually within normal limits.[8]

Intermediate phase. Plain films show soft tissue swelling at the involved joint, as well as poorly defined, small erosions in the cortex (juxta-articular and extra-articular locations).[1,8] As the disease progresses, the bone erosions become larger and may result in intra-osseous zones of radiolucency.[1,8] The erosions also often extend toward the subchondral bone.[8]

Late phase. Soft tissue swelling with or without calcifications can be seen with tophi.[3-8,12] The intra-osseous tophi are large and numerous with sclerotic margins. Joint space narrowing is usually seen, with or without chondrocalcinosis. Reactive bone formation occurs adjacent to the erosions producing "overhanging edges"[8] (Fig. 172). If untreated, the disease can progress to bone fragmentation/destruction, subluxation, and ankylosis.

Radiographic features of **gout involving the spine** may include erosions at the uncovertebral or facet joints, osteophytes, or spinal deformities with subluxations and pathologic fractures.[5,6]

On CT, tophi often have 160 Hounsfield units, which may be used for narrowing the differential diagnosis with respect to other joint diseases. Stippled calcifications in the tophi may be seen with *CT*.[3,4,6,7]

MRI Findings

Tophi have variable sizes and shapes and usually have low-intermediate signal on T1WI, FST2WI, and T2WI[1-6,8-10,12] (Figs. **170-174).** Zones of high signal on T2WI can be seen in tophi and may be secondary to regions with increased hydration and proteinaceous zones associated with the deposits of urate crystals.[8,10] Erosions of bone, synovial pannus, joint effusion, bone marrow, and soft tissue edema are readily seen with MRI.[8] MRI also depicts the extent of tophi involving the spine (disks, facet joints) as well as spinal canal or foraminal compromise.[1,2,5,6] Spinal involvement may extend over several adjacent segments.[5]

After Gd-contrast administration, tophi may be associated with heterogeneous, diffuse, or peripheral/marginal enhancement patterns.[1-6,8-10,12] Contrast enhancement seen associated with tophi is probably secondary to the hypervascular granulation tissue and reactive inflammatory cells in the synovium, and/or adjacent soft tissues.[1-6,8-10,12]

Differential Diagnosis

Rheumatoid arthritis, pigmented villonodular tenosynovitis, nodular synovitis, psoriasis, calcium pyrophosphate dihydrate (CPPD) deposition disease, septic arthritis, amyloidosis, sarcoidosis

Prognosis and Treatment

Conservative medical treatment with colchicine or allopurinol is usually effective.[8] Nonsteroidal anti-inflammatory drugs, intravenous colchicine, and/or intra-articular or systemic corticosteroids can be used to treat acute attacks of gout.[1,2,8] Allopurinol is typically used to dissolve tophi and prevent recurrent attacks.[1] Recombinant urate oxidase has been beneficial for chemotherapy-induced hyperuricemia.[8] Debulking of tophi may be necessary depending on the sizes and locations of the lesions.[8] Lesions in the carpal tunnel often require surgical decompression to alleviate pressure on the median nerve.[3] Patients with spinal gout causing neural compression and/or instability usually require surgical decompression and stabilization.[1,2]

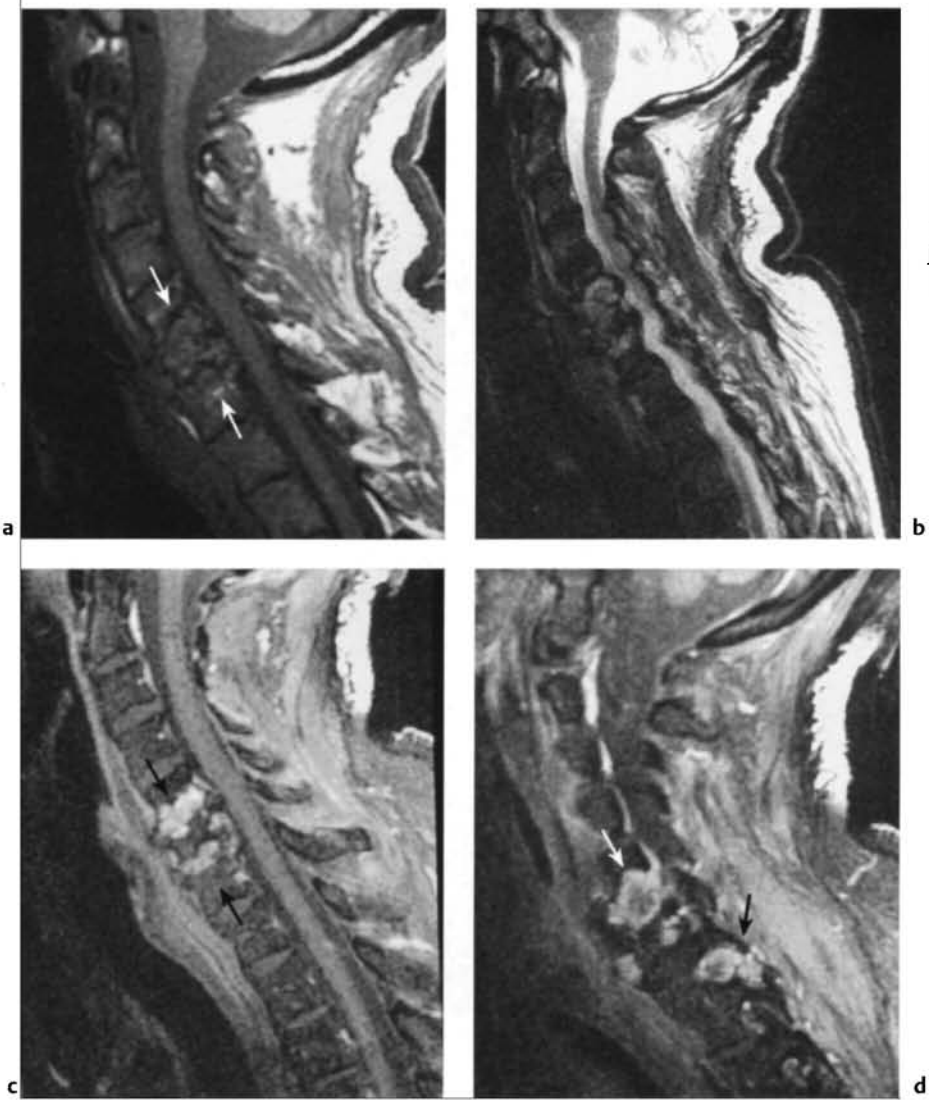

Figure **170a-d** A 60-year-old man with gout involving the spine. MRI shows erosions at the uncovertebral and facet joints at the C 5-6 and C 6-7 levels where there are zones of intermediate signal on sagittal T1 WI (**a**) and slightly high signal on sagittal FS T2WI (**b**). After Gd-contrast administration, heterogeneous contrast enhancement is seen at the sites of gout involving the uncovertebral joints and facet joints on sagittal FST1WI (**c, d**).

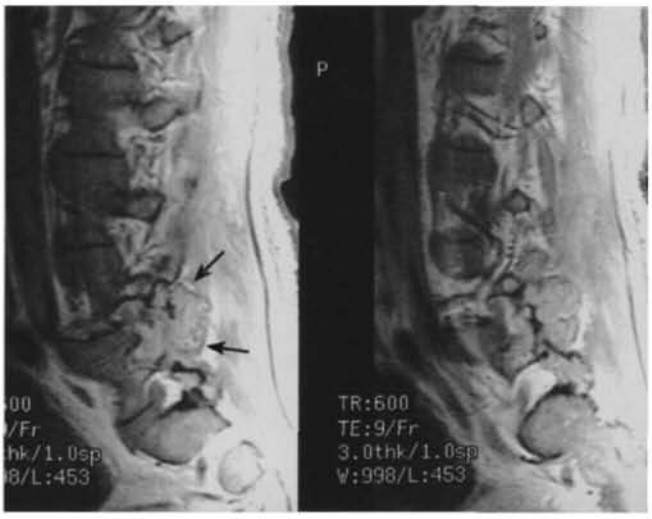

a

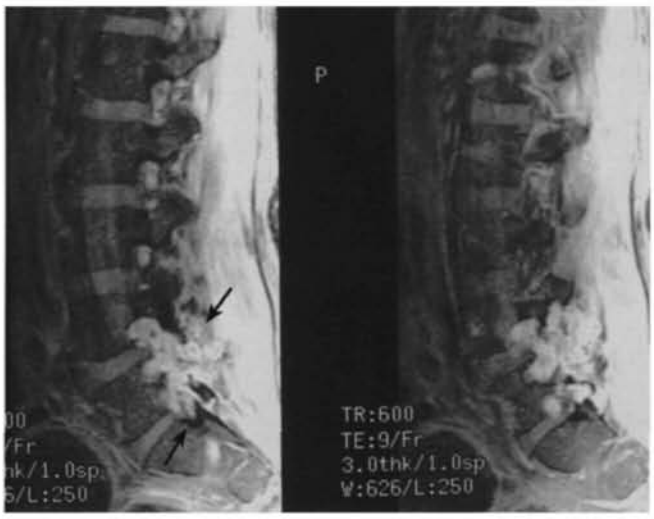

b

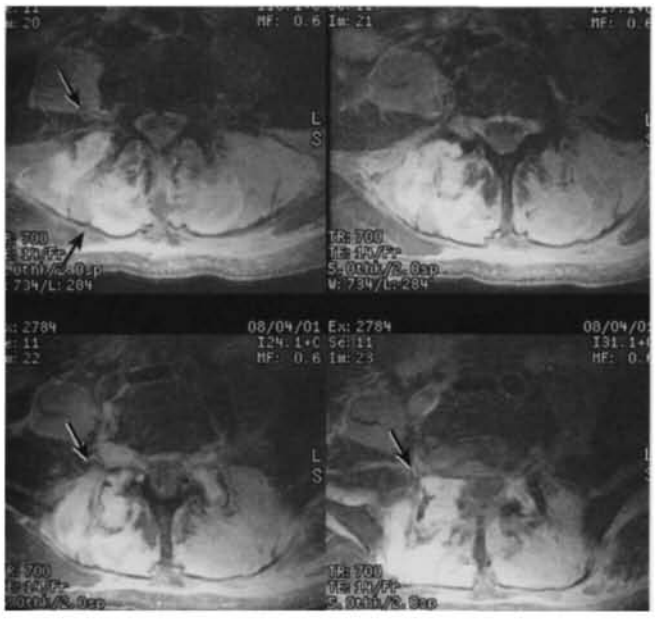

c

Figure **171 a-c** Gout involving the L4-5 facet joints. MRI shows erosions at the facet joints at zones of Gd-contrast enhancement on sagittal T1WI (**a**), and sagittal (**b**) and axial (**c**) FS T1WI.

a

b

Figure **172a-d** Gouty arthritis at the wrist. Radiograph (**a**) AP shows extensive erosive changes at the carpal bones and distal ulna. MRI shows a large fluid collection filled with debris which has intermediate signal on coronal T1WI (**b**) and mixed high, intermediate, and low signal on coronal T2WI (**c, d**). Extensive bone erosion and fragmentation are seen.

Figure 172 c, d

Figure **172c, d**

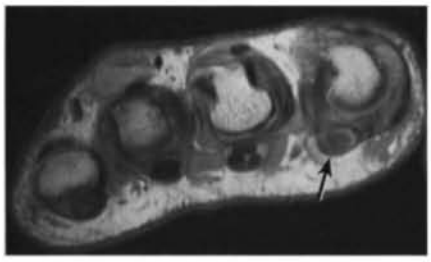

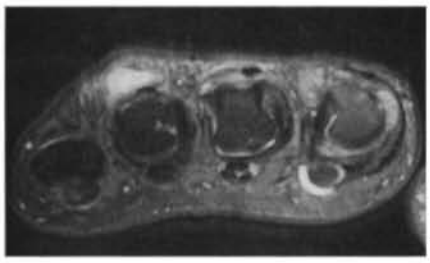

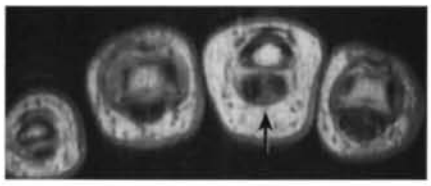

Figure **173 a-e** A 42-year-old man with gout involving the metacarpophalangeal joint of the second finger and distal interphalangeal joint of the third finger. AP radiograph (**a**) shows soft tissue swelling and erosions involving the juxta-articular cortex at the second and third metacarpophalangeal joints and at the distal interphalangeal joint of the third finger. MRI shows tophi involving the extensor tendon of the fourth digit, and flexor tendons and tendon sheaths of the second and third digits (**b-e**) The tophi have low and intermediate signal on coronal (**b, d**) T1WI, and mixed low and intermediate to slightly high signal on coronal (**c, e**) FS T2WI. These signal abnormalities also occur in the tendons at the sites of involvement. Fluid signal is also seen in the involved tendon sheaths.

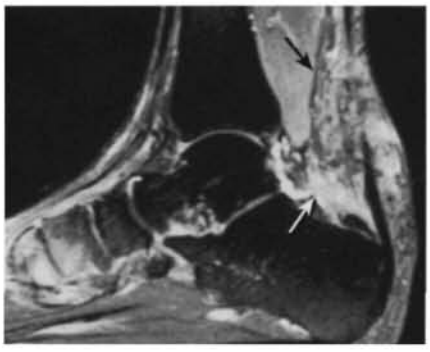

Figure **174a-d** A 47-year-old man with gout and a large tophus surrounding the Achilles tendon. The tophus has low and intermediate signal on sagittal (**a**) and axial (**c**) T1WI, and mixed high and low signal on sagittal (**b**) and axial (**d**) FST2WI.

Figure 174c, d >

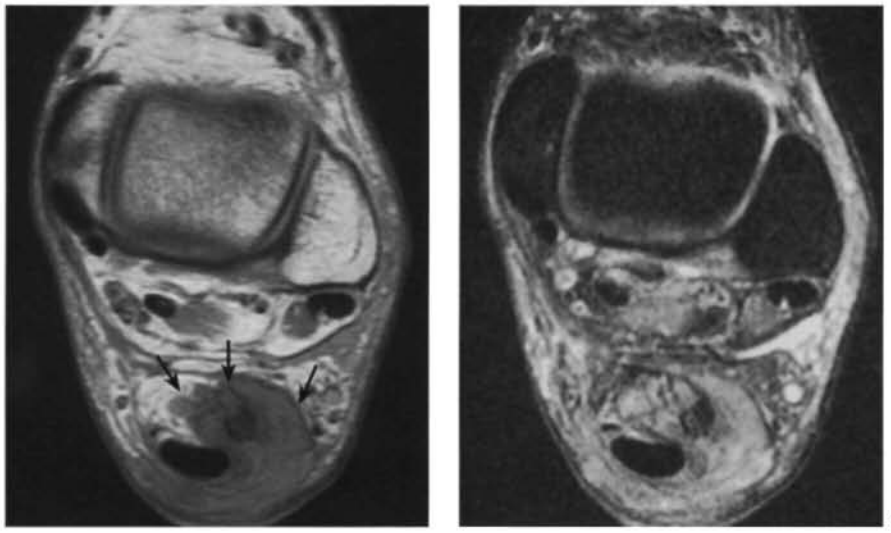

Figure **174c, d**

References

1 Barrett K, Miller ML, Wilson JT. Tophaceous gout of the spine mimicking epidural infection: case report and review of the literature. *Neurosurgery* 2001 ;48:1170-1172.

2 Bonaldi VM, Duong H, Starr MR, Sarazin L, Richardson J. Tophaceous gout of the lumbar spine mimicking an epidural abscess: MR features. *A]NR Am] Neuroradiol* 1996;17:1949-1952.

3 Chen CK, Chung CB, Yeh LR, et al. Carpal tunnel syndrome caused by tophaceous gout: CT and MR imaging features in 20 patients. *AJR Am J Roentgenol* 2000;175:655-659.

4 Chen CK, Yeh LR, Pan HB, et al. Intra-articular gouty tophi of the knee: CT and MR imaging in 12 patients. *Skeletal* Radio/ 1999;28: 75-80.

5 Duprez TP, Malghem J, VandeBerg BC, Noel HM, Munting EA, Maldague BE. Gout in the cervical spine: MR pattern mimicking diskovertebral infection. *AJNR Am J Neuroradiol* 1996;17:151-153.

6 Hsu CY, Shin TTF, Huang KM, Chen PQ, Sheu JJ, Li YW. Tophaceous gout of the spine: MR imaging features. *Clin Radiol* 2002;57:919-925.

7 Liu SZ, Yeh LR, Chou YJ, Chen CKH, Pan HB. Isolated intraoseeous gout in hallux sesamoid mimicking a bone tumor in a teenaged patient. *Skeletal Radiol* 2003;32:647-650.

8 Monu JUV, Pope TL Jr. Gout: a clinical and radiologic review. *Radiol Clin North Am* 2004;42:169-184.

9 Morrison WB, Ledermann HP, Schweitzer ME. MR imaging of inflammatory conditions of the ankle and foot. Magn *Reson Imaging Clin N Am* 2001:9:615-637.

10 Seidl G, Ulrich R, Trattnig S, et al. MR imaging in gout. *Radiologe* 1996:36:632-636.

11 Van Slyke MA, Moser RP, Madewell JE. MR imaging of periarticular soft-tissue lesions. *MRI Clin North Am* 1995:3:651-667.

12 Yu JS, Chung C, Recht M, Dailana T, Jurdi R. MR imaging of tophaceous gout. AJR Am J Roentgeno!1997;168:523-526.

A 33 Hemangioendothelioma (Also Referred to as Low-grade Hemangioendothelioma, Low-grade Hemangioendothelial Sarcoma, Low-grade Angiosarcoma, and Myxoid Angioblastoma)

ICD-O Code

Composite and Kaposi-form: 9130/1

Malignant endovascular papillary angioendothelioma and retiform: 9135/1

Epithelioid hemangioendothelioma: 9133/3

Definition

Hemangioendotheliomas are vasoformative/endothelial neoplasms that occur in soft tissues and bone.[1-31] Hemangioendotheliomas are considered to be low-grade, malignant neoplasms that are locally aggressive and rarely metastasize, compared with the high-grade endothelial tumors such as angiosarcoma.[1725] Hemangioendotheliomas are categorized into subtypes: epithelioid hemangioendothelioma, Kaposi-form hemangioendothelioma, papillary intralymphatic angioendothelioma (Dabska tumor), retiform hemangioendothelioma, composite hemangioendothelioma, and spindle cell hemangioendothelioma.[2-6,8,10,11,15,18-20.24-27,30]

Epithelioid hemangioendotheliomas are locally aggressive vascular tumors containing epithelioid endothelial cells organized in short cords or nests within myxohyaline stroma.[2,3,17,26,30-32] These tumors have metastatic potential.[30]

Kaposi-form hemangioendotheliomas are locally aggressive tumors with vascular differentiation and associated Kaposi-sarcoma-like fascicular patterns of atypical spindle cells.[27] These tumors, which rarely metastasize, can be associated with Kasabach-Merritt syndrome.[6,10,15,18,20]

Papillary angioendotheliomas (Dabska tumors) are locally aggressive vascular tumors which have lymphatic-like channels and papillary endothelial proliferation.[5] These tumors can occur within hemangiomas.[4,19]

Retiform hemangioendotheliomas are locally aggressive vascular tumors with elongated and narrow, arborizing blood vessels or channels lined by endothelial cells.[4]

Composite hemangioendotheliomas are locally aggressive tumors with vascular differentiation associated with various combinations of benign and malignant histologic zones.[25]

Spindle cell hemangioendotheliomas are primary benign vascular neoplasms that can be associated with Maffucci syndrome, Klippel-Trenaunay-Weber syndrome, early onset varicosities, and congenital lymph edema (Milroy disease).[7,11,15,24] These tumors reportedly have no metastatic potential and have been also been referred to as spindle cell hemangiomas for solitary lesions and spindle cell hemangiomatosis for multiple lesions.[24]

Frequency of Occurrence

Hemangioendotheliomas in bone. These tumors account for < 1 % of primary malignant bonetumors.[9,12,21-23,28,29] Lesions can be unifocal, or occur as multiple lesions in one or more bones.[12,17]

Hemangioendotheliomas in soft tissue. These tumors account for < 1 % of malignant tumors, and all soft tissue tumors.[14,16]

Age at Presentation

Hemangioendotheliomas in bone: from 10 to 82 years,[12,21-23,28,29] median = 36 to 47 years,[8,23] mean = 43 to 46 years.[9,12] Patients with multifocal lesions tend to be ~ 10 years younger on average than those with unifocal tumors.[12]

Hemangioendotheliomas in soft tissue: from 17 to 60 years, mean = 40 years.[14]

Epithelioid hemangioendotheliomas occur in adolescents, and in young and old adults.[15,30]

Kaposi-form hemangioendotheliomas frequently occur in infants and children during the first decade, but also occur in adults.[6,18,20,27] In one study, patients ranged in age from 2 weeks to 20 years, mean = 3.75 years.[18] These tumors have also been reported in adults as old as 64 years.[20]

Papillary angioendotheliomas (Dabska tumors) commonly occur in infants and children.[5] Approximately 25% occur in adults.[5]

Retiform hemangioendotheliomas commonly occur in young adults, but have been reported in older patients.[4]

Composite hemangioendotheliomas commonly occur in adults and occasionally in children.[25]

Spindle cell hemangioendotheliomas have been reported to range in age from 8 to 78 years, mean = 34 years, median = 32 years.[24]

Gender Ratio (M / F)

Hemangioendotheliomas in bone: 1.2 /1 to 2/1.[2-9,12,13,21-23.28.29]

Hemangioendotheliomas in soft tissue: 1 /1.4.[14,16]

Epithelioid hemangioendotheliomas: 1 /1[15,30]

Kaposi-form hemangioendotheliomas: 1.5 /1.[17]

Papillary angioendotheliomas (Dabska tumors): 1 /1.[5]

Retiform hemangioendotheliomas: 1 /1.[4]

Composite hemangioendotheliomas: 1 /1.[25]

Spindle cell hemangioendotheliomas: 1 /1.[24]

Location

Hemangioendotheliomas in bone. Tumors occur in the femur, tibia > humerus > vertebrae > ribs > feet > hands > skull, fibula > scapula > other bones.[2,12,13,17,23,29] Lesions can be located at or near the ends of long bones (epi-metaphyseal region) > diaphyseal > metaphyseal locations.[17,23]

Epithelioid hemangioendotheliomas in bone. These lesions have a multifocal distribution pattern in up to 64% of cases.[2,7,9,13,17,29] Multifocal lesions often involve a single limb or occur in one anatomic region.[7,9,12,13,17] Tumors in the spine are most commonly located in the vertebral body, although extension into the posterior elements is not uncommon.[1,3] Tumor extension into joints has been reported.[17]

Hemangioendotheliomas in soft tissue:

- **Epithelioid subtype.** This tumor often occur in the superficial or deep soft tissues of extremities.[15,30] Lesions can also occur in bone and viscera (liver and lung are common sites).[15] Over half of the tumors originate from a small vessel, which is often a vein.[15,30]
- **Kaposi-form subtype.** This tumor occurs in the skin, superficial or deep soft tissues of the trunk or extremities, as well the head and neck region, trunk, chest, mediastinum, retroperitoneum, and scrotum.[15,18,27]
- **Malignant endovascular papillary angioendothelioma (Dabska tumor).** This tumor occurs in skin, subcutaneous soft tissues, and bone. Most lesions occur in the extremities.[5]
- **Retiform hemangioendothelioma.** This tumor occurs in the skin and subcutaneous tissue. Lesions are often located in the distal extremities.[4]
- **Composite hemangioendothelioma.** This tumor commonly occurs in the distal extremities.[25]
- **Spindle cell hemangioendothelioma.** This tumor commonly occurs in the dermis/subcutis of the distal extremities.[24]

Signs and Symptoms

Hemangioendotheliomas in bone. Lesions are often associated with localized pain and occasionally with soft tissue swelling.[1,2,17,23,29] Lesions in the spine can result in myelopathy.[13] Pathologic fractures occur in up to 10 % of these tumors located in bone.[2,13,17] Tumors involving vertebrae can be associated with neck and back pain, as well as spinal cord compression.[1,3]

Hemangioendotheliomas in soft tissue. Lesions may present as solitary masses, with or without pain.[4-6,25,27,30] Lesions can range in size from less than 1 cm to 15 cm.[4-6,25,27,30]

Epithelioid hemangioendotheliomas. These neoplasms can be painful tumors in the superficial and/or deep soft tissues.[30] Tumors may be associated with edema and thrombophlebitis related to their frequent derivation from blood vessels.[30]

Kaposi-form hemangioendotheliomas. Those lesions that involve the superficial soft tissues can appear as violaceous or blue-red plaques or masses.[18,27,31] Kaposi-form hemangioendotheliomas in the deep soft tissues may erode bone or extend into lymph nodes, and retroperitoneal tumors may be associated with intestinal obstruction, ascites, and jaundice.[27] Large Kaposi-form hemangioendotheliomas can be associated with anemia and consumptive coagulopathy (Kasabach-Meritt syndrome or phenomenon) due to clot activation within the neoplastic vasculature.[18,27] Up to 56 % of patients with Kaposi-form hemangioendotheliomas present with Kasabach-Meritt syndrome or phenomenon.[18]

Malignant endovascular papillary angioendotheliomas (Dabska tumors). These tumors are often slow-growing, painless neoplasms that appear as a cutaneous nodule or plaque.[5]

Retiform hemangioendotheliomas. These neoplasms often appear as a blue-red cutaneous nodule or plaque.[4] Most of these tumors measure less than 3 cm.[4]

Composite hemangioendotheliomas. These tumors often appear as red-blue superficial nodules and may have associated lymph-edema.[25]

Spindle cell hemangioendotheliomas. These tumors often appear as one or more red or red-brown superficial nodules that most frequently occur in the distal extremities, ranging in size from less than 1 cm to 5 cm.[5,24] Spindle cell hemangioendotheliomas can be associated with multiple enchondromas (Maffucci syndrome), congenital lymphedema (Milroy syndrome), varicosities, and Klippel Trenaunay syndrome.[5,24]

Cross Pathologic Findings[4-6,1,,15,20,23,24]

Hemangioendotheliomas in bone. Tumors are often friable, firm, and/or soft-spongy, reddish-brown, and grossly bloody.[3,9,12,29] Epithelioid hemangioendotheliomas are typically soft and lobulated with associated zones of hemorrhage.[9]

Hemangioendotheliomas in soft tissue:

- **Epithelioid subtype (most common).** The tumors are often lobulated or ovoid, tan-pink or reddish vascular neoplasms.[30] This tumor can appear as a fusiform mass within a vein, simulating an organizing thrombus.[30]
- **Kaposi-form subtype.** Tumors often appear as slightly raised cutaneous purplish/violaceous lesions with irregular or poorly defined margins ranging in size from < 1 cm to 7 cm.[6,18,27] In the subcutaneous tissues, tumors can occur as gray-white, multinodular lesions with or without coalescence.[27] Tumors can invade adjacent muscle.[18]
- **Malignant endovascular papillary angioendothelioma (Dabska tumor).** Tumors can occur as cutaneous or intraosseous, purplish vascular lesions.[5,19] Tumors in the dermis and subcutaneous tissue often have ill-defined margins.[5]
- **Retiform hemangioendothelioma.** Tumors often appear as zones of swelling or induration of the dermis and subcutaneous soft tissues.[4]
- **Composite hemangioendothelioma.** Tumors often appear as red-blue, superficial nodules and may have associated lymph-edema.[25] The tumor nodules range in size from 0.7 to 6 cm.[25] Some of these tumors have ill-defined margins.[25]
- **Spindle cell subtype.** The tumors consist of one or more red-brown nodules which range in size from <1cm to 5cm.[5,24] Multiple lesions can occur as groups which may be separated by several centimeters.[5,24] Phleboliths and thrombi may be seen in some of these tumors.[5,24]

Histopathologic Findings

Hemangioendotheliomas in bone.[1-3,7-9,12,13,,17,19,29,32] Lesions have varying proportions of solid and vasoformative growth patterns, and contain variable amounts of well-formed blood vessels. Tumor cells have spheroid, ovoid, or cuboidal shapes and usually contain large ovoid or bilobed nuclei within eosinophilic cytoplasm. The cell nucleus is often eccentic or peripherally located

and may contain distinct nucleoli. Most tumors show low or absent mitotic activity. Spindle-shaped cells are occasionally present. Eosinophilic and lymphoplasmacytic inflammatory infiltrates can also occur, as well as small focal regions with myxoid or hyaline stroma.[8] Lesions typically permeate medullary bone.

Epithelioid subtype of hemangioendothelioma in bone. Lesions usually consist of cords or strands of spindle-shaped and plump epithelioid endothelial cells with eosinophilic cytoplasm and intracytoplasmic lumens (vacuoles) containing erythrocytes.[2,3,8,13,17] Tumor cells can occur in a myxoid and/or hyalinized stroma.[2,3,8,13] Mitotic activity is usually low. Only minimal well-formed vascular spaces are usually seen. Lesions are often multifocal.

Hemangioendotheliomas in bone can show immunoreactivity to vimentin, and endothelial markers (FVIIIRag, Ulex Europeaus agglutinin 1).[9,17] Immunoreactivity to epithelial membrane antigen and cytokeratins occurs in ~ 50 % of cases.[9]

Some epithelioid hemangioendotheliomas contain atypical cells with hyperchromatic nuclei and prominent nucleoli, spindle cells and primitive vascular differentiation, features associated with a worse prognosis.[9]

Hemangioendotheliomas in soft tissue:

- **Epithelioid subtype (most common).** Lesions consist of cords or strands of relatively uniform, plump to slightly-spindled endothelial cells with eosinophilic cytoplasm that are often referred to as "epithelioid" or "histocytoid."[30,31] The neoplastic cells show endothelial differentiation with intracytoplastic vacuoles containing red blood cells.[13,30] Tumor cells usually occur in a sulfated acidic matrix which can stain as light blue (chondroid-like) and/or pink.[30] Mitotic activity is usually low or absent.[30] Only a small number of well-formed vascular spaces are usually seen.[30] Osteoclastic giant cells and metaplastic bone may occasionally occur in these tumors.[30] Up to 33 % of hemangioendotheliomas have more aggressive histologic features such as prominent nuclear atypia, increased mitotic activity, and necrosis.[30] Epithelioid hemangioendotheliomas are usually immunoreactive to FLI 1 and vascular markers such as CD 31, CD 34, and von Willebrand factor.[30]
- **Kaposi-form subtype.** Lesions usually have nodular or lobular growth patterns containing densely packed, curved or straight fascicles of spindle-shaped cells associated with small vascular spaces.[6,10,18,27,31] Tumors vary in proportions of well canalized areas resembling capillary hemangiomas, and solid-appearing regions with minimal slitlike vascular channels.[6,10,18,27] The small vascular spaces may be lined by flat spindle-shaped cells or plump endothelial cells that are usually not immunoreactive to von Willebrand factor / VIII related antigen.[27] Tumor cells react positively to CD 31, CD 34, and FLI 1.[18,20,27] Mitotic activity is usually minimal.[18,27] Epithelioid or glomeruloid zones of spheroid cells with hyaline granules, small vacuoles, and hemosiderin are often scattered throughout these tumors.[18] The epithelioid or glomeruloid zones are associated with platelet trapping (as seen with CD 61-positive fibrin thrombi) and show immunoreactivity to smooth muscle actin.[18] Capillaries containing fibrin can be seen at the periphery.[27]
- **Malignant endovascular papillary angioendothelioma (Dabska tumor).** Lesions consist of anastomizing thin-walled vascular channels containing intraluminal papillary projections of endothelial cells overlying hyaline cores.[5,31] The typical endothelial cell has a high nuclear to cytoplasm ratio, and often contains an apically-positioned nucleus with minimal or no atypia, within a small volume of pink cytoplasm.[5,31] The nuclei may or may not have a grooved configuration, and some of these prominent nuclei can result in a bulge of the cell surface causing "hobnail" or "matchstick" cellular shapes.[5,31] Mitotic activity is typically low or absent.[5] Lesions can occur in bone or subcutaneous soft tissues and skin.[5] Tumor cells are often immunoreactive to von Willebrand factor, CD 31, and CD 34,[5] and may also be immunoreactive to vascular endothelial growth factor receptor-3.[5]
- **Retiform hemangioendothelioma.** These tumors contain narrow branching vascular channels lined by relatively uniform endothelial cells with prominent hyperchromatic nuclei and little cytoplasm.[4,31] Mitotic activity is rare.[4] Dense zones of endothelial cells may occur with or without peripheral sclerotic stroma.[4,31]
- **Composite subtype.** These tumors have portions that have histologic features similar to epithelioid hemangioendothelioma, retiform hemangioendothelioma, spindle cell hemangioendothelioma, and angiosarcoma.[25] These tumors usually show immunoreactivity to von Willebrand factor, CD 31, and CD 34.[25]
- **Spindle cell subtype.** Up to 58 % of these tumors are intravascular.[24] These tumors contain cavernous and collapsed vascular spaces lined with plump endothelial cells with cytoplasmic vacuolization or flattened endothelial cells when the vascular spaces are collapsed.[11,24] Endothelial cells react positively for Factor VIII RA, CD 31, and CD 34.[11] The vascular spaces are separated by spindled fibroblastic cells with low mitotic activity and minimal or no atypia.[24] The spindle cells react positively for vimentin and actin.[11]

Tumor Genetics

For epithelioid hemangioendothelioma a translocation [t(l;3(p36.3:q25)] has been reported.[15,30]

Findings on Plain Films (Roentgenograms) and Computed Tomography

Hemangioendotheliomas in bone.[1-3,7,9,13,17,19,21,23,26,29,31] Lesions are single or multiple, radiolucent zones in the medullary space, with or without cortical thinning (Fig. **176).** Most lesions have sharp, lobulated borders, with or without thin sclerotic margins. These neoplasms are associated with variable degrees of endosteal erosion, cortical thinning, cortical destruction, and osseous expansion. Matrix mineralization and periosteal reaction is uncommon.

Epithelioid hemangioendotheliomas in bone. Lesions have features that are similar to other types of hemangioendothelioma.[2,13,32] Lesions are usually radiolucent and well-defined in the medulla, although larger lesions (5-10 cm) can have a permeative radiolucent pattern. Cortical thinning and destruction can be seen with extra-osseous soft tissue extension. Epithelioid hemangioendotheliomas have a multifocal distribution pattern in up to 64 % of cases.[2,7,9,13,29,32] Multifocal lesions often involve a single limb or occur in one anatomic region.[7,9,12,13,32]

Hemangioendotheliomas in soft tissue[11,24,32] Soft tissue lesions may be observed, typically, without matrix mineralization.

MRI Findings

Hemangioendotheliomas in bone.[1-3,13,17,19,26,32] Lesions usually have sharp margins that may be slightly lobulated (Figs. **175, 176).** Lesions often have low-intermediate and/or high signal

on T1WI and PDWI, and heterogeneous intermediate-high signal on T2WI and FST2WI, with or without zones of low signal. Lesions can be multifocal. Extra-osseous extension of tumor through zones of cortical destruction can be seen. After Gd-contrast administration, lesions often show prominent heterogeneous enhancement.

Hemangioendotheliomas in soft tissue.[6] Lesions often have lobulated margins than can be either well-defined or irregular (Figs. 177). Lesions usually have intermediate signal on T1WI, and heterogeneous predominantly high signal on T2WI, with or without internal low-signal septations. Flow voids may be seen with the lesions. Erosions of adjacent bone may be seen from these neoplasms. After Gd-contrast administration, lesions often show heterogeneous prominent enhancement.

Differential Diagnosis

Hemangioendotheliomas in bone. For multifocal lesions: Langerhans cell histiocytosis, fibrous dysplasia, metastases, myeloma, lymphoma.[17] For solitary lesions: desmoplastic fibroma, nonossifying fibroma, Ewing sarcoma, osteosarcoma, fibrosarcoma, aneurysmal bone cyst, giant cell tumor, chronic osteomyelitis.

Hemangioendotheliomas in soft tissue. Metastatic carcinoma, melanoma, lymphoma, malignant fibrous histiocytoma, angiosarcoma, hemangiopericytoma, liposarcoma.

Prognosis and Treatment

Hemangioendotheliomas are considered to be low-grade, malignant, vasoformative tumors toward the benign end of the spectrum of vascular tumors, ranging from hemangiomas to the high-grade angiosarcomas.[4,5,7-9,12,17-20,23-25,27,29,30,32] Hemangioendotheliomas have better prognoses than angiosarcomas.[7,9,12,23,29,32] Grade 3 hemangioendotheliomas in bone, which contain atypical endothelial cells and nuclear pleomorphism, have a worse prognosis than lower grade tumors.[2] Hemangioendotheliomas in bone have been treated with preoperative embolization followed by surgical resection, with or without postoperative radiation and chemotherapy.[1-3,8,9,12,13,23] A local recurrence rate of 13 % has been reported, as well as a 31 % occurrence of regional and distant metastasis.[1,17] Secondary osteosarcomas can result from radiation of intra-osseous hemangioendotheliomas.[1]

For soft tissue hemangioendotheliomas, resection of these tumors with wide margins is usually performed with or without lymph node dissection.[4-6,13,15,18,24,27,31]

Patients with **epithelioid hemangioendotheliomas** have been reported to have a local recurrence rate of 15 %, metastatic rates up to 30%, and mortality rates up to 20 %.[15,30]

The prognosis for **Kaposi-form hemangioendothelioma** is poorer for large, intra-abdominal lesions associated with Kasabach-Merritt syndrome than those located in the superficial soft tissues with easier surgical access.[18,27] Tumors can occasionally spread to regional perinodal tissue, but typically do not metastasize to distant sites.[18,20] Mortality usually results from Kasabach-Merritt syndrome and not from metastatic disease.[18]

Papillary angioendotheliomas (Dabska tumors) have low rates of local recurrence and metastasis.[5]

Retiform hemangioendotheliomas have been reported to have local recurrences in up to 60% of patients, but low rates of metastasis.[4]

Composite hemangioendotheliomas have recurrence rates of ~50%.[25]

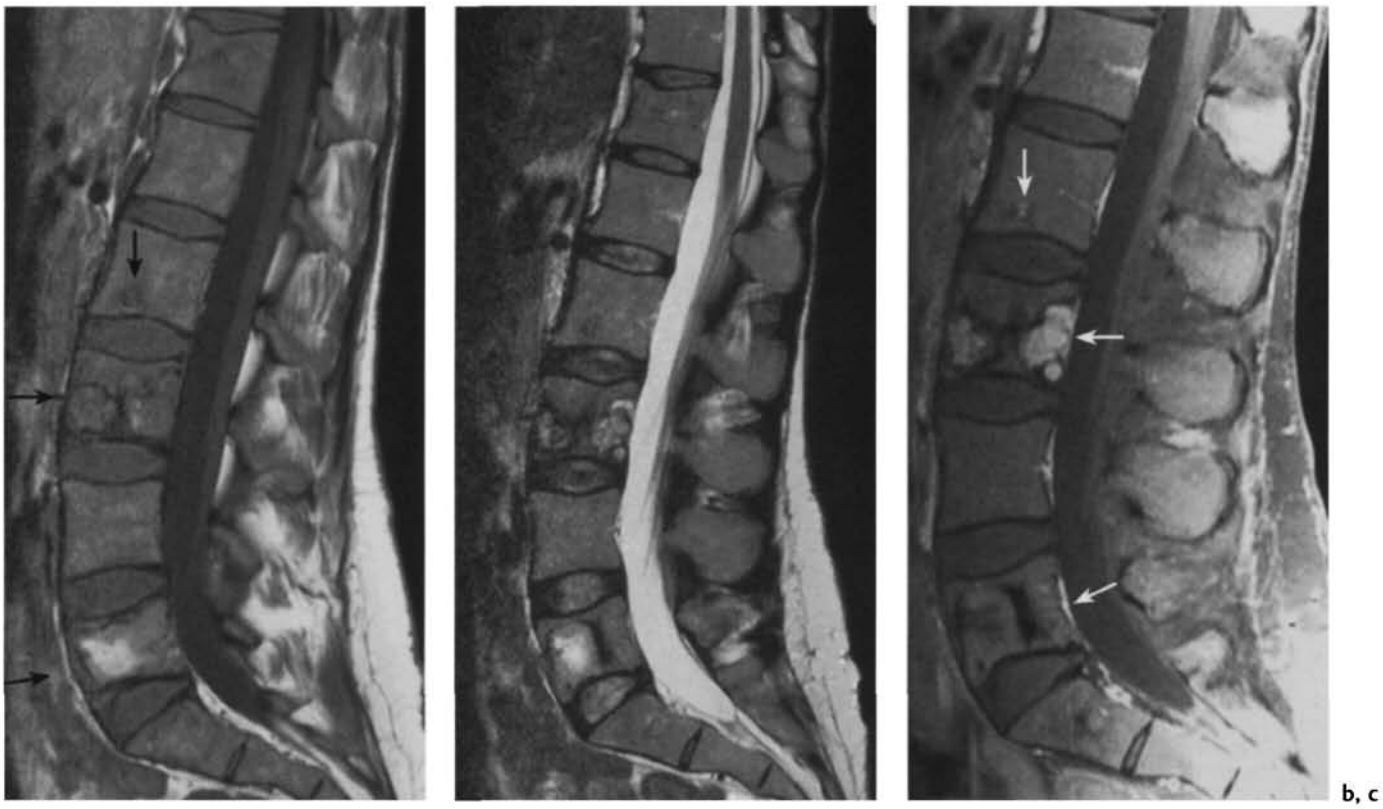

a b, c

Figure **175a-c** A 42-year old woman with multifocal hemangioendothelioma involving the L2, L3, and L5 vertebrae. The tumors have mixed low, intermediate, and high signal on sagittal T1WI (**a**) and sagittal T2WI (**b**). The lesions show heterogeneous and varying degrees of Gd-contrast enhancement on sagittal FST1WI (**c**).

a b

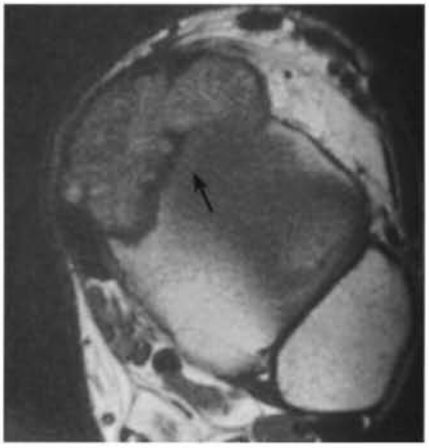

c d, e

f g

Figure **176a-g** A 19-year-old man with a multifocal hemangioendothelioma involving the distal tibia and talus. Oblique lateral (**a**) and oblique AP (**b**) radiographs show circumscribed radiolucent zones in the medullary portions of the tibia and talus associated with cortical thinning and expansion. The margins of the lesions are slightly lobulated. MRI shows the lesions to have low-intermediate signal on axial (**d**) T1WI, and heterogeneous high and intermediate signal on sagittal (**c**) T2WI, and axial (**e**) and coronal (**f**) FS T2WI. Cortical expansion is seen as well as extra-osseous tumor extension through sites of cortical disruption. Thin linear zones of low signal are seen at the medullary margins of the lesions. The lesions show prominent Gd-contrast enhancement on coronal (**g**) FST1WI.

Spindle cell hemangioendotheliomas have local recurrence in 58 % of patients, which have been reported to occur from months to 34 years after the original surgery.[24] Patients with spindle cell hemangioendothelioma typically do not have metastatic disease, although one patient with Maffucci syndrome developed an angiosarcoma at a different site from where the spindle cell hemangioendothelioma was located.[24]

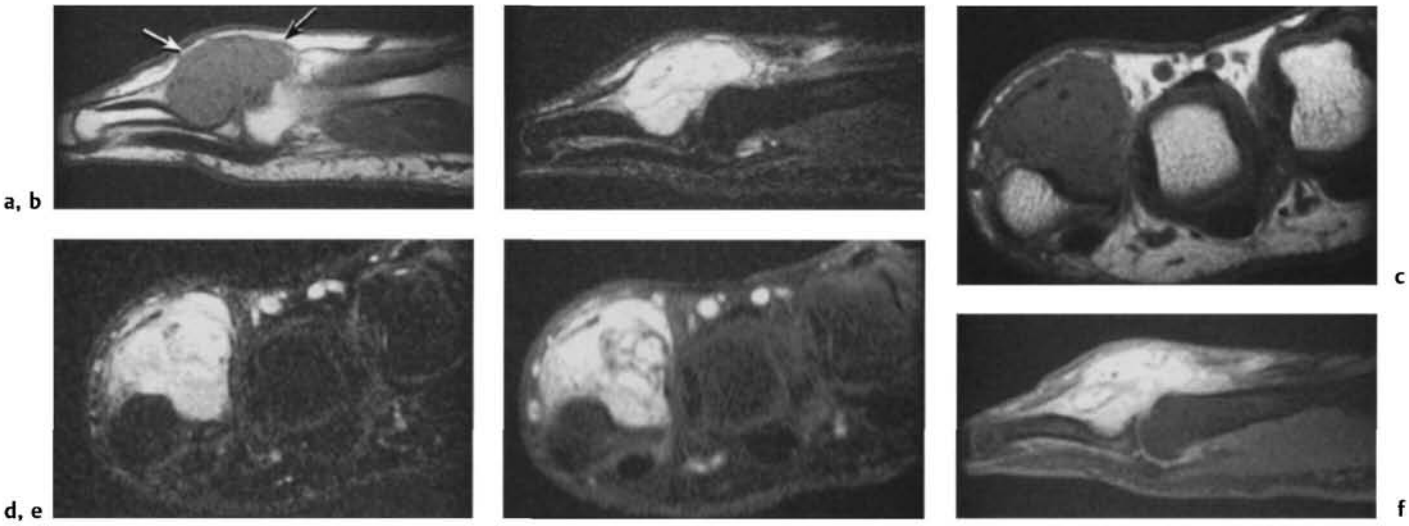

Figure **177a-f** A 36-year-old man with a hemangioendothelioma involving the dorsal soft tissues of the foot. MRI shows a circumscribed lesion with intermediate signal on sagittal (**a**) and coronal (**c**) T1WI, and high signal on sagittal (**b**) and coronal (**d**) FST2WI. Several small zones of low signal are seen on T1WI and FST2WI. The tumor shows prominent Gd-contrast enhancement on coronal (**e**) and sagittal (**f**) FS T1 WI. Erosion of adjacent cortical bone is present.

References

1 Aflatoon K, Staals E, Bertoni F, et al. Hemangioendothelioma of the spine. *Clin Orthop Relat Res* 2004;418:191-197.

2 Boutin RD, Spaeth HJ, Mangalik A, SellJJ. Epitheiioid hemangioendothelioma of bone. *Skeletal* Radiol1996;25(4}:391-395.

3 Brennan JW, Midha R, Ang LC, Perez-Ordonez B. Epitheiioid hemangioendothelioma of the spine presenting as cervical myelopathy: case report. *Neurosurgery* 2001:48:1166-1169.

4 Calonje E. Retiform haemangioendothelioma. In: Fletcher CDM, Unni KK, Mertens F, eds. *World Health Organization Classification of Tumours. Pathology and Genetics of Tumours of Soft Tissue and Bone* Geneva: IARC Press; 2002:165-166.

5 Calonje E. Papillary intralymphatic angioendothelioma. In: Fletcher CDM, Unni KK, Mertens F, eds. *World Health Organization Classification of Tumours. Pathology and Genetics of Tumours of Soft Tissue and Bone* Geneva: IARC Press: 2002:167

6 Cooper JG, Edwards SL, Holmes JD. Kaposiform haemangioendothelioma: case report and review of the literature. *Br] Plast Surg* 2002; 55:163-165.

7 Darby AJ. Vascular neoplasms of bone. In: Helliwell TR, ed. *Major Problems in Pathology: Pathology of Bone and Joint Neoplasms* 1st ed. Vol 37. Philadelphia, Pa: W.B. Saunders; 1999:330-343.

8 Evans HL, Raymond AK, Ayala AG. Vascular tumors of bone: a study of 17 cases other than ordinary hemangioma, with an evaluation of the relationship of hemangioendothelioma of bone to epithelioid hemangioma, epithelioid hemangioendothelioma, and high-grade angiosarcoma. Hum *Pathol* 2003;34:680-689.

9 Forest M. Vascular tumors. In: Forest M, Tomeno B, Vanel D, eds. *Orthopedic Surgical Pathology: Diagnosis of Tumors and Pseudotumoral Lesions of Bone and Joints* Edinburgh: Churchill Livingstone; 1998:345-362.

10 Hardisson D, Prim MP, DeDiego JI, Patron M, Escribano A, Rabanal I. Kaposiform hemangioendothelioma of the external auditory canal in an adult. *Head Neck* 2002;24:614-617.

11 Hisaoka M, Aoki T, Kouho H, Chosa H, Hashimoto H. Maffucci's syndrome associated with spindle cell hemangioendothelioma. *Skeletal Radial* 1997;26:191-194.

12 Huvos AG. Angiosarcoma of bone (epithelioid hemangioendothelioma; malignant hemangioendothelioma). In: Huvos Ag, ed. *Bone Tumors: Diagnosis, Treatment, and Prognosis* 2nd ed. Philadelphia, Pa: W.B. Saunders; 1991:579-598.

13 Ignacio EA, Palmer KM, Mathur SC, Schwartz AM, Olan WJ. Epithelioid hemangioendothelioma of the lower extremity. *Radiographics* 1999;19:531-537.

14 Kransdorf MJ. Malignant soft-tissue tumors in a large referral population: distribution of diagnoses by age, sex, and location. *AJR Am] Roentgenol* 1995;164:129-134.

15 Kransdorf MJ, Murphey MD. Vascular and lymphatic tumors. In: Kransdorf MJ, Murphey MD, eds. *Imaging of Soft Tissue Tumors* 2nd ed. Philadelphia, Pa: W.B. Saunders; 1997:2006:150-188.

16 Kransdorf MJ, Murphey MD. Soft tissue tumors in a large referral population: prevalence and distribution of diagnoses by age, sex, and location. In: In: Kransdorf MJ, Murphey MD, eds. *Imaging of Soft Tissue Tumors* 2nd ed. Philadelphia: W.B. Saunders; 2006:6-37.

17 Larochelle 0, Perigny M, Lagace R, Dion N, Giguere C. Epithelioid hemangioendothelioma of bone. *Radiographics* 2006:26:265-270.

18 Lyons LL, North PE, Lai FMM, Stoler MH, Folpe AL, Weiss SW. Kaposiform hemangioendothelioma. A study of 33 cases emphasizing its pathologic, immunophenotypic, and biologic uniqueness from juvenile hemangioma. *Am J Surg Pathol* 2004;28:559-568.

19 McCarthy EF, Lietman S, Argani P, Frassica FJ. Endovascular papillary angioendothelioma (Dabska tumor) of bone. *Skeletal Radiaol* 1999;28: 100-103.

20 Mentzel T, Mazzoleni G, Dei Tos AP, Fletcher CD. Kaposiform hemangioendothelioma in adults. Clinicopathologic and immunohistochemical analysis of three cases. *Am J Clin Pathol* 1997;108:450-455.

21 Mulder JD, Schutte HE, Kroon HM, Taconis WK. Introduction. In: *Radiologic Atlas of Bone Tumors* Amsterdam: Elsevier; 1993:3-6.

22 Mulder JD, Schutte HE, Kroon HM, Taconis WK. The diagnosis of bone tumors. In: *Radiologic Atlas of Bone Tumors* Amsterdam: Elsevier; 1993:9-46.

23 Mulder JD, Schutte HE, Kroon HM, Taconis WK. Hemangio-endothelioma and hemangio-endotheliosarcoma. In: *Radiologic Atlas of Bone Tumors* Amsterdam: Elsevier; 1993:241-248.

24 Perkins P, Weiss SW. Spindle cell hemangioendothelioma. An analysis of 78 cases with reassessment of its pathogenesis and biologic behavior. *Am J Surg Pathol* 1996;20:1196-1204.

25 Rubin BP. Composite haemangioendothelioma. In: Fletcher CDM, Unni KK, Mertens F, eds. *World Health Organization Classification of Tumours. Pathology and Genetics of Tumours of Soft Tissue and Bone* Geneva: IARC Press; 2002:168-169.

26 Rushing EJ, White JA, D'Alise MD, Chason DP, White CL, Bigio EH. Primary epithelioid hemangioendothelioma of the clivus. *Clin Neuropathol* 1998:17:110-114.

27 Tsang WYW. Kaposiform haemangioendothelioma. In: Fletcher CDM, Unni KK, Mertens F, eds. *World Health Organization Classification of Tumours. Pathology and Genetics of Tumours of Soft Tissue and Bone* Geneva: IARC Press; 2002:163-164.

28 Unni KK. Introduction and scope of study. In: *Dahlin's Bone Tumors-General Aspects and Data on 11* 087 Cases 5th ed. Philadelphia, Pa: Lippincott, Williams & Wilkins; 1996:1-9.

29 Unni KK. Hemagioendothelioma (hemangiosarcoma) and hemangiopericytoma. In: *Dahlin's Bone Tumors—General Aspects and Data on 11087 Cases* 5th ed. Lippincott, Williams & Wilkins; 1996:317-331.

30 Weiss SW, Bridge JA. Epithelioid haemangioendothelioma. In: Fletcher CDM, Unni KK, Mertens F, eds. *World Health Organization Classification of Tumours. Pathology and Genetics of Tumours of Soft Tissue and Bone* Geneva: IARC Press; 2002:173-174.

31 Weiss SW, Goldblum JR. Hemangioendothelioma: vascular tumors of intermediate malignancy. In: Weiss SW, Goldblum JR, eds. *Enzinger and* Weiss's *Soft Tissue Tumors* 4th ed. St. Louis, Mo: Mosby; 2001: 891-915.

32 Wenger DE, Wold LE. Malignant vascular lesions of bone: radiologic and pathologic features. *Skeletal* Radiol 2000;29:619-631.

A 34 Hemangiomas (Also Referred to as Vascular Hamartomas)

ICD-O Codes

Subcutaneous / deep soft tissue / bone: 9120/0

Capillary: 9131/0

Cavernous: 9121/0

Arteriovenous: 9123/0

Venous: 9122/0

Intramuscular: 9132/0

Synovial: 9120/0

Epithelioid: 9125/0

Definition

Hemangiomas are benign lesions of bone and soft tissues comprised of capillary, cavernous, and/or malformed venous vessels.[3,6,7,10,15,22,33] Hemangiomas have been considered to be a hamartomatous disorder.[3] Intramuscular hemangiomas consist of collections of benign vascular channels and varying amounts of mature adipose tissue in skeletal muscle.[3] Venous hemangiomas contain veins of differing sizes and wall thicknesses.[3] Arteriovenous hemangiomas are benign hemangiomas which also contain arteriovenous shunts.[3] Epithelioid hemangiomas are benign lesions with immature vessels lined with plump epithelioid endothelial cells.[9] Synovial hemangiomas represent benign proliferation of blood vessels in synovium.[3] Angiomatosis refers to a diffuse form of hemangiomas that can occur over a large area in soft tissues and/or bone, and often involves multiple tissue planes.[35] Angiomatosis may also contain lymphangiomatous portions."

Frequency of Occurrence

Hemangiomas in bone. Hemangiomas account for 2-4% of benign bone tumors and ~1 % of all bone tumors.[24-26,32,33] The number of intra-osseous hemangiomas is probably underestimated because of the frequent detection of incidental vertebral hemangiomas via the routine and widespread use of MR1 since the earlier reported data. Thirty to 40 % of angiomatosis cases involve only osseous structures.[17]

Hemangiomas in soft tissue. Hemangiomas account for 8 % of benign, soft tissue tumors and 5 % of all soft tissue tumors.[16-18] Hemangiomas are the fourth most common soft tissue tumor after lipoma, fibrous histiocytoma/dermatofibroma, and nodular fasciitis. Hemangiomas are the most frequent tumors of infancy and childhood.[7,16,22] Juvenile types of capillary hemangiomas occur in 1 of 200 births.[16] Sixty to 70 % of angiomatosis cases involve the soft tissues.[17]

Age at Presentation

Hemangiomas in bone: from 1 to 84 years, median = 33 years.[24-26,32,33]

Hemangiomas in soft tissue: froml to 65 years, mean = 32 years.[17,18]

Angiomatosis: usually presents in the first three decades.[17]

Gender Ratio (M / F)

Hemangiomas in bone: 2 /3.[24-26,32,33]

Hemangiomas in soft tissue: 1 /1.[17,18]

Location

Hemangiomas in bone.[1,24-26,32,33,36]: Hemangiomas commonly occur in the vertebrae followed by craniofacial bones > femur > tibia > fibula > humerus, scapula > phalanges > other bones. In vertebrae, hemangiomas occur in the vertebral body > vertebral body and pedicles > posterior elements.In long bones, hemangiomas occur in the diaphyseal portions > metadiaphyseal, epimetadiaphyseal locations.

Hemangiomas in soft tissue.[17,18] Hemangiomas occur in the hand and wrist > head and neck > trunk > lower extremity > upper extremity. Hemangiomas can occur in many different locations (orbits, liver, spleen, brain, tongue, scrotum, etc.). Many hemangiomas occur in the skin and subcutaneous soft tissues,[722] and also in synovium. Lesions can involve multiple adjacent muscles and adjacent fat. More than 50 % of cases of angiomatosis occur in the lower extremity.[35] Other common sites of angiomatosis include the chest wall, abdomen, upper extremity, and neck.[35]

Signs and Symptoms

Hemangiomas in bone. Intra-osseous hemangiomas are usually asymptomatic. Rarely, lesions may be associated with throbbing pain.[10,15,26,33] Pathologic fractures occur infrequently.[10,15,26,33] Neurologic signs and spinal canal compression can occur rarely, from epidural extension of vertebral hemangiomas or vertebral expansion related to intra-osseous hemangiomas.[11,13,21,27,31,36] Vertebral hemangiomas may enlarge and cause spinal cord compression during pregnancy.[31]

Hemangiomas in soft tissue. Hemangiomas can be deep or superficial soft tissue lesions which can have episodic changes in size.[7,16,35] Pain may be associated with intramuscular hemangiomas after exercise.[7,16] Lesions may enlarge during pregnancy.[716] Superficial hemangiomas can have a blue color as seen through the skin.[7,16] Large cavernous hemangiomas may be associated with functional platelet deficiency and congestive heart failure (Kasabach-Merritt syndrome).[7] Most juvenile capillary hemangiomas regress up to age 7 years.

Lesions with arteriovenous shunting. These arteriovenous hemangiomas can be associated with extremity enlargement, venous distention, elevated localized skin temperature, hypertension, bruit, and bradycardia after compression of the lesion (Branham sign).[7,16] Arteriovenous hemangiomas may slowly enlarge or appear abruptly.[7] Angiomatosis is often associated with pain and persistent swelling, which can vary in degree

with strenuous activity[17,35] Skin discoloration may be present at the sites involved with angiomatosis.[17] Angiomatosis may rarely be associated with gigantism and tissue hypertrophy.[17]

Cross Pathologic Findings

Hemangiomas in bone. Lesions can have a blue or brownish-red color, and are usually wellcircumscribed.[15,33] Osseous trabeculae are relatively decreased toward the central portion of the lesion.[15] Hemangiomas involving the skull may be associated with slight expansion (outer table > inner table).[15]

Hemangiomas in soft tissue

- **Capillary hemangiomas.** These are the most common type of hemangioma, usually located in the skin or mucous membranes. Capillary hemangiomas range from tiny lesions to large lesions: they can be flat, port-wine (pink to purplish) stains, or circumscribed sessile, lobulated, reddish lesions.[7,22]
- **Cavernous hemangiomas.** Lesions are usually soft and compressible; those near the skin surface can have red, blue, or purplish coloration.[7]
- **Arteriovenous hemangiomas (also referred to as racemose hemangioma or cirsoid aneurysm).** Lesions with arteriovenous shunting may appear as a collection of multiple enlarged pulsating blood vessels. Venous distention and extremity enlargement may be present.[7,16]
- **Angiomatosis** Multiple lesions range in size from 1 to 20 cm or greater, with variable color and mature adipose content.[35]

Histopathologic Findings

Hemangiomas in bone. Most hemangiomas in bone are the cavernous type, although portions of the lesions may have capillary components.[6,15,33] Lesions have decreased numbers of bony trabeculae.[6,10,15] The trabeculae that remain in the intraosseous hemangiomas are usually increased in thickness, likely representing a compensatory response to the decreased trabecular numbers relative to adjacent normal bone.[6,15] The endothelial cells lining the vascular spaces are often uniform, small, and flat.[15] Infrequently, lesions may have arteriovenous shunts with multiple arteries and veins of varying sizes and wall thickness.[15] Stroma containing fat are commonly seen in vertebral hemangiomas.[20,28] Endothelial cells are immunoreactive to vimentin, and often stain with antibodies to Factor VIII, CD 31, and CD34.[1]

Hemangiomas in soft tissue

- **Capillary hemangiomas.** Lesions are composed of small blood vessels lined by flattened endothelial cells.[16] Elastic stains show absence of an internal elastic lamina, allowing distinction from arteriovenous hemangiomas.[3]
- **Cavernous hemangiomas.** Lesions are composed of dilated vascular spaces lined by flattened endothelial cells. Cavernous hemangiomas often contain varying proportions of fat, fibrous tissue, smooth muscle, hemosiderin, thrombus, and/or myxoid stroma.[2-4] Elastic stains show absence of an internal elastic lamina, allowing distinction from arteriovenous hemangiomas.[3]
- **Arteriovenous hemangiomas (also referred to as racemose hemangioma or cirsoid aneurysm).** Lesions are composed of various proportions of arteriovenous shunts, and components similar to capillary and cavernous hemangiomas.[7,16] Elastic stains show an internal elastic lamina allowing distinction from venous hemangiomas.[3]
- **Angiomatosis.** Lesions can appear as mixed cavernous and capillary vessels with varying amounts of arteriovenous and mature adipose tissues, which infiltrate the adjacent tissues.[17,35]

Findings on Plain Films (Roentgenograms) and Computed Tomography

Hemangiomas in bone

- **Vertebral lesions.** Hemangiomas in the vertebrae may have decreased attenuation, with or without coarse vertical striations ("corduroy vertebra"), or honeycomb appearance[5,8,10,11,15,20,26,31,33] (Figs. **178,180).** With axial CT, a "polkadot" psttern csn be seen from the coarse, thickened vertical trabeculae.[5] Thin peripheral sclerotic rims can be sometimes seen with CT. Spinal stenosis occasionally occurs from expansion of vertebrae secondary to intra-osseous hemangioma.[36]
- **Skull lesions.** Hemangiomas in the skull may be expansile lesions with a radiating pattern of bony trabeculae oriented toward the center.[5,26]
- **Long bones and short tubular bones.** Hemangiorrms can be circumscribed or irregular radiolucent lesions with or without bony trabeculae.[5,26] Hemangiomas involving these bones may also be associated with expansion of the cortex.[5,26]

Hemangiomas in soft tissue. Radiographs can show a soft tissue mass with or without phleboliths[16] (Fig. **184).** CT usually shows a poorly defined lesion with attenuation similar to muscle, with or without phleboliths.[16] Enhancing vessels can sometimes be seen with CT as well as fat within the hemangiomas.[16] Sonography may show blood flow in the hemangiomas as well as acoustic shadowing from phleboliths.[16]

MRI Findings

Hemangiomas in Bone[5,8,11,20,21,26-28,31,36]

Hemangiomas in vertebrae are often well-circumscribed lesions (vertebral body > vertebral body and pedicles > posterior elements). Typically, hemangiomas have intermediate to high signal on T1WI, PDWI, T2WI, and FS T2WI (Figs. **178,179).** On T1WI, hemangiomas usually have signal equal to or greater than adjacent normal marrow secondary to fatty components. Hemangiomas usually show Gd-contrast enhancement (mild to prominent).

Rarely, atypical hemangiomas may be associated with extraosseous extension through zones of cortical disruption (Fig. **180).** These atypical hemangiomas in the spine may cause epidural compression of adjacent nerve roots or the spinal cord. They may lack adipose tissue, with resulting low-intermediate signal on Tl WI (Fig. **180).** Pathologic fractures associated with intra-osseous hemangiomas usually result in low-intermediate marrow signal on Tl WI.

Hemangiomas in Soft Tissue[2,4,12-14,19,23,29,30,34]

Hemangiomas in the soft tissues can range in size from less than 1 cm to involvement of a large portion of an extremity.

On T1WI, lesions can have either well-circumscribed margins with or without lobulations, such as commonly seen in the cutaneous forms, or irregular margins, commonly seen with intramuscular hemangiomas (Figs. **181-192).** On T1W1 and PDWI, hemangiomas usually have low-intermediate signal or heterogeneous low-intermediate and high signal. The high signal zones on Tl WI and PDWI can range from thin linear zones to thick irregular zones, and are most often secondary to fat and occasionally from slow-flowing blood within these lesions.

On T2WI, hemangiomas usually have distinct margins with or without lobulations, and high signal equal to or greater than

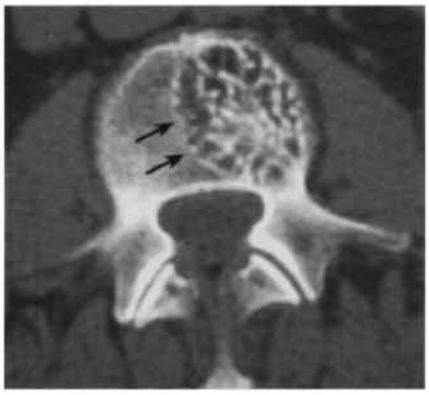

a

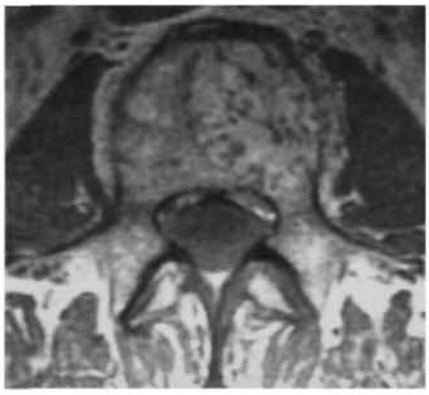

b

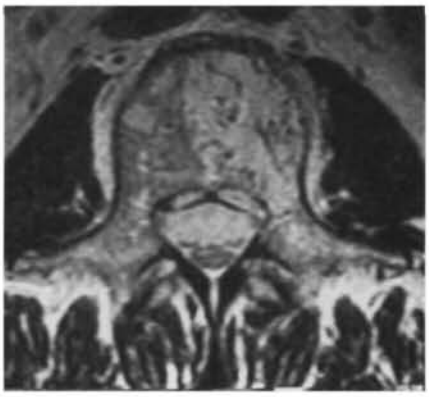

c

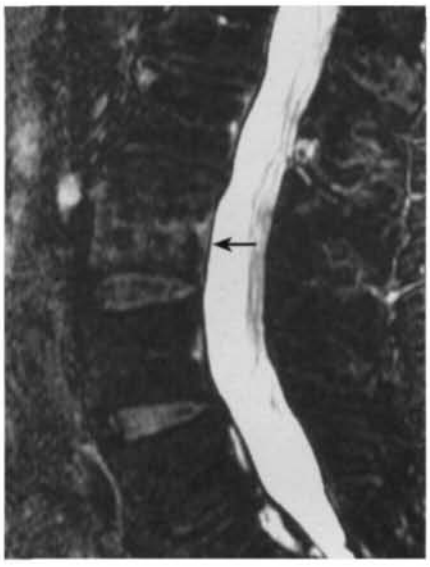

d

Figure **178a-d** Hemangioma in the L3 vertebral body. Axial CT (**a**) shows the hemangioma to have zones of decreased attenuation and coarse vertical striations ("corduroy vertebra") of bone in a honeycomb appearance surrounded by a thin peripheral sclerotic rim. Zones of low attenuation representing fat are seen in the lesion. The hemangioma has mostly high signal on axial PDWI (**b**), and axial T2WI (**c**). Small foci and curvilinear zones of low signal are seen representing thickened trabeculae. The lesion contains small zones of high signal on sagittal FST2WI (**d**), as well as zones of fat signal suppression.

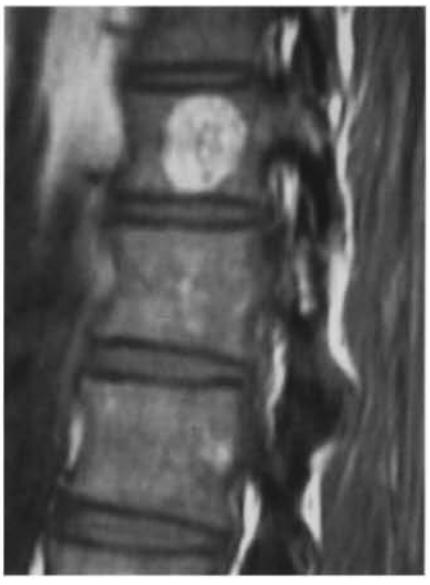

a, b

c

Figure **179a-c** Hemangioma in the T12 vertebral body. The spheroid lesion has mostly high signal on sagittal (**a**)T1WI, sagittal (**b**)T2WI, and sagittal (**c**) FST2WI.

Figure **180a-e** Hemangioma in the dorsal portion of the C 5 vertebral body which has low-intermediate signal on sagittal T1WI (**a**), and heterogeneous high signal on sagittal STIR (**b**). The lesion shows Gd-contrast enhancement on sagittal (**c**) and axial (**d**) FS T1WI, and shows extension through a zone of cortical disruption into the right anterior epidural soft tissues, as seen on axial postmyelographic CT (**e**). The intra-osseous portion of the lesion has coarsened bony trabeculae (**e**).

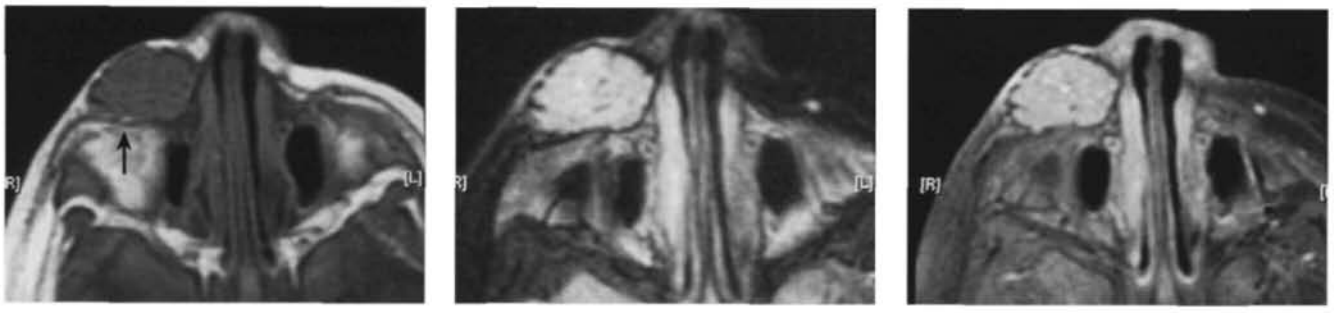

Figure **181 a-c** A 6-month-old female with a capillary hemangioma in the soft tissues of the face. The hemangioma has circumscribed margins and has mostly intermediate signal with small foci of low signal on axial T1WI (**a**). The hemangioma has mostly high signal on axial FS T2WI (**b**), surrounded by a thin rim of low signal. The hemangioma shows prominent Gd-contrast enhancement on FS T1WI (**c**).

Figure **182 a-c** A 9-month-old female with a capillary hemangioma superficial to the left parotid gland. The hemangioma has circumscribed margins and has intermediate signal on coronal (**a**) T1 WI. The hemangioma has high signal on axial (**b**) FS T2WI and shows prominent Gd-contrast enhancement on coronal (**c**) FS T1WI.

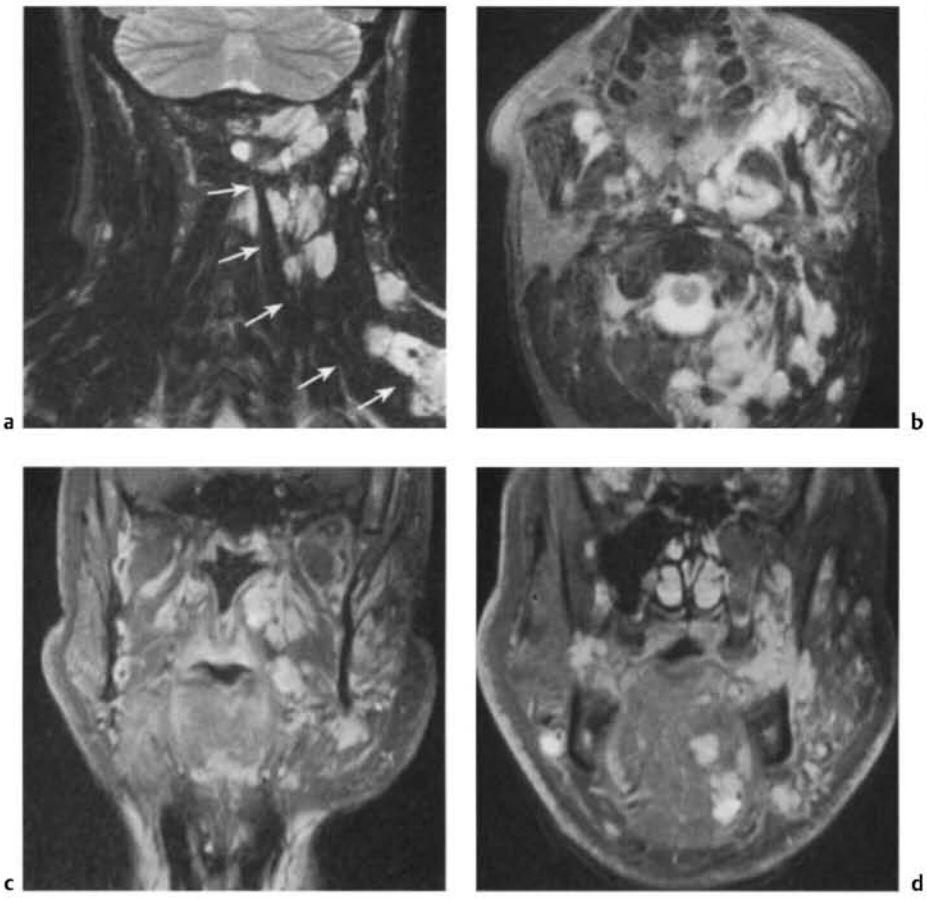

Figure **183a-d** A 22-year-old man with angiomatosis involving the soft tissues of the head and neck. The multifocal lesions involve multiple tissue planes and have high signal on coronal (**a**) and axial (**b**) FST2WI, and show moderate Gd-contrast enhancement on coronal and axial FST1WI (**c, d**).

adipose tissue in the field of view. Angiomatosis typically appears as multiple lesions that can occur over a large area in soft tissues with frequent involvement of multiple tissue planes (Fig. **183).** Intramuscular hemangiomas larger than 2 cm often have a striated high signal pattern on T2W1, secondary to parallel orientation of the vessels separated by fibrous and fatty septa within the lesions (Fig. **186).**

On FS T2WI, hemangiomas typically have high signal except for zones of fat within the lesions. Capillary hemangiomas are the common type in cutaneous and subcutaneous locations (Figs. **181,182),** whereas the intramuscular hemangiomas can be either cavernous or capillary types. Large vascular channels in intramuscular hemangiomas are more likely to be seen with the cavernous types of hemangiomas (Fig. **184).** The arteriovenous type of hemangiomas usually has large serpentine vessels representing dilated veins and sinusoidal spaces with high signal on T2WI and FS T2WI, as well as several flow voids from arteriovenous shunts (Fig. **189).** The cavernous and capillary types of intramuscular hemangiomas, however, can have similar or overlapping MR features. Zones of hemorrhage can sometimes be present in hemangiomas as well as phleboliths (Fig. **184).** Angiomatosis usually appears as multifocal, adjacent and/or contiguous lesions involving multiple tissues.

After Gd-contrast administration, hemangiomas usually show prominent contrast enhancement. The extent of Gd-contrast enhancement can differentiate the borders of hemangioma relative to edema.

Differential Diagnosis

Hemangiomas in vertebrae. Venous malformation, arteriovenous malformation, atypical lipoma, hemangioendothelioma, angiosarcoma, lymphangioma, fibrous dysplasia, Paget disease, atypical metastasis.

Hemangiomas in calvaria. Fibrous dysplasia, epidermoid cyst, eosinophilic granuloma, atypical lipoma, meningioma, hemangioendothelioma, angiosarcoma, metastasis.

Hemangiomas in long bones or short tubular bones. Atypical lipoma, aneurysmal bone cyst, giant cell tumor, metastasis, fibrous dysplasia, giant cell tumor.

Hemangiomas in soft tissue. Atypical lipoma, lymphangioma, venous malformation, arteriovenous malformation, hemangioendothelioma, angiosarcoma, angiomatoid malignant fibrous histiocytoma, extramedullary hematopoiesis, myxoid tu mors, post-traumatic hematomas, intramuscular tumors with hemorrhage, liposarcoma, muscle infarct.

Prognosis and Treatment

Hemangiomas in Bone

Intra-osseous hemangiomas are usually asymptomatic and often are incidental findings on imaging examinations. Occasionally, hemangiomas may be associated with pain, pathologic fractures, or spinal canal compression from epidural extension from vertebral hemangiomas, or vertebral expansion related to intra-osseous hemangiomas.[11,13,21,27,31,36] Patients with spinal cord compression typically have surgical decompression.[11] Radiation and/or embolization has been used for treatment of painful or recurrent vertebral hemangiomas.[11] Malignant degeneration to angiosarcoma is very rare.[1]

Figure **184a-d** A 14-year-old female with a hemangioma in the soft tissues of the forearm. AP radiograph (**a**) shows a soft tissue mass containing a phlebolith. The hemangioma has circumscribed lobulated margins and involves several muscles. The hemangioma has mostly intermediate signal on axial T1WI (**b**), and contains a zone of high signal from an area of hemorrhage. The lesion has mostly high signal on axial FS T2WI (**c**). Several prominent veins are also seen. The hemangioma shows prominent Gd-contrast enhancement on sagittal FS T1WI (**d**).

Hemangiomas in Soft Tissue

Capillary hemangioma. This is typically a juvenile type that usually involutes by age of 7 years.[16,22] Symptomatic lesions can be treated with steroid medication.[7,22]

Cavernous hemangioma. This type of hemangioma does not usually involute and may be followed conservatively. Symptomatic lesions can be treated with steroids medications, cryotherapy, intravascular injections of sclerosing solutions, and surgical excision.[5,9,11-13,16]

Arteriovenous hemangioma. Morbidity from these lesions can result from hypertension, venous distention and thrombosis, and bone erosion by adjacent pulsating blood vessels.[7,16] Surgical excision with or without preoperative embolization or ligation of the arterial supply is often performed.[7]

Angiomatosis. These lesions are considered benign, although can recur after surgery.[17,35] Metastatic disease and malignant degeneration have not been reported.[35] One notable exception is Mafucci syndrome, which is a type of angiomatosis that is associated with malignant potential and is mostly related to the co-existent intra-osseous chondroid lesions which undergo degeneration to chondrosarcomas in 15-56% of cases.[17] The hemangiomas in Maffuci syndrome can also degenerate into sarcomas in 3-5% of patients.[17]

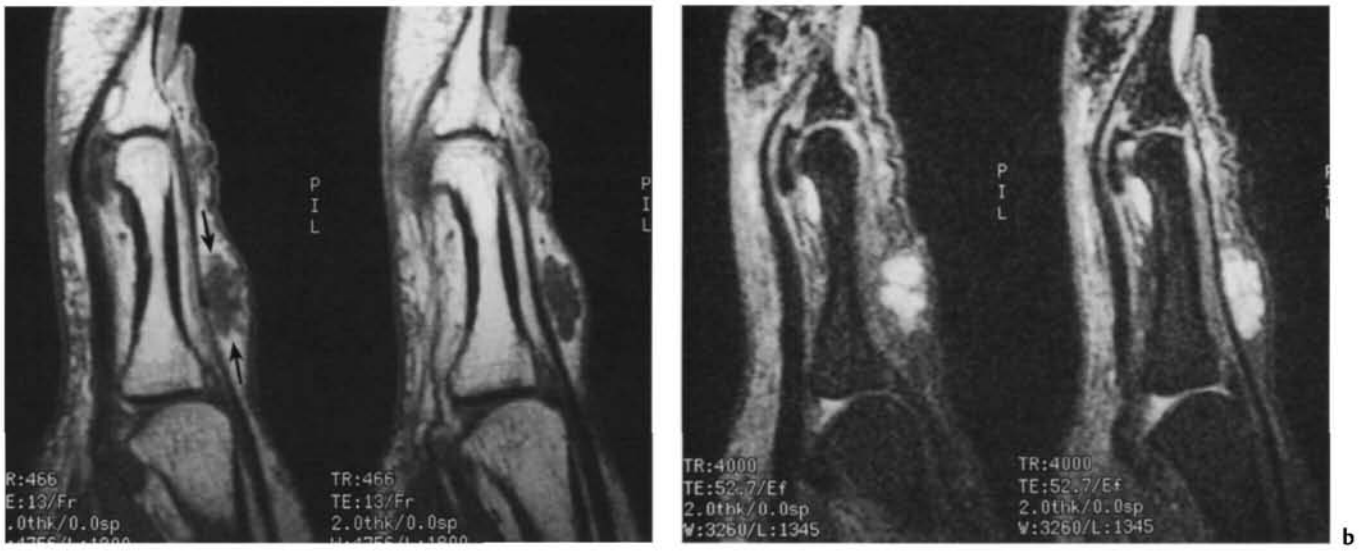

a b

Figure **185a, b** A 44-year-old woman with a hemangioma in the dorsal soft tissues of a finger. The hemangioma has circumscribed, slightly lobulated margins. The lesion has intermediate signal on sagittal (**a**) T1WI and high signal on sagittal (**b**) FS T2WI.

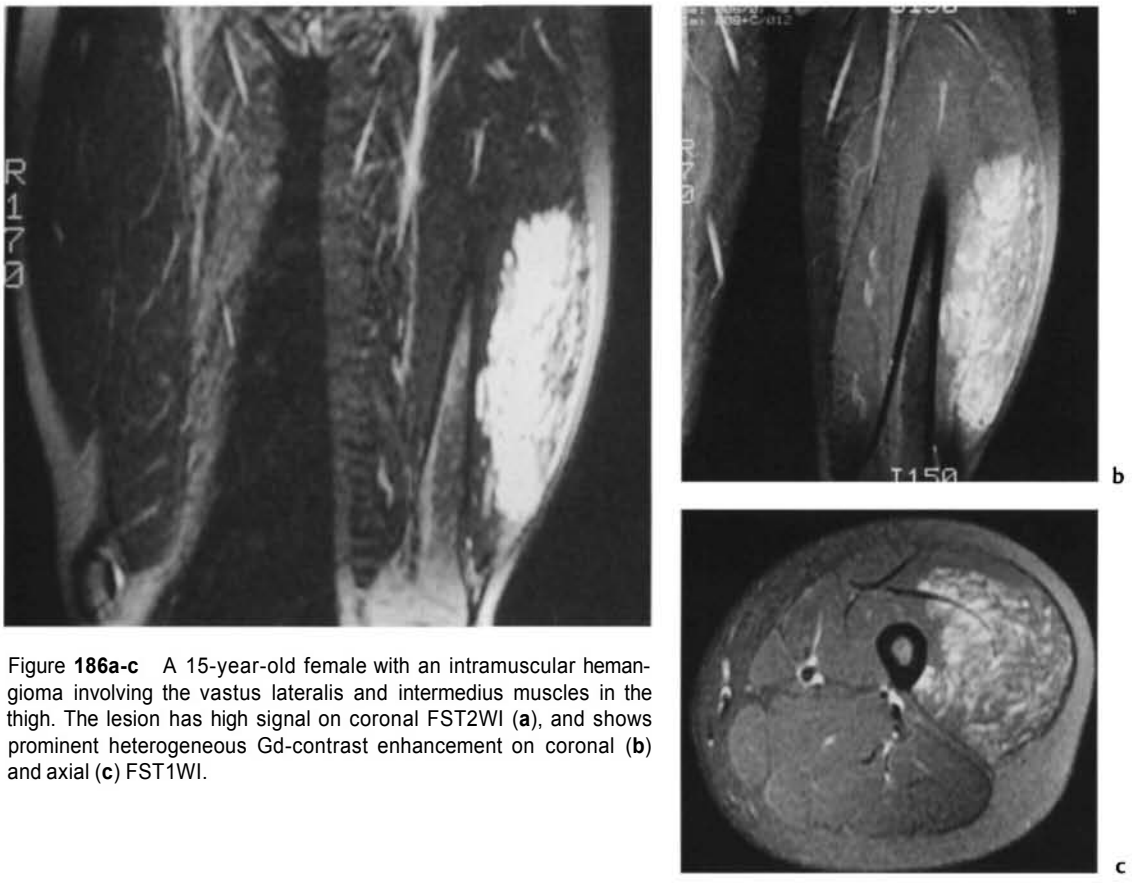

a b c

Figure **186a-c** A 15-year-old female with an intramuscular hemangioma involving the vastus lateralis and intermedius muscles in the thigh. The lesion has high signal on coronal FST2WI (**a**), and shows prominent heterogeneous Gd-contrast enhancement on coronal (**b**) and axial (**c**) FST1WI.

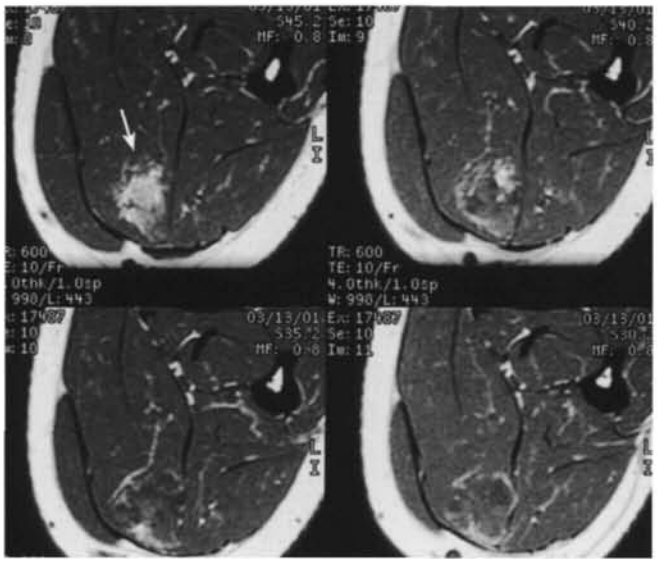

a

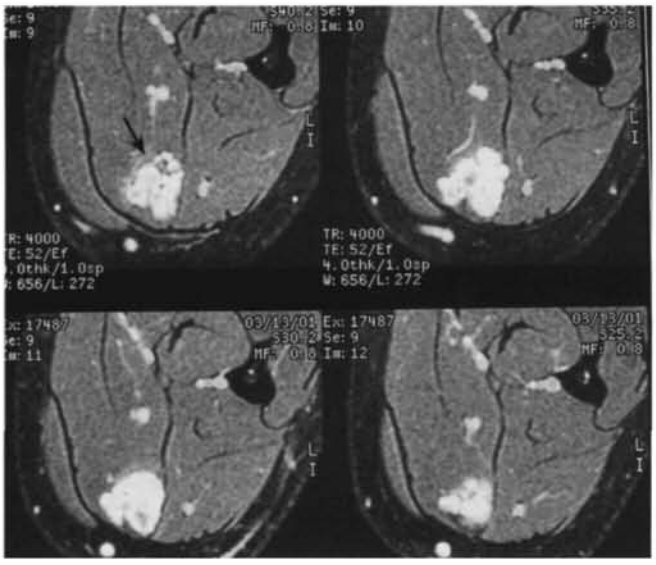

b

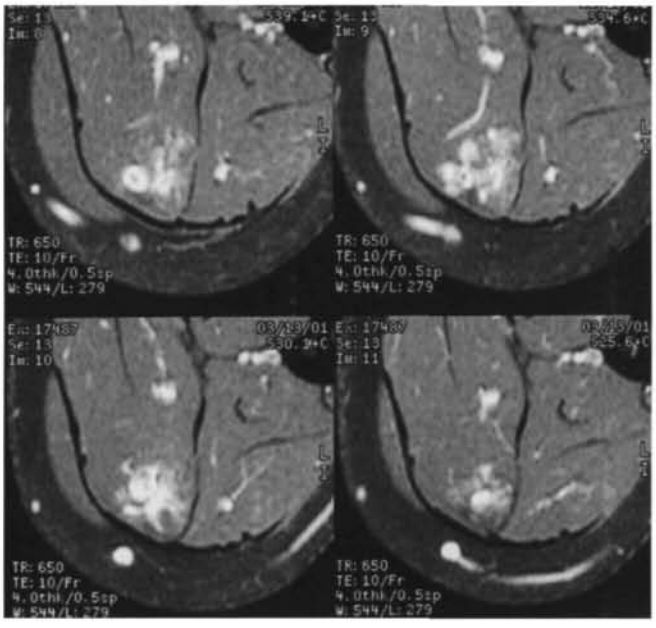

c

Figure **187a-c** Intramuscular hemangioma in the soleus muscle of the leg. The lesion has slightly lobulated margins and contains zones of intermediate and high signal on axial T1WI (**a**). The hemangioma has high signal on axial FS T2WI (**b**), and shows prominent heterogeneous Gd-contrast enhancement on axial FST1WI (**c**).

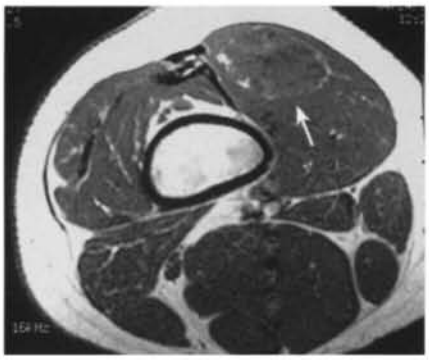

a, b

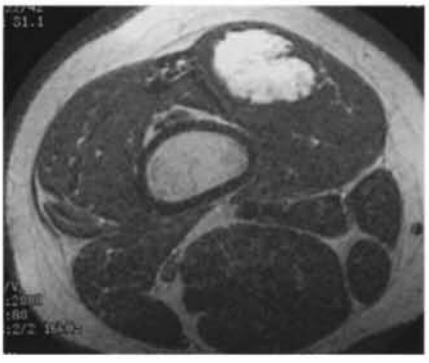

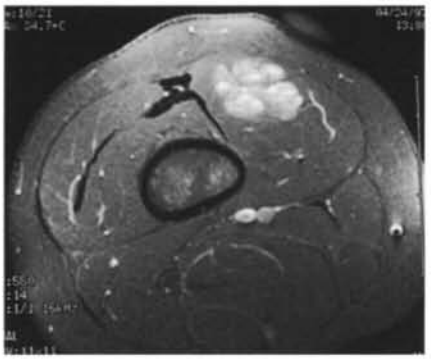

c

Figure **188a-c** A 7-year-old male with an intramuscular hemangioma in the vastus medialis of the distal thigh. The lesion has mostly intermediate signal on axial T1WI (**a**) and high signal on axial T2WI (**b**). The hemangioma shows heterogeneous Gd-contrast enhancement on axial FST1W! (**c**).

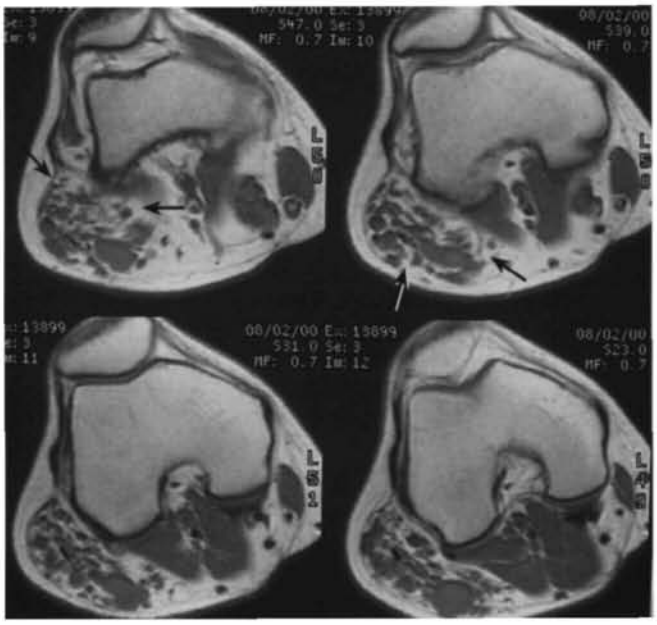

a

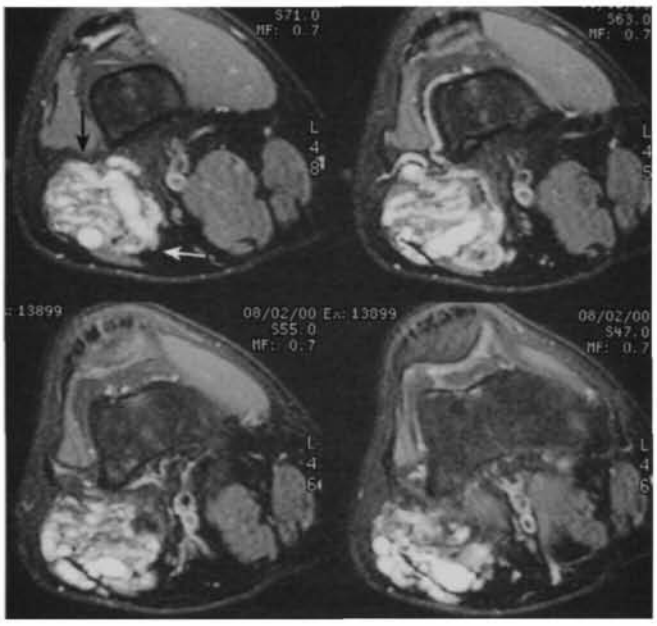

b

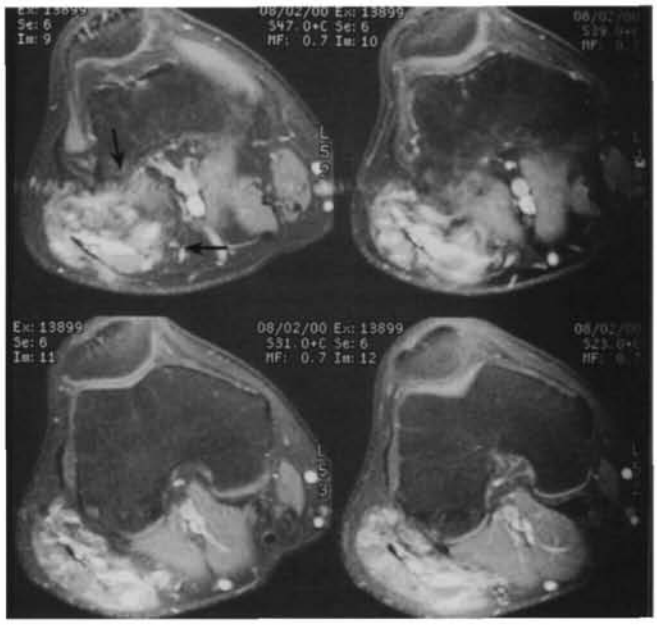

c

Figure **189a-c** An 18-year-old man with an arteriovenous type of hemangioma in the superficial soft tissues at the knee. The hemangioma contains fat and multiple vascular channels with intermediate signal on axial (**a**) T1WI. The hemangioma has mostly high signal on axial (**b**) FST2WI from dilated veins and sinuisoidal spaces, as well as several flow voids from sites of arteriovenous shunting. The hemangioma shows heterogeneous Cd-contrast enhancement on axial (**c**) FST1WI.

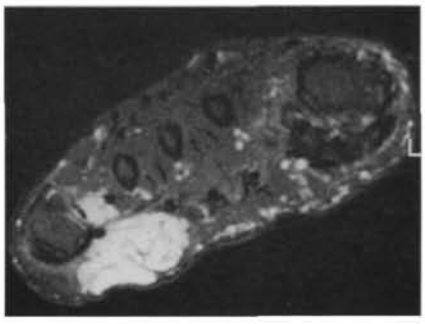

Figure **190** A 50-year-old woman with a hemangioma in the plantar soft tissues of the foot. The lesion has high signal on coronal FST2WI.

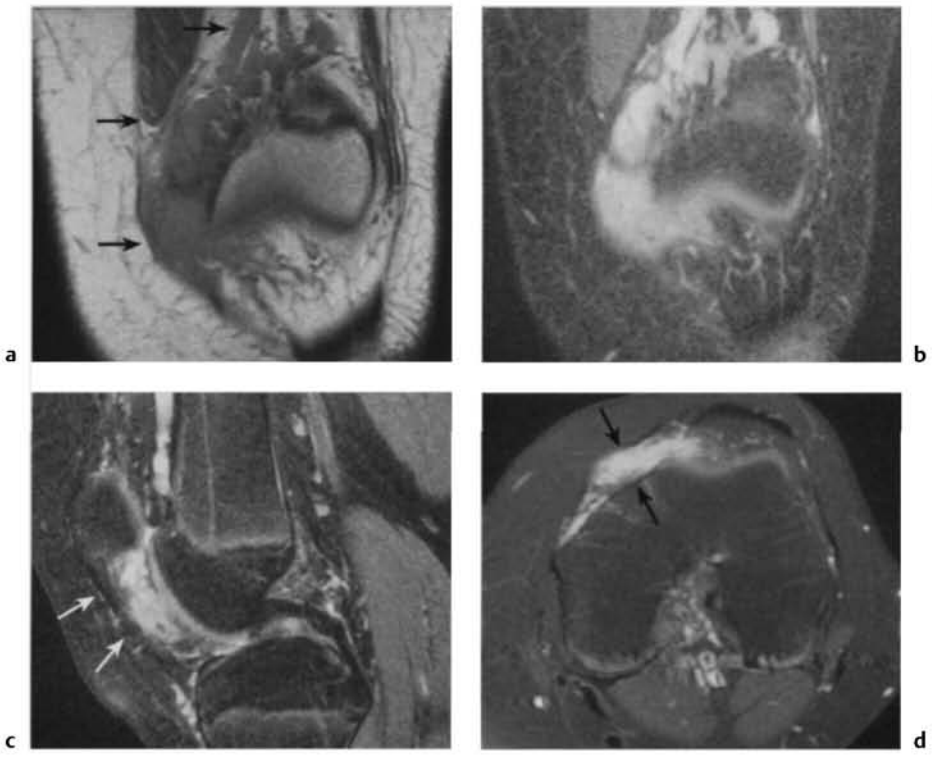

Figure **191 a-d** A 13-year-old female with a synovial hemangioma in the knee. The lesion has intermediate signal on coronal (**a**) PDWI, and high signal on coronal (**b**) and sagittal (**c**) FS T2WI. Multiple enlarged veins are seen adjacent to the hemangioma. The lesion shows prominent Gd-contrast enhancement on axial (**d**) FS T1WI.

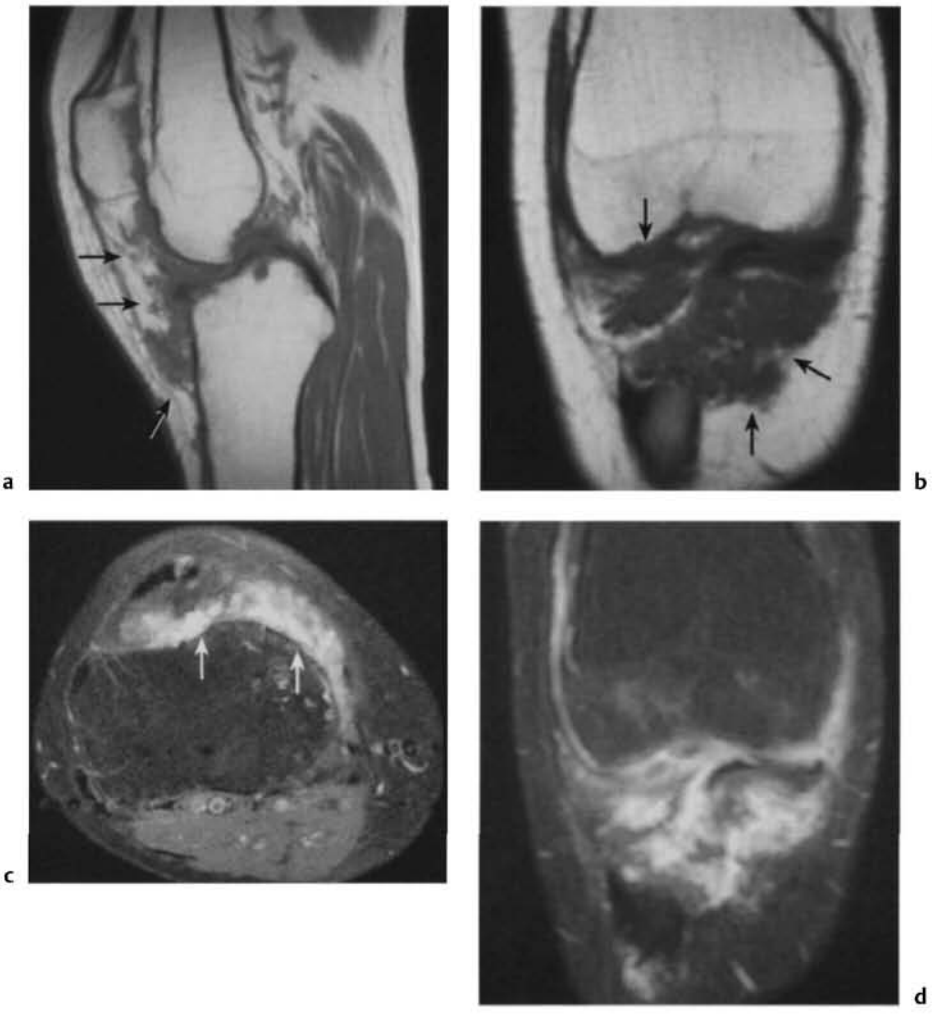

Figure **192a-d** A 46-year-old woman with a synovial hemangioma in the knee. The lesion has intermediate signal on sagittal (**a**) and coronal (**b**) T1WI. The hemangioma shows prominent Gd-contrast enhancement on axial (**c**) and coronal (**d**) FST1WI.

References

1 Adler CP, Wold L. Haemangioma and related lesions. In: Fletcher CDM, Unni KK, Mertens F, eds. *World Health Organization Classification of Tumours. Pathology and Genetics of Tumours of Soft Tissue and Bone* Geneva: IARC Press: 2002:320-321.

2 Buetow PC, Kransdorf MJ, Moser RP Jr, Jelinek JS, Berrey BH. Pictorial Essay—Radiologic appearance of intramuscular hemangioma with emphasis on MR imaging. *AJR Am J Roentgenol* 1990:154:563-567.

3 Calonje E. Haemangiomas. In: Fletcher CDM, Unni KK, Mertens F, eds. *World Health Organization Classification of Tumours. Pathology and Genetics of Tumours of Soft Tissue and Bone* Geneva: IARC Press; 2002:156-158.

4 Cohen EK, Kressel HY, Perosio T e t al. MR imaging of soft-tissue hemangiomas: correlation with pathologic findings. AJR *Am] Roentgenol* 1988:150:1079-1081.

5 Conway WF, Hayes CW. Miscellaneous lesions of bone. *Radiol Clin North Am* 1993:31:339-358.

6 Darby AJ. Vascular neoplasms of bone. In: Helliwell TR, ed. *Major Problems in Pathology: Pathology of Bone and Joint Neoplasms* 1st ed. Vol 37. Philadelphia, Pa: W.B. Saunders; 1999:330-338.

7 Das Gupta TK, Chaudhuri PK. Tumors of vascular and perivascular tissue. In: Das Gupta TK, Chaudhuri PK, eds. *Tumors of the Soft Tissues* 2nd ed. New York, NY: Appleton and Lange; 1998:407-440.

8 Djindjian M, Nguyen JP, Gaston A, Pavlovitch JM, Poirier J, Awad IA. Multiple vertebral hemangiomas with neurological signs-case report. J Neurosurg 1992;76:1025-1028.

9 Fetsch JF. Epithelioid haemangioma. In: Fletcher CDM, Unni KK, Mertens F, eds. *World Health Organization Classification of Tumours. Pathology and Genetics of Tumours of Soft Tissue and Bone* Geneva: IARC Press; 2002:159-160.

10 Forest M. Vascular tumors. In: Forest M, Tomeno B, Vanel D, eds. *Orthopedic Surgical Pathology: Diagnosis of Tumors and Pseudotumoral Lesions of Bone and Joints* Edinburgh: Churchill Livingstone; 1998:345-359.

11 Fox MW, Onofrio BM. The natural history and management of symptomatic and asymptomatic vertebral hemangiomas. *J Neurosurg* 1993;78:36-45.

12 Frassica FJ, Khanna JA, McCarthy EF. The role of MR imaging in soft tissue tumor evaluation: perspective of the orthopedic oncologist and musculoskeletal pathologist. *Magn Reson Imaging Clin N Am* 2000;8(4):915-927.

13 Golwyn DH, Cardenas CA, Murtagh FR, Balis GA, Klein JB. MRI of a cervical extradural cavernous hemangioma. *Neuroradiology* 1992; 34:68-69.

14 Marty MP. Imaging of pediatric foot disorders. *Radiol Clin North Am* 2001;39(4):733-748.

15 Huvos AG. Hemangioma of bone; lymphangioma of bone; diffuse skeletal angiomatosis and lymphangiomatosis; glomus tumor; "disappearing bone disease." *Bone Tumors: Diagnosis, Treatment, and Prognosis* 2nd ed. Philadelphia, Pa: W.B. Saunders; 1991:553-562.

16 Kransdorf MJ, Murphey MD. Vascular and lymphatic tumors. In: *Imaging of Soft Tissue Tumors 2nd* ed. Philadelphia, Pa: W.B. Saunders; 2006:150-188.

17 Kransdorf MJ, Murphey MD. Soft tissue tumors in a large referral population: prevalence and distribution of diagnoses by age, sex, and location. In: *Imaging of Soft Tissue Tumors* 2nd ed. Philadelphia, Pa: W.B. Saunders; 2006:6-37.

18 Kransdorf MJ. Benign soft-tissue tumors in a large referral population: distribution of specific diagnoses by age, sex, and location. *AJR Am J Roentgenol* 1995;164:395-402.

19 Laor T, Burrows PE. Congenital anomalies and vascular birthmarks of the lower extremities. *Magn Reson Imaging Clin N Am* 1998;6(3): 509-511.

20 Laredo JD, Assouline E, Gelbert F, Wybier M, Merland JJ, Tubiana JM. Vertebral hemangiomas: fat content as a sign of aggressiveness. *Radiology* 1990;177(2):467-472.

21 McAllister VL, Kendall BE, Bull JWD. Symptomatic vertebral hemangiomas. *Brain* 1975;98:71-80.

22 Metry DW. A newborn girl with large red plaque on her face. *Pediatr Ann* 200;35:423-426.

23 Meyer JS, Hoffer FA, Barnes PD, Mulliken JB. Pictorial Essay-Biological classification of soft-tissue vascular anomalies: MR correlation. *AJR Am J Roentgenol* 1991;157:559-564.

24 Mulder JD, Schutte HE, Kroon HM, Taconis WK. Introduction. In: *Radiologic Atlas of Bone Tumors* Amsterdam: Elsevier; 1993:3-6.

25 Mulder JD, Schutte HE, Kroon HM, Taconis WK. The diagnosis of bone tumors. In: *Radiologic Atlas of Bone Tumors* Amsterdam: Elsevier; 1993:9-46.

26 Mulder JD, Schutte HE, Kroon HM, Taconis WK. Hemangioma. In: *Radiologic Atlas of Bone Tumors Amsterdam:* Elsevier; 1993:507-516.

27 Paige ML, Hemmati M. Spinal cord compression by vertebral hemangioma. *Pediatr Radiol* 1977;6:43-45.

28 Ross JS, Masaryk TJ, Modic MT, Carter JR, Mapstone T, Dengel FH. Vertebral hemangiomas: MR imaging. *Radiology* 1987;165(1): 165-169.

29 Siegel MJ. Magnetic resonance imaging of musculoskeletal soft tissue masses. Radiol *Clin North Am* 2001;39(4):704-705.

30 Sundaram M, Sharafuddin Melhem JA. MR imaging of benign soft-tissue masses. In: Weatherall PT. Magn Reson *Imaging Clin N Am* 1995;3(4):613-614.

31 Tekkb'k IH, Acikgoz B, Sa9lam S, Önol B. Vertebral hemangioma symptomatic during pregnancy - Report of a case and review of the literature. *Neurosurgery* 1993;32(2):302-306.

32 Unni KK. Introduction and scope of study. In: *Dahlin's Bone Tumors-General Aspects and Data on 11087 Cases* 5th ed. Philadelphia, Pa: Lippincott, Williams & Wilkins; 1996:1-9.

33 Unni KK. Benign vascular tumors. In: Unni KK, ed. *Dahlin's Bone Tumors-General Aspects and Data on 11087 Cases* 5th ed. Philadelphia, Pa: Lippincott, Williams & Wilkins; 1996:307-315.

34 Van Slyke MA, Moser RP Jr, Madewell JE. MR imaging of periarticular soft-tissue lesions. *Magn Reson Imaging Clin N Am* 1995;3(4): 656-658.

35 Weiss SW. Angiomatosis. In: Fletcher CDM, Unni KK, Mertens F, eds. *World Health Organization Classification of Tumours. Pathology and Genetics of Tumours of Soft Tissue and Bone* Geneva: IARC Press; 2002:161.

36 Yochum TR, Lile RL, Schultz GD, Mick TJ, Brown CW. Acquired spinal stenosis secondary to an expanding thoracic vertebral hemangioma. *Spine* 1993;18(2):299-305.

A 35 Hemangiopericytoma

ICD-OCode

9150/1

Definition

Hemangiopericytomas are rare, benign and malignant tumors of presumed pericytic origin that show pericytic/myoid differentiation with variously shaped pericytic cells (oval, round, spindle-like) and adjacent irregular branching vascular spaces lined by endothelial cells.[7-11,22] Hemangiopericytomas can occur in soft tissues and less frequently in bone.[18]

Frequency of Occurrence

Hemangiopericytomas account for < 1 % of primary bone tumors, and < 1 % of primary tumors in the soft tissues.[12,14,16-18,20,21]

Age at Presentation

Most hemangiopericytomas occur in adults (90-95 %), and infrequently occur in children (5-10%).[12,14,1-19]

Hemangiopericytomas in adults:

- **Bone:** from 1 to 90 years, median = 40 years.[16-8]
- **Soft tissue:** from 22 to 73 years, mean = 44-46 years.[12-15]

Hemangiopericytomas in children:

- **Soft tissue:** less than 1 year to 20 years, median = 16 years.

Gender Ratio (m / F)[12,14,1-,19,21]

Hemangiopericytomas in adults: < 1 / 1 to 1 / 1.

Hemangiopericytomas in children: 2-3 / 1.

Location

Hemangiopericytomas in bone.[3,10,18,21] Tumors occur in the iliac bone > femur, humerus, tibia, craniofacial bones > vertebra, sacrum > other bones. Lesions are rarely multicentric.

Hemangiopericytomas in soft tissues.[2,3,12,14,19,22] Tumors occur in the lower extremity > trunk, retroperitoneum > head (skin, muscles, dura, intraventricular), neck > hip, buttocks > upper extremity > nasal cavity and paranasal sinuses.

Signs and Symptoms

Hemangiopericytomas in bone.[9-11,18,21] Patients can present with localized pain and/or regional tenderness (a few weeks to 1 year).

Hemangiopericytomas in soft tissues.[5-7,18,19] Tumors are often palpable, painless soft tissue masses. Pain can be a late symptom associated with an enlarging mass.[6,22] Tumors can cause symptomatic hypoglycemia secondary to secretion of insulin-like growth factors.[22] Tumors can also cause oncogenic osteomalacia.[22]

Cross Pathologic Findings[3-5,7-10,15,18,21]

Lesions are solid and/or spongy, friable, and sometimes have granular textures. Lesions are often brown and are surrounded by a pseudocapsule.[6] Small satellite nodular lesions may be seen adjacent to the primary tumor.[6]

Histopathologic Findings[3-10,18,21]

Hemangiopericytomas in bone and soft tissues have similar histologic features. Lesions consist of multisized vascular channels lined by a single layer of endothelial cells and surrounded by aggregates of pericytes (round, oval, or spindle-shaped cells). The pericytes have abundant eosinophilic cytoplasm. Pericytes are relatively uniform in low-grade lesions, but considerable cellular pleomorphism and high mitotic activity are often seen in high-grade malignant lesions.

Histologic features of hemangiopericytomas can overlap those of monophasic synovial sarcomas.[6] Hemangiopericytomas can be distinguished from synovial sarcomas because hemangiopericytomas typically lack immunoreactivity to epithelial membrane antigen (EMA) and keratins, whereas synovial sarcomas show immunoreactivity to these antigens.[6]

Hemangiopericytomas also show histologic and ultrastructural findings that are similar to extrapleural solitary fibrous tumors, and can show overlapping immunohistochemical reactivity to CD34, CD 99, and bcl-2 antigens[8,22] Hemangiopericytomas, however, usually lack findings typically seen with solitary fibrous tumors such as arrangements of long bundles of spindle cells with broad dense zones of hyalinization.[822]

Tumor Genetics

Chromosomal breakpoints at 12ql3-15 and 19ql3 have been reported in almost 50 % and 25 % of cases, respectively.[9] Other reported abnormalities include imbalances in 3p, 5q, 12 q, 13 q, 17 p, 17 q, 19 q, and chromosome 10, as well as t(12;19)(ql3;q!3).[9]

Findings on Plain Films (Roentgenograms) and Computed Tomography

Hemangiopericytomas in bone.[3,7,10,11,18,21] Hemangiopericytomas are usually radiolucent, intramedullary lesions. Borders of the lesions vary, from mostly distinct to indistinct or permeative. Mild sclerosis with slightly prominent bony trabeculae may occasionally be seen. Zones of cortical destruction and extraosseous tumor extension can be observed (Fig. **193).** Mild bony expansion occasionally occurs. Periosteal reaction is uncommon.

Hemangiopericytomas in soft tissues.[15] Tumors can appear as a soft tissue mass, rarely containing calcifications, and rarely associated with erosion of adjacent bone.

MRI Findings

Hemangiopericytomas in bone.[11] Intramedullary lesions can have associated cortical destruction and soft tissue extension. Lesions usually have low-intermediate signal on T1WI, inter-

mediate signal on PDWI, and slightly high-high signal on T2WI (Fig. **193).** On T1W1 and T2W1, thin tubular signal voids representing blood vessels may be seen within and/or at the periphery of tumors, as well as being arranged in "spoked-wheel"-type patterns. Hemangiopericytomas usually have moderate to prominent Gd-contrast enhancement (Fig. **193).**

Hemangiopericytomas in softtissues.[1,21,5,18]Hemangiopericytomas usually have well-defined margins, with or without lobulations. Lesions often have low-intermediate signal on T1WI, intermediate signal on PDWI, intermediate or slightly high-high signal onT2WI, and heterogeneous high signal on FST2WI (Figs. **194-197).** On T2WI, lesions may contain tubular signal voids centrally or peripherally, which probably represent tumor vessels (Fig. **194).** Intracranial lesions are typically extra-axial, and mostly involve the dura. Hemangiopericytomas can contain hemorrhagic zones with corresponding MR signal alteration (Fig. **197).** After Gd-contrast administration, hemangiopericytomas usually have moderate to prominent contrast enhancement in either a heterogeneous or homogeneous pattern (Figs. **194-196).**

a, b

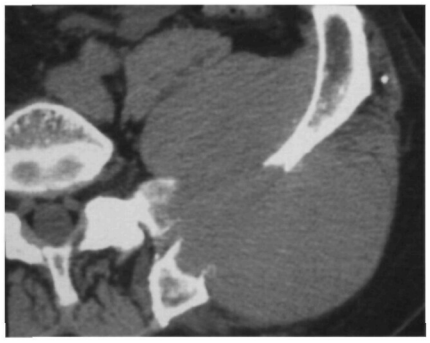

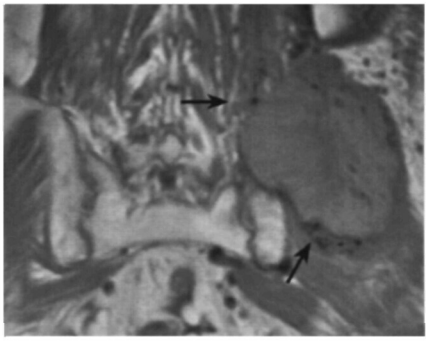

c

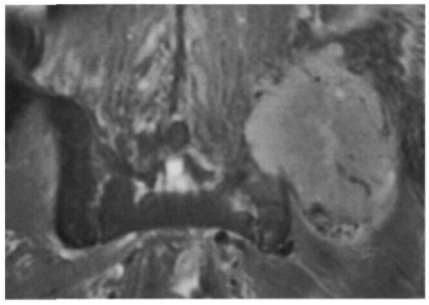

d, e

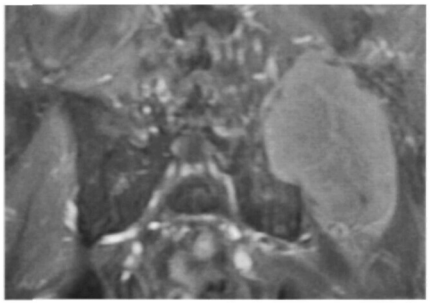

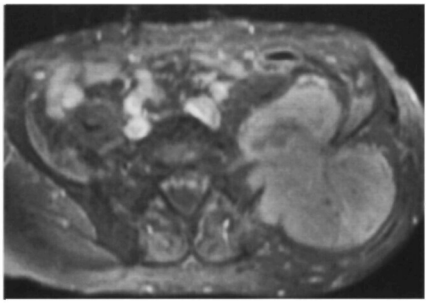

f

Figure **193 a-f** A 78 year old man with an intra-osseous hemangiopericytoma in the left iliac bone associated with destruction of cortical bone and extra-osseous extension. AP radiograph (**a**) shows a circumscribed radiolucent lesion. Axial CT image (**b**) shows the intra-osseous tumor with destruction of cortical bone and extra-osseous extension. The tumor has intermediate signal on coronal T1WI (**c**) and heterogeneous slightly high signal on coronal FST2WI (**d**). Multiple flow voids are seen within, and at the periphery of, the tumor. The tumor shows moderate Cd-contrast enhancement on coronal (**e**) and axial (**f**)FST1WI.

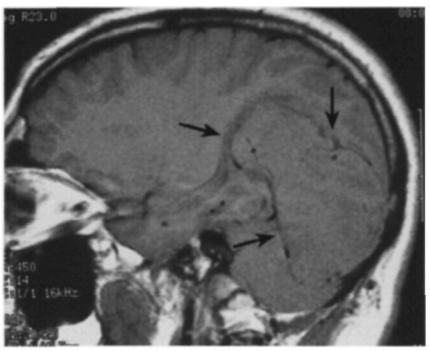

a, b

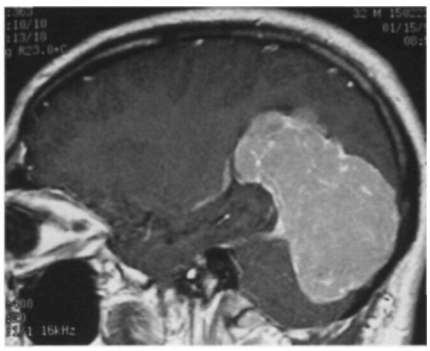

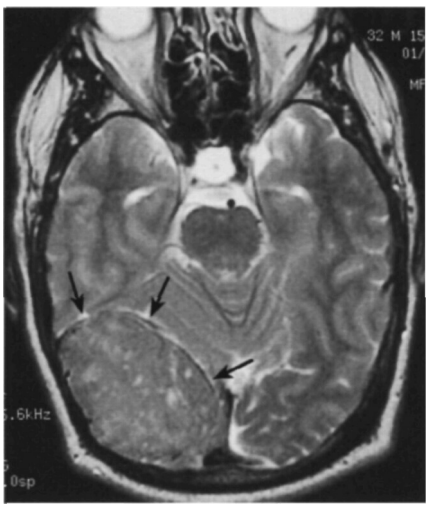

c

Figure **194a, b** A 32-year-old man with a hemangiopericytoma involving the tentorium. The tumor has well-defined, slightly lobulated margins, and has intermediate signal on sagittal T1WI (**a**), and intermediate and slightly high signal on axial T2WI (**c**) as well as small zones with high signal. The tumor shows prominent Gd-contrast enhancement on sagittal T1WI (**b**). Several prominent veins are seen at the peripheral portions of the tumor.

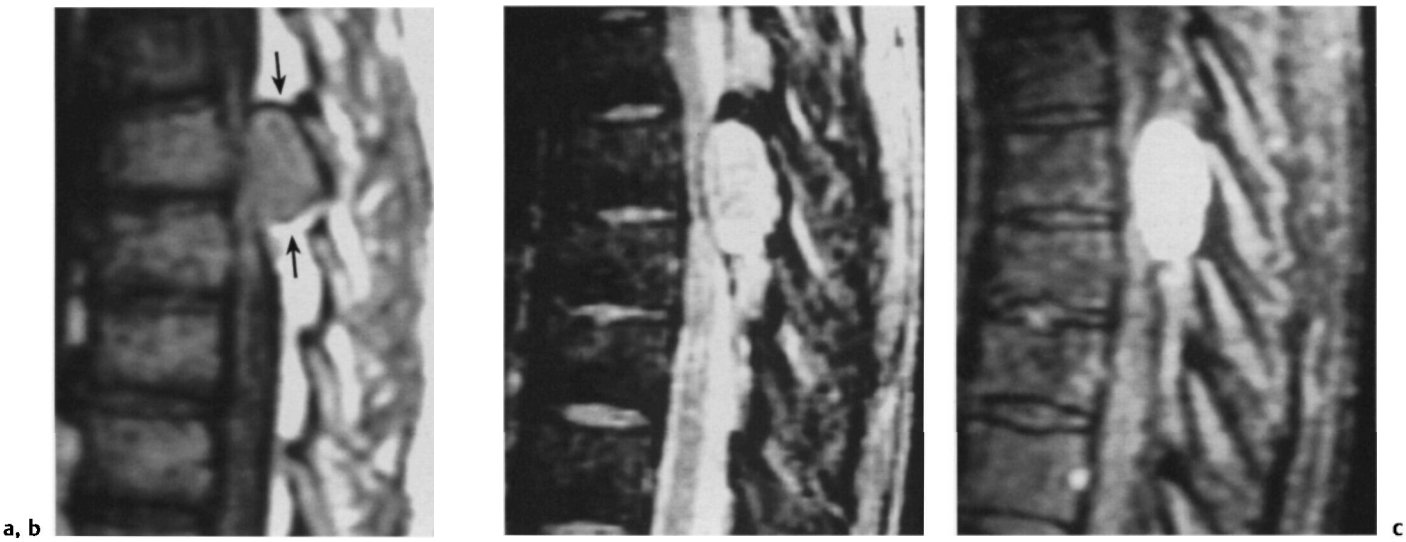

Figure **195a-c** Posterior epidural hemangiopericytoma involving the thoracic spine with spinal cord compression. The tumor has intermediate signal on sagittal T1WI **(a)** and high signal on sagittal T2WI (**b**). The tumor shows prominent Cd-contrast enhancement on sagittal (**c**) FST1WI.

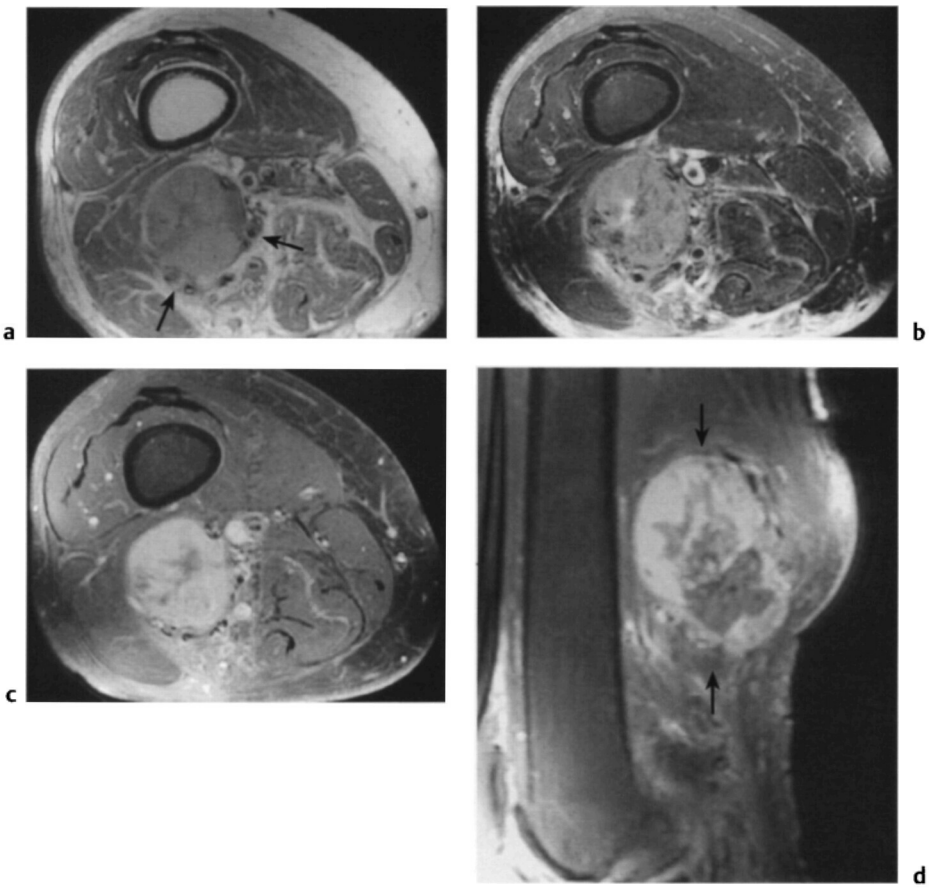

Figure **196a-d** A 75-year-old man with a hemangiopericytoma involving the dorsal soft tissues of the lower thigh. The tumor has intermediate signal on axial (**a**) T1WI, and mixed intermediate, slightly high and high signal on axial (**b**) FST2WI, as well as small foci of low signal. The tumor shows prominent heterogeneous Cd-contrast enhancement on axial (**c**) and sagittal (**d**) FST1WI.

Differential Diagnosis

Hemangiopericytomas in bone. Metastatic carcinoma, myeloma, eosinophilic granuloma, aneurysmal bone cyst, giant cell tumor, lymphoma, chondrosarcoma, Ewing sarcoma, osteosarcoma, fibrosarcoma.

Hemangiopericytomas in soft tissues. Solitary fibrous tumor, synovial cell sarcoma, malignant fibrous histiocytoma, liposarcoma, leiomyosarcoma, lymphoma, angiosarcoma, hemangioendothelioma, metastatic carcinoma, clear cell sarcoma.

Prognosis and Treatment[3,5-10,18]

Treatment often consists of wide resection with 2 cm of clear margins. Local recurrence and metastases are common for high-grade tumors, but can also occur in low-grade tumors. Preoperative radiation, radical excision, and chemotherapy

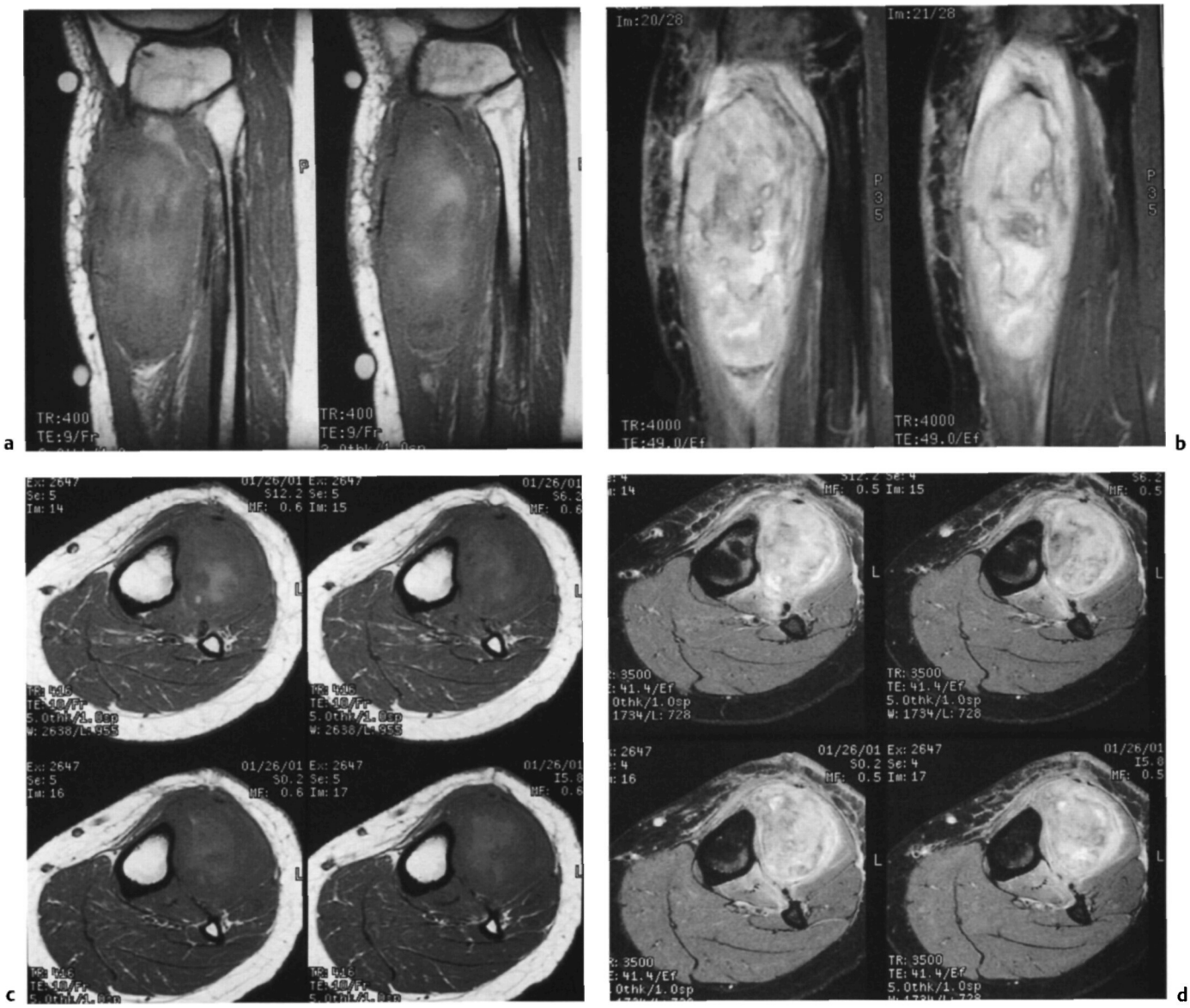

Figure **197a-d** A 29-year-old woman with a hemangiopericytoma involving the tibialis anterior, tibialis posterior, extensor digitorum longus, and popliteus muscles. The tumor has mostly intermediate signal on sagittal (**a**) and axial (**c**) T1 WI, as well as several zones of high signal at sites of hemorrhage. The tumor has mixed intermediate mostly high signal on sagittal (**b**) and axial (**d**) FST2WI, as well as foci and curvilinear zones of low signal.

have also been applied. Conventional hemangiopericytomas have recently been reported to have 2-year and 5-year survival rates of 93% and 86%, respectively.[6] Hemangiopericytomas in children less than 1 year old are less aggressive and more responsive to treatment than those that occur in older children and adults.[19]

References

1 Abrahams JM, Forman MS, Lavi E, Goldberg H, Flamm ES. Hemangiopericytoma of the third ventricle. case report. *J Neurosurg* 1999:90:359-362.

2 Chiechi MV, Smirniotopoulos JG, Mena H. Intracranial hemangiopericytomas: MR and CT features. *AJNR Am J Neuroradiol* 1996;17: 1365-1371.

3 Conway WF, Hayes CW. Miscellaneous lesions of bone. *Radiol Clin North Am* 1993;31:339-358.

4 Darby AJ. Vascular neoplasms of bone. In: Helliwell TR, ed. *Problems in Pathology: Pathology of Bone and Joint Neoplasms* 1st ed. Vol 37. Philadelphia, Pa: W.B. Saunders; 1999:330-338.

5 Das Gupta TK, Chaudhuri PK. Tumors of vascular and perivascular tissue. In: Das Gupta TK, Chaudhuri PK, eds. *Tumors of the Soft Tissues* 2nd ed. Stamford, Conn: Appleton & Lange; 1998:407-440.

6 Espat NJ, Lewis JJ, Leung D, et'al. Conventional hemangiopericytoma, modern analysis of outcome. *Cancer* 2002:95:1746-1751.

7 Forest M. Vascular tumors. In: Forest M, Tomeno B, Vanel D, eds. *Orthopedic Surgical Pathology: Diagnosis of Tumors and Pseudotumoral Lesions of Bone and Joints* Edinburgh: Churchill Livingstone; 1998:345-362.

8 Gengler C, Guillou L. Solitary fibrous tumor and haemangiopericytoma: evolution of a concept. *Histopathology* 2006;48:63-74.

9 Guillou L, Fletcher JA, Fletcher COM, Mandahl N. Extrapleural solitary fibrous tumour and haemangiopericytoma. In: Fletcher COM, Unni KK, Mertens F, eds. *World Health Organization Classification of Tumours. Pathology and Genetics of Tumours of Soft Tissue and Bone* Geneva: IARC Press; 2002:86-90.

10 Huvos AC. Hemangiopericytoma of bone. In: Huvos AG, ed. *Bone Tumors: Diagnosis, Treatment, and Prognosis* 2nd ed. Philadelphia, Pa: W.B. Saunders; 1991:591-593.

11 Juan CJ, Huang GS, Hsueh HH, Shen HJ, Chin SC, Hsiao HS. Primary hemangiopericytoma of the tibia: MR and angiographic correlation. *Skeletal Radiol* 2000;29:49-53.

12 Kransdorf MJ, Murphey MD. Soft tissue tumors in a large referral population: prevalence and distribution of diagnoses by age, sex, and location. In: *Imaging of Soft Tissue Tumors 2nd* ed. Philadelphia, Pa: W.B. Saunders; 2006:6-37.

13 Kransdorf MJ. Benign soft-tissue tumors in a large referral population: distribution of specific diagnoses by age, sex, and location. *AJR Am J Roentgenol* 1995;164:395-402.

14 Kransdorf MJ. Malignant soft-tissue tumors in a large referral population: distribution of diagnoses by age, sex, and location. *AJR Am J Roentgenol* 1995;164:129-134.

15 Kransdorf MJ, Murphey MD. Vascular and lymphatic tumors. In: *Imaging of Soft Tissue Tumors 2nd* ed. Philadelphia, Pa: W.B. Saunders; 2006:150-188.

16 Mulder JD, Schutte HE, Kroon HM, Taconis WK. Introduction.In: *Radiologic Atlas of Bone Tumors* Amsterdam: Elsevier; 1993:3-6.

17 Mulder JD, Schutte HE, Kroon HM, Taconis WK. The diagnosis of bone tumors. In: *Radiologic Atlas of Bone Tumors* Amsterdam: Elsevier; 1993:9-46.

18 Mulder JD, Schutte HE, Kroon HM, Taconis WK. Hemangiopericytoma. In: *Radiologic Atlas of Bone Tumors* Amsterdam: Elsevier; 1993:249-254.

19 Rodriguez-Galindo C, Ramsey K, Jenkins JJ, et al. Hemangiopericytoma in children and infants. *Cancer* 2000;88:198-204.

20 Unni KK. Introduction and scope of study. In: *Dahlin's Bone Tumors-General Aspects and Data on 11087* Cases 5th ed. Philadelphia, Pa: Lippincott, Williams & Wilkins; 1996:1-9.

21 Unni KK. Hemagioendothelioma (hemangiosarcoma) and hemangiopericytoma. In: *Dahlin's Bone Tumors—General Aspects and Data on 11087 Cases* 5th ed. Philadelphia, Pa: Lippincott, Williams & Wilkins; 1996:317-331.

22 Weiss SW, Goldblum JR. Perivascular tumors. In: Weiss SW, Goldblum JR, eds. *Enziger and Weiss's Soft Tissue Tumors* 4th ed. St. Louis, Mo: Mosby; 200:985-1035.

A 36 Hematoma, Morel–Lavallee Lesion, and Hemophilic Pseudotumor

Definition

Hematomas are extravascular collections of red and white blood cells. Hematomas can result from trauma, surgery, coagulopathy (hemophilia, thrombocytopenia, medications/coumadin/heparin), and sepsis. An acute hematoma is defined as one less than a few days in age. A subacute hematoma is from 1 week to 3 months in duration, and chronic hematomas are older than 3 months.[5] One form of chronic hematoma is the Morel-Lavallee lesion, which refers to an encapsulated lesion in the subcutaneous fat containing proteinaceous fluid from episodes of rebleeding caused by traumatic separaration of the subcutaneous fibrofatty tissue from adjacent vascularized fascia.[5] Hemophilic pseudotumors are chronic, slow-growing, encapsulated cystic lesions in bone or soft tissues secondary to recurrent hemorrhage that occur in 1-2% of patients with hemophilia.[26]

Location

Hematomas can occur in almost any location: subcutaneous, fascial, intramuscular, subperiosteal, intra-osseous, epidural, subdural, intra-axial (brain, spinal cord). Hemophilic pseudotumors in bone occur in the femur > pelvis > tibia > hand..[26] Hemophilic pseudotumors in soft tissue can be intramuscular, interfascial, and/or subcutaneous.[26]

Signs and Symptoms

Hematomas are often areas of painful or painless soft tissue swelling, with or without superficial bruising.

Cross Pathologic Findings

Hematomas appear as collections of clotted blood, often associated with soft tissue injury. Seromas may subsequently develop at site of hematomas.

Histopathologic Findings

Evolutionary changes are observed from clotted blood collections to subsequent organization associated with inflammatory cells and macrophages, to fibrovascular ingrowth (granulation), and eventual resolution with of without dystrophic calcifications or fibrosis. Atrophic changes can be seen in muscles from prior injuries associated with contusions and hematomas.

Findings on Plain Films (Roentgenograms) and Computed Tomography[4]

Plain Films

Plain films may show an area of soft tissue swelling and blurring of soft tissue planes.

Hemophilic pseudotumors in bone can occur in subperisoteal and/or intramedullary locations.[2,6] Subperiostal pseudotumors cause pressure erosions and remodeling of the underlying bone.[2,6] Intra-osseous pseudotumors can be radiolucent lesions of varying sizes with circumscribed margins, with or without expansion and thinning of cortical bone.[2,6]

Computed Tomography

Acute hematoma (<3 to 7 days). Acute hematomas often have attenuation slightly greater than muscle.

Subacute hematoma (1 week to 3 months). Subacute hematomas often have attenuation similar to, or less than, muscle.

Chronic hematoma (>3 months). Chronic hematomas often have attenuation similar to, or less than, muscle.

Intra-osseous pseudotumor. Lesions are radiolucent and of varying size with circumscribed margins, with or without expansion and thinning of cortical bone.[26] Crossing trabeculae within lesions, cortical thinning, and periosteal reaction are easily seen with CT.[26]

MRI Findings[1-7]

Acute hematoma (<3 to 7 days). Hematomas often have mostly intermediate signal that is similar to muscle on TlWI; and have mixed low-intermediate and/or high signal relative to muscle on PDW1, T2WI, and FST2W1. Poorly defined zones of high signal on PDWI, T2WI, and FST2WI may also be seen peripheral to the hematoma, representing adjacent edema.

Subacute hematoma (1 week to 3 months). Subacute hematomas can have high and/or intermediate signal on T1WI, and high signal on FST1WI, PDWI, T2WI, and FST2WI (Figs. **198-201, 203, 206, 207).** Peripheral and central zones of low signal on PDWI, T2WI, and FST2WI can be seen in mid to late subacute hematomas secondary to the presence of hemosiderin from breakdown of blood cells and oxidation/metabolism of hemoglobin. Mild, peripheral Gd-contrast enhancement may be seen.

Chronic hematoma (>3 months). Chronic hematomas can have high signal onT1WI, PDWI, T2WI, and FST2WI. A thin or thick peripheral rim of low signal on T2WI from hemosiderin can seen with chronic hematomas (Figs. **202, 204, 205).** Chronic hematomas often evolve eventually into zones with low-intermediate signal on T1WI and T2WI secondary to fibrosis and residual hemosiderin (Fig. **199).** The Morel-Lavellee form of persistent chronic hematoma is typically located in the subcutaneous fat of the proximal thigh and contains low, intermediate or high signal on TlWI and homogeneous or heterogeneous high signal on T2WI, surrounded by thin or slightly thick peripheral zones of low signal[5] (Fig. **202).** Lesions may show variable Gd-contrast enhancement.[4]

Hemophilic pseudotumor. This appears as circumscribed lesions in bone or soft tissues with well-defined margins. In soft tissues and bone, pseudotumors often have low signal margins onT1WI and T2WI, and have contents with low, intermediate, and/or high signal on T1WI and T2WI[26] (Fig. **208).** Intra-osseous lesions often have associated bone expansion with cortical thinning and perisoteal reaction.

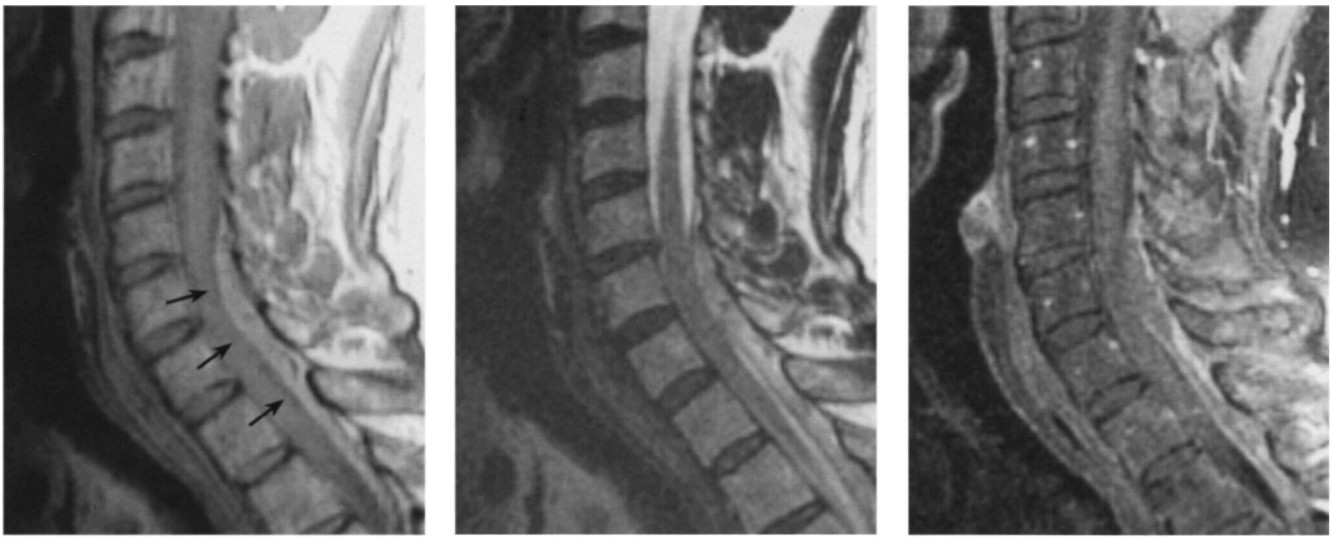

Figure **198a-c** A 60-year-old man with an epidural hematoma dorsally within the middle and lower cervical spinal canal as well as the upper thoracic spinal canal. The subdural hematoma has intermediate to slightly high signal on sagittal (**a**) PDWI. The hematoma has intermediate, slightly high and high signal on sagittal (**b**) T2WI. Peripheral Cd-contrast enhancement is seen on sagittal (**c**) FST1WI.

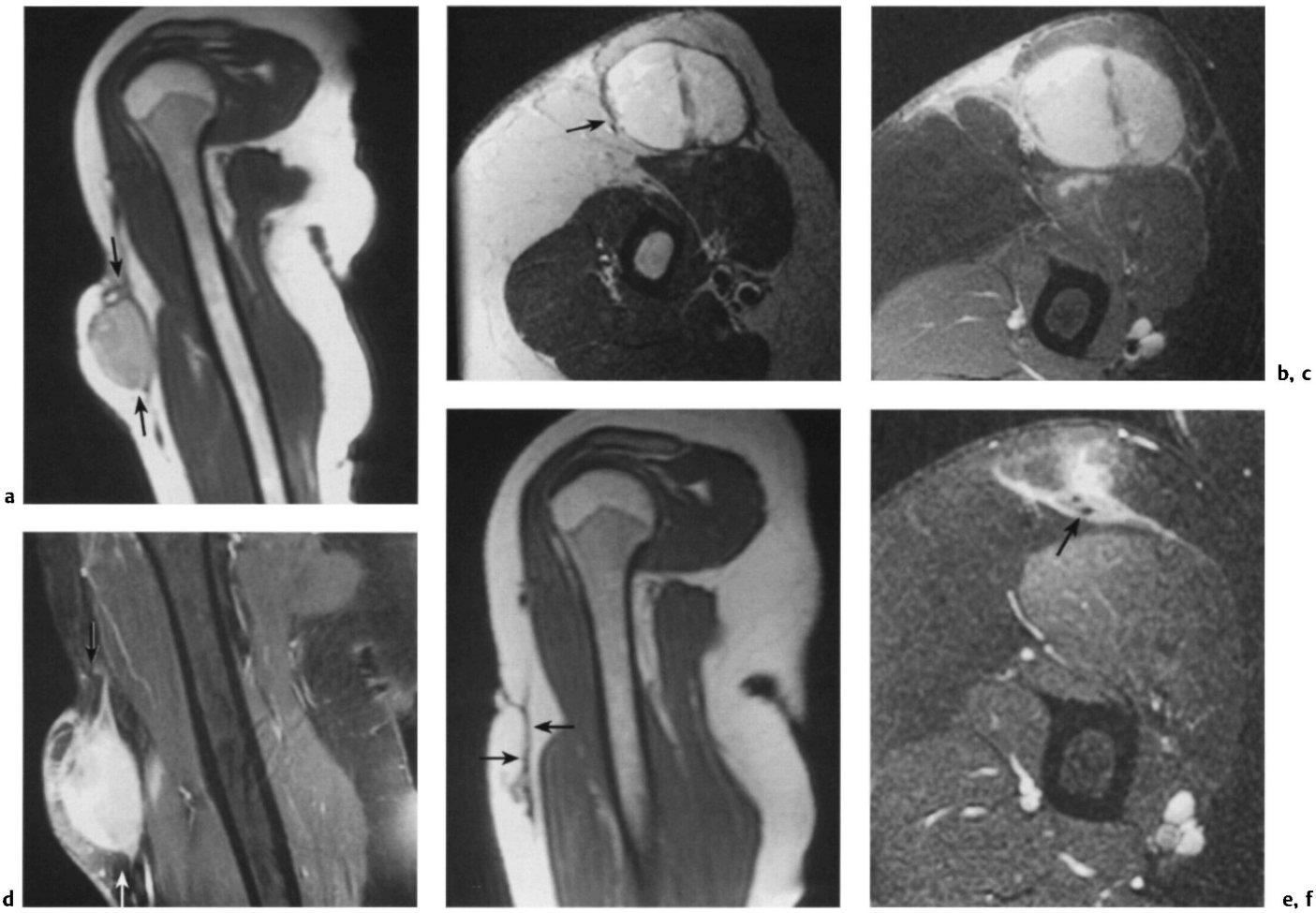

Figure 199a-f A 22-year-old woman with a subacute hematoma in the subcutaneous fat of the upper arm. The hematoma has slightly high signal, which is hyperintense relative to muscle on sagittal T1WI (**a**), and axial T2WI (**b**) surrounded by a rim of low signal. A single low signal septum is also seen. The hematoma has high signal centrally on axial (**c**) and sagittal (**d**) FST1 WI, and is surrounded by a thin peripheral zone of Cd-contrast enhancement. MR images 4 months later showed near complete resolution of the hematoma on sagittal T1WI (**e**), with residual irregular Gd-contrast enhancement on axial FST1WI (**f**).

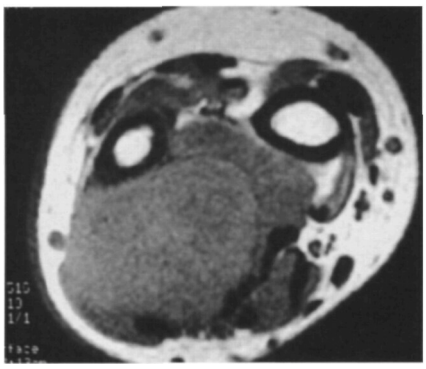

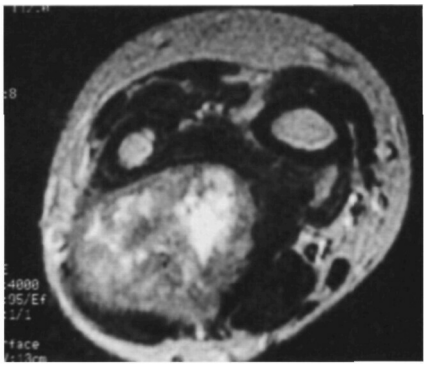

Figure **200 a, b** A 14-year-old female with a hematoma in the ventral soft tissues of the distal forearm. The hematoma has intermediate signal on axial T1WI (**a**), and heterogeneous intermediate, slightly high and high signal on axial T2WI (**b**), as well as several small foci of low signal.

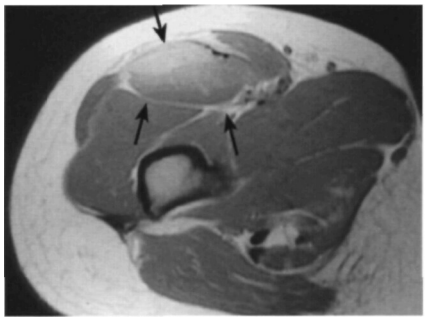

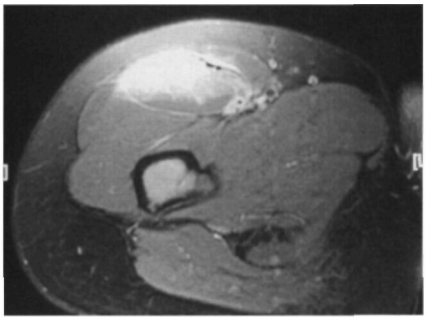

Figure **201 a, b** A 14-year-old female with an intramuscular hematoma in the rectus femoris muscle. The hematoma has irregular margins and has slightly high signal on axial PDWI(**a**)andaxialFST2WI(**b**).

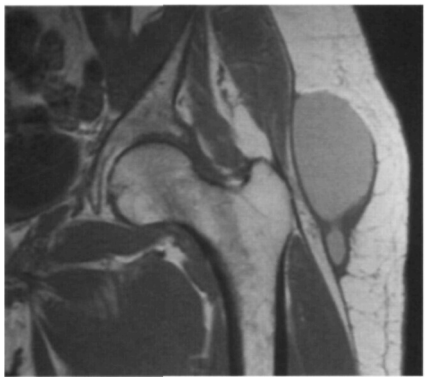

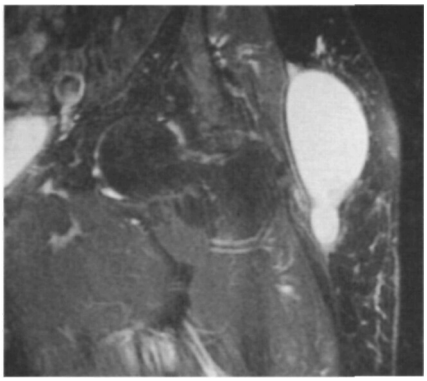

Figure **202 a, b** A 71-year-old woman with a chronic hematoma in the subcutaneous fat of the upper thigh, also referred to as a Morel-Lavallee lesion. The hematoma has intermediate signal on coronal T1WI (**a**), which is slightly hyperintense to muscle, and heterogeneous mostly high signal on coronal FST2WI (**b**). The hematoma is surrounded by a rim of low signal.

Figure **203 a, b** Subacute intramuscular hematoma involving the semitendinosus muscle in the upper thigh. The hematoma has heterogeneous slightly high, intermediate, and low signal on coronal (**a**) PDWI, and heterogeneous high, slightly high, and low signal on coronal (**b**) FST2WI.

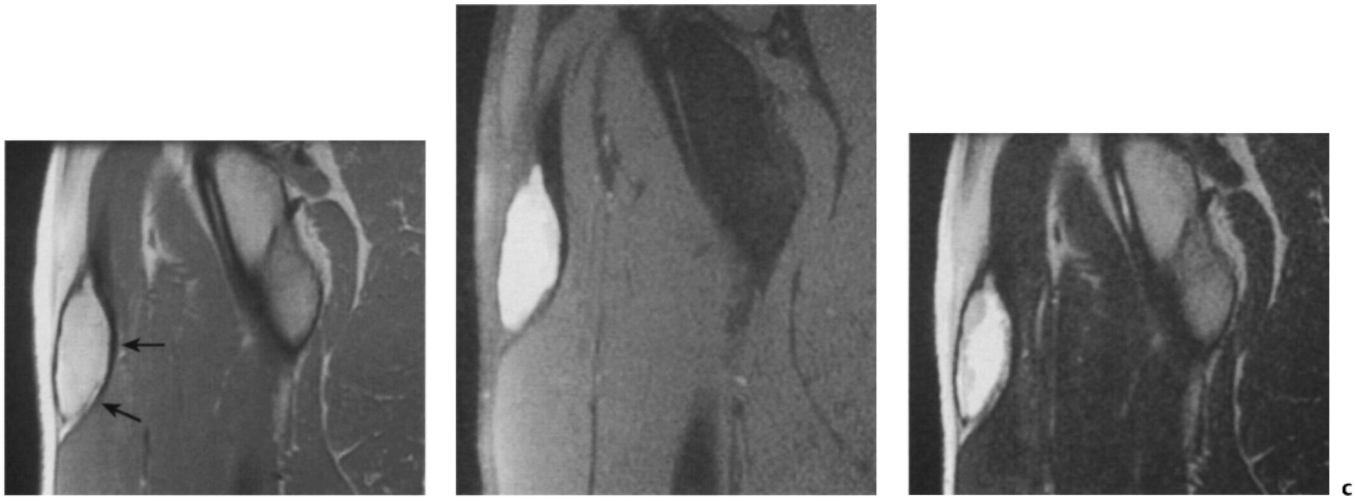

Figure **204a-c** A 31-year-old man with a chronic hematoma in the upper thigh which indents the ventral margin of the rectus femoris muscle. The hematoma has high signal on sagittal (**a**) PDWI and sagittal (**b**) FST1WI. The hematoma has mixed high and slightly high signal on sagittal (**c**) T2WI. The hematoma is surrounded by a rim of low signal on PDWI, FST1WI, and T2WI.

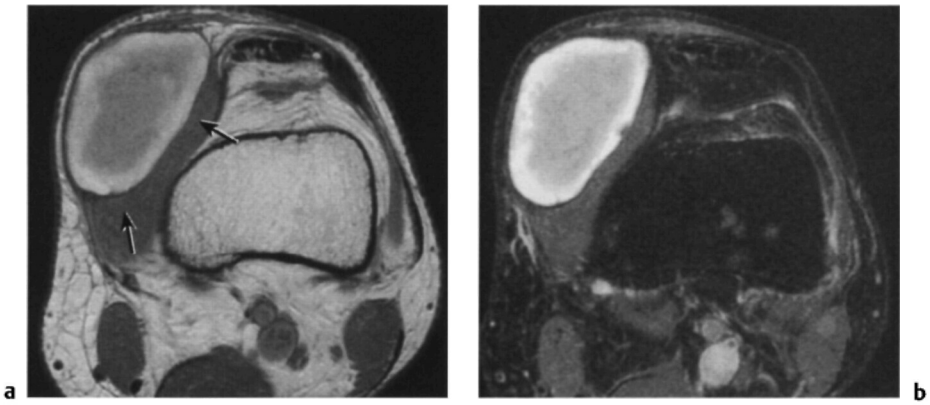

Figure **205 a, b** A 40-year-old woman with a chronic hematoma in the soft tissues at the medial knee. The hematoma has mixed high and intermediate signal on axial (**a**) PDWI, and high and slightly high signal on axial (**b**) FST2WI. The hematoma is surrounded by a rim of low signal on PDWI and FST2WI.

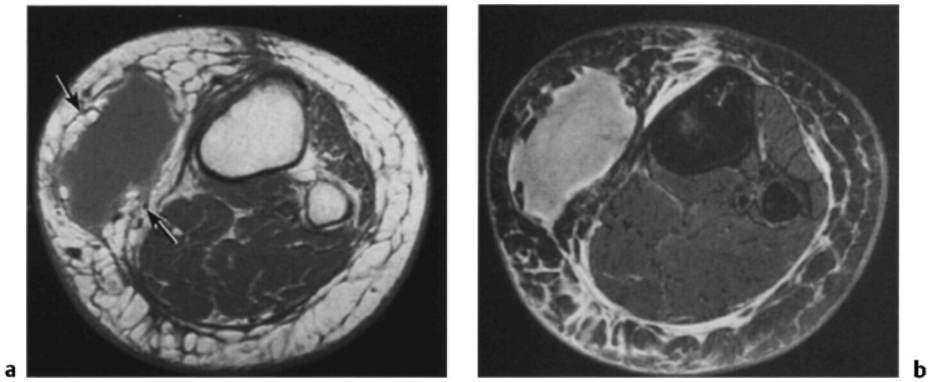

Figure **206a, b** A 55-year-old woman with a subacute hematoma in the subcutaneous fat of the upper medial leg. The hematoma has mostly low-intermediate signal centrally, with irregular peripheral zones of high signal on axial (**a**) T1WI. The hematoma has mostly high signal on axial (**b**) FST2WI.

Differential Diagnosis

Hematoma. Malignant or benign soft tissue tumor with hemorrhage, pseudoaneurysm, thrombosed aneurysm, myxoma, complex ganglion cyst, complex synovial cyst.

Intra-osseous hemophilic pseudotumor. Aneurysmal bone cyst, giant cell tumor, bone cyst, brown tumor, desmoplastic fibroma, plasmacytoma, metastatic lesion.[6]

Treatment

Conservative treatment with observation is routine for hematomas except for patients with compartment syndromes.

Hemophilic pesudotumors in bone or soft tissues can be treated conservatively with replacement therapy and immobilization.[2] Severe bone deformities secondary to intra-osseous pseudotumors may require surgery because of diminished structural integrity of bone and predisposition to pathologic fracture.

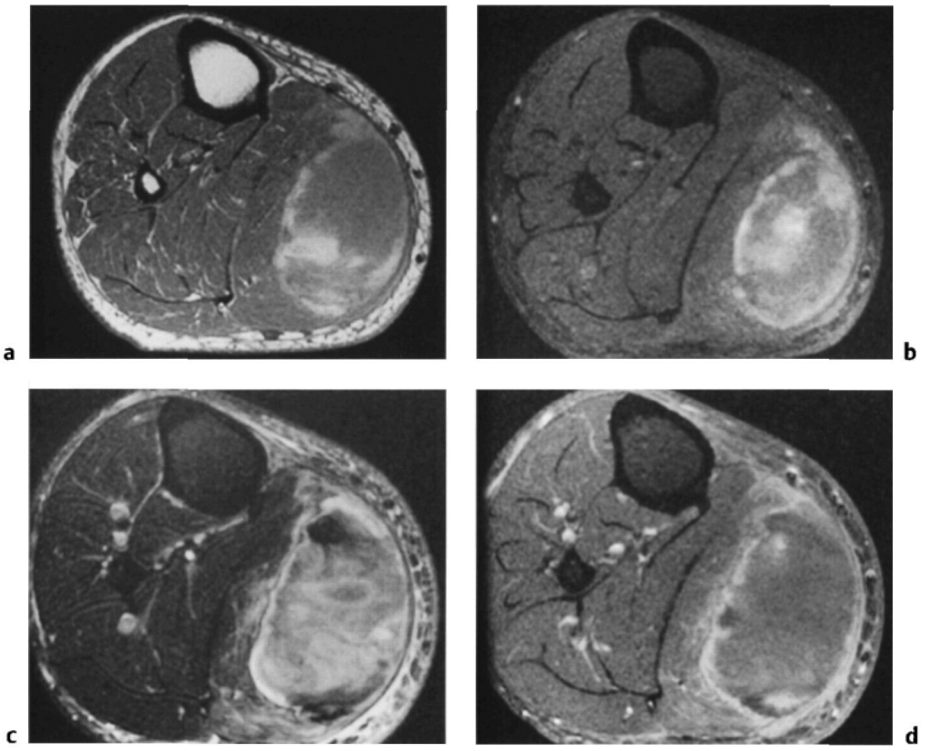

Figure **207a-d** A 50-year-old man with a subacute intramuscular hematoma in the medial gastrocnemius muscle in the upper leg. The hematoma has mixed intermediate and high signal on axial T1WI (**a**) and axial FST1WI (**b**). The hematoma has mixed high, slightly high signal, intermediate, and low signal on axial FST2WI (**c**). The hematoma shows irregular peripheral zones of Gd-contrast enhancement on axial FST1WI (**d**).

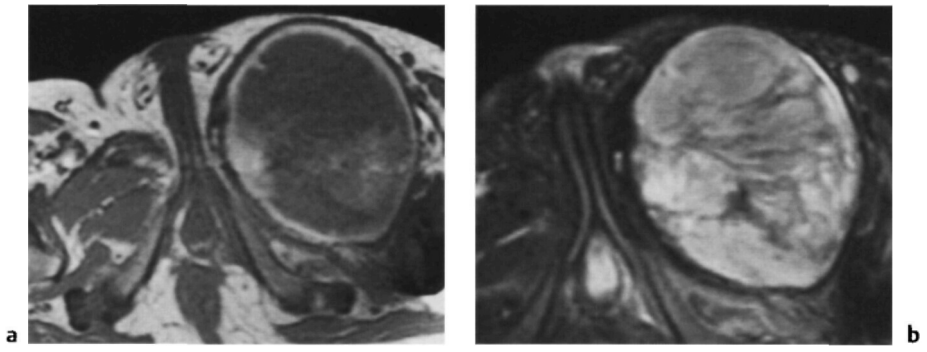

Figure **208a, b** A 45-year-old man with hemophilic pseudotumor involving the adductor muscles of the upper anterior thigh. The lesion has a thin margin of low signal and has contents with mixed intermediate and high signal on axial T1WI (**a**), and low, intermediate, and high signal on axial FST2WI(**b**).

References

1 Bush CH. The magnetic resonance imaging of musculoskeletal hemorrhage. *Skeletal Radial* 2000;29:l-9.

2 Jaovisidha S, Ryu KN, Hodler J, Schweitzer ME, Sartoris DJ, Resnick D. Hemophilic pseudotumor: spectrum of MR findings. *Skeletal Radial* 1997;26:468-474.

3 Jelinek J, Kransdorf MJ. MR imaging of soft-tissue masses. Mass-like lesions that simulate neoplasms. *Magn Reson Imaging Clin N Am* 1995;3:727-751.

4 Kransdorf MJ, Jelinek JS, Moser RP. Imaging of soft tissue tumors. Radiol *Clin North Am* 1993;31:359-372.

5 Kransdorf MJ, Murphey MD. Masses that may mimic soft tissue tumors. In: *Imaging of Soft Tissue Tumors* 2nd ed. Philadelphia, Pa: W.B. Saunders; 2006:511-572.

6 Park JS, Ryu KN. Hemophilic pseudotumor involving the musculoskeletal system: spectrum of imaging findings. *AJR Am J Roentgenol* 2004;183:55-61.

7 Rubin JI, Gomori JM, Grossman RI, Gefter WB, Kressel HY. High-field MR imaging of extracranial hematomas. *AJR Am J Roentgenol* 1987; 148:813-817.

A 37 Bone and Muscle Infarct (Also Referred to as Avascular Necrosis and Osteonecrosis)

Definition

Bone infarcts are zones of ischemic death involving bone trabeculae and marrow, which may be idiopathic or result from: trauma, corticosteroid treatment, chemotherapy, radiation treatment, occlusive vascular disease, collagen-vascular and other autoimmune diseases, metabolic storage diseases (Gaucher, etc.), sickle cell disease, thalassemia, hyperbaric events / Caisson disease, pregnancy, alcohol abuse, pancreatitis, infections, and lymphoproliferative diseases.[1-4,6,8-10-13,14,16]

Osteonecrosis is more common in fatty marrow than hematopoietic marrow. Avascular necrosis involving specific bones may have names such as: Legg-Calve-Perthes disease (femoral head), Kienbock disease (lunate), Preiser disease (scaphoid), Kohler disease (tarsal navicular), Freiberg infarction (metatarsal head), Panner disease (capitulum of humerus), and Thiemann disease (phalanges of hand). Muscle infarcts can result from similar causes to bone infarcts as well as diabetes and peripheral vascular disease.

Age at Presentation

Legg-Calve-Perthes disease (femoral head): from 3 to 12 years[12]

Kienbock disease (lunate): in adults, 20 to 40 years.

Preiser disease (scaphoid): in adults.

Freiberg infarction (metatarsal head): fromlS to 18 years.

Panner disease (capitulum of humerus): from 5 tolO years.

Thiemann disease (phalanges of hand): from 11 to 19 years.

Other sites of avascular necrosis: in children and adults.

Gender Ratio (M /F)

Legg-Calve-Perthes disease: typically affects boys.[12]

Freiberg infarction (metatarsal head): 1 / 4.

Panner disease (capitulum of humerus): typically affects boys.

Thiemann disease (phalanges of hand): M > F.

Other sites of avascular necrosis[8]: M > F.

Location

Bone infarcts occur in the proximal femur > distal femur > proximal tibia > proximal humerus > lunate, scaphoid > other bones.[8,16] Up to 60 % of bone infarcts are multiple.[8] In patients with Legg-Calve-Perthes disease, both hips are affected in 15 % of cases.[10] Muscle infarcts commonly occur in the lower extremities.

Signs and Symptoms

Patients can have localized pain or be asymptomatic.[8,10-16]

Histopathologic Findings[1,8,10,16]

In the early stages of avascular necrosis, bony trabeculae appear nonviable with "empty" lacunae lacking normal osteocytes which die within 48 hours. Fat cells in marrow become necrotic and die in 2-6 days.[1,8,16] After the initial phases of avascular necrosis, hemosiderin-laden histiocytes and fibroblasts are seen in the ischemic/infarcted regions. Progressive mineralization is also seen in the necrotic tissue. Eventually, granulation tissue and fibrosis appear at the borders of the infarct, and formation of new bone with osteoblastic activity occurs. If fractures occur in association with Osteonecrosis, areas of hemorrhage are typically seen in the early phases.

The weakest zone, which is prone to fracture, is located at the border between the avascular region and the vascularized region of attempted repair. At this junctional site, a hyperemic zone occurs with associated osteoporosis, which results in weakening of the mechanical bone strength and a decrease in the threshold for fracture. The overlying hyaline cartilage typically appears normal until subchondral fractures occur because its nutritional source is synovial fluid, unlike the underlying bone.

Periostitis can be seen with acute and subacute intramedullary bone infarcts.[15] Muscle infarcts usually show edematous and microangiopathic changes in the early phases followed by subsequent fatty replacement.

Findings on Plain Films (Roentgenograms) and Computed Tomography

Avascular necrosis of the hip:[1,4,10]

- **Stage 0.** No radiographic abnormalities are seen.
- **Stage I.** No radiographic abnormalities are seen, and radionuclide bone scans show decreased uptake.
- **Stage II.** Increased sclerosis is seen on plain films, radionuclide bone scans show increased uptake.
- **Stage IIIa.** Increased sclerosis is seen on plain films with subchondral lucency (crescent sign) without collapse; radionuclide bone scans show increased uptake. The subchondral lucency is usually indicative of the late pathologic phase of Osteonecrosis relative to the imaging findings.
- **Stage IIIb.** Increased sclerosis is seen on plain films as well as subchondral lucency with collapse; radionuclide bone scans show increased uptake.
- **Stage IV.** Increased sclerosis is seen on plain films as well as subchondral fracture bone fragmentation, and arthropathy; radionuclide bone scans show increased uptake.

Osteonecrosis in other bones. Findings seen with avascular necrosis in the hip are commonly seen with Osteonecrosis in other bones, with or without fracture.[1,4,10] Prominent sclerosis is seen in the later phases of Osteonecrosis. Near weight-bearing surfaces of long bones, Osteonecrosis can result in sclerosis as well as fragmentation, subchondral collapse and erosions, and secondary degenerative arthritis. Bone infarcts in metaphyseal

and diaphyseal regions of long bones often exhibit irregular peripheral zones of sclerosis within the marrow.

MRI Findings

Avascular necrosis of the hip.[1,4,10-12,15,17] Lesions often have a complex appearance on MRI. In the early phases of ischemia, diffuse, poorly defined zones of high signal may be seen on FST2WI which can overlap the MRI features of transient, painful bone marrow edema[7] (Fig. **215**). In zones of bone infarction, curvilinear zones of low signal on T1WI and T2WI representing zones of fibrosis are usually seen in the marrow. In addition to the above findings, irregular zones of low signal on T1WI and high signal on T2WI and FST2WI may be seen in the marrow, representing zones of fluid from edema, ischemia/infarction, or fracture" (Figs. **215-217**). Irregular zones with high signal on T1WI and T2WI can occasionally be seen, resulting from hemorrhage in combination with zones of fibrosis and fluid. A double-line sign (curvilinear adjacent zones of low and high signal on T2WI) is often seen at the edges of the infarcts, representing the borders of osseous resorption and healing (Figs. **216, 217**). Joint effusions can be seen in patients with osteonecrosis of the hip." After Gd-contrast administration, irregular enhancement can be seen from granulation tissue ingrowth.

Osteonecrosis in other bones.[4,5,9,10,12-15] The MRI features of osteonecrosis in other bones can overlap those with avascular necrosis of the hip. Metaphyseal and diaphyseal bone infarcts are less likely to be associated with fracture than infarcts near the weight-bearing ends of long bones (hip, distal femur, proximal tibia). Acute/early-subacute bone infarcts can show poorly defined intramedullary zones with increased signal on FS T2WI with corresponding Gd-contrast enhancement (Fig. **211**). Acute/

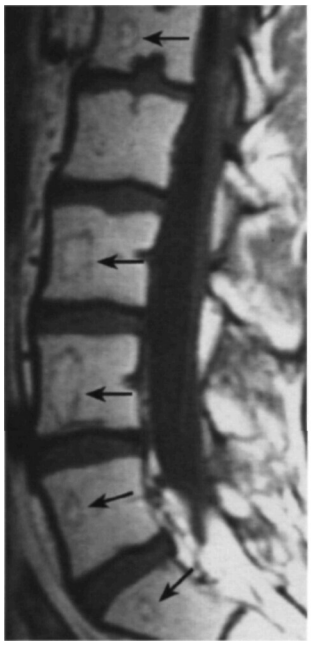

Figure **209** A 21-year-old woman with bone infarcts in multiple lumbar vertebral bodies related to prior radiation therapy. Thin curvilinear lines of low signal are seen in the marrow on sagittal T1WI. The adjacent marrow fat signal is preserved.

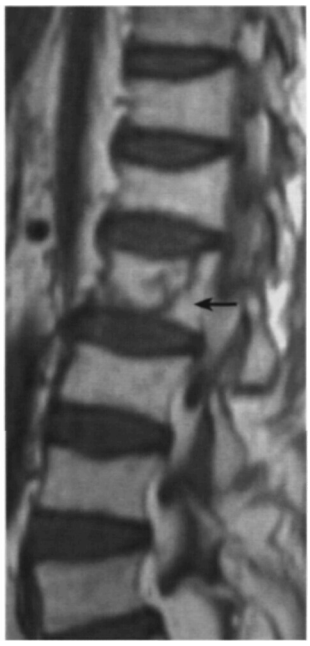

Figure **210** A 15-year-old male with a bone infarct in the L2 vertebral body secondary to prior radiation therapy. Thin curvilinear lines of low signal are seen in the marrow on sagittal T1 WI. The adjacent marrow fat signal is preserved. Remote compression fracture deformities are seen at the superior endplatesof the T12 through L4 vertebral bodies.

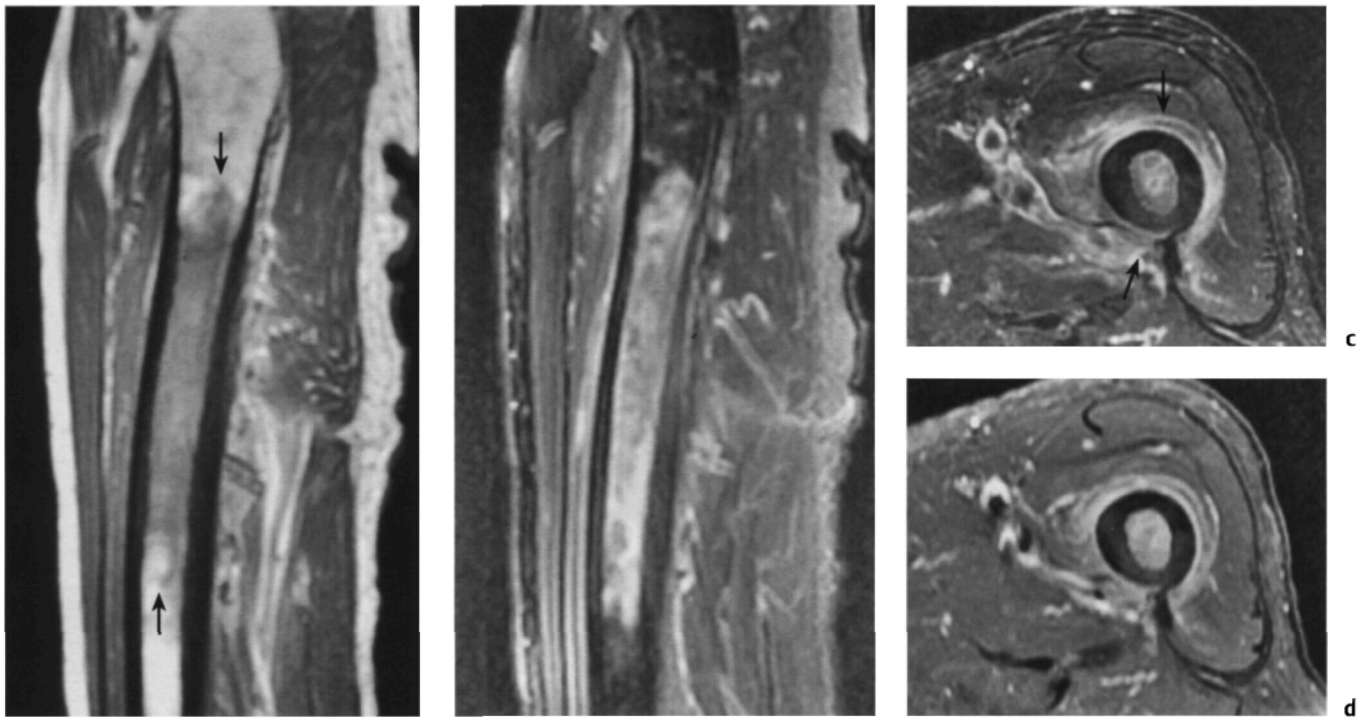

Figure **211a-d** A 76-year-old man with an acute/early-subacute intramedullary infarct involving the diaphyseal portion of the femur. The intramedullary lesion has intermediate signal on sagittal T1WI (**a**), and heterogeneous slightly high and high signal on sagittal (**b**) and axial (c) FST2WI. A thin linear zone of low signal representing elevated periosteum is seen superficial to the outer cortical margin associated with adjacent zones of increased signal on FST2WI (**b, c**) and Gd-contrast enhancement on axial FST1WI (**d**).

early-subacute intramedullary bone infarcts can also have associated periosteal elevation, with adjacent zones of Gd-contrast enhancement and increased signal on FST2WI in the juxtacortical extra-osseous soft tissues[15] (Fig. **211).** Poorly defined zones of subchondral high signal on T2WI may be seen with bone infarcts, which can overlap the MR features of bone contusions[5] and transient painful bone marrow edema[7] (Figs. **212-214).** In zones of bone infarction, curvilinear zones of low signal on T1WI and T2W1 representing zones of fibrosis are often eventually seen in the marrow (Figs. **209, 210, 212, 218-221).** A double-line sign (curvilinear adjacent zones of low and high signal on T2WI) can occur at the edges of the infarcts, representing the borders of osseous resorption and healing (Figs. **212, 218-221).** Irregular Gd-contrast enhancement in marrow can also be seen from granulation tissue ingrowth into zones of necrotic medullary bone. Late-phase bone infarcts involving the carpal bones often have prominent low signal on T1WI, as well as fragmentation, erosions of cartilage, and low signal in the adjacent radius representing degenerative sclerosis[10] (Figs. **213, 214**).

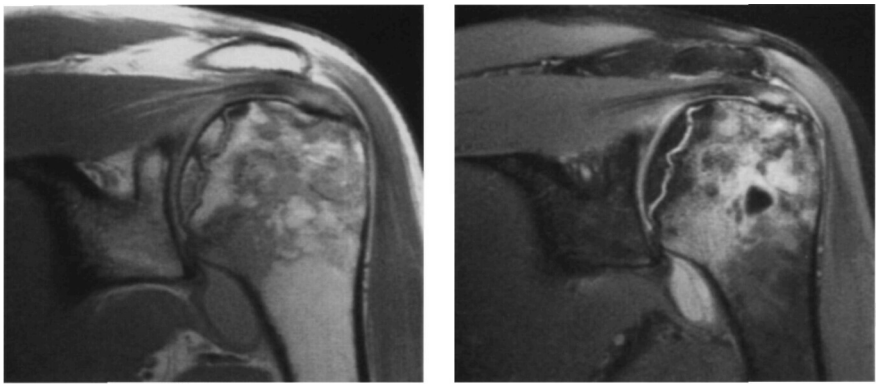

Figure **212 a, b** Ischemia and bone infarction involving the proximal humerus in a 50-year-old man. A small zone of bone infarction is seen in the subchondral bone of the upper medial humerus demarcated by two curvilinear zones of low signal separated by a thin zone of intermediate signal on coronal (**a**) PDWI. This thin intervening zone between the curvilinear zones of low signal has high signal on coronal (**b**) FS T2WI. A zone of bone ischemia involving the marrow of the humeral head is seen as a poorly defined region of high signal on coronal (**b**) FST2WI.

Figure **213a-c** Bone infarct involving the capitate. AP radiograph (**a**) shows increased density in the capitate. The zone of infarction in the marrow has intermediate and low signal on coronal (**b**) PDWI, and heterogeneous mostly high signal on coronal (**c**) FST2WI, as well as small zones of low signal.

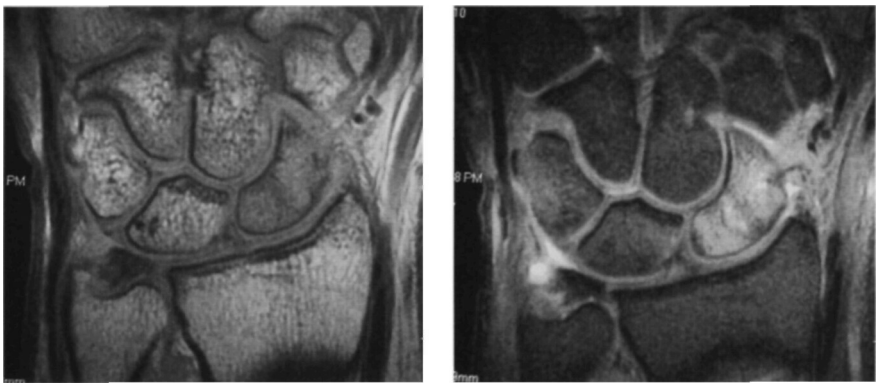

Figure **214a, b** Bone infarct in the scaphoid. The zone of infarction in the marrow has intermediate signal on coronal PDWI (**a**) and heterogeneous mostly high signal on coronal FST2WI(**b**).

a b, c

Figure **215** a-c A 50-year-old man with ischemic changes and infarction of the proximal femur. A small zone of bone infarction is seen in the subchondral bone of the upper femur, demarcated by a curvilinear zone of low signal on coronal PDWI (**a**). This thin zone of low signal is adjacent to zones of high signal in the marrow on FS T2WI (b). A poorly defined zone of Cd-contrast enhancement is seen in the involved marrow on coronal FST1WI (**c**), which probably represents granulation tissue ingrowth. A small joint effusion is present.

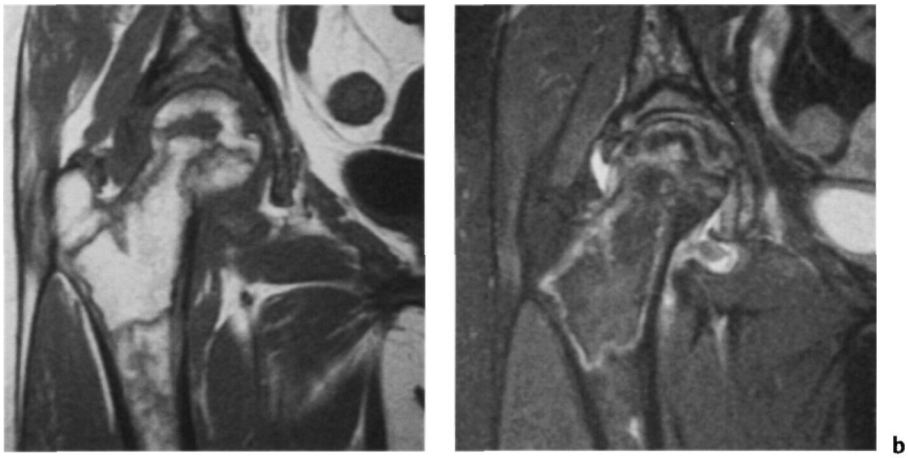

a b

Figure **216a, b** A 29-year-old woman with bone infarcts in both proximal femurs after chemotherapy for leukemia. Curvilinear zones of low signal on coronal PDWI (**a**) are seen, which are adjacent to zones of marrow with normal signal. A double-line sign consisting of curvilinear adjacent zones of low and high signal on coronal FST2WI (**b**) is seen at the edge of the infarct, representing the borders of osseous resorption and healing. A small joint effusion is present.

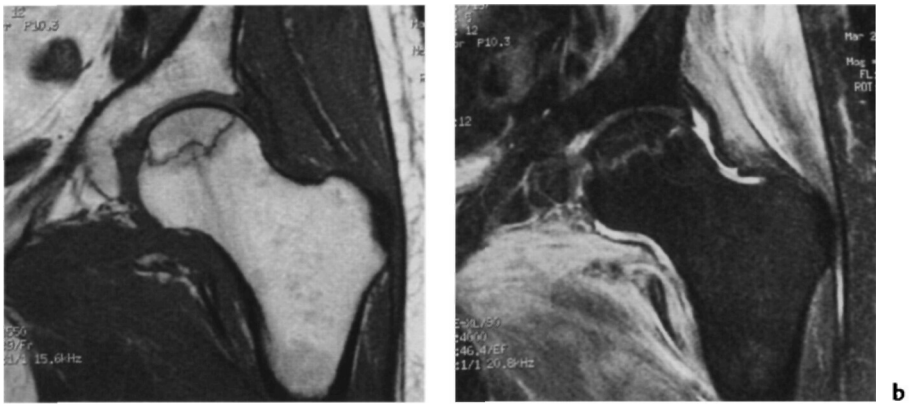

a b

Figure **217a, b** A 45-year-old man with a bone infarct in the subchondral marrow of the femoral head related to chemotherapy. Curvilinear zones of low signal on coronal PDWI (**a**) are seen which are adjacent to zones of marrow with normal signal. A double-line sign consisting of curvilinear adjacent zones of low and high signal on coronal FS T2WI (**b**) is seen at the edge of the infarct, representing the borders of osseous resorption and healing. A small joint effusion is present. Poorly defined zones of high signal on FST2WI are seen in the adjacent muscles from edematous changes.

Muscle infarcts. In the early phases of ischemia and infarction, poorly defined zones of increased signal on T2WI and FS T2W1 can be seen in the involved muscles. Fatty replacement of muscle tissue eventually occurs in many cases (Figs. **222, 223)**

Differential Diagnosis

Bone infarct. Bone contusion, transient painful bone marrow edema, intra-osseous lipoma, osteosarcoma, osteomyelitis, fibrous dysplasia, Paget disease.

Muscle infarct

- In early phases: myositis, contusion, hematoma, early deinnervation.
- In late phases: intramuscular lipoma, late stage of deinnervation.

Prognosis and Treatment

Legg-Calve-Perthes disease. Prognosis is dependent on how much of the femoral head is abnormally fissured: the greater the percentage over 50 %, the worse the prognosis.[10] Treatment

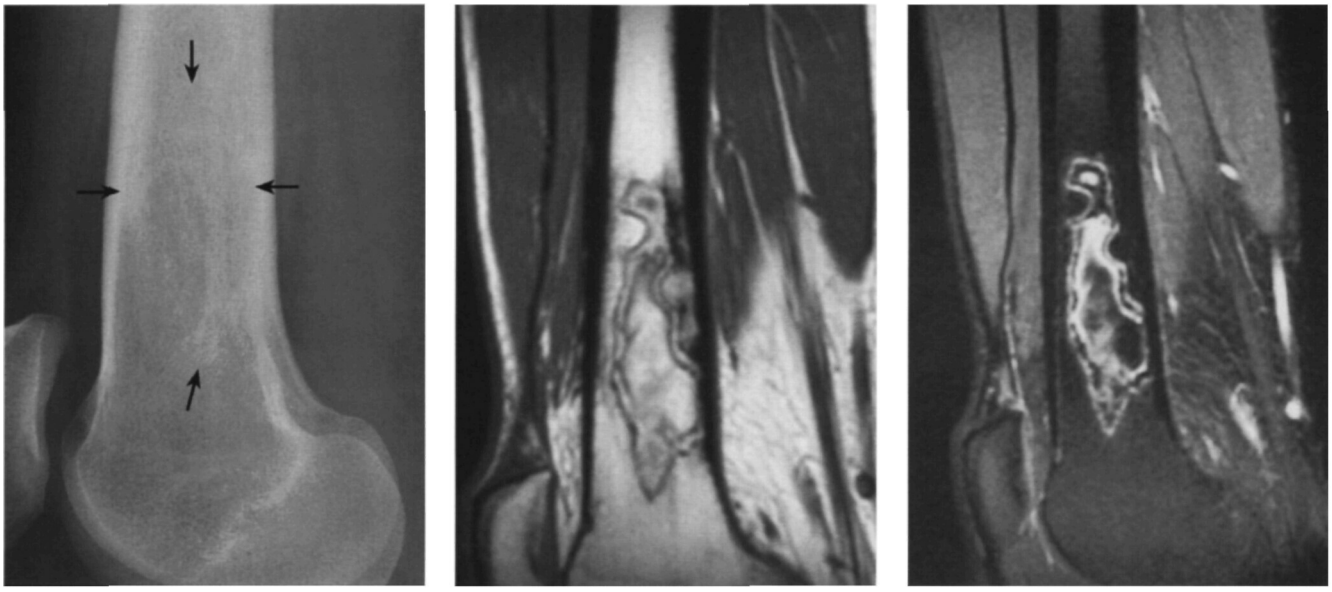

a b, c

Figure **218a-c** A 38-year-old man with sickle cell disease and a bone infarct in the distal femur. Lateral radiograph (**a**) shows a poorly defined zone of increased intramedullary density in the distal femur. Curvilinear parallel zones of low signal on sagittal (**b**) PDWI are seen which are adjacent to zones of marrow with normal signal. A double-line sign consisting of curvilinear adjacent zones of low and high signal on sagittal (**c**) FST2WI is seen at the edge of the infarct, representing the borders of osseous resorption and healing.

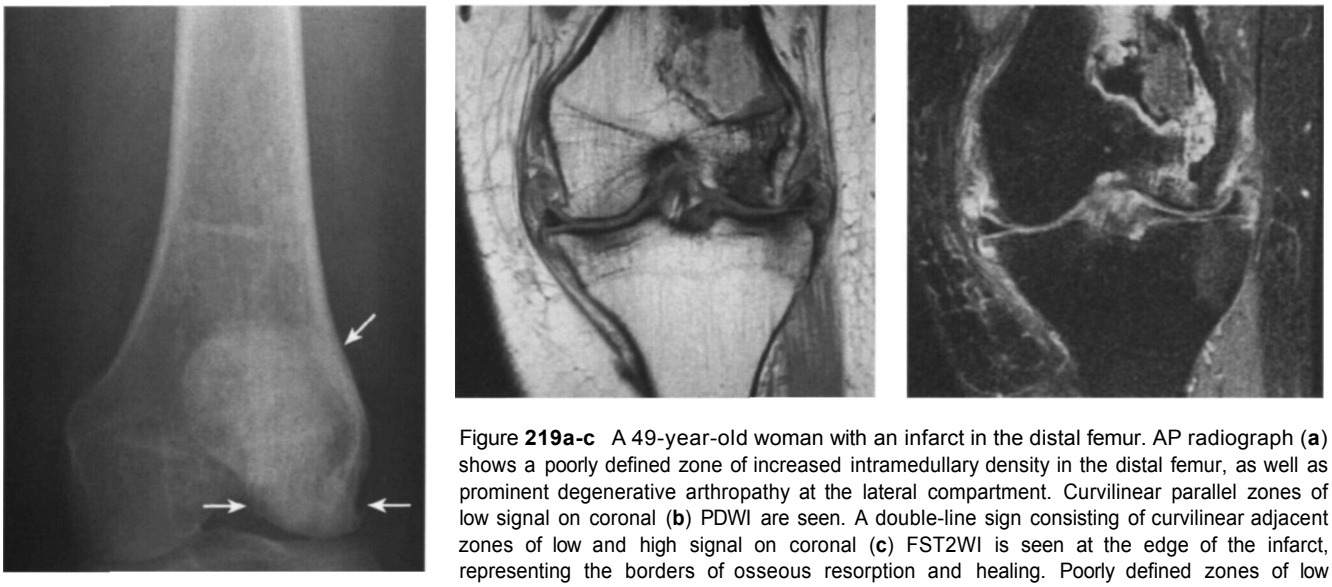

a b, c

Figure **219a-c** A 49-year-old woman with an infarct in the distal femur. AP radiograph (**a**) shows a poorly defined zone of increased intramedullary density in the distal femur, as well as prominent degenerative arthropathy at the lateral compartment. Curvilinear parallel zones of low signal on coronal (**b**) PDWI are seen. A double-line sign consisting of curvilinear adjacent zones of low and high signal on coronal (**c**) FST2WI is seen at the edge of the infarct, representing the borders of osseous resorption and healing. Poorly defined zones of low and intermediate signal on PDWI and heterogeneous high signal on FST2WI are also seen in the subchondral marrow, representing reactive edema from the degenerative arthropathy and osteonecrosis.

(varus derotational osteotomies, acetabular osteotomies) is controversial because of lack of long-term comparison studies.[12]

Avascular necrosis of the hip. Prognosis is dependent on how much of the femoral head has abnormal MR signal as well as fragmentation and degree of deformation of the femoral head. Prostheses of the femoral head with or without an acetabular component are routinely performed for osteonecrosis of the hip.

Osteonecrosis of other bones. Fractures secondary to bone infarcts are related to the size of lesions and proximity to the weight-bearing ends of long bones. Fractures resulting from bone infarcts may require joint replacements. Infarcts without fracture can be followed conservatively by observation.

Bone infarcts and tumors. Rare cases of sarcomatous transformation (osteogenic sarcoma, fibrosarcoma, arid malignant fibrous histiocytoma) from bone infarcts without radiation treatment history have been reported in patients older than 40 years).[8-16]

a

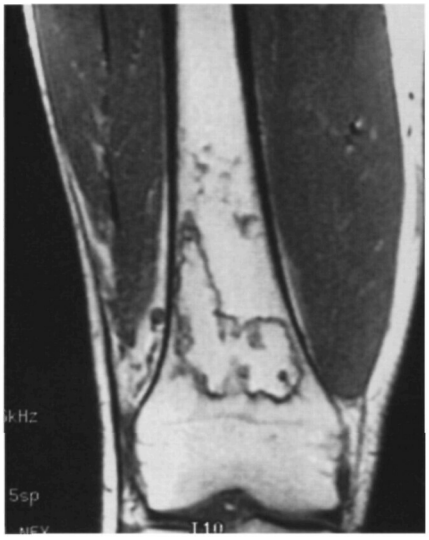

b, c

Figure **220**a-c A 31-year-old man with bone infarcts in the distal femur and proximal tibia related to chemotherapy for lymphoma. Lateral radiograph (**a**) shows poorly defined zones of increased intramedullary density in the distal femur and proximal tibia. Curvilinear parallel zones of low signal on coronal (**b**) T1WI are seen which are adjacent to zones of marrow with normal signal. A double-line sign consisting of curvilinear adjacent zones of low and high signal on coronal (**c**) FST2WI is seen at the edge of theinfarct, representing the borders of osseous resorption and healing.

a

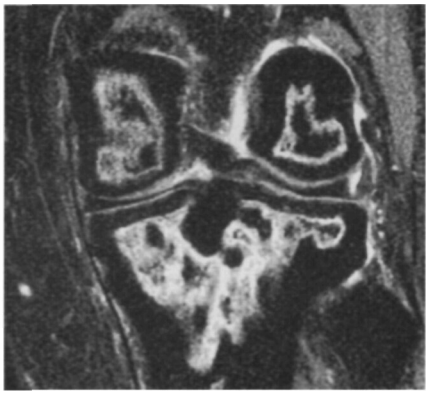

b

Figure **221 a, b** Bone infarcts in the distal femur and proximal tibia. Curvilinear parallel zones of low signal on coronal PDWI (**a**) are seen which are adjacent to zones of marrow with normal signal. A double-line sign consisting of curvilinear adjacent zones of low and high signal on coronal FST2WI (**b**) is seen at the edge of the infarct.

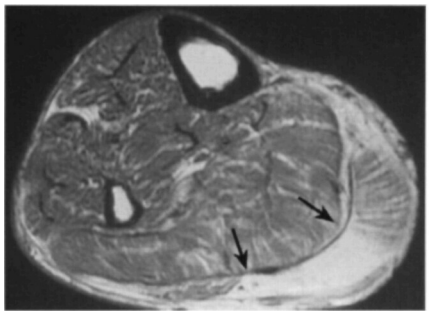

a

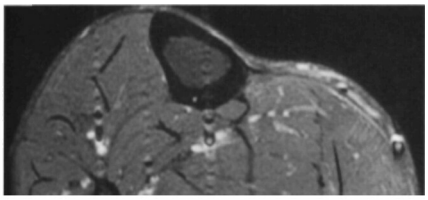

b

Figure **222a, b** A 56-year-old man with a nonacute infarct involving the medial gastrocnemius muscle. Zones with high signal on axial T1WI (**a**) are seen in the muscle secondary to fatty atrophy resulting from the infarct, which has corresponding low signal on axial FST1WI (**b**).

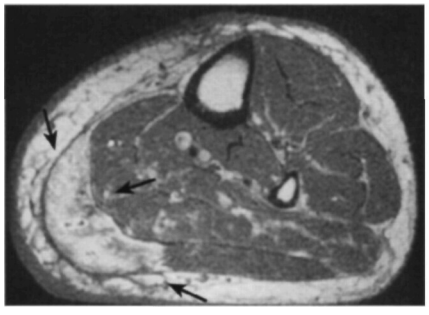

a

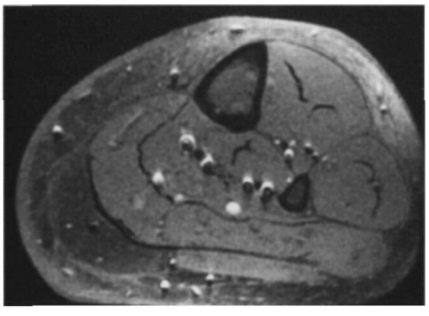

b

Figure **223 a, b** A 60-year-old man with a remote infarct involving the medial gastrocnemius muscle. There is diffuse high signal on axial T1WI (**a**) in the muscle secondary to fatty atrophy resulting from the infarct, which has corresponding low signal on axial FST1WI (**b**).

References

1 Andrews CL Evaluation of the marrow space in the adult hip. Radiographics 2000;20:S 27-S 42.

2 Assouline-Dayan Y, Chang C, Greenspan A, Shoenfeld Y, Gershwin ME. Pathogenesis and natrural history of osteonecrosis. *Semin Arthritis Rheum* 2002;32:94-124.

3 Balakrishnan A, Schemitsch EH, Pearce D, Mckee MD. Distinguishing transient osteoporosis of the hip from avascular necrosis. *CanJSurg* 2003;46:187-192.

4 Bluemke DA, Zerhouni EA. MRI of avascular necrosis of bone. Top Magn *Resort Imaging* 1996;8:231-246.

5 Boles CA, Ward WG. Loose fragments and other debris. Miscellaneous synovial and marrow disrders. Magn Reson *Imaging Clin N Am* 2000;8:371-390.

6 Coates PT, Tie M, Russ GR, Mathew TH. Transient bone marrow edema in renal transplantation: a distinct post-transplantation syndrome with a characteristic MRI appearance. *Am J Transplant* 2002;2:467-470.

7 Fernandez-Canton G, Casado 0, Capelastegui A, Astigarraga E, Larena JA, Merino A. Bone marrow edema syndrome of the foot: one year follow-up with MR imaging. *Skeletal Radiol* 2003;32:273-278

8 Forest M. Bone infarct. In: Forest M, Tomeno B, Vanel D, eds. *Orthopedic Surgical Pathology: Diagnosis of Tumors and Pseudotumoral Lesions of Bone and Joints* Edinburgh: Churchill Livingstone: 1998: 657-662.

9 Frush DP, Heyneman LE, Ware RE, Gissett GS. Ill MR features of soft-tissue abnormalities due to acute marrow infarction in five children with sickle cell disease. *AJR Am J Roentgenol* 1999:173:989-993.

10 Golimbu CN, Firoznia H, Raffi M. Avascular necrosis of the carpal bones. Magn Reson *Imaging Clin N Am* 1995;3:281-303.

11 Huang GS, Chan WP, Chang YC, Chang CY, Chen CY, Yu JS. MR imaging of bone marrow edema and joint effusion in patients with osteonecrosis of the femoral head: relationship to pain. A/RAmJRoentgenol 2003;181:545-549.

12 Hubbard AM. Imaging of hip pediatric disorders. *Radiol Clin North* Am 2001;39:721-732.

13 Kier R. Magnetic resonance imaging of plantar fasciitis and other causes of heel pain. Magn Reson *Imaging Clin N Am* 1994;2:97-107.

14 Terk MR, Esplin J, Lee K, Magre G, Coletti PM. MR imaging of patients with type 1 Gaucher's disease: relationship between bone and visceral changes. *AJR Am J Roentgenol* 1995;165:599-604.

15 Umans H, Haramati N, Flusser G. The diagnostic role of gadolinium enhanced MRI in distinguishing between acute medullary bone infarct and osteomyelitis. Magn Reson *Imaging* 2000:18:255-262.

16 Unni KK. Conditions that simulate primary neoplasms of bone. In: *Dahlin's Bone Tumors—General Aspects and Data on 11087 Cases* 5th ed. Philadelphia, Pa: Lippincott, Williams & Wilkins; 1996:355-432.

17 Vande Berg BC, Malghem J, Lecouvet FE, Noel H, Maldague B. MR imaging of bone infarction and epiphyseal osteonecrosis. *J Beige Radiol* 1997;80:243-250.

A 38 Kaposi Sarcoma (also Referred to as Angiosarcoma Multiplex, Kaposi Disease, Idiopathic Multiple Pigmented Sarcoma of the Skin, and Granuloma Multiplex Hemorrhagicum)

ICD-O Code

9140/3

Definition

Kaposi sarcoma is an endothelial tumor that is associated with human herpes virus 8 (HHV-8) infection.[5,6] These tumors are locally invasive and often are located in the cutaneous tissues, mucosa, lymph nodes, and/or visceral organs.[56] There are four types: classic indolent, endemic African, iatrogenic, and AIDS-associated. The classic indolent type is rare and typically occurs in the lower legs of elderly men of Mediterranean or Eastern European descent.[5,6] The endemic African type is fairly common and often occurs in the lower extremities or lymph nodes in middle-aged non-HIV infected men and children in equatorial Africa.[6] The iatrogenic type is fairly common and occurs in patients who are receiving immunosuppressive therapy.[6] The type of Kaposi sarcoma associated with AIDS is the most aggressive form and often involves the face, genitalia, and/or lower extremities.[6] The HHV-8 is present in all forms of Kaposi sarcoma.[6] Kaposi sarcoma in bone likely occurs from metastasis or direct extension from superficial lesions.[3]

Frequency of Occurrence

Kaposi sarcoma represents 1.2% of malignant soft tissue tumors.[4] The classic type of Kaposi sarcoma occurs with an incidence of 0.02-0.06 % of all malignant tumors.[1] Kaposi sarcoma is the most frequent tumor associated with AIDS.[1] Kaposi sarcoma rarely arises within bone.[8]

Age at Presentation

From 16 to > 85 years,[4] mean = 64.4 years.[4]

Gender Ratio (M/F)

2.4/1.[4]

Location

Soft tissue. Tumors occur in the foot and ankle > upper extremity, lower extremity > hand and wrist > head and neck > hip and buttocks > trunk.[4] These tumors are located in the cutaneous tissues, mucosa, lymph nodes, visceral organs, bones and muscles.[1-35-10] In patients with Kaposi sarcoma associated with AIDS, up to 35% occur in the mouth and oropharynx.[1]

Bone. Tumors occur in the axial skeleton > proximal or distal long bones > small tubular bones.[7-9]

Gross Pathologic Findings

Lesions can appear as reddish-blue, purplish, or dark brown nodules, macules, and/or plaques which can range in size from millimeters to several centimeters.[1,6] Some lesions may ulcerate.[6]

Histopathologic Findings

The histopathologic features of Kaposi sarcoma vary depending on the stage of development, which ranges from the early patch stage to the plaque and later nodular stages.[6] In the **patch stage,** there is proliferation of irregularly shaped vascular spaces that are oriented parallel to the epidermis.[6] These vascular spaces are lined by flattened or oval endothelial cells with minimal atypia.[6] Collagen bundles, extravasated erythrocyes, zones of hemosiderin, occasional lymphocytes, and plasma cells may occur around the vascular spaces.[6] In the **plaque stage,** the vascular spaces have more irregular contours compared with the patch stage and are surrounded by denser zones of inflammatory cells, extravascular red blood cells, siderophages, and hyaline globules from destroyed red blood cells.[6] In the **nodular phase,** well-defined nodules are composed of slit-shaped vascular spaces containing red blood cells; these lie adjacent to fascicles of spindle cells with mild atypia and mitotic activity, which are seen surrounded by peripheral ectatic blood vessels.[6] Hyaline globules may be present within or outside of the spindle cells.[6] All specimens show immunoreactivity to HHV-8.[6] Spindle cells are usually immunoreactive to CD 34 and CD 31, but not to factor VIII.[6]

Tumor Genetics

Recurrent gains have been reported for 11 q!3.[6]

Findings on Plain Films (Roentgenograms) and Computed Tomography

Soft tissue. Superficial lesions can be seen with CT as zones of skin thickening and/or soft tissue attenuation nodules, with or without extension into the subcutaneous tissues.[5]

Bone. Kaposi sarcoma likely results from metastatic disease or direct extension from adjacent lesions.[8,9] Kaposi sarcoma in bone typically appears as radiolucent intramedullary zones, which extend to the cortex with or without associated cortical erosion or destruction.[3,7,S]

MRI Findings[1,7,9,10]

Soft tissue. Kaposi sarcoma can appear as lesions with circumscribed or irregular margins that commonly involve the skin and superficial soft tissues, and mucosa.[1,5] Tumors often have low to intermediate signal on T1WI and PDWI; and slightly high to high signal on T2WI and FST2WI[1,5] (Fig. **224**). After Gd-contrast administration, lesions usually show moderate to marked enhancement.[1,5]

Bone. Kaposi sarcoma can appear as intramedullary lesions with circumscribed or irregular margins.[3,7,9] Zones of cortical destruction may be seen as well as tumor extension into the extra-osseous tissues[9]. Lesions often have low to intermediate signal on T1WI, slightly high to high signal on T2WI and FST2WI.[3,7,9] (Fig. **225**). After Gd-contrast administration, lesions can show moderate to marked enhancement. Peritumoral edema may also be seen.[9]

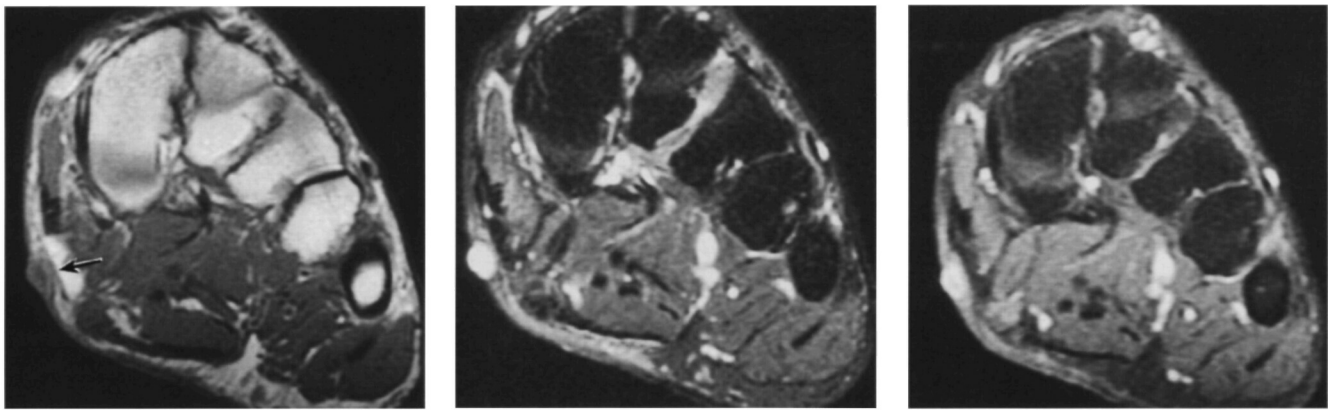

a, b c

Figure **224a-c** A 70-year-old man with Kaposi sarcoma involving the medial superficial soft tissues of the foot. The small tumor has circumscribed margins and has low to intermediate signal on coronal T1WI (**a**), and high signal on coronal FST2WI (**b**). The tumor shows prominent Gd-contrast enhancement on coronal FST1WI (**c**).

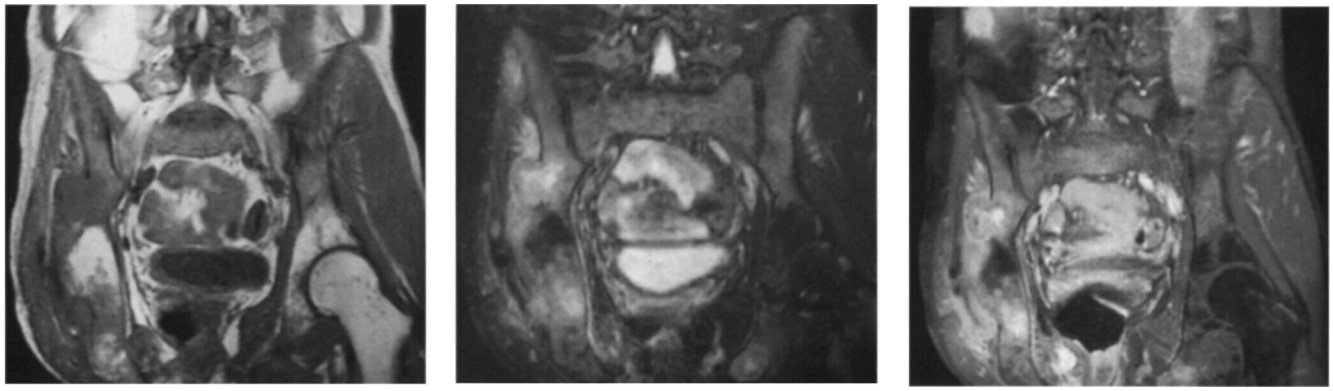

a, b c

Figure **225a-c** A 56-year-old man with metastatic Kaposi sarcoma to the bony pelvis after amputation of the right lower extremity. Multiple lesions with low-intermediate signal on coronal T1WI (**a**) and intermediate, slightly high and high signal on coronal FST2WI (**b**) are seen in the bony pelvis as well as in the soft tissues. These lesions show Cd-contrast enhancement on coronal FST1WI (**c**).

Differential Diagnosis

Hemangioendothelioma, hemangiopericytoma, angiosarcoma, leiomyoma, angiomyoma, dermatofibrosarcoma, neurofibroma, Schwannoma, bacillary (epithelioid) angiomatosis, lymphoma.

Prognosis and Treatment

The clinical course of Kaposi sarcoma depends on the type and extent of involvement.[6] The classic type that typically affects elderly men of Mediterranean or Eastern European descent usually has an indolent clinical course for 10-15 years.[6,8] Most of these patients die from other causes.[8] The endemic African type is more aggressive in children than in adults.[6,8] The endemic African type of Kaposi sarcoma in children can progress rapidly with extensive localized cutaneous growth as well as invasion of subcutaneous tissues and bone.[8] The iatrogenic type can be aggressive or indolent.[6] The type of Kaposi sarcoma associated with AIDS is the most aggressive form.[6] Bacterial myositis can occur concurrently with Kaposi sarcoma associated with AIDS.[2,10] Lesions can be treated with surgery, radiation, and/or chemotherapy.[6,7]

References

1 Atkinson DS Jr, Ptak T. Neuroradiology case of the day. Kaposi's sarcoma of the nasopharynx, oropharynx, and hypopharynx. *AJR Am J Roentgenol* 1999;173(3):804, 807-808.

2 Fleckenstein JL, Burns DK, Murphy FK, Jayson HT, Bonte FJ. Differential diagnosis of bacterial myositis in AIDS: evaluation with MR imaging. Radiology 1991;179(3):653-658.

3 Isenbarger DW, Aronson NE. Lytic vertebral lesions: an unusual manifestation of AIDS-associated Kaposi's sarcoma. C/m *Infect Dis* 1994;19(4):751-755.

4 Kransdorf MJ, Murphey MD. Soft tissue tumors in a large referral population: prevalence and distribution of diagnoses by age, sex, and location. In: *Imaging of Soft Tissue Tumors* 2nd ed. Philadelphia, Pa: W.B. Saunders; 2006:6-37.

5 Kransdorf MJ, Murphey MD. Vascular and lymphatic tumors. In: *Imaging of Soft Tissue Tumors* 2nd ed. Philadelphia, Pa: W.B. Saunders; 2006:150-188.

6 Lamovec J, Knuutila S. Kaposi sarcoma. In: Fletcher COM, Unni KK, Mertens F, eds. *World Health Organization Classification of Tumours. Pathology and Genetics of Tumours of Soft Tissue and Bone* Geneva: IARC Press; 2002:170-172.

7 Lombardo M, Girolomoni G, Spina V, Zambruno G, Giannetti A. Kaposi's sarcoma with primary bone lesions in an HIV-seronegative man. *Br J Dermatol* 1996;134(5):966-969.

8 Nguyen C, Lander P, Begin LR, Jarzem P, Grad R. AIDS-related Kaposi sarcoma involving the tarsal bones. *Skeletal Radiol* 1996;25:100-102

9 Pitson GA, Aw TJ, Rodger A Classical Kaposi's sarcoma involving bone. *Australas Radiol* 1999;43:391-393.

10 Wyatt SH, Fishman EK. CT/MRI of musculoskeletal complications of AIDS. *Skeletal Radiol* 1995;24(7):481-488.

A 39 Leiomyoma

ICD-OCode

Leiomyoma: 8890/0

Angioleiomyoma: 8894/0

Definition

Leiomyomas are benign, spindle cell tumors composed of mature smooth muscle bundles.[1-4,7,8] Ninety-five percent of leiomyomas involve the female genitourinary tract, and 3 % occur in the skin with the remainder in the gastrointestinal tract, bladder, and other sites.[9] Cutaneous leiomyomas (leiomyoma cutis) arise from the pilar arrector muscles of the skin, or from the network of muscle fibers in the deep dermis (genital leiomyomas).[1-4,7-9] Angioleiomyomas are tumors which contain mixtures of thick-walled vessels and smooth muscle cells.[9] Leiomyomas of deep soft tissues are benign, smooth muscle tumors which are typically larger and more histologically varied than the cutaneous leiomyomas.[9]

Frequency of Occurrence[5,6]

Soft tissue. Together, **leiomyomas and angioleiomyomas** represent ~2 to 5 % of benign musculoskeletal soft tissue tumors and 1 % of all musculoskeletal soft tissue tumors.[5.6.9] Cutaneous genital leiomyomas are twice as common as leiomyomas of pilar arrector origin.[9] **Leiomyomas of deep soft tissues** are uncommon.[9]

Bone. Leiomyomas of bone are rare tumors that represent < 1 % of benign tumors.

Age at Presentation

Cutaneous leiomyoma: from 14 to 67 years, mean = 40years.[56]

Angioleiomyoma: from 30 to 73 years, mean = 51 years.[5.6]

Leiomyoma of bone: usually occurs in adults over 30 years, and rarely occurs in children.[8]

Gender Ratio (M/F)

Cutaneous leiomyomas: 1 /2.[56]

Angioleiomyoma: 2 /1 to 1 /2.[3,5,6,9]

Leiomyoma of deep somatic soft tissue: 1 /1.[9]

Leiomyoma of body cavity or retroperitoneum: < 1 /1.[9]

Leiomyoma of bone: 1 /1.[8]

Location[1,2,5-7]

Soft tissue. Up to 98 % of leiomyomas occur in the uterus or gastrointestinal tract.[9] Elsewhere, leiomyomas occur in the hip and buttocks > foot and ankle > lower extremity > retroperitoneum >trunk, upper extremity > head and neck > other sites.[56]

- **Cutaneous leiomyoma (leiomyoma cutis).** Cutaneous leiomyomas arise from the pilar arrector muscle of the skin (extragenital sites) or muscle fibers of the deep dermis of the scrotum, labia, or nipple areola (genital leiomyoma).[9] Cutaneous leiomyomas of pilar arrector origin occur most frequently in the extensor surfaces of the extremities.[9]
- **Angioleiomyomas (vascular leiomyoma).** These tumors usually occur in the subcutis or deep dermis of the extremities (foot and ankle > lower extremity > hand and wrist > upper extremity > other sites), and account for about half of the superficial leiomyomas.[3,5,6,9]
- **Leiomyomas of deep soft tissues.** These tumors usually occur in the body cavities, retroperitoneum, and extremities.[9]

Bone. Leiomyomas have been reported in the mandible, maxilla > tibia > femoral neck > other sites.[28]

Signs and Symptoms[1,3,7.9]

Cutaneous leiomyomas. These slow-growing tumors often appear as brown-red to grayish papules of 1-2 cm in size.[9] Leiomyomas may be multiple and painful.[9] Multiple leiomyomas can be hereditary with an autosomal dominant inheritance.[3]

Angioleiomyomas. These are slow-growing lesions that are usually less than 2 cm in size and may have pain elicited from changes in temperature or pressure.,[39]

Leiomyomas of deep soft tissues. These lesions produce symptoms depending on their size and location.[9]

Leiomyomas of bone. Lesions may be associated with localized pain.[8]

Cross Pathologic Findings[1,7]

Cutaneous leiomyomas often appear as well-circumscribed, gray-white nodular lesions.[9] Superficial lesions are usually small, whereas leiomyomas in the deeper soft tissues/muscles can be large. Pilar leiomyomas occur in the dermal connective tissue and usually range in size from 1 to 2 cm.

Angioleiomyomas are usually well-defined, glistening gray-white nodules that occasionally may appear red, brown, or blue with or without small calcifications.[3,9]

Leiomyomas of deep soft tissues are usually gray-white lesions with or without myxoid or cystic changes.[9]

Leiomyomas of bone usually appear as firm, tan-gray tumors.[8]

Histopathologic Findings[1,3,7,9]

Cutaneous leiomyomas are composed of well-defined nodules of smooth muscle cells and thick-walled vessels, as well zones of myxoid change hyalinization, calcification, and/or fat.[9]

Angioleiomyomas (vascular leiomyomas) usually occur in the subcutaneous tissue and typically contain numerous thick-

walled vessels.[3,9] The smooth muscle cells are mature and well differentiated.[39] Mitotic figures are absent or rare.[3,9] Vascular channels vary in number and size.[3] The smooth muscle cells at the walls of the vascular channels merge with the smooth muscle cells between the vessels.[3] These lesions are often immunoreactive for a-smooth muscle actin, desmin, vimentin, and collagen type IV.[3]

Leiomyomas of deep soft tissues contain smooth muscle cells with blunt-ended fusiform nuclei in eosinophilic cytoplasm after staining with hematoxylin and eosin.[4] Tumor cells typically show no atypia, and little or no mitotic activity.[4] Calcifications and zones of myxoid changes and hyalinization are commonly seen in larger leiomyomas.[4] These lesions are often immunoreactive for a-smooth muscle actin, desmin, and h-caldesmon.[4]

Leiomyomas of bone contain interlacing bundles of uniform spindle cells without atypia.[8] Mitotic figures are rare.[8] These lesions are immunoreactive to a-smooth muscle actin and desmin.

Findings on Plain Films (Roentgenograms) and Computed Tomography[1,2,7]

Soft tissue. No findings are typically seen on plain films. CT may show a small subcutaneous lesion with soft tissue attenuation. Large leiomyomas in the deeper soft tissues may have zones of calcification and low attenuation from myxoid degeneration.

Bone. Leiomyomas in bone can appear as well-circumscribed, radiolucent abnormalities with or without thin sclerotic margins.[8] These lesions are usually 3 cm or less in diameter.[8]

MRI Findings[7]

Leiomyomas often are circumscribed lesions with intermediate signal on T1W1 and PDW1; and slightly high to high signal on T2WI and FST2WI (Figs. **226-228).** Large leiomyomas in the deep soft tissues may have zones of low signal on T2WI secondary to calcifications, or zones of high signal secondary to myxoid degeneration. After Gd-contrast administration, lesions usually show moderate to marked degrees of enhancement except at sites of calcification or myxoid degeneration. (Figs. **226-228).**

Differential Diagnosis

Soft tissue (cutaneous). Dermatofibroma, schwannoma, neurofibroma, giant cell tumor of tendon sheath, fibroma of the tendon sheath.

Deep soft tissue. Malignant fibrous histiocytoma, synovial sacoma, fibrosarcoma, leiomyosarcoma, liposarcoma.

Bone. Unicameral bone cyst, aneurysmal bone cyst, giant cell tumor, chondroblastoma, chondromyxoid fibroma, osteoblastoma, fibrous dysplasia, desmoplastic fibroma.

Prognosis and Treatment

Cutaneous leiomyomas do not undergo malignant transformation.[9] Leiomyomas of the superficial soft tissues can be observed for interval change or cured with excision for enlarging and/or symptomatic lesions.[9] Multiple lesions are difficult to completely resect, and have higher recurrence rates than solitary lesions.[9]

Angioleiomyomas are benign tumors and local excision is routinely performed.[3] Recurrence of these tumors is uncommon.[3,9]

Leiomyomas of deep soft tissues are routinely excised because of the potential overlap of imaging features with malignant soft tissue tumors.[4,9] These lesions are often cured with excision, although up to 6 % have local recurrence.[4]

Leiomyomas of bone are usually cured by excision.[8]

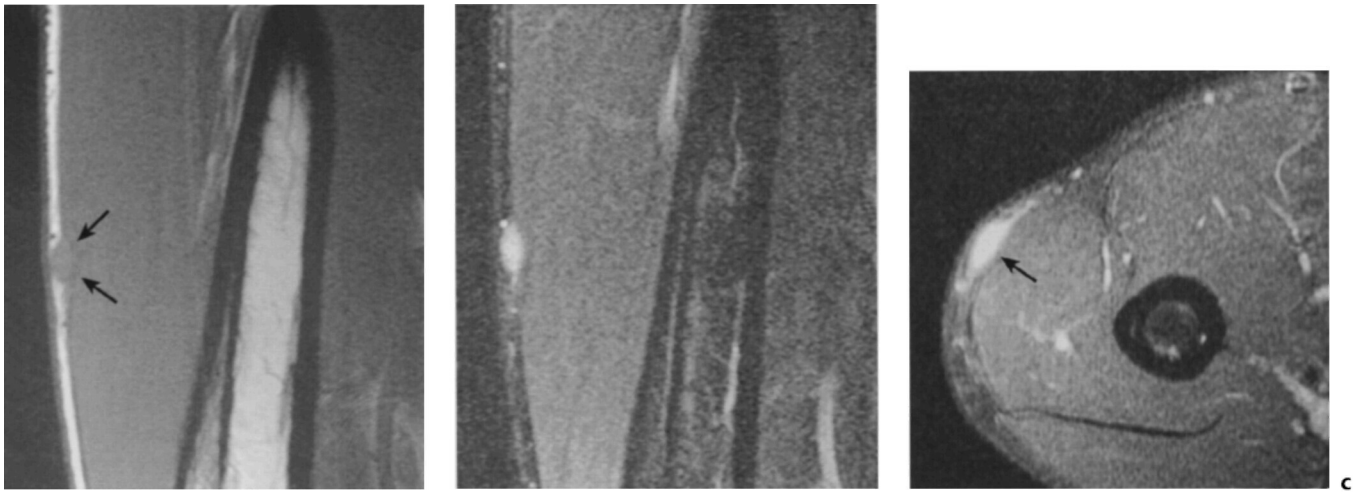

Figure **226a-c** A 22-year-old man with a leiomyoma in the subcutaneous fat of the lower leg. The small, circumscribed lesion has intermediate signal on sagittal T1WI (**a**) and slightly high to high signal on sagittal FST2WI (**b**). The lesion shows prominent Cd-contrast enhancement on axial FST1WI (**c**).

a, b

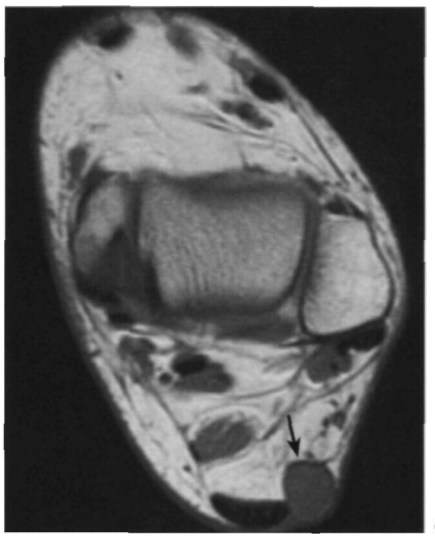

c

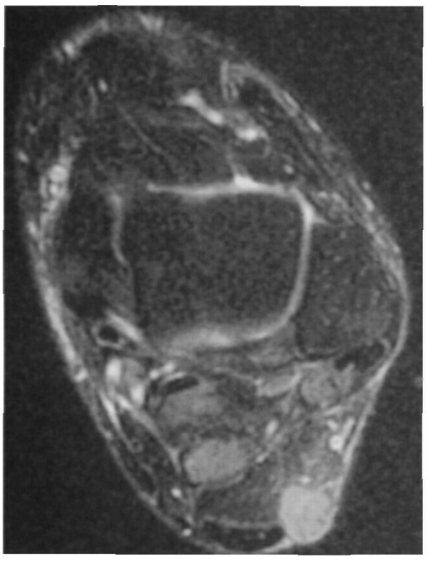

d

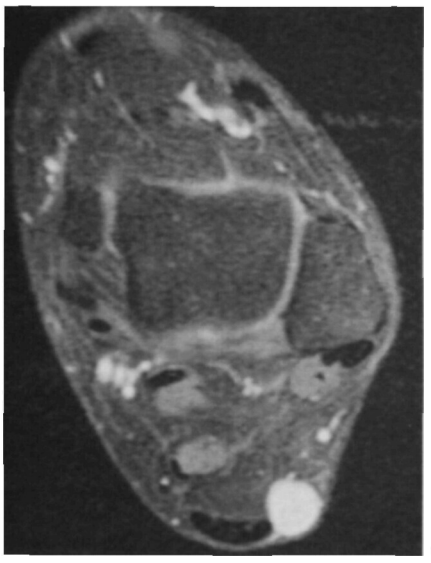

e

Figure **227a-e** A 60-year-old woman with a leiomyoma in the dorsal subcutaneous fat in the ankle region. The circumscribed lesion has intermediate signal on sagittal (**a**) and axial (**c**) T1 WI, and slightly high to high signal on sagittal (**b**) and axial (**d**) FST2WI. The lesion shows prominent Cd-contrast enhancement on axial (**e**) FST1WI.

a,b

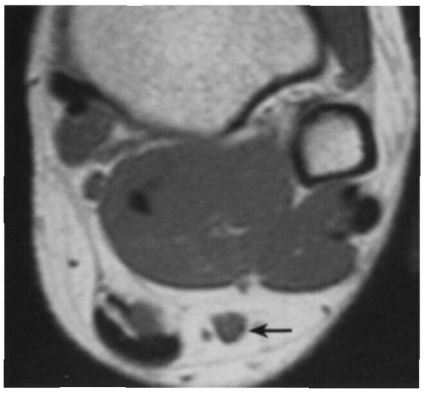

c

Figure **228a-e** A 15-year-old female with an angioleiomyoma involving a vein in the dorsal soft tissues of the ankle. The fusiform lesion has intermediate signal on sagittal (**a**) and axial (**c**) T1WI, and slightly high to high signal on sagittal (**b**) FST2WI. The lesion shows prominent Cd-contrast enhancement on axial FST1WI (**d, e**).

Figure **228 d,e** >

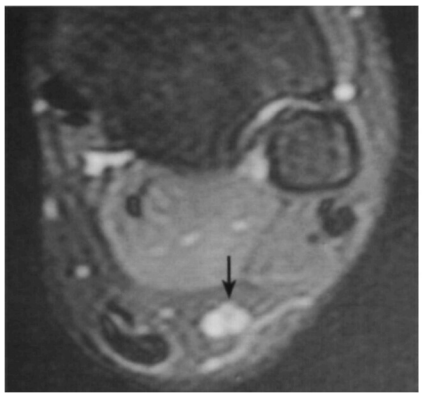

d

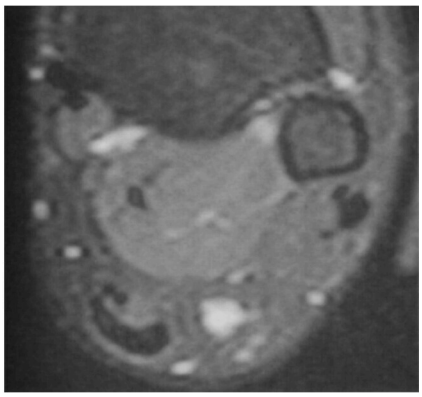

e

Figure **228d, e**

References

1 Das Gupta TK, Chaudhuri PK. Pathology of soft tissue sarcoma. In: Das Gupta TK, Chaudhuri PK, eds. *Tumors of the Soft Tissues* 2nd ed. Stamford, Conn: Appleton & Lange; 1998.

2 Forest M. Muscular tumors. In: Forest M, Tomeno B, Vanel D, eds. *Orthopedic Surgical Pathology: Diagnosis of Tumors and Pseudotumoral Lesions of Bone and Joints* Edinburgh: Churchill Livingstone; 1998:363-368.

3 Hashimoto H, Quade B. Angioleiomyoma. In: Fletcher COM, Unni KK, Mertens F, eds. *World Health Organization Classification of Tumours. Pathology and Genetics of Tumours of Soft Tissue and Bone* Geneva: IARC Press; 2002:128-129.

4 Hashimoto H, Quade B. Leiomyoma of deep soft tissue. In: Fletcher COM, Unni KK, Mertens F, eds. *World Health Organization Classification of Tumours. Pathology and Genetics of Tumours of Soft Tissue and Bone* Geneva: IARC Press; 2002.

5 Kransdorf MJ, Murphey MD. Soft tissue tumors in a large referral population: prevalence and distribution of diagnoses by age, sex, and location. In: *Imaging of Soft Tissue Tumors* 2nd ed. Philadelphia, Pa: W.B. Saunders; 2006:6-37.

6 Kransdorf MJ. Benign soft-tissue tumors in a large referral population: distribution of specific diagnoses by age, sex, and location. *AJR AmJRoentgenol* 1995;164:395-402.

7 Kransdorf MJ, Murphey MD. Muscle tumors. In: *Imaging of Soft Tissue Tumors* 2nd ed. Philadelphia, Pa: W.B. Saunders; 2006:298-327.

8 McCarthy E. Leiomyoma of bone. In: Fletcher COM, Unni KK, Mertens F, eds. *World Health Organization Classification of Tumours. Pathology and Genetics of Tumours of Soft Tissue and Bone* Geneva: IARC Press; 2002.

9 Weiss SW, Goldblum JR. Benign tumors of smooth muscle. In: Weiss SW, Goldblum JR, eds *Enzinger and Weiss's Soft Tissue Tumors* 4th ed. St. Louis, Mo: Mosby; 2001;695-726.

A 40 Leiomyosarcoma

ICD-O Code

8890/3

Definition

Leiomyosarcomas are malignant mesodermal tumors associated with smooth muscle differentiation.[1,3-10,16,17] Leiomyosarcomas arise de novo or occur after radiation treatment.[1] Soft tissue leiomyosarcomas are much more common than primary intra-osseous leiomyosarcomas.

Frequency of Occurrence

Soft tissue.[11,12] Leiomyosarcomas account for 8% of primary malignant soft tissue tumors and 3 % of all primary soft tissue tumors.[14,16]

Bone. Leiomyosarcomas account for < 1 % of primary bone tumors.[14,16]

Age at Presentation[1,5,9,11,12]

Soft tissue: from 35 to 79 years, mean = 58 years.

Bone: from 4 to 80 years, mean = 44-48 years.

Gender Ratio (M| F)[1,8,9,11,12,19]

1 /1, except for retroperitoneal tumors with ratio of 1 /1.5.[19]

Location

Soft tissue.[6,10-12] Tumors occur in the retroperitoneum > lower extremity > hip, buttocks > trunk > upper extremity > foot, ankle > other sites. Leiomyosarcomas may also arise in the walls of arteries or veins.

Bone.[17-9,13,16,17] Tumors occur in the distal femur > proximal tibia > mandible > maxilla > proximal humerus > iliac bone > proximal femur, distal tibia > vertebra > other bones. Most lesions are metaphyseal > epi-metaphyseal, diaphyseal locations.[7]

Signs and Symptoms[1,5,7-9,13,16,17]

Soft tissue. Tumors can present as localized soft tissue swelling with or without pain, days to years in duration.

Bone. Localized pain is the most frequent symptom. Lesions may be associated with pathologic fractures in 15 % of cases.[13] The duration of symptoms ranges from 2 weeks to 1 year.

Cross Pathologic Findings

Soft tissue.[1,3-5,1o] Leiomyosarcomas of soft tissue are often firm, white-gray, or yellowish. Lesions may have a whorled appearance.

Bone.[1,7-9,13,16-18] Lesions are tan-white and often contain zones of necrosis and cystic degeneration. Lesions may have a whorled appearance. Medullary destruction is typically seen. Zones of cortical destruction are observed in up to 95 % of lesions.[1] Extra-osseous soft tissue portions of tumor extending through zones of cortical destruction are seen in 83 % of lesions.[1] Lesions range in size from 2 to 12cm.[1,7] Sixteen percent of tumors involve the joint space[1]

Histopathologic Findings

Soft tissue.[3-6,10,19] Tumors are usually composed of interleaved bundles or fascicles of plump spindle cells containing fusiform or cigar-shaped nuclei, frequent paranuclear vacuoles, and eosinophilic cytoplasm associated with a myxoid or collagenized stroma. Mild to moderate nuclear pleomorphism is common with variable mitotic activity. Dystrophic calcifications may be seen. Leiomyosarcomas may contain rounded cells with vacuolar cytoplasm, and are labeled epithelioid leiomyosarcoma (malignant leiomyoblastoma), because of the appearance of these epithelioid smooth muscle cells.[3-6,10,19] Tumors are often immunoreactive to smooth muscle actin, desmin, and h-caldesmon.[6]

Bone.[1,7-9,13,15,16,18] Tumors are usually composed of interleaved bundles or fascicles of plump spindle cells containing fusiform or cigar-shaped nuclei and eosinophilic cytoplasm associated with a myxoid or collagenized stroma. Mild to moderate nuclear pleomorphism is common with variable mitotic activity. Areas of necrosis are seen in 30 % of tumors.[1] Lesions typically show permeative infiltration of bone associated with osteoclast-type giant cells. Cortical bone destruction is often observed. Lesions usually show immunoreactivity to common muscle actin (85 %), desmin (50 %), and type IV collagen, smooth muscle actin (100%), and vimentin (100%).' The epithelioid type of leiomyosarcomas may show focal immunoreactivity to cytokeratin, which can cause difficulty in excluding the possibility of metastatic carcinoma. In such cases, electron microscopy can help in distinguishing between these diagnoses.[1] Leiomyosarcomas can be graded on the basis of the degree of cellularity, cellular pleomorphism, mitotic activity, degree of necrosis, and extent of necrosis.[1]

Tumor Genetics

Various complex karyotypes have been reported for leiomyosarcomas.[6] Regions of chromosome losses have been reported such as 3p21-23, 8p21-pter, 13ql2-13, and 13q32-qter.[6] Rearrangements involving the RBI gene on chromosome 13 have been suggested to be involved in tumor formation.[6]

Findings on Plain Films (Roentgenograms) and Computed Tomography

Soft tissue.[1,10] Leiomyosarcomas appear as soft tissue lesions rarely containing mineralization evident on plain films and/or CT. Zones of low attenuation from necrosis or cystic change can also be seen with CT.

Bone.[1,2,7-9,13,16-18] Leiomyosarcomas are typically radiolucent, intra-osseous lesions with a permeative or moth-eaten pattern. Occasionally, a geographic radiolucent pattern may be seen. Mineralization in tumors is rarely seen.[2] Periosteal reaction is

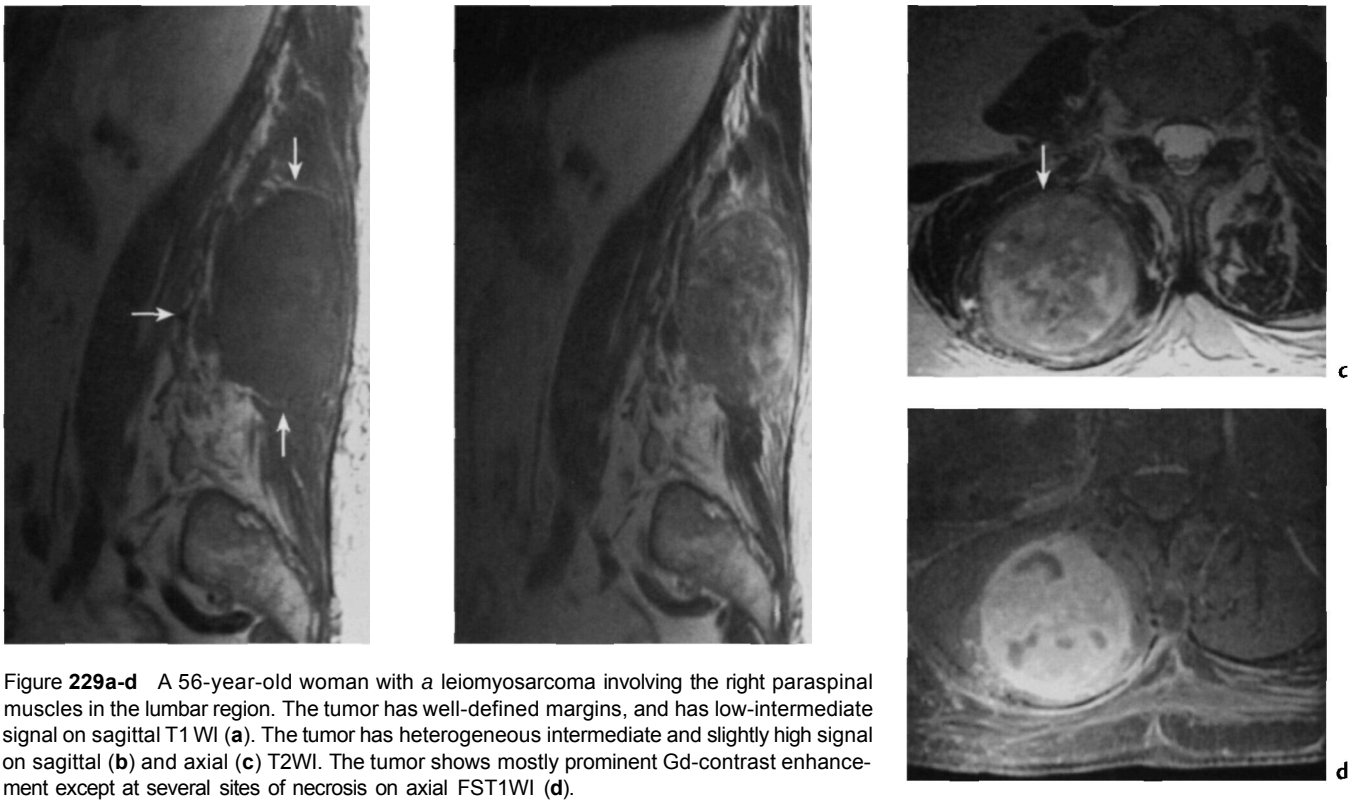

Figure **229a-d** A 56-year-old woman with *a* leiomyosarcoma involving the right paraspinal muscles in the lumbar region. The tumor has well-defined margins, and has low-intermediate signal on sagittal T1 WI (**a**). The tumor has heterogeneous intermediate and slightly high signal on sagittal (**b**) and axial (**c**) T2WI. The tumor shows mostly prominent Gd-contrast enhancement except at several sites of necrosis on axial FST1WI (**d**).

uncommon. CT readily shows zones of medullary and cortical destruction, and extra-osseous extension of tumors as well as mineralization (Fig. **234).** Pathologic fractures may be evident.[16]

MRI Findings

Soft tissue.[10] Lesions may have well-defined or irregular margins. Solid portions of the lesions usually have low-intermediate signal onT1WI and PDWI; and intermediate to slightly high or high signal on T2WI and FST2WI (Figs. **229-233).** Large lesions often have zones of necrosis or cystic change which have low signal on T1WI and high signal on T2W1. After Gd-contrast administration, solid portions of the lesions usually show moderate to marked enhancement. MRI can show zones of bone erosion or invasion.

Bone.[1,17]Lesions often have poorly defined margins. Lesions usually have low-intermediate signal on Tl Wl and PDWI; and intermediate to slightly high or heterogeneous high signal on T2WI and FST2WI (Fig. **234).** Zones of cortical destruction and extra-osseous tumor extension are common. After Gd-contrast administration, prominent heterogeneous enhancement is usually seen associated with these tumors.

Differential Diagnosis

Soft tissue. Malignant fibrous histiocytoma, synovial sarcoma, fibrosarcoma, dedifferentiated liposarcoma, Schwannoma, neurofibroma, malignant peripheral nerve sheath tumor, desmoid tumor, rhabdomyosarcoma, myofibrosarcoma.

Bone. Metastatic disease, myeloma, lymphoma, osteosarcoma, chondrosarcoma, fibrosarcoma, malignant fibrous histiocytoma.

Prognosis and Treatment

Soft tissue.[5,6,10,19] Leiomyosarcomas in the retroperitoneum are usually larger, metastasize more frequently, and have a worse prognosis than tumors in the peripheral soft tissues.[6,10,19] Metastases occur in the lungs > liver > soft tissue > bone > lymph node > gastrointestinal tract.[10,19] The 5-year survival rate for leiomyosarcomas is reported to be ~ 35 %.[10] The 5-year survival rate for leiomyosarcomas exclusive of retroperitoneal primary tumors has been reported to be 64 %.[19] Leiomyosarcomas in children have a more favorable prognosis than in adults, which may be related to the higher proportion of low-grade lesions in the pediatric population.[5] Treatment often includes surgery, radiation, and/or chemotherapy.

Bone.[1,7-9,13,16,17] Treatment usually consists of surgery with wide margins, if possible, or amputation. Preoperative and/or postoperative irradiation and/or chemotherapy have been used. Local recurrence occurs in 24 % of patients. Metastatic disease occurs in 27 % of patients, mostly located in the lungs with a small fraction involving bone. The overall survival rate is 77 % at 3 years and 68 % at 5 years. Up to 50 % of patients eventually die from leiomyosarcoma of bone.[13]

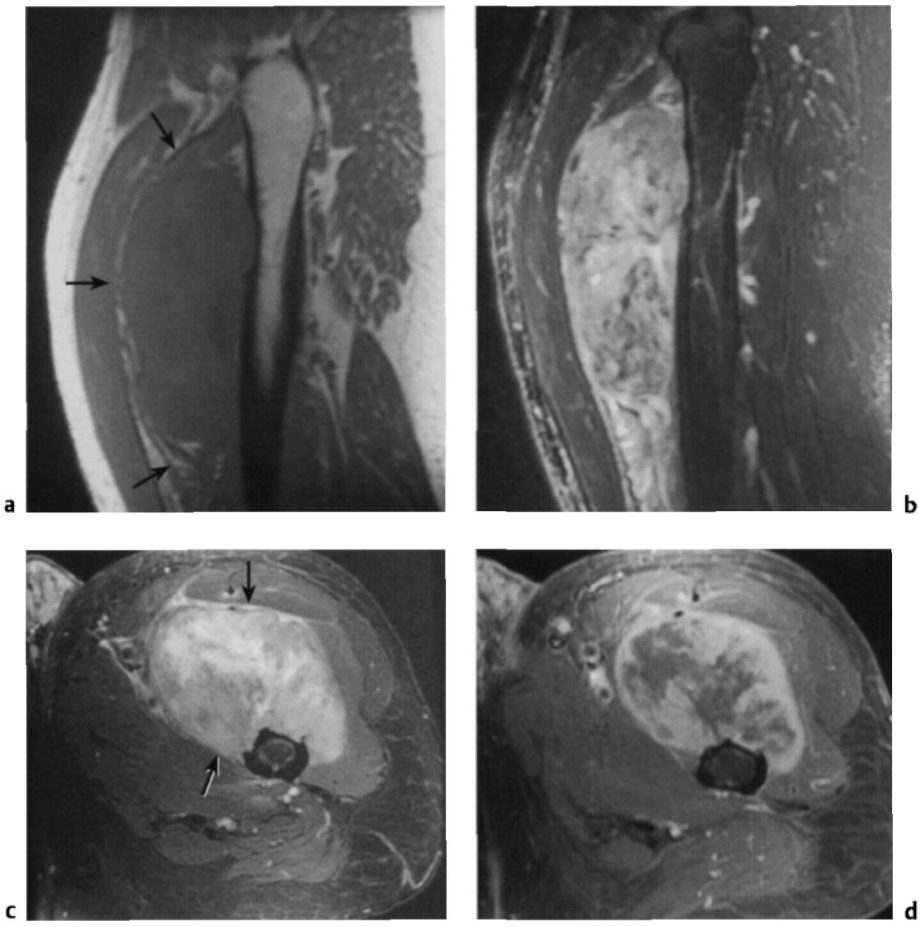

Figure **230a-d** A 55-year-old man with a leiomyosarcoma involving the muscles of the thigh. The tumor has circumscribed margins, and has low-intermediate signal on sagittal T1WI (**a**), and heterogeneous mostly high signal on sagittal (**b**) and axial (**c**) * FST2WI, as well as small zones of low signal. The tumor shows mostly prominent Cd-contrast enhancement, except at several sites of necrosis, on axial FST1WI (**d**). Erosion of outer cortical margin of the femur by the tumor is present.

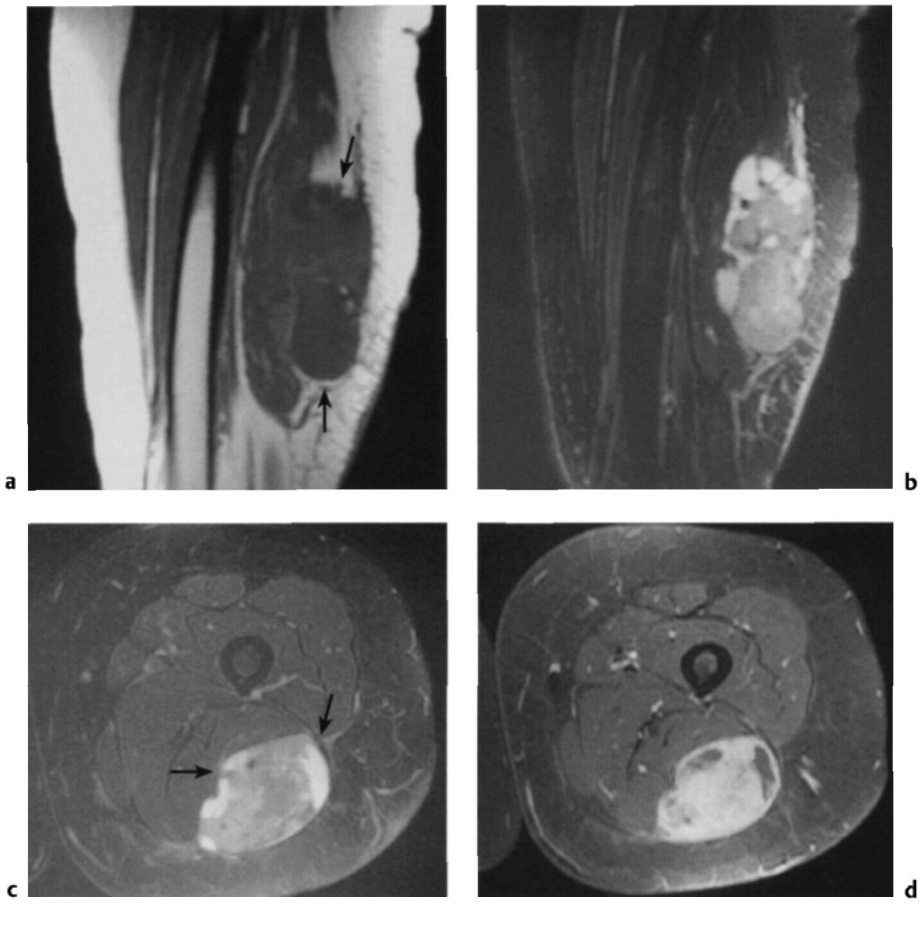

Figure **231 a-d** A 51-year-old woman with a leiomyosarcoma involving the biceps femoris muscle of the thigh. The tumor has circumscribed margins, and has low-intermediate signal on sagittal T1WI (**a**). The tumor has heterogeneous slightly high and high signal on sagittal (**b**) and axial (**c**) FST2WI, as well as small zones of low signal. The tumor shows mostly prominent Gd-contrast enhancement, except at several sites of necrosis, on axial FST1WI (**d**).

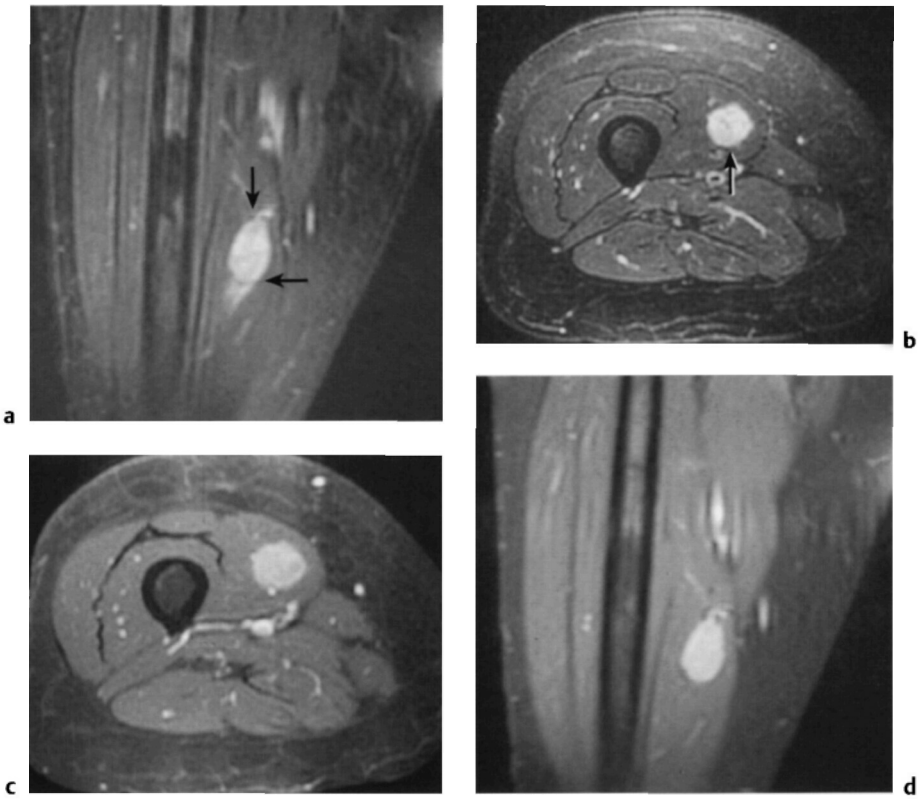

Figure **232a-d** A 62-year-old woman with a leiomyosarcoma involving the vastus medialis muscle of the thigh. The tumor has circumscribed margins, and has heterogeneous high signal on coronal (**a**) and axial (**b**) FST2WI. The tumor shows shdw Cd-contrast enhancement on axial (**c**) and coronal (**d**) FST1WI.

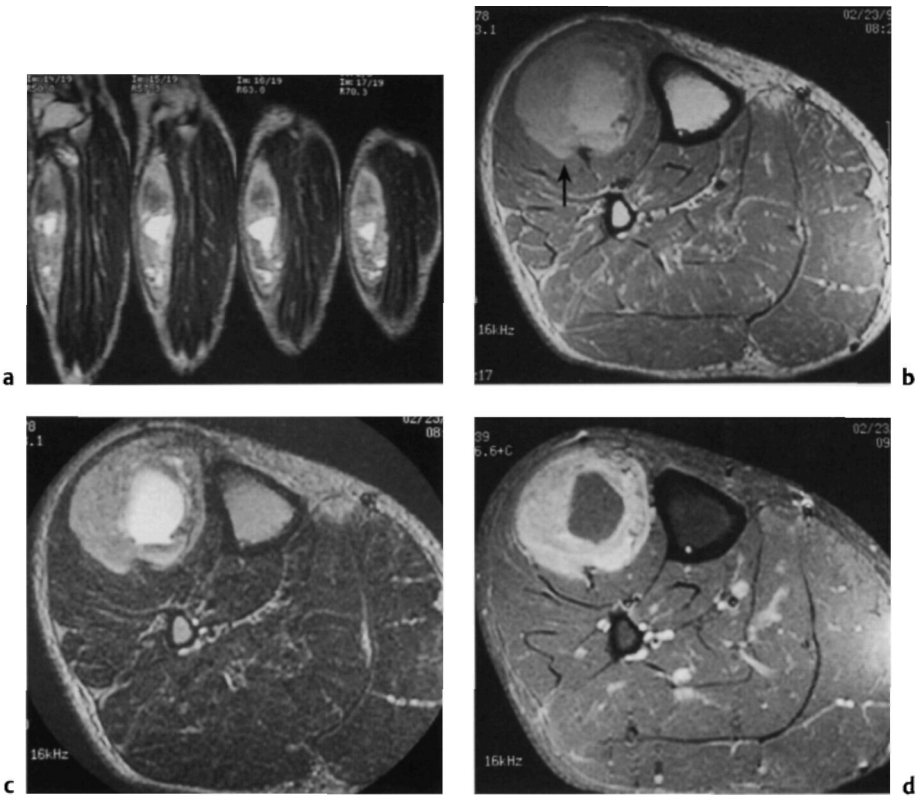

Figure **233 a-d** A 45-year-old man with a leiomyosarcoma involving the tibialis anterior and extensor digitorum longus muscles of the upper leg. The tumor has circumscribed margins, and has mixed low, intermediate, and high signal on sagittal (**a**) and axial (**c**) T2WI. The tumor has intermediate to slightly high signal on axial PDWI (**b**). The tumor shows mostly prominent Gd-contrast enhancement, except at sites of necrosis, on axial FST1WI(**d**)

a

Figure **234a-e** A 42-year-old man with leiomyosarcoma involving the proximal femur. Axial CT image (**a**) shows a radiolucent lesion associated with trabecular and cortical bone destruction with peripheral sclerosis. The tumor has mixed low and intermediate signal within the marrow on coronal (**b**) and axial (**c**) PDWI and heterogeneous high signal on coronal (**b**) and axial (**c**) T2WI. Zones of cortical destruction are seen with extra-osseous tumor extension. The tumor shows mostly prominent Gd-contrast enhancement except at sites of necrosis on axial (**d**) and coronal (**e**) FST1WI.

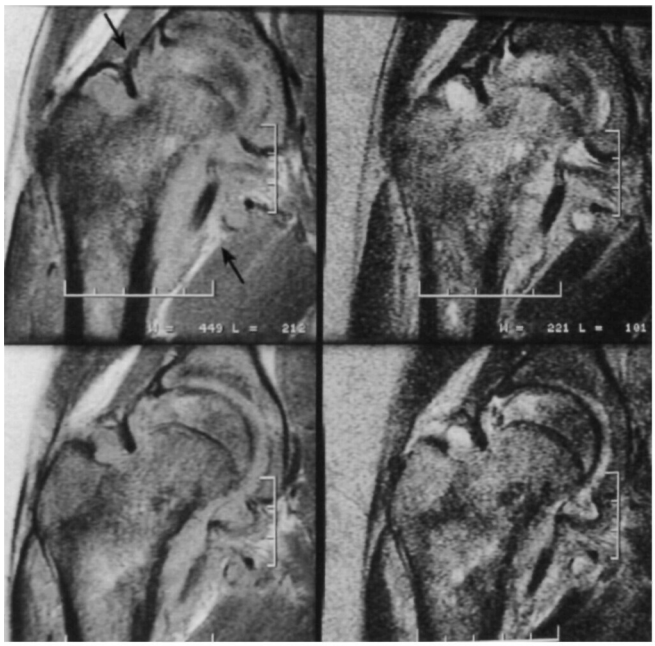

b

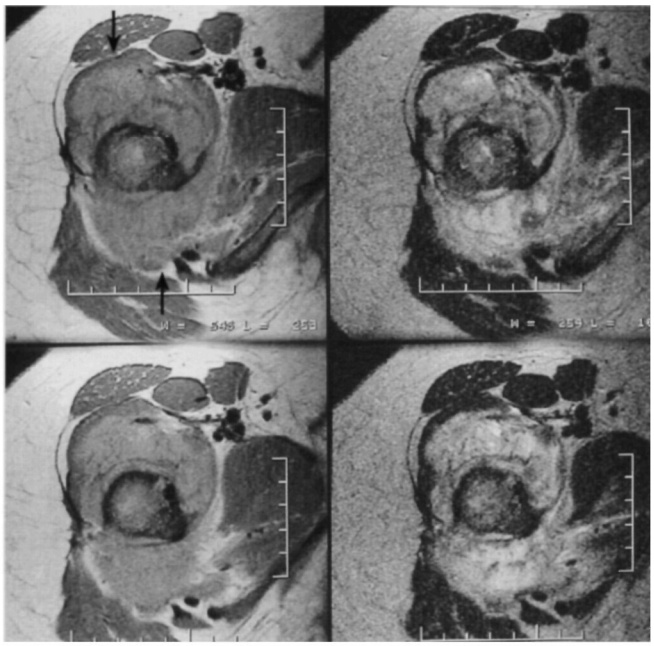

c

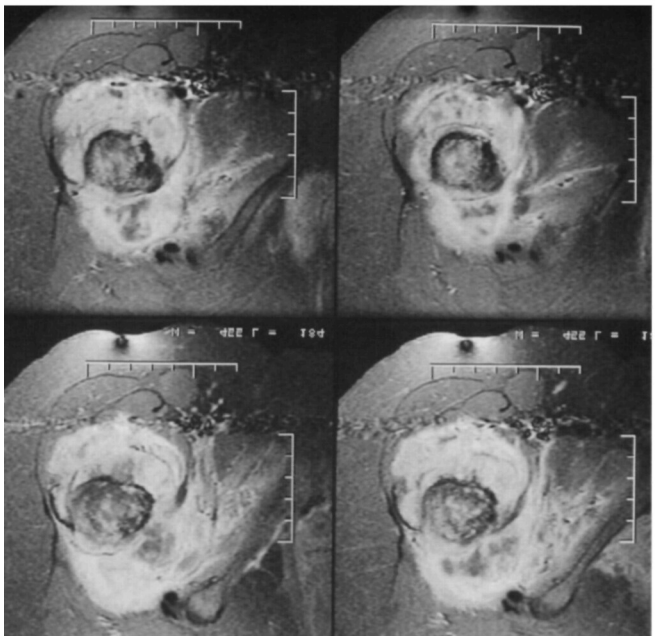

d

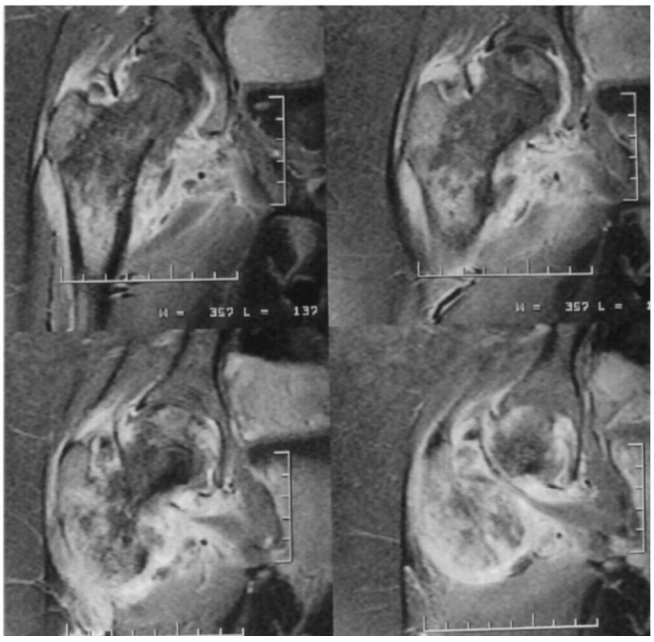

e

References

1 Antonescu CR, Erlandson RA, Huvos AG. Primary leiomyosarcoma of bone: a clinicopathologic, immunohistochemical, and ultrastructural study of 33 patients and a literature review. *Am J Surg Pathol* 1997; 21(11):1281-1294.

2 Bush CH, Reith JD, Spanier SS. Mineralization in musculoskeletal leiomyosarcoma: radiologic-pathologic correlation. *AJR Am J Roentgenol* 2003;180:109-113.

3 Chaudhuri B, Das Gupta TK. Pathology of soft tissue sarcoma. In: Das Gupta TK, Chaudhuri PK, eds. *Tumors of the Soft Tissues* 2nd ed. Stamford, Conn: Appleton & Lange; 1998:115-117.

4 Das Gupta TK, Chaudhuri PK. Tumors of the muscle tissue. In: Gupta TK, Chaudhuri PK, eds. *Tumors of the Soft Tissues* 2nd ed. Stamford, Conn: Appleton & Lange; 1998:313-325.

5 de Saint Aubain Somerhausen N, Fletcher C. Leiomyosarcoma of soft tissue in children: clinicopathologic analysis of 20 cases. *Am] Surg Pathol* 1999;23(7):755-763.

6 Evans HL, Shipley J. Leiomyosarcoma. In: Fletcher CDM, Unni KK, Mertens F, eds. *World Health Organization Classification of Tumours. Pathology and Genetics of Tumours of Soft Tissue and Bone* Geneva: IARC Press; 2002:131-134.

7 Forest M. Muscular tumors. In: Forest M, Tomeno B, Vanel D, eds. *Orthopedic Surgical Pathology: Diagnosis of Tumors and Pseudotumoral Lesions of Bone and Joints* Edinburgh: Churchill Livingstone; 1998:363-367.

8 Huvos AG. Miscellaneous tumors of soft tissue and bone. In: Huvos AG, ed. Bone Tumors Diagnosis, *Treatment, and Prognosis* 2nd ed. Philadelphia, Pa: W.B. Saunders; 1991;756-760.

9 Kilpatrick SE, Unni KK. Spindle cell lesions of bone. In: Helliwell TR, ed. Major *Problems in Pathology: Pathology of Bone and Joint Neoplasms* 1st ed. Vol 37. Philadelphia, Pa: W.B. Saunders;1999;37: 250-252.

10 Kransdorf MJ, Murphey MD. Muscle tumors. In: *Imaging of Soft Tissue Tumors* 2nd ed. Philadelphia, Pa: W.B. Saunders; 2006;298-327.

11 Kransdorf MJ, Murphey MD. Soft tissue tumors in a large referral population: prevalence and distribution of diagnoses by age, sex, and location. In: *Imaging of Soft Tissue Tumors* 2nd ed. Philadelphia, Pa: W.B. Saunders; 2006;6-37.

12 Kransdorf MJ. Malignant soft-tissue tumors in a large referral population: distribution of diagnoses by age, sex, and location. *AJR Am J Roentgenol* 1995;164:129-134.

13 McCarthy E. Leiomyosarcoma of bone. In: Fletcher CDM, Unni KK, Mertens F, eds. *World Health Organization Classification of Tumours. Pathology and Genetics of Tumours of Soft Tissue and Bone* Geneva: IARC Press; 2002:327

14 Mulder JD, Schutte HE, Kroon HM, Taconis WK. Introduction. In: *Radiologic Atlas of Bone Tumors* Amsterdam: Elsevier; 1993:3-6.

15 Mulder JD, Schutte HE, Kroon HM, Taconis WK. The diagnosis of bone tumors. In: *Radiologic Atlas of Bone Tumors* Amsterdam: Elsevier; 1993:9-46.

16 Mulder JD, Schutte HE, Kroon HM, Taconis WK. Leiomyosarcoma. In: Radio/ogic/4t/as *of Bone Tumors* Amsterdam: Elsevier; 1993:311-313.

17 Nishida J, Kato S, Shiraishi H, et al. Leiomyosarcoma of the lumbar spine: case report. Spine 2002;27(2):E42-E46.

18 Salisbury JR. Bone neoplasms containing epithelial and epithelioid cells. In: Helliwell TR, ed. *Major Problems in Pathology: Pathology of Bone and Joint Neoplasms* 1st ed. Vol 37. Philadelphia, Pa: W.B. Saunders; 1999:363.

19 Weiss SW, GoldblumJR. Leiomyosarcoma. In: Weiss SW, Goldblum JR, eds. *Enzinger and* Weiss's *Soft Tissue Tumors* 4th ed. St. Louis, Mo: Mosby; 2001:727-748.

A 41 Leukemia

ICD-O Codes

Acute lymphoblastic leukemia
- Precursor B lymphoblastic leukemia: 9835/3
- Precursor B lymphoblastic lymphoma: 9728/3

Chronic lymphocytic leukemia: 9823/3

Acute myelogenous leukemia: 9861/3

Chronic myelogenous leukemia: 9875/3

Hairy cell leukemia: 9940/3

Definition[1,4-6,12,18,26]

Leukemia represents a group of lymphoid neoplasms that have widespread involvement of the bone marrow as well as the frequent presence of tumor cells in peripheral blood. Unlike leukemia, lymphoma typically represents lymphoid neoplasms that arise as discrete masses. Lymphocytic leukemias and lymphoma may have overlapping clinical features and eventual distribution patterns.[1] All lymphoid neoplasms are monoclonal because they arise from a single transformed cell.[1]

In children and adolescents, acute lymphoblastic leukemia (ALL) is the most frequent type.[1] In adults, chronic lymphocytic leukemia (CLL) (small lymphocytic lymphoma) is the most common type of lymphocytic leukemia.

In addition to the lymphoblastic or lymphocytic leukemias; myelogenous leukemias represent neoplasms derived from abnormal myeloid progenitor cells that, if normal, would form erythrocytes, monocytes, granulocytes, and platelets. Acute myelogenous leukemia (AML) usually occurs in adolescents and young adults, and represents a small minority (-20%) of childhood leukemias. Chronic myelogenous leukemia (CIVIL) usually affects adults older than 25 years. Hairy cell leukemia is a rare, B cell neoplasm that accounts for 2 % of all leukemias and typically affects middle-aged men.[1,2,5]

Frequency of Occurrence[1,5,8,14,19,26]

Acute lymphoblastic leukemia: 3800 new cases per year in the United States, 3 per 100000 children per year. In adults, the incidence is 1 /100 000 per year.

Chronic lymphocytic leukemia: 7000 new cases per year in the United States, 10 per 100000 per year in patients older than 70 years, < 1 per 100 000 per year in patients under 50 years.

Acute myelogenous leukemia: 10 600 new cases per year in the United States, 2.3 per 100000 per year, 500 new cases in children per year.

Chronic myelogenous leukemia: 4400 new cases per year in the United States, 13 per 100 000 per year.

Hairy cell leukemia: accounts for ~2 % of all cases of leukemia.

Age at Presentation[1,5,8,14,19,26]

Acute lymphoblastic leukemia: children usually < 15 years, peak age = 4 years.

Chronic lymphocytic leukemia: adults >25 years, median = 60 years.

Acute myelogenous leukemia: peak ages between 15 and 39 years.

Chronic myelogenous leukemia: from 25 to 60 years, peak ages in 4th and 5th decades.

Hairy cell leukemia: peak in middle-aged adults.

Gender Ratio (M| F)[1,5,8,14,19,26]

Acute lymphoblastic leukemia: 1.4 /1

Chronic lymphocytic leukemia: 1.4 to 2 /1

Acute myelogenous leukemia: 1.3 /1

Chronic myelogenous leukemia: 1.3 /1

Hairy cell leukemia: 4 /1

Location[1,4-7,14,26]

Leukemic cells are typically seen in bone marrow and blood. Solitary or multifocal, lytic bone lesions can be seen with myelogenous leukemia (granulocytic sarcoma, chloroma). Granulocytic sarcomas are seen in the skull > spine > ribs > sternum.[7] In adults, normal femoral marrow is often fatty, and leukemic infiltration can be seen readily in this region. Localized or masslike collections of myelogemous leukemic cells in bone or soft tissues are referred to as chloromas/granulocytic sarcomas because of their greenish coloration. Chloromas can occur in the musculoskeletal soft tissues, orbits, cranial or spinal meninges, mediastinum, lung, gastrointestinal tract, breast, uterus, ovary, and prostate.[26] Hairy cell leukemia is a rare form that typically involves bone marrow, liver, and spleen.[1,5]

Signs and Symptoms

Acute lymphoblastic leukemia.[1,5,14] Patients may present with one or more of the following: fever (50%), pallor (45%), bleeding/bruising/petechiae (40%), bone/joint pain (35%), fatigue (30%), anorexia (25%), and/or abdominal pain. The duration of symptoms ranges from days to months. Generalized lymphadenopathy, splenomegaly, and hepatomegaly can result from infiltration of lymphoblasts. Symptoms (headaches) and signs (cranial nerve palsies) from disseminated leukemia in the meninges can also occur.

Chronic lymphocytic leukemia.[1,5,14] This is the most common indolent type of leukemia. CLL usually presents as an asymptomatic lymphocytosis in middle-aged and older adults. Hypo-y-globulinemia is common, which can predispose patients to

bacterial infections. With progressive marrow infiltration by CLL, cytopenias and/or immunosuppression may result in symptoms which, if present, include anorexia, weight loss, and fatigue.

Acute myelogenous leukemia.[1,5,19,26] Patients often present with nonspecific symptoms such as fever, fatigue, and spontaneous mucosal and cutaneous bleeding. Splenomegaly, hepatomegaly, lymphadenopathy, and sternal tenderness are common findings. Retinal hemorrhage is seen in 15% of patients. Symptoms usually range from weeks to months.

Chronic myelogenous leukemia.[1,5,19,26] Patients are often asymptomatic. Symptoms, if present, include fatigue, weight loss, malaise, and fever. Moderate splenomegaly and mild hepatomegaly may occur.

Hairy cell leukemia.[1,5] Patients can present with infections, including infection from atypical mycobacteria secondary to pancytopenia from marrow and splenic infiltration. Splenomegaly is commonly present, and sometimes hepatomegaly. Lymphadenopathy is uncommon.

Laboratory Findings

Acute lymphoblastic leukemia.[1,5,14] Anemia and thrombocytopenia are common. Leukocyte counts can be over 50000 per microliter in 22 % of cases.

Chronic lymphocytic leukemia.[1,5,14] The red cell and platelet counts are slightly decreased. Most patients have a lymphocytosis (absolute lymphocyte count of >4000/mm^3). Small lymphocytic lymphoma is the lymphomatous presentation of CLL, often without lymphocytosis.

Acute myelogenous leukemia.[1,5,19,26] Anemia, thrombocytopenia, and neutropenia are often present. Myeloblasts account for > 30% of white blood cells in blood and/or bone marrow establishing the diagnosis of AML. The median leukocyte count at presentation is 15 000 per microliter. Twenty percent of patients have leukocyte counts over 100 000 per microliter. Platelet counts less than 100 000 per microliter are seen in 75 % of patients at presentation.

Chronic myelogenous leukemia.[1,5,19,26] Patients may have elevated white blood counts with varying degrees of granulocyte immaturity. Initially, myeloblasts account for <10% of white blood cells (WBC) in circulating blood. After ~3 years, up to 50 % of patients undergo an accelerated phase with myeloblasts accounting for 10 to 19 % of WBC in blood and/or nucleated cells in bone marrow, and basophils > 20 %. A more aggressive phase is blast crisis or acute leukemia, in which blood or marrow blasts exceed 30% of circulating WBC or nucleated marrow cells, respectively.

Hairy cell leukemia.[1,5] Patients may have pancytopenia, granulocytopenia, or asymptomatic lymphocytosis. Bone marrow biopsy can be hypercellular with fibrosis.

Histopathologic Findings

Acute lymphoblastic leukemia.[1,5,14] Tumor cells are referred to as lymphoblasts, which are immature precursor B or T lymphocytes distributed within bone marrow with varying degrees of blood involvement. Eighty percent of ALLs are derived from B cells and 20 % from T cells.[4,13] Fifty-six percent of patients have leukocyte counts of greater than 10 000 per microliter, and 22 % have counts over 50 000 per microliter. Most children with ALL have bone marrow biopsies which show more than 60 % blasts (normal is less than 5%). As a result normal hematopoeisis is significantly impaired. Malignant precursor B and T cells are usually similar in appearance and can be distinguished by immunophenotyping. T-cell precursors may be immunoreactive to CD 1-8, and B-cell precursors to CD 10, CD 19-23. Ninety percent of ALL tumor cells have abnormal chromosomes (hyperploidy, pseudoploidy, and translocations such as t(12;21)(p!3;q22), +(l;19)(q23;p!3.3), t(4;ll)(q21;q23), and the Philadelphia chromosome-t(9;22)(q34;qll.2).

Chronic lymphocytic leukemia.[1,5,14] Numerous small round lymphocytes with scant cytoplasm are often seen in peripheral blood. Bone marrow biopsies typically show interstitial infiltrates or nonparatrabecular aggregates of small lymphocytes. Tumor cells can express B-cell markers CD 19 and 20, and occasionally a T-cell marker, CD 5. Chromosomal abnormalities associated with CLL include trisomy 12, and deletions of 13q12-14orllq.

Acute myelogenous leukemia.[1,5,19,26] Myeloblasts have fine nuclear chromatin, two to five nucleoli, and a greater amount of cytoplasm per cell compared with lymphoblasts. Azurophilic, peroxidase-positive granules are typically seen in the cytoplasm. Red-staining, rod-shaped structures in the cytoplasm called Auer rods are frequently seen. Using the F.A.B. (French, American, British) criteria; AML is divided into eight categories (MO-M7) based on the degree of blast maturation (MO-M3), blast lineage (M4-M7), and immunohistochemical reactivity. Chromosomal abnormalities such as translocations are seen in ~90% of AML patients.[1,19] Translocations include t(8;21)(q22;q22)+(15;17)(q22;q!2) and +(16;16)(pl3;q22).

Chronic myelogenous leukemia.[1,5,19,26] CML marrow typically shows hypercellularity with up to 100% cellularity. The hypercellularity is composed of myeloid and megakaryocytic lineages. Scattered storage histiocytes with wrinkled blue cytoplasm can be seen. Deposition of reticulin fibers is common, but marrow fibrosis is rare in the early phases of CML. Up to 95 % of patients with CML have a chromosomal translocation, typically t(9;22)(q34;qll) or Philadelphia chromosome, which affects the BCR gene on chromosome 9 and the ABL gene on chromosome 22.

Hairy cell leukemia.[1] Tumor cells have spheroid, ovoid or reniform nuclei with moderately pale blue cytoplasm and superficial hairlike projections. In bone marrow, the tumor cells are diffusely distributed in an extracellular matrix of reticulin fibrils. Within spleen, the tumor cells are usually diffusely distributed in red pulp. These hairy cells are usually immunoreactive to the B-cell markers of CD 19, CD 29, surface IgH, and the monocyte marker CD 11 c.

Findings on Plain Films (Roentgenograms) and Computed Tomography

Acute lymphoblastic leukemia.[4,17,18] Findings associated with ALL include diffuse osteopenia from proliferation of leukemic cells. In long bones and skull, focal or diffuse zones of demineralization may occur in the medullary space and cortex resulting from leukemic deposits or infarcts from vascular occlusion (Fig. **235**). Zones of bone infarction can also have increased attenuation (Fig. **235).** In children, thin radiolucent bands (2-15 mm) are often seen in the metaphysis secondary to de-

creased bone formation. In addition to the radiolucent metaphyseal bands, transverse lines of increased density may be seen in the metaphysis representing growth arrest lines or zones or provisional calcification (unabsorbed calcified cartilaginous matrix). Metaphyseal radiolucent bands are typically not seen in adults because of fusion of the growth plate. Zones of increased attenuation can also be seen with CT (Fig. **235).** Radiolucent zones may also be seen below the cortex in flat bones such as the ilium and ischium. A moth-eaten or permeative radiolucent pattern may be seen in the metaphyseal and diaphyseal regions of long bones.

Leukemic cells may destroy bone cortex. Leukemic cells that occur beneath the periosteum can result in formation of an elevated thin shell of periosteal new bone. Spontaneous fractures may occur at metaphyseal radiolucent bands. Vertebral body wedging may also be seen on lateral radiographs. Occasionally, focal or diffuse osteosclerotic changes may occur. Bone infarcts occur in ~ 15 % of patients with ALL

Chronic lymphocytic leukemia, acute myelogenous leukemia, and chronic myelogenous leukemia.[4,17] Diffuse osteoporosis can seen, as well as geographic radiolucent lesions (Fig. **237).** Focal radiolucent lesions in patients with AML may represent chloromas (granulocytic sarcoma), which can be associated with juxta-osseous soft tissue lesions.

Hairy cellleukemia.[1,2,10,24] Hairy cell leukemia may present with splenomegaly. Plain films are often unremarkable.

MRI Findings

Acute lymphoblastic leukemia.[6,15,16,18,25] Infiltration of ALL in marrow often appears as diffuse or poorly defined zones of low-intermediate signal on T1WI and PDWI, and intermediate-slightly high to high signal on FST2WI (Figs. **235, 236).** Focal or geographic regions with similar signal alteration can also be seen. Fractures and periosteal reaction may be associated with ALL After Gd-contrast administration, ALL is usually associated with increased enhancement on T1WI and FST1WI. Note should be made that Gd-contrast enhancement may be seen in normal vertebral marrow in children less than 7 years old.[18] Positive responses to chemotherapy can be monitored by quantitative decreases in bulk Tl values.[16,,25] Unlike the successful use of Tl values in the assessment of extent and degrees of initial or residual leukemic infiltration in marrow, discrimination of increased signal on T2WI secondary to leukemic infiltration compared with normal marrow in children is often variable and limited because of the high hematopoietic activity normally seen in the pediatric group with higher red/yellow marrow ratios compared with adults.

Chronic lymphocytic leukemia.[11,13,16] CLL can be associated with poorly defined or diffuse zones of low-intermediate signal on Tl WI and PDWI; and intermediate or slightly-high to high signal on FS T2WI in femoral, pelvic, and/or vertebral bone marrow (Figs. **237, 238).** Leukemic infiltration of the skull is associated with marrow signal on T1WI that is hypointense relative to cerebral white matter." The degree and extent of the marrow

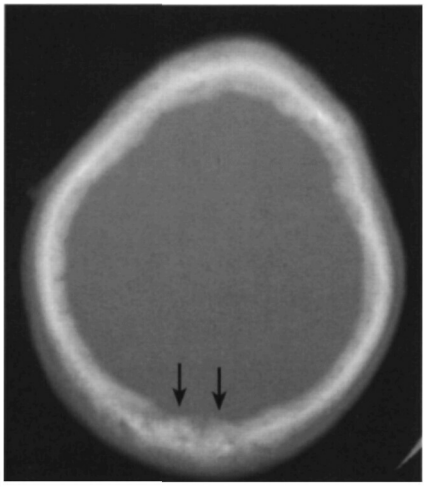

a

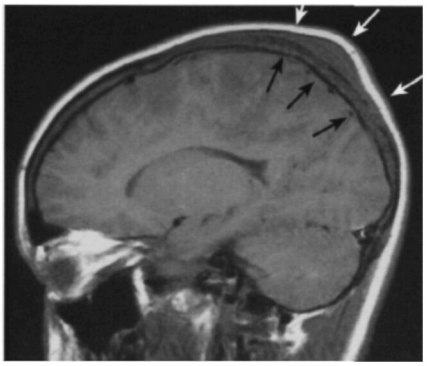

b

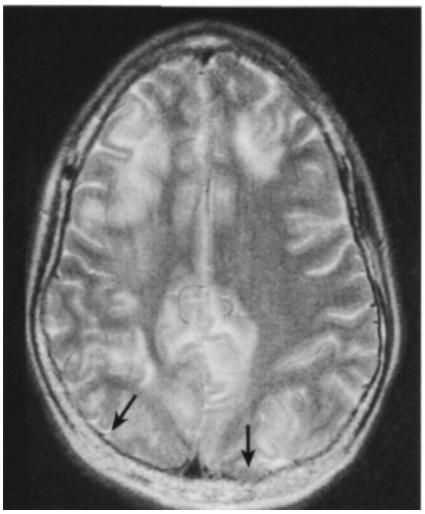

c

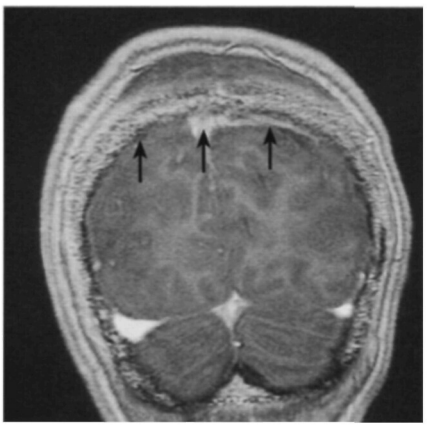

d

Figure **235a-d** A 12-year-old female with acute lymphoblastic leukemia involving the skull. Axial CT image (**a**) shows a poorly defined zone of radiolucency involving the calvarium, with associated small sites of destruction of the inner and outer tables. Leukemic involvement of the skull is seen as zones of low-intermediate signal in the marrow, as well as sites of destruction of the inner and outer tables, on sagittal T1WI (**b**). Neoplastic extension is seen into the scalp from the involved marrow through sites of cortical disruption. The leukemic infiltrates have heterogeneous high signal on axial T2WI (c). Poorly defined zones of high signal are also seen in the cerebral white matter secondary to posterior reversible encephalopathy syndrome related to chemotherapy. The leukemic tissue shows mild Cd-contrast enhancement on coronal T1WI (**d**).

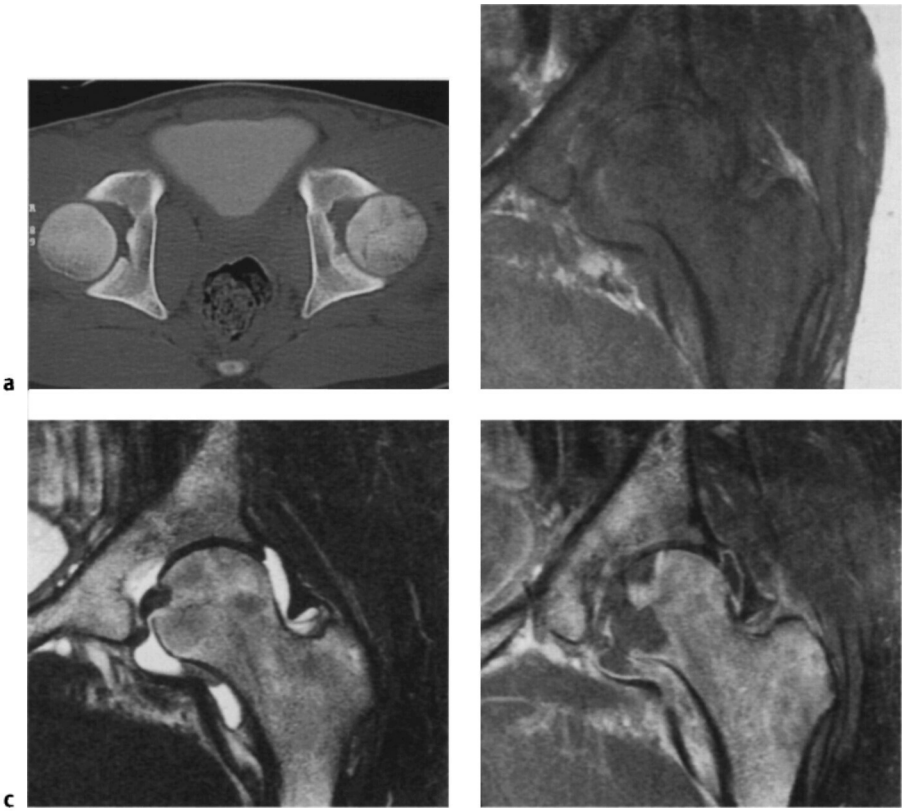

Figure **236a-d** A 16-year-old male with acute lymphoblastic leukemia involving the femur and bony pelvis. Axial CT image (**a**) shows increased attenuation within the proximal left femur with associated thin, linear, radiolucent zones secondary to superimposed bone infarction. The leukemic tissue in the marrow of the pelvis and femur has low-intermediate signal on coronal T1WI (**b**), and heterogeneous high signal on coronal (c) FST2WI. The leukemic tissue shows Cd-contrast enhancement on coronal FS T1 WI (**d**). Extension of leukemic tissue into the hip joint is also seen. Zones with no Gd-contrast enhancement in the femoral head represent sites of bone marrow ischemia/infarction.

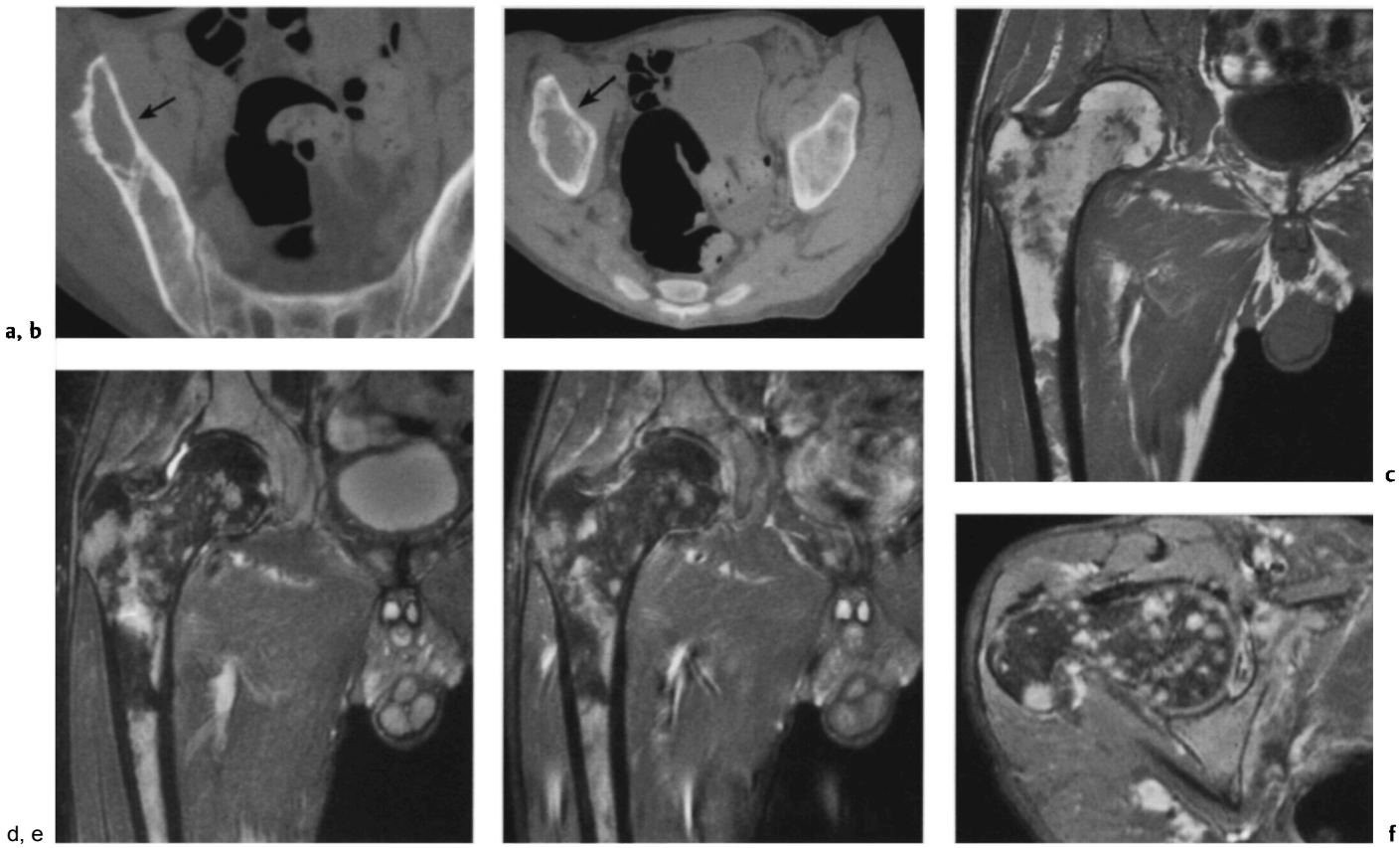

Figure **237 a-f** Chronic lymphocytic leukemia involving the marrow of a 61-year-old man. Axial CT images (**a**, **b**) show radiolucent zones in the right iliac bone and acetabulum from the leukemic deposits, as well as sites of cortical disruption and perpendicular periosteal reaction. Leukemic deposits are seen as irregular zones with low-intermediate signal on coronal T1WI (**c**), and slightly high or high signal on coronal FST2WI (**d**). The tumor shows Cd-contrast enhancement on coronal (**e**) and axial **(f)** FST1WI.

signal abnormality is related to the relative increases in blood and bone marrow lymphocytosis. After Gd-contrast administration, minimal to mild increased enhancement is often seen with higher stages of disease using the Binet staging (A, B, C) system. After chemotherapy, positive responses can be followed by changes in patterns of dynamic enhancement.

Acute myelogenousleukemia.[18,20-22,25] Infiltration of AML in marrow often appears as diffuse or poorly defined zones of low-intermediate signal on T1WI (hypointense relative to muscle) and PDWI; and intermediate to slightly high or high signal on FST2WI (hyperintense relative to muscle with STIR)[20] (Fig. **240-242).** Focal or geographic regions with similar signal alteration can also be seen with AML. After Gd-contrast administration, AML is usually associated with variable enhancement on FST1WI (Figs. **239-242).** Note should be made that Gd-contrast enhancement may be seen in normal vertebral marrow in children less than 7 years old.[18] Positive responses to chemotherapy can be monitored by qualitative changes in MR signal with STIR. Disease-free survival was reported to be shorter for patients with persistently high signal on FST2WI (STIR) after chemotherapy than those without.

Collections of myelogenous leukemic cells in soft tissues (chloromas/granulocytic sarcomas) have variable MRI findings. Chloromas are more common in AML compared with CML Lesions may be poorly defined or well-circumscribed. Lesions often have low-intermediate signal on T1WI and PDWI; and intermediate to high signal on T2WI and FST2WI, and moderate to marked Gd-contrast enhancement (Figs. **239, 240).** Chloromas may occur primarily in soft tissue or extend from intra-osseous lesions.

Chronic myelogenous leukemia.[9,12,23] Areas of CLL often show poorly defined zones of low-intermediate signal on T1WI and

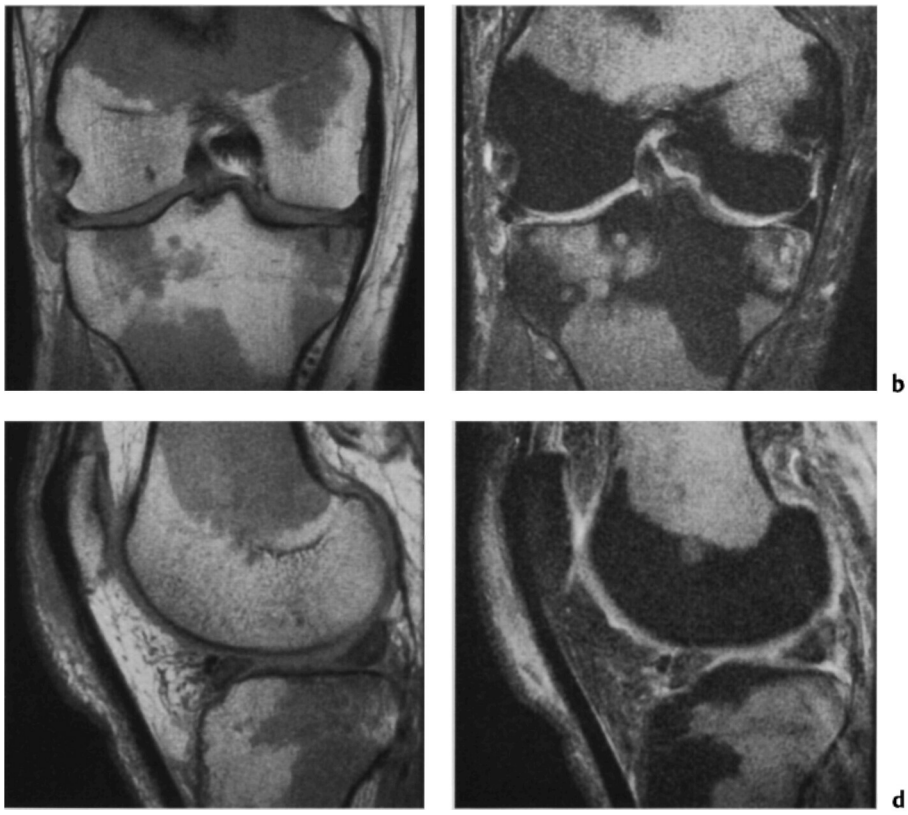

Figure **238 a-d** Chronic lymphocytic leukemia involving the marrow of a 66-year-old man. Leukemic deposits are seen as irregular zones with low-intermediate signal on coronal (**a**) and sagittal (**c**) PDWI, and slightly high and high signal on coronal (**b**) and sagittal (**d**) FST2WI.

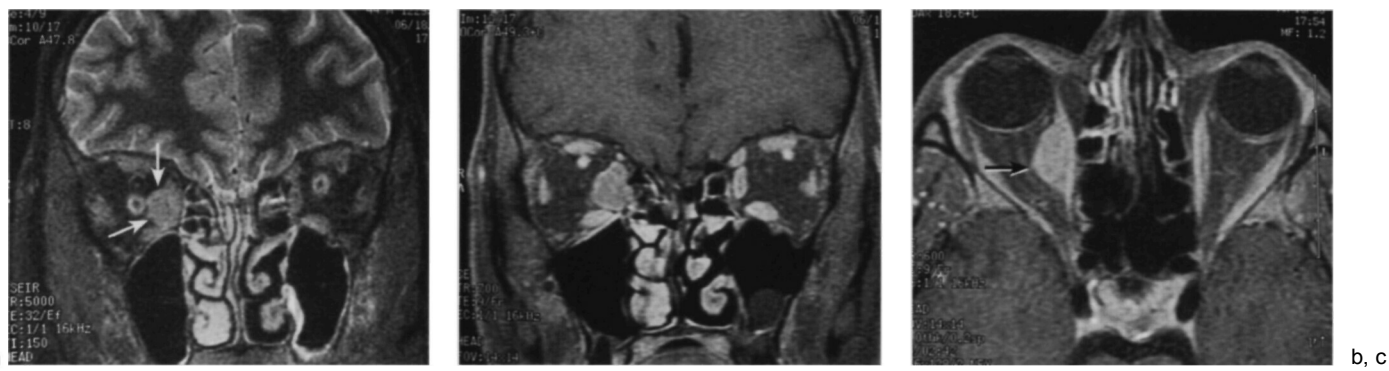

Figure **239a, b** A 44-year-old man with a chloroma/granulocytic sarcoma from acute myelogenous leukemia involving the medial rectus muscle. The chloroma has well-defined margins and has slightly high signal on coronal STIR (**a**). The chloroma shows Gd-contrast enhancement on coronal (**b**) and axial (**c**) FST1WI.

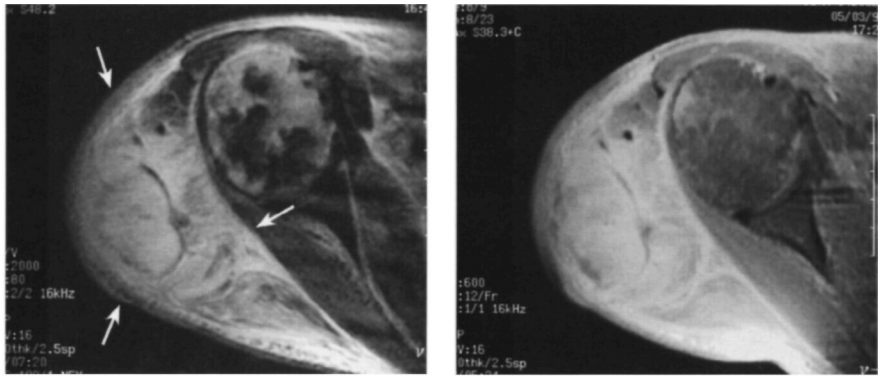

a, b

Figure **240a, b** A 69-year-old man with acute myelogenous leukemia involving the soft tissues at the right shoulder and right humerus. The leukemic tissue in the marrow of the humerus has heterogeneous slightly high signal on axial FST2WI (**a**). Leukemic involvement in the adjacent soft tissues has high signal on axial FST2WI (**a**) and irregular indistinct margins. The leukemic tissue in marrow shows minimal Cd-contrast enhancement whereas the leukemic involvement in the extra-osseous soft tissues shows prominent Cd-contrast enhancement on axial FST1WI(**b**).

a, b

\c, d

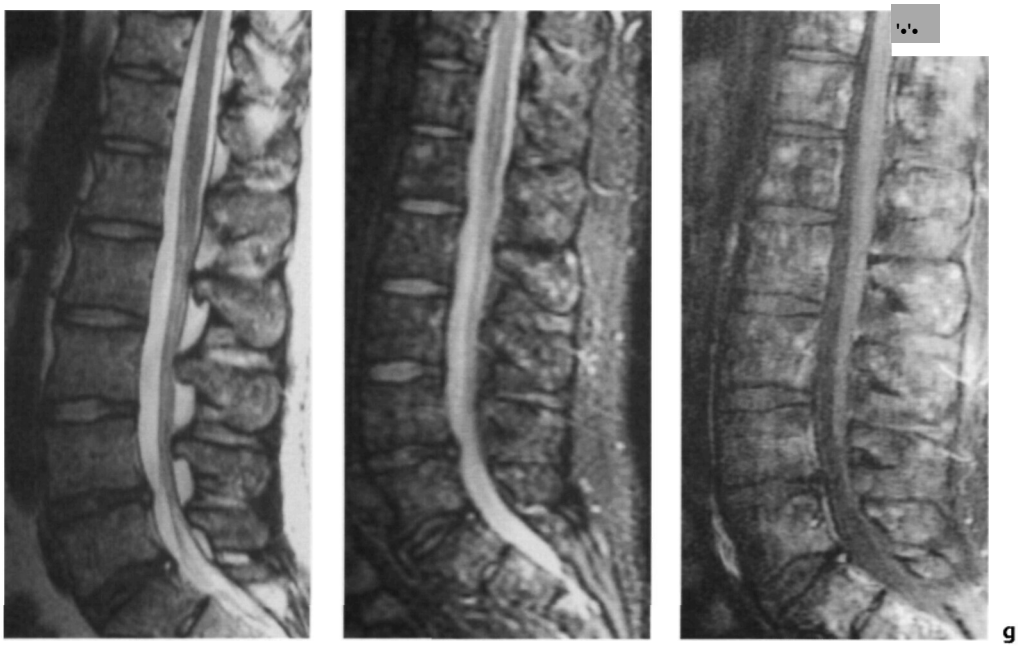

e, f

g

Figure **241 a-g** A 28-year-old man with acute myelogenous leukemia involving the marrow of the spine. The leukemic tissue has heterogeneous low-intermediate signal on sagittal T1WI (**a, d**), and heterogeneous intermediate, and slightly high signal on sagittal T2WI (**b, e**) and FST2WI (**f**). The leukemic tissue shows mild heterogeneous Cd-contrast enhancement on sagittal FST1WI (**c, g**).

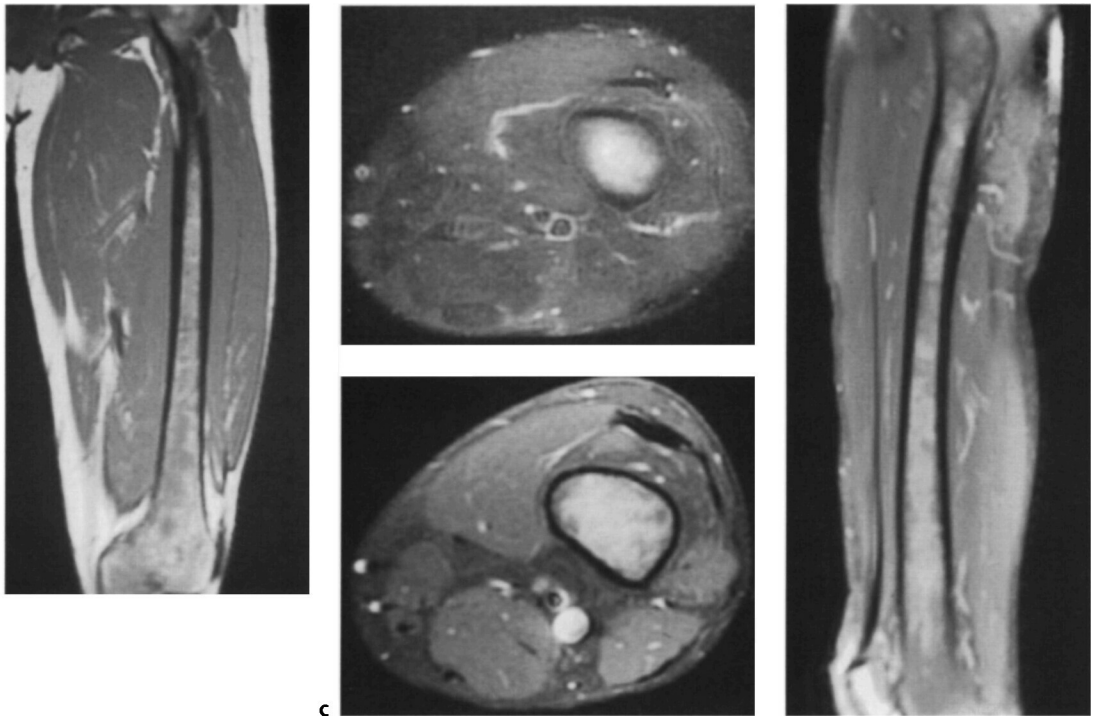

Figure **242 a-d** Acute myelogenous leukemia involving the marrow of the femur. The leukemic tissue has heterogeneous low-intermediate signal on coronal T1WI (**a**) and high signal on axial FST2WI(**b**). The leukemic tissue shows heterogeneous Gd-contrast enhancement on axial (**c**) and sagittal (**d**) FST1WI.

Figure **243 a, b** Chronic myelogenous leukemia involving the marrow of the spine. The leukemic tissue has heterogeneous low-intermediate signal on sagittal T1 WI (**a**) and heterogeneous low signal on sagittal T2WI (**b**).

PDWI; and low, intermediate to slightly high signal or high signal on FST2WI or STIR that can be hypointense, isointense, or hyperintense relative to muscle tissue in the field of view (Figs. **243,** 244). The extent and degree of marrow signal abnormality are often correlated to spleen size/enlargement, disease stage, response to therapy, and prognosis.[23] CLL involving marrow has been reported to be associated with avascular necrosis of the femoral head.[9,12] After Gd-contrast administration, CLL deposits may show mild or moderate enhancement. Successful chemotherapeutic responses often show conversion of marrow signal back to fat.[23]

Collections of myeloenous leukemic cells in soft tissues (chloromas) have variable MRI findings. Lesions may be poorly or well circumscribed. Lesions often have low-intermediate signal on T1WI and intermediate to high signal on T2W1 and FS T2WI, and show moderate to marked Gd-contrast enhancement.

Hairy cell leukemia[2,10,24] Areas of hairy cell leukemic infiltration can show poorly defined or geographic zones of low-intermediate signal on Tl WI, and intermediate to slightly high signal or high signal on FST2WI (STIR) that can be hypointense, isointense, or hyperintense relative to muscle tissue in the field of

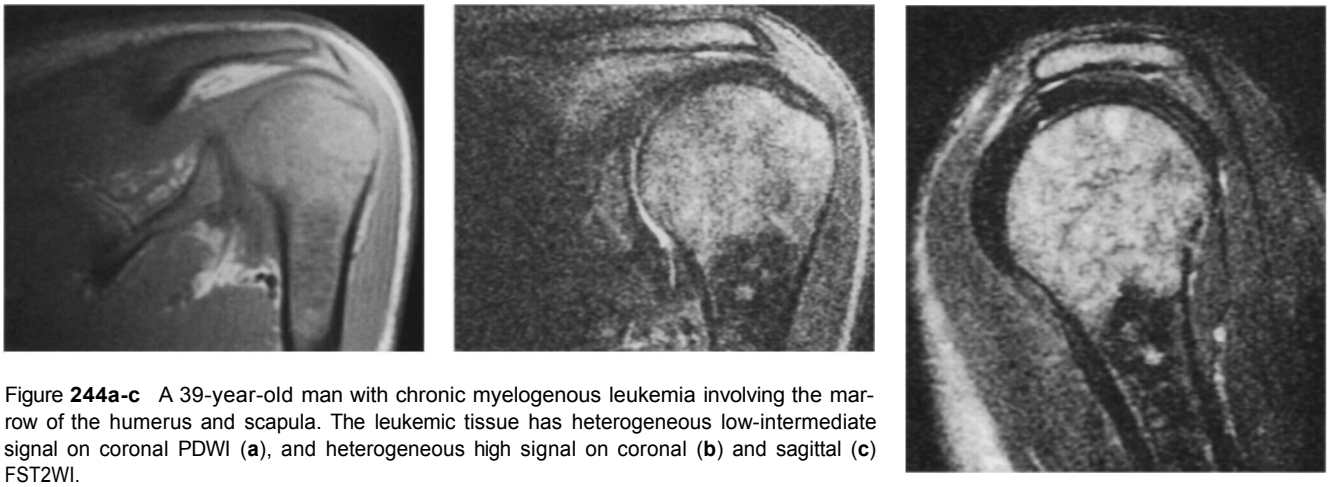

a, b c

Figure **244a-c** A 39-year-old man with chronic myelogenous leukemia involving the marrow of the humerus and scapula. The leukemic tissue has heterogeneous low-intermediate signal on coronal PDWI (**a**), and heterogeneous high signal on coronal (**b**) and sagittal (**c**) FST2WI.

view. Response to chemotherapy can be seen with normalization of MRI signal in the sites of leukemic infiltration.

Differential Diagnosis

Children.[17] Metastatic neuroblastoma, Ewing sarcoma, healing fracture, immobilization, hemolytic anemias, Langerhans cell histiocytosis, osteomyelitis, tuberculosis, congenital syphilis, vitamin C deficiency.

Adults. Metastatic disease, myeloma, myelodysplastic syndromes, lymphoma, healing fracture, eosinophilic granuloma, Erdheim-Chester disease.

Prognosis and Treatment

Acute lymphoblastic leukemia.[1,5,8,14] Prognosis is usually related to the risk category of disease at diagnosis. Features associated with favorable prognosis / good risk category in children with ALL include: ages between 1 and 10 years; leukocyte counts of less than 50 000 per microliter; cytogenetic findings of hyperploidy, t(12;21) or trisomies 4 and 10; and FAB LI cell type. Features associated with unfavorable prognosis in children with ALL include: ages of less than 1year or greater than 10 years; leukocyte counts of greater than 50000 per microliter; cytogenetic findings of t(9;22)(q34;qll.2), +(4;ll)(q21;q23), 11 q23; and FAB L3 cell type. ALL is considered as a heterogenous group of diseases. Combination chemotherapy is the main form of treatment for ALL. Maintenance chemotherapy is typically used after remission to prevent or decrease the likelihood of relapses. The 5-year, event-free survival rate is greater than 70 % of patients.[3] The 5-year survival rate for children under 15 years is 85 %.[8]

Chronic lymphocytic leukemia.[1,5] The prognosis of CLL is variable and depends on the clinical stage. Patients with trisomy 12 and deletions of 11 q have a poor prognosis. Median survival is ~ 5 years, but survival up to 10 years can occur. Chemotherapy is used for patients with symptomatic organ involvement, systemic symptoms, and cytopenia. CLL may also transform into more aggressive lymphoid neoplasms.

Acute myelogenous leukemia.[1,8,27] Chemotherapy can achieve complete remission in ~ 60 % of patients, but only 30 % of these remain disease-free after 5 years. Prognosis is related to the type of chromosomal abnormality associated with AML. Patients with t(8;21) and inv(16) have good prognoses, and those with t(15;17) have a moderately favorable prognosis. Poor prognosis is associated with complex karyotypes, multilineage dysplasia +(3;5)(q25;q34), +(2;11) +(1;7), major chromosomal deletions such as -7/del(7q), -5/del(5q), del(20q), -18, chromosomal gains such as +8, +9, +11, +19, +21, and abnormalities involving 3q21 and 3q26. Treatment of AML consists of induction chemotherapy and postremission management with intensive chemotherapy and allogenic or autologous bone marrow transplantation. The 5-year survival rate for children under 15 years is 45 %.[8] Patients with relapse less than 6 months after treatment have very poor outcomes. Patients with AML arising from a myelodysplastic syndrome also have a dismal prognosis.

Chronic myelogenous leukemia.[1,26] The clinical outcome of patients with CML is variable. Median survival is ~ 4 years. Ten percent of patients die within 2 years, and ~ 20 % per year afterwards. During the stable phase of the disease, CML can be controlled with low-dose chemotherapy. To enhance long-term survival and avoid blast crisis, allogenic bone marrow transplantation is performed during the stable phase of CML. Interferon has been show to suppress CML progenitor cells in the stable phase, but may cause graft versus host disease after bone marrow transplantation.

Hairy cell leukemia:[2,5,24] Hairy cell leukemia tends to be an indolent disease. Chemotherapy with purine analogs such as 2-chlorodeoxyadenosine or deoxycoformycin has proved effective in achieving long-term remissions of this disease in patients.[5]

References

1 Aster J, Kumar V. White cells, lymph nodes, spleen and thymus. In: Cotran RS, Kumar V, Collins T, eds. Pathologic Basis *of Disease* 6th ed. Philadelphia, Pa: W.B. Saunders; 1999:644-695.

2 Bentz M, Dohner H, Guckel F, et al. Assessment of bone marrow infiltration by magnetic resonance imaging in patients with hairy cell leukemia treated with pentosatin or alpha-interferon. *Leukemia* 1991:5:905-907.

3 Brunning RD, Borowitz M, Matutes E et al. Precursor B lymphoblastic leukemia/lymphoblastic lymphoma. In: Jaffe ES, Harris NL, Stein H, Vardinas JW eds. World *Health Organization Classification of Tumors. Tumors of Haematopoietic and lymphoid tissues.* IARC Press, Lyon 2001:111-114.

4 Diebold J. Bone involvement in Hodgkin's lymphoma, leukemias, myeloproliferative disorders and mastocytosis. In: Forest M.Tomeno B, Vanel D, eds. *Orthopedic Surgical Pathology: Diagnosis of Tumors and Pseudotumoral Lesions of Bone and Joints* Edinburgh: Churchill Livingstone; 1998:477-489.

5 Freedman AS, Nadler LM. Malignancies of lymphoid cells. In: Fauci AS, Braunwald E, Isselbacher KJ, et al, eds. *Harrison's Principles of Internal Medicine* 14th ed. New York, NY: McGraw-Hill; 1998: 695-712.

6 Hernandez RJ, Teo EL. Diffuse marrow disorders in children. *Magn Reson Imaging Clin N Am* 1998;6(3):605-626.

7 Huvos AG. Skeletal changes of acute and chronic leukemias in children and adults. In: Huvos AG, ed. *Bone Tumors: Diagnosis, Treatment, and Prognosis* 2nd ed. Philadelphia, Pa: W.B. Saunders; 1991: 640-645.

8 Jemal A, Thomas A, Murray T, Thun M. Cancer statistics 2002. *CA Cancer] Clin* 2002;52:23-47.

9 Kraemer M, Weissinger F, Kraus R, Beer M, Kunzmann V, Wilhelm M. Aseptic necrosis of both femoral heads as first symptom of chronic myelogenous leukemia. *Ann Hematol* 2003;82:44-46.

10 Lai A, Tallman MS, Soble MB, Golubovich I, Peterson L. Hairy cell leukemia presenting as localized skeletal involvement. *Leuk Lymphoma* 2002;43:2207-2211.

11 Lecouvet FE, VandeBerg BC, Michaux L, et al. Early chronic lymphocytic leukemia: prognostic value of quantitative bone marrow MR imaging findings and correlation with hematologic values. *Radiology* 1997:204:813-818.

12 Leone J, Vilque JP, Pignon B, et al. Aseptic necrosis of the femoral head as a complication of chronic myelogenous leukaemia. *Skeletal* Radio/ 1996:25:696-698.

13 Loevner LA, Tobey JD, Yousem DM, Sonners Al, Hsu WC. MR imaging characteristics of cranial bone marrow in adult patients with underlying systemic disorders compared with healthy control subjects. *AJNRAmJNeuroradiol* 2002;23:248-254.

14 Mahoney DH. Acute lymphoblastic leukemia. In: McMillan JA, DeAngelis CD, Feigin RD, Warshaw JB, eds. *Osik's Pediatrics: Principles and Practice* 3rd ed. Philadelphia, Pa: Lippincott, Williams & Wilkins; 1999:1493-1501.

15 Miller SL, Hoffer FA. Malignant and benign bone tumors. *Radial Clin North Am* 2001:39:673-699.

16 Moulopoulos LA, Dimopoulos MA. Magnetic resonance imaging of the bone marrow in hematologic malignancies. *Blood* 1997:90: 2127-2147.

17 Mulder JD, Schutte HE, Kroon HM, Taconis WK. Leukemia. In: *Radiologic Atlas of Bone Tumors* Amsterdam: Elsevier; 1993:373-378.

18 States LJ. Imaging of metabolic bone disease and marrow disorders in children. *Radial Clin North Am* 2001;39:749-772.

19 Steuber CP. Acute myeloid leukemia. In: McMillan JA, DeAngelis CD, Feigin RD, Warshaw JB, eds. Osik's *Pediatrics: Principles and Practice* 3rd ed. Philadelphia, Pa: Lippincott, Williams & Wilkins, 1999; 1501-1505.

20 Takagi S, Tanaka 0. Magnetic resonance imaging of femoral marrow predicts outcome in adult patients with acute myeloid leukaemia in complete remission. *BrjHaematol* 2002;117:70-75.

21 Takagi S, Tanaka 0. The role of magnetic resonance imaging in the diagnosis and monitoring of myelodysplastic syndromes or leukemia. *Leuk Lymphoma* 1996:23:443-450.

22 Tardivon AA, Vanel D, Munck JN, Bosq J. Magnetic resonance imaging of the bone marrow in lymphomas and leukemias. *Leuk Lymphoma* 1997:25:55-68.

23 Takagi S, Tanaka 0, Miura Y. Magnetic resonance imaging of femoral marrow in patients with myelodysplastic syndromes or leukemia. *Blood* 1995;86:316-322.

24 Thompson JA, Shields AF, Porter BA, et al. Magnetic resonance imaging of bone marrow in hairy cell leukemia: correlation with clinical response to alpha-interferon. *Leukemia* 1987;1:315-316.

25 Vande Berg BC, Michaux L, Scheiff JM, et al. Sequential quantitative MR analysis of bone marrow: differences during treatment of lymphoid versus myeloid leukemia. Radiology 1996;201:519-523.

26 Vardiman JW, Pierre R, Thiele J et al. Chronic myelogenous leukemia. In: Jaffe ES, Harris NL, Stein H, Vardiman JW eds. *World Health Organization Classification of Tumours. Tumours of Haematopoietic and Lymphoid Tissues.* IARL Press, Lyon 2001 ;20-26.

27 Wetzler M, Bloomfield CD. Acute and chronic myeloid leukemia. In: Fauci AS, Braunwald E, Isselbacher KJ, et al, eds. *Harrison's Principles of Internal Medicine* 14th ed. New York, NY: McGraw-Hill; 1998: 684-695.

A 42 Lipoblastoma

ICD-O Code

8881/0

Definition

Lipoblastomas are rare, benign mesenchymal tumors that contain embryonal white fat, and typically occur during infancy and early childhood.[1,6,15]

Frequency of Occurrence

Lipoblastomas represent < 1 % of benign soft tissue tumors.[9,10]

Age at Presentation

From < 1 year to 10 years, mean = 4-4.2 years.[1,9,10]

Gender Ratio (M f F)

1.6/1 to 3.8/1.[1,8,9,10]

Location

These lesions occur in the trunk > hip, buttock > lower extremity > foot and ankle, head and neck > proximal limb > upper extremity, retroperitoneum > other.[9] Lesions are often located in the superficial soft tissues.[7]

Signs and Symptoms

Patients usually present with an enlarging, painless, soft tissue mass.[1,8,15] Duration of symptoms ranges from months to several years.[1] Retroperitoneal lesions may be associated with episodes of emesis.[1] Lesions may be congenital.[1]

Cross Pathologic Findings

Tumors range in size from 1 to 21 cm.[1] Lesions may be lobulated, yellow, tan and white, pink, or red.[1] Gross specimens may show fibrous and gelatinous zones.[15]

Histopathologic Findings

Lesions are usually subdivided into lobules separated by fibrous septa containing spindle or stellate mesenchymal cells.[1,7,15] Lesions contain adipose cells in various stages of maturation, ranging from prelipoblasts to mature adipocytes.[1,7] Lipoblasts can have monovacuolated or multivacuolated cytoplasm lacking cytoplasmic granularity that is associated with hibernomas.[1] Prominent vascularity with a plexiform capillary network is seen in 80 % of specimens, and 54 % contain myxoid foci.[1] Cellular atypia and mitotic figures are typically absent.[1]

Lesion Genetics

Chromosomal rearrangements involving 8q11-13 with 3q12-13, 7p22, and 8q24 have been reported.[4,15] Gains of chromosome 8 have also been reported.[15] The COLIA2 / PLAG1 gene fusion produces a protein that may play a role in tumor genesis.[15]

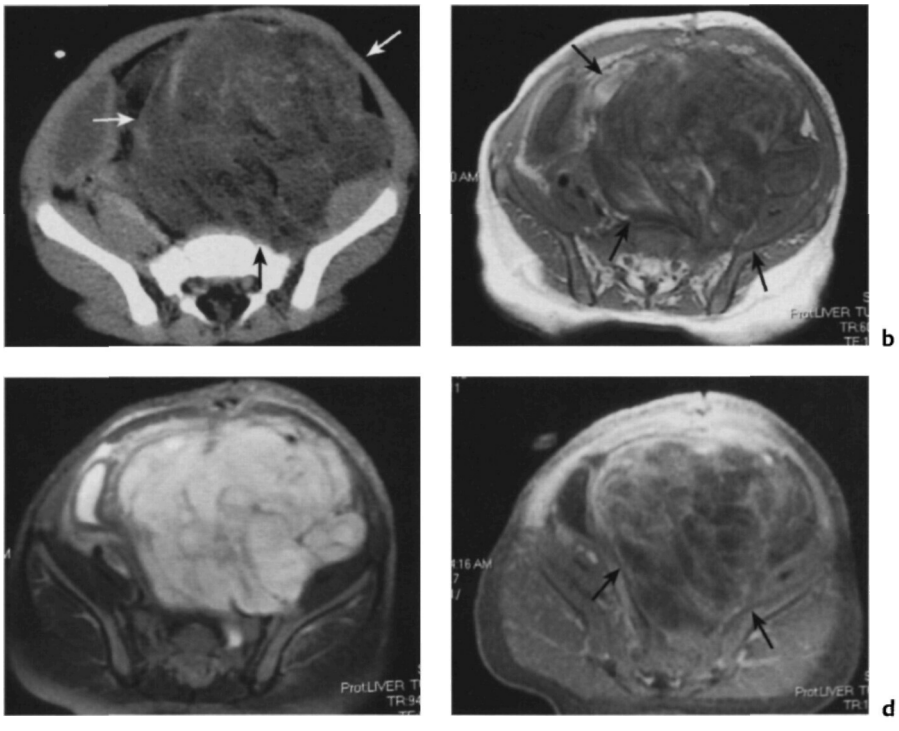

Figure **245a-d** A 1.5 year-old male with a large intra-abdominal and pelvic lipoblastoma. The lesion has heterogeneous attenuation with zones of soft tissue, fluid, and fat attenuation on axial CT (**a**). The lesion has mixed low-intermediate, intermediate, and high signal on axial T1WI (**b**), and heterogeneous mostly high signal with thin strands of low signal on axial FST2WI (**c**). The lesion shows heterogeneous Gd-contrast enhancement on axial FST1WI (**d**).

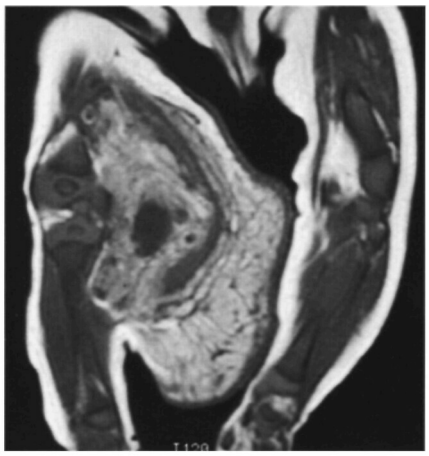

a, b

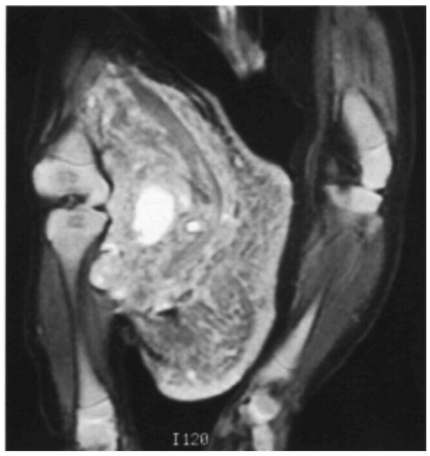

Figure **246** a-e A 3-month-old male with a large lipoblastoma involving the thigh. The lesion infiltrates adjacent muscles and subcutaneous tissues, and contains zones with MRI signal approximating that of fat on coronal T1WI (a). Many of the fatty zones have signal slightly lower than subcutaneous fat on T1WI, as well as higher signal on coronal STIR (b) and axial T2WI (c, d), resulting from the differing fat contents. Intralesional bands, septa, and/or nodular zones are seen with low-intermediate signal on T1WI and intermediate to slightly high signal on T2WI. The lesion shows heterogeneous Cd-contrast enhancement on axial FST1WI (e).

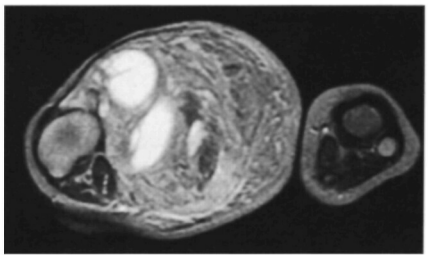

c, d

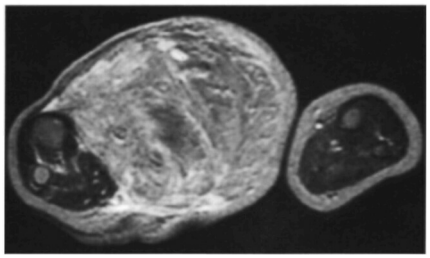

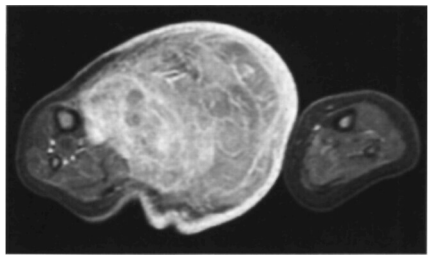

e

Findings on Plain Films (Roentgenograms) and Computed Tomography

Lipoblastomas can be seen on plain films as soft tissue masses that may contain zones of lower attenuation compared with adjacent muscles.[7] On CT, lipoblastomas often have zones with low attenuation comparable to subcutaneous fat[7,14] (Fig. 245). Thick or thin septa and/or nodular zones with soft tissue attenuation are often seen in lipoblastomas.

MRI Findings

Lesions are often circumscribed, although some have margins that infiltrate adjacent muscle or subcutaneous tissues.[5-7,14,16] Lesions typically contain zones with MRI signal approximating that of fat on T1WI and T2WI.[5-7,11,12,4] Fatty zones within the lesions may have signal slightly lower than subcutaneous fat on T1WI as well as slightly higher signal on FST2WI and STIR, resulting from the differing fat contents and shapes of immature lipoblasts compared with mature adipocytes" (Figs. **245, 246).** Intralesional bands, septa and/or nodular zones with low-intermediate to slightly high signal on T1WI and T2WI may be seen in large lesions.[6,14] Variable degrees of Gd-contrast enhancement may occur in the lesions, often in the nonlipomatosis portions (Figs. **245, 246).**

Differential Diagnosis

Lipoma, lipomatosis, liposarcoma, lymphangioma, hemangioma, hemangioendothelioma, hemangiopericytoma, angiosarcoma, lipofibromatosis, epidermoid cyst, dermoid cyst, teratoma.[3,4,7,8,11,12,14]

Prognosis and Treatment

Lipoblastomas are benign lesions that may represent hamartomas.[1] Lipoblastomas may mature into lipomas.[1,4,8,12] Lesions may regress spontaneously, or can be surgically excised.[4,6,12,13,14] Prognosis is usually excellent.[1,13,15]

References

1 Collins MH, Chatten J. Lipoblastoma/lipoblastomatosis: a clinicopathologic study of 25 tumors. *Am J Surg* Par/to/ 1997;21(10): 1131-1137.

2 Das Gupta TK, Chaudhuri PK. Tumors of the adipose tissue. In: Das Gupta TK, Chaudhuri PK, eds. *Tumors of the Soft Tissues* 2nd ed. Stamford, Conn: Appieton & Lange 1998:250-251.

3 Fetsch JF, Miettinen M, Laskin WB, Michal M, Enzinger FM. A clinicopathologic study of 45 pediatric soft tissue tumors with an admixture of adipose tissue and fibroblastic elements, and a proposal for classification as lipofibromatosis. *Am] Surg Pathol* 2000;24(11): 1491-1500.

4 Harrer J, Hammon G, Wagner T, Bolkenius M. Lipoblastoma and lipoblastomatosis: a report of two cases and review of the literature. *Eur J Pediatr Surg* 2001 ;ll(5):342-349.

5 Katz DS, Merchant N, Beaulieu CF, Blankenberg FG. Clinical image. Lipoblastoma of the thigh: MR appearance. *J Comput Assist Tomogr* 1996;20(6):1002-1003.

6 Ko SF, Shieh CS, Shih TY, et al. Case Report—Mediastinal lipoblastoma with intraspinal extension: MRI demonstration. *Magn Reson Imaging* 1998;16(4):445-448.

7 Kransdorf MJ, Moser RPJr, Meis JM, Meyer CA. From the Archives of the AFIP - Fat-containing soft-tissue masses of the extremities. *Radiographics* 1991;11(1):81-106.

8 Kransdorf MJ, Murphey MD. Lipomatous tumors. In: *Imaging of Soft Tissue Tumors* 2nd ed. Philadelphia, Pa: W.B. Saunders; 2006:80-149.

9 Kransdorf MJ, Murphey MD. Soft tissue tumors in a large referral population: prevalence and distribution of diagnoses by age, sex, and

location. In: *Imaging of Soft Tissue Tumors* 2nd ed. Philadelphia, Pa: W.B. Saunders; 2006:6-37.

10 Kransdorf MJ. Benign soft-tissue tumors in a large referral population: distribution of specific diagnoses by age, sex, and location. *AJR AmJRoentgenol* 1995;164:395-402.

11 Meyer JS, Dormans JP. Differential diagnosis of pediatric musculoskeletal masses. *Magn* Resort *Imaging Clin NAm* 1998;6(3): 541-571.

12 Mognato G, Cecchetto G, Carli M, et al. Is surgical treatment of lipoblastoma always necessary? *J Pediatr Surg* 2000;35(10):1511-1513.

13 Park CH, Kim KI, Lim YT, Chung SW, Lee CH. Ruptured giant intrathoracic lipoblastoma in a 4-month-old infant: CT and MR findings. *Pediatr* Radio/ 2000;30:38-40.

14 Reiseter T, Nordshus T, Borthne A, Roald B, Naess P, Schistad 0. Lipoblastoma: MRI appearances of a rare paediatric soft tissue tumour. *Pediotr Radial* 1999;29:542-545.

15 Sciot R, Mandahl N. Lipoblastoma. In: Fletcher COM, Unni KK, Mertens F, eds. *World Health Organization Classification of Tumours. Pathology and Genetics of Tumours of Soft Tissue and Bone* Geneva: IARC Press; 2002:26-27.

16 Siegel MJ. Magnetic resonance imaging of musculoskeletal soft tissue masses. *Radial Clin North Am* 2001 ;39(4):701-720.

A 43 Lipoma, Atypical Lipoma, and Hibernoma

ICD-OCode

Lipoma: 8850/0

Chondroid Lipoma: 8862/0

Spindle cell lipoma: 8857/0

Pleomorphic lipoma: 8854/0

Hibernoma: 8880/0

Definition

Lipomas are common, benign hamartomas composed of mature, white adipose tissue without cellular atypia.[6,8,12,28,29] Osseous or chondroid metaplasia with myxoid changes can be associated with lipomas.[5,14,16,20,28] These **atypical lipomas** have been labeled as **chondroid lipomas, osteolipomas, or benign mesenchymomas**[10,14,6,20,28] Chondroid lipomas are benign adipose tumors which contain mature fat, lipoblasts, and chondroid matrix.[14,28] **Spindle cell and pleomorphic lipomas** are lipoma variants which have overlapping histologic features of varying proportions of mature fat cells, spindle cells, hyperchromatic spheroid cells, collagen, and multinucleated giant cells.[2428] Lipomas with high content of fibrous tissue have been labeled as fibrolipomas.[5] **Hibernomas** are rare, benign lesions derived from brown adipose tissue intermixed with white adipose tissue.[5,9,15,23,28,29] Lipoma arborescens, also referred to as diffuse synovial lipoma, represents a disorder in which there are multiple villous or frond-like zones of fatty deposition in synovium within a joint, tendon sheath, and/or bursa.[17,28] Lipoma arborescens may be idiopathic, or occur in the setting of degenerative arthritis, collagen vascular disorders, or trauma.[17]

Frequency of Occurrence

Soft tissue. Lipomas are the most common soft tissue tumor, representing 10% of all soft tissue tumors and 16% of benign soft tissue tumors.[1928] The conventional form of lipoma accounts for ~50% of fatty soft tissue tumors.[18,19,28] Spindle cell lipomas account for 27 % of fatty soft tissue tumors.[18,19] Chondroid lipomas are rare variants of lipomas.[14] Hibernomas account for less than 2 % of fatty tumors.[923] Lipomas arborescens account for less than 1 % of lipomas.[17]

Bone. Lipomas in bone are rare lesions, representing ~0.1 % of bone tumors.[8,25-27,28,31,33,34] The prevalence of intra-osseous lipomas is markedly under-reported.[28]

Age at Presentation

Soft tissue:

- **Lipomas:** from 26 to 68 years, mean = 48 years.[18,19]
- **Spindle cell/pleomorphic lipomas:** from 37 to 74 years, mean = 56 years,[18,19] median 55 years.[24]
- **Hibernomas:** from 2 to > 75 years, mean = 38years,[9,21] 32 years.[18,19]
- **Lipomas arborescens:** from 9 to 66 years.[17]

Bone: from 5 to 85 years, median = 37 years, mean = 40years.[2,8,2S]

Gender Ratio (M f F)

Soft tissue:

- **Lipomas: 1 / 2.6.**[18,19]
- **Spindle cell/pleomorphic lipomas: 7/1.**[18,19]
- **Chondroid lipomas: 1 /4.**[14]
- **Hibernomas: < 1/1 to 1.4/1.**[1,9,18,19,23]
- **Lipomas arborescens: M > F.**[17]

Bone: 1/1 to4/3.[2,8,28]

Location

Soft tissue:

- **Lipomas.** These lesions occur in the trunk > head and neck > lower extremity > proximal limb > hip, buttock > upper extremity > hand, wrist.[18] Lipomas can be superficial within subcutaneous fat or deep-seated within muscle or other sites (labeled as heterotopic lipomas) within the body.[5,16,21] Lipomatosis refers to extensive infiltration of normal structures with mature adipose tissue, which can be confused grossly with low-grade liposarcoma.[5,15]
- **Spindle cell/pleomorphic lipomas.** These lesions frequently occur in the subcutaneous tissues of the posterior neck, trunk, and upper extremity.[18,19,24] These lesions have also been reported to occur in the scalp, hip and buttocks, hand and wrist, and lower extremities.[18,19,24]
- **Chondroid lipomas.** These lesions occur in the proximal extremities, trunk, head and neck.[14] These lesions often involve the deep soft tissues and muscles, and occasionally occur at the subcutis.[14]
- **Hibernomas.** These lesions are typically located in the subcutis.[23] Hibernomas occur in interscapular and periscapular locations > neck > axilla > thorax, chest wall > thigh.[1,5,13,15,18,19,23] Lesions in the extremities commonly occur within muscle,[1] thigh > shoulder > arm.[9]
- **Lipomas arborescens.** These abnormalities occur mostly in the knee joint, and are more frequently unilateral than bilateral.[17] Lipoma arborescens has also been reported to occur in the hip and wrist.[17]

Bone. Lesions occur in the calcaneus, femur > tibia > spine and pelvis, iliac bone > tibia > fibula > humerus > skull and mandible.[228] In long bones, the metaphyseal regions are common sites.[2] In the femur, intertrochanteric and subtrochanteric locations are common.[2,28,30] Lipomas rarely occur along the surface of bone, and are referred to as periosteal or parosteal lipomas.[5,15,28]

Signs and Symptoms

Soft tissue. Superficial lipomas are usually painless, palpable soft lesions. Deep-seated lipomas may cause mild extremity enlargement or no symptoms.[5,15] Spindle cell/pleomorphic lipomas are usually painless, movable, dermal or subcutaneous lesions.[24] Chondroid lipomas are usually painless masses.[14] Lipoma arborescens can occur as progressive and painless synovial thickening with intermittent effusions.[17] Hibernomas are slow-growing, painless tumors located in the subcutaneous soft tissues.[192328] The average duration observed for these painless masses is 30.6 months.[9]

Bone. Up to 70% of patients with intra-osseous lipomas present with pain.[2,28] Other intra-osseous lipomas are found as incidental findings.[2,8] Pathologic fractures associated with intra-osseous lipomas are rare.[8,28]

Cross Pathologic Findings

Soft tissue. Lipomas are soft, well-circumscribed tan or yellow lesions with lobular configurations, with or without peripheral encapsulation.[16,32] Subcutaneous lipomas are often encapsulated by a thin fibrous layer. Intramuscular lipomas, however, can be unencapsulated, and extend or infiltrate along muscle planes.[5]

- **Spindle cell / pleomorphic lipomas** are yellow and/or gray-white ovoid masses.[24]
- **Chondroid lipomas** are circumscribed, encapsulated yellow lesions that range in size from 2 to 7 cm.[14] These lesions can have associated hemorrhage.[14]
- **Hibernomas** are rare, benign lesions derived from brown adipose tissue.[1,5,9,13,15,23] Hibernomas can be yellow, reddish-brown to tan.[1,5,9] Mucoid zones and rare areas of hemorrhage can be seen.[9] Hibernomas range in size from 1 to 24cm, median =9.3 cm.[9,23]
- **Lipoma arborescens** often has a frondlike and/or villous configuration at the involved synovium.[17]

Bone. Lipomas are yellow-fatty, circumscribed and/or lobulated lesions.[8,28] Intra-osseous lipomas may contain cystic zones and/or calcifications.[8,28]

Histopathologic Findings

Soft tissue. Lipomas represent lesions derived from white adipose tissue,[5,6] and are typically composed of mature fat cells that are similar in size and shape.[16] The white adipose cell typically has a peripheral rim of cytoplasm containing a crescent-shaped nucleus adjacent to a single central vacuole containing a large droplet of neutral fat.[5] Lipomas have a vascular network that is not prominent microscopically because of compression by adjacent large adipose cells.[16] Thin septa of fibrous connective tissue can occur within lipomas.[16] Cellular atypia or mitoses are not typically seen. Occasionally, zones of hemorrhage, xanthomatous change, and/or myxomatous degeneration can occur in lipomas.[5] Mature adipocytes are immunoreactive to vimentin, S100 protein, and leptin.[29]

- **Spindle cell/pleomorphic lipomas.** Spindle cell and pleomorphic lipomas have overlapping histologic features of varying proportions of mature fat cells, spindle cells, hyperchromatic spheroid cells, collagen and multinucleated giant cells.[24] Spindle cell lipomas contain bands of bland spindle cells adjacent to fat cells and bundles of collagen. The spindle cells typically show no mitotic activity.[24] Pleomorphic lipomas show various combinations and proportions of spindle and round hyperchromatic cells, fat cells, multinucleated giant cells, mast cells, lymphocytes, plasma cells, and myxoid zones.[24] The spindle cells are immunoreactive to CD 34 and rarely to S100 protein.[24]
- **Chondroid lipomas** These tumors are benign adipose lesions composed of mature fat cells, univacuolated or multivacuoloated lipoblasts, myxoid and hyalinized chondroid matrix containing chondroitin sulfate.[14] The lipoblasts have small nuclei within cytoplasm containing small vacuoles with fat and glycogen.[14] These lesions are immunoreactive to vimentin, and occasionally to S100 protein.[14]
- **Hibernomas.** These are rare, benign lesions derived from brown adipose tissue.[1,5,9,16,23] Hibernomas are usually composed of polygonal brown fat cells containing small central nuclei, and the cytoplasm contains many mitochondria and multiple vacuoles with small fat droplets.[1,5,9,16,23] The brown fat cells vary from pale to eosinophilic.[9,23] Mitotic activity is typically absent.[9,23] Lobules of brown fat cells are separated by richly vascularized connective tissue containing nonmyelinated nerve fibers.[5,9] Variants of hibernomas contain myxoid stroma with a loose basophilic matrix (myxoid variant) or thick bundles of collagen fibers (spindle cell variant).[9,23] Up to 85 % of hibernomas can be immunoreactive to S100 protein.[9,23]
- **Lipoma arborescens.** This appears as zones of mature adipose tissue within the synovium with resultant frond like and/or villous projections with or without associated chronic inflammatory cells.[17,28]

Bone. Intra-osseous lipomas are lesions comprised of mature fat cells with limited fine, fibrovascular septa located in zones without medullary trabecular bone.[2,8,28] No cellular atypia or mitoses are seen.[2] Areas of fatty necrosis associated with foamy histiocytes may occur with or without ischemic bone formation, which appears as densely stained, woven bone with hematoxylin.[2,8,28] Zones of dystrophic calcifications may be present.[2828] Regions of myxoid degeneration and thin-walled cystic zones can also occur in intra-osseous lipomas.[2,8,28] A staging system has been proposed for intra-osseous lipomas:[2,28] stage 1 lesions contain mature adipose cells associated with fine bony trabeculae;[2,28,31] stage 2 lesions contain zones of infarction with areas of necrosis and foamy macrophages;[2,28,31] and stage 3 lesions contain mostly necrotic fat with calcifications, cystic zones, and reactive bone formation.[2,283,1]

Lesion Genetics

Three cytogenetic abnormalities have been reported for lipomas.[29] These cytogenetic aberrations involve 12ql3-15, 6p21-23, and loss of portions of 13 q.[29] The Alterations in the HMGIC gene located at 12 q!5 or HMGIY gene at 6 p21 -23 may be involved in lipoma formation.[29]

Chondroid lipomas have been associated with a balanced translocation, t(ll;16)(ql3;p!2-13).[14]

Hibernomas have been associated with abnormalities involving 11 q!3-21.[9,23]

Findings on Plain Films (Roentgenograms) and Computed Tomography

Soft tissue. Lipomas can occasionally be seen on plain films as zones of lower attenuation compared with adjacent muscles (Fig. **251).** On CT, lipomas usually have attenuation comparable to subcutaneous fat. Thin septa with soft tissue attenuation may be seen in the lipomas. **Atypical lipomas** are uncommon variants of lipomas, which can contain prominent zones of soft tissue attenuation in association with fatty portions, mimicking the imaging appearance of liposarcomas[10,15,16,28] (Fig. **252).**

- **Hibernomas** are circumscribed lesions with CT attenuation between fat and muscle[14,13,16,28] (Fig. **254).** Internal septations and zones with soft tissue attenuation may be present.[13,28] These lesions usually show variable and heterogeneous contrast enhancement.[1,13,16,28]
- **Lipoma arborescens** can appear as zones with fat attenuation within thickened synovium on CT.[17]

Bone. Intra-osseous lipomas are typically radiolucent intramedullary lesions with abrupt zones of transition[2,28,31] (Figs.

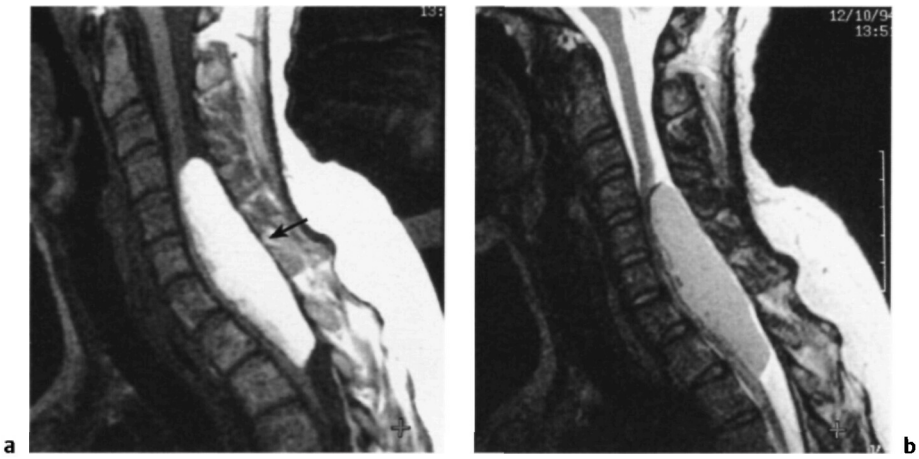

Figure **247 a, b** Intradural lipoma involving the dorsal portion of the cervical and upper thoracic spinal cord. The lipoma has high signal on sagittal T1WI (**a**), and slightly high signal on sagittal T2WI (**b**).

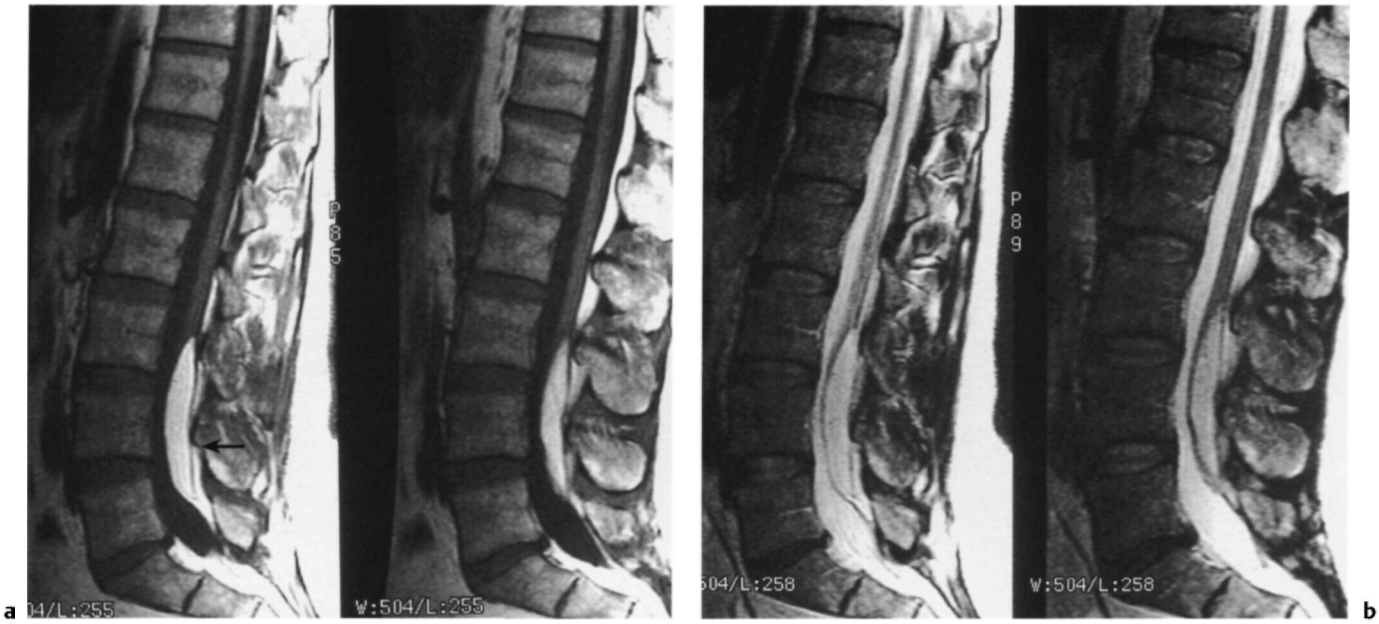

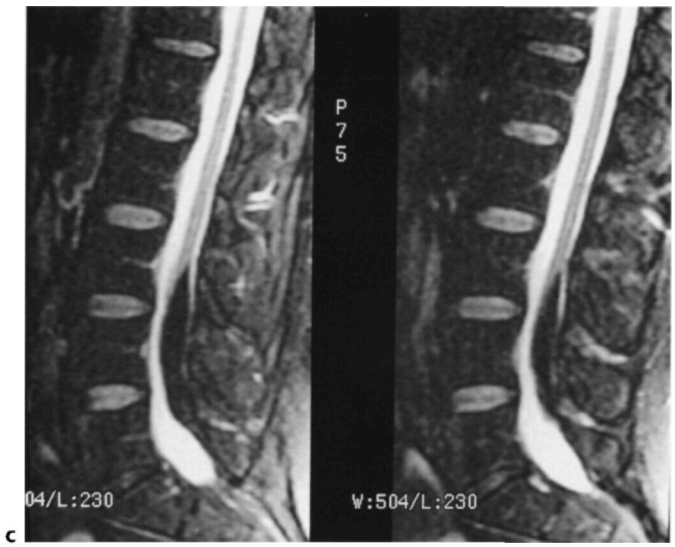

Figure **248 a-c** Intradural lipoma involving the dorsal portion of the lower spinal cord which is tethered at the L4 level. The posterior elements of the lumbar vertebrae are intact. The lipoma has high signal on sagittal (**a**) T1WI and slightly high signal on sagittal (**b**) T2WI. The signal of the lipoma is suppressed on sagittal (**c**) FST2WI.

258-261). Lesions range in size from 10 to 90mm, mean = 40 mm.[2] Marginal sclerosis is commonly seen with lipomas of the calcaneus (61 %), and to a lesser frequency with intra-osseous lipomas at other sites (38 %)[2] (Figs. **259-261).** Calcifications occur in more than half of intra-osseous lipomas, and are more frequently present in calcaneal lipomas than lipomas in other bones[2] (Figs. **259, 260).** Calcifications range in size from 1 to 22 mm.[2] CT can show fat attenuation within the lesions as well as cystic/necrotic zones and calcifications (Fig. **258).** Bone expansion occurs in only 14%, and is typically minimal.[2]

MRI Findings

Soft tissue. Superficial lipomas in subcutaneous fat often have circumscribed margins and have MRI signal comparable to subcutaneous fat on T1VVI, PDWI, T2WI, and FST2W1 (Fig. **249).** Nonencapsulated superficial lipomas have also been described.[28,32] Deep-seated lipomas may be localized within and/or between muscles[21,28] (Figs. **250, 251).** These lipomas can also infiltrate between muscle fibers which can produce a striated appearance.[16,21,28] Nonfatty, thin septa may be present within superficial or deep-seated lipomas.[10,11,5,16,21,28,30] These thin septa may show slightly high to high signal on FST2W1. Lipomas have

a

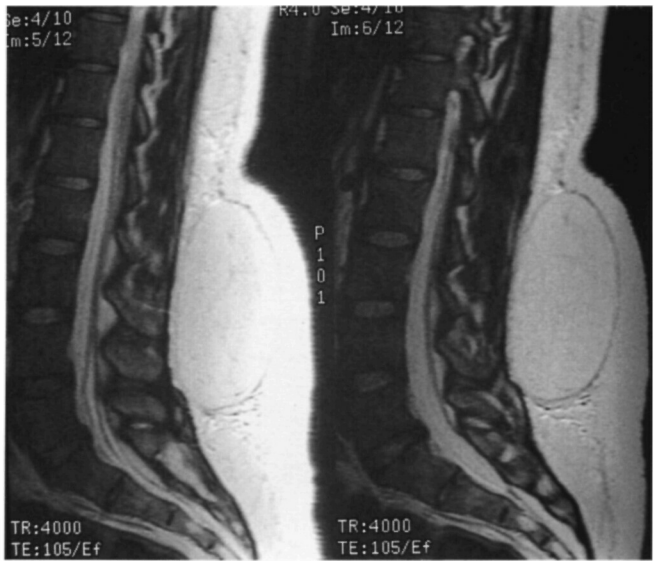

b

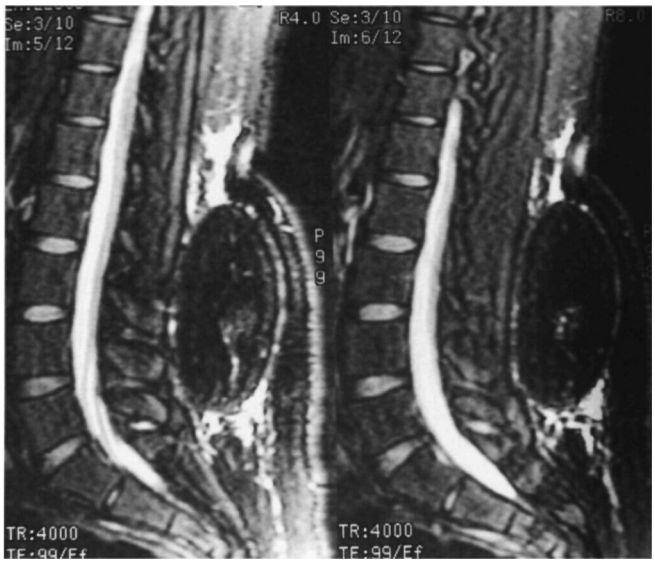

c

Figure **249a-c** 28-year-old woman with a lipoma in the dorsal subcubcutaneous fat superficial to the lumbar spine. The lipoma has high signal on sagittal T1 WI (**a**) and sagittal T2WI (**b**). The lipoma has a thin capsule of low signal. The signal of the lipoma is suppressed on sagittal FST2WI (**c**).

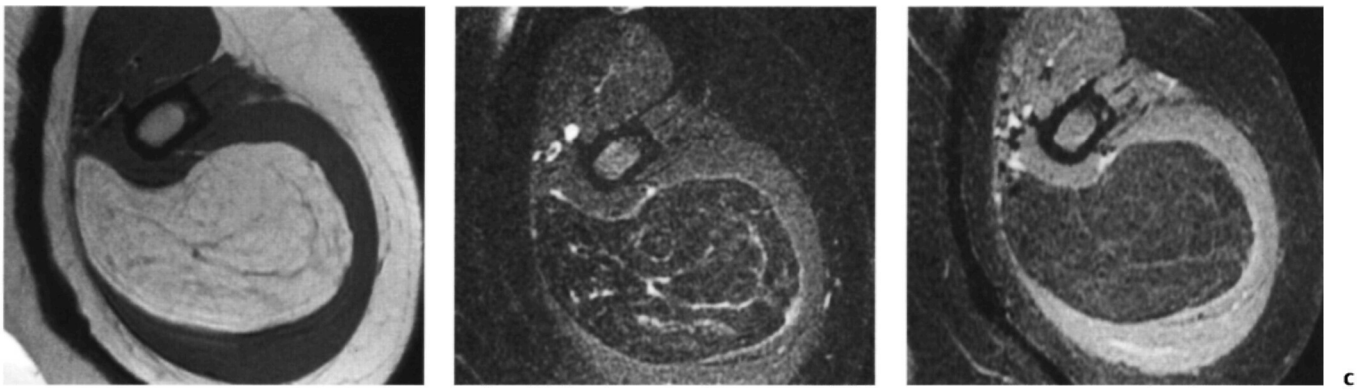

a, b c

Figure **250 a-c** A 43-year-old woman with an intramuscular lipoma in the triceps brachii muscle of the arm. The lipoma has high signal on axial (**a**) T1 WI. The fat signal of the lipoma is suppressed on axial (**b**) FST2WI. Thin septa are present within the lipoma, which show slightly high signal on FST2WI. No abnormal Cd-contrast enhancement is seen in the lipoma, except for minimal enhancement at several thin septa on axial (**c**) FST1WI.

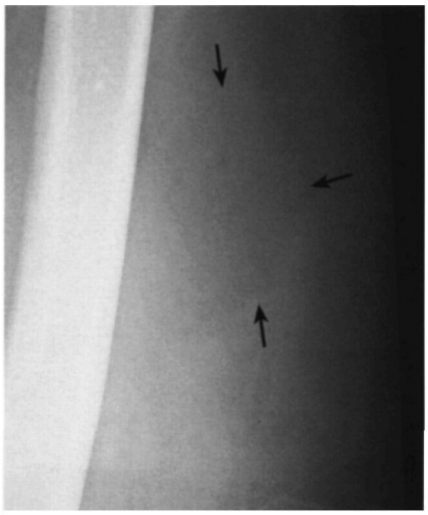

a

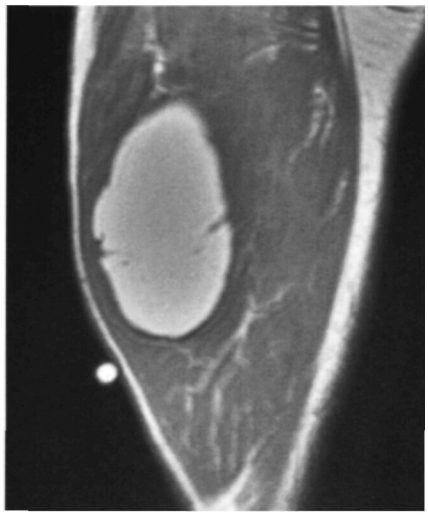

b

c

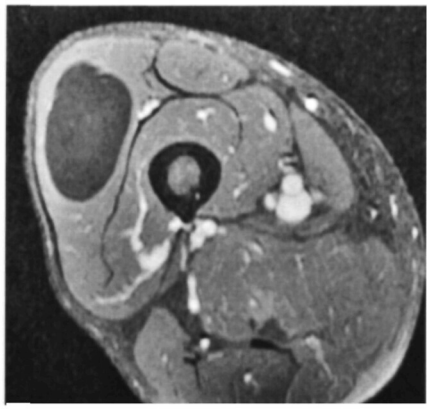

d

Figure **251 a-d** A 71-year-old man with an intramuscular lipoma in the vastus lateralis muscle of the thigh. Oblique radiograph (**a**) shows a circumscribed, radiolucent zone in the soft tissues. The lipoma has high signal on sagittal T1WI (**b**). The fat signal of the lipoma is suppressed on sagittal FST2WI (**c**). No abnormal Gd-contrast enhancement is seen in the lipoma on axial FST1WI (**d**).

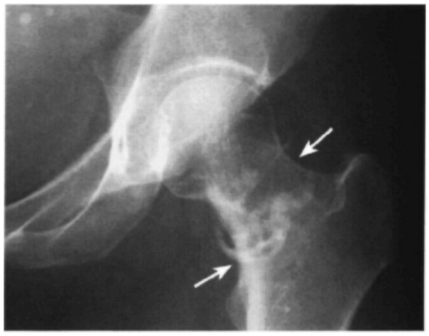

a

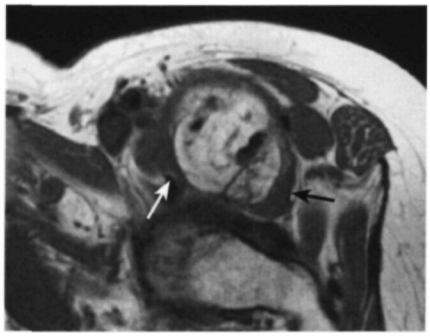

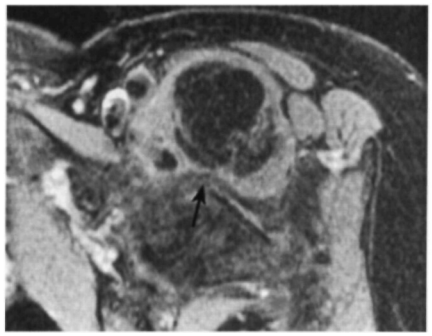

b, c

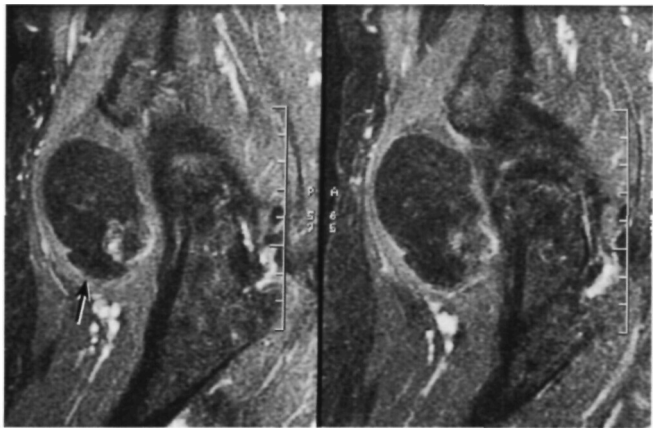

d

Figure **252a-d** A 55-year-old woman with an osteolipoma involving the iliopsoas muscle ventral to the proximal femur. AP radiograph (a) shows a lesion with dense peripheral and central mineralization. The lesion contains mostly fat signal on axial T1WI (**b**) as well curvilinear and small nodular zones of low signal. The signal of the fatty portions of the lesion is suppressed on axial (**c**) and sagittal (**d**) FST2WI, whereas several of the small nonfatty portions show intermediate to high signal.

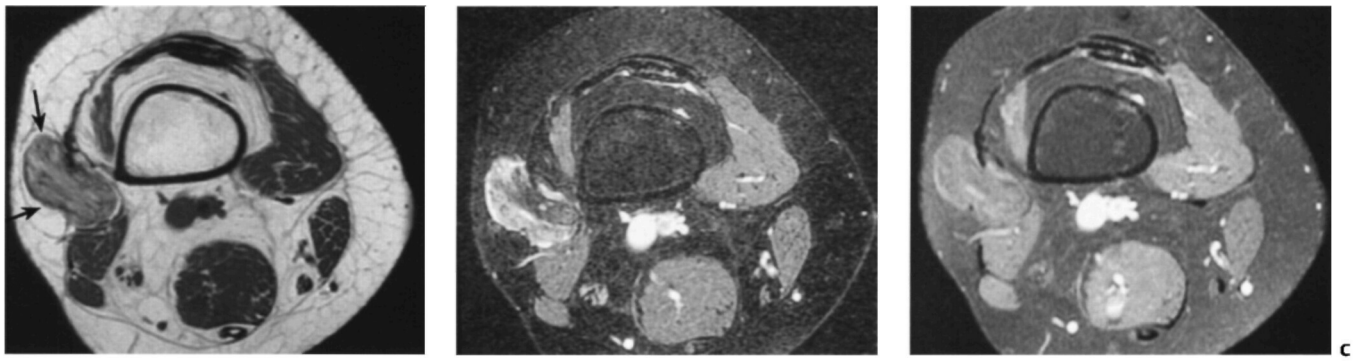

Figure **253a-c** A 57-year-old woman with a chondroid/myxoid lipoma in the soft tissues of the distal lateral thigh, which indents the biceps femoris muscle. The lesion has lobulated well-defined margins, and has heterogeneous low, intermediate, and high signal on axial (**a**) T1WI and axial (**b**) FST2WI. The lesion shows minimal Cd-contrast enhancement on axial FST1WI (**c**).

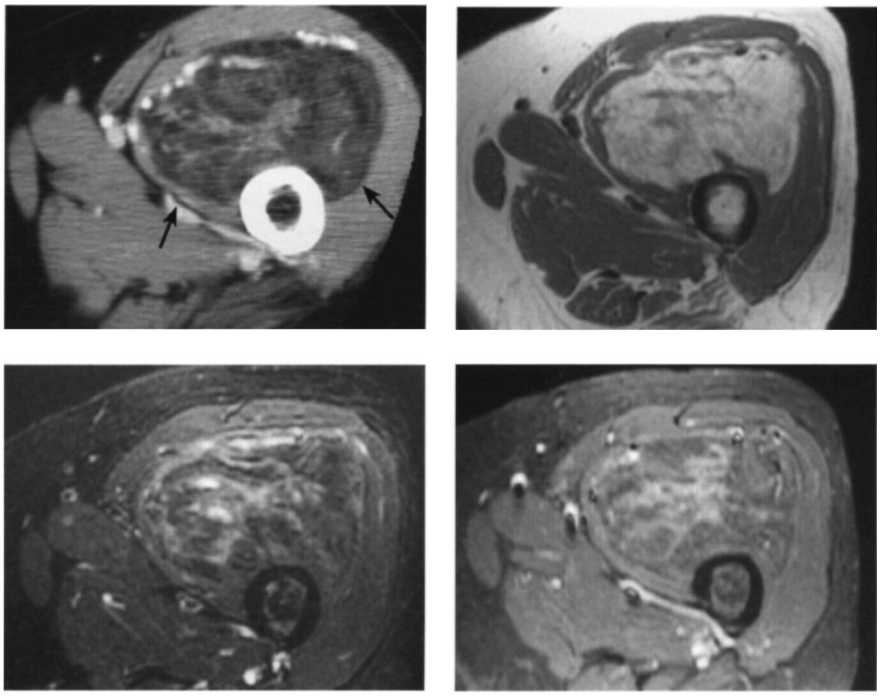

Figure **254a-d** 71-year-old woman with a hibernoma involving the vastus muscles of the proximal thigh. Axial CT image (**a**) shows the lesion to contain fat and irregular zones with soft tissue attenuation. The lesion has well-defined margins and contains mostly fat signal on axial T1WI (**b**), as well curvilinear and small nodular zones of low signal. The signal of the fatty portions of the lesion is suppressed on axial FST2WI (**c**), whereas nonfatty portions show intermediate to high signal on FST2WI. The nonfatty portions of the lesion show Gd-contrast enhancement on axial FST1WI (**d**).

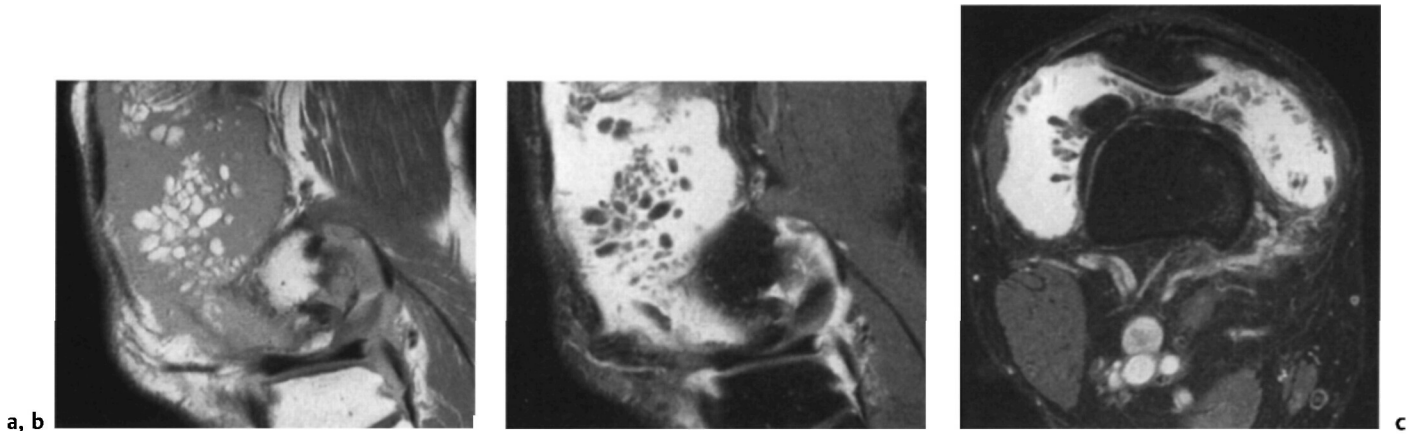

Figure **255 a-c** A 37-year-old man with lipoma arborescens at the knee. Multiple nodular and frondlike/villous deposits with fat signal are seen within hypertrophied synovium on sagittal PDWI (**a**). The fat signal is suppressed on sagittal (**b**) and axial (**c**) FST2WI. The hypertrophied fatty synovium is seen within a large joint effusion.

been reported to range in size from 3 to 25 cm, median = 10 cm, mean = 12.5 cm.[15] Lipomas can occur in the spine as intradural lesions attached to the dorsal aspect of the spinal cord, with or without tethering (Figs. **247, 248**); or associated with occult spinal dysraphism including abnormalities such as lipomyeloceles and lipomyelomeningoceles. After Gd-contrast administration, lipomas often show no enhancement (Fig. **251**). Minimal to mild enhancement may be seen along the thin, nonfatty septa (Fig. **250**).

- **Atypical lipomas** (chondroid lipomas, osteolipomas) are less common than the classic type, and may account for up to 31 % of lipomas.[15] Atypical lipomas may contain cystic/necrotic zones, calcifications, thick septa and/or nodular zones which may or may not show enhancement™ (Figs. **252, 253**). Most atypical lipomas contain more than 75% fat, whereas liposarcomas often have less than 75% fat.[15] Distinguishing between atypical lipomas and low-grade

Figure **256a-d** Intra-osseous lipomas in the L3 and L4 vertebral bodies. Two well-circumscribed intramedullary foci are seen which have high signal on sagittal T1WI (**a**) and sagittal T2WI (**b**), and are hyperintense relative to the adjacent marrow. The signal of these intra-osseous lipomas is suppressed on sagittal FST2WI (**c**). Neither of these lipomas show Cd-contrast enhancement on sagittal FST1WI (**d**).

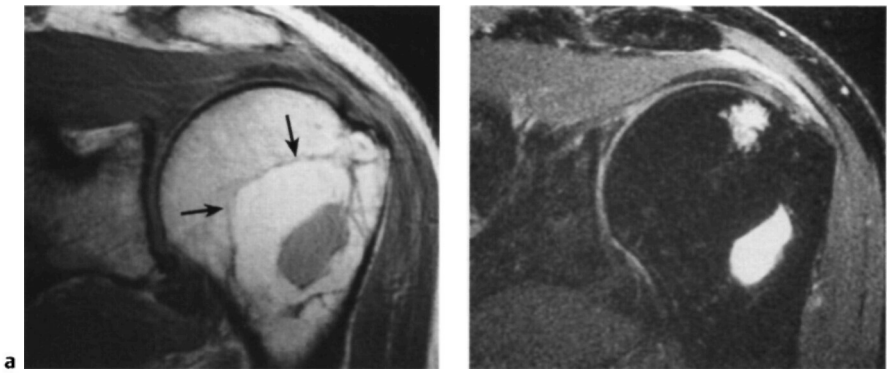

Figure **257 a, b** Intra-osseous lipoma in the proximal humerus. The lipoma is well circumscribed and has a peripheral thin border of low signal on coronal PDWI (**a**). The lipoma has mostly fat signal as well a smaller zone of necrosis. The fatty portion of the lesion has high signal on PDWI, which is suppressed on coronal FST2WI (**b**), whereas the zone of necrosis has intermediate signal on PDWI and high signal on FST2WI.

liposarcomas with MRI, however, can be difficult and challenging.™[30]

Hibernomas are typically well-defined soft tissue lesions that often have intermediate to high signal on T1WI (hypointense or isointense relative to fat), and slightly high signal onT2WI[13,28] (Fig. 254). Lesions can have slightly hyperintense signal relative to fat on FST2WI and STIR.[1,13] Mild signal heterogeneity, internal septations, and/or branching-serpentine, slow-flowing, vascular channels may be seen on T1WI andT2WI.[13,28] After Gd-contrast administration, hibernomas usually show enhancement.[1,7,13,28] Contrast enhancement seen within branching-serpentine vascular channels may distinguish these lesions from well-differentiated liposarcomas.[28] MR angiography may display vessels at the surface and/or within the hibernoma.[1] Related to the high metabolic rate of these tumors containing brown fat, increased uptake of Tc-99 m tetrofosmin and F-18 fluorodeoxyglucose has been reported.[4]

- **Lipomas arborescens** can appear as multiple, nodular or frondlike deposits with fat signal within hypertrophied synovium, often associated with a joint effusion[17] (Fig. **255**).

Bone. Intra-osseous lipomas are typically well circumscribed intramedullary lesions that have a peripheral thin border of low signal on T1WI, PDWI, and T2W1 in 74% of cases.[2,28,31] Intra-osseous lipomas often have high signal on T1WT and PDWI,

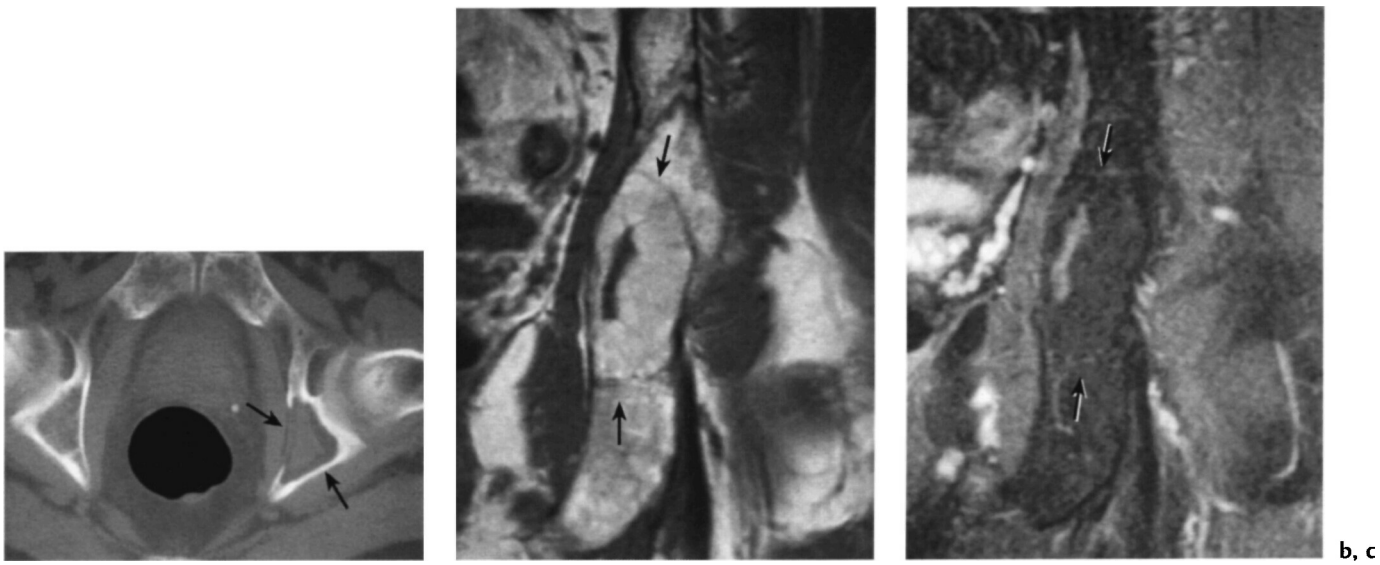

Figure **258a-c** A 55-year-old man with an intra-osseous lipoma in the ischium. Axial CT image (**a**) shows a circumscribed radiolucent lesion, which has low signal comparable to fat surrounding a central zone with fluid attenuation. The lipoma has mostly fat signal, as well a smaller zone of necrosis. The fatty portion of the lesion has high signal on coronal (**b**) T1WI, which is suppressed on coronal FST2WI (**c**), whereas the zone of necrosis has low- intermediate signal on T1 WI and high signal on FST2WI.

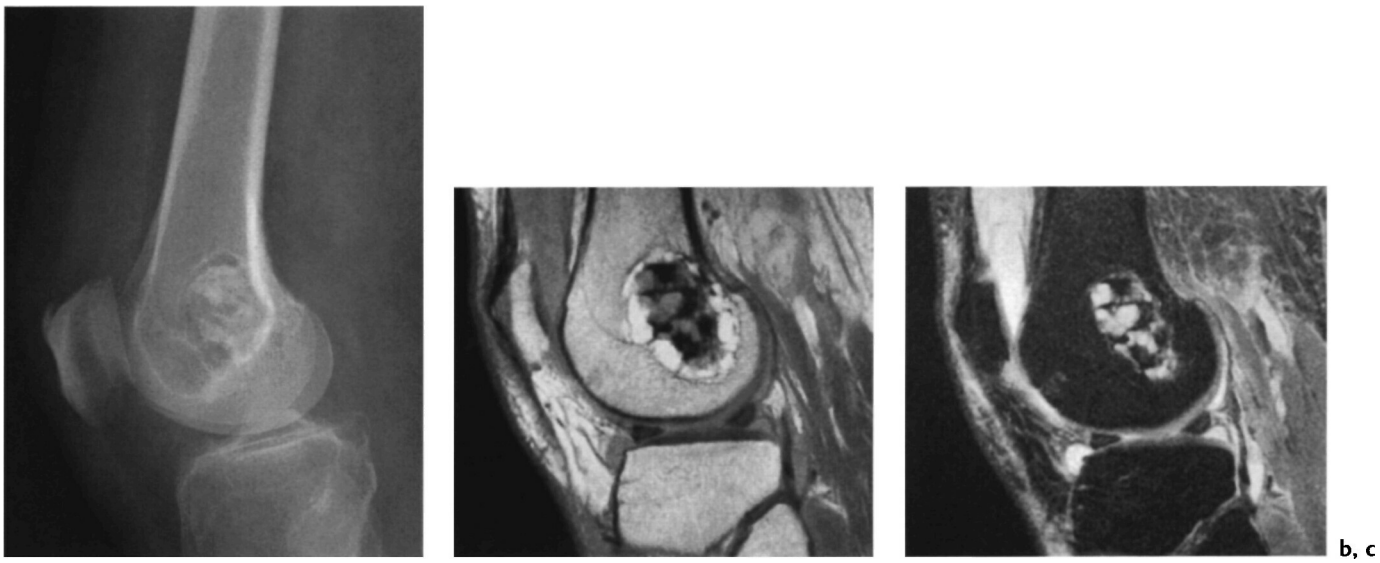

Figure **259a-c** A 74-year-old man with an intra-osseous lipoma in the distal femur. Lateral radiograph (**a**) shows a circumscribed intramedullary lesion containing dense amorphous calcifications surrounded by a sclerotic margin. The lipoma has high fat signal peripherally surrounding a central zone of low and intermediate signal on sagittal (b) PDWI. A thin rim of low signal is seen. The signal from the fat components of the lesion is suppressed on sagittal (**c**) FST2WI, whereas central zones of cystic change have high signal. In addition, zones of low signal on both PDWI and FST2WI correspond to internal calcifications seen on radiographs.

Figure **260 a-d** A 47-year-old woman with an intra-osseous lipoma of the calcaneus. Lateral radiograph (a) shows a circumscribed radiolucent lesion containing internal calcifications surrounded by a thin, peripheral, sclerotic margin. The lipoma has thin margins of low signal surrounding a central zone of mostly high fat signal as well as several zones of low signal on sagittal (**b**) and axial (**c**) T1 Wl. The fat signal of the lipoma is suppressed on axial (**d**) FST2WI. In addition, small internal zones of cystic change with high signal are seen on FS T2WI. Zones of low signal on both PDWI and FST2WI correspond to internal calcifications seen on radiographs.

and intermediate-high signal on T2WI, which is isointense to fat elsewhere in the field of view (Figs. **256-261).** Suppression of fat signal typically occurs with STIR and FST1WI or FST2WI. Cystic zones are seen in approximately two-thirds of intra-osseous lipomas and range in size from 2 to 35mm^2 (Figs. **257-261).** Calcifications, when present, usually appear as zones of low signal or signal void (Figs. **259, 260).**

Differential Diagnosis

Soft tissue lipoma. Liposarcoma, hemangioma, muscle infarct, muscle deinnervation, hibernoma, dermoid, epidermoid, fat necrosis.[3,22]

Bone. Hemangioma, fibrous dysplasia, unicameral bone cyst, aneurysmal bone cyst, bone infarct, enchondroma, chondrosarcoma, liposarcoma, liposclerosing myxofibrous tumors.[29]

Prognosis and Treatment

Soft tissue. Lipomas are often treated conservatively with observation.[29] Lipomas that cause disfigurement or limitation of patient movement can be surgically removed with good outcomes.[29] Atypical lipomas may require surgical removal because of potential confusion with liposarcoma.[14] Hibernomas are usually cured by excision.[1,9,23] Lipoma arborescens is typically treated with synovectomy.[17]

Bone. Intra-osseous lipomas are rarely associated with pathologic fractures.[8,12,34] Symptomatic intra-osseous lipomas can be treated with curettage and packing with bone chips.[8]

a

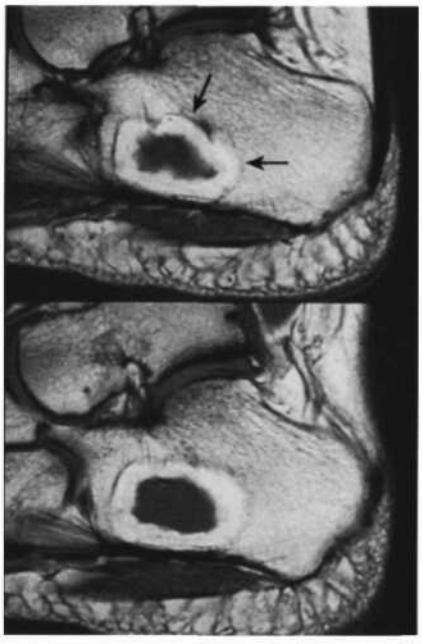

b

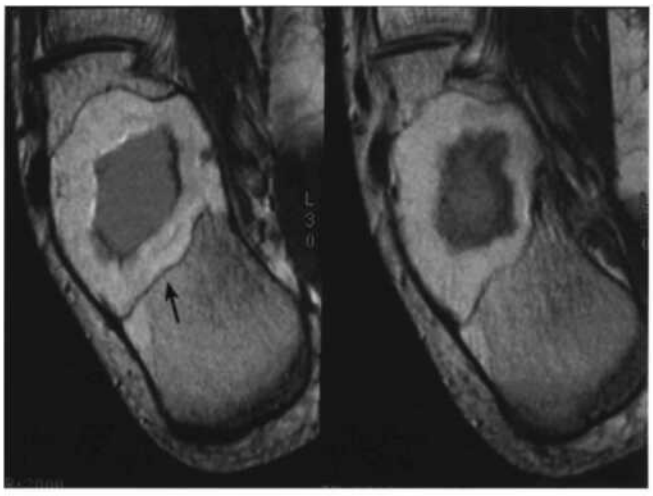

c

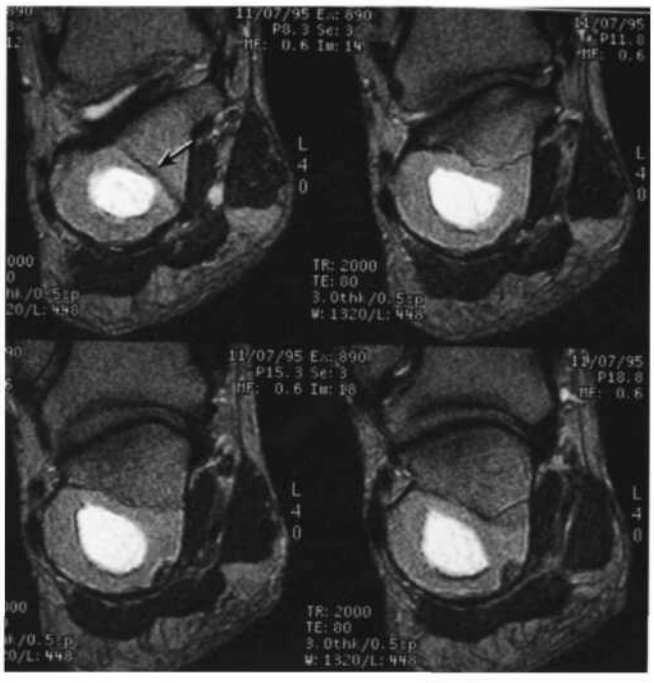

d

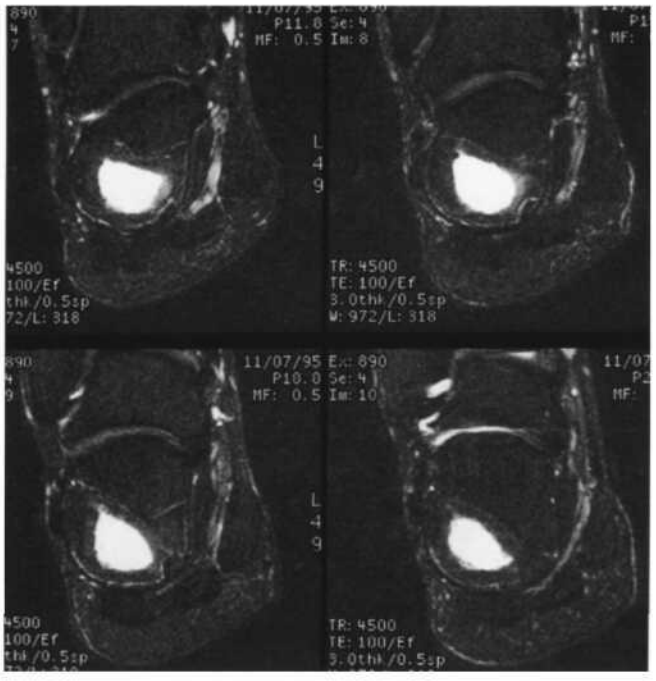

e

Figure **261 a-e** A 15-year-old female with an intra-osseous lipoma of the calcaneus. Lateral radiograph (**a**) shows a circumscribed radiolucent lesion surrounded by a thin, peripheral, sclerotic margin. The lipoma has thin margins of low signal surrounding a zone of high fat signal within which there is a zone with low-intermediate signal on sagittal T1WI (**b**), intermediate signal on axial PDWI (**c**) and high signal on coronal T2WI (**d**), representing an internal region of cystic change. The fat signal of the lipoma is suppressed on coronal FS T2WI (**e**), whereas the cystic region has high signal.

References

1 Anderson SE, Schwab C, Stauffer E, Banic A, Steinbach LS. Hibernoma: imaging characteristics of a rare benign soft tissue tumor. *Skeletal Radial* 2001 ;30:590-595.

2 Campbell RSD, Grainger AJ, Mangham DC, Beggs I, The J, Davies AM. Intraosseous lipoma: report of 35 new cases and a review of the literature. *Skeletal* Radiol *2003:32:209-222.*

3 Chan LP, Gee R, Keogh C, Munk PL. Imaging features of fat necrosis. *AJR AmJRoentgenol* 2003;181:955-959.

4 Chatterton BE, Menforth D, Coventry BJ, Cohen P. Hibernoma: intense uptake seen on Tc-99 m tetrofosmin and FDG positron emission tomographic scanning. *Clin Nud Med* 2002;27:369-370.

5 Das Gupta TK, Chaudhuri PK. Pathology of soft tissue sarcoma. In: Das Gupta TK, Chaudhuri PK, eds. *Tumors of the Soft Tissues* 2nd ed. Stamford, Conn: Appleton & Lange; 1998:63-200.

6 Das Gupta TK, Chaudhuri PK. Tumors of the adipose tissue. In: Das Gupta TK, Chaudhuri PK, eds. *Tumors of the Soft Tissues* 2nd ed. Stamford, Conn: Appleton & Lange; 1998:250-251.

7 Delia Volpe C, Salazard B, Casanova D, Vacheret H, Bartoli JF, Magalon G. Hibernoma of the antero-lateral thigh. *Br J Plast Surg* 2005; 58:859-861.

8 Forest M. Lipoma and liposarcoma. In: Forest M, Tomeno B, Vanel D, eds. *Orthopedic Surgical Pathology: Diagnosis of Tumors and Pseudotumoral Lesions of Bone and Joints.* Edinburgh: Churchill Livingstone; 1998:335-343.

9 Furlong MA, Fanburg-Smith JC, Miettinen M. The morphologic spectrum of hibernoma, a clinicopathologic study of 170 cases. *AmJSurg Pathol* 2001;25:809-814.

10 Gaskin CM, Helms CA. Lipomas, lipoma variants, and well-differentiated liposarcomas (atypical lipomas): results of MRI evaluations of 126 consecutive fatty masses. *AJR Am J Roentgenol* 2004;182: 733-739.

11 Hosono M, Kobayashi H, Fujimoto Y, et al. Septum-like structures in lipoma and liposarcoma: MR imaging and pathologic correlation. *Skeletal Radial* 1997;26:150-154.

12 Huvos AG. Miscellaneous tumors of soft tissue and bone. In: Huvos AC, ed. *Bone Tumors: Diagnosis, Treatment, and Prognosis* 2nd ed. Philadelphia, Pa: W.B. Saunders; 1991:713-766.

13 Kallas KM, Vaughan L, Haghighi P, Resnick D. Hibernoma of the left axilla; a case report and review of the literature. *Skeletal Radial* 2003;32:290-294.

14 Kindblom LG, Meis-Kindblom JM, Mandahl N. Chondroid lipoma. In: Fletcher CDM, Unni KK, Mertens F, eds. *World Health Organization Classification of Tumours. Pathology and Genetics of Tumours of Soft Tissue and Bone* Geneva: IARC Press; 2002:30.

15 Kransdorf MJ, Bancroft LW, Peterson JJ, Murphey MD, Foster WC, Temple HT. Imaging of fatty tumors: distinction of lipoma and well-differentiated liposarcoma. *Radiology* 2002;224:99-104.

16 Kransdorf MJ, Moser RPJr, Meis JM, Meyer CA. From the Archives of the AFIP _ Fat-containing soft-tissue masses of the extremities. Ra*diographics* 1991;11(1):81-106.

17 Kransdorf MJ, Murphey MD. Lipomatous tumors. In: *Imaging of Soft Tissue Tumors* 2nd ed. Philadelphia, Pa: W.B. Saunders; 2006:80-149.

18 Kransdorf MJ, Murphey MD. Soft tissue tumors in a large referral population: prevalence and distribution of diagnoses by age, sex, and location. In: *Imaging of Soft Tissue Tumors* 2nd ed. Philadelphia, Pa: W.B. Saunders; 2006:6-37.

19 Kransdorf MJ. Benign soft-tissue tumors in a large referral population: distribution of specific diagnoses by age, sex, and location. *AJR AmJRoentgenol* 1995:164:395-402.

20 Logan PM, Janzen DL, O'Connell JX, Munk PL, Connell DC. Chondroid lipoma: MRI appearances with clinical and histologic correlation. *Skeletal Radial* 1996;25:592-595.

21 Matsumoto K, Hukuda S, Ishizawa M, Chano T, Okabe H. MRI findings in intramuscular lipomas. *Skeletal Radial* 1999:28:145-152.

22 Meyer JS, Dormans JP. Differential diagnosis of pediatric musculoskeletal masses. *Magn Reson Imaging Clin NAm* 1998;6(3): 571-572.

23 Miettinen MM, Fanburg-Smith JC, Mandahl N. Hibernoma. In: Fletcher CDM, Unni KK, Mertens F, eds. *World Health Organization Classification of Tumours. Pathology and Genetics of Tumours of Soft Tissue and Bone* Geneva: IARC Press; 2002:33-34.

24 Miettinen MM, Fanburg-Smith JC, Mandahl N. Spindle cell lipoma / pleomorphic lipoma. In: Fletcher COM, Unni KK, Mertens F, eds. *World Health Organization Classification of Tumours. Pathology and Genetics of Tumours of Soft Tissue and Bone* Geneva: IARC Press; 2002:31-32.

25 Mulder JD, Schutte HE, Kroon HM, Taconis WK. Introduction. In: *Radiologic Atlas of Bone Tumors* Amsterdam: Elsevier; 1993:3-6.

26 Mulder JD, Schutte HE, Kroon HM, Taconis WK. The diagnosis of bone tumors. In: *Radiologic Atlas of Bone Tumors* Amsterdam: Elsevier; 1993:9-46.

27 Mulder JD, Schutte HE, Kroon HM, Taconis WK. Lipoma. In: *Radiologic Atlas of Bone Tumors* Amsterdam: Elsevier; 1993:551-553.

28 Murphey MD, Carroll JF, Flemming DJ, Pope TL, Gannon FH, Kransdorf MJ. Benign musculoskeletal lipomatous lesions. *Radiographics* 2004:24:1433-1466.

29 Nielsen GP, Mandahl N. Lipoma. In: Fletcher COM, Unni KK, Mertens F, eds. *World Health Organization Classification of Tumours. Pathology and Genetics of Tumours of Soft Tissue and Bone* Geneva: IARC Press; 2002:20-22.

30 Ohguri T, Aoki T, Hisaoka M, et al. Differential diagnosis of benign peripheral lipoma from well-differentiated liposarcoma on MR imaging: is comparison of margins and internal characteristics useful? *AJR Am J Roentgenol* 2003;180:1689-1694.

31 Propeck T, Bullard MA, Lin J, Martel W. Radiologic-pathologic correlation of intraosseous lipomas. *AJR Am J Roentgenol* 2000;175: 673-678.

32 Roberts CC, Liu PT, Colby TV. Encapsulated versus nonencapsulated superficial fatty masses: a proposed MR imaging classification. *AJR Am] Roentgenol* 2003; 180:1419-1422.

33 Unni KK. Introduction and scope of study. In: *Dahlin's Bone Tumors-General Aspects and Data on IT 087 Cases* 5th ed. Philadelphia, Pa: Lippincott, Williams & Wilkins; 1996:1-9.

34 Unni KK. Lipoma and liposarcoma In: *Dahlin's Bone Tumors—General Aspects and Data on 11087 Cases* 5th ed. Philadelphia, Pa: Lippincott, Williams & Wilkins, 1996:349-353.

A 44 Liposarcoma

ICD-OCode

Well-differentiated: 8851/3

Myxoid: 8852/3

Pleomorphic: 8854/3

Dedifferentiated: 8858/3

Round cell: 8853/3

Definition

Liposarcomas are malignant mesenchymal tumors containing portions showing differentiation into adipose tissue.[1,56,15,19] Liposarcomas are classified into five subtypes: well-differentiated (40-54 %), myxoid (23 %), pleomorphic (5-7 %), dedifferentiated (10%), and round cell (6%).[1,5,6,19,25]

Frequency of Occurrence

Liposarcomas represent ~ 14 % of malignant soft tissue tumors and 6 % of all soft tissue tumors.[16,18] Liposarcomas are the second most frequent sarcomas involving soft tissues in adults.[15] Primary liposarcoma in bone is very rare, with less than 40 reported cases in the literature.[8,11,20-22]

Age at Presentation

Soft tissue: from 18 to 78 years, mean = 47 years.[17] Liposarcoma is rare in children.[17]

- **Well-differentiated liposarcoma:** from 39 to 77 years, mean = 50 years.[18]
- **Myxoid liposarcoma:** from 18 to 67 years, mean = 42 years.[18]
- **Pleomorphic liposarcoma:** from 41 to 78 years, mean = 60 years.[18]
- **Dedifferentiated liposarcoma:** from 42 to 78 years, mean = 63 years.[18]
- **Round cell liposarcoma:** from 30 to 64 years, mean = 43 years.[18]

Bone: from 5 to 57 years, median = 31 years.[22]

Gender Ratio (M / F)

Well-differentiated liposarcoma: 1.4/1.[18]

Myxoid liposarcoma: 1.3 /1.[18]

Pleomorphic liposarcoma: 1 /1 to 1.5 /1.[18,19]

Dedifferentiated liposarcoma: 1.1 /1.[18]

Round cell liposarcoma: 1.6/l.[18]

Location

Liposarcomas typically occur in the soft tissues and rarely as primary tumors within bone.[22,30]

Soft tissue:

- **Well-differentiated liposarcoma.** Tumors are located in the lower extremity > retroperitoneum > trunk > hip and buttocks > trunk > proximal limb girdle > upper extremity > head and neck.[18] Liposarcomas in the extremities are commonly located in the deep intermuscular or periarticular planes, and occasionally in the subcutaneous soft tissues.[3]
- **Myxoid liposarcoma.** Tumors are located in the lower extremity > hip and buttocks > retroperitoneum > trunk > proximal limb girdle, foot and ankle > head and neck.[18]
- **Pleomorphic liposarcoma.** Tumors are located in the lower extremity (mostly thigh) > internal trunk > hip and buttocks > upper extremity > thoraco-abdominal wall.[9,18]
- **Round cell liposarcoma.** Tumors are located in the lower extremity > hip and buttocks > retroperitoneum, trunk, foot and ankle > other sites.[18]
- **Dedifferentiated liposarcoma.** Tumors are located in the retroperitoneum > lower extremity > hip and buttocks > trunk.[18]

Bone. Tumors have been reported in the humerus, femur, tibia, pelvic bones, and fibula.[22,31]

Signs and Symptoms

Soft tissue Liposarcomas in the extremities are often painless, palpable lesions.[1,5,6,9] Pain associated with lesions may occur in less than 15% of patients.[15] Liposarcomas are usually detected earlier in the extremities than retroperitoneum.[15] Pleomorphic liposarcomas often present as enlarging, firm, mass lesions.[19]

Cross Pathologic Findings

Liposarcomas of soft tissues tend to be larger lesions than lipomas. Liposarcomas have been reported to have an average largest dimension of 23.5 cm compared with 12.5 cm for lipomas.[13] Liposarcomas often appear as circumscribed tumors with a pseudocapsule. These tumors can have varying degrees of yellow, white or red coloration. Thick, fibrous septa often divide the tumors into small lobules. Recurrent liposarcomas often have indistinct margins.[3] Myxoid, pleomorphic, round cell, and dedifferentiated types of liposarcoma may have little or no evidence of fat on gross evaluation.[1,6,19] Dedifferentiated liposarcomas often show necrosis.[6] Pleomorphic liposarcomas are large, median = 10 cm, and often contain myxoid zones and/or regions of necrosis.[19]

Histopathologic Findings

Liposarcomas of soft tissues are typically subdivided into five types: well-differentiated, myxoid pleomorphic, myxoid, dedifferentiated, and round cell. In the extremities, well-differentiated liposarcomas account for 40-51 % of occurrences, myxoid

for 30 %, pleomorphic for 8 %, round cell for 8 %, and dedifferentiated for 3 %.[1,5,6,17,19] In the retroperitoneum, the well-differentiated type is more common than the pleomorphic type."

Well-differentiated liposarcomas are slow-growing tumors that rarely metastasize.[3,5] These liposarcomas can mimic lipomas grossly, but microscopically have thicker and more numerous fibrous septae containing fibroblastic spindle cells, atypical cells, and vacuolated lipoblasts surrounding variously sized lobules of fat.[5,24] Fat cells have nuclear atypia, and hyperchromatic stromal cells are seen in fibrous septa.[5] Monovacuolated and multivacuolated lipoblasts are often seen.[5] Adipocytic cells are immunoreactive to S 100 protein.[5]

Myxoid liposarcomas are composed of proliferating stellate and/or fusiform lipoblasts in varying stages of differentiation, signet cells containing lipids, variable myxoid matrix (mucopolysaccharide ground substance), and plexiform capillary network.[3] Mitotic activity is usually low. Osseous, cartilaginous and/or leiomyomatous metaplasia may occur in these tumors.[3] Fat content is usually less than 10-25% of tumor volume.[27] Tumor cells are usually immunoreactive to S 100 protein and aP2 protein (adipocyte lipid-binding protein).[1,33]

Pleomorphic liposarcomas contain various combinations of lipogenic and non-lipogenic zones.[9,19] The latter often have features similar to malignant fibrous histiocytoma, round cell liposarcoma, and/or epithelioid carcinoma.[9,19] These tumors have prominent cellular pleomorphism and contain varying proportions of malignant pleomorphic lipoblasts, pleomorphic spindle cells, and occasional giant cells which may or may not contain single or multiple lipid droplets.[3,7,9,19] Mitoses are common.[7,9,19] Variable degrees of necrosis are seen.[7,9,19] These tumors often have a disordered or storiform growth pattern in a myxoid stroma with a branching capillary network.[3,7,9,19] Most have infiltrative borders microscopically.[9] These tumors are immunoreactive to vimentin, and occasionally to S 100 protein.[19]

Round cell liposarcomas are composed of relatively uniform, small round cells with single naked round or slightly oval nuclei and scarce cytoplasm containing vacuoles with minimal intracellular lipid.[3,32,33] Tumor cells are often within a myxoid matrix, and are typically are not arranged in patterns.[3,32] Mitotic activity is often low.[3] Round cell liposarcomas have been considered to represent poorly differentiated myxoid liposarcomas.[7] Tumor cells are usually immunoreactive to S 100 protein and aP2 protein (adipocyte lipid-binding protein).[1,33]

Dedifferentiated liposarcomas occur most frequently in the retroperitoneum and are typically composed of two histologic types of liposarcoma: well-differentiated and poorly differentiated.[3,6,25] The poorly differentiated component is usually a high-grade sarcoma with histologic features that can often resemble malignant fibrous histiocytoma, fibrosarcoma, myofibrosarcoma, osteosarcoma, and/or chondrosarcoma.[6,25,28]

Tumor Genetics

Well-differentiated liposarcoma. These tumors have been reported to have ring and giant chromosomes which contain amplification of 12ql4-15 which includes the MDM2 gene.[5] Other sites amplified in these tumors include 12q21-22 and lq21-25.[5]

Myxoid liposarcoma. More than 90 % of myxoid liposarcomas have a translocation, [t(12;16)ql3;pll)], which results in the fusion of the DDIT3 gene at 12ql3 with the FUS gene at 16pll.[1,33] The DDIT3/FUS gene fusion is specific for myxoid and round cell liposarcomas.[1,33] Occasionally, another translocation, t(12;22)(ql3:q12), has been reported which results in fusion of the DDIT3 gene at 12 q13 with the EWS gene.[1,32]

Pleomorphic liposarcoma. These tumors show high chromosome counts and various chromosomal rearrangements, as well as ring, giant, and double-minute chromosomes.[19] Mutations involving the TP53 gene have been reported.[19]

Dedifferentiated liposarcoma. These tumors often have ring or giant chromosomes.[6] Amplification of 12 q!3-21 regions have been reported as well as MDM 2 and TP53 gene mutations[6]

Round cell liposarcoma. Most round cell liposarcomas have a translocation, [t(12;16)ql3;pll)], which results in the fusion of the DDIT3 gene at 12ql3 with the FUS gene at 16pll.[33] The DDIT3/FUS gene fusion is specific for myxoid and round cell liposarcomas.[1,33]

Findings on Plain Films (Roentgenograms) and Computed Tomography

Soft tissue. Liposarcomas can be occasionally seen on plain films as soft tissue masses, with or without zones of lower attenuation compared with adjacent muscles[25] (Figs. **264, 267).** On CT, liposarcomas often have zones with attenuation comparable to subcutaneous fat[25] (Fig. **264).** Thick septae and/or nodular zones with soft tissue attenuation are often seen in well-differentiated liposarcomas. Myxoid, pleomorphic, round cell, and dedifferentiated types of liposarcoma may have little or no fat visible on CT. Calcifications can occur in up to 30 % of dedifferentiated liposarcomas, and may be associated with zones of metaplasia (fibrosarcoma, myofibrosarcoma, osteosarcoma, chondrosarcoma).[25,28] Calcifications are uncommon in the other types of liposarcomas, occurring in up to 15%.[2S]

Bone. Liposarcomas involving bone are often radiolucent, intramedullary lesions that can have well-defined or poorly-defined margins associated with cortical thinning or destruction, lamellar periosteal reaction, and/or Codman triangle[22] (Fig. **262).**

MRI Findings

Soft tissue:

- **Well-differentiated liposarcoma.** MRI features commonly seen with these tumors include up to 75 % overall fat signal, thick nonadipose septae, and/or nodular non-adipose zones.[13,23-25] Thick septa or nodular, and/or patchy, nonadipose zones are more frequent in retroperitoneal and intermuscular or intra muscular tumors compared with those in subcutaneous locations.[24] The nonadipose zones can have low-intermediate signal on T1WI and PDWI; and low, intermediate, and/or high signal on T2WI (Fig. **263).** Tumor margins are usually smooth, well-defined, and/or tabulated.[2,23,24] MRI is useful for determining whether there is tumor invasion of neurovascular structures. After Gd-contrast administration, nonadipose portions of these tumors can show varying degrees of enhancement.[2,10,13,23,24]
  MRI features that are more commonly associated with well-differentiated liposarcomas than lipomas include male gen-

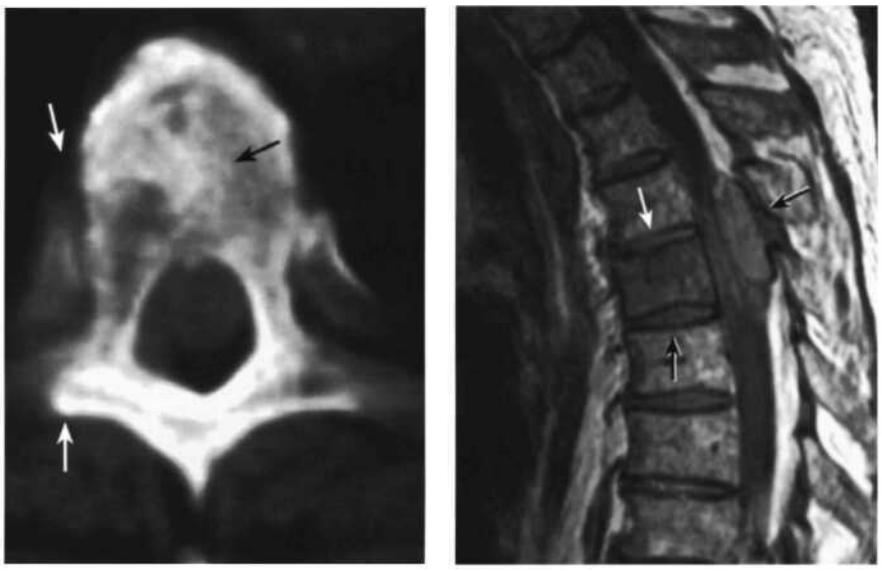

a, b

c, d

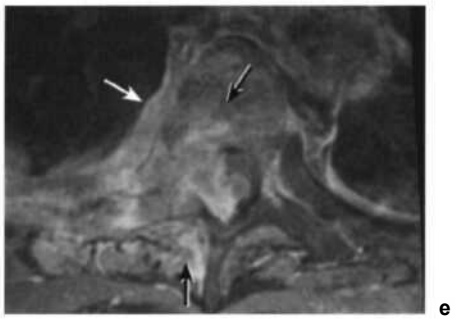

e

Figure **262a-e** An 81-year-old man with a pleomorphic liposarcoma involving the T4 vertebral body, right pedicle, right transverse process and right lamina. Axial CT image (**a**) shows an irregular radiolucent lesion in the right side of the vertebral body and right pedicle associated with irregular, marginal, sclerotic-bone reaction within the vertebral body. The tumor has heterogeneous low-intermediate signal on sagittal T1WI (**b**), and mixed intermediate and slightly high signal on sagittal T2WI (**c**). The tumor shows heterogeneous slightly prominent Cd-contrast enhancement on sagittal (**d**) and axial (**e**) FST1WI, and is associated with cortical bone destruction, extra-osseous tumor extension, and spinal cord compression.

der, large tumor size, and presence of Gd-contrast enhancing nonadipose, thick septa, or nodular/patchy zones.[2,13,24]

- **Myxoid liposarcoma.** These tumors usually have predominantly low signal on T1WI, and may contain smaller proportions of high signal in lacy, amorphous, and/or linear configurations secondary to fatty components[2,15,27] (Figs. **265, 266, 268, 269).** Approximately 90% of myxoid liposarcomas have tumor volumes which contain less than 26 % fat seen with MRI.[12] It has also been reported that up to 60 % of myxoid liposarcomas do not contain fatty zones evident on Tl WI.[12,27] These tumors can have heterogeneous or homogeneous high signal on PDWI and T2WI; some have a multiloculated pattern. Low signal septa may be present on T2WI. After Gd-contrast administration, these tumors typically show enhancement in varying degrees and patterns.[2,27] On rare occasions, these tumors may show no enhancement.[27] Tumors margins are often circumscribed with well-defined margins.[2,27] Recurrent tumors show enhancement 1 to 3 minutes after Gd-contrast administration, enabling distinction from seromas and hygromas which do not enhance.[27]
- **Pleomorphic liposarcoma.** These tumors often have well-defined or relatively well-defined margins, and have heterogeneous/mixed low, intermediate and/or high signal on T1WI, PDWI, and T2WI[2,12] (Fig. **264).** Typically, less than 26% of the tumor volumes of pleomorphic liposarcomas have fat signal.[12] After Gd-contrast administration, these tumors usually show prominent enhancement in a heterogeneous pattern[212]
- **Round cell liposarcoma.** These tumors can have relatively well-defined margins (72%) or poorly defined margins (28%), and have heterogeneous/mixed low, intermediate and/or high signal on T1WI, PDWI, and T2WI.[12,29] Approximately 90 % of round cell liposarcomas have tumor volumes which contain less than 26 % of fat seen with MRI.[12] After Gd-contrast administration, these tumors usually show prominent enhancement (61 %) in a heterogeneous pattern that may be globular or nodular.[12,29]
- **Dedifferentiated liposarcoma.** These tumors typically have a component with features of a well-differentiated liposarcoma as well as a focal nonlipomatous mass.[14,25] Dedifferentiated liposarcomas most frequently occur in the retroperitoneum and are large (mean =19.3 cm).[28] These tumors can have well-defined, relatively well-defined, and/or irregular/poorly defined margins.[25] Ninety percent have a lobu-

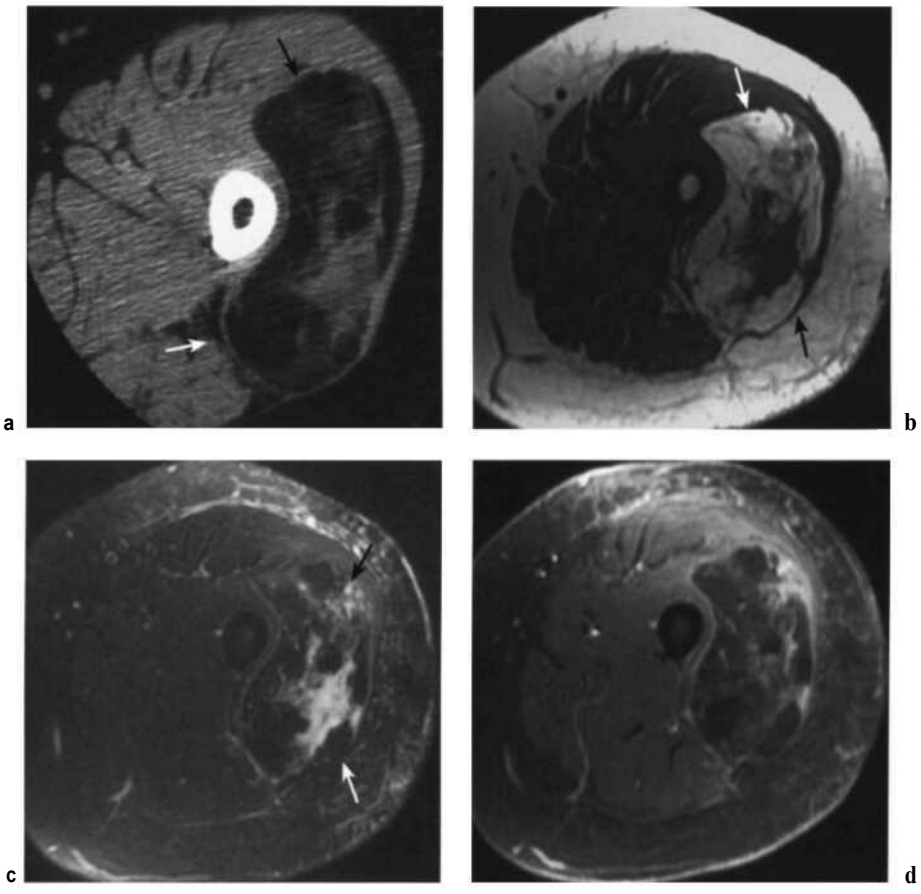

Figure **263a-d** A 57-year-old woman with a well-differentiated, low-grade liposarcoma involving the vastus lateralis muscle of the thigh. Axial CT image (**a**) shows the tumor to have circumscribed margins, and contains fat attenuation as well as thick irregular zones with intermediate soft tissue attenuation. The tumor has high fat signal on axial T1WI (**b**) as well as zones with low-intermediate signal. The nonfatty portions of the tumor have high signal on axial FST2WI (**c**), and show Gd-contrast enhancement on axial FST1WI(**d**).

lated morphology.[28] Variable percentages of fat are seen in these neoplasms. These tumors often have heterogeneous/mixed low, intermediate and/or high signal on T1WI, PDWI, and T2W1 (Fig. **267).** Hemorrhage and necrosis can be seen in the nonlipomatous portions.[25] After Gd-contrast administration, these tumors often show prominent enhancement in nonlipomatous portions in a heterogeneous or homogeneous pattern.[28]

Bone. Liposarcomas in bone can have intermediate and/or slightly high to high signal on T1WI and T2WI[23] (Fig. **262).** Tumors often show Gd-contrast enhancement[23] (Fig. **262).**

Differential Diagnosis

Lipoma, atypical lipoma, chondroid lipoma, hemangioma, muscle infarct, postradiation injury, deinnervation injury, lipomatosis.

For **myxoid, dedifferentiated, pleomorphic,** and **round cell liposarcomas:** malignant fibrous histiocytoma, synovial sarcoma, rhabdomyosarcoma, leiomyosarcoma, extraskeletal myxoid chondrosarcoma atypical lipoma, metastatic lesion, lymphoma, seromas, hygromas, epidermoid cyst, ganglion, intramuscular myxoma, fat necrosis.

Prognosis and Treatment

Well-differentiated liposarcomas. These tumors are usually treated with surgery with wide margins because of the high potential for local recurrence.[4,5,24] Metastatic disease is uncommon for this type of liposarcoma.[5,26] Liposarcomas in the retroperitoneum have a higher recurrence rate than those located in the extremities.[5,15] Amputation may be necessary is some extremity cases, particularly when there is evidence of tumor invasion of adjacent neurovascular structures.[4,12] The 5-year survival rate ranges from 83 to 90 % of patients.[4,26] The mortality rate for liposarcomas in the retroperitoneum is much higher than for tumors in the extremities.[5] Up to 80 % of patients with liposarcomas in the retroperitoneum die 10 to 20 years after diagnosis, with the median time to death between 6 and 11 years.[5]

Myxoid liposarcoma. These tumors are usually treated by surgery with wide margins.[4] The local recurrence rate for low-grade myxoid liposarcomas is 11 % and the 5-year survival ranges from 80 to 90 % of patients.[4,26] Adjuvant radiation has been beneficial.[4] Adverse outcomes are related to the presence of high histologic grade, necrosis, and overexpression of TP53.[1]

Pleomorphic liposarcoma. These tumors are considered high-grade sarcomas and frequently metastasize, most commonly to the lungs.[4,7,9,1,9,25,26] Treatment consists of surgery with neo-adjuvant or postoperative radiation and/or chemotherapy. The 5-year local recurrence and metastasis-free rates are 48% and 50 %, respectively.[9] The 5-year survival rate has been reported to range between 30 and 57 % of patients.[4,7,9,25,26] Factors associated with poor prognosis include patient age over 60 years, tumor size greater than 5 cm, truncal tumor location, tumor necrosis, more than 20 mitoses per high-power field, evidence of vascular invasion, and incomplete tumorectomy.[9,19]

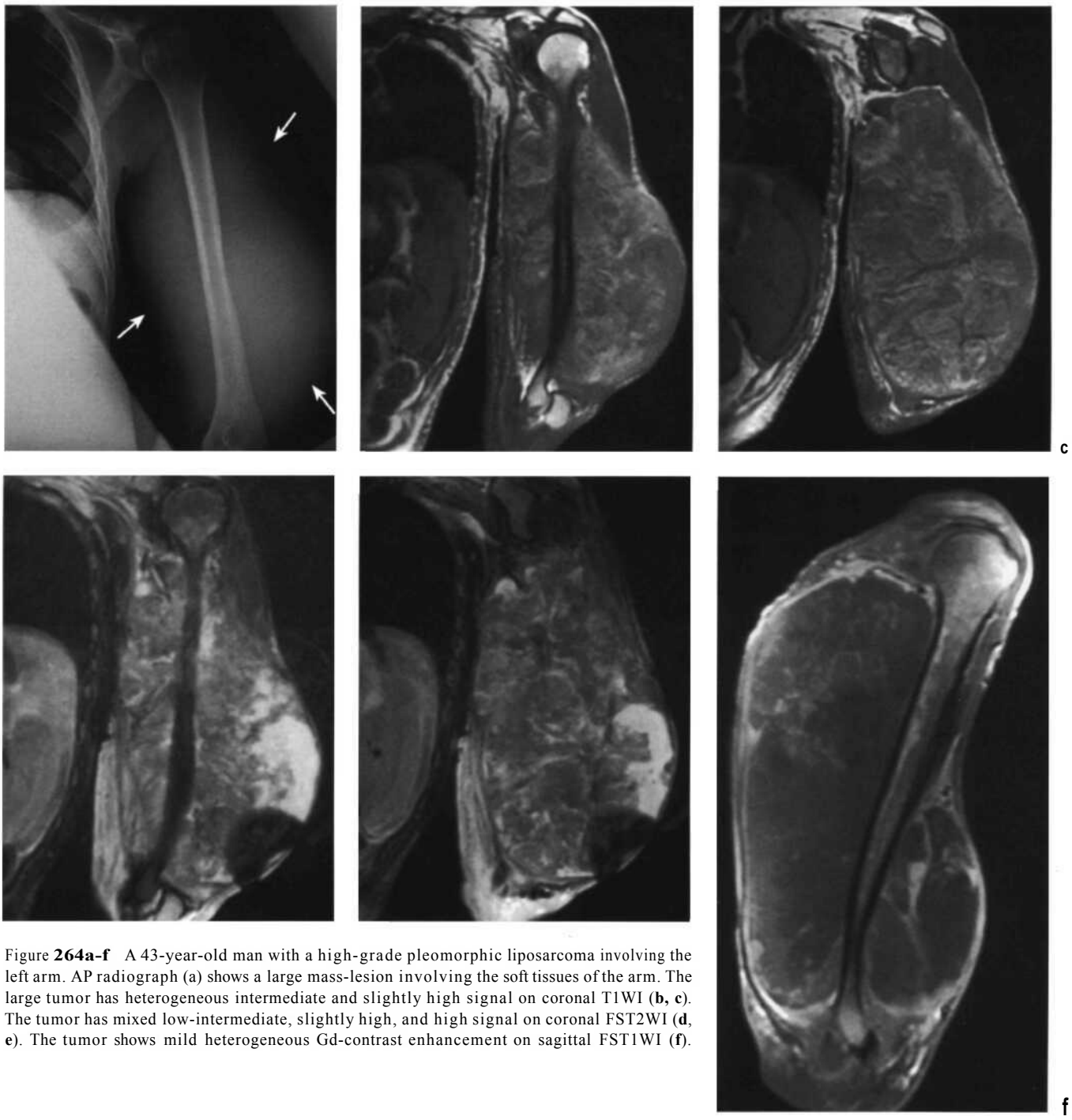

Figure **264a-f** A 43-year-old man with a high-grade pleomorphic liposarcoma involving the left arm. AP radiograph (a) shows a large mass-lesion involving the soft tissues of the arm. The large tumor has heterogeneous intermediate and slightly high signal on coronal T1WI (**b, c**). The tumor has mixed low-intermediate, slightly high, and high signal on coronal FST2WI (**d**, **e**). The tumor shows mild heterogeneous Gd-contrast enhancement on sagittal FST1WI (**f**).

Round cell liposarcoma. MRI findings associated with intermediate and high tumors include large tumor sizes of > 10cm, irregular tumor margins, absence of tumor capsule, presence of internal thick septa, and prominent globular or nodular Gd-contrast enhancement patterns.[29] Thin tumor capsules and thin internal septa are features usually associated with low-grade tumors.[29] These tumors are usually treated by surgery with wide margins.[4] The local recurrence rate ranges from 10 to 33% and the 5-year survival ranges from 25 to 80% of patients.[4,26,29]Patients with intermediate grade or high-grade lesions have a poorer prognosis than those with low-grade types.[29] Metastases can occur in up to 31 % of cases and have been reported in the peritoneal cavity, lung, bone, liver, retroperitoneum, and mediastinum.[29] Adjuvant radiation has been beneficial for some patients.[4]

Dedifferentiated liposarcoma. These tumors occur more frequently in the retroperitoneum than the extremities.[15] Treatment consists of surgery with neo-adjuvant or postoperative radiation and/or chemotherapy. Local recurrence occurs in 40 % of patients and metastatic disease occurs in 20 %.[6,15] For retroperitoneal dedifferentiated liposarcomas, the local recurrence rate was 83% and the metastatic rate was 30% at 3 years.[26] These patients usually have a poor prognosis.[15] Dedifferentiated liposarcoma is associated with a 6-fold increased risk of death compared with the well-differentiated type.[26] Mortality at *5* years is 30 %.[6]

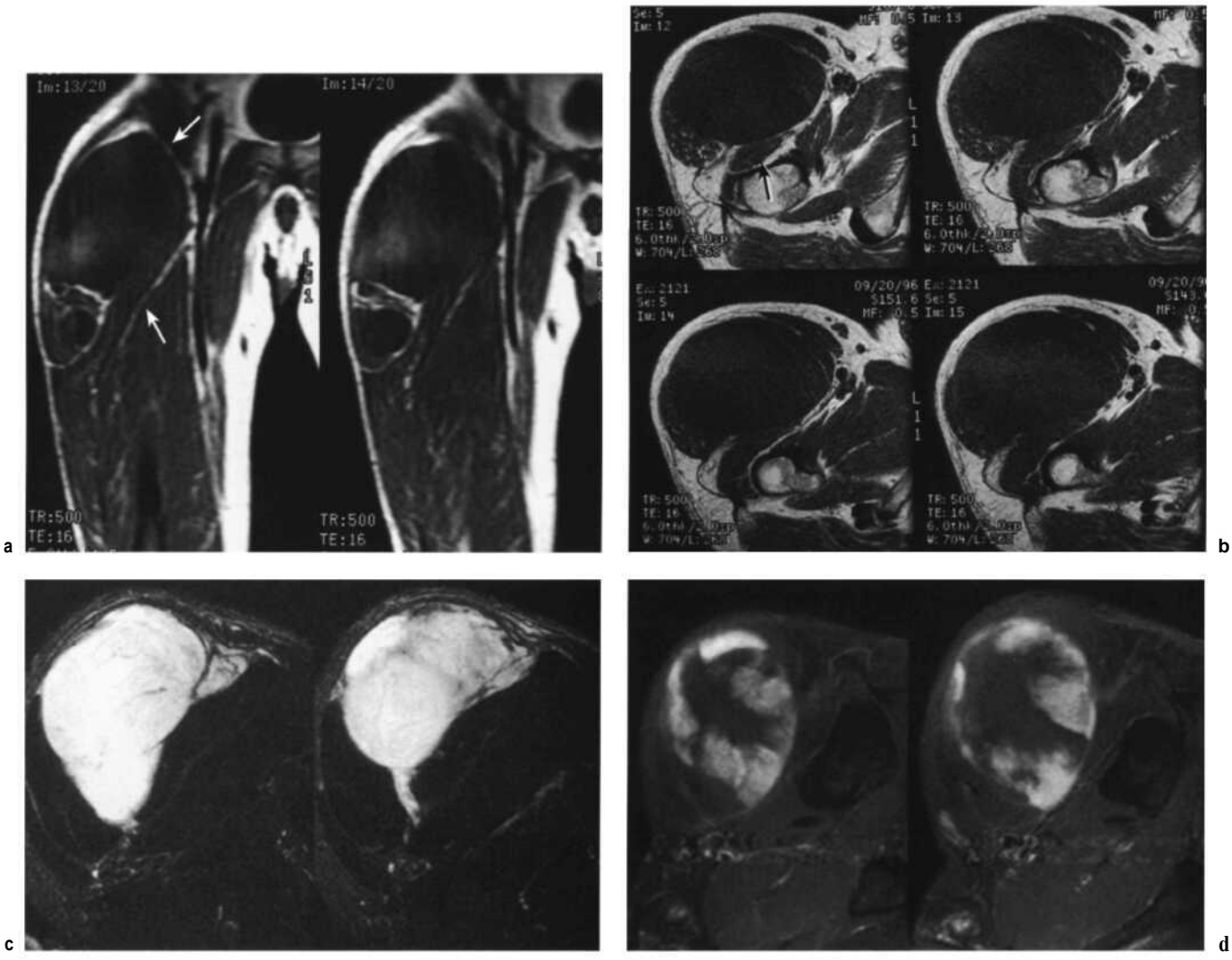

Figure **265 a-d** A 48-year-old man with a myxoid liposarcoma involving the upper thigh. This tumor has circumscribed margins and contains mostly low-intermediate signal as well as several small zones of high fat signal on coronal (**a**) and axial (**b**)T1WI. Most of the tumor has high signal on axial (**c**) FST2WI secondary to the myxoid regions. The signal from the small zones of fat is suppressed on sagittal FST2WI. The tumor shows heterogeneous Cd-contrast enhancement on axial (**d**) FST1WI.

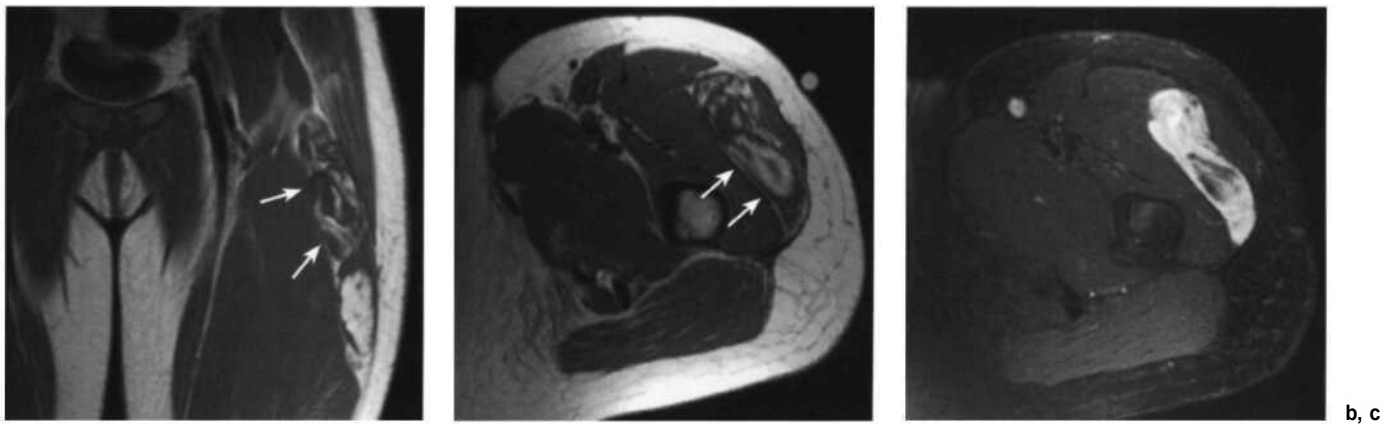

Figure **266a-c** A 13-year-old female with a myxoid liposarcoma involving the vastus lateralis muscle in the upper thigh. This tumor has circumscribed margins and contains both low-intermediate signal and high fat signal on coronal (**a**) and axial (**b**) T1WI. The signal from the small zones of fat signal is suppressed on axial FST2WI (**c**), whereas most of the tumor has high signal from the myxoid components.

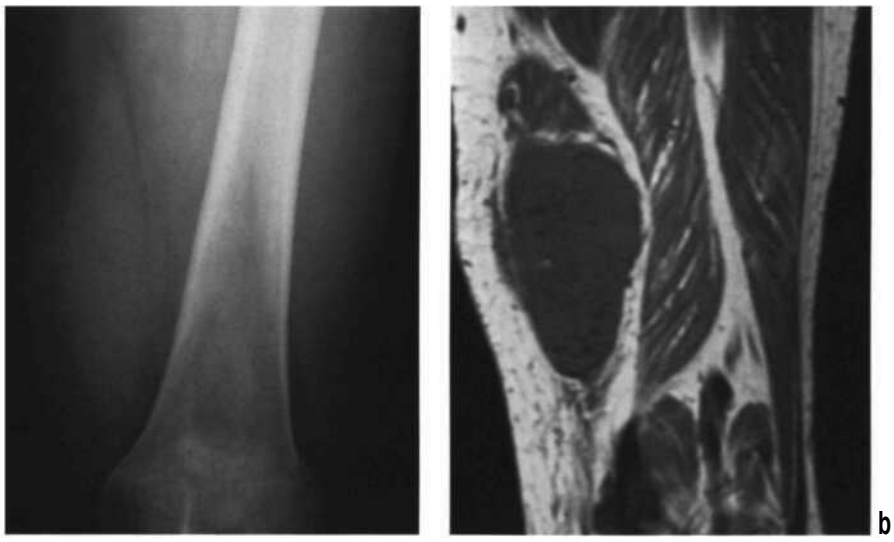

a b

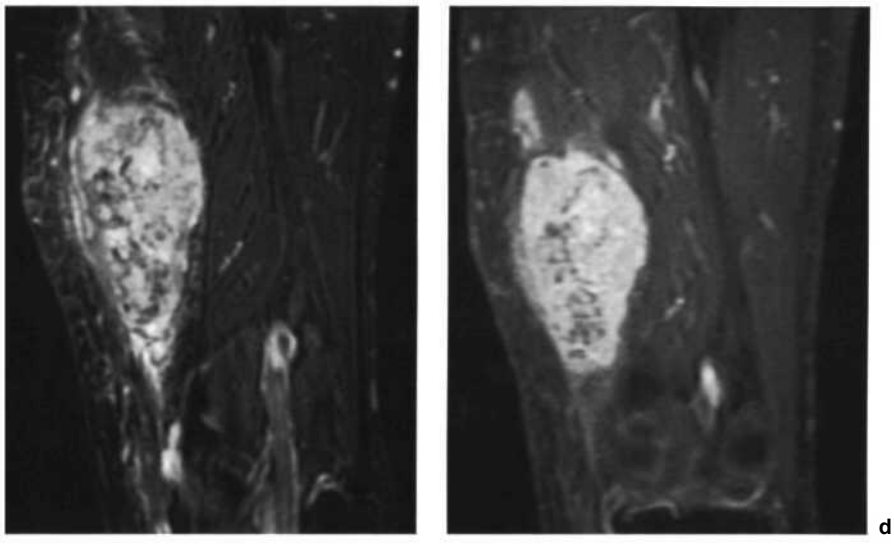

c d

Figure **267 a-c** A 71-year-old woman with a dedifferentiated liposarcoma in the distal thigh. AP radiograph (**a**) shows a large mass-lesion involving the soft tissues of the medial posterior distal thigh. The tumor has circumscribed margins and contains mostly low-intermediate signal on coronal (**b**) T1WI. Most of the tumor has high signal on coronal (**c**) FST2WI as well as small zones with low signal. The tumor shows prominent, slightly heterogeneous Gd-contrast enhancement on coronal (**d**) FST1WI.

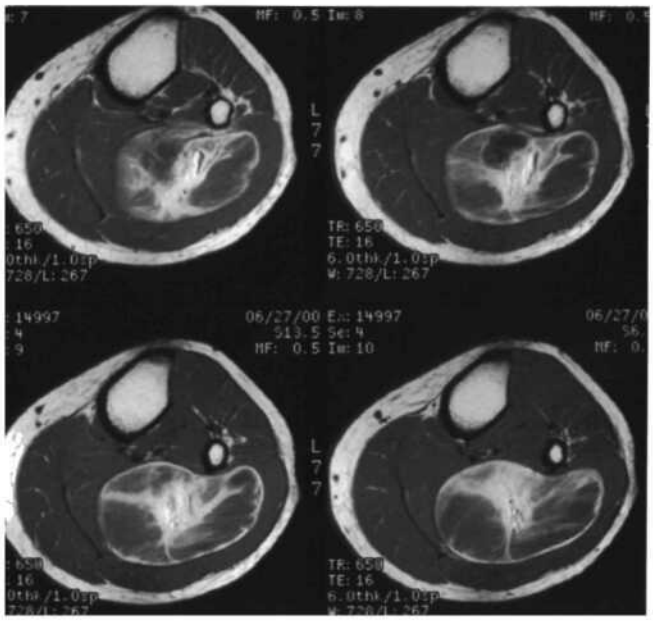

a

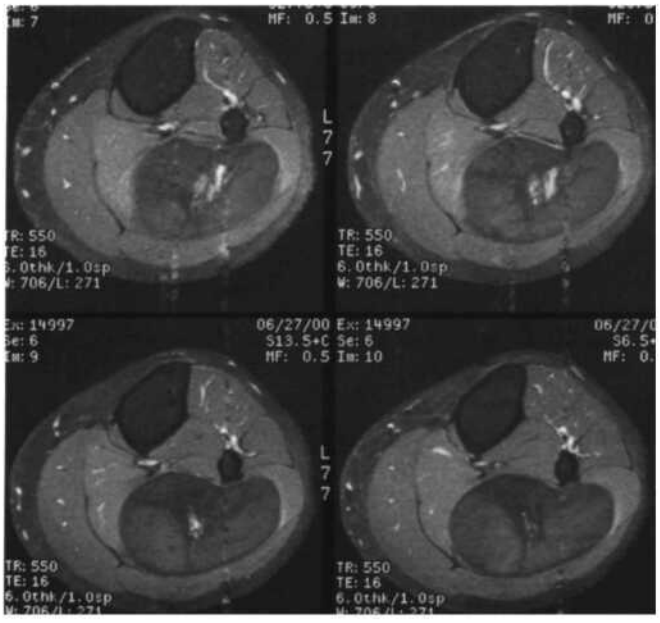

b

Figure **268a, b** A 34-year-old man with a myxoid liposarcoma involving the gastrocnemius muscles in the calf. The tumor has circumscribed margins and contains zones with low-intermediate signal as well as irregular zones of high fat signal on axial T1WI (a). The signal from the zones of fat is suppressed on axial FST1 Wl (**b**). Only a small central portion of the tumor shows Cd-contrast enhancement on axial FST1WI (**b**).

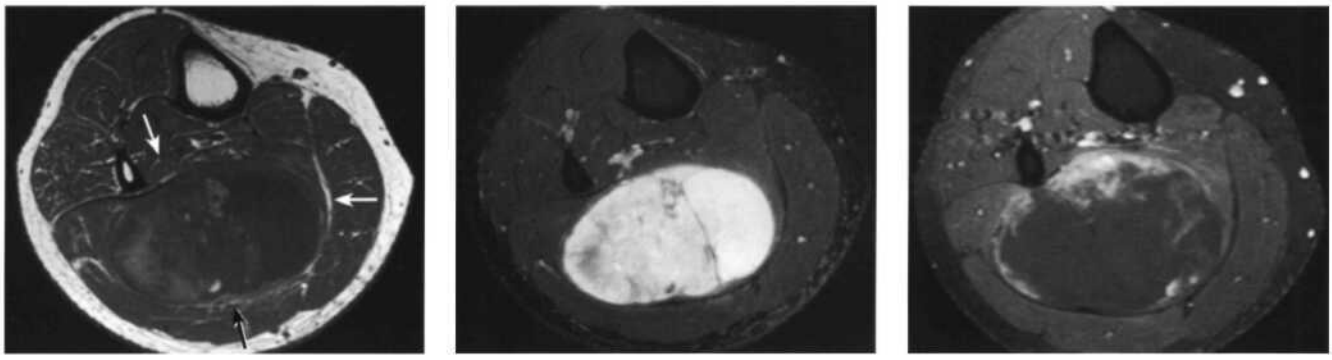

a b,c

Figure **269a-c** A 34-year-old woman with a myxoid liposarcoma in the posterior calf. The tumor has circumscribed margins and contains mostly low-intermediate signal on axial T1WI (a), as well as small irregular zones of high fat signal. Most of the tumor has high signal on axial FST2WI (**b**) secondary to the myxoid components. The signal from the zones of fat is suppressed on FST2WI. Only small portions of the tumor show Gd-contrast enhancement on axial FST1WI (**c**).

References

1 Antonescu C, Ladanyl M. Myxoid liposarcoma. In: Fletcher CDM, Unni KK, Mertens F, eds. *World Health Organization Classification of Tumours. Pathology and Genetics of Tumours of Soft Tissue and Bone* Geneva: IARC Press; 2002:40-43.

2 Arkun R, Memis A, Akalin T, Ustun EE, Sabah D, Kandiloglu G. Liposarcoma of soft tissue: MRI findings with pathologic correlation. *Skeletal Radial* 1997;26:167-172.

3 Chaudhuri B, Das Gupta TK. Pathology of soft tissue sarcoma. In: Das Gupta TK, Chaudhuri PK, eds. *Tumors of the Soft Tissues* 2nd ed. Stamford, Conn: Appleton & Lange; 1998:63-225.

4 Chaudhuri B, Das Gupta TK. Tumors of the adipose tissue. In: Das Gupta TK, Chaudhuri PK. *Tumors of the Soft Tissues* 2nd ed. Stamford, Conn: Appleton & Lange; 1998:229-263.

5 Dei Tos AP, Pedeutour F. Atypical lipomatous tumour / well-differentiated liposarcoma. In: Fletcher CDM, Unni KK, Mertens F, eds. *World Health Organization Classification of Tumours. Pathology and Genetics of Tumours of Soft Tissue and Bone* Geneva: IARC Press; 2002:35-37.

6 Dei Tos AP, Pedeutour F. Dedifferentiated liposarcoma. In: Fletcher COM, Unni KK, Mertens F, eds. *World Health Organization Classification of Tumours. Pathology and Genetics of Tumours of Soft Tissue and Bone* Geneva: IARC Press; 2002:38-39.

7 Downes KA, Goldblum JR, Montgomery EA, Fisher C. Pleomorphic liposarcoma: a clinicopathologic analysis of 19 cases. *Mod Pathol* 2001;14(3):179-184.

8 Forest M. Lipoma and liposarcoma. In: Forest M, Tomeno B, Vanel D, eds. *Orthopedic Surgical Pathology: Diagnosis of Tumors and Pseudotumoral Lesions of Bone and Joints* Edinburgh: Churchill Livingstone; 1998:335-343.

9 Gebhard S, Coindre JM, Michels JJ, et al. Pleomorphic liposarcoma: clinicopathologic, immunohistochemical, and follow-up analysis of 63 cases: a study from the French Federation of Cancer Centers Sarcoma Group. *AmJSurgPathol* 2002;26:601-616.

10 Hosono M, Kobayashi H, Fujimoto Y, et al. Septum-like structures in lipoma and liposarcoma: MR imaging and pathologic correlation. *Skeletal Radial* 1997;26:150-154.

11 Huvos AG. Miscellaneous tumors of soft tissue and bone. In: Huvos AC, ed. *Bone Tumors: Diagnosis, Treatment, and Prognosis* 2nd ed. Philadelphia, Pa: W.B. Saunders; 1991:713-766.

12 Jelinek JS, Kransdorf MJ, Shmookler BM, Aboulafia AJ, Malawer MM. Liposarcoma of the extremities: MR and CT findings in the histologic subtypes. *Radiology* 1993;186(2):455-459.

13 Kransdorf MJ, Bancroft LW, Peterson JJ, Murphey MD, Foster WC, Temple HT. Imaging of fatty tumors: distinction of lipoma and well-differentiated liposarcoma. *Radiology* 2002;224:99-104.

14 Kransdorf MJ, Meis JM, Jelinek JS. Dedifferentiated liposarcoma of the extremities: imaging findings in four patients. *AJR AmJ Roentgenol* 1993:161:127-130.

15 Kransdorf MJ, Moser RPJr, Meis JM, Meyer CA. From the Archives of the AFIP - Fat-containing soft-tissue masses of the extremities. *Radiographics* 1991;11(1):81-106.

16 Kransdorf MJ, Murphey MD. Soft tissue tumors in a large referral population: prevalence and distribution of diagnoses by age, sex, and location. In: *imaging of Soft Tissue Tumors* 2nd ed. Philadelphia, Pa: W.B. Saunders; 2006:6-37.

17 Kransdorf MJ, Murphey MD. Lipomatous tumors. In: Kransdorf MJ, Murphey MD, eds. *Imaging of Soft Tissue Tumors* 2nd ed. Philadelphia, Pa: W.B. Saunders; 2006:80-149.

18 Kransdorf MJ. Malignant soft-tissue tumors in a large referral population: distribution of diagnoses by age, sex, and location. *AJR Am] Roentgenol* 1995:164:129-134.

19 Mentzel T, Pedeutour F. Pleomorphic liposarcoma. In: Fletcher COM, Unni KK, Mertens F, eds. *World Health Organization Classification of Tumours. Pathology and Genetics of Tumours of Soft Tissue and Bone* Geneva: IARC Press; 2002:44-45.

20 Mulder JD, Schutte HE, Kroon HM, Taconis WK. Introduction. In: *Radiologic Atlas of Bone Tumors* Amsterdam: Elsevier; 1993:3-6.

21 Mulder JD, Schutte HE, Kroon HM, Taconis WK. The diagnosis of bone tumors. In: *Radiologic Atlas of Bone Tumors* Amsterdam: Elsevier; 1993:9-46.

22 Mulder JD, Schutte HE, Kroon HM, Taconis WK. Liposarcoma. In: *Radiologic Atlas of Bone Tumors* Amsterdam: Elsevier; 1993: 314-316

23 Murphey MD, Arcara LK, Farburg-Smith J. Imaging of musculoskeletal liposarcoma with radiologic-pathologic correlation. *Radiographics* 2005:25:1371-1395.

24 Ohguri T, Aoki T, Hisaoka M, et al. Differential diagnosis of benign peripheral lipoma from well-differentiated liposarcoma on MR imaging: is comparison of margins and internal characteristics useful? *AJR AmJ Roentgenol* 2003:180:1689-1694.

25 Peterson JJ, Kransdorf MJ, Bancroft LW, O'Connor MI. Malignant fatty tumors: classification, clinical course, imaging appearance and treatment. *Skeletal Radial* 2003:32:493-503.

26 Singer S, Antonescu C, Riedel E, Brennan MF. Histologic subtype and margin of resection predict pattern of recurrence and survival for retroperitoneal liposarcoma. *Ann Surg* 2003;238:358-371.

27 Sung MS, Kang HS, Suh JS, et al. Myxoid liposarcoma: appearance at MR imaging with histologic correlation. *Radiographics* 2000;20: 1007-1019.

28 Tateishi U, Hasegawa T, Beppu Y, Satake M, Moriyama N. Primary dedifferentiated liposarcoma of the retroperitoneum: prognostic significance of computed tomography and magnetic resonance imaging features. J *Comput Assist Tomogr* 2003;27:799-804.

29 Tateishi U, Hasegawa T, Beppu Y, Kawai A, Satake M, Moriyama N. Prognostic significance of MRI findings in patients with myxoid-round cell liposarcoma. *AJR Am J Roentgenol* 2004;182:725-731.

30 Unni KK. Introduction and scope of study. In: *Dahlin's Bone Tumors—General Aspects and Data on 11087 Cases* 5th ed. Philadelphia, Pa: Lippincott, Williams & Wilikins; 1996:1-9.

31 Unni KK. Lipoma and liposarcoma In: *Dahlin's Bone Tumors—General* .Aspects *and Data on 11087 Cases* 5th ed. Philadelphia, Pa: Lippincott, Williams & Wilkins; 1996:349-353.

32 Vicandi B, Jimenez-Hefferman J, Lopez-Ferrer P, Gonzalez-Peramato P, Viguer JM Cytologic features of round cell liposarcoma. A report on five patients. *Cancer* 2003:99:28-32 (Cancer Cytopathol).

33 Weiss SW, Goldblum JR. Liposarcoma In: Weiss SW, Goldblum JR, eds. *Enzinger and Weiss's Soft Tissue Tumors* 4th ed. St. Louis, Mo: Mosby; 2001:641 -693.

A 45

Liposclerosing Myxofibrous Tumor (Also Referred to as Polymorphic Fibro-osseous Lesion of Bone and Polymorphic Fibrocystic Disease of Bone)

Definition

Liposclerosing myxofibrous tumors are benign, fibro-osseous lesions that contain varying proportions with histologic features of lipoma, fibroxanthoma, myxoma, fibrous dysplasia, bone cyst, myxofibroma, fat necrosis, and/or ischemic ossification.[1-4] Most of these lesions occur in the intertrochanteric region of the femur.[1,3,4] Mutations involving the Arg-201 codon in exon 8 of the G-protein (guanine nucleotide-binding protein) a subunit are seen in these lesions as well as in fibrous dysplasia and McCune-Albright syndrome, suggesting that liposclerosing myxofibrous tumors represents a variant form of fibrous dysplasia.[2]

Frequency of Occurrence

These lesions are uncommon.

Age at Presentation

From 15 to 69 years, mean = 42 years.[1]

Gender (M f F)

1.2 /1.[1]

Location

Seventy-seven percent of these lesions are located in the intertrochanteric region of the femur.[1,3] Other sites include the femoral shaft (8%), iliac bone (8%), humerus (5%), and rib (2%).[1,2]

Signs and Symptoms

Approximately half of the patients with liposclerosing myxofibrous tumors present with pain ranging from weeks to l0 years in duration.[1] Pathologic fractures are seen in 10 %.[1,3] Forty-one percent of these lesions are detected as incidental findings on imaging studies.[1,3]

Cross Pathologic Findings

The appearance of these lesions is dependent on the proportions of components with features of lipoma, myxofibroma, fibroxanthoma (nonossifying fibroma), myxoma, fibrous dysplasia, bone cyst, Pagetoid changes, fat necrosis, ischemic ossification, and/or chondroma.[1,3,4]

Histopathologic Findings

Lesions contain a mixture of histologic elements including lipoma with or without mineralization, myxofibrous zones with or without curvilinear or woven bone ossicles, fibroxanthoma (nonossifying fibroma), myxoma, fibrous dysplasia, bone cyst, curvilinear ossicles with cement lines, fat necrosis with or without dystrophic calcifications, ischemic ossification, and/or chondroma.[1-4]

Lesion Genetics

Point mutations involving the Arg-201 codon in exon 8 of the G-protein a subunit were found for two cases of liposclerosing myxofibrous tumors.[2] Similar mutations are also seen in lesions of fibrous dysplasia and McCune-Albright syndrome, suggesting that liposclerosing myxofibrous tumors represent a variant form of fibrous dysplasia.[2]

Findings on Plain Films (Roentgenograms) and Computed Tomography

Lesions typically appear as well-defined radiolucent abnormalities that have sclerotic margins which are mild (10%), moderate (59%) or thick (31%)[1,3] (Figs. 270, 271). Mild expansile remodeling of bone is seen in 28 %.[1,3] Mineralization may be seen in these lesions.[1,3] Lipomatosis tissue is infrequently seen in these lesions with CT.[1,3]

MRI Findings

Lesions have well-defined margins with variable thickness of low signal borders on TlWl and T2WI.[1,3] Lesions often have low to intermediate signal on TlWI, and intermediate to high signal on T2WI and FST2VVI[1,3] (Figs. 270, 271). Small zones with MRI signal equal to fat may be seen at the periphery of these lesions. After Gd-contrast administration, absent or minimal enhancement may be seen.

Differential Diagnosis

Bone cyst, fibrous dysplasia, intra-osseous lipoma.

Prognosis and Treatment

Symptomatic lesions are treated with curettage, bone grafting, and fixation.[1-3] Malignant transformation (osteosarcoma, malignant fibrous histiocytoma) has been reported in up to 10% of these lesions.[1,3,4]

a

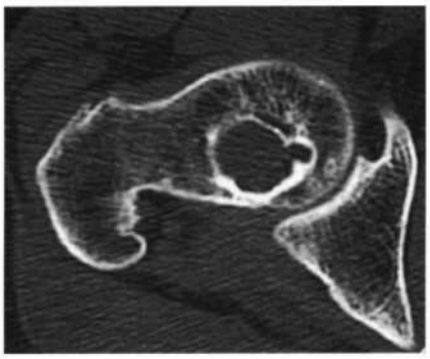

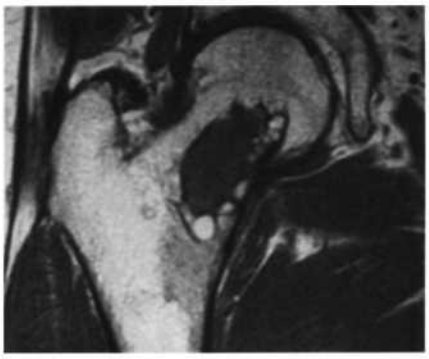

b, c

Figure 270a-f A 61-year-old man with a liposclerosing myxofibrous tumor in the intertrochanteric portion of the femur. AP radiograph (**a**) and axial CT image (**b**) show a well-defined radiolucent lesion with sclerotic margins. The lesion has well-defined margins with thin low signal on coronal T1WI (**c**). The internal portion of the lesion has mostly low-intermediate signal as well as small peripheral zones with high fat signal on coronal T1WI (**c**). The signal from the small zones of fat signal is suppressed on coronal FST2WI (**d**)and axial FST1 WI (**e**), whereas most of the lesion has high signal from the myxoid and fluid components. After Gd-contrast administration, only minimal peripheral enhancement is seen on axial FS T1WI(**f**).

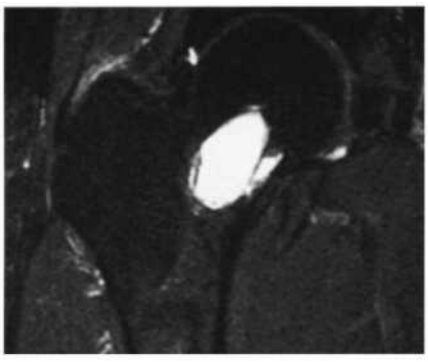

d

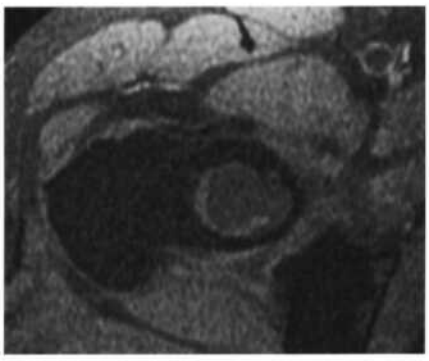

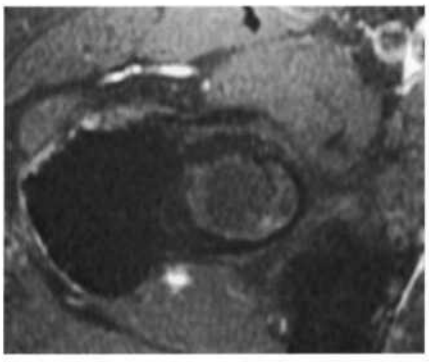

e, f

a

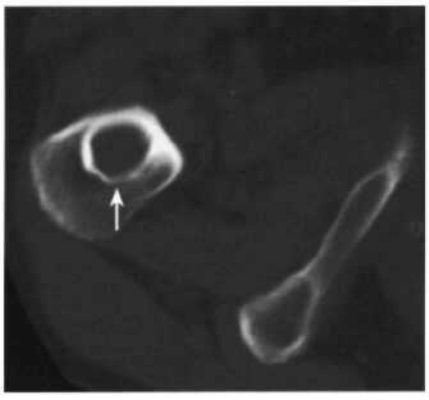

b

Figure **271 a-f** A 62-year-old man with a liposclerosing myxofibrous tumor in the intertrochanteric portion of the femur. AP radiograph (**a**) and axial CT image (**b**) show a well-defined radiolucent lesion with slightly thick sclerotic margins. The lesion has well-defined margins with slightly thick low signal on coronal (**c**) and axial (**e**) T1WI. The internal portion of the lesion has low-intermediate signal on T1 Wl. The lesion contains high signal from the myxoid and fluid components on coronal (**d**) and axial (**f**) FST2WI.

Figure **271 e, f** >

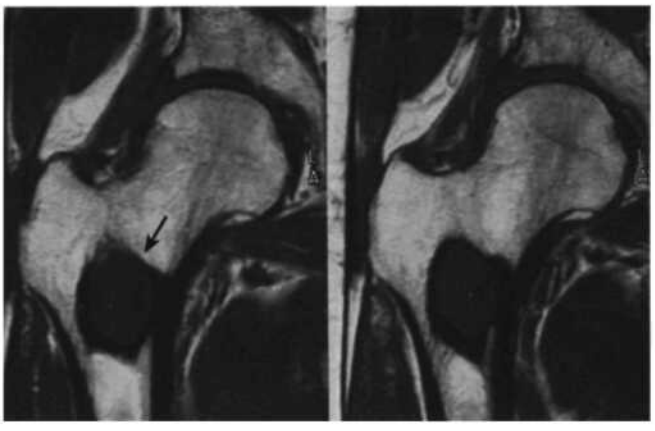

c

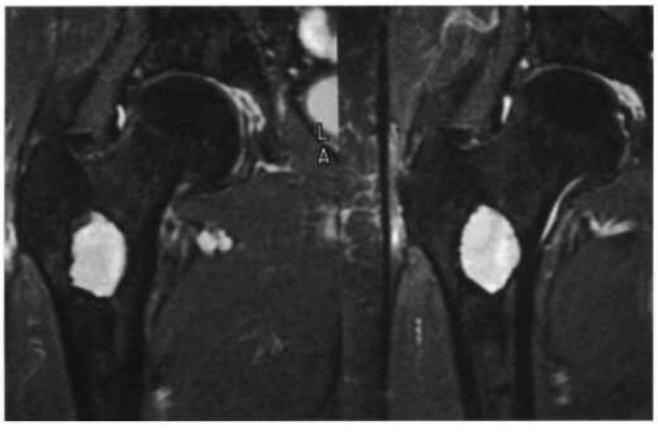

d

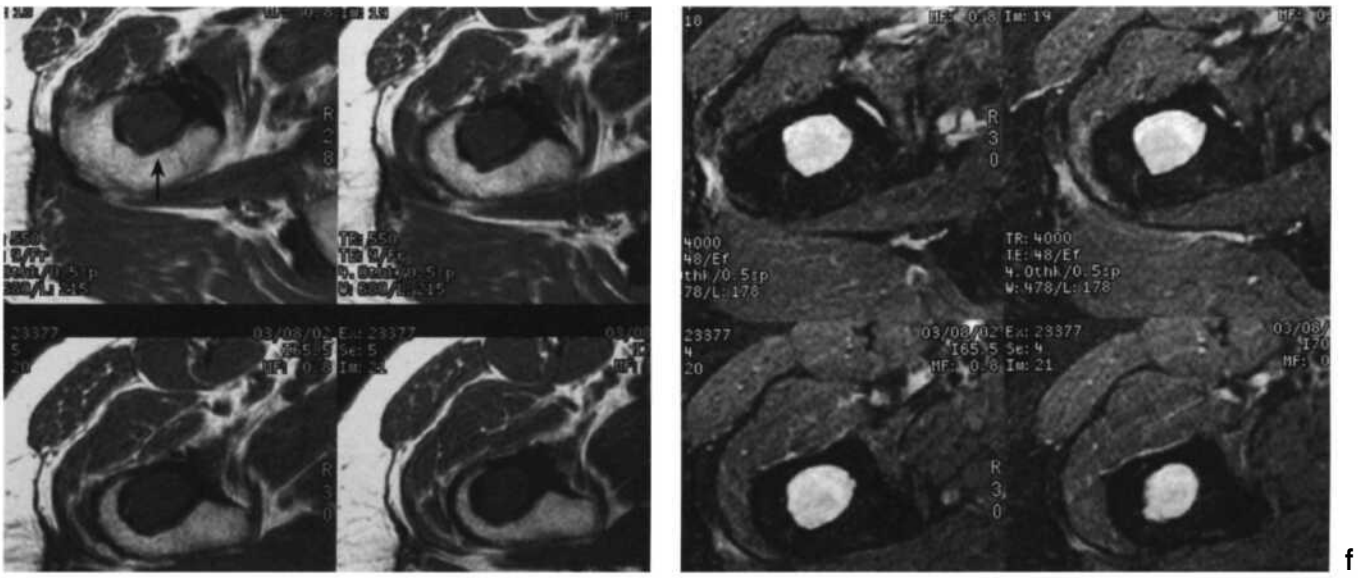

e f

Figure 271 e, f

References

1 Kransdorf MJ, Murphey MD, Sweet DE. Liposclerosing myxofibrous tumor: A radiologic-pathologic-distinct fibro-osseous lesion of bone with a marked predilection for the intertrochanteric region of the femur. *Radiology* 1999;212:693-698.

2 Matsuba A, Ogose A, Tokunaga K, et al. Activating Gs α mutation at the Arg^{201} codon in liposclerosing myxofibrous tumor. *Hum Pathol* 2003:34(11): 1204-1209.

3 Murphey MD, Carroll JF, Flemming DJ, Pope TL, Gannon FH, Kransdorf MJ. From the Archives of the AFIP: Benign musculoskeletal lipomatous lesions. *Radiographics* 2004;24(5):1433-1466.

4 Ragsdale BD. Polymorphic fibro-osseous lesions of bone: an almost site-specific diagnostic problem of the proximal femur. *Hum Pathol* 1993;24(5):505-512.

A 46 Lymphangioma (Also Referred to as Cystic Hygroma)

ICD-O Code

9170/0

Definition

Lymphangiomas are benign, vascular lesions that result from abnormal proliferation of lymphatic vessels.[2,4,6,11,17,18] Nearly all lymphangiomas occur in soft tissue, and only rarely in bone.[7] Lymphangiomas can be classified into three types based on the sizes of their lymphatic spaces: lymphangioma or cystic hygroma, cavernous lymphangioma, and capillary or simple lymphangioma.[20] All types are composed of endothelium-lined lymphatic channels interspersed among connective tissue stroma.[20] Congenital lymphangiomatosis (congential elephantiasis or Nonne-Milroy-Meige syndrome) refers to a rare, autosomal dominant disorder in which severe hypoplasia or aplasia of lymphatic channels results in enlargement of the involved anatomic sites.[11]

Another lesion, lymphangiohemangioma, contains elements of both lymphangioma and hemangioma.

Frequency of Occurrence

Lymphangiomas account for less than 1 % of benign soft tissue tumors,[12,13] and represent 5.6 % of all benign lesions of infancy and childhood.[20] Lymphangiomas can occur in association with Turner syndrome and Proteus syndrome.[2,10,11] Lymphangiomas rarely occur in bone.[7,15,16]

Age at Presentation

From 1 to 50 years, mean = 19 years.[13] Lymphangiomas can be congenital, with ~ 50 % present at birth.[20] Approximately 85 % are detected by age 2 years.[20]

Gender Ratio (M / F)

1/1 to 1.4/I.[13.20]

Location

Soft tissue Lymphangiomas are located in the head and neck > retroperitoneum > lower extremity > trunk > proximal limb > upper extremity > hand and wrist > mediastinum, other locations.[11,13,22]

- **Cystic lymphangiomas** are usually located in the head and neck, or axilla.[11]
- **Cavernous lymphangiomas** are often subcutaneous, located in the regions of the mouth, tongue, intramuscular septa, or salivary glands."
- **Capillary lymphangiomas** are typically small and located in the dermis and epidermis."
- **Lymphangiomatosis** typically appears as multifocal lesions that often involve multiple tissue planes."

Bone. Lymphangiomas in bone have been reported in the spine, ilium, long bones, and phalanges.[7] Lymphangiomatosis may involve both soft tissue and one or more bones."

Signs and Symptoms

Soft tissue. Cystic lymphangiomas are usually fluctuant lobular masses that are not attached to the skin and often occur in the head and neck region.[11,23] Transillumination can often be demonstrated with these lesions.[23]

Bone. Intra-osseous lymphangiomas may be associated with lymphangiomas in other skeletal sites as well as with viscera and other soft tissues, referred to as lymphangiomatosis.[7,17] Intra-osseous lymphangiomas can result in pathologic fractures.[7]

Gross Pathologic Findings

Soft tissue. Lesions can appear as multicystic spongy masses containing milky, yellow, or clear fluid.[2] Zones of recent or remote hemorrhage may be evident.

Bone. Lesions appear as intra-osseous lytic zones containing clear, milky or yellow fluid.[7]

Histopathologic Findings

Soft tissue. Lesions are comprised of variously sized, dilated, thin-walled lymphatic vessels. The vessels are lined with a flattened endothelium which may be surrounded by lymphoid aggregates.[2] Vessel contents may include proteinaceous fluid, lymphocytes, and erythrocytes.[2,4,6] Hemosiderin may be seen in the vessel walls.[2] Large-sized vessels may contain smooth muscle cells in the walls.[2] Stromal inflammation and fibrosis can occur over time.[2] Endothelial cells may be immunoreactive to factor VIII-rAg, CD 31, and CD 34.[2]

Bone. Lesions appear as cystic, cavernous spaces lined by a flattened layer of endothelial cells that may be associated with lymphoid aggregates.[7] Lesions are associated with progressive erosion and destruction of bone, and may result in skeletal deformities.[9]

Lesion Genetics

Cystic lymphangiomas can be associated with Turner syndrome.[2]

Findings on Plain Films (Roentgenograms) and Computed Tomography

Lymphangiomas in soft tissues often appear on CT as unilocular or multilocular cystic lesions filled with low-attenuation fluid, similar in attenuation to mucoid material (10-25 Hounsfield units), separated by thin or thick septa, with or without nodular zones with soft tissue attenuation.[11,21] Enhancement of septa and nodular zones can be seen with CT. Fluid-fluid levels and zones of high attenuation from hemorrhage may be seen with CT.[21] Calcifications are uncommon."

Findings on Ultrasound

Soft tissue. Lymphangiomas can appear as cystic or multicystic compressible lesions.[1] Lymphangiomas are usually avascular, unless the lesions are mixed lymphatic/venous malformations, which can show low-velocity arterial and/or venous flow within septa or stromal tissue on Doppler sonography.[1]

Bone. Lesions are usually radiolucent with abrupt zones of transition, with or without either sclerosis at borders or mild to moderate bone expansion.[9,11,17]

MRI Findings[3,8,11,19-24]

Lymphangiomas in soft tissue can be circumscribed lesions or have an infiltrative pattern with extension within and between muscles.[3,8,11,23] Lesions are often lobulated, containing single or multiple cystic zones which have predominantly low signal on T1W1, and high signal on T2WI and FST2WI[3,8,11,19,20,23] (Figs. **272-276).** Fluid-fluid levels and zones with high signal on T1WI and variable signal on T2WI may result from cysts containing hemorrhage, high protein concentration, and/or necrotic debris[3,11,20,21] (Fig. 273). Septa between the cystic zones can vary in thickness and Gd-contrast enhancement, and usu-

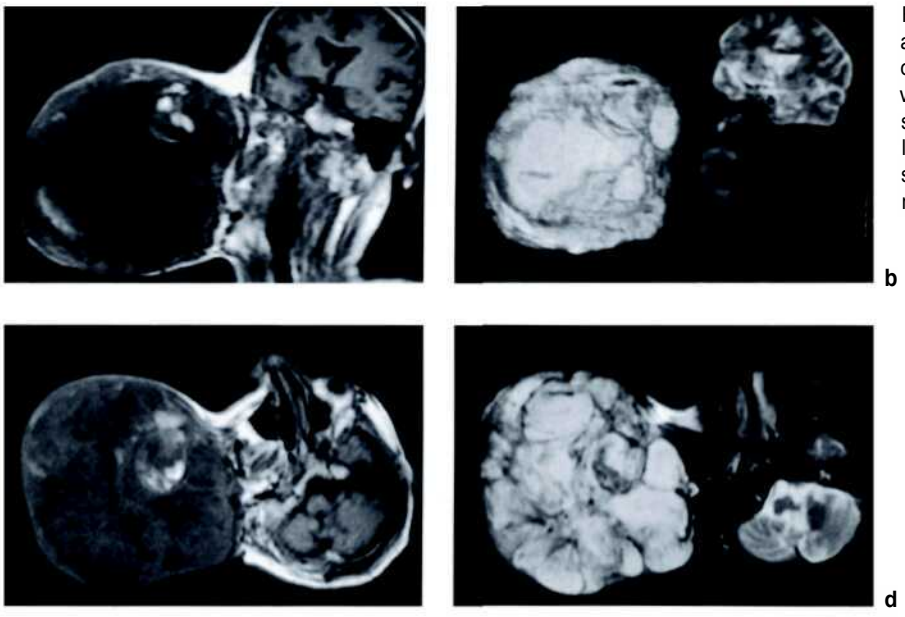

Figure **272 a-d** A large exophytic lymphangioma is seen extending from the right side of the face and neck, which contains zones with intermediate, low-intermediate, and high signal on coronal (a) and axial (c) T1WI. The lesion contains multiple lobules with high signal separated by low signal septa on coronal (**b**) and axial (**d**) FST2WI.

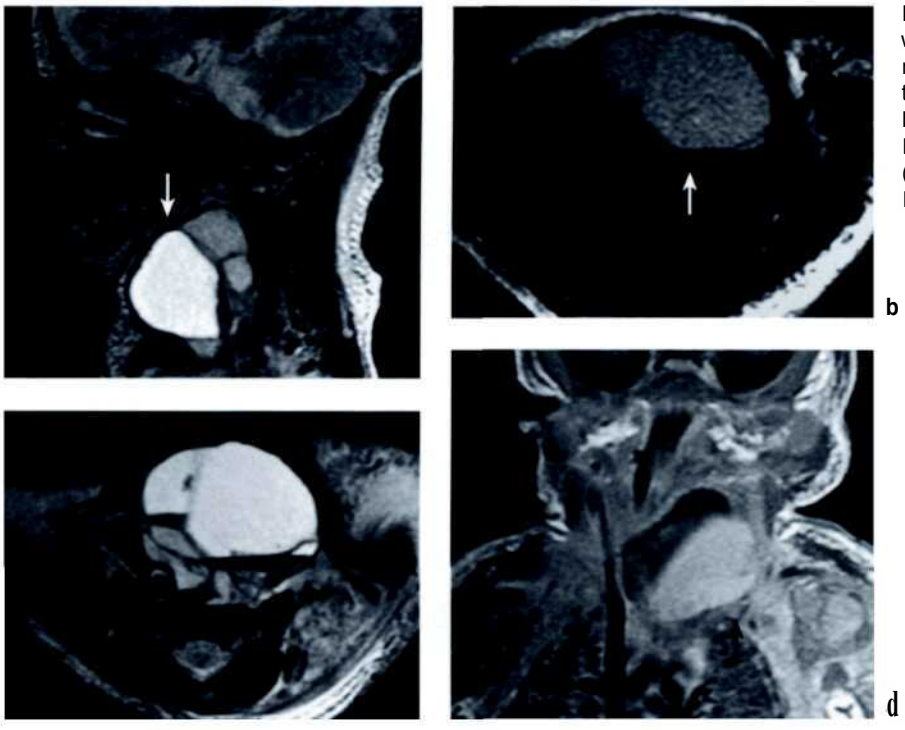

Figure **273 a-d** A 4-week-old male infant with a lymphangioma involving the upper neck with resultant rightward displacement of the trachea. The lesion contains multiple lobules containing low, intermediate, slightly high and high signal on sagittal (a) and axial (c) T2WI, and axial (**b**) and coronal (**d**) T1WI. Fluid-fluid levels are also seen on T2WI.

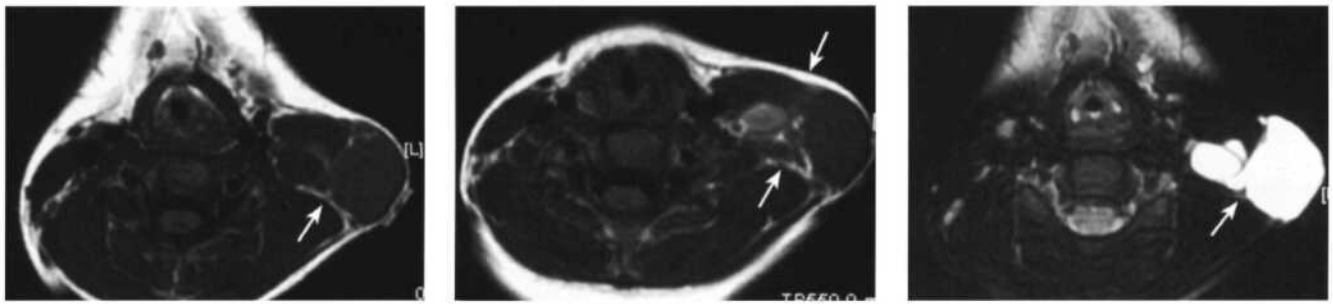

a, b c

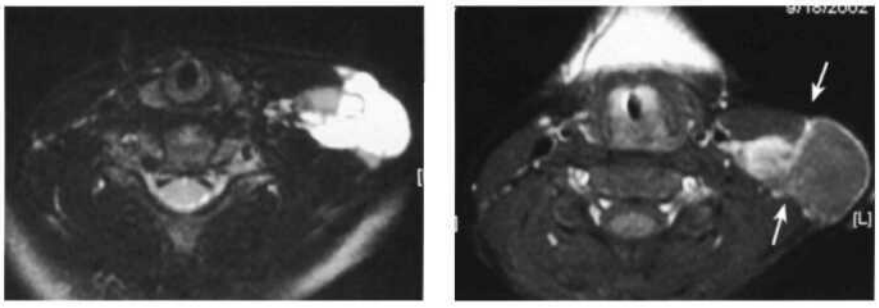

d, e

Figure **274 a-e** A 2-year-old male with a lumphangioma in the left side of the neck. The lesion contains mostly low-intermediate signal on axial T1WI (**a, b**), as well as several zones with high signal. The lesion contains multiple lobules with mostly high signal separated by low signal septa on axial FST2WI (**c, d**), as well as small zones with low and intermediate signal. Septal portions of the lesion show mild Cd-contrast enhancement on axial FST1WI (**e**).

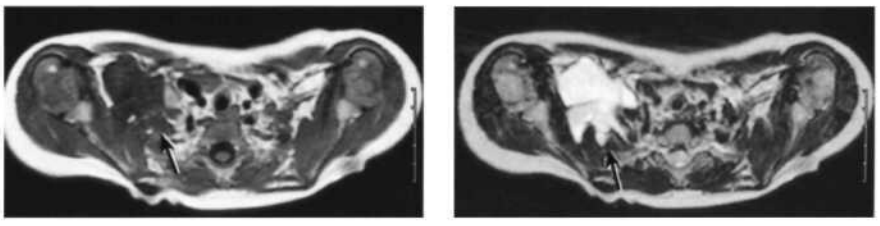

a, b

Figure **275 a, b** Lymphangioma in the right lower neck and thoracic inlet. A lobulated lesion is seen with intermediate signal on axial PDWI (**a**) and high signal on axial T2WI (**b**).

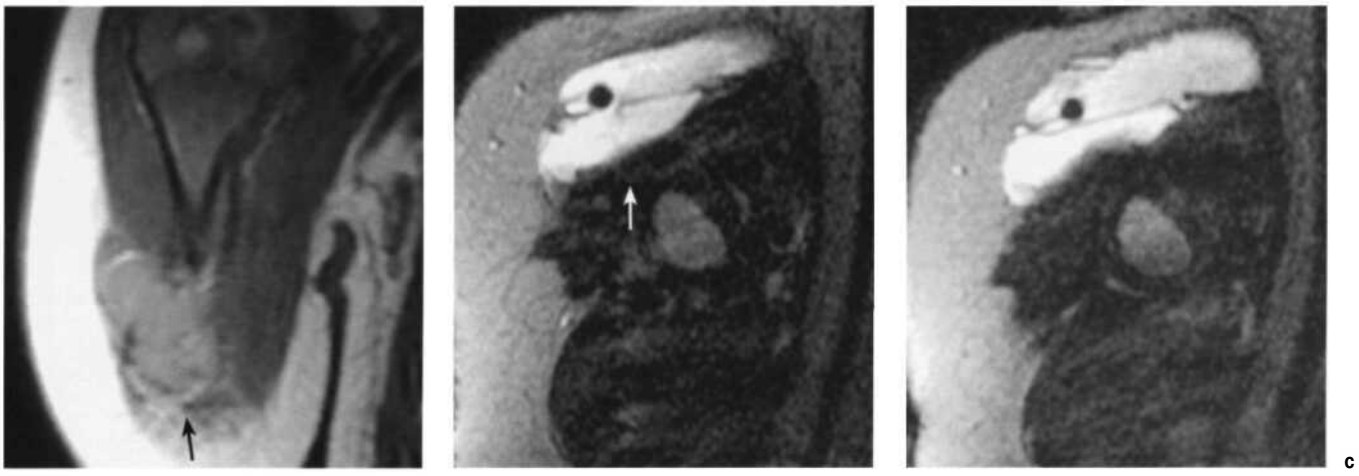

a, b c

Figure **276a-c** Lymphangioma in the right arm. A lobulated lesion with intermediate signal on coronal PDWI (**a**) and high signal on axial T2WI (**b, c**) is seen. Septa and a nodule of low signal are seen in the lesion on axial T2WI.

ally have low signal on T1WI and low to intermediate signal on T2W1 and FST2WI. Nodular zones within the lesions can have low-intermediate signal on T1WI, intermediate to high signal on T2WI, and variable degrees of Gd-contrast enhancement.[19]

Mediastinal lymphangiomas which occur in the fetus have been detected with prenatal MR imaging.[8]

Differential Diagnosis

Hemangioma, hemangioendothelioma, hemangiopericytoma, angiosarcoma, hematoma, lipoma, liposarcoma, lipoblastoma, myxoma.

Prognosis and Treatment

Lymphangiomas are considered to be benign lesions without malignant potential.[21] These lesions often enlarge and rarely regress.[23] Rapid or episodic enlargement may result from hemorrhage or infection.[23] These lesions may affect growth of adjacent bones or narrow the airway.[23] Lymphangiomas in soft tissue are often treated with surgery.[11,23] Complete resection may be limited when lymphangiomas infiltrate adjacent structures.[11,23] The recurrence rate is ~10 to 15 %.[11,23] Patients with lymphangiomas and lymphangiomatosis may respond favorably to interferon-α[18] Sclerotherapy has also been used.[14]

Lymphangiomas in bone can grow or regress. Larger lesions can be associated with pathologic fracture.[7] Intra-osseous lymphangiomas are usually treated with curettage, grafting, and sometimes radiation.[5,7]

References

1 Bellah R. Ultrasound in pediatric musculoskeletal disease. *Radial Clin North Am* 2001 ;39(4): 597-618.

2 Benham A. Lymphangiona. In: Fletcher CDM, Unni KK, Mertens F, eds. *World Health Organization Classification of Tumours. Pathology and Genetics of Tumours of Soft Tissue and Bone* Geneva: IARC Press; 2002:162-163.

3 Bissett GS III. MR imaging of soft-tissue masses in children. *Magn Reson Imaging Clin N Am* 1996;4(4):697-719.

4 Chaudhuri B, Das Gupta TK. Pathology of soft tissue sarcoma. In: Das Gupta TK, Chaudhuri PK, eds. Tumors *of the Soft Tissues* 2nd ed. 1998:63-200.

5 Darby AJ. Vascular neoplasms of bone. In: Helliwell TR, ed. *Major Problems in Pathology: Pathology of Bone* and Joint *Neoplasms* 1st ed. Vol 37. Philadelphia, Pa: W.B. Saunders; 1999:332, 335.

6 Das Gupta TK, Chaudhuri PK. Tumors of the lymphatic tissue. In: Gupta TK, Chaudhuri PK, eds. *Tumors of the Soft Tissues* 2nd ed. Stamford, Conn: Appleton & Lange; 1998:449-462.

7 Forest M. Vascular tumors. In: Forest M, Tomeno B, Vanel D, eds. *Orthopedic Surgical Pathology: Diagnosis of Tumors and Pseudotumoral Lesions of Bone and Joints* Edinburgh: Churchill Livingstone; 1998:345-362.

8 Hubbard AM. Magnetic resonance imaging of fetal thoracic abnormalities. *Top Magn Reson Imaging* 2001;12(l):18-24.

9 Huvos AC. Hemangioma of bone; lymphangioma of bone; diffuse skeletal angiomatosis and lymphangiomatosis; glomus tumor; "disappearing bone disease." In: *Bone Tumors: Diagnosis, Treatment, and Prognosis* 2nd ed. Philadelphia, Pa: W.B. Saunders; 1991:553-578.

10 Kloeppel R, Rothe K, Hoermann D, Schmidt F, Bennek J, Kahn T. Proteus syndrome. *J Comput Assist Tomogr* 2002;26(2):262-265.

11 Kransdorf MJ, Murphey MD. Vascular and lymphatic tumors. In: *Imaging of Soft Tissue Tumors* 2nd ed. Philadelphia, Pa: W.B. Saunders; 2006:150-188.

12 Kransdorf MJ, Murphey MD. Soft tissue tumors in a large referral population: prevalence and distribution of diagnoses by age, sex, and location. In: *Imaging of Soft Tissue Tumors* 2nd ed. Philadelphia, Pa: W.B. Saunders; 2006:6-37.

13 Kransdorf MJ. Benign soft-tissue tumors in a large referral population: distribution of specific diagnoses by age, sex, and location. *AJR Am J Roentgenol* 1995;164:395-402.

14 Ng EH, Shah VS, Armstrong DC, Clarke HM. Cavernous lymphangioma. *J Pediatr* 2001;138(1):146-148.

15 Mulder JD, Schutte HE, Kroon HM, Taconis WK. Introduction. In: *Radiologic Atlas of Bone Tumors* Amsterdam: Elsevier; 1993:3-6.

16 Mulder JD, Schutte HE, Kroon HM, Taconis WK. The diagnosis of bone tumors. In: *Radiologic Atlas of Bone Tumors* Amsterdam: Elsevier; 1993:9-46.

17 Mulder JD, Schutte HE, Kroon HM, Taconis WK. Lymphangioma. In: *Radiologic Atlas of Bone Tumors* Amsterdam: Elsevier; 1993:517-518.

18 Reinhardt MA, Nelson SC, Sencer SF, Bostrom BC, Kurachek SC, Nesbit ME. Treatment of childhood lymphangiomas with interferon. *J PediatrHematol Oncol* 1997;19(3):232-236.

19 Saito T, Kazumasa T, Tsuchiya K, Oda Y, Tsuneyoshi M, Iwamoto Y. Lymphangioma presenting as a dumbell tumor in the epidural space of the lumbar spine. *Spine* 1999:24:74-76.

20 Siegel MJ, Glazer HS, St Armour TE, Rosenthal DD. Lymphangiomas in children: MR imaging. *Radiology* 1989:170:467-470.

21 Som PM, Smoker WRK, Curtin HD, Reidenberg JS, Laitman J. Congenital lesions. In: Som PM, Curtin HD, eds. *Head and Neck Imaging* 4th ed. St. Louis, Mo: Mosby; 2003:1828-1864.

22 Sundaram M, Sharafuddin Melhem JA. MR imaging of benign soft-tissue masses. *Magn Reson Imaging Clin N Am* 1995;3(4):609-627.

23 Wever DJ, Heeg M, Mooyaart EL. Cystic hygroma of the shoulder region: a case report. *Clin Orthop Relat Res* 1997;338:215-218.

24 Winterer JT, Laubenberger J, Berger W, et al. Radiologic Findings in lymphangioma of the posterior tibial nerve. *J Comput Assist Tomogr* 1998:22(1):28-30.

A 47 Lymphoma

ICD-O Codes

Hodgkin lymphoma:
- Lymphocyte predominant: 9659/3
- Nodular sclerosis: 9663/3
- Mixed cellularity: 9652/3
- Lymphocyte depleted: 9653/3

Non- Hodgkin lymphoma:
- Lymphoblastic
  - Precursor B cell: 9728/3
  - Precursor T cell: 9837/3
- Burkitt: 9687/3
- Large cell: 9680/3
- Follicular: 9690/3
- Mantle cell: 9673/3
- Mycosis fungoides: 9700/3

Definition[1,4,14-16]

Lymphoma represents a group of lymphoid tumors whose neoplastic cells typically arise within lymphoid tissue (lymph nodes and reticuloendothelial organs). Unlike leukemia, lymphoma usually arises as discrete masses. Almost all primary lymphomas of bone are B cell non-Hodgkin lymphomas.[16]

Lymphomas are subdivided into Hodgkin disease (HD) and non-Hodgkin lymphoma (NHL). This distinction between HD and NHL is useful because of differences in clinical and histopathologic features, as well as treatment strategies. HD typically arises in lymph nodes and often spreads along nodal chains, whereas NHL frequently originates at extranodal sites and spreads in an unpredictable pattern.[1] Monoclonal antibodies have been used to characterize lymphoma with regard to possible types of tumor cell origin: immunoreactivity to CD 1-8 is often seen for T cells; CD 10,19-23 for B cells; CD 13-15,33 for monocyte or macrophage cells; CD 15,56 for natural killer (NK) cells; and CD45 for all leukocytes.[1]

The exact cell type that HD is derived from is not certain.[1,4] HD is divided into four main subtypes: nodular sclerosis (40-80%), mixed cellularity (20-40%), lymphocyte predominant (2-10%), and lymphocyte depleted (2-15%).[14]

The derivation of NHL is mostly from precursor B cells (~90 %), with the remainder derived from precursor T cells or NK cells. Various subtypes of NHL include lymphoblastic lymphoma, Burkitt lymphoma, large cell lymphoma, follicular lymphoma, mantle cell lymphoma, and mycosis fungoides.[1,14,26] The three predominant types of NHL in children are lymphoblastic lymphoma, Burkitt lymphoma, and large cell lymphoma. Follicular and large cell lymphoma account for approximately two-thirds of NHLs. Diffuse large cell lymphoma is the most common type of aggressive lymphoma in adults.[4,30] Various classification schemes for NHL have been proposed: Revised European-American Classification of Lymphoid Neoplasms (R. E.A.L.), Working Formulation, Kiel Classification, and Rappaport Terminology.[4]

R.E.A.L is used to categorize NHL regarding their B cell, T cell, and NK cell origins. Using the R.E.A.L, NHL and some leukemias have overlapping properties which have clinical relevance for treatment strategies.[4]

Frequency of Occurrence[10,18,21]

Hodgkin disease. An estimated 7000 new cases occur per year in the United States.[10] Infiltration of bone marrow occurs in 5-15% of them.[18]

Non-Hodgkin lymphoma. Some 53 900 new cases occur per year in the United States.[10] Infiltration of bone marrow occurs in 25-40 % of them.[18] Primary osseous NHL, also referred to as reticulum cell sarcoma, accounts for less than 2 % of primary malignant bone tumors.[21] T-cell lymphoma of the skin, mycosis fungoides, is rare with an incidence of 0.29 per 100000 population worldwide.[26]

Age at Presentation[1,14]

Hodgkin disease: children and adults, mean age = 32 years.[1,20,29]

Non-Hodgkin lymphoma:[20,21] children and adults.
- **Primary osseous NHL:** from 3 to 85 years, median = 35 years.
- **Secondary osseous NHL:** from 4 to 74 years, median = 30 years.
- **Lymphoblastic lymphoma** (28 % of childhood NHL): occurs in children > than adults); children are usually < 15 years old, peak = 4 years.
- **Burkitt lymphoma** (39 % of childhood NHL): occurs in children > adults.
- **Follicular lymphoma** (45 % of NHL): occurs in adults > children.
- **Large cell lymphoma** (20% of NHL): occurs in adults > children. For adults, median age = 60 years.
- **Mantle cell lymphoma** (3-9% of NHL): occurs in adults, peak age = 40-60 years.
- **Mycosis fungoides** (< 1 % of NHL): occurs in adults, median age = 50-60 years.

Gender Ratio (M / F)

Hodgkin disease: 1.1 / 1.[10]

Non-Hodgkin lymphoma: 1.1 /1.[10]

Location

Hodgkin disease.[1,4,21,27] HD usually presents as localized disease, and progresses along lymph nodes, followed by splenic, hepatic involvement, and eventually to other nonlymphoid tissues. Mediastinal adenopathy occurs in ~60 % of patients, followed by cervical/supraclavicular adenopathy. HD typically does not occur in bone as the initial site, but may occur in the later phases of disseminated disease.[21] Vertebral disease accounts for up to half of reported cases of HD involving bone followed by the ribs, pelvis, and femur.[21,27] Multiple bone lesions occur slightly more frequently than single bone lesions.[27]

Non-Hodgkin lymphoma.[4,21,27] Peripheral lymphadenopathy is commonly seen, as well as hepatic, splenic, and extranodal sites. Hepatic involvement occurs in up to 50% of patients with NHL at presentation. Primary lymphoma of the central nervous system, typically NHL, is uncommon. NHL often dis-

seminates hematogenously resulting in secondary osseous disease, and can involve bone by direct invasion from nodal or extranodal disease. Primary lymphoma of bone represents less than 5% of NHL, and is usually diffuse large B cell lymphoma. Burkitt lymphoma usually occurs at extranodal sites. African endemic Burkitt lymphoma can involve the mandible, as well as the kidneys, ovaries, and adrenal glands. Nonendemic Burkitt lymphoma often occurs as an abdominal mass (ileocecum, peritoneum). Mycosis fungoides is a T cell lymphoma that typically involves the skin with epidermal and dermal infiltration.[26]

Primary osseous NHL.[21] Lesions occur in the femur, pelvis > tibia > humerus > mandible > scapula > vertebrae, sternum, fibula > other bones. Twelve percent of primary osseous NHL occurs in multiple bones.[21] In tubular bones: diaphyseal > meta-diaphyseal > epi-metaphyseal, epi-metadiaphyseal > metaphyseal > epiphyseal sites.

Secondary osseous NHL.[21] Lesions occur in the femur > tibia > pelvis, clavicle > other bones. Nine percent of primary osseous NHL occurs in multiple bones.[21]

Signs and Symptoms

Hodgkin disease. Most patients have minimal or no symptoms.[4] Symptoms, if present, occur in -30% of patients and include low-grade fevers, night sweats, unexplained weight loss, fatigue, malaise, weakness, and pruritis. Thoracic disease may be associated with shortness of breath, cough, chest pain, compression of the superior vena cava, headaches, and hypertrophic osteoarthropathy. Abdominal disease may be accompanied with abdominal pain, ascites, and bowel dysfunction.

Non-Hodgkin lymphoma.[4,21] Many patients have painless peripheral lymphadenopathy.[4] Less than 20% of patients with NHL have systemic complaints (fever, night sweats, weight loss, fatigue, malaise, etc.) at presentation.[4] Hepatomegaly and splenomegaly are more commonly seen with NHL compared with HD. Most patients with primary and secondary bone lymphoma have NHL. Lymphoma involving bone can be associated with localized pain or pathologic fracture. Symptoms of patients with disease limited to a single bone location tend to be milder than those with secondary disease.[21] Spinal canal compression or foraminal disease may also result from extra-osseous extension of lymphoma from bone or epidural lymphoma. Mycosis fungoides usually appears as slowly growing skin patches and/or plaques.[26]

Cross Pathologic Findings

Hodgkin disease:

- **Bone.** HD is associated with irregular zones of medullary and cortical bone destruction. The bone cortex can be thinned or eroded, often associated with an extra-osseous soft-tissue lesion.[2,21] Hemorrhage and necrosis may occur in the specimens.[2,21]
- **Soft tissue.** Patients often have lymphadenopathy, splenic, and/or hepatic enlargement.

Non-Hodgkin lymphoma:

- **Bone.** NHL is associated with irregular zones of medullary bone destruction. The bone cortex can be thinned or distended, often associated with a white-gray or pink, firm and/or friable, soft tissue lesion.[2,21] Hemorrhage and necrosis may occur in the specimens[2,21]
- **Soft tissue.** NHL is often associated with lymphadenopathy, hepatomegaly, and/or splenomegaly. NHL more frequently involves bone than HD. Spinal canal compression and/or foraminal disease can result from extra-osseous extension of lymphoma from bone or epidural lymphoma. Mycosis fungoides usually appear as single or multiple skin plaques and/or patches.[26]

Histopathologic Findings

Hodgkin disease.[1,29] The true neoplastic cell of HD is the Reed-Sternberg cell, which is large (15-45 um), binucleate or bilobed, and surrounded by abundant cytoplasm. Multiple nuclei or multilobulated single nuclei may be present in the Reed-Sternberg cell. Variants of the Reed-Sternberg cell include (1) a mononuclear variant which has a single ovoid or spheroid nucleus with a large nucleolus, (2) a lacunar variant which has a multilobulated or folded nucleus and abundant cytoplasm, (3) lymphocytic and histiocytic variants which have polypoid nuclei. Reed-Sternberg cells are surrounded by various combinations of lymphocytes, macrophages, eosinophils, plasma cells, and fibrous bands/tissues.

- **Nodular sclerosis.**[1] This type of HD typically consists of frequent lacunar cells, occasional Reed-Sternberg cells in a background of T lymphocytes, eosinophils, macrophages, plasma cells, and collagenous fibrous bands which divide lymphoid tissue into nodules. Reed-Sternberg cells are immunoreactive to CD 15 and CD 30, but not to CD 45, B-cell and T-cell markers.
- **Mixed cellular.**[1] This type of HD has frequent classic and mononuclear Reed-Sternberg cells in a background of T lymphocytes, eosinophils, macrophages, and plasma cells. The mixture of cell types results in diffuse replacement of normal lymph structure. Reed-Sternberg cells are immunoreactive to CD 15 and CD 30.
- **Lymphocyte predominant.**[1] This type of HD has frequent lymphocytic and histiocytic variants of Reed-Sternberg cells in a background of reactive, small B cells. Eosinophils, neutrophils, plasma cells, and zones of fibrosis are infrequent. Reed-Sternberg cells are immunoreactive to CD 20 and CD 45, but not to CD 15 or CD 30.
- **Lymphocyte depleted.**[1] This type of HD has frequent Reed-Sternberg cells. Some of the lymphoma in this category may represent large cell NHL. Reed-Sternberg cells are immunoreactive to CD 15 and CD 30.

Non-Hodgkin lymphoma:

- **Lymphoblastic lymphoma.**[1] Affected lymph nodes contain a diffuse population of small lymphocytes (6-12 urn) which contain prominent, round to slightly irregular nuclei with little cytoplasm. The small, lymphocyte tumor cells are mixed with varying numbers of larger cells termed prolymphocytes, which may form loose aggregates called proliferation centers.[1] Tumor cells are often immunoreactive to CD 19 and CD 20, which are B-cell markers. Lymphoblastic lymphoma can be associated with trisomy 12, deletions of 11 q, and deletions of 13ql2-14; t(9;22)(q34;qll.2); t(12;21)(p13;q22); and t(l;19)(q23;p13.3).
- **Burkitt lymphoma.**[1] Lymph nodes are diffusely filled with tumor cells ranging in size from 10 to 25 uim. Tumor cells have spheroid or ovoid nuclei with several nucleoli, and moderate amounts of basophilic cytoplasm. Mitotic activity is often present, as well as apoptosis with associated macrophages ingesting cellular debris ("starry sky appearance").[1] Tumor cells are often immunoreactive to CD 10, CD 19, and CD 20. Burkitt lymphoma is often associated with transloca-

tions involving the *c-myc* gene on chromosome 8.[1] Burkitt lymphoma is endemic in Africa and often associated with Epstein Barr viral and HIV infections. Nonendemic Burkitt lymphoma, however, is associated with the Epstein Barr virus in only 20%.

- **Follicular lymphoma.**[1] Varying proportions of two types of tumor cells are usually seen in either nodular or nodular and diffuse distributions within lymph nodes. The more frequent of the two cell types are small cells with cleaved or indented nuclei with relatively small amounts of cytoplasm (termed small cleaved cells, centrocytes). The other type of tumor cells (referred to as centroblasts) are larger, with less densely staining chromatin and relatively greater amounts of cytoplasm than the small cleaved cells. Within bone marrow, paratrabecular aggregates are often manifest. Tumor cells are often immunoreactive to CD 10, CD 19, and CD 20. Follicular lymphoma is often associated with t(14;18)(q32;q21) and increased expression of BCL2 protein.[1]
- **Large cell lymphoma.**[1] Tumor cells typically occur diffusely within affected lymph nodes or within enlarging extranodal lesions (skin, brain, gastrointestinal tract, liver, spleen, Waldeyer ring, or bone). Tumor cells are relatively large (four to five times the size of normal lymphocytes), which can have ovoid/spheroid nuclei or multilobulated nuclei. Cells contain moderate basophilic or pale cytoplasm. Tumor cells are often immunoreactive to CD 19 and CD 20 and sometimes to CD 10, which are B-cell markers. Large cell lymphomas are associated with translocations such as t(14;18) and t(17)(p!3) and involve chromosome Sat the BCL6 locus.[1] Large cell lymphoma in patients with HIV may also be infected with herpes 8 virus, which has been implicated in formation of large cell lymphoma and Kaposi sarcoma in this patient group.[1]
- **Mantle cell lymphoma.** Tumor cells are usually small lymphocytes with ovoid, slightly irregular or cleaved nuclei. Tumor cells may be diffusely distributed within lymph nodes or appear in a somewhat nodular pattern with tumor cells replacing or surrounding B-cell follicles, called "mantle zone pattern"[1] Mantle cell lyphoma is immunoreactive to B-cell markers such as CD 19 and CD 20. A translocation, t(ll;14)(ql3;q32), is associated with mantle cell lymphoma in over 70% of cases.[1]
- **Mycosis fungoides.** Lesions often consist of collections of small to medium sized tumor cells with cerebrifrom nuclei with epidermis and/or dermis.[26] Tumor cells in the dermis may be associated with an inflammatory reaction consisting of small lymphocytes and eosinophils.[26] Spread to lymph nodes can occur.[26] Immunoreactivity has been reported to CD2, CD3, TCRbeta, CD5, CD4, as well as lack of immunoreactivity to CD7 and CD8.[26]

Findings on Plain Films (Roentgenograms) and Computed Tomography

Hodgkin disease:[9,12,21,24,27]

- **Bone.** HD typically does not occur in bone as the initial site, but may occur in the later phases of disseminated disease[21] (Fig. 282). Vertebral disease accounts for up to half of reported cases of HD involving bone followed by the ribs, pelvis, and femur.[21] HD within bone can appear as zones of radiolucency (30%), zones with increased density or attenuation (10%), or zones with mixed increased and decreased density-attenuation (60%)[21] (Fig. 282). Radiolucent zones can have a permeative or moth-eaten appearance, and/or well-defined margins.[21,27] Permeative radiolucent lesions may coalesce into more geographic radiolucent lesions over time. Zones of increased bone density represent reactive sclerosis or fibrosis, and are not secondary to bone formation.[21,27] Zones of sclerosis can be seen within or at the margins of the radiolucent zones. Zones of increased density can be seen as thickening of trabeculae, or can appear diffuse involving most of a vertebral body (ivory vertebra). Superficial erosions or zones of bone destruction can also occur from invasion from adjacent lymphadenopathy.
- **Soft tissue.** CT can show lymphadenopathy as well as splenic and hepatic involvement.[27]

Non-Hodgkin lymphoma:[5,9,12,16,21,22,24,27,30]

- **Bone.** NHL often appears as radiolucent, intramedullary lesions with a permeative or moth-eaten appearance, as well as involvement of the cortex[12,27] (Fig. 289). Zones of osteosclerosis may also be associated with areas of bone lysis in 24% of cases. Periosteal reaction can be seen in up to two-thirds of cases (Fig. 289). Extra-osseous extension

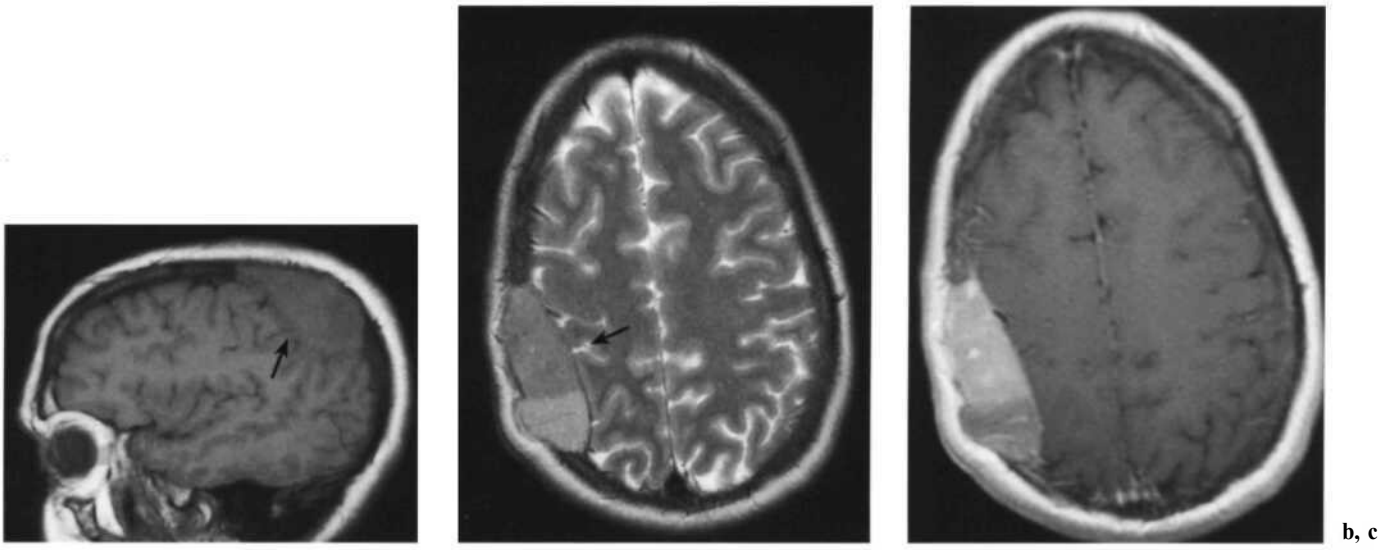

a b, c

Figure **277 a-c** A 46-year-old woman with diffuse, large B-cell non-Hodgkin lymphoma involving the skull and dura. The lesion has low-intermediate signal on sagittal T1 WI (a) and axial T2WI (**b**). The tumor shows heterogeneous moderate Gd-contrast enhancement on axial T1WI (c).

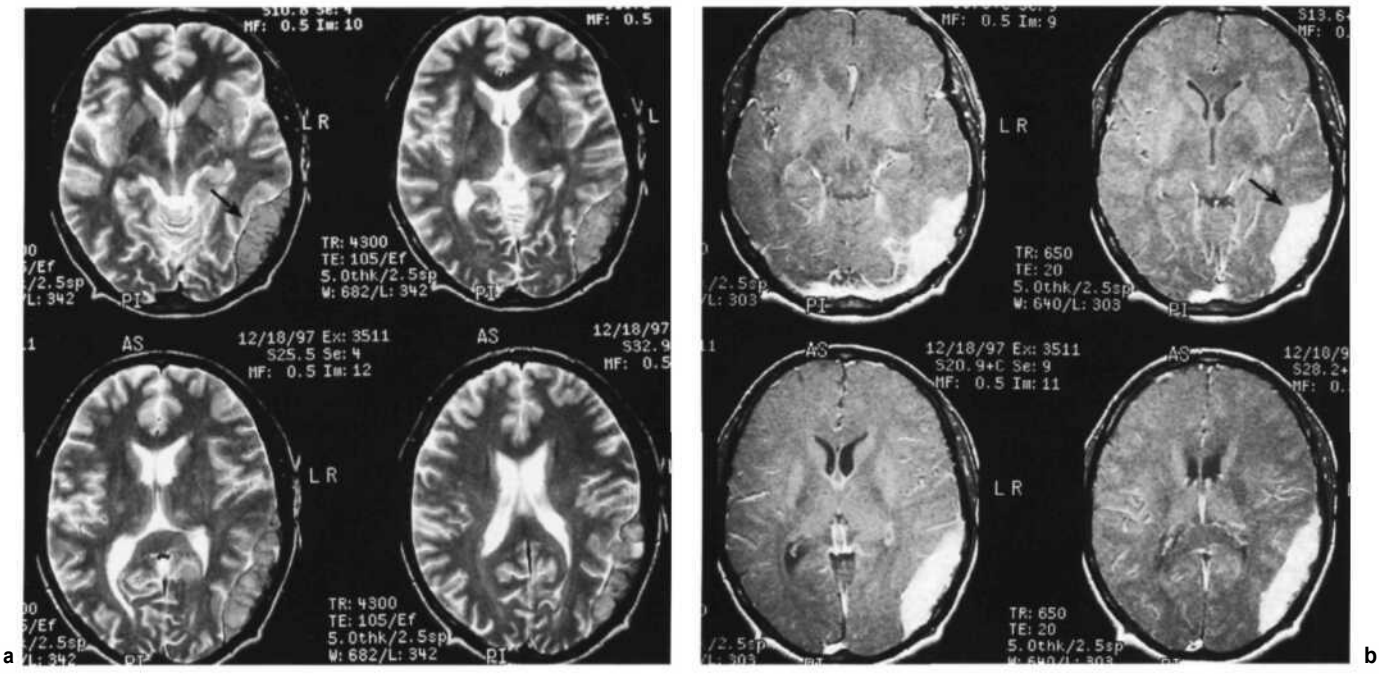

a b

Figure **278a, b** 26-year-old man with non-Hodgkin lymphoma involving the intracranial dura. The lesion has heterogeneous intermediate signal on axial T2WI (**a**). The tumor shows prominent enhancement on axial T1WI (**b**).

into the adjacent soft tissues can be seen with CT. Detached pieces of cortical bone or sequestra may be seen associated with extra-osseous tumor extension.[12,22,27] The soft tissue components of NHL typically do not contain calcifications. Successful treatment often results in remodeled bone which may overlap radiographic findings that can be seen with Paget disease.[16]

- **Soft tissue.** CT can readily show peripheral lymphadenopathy, hepatomegaly, and splenomegaly.[24] Spinal canal compression or foraminal disease can result from extra-osseous extension of lymphoma from bone or epidural lymphoma.

MRI Findings

Hodgkin disease:

- **Bone.**[18,27,31] HD within bone typically appears as intramedullary zones with low-intermediate signal on T1WI, and intermediate, slightly high, and/or high signal on T2WI, and high signal on FST2WI (Fig. **282).** Intramedullary lesions may have poorly defined or distinct margins. Multifocal lesions can be seen in long bones and vertebrae. Zones of cortical destruction may occur associated with extra-osseous soft tissue lesions. Most lesions show Gd-contrast enhancement. HD involving bone with associated sclerosis seen on plain films or CT usually have low signal on T1WI and variable/mixed signal on T2WI. Destruction of cortical and medullary bone may also occur from invasion from adjacent extra-osseous lymphadenopathy from HD. The detection of HD in bone with MRI has been reported to be useful for predicting disease relapse.[31]
- **Soft tissue.**[3,8,23] Lymphadenopathy from HD often has low-intermediate signal on T1WI (hypointense to fat and hyperintense to muscle on T1WI) ,and intermediate to slightly high signal on T2WI (hypointense or isointense to fat on T2W1).[23] Variability in MRI signal characteristics may be related to differing histologic features (such as the degree of fibrosis) for the subtypes of HD.[3,23] After Gd-contrast administration, extra-osseous HD can show enhancement to varying degrees. Epidural HD usually shows Gd-contrast enhancement and can cause spinal cord compression.[8]

During and shortly after treatment of HD, mediastinal lesions often have an increase in signal heterogeneity on T2W1.[3] After 6 months, successfully treated HD lesions in the mediastinum typically are decreased in size and have low signal on T1WI and T2WI.[3] Treated HD lesions that contain zones of high signal on T2WI may represent recurrent lymphoma.[3]

IMon-Hodgkin lymphoma:

- Bone.[5-7,12,16-18,27,28] NHL within bone typically appears as intramedullary zones with low-intermediate signal on T1WI and PDWI, and slightly high to high signal on T2WI and high signal on FST2WI (Figs. **277, 280, 281, 284, 285-290).** Zones of low signal on T1WI and T2WI may be secondary to fibrosis.[12] Intramedullary lesions may have poorly defined or distinct margins. Zones of cortical destruction may occur associated with extra-osseous soft tissue lesions. In some cases of NHL, intramedullary tumor may be associated with bulky extra-osseous lesions without extensive cortical destruction[7,12] (Fig. **289).** High resolution MRI in these cases shows thin, penetrating channels of tumor extending through bone cortex into the extra-osseous soft tissues.[7] In these cases, tumor cells were found to produce soluble cytokine mediators which increase osteoclastic bone resorption.[7]

NHL typically shows show Gd-contrast enhancement.[12] Destruction of cortical and medullary bone may also occur from invasion from adjacent extra-osseous NHL.

Evaluation of bone marrow in patients undergoing chemotherapy has shown sequential quantitative decreases in Tl values in patients with positive responses to treatment.[18] Rapid decreases of tumor volume including extra-osseous extent of neoplasm are usually seen with successful treatment.[16]

- **Soft tissue.**[7,11-13,23,24,27]NHL lesions in soft tissue often have low-intermediate signal on T1W1 and PDWI; intermediate to slightly high signal on T2WI; and intermediate-high signal on FSPDWI and FST2WI[11] (Figs. **283, 284, 291-293).** Variability in MRI signal characteristics may be related to differing histologic features (such as the degree of fibrosis) for the subtypes of NHL[3,23] After Gd-contrast administration, extra-osseous NHL usually shows enhancement in varying degrees. Epidural NHL usually shows Gd-contrast enhancement and can cause compression of the spinal cord or nerve roots exiting the spinal canal.[13] Intradural NHL can often be seen as irregular zones of Gd-contrast within the thecal sac surrounding the spinal cord and/or nerve roots (Fig. **281).** Paravertebral NHL can extend over multiple vertebral segments[27] (Figs. **279, 283).** NHL can infiltrate soft tissues such as muscle, nerves, dermis, and epidermis (Figs. **280,281,284, 285, 291-293)** as well as the intracranial dura (Figs. 277, 278). Mycosis fungoides can appear as single or multiple lesions involving the skin (Fig. **292).**

a

b

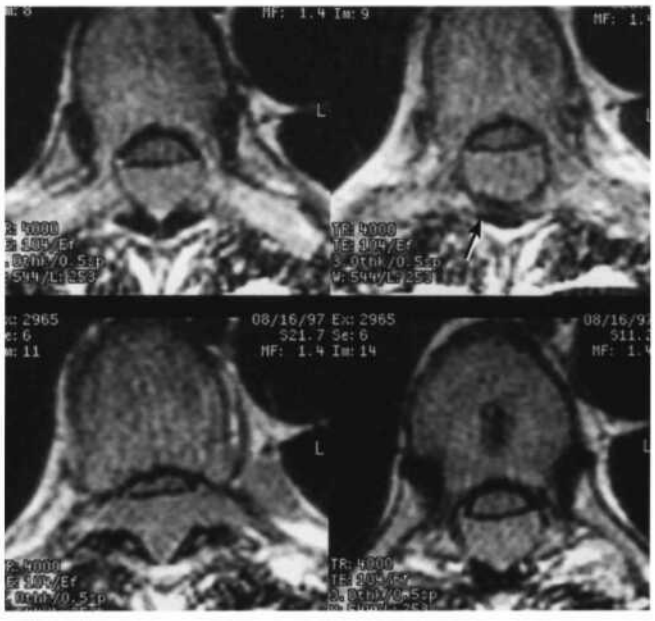

c

Figure **279a-c** Epidural non-Hodgkin lymphoma causing compression of the thoracic spinal cord. The epidural lesion has intermediate signal on sagittal T1WI (**a**), and sagittal (**b**) and axial (**c**) T2WI.

a

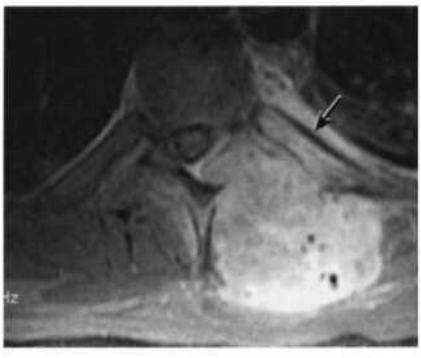

b

Figure **280a, b** A 23-year-old man with large cell non-Hodgkin lymphoma involving posterior vertebral elements and soft tissues at the thoracic spine with extension into the spinal canal. The tumor has heterogeneous intermediate, slightly high and high signal on axial T2WI, as well as several curvilinear zones of low signal (a). The tumor shows Gd-contrast enhancement on axial FST1WI (**b**).

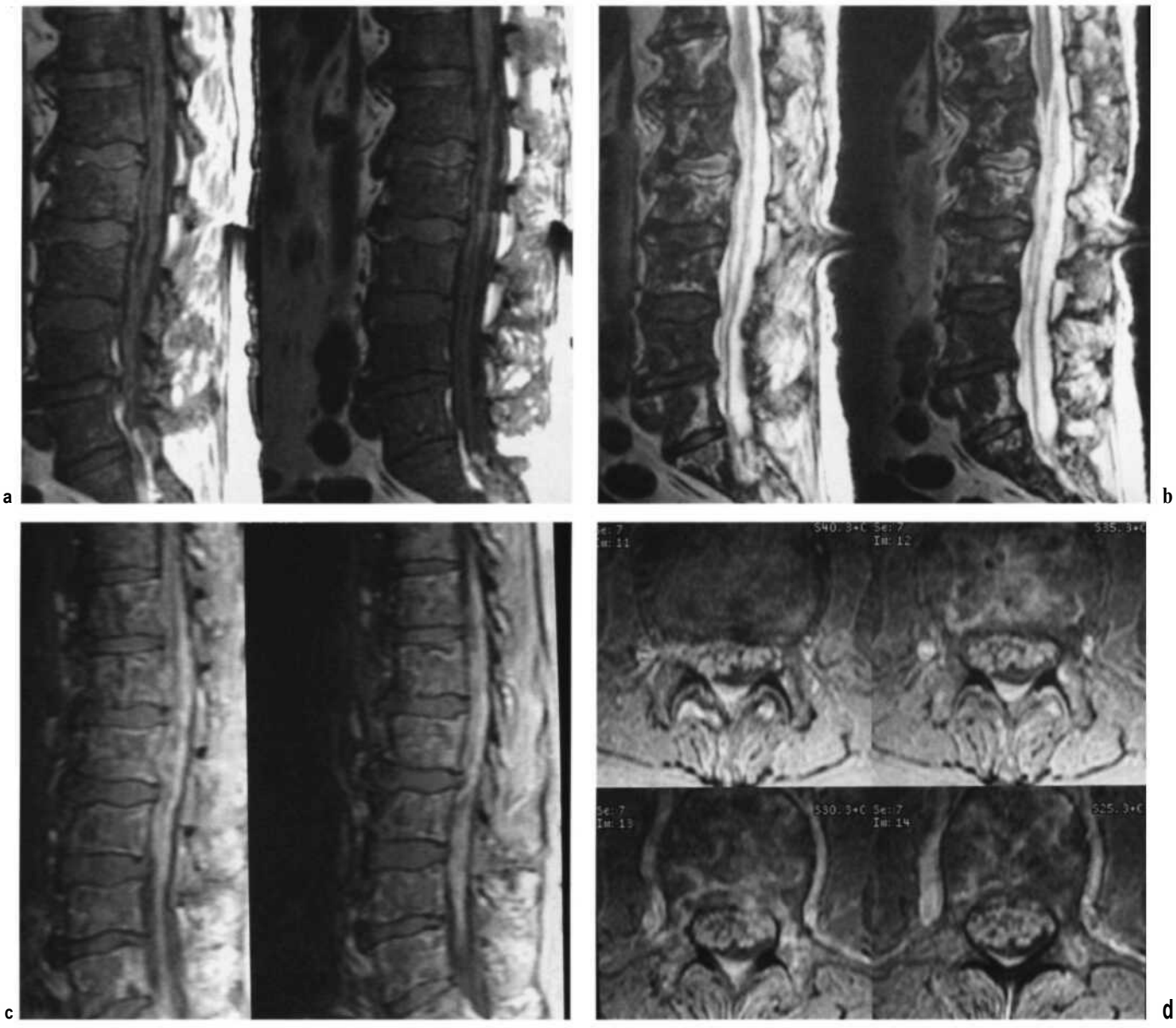

Figure **281 a-d** Non-Hodgkin lymphoma involving vertebral marrow as well as within the lumbar subarachnoid space. Diffuse low-intermediate signal on sagittal T1WI (a) is seen throughout the marrow. Heterogeneous mostly low signal is seen in the marrow on sagittal T2WI (**b**). Heterogeneous Gd-contrast enhancement is seen throughout the marrow as well as within the thecal sac on sagittal (c) and axial (**d**)FSTIWI.

Differential Diagnosis

Hodgkin disease:[4,21]

- **Bone.** Metastatic disease, myeloma, osteosarcoma, fibrosarcoma, malignant fibrous histiocytoma, eosinophilic granuloma / Langerhans cell histiocytosis, osteomyelitis.
- **Soft tissue.** Metastatic disease, infectious mononucleosis, toxoplasmosis, histoplasmosis, sarcoidosis, Langerhans cell histiocytosis, Castleman disease (angiofollicular lymphoid hyperplasia), post-transplantation lymphoproliferative disease.

Non-Hodgkin lymphoma:[4,12,21]

- **Bone.** Metastatic disease, myeloma, osteosarcoma, fibrosarcoma, malignant fibrous histiocytoma, eosinophilic granuloma / Langerhans cell histiocytosis, osteomyelitis, metastatic neuroblastoma (children), Ewing sarcoma (children).
- **Soft tissue.** Metastatic disease, sarcoidosis, lymphadenpathy from bacterial infection, viruses (infectious mononucleosis, HIV, CMV, rubella), parasites such as toxoplasmosis, Castleman disease (angiofollicular lymphoid hyperplasia), post-transplantation lymphoproliferative disease, Langerhans cell histiocytosis.

Prognosis and Treatment

Hodgkin disease:

- HD is often staged using the Ann Arbor Classification.[1,4,24]
  - Stage I includes involvement of a single lymph node region or single extralymphatic site.
  - Stage II includes involvement of two or more lymph node regions on the same side of the diaphragm, or limited involvement of contiguous extralymphatic sites.
  - Stage III includes involvement of lymph node regions on both sides of the diaphragm, with or without splenic involvement and/or or limited involvement of contiguous extralymphatic sites.
  - Stage IV includes multiple or disseminated foci.

- The 5-year survival rate for children under 15 years is 92 %.[10] Solitary bone lesions are treated with radiation.[21] Chemotherapy is used for patients with generalized disease.[21]

Non-Hodgkin lymphoma:

- NHL is often staged using the Ann Arbor Classification, as with HD.[14,24] This classification scheme, however, is less effective for NHL, which usually disseminates hematogenously rather than by contiguous lymphatic extension as typically occurs with HD.
- Only 10 % of patients with NHL have localized disease (stages I or II). These patients can be treated with localized radiation therapy.[4,19] The 5-year relapse-free survival is ~ 70 % for patients with stages I or II.[4] The uncommon form of NHL involving a single site in bone (reticulum cell sarcoma) is typically treated successfully with radiation or excision with wide margins, often followed by chemotherapy.[12,16,21]

The majority of patients with NHL have disseminated disease requiring systemic chemotherapy[4,21] Additional radiotherapy is often utilized for treatment of localized bulk disease.[4] Patients with advanced or recurrent disease have been treated with high-dose chemotherapy and autologous stem cell transplantation.[4]

The overall 5-year survival rate for adults and children with NHL is 53 %.[10] The 5-year survival rate for children with NHL under 15 years is 80 %.[10] Patients with aggressive NHL—such as diffuse, large B-cell lymphoma, aggressive T-cell lymphoma (rare), and AIDS-related lymphoma—are usually

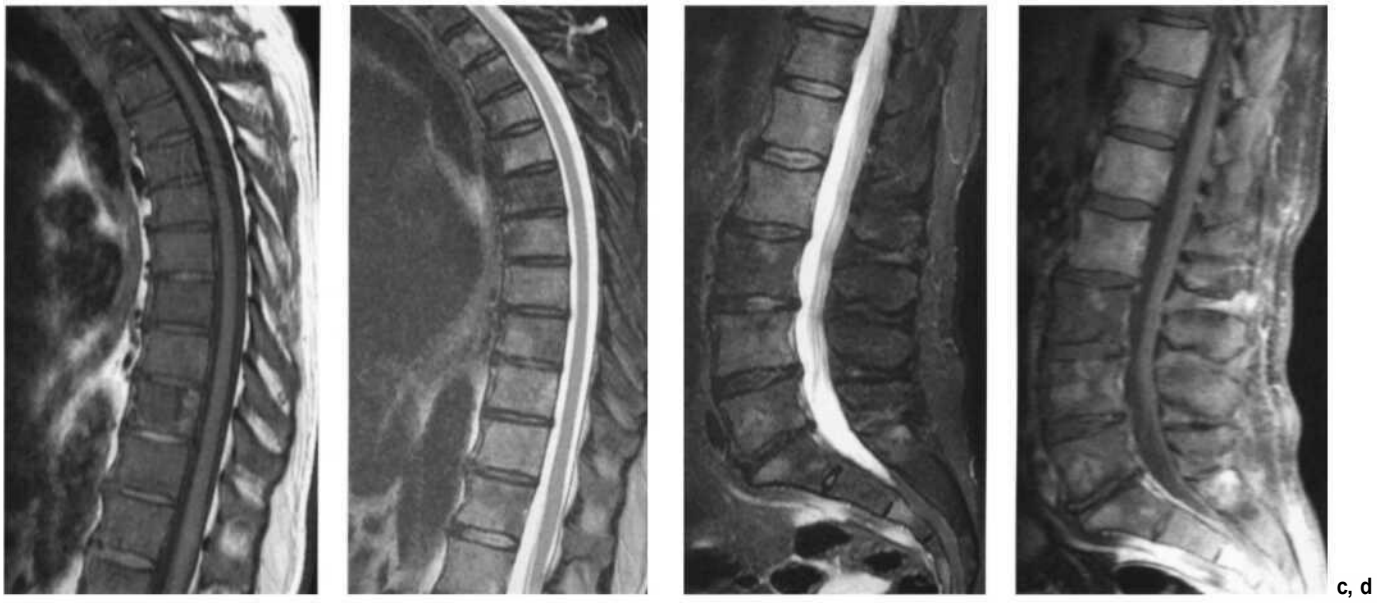

Figure **282 a-f** A 46-year-old man with Hodgkin lymphoma involving multiple thoracic and lumbar vertebrae, and sacrum. The lymphoma is seen as extensive, multiple, poorly defined zones in the marrow which have low-intermediate signal on sagittal (**a**) T1WI, slightly high signal on sagittal (**b, c**) FST2WI, and mild to moderate Gd-contrast enhancement on sagittal (**d**) FST1WI. Extensive, diffuse, osteosclerotic reaction is seen involving many thoracic and lumbar vertebrae on sagittal reconstructed CT (**e**). Sagittal positron emitting tomography (**f**) using F-18 fluorodeoxyglucose shows abnormal uptake in multiple vertebrae and sacrum secondary to the Hodgkin lymphoma.

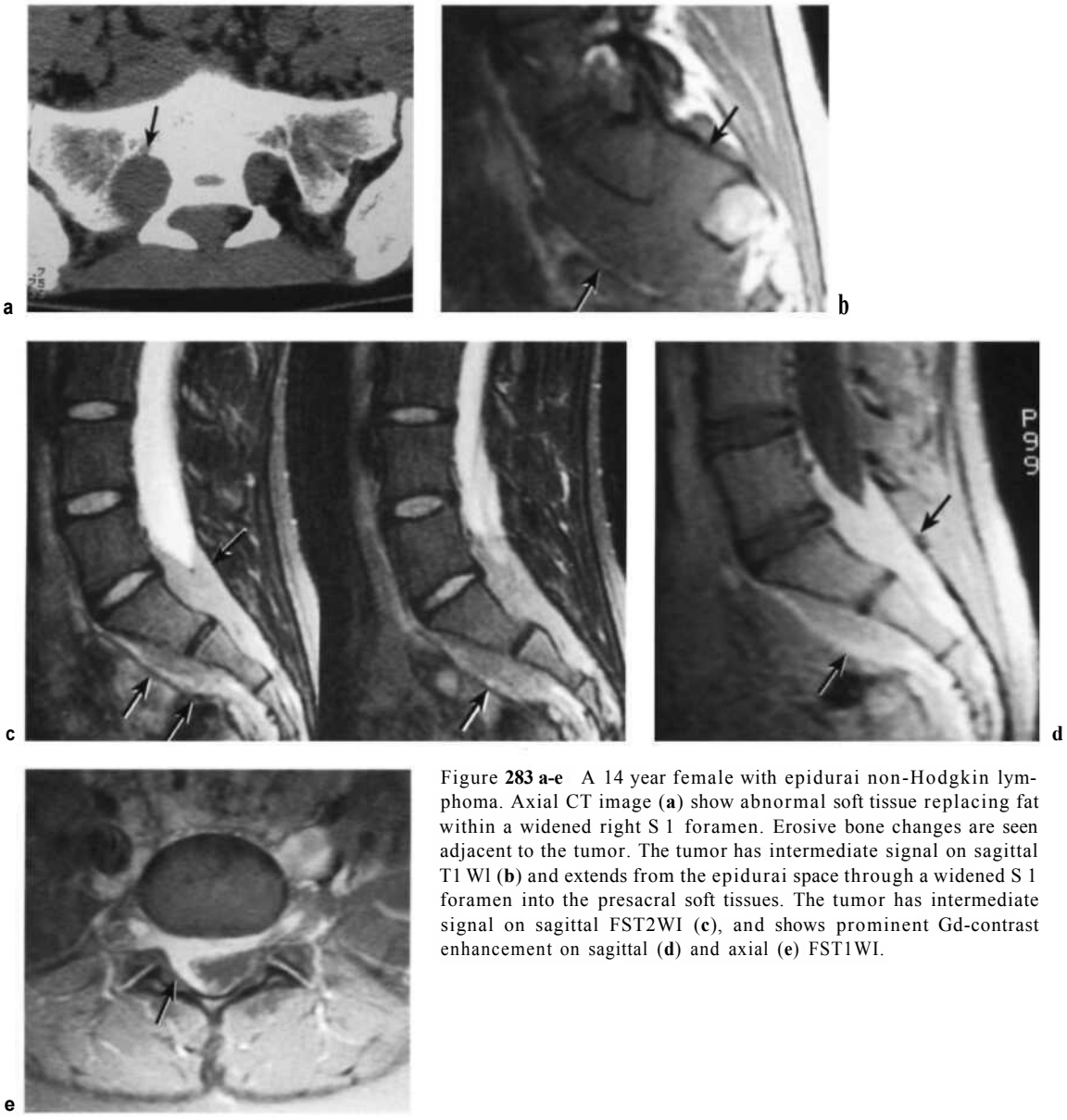

Figure **283 a-e** A 14 year female with epidurai non-Hodgkin lymphoma. Axial CT image (**a**) show abnormal soft tissue replacing fat within a widened right S 1 foramen. Erosive bone changes are seen adjacent to the tumor. The tumor has intermediate signal on sagittal T1 Wl (**b**) and extends from the epidurai space through a widened S 1 foramen into the presacral soft tissues. The tumor has intermediate signal on sagittal FST2WI (**c**), and shows prominent Gd-contrast enhancement on sagittal (**d**) and axial (**e**) FST1WI.

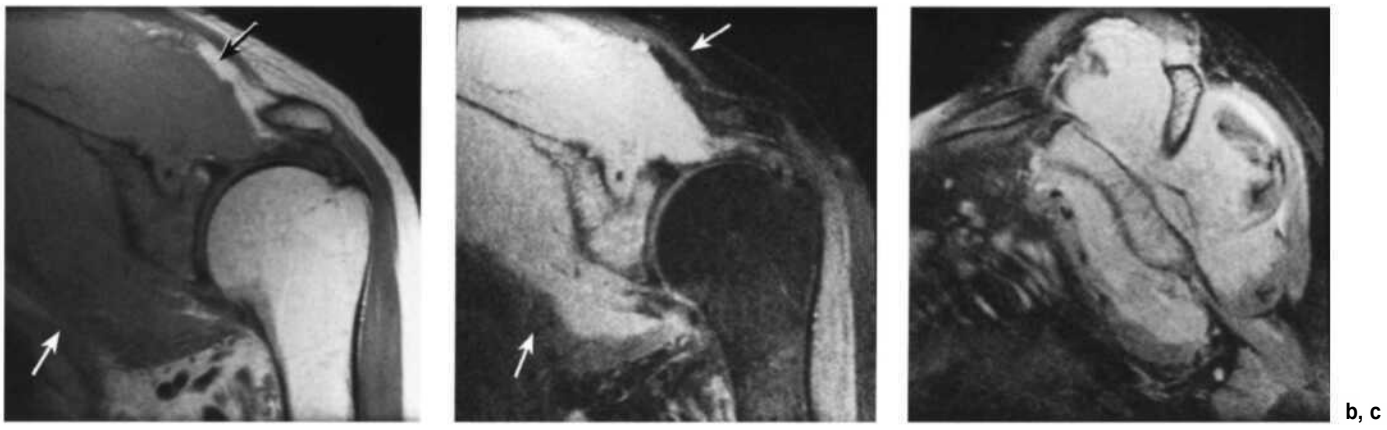

Figure **284a-c** A 66-year-old woman with non-Hodgkin lymphoma involving the marrow of the left scapula and adjacent soft tissues including the supraspinatus, infraspinatus, subscapularis, and teres minor muscles. The lymphoma has intermediate signal on coronal (a) PDWI, and high signal on coronal (**b**) and sagittal (**c**) FST2WI.

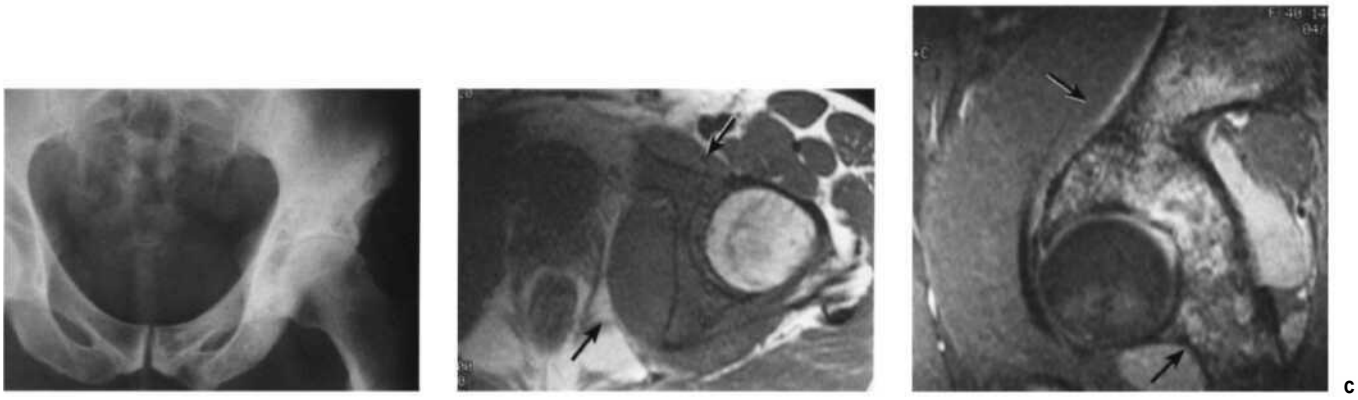

Figure **285a-c** A 40-year-old woman with large cell non-Hodgkin lymphoma involving the marrow of the left bony pelvis with extension into the extra-osseous soft tissues, including the hip joint. AP radiograph (a) shows a permeative radiolucent abnormality involving the left ischial and pubic bones. The lymphoma has low-intermediate signal on axial T1 Wl (**b**), with tumor extension into the extra-osseous soft tissues through sites of cortical disruption. Enhancing tumor is seen involving bone and extra-osseous soft tissues on postcontrast sagittal FST1WI (**c**).

Figure **286a-d** A 48-year-old woman with diffuse, large B-cell non-Hodgkin lymphoma involving the marrow of the left bony pelvis and proximal femur. AP radiograph (**a**) shows increased density in the femoral head as well as mild contour deformity and small osteophytes at the acetabulum. The lymphoma has low-intermediate signal within the marrow of the bony pelvis and proximal femur on coronal T1WI (**b**), and heterogeneous mostly high signal on coronal FST2WI (**c**). The lymphoma shows heterogeneous Gd-contrast enhancement on coronal FST1WI (**d**).

treated with aggressive multi-agent chemotherapy. Five-year survival rates range from 26 to 73 % for patients with aggressive NHL, depending upon which risk category the patient is assigned to. Features associated with increased or elevated risk include age over 60 years, limited response to first-line therapy, stages III or IV, and presence of more than one extranodal site of disease.[4] Prognosis in patients with mycoides fungosis is related to the extent of disease and clinical stage.[26] Extracutaneous dissemination of mycosis fungoides is typically a late event and usually occurs in those with extensive skin involvement.[26]

a

b

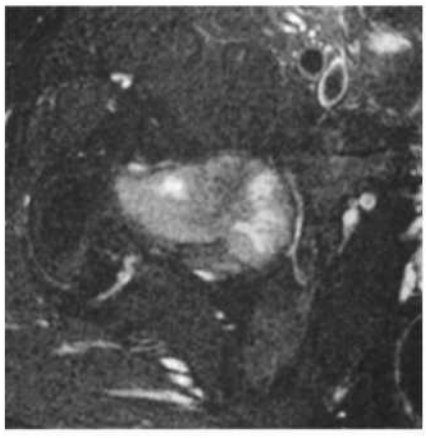

c

d

Figure **287 a-d** A 55-year-old man with non-Hodgkin lymphoma involving the marrow of the right proximal femur. AP radiograph (a) shows no definite abnormality. The lymphoma has low-intermediate signal within the marrow of the proximal femur on coronal T1WI (**b**), and heterogeneous mostly high signal on axial FST2WI (**c**). The lymphoma shows heterogeneous Gd-contrast enhancement on coronal FST1WI (**d**).

a

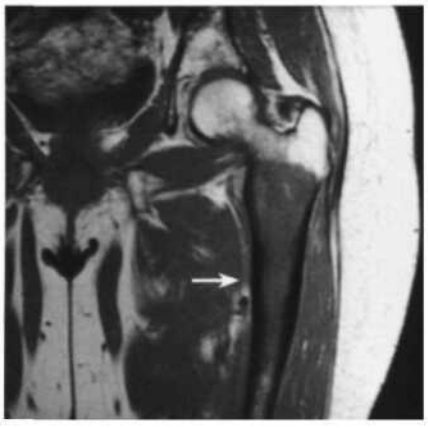

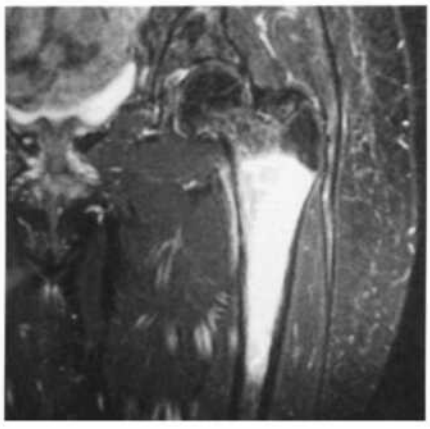

b, c

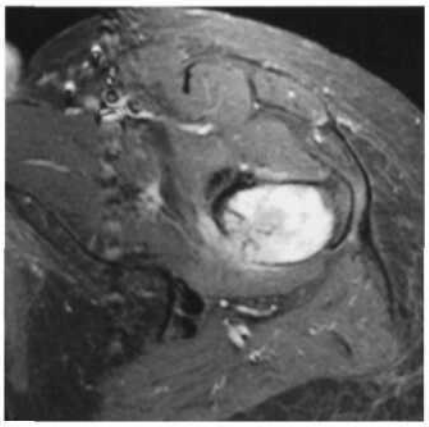

d

Figure **288 a-d** A 68-year-old woman with follicular, mixed small-cleaved and large-cell non-Hodgkin lymphoma involving the marrow of the proximal left femur. AP radiograph (a) shows a subtle, permeative radiolucent zone in the proximal shaft of the femur. The lymphoma has low-intermediate signal within the marrow of the proximal femur on coronal T1WI (**b**), and high signal on coronal FST2WI (c). The lymphoma shows Gd-contrast enhancement on axial FST1WI (**d**). The lymphoma is associated with cortical thinning and disruption with extra-osseus tumor extension.

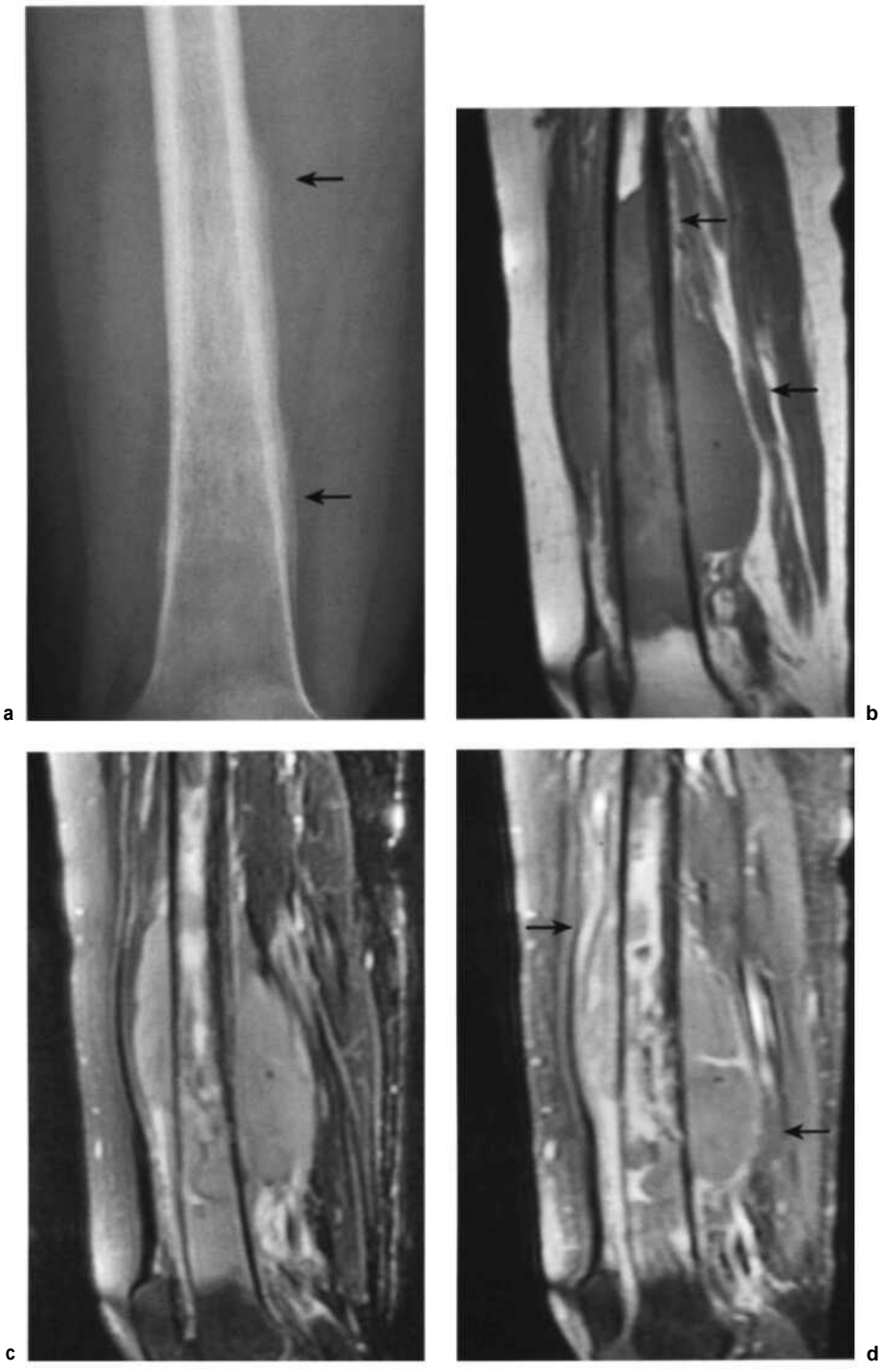

Figure **289a-d** A 36-year-old woman with large cell non-Hodgkin lymphoma involving the marrow of the distal femur. AP radiograph (a) shows permeative intramedullary radiolucent changes with zones of cortical disruption, multilayered periosteal reaction and Codman triangles. On MRI, the intramedullary tumor has slightly indistinct margins, and shows extensive extra-osseous tumor extension relative to the degree of cortical disruption. Elevated periosteum is seen with subjacent layered periosteal reaction caused by the tumor. The tumor has heterogeneous intermediate signal on sagittal T1WI (**b**), and heterogeneous slightly high and high signal on sagittal FST2WI (c). The tumor shows heterogeneous Gd-contrast enhancement on sagittal FST1WI (**d**).

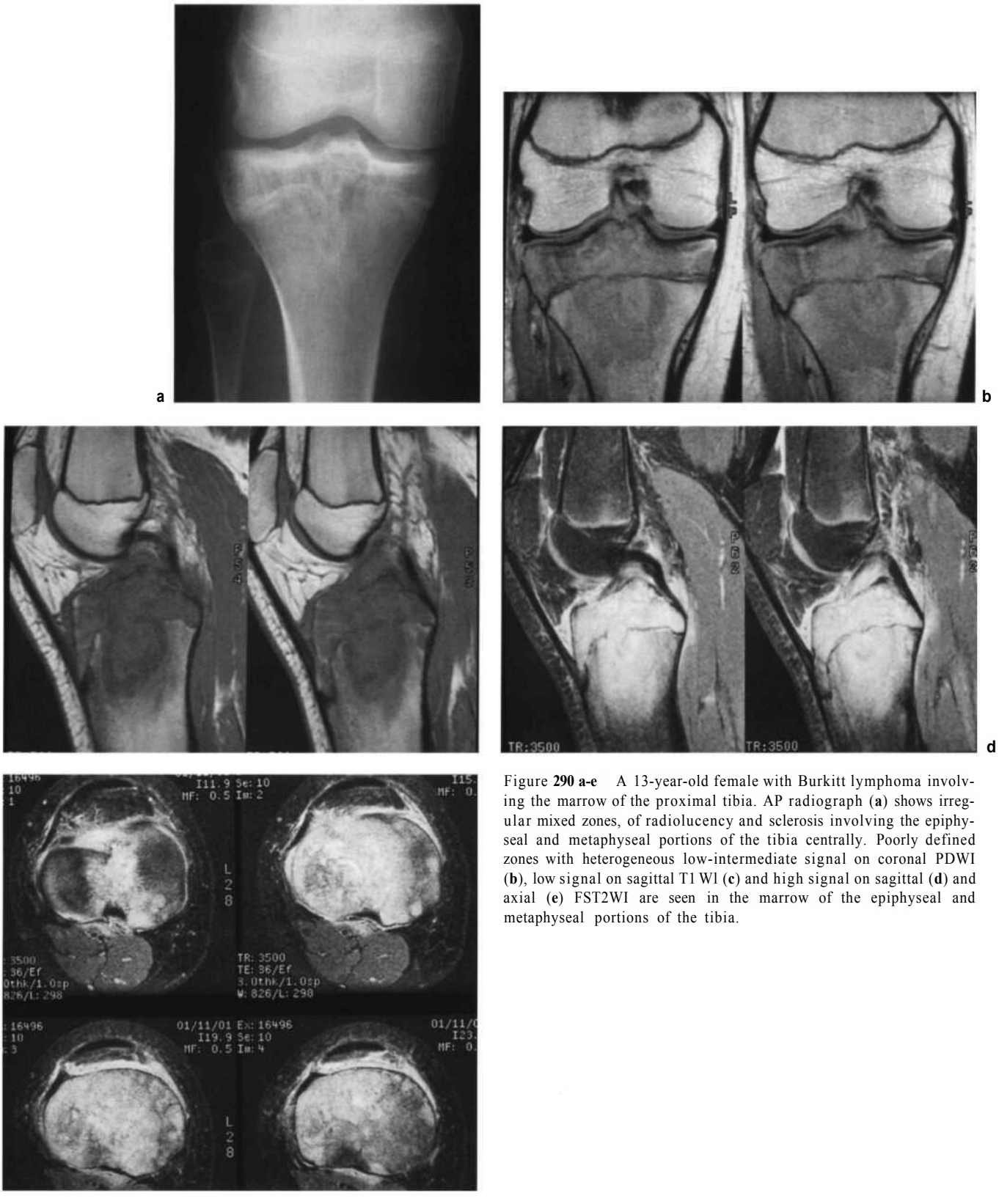

Figure **290 a-e** A 13-year-old female with Burkitt lymphoma involving the marrow of the proximal tibia. AP radiograph (**a**) shows irregular mixed zones, of radiolucency and sclerosis involving the epiphyseal and metaphyseal portions of the tibia centrally. Poorly defined zones with heterogeneous low-intermediate signal on coronal PDWI (**b**), low signal on sagittal T1 Wl (**c**) and high signal on sagittal (**d**) and axial (**e**) FST2WI are seen in the marrow of the epiphyseal and metaphyseal portions of the tibia.

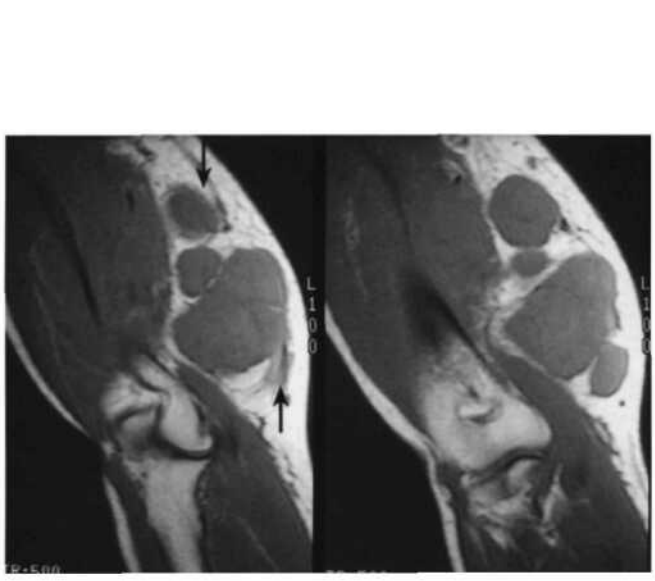

a

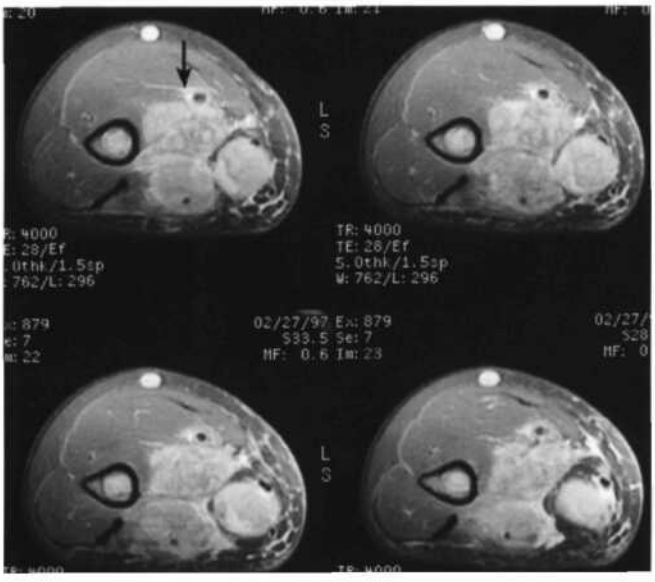

b

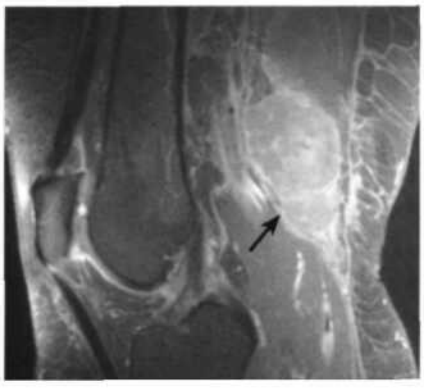

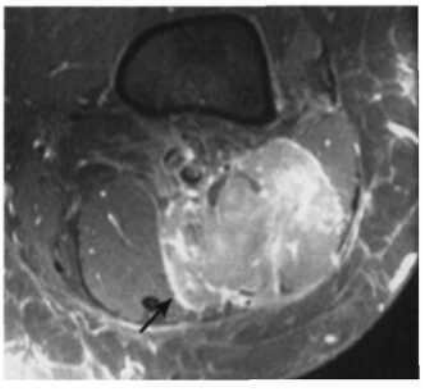

c, d

Figure **291 a-d** 66-year-old man with diffuse large B cell Non-Hodgkin lymphoma involving the subcutaneous fat, biceps brachii muscle, medial head of the triceps muscle and neurovascular bundle in the elbow region. Multiple nodular lesions with intermediate signal on coronal T1WI (**a**) are seen, which have heterogenous high signal on axial FS PDWI (**b**). A 51-year-old woman with diffuse, large B-cell non-Hodgkin lymphoma involving the posterior soft tissues at the distal thigh, which shows slightly heterogeneous Gd-contrast enhancement on sagittal (**c**) and axial (**d**)FSTIWI.

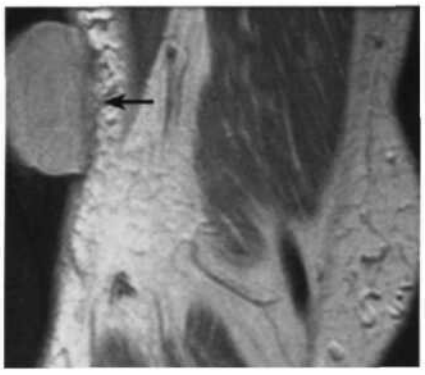

a

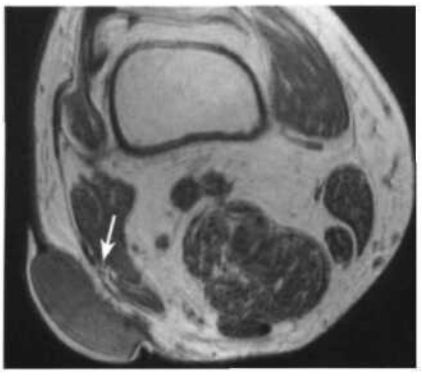

b

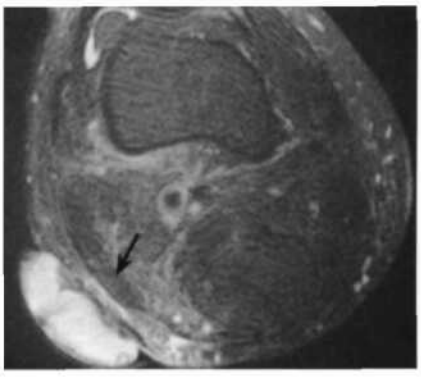

c

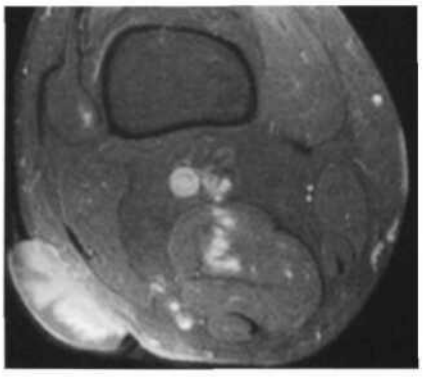

d

Figure **292a-d** A 62-year-old man with Tcell lymphoma (mycosis fungoides) involving the skin. The nodular lesion involves the epidermis and has intermediate signal on coronal PDWI (**a**) and axial T1WI (**b**), and heterogeneous high signal on axial FST2WI (**c**). The tumor shows heterogeneous Gd-contrast enhancement on axial FST1WI (**d**).

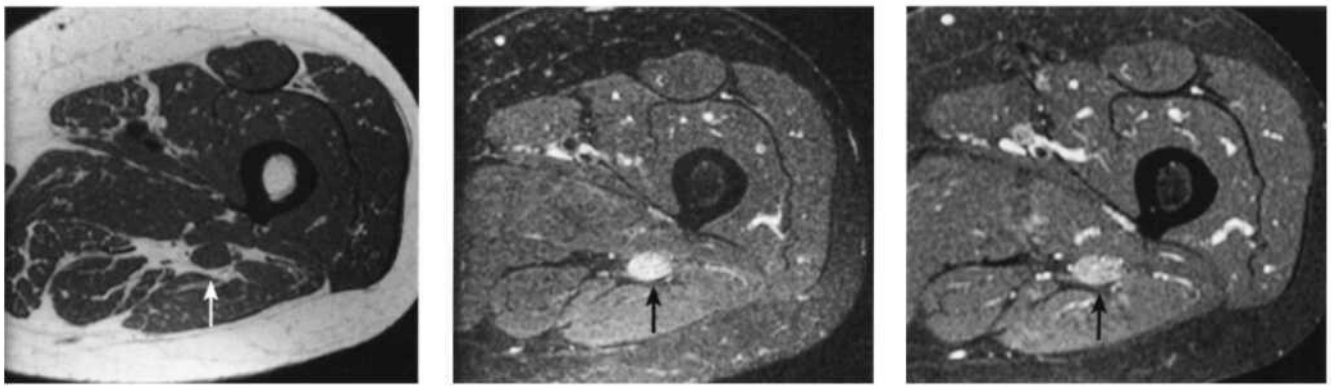

a b, c

Figure **293a-c** A 70-year-old woman with B cell non-Hodgkin lymphoma involving the sciatic nerve. The lymphoma has intermediate signal on axial T1WI (**a**) and high signal on axial FST2WI (**b**). The lesion shows Gd-contrast enhancement on axial FST1WI (c).

References

1 Aster J, Kumar V. White cells, lymph nodes, spleen and thymus. In: Cotran RS, Kumar V, Collins T, eds. *Pathologic Basis of Disease* 6th ed. Philadelphia, Pa: W.B. Saunders; 1999:644-695.

2 Diebold J. Primary lymphoma of bone. In: Forest M, Tomeno B, Vanel D, eds. *Orthopedic Surgical Pathology: Diagnosis of Tumors and Pseudotumoral Lesions of Bone and Joints* Edinburgh: Churchill Livingstone; 1998:467-474.

3 Erasmus JJ, McAdams P, Donnelly LF, Spitzer CE. MR imaging of mediastinal masses. *Magn Reson Imaging ClinN Am* 2000;8:59-89.

4 Freedman AS, Nadler LM. Malignancies of lymphoid cells. In: Fauci AS, Braunwald E, Isselbacher KJ, et al, eds. *Harrison's Principles of Internal Medicine* 14th ed. New York, NY: McGraw-Hill; 1998: 695-712.

5 Haussler MD, Fenstermacher MJ, Johnston DA, Harle TS. MRI of primary lymphoma of bone: cortical disorder as a criterion for differential diagnosis. J Magn Reson *Imaging* 1999:9:93-100.

6 Hernandez RJ, Teo EL. Diffuse marrow disorders in children. *Magn Reson Imaging Clin N Am* 1998;6(3):617-619.

7 Hicks DG, Gokan T, O'Keefe RJ, et al. Primary lymphoma of bone: correlation of magnetic resonance image features with cytokine production by tumor cells. Cancer 1995:75:973-980.

8 Higgins SA, Peschel RE. Hodgkin's disease with spinal cord compression. A case report and a review of the literature. Cancer 1995;75: 94-98.

9 Huvos AG. Skeletal manifestations of malignant lymphomas and leukemias. In: Huvos AG, ed. Bone Tumors: Diagnosis, *Treatment, and Prognosis* 2nd ed. Philadelphia, Pa: W.B. Saunders; 1991: 625-649.

10 Jemal A, Thomas A, Murray T, Thun M. Cancer statistics 2002. *CA Cancer] Clin* 2002;52:23-47.

11 Kransdorf MJ, Murphey MD. Masses that may mimic soft tissue tumors. In: *Imaging of Soft Tissue Tumors* 2nd ed. Philadelphia, Pa: W.B. Saunders; 2006:511-572.

12 Krishnan A, Sirkhoda A, Tehranzadeh J, Armin AR, Irwin R, Les K. Primary bone lymphoma: radiographic-MR imaging correlation. *Radiographics* 2003;23:1371-1387.

13 Mascalchi M, Torselli P, Falaschi F, DalPozzo G. MRI of spinal epidural lymphoma. Neuroradiology 1995;37:303-307.

14 McClain KL. Hodgkin's disease. In: McMillan JA, DeAngelis CD, Feigin RD, Warshaw JB, eds. Oski's Pediatrics: *Principles and Practice* 3rd ed. Philadelphia, Pa: Lippincott, Williams & Wilkins; 1999:1507-1509.

15 McClain KL. Non-Hodgkin's disease. In: McMillan JA, DeAngelis CD, Feigin RD, Warshaw JB, eds. Osfci's *Pediatrics: Principles and Practice* 3rd ed. Philadelphia, Pa: Lippincott, Williams & Wilkins; 1999: 1509-1511.

16 Mengiardi B, Honegger H, Hodler J, Exner UG, Csherhati MD, Bruhlmann W. Primary lymphoma of bone: MRI and CT characteristics during and after successful treatment. *AJR Am] Roentgenol* 2005;184:185-192.

17 Meyer JS, Dormans JP. Differential diagnosis of pediatric musculoskeletal masses. Magn Reson *Imaging Clin N Am* 1998;6(3):570-571.

18 Moulopoulos LA, Dimopoulos MA. Magnetic resonance imaging of the bone marrow in hematologic malignancies. *Blood* 1997;90: 2127-2147.

19 Mulder JD, Schutte HE, Kroon HM, Taconis WK. Introduction. In: *Radiologic Atlas of Bone Tumors* Amsterdam: Elsevier; 1993:3-6.

20 Mulder JD, Schutte HE, Kroon HM, Taconis WK. The diagnosis of bone tumors. In *Radiologic Atlas of Bone Tumors* Amsterdam: Elsevier; 1993:9-46.

21 Mulder JD, Schutte HE, Kroon HM, Taconis WK. Malignant Lymphoma. In: *Radiologic Atlas of Bone Tumors* Amsterdam: Elsevier; 1993:355-372.

22 Mulligan ME, Kransdorf MJ. Sequestra in primary lymphoma of bone: prevalence and radiologic features. *AJR Am J Roentgenol* 1993;160: 1245-1248.

23 Negendank WG, Al-Katib AM, Karanes C, Smith MR. Lymphomas: MR imaging contrast characteristics with clinical-pathologic correlations. *Radiology* 1990;177(1):209-216.

24 Parker BR. Leukemia and lymphoma in childhood. *Radial Clin North Am* 1997;35(6):1505-1515.

25 Perlman EJ. Ewing's sarcoma, lymphoma, and Langerhans' cell proliferations. In: Helliwell TR, ed. Major *Problems in Pathology: Pathology of Bone and Joint Neoplasms* 1st ed. Vol 37. Philadelphia, Pa: W.B. Saunders; 1999:290-292.

26 Ralfkiaer E, Jaffe ES. Mycosis fungoides and Sezary syndrome. In: Jaffe ES, Harris NL, Stein H, Vardiman JW, eds. Worfd *Health Organization Classification of Tumours. Tumours of Haematopoietic and Lymphoid Tissues* Geneva: IARC Press; 2001:216-220.

27 Resnick D, Haghighi P. Lymphoproliferative and myeloproliferative disorders. In: D. Resnick, ed. *Diagnosis of Bone and Joint Disorders* 5th ed. Philadelphia, Pa: W.B. Saunders; 2002:2291-2344.

28 Siegel MJ, Luker GD. Bone marrow imaging in children. Magn Reson Imaging Clin *NAm* 1996;4(4):782-783, 784.

29 Stein H, Delsol G, Piteri S. Classical Hodgkin lymphoma. In: Jaffe ES, Harris NL, Stein H, Vardiman JW, eds. Worfd *Health Organization Classification of Tumours. Tumours of Haematopoietic and Lymphoid Tissues.* Geneva IARC Press;2001:244-253.

30 Unni KK. Malignant lymphoma of bone (reticulum cell sarcoma). In: *Dahlin's Bone Tumors—General Aspects and Data on n 087 Cases* 5th ed. Philadelphia, Pa: Lippincott, Williams & Wilkins; 1996:237-248.

31 Varan A, Cila A, Buyukpamukcu M. Prognostic importance of magnetic resonance imaging in bone marrow involvement of Hodgkin disease. *Med Pediatr Oncol* 1999;32:267-271.

A 48

Malignant Fibrous Histiocytoma (Also Referred to as Malignant Histiocytoma, Xanthosarcoma, Malignant Fibrous Xanthoma, and Fibroxanthosarcoma)

ICD-O Codes

Pleomorphic malignant fibrous histiocytoma (undifferentiated high-grade pleomorphic sarcoma: 8830/3

Giant cell malignant fibrous histiocytoma (undifferentiated pleomorphic sarcoma with giant cells): 8830/3

Inflammatory malignant fibrous histiocytoma (undifferentiated pleomorphic sarcoma with prominent inflammation): 8830/3

Myxofibrosarcoma (myxoid malignant fibrous histiocytoma): 8811/3

Definition

Malignant fibrous histiocytoma (MFH) is a malignant tumor involving soft tissue and, rarely, bone that is likely derived from undifferentiated mesenchymalcells.[1-14,17,23,26] These malignant tumors contain cells with limited cellular differentiation such as mixtures of fibroblasts, myofibroblasts, histiocytelike cells, anaplastic giant cells, and inflammatory cells.'[1-14,17,23,27] MFH is considered the most common type of soft tissue sarcoma occurring as a complication of radiation treatment.[13,17] Histologic subtypes of MFH include (1) storiform-pleomorphic (50-60%), (2) myxoid (25%), (3) Giant cell (5-10%), and (4) inflammatory (5-10 %).[3,6-8,14,24,25]

Until recently, pleomorphic MFH was considered to be the most common sarcoma of soft tissues in adults.[3,6-8,19,20,28] The grouping of these tumors based on the concept of fibrohistiocytic differentiation has been challenged.[6-8,19] Pleomorphic MFH tumors are now considered to represent less than 5 % of adult sarcomas, and their definition has been restricted to those tumors without histologic, ultrastructural, and immunohistochemical features of myogenic differentiation.[6-8,19] The World Health Organization (WHO) now uses the term undifferentiated pleomorphic sarcoma for pleomorphic MFH. Myxofibrosarcoma is also the preferred term now for myxoid MFH.[19] Other subtypes in the new WHO Classification include giant cell malignant fibrous histiocytoma (undifferentiated pleomorphic sarcoma with giant cells) and inflammatory malignant fibrous histiocytoma (undifferentiated pleomorphic sarcoma with prominent inflammation).

Frequency of Occurrence

Soft tissue. MFH was previously considered to be the most common primary malignant tumor of the soft tissues. These tumors were reported to account for 24% of primary malignant soft tissue tumors and 10% of all primary soft tissue tumors.[16] Recent immunohistochemical studies have shown that many MFHs can be now be reclassified as various forms of myogenic sarcomas.[5-8] In 2002 the WHO revised the classification of MFH to exclude pleomorphic tumors exhibiting histologic, ultrastructural, and immunohistochemical features of myogenic differentiation.[5-8] As a result, pleomorphic MFH now represents a smaller group of undifferentiated pleomorphic sarcomas.[5-8]

Bone. Primary MFH in bone is rare, and represents between 1 and 5 % of primary malignant bone tumors and < 1 % to 3 % of all primary bone tumors.[21,25,26] MFH in bone can occur as primary bone tumors or secondary to pre-existing abnormalities such as Paget disease, bone infarct, or radiation injury.[25] Secondary MFH accounts for nearly 30 % of MFH in bone.[25]

Age at Presentation

Soft tissue: from 32 to 80 years, mean = 59 years.[15,16]

Bone: from 11 to 80 years, median = 48 years, mean = 55 years.[21]

Gender Ratio (M / F)

Soft tissue: 1.2 to 1.3/1.[7,15,16]

Bone: 1.2/1 to 1.4/1.[11,23,27]

Location

Soft tissue. Tumors occur in the lower extremity > upper extremity > trunk > hip and buttocks, retroperitoneum > proximal limb girdle, head and neck > foot and ankle > hand and wrist.[15,16]

Bone. Tumors occur in the femur > tibia > humerus > iliac bone > craniofacial bones > vertebra > scapula > other bones.[11,23,25] Metadiaphyseal > diaphyseal > metaphyseal > epi-metadiaphyseal > epi-metaphyseal.[23] Almost all primary MFHs in bone are solitary, although rare multifocal primary MFHs have been reported.[9,25]

Signs and Symptoms

Soft tissue. Patients often present with enlarging, painless lesions often ranging in size between 5 and 15 cm.[1,6,14] Lesions can be superficial or deep.[1,6,14] Retroperitoneal MFH can exceed 20 cm.[7]

Bone. Patients can have pain and swelling ranging from 1 week to 3 years, average = 5 months.[9,11,22,24] Pathologic fractures occur in 21-23% of cases.[9,11,18,23,25]

Cross Pathologic Findings

Soft tissue. MFHs are often circumscribed masses that may include fleshy or pale fibrous zones, with or without necrosis, hemorrhage, or myxoid changes.[3,7,8] Lesions can be permeative with ill-defined erosions of adjacent bone.[12] Some lesions may have yellow regions secondary to xanthoma cells.[3] Myxofibrosarcomas often contain multiple solid nodules and gelatinous zones with or without necrosis.[19] Giant cell MFHs tend to be large with necrosis and hemorrhage.[8] Inflammatory MFHs can be large and often contain xanthoma cells.[3]

Bone. MFHs in bone are typically medullary lesions associated with trabecular and cortical destruction as well as an extra-osseous soft tissue tumormass.[9,11,23,25] The extra-osseous compo-

nent may be multinodular with or without a pseudocapsule, or may be infiltrative.[22] Lesions can be tan, gray-white, gray-red, soft and/or firm.[9,11,12,23,25,27] Yellow zones secondary to lipid deposits may be present as well as hemorrhagic and necrotic areas.[9,11,23,25,27]

Histopathologic Findings

Soft tissue:[1346-8]

- **Pleomorphic malignant fibrous histocytoma (undifferentiated high-grade pleomorphic sarcoma.** Tumors often have heterogeneous cellularity with prominent cytologic and nuclear pleomorphism, and variable fibrous stroma.[7] Tumors often contain bizarre giant tumor cells, rounded histiocytelike cells and spindle cells which may have a storiform configuration[7]
- **Myxoid malignant fibrous histiocytoma (myxofibrosarcoma).** These tumors have a myxoid component containing hyaluronic acid which may account for more than 50 % of the tumor volume; as well as mixtures of spindle tumor cells, bizarre giant tumor cells, and spheroid histiocytic cells with foamy cytoplasm.[1419] Tumors can have a multinodular pattern with incomplete fibrous septa.[19] Elongated thin-walled blood vessels surrounded by tumor and/or inflammatory cells may be seen.[19] Higher grade tumors tend to contain more solid portions with spindled and pleomorphic tumor cells with high mitotic activity, as well as zones of necrosis and hemorrhage.[19] These tumors are now referred to as myxofibrosarcomas.[19]
- **Giant cell malignant fibrous histiocytoma.** These tumors consist of pleomorphic spindle or ovoid cells within a stroma containing numerous bizarre multinucleated giant cells." Areas of necrosis, hemorrhage, and/or osteoid formation may be present.[14]
- **Inflammatory malignant fibrous histiocytoma.** These tumors contain layers of xanthoma cells, inflammatory cells (neutrophils, eosinophils, lymphocytes, plasma cells), occasional large tumor cells with irregular hyperchromatic nuclei and prominent nucleoli, and pleomorphic tumor spindle cells in disorganized patterns within a hyalinized collagenous background.[3]
- **Storiform-pleomorphic malignant fibrous histiocytoma (description prior to new WHO system).** These tumors have heterogeneous cellularity within a fibrous stroma containing spindle cells (which can appear fibroblastic, myofibroblastic, smooth-muscle-like), bizarre giant cells, and spheroid histiocytic cells with foamy cytoplasm.[467] Tumor cells can occur in a storiform pattern with or without chronic inflammatory cells.[7] By definition, most tumor cells in MFH are poorly differentiated.[7] Using immunohistochemistry, tumors may show areas with varying degrees of differentiation (myogenic-leiomyosarcoma, rhabdomyosarcoma, liposarcoma, carcinoma, melanoma).[7] Osteoid and cartilage production are not present in MFH.[12]

Immunohistochemical Findings

Since 2002 the WHO now excludes the diagnosis of undifferentiated MFH when pleomorphic tumors exhibit histologic, ultrastructural, and immunohistochemical features of myogenic differentiation.[5-8] For example, leiomyosarcoma typically shows extensive positivity for smooth muscle actin (SMA) and pan muscle actin (HHF-35), and often desmin; but not to myosin and myoglobin.[6] Pleomorphic rhabdomyosarcomas are strongly positive for desmin, and often for fast myosin, myoglobin, and HHF-35, but rarely to SMA.[6] Pleomorphic myogenic sarcoma usually is reactive to desmin or SMA, but does not have the other histologic and immunophenotypic features of leiomyosarcoma or rhabdomyosarcoma.[6] Myofibroblastic sarcoma is reactive to HHF-35 or SMA, but not to desmin.[6] Using these and other criteria, MFH has become a less frequent diagnosis and is synonymous with undifferentiated pleomorphic sarcoma.[3,6-8]

Tumor Genetics

MFH is associated with varied heterogeneous chromosomal rearrangements within different portions of the tumors as well as triploid and teraploid chromosome numbers.[7] Losses of 2 p24-pter, 2 q32-qter, chromosomes 11,13, and 16 have been reported.[7] Mutations and/or deletions of TP53, RBI, and CDKN2A have been suggested to be involved in tumor development.[7]

Bone:[3,7,9-11,12,23,25,27]

- **Storiform-pleomorphic malignant fibrous histiocytoma.** These tumors have heterogeneous cellularity within a fibrous stroma containing spindle cells (which can appear fibroblastic, myofibroblastic, smooth-muscle-like), bizarre giant cells, and spheroid histiocytic cells with foamy cytoplasm.[467] Tumor cells can occur in a storiform pattern with or without chronic inflammatory cells.[7] By definition, most tumor cells in MFH are poorly differentiated.[7] Using immunohistochemistry, tumors may show areas with varying degrees of differentiation (myogenic-leiomyosarcoma, rhabdomyosarcoma, liposarcoma, carcinoma, melanoma).[7] Osteoid and cartilage production are not present in MFH.[12]
- **Myxoid malignant fibrous histiocytoma (myxofibrosarcoma).** These tumors have a myxoid component containing hyaluronic acid which is more than 50 % of the lesion volume; as well as spindle cells, bizarre giant cells, and spheroid histiocytic cells with foamy cytoplasm.[14]
- **Giant cell malignant fibrous histiocytoma.** These tumors consist of pleomorphic spindle or ovoid cells within a stroma containing numerous bizarre, multinucleated giant cells.[8] Areas of necrosis, hemorrhage and/or osteoid formation may be present.[14]
- **Inflammatory malignant fibrous histiocytoma.** These tumors contain layers of xanthoma cells, inflammatory cells (neutrophils, eosinophils, lymphocytes, plasma cells), occasional large cells with irregular hyperchromatic nuclei and prominent nucleoli, and pleomorphic spindle cells in disorganized patterns within a hyalinized collagenous background.[3]

Findings on Plain Films (Roentgenograms) and Computed Tomography

Soft tissue. MFH may be seen as soft tissue masses on plain films.[14] With CT, MFH can appear as large, lobulated tumors with attenuation similar to surrounding muscle as well as containing zones of low attenuation from myxoid material, necrosis, and/or prior hemorrhage.[1423] Punctate or curvilinear zones of mineralization may be seen with plain films or CT in the peripheral portions of MFH in up to 20 % of cases.[1424] Enhancement can be seen in the soft tissue portions of the tumors.[1424] MFH can be associated with erosion or invasion of adjacent bone cortex.[1424]

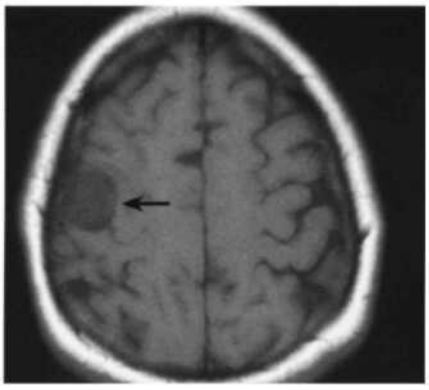
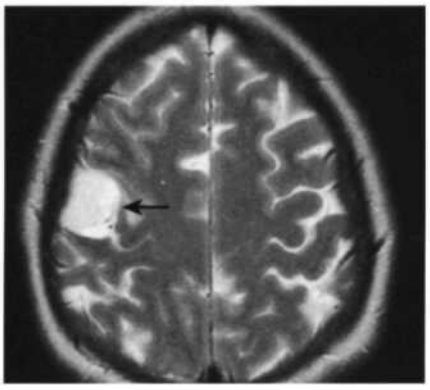
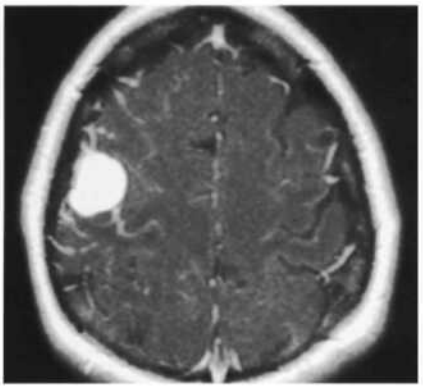

a, b c

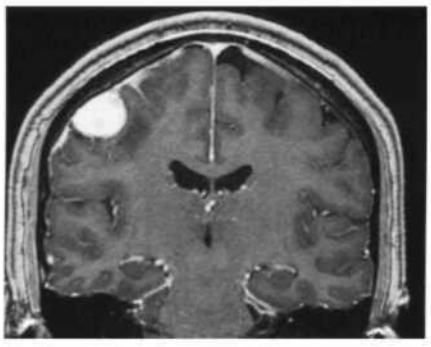

d

Figure **294a-d** A 35-year-old woman with a malignant fibrous histiocytoma involving the intracranial dura. The tumor has low-intermediate signal on axial T1 WI (**a**), and high signal on axial T2WI (**b**). The tumor shows prominent Gd-contrast enhancement on axial (**c**) and coronal (**d**)T1WI.

a b

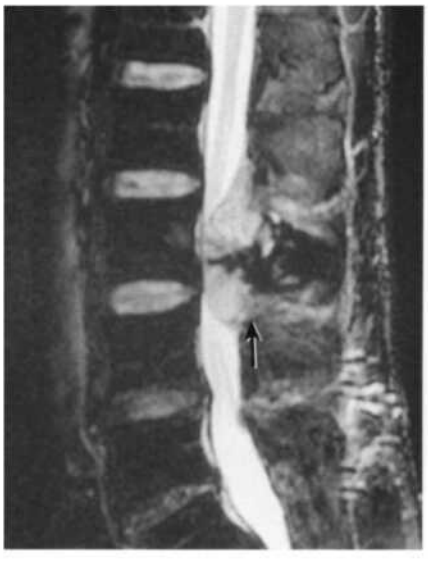

c d

Figure **295 a-d** A 56-year-old man with malignant fibrous histiocytoma involving the posterior elements at the L3 vertebra, with extra-osseous extension and spinal canal compression. The tumor has mixed low and intermediate signal on sagittal T1WI (**a**) and sagittal T2WI (**b**). The tumor has mixed low, intermediate, and slightly high signal on sagittal FST2WI (**c**). The tumor shows heterogeneous Cd-contrast enhancement on sagittal FST1WI (**d**).

Bone. MFH in bone often has a moth-eaten, permeative and/or partially geographic radiolucent pattern in the medullary compartment[18,23] (Fig. **296).** Irregular or regular zones of cortical destruction are seen in up to 91 % of cases.[23] Minimal periosteal reaction with a lamellar appearance may occur.[18,23] Zones of sclerosis or calcifications may occur within the lesions or at the periphery.[18,23]

MRI Findings

Soft tissue. MFHs are ovoid lesions with regular and/or irregular margins that are often located in muscle and/or subcutaneous tissue.[14,24] These lesions can also occur in less common locations such as the intracranial dura (Fig. **294).** High-grade MFH may have an infiltrative pattern with respect to adjacent soft tissues. Lesions usually have low-intermediate signal on T1WI, low-intermediate to slightly high signal on PDWI, and heterogeneous intermediate-high signal on T2WI[14,24,28] (Figs. **298-304).** The signal heterogeneity on Tl Wl and T2WI is often related to the presence and extent of fibrous components (low signal on Tl WI and T2WI), zones of hemorrhage (intermediate or high signal on T1WI; low, intermediate and/or high signal on T2W1), zones of necrosis and/or myxoid material (low signal on Tl WI and high signal on T2WI)[14,24] (Figs. **298-302, 304).** Calcifications, which occur in only 5-20% of cases of MFH, may be seen as zones of low signal on T1WI and T2WI.[24] Margins of lesions may be indistinct on T2WI for high-grade lesions. MFH can be associated with erosion, destruction, and invasion of adjacent bone.

After Gd-contrast administration, solid portions of lesions usually show heterogeneous, often prominent, enhancement.[14,24] Enhancing margins of lesions may be indistinct for high-grade lesions. MRI readily shows the relationship of tumor enhancement to nearby neurovascular bundles and adjacent bone.

Bone. MFHs are intramedullary lesions with irregular margins. Zones of cortical destruction and extra-osseous soft tissue masses are common.[18] Lesions usually have low-intermediate signal on T1WI (that is hypointense to normal marrow); low-intermediate signal on PDWI, and heterogeneous intermediate-high signal on T2WI and FST2WI[18] (Figs. **295-297).** Zones of acute or chronic hemorrhage seen with MRI occur in ~ 10 %. Fluid-fluid levels have not been described with MFH in bone.[18] Invasion of joints by MFH in bone can be seen with MRI in ~30%.[18] MFH may be associated with other bone lesions seen with MRI such as infarcts, bone cysts, chronic osteomyelitis, Paget disease, and other treated primary bone tumors.[18]

After Gd-contrast administration, lesions usually show heterogeneous, often prominent, enhancement. Enhancement is often greater at the periphery of the tumors than centrally.[18]

a

b,c

d

Figure **296a-d** A 55-year-old woman with malignant fibrous histiocytoma involving the humerus. AP radiograph (**a**) shows a permeative radiolucent lesion in the diaphyseal portion of the humerus with cortical erosion and expansion. The tumor involves the diaphyseal and metaphyseal marrow, and has heterogeneous low-intermediate signal on coronal (**b**) T1WI, and high signal on coronal (**c**) and axial (**d**) FST2WI. Tumor extension is seen into the adjacent soft tissues.

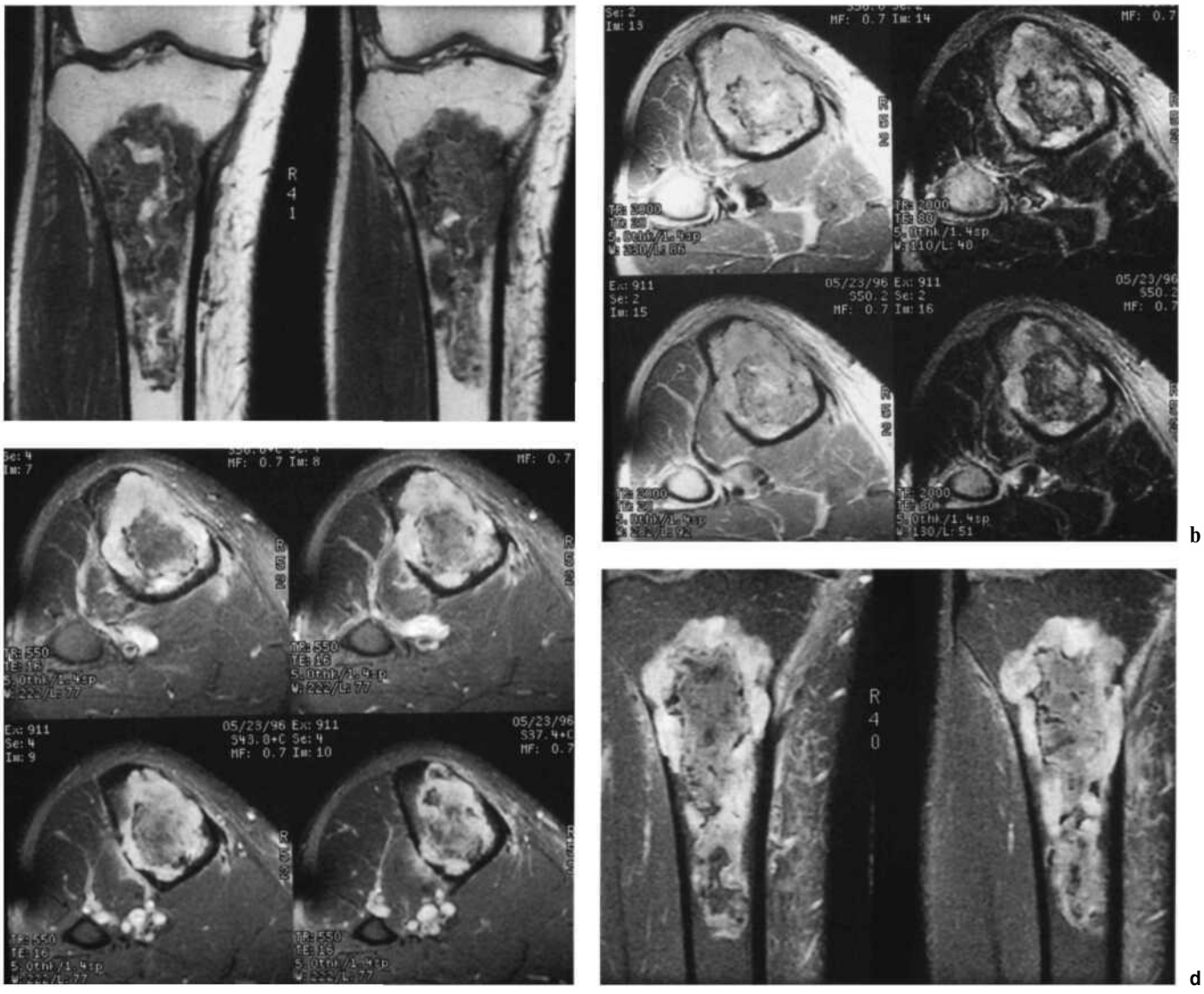

Figure **297 a-d** A 53-year-old man with malignant fibrous histiocytoma in the proximal tibia associated with a bone infarct. The lesion has circumscribed margins and contains mixed low and high signal on coronal T1WI (**a**), and mixed low, intermediate, and slightly high signal on axial PDWI and T2WI (**b**). The lesion shows heterogeneous Cd-contrast enhancement on axial (**c**) and coronal (**d**) FST1WI.

Differential Diagnosis

Soft tissue. Liposarcoma, leiomyosarcoma, malignant peripheral nerve sheath tumor, synovial sarcoma, fibrosarcoma, angiosarcoma, rhabdomyosarcoma, solitary metastatic lesion, epitheloid sarcoma, malignant hemangiopericytoma, clear cell sarcoma, malignant granular cell tumor, nodular fasciitis, organizing hematoma, proliferative myositis.

Bone:

- Adults: Metastatic carcinoma, plasmacytoma/myeloma, lymphoma, fibrosarcoma, osteomyelitis, chondrosarcoma, giant cell tumor, osteosarcoma.[18,23]
- Children: telangiectatic osteosarcoma, Ewing sarcoma, fibrosarcoma, osteomyelitis, eosinophilic granuloma, giant cell tumor.[18,23]

Prognosis and Treatment

Soft tissue:

- **Pleomorphic malignant fibrous histiocytoma.** The 5-year survival rate is 50-60 % of patients.[7] Treatment often consists of neoadjuvant chemotherapy and/or radiation followed by surgery.
- **Myxoid malignant fibrous histiocytoma (myxofibrosarcoma).** Using comprehensive immunohistochemical staining, nearly 56 % of myxoid MFH showed characteristics of myxofibrosarcoma.[6] Other myxoid MFH were also subclassified as leiomyosarcoma, liposarcoma, pleomorphic sarcoma, fibromyxoid sarcoma, and myxoid sarcoma.[6] Treatment usually consists of surgical excision with wide margins, preoperative or postoperative radiotherapy and/or chemotherapy.[167] The overall 5-year survival rate is 60-70% of patients.[19]

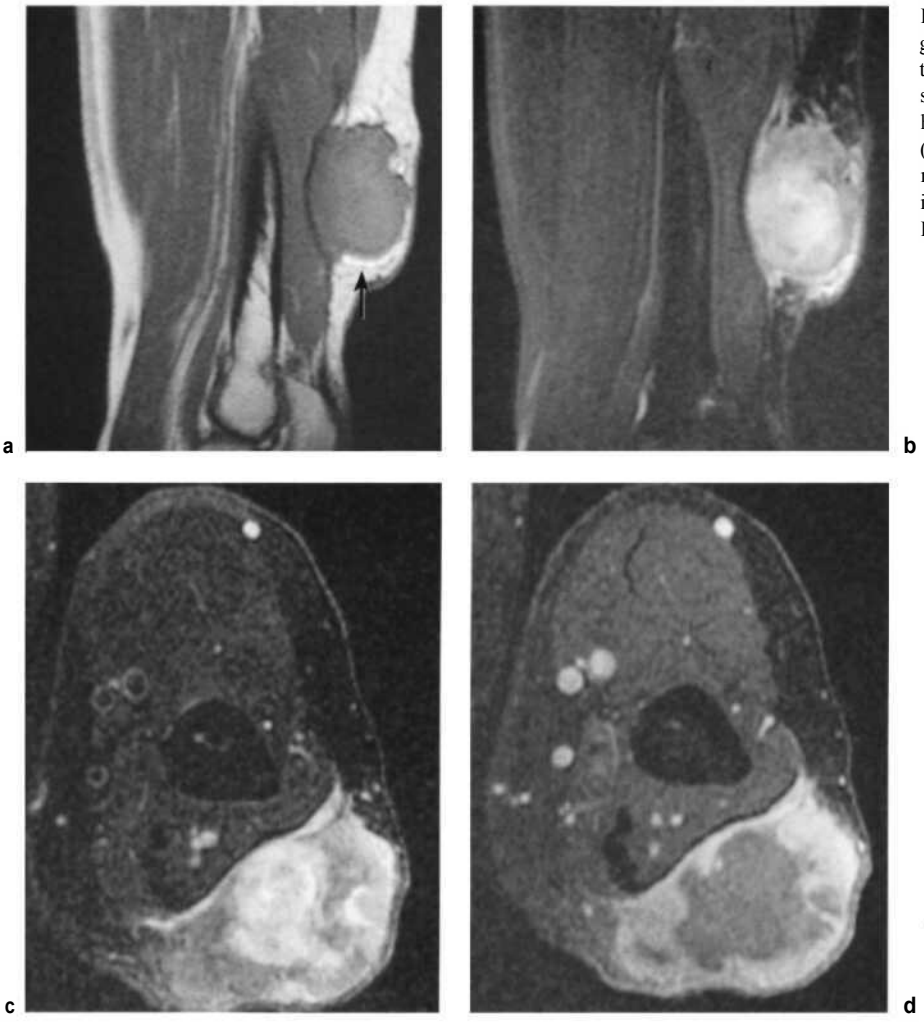

Figure **298a-d** A 77-year-old man with a giant cell malignant fibrous histiocytoma in the arm. The tumor has intermediate signal on sagittal (**a**) T1WI, and heterogeneous slightly high and high signal on sagittal (**b**) and axial (**c**) FST2WI. The tumor shows irregular peripheral Gd-contrast enhancement surrounding a central zone of necrosis on axial (**d**) FST1WI.

- **Giant cell malignant fibrous histiocytoma.** These tumors have similar prognoses to other pleomorphic sarcomas.[8] Treatment usually consists of surgical excision with wide margins, preoperative or postoperative radiotherapy, and/or chemotherapy.[167]
- **Inflammatory malignant fibrous histiocytoma.** Complete or near-complete surgical excision is often not possible because most inflammatory MFHs occur in the retroperitoneum, or intra-abdominal and deep soft tissues, and are large at the time of diagnosis, which limits surgical access.[3] As a result this type of MFH has a poor prognosis, with about two-thirds of patients dying from persistent or recurrent tumor.[3] Distant metastatic disease occurs in 25 *%?*
- **Storiform-pleomorphic malignant fibrous histiocytoma (prior to new WHO system).** Patients with high grade, pleomorphic MFH have a 5-year survival of 50-60 %.[7] Treatment usually consists of surgical excision with wide margins, preoperative or postoperative radiotherapy, and/or chemotherapy.[167] Using comprehensive immunohistochemical staining, nearly 50 % of MFHs may show myogenic differentiation.[6] MFH with myogenic differentiation has been associated with a poorer prognosis than other pleomorphic MFHs, necessitating more aggressive treatment.[6]

Bone. No correlation has been shown between clinical prognosis and the various subtypes of MFH in bone.[911] Prognosis, however, has been shown to be dependent on the histologic grade (degree of tumor differentiation, mitotic activity, tumor infiltration of adjacent tissues, degree of necrosis, nuclear pleomorphism) and stage (extent of tumor at diagnosis) of MFH.[11] Nearly 80 % of MFHs are high-grade tumors (grades III, IV). Low-grade MFH (grades I, II) are treated with surgery with wide margins.[11] High-grade MFHs are often treated with neoadjuvant chemotherapy followed by limb-sparing surgery.[1124] Resected high-grade MFH specimens that have zones of residual viable tumor may necessitate postsurgical chemotherapy.[1125] Metastases can occur in the lungs in up to 50% of patients, and in regional lymph nodes in 4%.[1125] Patients with low-grade MFH have a better prognosis (60% survival at 10years) than those with high-grade MFH (46% survival at 10years).[11,25] Patients with MFH secondary to other abnormalities have a 10-year survival of 36 %." Patients with MFH who are younger than 21 years have better survival rates than older patients.[11]

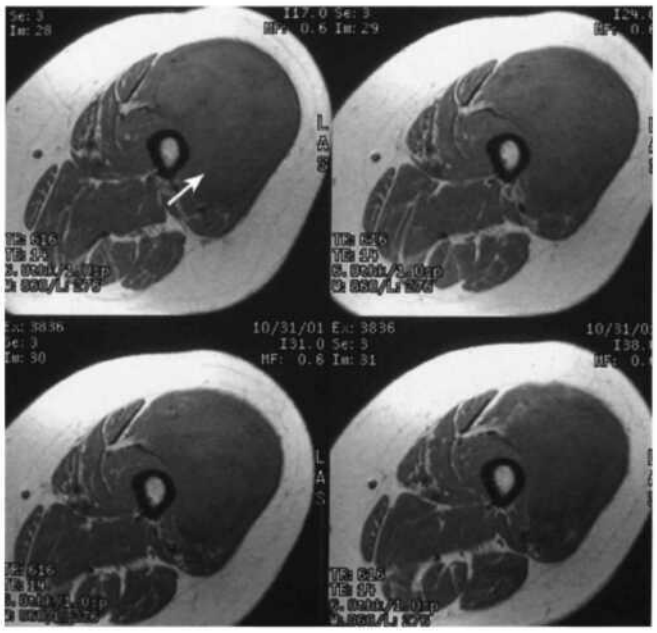

a

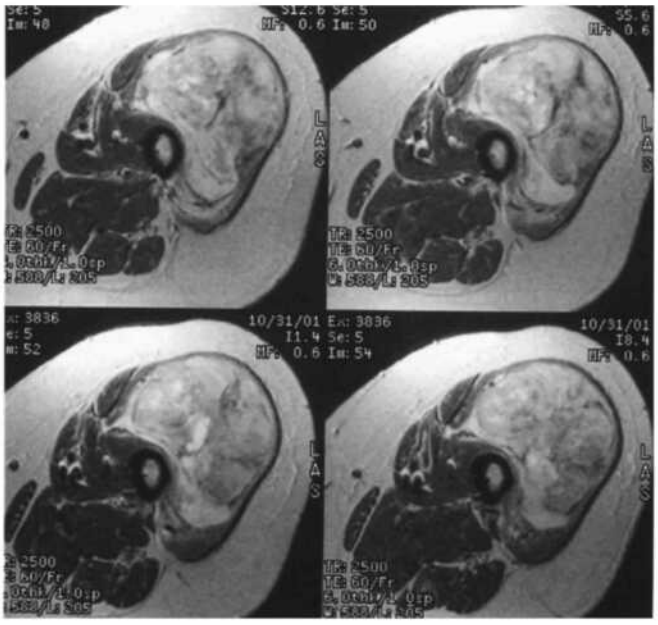

b

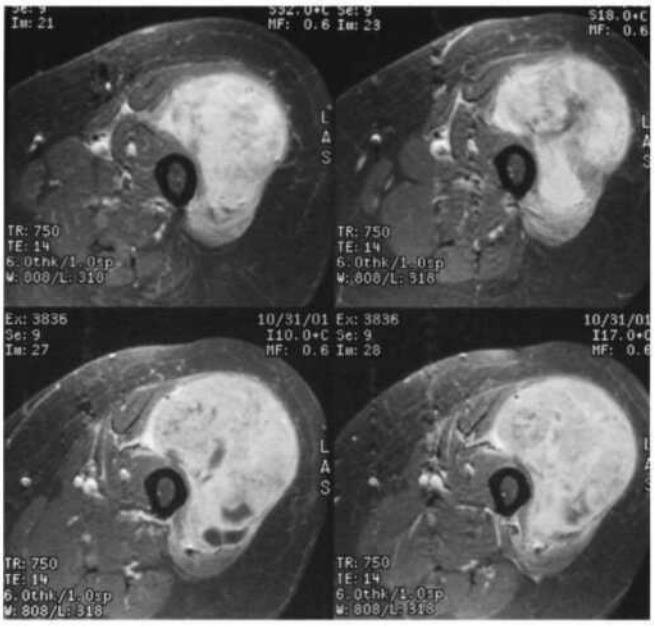

c

Figure **299a-c** A 66-year-old woman with a malignant fibrous histiocytoma involving the vastus lateralis muscle of the proximal thigh. The tumor has intermediate signal on axial T1WI (**a**), and heterogeneous slightly high and high signal on axial T2WI (**b**). The tumor shows irregular, prominent Cd-contrast enhancement as well as several nonenhancing zones of necrosis on axial FST1WI (**c**).

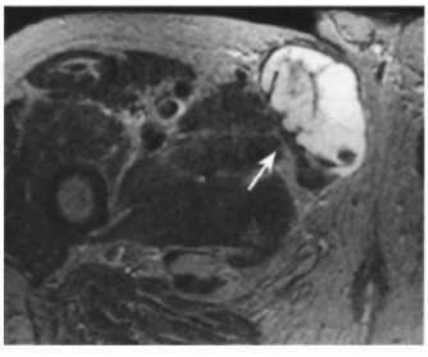

a, b

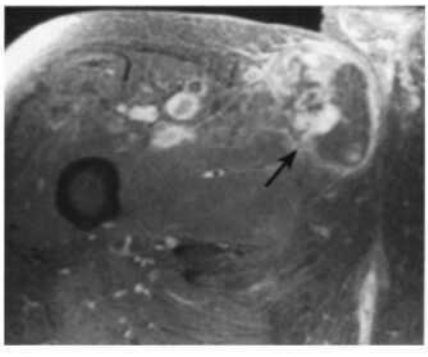

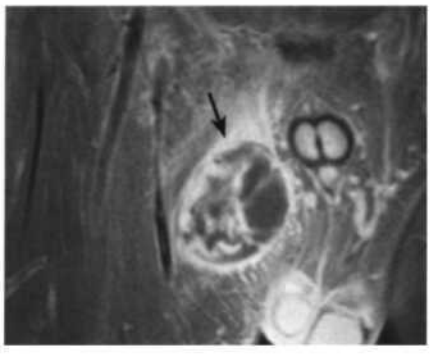

c

Figure 300a-c A 62-year-old man with a malignant fibrous histiocytoma involving the soft tissues in the right groin region. The tumor contains zones with slightly high and high signal on axial T2WI (**a**), as well several septa with low signal. The tumor shows zones with and without Gd-contrast enhancement on axial (**b**) and coronal (**c**) FST1WI.

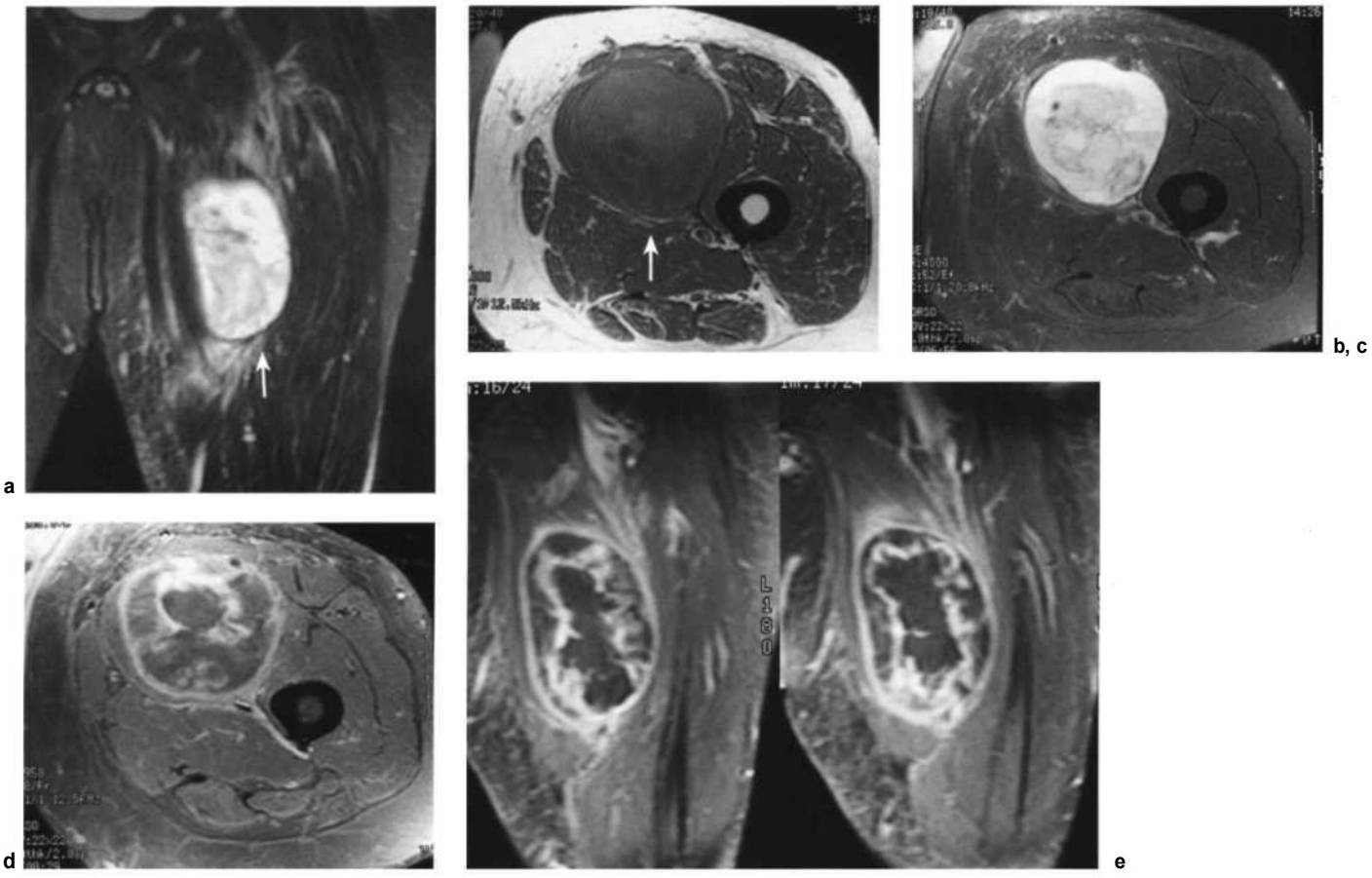

Figure **301 a-e** A 64-year-old man with a malignant fibrous histiocytoma involving the vastus medialis muscle of the upper medial thigh. The tumor contains zones with slightly high and high signal on coronal (a) and axial (c) FST2WI. The tumor has intermediate and slightly high signal on axial (**b**) PDWI. The tumor shows zones with and without Cd-contrast enhancement on axial (**d**) and coronal (**e**) FST1WI.

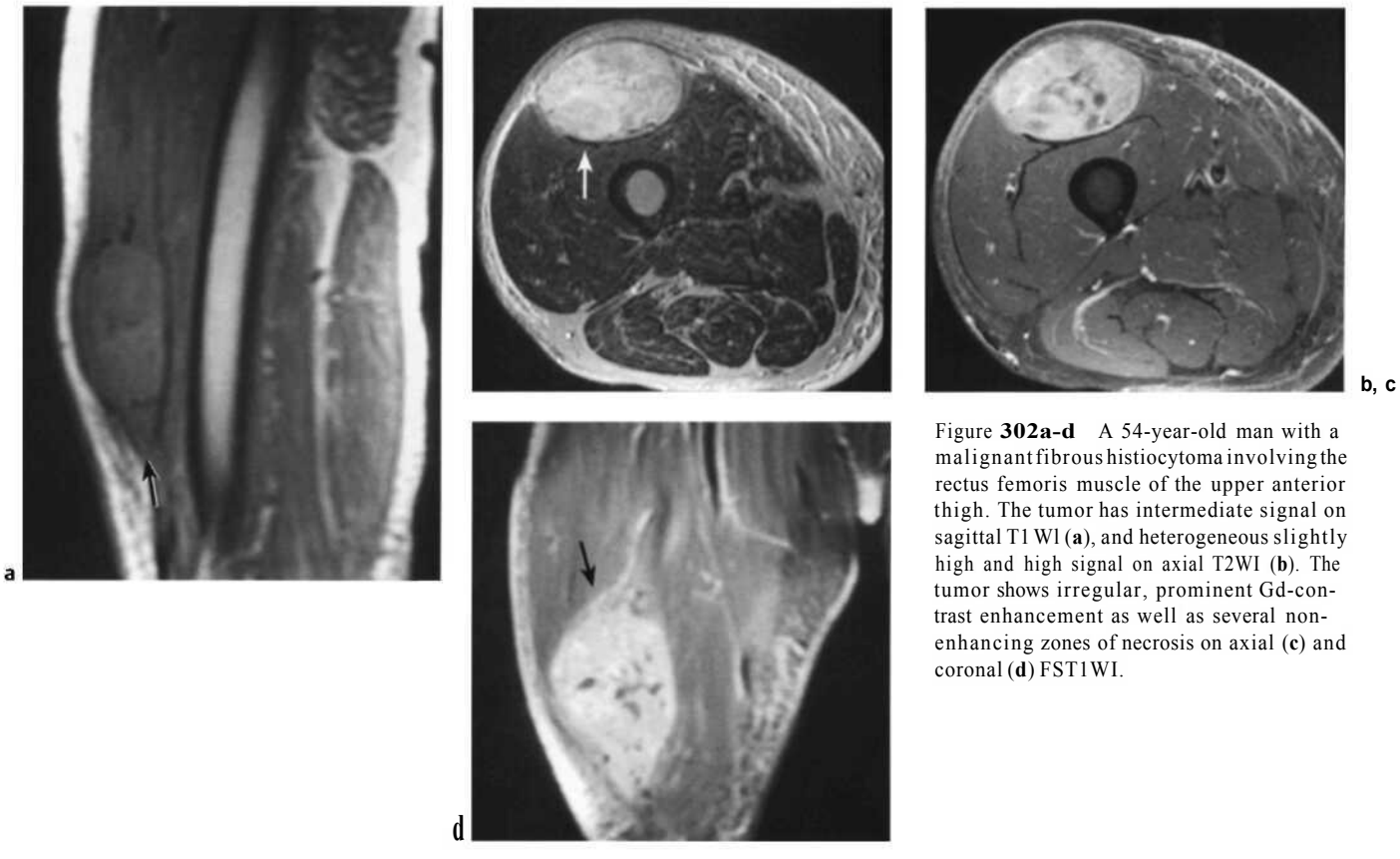

Figure **302a-d** A 54-year-old man with a malignant fibrous histiocytoma involving the rectus femoris muscle of the upper anterior thigh. The tumor has intermediate signal on sagittal T1 Wl (**a**), and heterogeneous slightly high and high signal on axial T2WI (**b**). The tumor shows irregular, prominent Gd-contrast enhancement as well as several non-enhancing zones of necrosis on axial (**c**) and coronal (**d**) FST1WI.

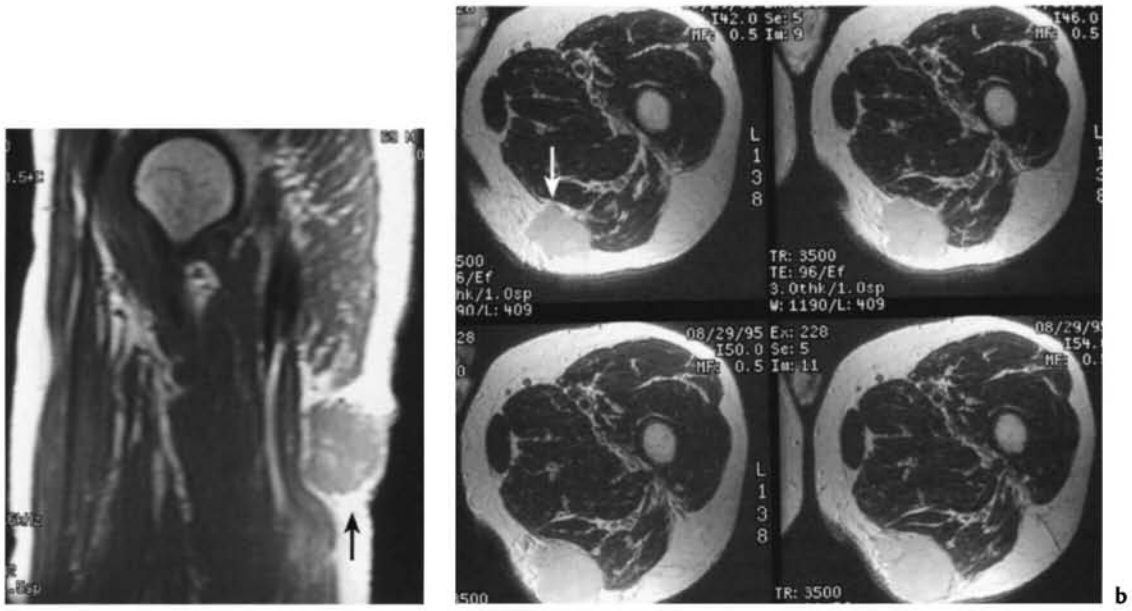

Figure **303a-c** A 69-year-old man with a malignant fibrous histiocytoma involving the subcutaneous fat of the posterior thigh. The tumor has intermediate signal on sagittal (**a**) T1WI, and high signal on axial (**b**) T2WI. The tumor shows slightly heterogeneous Gd-contrast enhancement on axial (**c**) FS T1WI.

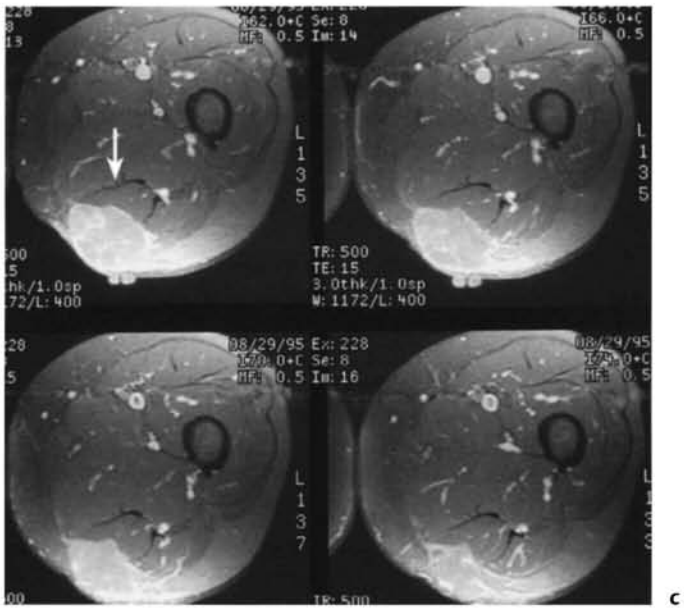

Figure **304a-c** A 79-year-old woman with a malignant fibrous histiocytoma involving the subcutaneous fat of the anterior leg. The tumor has low-intermediate signal on axial T1WI (**a**), and high signal on axial T2WI (**b**). The tumor shows zones with and without Gd-contrast enhancement on axial FST1WI (**c**).

References

1 Belal A, Kandil A, Allam A, et al. Malignant fibrous histiocytoma: a retrospective study of 109 cases. *Am J Clin Oncol* 2002;25(l):16-22.

2 Chaudhuri B, Das Gupta TK. Pathology of soft tissue sarcoma. In: Das Gupta TK, Chaudhuri PK, eds. Tumors *of the Soft Tissues.* 2nd ed. Stamford, Conn: Appleton & Lange; 1998:63-200.

3 Coindre JM. Inflammatory malignant fibrous histiocytoma/undifferentiated pleomorphic sarcoma with prominent inflammation. In: Fletcher CDM, Unni KK, Mertens F, eds. *World Health Organization Classification of Tumours. Pathology and Genetics of Tumours of Soft Tissue and Bone* Geneva: IARC Press; 2002:125-126.

4 Das Gupta TK, Chaudhuri PK. Tumors of the fibrous tissue. In: Das Gupta TK, Chaudhuri PK, eds. *Tumors of the Soft Tissues* 2nd ed. Stamford, Conn: Appleton & Lange; 1998:265-308.

5 Daw NC, Billups CA, Pappo AS, et al. Malignant fibrous histiocytoma and other fibrohistiocytic tumors in pediatric patients. The St. Jude Children's Research Hospital experience. *Cancer* 2003;97: 2839-2847.

6 Fletcher CD, Gustafson P, Rydholm A, Willén H, Akerman M. Clinicopathologic re-evaluation of 100 malignant fibrous histiocytomas: prognostic relevance of subclassification. *J Clin Oncol* 2001;19(12): 3045-3050.

7 Fletcher CDM, van den Berg E, Molenaar WM. Pleomorphic malignant fibrous histiocytoma/undifferentiated high grade pleomorphic sarcoma. In: Fletcher CDM, Unni KK, Mertens F, eds. *World Health Organization Classification of Tumours. Pathology and Genetics of Tumours of Soft Tissue and Bone* Geneva: IARC Press; 2002:120-122.

8 Fletcher COM. Giant cell malignant fibrous histiocytoma/undifferentiated pleomorphic sarcoma with giant cells. In: Fletcher CDM, Unni KK, Mertens F, eds. *World Health Organization Classification of Tumours. Pathology and Genetics of Tumours of Soft Tissue and Bone* Geneva: IARC Press; 2002:123-124.

9 Forest M. Malignant fibrous histiocytoma. In: Forest M, Tomeno B, Vanel D, eds. *Orthopedic Surgical Pathology: Diagnosis of Tumors and Pseudotumoral Lesions of Bone and Joints* Edinburgh: Churchill Livingstone; 1998:323-330.

10 Hanna SL, Fletcher BD. MR imaging of malignant soft-tissue tumors. *Magn Reson Imaging Clin North Am* 1995;3(4):629-650.

11 Huvos AG. Malignant fibrous histiocytoma. In: Huvos AG, ed. *Bone Tumors: Diagnosis, Treatment, and Prognosis* 2nd ed. Philadelphia, Pa: W.B. Saunders; 1991:497-517.

12 Kilpatrick SE, Unni KK. Spindle cell lesions of bone. In: Helliwell TR, ed. *Major Problems in Pathology: Pathology of Bone and Joint Neoplasms* 1st ed. Vol 37. Philadelphia, Pa: W.B. Saunders; 1999: 248-250.

13 Kransdorf MJ, Meis JM. Extraskeletal osseous and cartilaginous tumors of the extremities. *Radiographics* 1993;13:853-884.

14 Kransdorf MJ, Murphey MD. Malignant fibrous and fibrohistiocytic tumors. In: *Imaging of Soft Tissue Tumors* 2nd ed. Philadelphia, Pa: W. B. Saunders; 2006:257-297.

15 Kransdorf MJ, Murphey MD. Soft tissue tumors in a large referral population: prevalence and distribution of diagnoses by age, sex, and location. In: *Imaging of Soft Tissue Tumors* 2nd ed. Philadelphia, Pa: W.B. Saunders; 2006:6-37.

16 Kransdorf MJ. Malignant soft-tissue tumors in a large referral population: distribution of diagnoses by age, sex, and location. *AJR Am J Roentgenol* 1995:164:129-134.

17 Laskin WB, Silverman TA, Enzinger FM. Postradiation soft tissue sarcomas: an analysis of 52 cases. *Cancer* 1988;62:2330-2340.

18 Link TM, Haeussler MC, Poppek S, et al. Malignant fibrous histiocytoma of bone: conventional X-ray and MR imaging features. *Skeletal Radial* 1998;27:552-558.

19 Mentzel T, van den Berg E, Molenaar WM. Myxofibrosarcoma. In: Fletcher COM, Unni KK, Mertens F, eds. *World Health Organization Classification of Tumours. Pathology and Genetics of Tumours of Soft Tissue and Bone* Geneva: IARC Press; 2002:102-103.

20 Meyer JS, Dormans JP. Differential diagnosis of pediatric musculoskeletal masses. *Magn Reson Imaging Clin N Am* 1998;6(3):561-577.

21 Mulder JD, Schutte HE, Kroon HM, Taconis WK. Introduction. In: *Radiologic Atlas of Bone Tumors* Amsterdam: Elsevier; 1993:3-6.

22 Mulder JD, Schutte HE, Kroon HM, Taconis WK. The diagnosis of bone tumors. In *Radiologic Atlas of Bone Tumors* Amsterdam: Elsevier; 1993:9-46.

23 Mulder JD, Schutte HE, Kroon HM, Taconis WK. Malignant fibrous histiocytoma. In: *Radiologic Atlas of Bone Tumors* Amsterdam: Elsevier; 1993:227-239.

24 Munk PL, Sallomi DF, Janzen DL, et al. Malignant fibrous histiocytoma of soft tissue imaging with emphasis on MRI. *] Comput Assist Tomogr* 1998;22(5):819-826.

25 Steiner GC, Jundt G, Martignetti JA. Malignant fibous histiocytoma of bone. In: Fletcher CDM, Unni KK, Mertens F, eds. World *Health Organization Classification of Tumours. Pathology and Genetics of Tumours of Soft Tissue and Bone* Geneva: IARC Press; 2002:294-296.

26 Unni KK. Introduction and scope of study. In: *Dahlin'sBone Tumors-General Aspects and Data on* 31087 Cases 5th ed. Philadelphia, Pa: Lippincott, Williams & Wilkins; 1996:1-9.

27 Unni KK. Malignant (fibrous) histiocytoma. In: *Dahlin's Bone Tumors— General Aspects and Data on 11 087 Cases* 5th ed. Philadelphia, Pa: Lippincott, Williams & Wilkins; 1996:217-224.

28 Van Slyke MA, Moser RP Jr, Madewell JE. MR imaging of periarticular soft-tissue lesions. *Magn Reson Imaging Clin N Am* 1995;3(4): 651-667.

A 49 Meningioma

ICD-O Codes

Meningothelial: 9531/0

Fibrous (fibroblastic): 9532/0

Transitional (mixed): 9537/0

Psammomatous: 9533/0

Angiomatous: 9534/0

Atypical: 9539/1

Anaplastic: 9530/3

Microcystic: 9530/0

Secretory: 9530/0

Metaplastic: 9530/0

Chordoid: 9538/1

Clear cell: 9538/1

Papillary: 9538/3

Lymphoplasmacyte-rich: 9538/3

Rhabdoid: 9538/3

Definition

Meningiomas are benign, slow-growing tumors involving cranial and/or spinal dura, and are composed of neoplastic meningothelial (arachnoidal or arachnoid cap) cells.[2,9] Meningiomas are usually solitary and sporadic, but can also occur as multiple lesions in patients with neurofibromatosis type 2.[9] Most meningiomas are benign, although ~5% have atypical histologic features.[9] Anaplastic meningiomas are rare and account for less than 3 % of meningiomas.[9] Meningiomas can occur secondary to radiation treatment with latencies ranging from 19 to 35 years.[9] Most meningiomas arise within the neuraxis and are referred to as **primary neuraxial meningiomas**[4,15] Secondary meningiomas refer to primary neuraxial meningiomas that extend outside of the neuraxis, or metastasize.[4] Less frequently, meningiomas can arise outside of the neuraxis and are referred to as primary extraneuraxial or extradural meningiomas.[4,15] **Intra-osseous meningiomas** account for only 14 % of primary extraneuraxial meningiomas.[4]

Frequency of Occurrence

Meningiomas account for up to 26 % of primary intracranial tumors.[9] The annual incidence is 6 per 100 000 people worldwide.[9] The annual incidence of anaplastic (malignant) meningiomas is 0.17 per 100000 people.[9] Approximately 88% of meningiomas are intracranial or juxtacranial.[2] Approximately 12% of meningiomas involve the spine.[2] Meningiomas account for 25-46% of primary nonosseous spinal tumors." Primary extradural meningiomas account for 1-2% of all meningiomas.[15] Intra-osseous meningiomas account for 14 % of primary extraneuraxial meningiomas.[4]

Age at Presentation

Meningiomas have a peak occurrence in the 6th and 7th decades, although these tumors also occur in children and elderly patients.[9] Meningiomas frequently occur in adolescents and young adults with neurofibromatosis type 2. For intra-osseous meningiomas, the average age is 47 years.[4]

Gender Ratio (M | F)

Primary intracranial meningiomas: 1 / 2 to 2/3.[9]

Primary spinal neuraxial meningiomas: 1 /4.13

Primary extraneuraxial meningiomas: 3/5.

Intra-osseous meningiomas: 3 /7.[4]

Location

Tumors occur in the lateral endocranial dural surface > parasagittal/falcine > sphenoid and middle cranial fossa > frontobasal region > posterior cranial fossa, tentorium > spine (thoracic > cervical > lumbar) > intraventricular > orbit > ectopic or primary extraneuraxial meningiomas.[2,9,13] For spinal meningiomas, 87% are intradural, 9% are epidural, and 4% are both epidural and intradural.[13] Extradural spinal meningiomas rarely occur.[14] Within the spinal canal, meningiomas are anterior or anterolateral in 39 % of cases, posterior or posterolateral in 33 %, lateral in 22 %, and circumferential in 6 %.[13]

For primary extraneural meningiomas the frequency of occurrence is the orbit (58%) > skin (16%) > bone (14%) > paranasal sinuses (11 %) > others (1 %).[4] For intra-osseous meningiomas the frequency of occurrence is the middle ear > sphenoid ridge > frontal bone > roof of orbit.[4]

Signs and Symptoms

Meningiomas are slow-growing tumors which cause symptoms from compression of adjacent neural tissue.[9] Meningiomas account for 15 % of all symptomatic intracranial tumors and 33 % of all asymptomatic intracranial neoplasms.[2] Headaches, seizures, and focal neurologic deficits can be associated with intracranial meningiomas.[1,9] An orbital meningioma can cause visual loss by compression of the optic nerve.[2] Symptoms and signs associated with spinal meningiomas include: radicular pain for months or years (72%), paraparesis (76%), abnormal reflexes (78 %), sphincter dysfunction (37 %), sensory level deficit (39 %), paresthesia (28%), and paraplegia (4%).[13]

Cross Pathologic Findings

Meningiomas are circumscribed, firm, spheroid or slightly lobulated lesions which usually have a broad dural attachment.[9] Meningiomas may have a gritty texture from psammoma

bodies.[9] Occasionally, intracranial meningiomas may present as a flattened lesion, referred to as an en plaque meningioma.[9] Intracranial meningiomas may invade and occlude dural venous sinuses, as well as cause hyperostosis of adjacent skull from possible invasion.[9] Intracranial meningiomas may encase arteries as well as extend along foramina and/or the optic canal.[9]

Histopathologic Findings

Meningiomas can be classified into different subtypes such as meningothelial, fibrous (fibroblastic), transitional (mixed), psammomatous, angiomatous, atypical, and anaplastic.[9] The meningothelial, fibrous, and transitional types of meningioma are the most common of the intracranial meningiomas.[9] The meningothelial and psammomatous types of meningioma are the most common involving the spine.[13] Rare subtypes of meningioma include: microcystic, secretory, metaplastic, chordoid, clear cell, papillary, lymphoplasmacyte-rich, and rhabdoid.[9] Most meningiomas usually show immunoreactivity to epithelial membrane antigen and vimentin.[9] Secretory meningiomas are typically immunoreactive to carcinoembryonic antigen (CEA).[9]

Meningothelial meningioma. Tumor cells are uniform with oval nuclei that occur in lobules surrounded by thin, collagenous septae.[9] Whorls and psammoma bodies are common in this subtype.[9]

Fibrous meningioma. Tumors contain spindle-shaped cells as well as cells with oval nuclei.[9] Tumor cells are arranged in bands or fascicles with varying amounts of intercellular collagen and reticulin.[9] Psammoma bodies are infrequent in this subtype.[9]

Transitional (mixed) meningioma. The histologic features of this subtype are intermediate between the meningothelial and fibrous types.[9] Tumor cells occur in both lobules and fascicles.[9]

Psammomatous meningioma. These meningiomas contain meningothelial cells adjacent to abundant psammoma bodies,[9] which can be associated with extensive calcifications.[9]

Angiomatous meningioma. This type contains numerous blood vessels within a typical meningioma.[9]

Atypical meningioma. These meningiomas have increased mitotic activity (4 or more mitoses per 10 high-power fields), small cells with large nuclei, sheetlike growth pattern, and occasional zones of necrosis.[9]

Anaplastic meningioma. These meningiomas have abnormal increased mitotic activity (20 or more mitoses per 10 high-power fields), and malignant cytologic features resembling sarcoma, carcinoma, or melanoma.[9]

Microcystic meningioma. These meningiomas contain tumor cells within loose mucinous material simulating the appearance of small cysts.[9]

Secretory meningioma. These meningiomas show focal epithelial differentiation with cells containing eosinophilic material that is positive for periodic acid-Schiff stain.[9]

Metaplastic meningioma. These tumors (meningothelial, fibrous or transitional meningiomas) contain varying degrees of osseous, cartilaginous, myxoid, lipomatous, and/or xanthomatous changes.[9]

Chordoid meningioma. These tumors contain cells that resemble those in chordomas (eosinophilic vacuolated cells in a myxoid background).[9]

Clear cell meningioma: These neoplasms contain polygonal cells with glycogen-rich, clear cytoplasm.[9]

Papillary meningioma. These tumors are aggressive and invasive, and contain portions which have a perivascular pseudopapillary pattern.[9]

Lymphoplasmacyte-rich meningioma. These lesions contain both meningothelial cells and chronic inflammatory infiltrates.[9]

Rhabdoid meningioma. These tumors are aggressive, malignant meningiomas that contain rhabdoid cells, which are round cells with eccentric nuclei within an eosinophilic cytoplasm containing whorled intermediate filaments.[9]

Tumor Genetics

Meningiomas have been associated with cytogenetic findings of deletions involving chromosome 22.[9] Mutations in the NF-2 tumor suppressor gene on chromosome 22 have been found in 60% of sporadic meningiomas.[9]

Findings on Plain films and Computed Tomography

Primary neuraxial meningiomas.[1,2,4,7] On plain films, findings such as abnormal calcifications or bone erosion may be seen in up to 21 % of patients with intracranial meningiomas.[1] On CT, meningiomas commonly appear as spheroid or ovoid, dural-based extra-axial tumors which often have attenuation similar to or greater than brain parenchyma.[1,2,7] Meningiomas can contain calcifications which may vary from small amounts to a diffuse dense pattern.[Z] After contrast administration, meningiomas usually show prominent enhancement[12] (Fig. **305).** An enhancing dural tail may be seen with meningiomas on CT.[1,2] Some meningiomas have atypical features such as large cysts and metaplastic osseous, cartilaginous, and/or lipomatous changes.[1,2] Meningiomas can invade adjacent bone causing hyperostosis[1,2,9] (Fig. **305).**

Intra-osseous meningiomas. Tumors often have associated hyperostosis (59%), although radiolucency (osteolysis) occurs (35%) and mixed hyperostosis/osteolysis (6%)[4,15] (Fig. **313).** Expansion of bone is often seen with intra-osseous meningiomas.[4,15]

MRI Findings

Primary neuraxial meningiomas.[1-4,6,8-11,13] Meningiomas commonly appear as spheroid or ovoid, dural-based circumscribed extra-axial tumors which often have low to intermediate signal on T1WI, and intermediate to slightly high signal on PDWI and T2WI[1-5,7,9-12,14,15] (Figs. **305-312).** After Gd-contrast administration, meningiomas typically show prominent enhancement, often associated with a dural tail.[1,2] Calcifications within meningiomas often have correspondingly low signal on T1WI, PDWI, and T2WI (Fig. **311).**

Approximately 15% of meningiomas have atypical features secondary to cystic or necrotic zones or hemorrhage, as well as metaplastic zones containing fat, myxoid, chondroid, or osseous material.[2] Cystic and necrotic zones within meningiomas typically have low signal on T1WI and high signal on T2WI.[2,3,7] Necrotic zones can have restricted diffusion as seen with DWI

a

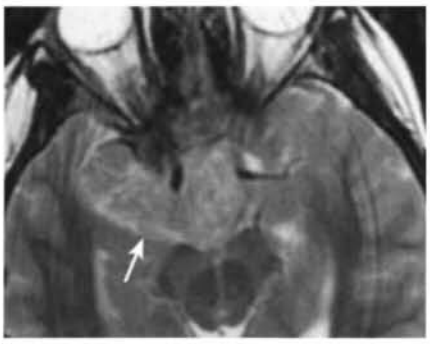

b, c

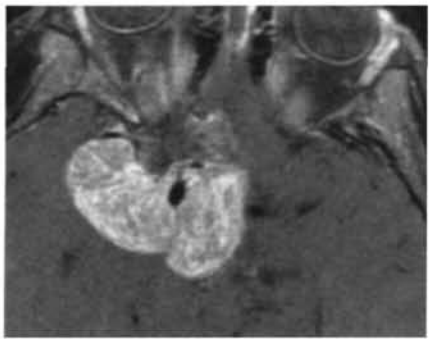

d

Figure **305 a-d** A 9-year old girl with neurofibromatosis type 2 with a large meningioma involving the right sphenoid bone. Axial CT image (**a**) shows the tumor to have prominent contrast enhancement. Axial CT image (**b**) shows reactive hyperostosis at the greater wing and right anterior clinoid process of the sphenoid bone from osseous invasion of the meningioma. The meningioma has heterogeneous intermediate signal on axial T2WI (**c**), and shows prominent heterogeneous Gd-contrast enhancement on axial FS T1WI (**d**). The hyperostotic bone has mixed low and intermediate signal on axial T2WI. Minimal irregular Gd-contrast enhancement is seen in the hyperostotic bone.

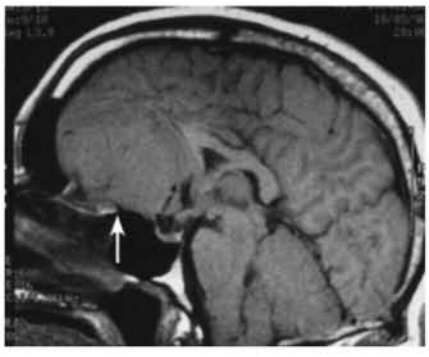

a

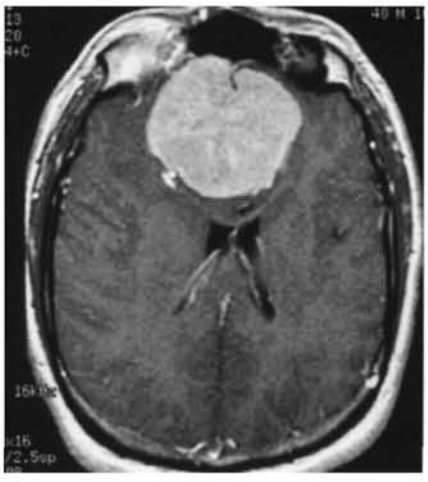

c

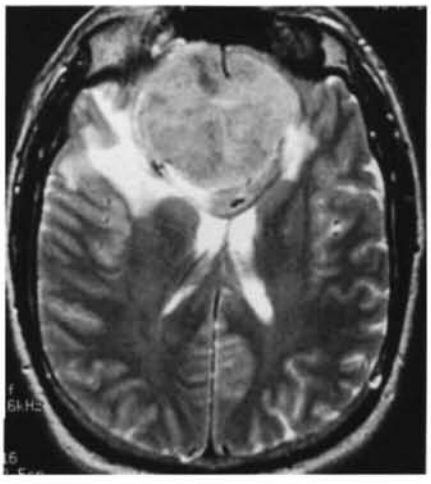

b

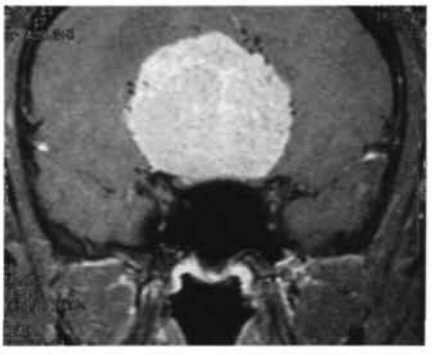

d

Figure **306a-d** A 40-year-old man with an olfactory groove meningioma. The dural-based extra-axial tumor has low-intermediate signal on sagittal T1 WI (**a**), and heterogeneous slightly high signal on axial T2WI (**b**), as well as several small zones of low signal. Edematous high signal changes on T2WI are seen in the brain compressed by the meningioma. The tumor shows prominent Gd-contrast enhancement on axial T1WI (**c**) and coronal FST1WI (**d**).

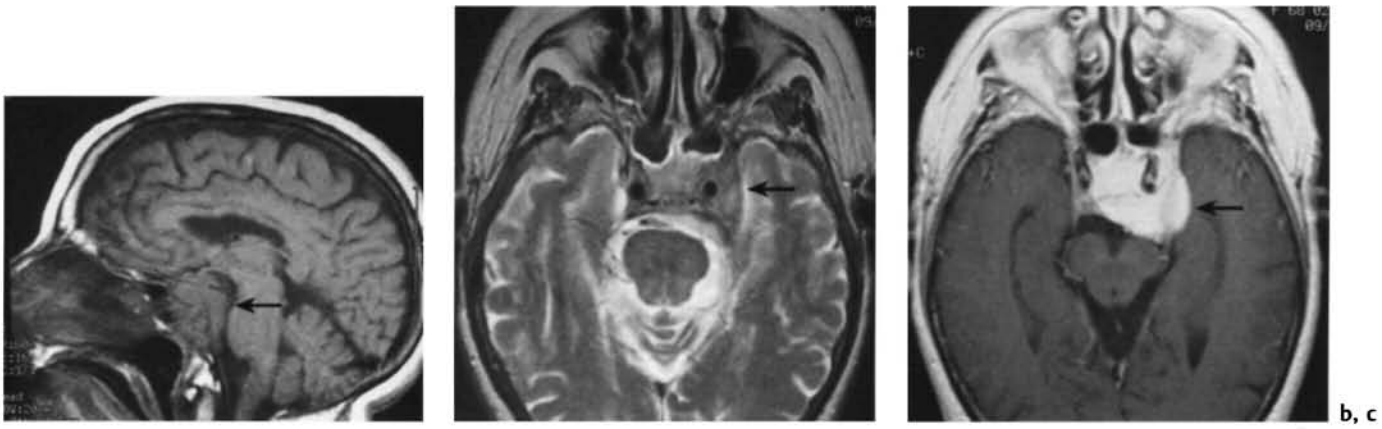

Figure **307a-c** A 68-year-old woman with a meningioma involving the anteromedial left middle cranial fossa, clivus, left cavernous sinus with encasement of the left internal carotid artery. The tumor has low-intermediate signal on sagittal T1WI (**a**), and heterogeneous intermediate signal on axial T2WI (**b**). The tumor shows prominent Gd-contrast enhancement on axial T1WI (**c**).

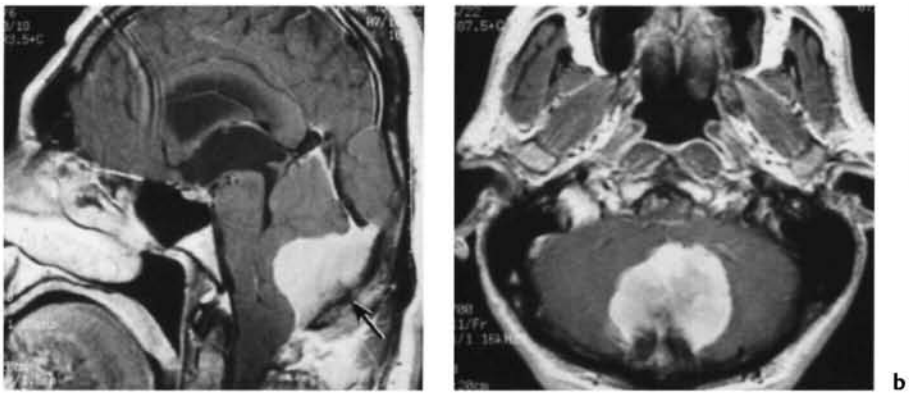

Figure **308a, b** A 46-year-old man with a meningioma along the floor of the posterior cranial fossa which displaces the cerebellar tonsils inferiorly through the foramen magnum. The tumor shows prominent Gd-contrast enhancement on sagittal (**a**) and axial (**b**)T1WI.

and apparent diffusion coefficient (ADC) images.[7] Cystic zones do not usually have restricted diffusion.[3,7] Lesions with necrosis, cysts, and/or calcifications typically show heterogeneous Gd-contrast enhancement.[27]

Edema in brain parenchyma was often found in association with meningiomas that have atypical features of slightly high to high signal on T2WI and indistinct margins with an invasive tumor-brain interface" (Fig. **306).**

Intracranial meningiomas may be associated with: encasement of arteries; extension through foramina; extension into dural venous sinuses with potential venous occlusion; extension into the cavernous sinuses or orbits; and hyperostosis of adjacent bone[2] (Figs. **305, 307).**

Spinal meningiomas have features on MRI that are similar to intracranial meningiomas.[5,12,14] Spinal meningiomas can cause spinal cord compression (Figs. **309-312).**

Hydrogen MR spectroscopy of meningiomas has shown these lesions to contain alanine and high concentrations of choline and glutamine/glutamate.[10]

Meningiomas typically have low concentrations of N-acetyl aspartate, creatine, and lipids.[10]

Intra-osseous meningiomas. Lesions often have low signal on T1WI and T2W1 within expanded bone. Gd-contrast enhancement may occur at the periphery of the tumors, which extend into the adjacent soft tissues (Fig. **313).** Chordoid intra-osseous meningiomas can have low signal on T1WI and high signal on T2W1 with prominent Gd-contrast enhancement.[15]

Differential Diagnosis

Primary neuraxial meningiomas. Metastatic lesion, lymphoma, hemangiopericytoma, leukemia, hematoma, ependymoma, Schwannoma, neurofibroma.

Intra-osseous meningiomas. Fibrous dysplasia, en plaque meningioma with hyperostosis, osteoma, Paget disease.[4]

Prognosis and Treatment[1,6,8,9,13]

Most symptomatic meningiomas can be treated with gross total resection.[9] Stereotactic radiosurgery has been used as an alternative to surgical resection. Fractionated, large-field conventional radiation has also been used in the treatment of intracranial meningiomas.[6] Spinal meningiomas can be completely resected using a posterior laminectomy approach in 92-98% of patients.[8]"

Approximately 20 % of benign meningiomas that have been completely resected recur after 20 years.[9] Atypical meningiomas and anaplastic menigiomas have recurrence rates of 40 % and 78%, respectively.[9] Anaplastic meningiomas are invasive tumors which can metastasize.[9] Anaplastic meningiomas typically lack progesterone receptors, have high mitotic indices, and high tumor grades.[9] These factors were found to be significant in shortening of the disease-free intervals.[9] Patients with anaplastic meningiomas have a poor prognosis with a median survival of less than 2 years.[9]

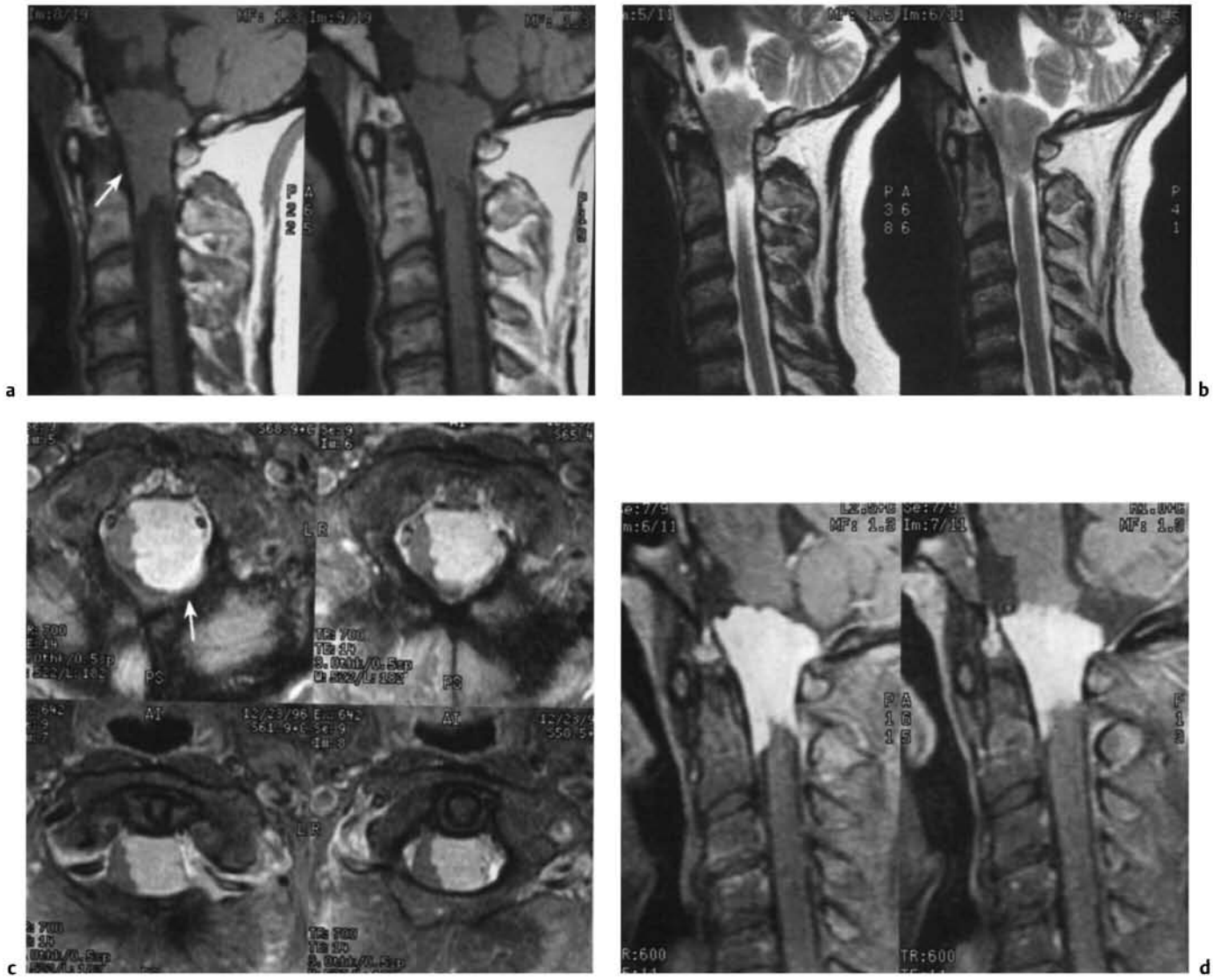

Figure **309 a-d** Meningioma at the cervicomedullary junction and C 1-2 level causing displacement and compression of the lower medulla and spinal cord. The tumor has low-intermediate signal on sagittal T1WI (**a**) and sagittal (**b**) T2WI. The tumor shows prominent Gd-contrast enhancement on axial (**c**) and sagittal (**d**) FS T1WI.

Figure **310a, b** A 67-year-old woman with a meningioma at the C 7 level causing compression of the spinal cord. The tumor has low-intermediate signal on sagittal T2WI (**a**) and shows prominent Gd-contrast enhancement on sagittal FS T1WI (**b**).

Figure **311a-c** Meningioma in the thoracic spinal canal causing compression of the spinal cord. The tumor has low signal centrally surrounded by intermediate signal on sagittal T1WI (**a**) and sagittal T2WI (**b**). (The low signal centrally corresponded to calcifications seen histologically.) The tumor shows heterogeneous mostly peripheral Gd-contrast enhancement on sagittal T1WI (**c**).

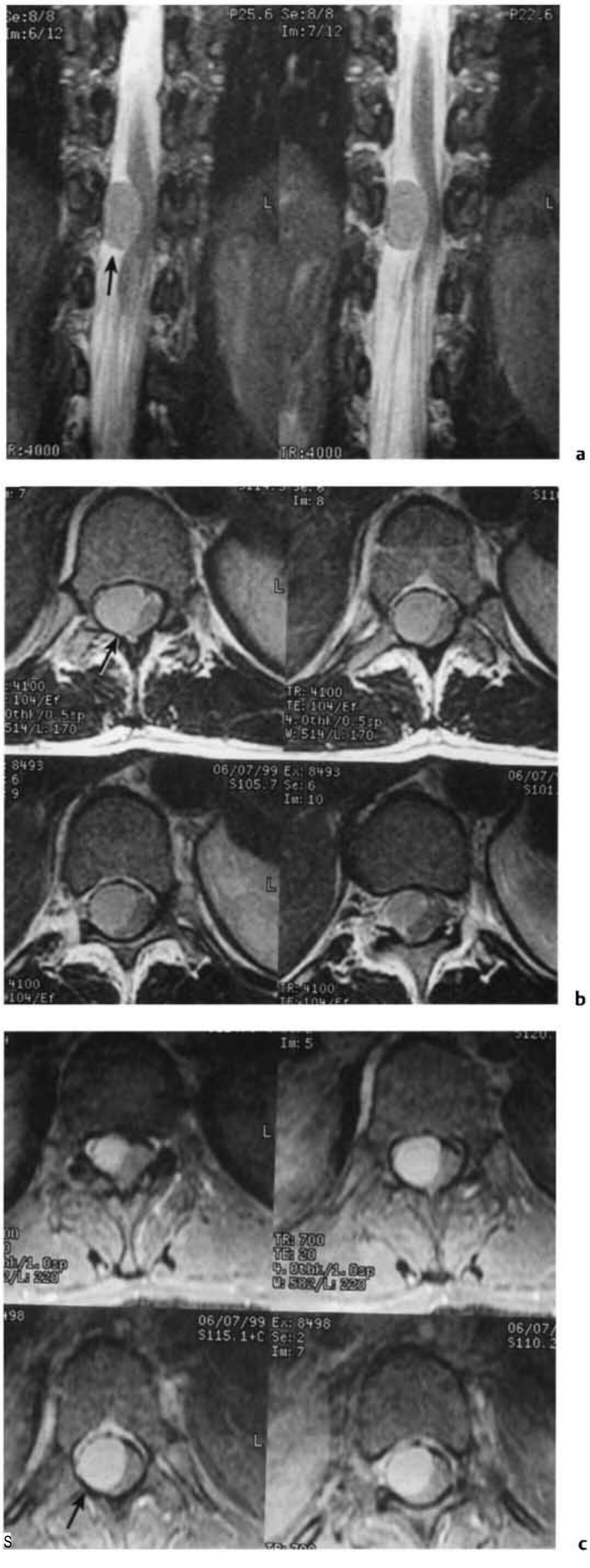

Figure **312a-c** A 43-year-old woman with a meningioma causing compression of the lower thoracic spinal cord. The tumor has intermediate to slightly high signal on coronal FS T2WI (**a**) and axial T2WI (b). The tumor shows prominent Gd-contrast enhancement on axial FST1WI(**c**). >

a, b 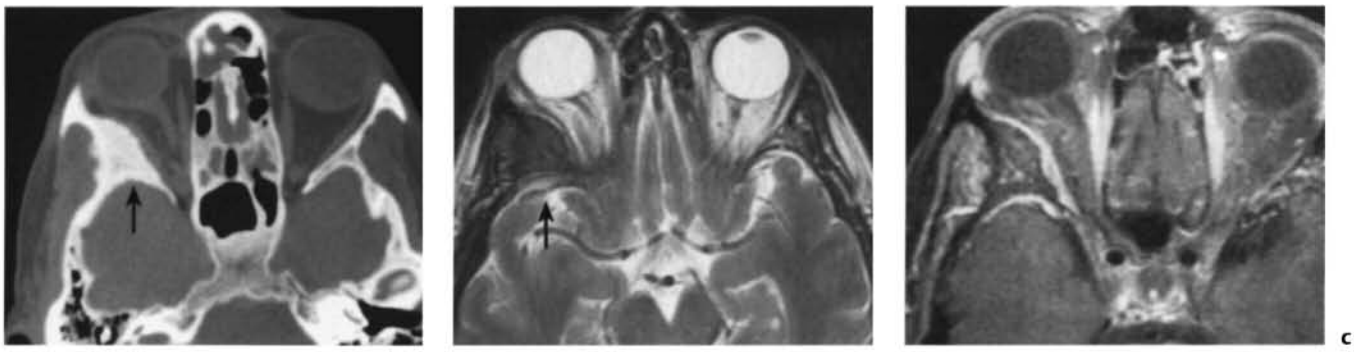 c

Figure **313 a-c** A 52-year old woman with an intra-osseous meningioma. Axial CT image (**a**) shows thickening and hyperostosis at the posterolateral wall of the right orbit. The intra-osseous meningioma has mostly low signal on axial T2WI (**b**) as well as thin zones of slightly high signal at sites of extra-osseous extension. The small zones of extra-osseous tumor at the lateral orbit and anterior middle cranial fossa show Gd-contrast enhancement on axial FST1WI (**c**).

References

1 Amirjamshidi A, Mehrazin M, Abbassioun K. Meningiomas of the central nervous system occurring below the age of 17: report of 24 cases not associated with neurofibromatosis and review of literature. *Childs Nerv Syst* 2000;16:406-416.

2 Buetow MP, Buetow PC, Smirniotopoulos JG. Typical, atypical, and misleading features in meningioma. *Radiographics* 1991;11(6): 1087-1106.

3 Chen TY, Lai PH, Ho JT, et al. Magnetic resonance imaging and diffusion-weighted images of cystic meningioma: correlating with histopathology. *Clin Imaging* 2004;28(1):10-19.

4 Daffner RH, Yakulis R, Maroon JC. Intraosseous meningioma. *Skeletal Radial* 1998;27:108-111.

5 Eastwood JD, Turner DA, McLendon RE, Provenzale JM. Diffusion-weighted MR imaging in a patient with spinal meningioma. *AJR Am J Roentgenol* 2001;177:1479-1481.

6 Flickinger JC, Kondziolka D, Maitz AH, Lunsford LD. Gamma knife radiosurgery of imaging-diagnosed intracranial meningioma. *Int J Radiat Oncol Biol Phys* 2003;56(3):801-806.

7 Harting *f,* Hartmann M, Bonsanto MM, Sommer C, Sartor K. Characterization of necrotic meningioma using diffusion MRI, perfusion MRI, and MR spectroscopy: case report and review of the literature. *Neuroradiology* 2004;46:189-193.

8 King AT, Sharr MM, Gullan RW, Bartlett JR. Spinal meningiomas: a 20-year review. *Br J Neurosurg* 1998;12(6):521-526.

9 Louis DN, Scheithauer BW, Budka H, von Deimling A, Kepes JJ. Meningiomas. In: Kleihues P, Cavenee WK, eds. *World Health Organization Classification of Tumours. Pathology and Genetics of Tumours of the Nervous System* Geneva: IARC Press; 2000:176-184.

10 Majos C, Alonso J, Aguilera C, et al. Utility of proton MR spectroscopy in the diagnosis of radiologically atypical intracranial meningiomas. *Neuroradiology* 2003;45:129-136.

11 Nakano T, Asano K, Miura H, Itoh S, Suzuki S. Meningiomas with brain edema radiological characteristics on MRI and review of the literature. *Clin Imaging* 2002;26:243-249.

12 Quekel LG, Versteege CW. The "dural tail sign" in MRI of spinal meningiomas. J *Comput Assist Tomogr* 1995;19(6):890-892.

13 Roux FX, Nataf F, Pinaudeau M, Borne G, Devaux B, Meder JF. Intraspinal meningiomas: review of 54 cases with discussion of poor prognosis factors and modern therapeutic management. *Surg Neurol* 1996;46(5):458-464.

14 Sato N, Sze G. Extradural spinal meningioma: MRI. *Neuroradiology* 1997;39:450-452.

15 Tokgoz N, Oner YA, Kaymaz M, Ucar M, Yilmaz G, Tali TE. Primary intraosseous meningioma: MR and CT appearance. *AJNR Am J Neuroradiol* 2005;26:2053-2056.

A 50 Metastatic Lesions

Definition

Metastatic lesions represent proliferating neoplastic cells that are located in sites or organs separated or distant from their origins. Metastatic lesions can disseminate hematogenously via arteries or veins, along cerebrospinal fluid pathways, along surgical tracts, and along lymphatic structures.

Frequency of Occurrence

Metastatic carcinoma is the most frequent malignant tumor involving bone.[11,12,14] In adults, metastatic lesions to bone occur most frequently from carcinomas of the lung, breast, prostate, kidney, thyroid, as well as from sarcomas.[10] Primary malignancies of the lung, breast, and prostate account for 80 % of bone metastases.[10,11]

The exact incidence of metastatic skeletal disease is unknown.[12] Up to 50% of patients who die from disseminated carcinoma have evidence of skeletal metastases at autopsy.[12] Almost 240,000 patients die in the United States each year from carcinoma of the lung, breast, prostate, kidney, and thyroid.[5] Using these data, up to 120,000 oncology patients who die each year may have metastatic skeletal disease. Metastatic skeletal disease has also been reported to occur in up to 30 % of all cancer cases.[4] Thirty percent of the 1,284,900 new cancer cases annually in the United States[5] is 385,470. By comparison, only 2400 primary malignant bone tumors occur in the United States per year.[5] Metastatic lesions may therefore occur from 50 to 161 times more frequently than primary bone tumors.[4-8,12] In children, osseous metastases usually result from neuroblastoma, rhabdomyosarcoma, osteosarcoma, Ewing sarcoma, leukemia, lymphoma, Wilm tumor, PNET, retinoblastoma, and medulloblastoma.[3,4,8]

Age at Presentation[8]

Adults > children.

Gender Ratio (M / F)

1.2/1.

Location

The distribution of metastatic lesions in bone is typically related directly to where red marrow predominates, such as the axial skeleton.[4] Up to 80 % of skeletal metastases involve the spine:[4] vertebrae > ribs > pelvic bones > skull > sternum, proximal femur > proximal humerus > other bones.

Skeletal metastases involving the skull or spine can invade the meninges with potential extension into the subarachnoid space and central nervous system.

Signs and Symptoms

Bone. Metastases involving bone may have associated pain, swelling, and pathologic fracture.[9]

Soft tissue. Swelling occurs with or without associated pain.

Histopathologic Findings

The histopathologic features of osseous metastases usually reflect the cytologic features of the primary tumor associated with osteoclasts and macrophages. Tumor cells in the marrow can increase osteoclastic and osteoblastic activity resulting in osteolysis or osteosclerosis.[4,14] Metastatic neoplastic cells can stimulate osteoclastic activity by secretion of various substances such as parathyroid hormone related proteins, prostaglandins, cytokines (interleukins and tumor necrosis factor), transforming growth factors a and (3, and procathepsin-D.[4,10] Tumor cells can also secrete cytokines that stimulate osteoblastic activity.[10] Increased osteoclastic activity resulting from metastatic neoplastic cells tends to dominate the increased osteoblastic activity.[4] Reactive immature woven bone can occur in up to 40 % of skeletal metastases.[4]

Confirmation of well or moderately differentiated metastatic adenocarcinoma or squamous cell carcinoma is not problematic.[12] The diagnosis of poorly differentiated or undifferentiated carcinoma can be confirmed in many cases using immunohistochemical reactivity to cytokeratins.[12] Evaluation of metastatic lesions for immunohistochemical reactivity to specific antigens (prostate specific antigen for prostate carcinoma, thyroglobulin antigen for thyroid carcinoma, etc.) can confirm the origins of these primary undifferentiated neoplasms.[12]

Findings on Plain Films (Roentgenograms) and Computed Tomography

Metastatic skeletal lesions in bone can have variable features on plain films and CT.[9] Most metastatic lesions (~90%) from carcinoma are radiolucent abnormalities involving the medullary portion of the bone and also the cortex with or without a soft tissue mass[9,14] (Figs. **317, 319-321).** Metastases involving the bone cortex alone without the medullary region can occur but are rare.[4] Margins of the metastatic lesions are often indistinct.[9] Sclerotic metastases are seen in 5 % of cases (Fig. **318),** and mixed radiolytic and radiosclerotic lesions are seen in 5%[9,14] (Fig. **323).** Radiolucent patterns associated with osseous metastases include: geographic (35%), moth-eaten (45%) and permeative (20 %).[9] Mild periosteal reaction may be seen in a 21 % of cases.[4,9,15] The most frequent patterns of perisoteal reaction associated with metastases include: disorganized type > Codman triangle > solid type.[15] Punctate or amorphous calcifications can be seen with metastases from mucinous adenocarcinomas.[4] Pathologic fractures can be associated with metastatic lesions involving tubular bones and vertebrae.

Osteolytic metastatic lesions are frequently observed from malignant tumors of the lung, breast, kidney, thyroid, gastrointestinal tract, larynx, cervix, bladder, ovary, and uterus.[4]

Osteosclerotic lesions can be seen from malignant tumors of the breast, lung (oat cell carcinoma, adenocarcinoma), bronchus and gastrointestinal tract (carcinoid), stomach (adenocarcinoma), colon (adenocarcinoma), pancreas (adenocarcinoma), testes (seminoma), ovary (seminoma), thyroid (medullary carcinoma), and cerebellum (medulloblastoma).[4]

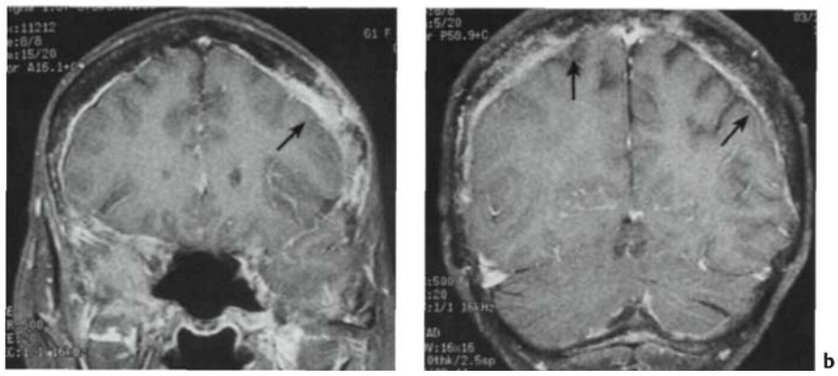

Figure **314a, b** A 61-year-old woman with metastatic breast carcinoma involving the skull. The poorly defined metastatic disease shows Cd-contrast enhancement on coronal (**a**) and axial (**b**) FST1WI, and extends from the marrow through zones of bone destruction at the inner and outer tables of the skull to involve the intracranial dura and soft tissues of the scalp.

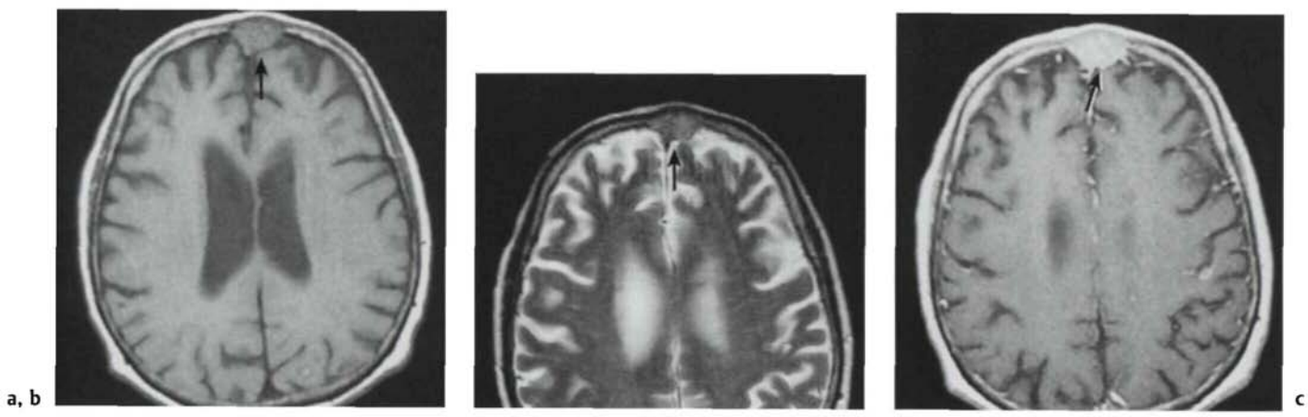

Figure **315a-c** Single metastatic lesion in the frontal bone from breast carcinoma. The tumor has circumscribed margins and extends from the marrow through zones of bone destruction. The tumor has intermediate signal on axial (**a**) T1WI, and axial T2WI (**b**). The tumor shows prominent Gd-contrast enhancement on axial T1WI (c).

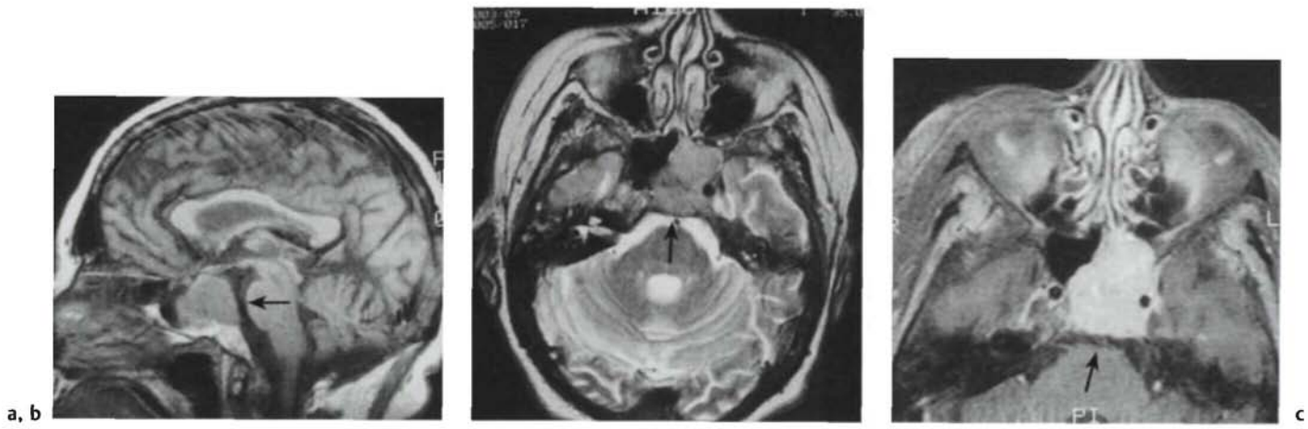

Figure **316a-c** Metastatic lesion in the clivus from breast carcinoma. The tumor has circumscribed margins and extends from the marrow through zones of bone destruction. The tumor has intermediate signal on sagittal T1WI (**a**) and slightly high signal on axial T2WI (**b**). The tumor shows prominent Gd-contrast enhancement on axial FST1WI (**c**).

MRI Findings[1,2,13]

Bone. Metastatic tumor within bone often appears as intramedullary zones with low-intermediate signal on T1WI, low-intermediate to slightly high signal on PDWI, intermediate, slightly high to high signal on T2WI and FST2WI (Figs. **314-317, 319-323).** Sclerotic lesions often have low signal on T1WI, and mixed low, intermediate, and/or high signal on T2W1 (Fig. **318).** The vertebral body is usually the earliest portion of the vertebra involved with metastatic tumor.[1]

Metastatic spinal lesions may be focal or involve most of a vertebra. In tubular bones, metastatic lesions are usually intramedullary with frequent cortical destruction and tumor extension into the extra-osseous soft tissues (Fig. **321).** Metastatic bone lesions may have poorly defined or distinct margins. Zones of cortical destruction often occur associated with ex-

tra-osseous soft tissue lesions. Pathologic fractures can be associated with metastatic lesions involving tubular bones and vertebrae. Pathologic compression fractures from metastases involving vertebral bodies often have convex bowing of the ventral and/or dorsal margins, unlike traumatic or osteopenic compression fractures which have sharply angulated cortical margins.[2] MRI is the main, noninvasive imaging modality for assessing spinal cord or spinal canal compression from metastatic tumor extension or pathologic vertebral fractures secondary to metastatic disease (Fig. **318).** Metastatic skeletal lesions usually show varying degrees of Gd-contrast enhancement.

Skeletal metastases involving the skull or spine can invade the meninges with potential extension into the subarachnoid space and central nervous system. Metastatic skeletal lesions

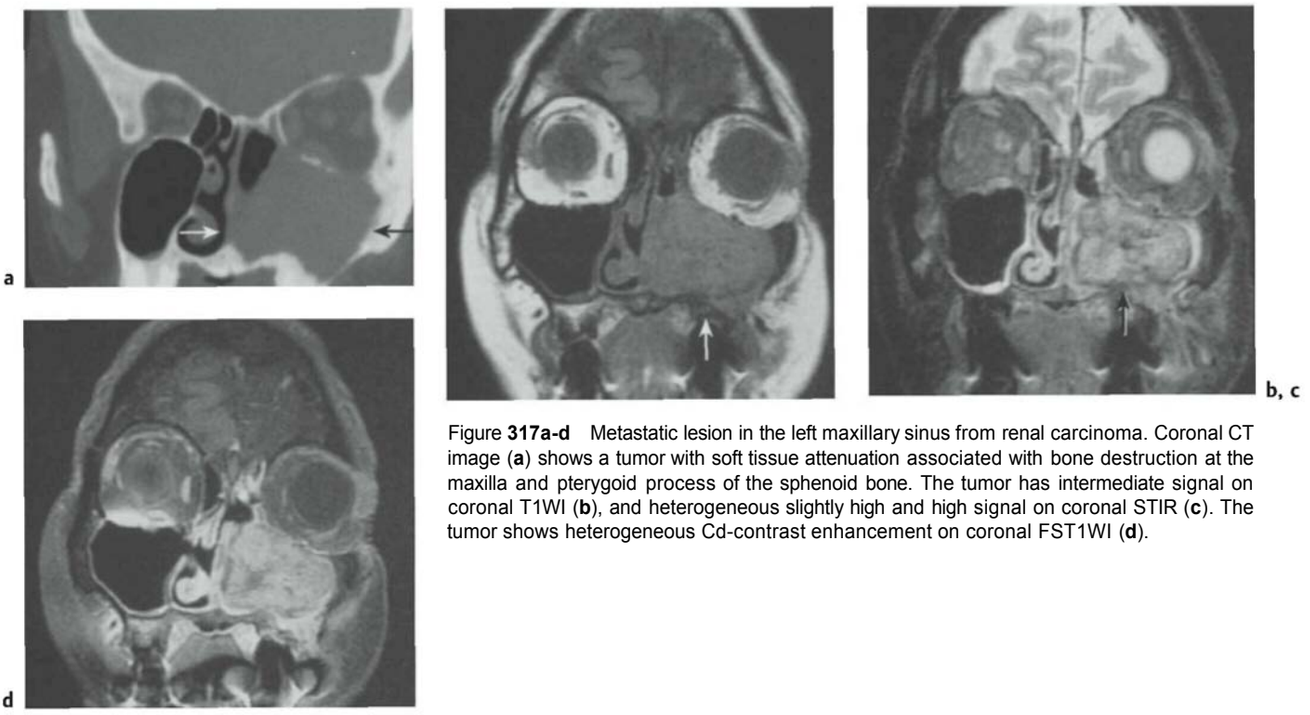

Figure **317a-d** Metastatic lesion in the left maxillary sinus from renal carcinoma. Coronal CT image (**a**) shows a tumor with soft tissue attenuation associated with bone destruction at the maxilla and pterygoid process of the sphenoid bone. The tumor has intermediate signal on coronal T1WI (**b**), and heterogeneous slightly high and high signal on coronal STIR (**c**). The tumor shows heterogeneous Cd-contrast enhancement on coronal FST1WI (**d**).

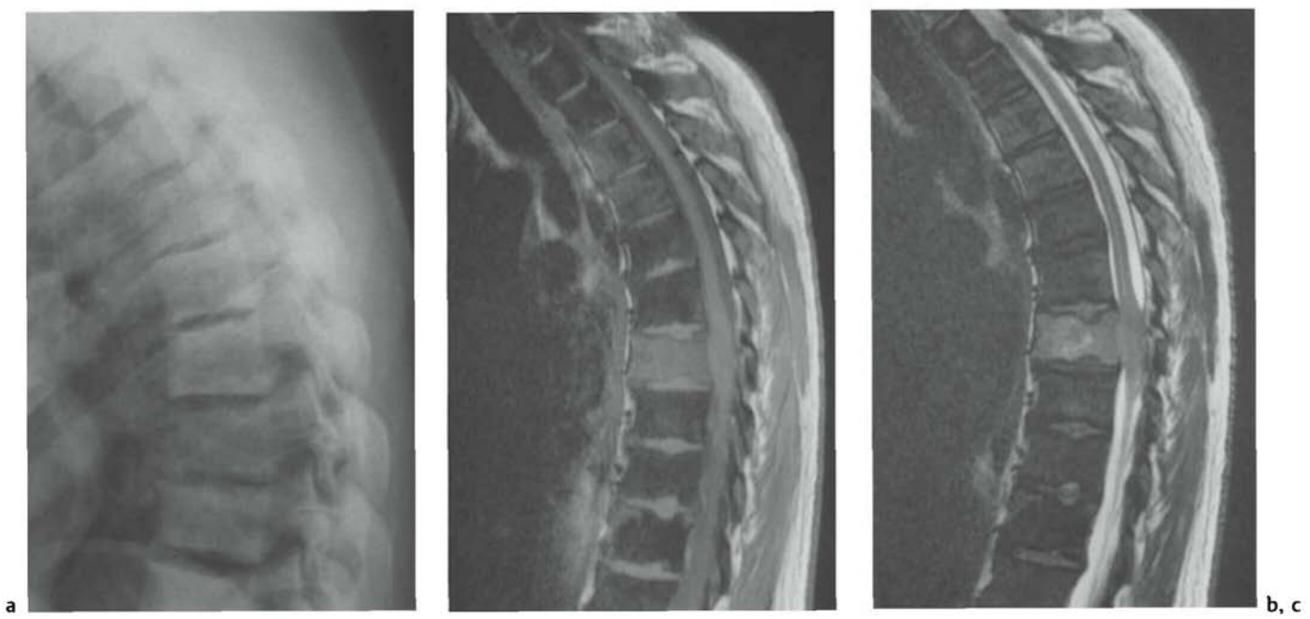

Figure **318a-c** A 57-year-old man with diffuse sclerotic metastases from prostate carcinoma involving the thoracic and lumbar spine. Lateral radiograph of the thoracic spine (**a**) shows diffuse increased density of the vertebrae. The neoplastic disease has mostly low signal on sagittal T1WI (**b**) and sagittal T2WI (**c**). One mid thoracic vertebral body has intermediate signal on T1WI and intermediate to slightly high signal on T2WI, and is associated with dorsal epidural tumor extension causing spinal cord compression.

invading the dura can appear as enhancing fusiform dural lesions (Fig. **314).** Extension of metastatic disease into the subarachnoid space can show Gd-enhancement within the sulci or basal cisterns adjacent to the brain, and/or Gd-enhancement adjacent to the spinal cord and nerve roots.

Soft tissue. Metastatic lesions in soft tissue can occur as lymphadenopathy, or as focal lesions with well-circumscribed, irregular, and/or poorly defined margins. Metastatic lesions often have low-intermediate signal on T1WI and PDWI, and intermediate to slightly high signal or high signal on T2WI and FST2W1 (Figs. **324-327).** Variability in MRI signal characteristics may be related to differing histologic features (such as necrosis, fibrosis, calcification, hemorrhage) of the metastatic lesions. After Gd-contrast administration, extra-osseous metastatic lesions can show varying degrees of enhancement.

Figure **319a-d** An 83-year-old woman with multiple metastases from breast carcinoma involving the lower spine. Lateral radiograph (**a**) shows multiple radiolucent lesions in the vertebrae. The extensive metastatic lesions have low-intermediate signal on sagittal T1WI (**b**) and sagittal T2WI (**c**), and are associated with prominent Cd-contrast enhancement on sagittal FST1WI (**d**).

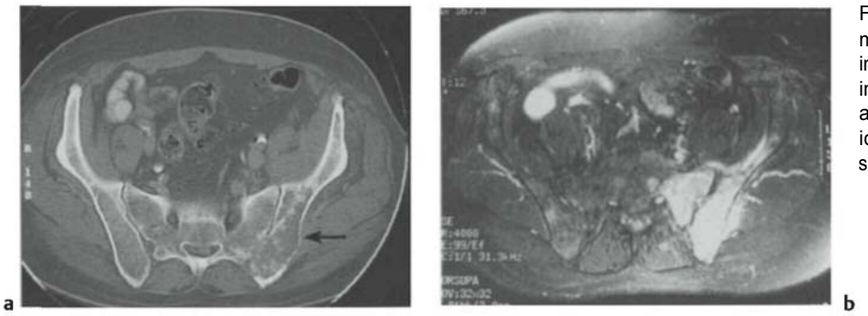

Figure **320a, b** A 65-year-old man with metastatic disease from lung carcinoma involving the sacrum and iliac bone. Axial CT image (**a**) shows a radiolucent lesion associated with destruction of trabecular and cortical bone. The metastatic tumor has high « signal on axial FST2WI (**b**).

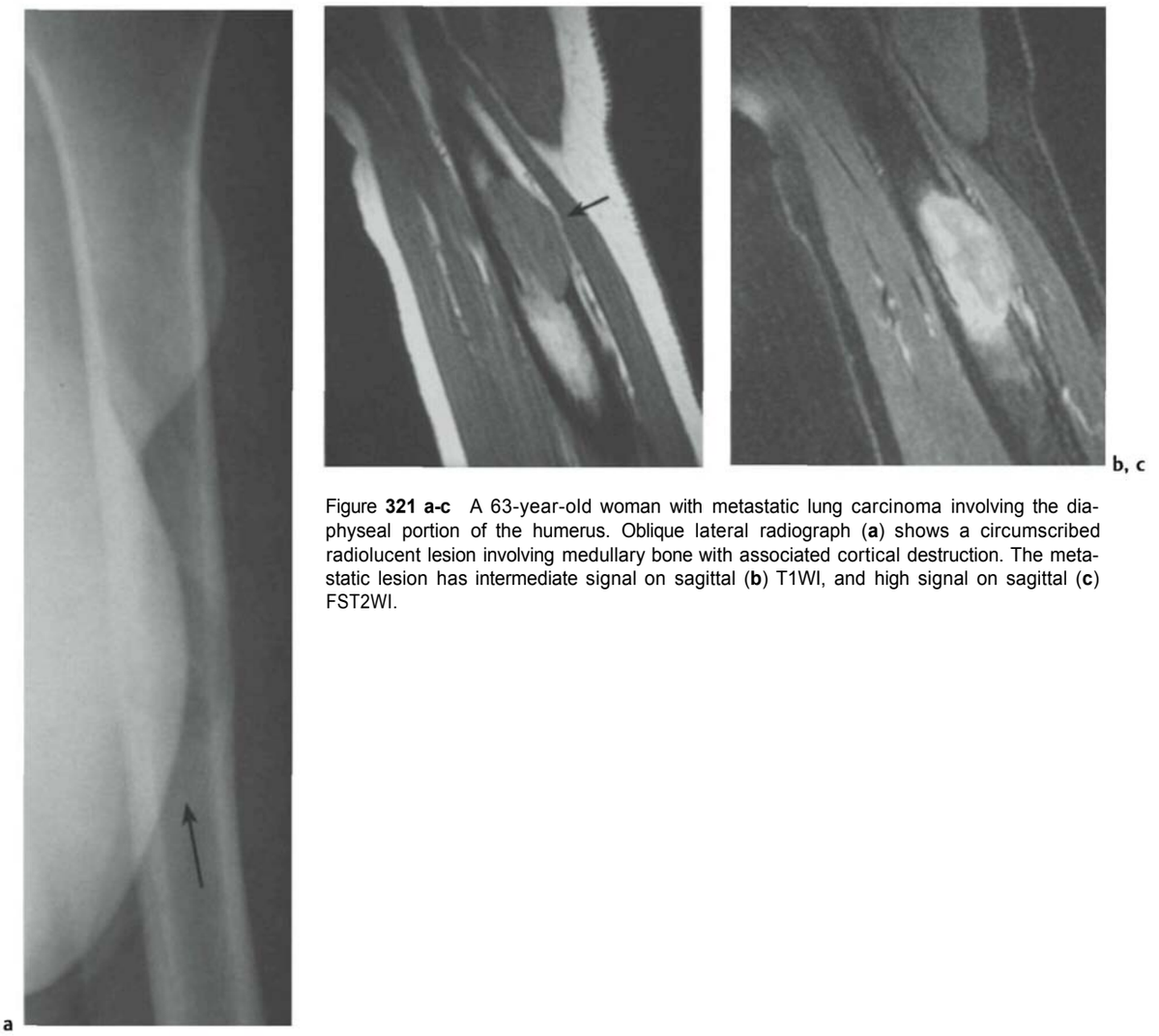

Figure **321 a-c** A 63-year-old woman with metastatic lung carcinoma involving the diaphyseal portion of the humerus. Oblique lateral radiograph (**a**) shows a circumscribed radiolucent lesion involving medullary bone with associated cortical destruction. The metastatic lesion has intermediate signal on sagittal (**b**) T1WI, and high signal on sagittal (**c**) FST2WI.

Differential Diagnosis

Adults:

- **Bone.** Myeloma, lymphoma, leukemia, giant cell tumor, osteosarcoma, chondrosarcoma, osteomyelitis, brown tumor.
- **Soft tissue.** Malignant fibrous histiocytoma, fibrosarcoma, liposarcoma, synovial sarcoma, lymphoma, leukemia, myeloma, rhabdomyosarcoma, leiomyosarcoma, malignant peripheral nerve sheath tumor, melanoma, dermatofibrosarcoma, Castleman disease (angiofollicular lymphoid hyperplasia), post-transplantation lymphoproliferative disease.

Children:

- **Bone.** Langerhans cell histiocytosis, lymphoma, leukemia, giant cell tumor, osteomyelitis, brown tumor.
- **Soft tissue.** Lymphoma, leukemia, Castleman disease (angiofollicular lymphoid hyperplasia), post-transplantation lymphoproliferative disease, malignant fibrous histiocytoma, fibrosarcoma, liposarcoma, synovial sarcoma.

a

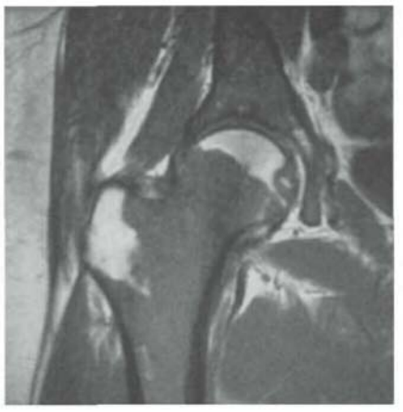

b, c

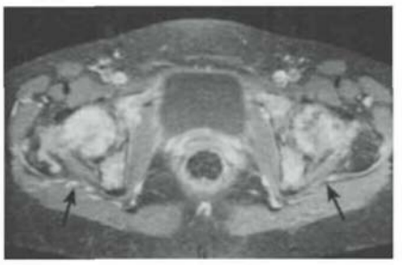

d

Figure **322a-d** A 53-year-old woman with metastatic disease involving the pelvic bones and proximal femurs. AP radiograph (**a**) shows no definite abnormalities. Metastatic tumor has low-intermediate signal in the marrow on coronal T1 WI (**b**), and high signal on coronal FST2WI (**c**). The metastatic tumor shows prominent Cd-contrast enhancement on axial FST1WI (**d**).

a

b, c

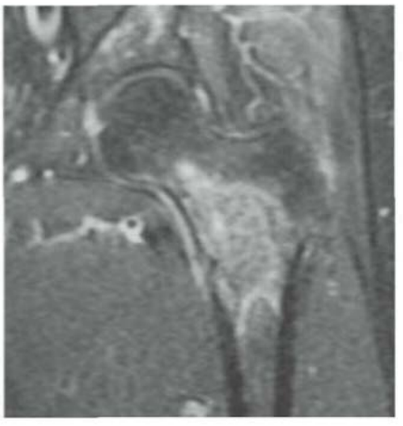

d

Figure **323a-d** A 57-year-old woman with metastatic breast carcinoma involving the proximal femur. AP radiograph (**a**) shows a radiolucent lesion in the intertrochanteric region, which is associated with peripheral sclerotic reaction as well as endosteal erosion. The tumor has mostly circumscribed margins and has low-intermediate signal on coronal T1WI (**b**), and heterogeneous high, slightly high, and low signal on coronal FS T2WI (**c**). The tumor shows heterogeneous Cd-contrast enhancement on coronal FST1WI(**d**).

Prognosis and Treatment

Patients with metastatic disease typically have a poor prognosis which is often dependent on the aggressiveness of the primary and secondary lesions. Systemic chemotherapy and/or radiation are often employed. High dose chemotherapy with bone marrow transplantation or stem cell rescue have also been used to treat metastatic disease. Orthopedic stabilization procedures with internal fixation devices can be useful for palliation.[10] Vertebroplasty or kyphoplasty procedures using injections of methyl methacrylate have been used for treatment of metastatic disease involving the spine.

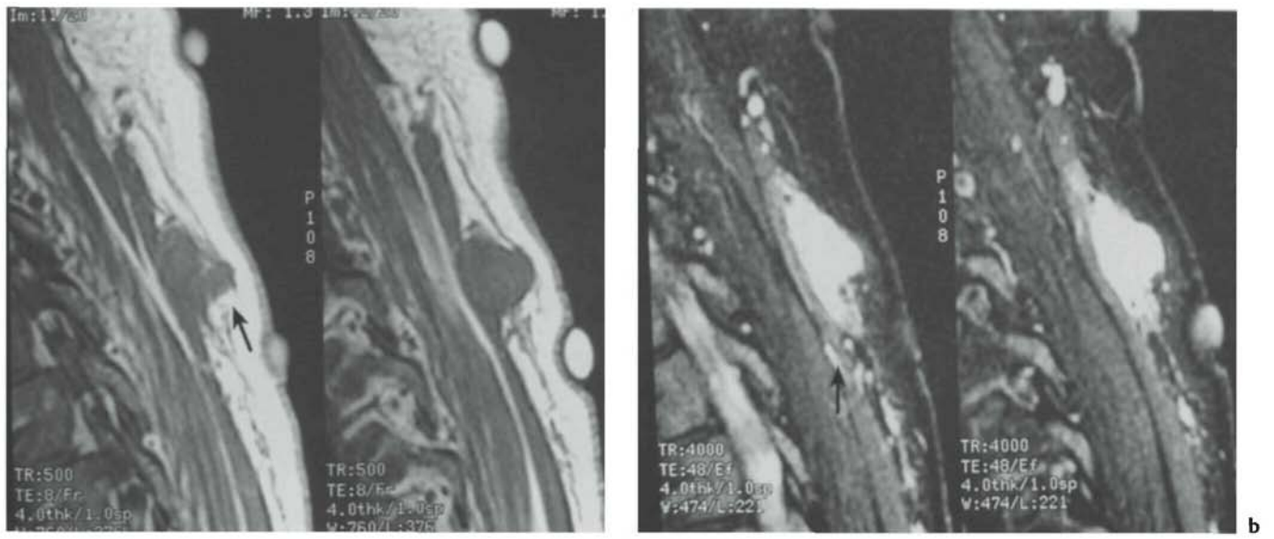

a b

Figure **324 a, b** Metastatic lesion from lung carcinoma involving the deep subcutaneous fat of the upper dorsal back. The tumor has low-intermediate signal on sagittal (**a**)T1WI, and high signal on sagittal (**b**)FST2WI.

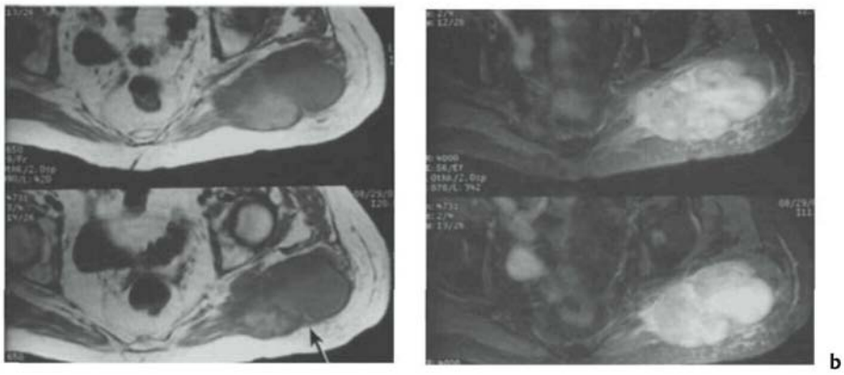

a b

Figure **325 a, b** A 70-year-old woman with metastatic lesion from renal carcinoma involving the left gluteus maximus. The tumor has mixed low-intermediate, intermediate, and slightly high signal on axial T1WI (**a**), and high signal on axial FST2WI (**b**).

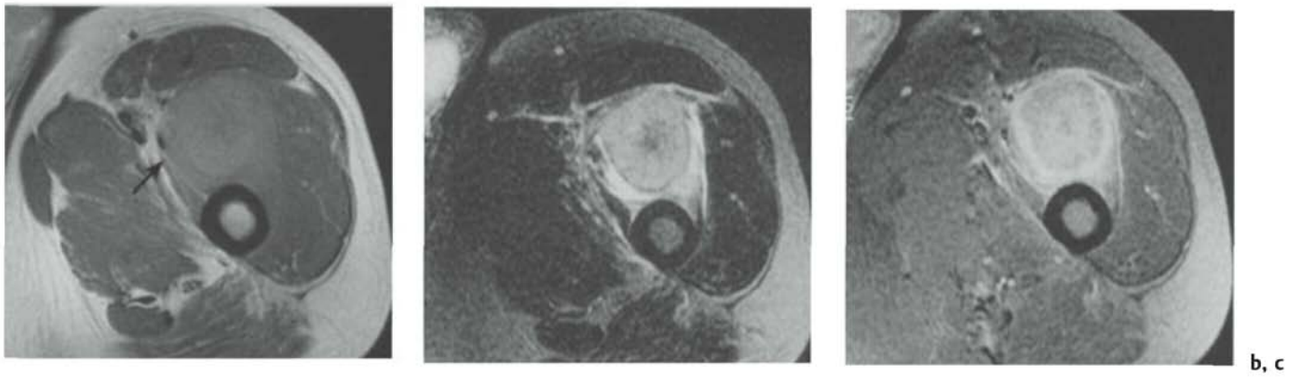

a b, c

Figure **326a-c** A 51-year-old man with a metastatic lesion from lung carcinoma involving the vastus intermedius muscle of the upper thigh. The tumor has intermediate to slightly high signal on axial PDWI (**a**), and heterogeneous high signal on FST2WI (**b**). The tumor shows prominent Gd-contrast enhancement on axial FST1WI (**c**).

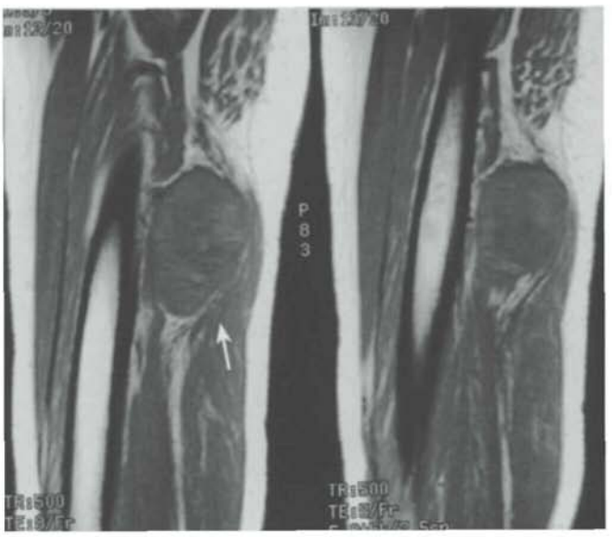

a

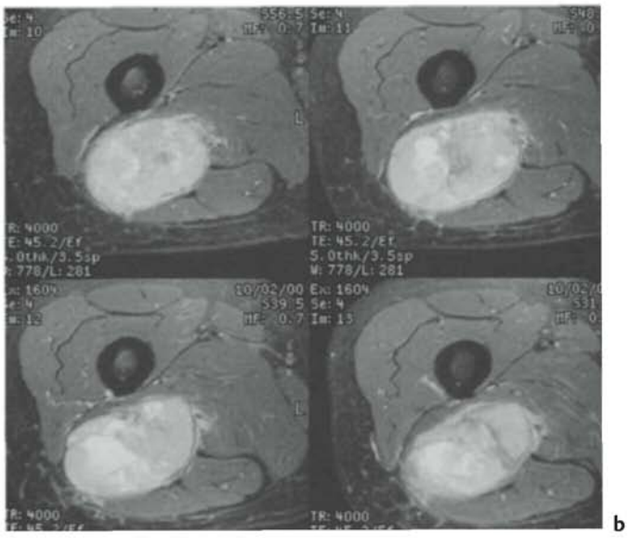

b

Figure **327 a, b** A 47-year-old woman with a metastatic melanoma involving the biceps femoris muscle of the posterior thigh. The tumor has low-intermediate signal on sagittal (**a**) T1WI, and heterogeneous mostly high signal on axial (**b**) FST2WI.

References

1 Algra PR, Heimans JJ, Valk J, Nauta JJ, Lachniet M, Van Kooten B. Do metastases in vertebrae begin in the body or the pedicles? Imaging study in 45 patients. *AJR Am J Roentgenol* 1992:158:1275-1279.

2 Baker LL, Goodman SB, Perkash I, Lane B, Enzmann DR. Benign versus pathologic compression fractures of vertebral bodies: assessment with conventional spin-echo, chemical shift, and STIR MR imaging. *Radiology* 1990;174(2):495-502.

3 Faerber EN, Roman NV. Central nervous system tumors of childhood. Radio/ *Clin North Am* 1997:35:1301-1328.

4 Forest M. Bone metastases. In: Forest M, Tomeno B, Vanel D, eds. *Orthopedic Surgical Pathology: Diagnosis of Tumors and Pseudotumoral Lesions of Bone and Joints* 1998:501-516.

5 Jemal A, Thomas A, Murray T, Thun M. Cancer statistics 2002. *CA CancerJ Clin* 2002:52:23-47.

6 Moser RP, Madewell JE. Metastatic bone disease. In: Tavers JM, Ferrucci JT, eds. *Radiology: Diagnosis-Imaging-Intervention* Vol 5. Philadelphia, PA: Lippincott, Williams & Wilkins; 2003:5:100(1-8).

7 Mulder JD, Schutte HE, Kroon HM, Taconis WK. Introduction. In: *Radiologic Atlas of Bone Tumors* Amsterdam: Elsevier: 1993:3-6.

8 Mulder JD, Schutte HE, Kroon HM, Taconis WK. The diagnosis of bone tumors. In: *Radiologic Atlas of Bone Tumors* Amsterdam: Elsevier; 1993:9-46.

9 Mulder JD, Schutte HE, Kroon HM, Taconis WK. Metastasis. In: Radiologic *Atlas of Bone Tumors* Amsterdam: Elsevier; 1993:337-351.

10 Patel SR, Benjamin RS. Sarcomas of soft tissue and bone. In: Fauci AS, Braunwald E, Isselbacher KJ, eds. *Harrison's Principles of Internal Medicine* 14th ed. New York, NY: McGraw-Hill; 1998:611-615.

11 Rosenberg A. Bones, joints and soft tissue tissues. In: Cotran RS, Kumar V, Collins T, eds. *Pathologic Basis of Disease* 6th ed. Philadelphia, Pa: W.B. Saunders; 1999:1215-1268.

12 Salisbury JR. Bone neoplasms containing epithelial and epithelioid cells. In: Forest M, Tomeno B, Vanel D, eds. *Orthopedic Surgical Pathology: Diagnosis of Tumors and Pseudotumoral Lesions of Bone and Joints* Edinburgh: Churchill Livingstone; 1998:345-368.

13 Schweitzer ME, Levine C, Mitchell DG, Gannon FH, Cornelia LG. Bull's-eyes and halos: useful MR discriminators of osseous metastases. *Radiology* 1993;188(l):249-252.

14 Unni KK. Conditions that commonly simulate primary neoplasms of bone. In: *Dahlin's Bone Tumors—General Aspects and Data on 11087 Cases* 5th ed. Philadelphia, Pa: Lippincott, Williams & Wilkins; 1996: 355-360.

15 Wenaden AET, Szyszko TA, Saifuddin A. Imaging of periosteal reactions associated with focal lesions of bone. *Clin* Radio/ 2005;60: 439-456.

A 51 Morton Neuroma

Definition

Morton neuromas are non-neoplastic lesions that result from perineural fibrosis of a plantar digital nerve near the metatarsal head.[1,3]

Age at Presentation

These lesions have the highest prevalence in the 5th to 6th decades.[7]

Gender Ratio

These lesions occur most frequently in women.[1,5,7] M / F ratios of 1 /18 have been reported.[3,5]

Location

Lesions occur at the plantar digital nerves near the metatarsal heads (between the third and fourth metatarsal heads > between the second and third metatarsal heads).[3,5,7]

Signs and Symptoms

Morton neuromas are frequently associated with ill-defined pain in the forefoot that can be elicited with exercise or the wearing of high-heeled shoes, and is often relieved with rest.[1,3,5,7,8] The pain may radiate into the toes or leg[1,3,5,7,8] Numbness, radiating pain, and/or tingling sensations often increase when wearing narrow shoes.[7,8] Removal of narrow shoes reduces these symptoms.[7,8] Morton neuromas larger than 5 mm are more symptomatic than smaller lesions.[8]

Gross Pathologic Findings

Morton neuromas often appear as fusiform enlargement of plantar digital nerves near the metatarsal heads.[3,5]

Histopathologic Findings

Lesions typically show interdigital perineural fibrosis with increased collagen content (Renaut bodies), and nerve degeneration with loss of myelinated fibers.[1,3,5] These lesions are often surrounded by inflammatory reaction.[1,3,5]

Findings on Plain Films (Roentgenograms) and Computed Tomography

Radiographs are usually unremarkable.[3] CT may show lesions with soft tissue attenuation.

MRI Findings

Lesions are located in the neurovascular bundle within the intermetatarsal space on the plantar side of the transverse metatarsal ligament.[5] The sizes of these lesions can vary based on patient positioning.[7] The transverse diameters of Morton neuromas were found to be larger when patients were imaged in the prone position compared with supine and upright weight-bearing positions.[7]

Lesions typically appear as a nodule with low-intermediate signal on T1WI and PDW1 that is isointense or slightly hyperintense relative to muscle[18] (Figs. **328-331).** Lesions often have low to intermediate signal on T2WI that is hypointense or isointense relative to fat[1-8] Lesions can have intermediate,

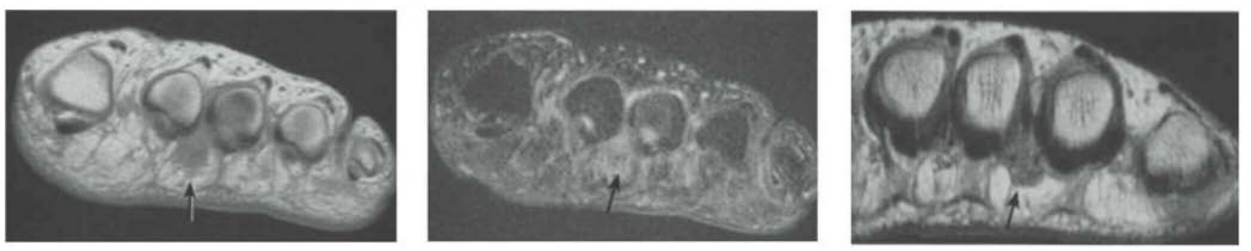

Figure **328 a, b** Morton neuroma between the second and third digits. The nodular lesion has intermediate signal on coronal PDWI (**a**), and slightly high signal on coronal FST2WI (**b**).

Figure 329 Morton neuroma between the third and fourth digits. The nodular lesion has low-intermediate signal on coronal T1WI.

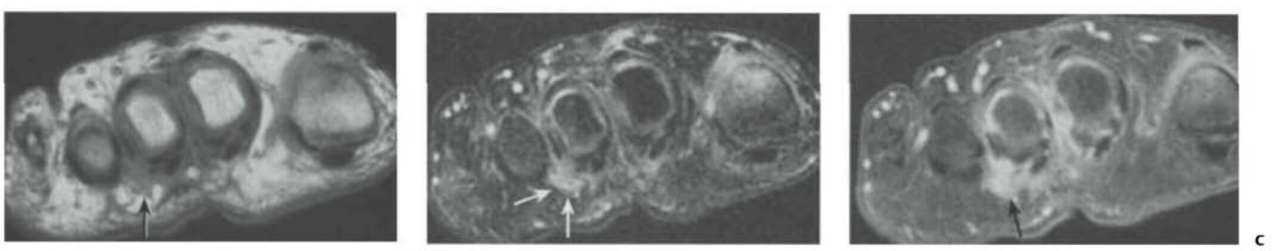

Figure **330 a-c** Morton neuroma between the third and fourth digits in a 48-year-old woman. The nodular lesion has intermediate signal on coronal PDWI (**a**), and high signal on coronal FST2WI (**b**). The lesion shows moderate Cd-contrast enhancement on coronal FST1WI (**c**).

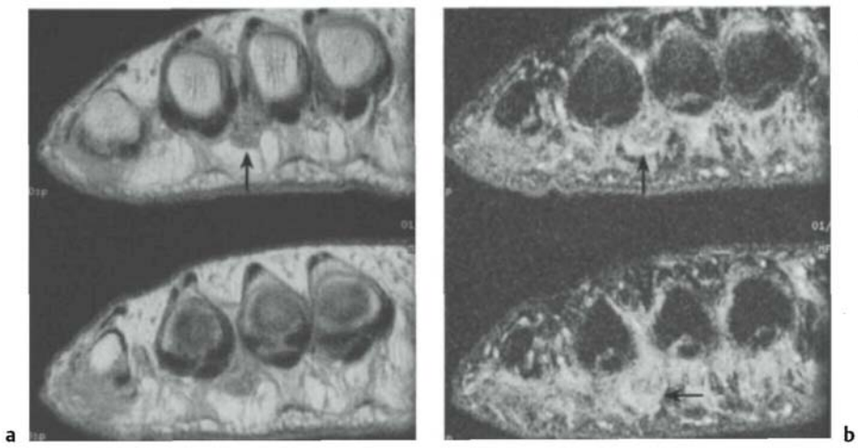

Figure **331 a, b** Morton neuroma between the third and fourth digits in a 58-year-old woman. The nodular lesion has low-intermediate signal on coronal PDWI (**a**), and high signal on coronal FST2WI (**b**).

slightly high or high signal on FST2WI[5] (Figs. **328-331).** After Gd-contrast administration, lesions can show enhancement which is often more conspicuous with fat-suppression[1,5,6] (Fig. **330).** Intermetatarsal bursal fluid is often associated with Morton neuromas.[2,3,5,8]

Differential Diagnosis

Giant cell tumor of the tendon sheath, pigmented villonodular synovitis, fibroma of the tendon sheath, Schwannoma.

Prognosis and Treatment

Treatment usually consists of modifying patients' shoes.[5] Steroid injections, ultrasound therapy, and/or surgical decompression by release of the transverse metatarsal ligament have been used to treat Morton neuromas.[5] Surgical resection of Morton neuromas is also performed for persistently symptomatic lesions that are more than 5 mm in diameter.[5,8] MR1 is useful for diagnosis of these lesions as well as determining the precise location for planning for the optimal surgical approach.[8]

References

1 Ashman CJ, Klecker RJ, Yu JS. Forefoot pain involving the metatarsal region: differential diagnosis with MR imaging. *Radiographics* 2001 ;21 (6): 1425-1440.

2 Erickson SJ, Canale PB, Carrera GF, et al. Interdigital (Morton) neuroma: high-resolution MR imaging with a solenoid coil. *Radiology* 1991;181(3):833-836.

3 Kransdorf MJ, Murphey MD. Neurogenic tumors. In: Kransdorf MJ, Murphey MD. *Imaging of Soft Tissue Tumors* 2nd ed. Philadelphia, Pa: W.B. Saunders; 2006:328-380.

4 Llauger J, Palmer J, Monill JM, Franquet T, Bague S, Roson N. MR imaging of benign soft-tissue masses of the foot and ankle. *Radiographics* 1998;18(6):1481-1498.

5 Murphey MD, Smith WS, Smith SE, Kransdorf MJ, Temple HT. From the archives of the AFIP. Imaging of musculoskeletal neurogenic tumors: radiologic-pathologic correlation. *Radiographics* 1999; 19(5): 1253-1280.

6 Terk MR, Kwong PK, Suthar M, Horvath BC, Colletti PM. Morton neuroma: evaluation with MR imaging performed with contrast enhancement and fat suppression. *Radiology* 1993:189(1):239-241.

7 Weishaupt D, Treiber K, Kundert HP, et al. Morton neuroma: MR imaging in prone, supine, and upright weight-bearing body positions. *Radiology* 2003)226:849-856.

8 Zanetti M, Strehle JK, Kundert HP, Zollinger H, Hodler J. Morton neuroma: effect of MR imaging findings on diagnostic thinking and therapeutic decisions. *Radiology* 1999;213:583-588.

A 52 Multiple Myeloma (Also Referred to as Myeloma, Kahler Disease, and Plasma Cell Neoplasm; Plasmacytoma Represents a Solitary Neoplastic Variant)

ICD-O Code

9732/3

Definition

Multiple myelomas are malignant tumors comprised of proliferating antibody-secreting plasma cells derived from single clones.[3,7,14] Plasma cells normally account for less than 5% of the cells in bone marrow. Multiple myeloma is primarily located in bone marrow.[3,7] A solitary myeloma or plasmacytoma is an infrequent variant in which a neoplastic mass of plasma cells occurs at a single site of bone or soft tissues.[1]

Frequency of Occurrence

An estimated 14600 new cases occur per year in the United States.[4] Multiple myeloma is the most common primary neoplasm of bone in adults.[3,15] Myeloma accounts for 44% of primary malignant bone tumors and 34% of all primary bone tumors.[15] Myeloma is the second most frequent hematologic cancer after non-Hodgkin lymphoma.[14] The prevalence of myeloma in the United States is 1 per 50 000 population.

Age at Presentation[11,15]

From 16 to 80 years, median = 60 years. Most patients are older than 40 years.

Gender Ratio (M / F)[4,16]

1.1/1 to 2.3/I

Location[12,14,16]

Tumors occur in the vertebrae > ribs > femur > iliac bone > humerus > craniofacial bones > sacrum > clavicle > sternum > pubic bone > tibia.[12,16] In tubular bones, tumors occur in the diaphyseal > metadiaphyseal > metaphyseal > epi-metaphyseal locations.[12] In vertebrae, tumors occur in the vertebral body and arch > vertebral body > arch.[12] Myeloma originates and proliferates in bone marrow.[14] In later phases of the disease, tumor cells can grow outside of the skeletal system.[14] Extra-osseous lesions occur in the lungs, oro-nasopharynx, nasal sinuses, liver, spleen, kidneys, and lymph nodes.[1]

Plasmacytomas represent ~5% of plasma cell tumors and have similar locations to multiple myeloma.

Signs and Symptoms

Bone pain is a common symptom in up to 70% of patients.[3,7,16] Pain often involves the spine and ribs, and is exacerbated by movement." The duration of the pain is usually less than 6 months.[3] Pathologic fractures can occur from the intra-osseous lesions.[1,3] Pathologic compression fractures involving vertebrae may result in kyphoscoliosis.[3] Symptoms associated with advanced disease include anemia, hypercalcemia, renal failure, and recurrent infections (pneumonia often from *Streptococcus pneumoniae, Staphylococcus aureus,* and *Klebsiella pneumoniae;* urinary tract infections from Gram-negative bacteria such as *Escherichia coli)* secondary to immunosuppression.[7,14]

Laboratory Findings

Neoplastic plasma cells produce an excess of complete immunoglobulins (Ig) (2 heavy and 2 light chains) as well as an excess of free heavy and light chains within plasma and extracellular fluid.[1] Monoclonal immunoglobulin (M-protein) in blood is detected with electrophoresis in 99% of patients with myeloma.[1] Excess light chains of Ig can be excreted into the urine and detected as proteinuria, referred to as Bence Jones proteins.[1]

Cytokines are associated with myeloma. Increased serum levels of the cytokine interleukin (IL)-6 produced by malignant plasma cells are associated with proliferation of myeloma and a poor prognosis.[1] Cytokines IL-1(ß as well IL-6 produced by myeloma cells stimulate osteoclastic bone lysis.[1] Moderate to severe anemia can occur.[16] Erythrocyte sedimentation rates are often increased.[16] Hypercalcemia occurs in up to 50% of patients.[16] Hyperviscosity of blood occurs in 7% from aggregation of M-proteins.[1]

Gross Pathologic Findings

Myeloma usually presents as multifocal, destructive bone lesions.[1] Lesions often appear as gray-white, soft nodules destroying or replacing bone marrow.[2,12] Coalescence of tumor nodules can result in a large multilobular lesion.[2]

Histopathologic Findings

Evaluation of the diseased bone marrow typically shows that plasma cells account for more than 30% of all marrow cells.[1] In marrow, malignant plasma cells can be distributed in a diffuse dense pattern within minimal stroma, consisting of thin fibrous septa with a reticulin meshwork pattern, and thin-walled blood vessels that may have associated hemorrhage.[1-3] Tumor cells may be also be arranged in aggregates, lobules, or strands separated by bands of collagen surrounding blood vessels.[1-3] In other cases, small nests of malignant plasma cells may be dispersed among adipose and/or hematopoietic cells, or along bone trabeculae.[2] Bone destruction may be associated with osteoclastic hyperplasia.[2]

Malignant plasma cells often have eccentric nuclei with a cartwheel pattern of thick chromatin, small or absent nucleolus, clear juxtanuclear halo secondary to a prominent Golgi apparatus, and basophilic cytoplasm that turns to a rose-red color in methyl-green, pyronine-stained solutions.[13] Monoclonal immunoglobulin within myeloma cells can be detected using immunofluorescence techniques with fluorescein and rhodamine.[3] Other cytologic plasma cell variants can occur such as: bizarre multinucleated cells, plasmablasts with mildly dense chromatin in a nucleus containing two or three nucleoli surrounded by a juxtanuclear halo from a Golgi apparatus and basophilic cytoplasm; immunoblasts containing a spheroid, pale nucleus with a prominent central nucleolus and basophilic cytoplasm; large proplasmocytes containing a pale nucleus and medium-sized central nucleolus; plasma cells with cleaved

nuclei; flame cells with bright red cytoplasm; and Mott cells with multiple blue droplets in the cytoplasm.[1-3]

A histologic staging system has been proposed for myeloma:[2] stage I is when <10% of the bone marrow is involved; stage II is when 20-50% of the bone marrow is involved; and stage III occurs with more than 50% involvement of the bone marrow.

Tumor Genetics

Using fluorescence in situ hybridization (FISH) techniques, DNA content abnormalities have been found in all cases of myeloma examined.[14] Rearrangements and translocations involving the immunoglobulin-associated locus at 14q32 can be seen with myeloma, as well as other B cell tumors.[14] Myeloma has been associated with t(4;14)(p!6;q32), t(ll;14)(ql3;q32), and t(6;14)(p21;q32). Deletions involving chromosome 13 are associated with decreased survival in patients with myeloma.[14]

Findings on Plain Films (Roentgenograms) and Computed Tomography

The most typical appearance of multiple myeloma consists of several or many radiolucent lesions of varying sizes in medullary bone.[2,3,10,12,13,16] Two-thirds of the radiolucent myeloma lesions have circumscribed smooth or lobulated margins, and the remaining third have lesions with indistinct borders[12] (Figs. **334, 336).** Minimal sclerosis can occasionally be seen at the margins of radiolucent myeloma lesions in bone[2,3,12] (Fig. **336).** Endosteal erosions can be seen associated with the osteolytic medullary lesions. Zones of cortical destruction can occur with or without fracture (Fig. **336).** Soft tissue masses secondary to extension from osseous myeloma can be seen with CT.

Multiple myeloma can also present as diffuse osteopenia which may be difficult to detect unless there is an associated pathologic fracture.[12] Myeloma involving the spine is associated with pathologic compression deformities involving vertebral bodies. Rarely, some untreated myeloma lesions can appear mostly sclerotic, and may be associated with various signs and symptoms such as polyneuropathy, hepatomegaly, splenomegaly, lymphadenopathy, endocrinopathy (amenorrhea, impotence, gynecomastia, hirsutism, diabetes), skin hyperpigmentation, hypertrichosis, and/or clubbing of the fingers.[3,12]

Osteosclerotic myeloma lesions occur in less than 3% of patients with myeloma, who tend to be slightly younger than patients with classical myeloma.[3] The features of this type of osteosclerotic myeloma have been referred to as POEMS, which is an acronym for the following clinical features: polyneuropathy, organomegaly, endocrinopathy, M-protein, and skin changes.[3] Plasmacytomas are usually radiolucent lesions that may be associated with bone expansion and mild periosteal reaction.[12]

MRI Findings

Multiple myeloma. Multiple myeloma typically appears as multiple intramedullary zones with low-intermediate signal on T1WI and PDW1; and intermediate, slightly high to high signal on T2W1, and slightly high to high signal on FST2WI (Figs. **337-341**). FS T2WI is important for detecting myeloma because intermediate and high signal heterogeneity on T1WI from red and yellow marrow, respectively, can be seen in normal vertebral marrow in elderly patients. Intramedullary lesions and corresponding signal abnormalities may be diffuse, focal with poorly defined or distinct margins, and/or in an extensive variegated pattern.[5,6,8-10] Multifocal lesions can be seen in long bones. Zones of cortical destruction may occur associated with extra-osseous soft tissue lesions. Lesions usually show Gd-contrast enhancement (Figs. **337,339,340).** Pathologic fractures can be seen in long bones. Myeloma involving vertebral bodies can be associated with compression fracture deformities and spinal cord compression (Fig. **338).**

Plasmacytoma. Lesions usually appear as intramedullary zones with low-intermediate signal on T1WI, low-intermediate to slightly high signal on PDWI, slightly high to high signal on T2WI, and high signal on FST2WI or STIR[5,8] (Figs. **332,334-336).** Intramedullary lesions may have poorly defined or distinct margins. Zones of cortical destruction may occur associated with extra-osseous soft tissue lesions. Lesions typically show moderate to prominent Gd-contrast enhancement (Figs. **332, 334-336).** Pathologic fractures can be seen in long bones. Plasmacytoma involving vertebral bodies can be associated with compression fracture deformities and spinal cord compression (Figs. **334, 335).**

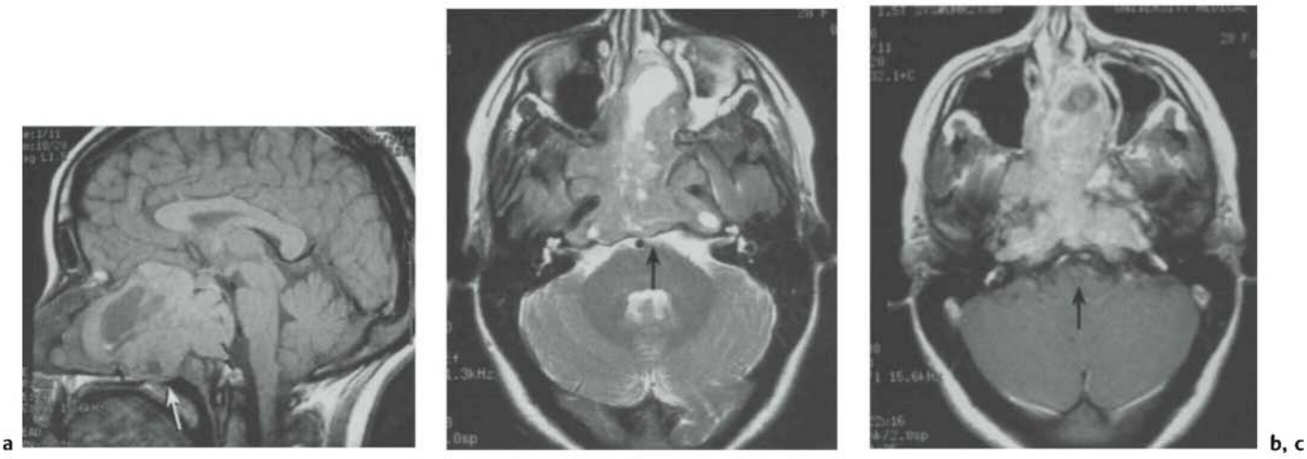

Figure **332 a-c** Plasmacytoma involving the nasal cavity, ethmoid and sphenoid sinuses, and skull base in a 28-year-old woman. The tumor has mixed zones of low and intermediate signal on sagittal T1WI (**a**), and zones of intermediate to slightly high signal and high signal on axial T2WI (**b**). The tumor shows prominent slightly heterogeneous Gd-contrast enhancement on axial T1WI (**c**).

a

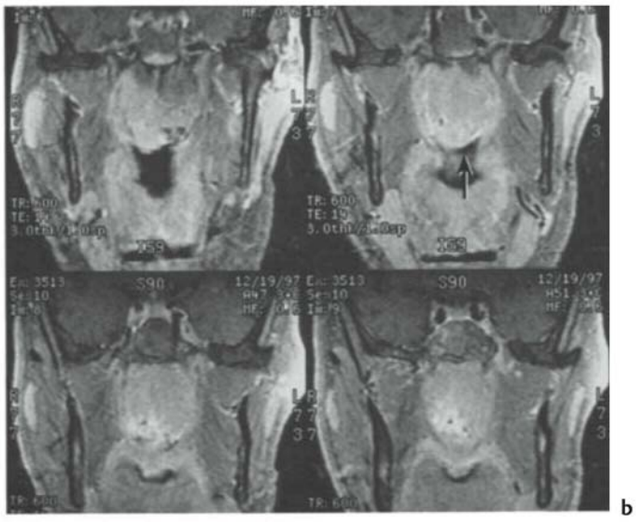

b

Figure **333 a, b** Plasmacytoma involving the soft tissues of the posterior nasopharynx. The tumor has heterogeneous intermediate, slightly high and high signal on sagittal T2WI (**a**), and shows mild to moderate Gd-contrast enhancement on coronal FST1WI (**b**).

a

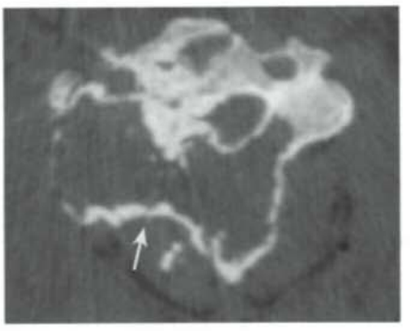

b, c

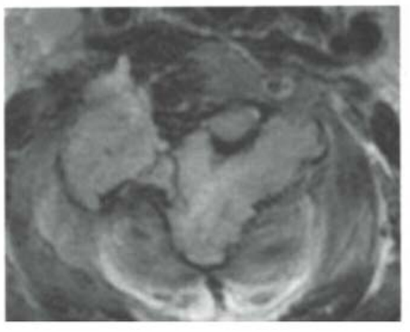

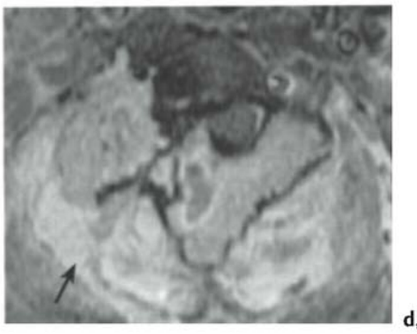

d, e

Figure **334a-e** A 51-year-old man with a plasmacytoma involving the posterior elements of the C 3 vertebra. Lateral radiograph (**a**) shows an expansile radiolucent lesion with thin sclerotic borders. Axial CT image (**b**) shows the expanded sclerotic margins on the right to be interrupted. The tumor has slightly high signal on sagittal (**c**) and axial (**d**) T2WI. The tumor shows heterogeneous Gd-contrast enhancement on axial (**e**) FST1WI. Tumor extension into the adjacent extra-osseous soft tissues is also seen.

Soft tissue. Extra-osseous multiple myelomas or plasmacytomas usually have low-intermediate signal on TlWI, and slightly high to high signal on T2WI, and high signal on FST2W1 (Fig. **333).** Extra-osseous myeloma or plasmacytoma usually occurs from extension from intra-osseous lesions (Figs. **332,334,337),** or less frequently arises from within the soft tissues. Lesions may have poorly defined or distinct margins. Most lesions show Gd-contrast enhancement. Zones of high signal on T2WI peripheral to the Gd-contrast enhancing portion of the lesion may represent zones of tumor invasion or perilesional edema.

Figure **335 a-c** Plasmacytoma involving a thoracic vertebral body with associated epidural extension and pathologic fracture. The tumor has diffuse low-intermediate signal on sagittal T1WI (**a**), and intermediate to slightly high signal on sagittal T2WI (**b**). The tumor shows prominent Gd-contrast enhancement on FST1WI (**c**). There is also evidence of tumor extension into the adjacent vertebral bodies.

Figure **336a-d** A 75-year-old woman with a plasmacytoma involving the proximal tibia. AP radiograph (**a**) shows multiple irregular, round, and oval radiolucent zones of various sizes, as well as zones of sclerosis and regions of cortical destruction. The tumor has low-intermediate signal on sagittal T1WI (**b**), and high signal on sagittal FST2WI (**c**). Intramedullary tumor margins are ill defined. The tumor shows prominent Gd-contrast enhancement on FST1WI (**d**). Tumor extension into the adjacent anterior soft tissues is seen through a zone of cortical bone destruction.

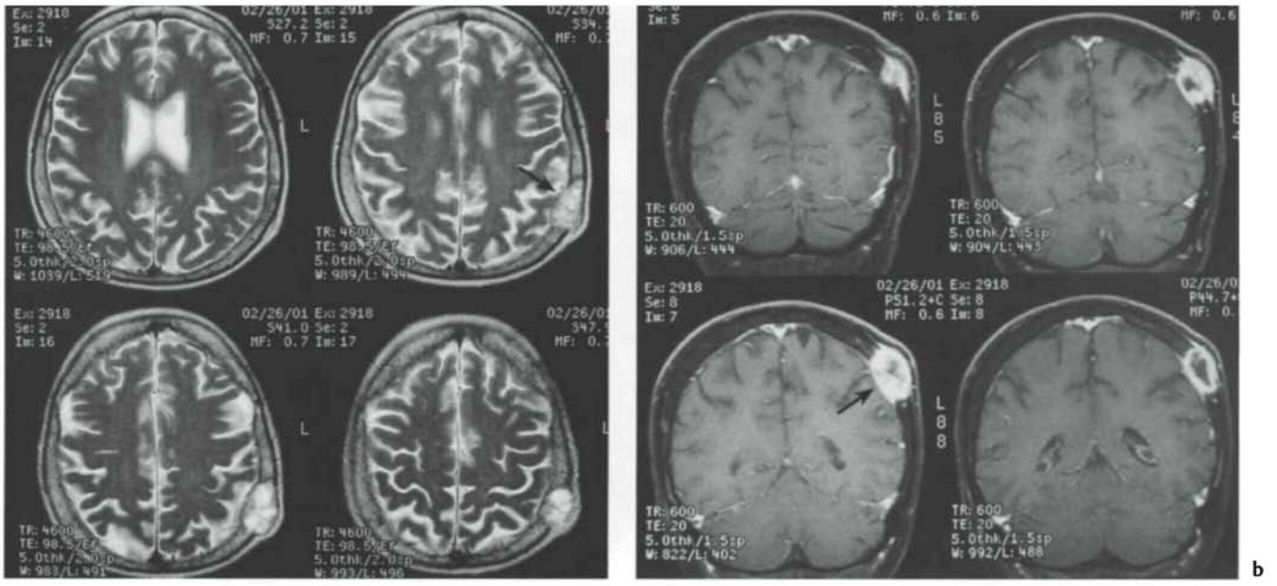

Figure **337 a, b** A .65-year-old woman with myeloma and a lesion involving the skull. The tumor has circumscribed margins, and has heterogeneous high signal on axial T2WI (**a**). The tumor shows irregular Cd-contrast enhancement on coronal FST1 WI (**b**).

Differential Diagnosis

Multiple myeloma. Metastatic disease, non-Hodgkin lymphoma, Langerhans cell histiocytosis, osteomyelitis.

Plasmacytoma. Metastatic disease, lymphoma, Langerhans cell histocytosis, giant cell tumor, fibrosarcoma, malignant fibrous histiocytoma, chondrosarcoma.

Prognosis and Treatment

The 5-year survival for multiple myeloma is 29 %.[4] Eleven thousand people die from myeloma in the United States per year.[14] Myeloma is usually fatal, although long remissions can sometimes result from high-dose chemotherapy and stem cell support.[14] Correlation of prognosis is reportedly high between tumor size and clinical stage.[2] Deletions involving chromosome 13 are associated with decreased survival in patients with myeloma.[14]

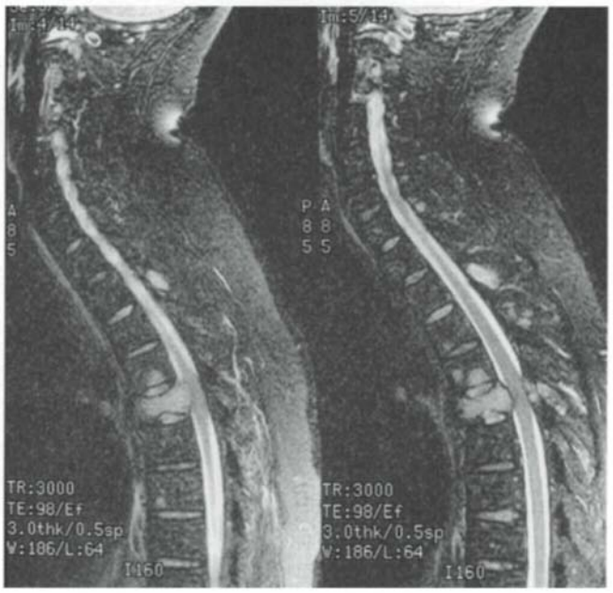

Figure 338 Multiple myeloma involving the spine, including one lesion in a thoracic vertebral body that has a pathologic fracture causing spinal cord compression. The lesions have high signal on sagittal FST2WI.

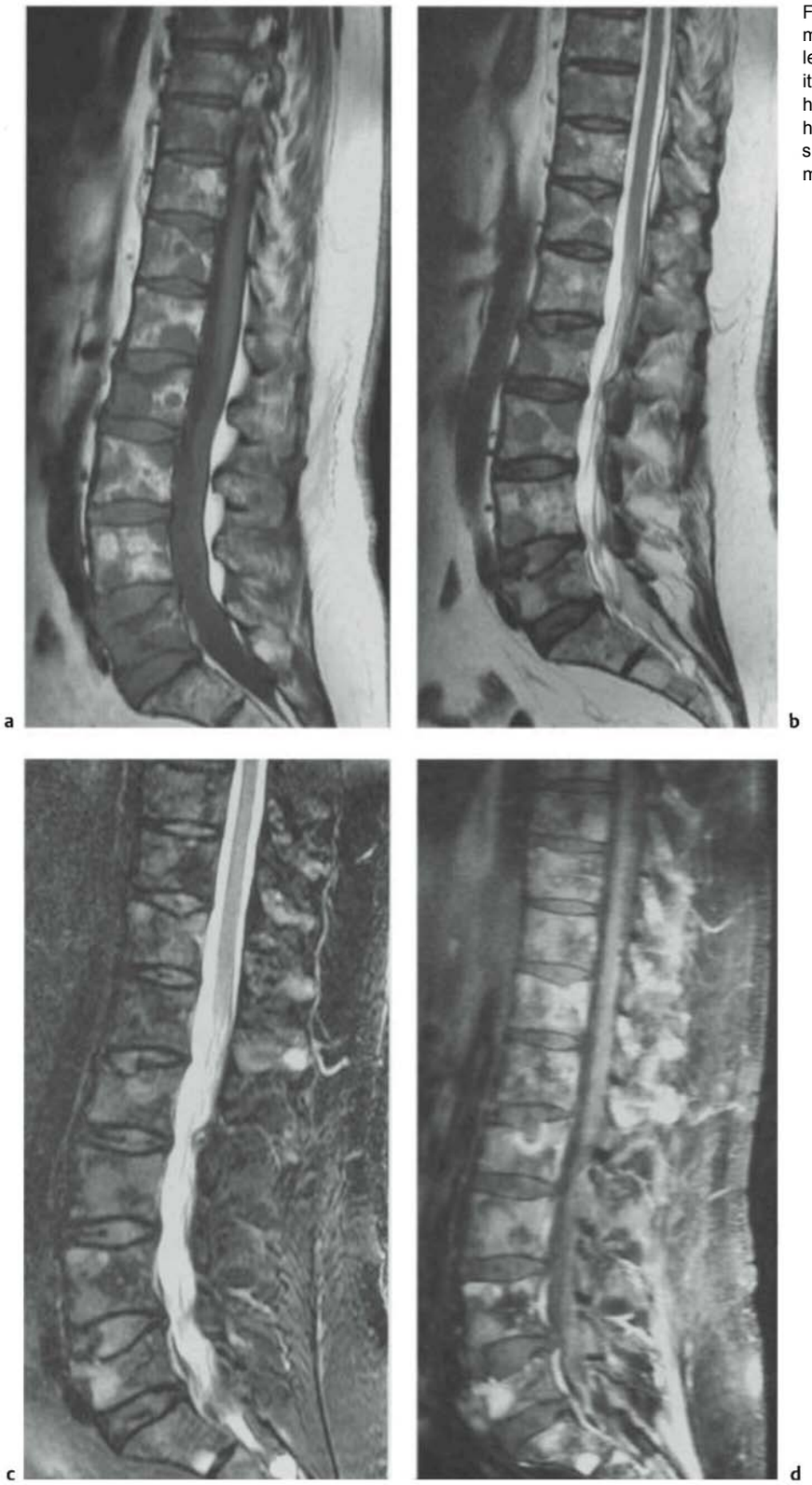

Figure **339a-d** Multiple myeloma involving multiple thoracic and lumbar vertebrae. The lesions have low-intermediate signal on sagittal T1WI (**a**), low-intermediate and slightly high signal on sagittal T2WI (**b**), and slightly high and high signal on FST2WI (**c**). The lesions show prominent Gd-contrast enhancement on sagittal FST1 WI (**d**).

a, b

c

Figure **340a-c**A 62-year-old woman with myeloma involving the marrow of the humerus and scapula. Radiograph (**a**) shows no definite abnormalities. Myeloma in the metadiaphyseal marrow of the humerus and marrow of the scapula has high signal on sagittal (**b**) and axial (**c**) FS T2WI.

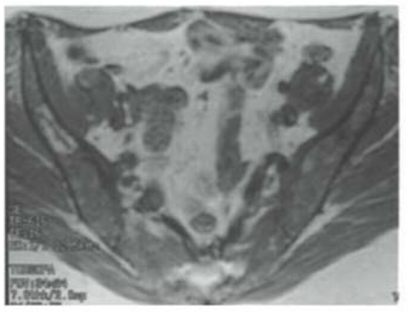

a

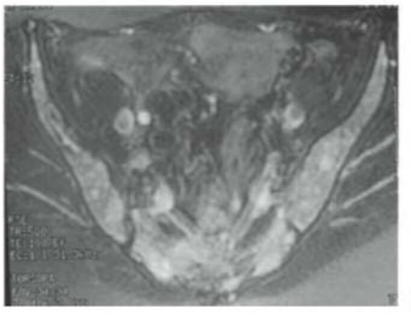

b

Figure **341 a, b** A 49-year-old woman with myeloma involving the marrow of the pelvis. Myeloma in the marrow of the pelvis has low-intermediate signal on axial T1 WI (**a**) and high signal on axial FST2WI (**b**).

References

1 Aster J, Kumar V. White cells, lymph nodes, spleen and thymus. In: Cotran RS, Kumar V, Collins T, eds. *Pathologic Basis of Disease* 6th ed. Philadelphia, Pa: W.B. Saunders; 1999:644-695.

2 Diebold J. Myeloma. In: Forest M, Tomeno B, Vanel D, eds. *Orthopedic Surgical Pathology: Diagnosis of Tumors and Pseudotumoral Lesions of Bone and Joints* Edinburgh: Churchill Livingstone; 1998:491-500.

3 Huvos AG. Multiple myeloma, including solitary osseous myeloma. In: Huvos AG. *Bone Tumors: Diagnosis, Treatment, and Prognosis* 2nd ed. Philadelphia, Pa: W.B. Saunders; 1991:653-676.

4 Jemal A, Thomas A, Murray T, Thun M. Cancer statistics 2002. *CA Cancer J Clin* 2002:52:23-47.

5 Lecouvet FE, Vande Berg BC, Michaux L, et al. Stage III multiple myeloma: clinical and prognostic value of spinal bone marrow MR imaging. *Radiology* 1998;209(3):653-660.

6 Libshitz HI, Malthouse SR, Cunningham D, MacVicar AD, Husband JE. Multiple myeloma: appearance at MR imaging. *Radiology* 1992; 182(3):833-837.

7 Longo DL. Plasma cell disorders. In: Fauci AS, Braunwald E, Isselbacher KJ, et al, eds. *Harrison's Principles of Internal Medicine* 14th ed. New York, NY: McGraw-Hill; 1998:712-718.

8 Moulopoulos LA, Dimopoulos MA. Magnetic resonance imaging of the bone marrow in hematologic malignancies. Btood 1997;90: 2127-2147.

9 Moulopoulos LA, Varma Datla GK, Dimopoulos MA, et al. Multiple myeloma: spinal MR imaging in patients with untreated newly diagnosed disease. *Radiology* 1992;185(3):833-840.

10 Moulopoulos LA, Gika D, Anagnostopoulos A. et al. Prognostic significance of magnetic resonance imaging of bone marrow in previously untreated patients with multiple Myeloma. *Ann Oncol* 2005; 16:1824-1828.

11 Mulder JD, Schutte HE, Kroon HM, Taconis WK, eds. The diagnosis of bone tumors. In: *Radiologic Atlas of Bone Tumors* Amsterdam: Elsevier; 1993:9-46.

12 Mulder JD, Schutte HE, Kroon HM, Taconis WK, eds. Myeloma. In: *Radiologic Atlas of Bone Tumors* Elsevier; 1993:275-291.

13 Resnick D, Haghighi P. Lymphoproliferative and myeloproliferative disorders. In: Resnick D, ed. *Diagnosis of Bone and Joint Disorders* 5th ed. Philadelphia, Pa: W.B. Saunders; 2002:2291-2344.

14 Shaughnessy J. Primer on medical genomics part IX: scientific and clinical applications of DNA microarrays - multiple myeloma as a disease model. *Mayo Clin Proc* 2003:78:1098-1109.

15 Unni KK. Introduction and scope of study. In: *Dahlin's Bone Tumors-General Aspects and Data on* 11087 Cases 5th ed. Philadelphia, Pa: Lippincott, Williams & Wilkins; 1996:1-9.

16 Unni KK. Myeloma. In: *Dahlin's Bone Tumors—General Aspects and Data on 11087 Cases* 5th ed. Philadelphia, Pa: Lippincott, Williams & Wilkins; 1996:225-236.

A 53

Myositis Ossificans (Also Referred to as Heterotopic Ossification, Reactive Mesenchymal Proliferation, Ossifying Hematoma, and Pseudomalignant Osseous Tumor of Soft Tissues)

Definition

Myositis ossificans represents localized, non-neoplastic, reparative extra-osseous lesions that are comprised of reactive hypercellular fibrous tissue, cartilage, and/or bone.[1,4,7,18,22] These lesions can arise secondary to trauma (myositis ossificans circumscripta, ossifying hematoma), although they may also occur without a history of prior injury (pseudomalignant osseous tumor of soft tissues).[4,7,18] Myositis ossificans progressiva is a fatal disorder that is congenital and hereditary, in which heterotopic ossification occurs simultaneously at multiple sites.[18]

Frequency of Occurrence

Myositis ossificans accounts for < 1% of benign, soft tissue tumors.[12,16]

Age at Presentation

From 3 to 87 years,[17,18] mean = 35 years,[12] median = 22 years.[17,18]

Gender Ratio (M / F)

1.2/1[12] to 2.2/1.[18]

Location

Lesions occur in the upper leg > trunk > proximal limb > upper extremity > hip/buttock, hand or wrist > temporalis or pterygoid muscles.[7,12,13]

Signs and Symptoms

Lesions may or may not be associated with a history of trauma (37%), coagulopathy, paraplegia, burns, abdominal surgical scars, total hip arthroplasties, injection sites, coma, tetanus, or chronic inflammation.[7,14,18,25] Some cases are idiopathic.[7,18,25] Lesions present as painless or painful masses observed within 2-3 weeks.[4,25] Over time, these lesions become progressively firmer.[18] Ossifying hematomas present as localized swellings of rapid onset that eventually evolve into firm masses over several weeks.[18] Lesions may regress, disappear, or remain stable in size.[4,7,18,25]

Gross Pathologic Findings

Lesions are often well-defined, ovoid, tan and/or whitish masses ranging in size from 2 to 12 cm (mean = 5 cm).[22] Peripheral portions of the lesions are typically gray-white, gritty, and firm secondary to a bone network.[4,22] Cystic zones containing a clear yellow fluid may also be present at the peripheral portions.[4] Centrally, lesions have usually soft glistening centers containing gelatinous and/or hemorrhagic material.[4,22] Lesions may be adjacent to the periosteum in ~ 50 % of cases.[4] Some lesions may eventually blend in with the periosteum and cortical bone.

Histopathologic Findings

Lesions observed within 3 weeks (early phase) usually show a central region of numerous proliferating fibroblasts, oriented randomly or in short fascicles.[4,22] Many normal-appearing mitotic figures are usually present.[4,22] The stroma is often highly vascular containing myxoid material, fibrin, extravasated blood cells, chronic inflammatory cells, osteoclastlike giant cells, and atrophic/injured myocytes.[4,20,22] Lesions subsequently show peripheral bone formation with osteoid rimmed by plump osteoblasts, cartilage with endochondral ossification, and vascular proliferation.[4,20] Older lesions show an outer region of maturing lamellar bone with peripheral osteoclasts surrounding regions of woven bone.[4] Some lesions fuse with the adjacent periosteum.[20,22] A central undifferentiated zone can persist for some time, and often transforms into a collagenous region that eventually ossifies with fatty or red marrow.[4,22] Lesions are often surrounded by a fibrous capsule.[22]

Findings on Plain Films (Roentgenograms) and Computed Tomography

The appearance of myositis ossificans on plain films and CT depends upon the ages of these lesions and their locations.[11,18,19] Lesions appear initially as poorly defined and/or localized soft tissue swelling, followed by progressive amorphous mineralization at the periphery by 2-4 weeks[3,4,11,18,19,21,23] (Fig. **342).** At 4 weeks, CT typically shows a rim of mineralization surrounding a central zone with low-intermediate attenuation[11,19] (Fig. **342).** A sharply circumscribed, peripherally ossified lesion is usually evident by 6-8 weeks[4,11,19,23] (Figs. **343-346).** Mature lesions typically have a dense peripheral ossification pattern, and some may show diffuse ossification[11,19,23] (Figs. **347, 348).**

Lesions located within muscle are typically ovoid or spheroid, and occasionally lacy.[18,19] Lesions near the cortical bone surfaces are often associated with a lamellar type of periosteal reaction[4,18,19,25] (Figs. **343, 344).** A thin, radiolucent zone may be seen between the lesion and adjacent bone cortex.[4,11,18,19] Some lesions may eventually show contiguity with adjacent bone cortex. Medullary bone is usually normal in appearance.[18,19] Multiple sites of heterotopic ossification are findings seen with myosificans ossificans progressiva (Fig. **348**).

MRI Findings[2,6,9-11,14,15,19,23,24]

The MRI features of myositis ossificans vary, depending on the age, location, and degree of mineralization/ossification.[2,11,15,19,23] Lesions less than 2 weeks from discovery typically have localized mass effect with poorly defined margins, heterogeneous low-intermediate or slightly high signal on T1WI, and heterogeneous slightly high to high signal on T2W1 and FST2W1.[3,5,9,11,19,23] Poorly defined zones of high signal on T2WI may be seen in the adjacent soft tissues.[2,8,9,11,14,23] Gd-contrast enhancement can be seen. After 2 weeks, curvilinear and/or amorphous zones of low signal on T2WI and FST2WI can be seen at the peripheral portions of the subacute lesions, resulting from mineralization/ossification[2,9,11,19,23] (Figs. **342).** This is

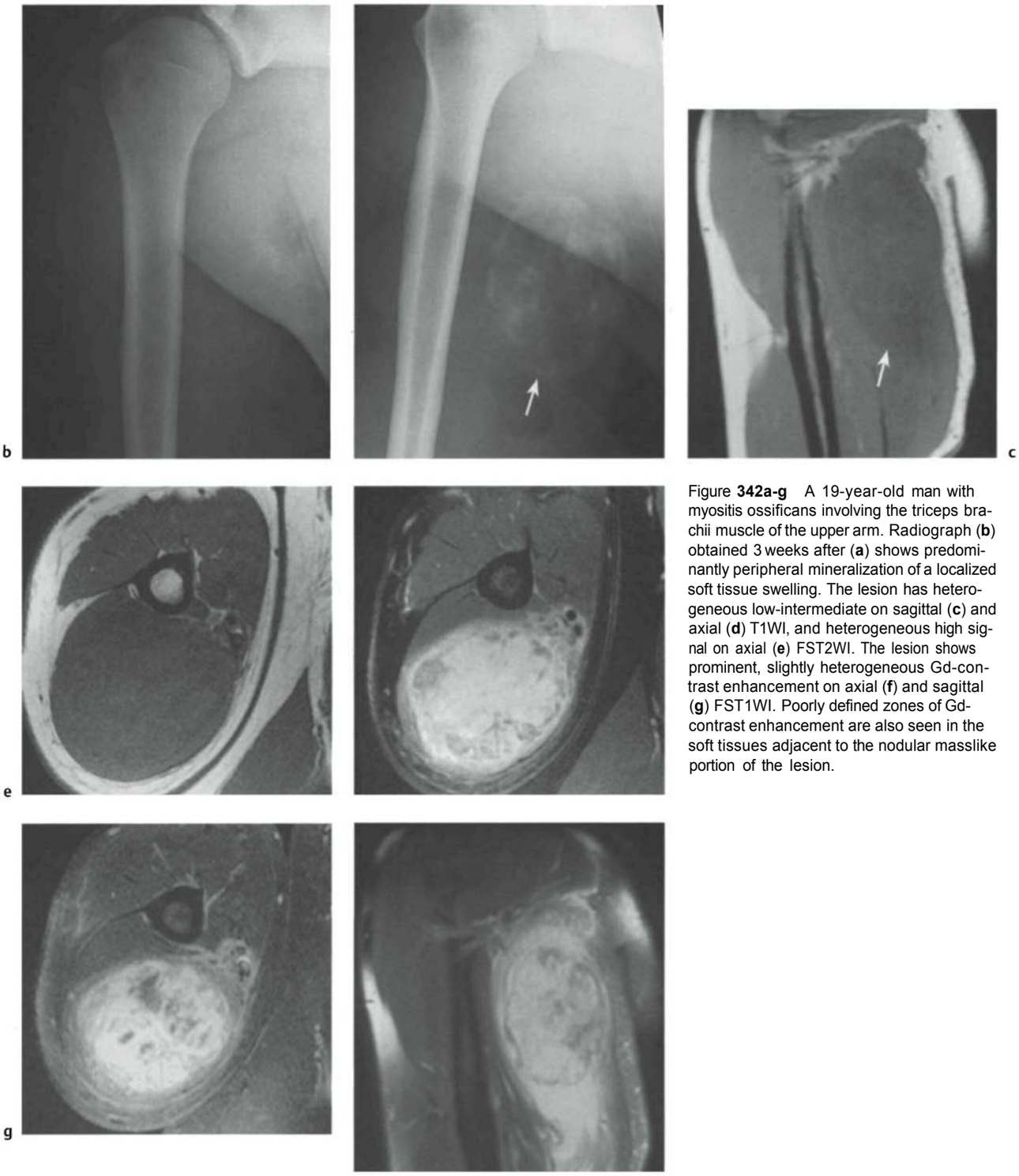

Figure **342a-g** A 19-year-old man with myositis ossificans involving the triceps brachii muscle of the upper arm. Radiograph (**b**) obtained 3 weeks after (**a**) shows predominantly peripheral mineralization of a localized soft tissue swelling. The lesion has heterogeneous low-intermediate on sagittal (**c**) and axial (**d**) T1WI, and heterogeneous high signal on axial (**e**) FST2WI. The lesion shows prominent, slightly heterogeneous Gd-contrast enhancement on axial (**f**) and sagittal (**g**) FST1WI. Poorly defined zones of Gd-contrast enhancement are also seen in the soft tissues adjacent to the nodular masslike portion of the lesion.

followed by progressive centripetal mineralization/ossification, which is manifested as irregular zones of low signal on T2WI.[3,11,19,23] During this process, heterogeneous Gd-contrast enhancement is typically seen[6,9,11,19,23] (Figs. **343-346).**

Hemorrhage and fluid-fluid levels may also occur within these lesions.[3,9,11,19,23] Old lesions usually have well-defined margins, and have variable low signal on T1WI, PDWI, and T2WI depending on the degree of mineralization/ossification, fibrosis, and hemosiderin deposition[9,11,19] (Fig. 347). Zones of high signal on T1WI and T2WI may occur from fatty marrow metaplasia[8,9,11,14,19,23] (Fig. 344). Gd-contrast enhancement in old, mature lesions is often minimal or absent.[11,23,24] Signal abnormalities within bone marrow are usually absent in patients with myositis ossificans, but may occasionally occur from associated post-traumatic edema or reactive bone changes.[6]

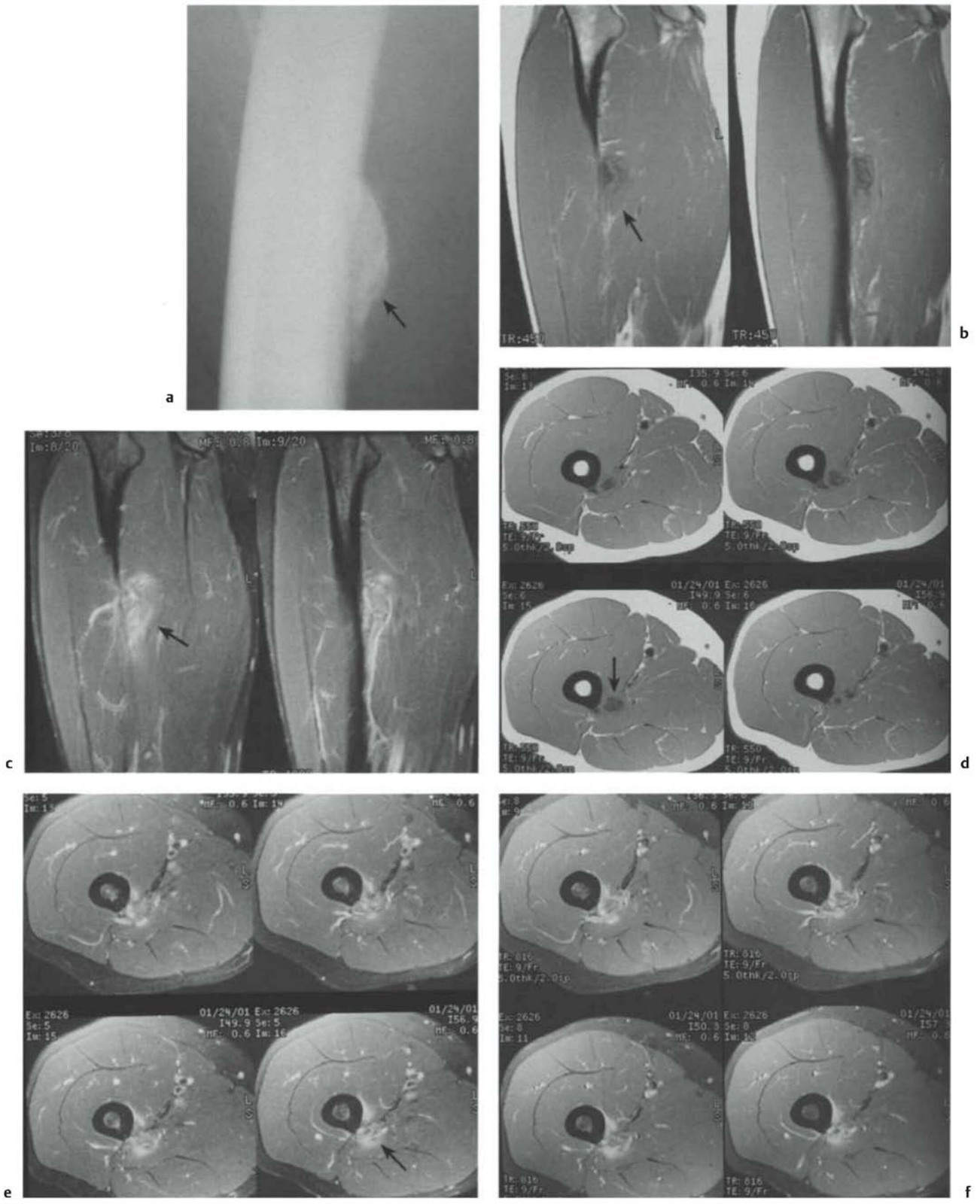

Figure **343 a-f** A 36-year-old man with myositis ossificans involving the proximal medial thigh adjacent to the femur. Radiograph (**a**) shows a thickened lamellar type of periosteal reaction adjacent to the outer cortical margin separated by a thin radiolucent zone. Bone cortex and medullary bone are normal in appearance. The lesion has low and intermediate signal on coronal (**b**) and axial (**d**) T1WI, and heterogeneous slightly high and high signal on coronal (**c**) and axial (**e**) FST2WI. The lesion shows irregular Gd-contrast enhancement on axial (**f**)FST1WI.

a

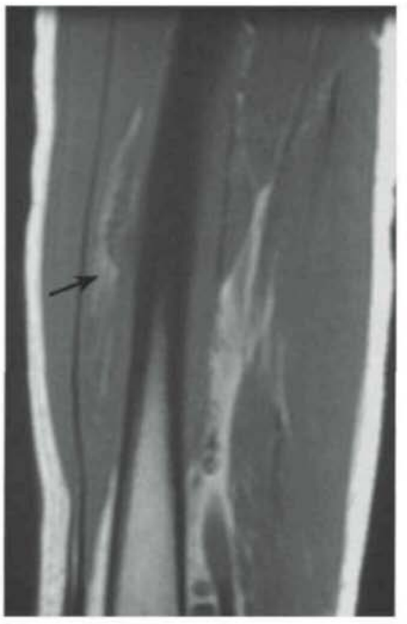

b, c

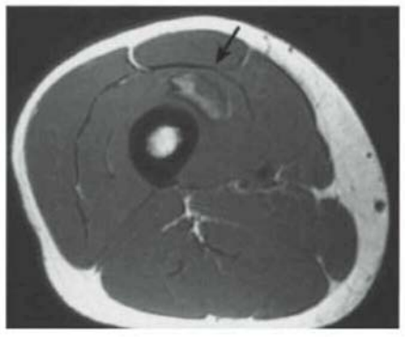

d

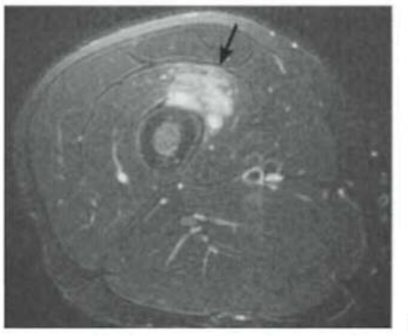

e

Figure **344a-e** A 14-year-old male with myositis ossificans involving the vastus intermedius muscle of the thigh adjacent to the femur. Radiograph (**a**) shows a thickened lamellar type of periosteal reaction adjacent to the outer cortical margin separated by a thin radiolucent zone. Bone cortex and medullary bone are normal in appearance. The lesion has low, intermediate, and high signal on sagittal (**b**) and axial (**d**) T1WI, and heterogeneous slightly high and high signal on sagittal (**c**) and axial (**e**) FST2WI.

a

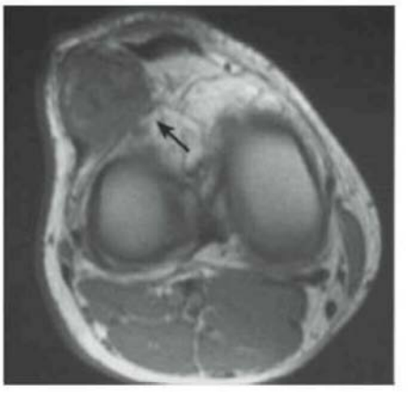

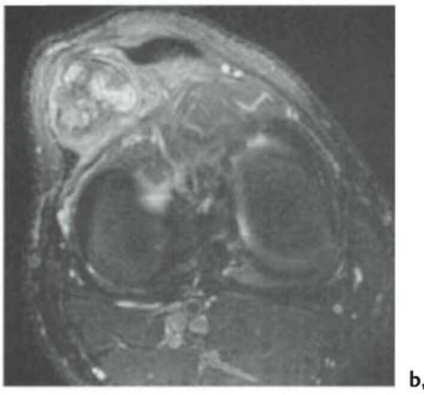

b, c

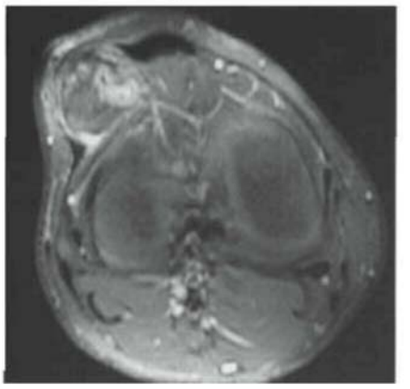

d

Figure **345a-d** A 15-year-old male with myositis ossificans involving the soft tissues anterior to the distal femur and lateral to the patellar tendon. Lateral radiograph (**a**) shows amorphous mineralization in the infrapatellar soft tissues. The ovoid lesion has intermediate signal on axial T1WI (**b**), and heterogeneous high, intermediate, and low signal on axial FST2WI (**c**). Poorly defined zones of high signal on FS T2WI are also seen in the soft tissues adjacent to the nodular masslike portion of the lesion The lesion shows heterogeneous Gd-contrast enhancement on axial FST1WI (**d**).

a

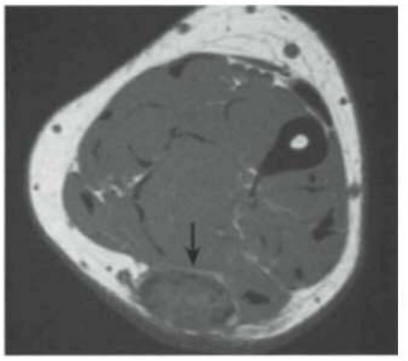

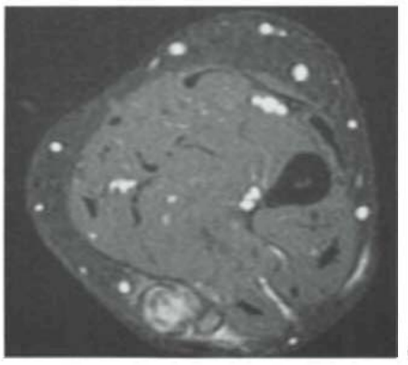

d

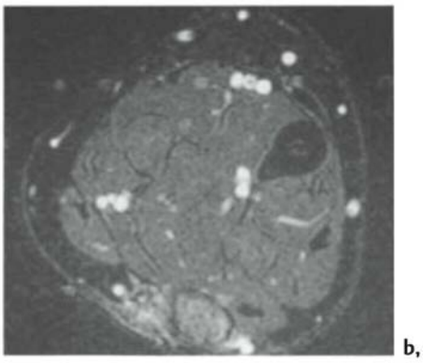

b, c

Figure **346a-d** A 27-year-old woman with myositis ossificans involving the soft tissues of the forearm after resection of the distal radius which contained a giant cell tumor. Radiograph (**a**) shows two spheroid zones with mostly peripheral mineralization. The lesions have low and intermediate signal on axial T1WI (**b**), and heterogeneous intermediate, low and slightly high signal on axial FS T2WI (**c**). The lesion shows heterogeneous Gd-contrast enhancement on axial FST1WI (**d**).

a

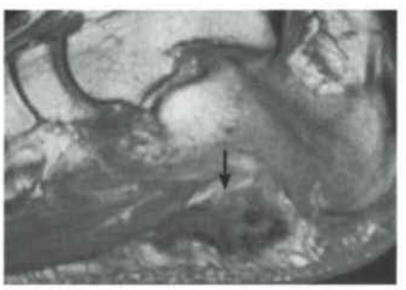

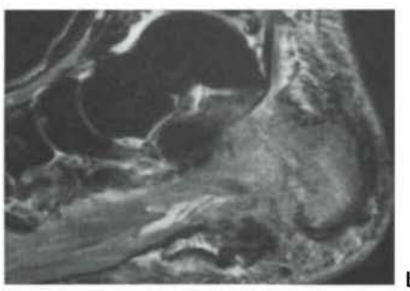

b, c

Figure **347 a-c** Myositis ossificans involving the plantar soft tissues of the foot. Radiograph (**a**) shows an irregular amorphous zone of mineralization. The lesion has low and intermediate signal on sagittal (**b**) T1WI; and heterogeneous low, high, and intermediate signal on sagittal (**c**) FST2WI.

Figure **348** Myositis ossificans progressiva in a 48-year-old woman. Radiograph shows multiple sites of heterotopic ossification.

Differential Diagnosis

Extra-osseous osteosarcoma, juxtacortical/parosteal osteosarcoma, fibrosarcoma, periosteal hematoma, periosteal lipoma.

Prognosis and Treatment

No definite examples of malignant degeneration have been reported.[4] Lesions may regress, disappear, or remain stable in size [4,7,18,20,25] Treatment often consists of surgical excision, and recurrence is rare.[4,20,22]

References

1 Das Gupta TK, Chaudhuri PK. Heterotopic bone and cartilage. In: Das Gupta TK, Chaudhuri PK, eds. Tumors *of the Soft Tissues* 2nd ed. Stamford, Conn: Appleton & Lange; 1998:463-471.

2 Ehara S, Shiraishi H, Abe M, Mizutani H. Reactive heterotopic ossification its patterns on MRI. *Clin Imaging* 1998;22(4):292-296.

3 Fletcher BD, Hanna SL. Pediatric musculoskeletal lesions simulating neoplasms. Magn *Resort Imaging Clin N Am* 1996;4(4):721-747.

4 Forest M. Myositis ossificans. In: Forest M, Tomeno B, Vanel D, eds. *Orthopedic Surgical Pathology: Diagnosis of Tumors and Pseudotumoral Lesions of Bone and Joints* Edinburgh: Churchill Livingstone: 1998:663-669.

5 Frassica FJ, Khanna JA, McCarthy EF. The role of MR imaging in soft tissue tumor evaluation: perspective of the orthopedic oncologist and musculoskeletal pathologist. Magn *Reson Imaging Clin N Am* 2000;8(4):915-927.

6 Gindele A, Schwamborn D, Tsironis K, Benz-Bohm G. Myositis ossificans traumatica in young children: report of three cases and review of the literature. *Pediatr Radiol* 2000:30:451-459.

7 Huvos AG. Miscellaneous tumors of soft tissue and bone. In: Huvos AG, ed. *Bone Tumors: Diagnosis, Treatment, and Prognosis* 2nd ed. Philadelphia, Pa: W.B. Saunders; 1991:745-751.

8 JelinekJ, Kransdorf MJ. MR imaging of soft-tissue masses: mass-like lesions that simulate neoplasms. *Magn Reson Imaging Clin N Am* 1995;3(4):728-729.

9 Kransdorf MJ, MeisJM.JelinekJS. Myositis ossificans: MR appearance with radiologic-pathologic correlation. *AJR Am J Roentgenol* 1991; 157:1243-1248.

10 Kransdorf MJ, Meis JM. Extraskeletal osseous and cartilaginous tumors of the extremities. *Radiographics* 1993:13:853-884.

11 Kransdorf MJ, Murphey MD. Extraskeletal osseous and cartilaginous tumors. In: *Imaging of Soft Tissue Tumors* 2nd ed. Philadelphia, Pa: W. B. Saunders; 2006:437-480.

12 Kransdorf MJ, Murphey MD. Soft tissue tumors in a large referral population: prevalence and distribution of diagnoses by age, sex, and location. In: *Imaging of Soft Tissue Tumors* 2nd ed. Philadelphia, Pa: W.B. Saunders; 2006;6-37.

13 Kransdorf MJ. Benign soft-tissue tumors in a large referral population: distribution of specific diagnoses by age, sex, and location. *AJR Am J Roentgenol* 1995;164:395-402.

14 May DA, Disler DG, Jones EA, Balkissoon AA, Manaster BJ. Abnormal signal intensity in skeletal muscle at MR imaging: patterns, pearls, and pitfalls. *Radiographics* 2000;20(Suppl 1):S295-S315.

15 Meyer JS, Dormans JP. Differential diagnosis of pediatric musculoskeletal masses. *Magn Reson Imaging Clin N Am* 1998;6(3}:561-577.

16 Mulder JD, Schutte HE, Kroon HM, Taconis WK. Introduction. In: *Radiologic Atlas of Bone Tumors* Amsterdam: Elsevier; 1993:3-6.

17 MulderJD, Schutte HE, Kroon HM, Taconis WK. The diagnosis of bone tumors. In: Radiologic Atlas *of Bone Tumors* Amsterdam: Elsevier; 1993:9-46.

18 Mulder JD, Schutte HE, Kroon HM, Taconis WK. Reactive mesenchymal proliferation. In: *Radiologic Atlas of Bone Tumors* Amsterdam: Elsevier; 1993:711-729.

19 Parikh J, Hyare H, Saifuddin A. The imaging features of post-traumatic myositis ossificans, with emphasis on MRI. *Clin Radial* 2002; 57:1058-1066.

20 Reid RP. Bone neoplasms and tumor-like lesions on the bone surface. In: Helliwell TR, ed. *Major Problems in Pathology: Pathology of Bone and Joint Neoplasms* 1st ed. Vol 37. Philadelphia, Pa: W.B. Saunders; 1999:215-235.

21 Ritchie DA, Davies AM. Imaging studies in bone neoplasia. In: Helliwell TR, ed. *Major Problems in Pathology: Pathology of Bone and Joint Neoplasms* 1st ed. Vol 37. Philadelphia, Pa: W.B. Saunders; 1999: 106-127.

22 Rosenberg AE. Myositis ossificans and fibrooseous pseudotumor of digits. In: Fletcher CDM, Unni KK, Mertens F, eds. *World Health Organization Classification of Tumours. Pathology and Genetics of Tumours of Soft Tissue and Bone* Geneva: IARC Press; 2002:52-54.

23 Siegel MJ. Magnetic resonance imaging of musculoskeletal soft tissue masses. *Radiol Clin North Am* 2001;39(4):710-711.

24 Sundaram M, Sharafuddin Melhem JA. MR imaging of benign soft-tissue masses. *Magn Reson Imaging Clin N Am* 1995;3(4):623-624.

25 Unni KK. Conditions that commonly simulate primary neoplasms of bone. In: *Dahlin's Bone Tumors—General Aspects and Data on* 11 *087* Cases 5th ed. Philadelphia, Pa: Lippincott, Williams & Wilkins; 1996: 395-399.

A 54 Myxoma

ICD-O Code

8840/0

Definition[1,4-6]

Myxomas are benign lesions that occur in soft tissues, and contain fibroblasts (spindle cells) and abundant mucoid material (glycosaminoglycans, other mucopolysaccharides). Mazabraud syndrome represents an association between polyostotic fibrous dysplasia and nearby single or multiple myxomas.[1,6] Myxomas can also be associated with mono-ostotic fibrous dysplasia.[7]

Frequency of Occurrence

Myxomas represent ~3% of benign soft tissue tumors/lesions and 2 % of all soft tissue tumors/lesions.[2,3]

Age at Presentation

These lesions occur in adults from 24 to 74 years,[3] average = 52 years.[3,5]

Gender Ratio (M /F)[3,5,6]

1/1.4 to 1/1.1

Location

Lesions occur in the lower extremity > hip, buttocks > upper extremity > trunk > head, neck > hand, wrist.[3,5,6] Most lesions are intramuscular (82 %).[5] Less frequent sites are intermuscular, subcutaneous, or juxta-articular.[5] Juxta-articular myxomas frequently occur near the knee.[1]

Signs and Symptoms[4-6]

Myxomas can present as slowly enlarging, firm, palpable lesions, which may be fluctuant and minimally mobile. Lesions can be associated with pain in ~ 50 % of patients.[5] Myxomas are most often solitary.[5]

Gross Pathologic Findings

Lesions are predominantly composed of gelatinous material and can range in size from 1 to 17 cm.[1,5,6] Cystic components may be present in more than half of myxomas, and can vary in size from small to large.[5] Lesion margins can be circumscribed (59 %) or somewhat indistinct (41 %).[5] A complete or incomplete pseudocapsule may be present in more than 75 % of lesions.[5] Muscle atrophy and edema can occur adjacent to intramuscular myxomas.[5]

Histopathologic Findings

Myxomas are usually composed of scattered spindle cells within an abundant mucoid substance (high mucin and low collagen contents) and loose reticulin network.[1,4,5] The bland spindle cells contain small nuclei and eosinophilic cytoplasm.[6] Mitotic activity, hyperchromasia, and necrosis are typically absent.[6] Lesions may show immunoreactivity to CD 34, desmin, and actin.[6]

Lesion Genetics

Mutations involving GNAS1 gene have been found in intramuscular myxomas.[6]

Findings on Plain Films (Roentgenograms), Ultrasonography, and Computed Tomography

On plain films, myxomas may be seen as soft tissue masses in ~45% of cases.[5] Calcifications are typically not seen with myxomas.[5] Sonographic examinations show myxomas to have defined margins and to be hypo-echoic relative to muscle.[5] Anechoic cystic zones are also seen in 83 % of the lesions.[5] On CT, myxomas usually have attenuation that is less than skeletal muscle and higher than water. Lesions often have defined margins, and typically show minimal or no enhancement on CT.[5]

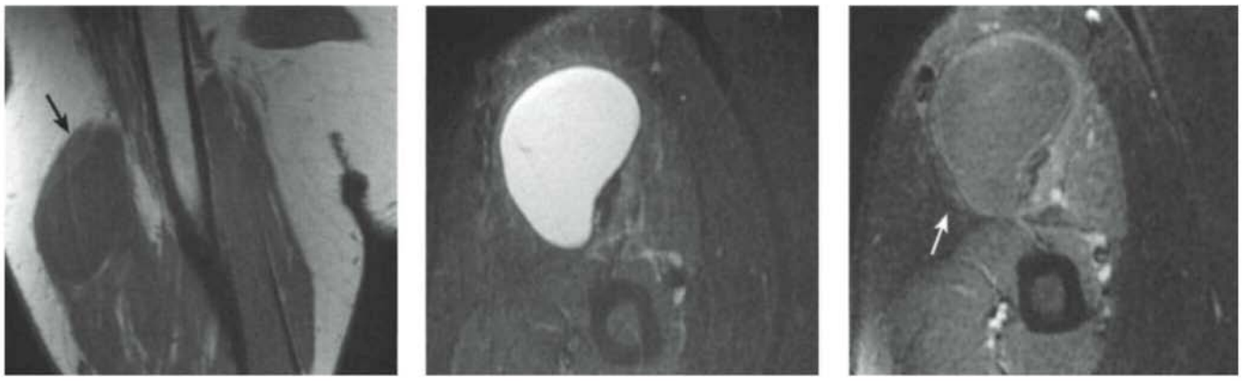

a, b c

Figure **349a-c** A 60-year-old man with a myxoma in the anterior soft tissues of the arm between the biceps brachii muscle and cephalic vein. The lesion has well-circumscribed margins, and has low-intermediate signal on T1WI (**a**) and high signal on axial FST2WI (**b**). The lesion shows no definite Gd-contrast enhancement on axial FST1WI (**c**).

MRI Findings

Lesions usually have low or low-intermediate signal on T1W1 and PDW1, and high signal on T2WI and FST2WI[1,4-6] (Figs. **349-351**). The high signal of these lesions on T2WI is secondary to their abundant myxoid extracellular stroma.[1,4-6] The high signal on T2W1 is homogeneous in 38 % of lesions, and either mildly or moderately heterogenous in the remainder.[5] Lesions can have well-defined or slightly indistinct margins.[4-6] A thin rim of high signal on T1WI may be seen surrounding intramuscular myxomas secondary to localized fatty atrophy[5] (Fig. **351**). Zones of edema seen as high signal on T2WI and FST2W1 in the soft tissues adjacent to myxomas may also be seen.[5]

After Gd-contrast administration, myxomas have been reported to show heterogeneous mild (76%) or moderate (24%) degrees of enhancement in noncystic portions[4,5] (Figs. **350,351**).

Differential Diagnosis

Hematoma, seroma, synovial cyst, ganglion, myxoid chondrosarcoma, myxoid liposarcoma, myxoid malignant fibrous histiocytoma, neurogenic tumors.[5]

Prognosis and Treatment

Surgical excision is usually curative.[1,6] Recurrence is uncommon, and metastatic lesions have not been reported.[1,6]

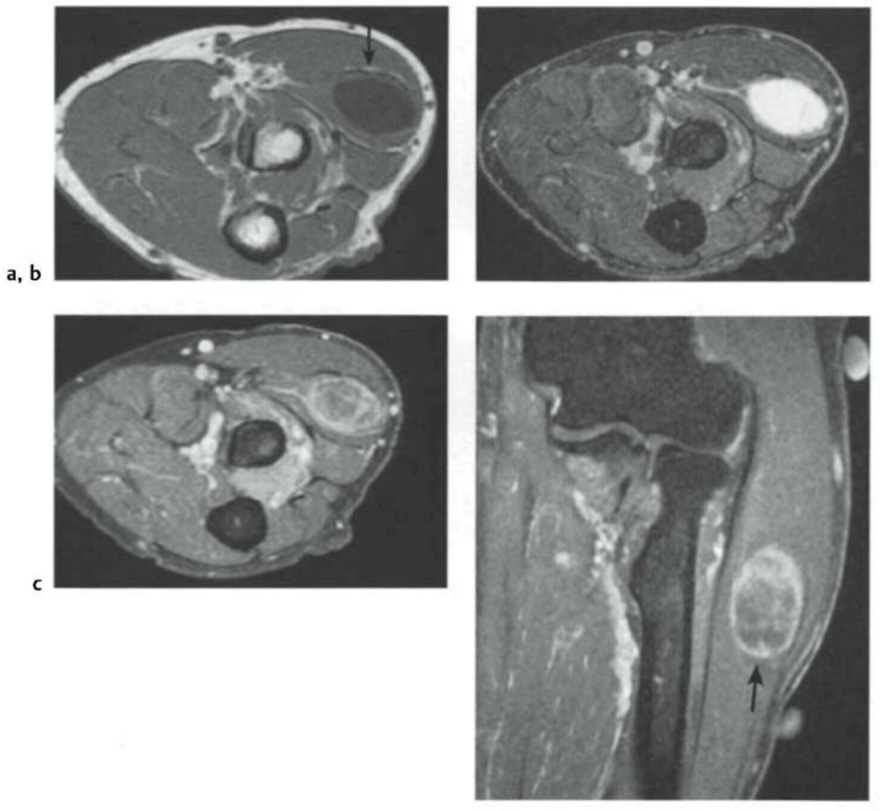

Figure **350a-d** A 77-year-old man with an intramuscular myxoma involving the extensor carpi radialis longus and brevis muscles of the proximal forearm. The lesion has mostly low signal on axial (**a**) T1WI. The lesion has high signal on axial (**b**) FST2WI. The lesion shows mild irregular Gd-contrast enhancement on axial (**c**) and coronal (**d**) FST1WI.

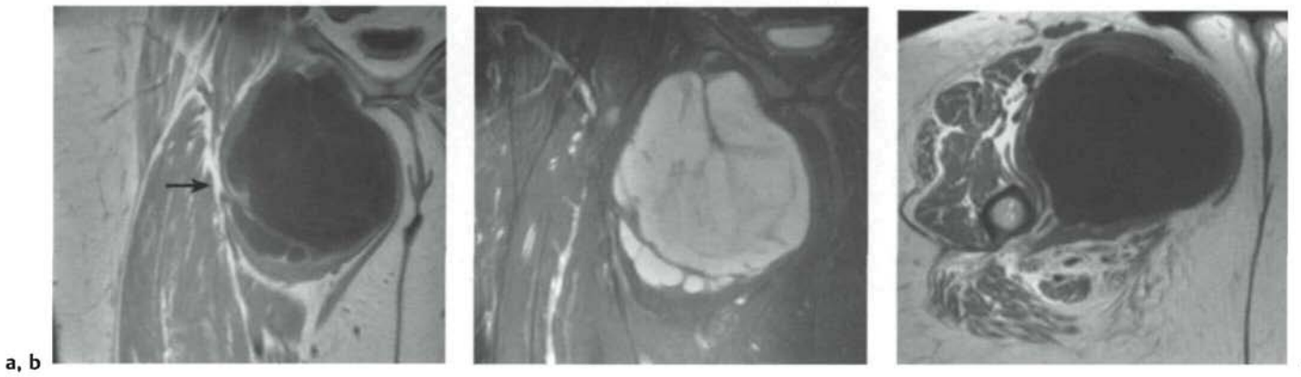

Figure **351 a-f** A 68-year-old woman with an intramuscular myxoma involving the adductor magnus muscle of the upper medial thigh. The lesion has mostly low signal as well as thin peripheral zones and septa with intermediate signal on coronal (**a**) and axial (**c**) T1WI. The lesion has mostly high signal as well as low signal septa on coronal (**b**) and axial (**d**) FST2WI. The septa show Cd-contrast enhancement on axial (**e**) and coronal (**f**) FST1WI.

Figure **351 e-f**

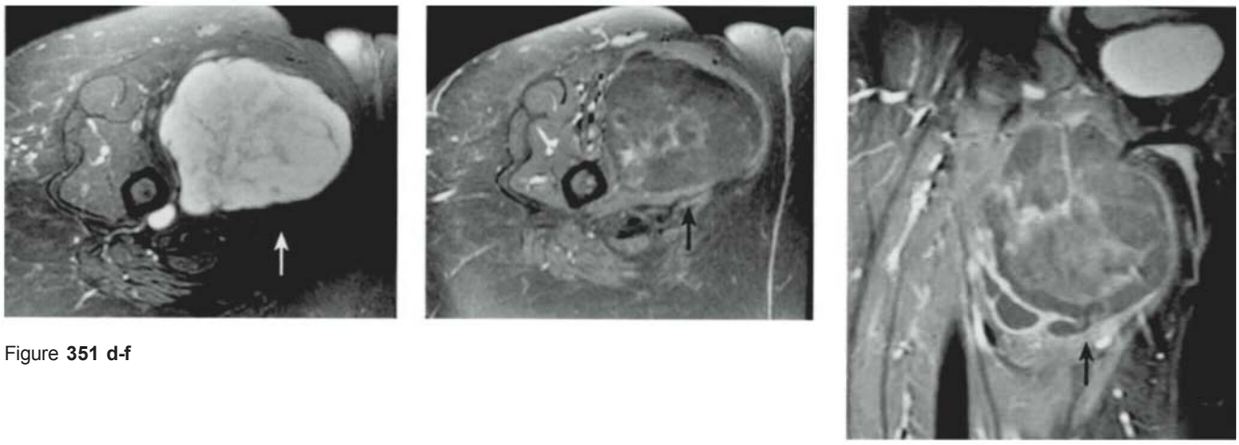

d, e

Figure **351 d-f**

References

1 Kransdorf MJ, Murphey MD. Tumors of uncertain histogenesis. In: *Imaging of soft tissue tumors* 2nd ed. Philadelphia, Pa: W.B Saunders; 2006:481-510.

2 Kransdorf MJ, Murphey MD. Soft tissue tumors in a large referral population: prevalence and distribution of diagnoses by age, sex, and location. In: *Imaging of Soft Tissue Tumors* 2nd ed. Philadelphia, Pa: W.B. Saunders; 2006:6-37.

3 Kransdorf MJ. Benign soft-tissue tumors in a large referral population: distribution of specific diagnoses by age, sex, and location. *AJR AmJRoentgenol* 1995;164:395-402.

4 Ly JQ, Bau JL, Beall DP. Forearm intramuscular myxoma. *AJR Am J Roentgenol* 2003;181:960.

5 Murphey MD, McRae GA, Fanburg-Smith JC, Temple HT, Levine AM, Aboulafia AJ. Imaging of soft-tissue myxoma with emphasis on CT and MR and comparison of radiologic and pathologic findings. Radiology 2002:225:215-224.

6 Nielsen G, Stenman G. Intramuscular myxoma. In: Fletcher COM, Unni KK, Mertens F, eds. *World Health Organization Classification of Tumours. Pathology and Genetics of Tumours of Soft Tissue and Bone* Geneva: IARC Press; 2002:186-187.

7 Sundaram M, McDonald DJ, Merenda G. Intramuscular myxoma: a rare but important association with fibrous dysplasia of bone. *AJR Am J Roentgenol* 1989:153:107-108.

A 55 Neuroblastoma, Ganglioneuroblastoma, and Ganglioneuroma

ICD-O Code

9500/3

Definition

Neuroblastomas, ganglioneuroblastomas, and ganglioneuromas are tumors of the sympathetic nervous system that consist of neuroectodermal cells derived from the neural crest.[6,9] (The neural crest normally gives rise to the adrenal gland and the sympathetic nervous system.)[3] These tumors vary in their degree of cellular maturation, grade of neuroblastic differentiation, and degree of Schwannian stromal development.[6,9] Neuroblastomas are the most malignant undifferentiated tumors in this group and are referred to as Schwannian stroma-poor.[6,9] Ganglioneuroblastomas are intermediate grade malignant tumors consisting of mature gangliocytes and immature neuroblasts.[6,9] Ganglioneuroblastomas are further classified as the intermixed subtype (Schwannian stroma-rich), or the nodular subtype (Schwannian stroma-rich / stroma-dominant and stroma-poor).[6,9] Ganglioneuromas are rare, benign lesions composed of ganglion cells and Schwannian stroma, and lack neuroblasts and mitotic figures.[6]

Frequency of Occurrence

Neuroblastoma and **ganglioneuroblastoma** are grouped together for clinical management purposes.[6] These tumors account for nearly 10% of all childhood cancer and are the third most common malignancies in the pediatric population after leukemia and tumors of the central nervous system.[3,6,9] The incidence is ~8 per million children under the age of 15 years per year worldwide.[6,9]

Ganglioneuromas have been reported to occur from 6 to 10 times less frequently than neuroblastomas.[6]

Age at Presentation

Neuroblastoma. From < 1 to 47 years.[4] Most neuroblastomas are sporadic.[9] Median age in the general population for sporadic neuroblastoma = 22 months.[6,9] Median age for patients with familial neuroblastoma = 9 months.[9] 96 % of neuroblastomas occur in the first decade and 3.5% occur in the second decade. Neuroblastoma accounts for up to 50 % of malignant tumors in the first month of life.[6]

Ganglioneuroblastoma. From 1 to 38 years,[4] median = 22 months.[5]

Ganglioneuroma. From 4 to 44 years,[5] median = 7 years.[6]

Gender Ratio (M /F)

Neuroblastoma: 1 /1.1.[4]

Ganglioneuroblastoma: 1 /1.1.[4]

Ganglioneuroma: 1 /1.1 to 1 /1.5.[5,6]

Location

Neuroblastoma and ganglioneuroblastoma. These tumors occur in the adrenal medulla (35-40%) > extra-adrenal retroperitoneum (25-35%) > posterior mediastinum (15-20%) > neck, pelvis (l-5%).[6,9] Neuroblastomas can occur at any site where sympathetic nervous tissue occurs.[6]

Ganglioneuroma. These tumors occur in the posterior mediastinum (41.5%) > retroperitoneum (37.5%) > adrenal gland (21 %) > neck (8%) > other sites such as bone, heart, spermatic cord, and intestine.[6]

Signs and Symptoms

Neuroblastoma and ganglioneuroblastoma. Patients can have localized pain, abdominal distention, shortness of breath, malaise, irritability, weight loss, and/or nerve root or spinal cord compression.[6,9] Up to 66% of patients have metastatic disease at the time of diagnosis.[6] Patients with metastatic disease may have multifocal pain, limping, and irritability (Hutchinson syndrome). Tumors involving the cervical sympathetic nerves can cause Horner syndrome (pupillary constriction, ptosis, facial anhidrosis, facial flushing).[6,9] Patients with mediastinal tumors may have opsoclonus-myoclonus (jerking movements of the eyes and extremities with or without cerebellar ataxia).[6] Patients may have diarrhea resulting from tumors secreting vasoactive intestinal polypeptide.[9] Tumors involving the orbits can cause proptosis.[9] Ondine curse (impairment of autonomic control of respiration) has also been reported in patients with neuroblastomas.[9] Up to 95 % of neuroblastomas and ganglioneuroblastomas secrete catecholamines such as vanillylmandelicacid(VMA)andhomovanillicacid(HVA).[6,9]Thesecatecholamines rarely cause symptoms.[6,9]

Ganglioneuroma. These tumors are often detected as incidental findings on imaging examinations.[6] Occasionally, patients may present with shortness of breath, abdominal pain, or cough.[6]

Gross Pathologic Findings

Neuroblastoma. These tumors range from 1 to 10cm, and are soft, gray, and/or tan.[9] Lesions may be encapsulated or have ill-defined margins.[9] Tumors may contain calcifications, cystic and/or hemorrhagic zones.[9]

Ganglioneuroblastoma. Tumors with the Schwannian stroma-rich subtype are usually firm and tan-white.[9] Tumors with the nodular subtype usually have one or more hemorrhagic foci associated with the stroma-poor portion, and zones of tan-gray in the stroma-rich components.[9]

Ganglioneuroma. Ganglioneuromas are usually firm and tan-white[9]

Histopathologic Findings

The categories and subtypes which follow accord with the recommendations of the International Neuroblastoma Pathology Committee.[9,10]

Neuroblastoma (Schwannian stroma-poor). These tumors contain groups or nests of neuroblasts separated by thin, stromal septa and minimal or absent Schwannian proliferation.[6,9] Neuroblasts are undifferentiated sympathetic cells, which are small and round with prominent dark nuclei and little surrounding cytoplasm.[6] There are three subtypes of neuroblastoma: undifferentiated, poorly differentiated, and differentiated.[9,10]

- **Undifferentiated type of neuroblastoma.** In order to to establish the diagnosis, identification often requires results from: immunohistochemical reactivity (positive for neuron specific enolase, synaptophysin, neurofilament protein, ganglioside GD2, chronogranin A, and tyrosine hydroxylase; negative for markers of other round-cell tumors); electron microscopy (dense neurosecretory granules measuring between 50 and 200 nm located at the cytoplasmic periphery, and cell processes containing neurotubules); and/or cytogenetics [deletion of the short arm of chromosome 1(1 p), trisomy of the long arm of chromosome 17 (17q)].[9]
- **Poorlydifferentiated type of neuroblastoma.** Tumors contain mostly undifferentiated neuroblasts (<5% show evidence of differentiation) within a neuropil background.[9]
- **Differentiated type of neuroblastoma.** Tumors contain neuroblasts (>5% with cytomorphologic evidence of differentiation toward ganglion cells) within an abundant neuropil background.[9] The neuroblasts of this type often have single, large, eccentric nuclei with vesicular chromatin and single nucleoli, and eosinophilic cytoplasm that is more than twice the diameter of the nuclei.[3]

Ganglioneuroblastoma

- **Intermixed (Schwannian stroma-rich) type of ganglioneuroblastoma.** Tumors contain small nests of neuroblasts in various stages of differentiation, maturing ganglion cells, and a neuropil background.[9]
- **Nodular (composite Schwannian stroma-rich/stroma-dominant and stroma-poor) types of ganglioneuroblastoma.** Tumors contain biologically different clones of neuroblasts with zones of hemorrhage in stroma-poor regions, as well as portions histologically similar to the intermixed (Schwannian stroma-rich) type of ganglioneuroblastoma, and ganglioneuroma (stroma-dominant).[9]

Ganglioneuroma. There are two types of ganglioneuroma: maturing and mature. The maturing type (stroma-rich, well differentiated) contains collections of differentiating neuroblasts and/or ganglion cells, mature ganglion cells, and a ganglioneuromatous stroma.[9] The mature type contains mature ganglion cells surrounded by satellite cells within mature Schwannian stroma with Schwann cells and perineural cells.[5]

Tumor Genetics

A chromosomal deletion and translocation, t(l;17) involving 1 p36, has been reported for neuroblastomas.[9] Abnormalities at 16pl2-13 have been found for patients with familial neuroblastoma.[9] Deletion of the short arm of 1 p, allelic loss of 11 q23, and trisomy for 17 q have been found in neuroblastomas,[9] as well as MYCN gene amplification linked to 2 p24.[9]

Findings on Plain Films (Roentgenograms) and Computed Tomography[1,3,6,8,9]

Neuroblastoma and ganglioneuroblastoma. These tumors can occur in the retroperitoneum, posterior mediastinum, pelvis, or neck.[6] With CT, these neoplasms can be ovoid or spheroid with distinct or indistinct margins.[6] Tumors usually have low-intermediate attenuation,[6] and calcifications can be seen in up to 90%.[3,6] Zones of low attenuation up to 4 cm in diameter can result from necrosis and/or hemorrhage.[6] These tumors can show mild to marked heterogeneous or homogeneous contrast enhancement.[6] The lesions can extend into the spinal canal, encase or compress vessels, or invade adjacent soft tissues, and/or bone.[6] Erosion and invasion of adjacent bone can occur with neuroblastomas.[6]

Ganglioneuroma. These tumors can appear as lesions in the posterior mediastinum, retroperitoneum, pelvis, or neck.[6] With CT, ganglioneuromas are well-circumscribed spheroid or ovoid tumors with low-intermediate attenuation ranging from 27 to 36 Hounsfield units;[6,8] fine and/or coarse calcifications can be seen in up to 60 % of them.[1,3,6,8] These tumors often show mild to moderate heterogeneous or homogeneous contrast enhancement.[1,6,8] The lesions can extend into the spinal canal.[8] Contrast enhancement has aided in discriminating tumor borders with adjacent tissues.[8]

MRI Findings[1,3,6,8]

Neuroblastoma and ganglioneuroblastoma. These tumors can have distinct or indistinct margins;[3,6,7] they often have low-intermediate signal on T1WI, and are hypointense or isointense relative to muscle[3,6,7] (Figs. **352-354).** Zones of high signal on T1WI may occur from sites of hemorrhage.[3,6] Lesions usually show homogeneous or heterogeneous intermediate, slightly high and/or high signal on T2WI and FST2WI.[3,6,7] Zones of high signal on T2WI may occur from sites of hemorrhage or necrosis.[6] Foci of low signal on T2WI may be seen secondary to calcifications and blood products.[6] Signal voids on T2WI may be seen within these tumors.[6] These tumors can show mild to marked heterogeneous Gd-contrast enhancement.[3,6] Ganglioneuromas do not typically show early contrast enhancement with dynamic MRI, although delayed images can show progressive enhancement.[6] MRI can show extension of these tumors into the spinal canal as well as into bone marrow[6] (Fig. **352).**

Ganglioneuroma. These tumors are well-circumscribed, spheroid or ovoid, with low-intermediate signal on T1WI, and are hypointense or isointense relative to muscle.[1,6,8] Lesions usually show homogeneous or heterogeneous intermediate, slightly high to high signal on T2WI and FST2W1[168] (Figs. **355, 356).** Small foci or strands of low signal on T2WI may be seen secondary to calcifications and fibrous tissue, respectively. These tumors can show mild to marked heterogeneous contrast enhancement.[1,6,8] Ganglioneuromas do not typically show early contrast enhancement with dynamic MRI, although delayed images can show progressive enhancement.[6] MRI can show extension of these tumors into the spinal canal.[6,8] Contrast enhancement of these neoplasms has aided in discriminating tumors margins enhancement with adjacent tissues.[8]

Radionuclear imaging[3,6,7]

Radionuclide studies can be used to detect primary neuroblastoma or ganglioneuroblastoma as well in the evaluation for metastatic disease.[3,6,7] Radiopharmaceutical agents such as the catecholamine analog 1-123 meta-iodobenzylguanidine (I-123 MIBG) and the somatostatin analog indium-Ill pentetriotide are taken up by catecholamine-producing primary and metastatic tumors such as neuroblastoma, ganglioneuroblastoma, ganglioneuroma, pheochromocytoma, medullary thyroid carcinoma, and carcinoid tumors.[6,7] Approximately 70 % of neuro-

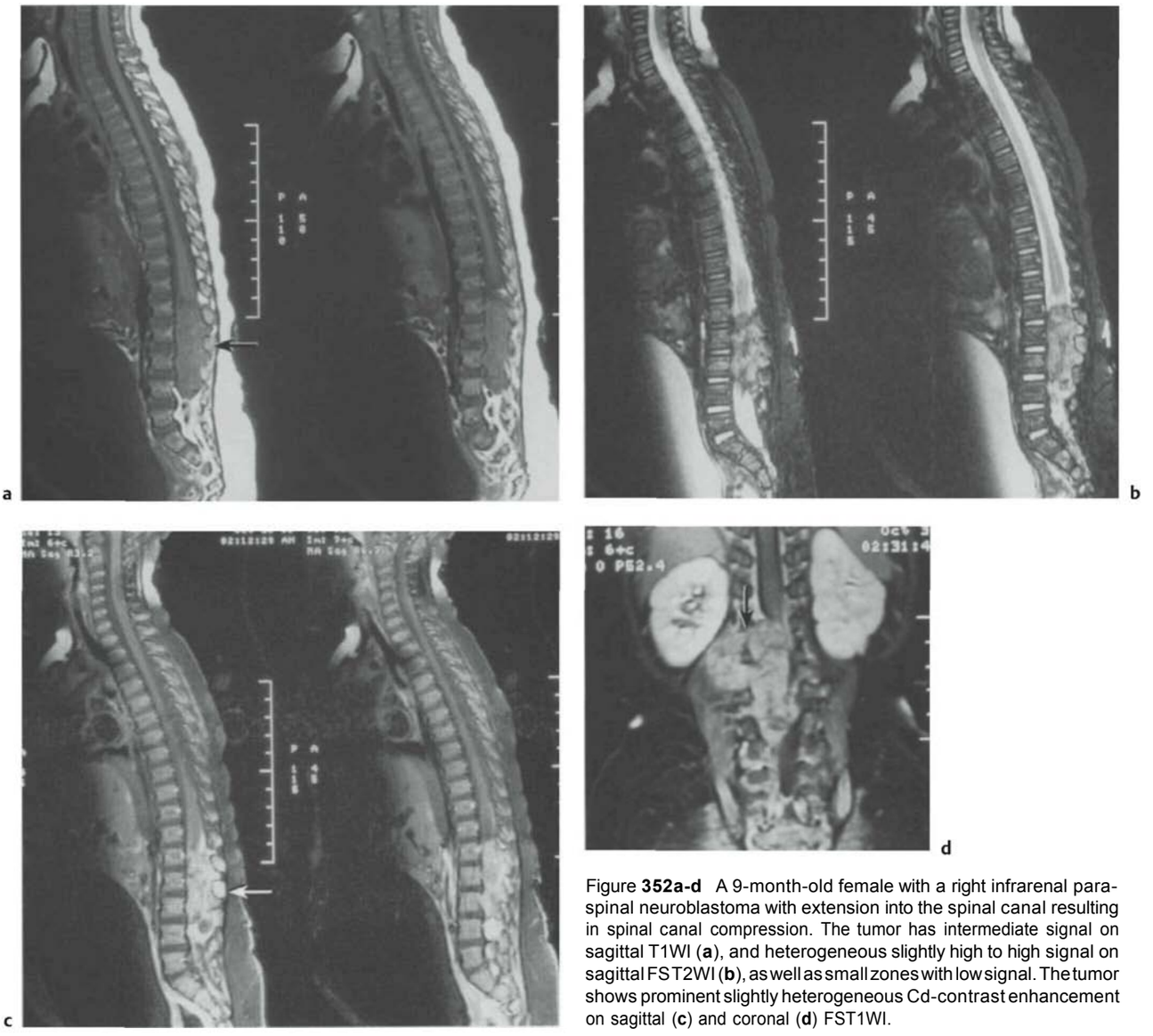

Figure **352a-d** A 9-month-old female with a right infrarenal paraspinal neuroblastoma with extension into the spinal canal resulting in spinal canal compression. The tumor has intermediate signal on sagittal T1WI (**a**), and heterogeneous slightly high to high signal on sagittal FST2WI (**b**), as well as small zones with low signal. The tumor shows prominent slightly heterogeneous Cd-contrast enhancement on sagittal (**c**) and coronal (**d**) FST1WI.

blastomas and ganglioneuroblastomas are I-123 MIBG-positive, despite the fact that up to 95 % of neuroblastomas and ganglioneuroblastomas secrete catecholamines.[6] MRI has been shown to have a higher sensitivity (86%) in detecting neuroblastoma lesions than I-123 M1BG scintigraphy (69 %), but the latter technique was shown to have a higher specificity (85 %) compared with MRI (77%). Using MRI and I-123 MIBG scintigraphy together increased the sensitivity and specificity for detection of neuroblastoma lesions to 99 % and 95 %, respectively.

Bone scanning using technetium-99 m methylene diphosphonate is also frequently employed to assess for metastatic skeletal disease, and is more sensitive than plain films.[6]

Differential Diagnosis

Metastatic disease, lymphoma, multiple myeloma/plasmacytoma, neurofibroma, Schwannoma, granulomatous disease (tuberculosis, sarcoid, fungal infection, etc), extramedullary hematopoeisis, pheochromocytoma, Wilm tumor, teratoma, intrathoracic goiter, intrathoracic desmoid, granular cell tumor, gastrointestinal stromal tumor.[1,3,6]

Prognosis and Treatment

The histologic features of neuroblastomas, ganglioneuroblastomas, and ganglioneuromas can be used for determining prognosis.[6,9] The Pediatric Oncology Group system is based on the degree of differentiation of tumor cells.[6,9] Neuroblastoma has less than 50 % of cellular differentiation, ganglioneuroblastoma has greater than 50 % cellular differentiation, and ganglioneuroma has 100% cellulardifferentiation.[6,9]Another classification is the modified Shimada system, which is based on cellular differentiation as well as patient age at diagnosis.[6,9,10]

The International Neuroblastoma Pathology Committee uses the Shimada system with several modifications.[9,10] Using this system, tumors are categorized into either favorable or unfavorable histologic groups.[9] Tumors with favorable histology include: neuroblastoma (Schwannian stroma-poor), poorly dif-

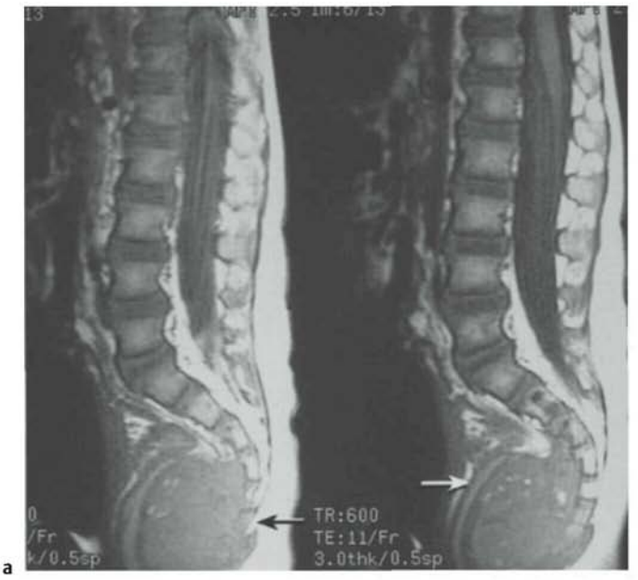

a

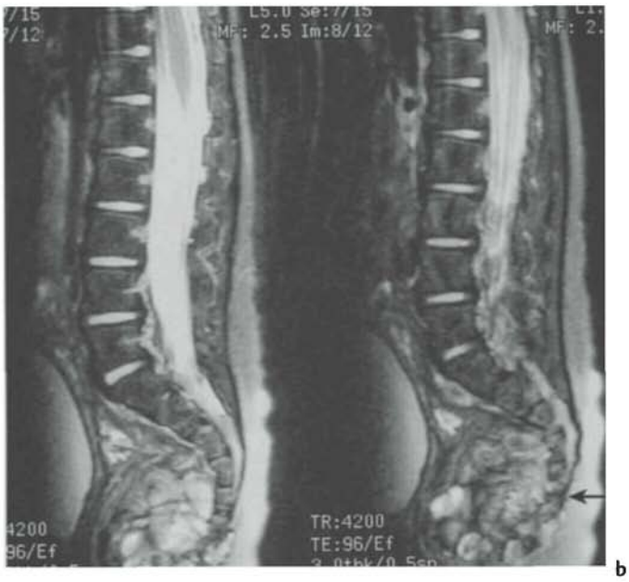

b

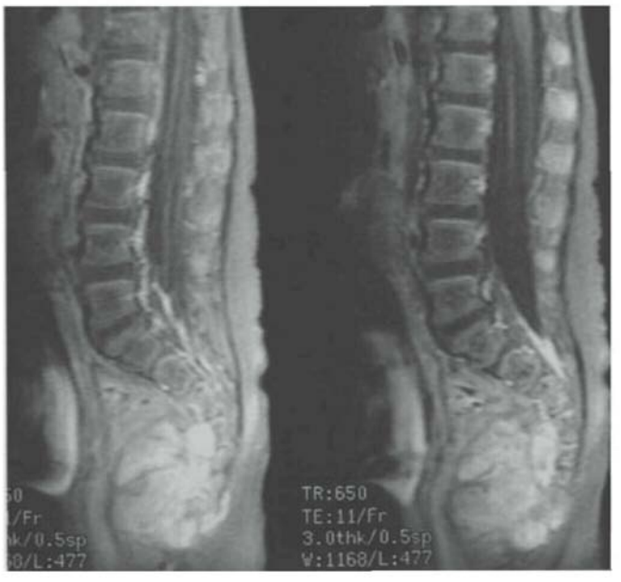

c

Figure **353a-c** A 1-year-old male with a neuroblastoma involving the presacral soft tissues. The tumor has lobular margins, and has intermediate signal with small foci with high signal on sagittal (**a**) T1 WI. The tumor contains zones with low, intermediate, slightly high and high signal on sagittal (**b**) FST2WI. The tumor shows heterogeneous Gd-contrast enhancement on sagittal (**c**) FST1WI.

ferentiated subtype with patient age < 1.5 years and < 200/5000 mitosis-karyorrhexis index (MKI); neuroblastoma (Schwannian stroma-poor) differentiating subtypes with patient age between 1.5 and 5 years and low MKI; ganglioneuroblastoma-intermixed (Schwannian stroma-rich) in older children; and ganglioneuroma (maturing and mature subtypes).[9,10] Tumors with unfavorable histology include: neuroblastoma (Schwannian stroma-poor) undifferentiated subtype; neuroblastoma (Schwannian stroma-poor) poorly differentiated subtype in patients of age between 1.5 and 5 years; neuroblastoma (Schwannian stroma-poor) with MKI > 200/5000; neuroblastoma (Schwannian stroma-poor) in patients of age > 5 years; ganglioneuroblastoma-nodular (composite Schwannian stroma-rich / stroma-dominant and stroma-poor).[9,10]

Other characteristics associated with poor prognosis include: cellular proliferative activity with K_r-67 protein expression scores > 25 %, serum VMA / HVA ratio of < 1, serum neuron-specific enolase > 100 ng/mL, serum ferritin > 150 ng/mL, serum lactate dehydrogenase > 1500 IU/L, amplification of the MYCN oncogene, and chromosome 1 p deletions.[9] The levels and types of catecholamines are often associated with the degree of tumor differentiation.[6] VMA is an immature precursor of epinephrine and norepinephrine, and is associated with less differentiated tumors than lesions containing HVA, which is a precursor of dopamine that is often associated with mature neuroblastomas and ganglioneuroblastomas.[6]

Staging of neuroblastomas is typically done with the International Neuroblastoma Staging System.[6,9] Stage 1 is defined as localized tumor at site of origin.[69] Stage 2A is incomplete gross excision of unilateral tumor.[6,9] Stage 2B is complete or incomplete excision of unilateral tumor with positive ipsilateral lymph nodes.[6,9] Stage 3 is tumor infiltrating across midline with or without positive lymph nodes, or unilateral tumor with positive contralateral lymph nodes, or midline tumor with positive bilateral lymph nodes.[6,9] Stage 4 is metastatic tumor to distant sites.[6,9] Stage 4S is localized tumor with metastatic disease to the liver, skin, and/or bone marrow in infants[6,9]

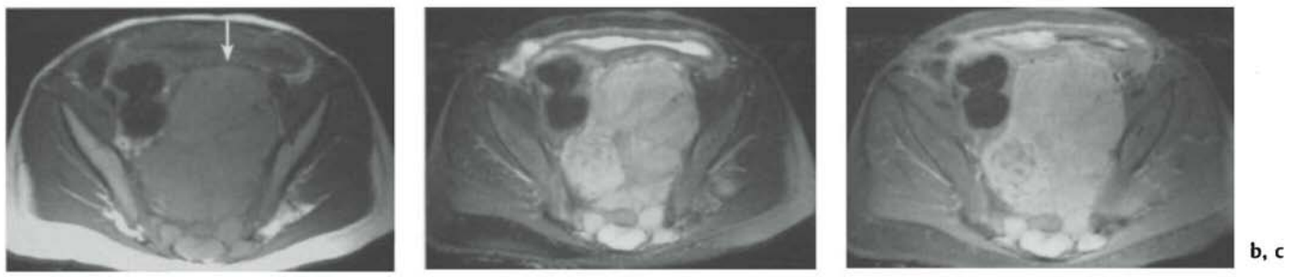

Figure **354a-c** A 2-year-old female with a ganglioneuroblastoma involving the presacral soft tissues. The tumor has lobular margins, and has intermediate signal on axial T1WI (**a**). The tumor contains zones mostly with slightly high and high signal, with strands of low signal on axial FST2WI (**b**). The tumor shows heterogeneous, prominent Gd-contrast enhancement on axial FST1 WI (**c**).

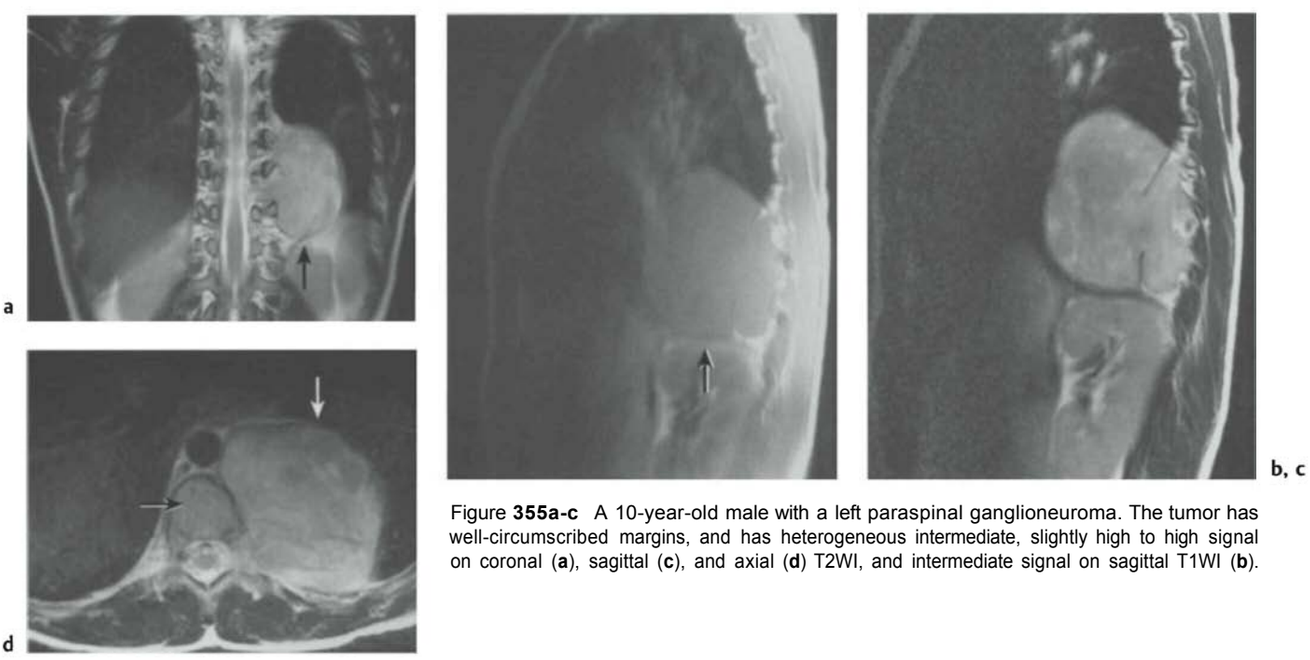

Figure **355a-c** A 10-year-old male with a left paraspinal ganglioneuroma. The tumor has well-circumscribed margins, and has heterogeneous intermediate, slightly high to high signal on coronal (**a**), sagittal (**c**), and axial (**d**) T2WI, and intermediate signal on sagittal T1WI (**b**).

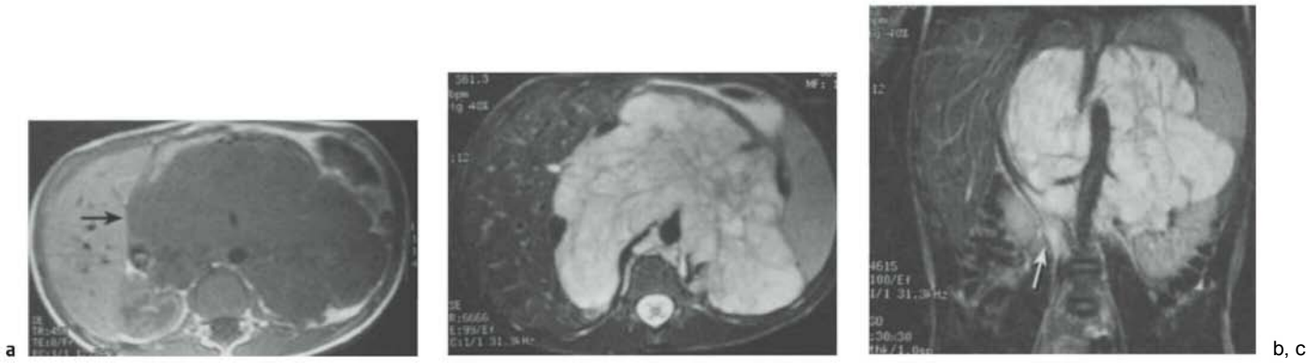

Figure **356a-c** A 9-year-old male with a large intra-abdominal ganglioneuroma. The tumor encases the aorta, and has intermediate signal on axial T1WI (**a**) and mostly high signal with strands of low signal on axial FST2WI (**b**) and coronal T2WI (**c**).

Neuroblastomas can be aggressive neoplasms and account for 15% of childhood cancer fatalities.[6] The 5-year survival rate for children below the age of 15 years with neuroblastoma is 71 %.[2] Infants with neuroblastoma that have tumor hyperploidy/triploidy, no tumor MYCN oncogene amplification, and no chromosome 1 p deletions have survival rates over 90 %.[9,10] Children older than 1 year with stages 3 and 4 neuroblastomas have 3-year event-free survival rates of 50% and 15%, respectively.[6] Low-risk and intermediate-risk neuroblastomas have a relatively favorable prognosis and are often treated with surgery alone.[6] Recurrent tumors are usually treated with surgery and chemotherapy.[6] Intermediate-risk and high-risk neuroblas-

tomas are treated with surgery and chemotherapy.[6] High-risk tumors may also require high-dose chemotherapy with bone marrow rescue.[6] Patients with stage 3 lesions may be treated with surgery or neoadjuvant chemotherapy to decrease viable tumor bulk prior to initial surgery.[6] Patients with stages 4 and 4S can be treated somewhat effectively with chemotherapy.[6] The role of surgery is controversial with regard to outcomes.[6] Radiation may be beneficial for patients with neuroblastoma and intracavitary lymph nodes.[6]

Metastases from neuroblastoma may occur in up to 66% of patients at diagnosis.[6] Metastatic lesions occur in bone followed by liver, lung, brain, and dura.[6]

Approximately 1-2% of neuroblastomas and ganglioneuroblastomas spontaneously undergo regression or maturation to more-mature neuroblastic tumors.[6] Stage 4S neuroblastomas are the most frequent type to undergo maturation followed by stage 1 and 2 tumors.[6]

Ganglioneuromas are typically treated with complete excision and infrequently show local recurrence.[6]

References

1 Forsythe A, Volpe J, Muller R. Posterior mediastinal ganglioneuroma. *Radiographics* 2004;24:594-597.

2 Jemal A, Thomas A, Murray T, Thun M. Cancer statistics 2002. *CA Cancer J Clin* 2002;52:23-47.

3 Kransdorf MJ, Murphey MD. Neurogenic tumors. In: *Imaging of Soft Tissue Tumors* 2nd ed. Philadelphia, Pa: W.B. Saunders; 2006: 328-380.

4 Kransdorf MJ. Malignant soft-tissue tumors in a large referral population: distribution of diagnoses by age, sex, and location. *AJR Am] Roentgenol* 1995;164:129-134.

5 Kransdorf MJ. Benign soft-tissue tumors in a large referral population: distribution of specific diagnoses by age, sex, and location. *AJR AmJ Roentgenol* 1995;164:395-402.

6 Lonergan GJ, Schwab CM, Suarez ES, Carlson CL. Neuroblastoma, gangioneuroblastoma, and ganglioneuroma: radiologic-pathologic correlation. *Radiographics* 2002;22:911-934.

7 Pfluger T, Schmied C, Porn U, et al. Integrated imaging using MRI and I-123 metaiodobenzylguanidine scinitigraphy in the diagnosis of pediatric neuroblastoma. *AJR Am] Roentgenol* 2003:181:1115-1124.

8 Scherer A, Niehues T, Engelbrecht V, Modder U. Imaging diagnosis of retroperitoneal ganglioneuroma in childhood. *Pediatr Radial* 2001; 31:106-110.

9 Schwab M, Shimada H, Joshi V, Brodeur GM. Neuroblastic tumours of adrenal gland and sympathetic nervous system. In: Kleihues P, Cavenee WK, eds. *World Health Organization Classification of Tumours. Pathology and Genetics of Tumours of the Nervous System* Geneva: IARC Press; 2000:153-161.

10 Shimada H, Umehara S, Monobe Yet al. International Neuroblastoma pathology classification for prognostic evaluation of patients with peripheral neuroblastic tumors. A report from the Children's Cancer Group. *Cancer* 2001 ;91:2451-2461.

A 56 Neurofibroma and Malignant Peripheral Nerve Sheath Tumor

ICD-O Code

9540/0

Definition

Neurofibromas are benign tumors of the peripheral nerve sheath that contain mixtures of Schwann cells, perineural-like cells, and interlacing fascicles of fibroblasts associated with abundant collagen.[9,26] Unlike Schwannomas, neurofibromas lack Antoni A and B regions and cannot be separated pathologically from the underlying nerve.[9,26] Neurofibromas can be localized (90%) or occur as diffuse or plexiform lesions.[9,16,26] The presence of multiple neurofibromas is a typical feature of neurofibromatosis type 1 (von Recklinghausen disease), which is an autosomal-dominant disorder resulting in mesodermal dysplasia and affecting multiple organ systems.[9,16,19,20,26] Neurofibromatosis type 1 (NF1) is one of the most common genetic diseases, the involved locus being on chromosome 17ql2.[15,17,24] Plexiform neurofibromas are associated with an increased risk of transformation into malignant peripheral nerve sheath tumors (MPNSTs).[12,27] Approximately 50% of MPNSTs occur in patients with NF1, followed by de novo evolution from peripheral nerves.[27] MPNSTs arise infrequently from Schwannomas, ganglioneuroblastomas, ganglioneuromas, and pheochromocytomas.[27]

Frequency of Occurrence

Solitary neurofibromas account for 5 % of primary benign soft tissue tumors and 3 % of all primary soft tissue tumors.[8,10]

The birth incidence of patients with autosomal-dominant NF1 is ~ 1 per 2500-4000.[12,16,19,25]

Age at Presentation

From 16 to 66 years, mean = 37 years.[8,10,14] Neurofibromas can occur in younger children and older adults.[26] NF1 often presents in childhood.[16,19]

Gender Ratio (M /F)

1.2/1.[10]

Location

Soft tissue:

- **Sporadic or solitary neurofibroma.** These lesions occur in the head and neck > lower extremity > trunk > upper extremity > hand and wrist > hip and buttock > foot and ankle > other sites.[10] In order of decreasing frequency, circumscribed cutaneous neurofibromas are more common than localized intraneural neurofibromas (peripheral nerve), plexiform neurofibromas, diffuse cutaneous neurofibromas, and localized gigantism-elephantiasis neuromatosa.[16,26]
- **Neurofibromatosis type 1.** Paraspinal, peripheral, and cutaneous neurofibromas are seen in most patients with NF1.[17] Localized neurofibromas are more frequent than diffuse and plexiform types.[16] Dermal neurofibromas occur more often than deep-seated, nodular (localized) neurofibromas.[25]
- **Malignant peripheral nerve sheath tumors.** Large and medium sized nerves of the buttock, thigh, upper arm and paraspinal region are common locations of MPNSTs.[27]

Bone. Neurofibromas rarely occur as intra-osseous lesions.[5] The mandible and maxilla are more frequent locations than long bones.[5] MPNSTs usually occur in the soft tissues and only rarely within bone.[22]

Signs and Symptoms

Localized neurofibromas are usually slow-growing and painless lesions.[16,26]

Diffuse neurofibromas often present as plaquelike thickenings of the skin.[16,26]

Plexiform neurofibromas may present as bands or cords of firm, soft tissue thickening, and may be associated with enlargement and/or severe disfigurement of the affected site.[16,25] The term **elephantiasis neuromatosa** refers to the situation where massive enlargement and disfigurement of an extremity results from a plexiform neurofibroma.[16]

Neurofibromatosis type 1:

- **Soft tissue.** Patients with NF1 usually have multiple neurofibromas as well as six or more pigmented cutaneous macules (cafe-au-lait spots), axillary or inguinal freckling, two or more melanocytic iris hamartomas (Lisch nodules), optic glioma, and/or intracranial / spinal astrocytoma.[16,19,20,25,26] Segmental hypertophy can occur in association with an underlying neurofibroma.[19] Plexiform neurofibromas may result in severe disfigurement of the affected site.[25]
- **Bone.** Osseous abnormalities occur in 25-40 % of patients with NF1.[16,20] Such patients can have sphenoid bone dysplasia, resulting in herniation of temporal lobe contents into the orbit, which may be associated with pulsatile proptosis and seizures.[16,19,25] Also seen with NF1 is osseous dysplasia involving long bones, which can result in bowing deformities, pathologic fractures, and pseudoarthroses.[16,19,20,25] NF1 is also associated with scoliosis, kyphosis, rib deformities ("ribbon ribs"), lambdoid suture defects, and dural ectasia.[16,19,20,25] Neurofibromas in soft tissue can erode or cause remodeling of the outer cortex of bone. Neurofibromas arising within bone are rare.[5,13,14]

Malignant peripheral nerve sheath tumors are progressively enlarging lesions with or without associated pain.[12,16,22,27] MPNSTs involving the spine may be associated with neurologic signs and symptoms.[12,16,27]

Gross Pathologic Findings

Localized neurofibromas often appear as nodular or fusiform, gray-white, circumscribed, firm lesions.[26]

Plexiform neurofibromas often appear as elongated fusiform and/or multinodular lesions which involve multiple trunks of a plexus or multiple fascicles or a large nerve.[16,26] They have been described as having a "bag of worms" appearance.[16,26] Plexiform

neurofibromas often extend beyond the epineurium into the adjacent soft tissues.[16]

Malignant peripheral nerve sheath tumors often appear as elongated fusiform and/or multinodular, gray or cream-colored, firm pseudoencapsulated lesions attached to medium or large sized nerves.[27] Lesions usually range from 5 to 10 cm and often contain zones of necrosis and hemorrhage.[27]

Histopathologic Findings

Sporadic neurofibromas. Neurofibromas that involve medium and large sized nerves are often confined to the nerve and enclosed by the epineurium.[26] Neurofibromas involving small nerves often extend diffusely into the adjacent dermis or other soft tissues.[26] Large, diffuse neurofibromas may contain melanotic cells and Wagner-Meissner-like corpuscles (tactilelike structures).[26] Plexiform neurofibromas contain tumor cells and collagen which extend along multiple nerves or fascicles.

- **Neurofibromas** are composed of neoplastic Schwann cells, perineurial-like cells, and interlacing fascicles of fibroblasts associated with abundant collagen.[9,16,26] Neurofibromas lack Antoni A and B regions which are typically seen with Schwannomas.[9,16,19,26] Neurofibromas cannot be separated pathologically from the underlying nerve.[9,16,26] Tumor cells contain nuclei which are ovoid, curved, or spindle-shaped.[26] Mitotic figures are rarely seen.[26] Cell processes are small, thin, and not usually observed with light microscopy.[26] Abundant collagen fibers are often seen in an Alcian-blue-positive myxoid matrix.[26] Blood vessels associated with neurofibromas lack hyalinization, which is commonly seen with Schwannomas.[26] Neurofibromas often show immunoreactivity to S-100 protein.[26]
- **Neurothekeoma,** also referred to as nerve sheath myxoma, is considered to be a neurofibroma with prominent myxoid matrix organized into lobules separated by fibrous connective tissue.[9,18]

Neurofibromatosis type 1:

- **Dermal neurofibromas** are circumscribed, nonencapsulated lesions consisting of Schwann cells, fibroblastlike cells, as well as: mast cells, lymphocytes, and endothelial cells.[25]
- **Deep-seated neurofibromas** are circumscribed, nonencapsulated lesions consisting of Schwann cells, fibroblastlike cells with adjacent extracellular collagen deposition.[25]
- **Plexiform neurofibromas** contain tumor cells and collagen that extend along multiple nerves or fascicles.[25,26]

Malignant peripheral nerve sheath tumors. Lesions usually have bands or fascicles of tightly packed hyperchromatic spindle cells with elongated nuclei and slightly eosinophilic cytoplasm.[27] Mitotic figures and zones of necrosis are commonly seen.[27] The density of neoplastic cells can vary within tumors.[27] Up to 15% of MPNSTs have epithelioid features and divergent differentiation.[27] Tumor invasion into adjacent soft tissues or bone is often seen by light microscopy.[27] Glandular MPNST is a variant which contains gland-forming epithelium.[27] MPNSTs with rhabdomyosarcomatous differentiation have been referred to as malignant **Triton tumor**[27]

Tumor Genetics

The NF1 locus is on chromosome 17q12 and contains the gene producing neurofibromin, which is a cytoplasmic RasGTPase-activating protein.[19,25] The NF1 gene is considered to be a classic tumor-suppressor gene in which both alleles need to be defective for tumor genesis.[19] Patients with NF1 have only one normal allele, so tumors will form if there are mutations or deletions in the remaining normal gene.[19]

Findings on Plain Films (Roentgenograms) and Computed Tomography

Neurofibromas may or may not be seen on radiographs as areas of localized soft tissue swelling. Neurofibromas may be associated with adjacent chronic bony changes such as widening of intervertebral foramina, scalloping of the dorsal or dorsal lateral aspects of vertebral bodies, and erosions at the caudal aspects of ribs.[11,15,20] Scoliosis and kyphosis may be seen.[15] Mesodermal dysplasia involving bone in patients with NF1 can result in thinning deformities of long bones which may be associated with pathologic fractures, pseudoarthroses, bowing deformities, as well as other growth disturbances.[15]

CT can demonstrate features associated with sphenoid dysplasia such as bony thinning or deficiency of the greater sphenoid wing, with or without expansion of the ipsilateral middle cranial fossa and proptosis.[6] Patients with sphenoid dysplasia usually have neurofibromas in the superficial temporal fossa contiguous with the abnormal temporo-squamosal suture.[6] CT scanning of localized neurofibromas usually shows circumscribed lesions with low and/or intermediate attenuation, which usually shows enhancement.[6,11,16] CT scanning of plexiform neurofibromas shows multilobulated lesions with low to intermediate attenuation.[11,16]

Rare, intra-osseous neurofibromas are radiolucent lesions without matrix mineralization, and may have thin sclerotic margins.[5] MPNSTs can appear as radiolucent lesions with cortical destruction (Fig. **368).**

MRI Findings

Localized neurofibromas are circumscribed ovoid or fusiform lesions with low-intermediate signal on T1W1, and intermediate to high signal on T2WI and FST2WT[1-4,6,7,11,12,17,20,21,23,24] **(Figs. 358-360, 362, 363).** After Gd-contrast administration, lesions typically show moderate to prominent enhancement.[1-4,6,7,9,11,12,17,20,21,23,24] Large lesions may show signal heterogeneity on T2WI and heterogeneous Gd-contrast enhancement. Neurofibromas involving spinal nerve roots may have a dumb-bell shape with or without associated chronic erosive changes of adjacent vertebrae.[7,11] Muscle atrophy in a nerve distribution pattern may occur in association with peripheral neurofibromas.[11] **Neurothekeomas** can occur as circumscribed lesions with low-intermediate signal on T1W1, high signal on T2WI, and heterogeneous Gd-contrast enhancement (Fig. **365).**[18]

Diffuse neurofibromas often appear as irregular infiltrative lesions with low-intermediate signal on T1WI, and mixed low-intermediate and/or high signal on T2W1 and FST2WT[6] (Fig. **364).**

Plexiform neurofibromas usually appear as curvilinear and multinodular lesions involving multiple nerve branches.[7,11,16] These lesions usually have low to intermediate signal on T1WI; and intermediate, slightly high to high signal on T2WI and FS T2WI, with or without bands or strands of low signal[11,16] (Figs. **357, 361).** On T2WI, lesions may show nodules with high signal surrounding a central region of low signal referred to as a "target sign"[7,11,16] After Gd-contrast administration, lesions typically show enhancement.[7]

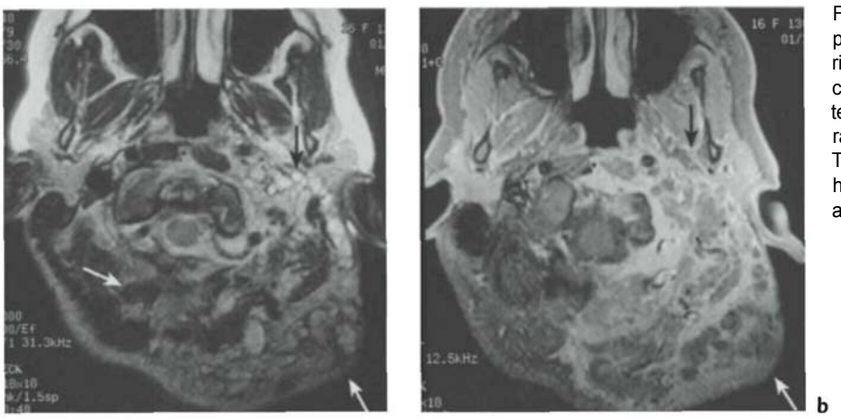

Figure **357 a, b** A 16-year-old female with a plexiform neurofibroma involving the posterior scalp and skull. The tumor appears as curvilinear and multinodular zones with intermediate, slightly high to high signal separated by curvilinear zones of low signal on ixial T2WI (**a**). The plexiform neurofibroma shows heterogeneous Cd-contrast enhancement on axial FSTIWI (**b**).

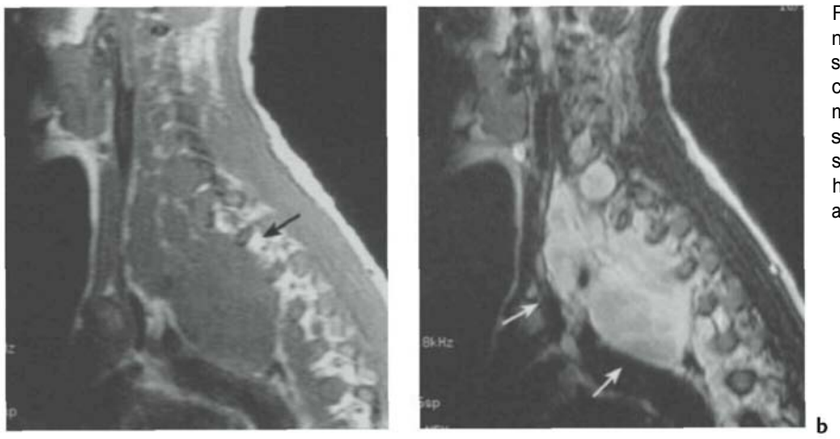

Figure **358 a-c** An 8-year-old male with neurofibromatosis type 1 and a large paraspinal neurofibroma extending into the spinal canal through a widened intervertebral foramen. The lesion has intermediate signal on sagittal T1WI (**a**), and heterogeneous high signal on sagittal T2WI (**b**). The lesion shows heterogeneous Cd-contrast enhancement on axial T1WI (**c**).

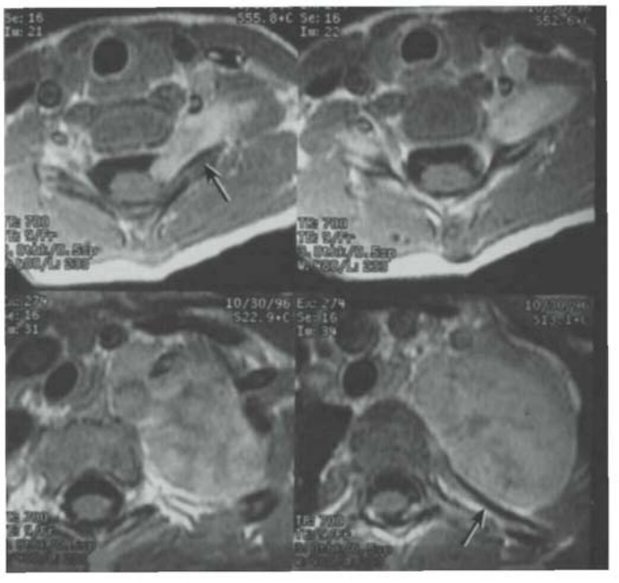

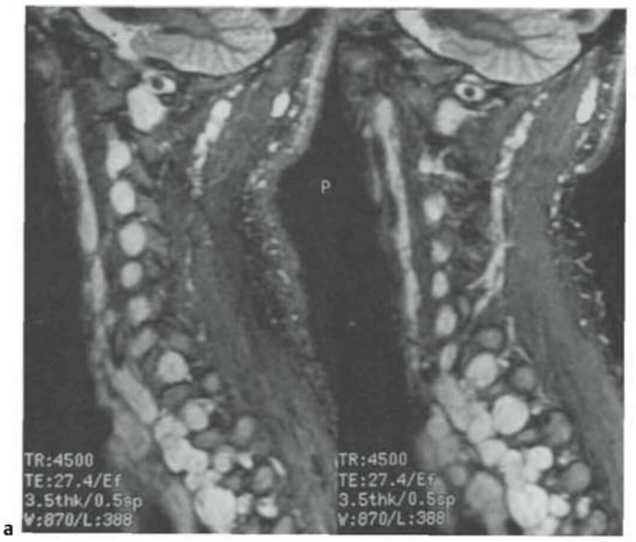

a

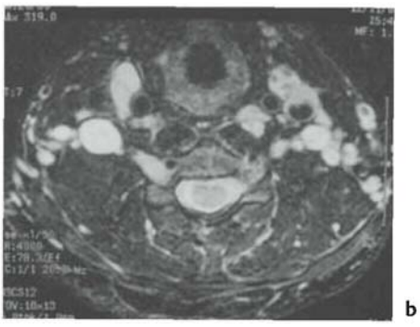

b

Figure **359 a, b** A 22-year-old man with neurofibromatosis type 1 and multiple neurofibromas involving the cervical and upper thoracic spine and soft tissues. The neurofibromas have high signal on sagittal (**a**) and axial (**b**)FST2WI.

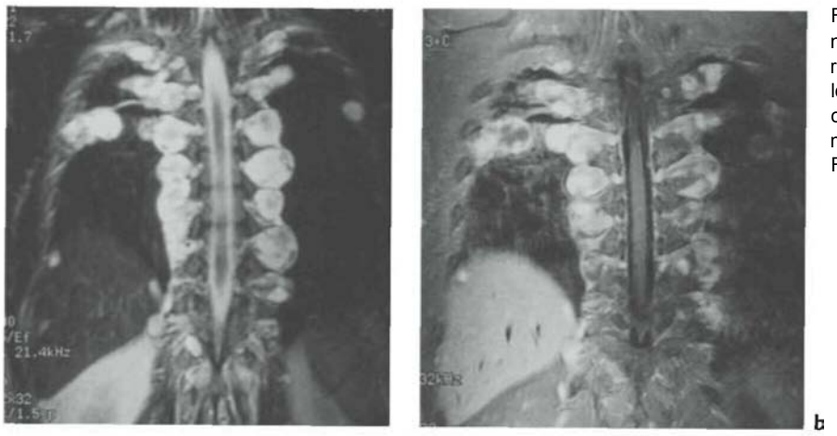

a b

Figure **360 a, b** A 39-year-old man with neurofibromatosis type 1 and multiple neurofibromas involving the thoracic spine. The lesions have heterogeneous mostly high signal on coronal FST2WI (**a**), and show heterogeneous Gd-contrast enhancement on coronal FST1WI (**b**).

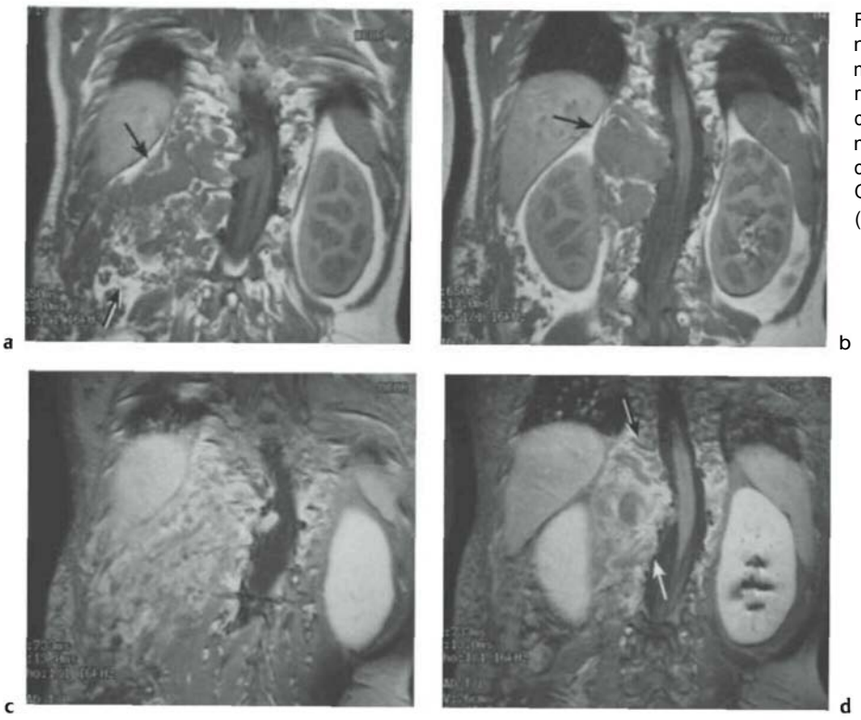

a b c d

Figure **361 a-d** A 2-year-old female with neurofibromatosis type 1 and a plexiform neurofibroma posterior and medial to the right kidney with extension into the spinal canal. The tumor appears as curvilinear and multinodular zones with intermediate signal on coronal T1WI (**a, b**), and heterogeneous Gd-contrast enhancement on coronal FST1WI (**c, d**).

Malignant peripheral nerve sheath tumors occur in ~10% of patients with NF1 and usually occur in pre-existing plexiform neurofibromas.[12] These lesions usually occur in soft tissue and have heterogeneous signal on T1WI, T2WI, and FST2WI, as well as heterogeneous Gd-contrast enhancement because of necrosis and hemorrhage[12] (Figs. **366-368).** Some MPNSTs are similar in appearance to benign nerve sheath tumors.[27] Rarely, MPNSTs can occur within bone and are associated with trabecular destruction, cortical destruction, and extra-osseous tumor extension (Fig. **368).**[22]

Differential Diagnosis

Schwannoma, leiomyosarcoma, rhabdomyosarcoma, Kaposi sarcoma, malignant fibrous histiocytoma, dermatofibrosarcoma, lymphoma, metastatic disease.

Prognosis and Treatment

Sporadic, localized, and diffuse neurofibromas. Treatment usually consists of complete surgical excision.[16] Recurrence of localized neurofibromas is uncommon.[16] Diffuse neurofibromas may recur if surgical excision does not include all of the poorly defined tumor margins.[16]

Neurofibromatosis type 1. Treatment usually consists of complete surgical excision of symptomatic lesions.[16] Neurofibromas may undergo transformation into MPNSTs.[16,25,27] The prevalence of malignant transformation ranges from 2 to 29 %.[7,16] Plexiform neurofibromas have a 5% risk of malignant transformation, whereas localized neurofibromas rarely show malignant progression.[7,25] Patients with NF1 have an increased risk of neurofibrosarcoma, rhabdomyosarcoma, non-Hodgkin lymphoma, lymphoblastic leukemia, melanoma, pheochromocytoma, duodenal carcinoid tumor, and adenocarcinoma of the ampulla of Vater.[19,25] Patients with NF1 also have a relative risk of chronic myelomonocytic leukemia that is 200 times greater than the general population.[19]

Malignant peripheral nerve sheath tumors. Treatment includes surgery with wide margins, neoadjuvant or postoperative chemotherapy and radiation.[16] Local recurrence and metastatic disease occurs in ~50 % of patients.[16] Five-year survival rates of 34-44% have been reported.[16,27] Paraspinal tumors have a worse prognosis than tumors in other locations.[27]

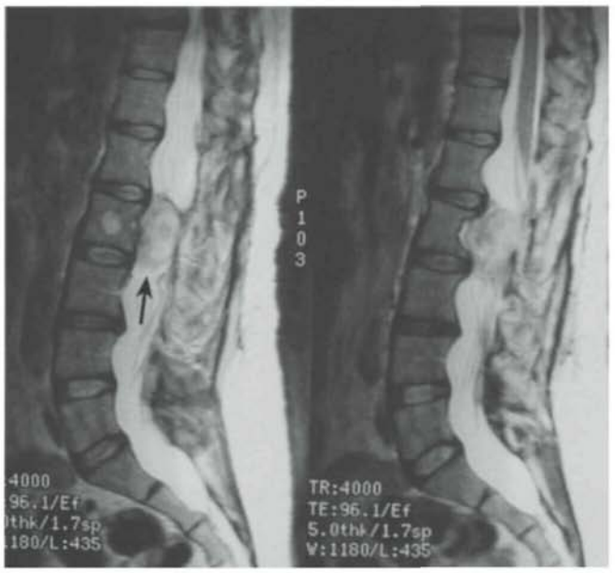

a

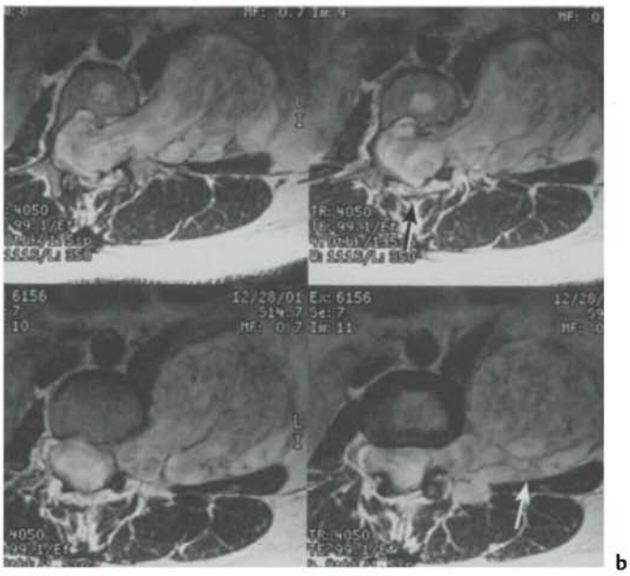

b

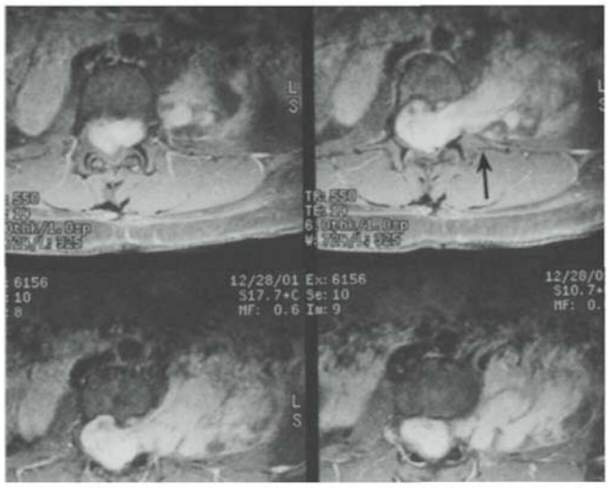

c

Figure **362 a-c** A 45-year-old woman with neurofibromatosis type 1 and a large left paraspinal neurofibroma extending through a widened intervertebral foramen, severely compressing the thecal sac. Note also the scalloping of the dorsal margins of the vertebral bodies from dural ectasia. The lesion has intermediate, slightly high to high signal with foci of low signal on sagittal (**a**) and axial (**b**) T2WI. The lesion shows heterogeneous Gd-contrast enhancement on axial FSTIWI(**c**).

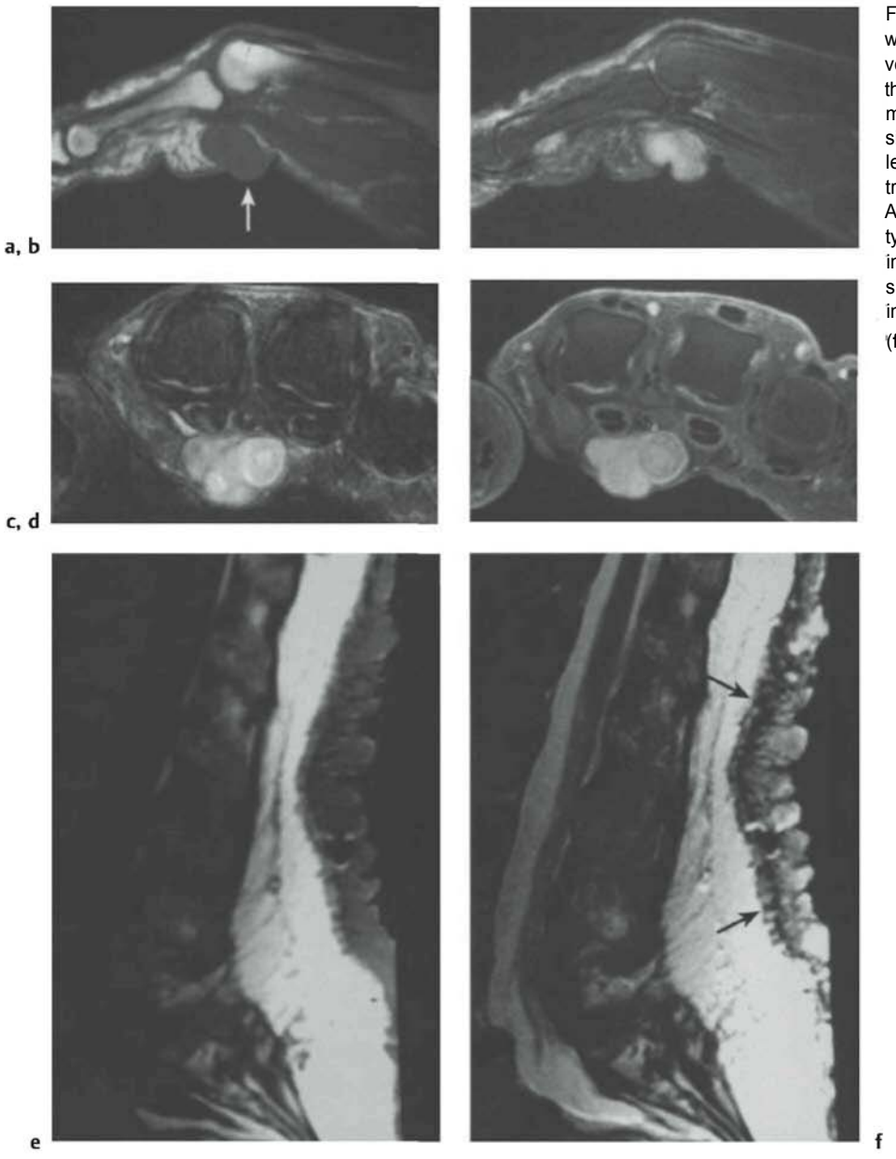

Figure **363** **(a-d)** An 81-year-old woman with a neurofibroma involving the soft tissues ventral to the metacarpophalangeal joint in the hand. The circumscribed lesion has intermediate signal on sagittal (**a**) T1WI, and high signal on sagittal (**b**) and axial (**c**) FST2WI. The lesion shows slightly heterogeneous Cd-contrast enhancement on axial (**d**) FST1WI. (**e, f**) A 68-year-old woman with neurofibromatosis type 1 and multiple cutaneous neurofibromas involving the skin, which have intermediate signal on sagittal T1WI (**e**) and heterogeneous intermediate to high signal on sagittal T2WI (**f**).

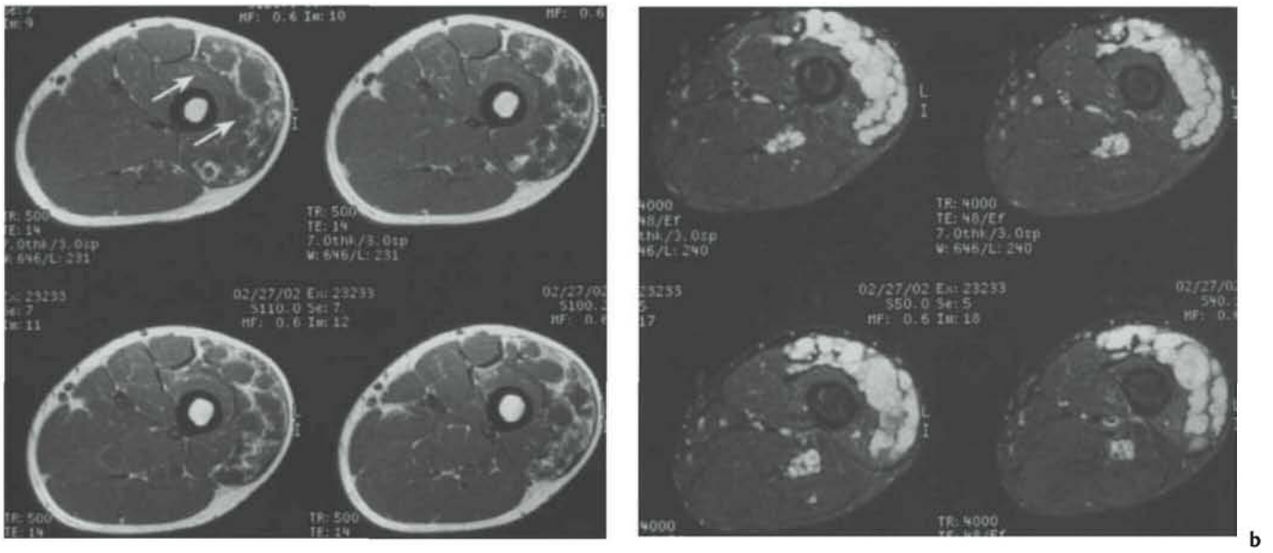

Figure **364a, b** A 13-year-old male with neurofibromatosis type 1 and multiple neurofibromas involving the vastus medialis muscle of the anterior thigh. The lesions have intermediate signal on axial T1WI (**a**) and have high signal on axial FST2WI (**b**).

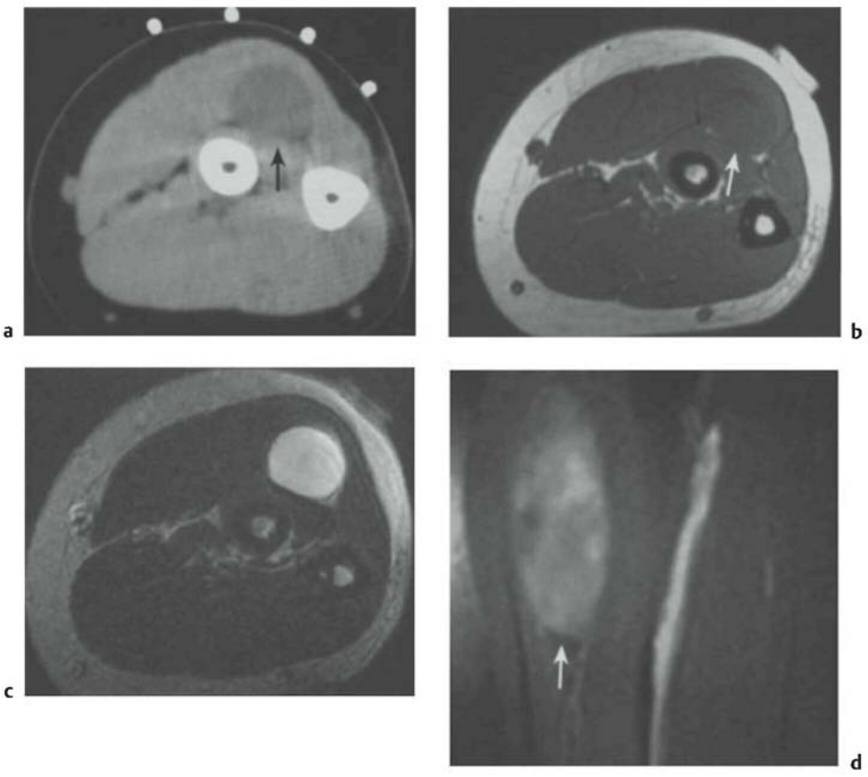

Figure **365 a-d** A 38-year-old man with a neurothekeoma involving the flexor digitorum superficialis muscle of the proximal forearm. Axial CT image (**a**) shows a circumscribed lesion with low-intermediate attenuation. The lesion has low-intermediate signal on axial T1WI (**b**), and high signal on axial T2WI (**c**). The lesion shows moderate heterogeneous Gd-contrast enhancement on sagittal FST1WI (**d**).

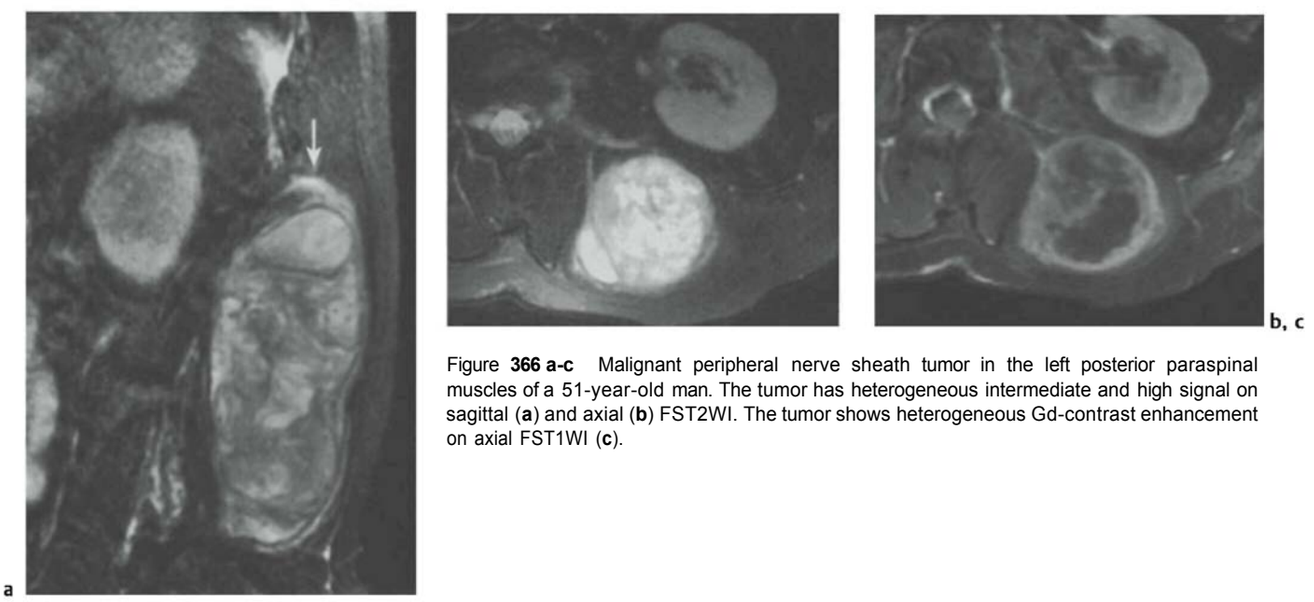

Figure **366 a-c** Malignant peripheral nerve sheath tumor in the left posterior paraspinal muscles of a 51-year-old man. The tumor has heterogeneous intermediate and high signal on sagittal (**a**) and axial (**b**) FST2WI. The tumor shows heterogeneous Gd-contrast enhancement on axial FST1WI (**c**).

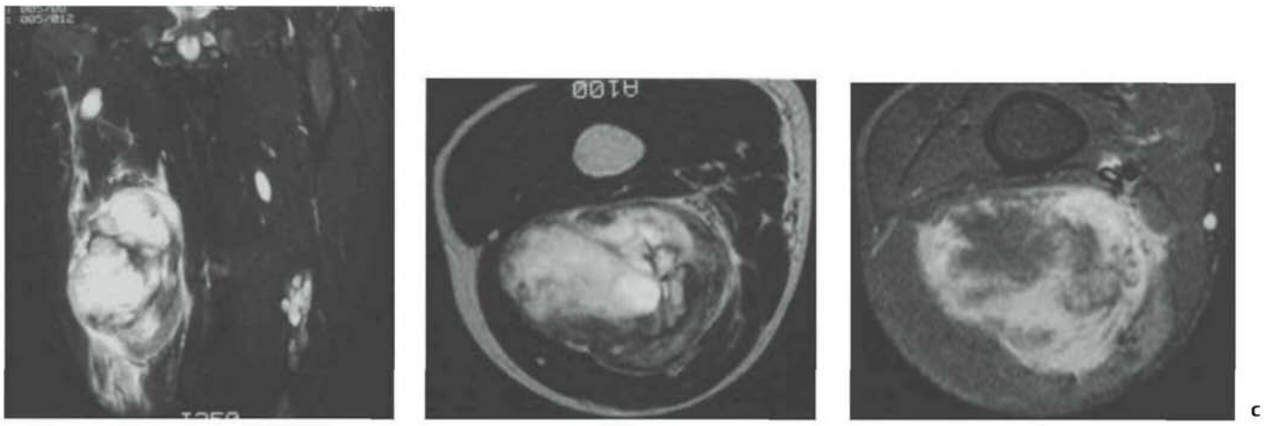

Figure **367 a-c** Malignant peripheral nerve sheath tumor in the posterior soft tissues of the thigh in a 19-year-old man with neurofibromatosis type 1 and multiple neurofibromas in both thighs. A large lesion is seen in the right thigh, which has heterogeneous mostly high signal with strands of low signal on coronal STIR (a). Poorly defined zones of high signal on STIR are seen in the soft tissues adjacent to the tumor. The tumor has mixed high, low and intermediate signal on axial T2WI (**b**). The tumor shows heterogeneous irregular Gd-contrast enhancement on axial FST1WI (**c**). Multiple, small, circumscribed nodular lesions with high signal on STIR are also seen in the soft tissues of both thighs, representing neurofibromas.

Figure **368 a-e** Intra-osseous malignant peripheral nerve sheath tumor in the proximal right femoral shaft of a 35-year-old man with neurofibromatosis type 1. AP radiograph (**a**) shows the intramedullary tumor to be radiolucent with ill-defined margins and associated with cortical disruption and periosteal reaction medially. On MRI, the intramedullary tumor has poorly defined margins and extends through a zone of cortical destruction into the adjacent soft tissues. The tumor has low-intermediate signal on coronal (**b**) T1WI, and heterogeneous high signal on axial FST2WI (**c**). The tumor shows heterogeneous Cd-contrast enhancement on axial (**d**) and coronal (**e**) FST1WI.

References

1 Aoki S, Barkovich AJ, Nishimura K, et al. Neurofibromatosis types 1 and 2: cranial MR findings. *Radiology* 1989;172:527-534.

2 Bancroft LW, Peterson JJ, Kransdorf MJ, Nomikos GC, Murphey MD. Soft tissue tumors of the lower extremities. *Radiol Clin North Am* 2002;40:991-1011.

3 Chung CJ, Armfield KB, Mukherji SK, Fordham LA, Krause WL. Cervical neurofibromas in children with NF-1. *Pediatr Radiol* 1999;29: 353-356.

4 Elster AD. Occult spinal tumors in neurofibromatosis: implications for screening. *AJR Am J Roentgenol* 1995;165:956-957.

5 Huang GS, Lee CH, Lee HS, Chang WC, Juan CJ, Chen CY. Solitary intraosseous neurofibroma of the tibia. *Skeletal Radiol* 2005 ;34: 303-306.

6 Jacquemin C, Bosley TM, Liu D, Svedberg H, Buhaliqa A. Reassessment of Sphenoid Dysplasia associated with neurofibromatosis type. *AJNR AmJNeuroradiol* 2002;23(4):644-648.

7 Khong PL, Goh Winnie HS, Wong Virginia CN, Fung CW, Ooi GC. MR imaging of spinal tumors in children with neurofibromatosis 1. *AJR AmJ Roentgenol* 2003;180(2):413-417.

8 Kransdorf MJ, Murphey MD. Soft tissue tumors in a large referral population: prevalence and distribution of diagnoses by age, sex, and location. In: Kransdorf MJ, Murphey MD, eds. *Imaging of Soft Tissue Tumors* 2nd ed. Philadelphia, Pa: W.B. Saunders; 2006:6-37.

9 Kransdorf MJ, Murphey MD. Neurogenic tumors. In: *Imaging of Soft Tissue Tumors* 2nd ed. Philadelphia, Pa: W.B. Saunders; 2006: 328-380.

10 Kransdorf MJ. Benign soft-tissue tumors in a large referral population: distribution of specific diagnoses by age, sex, and location. *AJR AmJ Roentgenol* 1995; 164:395-402.

11 Lin J, Martel W. Cross-sectional imaging of peripheral nerve sheath tumors. Characteristic signs on CT, MR imaging, and sonography. *AJR AmJ Roentgenol 2Q01;l76C[):75-82.*

12 Mautner VF, Friedrich RE, von Deimling A, et al. Malignant peripheral nerve sheath tumours in neurofibromatosis type 1: MRI supports the diagnosis of malignant plexiform neurofibroma. *Neuroradiology* 2003:45:618-625.

13 Mulder JD, Schutte HE, Kroon HM, Taconis WK. Introduction. In: *Radiologic Atlas of Bone Tumors* Amsterdam: Elsevier; 1993:3-6.

14 Mulder JD, Schutte HE, Kroon HM, Taconis WK. The diagnosis of bone tumors. In: *Radiologic Atlas of Bone Tumors* Amsterdam: Elsevier; 1993:9-46.

15 Mulder JD, Schutte HE, Kroon HM, Taconis WK. Neurofibroma. In: *Radiologic Atlas ofBone Tumors* Amsterdam: Elsevier; 1993:535-539.

16 Murphey MD, Smith WS, Smith SE, Kransdorf MJ, Temple HT. Imaging of musculoskeletal neurogenic tumors: radiologic-pathologic correlation. *Radiographics* 1999;19(5):1253-1280.

17 Muthukumar N. Segmental neurofibromatosis-induced spinaf cord compression. Case report. *J Neurosurg* 2001 ;95(Suppl 2):236-238.

18 O'Rourke H, Meyers SP, Katzman PJ. Neurothekeoma in the upper extremity, magnetic resonance imaging and computed tomography findings.^ *Comput Assist Tomogr* 2005;29:847-850.

19 Pollack IF, MulvihillJJ. Neurofibromatosis 1 and 2. *Brain Pathol* 1997; 7:823-836.

20 Restrepo CS, Riascos RF, Hatta AA, Rojas R. Neurofibromatosis type I. Spinal manifestations of a systemic disease. *J Comput Assist Tomogr* 2005;29:532-539.

21 Saifuddin A. Imaging tumours of the brachial plexus. *Skeletal Radial* 2003:32:375-387.

22 Smirniotopoulos JG, Murphy FM. The Phakomatoses. *AJNR Am J Neuroradiol* 1992;13:725-746.

23 Terry DC, Sauser DD, Gordon MD. Intraosseous malignant peripheral nerve sheath tumor in a patient with neurofibromatosis. *Skeletal Radial* 1998;27:346-349.

24 Thakkar SD, Feigen U, Mautner VF. Spinal tumours in neurofibromatosis type 1: an MRI study of frequency, multiplicity and variety. *Neuroradiology* 1999;41:625-629.

25 Von Deimling A, Foster R, Krone W. Neurofibromatosis type 1. In: Kleihues P, Cavenee WK, eds. *World Health Organization Classification of Tumours. Pathology and Genetics of Tumours of the Nervous System* Geneva: IARC Press; 2000:216-218.

26 Woodruff JM, Kourea HP, Louis DN, Scheithauer BW. Neurofibroma. In: Kleihues P, Cavenee WK, eds. *World Health Organization Classification of Tumours. Pathology and Genetics of Tumours of the Nervous System* Geneva: IARC Press; 2000:167-168.

27 Woodruff JM, Kourea HP, Louis DN, Scheithauer BW. Malignant peripheral nerve sheath tumour (MPNST). In: Kleihues P, Cavenee WK eds. *World Health Organization Classification of Tumours. Pathology and Genetics of Tumours of the Nervous System* Geneva: IARC Press; 2000:172-171.

A 57 Traumatic Neuroma

Definition

Traumatic neuromas are non-neoplastic lesions that result from complete or partial transaction of nerves. The proximal end of the damaged or transected nerve undergoes a benign proliferative process that can be painful.[2,3] Terminal neuromas refer to traumatic neuromas that result from transection or avulsion of nerves and occur 1-12 months after injury.[3] Spindle neuromas refer to focal swelling of intact nerves damaged by chronic friction or irritation.[3]

Location

These lesions often occur above a site of amputation such as involving the lower extremity.[3] Other sites include the oral cavity after tooth extraction.[3] These lesions also involve the brachial plexus and radial nerve.[3]

Signs and Symptoms

Traumatic neuromas may be palpable, firm, soft-tissue lesions[3] Palpation may cause pain.[3] Tapping of the lesion may induce pain (Tinel sign).[3]

Gross Pathologic Findings

Traumatic (terminal) neuromas appear as localized bulbous swellings at the proximal ends of avulsed, or partially/completely transected nerves.[3]

Histopathologic Findings

Traumatic neuromas are non-neoplastic disorganized masses of Schwann cells, axons, endoneurial, and perineurial cells within a dense collagenous matrix containing fibroblasts.[3] These lesions are not encapsulated.[3]

MRI Findings

Traumatic neuromas often appear as bulbous lesions at the end of a transected nerve (terminal neuroma) or as fusiform swelling of an intact nerve (spindle neuroma)[2,3] (Figs. 369-372). Lesions often have low-intermediate signal on T1WI, intermediate signal on PDW1, and mildly heterogeneous intermediate to high signal on T2W1 and FST2WL[1-3]

Differential Diagnosis

Schwannoma, neurofibroma, foreign body, granuloma, scar tissue, hematoma, heterotopic ossification.[2,3]

Prognosis and Treatment

Lesions may be treated with physical therapy and cortisone injection.[2,3] Surgical resection can be performed for lesions not responsive to conservative therapy.[2,3]

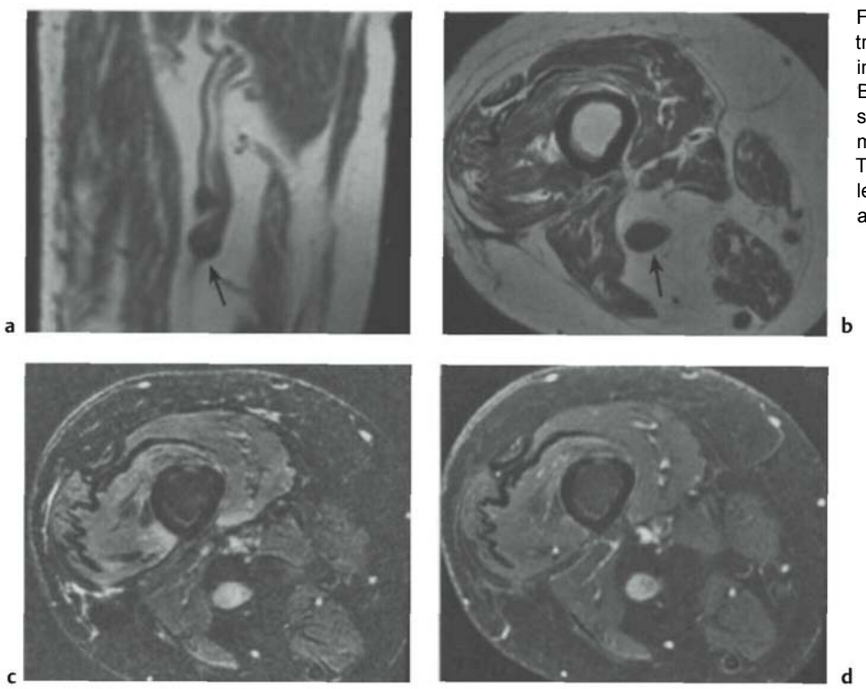

Figure **369a-d** A 60-year-old man with a traumatic neuroma involving the sciatic nerve in the thigh after an amputation of the leg. Bulbous dilatation of the distal transected sciatic nerve is seen which has low-intermediate signal on sagittal (**a**) and axial (**b**) T1WI, and high signal on axial FST2WI (**c**). The lesion shows Gd-contrast enhancement on axial FSTIWI(**d**).

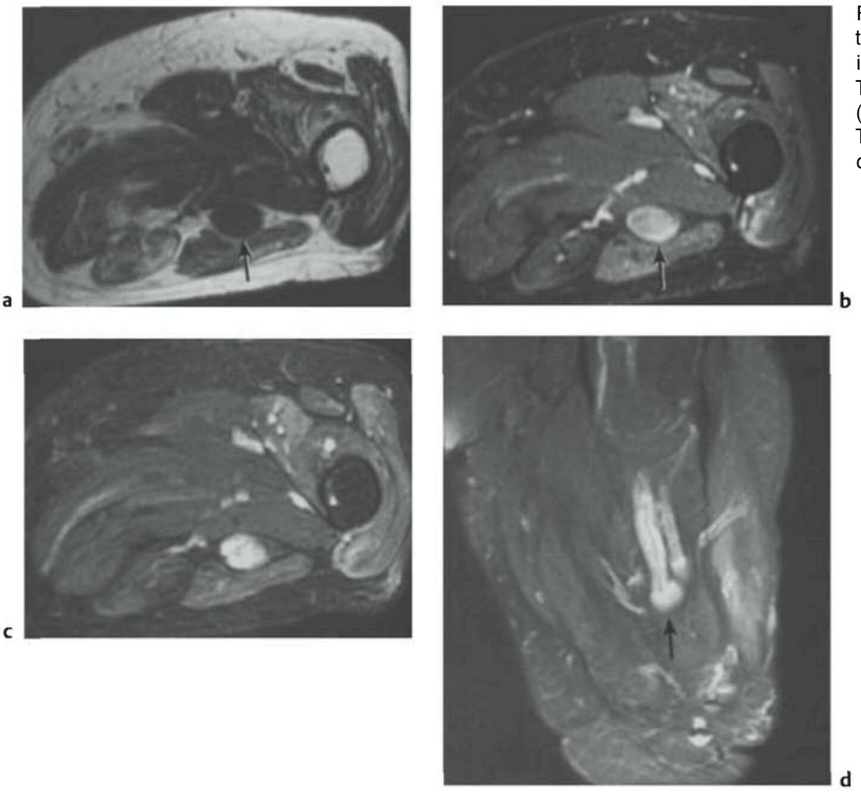

Figure **370a-d** A 33-year-old woman with a traumatic neuroma involving the sciatic nerve in the thigh after an amputation of the leg. The lesion has low- intermediate signal on axial (**a**) T1WI, and high signal on axial (**b**) FST2WI. The lesion shows Gd-contrast enhancement on axial (**c**) and sagittal (**d**) FST1WI.

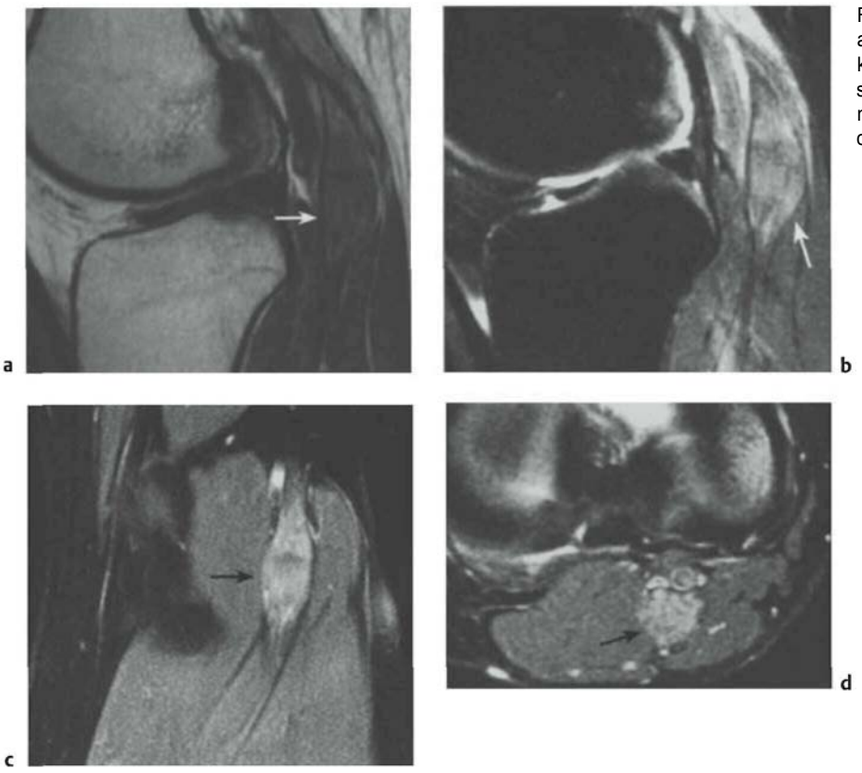

Figure **371 a-d** A 35-year-old woman with a traumatic spindle neuroma posterior to the knee. The fusiform lesion has intermediate signal on sagittal (**a**) PDWI, and heterogeneous mostly high signal on sagittal (**b**), coronal (**c**), and axial (**d**) FST2WI.

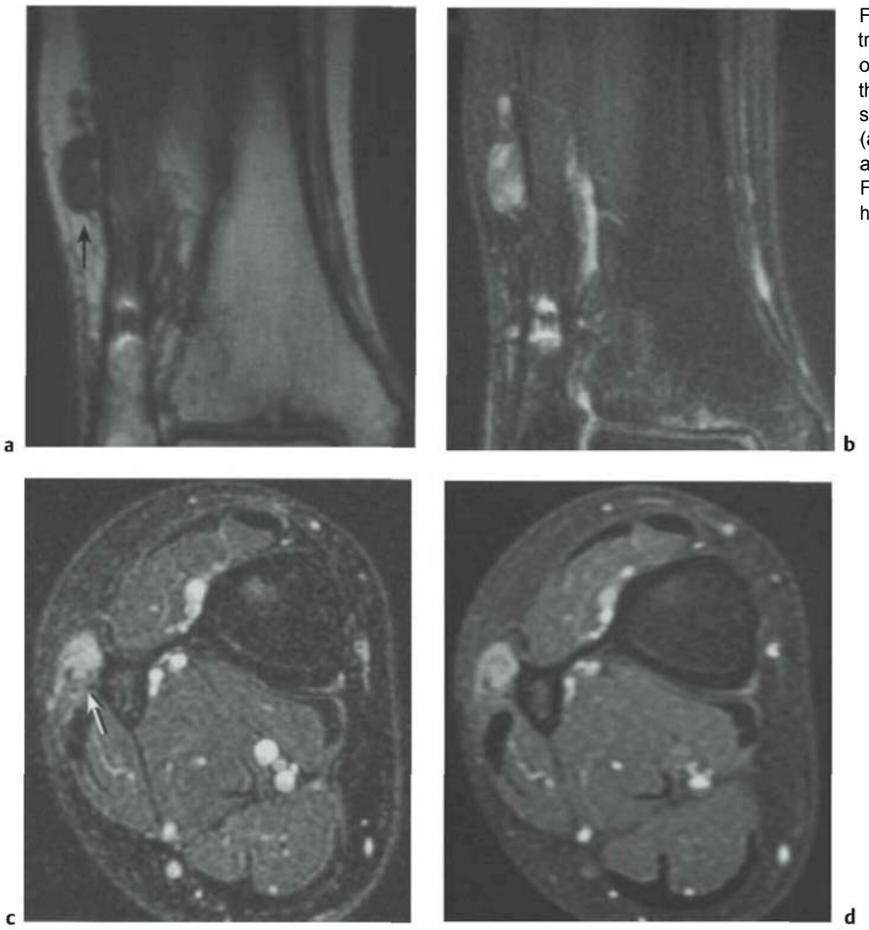

Figure **372 a-d** A 52-year-old woman with a traumatic neuroma involving the soft tissues of the distal lateral leg after a distal fracture of the fibula, requiring fixation. The bulbous lesion has low-intermediate signal on coronal (**a**) T1WI, and heterogeneous slightly high and high signal on coronal (**b**) and axial (**c**) FST2WI. The lesion shows Gd-contrast enhancement on axial FST1WI (**d**).

References

1 Boutin RD, Pathria MN, Resnick D. Disorders in stumps of amputee patients: MR imaging. *AJR Am J Roentgenol* 1998;171:497-501.

2 Kransdorf MJ, Murphey MD. Neurogenic tumors. In: *Imaging of Soft Tissue Tumors* 2nd ed. Philadelphia, Pa: W.B. Saunders; 2006: 328-380.

3 Murphey MD, Smith WS, Smith SE, Kransdorf MJ, Temple HT. From the archives of the AFIP. Imaging of musculoskeletal neurogenic tumors: radiologic-pathologic correlation. *Radiographics* 1999; 19 (5):1253-1280.

A 58 Osteochondroma (Also Referred to as Osteocartilaginous Exostosis)

ICD-O Code

Osteochondroma: 9210/0

Osteochondromatosis: 9210/1

Definition

Osteochondroma is a cartilage-capped, bony lesion that protrudes from the external cortex.[2,4,5,8,18,19,23,27] Beneath the cortex of an Osteochondroma is marrow and spongy bone that is contiguous with the marrow and cancellous bone of the underlying bone.[2,4,5,8,18,19,23,27] Osteochondromas can occur in irradiated bones, usually in children treated for Wilms tumor or neuroblastoma.[19] Approximately 15% of patients with Osteochondroma have multiple lesions, referred to as hereditary multiple exostoses, diaphyseal aclasis, or hereditary Osteochondromatosis.[8] Metachondromatosis is a rare familial syndrome in which multiple osteochondromas of the hands and feet occur in combination with enchondromas in the same bones, as well as periarticular ossifications and calcifications.[2]

In the past, sporadic, single osteochondromas have been considered to be developmental abnormalities rather than neoplasms.[8,23] Recent genetic studies have shown chromosomal and EXT gene mutations in sporadic and hereditary osteochondromas suggesting that both types of lesion are true neoplasms.[8]

Malignant transformation of osteochondromas occurs in less than 1 % of solitary lesions, and between 1 and 5 % of multiple osteochondromas.[2,7,8,19] Most of these malignant tumors are low-grade chondrosarcomas, although rare osteosarcomas have been reported.[2,7,19,21,23]

Frequency of Occurrence

Osteochondromas are common lesions, accounting for 14-35% of primary bone tumors and 5-8% of all primary bone tumors.[16,17,23,26,27] Osteochondromas may develop in up to 12 % of children who received radiation treatment of between 1500 and 5500 cGy for childhood malignancies such as neuroblastoma and Wilms tumor.[19,23] The osteochondromas usually develop from 3 to 17 years after irradiation,[19] mean = 5-12 years.

Age at Presentation

From 1 to 50 years, median = 20 years.[17,27] As many as 60-75% of patients are less than 20years.[17,27] Osteochondromas can present in older patients up to 84years.[4,17,26,27]

Gender Ratio (M /F)

1.7/1to2/1.[4,18,27]

Location

These lesions occur in the femur > humerus > tibia > pelvic bones > scapula > ribs > vertebrae > hands, feet.[4,18,27] The distal metaphysis of the femur and proximal metaphysis of the tibia together account for almost half of all osteochondromas.[4] In long bones the frequency of occurrence is metaphyseal/metadiaphyseal > diaphyseal > epiphyseal.[18,27] Osteochondroma involving the epiphysis is often categorized as dysplasia epiphysealis hemimelica (Trevor disease).[6,9] In vertebrae, lesions occur in the body more frequently than the posterior arch.[18] In patients with hereditary Osteochondromatosis, osteochondromas are often bilateral and relatively symmetric.[2]

Signs and Symptoms

Osteochondromas are often symptomless, and may present as a painless nodular swelling on the affected bone.[4,6,8,18,19,27] Some lesions are associated with mild to moderate pain, often secondary to irritation from distortion or compression of adjacent muscles, nerves, blood vessels, and tendons.[4,6,8,9,12,18,19,23,25,28,30] A bursa may develop over an Osteochondroma, and may be painful when inflamed.[8,18,19,27] Osteochondromas can have more pronounced pain secondary to fracture, infarction, or malignant degeneration.[4,6,8,19] Complications from osteochondromas are more frequent in patients with hereditary multiple exostoses than those with solitary lesions.[19] Malignant transformation of osteochondromas occurs in less than 1 % of solitary lesions, and between 1 and 5% for patients with multiple osteochondromas.[2,7,8,19] Malignant tumors can be associated with pain and increased growth in adults.[2,12,19] Malignant transformation of osteochondromas tends to occur most frequently at lesions located at the pelvis, hips, and shoulder.[6,19] Spinal osteochondromas may be associated with neural compression.[1,4,6,12,13,19,22,24]

Gross Pathologic Findings

Osteochondromas are usually between 1 and 10cm in size, rarely greater,[2,4,19] and can be pedunculated or sessile.[8,23,27] The protruding outer cortex of the Osteochondroma is typically covered by a shiny bluish-white cartilage cap.[2,4,8,19,23,27] The cartilaginous cap in adults after skeletal maturity often measures between 2 and 6 mm in thickness.[4,27] The cartilage cap in young patients before skeletal maturity can range between 10 and 30 mm in thickness.[19] The surface of the cartilaginous cap can be smooth, lobulated, and/or irregular.[2,23] Cartilaginous caps greater than 10-20 mm in thickness after skeletal maturity need to be carefully evaluated for malignant transformation into chondrosarcoma.[4,8,23,27] The marrow and spongy bone under the Osteochondroma is contiguous with the underlying marrow and cancellous bone.[4,8,27] A bursa may be seen over the osteochondroma.[4,8,27] Multiple osseous deformities and short stature are commonly present in patients with hereditary multiple exostoses.[6,9,19,29] Such deformities include ulnar shortening, radial head dislocation at the elbow, coxa valgus at the hip, genu valgus at the knee, valgus deformity at the ankle, and limb length discrepancies.[6,9,19,29]

Histopathologic Findings

The cartilaginous cap of an Osteochondroma consists of hyaline cartilage with endochondral ossification at the base.[2,4,8,23,27] The superficial portion of the cartilage cap contains chondrocytes in aggregates and lacunae.[4,8,23,27] Toward the base of a growing Osteochondroma, chondrocytes are arranged in columns similar to the physeal growth plate.[4,8,19,23,27] The chondrocytes at the base of the lesion show endochondral ossification.[2,8,19] Binucleate chondrocytes may occur in lacunae during growth.[2,4,19,27] A thin fibrous lining (perichondrium) over the cartilaginous cap represents the periosteum of the bone that is lifted up by the

osteochondroma.[2,8,19,27] At the conclusion of skeletal growth, the cartilaginous cap of an osteochondroma typically becomes replaced by bone covered by a thin layer of fibrous tissue containing few chondrocytes.[23] The medullary bone beneath an osteochondroma usually contains predominantly yellow rather than red marrow.[19]

Bursae over large osteochondromas have linings resembling synovium and may on occasion contain secondary synovial chondrometaplasia and/or fibrinous rice bodies.[2,20] Trauma to osteochondromas may result in fracture, as well as fibroblastic proliferation.[27]

Malignant transformation of osteochondromas occurs in less than 1 % of solitary lesions, and between 1 and 5 % for patients with multiple osteochondromas.[2,7,8,19] Features associated with malignant transformation of osteochondromas into chondrosarcomas include: cartilage cap thickness greater than 2cm, distorted architecture of cartilage cap, increased mitotic activity of chondrocytes and cellular atypia, thick fibrous bands, necrosis, and myxoid change.[8,19]

Lesion Genetics

The presence of multiple exostoses or osteochondromatosis is part of the autosomal-dominant syndrome of diaphyseal aclasis, in which there is failure of remodeling of the metaphysis into the diaphysis.[23] Diaphyseal aclasis has been associated with chromosomal deletions or translocations involving chromosome 1l, the long arm of chromosome 8, and the short arm of chromosome 19.[2,8,19,29] The mutated genes involved^ are EXT1, EXT2, and EXT3 located on chromosomes 8q24, 11 p!3, and 19 q, respectively.[7,8,19,23,29] Sporadic, single osteochondromas have also been shown to have cytogenetic abnormalities involving 8 q22-24.1, as well as aneuploidy in the cartilage caps, and loss of the 8 q24.1 locus by fluorescence in situ hybridization (FISH) techniques.[8] These findings suggest that even sporadic osteochondromas are true neoplasms.[8]

Findings on Plain Films (Roentgenograms) and Computed Tomography[2-4,6,9,15,18-20,24,27,29]

Osteochondromas typically show protrusion of cortical and medullary bone relative to adjacent cortical bone.[6,19] The bony protusion can have a narrow neck over which is a spheroid end (pedunculated osteochondroma), or can have a wide neck or base (sessile osteochondroma)[19] (Figs. **373-380, 384, 385).** Pedunculated osteochondromas often point in a direction away from the nearest joint.[19] On radiographs, visualization of the medullary continuity between osteochondroma and the under-

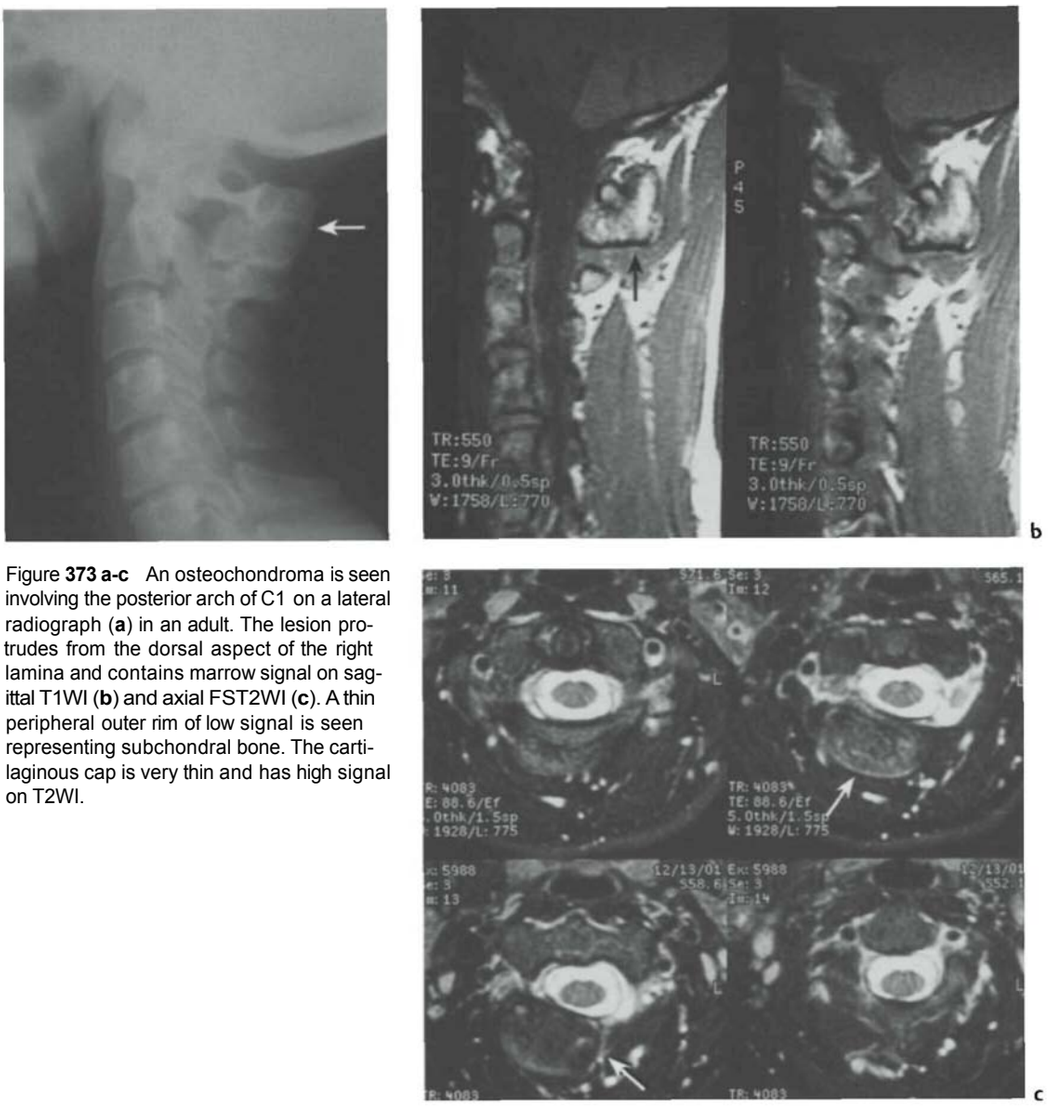

Figure **373 a-c** An osteochondroma is seen involving the posterior arch of C1 on a lateral radiograph (**a**) in an adult. The lesion protrudes from the dorsal aspect of the right lamina and contains marrow signal on sagittal T1WI (**b**) and axial FST2WI (**c**). A thin peripheral outer rim of low signal is seen representing subchondral bone. The cartilaginous cap is very thin and has high signal on T2WI.

lying bone is more readily demonstrated for the pedunculated than the sessile types.[19] CT, however, can easily show the marrow continuity for both pedunculated and sessile osteochondromas.[19] CT has also been useful for demonstrating and localizing the various degrees of endochondral mineralization seen in the marrow underlying osteochondromas, as well as enabling the measurement of the thicknesses of the cartilage caps.[19] The nonmineralized cartilage cap typically has attenuation lower than muscle because of its relatively higher water content.[19]

Osteochondromas can result in erosions, pseudoarthrosis, and/or synostosis with adjacent bones[9,19] (Fig. **374).** Bursae

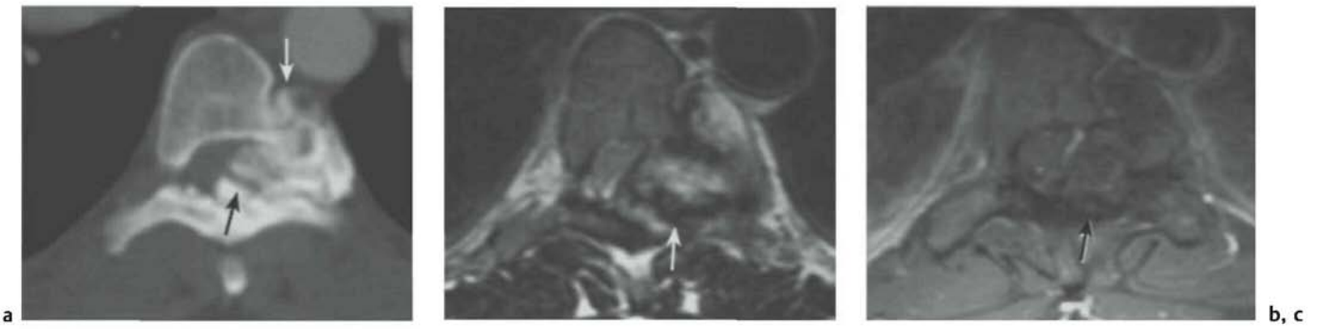

Figure **374a-c** A 43-year-old woman with an osteochondroma involving the left pedicle of a thoracic vertebra with extension of the lesion into the spinal canal resulting in compression of the spinal cord. Axial CT image (**a**) shows the osteochondroma extending into the left foramen and left side of the spinal canal. The lesion has central signal similar to marrow on axial T2WI (**b**) surrounded by a thin rim of low signal from subchondral bone. The cartilaginous cap is very thin and shows minimal Gd-contrast enhancement on axial FST1WI (**c**). A pseudoarthrosis is seen between the lesion and left lateral aspect of the vertebral body and left lamina.

Figure **375a-c** A 48-year-old man with an osteochondroma involving the left inferior articulating process of the L3 vertebra. Axial CT image (**a**) shows a sessile osteochondroma involving the outer left lamina, and inferior articulating process with associated degenerative changes at the facet joint. The medullary portion of osteochondroma is contiguous with the marrow of the adjacent bone, and has signal similar to marrow on axial PDWI (**b**) and axial T2WI (**c**). The lesion is surrounded by a thin rim of low signal from subchondral bone. The cartilaginous cap is very thin.

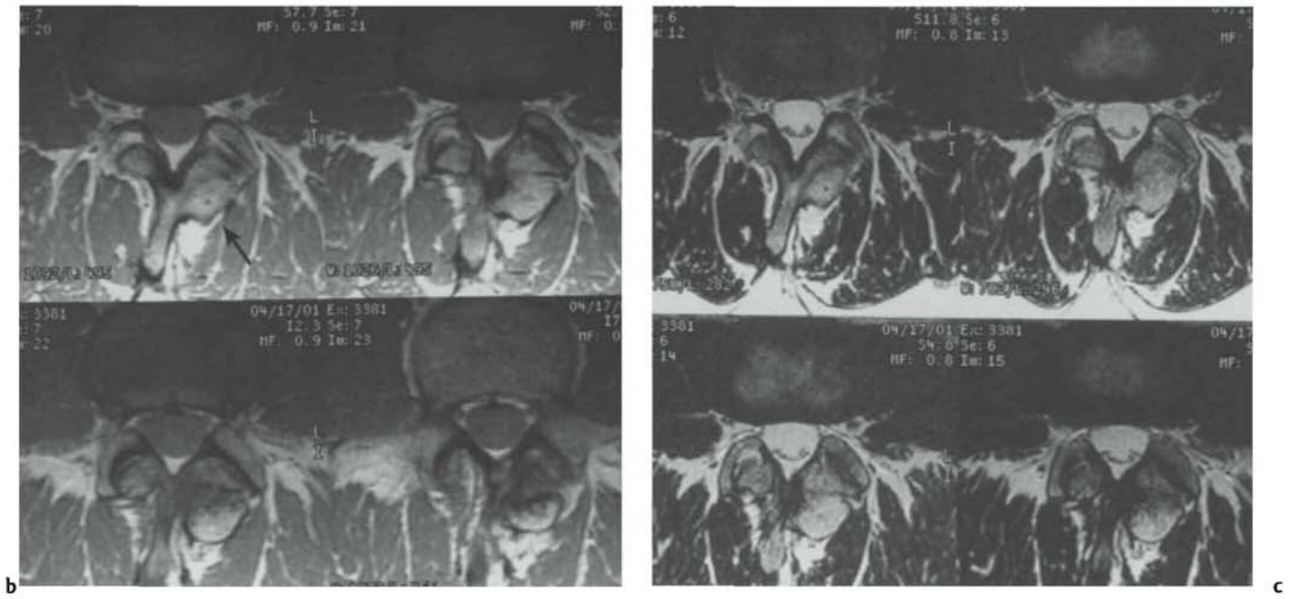

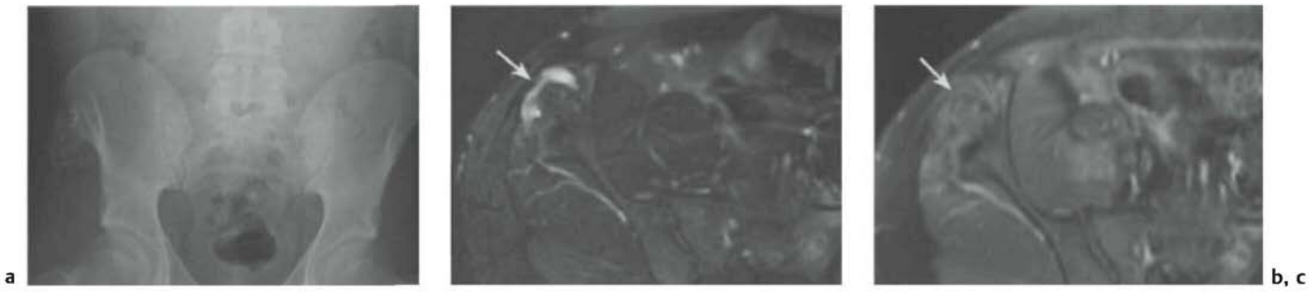

Figure **376a-c** A 20-year-old man with an osteochondroma arising from the right iliac bone. AP radiograph (**a**) shows protrusion of cortical and medullary bone relative to the cortical bone of the upper right iliac bone. The medullary portion of the pedunculated osteochondroma is contiguous with the marrow of the adjacent bone, and has signal similar to marrow on axial FST2WI (**b**). The lesion is surrounded by a thin rim of low signal from subchondral bone. The cartilaginous cap is very thin and shows minimal Cd-contrast enhancement on axial FST1 WI (**c**). A bursa with high signal on FST2WI is seen adjacent to the anterior portion of the osteochondroma.

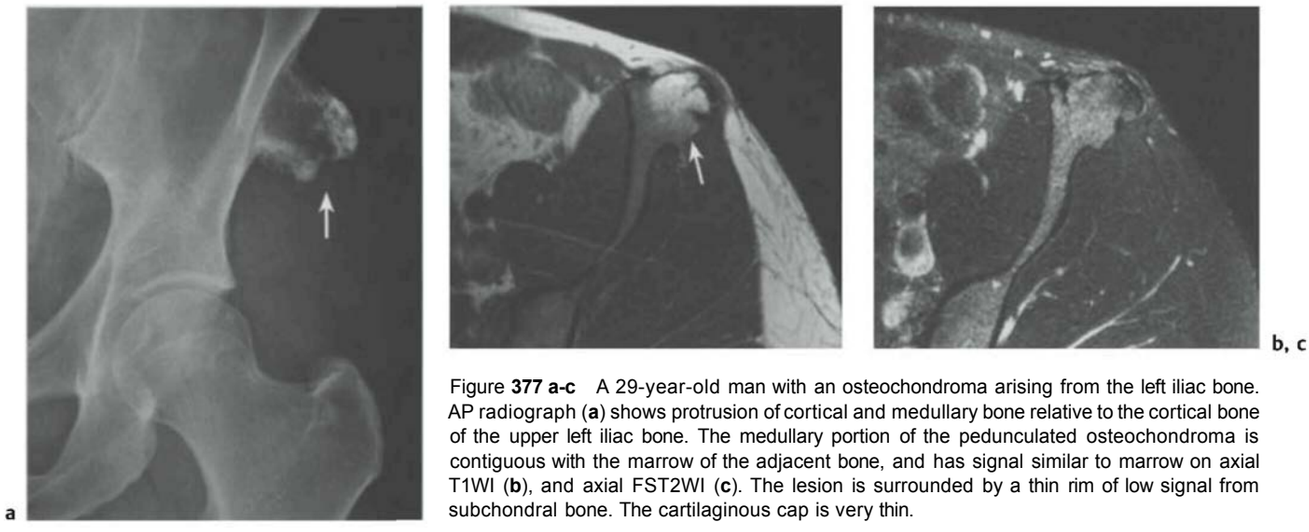

Figure **377 a-c** A 29-year-old man with an osteochondroma arising from the left iliac bone. AP radiograph (**a**) shows protrusion of cortical and medullary bone relative to the cortical bone of the upper left iliac bone. The medullary portion of the pedunculated osteochondroma is contiguous with the marrow of the adjacent bone, and has signal similar to marrow on axial T1WI (**b**), and axial FST2WI (**c**). The lesion is surrounded by a thin rim of low signal from subchondral bone. The cartilaginous cap is very thin.

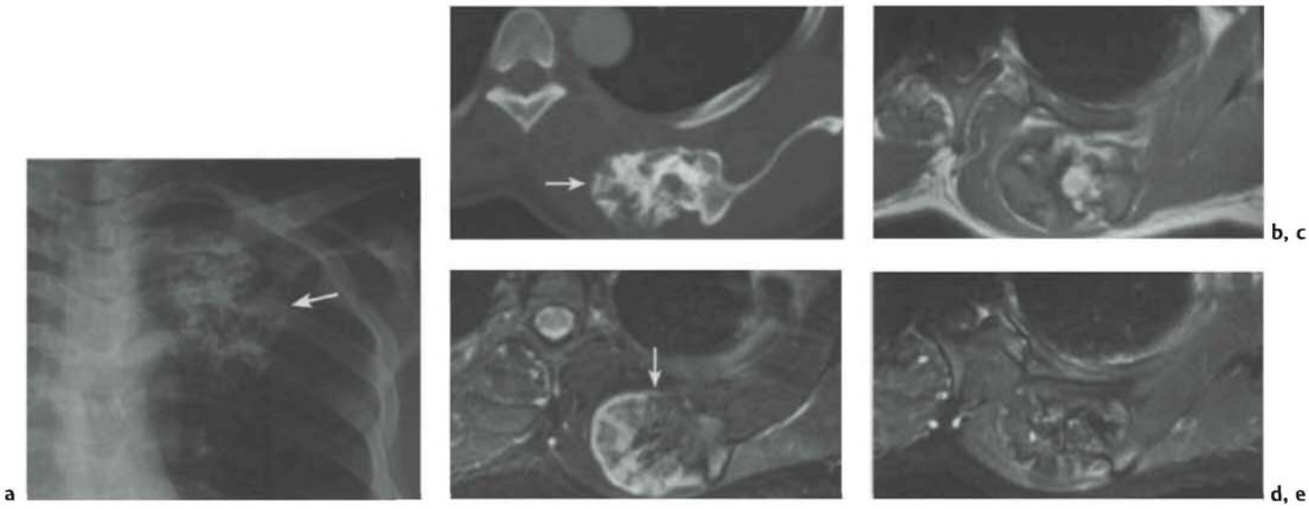

Figure **378a-e** A 43-year-old woman with a pedunculated osteochondroma arising from the left scapula. AP radiograph (**a**) and axial CT image (**b**) show protrusion of cortical and medullary bone relative to the cortical bone of the scapula as well as zones of endochondral mineralization seen in the marrow underlying the osteochondroma. The medullary portion of the pedunculated osteochondroma is contiguous with the marrow of the adjacent bone, and has signal similar to marrow on axial T1WI (**c**) and axial FST2WI (**d**). In addition, endochondral zones in the underlying marrow have low-intermediate signal on axial T1 WI (**c**) and mixed low, intermediate, and high signal on axial FST2WI (**d**). The lesion is surrounded by a thin rim of low signal from subchondral bone. The cartilaginous cap has high signal on FST2WI and is thin, measuring 2-4 mm in thickness. The cartilaginous cap and endochondral sites show minimal Gd-contrast enhancement on axial FST1 W (**e**).

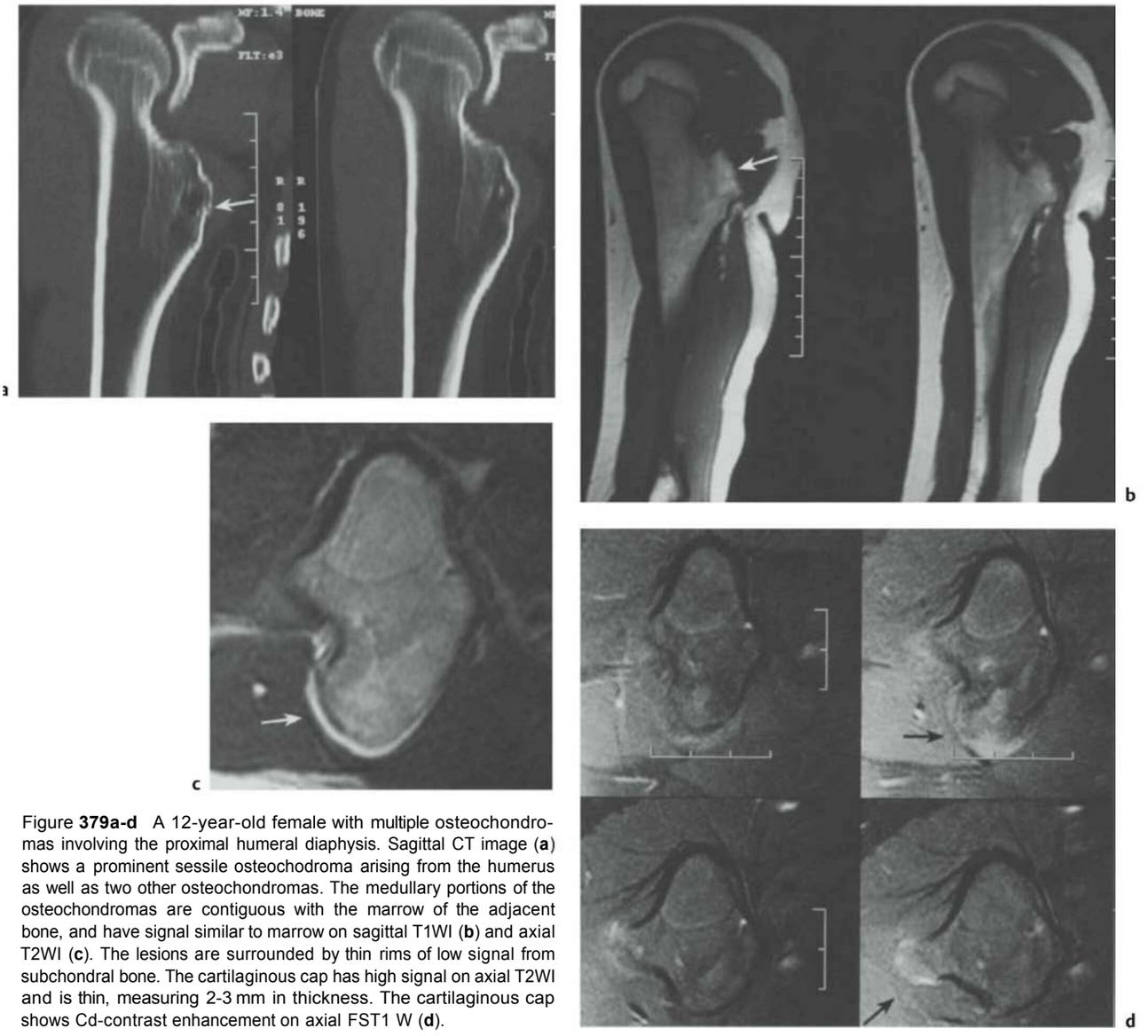

Figure **379a-d** A 12-year-old female with multiple osteochondromas involving the proximal humeral diaphysis. Sagittal CT image (**a**) shows a prominent sessile osteochodroma arising from the humerus as well as two other osteochondromas. The medullary portions of the osteochondromas are contiguous with the marrow of the adjacent bone, and have signal similar to marrow on sagittal T1WI (**b**) and axial T2WI (**c**). The lesions are surrounded by thin rims of low signal from subchondral bone. The cartilaginous cap has high signal on axial T2WI and is thin, measuring 2-3 mm in thickness. The cartilaginous cap shows Cd-contrast enhancement on axial FST1 W (**d**).

over large osteochondromas can contain secondary synovial osteochondromatosis.[20]

CT and radiographic features associated with malignant transformation of osteochondroma include: interval increase in lesion size with the cartilage cap measuring greater than 2 cm in thickness after skeletal maturation, zones of radiolucency within the lesion, irregular surface margins, areas of bone destruction, and prominent soft tissue mass[9,19] (Fig. **385).**

MRI Findings[1,3,5,6,9,11,13,14,18-20,28-30]

MRI readily depicts the cortical and medullary continuity of pedunculated and sessile osteochondromas.[13,19] Cortical bone has low signal on T1VVI, PDWI, T2WI, and FST2WI.[3,6,9,19,29] The medullary portion of osteochondroma is contiguous with the marrow of the adjacent bone, and typically has MRI signal comparable to fatty or yellow marrow with or without zones of low signal on Tl WI, PDWI, T2 Wl, and FS T2WI, resulting from various degrees of calcification or endochondral mineralization[3,9,19,29] (Figs. **373-385).** The cartilage cap typically has low signal on Tl WI, and high signal on PDWI, T2WI, and FST2WI.[3,19] In patients who have not reached skeletal maturity, signal heterogeneity can occur in the cartilage cap on PDWI, T2WI, and FS T2WI from nonmineralized cartilage, calcified cartilage, and ossification with fatty/yellow marrow.[19] A thin rim of low signal on T2WI may be seen at the outer margin of an osteochondroma, representing the perichondrium.[19] After Gd-contrast administration, cartilage caps can show enhancement in peripheral, nodular, and/or septal patterns.[3,19,22,29] Before skeletal maturation, osteochondromas can display a rapid early enhancement pattern.[3]

High signal on T2WI and FST2WI, and Gd-contrast enhancement, are often seen both in and adjacent to bursae that can occur in association with osteochondromas[3,6,9,12,30] (Fig. **382, 383).** Osteochondromas can result in erosions, pseudoarthrosis, and/or synostosis with adjacent bones[9,19] (Fig. **374).** Fractures involving osteochondromas typically show poorly defined areas of low signal on Tl WI, high signal on T2WI and FS T2WI,

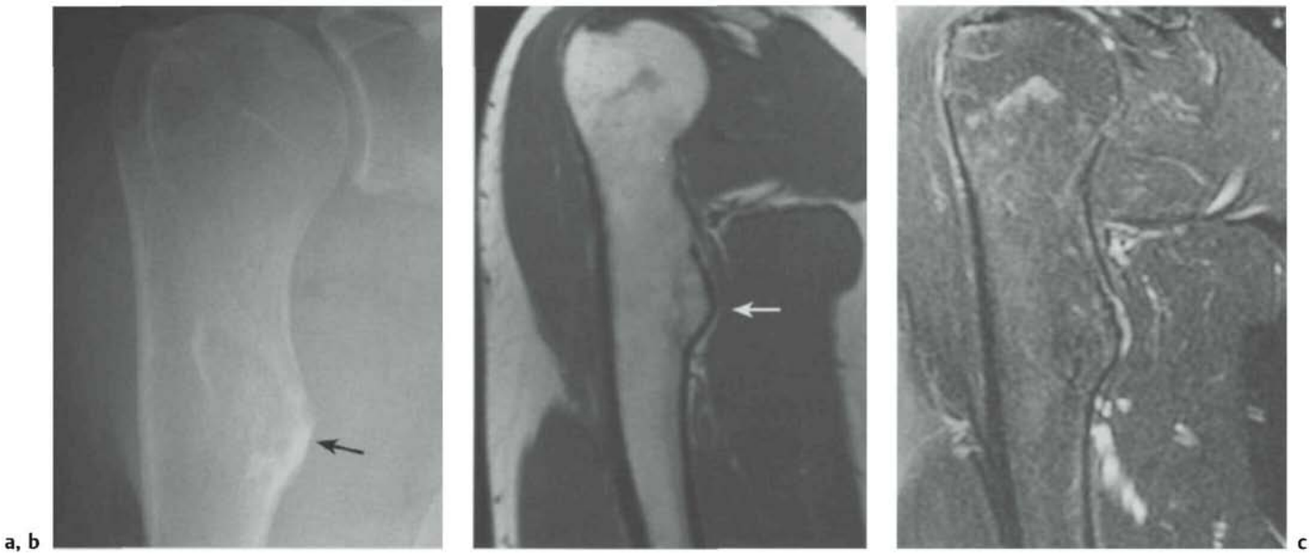

Figure **380a-c** A 35-year-old man with a sessile osteochondroma arising involving the proximal humeral diaphysis. Radiograph (**a**) shows protrusion of cortical and medullary bone relative to the cortical bone of the humerus. The medullary portion of the osteochondroma is contiguous with the marrow of the adjacent bone, and has signal similar to marrow on sagittal (**b**) T1WI and sagittal (c) FST2WI. The lesion is surrounded by a thin rim of low signal from subchondral bone. The cartilaginous cap has high signal on FST2WI and is thin, measuring 2 mm in thickness.

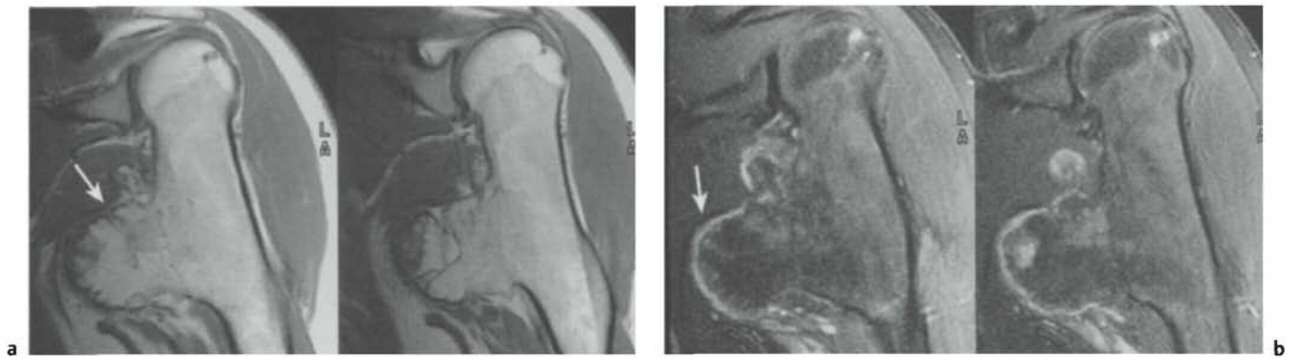

Figure **381 a, b** A 22-year-old man with multiple osteochondromas involving the proximal humeral diaphysis. The medullary portions of the osteochondromas are contiguous with the marrow of the adjacent bone, and have signal similar to marrow on coronal T1WI (**a**) and coronal FST2WI (**b**). The lesions are surrounded by thin rims of low signal from subchondral bone. The cartilaginous caps have high signal on FST2WI and are thin, measuring 2-3 mm in thickness.

and Gd-contrast enhancement.[12] Osteochondromas can cause compression of peripheral nerves resulting in secondary denervation muscular atrophy with fatty changes.[12] Increased signal on T2WI can be seen in muscles compressed and injured by adjacent osteochondromas.[28]

Spinal cord compression can be seen associated with osteochondromas extending into the spinal canal[19,22] (Fig. 374).

MRI can demonstrate vascular complications from osteochondromas such as pseudoaneurysm, venous and arterial thrombosis, and arterial rupture.[6,9,12,25,30]

MRI features associated with malignant transformation of osteochondroma include: cartilage cap more than 1.5cm thick in skeletally mature patients, interval increase in lesion size after skeletal maturation, irregular surface margins, areas of bone destruction, and prominent soft tissue mass[9,11,12,19,30] (Figs. **385, 386).**

Differential Diagnosis

Juxtacortical chondroma, chondrosarcoma, parosteal osteosarcoma, fracture deformity.[9,10,19]

Prognosis and Treatment

Treatment of symptomatic osteochondromas is usually by surgical resection including the periosteum[2,8,19] Recurrences occur in ~2 % of patients.[2,19] Multiple recurrences are often associated with malignancy.[8] Malignant transformation of osteochondromas occurs in less than 1 % of solitary lesions, and between 1 and 5 %, or higher, for patients with multiple osteochondromas.[2,7,8,19,23] Most of these malignant tumors are low-grade chondrosarcomas, and rare osteosarcomas have been reported.[2,7,19,21,23] Surveillance by clinical exam and imaging have been recommended for patients with multiple hereditary exostoses.[19]

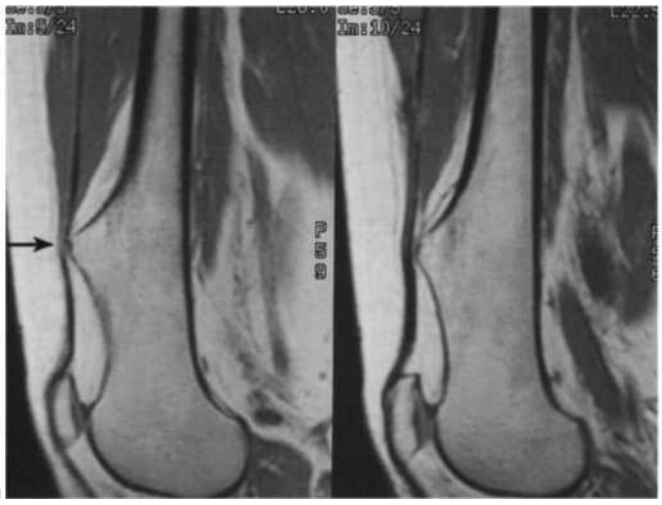

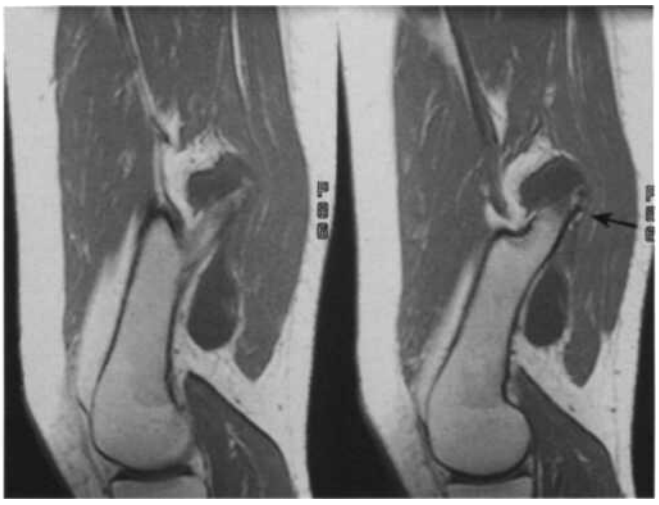

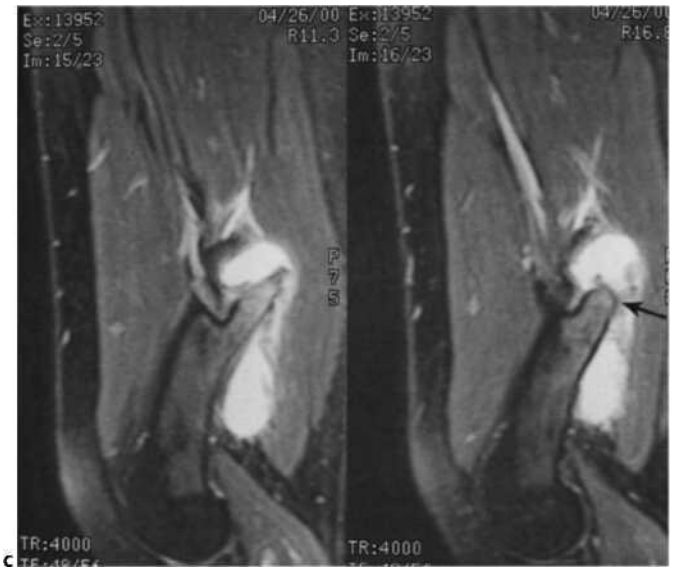

Figure **382 a-c** A 20-year-old woman with multiple osteochondromas involving the distal femoral diaphysis. The medullary portions of the osteochondromas are contiguous with the marrow of the adjacent bone, and have signal similar to marrow on sagittal (**a**, **b**) T1WI, and on sagittal **(c)** FS T2WI. The lesions are surrounded by thin rims of low signal from subchondral bone. The cartilaginous caps are very thin. The osteochondroma located at the dorsal surface of the femur is associated with a bursa containing fluid.

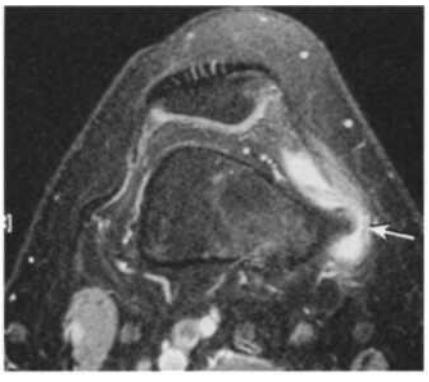

Figure **383a, b** A solitary osteochondroma located at the medial surface of the distal femoral metaphysis femur is associated with a bursa containing fluid. The medullary portion of the osteochondroma is contiguous with the marrow of the adjacent bone, and has signal similar to marrow on sagittal **(a)** PDWI and axial **(b)** FS T2WI. The lesion is surrounded by a thin rim of low signal from subchondral bone. The cartilaginous cap is very thin and is adjacent to a bursa containing fluid.

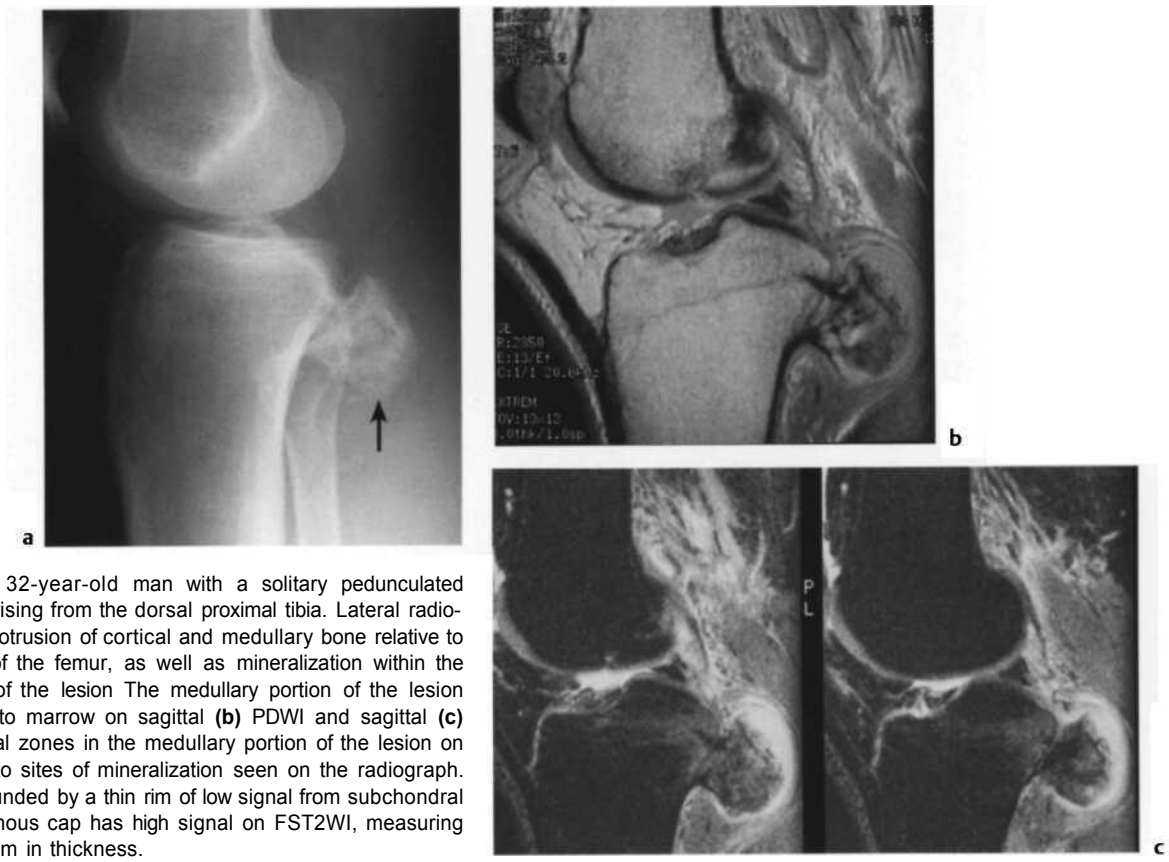

Figure **384a-c** A 32-year-old man with a solitary pedunculated osteochondroma arising from the dorsal proximal tibia. Lateral radiograph **(a)** shows protrusion of cortical and medullary bone relative to the cortical bone of the femur, as well as mineralization within the medullary portion of the lesion The medullary portion of the lesion has signal similar to marrow on sagittal **(b)** PDWI and sagittal **(c)** FST2WI. Low signal zones in the medullary portion of the lesion on PDWI correspond to sites of mineralization seen on the radiograph. The lesion is surrounded by a thin rim of low signal from subchondral bone. The cartilaginous cap has high signal on FST2WI, measuring between 2 and 4 mm in thickness.

Figure **385 a-c** A 30-year-old man who has multiple hereditary exostoses and a secondary low grade chondrosarcoma arising from an osteochondroma at the posterior right iliac bone. Axial CT image **(a)** shows multiple protrusions of cortical and medullary bone relative to the cortical bone of the pelvis representing benign osteochondromas, as well as a chondrosarcoma at the dorsal right iliac bone. The chondrosarcoma contains soft tissue attenuation and foci of chondroid mineralization associated with adjacent bone destruction. The chondrosarcoma has mostly intermediate signal on axial PDWI **(b),** as well as small foci with low and high signal. The tumor shows prominent heterogeneous Gd-contrast enhancement on axial FST1 WI **(b).**

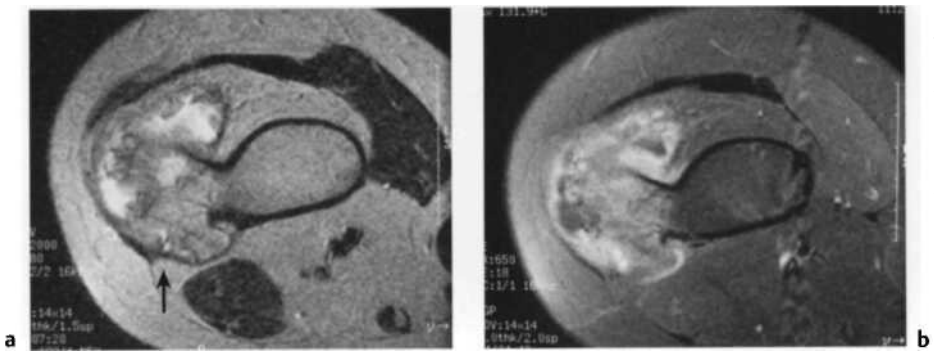

Figure **386a, b** An 18-year-old woman with a secondary low-grade chondrosarcoma arising from an osteochondroma at the distal femur. The tumor has indistinct margins with adjacent cortical and medullary bone, and has heterogeneous intermediate and high signal on axial T2WI (**a**). The tumor shows heterogeneous Gd-contrast enhancement on axial FST1WI (**b**). Zones of cortical destruction are seen.

References

1 Atabay H, Kuyucu Y, Korkmaz 0, Yplikcio31u AC. Myelopathy due to hereditary multiple exostoses**: CT** and MR studies. ***Clin Neurol Neurosurg*** 1996;98:186-188.

2 Forest M. Osteochondroma. In: Forest M, Tomeno B, Vanel D, eds. *Orthopedic Surgical Pathology: Diagnosis of Tumors and Pseudotumoral Lesions of Bone and joints* Edinburgh: Churchill Livingstone; 1998:177-188.

3 Geirnaerdt MJA, Hogendoorn PCW, Bloem JL, Taminiau AHM, van der Woude HJ. Cartilaginous tumors: fast contrast-enhanced MR imaging. *Radiology* 2000;214(2):539-546.

4 Huvos AG. Solitary and multiple osteochondromas and enchondromas; juxtacortical chondroma; Maffucci's disease. In: Huvos AG, ed. *Bone Tumors: Diagnosis, Treatment, and Prognosis* 2nd ed. Philadelphia, Pa: W.B. Saunders; 1991:253-264.

5 Jaramillo D, Laor T, Gebhardt MC. Pediatric musculoskeletal neoplasms: evaluation with MR imaging. *Magn Reson Imaging Clin N Am* 1996;4(4):749-770.

6 Karasick D, Schweitzer ME, Eschelman DJ. Pictorial Essay - Symptomatic osteochondromas: imaging features. *AJR Am J Roentgenol* 1997;168:1507-1512.

7 Kivioja A, Ervasti H, Kinnunen J, Kaitila I, Wolf M, Bohling T. Chondrosarcoma in a family with multiple hereditary exostoses. *J Bone Joint* Surg Br 2000;82(2):261 -266.

8 Khurana J, Abdul-Karim F, Bovee JVMG. Osteochondroma. In: Fletcher CDM, Unni KK, Mertens F, eds. *World Health Organization Classification of Tumours. Pathology and Genetics of Tumours of Soft Tissue and Bone* Geneva: IARC Press; 2002:234-236.

9 Lee KCY, Davies AM, Cassar-Pullicino VN. Imaging the complications of osteochondromas. *Clin Radial* 2002;57:18-28.

10 Lin J, Yao L, Mirra JM, Bahk WJ. Osteochondromalike parosteal osteosarcoma: a report of six cases of a new entity. *AJR Am J Roentgenol* 1998;170:1571-1577.

11 Martin C, Munk PL, O'Connell JX, Lee MJ, Masri B, Wambeek N. Malignant degeneration of an Osteochondroma with unusual intrabursal invasion. *Skeletal Radiol* 1999;28:540-543.

12 Mehta M, White LM, Knapp T, Kandel RA, Wunder JS, Bell RS. MR imaging of symptomatic osteochondromas with pathological correlation. *Skeletal Radiol* 1998;27:427-433.

13 Mermer MJ, Gupta MC, Salamon PB, Benson DR. Thoracic vertebral body exostosis as a cause of myelopathy in a patient with hereditary multiple exostoses. J Spinal *Disord Tech* 2002;15(2):144-148.

14 Meyer JS, Dormans JP. Differential diagnosis of pediatric musculoskeletal masses. Magn Reson *Imaging Clin N Am* 1998;6(3):561-577.

15 Miller SL, Hoffer FA. Malignant and benign bone tumors. *Radiol Clin North Am* 2001;39(4):695-696.

16 Mulder JD, Schutte HE, Kroon HM, Taconis WK. Introduction. In: *Radiologic Atlas of Bone Tumors* Amsterdam: Elsevier; 1993:3-6.

17 Mulder JD, Schutte HE, Kroon HM, Taconis WK. The diagnosis of bone tumors. In: *Radiologic Atlas of Bone Tumors* Amsterdam: Elsevier; 1993:9-46.

18 Mulder JD, Schutte HE, Kroon HM, Taconis WK. Cartilaginous exostosis. In: *Radiologic Atlas of Bone Tumors* Amsterdam: Elsevier; 1993:439-448.

19 Murphey MD, Choi JJ, Kransdorf MJ, Flemming DJ, Gannon FH. From the Archives of the AFIP _ Imaging of osteochondroma: variants and complications with radiologic-pathologic correlation. *Radiographics* 2000;20(5):1407-1434.

20 Peh WCG, Shek TWH, Davies AM, Wong JWK, Chien EP. Osteochondroma and secondary synovial osteochondromatosis. *Skeletal Radiol* 1999;28:169-174.

21 Pierz KA, Womer RB, Dormans JP. Pediatric bone tumors: osteosarcoma Ewing's sarcoma, and chondrosarcoma associated with multiple hereditary osteochondromatosis. J *Pediatr Orthop* 2001;21(3): 412-418.

22 Quirini GE, Meyer JR, Herman M, Russell EJ. Osteochondroma of the thoracic spine: an unusual cause of spinal cord compression. *AJNR AmJNeuroradiol* 1996;17:961-964.

23 Reid RP. Bone neoplasms and tumor-like lesions on the bone surface. In: Helliwell TR, ed. Major *Problems in Pathology: Pathology of Bone and Joint Neoplasms* 1st ed. Vol 37. Philadelphia, Pa: W.B. Saunders; 1999:227-229.

24 Sakai D, Mochida J, Toh E, Nomura T. Spinal osteochondromas in middle-aged to elderly patients. *Spine* 2002;27(23):E503-E506.

25 Sakamoto A, Tanaka K, Matsuda S, Harimaya K, Iwamoto Y. Vascular compression caused by solitary Osteochondroma: useful diagnostic methods of magnetic resonance angiography and Doppler ultrasonography. *J Orthop Sci* 2002;7(4):439-443.

26 Unni KK. Introduction and scope of study. In: *Dahlin's Bone Tumors-General Aspects and Data on* 11087 Cases 5th ed. Philadelphia, Pa: Lippincott, Williams & Wilkins; 1996:1-9.

27 Unni KK. Osteochondroma (osteocartilaginous exostosis). In: *Dahlin's Bone Tumors—General Aspects and Data on 11 087 Cases* 5th ed. Philadelphia, Pa: Lippincott, Williams & Wilkins; 1996:11-23.

28 Uri DS, Dalinka MK, Kneeland JB. Muscle impingement: MR imaging of a painful complication of osteochondromas. *Skeletal Radiol* 1996;25:689-692.

29 Vanhoenacker FM, Van Hul W, Wuyts W, Willems PJ, De Schepper AM. Hereditary multiple exostoses: from genetics to clinical syndrome and complications. *EurJ Radiol* 2001;40:208-217.

30 Woertler K, Lindner N, Gosheger G, Brinkschmidt C, Heindel W. Osteochondroma: MR imaging of tumor-related complications. *Eur Radiol* 2000; 10(5):832-840.

A 59 Osteofibrous Dysplasia (Also Referred to as Ossifying Fibroma of the Tibia and/or Fibula, Cortical Fibrous Dysplasia)

Definition

Osteofibrous dysplasia is a self-limited, benign, fibro-osseous lesion primarily involving the anterior midshaft of the tibia in children.[6,7,11,16,21] Osteofibrous dysplasias represent rare bone lesions that typically involve the cortex of the tibia and/or fibula in children and adolescents.[1421] Osteofibrous dysplasia has also been referred to as: Kempson-Campanacci lesion, congenital fibrous defect of the tibia, congenital osteitis fibrosa, congenital pseudoarthrosis, and intracortical fibrous dysplasia.

Frequency of Occurrence

These lesions account for < 1 % of primary bone lesions.

Age at Presentation

Congenital to 35 years, median age for males = 10 years, median age for females = 13.5 years.[16,19,20]

Gender Ratio (M / F)

1 / 1 to 1.2/1.[12,16,20]

Location

These lesions occur in the tibia (85%) > tibia and fibula (11 %) > fibula (4%).[16] Lesions occur in the mid-diaphysis (59%) > proximal third of diaphysis (29%) > distal third of diaphysis (7%) > proximal metaphysis (5%).[16] Osteofibrous dysplasia usually involves the anterior cortex of the tibia.[11,16,20] Medullary extension of osteofibrous dysplasia occurs in ~10%.[20]

Signs and Symptoms

These lesions can be asymptomatic.[14] Patients with osteofibrous dysplasia may present with localized pain (25-60%), localized swelling (9-43%), tibial protuberance and anterior bowing (6-13%), or pathologic fracture (13-37 %).[16,20,21]

Cross Pathologic Findings

osteofibrous dysplasia appears as pale-white, white-yellow, gray-tan, and/or reddish soft and/or firm, gritty tissue blending into surrounding cortical bone.[12,16,21] The involved bone cortex may be thinned or focally absent.[21] The perisoteum is usually intact.[21] A scleortic bony margin as seen with lesions that extend into medullary bone.[21] Lesions range in size from 3 cm to nearly the entire bone length.[16]

Histopathologic Findings

Osteofibrous dysplasia typically shows zones of irregularly shaped trabeculae of woven bone rimmed by well-defined osteoblasts within a stroma of benign, well-vascularized fibrous tissue.[16,7,14,16,21,22] The fibrous stroma consists of spindle cells with collagen production and variable myxoid material.[12,14,16,21] The spindle cells show immunopositivity for vimentin,[12,21] as well as neurofibromin (30%), and Schwann cell markers S-100 protein (53%), and Leu-7 (30%).[18] Mitoses are rarely seen.[12,14,16,21] The woven bony trabeculae show varying degrees of calcification and ossification.[12,14,16] A zonal pattern of bony trabeculae is seen in 86 % of specimens.[16] This zonal architecture consists of central regions with sparse, thin, immature trabeculae of woven bone within fibrous tissue that peripherally becomes progressively replaced by numerous, larger, and more-mature trabeculae that eventually anastomose and merge into lamellar bone of the adjacent bone cortex.[12,14,16,21] Cartilage and aggregates of epithelial cells are absent; and hemorrhage, cyst formation, giant cells, xanthomatous change, and hyalinization are rare.[21]

Osteofibrous dysplasia and fibrous dyplasia may share some patterns of formation.[17] Osteofibrous dysplasia can be distinguished from mono-ostotic fibrous dysplasia because its bony trabeculae are rimmed by osteoblasts and are composed of both woven and lamellar bone, which are features not seen with fibrous dysplasia.[4,9] Cytokeratin-positive cells are found in most cases of osteofibrous dysplasia and not in fibrous dysplasia.[12]

Osteofibrous dysplasia and fibrous dysplasia share some immunohistochemical expressions (c-fos, c-jun products, type 1 collagen, osteopontin); although these two disorders differ in their immunoreactivity to osteonectin (osteofibrous dysplasia=82%, fibrous dysplasia=5%).[17] Osteofibrous dysplasia can show immunoreactivity to neurofibromin and S-100 protein, whereas fibrous dysplasia does not.[18]

In some cases, immunoreactivity of osteofibrous dysplasia for cytokeratin subtypes can be similar to adamantinoma.[10,12,21] These cases of osteofibrous dysplasia are often referred to as osteofibrous dysplasia-like adamantinoma.[21]

Lesion Genetics

Cytogenetic abnormalities associated with osteofibrous dysplasia include trisomy for chromosomes 7, 8, 12, and 22.[5,21]

Findings on Plain Films (Roentgenograms) and Computed Tomography

Osteofibrous dysplasia typically appears as multifocal, circumscribed, radiolucent zones with sclerotic margins seen in bone cortex.[1-8,11-16,19-22] (Figs. **387-390).** The radiolucent lesions may have a "saw tooth" appearance.[14] Unifocal, radiolucent, cortical lesions occur infrequently.[12] The outer and inner sclerotic margins range from thick to thin.[16] The expanded inner sclerotic margins may cause narrowing of the medullary canal.[7] The radiolucent lesions are often eccentric within bone cortex, measure more than 3 cm in length and usually involve between 10 and 40% of the bone length.[16] The radiolucent zones may rarely have a hazy or ground glass appearance, similar to fibrous dysplasia.[7,12,16] The involved cortex can be thickened.[16] Anterior bowing deformities of the tibia may occur.[12,16] No juxtacortical soft tissue lesions are seen.[16] Pathologic fractures occur in 13 % of cases, and are associated with periosteal reaction.[16] Pseudoarthroses may result from pathologic fractures.[3] CT can demonstrate the degree of medullary narrowing.[12]

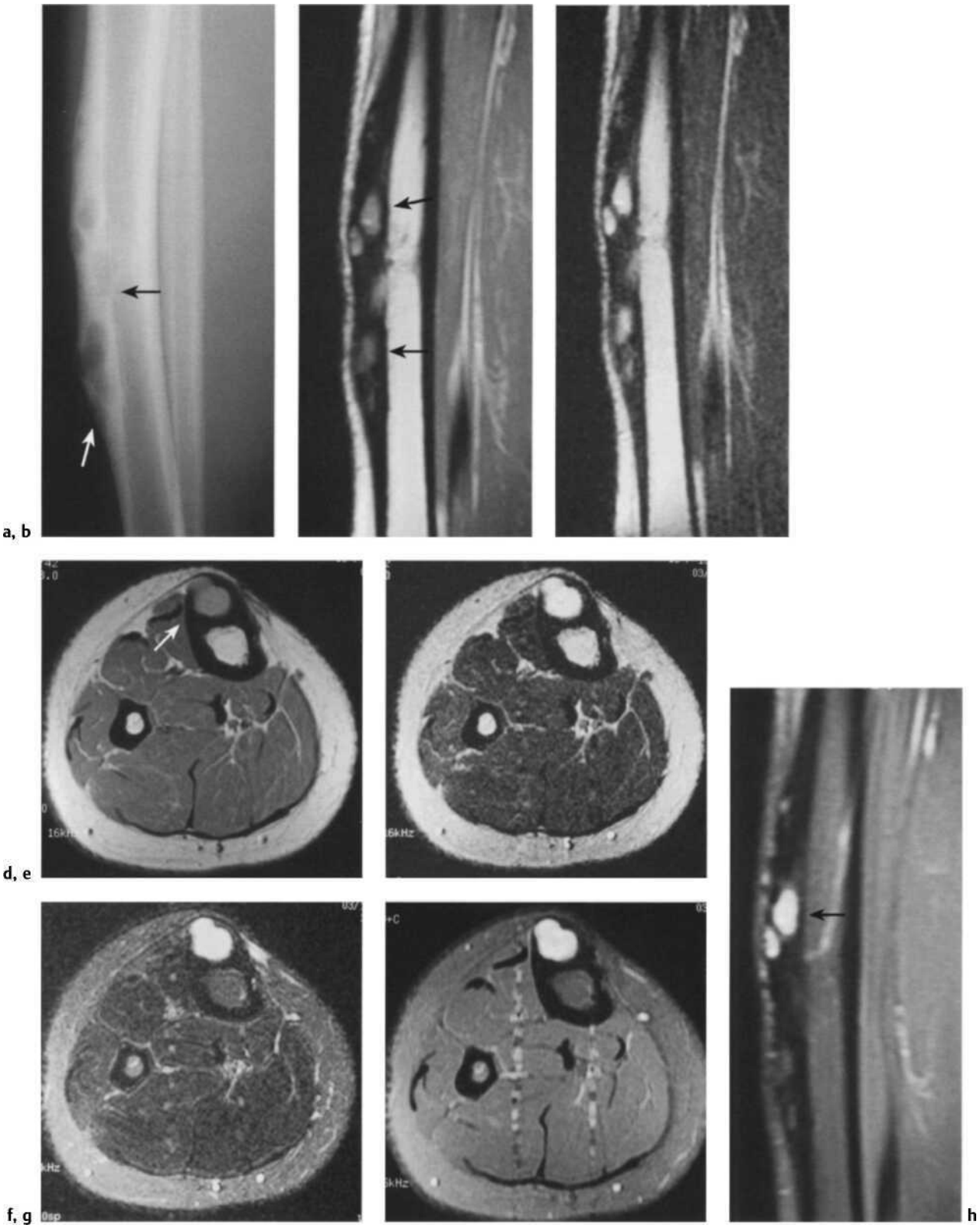

Figure **387 a-h** A 15-year-old female with osteofibrous dysplasia involving the anterior cortex of the tibial diaphysis. Lateral radiograph **(a)** shows thickening of the anterior tibial cortex, within which are multiple, various-sized, circumscribed radiolucent zones. Mild anterior tibial bowing is seen. Within the thickened anterior tibial cortex, there are multiple irregular zones with low-intermediate signal on sagittal T1WI **(b),** intermediate to slightly high signal on axial PDWI **(d),** and high signal on sagittal **(c)** and axial **(e)** T2WI and axial **(f)** FST2WI. Zones of low signal on T1WI and T2WI are seen superficial and deep to the lesions, representing sclerotic bone reaction. The outer cortical margin is expanded and thinned. The intracortical foci show prominent Gd-contrast enhancement on axial **(g)** and sagittal **(h)** FST1WI.

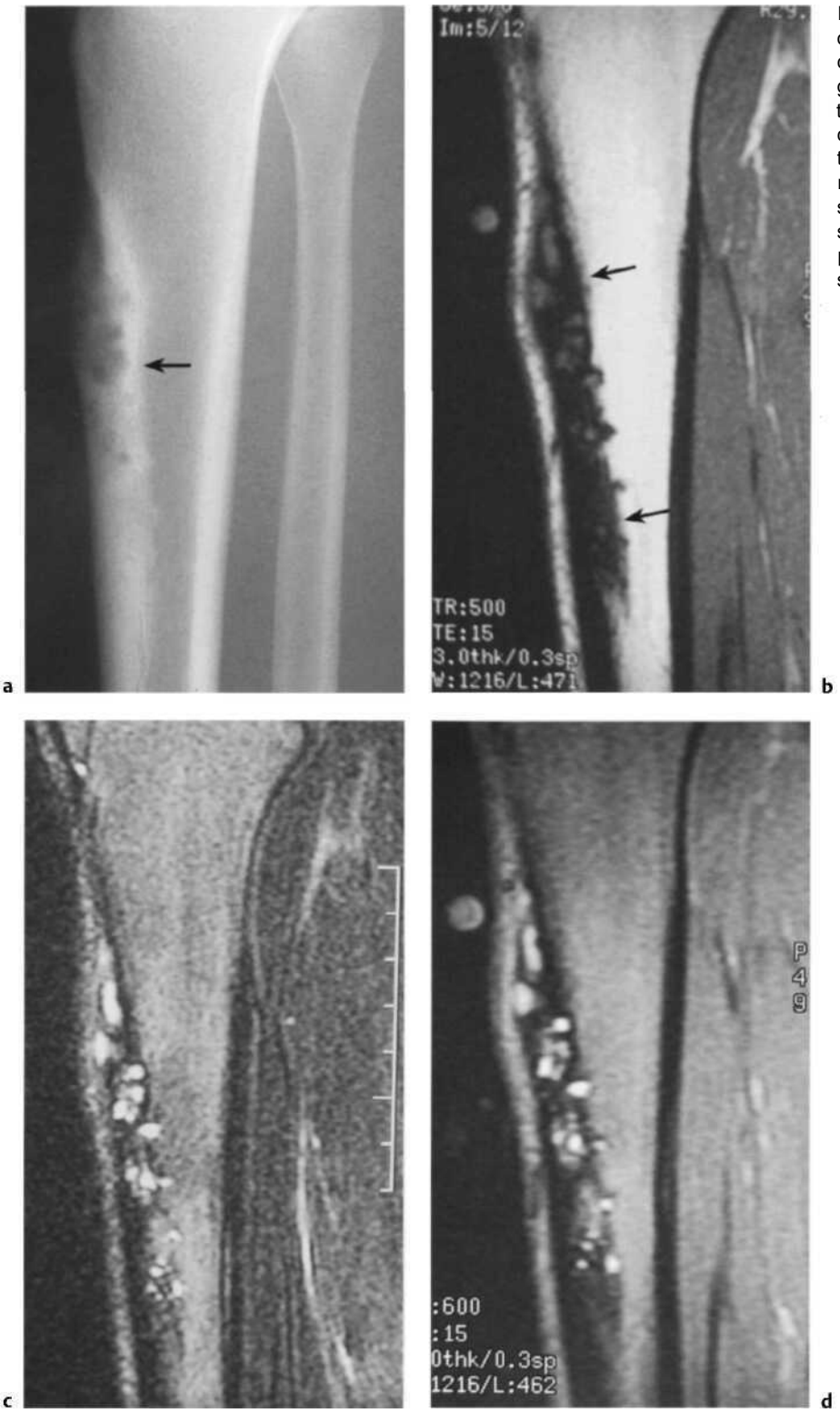

Figure **388a-d** A 17-year-old female with osteofibrous dysplasia involving the anterior cortex of the tibial diaphysis. Lateral radiograph **(a)** shows thickening of the anterior tibial cortex, within which are multiple, small, circumscribed radiolucent zones. Within the thickened anterior tibial cortex, there are multiple small zones with low-intermediate signal on sagittal T1WI **(b),** and high signal on sagittal FS T2WI **(c)**. The intracortical foci show prominent Gd-contrast enhancement on sagittal FST1WI **(d).**

MRI Findings[2,11,15]

Osteofibrous dysplasia often shows multiple irregular intracortical zones of low-intermediate signal on Tl W images, intermediate to slightly high signal on PDWI, and high signal on T2W1 and FST2WI separated by irregular zones of low signal on T1W1 and T2WI, the latter representing sclerotic cortical bone[2,11,15] (Figs. **387-390).** Unifocal lesions are less common. Zones of low signal on T1WI and T2WI of varying thickness are typically seen superficial and deep to the lesions, representing sclerotic bone reaction.[2,11] The outer cortical margins can be expanded and markedly thinned.[2] Medullary narrowing can be severe from extension of osteofibrous dysplasia arising from the cortex.[11]

After Gd-contrast administration, the intracortical lesions usually show prominent enhancement. MRI can depict the

a

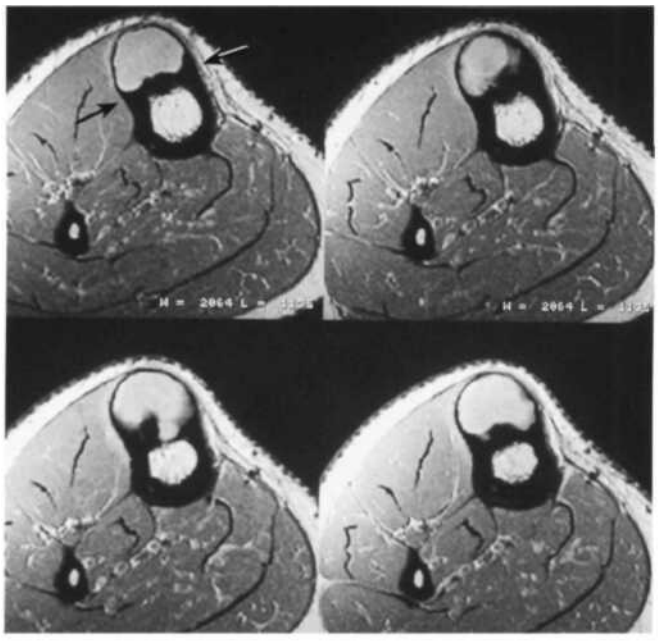

b

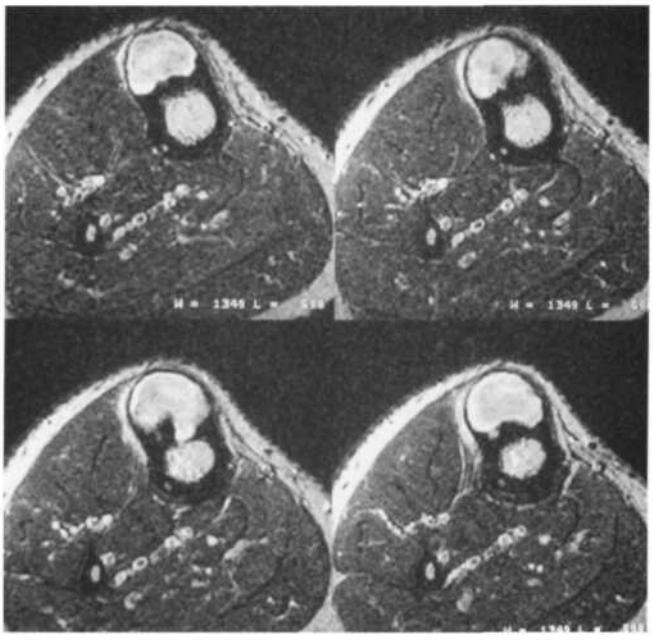

c

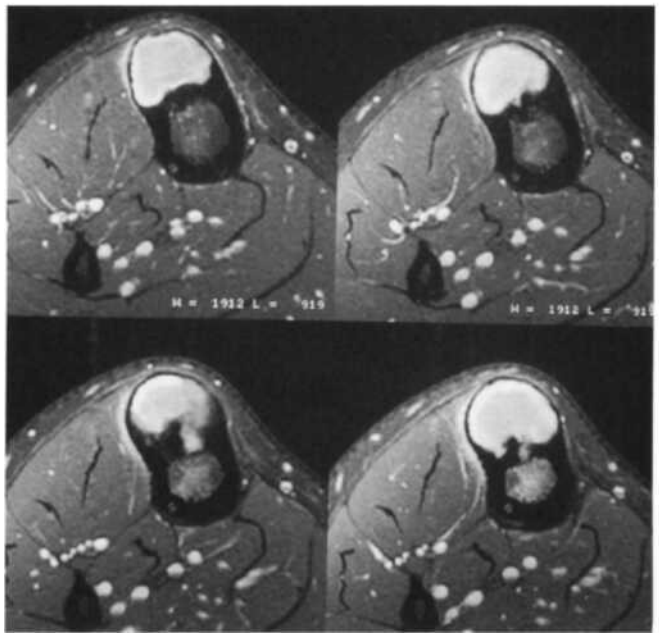

d

Figure **389a-d** An 18-year-old female with a post-traumatic fracture through osteofibrous dysplasia involving the anterior cortex of the tibial diaphysis. Lateral radiograph **(a)** shows thickening and expansion of the anterior tibial cortex, within which are multiple, various-sized, circumscribed radiolucent zones, as well as a fracture. Within the thickened anterior tibial cortex above the fracture, there are zones with intermediate to slightly high signal on axial PDWI **(b)**, and high signal on axial T2WI **(c)**. The outer cortical margin is expanded and markedly thinned. The intracortical foci show prominent Gd-contrast enhancement on axial **(d)** FST1WI.

extent of medullary narrowing. No extra-osseous soft tissue masses are seen. Thin juxtacortical/periosteal enhancement may be seen in lesions with thinned and expanded cortical margins.

Prominent, diffuse high signal on T2W1 and marrow enhancement are seen for lesions with acute/subacute pathologic fractures. Prominent periosteal/juxtacortical Gd-contrast enhancement is typically seen with lesions complicated by pathologic fractures.

Differential Diagnosis

Fibrous dysplasia, adamantinoma, metastatic disease, osteomyelitis, eosinophilic granuloma, healing fracture.

Prognosis and Treatment

Osteofibrous dysplasia often shows gradual, slow growth in children, which attenuates at 15 years of age.[21] Osteofibrous dysplasia may spontaneously resolve.[12,21] The subtype referred

a

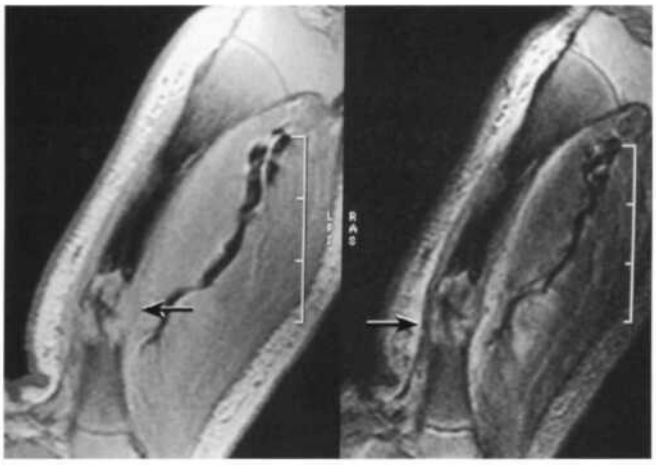

b

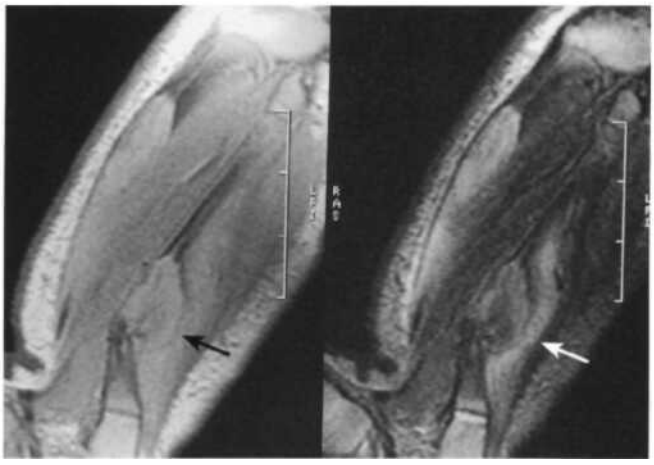

c

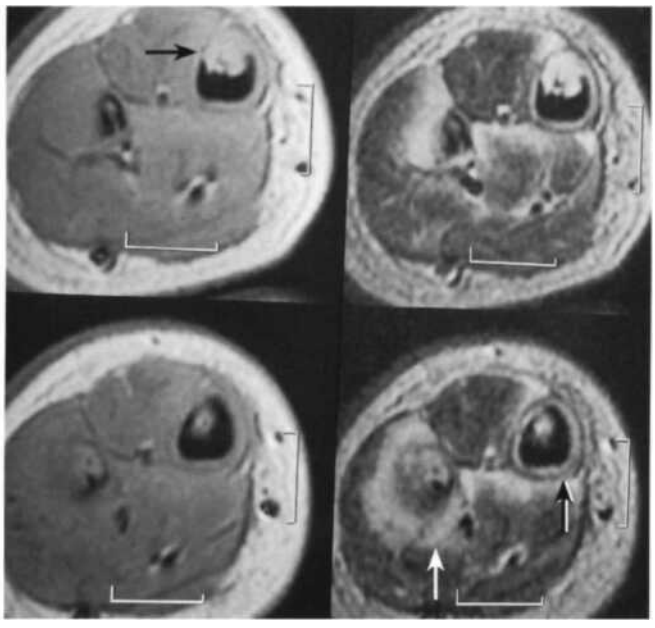

d

Figure **390 a-f** A 6-day-old neonate with pathologic fractures secondary to osteofibrous dysplasia involving the distal diaphyseal portions of the tibia and fibula. Radiograph (**a**) through a cast shows pathologic fractures at zones of radiolucency, expansion, and cortical irregularity at the distal fibula and tibia. The lesion in the tibia involves medullary bone and is associated with thinning and marked expansion of bone cortex on sagittal (**b**, left image) and axial (**d,** left images) PDWI, and sagittal (**b**, right image) and axial (**d**, right images) T2WI. The outer cortical margin is expanded and markedly thinned. Similar findings are seen at the lesion involving the fibula (**c, d**). Both lesions have heterogeneous intermediate to slightly high signal and low signal on PDWI, and mixed low, intermediate, and high signal on T2WI. Irregular zones of prominent Gd-contrast enhancement are seen at both lesions on axial FST1 WI (**e, f**), which is likely due in part to the pathologic fractures associated with the lesions.

Figure **390e-f** t>

to as osteofibrous dysplasia-like adamantinoma may show slow progressive growth, but rarely progresses to classic adamantinoma.[21] In children less than 15 years of age, surgery for osteofibrous dysplasia is performed for pseudoarthroses, accentuated tibial bowing, and/or extensive lesions that are prone to fracture or have already fractured.[7,12,16] Surgery consists of either curettage with cryosurgery and bone grafting or excision with wide margins followed by bone grafting.[12,14,23]

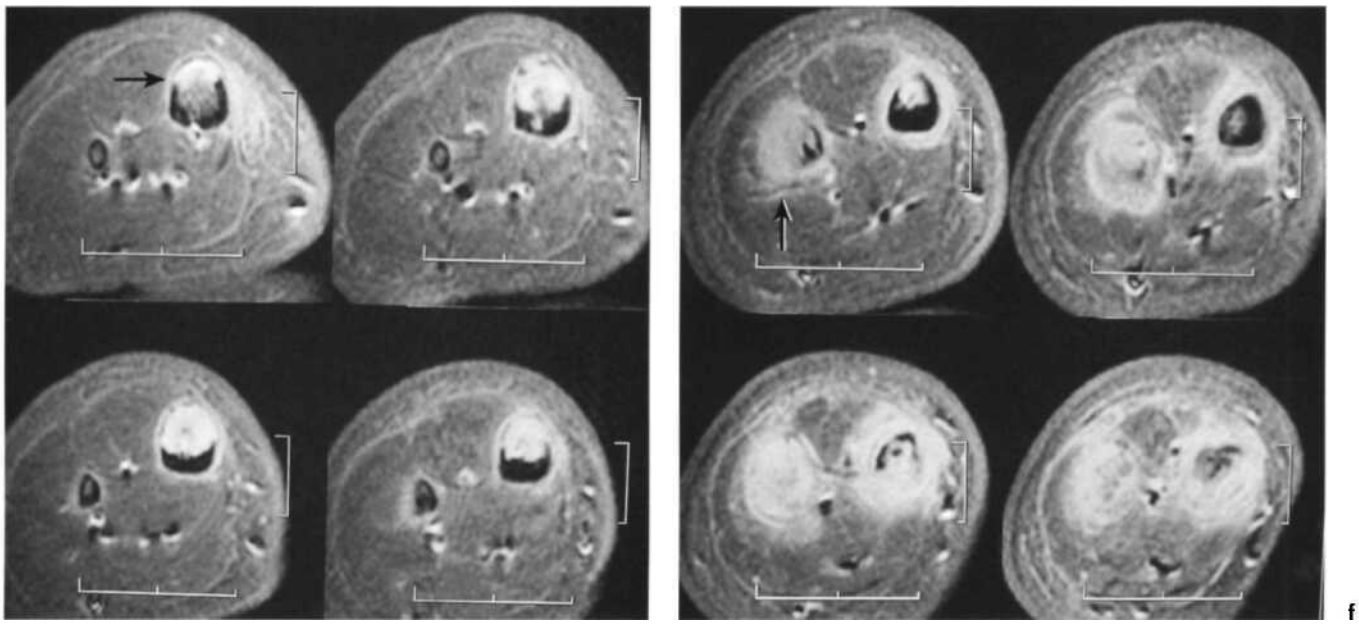

e f

Figure **390 e-f**

References

1 Alguacil-Garcia A, Alonso A, Pettigrew NM. Osteofibrous dysplasia (ossifying fibroma) of the tibia and fibula and adamantinoma. *AmJ Clin Pathol* 1984;82:470-474.

2 Anderson MJ, Townsend DR, Johnston JO, Bohay DR. Osteofibrous dysplasia of the newborn.J Bone Joint Surg *Am* 1993;75(2):265-267.

3 Blackwell JB, McCarthy SW, Xipell JM, Vernon-Roberts B, Duhig RET. Osteofibrous dysplasia of the tibia and fibula. *Pathology* 1988;20: 227-233.

4 Bloem JL, van der Heul RO, Schuttevaer HM, Kuipers D. Fibrous dysplasia vs adamantinoma of the tibia: differentiation based on discriminant analysis of clinical and plain film findings. *AJR Am] Roentgenol* 1991; 156:1017-1023.

5 Bridge JA, Dembinski A, DeBoer J, Travis J, NeffJR. Clonal chromosomal abnormalities in Osteofibrous dysplasia. Implications for histopathogenesis and its relationship with adamantinoma. Cancer 1994; 73:1746-1752.

6 Campanacci M. Osteofibrous dysplasia of long bones. A new clinical entity. *ItalJ Orthop Traumatol* 1976;2:221-237.

7 Campanacci M, Laus M. Osteofibrous dysplasia of the tibia and fibula. *J Bone Joint Surg Am* 1981:63:367-375.

8 Campbell CJ, Hawk T. A variant of fibrous dysplasia (osteoflbrous dysplasia). *J Bone Joint Surg Am* 1982;64:231-236.

9 Conway WF, Hayes CW. Miscellaneous lesions of bone. *Radiol Clin North Am* 1993;31:339-358.

10 Czerniak B, Rojas-Corona RR, Dorfman HD. Morphologic diversity of long bone adamantinoma: the concept of differentiated (regressing) adamantinoma and its relationship to Osteofibrous dysplasia. Cancer 1989;64:2319-2334.

11 Dominguez R, Saucedo J, Fenstermacher M. MRI findings in osteofibrous dysplasia. Magn Reson *Imaging* 1989;7:567-570.

12 Forest M. Osteofibrous dysplasia. In: Forest M, Tomeno B, Vanel D, eds. *Orthopedic Surgical Pathology: Diagnosis of Tumors and Pseudotumoral Lesions of Bone and Joints* Edinburgh: Churchill Livingstone; 1998:613-620.

13 Hindman BW, Bell S, Russo T. Zuppan. Neonatal Osteofibrous dysplasia: report of two cases. *Pediatr Radiol* 1996;26:303-306.

14 Huvos AG. Ossifying fibroma and fibrous dysplasia. In: Huvos AC, ed. *Bone Tumors: Diagnosis, Treatment and Prognosis* 2nd ed. Philadelphia, Pa: W.B. Saunders; 1991;13-29.

15 Kahn LB. Adamantinoma, osteoflbrous dysplasia and differentiated adamantinoma. *Skeletal Radiol* 2003;32:245-258.

16 Park YK, Unni KK, McLeod RA, Pritchard DJ. Osteofibrous dysplasia: clinicopathologic study of 80 cases. *Hum Pathol* 1993;24:1339-1347.

17 Sakamoto A, Oda Y, Iwamoto Y, Tsuneyoshi M. A comparative study of fibrous dysplasia and osteoflbrous dysplasia with regard to expressions of c-fos and c-jun products and bone matrix proteins: a clinicopathologic review and immunohistochemical study of c-fos, c-jun, type I collagen, osteonectin, osteopontin, and osteocalcin. *Hum Pathol* 1999;30:1418-1426.

18 Sakamoto A, Oda Y, Oshiro Y, Tamiya S, Iwamoto Y, Tsuneyoshi M. Immunooexpression of neurofibromin, S-100 protein, and leu-7 and mutation analysis of the NF1 gene at codon 1423 in osteoflbrous dysplasia. *Hum Pathol* 2001;32:1245-1251.

19 Smith NM, Byard RW, Foster B, Morris L, Clark B, Bourne AJ. Congenital ossifying fibroma (osteofibrous dysplasia) of the tibia- a case report. Pediatr Radiol 1991 ;21:449-451.

20 Sweet DE, Vinh TN, Devaney K. Cortical osteofibrous dysplasia of long bone and it relationship to adamantinoma. A clinicopathologic study of 30 cases. *AmJ Surg Pathol* 1992:16:282-290.

21 Vigorita VJ, Ghelman B, Hogendoorn PCW. Osteofibrous dysplasia. In: Fletcher COM, Unni KK, Mertens F, eds. *World Health Organization Classification of Tumours. Pathology and Genetics of Tumours of Soft Tissue and Bone* Geneva: IARC Press; 2002:343-344.

22 Unni KK. Conditions that commonly simulate primary neoplasms of bone. In: *Dahlin's Bone Tumors—General Aspects and Data on* 11087 Cases 5th ed. Philadelphia, Pa: Lippincott, Williams & Wilkins; 1996: 355-432.

23 Wang JW, Shih CH, Chen WJ. Osteofibrous dysplasia (ossifying fibroma of long bones). A report of four cases and review of the literature. Clin *Orthop RelatRes* 1992;278:235-243.

A 60 Osteoid Osteoma

ICD-OCode

9191/0

Definition

Osteoid osteoma is a benign, osteoblastic lesion comprised of a circumscribed nidus less than 1.5cm in size, and is usually surrounded by reactive bone formation.[6,9.11-13,17,18,22] These lesions are usually painful and have limited growth potential.[1 6,9.11-13,17.18,22]

Frequency of Occurrence

Osteoid osteoma accounts for 11-13 % of primary benign bone tumors and 3-4% of all primary bone tumors.[15,16,21]

Age at Presentation

From 6 to 30 years, median = 17 years.[9,15] Approximately 75% occur in patients under 25 years old.[9] Rare cases have been reported in older adults up to 72years old.[15,21]

Gender Ratio (M/F)

2.2 / 1 to 4/1.[9,17,22]

Location

Lesions occur in the femur (proximal > mid, distal) > tibia > feet, hands > humerus > vertebrae (lumbar > cervical, thoracic) > iliac bone > sacrum > radius, ulna > other sites.[91,17,22] More than 50 % of lesions occur in the femur and tibia.[91722] Lesions are most frequently located in the cortex (intracortical) and at the subperiosteum/bone surface,[10] and rarely at the endosteal surface.[9,10,17,22] Osteoid osteomas in the small tubular bones of the hands and feet commonly occur in medullary bone.[9,17,22] Lesions in tubular bones are usually located eccentrically within the cortex (47-80%), at the outer original bone surface (subperiosteum) (15-47 %), or medullary bone (5 %).[10,17] In long bones, most lesions are located in the diaphysis followed by the metaphysis.[10,17] Osteoid osteomas are located in the epiphysis in only 5%.[9,17] Lesions are located more frequently in the proximal portions of long bones than the middle and distal regions.[17] Vertebral lesions usually involve the neural arch, spinous and transverse processes.[9,17]

Signs and Symptoms

Patients often present with localized, gradually progressive bone pain which is worse at night.[6,9,11,17,22] The pain is relieved by salicylates in 70% of patients.[6,9,17,22] The relief of pain by salicylates is less for intracapsular lesions than extracapsular ones.[8] The pain may eventually become constant and interfere with sleep.[9,11] The duration of symptoms before diagnosis often varies from weeks to several years.[6,9,22] Lesions located near the ends of tubular bones can be associated with referred pain to adjacent joints.[622] Vasomotor disturbances, such as localized increased perspiration and increased skin temperature, can be associated with the bone pain.[9] Approximately 5 % of lesions, however, are not associated with pain.[6,9]

Osteoid osteomas have been associated with increased bone lengths, scoliosis associated with pain and muscle spasms, contractures, atrophy of adjacent muscles, and decreased muscle stretch reflexes.[11,22] Intra-articular osteoid osteomas can be associated with joint effusion, synovitis, capsular contracture, restriction of joint motion, and/or advanced epiphyseal development.[6,9,11]

Cross Pathologic Findings

Osteoid osteomas typically are small (<1.5cm), spheroid or ovoid, reddish-brown, gritty, or granular circumscribed lesions within cortex surrounded by prominent adjacent sclerotic bone.[6,9,1117,22] Lesions with relatively greater degrees of calcification typically are yellow-white.[6]

Histopathologic Findings

The nidus, or central region of osteoid osteoma, rarely exceeds 1 cm in size, and consists of vascularized connective tissue with differentiated osteoblastic activity from osteoblasts with plump nuclei.[6,9,11,17,18,22] The osteoblasts lack nuclear pleomorphism, allowing for discrimination from the diagnostic possibility of osteosarcoma.[6,9,11,18,22] Within the nidus, interlacing networks of osteoid and bony trabeculae with variable amounts of mineralization are usually seen.[6,9,17,18,22] The trabeculae in the nidus range from thin to broad, and often have irregular orientations and anastomoses.[6,9,11,17,18,22] The central portion of the nidus may be the site of greatest mineralization.[6,22] Osteoclasts may be present, but are rarely positioned next to mineralized osteoid.[6] Occasional scattered lymphocytes and plasma cells may be present.[6] Cartilage formation is typically absent in osteoid osteomas.[9,11,22] Thickened hypervascular sclerotic cortical bone usually surrounds the nidus.[6,9,11,17,18,22] The degree of osteosclerosis tends to be greater toward the outer cortical surface than toward the medullary side."

Lesions have been categorized into three evolutionary phases.[6,9] Early or initial stage lesions have densely packed osteoblasts in highly vascularized stroma within the nidus.[6,9] Intermediate stage lesions contain osteoblasts interspersed amongst intercellular substance (osteoid) containing trabeculae with various degrees of calcification.[6,9] Late or mature stage lesions have atypical compact trabeculae of bone that does not have the characteristic appearance of either woven or lamellar bone.[6,9] Intra-articular lesions usually have associated joint effusions, and lymphofollicular synovitis (synovial proliferation with lymphocytes and plasma cells).[6] Bone marrow adjacent to and near osteoid osteomas often shows replacement of marrow fat with fibrovascular tissue and inflammatory cells mostly consisting of plasma cells.[2] Intra-articular osteoid osteomas are associated with a lymphofollicular synovial inflammatory reaction.[20]

Lesion Genetics

Abnormalities involving chromosome band 22 q 13 and loss of the distal portion of 17 q have been reported.[11]

Findings on Plain Films (Roentgenograms)[6,9,10,1214,17,22] and Computed Tomography[12,4,8,10,12]

Cortical osteoid osteoma. An intracortical or cortical osteoid osteoma typically appears on radiographs as a region of dense fusiform osteosclerosis within which there is a small, circumscribed, spheroid or ovoid, radiolucent zone (nidus) measuring less than 1.5 cm.[6,9,12,14,17,22] The nidus usually has sharp margins (narrow zones of transition) from the adjacent region of osteosclerosis.[6,9,12,4,17,22] CT is useful in defining the nidus in lesions in which dense osteosclerosis obscures the nidus on radiographs[10,17] (Fig. **395).** Various amounts of mineralization (amorphous, punctate, ringlike, or focally dense in the central portion) can be seen with CT in the nidus in 50% of cases.[12]

Subperiosteal osteoid osteoma. A subperisosteal osteoid osteoma typically appears on radiographs as a region of dense fusiform osteosclerosis within which there is a small, circumscribed, spheroid or ovoid, radiolucent zone (nidus) measuring less than 1.5 cm.[6,9,12,14,17,22] The nidus usually has sharp margins (narrow zones of transition) from the adjacent region of osteosclerosis, and is located at the external surface of the original cortical margin[6,9,10,12,14,17,22] (Figs. **393,394).** CT is useful in defining the nidus in lesions in which dense osteosclerosis obscures the nidus on radiographs.[10,17] The nidus of osteoid osteoma is usually well-defined and typically has decreased attenuation.[12] Various amounts of mineralization (amorphous, punctate, ringlike, or focally dense in the central portion) can be seen with CT in the nidus in 50% of cases.[12]

Endosteal osteoid osteoma. An endosteal osteoid osteoma typically appears on radiographs as a region of dense fusiform osteosclerosis within which there is a small, circumscribed, spheroid or ovoid, radiolucent zone (nidus) measuring less than 1.5cm[6,9,12,14,17,22] (Fig. **391).** The nidus usually has sharp margins (narrow zones of transition) from the adjacent region of osteosclerosis, and is located at the inner surface of the original cortical margin.[6,9,10,12,14,17,22] CT is useful in defining the nidus in lesions in which dense osteosclerosis obscures the nidus on radiographs.[10,17] Various amounts of mineralization (amorphous, punctate, ringlike, or focally dense in the central portion) can be seen with CT in the nidus in 50 % of cases.[12]

Intra-articular osteoid osteomas. Intra-articular osteoid osteomas can be subperiosteal, intracortical, endosteal, or cancellous (intramedullary).[9,12,17,20,22] Since cancellous bone predominates at the ends of long bones, many intramedullary osteoid osteomas occur in juxta-articular/intracapsular locations such as the hip.[12,17,20] Cancellous osteoid osteomas also commonly occur in the small tubular bones of the hands and feet.[9,17,22] Intracapsular osteoid osteomas can have minimal or no associated cortical or periosteal osteosclerosis.[4,8,12,17,20] The lack of periosteal osteosclerosis associated with intra-articular osteoid osteoma is because intracapsular periosteum is not capable of forming a proliferative sclerotic response, unlike extracapsular periosteum.[4,8,12] Occasionally, mild periosteal reaction may be seen outside of the joint from an intracapsular osteoid osteoma.[8,12] Features associated with intracapsular osteoid osteomas include: joint widening from synovitis and/or joint effusion, regional osteopenia, widening and shortening of the femoral neck, decreased height of the femoral capital epiphysis, and variable reactive medullary sclerosis[2,4,8,12,20] (Fig. **392).** The degree of medullary sclerosis is greater for lesions at the elbow than at the hip.[12,14] CT is useful for identifying the nidus of cancellous osteoid osteoma.[12] Various amounts of mineralization (amorphous, punctate, ringlike, or focally dense in the central portion) can be seen with CT in the nidus in 50 % of cases.[4,12]

MRI Findings[2-8,10,12,14,20,23,24]

Cortical osteoid osteoma. An intracortical or cortical osteoid osteoma typically shows dense fusiform thickening of the cortex that has mostly low signal on Tl W, T2WI, and FST2W1.[2,3,5,10,12,23] Within the thickened cortex, a small spheroid or ovoid zone (nidus) measuring less than 1.5cm is seen.[2,3,10,12] The nidus can have irregular, distinct or indistinct margins relative to the adjacent region of cortical thickening.[2,3,10,12] The nidus can have low-intermediate signal on T1WI and PDWI, and low-intermediate or high signal on T2W1 and FST2WI[2,3,10,20] (Fig. **395).** Calcifications in the nidus can be seen as low signal on T2WI.[210] After Gd-contrast administration, variable degrees of enhancement are seen at the nidus.[2,10,20,23]

Poorly defined zones of marrow signal alteration consisting of low-intermediate signal on T1WI, high signal on T2WI and FST2WI, and corresponding Gd-contrast enhancement are commonly seen adjacent to and near osteoid osteomas in up to 63% of cases.[2,5,20,23,24] The MRI findings were found to be related to replacement of marrow fat with fibrovascular tissue and inflammatory cells.[2] Linear, amorphous and/or focal regions of high signal on FS T2WI and Gd-contrast enhancement were also seen in the soft tissues adjacent to the external bone surface involved by osteoid osteoma in up to 47 % of cases, and resulted from soft tissue inflammation and increased vascularity.[2,5,20,23]

Subperiosteal osteoid osteoma. A subperisosteal osteoid osteoma typically shows dense fusiform thickening of the cortex, which has mostly low signal on Tl W, PDWI, T2W1, and FS - T2W1[10] (Figs. **393,394).** Within the thickened cortex, a spheroid or ovoid zone (nidus) measuring less than 1.5 cm is seen in the region of the original external surface of bone cortex.[12] The nidus can have irregular, distinct or indistinct margins relative to the adjacent region of cortical thickening.[2,3,10,12] The nidus can have low-intermediate signal on T1WI and PDWI, and low-intermediate or high signal on T2WI and FST2WI.[2,3,10,12,20] Calcifications in the nidus can be seen as low signal on T2WI.[2,10] After Gd-contrast administration, variable degrees of enhancement are seen at the nidus.[2,10,20,23]

Poorly defined zones of marrow signal alteration consisting of low-intermediate signal on Tl WI, high signal on T2WI and FST2WI, and corresponding Gd-contrast enhancement are commonly seen adjacent to and near osteoid osteomas in up to 63 % of cases.[2,5,20,23,24] The MRI findings were found to be related to replacement of marrow fat with fibrovascular tissue and inflammatory cells.[2] Linear, amorphous and/or focal regions of high signal on FST2WI and Gd-contrast enhancement were also seen in the soft tissues adjacent to the external bone surface involved by osteoid osteoma in up to 47 % of cases, and resulted from soft tissue inflammation and increased vascularity.[2,5,20,23]

Endosteal osteoid osteoma. An endosteal osteoid osteoma typically shows dense fusiform thickening of the cortex, which has mostly low signal on T1W, T2WI, and FST2WI. Within the thickened cortex, a small spheroid or ovoid zone (nidus) measuring less than 1.5 cm is seen in the region of the inner surface of bone cortex.[12] The nidus can have irregular, distinct or indistinct margins relative to the adjacent region of cortical thickening.[2,3,10,12] The nidus can have low-intermediate signal on T1WI and PDWI, and low-intermediate or high signal on T2WI and FST2WI[2,3,10,12,20] (Fig. **391).** Various amounts of mineralization in

a

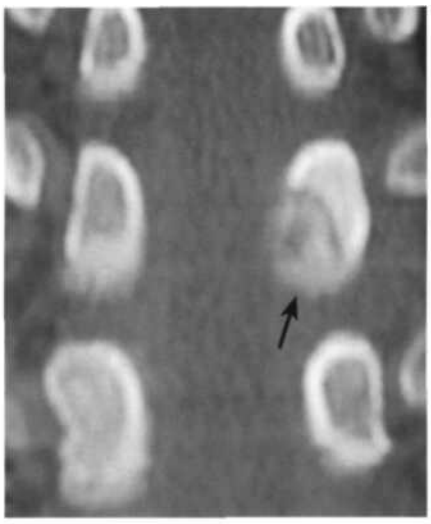
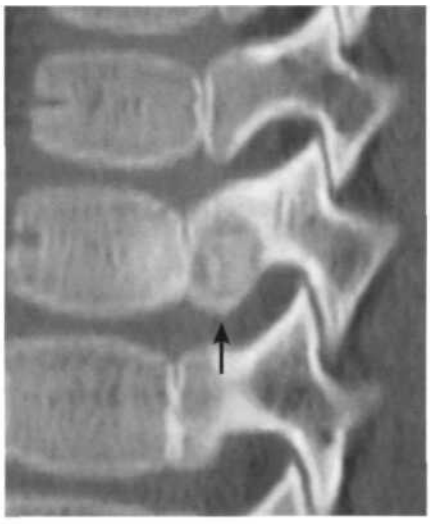
b, c

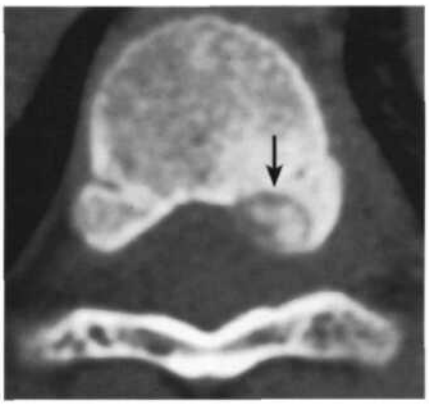
d

e, f

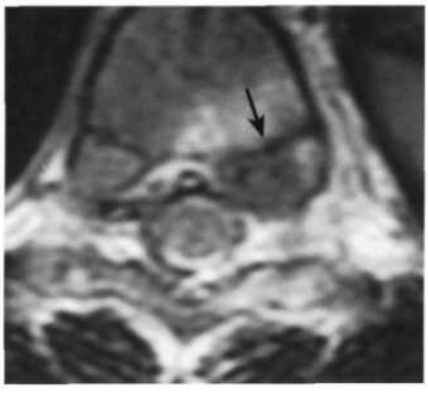
g

h

i

Figure **391 a-i** A 5-year-old female with an endosteal-cancellous osteoid osteoma involving the left pedicle of the T10 vertebra. AP radiograph (a) shows increased density within the left T10 pedicle and slight cortical irregularity. Coronal (**b**), sagittal (**c**), and axial (**d**) CT images show a circumscribed intramedullary lesion with low attenuation surrounding a zone of mineralization/calcification. Sclerotic increased attenuation is seen in the medullary bone adjacent to lesion. The lesion has intermediate signal surrounding a small zone of low signal bordered by a peripheral region of low signal on sagittal T1 WI (**e**). The lesion has low and intermediate signal on sagittal (**f**) and axial (**g**) T2WI surrounded by high signal. The lesion shows prominent Gd-contrast enhancement on axial FST1WI (**h**) and sagittal T1WI (**i**). In addition, poorly defined zones of Gd-contrast enhancement are seen in the marrow adjacent to the lesion, as well as in the extraosseous soft tissues.

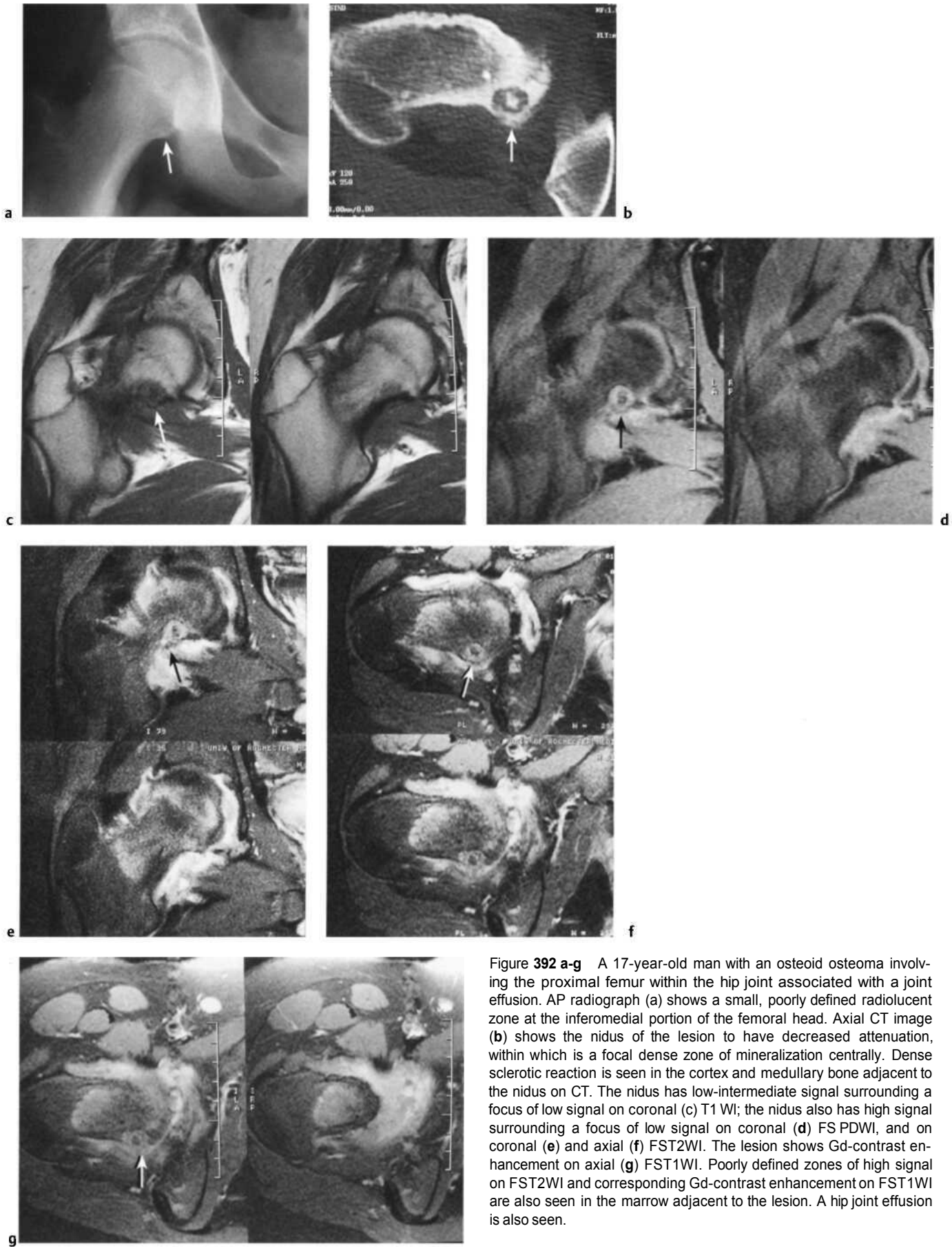

Figure **392 a-g** A 17-year-old man with an osteoid osteoma involving the proximal femur within the hip joint associated with a joint effusion. AP radiograph (a) shows a small, poorly defined radiolucent zone at the inferomedial portion of the femoral head. Axial CT image (**b**) shows the nidus of the lesion to have decreased attenuation, within which is a focal dense zone of mineralization centrally. Dense sclerotic reaction is seen in the cortex and medullary bone adjacent to the nidus on CT. The nidus has low-intermediate signal surrounding a focus of low signal on coronal (c) T1 WI; the nidus also has high signal surrounding a focus of low signal on coronal (**d**) FS PDWI, and on coronal (**e**) and axial (**f**) FST2WI. The lesion shows Gd-contrast enhancement on axial (**g**) FST1WI. Poorly defined zones of high signal on FST2WI and corresponding Gd-contrast enhancement on FST1WI are also seen in the marrow adjacent to the lesion. A hip joint effusion is also seen.

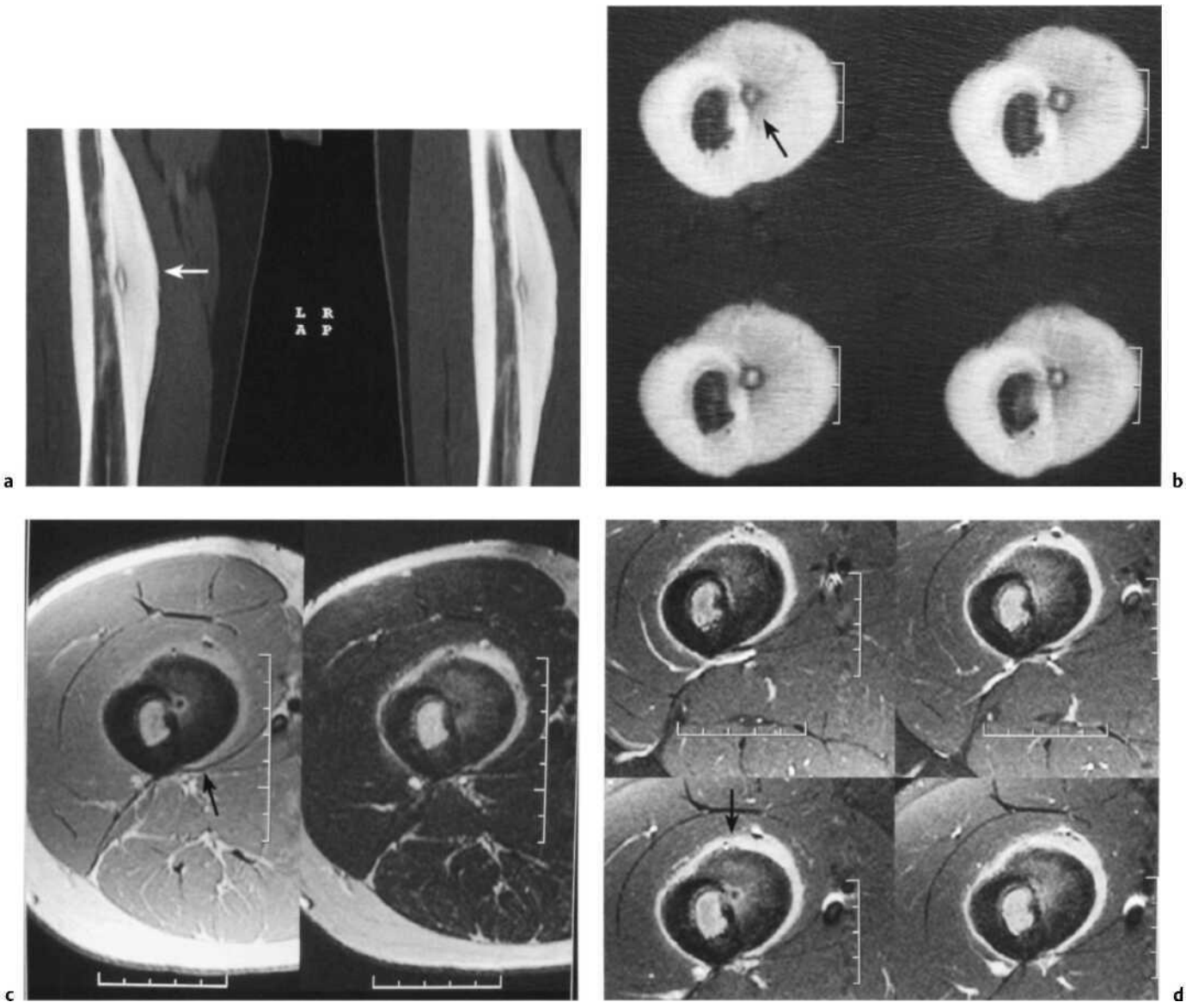

Figure **393**a-d A 15-year-old male with a subperiosteal osteoid osteoma involving the diaphyseal portion of the femur. Coronal (a) and axial (b) CT images show dense fusiform osteosclerosis, within which is a small, circumscribed, ovoid radiolucent zone (nidus) with sharp margins which contains a central focus of calcification. The nidus has intermediate signal on axial PDWI (c, left image), and high signal on axial T2WI (c, right image). The small central calcification in the nidus has low signal. The thickened cortex adjacent to the nidus has low and intermediate signal on T2WI, and is associated with periosteal reaction with high signal. The nidus shows Gd-contrast enhancement on axial FST1 WI (**d**). Prominent Gd-contrast enhancement is seen at the periosteal reaction, and mild diffuse enhancement is seen in the cortical thickening adjacent to the enhancing nidus.

the nidus can be seen as areas with low signal on T1WI and T2WI.[2,10]

Poorly defined zones of marrow signal alteration consisting of low-intermediate signal on T1WI, high signal on T2WI and FST2WI, and corresponding Gd-contrast enhancement are commonly seen adjacent to and near osteoid osteomas in up to 63% of cases.[2,5,20,23,24] The MRI findings were found to be related to replacement of marrow fat with fibrovascular tissue and inflammatory cells.[2] Linear, amorphous and/or focal regions of high signal and Gd-contrast enhancement were also seen in the soft tissues adjacent to the external bone surface involved by osteoid osteoma in up to 47% of cases, and resulted from soft tissue inflammation and increased vascularity.[2,5]

Intra-articular osteoid osteoma. Intra-articular osteoid osteomas can be subperiosteal, intracortical, endosteal, or cancellous (intramedullary).[9,12,17,20,23] Intracapsular osteoid osteomas can have minimal or no associated cortical or periosteal osteosclerosis.[4,8,12,17,20] The lack of periosteal osteosclerosis associated with intra-articular osteoid osteoma is because intracapsular periosteum is not capable of forming a proliferative sclerotic response, unlike extracapsular periosteum.[4,8,12] Occasionally, mild periosteal reaction may be seen outside of the joint from an intracapsular osteoid osteoma.[8,12]

The nidus of cancellous osteoid osteoma may have irregular, distinct or indistinct margins.[8,12] The nidus can have low-intermediate signal on T1WI and PDWI, and low-intermediate or high signal on T2WI and FS T2WI[2–4,10,20] (Fig. **392**). Calcifications in the nidus can be seen as low signal on T2WI.[2,4,10] After Gd-contrast administration, variable degrees of enhancement are seen at the nidus.[2,10,20,23] Features associated with intracapsular osteoid osteomas include: joint widening from synovitis and/or

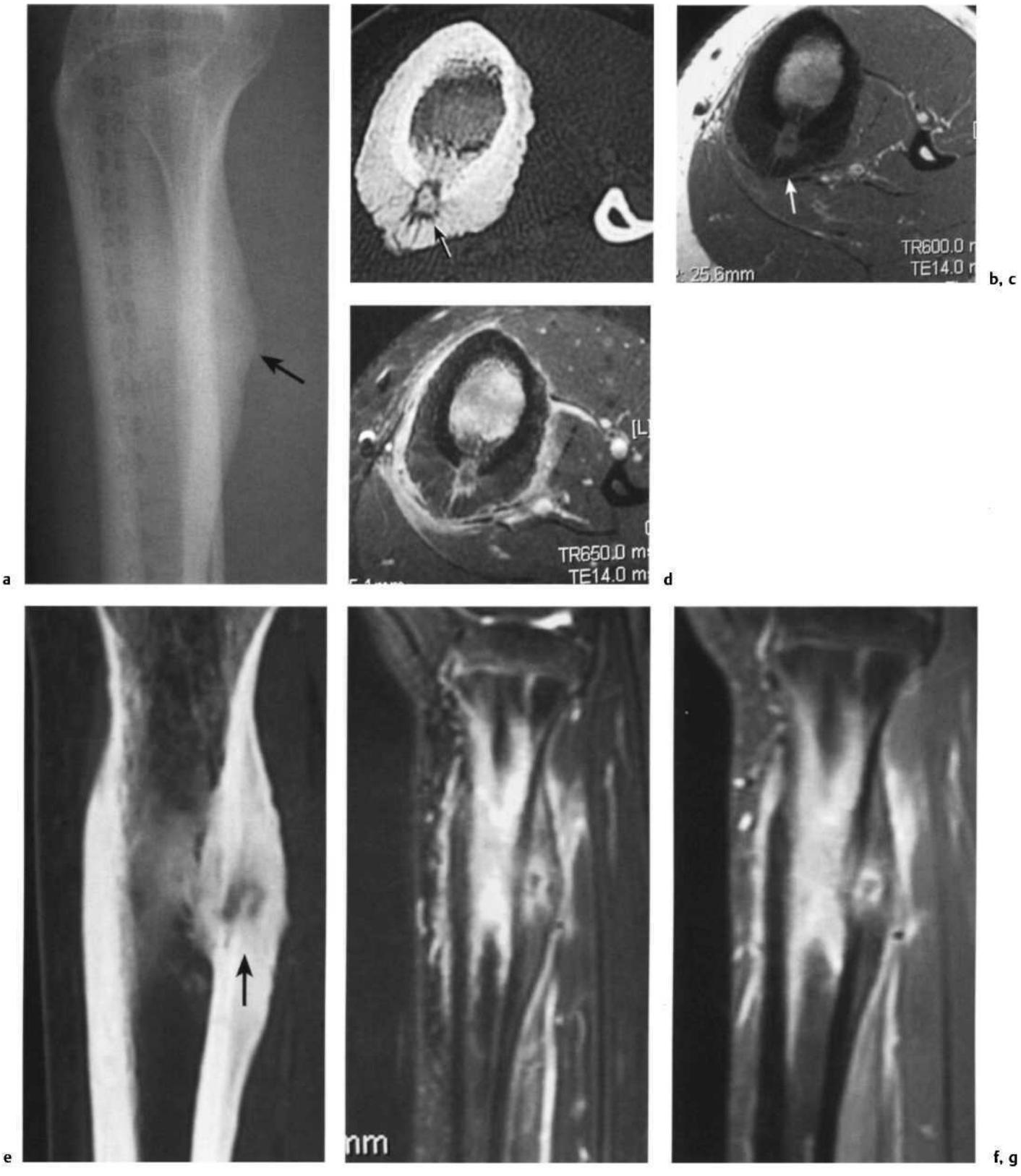

Figure **394a-g** A 15-year-old female with a subperiosteal osteoid osteoma involving the proximal tibia. Lateral radiograph (**a**) shows fusiform osteosclerotic thickening of the posterior tibial cortex. Axial (**b**) and sagittal (**e**) CT images show dense fusiform osteosclerosis, within which is a small circumscribed radiolucent zone (nidus) with sharp margins which contains a central calcification. The nidus has intermediate signal on axial T1WI (**c**), and high signal on sagittal FST2WI (**f**). The small central calcification in the nidus has low signal on T1 WI and FS T2WI. The thickened cortex adjacent to the nidus has low and slightly high signal on FST2WI, and is associated with periosteal reaction with high signal. The nidus shows Gd-contrast enhancement on axial (**d**) and sagittal (**g**) FST1WI. Prominent Gd-contrast enhancement is seen at the periosteal reaction, and mild diffuse enhancement is seen in the cortical thickening adjacent to the enhancing nidus. Poorly defined zones of high signal on FST2WI and corresponding Gd-contrast enhancement on FS T1 WI are also seen in the marrow adjacent to the lesion.

a, b

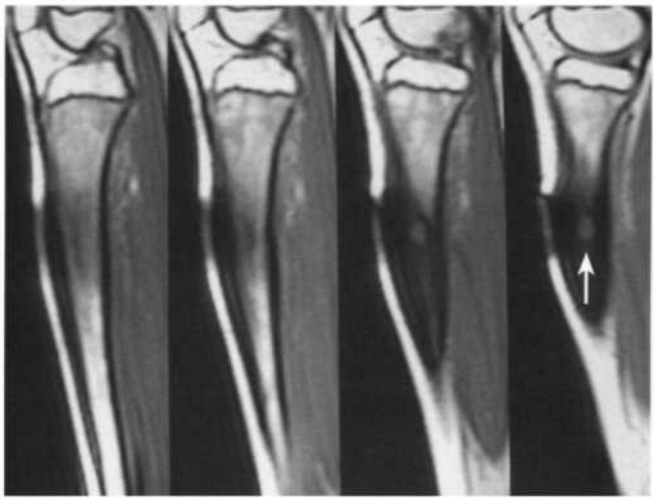

c

Figure **395 a-f** A 9-year-old female with a cortical osteoid osteoma involving the proximal tibia. AP (**a**) and lateral (**b**) radiographs show fusiform thickening of the anteromedial tibial cortex. The nidus has low-intermediate signal on sagittal T1WI (**c**), intermediate signal on axial PDWI (**d**), and intermediate to slightly high signal on axial T2WI (**e**). The small central calcification in the nidus has low signal on T1 WI and FST2WI. The thickened cortex adjacent to the nidus has low, intermediate, and slightly high signal on T2WI. The nidus shows Gd-contrast enhancement on axial FST1WI (**f**). Prominent Gd-contrast enhancement is seen with the associated periosteal reaction, and mild diffuse enhancement is seen in the cortical thickening adjacent to the nidus. Poorly defined zones of high signal on T2WI and corresponding Gd-contrast enhancement on FST1WI are also seen in the marrow adjacent to the lesion.

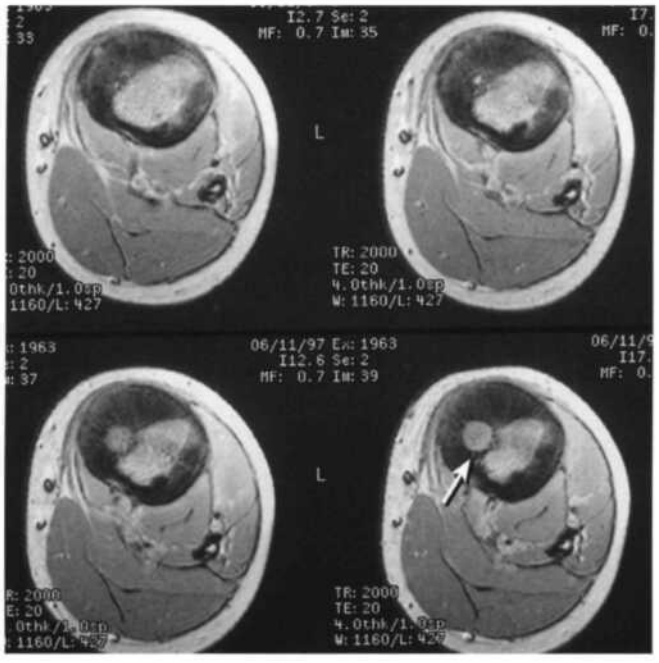

d

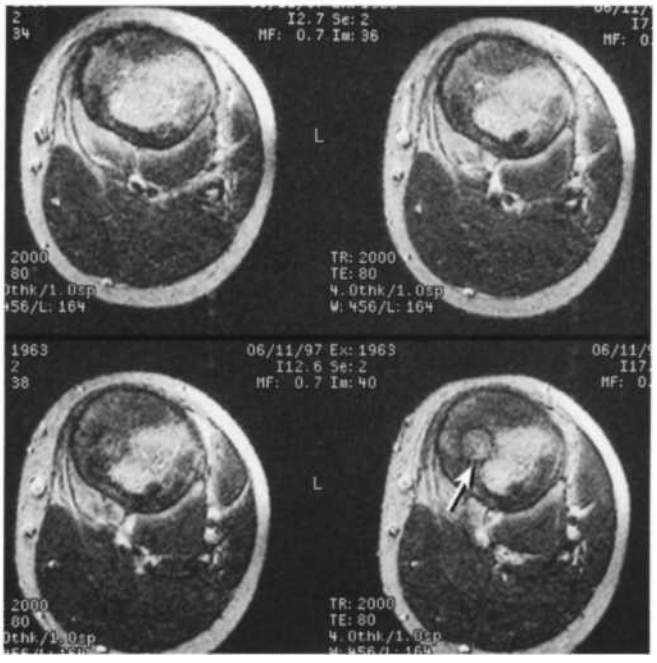

e

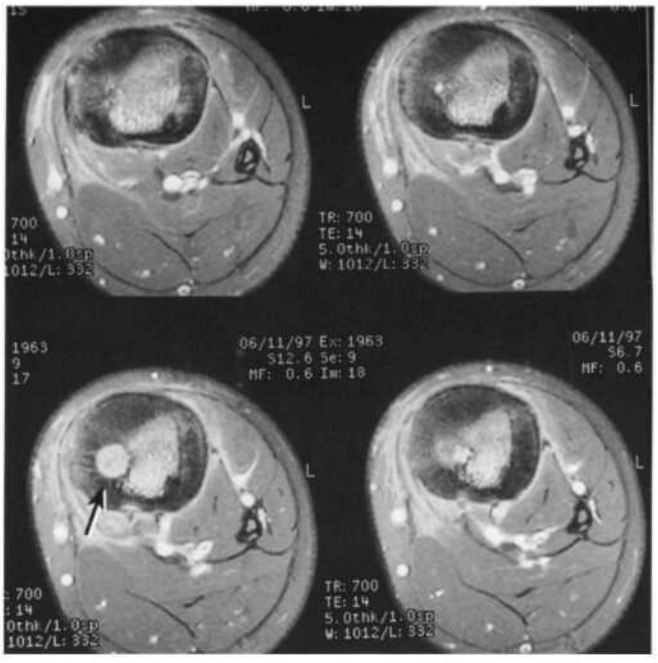

f

joint effusion (Fig. **392),** widening and shortening of the femoral neck, and decreased height of the femoral capital epiphysis[2,4,8,12,20] Poorly defined marrow zones with low signal on T1WI, high signal on T2W1 and FST2WI, and corresponding Gd-contrast enhancement representing edema and/or inflammation are usually seen adjacent to cancellous osteoid osteomas.[2,5,8,20,23] The extent and degree of the marrow signal alteration tends to be greater for cancellous osteoid osteomas compared with cortical osteoid osteomas,[5] as well as for intra-articular lesions at the elbow compared with the hip.[12,14]

Differential Diagnosis

Cortical and subperiosteal osteoid osteoma. Osteoblastoma, healing stress fracture, Brodie abscess, sclerosing osteomyelitis, parosteal osteosarcoma, osteofibrous dysplasia, adamantinoma fibrous cortical defect, osteoma.[12,7]

Cancellous (intramedullary) osteoid osteoma Osteoblastoma, healing stress fracture, Brodie abscess, sclerosing osteomyelitis, bone island, osteoblastic metastatic lesion, hemangioma[612]

Intra-articular osteoid osteoma. Osteoblastoma, Brodie abscess, eosinophilic granuloma, inflammatory synovitis (rheumatoid arthritis, etc.), septic joint, tuberculous arthritis, Legg-Calve-Perthes disease, enchondroma, osteochondritis dissecans, synovial pit.[4,12,17,20]

Prognosis and Treatment

Osteoid osteomas have variable clinical courses.[6] Lesions can persist with symptoms for years or may involute.[6] There are no reports of definite malignant transformation.[6] Intra-articular osteoid osteomas are associated with a lymphofollicular synovial inflammatory response which may cause injury to articular cartilage and result in osteoarthritis.[20] Complete surgical excision (en bloc resection) typically results in cure and abrupt termination of symptoms.[6,12,22] Localization of the nidus before surgery can be difficult; and CT guidance techniques, intraoperative radiography, and intraoperative identification of lesions with ultraviolet light after the preoperative administration of tetracylcine have been utilized for this purpose.[6,12,19] CT-guided percutaneous radio frequency ablation has been recently shown to be effective and safe for treating osteoid osteomas.[19] Thickened reactive bone can persist or regress after removal or ablation of the nidus.[16,12]

References

1 Assoun J, Railhac JJ, Bonnevialle P, et al. Osteoid osteoma: percutaneous resection with CT guidance. Radiology 1993;188(2):541-547

2 Assoun J, Richardi G, Railhac JJ, et al. Osteoid osteoma: MR imaging versus CT. Radiology 1994;191(l):217-223.

3 Bell RS, O'Connor GD, Waddell JP. Importance of magnetic resonance imaging in osteoid osteoma: a case report. *CanJSurg* 1989;32(4): 276-278.

4 Ebrahim FS, Jacobson JA, Lin J, Housner JA, Hayes CW, Resnick D. Intra-articular osteoid osteoma: sonographic findings in three patients with radiographic, CT, and MR imaging correlation. *AJR Am J Roentgenol* 2001 ;177:1391-1395.

5 Ehara S, Rosenthal DI, Aoki J, et al. Peritumoral edema in osteoid osteoma on magnetic resonance imaging. *Skeletal Radiol* 1999;28: 265-270.

6 Forest M. Osteoid osteoma and Osteoblastoma. In: Forest M, Tomeno B, Vanel D, eds. Orthopedic Surgical Pathology: Diagnosis *of Tumors and Pseudotumoral Lesions of Bone and Joints* Edinburgh: Churchill Livingstone; 1998:79-98.

7 Glass RB, Poznanski AK, Fisher MR, Shkolnik A, Dias L. MR imaging of osteoid osteoma. *J Comput Assist Tomogr* 1986; 10(6): 1065-1067.

8 Goldman AB, Schneider R, Pavlov H. Osteoid osteomas of the femoral neck: report of four cases evaluated with isotopic bone scanning, CT, and MR imaging. *Radiology* 1993;186(l):227-232.

9 Huvos AG. Osteoid osteoma. In: Huvos AG, ed. Bone *Tumors: Diagnosis, Treatment, and Prognosis* 2nd ed. Philadelphia, Pa: W.B. Saunders; 1991:49-60.

10 Kayser F, Resnick D, Haghighi P, et al. Evidence of the subperiosteal origin of osteoid osteomas in tubular bones: analysis by CT and MR imaging. *AJR Am J Roentgenol* 1998;170:609-614.

11 Klein MJ, Parisien MV, Schneider-Stock R. Osteoid osteoma. In: Fletcher CDM, Unni KK, Mertens F, eds. *World Health Organization Classification of Tumours. Pathology and Genetics of Tumours of Soft Tissue and Bone* Geneva: IARC Press; 2002:260-261.

12 Kransdorf MJ, Stull MA, Gilkey FW, Moser RP Jr. From the Archives of the AFIP-Osteoid osteoma. *Radiographics* 1991;ll(4):671-696.

13 Miller SL, Hoffer FA. Malignant and benign bone tumors. Radiol Clin *North Am* 2001;39(4):673-699.

14 Moser RP Jr, Kransdorf MJ, Brower AC, et al. Osteoid osteoma of the elbow-a review of six cases. *Skeletal Radiol* 1990;19:181-186.

15 Mulder JD, Schutte HE, Kroon HM, Taconis WK. Introduction. In: Radioiogic Atlas *of Bone Tumors* Amsterdam: Elsevier; 1993:3-6.

16 Mulder JD, Schutte HE, Kroon HM, Taconis WK. The diagnosis of bone tumors. In: *Radioiogic Atlas of Bone Tumors* Amsterdam: Elsevier; 1993:9-46.

17 Mulder JD, Schutte HE, Kroon HM, Taconis WK. Osteoid osteoma. In: Radioiogic *Atlas of Bone Tumors* Amsterdam: Elsevier; 1993:385-397.

18 Pringle Jean AS. Bone-forming neoplasms arising within bone. In: Helliwell TR, ed. Major *Problems in Pathology: Pathology of Bone and Joint Neoplasms* 1st ed. Vol 37. Philadelphia, Pa: W.B. Saunders; 1999: 168-171.

19 Rosenthal DI, Hornicek FJ, Torriani M, Gebhardt MC, Mankin HJ. Osteoid osteoma: percutaneous treatment with radiofrequency energy. Radiology 2003;229:171-175.

20 Spouge AR, Thain Lisa MF. Osteoid osteoma: MR imaging revisited. Clin Imaging 2000;24:19-27.

21 Unni KK. Introduction and scope of study. In: *Dahlin'sBone Tumors-General Aspects and Data on* 17087 Cases 5th ed. Philadelphia, Pa: Lippincott, Williams & Wilkins; 1996:1-9.

22 Unni KK. Osteoid osteoma. In: *Dahlin's Bone Tumors—General Aspects and Data on 11087 Cases* 5th ed. Philadelphia, Pa: Lippincott, Williams & Wilkins; 1996:121-130.

23 Woods ER, Martel W, Mandell SH, Crabbe JP. Reactive soft-tissue mass associated with osteoid osteoma: correlation of MR imaging features with pathologic findings. Radiology 1993;186(l):221-225.

24 Yeager BA, Schiebler ML, Wertheim SB, et al. Case Report-MR imaging of osteoid osteoma of the talus. J Comput Assist *Tomogr* 1987; 11(5):916-917.

A 61 Osteoblastoma (Also Referred to as Ossifying Giant Cell Tumor and Giant Osteoid Osteoma)

ICD-O Code

9200/0

Definition

Osteoblastomas are rare, benign, bone-forming tumors that are histologically related to osteoid osteomas.[2,3,5,8,14,15,19] Osteoblastomas are larger than osteoid osteomas and show progressive enlargement.[2,3,5,8,14,15,19] Osteoblastomas typically produce well-vascularized osteoid with woven bone spicules surrounded by osteoblasts.[2,3,5,8,14,15,19]

Frequency of Occurrence

Osteoblastomas account for 3-6% of primary benign bone tumors and from < 1 to 2 % of all primary bone tumors.[6,7,18]

Age at Presentation

From 1 to 30 years, median = 15 years,[7] mean age = 20 years.[2] Approximately 90 % of lesions occur in patients less than 30 years old.[3] Osteoblastomas occasionally occur in older adults up to 78years old.[3,7,18]

Gender Ratio (M / F)

2/1 to 2.6/1.[3,8,19]

Location

Lesions occur in the vertebrae > craniofacial bones > femur > tibia > talus > sacrum > small bones of hands and feet > humerus > radius > ulna.[3,8,19] In vertebrae, lesions are located in the arch > vertebral body and arch > vertebral body.[4,8,19] In tubular bones, lesions are located in the diaphysis > metaphysis > metadiaphysis > epi-metadiaphysis > epiphysis.[8]

Signs and Symptoms

Up to 87 % of patients with Osteoblastomas can have localized, dull-aching pain.[3,4,8,15,19] The duration of pain symptoms ranges from 1 week to 72 months, median = 6 months,[48] average = 2 years.[19] Unlike osteoid osteoma, the pain associated with osteoblastoma is not typically worse at night or very responsive to salicylates.[2-58] Progressive swelling and local tenderness may occur at the site of osteoblastoma.[3,8] Vertebral lesions can be associated with progressive nerve root and/or spinal cord compression, gait disturbance, scoliosis concave to the affected side, and/or muscle spasms.[2-4,8-10,13-15-16-19]

Osteoblastomas in the appendicular skeleton may be associated with limp and muscle atrophy.[3,8] Lesions in the mandible or maxilla can be associated with prominent localized tooth pain and swelling.[3,5] Osteoblastoma in the skull base has been reported to cause progressive blindness from compression of the optic chiasm and orbital invasion.[21] Osteoblastomas can be associated with tumor-induced osteomalacia.[2,19]

Cross Pathologic Findings

Lesions are often well-circumscribed and vary in size from 2 to 12 cm.[2,3,,5,19] Most of these tumors are removed by curettage and whole gross specimens are rarely available.[19] The specimens obtained are hemorrhagic, red-brown or purple-red, friable, soft and gritty in texture resulting from lesion vascularity, and osteoid with various calcifications.[3,5,8,15,19] Zones of cystic degeneration often occur in larger tumors.[3] Older lesions can be associated with cortical expansion with a thin sclerotic rim.[19] The borders of lesions with medullary bone are usually sharp with or without reactive sclerotic bone.[5,19] Tumors may have associated aneurysmal bone cysts.[2,5]

Histopathologic Findings

Osteoblastomas are composed of vascularized connective tissue and abundant osteoid, with differentiated osteoblastic activity from osteoblasts with plump nuclei.[3,5,15] Occasional mitoses are seen in osteoblasts, but they are not atypical.[5] Osteoblasts are mononucleated or occasionally binucleated.[2] The nucleus within an osteoblast is usually eccentric, and there is abundant cytoplasm.[2] Osteoblastomas often show immunoreactivity to osteonectin, which is a glycoprotein associated with differentiated osteogenic cells.[2] Tumors contain woven bone spicules and/or trabeculae, usually surrounded by a single layer of osteoblasts with occasional zones of pseudostratification.[1,3,5,15] The trabeculae and woven bone spicules occur in irregular arrangements.[3,5,15] Occasional zones of lamellar maturation may be seen.[1] Loosely arranged fibrovascular stroma containing spindle cells, vascular channels, and osteoclasts is often observed amongst the osseous trabecular network.[3,15] Scattered multinucleated giant cells are often present around vascular channels and extravasated blood.[3,5] Occasional scattered lymphocytes and plasma cells may be present.[6] Cartilage formation rarely occurs in Osteoblastomas.[5,19] Approximately 6% of Osteoblastomas have foci of cartilage maturing into bone.[19] Enlarged blood-filled spaces lined by fibrovascular tissue without endothelial cells, similar to aneurysmal bone cysts, can occur in Osteoblastomas.[3,5] Secondary aneurysmal bone cysts occur in up to 16 % of Osteoblastomas.[2] Osteoblastomas usually have sharp margins, except for ~15% which have a permeative pattern of tumor growth.[1,3,5] The less frequent Osteoblastomas with permeative margins are usually located in short and flat bones, and tibia.[1] Features typically associated with osteoblastoma that allow distinction from osteosarcoma include: sharply circumscribed margins; lack of increased mitotic activity and nuclear pleomorphism of osteoblasts; appearance of bony trabeculae within loose connective tissue; single layer of osteoblasts surrounding bony trabeculae; and lack of tumor permeation into adjacent normal bone.[1,3,5,19]

Epithelioid Osteoblastomas represent a subtype of osteoblastomas which contain large osteoblasts with large nuclei and nucleoli, and occasional mitoses, and account for 16% of cases.[1,5] These Osteoblastomas have the same clinical course and outcome as the other Osteoblastomas.[1,2]

Lesion Genetics

Various chromosomal rearrangements have been reported including hypodipolid and hyperdiploid chromosome numbers.[5]

Findings on Plain Films (Roentgenograms) and Computed Tomography

Osteoblastomas usually appear as circumscribed radiolucent lesions measuring greater than 1.5cm associated with surrounding osteosclerosis[2-4,8,9,13,14,16,17,19,21] (Figs. **396, 398, 399).** The radiolucent lesions typically arise in the medulla of bone and may or may not contain internal calcifications[2-4,8,9,13,14,16,17,19,21] (Fig. **400).** Spinal lesions are typically associated with bony expansion with thin peripheral sclerotic rims and variable internal mineralization[2-4,8,9,13,14,16,17,19,21] (Figs. **396, 397).** In tubular bones, osteoblastomas typically are circumscribed radiolucent lesions with or without central mineralization and adjacent reactive bone sclerosis[8] (Fig. **399, 400).** Solid or multilamellar (onion skin) periosteal reaction is seen in most osteoblastomas in long bones.[8] Approximately 10% of osteoblastomas have an aggressive growth pattern with irregular cortical bone destruction, permeative poorly defined margins, infiltration/invasion of adjacent tissues, and variable amounts of mineralization.[2-4,8,9,13,14,16,17,19,21] CT is superior to plain films for evaluation of tumor extent and thinned sclerotic rims, as well as presence of matrix mineralization.[4]

MRI Findings

Osteoblastomas often appear as a spheroid or ovoid zone measuring greater than 1.5-2 cm located within medullary bone.[4,8-13,17,20,21] The lesions can have irregular, distinct, or indistinct margins. Osteoblastomas often have low-intermediate signal on T1W1, low-intermediate to slightly high signal on PDW1, and low-intermediate and/or high signal on T2WI and FST2WI[4,8-13,17,20,21] (Figs. **396-400).** Calcifications or areas of mineralization can be seen as zones of low signal on T2W[9,12,17] (Figs. **396, 398).** After Gd-contrast administration, osteoblastomas show variable degrees of enhancement[10,11,17,21] (Figs. **396-400).** Zones of thickened cortical bone and medullary sclerosis that are often seen adjacent to osteoblastomas typically show mostly low signal on T1W, T2W1, and FST2W1.[4,9,13,17] Poorly defined zones of marrow signal alteration consisting of low-intermediate signal on T1WI, high signal on T2W1 and FST2WI, and corresponding Gd-contrast enhancement can be seen in the marrow adjacent to osteoblastomas as well as within the extra-osseous soft tissues[4,9,10,12,17] (Figs. **396,398,400).**

The MRI findings are related to replacement of marrow fat with fibrovascular tissue and inflammatory cells.[9-22] Linear, amorphous and/or focal regions of high signal on FS T2WI and Gd-contrast enhancement can be seen in the soft tissues adjacent to the tumors, resulting from soft tissue inflammation and increased vascularity, as well as from tumor extension.[4,9,10,13,17] Fluid-fluid levels and aneurysmal bone cysts may be seen in association with osteoblastomas[20] (Fig. **399).** MRI is useful in

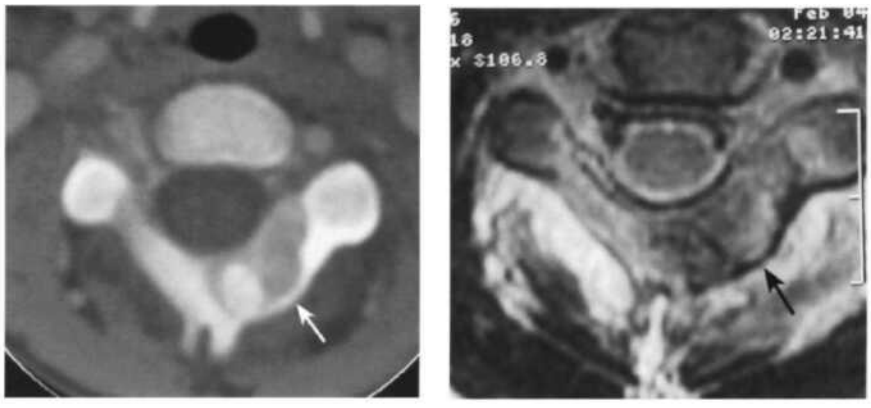

a, b

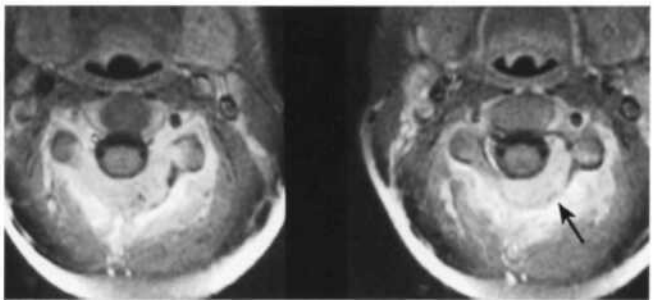

c

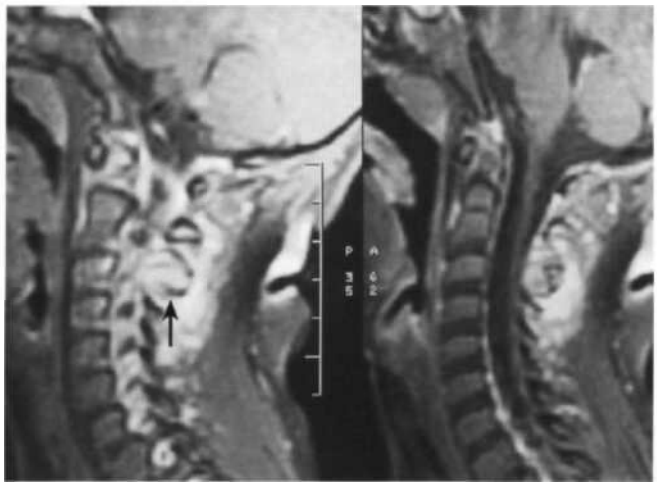

d

Figure **396a-d** A 4-year-old female with an osteoblastoma involving the left lamina of the C3 vertebra. Axial CT image (**a**) shows a circumscribed radiolucent lesion with an internal calcification. Sclerotic reaction is seen in the adjacent bone. Bony expansion with thin, peripheral, sclerotic rims are seen. The lesion has heterogeneous low-intermediate on axial T2WI (**b**), surrounded by poorly defined zones of high signal. The lesion shows prominent Gd-contrast enhancement on axial (**c**) and sagittal (**d**) FST1WI. Poorly defined zones of Gd-contrast enhancement are also seen in the marrow and soft tissues adjacent to the osteoblastoma.

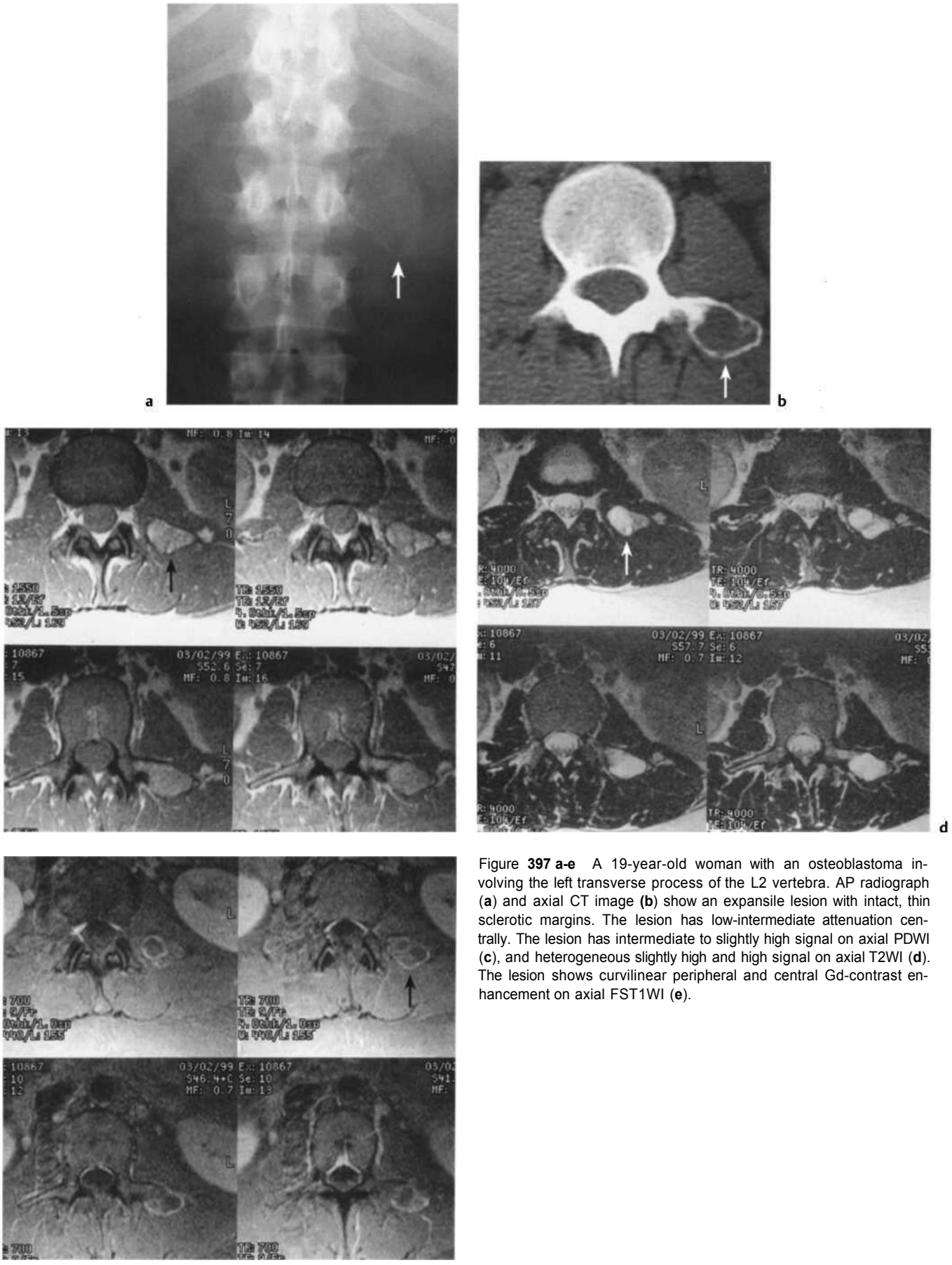

Figure **397 a-e** A 19-year-old woman with an osteoblastoma involving the left transverse process of the L2 vertebra. AP radiograph (**a**) and axial CT image **(b**) show an expansile lesion with intact, thin sclerotic margins. The lesion has low-intermediate attenuation centrally. The lesion has intermediate to slightly high signal on axial PDWI (**c**), and heterogeneous slightly high and high signal on axial T2WI (**d**). The lesion shows curvilinear peripheral and central Gd-contrast enhancement on axial FST1WI (**e**).

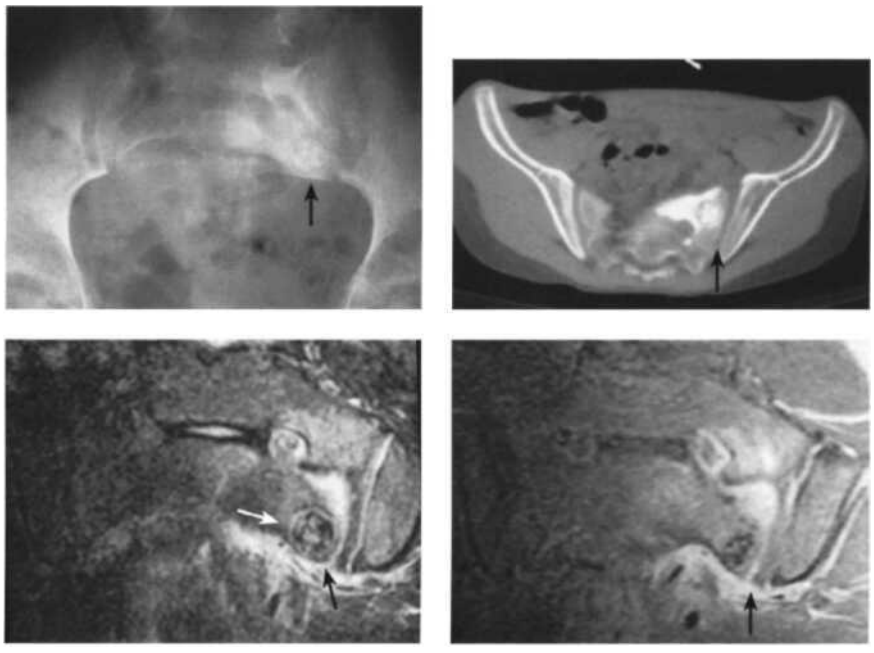

Figure **398a-d** A 12-year-old male with an osteoblastoma involving the inferior portion of the left sacral alum. AP radiograph (**a**) and axial CT image (**b**) show a radiolucent lesion containing a dense calcfication surrounded by thin sclerotic margins. Prominent dense sclerotic reaction is seen in the bone adjacent to the lesion on CT. The lesion has intermediate to slightly high signal peripherally, surrounding a central zone with low and slightly high signal on coronal FST2WI (**c**). The lesion shows mild to moderate Cd-contrast enhancement on coronal FST1 WI (**d**). Poorly defined zones of high signal on T2WI and corresponding Gd-contrast enhancement are seen in the marrow and soft tissues adjacent to the osteoblastoma.

Figure 399a-c A 39-year-old man with an osteoblastoma involving the proximal tibia. AP radiograph (**a**) shows a circumscribed radiolucent lesion with thin sclerotic margins. The intramedullary osseous lesion has heterogeneous intermediate signal on coronal T1WI (**b**), and extends into the soft tissues laterally through a zone of cortical destruction. The lesion has heterogeneous signal with zones of low, intermediate, and high signal on axial PDWI (**c**, left images) and T2WI (c, right images), as well as multiple fluid-fluid levels from secondary aneurysmal cyst formation. The tumor causes expansion and irregular thinning of the dorsal margin of the proximal tibia. A thin, low signal margin is seen at the border of the tumor with medullary bone. The lesion shows prominent heterogeneous Gd-contrast enhancement on axial (**d**) and coronal (**e**) FST1WI.

Figure **399 d,e** >

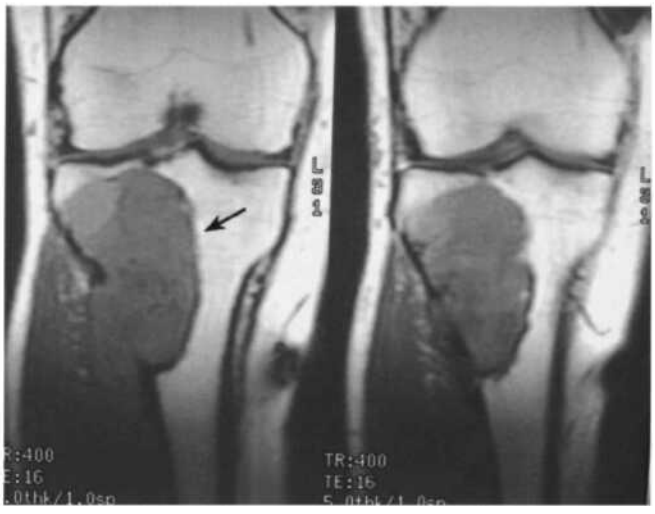

b

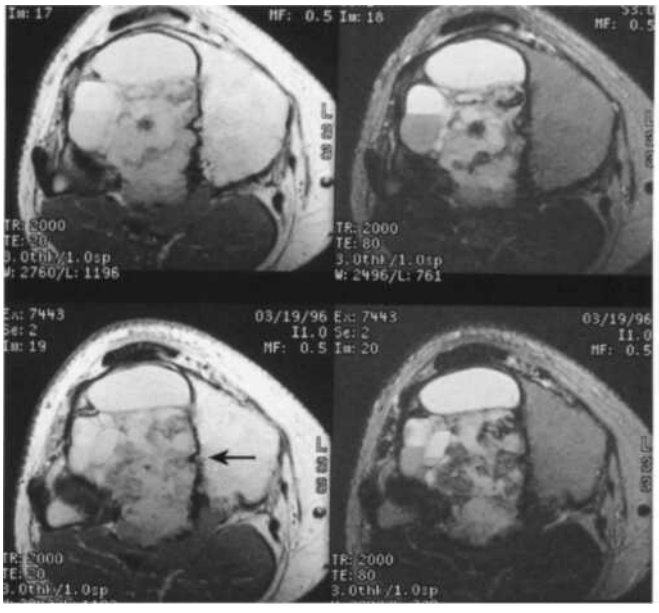

c

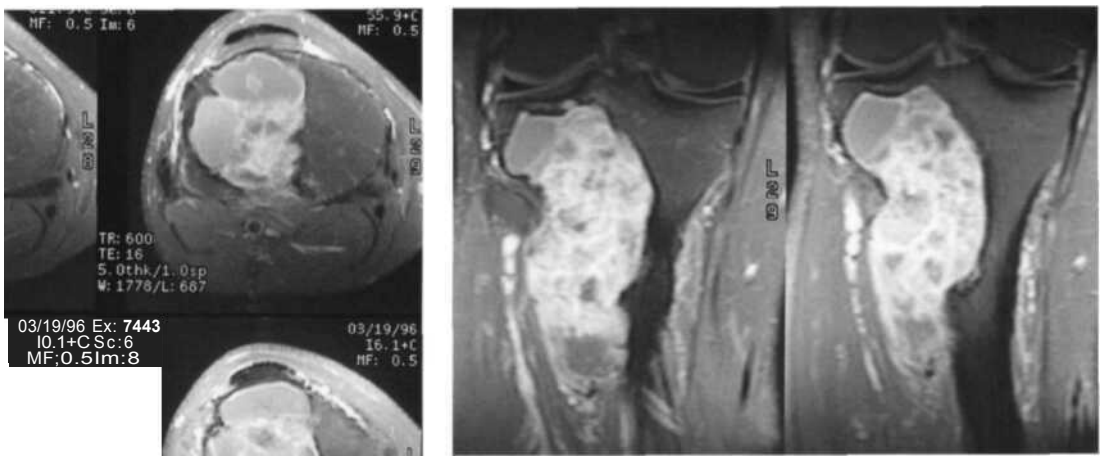

Figure **399 d, e**

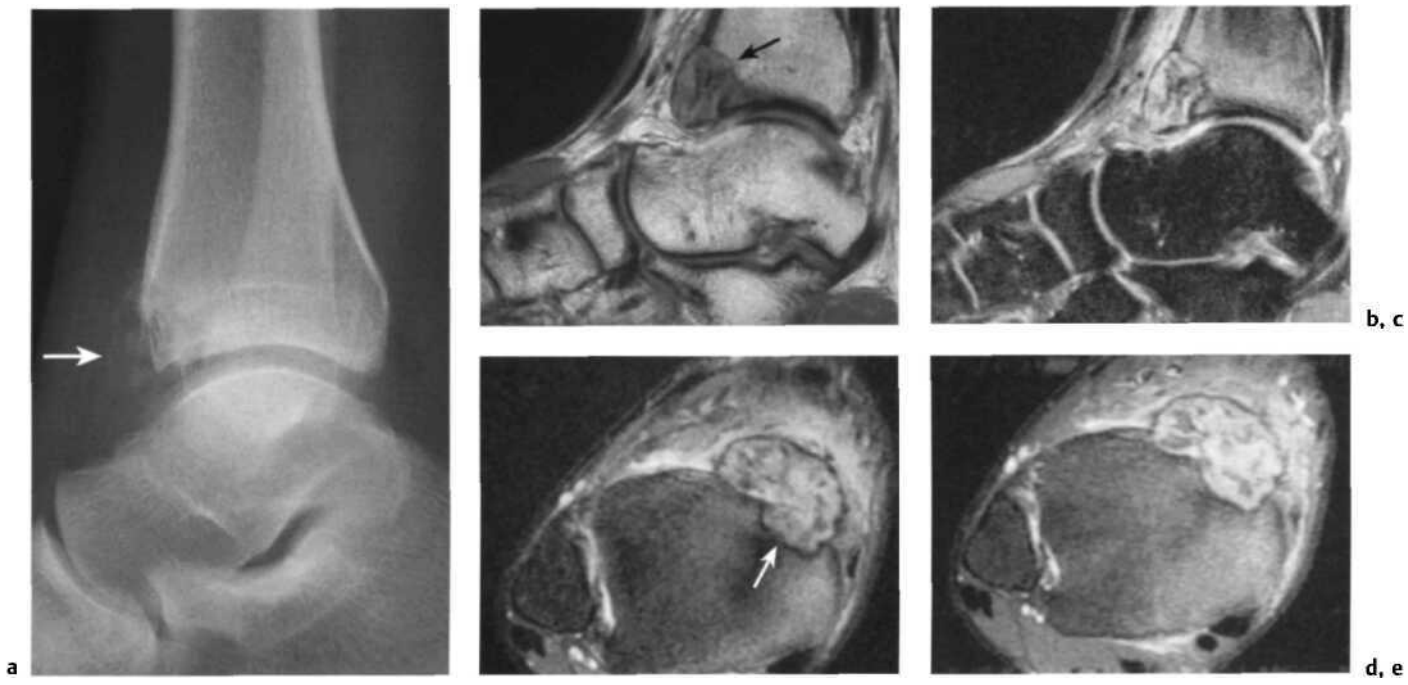

Figure **400a-d** A 24-year-old man with an osteoblastoma involving the distal tibia. Lateral radiograph (**a**) shows a circumscribed, slightly expansile radiolucent lesion with thin, slightly sclerotic margins. The lesion has heterogeneous low and intermediate signal on sagittal T1 WI (**b**), and heterogeneous signal with zones of high and low signal on sagittal (**c**) and axial (**d**) FS T2WI. A thin rim of low signal is seen at the periphery of the tumor and at the border with medullary bone. The tumor causes expansion and irregular thinning of the anterior cortical margin of the distal tibia. The lesion shows prominent heterogeneous Gd-contrast enhancement on axial (**e**) and sagittal **(f**) FST1WI. Poorly defined zones of high signal on T2WI and corresponding Gd-contrast enhancement are seen in the marrow and soft tissues adjacent to the osteoblastoma.

discriminating tumor tissue from adjacent reactive edema.[4,9] MRI also provides critical information regarding the extent of spinal osteoblastomas and the presence of spinal canal and foraminal compression.[4,9,10,12,13,17]

Differential Diagnosis

Osteoid osteoma, aneurysmal bone cyst, giant cell tumor, chondrosarcoma, osteosarcoma, chondroblastoma, metastatic lesion, eosinophilic granuloma, osteomyelitis, sarcoid.

Prognosis and Treatment

Osteoblastomas are benign tumors with varying degrees of progression. The degree of aggressive growth is not related to histologic features, but is related to tumor location.[1] Osteoblastomas in short and flat bones were more aggressive than lesions in long bones.[1] Osteoblastomas are usually treated with curettage, although large lesions often require excision.[5,8,13,15,19] With complete surgical removal, prognosis is typically excellent with a low rate of recurrence.[2,5,8] Cryosurgery may be useful for treating tumor beyond the surgical margins.[8] Malignant transformation of osteoblastomas is considered rare.[2,19] Radiation is not routinely utilized because of the potential for malignant transformation.[13,15,19] Radiation is usually used only for aggressively growing tumors or recurrent lesions.[3] Chemotherapy may be of benefit for large lesions, recurrent aggressive tumors, or those that are surgically inaccessible.[2]

References

1 Delia Rocca C, Huvos AG. Osteoblastoma: varied histologic presentations with a benign clinical course. An analysis of 55 cases. *Am J SurgPathol* 1996;20:841-850.

2 Forest M. Osteoid osteoma and osteoblastoma. In: Forest M, Tomeno B, Vanel D, eds. *Orthopedic Surgical Pathology: Diagnosis of Tumors and Pseudotumoral Lesions of Bone and Joints* Edinburgh: Churchill Livingstone; 1998:79-98.

3 Huvos AG. Osteoblastoma. In: Huvos AG, ed. *Bone Tumors: Diagnosis, Treatment, and Prognosis* 2nd ed. Philadelphia, Pa: W.B. Saunders; 1991:67-80.

4 Kroon HM, Schurmans J. Osteoblastoma: clinical and radiologic findings in 98 new cases. *Radiology* 1990;175(3):783-790.

5 Malcolm AJ, Schiller AL, Schneider-Stock R. Osteoblastoma. In: Fletcher COM, Unni KK, Mertens F, eds. *World Health Organization Classification of Tumours. Pathology and Genetics of Tumours of Soft Tissue and Bone* Geneva: lARC Press; 2002:262-263.

6 Mulder JD, Schutte HE, Kroon HM, Taconis WK. Introduction. In: *Radiologic Atlas of Bone Tumors* Amsterdam: Elsevier; 1993:3-6.

7 Mulder JD, Schutte HE, Kroon HM, Taconis WK. The diagnosis of bone tumors. In: *Radiologic Atlas of Bone Tumors* Amsterdam: Elsevier; 1993:9-46.

8 Mulder JD, Schutte HE, Kroon HM, Taconis WK. Osteoblastoma. In: *Radiologic Atlas of Bone Tumors* Amsterdam: Elsevier; 1993: 399-418.

9 Murphey MD, Andrews CL, Flemming DJ, Temple HT, Smith WS, Smirniotopoulos JG. Primary tumors of the spine: radiologic-pathologic correlation. *Radiographics* 1996:16:1131-1158.

10 Obenberger J, Seidl Z, Plas J. Osteoblastoma in a lumbar vertebral body. *Neuroradiology* 1999;41:279-282.

11 Orbay T, AtaoSlu 0, Taly ET, Kaymaz M, Alp H. Vertebral osteoblastoma: are radiologic structural changes necessary for diagnosis? *SurgNeurol* 1999;51:426-429.

12 Őzkal E, Erongun U, çakir B, Acar 0, Uygun A, Bitik M. CT and MR imaging of vertebral osteoblastoma—a report of two cases. *Clin Imaging* 1996;20(1):37-41.

13 Ozaki T, Liljenqvist U, Hillman A, et al. Osteoid osteoma and osteoblastoma of the spine: experiences with 22 patients. *Clin Orthop Relat Res* 2002;397:394-402.

14 Papagelopoulos PJ, Galanis EC, Sim FH, Unni KK. Clinicopathologic features, diagnosis, and treatment of osteoblastoma. *Orthopedics* 1999;22:244-247.

15 Pringle Jean AS. Bone-forming neoplasms arising within bone. In: Helliwell TR, ed. Major *Problems in Pathology: Pathology of Bone and Joint Neoplasms.* 1 st ed. Vol 37. Philadelphia, Pa: W.B. Saunders, 1999: 168-171.

16 Saifuddin A, White J, Sherazi Z, Shaikh MI, Natali C, Ransford AO. Osteoid osteoma and osteoblastoma of the spine. Factors associated with the presence of scoliosis. *Spine* 1998;23:47-53.

17 Shaikh MI, Saifuddin A, Pringle J, Natali C, Sherazi Z. Spinal osteoblastoma: CT and MR imaging with pathological correlation. *Skeletal* Radio/1999;28:33-40.

18 Unni KK. Introduction and scope of study. In: *Dahlin's Bone Tumors-General Aspects and Data on 11*087 Cases 5th ed. Philadelphia, Pa: Lippincott, Williams & Wilkins; 1996:1-9.

19 Unni KK. Benign osteoblastoma (giant osteoid osteoma). In: *Dahlin's Bone Tumors-General Aspects and Data on 11087 Cases* 5th ed. Philadelphia, Pa: Lippincott, Williams & Wilkins; 1996:131-142.

20 Vilanova JC, Dolz JLI, Maestro de Leon JL, Aparicio A, Aldoma J, Capdevila A. MR imaging of a malignant schwannoma and an osteoblastoma with fluid-fluid levels. Report of two new cases. *Eur Radiol* 1998;8:1359-1362.

21 Wang YC, Huang JS, Wu CJ, Jeng CM, Fan JK, Resnick D. A huge osteoblastoma with aneurysmal bone cyst in skull base. *Clin Imaging* 2001 ;25:247-250.

22 Yamamura S, Sato K, Sugiura H, et al. Prostaglandin levels of primary bone tumor tissues correlate with peritumoral edema demonstrated by magnetic resonance imaging. Cancer 1997;79:255-261.

A 62 Osteoma, Enostosis, Osteopoikilosis, and Melorheostosis

Definition

Osteomas are benign primary bone tumors composed of dense, lamellar, woven and/or compact cortical bone that is usually located at the surface of bones.[3,5,11] Rarely, intramedullary osteomas also occur.[5] Multiple osteomas usually occur in Gardner syndrome, which is an autosomal-dominant disorder that is associated with intestinal polyposis, fibromas, and desmoid tumors.[3,5,15]

Enostoses (bone islands) are non-neoplastic intramedullary zones of mature compact bone composed of lamellar bone, which are considered to be developmental anomalies resulting from localized failure of bone resorption during skeletal maturation.[3]

Osteopoikilosis (osteopathia condensans disseminata or spotted bone disease) is a sclerosing bone dysplasia in which numerous small, round or oval, radiodense foci are seen in medullary bone giving the appearance of multiple bone islands.

Melorheostosis is a rare, nonhereditary, sclerosing mesodermal dysplasia in which there is irregular smooth sclerotic thickening of cortical bone in a "dripping or flowing candle-wax" configuration.[4] The abnormality localizes in regions of innervation of spinal sensory nerves and correlates with those sclerotomes and myotomes.[8]

Frequency of Occurrence

Osteomas account for < 1 % of benign primary bone tumors.[9™]

Enostoses occur in 1 % of the adult population.[3]

Osteopoikilosis is a rare disorder.[4]

Melorheostosis is a rare disorder.[4]

Age at Presentation

Osteoma: fromlS to 74 years, most frequent in the 6th decade.[5]

Enostosis: usually occurs in adults, rarely in children[3]

Osteopoikilosis: can occur at any age.[4]

Melorheostosis: usually occurs in children and young adults.[4] As many as 40-50 % of cases occur in the first 20 years of life.[8]

Gender Ratio (M/F)

Osteoma: 1 / 3.[5]

Enostosis: 1 /1.[3]

Osteopoikilosis: 1 /l.[4]

Melorheostosis: 1 /1.[4]

Location

Osteomas usually involve membranous bone, and are most often located at the surfaces of the skull and facial bones.[35] Osteomas typically protrude from the outer table of the skull, but may occasionally protrude from the inner table.[1,11] Osteomas infrequently occur in long bones and have been referred to as parosteal osteomas.[15] Rarely, osteomas can occur in soft tissues.[3,6]

Enostoses occur in medullary bone of the pelvis, femur, humerus, ribs, vertebrae, and other bones.[3] In long bones, enostoses often occur in the epiphyseal or metaphyseal regions.[3]

Osteopoikilosis occurs in medullary bone of the pelvis, femur, tibia, fibula, carpus, tarsus, hands, and feet.[4] Foci rarely occur in the skull, facial bones, ribs, and vertebrae.[4]

Melorheostosis may involve one bone (mono-ostotic) or multiple bones (polyostotic).[4] One or multiple adjacent bones are often affected in a sclerotomal distribution. The lower limb is a common location, but lesions also have been reported in the pelvis, humerus, ulna, hands, and feet.[4] The abnormality may extend across synovial joints.[8] Lesions rarely occur in the spine, ribs, and craniofacial bones.[4]

Signs and Symptoms

Osteomas are usually painless, hard lesions along a bone surface with duration of 1-2 years.[5,15] Osteomas in the paranasal sinuses are usually asymptomatic except for rare cases when there is obstruction of mucous drainage.[5] Osteomas involving the orbit can produce proptosis.[15] Osteomas in the middle-ear can result in conductive hearing loss.[5]

Enostoses are typically asymptomatic.[3]

Osteopoikilosis is usually asymptomatic.[4] In 25 % of patients, bone lesions may be associated with subcutaneous nodules, keloid formation, and sclerodermalike lesions (Buschke-Ollendorff syndrome). Osteopoikilosis may also occur in association as an overlap syndrome with other sclerosing bone dysplasias such as melorheostosis and osteopathia striata.[4]

Melorheostosis can be asymptomatic, although patients may have pain, limitation of motion, joint contractures, muscle atrophy, and limb length discrepancy.[4] The lower extremity is more frequently involved than the upper extremity. Melorheostosis may be occasionally associated with skin lesions and vascular anomalies. Melorheostosis in the spine may result in back pain as well as fusion over several levels.[8]

Cross Pathologic Findings

Osteomas are elongated or lobular, dense, ivorylike lesions covered by a periosteal membrane.[3] Osteomas vary in size from 2 to 20 cm, but most do not exceed 6 cm.[3]

Enostoses are small, white, spheroid or ovoid masses ranging in size from 1 to 15mm.[3]

Osteopoikilosis appears as multiple small, white, spheroid or ovoid masses of sclerotic bone which are similar to enostoses.[4]

Melorheostosis are elongated, wavy, and ivorylike lesions contiguous with bone cortex.[4] Lesions may be associated with ossification in adjacent soft tissues.[6]

Histopathologic Findings

Osteomas are usually composed of dense, mature lamellar or compact cortical bone.[3] The periosteal surface of osteomas usually have layers of lamellar bone, whereas deeper portions may contain a coarse mosaic pattern of lamellar bone.[5] Haversian systems and cement lines similar to Paget disease may be present in osteomas.[3,13] Osteomas are usually covered by a thin layer of spindle cells without cellular atypia.[3,13] No cartilage is present in osteomas.[13]

Trabecular or spongy osteomas can occur in medullary bone or in a subperiosteal location.[5] These osteomas have a predominant, cancellous trabecular architecture containing fatty marrow surrounded by a cortical bony margin.[5]

Intramedullary osteomas can radiographically resemble bone islands (enostoses).[3,5]

Enostoses are non-neoplastic zones of mature compact bone composed of lamellar bone surrounded by small blood vessels within spongiosa.[3,5] Bone islands are considered to be developmental anomalies in which there is focal localized failure of bone resorption during skeletal maturation.[3]

Osteopoikilosis has histologic features similar to enostoses with foci of sclerotic compact bone with some Haversian systems.[4]

Melorheostosis consists of variable degrees of cortical thickening composed of chondroid islands surrounded by dense lamellar and woven bone with irregularly distributed, normal-appearing Haversian systems.[4] Additional findings associated with melorheostosis include peripheral zones of fibrocartilage with irregular surface fibrillation as well as soft tissue abnormalities consisting of osseous, chondroid, vascular, and fibrocartilaginous tissue in up to 76 % of cases.[6,8]

Findings on Plain Films (Roentgenograms) and Computed Tomography

Surface osteomas appear on radiographs and CT as dense, round or ovoid lesions with well-circumscribed margins that are contiguous with cortical bone, and inner or outer tables of the skull.[1-3,5-7,11,12,14,15] Osteomas can attach to bone via a neck or a broad base, both of which are dense, unlike parosteal osteosarcomas.[1,14] CT shows contiguity of surface osteomas with underlying bone without a cleavage plane[6] (Fig. **401).** The surface of osteomas is usually smooth or lobulated[3,5,14] (Figs. **401, 402).** Large osteomas may contain small internal zones of intermediate attenuation on CT.[1] Zones of bone destruction or associated mass lesions of soft tissue are not associated with osteomas.[3,14] Perisosteal reaction is not associated with osteomas except in cases with coincidental antecedent trauma.[14] Intramedullary osteomas resemble bone islands.[35]

Enostoses typically appear as a circumscribed, radiodense, ovoid or spheroid focus in medullary bone, which may or may not contact the endosteal surface of cortical bone[3] (Fig. **403).** Enostoses that are larger than 2cm are referred to as "giant bone islands."[3]

Osteopoikilosis typically appears as multiple circumscribed, radiodense, ovoid or spheroid foci in medullary bone that usually measure 3-5 mm[4] (Fig. **404).** The long axis of the foci

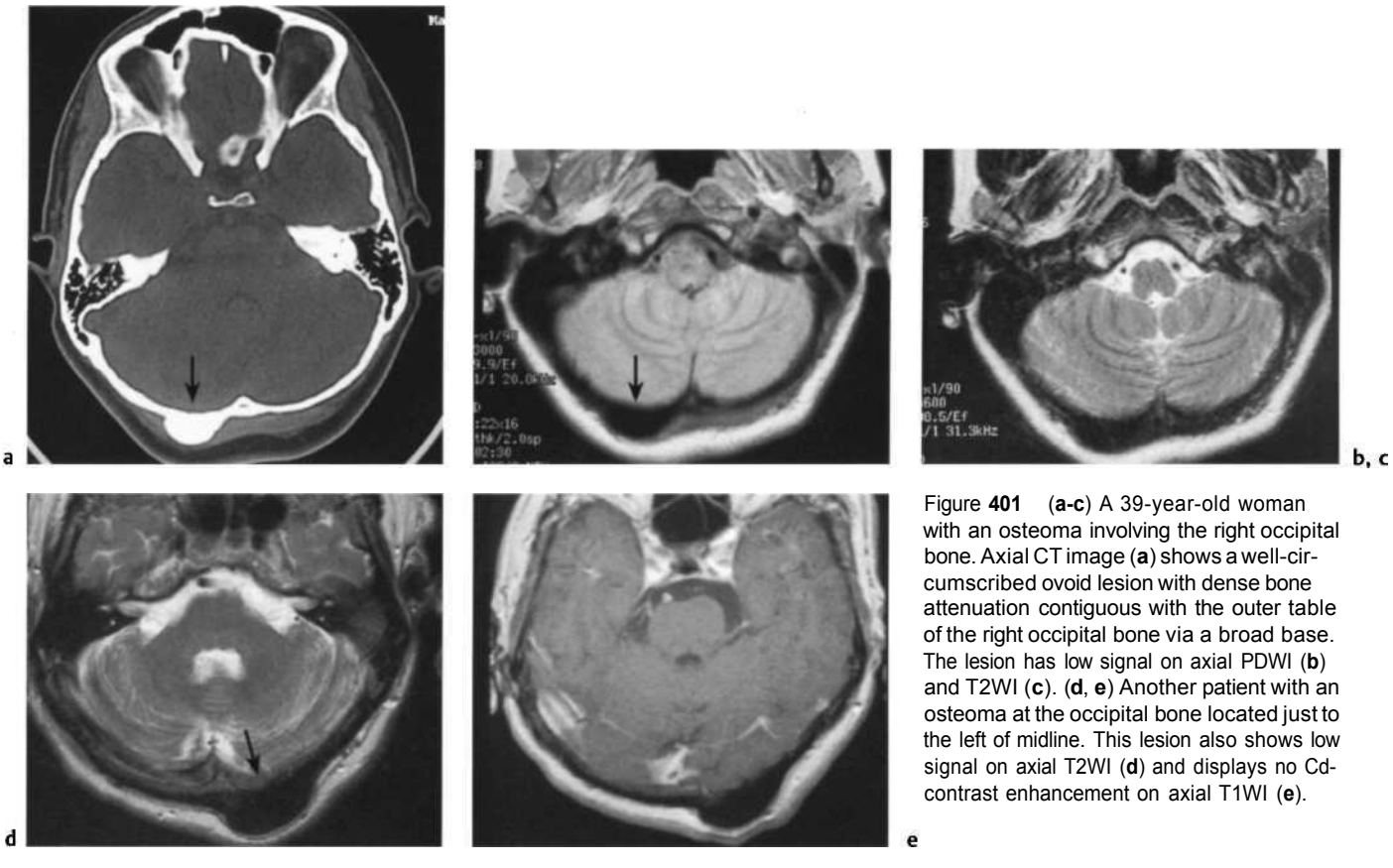

Figure **401** (**a-c**) A 39-year-old woman with an osteoma involving the right occipital bone. Axial CT image (**a**) shows a well-circumscribed ovoid lesion with dense bone attenuation contiguous with the outer table of the right occipital bone via a broad base. The lesion has low signal on axial PDWI (**b**) and T2WI (**c**). (**d**, **e**) Another patient with an osteoma at the occipital bone located just to the left of midline. This lesion also shows low signal on axial T2WI (**d**) and displays no Cd-contrast enhancement on axial T1WI (**e**).

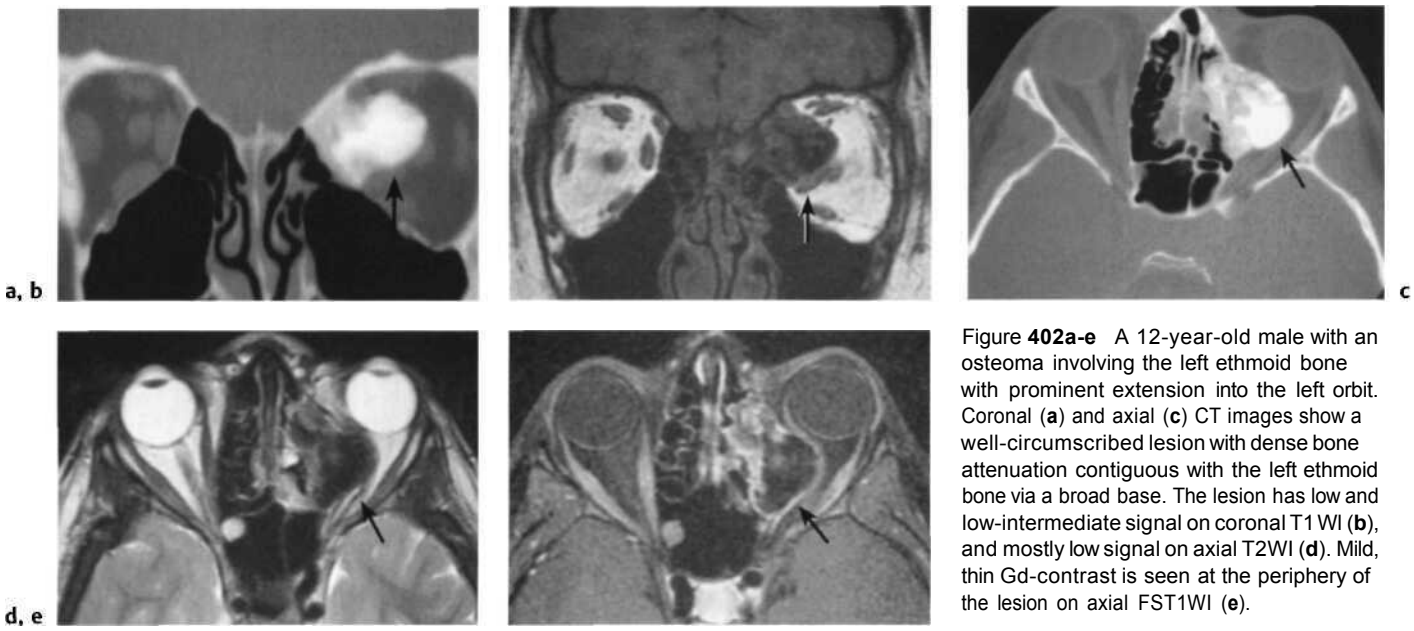

Figure **402a-e** A 12-year-old male with an osteoma involving the left ethmoid bone with prominent extension into the left orbit. Coronal (**a**) and axial (**c**) CT images show a well-circumscribed lesion with dense bone attenuation contiguous with the left ethmoid bone via a broad base. The lesion has low and low-intermediate signal on coronal T1 WI (**b**), and mostly low signal on axial T2WI (**d**). Mild, thin Gd-contrast is seen at the periphery of the lesion on axial FST1WI (**e**).

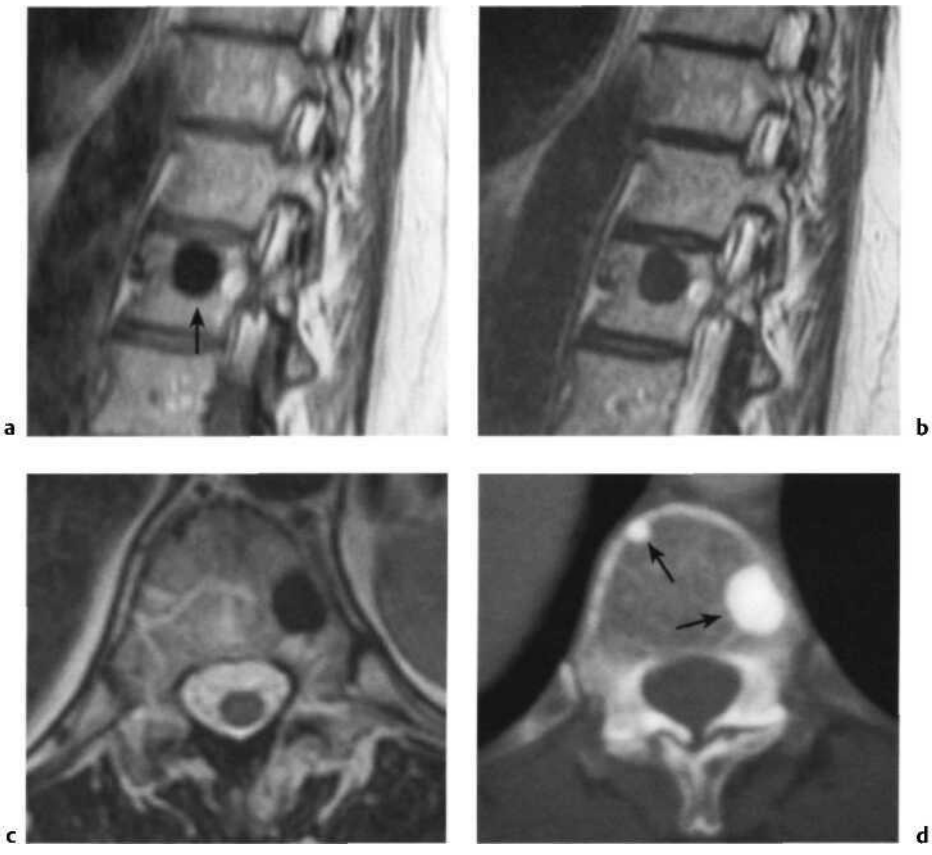

Figure **403a-d** A 68-year-old woman with two bone islands in the T12 vertebral body. The bone islands have well-circumscribed margins and have low signal on sagittal T1 WI (**a**), and sagittal (**b**) and axial (**c**) T2WI. The bone islands have uniform high attenuation on axial CT (**d**).

are often parallel to the adjacent bone trabeculae.[4] Some foci may contact the endosteal surface of cortical bone.[4]

Melorheostosis typically appears as wavy, eccentric, well-defined zones of dense cortical hyperostosis, which is often associated with narrowing of the medullary cavity[48] (Fig. **404).**

Radionuclide Bone Scan

Osteomas typically do not show increased radiopharmaceutical accumulation during early vascular and blood pool phases, but may show mild increased uptake on delayed images.[7] Melorheostosis may show radiopharmaceutical uptake on bone scintigraphy.[4]

MRI Findings

Osteomas typically appear as well-circumscribed zones of dense bone with mostly low signal on Tl Wl, PDWI, T2WI, and FST2WT (Figs. **401, 402).**[7] Zones of bone destruction or associated mass-lesions of soft tissue are not associated with osteomas.[3,14] Perisosteal reaction is not associated with osteomas

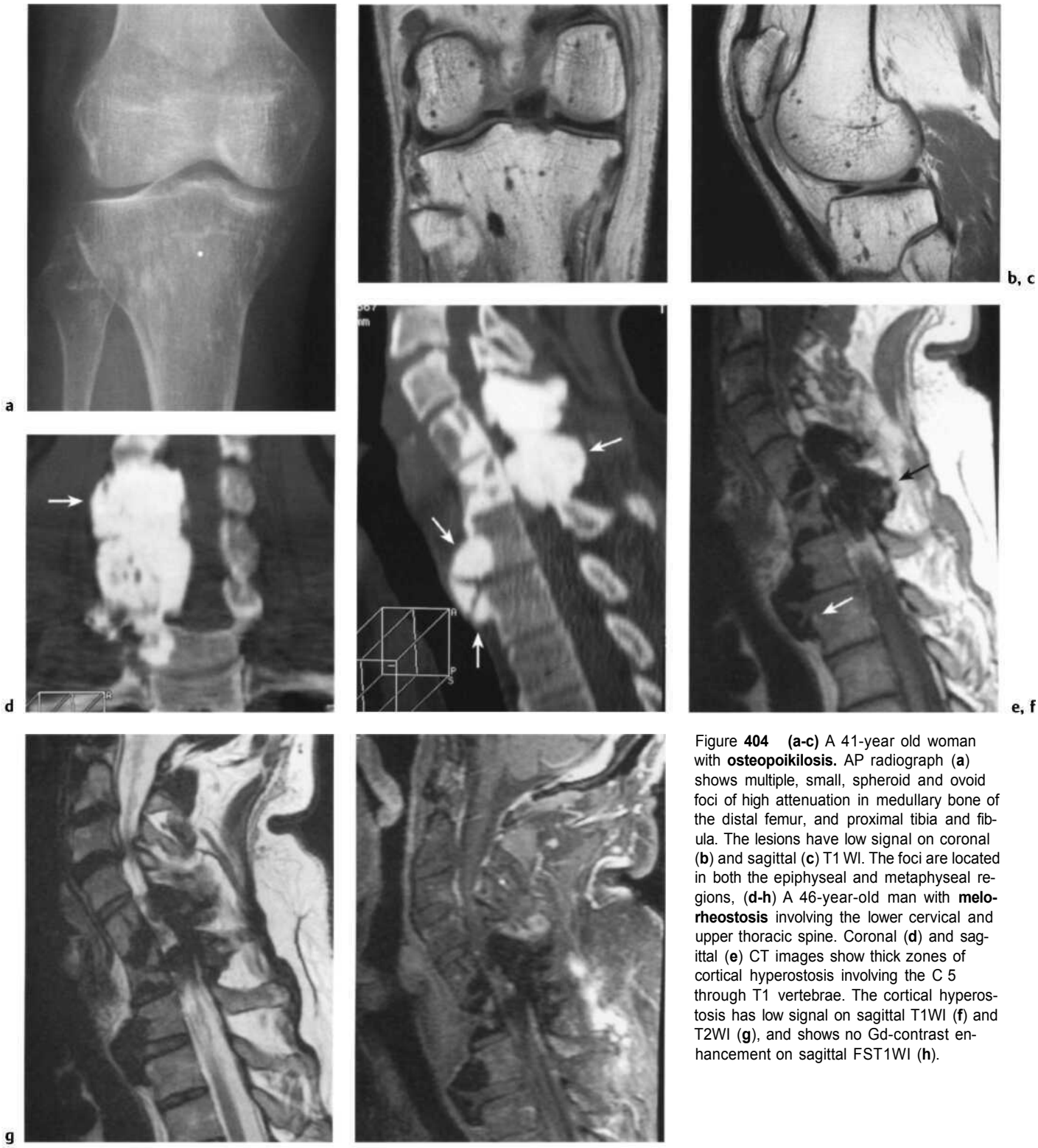

Figure **404** **(a-c)** A 41-year old woman with **osteopoikilosis.** AP radiograph (**a**) shows multiple, small, spheroid and ovoid foci of high attenuation in medullary bone of the distal femur, and proximal tibia and fibula. The lesions have low signal on coronal (**b**) and sagittal (**c**) T1 WI. The foci are located in both the epiphyseal and metaphyseal regions, (**d-h**) A 46-year-old man with **melorheostosis** involving the lower cervical and upper thoracic spine. Coronal (**d**) and sagittal (**e**) CT images show thick zones of cortical hyperostosis involving the C 5 through T1 vertebrae. The cortical hyperostosis has low signal on sagittal T1WI (**f**) and T2WI (**g**), and shows no Gd-contrast enhancement on sagittal FST1WI (**h**).

except in cases with coincidental antecedent trauma.[14] Enostoses (intramedullary osteomas) can resemble bone islands.

Enostoses typically have low signal comparable to cortical bone on all pulse sequences[3] (Fig. **403).**

Osteopoikilosis typically appears as multiple foci with low signal comparable to cortical bone on all pulse sequences (Fig. **404).**

Melorheostosis usually appears as elongated wavy zones of thickened bone cortex with low signal on T1WI, PDWI, and T2WI[68] (Fig. **404).** No Gd-contrast enhancement is typically seen at the cortical hyperostosis (Fig. **404).** Narrowing of the medullary canal of bone is often seen. Soft tissue lesions may also occur adjacent to the cortical lesions, which have mixed signal on T1WI and T2WI.[6]

Differential Diagnosis

Osteoma. Parosteal osteosarcoma, osteochondroma, osteoid osteoma, osteoblastoma, healing stress fracture, fibrous dysplasia, osteofibrous dysplasia/ossifying fibroma, melorheostosis, end-stage myositis ossificans, hyperostosis related to a meningioma.

Enostosis. Calcified nidus of osteoid osteoma, osteoblastoma, osteoblastic metastases, sclerotic steosarcoma (giant bone island).[3]

Osteopoikilosis. Osteoblastic metastases, mastocytosis.

Melorheostosis. Osteoma, healing stress fracture, tumoral calcinosis, tumoral calcium pyrophosphate dehydrate deposition disease, osteofibrous dysplasia, heteroropic ossification, involuted or treated osteoid osteoma, parosteal and periosteal osteosarcoma.

Prognosis and Treatment

Surgical excision resulting in cure is usually performed only for symptomatic osteomas.[3,5,13] Enostoses and Osteopoikilosis are not treated.[3,4] Melorheostosis lesions may have a slowly progressive course.[4] Surgical treatment is usually reserved for symptomatic lesions.[4]

References

1 Avrahami E, Even I. Osteoma of the inner table of the skull—CT diagnosis. *Clin Radiol* 2000;55:435-438.

2 Chikuda H, Goto T, Ishida T, lijima T, Nakamura K. Juxtacortical osteoma of the ulna. *] Orthop Sci* 2002;7:721-723.

3 Forest M. Osteoma and bone island. In: Forest M, Tomeno B, Vanel D, eds. *Orthopedic Surgical Pathology: Diagnosis of Tumors and Pseudotumoral Lesions of Bone and Joints* Edinburgh: Churchill Livingstone; 1998:71-77.

4 Forest M. Osteopoikilosis and melorheostosis. In: Forest M, Tomeno B, Vanel D, eds. *Orthopedic Surgical Pathology: Diagnosis of Tumors and Pseudotumoral Lesions of Bone and Joints* Edinburgh: Churchill Livingstone; 1998:627-637.

5 Huvos AE. Osteoma and Gardner's syndrome. In: Huvos AE, ed. *Bone Tumors: Diagnosis, Treatment and Prognosis* 2nd ed. Philadelphia, Pa: W.B. Saunders; 1991:1-7.

6 Kransdorf MJ, Murphey MD. Extraskeletal osseous and cartilaginous tumors. In: *Imaging of Soft Tissue Tumors* 2nd ed. Philadelphia, Pa: W.B. Saunders; 2006:437-480.

7 Lambiase RE, Levine SM, Terek RM, Wyman JJ. Long bone surface osteomas: imaging features that may help avoid unnecessary biopsies. *AJR Am J Roentgenol* 1998;171:775-778.

8 Motimaya AM, Meyers SP. Melorheotosis of the cervical and upper thoracic spine: radiographic, CTand MRI findings. *AJNR Am J Neuroradiol* 2006;27(6):1198-1200.

9 Mulder JD, Schutte HE, Kroon HM, Taconis WK. Introduction. In: *Radiologic Atlas of Bone Tumors.* Amsterdam: Elsevier; 1993:3-6.

10 Mulder JD, Schutte HE, Kroon HM, Taconis WK. The diagnosis of bone tumors. In: *Radiologic Atlas of Bone Tumors.* Amsterdam: Elsevier; 1993:9-46.

11 Mulder JD, Schutte HE, Kroon HM, Taconis WK. Osteoma. In: *Radiologic Atlas of Bone Tumors* Amsterdam: Elsevier; 1993: 381-384.

12 Peyser AB, Makley JT, Callewart CC, Brackett B, Carter JR, Abdul-Karim FW. Osteoma of the long bones and the spine. A study of eleven patients and a review of the literature. *J Bone Joint Surg Am* 1996;78(8):1172-1180.

13 Reid RP. Bone neoplasms and tumor-like lesions on the bone surface. In: Helliwell TR, ed. *Major Problems in Pathology: Pathology of Bone and Joint Neoplasms* 1st ed. Vol 37. Philadelphia, Pa: W.B. Saunders; 1999:215-233.

14 Sundaram M, Falbo S, McDonald D, Janney C. Surface osteomas of the appendicular skeleton. *AJR Am] Roentgenol* 1996;167:1529-1533.

15 Unni KK. Osteoma. In: *Dahlin's Bone Tumors—General Aspects and Data on 11087 Cases* 5th ed. Philadelphia, Pa: Lippincott, Williams & Wilkins; 1996:117-120.

A 63 Osteomyelitis

Definition

Osteomyelitis is a disorder in which there is infection of bone and, commonly, the adjacent soft tissues. Osteomyelitis can result from hematogenous spread of microorganisms as well as from trauma-direct inoculation, extension from adjacent tissues, and complications from surgery.[3,14,23] Bacteria are the most common infectious organisms.[16] *Staphylococcus aureus* and *Streptococcus pyogenes* are the most common bacterial infections involving bone.[14,16,18,19,23] Osteomyelitis can also result from other bacteria such as *Pseudomonas aeruginosa, Escherichia coli,* and *Klebsiella* spp., which occur in intravenous drug abusers, streptococcal organisms in patients with endocarditis, and *Haemophilis aprophilus* in patients with meningitis.[18,19,23] *Haemophilus influenzae* and group B Streptococci are frequent pathogens causing osteomyelitis in neonates, and Salmonella is a frequent cause of osteomyelitis in patients with sickle cell disease.[18] Recently, osteomyelitis from *Haemophilus influenzae* has declined because of the use of the *Haemophilus influenzae* type B vaccine.[19] Almost any bacteria can cause osteomyelitis, given the appropriate situation.[23] Osteomyelitis can also result from other organisms such as Mycobacteria tuberculosis, fungi, parasites, and viruses.[4,18,19,23] Mycobacteria tuberculosis caused an estimated 8.8 million new infections worldwide in 2005 (World Health Organization), and osteoarticular tuberculosis occurs in up to 3 % of this group.[15] Musculoskeletal tuberculosis is endemic in China, India, South Africa, and the Near East; and it also occurs in immunocompromised patients.[15] Fungal osteomyelitis usually occurs in immunocompromised patients, with Candida and Aspergillus being the most common organisms.[12] *Coccidioides immitis* also causes osteomyelitis in 10-20% of immunocompetent patients infected with this fungus.[4,22] Pa tients with HIV infection occasionally develop osteomyelitis, with *Staphylococcus aureus* and Salmonella accounting for most cases.[2,19] Less frequently, organisms such as *Neisseria gonorrhea, Cryptococcus neoformans,* and *Nocardia* asteroides have also been reported to cause osteomyelitis in HIV-infected patients.[2,19]

Chronic recurrent multifocal osteomyelitis is an inflammatory disease involving bone of unknown etiology which typically affects children and adolescents.[17] Multiple metaphyseal osteolytic lesions associated with localized plasma cell proliferation occur and regress, and may be associated with pyoderma gangrenosum and ulcerative colitis."

Neoplasms in bone occur in 0.2-1.7% of cases of osteomyelitis.[6,19] Most of these tumors occur in the setting of chronic osteomyelitis and are usually epidermoid carcinomas.[6]

Age at Presentation

Pyogenic osteomyelitis frequently occurs in children and adolescents.[9,16] Immunocompromised patients, intravenous drug abusers, and patients with diabetes have an increased risk for osteomyelitis.[14,16] Pyogenic spondylodiskitis typically affects men over the age of 50years, median = 67 years.[14,23]

Location

Pyogenic osteomyelitis. Common sites of infection include femur, tibia, humerus, fibula, radius, vertebra, iliac bone, mandible, and rib.[16] The initial location of osteomyelitis within specific bones is usually related to the configuration, size, and distribution of the vascular supply, which varies with patient age.[18] In neonates, metaphyseal vessels penetrate the physeal plate, and osteomyelitis often involves the metaphysis and/or epiphysis.[18,19] Epiphyseal osteomyelitis can extend into the joint, resulting in septic arthritis and articular damage or destruction.[18,19] In children, osteomyelitis in long bones occurs most frequently in the metaphysis because of the rich vascular supply and lack of contiguity with epiphyseal vessels, resulting in increased susceptibility to blood-borne pathogens.[9,16,18,19] After growth plate closure, metaphyseal and epiphyseal vessels reunite.[18,19] In adults, osteomyelitis can occur near the ends of long bones or diaphysis.[16,18,19] Pedal osteomyelitis can result from direct extension of soft tissue infections associated with foot ulcers, and are often located at the fifth and first metatarsophalangeal joints.[10] Osteomyelitis can involve different portions of the skull that may be related to sites of extension from sinus infections, otitis externa, mastoiditis, chronic periodontal disease, surgery, and traumatic injuries.[3,22]

Brodie abscess refers to a small (1-4 cm diameter) abscess (subacute osteomyelitis) in long bones that is typically walled-off by sclerotic bone and often involves the cortex.[6,18,19] These lesions account for up to 5 % of osteomyelitis cases,[6] with frequency of occurrence in tibia (50%) > femoral neck > other sites.[6]

Sclerosing osteomyelitis of Carre is a chronic bone infection that usually involves the mandible or shafts of long bones and is associated with extensive new bone formation which often obscures the involved osseous structure.[6,18,19]

,Pyogenic spondylodiskitis represents up to 4% of all cases of osteomyelitis,[23] and occurs in lumbar > thoracic > cervical, sacral locations.[23] Hematogenous vertebral osteomyelitis usually begins in richly vascularized subchondral bone adjacent to the vertebral endplate via nutrient arteries or Batson venous plexus.[14,23] The infection can spread by extension across the disk to involve the adjacent vertebral body, along longitudinal spinal ligaments, or hematogenously through interconnecting spinal arteries and veins.[14]

Tuberculous osteomyelitis occurs most frequently in the vertebrae (thoracic > lumbar > cervical) > knees > hips.[15,18] Spinal tuberculosis usually involves the two or more adjacent vertebral bodies, near the endplates initially, and less frequently in the posterior elements.[15] Extra-axial tuberculous osteomyelitis is usually mono-ostotic.[15] Tuberculous arthritis can result from extension from adjacent osteomyelitis (hip and knee > sacroiliac joint > shoulder > elbow > ankle).[15]

Signs and Symptoms

Pyogenic osteomyelitis. Patients can have localized pain, tenderness, swelling, malaise, fever, chills, elevated erythrocyte sedimentation rate, elevated serum C-reactive protein, leukocytosis, and/or bacteremia.[3,16,18] Patients with osteomyelitis of the skull base may have headaches and cranial neuropathies.[3]

Pyogenic spondylodiskitis (vertebral osteomyelitis/diskitis). Patients can have back pain, localized tenderness and/or rigidity, malaise, fever, chills, elevated erythrocyte sedimentation rate, elevated serum C-reactive protein, leukocytosis, and/or bacteremia.[23] Because of the nonspecificity of symptoms, diagnosis is often delayed.[23] Epidural abscesses or pathologic compression fractures from vertebral osteomyelitis can cause spinal cord and/or nerve root compression.[23] Epidural abscesses often result in localized and/or diffuse pain that can be more disabling than the associated neurologic deficits.[23]

Tuberculous osteomyelitis. Patients can have localized pain and tenderness, stiffness, low-grade fevers, chills, and weight loss.[15,18] Tuberculous osteomyelitis involving the spine is referred to as Pott disease.[15] Vertebral deformities resulting from destructive changes of involved vertebrae can result in kyphosis and/or scoliosis.[15,18] Up to 10% of patients with tuberculous vertebral osteomyelitis have significant neurologic complications such as paraparesis or paraplegia.[15] Patients with extra-axial tuberculous osteomyelitis may present with chronic progressive bone pain over months or years that is nonresponsive to analgesics.[15] Cold abscesses associated with tuberculous osteomyelitis often show soft tissue swelling without other features of inflammation.[15]

Pathologic Findings

The pathologic features of osteomyelitis depend on the age or stage (acute, subacute, or chronic) of the infection.[14,18]

Pyogenic Osteomyelitis

In the **acute phase of pyogenic osteomyelitis,** bacteria proliferate resulting in an early inflammatory response that consists of exudative, edematous, and ischemic changes in bone marrow.[14,18,19] Purulent material extends into vascular channels in bone resulting in increased intra-osseous pressure, impaired blood flow, and ischemic necrosis of bone.[19] Histologic examination typically shows microorganisms (bacteria), polymorphonuclear cells, and thrombosed blood vessels.[19] Lysosomal activation of polymorphonuclear cells and cytokines (interleukin (IL)-l, IL-6, IL-11, and tumor necrosis factor) released by inflammatory cells and bone cells results in necrosis and osteolysis of entrapped bony trabeculae.[14,18,19] The bacteria, inflammatory response, and increased pressure spread along the marrow, as well as extend through the cortex via the Haversian system and Volkman canals to the subperiosteal space.[18,19]

In long bones, extension of the infection through the cortex to the bone surface can result in a periosteal abscess, which lifts the periosteum.[18] Elevation of the periosteum by the inflammatory tissue can be prominent in infants and children.[19] Periosteal abscesses can extend for long distance along the shafts of tubular bones with potential impairment of the blood supply predisposing to segmental bone ischemia and necrosis.[18,19] The periosteum is more firmly attached to bone in adults than in children.[19] As a result there is typically minimal periosteal elevation from ostemyelitis in adults compared with the pediatric population.[19] Periosteal abscesses can secondarily increase the extent and degree of ischemia, resulting in a zone of segmental bone necrosis or sequestrae.[18] Rupture of the periosteal abscess can result in a sinus tract.[18] Involvement of the periosteum by osteomyelitis often leads to extension of the infection into the adjacent soft tissues.[19] Extension of the infection into an adjacent joint can result in chondrolysis and articular deformity from proteolytic degradation and oxygen radicals produced by the host phagocytic reaction against the infectious microorganisms.[19] Other complications of osteomyelitis in children include: premature closure of the physeal plate with growth disturbance, slipped epiphyses, pathologic fractures, and potential for sepsis and chronic infection.[19]

In the **subacute phase of pyogenic osteomyelitis,** chronic inflammatory cells increase in number and the pyogenic process becomes more localized.[13,18,19] Fibrovascular or granulation tissue ingrowths progressively occur at sites of osteoclastic activity and trabecular necrosis, and deposition of reactive bone occurs at the periphery forming an intra-osseous abscess.[13,18,19] A **Brodie abscess** represents a common form of subacute osteomyelitis, in which an intra-osseous radiolucent abscess in long bones is typically walled-off by sclerotic bone and often involves the cortex with or without a sinus tract.[6,18]

Chronic osteomyelitis

Decreased blood supply to bone secondary to the infection can result in a zone of osseous necrosis that lacks living osteocytes.[19] This zone of devitalized necrotic bone (also referred to as the sequestrum) is typically surrounded by granulation tissue.[19] A peripheral zone of reactive or reparative bone formation (involucrum) often forms around the sequestrum.[18,19] Drainage from the sequestrum into the extra-osseous soft tissues can occur through a tract (referred to as cloaca) or multiple tracts through the involucrum.[19] **Sclerosing osteomyelitis of Carre** is a form of chronic osteomyelitis in which there is prominent cortical thickening and periosteal reaction that can obscure the underlying bone.[6,18,19]

Tuberculous Osteomyelitis

Osteomyelitis resulting from tuberculosis usually occurs by hematogeneous spread.[15] Tuberculous osteomyelitis tends to be associated with greater medullary extension, osseous necrosis and destruction than pyogenic osteomyelitis.[18] Tuberculous osteomyelitis involving the spine (Pott disease) often extends into the adjacent soft tissues forming abscesses, referred to as cold abscesses.[15,18] Specimens from sites of tuberculous osteomyelitis show friable, light-gray, necrotic material containing acid-fast bacilli on smears, caseating granulomata, fibrosis, and positive cultures.[15,20] Bone biopsies are more accurate for detection of tuberculous osteomyelitis than fine needle aspirates.[15]

Findings on Plain Films (Roentgenograms) and Computed Tomography

Pyogenic osteomyelitis. Findings on plain films are typically absent until 10-21 days after the onset of symptoms.[13,16,19,22] These findings include: geographic zones of lucency involving medullary and/or cortical bone; indistinct or distinct lesion margins with or without reactive sclerosis; periosteal bone formation (one or more smooth uninterrupted lamellae) that is more prominent in children than adults; and soft tissue swelling[6,13,16,19,22] (Figs. **406, 413**). Sunburst periosteal reaction and Codman triangles are atypical for osteomyelitis.[1619] Occasionally, lesions can have a moth-eaten or permeative radiolucent pattern.[16,19] A **Brodie abscess** represents a form of subacute osteomyelitis in which a circumscribed spheroid or sinusoid intramedullary radiolucent abscess has sharp margins surrounded by a zone of reactive sclerosis[16,19] (Figs. **414, 415).** In chronic osteomyelitis, the bone is often expanded and remodeled with a thickened cortex.[22] A narrow zone of transition is often seen between the sites of chronic osteomyelitis and normal adjacent bone.[22] CT is the optimal method for demonstrating sites of cortical destruction, bone sequestra, and marrow calcifications and sclerotic reaction.[22]

Chronic sclerosing osteomyelitis. Radiolucent zones are typically surrounded by enlarged thickened bone without sequestration or fistulas.[6,16]

Pyogenic spondylodiskitis. About 10-14 days after the onset of symptoms, plain films can show blurring of the endplates of the vertebral bodies, decreased disk space height, and medullary bone destruction.[23] Late changes can be seen as compression deformities, kyphosis, and/or scoliosis.[23] Reactive sclerosis may eventually occur.[23] CT is superior to plain films in detecting and defining the extent of bone destruction, and paravertebral and intraspinal extension of the infection.[23]

Tuberculous osteomyelitis. The spine is the most frequent location for musculoskeletal tuberculosis, and accounts for more than 50% of cases.[7,15] Findings on plain films may not occur until up to 6 months after the onset of symptoms when more than 50 % of trabecular bone may be eroded.[15] Plain films can show erosions and/or blurring of the endplates of the vertebral bodies, medullary bone destruction, paravertebral soft tissue masses, and asymmetry of the psoas shadows.[12,15] Narrowing of the disk space may be minimal.[12,15] Late changes can be seen as compression deformities, kyphosis, and/or scoliosis.[15] Outside of the spine, tuberculous osteomyelitis is often initially localized in the metaphyseal portions of long bones.[15] In children, the infection rarely crosses the physeal plate.[15] Findings associated with tuberculous osteomyelitis include: soft-tissue swelling; zones of medullary radiolucency usually without prominent reactive sclerosis; minimal periosteal reaction; and zones of cortical erosion/destruction with or without extension into nearby joints or extra-osseous soft tissues.[15,20] Tuberculous arthritis may be associated with joint swelling; periarticular osteoporosis and osseous erosions.[15]

CT is superior to plain films in detecting and defining the extent of bone destruction and fragmentation, as well as paravertebral and epidural abscesses which may be associated with calcifications or displaced bone fragments[15] (Figs. 410, 412). With CT, paravertebral and epidural abscesses may have irregular thick rims of soft tissue attenuation surrounding central zones with lower attenuation.[15]

Fungal osteomyelitis. Various fungi (Monosporium, Aspergillus, Penicillium, Streptomyces, Madurella, Caephalosporium, etc.) cause chronic granulomatous infections of the feet (Madura foot), which can secondarily involve adjacent bone resulting in radiolucent lesions, sclerosis, periostitis, progressive fragmentation, and/or sinus tracts.[4] Sporotrichosis is a chronic fungal disease *(Sporothrix schenckii)* of the skin which can also involve adjacent bones and joints with radiolucent bone lesions, subchondral erosions, joint space narrowing, effusions, and soft tissue swelling.[4]

Blastomycosis can cause osteomyelitis hematogeneously or by direct extension, as is often associated with lung, skin, and joint abnormalities.[4] Features associated with osteomyelitis from blastomycosis include superficial cortical erosions from cutaneous lesions, and cystic-appearing or moth-eaten radiolucent zones with or without sclerotic margins and perisostitis.[4] Spinal infections may be associated with paravertebral abscesses that cause spinal cord compression.[4] Coccidioidomycosis infections typically involve the lung. Up to 20 % have granulomatous lesions in bone, which are seen as multiple, well-defined, radiolucent foci in the metaphyses of long bones and bony prominences, with or without periostitis.[4,22] Coccidioidomycosis involving the spine usually involves more than one vertebra.[4] Fungal infections involving bone from Histoplasmosis, Aspergillosis, Candidiasis, Cryptococcus, and Mucormycosis usually result in radiolucent lesions.[4] In immunocompromised patients, fungal osteomyelitis occurs most frequently from Aspergillosis and Candidiasis.[12]

Radionuclide Bone Scan

Pyogenic osteomyelitis. Radionuclide bone scans using technetium-99m methylene diphosphonate have been reported to give an accuracy up to 90 % for osteomyelitis in patients with more than 2 days of symptoms.[23] The combination of gallium-67 citrate scans and technetium-99 m methylene diphosphonate scans has been reported to give an accuracy up to 94 % for osteomyelitis.[23] Indium-1ll-labeled white blood cells or technetium-99 m hexamethylpropyleneamine oxime (HMPAO)-labeled white blood cells are also useful for detecting osteomyelitis, and have been shown to have higher specificities than conventional bone scans because of the association of the radiopharmaceutical agent with white blood cells.[19] The combined accuracy of technetium-99 m methylene diphosphonate and Indium-lll-labeled white blood cells is higher for detecting osteomyelitis in the appendicular skeleton compared with the axial skeleton.[22] A major limitation of nuclear medicine is the lack of spatial resolution in defining the exact extent and location of the infection and associated anatomic complications.[19]

MRI Findings

Pyogenic Osteomyelitis

In the acute phase of hematogenous pyogenic osteomyelitis, poorly defined zones of low or low-intermediate signal on T1WI; low-intermediate to slightly high signal on PDW1; and high signal on T2W1, STIR and FST2WI are seen in the marrow[3,7-11,13,17,19,21,2,22] (pigs. **405-407, 409, 413, 416, 417**). A wide zone of transition between normal bone and edematous and infected bone is typically seen in acute osteomyelitis.[19] Loss of definition of the low-signal line of the cortical margins is often observed on Tl WI, T2WI, STIR, and FST2WI.[3,7,8,10,11,13,17,19,22] After Gd-contrast administration, irregular zones of contrast enhancement are seen in the involved marrow on FSTIWI.[3,7,8,10,11,13,17,19,22] The sensitivity of MRI for detecting acute osteomyelitis has been reported to range from 82 to 100%, and the specificity from 75 to 96 %.[19]

Irregular and/or circumscribed zones of high signal on T2WI and FST2WI with corresponding diffuse and/or peripheral/marginal Gd-contrast enhancement can be seen in the extra-osseous soft tissues adjacent to intra-osseous sites of acute osteomyelitis, representing extension of the infectious process with or without abscess formation.[19,21] Subperiosteal fluid collections (abscesses) can be seen in patients with acute osteomyelitis, and typically have low signal on Tl WI and intermediate to high signal on T2WI, STIR, and FST2WI.[19] In the opposite direction, direct extension of infection from soft tissues to bone usually results in the initial localization of signal alteration (high signal on T2WI, STIR and FST2WI) and Gd-contrast enhancement in the periosteum and cortex prior to involvement of the marrow.[10,19,22] Foot ulcers are common complications of diabetes.[10,11,19] Pedal osteomyelitis can result from direct extension of infections associated with foot ulcers in -15% of patients.[10,11,19] Up to one-third of patients with advanced pedal infections also have septic arthritis.[10]

In the **subacute phase of pyogenic osteomyelitis,** chronic inflammatory cells increase in number and the pyogenic process becomes more localized than acute osteomyelitis.[13,18,19] The zone of transition between normal and abnormal bone is sharper and more well-defined in subacute and chronic osteo-

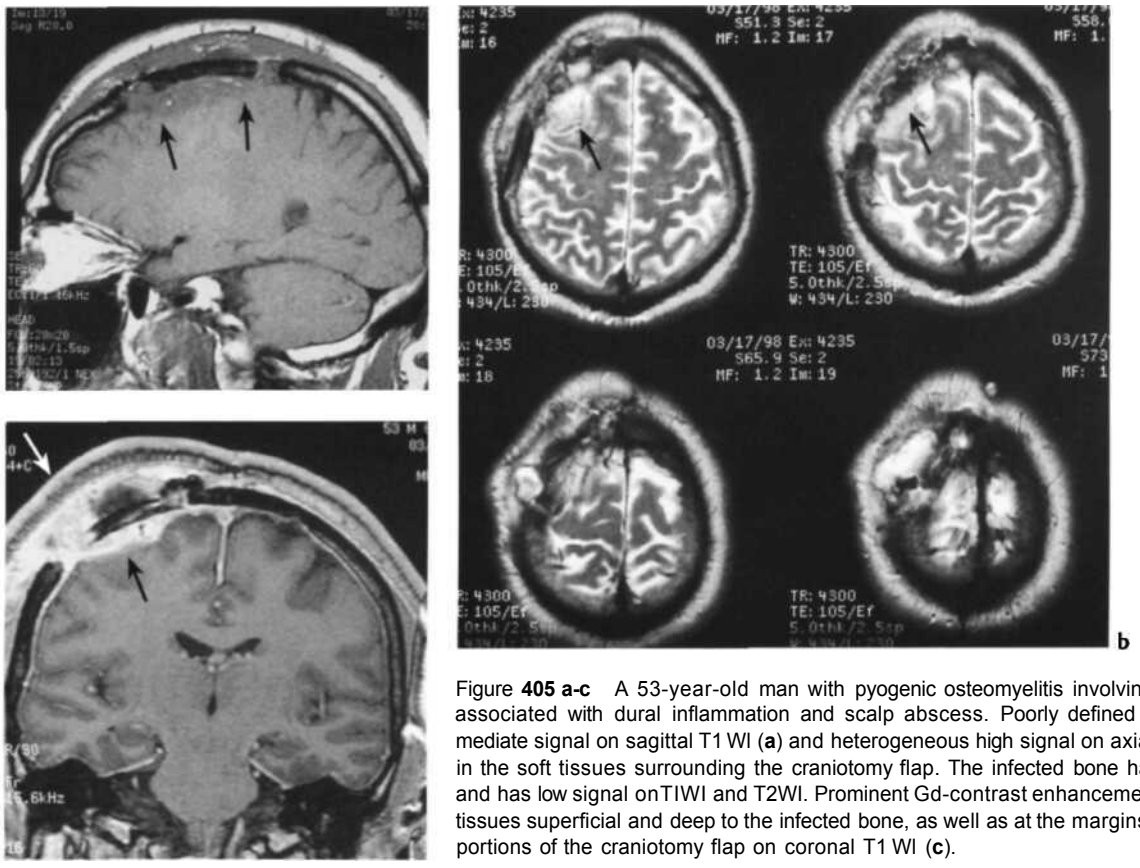

Figure **405 a-c** A 53-year-old man with pyogenic osteomyelitis involving a craniotomy flap associated with dural inflammation and scalp abscess. Poorly defined zones of low-intermediate signal on sagittal T1 WI (**a**) and heterogeneous high signal on axial T2WI (**b**) are seen in the soft tissues surrounding the craniotomy flap. The infected bone has irregular margins and has low signal onTIWI and T2WI. Prominent Gd-contrast enhancement is seen in the soft tissues superficial and deep to the infected bone, as well as at the margins and intramedullary portions of the craniotomy flap on coronal T1 WI (**c**).

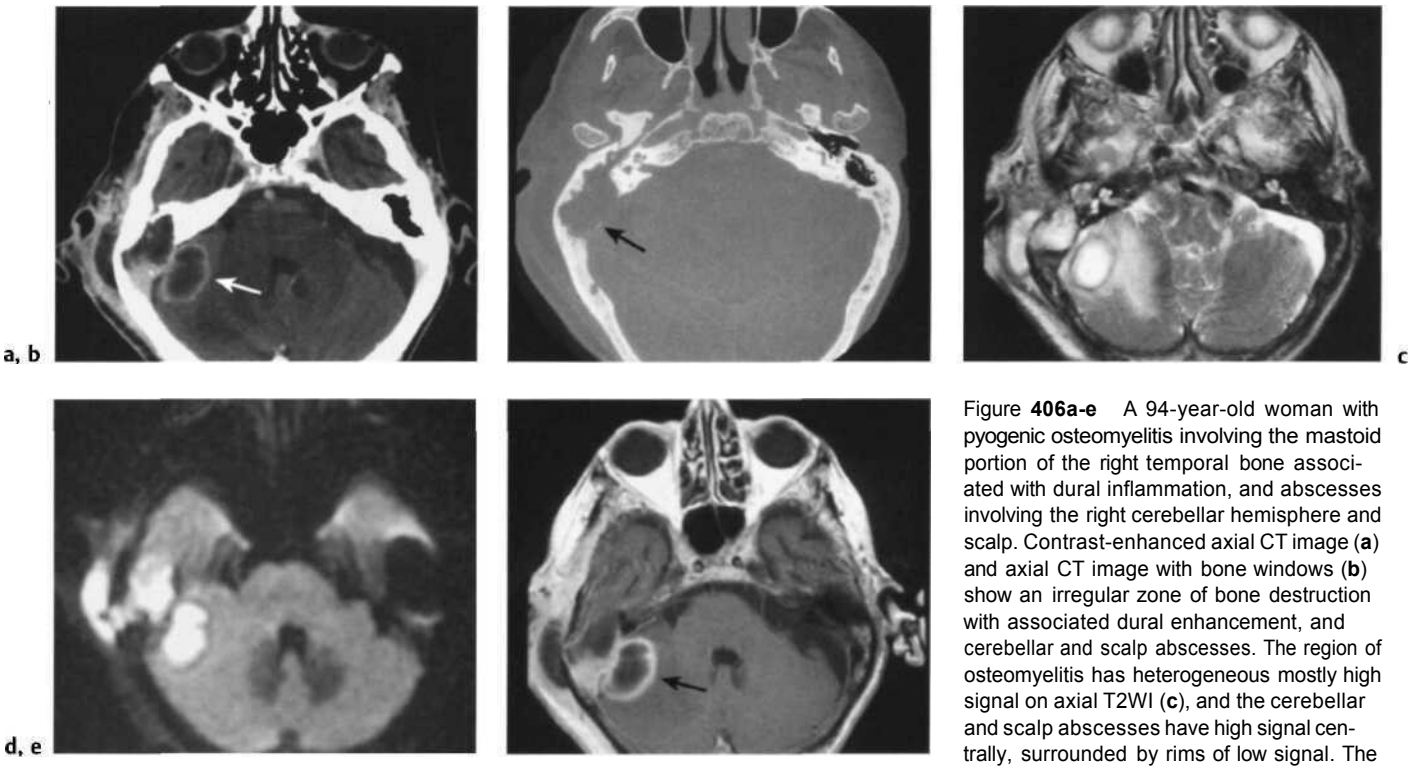

Figure **406a-e** A 94-year-old woman with pyogenic osteomyelitis involving the mastoid portion of the right temporal bone associated with dural inflammation, and abscesses involving the right cerebellar hemisphere and scalp. Contrast-enhanced axial CT image (**a**) and axial CT image with bone windows (**b**) show an irregular zone of bone destruction with associated dural enhancement, and cerebellar and scalp abscesses. The region of osteomyelitis has heterogeneous mostly high signal on axial T2WI (**c**), and the cerebellar and scalp abscesses have high signal centrally, surrounded by rims of low signal. The zones of osteomyelitis, scalp and cerebellar abscesses have high signal on diffusion-weighted imaging (**d**) from restricted diffusion. The abscesses are surrounded by irregular zones of Gd-contrast enhancement on axial T1WI (**e**).

myelitis than with acute osteomyelitis.[19] A **Brodie abscess** represents a type of subacute osteomyelitis in long bones in which there is an intraosseous lesion (abscess) that usually appears as a central zone with low to intermediate signal on T1WI and slightly high to high signal on T2WI surrounded by two rings, and an outer poorly-defined zone or halo with low to intermediate signal on TlWI and high signal on T2WI, FS T2W1, and STIR[13,19,22] (Figs. **414, 415**). The inner ring surrounding the abscess represents vascularized granulation tissue containing inflammatory cells connective tissues, and usually has low to intermediate signal on T1WI (similar to muscle, and greater than the abscess contents) and high signal on T2WI.[13] This inner ring usually shows Gd-contrast enhancement and has been referred to as the "penumbra sign."[13] The outer ring that usually occurs results from fibrotic reaction and sclerosis, and often has low signal on T1WI and T2WI.[13] Peripheral to these two rings, the poorly defined halo representing reactive edema often has low signal on T1WI, and low, intermediate, and/or high signal on T2WI and FST2WI.[13,22] The peripheral halo typically shows contrast enhancement.[19] A sinus tract may be seen extending through thickened cortex adjacent to the intra-osseous abscess.[6,18]

In the **chronic active phase of pyogenic osteomyelitis,** findings commonly seen with MR1 include: intra-osseous abscesses, sequestra, cloacae, subperiosteal fluid collections, and cortical thickening.[22] A narrow zone or rim of low signal on T1WI and T2WI is seen in 93% of cases separating the site of chronic osteomyelitis from normal adjacent bone marrow.[22] Within this rim, a zone with low-intermediate signal on T1WI and heterogeneous intermediate, slightly high, to high signal is

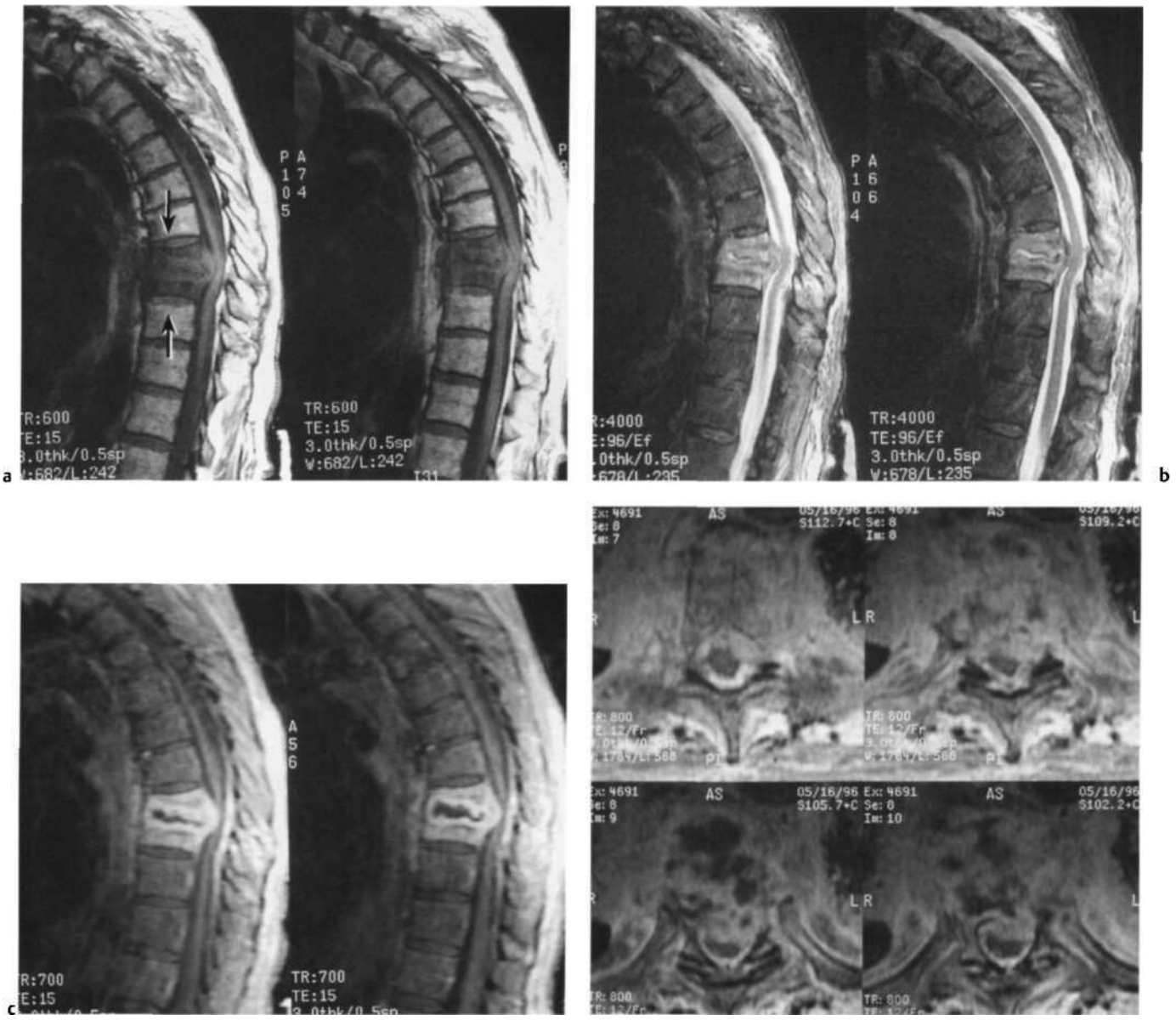

Figure **407a-e** A 77-year-old woman with pyogenic osteomyelitis involving two adjacent thoracic vertebral bodies and infection of the intervening disk. Poorly defined zones of low signal on sagittal T1WI (**a**) and high signal on sagittal FST2WI (**b**) are seen throughout the marrow of the vertebral bodies and intervening disk. Loss of definition of the low signal line of the endplates of the vertebral bodies is seen on T1WI and FST2WI. After Gd-contrast administration, prominent diffuse contrast enhancement is seen in the involved marrow on sagittal (c) and axial (d) FST1WI. Abnormal contrast enhancement is seen at the margins of the disk, as well as in paraspinal and epidural locations representing phlegmon/early epidural abscess formation. The inflammatory epidural lesion surrounds and indents the ventral margin of the spinal cord representing spinal cord compression.

usually seen representing the intra-osseous infection or abscess that may contain foci of low signal on T1WI and T2WI from sequestra.[22] After Gd-contrast administration, irregular zones of enhancement may be seen in active chronic osteomyelitis.[22] Cloacae and sinus tracts can appear as linear or curvilinear zones with high signal on T2WI and Gd-contrast enhancement involving the cortex and extraosseous soft tissues.[22] Cortical thickening usually has low signal on T2WI.

The role of MR1 in the follow-up evaluation for response to treatment of osteomyelitis can be limited because the MRI features of sympathetic edema overlap those of purulent material.[22] Healing of chronic osteomyelitis can be observed as progression of abnormal signal within involved bone toward fatty marrow signal characteristics.[22]

Pyogenic Spondylodiskitis

In the acute phase, poorly defined zones of low signal on T1WI and high signal on T2WI and FS T2WI are seen in the marrow adjacent to the endplates of adjacent vertebral bodies[7,12,14,23] (Figs. **407, 409).** Abnormally high signal on T2WI and FST2WI

Figure **408 a-d** Osteomyelitis from *Coccidioides immitis* involving three adjacent thoracic vertebral bodies and intervening discs. Poorly defined zones of low signal are seen in the marrow of three adjacent vertebral bodies and intervening disks on sagittal T1WI (**a**), and heterogeneous low, intermediate, slightly high and high signal on sagittal T2WI (**b**), as well as heterogeneous mostly high signal on sagittal FST2WI (**c**). Loss of definition of the low-signal lines of the vertebral body endplates is seen on TI WI, T2WI, and FS T2WI. After Gd-contrast administration, irregular contrast enhancement is seen in the involved marrow on sagittal T1WI (**d**). Abnormal irregular contrast enhancement is seen at the margins of the involved disks.

is also seen in 90 % of the intervening disks.[12,14,23] Loss of definition of the low-signal line of the endplates of the vertebral bodies is usually observed on T1WI, T2WI, and FST2WI.[7,12,14,23] After Gd-contrast administration, irregular contrast enhancement is seen in the involved marrow on FSTIWI.[7,23] Abnormal contrast enhancement of the intervening disk can occur in various patterns (diffuse, patchy/nonconfluent, thin or thick peripheral).[7,23]

MR1 is useful for detecting epidural and paravertebral abscesses and phlegmons.[14,23] Epidural abscesses and phlegmons can have variable mixed signal, but abscesses often have low to intermediate signal on T1WI and PDWI, and high signal on T2WI and FST2WI.[14,23] After Gd-contrast administration, epidural abscesses typically show linear peripheral enhancement surrounding low to intermediate signal exudates on FSTIWI.[23] Unlike abscesses, an epidural phlegmon usually shows diffuse Gd-contrast enhancement.[23]

Positive responses to therapy usually result in progressive increases in fatty marrow signal and decreased abnormal contrast enhancement of the involved marrow.[23]

Tuberculous Osteomyelitis[1,5,7,15,20]

In **tuberculous spondylodiskitis,** poorly defined zones of low signal on T1WI and high signal on T2WI and FST2WI are seen in the marrow adjacent to the endplates of multiple vertebral bodies (60%), less than or equal to two adjacent vertebral bodies (40 %).[715] Loss of definition of the low signal line of the endplates of the vertebral bodies is usually observed on Tl WI, T2WI, and FST2WI™ (Figs. **410, 411).** Abnormal high signal on T2WI and FST2WI is also seen in 80% of the intervening disks,

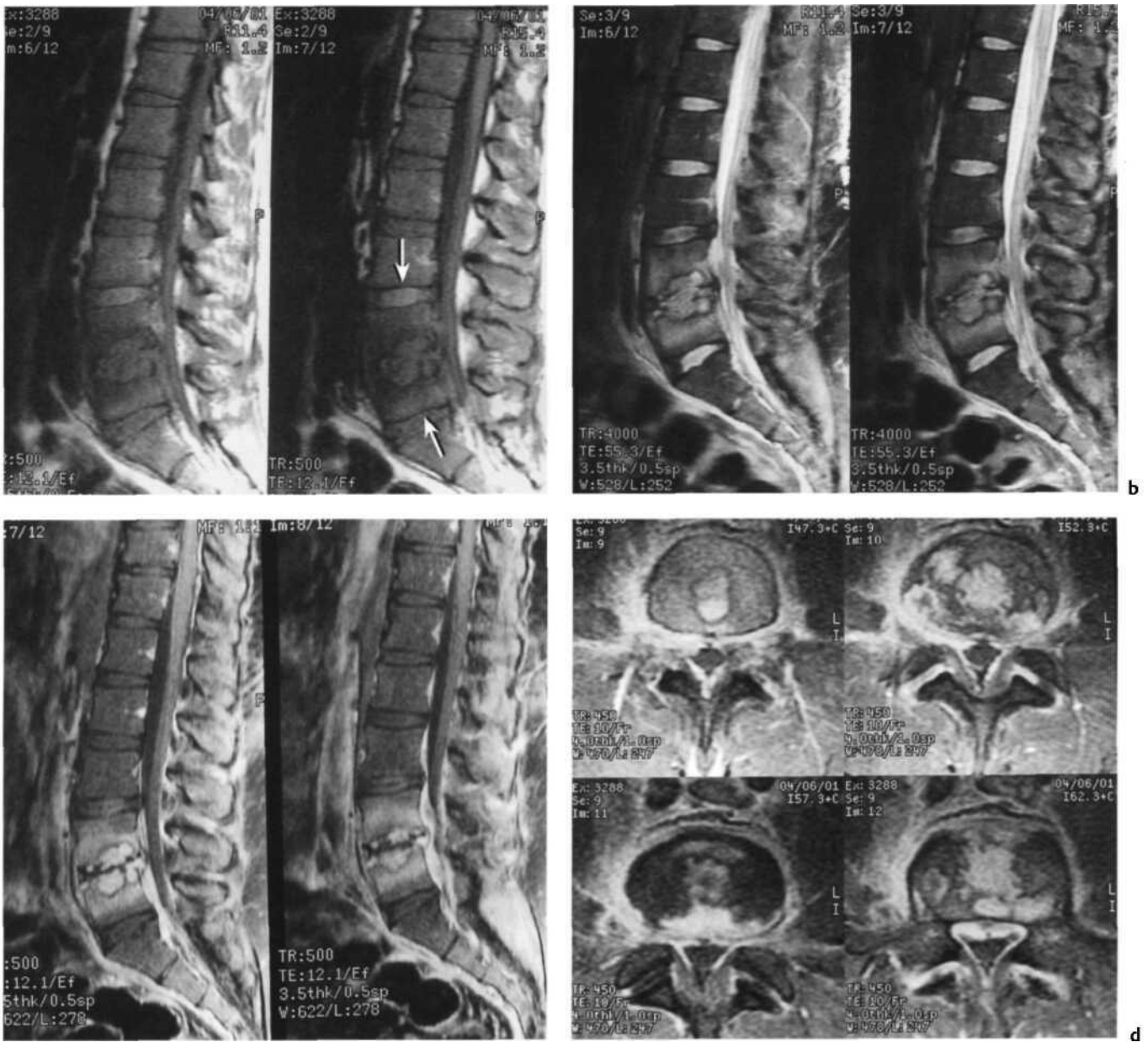

Figure **409a-d** A 34-year-old man with pyogenic osteomyelitis involving the L4 and L5 vertebral bodies and intervening disk. Poorly defined zones of low signal on sagittal T1WI (**a**) and heterogeneous high signal on sagittal FST2WI (**b**) are seen in the marrow of the adjacent vertebral bodies. Abnormal high signal on FS T2WI is seen in the intervening disk. Loss of definition of the low-signal lines of the vertebral body endplates is seen on T1WI and FST2WI. After Gd-contrast administration, irregular contrast enhancement is seen in the involved marrow on sagittal (**c**) and axial (**d**) FST1WI. Abnormal contrast enhancement is also seen in the intervening disc, as well as in the anterior epidural soft tissues causing spinal canal compression.

although the disk abnormalities may appear later relative to the extent of bone marrow lesions compared with pyogenic osteomyelitis.[7,15] After Gd-contrast administration, irregular contrast enhancement is seen in the involved marrow on FST1WI.[7,15] Abnormal contrast enhancement of the intervening disk can occur in various patterns (diffuse, patchy/nonconfluent, heteorgeneous, thin or thick peripheral).[7,15]

In tuberculous spondylodiskitis, other features seen with MRI include subligamentous spread of the infection over more than three vertebral levels (85 %), well-defined paraspinal zones of abnormal signal (95 %), and paraspinal or intra-osseous abscesses with thin and smooth Gd-contrast-enhancing walls (95 %).[7] Unlike tuberculous spondylodiskitis, paraspinal or intra-osseous abscesses with thin and smooth enhancing margins were found in only in 15% of cases with pyogenic osteomyelitis.[7] Whereas 35 % of cases of pyogenic vertebral osteomyelitis had paraspinal or intra-osseous abscesses with thick and irregular enhancing margins, these findings were not observed with tuberculous spondylodiskitis.[7]

In extra-axial tuberculous osteomyelitis, poorly defined zones with low signal on T1WI, and low-intermediate, slightly high, and/or high signal onT2WI and FST2WI are typically seen

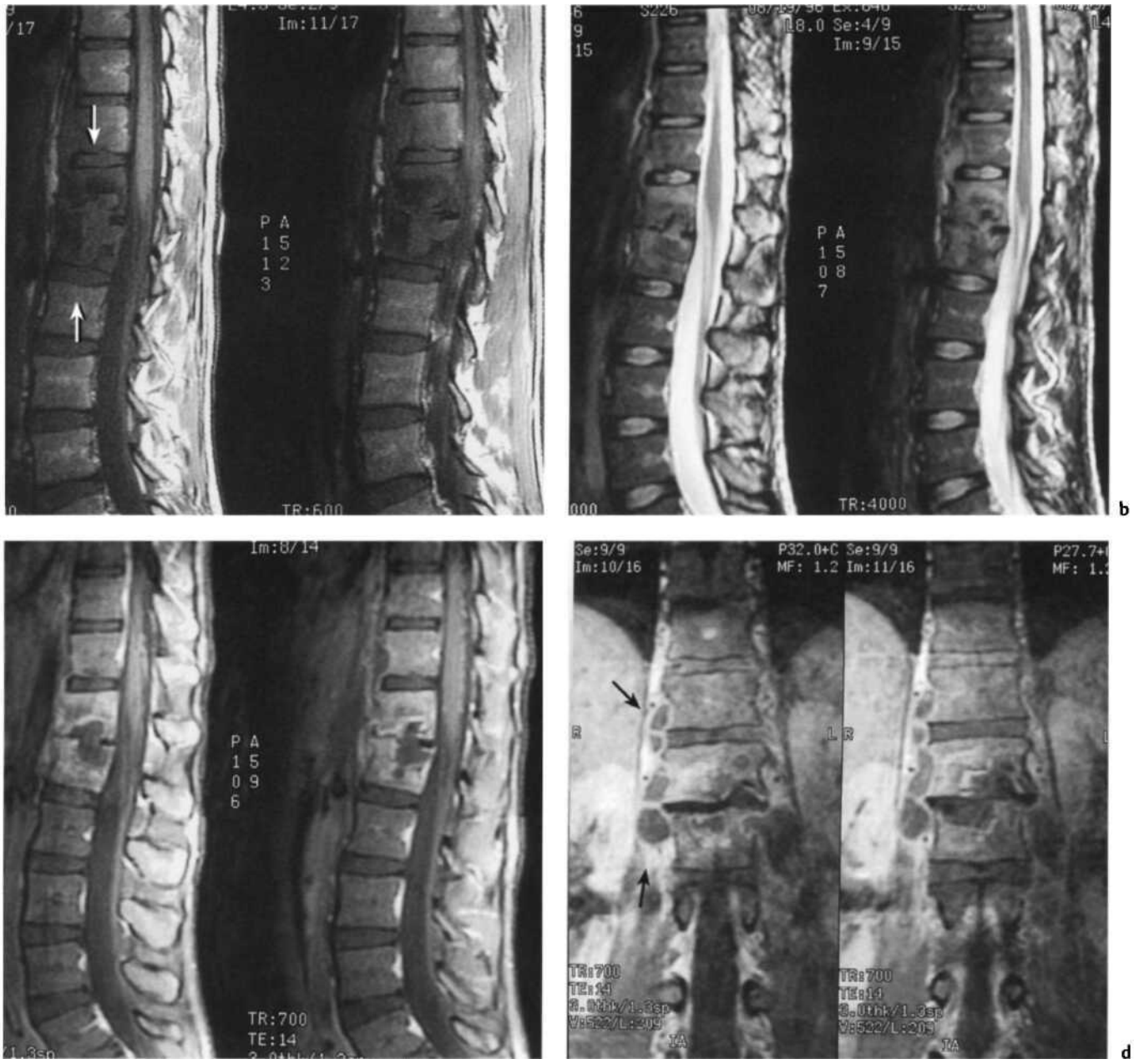

Figure **410a-f** A 23-year-old man with tuberculous osteomyelitis involving the T12 and L1 vertebral bodies and intervening disk, as well as paraspinal cold abscesses. Poorly defined zones of low signal on sagittal T1WI (**a**) and heterogeneous intermediate, slightly high and high signal on sagittal T2WI (**b**) are seen in the marrow adjacent to the endplates of the adjacent vertebral bodies and intervening disk. Loss of definition of the low-signal lines of the vertebral body endplates is seen on T1WI and T2WI. After Gd-contrast administration, irregular contrast enhancement is seen in the involved marrow and peripheral portions of the disk on sagittal (**c**), coronal (**d**), and axial (**e**) FST1WI. Also, subligamentous spread of the paraspinal abscesses over 3 vertebral levels is evident (**d**). The paraspinal abscesses shows peripheral rims of Gd-contrast enhancement (**d, e**). The intra-osseous infection is manifested by zones of radiolucency with slightly irregular sclerotic borders on axial CT images (**f**).

Figure 41Oe,f >

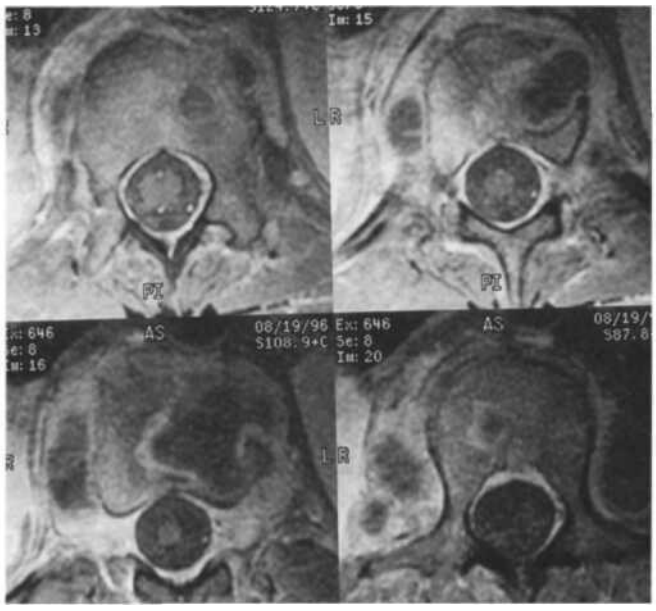

e

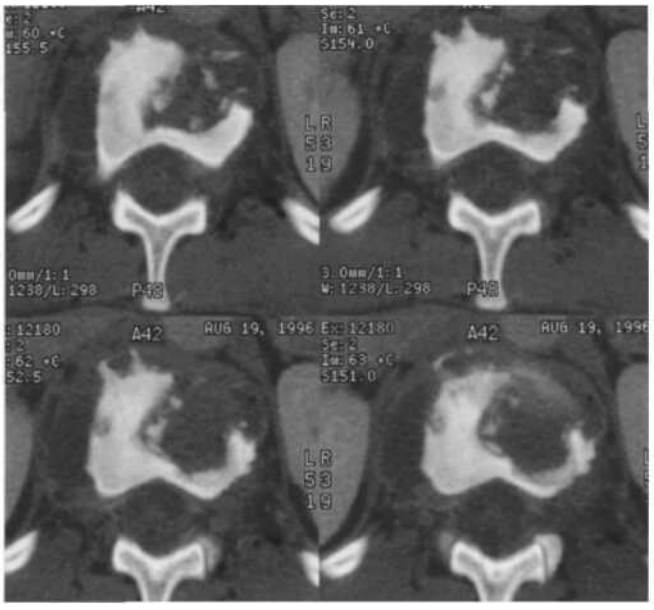

f

Figure **410** e, f

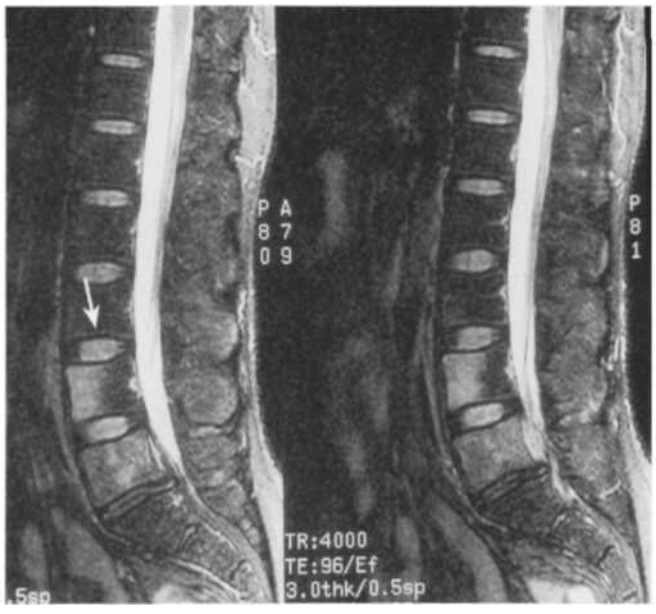

a

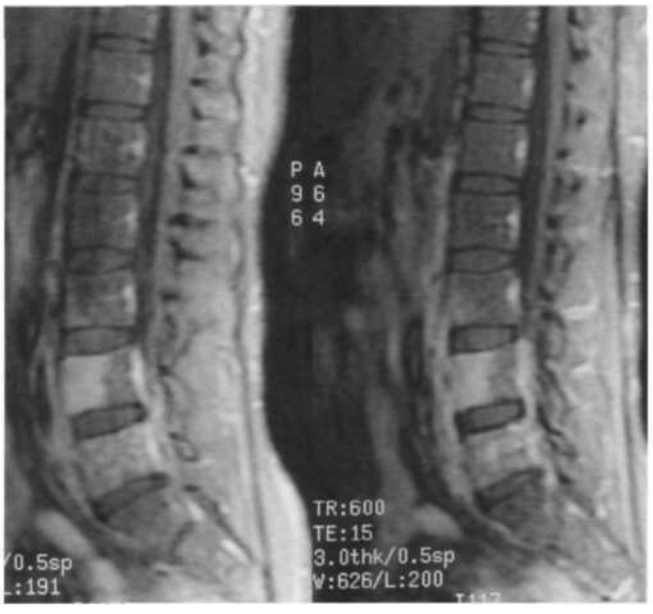

b

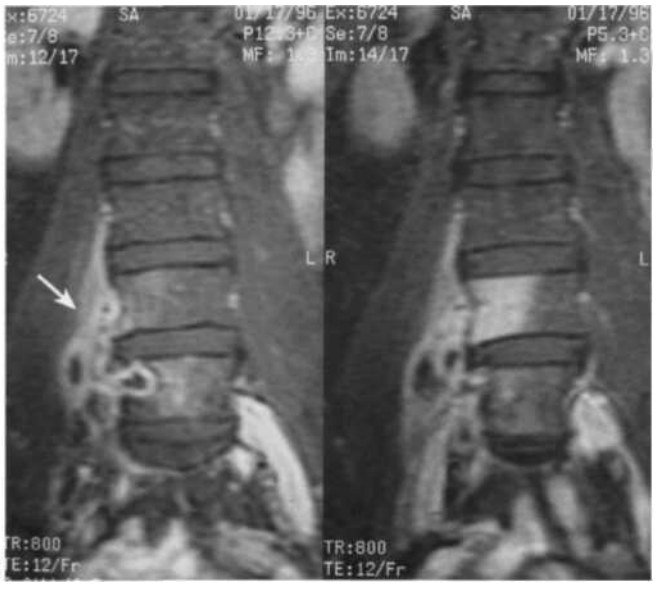

c

Figure **411a-c** A 35-year-old man with tuberculous osteomyelitis involving the L4 and L5 vertebral bodies and paraspinal cold abscesses. Poorly defined zones of high signal on sagittal FS T2WI (**a**) are seen in the marrow of adjacent vertebral bodies. No abnormal signal is seen at the intervening disk. The endplates appear intact. After Gd-contrast administration, irregular contrast enhancement is seen in the involved marrow on sagittal (**b**) and coronal (**c**) FST1WI. Also, subligamentous spread of the paraspinal abscesses is evident as irregular peripheral zones of Gd-contrast enhancement (**c**).

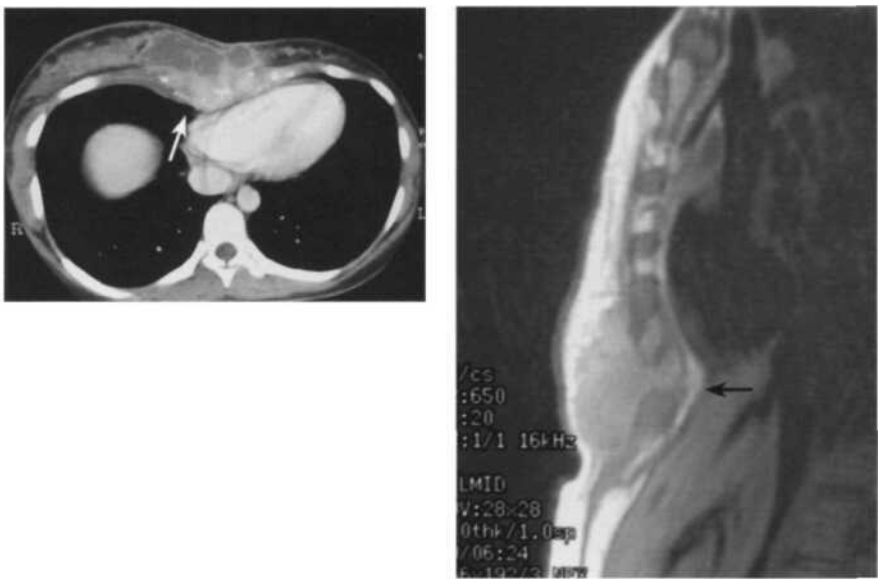

Figure **412 a, b** A 28-year-old woman with tuberculous osteomyelitis involving the sternum. Axial CT image (**a**) shows destructive changes at the sternum associated with an inflammatory mass with soft tissue and fluid attenuation. The inflammatory mass has low-intermediate signal on sagittal (**b**) T1WI.

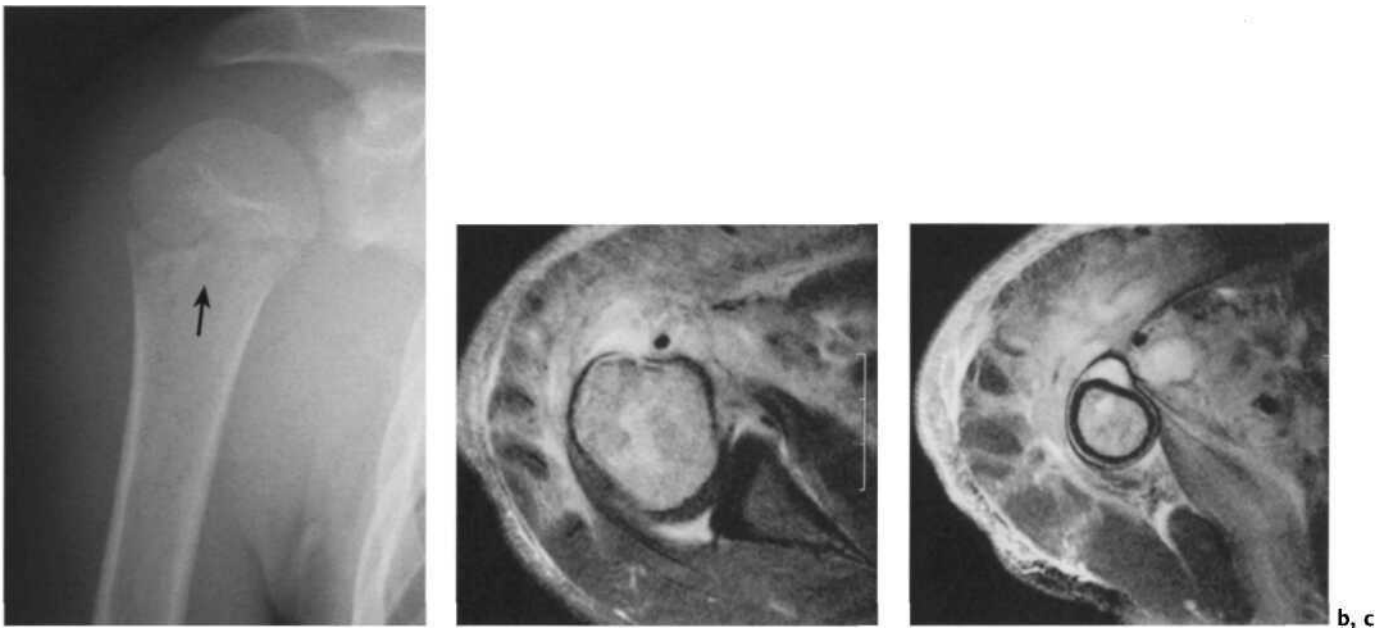

Figure **413a-d** A 9-year-old male with pyogenic osteomyelitis involving the proximal humerus as well as infection of the adjacent soft tissues. AP radiograph (**a**) shows small radiolucent zones in the metaphysis. Extensive abnormal high signal on axial FST2WI (**b, c**) is seen in the marrow of the humerus and adjacent superficial soft tissues representing osteomyelitis, myositis, and cellulitis. Abnormal Gd-contrast enhancement is seen at the sites of infection of the bone and soft tissues on axial FST1WI (**d**), as well as nonenhancing sites representing abscess formation. A subperiosteal abscess is also seen on axial FST2WI (**c**) and postcontrast FST1WI (**d**).

in the involved marrow[1,5,7,15,20] (Fig. **412**). In some cases, a rim of intermediate to slightly high signal on T1WI may be seen surrounding a central zone of low signal.[20] Poorly defined zones of marrow edema with high signal on T2WI and FST2WI are seen peripheral to the sites of intra-osseous tuberculous osteomyelitis in 89 % of patients.[20] Zones of cortical disruption are seen in 73 %.[20] Abscesses and zones of edema in the extra-osseous soft tissues are seen in 73 % and 91 % of patients, respectively.[20] After Gd-contrast administration, lesions may show a peripheral rim enhancement pattern and/or zones with diffuse or heterogeneous enhancement.[1,20] Nonenhancing central zones within the lesions may be secondary to areas of necrosis.[1] Gd-contrast enhancement can also be seen in the extra-osseous soft tissues representing myositis and/or cellulitis.[1,20]

Fungal osteomyelitis[4,12,22]

In fungal vertebral ostemyelitis, poorly defined zones of low signal on T1WI, and slightly high signal on T2WI and FST2W1 are seen in the marrow adjacent to the endplates of single or adjacent vertebral bodies[12] (Fig. **408).** Involvement of the intervening disk may occur late in the process as with tuberculosis spondylodiskitis.[12] Abnormal, slightly high signal on T2WI and FST2WI may be seen in the intervening disks, although the degree of signal alteration is often less than with pyogenic infections.[12] Loss of definition of the low signal line of the endplates of the vertebral bodies may be observed on T1WI, T2WI, and FST2WI.[12]

In long and flat bones, poorly defined zones of low signal on T1WI and slightly high to high signal on T2WI, STIR, and FST2WI are seen in the marrow.[4,12] A wide zone of transition between normal bone and edematous and infected bone is typically seen." Loss of definition of the low signal line of the cortical margins is often observed on T1WI, T2W1, STIR, and FST2WI.[4] After Gd-contrast administration, irregular zones of contrast enhancement are usually seen in the involved marrow on FST1WI.[4]

Differential Diagnosis

Osteomyelitis. Osteosarcoma, Ewing sarcoma, metastatic tumor, lymphoma, eosinophilic granuloma, chordoma (spinal lesions), neuropathic arthropathy.

Brodie abscess. Bone cyst, ganglion cyst, eosinophilic granuloma, chondroblastoma, enchondroma, metastatic lesion, chondrosarcoma, rheumatoid arthritis, intra-osseous gout.[6,18]

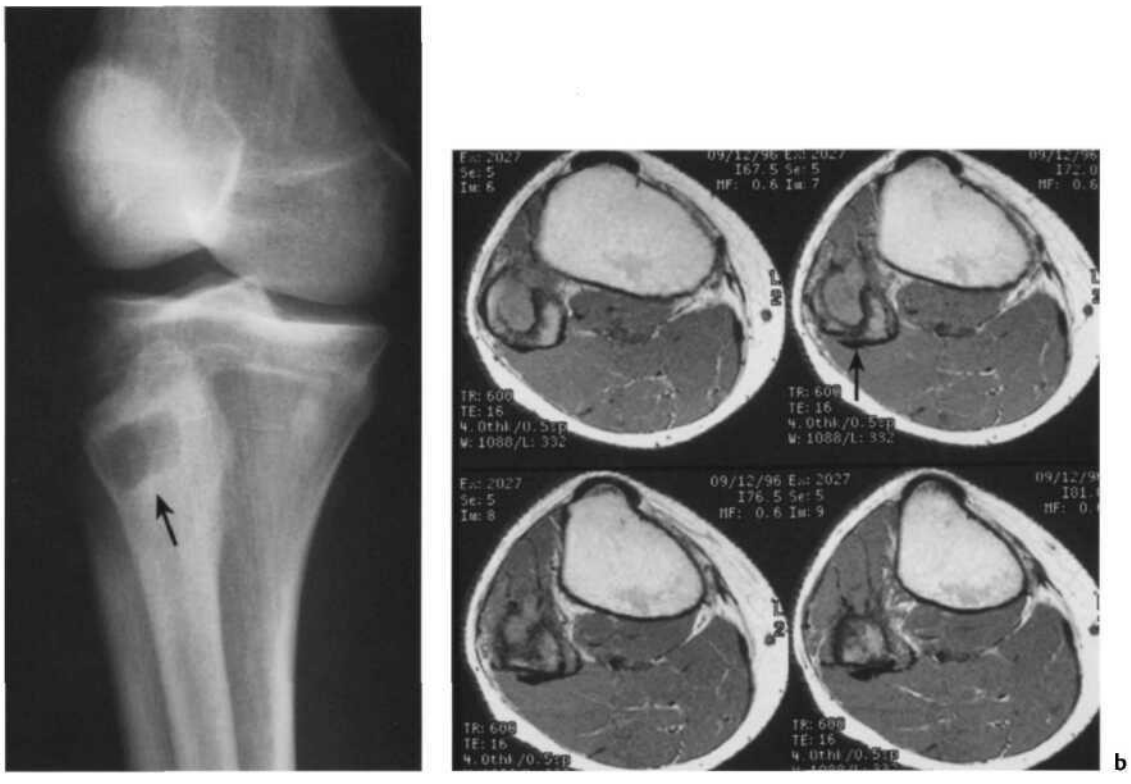

Figure **414a-d** A 20-year-old man with osteomyelitis and Brodie abscess involving the proximal fibula. Oblique radiograph (**a**) shows a well-circumscribed radiolucent lesion in the proximal fibula that is surrounded by sclerotic reaction. A central zone with low to intermediate signal on axial T1WI (**b**) and high signal on axial T2WI (**c**) is surrounded by two rings, and an outer, poorly defined zone with intermediate signal on T1W1 and slightly high to high signal on T2WI. The central portion of the lesion shows prominent Gd-contrast enhancement on axial FST1WI (**d**). A sinus tract is seen extending through the fibular cortex anteriorly into the extra-osseous soft tissues.

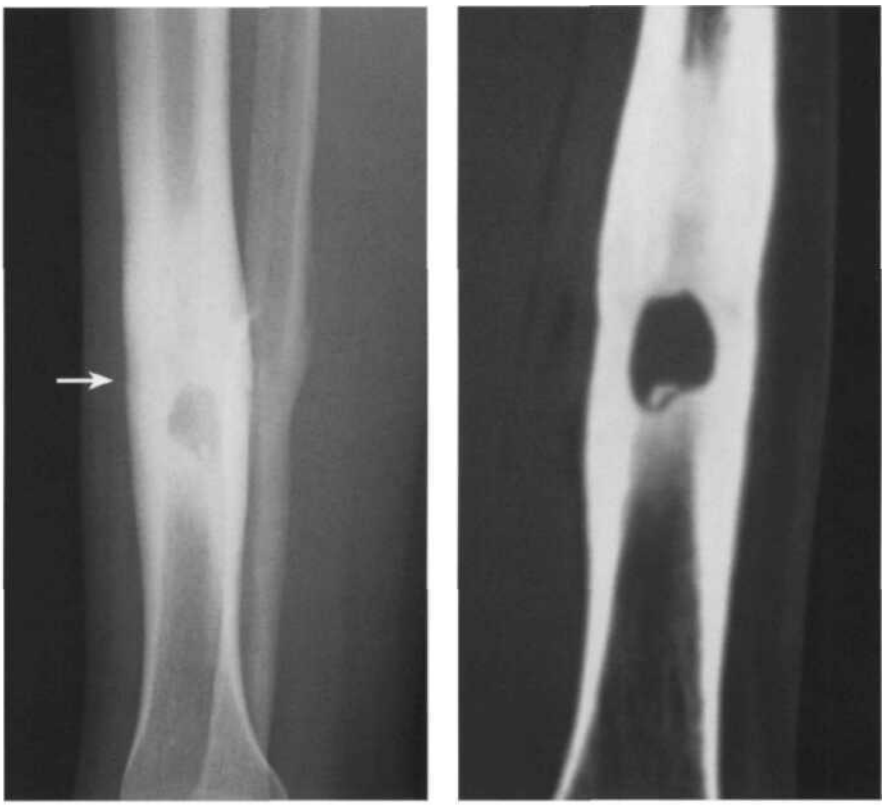

a, b

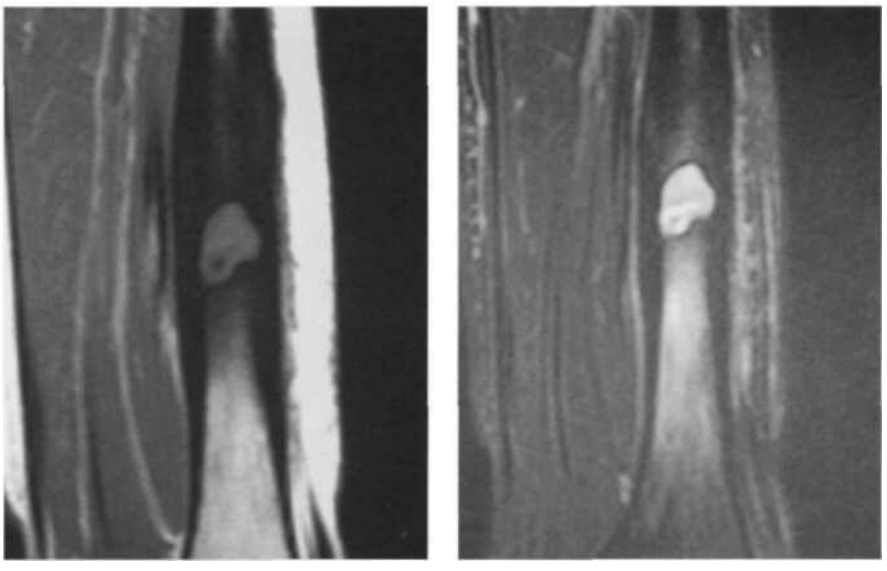

c, d

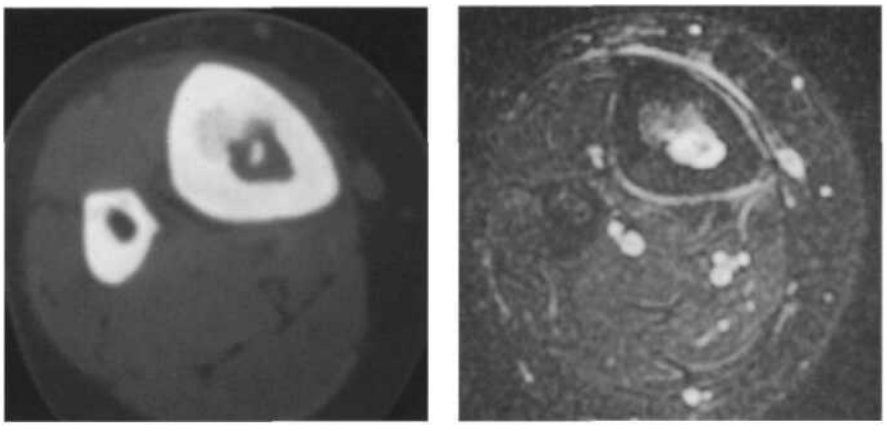

e, f

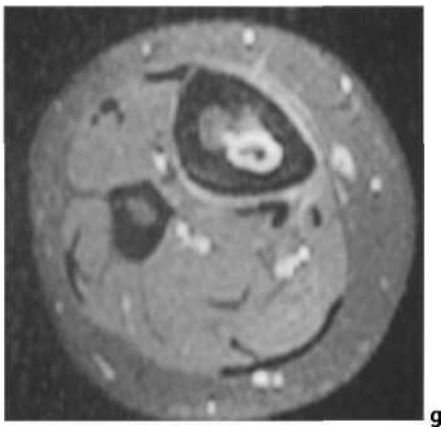

g

Figure **415a-g** A 21-year-old woman with osteomyelitis and Brodie abscess involving the distal diaphysis of the tibia. Oblique radiograph (**a**), and coronal (**b**) and axial (**e**) CT images show a well-circumscribed radiolucent lesion containing a bone fragment (sequestrum) that is surrounded by sclerotic reaction. The intramedullary abscess has intermediate signal on coronal (**c**) PDWI and is surrounded by a poorly defined zone of low signal. The abscess has high signal on coronal (**d**) and axial (**f**) FST2WI, and is surrounded by a poorly defined zone of high signal in the adjacent marrow. A thin periosteal zone of high signal is also seen (**f**). Irregular Gd-contrast enhancement is seen at the pe riphery of the abscess on axial (**g**) FST1 WI.

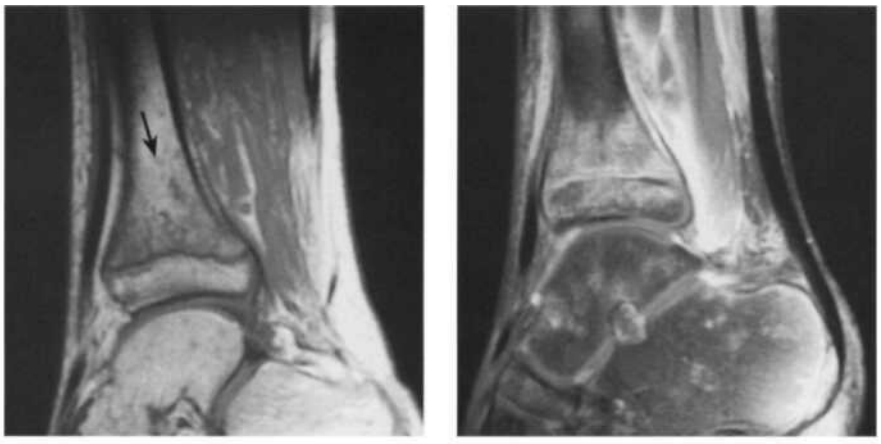

Figure **416a, b** A 9-year-old female with pyogenic osteomyelitis involving the distal metaphyseal portion of the tibia, as well as infection of the adjacent soft tissues. A poorly defined zone of low-intermediate signal on sagittal T1WI (**a**) is seen in the marrow of the distal tibial metasphysis. Poorly defined zones of abnormal Gd-contrast enhancement are seen in the epi-metaphyseal marrow of the distal tibia as well as in the adjacent soft tissues on sagittal FSTIWI(**b**).

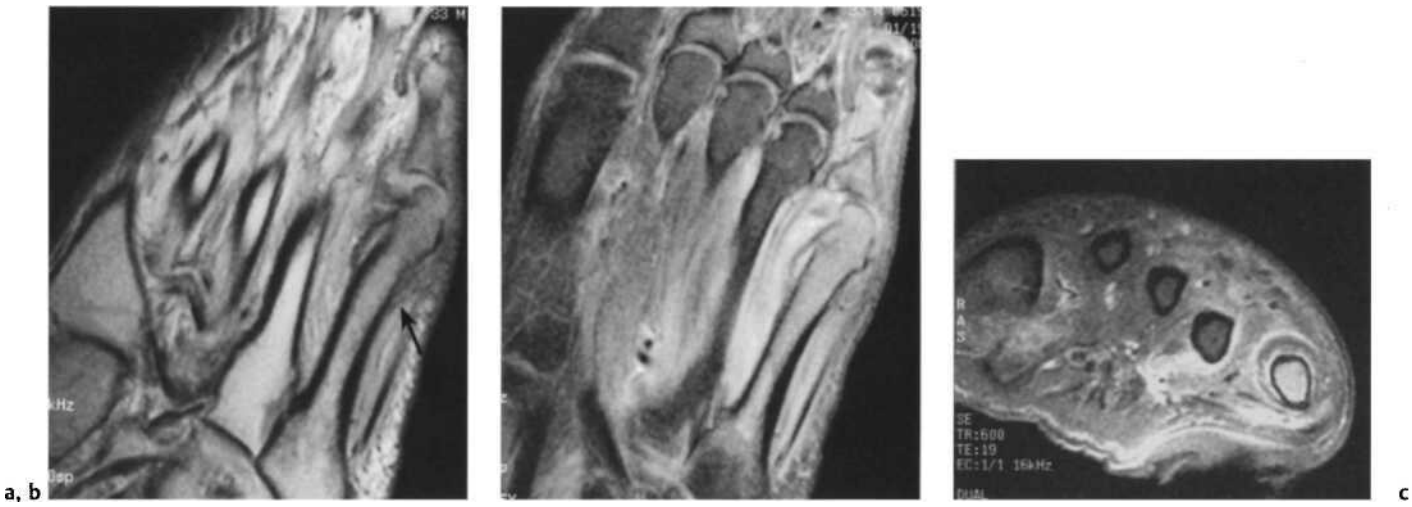

Figure **417a-c** A 33-year-old man with pyogenic osteomyelitis involving the fifth metatarsal head and adjacent proximal phalanx, as well as septic arthritis. The infected marrow has intermediate signal on axial T1WI (**a**). Diffuse abnormal Gd-contrast enhancement is seen in the marrow of the metatarsal head and proximal phalanx on axial (**b**) and coronal (**c**) FST1WI, as well as in the joint and extra-osseous soft tissues representing sites of infection and inflammation.

Prognosis and Treatment

Pyogenic osteomyelitis. Treatment usually consists of antiobiotic therapy with or without surgical drainage or debridement.[1823] Chronic osteomyelitis can result when there has been an extensive delay in diagnosis, extensive bone necrosis, inadequate antiobiotic therapy, inadequate surgical debridement, and/or immunocompromised or weakened host defenses.[18] Recurrent acute osteomyelitis may occur in the setting of chronic osteomyelitis.[18] Chronic osteomyelitis can be associated with pathologic fractures, sepsis, endocarditis, secondary amyloidosis, and squamous cell carcinoma in sinus tracts.[18]

Tuberculous osteomyelitis. Treatment of tuberculous osteomyelitis usually consists of rapid utilization of appropriate antimicrobial agents.[15] With medical treatment, most osseous manifestations show resolution.[15] Athrodesis may be necessary in cases with extensive bone destruction.[15] Spinal surgery may be necessary for stabilization of destructive lesions involving vertebrae and evacuation of epidural abscesses.[15] Paravertebral abscesses can be drained surgically or by image-guided percutaneous methods.[15]

Fungal osteomyelitis Treatment of fungal osteomyelitis is similar to that for pyogenic and tyberculous osteomyelitis.

References

1 Atasoy C, Oztekin PS, Ozdemir N, Sak SD, Erden I, Akyar S. CTand MRI in tuberculous sternal osteomyelitis: a case report. C/in *Imaging* 2002;26(2):112-115.

2 Bureau NJ, Cardinal E. Imaging of musculoskeletal and spinal infections in AIDS. Radiol Cfin *North Am* 2001;39(2):343-355.

3 Chang PC, Fischbein NJ, Holliday RA. Central skull base osteomyelitis in patients without otitis externa: imaging findings. *AJNR Am J* Neuroradiol 2003;24(7):1310-1316.

4 Chhem RK, Wang S, Jaovisidha S, et al. Imaging of fungal, viral, and parasitic musculoskeletal and spinal diseases. *Radiol Clin North Am* 2001;39:357-378.

5 De Vuyst D, Vanhoenacker F, Gielen J, Bernaerts A, De Schepper AM. Imaging features of musculoskeletal tuberculosis. *Eur Radial* 2003; 13(8):1809-1819.

6 Forest M. Osteomyelitis. In: Forest M, Tomeno B, Vanel D, eds. Orthopedic Surgical *Pathology: Diagnosis of Tumors and Pseudotumoral Lesions of Bone and Joints* Edinburgh: Churchill Livingstone; 1998: 573-578.

7 Jung NY, Jee WH, Ha KY, Park CK, Byun JY. Discrimination of tuberculous spondylitis from pyogenic spondylitis on *MRl.AJRAmJRoentgenol* 2004;182:1405-1410.

8 Karchevsky M, Schweitzer ME, Morrison WB, Parellada JA. MRI findings of septic arthritis and associated osteomyelitis in adults. *AJR Am JRoentgenol* 2004;182(1):119-122.

9 Kleinman PK. A regional approach to osteomyelitis of the lower extremities in children. Radio/ *Clin North Am* 2002;40(5):1033-1059.

10 Ledermann HP, Morrison WB, Schweitzer ME. MR image analysis of pedal osteomyelitis: distribution, patterns of spread, and frequency of associated ulceration and septic arthritis. *Radiology* 2002;223(3): 747-755.

11 Ledermann HP, Morrison WB, Schweitzer ME. Pedal abscesses in patients suspected of having pedal osteomyelitis: analysis with MR imaging. *Radiology* 2002;224(3):649-655.

12 Mahboubi S, Morris MC. Imaging of spinal infections in children. Radiof *Clin North Am* 2001;39(2):215-222.

13 Marui T, Yamamoto T, Akisue T, et al. Subacute osteomyelitis of long bones: diagnostic usefulness of the "penumbra sign" on MRI. *Clin Imaging* 2002;26(5):314-318.

14 Meyers SP, Wiener SN. Diagnosis of hematogenous pyogenic vertebral osteomyelitis by magnetic resonance imaging. *Arch Intern Med* 1991;151:683-687.

15 Moore SL, Rafii M. Imaging of musculoskeletal and spinal tuberculosis. Radiol *Clin North Am* 2001;39:329-342.

16 Mulder JD, Schutte HE, Kroon HM, Taconis WK. Osteomyelitis. In: *Radiologic Atlas of Bone Tumors* Amsterdam: Elsevier; 1993:671-680.

17 Oudjhane K, Azouz EM. Imaging of osteomyelitis in children. Radio/ *Clin North Am* 2001 ;39(2):251-266.

18 Rosenberg A. Bones, joints, and soft tissue tumors. In: Cotran RS, Kumar V, Collins T. *Pathologic Basis of Disease* 6th ed. Philadelphia, Pa: W.B. Saunders; 1999:1215-1267.

19 Santiago Restrepo C, Gimenez CR, McCarthy K. Imaging of osteomyelitis and musculoskeletal soft tissue infections: current concepts. *Rheum Dis Clin North Am* 2003;29(1):89-109.

20 Sharma P. MR features of tuberculous osteomyelitis. *Skeletal Radial* 2003;32(5):279-285.

21 Struk DW, Munk PL, Lee MJ, Ho SG, Worsley DF. Imaging of soft tissue infections. Radio/ *Clin North Am* 2001;39(2):277-303.

22 Tehranzadeh J, Wong E, Wang F, Sadighpour M. Imaging of osteomyelitis in the mature skeleton. *Radial Clin North Am* 2001;39(2): 223-250.

23 Varma R, Lander P, Assaf A. Imaging of pyogenic infectious spondylodiskitis. Radio/ *Clin North Am* 2001 ;39:203-213.

24 Tuberculosis, Media Center, World Health Organization www.who.int/mediacentre

A64 Osteosarcoma (Also Referred to as Osteogenic Sarcoma and Osteoblastic Sarcoma)

Osteoblastic Osteosarcoma: 9180/3

Chondroblastic Osteosarcoma: 9181/3

Fibroblastic Osteosarcoma: 9182/3

Common mixed type Osteosarcoma: 9180/3

Telangiectatic Osteosarcoma: 9183/3

Small cell Osteosarcoma: 9185/3

Low-grade central Osteosarcoma: 9187/3

Parosteal Osteosarcoma: 9192/3

Periosteal Osteosarcoma: 9193/3

High-grade surface Osteosarcoma: 9194/3

Secondary osteosarcoma: 9180/3

Paget osteosarcoma: 9184/3

Postradiation osteosarcoma: 9180/3

Extraskeletal osteosarcoma: 9180/3

Osteosarcoma is a malignant tumor comprised of proliferating neoplastic spindle cells that produce osteoid and/or immature tumoral bone.[1,14,19,20,42,50,63] Osteosarcoma most commonly occurs within bone (intra-osseous osteosarcoma). Less frequently, juxtacortical or parosteal osteosarcomas occur, which represent malignant sarcomas that arise on the external surface of bone.[20,42,69] Periosteal sarcoma has been proposed to represent a variant of parosteal osteogenic sarcoma that contains cartilaginous zones.[2] "Rarely, osteogenic sarcomas can also occur as extraskeletal primary lesions in the soft tissues[10,11,29,30,44,54] or within bone cortex.[25,44] Osteosarcomas can occur de novo, or arise as secondary lesions associated with Paget disease (accounts for 67-90 % of secondary osteosarcoma), radiation treatment/exposure (accounts for 6-22 %), fibrous dysplasia, retinoblastoma, osteogenesis imperfecta, chronic osteomyelitis, and myositisossificans.[5,16,19,27,33,34,44,48] Rare, congenital and inherited syndromes that can result in an increased incidence of osteosarcoma include autosomal-dominant Li-Fraumeni syndrome, autosomal-dominant hereditary retinoblastoma, autosomal-recessive Bloom syndrome, autosomal-recessive Rothmund-Thomson syndrome, autosomal-recessiveWerner syndrome, and autosomal-dominant familial expansile osteolysis.

Frequency of Occurrence

Intra-osseous osteosarcoma: from 0.11 to 1.0 per 100000 per year.[19] Accounts for up to 91-95% of osteosarcomas.[40,42,63,64]

Telangiectatic Osteosarcoma: these tumors are rare, although they have been reported to account for up to 12 % of osteosarcomas.[40,43]

Parosteal Osteosarcoma: these tumors account for 4-6% of osteosarcomas.[15,42,52,63,64]

Periosteal Osteosarcoma: these tumors accounts for 1-2% of osteosarcomas.[15,42,51,63,66]

Intracortical Osteosarcoma: these tumors are very rare.[25,44]

Extraskeletal Osteosarcoma: these tumors accounts for 1-4% of osteosarcomas;[10,11,40,42] and ~1 to 2% of malignant soft tissue tumors.[28,44,54]

Postradiation Osteosarcoma: these tumors account for 3.4-5.5 % of osteosarcomas.[16]

Age at Presentation[19,41,63]

From 2 to 92 years, median = 16-39 years, mean = 25 years. Over 60 % of osteogenic sarcomas occur in the 1 st two decades. Osteogenie sarcoma has two age peaks of incidence: the larger peak occurs between the ages of 10 and 20 years and accounts for over half of the cases; the second smaller peak occurs in adults over 60 years old and accounts for ~ 10 % of the cases.[19] Extra-osseous osteosarcoma typically occurs in adults, whereas intra-osseous osteosarcoma mostly affects patients under 20 years of age.

Intra-osseous osteosarcoma: from 2 to 92years, median = 17 years.[41]

Telangiectatic osteosarcoma: from 4 to 83 years, mean = 24years.[43]

Parosteal osteosarcoma: from 6 to 80 years, median = 27 years.[41,64]

Periosteal osteosarcoma: from 11 to 57 years, median = 17 to 24years.[41,44,63]

Extraskeletal osteosarcoma: from 16 to 86 years, median = 39 years, mean = 57 years.[28,29,41]

Gender Ratio (M/F)

1.36/I to 2/1.[14,63]

Intraosseous osteosarcoma: 1.4/1 to 2/I.[14,42,63]

Telangiectatic osteosarcoma: 2.1 /1.[43]

Parosteal osteosarcoma: 1/1 to 1/1.8;[42,64] 1/3 for rare primary tumors that involve the calvaria.[31]

Periosteal osteosarcoma: 1 /1.6 to 1.8 /1.[42,45,63]

Extraskeletal osteosarcoma: 1.7 /1 to 1.9 /1.[28]

Paget osterosarcoma: 2/1.[16]

Location

Osteosarcomas can occur in three locations. Osteosarcomas within bone (intra-osseous Osteosarcomas) account for 91-95% of all these neoplasms.[42] Osteosarcomas can occur along the surface of bone (5-8% of Osteosarcomas) and at extra-osseous sites (1 % of Osteosarcomas).[42]

Intra-osseous osteosarcoma. Tumors occur in the distal femur > proximal tibia > proximal humerus > craniofacial bones > pelvic bones > proximal femur > proximal fibula > distal tibia > ribs > scapula > vertebra > sacrum > other bones.[21,22,42,63] Lesions occur in the metadiaphyseal > metaphyseal > diaphyseal > epi-metadiaphyseal > epi-metaphyseal locations.[42] Approximately 4 % of primary Osteosarcomas arise from the vertebrae (thoracic > lumbar > cervical).[22] Most vertebral tumors arise from the posterior elements with extension into the vertebral body.[22] Tumors rarely involve just the vertebral body.[22] Tumors in the sacrum often involve both the body and sacral ala.[22] Multifocal osteosarcoma (also referred to as osteosarcomatosis, multiple sclerotic osteosarcoma, and synchronous mulitcentric osteosarcoma) represents a situation in which multiple osseous foci of osteosarcoma occur at presentation.[7,36,34] The favored theory is that multifbcal osteosarcoma is secondary to rapidly progressive metastatic disease rather than multiple, primary, synchronous Osteosarcomas.[7,44] Paget osteosarcoma can potentially occur in any bone affected by Paget disease.[16] Paget Osteosarcomas have been reported in the femur, humerus and tibia in ~ 67 % of cases, and pelvis, skull or pelvis for most of the remainder.[16] Postradiation Osteosarcomas can potentially occur in any irradiated bone with the pelvis and shoulder being the most common sites.[16]

- **Telangiectatic osteosarcoma.** Tumors commonly involve the femur (50%) followed by the tibia (25%), humerus (10%), iliac bone (5%), as well as in the sacrum, lumbar vertebra, scapula, and fibula.[19,33,43,44] In long bones, 83% of lesions occur in the metaphysis and 17 % occur in the diaphyseal region.[43] Up to 83 % of tumors centered in the metaphysis extend into the epiphyseal region.[43]

Juxtacortical or Surface osteosarcoma:

- **Parosteal osteosarcoma.** Tumors occur in the distal femur > proximal humerus > proximal tibia > distal tibia > ribs > fibula > radius > other bones.[42,64] Tumors occur in the metadiaphyseal > diaphyseal > metaphyseal > epi-metadiaphyseal locations.[42,44] Parosteal Osteosarcomas occasionally occur in the facial bones such as the mandible, and only rarely involve the calvarial bones.[31]
- **Periosteal osteosarcoma.** Tumors occur in the femur > tibia > humerus > other bones.[42,63] Tumors occur in the diaphyseal region most frequently compared with other sites.[42]

Intracortical osteosarcoma. Tumors usually occur in the femur or tibia.[25,44]

Extraskeletal osteosarcoma. Tumors occur in the lower extremity > trunk > hips and buttocks, retroperitoneum > upper extremity > other sites.[11,28,29] Ninety percent occur in the deep soft tissues with the remainder in the subcutaneous or superficial soft tissues.[29,30]

Signs and Symptoms[14,19,63]

Bone. Patients can have sudden or relatively rapid onset of varying degrees of pain, swelling, palpable mass, and limitation of joint mobility.[14,19,63] Slowly progressing pain and tenderness can also occur. Duration of symptoms typically ranges from weeks to months.[63] Lesions can also be detected as incidental findings on radiographic examinations after trauma. Osteosarcomas are rarely associated with pathologic fractures.[14,19,22] Lesions can also present as a palpable, painful mass.[63] Primary vertebral osteosarcoma invades the spinal canal in up to 84 % of cases, and can result in spinal cord or neural compression.[22] Paget osteosarcoma can be associated with pain, swelling, pathologic fracture (up to 20%), and elevated serum alkaline phosphatase.[16]

Soft tissue. Patients with superficial lesions often have an enlarging, palpable, soft tissue mass with or without pain and tenderness.[29,30] Deep lesions (retroperitoneum, etc.) may present with symptoms related to compression and/or displacement of other organs.

Cross Pathologic Findings

Bone

Intra-osseous osteosarcoma. Osteosarcomas are intramedullary tumors, often associated with zones of cortical destruction and periosteal elevation due to a extra-osseous tumor extension. Lesions can be yellow-white, gray-white (fibrous component), and/or blue-gray (tumoral cartilage).[14,42,50,63] Lesions can vary: they can be soft and fleshy, or firm and fibrous containing irregular zones of ossification and chondroid material, or hard and densely ossified zones.[14,42,50,63] Undifferentiated osteosarcomas are usually fleshy and soft.[14] Various combinations of the aforementioned findings often occur.[14,42,63] Zones of necrosis, cyst formation, and hemorrhage often occur in the soft tissue portions of Osteosarcomas.[14,63] Telangiectatic Osteosarcomas are typically osteolytic with a cystic/necrotic zone or zones containing blood and necrotic debris similar in appearance to an aneurysmal bone cyst.[14;43;63]

Juxtacortical osteosarcoma:

- **Parosteal osteosarcoma.** Lesions are ovoid or spherical, gray-white, ossified masses that are adherent to the shafts of bone.[42,65] These tumors also can encircle bone.[20,42,52] Tumors can be large measuring up to 25 cm.[20] Tumors are often well-circumscribed and may have a pseudocapsule continuous with the periosteum.[20,42] Softer portions can be seen at the periphery which may infiltrate adjacent soft tissue or muscle.[52] Cartilaginous zones are seen in half of the tumors.[52] Cortical involvement and tumor extension into the medullary space can be seen in up to 50 %.[15,20] The base of the tumor is usually densely ossified, whereas the peripheral portions of the tumors show less dense ossification with relatively greater amounts of fibrous and/or cartilaginous zones.[20] Lesions frequently involve the distal dorsal portion of the femoral shaft near the metaphysis (40-70 %), as well as the humerus (15%) and proximal tibia (10%).[3,14,20,42]
- **Periosteal osteosarcoma.** These tumors occur at the surface of bone and often appear as well demarcated lobules of cartilage containing white spicules of bone.[42,45,52,63] Variable infiltration of cortical bone is typical.[42,45] These lesions often involve the proximal diaphysis of the tibia and femur, and rarely involve flat bones.[14,19,42]

Intracortical osteosarcoma. These very rare Osteosarcomas are associated with intracortical bone lysis from tumors containing mineralized osteoid, and cortical expansion/destruction.[25,44]

Soft tissue

Lesions may have poorly defined margins or appear circumscribed with a pseudocapsule.[2930] Tumors may also have irregular borders that are adherent or fixed to adjacent tissue. Hemorrhage and necrosis are often present.[29,30]

Histopathologic Findings

Bone

Osteogenic sarcomas can be classified into subtypes based upon the predominant histologic features of cell types and stromal differentiation (osteoblastic, chondroblastic, fibroblastic, common mixed, telangiectatic, and small cell).[14,19,45,49,63] Osteosarcomas often exhibit histologic variability within the lesions, complicating classification into subtypes.[19] Osteoclast-like giant cells or epithelioid-appearing cells may be present in osteosarcomas.[63] Perisosteal elevation is often seen secondary to tumor invasion and cortical perforation.[63] The elevated periosteum is a thick, resistant barrier that may enclose the extra-osseous tumor extension through zones of cortical destruction or perforation.[49]

- **Osteoblastic *type.*[14,63]** This subgroup of osteosarcomas accounts for up to 50 % of osteosarcomas.[63] Lesions contain a lacelike network of tumor osteoid between neoplastic cells. With the May-Grunwald-Giemsa stain, the osteoid matrix has an amorphous pink fibrillary appearance.[14] Tumor cells are usually large, round or polygonal containing large nuclei and pink cytoplasm.[14] Nuclei often have irregular margins containing coarse chromatin and prominent nucleoli.[1463] Increased mitotic activity is frequent as well as multinucleated tumor cells and other types of nuclear atypia.[14,63] Calcifications can occur focally or as thin interconnecting trabeculae within the tumor matrix.[14,63] Dense sclerosis can occur from extensive tumor matrix filling the marrow and obscuring neoplastic cells, as well as in tumor extending between preexisting bone trabeculae.[63] Immunoreactivity to collagen type I can be seen in osteoblastic regions.[14]
- ***Chondroblastic* type.[14,63,66]** Chondroblastic osteosarcomas account for ~ 25 % of osteosarcomas. These osteosarcomas contain chondroid zones which can be distributed as small scattered foci, lobules, or in a diffuse pattern. The chondroid neoplastic zones often contain spindle-shaped cells, similar in appearance to neoplastic cells in other portions of the tumor.[14,63,66] Cartilaginous lobules can have a hyaline or myxoid matrix within which are fine bony trabeculae.[14,63] Spindle-shaped cells are prominent in number at the periphery of the lobules where osteoid matrix can also be found.[14,63,66] Enchondral ossification and metaplastic bone formation are commonly seen in chondroblastic osteosarcoma.[14] Immunoreactivity to S-100, and collagen types II and V can be seen in chondroblastic regions.[14]
- ***Fibroblastic type.*** Fibroblastic osteosarcomas represent up to 25 % of osteosarcomas.[14,62] These osteosarcomas contain spindle-shaped cells often arranged in a herringbone pattern in a limited collagen matrix.[14,63,66] Immunoreactivity to collagen type IV can be seen in fibroblastic regions.[14]
- **Common *mixed type.*** These osteosarcomas contain undifferentiated zones and areas with osteoblastic, chondroblastic, and fibroblastic differentiation.[49]
- ***Telangiectatic type.*** Telangiectatic osteosarcomas account for 2-12% of osteosarcomas.[14,37,42,43,63] These lesions are typically osteolytic with cystic/necrotic zones containing blood, necrotic debris, malignant cells, reactive giant cells, and hemosiderin-laden macrophages.[14,63] Unlike aneurysmal bone cysts, malignant cells with increased mitotic activity are seen lining septa and the walls of the cystic/necrotic spaces.[14,63] Minimal or no osteoid matrix is present.[14,63]
- **Small *cell type.*** Small cell osteosarcomas account for approximately 1.5-4% of osteosarcomas.[14,26,63] These tumors typically consist of sheets of round, small cells in an osteoid matrix associated with permeative bone destruction.[14,26,63] Tumor cells can appear round or oval with a large nucleus containing finely dispersed chromatin.[14,62] Mitotic activity ranges from 3 to 5 per HPF.[26] Tumor cells may also have spindle shapes.[26] Neoplastic cells of small cell osteosarcoma may resemble tumor cells in Ewing sarcoma or large cell lymphomas.[14,26,63] Tumor cells are often immunoreactive to CD 99, osteonectin, osteocalcin, alkaline phosphatase, smooth muscle actin, Leu-7, KP1, and vimentin.[14,26]

Juxtacortical osteosarcoma:

- **Parosteal osteosarcoma.[15,20,52,64,65]** Lesions often consist of elongated or ribbonlike trabeculae of osteoid and woven bone separated by a stoma containing a low density of spindlelike cells.[15,52,65] The spindlelike cells have minimal cytologic atypia and occasional mitoses.[15,65] Foci of low-grade, tumoral cartilage with irregular arrangements of chondrocytes are seen in half of cases.[15,64] Disorganized trabeculae of woven bone lacking osteoblast rimming are often seen at the peripheral outer portions of the lesions.[15,52] A progressive pattern of increasingly well-formed trabeculae with osteoblastic rimming is often seen toward the base of the tumor.[15,52] Calcified tissue can have a lamellar pattern appearing as cement lines similar to findings with Paget disease.[15,52] Well-differentiated tumoral bone may be difficult to distinguish from reactive bone near the cortical margins.[15] Cortical involvement and tumor extension into the medullary space can be seen in up to 50 % of cases.[15,20] Parosteal osteosarcomas can be graded into well-differentiated tumors, high-grade surface tumors, and dedifferentiated tumors.[15] Well-differentiated tumors account for ~ 60 to 82 % of parosteal osteosarcomas.[19,64] The less common, dedifferentiated type of parosteal osteosarcoma typically contains a second type of tumor cell such as seen in fibrosarcoma, malignant fibrous histiocytoma, etc.[44] Zones of high-grade, spindle cell sarcoma forming osteoid, often with malignant cartilage containing chondrocytes with anaplastic and/or duplicated nuclei, can be seen in dedifferentiated parosteal osteosarcoma.[44,64] Approximately 10% of parosteal osteosarcomas are, or become, dedifferentiated.[33]
- **Periosteal osteosarcoma.[2,15,42,45,52,64]** Histologic features are often similar to moderately differentiated chondroblastic osteosarcoma.[63] These tumors are often covered by periosteum associated with immature cells.[15,42] Bone spicules are seen at sites of periosteal reaction.[15,45] Tumors consist of lobules of malignant-appearing cartilage separated and surrounded by malignant spindle-shaped cells within an osteoid matrix.[2,42,52,63] Enchondral ossification can be seen in the central portions of the chondroid lobules.[15] Tumor may extend into Haversian canals and bone marrow.[15]
- **Intracortical osteosarcoma.** Osteosarcomas rarely arise within bone cortex and are often a sclerosing variant, with or without foci, of fibrosarcoma and/or chondrosarcoma.[25,44] These tumors do not usually invade the medullary space.[25,44]
- **Extra-osseous osteosarcoma.** Tumors contain variable amounts of osteoid and bone, cartilage, and calcifications.[8,11,29,30] Extraskeletal osteosarcomas can have histologic patterns similar to those for intra-osseous osteosarcomas (osteoblastic, chondroblastic, fibroblastic, telangiectatic, and small cell types).[11,29,305,4] Margins of the tumors are usually poorly defined with evidence of invasion of adjacent tissue.[29,30] Serum alkaline phosphatase is usually elevated above the normal range.[8]

Tumor Genetics

Intra-osseous osteosarcoma. Conventional osteosarcomas have been reported to have chromosomal abnormalities in regions 1 pll-13,1 qll-12,1 q21-22,11 p14-15,14pll-13,15pll-13, 17 p, and 19ql3.[50] Loss of heterozygosity involving chromosome arms 3 q, 13 q, 17 p and 18 q have been reported.[50] Gain of 8 q24, which includes the MYC gene, is detected in 50 % of osteosarcomas, and is associated with a worse prognosis.[50] Translocations, mutations, or deletions involving the RBI gene at 13 q!4 (as can be seen in hereditary retinoblastoma) and the P53 tumor suppressor gene at 17pl3 have been found in osteosarcomas, as can be seen in Li-Fraumeni syndrome.[1,14] Amplified genes associated with osteosarcoma include MDM2at 12ql3-14 and PRIMl.[50] Amplified genes associated with aggressive osteosarcoma include CDK4 and MDM 2.[50] Rare, congenital and inherited syndromes that can result in an increased incidence of osteosarcoma include: autosomal-dominant Li-Fraumeni syndrome (TP53 germline mutation on chromosome 17ql3, and CHEK2 gene on chromosome 22qll); autosomal-dominant hereditary retinoblastoma (abnormalities involving the RBI tumor suppressor gene on chromosome 13ql4); autosomal-recessive Bloom syndrome (BLM gene on chromosome 15 q26); autosomal-recessive Rothmund-Thomson syndrome (RECQL4 gene on chromosome 8q24); autosomal-recessiveWerner syndrome (WRN gene on chromosome 8pll-12), and autosomal-dominant familial expansile osteolysis (TNFRSFHA gene on chromosome 18q21).

Telangiectatic osteosarcoma. These tumors have been reported to have various complex chromosomal alterations.[37]

Parosteal osteosarcoma. These tumors have been reported to have supernumerary ring chromosomes with amplifications of 12 q13-15, as well as the SAS, CDK4, and MDM 2 genes.[65]

Periosteal osteosarcoma. These tumors have been reported to have various complex chromosomal alterations as well as gains of chromosome 17.[2]

Extraskeletal osteosarcoma. These tumors have been reported to have complex chromosomal alterations which overlap those of osteosarcomas involving bone.[54]

Findings on Plain Films (Roentgenograms) and Computed Tomography

Bone

Intra-osseous osteosarcoma. Findings on plain films vary considerably depending on the amounts of bone destruction and osteoid matrix mineralization.[32,43,53,63] Intra-osseous osteosarcomas can range from mostly radiolucent intramedullary lesions (25–43 %) to predominantly sclerotic lesions (25-47%), with the remainder in between.[14,19,42] Zones of intramedullary and extra-osseous sclerosis/calcifications in osteosarcoma from tumor-induced bone formation can have irregular, partially-rounded, poorly defined borders that have been referred to as "cumulus cloud" and/or disorganized appearance" (Figs. **418, 419, 421, 423, 425-428, 430).** Matrix mineralization/calcification can also have a ground-glass or ivory pattern.[14,22] Osteosarcomas within vertebral bodies can produce dense osteoid matrix mineralization resulting in an "ivory vertebra" appearance.[22] Ringlike or arclike calcifications may be seen in the cartilaginous portions of osteosarcoma if present.[14] Calcified osteoid matix within osteosarcoma is also frequently seen at sites of extra-osseous tumor extension[19,49] (Figs. **418, 421, 423, 424, 426, 428, 430).** Osteosarcomas are often located at the meta-diaphyseal or metaphyseal regions.[41,62] Osteosarcomas can involve the physeal plate and extend into epiphysis.[1944] Articular cartilage is often a barrier to intra-articular extension of osteosarcoma.[15]

Intra-osseous osteosarcomas usually have poorly defined margins. Intramedullary tumors are often associated with zones of cortical destruction.[44,55] Extra-osseous tumor extension with or without ossifying tumor-induced calcifications is commonly seen with plain films and CT. Periosteal elevation may be seen within 3 weeks after occurrence.[14] Interrupted lamellated ("onion-skin") and/or spiculated (perpendicular, divergent, sunburst, disorganized) zones of perisosteal reaction are often seen secondary to tumor invasion and perforation of bone

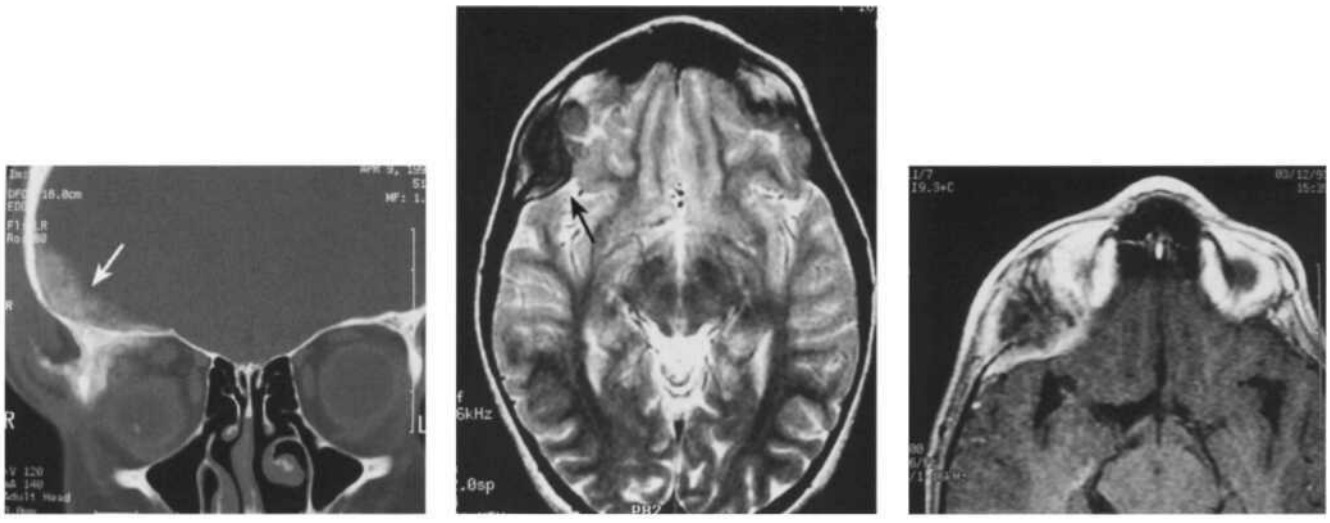

a, b

Figure **418 a–c** A 10-year-old female with osteosarcoma involving the right zygoma, sphenoid, and frontal bones. Coronal CT (a) image shows the intra-osseous tumor to have irregular zones of high attenuation as well as sites of cortical irregularity. Tumor extension occurs into the orbit inferiorly, masticator space laterally, and intracranially superiorly, within which are amorphous "cloud-like" zones of calcifying tumor osteoid. The tumor has mixed low, intermediate, and slightly high signal on axial T2WI (b), and shows irregular, mostly peripheral Cd-contrast enhancement on axial T1 WI (c)

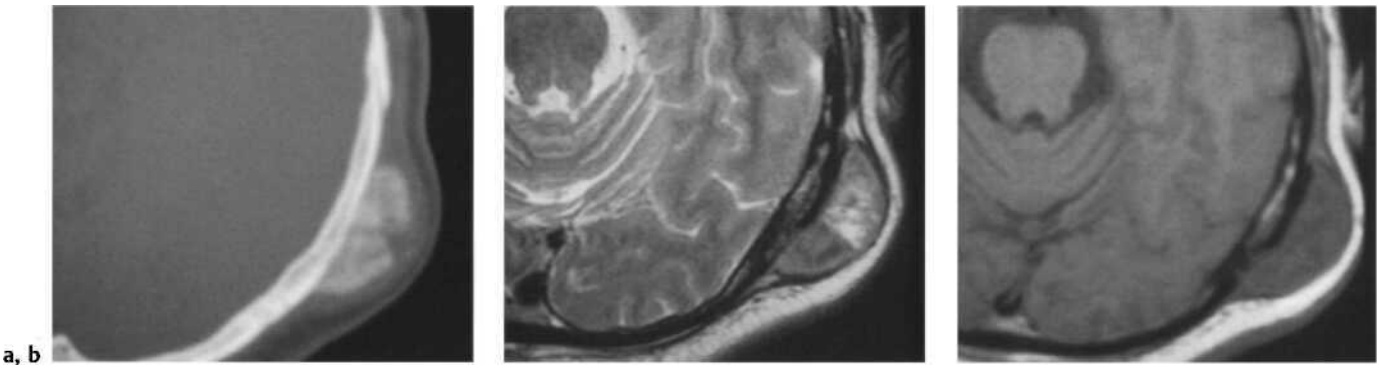

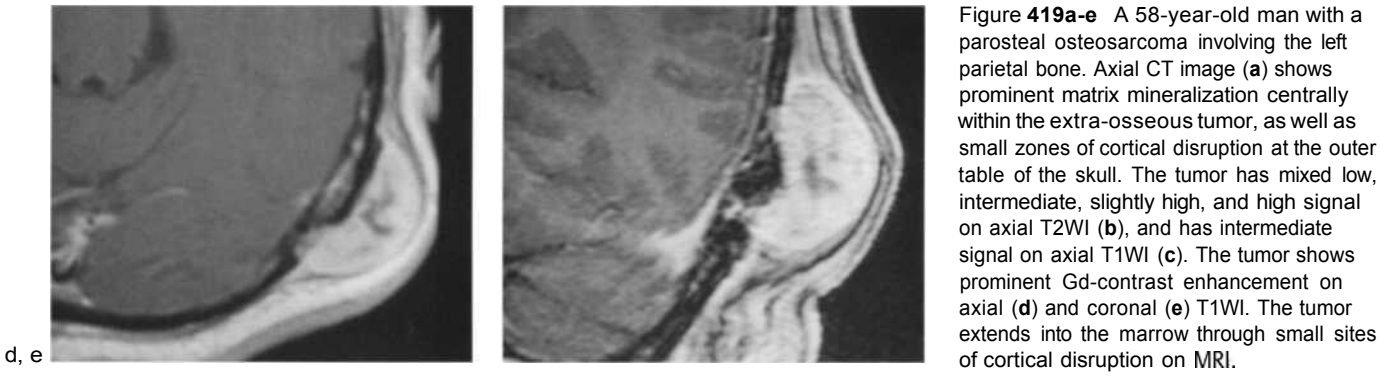

Figure **419a-e** A 58-year-old man with a parosteal osteosarcoma involving the left parietal bone. Axial CT image (**a**) shows prominent matrix mineralization centrally within the extra-osseous tumor, as well as small zones of cortical disruption at the outer table of the skull. The tumor has mixed low, intermediate, slightly high, and high signal on axial T2WI (**b**), and has intermediate signal on axial T1WI (**c**). The tumor shows prominent Gd-contrast enhancement on axial (**d**) and coronal (**e**) T1WI. The tumor extends into the marrow through small sites of cortical disruption on MRI.

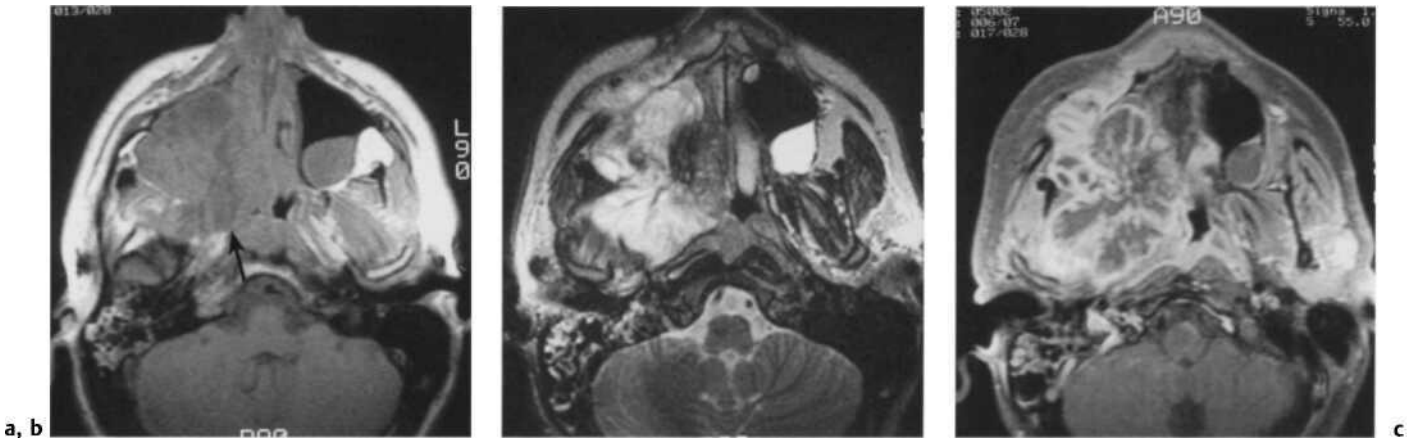

Figure **420 a–c** Osteosarcoma involving the right maxilla and sphenoid bones The tumor has low and intermediate signal on axial T1 WI (**a**), and mixed low, intermediate, and high signal on axial T2WI (**b**). The tumor is associated with bone destruction and extension into the infratemporal fossa, right nasal cavity, nasopharynx, and right masticator space. The tumor shows prominent heterogeneous Gd-contrast enhancement on axial FS T1WI (**c**).

cortex[14,44,59,63,68] (Figs. **423-426, 428, 430, 432).** Triangular zones of periosteal reaction (Codman triangles) can be seen at the borders of zones of cortical destruction and extra-osseous tumor extension[14,19,59,62,68] (Figs. **423**, **424**). Various combinations of interrupted periosteal reaction can occur with the same tumor. Elevated periosteum displaced by extra-osseous extension of osteosarcoma is a strong barrier that may initially constrain these malignant tumors.[49,63] Distinction between osteosarcoma enclosed by elevated periosteum and extra-osseous soft-tissue tumor extension or invasion may be difficult on radiographic examinations.[49] CT is useful for determining the intramedullary extent of osteosarcoma, and for planning biopsies.[19]

Telangiectatic osteosarcomas and small cell osteosarcomas are typically radiolucent lesions which often have indistinct margins, cortical destruction, and periosteal reaction[3,14,37,43,44,63] (Fig. **431, 432).** Telangiectatic osteosarcomas can have the appearance of an expansile pseudocystic lesion similar to an aneurysmal bone cyst[3,14,43,44,59,63] (Fig. **431**).

Parosteal osteosarcoma.[3,15,20,23,31,38,42,44,52,64,65,67,70] These tumors usually have prominent extra-osseous masses with borders which may be circumscribed, lobulated, and/or poorly defined. Matrix calcifications are usually seen centrally and to lesser extent peripherally (Figs. **419**, **435**). The degree of matrix calcification within these tumors is related to the amounts of mineralized osteoid produced by tumor cells. Calcifications are also seen where there is continuity or attachment of these tumors to the outer surface of bone cortex via a stalk or broad zone. The involved cortex can have prominent thickening or relatively normal thickness. Thickening of the inner cortex may represent

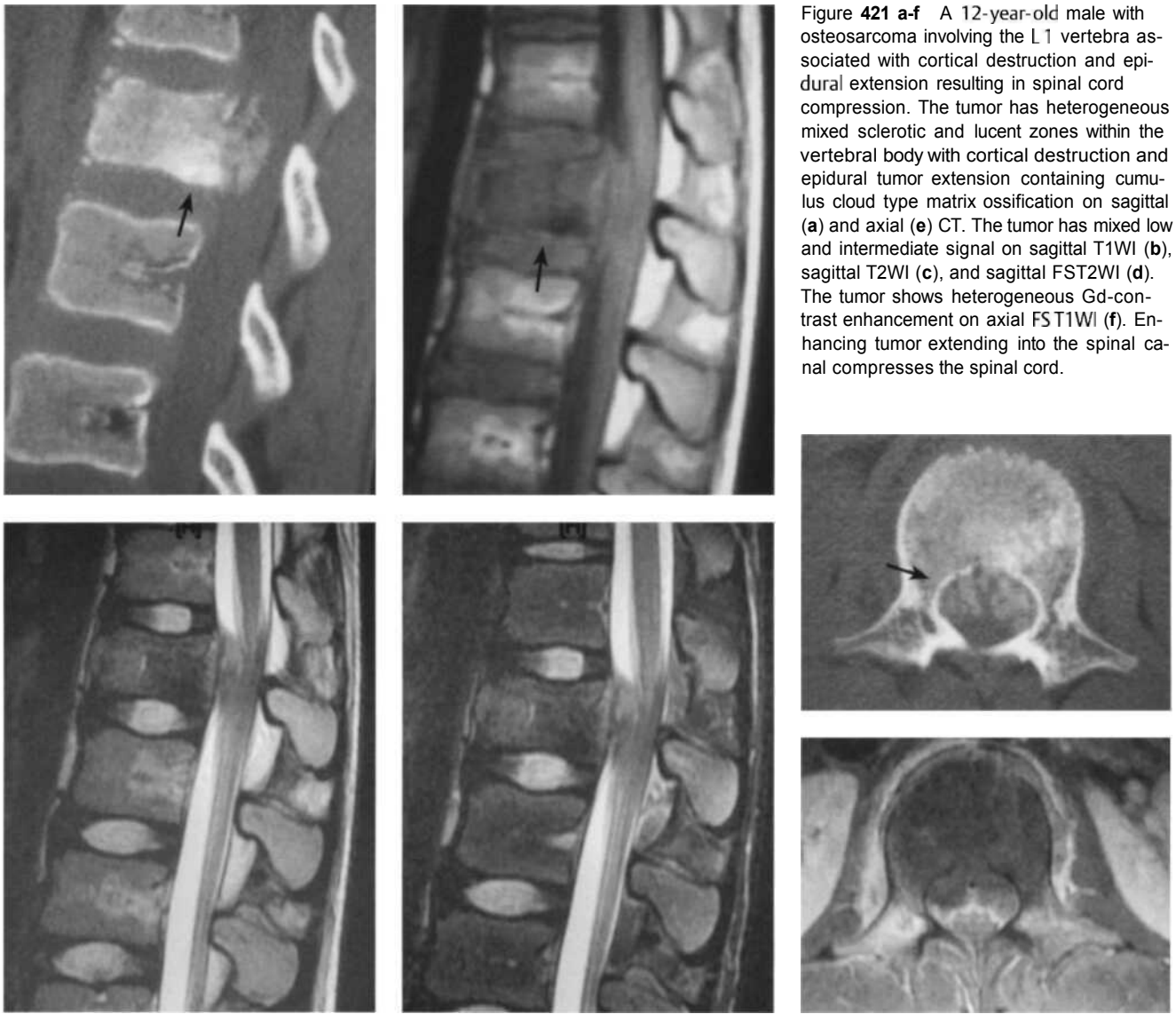

Figure **421 a-f** A 12-year-old male with osteosarcoma involving the L1 vertebra associated with cortical destruction and epidural extension resulting in spinal cord compression. The tumor has heterogeneous mixed sclerotic and lucent zones within the vertebral body with cortical destruction and epidural tumor extension containing cumulus cloud type matrix ossification on sagittal (**a**) and axial (**e**) CT. The tumor has mixed low and intermediate signal on sagittal T1WI (**b**), sagittal T2WI (**c**), and sagittal FST2WI (**d**). The tumor shows heterogeneous Gd-contrast enhancement on axial FS T1WI (**f**). Enhancing tumor extending into the spinal canal compresses the spinal cord.

Figure **422** A 17-year-old male with small cell osteosarcoma involving the right iliac bone and sacrum. The tumor shows prominent heterogeneous Gd-contrast enhancement on coronal FS T1WI, as well as nonenhancing central zones of necrosis. Tumor extends from the marrow into the adjacent soft tissues through sites of cortical destruction.

intramedullary tumor extension. These tumors often grow proximally and distally adjacent to the cortex where there may be a radiolucent line. Axial CT can easily demonstrate tumor encircling bone as well as intramedullary extension.

Periosteal osteosarcoma.[2,3,15,20,39,42,44,45,52,63,67] These tumors involve the bone cortex, which is irregularly calcified from reactive bone formation (Fig. **436).** A shallow zone of cortical bone erosion or destruction may occur with borders of thickened cortical bone. Striated or lamellated zones of periosteal mineralization may be present, near the zone of erosion. A soft tissue mass containing varying amounts of calcification as coarse or fine striations, arclike or ringlike, is often seen, mostly in the central portion.

Intracortical osteosarcoma. These tumors show a zone of radiolucency in bone cortex containing mineralized osteoid. Tumors can have thickened sclerotic margins, and usually do not extend into the medullary space.[25,44]

Secondary osteosarcoma.[3,42,44] Secondary osteosarcomas usually show combinations of findings associated with intra-osseous osteosarcomas superimposed upon the primary abnormalities (Paget disease, radiation injury, fibrous dysplasia, osteogenesis

imperfecta, chronic osteomyelitis, etc.). Secondary osteosarcomas may occur from malignant transformation of benign lesions or tumors.

Extra-osseous osteosarcoma. Tumors can appear as masses in the soft tissues on plain films. In ~50% of cases, tumors contain irregular zones of dense mineralization visible on plain films or increased attenuation seen with CT.[10,11,29,30] Zones of low attenuation in tumors representing areas of necrosis can be seen with CT.[10,29,30] Margins of the tumors can be indistinct or circumscribed on CT.

MRI Findings

Intra-osseous osteosarcoma.[3,5,9,12,13,18,22,32,33,38,39,43,44,46,47,50,51,56–61] Intra-osseous osteosarcomas are intramedullary tumors that often have poorly defined margins and usually involve the metaphysis or metaphyseal equivalent regions. Tumors often extend into the diaphysis, and up to 88% extend through the physeal plate into the epiphysis[44] (Figs. **423-433).** Primary intra-osseous osteosarcomas can also involve the skull, facial bones, vertebrae, and pelvis (Figs. **418,420-422).** These tumors usually have low-intermediate signal on T1WI. Zones of low signal often correspond to areas of tumor calcification/mineralization and/or necrosis. Zones of necrosis typically have high signal on T2WI, whereas mineralized zones usually have low signal on T2WI. Tumors can have variable MRI signal on PDWI, T2WI, and FST2WI depending upon the relative proportions, distributions, and locations of calcified/mineralized osteoid, chondroid, fibroid, hemorrhagic, and necrotic components (Figs. **418, 420-433).** Tumors may have low, low-intermediate, intermediate to high signal on T2WI and FS T2WI. Low signal on T1WI and T2WI from matrix mineralization can vary from small to large amounts.[44]

Intramedullary osteosarcomas often have zones of cortical destruction through which tumors extend toward the extra-osseous soft tissues under an elevated periosteum. Lamellated, speculated, and disorganized zones of tumor-induced bone formation can occur under the perisosteal elevation. Low signal from tumoral bone formation may have a divergent ("sunburst") pattern, perpendicular ("hair on end") pattern, or disorganized or complex appearance.[66] Triangular zones of periosteal elevation (Codman triangles) can be seen at the borders of zones of cortical destruction and tumor extension.[68] Periosteal elevation secondary to tumor invasion and cortical perforation is often seen on pathologic examination.[63] The elevated periosteum is a thick, resistant barrier, often enclosing tumor extension through zones of cortical destruction or perforation.[49] With MRI, a thin zone of low signal on T1WI and T2WI may seen at the peripheral border of the extra-osseous tumor in-

a

b, c

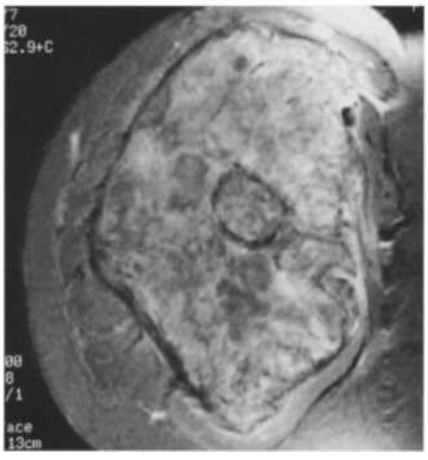

d

Figure **423 a–d** A 12-year-old female with a high-grade osteosarcoma involving the proximal metaphysis and diaphysis of the humerus. Radiograph (**a**) shows a mixture of "moth-eaten" radiolucent pattern of bone destruction plus osteoid matrix mineralization within the metadiaphyseal portion of the humerus. Multiple sites of cortical destruction are seen associated with extra-osseous tumor extension containing an irregular disorganized pattern of tumor-induced bone formation. In addition, a Codman triangle of interrupted perisoteal reaction is seen at the inferior border of cortical destruction and tumor extension. With MRI, extensive signal abnormality is seen in the marrow as well as multiple sites of cortical destruction through which tumor extends into the extra-osseous soft tissues. The intra-osseous and extra-osseous portions of the tumor have zones with low, low-intermediate, and slightly high signal on coronal (**b**) T1 WI, and mixed low, intermediate, and high signal on axial (**c**) T2WI. A thin, slightly irregular zone of low signal on T1 WI and T2WI is seen at portions of the peripheral border of the extra-osseous tumor. The tumor shows markedly heterogeneous Cd-contrast enhancement in both the intra-osseous and extra-osseous portions on axial (d) FST1WI.

a

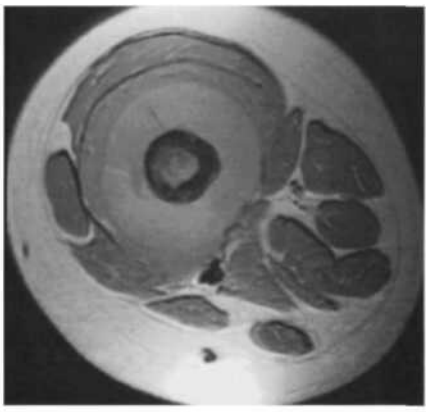

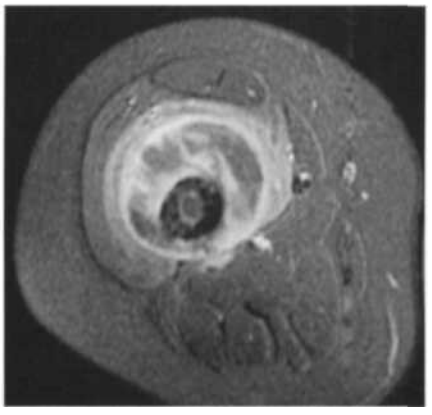

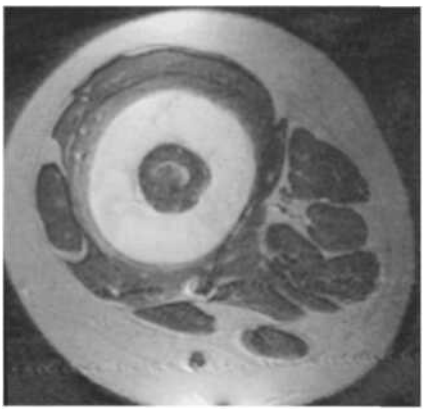

b, c

Figure **424 a–d** A 10-year-old female with a chondroblastic osteosarcoma involving the proximal diaphysis of the femur. AP radiograph (**a**) shows osteoid matrix mineralization from intramedullary tumor associated with interrupted perpendicular and lamellated periosteal reaction. A Codman triangle is seen at the upper border of tumor extension. With MRI, tumor extends from the marrow into the extra-osseous soft tissues via small irregular zones of cortical disruption. The intramedullary tumor has low-intermediate signal on axial PDWI (**b**), whereas circumferential extra-osseous tumor has mostly intermediate signal. Intramedullary tumor has mostly low signal on axial T2WI (**c**), whereas extra-osseous tumor has mostly high signal. Irregular thin strands of low signal are seen in the extra-osseous tumor representing perpendicular periosteal reaction. Irregular Cd-contrast enhancement is seen mostly in the extra-osseous tumor on axial FS T1WI (**d**).

a

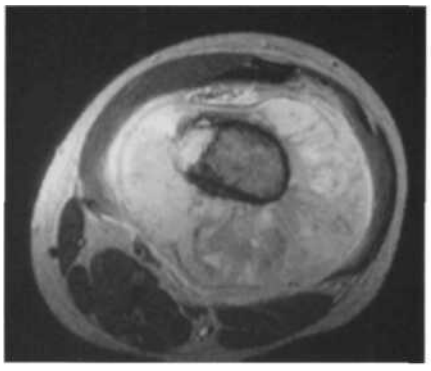

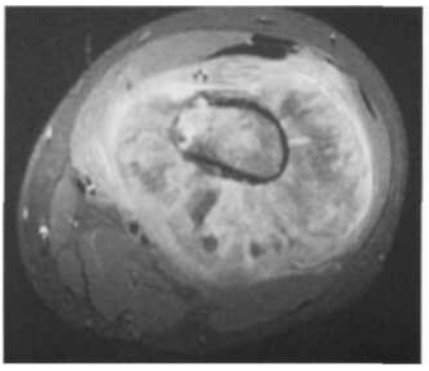

b, c

Figure **425 a-c** Lateral radiograph (**a**) shows dense osteoid matrix mineralization from intramedullary tumor associated with interrupted lamellated periosteal reaction. With MRI, tumor extends from the marrow into the extra-osseous soft tissues via zones of cortical disruption. The intramedullary tumor has low-intermediate signal and high signal on axial T2WI (**b**), whereas circumferential extra-osseous tumor has mostly high signal, as well as irregular zones with low signal representing tumor-induced bone formation. A thin, slightly irregular zone of low signal on T1 WI and T2WI is seen at portions of the peripheral border of the extra-osseous tumor representing a partially intact, elevated periosteum. Irregular Cd-contrast enhancement is seen at both the intramedullary and extra-osseous tumor on axial FST1WI (**c**). Tumor is seen extending into the knee joint.

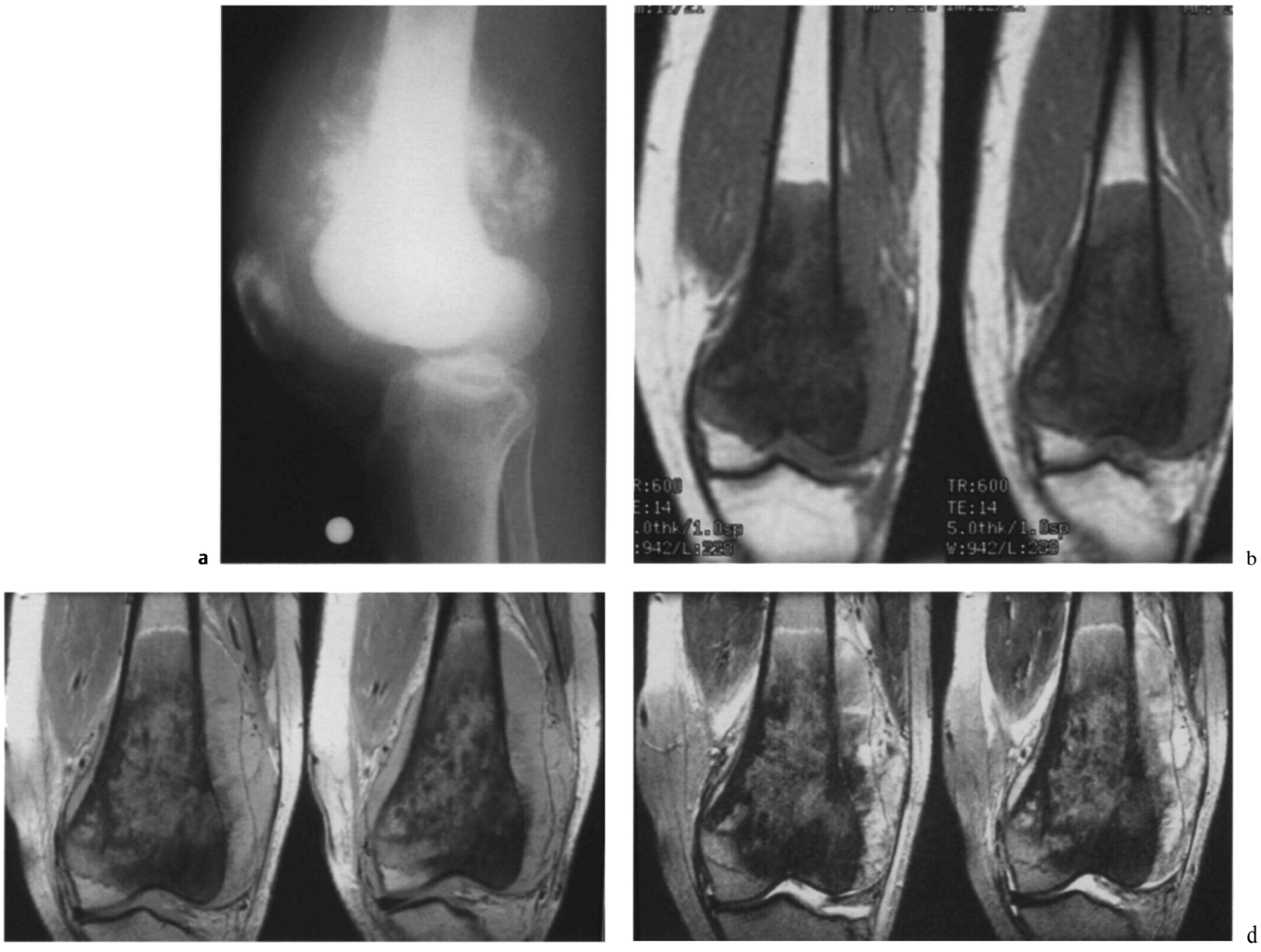

Figure **426 a-d** A 19-year-old woman with a high-grade osteosarcoma of the distal metaphysis and epiphysis of the femur. Lateral radiograph **(a)** shows dense osteoid matrix mineralization from intramedullary tumor as well as a "cumulus cloud" or "sunburst appearance" of tumor-induced bone formation / periosteal reaction in the extra-osseous portion of the osteosarcoma. With MRI, tumor extends from the marrow into adjacent extra-osseous tissues via zones of cortical disruption. The intramedullary tumor has low-intermediate signal on coronal **(b)** T1WI, whereas extra-osseous tumor has mostly intermediate signal. The intramedullary tumor has heterogeneous low and intermediate signal on coronal **(c)** PDWI, whereas extra-osseous tumor has mostly intermediate signal. Intramedullary tumor has mixed low, intermediate, and slightly high signal on coronal **(d)** T2WI, whereas extra-osseous tumor has mixed signal as well as zones with high signal. Irregular amorphous perpendicular and divergent bands and strands of low signal are seen in the extra-osseous tumor, representing tumor-induced bone formation/periosteal reaction. A thin, slightly irregular zone of low signal on **T1 WI** and T2WI is seen at portions of the peripheral border of the extra-osseous tumor, representing the elevated periosteum.

volving long bones representing the elevated periosteum, which may be partially intact (Figs. **423-428).** Extra-osseous tumor extension may be seen beyond the elevated periosteal membrane (Figs. **425-428).** MRI is highly sensitive in detecting joint invasion by osteosarcoma.[56]

Areas of hemorrhage in osteosarcomas can have high signal on both T1WI and T2W1. Fluid-fluid levels can also be seen secondary to hemorrhage and/or necrosis.[4461]
After GD-contrast administration, osteosarcomas typically show prominent enhancement in non-mineralized/calcified portions of the tumors.

- **Telangiectatic osteosarcomas.** These tumors represent an uncommon subtype of osteosarcoma that are associated with prominent blood-filled cysts and vessels comprising -90% of the mass.[192233434459] These tumors often have heterogeneous high signal on T2WI and FS T2WI, as well as zones of high signal on T1WI and PDWI corresponding to areas of hemorrhage[22,43,44] (Figs. **431, 432).** Fluid-fluid levels are frequently seen with these osteosarcomas[22,43,44] (Fig. **432).** Solid portions of the tumor usually show prominent Gd-contrast enhancement.[43,44]

  Preoperative evaluation of tumor extent.[13,39,46,57] Intra-osseous margins of osteosarcomas are more accurately determined with T1WI than FST2WI because of the latter technique's lower threshold in detecting peritumoral edema/inflammation that can obscure tumor borders.[13,39,46] In addition, peritumoral edema/inflammation is also detected as Gd-contrast enhancement which can also obscure intra-osseous and extra-osseous tumor margins.[57] Dynamic Gd-contrast enhanced MRI, however, can usually distinguish between tumor margins and peritumoral edema/inflammation because osteosarcomas show more rapid enhancement patterns than peritumoral edema/inflammation.[13]
- **Response to chemotherapy.**[4.9.12.13.18.33.39.51.55.58] Many patients now receive treatment for osteosarcoma consisting of neo-

a

b, c

Figure **427 a-c** A 15-year-old female with a high-grade osteosarcoma of the distal metaphysis and epiphysis of the femur. Lateral radiograph **(a)** shows dense osteoid matrix mineralization with a "cumulus cloud appearance" from intramedullary tumor. The intramedullary tumor has heterogeneous low and intermediate signal on sagittal T1WI **(b)**, whereas extra-osseous tumor seen lateral and posterior to the cortex has mostly intermediate signal. A thin, slightly irregular zone of low signal on T1 WI is seen at portions of the peripheral border of the extra-osseous tumor. Cd-contrast enhancement is seen at both the intramedullary and extra-osseous tumor on sagittal FST1WI **(c)**. Tumor is also seen extending beyond the elevated periosteum into the knee joint.

a, b

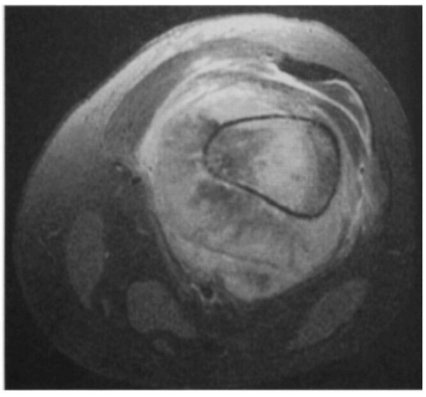

d

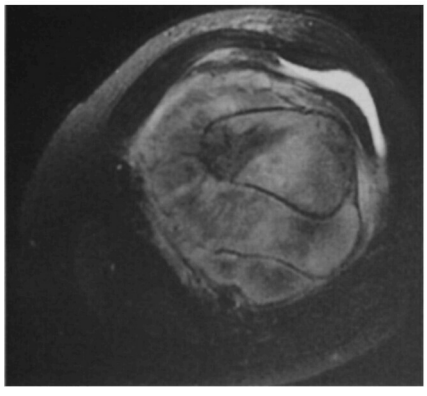

c

Figure **428 a-d** An 8-year-old male with an osteosarcoma of the distal metaphysis and epiphysis of the femur. Lateral radiograph **(a)** shows irregular osteoid matrix mineralization within intramedullary and extra-osseous tumor, as well as sites of cortical disruption. With MRI, tumor extends from the marrow into adjacent extra-osseous tissues via multiple zones of cortical disruption The intramedullary and extra-osseous tumor has heterogeneous slightly high, intermediate, and low signal on sagittal **(b)** and axial **(c)** FST2WI. Irregular amorphous, divergent, and perpendicular bands and strands of low signal are seen in the extra-osseous tumor, representing tumor-induced bone formation/periosteal reaction. A thin, slightly irregular zone of low signal on T1 WI is seen at portions of the peripheral border of the extra-osseous tumor, representing a partially intact elevated periosteum. Heterogeneous Cd-contrast enhancement is seen at both the intramedullary and extra-osseous tumor on axial **(d)** FST1WI. Tumor is also seen extending beyond the elevated periosteum into the knee joint.

adjuvant (preoperative) chemotherapy to decrease tumor bulk prior to limb-sparing surgery or amputation. The extent of chemotherapy-induced tumor necrosis is highly correlated with local control and patient survival.[51] Positive responses to chemotherapy can be estimated with regional Gd-contrast access correlated with tumor size.[51] Viable tumor can be discriminated from zones of chemotherapy-induced tumor necrosis with dynamic contrast-enhanced MRI because residual tumor shows rapid enhancement patterns unlike tumor necrosis.[4,9,12,13,18,51,58]

Patients undergoing chemotherapy for osteosarcoma may be treated with granulocyte colony-stimulating factor (GCSF), which stimulates the production and function of normal myeloid cells to minimize neutropenia and immunosuppression associated with chemotherapy.[13.39.55] GCSF can result in reconversion from fatty to hematopoeitic (red) marrow.[13,39,55] Zones of marrow reconversion may mimic findings of metastatic disease and obscure intra-osseous tumor margins.[13,39.55]

Juxtacortical osteosarcoma:

- **Parosteal osteosarcoma.**[15,17,20,24,33,,4,65,67,69,70] Parosteal osteosarcomas occur at the surface of bone and extend outward with well-defined and/or indistinct margins. The portions of these tumors that extend toward the Juxtacortical soft tissues typically have mixed soft tissue and mineralized components. The mineralized portions of these tumors tend to be dense centrally and at the sites of contiguity (broad-based or stalklike) with the outer cortical margins. The mineralized portions of these tumors usually have low signal on T1WI, PDWI, T2WI and FS PDWI and FST2WI (Figs. **419, 434, 435).** The soft tissue portions of these tumors often have low-intermediate signal on T1WI, intermediate to slightly high or high signal on T2WI, and high signal on FSPDWI and FST2WI (Figs. **419, 434, 435**). Poorly defined, nonmineralized portions of these tumors measuring > 1 cm^3 can represent high-grade foci, and their localization may be useful for planning of biopsies.[17,24,44] Areas of hemorrhage, cystic change, and/or necrosis with or without associated fluid-fluid levels may be present. Zones with hemorrhage, or cystic and/or necrotic regions with proteinaceous contents, may have high signal on T1WI. Tumor extension into the medullary space seen with MRI can occur in up to 50%.[15,20,44] After Gd-contrast administration, nonnecrotic or nonmineralized soft tissue portions of these tumors usually show enhancement as well as sites of invasion into the medullary space and adjacent soft tissues.
- **Periosteal osteosarcoma.** These tumors usually involve the diaphyseal regions with associated cortical thickening manifest as low signal on T1WI and T2WI.[44,45] A lesion with a broad base along the outer cortex is typically seen extending outward and toward the adjacent soft tissues. Cortical thickening associated with these tumors is often thinner or eroded at the center or base of the protruding mass. Periosteal reaction, seen as linear zones of low signal on Tl WI and T2WI, can be associated with these tumors, as well as Codman triangles).[44.45] These tumors can involve 50% or more of the bone circumference.[44.45] These tumors often have low-intermediate signal on T1WI and heterogenous slightly high to high signal on T2W1 and FST2WI (Fig. **436).** Tumor extension into the marrow is uncommon, and when present is usually seen associated with a zone of cortical destruction.[44.45]
- **Intracortical osteosarcoma.** These tumors show a zone of intermediate signal on Tl WI in bone cortex without extension into the medullary space.[25] The outer cortical margin can be expanded with zones of cortical destruction.[25] Tumors can have thickened sclerotic margins, and usually do not extend into the medullary space.[25,44]
- **Secondary osteosarcoma.** Secondary osteosarcomas usually show combinations of findings associated intra-osseous osteosarcomas superimposed upon the primary abnormalities (Paget disease, radiation injury, fibrous dysplasia, osteogenesis \imperfecta, chronic osteomyelitis, etc.) (Fig. **433).**

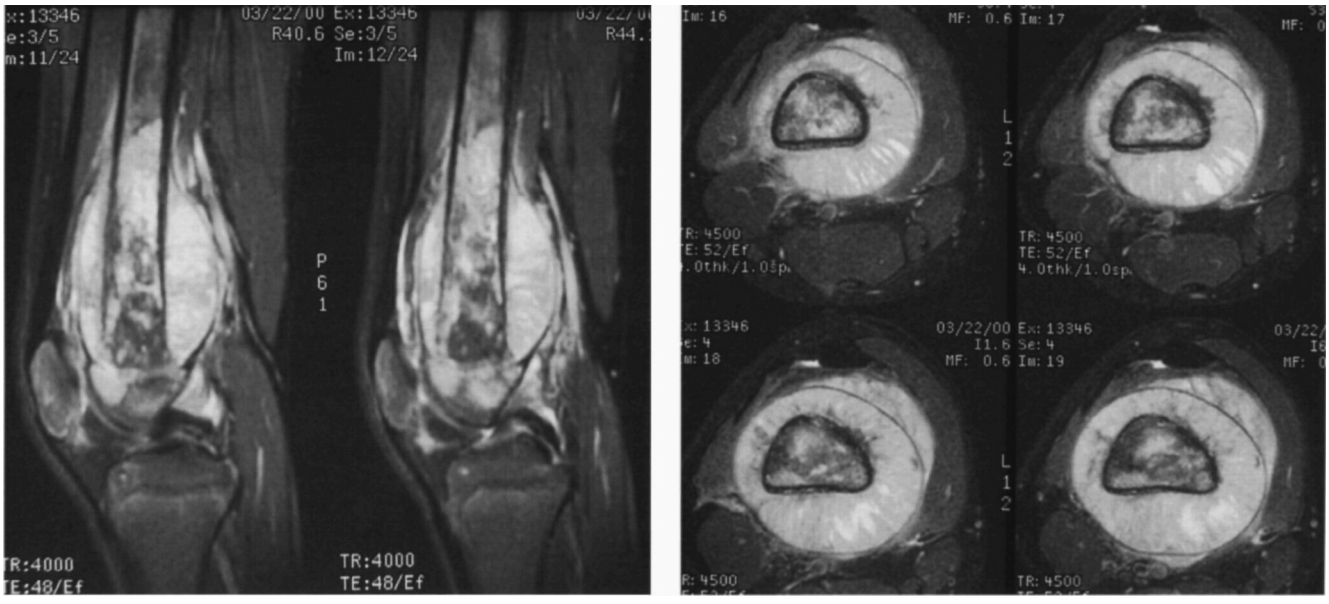

b

Figure **429 a, b** A 9-year-oid female with a chondroblastic osteosarcoma involving the distal diaphysis, metaphysis, and epiphysis of the femur. Tumor extends from the marrow into adjacent extra-osseous tissues via multiple zones of cortical disruption. The intramedullary and extra-osseous tumor has heterogeneous high, intermediate, and low signal on sagittal **(a)** and axial **(b)** FST2WI. Irregular amorphous, divergent, and perpendicular bands and strands of low signal are seen in the extra-osseous tumor, representing tumor-induced bone formation/periosteal reaction. A thin, slightly irregular zone of low signal on T2WI is seen at the peripheral border of the extra-osseous tumor, representing a partially intact elevated periosteum. Tumor is also seen extending beyond the elevated periosteum into the knee joint.

a

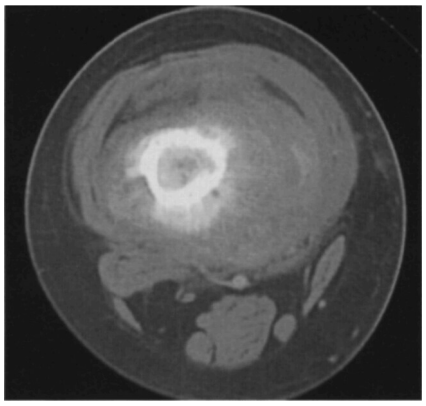

b

Figure **430a-e** An 8-year-old female with a small cell osteosarcoma involving the distal diaphysis, metaphysis, and epiphysis of the femur. Coronal **(a)** and axial **(b)** CT images show tumor-induced bone formation/periosteal reaction with a sunburst/divergent pattern of mineralization within the extra-osseous portions of the tumor. The tumor has heterogeneous intermediate signal on sagittal (c) T1WI and heterogeneous mostly high signal on sagittal FST2WI **(d)**. Prominent heterogeneous Gd-contrast enhancement is seen at both the intramedullary and extra-osseous tumor on sagittal FST1WI **(e)**.

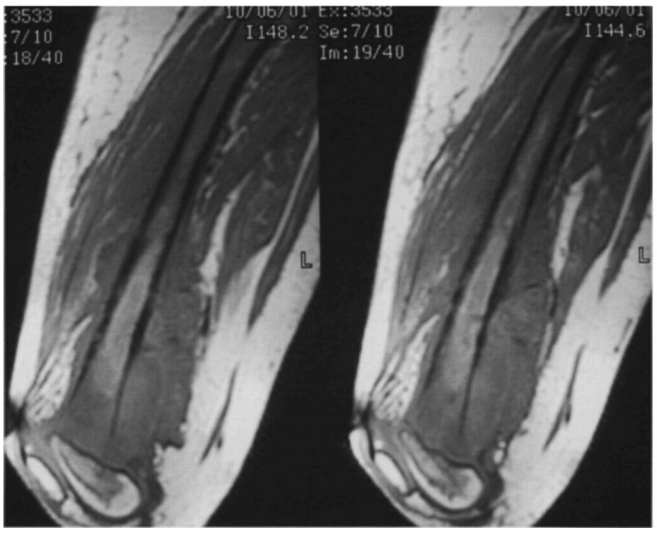

c

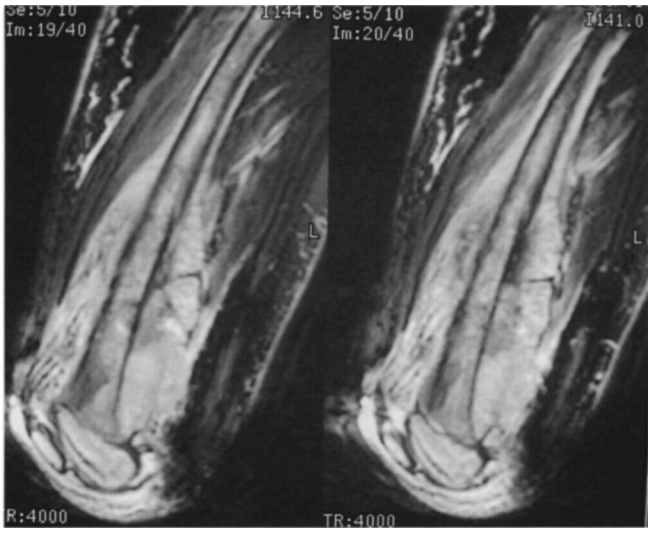

d

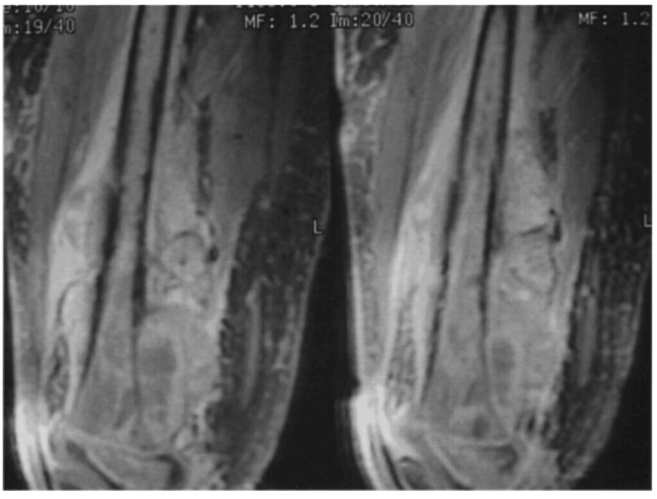

e

Secondary osteosarcomas may occur from malignant transformation of benign lesions or tumors (**Fig. 437**).

Extra-osseous osteosarcoma.[10,11,29,30,53] Tumors are often large at presentation (average = 9 cm).[44] Tumors can have irregular, poorly defined, or well-circumscribed margins. Tumors often have heterogeneous signal on most MRI pulse sequences (Figs. **438-440).** Tumors can have various combinations of zones with low, intermediate, and/or high signal onTlWI, PDW1, T2WI, and FST2WI depending on the presence and extent of hemorrhage and/or necrosis within the lesions (Fig. **440).** OnT2WI and FST2WI, tumors often have heterogenous predominantly high signal. Fluid-fluid levels may be present at sites of hemorrhage or necrosis" (Fig. **440).** Peripheral, nonenhancing, high signal on T2WI may occur and represent zones of edema and/or tumor invasion within adjacent tissues. After Gd-contrast administration, tumors often show heterogenous patterns of enhancement. Solid portions of the tumors often show moderate or prominent enhancement. Margins of the enhancing tumor can be irregular. Enhancing satellite lesions may be present.[29,30]

a, b

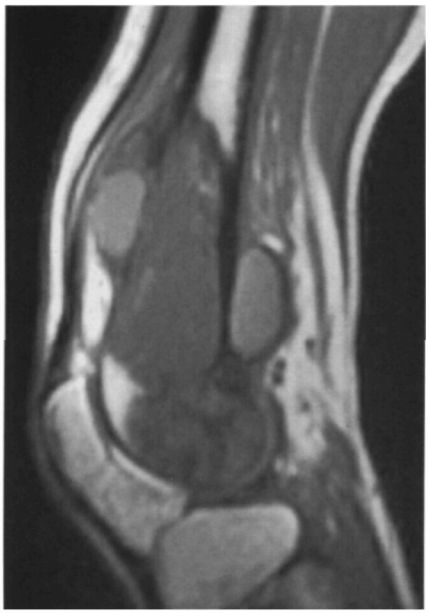

c

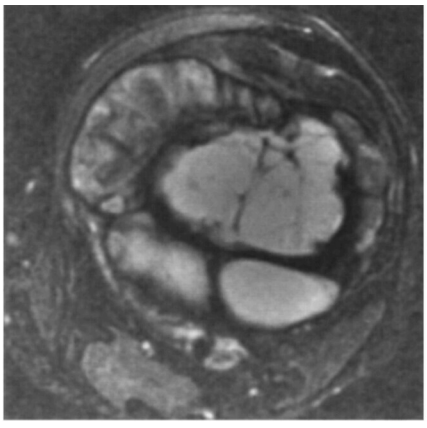

d, e

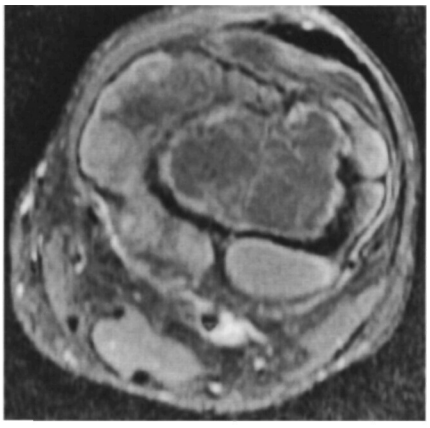

Figure **431 a-e** An 18-year-old man with a telangiectatic osteosarcoma involving the distal diaphysis, metaphysis, and epiphysis of the femur. AP radiograph **(a)** shows the tumor to have an expansile pseudocystic appearance similar to an aneurysmal bone cyst. The tumor extends into the extra-osseous soft tissues though sites of cortical destruction and contains multiple zones of high signal on coronal **(b)** and axial **(d)** FST2WI separated by septa and irregular thickened regions of low signal. The tumor contains zones with low, intermediate, and slightly high signal on sagittal **(c)** T1WI. The tumor shows irregular Cd-contrast enhancement on axial **(e)** FST1WI.

Differential Diagnosis

Bone

Intraosseous osteosarcoma. Chondrosarcoma, Ewing sarcoma, metastatic lesion, fibrosarcoma, malignant fibrous histiocytoma, chondromyxoid fibroma, bone infarct, osteoblastoma, giant cell tumor, aneurysmal bone cyst, osteomyelitis.[19,35,38,42]

Juxtacortical osteosarcoma.[8,42,44,45] Chondrosarcoma, juxtacortical chondroma, benign parosteal osteoma, Ewing sarcoma, cortical fibrous dysplasia, osteofibrous dysplasia, myositis ossificans

Soft tissue[6,8]

Malignant fibrous histiocytoma, fibrosarcoma, extra-osseous Chondrosarcoma, synovial sarcoma, malignant peripheral nerve sheath tumor, liposarcoma, metastatic disease, plasmacytoma, lymphoma, leukemia (chloroma), myositis ossificans.

Prognosis and Treatment

Intra-osseous osteosarcoma. Current treatment consists of neoadjuvant or preoperative chemotherapy.[14,50,63] The extent of tumor necrosis caused by chemotherapy has been shown to be correlated with prognosis.[50] In patients whose tumors show only minimal tumor necrosis, chemotherapy is either intensified or modified. Limb-sparing surgery is often performed after primary (neoadjuvant) chemotherapy. Amputations, however, are occasionally necessary. Using these protocols, 5-year survival ranges from 60 to 80% of patients.[14,50] Local recurrence occurs in ~5 %. Prognosis has not been correlated to histologic grading, although tumors more than 10cm in diameter occurring in the trunk, pelvis, and proximal femur have poorer prognoses than osteosarcomas located elsewhere.[14] Metastatic lesions usually disseminate hematogenously and to a lesser extent via the lymphatic system.[7,14,19,44] Metastatic disease occurs most often in the lung (90 %).[14] Patients with pulmonary meta-

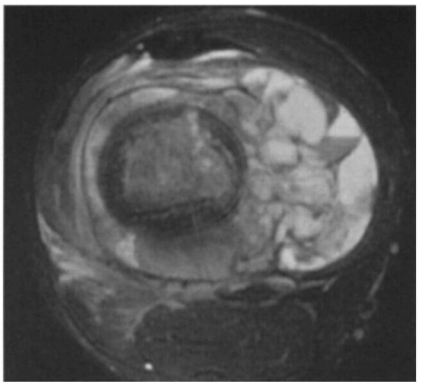

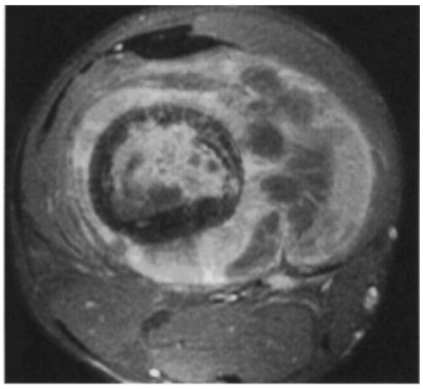

a, b c d

Figure **432a-d** A 12-year-old male with a telangiectatic osteosarcoma of the distal femur. AP radiograph **(a)** shows the intramedullary portion of the tumor to have mixed lucent and sclerotic zones. Lamellated periosteal reaction is seen as well as Codman triangles on one side. The tumor extends into the extra-osseous soft tissues though sites of cortical destruction and contains mixed signal with zones of high, slightly high, intermediate, and low signal on coronal **(b)** and axial **(c)** FST2WI. Multiple fluid-fluid levels are seen in the tumor. The tumor shows irregular Cd-contrast enhancement on axial **(d)**FSTIWI.

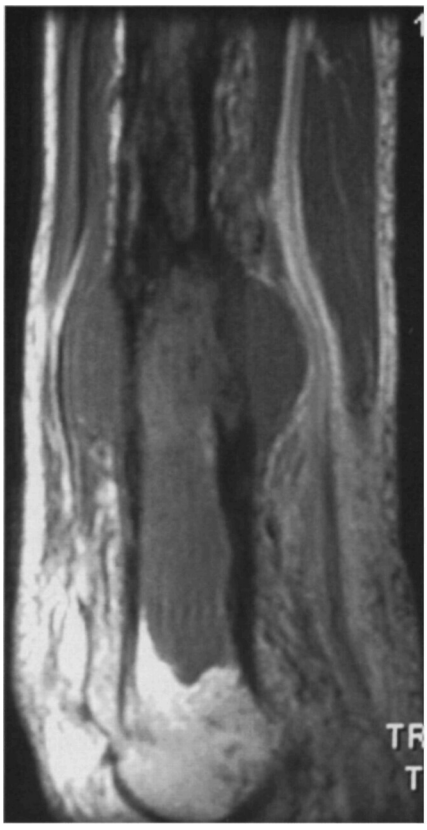

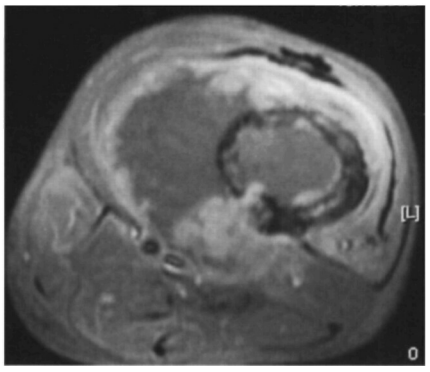

a b

Figure 433a, b A 71-year-old woman with Paget disease and a secondary osteosarcoma in the distal diaphyseal portion of the femur. The tumor extends from the marrow into the extra-osseous soft tissues though zones of cortical destruction, and contains low-intermediate signal on sagittal T1WI (a). The tumor shows heterogeneous, irregular Gd-contrast enhancement on axial FST1WI (b).

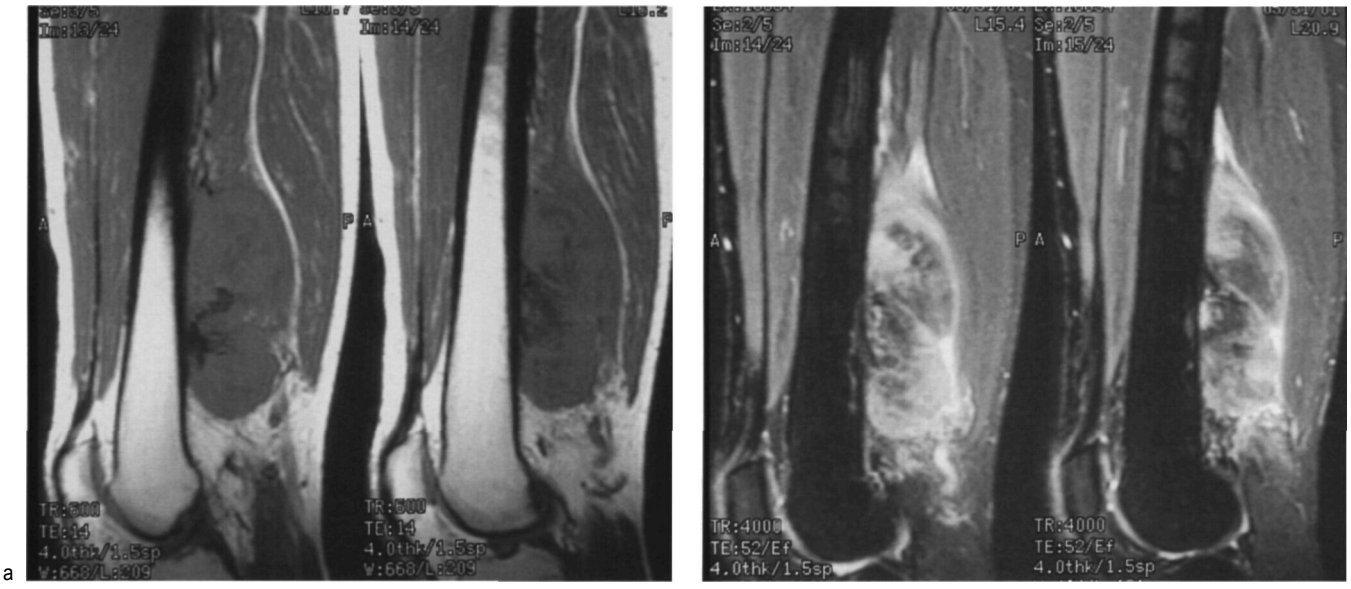

a

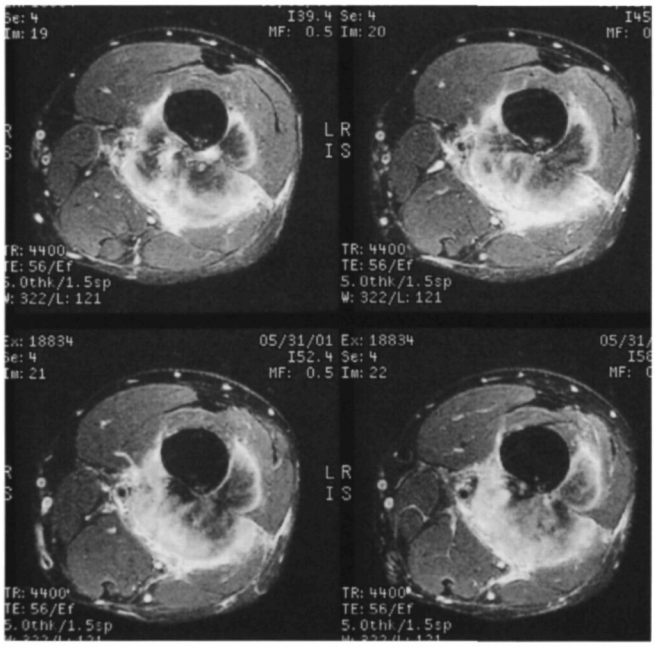

c

Figure **434**a-c A 36-year-old woman with a parosteal osteosarcoma located along the dorsal outer cortical surface of the distal diaphyseal portion of the femur. The tumor has intermediate and low signal on sagittal (a)T1WI, and heterogeneous low and high signal on sagittal (b) and axial (c) FST2WI.

stases from osteosarcoma have poor prognoses with reported mortality rates of 80-90 %.[50] Metastatic lesions also involve bone, pleura, and heart.[14] Multifocal osteosarcoma is considered to represent rapidly progressive metastatic osseous disease, which is associated with an extremely poor prognosis.[7,44]

- **Secondary osteosarcoma.** Osteosarcomas can occur as secondary lesions related to fibrous dysplasia (0.5-2.5% frequency), radiation treatment/exposure (0.2-4% prevalence), Paget disease (0.2-1 % incidence in solitary Paget disease, 5-10% incidence with multifocal or widespread Paget disease), bone infarcts, retinoblastoma, and Wilm tumor.[3,15,16,19,42] Prognosis for secondary osteosarcomas is poor for tumors located in the spine, pelvis, and shoulder.[15,16,20] The 5-year survival for tumors in the extremities is 68% compared with 28 % for axial tumors.[16] Paget osteosarcoma is associated with metastases in 25% of cases, and a very poor prognosis with a 5-year survival rate of 11 %.[16]

Juxtacortical osteosarcoma:

- **Parosteal osteosarcoma.** Treatment typically includes resection with wide margins or amputation.[15,64,65] The 5-year survival is 91 %,[65] and the 10-year survival rate is 80 %.[15] Intramedullary extension does not adversely affect prognosis unless there are undifferentiated zones.[15,65] Metastatic disease is related to the presence of dedifferentiated zones in parosteal osteosarcomas.[15] Metastatic disease most often involves the lungs.[15] Parosteal osteosarcomas involving the bones of the calvaria can have an excellent outcome after en bloc tumor resection.[31]
- **Perisosteal osteosarcoma.** Treatment usually includes surgical resection with wide margins.[215] Intramedullary extension does not adversely affect prognosis.[15] Local recurrence occurs in ~ 13 %.[15] Metastatic disease, usually to the lungs, occurs in up to 20 % of cases.[15]
- **High-grade surface osteosarcoma.** Prognosis of these tumors is related to the responses to chemotherapy.[68]

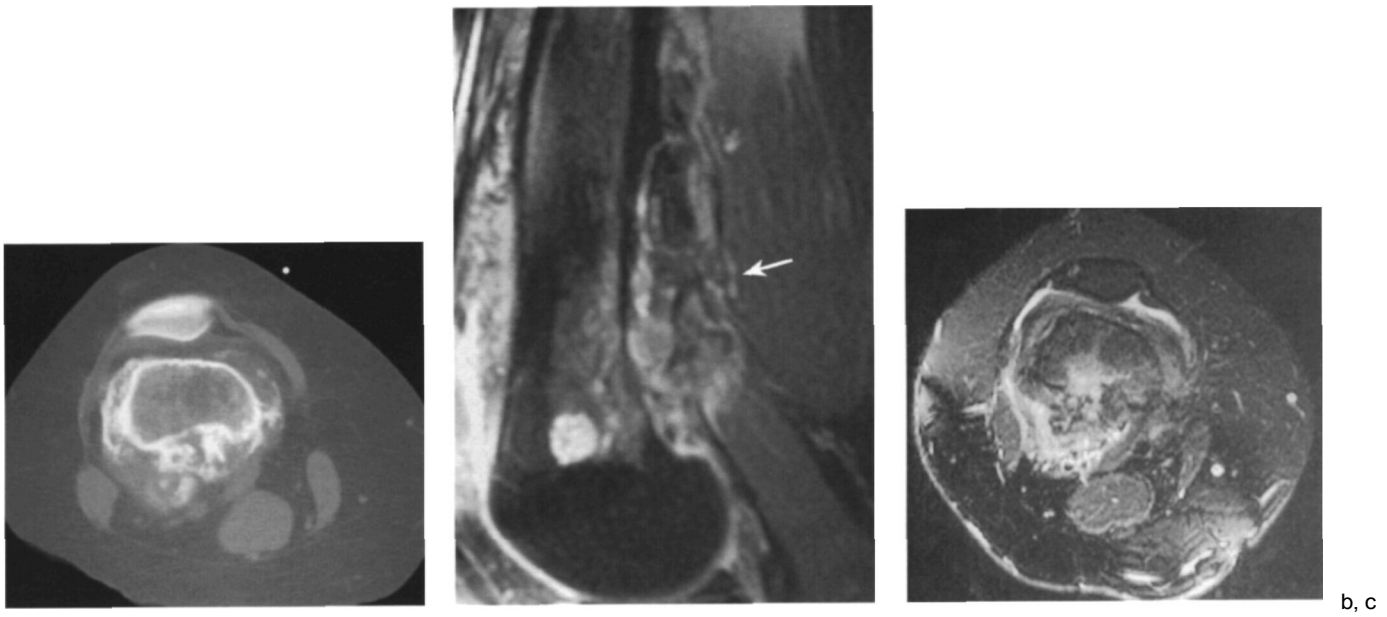

a b, c

Figure 435 a-c A 45-year-old woman with parosteal osteosarcoma involving the distal femur. Axial CT image (a) shows soft tissue tumor containing mineralized osteoid along the dorsal, medial, and lateral outer margins of the bone cortex. Small zones of cortical erosion are seen. Slight thickening of the inner cortex is also seen at several sites. The tumor has mixed low, intermediate, slightly high, and high signal on sagittal (b) and axial (c) FST2WI. The tumor extends into the marrow through a zone of cortical destruction. The mineralized portions of this tumor have low signal on axial FS T2WI.

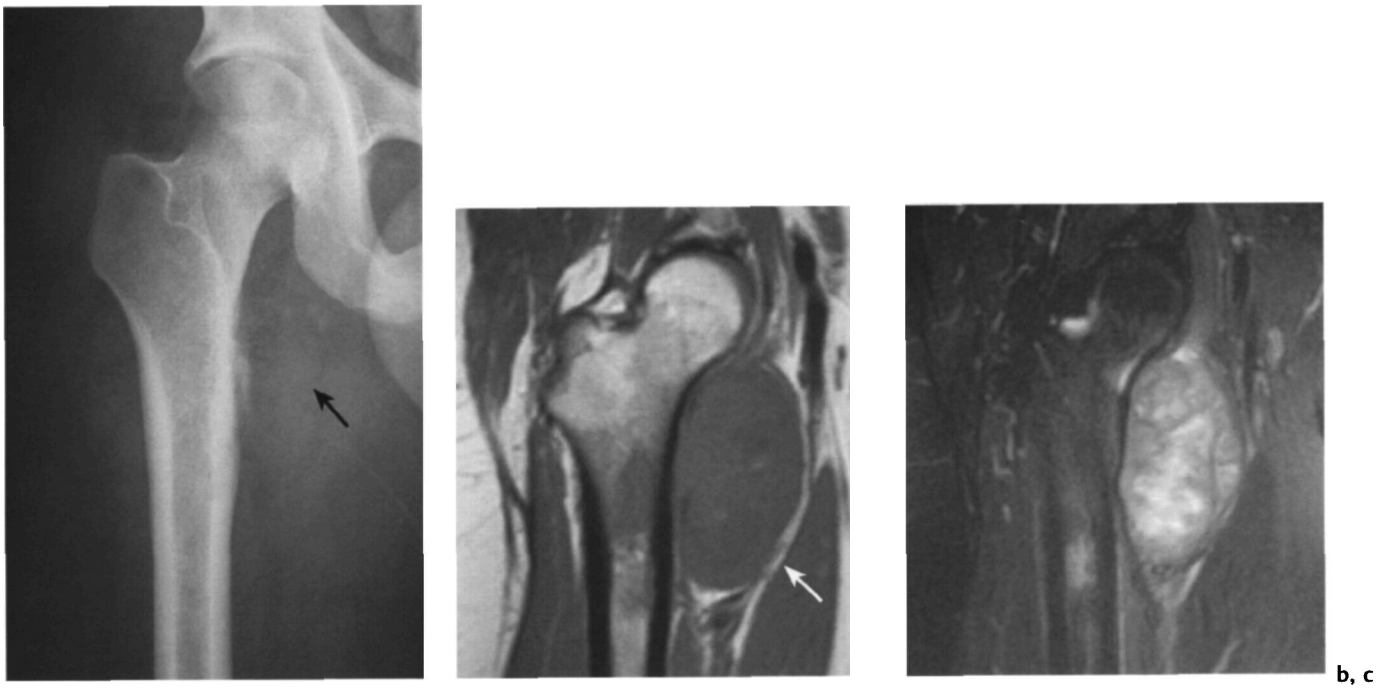

a **b, c**

d

Figure **436 a-d** A 26-year-old man with a periosteal osteosarcoma involving the anteromedial surface of the proximal femur. AP radiograph (**a**) shows an extra-osseous tumor containing mineralized osteoid as well as interrupted lameilated periosteal reaction adjacent to the femur. The tumor has low-intermediate signal on coronal (**b**) T1WI, and has mixed intermediate, slightly high, and high signal on coronal (**c**) FST2WI. The tumor shows heterogeneous Cd-contrast enhancement on axial (**d**) FST1WI. The tumor is associated with erosion of the outer cortical margin of the adjacent femur.

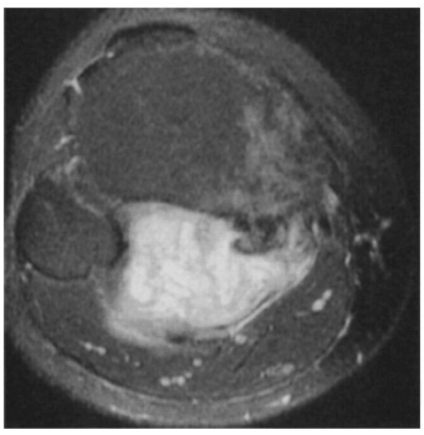

a

b

Figure **437a, b** A 49-year-old man with an osteochondroma at the dorsal upper tibia associated with a mixed osteosarcoma and chondrosarcoma. The tumor has heterogeneous mostly high signal on axial (**a**) and sagittal (**b**) FST2WI.

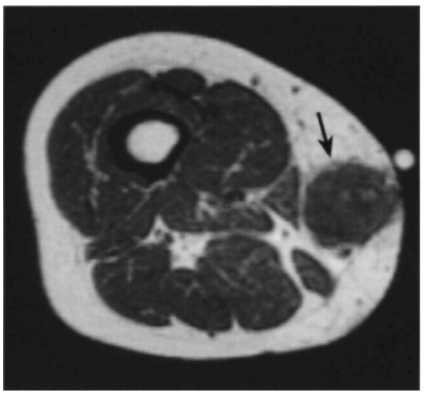

a

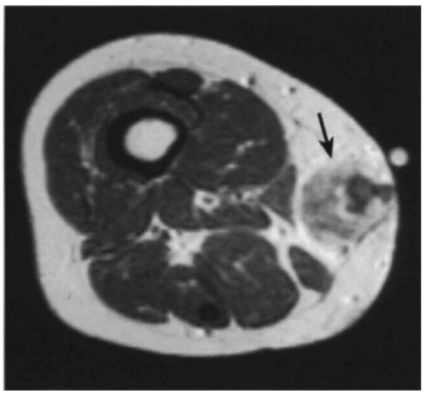

b

Figure **438a, b** A 47-year-old woman with an extra-osseous osteosarcoma in the subcutaneous fat of the medial thigh. The tumor has slightly irregular margins, and has low signal on axial T1WI (**a**). The tumor shows heterogeneous Cd-contrast enhancement on axial T1WI (**b**).

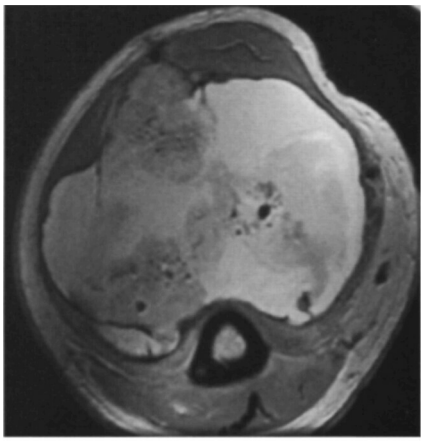

a

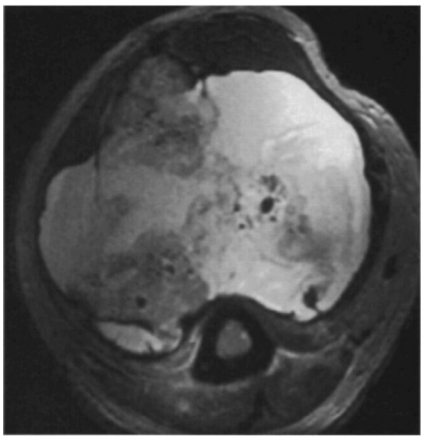

b

Figure **439** a-d A 54-year-old man with an extra-osseous osteosarcoma in the ventral soft tissues of the distal arm. The tumor has an irregular thin margin of low signal within which are zones with low, intermediate, and high signal on axial PDWI (**a**) and axial T2WI (**b**). The tumor shows heterogeneous Cd-contrast enhancement on axial (**c**) FST1WI.

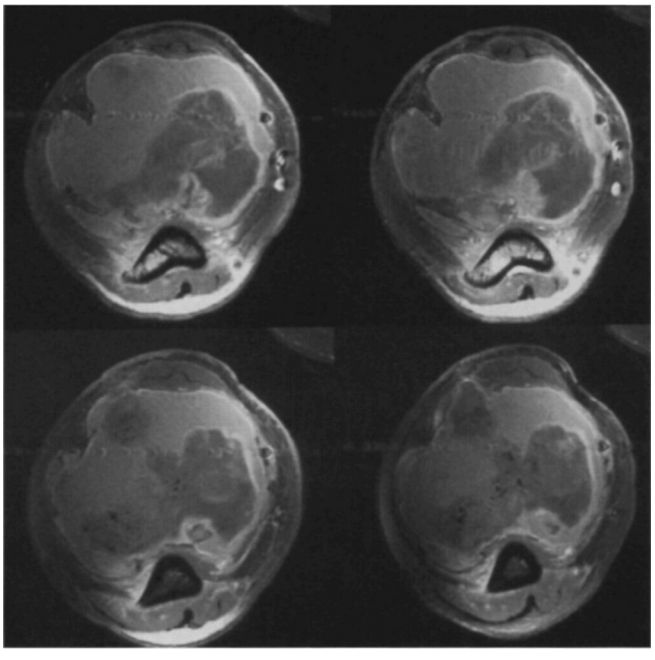

c

a

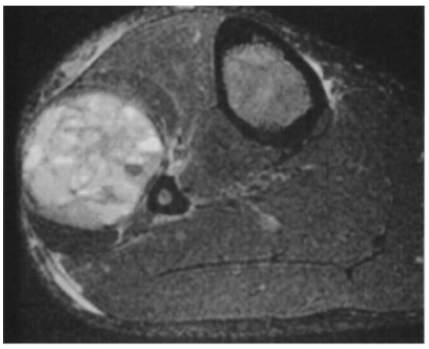

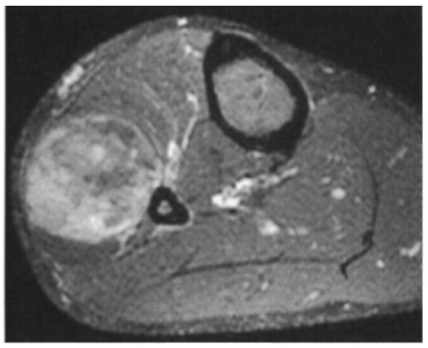

b, c

Figure **440 a-c** A 32-year-old man with an extra-osseous osteosarcoma involving the extensor digitorum longus muscle and peronerus longus and brevis muscles of the proximal lateral leg. The tumor has heterogeneous intermediate and high signal on coronal T1WI (**a**), and heterogeneous mostly high signal on axial FST2WI (**b**) as well as septa with low signal and fluid-fluid levels with high and low signal. The zones of high signal on T1WI and fluid-fluid levels represent sites of hemorrhage within the tumor. The tumor shows heterogeneous Gd-contrast enhancement on axial FST1WI (**c**).

Extraskeletal osteosarcoma. Patients with extraskeletal osteosarcoma usually have a poor prognosis. Up to 90 % of extraskeletal osteosarcomas develop local recurrences and/or metastases [10,11,29,30] Median time to recurrence is usually 1 year or less.[29,30] Metastatic lesions are most frequent to the lungs (over 80 %), and to a lesser degree involve lymph nodes, liver, bone, and subcutaneous tissues.[28,29] Extraskeletal osteosarcomas measuring less than 5 cm have slightly better prognosis than larger tumors.[10,11,29,30] Prognosis is very poor for extraskeletal osteosarcomas arising in an irradiated area.[8] Over half of patients with extraskeletal osteosarcoma die within 3 years,[29,30] and 75 % are dead at 5 years.[54] Treatment usually consists of amputation or surgical resection with wide margins in patients without metastatic disease.[8,44] To date, radiation and chemotherapy have not proved beneficial.[8,11]

References

1 Athanasou NA. Cell and organ culture in the understanding of bone and its neoplasms. In: Helliwell TR, ed. *Major Problems in Pathology: Pathology of Bone and Joint Neoplasms* 1 st ed. Vol 37. Philadelphia, Pa: W.B. Saunders; 1999:39-44.

2 Ayala AG, Czerniak B, Raymond AK, Knuutila S. Periosteal osteosarcoma. In: Fletcher CDM, Unni KK, Mertens F, eds. *World Health Organization Classification of Tumours. Pathology and Genetics of Tumours of Soft Tissue and Bone* Geneva: IARC Press; 2002:282-283.

3 Bloem JL, Kroon HM. Osseous lesions. Radio! *Clin North Am* 1993;31: 261-278.

4 Bonnerot V, Charpentier A, Frouin F, Kalifa C, Vanel D DE Paola R. Factor analysis of dynamic magnetic resonance imaging in predicting the response of osteosarcoma to chemotherapy. Invest *Radial* 1992;27(10):847-855.

5 Chan LL, Czerniak BA, Ginsberg LE. Radiologic-Pathologic Conferences of The University of Texas M.D. Anderson Cancer Center—Radiation-induced osteosarcoma after bilateral childhood retinoblastoma. *AJR Am J Roentgenol* 2000;174(5):1288.

6 Crim JR, Seeger LL, Yao L, Chandnani V, Eckardt JJ. Diagnosis of soft-tissue masses with MR imaging: can benign masses be differentiated from malignant ones? *Radiology* 1992;185(2):581-586.

7 Daffner RH, Kennedy SL, Fox KR, Crowley JJ, Sauser DD, Cooperstein LA. Synchronous multicentric osfeosarcoma: the case for metastases. *Skeletal Radial* 1997;26:569-578.

8 Das Gupta TK, Chaudhuri PK. Heterotopic bone and cartilage. In: Das Gupta TK, Chaudhuri PK, eds. *Tumors of the Soft Tissues* 2nd ed. Stamford, Conn: Appleton & Lange; 1998:464-465.

9 de Baere T, Vanel D, Shapeero LG, Charpentier A, Terrier P, di Paola M. Osteosarcoma after chemotherapy: evaluation with contrast material-enhanced subtraction MR imaging. *Radiology* 1992;185(2): 587-592.

10 Doud TM, Moser RP Jr, Giudici Michaela AI, Frauenhoff EE, Maurer RJ. Case report 704. *Skeletal Radial* 1991;20:628-632.

11 Dubec JJ, Munk PL, O'Connell JX, et al. Soft tissue osteosarcoma with telangiectatic features: MR imaging findings in two cases. *Skeletal Radial* 1997;26:732-736.

12 Erlemann R, Sciuk J, Bosse A, et al. Response of osteosarcoma and Ewing's sarcoma to preoperative chemotherapy: assessment with dynamic and static MR imaging and skeletal scintigraphy. *Radiology* 1990;175(3):791-796.

13 Fletcher BD. Imaging pediatric bone sarcomas: diagnosis and treatment-related issues. Radio/ Cfin *North Am* 1997;35(6):1477-1479.

14 Forest M. Osteosarcoma. In: Forest M, Tomeno B, Vanel D, eds. *Orthopedic Surgical Pathology: Diagnosis of Tumors and Pseudotumoral Lesions of Bone and Joints* Edinburgh: Churchill Livingstone; 1998: 103-131.

15 Forest M. Osteosarcoma: variants. In: Forest M, Tomeno B, Vanel D, eds. *Orthopedic Surgical Pathology: Diagnosis of Tumors and Pseudotumoral Lesions of Bone and Joints* Edinburgh: Churchill Livingstone; 1998:137-170.

16 Forest M, De Pinieux G, Knuutila S. Secondary osteosarcomas. In: Fletcher COM, Unni KK, Mertens F, eds. *World Health Organization Classification of Tumours. Pathology and Genetics of Tumours of Soft Tissue and Bone* Geneva: IARC Press; 2002:277-278.

17 Futani H, Okayama A, Maruo S, Kinoshita G, Ishikura R. The role of imaging modalities in the diagnosis of primary dedifferentiated parosteal osteosarcoma. J Orthop *Sci* 2001;6:290-294.

18 Holscher HC, Bloem JL, Vanel D, et al. Osteosarcoma: chemotherapy-induced changes at MR imaging. Radiology 1992;182(3):839-844.

19 Huvos AG. Osteogenic sarcoma. In: Huvos AC, ed. *Bone Tumors: Diagnosis, Treatment, and Prognosis* 2nd ed. Philadelphia, Pa: W.B. Saunders; 1991:85-155.

20 Huvos AG. Juxtacortical osteogenic sarcoma. In: Huvos AG, ed. Bone *Tumors: Diagnosis, Treatment, and Prognosis* 2nd ed. Philadelphia, Pa: W.B. Saunders; 1991:157-177.

21 Huvos AG. Osteogenic sarcoma of the craniofacial bones. In: Huvos AG, ed. *Bone Tumors: Diagnosis, Treatment, and Prognosis* 2nd ed. Philadelphia, Pa: W.B. Saunders; 1991:179-200.

22 Ilaslan H, Sundaram M, Unni KK, Shives TC. Primary vertebral osteosarcoma: imaging findings. *Radiology* 2004;230:697-702.

23 Inwards CY, Knuutila S. Low grade central osteosarcoma. In: Fletcher COM, Unni KK, Mertens F, eds. *World Health Organization Classification of Tumours. Pathology and Genetics of Tumours of Soft Tissue and Bone* Geneva: IARC Press; 2002:275-276.

24 Jelinek JS, Murphey MD, Kransdorf MJ, Shmookler BM, Malawer MM, Hur RC. Parosteal osteosarcoma: value of MR imaging and CT in the prediction of histologic grade. *Radiology* 1996;201(3):837-842.

25 Johnston JO, Helms CA, Weidner N. Posterior thigh pain in a 42-year-old woman, din *Orthop RelatRes* 1996:327:305-307, 311-312.

26 Kalil R, Bridge JA. Small cell osteosarcoma. In: Fletcher COM, Unni KK, Mertens F, eds. *World Health Organization Classification of Tumours. Pathology and Genetics of Tumours of Soft Tissue and Bone* Geneva: IARC Press; 2002:273-274.

27 Konishi E, Kusuzaki K, Murata H, Tsuchihashi Y, Beabout JW, Unni KK. Extraskeletal osteosarcoma arising in myositis ossificans. *Skeletal Radiol* 2001;30:39-43.

28 Kransdorf MJ. Malignant soft-tissue tumors in a large referral population: distribution of diagnoses by age, sex, and location. *AJRAmJ Roentgenol* 1995;164:129-134.

29 Kransdorf MJ, Meis JM. Extraskeletal osseous and cartilaginous tumors of the extremities. *Radiographics* 1993:13:853-884.

30 Kransdorf MJ, Murphey MD. Extraskeletal osseous and cartilaginous tumors. In: *Imaging of Soft Tissue Tumors* 2nd ed. Philadelphia, Pa: W.B. Saunders; 2006:437-480.

31 Kumar R, Moser RP Jr, Madewell JE, Edeiken J. Parosteal osteogenic sarcoma arisning in cranial bones: clinical and radiologic features in eight patients. *AJR Am J Roentgenol* 1990:155:113-117.

32 Lee SY, Cho WH, Song WS, Park JH. Different radiological findings with the same pathologic diagnosis due to different age in primary osteosarcoma. *Acta Radiol* 2006;47:841-844.

33 Logan PM, Mitchell MJ, Munk PL Pictorial Essay—Imaging of variant osteosarcomas with an emphasis on CT and MR imaging. *AJR Am J Roentgenol* 1998;171:1531-1537.

34 Lopez-Ben R, Pitt MJ, Jaffe KA, Siegal GP. Osteosarcoma in a patient with McCune-Albright syndrome and Mazabraud's syndrome. *Skeletal Radiol* 1999;28:522-526.

35 Macdonald D, Fornasier V, Holtby R. Chondromyxoid fibroma of the acromium with soft tissue extension. *Skeletal Radiol* 2000;29: 168-170.

36 Mahoney JP, Spanier SS, Morris JL Multifocal osteosarcoma: a case report with review of the literature. *Cancer* 1979:44:1897-1907.

37 Matsuno T, Okada K, Knuutila S. Telangiectatic osteosarcoma. In: Fletcher COM, Unni KK, Mertens F, eds. *World Health Organization Classification of Tumours. Pathology and Genetics of Tumours of Soft Tissue and Bone* Geneva: IARC Press; 2002:271-272.

38 Meyer JS, Dormans JP. Differential diagnosis of pediatric musculoskeletal masses. *Magn Reson Imaging Clin N Am* 1998;6(3):569-570.

39 Miller SL, Hoffer FA. Malignant and benign bone tumors. *Radiol Clin North Am* 2001;39(4):673-675, 680, 682.

40 Mulder JD, Schutte HE, Kroon HM, Taconis WK. Introduction. In: *Radiologic Atlas of Bone Tumors* Amsterdam: Elsevier; 1993:3-6.

41 Mulder JD, Schutte HE, Kroon HM, Taconis WK. The diagnosis of bone tumors. In: *Radiologic Atlas of Bone Tumors* Amsterdam: Elsevier; 1993:9-46.

42 Mulder JD, Schutte HE, Kroon HM, Taconis WK. Osteosarcoma. In: *Radiologic Atlas of Bone Tumors* Amsterdam: Elsevier; 1993:49-137.

43 Murphey MD wan Jaovisidha S, Temple HT, Gannon FH, Jelinek JS, Malawer MM. Telangiectatic osteosarcoma: radiologic-pathologic comparison. Radiology 2003;229:545-553.

44 Murphey MD, Robbin MR, McRae GA, Flemming DJ, Tempel HT, Kransdorf MJ. From the Archives of the AFIP—The many faces of osteosarcoma. Radiographics 1997;17(5):1205-1231.

45 Murphey MD, Jelinek JS, Temple HT, Flemming DJ, Gannon FH. Imaging of periostea! osteosarcoma: radiologic-pathologic comparison. *Radiology* 2004;233:129-138.

46 Onikul E, Fletcher BD, Parham DM, Chen G. Accuracy of MR imaging for estimating intraosseous extent of osteosarcoma. *AJR Am J Roentgenol* 1996;167:1211-1215.

47 Pierz KA, Womer RB, Dormans JP, Stanitski CL. Pediatric bone tumors: osteosarcoma Ewing's sarcoma, and chondrosarcoma associated with multiple hereditary osteochondromatosis.*J Pediatr* Orthop 20031;21(3):412-418.

48 Potepan P, Luksch R, Sozzi G, et al. Multifocal osteosarcoma as a second tumor after childhood retinoblastoma. *Skeletal Radiol* 1999; 28:415-421.

49 Pringle JAS. Bone-forming neoplasms arising within bone. In: Helliwell TR, ed. Major *Problems in Pathology: Pathology of Bone and Joint Neoplasms.* 1st ed. Vol 37. Philadelphia, Pa: W.B. Saunders; 1999: 168-191.

50 Raymond AK, Ayala AG, Knuutila S. Conventional osteosarcoma. In: Fletcher CDM, Unni KK, Mertens F, eds. World Heafth Organization *Classification of Tumours. Pathology and Genetics of Tumours of Soft Tissue and Bone* Geneva: IARC Press; 2002:264-270.

51 Reddick WE, Wang S, Xiong X, et al. Dynamic magnetic resonance imaging of regional contrast access as an additional prognostic factor in pediatric osteosarcoma. *Cancer* 2001 ;91(12):2230-2237.

52 Reid RP. Bone neoplasms and tumor-like lesions on the bone surface. In: Helliwell TR. *Major Problems in Pathology: Pathology of Bone and Joint Neoplasms* 1st ed. Vol 37. Philadelphia, Pa: W.B. Saunders 1999: 225-226.

53 Robinson LH, Pitt MJ, Jaffe KA, Siegal GP. Small cell osteosarcoma of the soft tissue. *Skeletal Radiol* 1995 ;24:462-465.

54 Rosenberg AE, Helm S. Extraskeletal osteosarcoma. In: Fletcher COM, Unni KK, Mertens F, eds. World *Health Organization Classification of Tumours. Pathology and Genetics of Tumours of Soft Tissue and Bone* Geneva: IARC Press; 2002:182-183.

55 Ryan SP, Weinberger E, White KS, et al. MR imaging of bone marrow in children with osteosarcoma: effect of granulocyte colony-stimulating factor. AJR *Am J Roentgenol* 1995;165:915-920.

56 Schima W, Amann G, Stiglbauer R, et al. Preoperative staging of osteosarcoma: efficacy of MR imaging in detecting joint involvement. *AJR Am J Roentgenol* 1994:163:1171-1175.

57 Seeger LL, Widoff BE, Bassett LW, Rosen G, Eckardt JJ. Preoperative evaluation of osteosarcoma: value of gadopentetate dimeglumine-enhanced MR imaging. *AJR Am J Roentgenol* 1991;157:347-351.

58 Shapeero LG, Vanel D. Imaging evaluation of the response of high-grade osteosarcoma and Ewing's sarcoma to chemotherapy with emphasis on dynamic contrast-enhanced magnetic resonance imaging. *Semin Musculoskelet Radiol* 2000;4(1): 137-146.

59 Spina V, Montanari N, Romagnoli R. Malignant tumors of the osteogenic matrix. *EurJ Radiol* 1998;27:S98-S 109.

60 Sundaram M, Totty WG, Kyriakos M, McDonald DJ, Merkel K. Imaging findings in pseudocystic osteosarcoma. *AJR Am J Roentgenol* 2001; 176:783-788.

61 Tsai JC, Dalinka MK, Fallon MD, Zlatkin MB, Kressel HY. Fluid-fluid level: a nonspecific finding in tumors of bone and soft tissue. Radiology 1990;175(3):779-782.

62 Unni KK. Introduction and scope of study. In: Unni KK, ed. *Dahlin's Bone Tumors—General Aspects and Data on 11087 Cases* 5th ed. Philadelphia, Pa: Lippincott, Williams & Wilkins; 1996:1-9.

63 Unni KK. Osteosarcoma. In: *Dahlin's Bone Tumors—General Aspects and Data on* 71087 Cases 5th ed. Philadelphia, Pa: Lippincott, Williams & Wilkins; 1996:143-183.

64 Unni KK. Parosteal Osteosarcoma (juxtacortical osteosarcoma). In: *Dahlin's Bone Tumors—General Aspects and Data on 11087 Cases* 5th ed. Philadelphia, Pa: Lippincott, Williams & Wilkins; 1996: 185-196.

65 Unni KK, Knuutila S. Parosteal osteosarcoma. In: Fletcher COM, Unni KK, Mertens F, eds. World *Health Organization Classification of Tumours. Pathology and Genetics of Tumours of Soft Tissue and Bone* Geneva: IARC Press 2002: 279-281.

66 Vacher-Lavenu MC. Electron microscopy. In: Forest M, Tomeno B, Vanel D, eds. *Orthopedic Surgical Pathology: Diagnosis of Tumors and Pseudotumoral Lesions of Bone and Joints* Edinburgh: Churchill Livingstone; 1998:48-52.

67 Vanel D, Picci P, De Paolis M, Mercuri M. Radiological study of 12 high-grade surface osteosarcomas. *Skeletal Radiol* 2001 ;30:667-671.

68 Wenaden AET, Szyszko TA, Saifuddin A. Imaging of periosteal reactions associated with focal lesions of bone. *Clin Radial* 2005;60: 439-456.

69 Wold L, McCarthy E, Knuutila S. High grade surface osteosarcoma; Unni KK, Knuutila S. Parosteal osteosarcoma. In: Fletcher COM, Unni KK, Mertens F, eds. *World Health Organization Classification of Tumours. Pathology and Genetics of Tumours of Soft Tissue and Bone* Geneva: IARC Press: 2002:284-285.

70 Yu JS, Weis LD. MR imaging of parosteal osteosarcoma in two skeletally immature patients. *Clin Imaging* 1997:21(1):63-68.

A65 Paget Disease (Also Referred to as Osteitis Deformans)

Definition

Paget disease is a chronic skeletal disease in which there is disordered bone resorption and woven bone formation resulting in osseous deformity.[1,2,4,6,11] paramyxovirus may be an etiologic agent for this disease.[2] Paget disease is polyostotic in up to 66 % of patients,[7] and is associated with a risk of less than 1 % for developing secondary sarcomatous changes: osteosarcoma (60%) > fibrosarcoma > malignant fibrous histiocytoma > undifferentiated sarcomas, chondrosarcoma.[1-57-10] Giant cell tumors are rare complications of Paget disease and are usually benign.[1] Paget disease is rarely associated with multiple myeloma, metastatic disease, leukemia, Hodgkin disease, and non-Hodgkin lymphoma.[1611]

Frequency of Occurrence

Paget disease affects 2.5-5 % of Caucasians older than 55 years, and 10 % of those over the age of 85 years.[26] Paget disease is the second most common bone disease in older adults after osteoporosis.[2] The incidence of secondary sarcomas in Paget disease ranges from 0.7 to 0.95 %.[3]

Age at Presentation

Paget disease typically affects adults, with 90 % of cases occurring in patients older than 40 years.[7] Patients with Paget sarcoma range from 39 to 85 years, median = 66 years,[5] median = 64 years.[34]

Gender Ratio (M /F)

Paget disease: 1.5/1.[7]

Paget sarcoma: 2/1.[5]

Location

Paget disease: Lesions occur in the vertebrae (lumbar > thoracic > cervical) > sacrum, pelvic bones > femur > skull > tibia > clavicle > humerus > ribs > other bones.[1,4,7,10]

Paget sarcoma. Lesions occur in the femur > humerus > pelvis > tibia > skull and facial bones > scapula> vertebra.[5] Approximately 65 % of Paget sarcomas are located in long bones such as the femur, humerus, and tibia.[3] The next most frequent sites are flat bones such as the pelvis, skull, and scapula.[3] Paget sarcoma usually arises in medullary bone.[3] Multifocal osteosarcoma occurs in 17% of cases.[3]

Signs and Symptoms

Paget disease is frequently asymptomatic, and is often detected incidentally on plain films.[279] Paget disease can also be associated with pain, bone deformity, fracture, spinal stenosis, and cranial neuropathy from basilar invagination or foraminal narrowing.[279] Symptoms such as pain and pathologic fractures may also result from sarcomatous degeneration, which occurs in less than 1 % of patients with Paget disease.[2379]

Gross Pathologic Findings

Paget disease. The involved bone shows irregular thickening of cortical bone and coarsened trabecular bone.[1,4,10] On cut section, there is a loss of distinction between Haversian and cancellous bone.[110] Numerous vessels are seen in the periosteum.[1] Bone marrow appears fibrous with increased vascularity.[1] Fibrous tissue within marrow can appear cystlike, lacking bony trabeculae.[1]

Paget sarcoma. The appearance of the involved bone typically shows findings characteristic of Paget disease plus a lesion associated with cortical destruction and soft tissue extension.[3 5]

Histopathologic Findings

Paget disease. Specimens show abnormal remodeling of bone with increased osteoclastic resorption followed by osteoblastic reaction that results in production of immature woven bone (primary bone).[1410] Paget disease often undergoes stages of osteoclastic hyperactivity with subsequent osteoblastic active phases followed by quiescent periods with inactive bone resorption and formation.[1,4,10] During the active phases of Paget disease, elevated serum levels of alkaline phosphatase and elevated urinary excretion of hydroxyproline are found.[14] Abnormal bone is usually seen composed of thickened trabeculae adjacent to bone marrow that is replaced with fine, fibrovascular connective tissue.[1,4,10] Osteoclasts are often numerous.[9] The bone trabeculae typically have a puzzlelike or mosaic pattern.[1,4,10] Bone trabeculae may be separated by basophilic (blue) lines termed "cement lines."[1,4,10] In addition to separating zones of trabecular bone, cement lines are also seen where there are discontinuous collagen fibers.[110] Using electron microscopy, intranuclear inclusions similar in appearance to paramyxovirus of the measles group are usually seen in osteoclasts in Paget disease and not in normal bone.[1]

Paget sarcoma. Up to 60 % of Paget sarcomas are osteogenic sarcomas followed by fibrosarcomas (19%).[4] Other sarcomas associated with Paget disease include undifferentiated sarcomas, malignant fibrous histiocytomas, chondrosarcomas, and hemangiosarcomas.[1-5,8-10]

Tumor Genetics

Abnormalities involving the chromosome arm 18 q have been found in Paget disease and sporadic osteosarcomas.[3]

Findings on Plain Films (Roentgenograms) and Computed Tomography

Paget disease. Findings on plain films and CT include osseous expansion, thick coarsened trabeculae, cortical thickening, and indistinctness or irregularity at the border between cortical and medullary bone.[1,2,4,7-11] (Figs. **441-444, 446, 447**). At the skull, irregular patterns of lucent and sclerotic changes involving the diploic space are usually seen, as well as the inner and outer tables (Figs. **441,442).** The interface between the diploic space and the inner and outer tables is often obscured, and osseous expansion commonly occurs to various degrees.

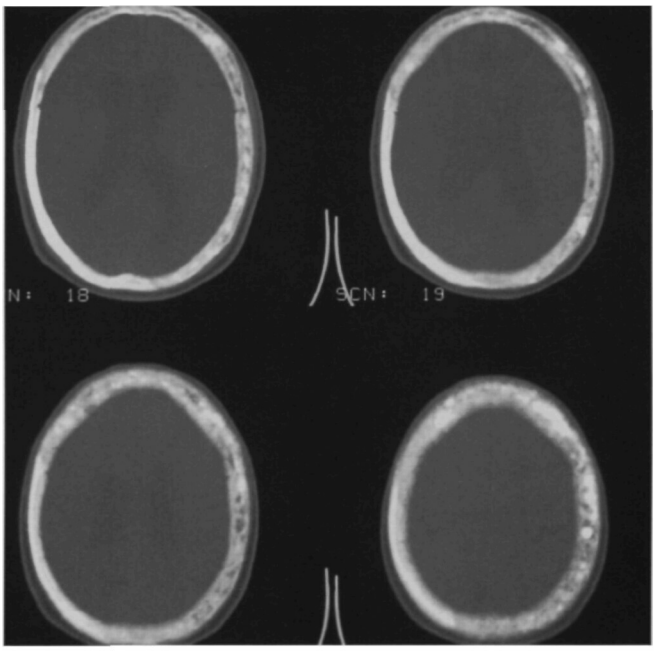

a

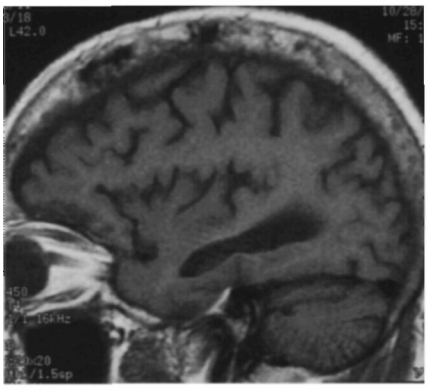

b

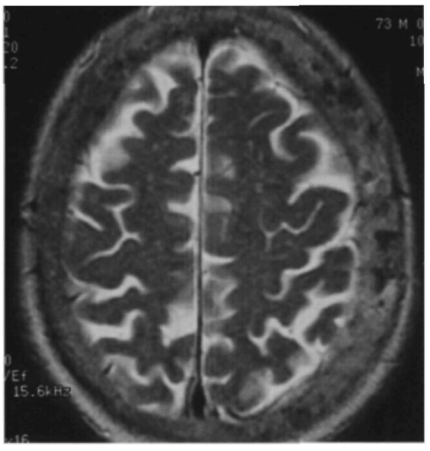

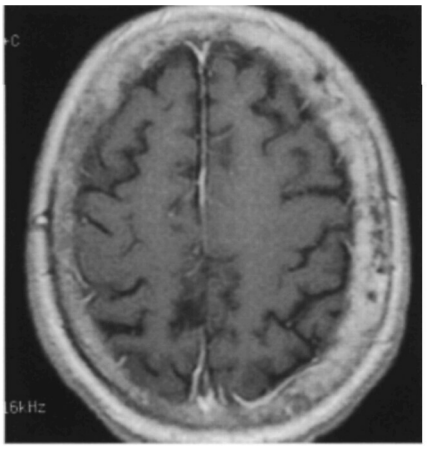

c, d

Figure **441 a-d** A 73-year-old man with Paget disease involving the skull. Axial CT images (**a**) show an irregular pattern of lucent and sclerotic changes involving the diploic space as well as the inner and outer tables of the skull. The interface between the diploic space and the inner and outer tables is obscured, and there is osseous expansion. The marrow has mixed low and high signal on sagittal T1 WI (**b**), and low and intermediate signal on axial T2WI (**c**). Irregular/indistinct borders are seen between the marrow and inner and outer tables of the skull. Irregular Cd-contrast enhancement is seen at the involved bone on axial T1WI (**d**).

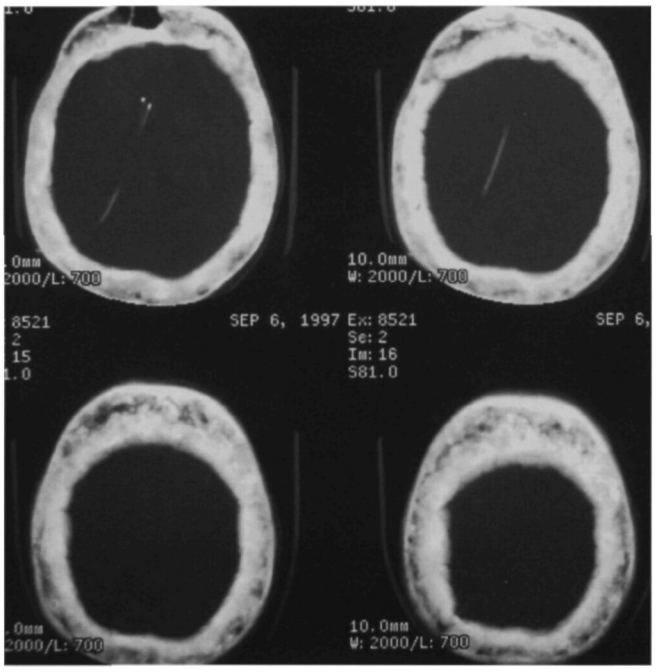

a

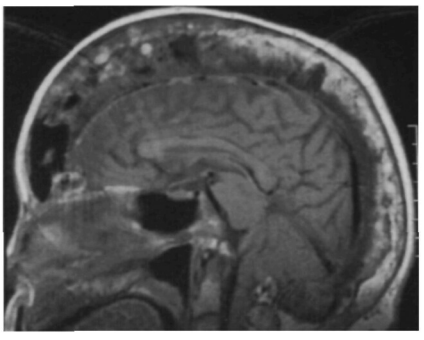

b

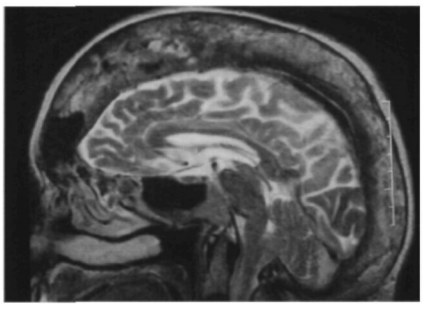

c

Figure **442 a-c** An 81-year-old woman with Paget disease involving the skull with associated basilar impression. Axial CT images (**a**) show an irregular pattern of lucent and sclerotic changes involving the diploic space as well as the inner and outer tables of the skull. The interface between the diploic space and the inner and outer tables is obscured, and there is marked osseous expansion. The marrow has mixed low, intermediate, and high signal on sagittal (**b**) T1WI and sagittal (**c**) T2WI. Irregular/indistinct borders are seen between the marrow and inner and outer tables of the skull.

a

Figure **443 a-d** Paget disease involving the L4 vertebra. Lateral radiograph (**a**) shows diffuse increased density of an enlarged L4 vertebra, also referred to as "ivory vertebra." The L4 vertebra has mostly low signal on sagittal T1WI (**b**), sagittal T2WI (**c**), and axial PDWI (**e**), as well as several small zones with slightly high signal. The L4 vertebra has heterogeneous low-intermediate, slightly high, and high signal on sagittal FST2WI (**d**).

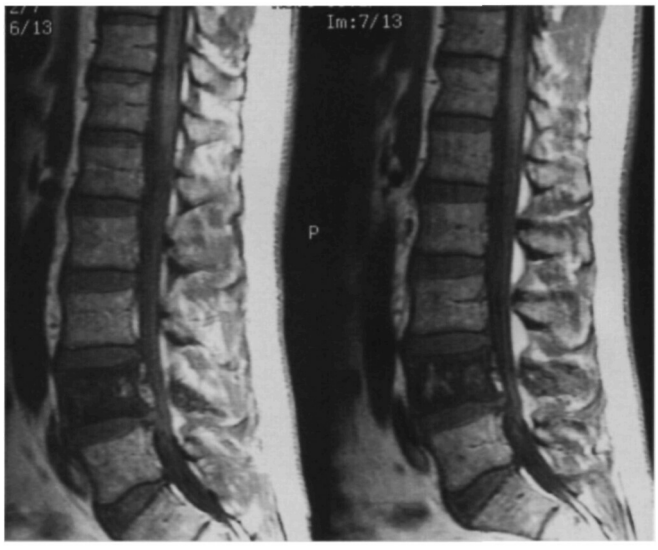

b

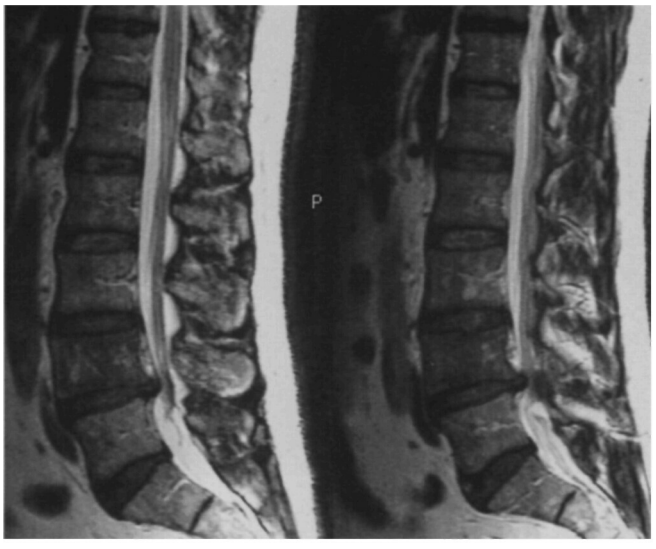

c

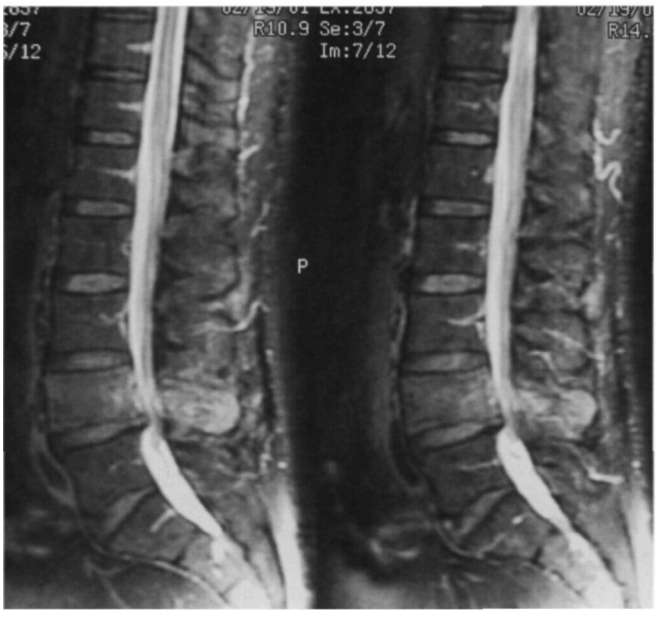

d

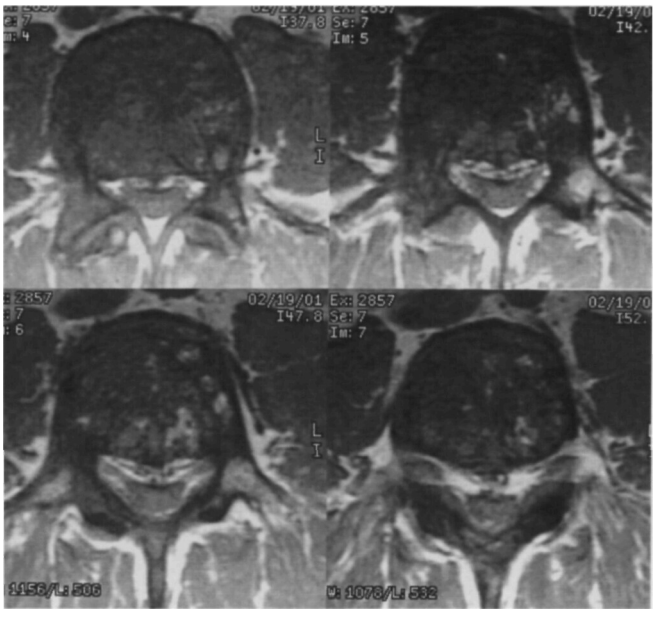

e

a

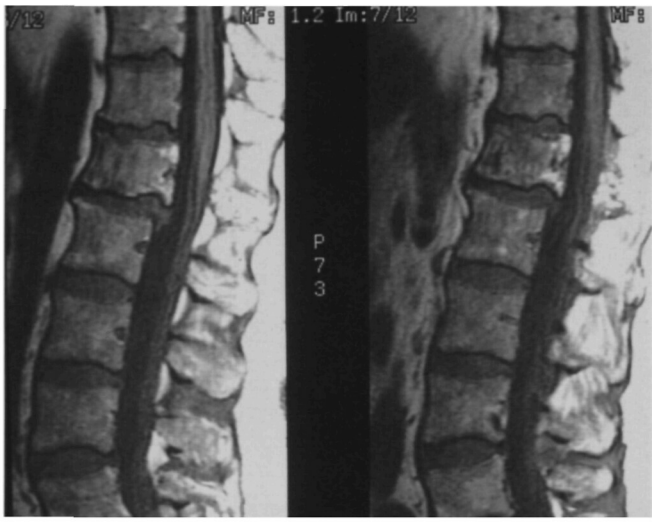

b

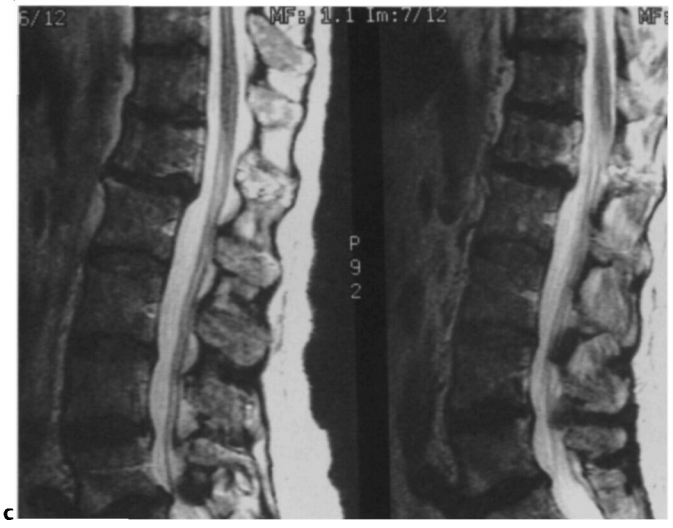

c

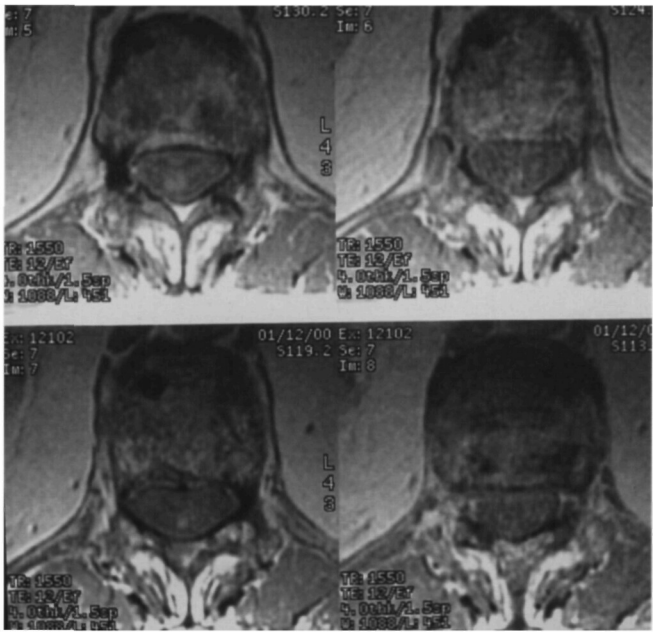

d

Figure **444 a-c** Paget disease involving the L1 vertebra. Lateral radiograph (a) shows slight irregularity/indistinctness between the cortical margins and marrow as well as coarsened intramedullary trabecula. The LI vertebra is slightly enlarged, and has a mixed pattern of low, intermediate, and high signal in the marrow on sagittal T1WI (**b**), sagittal T2WI (**c**), and axial PDWI (**d**). Indistinctness between the cortex and marrow is seen on PDWI.

The initial or active phase of Paget disease is typically associated with a zone of radiolucency secondary to intense osteoclastic activity.[1,2,6] (Fig. **448).** The osteolysis during the initial phases can appear as flame-shaped radiolucencies in long bones, or as circumscribed radiolucent zones in the skull—osteoporosis circumscripta.,[1,11] In the intermediate phase of Paget disease, there is a mixture of osteolysis and osteosclerosis secondary to co-existent decreasing osteoclastic and increasing osteoblastic activity.[1,2,6,10,11] In the late or inactive phases of Paget disease, osteoblastic activity decreases, and osteosclerotic findings predominate resulting in osseous expansion, cortical thickening, and coarsened trabeculae along stress lines.[1,2,6] Because of decreased stress resistance of bone affected by Paget disease, bone deformities such as varus bowing of the proximal femur, fractures, spinal stenosis, and basilar invagination can occur.

Paget disease involving the spine can result in findings such as enlargement of the affected vertebra with thick coarsened primary trabeculae, marginal vertebral sclerosis in a "picture-frame pattern," and/or diffuse increased attenuation (ivory vertebra)[6,7] (Figs. **443-445).** Lytic Paget disease of the spine is rare.[7]

CT is superior to plain films in the diagnosis of complications related to Paget disease such as fractures, spinal stenosis, and secondary neoplasms.[2] CT is also useful for complications of Paget disease involving the skull such as platybasia, basilar invagination, and foraminal encroachment.[2]

Paget sarcoma. Findings associated with Paget sarcoma include irregular zones of radiolucency and/or sclerosis in medullary and/or cortical bone, cortical disruption, and a soft tissue mass-lesion.[1-5-8-10]

MRI Findings

Paget disease: The MRI features of Paget disease vary based on the phases of the disease.[2,6,7,9,11] In the initial and intermediate phases of Paget disease, thickening of the involved cortex is seen.[2,6,7,9,11] The thickened cortex typically has low to intermedi-

a, b

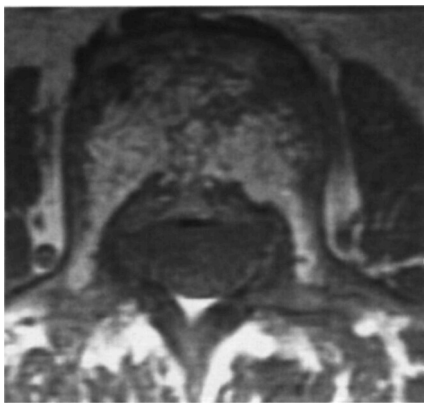

c

Figure **445 a-c** Paget disease involving the L2 vertebra. The lesion has a thickened cortex with low-intermediate signal representing marginal sclerosis ("picture frame pattern") surrounding high-signal fatty marrow containing coarsened trabecula on sagittal T1WI (**a**), sagittal T2WI (**b**), and axial PDWI (**c**).

a, b

c

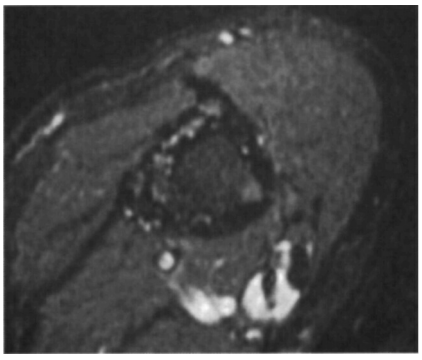

d

Figure **446 a-d** Paget disease involving the humerus of a 62-year-old man. Radiograph (**a**) shows osseous expansion, thick coarsened trabecula, cortical irregularity and thickening, and indistinctness at the border between cortical and medullary bone. The involved cortical bone is irregularly thickened on coronal (**b**) T1WI. The involved cortical bone has mixed low and slightly high signal on coronal (**c**) and axial (**d**) FST2WI.

ate signal on T1WI and PDWI; and often has various combinations of low, intermediate, slightly high and/or high signal on T2WI andFST2WT[6,11](Figs. **446, 448**). Cortical zones with intermediate to high signal on T2WI are probably secondary to sites of bone resorption and remodeling, which contain cellular or other marrow elements" Prominent vessels may be seen at the outer cortical margins.[1,6,11] After Gd-contrast administration, irregular enhancement can be seen in the thickened cortex." Marrow signal during the initial phases of Paget disease can be within normal limits, or slightly increased in a V-shape on FST2W1 secondary to fibrovascular tissue replacement of normal marrow, and/or dilated blood vessels with slow flow."

In the late or inactive phases of Paget disease, typical findings include osseous expansion, cortical thickening, decreased diameter of the medullary canal, and coarsened trabeculae along stress lines[2,6,7,9,11] (Figs. **441-444,447**). The zones of cortical thickening usually have low signal on T1W1 and T2WI[2679]" (Figs. **445, 447**). The inner margins of the thickened cortex can be irregular, indistinct, or slightly lobulated.[2679]" Thick, linear intramedullary zones of low signal on T1WI and T2WI

a

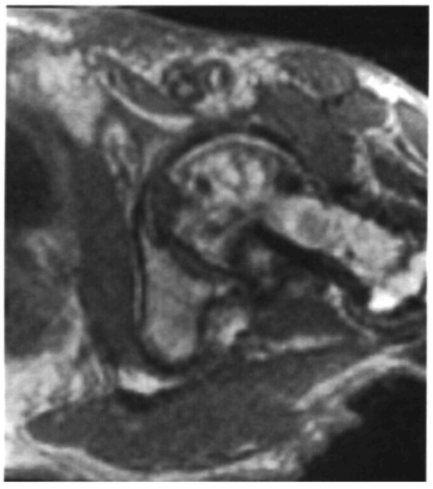

b

Figure **447 a, b** Paget disease involving the proximal femur of a 71 -year-old woman. AP radiograph (**a**) shows osseous expansion with varus bowing deformity, thick coarsened trabecula, cortical irregularity and thickening, and indistinctness at the border between cortical and medullary bone. The involved bone has irregularly thickened cortical and trabecular bone on axial T1WI (**b**).

a, d

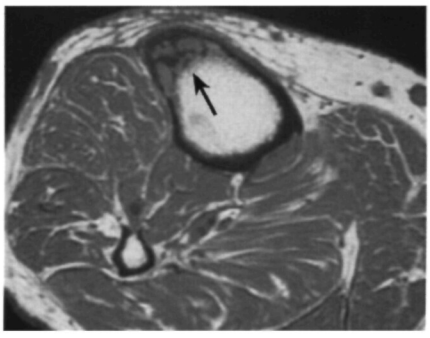

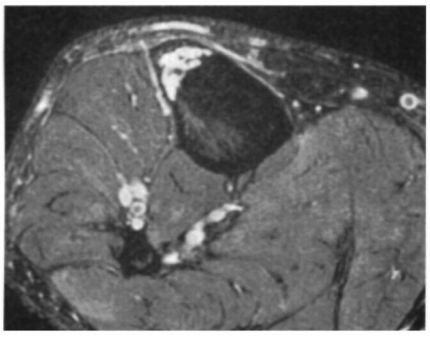

b, c

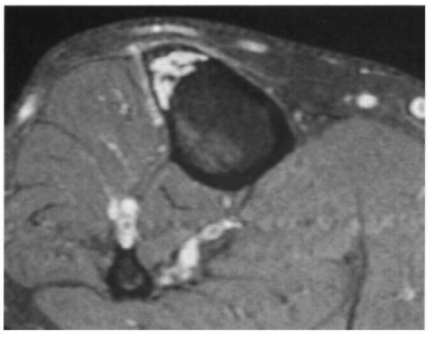

e

Figure **448**a-e A 76-year-old man with an active lytic phase of Paget disease involving the anterior cortex of the proximal tibia. Lateral radiograph (a) shows a circumscribed radiolucent zone involving the anterior cortex of the proximal tibia. The lesion involves an expanded bone cortex and has mixed low and intermediate signal on axial T1 WI (b), and mixed high and low signal on axial FS T2WI (c). The lesion shows prominent Cd-contrast enhancement on axial (d) and sagittal (e) FST1WI.

a

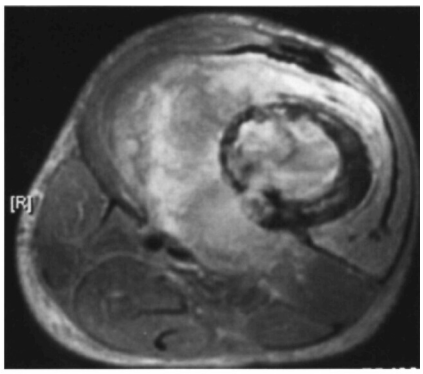

b

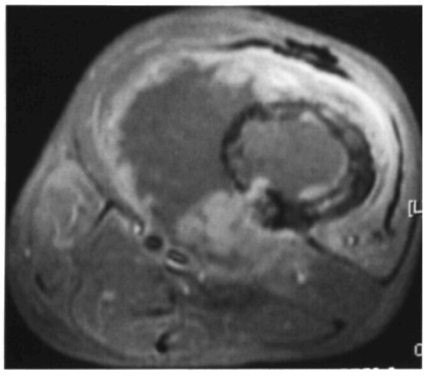

c

Figure **449 a-c** A 71-year-old woman with Paget disease involving the distal femur as well as a secondary osteosarcoma. The tumor has low-intermediate signal on sagittal (**a**) T1WI and heterogeneous mostly high signal on axial T2WI (**b**). The tumor extends from the marrow through zones of cortical destruction into the extra-osseous soft tissues, and shows heterogeneous Cd-contrast enhancement on axial FST1WI(**c**).

can be seen secondary to thickened bone trabeculae" (Figs. **443-445, 467).** Marrow in late or inactive phases of Paget disease can (1) have signal similar to normal marrow, (2) contain focal areas of fat signal, (3) have low signal on T1WI and T2W1 secondary to regions of sclerosis, (4) have areas of high signal on FST2WI from edema or persistent fibrovascular tissue, or (5) various combinations of the aforementioned.[6,11] Areas of high signal on FS T2W1 associated with linear zones of low signal on T1WI and T2WI may occur secondary to insufficiency fractures.[11]

Paget sarcoma. Findings associated with Paget sarcoma include irregular zones of destruction involving medullary and/or cortical bone, cortical disruption, and a soft tissue mass-lesion.[6,11] The involved marrow typically has low to intermediate signal on T1WI and PDW1, and low to high signal on T2W1[6,9,11] (Fig. **449).** MR1 has proven useful in the evaluation of large areas of osteolysis in Paget disease seen with plain films.[6,9,11] Zones of .osteolysis with low signal on T1W1 were found most likely to represent areas of malignant degeneration, whereas the presence of fat signal typically ruled out this possibility.[6,9,11] After Gd-contrast administration, abnormal enhancement is typically seen in the marrow involved with Paget sarcoma, as well as in the extra-osseous tumor extension."

Differential Diagnosis

Fibrous dysplasia, myeloma, metastatic disease, lymphoma, leukemia, Ewing sarcoma, osteomyelitis, eosinophilic granuloma.

Prognosis and Treatment

Paget disease. Patients with Paget disease can be treated medically with inhibitors of osteoclast activity such as calcitonin and biphosphonates.[2] Despite the beneficial results from these drugs, Paget disease typically progresses.[2] Complications from Paget disease often depend on the location and extent of the affected bone.[2]

Paget sarcoma. The prognosis of patients with Paget sarcoma is poor.[5,8,10] Patients with multifocal tumor have a worse prognosis than those with unifocal disease.[3] Paget sarcoma involving the skull or pelvis has a 5-year survival of 11 %.[3] Metastatic disease is found in 25 % of patients at the time of diagnosis.[3] Radiation is effective in reducing pain associated with Paget sarcoma in 50% of patients, but does not improve survival.[4] Patients less than 60 years old with mono-ostotic Paget sarcomas involving long bones have a slightly better survival rate after intensive therapy including surgery, amputation, chemotherapy, and radiation.[3]

References

1 Amouroux J. Paget's disease. In: Forest M, Tomeno B, Vanel D, eds. *Orthopedic Surgical Pathology: Diagnosis of Tumors and Pseudotumoral Lesions of Bone and Joints* Edinburgh: Churchill Livingstone; 1998:589-594.

2 Boutin RD, Spitz DJ, Newman JS, Lenchik L, Steinbach LS. Complications in Paget Disease at MR imaging. *Radiology* 1998:209:641-651.

3 Forest M, De Pineux G, Knuutila S. Secondary osteosarcomas. In: Fletcher COM, Unni KK, Mertens F, eds. *World Health Organization Classification of Tumours. Pathology and Genetics of Tumours of Soft Tissue and Bone* Geneva: IARC Press: 2002:277-278.

4 Huvos AG. Tumors associated with Paget's disease of bone. In: Huvos AG, ed. *Bone Tumors: Diagnosis, Treatment, and Prognosis* 2nd ed. Philadelphia, Pa: W.B. Saunders; 1991:201-222.

5 Mulder JD, Schutte HE, Kroon HM, Taconis WK. Paget's sarcoma. In: *Radiologic Atlas of Bone Tumors.* Amsterdam: Elsevier; 1993: 323-328.

6 Roberts MC, Kressel HY, Fallon MD, Zlatkin MB, Dalinka M. Paget disease: MR imaging findings. *Radiology* 1989;173:341-345.

7 Saifuddin A, Hassan A. Paget's Disease of the spine: unusual features and complications. *Clin Radial* 2003;58:102-111.

8 Salvati M, Clappetta P, Capoccia G, Capone R, Raco A. Osteosarcoma of the skull. Report of a post-Paget and post-radiation case in an elderly woman. *Neurosurg Rev* 1994;17:73-76.

9 Sundaram M, Khanna G, El-Khoury GY. Tl-weighted MR imaging for distinguishing large osteolysis of Paget's disease from sarcomatous degeneration. *Skeletal* Radio/ 2001 ;30:378-383.

10 Unni KK. Conditions that commonly simulate primary neoplasms of bone. In: *Dahlin's Bone Tumors—General Aspects and Data on 11087 Cases* 5th ed. Philadelphia, Pa: Lippincott, Williams & Wilkins: 1996: 355-432.

11 Whitten CR, Saifuddin A. MRI of Paget's Disease of bone. *Clin Radial* 2003:58:763-769.

A 66

Paraganglioma (Also Referred to as Chemodectoma for Carotid Body Tumor and Glomus Jugulare Tumor for Jugulotympanic Paragangliomas)

ICD-O Code

8680/1

Definition

Extra-adrenal paragangliomas are benign encapsulated neuroendocrine tumors that arise from neural crest cells associated with autonomic ganglia (paraganglia) throughout the body.[7,13] Extra-adrenal paraganglia can be associated with the parasympathetic system and function as chemoreceptors located near nerves and blood vessels, usually in the head, neck, and anterior mediastinum.[7,10] Extra-adrenal paraganglia can also be associated with the sympathetic system, typically in the posterior mediastinum, and retroperitoneum.[7] Extra-adrenal paragangliomas are hormonally inactive in 97% of pateints.[4™] The infrequent extra-adrenal paragangliomas that are hormonally active (functional paraganglioma) usually involve the sympathetic system and secrete catecholamines, which can cause hypertension and tachycardia similarly to pheochromocytomas (paragangliomas of the adrenal gland).[4,10] A small number of paragangliomas (2-13 %) have malignant behavior with metastatic disease.[10]

Familial paragangliomas represents an autosomal-dominant syndrome with incomplete penetrance, which predisposes those affected to develop one or more paragangliomas.[10] Deactivation of a tumor suppressor gene on the long arm of chromosome 11 has been implicated.[10]

Frequency of Occurrence

Extra-adrenal paragangliomas represent less than 1 % of benign primary tumors of the soft tissues.[6] Paragangliomas represent 0.6 % of tumors involving the head and neck, and 0.03 % of all neoplasms.[10] Familial paragangliomas account for 7-9 % of paragangliomas.[10]

Age at Presentation

From 24 to 70 years, mean = 47 years.[6] For carotid body tumors, the peak prevalence is 45-50 years.[10] For glomus jugulotympanicum and vagal paragangliomas, the peak age of presentation is in the 5th to 6th decades.[10] For cauda equina, patients range from 13 to 70 years.[3,11]

Gender Ratio (M / F)

1/1.3.[6]
Carotid body tumors: 1 / 1.[10]
Vagal paragangliomas: 1 / 2.7.[10]
Clomus jugulare/tympanicum tumors: 1 / 4 to 1 / 6[10]

Location

Paragangliomas occur most frequently in the adrenal glands and are referred to as pheochromocytomas and are not discussed further in this text.[3] For **extra-adrenal paragangliomas,** frequency of occurrence is head and neck > retroperitoneum > hip, buttock, lower extremity, spinal canal.[6] Up to 80 % of all extra-adrenal paragangliomas are carotid body tumors or glomus jugulare / tympanicum tumors.[10] Vagal paragangliomas account for ~ 5 % of extra-adrenal paragangliomas.[10] For spinal paragangliomas, the lumbosacral spine is the most frequent location.[T3,15] Other less common paragangliomas have been reported in the pineal region, sella turcica, petrous ridge, thyroid, tracheobronchial tree, mediastinum, pericardium, heart (atrial septum), retroperitoneum, gastrointestinal tract, and pancreas.[3,10,12,14]

More than one paraganglioma per person may occur in sporadic cases, whereas multicentric parangliomas are commonly seen in patients with familial paragangliomas.[10] Sporadic paragangliomas may occur in both carotid bodies in 5% of cases.[10] Up to 38% of patients with familial paragangliomas have bilateral carotid body tumors.[10]

Signs and Symptoms

Extra-adrenal paragangliomas. These are neuroendocrine tumors that are not hormonally active in 97 % of cases.[4,10] The infrequent hormonally active or functional extra-adrenal paragangliomas secrete catecholamines that can cause headaches, hypertension, tachycardia, and/or palpitations.[4,10]

- **Carotid body tumor.** These paranganglioma are usually painless, movable, slow-growing lesions in the lateral neck.[10] Carotid body tumors typically transmit pulsations, and may be associated with a bruit.[10] These tumors are often asymptomatic, although can be associated with hoarseness, dysphagia, tongue paresis, stridor, and/or vertigo.[10]
- **Vagal paraganglioma.** Vagal paragangliomas are painless, slow-growing lesions in the lateral neck. These tumors are located posterior to the angle of the mandible in up to 83 % of patients, or as an intraoral lesion.[10] Neurologic deficits such as palsies involving the vagus, hypoglossal, glossopharyngeal, and/or accessory nerves can occur as late manifestations in 20-50 % of enlarging vagal paragangliomas.[10] Horner syndrome is seen in 25 % of vagal paragangliomas.[10] Hoarseness and/or vocal cord paralysis may rarely be associated with these tumors.[10]
- **Clomus jugulare/tympanicum tumors.** Glomus jugulare tumors can be associated with Horner syndrome as well as palsies involving cranial nerves IX, X, XI, and XII.[10] Patients may have motor paralysis of cranial nerves IX, X, and XI, which is referred to as the Vernet (jugular foramen) syndrome.[10] The Collet-Sicard syndrome (Vernet syndrome with palsy also involving the hypoglossal nerve) can also occur with glomus jugulare tumors.[10] Glomus tympanicum tumors are usually associated with pulsatile tinnitus and a retrotympanic vascular mass.[10] In addition, these tumors may be associated with vertigo and conductive hearing loss.[10]

Paragangliomas involving the spinal canal

- **Paragangliomas of the cauda equina:** patients can present with lumbar pain, sensory or motor deficits of the lower extremities, bowel and bladder dysfunction[3,11] The duration of symptoms can range from days to years.[3,11,15]
- **Extradural paragangliomas of the spine:** patients can present with back pain and/or sensory or motor deficits.[3,4,15]

Cross Pathologic Findings

Paragangliomas are ovoid and/or tabulated, gray-tan, or red/brown/purplish lesions that are usually enclosed by a delicate fibrous pseudocapsule.[10,13] The lesions range in size from 1 to 13 cm.[10,13] The cut surface of these lesions often shows multiple blood vessels.[10] Zones of necrosis or cystic change are occasionally seen in these tumors.[10,13]

Histopathologic Findings

Paragangliomas are well-differentiated neoplasms containing biphasic or biphenotypic collections of chief cells (type I) arranged in nests or lobules *(zellballen)* surrounded by single layers of sustentacular cells (type II).[7,10,13] The chief cells are round or polygonal in shape, and contain spheroid or ovoid nuclei with finely stippled chromatin within granular eosinophilic cytoplasm.[7,10,13] Sustentacular cells surrounding the lobules of chief cells usually have spindle shapes with long cytoplasmic processes that can mimic pericytes.[10,13] Surrounding the chief and sustentacular cells is a fibrovascular stroma containing endothelial cells, vascular pericytes, and nerve fibers.[10,13]

Some minor histologic differences have been described for Paragangliomas in different locations.[10,13] For example, carotid body tumors often have more hyalinization and vascularity than vagal paragangliomas.[10,13] Up to half of paragangliomas involving the cauda equina contain ganglion cells and cells that have varying features between chief and ganglion cells.[13]

Histologic features of paragangliomas associated with aggressive growth behavior include central necrosis, vascular invasion, and mitoses.[10,13] The only reliable indicator for malignant paragangliomas has been evidence of metastasis.[10]

Paragangliomas often show immunoreactivity for synaptophysin, chromographin, neurofilament proteins, and neuron-specific enolase by chief cells, and for S-100 protein by sustentacular cells.[10,13] Paragangliomas of the cauda equina may show immunoreactivity to serotonin, somatostatin, leukephalin, metakephalin, and paranuclear cytokeratin.[13]

Tumor Genetics

Abnormalities at Ilq22.3-q23, 11 q!3.1, and Il qll-q23 have been found for carotid body tumors, and at 3 p21 for extra-adrenal paragangliomas and 40 % of pheochromocytomas.[13]

Findings on Plain Films (Roentgenograms) and Computed Tomography

Paragangliomas appear as lesions with soft tissue attenuation which show prominent enhancement.[5,6,8,12,14] Paragangliomas often show zones of osseous destruction adjacent to lesions at the skull base or middle ear (Fig. **450).** Paragangliomas involving the spine may show chronic erosion of vertebrae.[11]

MRI Findings

Paragangliomas are circumscribed ovoid or fusiform lesions with low-intermediate signal on T1WI and PDWI, and intermediate to high signal on T2WI and FST2WT[1,3-5,7-15] (Figs. **450-453).** Variable degrees of multiple tortuous and/or punctate zones of signal void or low signal on PDWI, T2WI, and FS T2WI are often seen within paragangliomas that are greater than 1 cm, and represent intratumoral vessels"[1,3-5,7-15] (Figs. **450, 451**). This appearance on T2WI has been referred to as a "salt and pepper" pattern, with the pepper representing flow voids and salt representing hemorrhage or slow flow in vessels.[10] Lesions may also show signal heterogeneity on T2WI secondary to cyst formation and/or hemorrhage.[10,11]

- **Carotid body paragangliomas** typically splay the proximal external carotid artery from the internal carotid artery[7,10] (Figs. **451,452**).

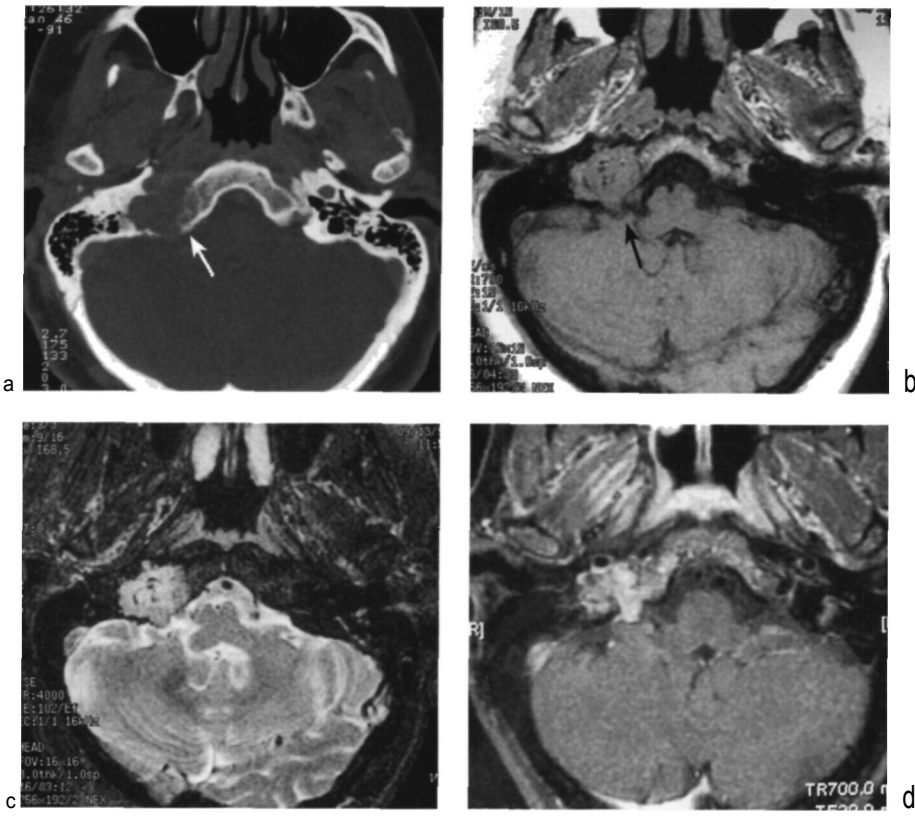

Figure **450a-d** A 55-year-old woman with a jugular bulb paraganglioma (glomus jugulare). Axial CT image (**a**) shows erosive changes at the jugular foramen secondary to an enhancing soft tissue tumor. The tumor has intermediate signal on axial T1WI (**b**) and heterogeneous high and slightly high signal on axial FST2WI (**c**). Multiple tortuous and punctate zones of signal void are seen on T1WI and FST2WI representing intratumoral vessels. The tumor shows prominent Gd-contrast enhancement on axial FST1WI (**d**).

- **Spinal paragangliomas** range in size from 2 to 9 cm, can be ovoid, spheroid, or lobulated, and intradural and/or extradural[3,4,11,15] (Fig. **453**). Spinal cord cysts may occur secondarily from intradural paragangliomas at the cauda equina.[3]

After Gd-contrast administration, lesions typically show moderate to prominent enhancement.[1,3,7,9-11] Paragangliomas usually show rapid and intense Gd-contrast enhancement.[1,10] Using time-resolved analysis, paragangliomas show early enhancement from the early bolus arrival within these vascularized tumors, and subsequent prolonged washout secondary to blood pooling.[1]

Differential Diagnosis

Carotid body tumor. Schwannoma, neurofibroma, lymphoma, metastatic lesion, abscess, venous thrombosis.[10]

Clomus jugulare tumor. Schwannoma, neurofibroma, meningioma, lymphoma, metastatic lesions, dehiscent jugular bulb, jugular vein thrombosis, Langerhans' cell histiocytosis.[2,10]

Clomus tympanicum tumor. Cholesteatoma, cholesterol granuloma, squamous cell carcinoma, adenocarcinoma, sarcomas, facial nerve schwannomas, endolymphatic sac tumor.[10]

Vagal paraganglioma. Schwannoma, neurofibroma, lymphoma, metastatic lesion.

Spinal paraganglioma. Schwannoma, neurofibroma, ependymoma, meningioma, lymphoma, metastatic lesion.[3]

Prognosis and Treatment

Paragangliomas are usually benign tumors with favorable outcomes.[10,13] Preoperative embolization can be performed to limit bleeding of these vascular tumors during surgery.[10] Embolization is recommended to be done between 2 days and 2 weeks before surgery to minimize initial edematous reaction and avoid recanalization of the treated tumors.[10] CT and/or MRI are used to plan for the optimal surgical approaches for glomus jugulare / tympanicum tumors and vagal paragangliomas.[10] For surgical resection of carotid body tumors, complications include cranial nerve deficits (up to 44%), perioperative stroke (< 1 %), and mortality (< 1 %).[10] Complications associated with resection of vagal paragangliomas include paresis/paralysis of cranial nerves, typically the vagus nerve (~60%).[10] Because of their surgically challenging locations, complete resection of glomus jugulare tumors is difficult to achieve, and up to 50 % recur locally.[13] In patients with paragangliomas that are partially resected or cannot be surgically removed, radiation has been used with excellent palliation.[10]

The metastatic rates for paragangliomas depend on the location of the tumors.[13] Para-aortic paragangliomas have metastatic rates of 28-42 %, whereas the metastatic rates for carotid body and glomus jugulare tumors range from 2 to 9%.[13] Malignant paragangliomas can be treated with surgery and radiation.[10] Metastatic disease has been reported to the lungs, pleura, vertebrae, skull, meninges, lymph nodes, liver, heart, pancreas, and skin.[10] Paragangliomas involving the cauda equina can be cured by surgical excision, although 4% recur and rare tumor dissemination into the cerebrospinal fluid has been reported.[13]

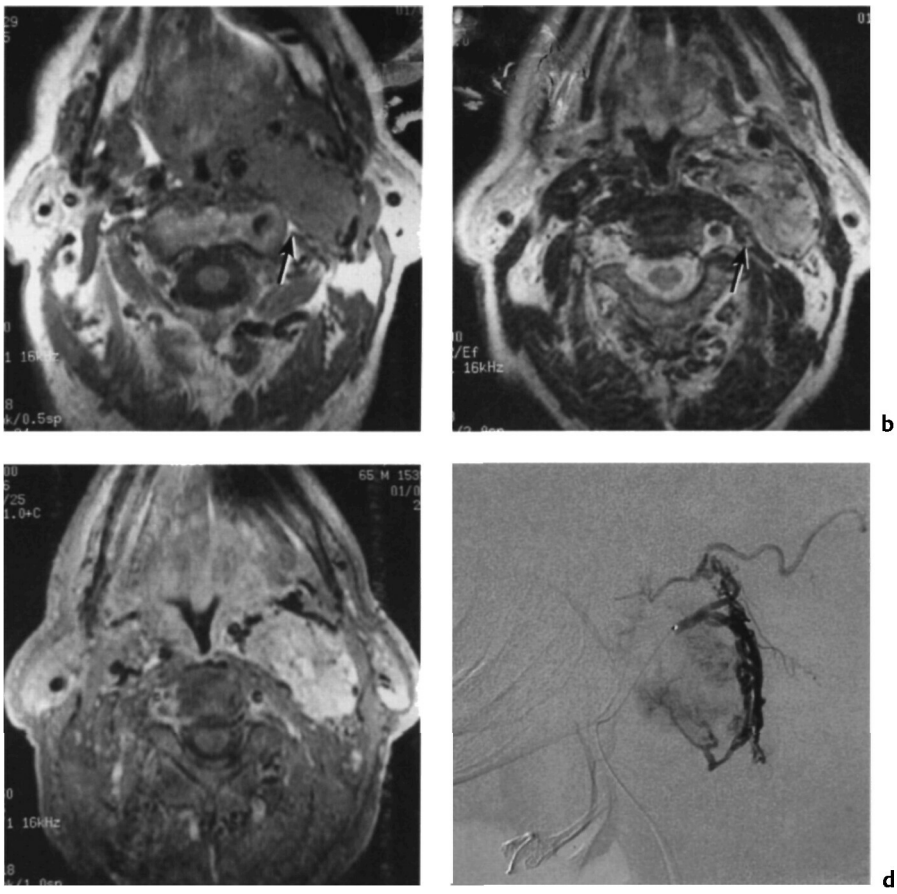

Figure **451 a-d** A 65-year-old man with a paraganglioma at the left common carotid artery bifurcation in the neck, also referred to as a carotid body tumor. The ovoid tumor splays the proximal external carotid artery from the internal carotid artery, and has intermediate signal on axial T1WI (**a**) and heterogenous slightly high and intermediate signal on axial T2WI (**b**). The tumor shows prominent Gd-contrast enhancement on axial FST1WI (**c**). Multiple tortuous and punctate zones of signal void are seen within the peripheral and central portions of the tumor on T1WI, FST2WI, and postcontrast FST1WI, representing blood vessels as seen on a conarteriogram (d).

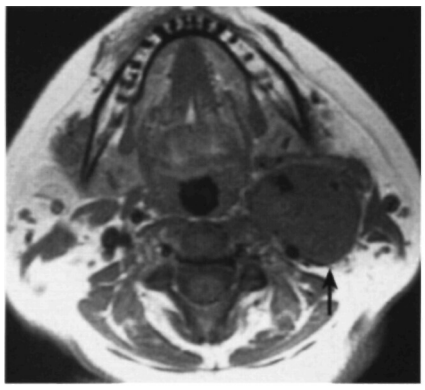

a

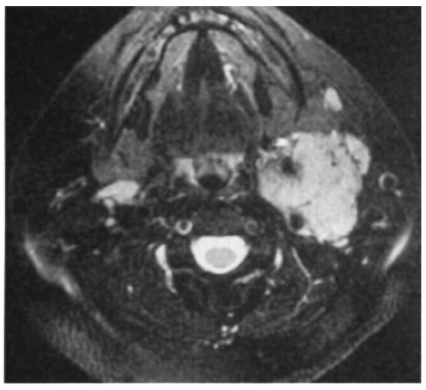

b

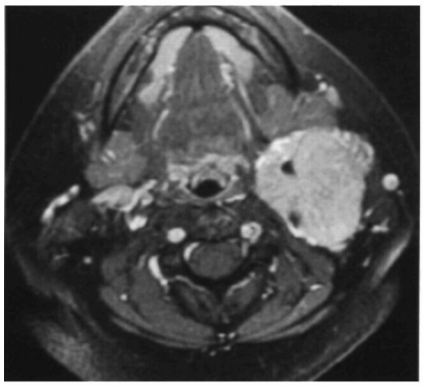

c

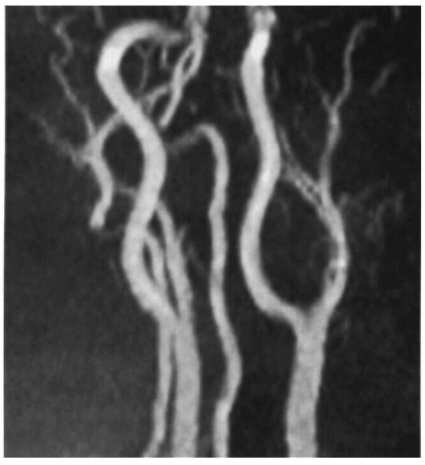

d

Figure **452 a-d** A 27-year-old woman with a paraganglioma (carotid body tumor) at the left common carotid artery bifurcation. The ovoid tumor has intermediate signal on axial T1WI (**a**), and heterogenous mostly high signal on axial FST2WI (**b**). The tumor shows prominent Gd-contrast enhancement on axial FST1WI (**c**). The tumor splays the proximal external carotid artery from the internal carotid artery as seen on an image from a 2 D time-of-flight MR angiogram (**d**).

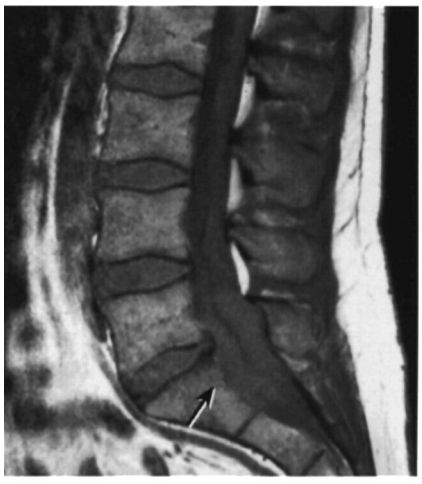

a

b

c

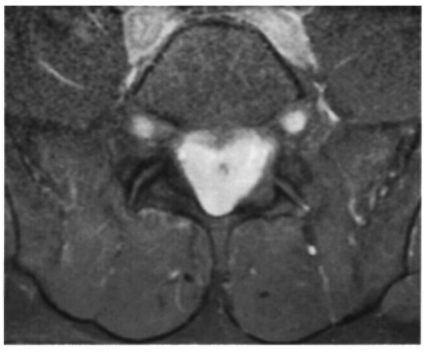

d

Figure **453a-d** A 33-year-old man with an intradural paraganglioma in the distal lumbar thecal sac. The lesion has low-intermediate signal on sagittal T1WI (**a**), and heterogeneous intermediate to slightly high signal on sagittal T2WI (**b**). The tumor shows prominent Cd-contrast enhancement on sagittal (**c**) and axial(**d**)FST1WI.

References

1 Arnold SM, Strecker R, Scheffler K, et al. Dynamic contrast enhancement of paragangliomas of the head and neck: evaluation with time-resolved 2D MR projection angiography. *Eur Radial* 2003;13(7): 1608-1611.

2 Eldevik OP, Gabrielsen TO, Jacobsen EA. Imaging findings in schwannomas of the jugular foramen. *AJNR Am J Neuroradiol* 2000;21(6): 1139-1144.

3 Faro SH, Turtz AR, Koenigsberg RA, Mohamed FB, Chen CY, Stein H. Paraganglioma of the cauda equina with associated intramedullary cyst: MR findings. *AJNR Am* JNeuroradioM997;18(8):1588-1590.

4 Jeffs GJ, Lee GY, Wong GT. Functioning paraganglioma of the thoracic spine: case report. *Neurosurgery* 2003;53(4):992-994; discussion 954-955.

5 Kransdorf MJ. Benign soft-tissue tumors in a large referral population: distribution of specific diagnoses by age, sex, and location. *AJR AmJRoentgenol* 1995:164:395-402.

6 Kransdorf MJ, Murphey MD. Neurogenic tumors. In: *Imaging of Soft Tissue Tumors* 2nd ed. Philadelphia, Pa: W.B. Saunders; 2006: 328-380.

7 Lee KY, Oh YW, Noh HJ, et al. Extraadrenal paragangliomas of the body: Imaging features. *AJR Am J Roentgenol* 2006; 187:492-504.

8 Magliulo G, Zardo F, Varacalli S, D'Amico R. Multiple paragangliomas of the head and neck. *An Otorrinolaringol Ibero Am.* 2003;30(1): 31-38.

9 Noujaim SE, Pattekar MA, Cacciarelli A, Sanders WP, Wang AM. Paraganglioma of the temporal bone: role of magnetic resonance imaging versus computed tomography. Top *Magn Reson Imaging* 2000;11(2):108-122.

10 Rao AB, Koeller KK, Adair CF. Paragangliomas of the head and neck: radiologic-pathologic correlation. *Radiographics* 1999;19: 1605-1632.

11 Rees JH, Smirniotopoulos JG, Moran C, Mena H. Paragangliomas of the cauda equina. Imaging features with radiologic-pathologic correlation. *J Neuroradiol* 1996;2:242-250.

12 Rha SE, Byun JY. Jung SE, Chun HJ, Lee HG, Lee JM. Neurogenic tumors in the abdomen: tumor types and imaging characteristics. Radiographics 2003;23(l):29-43.

13 Soffer D, Scheithauer BW. Paraganglioma. In: Kleihues P, Cavenee WK, eds. *World Health Organization Classification of Tumours. Pathology and Genetics of Tumours of the Nervous System* Geneva: IARC Press; 2000:112-114.

14 Somasundar P, Krouse R, Hostetter R, Vaughan R, Covey T. Paragangliomas - A decade of clinical experience. *J Surg Oncol* 2000; 74:286-290.

15 Sundgren P, Annertz M, Englund E, Stromblad LG, Holtas S. Paragangliomas of the spinal canal. *Neuroradiology* 1999;41(10):788-794.

Pigmented Villonodular Synovitis

Definition

Pigmented villonodular synovitis (PVNS) represents benign, intra-articular lesions of proliferative synovium (tendon sheaths, joints, and bursae) containing zones of recent or remote hemorrhage.[3,4,12,13] PVNS has similar histopathologic features to giant cell tumors of the tendon sheath / nodular synovitis, although PVNS lesions have frondlike or villous growth patterns and contain large amounts of hemosiderin.[3,4,6,9]

Frequency of Occurrence

These lesions account for < 1! of benign and all soft tissue tumors.[7]

Age at Presentation

From 9 to74 years, mean = 38 years, median = 32 years.[7,8,10,11] Most patients present with PVNS between the 3rd and 4th decades.[9-11] In children, PVNS may occur secondary to joint hemorrhage from disorders such a synovial hemangioma or hemophilia.

Gender Ratio (M |F)

I/1[9] to 1.4*II*.

Location

PVNS lesions are typically intra-articular abnormalities and are most commonly seen in the knee (80 %).[9] Lesions are most often mono-articular. Other locations in order of decreasing frequency include the lower extremity > foot and ankle > hand and wrist > hip > shoulder > elbow.[7] PVNS may extend into periarticular soft tissues, adjacent joints, and adjacent bursae.

Signs and Symptoms

PVNS is often associated with slowly progressing, intermittent pain involving a single joint.[6,9] PVNS may be associated with joint stiffness or locking.[6,9] A joint effusion is usually present.[6,9]

Gross Pathologic Findings

PVNS can be localized solitary lesions or appear as multifocal or diffuse synovial lesions. Lesions usually have irregular margins with frondlike projections.[9] PVNS usually has reddish coloration.[3,4,9,12,13]

Histopathologic Findings

Lesions consist of synovial proliferation with fibrous collagenous tissue and varying amounts of scattered multinucleated giant cells, macrophages, round/polygonal cells, fibroblasts, and xanthoma cells.[3,4,9,12,13] Considerable amounts of hemosiderin are usually present.[3,4,9,12,13] Zones of hyalinization and fibrosis are often present in long-standing PVNS.[9] Joint effusions are usually serosanguineous or xanthochromic.[9]

Lesion Genetics

Rearrangements of 1 pll-13 and 16q24, as well as the translocation of t(l;2)(p22;q35-37) have been reported.[3]

Findings on Plain Films (Roentgenograms) and Computed Tomography

Periarticular soft tissue swelling without mineralization is often seen on plain films in patients with PVNS[1,6,9,12] (Figs. **454,456).** CT can show joint effusions, periarticular soft-tissue PVNS lesions, and subtle bone erosions.[6,9] Long-standing or extensive PVNS is often associated with areas of lucency in bone cortex and medullary cavity, with or without reactive sclerosis.[6,9,12] PVNS lesions often involve bones on both sides of joints.[6,9]

MRI Findings

PVNS often appears as irregular, multinodular, and/or diffuse thickening of synovium.[6,8,9] Occasionally PVNS occurs as single, nodular, intra-articular lesions. Lesions often have low or low-intermediate signal on T1WI, PDWI, and T2WI[6,8,9] (Figs. **454-456).** Areas of low signal on T2WI and T2*WI are secondary to hemosiderin in PVNS.[6,8,9,14] Areas of slightly high to high signal on T2WI and FST2WI can also occur from edema and/or inflammatory reaction.[69] Joint effusions are usually present, rarely with fluid-fluid levels (Fig. 455). After Gd-contrast administration, PVNS usually shows enhancement in homogeneous, heterogeneous, and/or septal patterns.[9]

Differential Diagnosis

Intra-articular giant cell tumor of the tendon sheath, rheumatoid arthritis, gout, synovial hemangioma with recent hemorrhage, hemophilia, synovial hyperplasia secondary to degenerative joint disease, primary noncalcified synovial chondromatosis.[1-3,5-6,8-9,12,13]

Prognosis and Treatment

PVNS is usually treated with arthroscopic or surgical synovectomy.[4,9,12] Radiation is sometimes used when the abnormal synovial tissue is less than 5 mm in size.[9] PVNS can recur in up to 50% of patients.[9]

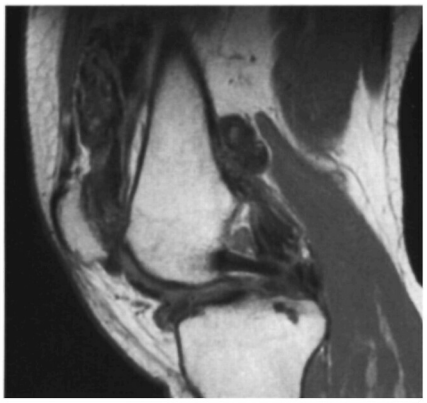

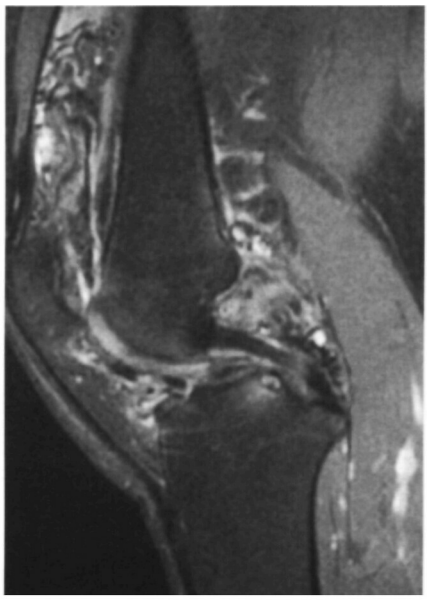

a, b

c

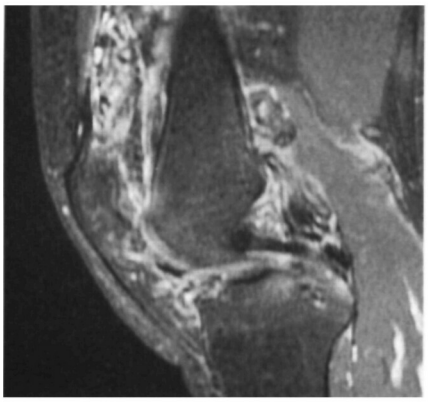

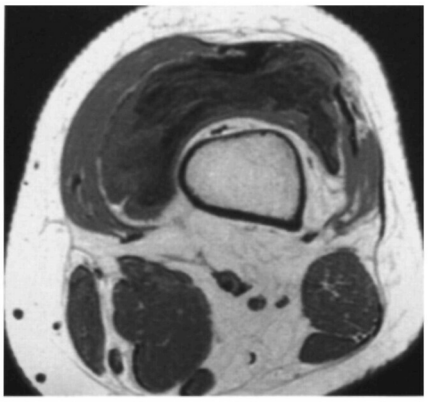

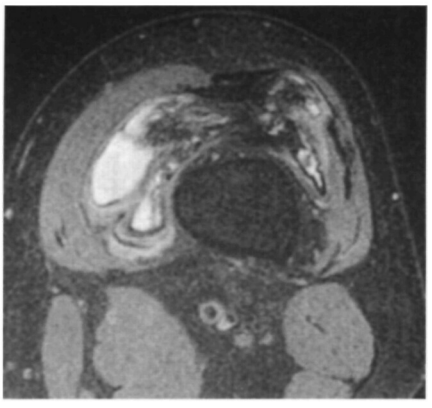

d, e

f

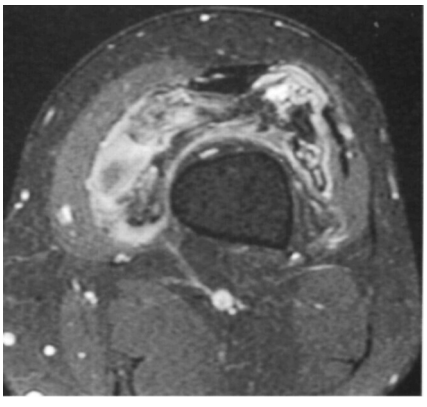

g

Figure **454a-f** A 36-year-old woman with pigmented villonodular synovitis involving the knee. Lateral radiograph (**a**) shows zones of soft tissue swelling in the suprapatellar portions of the knee joint. Poorly defined and ovoid zones with heterogeneous intermediate and low signal on sagittal (**b**) and axial (**e**) T1 WI are seen in the anterior and posterior portions of the knee joint; also seen with heterogeneous intermediate, slightly high, and low signal on sagittal (**c**) and axial (**f**) FST2WI. Heterogeneous Gd-contrast enhancement of the lesions is seen on sagittal (**d**) and axial (**g**) FST1WI.

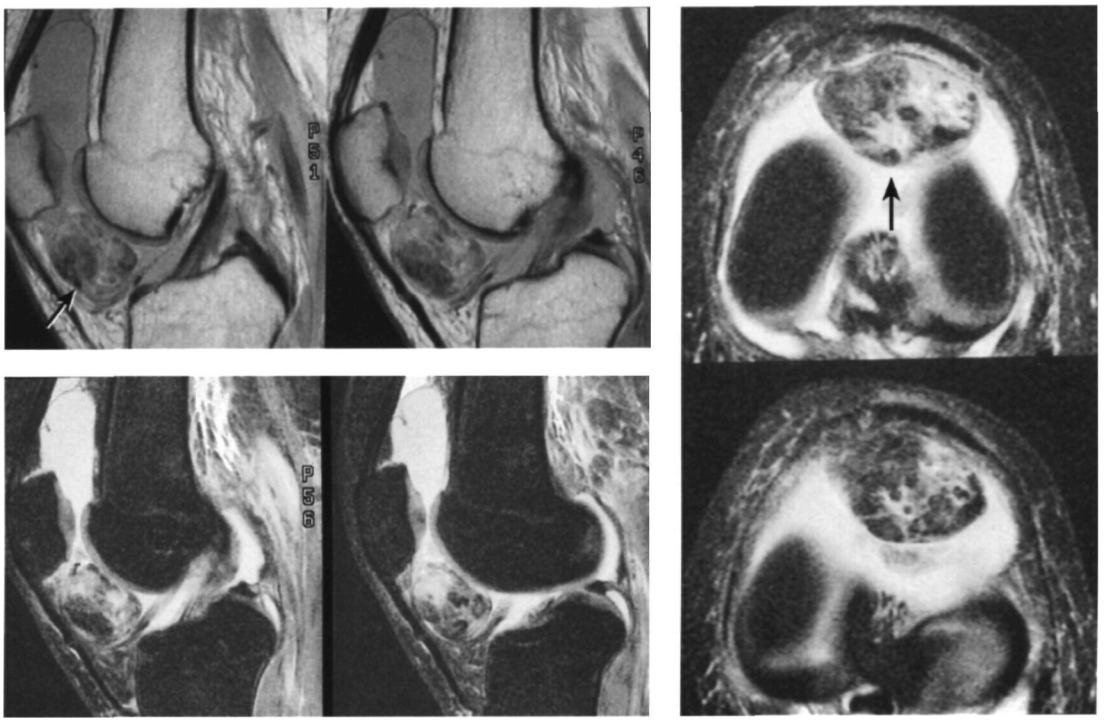

a

b

c

Figure **455a-c** A 22-year-old woman with pigmented villonodular synovitis involving the knee. A circumscribed zone with heterogeneous intermediate and low signal on sagittal (**a**) PDWI, and heterogeneous intermediate, high and low signal on sagittal (**b**) and axial (**c**) FST2WI is seen in the anterior-inferior portion of the knee joint. A large joint effusion is also present.

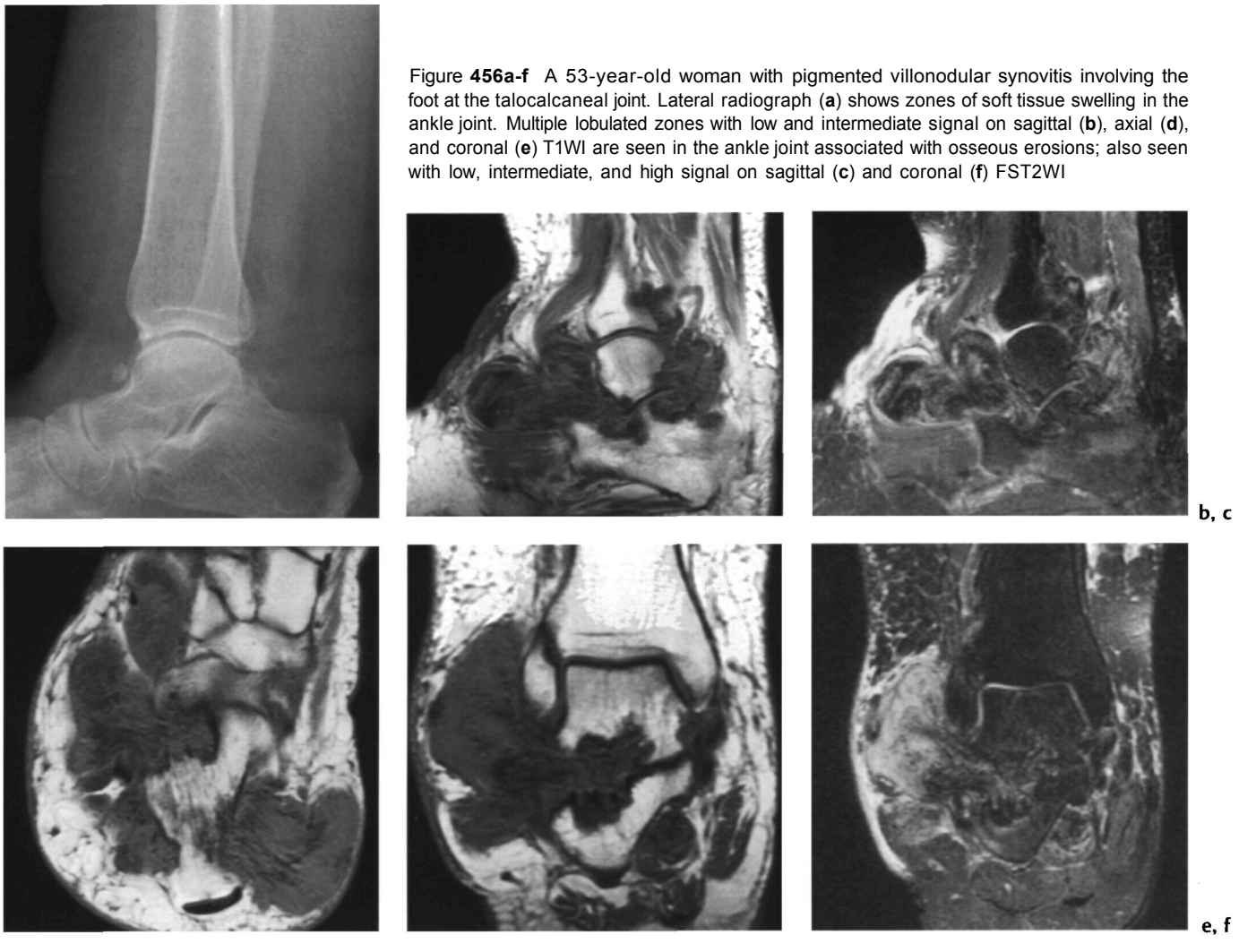

a

b, c

d

e, f

Figure **456a-f** A 53-year-old woman with pigmented villonodular synovitis involving the foot at the talocalcaneal joint. Lateral radiograph (**a**) shows zones of soft tissue swelling in the ankle joint. Multiple lobulated zones with low and intermediate signal on sagittal (**b**), axial (**d**), and coronal (**e**) T1WI are seen in the ankle joint associated with osseous erosions; also seen with low, intermediate, and high signal on sagittal (**c**) and coronal (**f**) FST2WI

References

1 Bancroft LW, Peterson JJ, Kransdorf MJ, Nomikos GC, Murphey MD. Soft tissue tumors of the lower extremities. *Radial Clin North Am* 2002:40:991-1011.

2 Crotty JM, Monu JUV, Pope TL Jr. Synovial osteochondromatosis. Radio/ *Clin North Am* 1996;34(2):327-342.

3 de St. Aubain Somerhausen N, Dal Cin P. Diffuse-type giant cell tumor. In: Fletcher COM, Unni KK, Mertens F, eds. *World Health Organization Classification of Tumours. Pathology and Genetics of Tumours of Soft Tissue and Bone* Geneva: IARC Press: 2002:112-114.

4 Helliwell TR, Ritchie DA. Tumors and tumor-like lesions ofjoints and juxta-articular bone. In: Helliwell TR, ed. *Major Problems in Pathology: Pathology of Bone and Joint Neoplasms.* 1st ed. Vol 37. Philadelphia, Pa: W.B. Saunders; 1999:369-393.

5 JelinekJS, Kransdorf MJ, Shmookler BM, Aboulafia AA, Malawer MM. Giant cell tumor of the tendon sheath: MR findings in nine cases. *AJR Am] Roentgenol* 1994;162:919-922.

6 Jelinek JS, Kransdorf MJ, Utz JA, et al. Imaging of pigmented villonodular synovitis with emphasis on MR imaging. *AJR AmJ Roentgenol* 1989:152:337-342.

7 Kransdorf MJ. Benign soft-tissue tumors in a large referral population: distribution of specific diagnoses by age, sex, and location. *AJR AmJ Roentgenol* 1995:164:395-402.

8 Kransdorf MJ, Murphey MD. Synovial tumors. In: *Imaging of Soft Tissue Tumors* 2nd ed. Philadelphia, Pa: W.B. Saunders; 2006: 381-436.

9 Llauger J, Palmer J, Roson N, Cremades R, Bague S. Pictorial Essay-Pigmented villonodular synovitis and giant cell tumors of the tendon sheath: radiologic and pathologic features. *AJR Am] Roentgenol* 1999; 172:1087-1091.

10 Mulder JD, Schutte HE, Kroon HM, Taconis WK. Introduction. In: *Radiologic Atlas of Bone Tumors* Amsterdam: Elsevier; 1993:3-6.

11 Mulder JD, Schutte HE, Kroon HM, Taconis WK. The diagnosis of bone tumors. In: *Radiologic Atlas of Bone Tumors* Amsterdam: Elsevier: 1993:9-46.

12 Mulder JD, Schutte HE, Kroon HM, Taconis WK. Pigmented villonodular synovitis. In: *Radiologic Atlas of Bone Tumors* Amsterdam: Elsevier; 1993:689-695.

13 Unni KK. Conditions that commonly simulate primary neoplasms of bone. In: *Dahlin's Bone Tumors—General Aspects and Data on* II087 Coses 5th ed. Philadelphia, Pa: Lippincott, Williams & Wilkins; 1996:355-432.

14 Weatherall PT. Benign and malignant masses. *Magn Reson Imaging Clin NAm* 1995:3:669-694.

A 68 Pleomorphic Hyalinizing Angiectatic Tumor

Definition

Pleomorphic hyalinizing angiectatic tumors (PHATs) are non-metastasizing tumors that contain a spindle cell neoplastic stroma lacking mitotic activity that surrounds aggregates of thin-walled ectatic vessels lined with fibrin.[1-5]

Frequency of Occurrence

PHATs are rare lesions[8] and account for < 1 % of soft tissue tumors.

Age at Presentation

These tumors usually occur in adults ranging in age from 32 to 83 years, mean = 58.5 years.[3,7]

Gender (M / F)

1/1 to 1/1.7.[3,7,8]

Location

More than 50 % of PHATs involve the subcutaneous tissues of the lower extremity.[6-8] Others have been reported to occur in the subcutaneous tissues of the chest wall, axilla, back, buttock, and arm, as well as within skeletal muscle of the shoulder thigh and chest wall.[1,2,7,8]

Signs and Symptoms

PHATs are slow-growing neoplasms that present as areas of localized swelling in the superficial soft tissues.[3,7,8]

Cross Pathologic Findings

PHATS are usually white-tan and/or maroon, lobulated, non-encapsulated lesions with infiltrative margins.[7,8] PHATs range in size from 2 to 8 cm.[3-6,8]

Histopathologic Findings

PHATs usually have a stroma of plump, spindled and spheroid cells with hyperchromatic pleomorphic nuclei that may contain intranuclear cytoplasmic inclusions.[1-8] Mitotic activity is minimal or absent (< 1 mitosis per 50 HPF).[7,8] Within the stroma, collections of ectatic thin-walled vessels are seen that range in size from microscopic to macroscopic.[6-8] The inner margins of these vessels are lined with hyaline fibrin material adjacent to endothelial cells.[6-8] PHATs may also contain eosinophils, mast cells, plasma cells, and psammoma bodies.[7] PHATs are often immunoreactive to vimentin and vascular endothelial growth factor; and occasionally to CD 34, epithelial membrane antigen, CD 99, and factor Xllla,[2-8] but are typically not immunoreactive to S100 protein, actin, desmin, cytokeratin, CD 31, and von Willebrand factor.[78]

Tumor Genetics

PHATs have been reported to have a diploid histogram as determined with DNA flow cytometry.[3]

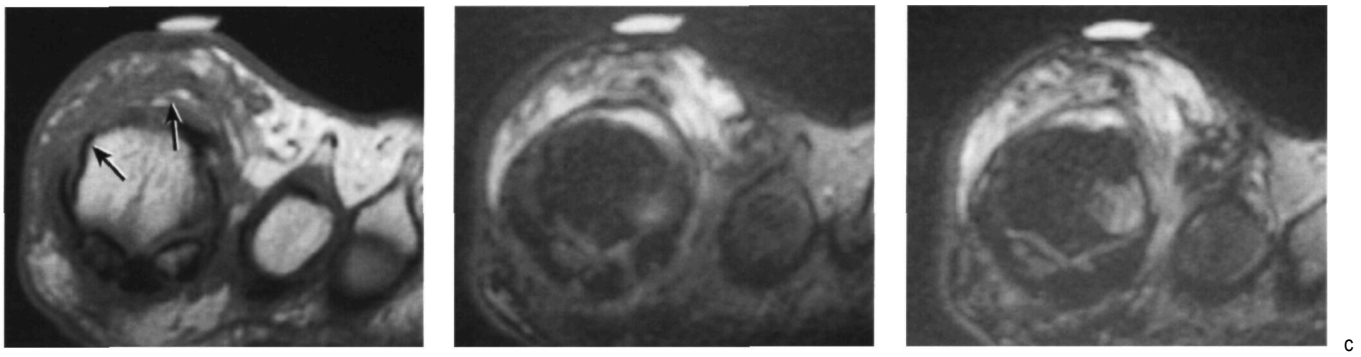

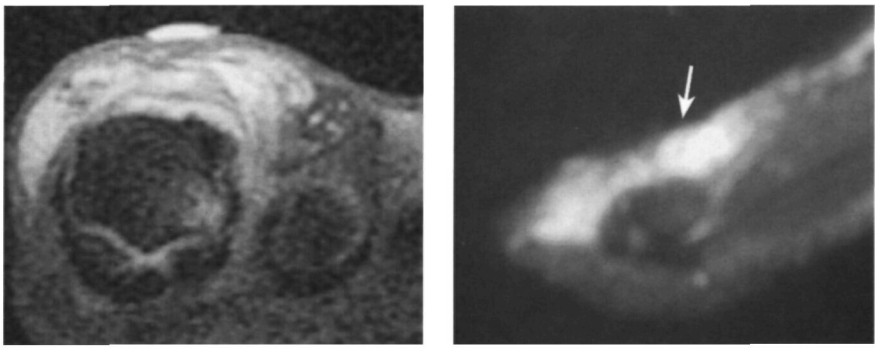

Figure **457a-d** A 42-year-old woman with a pleomorphic hyalinizing angiectatic tumor involving the dorsal superficial soft tissues of the foot adjacent to the region of the first metatarsal-phalangeal joint. The tumor has lobulated and irregular/indistinct margins. The tumor has low to intermediate signal on coronal T1WI (**a**), and heterogeneous slightly high and high signal on coronal FS T2WI (**b, c**). Linear and curvilinear zones of low signal on FST2WI are seen in the lesion. The tumor shows prominent Gd-contrast enhancement on coronal (**d**) and sagittal (**e**) FST1WI.

Findings on Plain Films (Roentgenograms) and Computed Tomography

Lesions are often not seen on radiographs. PHATs may be seen as irregular zones of soft tissue attenuation in the subcutaneous soft tissues, with occasional calcifications on CT.

MRI Findings

PHATs can appear as lesions in the superficial soft tissues with lobulated and/or irregular/indistinct margins. Lesions can have low to intermediate signal on Tl WI and PDW1, and slightly high to high signal on T2WI and FST2WI (Fig. 457). Linear or curvilinear zones of low signal on T2WI and FST2WI can be seen within these tumors. After Gd-contrast administration, PHATs can show prominent enhancement.

Differential Diagnosis

Hemangioma, hemangioendothelioma, Schwannoma, neurofibroma, Kaposi sarcoma, solitary fibrous tumor.[278]

Prognosis and Treatment

Up to 50 % of PHATs recur locally.[78] Metastatic disease from PHATs has not been reported.[6-8] Treatment usually consists of wide local excision.[18]

References

1 Fujiwara M, Yuba Y, Wada A, Ozawa T, Tanaka T. Pleomorphic hyalinizing angiectatic tumor of soft parts: report of a case and review of the literature.; Dermaro/ 2004;31(5):419-423.

2 Fukunaga M, Ushigome S. Pleomorphic hyalinizing angiectatic tumor of soft parts. *Pathol Int* 1997;47(ll):784-788.

3 Groisman CM, Bejar J, Amar M, Ben-Izhak 0. Pleomorphic hyalinizing angiectatic tumor of soft parts. Immunohistochemical study including the expression of vascular endothelial growth factor. *Arch Pathol lab Med* 2000;124:423-426.

4 Matsumoto K, Yamamoto T. Pleomorphic hyalinizing angiectatic tumor of soft parts: a case report and literature review. *Pathol Int* 2002;52(10):664-668.

5 Silverman JS, Dana MM. Pleomorphic hyalinizing angiectatic tumor of soft parts: immunohistochemical case study shows cellular composition by CD 34+ fibroblasts and factor XIlla+ dendrophages. *J Cutan Pathol* 1997;24(6):377-383.

6 Smith ME, Fisher C, Weiss SW. Pleomorphic hyalinizing angiectatic tumor of soft parts. A low-grade neoplasm resembling neurilemoma. *AmJSurgPathol* 1996;20(l):21-29.

7 Weiss SW. Pleomorphic hyalinizing angiectatic tumour of soft parts. In: Fletcher COM, Unni KK, Mertens F, eds. *World Health Organization Classification of Tumours. Pathology and Genetics of Tumours of Soft Tissue and Bone* Geneva: IARC Press; 2002:191.

8 Weiss SW, Goldblum JR. Benign soft tissue tumors and pseudotumors of miscellaneous type. In: Weiss SW, Goldblum JR, eds. *Enzinger and Weiss's Soft Tissue Tumors* 4th ed. St. Louis, Mo: Mosby; 2001: 1419-1481.

A 69 Rhabdomyosarcoma (Also Referred to as Myosarcoma, Malignant Rhabdomyoma, Rhabdosarcoma, and Embryonal Sarcoma)

ICD-OCode

Embryonal: 8910/3

Alveolar: 8920/3

Pleomorphic: 8901/3

Definition

Rhabdomyosarcomas are malignant mesenchymal tumors with rhabdomyoblastic differentiation that occur primarily in soft tissue, and only very rarely in bone.[1119202223] There are three subgroups of rhabdomyosarcoma: embryonal (50-70%), alveolar (18-45%), and pleomorphic (5-10 %)."[19]-[23] Embryonal and alveolar rhabdomyosarcomas occur primarily in children, and pleomorphic rhabdomyosarcomas occur mostly in adults.[1119202223] Embryonal rhabdomyosarcomas have phenotypic and biologic features of embryonal muscle.[22] Alveolar rhabdomyosarcomas are round cell neoplasms that show partial skeletal muscle differentiation.[23] Pleomorphic rhabdomyosarcomas contain bizarre, spheroid, and spindle cells which show skeletal muscle differentiation.[19]

Frequency of Occurrence

Rhabdomyosarcomas represent ~ 2 % of primary malignant soft tissue tumors and < 1 % of all primary soft tissue tumors.[13] These tumors account for 19% of soft tissue sarcomas in children." Rhabdomyosarcomas occur in 4.6 per million children, below 15 years old, in the United States.[22] Embryonal rhabdomyosarcomas occur in 3 per million children below 15 years old.[22]

Age at Presentation

From 2 to 40 years, mean = 18 years.[13] Embryonal rhabdomyosarcomas occur primarily in children less than 10 years old.[22] Alveolar rhabdomyosarcomas occur in children of all ages, median = 6.8-9 years.[23] Pleomorphic rhabdomyosarcomas typically occur in adults, median age in the 6th decade.[19]

Gender Ratio (M f F)

1:1/1 to 1.7/I.[11]-[1322]

Location

These tumors occur in the head and neck > lower extremity > trunk > upper extremity, retroperitoneum > hip and buttocks > hand and wrist > proximal limb girdle > foot and ankle > spine.[13,22,23] Alveolar and pleomorphic rhabdomyosarcomas occur frequently in the extremities.[1923] Embryonal rhabdomyosarcomas occur mostly in the head and neck (47 %) followed by the genitourinary system (bladder, prostate, paratesticular soft tissues) > retroperitoneum > visceral organs (liver, kidney, heart, lungs) > trunk > appendicular skeleton.[22] The spindle cell variants of embryonal rhabdomyosarcoma are often located in scrotal soft tissues, and head and neck.[22] The botryoid variants of embryonal rhabdomyosarcoma typically occur in submucosal locations (urinary bladder, biliary tract, pharynx, conjunctiva, auditory canal).[22]

Signs and Symptoms

Embryonal rhabdomyosarcoma. Lesions present as rapidly growing masses that often manifest symptoms by compression of adjacent structures (proptosis and/or diplopia related to orbital lesions, sinusitis from nasal or nasopharyngeal tumors, urinary obstruction from genitourinary tumors, jaundice from hepatic or biliary tumors, parathesias or paresis from paraspinal tumors, etc.).[22,29]

Alveolar rhabdomysarcoma. Lesions often present as rapidly growing masses in the extremities, or with proptosis and diplopia from orbital tumors, sinusitis from sinonasal tumors, constipation from perirectal tumors, parathesias or paresis from paraspinal tumors, etc.[23]

Pleomorphic rhabdomyosarcoma. Lesions often occur as painful, rapidly growing masses in the extremities.[19]

Cross Pathologic Findings

Embryonal rhabdomyosarcoma. Tumors are fleshy, tan lesions with poorly defined margins.[22] The spindle cell variants of embryonal rhabdomyosarcoma are firm, fibrous, tan-yellow tumors that often have a whorled pattern on cut surfaces.[22] The botryoid variants of embryonal rhabdomyosarcoma have polypoid configurations with clusters of sessile or pendulous nodules near epithelial surfaces.[22]

Alveolar rhabdomysarcoma. Tumors are often fleshy and fibrous, gray-tan, or gray-white lesions.[223] Zones of necrosis or cystic change can be present.[2]

Pleomorphic rhabdomyosarcoma. Tumors are circumscribed and/or poorly marginated, white-gray-red lesions with variable amounts of hemorrhage and/or necrosis.[219] Lesions are often large (5-15 cm) and frequently have a fibrous pseudocapsule.[419]

Histopathologic Findings

Embryonal rhabdomyosarcoma. Tumors are composed of primitive mesenchymal cells (rhabdomyoblasts) in various stages of myogenesis.[2,22] The less differentiated cells appear as stellate cells with central oval nuclei within pale, slightly amphophilic cytoplasm.[22] A high rate of mitosis is usually observed.[224] As lesions become more differentiated, tumor cells tend to have more elongated shapes with darker eosinophilic cytoplasm.[22] Other tumor features associated with more advanced stages of myogenesis include multinucleated cells, prominent eosinophilia, cytoplasmic cross-striations, and myotube forms.[22] The distribution and density of tumor cells varies within loose myxoid tissue containing minimal interstitial collagen, some-

what similar in appearance to embryonic muscle.[222] Poorly differentiated tumors show undifferentiated cells with hyperchromatic nuclei and nucleoli, high mitotic activity, and minimal cytoplasm.[2]

- **The botryoid variant** of embryonal rhabdomyosarcoma contains myxoid stroma with small, round rhabdomyoblasts with high mitotic activity arranged as linear aggregates (each 2 to 4 cell-layers thick) adjacent to an epithelial surface.[22224] The cell layering feature of these tumors resembles the growth layers of a tree-trunk in cross-section, and have been referred to as "cambium" layers.[2]
- **The spindle cell variant** of embryonal rhabdomyosarcoma contains spindle cells with blunted central nuclei, which may resemble smooth muscle cells.[2224] Tumor cells may be arranged in whorls, fascicles, and/or waves, as well as storiform patterns.[2224] Embryonal rhabdomyosarcomas usually show immunoreactivity to MyoD 1 and myogenin.[22,24] These tumors show variable reactivity to vimentin, actin, and desmin depending on the degree of differentiation of the rhabdomyoblasts.[2224]

Alveolar rhabdomysarcoma. These tumors contain round or oval cells with primitive myoblastic features.[223] Tumor cells are often arranged in nests separated by fibrovascular septa.[223] Rhabdomyoblasts that are adjacent to the fibrous septa may be arranged in a pseudoglandular or alveolar pattern.[224] Giant cells with rhabdomyoblastic differentiation also occur.[23] The solid variant of alveolar rhabdomyosarcomas contains sheets of round rhabdomyoblasts without fibrovascular stroma.[23] Another variant of alveolar rhabdomyosarcoma is the mixed embryonal/alveolar type that has features of both.[23] Anaplasia is a usual feature for these tumors.[24] Alveolar rhabdomyosarcomas usually show immunoreactivity to MyoDl and myogenin.[23] These tumors show variable reactivity to vimentin, actin, and desmin depending on the degree of differentiation of the rhabdomyoblasts.[23]

Pleomorphic rhabdomyosarcoma. These tumors contain pleomorphic rhabdomyoblasts which can have round, spindled, straplike, tadpole, polygonal, and/or racquetlike shapes.[2419] Multinucleated cells with vesicular nuclei containing prominent nucleoli within abundant eosinophilic cytoplasm also occur in these tumors.[2419] Cross-striations are rare.[24] Pleomorphic rhabdomyosarcomas can be subdivided into three morphologic variants.[4] The classic variant consists of sheets of multinucleated polygonal pleomorphic rhabdomyoblasts.[419] The round cell variant contains multinucleated polygonal pleomorphic rhabdomyoblasts in a background of round rhabdomyoblasts.[4] The spindle cell variant contains pleomorphic spindled rhabdomyoblasts in storiform patterns with scattered, large, multinucleated pleomorphic rhabdomyoblasts.[4] Pleomorphic rhabdomyosarcomas usually show lesser immunoreactivity to MyoD 1 (53 %) and myogenin (56%) compared with embryonal and alveolar rhabdomyosarcomas.[19] These tumors show variable reactivity to vimentin, actin, and desmin.[419]

Tumor Genetics

Embryonal rhabdomyosarcomas often show allelic loss in 11p15.[52224] Rearrangements of 1p11-q11 and 12q13 have been reported.[22] Inactivation mutations involving TP53 and CDKN2A, and activating mutations involving RAS genes have been found in some cases.[22]

Alveolar rhabdomyosarcomas often show translocations such as t(2;13)(q35;q!4), or t(l;13)(p36;ql4).[52324] In these translocations, the PAX3 gene on chromosome 2 or the PAX7 gene on chromosome 1 fuse with the transcription factor FKHR gene on chromosome 13.[23] The resulting chimeric proteins activate downstream transcriptional products and exert oncogenic effects.[23]

Pleomorphic rhabdomyosarcomas have complex karyotypes, and lack t(l;13) and t(2;13) translocations that are seen with alveolar rhabdomyosarcomas.[19]

Findings on Plain Films (Roentgenograms) and Computed Tomography[7,10,11-17,20,29]

Rhabdomyosarcomas may not be seen on plain films. When visible on radiographs, soft tissue lesions can have circumscribed and/or poorly defined margins. Rhabdomyosarcoma can be associated with erosion and/or destruction of bone cortex and/or medullary invasion. When present, intra-osseous tumor invasion is typically seen as radiolucent zones.[20] With CT, soft tissue lesions usually can have circumscribed or irregular margins.[10-14,16-17] Calcifications are uncommon. Tumors can have mixed CT attenuation with solid zones of soft tissue attenuation, cystic-appearing and/or necrotic zones, and occasional foci of hemorrhage.[11]

MRIFindings[6-8-10-11-16-18-20,28-29]

Tumors are often ovoid and/or lobulated lesions with circumscribed and/or poorly-defined margins. Tumors typically have low-intermediate signal on TlWl and FSTIWI[6810111416-18202823] (Figs. **458-462).** Zones of high signal on TlWl may be seen resulting from areas of hemorrhage[1116] (Fig. 458). Lesions usually have heterogeneous signal, that is, various combinations of intermediate, slightly high, and/or high signal, on T2WI and FST2WI[6-8,10,11,14,16-18,20,28,29] (Figs. **458-462).** Poorly defined zones of edema may occur in the soft tissues adjacent to the tumors.[8] Tumors are often associated with destructive changes of adjacent bone.[141617] After Gd-contrast administration, tumors show variable degrees of enhancement in various patterns[810141617] (Figs. **458-462).**

Differential Diagnosis

Liposarcoma, malignant fibrous histiocytoma, leiomyosarcoma, synovial sarcoma, malignant nerve sheath tumor, fibrosarcoma, angiosarcoma, metastatic carcinoma or neuroblastoma, hemangiopericytoma, clear cell sarcoma, nodular fasciitis, hematoma, proliferative myositis.

Prognosis and Treatment

Embryonal rhabdomyosarcoma. Treatment usually consists of surgical excision or amputation, neoadjuvant and/or postoperative chemotherapy, and radiation.[1925-273031] Staging using the Intergroup Rhabdomyosarcoma Study/Postsurgical Clinical Grouping System is predictive of outcome.[2122] Approximately 30 % of children with rhabdomyosarcoma are considered low risk for treatment failure, and 70% have intermediate risk (tumors in unresectable locations, presence of metastatic disease at diagnosis in patients less than 10 years old).[17] The 5-year overall survival rates are 64 %, 95 %, and 88 % for the embryonal,

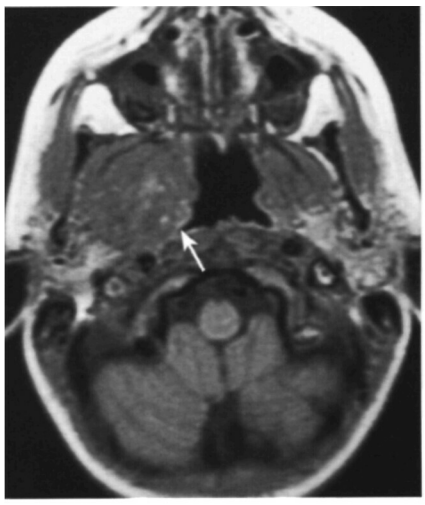

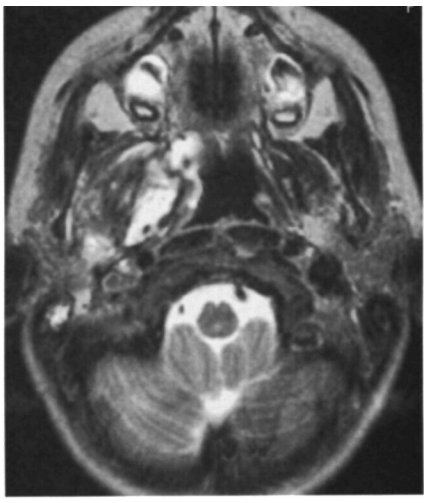

b

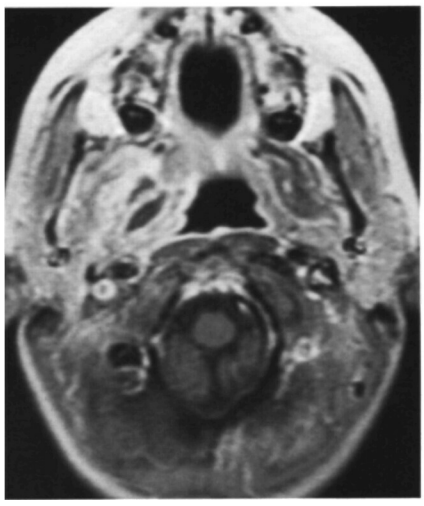

d

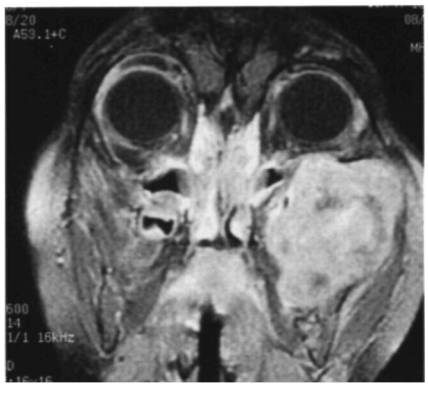

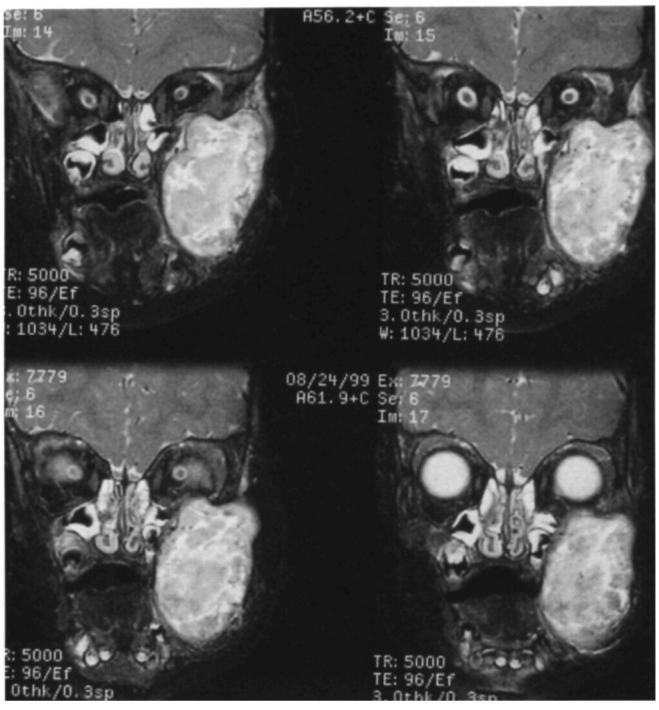

Figure **458**a-d A 14-year-old female with an embryonal rhabdomyosaroma in the submucosal portion of the right nasopharynx. The ovoid tumor has mostly intermediate signal with small foci of high signal on axial T1WI (a). The tumor has heterogeneous high, intermediate, and low signal on axial T2WI (458 b), and shows heterogeneous Gd-contrast enhancement with indistinct margins on axial (c) and coronal (d) T1WI.

Figure 459 a-c An 18-month-old male with an embryonal rhabdomyosarcoma involving the left maxilla and orbit. The tumor has mostly intermediate signal on sagittal T1WI (a), and heterogeneous mostly high signal on coronal FST2WI (b). The tumor shows heterogeneous Cd-contrast enhancement on coronal FST1WI (c). The tumor is associated with bone erosion and destruction.

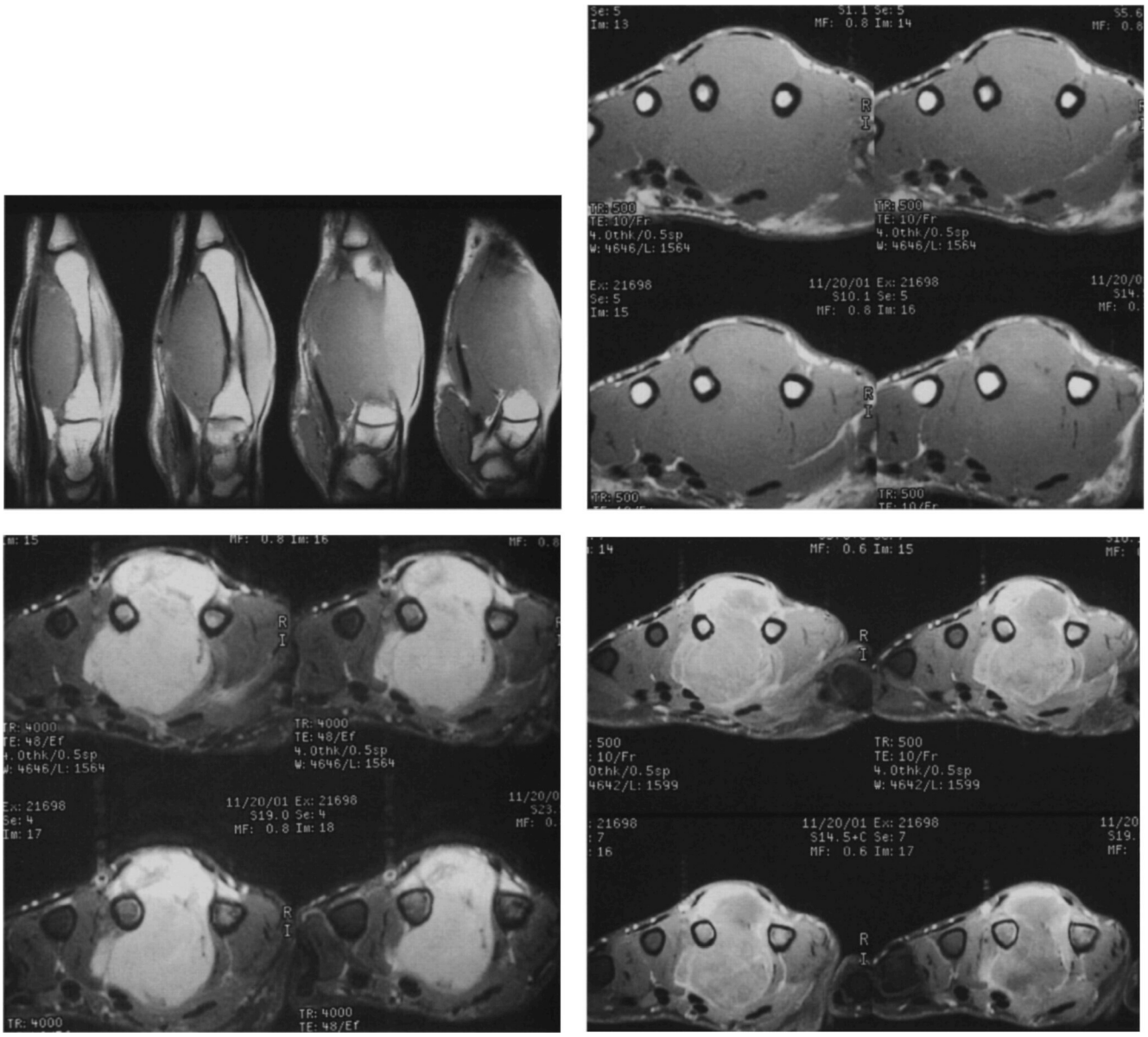

Figure **460 a-d** A 23-year-old man with an alveolar rhabdomyosarcoma involving the soft tissues between the second and third metacarpal bones. The tumor has intermediate signal on sagittal (**a**) and axial (**b**) T1WI, and high signal on coronal FST2WI (**c**). The tumor shows heterogeneous Cd-contrast enhancement on coronal FST1WI (**d**). The tumor is associated with erosion of adjacent bones.

botryoid/embryonal subtype, and spindle-cell embryonal subtype, respectively.[21] Up to 20 % of patients have metastatic disease at diagnosis.[817] The presence of ,metastatic rhabdomyosarcoma at diagnosis is associated with a 5-year survival of only 20 %.[17] Metastatic disease occurs at one site in 50 % of patients.[17] Common sites of metastatic rhabdomyosarcoma include lung, bone marrow, and lymph nodes.[11,17,28]

Alveolar rhabdomysarcoma. Alveolar rhabdomyosarcomas are high-grade tumors that are more aggressive than the embryonal type[21,23] Treatment usually consists of surgical excision or amputation, neoadjuvant and/or postoperative chemotherapy, and radiation.[1,9,25_27,30,31] Staging using the Intergroup Rhabdomyosarcoma Study/Postsurgical Clinical Grouping System is predictive of outcome. The 5-year overall survival is 53 %.[21]

Pleomorphic rhabdomyosarcoma. The prognosis for patients with these tumors is poor.[3,4,19,21] Treatment usually consists of surgical excision or amputation, neoadjuvant and/or postoperative chemotherapy, and radiation.[3,30,31] Local recurrence occurred in 45 % patients in a mean time of 9 months after diagnosis.[4] Fifty-five percent of patients had metastatic disease from 1 to 36 months after diagnosis, mean = 15 months." Seventy percent of patients died of disease in a mean time of 20 months (range: 1-108 months) after diagnosis.[4]

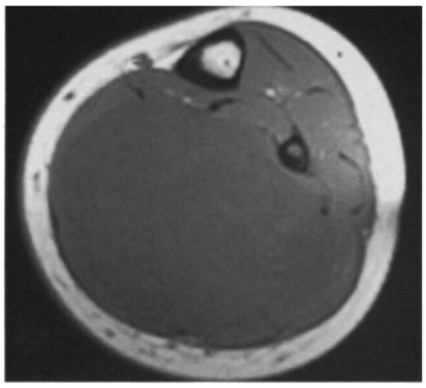

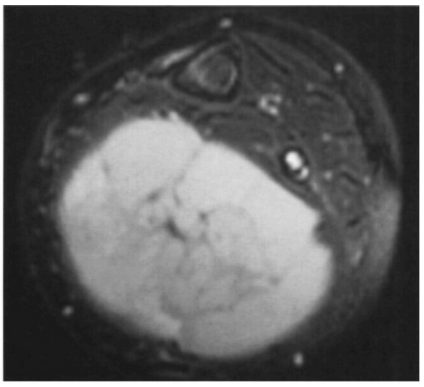

b

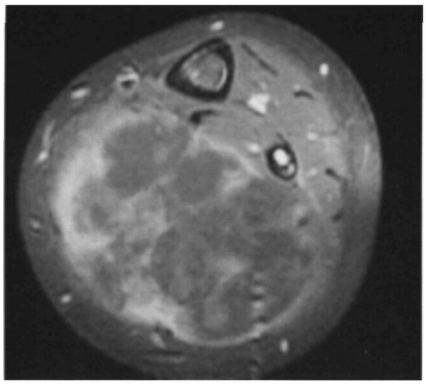

c

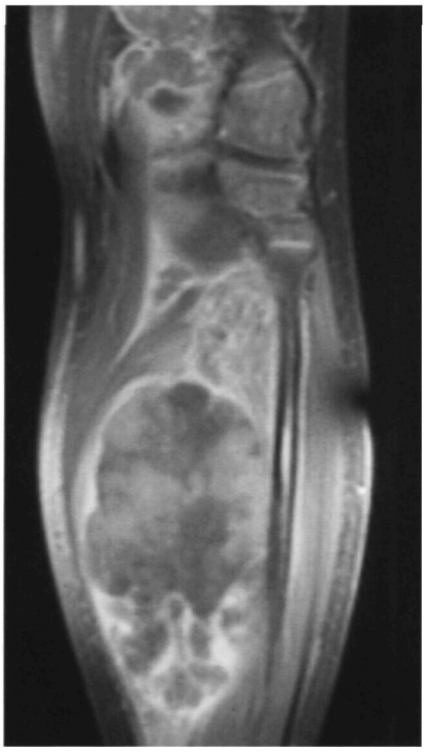

d

Figure **461 a-d** A 2.5-year-old female with an embryonal rhabdomyosarcoma involving the posterior calf. The tumor has intermediate signal on axial T1 WI (**a**), and mostly high signal with strands of low signal on axial FST2WI (**b**). The tumor shows heterogeneous, irregular, peripheral and central Gd-contrast enhancement on axial (**c**) and coronal (**d**) FST1 WI. The tumor is associated signal alteration of the adjacent fibula. Metastatic disease is seen in the popliteal soft tissues.

a

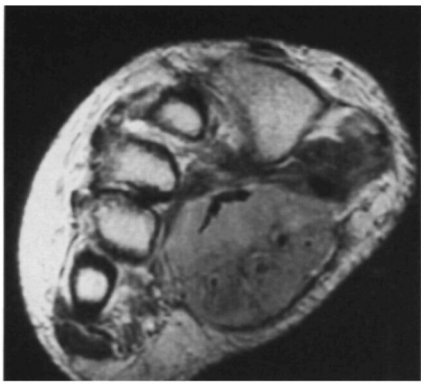

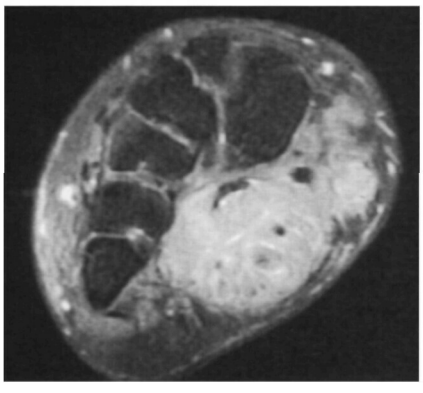

c

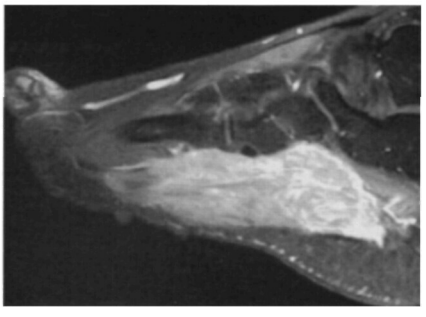

d

Figure **462 a-d** A 20-year-old woman with an alveolar rhabdomyosarcoma involving the plantar soft tissues with encasement of multiple tendon sheaths. The tumor has heterogeneous slightly high signal with strands of low signal on sagittal (**a**) and coronal (**b**) T2WI. The tumor shows prominent Cd-contrast enhancement on coronal (**c**) and sagittal (**d**) FST1WI.

References

1 Breitfeld PP, Lyden E, Raney RB, et al. Ifosfamide and etoposide are superior to vincristine and melphalan for pediatric metastatic rhabdomyosarcoma when administered with irradiation and combination chemotherapy: a report from the Intergroup Rhabdomyosarcoma Study Group.*] Pediatr Hematol Oncol* 2001;23(4):225-233.

2 Das Gupta TK Chaudhuri PK. Pathology of soft tissue sarcoma. In: Das Gupta TK, Chaudhuri PK, eds. *Tumors of the Soft Tissues* 2nd ed. Stamford, Conn: Appleton & Lange; 1998:63-200.

3 Ferrari A, Dileo P, Casanova M, et al. Rhabdomyosarcoma in adults. A retrospective analysis of 171 patients treated at a single institution. *Cancer* 2003;98(3):571-580.

4 Furlong MA, Mentzel T, Fanburg-Smith JC. Pleomorphic rhabdomyosarcoma in adults: a clinicopathologic study of 38 cases with emphasis on morphologic varaiants and recetn muscle-specific markers. Mod *Pathol* 2001:14:595-603.

5 Gil-Benso R, Lopez-Gines C, Carda C, et al. Cytogenetic and molecular findings related to rhabdomyosarcoma. An analysis of seven cases. *Cancer Genet Cytogenet* 2003:144:125-133.

6 Hanna SL, Fletcher BD. MR imaging of malignant soft-tissue tumors. In: *Magn Reson Imaging Clin North Am* 1995;3(4):644-646.

7 Huvos AG. Miscellaneous tumors of soft tissue and bone. In: Huvos AC, ed. *Bone Tumors: Diagnosis, Treatment, and Prognosis* 2nd ed. Philadelphia, Pa: W.B. Saunders;1991:745-766.

8 Kim EE, Valenzuela RF, Kumar AJ, Raney RB, Eftekari F. Imaging and clinical spectrum of rhabdomyosarcoma in children. *Clin Imaging* 2000:24:257-262.

9 Komdeur R, Klunder J, van der Graaf Winette TA, et al. Multidrug resistance proteins in rhabdomyosarcomas. Comparison between children and adults. *Cancer* 2003;97(8):1999-2005.

10 Koenigsberg RA, Noah R, Turtz A, et al. Rhabdomyosarcoma of the paranasal sinuses in an adult. *Clin Imaging* 1995;19:234-236.

11 Kransdorf MJ, Murphey MD. Muscle tumors. In: Kransdorf MJ, Murphey MD, eds. *Imaging of Soft Tissue Tumors* 2nd ed. Philadelphia, Pa: W.B. Saunders; 2006:298-327.

12 Kransdorf MJ, Murphey MD. Soft tissue tumors in a large referral population: prevalence and distribution of diagnoses by age, sex, and location. In: Kransdorf MJ, Murphey MD, eds. *Imaging of Soft Tissue Tumors* 2nd ed. Philadelphia, Pa: W.B. Saunders; 2006:6-37.

13 Kransdorf MJ. Malignant soft-tissue tumors in a large referral population: distribution of diagnoses by age, sex, and location. *AJR Am] Roentgenol* 1995:164:129-134.

14 Lee JH, Lee MS, Lee BH, et al. Rhabdomyosarcoma of the head and neck in adults: MR and CT findings. *AJNR Am J Neuroradiol* 1996;17: 1923-1928.

15 Lucas DR, Ryan JR, Zapulski MM, Ravindranath Y ortman B. Primary embryonal rhabdomyosarcoma of long bone. Case report and review of the literature. *Am J Surg Pathol* 1996;20:239-244.

16 Mafee MF, Pai E, Philip B. Rhabdomyosarcoma of the orbit. Evaluation with MR imaging and CT. Radio/ *Clin North Am* 1998:36:1215-1227.

17 McCarville MB, Spunt SL, Pappo AS. Rhabdomyosarcoma in pediatric patients. *AJR Am J Roentgenol* 2001 ;176:1563-1569.

18 Meyer JS, Dormans JP. Differential diagnosis of pediatric musculoskeletal masses. *Magn Reson Imaging Clin N Am* 1998;6(3):574-575.

19 Montgomery E, Barr FG. Pleomorphic rhabdomyosarcoma. In: Fletcher COM, Unni KK, Mertens F, eds. *World Health Organization Classification of Tumours. Pathology and Genetics of Tumours of Soft Tissue and Bone* Geneva: IARC Press; 2002:153-154.

20 Mulder JD, Schutte HE, Kroon HM, Taconis WK. Rhabdomyosarcoma. In: *Radiologic Atlas of Bone Tumors* Amsterdam: Elsevier; 1993: 305-309.

21 Oliveira AM, Nascimento AG. Grading in soft tissue tumors: principles and problems. *Skeletal Radiol* 2001;30:543-559.

22 Parham DM, Barr FG. Embryonal rhabdomyosarcoma. In: Fletcher COM, Unni KK, Mertens F, eds. *World Health Organization Classification of Tumours. Pathology and Genetics of Tumours of Soft Tissue and Bone* Geneva: IARC Press; 2002:146-149.

23 Parham DM, Barr FG. Alveolar rhabdomyosarcoma. In: Fletcher COM, Unni KK, Mertens F, eds. *World Health Organization Classification of Tumours. Pathology and Genetics of Tumours of Soft Tissue and Bone* Geneva: IARC Press; 2002:150-152.

24 Qualman SJ, Bowen J, Parham DM, Branton PA, Meyer WH. Protocol for the examination of specimens from patients (children and young adults) with rhabdomyosarcoma. *Arch Pathol Lab Med* 2003;127: 1290-1297.

25 Raney RB, Anderson JR, Barr FG, et al. Rhabdomyosarcoma and undifferentiated sarcoma in the first two decades of life: a selective review of intergroup rhabdomyosarcoma study group experience and rationale for Intergroup Rhabdomyosarcoma Study *V. J Pediatr Hematol Oncol* 2001;23(4):215-220.

26 Schalow EL, Broecker BH. Role of surgery in children with rhabdomyosarcoma. *Med Pediatr Oncol* 2003;41:l-6.

27 Schuck A, Mattke AC, Schmidt B, et al. Group II rhabdomyosarcoma and rhabdomyosarcomalike tumors: is radiotherapy necessary? *] Clin Oncol* 2004;22(1):143-149.

28 Siegel MJ. Magnetic resonance imaging of musculoskeletal soft tissue masses. Radio/ *Clin North Am* 2001 ;39:701-720.

29 Tsitsopoulos PD, Tsonidis CA, Nanasis KA, Tsoleka KD, Tavridis GN. Unusual course of an epidural rhabdomyosarcoma of the upper thoracic spine. *Acta Neurochir (Wien)* 1995;135:198-200.

30 Wolden SL, La TH, LaQuaglia MP, Meyers PA, Kraus DH, Wexler LH. Long-term results of three-dimensional conformal radiation therapy for patients with rhabdomyosarcoma. *Cancer* 2003;97(1):179-185.

31 Zagars GK, Ballo MT, Pisters Peter WT, et al. Prognostic factors for patients with localized soft-tissue sarcoma treated with conservation surgery and radiation therapy. An analysis of 1225 patients. *Cancer* 2003;97(10):2530-2543.

A 70 Rheumatoid Arthritis

Definition

Rheumatoid arthritis is a chronic, multisystem disease of unknown etiology in which there is persistent inflammatory synovitis that typically involves peripheral joints in a symmetric distribution.[7] The inflammatory synovitis associated with rheumatoid arthritis typically results in progressive destruction of cartilage and bone, leading to joint dysfunction.[14] Genetic factors associated with rheumatoid arthritis include HLA genes from the class II major histocompatibility complex, and genes controlling antigen receptors on T cells and immunoglobulin heavy and light chains.[7] Up to 70 % of patients have the gene product HLA-DR4.[7] Rheumatoid arthritis has also been associated with HLA-DR1 and HLA-Dwl6 in others.[7] Juvenile rheumatoid arthritis is the most frequent rheumatic disorder in children, but is less common than the adult form.[4] A new classification scheme by the International League for Rheumatology incorporates juvenile rheumatoid arthritis and juvenile chronic arthritis under the term "juvenile idiopathic arthritis."[6] Felty's syndrome is a disease that consists of chronic rheumatoid arthritis with high titers of rheumatoid factor, neutropenia (< 1500 polymorphonuclear white blood cells per microliter of blood), splenomegaly, as well as occasional thrombocytopenia and anemia.[7]

Frequency of Occurrence

Rheumatoid arthritis affects ~ 1 % of the world population.[14] The prevalence has been reported to range from 0.3 to 2.1 % of the population.[7] The incidence of juvenile rheumatoid arthritis ranges from 6 to 19.6 cases per 100 000."

Age at Presentation

Eighty percent of adult patients present between the ages of 35 and 50 years.[7] In patients with juvenile rheumatoid arthritis, patients range from 5 to 16 years, mean = 10.2 years.[4]

Gender Ratio (M |F)

Adults: 1/3.[7]

Children: 1/2.3.[4]

Location

Rheumatoid arthritis:

- **Adults.** The disease usually involves diarthrodial joints.[7] Common sites include: the proximal and middle interphalangeal and metacarpophalangeal joints, wrist, elbow, knee, shoulder, ankle, subtalar joints, and forefoot.[17] Rheumatoid arthritis may occasionally involve the atlantoaxial joint and mid-cervical levels, and rarely affects the thoracic and lumbar spine.[711] Rheumatoid arthritis can also involve tendons, tendon sheaths, and bursae.[1]
- **Children.** The knee is the most common site affected.[4] Synovial hypertrophy in the knee occurs in the suprapatellar bursa > intercondylar notch > Hoffa fat pad > posterior femoral recess > posterior tibial recess.[5,6]

Rheumatoid nodules. Common locations include olecranon bursa, proximal ulna, Achilles tendon, and occiput.[7]

Signs and Symptoms

Rheumatoid arthritis is a chronic polyarthritis that is often diagnosed within .1-2 years, mean = 9 months, after onset of symptoms.[7] Patients can have pain, swelling, tenderness, and morning stiffness for more than 1 hour at the involved joints.[7] In late stages of the disease, patients may have bony or fibrous ankylosis as well as deformities from soft tissue contractures.[7] Up to 30 % have rheumatoid nodules.[7] Synovitis at the cervical spine can result in subluxation and instability at the atlantoaxial joint and mid-cervical levels.[7]

Histopathologic Findings

Features associated with rheumatoid arthritis include hypertrophy and hyperplasia of synovial cells at the intima and subsynovial tissue associated with neovascularization, thrombosis, edema, collections of B cells and antibody-producing plasma cells, and perivascular collections of mononuclear T cells (CD4+ > CD 8+ T cells).[27] Plasma cells produce the autoantibody rheumatoid factor as well as polyclonal immunoglobulins.[7] T cells produce interleukins 2, 6, and 10; interferon *y,* granulocyte-macrophage colony stimulating factor, and tumor necrosis factor a[7] Activated macrophages produce interleukins 1,6,7, and 10, as well as interferon gamma, granulocyte-macrophage colony stimulating factor, and tumor necrosis factor a[7] These immune modulators (also referred to as cytokines and chemoldnes) are responsible for the inflammatory synovial pathology associated with rheumatoid arthritis." Activated fibroblasts producing collagenase, proteases, and cathepsins are present in the synovial lining and subsynovial tissue at the bone-cartilage interface where progressive cartilage degradation occurs.[2,7,14] In addition to the chronic inflammatory synovitis associated with rheumatoid arthritis, acute inflammation with polymorphonuclear leukocytes and exudates also occurs in the involved joints from complement activation, anaphylatoxins, and chemotactic factors.[7]

Rheumatoid nodules vary in size and contain an outer zone of granulation surrounding a middle zone of macrophages which express HLA-DR antigens, and a central zone of necrotic material with collagen fibrils and cellular debris.[7]

Findings on Plain Films (Roentgenograms) and Computed Tomography

Early findings include juxta-articular osteopenia during the first weeks or months, followed by loss of articular cartilage and bone erosions.[6,7] Serial radiographs can be of value in monitoring disease progression.[6] In later phases of the disease pannus can be associated with extensive erosions of the bone cortex as well as excavation into the marrow, resulting in zones of cystic degeneration (Figs. **466,467,470).** In the cervical spine, erosions of the dens and atlas can be seen resulting from pannus at the C1-C2 articulation, as well as upward subluxation of C 2 secondary to involvement of the transverse ligament (Fig. **463).**

MRI Findings

MRI has been shown to be superior to conventional radiographs in the detection and visualization of the synovial and osseous changes associated with the early phases of rheumatoid arthritis.[3,5,6,10] In the early phases in adults, MRI findings of active synovitis and bone erosions have been shown, respectively, in the wrist in 93 % and 80 %, in the metacarpophalangeal joints in 90% and 77%, and in the feet in 97% and 77%.' In patients with juvenile rheumatoid arthritis, synovial hypertrophy (mean = 4.8 mm) and joint effusions in the knee are the most frequent early findings.[4,5]

Hypertrophied synovium can be diffuse, nodular, and/or villous, and usually has low to intermediate or intermediate signal on T1WI and PDWI[4,6,11,14] Figs. **463, 464, 466-472).** On T2WI, hypertrophied synovium can have low to intermediate, intermediate, and/or slightly high to high signal that is typically lower than joint fluid.[4,6,11,14] The signal heterogeneity of hypertrophied synovium on T2WI is secondary to the variable amounts of vascularity, fibrin, hemosiderin, and fibrosis.[6]

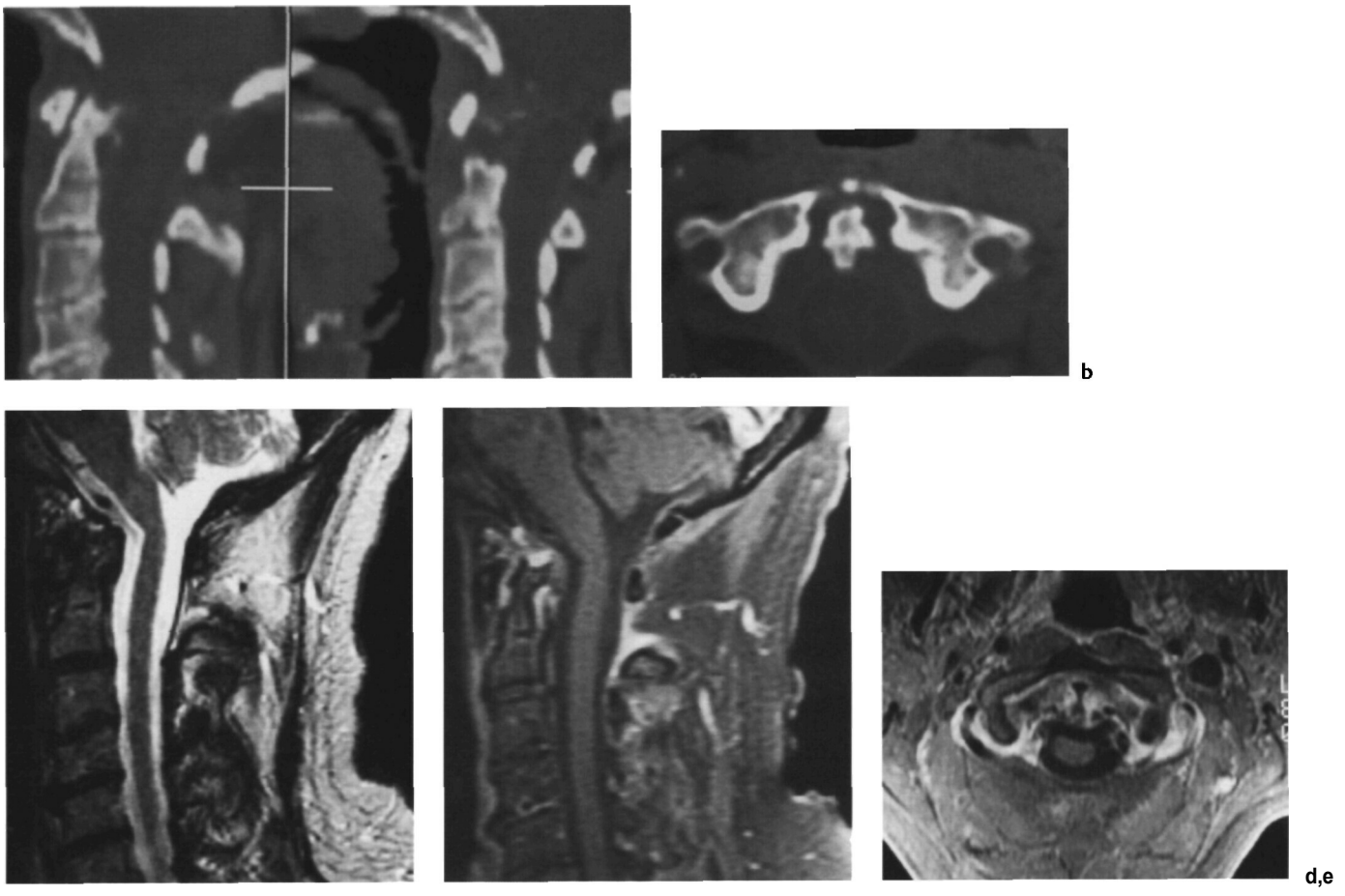

Figure **463 a-e** Pannus from rheumatoid arthritis causing erosive changes at the upper dens and atlas as seen on sagittal (**a**) and axial (**b**) CT images. The pannus has low-intermediate signal on sagittal T2WI (**c**), and shows Cd-contrast enhancement on sagittal (**d**) and axial (**e**) FST1WI.

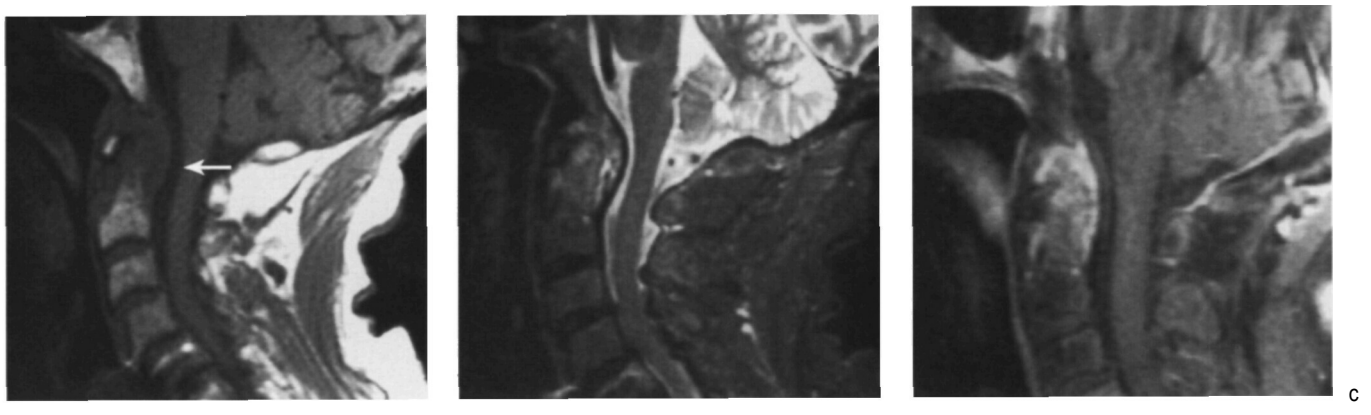

Figure 464 a-c A 72-year-old woman with pannus from rheumatoid arthritis causing erosive changes at the upper dens and atlas. The low-signal line of bone cortex at the upper dens is markedly thinned and eroded on sagittal T1WI (**a**) and FST2WI (**b**). The pannus and adjacent marrow have low-intermediate signal on T1WI and heterogeneous intermediate to slightly high signal on FST2WI. The pannus and adjacent marrow show Gd-contrast enhancement on sagittal FST1WI(**c**).

Chronic fibrotic nonvascular synovium usually has low signal on T1WI and T2WI.[6,14] After Gd-contrast administration, hypertrophied synovium can show prominent homogeneous or variable heterogeneous enhancement[4,6,11,14] (Figs. **463, 464, 469, 471).** Using dynamic Gd-contrast enhanced MRI, the rate of early contrast enhancement and relative enhancement rates of synovial membranes were found to be significantly higher for patients with active rheumatoid arthritis than those with inactive disease and controls.[2,14] It has been recommended that Gd-contrast MRI should be performed within 5 minutes of administration to optimize the contrast between the inflamed synovium and synovial fluid.[6,14] This is because synovial fluid enhancement normally begins within minutes, plateaus after 30 minutes, and persists for 1 hour.[14]

Joint effusions can be seen in both juvenile and adult rheumatoid arthritis.[4,6,13,14] The sizes of joint effusions and synovial thickness are often directly related to the clinical activity of rheumatoid arthritis.[6] Clinical improvement has been shown to be related to reductions in effusion size.[6]

In later phases of rheumatoid arthritis, MRI can show continued diffuse and/or localized zones of synovial hypertrophy; soft tissue swelling; zones of erosion, and/or destruction of hyaline cartilage, menisci, subchondral bone, tendons, ligaments; bursal fluid collections containing "rice bodies," other extra-articular cysts, intra-osseous cysticlike areas, joint effusion, and rheumatoid nodules[6,8,9,13,14] (Figs. **466-472).** Rheumatoid nodules occur in adults and are not typically seen in

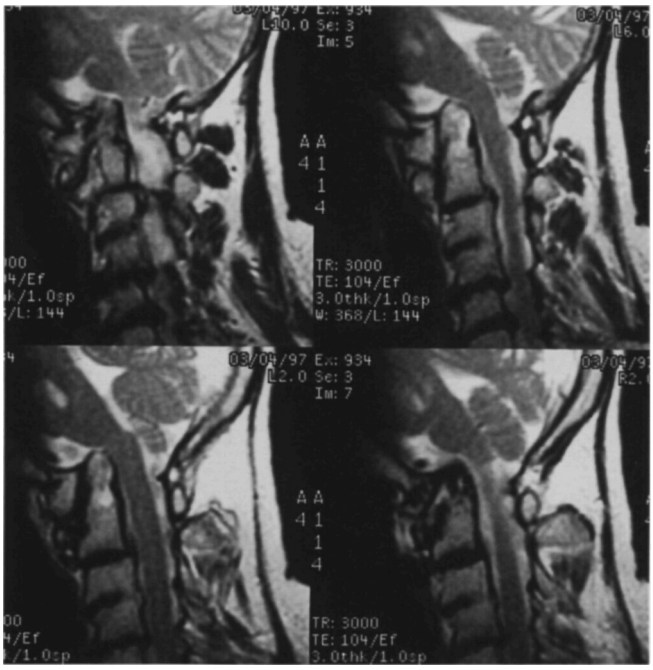

Figure **465** Basilar impression (secondary basilar invagination) resulting from destruction of the transverse ligament from pannus at the atlantodens articulation. The dens is subluxed upward through the foramen magnum on sagittal T2WI.

a

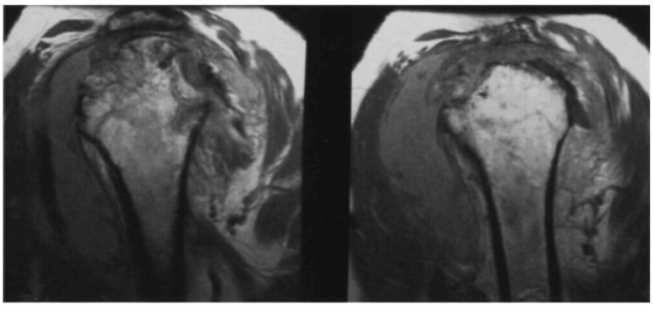

b

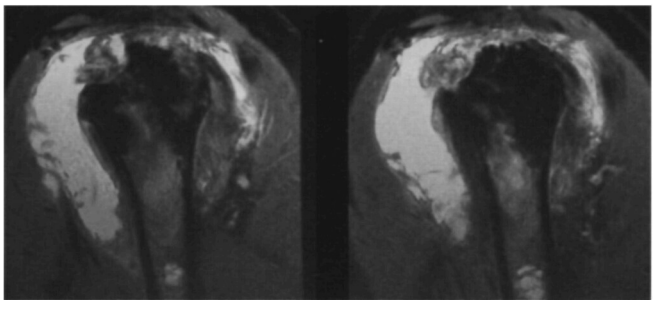

c

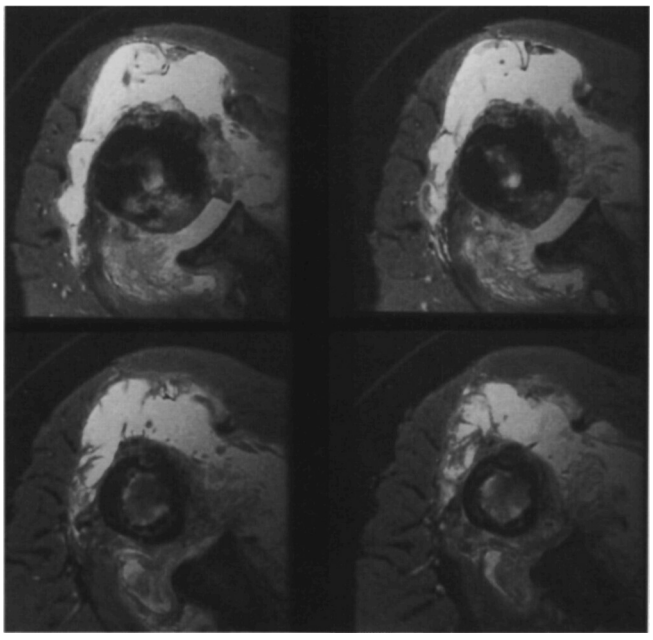

d

Figure **466 a-d** Rheumatoid arthritis involving the shoulder with pannus formation associated with erosions into the humeral head. AP radiograph (**a**) shows erosions and contour irregularity at the humeral head. With MRI, extensive erosive changes are seen at the hyaline cartilage of the glenohumeral joint. Pannus with irregular margins is seen at sites of bone erosions within a large joint effusion. The pannus has heterogeneous low-intermediate signal on sagittal PDWI (**b**), and mixed intermediate, slightly high, high and low signal on sagittal (**c**) and axial (**d**) FST2WI. Zones of increased signal on FST2WI are also seen in the marrow of the humerus near sites of cortical erosions.

a

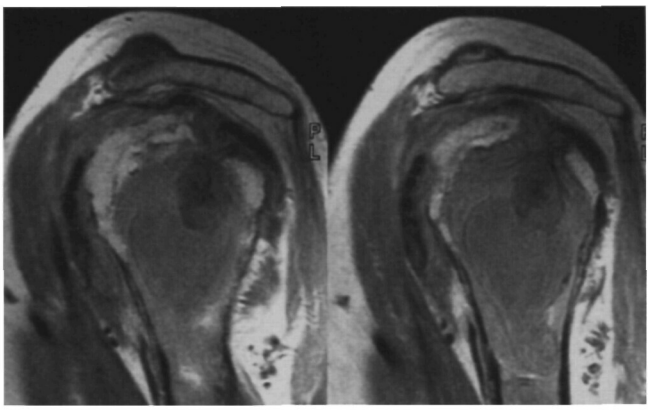

b

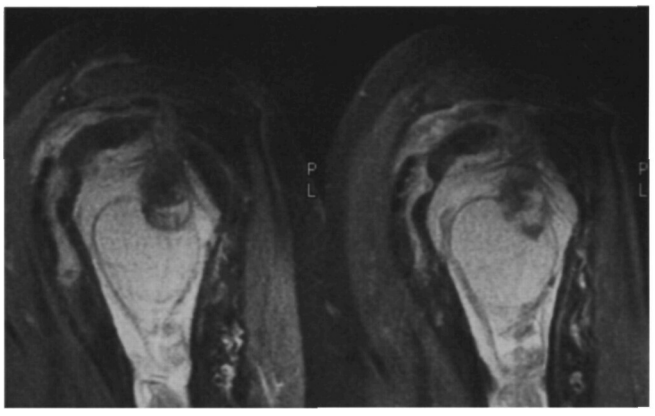

c

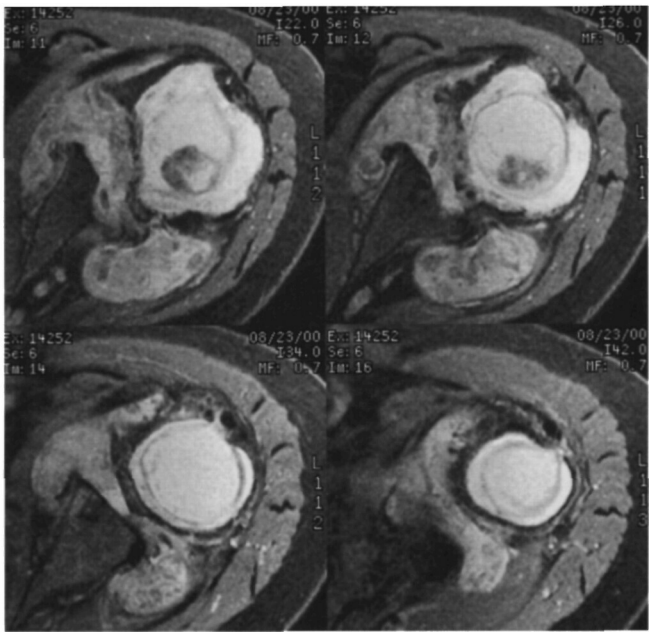

d

Figure **467a-d** A 45-year-old woman with rheumatoid arthritis involving the shoulder with pannus formation causing erosions into the humeral head, with a resultant intra-osseous cystic zone as seen on an AP radiograph (**a**). With MRI, pannus with irregular margins is seen at sites of bone erosions within a large joint effusion. Extensive erosive changes are seen at the hyaline cartilage. The pannus has heterogeneous low-intermediate signal on sagittal (**b**) PDWI, and mixed intermediate, slightly high, high and low signal on sagittal (**c**) and axial (**d**) FST2WI. A large zone with high signal on FST2WI is seen in the marrow of the humerus, representing an intra-osseous cyst.

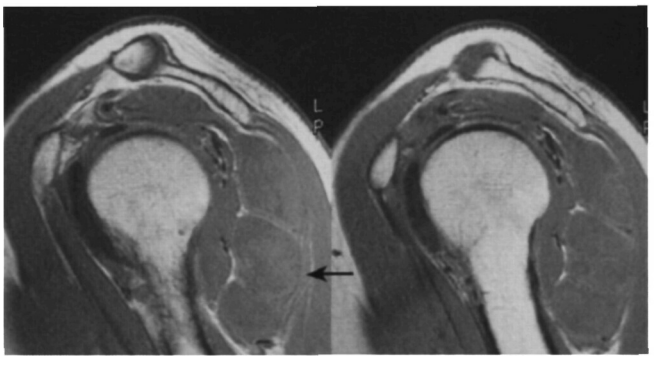

a

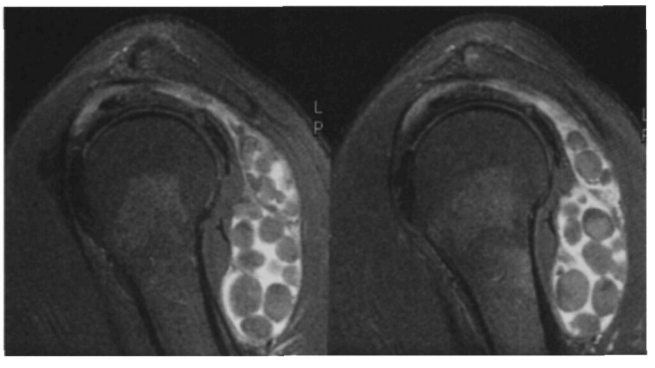

b

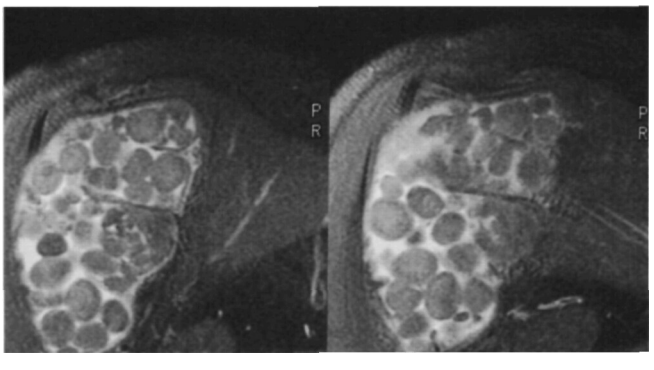

c

Figure **468a-c** A 56-year-old woman with rheumatoid arthritis involving the shoulder with hypertrophied synovium appearing as "rice bodies." The ovoid and spheroid zones of synovial proliferation have intermediate signal on sagittal PDWI (**a**), and sagittal (**b**) and coronal (**c**) FST2WI, and are located within a large effusion in the subdeltoid bursa.

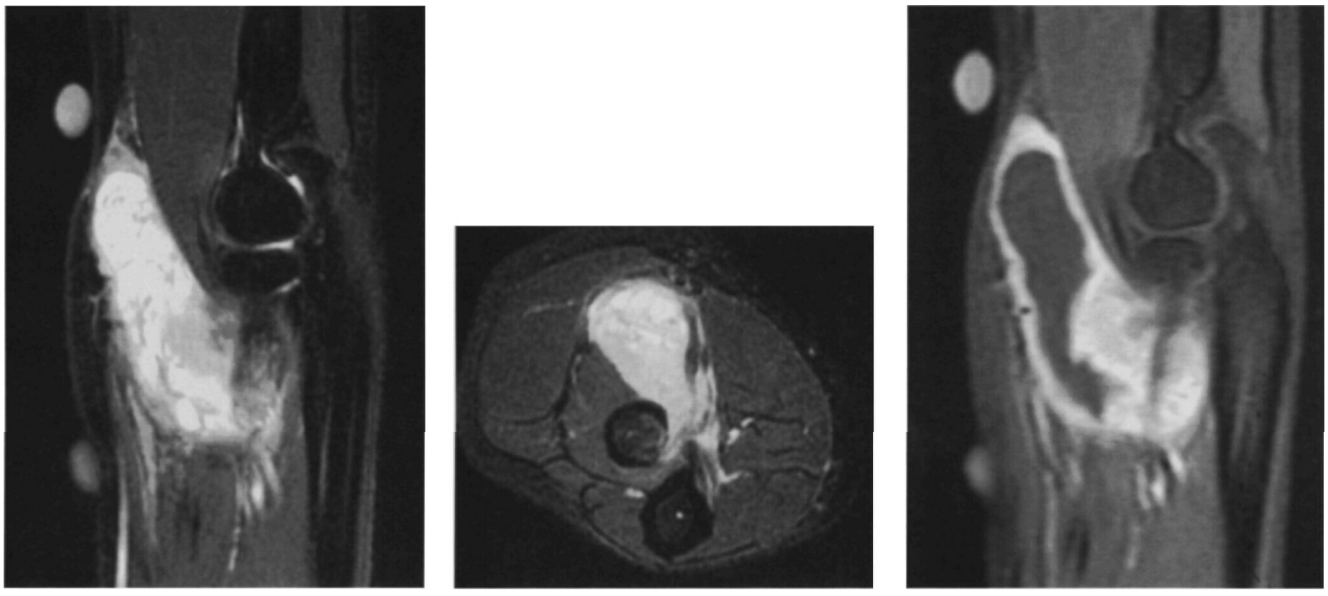

a b, c

Figure **469 a-c** 37-year-old woman with an inflammatory lesion from rheumatoid arthritis involving the antecubital bursa and biceps brachii muscle and tendon. The lesion has heterogeneous high signal on sagittal (**a**) and axial (**b**) FST2WI. The lesion shows heterogeneous Gd-contrast enhancement on sagittal (**c**) FST1WI. The lesion causes erosion of the cortex of the adjacent radius.

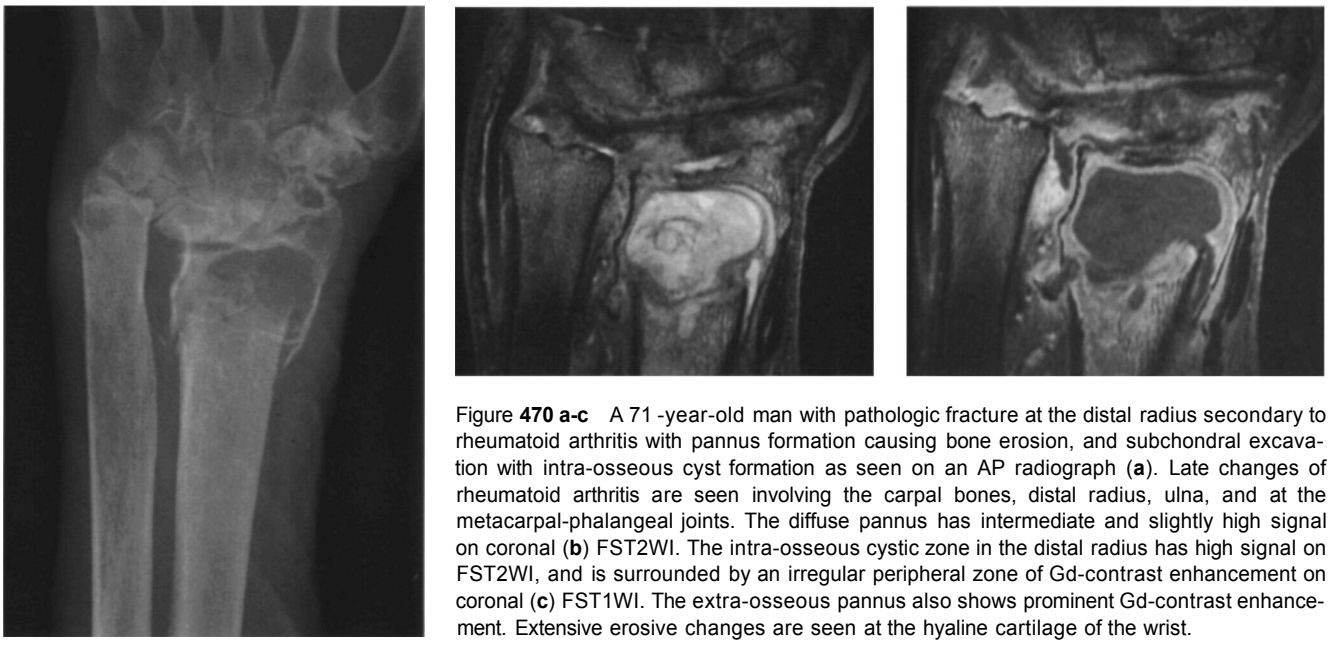

a b, c

Figure **470 a-c** A 71 -year-old man with pathologic fracture at the distal radius secondary to rheumatoid arthritis with pannus formation causing bone erosion, and subchondral excavation with intra-osseous cyst formation as seen on an AP radiograph (**a**). Late changes of rheumatoid arthritis are seen involving the carpal bones, distal radius, ulna, and at the metacarpal-phalangeal joints. The diffuse pannus has intermediate and slightly high signal on coronal (**b**) FST2WI. The intra-osseous cystic zone in the distal radius has high signal on FST2WI, and is surrounded by an irregular peripheral zone of Gd-contrast enhancement on coronal (**c**) FST1WI. The extra-osseous pannus also shows prominent Gd-contrast enhancement. Extensive erosive changes are seen at the hyaline cartilage of the wrist.

children.[6] Zones of cartilage erosion and/or loss can be seen with T2WI and FSPDWI.[6,14]MRI is a sensitive imaging technique for detecting erosive bony changes,[6,10-12 M] and has been shown to detect these changes up to 1 year earlier than conventional radiography.[10] Erosive changes in subchondral bone appear as zones of low signal on T1WI and high signal on T2WI.[6,13,14] Contrast enhancement is often seen within the erosions.[14] Bone marrow edema is often seen in the bone marrow near the involved joints, and is best visualized with STIR and FST2WI.[6]

Rheumatoid synovium can involve tendon sheaths, tendons, and ligaments[6,8,9,13,14] (Fig. **471).** With tendon and ligament involvement, abnormal increased signal is seen on PDWI and T2WI.[14] Tendons and ligaments may be thickened from partial tearing, or thinned.[14] Progression of disease can lead to tendon rupture.[14] Tenosynovitis is usually seen with fluid and hypertrophied synovium within tendon sheaths.[14]

Rheumatoid arthritis involving the cervical spine often occurs at the atlantoaxial joint where there is synovial hypertrophy, erosions of the upper dens and atlas, and widening of the atlanto-dens distance (>5mm) secondary to laxity of the transverse ligament and/or pannus[6,11,14] (Figs. **463-465).** Basilar impression (secondary basilar invagination) can occur from destruction of the transverse ligament by pannus at the atlanto-dens articulation resulting in upward subluxation of the dens (Fig. **465).** Involvement of the apohyseal joints can result in bony fusion, which occurs most frequently at the C2-C3 level.[6]

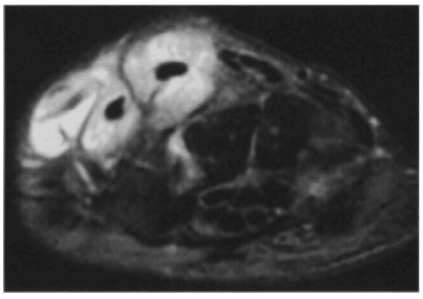

a

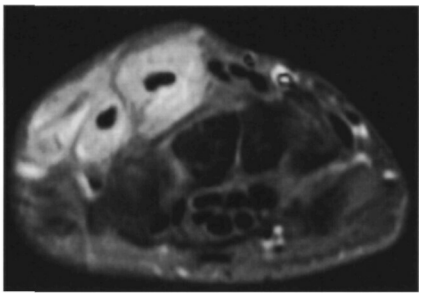

b

Figure **471 a, b** A 48-year-old woman with rheumatoid arthritis. Hypertrophied synovium (pannus) is seen in the tendon sheaths of the extensor carpi radialis brevis and longus tendons. The pannus has heterogeneous intermediate to high signal on axial FST2WI (**a**). The pannus shows prominent Cd-contrast enhancement on axial FST1WI (**b**).

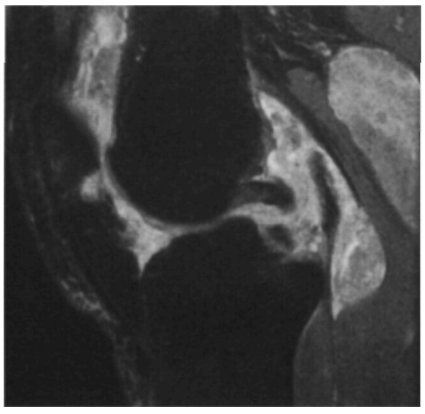

Figure 472 A 41-year-old woman with rheumatoid arthritis involving the knee with hypertrophied synovium in the joint as well as in a Baker cyst. The pannus has intermediate to slightly high signal on sagittal FST2WI. Erosions of the hyaline cartilage and a joint effusion are also seen.

Differential Diagnosis

Infection, reactive arthritis, other inflammatory arthropathies, hemophilia, nodular synovitis, pigmented villonodular synovitis.

Prognosis and Treatment

Features associated with a worse prognosis include: radiographic findings of bone erosions at diagnosis; gender (females greater than males); persistent active disease for more than 1 year; and high titers of rheumatoid factor, C-reactive protein, and haptoglobin.[7] Up to 70 % of patients have abnormal radiographic findings at involved joints.[7] Joint function is most affected in the first 2 years.[7] Treatment often consists of various combinations of nonsteroidal anti-inflammatory drugs, glucocorticoids, disease modifying antirheumatic drugs (D-penicillamine, sulfasalazine, methotrexate, and antimalarials), immunosuppressive and cytotoxic drugs (cyclophosphamide, azathioprine, cyclosporin, etc.), and newer drugs such as antibodies against tumor necrosis factor.[7] Complications such as gastrointestinal bleeding and infection can occur from analgesic and immunosuppressant treatment.[7] Other complications include osteonecrosis, stress fracture, and tendon ruptures.[9] MRI is now the optimal imaging method to assess responses to treatment.[14] Pannus at the atlantoaxial joint can lead to subluxations with compression of the brainstem, spinal cord and/or vertebral arteries.[14] Surgical fusion may be required to decompress and stabilize the spine in these situations.[14]

References

1 Boutry N, Larde A, Lapegue F, Solau-Gervais E, Flipo RM, Gotten A. Magnetic resonance imaging appearance of the hands and feet in patients with early rheumatoid arthritis. *J Rheumatol* 2003;30: 671-679.

2 Cimmino MA, Innocent! S, Livrone F, Magnaguagno F, Silvestri E, Garlaschi G. Dynamic gadolinium-enhanced magnetic resonance imaging of the wrist in patients with rheumatoid arthritis can discriminate active from inactive disease. *Arthritis Rheum* 2003;48(5): 1207-1213.

3 Goldbach-Mansky R, Mahadevan V, Yao L, Lipsky PE. The evaluation of bone damage in rheumatoid arthritis with magnetic resonance imaging. C/in *Exp Rheumatol* 2003; 21(5, Suppl 31)S50-S53.

4 Gylys-Morin VM, Graham TB, Blebea JS, et al. Knee in early juvenile rheumatoid arthritis: MR imaging findings. *Radiology* 2001 ;220: 696-706.

5 Johnson K, Wittkop B, Haigh F, Ryder C, Gardner-Medwin JM. The early magnetic resonance imaging features of the knee in juvenile idiopathic arthritis. C/in Radio/ 2002;57:466-471.

6 Johnson K, Gardner-Medwin J. Childhood arthritis: classification and radiology. Cfin Radio/ 2002;57:47-58.

7 Lipsky PE. Rheumatoid arthitis. In: Fauci AS, Braunwald E, Isselbacher KJ, et al, eds. *Harrison's Principles of Internal Medicine* 14th ed. New York, NY: McGraw-Hill; 1998:1880-1888.

8 Moran M, Fang C, Paul A. Rheumatoid arthritis presenting as an invasive soft-tissue tumour. *Arch Orthop Trauma Surg* 2002;122 (9-10):538-540.

9 Narvaez JA, Narvaez J, Roca Y, Aguilera C. MR imaging assessment of clinical problems in rheumatoid arthritis, fur *Radial* 2002;12(7): 1819-1828.

10 Ostergaard M, Hansen M, Stoltenberg M, et al. New radiographic bone erosions in the wrists of patients with rheumatoid arthritis are detectable with magnetic resonance imaging a median of two years earlier. Arthritis *Rheum* 2003;48(8):2128-2131.

11 Stiskal MA, Neuhold A, Szolar DH, et al. Rheumatoid arthritis of the craniocervical region by MR imaging: detection and characterization. *AJRAm] Roentgenol* 1995; 165:585-592.

12 Taouli B, Zaim S, Peterfy CG, et al. Rheumatoid arthritis of the hand and wrist: comparison of three imaging techniques. *AJR Am J Roentgenol* 2004;182(4):937-943.

13 Wakefield RJ, Kong KO, Conaghan PG, Brown AK, O'Connor PJ, Emery P. The role of ultrasonography and magnetic resonance imaging in early rheumatoid arthritis. C/in *Exp Rheumatol* 2003; 21(5, Suppl 31)S42-S49.

14 Winalski CS, Palmer WE, Rosenthal DI, Weissman BN. Magnetic resonance imaging of rheumatoid arthritis. Radio/ C/in North *Am* 1996;34:243-258.

Sarcoid

Definition

Sarcoidosis is a chronic systemic granulomatous disease of unknown etiology in which noncaseating granulomas occur in various tissues and organs.[1,3,5,7,9,10] Sarcoidosis appears to be related to an abnormal or exaggerated cellular immune response induced by T helper cells to antigens or self-antigens, resulting in the collection of large numbers of activated T cells in the affected tissue.[2]

Frequency of Occurrence

Sarcoidosis is relatively common with a prevalence of between 10 and 40 per 100000 population in the United States.[2] Most patients in the United States with Sarcoidosis are African-Americans, in whom the disease occurs 10 to 17 times more frequently than in Caucasians.[2]

Age at Presentation

Most patients present between the ages of 20 and 40 years.[2]

Gender Ratio

Males are affected slightly less than females.[2]

Location

Lesions commonly occur in the lungs, lymph nodes (mediastinal and hilar > neck and abdomen), liver, spleen, skin and eyes.[1,5,7] Sarcoid involving the skeleton occurs in 1-15% of patients with sarcoidosis.[57] Bones of the hands and feet are common sites of involvement, but any bone can be affected.[2] Sarcoid involving the spine often occurs as multiple lesions, with the thoracic spine being the most common location.[1] Sarcoid can also involve muscles, joints, tendons and tendon sheaths, and subcutaneous fat.[2,7] Sarcoid involving joints can cause a granulomatous synovitis (Lofgren syndrome) and usually involves multiple joints.[7]

Signs and Symptoms

The clinical manifestations of this systemic disease depend on the extent and organs involved. Asymptomatic sarcoid occurs in up to 20% of cases.[2] Acute or subacute sarcoid occurs in 20-40 % of cases and is associated with constitutional symptoms such as fever, malaise, and weight loss over several weeks.[2] The insidious form of sarcoid accounts for 40-70 % of cases and develops over months.[2] Patients present with respiratory complaints from pulmonary involvement usually without associated constitutional symptoms.[2] Patients with the insidious form of sarcoid account for most cases of chronic sarcoid.[2] Patients with musculoskeletal sarcoid may be asymptomatic or present with bone and joint pain, and soft tissue swelling.[3,7] Pain associated with musculoskeletal sarcoid is usually unresponsive to analgesics and nonsteroidal anti-inflammatory drugs.[9] Patients with sarcoid involving the spine may present with pain with or without compression of the spinal cord and/or nerve roots[1,3,9]

Cross Pathologic Findings

Sarcoid can appear as solid, gray-pinkish soft tissue.[1]

Histopathologic Findings

In the early phase of sarcoid, focal accumulations of mononuclear inflammatory cells such as T helper lymphocytes and mononuclear phagocytes occur.[2] Subsequently, aggregates of macrophages, epithelioid cells, and multinucleated giant cells form a sarcoid granuloma at the involved site.[2] The sarcoid granuloma has a compact configuration composed of mononuclear phagocytes, multinucleated giant cells, and fine collagen fibrils surrounded by rim of T helper-inducer lymphocytes and occasional B lymphocytes.[2] With effective therapy, the mononuclear inflammation is reduced and replaced by centripetal fibroblastic proliferation, resulting in progressive fibrosis and scar formation.[2] Distortion and direct physical damage from the sarcoid granulomas can cumulatively affect the function of the involved tissue or organ.[2] Sarcoid granulomas, however, are not typically associated with the release of mediators that cause damage to cells and extracellular matrix in the involved tissue or organ.[2] The diagnosis of sarcoid is made by demonstration of noncaseating granulomas and the exclusion of other causes.[29]

Findings on Plain Films (Roentgenograms) and Computed Tomography

Bone[1AS_7A1o]

In small bones, lesions often have coarse trabeculation involving medullary and/or cortical bone, and are often described as having a "lacy" radiolucent appearance.[37] These radiolucent lesions may be associated with pathologic fractures.[7] Sarcoid lesions in **long bones** or involving the axial skeleton can be radiolucent with or without sclerotic margins, mixed radiolucent and sclerotic, or predominantly osteosclerotic.[13,9,10] Some sarcoid lesions are occult on plain films.[3,7,9]

MRI Findings

Bone

In **small bones,** lesions usually appear as intramedullary zones with low to intermediate signal on T1WI and slightly high to high signal on T2WI, FS PDWI, and FS T2WI.[7] Erosions and zones of destruction are often seen involving the adjacent bone cortex as well as periosseous extension of the granulomatous process.[7] Fine perpendicular lines of low signal on T1WI may be seen extending outward from the region of eroded or destroyed cortex, representing collagen separating periosseous extension of granulomas.[7] After Gd-contrast administration, lesions typically show moderate to prominent enhancement.[7]

In **long bones and axial skeleton,** sarcoid lesions are often multiple with variable sizes, or solitary within marrow.[37] Zones of cortical destruction associated with intramedullary lesions are uncommon, unlike sarcoid involving small bones.[7] Lesions can have circumscribed and/or indistinct margins within marrow.[37] Irregular confluent or patchy zones as well as a diffuse stippled patterns of signal alteration in marrow have also been described for skeletal sarcoid.[7] Lesions usually have low to intermediate signal on T1WI and PDWI, and often have slightly

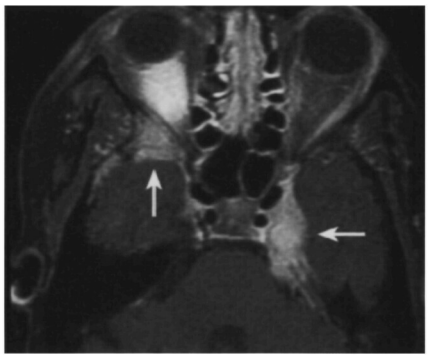

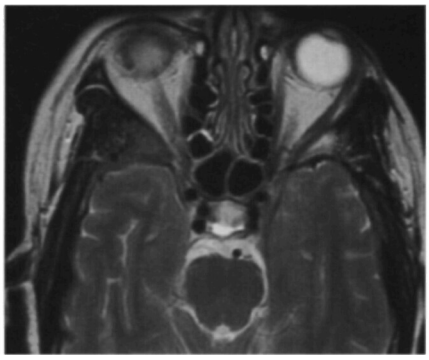

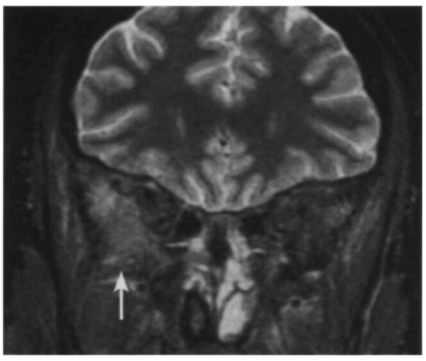

a, b c

Figure **473a-c** A 55-year-old woman with sarcoidosis and an intra-osseous lesion involving the greater wing of the right sphenoid bone. In addition, a sarcoid lesion is also present in the subarachnoid space at the left cerebellopontine angle cistern and left trigeminal cistern with encasement of the left trigeminal nerve. Both lesions show Cd-contrast enhancement on axial FST1WI (**a**). The intra-osseous lesion has intermediate signal on axial T2WI (**b**) and intermediate to slightly high signal on coronal STIR (**c**). Erosion of the cortical margins of the sphenoid bone with associated Cd-contrast enhancing dural reaction is also seen.

a, b

Figure **474a-d** A 50-year-old man with sarcoidosis and multiple intra-osseous spinal lesions. Technetium-99m diphosphonate bone scan (**a**) shows multiple foci of radiopharmaceutical accumulation in the vertebrae and ribs. Multiple zones of low-intermediate signal on sagittal T1 WI (**b**) and slightly high signal on sagittal FST2WI (**c**) are seen in multiple vertebrae. The lesions show prominent Gd-contrast enhancement on sagittal FST1WI (**d**).

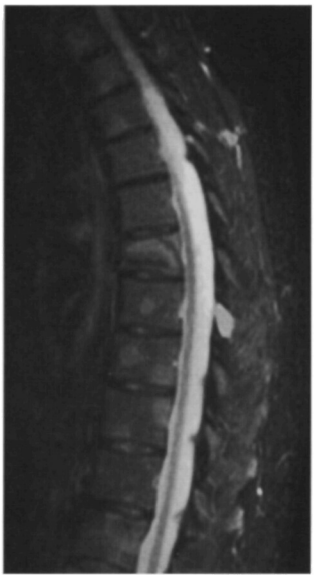

c, d

high to high signal on T2WI and FST2WI[3,7,9] (Fig. **474**). Occasional lesions may also have low or intermediate signal on T2WI.[5,7] Focal areas with MRI signal similar to fat are seen in some lesions in long bones.[7] Lesions with low signal on T2WI correspond to plain film and CT findings of osteosclerosis.[59] After Gd-contrast administration, enhancement of the lesions is typically seen[7,9] (Fig. **474**). The degree of Gd-contrast enhancement can range from minimal to prominent, and occur in diffuse, heterogeneous, and/or peripheral ringlike patterns.[3,7,9] Involvement of intervertebral discs by sarcoid is uncommon.[9]

In **the skull,** sarcoid lesions are typically within the marrow and may be associated with bone expansion and/or erosions or areas of destruction of the inner and/or outer tables with extension intracranially or into the extracranial soft tissues[7] (Fig. 473). Lesions usually have low-intermediate signal on T1WI, and intermediate to high signal on T2WI.[7] After Gd-contrast administration, enhancement of the lesions is typically seen.[7]

Soft tissue

Sarcoid can involve muscles as discrete lesions in 1.4% of cases.[7] Lesions are often nodular with low to intermediate signal on T1WI and PDWI, and intermediate to high signal on T2WI and FST2WT (Fig. 475). Some lesions have a central area of low signal on T2WI.[7] After Gd-contrast administration, enhancement of the lesions is typically seen.[7] Gd-contrast enhancement may be diffuse within the lesions or more prominent periph-

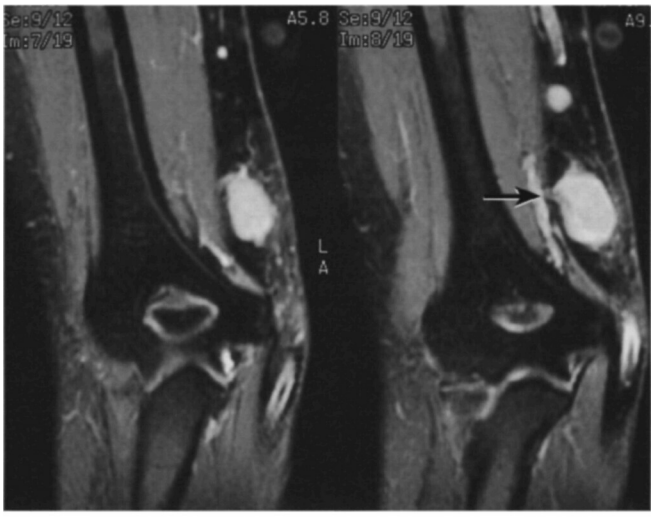

a

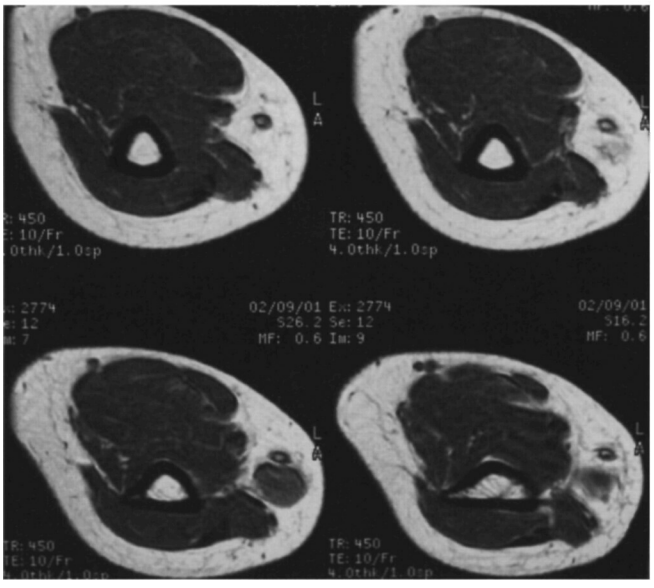

b

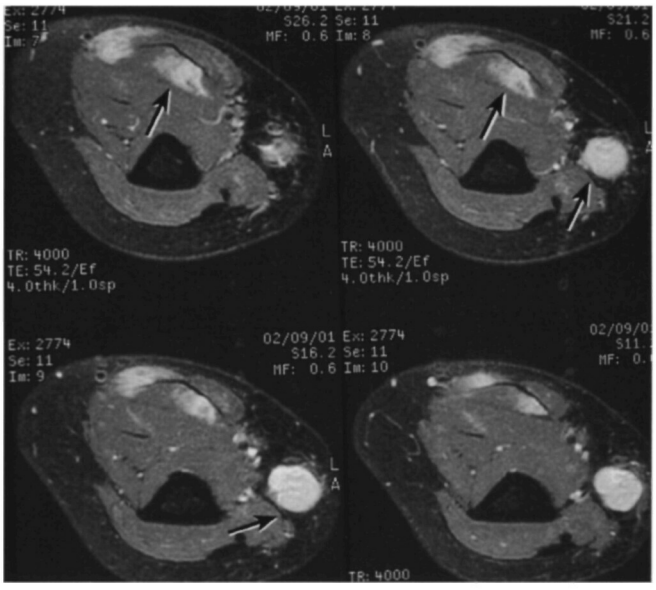

c

Figure **475**a-c A 49-year-old woman with sarcoid granulomas in the subcutaneous fat and within the biceps brachii muscle at the distal arm. The lesions show slightly irregular margins, and have high signal on coronal (**a**) and axial (**c**) FST2WI, and low to intermediate signal on axial T1WI (**b**).

erally than centrally.[7] Fatty muscle atrophy may occur as a result of sarcoidal myopathy.[7]

Sarcoid granulomas can also occur in subcutaneous fat and may be associated with superficial adenopathy[7] (Fig. **475**). Lesions are often nodular with low to intermediate signal on T1WI, and intermediate to high signal on T2WI.[7] Some lesions have a central area of low signal on T2WI.[7] After Gd-contrast administration, enhancement of the lesions is typically seen.[7]

Differential Diagnosis

Bone. Metastatic disease, eosinophilic granuloma, osteomyelitis, lymphoma, Erdheim-Chester disease, tuberous sclerosis, myeloma, tuberculosis.[7]

Soft tissue. Lymphoma, metastatic disease, tophus, pannus, xanthoma.[7]

Prognosis and Treatment

The prognosis in sarcoidosis is generally favorable.[2] Approximately 50% of patients have mild, stable, organ dysfunction induced by damage prior to treatment.[2] In 50% of cases, sarcoid clears spontaneously.[2] Up to 20% of patients have active or recurrent disease.[2] Approximately 10% of patients with sarcoid die as a direct result of this disease.[2] Glucocorticoids, calcitonin therapy, and methotrexate have been shown to be effective in the treatment of sarcoidosis.[2,6,9] Recurrent sarcoid involving the spine can result in instability requiring surgical fusion.[10]

References

1 Bundens DA, Rechtine GR. Sarcoidosis of the spine. Case report and literature review. Spine 1986;11(3):209-212.

2 Crystal RG. Sarcoidosis. In: Fauci AS, Braunwald E, Isselbacher KJ, et al., eds. *Harrison's Principles of Internal Medicine* 14th ed. New York, NY: McGraw-Hill: 1998:1922-1928.

3 Fisher AJ, Gilula LA, Kyriakos M, Holzaepfel CD. MR imaging changes of lumbar vertebral sarcoidosis. *AJR Am J Roentgenol* 1999;173: 354-356.

4 Franco M, Passeron C, Tieulie N, Verdier JF, Benisvy D. Long-term radiographic follow-up in a patient with osteosclerotic sarcoidosis of the spine and pelvis. Rev *Rhum Engl Ed* 1998;65(10):586-590.

5 JelinekJS, Mark AS, Barth WF. Sclerotic lesions of the cervical spine in sarcoidosis. *Skeletal* Radio! 1998:27(12):702-704.

6 Mana J, Gomez-Vaquero C, Dorca J, Pujol R. Vertebral and rib sarcoidosis: long-term clinical remission with methotrexate. *Clin Rheumatol* 1999;18(6):492-494.

7 Moore SL, Teirstein AE. Musculoskeletal sarcoidosis: spectrum of appearances at MR imaging. *Radiographics* 2003;23:1389-1399.

8 Poyanli A, Poyanli 0, Sencer S, Akan K, Sayrak H, .Acunas B. Vertebral sarcoidosis: imaging findings. .*EurRadiol* 2000:10(1):92-94.

9 Rua-Figueroa I, Gantes MA, Erausquin C, Mhaidii H, Montesdeoca A. Vertebral sarcoidosis: clinical and imaging findings. Semin *Arthritis Rheum* 2002;31(5):346-352.

10 Sundaram M, Place H, Shaffer WO, Martin DS. Progressive destructive vertebral sarcoid leading to surgical fusion. *Skeletal Radial* 1999; 28(12):717-722.

A 72 Schwannoma (Also Referred to as Neurilemoma and Neurinoma)

ICD-O Code

9560/0

Definition

Schwannomas are benign, encapsulated tumors that contain differentiated neoplastic Schwann cells.[26] Multiple schwannomas are often associated with neurofibromatosis type 2 (NF2), which is an autosomal-dominant disease involving a gene at chromosome 22q12.[29111S1£,232526] In addition to schwannomas, patients with NF2 can also have multiple meningiomas, gliomas, ependymomas, neurofibromas, and juvenile posterior subcapsular cataracts.[2,9,8,19,23,26] Schwannomatosis refers to a rare genetic disorder that is associated with multiple subcutaneous schwannomas.[26]

Frequency of Occurrence

Schwannomas account for 5 % of benign, primary soft tissue tumors and 3 % of all primary soft tissue tumors.[56] Schwannomas represent 8 % of primary intracranial tumors and 29 % or primary spinal tumors.[2026] As many as 63-89 % of patients with NF2 have spinal tumors: schwannomas, ependymomas, meningiomas, and ependymomas.[18] Extramedullary tumors are more frequent than intramedullary tumors in patients with NF2.[18]

The incidence of NF2 is 1 per 37 000 to 1 per 50 000 newborns worldwide.[91119] Up to half of NF2 cases are caused by germline mutations.[9]

Age at Presentation

From 22 to 72years, mean = 46years.[56] Peak incidence is in the 4th to 6th decades.[26] With NF2, many patients present in the 3rd decade with bilateral vestibular schwannomas.[9]

Gender Ratio (M/F)

Schwannomas in the extremities: 1.3 /1.[6]

Intracranial schwannomas: 1 / 1 to 1 / 2.[9]

Location

Schwannomas occur intracranially as extra-axial tumors involving cranial nerves.[239-1117-19,232526] Schwannomas commonly involve the peripheral nerves of the head and neck, and also occur as extramedullary tumors in the spine.[239-1117-20232526] Schwannomas rarely occur within brain or spinal cord.[20,26] Schwannomas most frequently involve sensory nerves, and occasionally involve motor or autonomic nerves.[26]

Schwannomas are also commonly located in the soft tissues of the extremities, and rarely occur within bone.[1416] For **schwannomas in the extremities** the decreasing frequency of occurrence is lower extremity > trunk > upper extremity > retroperitoneum > head and neck > foot and ankle > hand and wrist > hip and buttocks > other sites.[6]

Rare, **intra-osseous schwannomas** have been reported in the mandible, tibia, scapula, maxilla, vertebral bodies, femur, metacarpal bones, and humerus.[121316]

Signs and Symptoms

Vestibular schwannomas are associated with progressive sensorineural hearing loss, tinnitus, and facial parathesias.[1926]

Nonvestibular schwannomas can be associated with cranial nerve dysfunction secondary to compression of the specifically-involved cranial nerve.[9] Usually sensory nerves are affected more than motor nerves.[9]

Spinal schwannomas can be associated with compression of the spinal cord or dorsal nerve roots.[1922] Spinal schwannomas may be detected as incidental findings on MRI or CT examinations.[26]

Schwannomas in the extremities can present as painless, slow-growing lesions that are usually less than 10 cm in size.[1526] Large schwannomas can cause pain and neurologic symptoms.[15]

Cross Pathologic Findings

Schwannomas are often encapsulated, tan and/or yellow lesions that may contain cystic zones and/or hemorrhage.[26] Necrosis is typically absent.[26] Infarction of schwannomas can occur rarely.[22]

Histopathologic Findings

Schwannomas contain spindle-shaped neoplastic Schwann cells with ovoid nuclei within abundant slightly eosinophilic cytoplasm.[26] Nuclear pleomorphism and infrequent mitotic figures may be seen occasionally.[26] Tumor cells can have two types of arrangements (Antoni A and Antoni B).[1526] Varying proportions of Antoni A and B regions are often seen within each schwannoma.[15] The Antoni A pattern occurs when the elongated tumor cells are densely packed in fascicles with or without nuclear pallisading (parallel arrays of tumor cell nuclei).[26] Cytoplasmic processes and hypereosinophilic basement membranes between regions of nuclear pallisading are referred to as Verocay bodies. The Antoni B pattern occurs when there is a low density of tumor cells within a loose meshwork of myxoid and/or xanthomatous material.[26] Schwannomas typically show immunoreactivity to S-100 protein, and may show reactivity to Leu-7 and glial fibrillary acidic protein.[26] Large schwannomas often have degenerative features such as fibrosis, cyst formation, hemorrhage, and/or calcification.[15] Malignant transformation of schwannomas is rare.[1526]

Several variant subtypes of schwannoma occur.[26] **Cellular schwannomas** are variant hypercellular tumors containing only Antoni A tissue without Verocay bodies.[26] **Melanotic schwannomas** are pigmented and contain melanosomes.[26] **Plexiform schwannomas** are rare variants which occur predominantly in the skin, and are associated with NF2 and schwannomatosis.[26]

Lesion Genetics

Multiple schwannomas are often associated with NF2, which is an autosomal-dominant disease involving a gene at chromosome 22ql2[2,9-11,18,19,23,25,26] The gene product is referred to as schwannomin or merlin (a moesin-, ezrin-, and radixin-Hke protein) which encodes a polypeptide that is involved in linking plasma membrane proteins to cytoskeletal elements.[19] The NF2 gene is considered to be a classic tumor suppressor gene in which both alleles need to be defective for tumorigenesis.[19] Patients with NF2 have only one normal allele, so tumors will form if there are mutations or deletions in the remaining normal gene.[19]

Findings on Plain Films (Roentgenograms) and Computed Tomography s.[8].'"-[16]

Schwannomas may or may not be seen on radiographs as areas of localized soft tissue swelling.[3,8,14-16] Schwannomas may be associated with adjacent chronic bony changes such as widening of intervertebral foramina, and scalloping of the dorsal or dorsal lateral aspects of vertebral bodies. CT of schwannomas usually shows circumscribed lesions with low and/or intermediate attenuation, which usually show enhancement.[3,8,14,15] Large lesions often have areas of low attenuation secondary to cystic degeneration and/or prior hemorrhage.[8,15] Dystrophic calcifications can be seen with long-standing schwannomas.[8] Rarely, schwannomas can occur as intra-osseous lesions.[14,16] Intra-osseous schwannomas are usually well-defined, radiolucent lesions that are only rarely associated with pathologic fracture.[16]

MRIFindings[1-4,7-9,15,16,19-22,24]

Schwannomas are circumscribed, ovoid or fusiform lesions with low-intermediate signal on T1VVI, intermediate signal on PDWI, and intermediate to high signal on T2W1 and FS T2WT-[4,8,9,15,16,19,22] (Figs. **476-482).** After Gd-contrast administration, lesions typically show moderate to prominent enhancement (Figs. **476-482).** Schwannomas involving spinal nerve roots may be associated chronic erosive changes of adjacent vertebrae. Rare schwannomas that are acutely infarcted may not show Gd-contrast enhancement.[22] Lesions may show signal heterogeneity on T2WI and heterogeneous Gd-contrast enhancement secondary to cyst formation, hemorrhage, fibrous/collagenous zones, and/or dense cellularity. Signal heterogeneity on T2WI tends to occur frequently in large schwannomas. Malignant schwannomas (malignant peripheral nerve sheath tumors) can be large lesions which have heterogeneous signal on T1WI, T2WI, and FST2WI; as well as heterogeneous Gd-contrast enhancement because of necrosis and hemorrhage (Figs. **483, 484).** These tumors can have irregular margins and associated invasion of adjacent structures (Fig. **483).**

Differential Diagnosis

VestibularSchwannoma. Neurofibroma,meningioma,ependymoma, paraganglioma, metastatic disease, nodular extra-axial granulomas (sarcoid, tuberculosis).

Nonvestibular intracranial schwannoma. Neurofibroma, meningioma, ependymoma, choroid plexus papilloma, choroid plexus carcinoma, paraganglioma, metastatic disease, nodular extra-axial granulomas (sarcoid, tuberculosis).

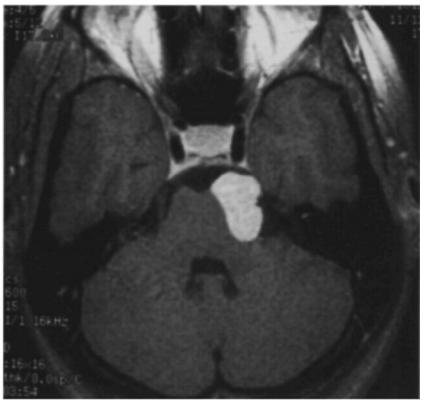

Figure **476a, b** A 17-year-old female with a Schwannoma involving the left trigeminal nerve. The extra-axial lesion has circumscribed margins and has high signal on axial T2WI (**a**). The tumor shows prominent Gd-contrast enhancement on axial FST1WI (**b**).

Figure 477 a, b A 28-year-old woman with a Schwannoma involving the vestibular nerve (acoustic neuroma). The extra-axial lesion in right cerebellopontine angle cistern extends into, and widens, the right internal auditory canal. The lesion has heterogeneous mostly high signal on axial T2WI (**a**), and shows prominent Gd-contrast enhancement on axial FST1WI (**b**).

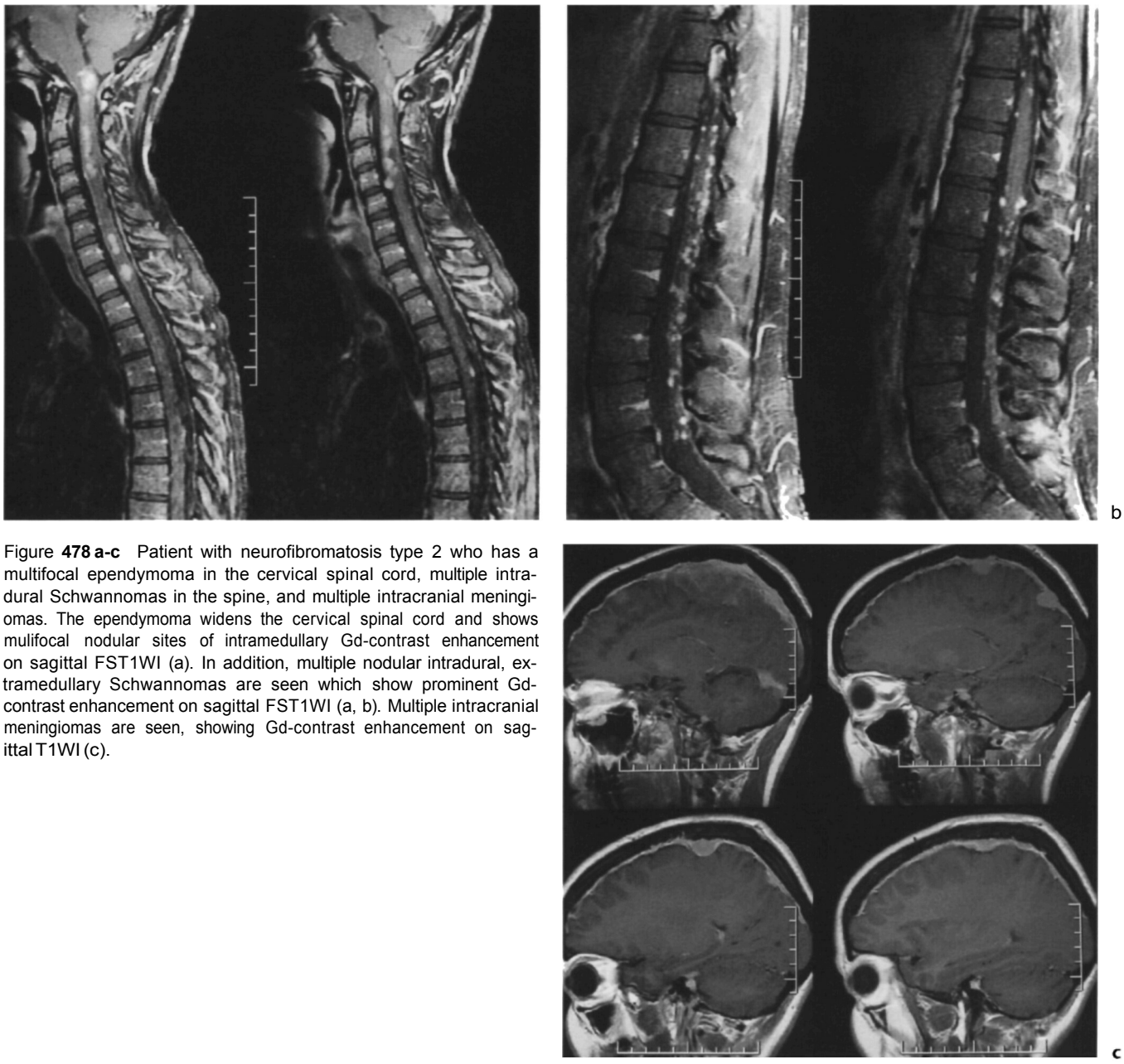

Figure **478 a-c** Patient with neurofibromatosis type 2 who has a multifocal ependymoma in the cervical spinal cord, multiple intradural Schwannomas in the spine, and multiple intracranial meningiomas. The ependymoma widens the cervical spinal cord and shows mulifocal nodular sites of intramedullary Gd-contrast enhancement on sagittal FST1WI (a). In addition, multiple nodular intradural, extramedullary Schwannomas are seen which show prominent Gd-contrast enhancement on sagittal FST1WI (a, b). Multiple intracranial meningiomas are seen, showing Gd-contrast enhancement on sagittal T1WI (c).

Spinal schwannoma. Neurofibroma, meningioma, ependymoma, paraganglioma, ganglioneuroma, neuroblastoma, ganglioneuroblastoma.

Schwannoma in the extremities. Neurofibroma, malignant nerve sheath tumor, neurofibrosarcoma, leiomyoma, synovial sarcoma, leiomyosarcoma, rhabdomyosarcoma, Kaposi sarcoma, malignant fibrous histiocytoma, lymphoma, metastatic disease.

Prognosis and Treatment

Schwannomas are benign, slow-growing tumors that rarely show malignant transformation.[15-26]

Vestibular schwannomas have variable growth rates, and patients may or may not have irreversible hearing loss at diagnosis. Patients are usually treated with surgery or stereotactic radiosurgery. Vestibular schwannomas in patients with NF2 are often treated with surgery, even when these lesions are small, to preserve hearing or minimize hearing loss."

Nonvestibular cranial nerve schwannomas have unpredictable growth rates.[19] Surgical resection or stereotactic radiosurgery is typically performed for large lesions with progressive growth and/or associated neural compression.[19]

Spinal schwannomas are typically treated with surgical resection, for tumors causing compression of the spinal cord or nerves.[19] Resection of spinal schwannomas can usually be achieved with minimal neurologic morbidity because these tumors typically arise from only a single nerve fascicle.[19] In patients with NF2, extramedullary tumors were more frequent and associated with a higher rate of surgery than intramedullary tumors.[18]

Schwannomas in the extremities are typically treated by surgical excision.[15] Schwannomas can be usually separated and removed from the nerve after incision of the epineurium resulting in preservation of nerve function.[15]

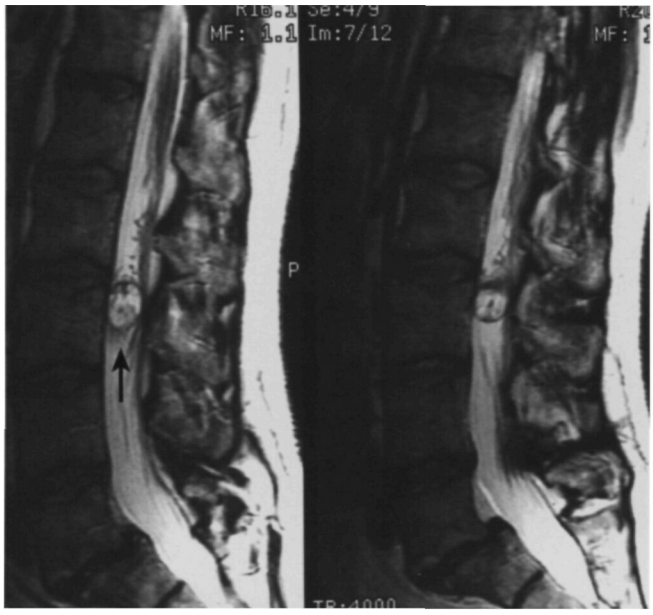

a

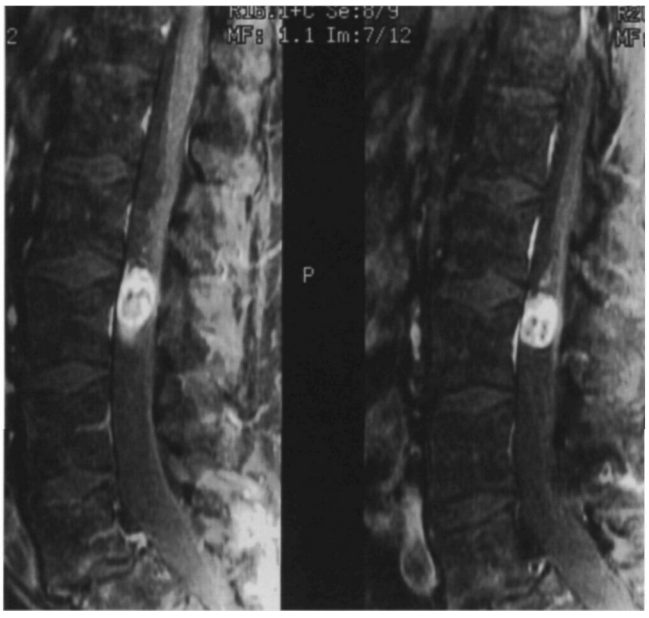

b

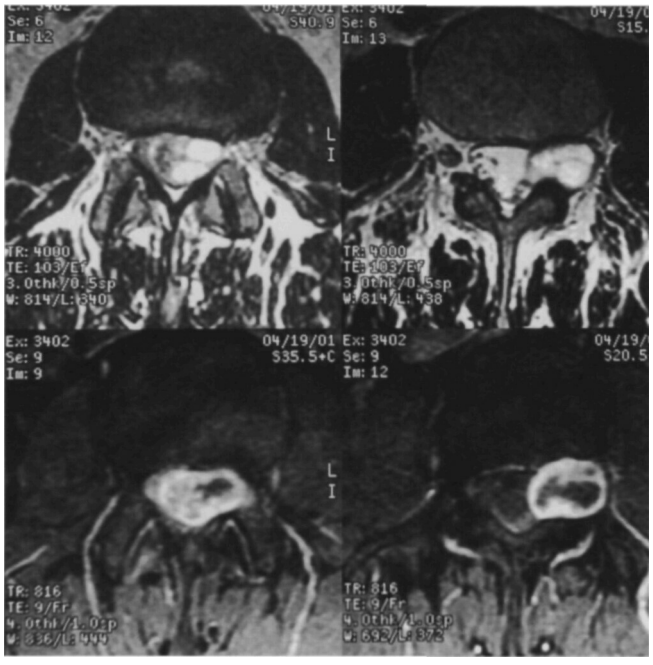

c

Figure **479 a-c** Solitary intradural Schwannoma in the lumbar spine at the upper L3 level. The lesion has heterogeneous high signal on sagittal (**a**) and axial (**c**, upper images) T2WI, and shows prominent heterogeneous Cd-contrast enhancement on sagittal (**b**) FST1WI and axial FS T1WI (c, lower images).

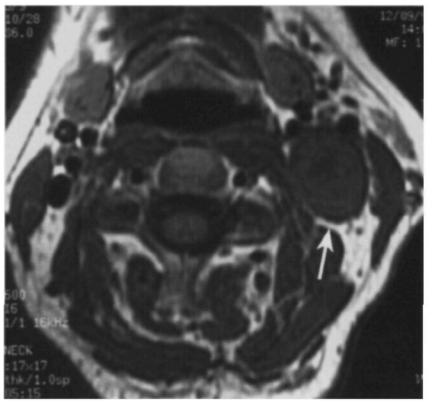

a, b

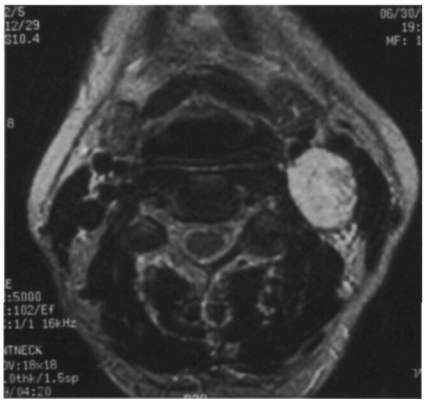

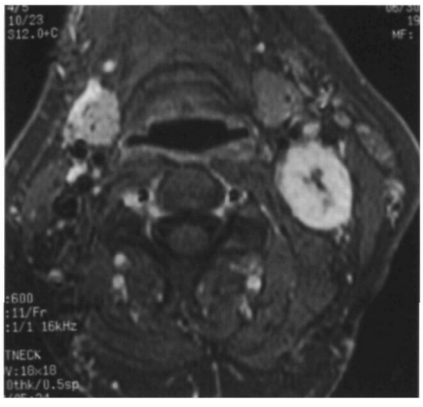

c

Figure **480a-c** A 47-year-old woman with a Schwannoma in the neck displacing the carotid arteries anteriorly. The circumscribed lesion has low-intermediate signal on axial T1WI (**a**) and has high signal on axial T2WI (**b**). The Schwannoma shows prominent Cd-contrast enhancement on axial (**c**) FST1WI.

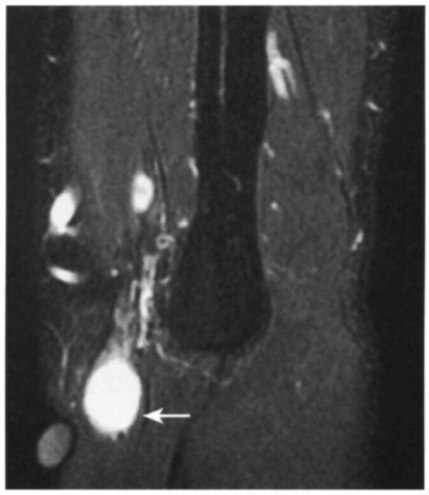

a

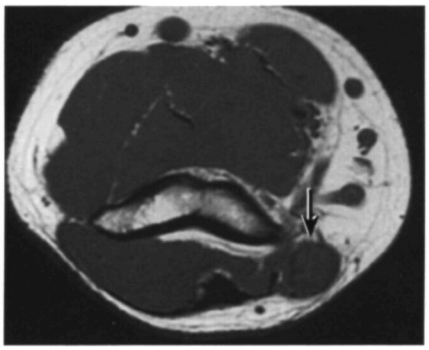

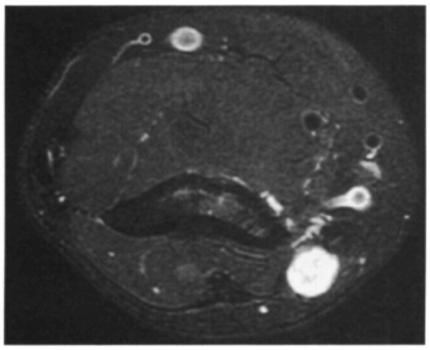

b, c

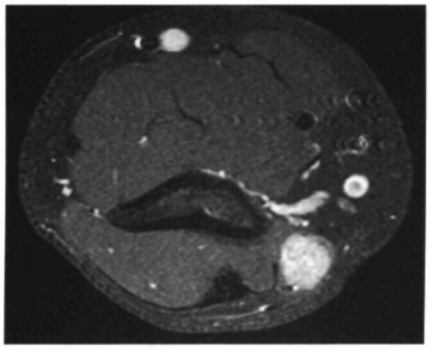

d

Figure **481 a-d** A 37-year-old man with a Schwannoma in the proximal forearm. A well-circumscribed ovoid lesion is seen at the ulnar nerve, which has high signal on coronal (**a**) and axial (**c**) FST2WI, and intermediate signal on axial (**b**) T1WI. The Schwannoma shows prominent Gd-contrast enhancement on axial (**d**) FST1WI. Slight thickening of the median nerve is seen distal to the Schwannoma.

a

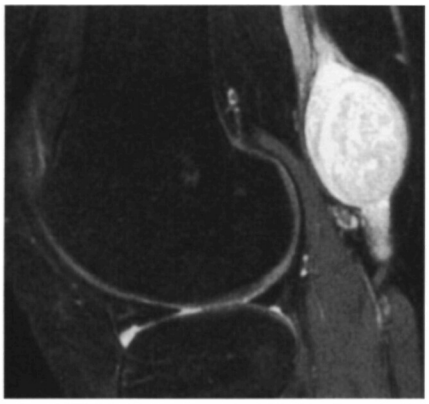

b

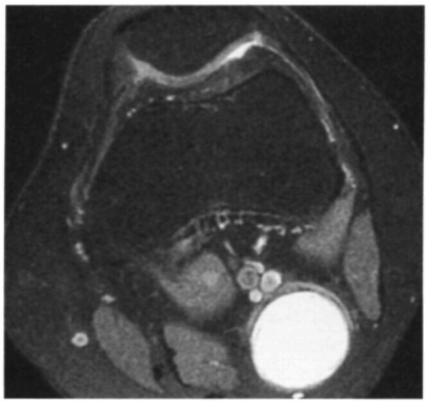

c

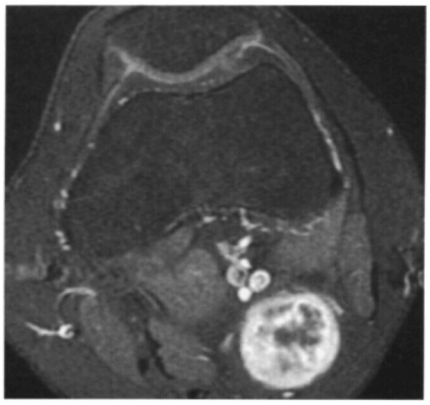

d

Figure **482 a-d** A 17-year-old female with a Schwannoma involving the tibial nerve at the dorsal knee. A well-circumscribed ovoid lesion is seen along the nerve, which has intermediate signal on sagittal (**a**) PDWI, and high signal on sagittal (**b**) and axial (**c**) FS **T2WI**. The Schwannoma shows prominent Gd-contrast enhancement on axial (**d**) FS **T1WI**. Slight thickening of the tibial nerve is seen proximal and distal to the Schwannoma.

Figure **483** A 49-year-old man with a malignant peripheral nerve sheath tumor arising from a benign Schwannoma. The large left paraspinal tumor shows irregular Gd-contrast enhancement. Small zones of abnormal contrast enhancement are seen in two vertebral bodies secondary to tumor invasion.

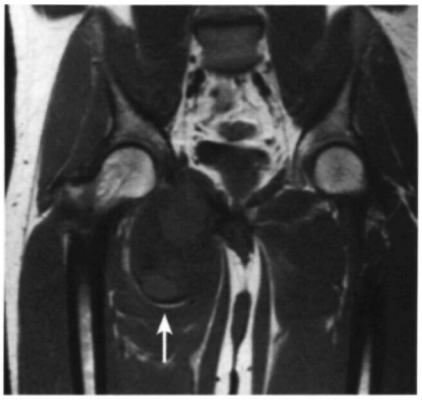

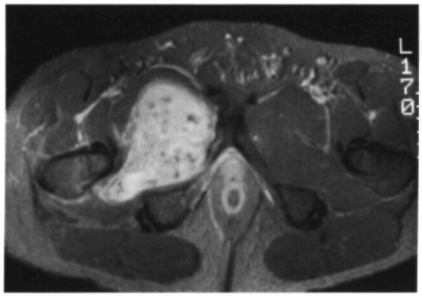

c

a, b

Figure **484a-c** A 48-year-old man with a malignant peripheral nerve sheath tumor (malignant Schwannoma) in the upper medial right thigh and groin region. The lesion has mixed intermediate and slightly high signal on coronal T1WI (**a**), and high signal on coronal STIR (**b**). High signal zones within the tumor on T1WI represent sites of hemorrhage. The tumor shows mildly heterogeneous, prominent Gd-contrast enhancement on axial FST1WI (**c**).

References

1 Abe T, Kawamura N, Homma H, Sasaki K, Izumiyama H, Matsumoto K. MRI of orbital schwannomas. *Neuroradiology* 2000;42(6): 466-468.

2 Aoki S, Barkovich AJ, Nishimura K, et al. Neurofibromatosis types 1 and 2: cranial MR findings. *Radiology* 1989;172:527-534.

3 Aydin K, Maya MM, Lo William WM, Brackmann DE, Kesser B. Jacobson's nerve schwannoma presenting as middle ear mass. AJNRAmJNeuroradiol 2000;21(7):1331-1333.

4 Kang HJ, Shin SJ, Kang ES. Schwannomas of the upper extremity. *JHandSurg* 2000;25(6):604-607.

5 Kransdorf MJ, Murphey MD. Soft tissue tumors in a large referral population: prevalence and distribution of diagnoses by age, sex, and location. In: Kransdorf MJ, Murphey MD, eds. *Imaging of Soft Tissue Tumors* 2nd ed. Philadelphia, Pa: W.B. Saunders; 2006:6-37.

6 Kransdorf MJ. Benign soft-tissue tumors in a large referral population: distribution of specific diagnoses by age, sex, and location. *AJR AmJRoentgenol* 1995;164:395-402.

7 Kransdorf MJ, Murphey MD. Neurogenic tumors. In: *Imaging of Soft Tissue Tumors* 2nd ed. Philadelphia, Pa: W.B. Saunders; 2006: 328-380.

8 Lin J, Martel W. Cross-sectional imaging of peripheral nerve sheath tumors. Characteristic signs on CT, MR imaging, and sonography. *AJR AmJRoentgenol* 2001;176(l):75-82.

9 Louis DN, Stemmer-Rachamimov AO, Wiestler OD. Neurofibromatosis type 2. In: Kleihues P, Cavenee WK, eds. *World Health Organization Classification of Tumours. Pathology and Genetics of Tumours of the Nervous System* Geneva: IARC Press; 2000:219-222.

10 Martuza RL, Eldridge R. Neurofibromatosis 2 (bilateral acoustic neurofibromatosis). *NEnglJMed* 1988;318(ll):684-688.

11 Mautner VF, Tatagiba M, Lindenau M, et al. Spinal tumors in patients with neurofibromatosis type 2: MR imaging study of frequency, multiplicity, and variety. *AJRAmJRoentgenol* 1995;165:951-955.

12 Mulder JD, Schutte HE, Kroon HM, Taconis WK, eds. Introduction, In: *Radiologic Atlas of Bone Tumors* Amsterdam: Elsevier; 1993:3-6.

13 Mulder JD, Schutte HE, Kroon HM, Taconis WK, eds. The diagnosis of bone tumors. In *Radiologic Atlas of Bone Tumors* Amsterdam: Elsevier; 1993:9-46.

14 Mulder JD, Schutte HE, Kroon HM, Taconis WK, eds. Neurilemmoma. In: *Radiologic Atlas of Bone Tumors* Amsterdam: Elsevier; 1993: 529-534.

15 Murphey MD, Smith WS, Smith SE, Kransdorf MJ, Temple HT. Imaging of musculoskeletal neurogenic tumors: radiologic-pathologic correlation. *Radiographics* 1999;19(5):1253-1280.

16 Mutema GK, Sorger J. Intraosseous schwannoma of the humerus. *Skeletal Radiol* 2002;31:419-421.

17 Muthukumar N. Segmental neurofibromatosis-induced spinal cord compression. Case report. *J Neurosurg* 2001; **95**(2, Suppl)236-238.

18 Patronas NJ, Courcoutsakis N, Bromley CM, Katzman GL, MacCollin M, Parry DM. Intramedullary and spinal canal tumors in patients with neurofibromatosis 2: MR imaging findings and correlation with genotype. *Radiology* 2001;218(2}:434-442.

19 Pollack IF, MulvihillJJ. Neurofibromatosis 1 and 2. *Brain Pathol* 1997; 7:823-836.

20 Riffaud L, Morandi X, Massengo S, Carsin-Nicol B, Heresbach N, Guegan Y. MRI of intramedullary spinal schwannomas: case report and review of the literature. *Neuroradiology* 2000;42:275-279.

21 Saifuddin A. Imaging tumours of the brachial plexus. *Skeletal Radiol* 2003;32:375-387.

22 Shrier DA, Rubio A, Numaguchi Y, Powers JM. Infarcted spinal schwannoma: an unusual MR finding. *AJNR Am J Neuroradiol* 1996; 17:1566-1568.

23 Smirniotopoulos JG, Murphy FM. The Phakomatoses. *AJNR Am J Neuroradiol* 1992;13:725-746.

24 Stone JA, Cooper H, Castillo M, Mukherji SK. Malignant schwannoma of the trigeminal nerve. *AJNR Am J Neuroradiol* 2001;22(3): 505-507.

25 Wertelecki W, Rouleau GA, Superneau DW, et al. Neurofibromatosis 2: clinical and DNA linkage studies of a large kindred. N *EnglJ Med* 1988;319(5):278-283.

26 Woodruff JM, Kourea HP, Louis DN, Scheithauer BW. Schwannoma. In: Kleihues P, Cavenee WK, eds. *World Health Organization Classification of Tumours. Pathology and Genetics of Tumours of the Nervous System* Geneva: IARC Press; 2000:164-166.

A 73 Synovial Chondromatosis (Also Referred to as Primary and Secondary Chondromatosis, and Synovial Chondrometaplasia), and Synovial Osteochondromatosis

Definition

Primary synovial Chondromatosis is a benign disorder in which there is nodular cartilaginous metaplastic proliferation in synovium of joints.[1.4.8.10.11.14] The cartilaginous nodules can become detached forming intra-articular loose bodies.[1] Metaplasia of connective tissue into cartilage can also occur in bursae (capsular/para-articular chondroma) and in tendon sheaths (tenosynovial chondroma).[1.4.8.10.11.14]

Secondary synovial Chondromatosis occurs in the setting of other joint disorders such as degenerative osteoarthrosis, avascular necrosis, osteonecrosis, osteochondritis dissecans, trauma/osteochondral fractures, tuberculosis, neuropathic osteoarthropathy, and presence and/or surgery of osteochondromas.[4.9.13] In secondary synovial Chondromatosis, cartilaginous loose bodies arise from avulsion of hyaline cartilage into the joint.[4.14] As with primary synovial Chondromatosis, these loose bodies can enlarge via nutrient supply from synovial fluid.

Solitary lesions can occur in both primary and secondary disorders and are referred to as **synovial chondromas** With progressive osseous metaplasia of synovial chondromas or with loose cartilaginous fragments, which can be seen as calcifications/mineralization on radiographs and CT, both primary and secondary Chondromatosis are then be appropriately referred to as **primary or secondary synovial osteochondromatosis.**

Frequency of occurrence

Primary synovial chondromatosis: less than 1 % of benign, soft tissue tumors[7]

Age at Presentation

Synovial chondromatosis occurs most frequently between the ages of 25 to 65 years, mean = 44years.[7.9] Synovial chondromatosis can also occur in children and older adults.[11]

Gender Ratio (M/F)

1.7/1 to 2/1'-[4.7]

Location

Intra-articular sites are more common than **extra-articular sites** (bursae, tendon sheaths). In intra-articular sites, lesions occur in the knee joint (50-70%) > hip, elbow > shoulder > wrist, ankle > small joints > spinal synovial joints.[1.2.4.9.11] At extra-articular sites, lesions occur in the hand, wrist > foot and ankle.[4.7.11]

Signs and Symptoms

Patients with synovial chondromatosis and osteochondromatosis can have pain (85%), decreased range of motion (55%), swelling (42%), muscle atrophy (20%), palpable nodules (20%), and/or stiffness or locking of joints (5%).[1.4.10.12] Signs and symptoms often range in duration from months to years.[9] Painful disability may result after several years from secondary osteoarthritis.[1]

Cross Pathologic Findings

In primary synovial chondromatosis, lesions usually appear as glistening, white-blue nodules that occur within the joint or attached to synovium.[1.10.14] The lesions can have various shapes: ovoid, spheroid, polyhedral, or multilobulated.[1.10.14] The nodules usually range in size from less than 1 mm to 3 cm.[4] Occasionally, larger lesions have been reported.[4] Large solitary lesions have been referred to as synovial chondromas.[1.4.11]

Cartilaginous and osteocartilaginous loose bodies are firm and white, and can occur in the joint or within synovium.[14]

Histopathologic Findings

The nodules of primary synovial chondromatosis typically consist of hyaline and fibrillar cartilage containing clusters of chondrocytes with plump, pleomorphic nuclei within abundant, solid chondroid matrix.[1.10.11.14] Mild to moderate nuclear atypia is seen in up to two-thirds of specimens.[9] Binucleate cells may occur.[1.10.11.14] Mitoses, however, are uncommon.[1.10.14] The nodules are often covered by a fine fibrous layer or synovium.[10] The synovial membrane can also be thickened and show villous formation.[9] Osteoclastlike giant cells and chondroblasts may occur at the periphery of the nodules.[9] Cartilaginous nodules may eventually become invaded by blood vessels with progressive conversion to bone by endochondral ossification with resultant fatty internal marrow.[9.10] Calcification/ossification often occurs in patchy irregular patterns.[9]

Cartilaginous and osteochondral loose bodies associated with secondary synovial Chondromatosis and osteochondromatosis contain cartilage arranged in layers, and these loose bodies lack the clustered chondrocyte arrangements and nuclear changes (plump and/or binucleated nuclei with mild to moderate nuclear pleomorphism) seen with primary synovial chondromatosis.[9.14] Calcifications/ossifications typically occur in ringlike or zonal patterns.[9]

Lesion Genetics

Rearrangements involving 1 pl3-p22 have been reported.[10]

Findings on Plain Films (Roentgenograms) and Computed Tomography

Synovial osteochondromatosis typically appears as multiple nodules of various sizes with varying degrees of mineralization/calcification and ossification.[1.4.5.8-13] Large ossified lesions may show bony trabeculation with central radiolucent bone marrow.[4] Small calcifications are seen better with CT than radiographs.[9]

With primary synovial chondromatosis, the lesions are relatively similar in size, and are scattered within the joint[4] (Fig. **485).** With secondary synovial chondromatosis and osteochondromatosis, the chondral and osteochondral bodies are fewer in number and are more variable in size relative to the lesions occurring with primary synovial chondromatosis[4] (Figs. **485-487).** In addition, radiographs and CT usually show the primary joint abnormality preceding and co-existing with secondary synovial chondromatosis.[4]

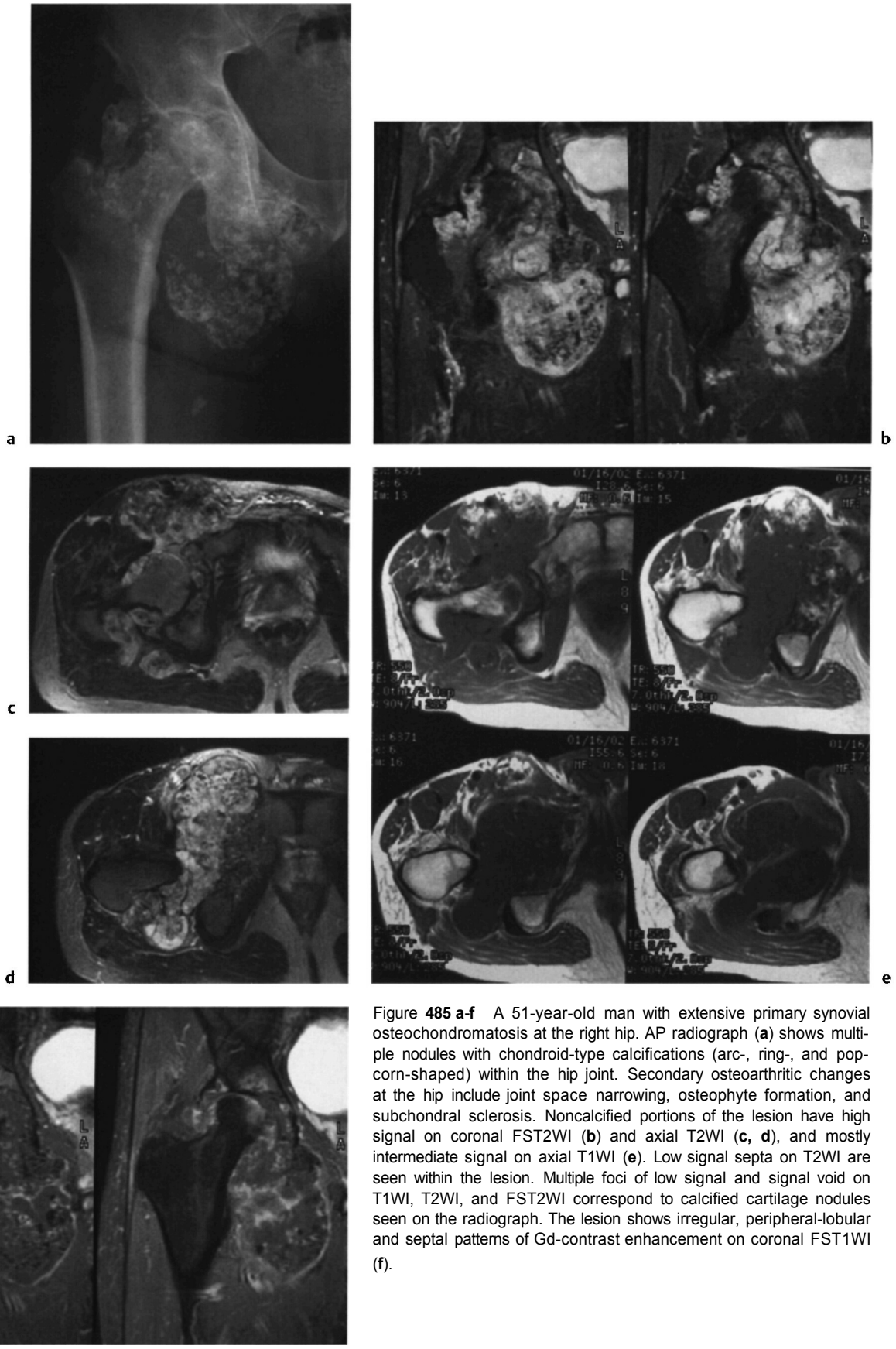

Figure **485 a-f** A 51-year-old man with extensive primary synovial osteochondromatosis at the right hip. AP radiograph (**a**) shows multiple nodules with chondroid-type calcifications (arc-, ring-, and popcorn-shaped) within the hip joint. Secondary osteoarthritic changes at the hip include joint space narrowing, osteophyte formation, and subchondral sclerosis. Noncalcified portions of the lesion have high signal on coronal FST2WI (**b**) and axial T2WI (**c, d**), and mostly intermediate signal on axial T1WI (**e**). Low signal septa on T2WI are seen within the lesion. Multiple foci of low signal and signal void on T1WI, T2WI, and FST2WI correspond to calcified cartilage nodules seen on the radiograph. The lesion shows irregular, peripheral-lobular and septal patterns of Gd-contrast enhancement on coronal FST1WI (**f**).

Up to 30 % of lesions may not show calcifications on radiographs.[4.9] Noncalcified synovial chondromas may present as circumscribed mass-lesions with or without lobulated margins.[4.11]

Later stages of synovial chondromatosis and osteochondromatosis can be associated with secondary osteoarthritis manifest by joint effusion, joint space narrowing, osteophyte formation, and/or subchondral sclerosis.[1.4.11]

MRI Findings

The MRI features of primary and secondary synovial chondromatosis and osteochondromatosis are dependent on the relative proportions of cartilage, calcified cartilage, and mineralized osseous tissue within the lesions[2,4-6,8-10,12] (Figs. **485-489).** For synovial osteochondromatosis, calcifications result in low signal on T1WI, PDWI, T2WI, and FST2WI[2,4-6,8-10,12] (Figs. **485-488).** Synovial osteochondromas with extensive calcification can appear as lesions with signal void[6] (Figs. **486, 488).** Synovial chondromas with ossification can have peripheral low signal on T1WI and T2WI surrounding a central region with fat signal.[4,6] Noncalcified portions of the lesions and synovial chondromas typically have low to intermediate signal on TlWI that is isointense or hyperintense relative to muscle, intermediate signal on PDWI, and slightly high to high signal on T2WI and FST2WI[2,4-6,8-10,12] (Figs. **485,489).** Low signal septae on T2WI can be seen within the lesions[2,4-6,8-10,12] (Figs. **485, 489).** After Gd-contrast administration, synovial chondromas and osteochondromas can show irregular, thin-peripheral and/or septal enhancement.[2,4,13]

a

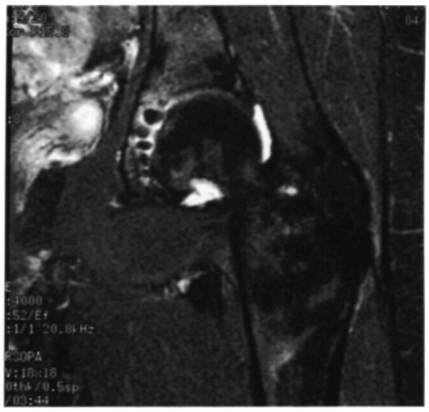

b, c

Figure **486a-c** A 41-year-old woman with secondary synovial osteochondromatosis at the left hip. AP radiograph (**a**) shows multiple calcified nodules within the medial portion of the left hip joint. Foci of low signal on coronal (**b**) T1WI and coronal (**c**) FST2WI are seen within the medial portion of the hip joint, which correspond to calcified cartilage nodules seen on the corresponding radiograph.

a

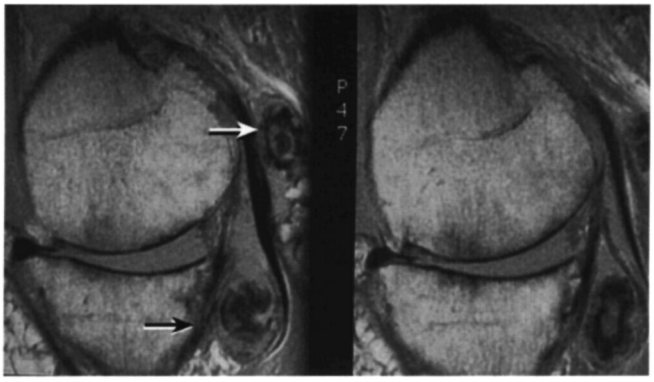

b

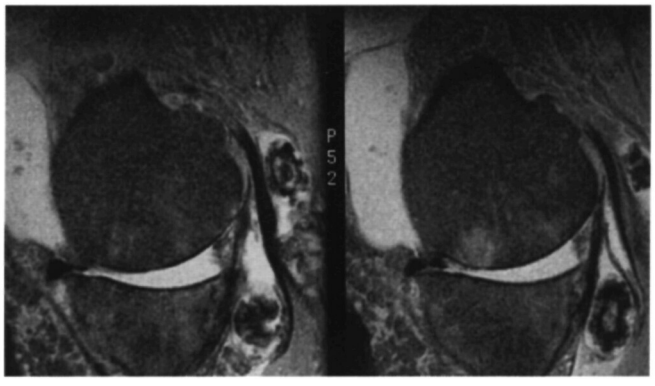

c

Figure **487 a-c** Secondary synovial osteochondromatosis at the knee. Lateral radiograph (**a**) shows multiple, various-sized nodules with calcifications within soft tissue thickening at the knee. Secondary osteoarthritic changes at the knee include joint space narrowing, osteophyte formation, and subchondral sclerosis. The nodules have mixed low and intermediate signal on sagittal PDWI (**b**) and mixed low, intermediate, and slightly high signal on sagittal FST2WI (**c**). Osteophytes, thickened synovium, degenerative thinning of the hyaline cartilage, and a large joint effusion are also seen.

Figure **488a-d** A 56-year-old woman with secondary synovial osteochondromatosis at the knee. AP (**a**) and lateral (**b**) radiographs show multiple, various-sized nodules which have mineralization/calcification. The nodules have mixed low and intermediate signal on sagittal PDWI (**c**) and mixed low, intermediate, and slightly high signal on sagittal FS T2WI (**d**). Degenerative thinning of the hyaline cartilage as well as a focal defect are seen at the lateral femoral condyle. A moderate joint effusion is present.

Differential Diagnosis

Rheumatoid arthritis (rice bodies) and other mono-articular inflammatory arthritides, PVNS, nodular synovitis, gout, tumoral calcinosis, pyogenic or fungal septic arthritis.[1,3,4,11]

Prognosis and Treatment

Synovial chondromatosis and osteochondromatosis are self-limited disorders that can be corrected by surgical removal of the synovial chondromas and osteochondromas with synovectomy.[1,10,11,14] Local recurrence can occur after incomplete synovectomy.[1,10,14] Erosive changes resulting in secondary osteoarthritis can occur in bone adjacent to synovial chondromas and osteochondromas.[1,10,14] Chondrosarcomas have been reported to rarely occur in the setting of synovial chondromatosis.[10,14]

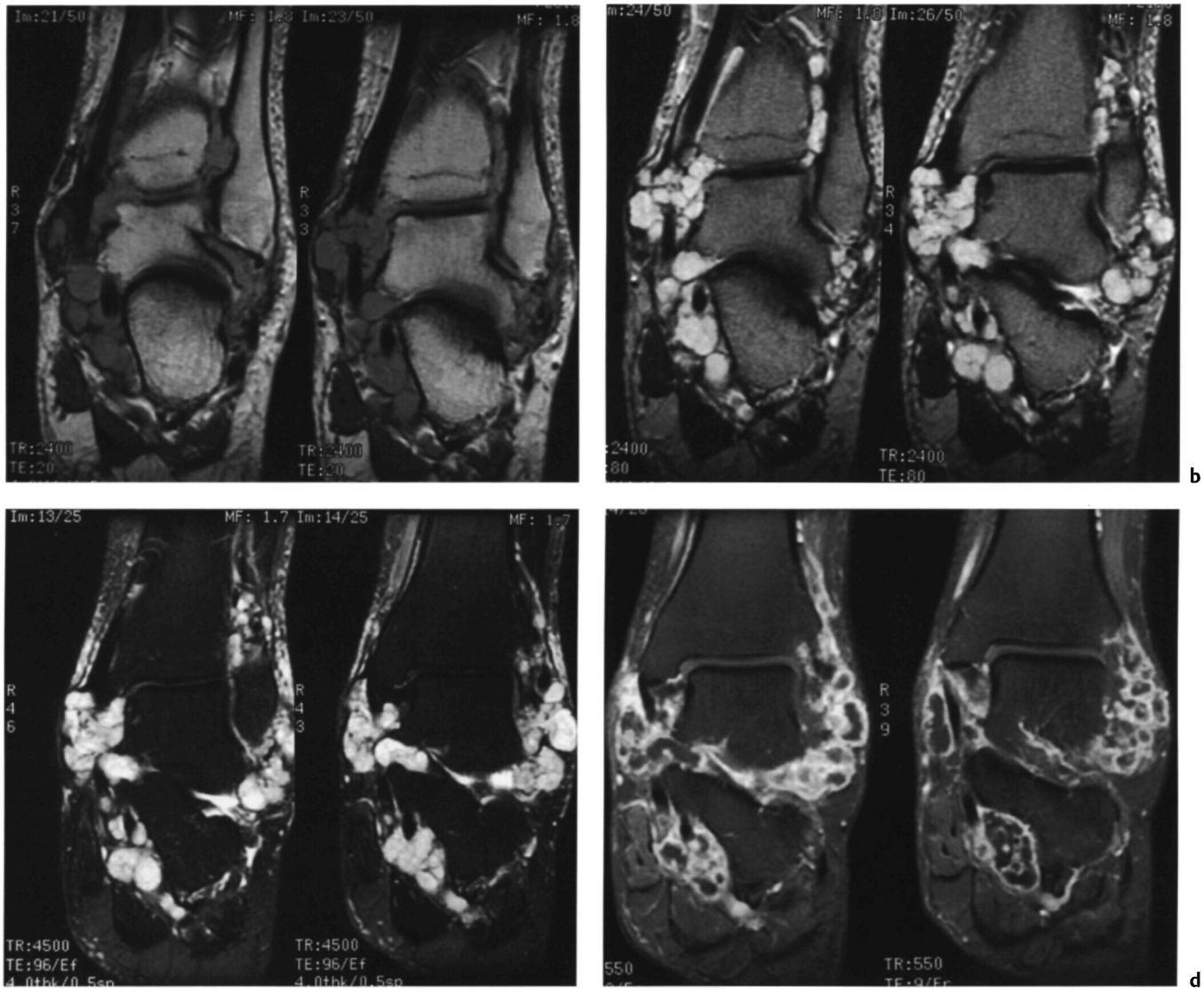

Figure **489 a-d** Primary synovial chondromatosis at the ankle. Multiple tabulated zones are seen at the ankle joint and tendon sheaths that have intermediate signal on coronal PDWI (**a**), and high signal on coronal T2WI (**b**) and coronal (**c**) FST2WI. The lobules have thin margins of low signal on PDWI, T2WI, and FS T2WI. The lesion shows irregular, peripheral-lobular and septal patterns of Gd-contrast enhancement on coronal FST1WI (**d**).

References

1 Amouroux J. Synovial chondromatosis. In: Forest M, Tomeno B, Vanel D, eds. *Orthopedic Surgical Pathology: Diagnosis of Tumors and Pseudotumoral Lesions of Bone and Joints* Edinburgh: Churchill Livingstone; 1998:693-703.

2 Birchall D, Khangure MS, Spagnolo DV. Vertebral synovial osteochondromatosis with compressive myelopathy. *Spine* 1999;24(9): 921-923.

3 Chen A, Wong LY, Sheu CY, Chen BF. Distinguishing multiple rice body formation in chronic subacromial-subdeltoid bursitis from synovial chondromatosis. *Skeletal* Radiol 2002;31:119-121.

4 Crotty JM, Monu Johnny UV, Pope TL Jr. Synovial osteochondromatosis. *Radiol Clin North Am* 1996;34(2):327-342.

5 Kim SH, Hong SJ, Park JS, Cho JM, Kim EY, Park JS. Idiopathic synovial osteochondromatosis of the hip: radiographic and MR appearances in 15 patients. *Korean J Radiol* 2002;3(4):254-259.

6 Kramer J, Recht M, Deely DM, et al. MR appearance of idiopathic synovial osteochondromatosis. *J Comput Assist Tomogr* 1993;17(5): 772-776.

7 Kransdorf MJ. Benign soft-tissue tumors in a large referral population: distribution of specific diagnoses by age, sex, and location. *AJR Am J Roentgenol* 1995;164:395-402.

8 Kransdorf MJ, Murphey MD. Synovial tumors. In: *Imaging of Soft Tissue Tumors* 2nd ed. Philadelphia, Pa: W.B. Saunders; 2006: 381-436.

9 Kyriakos M, Totty WG, Riew KD. Synovial chondromatosis in a facet joint of a cervical vertebra. *Spine* 2000;25(5):635-640.

10 Miller MV, King A, Mertens F. Synovial chondromatosis. In: Fletcher CDM, Unni KK, Mertens F, eds. *World Health Organization Classification of Tumours. Pathology and Genetics of Tumours of Soft Tissue and Bone* Geneva: IARC Press; 2002:246.

11 Mulder JD, Schutte HE, Kroon HM, Taconis WK. Extraosseous chondroma. In: *Radiologic Atlas of Bone Tumors* Amsterdam: Elsevier; 1993:449-460.

12 Narváez JA, Narváez J, Ortega R, De Lama E, Roca Y, Vidal N. Hypointense synovial lesions on T2-weighted images: differential diagnosis with pathologic correlation. *AJR Am J Roentgenol* 2003;181: 761-769.

13 Peh WC, Shek TW, Davies AM, Wong JW, Chien EP. Osteochondroma and secondary synovial osteochondromatosis. *Skeletal Radiol* 1999; 28:169-174.

14 Unni KK. Chondroma. In: *Dahlin's Bone Tumors—General Aspects and Data in 11087 Cases* 5th ed. Philadelphia, Pa: Lippincott, Williams & Wilkins; 1996:25-45.

A 74 Synovial Cyst

Definition

Synovial cysts are synovium-lined fluid collections that frequently occur at or near joints of the extremities, occasionally occur at facet joints of the spine, as well as bursae and tendon sheaths.[1,6,8] In adults, synovial cysts are often associated with osteoarthritis, rheumatoid arthritis, and trauma.[1]

Frequency of Occurrence

Popliteal cyst (Baker cyst). The prevalence of popliteal cysts ranges from 5 to 19 %.[3,6,12,13] In children, the prevalence is 6.3 %.[3]

Spinal synovial cyst. The prevalence rates for synovial cysts arising anteriorly and posteriorly from the facet joint have been reported to be 2.3 % and 7.3 %,[4] respectively.

Age at Presentation

Popliteal cyst (Baker cyst): from 1 to 64 years, mean = 43 years.[3,13]

Spinal synovial cyst: from 27 to 94 years, median = 64 years,[3] average = 66 years.[7]

Gender Ratio (M / F)

Popliteal cyst: 1 / 1

Spinal synovial cyst: 1 /1 to 4 / 3 for synovial cysts arising from the anterior margins of the facet joints.[4,7] For synovial cysts that occur at the dorsal margins of the facet joints, a 7/15 ratio has been reported.[4]

Location

Extremities. Most lesions occur at the knee, wrist, shoulder and hip, ankle and foot.[6,8] Popliteal cysts, also referred to as Baker cysts, are synovial cysts that occur at the knee posteriorly. Popliteal cysts represent focal distentions of the gastrocnemius/semimembranosus bursa, which are located between the tendons of the medial head of the gastrocnemius muscle and semimembranosus muscle.[6,12] Synovial cysts also occur as juxta-articular synovium-lined fluid collections at other joints, or arise from bursae or tendon sheaths.[6]

Spine. Seven percent of spinal synovial cysts are bilateral.[8] Synovial cysts arise from either the ventral or dorsal margins of the facet joints.[4] Dorsal or posterior synovial cysts are more common than synovial cysts arising from the ventral margins of facet joints.[4] The lumbar spine is the most common location for spinal synovial cysts: L4-5> L5-S1, L3-4> others.[4,7,8]

Signs and Symptoms

Popliteal cyst (Baker cyst). Popliteal cysts can be asymptomatic or present with popliteal pain and/or swelling.[3,6,12] In adults, popliteal cysts are often associated with other joint abnormalities such as meniscal tears, chondral injuries or degeneration, and anterior cruciate ligament tears.[12] In children, Baker cysts were not found to be associated with increased joint fluid, anterior crucial ligament or meniscal tears,[3] but did occasionally occur with synovial disease (juvenile rheumatoid arthritis, infection), and chondral abnormalities such as osteochondritis dissecans.[3,12]

Synovial cysts at other joints, bursae, and tendon sheaths. Synovial cysts can be asymptomatic or present with localized pain and/or swelling.[1]

Spine. Synovial cysts arising from the anterior margins of facet joints can present with painful radiculopathy (85 %), neurogenic single or multiroot claudication (44 %), sensory loss (43 %), and motor weakness (27%).[2,4,5,7,9,10]

Pathologic Findings

Synovial cysts are lined with flattened or cuboid synovial cells, and typically contain clear fluid.[1,8] Synovial cysts usually communicate with an articular cavity or tendon sheath.[8] Spinal synovial cysts are usually associated with facet joint osteoarthritis.[4] Unlike synovial cysts, ganglion cysts (also referred to as pseudosynovial cysts) and meniscal cysts are periarticular cyst-like lesions that are lined by spindle-shaped cells and contain a mixed gelatinous liquid or myxoid material.[6,8,13] Ganglion cysts are not lined by synovium.[6813] Ganglion cysts typically lack communication with an articular cavity and likely arise by myxomatous degeneration of periarticular connective tissue.[6]

Findings on Computed Tomography

Popliteal cysts. These lesions usually are well-circumscribed and have contents with fluid attenuation.[6,12]

Synovial cysts. These lesions are usually well-circumscribed with thin peripheral margins.[1] Cyst contents usually approximate water attenuation.[1] Occasionally, gas or calcifications may occur within spinal synovial cysts.[1]

MRI Findings

Spinal synovial cysts. These lesions are spheroid or ovoid, circumscribed collections that protrude beyond the margins of the facet joints.[2,4,5] Spinal synovial cysts that arise from the anterior margins of the facet joint range in size from 2 to 9mm, median = 6 mm.[4] Spinal synovial cysts that arise from the dorsal margins of the facet joint range from 3 to 14 mm, median = 6.5 mm.[4] Spinal synovial cysts typically show a site of communication with the adjacent facet joint.

The contents of the spinal synovial cyst usually have low to intermediate signal on T1WI and PDWI, and high signal on T2WI and FST2WI[245] (Figs. **490-492).** A thin, or slightly thick, rim of low signal on T2WI and FST2WI is typically seen at the periphery of the cysts.[1,2,4,5] Some synovial cysts may have intermediate to high signal on T1WI, and/or intermediate or low signal on T2WI secondary to calcifications, cartilage formation, and/or hemorrhage.[1] After Gd-contrast administration, thin marginal enhancement may be seen (Fig. **492).**

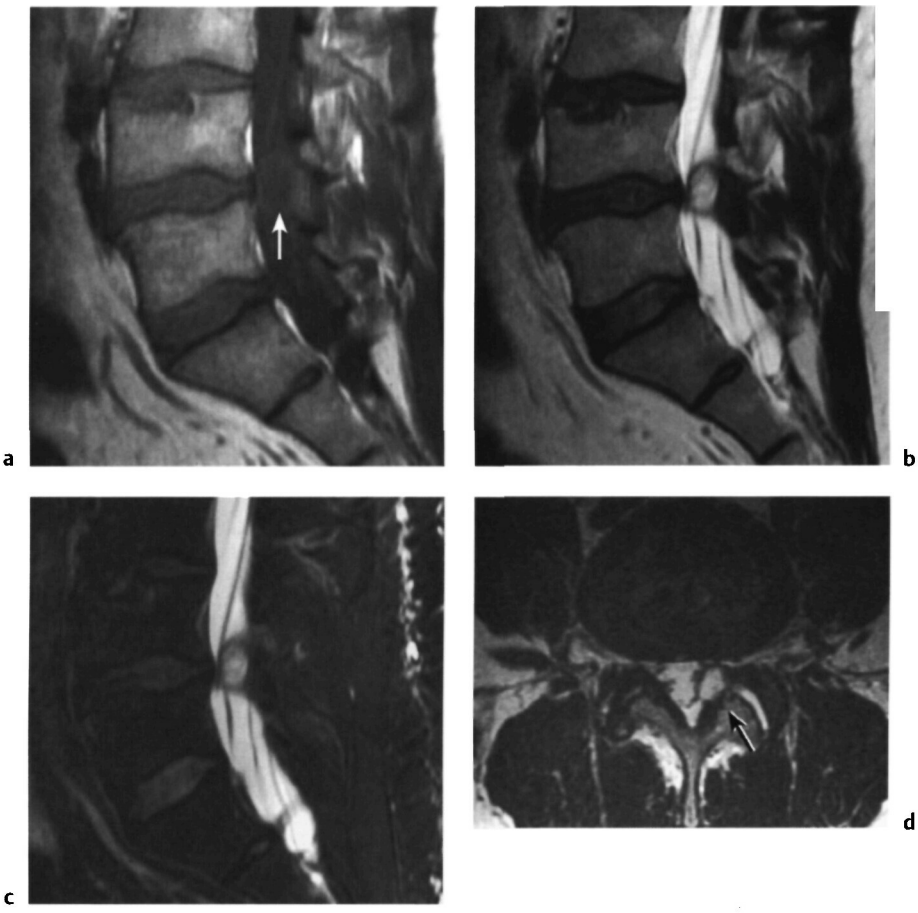

Figure **490 a-d** a 51-year-old man who has a synovial cyst extending from the medial aspect of the left L4-5 facet joint which mildly compresses the lateral margin of the thecal sac. The ovoid lesion has circumscribed margins, and contains low to intermediate signal on sagittal T1WI (**a**), slightly high to high signal on sagittal (**b**) and axial (**d**) T2WI, and sagittal FST2WI (**c**). A thin rim of low signal on T2WI and FST2WI is seen at the periphery of the lesion.

Popliteal cysts. Baker cysts usually measure less than 30 mm." These lesions typically have well-circumscribed margins, and have contents with low signal on T1WI and high signal on T2WI and FS T2WI[3,12] (Fig. **494).** A low-signal membrane on T2WI may be seen partially separating the semimembranous and gastrocnemius components of the popliteal cyst.[12] Most popliteal cysts are unilocular,[12] but occasionally are multilocular.[12] A small communication can often be seen be seen extending from the popliteal cyst to the subgastrocnemius bursa.[3] After Gd-contrast administration, thin marginal enhancement can be seen. Large popliteal cysts can rupture resulting in poorly-defined zones of high signal on T2WI and FST2WI in the adjacent soft tissues.[12] Ruptured popliteal cysts can produce symptoms similar to deep venous thromboses, although these two disorders can be distinguished by their differing MRI features.

Other synovial cysts. Synovial cysts that occur in other soft tissues have circumscribed margins and contain low signal on T1WI, and high signal on T2WI and FST2W1 (Figs. **493, 495).** After Gd-contrast administration, thin marginal enhancement can be seen (Fig. **495).**

Differential Diagnosis

Popliteal cyst. Ganglion cyst, seroma, meniscal cyst, bursitis.[1213]

Spinal synovial cyst. Ganglion cyst, seroma, ligamentum flavum cyst.[4]

Prognosis and Treatment

Popliteal cyst. Treatment of symptomatic Baker cysts is usually nonsurgical and often includes rest, leg elevation, nonsteroidal anti-inflammatory drugs, cold packs, fluid aspiration, and/or corticosteroid injection.[12] Correction of associated internal derangements of joints may cause regression or resolution of popliteal cysts.[12] Surgical excision is usually reserved for very symptomatic popliteal cysts that do not respond satisfactorily to conservative treatment.[12]

Spinal synovial cyst. Symptomatic spinal synovial cysts can be treated with conservative therapy that may include patient immobilization, intra-articular injection of steroids, and/or cyst aspiration.[2,10] Occasionally, spinal synovial cysts may spontaneously regress or have a relapsing-remitting course.[2,5,11] Conservative therapyis often ineffective, however, for radiculopathy caused by spinal synovial cysts.[10] Successful treatment of symptomatic spinal synovial cysts is usually achieved by complete surgical excision, including removal of the synovial membrane." [10] Spinal synovial cysts can also be treated with minimally invasive surgery using a tubular retractor system guided by an endoscope.[9] Spinal synovial cysts can occur at multiple sites in the same patient over a short period.[8] Postoperative MRI has been recommended to evaluate for synovial cysts at other sites in patients who have recurrent sciatica after prior synovial cyst resection.[8]

a

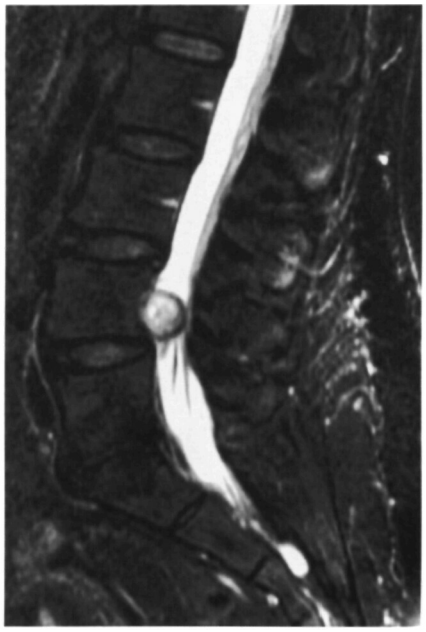

b

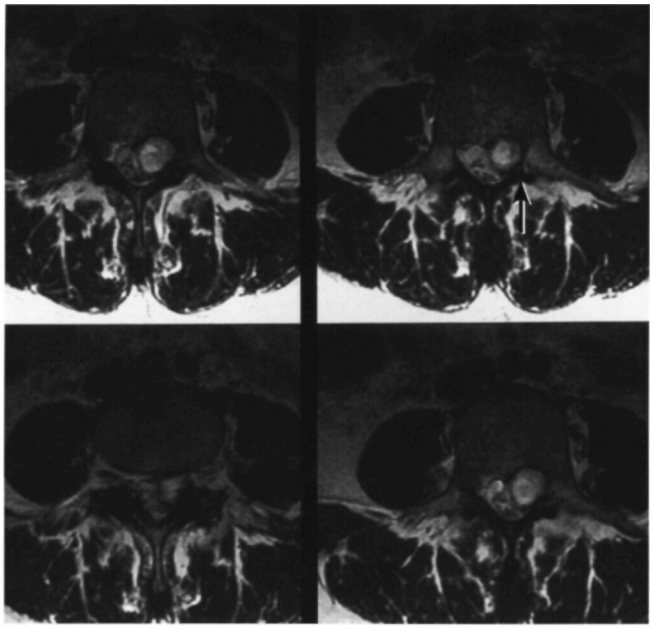

c

Figure **491 a-c** A synovial cyst is seen extending from the medial aspect of the left L4-5 facet joint that results in compression of the thecal sac and scalloped erosive deformity of the dorsal aspect of the L4 vertebral body. The spheroid lesion has circumscribed margins, and contains slightly high to high signal on sagittal (**a**) and axial (**c**) T2WI, and high signal on sagittal FST2WI (**b**). A thin rim of low signal on T2WI and FST2WI is seen at the periphery of the lesion.

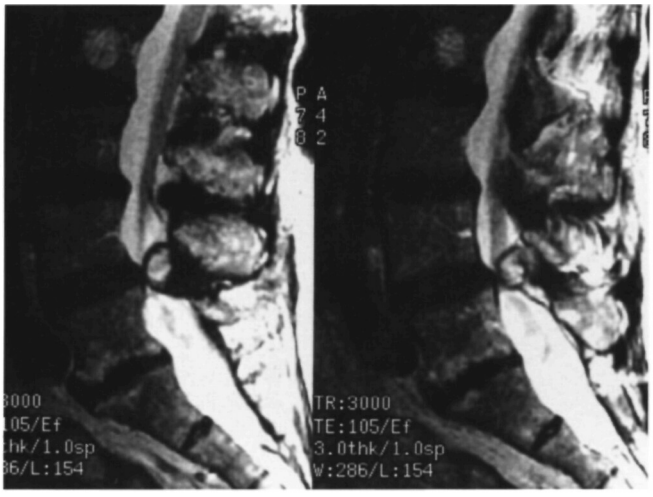

a

b

Figure **492 a, b** A synovial cyst is seen extending from the L4-5 facet joint that results in compression of the thecal sac. The synovial cyst has high signal centrally surrounded by a thin rim of low signal on sagittal T2WI (**a**). A thin rim of marginal Gd-contrast enhancement is seen on sagittal FST1WI (**b**). A hemangioma is also seen in the L2 vertebral body.

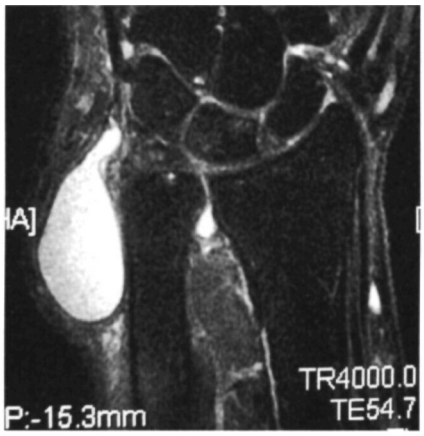

a

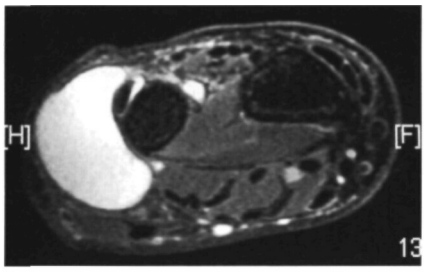

b

Figure **493 a, b** A synovial cyst is seen superficial to the extensor carpi ulnaris tendon at the ulnar aspect of the wrist. The circumscribed lesion has homogeneous high signal on coronal (**a**) and axial (**b**) FST2WI.

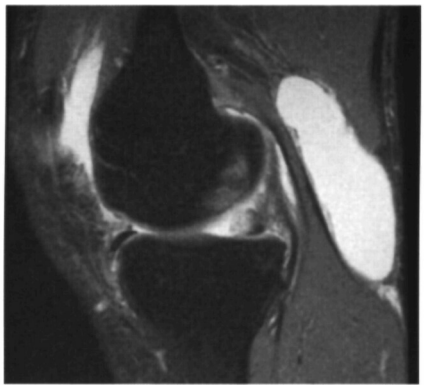

a

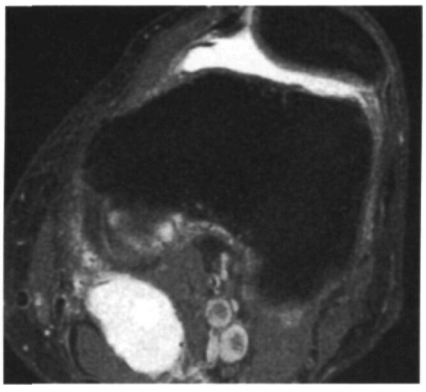

b

Figure **494 a, b** A Baker cyst (synovial cyst) is seen at the semimembranosus, semitendinosus, gastrocnemius bursa. The circumscribed lesion has homogeneous high signal on sagittal (**a**) and axial (**b**) FST2WI. A small joint effusion is also present.

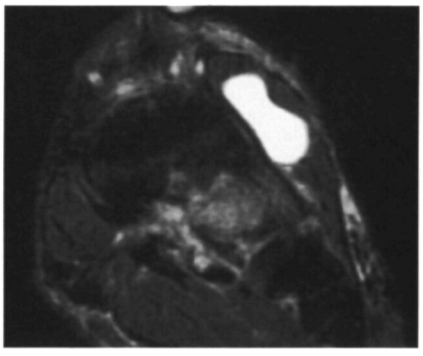

a

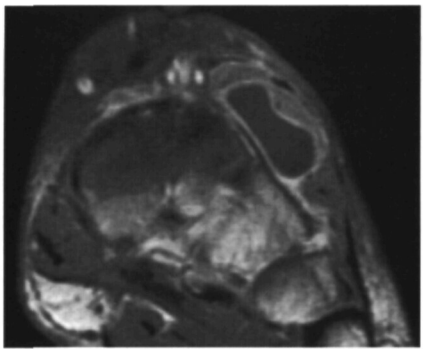

b

Figure **495 a, b** A synovial cyst is seen adjacent to the extensor digitorum longus and brevis tendons. The circumscribed lesion has homogeneous high signal on coronal FST2WI (**a**). A thin rim of marginal Gd-contrast enhancement is seen on coronal FST1WI (**b**).

References

1 Bergemer AM. Benign tumors and cysts of synovium. In: Forest M, Tomeno B, Vanel D, eds. *Orthopedic Surgical Pathology: Diagnosis of Tumors and Pseudotumoral Lesions of Bone and Joints* Edinburgh: Churchill Livingstone; 1998:673-677.

2 Bozzao A, Floris R, Fraioli C, Ticca L, Simonetti G. Relapsing-remitting bilateral synovial cysts of the lumbar spine. A case report. Neuro-*radiology* 2001;43:1076-1078.

3 De Maeseneer M, Debaere C, Desprechins B, Osteaux M. Popliteal cysts in children: prevalence, appearance and associated findings at MR imaging. *Pediatr Radiol* 1999;29:605-609.

4 Doyle AJ, Merrilees M. Synovial cysts of the lumbar facet joints in a symptomatic population: prevalence on magnetic resonance imaging. *Spine* 2004;29(8):874-878.

5 Houten JK, Sanderson SP, Cooper PR. Spontaneous regression of symptomatic lumbar synovial cysts. Report of three cases. *J Neurosurg 2003;* **99**(2, Suppl)235-238.

6 Kransdorf MJ, Murphey MD. Synovial tumors. In: *Imaging of Soft Tissue Tumors* 2nd ed. Philadelphia, Pa: W.B. Saunders; 2006: 381-436.

7 Lyons MK, Atkinson John LD, Wharen RE, Deen HG, Zimmerman RS, Lemens SM. Surgical evaluation and management of lumbar synovial cysts: the Mayo Clinic experience. *J Neurosurg* 2000; 93(1, Suppl) 53-57.

8 Pirotte B, Gabrovsky N, Massager N, Levivier M, David P, Brotchi J. Synovial cysts of the lumbar spine: surgery-related results and outcomeJ Neurosurg 2003;99(Suppl 1):S 14-S19.

9 Sandhu FA, Santiago P, Fessler RG, Palmer S. Minimally invasive surgical treatment of lumbar synovial cysts. *Neurosurgery* 2004; 54(1):107-111; discussion 111-112.

10 Shah RV, Lutz GE. Lumbar intraspinal synovial cysts: conservative management and review of the world's literature. *SpineJ* 2003;3(6): 479-488.

11 Swartz PG, Murtagh FR. Spontaneous resolution of an intraspinal synovial cyst. *AJNR Am J Neuroradiol* 2003;24(6):1261-1263.

12 Torreggiani WC, Al-Ismail K, Munk PL, et al. The imaging spectrum of Baker's (popliteal) cysts. *Clin Radiol* 2002;57:681-691.

13 Tschirch FT, Schmid MR, Pfirrmann CW, Romero J, Hodler J, Zanetti M. Prevalance and size of meniscal cysts, ganglionic cysts, synovial cysts of the popliteal space, fluid-filled bursae, and other fluid collections in asymptomatic knees on MR Imaging. *AJR Am] Roentgenol* 2003;180:1431-1436.

A 75 Synovia! Sarcoma (Also Referred to as Carcinosarcoma and Spindle Cell Carcinoma of Soft Tissue)

ICD-O Code

9040/3

Definition

Synovial sarcomas are mesenchymal tumors comprised of spindle cells and cells with varying degrees of epithelial differentiation.[1,2,5,7-9,11,13,27] More than 90 % of these tumors are associated with a chromosomal translocation, t(X;18)(pll;q11).[2,11,13,16,20,27,30] These tumors can occur at any site. Although synovial sarcoma may resemble synovial tissue at light microscopy, there is no association between synovial sarcoma and synovium.[11,17] Synovial sarcoma does not arise from synovial tissue or show features of synovial differentiation." Synovial sarcomas usually show epithelial differentiation, which is not typically found with synovial tissue.[11,17]

Frequency of Occurrence

Synovial sarcomas account for 5 % of malignant, primary soft tissue tumors, and 2 % of all primary soft tissue tumors.[18,19,24] Synovial sarcomas may rarely occur secondary to prior radiation treatment.[37]

Age at Presentation

From 14 to 58 years, mean = 32 years.[19] Synovial sarcoma has been reported to occur in patients up to 83 years old.[14,25,36] Less than 10% of synovial sarcomas, however, occur in adults over 60 years.[5]

Gender Ratio (M/F)

1 / 1 [14,19,36]

Location

Tumors occur in the lower extremity > foot and ankle > upper extremity > hip, buttocks > hand, wrist > trunk > head and neck > other sites.[19,26]

Signs and Symptoms

Synovial sarcomas often present as painless, slow-growing masses, or with dull-aching pain.[8,11] The duration of slow, progressive symptoms is commonly of 2-4years.[11]

Cross Pathologic Findings

Tumors usually range between 3 and 18cm, and are circumscribed, tan and/or gray, soft and/or firm, depending on the degree of fibrous stroma or calcifications, and/or necrosis.[17,11] Areas of recent or remote hemorrhage may be seen.[28] These tumors often have a pseudocapsule of compressed adjacent tissue.[7]

Histopathologic Findings

Tumors can be monophasic or biphasic, and/or poorly differentiated.[1,7,11,17] Biphasic tumors have varying proportions of fibroblastlike spindle cells and epithelial cell components." The spindle cells are often uniform, plump, and small with indistinct cell borders, and contain pale-staining nuclei within sparse cytoplasm.[7,11] Small amounts of type III collagen may be seen surrounding the spindle cells,[7] which are often arranged in a herringbone pattern and/or irregular nodular arrangements.[7] Mitoses and necrosis are often infrequent except in poorly differentiated tumors." The epithelial cells are relatively large ovoid or spheroid cells containing ovoid nuclei and abundant cytoplasm.[7,11] The epithelial cells may be organized into glandular appearing zones with lumina and papillary structures, as well as in rounded clusters or solid cords." Myxoid changes may occur focally within these tumors." Squamous metaplasia with keratinization is infrequently seen associated with the epithelial components.[7,11]

In monophasic tumors, either the spindle cell or epithelial cell types predominate.[7,11] Calcifications are seen in up to 33 %.[11] Up to 90% of synovial sarcomas show immunoreactivity to cytokeratins in the epithelial components."

Immunoreactivity to epithelial membrane antigen is frequently found for poorly differentiated synovial sarcoma." In the spindle cells, immunoreactivity is often found for BCL2, calponin, actin, and vimentin.[11]

Tumor Genetics

More than 90% of synovial sarcomas have a chromosomal translocation, t(X;18) (pll;qll).[2,11,13,16,20,30] For tissue specimens in which the histologic diagnosis of synovial sarcoma overlaps other tumor types, cytogenetic analysis and/or detection of the SYT-SSX transcripts produced from the t(X;18) (pll ;qll) translocation using the polymerase chain reaction can establish the diagnosis of synovial sarcoma.[6,9]

Findings on Plain Films (Roentgenograms) and Computed Tomography [1,10,17,22,26,27,33]

Synovial sarcomas may not be seen on plain films in 50-90 % of cases.[17,26,27] When visible on radiographs, soft tissue lesions can have circumscribed and/or poorly defined margins.[10] Synovial sarcoma can be associated with erosion of bone cortex and/or medullary invasion in 11-50% of patients.[17,26,34] When present, intra-osseous tumor invasion was typically seen as radiolucent zones (geographic in 50 %, moth-eaten in 35 %, or permeative in 15 %), with occasional mild sclerosis.[26] With CT, tumors can have well-defined margins[10,22,26,28,33] (Figs. **498, 500).** Calcifications may occur in up to 30% of tumors, and often tend to be peripherally located.[1,17,22,26] The calcifications are often fine and amorphous, although can rarely be large[1] (Figs. **498, 500).** Tumors often have mixed CT attenuation with solid zones of soft tissue attenuation, cystic-appearing zones, and/or necrotic zones[17,22,28] (Figs.498,500**).** occasionally, zones of hemorrhage may be present.[17,22,28]

MRIFindings[3,4,10,12,17,22,23,27-29,33,3638,39]

Tumors are often ovoid and/or lobulated lesions ranging in size from 1 to 18cm, mean = 7.5-8.8 cm, median = 12 cm.[14,28,36,38] Tumors margins are well-defined in over 90 % of cases.[14,36] From 63 to 73 % of tumors are located within 5-7 cm of a joint.[14,36]Tumors often have low-intermediate signal on T1WI and FST1WI, and up to 73 % contain small zones of high signal secondary to hemorrhage[14,36] (Figs. **497, 500, 501).** Multiloculated, cystic-appearing zones are present in 77% of lesions[14,36] (Figs. **496-501).** Lesions typically have heterogeneous signal (various combinations of intermediate, slightly high, high, and/or low signal) on PDWI, T2W1, and FST2WI in over 80% of cases[12,14,17,22,23,27-29,33,36,39] (Figs. **496-501).** Up to 35% of tumors show a triple signal pattern on T2WI.[14,17] Zones of low signal on T2WI may occur from calcifications. Uncommon, small tumors less than 5 cm in

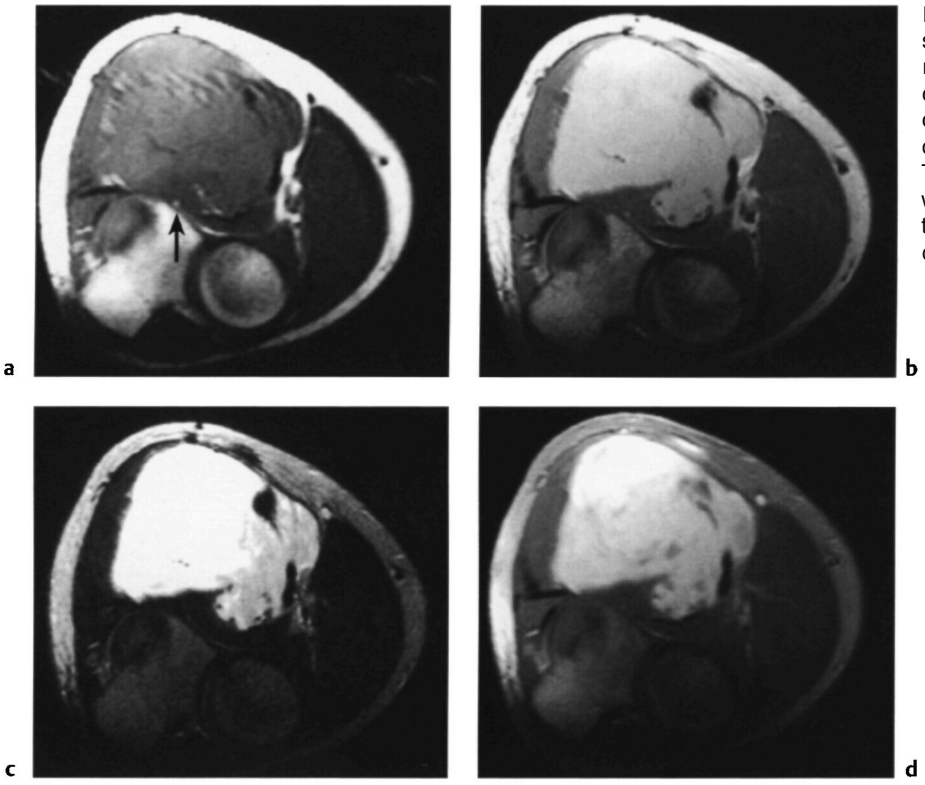

Figure **496a-d** A 14-year-old male with a synovial sarcoma involving the brachialis muscle and soft tissues at the elbow. The circumscribed tumor has intermediate signal on axial T1WI (**a**), slightly high to high signal on axial PDWI (**b**), and high signal on axial T2WI (**c**). Thin septa of low signal are seen within the tumor on PDWI and T2WI. The tumor shows prominent heterogeneous Gd-contrast enhancement on axial FST1WI (**d**).

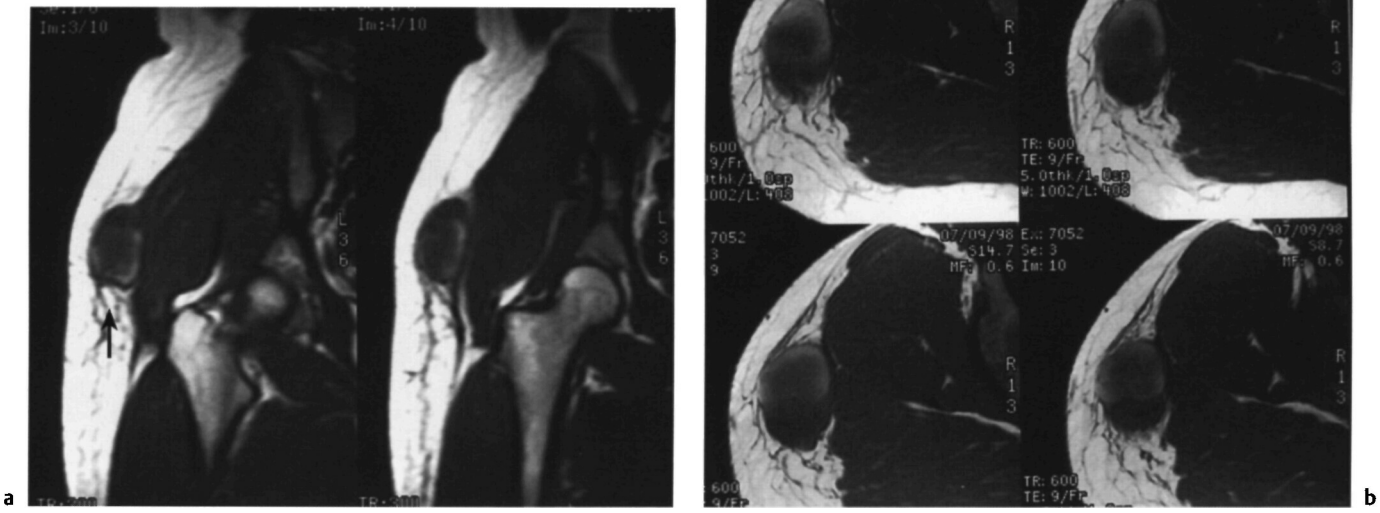

Figure **497a-d** A 23-year-old woman with a synovial sarcoma involving the subcutaneous fat of the upper lateral thigh. The tumor has mixed intermediate and high signal on coronal (**a**) and axial (**b**) TIWI.and high signal on axial FST2WI (**c**). Thin septa of low signal are seen within the tumor on FST2WI. The tumor shows heterogeneous irregular Gd-contrast enhancement on axial (**d**) FST1WI. The enhancing tumor margins are slightly irregular.

Figure **497 c, d** >

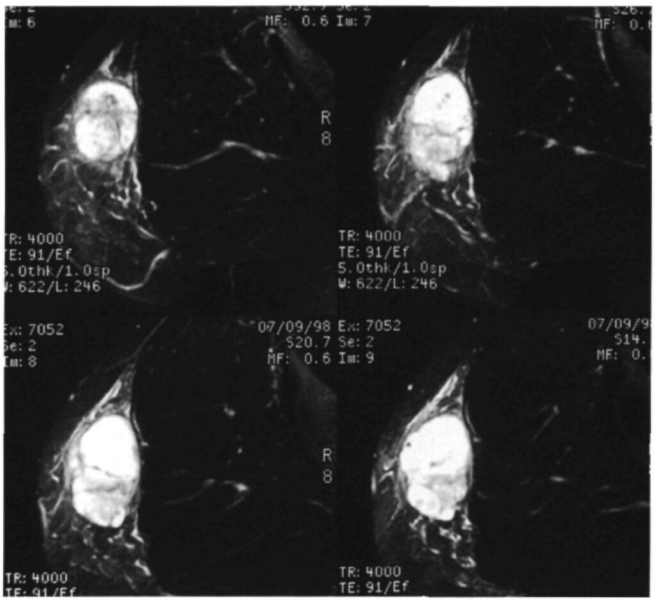

c

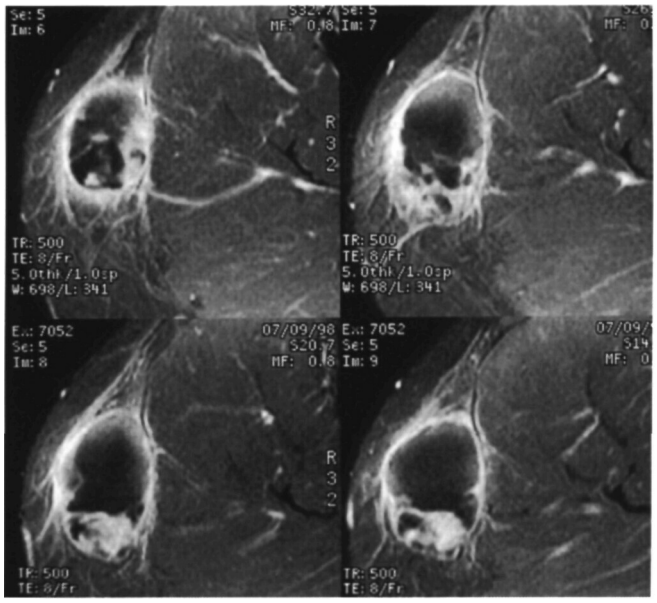

d

Figure 497 c, d

a, b

c

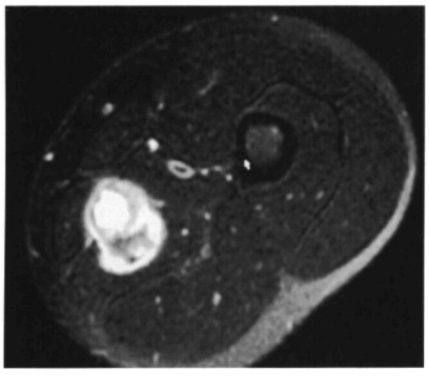

d

e, f

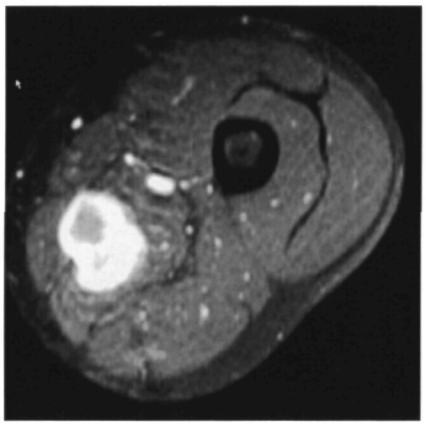

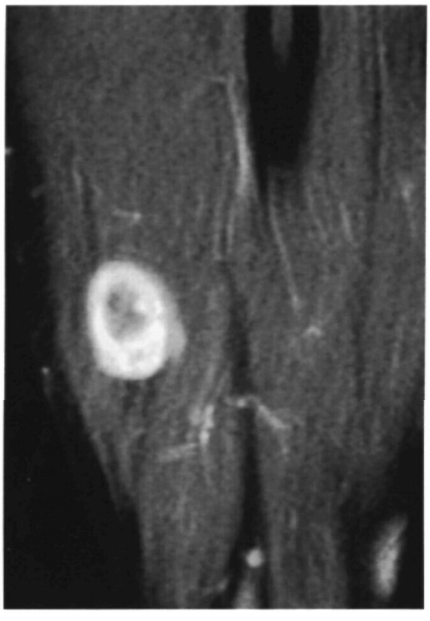

Figure **498a-f** A 15-year-old male with a synovial sarcoma in the medial lower thigh located deep to the sartorius and gracilis muscles, and involving the semimembranosus muscle. The tumor has circumscribed margins, and has intermediate signal on sagittal T1WI (**a**), and heterogeneous mostly high signal on coronal T2WI (**b**) and axial FST2WI (**d**). A cystic zone with high signal on T2WI is seen within the lesion. Axial CT image (**c**) shows the tumor to have intermediate attenuation as well as irregular calcifications and a cysticlike zone. The tumor shows prominent heterogeneous Gd-contrast enhancement on axial (**e**) and coronal (**f**) FST1WI.

size often have lesser degrees of signal heterogeneity on Tl WI and T2WI compared with the more common, larger lesions.[14] Fluid-fluid levels on T2WI are seen in 18% of synovial sarcomas.[14,36] No differences were found in the MRI features of monophasic and Diphasic synovial sarcomas.[14]

After Gd-contrast administration, tumors usually show dynamic enhancement in various patterns (peripheral, heterogeneous, or diffuse)[38] (Figs. **496-501).** Synovial sarcomas typically show rapid contrast enhancement within 7 seconds after arterial enhancement, which is a feature associated with malignant musculoskeletal tumors.[38] Synovial sarcomas with cystic zones show heterogeneous enhancement of solid portions and septa.[28,36]

Synovial sarcomas are seen to contact the surface of bone in 50-59 % of cases.[14,36] Erosion, destruction, and/or invasion of adjacent bone by synovial sarcoma has been reported in 21-23% of cases.[14,36]

Differential Diagnosis[1,11,14,17,22,28,29,39]

Metastatic carcinoma, liposarcoma, malignant fibrous histiocytoma, leiomyosarcoma, malignant peripheral nerve sheath tumor, melanoma, dermatofibrosarcoma, fibrosarcoma, angiosarcoma, rhabdomyosarcoma, epitheloid sarcoma, malignant hemangiopericytoma, clear cell sarcoma, nodular fasciitis, myositis ossificans, proliferative myositis.

Prognosis and Treatment[5-8,11,16,20,21,30-32,35]

Treatment usually consists of surgical resection with wide margins, occasional amputation, and radiation.[8,11,31,32] Prognosis is not different for either monophasic or biphasic synovial sarcomas.[11] Pediatric patients with synovial sarcoma have better outcomes than adults with these neoplasms.[11] Synovial sarcoma in children is associated with 5-year overall survival rates of 75-80 %, event-free survival rate of 72 %, and 5-year progression-free survival rate of 88 %.[31,32] Tumor size > 5 cm, > 10 mitoses per HPF, and presence of necrosis and/or neoplastic invasion of bone and/or adjacent soft tissues are associated with adverse prognosis.[11,21,32] Synovial sarcoma of the head and neck typically occurs in young people and is associated with a poor prognosis and a 5-year overall survival rate of 40 %.[15] Neoadjuvant or postoperative chemotherapy combined with radiation and surgical excision or amputation can result in local control and long-term survival (5-year survival rate up to 80%) in adults with synovial sarcoma of the extremities.[35] Poorly differentiated synovial sarcomas are aggressive neoplasms which frequently metastasize (lungs, bone, lymph nodes), and are associated with a poor prognosis (mean survival of 33 months).[11]

The types of chromosomal translocations associated with nearly all synovial sarcomas involve the fusion of the SYT gene at 18qll with the SSX1, SSX2, or SSX4 genes at Xpll. The different types of these translocations have been recently shown to affect prognosis.[20,30] Synovial sarcomas with the SYT-SSX1 fusion gene have a reduced overall 5-year survival (53 %) compared with synovial sarcomas with the SYT-SSX2 fusion gene (73 %).[20,30] Synovial sarcomas with the SYT-SSX1 fusion were shown to have a higher metastatic rate than tumors with the SYT-SSX2 fusion.[30] The 5-year metastasis-free survival for patients with SYT-SSX1 was only 42 % compared with 89% for patients with SYT-SSX2.[30] The SYT-SSX fusion type was found to be the single most significant prognostic factor for patients with localized disease at diagnosis.[20]

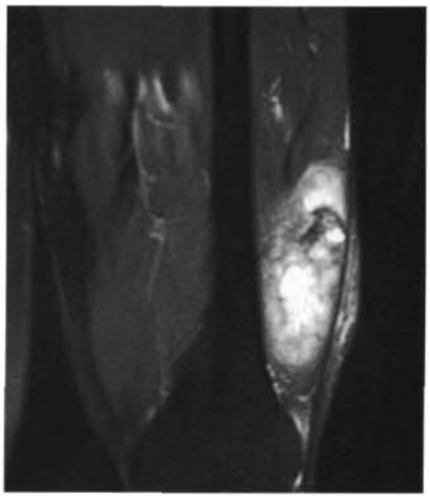

a

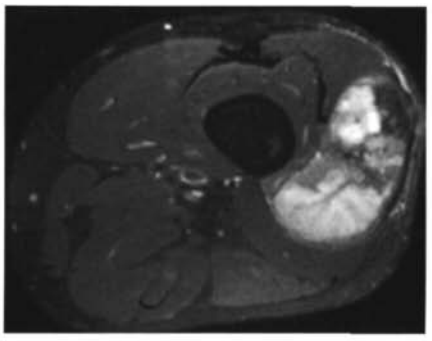

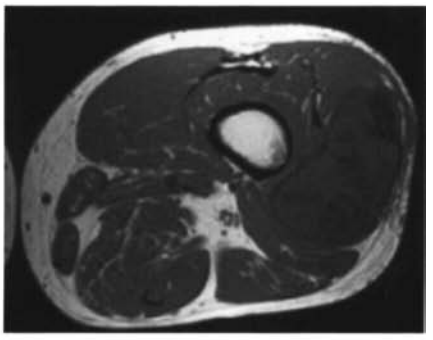

b, c

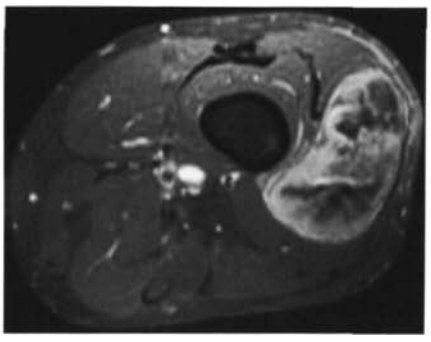

d

Figure **499a-d** A 59-year-old man with a synovial sarcoma in the lateral lower thigh involving the vastus lateralis muscle. The tumor has irregular margins, and has heterogeneous mostly high signal with zones of low and intermediate signal on coronal (**a**) and axial (**b**) FST2WI. The tumor has low and intermediate signal on axial T1WI (**c**). The tumor shows prominent heterogeneous Gd-contrast enhancement on axial FST1WI (**d**).

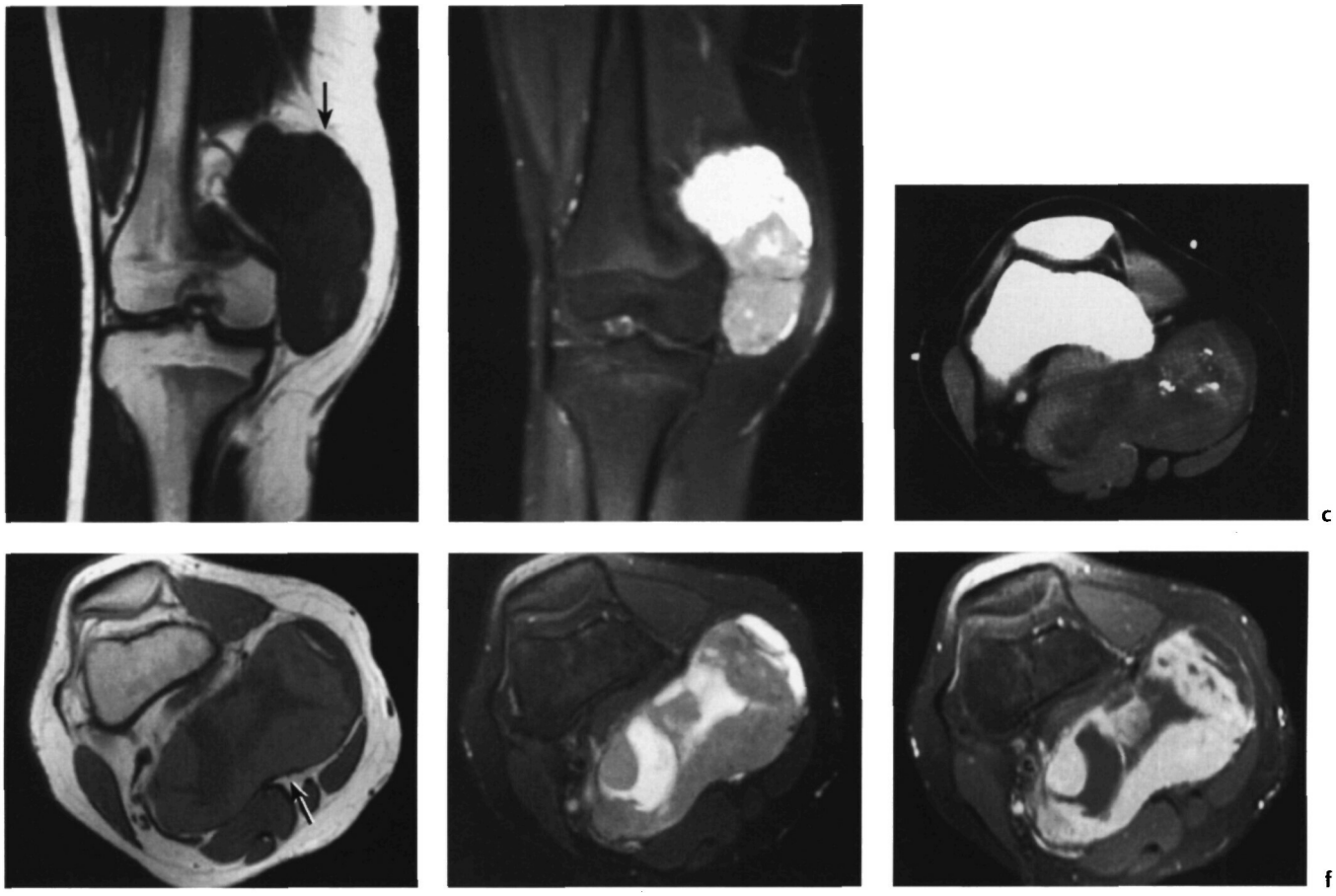

Figure **500a-f** A 15-year-old male with a synovial sarcoma involving the dorsal soft tissues at the knee located deep to sartorius, gracilis, and semimembranosus muscles. The tumor has slightly lobulated margins, and has low and intermediate signal on coronal (**a**) and axial (**d**) T1WI as well as a small zone of high signal from hemorrhage. The tumor has heterogeneous slightly high and high signal on coronal (**b**) and axial (**e**) FST2WI. Axial CT image (**c**) shows the tumor to have intermediate attenuation as well as irregular calcifications and cysticlike zones. The tumor shows prominent heterogeneous Gd-contrast enhancement on axial FST1WI (**f**).

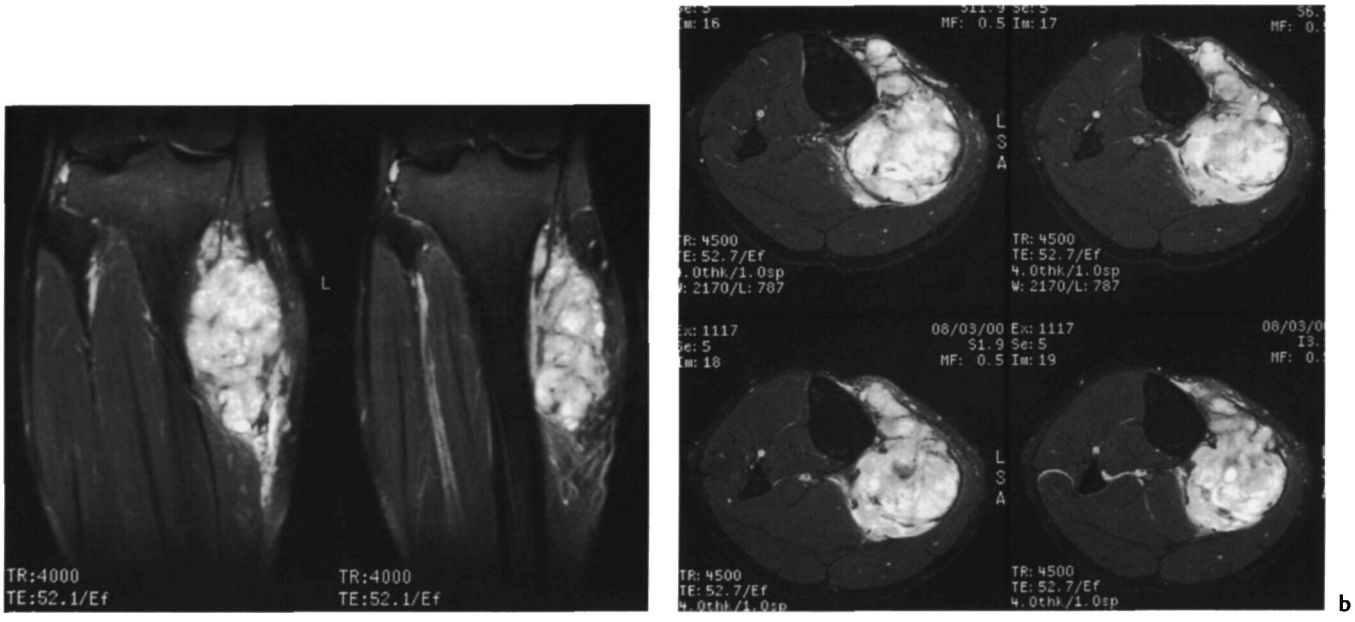

Figure **501 a-d** A 26-year-old man with a synovial sarcoma involving the medial portion of the soleus muscle and adjacent soft tissues of the upper medial leg adjacent to the proximal tibia. The tumor has lobulated, slightly irregular margins and has heterogeneous mostly high signal with septa and zones of low signal on coronal (**a**) and axial (**b**) FST2WI. The tumor has mostly has intermediate signal on axial T1 WI (**c**) as well as zone of high signal from hemorrhage. The tumor shows prominent heterogeneous Gd-contrast enhancement on axial FSTIWI(**d**).

Figure **501 c, d** >

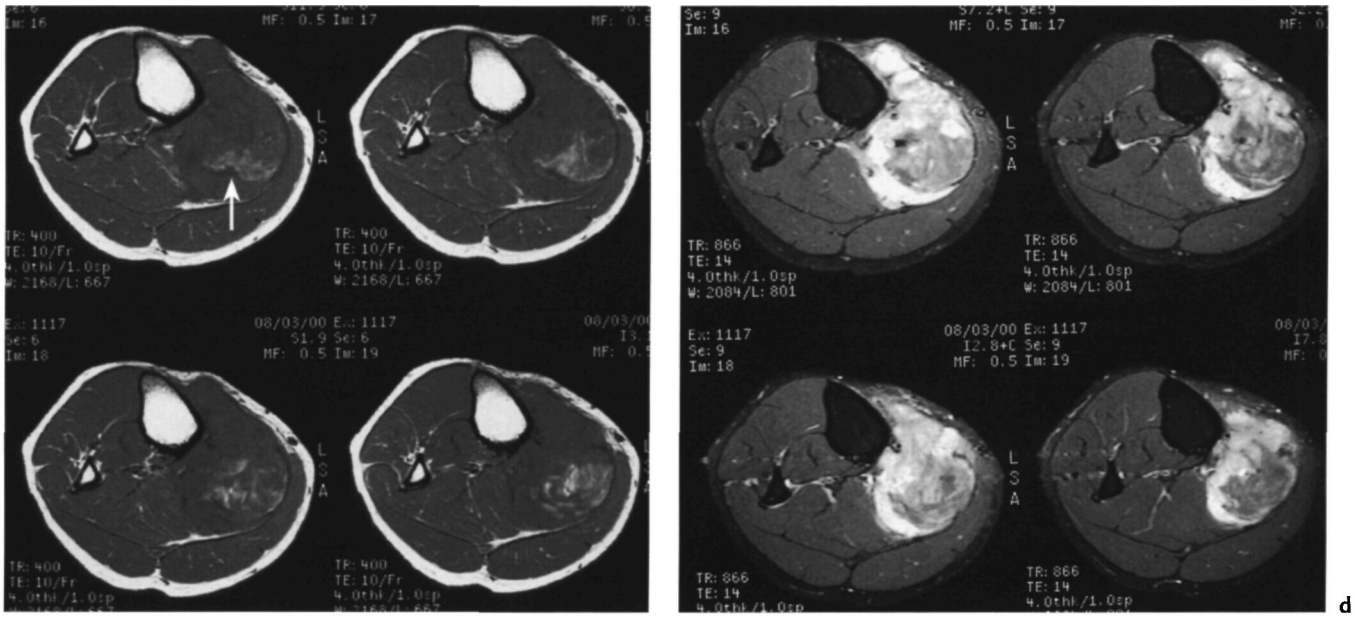

c d

Figure **501 c, d**

References

1 Amouroux J. Synovial sarcoma. In: Forest M, Tomeno B, Vanel D, eds. *Orthopedic Surgical Pathology: Diagnosis of Tumors and Pseudotumoral Lesions of Bone and Joints* Edinburgh: Churchill Livingstone; 1998:705-712.

2 Antonescu CR, Kawai A, Leung DH, et al. Strong association of SYT-SSX fusion type and morphologic epithelial differentiation in synovial sarcoma. *Diagn MolPathol* 2000;9(l):l-8.

3 Bergman AG. Synovial lesions of the hand and wrist. Magn *Reson Imaging ClinNAm* 1995;3:265-279.

4 Bui-Mansfield LT, Kaplan KJ, Boardman J. Synovial sarcoma of the chest wall. *AJR Am J Roentgenol* 2002;179:880.

5 Chan JA, McMenamin ME, Fletcher COM. Synovial sarcoma in older patients: clinicopathological analysis of 32 cases with emphasis on unusual histological features. *Histopathology* 2003;43:72-83.

6 Coindre JM, Pelmus M, Hostein I, Lussan C, Bui BN, Guillou L Should molecular testing be required for diagnosing synovial sarcoma? A prospective study of 204 cases. *Cancer* 2003;98(12):2700-2707.

7 Das Gupta TK, Chaudhuri PK. Pathology of soft tissue sarcomas. In: Das Gupta TK, Chaudhuri PK, eds. *Tumors of the Soft Tissues* 2nd ed. Stamford, Conn: Appleton *&* Lange; 1998:63-200.

8 Das Gupta TK, Chaudhuri PK. Tumors of the synovial tissue. In: Das Gupta TK, Chaudhuri PK, eds. Tumors *of the Soft Tissues* 2nd ed. Appleton and Lange Pubs.; 1998:397-404.

9 de Silva MVC, McMahon AD, Paterson L, Reid R. Identification of poorly differentiated synovial sarcoma: a comparison of clinicopathological and cytogenetic features with those of typical synovial sarcoma. *Histopathology* 2003;43:220-230.

10 Duran-Mendicuti A, Costello P, Vargas SO. Primary synovial sarcoma of the chest: radiographic and clinicopathologic correlation.*J Thorac Imaging* 2003;18(2):87-93.

11 Fisher C, de Bruijn DRH, van Kessel AG. Synovial sarcoma. In: Fletcher CDM,Unni KK, Mertens F, eds. *World Health Organization Classification of Tumours. Pathology and Genetics of Tumours of Soft Tissue and Bone* Geneva: IARC Press; 2002:200-204.

12 Harty MR Imaging of pediatric foot disorders. *Radiol Clin North Am* 2001;39(4):743-744.

13 Helliwell TR, Ritchie DA. Tumors and tumor-like lesions ofjoints and juxta-articular bone. In: Helliwell TR, ed. *Major Problems in Pathology: Pathology of Bone and Joint Neoplasms* 1st ed. Vol 37. Philadelphia, Pa: W.B. Saunders; 1999:380-381.

14 Jones BC, Sundaram M, Kransdorf MJ. Synovial sarcoma: MR imaging findings in 34 patients. *AJR Am J Roentgenol* 1993;161(4):827-830.

15 Kartha SS, Bumpous JM. Synovial cell sarcoma: diagnosis, treatment, and outcomes. *Laryngoscope* 2002;112(11):1979-1982.

16 Kawai A, WoodruffJ, HealeyJH, Brennan MF, Antonescu CR, Ladanyi M. SYT-SSX gene fusion as a determinant of morphology and prognosis in synovial sarcoma. N *EnglJ Med* 1998:338:153-160.

17 Kransdorf MJ, Murphey MD. Synovial tumors. In: *Imaging of Soft Tissue Tumors.* 2nd ed. Philadelphia, Pa: W.B. Saunders; 2006: 381-436.

18 Kransdorf MJ, Murphey MD. Soft tissue tumors in a large referral population: prevalence and distribution of diagnoses by age, sex, and location. In: *Imaging of Soft Tissue Tumors* 2nd ed. Philadelphia, Pa: W.B. Saunders; 2006:6-37.

19 Kransdorf MJ. Malignant soft-tissue tumors in a large referral population: distribution of diagnoses by age, sex, and location. *AJR Am J Roentgenol* 1995;164:129-134.

20 Ladanyi M, Antonescu CR, Leung DH, et al. Impact of SYT-SSX fusion type on the clinical behavior of synovial sarcoma: a multi-institutional retrospective study of 243 patients. *Cancer Res* 2002;62: 135-140.

21 Lewis JJ, Antonescu CR, Leung DH, et al. Synovial sarcoma: a multivariate analysis of prognostic factors in 1l2 patients with primary localized tumors of the extremity. *J Clin Oncol* 2000;18(10): 2087-2094.

22 McCarville MB, Spunt SL, Skapek SX, Pappo AS. Synovial sarcoma in pediatric patients. *AJR Am J Roentgenol* 2002;179:797-801.

23 Meyer JS, Dormans JP. Differential diagnosis of pediatric musculoskeletal masses. *Magn Reson Imaging Clin N Am* 1998;6(3):574-575.

24 Mulder JD, Schutte HE, Kroon HM, Taconis WK. Introduction. In: *Radiologic Atlas of Bone Tumors* Amsterdam: Elsevier; 1993:3-6.

25 Mulder JD, Schutte HE, Kroon HM, Taconis WK. The diagnosis of bone tumors. In: *Radiologic Atlas of Bone Tumors* Amsterdam: Elsevier; 1993:9-46.

26 Mulder JD, Schutte HE, Kroon HM, Taconis WK. Synovial sarcoma. In: *Radiologic Atlas ofBone Tumors* Amsterdam: Elsevier; 1993:295-304.

27 Murphey MD, Gibson MS, Jennings BT, Crespo-Rodriguez AM, Fanburg-SmithJF, Gajewski DA. Imaging of synovial sarcoma with radiologic-pathologic correlation. *Radiographics* 2006;26:1543-1565.

28 Nakanishi H, Araki N, Sawai Y, et al. Cystic synovial sarcomas: imaging features with clinical and histopathologic correlation. *Skeletal - Radiol* 2003;32:701-707.

29 Narvaez JA, Narvaez J, Aguilera C, De Lama E, Portabella F. MR imaging of synovial tumors and tumor-like lesions. *Eur Radiol* 2001;11(12):2549-2560.

30 Nilsson G, Skytting B, Xie Y, et al. The SYT-SSX1 variant of synovial sarcoma is associated with a high rate of tumor cell proliferation and poor clinical outcome. *Cancer Res* 1999;59:3180-3184.

31 Okcu MF, Despa S, Choroszy M, et al. Synovial sarcoma in children and adolescents: thirty three years of experience with multimodal therapy. *Med Pediatr Oncol* 2001 ;37(2):90-96.

32 Okcu MF, Munsell M, Treuner J, et al. Synovial sarcoma of childhood and adolescence: a multicenter, multivariate analysis of outcome. *J Clin Oncol* 2003;21:1602-1611.

33 Rangheard AS, Vanel D, Viala J, Schwaab G, Casiraghi 0, Sigal R. Synovial sarcomas of the head and neck: CT and MR imaging findings of eight patients. *AJNR Am J Neuroradiol* 2001 ;22:851-857.

34 Salisbury JR. Bone neoplasms containing epithelial and epithelioid cells. In: Helliwell TR, ed. *Major Problems in Pathology: Pathology of Bone and Joint Neoplasms* 1st ed. Vol 37. Philadelphia, Pa: W.B. Saunders; 1999:345-368.

35 Ulmer C, Kettelhack C, Tunn PU, Reichardt P, Schlag PM. Synovial sarcoma of the extremities. Results of surgical and multimodality therapy. Orirurg 2003;74:370-374.

36 Valenzuela RF, Kim EE, Seo JG, Patel S, Yasko AW. A revisit of MR1 analysis for synovial sarcoma. *Clin Imaging* 2000;24:231-235.

37 van de Rijn M, Barr FG, Xiong QB, Salhany KE, Fraker DL, Fisher C. Radiation-associated synovial sarcoma. *Hum Pathol* 1997;28: 1325-1328.

38 van Rijswijk CSP, Hogendoorn PCW, Taminiau AHM, Bloem JL. Synovial sarcoma: dynamic contrast-enhanced MR imaging features. *Skeletal Radiol* 2001 ;30:25-30.

39 Van Slyke MA, Moser RP Jr, Madewell JE. MR imaging of periarticular soft-tissue lesions. *Magn Reson Imaging Clin N Am* 1995 ;3(4): 664-665.

A 76 Teratoma

ICD-O Code

Mature: 9080/0

Immature: 9080/3

Teratoma with malignant transformation: 9084/3

Definition

Teratomas are neoplasms that arise from displaced embryonic germ cells (multipotential germinal cells), and contain various combinations of cells and tissues derived from more than one germ layer (endoderm, mesoderm, ectoderm).[3,6,10,17]

Frequency of Occurrence

Extragonadal teratomas account for less than 5 % of pediatric neoplasms.[17] Teratomas are the most common congenital neoplasm, defined as occurring in the first 2 months of life, and account for 36 % of congenital tumors.[17] The prevalence of sacrococcygeal teratomas is 1 per 30000 to 1 per 43000 live births.[5,10] The incidence of congenital teratomas of the head and neck ranges from 1 per 20 000 to 1 per 40 000 live births in the United States.[3]

Age at Presentation

Childhood teratomas: up to 49 % of cases occur in the newborn period.[17]

- **Teratomas of the head and neck:** up to 75 % of cases present in the first year of life.[17]
- **Intracranial teratomas:** patients have been reported to have median ages between 2.5 and 13 years.[15,17]

Gender Ratio (M / F)

Sacrococcygeal teratomas: 1 / 3 to 1 / 6.7.[10,17]

Craniofacial teratomas: 1/1 to 2 /1.[17]

Pineal teratomas: 8 /1.[17]

Location

Childhood teratomas are primarily extragonadal and occur in the sacrococcygeal region (59-65 %) > spine > extracranial head and neck (5%) > intracranial (pineal gland, suprasellar cistern, intra-axial within the cerebral hemipheres).[3,10,17] In the first 2 months, up to 82% of teratomas are sacrococcygeal, and 14% are in the head and neck region.[10,17] Spinal teratomas are usually intradural, extramedullary lesions and are rarely extradural within the spinal canal.[6] Mediastinal teratomas occur most frequently in the anterior mediastinum (82%), multiple compartments (14%), posterior mediastinum (3 %), and middle mediastinum (1 %).[11]

Most adult teratomas are gonadal.[17]

Signs and Symptoms

In the newborn period, extracranial head and neck teratomas can be associated with feeding problems and respiratory difficulties.[3,17] Sacrococcygeal teratomas often present as a palpable exophytic mass.[10] Sacrococcygeal teratomas can be associated with other congenital anomalies in 18% of cases, such as hindgut malformation (imperforate anus), sacral dysgenesis, spinal dysraphism, gastroschisis, and others.[10] Sacrococcygeal teratomas diagnosed in utero can be associated with obstetric complications and cardiac compromise.[9] Intracranial teratomas can be associated with seizures, hydrocephalus, and/or developmental delay.[17]

Cross Pathologic Findings

Sacrococcygeal teratomas are usually encapsulated midline lesions ranging in size from 1 to 30cm (mean = 8 cm), which contain gray-tan nodules of soft tissue, and zones with hemorrhage, calcifications, cartilage, bone, teeth, fat, and serous, sebaceous and/or myxoid material.[10]

Histopathologic Findings

Benign teratomas contain mostly mature tissues (>50%), and lesser amounts of immature tissues.[17] Teratomas have heterogeneous histologic features, and can contain various forms of mature tissues with variable states of organoid development.[17] Nearly 90 % of childhood teratomas contain derivatives from all three germ layers.[17] Up to 40 % of childhood teratomas contain immature tissues.[17] Most childhood teratomas in the head and neck contain neuroectodermal elements,[17] as do approximately 34% of sacrococcygeal teratomas.[17] Cervical teratomas frequently contain thyroid tissue.[17]

Malignant extragonadal teratomas occur in older children.[17] There are three types of malignant teratomas.[17] The first group is teratoma with germ cell tumor (seminoma, embryonal carcinoma, choriocarcinoma, endodermal sinus tumor).[17] The second group is teratoma with nongerminal malignant tissue (carcinoma, sarcoma).[17] The third group is immature teratoma with embryonic elements associated with metastatic disease.[10,17]

Tumor Genetics

Germ cell tumors have been found to have extranumerary X chromosomes, amplification of 1q21-lqter, aberrations involving chromosome 12, and TP53 mutations.[13]

Findings on Plain Films (Roentgenograms) and Computed Tomography

Teratomas usually have circumscribed margins, which may be lobulated. Lesions may contain various combinations and proportions of zones with soft tissue, water/serous, and/or fat attenuation.[4,7,8,10-12,14,16,17] Cystic zones may have a multiloculated appearance.[11,17] Amorphous, clumplike, and/or curvilinear calcifications may be seen in teratomas as well as fat-fluid levels[4,10,11,17] (Fig. **502).** Teeth and zones of bone formation may occur.[1,4] After contrast administration, enhancement is usually

seen in solid portions and septa.[11,17] Invasion of adjacent tissue and bone destruction, as well as metastases, are findings associated with malignant teratomas.[10]

MRI Findings

Teratomas usually have circumscribed margins, which may be lobulated. Lesions may contain various combinations and proportions of zones with low, intermediate, and/or high signal on T1WI, PDW1, T2WI and FST2WI[1,3,4,7,9-12,16,17,19] (Figs. **502-504).** Cystic zones may have a multiloculated appearance[10,17] (Fig. **504).** Teeth and zones of bone formation, as well as amorphous, clumplike, and/or curvilinear calcifications with low signal on T1WI, PDWI, T2WI, and FST2WI may be seen in teratomas[4] (Fig. **502).** Fluid-fluid and fat-fluid levels may be seen within teratomas.[17] Flow voids may be seen within teratomas resulting from vessels within and supplying the tumors.[10] After Gd-contrast administration, enhancement is usually seen in solid portions and septa.[17] Invasion of adjacent tissue and bone destruction, as well as metastases, are findings associated with malignant teratomas.[10]

Differential Diagnosis

Sacrococcygeal teratoma. Neuroblastoma, ganglioneuroblastonna, dermoid, epidermoid, meningocele, lymphoma, hemangioma, lipoma.[10]

Teratoma in the spine. Dermoid, epidermoid, lipoma, ependymoma, schwannoma, neurofibroma.

Teratoma in the neck. Lymphangioma (cystic hygroma), dermoid, epidermoid, lymphoma, lymphadenitis, branchial cleft cyst, congenital goiter, thyroglossal duct cyst.[3,17]

Teratoma in the nasopharynx. Dermoid, lymphangioma, hemangioma, rhabdomyosarcoma, chondroma, chordoma, Rathke pouch cyst, neurofibroma.[3]

Prognosis and Treatment

Sacrococcygeal teratomas. Benign lesions are treated with complete resection and coccygectomy with subsequent reconstruction of the pelvic floor.[5,10] Malignant tumors are treated

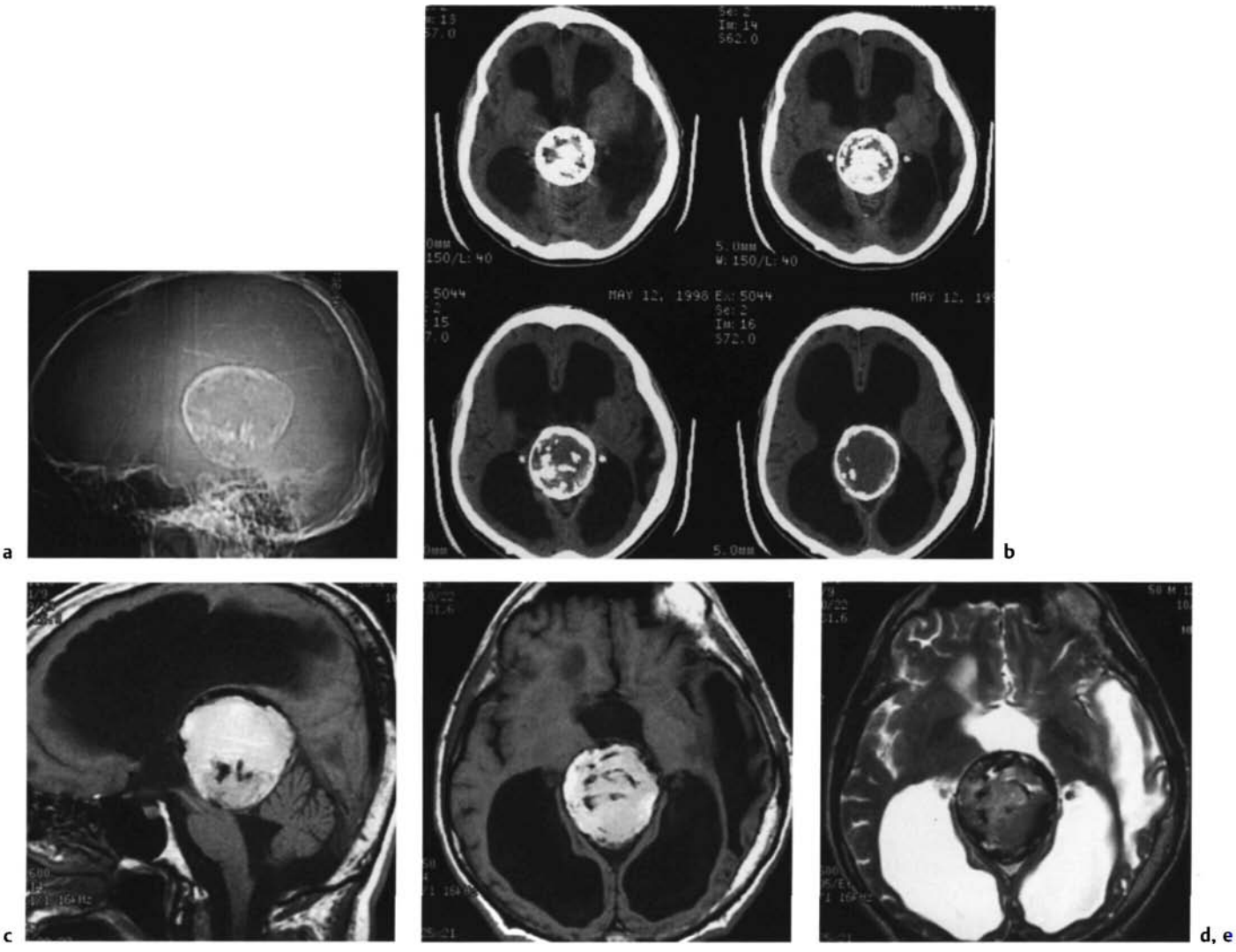

Figure 502 a-e A 50-year-old man with an intracranial teratoma in the pineal recess. Lateral radiograph (**a**) and axial CT image (**b**) show a spheroid lesion, which has thick peripheral and dense amorphous central calcifications. The lesion has a peripheral rim of low signal on sagittal (**c**) and axial (**d**) T1WI and axial (**e**) T2WI, corresponding to the peripheral rim of calcification seen on CT. The contents of the lesion have mostly high signal as well as small zones of low signal on T1WI, and mixed low, intermediate, slightly high and high signal on T2WI.

a

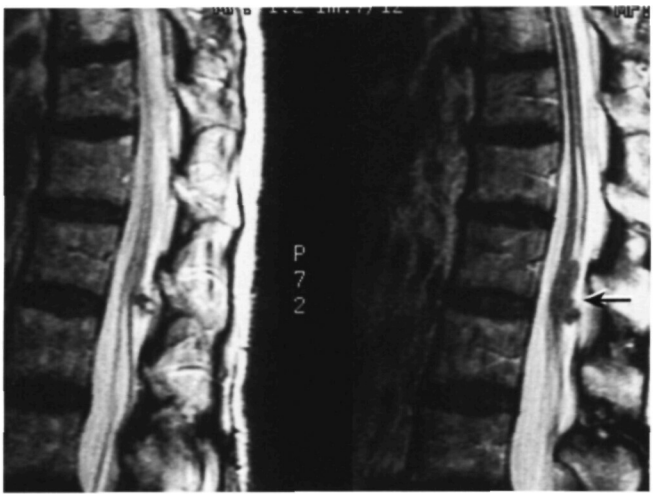

b

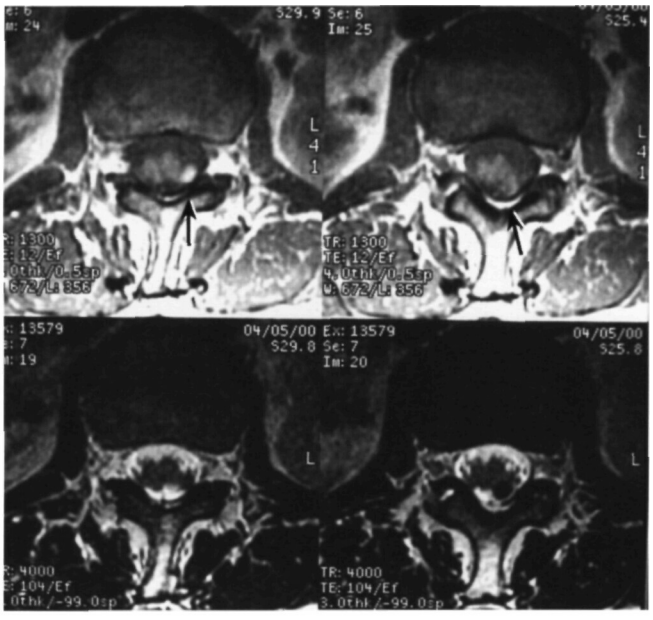

c

Figure **503a-c** A 77-year-old woman with a small intradural teratoma at the dorsal left aspect of the conus medullaris. The lesion has intermediate and high signal on sagittal T1WI (**a**) and axial PDWI (**c,** upper images), and mostly low-intermediate signal on sagittal (**b**) and axial (**c,** lower images) T2WI.

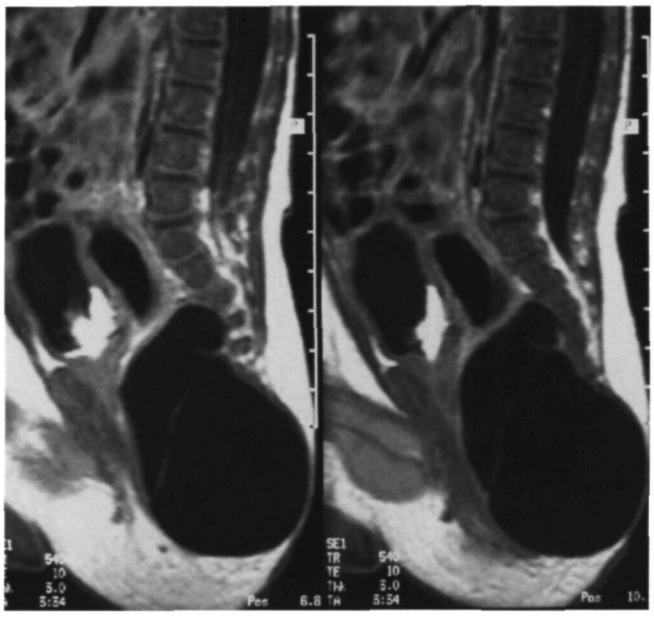

a

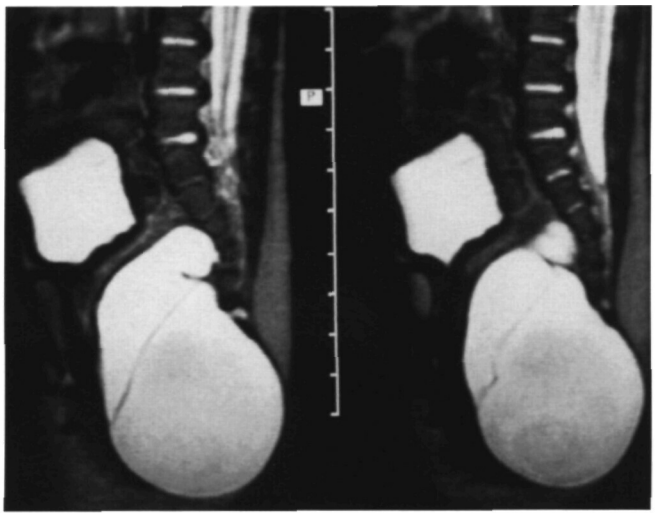

b

Figure **504a, b** Sacrococcygeal teratoma in a 2-month-old male infant. The large lesion has low signal on sagittal (**a**) T1WI, and high signal on sagittal T2WI (**b**). Two thin septa are seen within the lesion.

with surgical excision, and chemotherapy.[10,18] Monitoring of serum α-fetoprotein is used to assess for residual or recurrent disease.[18]

Teratomas in the spine. Benign teratomas in the spine are usually treated with surgery, although complete removal is difficult because these lesions are often adherent to intrathecal nerve roots and/or spinal cord.[2] A recurrence rate of 10% has been reported in a mean follow-up period of 25 months for both total and subtotal resection of spinal teratomas.[2] Malignant teratomas of the spine are treated with surgery and radiation.[2]

Teratomas of the head and neck. Benign lesions are treated with surgical resection.[3] Monitoring of serum α-fetoprotein is used to assess for residual or recurrent disease.[3] Malignant tumors are treated with surgical excision, and chemotherapy.

Intracranial teratomas. Benign lesions and malignant tumors are treated with surgical excision.[15] Adjuvant chemotherapy and radiation are used depending on the histologic subtypes.[15]

References

1 Acar 0, Guney 0, Eser 0. Epidural thoracal teratoma in a 7-month-old girl. *Childs Nerv Syst* 2003;19(2):126-128.

2 Allsopp G, Sgouros S, Barber P, Walsh AR. Spinal teratoma: is there a place for adjuvant treatment? Two cases and a review of the literature. *Br J Neurosurg* 2000;14(5):482-488.

3 April MM, Ward RF, Garelick JM. Diagnosis, management, and follow-up of congenital head and neck teratomas. *Laryngoscope* 1998; 108(9):1398-1401.

4 Bavbek M, Altinors N, Caner H, et al. Giant posterior fossa teratoma. *Childs Nerv Syst* 1999;15(6-7):359-361.

5 Bull J Jr, Yeh KA, McDonnell D, Caudell P, Davis J. Mature presacral teratoma in an adult male: a case report. *Am Surg* 1999;65(6): 586–591.

6 Choi SJ, Choi HJ, Hong JT, et al. Intraspinal extradural teratoma mimicking neural sheath tumor in infant. *Childs Nerv Syst* 2004; 20(2):123-126.

7 Erasmus JJ, McAdams HP, Donnelly LF, Spritzer CE. MR imaging of mediastinal masses. *Magn Resort Imaging Clin N Am* 2000;8(1): 59-89.

8 Foshager MC, Hood LL, Walsh JW. Masses simulating gynecologic diseases at CT and MR imaging. *Radiographics* 1996;16(5):1085-1099.

9 Hedrick HL, Flake AW, Crombleholme TM, et al. Sacrococcygeal teratoma: prenatal assessment, fetal intervention, and outcome. *J Pediatr Surg* 2004;39(3):430-438.

10 Keslar PJ, Buck JL, Suarez ES. Germ cell tumors of the sacrococcygeal region: radiologic-pathologic correlation. *Radiographics* 1994; 14(3): 607-620.

11 Moeller KH, Rosado-de-Christenson ML, Templeton PA. Mediastinal mature teratoma: imaging features. *AJR Am J Roentgenol* 1997; 169(4):985-990.

12 Ribeiro PR, Guys JM, Lena G. Sacrococcygeal teratoma with an intradural and extramedullary extension in a neonate: case report. *Neurosurgery* 1999;44(2):398-400.

13 Rosenblum MK, Matsutani M, Van Meir EG. CNS germ cell tumors. In: Kleihues P, Cavenee WK, eds. *World Health Organization Classification of Tumours. Pathology and Genetics of Tumours of the Nervous System* Geneva: IARC Press; 2000:208-214.

14 Sasaka K, Kurihara Y, Nakajima Y, et al. Spontaneous rupture: a complication of benign mature teratomas of the mediastinum. *AJR Am] Roentgenol* 1998;170(2):323-328.

15 Sawamura Y, Kato T, Ikeda J, Murata J, Tada M, Shirato H. Teratomas of the central nervous system: treatment considerations based on 34 cases J Neurosurg 1998;89(5):728-737.

16 Sigal R, Ousehal A, Pharaboz C, Leridant A, Bosq J, Vanel D. Nasopharyngeal teratoma: CT and MR findings. *Eur Radiol* 1997;7(l):96-98.

17 Smirniotopoulos JG, Chiechi MV. Teratomas, dermoids, and epidermoids of the head and neck. *Radiographics* 1995;15(6):1437-1455.

18 Wakhlu A, Misra S, Tandon RK, Wakhlu AK. Sacrococcygeal teratoma. *Pediatr Surg Int* 2002;18(5-6):384-387.

19 Yamashita Y, Hatanaka Y, Torashima M, Takahashi M, Miyazaki K, Okamura H. Mature cystic teratomas of the ovary without fat in the cystic cavity: MR features in 12 cases. *AJR Am J Roentgenol* 1994; 163(3):613-616.

A 77 Xanthoma

Definition

Xanthomas represent localized accumulations of lipids within normal structures such as tendons, skin, and bone.[3,5,6] Xanthomas are considered reactive lesions and are not true neoplasms.[3,5] Xanthomas usually occur in the setting of hypercholesterolemia and types 1, II, and III hyperlipoproteinemia.[3,5] Xanthomas can also occur in patients with cerebrotendinous xanthomatosis, which is an autosomal-recessive lipid storage disease affecting bile acid synthesis, resulting in accumulation of cholesterol and cholestanol in various tissues.[1,2,5,6]

Age at Presentation

Xanthomas resulting from hypercholesterolemia usually occur in adults. Xanthomas can also occur in children with cerebrotendinous xanthomatosis.[1]

Location

Lesions occur in the skin and subcutaneous tissues > tendons (Achilles, most commonly) > synovium > bone.[5] Xanthomas have also been reported in the spinal leptomeninges.[4]

Signs and Symptoms

Xanthomas may be single or multiple, and are usually found as painless, localized swelling in the skin or tendon.[3,5] Patients with cerebrotendinous xanthomatosis usually present with xanthomas as well as bilateral cataracts, diarrhea, and neurologic deficits such as cerebellar and pyramidal dysfunction, dementia, epilepsy, and polyneuropathy.[1,5] The neurologic deficits result from the accumulation of cholestanol in the central nervous system, and systemically.[1,2,5]

Cross Pathologic Findings

Xanthomas can be localized or diffuse lipid deposits within tendons and other soft tissues.[5] In the brain, lesions occur in the dentate nucleus and adjacent white matter, basal ganglia, internal capsules, brain stem, and spinal cord.[1,2] Cerebral and cerebellar atrophy also occur frequently.[1,2]

Histopathologic Findings

Xanthomas in tendons contain sheets of foamy histiocytes containing cholesterol, cholesterol esters, phospholipids and triglycerides, and fibrosis.[5,6] Using polarized light microscopy, cholesterol appears as birefringent crystals.[5] Calcifications rarely occur in xanthomas.[5]

Findings on Plain Films (Roentgenograms) and Computed Tomography

On plain films, xanthomas can appear as localized or diffuse, soft tissue swelling.[3,5] Rarely, calcifications can also be seen.[5] Xanthomas can be associated with erosion of adjacent bone.[5] Rarely, xanthomas can occur within bone and appear as osteolytic lesions partially surrounded by sclerotic bone.[7]

MRI Findings

Xanthomas in tendons often appear as zones of fusiform enlargement with diffuse heterogeneous signal[3,5,6] (Figs. **505,506).**

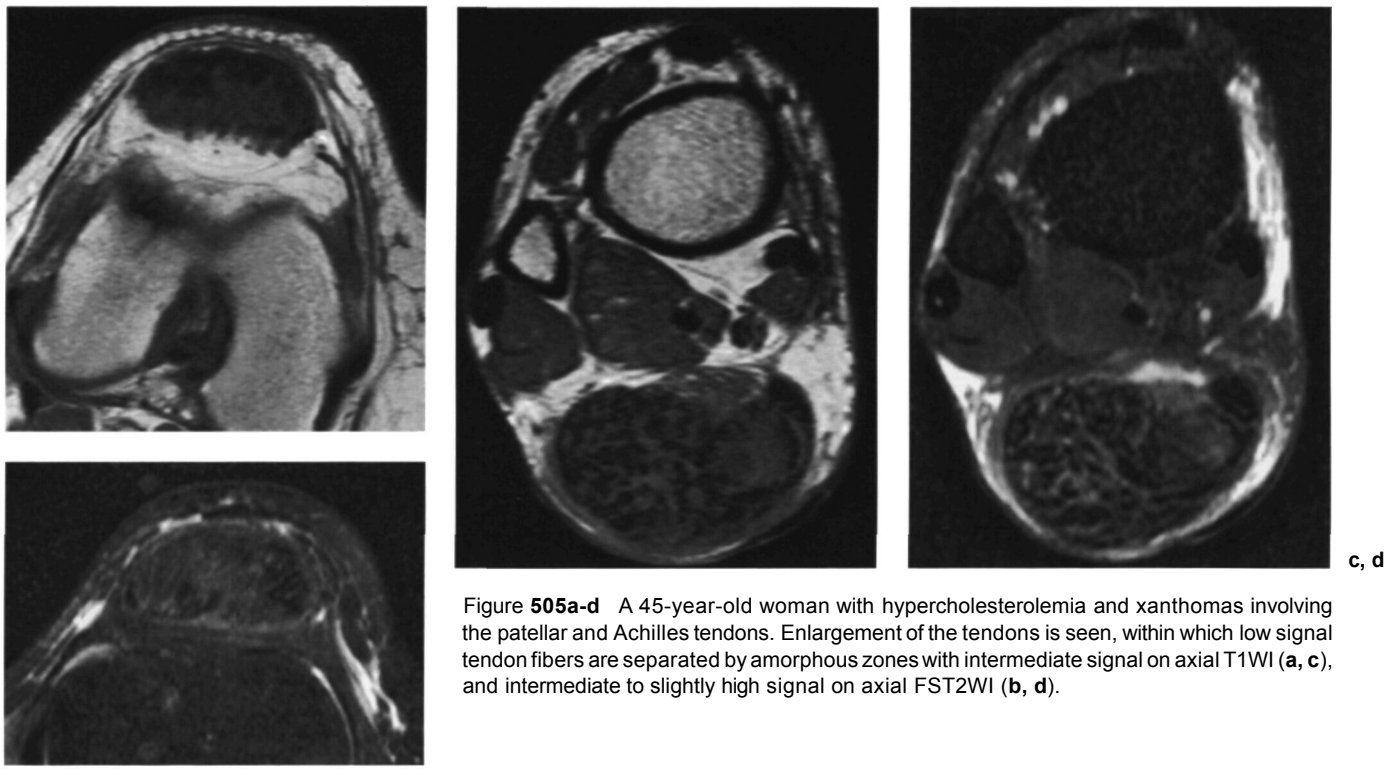

Figure **505a-d** A 45-year-old woman with hypercholesterolemia and xanthomas involving the patellar and Achilles tendons. Enlargement of the tendons is seen, within which low signal tendon fibers are separated by amorphous zones with intermediate signal on axial T1WI (**a, c**), and intermediate to slightly high signal on axial FST2WI (**b, d**).

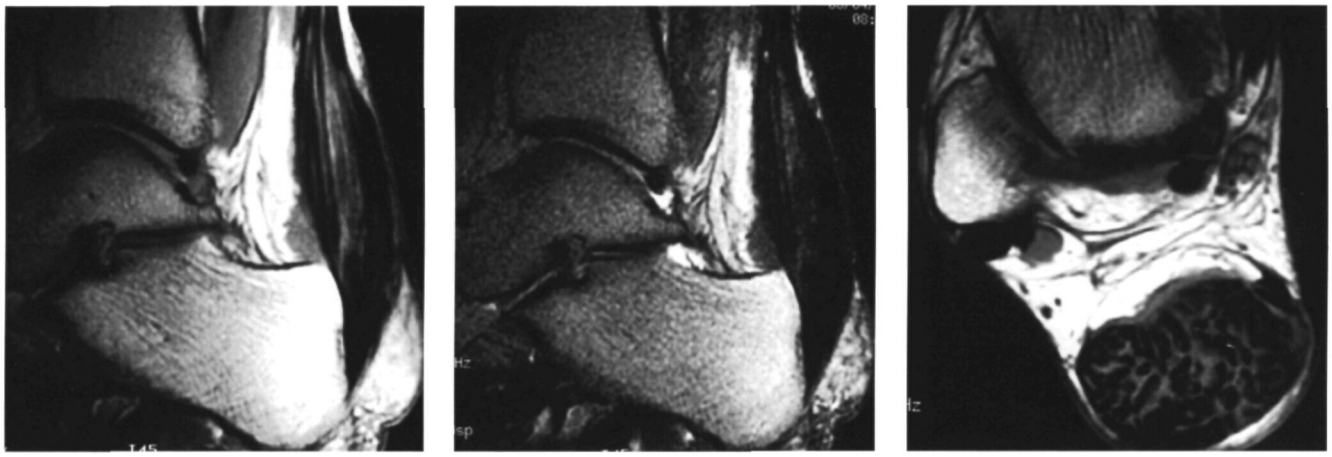

a b, c

Figure **506a-c** Xanthoma involving the Achilles tendon in a 33-year-old woman with hypercholesterolemia. Fusiform enlargement of the tendon is seen, within which low signal tendon fibers are separated by amorphous zones with intermediate to slightly high signal on sagittal PDWI (**a**), and sagittal (**b**) and axial (**c**) T2WI.

Xanthomas usually contain multiple, longitudinally oriented linear zones or striations of low signal tendon fibers separated by amorphous zones with intermediate signal on T1WI and PDWI, and intermediate to slightly high signal on T2WI and FST2WI[3,5] (Fig. **506).** On axial images, xanthomas often have a stippled or reticulated pattern on T1WI and T2WI resulting from collagen bundles with low signal surrounded by a zone of higher signal due to lipid deposits, foamy histiocytes and inflammatory reaction[3,5,6] (Figs. **505, 506).** Intra-osseous xanthomas can have low-intermediate and/or high signal on T1WI and T2WI.[7]

Differential Diagnosis

Tendon xanthoma. Partial tendon tear, tendonitis, gout.

Intra-osseous xanthoma. Bone cyst, intra-osseous lipoma, osteoblastoma, sarcoid, Erdheim-Chester disease, eosinophilic granuloma.[7]

Prognosis and Treatment

Xanthomas are often treated conservatively, and can regress with improvement in the patient's hyperlipoprteinemia status.[5] Large xanthomas in tendons, however, may require surgical intervention.[5]

References

1 Barkhof F, Verrips A, Wesseling P, et al. Cerebrotendinous xanthomatosis: the spectrum of imaging findings and the correlation with neuropathologic findings. *Radiology* 2000;217(3):869-876.

2 Dotti MT, Federico A, Signorini E, et al. Cerebroterfdinous xanthomatosis (van Bogaert-Scherer-Epstein disease): CT and MR findings. *AJNR Am] Neuroradiol* 1994;15(9): 1721-1726.

3 Kelman CG, Disler DG, Kremer JM, Jennings TA. Xanthomatous infiltration of ankle tendons. *Skeletal Radiol* 1997;26:256-259.

4 Kim DS, Kim TS, Choi JU. Intradural extramedullary xanthoma of the spine: a rare lesion from the dura mater of the spine: case report. *Neurosurgery* 1996;39(1):182-185.

5 Kransdorf MJ, Murphey MD. Benign fibrous and fibrohistiocytic tumors. In: *Imaging ofSoft Tissue Tumors* 2nd ed. Philadelphia, Pa: W.B. Saunders; 2006:189-256.

6 Smithard A, Lamyman MJ, McCarthy CL, Gibbons CLMH, Cooke PJ, Athanasou N. Cerebrotendinous xanthomatosis presenting with bilateral Achilles tendon xanthomata. *Skeletal Radiol* 2007;36: 171-175.

7 Yamamoto T, Kawamoto T, Marui T, et al. Multimodality imaging features of primary xanthoma of the calcaneus. *Skeletal Radiol* 2003;32:367-370.

Subject Index

Page numbers is italics denote figures

A

abdominal
  desmoids 396
abscess(es)
  Brodie *see* Brodie abscess
  cold, tuberculous osteomyelitis 680, 686, 687
  deep to subcutaneous fat 276,277
  epidural 72, 72, 685
  periosteal 680
  superficial soft tissue 298, 299
acute bone marrow edema syndromes *see* transient bone marrow edema
acute gouty arthritis 479
acute lymphoblastic leukemia (ALL)
  age at presentation 531
  Bcell 532
  children 532-533
  computed tomography findings 532-533, 533, 534
  definition 531
  frequency of occurrence 531
  Gd-contrast enhancement 533
  genetics 532
  histopathologic findings 532
  immunophenotyping 532
  laboratory findings 532
  MRI findings 533, 533, 534
    cortical destruction and extraosseous extension 100,100,132, J33
    marrow signal 230,230, 533, 533, 534
    outer bone surface 100, 100
  plain film (roentgenogram) findings 532-533
  prognosis 538
  radiolucent zones 533
  signs/symptoms 531
  Tcell 532
  treatment 538
acute myelogenous leukemia (AML)
  age at presentation 531
  computed tomography findings 533
  definition 531
  frequency of occurrence 531
  histopathologic findings 532
  laboratory findings 532
  MRI findings 535, 535, 536, 537
    abnormal marrow signal 230, 231
    deep to subcutaneous fat 262
  plain film (roentgenogram) findings 533
  prognosis 538
  signs/symptoms 532
  spinal 41
  treatment 538
acute transient bone marrow edema *see* transient bone marrow edema
adamantinoma 325-327
  classic type 325
  definition 325
  differential diagnosis 326
  genetics 7, 325
  gross pathologic findings 325
  histopathologic findings 325
  location 325
  MRI findings 325,326
    cortical bone expansion 106,107,126, 127, 326
  osteofibrous dysplasia type 325, 658
  plain film (roentgenogram) findings 325, 326
  prognosis 326
  signs/symptoms 325
  treatment 326
adamantinoma of long bones *see* adamantinoma
adenoid cystic carcinoma 22,23
adenoma, pleomorphic 288
adiopocytic tumors, WHO classification 3
adiposis dolorosa (Dercum syndrome) 266, 312
aggressive fibromatosis
  definition 396
  MRI findings 401
aggressive mastocytosis (mastocytosis category III) 232
AIDS-related lymphoma 578
algodystrophy 218
alkaline phosphatase 7
allopurinol 480
alveolar rhabdomyosarcoma
  definition 732
  genetics 733
  giant cell variant 733
  gross pathologic findings 732
  histopathologic findings 733
  location 732
  mixed embryonal/alveolar type 733
  MRI findings 735, 736
  prognosis 735
  signs/symptoms 732
  treatment 735
ameloblastoma 28,28
  bone expansion 124,125,146,147
  cortical thinning 124,125,146,147
American Joint Committee on Cancer (AJCC), bone tumor classification system 10-12
amyloidoma
  deep to subcutaneous fat 275
  spinal 60, 61
  superficial soft tissue 298
amyloidosis 275
anaplastic meningioma 594
  histopathologic findings 595
  prognosis 597
  treatment 597
anemias, inherited 212,212, 213
aneurysm
  deep to subcutaneous fat 275
  giant 275
  saccular *see* saccular aneurysm
  skull 32,33
  superficial soft tissue 298, 298, 299
aneurysmal bone cysts (ABCs)
  age at presentation 328
  chondroblastoma and 348, 350
  computed tomography findings 328, 329
  definition 328
  differential diagnosis 330
  frequency of occurrence 328
  gender ratio 328
  genetics 328
  giant cell tumor of bone and 463, 466
  gross pathologic findings 328
  hands/feet 202,203
  histopathologic findings 328
  intramedullary, abnormal marrow signal 154,155
  location 328
  MRI findings 328-330,329, 330, 331,332
    intact cortical margin expansion 118, 119
    intramedullary metadiaphyseal lesions 178,178
    well-circumscribed margins 142,143
  osteoblastoma and 668, 669, 671-672
  plain film (roentgenogram) findings 328, 329, 330, 331, 332
  prognosis 330
  radionuclide bone scans 328
  signs/symptoms 328
  skull/facial bones 30,30
  solid *see* giant cell reparative granuloma
  spinal 46, 47
  treatment 330
angioendothelioma *see* angiosarcoma
angiofibroma 340-341
  age at presentation 340
  computed tomography findings 340
  definition 340
  differential diagnosis 340
  extension 340
  frequency of occurrence 340
  gender ration 340
  gross pathologic findings 340
  histopathologic findings 340
  location 340
  MRI findings 340, 341
  plain film (roentgenogram) findings 340
  prognosis 340
  recurrence 340
  signs/symptoms 340
  treatment 340
angiofibrosarcoma *see* angiosarcoma
angioglomoid tumor *see* glomus tumor
angioleiomyomas 291, 521
  age at presentation 521
  gross pathologic findings 521
  histopathologic findings 521-522
  location 521

angioleiomyomas
MRI findings *523-524*
prognosis 522
treatment 522
angiolipoma, spinal 316
angiomatoid fibrous histiocytoma (AFH) 342-343
age at presentation 342
definition 342
differential diagnosis 343
frequency of occurrence 342
genetics 342-343
gross pathologic findings 342
histopathologic findings 342
location 342
MRI findings 294, 294, 342, 343
signs/symptoms 342
treatment 343
angiomatoid malignant fibrous histiocytoma *see* angiomatoid fibrous histiocytoma (AFH)
angiomatosis
definition 491
gross pathologic findings 492
histopathologic findings 492
MRI findings *494,495*
signs/symptoms 491-492
treatment 496
angiomatous meningioma 595
angiosarcoma 264, 265, 344-346
age at presentation 344
computed tomography findings 344
definition 344
differential diagnosis 344
frequency of occurrence 344
gender ratio 344
genetics 344
gross pathologic findings 344
histopathologic findings 344
location 344
MRI findings
bone 344
soft tissue 284,344,345
plain film (roentgenogram) findings 344
prognosis 345
signs/symptoms 344
treatment 345
angiosarcoma multiplex *see* Kaposi sarcoma
Ann Arbor Classification
Hodgkin disease 575-576
non-Hodgkin lymphoma 576
anorexia 220, 221
arachnoidal (meningothelial, arachnoid cap) cells 594
arachnoid cap (arachnoidal, meningothelial) cells 594
arachnoid cyst
outer bone surface 84, 85
skull/facial bones 30, *31*
spinal 48,49
arteriovenous hemangioma 491 -492
gross pathologic findings 492
histopathologic findings 492
MRI findings 499
treatment 496
atypical hemangioma 130,131, 492, 494
atypical lipoma 543-553
computed tomography findings 544
definition 543
genetic abnormalities 9
MRI findings 314, 314, 547, 548, 549-550
deep to subcutaneous fat 266, 267
plain film (roentgenogram) findings 544, 547
treatment 551
see also individual types
atypical meningioma 595
Auer rods 532
avascular necrosis *see* bone infarct
avascular necrosis of the hip
computed tomography findings 512
ischemia 513, 515
location 512
MRI findings 513,515
plain film (roentgenogram) findings 512
prognosis 516
avulsed nerve root 305, 307

B

bacterial infection, osteomyelitis 679
Baker cyst *see* popliteal cyst
Bartonella henselae 300
Bence Jones protein 611
benign fibrous histiocytoma *see* fibroxanthoma
benign mesenchymomas 543
benign synovioma *see* giant cell tumor of the tendon sheath
Binet staging (A.B.C) system, chronic lymphocytic leukemia 535
bizarre parosteal osteochondromatous proliferation 200,201
blastomycosis, fungal osteomyelitis 681
Bloom syndrome 696
bone
formation 2
tumor-induced *see* periosteal reaction
MRI appearance 2
remodeling 2
tissue markers 7
bone bruise 150, 151, 168, 169
bone contusion 150, 151, 168, 169
bone cortex thickening lesions 104-116
benign 104
malignant 106
bone cyst *see* unicameral bone cysts (UBCs)
bone infarct 512-518
age at presentation 512
carpal bones 514, 514
computed tomography findings 512-513
definition 512
differential diagnosis 515
double-line sign 144, 513, 514, 515, 516, 517
"empty" lacunae 512
fractures 512
FST2WI 514, 514
gender ratio 512
hands/feet 208, 208
histopathologic findings 512
location 512
MRI findings 513, 513-515, 514, 516, 517
diffuse, multiple, poorly defined signal 218,219
intramedullary, tubular bone ends 168, 169
intramedullary, well-circumscribed margins 144, 145
intramedullary diaphyseal lesion 189, 189
intramedullary metadiaphyseal lesions 182, 182
zones of fibrosis 513, 514, 514
periostitis 94, 94, 512
plain film (roentgenogram) findings 512-513, 517
prognosis 515-516
spinal 60, 513, 514
treatment 515-516
tumors and 516
bone ischemia
acute 150, 151
subacute 150,151
bone islands *see* enostoses
bone lesions
outer surface involvement 76-103
benign lesions 76-94
malignant lesions 95-102
tumorlike, frequency of occurrence 11
bone marrow
abnormal signaling 211-235
malignant 227-233
nonmalignant 211-226
degenerative disk disease 54, 55
hematopoeitically-inactive fatty (yellow) 2
hyperplasia, exogenous erythropoietin 214, 214
MRI appearance 2
red (hematopoeitic) 2
transient edema see transient bone marrow edema
bone pain
multiple myeloma 611
osteoid osteoma 660
bone tumors
classification 2-5
genetic abnormalities 7-8
grading 10-12
imaging evaluation 13-15
immunohistochemical markers 3, 5-7
MRI 14-15
differential diagnosis 14
occurrence 9, 10, 11
benign lesions 10
malignant lesions 9, 10
primary malignant, intra-articular extension 256, 257
radiography 13-14
patterns 14
staging 10-12
see also individual tumors
bony spurs (osteophytes) 76, 76
Branham sign 491
Brodie abscess
computed tomography findings 680, 690
differential diagnosis 689
location 679
MRI findings 112, 683, 689, 690
pathologic findings 680
plain film (roentgenogram) findings 680, 689
brown tumor
abnormal marrow signal 156

cortical destruction and extraosseous extension 130
intact cortical margin expansion 122
well-circumscribed margins 144
bruit, carotid body tumor 721
Burkitt lymphoma
age at presentation 570
histopathologic findings 571
location 571
MRI findings 158, 581
plain film (roentgenogram) findings 58J
"starry sky appearance" 571
bursae, osteochondroma 646, 649, 650, 651
Buschke-Ollendorff syndrome 674

C

cachexia 221
café-au-lait spots
fibrous dysplasia 449
McCune-Albright syndrome 449, 450
neurofibromatosis type 1 633
Caffey disease (noninterrupted periosteal reaction from infantile cortical hyperostosis) 92
calcification 14
calcific tendinitis 90, 91
calcifying zone, bone 2
calcium pyrophosphate dihydrate deposition disease (CPPD) 252, 252
symptomatic (pseudogout) 252
cancellous osteoid osteoma 661, 664, 667
capillary hemangioma
gross pathologic findings 492
histopathologic findings 492
MRI findings *494,* 495
treatment 496
capillary (simple) lymphangioma 566
capsular chondroma 753
carcinoembryonic antigen (CEA) 7
carotid body tumor
age at presentation 721
differential diagnosis 723
histopathologic findings 722
MRI findings 722, 723, 724
signs/symptoms 721
see also paraganglioma
cartilage containing lesions 236-246
benign 236-240
malignant 240-246
WHO classification 3
see also individual lesions/tumors
cat-scratch disease 300, 301
cauda equina paraganglioma 721, 723
causalgia (complex regional pain syndrome type 2) 218
cavernous hemangioma 492, 496
cavernous lymphangioma 566
cell proliferation evaluation 7
cellulitis, bone infection and 88
"cement lines" 713
central chondroma *see* enchondroma
centroblasts, follicular lymphoma 572
centrocytes, follicular lymphoma 572
cephaloceles 34, 35
cephalohematoma 34
cerebrotendinous xanthomatosis 774
chemodectomas *see* carotid body tumor; paraganglioma
chemokines, rheumatoid arthritis 738
cherubism 449
chief cells, paraganglioma 722
chloromas
location 531
MRI findings 535, 535, 536, 537
cholesteatomas, acquired 390
cholesterol granuloma 32, 33
chondroblastic osteosarcoma 244, 245, 700
chondroblastoma 26, 27, 347-351
age at presentation 347
aneurysmal bone cysts and 348, 350
bone marrow 152, 153, 347, 348, 349, 350, 351
calcification 347
"chicken wire/lattice-like" pattern 347
computed tomography findings 347, 348
definition 347
differential diagnosis 348
frequency of occurrence 347
gender ratio 347
genetics 347
gross pathologic findings 347
hands/feet 204, 205
histopathologic findings 347
immunohistochemistry 347
within joints 254, 255
location 347
malignant see clear cell chondrosarcoma
MRI findings 237, 347-348, 348, 349, 350, 351
intramedullary, intact cortical margin expansion 124, 125
intramedullary, tubular bone ends 164, 165
plain film (roentgenogram) findings 347, 349, 350
prognosis 348
radionuclide bone scan 347
recurrence 348
signs/symptoms 347
spinal 42, 347, 348
treatment 348
chondrocalcinosis 252
chondroid chordomas
cartilage containing 246, 246
histopathologic findings 379
MRI findings 134, 380
chondroid lipomas
definition 543
frequency of occurrence 543
genetics 544
gross pathologic findings 544
histopathologic findings 544
location 543
MRI findings 240, 240, 548, 549-550
signs/symptoms 543
see also atypical lipoma
chondroma
capsular 753
central *see* enchondroma
genetics 8
intramedullary type *see* enchondroma
intra-osseous see enchondroma
juxtacortical *see* juxtacortical chondroma
periosteal *see* juxtacortical chondroma
surface *see* juxtacortical chondroma
synovial 238, 248, 753
tenosynovial 753
chondromyxoid fibroma 364-367
age at presentation 364
cartilage containing 238, 238
computed tomography findings 364
definition 364
differential diagnosis 364
frequency of occurrence 364
genetics 364
gross pathologic findings 364
hands/feet 202, 202
histopathologic findings 364
location 364
MRI findings 364, 365, 366
intact cortical margin expansion 122, 123
intramedullary, tubular bone ends 164, 165
intramedullary metadiaphyseal lesions 178, 179
outer bone surface 78, 79
plain film (roentgenogram) findings 364, 365, 366
prognosis 364
radionuclide bone scans 364
"ridges" and "septa" 364
sign/symptoms 364
treatment 364
chondro-osseous tumors, WHO classification 4
chondrosarcoma 366-368
age at presentation 368
cartilaginous cap 375
classification 368
clear cell *see* clear cell chondrosarcoma
computed tomography findings 369-371, 370, 373, 374
conventional
histopathologic findings 369
location 368
dedifferentiated *see* dedifferentiated chondrosarcoma
definition 368
differential diagnosis 376
extraosseous 267
deep to subcutaneous fat 266
superficial soft tissue 286, 287
frequency of occurrence 368
gender ratio 368
genetics 7, 8, 369
grading 369
gross pathologic findings 368-369
hands/feet 209, 209
histologic variants 368
histopathologic findings 369
1CD-0 codes 368
location 368
malignant *see* clear cell chondrosarcoma
mesenchymal *see* mesenchymal chondrosarcoma
MRI findings 240, 241, 370, 371, 371-376, 372, 373, 374, 375
contrast enhancement 371-373
intramedullary, abnormal marrow signal 158, 159
intramedullary, cortical destruction and extraosseous extension 134, 135
intramedullary, tubular bone ends 172, 173

chondrosarcoma
MRI findings
intramedullary, well-circumscribed margins 148, 149
intramedullary diaphyseal lesion 196, 197
intramedullary metadiaphyseal lesions 186, *187*
myxoid *see* myxoid chondrosarcoma
outer bone surface involving 96, 97
periosteal *see* periosteal chondrosarcoma
peripheral *see* peripheral chondrosarcoma
plain film (roentgenogram) findings 369-371, 371, 372, 373, 374
primary 240, 368
prognosis 376-377
radionuclide bone scans 371
secondary 240
from osteochondroma 244, 245
signs/symptoms 368
skull/facial bones 20, 21
spinal 42, 43
synovial 256
treatment 376-377
see also individual types
chordoid meningioma 595
chordoid sarcoma *see* myxoid chondrosarcoma
chordoma 379-382
age at presentation 379
chondroid *see* chondroid chordomas
computed tomography findings 379, 381
dedifferentiated 379
definition 379
differential diagnosis 380
frequency of occurrence 379
genetics 7, 379
gross pathologic findings 379
histopathologic findings 379
location 379
metastases 381
MRI findings 379-380, 380, 381, 382
cortical destruction and extraosseous extension 134, 135
outer bone surface 96, 97
plain film (roentgenogram) findings 379
prognosis 381
radionuclide bone scans 379
sacrococcygeal 379, 382
sarcomatoid 379
signs/symptoms 379
skull/facial bones 20, 20
spheno-occipital 379, 380, 380, 381
treatment 381
vertebral 42, 43, 379, 380, 381
choriocarcinoma 770
chroniclymphocyticleukemia(CLL)
age at presentation 531
computed tomography findings 533, 534
definition 531
frequency of occurrence 531
histopathologic findings 532
laboratory findings 532
MRI findings 533-535, 534, 535
diffuse, multiple, poorly defined signal 230, 230
plain film (roentgenogram) findings 533
prognosis 538
signs/symptoms 531-532
treatment 538
chronic myelogenous leukemia (CML)
age at presentation 531
definition 531
frequency of occurrence 531
histopathologic findings 532
MRI findings 535-537, 537, 538
diffuse, multiple, poorly defined signal 230, 231
plain film (roentgenogram) findings 533
prognosis 538
signs/symptoms 532
treatment 538
chronic myeloproliferative disease (CMPD) 232, 233
chronic recurrent multifocal osteomyelitis 679
chronic tophaceous gout 479
cirsoid aneurysm *see* arteriovenous hemangioma
clear cell chondrosarcoma
computed tomography findings 371
gross pathologic findings 368
histopathologic findings 369
location 368
MRI findings 242, 373
plain film (roentgenogram) findings 371
prognosis 377
treatment 377
clear cell meningioma 595
clear cell sarcoma
deep to subcutaneous fat 262, 263
genetic abnormalities 8
c-myc gene 572
coccidioidomycosis infection, fungal osteomyelitis 681
Codman triangles 14, 100, 101
Ewing sarcoma 416, 417, 419, 420
osteosarcoma 134, 184, 697, 699, 699, 700
periosteal osteosarcoma 96, 703
pyogenic osteomyelitis 680
telangiectatic osteosarcoma 706
COL 1A1 gene 383
cold-sensitivity test 476
collagen 7
Collet-Sicard syndrome 721
complex regional pain syndrome type 1 218
complex regional pain syndrome type 2 (causalgia) 218
composite hemangioendotheliomas
age at presentation 484
definition 484
gross pathologic findings 485
histopathologic findings 486
location 485
prognosis 487
signs/symptoms 485
congenital elephantiasis 566
congenital fibrous defect of the tibia *see* osteofibrous dysplasia
congenital lymphangiomatosis 566
congenital osteitis fibrosa *see* osteofibrous dysplasia
congenital pseudoarthrosis *see* osteofibrous dysplasia
contrast-enhanced MRI
musculoskeletal lesions 14
soft tissue tumors 14
cortical desmoid 438-448
age at presentation 438
computed tomography findings 442, 446
definition 438
frequency of occurrence 438
gross pathologic findings 438
histopathologic findings 439
location 438
MRI findings 80, 81, 443, 446, 447
plain film (roentgenogram) findings 442, 447
signs/symptoms 438
treatment 444
cortical fibrous dysplasia *see* osteofibrous dysplasia
cortical osteoid osteoma
computed tomography findings 661
differential diagnosis 667
MRI findings 661, 666
marrow signal 661
plain film (roentgenogram) findings 661, 666
cranial fasciitis 423
cystic hygroma *see* lymphangioma
cytokeratins 7
cytokines
metastatic lesions 601
multiple myeloma 611
rheumatoid arthritis 738

D

Dabska tumor *see* papillary hemangioendothelioma
DDIT3/FUS gene fusion, liposarcoma 555
DDIT3 gene, liposarcoma 555
dedifferentiated chondrosarcoma
computed tomography findings 371, 374
gender ratio 369
histopathologic findings 369, 379
location 368
MRI findings 242, 243, 372, 374, 375
plain film (roentgenogram) findings 371
prognosis 377
treatment 377
dedifferentiated chordoma 379
dedifferentiated liposarcoma
age at presentation 554
differential diagnosis 557
genetics 555
histopathologic findings 555
location 554
MRI findings 320, 556-557, 560
deep to subcutaneous fat 260, 261
plain film (roentgenogram) findings 560
prognosis 558
superficial soft tissue 280
treatment 558
degenerative disk disease, marrow changes 54, 55
deoxyhemoglobin 2
Dercum syndrome (adiposis dolorosa) 266, 312
dermatofibrosarcoma (DPS) 383-385
age at presentation 383
computed tomography findings 383
definition 383
differential diagnosis 383
frequency of occurrence 383

genetics 383
gross pathologic findings 383
histopathologic findings 383
location 383
MRI findings 280, 280, 383, *384*
plain film (roentgenogram) findings 383
prognosis 383-384
signs/symptoms 383
treatment 383-384
dermatofibrosarcoma protuberans (DFSP)
age at presentation 383
computed tomography findings 383
definition 383
differential diagnosis 383
frequency of occurrence 383
genetics 8, 383
gross pathologic findings 383
histopathologic findings 383
location 383
MRI findings 280, 383, *384*
plain film (roentgenogram) findings 383
signs/symptoms 383
treatment 383
dermatomyositis 386-389
age at presentation 386
calcification 386
computed tomography findings 386
definition 386
differential diagnosis 387
frequency of occurrence 386
gross pathologic findings 386
histopathologic findings 386
hydrogen MR spectroscopy 387
juvenile 386
location 386
MRI findings *386,* 386-387, 387, 388
active inflammation 387, 387
deep to subcutaneous fat 278, 278
low signal zones 386, 387, 387, 388
plain film (roentgenogram) findings 386, 386, 387, 388
prognosis 389
signs/symptoms 386
treatment 389
dermoid 390-395
age at presentation 390
computed tomography findings 391, 392
congenital 390
definition 390
differential diagnosis 395
fat containing 316, 317
frequency of occurrence 390
gross pathologic findings 390
histopathologic findings 390
location 390
MRI findings 391, *391, 392*
plain film (roentgenogram) findings 391
rupture 390, 391, 392
signs/symptoms 390
skull/facial bones 28, 29
spinal 50, 50, 390
superficial soft tissue 296, 391, 392
treatment 395
desmoid tumor 396-403
abdominal 396
age at presentation 396
children 396, 397
computed tomography findings 397-398
cortical *see* cortical desmoid
deep to subcutaneous fat 272, 273, 397, 398, 399, 400, 401
definition 396
differential diagnosis 399
frequency of occurrence 396
gender ratio 396
genetics 9, 397
gross pathologic findings 397
histopathologic findings 397
location 396-397
bone 396
soft tissue 396-397
MRI findings 398-399
paraspinal 70, 70
plain film (roentgenogram) findings 397-398
prognosis 399
signs/symptoms 397
superficial soft tissue 291, 293, 397, 398, 399
treatment 399
desmoid tumor with bone *see* desmoid tumor
desmoplastic fibroma
age at presentation 396
computed tomography findings 398, 398
definition 396
differential diagnosis 399
gender ratio 396
gross pathologic findings 397
histopathologic findings 397
location 396
MRI findings 398, 398-399
intramedullary, intact cortical margin expansion 124, 125
intramedullary, well-circumscribed margins 146, 147
plain film (roentgenogram) findings 398
prognosis 399
treatment 399
desmoplastic small round cell tumor 8
diaphyseal aclasis 645, 646
diffuse idiopathic skeletal hyperostosis (DISH) 76
diffuse neurofibroma
MRI findings 634, 638
prognosis 637
signs/symptoms 633
treatment 637
diffuse synovial lipoma *see* lipoma arborescens
diffusion-weighted imaging 1
distal femoral cortical irregularity *see* cortical desmoid
Dupuytren contracture
age at presentation 396
frequency of occurrence 396
gender ratio 396
gross pathologic findings 397
histopathologic findings 397
location 396
MRI findings 398
prognosis 399
treatment 399
dural ectasia 62, 62
dysplasia epiphysealis hemimelica (Trevor disease) 645

E

elastofibroma 404-405
age at presentation 404
"beads on a string" appearance 404
computed tomography findings 404
definition 404
differential diagnosis 404
frequency of occurrence 404
genetics 404
gross pathologic findings 404
histopathologic findings 404
location 404
MRI findings 404, 405
"pipe-cleaner" appearance 404
plain film (roentgenogram) findings 404
signs/symptoms 404
treatment/prognosis 404
elephantiasis neuromatosa 633
embryonal carcinoma 770
embryonal rhabdomyosarcoma
age at presentation 732
botryoid variant 732, 733
definition 732
frequency of occurrence 732
genetics 733
gross pathologic findings 732
histopathologic findings 732-733
location 732
MRI findings 734, 736
prognosis 733-735
signs/symptoms 732
spindle cell variant 732, 733
treatment 733-735
embryonal sarcoma see rhabdomyosarcoma
enchondroma
age at presentation 352
computed tomography findings 352
definition 352
differential diagnosis 357
feet 199, *199*
frequency of occurrence 352
gender ratio 352
genetics 352
gross pathologic findings 352
hands 199,199
histopathologic findings 352
location 352
malignant transformation 357
MRI findings 236, 237, 353, 354, 355, 357
delayed enhancement 357
intact cortical margin expansion 122, *123*
intramedullary, well-circumscribed margins 141, 141
intramedullary diaphyseal lesions 190, 191
intramedullary metadiaphyseal lesions 176, 177
tubular bone ends 163, 163
plain film (roentgenogram) findings 352, 353, 354, 355, 356
prognosis 357
signs/symptoms 352
skull/facial bones 26, 27
spinal 42
treatment 357
enchondromatosis 190
endodermal cyst 50, 51

endodermal sinus tumor 770
endolymphatic sac cystadenoma 26, 27
endosteal osteoid osteoma
  computed tomography findings 661, 662, 663
  MRI findings 662, 663, 663-664, 666
    marrow signal 664
  plain film (roentgenogram) findings 661, 662, 663
endothelial tumor markers 5
enostoses 674-678
  age at presentation 674
  computed tomography findings 675, 676
  definition 674
  differential diagnosis 678
  frequency of occurrence 674
  gender ratio 674
  gross pathologic findings 674
  hands/feet 202
  histopathologic findings 675
  location 674
  MRI findings 146,147, 676, 677
  plain film (roentgenogram) findings 675
  spinal 52, 53
  treatment 678
en plaque meningioma 595
eosinophilic granuloma 30, 31, 406-412
  age at presentation 406
  computed tomography findings 407, 407, 408, 409
  definition 406
  differential diagnosis 410
  flat bones 407
  frequency of occurrence 406
  gross pathologic findings 406
  hands/feet 206
  histopathologic findings 407
  immunohistochemistry 407
  within joints 252, 253
  location 406
  long bones 407
  mandible 407
  MRI findings 407, 407, 408, 409, 410, 411, 412
    abnormal marrow signal 152, 153
    bone cortex eroding 88, 89, 128, 129
    diffuse, multiple, poorly defined signal 222
    Gd-contrast enhancement 407, 410
    intramedullary diaphyseal lesions 192, 192
    intramedullary metadiaphyseal lesions 182, 183
    tubular bone ends 170, 174
  plain film (roentgenogram) findings 407, 411, 411-412
  prognosis 410
  radionuclide bone scans 407
  signs/symptoms 406
  skull 407, 407
  spinal 58, 59, 407, 409-410, 410
  treatment 410
ependymoma, paraspinal 64, 64
epidermoid 390-395
  age at presentation 390
  bone erosion 391
  computed tomography findings 391, 393
  congenital 390
  definition 390
  differential diagnosis 395
  frequency of occurrence 390
  gross pathologic findings 390
  histopathologic findings 390
  MRI findings 296, 297, 391, 393, 394
  plain film (roentgenogram) findings 391
  rupture 390
  secondary 390
  signs/symptoms 390
  skull/facial bones 28, 29
  spinal 50
  treatment 395
epidural abscess 72, 72, 685
epidural hematoma 72, 73
epidural lipomatosis 316, 316
epiphyseal osteomyelitis 679
epithelial markers 7
epithelial membrane antigen (EMA) 7
epithelioid hemangioendothelioma
  age at presentation 484
  bone 485
  computed tomography findings 486
  definition 484
  gross pathologic findings 485
  histopathologic findings 486
  plain film (roentgenogram) findings 486
  prognosis 487
  signs/symptoms 485
  soft tissue 485
epithelioid hemangioma 491
epithelioid leiomyosarcoma (malignant leiomyoblastoma) 525
epithelioid osteoblastoma 668
epithelioid sarcoma 288, 288
Epstein Barr virus, Burkitt lymphoma 572
Erdheim-Chester disease 413-415
  age at presentation 413
  computed tomography findings 413
  definition 413
  differential diagnosis 415
  dura 415
  gross pathologic findings 413
  histopathologic findings 413
  location 413
  marrow involvement 414
  MRI findings 413-415
    bone 413, 414
    diffuse, multiple, poorly defined signal 224, 224
    orbital 413, 414
  orbital involvement 413
  plain film (roentgenogram) findings 413, 414
  prognosis 415
  signs/symptoms 413
  treatment 415
erythroid hyperplasia, spinal 59
esthesioneuroblastoma 22, 23
Ewing sarcoma 416-422
  age at presentation 416
  computed tomography findings 417, 417, 418
  definition 416
  differential diagnosis 421
  extra-osseous masses 266, 266, 286, 417, 417, 418, 419, 419, 420
  extraskeletal *see* primitive neuroectodermal tumor
  frequency of occurrence 416
  genetics 7, 416
  gross pathologic findings 416
  "hair on angles" appearance 417
  "hair on end" appearance 172, 419
  hands/feet 209
  histopathologic findings 416
  location 416
  metastatic disease 421
  "moth-eaten" appearance 417
  MRI findings 417, 418, 419-421, 420, 421
    abnormal marrow signal 160, 161
    cortical destruction and extraosseous extension 134, 135
    intramedullary, tubular bone ends 172, 173
    intramedullary diaphyseal lesion 196, 197
    intramedullary metadiaphyseal lesions 186, 187
    post-chemotherapy 421
  "onion-skin" appearance 417, 419, 420
  plain film (roentgenogram) findings 417, 418, 419, 420, 421
  prognosis 421-422
  radionuclide bone scans 417
  signs/symptoms 416
  skull/facial bones 20, 21
  soft tissue 416, 417, 417
    genetic abnormalities 8
  spinal 44, 44, 417
  treatment 421-422
  WHO classification 3
Ewing tumors 416
extradural meningioma 594
extragnathic adamantinoma *see* adamantinoma
extramedullary hematopoiesis
  sickle cell disease and 130, 131
  spinal 60, 60
extraskeletal osteosarcoma
  age at presentation 693
  computed tomography findings 699
  frequency of occurrence 693
  genetics 696
  histopathologic findings 695
  location 694
  metastasis 710
  MRI findings 264, 265, 704, 704, 705, 709, 710
  plain film (roentgenogram) findings 699
  prognosis 710
  superficial soft tissue 286, 286
  treatment 710

F

F.A.B (French, American, British) criteria, acute myelogenous leukemia 532
facial bone tumors/tumor-like lesions 18-37
  acquired 32-34
  benign neoplasms 24-28
  congenital abnormalities 34-36
  inflammatory lesions 30-32
  malignant neoplasms 18-23
  traumatic 34
  see also individual lesions
familial paraganglioma 721

fat containing lesions 312-321
benign 312-319
congenital 312
malignant 320
see also individual lesions
feet, osseous tumors/tumorlike lesions 199-210
benign 199-208
malignant 208-209
Felty's syndrome 738
fibroblastic tumors, WHO classification 4
fibrocartilaginous dysplasia *see* fibrous dysplasia
fibrogenic tumors, WHO classification 3
fibrohistiocystic tumors, WHO classification 3, 4
fibrolipoma 266, 543
fibrolipomatous hamartoma 426-427
"coaxial cables" 308, 426
computed tomography findings 426
definition 426
differential diagnosis 426
frequency of occurrence 426
gross pathologic findings 426
histopathologic findings 426
location 426
MRI findings 308, 308, 426, 427
neural sheath lipoma vs. 426
plain film (roentgenogram) findings 426
prognosis 426
signs/symptoms 426
treatment 426
ulnar nerve 426
fibrolipomatous hamartoma of nerve 314, *315*
fibroma
chondromyxoid *see* chondromyxoid fibroma
desmoplastic *see* desmoplastic fibroma
nonossifying *see* nonossifying fibroma (NOF)
fibroma of the tendon sheath 278, 428-429
age at presentation 428
bone cortex erosion 428, 429
computed tomography findings 428
definition 428
differential diagnosis 429
frequency of occurrence 428
gross pathologic findings 428
hands/feet *428, 428, 429*
histopathologic findings 428
location 428
MRI findings *428,* 428-429, 429
Gd-contrast enhancement 428, 429, 429
superficial soft tissue 302, 303
plain film (roentgenogram) findings 428
prognosis 429
signs/symptoms 428
treatment 429
fibromatosis *see* desmoid tumor
fibromatosis coli
age at presentation 396
computed tomography findings 398
definition 396
frequency of occurrence 396
gender ratio 396
gross pathologic findings 397
histopathologic findings 397
location 397
MRI findings 398, 402
prognosis 399
treatment 399
fibromyxoid sarcoma 433, 434
fibro-osseous dysplasia *see* fibrous dysplasia
fibrosarcoma 433-437
amputation 436
bone
abnormal marrow signal 160
age at presentation 433
computed tomography findings 434
cortical destruction and extraosseous extension 136, *137*
diaphyseal lesions 196
differential diagnosis 436
frequency of occurrence 433
grading 434
gross pathologic findings 433-434
"herringbone pattern" 434
histopathologic findings 434
intramedullary, tubular bone ends 174
location 433
metadiaphyseal lesions 186
"moth-eaten" appearance 434
MRI findings 434, 435
plain film (roentgenogram) findings 434
prognosis 436
signs/symptoms 433
treatment 436
deep to subcutaneous fat 258
definition 433
genetics 434
infantile 433, 434, 436
postradiation 434
soft tissue
age at presentation 433
computed tomography findings 434
differential diagnosis 436
differentiated 434
frequency of occurrence 433
gross pathologic findings 434
histopathologic findings 434
location 433
MRI findings 435, 435, 436
plain film (roentgenogram) findings 434
prognosis 436
signs/symptoms 433
treatment 436
undifferentiated 434
spinal 435
fibrosarcoma, infantile 8
fibrosarcomatous variant of DFSP (FS-DFSP) 383, 384
fibrous cortical defect (FCD) 438-448
age at presentation 438
computed tomography findings 439
definition 438
differential diagnosis 443
frequency of occurrence 438
gross pathologic findings 438
histopathologic findings 439
intramedullary, intact cortical margin expansion 118
location 438
MRI findings 80, 80, 439, 440, 442
plain film (roentgenogram) findings 439, 439, 440
signs/symptoms 438
stress fracture and 440
fibrous dysplasia 449-455
age at presentation 449
bone deformity ("shepherd's crook") 449, 452
computed tomography findings 450, 450-452, 451, 453
definition 449
differential diagnosis 454
frequency of occurrence 449
genetics 450
gross pathologic findings 450
"ground-glass" appearance 450, 450, 451, 452, 453
hands/feet 206, 207
histopathologic findings 450
immunohistochemistry 654
malignant change 454-455
mono-ostotic 117, 449
location 449
MRI findings 450, 451, 452, 452-454, 453, 454
bone cortex thickening 108, 109
Gd-contrast enhancement 452-454
intact cortical margin expansion 117, *117*
intramedullary, well-circumscribed margins 141, *141*
intramedullary diaphyseal lesion 190, *191*
intramedullary metadiaphyseal lesions 180, *181*
osteofibrous dysplasia vs. 654
pathologic fractures 449
plain film (roentgenogram) findings 450-452, 451, 453
polyostotic 117, 226, 226, 449
prognosis 454-455
radionuclide bone scans 452
signs/symptoms 449-450
skull/facial bones 34, 35
treatment 454-455
fibrous meningioma 595
fibrous xanthoma *see* giant cell tumor of the tendon sheath
fibroxanthoma 438-448
age at presentation 438
computed tomography findings 439
definition 438
frequency of occurrence 438
gross pathologic findings 438
histopathologic findings 439
location 438
MRI findings 190, 443, 445
plain film (roentgenogram) findings 439, 445
signs/symptoms 438
treatment 444
fibroxanthosarcoma *see* malignant fibrous histiocytoma (MFH)
FLAIR, epidermoids 391
florid synovitis (diffuse-type giant cell tumor of the tendon sheath) 469, 470, 474
fluorosis 222

FNCLCC (French Federation Nationale des Centres de Lutte Contre le Cancer) system, soft tissue tumor staging 12, 13
foamy macrophages, Erdheim-Chester disease 413
focal aneurysm *see* saccular aneurysm
focal fibrocartilaginous dysplasia 110, *110*
follicular lymphoma
age at presentation 570
histopathologic findings 572
fracture
abnormal marrow signal 152, 153
healed, bone cortex thickening 110, 111
healing, bone cortex thickening 110, 113
intramedullary, tubular bone ends 168, *168*
within joints 252, 253
skull/facial bones 34
spinal 54, 55
Freiberg infarction 218, 512
French, American, British (F.A.B.) criteria, acute myelogenous leukemia 532
functional paraganglioma 721
fungal osteomyelitis 679
computed tomography findings 681
MRI findings 684, 689
plain film (roentgenogram) findings 681
treatment 691
FUS/ATF1 protein 342-343

G

ganglia 272
ganglion, intra-osseous *see* intra-osseous ganglion
ganglion cyst 759
deep to subcutaneous fat 272, 273
outer bone surface 76, 77
superficial soft tissue 294, 295
ultrasonography 457
ganglioneuroblastoma 627-632
age at presentation 627
computed tomography findings 628
definition 627
frequency of occurrence 627
gender ratio 627
gross pathologic findings 627
histopathologic findings 628
intermixed 628
location 627
MRI findings 628, 631
nodular 628
paraspinal 68
peripheral nervous tissue 310
plain film (roentgenogram) findings 628
prognosis 632
radionuclear imaging 628-629
signs/symptoms 627
subtypes 627
ganglioneuroma 627-632
age at presentation 627
computed tomography findings 628
definition 627
frequency of occurrence 627
gender ratio 627
gross pathologic findings 627
histopathologic findings 628
location 627
mature type 628
maturing type 628
MRI findings 628, 631
paraspinal 68, 69
peripheral nervous tissue 308, 309
plain film (roentgenogram) findings 628
prognosis 632
signs/symptoms 627
treatment 632
Gardner syndrome 202
gastrointestinal stromal tumor 8
Gaucher cells 126, 220
Gaucher disease 126, 126, 220, 221
genital leiomyoma 521
geode 456-461
age at presentation 456
definition 456-461
differential diagnosis 458
frequency of occurrence 456
gross pathologic findings 456
histopathologic findings 456-457
intramedullary, tubular bone ends 166, 166
intramedullary, well-circumscribed margins 144, 145
location 456
MRI findings 457, 457, 458
plain film (roentgenogram) findings 457, 457, 458
signs/symptoms 456
geographic destructive pattern (type 1), bone tumors 14
germ cell tumor 770
giant aneurysm 275
giant bone islands 675
giant cell(s) 121
giant cell malignant fibrous histiocytoma
genetics 585
gross pathologic findings 584
histopathologic findings 585
MRI findings *589*
prognosis 589
treatment 589
giant cell reaction to foreign body 276, 300
giant cell reparative granuloma
hands/feet 202, 203
location 328
MRI findings 328-330, 332-333
abnormal marrow signal 154, 155
intact cortical margin expansion 120, 120
intramedullary, well-circumscribed margins 142, 143
intramedullary metadiaphyseal lesions 178, 179
plain film (roentgenogram) findings 332-333
skull/facial bones 30, 30
giant cell tumor
hands/feet 204, 205
intramedullary, abnormal marrow signal 154, 154
intramedullary, tubular bone ends 164, 165
intramedullary, well-circumscribed margins 146, 147
intramedullary metadiaphyseal lesions 178, 179
nonmalignant 86, 87, 130, 130
ossifying *see* osteoblastoma
spinal 46, 46
WHO classification 3
giant cell tumor of bone 462-468
age at presentation 462
aneurysmal bone cyst and 463, 466
"benign" 462
children 462
computed tomography findings 463, 466, 467
definition 462
differential diagnosis 463-464
frequency of occurrence 462
gender ratio 462
genetics 462-463
grading 462
gross pathologic findings 462
histopathologic findings 462
joint extension and 254, 255
location 462
long bones 463
metastases 462, 465
MRI findings 463, 463, 464, 465, 466, 467
Gd-contrast enhancement 463
intramedullary, intact cortical margin expansion 121, 121
plain film (roentgenogram) findings 463, 465
prognosis 464-465
radionuclide scans 463
recurrence 464
signs/symptoms 462
spinal cord compression 463
treatment 464-465
zones of enhancement 463, 465, 467
giant cell tumor of soft tissue 469-475
definition 469
frequency of occurrence 469
location 469
giant cell tumor of the tendon sheath 469-475
age at presentation 469
computed tomography findings 470
differential diagnosis 470
diffuse-type (florid/proliferative synovitis) 469, 470, 474
frequency of occurrence 469
genetics 470
gross pathologic findings 469
histopathologic findings 469-470
within joints 249, 249
location 469
MRI findings 470, 470, 471, 472, 473, 474
deep to subcutaneous fat 278, 279
outer bone surface involving 86, 87
plain film (roentgenogram) findings 470, 474
prognosis 473
recurrence 473
signs/symptoms 469
superficial soft tissue 302, 303
treatment 473
type I 469
type II 469
giant collagen rosettes 434
giant osteoid osteoma *see* osteoblastoma
glomangioma 476
see also glomus tumor
glomangiomyoma 476

glomangiosarcoma (malignant glomus tumor) 476, 477, 478
glomus bodies 291, 476
glomus body tumor
  hands/feet 204, 205
  superficial soft tissue 291, 293
glomus jugulare 26, 27
glomus jugulare tumor
  age at presentation 721
  differential diagnosis 723
  signs/symptoms 721
glomus tumor 476-478
  age at presentation 476
  bone erosion 476
  categorization 476
  computed tomography findings 477
  definition 476
  differential diagnosis 478
  extradigital 476
  fingers 476
  frequency of occurrence 476
  genetics 477
  gross pathologic findings 476
  histopathologic findings 476-477
  location 476
  malignant (glomangiosarcoma) 476, 477, 478
  MRI findings 477, 477
    Gd-contrast enhancement 477, 477
    outer bone surface involving 86, *87*
  plain film (roentgenogram) findings 477
  prognosis 478
  signs/symptoms 476
  solid 476
  treatment 478
glomus tympanicum tumor
  differential diagnosis 723
  signs/symptoms 721
glycogen storage disease type 1A 220
glycogen storage disease type 1B 220
GNAS1 gene 450
Gottron papules 386
gout 479-483
  age at presentation 479
  clinical phases 479
  computed tomography findings 479-480
  deep to subcutaneous fat 276
  definition 479
  differential diagnosis 480
  exacerbations 479
  frequency of occurrence 479
  gross pathologic findings 479
  hands/feet 206, 207
  histopathologic findings 479
  within joints 250, 253
  location 479
  MRI findings 480, 480, *481, 482, 483*
  plain film (roentgenogram) findings 479-480, 482
    "over-hanging" edges 479, *481*
  prevalence 250
  primary 250, 479
  prognosis 480
  secondary 479
  spinal 479-480, 480, 480, 481
  superficial soft tissue 300, 301
  treatment 480
gouty arthritis, acute 479
G-protein mutations 563
granular cell tumor
  peripheral nervous tissue 305, 307
  superficial soft tissue 291, 293
granulocyte colony stimulating factor (G-CSF)
  diffuse, multiple, poorly defined signal 214
  osteosarcoma 703
granulocyte/macrophage colony stimulating factor (G/M-CSF) 215
granulocytic sarcomas *see* chloromas
granuloma annulare 300
granuloma multiplex hemorrhagicum *see* Kaposi sarcoma
ground state 1
gyromagnetic ratio 1

H

Haemophilus influenzae, osteomyelitis 679
hairy cell leukemia
  age at presentation 531
  definition 531
  frequency of occurrence 531
  histopathologic findings 532
  laboratory findings 532
  MRI findings 537-538
  plain film (roentgenogram) findings 533
  prognosis 538
  signs/symptoms 532
  treatment 538
hands, osseous tumors/tumorlike lesions 199-210
  benign 199-208
  malignant 208-209
Hand-Schüller-Christian disease
  age at presentation 406
  frequency of occurrence 406
  gross pathologic findings 406
  location 406
  prognosis 410
  signs/symptoms 406
  treatment 410
head and neck teratoma 770, 773
hemangioendothelioma 484-490
  age at presentation 484
  composite *see* composite hemangioendotheliomas
  computed tomography findings 486
  deep to subcutaneous fat 264
  definition 484
  differential diagnosis 487
  epithelioid *see* epithelioid hemangioendothelioma
  frequency of occurrence 484
  gender ratio 484
  genetics 486
  gross pathologic findings 485
  high-grade *see* angiosarcoma
  histopathologic findings 485-486
  immunohistochemistry 486
  Kaposi-form *see* Kaposi-form hemangioendotheliomas
  location 485
  malignant *see* angiosarcoma
  MRI findings
    bone 486, 486-487, 487, 488
    cortical destruction and extraosseous extension 136, 337
    intact cortical margin expansion 126
    outer bone surface 96, 97
    soft tissue 284, 285, 487, 489
    tubular bone ends 174, 375
  papillary *see* papillary hemangioendothelioma
  plain film (roentgenogram) findings 486, 488
  prognosis 487-488
  retiform *see* retiform hemangioendothelioma
  signs/symptoms 485
  spinal 48, 48
  spindle cell *see* spindle cell hemangioendotheliomas
  subtypes 484
  treatment 487-488
hemangioendotheliosarcoma *see* angiosarcoma
hemangioma 491-501
  age at presentation 491
  arteriovenous *see* arteriovenous hemangioma
  atypical 130, 333, 492, 494
  capillary *see* capillary hemangioma
  cavernous 492, 496
  computed tomography findings 492, 494
  "corduroy vertebrae" 493, 494
  definition 491
  differential diagnosis 495
  epithelioid 491
  fat containing 316, 317
  frequency of occurrence 491
  gross pathologic findings 492
  hands/feet 204
  histopathologic findings 492
  intramuscular 491, 495, 497, 498
  location 491
  long bones 493
  MRI findings
    bone 316, 492, 493
    deep to subcutaneous fat 268, 269
    intact cortical margin expansion 124
    intramedullary, well-circumscribed margins 140, 340
    intramedullary metadiaphyseal lesions 180
    soft tissue 290, 290, 316, 492-495, 494, 495, 496, 497, 499
  ossifying 24, 25
  plain film (roentgenogram) findings
    bone 492
    soft tissue 492, 496
  prognosis 495-496
  signs/symptoms 491
  skull/facial bones 24, 25, 493
    differential diagnosis 495
  synovial 252, 252, 491, 500
  treatment 495, 496
  tubular bones 493
  ultrasonography 492
  venous 491
  vertebral 46, 47, 492, 493, 494
    differential diagnosis 495
hemangiopericytoma 502-506
  age at presentation 502
  children 502, 505
  computed tomography findings 502
  deep to subcutaneous fat 264, 265

hemangiopericytoma
definition 502
differential diagnosis 504
frequency of occurrence 502
genetics 502
gross pathologic findings 502
histopathologic findings 502
location 502
MRI findings
bone 502-503, 503
soft tissue 503, 503, 504, 505
paraspinal 70
plain film (roentgenogram) findings 502, 503
prognosis 504-505
signs/symptoms 502
skull/facial bones 22, 23
spinal 48, 49
"spoked-wheel" patterns 503
synovial sarcoma vs. 502
treatment 504-505
hemangiosarcoma *see* angiosarcoma
hemarthrosis 252
hematoma 507-511
acute 272, 296, 507
MRI findings 507
chronic 272, 296, 507
MRI findings 509, 509, 5JO
computed tomography findings 507
deep to subcutaneous fat 272, 273
definition 507
differential diagnosis 510
epidural 72, 73
gross pathologic findings 507
histopathologic findings 507
location 507
ossifying *see* myositis ossificans
plain film (roentgenogram) findings 507
signs/symptoms 507
subacute 272, 273, 296, 297, 507
MRI findings 507, 508, 509, 530, 533
subperiosteal 90, *91*
superficial soft tissue 296, 297
treatment 510
hematopoeitically-inactive fatty (yellow) marrow 2
hematopoietic disorders
skull/facial bones 34, 35
spinal 58, 59
hematopoietic marrow *see* red marrow
hematopoietic tumors, WHO classification 3
hemochromatosis, multiple transfusions 214, 215
hemoglobin S 212
hemophilic pseudotumor 507-511
computed tomography findings 507
definition 507
differential diagnosis 510
location 507
MRI findings 507, *511*
intramedullary, intact cortical margin expansion 126
intramedullary, well-circumscribed margins 146
outer bone surface 90
plain film (roentgenogram) findings 507
treatment 510
hemorrhage 2
hereditary multiple exostoses 645, 646
hereditary osteochondromatosis 645, 646
herpes 8 virus, large cell lymphoma 572
heterotopic lipoma 543
heterotopic ossification *see* myositis ossificans
hiatal hernia 74, 74
hibernoma 543-553
age at presentation 543
computed tomography findings 544, 548
deep to subcutaneous fat 268, 268
definition 543
frequency of occurrence 543
genetics 9, 544
gross pathologic findings 544
histopathologic findings 544
location 543
MRI findings 314, 335, 548, 550
myxoid variant 544
plain film (roentgenogram) findings 544
signs/symptoms 543
spindle cell variant 544
treatment 551
high-grade hemangioendothelioma *see* angiosarcoma
high-velocity injuries 296
Hildreth sign 476
histiocytes (Langerhans' cells) 128, 406
histiocytic markers 6
histiocytosis X *see* eosinophilic granuloma
HIV infection, osteomyelitis 679
HLA-DR4, rheumatoid arthritis 738
Hodgkin disease (HD)
age at presentation 570
computed tomography findings 572
definition 570
differential diagnosis 575
frequency of occurrence 570
gross pathologic findings 571
histopathologic findings 571
location 570
lymphadenopathy 260, 282
lymphocyte depleted 571
lymphocyte predominant 571
mixed cellular 571
MRI findings 573-574
bone 573, 576
cortical destruction and extraosseous extension 132
Gd-contrast enhancement 573
intramedullary diaphyseal lesion 194
marrow signal 158, 228, 229
soft tissue 573
plain film (roentgenogram) findings 572
prognosis 575-576
signs/symptoms 571
staging 575-576
subtypes 570
treatment 576
Horner syndrome
glomus tumors 721
neuroblastoma 627
vagal paraganglioma 721
Hutchinson syndrome 627
hydrogen MR spectroscopy
dermatomyositis 387
meningioma 597
hydrogen nucleus 1
hypercholesterolemia, xanthomas 774, 774, 775
hyperemia 2
hypertrophic zone, bone 2
hyperuricemia 479
hypervitaminosis A 222
hypervitaminosis D 222
hypoglycemia, hemangiopericytoma 502
hypoparathyroidism 217
hypothenar hammer injury 298, 299
hypovitaminosis C (scurvy) 93, 115

I

idiopathic multiple pigmented sarcoma of the skin *see* Kaposi sarcoma
immunoblasts 611
infiltrative fasciitis *see* nodular fasciitis
inflammatory malignant fibrous histiocytoma
genetics 585
gross pathologic findings 584
histopathologic findings 585
prognosis 589
treatment 589
inflammatory myofibroblastic tumor 8
inflammatory synovitis 738
Intergroup Rhabdomyosarcoma Study Postsurgical Clinical Grouping System 733
interleukins, rheumatoid arthritis 738
International League for Rheumatology 738
International Neuroblastoma Pathology Committee 627, 629-630
intra-articular lipoma 254, 255
intra-articular nodular synovitis, pigmented villonodular synovitis vs. 469
intra-articular osteoid osteoma 660
computed tomography findings 661, 663
differential diagnosis 667
MRI findings 663, 664-667
plain film (roentgenogram) findings 661, 663
intracortical fibrous dysplasia *see* osteofibrous dysplasia
intracortical osteosarcoma
computed tomography findings 698
gross pathologic findings 694
histopathologic findings 695
location 694
MRI findings 703
plain film (roentgenogram) findings 698
intramedullary lesions
cortical destruction and extraosseous extension and 128-139
malignant 132-136
nonmalignant 128-130
intact cortical margin expansion 117-127
benign lesions 117-126
malignant 126
solitary, abnormal marrow signals 150-162
benign 150-156
malignant 156-160
solitary, metadiaphyseal 176-188
benign 176-182
malignant 184-186
solitary, tubular bone ends 163-175
benign 163-170

malignant 170-174
solitary, well-circumscribed margins 140-149
benign 140-146
malignant 146-148
solitary diaphyseal 189-198
benign 189-192
malignant 192-196
intramedullary primary sarcoma 98, 99
intraneural lipoma *see* fibrolipomatous hamartoma
intraosseous calcific tendinopathy 166, 167
intra-osseous chondroma *see* enchondroma
intra-osseous extension of inflammatory synovium/pannus 166, 167
intra-osseous ganglion
age at presentation 456
computed tomography findings 457
definition 456
differential diagnosis 458
frequency of occurrence 456
gross pathologic findings 456
histopathologic findings 457
intramedullary, tubular bone ends 166, 167
intramedullary, well-circumscribed margins 144, 145
location 456
MRI findings 457, 458, 459
plain film (roentgenogram) findings 457
signs/symptoms 456
treatment 459
intra-osseous lipoma
age at presentation 543
calcification 312, 545, 550, 551, 551
computed tomography findings 544-545, 550
differential diagnosis 551
frequency of occurrence 543
gross pathologic findings 544
histopathologic findings 544
location 543
MRI findings 312, 313, 549, 550, 550-551, 551, 552
intramedullary, well-circumscribed margins 144, 145
intramedullary metadiaphyseal lesions 180, 180
tubular bone ends 164, 165
plain film (roentgenogram) findings 544-545, 550, 552
signs/symptoms 544
staging system 544
treatment 551
intra-osseous osteosarcoma
amputation 705
bone cortex thickening 106, 107
chemotherapy 705
computed tomography findings 696, 696-697
"cumulus cloud" appearance 696, 701, 702
definition 693
differential diagnosis 705
frequency of occurrence 693
genetics 696
gross pathologic findings 694
hair on end pattern 699
"ivory vertebrae" appearance 696
location 694
metastasis 705-707
MRI findings 696, 697, 698, 699, 699-703, 700, 701, 702, 703, 704, 705, 706, 707
intramedullary, tubular bone ends 172, 173
plain film (roentgenogram) findings 696-697, 698, 699, 700, 701, 702
prognosis 705-707
signs/symptoms 694
sunburst pattern 699, 701
treatment 705-707
intravascular fasciitis 423
inversion recovery techniques 2
iron deposition, multiple transfusions 214, 215
ivory vertebrae 40
intra-osseous osteosarcoma 696
Paget disease 715, 716

J

Jaffe-Campanacci syndrome 438
joint tumors/tumor-like lesions 247-257
benign 247-254
WHO classification 3
joint tumours/tumour-like lesions
malignant 254-256
see also individual types
jugular foramen (Vernet) syndrome 721
jugulotympanic paraganglioma *see* glomus jugulare tumor
JUN oncogene 463
juvenile dermatomyositis 278
juvenile idiopathic arthritis *see* juvenile rheumatoid arthritis
juvenile intracortical adamantinoma *see* adamantinoma
juvenile nasopharyngeal angiofibroma *see* angiofibroma
juvenile rheumatoid arthritis 738
frequency of occurrence 738
MRI findings 739
juxta-articular bone cyst *see* intra-osseous ganglion
juxtacortical chondroma 359-363
age at presentation 359
bone cortex thickening 104, 105
computed tomography findings 359, 360, 369
definition 359
differential diagnosis 359
frequency of occurrence 359
genetics 359
gross pathologic findings 359
hands/feet 200
histopathologic findings 359
location 359
MRI findings 236, 237, 359, 360, 361, 362, 363, 373, 374
outer bone surface 78, 79
periosteal thickening 359
plain film (roentgenogram) findings 359, 360, 361, 369
signs/symptoms 359
subperiosteal 359, 362-363
treatment/prognosis 359
juxtacortical chondrosarcoma *see* periosteal chondrosarcoma
juxtacortical osteosarcoma
differential diagnosis 705
histopathologic findings 695
location 694
MRI findings 703
prognosis 707
treatment 707
juxtacortical/parosteal chondroma *see* juxtacortical chondroma

K

Kahler disease *see* multiple myeloma
Kaposi disease *see* Kaposi sarcoma
Kaposi-form hemangioendotheliomas
age at presentation 484
definition 484
histopathologic findings 486
location 485
prognosis 487
signs/symptoms 485
Kaposi sarcoma 519-520
age at presentation 519
AIDS-associated 519, 520
bone 519
classic indolent type 519, 520
definition 519
differential diagnosis 520
endemic African type 519, 520
frequency of occurrence 519
genetics 519
gross pathologic findings 519
histopathologic findings 519
iatrogenic 519, 520
location 519
metastatic 520
MRI findings 519, 520
nodular stage 519
patch stage 519
plain film (roentgenogram) findings 519
plaque stage 519
prognosis 520
soft tissue 286, 287, 519
treatment 520
Kasabach-Merittsyndrome/phenomenon 485, 491
Kempson-Campanacci lesion *see* osteofibrous dysplasia
Kienbock disease 218, 512
Kimura disease 302
Kohler disease 218, 512

L

Langerhans' cell histiocytosis *see* eosinophilic granuloma
Langerhans' cells (histiocytes) 128, 406
large cell lymphoma
age at presentation 570
histopathologic findings 572
Larmor equation 1
Larmor frequency 1
Legg-Calvé-Perthes disease 218, 512
prognosis 515-516
treatment 515-516
leiomyoma 521-524
age at presentation 521
bone 521, 522
computed tomography findings 522

leiomyoma
cutaneous *see* leiomyoma cutis
deep soft tissue 521, 522
definition 521
differential diagnosis 522
frequency of occurrence 521
gender ratio 521
genetics 9
gross pathologic findings 521
histopathologic findings 521-522
MRI findings 522, 522, 523, 524
plain film (roentgenogram) findings 522
signs/symptoms 521
superficial soft tissue 291, 293
vascular *see* angioleiomyomas
leiomyoma cutis (cutaneous leiomyoma)
age at presentation 521
definition 521
differential diagnosis 522
gross pathologic findings 521
histopathologic findings 521
location 521
MRI findings 291
prognosis 522
signs/symptoms 521
treatment 522
leiomyosarcoma 525-530
age at presentation 525
children 526
computed tomography findings
bone 525-526, 529
soft tissue 525
deep to subcutaneous fat 262, 263
definition 525
differential diagnosis 526
epithelioid 525
frequency of occurrence 525
genetics 8, 525
grading 525
gross pathologic findings 525
histopathologic findings 525
immunohistochemical findings 585
immunoreactivity 525
location 525
metastases 526
MRI findings
bone 526, 529
soft tissue 284, 285, 526, 526, 527, 528
paraspinal 71
plain film (roentgenogram) findings
bone 525-526
soft tissue 525
prognosis 526
signs/symptoms 525
treatment 526
leontiasis ossea 449
Letterer-Siwe disease 406, 410
leukemia 531-539
age at presentation 531
chemotherapy 538
computed tomography findings 532-533
definition 531
differential diagnosis 538
frequency of occurrence 531
gender ratio 531
histopathologic findings 532
intra-articular extension 256
laboratory findings 532
leukocyte count 532
location 531
lymphoma vs. 531
MRI findings 533-538
abnormal marrow signal 156
cortical destruction and extraosseous extension 132, 133
deep to subcutaneous fat 262, 262
diffuse, multiple, poorly defined signal 230, 230, 231
intramedullary, tubular bone ends 172
outer bone surface involving 100, 300
plain film (roentgenogram) findings 532-533
prognosis 538
sign/symptoms 531-532
skull/facial bones 18, 19
spinal 40, *41*
treatment 538
leukemia cutis 282
leukocyte differentiation antigens 5-6
Lichtenstein-Jaffe disease *see* fibrous dysplasia
Li-Fraumeni syndrome 696
lipoblastoma
age at presentation 540
computed tomography findings 540, 541
deep to subcutaneous fat 268, 269
definition 540
differential diagnosis 541
fat containing 314, 315
frequency of occurrence 540
gender ratio 540
genetics 9, 540
gross pathologic findings 540
histopathologic findings 540
location 540
MRI findings 540, 541
paraspinal 71, 71
plain film (roentgenogram) findings 541
prognosis 541
signs/symptoms 540
superficial soft tissue 288, 289
treatment 541
lipoblasts 540
lipofibroma *see* fibrolipomatous hamartoma
lipofibromatous hamartoma *see* fibrolipomatous hamartoma
lipogenic tumors, WHO classification 3
lipoma 543-553
atypical *see* atypical lipoma
bone *see* intra-osseous lipoma
deep to subcutaneous fat 266, 267
definition 543
fat containing 313
Gd-contrast enhancement 546, 547, 549
gender ratio 543
genetics 9, 544
hands/feet 202, 203
heterotopic 543
intra-articular 254, 255
intradural 312, 313, 545, 549
myxoid 548
parosteal *see* parosteal lipoma
periosteal *see* parosteal lipoma
pleomorphic *see* pleomorphic lipoma
soft tissue *see* soft tissue lipoma
spinal 312
spindle cell *see* spindle cell lipoma
lipoma arborescens
age at presentation 543
computed tomography findings 544
definition 543
frequency of occurrence 543
gross pathologic findings 544
histopathologic findings 544
within joints 254, 255
location 543
MRI findings 318, 319, 548, 550
signs/symptoms 543
treatment 551
lipomatosis 312
deep to subcutaneous fat 266, 267
definition 543
diffuse type 266, 312
epidural 316, 316
multiple symmetric (Madelung disease) 312
lipomatosis of the nerve *see* fibrolipomatous hamartoma
lipomatous hamartoma *see* fibrolipomatous hamartoma
lipomyelocele 312, 313
lipomyelomeningocele 62, 63, 312
liposarcoma 554-562
age at presentation 554
calcification 555
computed tomography findings
bone 555
soft tissue 555, 556
dedifferentiated *see* dedifferentiated liposarcoma
definition 554
differential diagnosis 557
frequency of occurrence 554
gender ratio 554
genetics 8, 555
gross pathologic findings 554
histopathologic findings 554-555
location 554
MRI findings 320, 320, 321
bone 138, 138, 557
soft tissue 280, 281, 555-557
myxoid *see* myxoid liposarcoma
paraspinal 71
plain film (roentgenogram) findings
bone 555
soft tissue 555, 558, 560
pleomorphic *see* pleomorphic liposarcoma
prognosis 557-558
pseudocapsule 554
round cell *see* round cell liposarcoma
signs/symptoms 554
subtypes 554
treatment 557-558
well-differentiated *see* well-differentiated liposarcoma
liposclerosing myxofibrous tumor 563-565
age at presentation 563
computed tomography findings 563, 564
definition 563
differential diagnosis 563
frequency of occurrence 563
genetics 563
gross pathologic findings 563
histopathologic findings 563

liposclerosing myxofibrous tumor
intramedullary, well-circumscribed margins 142, 342
intramedullary metadiaphyseal lesions 180, 281
location 563
MRI findings 318, 319, 563, 564, 565
plain film (roentgenogram) findings 563, 564
prognosis 563
signs and symptoms 563
treatment 563
Lisch nodules 633
Lofgren syndrome 744
longitudinal relaxation 1
loose bodies, synovial chondromatosis 753
Love's test 476
low-grade angiosarcoma *see* hemangioendothelioma
low-grade hemangioendothelial sarcoma *see* hemangioendothelioma
low-grade hemangioendothelioma *see* hemangioendothelioma
lymphangiohemangioma 566
lymphangioma 566-569
age at presentation 566
capillary (simple) 566
cavernous 566
computed tomography findings 566
deep to subcutaneous fat 268, 567, 568
definition 566
differential diagnosis 568
genetics 566
gross pathologic findings 566
histopathologic findings 566
intra-osseous 566
location 566
MRI findings 567, 567, 568
prognosis 568-569
signs/symptoms 566
simple 566
superficial soft tissue 290, 567
treatment 568-569
types 566
ultrasound findings 567-568
lymphangiomatosis, congenital 566
lymphoadenopathic mastocytosis with eosinophilia (mastocytosis category III) 232
lymphoblastic lymphoma
age at presentation 570
histopathologic findings 571
lymphoblasts 532
lymphoma 570-583
age at presentation 570
AIDS-related 578
definition 570
differential diagnosis 575
frequency of occurrence 570
gender ratio 570
gross pathologic findings 571
histopathologic findings 571
intra-articular extension 256, 256
location 570-571
lymphadenopathy 68
MRI findings 573-574
abnormal marrow signal 158, 158
cortical destruction and extraosseous extension 132, 133
deep to subcutaneous fat 260, 261
intramedullary, well-circumscribed margins 148, 149
intramedullary diaphyseal lesion 194, 194
intramedullary metadiaphyseal lesions 184, 185
outer bone surface 98, 99
superficial soft tissue 282, 282, 283
tubular bone ends 172, 173
paraspinal 68, 69
prognosis 575-578
signs/symptoms 571
skull/facial bones 18, 29
spinal 40, 40, 41
treatment 575-578
lymphoma of nerve 310, 310
lymphoplasmacyte-rich meningioma 595
lymphoplasmacytic lymphoma 232, 233

M

macrodystrophia lipomatosa 426
macrophage colony stimulating factor (M-CSF) 214
Madelung disease (multiple symmetric lipomatosis) 312
Madura foot 681
Maffucci disease 122, 190
frequency of occurrence 352
genetics 352
hands 199, 299
Maffucci syndrome
age at presentation 352
definition 352
gender ratio 352
location 352
malignant transformation 357
MRI findings 357, 357
diffuse, multiple, poorly defined signal 224, 225
plain film (roentgenogram) findings 352
prognosis 496
magnetic moment 1
magnetic resonance imaging (MRI) 1-2
bone tumors 14-15
contraindications 1
image generation 1
indications 1
planes 1
scanner components 1
signal generation 1
soft tissue contrast 1
soft tissue tumors 14-15
magnetic resonance spectroscopy 1
malabsorption syndrome 222
malignancy related vertebral fracture 54, 55
malignant chondroblastoma *see* clear cell chondrosarcoma
malignant chondrosarcoma *see* clear cell chondrosarcoma
malignant endovascular papillary angioendotheliomas *see* papillary hemangioendothelioma
malignant fibrous histiocytoma (MFH) 136, 137, 584-593
age at presentation 584
computed tomography findings
bone 587
soft tissue 585
definition 584
differential diagnosis 588
frequency of occurrence 584
gender ratio 584
genetics 8, 585
giant cell *see* giant cell malignant fibrous histiocytoma
grading 589
gross pathologic findings 584-585
histopathologic findings 585
immunohistochemical findings 585
location 584
metastases 589
MRI findings
abnormal marrow signal 160, 162
bone 587, 587, 588
deep to subcutaneous fat 258, 258-266
Gd-contrast enhancement 586, 587, 590
hemorrhage 587
intramedullary, tubular bone ends 174
intramedullary diaphyseal lesion 196
intramedullary metadiaphyseal lesions 186, 288
soft tissue 586, 587, 589, 590, 591, 592
myxoid *see* myxofibrosarcoma
plain film (roentgenogram) findings
bone 587, 587
soft tissue 585
pleomorphic *see* pleomorphic malignant fibrous histiocytoma
prognosis 588-589
radiation treatment-induced 584
signs/symptoms 584
spinal 44, 45
storiform-pleomorphic 585, 589
subtypes 584
superficial soft tissue 280, 281
treatment 588-589
WHO classification 584
malignant fibrous xanthoma *see* malignant fibrous histiocytoma (MFH)
malignant giant cell tumor
intramedullary, abnormal marrow signal 160, 261
intramedullary, cortical destruction and extraosseous extension 136, 137
intramedullary, tubular bone ends 174, 175
intramedullary, well-circumscribed margins 148
malignant hemangioendothelioma *see* angiosarcoma
malignant hemangiopericytoma 8
malignant histiocytoma *see* malignant fibrous histiocytoma (MFH)
malignant leiomyoblastoma (epithelioid leiomyosarcoma) 525
malignant peripheral nerve sheath tumor (MPNSTs) 308, 309, 633-641
computed tomography findings 634
deep to subcutaneous fat 262, 263
definition 633
genetic abnormalities 8
glandular 634
gross pathologic findings 634
histopathologic findings 634

malignant peripheral nerve sheath tumor (MPNSTs)
location 633
MRI findings 637, 639, 640, 748, 752
paraspinal 67, 67
plain film (roentgenogram) findings 634, 640
prognosis 637
signs/symptoms 633
STIR 640
superficial soft tissue 284, 284
treatment 637
malignant rhabdomyoma see rhabdomyosarcoma
malnutrition, serous marrow atrophy 220, 223
mantle cell lymphoma
age at presentation 570
histopathologic findings 572
Marfan syndrome 62
mastocytosis 232
Mazabraud syndrome
definition 449, 624
location 449
prognosis 455
McCune-Albright syndrome
computed tomography findings 453
definition 449
MRI findings 226, 453
signs/symptoms 450
mediastinal teratoma 770
melanoma
immunohistochemical markers 6
superficial soft tissue 282
melanoma of soft parts *see* clear cell sarcoma
melorheostosis 674-678
age at presentation 674
bone cortex thickening 110, *111*
computed tomography findings 676, 677
definition 674
differential diagnosis 678
"dripping/flowing candle wax" appearance 674
frequency of occurrence 674
gender ratio 674
gross pathologic findings 675
histopathologic findings 675
location 674
MRI findings 677, 677
outer bone surface 82, 83
plain film (roentgenogram) findings 676
signs/symptoms 674
spinal 52, 53
treatment 678
meningioma 594-600
age at presentation 594
anaplastic *see* anaplastic meningioma
angiomatous 595
atypical 595
chordoid 595
clear cell 595
computed tomography findings 595, 600
definition 594
differential diagnosis 597
en plaque 595
extradural 594
fibrous 595
frequency of occurrence 594
gender ratio 594
genetics 595
gross pathologic findings 594-595
histopathologic findings 595
hydrogen MR spectroscopy 597
intracranial 595
MRI findings 596, 597, 597
intra-osseous 594
computed tomography findings 595, 600
differential diagnosis 597
MRI findings 597, 600
location 594
lymphoplasmacyte-rich 595
meningothelial 595
metaplastic 595
microcystic 595
MRI findings 595-597
outer bone surface 84, 85
neurofibromatosis type 2 25, 596
orbital 594
papillary 595
paraspinal 67, 67
plain film (roentgenogram) findings 595
primary extraneuraxial 594
primary neuraxial *see* primary neuraxial meningioma
prognosis 597
psammomatous 595
rhabdoid 595
secondary 594
secretory 595
signs/symptoms 594
skull/facial bones 24, 24, 25
spinal 594, 596, 598, 599
subtypes 595
transitional (mixed) 595
meningoceles 34, 62, 62
meningoencephaloceles 34, 35
meningothelial (arachnoidal, arachnoid cap) cells 594
meningothelial meningioma 595
meniscal cyst *see* ganglion cyst
Merkel cell tumor
peripheral nervous tissue 310, *311*
superficial soft tissue 286, 287
merlin (schwannomin) gene product 748
mesenchymal chondrosarcoma
computed tomography findings 371
histopathologic findings 369
location 368
MRI findings 244, 244, 375, 376
plain film (roentgenogram) findings 371
prognosis 377
treatment 377
mesenchymal markers 7
mesenchymomas 543
mesothelioma 8
metachondromatosis 122, 190, 224
definition 352, 645
frequency of occurrence 352
metaphyseal fibrous defect *see* fibrous cortical defect (FCD)
metaplastic meningioma 595
metastatic lesions 601 -608
age at presentation 601
children 601, 605
computed tomography findings 601, 603
cortical destruction 602-603
deep to subcutaneous fat 260, 261
definition 601
diagnosis 601
differential diagnosis 605
diffuse, multiple, poorly defined and/or multifocal zones of abnormal marrow signal 227, 227
dural 602, 603-604
frequency of occurrence 601
Gd-contrast enhancement 602
hands/feet 208
histopathologic findings 601
intramedullary, tubular bone ends 170
intramedullary diaphyseal lesion 192, 193
intramedullary metadiaphyseal lesions 184, 185
location 601
MRI findings 602, 602-604
bone 602, 602-604, 603, 604, 605
soft tissue 604, 607, 608
occurrence 9
osteoclastic activity 601
outer bone surface involving 98, 99
paraspinal 70
pathologic fractures 603
plain film (roentgenogram) findings 601, 604, 606
prognosis 607
radiolucent patterns 601
sclerotic 601, 603
signs/symptoms 601
skeletal 601
meninges invasion 603-604
soft tissue 601
superficial soft tissue 280, 281
treatment 607
tubular bones 602
metastatic tumor
intra-articular extension 254
intramedullary, abnormal marrow signal 156, 157
intramedullary, cortical destruction and extraosseous extension 132, 133
intramedullary, intact cortical margin expansion 126, 127
intramedullary, well-circumscribed margins 146, 147
skull/facial bones 18, 18
spinal 38, 38
methemoglobin 2
1-123-MIBG scintigraphy, neuroblastoma 629
MIC2 gene 416
microcystic meningioma 595
monoclonal antibodies 570
monoclonal immunoglobulin (M-protein), multiple myeloma 611
Morel-Lavallee lesion 507-511
definition 507
MRI findings 509, 509
superficial soft tissue 296, 506
Morton neuroma 305, 307, 609-610
age at presentation 609
computed tomography findings 609
definition 609
differential diagnosis 610
gender ratio 609
gross pathologic findings 609

histopathologic findings 609
location 609
MRI findings 609, 609-610, 610
fat-suppression 609, 610
plain film (roentgenogram) findings 609
signs/symptoms 609
treatment 610
"moth-eaten" radiolucent pattern (type 2), bone tumors 14
M-protein (monoclonal immunoglobulin), multiple myeloma 611
MR angiography 1
hibernoma 550
multiple enchondromatosis 224, 225
multiple myeloma 611-617
age at presentation 611
computed tomography findings 612, *613, 614*
deep to subcutaneous fat 260
definition 611
differential diagnosis 615
extra-osseous 611
frequency of occurrence 611
genetics 612
gross pathologic findings 611
hands/feet 208
histopathologic findings 611-612
intra-articular extension 254, 255
laboratory findings 611
location 611
MRI findings 612, 635, 626, 617
abnormal marrow signal 156, 157
cortical destruction and extraosseous extension 132, 133
diffuse, multiple, poorly defined signal 228, 228
Gd-contrast enhancement 612, 615, 616, 617
intramedullary diaphyseal lesions 194
intramedullary metadiaphyseal lesions 184
outer bone surface involving 98, 99
soft tissue 612, 613, 613, 615
osteosclerotic 612
pathologic fractures 611
plain film (roentgenogram) findings 612, 617
prognosis 615
signs/symptoms 611
skull/facial bones 18, 19
solitary *see* plasmacytoma
staging system 612
treatment 615
vertebral 38, 39, 612, 615
multiple sclerotic osteosarcoma 694
multiple transfusions 214
muscle denervation 318, 319
muscle infarct 318, 319, 512-518
definition 512
differential diagnosis 515
histopathologic findings 512
location 512
MRI findings 515, 517
musculoskeletal lesions, contrast-enhance MRI 14
musculoskeletal system sarcomas 10
musculoskeletal tuberculosis 679
Musculoskeletal Tumor Society (MSTS), bone tumor staging system 12
mycosis fungoides
age at presentation 570
histopathologic findings 572
location 571
MRI findings 283, 574, 582
prognosis 578
myeloblasts 230
myelocele 60
myelodysplastic syndromes (MDS) 230, 231
myeloma *see* multiple myeloma
myelomeningocele 60, 61
myoepithelial carcinoma 288, 289
myofibroblastic sarcoma 585
myofibroblastic tumors, WHO classification 4
myosarcoma *see* rhabdomyosarcoma
myositis
bone infection and 88, 89
deep to subcutaneous fat 276, 277
myositis ossificans 618-623
age at presentation 618
computed tomography findings 618
definition 618
differential diagnosis 622
frequency of occurrence 618
gross pathologic findings 618
histopathologic findings 618
location 618
mineralization/ossification 274
MRI findings 618-619, 620, 621, 622
cortical thickening 108, 108
deep to subcutaneous fat 274, 274
Gd-contrast enhancement 619, 620, 621, 622
mineralization/ossification 618, 619
outer bone surface 82, 83
plain film (roentgenogram) findings 618, 619, 620, 621, 622
prognosis 622
signs/symptoms 618
superficial soft tissue 296, 297
treatment 622
myositis ossificans circumscripta 618
myositis ossificans progressiva 618
myxofibrosarcoma
deep to subcutaneous fat 258, 258
definition 433, 584
genetics 585
gross pathologic findings 584
histopathologic findings 434, 585
MRI findings 435, 436
prognosis 588
subclassification 588
treatment 588
myxoid angioblastoma *see* hemangioendothelioma
myxoid chondrosarcoma
computed tomography findings 371, 376
gross pathologic findings 369
histopathologic findings 369
location 368
MRI findings 242, 242, 243, 373, 376
plain film (roentgenogram) findings 371, 373
prognosis 377
treatment 377
myxoid lipoma 548
myxoid liposarcoma
age at presentation 554
differential diagnosis 557
genetics 555
histopathologic findings 555
location 554
MRI findings 320, 321, 559, 560, 561
deep to subcutaneous fat 259, 259
superficial soft tissue 280, 281
prognosis 557
treatment 557
myxoid malignant fibrous histiocytoma *see* myxofibrosarcoma
myxoma 624-626
age at presentation 624
computed tomography findings 624
cystic components 624
deep to subcutaneous fat 272, 273
definition 624
differential diagnosis 625
frequency of occurrence 624
genetics 9, 624
gross pathologic findings 624
histopathologic findings 624
location 624
MRI findings 624, 625, 625, 626
plain film (roentgenogram) findings 624
prognosis 625
signs/symptoms 624
superficial soft tissue 294, 624, 625
treatment 625
ultrasonography 624

N

nasopharyngeal carcinoma 22, 22, 23
nasopharyngeal teratoma 771
NCI (United Stated National Cancer Institute) system, soft tissue tumor staging 12
nerve lipoma *see* fibrolipomatous hamartoma
nerve root avulsion 305, 307
nerve sheath myxoma *see* neurothekeoma
nerve sheath tumor
deep to subcutaneous fat 270, 270, 271
markers 6
superficial soft tissue 291, 292
neural fibrolipoma *see* fibrolipomatous hamartoma
neural placode 60, 312
neural tumor markers 6
neural tumors, WHO classification 3
neurilemmoma *see* schwannoma
neurinoma *see* schwannoma
neuroblastoma 627-632
age at presentation 627
chemotherapy 632
children 631
computed tomography findings 628
definition 627
differential diagnosis 629
frequency of occurrence 627
gender ratio 627
genetics 8, 628
gross pathologic findings 627
histopathologic findings 628
location 627
metastases 632
MRI findings 310, 310, 628, 629, 631
paraspinal 68, 69, 310

neuroblastoma
peripheral nervous tissue 310, 310
plain film (roentgenogram) findings 628
prognosis 629-632
radionuclear imaging 628-629
signs/symptoms 627
staging 630
treatment 629-632
neuroblasts 628
neuroendocrine-specific markers 6
neuroenteric cyst 50, *51*
neurofibroma 633-641
age at presentation 633
computed tomography findings 634
definition 633
differential diagnosis 637
diffuse *see* diffuse neurofibroma
dumb-bell shape spinal nerve roots 638
frequency of occurrence 633
genetic abnormalities 9
gross pathologic findings 633
histopathologic findings 634
intra-osseus 634
localized 84, *84,* 291, 292
location 633
MRI findings 634-637, 635, 636, 637, 638
Gd-contrast enhancement 634, 638
outer bone surface 84, *84, 85*
paraspinal 64, 65
peripheral nervous tissue 305, 306
plain film (roentgenogram) findings 634
plexiform *see* plexiform neurofibroma
prognosis 637
signs/symptoms 633
skull/facial bones 36
treatment 637
neurofibromatosis type 1 (NF1)
bone 112, 313, 633
malignant peripheral nerve sheath tumor 262
neurofibroma in 84, 633
histopathologic findings 634
location 633
MRI findings 635, 636, 637, 638
outer bone surface involving 93, 93
prognosis 637
signs/symptoms 633
skull/facial bones 36, 36
soft tissue 633
treatment 637
neurofibromatosis type 2 (NF2)
incidence 747
meningioma 25, 596
schwannoma 747
neurogenic edema 318
neurothekeoma
computed tomography findings 639
deep to subcutaneous fat 270, 271
histopathologic findings 634
MRI findings 305, 307, 634, 639
NF-2 gene 595, 748
nidus 104
NME2 oncogene, giant cell tumor of bone 463
nodular fasciitis 423-425
age at presentation 423
computed tomography findings 423, 424
definition 423
differential diagnosis 423
frequency of occurrence 423
genetics 423
gross pathologic findings 423
histopathologic findings 423
immunohistochemistry 423
location 423
MRI findings 423, 424
deep to subcutaneous fat 268, 269
superficial soft tissue 290, 424
plain film (roentgenogram) findings 423
prognosis 423
signs/symptoms 423
treatment 423
nodular sclerosis 571
nodular synovitis *see* giant cell tumor of the tendon sheath
nodular tenosynovitis *see* giant cell tumor of the tendon sheath
non-Hodgkin lymphoma (NHL)
age at presentation 570
chemotherapy 578
classification schemes 570
computed tomography findings
bone 572-573, 577
soft tissue 573, 577
definition 570
differential diagnosis 575
frequency of occurrence 570
gross pathologic findings 571
histopathologic findings 571-572
intra-articular extension 256
location 571
lymphadenopathy 260, 282
MRI findings
abnormal marrow signal 158, 228,229
bone 572, 573, 573-574, 575, 577, 578, 579, 580, 581
cortical destruction and extraosseous extension 132, 133
diffuse, multiple, poorly defined signal 228, 229
Gd- contrast enhancement 579
intramedullary diaphyseal lesion 194, 194
intramedullary metadiaphyseal lesions 184, 185
soft tissue 282, 282, 574, 577, 578, 582, 583
tubular bone ends 173
paraspinal 69
peripheral nervous tissue 310, 310
plain film (roentgenogram) findings 578, 579, 580
bone 572-573, 580
moth-eaten appearance 572
primary osseous 570, 571
prognosis 576-578
secondary osseous 570, 571
signs/symptoms 571
skull/facial bones 19
spinal cord 574, 574, 575, 577
staging 576
subtypes 570
treatment 576-578
vertebral 40, 41, 574, 574-575
Nonne-Milroy-Meige syndrome 566
nonossifying fibroma (NOF) 438-448
age at presentation 438
computed tomography findings 439
definition 438
differential diagnosis 443
frequency of occurrence 438
gross pathologic findings 438
histopathologic findings 439
location 438
MRI findings 80, *81 441, 442,* 442-443, 443, *444, 445*
cortical margin expansion 118,119
intramedullary metadiaphyseal lesions 176, 176
well-circumscribed margins 140, 140
plain film (roentgenogram) findings 439, 441, 442, 445
prognosis 444
signs/symptoms 438
treatment 444
nonsteroidal anti-inflammatory drugs, rheumatoid arthritis 743
notochordal tumors, WHO classification 3

O

Oilier disease 122, 190
age at presentation 352
definition 352
frequency of occurrence 352
gender ratio 352
genetics 352
location 352
MRI findings 224, 225, 356
Ondine curse 627
opsoclonus-myoclonus 627
ossifying fasciitis 423
ossifying fibroma of the fibula *see* osteofibrous dysplasia
ossifying fibroma of the tibia *see* osteofibrous dysplasia
ossifying giant cell tumor *see* osteoblastoma
ossifying hemangioma 24, 25
ossifying hematoma *see* myositis ossificans
osteitis condensans 217, 217
osteoarthritic cyst *see* geode
osteoblastic sarcoma *see* osteosarcoma
osteoblastoma 668-673
age at presentation 668
aneurysmal bone cysts and 668, 669, 671-672
calcification 669, 669, 670
cartilage formation 668
computed tomography findings 669, 669, 670, 671
cryosurgery 673
definition 668
differential diagnosis 673
epithelioid 668
frequency of occurrence 668
genetics 669
gross pathologic findings 668
hands/feet 200, 201
histopathologic findings 668
location 668
marrow fat 669
MRI findings 669, 669-673, 670, 671, 672
abnormal marrow signal 156,157
cortical thickening 104, 105
Gd-contrast enhancement 669, 670, 671, 672

intact cortical margin expansion 122, 123
intramedullary, tubular bone ends 164,165
periosteal reaction 669
plain film (roentgenogram) findings 669, 670, 671, 672
prognosis 673
radiation therapy 673
signs/symptoms 668
skull/facial bones 26, 27, 668
treatment 673
vertebral 44, *45,* 668
osteocalcin 7
osteocartilaginous exostosis *see* osteochondroma
osteochondritis dissecans 168,169
osteochondroma645-653
age at presentation 645
bursae 646, 649, 650, 651
cartilage containing 236, 237, 645
children 645
computed tomography findings 646-649, 647, 648, 649, 652
definition 645
differential diagnosis 650
fractures 649-650
frequency of occurrence 645
genetics 645, 646
gross pathologic findings 645
hands/feet 200,201
histopathologic findings 645-646
location 645
malignant transformation 645, 646, 650
MR1 features 650, 652
MRI findings 646, 647, 648, 649, 649-650, 650, 651, 652
Gd-contrast enhancement 649
intramedullary, intact cortical margin expansion 117, 117
outer bone surface 78, 78
pedunculated 646, 648, 652
perichondrium 645-646
plain film (roentgenogram) findings 646, 646-649, 648, 650, 652
post-neuroblastoma treatment 645
post-Wilm tumor treatment 645
prognosis 650
pseudoarthrosis 647, 647, 649
sessile 646, 649, 650
signs/symptoms 645
spinal cord compression 647, 650
synovia! 238, 247, 247
treatment 650
vertebral 46, 47, 645
osteochondromatosis, synovial see synovial osteochondromatosis
osteoclasts 668
osteofibrous dysplasia 654-659
age at presentation 654
bone cortex thickening 108, 109
children 658
computed tomography findings 654-656
definition 654
differential diagnosis 657
fibrous dysplasia vs. 654
frequency of occurrence 654
Gd-contrast enhancement 656-657
genetics 654
gross pathologic findings 654
histopathologic findings 654
immunohistochemistry 654
intramedullary, intact cortical margin expansion 124, 125
location 654
marrow enhancement 657
MRI findings 655, 656, 656-657, 657, 658-659
pathologic fractures 654-656
plain film (roentgenogram) findings 654-656, 655, 656, 657, 65S
prognosis 657-658
radiolucent zones 654
"saw tooth" appearance 654
signs/symptoms 654
treatment 657-658
osteofibrous dysplasia-like adamantinoma 325, 658
osteogenic sarcoma *see* osteosarcoma
osteogenic tumors, WHO classification 3
osteoid osteoma 660-667
age at presentation 660
bone marrow 660
cancellous 661, 664, 667
computed tomography findings 661
cortical *see* cortical osteoid osteoma
cortical bone thickening 104, 105, 660
definition 660
differential diagnosis 667
en bloc resection 667
endosteal *see* endosteal osteoid osteoma
evolutionary phases 660
frequency of occurrence 660
genetics 660
giant *see* osteoblastoma
gross pathologic findings 660
hands/feet 200,201
histopathologic findings 660
intra-articular *see* intra-articular osteoid osteoma
intracapsular 661, 664
intracortical see cortical osteoid osteoma
location 660
MRI findings 661-667
marrow signal 154, 155
nidus (central region) 660
periosteal 78, 79
plain film (roentgenogram) findings 661
prognosis 667
signs/symptoms 660
skull/facial bones 26, 27
spinal 44, 45
subperiosteal *see* subperiosteal osteoid osteoma
treatment 667
tubular bones 660
osteolipomas 543
MRI findings 547, 549-550
osteoma 674-678
age at presentation 674
computed tomography findings 675, 675, 676
definition 674
differential diagnosis 678
frequency of occurrence 674
gender ratio 674
gross pathologic findings 674
histopathologic findings 675
location 674
MRI findings 675, 676, 676-677
cortical thickening 104, 105
outer bone surface 80, 81
multiple 80
parosteal 674
plain film (roentgenogram) findings 675
radionuclide bone scan 676
signs/symptoms 674
skull/facial bones 28, 29
trabecular/spongy 675
treatment 678
osteomyelitis 679-692
acute 152, 170, 206
age at presentation 679
bone neoplasms and 679
chronic 690
bone cortex thickening 112, 113
MRI findings 689
pathologic findings 680
plain film (roentgenogram) findings 689
chronic recurrent multifocal 679
computed tomography findings 680-681, 690
definition 679
differential diagnosis 689
epiphyseal 679
etiology 679
fungal *see* fungal osteomyelitis
hands/feet 206, 207
location 679
MRI findings 690
abnormal marrow signal 152, 153
cortical destruction and extraosseous extension 128, 128
diffuse, multiple, poorly defined signal 222,223
intramedullary diaphyseal lesions 192, 193
intramedullary metadiaphyseal lesions 182, 183
outer bone surface 88, 89
tubular bone ends 170, 171
pathogens 679
pathologic findings 680
pedal 679, 681
plain film (roentgenogram) findings 680-681
pyogenic *see* pyogenic osteomyelitis
radionuclide bone scan 681
signs/symptoms 679-680
subacute 112, 152, 170, 206
see also Brodie abscess
tuberculous *see* tuberculous osteomyelitis
osteonecrosis *see* bone infarct
osteonectin 7
osteoblastoma 668
osteopathia condensans disseminata *see* osteopoikilosis
osteopenic vertebral fracture 54, 55
osteopetrosis 220, 221
osteophytes (bony spurs) 76, 76
osteopoikilosis 674-678
age at presentation 674
computed tomography findings 675-676,677
definition 674

osteopoildlosis
  differential diagnosis 678
  frequency of occurrence 674
  gender ratio 674
  gross pathologic findings 675
  histopathologic findings 675
  location 674
  MRI findings 677, 677
    diffuse, multiple, poorly defined signal 226, 226
  plain film (roentgenogram) findings 675-676, 677
  signs/symptoms 674
  treatment 678
osteoporosis, transient of the hip *see* transient bone marrow edema
osteosarcoma 693-712
  age at presentation 693
  chondroblastic 244, 245, 695, 700
  common mixed 695
  computed tomography findings 696-699
  definition 693
  differential diagnosis 705
  extraosseous *see* extraskeletal osteosarcoma
  fibroblastic 695
  frequency of occurrence 693
  gender ratio 693
  genetics 7, 696
  gross pathologic findings 694-695
    soft tissue 695
  "hair on end" pattern 184
  hands/feet 209
  histopathologic findings 695
  ICD-0 coded 693
  intracortical *see* intracortical osteosarcoma
  intramedullary 699, 700
  intra-osseous *see* intra-osseous osteosarcoma
  juxtacortical *see* juxtacortical osteosarcoma
  location 694
  MRI findings 699-704
    abnormal marrow signal 158, 159
    cortical destruction and extraosseous extension 134, 134
    intramedullary diaphyseal lesion 195, J95
    intramedullary metadiaphyseal lesions 184, 185
    preoperative evaluation 701
    response to chemotherapy 701-703
  multifocal 694
  multiple sclerotic 694
  osteoblastic 695
  Paget 694, 706
  parosteal *see* parosteal osteosarcoma
  periosteal *see* periosteal osteosarcoma
  plain film (roentgenogram) findings 696-699
  postradiation 693
  prognosis 705-710
  secondary 693, 698-699, 707
    MRI findings 703-704, 706, 709
  signs/symptoms 694
  skull/facial bones 20, 23
  small cell *see* small cell osteosarcoma
  spinal 42, 43
  subtypes 695
  "sunburst" pattern 184
  synchronous multicentric 694
  telangiectatic *see* telangiectatic osteosarcoma
  treatment 705-710
osteosarcomatosis 694
osteosclerotic myeloma 612
oxyhemoglobin 2

P

p53 protein 7
pachydermoperiostosis 90, 114
Paget disease 713-720
  active/initial phase 716, 738
  age at presentation 713
  basilar impression 734
  bone deformities 716, 738
  computed tomography findings 713-716, 714
  definition 713
  differential diagnosis 719
  frequency of occurrence 713
  genetics 713
  gross pathologic findings 713
  histopathologic findings 713
  intermediate phase 716
  ivory vertebrae 775, 716
  late/inactive phase 716
  location 713
  MRI findings 774, 775, 776, 716-719
    cortical thickening 112, 113, 716-718, 737, 738
    diffuse, multiple, poorly defined signal 216
    marrow signal 734, 718
  "picture frame pattern" 716, 737
  plain film (roentgenogram) findings 775, 716, 717, 778/
  prognosis 719
  skull/facial bones 34, 34
  treatment 719
Paget osteosarcoma 694, 706
Paget sarcoma
  computed tomography findings 716
  gross pathologic findings 713
  histopathologic findings 713
  location 713
  MRI findings 719, 779
    abnormal marrow signal 160, 167
    cortical destruction and extraosseous extension 138, 139
    intramedullary diaphyseal lesion 196, 797
  plain film (roentgenogram) findings 716
  prognosis 719
  signs/symptoms 713
  treatment 719
palmar fibromatosis *see* Dupuytren contracture
Panner disease 218
papillary hemangioendothelioma
  age at presentation 484
  definition 484
  gross pathologic findings 485
  histopathologic findings 486
  "hobnail" cellular shapes 486
  location 485
  "matchstick" cellular shapes 486
  prognosis 487
  signs/symptoms 485
papillary meningioma 595
paraganglia 270, 721
paraganglioma 721-725
  age at presentation 721
  computed tomography findings 722, 722
  definition 721
  differential diagnosis 723
  embolization 723
  familial 721
  frequency of occurrence 721
  functional 721
  genetics 722
  gross pathologic findings 722
  histopathologic findings 722
  jugulotympanic *see* glomus jugulare tumor
  location 721
  metastasis 723
  MRI findings 722, 722-724, 723, 724
    deep to subcutaneous fat 270, 271
    Gd-contrast enhancement 723
    intratumoral vessels 722, 722, 723
    "salt and pepper" pattern 291, 722
  paraspinal 68, 68
  peripheral nervous tissue 308, 309
  plain film (roentgenogram) findings 722
  prognosis 723
  signs/symptoms 721
  skull/facial bones 26, 27
  spinal *see* spinal paraganglioma
  sporadic 721
  superficial soft tissue 291
  surgical complications 723
  treatment 723
  vagal *see* vagal paraganglioma
paranasal sinus mucocele 32, 32
parasitic infection
  deep to subcutaneous fat 276, 277
  superficial soft tissue 300
paraspinal tumors/tumour-like lesions 64-75
  primary sarcomas 71, 73
parosteal lipoma
  bone cortex thickening 104
  location 543
  outer bone surface 82
parosteal osteoma 674
parosteal osteosarcoma 95, 95
  age at presentation 693
  computed tomography findings 697, 708
  dedifferentiated 695
  frequency of occurrence 693
  genetics 7, 696
  gross pathologic findings 694
  histopathologic findings 695
  metastasis 707
  MRI findings 697, 703, 707, 708
    bone cortex thickening 106, 107
  plain film (roentgenogram) findings 697
  prognosis 707
  treatment 707
  well-differentiated 695
Parsonage-Turner syndrome 318
pedal osteomyelitis 679, 681
Pediatric Oncology Group system, neuroblastoma 629

penumbra sign 112, 683
perfusion imaging 1
pericytes 502
pericytic tumors, WHO classification 4
perineural cyst *see* Tarlov cyst
perineural lipoma *see* fibrolipomatous hamartoma
periosteal abscess, pyogenic osteomyelitis 680
periosteal chondroma *see* juxtacortical chondroma
periosteal chondrosarcoma
definition 368
gross pathologic findings 368
histopathologic findings 369
location 368
MRI findings 242, 243
prognosis 376
treatment 376
periosteal desmoid *see* cortical desmoid
periosteal ganglion
age at presentation 456
computed tomography findings 457
definition 456
differential diagnosis 459
frequency of occurrence 456
gross pathologic findings 456
histopathologic findings 457
location 456
MRI findings 457, 460
plain film (roentgenogram) findings 457, 460
signs/symptoms 456
treatment 459
periosteal lipoma *see* parosteal lipoma
periosteal osteoid osteoma 78, 79
periosteal osteosarcoma
age at presentation 693
cartilage containing 244, 245
computed tomography findings 698
definition 693
frequency of occurrence 693
genetics 696
gross pathologic findings 694
histopathologic findings 695
location 694
MRI findings 703, 708
outer bone surface involving 96, 96
plain film (roentgenogram) findings 698, 708
prognosis 707
treatment 707
periosteal reaction 14
"hair on end"/perpendicular-oriented spicules 102, 702
interrupted
disorganized pattern 100, 101
sunburst/divergent pattern 100, 703
noninterrupted
bone formation and thyroid acropachy 115
hypervitaminosis A 92, 115
hypovitaminosis A 93, 115
hypovitaminosis C (scurvy) 93, 115
infantile cortical hyperostosis (Caffey disease) 92, 114
primary hypertrophic osteoarthropathy (pachydermoperiostosis) 90, 114
secondary hypertrophic osteoarthropathy 90, 114, 114
stress fracture-related 90, 93
venous stasis 92, 92
"onion skin"/multilayered/multilamellated 102, 102
periosteum, MRI appearance 2
periostitis, bone infarct 94, 94, 512
peripheral chondrosarcoma
computed tomography findings 369, 375
histopathologic findings 369
location 368
MRI findings 373, 375
plain film (roentgenogram) findings 369
prognosis 376
treatment 376
peripheral nervous tissue lesions 305-311
benign 305-308
malignant 308-314
perivascular tumors 4
"permeative" radiolucent pattern (type 3), bone tumors 14
pheochromocytomas 721
Philadelphia chromosome 532
physaliferous cells 379
pigmented villonodular synovitis (PVNS) 726-729
age at presentation 726
computed tomography findings 726
definition 469, 726
differential diagnosis 726
frequency of occurrence 726
genetics 726
gross pathologic findings 726
histopathologic findings 726
intra-articular nodular synovitis vs. 469
joint effusion 726, 728
within joints 248, 249
location 726
MRI findings 726, 727, 728
deep to subcutaneous fat 278, 279
outer bone surface 86, 87, 88, 89
plain film (roentgenogram) findings 726, 727, 728
prognosis 726
signs/symptoms 726
treatment 726
pituitary adenoma 26, 27
plantar fibromatosis
age at presentation 396
frequency of occurrence 396
gender ratio 396
gross pathologic findings 397
histopathologic findings 397
MRI findings 398, 399
prognosis 399
treatment 399
plasma cells, rheumatoid arthritis 738
plasmacytoma
computed tomography findings 612
definition 611
differential diagnosis 615
hands/feet 208
location 611
MRI findings 612, 612, 613, 614
abnormal marrow signal 156, 157
cortical destruction and extraosseous extension 132
intramedullary, tubular bone ends 170, 171
intramedullary diaphyseal lesions 194, 194
intramedullary metadiaphyseal lesions 184
well-circumscribed margins 148, 148
outer bone surface involving 98
plain film (roentgenogram) findings 612, 674
skull/facial bones 18, 19
spinal 38, 39
pleomorphic adenoma 288
pleomorphic carcinoma 288
pleomorphic hyalinizing angiectatic tumor (PHATs) 730-731
age at presentation 730
computed tomography findings 731
definition 730
differential diagnosis 731
genetics 730
gross pathologic findings 730
histopathologic findings 730
location 730
MRI findings 294, 295, 730, 731
plain film (roentgenogram) findings 731
prognosis 731
signs/symptoms 730
treatment 731
pleomorphic lipoma 266, 314, 543
age at presentation 543
gross pathologic findings 544
histopathologic findings 544
location 543
signs/symptoms 543
pleomorphic liposarcoma
age at presentation 554
computed tomography findings 556
differential diagnosis 557
genetics 555
histopathologic findings 555
location 554
MRI findings 320, 323, 556, 556, 558
deep to subcutaneous fat 260, 261
plain film (roentgenogram) findings 558
prognosis 557
superficial soft tissue 280
pleomorphic malignant fibrous histiocytoma
definition 584
frequency of occurrence 584
histopathologic findings 585
prognosis 588
treatment 588
pleomorphic myogenic sarcoma 585
pleomorphic rhabdomyosarcoma
age at presentation 732
classic variant 733
definition 732
genetics 733
gross pathologic findings 732
histopathologic findings 733
immunohistochemical findings 585
location 732
prognosis 735
round cell variant 733
signs/symptoms 732
spindle variant 733
treatment 735

plexiform neurofibroma
"bag of worms" appearance 633
definition 633
gross pathologic findings 633-634
histopathologic findings 634
MRI findings 84, 85, 634, 635, 636
deep to subcutaneous fat 270, 273
peripheral nervous tissue 305, 306
signs/symptoms 633
superficial soft tissue 291, 292
"target sign" 634
plexiform schwannoma 747
pneumonia, paraspinal 74, *74*
POEMS 612
polycythemia vera (PCV) 232, 233
polymorphic fibrocystic disease of bone *see* liposclerosing myxofibrous tumor
polymorphic fibro-osseous lesion of bone *see* liposclerosing myxofibrous tumor
popliteal cyst
age at presentation 759
children 759
computed tomography findings 759
differential diagnosis 760
frequency of occurrence 759
location 759
MRI findings 743, 760, 762
prognosis 760
ruptured 760
signs/symptoms 759
treatment 760
positron emitting tomography, Hodgkin disease 576
postradiation osteosarcoma 693
Pott disease 680
Preiser disease 218, 512
primary chondromatosis *see* synovial chondromatosis
primary extraneuraxial meningioma 594
primary neuraxial meningioma 594
computed tomography findings 595, 596
differential diagnosis 597
MRI findings 595-597, 596, 597, 598, 599
atypical features 595
calcification 595, 597, 598
edema 596, 597
plain film (roentgenogram) findings 595
primitive neuroectodermal tumor (PNET)
extracranial 308
definition 416
histopathologic findings 416
genetic abnormalities 7, 8
peripheral nervous tissue 308, 309
WHO classification 3
proliferating zone, bone 2
proliferative fasciitis *see* nodular fasciitis
proliferative synovitis (diffuse-type giant cell tumor of the tendon sheath) 469, 470, *474*
psammomatous meningioma 595
pseudoangiomatoid spaces 342
pseudoarthrosis, congenital *see* osteofibrous dysplasia
pseudogout 252
pseudohypoparathyroidism 217
pseudomalignant osseous tumor of soft tissue see myositis ossificans
pseudomeningocele, postsurgical 32, 33
pseudo-pseudohypoparathyroidism 217
pseudosarcomatous fasciitis *see* nodular fasciitis
pseudosarcomatous fibromatosis *see* nodular fasciitis
pseudosynovial cyst *see* ganglion cyst
pyogenic osteomyelitis
acute phase 680
children 679, 680
chronic active phase 683-684
computed tomography findings 680, 682
epidural abscess 72, 685
inflammation 680
location 679
long bones 680
MRI findings 681-684, 682, 683, 684-685, 685, 688, 691
Gd-contrast enhancement 681
treatment response evaluation 684
pathologic findings 680
periosteal abscess 680
phlegmons 685
plain film (roentgenogram) findings 680, 688
prognosis 691
radionuclide bone scan 681
signs/symptoms 680
skull/facial bones 30, 33
subacute phase 680, 681-683
treatment 691
vertebral 56, 56
pyogenic spondylodiskitis
computed tomography findings 681
location 679
plain film (roentgenogram) findings 681
signs/symptoms 680
pyogenic vertebral diskitis 56

Q

quadrilateral space syndrome 318

R

racemose hemangioma *see* arteriovenous hemangioma
radiation injury 224, 224
radiofrequency (RF) coils 1
radiography, bone tumors 13-14
reactive mesenchymal proliferation *see* myositis ossificans
red marrow 2
reconversion 211, 211
Reed-Sternberg cell 571
reflex sympathetic dystrophy (RSD) 218
regional migratory osteoporosis *see* transient bone marrow edema
renal osteodystrophy 216, 216
resting zone, bone 2
reticulum cell sarcoma 578
retiform hemangioendothelioma
age at presentation 484
gross pathologic findings 485
histopathologic findings 486
location 485
prognosis 487
signs/symptoms 485
retinoblastoma 696
retroperitoneal fibrosis 74
Revised European-American Classification of Lymphoid Neoplasms (R.E.A.L), non-Hodgkin lymphoma 570
rhabdoid meningioma 595
rhabdoid tumor, genetics 8
rhabdomyoblasts 732, 733
rhabdomyosarcoma 732-737
age at presentation 732
alveolar *see* alveolar rhabdomyosarcoma
computed tomography findings 733
definition 732
differential diagnosis 733
embryonal *see* embryonal rhabdomyosarcoma
frequency of occurrence 732
genetics 9, 733
gross pathologic findings 732
histopathologic findings 733
location 732
MRI findings 733, 734, 735, 736
deep to subcutaneous fat 264, 265
Gd-contrast enhancement 733, 734, 735, 736
hemorrhage 733, 734
superficial soft tissue 284, 285
plain film (roentgenogram) findings 733
pleomorphic *see* pleomorphic rhabdomyosarcoma
prognosis 733-735
signs/symptoms 732
skull/facial bones 22, 734
subtypes 732
superficial soft tissue 284, 285
treatment 733-735
rhabdosarcoma *see* rhabdomyosarcoma
rheumatoid arthritis 738-743
age at presentation 738
bone erosion 742
computed tomography findings 738, 739
definition 738
differential diagnosis 743
frequency of occurrence 738
genetics 738
histopathologic findings 738
hypertrophied synovium 250, 739, 739, 740, 741, 742, 743
inflammatory lesions 276, 277
joint effusions 740
ligament involvement 742
location 738
MRI findings 739, 739-742, 740, 741, 742, 743
basilar impression 740, 742
bone erosion 739
deep to subcutaneous fat 276, 277
Gd-contrast enhancement 739, 740, 742
within joints 250, 250, 253
late phases 740, 740, 743, 742, 743
plain film (roentgenogram) findings 738, 740, 743, 742
"rice bodies" 250, 253, 740, 743
signs/symptoms 738
spinal 58, 58, 739, 740, 742
superficial soft tissue 302, 303
synovitis 738
tendons 742
tendon sheaths 742, 743
treatment 743

rheumatoid factor 743
rheumatoid nodules 738, 740-742
rheumatoid pannus 88, 89
Rothmund-Thomson syndrome 696
round cell liposarcoma 555
  age at presentation 554
  differential diagnosis 557
  histopathologic findings 555
  location 554
  MRI findings 260, 320, 556
  prognosis 558
  superficial soft tissue 280
  treatment 558
rugger jersey vertebrae 216, 216

S

S-100 protein 6
saccular aneurysm
  deep to subcutaneous fat 275
  superficial soft tissue 298
sacral insufficiency fractures, bilateral 218, *219*
sacrococcygeal teratoma 770
  differential diagnosis 771
  MRI findings 772
  prognosis 771-773
  teratoma 771-773
sacroiliitis, bilateral 218, 279
sarcoid 744-746
  acute 744
  asymptomatic 744
  computed tomography findings 744
  definition 744
  differential diagnosis 746
  gross pathologic findings 744
  histopathologic findings 744
  insidious 744
  "lacy" radiolucent appearance 744
  location 744
  MRI findings 744-746
    axial skeleton 74-745
    bone 744-745, 745
    deep to subcutaneous fat 276, 277
    Gd-contrast enhancement 745, 745
    long bones 744-745
    skull 745, 745
    small bone 744
    soft tissue 745-746, 746
    superficial soft tissue 300, *301*
  musculoskeletal 744
  plain film (roentgenogram) findings 744
  prognosis 746
  signs/symptoms 744
  spinal 744
  subacute 744
  treatment 746
sarcoid granuloma 744
  subcutaneous fat 746, 746
sarcoidosis
  axial skeleton 222
  definition 744
  etiology 222
  frequency of occurrence 744
  hands/feet 206
  long bones 222
  MRI findings
    abnormal marrow signal 152
    cortical destruction and extraosseous extension 128, 129
    diffuse, multiple, poorly defined signal 222, 223
  skull/facial bones 32, 32
  small bones 222
  spinal 58, 59
sarcoma
  clear cell see clear cell sarcoma
  epithelioid 288, 288
  fibromyxoid 433, 434
  musculoskeletal system 10
  myofibroblastic 585
  pleomorphic myogenic 585
  soft tissue, bone eroding 98, 98
sarcomatoid chordoma 379
Schwann cells 270
schwannoma 747-752
  age at presentation 747
  Antoni A pattern 747
  Antoni B pattern 747
  cellular 747
  computed tomography findings 748
  definition 747
  differential diagnosis 748-749
  extremities 747, 749
  frequency of occurrence 747
  genetics 9, 747
  gross pathologic findings 747
  histopathologic findings 747
  intra-osseous 747
  location 747
  malignant *see* malignant peripheral nerve sheath tumor (MPNSTs)
  melanotic 747
  MRI findings 748, 748, 749, 750, 751
    deep to subcutaneous fat 270, 270
    Gd-contrast enhancement 748, 749, 750, 751
    superficial soft tissue 291, 292
  nonvestibular
    differential diagnosis 748
    prognosis 749
    signs/symptoms 747
    treatment 749
  outer bone surface 82, 83
  paraspinal 66, 66
  peripheral nervous tissue 305, 306
  plain film (roentgenogram) findings 748
  plexiform 747
  prognosis 749
  signs/symptoms 747
  spinal *see* spinal schwannoma
  subtypes 747
  treatment 749
  vestibular *see* vestibular schwannoma
schwannomatosis 747
schwannomin (merlin) gene product 748
sclerosing epithelioid fibrosarcoma 433, 434, 435
sclerosing osteomyelitis of Garre 112
  location 679
  pathologic findings 680
  plain film (roentgenogram) findings 681
scurvy (hypovitaminosis C) 93, 115
sebaceous cyst 294, 295
sebaceous glands 294
secondary chondromatosis *see* synovial chondromatosis
secretory meningioma 595
seminoma 770
sequestrum 680
seroma *see* hematoma
Shimada classification system, neuroblastoma 629
shoulder girdle lipomatosis 266, 312
sickle cell anemia
  bone infarct *183*
  diffuse, multiple, poorly defined and/or multifocal zones of abnormal marrow signal 212,232
  extramedullary hematopoiesis 130, 131
  skull/facial bones 35
sideroblastic anemia 212
simple bone cyst *see* unicameral bone cysts (UBCs)
simple (capillary) lymphangioma 566
sinonasal carcinoma 22, 23
sinus tract 683, 689
skeletal muscle tumors, WHO classification 4
skull fractures 34
skull tumors/tumor-like lesions 18-37
  acquired 32-34
  benign neoplasms 24-28
  congenital abnormalities 34-36
  inflammatory lesions 30-32
  malignant neoplasms 18-23
  traumatic 34
small cell osteosarcoma
  computed tomography findings 697
  MRI findings 698, 704
  plain film (roentgenogram) findings 697
small lymphocytic lymphoma *see* chronic lymphocytic leukemia (CLL)
smooth muscle tumors, WHO classification 3, 4
soft tissue ganglion
  age at presentation 456
  computed tomography findings 457
  definition 456
  differential diagnosis 459
  frequency of occurrence 456
  gross pathologic findings 456
  histopathologic findings 457
  location 456
  MRI findings 458, 459, 460, 461
  plain film (roentgenogram) findings 457
  signs/symptoms 456
  treatment 459
soft tissue lipoma
  age at presentation 543
  computed tomography findings 544
  differential diagnosis 551
  frequency of occurrence 543
  gross pathologic findings 544
  histopathologic findings 544
  location 543
  MRI findings 312, 313, 546, 546-549, 547
    deep 546, 546, 547
    superficial 288, 289, 546, 546
  plain film (roentgenogram) findings 544, 547
  signs/symptoms 543
  treatment 551
soft tissue sarcoma, bone eroding 98, 98

soft tissue tumors/tumor-like lesions
deep to subcutaneous fat 258-279
inflammatory 276-278
neoplastic benign 266-272
neoplastic malignant 258-266
tumor-like lesions 272-275
frequency of occurrence 10
benign tumors 10, 11
malignant tumors 11
genetic abnormalities 8-9
grading 12
imaging evaluation 13-15
immunohistochemical markers 3, 5-7
MRI 14-15
staging 12
superficial 280-304
inflammatory 298-302
neoplastic-benign 288-294
neoplastic-malignant 280-288
tumor-like lesions 294-298
WHO classification 3-5
solitary bone cyst *see* unicameral bone cysts (UBCs)
solitary fibrous tumor (SFT) 430-432
age at presentation 430
computed tomography findings 430, 437
definition 430
differential diagnosis 430
extrapleural 430
frequency of occurrence 430
genetics 430
gross pathologic findings 430
histopathologic findings 430
immunoreactivity 430
location 430
malignant 430
MRI findings 430, *431*
deep to subcutaneous fat 270, *271*
plain film (roentgenogram) findings 430
prognosis 430
signs/symptoms 430
treatment 430
spina bifida 62, 63, 312
spinal angiolipoma 316
spinal paraganglioma
differential diagnosis 723
extradural 721
location 721
MRI findings 723, 724
spinal schwannoma
differential diagnosis 749
MRI findings 750
prognosis 749
signs/symptoms 747
treatment 749
spinal synovial cyst
age at presentation 759
differential diagnosis 760
frequency of occurrence 759
location 759
MRI findings 52, 52, 76, 759, 760, 761
postoperative MRI 760
prognosis 760
signs/symptoms 759
treatment 760
spinal teratoma 770
differential diagnosis 771
prognosis 773
treatment 773
spinal tumors/tumorlike lesions 38-63
congenital 60-62
degenerative changes 54
hematopoietic 58-60
infection 56-58
inflammation 56-58
neoplasms 38-48
traumatic 54
spindle cell(s) 272
spindle cell hemangioendotheliomas
age at presentation 484
definition 484
gross pathologic findings 485
histopathologic findings 486
location 485
prognosis 487
signs/symptoms 485
spindle cell lipoma 266, 314
age at presentation 543
definition 543
frequency of occurrence 543
genetic abnormalities 9
gross pathologic findings 544
histopathologic findings 544
location 543
signs/symptoms 543
spindle neuroma 305
spin lattice relaxation 1
spin spin relaxation 1
sporotrichosis, osteomyelitis 681
spotted bone disease *see* osteopoildlosis
squamous cell sarcoma 282, 2S3
Staphylococcus aureus, osteomyelitis 679
STIR, malignant peripheral nerve sheath tumor 640
storiform-pleomorphic malignant fibrous histiocytoma 585, 589
Streptococcus pyogenes, osteomyelitis 679
stress fracture
intramedullary diaphyseal lesion 189, *189*
intramedullary metadiaphyseal lesions 180, *181*
stromal cells, giant cell tumor of bone 462
subchondral cyst *see* geode
subperiosteal hematoma 90, *91*
subperiosteal osteoid osteoma
computed tomography findings 661, 664, 665
differential diagnosis 667
MRI findings 661, 665, 666
plain film (roentgenogram) findings 661, 664, 665
Sucquet-Hoyer canal 476
Sudek atrophy 218
surface chondroma *see* juxtacortical chondroma
sustentacular cells, paraganglioma 722
syndromes of hyperostosis, osteitis, and skin lesions (SAPHO syndrome) 93, 115
synovial cell sarcoma
deep to subcutaneous fat 262, 263
superficial soft tissue 282, 2S3
synovial chondroma 238, 248, 753
synovial chondromatosis 753-757
age at presentation 753
calcification 754, 755, 756
computed tomography findings 753-754
definition 753
differential diagnosis 757
frequency of occurrence 753
gross pathologic findings 753
histopathologic findings 753
within joints 248, 248, 249
location 753
MRI findings 754, 755, 756, 757
plain film (roentgenogram) findings 753-754, 754, 755, 756
primary 239, 248, 248, 249, 753, 754, 757
prognosis 757
secondary 238, 248, 753, 756
signs/symptoms 753
treatment 757
synovial chondrometaplasia *see* synovial chondromatosis
synovial chondrosarcoma 256
synovial cyst 759-762
age at presentation 759
computed tomography findings 759
definition 759
differential diagnosis 760
frequency of occurrence 759
location 759
MRI findings 759-760, 760, 760, 761, 762
outer bone surface 76, 77
pathologic findings 759
prognosis 760
signs/symptoms 759
spinal *see* spinal synovial cyst
treatment 760
synovial granulomas 479
synovial hemangioma 252, 253, 491, 500
synovial lipoma, diffuse *see* lipoma arborescens
synovial osteochondromas 238, 247, 247
synovial osteochondromatosis
definition 753
within joints 247, 247
MRI findings 238
primary 247
prognosis 753-757, 757
secondary 247
treatment 757
synovial sarcoma 763-769
age at presentation 763
calcification 763
children 766
computed tomography findings 763, 765, 767
definition 763
differential diagnosis 766
frequency of occurrence 763
genetics 9, 763, 766
gross pathologic findings 763
head and neck 766
hemangiopericytoma vs. 502
histopathologic findings 763
intra-osseous tumor invasion 763
location 763
monophasic 763
MRI findings 764, 764-766, 765, 766, 767, 768
Gd-contrast enhancement 764, 765, 766, 766, 767
hemorrhage 764, 764-765, 767, 768
plain film (roentgenogram) findings 763
prognosis 766

signs/symptoms 763
treatment 766
SYT-SSX1 fusion gene 763, 766

T

Tl relaxation 1
T2 relaxation 1
"target sign," plexiform neurofibroma 84, 634
Tarlov cyst
outer bone surface 84, *85*
spinal 48, 49
T cell lymphoma *283*
telangiectatic osteosarcoma
age at presentation 693
computed tomography findings 697
frequency of occurrence 693
genetics 696
gross pathologic findings 694
histopathologic findings 695
location 694
MRI findings 701, 705, 706
plain film (roentgenogram) findings 697, 705, 706
telomeric association, giant cell tumor of bone 462-463
tenosynovial chondroma 753
tenosynovial giant cell tumor *see* giant cell tumor of the tendon sheath
tenosynovitis 302
teratoma 770-773
age at presentation 770
benign 770
computed tomography findings 770-771, 771
congenital 770
definition 770
differential diagnosis 771
extragonadal 770
fat containing 318, 319
frequency of occurrence 770
genetics 770
gross pathologic findings 770
head and neck 770, 773
histopathologic findings 770
immature 770
intracranial 770, 773
location 770
malignant 770
MRI findings 318, 319, 771, 771, 772
paraspinal 72, 73
plain film (roentgenogram) findings 770-771, 771
prognosis 771-772
sacrococcygeal *see* sacrococcygeal teratoma
signs/symptoms 770
treatment 771-773
terminal neuroma 305
thalassemia 212,213
p-thalassemia 212
p-thalassemia 213
Thiemann disease 512
thyroid dermopathy 92
Tinelsign 642
tinnitus, glomus tumors 721
TNM system, soft tissue tumor staging 12, 13
tophi 479
hands/feet 206, 207
within joints 250, 251
MRI findings *482-483*
superficial soft tissue 300, 301
transfusions, multiple 214
transient bone marrow edema
abnormal marrow signal 150, 151
biopsy 150
intramedullary, tubular bone ends 168, 169
therapy 150
transient osteoporosis of the hip *see* transient bone marrow edema
transverse relaxation 1
traumatic neuroma 307, 642-644
definition 642
differential diagnosis 642
gross pathologic findings 642
histopathologic findings 642
location 642
MRI findings 642, 642, 643, 644
peripheral nervous tissue 305, 307
prognosis 642
signs/symptoms 642
treatment 642
traumatic vertebral fracture 54, 55
Trevor disease (dysplasia epiphysealis hemimelica) 645
Triton tumor 634
tuberculous osteomyelitis
cold abscesses 680, 686, 6S7
computed tomography findings 681, *686-687, 688*
epidural abscess 72
extra-axial 679, 686-689
location 679
MRI findings 685-689, 686-687, *688*
pathologic findings 680
plain film (roentgenogram) findings 681
prognosis 691
signs/symptoms 680
spinal 680
treatment 691
vertebral 57, 57
tuberculous spondylodiskitis 685-686, 686, 687
tumoral calcinosis 275, 275
tumors of uncertain differentiation, WHO classification 4-5
Turcot syndrome 400

U

undifferentiated pleomorphic sarcoma *see* malignant fibrous histiocytoma
unicameral bone cysts (UBCs) 334-339
age at presentation 334
computed tomography findings 334
definition 334
differential diagnosis 334
"fallen-leaf fracture fragments 334, 337
frequency of occurrence 334
genetics 334
gross pathologic findings 334
hands/feet 204, 205
histopathologic findings 334
location 334
MRI findings 334, 335, 336, 337, 33S, 339
intramedullary, intact cortical margin expansion 118, 119
intramedullary, well-circumscribed margins 142, 143
intramedullary metadiaphyseal lesions 176, 177
pathologic fractures 334, 338, 339
plain film (roentgenogram) findings 334, 335, 336, 337, 338, 339
prognosis 338
signs/symptoms 334
treatment 338
United Stated National Cancer Institute (NCI) system, soft tissue tumor staging 12
urate levels, gout 479

V

vagal paraganglioma
age at presentation 721
differential diagnosis 723
histopathologic findings 722
location 721
signs/symptoms 721
vascular hamartomas *see* hemangioma
vascular leiomyoma *see* angioleiomyomas
vascular tumors, WHO classification 3, 4
vasomotor disturbances, osteoid osteoma 660
venous hemangioma 491
Vernet (jugular foramen) syndrome 721
Verocay bodies 747
vertebral fractures 54, 55
traumatic 54, 55
vertebral osteomyelitis/diskitis *see* pyogenic spondylodiskitis
vestibular schwannoma
differential diagnosis 748
prognosis 749
signs/symptoms 747
treatment 749
vimentin 7
vitamin A intoxication 92
von Recklinghausen disease *see* neurofibromatosis type 1

W

Waldenstrom macroglobulinemia 232, 233
well-differentiated liposarcoma 320, 320
age at presentation 554
amputation 557
computed tomography findings 557
genetics 555
histopathologic findings 555
location 554
MRI findings 555-556, 557
deep to subcutaneous fat 259, 259
prognosis 557
superficial soft tissue 280
treatment 557
Werner syndrome 696
WHO *see* World Health Organization (WHO)
World Health Organization (WHO)
bone tumor classification 3
soft tissue tumor classification 3

X

xanthelasmas 413
xanthoma 774-775
  age at presentation 774
  computed tomography findings 774
  deep to subcutaneous fat 278
  definition 774
  differential diagnosis 775
  fat containing 318, 774, 775
  fibrous *see* giant cell tumor of the tendon sheath
  gross pathologic findings 774
  histopathologic findings 774
  location 774
  MRI findings 774, 774-775, 775
  plain film (roentgenogram) findings 774
  prognosis 775
  signs/symptoms 774
  superficial soft tissue 302, 774, 775
  tendons 278, 302, 774, 775
  treatment 775
xanthoma cells 439, 469
xanthosarcoma see malignant fibrous histiocytoma (MFH)

Y

yellow (hematopoeitically-inactive fatty) marrow 2

Z

zeballen 722
zone of provisional calcification 2